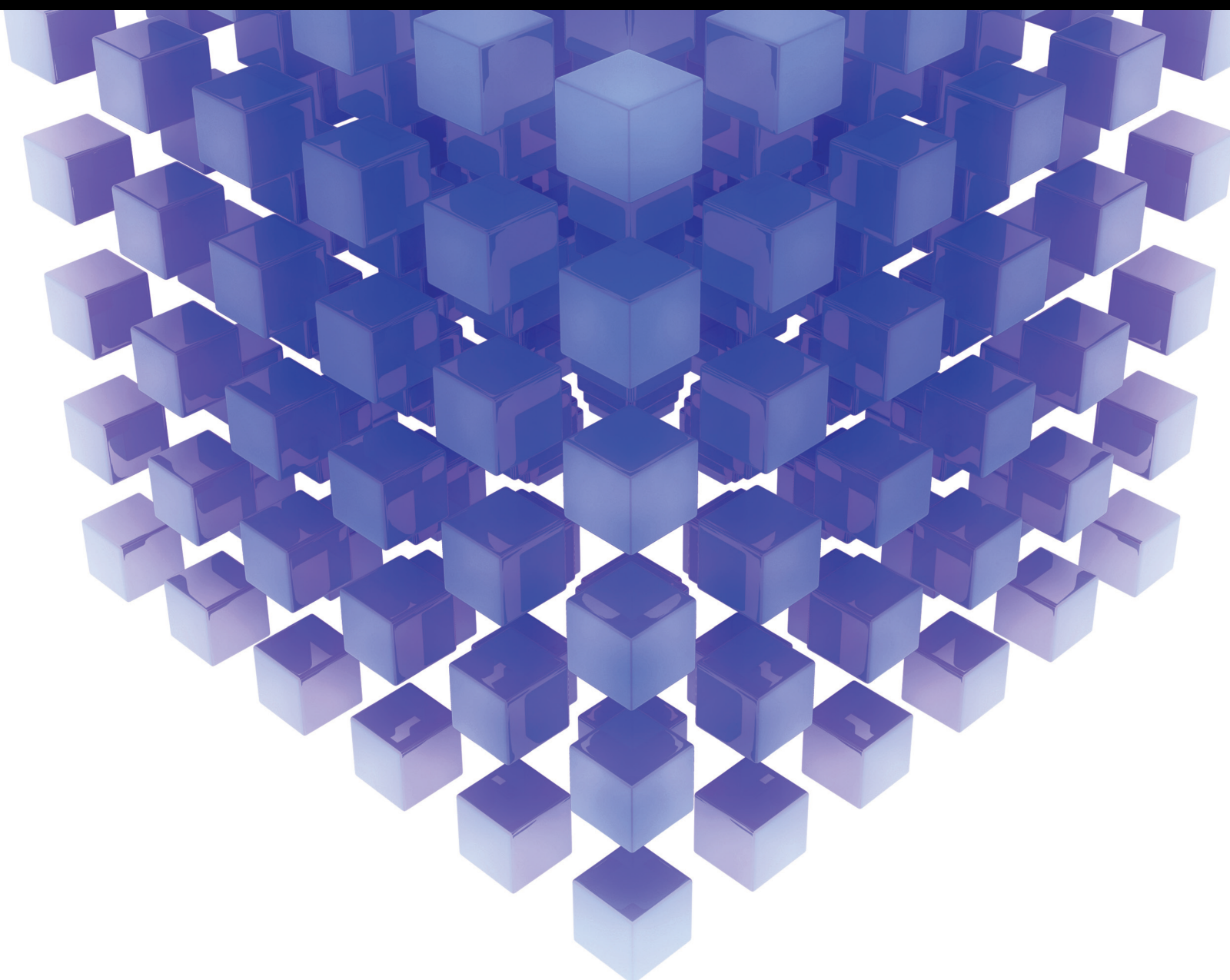


Mathematical Problems in Engineering

Artificial Intelligence Edge Computing for Innovative Applications

Lead Guest Editor: Wei Liu

Guest Editors: Xuefeng Shao and Yuan-Jun Zhao





Artificial Intelligence Edge Computing for Innovative Applications

Mathematical Problems in Engineering

Artificial Intelligence Edge Computing for Innovative Applications

Lead Guest Editor: Wei Liu


Guest Editors: Xuefeng Shao and Yuan-Jun Zhao



Copyright © 2023 Hindawi Limited. All rights reserved.

This is a special issue published in “Mathematical Problems in Engineering.” All articles are open access articles distributed under the Creative Commons Attribution License, which permits unrestricted use, distribution, and reproduction in any medium, provided the original work is properly cited.

Chief Editor

Guangming Xie , China

Academic Editors

Kumaravel A , India
Waqas Abbasi, Pakistan
Mohamed Abd El Aziz , Egypt
Mahmoud Abdel-Aty , Egypt
Mohammed S. Abdo, Yemen
Mohammad Yaghoub Abdollahzadeh
Jamalabadi , Republic of Korea
Rahib Abiyev , Turkey
Leonardo Acho , Spain
Daniela Addessi , Italy
Arooj Adeel , Pakistan
Waleed Adel , Egypt
Ramesh Agarwal , USA
Francesco Aggogeri , Italy
Ricardo Aguilar-Lopez , Mexico
Afaq Ahmad , Pakistan
Naveed Ahmed , Pakistan
Elias Aifantis , USA
Akif Akgul , Turkey
Tareq Al-shami , Yemen
Guido Ala, Italy
Andrea Alaimo , Italy
Reza Alam, USA
Osamah Albahri , Malaysia
Nicholas Alexander , United Kingdom
Salvatore Alfonzetti, Italy
Ghous Ali , Pakistan
Nouman Ali , Pakistan
Mohammad D. Aliyu , Canada
Juan A. Almendral , Spain
A.K. Alomari, Jordan
José Domingo Álvarez , Spain
Cláudio Alves , Portugal
Juan P. Amezcua-Sanchez, Mexico
Mukherjee Amitava, India
Lionel Amodeo, France
Sebastian Anita, Romania
Costanza Arico , Italy
Sabri Arik, Turkey
Fausto Arpino , Italy
Rashad Asharabi , Saudi Arabia
Farhad Aslani , Australia
Mohsen Asle Zaem , USA

Andrea Avanzini , Italy
Richard I. Avery , USA
Viktor Avrutin , Germany
Mohammed A. Awadallah , Malaysia
Francesco Aymerich , Italy
Sajad Azizi , Belgium
Michele Baccocchi , Italy
Seungik Baek , USA
Khaled Bahlali, France
M.V.A Raju Bahubalendruni, India
Pedro Balaguer , Spain
P. Balasubramaniam, India
Stefan Balint , Romania
Ines Tejado Balsera , Spain
Alfonso Banos , Spain
Jerzy Baranowski , Poland
Tudor Barbu , Romania
Andrzej Bartoszewicz , Poland
Sergio Baselga , Spain
S. Caglar Baslamisli , Turkey
David Bassir , France
Chiara Bedon , Italy
Azeddine Beghdadi, France
Andriette Bekker , South Africa
Francisco Beltran-Carbajal , Mexico
Abdellatif Ben Makhlof , Saudi Arabia
Denis Benasciutti , Italy
Ivano Benedetti , Italy
Rosa M. Benito , Spain
Elena Benvenuti , Italy
Giovanni Berselli, Italy
Michele Betti , Italy
Pietro Bia , Italy
Carlo Bianca , France
Simone Bianco , Italy
Vincenzo Bianco, Italy
Vittorio Bianco, Italy
David Bigaud , France
Sardar Muhammad Bilal , Pakistan
Antonio Bilotta , Italy
Sylvio R. Bistafa, Brazil
Chiara Boccaletti , Italy
Rodolfo Bontempo , Italy
Alberto Borboni , Italy
Marco Bortolini, Italy

Paolo Boscariol, Italy
Daniela Boso , Italy
Guillermo Botella-Juan, Spain
Abdesselem Boulkroune , Algeria
Boulaïd Boulkroune, Belgium
Fabio Bovenga , Italy
Francesco Braghin , Italy
Ricardo Branco, Portugal
Julien Bruchon , France
Matteo Bruggi , Italy
Michele Brun , Italy
Maria Elena Bruni, Italy
Maria Angela Butturi , Italy
Bartłomiej Błachowski , Poland
Dhanamjayulu C , India
Raquel Caballero-Águila , Spain
Filippo Cacace , Italy
Salvatore Caddemi , Italy
Zuowei Cai , China
Roberto Caldelli , Italy
Francesco Cannizzaro , Italy
Maosen Cao , China
Ana Carpio, Spain
Rodrigo Carvajal , Chile
Caterina Casavola, Italy
Sara Casciati, Italy
Federica Caselli , Italy
Carmen Castillo , Spain
Inmaculada T. Castro , Spain
Miguel Castro , Portugal
Giuseppe Catalanotti , United Kingdom
Alberto Cavallo , Italy
Gabriele Cazzulani , Italy
Fatih Vehbi Celebi, Turkey
Miguel Cerrolaza , Venezuela
Gregory Chagnon , France
Ching-Ter Chang , Taiwan
Kuei-Lun Chang , Taiwan
Qing Chang , USA
Xiaoheng Chang , China
Prasenjit Chatterjee , Lithuania
Kacem Chehdi, France
Peter N. Cheimets, USA
Chih-Chiang Chen , Taiwan
He Chen , China



































Kebing Chen , China
Mengxin Chen , China
Shyi-Ming Chen , Taiwan
Xizhong Chen , Ireland
Xue-Bo Chen , China
Zhiwen Chen , China
Qiang Cheng, USA
Zeyang Cheng, China
Luca Chiapponi , Italy
Francisco Chicano , Spain
Tirivanhu Chinyoka , South Africa
Adrian Chmielewski , Poland
Seongim Choi , USA
Gautam Choubey , India
Hung-Yuan Chung , Taiwan
Yusheng Ci, China
Simone Cinquemani , Italy
Roberto G. Citarella , Italy
Joaquim Ciurana , Spain
John D. Clayton , USA
Piero Colajanni , Italy
Giuseppina Colicchio, Italy
Vassilios Constantoudis , Greece
Enrico Conte, Italy
Alessandro Contento , USA
Mario Cools , Belgium
Gino Cortellessa, Italy
Carlo Cosentino , Italy
Paolo Crippa , Italy
Erik Cuevas , Mexico
Guozeng Cui , China
Mehmet Cunkas , Turkey
Giuseppe D'Aniello , Italy
Peter Dabnichki, Australia
Weizhong Dai , USA
Zhifeng Dai , China
Purushothaman Damodaran , USA
Sergey Dashkovskiy, Germany
Adiel T. De Almeida-Filho , Brazil
Fabio De Angelis , Italy
Samuele De Bartolo , Italy
Stefano De Miranda , Italy
Filippo De Monte , Italy

José António Fonseca De Oliveira
Correia , Portugal
Jose Renato De Sousa , Brazil
Michael Defoort, France
Alessandro Della Corte, Italy
Laurent Dewasme , Belgium
Sanku Dey , India
Gianpaolo Di Bona , Italy
Roberta Di Pace , Italy
Francesca Di Puccio , Italy
Ramón I. Diego , Spain
Yannis Dimakopoulos , Greece
Hasan Dinçer , Turkey
José M. Domínguez , Spain
Georgios Dounias, Greece
Bo Du , China
Emil Dumic, Croatia
Madalina Dumitriu , United Kingdom
Premraj Durairaj , India
Saeed Eftekhar Azam, USA
Said El Kafhali , Morocco
Antonio Elipe , Spain
R. Emre Erkmen, Canada
John Escobar , Colombia
Leandro F. F. Miguel , Brazil
FRANCESCO FOTI , Italy
Andrea L. Facci , Italy
Shahla Faisal , Pakistan
Giovanni Falsone , Italy
Hua Fan, China
Jianguang Fang, Australia
Nicholas Fantuzzi , Italy
Muhammad Shahid Farid , Pakistan
Hamed Faruqi, Iran
Yann Favennec, France
Fiorenzo A. Fazzolari , United Kingdom
Giuseppe Fedele , Italy
Roberto Fedele , Italy
Baowei Feng , China
Mohammad Ferdows , Bangladesh
Arturo J. Fernández , Spain
Jesus M. Fernandez Oro, Spain
Francesco Ferrise, Italy
Eric Feulvarch , France
Thierry Floquet, France

Eric Florentin , France
Gerardo Flores, Mexico
Antonio Forcina , Italy
Alessandro Formisano, Italy
Francesco Franco , Italy
Elisa Francomano , Italy
Juan Frausto-Solis, Mexico
Shujun Fu , China
Juan C. G. Prada , Spain
HECTOR GOMEZ , Chile
Matteo Gaeta , Italy
Mauro Gaggero , Italy
Zoran Gajic , USA
Jaime Gallardo-Alvarado , Mexico
Mosè Gallo , Italy
Akemi Gálvez , Spain
Maria L. Gandarias , Spain
Hao Gao , Hong Kong
Xingbao Gao , China
Yan Gao , China
Zhiwei Gao , United Kingdom
Giovanni Garcea , Italy
José García , Chile
Harish Garg , India
Alessandro Gasparetto , Italy
Stylianios Georgantzinou, Greece
Fotios Georgiades , India
Parviz Ghadimi , Iran
Ştefan Cristian Gherghina , Romania
Georgios I. Giannopoulos , Greece
Agathoklis Giaralis , United Kingdom
Anna M. Gil-Lafuente , Spain
Ivan Giorgio , Italy
Gaetano Giunta , Luxembourg
Jefferson L.M.A. Gomes , United Kingdom
Emilio Gómez-Déniz , Spain
Antonio M. Gonçalves de Lima , Brazil
Qunxi Gong , China
Chris Goodrich, USA
Rama S. R. Gorla, USA
Veena Goswami , India
Xunjie Gou , Spain
Jakub Grabski , Poland

Antoine Grall , France
George A. Gravvanis , Greece
Fabrizio Greco , Italy
David Greiner , Spain
Jason Gu , Canada
Federico Guarracino , Italy
Michele Guida , Italy
Muhammet Gul , Turkey
Dong-Sheng Guo , China
Hu Guo , China
Zhaoxia Guo, China
Yusuf Gurefe, Turkey
Salim HEDDAM , Algeria
ABID HUSSANAN, China
Quang Phuc Ha, Australia
Li Haitao , China
Petr Hájek , Czech Republic
Mohamed Hamdy , Egypt
Muhammad Hamid , United Kingdom
Renke Han , United Kingdom
Weimin Han , USA
Xingsi Han, China
Zhen-Lai Han , China
Thomas Hanne , Switzerland
Xinan Hao , China
Mohammad A. Hariri-Ardebili , USA
Khalid Hattaf , Morocco
Defeng He , China
Xiao-Qiao He, China
Yanchao He, China
Yu-Ling He , China
Ramdane Hedjar , Saudi Arabia
Jude Hemanth , India
Reza Hemmati, Iran
Nicolae Herisanu , Romania
Alfredo G. Hernández-Díaz , Spain
M.I. Herreros , Spain
Eckhard Hitzer , Japan
Paul Honeine , France
Jaromir Horacek , Czech Republic
Lei Hou , China
Yingkun Hou , China
Yu-Chen Hu , Taiwan
Yunfeng Hu, China
Can Huang , China
Gordon Huang , Canada
Linsheng Huo , China
Sajid Hussain, Canada
Asier Ibeas , Spain
Orest V. Iftime , The Netherlands
Przemyslaw Ignaciuk , Poland
Giacomo Innocenti , Italy
Emilio Insfran Pelozo , Spain
Azeem Irshad, Pakistan
Alessio Ishizaka, France
Benjamin Ivorra , Spain
Breno Jacob , Brazil
Reema Jain , India
Tushar Jain , India
Amin Jajarmi , Iran
Chiranjibe Jana , India
Łukasz Jankowski , Poland
Samuel N. Jator , USA
Juan Carlos Jáuregui-Correa , Mexico
Kandasamy Jayakrishna, India
Reza Jazar, Australia
Khalide Jbilou, France
Isabel S. Jesus , Portugal
Chao Ji , China
Qing-Chao Jiang , China
Peng-fei Jiao , China
Ricardo Fabricio Escobar Jiménez , Mexico
Emilio Jiménez Macías , Spain
Maolin Jin, Republic of Korea
Zhuo Jin, Australia
Ramash Kumar K , India
BHABEN KALITA , USA
MOHAMMAD REZA KHEDMATI , Iran
Viacheslav Kalashnikov , Mexico
Mathiyalagan Kalidass , India
Tamas Kalmar-Nagy , Hungary
Rajesh Kaluri , India
Jyottheswara Reddy Kalvakurthi, India
Zhao Kang , China
Ramani Kannan , Malaysia
Tomasz Kapitaniak , Poland
Julius Kaplunov, United Kingdom
Konstantinos Karamanos, Belgium
Michal Kawulok, Poland

Irfan Kaymaz , Turkey
Vahid Kayvanfar , Qatar
Krzysztof Kecik , Poland
Mohamed Khader , Egypt
Chaudry M. Khalique , South Africa
Mukhtaj Khan , Pakistan
Shahid Khan , Pakistan
Nam-Il Kim, Republic of Korea
Philipp V. Kiryukhantsev-Korneev ,
Russia
P.V.V Kishore , India
Jan Koci , Czech Republic
Ioannis Kostavelis , Greece
Sotiris B. Kotsiantis , Greece
Frederic Kratz , France
Vamsi Krishna , India
Edyta Kucharska, Poland
Krzysztof S. Kulpa , Poland
Kamal Kumar, India
Prof. Ashwani Kumar , India
Michal Kunicki , Poland
Cedrick A. K. Kwuimy , USA
Kyandoghere Kyamakya, Austria
Ivan Kyrchei , Ukraine
Márcio J. Lacerda , Brazil
Eduardo Lalla , The Netherlands
Giovanni Lancioni , Italy
Jaroslaw Latalski , Poland
Hervé Laurent , France
Agostino Lauria , Italy
Aimé Lay-Ekuakille , Italy
Nicolas J. Leconte , France
Kun-Chou Lee , Taiwan
Dimitri Lefebvre , France
Eric Lefevre , France
Marek Lefik, Poland
Yaguo Lei , China
Kauko Leiviskä , Finland
Ervin Lenzi , Brazil
ChenFeng Li , China
Jian Li , USA
Jun Li , China
Yueyang Li , China
Zhao Li , China































Zhen Li , China
En-Qiang Lin, USA
Jian Lin , China
Qibin Lin, China
Yao-Jin Lin, China
Zhiyun Lin , China
Bin Liu , China
Bo Liu , China
Heng Liu , China
Jianxu Liu , Thailand
Lei Liu , China
Sixin Liu , China
Wanquan Liu , China
Yu Liu , China
Yuanchang Liu , United Kingdom
Bonifacio Llamazares , Spain
Alessandro Lo Schiavo , Italy
Jean Jacques Loiseau , France
Francesco Lolli , Italy
Paolo Lonetti , Italy
António M. Lopes , Portugal
Sebastian López, Spain
Luis M. López-Ochoa , Spain
Vassilios C. Loukopoulos, Greece
Gabriele Maria Lozito , Italy
Zhiguo Luo , China
Gabriel Luque , Spain
Valentin Lychagin, Norway
YUE MEI, China
Junwei Ma , China
Xuanlong Ma , China
Antonio Madeo , Italy
Alessandro Magnani , Belgium
Toqeer Mahmood , Pakistan
Fazal M. Mahomed , South Africa
Arunava Majumder , India
Sarfranz Nawaz Malik, Pakistan
Paolo Manfredi , Italy
Adnan Maqsood , Pakistan
Muazzam Maqsood, Pakistan
Giuseppe Carlo Marano , Italy
Damijan Markovic, France
Filipe J. Marques , Portugal
Luca Martinelli , Italy
Denizar Cruz Martins, Brazil

Francisco J. Martos , Spain
Elio Masciari , Italy
Paolo Massioni , France
Alessandro Mauro , Italy
Jonathan Mayo-Maldonado , Mexico
Pier Luigi Mazzeo , Italy
Laura Mazzola, Italy
Driss Mehdi , France
Zahid Mehmood , Pakistan
Roderick Melnik , Canada
Xiangyu Meng , USA
Jose Merodio , Spain
Alessio Merola , Italy
Mahmoud Mesbah , Iran
Luciano Mescia , Italy
Laurent Mevel , France
Constantine Michailides , Cyprus
Mariusz Michta , Poland
Prankul Middha, Norway
Aki Mikkola , Finland
Giovanni Minafò , Italy
Edmondo Minisci , United Kingdom
Hiroyuki Mino , Japan
Dimitrios Mitsotakis , New Zealand
Ardashir Mohammadzadeh , Iran
Francisco J. Montáns , Spain
Francesco Montefusco , Italy
Gisele Mophou , France
Rafael Morales , Spain
Marco Morandini , Italy
Javier Moreno-Valenzuela , Mexico
Simone Morganti , Italy
Caroline Mota , Brazil
Aziz Moukrim , France
Shen Mouquan , China
Dimitris Mourtzis , Greece
Emiliano Mucchi , Italy
Taseer Muhammad, Saudi Arabia
Ghulam Muhiuddin, Saudi Arabia
Amitava Mukherjee , India
Josefa Mula , Spain
Jose J. Muñoz , Spain
Giuseppe Muscolino, Italy
Marco Mussetta , Italy

Hariharan Muthusamy, India
Alessandro Naddeo , Italy
Raj Nandkeolyar, India
Keivan Navaie , United Kingdom
Soumya Nayak, India
Adrian Neagu , USA
Erivelton Geraldo Nepomuceno , Brazil
AMA Neves, Portugal
Ha Quang Thinh Ngo , Vietnam
Nhon Nguyen-Thanh, Singapore
Papakostas Nikolaos , Ireland
Jelena Nikolic , Serbia
Tatsushi Nishi, Japan
Shanzhou Niu , China
Ben T. Nohara , Japan
Mohammed Nouari , France
Mustapha Nourelfath, Canada
Kazem Nouri , Iran
Ciro Núñez-Gutiérrez , Mexico
Włodzimierz Ogryczak, Poland
Roger Ohayon, France
Krzysztof Okarma , Poland
Mitsuhiro Okayasu, Japan
Murat Olgun , Turkey
Diego Oliva, Mexico
Alberto Olivares , Spain
Enrique Onieva , Spain
Calogero Orlando , Italy
Susana Ortega-Cisneros , Mexico
Sergio Ortobelli, Italy
Naohisa Otsuka , Japan
Sid Ahmed Ould Ahmed Mahmoud , Saudi Arabia
Taoreed Owolabi , Nigeria
EUGENIA PETROPOULOU , Greece
Arturo Pagano, Italy
Madhumangal Pal, India
Pasquale Palumbo , Italy
Dragan Pamučar, Serbia
Weifeng Pan , China
Chandan Pandey, India
Rui Pang, United Kingdom
Jürgen Pannek , Germany
Elena Panteley, France
Achille Paolone, Italy

George A. Papakostas , Greece
Xosé M. Pardo , Spain
You-Jin Park, Taiwan
Manuel Pastor, Spain
Pubudu N. Pathirana , Australia
Surajit Kumar Paul , India
Luis Payá , Spain
Igor Pažanin , Croatia
Libor Pekař , Czech Republic
Francesco Pellicano , Italy
Marcello Pellicciari , Italy
Jian Peng , China
Mingshu Peng, China
Xiang Peng , China
Xindong Peng, China
Yuexing Peng, China
Marzio Pennisi , Italy
Maria Patrizia Pera , Italy
Matjaz Perc , Slovenia
A. M. Bastos Pereira , Portugal
Wesley Peres, Brazil
F. Javier Pérez-Pinal , Mexico
Michele Perrella, Italy
Francesco Pesavento , Italy
Francesco Petrini , Italy
Hoang Vu Phan, Republic of Korea
Lukasz Pieczonka , Poland
Dario Piga , Switzerland
Marco Pizzarelli , Italy
Javier Plaza , Spain
Goutam Pohit , India
Dragan Poljak , Croatia
Jorge Pomares , Spain
Hiram Ponce , Mexico
Sébastien Poncet , Canada
Volodymyr Ponomaryov , Mexico
Jean-Christophe Ponsart , France
Mauro Pontani , Italy
Sivakumar Poruran, India
Francesc Pozo , Spain
Aditya Rio Prabowo , Indonesia
Anchasa Pramuanjaroenkij , Thailand
Leonardo Primavera , Italy
B Rajanarayan Prusty, India

Krzysztof Puszynski , Poland
Chuan Qin , China
Dongdong Qin, China
Jianlong Qiu , China
Giuseppe Quaranta , Italy
DR. RITU RAJ , India
Vitomir Racic , Italy
Carlo Rainieri , Italy
Kumbakonam Ramamani Rajagopal, USA
Ali Ramazani , USA
Angel Manuel Ramos , Spain
Higinio Ramos , Spain
Muhammad Afzal Rana , Pakistan
Muhammad Rashid, Saudi Arabia
Manoj Rastogi, India
Alessandro Rasulo , Italy
S.S. Ravindran , USA
Abdolrahman Razani , Iran
Alessandro Reali , Italy
Jose A. Reinoso , Spain
Oscar Reinoso , Spain
Haijun Ren , China
Carlo Renno , Italy
Fabrizio Renno , Italy
Shahram Rezapour , Iran
Ricardo Rianza , Spain
Francesco Riganti-Fulginei , Italy
Gerasimos Rigatos , Greece
Francesco Ripamonti , Italy
Jorge Rivera , Mexico
Eugenio Roanes-Lozano , Spain
Ana Maria A. C. Rocha , Portugal
Luigi Rodino , Italy
Francisco Rodríguez , Spain
Rosana Rodríguez López, Spain
Francisco Rossomando , Argentina
Jose de Jesus Rubio , Mexico
Weiguo Rui , China
Rubén Ruiz , Spain
Ivan D. Rukhlenko , Australia
Dr. Eswaramoorthi S. , India
Weichao SHI , United Kingdom
Chaman Lal Sabharwal , USA
Andrés Sáez , Spain

Bekir Sahin, Turkey
Laxminarayan Sahoo , India
John S. Sakellariou , Greece
Michael Sakellariou , Greece
Salvatore Salamone, USA
Jose Vicente Salcedo , Spain
Alejandro Salcido , Mexico
Alejandro Salcido, Mexico
Nunzio Salerno , Italy
Rohit Salgotra , India
Miguel A. Salido , Spain
Sinan Salih , Iraq
Alessandro Salvini , Italy
Abdus Samad , India
Sovan Samanta, India
Nikolaos Samaras , Greece
Ramon Sancibrian , Spain
Giuseppe Sanfilippo , Italy
Omar-Jacobo Santos, Mexico
J Santos-Reyes , Mexico
José A. Sanz-Herrera , Spain
Musavarah Sarwar, Pakistan
Shahzad Sarwar, Saudi Arabia
Marcelo A. Savi , Brazil
Andrey V. Savkin, Australia
Tadeusz Sawik , Poland
Roberta Sburlati, Italy
Gustavo Scaglia , Argentina
Thomas Schuster , Germany
Hamid M. Sedighi , Iran
Mijanur Rahaman Seikh, India
Tapan Senapati , China
Lotfi Senhadji , France
Junwon Seo, USA
Michele Serpilli, Italy
Silvestar Šesnić , Croatia
Gerardo Severino, Italy
Ruben Sevilla , United Kingdom
Stefano Sfarra , Italy
Dr. Ismail Shah , Pakistan
Leonid Shaikhet , Israel
Vimal Shanmuganathan , India
Prayas Sharma, India
Bo Shen , Germany
Hang Shen, China

Xin Pu Shen, China
Dimitri O. Shepelsky, Ukraine
Jian Shi , China
Amin Shokrollahi, Australia
Suzanne M. Shontz , USA
Babak Shotorban , USA
Zhan Shu , Canada
Angelo Sifaleras , Greece
Nuno Simões , Portugal
Mehakpreet Singh , Ireland
Piyush Pratap Singh , India
Rajiv Singh, India
Seralathan Sivamani , India
S. Sivasankaran , Malaysia
Christos H. Skiadas, Greece
Konstantina Skouri , Greece
Neale R. Smith , Mexico
Bogdan Smolka, Poland
Delfim Soares Jr. , Brazil
Alba Sofi , Italy
Francesco Soldovieri , Italy
Raffaele Solimene , Italy
Yang Song , Norway
Jussi Sopanen , Finland
Marco Spadini , Italy
Paolo Spagnolo , Italy
Ruben Specogna , Italy
Vasilios Spitas , Greece
Ivanka Stamova , USA
Rafał Stanisławski , Poland
Miladin Stefanović , Serbia
Salvatore Strano , Italy
Yakov Strelniker, Israel
Kangkang Sun , China
Qiuqin Sun , China
Shuaishuai Sun, Australia
Yanchao Sun , China
Zong-Yao Sun , China
Kumarasamy Suresh , India
Sergey A. Suslov , Australia
D.L. Suthar, Ethiopia
D.L. Suthar , Ethiopia
Andrzej Swierniak, Poland
Andras Szekrenyes , Hungary
Kumar K. Tamma, USA

Yong (Aaron) Tan, United Kingdom
Marco Antonio Taneco-Hernández , Mexico
Lu Tang , China
Tianyou Tao, China
Hafez Tari , USA
Alessandro Tasora , Italy
Sergio Teggi , Italy
Adriana del Carmen Téllez-Anguiano , Mexico
Ana C. Teodoro , Portugal
Efstathios E. Theotokoglou , Greece
Jing-Feng Tian, China
Alexander Timokha , Norway
Stefania Tomasiello , Italy
Gisella Tomasini , Italy
Isabella Torricollo , Italy
Francesco Tornabene , Italy
Mariano Torrisi , Italy
Thang nguyen Trung, Vietnam
George Tsiatas , Greece
Le Anh Tuan , Vietnam
Nerio Tullini , Italy
Emilio Turco , Italy
Ilhan Tuzcu , USA
Efstratios Tzirtzilakis , Greece
FRANCISCO UREÑA , Spain
Filippo Ubertini , Italy
Mohammad Uddin , Australia
Mohammad Safi Ullah , Bangladesh
Serdar Ulubeyli , Turkey
Mati Ur Rahman , Pakistan
Panayiotis Vafeas , Greece
Giuseppe Vairo , Italy
Jesus Valdez-Resendiz , Mexico
Eusebio Valero, Spain
Stefano Valvano , Italy
Carlos-Renato Vázquez , Mexico
Martin Velasco Villa , Mexico
Franck J. Vernerey, USA
Georgios Veronis , USA
Vincenzo Vespri , Italy
Renato Vidoni , Italy
Venkatesh Vijayaraghavan, Australia

Anna Vila, Spain
Francisco R. Villatoro , Spain
Francesca Vipiana , Italy
Stanislav Vitek , Czech Republic
Jan Vorel , Czech Republic
Michael Vynnycky , Sweden
Mohammad W. Alomari, Jordan
Roman Wan-Wendner , Austria
Bingchang Wang, China
C. H. Wang , Taiwan
Dagang Wang, China
Guoqiang Wang , China
Huaiyu Wang, China
Hui Wang , China
J.G. Wang, China
Ji Wang , China
Kang-Jia Wang , China
Lei Wang , China
Qiang Wang, China
Qingling Wang , China
Weiwei Wang , China
Xinyu Wang , China
Yong Wang , China
Yung-Chung Wang , Taiwan
Zhenbo Wang , USA
Zhibo Wang, China
Waldemar T. Wójcik, Poland
Chi Wu , Australia
Qihong Wu, China
Yuqiang Wu, China
Zhibin Wu , China
Zhizheng Wu , China
Michalis Xenos , Greece
Hao Xiao , China
Xiao Ping Xie , China
Qingzheng Xu , China
Binghan Xue , China
Yi Xue , China
Joseph J. Yame , France
Chuanliang Yan , China
Xinggang Yan , United Kingdom
Hongtai Yang , China
Jixiang Yang , China
Mijia Yang, USA
Ray-Yeng Yang, Taiwan

Zaoli Yang , China
Jun Ye , China
Min Ye , China
Luis J. Yebra , Spain
Peng-Yeng Yin , Taiwan
Muhammad Haroon Yousaf , Pakistan
Yuan Yuan, United Kingdom
Qin Yuming, China
Elena Zaitseva , Slovakia
Arkadiusz Zak , Poland
Mohammad Zakwan , India
Ernesto Zambrano-Serrano , Mexico
Francesco Zammori , Italy
Jessica Zangari , Italy
Rafal Zdunek , Poland
Ibrahim Zeid, USA
Nianyin Zeng , China
Junyong Zhai , China
Hao Zhang , China
Haopeng Zhang , USA
Jian Zhang , China
Kai Zhang, China
Lingfan Zhang , China
Mingjie Zhang , Norway
Qian Zhang , China
Tianwei Zhang , China
Tongqian Zhang , China
Wenyu Zhang , China
Xianming Zhang , Australia
Xuping Zhang , Denmark
Yinyan Zhang, China
Yifan Zhao , United Kingdom
Debao Zhou, USA
Heng Zhou , China
Jian G. Zhou , United Kingdom
Junyong Zhou , China
Xueqian Zhou , United Kingdom
Zhe Zhou , China
Wu-Le Zhu, China
Gaetano Zizzo , Italy
Mingcheng Zuo, China

Contents

Retracted: Mathematical Model of Quantitative Evaluation of Financial Investment Risk Management System

Mathematical Problems in Engineering

Retraction (1 page), Article ID 9893832, Volume 2023 (2023)

Retracted: The Influence of the Network Evolutionary Game Model of User Information Behavior on Enterprise Innovation Product Promotion Based on Mobile Social Network Marketing Perspective

Mathematical Problems in Engineering

Retraction (1 page), Article ID 9875082, Volume 2023 (2023)

Retracted: Embedded Demand, Policy Supply, and the Urban Spatial Effect of the Transformation of the New Generation of Migrant Workers into Citizens

Mathematical Problems in Engineering

Retraction (1 page), Article ID 9846094, Volume 2023 (2023)

Retracted: Promotion Strategy of Low-Carbon Consumption of Fresh Food Based on Willingness Behavior

Mathematical Problems in Engineering

Retraction (1 page), Article ID 9820721, Volume 2023 (2023)

Retracted: An Accurate Method of Determining Attribute Weights in Distance-Based Classification Algorithms

Mathematical Problems in Engineering

Retraction (1 page), Article ID 9762363, Volume 2023 (2023)

Retracted: Application of Boiler Optimization Monitoring System Based on Embedded Internet of Things

Mathematical Problems in Engineering





Retraction (1 page), Article ID 9785879, Volume 2023 (2023)

Analysis on Spatial Characteristics and the Adaptation Mechanism of Miao Traditional Settlement in Qiandongnan, China

Yalun Lei , Hongtao Zhou , Meng Wang, and Chuan Wang

Research Article (11 pages), Article ID 6293833, Volume 2022 (2022)

Evaluation of China's High-Advanced Industrial Policy: A PMC Index Model Approach

Ying Tian , Kai Zhang , Jiayi Hong , and Fanglin Meng 

Research Article (13 pages), Article ID 9963611, Volume 2022 (2022)

A Miniaturized Electrochemical Nitrate Sensor and the Design for Its Automatic Operation Based on Distributed Model

Zhenxing Ren  and Yang Li 









Research Article (9 pages), Article ID 6028110, Volume 2022 (2022)

Application of Artificial Intelligence Technology in Cross-Cultural Communication of Intangible Cultural Heritage

Jiankun Zhang  and Yanhui Jing



Research Article (12 pages), Article ID 6563114, Volume 2022 (2022)

Effect of Farmland Transfer on Poverty Reduction under Different Targeted Poverty Alleviation Patterns Based on PSM-DID Model in Karst Area of China

Yan Liu , Maoqiang Wang , Zhu Qian , Baolin Hou , Xi Chen , Qinghua Lei , Lu He , and Longxue Zhao 


Research Article (13 pages), Article ID 9143080, Volume 2022 (2022)

A Star Pattern Recognition Algorithm Based on the Radial Companion-Circumferential Feature

Weiwei Zhao , Baoqiang Li , and Xiuyi Li

Research Article (10 pages), Article ID 1857481, Volume 2022 (2022)

Modeling and Simulation of Theoretical Digging Force of an Excavator Based on Arbitrary Posture

Zuhe Qin 


Research Article (7 pages), Article ID 8030349, Volume 2022 (2022)

Development of Physical Education Network Course Resources Based on Intelligent Sensor Network

Moutao Li, Ditao Song , and Xiaoyong Hu


Research Article (8 pages), Article ID 9934524, Volume 2022 (2022)

Research on Influencing Factors of Consumption and Purchase Intention of Camellia Oil in Coastal Areas Based on Logistics Model

Xue Wu 


Research Article (10 pages), Article ID 7028499, Volume 2022 (2022)

Financial Shared Services Empower the Real Economy: The Evidence from China

Xue Chen 


Research Article (12 pages), Article ID 2087054, Volume 2022 (2022)

The Relationship between Social Entrepreneurship Capability of SOM Neural Network Algorithm and New Enterprise Performance

Tianhua Li 



Research Article (12 pages), Article ID 8072941, Volume 2022 (2022)

One Person Plays Multiple Roles: The Diversified Roles and Functions of Convention Project Hosts by SEM Methods

Jie Zhou , Mengjie Zhao, and Qi Yang

Research Article (12 pages), Article ID 7680005, Volume 2022 (2022)


An RBF Neural Network Clustering Algorithm Based on K-Nearest Neighbor

Jitao Li , Chugui Xu, Yongquan Liang, Gengkun Wu , and Zhao Liang


Research Article (9 pages), Article ID 1083961, Volume 2022 (2022)

Contents



Influence of Management Education on Enterprise Scientific and Technological Innovation Based on K-Means Clustering Algorithm

Jun Ma , Zhigang Li, Zichan Liu, Shan Zhang, and Wenling Lai
Research Article (12 pages), Article ID 9030862, Volume 2022 (2022)


Research on Institutional Investors and Executive Compensation Stickiness Based on Fixed Effect Model: A Case Study of Chinese Listed Companies

Yizhao Hong 
Research Article (13 pages), Article ID 1402891, Volume 2022 (2022)


Analysis on Vibroacoustic Fatigue Life of Empennage in a Hypersonic Vehicle

Wang Hongxian , Zhang Ming, and Nie Hong 
Research Article (15 pages), Article ID 7027528, Volume 2022 (2022)

Artificial Intelligence-Based Drug Production Quality Management Data

Chenggong Yu 
Research Article (14 pages), Article ID 4089917, Volume 2022 (2022)

Research on Optimization of Structural Parameters of Equipment Cabin Bottom Cover

Hua Zou , Qifeng Wu, and Yonggui Zhang
Research Article (13 pages), Article ID 6204795, Volume 2022 (2022)


Design and Implementation of an Interactive English Translation System Based on the Information-Assisted Processing Function of the Internet of Things

Liya Mo 
Research Article (13 pages), Article ID 2722923, Volume 2022 (2022)

Implementation of Creator-Based Virtual Simulation in News Interview

Wen Zhou 
Research Article (11 pages), Article ID 1359170, Volume 2022 (2022)


Human Capital Digital Incentive Mechanism Construction Based on Deep Learning

Jie He and Jianhua Zhang 
Research Article (12 pages), Article ID 6180883, Volume 2022 (2022)


Mathematics Deep Learning Teaching Based on Analytic Hierarchy Process

Yonghua Duan 
Research Article (10 pages), Article ID 3070791, Volume 2022 (2022)

Monetary Policy, Fiscal Policy, and Capital Structure Dynamic Adjustment: Evidence from Chinese Listed Companies


Liangwei Wan 
Research Article (12 pages), Article ID 8040641, Volume 2022 (2022)

Development and Application of an Expert Decision-Making System for Personalized Exercise Prescriptions for Children with Special Physiques

Li-Fang Zhang, Chun-Long Fang, and Liang Zhou 


Research Article (10 pages), Article ID 5417473, Volume 2022 (2022)

Brainwave Acquisition Terminal Based on IoT Smart Sensor for English Listening Test

Juan Bi 


Research Article (11 pages), Article ID 3738897, Volume 2022 (2022)

New Technological Measures of Sustainable Buildings in Triple Bottom-Line Analysis

Yi Ding 

Research Article (14 pages), Article ID 7750056, Volume 2022 (2022)

[Retracted] Application of Boiler Optimization Monitoring System Based on Embedded Internet of Things

Haiqing Zhang , Mingxiang Qiu, Xingjiang Yu, Yujiao Wu, and Yinhong Ma


Research Article (12 pages), Article ID 9974393, Volume 2022 (2022)

Construction of Rural Governance Digital Driven by Artificial Intelligence and Big Data

Ruolan Huang 

Research Article (13 pages), Article ID 8145913, Volume 2022 (2022)

Deep Collaborative Filtering: A Recommendation Method for Crowdfunding Project Based on the Integration of Deep Neural Network and Collaborative Filtering

Pei Yin , Jing Wang, Jun Zhao, Huan Wang, and Hongcheng Gan


Research Article (15 pages), Article ID 4655030, Volume 2022 (2022)

Special-Purpose English Teaching Reform and Model Design in the Era of Artificial Intelligence

Yali Ruan 


Research Article (12 pages), Article ID 3068136, Volume 2022 (2022)

Statistics and Analysis of Effective Data on Online Teaching of College English Audiovisual Teaching

Kerong Wang 


Research Article (7 pages), Article ID 8956891, Volume 2022 (2022)

Research on Optimization of the AGV Shortest-Path Model and Obstacle Avoidance Planning in Dynamic Environments

Ruixi Liu 

Research Article (14 pages), Article ID 2239342, Volume 2022 (2022)


Economic Policy Uncertainty, Investor Sentiment, and Stock Price Synchronisation: Evidence from China

Jing Wu 

Research Article (8 pages), Article ID 7830668, Volume 2022 (2022)


Contents

Lightweight Fall Detection Algorithm Based on AlphaPose Optimization Model and ST-GCN

Hongtao Zheng and Yan Liu 





Research Article (15 pages), Article ID 9962666, Volume 2022 (2022)

Improvement and Optimization of a 3D Reconstruction Algorithm for SEM Images of Porous Materials

Cheng Cheng , Ning Dai, and Tao Tang


Research Article (9 pages), Article ID 2904178, Volume 2022 (2022)

Understanding the Impact of Rural Returnees' Hometown Identity on Their Successful Entrepreneurship with the Operations Research Framework

Feihan Sun , Xumei Miao , Xiaoyan Feng , and Chongliang Ye 


Research Article (13 pages), Article ID 6142477, Volume 2022 (2022)

Application of Computer 3D Modeling Technology in the Simulation Design of Modern Garden Ecological Landscape

Zhiyong Tian 

Research Article (9 pages), Article ID 7033261, Volume 2022 (2022)

Color Matching in Children's Room Based on Computer Interactive Experience

Jia Huang 


Research Article (10 pages), Article ID 7077711, Volume 2022 (2022)

Smart Mobile Information Systems on the Key Systems of Blockchain Privacy Protection

Xiaobo Wei 


Research Article (8 pages), Article ID 5126326, Volume 2022 (2022)

Application of Conditional Random Field Model Based on Machine Learning in Online and Offline Integrated Educational Resource Recommendation

Erqi Zeng 


Research Article (9 pages), Article ID 5746671, Volume 2022 (2022)

Brand Preference Prediction Method of Cross-Border E-Commerce Consumers Based on Potential Tag Mining

Xujie Qin 

Research Article (8 pages), Article ID 4654660, Volume 2022 (2022)

Data Mining and Economic Application in the Age of Financial Big Data: A Case Study of Shadow Banking and Interest Rate Liberalization in China

Shi Liang 


Research Article (8 pages), Article ID 9634999, Volume 2022 (2022)

Construction of Data Mining Analysis Model in English Teaching Based on Apriori Association Rule Algorithm

Shufei Wang 


Research Article (13 pages), Article ID 6875207, Volume 2022 (2022)

[Retracted] Mathematical Model of Quantitative Evaluation of Financial Investment Risk Management System

Xiaoling Wang 


Research Article (14 pages), Article ID 2439549, Volume 2022 (2022)

A Semantic Model of Internet of Things for Intelligent Translation and Learning

Nan Wei 


Research Article (11 pages), Article ID 1651288, Volume 2022 (2022)

Regional Financial Economic Data Processing Based on Distributed Decoding Technology

HuiLi Zhang 


Research Article (13 pages), Article ID 9692047, Volume 2022 (2022)

Effects and Appraisal of Grain Subsidy Policy Based on Statistical Analysis

Xiaoya Hu 


Research Article (10 pages), Article ID 2893486, Volume 2022 (2022)

[Retracted] Embedded Demand, Policy Supply, and the Urban Spatial Effect of the Transformation of the New Generation of Migrant Workers into Citizens

Lin Yu , Jianbing Yin, and Wei Qiao


Research Article (13 pages), Article ID 4323308, Volume 2022 (2022)

Increase in Suspended Sediment Contents by a Storm Surge in Southern Bohai Sea, China

Yongqiang Zhang, Yongfu Sun , Zejian Hu, Shuhua Bian, Congbo Xiong, Jianqiang Liu, Wanqing Chi, and Wanjun Zhang

Research Article (11 pages), Article ID 9585386, Volume 2022 (2022)

Construction of a Multimedia Education Resource Security Model Based on Multistage Integration

Lina Yuan 

Research Article (11 pages), Article ID 3624360, Volume 2022 (2022)

A Two-Level Integrated Scheduling Strategy for Vehicle-Network Synergy considering New Energy Consumption

Yifei Gao 

Research Article (13 pages), Article ID 6989785, Volume 2022 (2022)

[Retracted] Promotion Strategy of Low-Carbon Consumption of Fresh Food Based on Willingness Behavior

Zhao Zhao, Xiaqing Zhong , and Yuqing Zhu

Research Article (10 pages), Article ID 9571424, Volume 2022 (2022)

[Retracted] An Accurate Method of Determining Attribute Weights in Distance-Based Classification Algorithms

Fengtao Liu  and Jialei Wang

Research Article (15 pages), Article ID 6936335, Volume 2022 (2022)


Contents

The Network Transmission Path Risk Assessment and Application of Chemical Substances in Toys

Sainan Zhang  and Yuncai Ning


Research Article (10 pages), Article ID 2702325, Volume 2022 (2022)

Computer Digital Technology Combined with Dynamic Visual Communication Sensors in Target Tracking with Big Data

Zhihui Han  and Jianhua Zhao


Research Article (9 pages), Article ID 6713007, Volume 2022 (2022)

Improvement of English Teaching Process Management Based on Intelligent Data Sampling

Jin Cheng 



Research Article (12 pages), Article ID 2783725, Volume 2022 (2022)

Analysis of Public Mental Health Status and Exploration of Social Anxiety in the Context of Epidemic

Yuanxin Lu 


Research Article (10 pages), Article ID 6388212, Volume 2022 (2022)

Enterprise Financing Risk Analysis and Internal Accounting Management Based on BP Neural Network Model

Haojie Liao , Huabo Yue , Yibin Lin, Dong Li, and Lei Zhang


Research Article (13 pages), Article ID 8627185, Volume 2022 (2022)

Analysis of Music Teaching in Basic Education Integrating Scientific Computing Visualization and Computer Music Technology

Yanyan Zhao 


Research Article (12 pages), Article ID 3928889, Volume 2022 (2022)

Modeling and Analysis of the Impact of Information and Communication Technology on Household Consumption Expenditure in Different Regions

Chaozhi Fan , Siong Hook Law, Saifuzzaman Ibrahim, and N. A. M. Naseem


Research Article (11 pages), Article ID 5778788, Volume 2022 (2022)

Research on the Development Path of Manufacturing Industry and Its Economic Effect Based on Computational Visualization

Shiyuan Zhou , Zhixiong Liao, and Xiaoqin Yang


Research Article (12 pages), Article ID 1762561, Volume 2022 (2022)

Optimization of the Index System of the Sports Social Organization Development Ability Relying on Image Optimization, Recognition, and Simulation

Wei Sun 


Research Article (11 pages), Article ID 5638797, Volume 2022 (2022)

Construction of Enterprise Financial Early Warning Model Based on Intelligent Mathematical Model

Jing Cheng, Xiaofan Lu, and Xionggang Zhang 


Research Article (12 pages), Article ID 5230147, Volume 2022 (2022)

Evaluation of Multimedia Classroom Teaching Effectiveness Based on RS-BP Neural Network

Nan Xie 

Research Article (8 pages), Article ID 9416634, Volume 2022 (2022)

The Construction of College Sports Culture Based on Intelligent Information Management Technology

Baihua Luo 

Research Article (10 pages), Article ID 7197653, Volume 2022 (2022)

Evaluation of Urban Park Landscape Satisfaction Based on the Fuzzy-IPA Model: A Case Study of the Zhengzhou People's Park

Lei Feng  and Jie Zhao


Research Article (7 pages), Article ID 2116532, Volume 2022 (2022)

[Retracted] The Influence of the Network Evolutionary Game Model of User Information Behavior on Enterprise Innovation Product Promotion Based on Mobile Social Network Marketing Perspective

Tingting Liu , Xiaofei He , Xin Guo , and Yi Zhao 

Research Article (12 pages), Article ID 1416488, Volume 2022 (2022)

PLS-SEM Model of Integrated Stem Education Concept and Network Teaching Model of Architectural Engineering Course

Ping Wang 


Research Article (10 pages), Article ID 7220957, Volume 2022 (2022)

Mathematical Problems in Engineering Landscape Ecological Security Assessment and Ecological Pattern Optimization of Inland River Basins in Arid Regions: A Case Study in Tarim River Basin

Yuanrui Mu  and Wei Shen 


Research Article (17 pages), Article ID 9476860, Volume 2022 (2022)

Correction of Chinese Dance Training Movements Based on Digital Feature Recognition Technology

LinJuan Zhang 


Research Article (11 pages), Article ID 1150051, Volume 2022 (2022)

Research on Intelligent Campus and Visual Teaching System Based on Internet of Things

Tao Xu , Zhi-hong Wang, and Xian-qi Zhang

Research Article (10 pages), Article ID 4845978, Volume 2022 (2022)

Pedestrian Fall Event Detection in Complex Scenes Based on Attention-Guided Neural Network

Peng Geng, Hui Xie, Houqin Shi, Rui Chen , and Ying Tong

Research Article (10 pages), Article ID 4110246, Volume 2022 (2022)


Personalized Music Hybrid Recommendation Algorithms Fusing Gene Features

Yixiao Cao  and Peng Liu

Research Article (8 pages), Article ID 9209022, Volume 2022 (2022)


Contents

Substation Equipment Spare Parts' Inventory Prediction Model Based on Remaining Useful Life

Bing Tang, Zhenguo Ma, Keqi Zhang, Danyi Cao, and Jianyong Zhang 


Research Article (11 pages), Article ID 3396850, Volume 2022 (2022)

A Recognition Method Based on Speech Feature Parameters-English Teaching Practice

Lili Zhu, Xiujing Yan , and Jing Wang

Research Article (11 pages), Article ID 2287468, Volume 2022 (2022)

Ray Tracing Acceleration Algorithm Based on FaceMap

Jian Wang, Hui Xiao, and Hongbin Wang 

Research Article (16 pages), Article ID 8961577, Volume 2022 (2022)

Research on University Innovation and Entrepreneurship Resource Database System Based on SSH2

Libo Wu, Lili Feng , and Jianna Yan


Research Article (9 pages), Article ID 1168796, Volume 2022 (2022)

Digital Transformation of Listed Agricultural Companies in China: Practice, Performance, and Value Creation

Ying Yang and Wenqin Cui 

Research Article (9 pages), Article ID 4429937, Volume 2022 (2022)

Research on Basic Information of Enterprise Electronization under the Background of Big Data

Qihang Wang 


Research Article (11 pages), Article ID 3751828, Volume 2022 (2022)

Research and Application of Haar Wavelet Transformation in Train Positioning

Pengfei Wang  and Xiuhui Diao

Research Article (14 pages), Article ID 6545817, Volume 2022 (2022)

Thermal Analysis of Axial-Flux Permanent Magnet Motors for Vehicles Based on Fast Two-Way Magneto-Thermal Coupling

Xiaoting Zhang , Bingyi Zhang, Xin Chen, and Simeng Zhong

Research Article (15 pages), Article ID 1880912, Volume 2022 (2022)

Influence of Vertical Downward Annulus Eccentricity on Steam-Water Two-Phase Flow Pressure Drop

Chuan Ma , Xiaoyan Liu, Haiqian Zhao, and Guangfu Cui

Research Article (12 pages), Article ID 7682520, Volume 2022 (2022)

Judgment of Athlete Action Safety in Sports Competition Based on LSTM Recurrent Neural Network Algorithm

Yanying Liu, Lijun Wang , Yuanjin Tang , and Bo Ren

Research Article (13 pages), Article ID 1758198, Volume 2022 (2022)

Global COVID-19 Epidemic Prediction and Analysis Based on Improved Dynamic Transmission Rate Model with Neural Networks

Yanyu Ding, Jiaxing Li, Weiliang Song, Xiaojin Xie, and Guoqiang Wang 
Research Article (12 pages), Article ID 4849928, Volume 2022 (2022)


Pattern Recognition Characteristics and Neural Mechanism of Basketball Players' Dribbling Tactics Based on Artificial Intelligence and Deep Learning

Xuhui Song and Linyuan Fan 
Research Article (11 pages), Article ID 1673969, Volume 2022 (2022)

Computer Analysis and Automatic Recognition Technology of Music Emotion

Yuehua Xiang 
Research Article (9 pages), Article ID 3145785, Volume 2022 (2022)

Continuance Intention Mechanism of Middle School Student Users on Online Learning Platform Based on Qualitative Comparative Analysis Method

Guomin Chen, Pengrun Chen, Wenxia Huang, and Jie Zhai 
Research Article (12 pages), Article ID 3215337, Volume 2022 (2022)

Retraction

Retracted: Mathematical Model of Quantitative Evaluation of Financial Investment Risk Management System

Mathematical Problems in Engineering

Received 13 September 2023; Accepted 13 September 2023; Published 14 September 2023

Copyright © 2023 Mathematical Problems in Engineering. This is an open access article distributed under the Creative Commons Attribution License, which permits unrestricted use, distribution, and reproduction in any medium, provided the original work is properly cited.

This article has been retracted by Hindawi following an investigation undertaken by the publisher [1]. This investigation has uncovered evidence of one or more of the following indicators of systematic manipulation of the publication process:

- (1) Discrepancies in scope
- (2) Discrepancies in the description of the research reported
- (3) Discrepancies between the availability of data and the research described
- (4) Inappropriate citations
- (5) Incoherent, meaningless and/or irrelevant content included in the article
- (6) Peer-review manipulation

The presence of these indicators undermines our confidence in the integrity of the article's content and we cannot, therefore, vouch for its reliability. Please note that this notice is intended solely to alert readers that the content of this article is unreliable. We have not investigated whether authors were aware of or involved in the systematic manipulation of the publication process.

Wiley and Hindawi regrets that the usual quality checks did not identify these issues before publication and have since put additional measures in place to safeguard research integrity.

We wish to credit our own Research Integrity and Research Publishing teams and anonymous and named external researchers and research integrity experts for contributing to this investigation.

The corresponding author, as the representative of all authors, has been given the opportunity to register their agreement or disagreement to this retraction. We have kept a record of any response received.

References

- [1] X. Wang, "Mathematical Model of Quantitative Evaluation of Financial Investment Risk Management System," *Mathematical Problems in Engineering*, vol. 2022, Article ID 2439549, 14 pages, 2022.

Retraction

Retracted: The Influence of the Network Evolutionary Game Model of User Information Behavior on Enterprise Innovation Product Promotion Based on Mobile Social Network Marketing Perspective

Mathematical Problems in Engineering

Received 13 September 2023; Accepted 13 September 2023; Published 14 September 2023

Copyright © 2023 Mathematical Problems in Engineering. This is an open access article distributed under the Creative Commons Attribution License, which permits unrestricted use, distribution, and reproduction in any medium, provided the original work is properly cited.

This article has been retracted by Hindawi following an investigation undertaken by the publisher [1]. This investigation has uncovered evidence of one or more of the following indicators of systematic manipulation of the publication process:

- (1) Discrepancies in scope
- (2) Discrepancies in the description of the research reported
- (3) Discrepancies between the availability of data and the research described
- (4) Inappropriate citations
- (5) Incoherent, meaningless and/or irrelevant content included in the article
- (6) Peer-review manipulation

The presence of these indicators undermines our confidence in the integrity of the article's content and we cannot, therefore, vouch for its reliability. Please note that this notice is intended solely to alert readers that the content of this article is unreliable. We have not investigated whether authors were aware of or involved in the systematic manipulation of the publication process.

Wiley and Hindawi regrets that the usual quality checks did not identify these issues before publication and have since put additional measures in place to safeguard research integrity.

We wish to credit our own Research Integrity and Research Publishing teams and anonymous and named external researchers and research integrity experts for contributing to this investigation.

The corresponding author, as the representative of all authors, has been given the opportunity to register their

agreement or disagreement to this retraction. We have kept a record of any response received.

References

- [1] T. Liu, X. He, X. Guo, and Y. Zhao, "The Influence of the Network Evolutionary Game Model of User Information Behavior on Enterprise Innovation Product Promotion Based on Mobile Social Network Marketing Perspective," *Mathematical Problems in Engineering*, vol. 2022, Article ID 1416488, 12 pages, 2022.

Retraction

Retracted: Embedded Demand, Policy Supply, and the Urban Spatial Effect of the Transformation of the New Generation of Migrant Workers into Citizens

Mathematical Problems in Engineering

Received 13 September 2023; Accepted 13 September 2023; Published 14 September 2023

Copyright © 2023 Mathematical Problems in Engineering. This is an open access article distributed under the Creative Commons Attribution License, which permits unrestricted use, distribution, and reproduction in any medium, provided the original work is properly cited.

This article has been retracted by Hindawi following an investigation undertaken by the publisher [1]. This investigation has uncovered evidence of one or more of the following indicators of systematic manipulation of the publication process:

- (1) Discrepancies in scope
- (2) Discrepancies in the description of the research reported
- (3) Discrepancies between the availability of data and the research described
- (4) Inappropriate citations
- (5) Incoherent, meaningless and/or irrelevant content included in the article
- (6) Peer-review manipulation

The presence of these indicators undermines our confidence in the integrity of the article's content and we cannot, therefore, vouch for its reliability. Please note that this notice is intended solely to alert readers that the content of this article is unreliable. We have not investigated whether authors were aware of or involved in the systematic manipulation of the publication process.

In addition, our investigation has also shown that one or more of the following human-subject reporting requirements has not been met in this article: ethical approval by an Institutional Review Board (IRB) committee or equivalent, patient/participant consent to participate, and/or agreement to publish patient/participant details (where relevant).

Wiley and Hindawi regrets that the usual quality checks did not identify these issues before publication and have since put additional measures in place to safeguard research integrity.

We wish to credit our own Research Integrity and Research Publishing teams and anonymous and named external

researchers and research integrity experts for contributing to this investigation.

The corresponding author, as the representative of all authors, has been given the opportunity to register their agreement or disagreement to this retraction. We have kept a record of any response received.

References

- [1] L. Yu, J. Yin, and W. Qiao, "Embedded Demand, Policy Supply, and the Urban Spatial Effect of the Transformation of the New Generation of Migrant Workers into Citizens," *Mathematical Problems in Engineering*, vol. 2022, Article ID 4323308, 13 pages, 2022.

Retraction

Retracted: Promotion Strategy of Low-Carbon Consumption of Fresh Food Based on Willingness Behavior

Mathematical Problems in Engineering

Received 13 September 2023; Accepted 13 September 2023; Published 14 September 2023

Copyright © 2023 Mathematical Problems in Engineering. This is an open access article distributed under the Creative Commons Attribution License, which permits unrestricted use, distribution, and reproduction in any medium, provided the original work is properly cited.

This article has been retracted by Hindawi following an investigation undertaken by the publisher [1]. This investigation has uncovered evidence of one or more of the following indicators of systematic manipulation of the publication process:

- (1) Discrepancies in scope
- (2) Discrepancies in the description of the research reported
- (3) Discrepancies between the availability of data and the research described
- (4) Inappropriate citations
- (5) Incoherent, meaningless and/or irrelevant content included in the article
- (6) Peer-review manipulation

The presence of these indicators undermines our confidence in the integrity of the article's content and we cannot, therefore, vouch for its reliability. Please note that this notice is intended solely to alert readers that the content of this article is unreliable. We have not investigated whether authors were aware of or involved in the systematic manipulation of the publication process.

In addition, our investigation has also shown that one or more of the following human-subject reporting requirements has not been met in this article: ethical approval by an Institutional Review Board (IRB) committee or equivalent, patient/participant consent to participate, and/or agreement to publish patient/participant details (where relevant).

Wiley and Hindawi regrets that the usual quality checks did not identify these issues before publication and have since put additional measures in place to safeguard research integrity.

We wish to credit our own Research Integrity and Research Publishing teams and anonymous and named external researchers and research integrity experts for contributing to this investigation.

The corresponding author, as the representative of all authors, has been given the opportunity to register their agreement or disagreement to this retraction. We have kept a record of any response received.

References

- [1] Z. Zhao, X. Zhong, and Y. Zhu, "Promotion Strategy of Low-Carbon Consumption of Fresh Food Based on Willingness Behavior," *Mathematical Problems in Engineering*, vol. 2022, Article ID 9571424, 10 pages, 2022.

Retraction

Retracted: An Accurate Method of Determining Attribute Weights in Distance-Based Classification Algorithms

Mathematical Problems in Engineering

Received 13 September 2023; Accepted 13 September 2023; Published 14 September 2023

Copyright © 2023 Mathematical Problems in Engineering. This is an open access article distributed under the Creative Commons Attribution License, which permits unrestricted use, distribution, and reproduction in any medium, provided the original work is properly cited.

This article has been retracted by Hindawi following an investigation undertaken by the publisher [1]. This investigation has uncovered evidence of one or more of the following indicators of systematic manipulation of the publication process:

- (1) Discrepancies in scope
- (2) Discrepancies in the description of the research reported
- (3) Discrepancies between the availability of data and the research described
- (4) Inappropriate citations
- (5) Incoherent, meaningless and/or irrelevant content included in the article
- (6) Peer-review manipulation

The presence of these indicators undermines our confidence in the integrity of the article's content and we cannot, therefore, vouch for its reliability. Please note that this notice is intended solely to alert readers that the content of this article is unreliable. We have not investigated whether authors were aware of or involved in the systematic manipulation of the publication process.

Wiley and Hindawi regrets that the usual quality checks did not identify these issues before publication and have since put additional measures in place to safeguard research integrity.

We wish to credit our own Research Integrity and Research Publishing teams and anonymous and named external researchers and research integrity experts for contributing to this investigation.

The corresponding author, as the representative of all authors, has been given the opportunity to register their agreement or disagreement to this retraction. We have kept a record of any response received.

References

- [1] F. Liu and J. Wang, "An Accurate Method of Determining Attribute Weights in Distance-Based Classification Algorithms," *Mathematical Problems in Engineering*, vol. 2022, Article ID 6936335, 15 pages, 2022.

Retraction

Retracted: Application of Boiler Optimization Monitoring System Based on Embedded Internet of Things

Mathematical Problems in Engineering

Received 1 August 2023; Accepted 1 August 2023; Published 2 August 2023

Copyright © 2023 Mathematical Problems in Engineering. This is an open access article distributed under the Creative Commons Attribution License, which permits unrestricted use, distribution, and reproduction in any medium, provided the original work is properly cited.

This article has been retracted by Hindawi following an investigation undertaken by the publisher [1]. This investigation has uncovered evidence of one or more of the following indicators of systematic manipulation of the publication process:

- (1) Discrepancies in scope
- (2) Discrepancies in the description of the research reported
- (3) Discrepancies between the availability of data and the research described
- (4) Inappropriate citations
- (5) Incoherent, meaningless and/or irrelevant content included in the article
- (6) Peer-review manipulation

The presence of these indicators undermines our confidence in the integrity of the article's content and we cannot, therefore, vouch for its reliability. Please note that this notice is intended solely to alert readers that the content of this article is unreliable. We have not investigated whether authors were aware of or involved in the systematic manipulation of the publication process.

Wiley and Hindawi regrets that the usual quality checks did not identify these issues before publication and have since put additional measures in place to safeguard research integrity.

We wish to credit our own Research Integrity and Research Publishing teams and anonymous and named external researchers and research integrity experts for contributing to this investigation.

The corresponding author, as the representative of all authors, has been given the opportunity to register their agreement or disagreement to this retraction. We have kept a record of any response received.

References

- [1] H. Zhang, M. Qiu, X. Yu, Y. Wu, and Y. Ma, "Application of Boiler Optimization Monitoring System Based on Embedded Internet of Things," *Mathematical Problems in Engineering*, vol. 2022, Article ID 9974393, 12 pages, 2022.

Research Article

Analysis on Spatial Characteristics and the Adaptation Mechanism of Miao Traditional Settlement in Qiandongnan, China

Yalun Lei ¹, Hongtao Zhou ¹, Meng Wang,² and Chuan Wang³

¹College of Design and Innovation, Tongji University, Shanghai 200092, China

²Shanghai Academy of Fine Arts, Shanghai University, Shanghai 200444, China

³School of Design and Fashion, Zhejiang University of Science and Technology, Hangzhou 310023, China

Correspondence should be addressed to Hongtao Zhou; zhouhongtao@tongji.edu.cn

Received 7 July 2022; Accepted 9 September 2022; Published 4 October 2022

Academic Editor: Wei Liu

Copyright © 2022 Yalun Lei et al. This is an open access article distributed under the Creative Commons Attribution License, which permits unrestricted use, distribution, and reproduction in any medium, provided the original work is properly cited.

In the farming era, the ancestors of Miao moved to a mountainous area in Qiandongnan to avoid wars. When they started their settlement construction, people gave priority to how to deal appropriately with the great survival pressure they were facing. This paper uses the methods GIS spatial analysis, morphological index, and spatial syntax to explain the spatial characteristics of Miao traditional settlements from the perspective of both regional scale and individual settlement and explores the adaptation mechanism. The results show that (1) spatial distribution of settlements shows a tendency of agglomeration and significant spatial heterogeneity; the maximum kernel density is in the Leikaitai area, which is featured by an inclined “T” shape; (2) settlements are concentrated in areas mainly around Qingshui River and Duliu River, with an elevation of 500–1000 m, terrain relief of 10–20 m, and the slope of 5–15°; (3) the external boundary of settlement is mainly finger-shaped and buildings showed a large concentration of small distribution; and (4) settlements have generally formed an overall landscape pattern of “mountain-water-field-forest-building,” with the space center appearing inside the settlements and the road connecting the outside of the settlement. This paper summarizes the intrinsic relationship among settlements’ spatial characteristics, the natural environment, and the social and economic environment and concludes the internal morphological evolution of the settlement which has shifted from survival adaptability to active search for development. The results of this research can provide a valuable reference for traditional settlement protection, utilization, and sustainable development.

1. Introduction

In the 1950s, French geographer Mark Sone proposed the theory that geographical conditions determine the survival mode [1], in which settlement construction occupies a vital part and serves as the main space carrier [2]. Also, traditional settlements are regarded as witnesses of historical processes and carriers of cultural inheritance. They have important social, cultural, aesthetic, and tourism values [3, 4]. Particularly, as an essential part of traditional settlements, ethnic minority settlements are able to reflect the survival logic and historical culture of ethnic minorities [5]. They are the main resources for inheriting the excellent Chinese traditional culture and developing tourism in mountainous

areas. However, with the acceleration of urbanization and the development of tourism in rural areas, the spaces of traditional settlements are suffering various degrees of destruction and decay, such as ecological degradation, functional decline, and construction destruction [6, 7]. In 2018, the Chinese government proposed implementing rural revitalization and protecting traditional regional culture, which made it clear that the protection and inheritance of traditional settlements are of great significance [8]. Therefore, the sustainable development of traditional settlements has become a hot topic in the Chinese academic world.

Western academia, especially Poland architects, had studied the spatial characteristics of traditional settlements in rural areas and concluded that the traditional settlement

was a distribution of types and density depending on both natural and socioeconomic conditions [9–11]. The natural factors are regarded as the elementary role where the outset of traditional settlement is concerned [12]. Socioeconomic factors shape the spatial structure of the settlement system, especially for individual settlements [13, 14]. However, from the regional scale perspective to individual settlement, the quantitative analysis of the spatial characteristics of traditional settlements and their adaptation factors is not enough. Most researches are limited to the spatial organization, construction techniques, building decoration, and cultural connotation of settlements. There is a lack of systematic research on the spatial distribution, morphological characteristics, and adaptation mechanisms of settlements.

Based on the specific geographical environment of Qiandongnan, this research uses analysis methods of GIS, morphological index, and spatial syntax to investigate the relationship among the regional environment, the spatial distribution, the morphological characteristics, and internal spatial organization of the traditional settlement. It is found that the construction of Miao traditional settlements is formally rooted in the local area, adapted to, and cleverly used natural processes, and the final formation of the overall “mountain-water-field-forest-building” spatial pattern was the core requirement of Miao people’s survival and reproduction.

Today, the survival pressure of Miao people is greatly reduced, and they can go out to work and engage in tourism service industries and handicrafts to obtain survival security. The most important “field” factor in the past was no longer important to Miao people. Therefore, the adaptation mechanisms of cherishing fields, protecting mountains and forests, and respecting traditional rituals and beliefs formed in the entire settlement over hundreds of years are being eroded.

In response, the research focuses on the evolution processes and adaptation mechanism of spatial settlement structure to discuss possible solutions and seek out ways to strengthen the reuse of resources and cultural preservation in the process of rural revitalization and tourism to provide valuable enlightenment for traditional settlements restructuring, utilization, and sustainable development.

2. Study Area and Method

2.1. Study Area. Qiandongnan is located in the transitional zone from the Yunnan-Guizhou Plateau to Xianggui hills and basins in China, with continuous peaks and ridges. Karst is widespread in the territory and forms a particular karst ecosystem. The study area has jurisdiction over 15 county-level units, including Cenggong, Zhengyuan, Shibing, Huangping, Sansui, Majiang, Taijiang, Jianhe, Pingjing, Danzai, Leishan, Rongjiang, Liping, Congjiang, and Kaili. Qiandongnan is a specific area for studying Miao traditional settlements. The total population of Miao in China is 8,940,100, of which 3,799,500 live here. Its geographical location is 107°17′–109°35′ E, 25°19′–27°31′ N, and its land area is 30337 km².

2.2. Data Sources. Four main categories of data sources are included in this study: (1) the list of minority characteristic villages from the official website of the People’s Government of Guizhou province; as of August 2021, 314 settlements in the study area have been selected into the list of ethnic minority villages in Guizhou province; and the geographic coordinates were calibrated using Google Earth; (2) the vector map, elevation, and river system of the administrative boundary of Qiandongnan are provided by the Chinese Resources and Environment Science and Data Center; (3) the space syntax graph of traditional settlements was obtained from calculations of AutoCAD and Depthmap; (4) the drawing of overall landscape composition pattern map from field investigation and villager’s interview; and (5) social and economic data were acquired from statistical yearbooks.

2.3. Methods

2.3.1. The Nearest Average Neighbor Ration. Thinking of the traditional settlements as abstract points in space, these settlements will present three spatial distribution patterns: discrete, random, and agglomeration. The nearest average neighbor index (R) method is used to identify the spatial distribution of traditional settlements, and the result shows the degree of mutual proximity of traditional settlements in the geographic space [15]. The R index can be calculated as follows:

$$R = \frac{\overline{r1}}{rE} \quad (1)$$

2.3.2. The Kernel Density Estimation. The kernel density estimation (KDE) method is the most widely used non-parametric estimation method in spatial point pattern analysis. It is used to calculate the aggregation of elements in its entire area. The greater the KDE value, the higher the degree of aggregation of settlements. The KDE can be calculated as follows:

$$f(x) = \frac{1}{nh} \sum_{i=1}^n k\left(\frac{x-x_i}{h}\right), \quad (2)$$

where $f(x)$ denotes the estimated density at the location, h is the bandwidth or kernel size, n is the number of traditional settlements, K is the kernel function, and $(x-x_i)$ is the distance from the location to the measuring point x_i [16].

2.3.3. Boundary Morphology Index. The settlement boundary morphology can be classified into three types: cluster, band, and finger shape. Boundary morphology is illustrated in the subject using the length-width ratio, void-solid ratio, radian, and concave-convex degree [17].

- (1) The length-width ratio of the shape index (λ) reveals the narrowness of the settlement boundary morphology. Set $\lambda = 2$ as the critical point; when $\lambda > 2$, the settlement is the central control feature of the group,

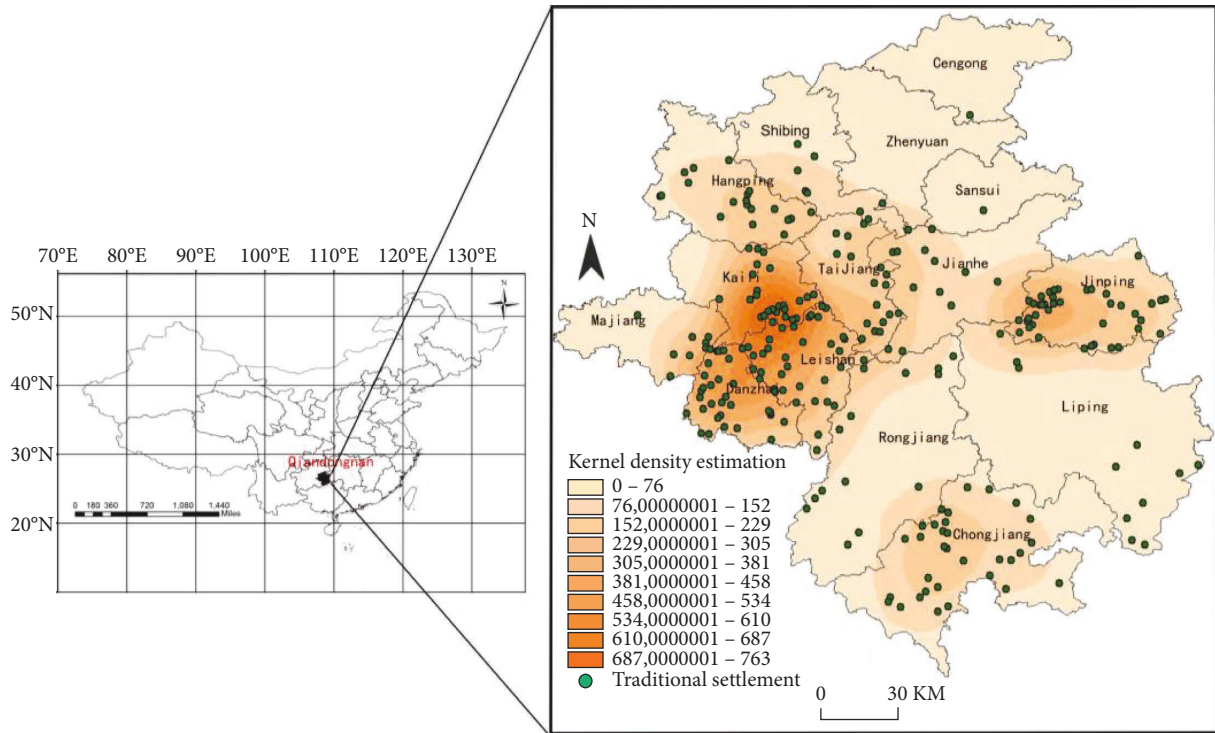


FIGURE 1: The kernel density distribution of Miao traditional villages in the study area.

and between 1.5 and 2, the settlements are either atypical clusters or atypical belts, becoming clusters with a tendency towards belts.

- (2) The minimum value of the shape index (S) is 1. The closer the value is to 1, the closer the graph is to the circle. The larger the value, the greater the difference between the shape and the circle, and the more complex and irregular. Thus, the boundary characteristics of traditional settlements can be calculated as follows:

$$S = \frac{P}{(1.5\lambda - \sqrt{\lambda + 1.5})} \sqrt{\frac{\lambda}{A\pi}} \quad (3)$$

where P means the circumference, and A is the area of the settlement.

2.3.4. The Space Syntax Technique. Use the remote sensing images of six typical traditional settlements in 2021 to make the base map, then draw the road axis map in AutoCAD, and import it into “Depthmap” software to analyze the topological relationship, obtain the spatial integration and control degree, and then do the traditional settlement quantitative analysis of internal organization characteristics [18].

The global integrated axis map can reproduce the spatial structure of traditional settlements. Then, the chromatographic analysis of the axis reflects the level of spatial visibility and accessibility. The red area has the highest spatial visibility and accessibility, the yellow area is the second, and the blue area is the third.

3. Results

3.1. Spatial Distribution Characteristics

3.1.1. Density Analysis of the Spatial Distribution. Using the average nearest neighbor tool under the spatial statistics module of ArcGIS 10.21, it was calculated that the actual distance of traditional settlements was 13.79 km, the expected average distance was 43.90 km, the nearest neighbor ratio was 0.31, and the significance $P < 0.01$, Z value was -23.34 , the result shows that traditional settlements presented an agglomeration spatial morphology (Figure 1).

The traditional settlements presented typical unbalanced characteristics in space, mainly concentrated in the central and western regions, accounting for 66.20% of all settlements. In contrast, the least were distributed in Zhenyuan, Cengong, and Sansui, accounting for only 1.37% of the total.

From the perspective of the spatial distribution of KDE, the KDE of traditional settlements formed a spatial distribution pattern of primary centers and secondary centers, which were similar to the “ T ” character. The first-level center was the junction of Leishan, northern Danzhai, and southern Kaili. The secondary centers spread around the first-level center to east Jinping and showed decreasing grades whereas the lowest values of traditional settlements KDE were located in Zhenyuan, Cengong, Sansui.

3.1.2. Elevation Analysis of Spatial Distribution. Miao is a typical alpine ethnic group, and mountains constitute the natural environment and basic skeleton of their settlements. The traditional settlements were concentrated at an altitude

TABLE 1: Elevation statistics of Miao traditional settlements in the study area.

Elevation (M)	Number	Percentage	Land area (km ²)	Percentage
91–500	41	13.05	41.76	20.38
500–1000	217	69.10	148.18	71.84
1000–1500	38	12.10	13.02	6.31
1500–2178	18	5.73	4.20	1.94

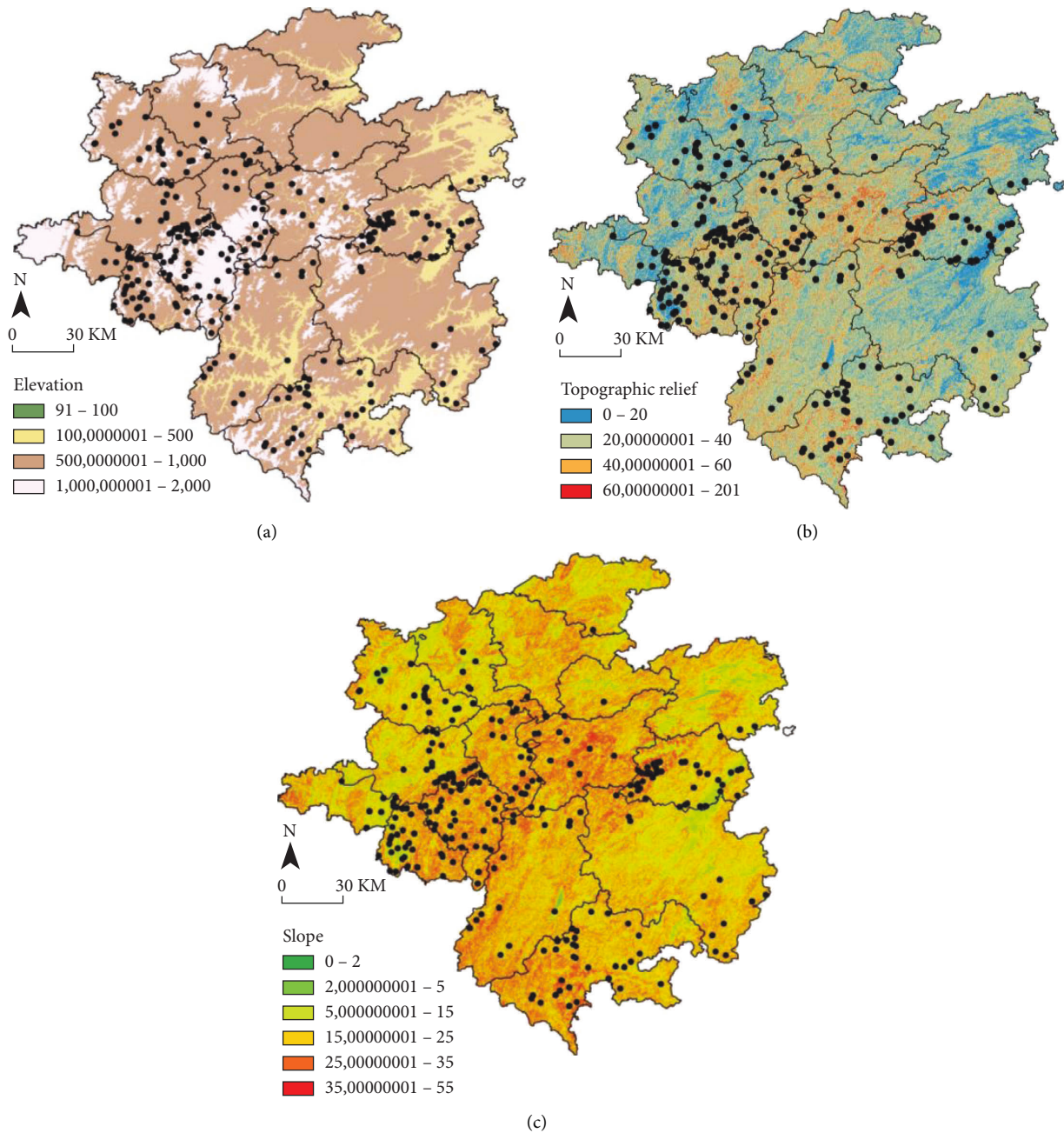


FIGURE 2: Topographic map: (a) elevation map; (b) topographic map; and (c) slope map.

of 500–1000 M, with 217, accounting for 84.07% of the total. Instead, only 18 settlements with an altitude of more than 1500 M accounted for 4.14% of the total, and 41 settlements

with an altitude of <500 M accounted for 12.10% of the total (Table 1, Figure 2(a)). As the altitude increases, the number of settlements decreases, and the settlement patch areas

TABLE 2: Slope statistics of Miao traditional settlements in the study area.

Slope classification	Slope (°)	Number	Percentage
Flat to almost undulating	0–5	29	9.24
Gently inclined	5–15	153	48.72
Moderately inclined	15–25	78	24.84
Steep	25–45	54	17.19
Very steep	>45	0	0

reach a peak between 500 and 1000 M above the sea level. Furthermore, the total area of settlements in this altitude range was 148.18 km², accounting for 71.84%.

3.1.3. Topographic Relief Analysis of the Spatial Distribution. The Miao traditional settlements were concentrated in flat dams and hilly areas with a topographic relief of 10–20 M, accounting for 69.42% (Figure 2(b)). In contrast, in areas where topographic relief >60 M had a significant drop, geological disasters such as mudslides, avalanches, and landslides were more frequent, and soil erosion was more serious.

3.1.4. Slope Analysis of the Spatial Distribution. To analyse the effect of slope on the location of Miao traditional settlements, we divided the slope of the study area into five grades according to the division plan of the Geomorphological Survey and Cartography Committee of the International Society [19]. The study found that the spatial distribution of traditional settlements grew firstly and then decreased with the increase in slope. Traditional settlements mainly concentrated in the gently inclined area and were more minor in the flat to the almost undulating area (Table 2 and Figure 2(c)) because the area with a slope of 0–5° in the study was relatively small. Moreover, the area with a slope of 5°–15° has apparent undulations. But it has specific soil resources. Moreover, the agricultural area accounts for 39.54% of the total, so there are 153 traditional settlements. At the same time, the area with a slope >25° had intense soil erosion, barren soil, and highly fragile ecology, which was not suitable for farming activities and settlement construction.

3.1.5. River System Analysis of the Spatial Distribution. The abundant rainfall and river systems in the study area have a certain influence on traditional settlements' site selection and agricultural production. To analyse the effect of the river on the spatial distribution of traditional settlements, we measured the river to traditional settlements distance by the Hydrology model of GIS (Table 3 and Figure 3(a)). As a result, from along the river to distances >1500 M and <500 M, the number of traditional settlements showed a gradual decrease. The most significant number of traditional settlements was 500–1500 M away from the river, accounting for 47.45% of the total, followed by 1–500 M and 1500–2000 M, which accounted for 26.75%, 13.38%, respectively. Besides, buildings along the river system of Qingshui and Dulu were a common feature shared by traditional settlements (Figure 3(b)).

3.2. External Spatial Morphology Characteristics

3.2.1. The External Boundary. In order to plot the traditional settlements boundary, we assumed the distance of 30 M as the farthest distance wherein faces, clothing, and behavior of people could be recognized. The morphological characteristics and relevant indexes of the six typical settlements were computed scientifically and summarized in Table 4.

The calculation results for λ and S reflected the narrow extension and concave-convex degree. First, $S \geq 2$, the external boundary morphology exhibited a zonal plane characteristic, while a finger-shaped tendency occurred given the effect of the landform environment. Second, when $\lambda < 1.5$, the morphology was finger-shaped and tended to clump, such as Yemeng, Nanmeng, and Wudong. Third, $\lambda \geq 2$, they were finger-shaped and tended to band, such as Zhangao, Basha, $1.5 \leq \lambda < 2$, and it was finger-shaped with no clear tendency, like Getou. The settlements with finger-shaped external boundaries were commonly found in Qiandongnan.

3.2.2. The Structural Characteristics of the Buildings. Miao peoples followed the principles of natural factors to arrange and integrate the internal space of settlement in an orderly manner according to their own survival needs and a particular logical relationship (Figure 4).

Firstly, the structure of buildings presented a clustered pattern that was a distributed morphology of large concentration and small dispersion. The buildings' structures in the area were gathered together in the form of a group, which could be defined as a "reunion type." Then, according to the number of building groups, it could be divided into "single reunion" and "multiple reunions." "Single-group" refers to a settlement with only one large concentrated area of building structure, such as Getou, Wudong, and Yemeng, while "multigroups" refers to the structure of a settlement group with two or more concentrated areas, such as Nanmeng, Basha, Zhangao, which were formed by the combination of several small settlements. The structural characteristics of the buildings were still large concentration and small dispersion, but there are multiple large concentration areas instead of one.

Secondly, the distance between the individual building was small, and they were close to each other in a staggered or parallel manner, forming a compact space feature. When the settlement expands, new buildings always fill in the gaps inside or outside the settlement to improve the compactness of the space. It can be seen that the spatial characteristics of the compact buildings not only stay in the present but also will continue over time.

TABLE 3: The statistics between Miao traditional settlements and the river buffer zone.

Nearest water distance (M)	0–100	100–500	500–1500	1500–2000	>2000
Number	30	84	149	42	9
Percentage	10.46	26.75	47.45	13.38	2.86

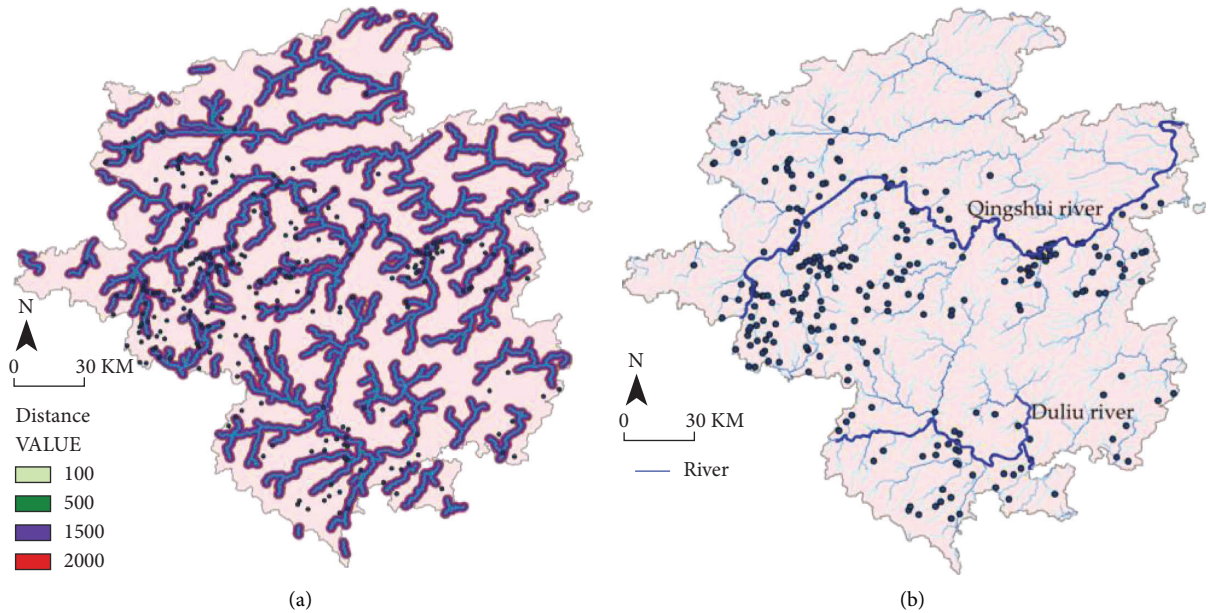


FIGURE 3: Water system distribution map: (a) water buffer map and (b) river distribution map.

TABLE 4: Statistics on the external boundary of typical settlements.

Settlements	P (m)	A (m ²)	λ	s	Boundary characteristics
Zhangao	2545	30805	8.73	6.91	Finger-shaped with a tendency to banded
Nanmeng	9136	41454	1.21	12.57	Finger-shaped with a tendency to clump
Getou	2561	30360	1.66	3.95	Finger-shaped with no clear tendency
Yemeng	1303	23034	1.34	2.37	Finger-shaped with a tendency to lump
Wudong	1894	40452	1.47	2.58	Finger-shaped with a tendency to lump

3.2.3. Overall Landscape Composition Pattern. After the initial exploration and a long process of evolution, Miao traditional settlements in Qiandongnan had generally formed an overall landscape pattern of “mountain-water-field-forest-building.” The results show (Figure 5) those as follows: (1) Mountains and rivers together shape the natural background of the settlement landscape, forming a “trough” flat land along the river; (2) open up fields in flat land and draw water from rivers for irrigation; (3) planting forests on the mountains; (4) the dwelling house is built at the foot of the mountain to ensure that it “occupies the mountain but not the cultivated land.”

3.3. Syntactic Analysis of Internal Spatial Morphology Characteristics. To analyse the visibility and accessibility of the internal spatial organization of traditional settlements, we selected global angular distance (Ang N), and two morphological variables, including the global average

integration degree and the global control degree, to analyze the spatial organization of settlements.

3.3.1. Integration. The global average integration degree of Wudong and Getou were $R_n0.47$ and $R_n0.44$, respectively, (Figure 6(a)), and the red and yellow axes with high integration were mostly enclosed in important nodes, such as Lushenping, Huzhai tree, shelter bridge, and pond. These critical nodes had morphological control and dominance and were the core of the settlement’s humanistic spirit. Moreover, significant celebrations, ceremonies, meetings, and other public activities were usually held here, which gives it the characteristic of being powerful and the nature of “public domain.” In addition, the global average integration degrees of Nameng, Basha, Zhangao, and Yemeng were $R_n0.28$, $R_n0.26$, $R_n0.21$, and $R_n0.20$, respectively, which were lower and higher spatial dispersion values. As a result, the most integrated axis was the roads that connect the

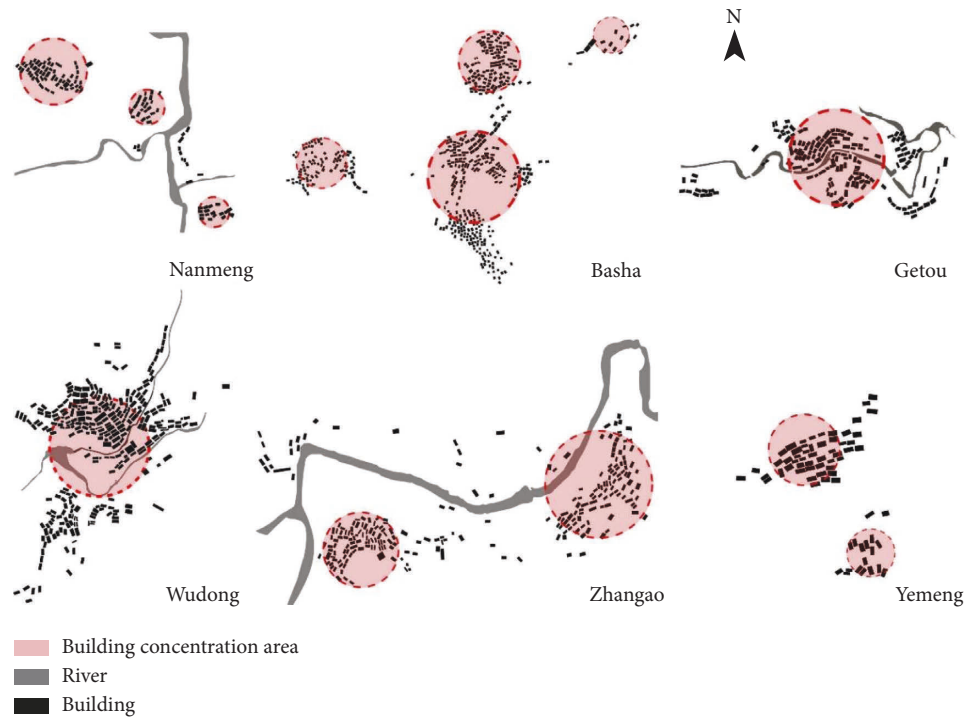


FIGURE 4: The aggregation analysis map of typical sample buildings.

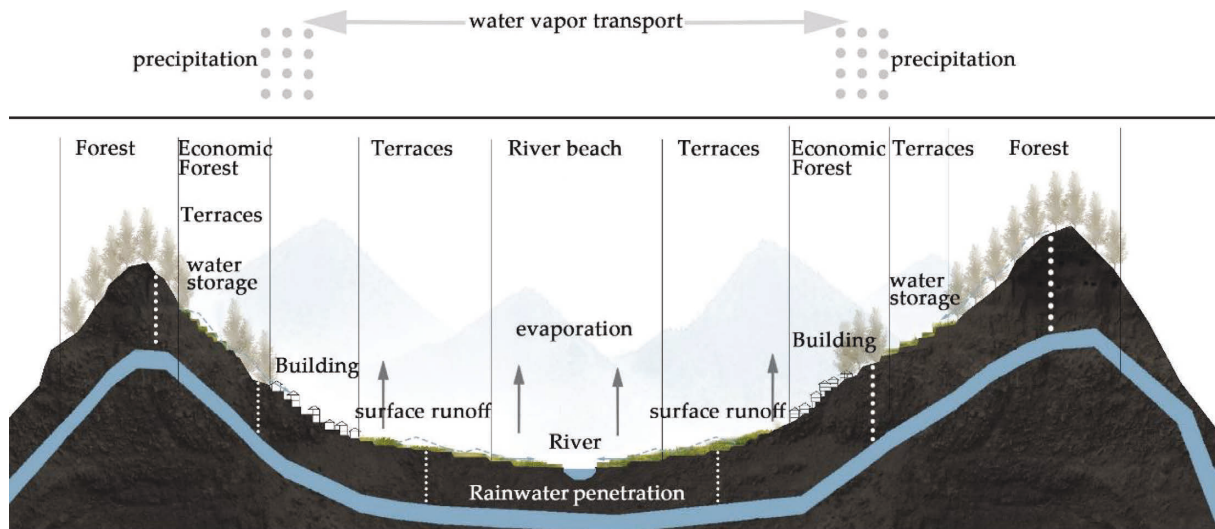


FIGURE 5: The overall landscape pattern analysis map of typical sample settlements.

outside of the settlements, and its functions are closely related to life laid out along the roads. Moreover, these settlements have no core spaces surrounded by several highly integrated axes.

3.3.2. *Control.* The global control degree analysis shows that most traditional settlements presented light green or blue short lines on the control axis (Figure 6(b)), which means that the global control degree of the main streets was low because there are many turns of streets and lanes dividing the axis of the main street into multiple short lines. In contrast, the connection between these streets or lanes was

single, making the settlement's internal space structure more private and defensive. Moreover, the space has a certain degree of change and interest. Consistent with the global average integration degree of settlements, the most controlled axis in the six typical settlements was still the core area of important nodes or the roads connected to the outside.

4. Discussion

In this study, we demonstrated that the spatial distribution and morphological characteristics of Miao traditional

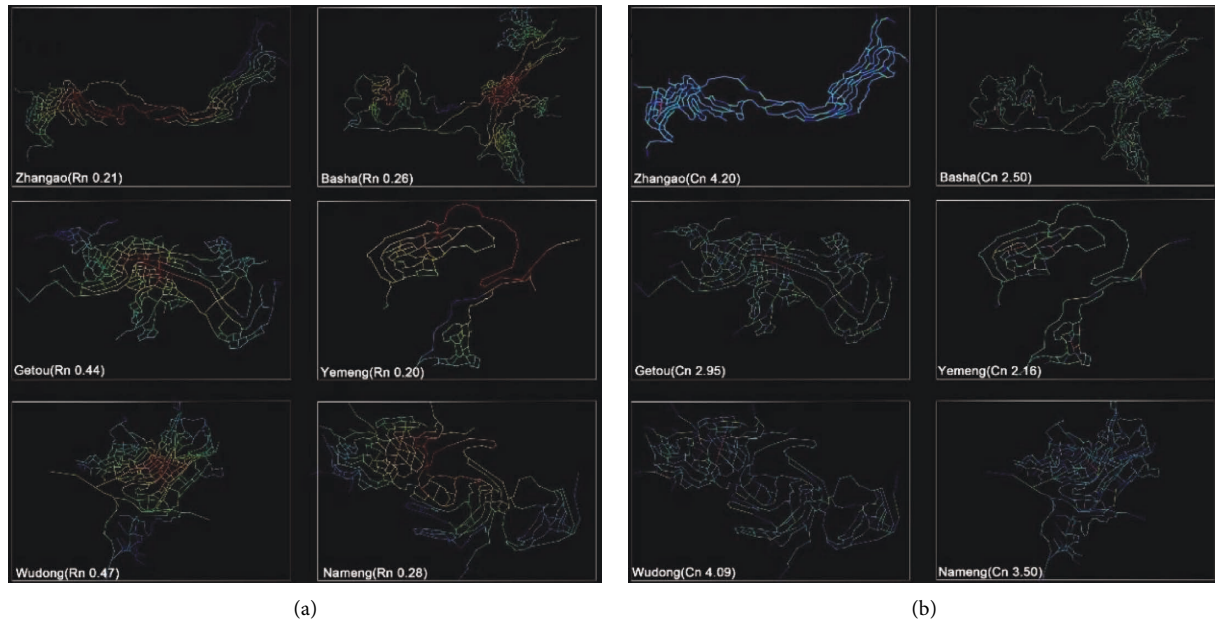


FIGURE 6: The spatial syntactic analysis map. (a) The global integration map of settlements. (b) The global control map of settlements.

settlements was a survival process of constantly adapting to the harsh natural environment and coping with changes in internal and external conditions in different periods, which was an external manifestation of the joint effect of the natural environment, social environment, and economic environment [20]. However, due to the development of tourism, the implementation of the rural revitalization policy, and the changes in the production and lifestyle, the internal and external conditions for the formation and development of traditional settlements are changing. The traditional settlements and their adaptation mechanisms face multiple challenges (Figure 7).

4.1. Natural Environment and Settlement Spatial Distribution.

The natural environment is the material basis for the survival and development of traditional settlements. Traditional settlements are located in the mountains area of Qian-dongnan, a fragile karst natural ecosystem with broken terrain, limited natural resources, changeable climate, and jointly impacted the spatial distribution of the seat of the settlement.

In the early stage of settlements formation, most settlements were located areas with an altitude of 50–1000 M, sloping gentle slopes of 5°–15°, and topographic relief of 10–20 M were easy to defend and difficult to attack and had a relatively good geographical environment, suitable for agricultural production activities with a low cost of living. In contrast, most of the northeast and southeast region had dangerous terrain, deep canyons, and poor soil. So the number of traditional settlements was relatively small.

After determining the selection and layout of the settlements, the ancestor of Miao began the overall management of the settlement environment, transforming the natural environment, opening up fields, and

planting economic trees, finally forming a landscape pattern of “mountain-water-forest-field-building.” It has been gradually formed after several generations of Miao people’s continuous exploration, construction, and adjustment. In this pattern, firstly, mountains surrounding the settlements provide shelter for living, and streams flowing in the fields provide for drinking and convenient field irrigation. Secondly, the fields make full use of the flat land in the mountains to provide people with the most basic food security, and the forests cover the mountains to maintain the ecology and protect the settlements from natural disasters, such as mudslides. Thirdly, the settlement houses are built in the mountains and will never invade the cultivated lands. As the population grows, the settlements continue to develop based on the unique natural conditions, presenting the following three modes:

- (1) *Natural growth within the original settlement pattern.* The population growth rate was still within the ecological capacity of the settlement, and the buildings were distributed along the contour lines, which formed a random and orderly group space. Its external boundary broke the balanced form of clusters or bands and extended in different directions and developed into finger shapes, and this is because the ravine of surrounding mountains made the environment and space resources uneven in all directions, and new buildings will always choose relatively flat and livable land followed natural environment as much as possible.
- (2) *Relying on the “multigroup” growth of the original settlement pattern.* There were some available lands for reclaiming in the settlement area, but the original settlement’s construction land was insufficient.

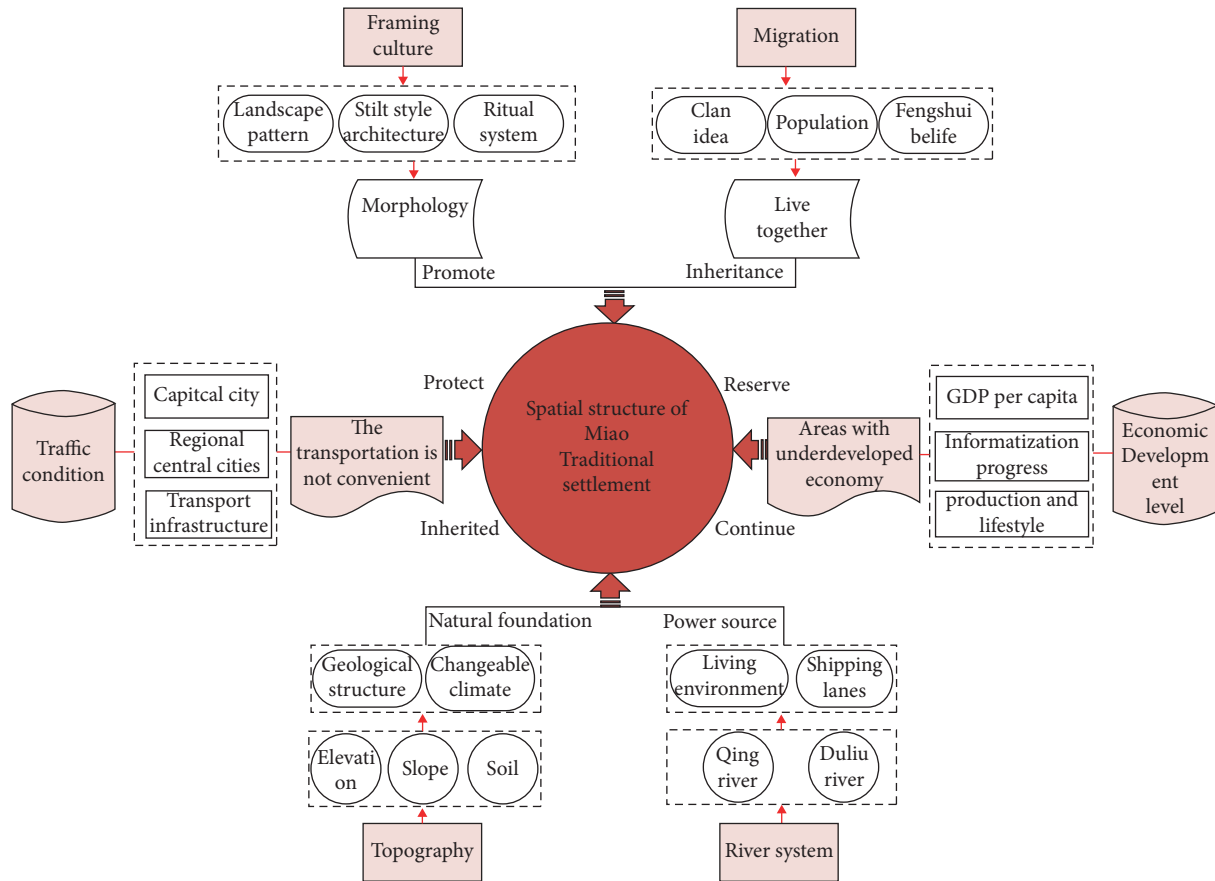


FIGURE 7: Adaptation mechanism for spatial evolution of Miao traditional settlement.

(3) Find a new location along the river to build a new settlement, then form a “branding” layout. When the lands of settlements were not enough to support the population growth, the residence would generally find a suitable location near the Qingshui and Duliu rivers to rebuild a new settlement. The rivers provided sufficient water for agricultural production and living in newly built settlements and served as important navigation between the Miao settlements and the Han areas, bringing agricultural production technology and living materials to Miao from Han areas.

4.2. Social Environment and Settlement Internal Space Organization. The social environment plays a guiding and controlling role in the evolution of traditional settlement spaces. Social environmental factors, such as clan ideas, “Fengshui” beliefs, and ritual systems, have affected the architectural layout, the spatial growth of streets, lanes, and bridges, the function of public space, and the formation of the morphology of traditional settlements.

Due to wars, ethnic oppression, and other reasons, the Miao people were forced to migrate from the plains and lakes to settle in the mountains. This migration was oppressive. However, the painful history of migration has not

diminished the national consciousness of the Miao people. The authority of the Miao clan, the sense of belonging to the migration, the common defense needs, and the consistent “Fengshui” beliefs and other group ideologies urged the Miao groups to live together in the same family or the same clan. Hence, the festival activities in the Miao culture are vibrant, and various activities had specific venues, such as Lushenping, Huzhai tree, Fengyu bridge, and pond, which were closely related to the process of ritual activities and created an orderly space. For example, the Miao ancestor chooses a flat open space in the internal space of settlements to build “Lushengping.” Its location was often in the center of the settlements space. The accessibility and the global average integration degree were also the highest based on the syntactic analysis of the six typical traditional settlements. As a matter of fact, “Lushengping” was usually used as a space for Miao people’s daily communication opportunities. But it has a very sacred meaning in festivals and has become an important cultural symbolic place to connect “ancestors and future generations.”

After the traditional settlements were formed, people started to reclaim fields, build houses, and expand the scale when the ecological capacity permitted. Once the original agglomeration point reached saturation, it became an important task for the Miao people to separate the surplus population and open up new strongholds. Then, settlements

were separated by clan ideas and “Fengshui” beliefs, and its branches were relocated to other surrounding spaces to multiply and develop. The spreads were like cell division, with new agglomeration points growing continuously and then a new round of fission. In brief, the internal spatial organization of settlements linked by social environment factors is the core of controlling the spatial order.

4.3. Economic Rise and Fall and Settlements Spatial Morphology Protection. Backward economic development has a positive impact on the protection of traditional settlements. Per capita GDP, per capita disposable income, and transportation convenience restrict the development scale and capacity of the settlement [21]. The settlements space formed during the agricultural cultivation period, and accordingly, its initial development depended on the scale of agricultural land. Although the settlement has formed the “mountain-water-forest-field-building” production space in the adjustment process, its production capacity can still only meet the basic survival needs, and Miao people mostly rely on self-sufficient small farmers to live. Before 1949, there were almost no current traffic conditions to contact the outside world, which also allowed many settlements to maintain traditional spatial characteristics and the wisdom of ancients [22].

In recent years, with the transformation of the rural economy, informatization, and tourism advancement, the settlements far away from the city and with inconvenient transportation were hit by unprecedented impact. The inherent production and lifestyles of settlements could no longer meet the needs of the younger generation, which caused the younger generation, especially the young and middle-aged laborers, to leave their homes. And eventually, the settlements disappeared. In addition, due to the continuous advancement of urbanization and the rural tourism industry, in the settlements that were relatively close to the urban space, a large number of new buildings arose, expanded to flat land and roads, and occupied farmland, which broke the overall pattern of “mountain-water-forest-field-building,” and made the original settlements become hollowed out. What’s more, this disorderly construction might bring about the demise of traditional settlements or the presence of totally new Miao settlements with no characteristics.

In contrast, the areas with poor social and economic development were subjected to many restrictions on contact with the outside world and were weaker from foreign cultural invasions. As a result, the settlements could continue their unique customs and habits, and spatial characteristics, such as buildings structures, boundary morphology, spatial distribution, and overall landscape pattern, got the possibility to be inherited and developed.

5. Conclusion

This paper uses spatial analysis methods to disclose the internal logic of the formation, organization scientifically, and the growth of Miao traditional settlements space from

the spatial distribution at the regional level to the micro-level settlement morphological characteristics, which are of specific reference value to policies and plans related to the conservation, utilization, and sustainable development of traditional settlements. The results show those as follows:

- (1) The spatial distribution of traditional settlements are affected by the comprehensive effects of the natural environment, social environment, and economic environment, mainly distributed areas with altitudes of 500–1000 M, terrain undulations of 10–20 M, slopes of 5°–25°, near the Qingshui river and Dulu river, and with backward economy and transportation.
- (2) Traditional settlements from a T-shaped structure in the overall regional spatial distribution pattern present a spatial distribution pattern of dense central and sparse northeast. The first-level center of the density pattern is the junction of Leishan, northern Danzhai, and southern Kaili. The “finger-shaped” form is the most common form of the external boundary of settlements.
- (3) The structure of traditional buildings shows a feature of large concentration and small dispersion and can be divided into “single-group” and “multigroup.” Moreover, these settlements generally formed an overall landscape pattern of “mountain-water-field-forest-building,” which is the basic space guarantee for survival and reproduction in the face of survival pressure.
- (4) External forces such as the natural environment, social economy, and technology are the basis for the formation and pattern evolution of the traditional settlement space and are also an important driving force that affects the transformation of the settlement space. The internal driving force, such as social culture, is vital for controlling the functional organization and continuing the spatial form.

At present, China has been in the process of rural revitalization, and excessive and disorderly constructions not only continue to invade and occupy rural land but also lead to some traditional settlements being demolished and becoming tourist towns. With the rise of social space research, traditional settlements should not be limited to traditional material spaces, and more attention should be paid to the accompanying social space research. Traditional settlements are caused by the spatial projection of people’s social activities and their organizational methods. The transformation of social structure will inevitably lead to the renewal of settlements space. Based on this cognition, follow-up research is needed to strengthen the interaction and coupling relationship between social structure and the evolution of settlements.

Data Availability

Four main categories of data sources are included in this study: (1) the list of minority characteristic villages from the

official website of the People's Government of Guizhou province; as of August 2021, 314 settlements in the study area have been selected into the list of ethnic minority villages in Guizhou province and; the geographic coordinates were calibrated using Google Earth; (2) the vector map, elevation, and river system of the administrative boundary of Qain-dongnan are provided by the Chinese Resources and Environment Science and Data Center; (3) the space syntax graph of traditional settlements was obtained from calculations of AutoCAD and Depthmap; (4) the drawing of overall landscape composition pattern map from field investigation and villager's interview; and (5) social and economic data were acquired from statistical yearbooks.

Conflicts of Interest

The authors declare that there are no conflicts of interest in the paper.

References

- [1] R. M. Adams and J. H. Steward, "Theory of Culture Change The Methodology of Multilinear Evolution Julian H Steward University of Illinois Press Urbana 1955 244 pp 5 tables \$4.00," *American Antiquity*, vol. 22, no. 2 Part 1, pp. 195-196, 1956.
- [2] R. W. Lacey, V. G. Alder, and W. A. Gillespie, "The survival of *Staphylococcus aureus* on human skin. An investigation using mixed cultures," *British Journal of Experimental Pathology*, vol. 51, no. 3, pp. 305-313, 1970.
- [3] U. Schirpke, F. Timmermann, U. Tappeiner, and E. Tasser, "Cultural ecosystem services of mountain regions: Modelling the aesthetic value," *Ecological Indicators*, vol. 69, pp. 78-90, 2016.
- [4] D. Mantey and P. Sudra, "Types of suburbs in post-socialist Poland and their potential for creating public spaces," *Cities*, vol. 88, pp. 209-221, 2019.
- [5] K. Daugstad, K. Rønningen, and B. Skar, "Agriculture as an upholder of cultural heritage? Conceptualizations and value judgements—A Norwegian perspective in international context," *Journal of Rural Studies*, vol. 22, no. 1, pp. 67-81, 2006.
- [6] A. A. Adewumi, "Cultural heritage protection and disaster risk management in Nigeria: Legal framework for promoting coherence and efficiency," *Art, Antiquity and Law*, vol. 23, p. 69, 2018.
- [7] R. M. Olalekan, O. Adedoyin O, E. A. Williams, M. B. Christianah, and O. Modupe, "The roles of all tiers of government and development partners in environmental conservation of natural resource: a case study in Nigeria," *MOJ Ecology & Environmental Sciences & Environmental Sciences*, vol. 4, no. 3, pp. 114-121, 2019.
- [8] "China Social Science," http://www.cssn.cn/mzx/202011/t20201109_5213095.shtml.
- [9] J. Bański and M. Wesołowska, "Transformations in housing construction in rural areas of Poland's Lublin region—Influence on the spatial settlement structure and landscape aesthetics," *Landscape and Urban Planning*, vol. 94, no. 2, pp. 116-126, 2010.
- [10] P. Angelstam, T. Yamelynets, M. Elbakidze, B. Prots, and M. Manton, "Gap analysis as a basis for strategic spatial planning of green infrastructure: a case study in the Ukrainian Carpathians," *Écoscience*, vol. 24, no. 1-2, pp. 41-58, 2017.
- [11] A. Wasilewski and K. Krukowski, "Land Conversion for Suburban Housing: A Study of Urbanization Around Warsaw and Olsztyn, Poland," *Environmental Management*, vol. 34, no. 2, pp. 291-303, 2004.
- [12] M. Sevenant and M. Antrop, "Settlement models, land use and visibility in rural landscapes: Two case studies in Greece," *Landscape and Urban Planning*, vol. 80, pp. 362-374, 2007.
- [13] A. Kaya, "Interpreting vernacular settlements using the spatial behavior concept," *Gazi University Journal of Science*, vol. 33, no. 2, pp. 297-316, 2020.
- [14] T. Sporna and R. Krzysztofik, "Inner'suburbanisation—Background of the phenomenon in a polycentric, post-socialist and post-industrial region. Example from the Katowice conurbation, Poland," *Cities*, vol. 104, Article ID 102789, 2020.
- [15] H. Pretzsch, "Analysis and modeling of spatial stand structures. Methodological considerations based on mixed beech-larch stands in Lower Saxony," *Forest Ecology and Management*, vol. 97, no. 3, pp. 237-253, 1997.
- [16] M. C. Jones, "Simple boundary correction for kernel density estimation," *Statistics and Computing*, vol. 3, pp. 135-146, 1993.
- [17] Y. Zhang, S. Baimu, J. Tong, and W. Wang, "Geometric spatial structure of traditional Tibetan settlements of Degger County, China: A case study of four villages," *Frontiers of Architectural Research*, vol. 7, no. 3, pp. 304-316, 2018.
- [18] S. Bafna, "Space syntax: A brief introduction to its logic and analytical techniques," *Environment and Behavior*, vol. 35, no. 1, pp. 17-29, 2003.
- [19] P. Brandolini, C. Cappadonia, G. M. Luberti et al., "Geomorphology of the Anthropocene in Mediterranean urban areas," *Progress in Physical Geography: Earth and Environment*, vol. 44, no. 4, pp. 461-494, 2020.
- [20] S. Kamal and V. Lim, "Forest reserve as an inclusive or exclusive space? Engaging orang asli as stakeholder in protected area management," *Journal of Tropical Forest Science*, vol. 31, no. 3, pp. 278-285, 2019.
- [21] Y. Li, Y. Liu, H. Long, and W. Cui, "Community-based rural residential land consolidation and allocation can help to revitalize hollowed villages in traditional agricultural areas of China: Evidence from Dancheng County, Henan Province," *Land Use Policy*, vol. 39, pp. 188-198, 2014.
- [22] J. Xu, M. S. Yang, C. P. Hou, Z. L. Lu, and D. Liu, "Distribution of rural tourism development in geographical space: a case study of 323 traditional villages in Shaanxi, China," *European Journal of Remote Sensing*, vol. 54, no. sup2, pp. 318-333, 2021.

Research Article

Evaluation of China's High-Advanced Industrial Policy: A PMC Index Model Approach

Ying Tian ¹, Kai Zhang ¹, Jiayi Hong ¹ and Fanglin Meng ²

¹School of Management, University of Shanghai for Science and Technology, Shanghai 200093, China

²School of Business, Shanghai Sanda University, Shanghai 201209, China

Correspondence should be addressed to Kai Zhang; 1913120134@st.usst.edu.cn

Received 1 July 2022; Accepted 15 September 2022; Published 30 September 2022

Academic Editor: Wei Liu

Copyright © 2022 Ying Tian et al. This is an open access article distributed under the Creative Commons Attribution License, which permits unrestricted use, distribution, and reproduction in any medium, provided the original work is properly cited.

High-advanced industries upgraded by digital empowerment have gradually become an important support industry. Therefore, various provinces in China have issued relevant policies to support the prosperous of the digital economy and high-advanced industries. The collection and analysis of high-advanced industrial policy help to scientifically evaluate industrial policies and formulate scientific policy optimization paths. Based on a total of 168 high-advanced industrial policy documents from 26 cities in the Yangtze River Delta region from 2009–2021, this study adopts the PMC-Index model to evaluate the high-advanced industry policies in the digitalization context quantitatively. 12 representative high-advanced industry policy texts were selected for specific analysis. In addition, this study visualizes the measurement results of the internal structure and policy effectiveness of policies by PMC-Surface diagrams and then concludes that the design of high-advanced industry policies was relatively reasonable overall, with 11 policies rated as “Good Consistency” and only one “Acceptable Consistency.” The sample policies lack reasonable arrangements for different period plans, lack incentives, or have relatively single incentives. The policy influence among cities in the Yangtze River Delta urban agglomerations is small, and the integration trend is not apparent. There is a particular gap in the scores between Shanghai, Zhejiang, Jiangsu, and Anhui province. This study provides references and suggestions for formulating and revising high-advanced industrial policies.

1. Introduction

Digital technology is dramatically changing industrial production and organizational activities [1, 2]. The digitization of industries is providing the impetus for economic development in various countries. Each country has different directions and motivations for using digital technology to promote economic development, so the impact of digitization on national economies is also different [3]. Digitization refers to using digital technology to create new business models, new business formats, and industrial production models, thereby improving product quality, production quantity, and production efficiency [4]. Digitization empowers and embeds industries to help industrial transformation and technological innovation [5, 6].

China is gradually shifting its economic focus from rapid GDP growth to high-quality economic development,

considering transforming from the world's factory to an innovative powerhouse with leading-edge technologies [7]. China needs to transform and upgrade its industry with the help of the digital empowerment of industry [8]. The high-advanced industry, closely linked to digitalization, has become the main target of industrial transformation and upgrading [9]. High-advanced industries characterized by high technological knowledge density, high intensity of R&D investment, and high added value have gradually become essential support industries for national economic development and are an important symbol of a country's core competitiveness [10]. This study takes the advanced industry proposed by the American Brookings Institution as the core definition of a high-advanced industry. The study “America's Advanced Industries,” released by the Brookings Institution in February 2015, states that industries that meet the following two criteria are defined as the high-advanced

industry: First, the industry must use at least 80% of the expenditure for research and development each year. Each worker must spend more than \$ 450 on research and development. Secondly, the proportion of workers in the industry that requires high-level STEM (science, technology, engineering, and mathematics education) knowledge should also be higher than the national average, or 21% of all workers [11].

For the sake of meeting the trend of digital economy and realizing the transformation from low advanced industries to high advanced industries, the governments of various regions in China have adopted relevant industrial policies. However, in the policy playing a role, there are also some problems: the security measures and incentives of the policy are ineffective, there is a lack of mechanism for policy implementation and supervision, the content of the policy is incomplete, and the effect of policy implementation is not obvious. Therefore, it is necessary to scientifically evaluate and judge the high-advanced industrial policy, test the effectiveness of the policy, reasonably allocate the policy resource base, and provide a scientific governance basis [12].

The PMC-Index model can evaluate policies based on establishing a system of relevant indicators and calculate each policy's score composition to effectively evaluate policies [13]. This study creatively puts forward the concept of China's high-advanced industry, evaluates the effectiveness of policies by the PMC-Index model, taking the Yangtze River Delta region of China as an example.

The remaining structure of this study is as follows. Section 2 reviews the relevant literature. Section 3 introduces the research samples and research methods. Section 4 demonstrates the empirical results and analysis. Section 5 puts forward the conclusions and limitations.

2. Literature Review

Existing research on high-advanced industry mainly focuses on three categories. One is the research conducted with high-advanced industry as the subject term. Since the concept of the high-advanced industry mentioned above is not clearly defined, fewer studies directly use the high-advanced industry as a subject term [14]. The second is the study of a specific industry in the high-advanced industry [15]. Wu et al. processed and modeled the data through spatial econometric models to derive the impact of regional financial resources on the cluster of high-advanced horizontal service industries [16]. The third is the study of strategic emerging industries [17]. Prud'homme examined technological specialization in strategic emerging industries and found that China's economic decentralization system ensures, to some extent, the effectiveness of provincial industrial policy making [18].

Policy evaluation is the development of appropriate evaluation criteria through scientific methods to examine policies in multiple dimensions and provide references for policy improvement and new policy development. It can assess the usefulness and value of the policy itself and check the results and effectiveness of its implementation [19]. The first policy evaluation studies were the five-category

assessment model proposed by Suchman [20] and the "Three E" Evaluation Model Architecture proposed by Poland [21]. Jun proposed a classical policy evaluation approach to policy analysis through causality [22]. At present, the commonly used policy evaluation methods include the hierarchical analysis process (HAP), BP neural network, and fuzzy comprehensive evaluation method [23, 24].

The policy modeling consistency index (PMC-Index) model was proposed by Estrada, which can evaluate any social policy to analyze the results and impacts of implementation and the reasons for the results or impacts [25]. The model provides policy researchers with a new tool for policy analysis that can detect policy strengths and weaknesses. The model has been applied to the evaluation of the arable land protection policy [26], pork price policy evaluation [13], and the new energy vehicle policy evaluation [27].

3. Materials and Method

3.1. Data Source and Sample Selection. To obtain high-advanced industry policy texts in a digital context systematically and comprehensively, the following search strategy is used in this study. Taking 2009 as the policy starting point, the policy and regulation databases such as "Beida Fabao" (<http://www.pkulaw.cn/>) and "Beida Fayi" (<http://www.lawyee.net/>) were used as data sources, supplemented by the official websites of cities in the Yangtze River Delta. We searched for "high-advanced industry" and "digitalization" as keywords to filter the policy texts of high-advanced industry in the context of digitalization in each city of the Yangtze River Delta. After the above screening, 168 policy texts were retrieved from 26 cities in the Yangtze River Delta region from January 1, 2009, to April 19, 2021. Based on the retrieved policies, these policy texts were sorted out to eliminate those that were irrelevant and repetitive to high-advanced industries, and finally, 44 policy texts with strong relevance were screened out.

3.2. Establishment of PMC-Index Model. As shown in Figure 1, there are five steps to construct the PMC-Index model: Policy text mining is used to classify variables, identify parameters, and then determine this evaluation system's main variables and subvariables. Multi-input-output tables are then constructed based on variable classification and parameter identification to form the framework for data analysis. The results are further analyzed by calculating the PMC-Index to quantify the analysis and visualize the PMC-Surface diagram.

3.2.1. Word Division and Word Frequency Statistics. In this study, the policy text is processed with the help of the text mining tool ROST software. First, the core keywords of the policy text are obtained by reading the policy text, and then the keywords are imported into the word separation table of ROST for the next word separation and word frequency statistics. Next, 44 high-advanced industry policy texts were input into the ROST, and the obtained text sets are word-

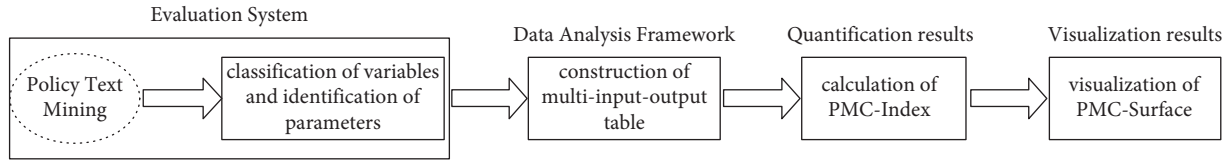


FIGURE 1: PMC-index model construction framework.

sorted and word frequencies are counted in the order from highest to lowest. Since ROST software automatically identifies keywords with no practical meaning, it is necessary to filter out high-frequency words such as “provide” and “above” that have no practical meaning for policy analysis. After eliminating the redundant words, the valid keywords are screened out and a list of the top 50 keywords in terms of word frequency is compiled as shown in Table 1.

3.2.2. *Analysis of Social Networks.* Reimport statistical keywords above into the Rost software and extract the high-frequency words and row features from the cooccurrence matrix. Based on the cooccurrence matrix, the visualization network diagram of China’s high-advanced industrial policy is drawn by Ucinet software.

As shown in Figure 2, each node represents a keyword, and the line between nodes represents the existence of a correlation between two nodes. In the social network, the node at the center is more important, can be interconnected with more nodes, and has more influence on the whole social network. In this social network, technology, innovation, R&D, etc., are at the center position, indicating that these keywords have a vital influence on the policy guidance in high-advanced industries. The digitization of high-advanced industry and technological innovation are inseparable. Relying on R&D to increase the added value of technology can realize the transformation and digitization of technology from low-advanced to high-advanced and realize industrial layout and growth. Keywords around the center are talent, market, entrepreneurship, industry chain, etc. That is, the transformation and digitalization of high-advanced industry cannot be separated from the support of talents, the improvement of the market, the vitality of entrepreneurship, and the construction of the industrial chain. Talents bring intellectual capital to the high-advanced industries. The perfection and development of the market realize the supply and demand balance. Entrepreneurship brings new growth points, creates a new pattern of high-advanced industrial chain development through industrial complementary cooperation, and lays out the industrial chain around the innovation chain, so as to enhance international competitiveness. These keywords are in between the central and marginal positions and have a relatively strong influence. They are both influenced by main keywords and can influence marginal keywords. The keywords in marginal positions are less influential and have even weaker interconnections with other keywords.

TABLE 1: Key words of China’s high-advanced industry regulation policy text.

Number	Keyword	Frequency
1	Technique	4815
2	Enterprise	4311
3	Innovation	3674
4	Technology	2782
5	Service	1874
6	Industry	1758
7	Research and development	1573
8	Project	1317
9	Manufacturing	1238
10	Nurturing	1068
11	Engineering	1058
12	Equipment	1057
13	Key	1019
14	Economy	1011
15	Center	978
16	Talents	973
17	Material	934
18	Resource	928
19	System	927
20	Management	810
21	New	764
22	Development	754
23	Intelligence	740
24	Entrepreneurship	731
25	Mechanism	719
26	Research	684
27	Software	659
28	Bases	643
29	Core	632
30	Encourage	629
31	Environment	627
32	Policy	626
33	Institution	623
34	Industrialization	615
35	Basis	593
36	Integration	593
37	New energy	590
38	Market	583
39	Scope	549
40	Investment	536
41	Feature	531
42	Planning	527
43	Strategic emerging industry	527
44	Gather	517
45	Cooperation	495
46	Breakthrough	492
47	Strategy	492
48	Electronic	486
49	Energy saving	482
50	Biology	477

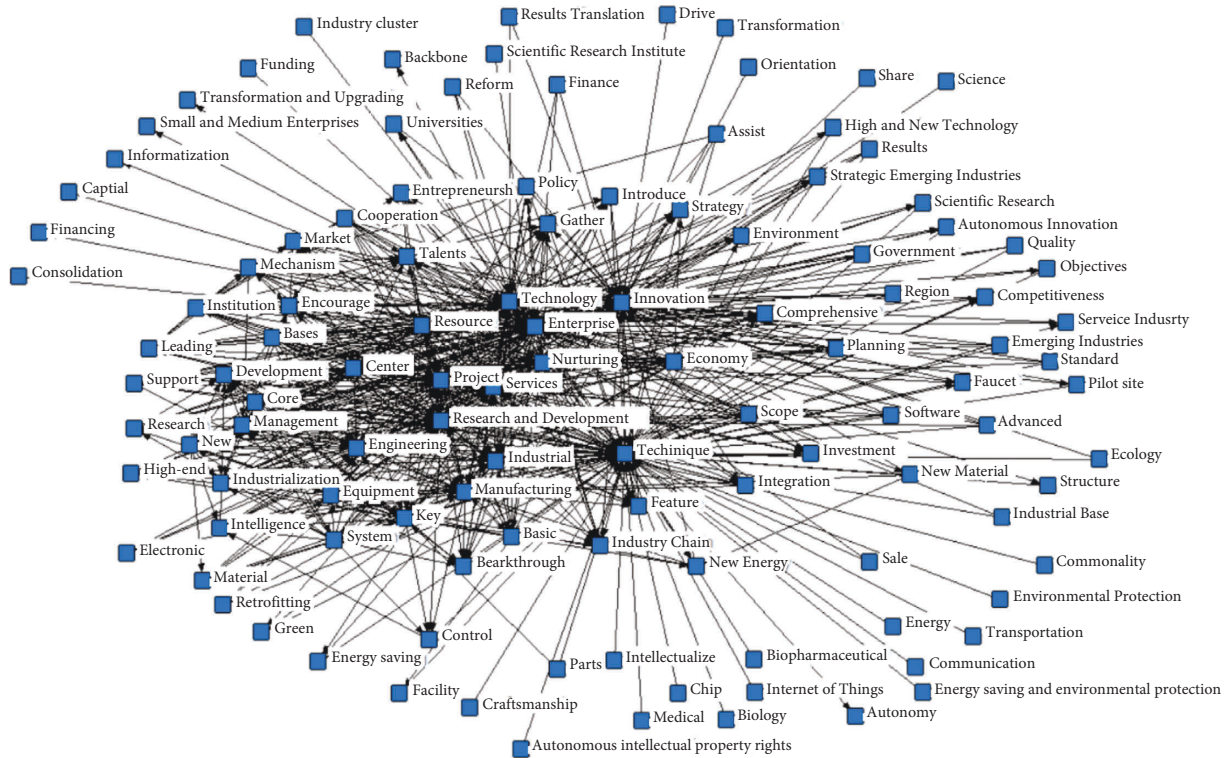


FIGURE 2: The social network of China's high-advanced industry regulation policy.

3.2.3. Classification of Variables and Identification of Parameters. Based on Jin's policy evaluation variables proposed by Jin [24] and the words combined with high-frequency of policy texts and their social networks analysis results, 10 main variables and 38 subvariables are set and shown in Table 2.

The 10 main variables are as follows: (X_1) Policy type; (X_2) Policy timeliness; (X_3) Policy function; (X_4) Incentives; (X_5) Policy area; (X_6) Policy evaluation; (X_7) Policy focus; (X_8) Policy object; (X_9) Policy level and (X_{10}) Public policy. Policy type (X_1) is to evaluate whether the policy has a predictive, supervisory, advisory, descriptive, and guiding role for high-advanced industries. Policy timeliness (X_2) is to judge whether the policy has the effective duration of long-term, short-term, medium-term, or less than 1 year. Policy function (X_3) is to reveal the purpose of policy introduction and to judge whether the policy can improve the industry's quality level, promote the industry's restructuring, and promote innovation within the industry for the high-advanced industry. Incentives (X_4) refers to incentive measures of the smooth implementation and the active cooperation of policy recipients, including talent introduction, tax subsidies, R&D subsidies, and other incentive measures. Policy area (X_5) is a division based on economic, social, scientific, political, environmental, and other areas to judge the areas covered by the policy. Policy evaluation (X_6) is to evaluate the reasonableness of the policy based on four aspects: adequate basis, a clear objective, a scientific program, and explicit content. Policy focus (X_7) is to examine the focus

involved in the policy content, including innovation, talent training, the transformation of results, market leadership, and other focus. Policy object (X_8) is the object of policy action, including enterprises, financial institutions, regulatory authorities, and other objects. Policy level (X_9) indicates the scope of policy implementation, which is divided into three levels: regional cluster, province, and industry. Public policy (X_{10}) reflects whether the policy is publicly released.

If the policy text has the same content as the subvariables, the parameter of the subvariables is set to "1;" otherwise, it is set to "0." After setting the main variable and subvariable, use the text mining method to score the variables. The variable scoring criteria are shown in Table 3.

3.2.4. Constructing Multi-Input-Output Table. This study stores, calculates, and analyzes data through multi-input-output tables and uses policy variables to evaluate the effect of the results.

3.2.5. Calculation of the PMC-Index. Step 1: place the main variables and subvariables into a multi-input-output table. Step 2: evaluate the subvariables based on the variable scoring criteria for text mining. Expression (1) is used to determine the subvariables to be evaluated. Step 3: integrate the values of each subvariable obtained in step 2 according to Expression (1) and calculate the value of variables. Step 4: measure the final PMC-Index according to Expression (2).

$$X \sim N[0, 1],$$

$$X = XR: [0 \sim 1],$$

(1)

$$X_a = \left(\sum_{b=1}^n \frac{X_a b}{T(X_a b)} \right) \quad a = 1, 2, 3, 4, 5 \dots,$$

a = main variables; b = subvariables:

$$\begin{aligned} \text{PMC - Index} = & X_1 \left(\sum_{o=1}^5 \frac{X_1 o}{5} \right) + X_2 \left(\sum_{p=1}^4 \frac{X_2 p}{4} \right) + X_3 \left(\sum_{q=1}^3 \frac{X_3 q}{3} \right) + X_4 \left(\sum_{r=1}^4 \frac{X_4 r}{4} \right) + \\ & X_5 \left(\sum_{s=1}^6 \frac{X_5 s}{6} \right) + X_6 \left(\sum_{t=1}^4 \frac{X_6 t}{4} \right) + X_7 \left(\sum_{u=1}^5 \frac{X_7 u}{5} \right) + X_8 \left(\sum_{v=1}^4 \frac{X_8 v}{4} \right) + X_9 \left(\sum_{w=1}^3 \frac{X_9 w}{3} \right) + X_{10}. \end{aligned} \quad (2)$$

3.2.6. *Evaluation the Consistency of Policy Value.* The PMC index value can reflect the strategic model’s consistency level. As shown in Table 4, when the PMC index value is 0–4.99, the consistency of policy is low. When the PMC index value is 5–6.99, the consistency of policy is acceptable. When the PMC index value is 7–8.99, the consistency of policy is good. When the PMC index value is 9–10, the consistency of policy is entirely perfect. The higher the PMC index value is, the more perfect the content of the policy text is. Then, the policy can have strong operability in practice.

To make the policy assessment more objective and reduce subjective errors, the corresponding score is increased only when the assessment indicators are clearly and explicitly described in the policy text; otherwise, no points are added. When there are indeterminable or highly subjective assessment indicators, discuss them with other researchers before deciding whether to add points. This will make the assessment results more objective and have higher credibility.

3.2.7. *Visualization of the PMC-Surface.* By visualizing the PMC index value, this study draws a PMC surface diagram, which can intuitively and clearly perspective the policy model, so as to judge the effectiveness of the policy. Draw PMC surface diagram according to PMC matrix in Expression (3). PMC matrix is a 3×3 matrix mainly composed of nine variables, namely (X_1-X_9) . Because the number of rows and columns in the matrix are the same, these variables have a certain balance and symmetry. Among them, $X_1, X_2,$ and X_3 are series 1, $X_4, X_5,$ and X_6 are series 2, $X_7, X_8,$ and X_9 are series 3.

$$\text{PMC - Surface} = \begin{pmatrix} X_1 & X_2 & X_3 \\ X_4 & X_5 & X_6 \\ X_7 & X_8 & X_9 \end{pmatrix}. \quad (3)$$

4. Results

Considering that the policy priorities issued by government agencies and the commonality and respective characteristics of policies in different regions are different, this study selects 12 representative policy texts according to the provinces or municipalities to which the Yangtze River Delta cities belong. As shown in Table 5, $P_1 - P_3$ is the policy of Shanghai, $P_4 - P_6$ is the policy of Anhui, $P_7 - P_9$ is the policy of Jiangsu, and $P_{10} - P_{12}$ is the policy of Zhejiang.

According to the PMC index model of the above high-advanced industrial policy evaluation, this study uses the text mining method to construct multi-input-output tables for 12 policies and thus calculates scores for each policy. Finally, the PMC-Index and evaluation level of the policies is constructed and shown in Table 6.

As shown in Table 6, the mean value of the 12 policies is 8.09. Among the 12 policies, only the level of P_5 is acceptable, while the level of the PMC-Index for the rest of the policies is good. The overall quality of the 12 policies is excellent. No low consistency policies, with a certain degree of scientific and rationale, can provide guidance for the rapid growth of the high-advanced industry. Nevertheless, the lack of perfect, consistency policies also mean there is still a need and room for further improvement in the design of the policies in terms of content. According to the policies divided by different regions, the mean PMC-Index of Shanghai is 8.24, the mean PMC-Index of Anhui is 7.57, the mean PMC-Index of Jiangsu is 8.35, and the mean PMC-Index of Zhejiang is 8.20. The policy with the highest PMC-Index score is in Jiangsu province, Zhejiang and Shanghai, while Anhui’s policy performs poorly compared to other provinces.

To facilitate comparisons between policies, this study plots PMC-Surface for each of the 12 policies by using PMC-

TABLE 2: High-advanced industry policy evaluation variable settings.

Main variables	Sub variables	References
(X ₁) policy type	(X ₁₋₁) predictive role (X ₁₋₂) supervisory role (X ₁₋₃) advisory role (X ₁₋₄) descriptive role (X ₁₋₅) guiding role	[24]
(X ₂) policy timeliness	(X ₂₋₁) long term (>5 years) (X ₂₋₂) medium term (3–5 years) (X ₂₋₃) short term (1–3 years) (X ₂₋₄) less than 1 year (<1 years)	[24]
(X ₃) policy function	(X ₃₋₁) improving the quality of industry (X ₃₋₂) promoting industrial restructuring (X ₃₋₃) promoting technology innovation	Due to social network
(X ₄) incentives	(X ₄₋₁) talent introduction (X ₄₋₂) tax subsidy (X ₄₋₃) R&D subsidy (X ₄₋₄) other	Due to social network
(X ₅) policy area	(X ₅₋₁) economy (X ₅₋₂) society (X ₅₋₃) technology (X ₅₋₄) politics (X ₅₋₅) environment (X ₅₋₆) other	[24]
(X ₆) policy evaluation	(X ₆₋₁) adequate basis (X ₆₋₂) clearly defined goals (X ₆₋₃) scientific programs (X ₆₋₄) detailed content	[12]
(X ₇) policy focus	(X ₇₋₁) technological innovation (X ₇₋₂) talent cultivation (X ₇₋₃) achievement transformation (X ₇₋₄) market-leading (X ₇₋₅) other	Due to social network
(X ₈) policy object	(X ₈₋₁) enterprise (X ₈₋₂) financing institution (X ₈₋₃) management department (X ₈₋₄) other	[12]
(X ₉) policy level	(X ₉₋₁) regional cluster (X ₉₋₂) province (X ₉₋₃) industry	[24]
(X ₁₀) public policy		[12]

Index and PMC-Matrix and conducts a detailed analysis which are shown in Figures 3(a)–3(l). The different colors in the graph represent different segments, with a depression indicating that the variable has a lower score than the other variables and a bump indicating that the variable has a higher score than the other variables.

Most of the 10 main variables scored high and achieved good performance. Among them, X₁₀ (Public policy) has a score of 1 with perfect consistency, which is since the implementation of the country's policies is based on the people, so an open-ended approach is taken to the policies. In comparison, X₂ (Policy timeliness) and X₄ (Incentives) have poorer scores, which differ significantly from the mean. Since most of these policy texts play a guiding role in the policy implementation, the specific arrangements for

different periods are not described in great detail. It is also because these policy texts describe the policy in general terms that they do not describe in detail the incentives for the development of the high-advanced industry. Relevant institutions need to improve these, make more detailed and reasonable arrangements for the content of the policy texts, and add some incentives to make the guidance and role of the policy text clearer. To facilitate the comparison of the degree of depression between each principal variable, plot the average depression index of each principal variable in the PMC-Surface as a radar plot in Figure 4. In Figure 4, the mean values of concavity indices for X₂ and X₄ are 0.60 and 0.52, respectively, which are significantly more concave than the other main variables. The mean value of the depression index for X₉ is similarly higher than the overall

TABLE 3: Variable scoring criteria.

	Variables	Scoring criteria
X_1	(X_{1-1}) predictive role	If the policy is predictive, it is 1. If not, it is 0.
	(X_{1-2}) supervisory role	If the policy is regulatory, it is 1. If not, it is 0.
	(X_{1-3}) advisory role	If the policy makes recommendations, it is 1. If not, it is 0.
	(X_{1-4}) descriptive role	If the policy is descriptive, it is 1. If not, it is 0.
	(X_{1-5}) guiding role	If the policy is instructive, it is 1. If not, it is 0.
X_2	(X_{2-1}) long term	If the policy involves long-term content (more than 5 years), it is 1. If not, it is 0.
	(X_{2-2}) medium term	If the policy involves medium-term content (3–5 years), it is 1. If not, it is 0.
	(X_{2-3}) short term	If the policy involves short-term content (1–3 years), it is 1. If not, it is 0.
	(X_{2-4}) within 1 year	If the policy involves the content within 1 years, it is 1. If not, it is 0.
X_3	(X_{3-1}) improving the quality of industry	If the policy has elements to improve the quality of the industry, it is 1. If not, it is 0.
	(X_{3-2}) promoting industrial restructuring	If the policy has elements to promote industrial restructuring, it is 1. If not, it is 0.
	(X_{3-3}) promoting technology innovation	If the policy has elements to promote technology innovation, it is 1. If not, it is 0.
X_4	(X_{4-1}) talent introduction	If the policy involves talent introduction incentives, it is 1. If not, it is 0.
	(X_{4-2}) tax subsidy	If the policy involves tax subsidy incentives, it is 1. If not, it is 0.
	(X_{4-3}) R&D subsidy	If the policy involves R&D subsidy incentives, it is 1. If not, it is 0.
	(X_{4-4}) other	If the policy involves other incentives, it is 1. If not, it is 0.
X_5	(X_{5-1}) economy	If the policy is related to the economic field, it is 1. If not, it is 0.
	(X_{5-2}) society	If the policy is related to the social field, it is 1. If not, it is 0.
	(X_{5-3}) technology	If the policy is related to the technology field, it is 1. If not, it is 0.
	(X_{5-4}) politics	If the policy is related to the political field, it is 1. If not, it is 0.
	(X_{5-5}) environment	If the policy is related to the environmental field, it is 1. If not, it is 0.
	(X_{5-6}) other	If the policy is related to the other field, it is 1. If not, it is 0.
X_6	(X_{6-1}) adequate basis	If the policy is well founded, it is 1. If not, it is 0.
	(X_{6-2}) clearly defined goals	If the policy is clear, it is 1. If not, it is 0.
	(X_{6-3}) scientific programs	If the policy is scientific, it is 1. If not, it is 0.
	(X_{6-4}) detailed content	If the policy is exhaustive, it is 1. If not, it is 0.
X_7	(X_{7-1}) technological innovation	If the policy pays attention to technological innovation, it is 1. If not, it is 0.
	(X_{7-2}) talent cultivation	If the policy pays attention to talent cultivation, it is 1. If not, it is 0.
	(X_{7-3}) achievement transformation	If the policy pays attention to achievement transformation, it is 1. If not, it is 0.
	(X_{7-4}) market-leading	If the policy pays attention to market-leading, it is 1. If not, it is 0.
	(X_{7-5}) other	If the policy pays attention to other, it is 1. If not, it is 0.
X_8	(X_{8-1}) enterprise	If the policy involves enterprises, it is 1. If not, it is 0.
	(X_{8-2}) financing institution	If the policy involves financing institutions, it is 1. If not, it is 0.
	(X_{8-3}) management department	If the policy involves management departments, it is 1. If not, it is 0.
	(X_{8-4}) other	If the policy involves other, it is 1. If not, it is 0.
X_9	(X_{9-1}) regional cluster	If the policy focuses on Yangtze river delta, it is 1. If not, it is 0.
	(X_{9-2}) province	If the policy focuses on a province, it is 1. If not, it is 0.
	(X_{9-3}) industry	If the policy involves an industry, it is 1. If not, it is 0.
X_{10}		If the policy is open, it is 1. If not, it is 0.

TABLE 4: Policy evaluation criteria.

PMC-index	0–4.99	5–6.99	7–8.99	9–10
Evaluation	Low	Acceptable	Good	Perfect

mean. The concavity indices of the remaining main variables are all smaller than the mean, indicating that these policy texts are more consistent and dominant in these areas.

When divided by region, there is convergence in the approach of policies introduced by local institutions, and there is some similarity in the values of the resulting PMC-Index. However, there is some variability in the PMC-Index of policies between regions. At a macro level, this is due to the economic, political, and cultural influences of different regions, which lead to differences in the level of policies

introduced. At a micro level, the level of policies introduced is limited by the scope of authority of different institutions and their level of competence.

Most of the 12 policy texts have good consistency with a mean value of 1.91 for the degree of concavity of the PMC-Surface. Only the policy level of P_5 is acceptably consistent, and the degree of depression is much greater than the average degree of depression. This study compares the P_5 with the best-performing P_{10} to compare where the gap exists between the two, and to arrive at the same advantages or disadvantages. As shown in Figure 5, P_5 has a particular gap with P_{10} overall. The scores of the main variables X_1 , X_9 , and X_{10} of P_5 are the same as P_{10} , but the scores of the remaining main variables of P_5 are lower than P_{10} .

X_2 (Policy timeliness). In P_5 , there is only a medium-term plan for the next 5 years, not a long-term plan or a more detailed plan for the short term. P_{10} has not only a 5-year

TABLE 5: High-advanced industry representative policy summary.

Policy	Policy name	Institution	Release date
P_1	Qingpu district to accelerate the implementation of high-tech industrialization.	Shanghai Qingpu district people's government	July 31, 2009
P_2	Supply-side structural reform to promote industrial stability and growth of the structure and transformation.	Shanghai municipal people's government	April 29, 2016
P_3	Shanghai strategic emerging industries development "the 12th five-year plan."	Shanghai municipal people's government	January 4, 2012
P_4	The 12th five-year plan for industrial development of Hefei.	The general office of Hefei municipal people's government	June 23, 2011
P_5	Accelerating the implementation of industrial transformation and upgrading.	Anqing municipal people's government	July 27, 2016
P_6	Accelerating the cultivation of strategic emerging industries.	The office of Wuhu municipal people's government	June 14, 2011
P_7	Suzhou city emerging industries multiplier development plan (2010~2012).	Suzhou municipal people's government of Jiangsu province	November 25, 2010
P_8	The Nanjing action plan for promoting innovation, promoting industrial transformation, and developing an innovative economy.	The CPC Nanjing municipal committee and the Nanjing municipal people's government	March 12, 2010
P_9	The 13th five-year plan strategic emerging industries development plan of Nantong city	Nantong municipal government office	December 28, 2016
P_{10}	The 13th five-year plan for the development of industry and information economy in Hangzhou"	The general office of Hangzhou municipal people's government	December 15, 2016
P_{11}	The 13th five-year industrial development plan	Shaoxing city people's government on the issuance of Shaoxing city	June 15, 2016
P_{12}	Accelerating Hangzhou guiding opinions on intelligent manufacturing for industrial transformation and development.	Hangzhou municipal people's government	August 21, 2015

TABLE 6: PMC-Index and evaluation level of 12 China's high-advanced industrial policies.

Main variables	P_1	P_2	P_3	P_4	P_5	P_6	P_7	P_8	P_9	P_{10}	P_{11}	P_{12}	Average
X_1	0.80	0.80	0.80	0.80	1.00	1.00	0.80	0.80	0.80	1.00	1.00	0.80	0.87
X_2	0.50	0.50	0.25	0.25	0.25	0.25	0.50	0.75	0.25	0.50	0.50	0.25	0.40
X_3	0.67	1.00	1.00	1.00	0.67	1.00	1.00	1.00	1.00	1.00	1.00	0.67	0.92
X_4	0.75	0.50	0.75	0.00	0.25	0.50	0.50	0.50	0.50	0.75	0.50	0.25	0.48
X_5	1.00	1.00	1.00	1.00	0.83	1.00	1.00	1.00	1.00	1.00	1.00	0.83	0.97
X_6	1.00	1.00	1.00	1.00	0.75	1.00	1.00	1.00	1.00	1.00	1.00	0.75	0.96
X_7	0.60	0.80	1.00	0.60	0.80	1.00	0.80	1.00	1.00	1.00	1.00	0.80	0.87
X_8	1.00	1.00	1.00	1.00	0.75	1.00	0.75	0.75	1.00	1.00	1.00	1.00	0.94
X_9	0.67	0.67	0.67	0.67	0.67	0.67	0.67	1.00	0.67	0.67	0.67	0.67	0.70
X_{10}	1.00	1.00	1.00	1.00	1.00	1.00	1.00	1.00	1.00	1.00	1.00	1.00	1.00
Total score	7.99	8.27	8.47	7.32	6.97	8.42	8.02	8.80	8.22	8.92	8.67	7.02	8.09
Ranking	9	6	4	10	12	5	8	2	7	1	3	11	—
Level	Good	Good	Good	Good	Acceptable	Good	Good	Good	Good	Good	Good	Good	—

medium-term plan but also a long-term plan beyond 5 years, but the description of the short-term plan is still missing in P_{10} .

X_3 (Policy function). P_5 contains the content of promoting the quality of the industry and scientific and technological innovation, but there is no clear proposal for restructuring the industry. On this issue, P_5 does not keep pace with the times and makes strategies to improve the industrial structure. P_{10} 's policy features are much more

comprehensive, providing more detailed descriptions of each of these directions.

X_4 (Incentives). Regarding incentives, P_5 only mentions making corresponding financial subsidies, and there are no more incentives to encourage the development of the high-advanced industry. While in P_{10} , not only financial subsidies and loan subsidies are mentioned, but also talent introduction and tax subsidies, which are more conducive to accelerating the development of the high-advanced

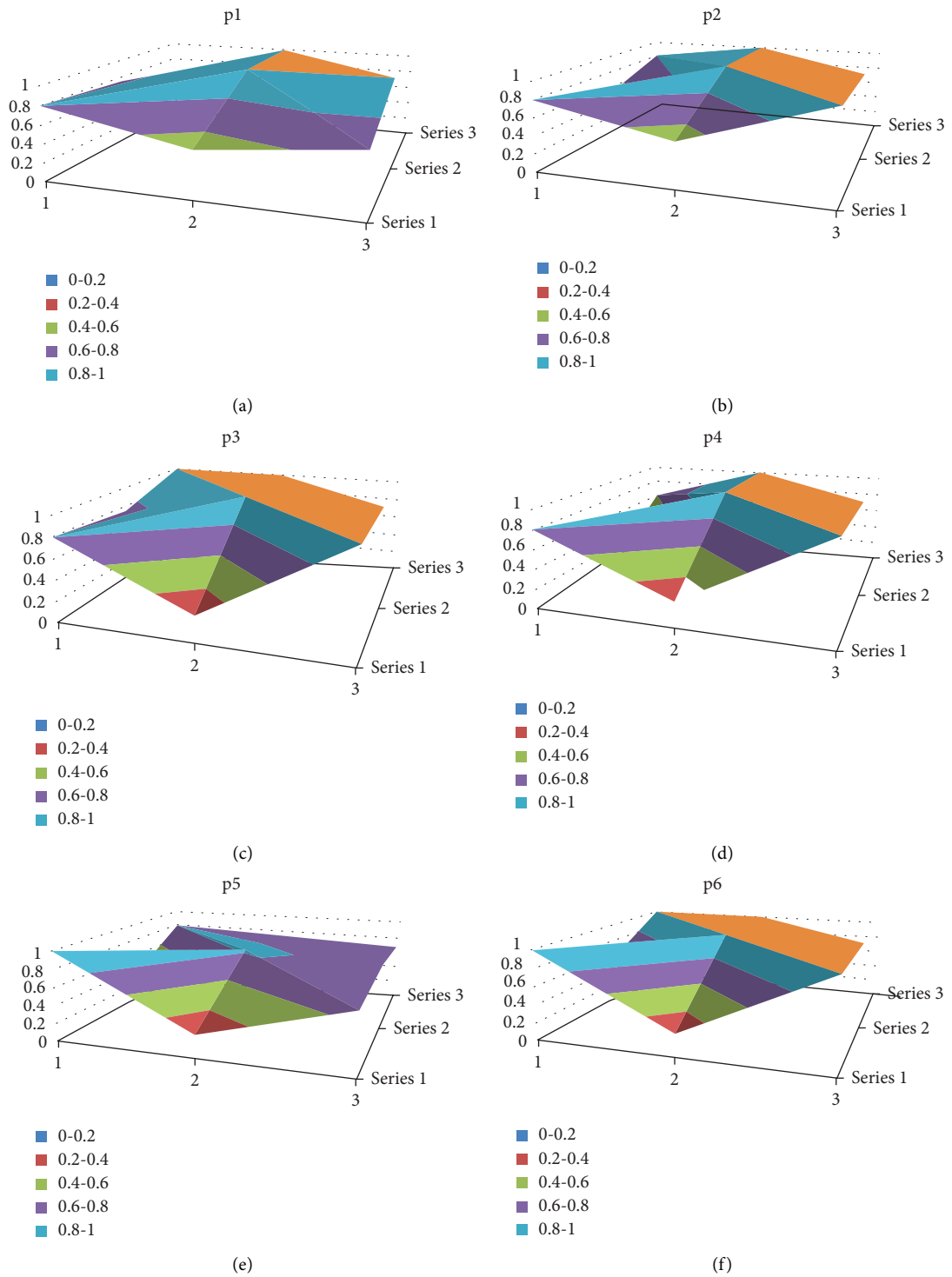


FIGURE 3: Continued.

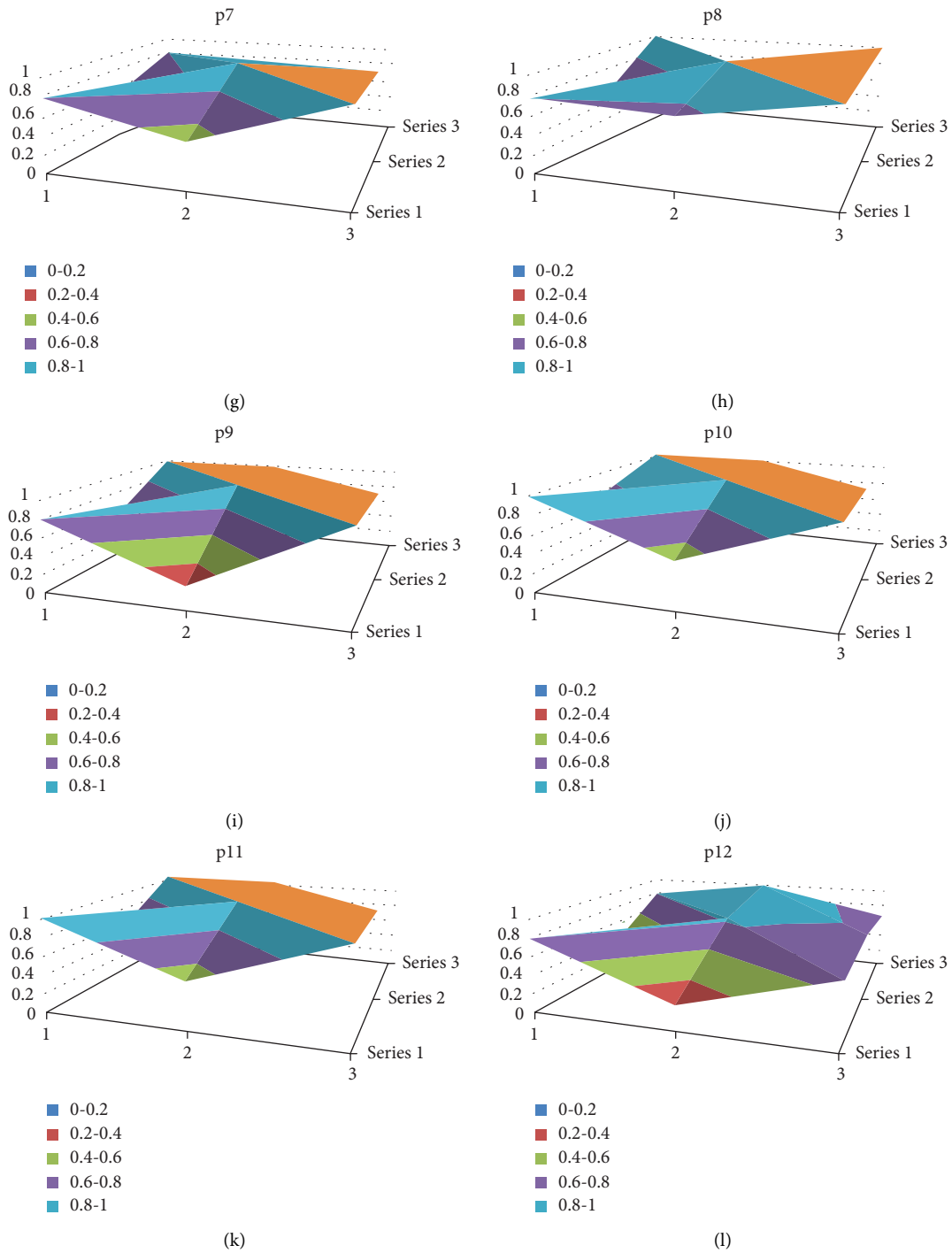


FIGURE 3: (a) P_1 , (b) P_2 , (c) P_3 , (d) P_4 , (e) P_5 , (f) P_6 , (g) P_7 , (h) P_8 , (i) P_9 , (j) P_{10} , (k) P_{11} , (l) P_{12} .

industry. Nevertheless, P_{10} still has no content about R&D subsidies, lacking emphasis and focus on science and technology R&D.

X_5 (Policy area). P_5 covers various areas such as economy, politics, ecology, etc., but the description of the social

area is less clear, so it does not get the corresponding score. P_{10} , on the other hand, clearly articulated each area and received a score of 1.

X_6 (Policy evaluation). P_{10} has sufficient basis, clear objectives, scientific arrangement, and detailed description.

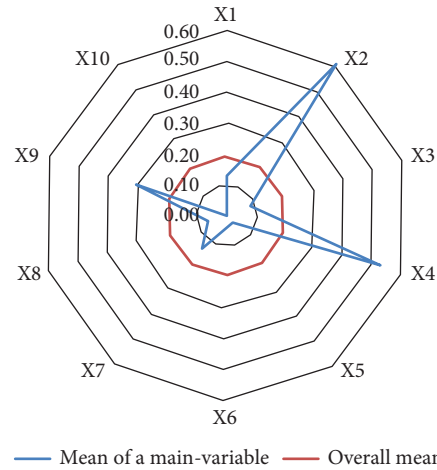


FIGURE 4: Radar chart of main variables depression index.

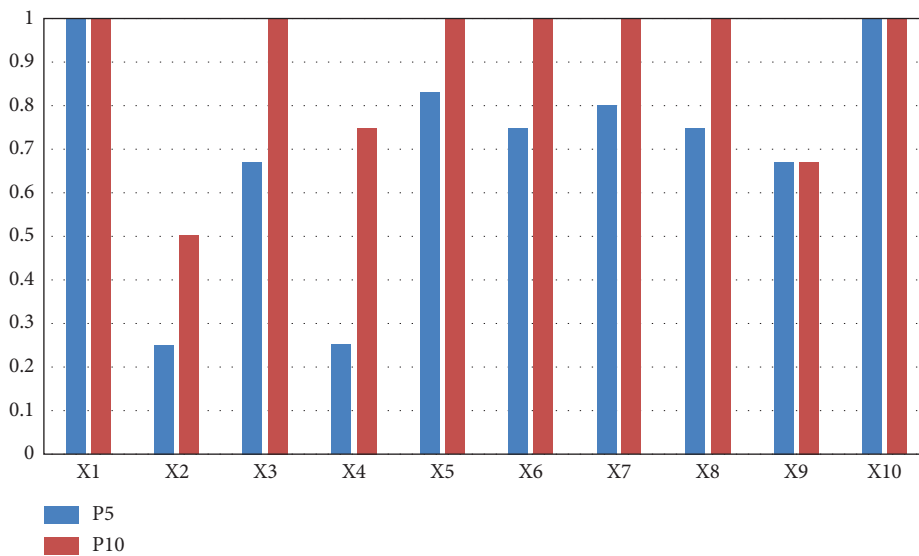


FIGURE 5: Scores of each main-variable for P_5 and P_{10} .

The content of P_5 seems to be general and cursory, and the short length does not describe clearly in detail, but other aspects of the performance are not bad.

X_7 (Policy focus). The content of P_5 has the focus on policies such as innovation, the transformation of achievements, and market leadership. In addition to these elements, P_{10} also mentions the introduction of human resources and the importance of being people-oriented.

X_8 (Policy object). P_5 mentions enterprises, financial institutions, management agencies, and other policy objects, but the descriptions are cursory and there are no other policy objects. P_{10} then clearly and explicitly states these policy objects, on top of which other policy objects such as service organizations are also mentioned.

5. Discussion and Conclusions

5.1. Conclusion and Implications. This study adopts the content analysis method and text mining method, combined with the PMC-Index model to evaluate high-advanced industry policies in Yangtze River Delta region quantitatively and selects 12 representative high-advanced industry policy texts for specific analysis. The study found that the design of high-advanced industry policies was relatively reasonable overall, with 11 policies rated as “Good Consistency” and only one policy rated as “Acceptable Consistency.” In general, the high-advanced industrial policy has, to some extent, promoted the industrial restructuring and the development of high-

advanced industry in China, but there are still some problems to be improved.

First, the policy lacks reasonable arrangements for different period plans. The mean value of X_2 (policy duration) is only 0.4, and most of the policy samples have only planned arrangements for one or two periods. Although the formulation is detailed and precise, there is no mention of arrangements for other periods. The establishment of planning arrangements for different periods is beneficial for enterprises, local governments, and relevant departments to have clear objectives at different periods of high-advanced industrial development. It also needs to optimize “guidance” in X_1 and “detailed content” in X_6 .

Second, the sample policies lack incentives or have relatively single incentives. Most of the sample policies contain incentives in the form of financial subsidies and loan subsidies, but almost all of them do not mention R&D subsidies, reflecting China’s insufficient incentive policy support for R&D in high-advanced industries. The level of R&D subsidies in China has increased in recent years, but most of them are provided directly to state-owned enterprises, with only a tiny percentage allocated to private and triple-funded enterprises. As a result, there is little mention of R&D subsidies in the sample policies. In the subsequent policy development and modification, attention should be paid to the related issues, and resources should be allocated rationally to improve the effectiveness of incentives.

Third, the policy influence among cities in the Yangtze River Delta urban agglomerations is small, and the integration trend is not apparent. The score for the subvariable “regional cluster” in X_9 is almost 0. The synergy effect of high-advanced industry policies between different regions is relatively low, and the advantages of integrated development of the Yangtze River Delta urban agglomerations have not been shown. There is a certain gap in the scores of high-advanced industrial policies between Shanghai, Zhejiang, Jiangsu, and Anhui. The policy with the highest PMC-Index score is in Jiangsu, Zhejiang, and Shanghai, while Anhui’s policy performs poorly compared to other provinces’ policies, which means there is still a need and room for further improvement in the design of the policies in terms of content. Partners between urban agglomerations can benefit from the dynamic synergies of mutual growth through reciprocity, knowledge exchange, and realizing significant economies of scope.

5.2. Limitation. There are still some limitations in this study. First, further research is still needed for the dimensionality and extension of the variable selection [28–32]. On the one hand, some variables with universal applicability can be set according to the basic attributes of the policy [33]. On the other hand, some variables with targeted nature can be set out according to the special attributes of the studied policies, which can be analyzed for specific directions [34]. Second, although this study integrates the results of content analysis and text mining, the evaluation of policies and the set of variables are still somewhat subjective [35, 36]. Third,

because the PMC-Index model needs to take into account all global variables, the model does not enable a detailed analysis for a particular direction.

Data Availability

The data supporting the conclusions of this research can be obtained from the corresponding author upon request.

Conflicts of Interest

The authors declare that there are no conflicts of interest in this study.

Acknowledgments

This work was supported by the Youth Project of Shanghai Philosophy and Social Sciences Planning (2020) (Grant no. 2020EJB001), the Project of Research Center for Cultural Industry Development of Sichuan Provincial Key Research Base of Social Sciences (2020) (Grant no. WHCY2020A01), the Teacher Development Research Project of the University of Shanghai for Science and Technology (2022) (Grant no. CFTD223013), and the Ministry of Education Industry-University Cooperation Collaborative Education Project (2022).

References

- [1] B. D’Ippolito, A. Messeni Petruzzelli, and U. Panniello, “Archetypes of incumbents’ strategic responses to digital innovation,” *Journal of Intellectual Capital*, vol. 20, no. 5, pp. 662–679, 2019.
- [2] R. Ceipek, J. Hautz, A. M. Petruzzelli, A. De Massis, and K. Matzler, “A motivation and ability perspective on engagement in emerging digital technologies: the case of Internet of Things solutions,” *Long Range Planning*, vol. 54, no. 5, Article ID 101991, 2021.
- [3] N. K. Hanna, “Mastering digital transformation,” *Mastering Digital Transformation (Innovation, Technology, and Education for Growth)*, Emerald Publishing, Bingley, UK, 2016.
- [4] V. Parida, D. Sjödin, and W. Reim, “Reviewing literature on digitalization, business model innovation, and sustainable industry: past achievements and future promises,” *Sustainability*, vol. 11, no. 2, p. 391, 2019.
- [5] T. J. Sturgeon, “Upgrading strategies for the digital economy,” *Global Strategy Journal*, vol. 11, no. 1, pp. 34–57, 2019.
- [6] H. Wen, Q. Zhong, and C. C. Lee, “Digitalization, competition strategy and corporate innovation: e,” *International Review of Financial Analysis*, vol. 82, Article ID 102166, 2022.
- [7] Y. Yang, M. Liang, S. Sun, and Y. Zou, “Strengthening top-down design? Mapping science, technology and innovation policy developments in China in the age of COVID-19,” *Asian Journal of Technology Innovation*, pp. 1–22, 2022.
- [8] S. Zeng, J. Zhou, C. Zhang, and J. M. Merigó, “Intuitionistic fuzzy social network hybrid MCDM model for an assessment of digital reforms of manufacturing industry in China,” *Technological Forecasting and Social Change*, vol. 176, Article ID 121435, 2022.
- [9] O. Ellingsen and K. E. Aasland, “Digitalizing the maritime industry: a case study of technology acquisition and enabling

- advanced manufacturing technology,” *Journal of Engineering and Technology Management*, vol. 54, pp. 12–27, 2019.
- [10] J. Ye, Q. Wan, R. Li, Z. Yao, and D. Huang, “How do R&D agglomeration and economic policy uncertainty affect the innovative performance of Chinese high-tech industry?” *Technology in Society*, vol. 69, Article ID 101957, 2022.
- [11] M. Muro, J. Rothwell, S. Andes, K. Fikri, and S. Kulkarni, *America’s Advanced Industries: What They Are, where They Are, and Why They Matter*, Brookings, Washington, DC, USA, 2015.
- [12] Y. A. Zhang and Z. Geng, “The quantitative evaluation of regional science and technology innovation policy: based on the index of PMC model,” *Science and Technology Management Research*, vol. 35, pp. 26–31, 2015.
- [13] Y. Li, R. He, J. Liu, C. Li, and J. Xiong, “Quantitative evaluation of China’s pork industry policy: a PMC index model approach,” *Agriculture*, vol. 11, no. 2, p. 86, 2021.
- [14] X. Liu and T. Buck, “Innovation performance and channels for international technology spillovers: evidence from Chinese high-tech industries,” *Research Policy*, vol. 36, no. 3, pp. 355–366, 2007.
- [15] T. Li, L. Liang, and D. Han, “Research on the efficiency of green technology innovation in China’s provincial high-end manufacturing industry based on the Raga-PP-SFA model,” *Mathematical Problems in Engineering*, vol. 2018, Article ID 9463707, 13 pages, 2018.
- [16] D. Wu, X. Tong, L. Liu, and J. Wang, “Do regional financial resources affect the concentration of high-end service industries in Chinese cities?” *Finance Research Letters*, vol. 42, Article ID 101935, 2021.
- [17] C. Miao, D. Fang, L. Sun, Q. Luo, and Q. Yu, “Driving effect of technology innovation on energy utilization efficiency in strategic emerging industries,” *Journal of Cleaner Production*, vol. 170, pp. 1177–1184, 2018.
- [18] D. Prud’homme, “Dynamics of China’s provincial-level specialization in strategic emerging industries,” *Research Policy*, vol. 45, no. 8, pp. 1586–1603, 2016.
- [19] I. Sanderson, “Evaluation, policy learning and evidence-based policy making,” *Public Administration*, vol. 80, no. 1, pp. 1–22, 2002.
- [20] E. Suchman, *Evaluative Research: Principles and Practice in Public Service and Social Action Programs*, Russell Sage Foundation, Manhattan, NY, USA, 1968.
- [21] O. F. Poland, “Program evaluation and administrative theory,” *Public Administration Review*, vol. 34, no. 4, p. 333, 1974.
- [22] W. E. N. Jun, “Fuzzy comprehensive evaluation of risk in airline safety system,” *Journal of Safety Science and Technology*, vol. 6, no. 1, pp. 44–48, 2010.
- [23] S. Wang, Y. Wang, and L. I. Chao, “Application of BP neural network in inherent safety degree evaluation of aviation maintenance personnel,” *Journal of Safety Science and Technology*, vol. 6, no. 6, pp. 35–39, 2010.
- [24] J. L. Jin, Y. M. Wei, and J. Ding, “Fuzzy comprehensive evaluation model based on improved analytic hierarchy process,” *Journal of Hydraulic Engineering*, vol. 3, no. 3, pp. 65–70, 2004.
- [25] M. A. Ruiz Estrada, “Policy modeling: definition, classification and evaluation,” *Journal of Policy Modeling*, vol. 33, no. 4, pp. 523–536, 2011.
- [26] B. Kuang, J. Han, X. Lu, X. Zhang, and X. Fan, “Quantitative evaluation of China’s cultivated land protection policies based on the PMC-Index model,” *Land Use Policy*, vol. 99, Article ID 105062, 2020.
- [27] T. Yang, C. Xing, and X. Li, “Evaluation and analysis of new-energy vehicle industry policies in the context of technical innovation in China,” *Journal of Cleaner Production*, vol. 281, Article ID 125126, 2021.
- [28] L. Yan, S. Yin-He, Y. Qian, S. Zhi-Yu, W. Chun-Zi, and L. Zi-Yun, “Method of reaching consensus on probability of food safety based on the integration of finite credible data on block chain,” *IEEE Access*, vol. 9, pp. 123764–123776, 2021.
- [29] S. Liu, J. Zhang, B. Niu, L. Liu, and X. He, “A novel hybrid multi-criteria group decision-making approach with intuitionistic fuzzy sets to design reverse supply chains for COVID-19 medical waste recycling channels,” *Computers & Industrial Engineering*, vol. 169, Article ID 108228, 2022.
- [30] J. Yan, H. Jiao, W. Pu, C. Shi, J. Dai, and H. Liu, “Radar sensor network resource allocation for fused target tracking: a brief review,” *Information Fusion*, vol. 86–87, pp. 104–115, 2022.
- [31] W. Zheng, X. Liu, and L. Yin, “Research on image classification method based on improved multi-scale relational network,” *PeerJ Computer Science*, vol. 7, p. e613, 2021.
- [32] Z. Ma, W. Zheng, X. Chen, and L. Yin, “Joint embedding VQA model based on dynamic word vector,” *PeerJ Computer Science*, vol. 7, p. e353, 2021.
- [33] W. Zheng, L. Yin, X. Chen, Z. Ma, S. Liu, and B. Yang, “Knowledge base graph embedding module design for Visual question answering model,” *Pattern Recognition*, vol. 120, Article ID 108153, 2021.
- [34] L. Yao, X. Li, R. Zheng, and Y. Zhang, “The impact of air pollution perception on urban settlement intentions of young talent in China,” *International Journal of Environmental Research and Public Health*, vol. 19, no. 3, p. 1080, 2022.
- [35] B. Wu, A. Monfort, C. Jin, and X. Shen, “Substantial response or impression management? Compliance strategies for sustainable development responsibility in family firms,” *Technological Forecasting and Social Change*, vol. 174, Article ID 121214, 2022.
- [36] P. Ghimire, “Digitalization of indigenous knowledge in Nepal—review article,” *Acta Informatica Malaysia*, vol. 5, no. 2, pp. 42–47, 2021.

Research Article

A Miniaturized Electrochemical Nitrate Sensor and the Design for Its Automatic Operation Based on Distributed Model

Zhenxing Ren ^{1,2} and Yang Li ³

¹School of Mechanical Engineering, Chengdu University, Chengdu 610106, Sichuan, China

²Key Laboratory of Highway Engineering of Ministry of Education, Changsha University of Science and Technology, Changsha 410114, Hunan, China

³Aerospace Information Research Institute, Chinese Academy of Sciences, Beijing 100190, China

Correspondence should be addressed to Zhenxing Ren; renzhenxing@cdu.edu.cn and Yang Li; liyong.cas@aircas.ac.cn

Received 5 June 2022; Accepted 15 July 2022; Published 29 September 2022

Academic Editor: Wei Liu

Copyright © 2022 Zhenxing Ren and Yang Li. This is an open access article distributed under the Creative Commons Attribution License, which permits unrestricted use, distribution, and reproduction in any medium, provided the original work is properly cited.

As one of the most common inorganic ions in daily food and ecological environment, nitrate (NO_3^-) is potentially harmful to both environment and humans. Therefore, the detection of nitrate concentration is quite important. Chemical sensors, as analytical measurement tools, usually demonstrate high selectivity, fast analysis speed, simple structure, convenient operation, and low cost and are considered to be a promising method for ion identification and detection. In this paper, a miniaturized electrochemical electrode is fabricated based on the microfabrication technology, and an electrochemical sensor for the detection of nitrate concentration in water is developed by combining the deposition technology of nanometal particles with electrochemical analysis technique. The developed electrochemical sensor utilizes electrochemical deposition to prepare a copper (Cu) granular sensitive film with a branch-cluster structure on the surface of a circular working electrode (Pt). Using copper's characteristics of electrocatalytic reduction of NO_3^- in the acid solution environment ($\text{pH} = 2$), the concentration of NO_3^- in the water sample was calculated by measuring the reduction current on the working electrode when the electrocatalytic reduction reaction of NO_3^- occurred on the surface of the copper-sensitive membrane. The sensitive film is characterized and detected both with the scanning electron microscope (SEM) and X-ray diffraction analysis (XRD) technique; and the microsensor is used to detect nitrate standard samples; a high detection sensitivity ($24.9 \mu\text{A}/\text{mmol}\cdot\text{L}^{-1}$) is achieved in the concentration range of 0.0 to 3.0 mmol/L. At the same time, a MEMS three-electrode sensor without gold wire bonding and insulating glue packaging is designed, and an automatic detection system is constructed with a STM32f103 microcontroller as the controller to realize the automated detecting process for nitrate ions. At the same time, a distributed system is constructed, which can describe the nitrate concentration in every position of the water area and realize the monitoring of the whole water area. The detection system can meet the working environment under most conditions and has practical significance.

1. Introduction

Nowadays, nitrate is one of the most prevalent pollutants in surface and groundwater throughout the world. In recent decades, with the fast development of large-scale industry and agriculture as well as the rapid expansion of urban population, the level of nitrate pollution continues to increase in both developed and developing countries. Nitrate is highly soluble and migrates very fast in water or in the atmosphere. Once the nitrates generated in industrial and

agricultural production enter the natural environment, they will diffuse widely with various water currents or atmospheric circulation activities. As a result, the nitrate concentration in natural water bodies is on the rise and has become a significant environmental pollution problem [1]. Many studies have proved that excessive nitrate content in water will cause serious environmental pollution and physiological diseases [2, 3]. For example, in terms of environmental pollution, nitrates will gather in local waters after flowing into lake waves with rivers. They, together with

other pollutants, cause eutrophication of water bodies and even lead to cyanobacteria outbreaks in severe cases. As for health hazards, nitrates are harmful to human health mainly through drinking water contamination. Long-term consumption of drinking water containing excessive nitrates will cause changes in blood components, which in turn induce diseases such as muscle cramps, methemoglobinemia, and even gastric cancer [2, 4]. Hence, all countries have implemented strict restrictions on the content of nitrate in drinking water [5–7]. Whether from the perspective of environmental protection or the building of healthy life, it is of great significance to establish a simple, sensitive, and accurate nitrate detection method.

At present, the commonly used nitrate ion detection methods mainly include spectrophotometry, chromatography, chemiluminescence, capillary electrophoresis, electrochemical detection, and so on [8–10]. Among them, detection methods based on optical principles usually feature the merits of low detection limit, high precision, and good sensitivity. However, there are also problems such as large instrument size, high price, complex sample preprocessing, and long time-consuming. And there are two kinds of smaller nitrate ion sensors, pen sensors and hand-held testers. In contrast, the detection method based on the electrochemical principle has the advantages of simple instrument, convenient operation, less reagents required, and easy integration with the detection circuit, which is considered to be a new type of nitrate detection method with great development prospects [11–13].

In this paper, a miniature electrochemical sensing electrode was prepared based on MEMS technology, and a copper-sensitive film was prepared on the surface of the working electrode (Pt) by potentiostatic deposition. In this way, a miniature electrochemical sensor was constructed and used for the detection of nitrate ions in water. At the same time, a novel microsensor packaging-free system is designed for the difficult packaging of MEMS technology. It does not need to use metal wires for welding and builds an automatic detection system with STM32f103 microcontroller as the controller to realize the automated detecting process for nitrate.

2. Preparation of Microsensors

2.1. Instruments and Reagents. The instruments used are Camry Reference-600 electrochemical analyzer (USA, Gamry); AUW electronic balance (Japan, Shimadzu); Direct-Q3UV high-purity water machine (USA, Millipore); digital pH meter (Shanghai Zhiguang Instrument Co., Ltd., pHS-25 type); and S-4800 scanning electron microscope (FE-SEM, Japan, Hitachi).

Reagents used are $\text{CuSO}_4 \cdot 5\text{H}_2\text{O}$, Na_2SO_4 , NaNO_3 , and 98% H_2SO_4 (Beijing Chemical Reagent Company); nitrate standard sample 50 mg/L (Beijing, Institute of Standardization, Ministry of Environmental Protection). Chemicals and solvents are of analytical grade, and experimental water is 30 M Ω cm deionized water. Unless otherwise specified, all solutions are obtained by dissolving quantitative solid reagents in deionized

water at room temperature of 25°C. All experiments were completed in a three-electrode system, the reference electrode was Ag/AgCl reference electrode (CHI111, China, Shanghai Chenhua), and the working electrode and counter electrode were laboratory-made miniature sensing electrodes.

2.2. Preparation of Sensing Electrodes. The fabrication process of miniature electrochemical sensing electrodes has been reported in detail in other papers [14, 15]. It mainly uses photolithography, sputtering, lift-off, scribing, packaging, and other process steps, which can realize the batch preparation of sensing electrodes to ensure the consistency of different electrodes. The specific structure of the sensor is mainly a micrometal electrode system prepared by MEMS technology, and a polymer layer sensitive to specific materials is prepared on the working electrode by the electrochemical method. The prepared microsensing electrode is shown in Figure 1(a): the working electrode and the counter electrode which is usually made of Pt [16–18] are in symmetrical circular-ring structures, and the area of the working electrode is 1.0 mm²; the whole size is 10 mm × 10 mm; the electrode is attached to the printed circuit board, soldered to the gold finger on the PCB using gold wire, sealed to the PCB with insulating glue, as shown in Figure 1(b), and then dried at 60°C for 12 hours.

2.3. Preparation of Copper-Sensitive Film. The encapsulated microsensing electrodes were immersed in copper sulfate solution (pH = 2.0, 100 mmol/L CuSO_4). Electrochemical deposition was performed on the working surface of the microelectrode using Chronoamperometry Scan through an electrochemical workstation (deposition time was 160 s, and deposition potential was -0.3 V). In order to prevent the deposited copper from being oxidized in the air after the deposition is completed, the surface of the electrode is rinsed with deionized water, and the electrode is placed in deionized water for preservation. When using the potentiostatic method to modify the electrode, the electrochemical deposition curve is shown in Figure 2.

2.4. Package-Free System for Miniature Sensors. MEMS is a key technology for the preparation of modern microsensors, and three-electrode microsystems are commonly used electrochemical sensors based on MEMS technology, featuring simple preparation, easy batch production, and stable performance. However, in the actual preparation process, it is necessary to use gold wire pressure welding. At the same time, the gold wire is easy to break when packaged with insulating glue, and the efficiency is low. Therefore, this paper designs a MEMS three-electrode sensor without gold wire bonding and insulating glue packaging, as shown in Figure 3.

In this paper, the screws inserted through the fixing hole make the electrode on the pressing device closely fit with the microelectrode system, so as to ensure that the electrode is closely combined with the external circuit. The pressing device and the unique groove design of the microelectrode in

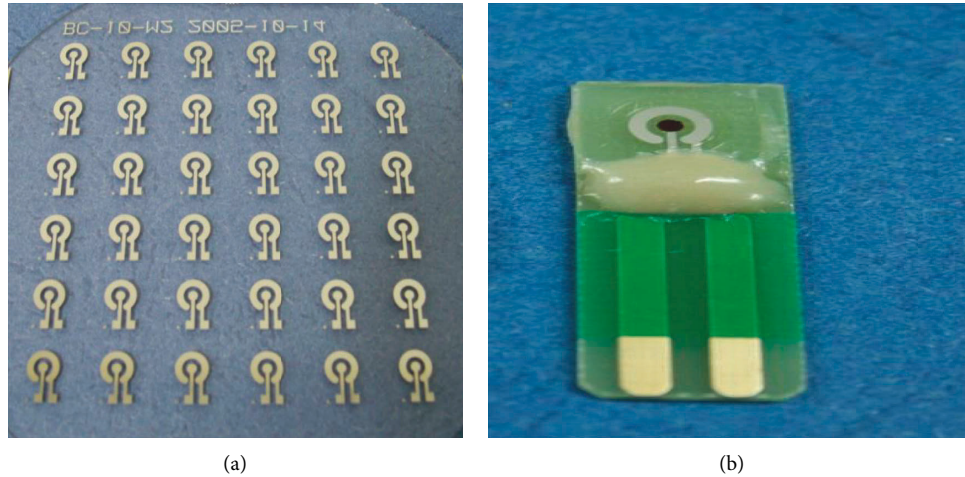


FIGURE 1: Photo of sensing electrodes: bulk-fabricated sensing electrodes. (a) Unpackaged electrodes. (b) Packaged electrode on PCB.

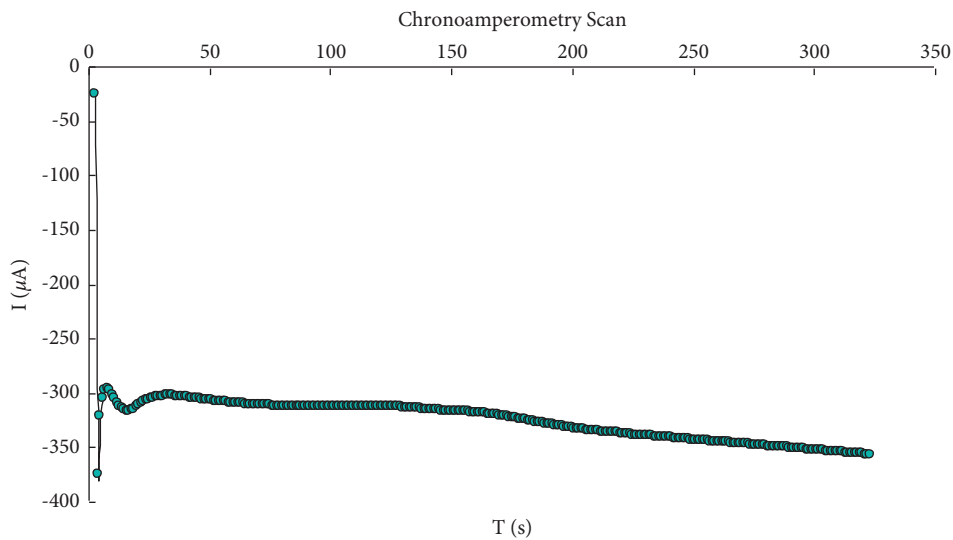


FIGURE 2: Potentiostatic deposition scanning curve: potential -0.3 V ; time 160 s.

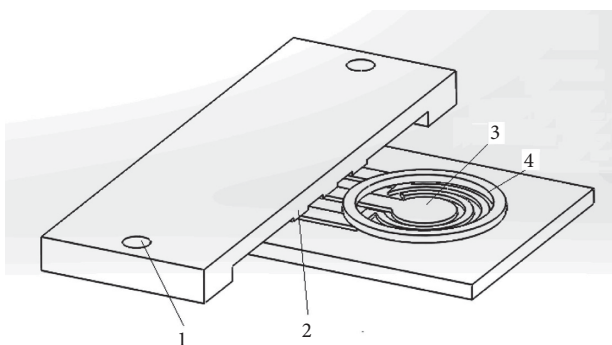


FIGURE 3: (1) Fixing hole, (2) screen-printed electrode, (3) microelectrode system, and (4) microreaction tank.

the PCB and the conductive glue instead of the gold wire are used. In this way, it effectively avoids the disadvantages of the existing three-electrode microsensor system that need to

use a gold wire ball bonding machine for pressure bonding, the use of insulating glue to make the gold wire easy to break and fall off, and the low efficiency of the use of insulating glue, which improves the reliability, avoids the sensors to be a disposable chip, and is convenient for the regeneration and the reuse of the sensors.

2.5. Automatic Detection System and Model Analysis. Usually the detection takes place in a large place such as a lake, so the automatic detection system consists of several automatic detection subunits (SUa) and a main processing unit (MU); each automatic detection unit consists of a single-chip microcontroller and has an identity code, while using the wireless transmission module for signal transmission to the main processing unit [19, 20]. The main processing unit collects and processes the information. This information includes the temperature, the automatic detection unit ID number, and the structure of the system as shown in Figure 4. The contact method between subunits

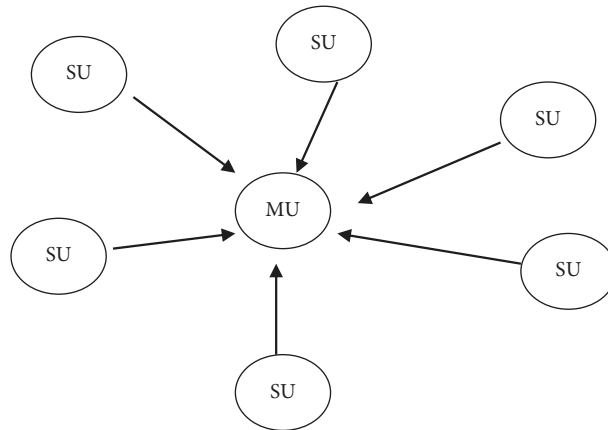


FIGURE 4: Schematic model of node structure of automatic detection system.

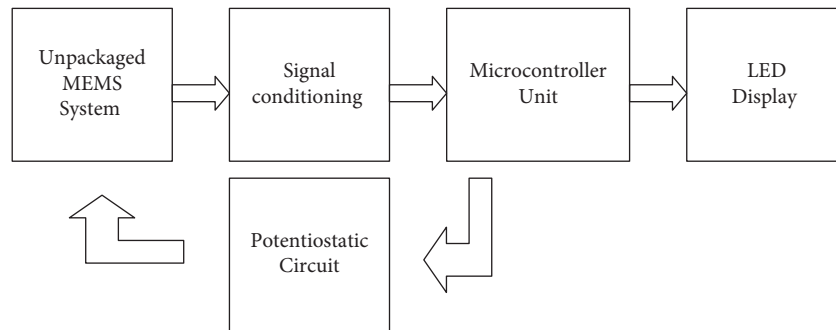


FIGURE 5: Structure and composition diagram of the automatic detection system.

and main processing unit was bluetooth communication mode.

In order to satisfy the online automatic detection of nitrate microsensor based on MEMS technology, the system consists STM32f103 microcontroller as controller, HX711 as signal converter, signal conditioning circuit and constant potential circuit, unpackaged MEMS system, and display circuit, as shown in Figure 5. The controller applies a constant voltage to the electrochemical sensor in the MEMS system through the potentiostatic circuit, so that the sensor generates a current signal, which is carefully processed by the signal conditioning circuit and converted into a voltage signal.

The TU is a signal transmission unit; usually a fixed monitored water area has multiple transmission units, each of which is responsible for receiving the signal from the attached MU, as shown in Figure 6; the signal is processed and sent to the central processing unit for storage and display. Tu is composed of signal receiving circuit, memory circuit, and signal transmitting circuit.

In the wireless data acquisition model as shown in Figure 7, each SU unit has an identification tag, which only communicates with the adjacent MU one-to-one. The MU receives the detection data, and the TU unit will also receive the data of the nearby MU unit one-to-one, and the data are transmitted wirelessly to the central control room for display.

3. Results and Discussion

3.1. Micromorphological Characterization and Material Analysis of Sensitive Materials. Scanning electron microscope (SEM) was used to observe the microscopic topography of the electrodeposited working electrode surface. As shown in Figure 8, a layer of loose branch-like structure was formed on the surface of the platinum working electrode after the potentiostatic deposition treatment. In the local magnified image, it can be found that the surface of the working electrode has been completely covered by the granular material. There are also branch-like protruding structures locally, which are formed by interconnected particles with a particle size of about 200 nm and protruding upwards from the electrode surface and depositing continuously along a certain spatial direction.

In order to investigate the composition of the materials generated on the electrode surface after electrodeposition treatment, X-ray diffraction analysis (XRD) was performed on the surface of the working electrode. The results of XRD analysis are shown in Figure 9. It can be found that there are 5 characteristic peaks in the XRD test pattern, and the comparison material spectrum shows that three of them are characteristic peaks of platinum (Pt), which is the property of the platinum material of the working electrode; the other

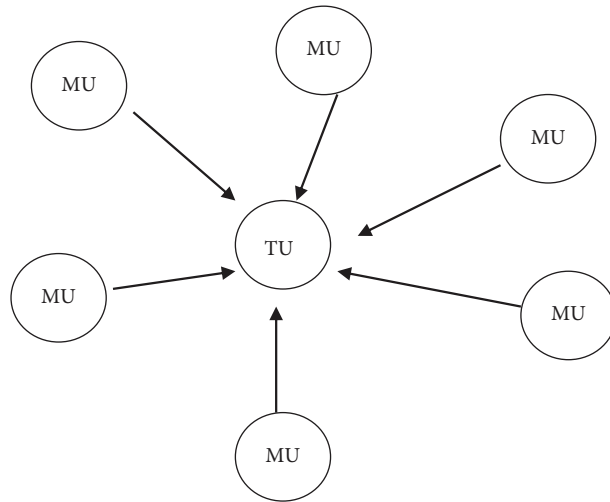


FIGURE 6: Structure and composition model of the automatic detection system.

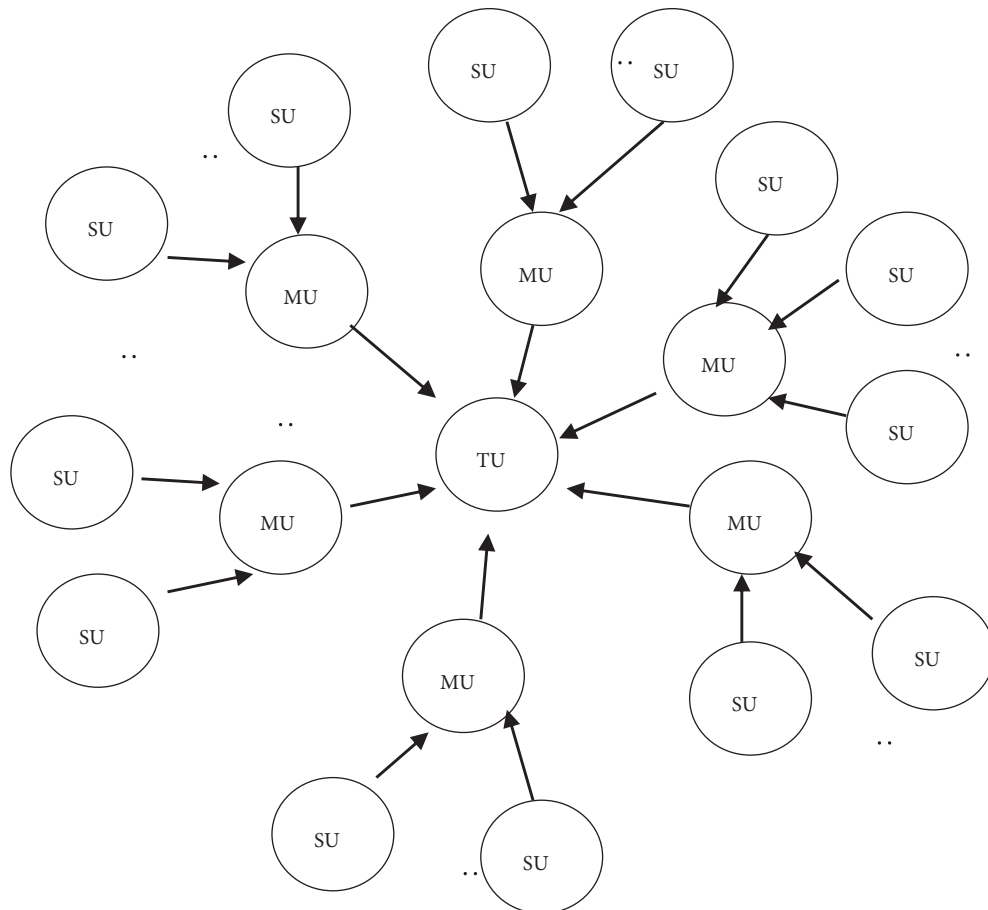


FIGURE 7: Structure and composition model of the wireless data acquisition system.

two peaks are characteristic peaks of (111) and (200) orientations of copper (Cu), indicating that the modified layer prepared by the potentiostatic deposition method is made of metallic copper rather than its related oxides.

3.2. *Electrochemical Detection Performance of the Microsensor for Nitrate Ions.* The current response characteristics of the microsensing electrodes modified by constant voltage deposition to different concentrations of nitrate standard

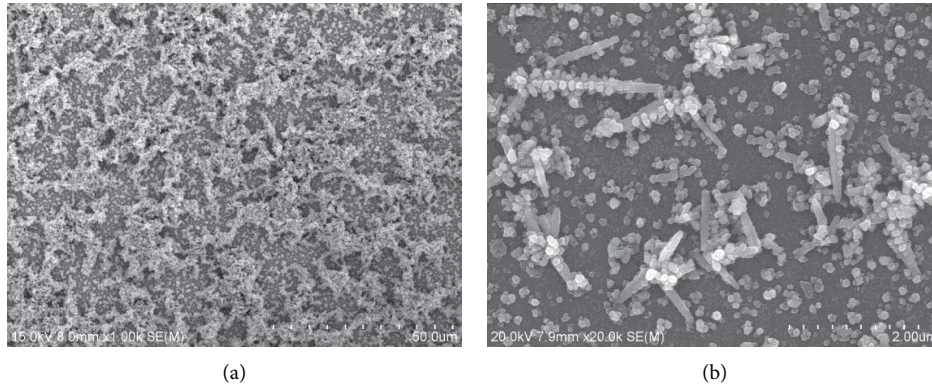


FIGURE 8: The SEM image of the surface on the working electrode after electrochemical deposition process with deposition potential -0.3 V and deposition time 160 s. (a) $\times 1000$ times. (b) $\times 20000$ times.

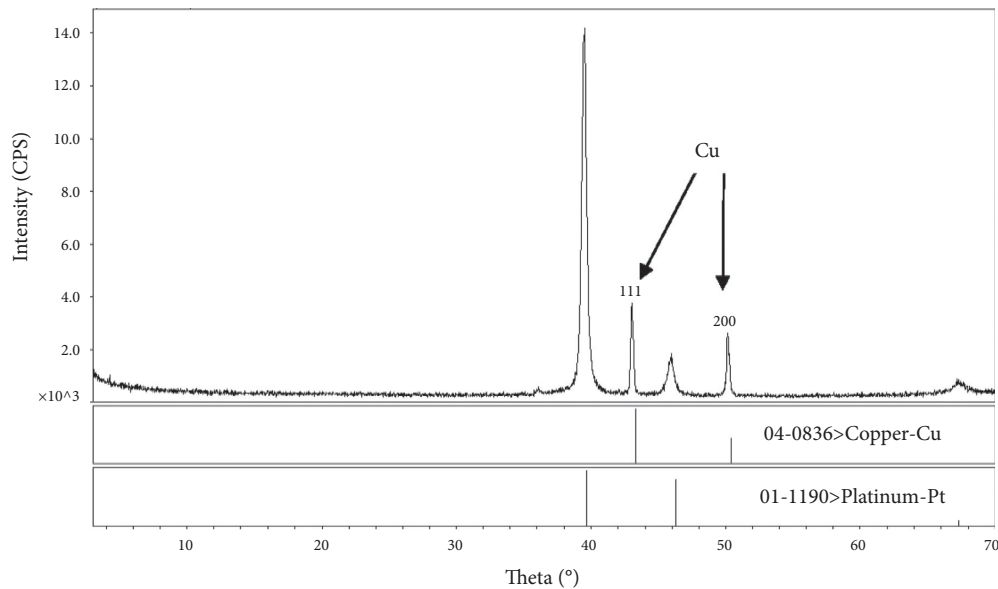


FIGURE 9: X-ray diffraction analysis of the modified layer material: deposition potential of -0.3 V; deposition time of 160 s.

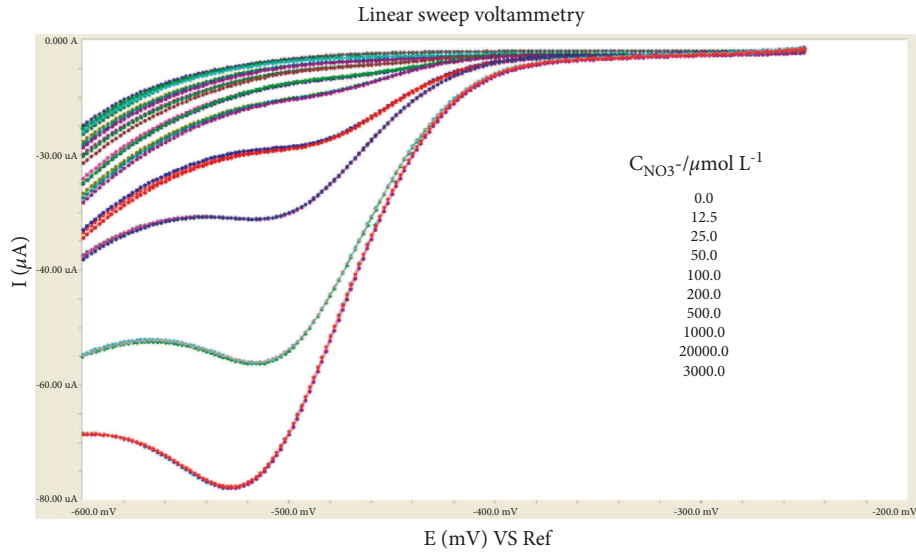
solutions were analysed by voltage linear scanning. In all experiments, 0.1 mol/L Na_2SO_4 solution with $\text{pH} = 2.0$ was used as the supporting electrolyte, and the microsensor was immersed in the test solution containing different concentrations of NO_3^- for linear scanning test, and the relationship between the concentration of NO_3^- and the reduction peak current was investigated. Figure 10(a) is the linear scan response curve of the microsensor in different concentrations (0.0 – 3.0 mmol/L) of standard nitrate. It is found that from the figure that the current response signal of the sensor increases with the increasing NO_3^- concentration in the test solution.

Literature studies [6, 21] have shown that applying a voltage to the surface of the copper nanoparticles converts the nitrate into ammonium ions, generating an electric current in the process. The nitrate concentration can be reflected by measuring the current. During the experiment, a total of 10 concentrations were measured and these concentration-current data sets were obtained, and the I–C relationship curve was plotted based on

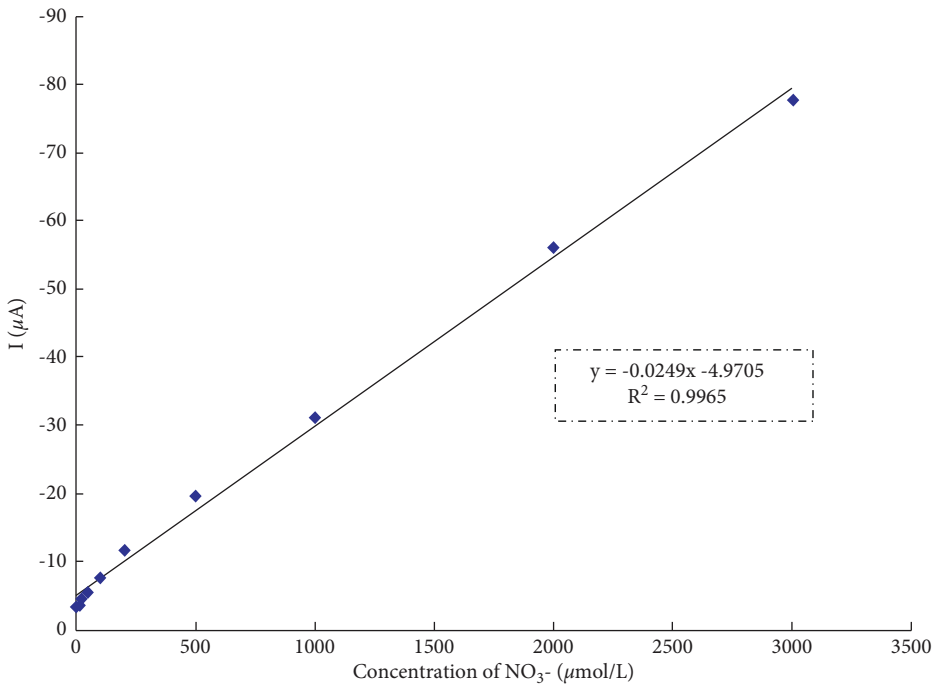
these data. Figure 10(b) is the fitting relationship curve between the corresponding reduction current value in the linear scan curve and the NO_3^- concentration in the test solution when the reduction potential is -600 mV. It is found that there is a good linear relationship between the reduction current value and the NO_3^- concentration value in the concentration range of 0.1 – 3.0 mmol/L. The result indicates that the detection of nitrate concentration can be realized by measuring the magnitude of the reduction current via the developed miniature electrochemical sensor. The current is related to the rate of the scanning voltage and the area of the working electrode [22]. The functional relationship between the peak current value obtained by linear fitting and the nitrate concentration is

$$y \left[\frac{\mu\text{A}}{\text{mmolL}^{-1}} \right] = -0.0249x - 4.9705, \quad (1)$$

$$R_1^2 = 0.9965.$$



(a)



(b)

FIGURE 10: Response curve of the miniature electrochemical sensor. (a) Linear scan curves in different nitrate solution concentrations. (b) Linear fit curve: scan rate of 50 mV/s.

The microsensor modified by the potentiostatic deposition method also demonstrated good repeatability and anti-interference when testing nitrate ions. Except for nitrite ions, the common ions in water did not significantly interfere with the test results [10]. The microsensor was tested three times for each nitrate standard sample, namely, 1.0 mmol/L, 2.0 mmol/L, and 3.0 mmol/L, and the maximum relative standard deviation RSD was less than 5%. The detection limit was $10 \mu\text{mol/L}$ ($S/N = 3$).

3.3. Reuse of Electrochemical Sensors. The sensor studied in this paper is fabricated by using MEMS technology on silicon substrate. The manufacturing process can be described by sputtering a layer of silicon dioxide insulating layer on which the electrode pattern is etched by light, and then a layer of platinum metal is sputtered by sputtering process, and the final electrodes are made by stripping technique. The sensors are made of working electrode and counter electrode. On the working electrode, the sensitive material of the sensor is

polymerized on the working electrode by an electrochemical analysis instrument to form a nitrate-sensitive sensor. When a new sensitive material needs to be polymerized, most of the sensitive materials are dissolved by concentrated nitric acid, and the oxygen plasma is used to strike the metal surface for removing the sensitive material completely, so that the sensor can be used repeatedly. At the same time, the sensor is designed to be used more frequently by unusing with gold wire and insulating glue.

4. Conclusion

In this paper, a microelectrochemical sensing electrode was fabricated by micromachining technology. Combined with electrochemical potentiostatic deposition technology, it prepared a copper-sensitive film with a branch-like structure on the surface of the platinum working electrode. The electrocatalytic reduction characteristics of copper were used to nitrate ions in an acidic solution and realized the detection of nitrate concentration in the solution. Good detection sensitivity and linearity were obtained in the standard concentration range of 0.0 mmol/L to 3.0 mmol/L. At the same time, a new package-free microsensor system was developed, using STM32f103 microcontroller as the controller and HX711 as the signal converter to build an automatic nitrate detection system, realizing the advantages of miniaturization of detection, fast response, and less detection reagent consumption. The new structure was adopted, which can avoid the defects caused by the golden wire connection between the traditional sensor and the external circuit, and prolong the reliability, stability, and life of the sensor. It has high value to realize the development of low cost and portable nitrate detector for environmental monitoring and food safety detection. It also makes sense that a distributed detection system was built, and a main processing unit was used to collect the automatic detection units with sensors around them, and the collected data were transmitted to the nearby signal transmission unit to realize real-time data transmission. Because the electrode system adopts MEMS technology for mass production, its cost is lower than the existing sensors, which greatly reduces the cost of the whole system, and the consistency and reliability of the electrode system can be guaranteed.

Data Availability

All data included in this study are available upon request to the corresponding author.

Conflicts of Interest

The authors declare that they have no conflicts of interest.

Acknowledgments

The project was supported by Open Fund of the Key Laboratory of Highway Engineering of Ministry of Education (Changsha University of Science and Technology).

References

- [1] X. Zhang, *Electrocatalysis of Polypyrrole Nanowires-Modified Electrode-Electrocatalytic Reduction of Nitrate Ions*, Tianjin University, Tianjin, China, 2006.
- [2] R. Desai, M. Marti Villalba, N. S. Lawrence, and J. Davis, "Green approaches to field nitrate analysis: an electroanalytical perspective," *Electroanalysis*, vol. 21, no. 7, pp. 789–796, 2009.
- [3] M. Mehmandoust, P. Pourhakkak, G. Tiris, and N. Erk, "A reusable and sensitive electrochemical sensor for determination of idarubicin in environmental and biological samples based on NiFe₂O₄ nanospheres anchored N-doped graphene quantum dots composite; an electrochemical and molecular docking investigation," *Environmental Research*, vol. 212, 2022.
- [4] H. Lu, B. He, and B. Gao, *Emerging electrochemical sensors for life healthcare*, vol. 2, pp. 175–181, 2021.
- [5] M. J. Moorcroft, J. Davis, and G. C. Richard, "Detection and determination of nitrate and nitrite: a review," *Talanta*, vol. 54, no. 5, pp. 785–803, 2001.
- [6] J. C. M. Gamboa, R. C. Pena, and M. Bertotti, "A renewable copper electrode as an amperometric flow detector for nitrate determination in mineral water and soft drink samples," *Talanta*, vol. 80, no. 2, pp. 581–585, 2009.
- [7] D. Kim, I. B. Goldberg, and J. W. Judy, "Microfabricated electrochemical nitrate sensor using double-potential-step chronocoulometry," *Sensors and Actuators B: Chemical*, vol. 135, no. 2, pp. 618–624, 2009.
- [8] J. H. Liang, Y. F. Zheng, and Z. J. Liu, "Nanowire-based Cu electrode as electrochemical sensor for detection of nitrate in water," *Sensors and Actuators B: Chemical*, vol. 232, pp. 336–344, 2016.
- [9] L. Y. Yu, Q. Zhang, Q. Xu et al., "Electrochemical detection of nitrate in PM_{2.5} with a copper-modified carbon fiber micro-disk electrode," *Talanta*, vol. 143, pp. 245–253, 2015.
- [10] M. W. Kim, Y. H. Kim, J. Bal et al., "Rational design of bienzyme nanoparticles-based total cholesterol electrochemical sensors and the construction of cholesterol oxidase expression system," *Sensors and Actuators B: Chemical*, vol. 349, Article ID 130742, 2021.
- [11] I. S. Silva, W. R. Araujo, T. R. L. C. Paixão, and L. Angnes, "Direct nitrate sensing in water using an array of copper microelectrodes from flat flexible cables," *Sensors and Actuators B: Chemical*, vol. 188, pp. 94–98, 2013.
- [12] L. Wei, X. Huang, J. Yang et al., "A high performance electrochemical sensor for carbendazim based on porous carbon with intrinsic defects," *Journal of Electroanalytical Chemistry*, vol. 915, Article ID 116370, 2022.
- [13] A. Khuntia, A. S. Kumawat, and M. Kundu, "Detection of pesticide using Cu-rGO modified electrochemical sensor," *Materials Today Proceedings*, vol. 62, no. 5, pp. 6227–6231, 2022.
- [14] L. Yang, J. Sun, J. Wang, C. Bian, and J. Tong, "Research on nitrate microsensor based on current pulse deposition," *Analytical Chemistry*, vol. 1, no. 43, pp. 98–104, 2015.
- [15] L. Yang, J. Sun, C. Bian, J. Tong, and S. Xia, "Research on nitrate microsensor based on copper nanoclusters," *Analytical Chemistry*, vol. 39, no. 11, pp. 1621–1628, 2011.
- [16] S. Lee, Y. Kang, and A. Jihwan, "Atomic layer deposited Pt nanoparticles on functionalized MoS₂ as highly sensitive H₂ sensor," *Applied Surface Science*, vol. 571, Article ID 151256, 2021.

- [17] L. Jing, G. Zhou, and Y. Zhu, "Highly sensitive, flexible and wearable piezoelectric motion sensor based on PT promoted β -phase PVDF," *Sensors and Actuators A: Physical*, vol. 337, 2022.
- [18] A. V. Almaev, V. I. Nikolaev, and N. N. Yakovlev, "Hydrogen sensors based on Pt/ α -Ga₂O₃:Sn/Pt structures," *Sensors and Actuators B: Chemical*, vol. 364, 2022.
- [19] J. Alshudukhi and K. Yadav, "Survivability development of wireless sensor networks using neuro fuzzy-clonal selection optimization," *Theoretical Computer Science*, vol. 922, no. 4, pp. 25–36, 2022.
- [20] K. M. Anup, G. Debasis, and K. D. Ashok, "Secure user authentication mechanism for IoT-enabled Wireless Sensor Networks based on multiple Bloom filters," *Journal of Systems Architecture*, vol. 120, Article ID 102296, 2021.
- [21] T. R. L. C. Paixao, J. L. Cardoso, and M. Bertotti, "Determination of nitrate in mineral water and sausage samples by using a renewable in situ copper modified electrode," *Talanta*, vol. 71, no. 1, pp. 186–191, 2007.
- [22] D. Kim, I. B. Goldberg, and J. W. Judy, "Chronocoulometric determination of nitrate on silver electrode and sodium hydroxide electrolyte," *Analyst*, vol. 132, no. 4, pp. 350–357, 2007.

Research Article

Application of Artificial Intelligence Technology in Cross-Cultural Communication of Intangible Cultural Heritage

Jiankun Zhang  and Yanhui Jing

Department of Basic Education, Lanzhou Resources and Environment Voc-Tech University, Lanzhou 730021, Gansu, China

Correspondence should be addressed to Jiankun Zhang; jiankun_z@cmu.ac.th

Received 13 July 2022; Revised 12 August 2022; Accepted 24 August 2022; Published 27 September 2022

Academic Editor: Wei Liu

Copyright © 2022 Jiankun Zhang and Yanhui Jing. This is an open access article distributed under the Creative Commons Attribution License, which permits unrestricted use, distribution, and reproduction in any medium, provided the original work is properly cited.

Intercultural communication not only promotes the emergence and development of multiculturalism but also promotes cultural exchanges on a global scale. China has rich resources and a long history. Because of its unique national characteristics, it is even more famous and unique in the world today. However, with the transformation of society, cross-cultural dissemination and blending are inevitable. Intangible cultural heritage is an important cultural form, and its international dissemination is increasingly attracting people's attention. The spontaneous inheritance mode of intangible cultural heritage, which is mainly based on oral and heart teaching, has been unable to adapt to the development of society and has gradually moved away from people's sight. How to better protect and inherit intangible cultural heritage is an important topic in the field of current cultural exchanges. However, due to the particularity of intangible culture, especially its abstract nature, it is difficult to show it to the public, which makes it difficult to protect and promote intangible cultural heritage. The application of the advantages of artificial intelligence technology to the dissemination of intangible cultural heritage is to solve these problems, which can not only make it innovative in protection but also promote its sustainable development to a certain extent. This paper discusses the application of artificial intelligence technology in the protection and dissemination of intangible cultural heritage from multiple perspectives and points out that the advantage of artificial intelligence is that although it cannot be creatively inherited, it can be reproduced in a historical moment, so as to meet people's needs for intangible cultural heritage. It can also be found in the questionnaire for the visitors that 66% of the visitors prefer to learn about the intangible cultural heritage through experience and feel that the personal experience is more intuitive and interesting. Artificial intelligence technology has great advantages in disseminating intangible cultural heritage.

1. Introduction

Currently, intangible cultural heritage is an international topic that has attracted the attention of domestic and overseas people. With its global endangerment, the intangible cultural heritage is in a difficult place for its survival. Especially now that many tourist attractions are over-exploited and commercialized and some intangible cultural heritage items have already existed in name only, it is urgent to call on the public to pay more attention to intangible cultural heritage. In the protection of intangible cultural assets, dissemination and promotion are the primary tasks of preserving intangible culture assets, while realizing preservation is the eventual starting point and destiny. The conservation and transfer of intangible and cultural heritage not only is in the form of

words, figures, and recordings but also can be disseminated in an increasingly versatile way. It makes up for the feelings given to later generations by a single text and photo record. It dynamically reproduces the historical features at that time, makes the viewer feel more immersive, and can more vividly spread the intangible cultural heritage. It also makes the audience more willing to accept this form of communication and achieves the effect of entertaining. It combines cultural communication and entertainment very appropriately. In the collision of global cultures, it is undoubtedly of great significance to further enhance the country's cultural soft power.

Intangible culture is the weakest part of living culture. The cultural differences between different countries and ethnic groups are the inevitability of cross-cultural

communication, and it is also the result that cross-cultural communication is difficult to penetrate into the hearts of the people. Based on the “use and satisfaction theory,” Yun established an evaluation model for the dissemination and identification of intangible cultural heritage popular science publications. Based on surveys of experts and general audiences, the weighted scores for the model are obtained. The results are presented below. In the assessment module of dissemination and evaluation of popular science and culture related publications of subtangible cultural property, various levels of access and validation factors impact the identified recipients. Among these factors, the audience's ability to understand the channel, whether it can be clearly presented, and the skills and knowledge to integrate into the relevant context have a significant impact on the dissemination of intangible cultural heritage publications. It can not only help the audience to acquire knowledge but also make the audience interested and combine the new media with itself [1]. Manera conducted a cross-cultural exchange analysis of the clinical structure of the Urok practice of the Bago tribe in Kalinga province, Philippines. Urok refers to the custom of offering financial relief to each tribal group member during times of marriage, residency, and death, developing a community identity worthy of acceptable and honorable representation from the outside of the tribe. The intercultural exchange was used to conduct a critical analysis of the cultural fabric of the Urok custom of the Bago tribe. It investigates how members of Aboriginal communities have used their first-hand experiences to model Urok customs, particularly their implications for alleviating the economic hardships of community members. Important findings include the following topics. (a) Urok is the value of true mutual love and coexistence in the sociocultural sense. (b) Urok is seen not only as a material aid but also as a portrait of a harmonious relationship. (c) Urok is a form of moral compassion, an act of restraint. In general, the cross-cultural communication of the Bago tribe is revealed in the practice of Urok, whose cultural structure creates an image of unity and mutual aid in the Bago. Undoubtedly, Urok becomes an important part of community life because it is rooted in the value of “panakikadwa” (partnership), resulting in reciprocity and camaraderie [2]. Khaydarova studied the peculiarities of forming linguistic and literacy abilities of students in the teaching process of English and worked on the problem of forming the linguistic to cultural abilities when acquiring English. The elements and a structure of verbal and cultural proficiency are formed on the basis of auditory texts, and the major types of skills, knowledge, and skills falling within their framework are presented, as well as some approach and receptive techniques to form their structure. The relevance of the purposes of foreign education is associated with the students' formation of these kinds of knowledge, skills, and abilities, the mastering of which allows them to become familiar with the national values of the country they are attending and to practically use the foreign language on the basis of intercultural intelligibility and knowledge. The sum of these kinds of knowledge, skills, and capacities makes up the sociability of a student. The notion of interpersonal competence is the result of an attempt to

draw a line somewhere between one's intellectual skills and basic interpersonal ability. Based on the communicative law, it is necessary to develop students' ability to communicate in a foreign language or, in the other words, to acquire communicative competence in the process of teaching foreign languages. Communicative competence is the ability to use all types of language activities: reading, listening, speaking (monologue and dialogue), and writing [3]. As an important part of modern society, intercultural dialogue should help one's self-identification in cultural space. SerEGINA proved the necessity of multiculturalism—learning a secondary tongue in the Russian higher learning experience system. By analyzing and making comparisons of trials of learning a second language, the research results defined effective teaching methodology and modalities. In the process, the research foreshadowed a number of effective forms of teaching and pointed out the ways to achieve them. In other words, the results of the study are likely to help determine effective strategies for teaching foreign languages at the local and global level but are not very practical [4].

AI translation provides users with the means to turn any text—from phrases to books—into recognizable expressions. Yanisky-Ravid and Shlomit discussed the thriving possibilities of AI online translation as an accessibility tool in the era of 3A (advanced, autonomous, and AI systems), whose users are data providers and feedback providers. Therefore, they contribute to the programming and improvement process of these translation tools. The real worry resulting from admitting this new area, conversely, stems from the mischievous use of AI, frequently hidden. Such hidden facets include embedded all kinds of biases such as ethnicity, gender, race, color, religions, or ethnic origin, which are always included in a discussion of the problematic systemic flaws of AI systems [5]. Human-machine communication has become a new relational context in education and should be the focus of teaching research in the coming years. As AI and robots provide personalized instruction, the role of teachers may shift to those of supervisors, designing and selecting machine-guided instruction, monitoring student progress, and providing support. Chad et al. believed that it is important to bring the emotion of teaching researchers to these issues involving machine agents, both inside and outside the traditional classroom walls [6]. Artificial intelligence (AI) has gained momentum and importance in society over the past few years, and Luttrell et al. provided an opportunity for greater dialogue between the greater social and digital media community of inquiry and those invested in using focused and productively focused ways to answer critical questions associated with these areas. Five critical considerations are raised in educational efforts to sustain the future of the communication classroom, particularly on this topic, that will move the discourse forward. These considerations are designed to engage the scholars in intellectually engaging dialogue and to provide a tentative foundation for the direction of dissemination education. They are not implied to be an elaborate list, but rather to initiate discussions in teaching and research that tackle the impact of new and emerging technologies on the field and what can be built into media and dissemination curricula to prepare

educators and students [7]. These studies provide a detailed analysis of the cross-cultural transmission of intangible cultural heritage. It is undeniable that these studies have greatly promoted the development of the corresponding fields. One can learn a lot from methodology and data analysis. However, there are relatively few studies combining artificial intelligence technologies, and it is not thorough enough, and it is necessary to fully apply these technologies to the research in this field.

Intangible cultural heritage contains the essence of a large number of national traditional culture. This article conducted a survey of a group of arts and crafts museums. For local tourists, 50% of them learned about relevant intangible cultural heritage through friends and came to visit. The acquisition of foreign tourists is relatively scattered, mainly through newspapers (23%), Internet information (38%), and other media and friends (20%) to visit. For local audiences who have emotional resonance and a sense of identity in their own history and culture, 43% of the visitors' main purpose of visiting is to increase their knowledge, and most of them will visit the museum for 1 to 3 hours. 66% of the visitors hope to understand the intangible cultural heritage culture through experience and feel that the personal experience is more intuitive, and 65% of the visitors are highly satisfied with the display and exhibits.

2. Deconstruction of the Application of Artificial Intelligence Technology in the Cross-Cultural Communication of Intangible Cultural Heritage

Intangible cultural heritage means conventional aspects of culture that exist in an immaterial form, are strongly linked to people's daily lives, and are handed down from a generation to another. Intangible cultural heritage is produced and spread among the people. It is the product of social development to a certain stage, the crystallization of collective or individual social practice, and an important part of traditional culture. To a certain extent, it reflects the national sentiment and aesthetic taste of a place. Intangible cultural heritage includes oral tradition, traditional performed arts, folklore events and festivals, traditional folk knowledge and practices, traditional craft techniques, and cultural spaces associated with these expressions of traditional culture [8, 9]. Most of the intangible cultural heritage relies on physical objects that reflect their spirit, values, and meaning through a material medium or vehicle. With the increasing trend of international integration, intangible cultural heritage has gradually become an international topic. Figure 1 shows the scope of intangible cultural heritage [10].

China is the world's third largest cultural heritage country. It officially joined the protection of intangible cultural heritage in 2004. At present, three batches of national intangible cultural heritage lists (including two batches of expanded lists) have been publicly released, including a total of 10 categories of items (as shown in Table 1) [11].

As shown in Figure 2, the intangible cultural heritage culture is regarded as a cultural information space. The cultural information space can be divided into three layers, namely, the inner layer, the middle layer, and the outer layer. The inner layer reflects people's spiritual and ideological needs and is generally an intangible non-material culture, which is embodied in the core cultural concepts, values, storytelling, and cultural characteristics [12, 13]. The inner layer of the core expands outward to the outer material culture carrier, which is a cultural element that is easier to be extracted. For example, Dongyang woodcarving is a traditional art in Dongyang City, Zhejiang Province, and one of the national intangible cultural heritages. It can be analyzed in terms of specific theme, color, texture, shape, texture, component composition, etc. Between the inside and the outside is the immaterial core cultural memetic information that is encoded, transmitted, and decoded. In the dissemination of intangible culture, this process of encoding, transmitting, and decoding will be repeated repeatedly. This process is smooth, which is the successful replication of memes. If the deviation or delivery fails due to various reasons, the meme will mutate or disappear [14]. It must be pointed out that non-material cultural factors and their related factors cannot all become non-material cultural memes, and non-material cultural factors must possess the above-mentioned three characteristics of inheritance, variation, and selection to be considered as their memes [15].

Since intangible cultural heritage is a living culture rooted in national soil and a developing living culture, it has the characteristics of dependence and activity, so it cannot be separated from the subjective initiative of human beings, and the main body of inheritance has its core role [16]. The main body of intangible cultural heritage inheritance has its own unique craftsmanship and techniques. For example, local folk paper-cuts, clay sculptures, wood carvings, brocades, Thangkas, and other works have their own unique expression techniques. They are all passed down to the present day through the skilled craftsmanship and creativity of the inheritors [17].

In the cross-cultural dissemination of intangible cultural heritage, different cultural backgrounds and their own time factors make the dissemination of intangible cultural heritage into a dilemma [18]. Intangible cultural heritage has a strong cultural atmosphere of ritual and music, and its cultural structure has many spiritual connotations, and there are many factors that affect the effect of cross-cultural communication, such as outlook on life, legal norms, values, and ways of thinking. Each era has its own cultural form and characteristics, and there is a natural "generation gap" between the cultural form as "heritage" and the characteristics of the era of informatization and modernization [19]. For example, some people believe that, as a product of farming civilization, shadow play can no longer meet the aesthetic needs and values of modern people, and it is difficult to escape the historical fate of extinction. The success of intercultural communication is related not only to the scope of communication but also to whether the intercultural system is easily recognized by people in other countries.

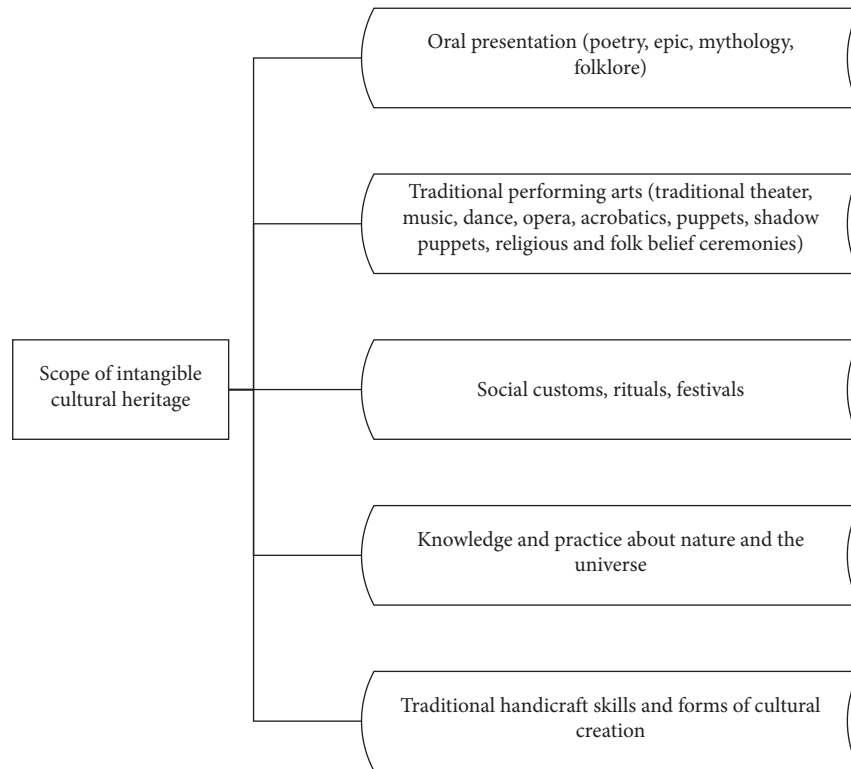


FIGURE 1: Scope of intangible cultural heritage.

TABLE 1: Statistics on the list of intangible cultural heritage.

Category	Number of items	Category	Number of items
Folk literature	145	Folk music	188
Traditional drama	219	Music and arts	139
Folk art	144	Traditional medicine	33
Traditional handcraft	264	Folklore	183
Traditional sports and acrobatics	82	Folk dance	140

Figure 3 shows a ladder model of cultural communication effect.

Artificial intelligence technology refers to the intelligent behavior of artificial objects, including perception, reasoning, learning, communication, and behavior in complex situations [20]. It is a variety of technical means such as computer, image, simulation, language, multimedia, network, data, virtual reality, and so on and provides an effective auxiliary means for human beings [21]. With the development of artificial intelligence technology, the interaction between people and intelligent machines is getting closer and closer. In some ways, people have been able to perform human-computer interaction in real time, providing better services for people's daily life and production. Using artificial intelligence technology to protect intangible cultural heritage and using artificial intelligence technology to spread intangible cultural heritage, its advantages in the process of dissemination are as follows [22]:

- (1) Objective and true: digitally record the text, figures, and sounds of intangible cultural heritage, so as to

restore the historical style of the time to the greatest extent and fully display its artistic characteristics and expression techniques. These intangible cultural heritages can also be permanently preserved [23].

- (2) Various forms: when the audience understands the knowledge of intangible cultural heritage, they are no longer limited to the understanding of words but can selectively expand to various communication methods such as images, sounds, videos, and so on. It deepens people's understanding and recognition of intangible cultural heritage.
- (3) Convenient storage: the unique storage information function of new media can systematically organize and preserve a large number of long-standing and fragmented intangible cultural heritage and save massive and rich intangible cultural heritage at a very low cost. Especially the arrival of the 4G era will also bring more convenience to the dissemination of intangible cultural heritage.

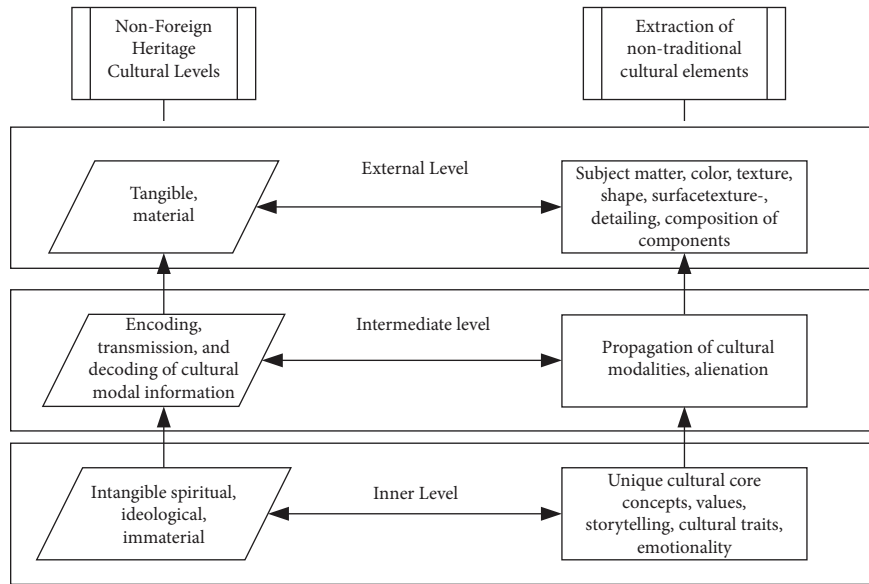


FIGURE 2: Intangible cultural heritage information space.

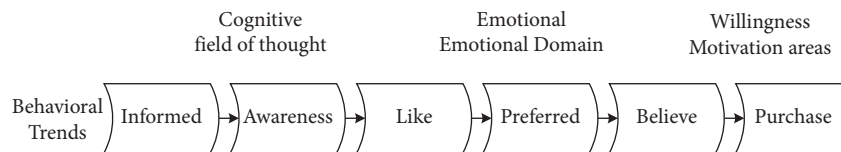


FIGURE 3: Propagation effect ladder model.

- (4) Interactive function: the interaction of new media such as the Internet and mobile phones has deepened the public’s understanding and understanding of intangible cultural heritage culture, especially smart phones, which facilitates online and offline support and interaction, thus broadening the audience of intangible cultural heritage. It is convenient for the audience to deepen their understanding of intangible cultural heritage and expand the influence of intangible cultural heritage.
- (5) Entertainment: with the change of society, the audience cannot accept dogmatic indoctrination but is willing to accept novel, unique, and entertaining forms to accept new things. Intangible cultural heritage spreads intangible cultural heritage through humorous and vivid animation images, vividly displays the content of intangible cultural heritage, and enriches the form of dissemination of intangible cultural heritage. It can gradually change the people’s outdated views on intangible cultural heritage, stimulate the audience’s interest, increase their attention, and make them more easily and happily accept and understand intangible cultural heritage knowledge.

Human-computer interaction is the information exchange between humans and computers. It includes the

two-way information exchange between humans and computers. It is a key technology in the field of artificial intelligence. Using artificial intelligence software, it gets rid of the limitations of traditional keyboard, mouse, and other input methods and can use body language, such as voice, gestures, and so on [24, 25]. In a virtual environment, people can make corresponding actions according to your own commands, giving people an immersive illusion. Most of its technology is implemented by sensors. The digital dissemination of intangible cultural heritage can be displayed through various platforms, thereby shortening the distance between intangible cultural heritage and the public.

Virtual reality (VR) is a device-implemented technology that has more features in actual use, including immersion, multisensory, conceptual, and interactive. The basic realization of virtual reality technology is computer simulation of virtual environment to give people a sense of environmental immersion. By using virtual reality technology to carry on the inheritance and dissemination of intangible cultural heritage culture, users can have a feeling of “operability,” breaking through the limitations of traditional static display of intangible cultural heritage, and realizing multilevel and multidirectional virtual scene reproduction to achieve inheritance and dissemination of culture. Figure 4 highlights the use of virtual reality technology to pass on and spread intangible culture.

Panoramic video is one of the most important components of virtual reality. Due to the ultra-high-definition resolution and multiangle information required for panoramic images to immerse users in it, the amount of information in panoramic videos may be dozens of times higher than ordinary videos. Taking 4KRGB (red-green-blue) 360° panoramic video as an example, its full viewing angle resolution needs to reach 7680×3840 pixels, which is 32 times that of ordinary 720P video, and the processing and transmission delay will be greatly increased. This puts forward high demands on the processing and transmission capabilities of the system. The network requirements for virtual reality video are shown in Table 2.

In the video transmission system, the judgment of video quality will be affected by many factors, such as video acquisition, encoding, transmission, decoding, rendering, playback process, and so on, which can be measured by objective data monitoring or subjective experience testing. Objective methods will evaluate the quality of videos by building a mathematical model of the human visual system. In image and video processing, peak signal to noise ratio (PSNR) is the most commonly used objective quality assessment metric. PSNR is compared pixel by pixel between the reference image and the distorted image, and finally a peak SNR map is generated. This process does not need to consider what the image content actually represents. For the decoded image pixel component/d, the mean square error (MSE) of the original image pixel component I is calculated as

$$MSE = \frac{\sum_{i=0}^{P-1} \sum_{j=0}^{Q-1} (I(i, j) - I_d(i, j))^2}{M \times N}. \quad (1)$$

Among them, each frame has $M \times N$ pixels, and $I(i, j)$ and $I_d(i, j)$ are the luminance pixels at position (i, j) in the image. PSNR is the logarithmic ratio between the maximum value of the received signal and the maximum value of the background noise (MSE), so the PSNR value is calculated as follows:

$$PSNR = 10 \times \log \frac{(2^B - 1)^2}{MSE}. \quad (2)$$

Among them, B is the bit depth of the image sample. If each sample uses 8 bits to represent pixels, then

$$PSNR = 10 \times \log \frac{255^2}{MSE}. \quad (3)$$

Doing the PSNR calculation for each frame in the above form can be 50% slower than encoding the same video.

Calculate the weighted mean square error and WMSE of each pixel, as shown in the following formula.

$$WMSE = \frac{1}{\sum_{i=0}^{P-1} \sum_{j=0}^{Q-1} w(i, j)} \sum_{i=0}^{P-1} \sum_{j=0}^{Q-1} \Delta^2 w(i, j). \quad (4)$$

Among them, $M \times N$ represents the resolution of the 2D planar virtual reality image after projection.

$$\Delta = y(i, j) - \hat{y}(i, j), \quad (5)$$

where $y(i, j)$ and $\hat{y}(i, j)$ represent the value of the original image and the reconstructed image at pixel (i, j) , respectively, and Δ^2 represents the variance of the absolute values of the two.

$$w(i, j) = \cos \frac{(i + 0.5 - P/2)\pi}{P} \times \cos \frac{(j + 0.5 - Q/2)\pi}{Q}. \quad (6)$$

The user-perceived video quality $q(R_c)$ can be expressed as

$$q(R_c) = 10 \log \left(\frac{(2^I)^2}{WMSE} \right). \quad (7)$$

Among them, I represents the bit depth of the initial video (image color depth), that is, the number of bits used to define each pixel, and commonly used values are 8, 10, 12, etc.. The larger the value of this parameter is, the larger the pixel value range of the image is and the richer the color that the image can present.

By using a Gaussian function to fit the viewing angle and the MOS (mean option score) curve obtained by subjective ratings of the quality of six different videos viewed by 50 first-time participants, the quantitative relationship expression between viewer QoE and viewing angle and blocking scheme can be obtained:

$$R = 60 - N + (N - 1) \times e^{-0.5 \times (h - 2/6N)^2}. \quad (8)$$

Among them, R represents the QoE value, h represents the viewing angle, and N represents the corresponding parameter of the selected blocking scheme.

Kalman filtering is a method of using the state formula of a linear system to perform a recursive operation on the previous prediction and observation data to obtain a posterior system state value. The algorithm consists of two steps, one is to estimate the current system state according to the last estimated value, and the other is to adjust the existing predicted value according to the Kalman gain coefficient to obtain a more accurate prediction.

The state variable to be estimated is defined as $x \in R^n$, which can be expressed as a stochastic difference formula in a linear system:

$$x_c = A_{c-1} x_{c-1} + B u_{c-1} + w_{c-1}. \quad (9)$$

Define the observed variable $z \in R^m$, and the measurement formula is

$$z_c = H x_c + v_c. \quad (10)$$

Among them, w_c and v_c represent process excitation noise and observation noise, so the essence of Kalman filtering is to reduce the influence of noise signals of w_c and v_c in the calculation process and obtain the optimal estimated value of x_c .

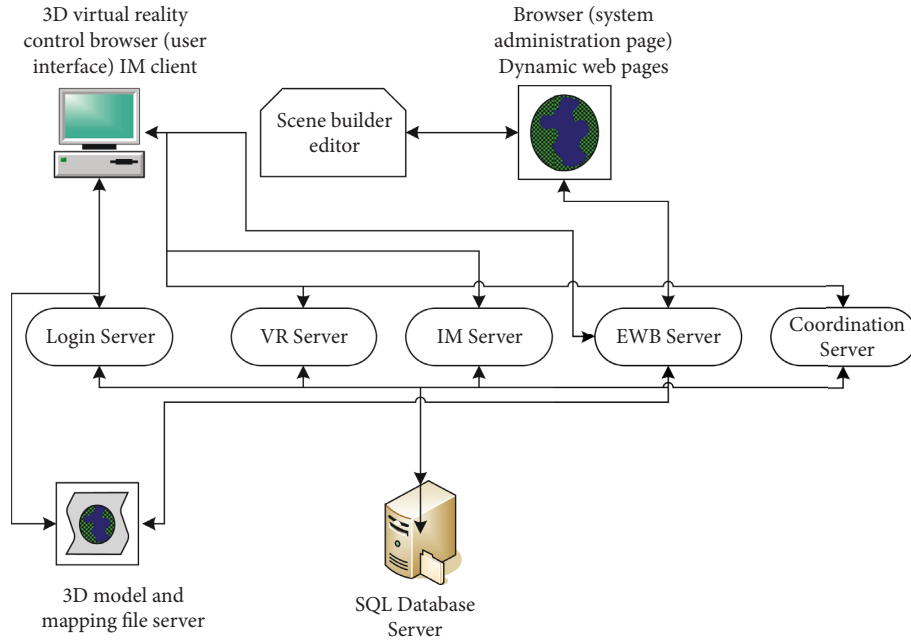


FIGURE 4: System structure figure.

TABLE 2: Network transmission requirements for virtual reality video.

Different VR levels	Para-VR (no immersion)	Entry-level VR (partial immersion)	Optimized VR (deep immersion)	Ultimate VR (full immersion)
Bandwidth requirements	25Mbit/s	100Mbit/s	420Mbit/s	2.4Gbit/s
RTT requirements	40 ms	30 ms	20 ms	10 ms
Packet loss ratio requirements	$1.4E-4$	$1.5E-5$	$2.0E-6$	$5.5E-8$

Definition $\hat{x}_{\bar{c}} \in R^n$ (-represents prior, ^ represents estimation) is the prior state estimate of the c -th step when the state before the c -th step is known, and definition $\hat{x}_{\bar{c}} \in R^n$ is the posterior state estimate of the c -th step when the measured variable z_c is known. This defines the prior estimation error and the posterior estimation error:

$$\begin{aligned} e_{\bar{c}} &= x_c - \hat{x}_{\bar{c}}, \\ e_c &= x_c - \hat{x}_c. \end{aligned} \quad (11)$$

The covariance of the prior estimation error is

$$P_{\bar{c}} = E[e_{\bar{c}}e_{\bar{c}}^T]. \quad (12)$$

The covariance of the posterior estimation error is

$$P_c = E[e_c e_c^T]. \quad (13)$$

In order to find the optimal value of x , the posterior variance must be minimized, and then the Kalman filter is used to weight the existing estimates and observations to obtain the posterior estimate (K is the Kalman gain).

$$\hat{x}_c = \hat{x}_{\bar{c}} + K(z_c - H\hat{x}_{\bar{c}}). \quad (14)$$

3. Experiments on the Application of Artificial Intelligence Technology in the Cross-Cultural Communication of Intangible Cultural Heritage

The digital interactive experience-type intangible cultural heritage culture is a multifunctional smart museum that emerged after the revival of modern culture. Under the action of AR full-sensing experience technology, virtual figures are introduced into the real world, so that people can feel the charm of traditional culture from all angles. Through the impact of 3D visual effects, the auditory impact of multichannel audio and video, the tactile impact of the scene, the impact of smell, and the impact of taste, people can experience the intangible cultural heritage in an all-round way. Coupled with the AR full-sensing model, various scenarios can be switched according to the user's preferences and requirements to meet the needs of users. In order to strengthen the protection of intangible cultural heritage and promote the development of intangible cultural heritage in the tourism industry, we must adhere to the principles of prioritizing protection, rational

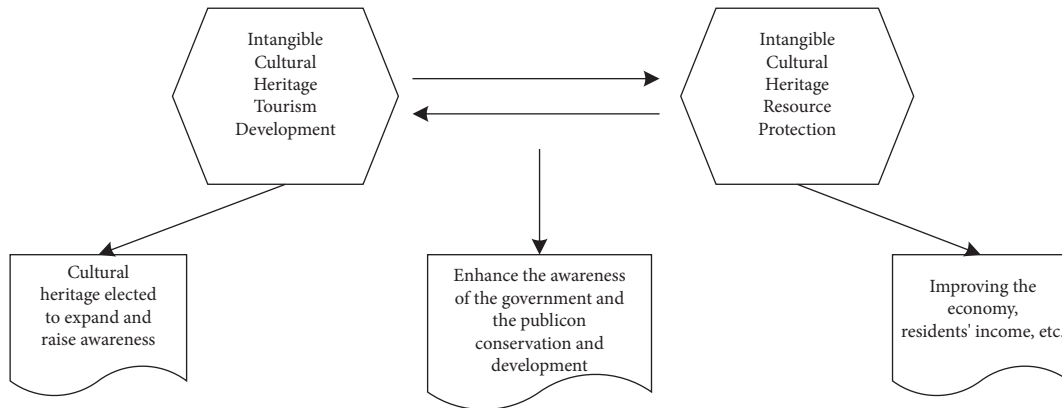


FIGURE 5: Interaction and impact of intangible cultural heritage protection and museum development.

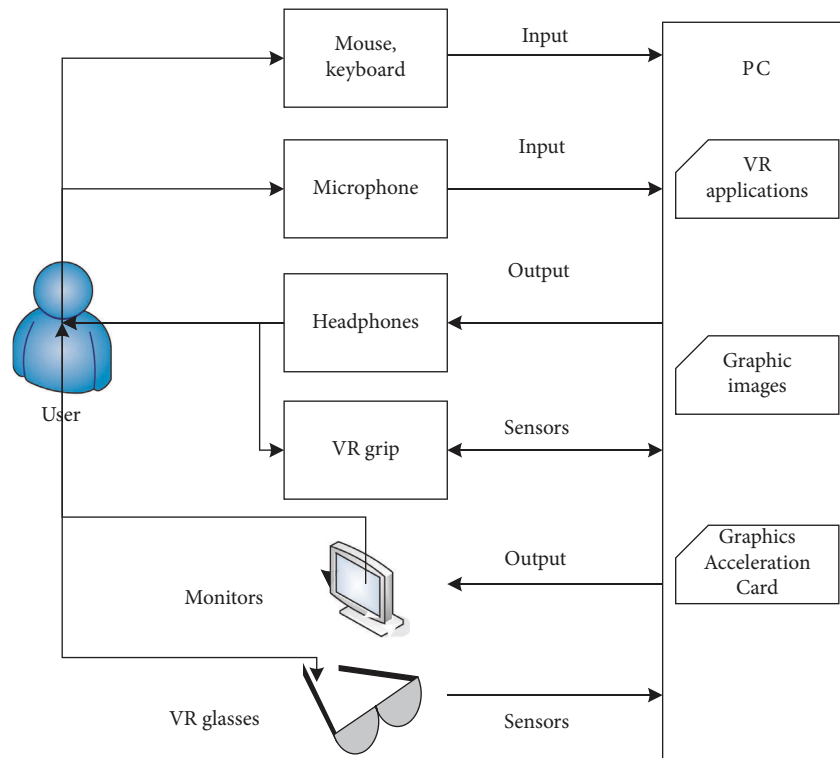


FIGURE 6: Architecture of a virtual reality system.

utilization, inheritance and development, protection first, and development second. In order to achieve a double harvest of intangible cultural heritage protection and tourism development, in the entire process of intangible cultural heritage tourism development, people should also focus on the organic combination of development and protection. On the premise of doing a good job in protection, scientific development can be carried out to achieve sustainable development of intangible cultural heritage and enrich cultural background, as shown in Figure 5.

Developers can use computers or workstations to achieve simulation effects, use computer input and output devices to control visual and physical sensations, and allow users to

enter a virtual 3D simulation environment. At the same time, it can also change with the movement of the user, bringing an immersive feeling to the user, as shown in Figure 6.

Intangible cultural heritage is highly valued in today's cultural communication. This paper conducts a survey on a group of arts and crafts museums and also conducts a questionnaire survey on the public. In the survey, a total of 200 visitors of different ages are randomly selected for questionnaire survey. As shown in Table 3, from the statistics of the questionnaire results, the arts and crafts museum group has a relatively wide audience, among which the youth and middle-aged and young people account for more than half.

TABLE 3: Basic information of the respondents.

Age group of visitors	Number of people	Proportion (%)
<18	20	10
18–25	24	12
25–35	40	20
35–65	76	38
>65	20	10

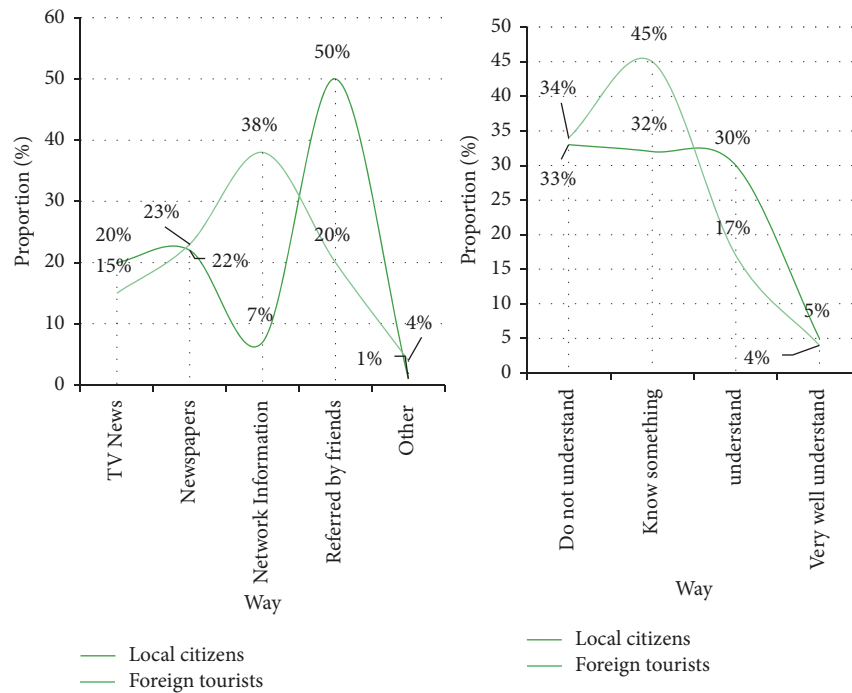


FIGURE 7: Visitors' access to information.

4. Data Deconstruction in the Cross-Cultural Communication of Intangible Cultural Heritage

In order to understand the effects of various dissemination channels of intangible cultural heritage, statistics were made on the ways of information acquisition by visitors, as shown in Figure 7.

It can be seen from Figure 7 that for local tourists, they mainly come to visit relevant intangible cultural heritage through the introduction of friends, accounting for 50%. The acquisition of foreign tourists is relatively scattered, mainly through newspapers (23%), Internet information (38%), and other media and friends (20%) to visit. It can be seen that the proportion of visitors who know very well is very small, no more than 5%.

Intangible cultural heritage is limited by the natural environment. China has a vast territory, a large population, and different living habits, forming the diversity of Chinese culture. Figure 8 shows the statistical result of the visitor's visit purpose and stay time.

As can be seen from Figure 8, for local audiences who have emotional resonance and a sense of identity in their own history and culture, the main purpose of their visit is to increase their knowledge, accounting for 43%, and most of them will visit the museum for 1 to 3 hours.

According to the progress of technology, information technology, figure processing, and VR technology have gradually revealed their unique charm. Digital restoration and reproduction provide advanced and better means of preservation for the transmission and spreading of inter-material cultural heritage. The statistics resulted in Figure 9 in order to examine the public's position on the succession of science and technology and the diffusion of subtangible cultural assets.

It can be seen from Figure 9 that 66% of the visitors prefer to learn about intangible cultural heritage culture through experience and feel that the personal experience is more intuitive and interesting. This provides a broad market prospect for the improvement of virtual intangible cultural heritage experience. The audience generally believes that the on-site display of traditional handicrafts is the biggest

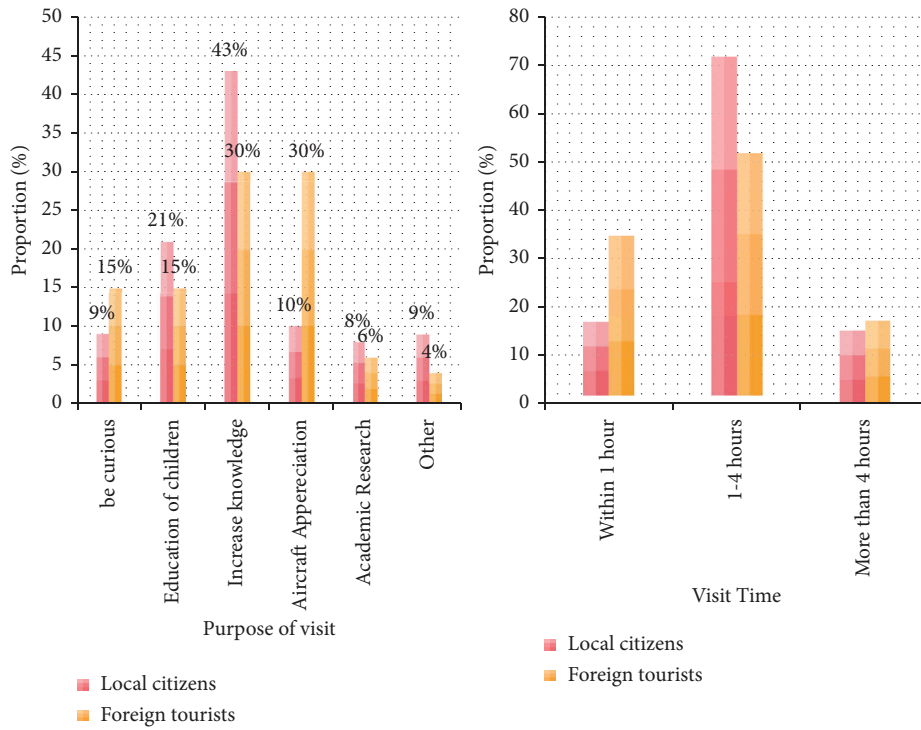


FIGURE 8: Visitor's purpose and stay time.

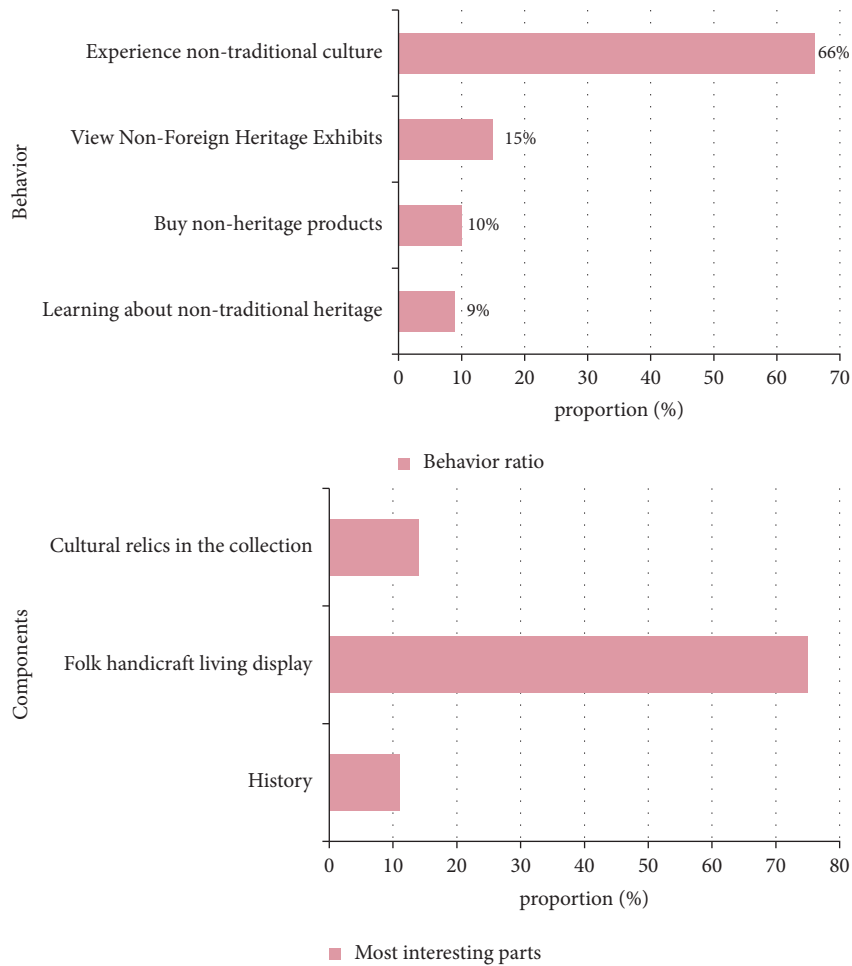


FIGURE 9: Proportion of participation in intangible cultural heritage.

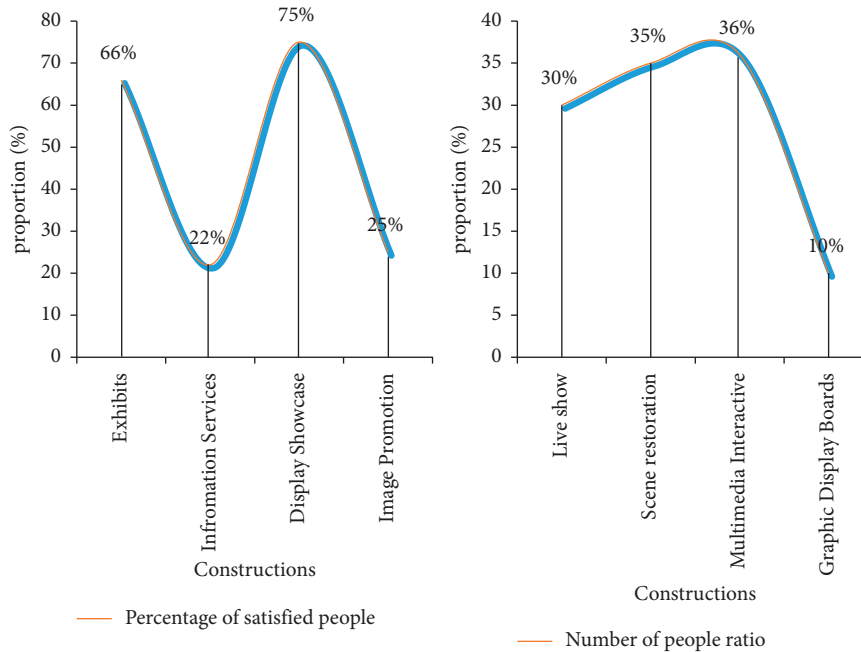


FIGURE 10: What visitors are satisfied with and what they think needs improvement.

attraction of the museum, and they hope to strengthen the on-site display content and scene creation during the display process. At the same time, they also affirmed the important role of the handicraft life exhibition hall in the protection and inheritance of intangible cultural heritage. Figure 10 shows the parts that visitors are satisfied with and the parts that need to be improved.

From Figure 10, it can be seen that the audience’s satisfaction with the display and exhibits is high, reaching more than 65%. 36% of the visitors believe that multimedia interaction needs to be strengthened, and 35% of the people think that the scene restoration needs to be strengthened.

5. Conclusions

With the development of the times, the Internet has become the most efficient and convenient way for cross-cultural communication. The globalization of economy and culture is also a good opportunity for intangible cultural heritage to realize cross-cultural dissemination. This paper studies the application of artificial intelligence technology to the cross-cultural dissemination of intangible cultural heritage in order to better protect and promote intangible cultural heritage culture. The cross-cultural dissemination of artificial intelligence technology in non-material culture is not only a means of attracting consumers but also a high-tech technology that is truly, comprehensively, and deeply applied to venues. With the application of artificial intelligence technology, the protection and utilization of Chinese folk intangible cultural heritage is being carried out in an orderly manner, and the revival and prosperity of national traditional culture is imminent. Intangible cultural heritage is a living fossil of human civilization. People all over the world use various means and methods to record, disseminate, and

preserve ancient intangible cultural heritage. Intangible cultural heritage is the crystallization of Chinese wisdom and civilization and an important cultural resource for the development of human society. On the basis of inheriting the national culture, through the power of the government, the media, and the people, the Chinese cultural concept, way of thinking, way of life, art form, etc. are transmitted to the outside world, thereby reducing misreading, rejection, anxiety, and conflict between cultures and realizing understanding, adaptation, identification, and integration between cultures.

Data Availability

The datasets generated and/or analyzed during the current study are not publicly available due to sensitivity and data use agreement.

Conflicts of Interest

The authors declare that they have no conflicts of interest.

References

- [1] Y. Zhu, H. Ye, and S. Tang, “Research on communication identification of intangible cultural heritage popular science publication based on AHP and entropy method,” *Open Journal of Social Sciences*, vol. 05, no. 08, pp. 199–208, 2017.
- [2] A. B. Manera, R. T. Vecaldo, and A. Com, “Cultural structuring of Urok practice: an intercultural communication of the Bago tribe in Kalinga province, Philippines,” *International Journal of Psychosocial Rehabilitation*, vol. 24, no. 6, pp. 13193–13217, 2020.
- [3] U. P. Khaydarova, “Intercultural communication as a pattern of learning content in linguocultural competence,” *Academy*

- Journal of Educational Sciences*, vol. 2, no. 1, pp. 783–788, 2021.
- [4] T. Seregina, S. Zubanova, V. Druzhinin, and G. Shagivaleeva, “The role of language in intercultural communication,” *Space and Culture India*, vol. 7, no. 3, pp. 243–253, 2019.
- [5] R. Yanisky and S. Shlomit, “From the myth of babel to google translate: confronting malicious use of artificial intelligence—copyright and algorithmic biases in online translation systems,” *Seattle University Law Review*, vol. 43, no. 1, p. 4, 2019.
- [6] E. Chad, A. Edwards, P. R. Spence, and X. Lin, “I, teacher: using artificial intelligence (AI) and social robots in communication and instruction,” *Communication Education*, vol. 67, no. 4, pp. 473–480, 2018.
- [7] R. Luttrell, A. Wallace, C. Mccollough, and J. Lee, “The digital divide: addressing artificial intelligence in communication education,” *Journalism and Mass Communication Educator*, vol. 75, no. 4, pp. 470–482, 2020.
- [8] I. Nyshchak, M. Kurach, G. Buchkivska, V. Greskova, and N. Nosovets, “Didactic opportunities of information and communication technologies in graphic training of future technology teachers,” *BRAIN: Broad Research in Artificial Intelligence and Neuroscience*, vol. 11, no. 2, pp. 104–123, 2020.
- [9] S. M. Aljaberi and S. Ali, “Integration of cultural digital form and material carrier form of traditional handicraft intangible cultural heritage, fusion,” *Practice and Applications*, vol. 5, no. 1, pp. 21–30, 2021.
- [10] O. M. Shekoni, A. N. Hasan, and T. Shongwe, “Applications of artificial intelligence in powerline communications in terms of noise detection and reduction: a review,” *Australian Journal of Electrical and Electronics Engineering*, vol. 15, no. 1–2, pp. 29–37, 2018.
- [11] S. B. Lee, “Chatbots and communication: the growing role of artificial intelligence in addressing and shaping customer needs,” *Business Communication Research and Practice*, vol. 3, no. 2, pp. 103–111, 2020.
- [12] M. H. Shin, “The effects of communication strategies for EFL students (Applying artificial intelligence),” *Journal of Advanced Research in Dynamical and Control Systems*, vol. 10, no. 3, pp. 126–130, 2018.
- [13] J. Y. Hong, H. Ko, L. Mesicek, and M. B. Song, “Cultural Intelligence as Education Contents: Exploring the Pedagogical Aspects of Effective Functioning in Higher Education,” *Concurrency and Computation Practice and Experience*, vol. 12, 2019.
- [14] L. Vm, “Artificial intelligence at health care industry name-likitha vm reg.No-20bec0614 school of electronics and communication engineering vit vellore introduction,” *International Journal of Humanities, Arts, Medicine and Science*, vol. 5, no. 3, pp. 39–42, 2021.
- [15] S. Lehman-Wilzig, H. T. Dyer, and S. Lehman-Wilzig, “Book Review: an introduction to communication and artificial intelligence,” *New Media & Society*, vol. 22, no. 7, pp. 1329–1330, 2020.
- [16] J. Malankowski and D. S. Majewicz, “Communicating with metaphors: a cross-cultural analysis of technology forums,” *Iberica*, vol. 36, pp. 43–68, 2018.
- [17] K. Choden, K. K. Bagchi, G. J. Udo, P. J. Kirs, and G. Frankwick, “The influence of cultural values on information and communication technology (ict) diffusion levels: a cross-national study,” *Journal of Global Information Technology Management*, vol. 22, no. 4, pp. 243–256, 2019.
- [18] S. S. A. Guan, T. A. Bui, and W. Ho, “Considering cultural factors in emerging adult use of communication technologies: culture in technology use,” *International Journal of Information Communication Technologies and Human Development*, vol. 9, no. 3, pp. 14–28, 2017.
- [19] R. Li, Z. Zhao, X. Zhou et al., “Intelligent 5G: when cellular networks meet artificial intelligence,” *IEEE Wireless Communications*, vol. 24, no. 5, pp. 175–183, 2017.
- [20] K. Mohamed, A. S. Abd Aziz, and N. A. Mohd Noor, “Legal analysis for protection of intangible cultural heritage in Malaysia,” *International Journal of Law Government and Communication*, vol. 5, no. 19, pp. 10–20, 2020.
- [21] A. Jeavons, “What is artificial intelligence?” *Research World*, vol. 65, p. 75, 2017.
- [22] D. Hassabis, D. Kumaran, C. Summerfield, and M. Botvinick, “Neuroscience-inspired artificial intelligence,” *Neuron*, vol. 95, no. 2, pp. 245–258, 2017.
- [23] A. Bundy, “Preparing for the future of artificial intelligence,” *AI & Society*, vol. 32, no. 2, pp. 285–287, 2017.
- [24] Z. Lv, X. Li, and W. Li, “Virtual reality geographical interactive scene semantics research for immersive geography learning,” *Neurocomputing*, vol. 254, pp. 71–78, 2017.
- [25] C. Grange and H. Barki, “The nature and role of user beliefs regarding a website’s design quality,” *Journal of Organizational and End User Computing*, vol. 32, no. 1, pp. 75–96, 2020.

Research Article

Effect of Farmland Transfer on Poverty Reduction under Different Targeted Poverty Alleviation Patterns Based on PSM-DID Model in Karst Area of China

Yan Liu ¹, Maoqiang Wang ¹, Zhu Qian ², Baolin Hou ¹, Xi Chen ¹, Qinghua Lei ¹,
Lu He ¹ and Longxue Zhao ¹

¹School of Geography and Environmental Science, Guizhou Normal University, Guiyang, Guizhou 550025, China

²School of Planning, University of Waterloo, 200 University Avenue West Waterloo, ON N2L 3G1, Waterloo, ON, Canada

Correspondence should be addressed to Yan Liu; 465153909@qq.com

Received 8 July 2022; Accepted 17 August 2022; Published 19 September 2022

Academic Editor: Wei Liu

Copyright © 2022 Yan Liu et al. This is an open access article distributed under the Creative Commons Attribution License, which permits unrestricted use, distribution, and reproduction in any medium, provided the original work is properly cited.

Rural farmland transfer is a key factor in the successful implementation of targeted poverty alleviation strategies in China. In this paper, a multidimensional index system with 15 indicators from five dimensions, namely, natural, human, physical, financial, and social capital was established. It analyzed the effect of farmland transfer on poverty alleviation under four typical poverty alleviation models implemented in a karst area in China by using Propensity Score Matching (PSM) and Difference-in-Difference (DID) to analyze 467 rural households questionnaire responses from five representative villages in Guizhou Province. The results show that different models had different effects on poverty reduction. In the model of "three changes" + relocation for poverty alleviation + rural tourism + poor households, farmland transfer was the most effective in poverty alleviation, as attested by its average treatment effect on the treated (ATT) value of 0.44. Rural households' nonfarm income increased significantly to develop rural tourism after relocation from inhospitable areas. In the model of "farmland lease/shareholding" + cooperative + enterprise + poor households, farmland transfer had a moderate effect on poverty alleviation, with an ATT value of 0.06. Its effect on the total income of rural households was the lowest among the four models. This study's results can provide a theoretical reference for solidifying the benefits of poverty alleviation and rural revitalization strategies in karst areas.

1. Introduction

Farmland transfer is one of the main contents of rural land system reform and the core of rural development and the steady promotion of agriculture, rural areas, and farmers [1–3], essentially becoming one of the keys to the success of targeted poverty alleviation in rural areas of China [4–6]. The Third Plenary Session of the 18th Central Committee of the Communist Party of China first proposed to entitle farmer households to occupy use benefits and transfer the right of contracted land, and in November 2014, the General Office of the Central Committee of the Communist Party of China and the General Office of the State Council published the "Opinions on guiding the orderly transfer of rural land management rights to develop an appropriate scale of

agricultural operations," which clearly defined the "three rights division" (i.e., division of ownership rights, contracting rights, and management rights) to rural land and provided guidance for the orderly transfer of land management rights [7]. In these policy contexts, whether the farmland transfer can be driven the farmer households to increase their income in a diversified way? Whether it can alleviate the poverty of farmer households.

Farmland transfer plays a more important role in poverty alleviation and development [8, 9]. Some studies have been conducted on the poverty reduction effect of farmland transfer from different perspectives. The transfer of farmland can significantly increase the family income because it will release surplus labor [10, 11]. A healthy and stable land rental market has a positive impact on the

increase of farmers' income [12, 13]. It also helps to reduce the poverty vulnerability of farmer households, and with the increase of the transfer area, the reduction effect is better [14]. However, some thought farmland transfer may lead to the polarization of land management scale; that is, the landless farmer households and a large grain of farmer households coexist, damaging the interests of small-scale farmer households and increasing the gap between the rich and the poor [15, 16].

An active response to the newly introduced national land policies in various locations throughout China resulted in the development of different targeted poverty alleviation models (e.g., "three changes" + farmland transfer + company + poor farmer households) based on farmland transfer [6]. Especially in the karst area of Guizhou Province, perfecting rural land property rights and encouraging farmland transfer are more effective ways to get rid of poverty [5, 17]. Studies have proved that large-scale farmland transfer can promote agricultural efficiency and increase farmer households' income [18–20]. However, the natural conditions, resource endowment, and economic development of different regions will affect farmland transfer and its effect [21, 22]. The difference in land quality [22, 23], geographical location [11], transaction cost [24], and farmer households' behavior [25] have an impact on the poverty reduction effect of farmland transfer.

In the karst area, a fragile eco-environment, high degree of land fragmentation, decentralized production and management, and a single livelihood model of farmer households directly restrict the local farmland transfer [26]. The excessive restriction and intervention of the local system on farmland property rights in karst mountainous areas make farmers control their enthusiasm in the capital, labor input, and farmland transfer [27, 28]. Farmer households' willingness and behavior also have a fundamental impact on the scale, speed, mechanism, and mode selection of land-transfer-in karst areas. Therefore, in recent years, Chinese policies have had a strong guiding effect on farmer households' land use behavior in rocky areas, especially targeted poverty alleviation policy has a very obvious effect on effective rural land transfer [29–31].

There are regional differences in the effectiveness of farmland transfer under targeted poverty alleviation strategies because of the impact of the natural and geographical environment, the abundance of resources, the local economic and social conditions, and other factors unique to each area [32, 33]. It is worthy of attention how to choose a suitable targeted poverty alleviation model to better guide farmer households' farmland transfer and how to reform the system of rural land transfer in coordination with the existing policies of benefiting farmer households. Therefore, this study examines the effect of farmland transfer under different models of targeted poverty alleviation in karst areas based on a comprehensive consideration of the unique background of five villages in Guizhou Province.

2. Research Data and Methods

2.1. Study Area. Guizhou Province is located in Southwest China, the transition area between the Eastern Yunnan Plateau and the Western Hunan Hilly in the east of Yunnan-Guizhou Plateau, with an average altitude of 1104m. It has a subtropical humid monsoon climate, with a land area of 176128 km², accounting for about 1.8% of China's land area, karst landform 73%, plateau mountains 87%, hills 10%, and basins 3%. The total population will be 38,562,148 in 2020, and the urbanization rate will be 49.02%. The number of poor rural people was 9.23 million in Guizhou Province in 2013, and the incidence of poverty was 26.8%, which was about 3.7 times the incidence of rural poverty in China. The highest poverty rate was 37.7%, and the lowest was 0.7% in counties [33]. By the end of 2020, all 66 poverty-stricken counties in the province, 9.23 million people have been lifted out of poverty, 1.92 million people have moved out of the mountains and moved to other places for poverty alleviation and resettlement, 1.8327 million people have been included in the social assistance, and "no missing a poverty person or family" has been fully implemented to achieve the goal.

The cases selection is mainly based on the following two factors: ① The villages are mainly agricultural production with similar population density, and all of them boost poverty alleviation projects through land circulation, which has a certain demonstration effect in the local area; ② Each village is 5–10 km² away from the town center, the karst mountain area has obvious landform, similar resources, and traffic conditions, and the poverty characteristics of villages are representative of the region. The study area was selected and consisted of five typical villages in Guizhou Province in China: Machang Village in Guiyang City, Haiping Village in Liupanshui City, Luzhi Village, and Tangyue Village in Anshun City, Diba Village in Qiandongnan Prefecture (Figure 1).

2.2. Data Collection. The data were collected through questionnaires and interviews to investigate five villages in Guizhou from July to September of 2020 in order to analyze better the difference in poverty reduction effect of farmland transfer under different targeted poverty alleviation models. The questionnaires were refined following a pilot survey. Multistage sampling was adopted to reduce variations and improve sampling efficiency [35, 36]. Study sites selection considered the typicality, spatial distribution, and land quality of various sites and selected villages in both flatland and mountainous areas. Systematic random sampling was used for sample selection to avoid systematic errors caused by subjective factors. A total of 500 questionnaires and conducted in-depth interviews, including 18 interviews with village cadres. Excluding duplicate and missing samples, 467 valid samples (an efficiency rate of 93.4%) collected information on farmland transfer, natural capital, human capital, physical capital, financial capital, and social capital of farmer household.

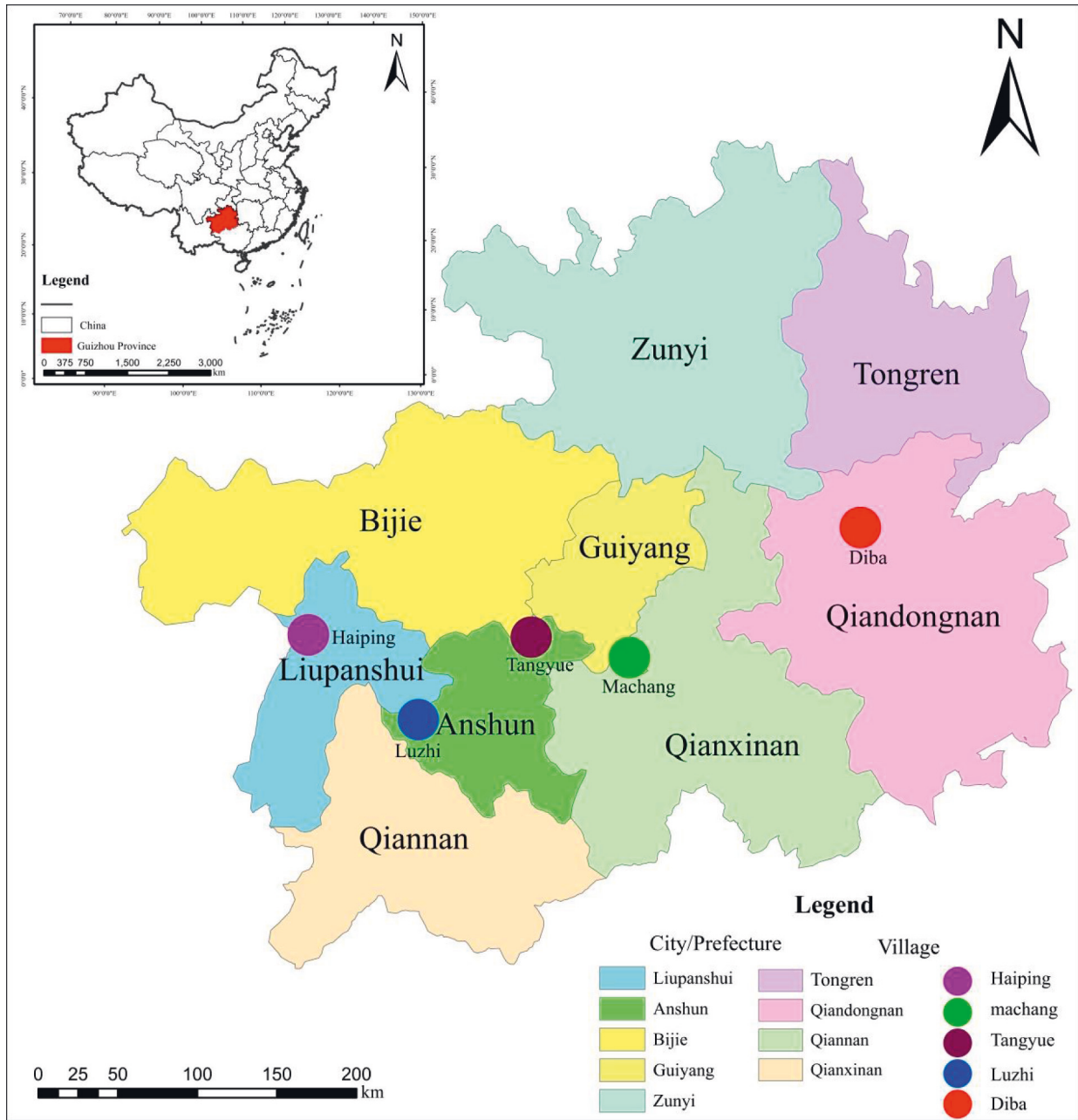


FIGURE 1: The study areas.

The statistical analysis of the selected samples shows that the proportion of men and women who were interviewed in this study was relatively balanced: men accounted for 54.6% of the respondents, and women accounted for 45.4%, which is quite representative of the studied population (Table 1). Among effective samples, interviews with village cadres accounted for 3.9% of all respondents. The proportion of farmer households with incomes below RMB 10,000 and above RMB 70,000 was relatively small, accounting for 12.6% and 12.2% of all respondents, respectively; most farmer households' incomes were distributed in the moderate ranges of RMB 10,000–25,000 and RMB 25,000–50,000. The survey also found that the education level of farmer households was low, with 60.4% having only

elementary education or below; there were 253 respondents who had rented out (transfer-out) their land, 57 respondents who had rented land from others (transfer-in) and 167 who had not participated in farmland transfer. The proportion of respondents participating in farmland transfer was relatively high, accounting for 66.4% of all respondents.

The statistical data in Table 2 shows that the minimum and maximum per-capita area of arable land is 0.2 mu and 4 mu, respectively; the maximum farmland transfer was done by a group leader in one of the surveyed villages. The leader contracted out 80 mu of land for chili pepper cultivation; the average farmland transfer was 4.19 mu. In 2014 and 2019, the minimum per-capita net income was RMB 2300 and RMB 4050, respectively, the maximum per-capita net income was

TABLE 1: Questionnaire statistics ($N = 467$).

Item	Variable	N	Proportion (%)
Gender	Male	255	54.6
	Female	212	45.4
Respondents	Nonregistered card Farmer household Holders	381	81.6
	Poor farmer household cardholders	86	18.4
Income level (RMB)	10,000 or less	59	12.6
	10,000–24,000	144	30.9
	25,000–49,000	143	30.6
	50,000–69,000	64	13.7
	70,000 or above	57	12.2
Education level	Elementary or lower	282	60.4
	Middle school	134	28.6
	High school and above	51	11.0
Farmland transfer	Transfer-out	253	81.7
	Transfer-in	57	18.3

TABLE 2: Sample statistical data.

Variable	Minimum value	Maximum value	Average value	Standard deviation
Per-capita arable land area (mu)	0.200	4.000	1.172	0.489
Arable land ratio	0.250	0.802	0.480	0.000
Transferred land area (mu)	0.000	80.000	4.190	5.280
Family members in the labor force	1.000	6.000	3.250	1.370
Average labor force age	1.000	4.000	2.663	0.706
Family savings (RMB)	0.500	6.000	0.892	1.425
2014 per-capita net income (RMB)	2,300.000	8,300.000	6,918.053	6,994.852
2019 per-capita net income	4,050.000	10,000.000	9,122.539	7,475.376
Agricultural income to total income ratio in 2014 (RMB)	0.300	1.000	0.464	0.335
Agricultural income to total income ratio in 2019 (RMB)	0.000	0.250	0.369	2.336
Frequency of participation in professional cooperatives (times)	0.000	2.000	0.148	0.403
Nonagricultural work time (Hour)	0.000	9.000	5.682	2.581

RMB 8,300 and RMB 10,000, respectively, and the average income was RMB 6918 and RMB 9122, respectively.

2.3. The PSM-DID Model. Propensity score matching (PSM) is a statistical analysis method used to process observational research data in a way that reduces the bias due to confounding variables between the experimental and control groups [34]. The DID model was used to evaluate the net effect of poverty alleviation policy implementation. There are significant differences between farmer households in the treatment group with farmland transfer and those in the control group without farmland transfer. The assessment results will be affected by selection bias if the Difference-in-Differences (DID) model is applied directly to evaluate the effect of the farmland transfer policy. The farmland transfer effect in the targeted poverty alleviation model is compared against a set of evaluation variables to eliminate the interference factors and hidden bias between different groups. The model contains some unmeasurable variables at different times. Therefore, the PSM method is simultaneously combined with DID model (PSM-DID).

Five dimensions were selected, namely natural capital, human capital, physical capital, financial capital, and social capital, with per-capita net income as the explained variable and farmland transfer as the predictor variable. DID model was used to perform multiple linear regression (MLR) on the

selected indicators and calculated the propensity scores for three types of rural residents under different modes: farmland transfer, land in-flow, and land out-flow. The specific steps are as follows.

Estimate the propensity scores: The conditional probability of a farmer household participating in farmland transfer is estimated by the following:

$$PS_m = \Pr[L_m = 1 | X_m] = E[L_m = 1 | X_m]. \quad (1)$$

PS_m is the propensity score, which represents the probability of the sample receiving a treatment given under a set of conditions X . When $L_m = 1$, which indicates participation in farmland transfer, then the propensity score is $P(X) = \Pr(L_m = 1 | X)$. When the PSM assumptions are met, the average annual income of the experimental group $E[\text{experimental group } [L_m = 1, P(X)]]$ and the average annual income of the control group $E[\text{control group } [L_m = 0, P(X)]]$ can be compared in (1).

A multiple linear regression model was established in equation (2). The model is as follows:

$$y_{it} = \beta_0 + \beta_1 \text{Tour}_{it} + \beta_2 \text{Tour}_{it} + \beta_3 \text{Tour}_{it} \text{year}_{it} + \alpha x_{it} + \varepsilon_{it}, \quad (2)$$

where y_{it} is the multidimensional poverty index at time t ; a dummy variable $\text{Tour}_{it} = \{(0, 1)\}$ represents whether farmer household i participates in farmland transfer at time t

(yes = 1, no = 0); Year_{it} is a dummy variable for time, using the time of the targeted poverty alleviation implementation as a reference (0 if 2014 and 1 if 2019); β₀, β₁, β₂, β₃, and α are parameters; χ_{it} is a vector set of other unobservable variables that not only affect whether a farmer household enjoys the benefits of the targeted poverty alleviation policy but also affect the effectiveness of the policy's implementation; for farmer households in the control group and the treatment group, the two time period parameters are β₁ and β₂+β₃, respectively, where β₃ is the estimated value of the double difference, which is the net effect of farmland transfer-in on the targeted poverty alleviation model under consideration on the multidimensional poverty alleviation of farmer households, and ε_{it} is the residual term.

The average treatment effect on the treated (ATT): the PSM results are used to calculate the difference in the effect of farmer households' poverty alleviation (expressed by demand intensity); that is, for the experimental and control groups of farmer households, so as to obtain the effect of farmland transfer (farmland transfer-in and farmland transfer-out) on farmer households' targeted poverty alleviation in different models as follows:

$$ATT = \frac{1}{n} \sum_i \in R_1 \cap U_p (y_i^1 - y_{i,t_0}^1). \quad (3)$$

The average treatment effect (ATE): the average treatment effect of the matching control group is calculated. The above PSM methods are used to calculate the ATE of the control group as follows:

$$ATE = \frac{1}{n} \sum_j \in R_0 \cap U_p (y_{j,t_1}^0 - y_{j,t_0}^0), \quad (4)$$

where t₀ and t₁, respectively, represent the years before and after the implementation of targeted poverty alleviation policy; y_i¹ and y_{i,t₀}¹ are outcome variables of a sample farmer household i in an area with targeted poverty alleviation at times t₀ and t₁, respectively; y_{j,t₁}⁰ and y_{i,t₀}¹ are outcome variables of a sample farmer household j in an area without farm transfer at times t₀ and t₁, respectively.

The PSM-DID results (ATT) are as follows:

$$\begin{aligned} \widehat{ATT} &= \frac{1}{N^T} \sum_j \varepsilon R_1 (y_{i,t_1}^1 - y_{i,t_0}^0) - \sum_j \varepsilon R_0 \cap U_p W(i, j) (y_{j,t_1}^0 - y_{j,t_0}^0), \\ W(i, j) &= \frac{F[(P_j - P_i)/D]}{\sum_m \varepsilon R_0 F[(P_m - P_i)/D]}. \end{aligned} \quad (5)$$

w(i, j) is the weight vector; F(·) is the kernel density function; P_i is the propensity score of sample i in the control group; P_j is the propensity score of sample j in the treatment group; D is a bandwidth parameter.

Assess the significance of the poverty alleviation effect: using the average consumption level as a measure of poverty in rural areas and based on the field investigation results of rural conditions, we derived a set of significance assessment intervals (Table 3) to illustrate the effect of farmland transfer on farmer households' income under different targeted poverty alleviation models.

2.4. *Independent Variables.* Based on the principles of the sustainable livelihood framework, a multidimensional poverty alleviation index system with the following categories of variables was established: natural capital (N), human capital (H), physical capital (P), financial capital (F), and social capital (S). The specific meaning and values of each variable as they relate to the studied areas and farmland transfer conditions were assigned based on the field investigation results and were shown in Table 4.

3. Results

3.1. *Farmland Transfer-in Targeted Poverty Alleviation Models.* Driven by the targeted poverty alleviation policy, Guizhou has formed various models of farmland transfer, among which the following four models are typical.

3.1.1. *Farmland Shareholding + Enterprise + Village Collective/Cooperative + Alluvial Plain Farming + Poor Farmer Household (Model 1).* Model 1 is the primary model of farmland transfer-in Machang Village (Figure 2). In this model, farmland transfer allows for the expansion of the scale of operations to achieve industrial scale, thereby aiding targeted poverty alleviation. In 2020, about 250 mu of Machang's land was subject to farmland transfer. Under the government's guidance, various companies and cooperatives in the village have contracted with the local farmer households to pay RMB 1500/year/leased mu. After the farmland transfer, farmer households have been able to work as seasonal labor to obtain additional income, and this further promotes poverty alleviation.

The farmland transfer-in Machang mainly involved local enterprises. The contract period ranged from five to 15 years. The implementation of this model has allowed for the consolidation of the entire village's idle land resources into large-scale farms for cultivating green onions, ginger, and other industrial crops. After the implementation of farmland transfer policies, the economic conditions in the village improved. The village has become a base for blueberry farming and a sight-seeing destination for mountain tea farm tours. In addition, a rural-ecosystem sight-seeing garden and a 500-mu alluvial plain green-onion farm have been established in the village. These developments have led to the opening of the "Yunxia Nonggeng," an agritourism farm and guesthouse, where the superiority of the locally grown green onions, tea, and rice is further promoted. The current per-capita annual income of the village is about RMB 18,000 yuan. Local farmer households have been encouraged to participate in the construction of a 3000-mu alluvial plain farm planned for 2020 so that they can obtain income from nonagricultural labor.

3.1.2. *Farmland Shareholding + Village Party Organization + Enterprise + Poor Farmer Household (Model 2).* Model 2 is a model in Tangyue Village (Figure 3), in which the village party organization effectively took the lead in a large-scale farmland transfer while actively supporting the development of modern agriculture and promoting the

TABLE 3: Significance level.

Significance level	Farmland transfer-in	Farmland transfer-out	Farmland transfer
Highly significant	>0.010	>0.030	>0.040
Quite significant	0.006 ~ 0.010	0.021 ~ 0.030	0.026 ~ 0.040
Moderately significant	0.003 ~ 0.005	0.011 ~ 0.020	0.016 ~ 0.025
Weakly significant	0 ~ 0.002	0.006 ~ 0.010	0.006 ~ 0.015
Not significant	<0	<0.005	<0.005

TABLE 4: Evaluation index system.

	Variable	Variable meaning
Natural capital (N)	Per-capita arable land area (N_1)	Total arable land area of interviewed households/family size
	Proportion of arable land (N_2)	Arable land area/total land area
	Transportation conditions (N_3)	Local transportation convenience of interviewed households, 4 = very good, 3 = good, 2 = fair, 1 = poor
Human capital (H)	Number of family members in labor force (H_1)	Total number of household members in labor force/person
	Average age of labor force (H_2)	The actual average age/years of labor force of the interviewed family
	Average education level of labor force (H_3)	Average length-of-education/years of labor force of the interviewed family
	Registered poor household card holder (H_4)	0 = No, 1 = Yes
Physical capital (P)	Family Savings (P_1)	Interviewed household's amount of savings/RMB 10,000
	Average annual income per resident (P_2)	Total annual income of interviewed family members/RMB 10,000
Financial capital (F)	Agricultural equipment value (F_1)	Total value of machinery used by interviewed households for agricultural production/RMB 10,000
	Ratio of agricultural income to total income (F_2)	The ratio of households' agricultural income to total income
Social capital (S)	Participation in professional cooperatives (S_1)	Participation frequency of interviewed family in professional cooperatives/times
	Participation in agricultural training (S_2)	Participation frequency of interviewed family in agricultural training/times
	Nonagricultural profitable working hours (S_3)	The total time of nonagricultural profitable employment carried out by the interviewed household/months

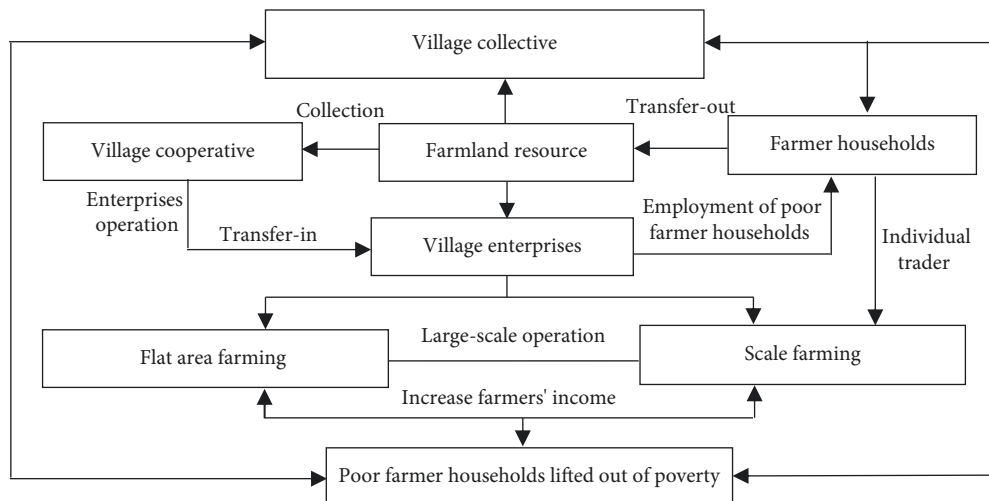


FIGURE 2: Farmland shareholding + enterprise + village collective/cooperative + alluvial plain farming + poor farmer household.

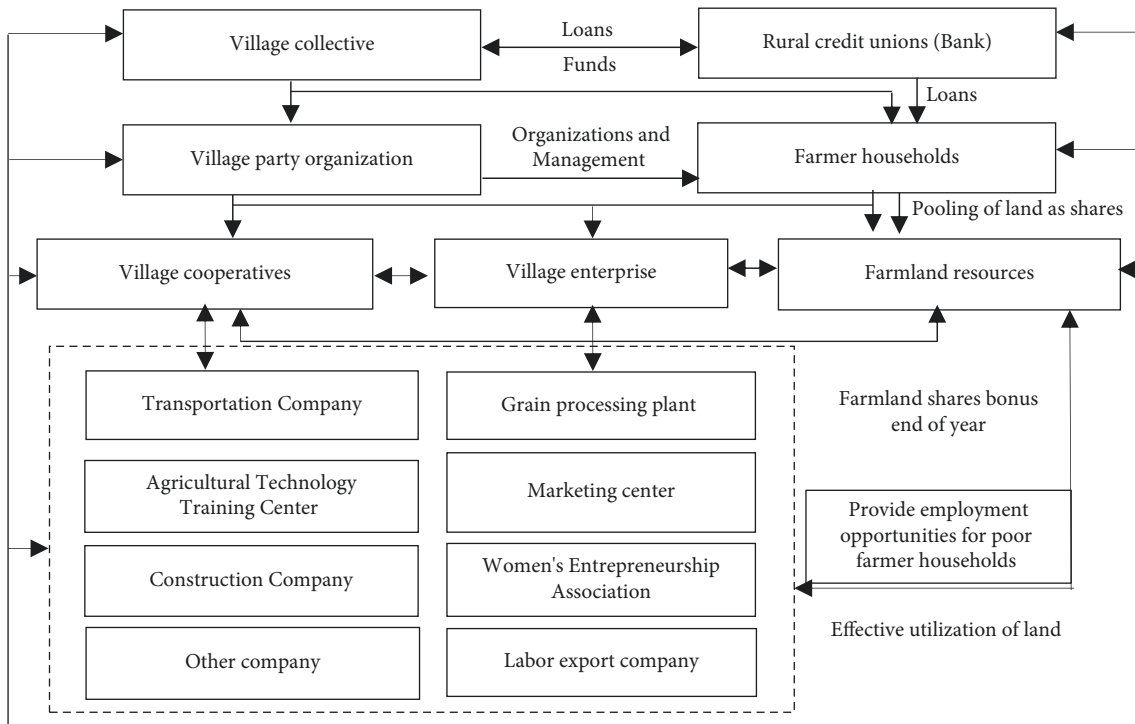


FIGURE 3: Farmland shareholding + village Party organization + enterprises + cooperative + poor farmer households.

village’s self-governance reform. In this model, farmer households (including poor residents) receive dividends from the land they have contracted to the Golden Land Cooperative. In turn, the cooperative works with different enterprises to develop modern agriculture and build various grain processing plants, creating a rural economic powerhouse and spurring the development of other industries in the village. It has also established seven organizations, including a marketing center and an agricultural training center. The successful implementation of this model has helped to diversify farmer households’ livelihood sources, improve the villagers’ living standards, promote rural agriculture, and substantially reduce the number of migrant workers, thereby reducing the problem of "rural hollowing" and allowing poor residents to lift themselves out of poverty.

Based on statistical data, the total area of Tangyue Village is 4881 mu, and almost all of these have been invested in cooperative shares: 921 farmer households have become shareholders with a collective 5230 shares between them. The dividends obtained from land shareholding are split between the cooperative, the village collective, and the villagers using a 3 : 3:4 ratio, respectively. In 2016, the cooperative used three small-scale water conservancy projects and more than 400 mu of forest land to obtain mortgage loans from rural credit unions; the number of dividends received by the village collective and cooperative was RMB 1,214,700 yuan, and the members’ dividends amounted to RMB 896,000 yuan, of which the highest amount was RMB 8,960, and the lowest was RMB 1840. By the end of 2019, the village’s collective economy had exceeded RMB 6.38 million, and the per-capita disposable income had surpassed RMB 20,000.

3.1.3. "Three Changes" + Relocation For Poverty Alleviation + Rural Tourism + Poor Farmer Households (Model 3). In model 3, farmer households receive guidance on how to use their land resources for investment to transform their village into a unique tourist destination featuring the cultural heritage of the Yi ethnic group through the "three changes" reforms (i.e., resources changes into assets, capital changes into share capital, farmer household change into shareholder) in Haiping Village (Figure 4). The model also includes a relocation program for poverty-stricken individuals to facilitate their employment, offering guidance on how to start a business and ensuring a continuous sustainable source of income for rural households. The government grants subsidies to poor households as shares. The Yeyuhai Management Committee has used joint share construction to build a mountain tourism resort; the dividend income is divided between the resort management committee and the village collective based on a 7 : 3 ratio, with 50% of the 30% village collective dividend income being distributed to farmer households. Also, to ensure that poor households maintain basic income, several types of employment were provided, effectively integrating tourism development with poverty alleviation and creating a positive environment for both tourism and living. This distinctive model has become known as the Haiping model.

3.1.4. Farmland Shareholding + Cooperatives + Poor Farmer Household (Model 4). Luzhi Village has used model 4 to lease out consolidated land to local enterprises and cooperatives for agricultural industry projects, including Guanling Cattle Farms, Rosa roxburghii (Chestnut rose), or pearl

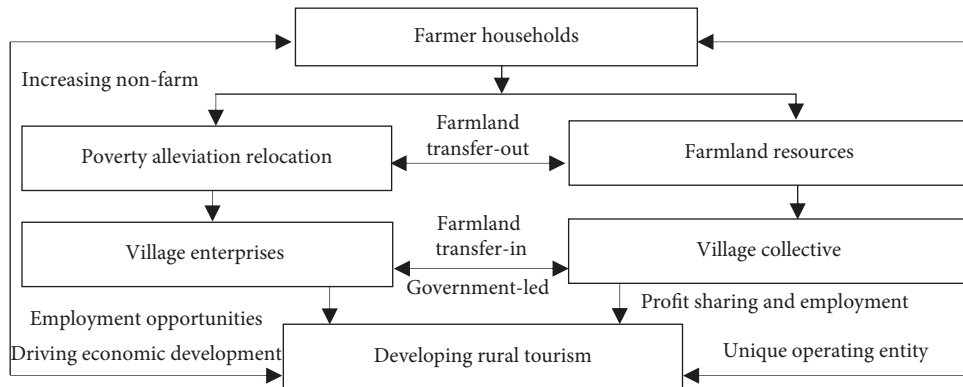


FIGURE 4: "Three changes" + relocation for poverty alleviation + rural tourism + poor farmer household.

barley plantations (Figure 5). These projects have involved 110 poor farmer households and 50 nonpoor farmer households. The village has effectively solved the problems of idle farmland and wasted land resources while providing farmer households with employment opportunities and reducing the number of migrant workers. Consequently, farmer households have a larger share of profits. In the barley cultivation project, barley seed was provided by the government and was planted on 60 mu (1 mu = 0.667 ha) of land provided by the village cooperative.

Diba Village used the same model to establish farming cooperatives for cultivating lucid Ganoderma, chili pepper, ginger, and tea. Poor farmer households can lease out their land for RMB 500 per mu per year to enter the cooperative and receive dividends of RMB 100~1500 per household each year, based on the invested land area. The entire village has transferred more than 1200 mu of land, of which 100 mu of forest land was used for Lizhi mushroom cultivation, 310 mu of forest land for chili pepper farming, 200 mu for tea, and 600 mu for ginger. Farmer households join cooperatives by leasing out their land for large-scale cultivation of ginger, chili peppers, lucid Ganoderma, and other cash crops. The cooperative buys crops from poor farmer households at market prices and sells them by order through different companies to outside markets. In the first half of 2020, tea sales reached RMB 130,000 and the sales of Lizhi mushrooms exceeded RMB 53,000.

3.2. The Net Effect of Farmland Transfer on Farmer Household Households' Income

3.2.1. The Influence Of Farmland Transfer On Farmer Household's Income. The net effect of farmland transfer on farmer household households' income is remarkable. Table 5 shows that the farmland transfer and nonfarm profitable labor time have a significant positive effect on the per-capita net income (given in logarithm form). Similarly, head of farmer household education, per-capita arable land area, number of family members in the labor force, household savings, and average annual household income have a significant positive effect on the per-capita net income. On the other hand, whether the resident is a registered poor

cardholder and the ratio of agricultural income to total income has a significant negative effect on the per-capita net income. However, transportation conditions, the value of agricultural machinery, the superiority of social relations, the average age of the labor force, the proportion of arable land, the frequency of participation in professional cooperatives, and the frequency of participation in agricultural training had no significant effect on the per-capita net income.

3.2.2. The Influence Of Farmland Transfer On Farmers' Livelihood Capital. The indicators that affect farmer households' income are used as matching variables to analyze the poverty reduction effect of farmland transfer; the nontransfer households are used as the control group, and the farmland transfer households as the experimental groups. The ATT difference before matching is 2080.9, and the ATT difference after matching is 2085.8 s (Table 6). The poverty reduction effects of the five livelihood capitals are different. Farmland transfer has a significant effect on poverty reduction of physical capital, human capital, and social capital, 0.22, 0.37, and 5.732, respectively. The effect of farmland transfer on natural and financial capital is not significant.

3.3. The Difference between Farmland Transfer-In and Transfer-Out. The effect of farmland transfer is obvious (Table 7). The average income for farmland transfer residents (experimental group) and nontransfer residents was RMB 9993.381 and RMB 9934.427, respectively, with a standard deviation of 0.07% < 20% after matching, indicating a good match. The difference in the average treatment effect (ATT) between the two groups is 4.954, and the income level of land-transfer farmer households exceeds that of nontransfer farmer households by 88.568.

When the transfer-out farmer household is taken as the experimental group, and the nontransfer farmer household is taken as the control group, before matching, the average income of the experimental and the control group is 12100.600 and 9934.427, respectively, a difference of 2166.168; and after matching, the average income of the

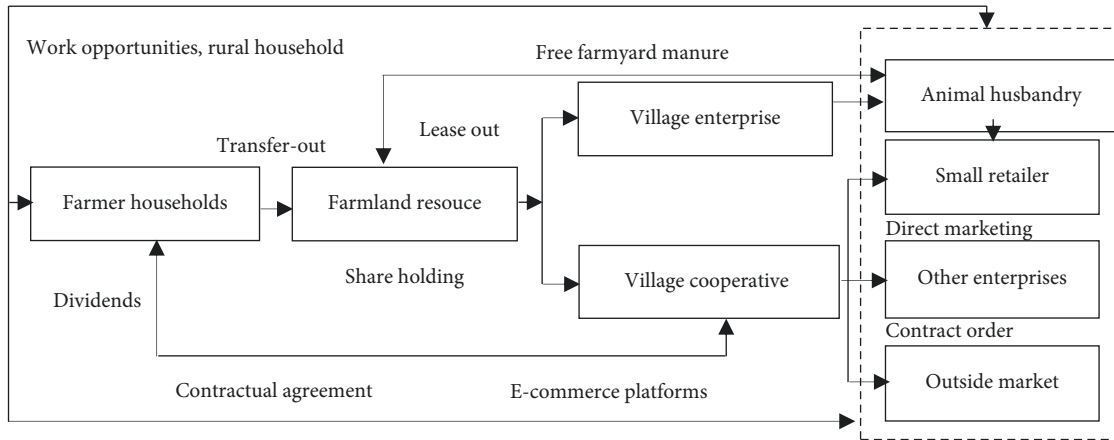


FIGURE 5: Farmland shareholding + cooperatives + enterprises + poor farmer households.

TABLE 5: The net effect of farmland transfer on farmer household households' income.

Variables	Unstandardized Coefficients		Standardized Coefficients		t	p	VIF
	B	SE	B	SE			
T	8.836	0.195	—	—	45.201	0.001	—
N1	0.126	0.048	0.088	0.048	2.608	0.01**	1.198
N2	0.089	0.041	0.005	0.041	0.129	0.01**	1.398
N3	0.005	0.041	0.005	0.041	0.129	0.865	1.322
H1	-0.043	0.034	-0.039	0.034	-1.251	0.212	1.048
H2	0.305	0.025	-0.442	0.025	-12.23	0.001***	1.376
H3	0.03	0.03	0.035	0.03	1.006	0.316	1.274
H4	0.026	0.012	0.076	0.012	2.211	0.028**	1.24
H4	-0.028	0.013	0.046	0.013	1.201	-0.023**	1.524
P1	0.028	0.014	-0.07	0.014	-2.008	0.046*	1.27
P2	0.000	0.000	0.915	0.000	23.17	0.001***	1.644
F1	0.029	0.028	-0.342	0.028	0.782	0.321	1.052
F2	-0.027	0.013	-0.071	0.013	-2.178	0.03**	1.137
S1	0.072	0.051	0.044	0.051	1.419	0.157	1.027
S2	-0.01	0.048	-0.007	0.048	-0.218	0.828	1.023
S3	0.086	0.023	0.007	0.023	0.312	0.003***	1.257

Note.***, **, * indicate significance levels under 0.01, 0.05, and 0.1, respectively.

TABLE 6: The influence of farmland transfer on farmers' livelihood capital.

Status	Experimental group	Control group	ATT	N				H				P		F	S
				N1	H1	H3	H4	P1	P2	F2	S3				
Before matching	12020.2	9934.4	2080.9	0.4	-0.2	0.02	0.18	0.05	2611.4	-0.8	6.58				
After matching	12020.2	9939.3	2085.8	0.03	0.2	0.35	-0.2	0.22	1939.9	0.07	5.73				

experimental and the control group is 10129.350 and 10069.021, with the ATT value of 60.325, which shows that significant changes occurred after matching. After farmland transfer-in, farmer households' income increased to a certain extent, but the magnitude of the increase was not large. When the transfer-out farmer households are taken as the experimental group and the nontransfer farmer households as the control group, the ATT value after matching exceeds 20% with a significance level of 5%, indicating a good match and a significant increase in income after matching.

3.4. The Effect of Farmland Transfer under Various Targeted Poverty Reduction Models. The modes of different targeted poverty alleviation have different poverty reduction effects of land transfer. Model 3 ("three changes" + relocation for poverty alleviation + rural tourism + poor household) has the highest effect on poverty reduction, ATT of farmland transfer effect, farmland transfer-out effect, and farmland transfer-in effect is 0.44, 0.032, and 0.012, respectively. ATT of farmland transfer-out effect in model 1 (Land lease/shareholding + enterprise + village collective/cooperative + alluvial plain agriculture +

TABLE 7: Differences in poverty reduction effect of farmland transfer-in and transfer-out.

Samples	Status	Experimental group	Control group	Standard deviation (%)	ATT	t-after	p-value
Entire sample group	Before matching	12020.3	9934.427	29.63	2085.869	2.035	0.044
	After matching	9939.381	9934.427	0.07	4.954	0.004	0.997
Transfer-in farmer household	Before matching	12100.6	9934.427	30.71	2166.168	2.086	0.039
	After matching	10129.3	10069.021	0.90	60.325	0.052	0.959
Transfer-out farmer household	Before matching	11131.28	9934.430	17.23	1196.85	0.606	0.551
	After matching	11131.28	9444.411	26.84	1686.866	0.710	0.484

TABLE 8: Differences in the effect of farmland transfer under different targeted poverty alleviation models.

Model	All samples			Transfer-out			Transfer-in		
	Experimental group	Control group	ATT	Experimental group	Control group	ATT	Experimental group	Control group	ATT
Model 1	8.476	8.466	0.010	8.483	8.466	0.007	8.470	8.466	0.003
Model 2	8.490	8.471	0.019	8.482	8.471	0.011	8.478	8.471	0.007
Model 3	7.979	7.935	0.044	7.967	7.935	0.032	7.947	7.935	0.012
Model 4	8.289	8.283	0.006	8.302	8.283	0.019	8.270	8.283	-0.013

farmer household/poor household) has the lowest effect on poverty reduction with 0.007. ATT of farmland transfer-in effect in model 4 (land lease/shareholding + cooperative + enterprise + poor household) is the lowest of all (Table 8).

3.5. The Effect of Poverty Reduction in Different Regions.

Based on the comprehensive analysis of the effect of farmland transfer on poverty alleviation in five different dimensions of capital, we were able to examine the regional differences in poverty alleviation strategies and reveal the spatial distribution of the different poverty alleviation models selected in this study (Figure 6). In terms of the effect of different poverty alleviation models on different types of capital, based on their effect on natural capital, the models can be arranged as Luzhi > Haiping > Tangyue > Diba > Machang; in terms of the effect on human capital, the Machang model is the best and Diba model is the worst; in terms of the effect on physical capital, the difference between all five villages was not significant; in terms of the effect on financial capital, Luzhi was the worst and Haiping was the best; and in terms of the effect on social capital, Machang was the worst, and the difference between the remaining villages was not significant.

4. Discussion

The effect of different types of capital factors in farmland transfer has different effects on farmer households' income. The ATT of the influence of farmland transfer on farmers' livelihood capital is different before matching and after matching (2080.9 and 2085.8). Farmland transfer can help farmer households increase their income, provided there is no interference from other factors.

The poverty reduction effect in terms of natural and financial capital factors is not significant. In karst mountain regions, the soil quality is poor, the degree of land fragmentation is high, and large-scale mechanized farming is difficult. Therefore, farmland transfer is mainly distributed in a small areas. In terms of human capital factors, the number of family members in the labor force and their education level significantly affect farmer households' income. The overall economic situation and the average annual income of farmer households increase in terms of physical capital factors, the poverty reduction effect is significant, and in terms of social dimension factors, the effect of farmland transfer on poverty reduction is significant due to the increase of nonagricultural profitable work time.

Compared with farmland nontransfer, the poverty reduction effect of farmland transfer is better, and the effect of transfer-out is more significant than that of transfer-in. On the one hand, Farmland transfer-out allows for a reasonable allocation of idle, inefficiently utilized, and wasted land so as to maximize the effectiveness of land resources, which is conducive to improving farmer households' income. Collective farming after farmland transfer has similar benefits to large-scale production because it allows for the optimized allocation of resources and improved production effectiveness, thereby increasing farmer households' income. On the other hand, the effect of transfer-in on poverty reduction is weak because transfer-in farmland requires adequate human resources, and with the limited labor force and low education level of farmer households [35]. It is difficult to form a large-scale agricultural industry, so poor farmer households' farmland allows them to lift themselves from poverty by transfer-out their farmland to agricultural cooperatives, companies, and village collectives. However,

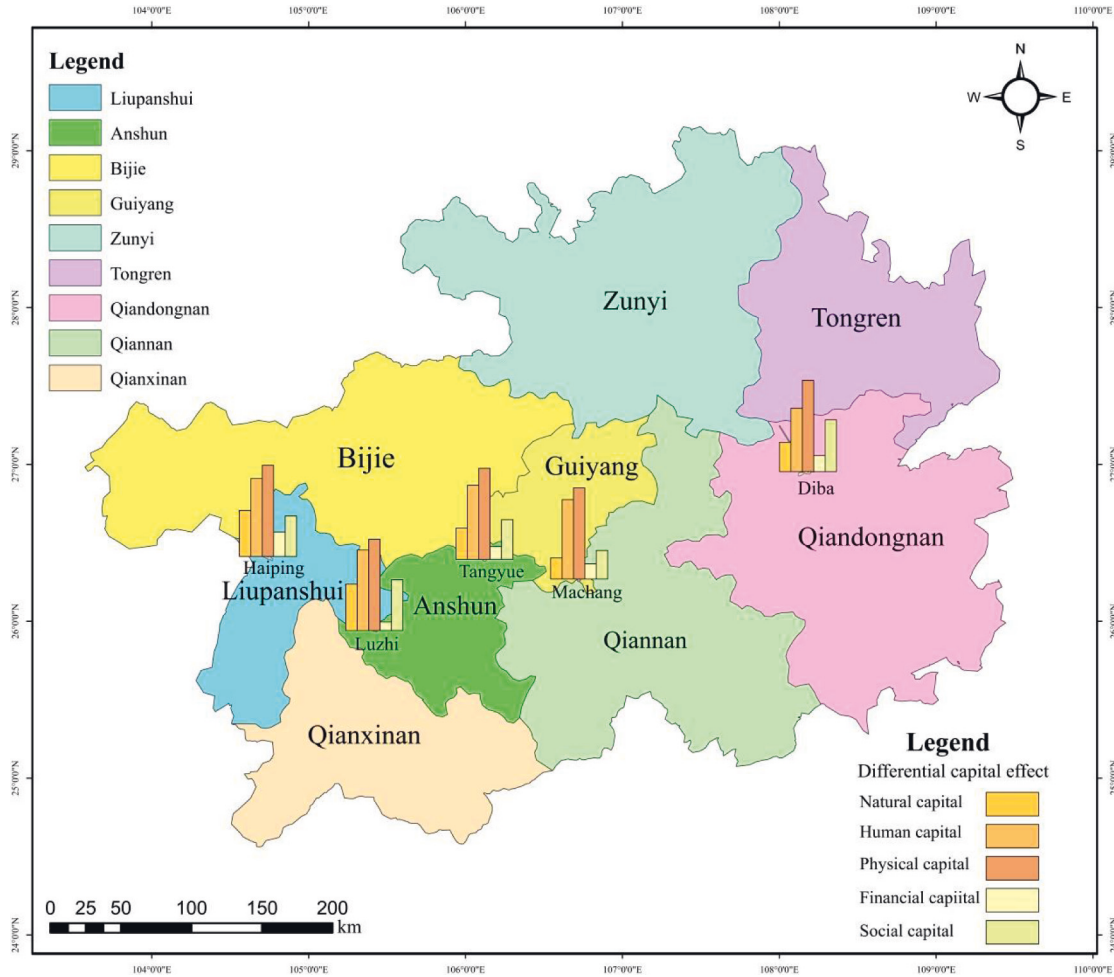


FIGURE 6: Spatial differences in poverty alleviation effect of different models.

farmland transfer-out is subject to market-related risks and fluctuations, which makes the farmer households' income from land lease relatively unstable.

The effect of different types of farmland transfer under different poverty alleviation models varies. The rapid development of tourism in karst mountainous areas has spurred the development of local cultural-tourism destinations, which has supported targeted poverty alleviation, resulting in effective poverty reduction. In model 2, poverty alleviation is achieved effectively through agricultural industry development based on land shareholding and by establishing training centers where farmer households can acquire new knowledge and skills required to continually improve their economic situation. However, model 4 reflects the lack of innovation in farmland transfer methods in economically underdeveloped areas. It is difficult for farmers to obtain income from farmland transfers. This study analyzes the poverty reduction effect of farmland transfer under different typical targeted poverty alleviation models so as to provide a reference for promoting land system reform, improving the land market, and increasing land use efficiency in karst mountain areas. This study has important theoretical and practical guidance for the successful

implementation of poverty alleviation strategies and preventing the recurrence of poverty.

5. Policy Implications

To solve the issues of poverty reduction effect of farmland transfer-in different models, some policies can be proposed. Firstly, the system of farmland transfer should be improved. It promotes the redistribution of productive resources and income of farmer households and plays an important role in the reform of rural land property rights. It is also conducive to the reasonable and effective transfer of farmland use rights, solving the problems of agriculture, rural area, and farmer household, promoting the construction of agricultural industrialization and intensive management, and promoting farmland transfer to boost targeted poverty alleviation. Thus, comprehensively establishing and improving farmland transfer management agencies and free-style farmland transfer behavior should be standardized to increase the enthusiasm of farmland transfer business households. Secondly, the local government should fully mobilize farmer households to participate in the enthusiasm for farmland transfer. Arouse the initiative of leading

enterprises and professional cooperatives to develop industries to stimulate their vitality so as to increase the income of poor farmer households and achieve the goal of poverty alleviation by industry. Thirdly, the targeted poverty alleviation models should be optimized. Appropriate targeted poverty alleviation models are selected or adjusted according to the economic development and resource endowment of different regions. A sustainable targeted poverty alleviation model can effectively guarantee farmer households' income and prevent poor farmer households from falling back into poverty.

6. Conclusion

In this study, Propensity Score Matching (PSM) and Difference-in-Differences (DID) methods were used to analyze the effect of farmland transfer under different models of targeted poverty reduction from the aspect of five different types of capital. The results show that farmland transfer has a significant poverty reduction effect on farmer households that they transfer in and transfer out their land and that both types of transfer play an important role in promoting the growth of farmer households' property. However, the overall effect of farmland transfer-out on poverty reduction is more significant than farmland transfer effectively improves farmer households' nonfarm income. The model of "three changes" + relocation for poverty alleviation + rural tourism + poor household has the most significant effect on poverty reduction. The remarkable results in poverty alleviation are achieved through capitalizing on local natural resources and seizing opportunities to develop unique types of industries, which require a large-scale transfer of labor force, further promoting farmland transfer. Model of land lease/shareholding + cooperative + enterprise + poor household has an insignificant effect. Therefore, there are too many restrictive factors in some areas, and the poverty reduction effect is relatively weak. Some policy suggestions are also proposed: choose a suitable development model according to regional differences and resource endowment. The results of this study are limited by the lack of diversity in the selected poverty reduction models. At the same time, the study fails to fully consider how to reduce the regional differences in poverty reduction, so further research is recommended.

Data Availability

The data used to support the findings of this study are included within the article.

Conflicts of Interest

The authors declare that they have no conflicts of interest.

Acknowledgments

This research was funded by the National Social Science Foundation of China (File number: 19BGL180) and the Insight Grant from the Social Sciences and Humanities Research Council of Canada (File number: 435-2018-0953).

References

- [1] B. Z. Su, Y. H. Li, L. Li, and Y. Wang, "How does nonfarm employment stability influence farmers' farmland transfer decisions? Implications for China's land use policy," *Land Use Policy*, vol. 74, pp. 66–72, 2018.
- [2] H. Cao, X. Q. Zhu, W. Heijman, and K. Zhao, "The impact of land transfer and farmers' knowledge of farmland protection policy on pro-environmental agricultural practices: the case of straw return to fields in Ningxia, China," *Journal of Cleaner Production*, vol. 277, Article ID 123701, 2020.
- [3] Y. Zhou, X. H. Li, and Y. S. Liu, "Rural land system reforms in China: history, issues, measures and prospects," *Land Use Policy*, vol. 91, Article ID 104330, 2020.
- [4] Y. S. Liu, J. L. Liu, and Y. Zhou, "Spatio-temporal patterns of rural poverty in China and targeted poverty alleviation strategies," *Journal of Rural Studies*, vol. 52, pp. 66–75, 2017a.
- [5] Y. S. Liu, L. L. Zou, and Y. S. Wang, "Spatial-temporal characteristics and influencing factors of agricultural eco-efficiency in China in recent 40 years," *Land Use Policy*, vol. 97, Article ID 104794, 2020.
- [6] J. Yu, Y. Liu, M. Yu, C. Cui, R. Wang, and Y. Wu, "Evaluation of targeted poverty alleviation models under the "three changes" rural reform: a case study of Guizhou's four types of "three changes" reform models," *Journal of Guizhou Normal University (Natural Science Edition)*, vol. 38, no. 04, pp. 26–34, 2020.
- [7] T. B. Udimal, E. Liu, M. Luo, and Y. Li, "Examining the effect of land transfer on landlords' income in China: an application of the endogenous switching model," *Heliyon*, vol. 6, no. 10, p. e05071, 2020.
- [8] W. Liu and Z. Li, "Operating performance for the modes of rural farmland transfer and strategies in new times," *Economic Geography*, vol. 31, no. 02, pp. 300–304, 2011.
- [9] C. Y. Li, Y. Jiao, T. Sun, and A. R. Liu, "Alleviating multi-dimensional poverty through land transfer: evidence from poverty-stricken villages in China," *China Economic Review*, vol. 69, Article ID 101670, 2021.
- [10] T. Reardon, "Using evidence of household income diversification to inform study of the rural nonfarm labor market in Africa," *World Development*, vol. 25, no. 5, pp. 735–747, 1997.
- [11] M. Varga, "Poverty reduction through land transfers? The World Bank's titling reforms and the making of "subsistence" agriculture," *World Development*, vol. 135, Article ID 105058, 2020.
- [12] S. Kimura, K. Otsuka, T. Sonobe, and S. Rozelle, "Efficiency of land allocation through tenancy markets: evidence from China," *Economic Development and Cultural Change*, vol. 59, no. 3, pp. 485–510, 2011.
- [13] Z. Yang, X. L. Ma, and P. X. Zhu, "Land transfer and income change of peasants," *China Population Resource and Environment*, vol. 27, no. 5, pp. 111–120, 2020.
- [14] X. M. Chen, "Analysis of the impact of contracted land transfer on farmers welfare," *Journal of Chinese Agricultural Mechanization*, vol. 41, no. 3, pp. 192–200, 2020.
- [15] L. Z. Xiao and B. Zhang, "Land transfer and expansion of rural residents income gap," *Collected Essays on Finance and Economics*, no. 9, pp. 10–18, 2017.
- [16] C. L. Shi, J. Luan, and J. F. Zhu, "Land transaction and farmers income: an analysis based on Chinese eight provinces survey data," *Economic Review*, no. 5, pp. 152–166, 2017.
- [17] K. L. Peng, C. Yang, and Y. Chen, "Land transfer in rural China: incentives, influencing factors and income effects," *Applied Economics*, vol. 52, no. 50, pp. 5477–5490, 2020.

- [18] X. Wang and C. Sun, "Decomposition and spatial difference analysis of poverty alleviation effect in county-level cities of China from 1996 to 2008," *Economic Geography*, vol. 31, no. 06, pp. 888–894, 2011.
- [19] H. Jiang and Z. Liu, "Analysis of coupling coordination of public policy, agricultural development and poverty alleviation in underdeveloped areas: an empirical study based on Guizhou, Yunnan and Anhui data analysis," *Economic Geography*, vol. 36, no. 11, pp. 132–140, 2016.
- [20] J. Gao and Ge. Song, "The effect of rural labor transfer scale on agricultural farmland transfer," *Economic Geography*, vol. 40, no. 8, pp. 172–178, 2020.
- [21] X. Wei, W. Cao, X. Liu, J. Wang, and N. Shi, "Research on multidimensional poverty reduction effect of fiscal decentralization," *Economic Geography*, vol. 1, no. 21, 2020.
- [22] Y. Liu, "Household livelihood choices under the different environment in the karst area: a case study of Anshun City, southwest of China," *Environmental Research*, vol. 197, Article ID 111171, 2021.
- [23] Z. Zou, G. Song, and L. Chen, "The effect of farmland use right transfer on land productivity in main grain-producing area of Heilongjiang Province," *Economic Geography*, vol. 37, no. 04, pp. 176–181, 2017.
- [24] K. Deininger and S. Jin, "The potential of land rental markets in the process of economic development: evidence from China," *Journal of Development Economics*, vol. 78, no. 1, pp. 241–270, 2005.
- [25] E. Karali, M. D. A. Rounsevell, and R. Doherty, "Integrating the diversity of farmers' decisions into studies of rural land-use change," *Procedia Environmental Sciences*, vol. 6, pp. 136–145, 2011.
- [26] G. H. Wan and E. Cheng, "Effects of land fragmentation and returns to scale in the Chinese farming sector," *Applied Economics*, vol. 33, no. 2, pp. 183–194, 2001.
- [27] X. Liu, Y. Li, Y. Wang, Z. Guo, and F. Zheng, "Geographical identification of poverty in county space: a case study of Jingyuan County in Ningxia," *Acta Geographica Sinica*, vol. 72, no. 3, pp. 545–557, 2017b.
- [28] B. A. Legesse, K. Jefferson-Moore, and T. Thomas, "Impacts of land tenure and property rights on reforestation intervention in Ethiopia," *Land Use Policy*, vol. 70, pp. 494–499, 2018.
- [29] W. Xiuqin, C. Yunlong, and Z. Tao, "Effects of land use/land cover changes on rocky desertification: a case study of a small karst catchment in southwestern China," *Energy Procedia*, vol. 5, pp. 1–5, 2011.
- [30] C. Liu, J. Huang, J. Gong, and B. Xie, "Provincial differences and influencing factors of targeted poverty alleviation in China," *Geographical Sciences*, vol. 38, no. 7, pp. 1098–1106, 2018.
- [31] H. W. Zhang, Z. Q. Wang, J. F. Liu, J. Chai, and C. Wei, "Selection of targeted poverty alleviation policies from the perspective of land resources-environmental carrying capacity," *Journal of Rural Studies*, vol. 93, pp. 318–325, 2022.
- [32] Y. Liu, X. J. Huang, H. Yang, and T. Y. Zhong, "Environmental effects of land-use/cover change by urbanization and policies in Southwest China karst area—a case study of Guiyang," *Habitat International*, vol. 44, pp. 339–348, 2014.
- [33] H. You and X. Zhang, "Sustainable livelihoods and rural sustainability in China: ecologically secure, economically efficient or socially equitable?" *Resources, Conservation and Recycling*, vol. 120, pp. 1–13, 2017.
- [34] Y. M. Wang, M. X. Wang, and D. T. Wu, "Spatial patterns and determinants of rural poverty: a case of Guizhou Province, China," *Scientia Geographica Sinica*, vol. 37, no. 2, pp. 217–227, 2017.
- [35] W. G. Cochran, "Sampling Techniques third edition," *New York: Wiley*, p. 1977, 1953.
- [36] A. Soltani, A. Angelsen, T. Eid, M. S. N. Naieni, and T. Shamekhi, "Poverty, sustainability, and household livelihood strategies in Zagros, Iran," *Ecological Economics*, vol. 79, pp. 60–70, 2012.
- [37] M. Mendola, "Agricultural technology adoption and poverty reduction: a propensity-score matching analysis for rural Bangladesh," *Food Policy*, vol. 32, no. 3, pp. 372–393, 2007.
- [38] J. K. S. Kung, "Off-farm labor markets and the emergence of land rental markets in rural China," *Journal of Comparative Economics*, vol. 30, no. 2, pp. 395–414, 2002.

Research Article

A Star Pattern Recognition Algorithm Based on the Radial Companion-Circumferential Feature

Weiwei Zhao ¹, Baoqiang Li ², and Xiuyi Li¹

¹Civil Aviation Flight University of China, Guanghan 618300, Sichuan, China

²Xi'an Aeronautical Polytechnic Institute, Xi'an 710000, Shanxi, China

Correspondence should be addressed to Baoqiang Li; 15525054008@163.com

Received 6 July 2022; Accepted 13 August 2022; Published 13 September 2022

Academic Editor: Wei Liu

Copyright © 2022 Weiwei Zhao et al. This is an open access article distributed under the Creative Commons Attribution License, which permits unrestricted use, distribution, and reproduction in any medium, provided the original work is properly cited.

Attitude measurement is an important core technology of vehicle flight. It is of great significance to ensure the vehicle's accurate orbit entry and orbit change, high-performance flight, reliable ground communication, high-precision ground observation, and successful completion of various space missions. Star sensor is the core component to realize an autonomous attitude measurement of the vehicle. Autonomous star map recognition is a key technology in star sensor technology, and it is also the focus and difficulty of research. When the star sensor enters the initial attitude acquisition mode, according to the algorithm, the star sensor can quickly obtain the initial attitude and enter the normal working mode. This paper proposes a star pattern recognition algorithm based on the radial companion-circumferential feature with a noise compensation code to address the low recognition rate caused by position noise in the process of constructing star patterns in the traditional star pattern recognition algorithm based on the radial feature. In order to solve the problem of slow matching search speed, a maximum matching number algorithm has been innovatively adopted, which can improve the search efficiency in the process of star pattern recognition. Thus, the capacity of the star pattern recognition feature library is effectively reduced, and the stability and recognition rate of the improved star pattern recognition algorithm are further improved. The improved star pattern recognition algorithm first establishes radial and circumferential feature vectors based on the bit vector, then adds the noise compensation code according to the companion star position error, then modifies the radial and circumferential feature vectors, and finally calculates the minimum similarity difference between the feature vector of the star pattern observed by the star sensor and the feature vector of the navigation star in the feature library to obtain the unique star pattern recognition result. The identification star database adopts the maximum matching number algorithm, which can improve the search efficiency, reduce the amount of redundant matching, and shorten the matching time. The simulation results show that even in the presence of star position and magnitude noise, the improved star pattern recognition algorithm with radial companion-circumferential feature maintains a high recognition rate of more than 97 percent, demonstrating that the algorithm's robustness is superior to other algorithms. The revised method described in this work outperforms the classic triangle algorithm and the radial feature star pattern recognition algorithm without compensation code in terms of algorithm robustness, recognition success rate, and recognition time.

1. Introduction

Star sensor, which is currently the most precise space attitude measuring equipment, can perform tasks such as star pattern acquisition, centroid extraction, star pattern identification, and attitude determination. It is crucial in aeronautical and navigational technology to use astronomical starlight. [1]. Automatic star pattern recognition is a key technology in star sensor technology, as shown in Annex 1.

At present, star pattern recognition algorithms proposed for star sensors mainly include the triangle angular distance matching algorithm, the main star recognition method [2, 3], the probability statistics method [4], the polygon angular distance matching algorithm [5], and the grid algorithm [6, 7]. Among them, the triangle algorithm is good, and the main star recognition method is the most widely used [8, 9]. Although the triangle algorithm is simple to implement, due to the drawbacks of a large amount of star

point angular distance calculation and many times of angular distance redundant matching, many scholars have proposed two main directions for improvement, such as improving the recognition success rate and reducing the recognition time to meet real-time performance. The improved methods include various improved triangle algorithms [10, 11], quadrilateral algorithms [12], grid algorithms [13], KMP algorithms [14], connected clustering star recognition algorithms, and character matching based algorithms [15]. In order to reduce the matching times, star library search algorithms such as the K vector method [16] and the P vector method have been proposed, which can improve the search efficiency of the triangle algorithm [17]. The literature [18] saves the star diagonal distance and tolerance set of triangles by constructing a two-dimensional linked list array, which avoids the repeated calculation and search process of star diagonal distance by building a hash table, changing the matching mode of star diagonal distance, reducing the number of star diagonal distance matching, and greatly reducing the time complexity of triangular star pattern recognition. Reference [19] proposed a star pattern recognition algorithm based on the star triangle. The corresponding pattern vector is constructed according to the star triangle, arranged in ascending order according to the circumference of the triangle, and the auxiliary index vector is constructed to improve the search efficiency. Literature [20] proposed an all-sky autonomous, fast triangle recognition algorithm independent of magnitude information. By constructing the maximum internal angle of the triangle and its two sides as matching feature triangles, an all-sky navigation feature library is established. The hash function is constructed according to the maximum internal angle value of the generated feature library and is stored in blocks.

This paper improves the radial feature of the star map, constructs the feature vector based on the radial companion feature in the form of the bit vector, and adds the angular distance information between companion stars and the compensation information of position noise to the feature vector, so as to effectively reduce the impact of position noise, magnitude noise, and interfering stars on the construction of the star pattern and reduce recognition failures due to star pattern construction errors. In this paper, an improved radial companion-circumferential feature star pattern recognition model based on the compensation code is constructed. The maximum matching number algorithm can split and create the navigation star database in a reasonable manner, substantially reducing the database's size and improving the search efficiency without compromising the recognition rate. At the same time, compared with the traditional triangle algorithm and the radial characteristic star pattern recognition algorithm without the compensation code, the recognition success rate of the improved method is higher than that of the traditional radial characteristic star pattern recognition algorithm and the traditional triangle algorithm under the same conditions of star position noise and magnitude (brightness) noise, which can effectively reduce the data capacity of the navigation star database and shorten the star pattern recognition time.

2. Construction of the Star Pattern Recognition Model under Different Feature Modes

2.1. Star Pattern Recognition of Traditional Radial Features. The radial feature star pattern recognition algorithm refers to a star pattern recognition algorithm that classifies other stars (called companion stars) in a certain neighbourhood of the observation star (or navigation star) according to their radial distance from the observation star as the feature pattern of the observation star [21].

The radial feature composition method is as follows: take the observation star S as the center, make a circular neighbourhood with R_r as the radius, and divide the neighbourhood of S into N_{\max} rings along the radial direction. N_{\max} is the effective digits of the radial feature vector. The radial feature diagram is shown in Figure 1.

$$N_{\max} = \frac{R_r}{e}. \quad (1)$$

The angular distance between S and A is marked as V_{sa} , the angular distance information is discretized, and its discrete value is marked as V_{sa}^* ; then,

$$v_{sa}^* = \frac{v_{sa}}{e} + 1. \quad (2)$$

According to the dispersion value of the angular distance information, the position $[V_{sa}]$ in the radial feature vector of the observed star can be determined to be 1 from (3). For example, if the star's angular distance dispersion value to SA is 27.25, then point 27 in the observed star's radial feature vector will be 1. Figure 2 shows a schematic representation of the radial feature pattern's creation.

$$V_{sa} = \text{floor}(v_{sa}^*). \quad (3)$$

The angular distance between companion stars A and B may be calculated using the same method and the spatial distribution relationship between companion stars in the vicinity of observation stars, and its discrete value V_{sa}^* is as follows:

$$v_{sa}^* = \frac{v_{sa}}{2e} + 1. \quad (4)$$

Then, the bit (set to 1) in the eigenvector of the observation star companion star can be determined according to formula (3). According to Figure 3, the maximum angular distance between companion stars is $2rR$, and the divisor in formula (4) is set to $2e$ to ensure that the number of bits of radial eigenvector of the observation star and the companion star eigenvector is the same. The construction method of the observation star companion feature vector is shown in Figure 3.

2.2. Triangular Star Pattern Identification. A common isomorphic star map recognition algorithm of a subgraph is the triangular star pattern identification technique. It has the advantage of high reliability and is still widely used in engineering practice [22].

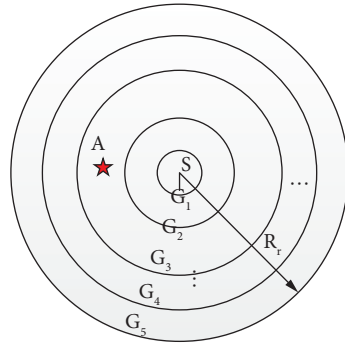
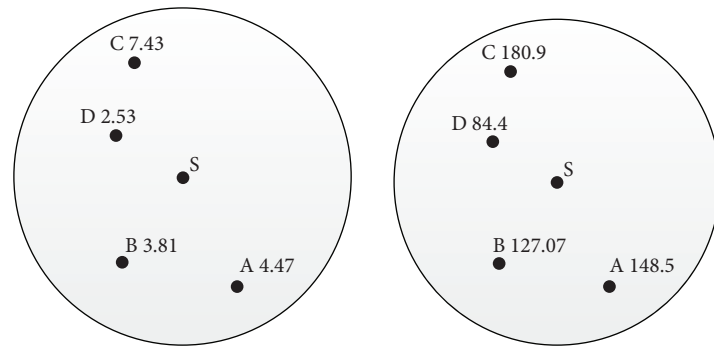


FIGURE 1: Schematic diagram of the radial feature.



Angular distance between observation star and companion star

Discrete value of angular distance information

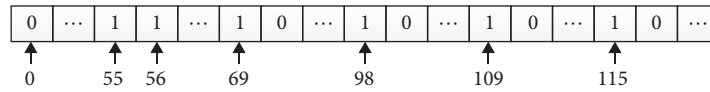
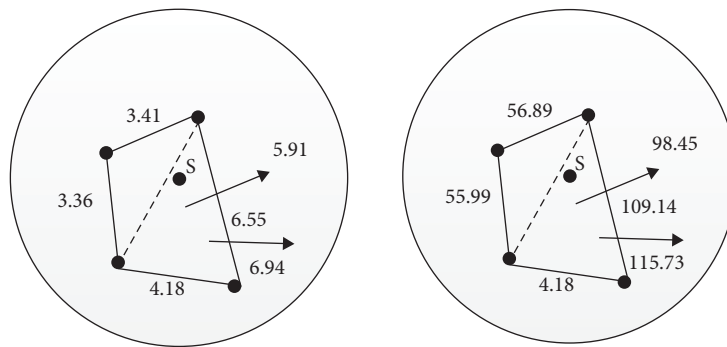


FIGURE 2: Construction diagram of the radial feature mode.



The angle between the observation star and the companion star.

The angle between the observation star and the companion star.

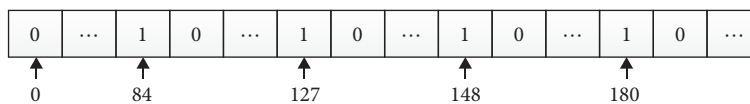


FIGURE 3: Construction method of the companion star eigenvector of the observation star.

The implementation process of the triangular star pattern recognition algorithm is to select three noncolinear stars from the real-time star pattern of the star sensor to form a star triangle to be recognized. By comparing with the star triangles in the navigation star catalog, the star pattern recognition is completed under the matching constraints.

However, in the process of triangular star map recognition, star points need to be traversed, where there is redundant matching and false matching, and the recognition efficiency is low [23, 24].

2.3. Construction of the Radial Companion Circumferential Feature Mode Based on the Compensation Code. Firstly, the observation star circumferential feature mode is established. The construction of the observation star circumferential feature mode is shown in Figure 4, and the construction method is as follows:

- (i) As shown in the figure, take S as the main star to determine the circumferential mode of radius R_c (this paper takes T_1 , T_2 , and T_3 as companion stars for example);
- (ii) Taking the main star S as the center, calculate the included angles $\angle T_1ST_2$, $\angle T_2ST_3$, and $\angle T_3ST_1$ between companion stars, respectively;
- (iii) Taking the side with the minimum companion angle (the ST_1) as the starting edge, the circular neighbourhood is divided in the circumferential direction, and the circumference is equally divided into 8 quadrants;
- (iv) According to the distribution of companion stars in each quadrant, an 8 bit vector V is formed in a counterclockwise direction. As shown in the figure, $V = [11001000]$, the circumferential distribution feature of S is the vector V .

Based on the radial companion feature pattern [25], the circumferential feature pattern is introduced. Although it can well describe the finer feature distribution relationship of star points, position noise is still easy to interfere with this feature. In this paper, a position noise compensation code is added to the radial companion-circumferential feature mode to compensate for the companion drift caused by position noise. As can be seen from Figure 5, the discrete value of the angular distance between observation star S and companion star A is at the boundary of ring 76 and ring 77. In order to compensate for the adverse effect of position noise on identification, it can be assumed that companion star A is in ring 76 and ring 77 at the same time. In order to control the number of compensation codes added, a threshold can be set, that is, $\delta_L = 0.3$, $\delta_H = 0.7$. Only if the decimal of the angular distance dispersion of S and A is less than σ_L or greater than σ_H , add a compensation code (set it to "1") in bit $[v_{sa}] - 1$ orbit $[v_{sa}] + 1$ of the eigenvector.

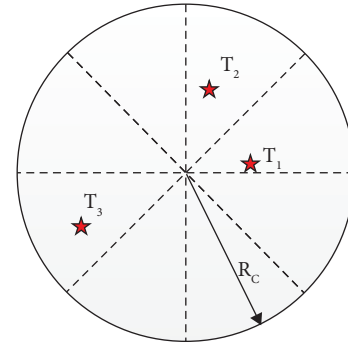


FIGURE 4: Construction diagram of the observation star circumferential pattern mode.

3. Improved Star Pattern Recognition of Radial Companion-Circumferential Features

3.1. Establishment of Feature Database. There are two elements in a navigation database: a navigation star catalog and a navigation star feature database. A navigation star catalog is a simple star catalog created by choosing navigation stars from the basic star catalog that fall within a specific brightness range and combining their position (right ascension and right latitude) and brightness information. In addition to the navigation star catalog, the feature extraction technique requires the creation of a navigation star feature database. The following features are part of the experimental feature library

- (i) Annex 2 provides a simple catalog. The table is a $4908 * 4$ matrix, with the first column containing the star number, followed by numbers 1 through 4908; the second column containing the star's right ascension data; the third column containing the star's declination data (unit of right ascension and declination data: angle); and the fourth column containing the star's magnitude data. Smaller storage and faster matching speeds can be obtained by simplifying the star list while retaining the same recognition rate. Table 1 shows the precise simplification findings;
- (ii) In Annex 3, A_{xx} to H_{xx} represent the star point numbers in the star map in turn. The data is a $3 * 3$ matrix that stores the picture coordinate system location information for the N star image points. The first column is the star image point number; the second column is the image coordinate system's x-axis coordinate of the star image point centroid center; and the third column is the image coordinate system's y-axis coordinate of the star image point centroid center. The field of view of the star sensor is $20 * 20$, and the number of pixels is $1024 * 1024$.

The technique is based on a comparison of the star map and the vector characteristics of the stars in the library with the highest number of matches. The eigenvalues of the actual

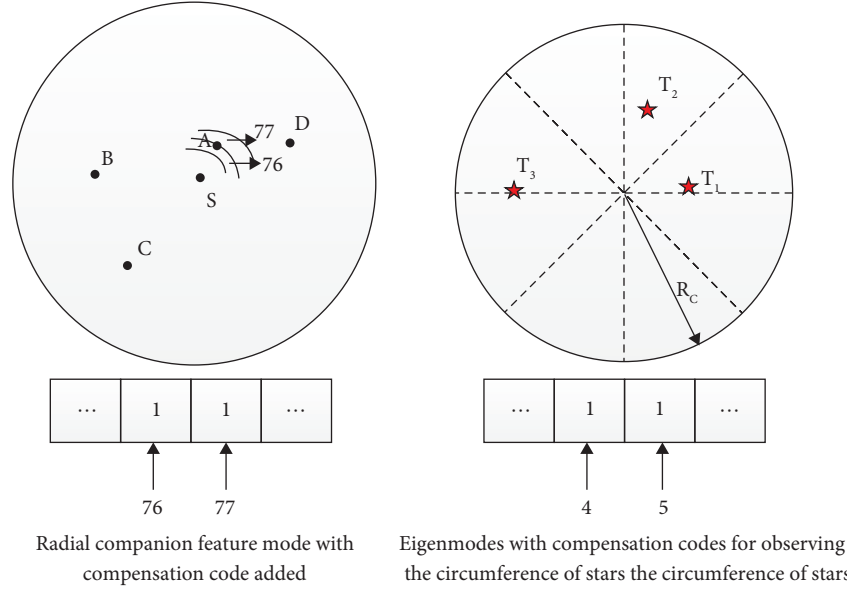


FIGURE 5: Radial circumferential companion feature mode with compensation code added.

TABLE 1: Simplified Tycho_2-star catalog.

Asterisk	Simplified catalog		Magnitude (ordered star)
	Right ascension	Declination	
No. 1	α_1	δ_1	...
...
No. M	α_M	δ_M	...

must be present in the library, and the number of matches for the eigenvalues of known stars in the navigation library (as shown in Figure 6) is much greater than the number of matches for the eigenvalues of false stars, so the maximum number of matches identification method is used.

Using this method, a navigation star feature database characterized by angular distance is constructed. Compared with the traditional database construction method, this method eliminates a large number of redundant eigenvalues and greatly reduces the storage space.

3.2. Improved Star Pattern Recognition Algorithm of Radial Companion- Circumferential Feature. When the improved matching group star map recognition model encounters the error problem caused by position noise, the star map recognition efficiency is low, the matching speed is slow, and there will be a certain misjudgment rate. To solve this problem, a radial companion-circumferential feature star pattern recognition model with a compensation code is constructed. The feature vector of the navigation star is represented by the model in the form of a bit vector. The radial feature of the observation star, the circumferential feature of the observation star, and the position feature of the companion star of the observation star make up the feature vector.

The radial companion feature is used to complete the initial matching and narrow the search range in the process of radial companion annular star map recognition based on compensation code, and then the observation star is

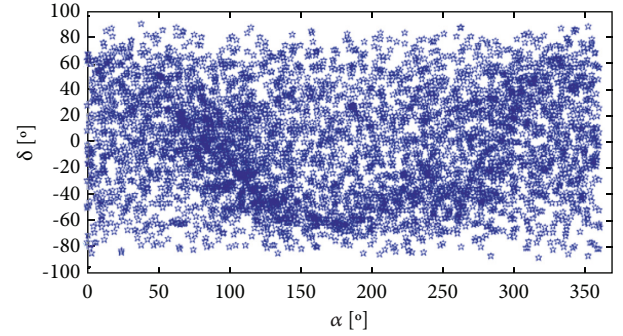


FIGURE 6: Star point distribution of all navigation stars.

uniquely identified by screening according to the correlation of the position information of each star point in the field of view. T_f is defined as the minimum similarity difference between the navigation star feature vector and the observation star feature vector in the feature library. The observation star whose minimum similarity difference is not greater than the threshold F is selected as the candidate star.

$$f_T = \left[T_s - \sum_{i=1}^{N_{\max}} S'(i) \right]^2 + \left[T_a - \sum_{j=1}^{N_{\max}} C'(j) \right]^2 + \left[T_v - \sum_{k=1}^8 V'k \right]^2, \quad (5)$$

$$\begin{cases} T_s = \sum_{i=1}^{N_{\max}} S(i) \& S'(i), \\ T_a = \sum_{j=1}^{N_{\max}} C(j) \& C'(j), \\ T_v = \sum_{k=1}^8 V(k) \& V'(k), \end{cases}$$

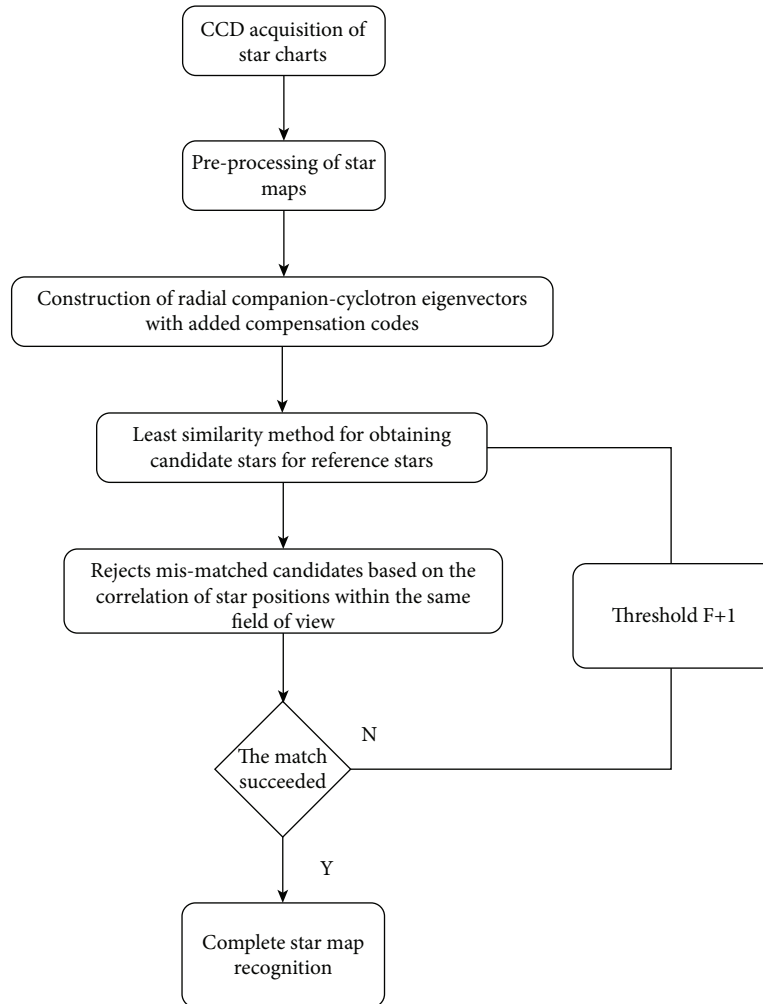


FIGURE 7: The star pattern recognition process of radial companion-circumferential feature based on the compensation code.

where $S(i)$ is the i th bit of the observation star's radial feature vector and $S(i)$ is the i th bit of the navigation star library's radial feature vector. $C(j)$ is the j -th bit of the observation star's companion star feature vector, and $C(j)$ is the j -th bit of the navigation star library's companion star feature vector. The k -th bit of the annular feature vector of the observation star is represented by $V(k)$, and the k -th bit of the annular feature vector in the navigation star library is represented by $V(k)$. Equation (6) determines the candidate stars.

$$f_T \leq F. \quad (6)$$

The candidate stars are obtained by the minimum similarity difference method, and other constraints should be considered, such as the star's angular distance being less than the field angle. The specific methods are as follows in Figure 7 below: screen the preprocessed star map and adjust the threshold F ; if the selected candidate stars are unique, the candidate stars are uniquely matched to complete the star pattern identification; if the candidate stars obtained by screening are not unique, it is necessary to reduce the value of F for screening; if no candidate star can be obtained

through screening, increase the value of F and repeat the above process to match the candidate star uniquely.

4. The Experimental Results and Analysis

The experimental data are shown in the supplementary material files (available here), which come from the national postgraduate mathematical modeling competition of China. The performance of the improved star pattern recognition algorithm based on radial companion-circumferential feature is evaluated in order to verify the effectiveness, timeliness, robustness, and storage space requirements of the improved star pattern recognition algorithm based on radial companion-circumferential feature. In the known star pattern, the experiment should match the star number corresponding to each star picture point. The point spread function approach of Gaussian surface fitting is used for star image processing, while the neighborhood means of the filtering method are used for picture denoising. To extract the recorded star coordinate data, the star pattern is first filtered, and three-star pattern recognition algorithms are then run in conjunction with the navigation star data in the field of view.

TABLE 2: Identification results.

Number of star image points in the star pattern	Star number	Number of star image points in the star pattern	Star number
G01	1525	G22	1603
G02	1572	G23	1415
G03	1443	G24	1692
G04	1748	G25	1453
G05	1780	G26	1432
G06	1675	G27	1492
G07	1720	G28	1488
G08	1503	G29	1648
G09	1634	G30	1646
G10	1577	G31	1566
G11	1757	G32	1688
G12	1586	G33	1655
G13	1536	G34	1505
G14	1610	G35	1373
G15	1681	G36	1576
G16	1606	G37	1545
G17	1670	G38	1424
G18	1477	G39	1375
G19	1790	G40	1825
G20	1502	G41	1401
G21	1631	G22	1603

4.1. *The Results of Simulation Star Pattern Experiment.* Process any star map, extract the star point coordinate data, and identify the star pattern in combination with the navigation star data in the field of view. Features are used for the initial identification of star points. Table 2 shows the results of the initial identification (due to space constraints, only some initial identification results are given here).

The star pattern in Figure 8 is recognized in the experiment, and the matching numbers of star image points and stars are listed in Table 2. All-stars in the field of view of star pattern 1 are indicated by “*,” and stars in the field of vision of star pattern 1 are highlighted with red boxes.

Figure 8 shows that three stars are not visible in the area of vision. These three stars are at the edge of the field of vision, as seen in the diagram. They do not appear in the field of vision because the spacecraft’s attitude moves around the optical axis of the star sensor, preventing stars that should appear at the edge of the field of view from entering it. The three models can successfully perform the recognition task in the experiment. In the problem of the broad field of view multistar image point matching, it was discovered that the star pattern recognition model of radial companion-circumferential pattern with the compensating code has greater calculation efficiency when compared to the computation speed.

4.2. *Comparison and Analysis of Simulation Results.* First, add the noise to the star pattern created by the simulation at the start point position, with a mean value of 0 and a standard deviation of 3 pixels, and follow the Gaussian distribution (0.015 mm is 1 pixel long). Observe the star pattern recognition results of the three recognition algorithms and count the recognition rate. Figure 9 shows the comparison of the results.

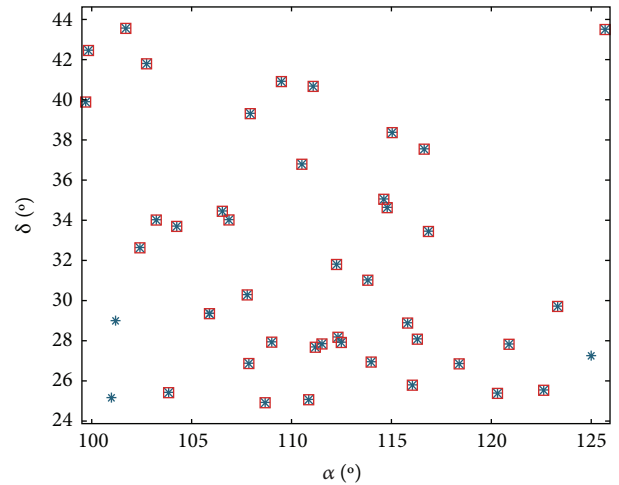


FIGURE 8: Stars in the field of view.

Then, to the star pattern created by the simulation on the magnitude, add noise with a mean of 0 and a standard deviation ranging from 0 to 1 Mv, and follow the Gaussian distribution. Observe the recognition results of the star pattern by the three recognition algorithms and count the recognition rate. Figure 10 shows the comparison of the results.

Finally, the recognition time is counted. Under the same conditions, the three algorithms match and recognize 900 simulated star patterns without noise, calculate the average time of each algorithm, and count the average matching time rounded up every 100, as shown in Table 3.

It can be concluded from Table 3 that compared with the triangle algorithm, the improved recognition algorithm proposed in this paper improves the recognition time by 640 ms, is better than the matching group algorithm, and

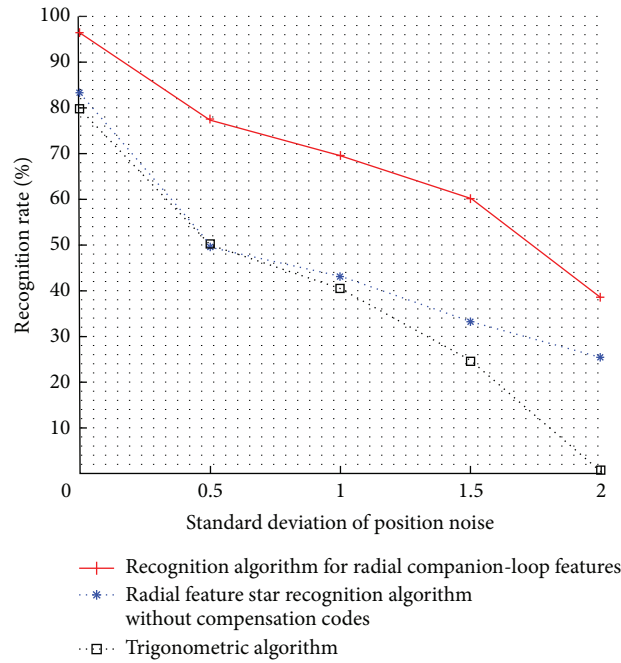


FIGURE 9: Effect of position noise on the recognition rate.

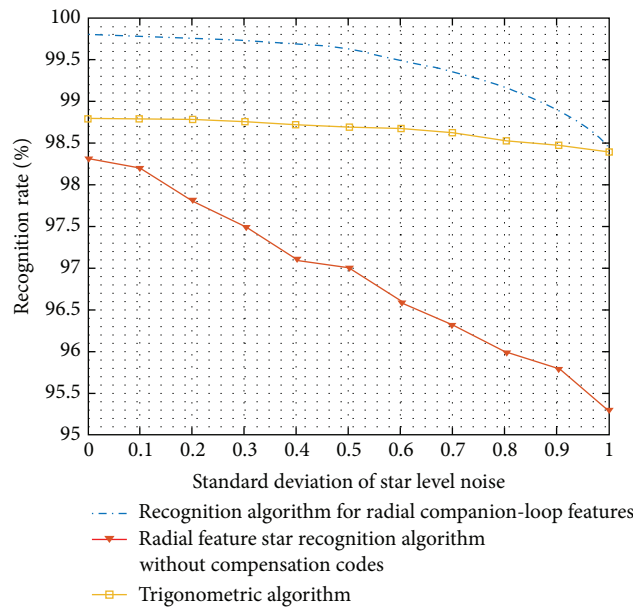


FIGURE 10: Effect of magnitude noise on the recognition rate.

TABLE 3: Comparison of recognition time of three recognition algorithms.

Algorithm	The traditional triangle algorithm	The radial feature star pattern recognition algorithm without the compensation code	The star pattern recognition algorithm based on the radial companion- circumferential feature
Identification time(ms)	800	700	160

maintains a fast recognition speed. It shows that the improved maximum matching number algorithm can reduce the matching redundancy and recognition time. In addition, the algorithm can reduce the storage space of the star database and improve the rate of recognition success.

5. Conclusion

A star pattern identification method with a radial companion ring feature and a compensation code is proposed in this work. The algorithm adds the compensation

information for position noise on the basis of star radial feature, reduces the influence of position noise, and stores the feature vector based on radial companion feature in the form of a bit vector, which greatly reduces the memory requirement of the algorithm.

In terms of matching, this method uses a recognition algorithm based on the maximum matching number, which improves search efficiency significantly. In order to reduce the matching rate due to the influence of interference stars and the nonuniqueness of matching star pairs, this method adopts logic and operations, which greatly reduces the recognition time of the algorithm.

The suggested approach is more resilient to position and magnitude noise than the other two traditional algorithms, and the average recognition time is also improved to some extent, according to the experimental findings of simulated star patterns. The recognition success rate of this method may reach more than 97 percent in simulation.

Data Availability

The data come from the national postgraduate mathematical modeling competition in China. The data used to support the findings of this study are included within the supplementary information files.

Conflicts of Interest

The authors declare that they have no conflicts of interest.

Acknowledgments

This work was supported by the National Natural Science Foundation of China (U2133209).

Supplementary Materials

Annex 1 is the relevant background of this project. Annex 2 provides a simple catalog. The table is a matrix in which the first column is the number of stars, numbered from 1 to 4908; the second column is the right ascension data of stars; the third column is the right ascension data of stars (right ascension and right ascension data unit: angle); and the fourth column is the magnitude information of stars. Annex 3 contains 8-star map data. For the sake of distinction, the numbers are represented by axx~hxx in turn. Taking C as an example, the data is a matrix, which records the position information of 7-star image points in the image coordinate system. The first column is the star image point number (numbers are c01~c07 in turn), the second column is the x -axis coordinate of the star image point centroid center in the image coordinate system, and the third column is the y -axis coordinate of the star image point centroid center in the image coordinate system. The field of view of the star sensor recorded in A~F files is $12^\circ \times 12^\circ$, and the number of pixels is 512×512 . The field of view of the star sensor recorded in G and H files is $20^\circ \times 20^\circ$, and the number of pixels is 1024×1024 . . (Supplementary Materials)


References

- [1] S. Shi, X. Lei, and C. Yu, "Overview of triangle recognition algorithms in star map," *Photoelectric Technology Application*, vol. 29, no. 5, pp. 1–6, 2014.
- [2] R. W. H. V. Bezooijen, "True-sky demonstration of an autonomous star tracker," *Proceedings of SPIE - The International Society for Optical Engineering*, vol. 2221, pp. 156–168, 1994.
- [3] H. Wang, Z. Fei, and C. Zhang, "Improved star pattern recognition algorithm based on host star," *Optics and Precision Engineering*, vol. 17, no. 1, pp. 220–224, 2009.
- [4] D. S. Mehta, S. Chen, and K. S. Low, "A rotation-invariant additive vector sequence-based star pattern recognition," *IEEE Transactions on Aerospace and Electronic Systems*, vol. 55, no. 2, pp. 689–705, 2019.
- [5] G. Wang, J. Li, and X. Wei, "Star identification based on hash map," *IEEE Sensors Journal*, vol. 18, no. 4, pp. 1591–1599, 2018.
- [6] C. Padgett and K. Kreutz-Delgado, "A grid algorithm for autonomous star identification," *IEEE Transactions on Aerospace and Electronic Systems*, vol. 33, no. 1, pp. 202–213, 1997.
- [7] H. Qian, L. Sun, J. Cai, and W. Huang, "An extended grid algorithm for star pattern recognition," *Journal of Harbin Institute of Technology*, vol. 47, no. 2, pp. 110–116, 2015.
- [8] H. Zhu, B. Liang, and T. Zhang, "A robust and fast star identification algorithm based on an ordered set of points pattern," *Acta Astronautica*, vol. 148, pp. 327–336, 2018.
- [9] M. S. Arani, A. Toloei, and Z. Eghbaleh, "A geometric star identification algorithm based on triple triangle pattern," in *Proceedings of the 2015 7th International Conference on Recent Advances in Space Technologies (RAST)*, June 2015.
- [10] C. Lv, J. Zhou, Y. He, and X. Lu, "An improved fast star pattern recognition algorithm," *Computer Measurement & Control*, vol. 18, no. 6, pp. 1390–1393, 2010.
- [11] G. Zhang, W. Xinguo, and J. Jiang, "An improved method of triangle star pattern recognition," *Acta Aeronautica Sinica*, vol. 27, no. 6, pp. 1150–1154, 2006.
- [12] T. Lin, J. Zhou, X. Zhang, G. Jia, and J. Qian, "Quadrilateral all-sky autonomous star pattern recognition algorithm," *Journal of Astronautics*, vol. 21, no. 2, pp. 82–85, 2000.
- [13] J. Yang, G. Zhang, and J. Jiang, "P-vector to realize fast star pattern recognition method," *Acta Aeronautica Sinica*, vol. 28, no. 4, 2007.
- [14] B. Li, Y. Zhang, H. Li, and S. Xu, "Improved method for star image recognition of star sensor using KMP algorithm," *Opto-Electronic Engineering*, vol. 31, no. 2, 2004.
- [15] S. Xu, B. Li, Y. Zhang, and H. Li, "Navigation library storage method for star map recognition using character matching," *Journal of Harbin Institute of Technology*, vol. 37, no. 6, 2005.
- [16] F. Xing, Y. Zheng, and Y. Dong, "Fast star pattern recognition algorithm based on navigation star field and K vector," *Journal of Astronautics*, vol. 31, no. 10, pp. 2302–2308, 2010.
- [17] Q. Fan and X. Zhong, "A triangle voting algorithm based on double feature constraints for star sensors," *Advances in Space Research*, vol. 61, no. 4, pp. 1132–1142, 2018.
- [18] L. Zhang, Yu Zhou, R. Lin, and Z. Zhang, "A Fast triangle star Pattern Recognition Algorithm," *Applied Optics*, vol. 39, 2018.
- [19] X. Sun, H. Wang, and J. Lu, "A star pattern recognition algorithm based on star triangle," *Sensors and Microsystems*, vol. 28, no. 12, pp. 8–10, 2009.

- [20] T. Zhang, J. Guo, and B. Yang, "Triangular star pattern recognition algorithm based on maximum internal angle," *Optics and Precision Engineering*, vol. 25, no. 1, 2017.
- [21] C. Li, Y. Yuan, and D. Wang, "Efficient star pattern recognition method based on feature pattern matching method," *China Space Science and Technology*, vol. 36, no. 6, pp. 9–16, 2016.
- [22] P. He, "An improved triangle recognition algorithm," *Ship Electronic Engineering*, vol. 32, no. 4, pp. 42–44, 2012.
- [23] W. Zheng, *Research on All-Sky Autonomous Hierarchical Algorithm Based on star sensor*, Changchun: Changchun Institute of Optics, Fine Mechanics and Physics, Chinese Academy of Sciences, Changchun, China, 2003.
- [24] X. Cui, H. Wang, C. Chen, and J. Lu, "Star selection strategy and realization in star triangle recognition," *Journal of Chinese Inertial Technology*, vol. 20, no. 3, pp. 296–299, 2012.
- [25] Y. Gao, *Research on Narrow Field Astronomical Positioning Technology*, University of Chinese Academy of Sciences, Beijing, China, 2019.

Research Article

Modeling and Simulation of Theoretical Digging Force of an Excavator Based on Arbitrary Posture

Zuhe Qin 

School of Mechanical Engineering, Guangxi Technological College of Machinery and Electricity, Nanning, China

Correspondence should be addressed to Zuhe Qin; 8002016023@gxcme.edu.cn

Received 28 June 2022; Revised 4 August 2022; Accepted 9 August 2022; Published 10 September 2022

Academic Editor: Wei Liu

Copyright © 2022 Zuhe Qin. This is an open access article distributed under the Creative Commons Attribution License, which permits unrestricted use, distribution, and reproduction in any medium, provided the original work is properly cited.

Theoretical digging force is an important performance parameter of the hydraulic excavator. Due to the multi-linkage mechanism, the digging posture of an excavator is ever-changing; thus, it is not easy to calculate the theoretical digging force. Traditionally, the theoretical digging force is calculated by selecting a limited number of postures of the excavator based on experience, which cannot reflect the force condition of each posture in the excavation process. In order to calculate the theoretical digging force of any posture in the excavation process, this paper uses the principle of the analytical method to establish a theoretical excavation force mathematical model of bucket excavation and uses Matlab software to solve the theoretical excavation force mathematical models. In order to verify the model's correctness, the experimental method is used to determine the actual maximum excavation force of the excavator. The test results showed that there was little difference between the actual maximum digging force and the theoretical maximum digging force, which verified the correctness of the theoretical digging force mathematical models and provided a theoretical digging force calculation method and reference for the structural design and optimization of the excavator.

1. Introduction

Theoretical digging force is an important index to measure the performance of the hydraulic excavator as well as the basis for calculating the power of the hydraulic system and the power system. Therefore, theoretical digging force is the most important performance parameter concerned by the designer in the design stage of the excavator [1]. In addition, it is also one of the boundary conditions for the structural finite element analysis of the working device of the excavator and other components. Therefore, it is extremely important to obtain the accurate theoretical digging force. There are countless digging postures during excavator operation. The theoretical digging force varies with different digging postures. It is very complicated to calculate the theoretical digging force. It is almost impossible to manually calculate the theoretical digging force corresponding to each digging posture. Therefore, the traditional calculation method of theoretical digging force selects the typical working conditions and postures of the excavator according to experience and then conducts a general survey and calculation

with the analytical method [2]. This calculation method is limited by only calculating the digging force of a limited number of digging postures, and the posture of the maximum digging force of the excavator is often difficult to determine accurately. Therefore, the traditional calculation method cannot fully master the stress condition of the excavator [3], and the calculation result may not be the maximum theoretical digging force of the excavator.

Based on the limitations of the traditional calculation method of theoretical digging force, this paper used the principle of the analytical method to establish the theoretical digging force mathematical model of bucket digging and the theoretical digging force mathematical model of bucket rod digging, respectively. The theoretical digging force mathematical models could calculate the theoretical digging force of any posture of the excavator. Matlab software was used to solve the theoretical digging force mathematical models and draw the theoretical digging force map, so as to more intuitively reflect the stress state of the excavator in the whole digging posture. In order to verify the correctness of the theoretical digging force mathematical models, the

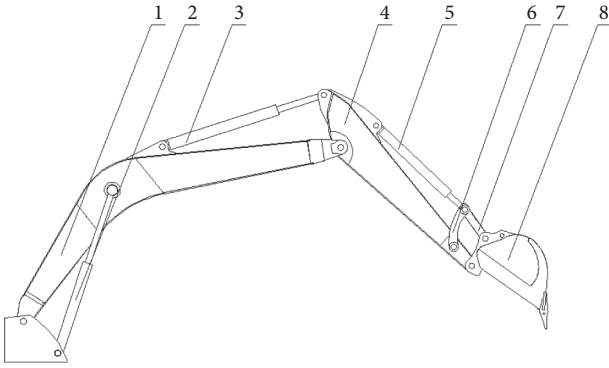


FIGURE 1: Structure of the working device. (1) bionic boom, (2) hydraulic cylinder of bionic boom, (3) hydraulic cylinder of bucket rod, (4) bucket rod (5) hydraulic cylinder of bucket, (6) swinging rod, (7) linkage, and (8) bucket.

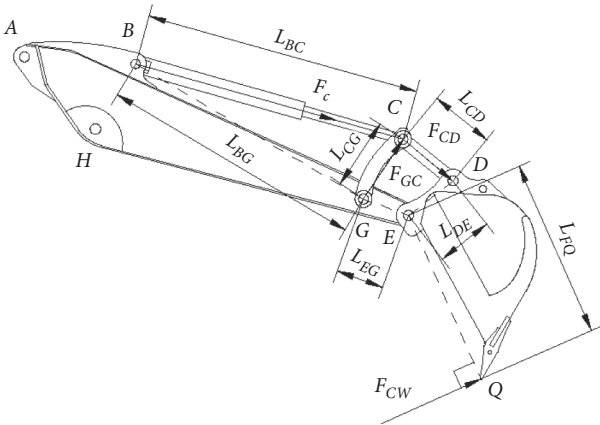


FIGURE 2: Force analysis of the bucket digging device.

maximum theoretical digging force of the excavator was tested on the spot. The test data showed that there was little difference between the measured maximum digging force and the theoretical maximum digging force, which verified the correctness of the theoretical digging force mathematical models and provided the basis and reference for calculation of the theoretical digging force for the structural design and improvement of the excavator.

2. Establishment of Theoretical Digging Force Mathematical Models

During excavator operation, the bucket teeth cut into the soil and the tips of the bucket teeth are affected by soil resistance, which is called the digging resistance. The digging resistance and the theoretical digging force are in the action-and-reaction relationship, and the theoretical digging force of the excavator is obtained by solving the digging resistance. A digging posture will be formed as long as the hydraulic cylinder moves a unit length during excavator operation. An infinite number of digging postures can be formed within the stroke range of the hydraulic cylinder. When establishing the theoretical digging force mathematical models, an arbitrary digging posture within the stroke range of the

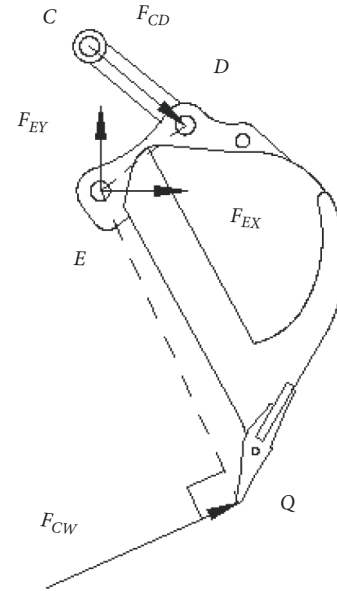


FIGURE 3: Force analysis of separated linkage and the bucket.

hydraulic cylinder was taken as the research object without considering the self-weight of the working device and the weight of the soil in the bucket, and the efficiency of the hydraulic system and linkage mechanism [4], The structure of the working device of the excavator is shown in Figure 1.

2.1. Establishment of the Theoretical Digging Force Mathematical Model of Bucket Digging. When the excavator operates in the way of bucket digging, the bucket hydraulic cylinder drives the bucket to move, the hydraulic cylinder of the bucket rod and the hydraulic cylinder of the bionic boom are in the locked state, and the bucket teeth tips are affected by the digging resistance F_{CW} and perpendicular to the EQ connecting direction. The stress is shown in Figure 2, wherein, A is the hinge point formed by the hydraulic cylinder of bucket rod and the bucket rod, B is the hinge point formed by the hydraulic cylinder of bucket rod and the bucket rod, C is the hinge point formed by the hydraulic cylinder of the bucket and the swinging rod and linkage, D is the hinge point formed by the linkage and the bucket, E is the hinge point formed by the bionic boom and the bucket, G is the hinge point formed by the bionic boom and the swinging rod, H is the hinge point formed by the bionic boom and the bucket rod, and F_c is the thrust of the hydraulic cylinder of the bucket. The thrust F_c can be divided into two components of F_{CD} and F_{GC} , in which the component F_{CD} is along the hinge points C and D , and the component F_{GC} is along the hinge points G and C , as shown in the figure. Based on the principle of vector decomposition, the following is deduced as

$$\vec{F}_C = \vec{F}_{CD} + \vec{F}_{GC}. \quad (1)$$

The moments of the thrust F_c of the hydraulic cylinder of the bucket before and after decomposition to the hinge point G are the same, as given in the following formula:

$$F_C \cdot L_{BG} \cdot \sin \angle CBG = F_{C D} \cdot L_{CG} \cdot \sin \angle DCG. \quad (2)$$

The big chamber thrust F_C of the hydraulic cylinder of the bucket is calculated by the following formula:

$$F_C = P_0 \cdot A_1 = \frac{\pi \cdot D_1^2}{4} \cdot P_0. \quad (3)$$

The stress by taking the linkage and the bucket as research objects is shown in Figure 3. For the hinge point E , based on the principle of moment balance, the following is deduced as

$$F_{CW} \cdot L_{EQ} = F_{C D} \cdot L_{DE} \cdot \sin \angle CDE. \quad (4)$$

The following is deduced by substituting formulas (2) and (3) into formula (4), we get

$$F_{CW} = \frac{\pi \cdot D_1^2 \cdot L_{BG} \cdot \sin \angle CBG \cdot L_{DE} \cdot \sin \angle CDE}{4 \cdot L_{CG} \cdot \sin \angle DCG \cdot L_{EQ}} \cdot P_0, \quad (5)$$

where L_{BG} is the the distance between the hinge points B and G ; L_{CG} is the the distance between the hinge points C and G ; L_{DE} is the the distance between the hinge points D and E ; L_{EQ} is the the distance between the hinge points E and Q ; P_0 is the rated pressure of the hydraulic system; and D_1 is the inner diameter of the hydraulic cylinder of the bucket.

For formula (5), $\angle CBG$, $\angle CDE$, and $\angle DCG$ change with the digging posture, and they are all the functions of the length of the hydraulic cylinder of the bucket. Therefore, the digging posture angle function is established with the length L_{BC} of a hydraulic cylinder as the independent variable. According to the triangle cosine theorem, the following is deduced as

$$\angle CBG = \arccos \left(\frac{L_{BC}^2 + L_{BG}^2 - L_{CG}^2}{2 \cdot L_{BC} \cdot L_{BG}} \right), \quad (6)$$

$$\angle CDE = \arccos \left(\frac{L_{C D}^2 + L_{DE}^2 - L_{CE}^2}{2 \cdot L_{C D} \cdot L_{DE}} \right), \quad (7)$$

$$\angle DCG = \arccos \left(\frac{L_{C D}^2 + L_{CG}^2 - L_{DG}^2}{2 \cdot L_{C D} \cdot L_{CG}} \right), \quad (8)$$

$$\angle BGC = \arccos \left(\frac{L_{BG}^2 + L_{CG}^2 - L_{BC}^2}{2 \cdot L_{BG} \cdot L_{CG}} \right), \quad (9)$$

$$\begin{aligned} \angle DEG &= \angle CEG + \angle CED \\ &= \arccos \left(\frac{L_{CE}^2 + L_{EG}^2 - L_{CG}^2}{2 \cdot L_{CE} \cdot L_{EG}} \right) \\ &\quad + \arccos \left(\frac{L_{CE}^2 + L_{DE}^2 - L_{C D}^2}{2 \cdot L_{CE} \cdot L_{DE}} \right), \end{aligned} \quad (10)$$

$$L_{CE} = \sqrt{L_{CG}^2 + L_{EG}^2 - 2 \cdot L_{CG} \cdot L_{EG} \cdot \cos(\angle BGE - \angle BGC)}, \quad (11)$$

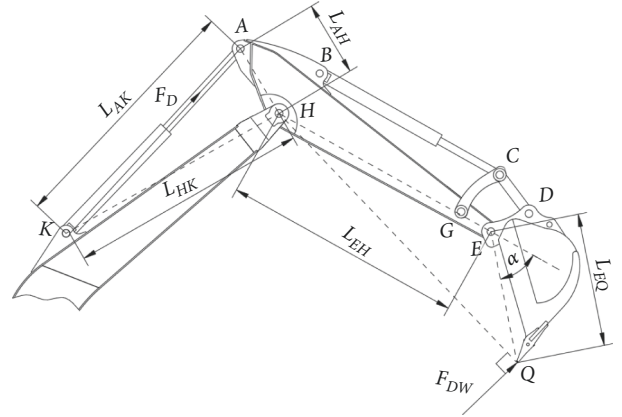


FIGURE 4: Force analysis of the bucket rod digging device.

$$L_{DG} = \sqrt{L_{EG}^2 + L_{DE}^2 - 2 \cdot L_{EG} \cdot L_{DE} \cdot \cos \angle DEG}, \quad (12)$$

where L_{BC} is the the distance between the hinge points B and C ; $L_{C D}$ is the the distance between the hinge points C and D ; L_{CE} is the the distance between the hinge points C and E ; L_{EG} is the the distance between the hinge points E and G ; L_{DG} is the the distance between the hinge points D and G .

The theoretical digging force mathematical model of bucket digging can be obtained by substituting formulas (6-12) into formula (5). When the hydraulic cylinder of the bucket expands and contracts within its stroke range, the theoretical digging force of any digging posture can be solved by using the theoretical digging force mathematical model, so as to obtain the theoretical digging force of any posture during bucket digging.

2.2. Establishment of the Theoretical Digging Force Mathematical Model of Bucket Rod Digging. For bucket rod digging operation, the theoretical digging force generated by the hydraulic cylinder of the bucket rod is related to the stroke of the hydraulic cylinder of the bucket rod and the rotation angle α , that is, the stroke of the bucket hydraulic cylinder. During bucket rod digging, the hydraulic cylinder of the bucket rod drives the bucket rod to move, and the bucket rod drives the bucket to move to dig. Both the hydraulic cylinder of bionic boom and the hydraulic cylinder of the bucket are locked. The theoretical digging force F_{DW} is equal to the digging resistance of the bucket teeth tips in the opposite direction and is perpendicular to the straight line HQ (the connecting line between the hinge point H and the bucket teeth tips Q). The digging resistance force arm is L_{HQ} , as shown in Figure 4, and K is the hinge point formed by the hydraulic cylinder of the bucket rod and the bionic boom. For the hinge point H , according to the principle of moment balance, the following is deduced as

$$F_D \cdot L_{HK} \cdot \sin \angle AKH = F_{DW} \cdot L_{HQ}. \quad (13)$$

Then the theoretical digging force during bucket rod digging is

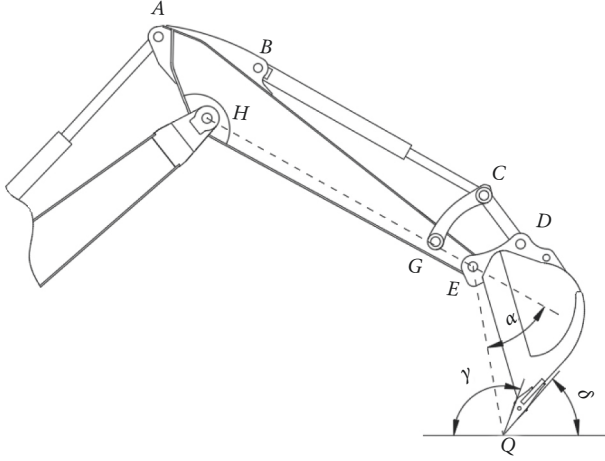


FIGURE 5: The cutting angle of the front edge of the bucket teeth and the rear cutting angle.

$$F_{DW} = \frac{F_D \cdot L_{HK} \cdot \sin \angle AKH}{L_{HQ}}. \quad (14)$$

In formula (14), $\angle AKH$ varies with the digging posture and is a function of the length of the hydraulic cylinder of the bucket rod. According to the triangle cosine theorem, the following is deduced as

$$\angle AKH = \arccos\left(\frac{L_{AK}^2 + L_{HK}^2 - L_{AH}^2}{2 \cdot L_{AK} \cdot L_{HK}}\right), \quad (15)$$

$$L_{HQ} = \sqrt{L_{EH}^2 + L_{EQ}^2 - 2 \cdot L_{EH} \cdot L_{EQ} \cdot \cos(\pi - \alpha)}. \quad (16)$$

The big chamber thrust F_D of the hydraulic cylinder of the bucket rod is calculated by the following formula:

$$F_D = P_0 \cdot A_2 = \frac{\pi \cdot D_2^2}{4} \cdot P_0. \quad (17)$$

The theoretical digging force mathematical model during bucket rod digging is deduced by substituting formulas (15), (16), and (17) into formula (14):

$$F_{DW} = \frac{\pi \cdot D_2^2 \cdot L_{HK} \cdot \sin \angle AKH}{4 \cdot \sqrt{L_{EH}^2 + L_{EQ}^2 - 2 \cdot L_{EH} \cdot L_{EQ} \cdot \cos(\pi - \alpha)}} \cdot P_0, \quad (18)$$

where L_{HK} is the the distance between the hinge points H and K ; L_{EH} is the the distance between the hinge points E and H ; α is the the rotation angle of the bucket relative to the bucket rod; D_2 is the inner diameter of hydraulic cylinder of the bucket rod.

As shown in Figure 5, the included angle formed γ by the front side of the bucket teeth and the horizontal line is called the cutting angle of the front edge of the bucket teeth, and the included angle δ formed by the rear side of the bucket teeth and the horizontal line is called the rear cutting angle. For bucket rod digging, the change of the rotation angle α will change the size of the cutting angle of the front edge of the bucket teeth and the rear cutting angle. From Figure 5, it

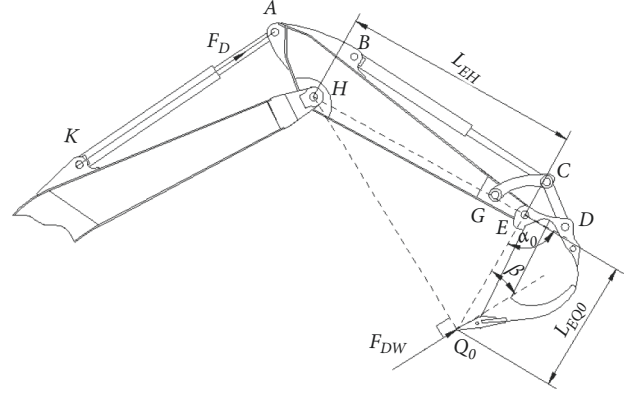


FIGURE 6: Critical posture of bucket rod digging.

can be seen that normal digging can be carried out only when the rear cutting angle is greater than 0° in which the bucket teeth tips contact the soil before the bottom of the bucket. When the bucket rotation angle α turns to the position as shown in Figure 6, the bottom of the bucket contacts the soil first, the bucket teeth tips cannot contact the soil, and the bucket rod cannot excavate normally. This posture is called the critical posture of bucket rod excavation, and the rotation angle of the bucket relative to the bucket rod is called the critical rotation angle α_0 . When $\alpha < \alpha_0$, that is, the length of the bucket hydraulic cylinder is less than that of the hydraulic cylinder in the critical posture, there is a rear cutting angle of digging, the bucket teeth tips contact the soil first, and the bucket rod can excavate normally. When $\alpha \geq \alpha_0$, that is, the length of the hydraulic cylinder of the bucket is greater than or equal to the that of the hydraulic cylinder in the critical posture, the rear cutting angle is less than or equal to 0, so the bucket rod cannot dig normally.

The following is deduced in the critical posture as

$$\alpha_0 = \pi - \angle HEQ_0, \quad (19)$$

$$\angle HEQ_0 = \arccos\left(\frac{L_{EH}^2 + L_{EQ_0}^2 - L_{HQ_0}^2}{2 \cdot L_{EH} \cdot L_{EQ_0}}\right), \quad (20)$$

$$L_{HQ_0} = L_{EQ_0} \cdot \cos\left(\frac{\pi}{2} - \beta\right) + \sqrt{L_{EH}^2 - \left[L_{EQ_0} \cdot \sin\left(\frac{\pi}{2} - \beta\right)\right]^2}, \quad (21)$$

where α_0 is the critical rotation angle of bucket and β is the included angle between the EQ_0 connecting line and the bucket teeth.

The critical rotation angle α_0 of the bucket under the critical posture can be solved by substituting formulas (20) and (21) into formula (19). When $\alpha < \alpha_0$ and $L_{HQ} > L_{HQ_0}$, there is a rear cutting angle of digging. At this time, the bucket rod can dig normally, that is, once the hydraulic cylinder of the bucket changes one unit length every time within the range of critical rotation angle α_0 , the hydraulic cylinder of the bucket rod expands and contracts within its stroke range for digging. In bucket rod digging, the

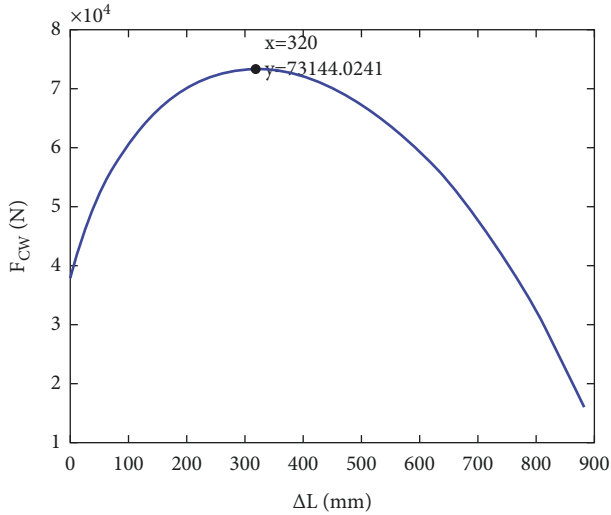


FIGURE 7: Relationship between theoretical digging force of bucket digging and stroke of the hydraulic cylinder of the bucket.

theoretical digging force of any posture within the range of the critical rotation angle can be obtained with formula (18).

2.3. Solution of the Theoretical Digging Force Mathematical Model. In order to accurately and quickly solve the theoretical digging force, the powerful computing function and the convenient programming method of Matlab numerical calculation software were used to transform the theoretical digging force mathematical model into the Matlab programming language and then realize the programming and automatic solution of the theoretical digging force, and the theoretical digging force was drawn into intuitive map output.

2.4. Solution of Theoretical Digging Force of Bucket Digging. The installation distance of the hydraulic cylinder of the bucket was 1378 mm and the stroke was 885 mm, i.e., $L_{BC} = [1378 \sim 2263]$. The other information were as follows: inner cylinder diameter: $D_1 = 90$ mm; rated pressure of hydraulic system: $P_0 = 34.3$ MPa; $L_{BG} = 1834.6$ mm; $L_{CG} = 495$ mm; $L_{DE} = 390$ mm; $L_{EQ} = 1239$ mm; $L_{CD} = 450$ mm; $L_{EG} = 332$ mm; $\angle BGE = 169^\circ$. The Matlab program was compiled and solved according to the theoretical digging force mathematical model of the bucket, and the relevant data and initial values were substituted into the program for automatic solution, so as to obtain the theoretical digging force of any posture during bucket digging, as shown in Figure 7. It can be seen from the figure that when the bucket hydraulic cylinder stroke is 320 mm (i.e., the length of the hydraulic cylinder of the bucket is 1698 mm), the theoretical digging force of the hydraulic cylinder of the bucket reaches the maximum value of 73.144 KN.

2.5. Solving of Theoretical Digging Force of Bucket Rod Digging. The installation distance of the hydraulic cylinder of the bucket rod was 1700 mm and the stroke was 1175 mm, i.e.,

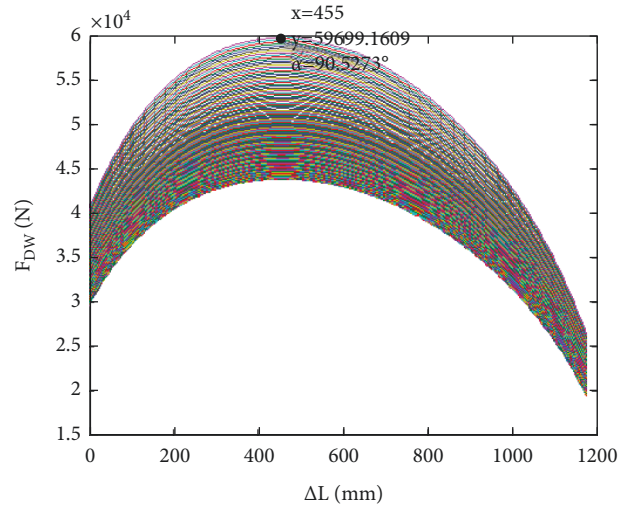


FIGURE 8: Relationship between theoretical digging force of bucket rod digging and stroke of the hydraulic cylinder of the bucket rod.

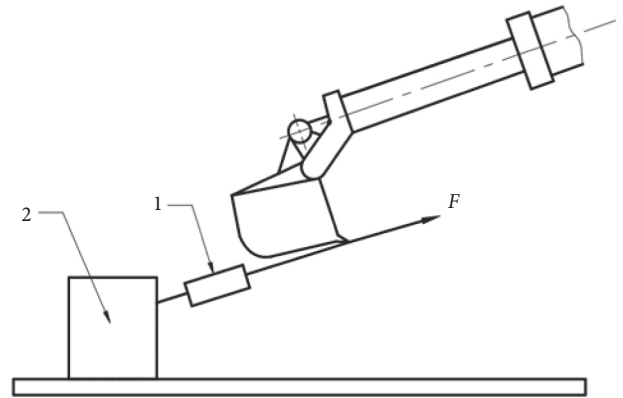


FIGURE 9: Principle of the maximum theoretical digging force test.



FIGURE 10: Test of maximum theoretical digging force.

$L_{AK} = [1700 \sim 2875]$. The other information were as follows: inner cylinder diameter: $D_2 = 90$ mm; rated pressure of hydraulic system: $P_0 = 34.3$ MPa; $L_{HK} = 2267$ mm; $L_{AH} = 700$ mm; $L_{EH} = 2250$ mm; $L_{EQ} = 1239$ mm. The Matlab solution program was compiled according to the theoretical digging force mathematical model of the bucket rod, and the relevant data and initial values were substituted into the program for solution, so as to obtain the theoretical digging force of any posture during bucket rod digging, as

TABLE 1: Comparison between measured values and theoretical values of maximum theoretical digging force.

Maximum digging force	Engine rotation speed/rpm	Length of hydraulic cylinder of bucket/mm	Length of hydraulic cylinder of bucket rod/mm	1st test value/KN	2nd test value/KN	3rd test value/KN	Average/KN	Calculate value/KN	Error rate (%)
Maximum digging force of bucket	2060	1698	--	68.5	68.2	69.1	68.6	73.144	6.60
Maximum digging force of bucket rod	2060	2155	2132	56.1	56.6	56.4	55.2	59.699	8.20

Note: error rate = calculated value of maximum theoretical digging force – tested value of maximum theoretical digging force/tested value of maximum theoretical digging force.

shown in Figure 8. It can be seen from the figure that when the stroke of the hydraulic cylinder of the bucket rod is 455 mm (the length of the hydraulic cylinder of the bucket rod is 2155 mm) and the rotation angle of the bucket is 90.5° , the theoretical digging force of the hydraulic cylinder of the bucket rod reaches the maximum value of 59.699 KN.

3. Test of Maximum Theoretical Digging Force

In order to verify the correctness of the theoretical digging force mathematical model, the test method is used to test the maximum theoretical digging force of the excavator. The test value and the calculated value of the maximum theoretical digging force are analyzed and compared to verify the correctness of the theoretical digging force mathematical models. The mathematical models are wrong when the error rate of the calculated value exceeds 10%, or else, they are correct. The principle of maximum theoretical digging force test is shown in Figure 9. The mechanical sensor dynamometer is used for testing. The excavator model is completely consistent with the excavator model used to calculate the theoretical digging force. The test process is as follows:

- (1) Adjust the excavation posture of the excavator to the maximum theoretical excavation force posture.
- (2) Connect the steel wire rope at one end of the dynamometer to the bucket, and the steel wire rope at the other end to the fixture and make the dynamometer in a tension state.
- (3) Adjust the engine speed to the rated pressure of the hydraulic system and keep this state for a certain time and record the reading value of the dynamometer.

Repeat the test for 3 times and take the average value as the test value of the maximum digging force. The test site is shown in Figure 10, and the test results are shown in Table 1.

The above test data show that the error between the calculated value of the maximum theoretical digging force and the measured value of the maximum digging force of bucket digging is 4.5 KN, and the error between the calculated value of the maximum theoretical digging force and the measured value of the maximum digging force of bucket rod digging is 3.3 KN. Since the calculation of the theoretical digging force did not consider the factors such as the back

pressure of the hydraulic cylinder, the friction at hinge points and the efficiency of linkage, and the thrust of the hydraulic cylinder needs to overcome the useless work factors such as the back pressure of the hydraulic cylinder and the friction at each hinge point in the test process, the measured value is smaller than the theoretical value, but the error is within a small range. Therefore, it can be considered that the calculated value of the maximum theoretical digging force is consistent with the test value. It shows that the calculation method of theoretical digging force is correct and feasible and further verifies the correctness of the theoretical digging force mathematical models.

4. Conclusion

To solve the limitations of the traditional calculation method of the theoretical digging force of the hydraulic excavator, this paper established the theoretical digging force mathematical models by using the principle of the analytical method and solved it by using Matlab software. Firstly, the theoretical digging force mathematical models of two digging methods of the excavator were established, which were then transformed into the Matlab programming language. The complicated manual solving of the theoretical digging force mathematical models was solved by using the powerful computing function of computer, and the theoretical digging force under any excavator posture was rapidly calculated. The maximum theoretical digging force of the excavator was tested on site in order to verify the correctness of the established theoretical digging force mathematical models. The test data show that the errors between the measured values and calculated values of the maximum theoretical digging force of bucket digging and bucket rod digging were small, which further verifies the correctness of the theoretical digging force mathematical models. The theoretical digging force mathematical models can calculate the theoretical digging force of any digging posture. The calculation program of theoretical digging force mathematical models can help the engineers of excavator manufacturers calculate the digging force quickly. The engineers only need to input the structural parameters of the excavator, the rated pressure of the hydraulic system, and other parameters to calculate the theoretical digging force quickly, which greatly improves the design efficiency.

Based on the theoretical digging force mathematical models established in this paper, the later research work will use Matlab software, Visual Basic programming language, and other software to develop a program for calculating theoretical digging force, so as to provide convenient services for enterprise engineers to calculate the digging force accurately and rapidly. The application of lightweight technology in the field of construction machinery will also be paid more and more attention as energy conservation and environmental protection have been paid more and more attention all over the world. Lightweight plays a vital role in reducing oil consumption, reducing emissions, and improving performance of excavators. Therefore, the future research will focus on the lightweight research around excavators, optimize theoretical digging force, and improve the performance of excavators.

However, there are also deficiencies in this paper. Only single hydraulic cylinder digging was considered when the theoretical digging force mathematical models were established, and when digging, the composite digging method was often adopted, i.e., the hydraulic cylinder of bucket rod and the hydraulic cylinder of the bucket drove the buckets to dig at the same time. It is more complex to establish the theoretical digging force mathematical models of the composite digging method, thus, in-depth research will be carried out on the composite digging method of the excavator, and we will try to establish the theoretical digging force mathematical models of the composite digging method in the follow-up work. [5–15].

Data Availability

The data are available from the corresponding author upon request.

Conflicts of Interest

The author declares that they have no conflicts of interest.

Acknowledgments

This research was funded by Project for “Improving Young and Middle-Aged Teachers’ Basic Scientific Research Ability in Universities and Colleges of Guangxi Province”, grant no. 2020KY32009, and Project of “Guangxi Vocational Education CNC Technology Major and Professional Group Development Research Base” of Guangxi Vocational Education Professional Development Research Base.

References

- [1] Q. Shi, J. Lian, and M. Lin, “Determination of the maximum theoretical digging force of excavator,” *Journal of Taiyuan University of Science and Technology*, vol. 28, no. 1, pp. 32–36, 2007.
- [2] Y. Zhang, Y. She, and X. Ning, “Analysis of maximum digging force of hydraulic excavator working device based on virtual prototype,” *Mechanical & Electrical Engineering Magazine*, vol. 31, no. 9, pp. 1132–1135, 2014.
- [3] H. Chen and W. Li, “Research on digging force and optimization of arm structure of multi-functional demolition and digging robot,” *Construction Machinery and Equipment*, vol. 50, no. 11, pp. 55–60, 2019.
- [4] Qi Zu, Y. Zhao, and Z. Liu, “Kinematics Analysis of a new face-shovel hydraulic excavator in mining machine tool,” *Hydraulics*, vol. 48, no. 2, pp. 114–118, 2020.
- [5] B. P. Patel and J. M. Prajapati, “Evaluation of bucket capacity, digging force calculations and static force analysis of mini hydraulic backhoe excavator,” *Machine Design*, vol. 4, no. 1, pp. 59–66, 2012.
- [6] Z. Ren, J. Wang, Z. Zou, Y. Wang, and H. Zhu, “Modeling of the limiting digging force of hydraulic excavator based on resistance characteristics,” *Mechanics*, vol. 25, no. 5, pp. 357–362, 2019.
- [7] V. Panov and R. Mitrev, “Theoretic-experimental approach to computation of digging force,” *Metals and Alloys*, vol. 9, no. 2, pp. 59–66, 2008.
- [8] SAE J1179: *Hydraulic Excavator and Manipulator Digging Forces*, 2008.
- [9] A. Wilkinson and A. De Gennaro, “Digging and pushing lunar regolith: c,” *Journal of Terramechanics*, vol. 44, no. 2, pp. 133–152, 2007.
- [10] Y. Cheng, “Research on the Optimization of the Working Mechanism and the Bionic Boom of the Excavator,” Master’s Degree Thesis, Jilin University, Changchun, China, 2013.
- [11] W. Liu, H. Zhou, and W. Wu, “Simulation analysis of digging force and hinge point force of excavator working device,” *Mechanical Science and Technology for Aerospace Engineering*, vol. 34, no. 10, pp. 1482–1487, 2015.
- [12] G. Zhang, C. Xiao, and Q. Tan, “Dynamic analysis and simulation of excavator working device based on virtual prototype technology,” *Journal of Central South University*, vol. 45, no. 6, pp. 1827–1833, 2014.
- [13] C. Jin, Z. H. Ren, L. Lv, and B. Yong, “Modeling of compound digging force of hydraulic excavator based on resistance characteristics,” *Journal of Northeastern University*, vol. 36, no. 7, pp. 1015–1019, 2015.
- [14] C. Jin, W. Li, and S. Zhang, “Experimental study on digging resistance of large mining shovel hydraulic excavator,” *China Mechanical Engineering*, vol. 19, no. 5, pp. 518–521, 2008.
- [15] H. M. Zhu, “Digging performance analysis and digging force calculation for hydraulic excavator,” *Chemical Equipment Technology*, vol. 28, no. 4, 2007.

Research Article

Development of Physical Education Network Course Resources Based on Intelligent Sensor Network

Moutao Li,¹ Ditao Song ,² and Xiaoyong Hu³

¹College of Physical Education, Huangshan College, Huangshan 245041, Anhui, China

²College of Physical Education, Guangxi Science & Technology Normal University, Laibin 546199, Guangxi, China

³Institute of Physical Education, Guiyang College, Guiyang 550005, Guizhou, China

Correspondence should be addressed to Ditao Song; songditao@gxstnu.edu.cn

Received 20 April 2022; Revised 2 June 2022; Accepted 23 June 2022; Published 8 September 2022

Academic Editor: Xuefeng Shao

Copyright © 2022 Moutao Li et al. This is an open access article distributed under the Creative Commons Attribution License, which permits unrestricted use, distribution, and reproduction in any medium, provided the original work is properly cited.

Judging from the current online teaching practice of higher physical education basic theory courses, there are many problems such as lagging theory, unclear models, confusing mechanisms, outdated methods, and lack of resources, resulting in the low interest of students. Basic theory courses are studied. The phenomenon of skipping class and being late is common, which seriously affects the improvement of the comprehensive quality of physical education students. Therefore, it has become an urgent problem for the majority of higher sports workers to develop learning resources for basic physical education courses and realize the innovation and application of the teaching mode of higher sports online courses. Compared with the traditional teaching method, the students' physical education teaching performance is improved by about 30%, and their personality is fully developed. Linking teacher performance to changes in student performance parameters can effectively improve teacher motivation. This shows that under the background of intelligent sensor network, the physical education network course can effectively improve the teaching efficiency.

1. Introduction

With the accelerated pace of educational informatization, the ability to be familiar with modern educational technology, personal information, and information literacy has become a must-have quality for people. As a reserve force for future social development, students urgently need to improve their educational level [1]. Colleges and universities have begun to focus on improving students' educational technology capabilities. Starting from the enhancement of physical fitness, it should be combined with the "National Physical Exercise Standards"; it should conform to the students' understanding and the law of growth and development; according to the actual situation and the needs of future development, pay attention to training modern sports techniques. At the same time, it is necessary to focus on cultivating students' comprehensive quality, innovation ability, and information ability, so that they can adapt to new teaching methods; modern educational technology should be integrated into

teaching to help students develop good information literacy. The ability to develop information-based teaching enables them to actively use the concepts of modern educational technology after entering the society and to improve the ability and practical ability to use information technology [2, 3].

Smart sensors are devices with information capabilities. Smart sensors with multiple processors capable of receiving, processing, and exchanging information are the product of the integration process of sensors and microprocessors [4]. Compared with traditional sensors, smart sensors have the following three characteristics: use software processes for high-resolution information retrieval at low cost; measure the performance of training programs; and have multiple functions [5]. Smart sports are to use smart sports equipment to make traditional sports intelligent or online games real. Compared with simple sports, the blessing of smart equipment can make sports experience more data-based, professional, and entertaining.

For online jobs, there are also many training jobs for domestic and foreign professionals. Based on the research and analysis of the current situation of online and offline, Zha and Zhang [6] proposed an online and offline training mode based on the mobile social network. This model deepens the relationship between teachers and students. Communication and collaboration also promote the implementation of online and offline training standards [6]. When implementing the offline e-learning model, Yue and Zhou [7] use WeChat as a forum, combine modern information technology with traditional training methods, and explore offline writing exercises. The offline teaching method is implemented with the support of WeChat school guidelines [7]. It is considered that integrated learning is a new learning mode, which can not only overcome some shortcomings of online learning but also break the existing traditional academic mode and make the two learning modes merge with each other [8]. Effective analysis of student performance data to understand the characteristics and weaknesses of student learning was pioneered by Chen and Chen [9], providing a scientific basis for teachers to better understand students and apply knowledge to instructional management systems. While these studies add to our understanding of e-learning on the one hand, our understanding of the test data is still insufficient. Findings from small samples of researchers and policymakers are not generally credible enough. Therefore, we optimize sports network course resources based on intelligent sensor network research.

The network-based learning method has been accepted by people and has even reached the point where it is impossible to live, produce, and learn without the network. The article establishes a network teaching platform to realize the complementation of “in-class” and “out-of-class”. In the process of implementing physical education courses, teachers are required to upload various teaching documents, courseware, and assignments to the online teaching platform and make full use of the school’s online teaching platform to implement teaching, which can not only enrich classroom information but also allow students to learn outside of class. Self-study provides a network environment for teachers and students to interact with teachers and students in basic theoretical courses and expands the teaching space. Various forms of online teaching activities are carried out to achieve “online” and “offline” interaction. In the implementation process of sports theory, the online classroom is fully used for online learning, and representative questions are answered “online” through “forum”, “Q&A,” and other columns, so that students can learn in time and answer through QQ, e-mail, MSN, and other methods. The problems of individual students make students feel that the teacher is around at any time, shorten the distance between teachers and students, provide students with timely and rich information under limited time and limited teacher conditions, and make up for the shortage of teachers. Online course resources are developed to realize the combination of “theory” and “practice”. According to the characteristics of physical education, with the help of modern teaching technology, we develop and

update teaching resources and enrich teaching content. In the teaching of sports theory, the use of sports technical action pictures, animations and videos, or multimedia materials of experimental operations visualizes the boring theory, increases students’ interest in learning, increases teachers’ teaching fun, and extends the deficiencies of teaching materials.

2. The Entry Point of Resource Development and Its Management Performance Evaluation Research Method

2.1. Online Courses. With the rapid development of online learning and the deepening of online interpersonal communication training exchanges, a large amount of structured data—also available—are available on many training platforms [10]. There are different types of data. People use submissions in lieu of allegations behind it [11, 12]. Educational data mining refers to extracting unique academic data, making complex academic data useful information that students can better understand, make course decisions for us, and improve vocational training. Let’s be better [13]. Carrying out online physical education can effectively develop the physical quality of students, cultivate students’ good exercise habits, and enhance their awareness of actively participating in physical exercise.

The control system considers the controller’s self-efficacy and control method to be improved relative to the control level [14]. The scale of control is limited, and the number of directors who can effectively and directly control its headquarters is also limited [15]. Any control system has a certain controller. In an organization, the control system obeys the controller, and the control system and the controller complement each other. If the control area is expanded, the administrator shall prevail; that is, the control level shall be reduced. If the control size is reduced, performance will be degraded, and the control size must be increased to improve performance [16].

Figure 1 shows the different assessment methods for students. The so-called flat housing means that the steering system has fewer control levels and a wider control range. The flat housing features a refined control hierarchy. It is a “one-to-many” organizational structure in which the controller directly faces the system. The correct way is the opposite.

$$M = \frac{x}{(x + i + 1)},$$

$$P_{LA} = L_A + \left[\frac{D_A - (L_A + 1)}{C_{\text{skip}}(d)} \right] \times C_{\text{skip}}(d) + 1, \quad (1)$$

$$d(x_i, x_j) = \sqrt{(|x_{i1} - x_{j1}|^2 + |x_{i2} - x_{j2}|^2 + \dots + |x_{in} - x_{jn}|^2)}.$$

Among them, M refers to the performance evaluation system, PLA refers to the performance evaluation organization, and $d(x_i, x_j)$ refers to the performance evaluation index.

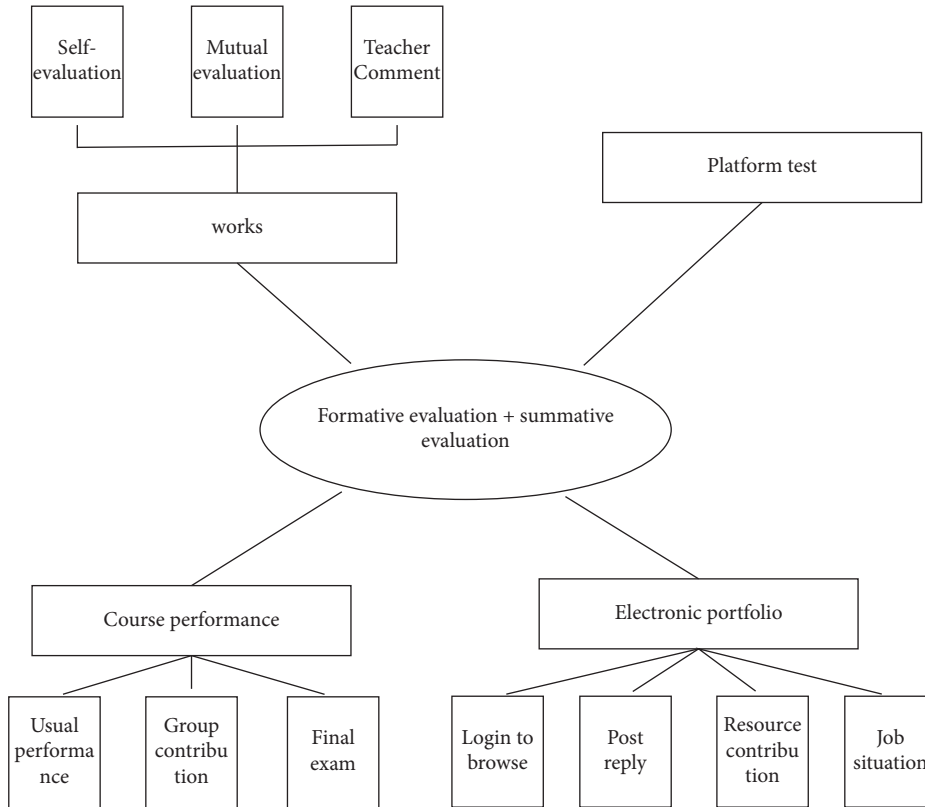


FIGURE 1: Multiple assessment methods.

Combined with the characteristics of the performance evaluation system, promote relevant statistical functions

$$W = \frac{N_1 r_1^2}{2} + \frac{N_2 r_2^2}{2} + N_2 d_2^2 + \left(\frac{N_3 r_3^2}{2} + N_3 d_3^2 \right) * 0.1 + \frac{2}{3} N. \quad (2)$$

Therefore, the range of control and the level of control show an inverse relationship when confirmed by the controller. The key is the management recommendations adopted by the company's top management and the management model determined by the company. Leaders have high personal strengths and strong combined skills. They can quickly get the gist of a situation, give appropriate guidance on contextual requirements, and keep authorities informed, reducing the number of contacts with each supervisor. Over time, its management scope will continue to expand.

2.2. Online Sports Courses. With the progress of science and technology in our country, the compilation of educational information sources has been paid more and more attention, which is also the reason for the continuous change of the current curriculum model. In the teaching of sports online, teachers should make reasonable use of information technology to make students have a more profound grasp of sports theory. Therefore, online services are of great interest to educators. So what is an online service? How should the concept of online work be defined? The authors suggest a

number of relevant resources to ensure that online services are also built into the curriculum, allowing students to experience training beyond the interaction of the learning community. However, online services have unique advantages over traditional educational services. They are based on modern technology and spread over the Internet to achieve educational goals.

Online services are the result of modern curriculum development and an important introduction of information technology in the field of curriculum technology. It is an online education model created by the combination of network technology, multitechnology, and digital technology. Such educational activities can be done in a one-to-one or one-to-one learning program. Multiparty sharing of resources is conducive to making full use of materials. This method is more innovative and has rich educational content, which can increase students' interest in writing. Most importantly, such educational activities are not just for students. It can benefit more people and is an important way to learn new teaching methods. At the same time, we use multimedia development to create learning content, teaching methods, and teaching space for sports activities. With the help of the Internet, audio, video, games, pictures, etc. are shared with students. The large capacity, rich and diverse forms, and high sharing characteristics of network information resources can play an important role in college education, especially physical education, which has important and unique significance. Therefore, the sports

network service introduces a new way of sports training, introducing the characteristics of modern information technology.

- (1) The transmission speed is fast, and the distribution is strong. Implement online training services and determine distribution. If the network is available and mobile, you can also learn about useful educational activities for students to train outside of school hours to help students manage their time.
- (2) Strong communication skills, easy to learn and communicate: Communication means that students can exchange knowledge with each other on the Internet. Even two strangers can still discuss and exchange knowledge over the Internet. This is an important part of online education services.
- (3) Virtual, long-term: In the traditional course model, students and teachers stay in the same classroom to study and communicate, which limits the number of students who take the course, hoping that more students will learn more. Teachers need to lecture frequently, which increases the effectiveness of teachers' teaching.
- (4) Improve information sources: In today's information age, students can gain understanding from many aspects. The source of knowledge no longer comes from textbooks or teacher lectures as it once did. Multimedia can be used as other means of acquiring knowledge from many sources. Due to the development of modern technology, the diversification and rich applications of these information sources have been developed.
- (5) Can meet the individual requirements of students: Students can choose according to their preferences or training time. They are not limited to the only educational activities ordered by the school. Online services can provide comprehensive rewards for students' freedom. When studying, it is more important to choose training activities according to your own preferences, which can improve the academic performance of the class, and also help students to a certain extent, and help students develop personal training plans.

Table 1 shows the differences between online learning and traditional learning. An online learning environment may also be referred to as an online learning environment. It is based on computer technology and usually comes with training resources and online training forums. Compared with the local offline classroom, the online learning community of the learning community is more free in time and space, and these learning resources are rich and can be distributed quickly. Different platforms and resources provide a platform to help teachers and students practice online.

2.3. Teaching of Sports Online Courses. Sports' networking is a topic where science and practice are closely integrated. Therefore, teachers should choose issues closely related to

students' learning and lifestyle for online education, so as to improve students' understanding of information technology and work knowledge. At the same time, teachers should encourage students to apply technology to life coaching or learning other subjects, so that students can apply powerful knowledge, exert their problem-solving ability, and lay a foundation for the cultivation of students' life. Learn the ability to climb. For the analysis, judgment, and optimization of the motion network algorithm, we use the following equation to calculate

$$t(s) = \exp\left(-\int_0^s \kappa(t)dt\right), \quad (3)$$

as we can see

$$\partial = 1 - t(s) = 1 - \exp\left(-\int_0^s k(t)dt\right). \quad (4)$$

When Δs approaching zero,

$$\frac{dI}{ds} = T(s) * \rho(s) * A = T(s) * \kappa(s), \quad (5)$$

$$I(s) = I_0 + \int_0^s g(t)dt.$$

The general formula we use for this is as follows:

$$x(k+1) = Ix(k) + Jv(k), k = 1, 2, \dots \quad (6)$$

The power has the following performance indicators:

$$K = \sum_{k=1}^{\infty} [x^i(k)Jx(k) + r^i(k)cJ], \quad (7)$$

where the power matrix Q is

$$Q = \frac{1}{2a^2r^{-1}} \left(\frac{2b^2}{a^2r^{-1}} p - t \right)^{-1} [a^2r^{-1}t^2 + 2(1-b^2)t], \quad (8)$$

$$Q = \frac{1}{2a^2r^{-1}} \left(\frac{2b^2}{a^2r^{-1}} t - L \right)^{-1} [a^2r^{-1}L^2 + 2(1-a^2)L].$$

Introducing the parameter and power weighting factor Q gives

$$\left(\frac{2b^2}{a^2r^{-1}} I_x - t \right) Q = \frac{1}{2} t^2 + \frac{1-b^2}{a^2r^{-1}} t. \quad (9)$$

Delivered by recipe

$$Q^2 + \frac{2(1+b^2)}{a^2r^{-1}} Q + \frac{(1+b^2)^2}{(a^2r^{-1})^2} I_x = \left(Q + t + \frac{1-b^2}{a^2r^{-1}} I_x \right)^2. \quad (10)$$

3. Research Experiment on the Entry Point of Resource Development and Its Management Performance Evaluation

3.1. Subjects. The six classes were selected according to the physical education level of a university in the city and were

TABLE 1: The difference between online learning and traditional teaching.

1	Number of learners	Basically unlimited	Limited by the environment
2	Study location	No space restrictions	Fixed study place
3	Actual	Comparing men to start hands-on activities	Easy to carry out practical activities
4	Learning feedback	Multi-channel	Single mechanism
5	Study time	Flexible	Fixed time
6	Learning resources	Multimedia	Easier
7	Learning evaluation	Easy-to-implement processes and summative assessments	Summative evaluation

divided into traditional teaching groups, general e-learning groups, and e-learning groups based on electronic sensors. When students teach online through e-learning, each group selects a group leader and creates a message group to facilitate learning and discussion among group members. Teachers publish this handbook prior to the start of the course and provide students with related microvideos, training pages, and other resources.

3.2. Data Preprocessing. For the test system and the tutorial, the integration method is used for clustering, and the k value and $dk = 2, 3, 4,$ and 5 are selected, respectively, and then, the clustering is performed in turn. The results are shown in Table 2.

It can be seen that when k is 3, the GA arrow reaches its maximum value. So the optimal number of clusters for this dataset is 3. This clustering model currently has high overall performance and is an ideal compiler for this dataset.

3.3. Entry Point for Students. At the same time, through the construction of curriculum resources, it can better encourage students to learn actively and independently, encourage teachers to learn new knowledge, expand teaching space and time, and solve problems such as insufficient teachers and insufficient facilities.

4. Experimental Analysis of Resource Development Entry Point and Management Performance Evaluation Research

4.1. Students Understand. The statistics are based on the knowledge base of physical education. The sports knowledge and sports identification data system consist of 343 instances, with a sample size of 6 and a total of 2 classes; the data system for practice techniques consists of 762 examples, with a sample size of 8 and the correct number of classes of 2. The motion parameter data system consists of 702 samples, with a sample size of 9 and a maximum number of classes of 2. The results are shown in Table 3.

Comparing the performance with the experimental results shown in Table 3, it can be seen that for all three datasets, the GA ratio can find the exact number of clusters, while the traditional DBSCAN index cannot find the exact number of clusters. The CLIKU index of each dataset can only find the number of clusters of the motion knowledge dataset but not the ideal motion parameters and the number of clusters of the motion knowledge dataset.

TABLE 2: GA indices at different K values.

K	N	Number of samples	Genetic algorithm
2	175	265	0.664
3	263	265	0.989
4	227	265	0.858
5	235	265	0.564

The most important athletic ability knowledge is sports-related knowledge, that is, understanding athletic ability. The knowledge most relevant to athletic ability is exercise-related knowledge, that is, understanding athletic ability. Ten relevant topics were randomly selected, namely “health,” “physical exercise,” “physical fitness,” “lifestyle,” “aerobic exercise,” and “lack of physical exercise,” “Conclusion” and “Conclusion,” “BMI,” “Health Equivalence,” and “Physical Activity Guidelines”—these terms are very similar to those used in sports. Therefore, studying students’ attitudes towards their use can show their knowledge of sports. The result is shown in Figure 2.

Figure 3 shows that 55.2% of the respondents understood the term “health,” followed by “exercise” at 46.2%, “body” at 45.6%, and “lifestyle” at 39.2%. The three least understood terms were “obesity,” “fitness,” and “inactivity,” accounting for 33.0%, 24.2%, and 28.8%, respectively. Not everyone understands these terms because all of them are business rules. Conscious memory is not easy to understand.

An important role of exercise is to maintain good health, and physical fitness plays an important role in health. The 20 questions on physical fitness are multiple-choice questions, each correct answer will score 2 points, and no wrong answers are allowed. The total score is 40 points. To better analyze the students’ grades, their scores were converted to 100 points, and the results are shown in Table 4.

4.2. Student Differences. Statistics are based on the sports lives of nonformal students and disaggregated by gender for women and men to understand current understanding of sports network activity. The size of the male head is shown in Figure 4.

As can be seen from Figure 4, the ability of boys before the multifunctional vocational training is not deep, and the average is 2, which does not meet the requirements of art students. To judge whether students meet the requirements, we also calculated student performance at the following six levels, as shown in Figure 2.

As can be seen from Figure 2, there is no significant difference between the student’s control and the male

TABLE 3: Experimental comparison solution results.

Data set	Sample	Sample size	Correct number of classes	Optimal number of clusters		
				DBS scan	Group	Genetic algorithm
Grade	3 52	5	3	1 7	1	5
Consciousness	754	7	4	18	18	4
Participate	702	10	2	17	6	2

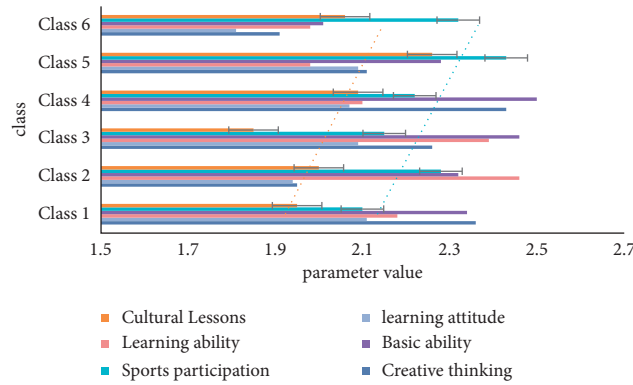


FIGURE 2: Schoolgirl's mastery.

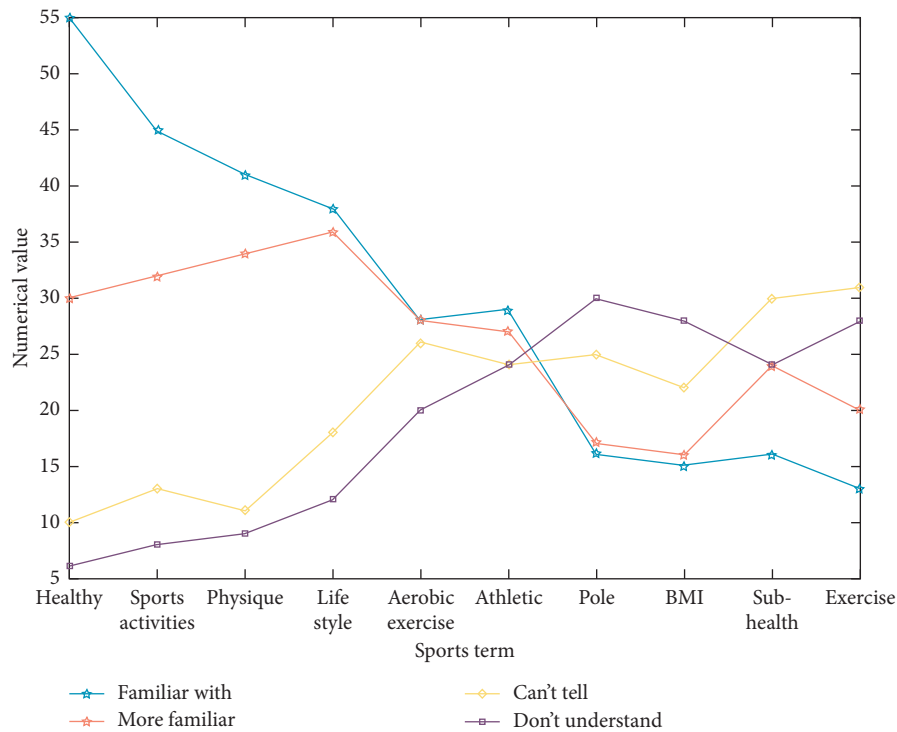


FIGURE 3: Cognition of sports terminology.

TABLE 4: College students' awareness of sports knowledge.

	90–100	80–89	70–79	60–69	<60
Number	45	324	421	256	68
Percentage	3.54	36.5	42.65	21.65	6.51

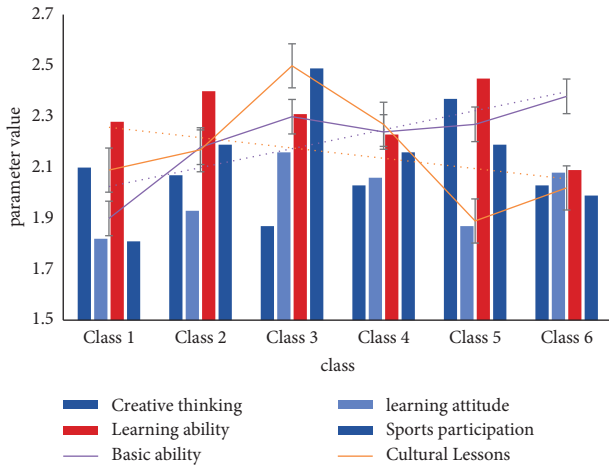


FIGURE 4: Male students' artistic mastery.

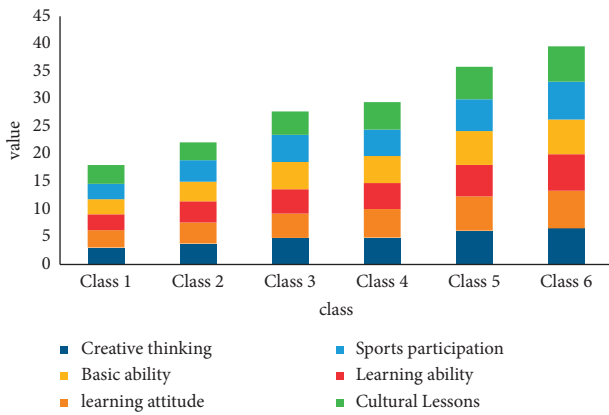


FIGURE 5: After learning the parameters.

student's control, and the mean is around 2. The data after the study are shown in Figure 5.

As can be seen from Figure 5, we can confirm that after training, students' athletic ability has made good progress, and sensor-based online learning can achieve better results than these two teaching methods. It can be seen that if you want to create a good entry point for online sports service resources, you can start from the places that students are interested in.

4.3. *Parameter Changes.* The specific data are shown in Figure 6.

Course quality statistics are also provided, as shown in Figure 7.

At the same time, through the construction of curriculum resources, it can better encourage students to learn actively and independently, encourage teachers to learn new knowledge, expand teaching space and time, and solve problems such as insufficient teachers and insufficient facilities. Network teaching research is to realize the combination of "teaching" and "research". In order to better explore the laws, principles, and methods of physical education theory of the teaching practice and solve the problems

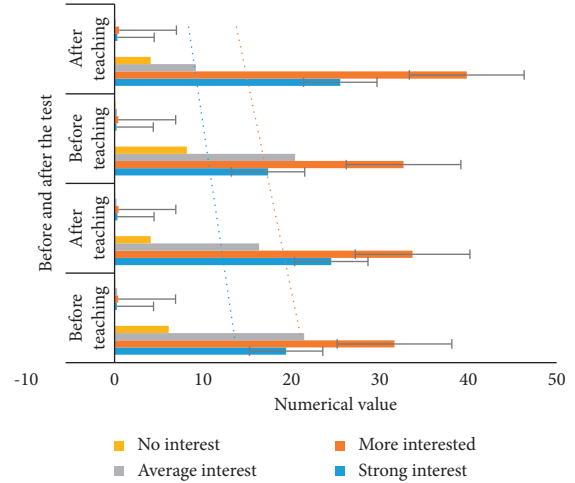


FIGURE 6: Changes in student interests.

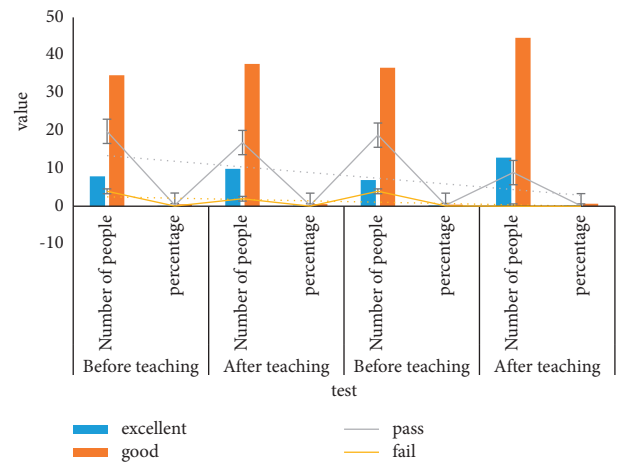


FIGURE 7: Students' sports scores before and after the experiment.

that need to be solved in teaching, we have carried out a lot of "curriculum construction" in the teaching process of physical education theory. Exploration and research were carried out, and the results were applied to the teaching practice of physical education theory courses, helping teachers to better carry out network teaching, allowing students to better use the network for autonomous learning, and improving teaching quality [16].

5. Conclusion

Develop online teaching resources for sports theory courses to enrich teaching content. Its experimental data showed that 55.2% of the respondents understood the word "health," followed by 46.2% "exercise," 45.6% "body," and 39.2% "lifestyle." It can be seen that at present, the theory course teaching team of our school has integrated the advantages of traditional classroom learning and online self-study, constructed the network teaching mode of sports theory course, and developed multimedia courseware and video of sports theory course. The school network platform implements

online teaching and realizes the complementation of “in-class” and “extra-curricular”, the interaction between “online” and “offline”, and the combination of “theory” and “practice” to maximize the sharing of high-quality teaching resources. It solves the problem of insufficient learning interest of teachers and students, expands the time and space of students’ learning, overcomes the contradiction between “learning and training” to a certain extent, fully embodies “people-oriented”, and realizes personalized and autonomous learning. Teaching and learning improve the learning effect of physical education students. The combination of “theory” and “practice” is the key to the teaching of theory courses in sports majors. In the process of the construction of sports theory curriculum resources, relevant teaching reform research should be actively carried out, and the ways of opening high-quality curriculum resources and quality sports products to the society should be analyzed. The effect of the course, the implementation of the online course construction project, and the update and maintenance of the course network resources have accumulated valuable practical experience, promoted the sustainable development of online teaching, and promoted the combination of teaching and science. Research and realize that the teaching reform project originates from teaching practice, and the teaching reform results serve the virtuous circle of teaching practice.

Data Availability

No data were used to support this study.

Conflicts of Interest

The authors declare that they have no conflicts of interest.

Acknowledgments

This work was supported by the Key Research Project of Social Sciences and Humanities in Anhui Province (Project Number: SK2017A0386): Research on the inheritance and protection of intangible cultural heritage-take “Huizhou seasonal dancing” as an example.

References

- [1] C. Yan, “Research on high school men’s basketball training strategies and methods based on neural network model,” *Journal of Computational and Theoretical Nanoscience*, vol. 13, no. 12, pp. 10059–10063, 2016.
- [2] C. H. Landry, K. S. Allan, K. A. Connelly, K. Cunningham, L. J. Morrison, and P. Dorian, “Sudden cardiac arrest during participation in competitive sports,” *New England Journal of Medicine*, vol. 377, no. 20, pp. 1943–1953, 2017.
- [3] S. Liddell, “IP broadcast media and music industry workflows in Sweden,” *Journal of the Audio Engineering Society*, vol. 64, no. 10, p. 815, 2016.
- [4] Y. Karaka and B. Phyllis, “Value orientation of middle school students’ physical education and physical education curriculum,” *Kuramsal Eğitimbilim*, vol. 13, no. 4, pp. 716–730, 2020.
- [5] E. Claudia, “Siegfried and others. Sports participation in the life course,” *European Journal of Sport and Society*, vol. 8, no. 1-2, pp. 45–63, 2016.
- [6] Z. Zha and X. Zhang, “Study on the dynamic development of folk custom sports and inheritance innovation in heilongjiang Province,” *International Journal of Multimedia and Ubiquitous Engineering*, vol. 11, no. 5, pp. 377–386, 2016.
- [7] T. Yue and Yu Zou, “Online teaching system of sports training based on mobile multimedia communication platform,” *International Journal of Mobile Computing and Multimedia Communications*, vol. 10, no. 1, pp. 32–48, 2019.
- [8] X. Yang, X. Jiang, L. Rong, and Z. Xu, “A sports teaching mode based on social networking service teaching resources,” *International Journal of Emerging Technologies in Learning (iJET)*, vol. 15, no. 08, p. 180, 2020.
- [9] R. Chen and S. Chen, “Online cooperative teaching mode based on self-direction theory in method of sport science research,” *International Journal of Emerging Technologies in Learning (iJET)*, vol. 15, no. 22, p. 24, 2020.
- [10] W. J. Smile, J. A. Hawley, and D. M. Camera, “The effect of skeletal muscle energy availability on the protein turnover response to exercise,” *Journal of Experimental Biology*, vol. 219, no. 2, pp. 214–225, 2016.
- [11] D. Hellier and E. Novi-Williams, “Telemundo says World Cup broadcast stolen in Middle East,” *World Intellectual Property Report*, vol. 32, no. 7, pp. 10–11, 2018.
- [12] T. Dragon, “Application research of athlete pose tracking,” *Algorithm Based on Deep Learning Journal of Environmental Intelligence and Humanized Computing*, vol. 11, no. 9, pp. 3649–3657, 2020.
- [13] Y. Jia, “Research on the teaching quality, sports enjoyment and learning satisfaction of college basketball courses,” *Asian Journal of Education and Social Research*, vol. 1, no. 1, pp. 1–12, 2018.
- [14] R. Devrilmez, E. Çiy, D. Bilgiç, and M. Dervent, “Turkish validity and reliability of physical education and sport course exam anxiety scale,” *Journal of Physical Education and Sports Studies*, vol. 13, no. 1, pp. 1–13, 2021.
- [15] M. Olena, “Formation of a test system for controlling the preparedness of players in team sports games,” *Sport Science and Human Health*, vol. 4, no. 2, pp. 88–101, 2020.
- [16] W. Sun and Y. Gao, “The design of university physical education management framework based on edge computing and data analysis,” *Wireless Communications and Mobile Computing*, vol. 2021, no. 2, pp. 1–8, 2021.

Research Article

Research on Influencing Factors of Consumption and Purchase Intention of Camellia Oil in Coastal Areas Based on Logistics Model

Xue Wu 

School of Economics and Management, Kaili University, Guizhou, Kaili City, China

Correspondence should be addressed to Xue Wu; wuxuesisi@xs.ustb.edu.cn

Received 25 July 2022; Accepted 18 August 2022; Published 1 September 2022

Academic Editor: Wei Liu

Copyright © 2022 Xue Wu. This is an open access article distributed under the Creative Commons Attribution License, which permits unrestricted use, distribution, and reproduction in any medium, provided the original work is properly cited.

Camellia oil contains a variety of active substances, which have the functions of strengthening the heart and lowering cholesterol, and can prevent a variety of cardiovascular and cerebrovascular diseases caused by vascular sclerosis edible oil. Based on the logistics model, this paper builds a research model on the influencing factors of consumption and purchase intention and analyzes the coastal areas of camellia oil. Using this model, it makes an empirical analysis and research on the differences in the purchase intention and influencing factors of different consumers of camellia oil. Based on the results of empirical analysis, the main research conclusions of this paper are extracted, including the influencing factors of consumers' camellia oil purchase willingness and the differences in the influencing factors of consumers' camellia oil purchase willingness under different income levels, and put forward some corresponding measures and policy suggestions in a targeted manner. Based on the research model of the influencing factors of purchase intention established by logistic algorithm, this paper analyzes the coastal areas of Chashan oil and finds that the factors affecting consumers' purchase intention are positively related to education and personal monthly income and negatively related to gender. "Educational education" is significant at 1% and has a positive correlation with a coefficient of 0.864; personal income is significant at 5% with a coefficient of 0.762; for gender, it is negatively correlated with a coefficient of -0.259, indicating that other variables remain unchanged. Education can promote consumers' willingness to buy camellia oil, and consumers with higher education are more likely to buy camellia oil. In the same regression prediction model, the regression prediction efficiency of this model is better. In general, this shows that the model in this paper has certain superior performance.

1. Introduction

Food safety is an important issue related to the stability and economic development of any country. Edible oil is an important part of diet, necessarily consumable for people's life, and an indispensable food ingredient in people's daily diet. Camellia oil is one of the traditional edible oils of residents, with high nutritional value. It not only is edible, but also has medicinal value and can be used as a beauty and skin care product. Its structure is very similar to that of olive oil, especially monounsaturated fatty acids, and its component content is slightly higher than that of olive oil, while the price of camellia oil is only about 1/3 of that of olive oil. It conforms to the Mediterranean dietary pattern generally recommended by nutritionists all over the world today and

has a certain competitive advantage in the international market. It is of great significance to improve dietary structure and national physical quality. Camellia oil contains a variety of active substances, which have the functions of strengthening heart and lowering cholesterol, and can prevent a variety of cardiovascular and cerebrovascular diseases caused by arteriosclerosis. Therefore, it is called "Changshou oil," and it is a healthy high-grade edible oil promoted by FAO [1]. Camellia oil cultivation has the advantage of not occupying cultivated land, so developing camellia oil industry has become an important deployment of edible oil safety strategy [2]. With the growth of oil planting area slowing down and shrinking, more and more countries have increased their dependence on the world edible oil market, and many countries' dependence on

foreign countries is as high as 60%. Faced with a large population and a small cultivated land area per capita in some countries, the grain and oil provided by the traditional grain industry cannot meet the market demand of the country well. With the adjustment of agricultural structure and the acceleration of urbanization, various factors that perplex the grain and oil security still exist [3]. After several years' development, camellia oil has been known by more and more people, but compared with the camellia oil industry, which is developing faster and faster, we are still faced with a relatively cold camellia oil market. On the one hand, the sustainable development of camellia oil industry depends on increasing productivity, expanding production scale and improving production efficiency to increase supply. On the other hand, it is necessary to increase the market demand and increase the market share of camellia oil [4]. However, with the expansion of *Camellia oleifera* planting area, the continuous improvement and promotion of *Camellia oleifera* oil production technology have led to the continuous increase of output and market supply. At the same time, people's lack of knowledge of *Camellia oleifera* and *Camellia oleifera* oil will lead to insufficient demand in *Camellia oleifera* oil market, which may lead to the situation of oversupply, which will eventually lead to waste of resources and damage to the interests of *Camellia oleifera* oil operators, and then make the industry gradually decline [5]. Therefore, it is urgent to promote and expand the market of edible oil. Based on the logistics model, this paper builds a research model of influencing factors of consumption purchase intention, analyzes the coastal areas of camellia oil, and makes an empirical analysis and research on differences of purchasing intention and influencing factors of different consumers.

Based on the logistics model, this paper studies the influencing factors of consumption and purchase intention in the coastal areas of camellia oil. The innovations of this paper are as follows:

- (1) Innovation of research perspective. From the current research of scholars, the research on the development of camellia oil industry is mostly conducted from the perspective of producers. The innovation of this paper is from the perspective of consumers, through the investigation and analysis of consumers' willingness to buy camellia oil.
- (2) Taking the theory of planned behavior as the theoretical analysis basis, this paper puts forward research hypotheses for the model and then empirically tests the hypotheses based on the actual survey data by using the structural equation model, which further expands the application field of the theory of planned behavior and makes up for the theoretical gap in the study of consumers' willingness to buy camellia oil.
- (3) This paper introduces the thinking framework of logistic model into the field of camellia oil, focuses on exploring and analyzing the influencing factors of consumers' purchase intention in coastal areas,

establishes logistic model regression to analyze the main factors affecting consumers' purchase of camellia oil, and puts forward countermeasures and suggestions to promote camellia oil consumption through the research conclusions.

2. Related Work

Camellia oil is a kind of woody edible oil plant planted only in China. It has a long history of cultivation and utilization in China, which has lasted for more than 2300 years. It mainly grows in the hilly areas of southern China. In China, it is mainly planted in some coastal cities: Fujian, Guangdong, Guangxi, etc. [6]. Some Chinese scholars have studied the consumption of camellia oil in the market as follows: Ahmed et al. have concluded that camellia oil is well used in the fields of edible industry, medicine, pharmacy, chemical industry, cosmetics, and so on [7]. The tea industry has a long industrial chain. From planting to processing and sales, tea has high economic value. It can be used not only in the deep processing and production of *Camellia oleifera*, skin care products, and nutrition and healthcare products, but also in the production of feed, fertilizer, cleaning products, and refined tea saponins, which are processed by the remaining materials. By analyzing that *Camellia oleifera* can be planted and harvested for many years, and that *Camellia oleifera* production can produce a variety of economic and ecological benefits, Zhong and Lou pointed out that *Camellia oleifera* oil has broad market potential. Due to the lack of consumer awareness, the current market demand is insufficient, which needs further publicity and promotion by government and enterprises [8]. Zhu et al. analyzed the growth characteristics, suitable planting areas, and other natural characteristics of *Camellia oleifera*, and put forward the important role of *Camellia oleifera* cultivation technology and science and technology promotion. In the 1960s, consumer behavior research began to become a new research field [9]. Among them, the research on the theoretical basis of consumer behavior mainly has the following views: the rational behavior theory proposed by Han et al. can widely and effectively predict the consumer psychology and behavior of consumers. According to TRA theory, consumers can rationally find a way to maximize their own utility to guide their consumption behavior. In a narrow sense, consumer behavior refers to all kinds of behaviors that people perform when consumers obtain the goods they need, such as comparison, selection, purchase, and use [10]. Zhou et al. believe that consumer behavior is the decision-making process when consumers choose and finally buy their favorite products, and point out that consumer behavior is the physical and mental activities of purchasing and consuming products [11]. Xiang et al. emphasized that different health conditions of individual consumers will have a certain impact on their acquisition of consumption information. It is believed that purchase intention is related to behavior habits, which is an indicator to measure whether consumers will have further consumption behavior, and can be used to

predict consumers' consumption behavior [12]. Zhou et al. pointed out that consumer behavior is related to the concept of consumption lifestyle. He pointed out that there is a significant internal correlation between demographic and psychological statistical characteristics and consumption behavior. The research shows that the relationship between demographic characteristics, such as gender, age, and education level, and consumption behavior is complex, and whether there is a significant impact between them and consumption behavior is still uncertain [13]. Chun et al. believe that more efficient and accurate prediction should be based on purchase intention, and point out that when consumers have high uncertainty about products and many input factors, it is difficult to make rational decisions, and they often reduce uncertainty by establishing relationships [14]. With the rapid development of database technology and information technology, enterprise managers can use information technology to better understand consumer behavior.

In the research process, the related theoretical research results of camellia oil were comprehensively reviewed and sorted, and the main points were comprehensively sorted out and summarized. Among them, the collection of literature mainly includes a review of the camellia oleifera industry, the background of the camellia oleifera industry based on the large grain and oil safety strategy, and the research status of the camellia oleifera industry. From the perspective of research content, the existing research literature still stays at the qualitative description of the development significance and problems of the Camellia oleifera industry, lacking the support of sufficient survey data and the overall clear description of the current situation of industrial development. The development of Camellia oleifera industry is mainly carried out from the perspective of producers, and there is less research from the perspective of consumers. Therefore, the article starts from the consumption of camellia oil, introduces the thinking framework of the logistic model in the field of camellia oil, focuses on the exploration and analysis of the influencing factors of consumers' purchase intention in coastal areas, establishes the logistic model regression for empirical analysis, and finally proposes the promotion of countermeasures and suggestions for the consumption of camellia oil.

3. Methodology

3.1. Concept and Theoretical Basis of Camellia Oil Consumption and Purchase Intention. Camellia oleifera is a unique woody edible vegetable oil tree species in China. It has a long history of more than 2,300 years of cultivation and utilization in the country. The hilly areas of southern China are the main planting areas. The planting provinces are Hunan, Jiangxi, Fujian, Guangdong, Guangxi, etc. [15]. Camellia seeds can be processed into edible oil. Camellia oil is bright in color, fragrant in taste, and rich in nutrition. It is a high-quality edible oil in China. Camellia oil can also be referred to as camellia oil. The whole body of camellia oil is a treasure. It can be used as lubricating oil and anti-rust oil. At the same time, tea cakes can be used for daily necessities such

as washing and cleaning. The peel can be used to extract tannin extract. It is suitable for planting in warm and humid climates, 16–18 degrees Celsius, and the average annual temperature, and the average temperature during the flowering period is 12–13 degrees Celsius. The annual precipitation should be more than 1000 mm, and it is advisable to plant in the deep acidic soil. Camellia oil, commonly known as camellia oil, is a pure natural high edible vegetable oil made from camellia seeds, with bright color, high fragrance, and high nutritional value [16]. More than 90% of the world's camellia oil products come from China. According to historical records, as early as the first 100 years of the Han Dynasty, China began to plant tea. At present, the area of camellia planting in the country is about 45 million mu, with an annual output of about 1 million tons of camellia seeds and an annual output of over 270,000 camellia oil [17]. The camellia oil industry refers to the concentrated and contiguous planting of camellia oleifera, the comprehensive utilization of camellia oleifera oil, and nutritional healthcare products, skin care products, and other products through intensive and deep processing, forming an industrial chain based on camellia oleifera. Its structure is shown in Figure 1.

General academic understanding: the meaning of consumer behavior is the meaning of consumer purchase, the decision-making process of using consumer goods or receiving services before taking various actions, and determining these actions [18]. From the definition, it can be seen that consumer behavior includes not only all kinds of actions taken to buy, use consumer goods, or receive services, but also the decision-making process before actions. The decision-making process of consumers' final consumption behavior needs to go through a series of comprehensive psychological and thinking activities, which are influenced by advertising, culture, folklore, economy, personal cognition, and other aspects [19].

The planning behavior theory can be traced back to 1963. American scholar Fish Bein. M put forward the multi-attribute attitude theory and analyzed the relationship between attitude and behavior. With the rapid development of the theory of planned behavior, it has been successfully and widely used in many fields of behavior research. According to the planning theory, behavioral intention is the direct factor that determines behavior, while behavioral intention is influenced by three variables: behavioral attitude, subjective norms, and perceived behavioral control. The relationship among these factors is shown in Figure 2.

The theory of consumer purchasing behavior is a theory mainly used in the study of factors affecting consumer cognition and purchase intention. Consumer buying behavior refers to the process activities in which people seek, select, purchase, use, and dispose of products and services to meet their needs and desires, including the subjective psychological activities of consumers and the objective material camellia oil activities. The purchase behavior of consumers is regarded as a decision-making process. Part of this decision-making process can be observed, such as the statistical characteristics of consumers, the behavior of consumers to buy or not to buy, and the specific products

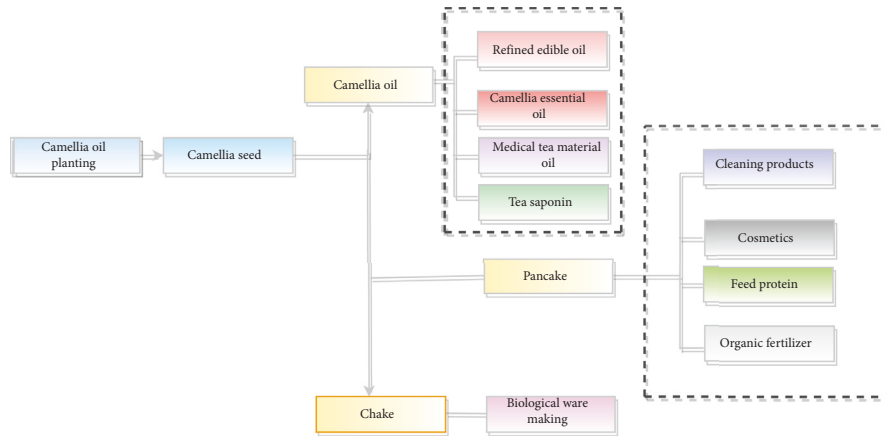


FIGURE 1: Structure of the camellia oil industry chain.

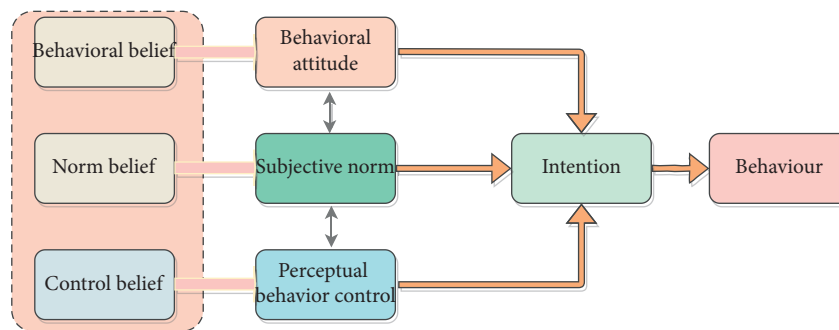


FIGURE 2: The theoretical structure model diagram of planned behavior.

bought by camellia oil. The premise for tea oil consumers to buy tea oil is to have sufficient understanding of tea oil and generate purchase intention. The factors that affect the impact of camellia oil on consumers' purchase of tea oil include the price of tea oil, the degree of understanding of tea oil products, the atmosphere in which consumers use camellia oil, etc. Consumers' understanding of tea oil and their willingness and behavior to buy tea oil involve two aspects: information asymmetry and transaction cost.

In order to confirm the reliability and effectiveness of the questionnaire, this paper uses internal to measure the reliability of the questionnaire and uses SPSS16.0 to analyze the reliability of the observed variables of four potential variables: behavior attitude, subjective norms, perceived behavior control, and purchase intention. It can be seen that Cronbach's value is between 0.656 and 0.837, and the overall Cronbach's value of the questionnaire is 0.801. The questionnaire has good internal consistency. The reliability, validity, and exploratory factors are shown in Table 1.

When analyzing the convergent validity and discriminant validity of the observed variables under the common factor, the factor weighted value in confirmatory factor analysis, also called factor loading, has different criteria for judging factor loading. Some experts suggest that the standardization factor loading should be above 0.3. Some experts suggest that it should be above 0.4, but it is usually less than 1. The article draws on the standard of 0.3 to 1.0; the standard factor loading coefficient of the variable "I buy" is

0.076, the standard factor loading coefficient of the variable "opinions of relatives and friends will affect my purchase" is 0.269, and the criterion "low income level limits my purchases" has a loading factor of 0.295 in the perceived behavior control variable.

This article is mainly based on the theory of consumer behavior, combined with the existing scholars' research on cognitive influencing factors. The selected variables are consumers' personal characteristics, including gender, age, education, personal income, and marital status. The variables of consumer family characteristics are mainly the number of family members, the regional characteristics, that is, whether they come from the main camellia producing areas in the coastal areas, and the level of health care. The variable names, values, meanings, and symbols are shown in Table 2.

This paper expects that among these eight variables, the level of health concern, the characteristics of the place of origin, and the personal monthly income will show a strong correlation with cognition, and they are all positively correlated. One of the major features of camellia oil is that it has high nutritional value and health benefits. Therefore, the more concerned people are about their own health, the more likely they are to be interested in camellia oil, and the more likely they are to know about camellia oil. It is also a very reasonable explanation that consumers in the region have greater exposure to camellia oil than consumers in nonmain producing areas; since the current market price of camellia

TABLE 1: Reliability, validity, and exploratory factor analysis.

Potential variable	Potential variable	Standard load	Cronbach's alpha
Behavioral attitude (AB)	Camellia oil has high nutritional and healthcare value (X_1)	0.577	0.656
	Camellia oil tastes good (X_2)	0.378	
	Camellia oil is clean and sanitary (X_3)	0.468	
	Camellia oil has high cost performance (X_4)	0.635	
	Camellia oil has high quality and relatively reasonable price (X_5)	0.543	
Subjective norm (SN)	National authority certification will affect my purchase (X_6)	0.685	0.658
	Experts' opinions will influence my purchase (X_7)	0.785	
	The information spread by the media will affect my purchase (X_8)	0.541	
	My family's opinions will influence my purchase (X_9)	0.076	
	My friends' opinions will influence my purchase (X_{10})	0.258	
	Income level restricts my purchase (X_{11})	0.269	
Perceptual behavior control (PBC)	Have purchasing autonomy (X_{12})	0.295	0.578
	Can identify the quality of camellia oil (X_{13})	0.502	
	Convenient to buy camellia oil (X_{14})	0.438	
	The certification mark cannot be recognized (X_{15})	0.513	
Buying inclination (BI)	Willing to buy camellia oil (X_{16})	0.815	0.837
	Meet my needs (X_{17})	0.875	
	When purchasing edible oil, camellia oil will be selected (X_{18})	0.422	

TABLE 2: Variable names, values, meanings, and symbols.

Variable classification	Variable name	Value and meaning	Representative symbol
Personal characteristic	Gender	1 = male; 0 = female	N1
	Age	Numerical variable	N2
	Marital status	1 = yes; 0 = no	N3
	Academic degree	1 = primary school and below; 2 = junior high school; 3 = high school	N4
	Personal monthly income	3 = (2000, 3000); 4 = (3000, 4000); 5 = 5000 yuan and above	N5
Family characteristics	Number of households	Numerical variable	N6
Regionalism	Are they from coastal areas?	1 = yes; 0 = no	N7
Attention level to health	Degree of concern	1 = no attention; 2 = occasional attention; 3 = more attention; 4 = very concerned	N8

oil is still relatively high, and it is positioned as a high-end edible oil, the lower the income level, the less likely people will buy high-end edible oil, the less chance they will know about camellia oil.

At present, the coverage of camellia oil in the market is relatively low, and many consumers are unaware of camellia oil, let alone have an understanding of camellia oil. According to the survey, the existing edible oil testing equipment and technology are still unable to monitor the quality and authenticity of camellia oil. If the water content is less than 10%, it is basically difficult to detect. Mixing other oils into camellia oil for profiteering, in a better case, is to use soybean oil, etc., and even worse is to use gutter oil mixed with camellia oil, which will not only disturb the order of the edible oil market, but more importantly, it will threaten the food safety and health of consumers. The efficacy of camellia oil is shown in Figure 3.

At present, many related studies have confirmed that camellia oil has high nutritional and healthcare value. Unsaturated fatty acids are essential fatty acids for human body, which can regulate blood lipids, clear thrombi,

enhance immunity, maintain retina, nourish brain, improve arthritis symptoms, and relieve pain. According to research, it is known that olive oil contains 75%–90% unsaturated fatty acids, while camellia oil contains 85%–97% unsaturated fatty acids, which is even higher than olive oil. In addition, camellia oil also contains linoleic acid, linolenic acid, squalene, tea polyphenols, camellia saponin, camellia saponin E, and other substances, which are of great help to people's health. However, many consumers do not know it. Even if they do, because the specific embodiment of the nutritional value of camellia oil needs a long-term continuous process, it is difficult for consumers who have not eaten camellia oil for a long time to confirm these values. On the one hand, information asymmetry is also one of the obstacles to the development of camellia oil market.

3.2. *Relevant Theorems about the Logistics Model.* In the conventional regression model, the dependent variable is an interval (quantitative) variable, and theoretically it is required to obey the assumption of normal distribution line

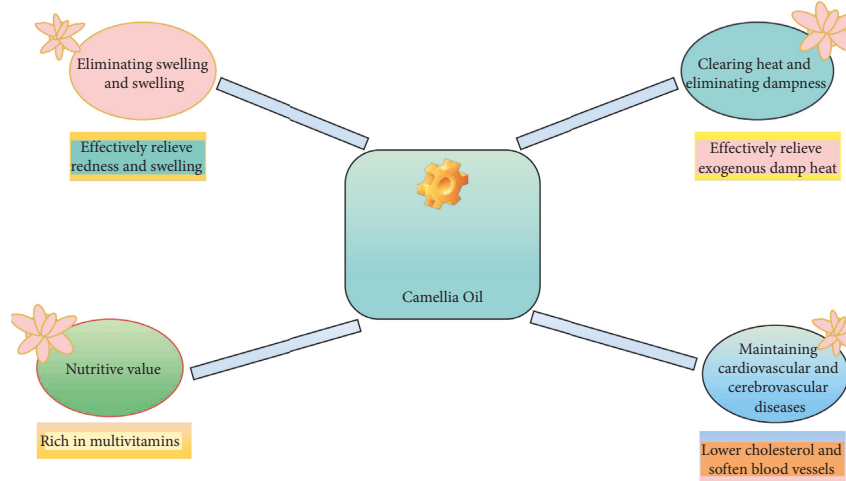


FIGURE 3: Effect map of camellia oil.

(linear, independent, normal, equal variance). However, the main difference between logistic regression model and conventional regression model lies in the different types of dependent variables. Logistic regression model can be used to predict the probability of each classification of a categorical variable. The dependent variable is categorical variable, and the independent variable can be interval variable, categorical variable, or the mixture of interval and categorical variables. According to the different categories of dependent variables, it can be divided into binary logistic regression analysis and multivariate logistic regression analysis. In multivariate logistic regression model, dependent variables can take multiple values, and in binary logistic regression model, dependent variables are binary values.

Let P represent the probability of an event occurring, then its value is $[0, 1]$, and $1 - p$ represents the probability that the event does not occur. Usually the ratio of the probability of a certain result to the probability of not appearing is called the ratio, and some are also translated as the advantage, the ratio, that is, odds = $P/(1 - p)$, whichever is the logarithm $\ln(\text{odds}) = \ln P/(1 - p)$. This process is logit transformation, denoted as $\text{logit}(P)$, then the value range of $\text{logit}(P)$ is $(-\infty, +\infty)$. Taking $\text{logit}(P)$ as the dependent variable, a logistic regression model containing m independent variables is established as follows:

$$\text{logit}(P) = \alpha + \beta_1 x_1 + \cdots + \beta_m x_m. \quad (1)$$

Specifically, the logit model uses the cumulative distribution function of a standardized distribution, or C.D.F. for short, to transform values so that the index is between 0 and 1. Its form is

$$P_i = F(y_i) = F(\beta X_i + \alpha) = \frac{1}{1 + e^{-y_i}} + \frac{1}{1 + e^{-(\alpha + \beta X_i)}}. \quad (2)$$

For a given X_i , P_i represents the probability of a certain choice made by the corresponding individual. Continue to make the following transformation to

$$P_i(1 + e^{-y_i}) = 1. \quad (3)$$

Among them, $X_i (i = 1, 2, \dots, m)$ is the independent variable, and the parameter α in the model is a constant term, which represents the natural logarithm of the ratio (the ratio of the probability of $Y = 1$ to $Y = 0$) when the independent variables are all 0, and the parameter β_i is the regression model of the model. The coefficient represents the change in the natural logarithm value of the odds ratio (OR) caused by an increase in the value of the independent variable by one unit when the values of the other independent variables remain unchanged:

$$e^{-y_i} = \frac{1}{P_i} - 1 = \frac{1 - P_i}{P_i}. \quad (4)$$

Take the reciprocal and then the logarithm to get

$$y_i = \ln\left(\frac{1 - P_i}{P_i}\right). \quad (5)$$

So, we have

$$\ln\left(\frac{1 - P_i}{P_i}\right) = y_i = \alpha + \beta X_i. \quad (6)$$

In the logistic regression model, the dependent variable is the logarithm of a specific selection probability ratio, and its advantage lies in transforming the problem of predicting probability on the $[0, 1]$ interval into the problem of predicting the selection ratio of an event on the real number axis. In fact, the value of $\text{logit}(P)$ takes 0.5 as a symmetrical point and is distributed in the range of 0 to 1, and the corresponding size of $\text{logit}(P)$ is

$$\begin{aligned} P = 0 \quad \text{logit}(P) &= \ln\left(\frac{0}{1}\right) = -\infty; \\ P = 0.5 \quad \text{logit}(P) &= \ln\left(\frac{0.5}{0.5}\right) = 0; \\ P = 1 \quad \text{logit}(P) &= \ln\left(\frac{1}{0}\right) = +\infty. \end{aligned} \quad (7)$$

This shows that the change of the explanatory variable relative to $P_i = 0.5$ has a greater impact on the change of the probability. On the contrary, the change of the X_i value near 0 and 1 relative to P_i has less effect on the change of the probability.

Since the dependent variable is a binary variable, the error of the logistic model should obey the binomial distribution, not the normal distribution. Therefore, the model is actually no longer suitable for parameter estimation by the least squares method in the previous general linear model, and the maximum likelihood method is currently used for parameter estimation.

First, a random experiment with two parameters (α and β) is analyzed, assuming that the model used for estimation is as follows:

$$P_i = \frac{1}{1 + e^{-(\alpha + \beta X_i)}} = \frac{1}{1 + e^{-Y_i}} \quad (8)$$

In the sample, P_i is unobservable, and compared with the value of X_i , only the information that the value of Y_i is most likely to be 0 or 1 can be obtained. The starting point of maximum likelihood estimation is to find the estimated values of sample observations α and β . From the sample, if the first choice happens n times, the second choice happens $N-n$ times. Then, let the probability of choosing the first option be P_i , and the probability of taking the second option be $(1 - P_i)$. Rearrange the sample data so that the first n observations are the first choice, the last $N - n$ observations are the second choice, and the obtained likelihood function is

$$\begin{aligned} L(\alpha, \beta) &= P(y_1, y_2, \dots, y_N) \\ &= P(y_1)P(y_2)P(y_3) \dots P(y_N) \\ &= \prod_{i=1}^n P_i \prod_{i=n+1}^N 1 - P_i. \end{aligned} \quad (9)$$

The maximum likelihood estimators of α and β can be obtained. They are consistent and asymptotically valid, and both are asymptotically normal.

4. Result Analysis and Discussion

In logistic regression analysis, if there is a strong correlation between variables, the regression equation will be taken into account.

Estimation brings difficulties, inaccurate parameters, and unusable models. This study reduces explanatory variables through factor analysis.

At the same time, it will not reduce the information obtained, and eliminate the multicollinearity among variables. Through SPSS statistical software, KMO value and Bartlett sphericity of the items were tested. The results are shown in Figure 4.

The KMO value of this test is 0.720. According to the KMO test standard described by Kaiser, $KMO > 0.7$ is more suitable combined factor analysis. Bartlett's test of sphericity is significant ($P = 0.001$) with an approximate chi-square of 305.691, satisfying conditions for factor analysis. To analyze

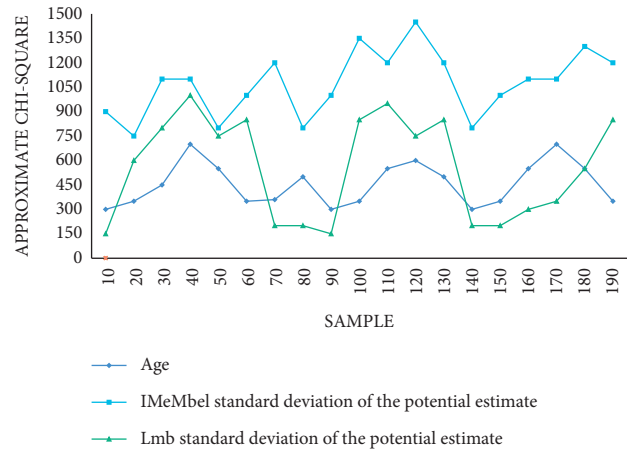


FIGURE 4: KMO value and Bartlett's sphericity test results.

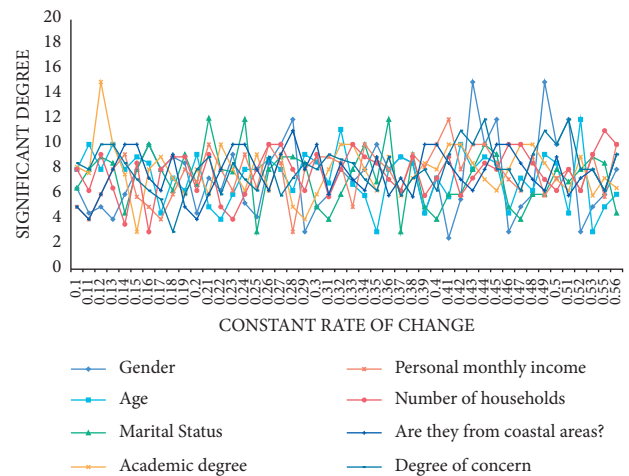


FIGURE 5: Comparison of significance levels with changes in understanding.

the sample data of the coastal area survey, the consumer's understanding of *Camellia oleifera* is used as the dependent variable, the entry method is used in the data processing process, the variables defined in Table 2 are used as the independent variables, the logistic model regression is used for analysis, and the test results are shown in Figure 5.

The observation shows that only gender, age, educational background, personal income, whether the number of family members comes from coastal areas, and consumers' attention to their own health are significant, among which 10% of them show positive correlation, with a coefficient of 0.202. It shows that the more concerned consumers are about their health, the more likely they are to know about tea oil. This result is because tea oil is not only a high-grade edible oil, but also a good nutritional health product. With the improvement of life quality, consumers' health is getting more and more attention. Consumers are no longer troubled by food and clothing, but more about their own health problems. On the one hand, it is related to the law of life, and on the other hand, it is closely related to our usual diet. In the model, the gender variable is significant at 5%, with a coefficient of

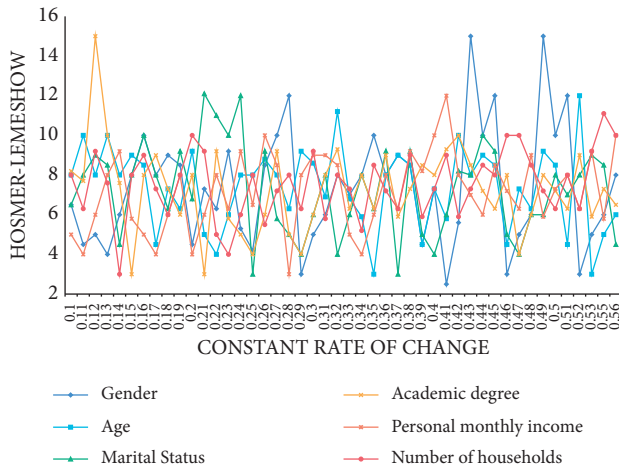


FIGURE 6: Comparison of significance levels after pruning variables.

0.625, which means that male consumers have a higher chance to know about tea oil than female consumers when other variables are constant, which is an unexpected result of the author. In the model, the variable of whether it comes from coastal areas is significant at 2%, with a coefficient of 1.112, which indicates that consumers from main producing areas have a lower chance to know about tea oil than consumers from nonmain producing areas when other variables are constant. This result is contrary to common sense. Generally speaking, consumers from the main camellia oil-producing areas in coastal areas have a greater chance to contact camellia oil, and there should be more opportunities to learn about camellia oil. Cronbach's alpha value is 0.544. Compared with Cronbach's alpha value of a certain item deleted in Table 2, it is found that Cronbach's alpha value can reach 0.612 after removing N7 and N8, which makes the designed scale have a better reliability structure. Therefore, before the model analysis, N7 and N8 are eliminated and the remaining six explanatory variables are selected to analyze the influencing factors of consumers' purchase intention of tea oil, as shown in Figure 6.

After excluding the variables, the coefficient only reflects the direction of change in the regression, so we can study the positive and negative effects of changes in independent variables on consumer behavior. From the perspective of consumers, although most household daily affairs are still men, the decision-makers of daily necessity purchase are still men. There are still differences in shopping concepts between men and women. Men are more likely to be curious about and try new things. Therefore, male consumers of tea oil, a relatively new edible oil, have more opportunities to contact. From the perspective of consumer psychology, women are more willing to buy products that are generally familiar and have relatively stable psychological products with low prices and good taste. The results show that there is not much difference. It shows that with the progress and development of society, women's status in the family has been paid more and more attention and improved. Access to information and understanding of facts is no longer always

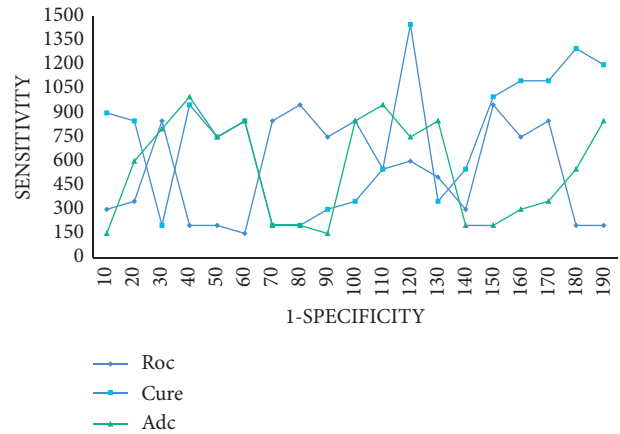


FIGURE 7: Logistic regression prediction model ROC curve.

later than men, as in the past. At the same time, they also have their own thinking, opinions, and decision-making power. The AUC of the prediction model probability is 0.913. According to the ROC curve, the critical value of P is 0.15, which is ideal. Its willingness to buy and attention are 84.44% and 75.6%, respectively.

The ROC curve of the prediction probability p of the logistic regression prediction model is shown in Figure 7.

With the increase of academic qualifications and higher education level, consumers' cognition of life is different. The higher the education level, the more concerned you may be about your own health and the more eager you are to improve your quality of life. Tea is a fast-moving consumer product. When consumers consider whether to buy it or not, it is based on their consumption preferences. Consumers with high academic qualifications are more inclined to buy goods with high nutritional value and good quality. In addition, consumers with a high degree of education, on the other hand, should get a better job treatment, and generally, their income level is relatively higher, so their willingness to pay and purchasing power are also relatively higher, so price is not their primary consideration.

The experimental results of this chapter show that the research model of influencing factors of purchasing intention based on logistic algorithm is used to analyze the coastal areas of Chashan oil, and it is found that the factors influencing consumers' purchasing intention are positively related to education and personal monthly income, and negatively related to gender, among which the variable "education" is significant above 1%, with a positive correlation coefficient of 0.864, and personal income is significant above 5%, with a coefficient of 0.762. There is a negative correlation between sex, with a coefficient of -0.259 , which indicates that education can promote consumers' willingness to buy tea oil with other variables unchanged, and the higher the education, the more likely consumers are to buy tea oil. In addition, in the same regression prediction model, the regression prediction efficiency of this model is better. Generally speaking, this model has certain superior performance.

According to the results of the above analysis, this paper puts forward some effective suggestions to promote the

market demand of camellia oil. First, we can increase publicity and raise public awareness. Compared with olive oil with the same positioning, the market share of tea oil is low, and the market awareness is low. Awareness is the premise of purchasing tea oil. Only by improving consumers' awareness of tea oil can the market demand of tea oil be increased and consumers' purchase of tea oil be promoted. In order to improve consumers' demand for tea oil, the government and enterprises should fully cooperate, make use of various media, popular science bases, and other forms, vigorously publicize the excellent characteristics and unique effects of tea oil in various public places as much as possible, guide scientific and healthy eating habits and rational consumption, and create favorable market conditions for the development of *Camellia oleifera* industry. It is necessary to actively support the development of leading enterprises in various places, continuously improve the ability of product research and development and scientific and technological innovation, vigorously develop functional tea oil products that meet the needs of domestic and foreign markets, and make tea oil rank among the international high-grade oils from regional small-variety edible oils, so as to enhance its popularity and market share, and make tea oil everywhere in the edible oil market. Second, at the same time, when promoting tea oil, there should be focused publicity. At present, tea oil publicity focuses on "health." Some publicity has the effect of beautifying, some publicity has the effect of preventing "three highs," some publicity focuses on regulating immunity, etc., which makes the publicity confusing. Consumers' recognition of tea oil is not high, and their memory is not deep. However, there are many edible oils, including olive oil, on the market that focus on health. Focus on the healthcare value of tea oil, and publicize that it can prevent "three highs," promote lactation and growth, and prevent atherosclerosis. Third, financial and technical support should be increased, and an effective cooperation mechanism can be formed between enterprises. For example, some enterprises have advantages in the cultivation and planting of *camellia oleifera*, some enterprises have done a good job in pressing *camellia oleifera* seeds to make primary tea oil, and some tea oils have done a good job in leaching and deodorizing tea oil. Then, these enterprises can get together, and each enterprise can work together with different divisions of labor, from one link to another. In this way, it can not only avoid the small development of the enterprise itself, but also each can spend more energy in each link to make it more refined and better, and the finished tea oil produced by the company will be better and more labor-saving than that produced by itself from beginning to end.

5. Conclusions

Under the background that the state and the government vigorously promote the development of *Camellia oleifera* industry, in order to continuously expand the market demand on the premise of ensuring the steady progress of the *Camellia oleifera* market, it is necessary to form a relative balance between the supply and demand of *Camellia*

oleifera. Due to the good planting and processing of *Camellia oleifera*, the development momentum is sufficient, and the supply capacity of *Camellia oleifera* is good, but the market demand capacity does not form an effective balance with it. Under such circumstances, if the tea oil supply continues to increase but the tea oil market demand cannot be improved, the healthy development of the tea oil industry will be affected. Through logistic regression model, this paper finds that the factors that affect consumers' understanding of tea oil include gender and age. The positive correlation is gender and health concern, and the negative correlation is age. Based on the research model of influencing factors of purchase intention established by logistic algorithm, this paper analyzes the coastal areas of Chashan oil. It is found that the factors that affect consumers' purchase intention are positively related to education and personal monthly income, and negatively related to gender. For the variable "academic history," it is significant at 1% and positively related, with a coefficient of 0.864. For personal income, it is significant at 5%, with a coefficient of 0.762, and negatively related to gender. The coefficient is -0.259 , indicating that education can promote consumers' willingness to buy tea oil when other variables remain unchanged. Consumers with higher education are more likely to buy tea oil. In addition, in the same regression prediction model, the regression prediction efficiency of this model is better. In general, this shows that this model has certain superior performance.

Data Availability

The data used to support the findings of this study are available from the author upon request.

Conflicts of Interest

The author declares no conflicts of interest.

Acknowledgments

This work was supported by 2020 Carey College "Outstanding School-Running Characteristics" Special Project (Engineering and Practical Project): Research on Value Cognition and Purchase Behavior of *Camellia* Oil in Southeast Guizhou—Based on Consumer Survey (Project No.: 2020gkzs02); 2020 Carey College Special Project "Response, Governance and Impact of New Coronary Pneumonia Epidemic and Other Public Health Events": Empirical Investigation and Research on the Impact of New Coronary Pneumonia on Key Industries in Guizhou (Project No.: YQZX201902); and 2019 Special Project of "Doctoral Professor Service Group" of Carey College: Investigation and Research on *Camellia* Oil Industry in Qiandongnan Prefecture (Project No.: BJFWT201902).

References

- [1] M. Wu, M. Du, H. Wen, W. Q. Wang, J. Tang, and L. R. Rhen, "Effects of n-6-enriched soybean oil, enriched olive oil and camellia oil on body weight and cardiometabolism in Chinese

- women: a 3-month double-blind randomized control Feeding Test,” *Food and Function*, vol. 2022, no. 6, pp. 98–105, 2022.
- [2] Li Deng, F. Que, H. Wei, G. Xu, X. Dong, and H. Zhang, “Solubilization of tea seed oil in a food-grade water-dilutable microemulsion,” *Plos One*, vol. 10, no. 5, Article ID e0127291, 2015.
- [3] M. Nakpathom, B. Somboon, N. Narumol, and R. Mongkhorrattanasit, “Fruit shells of *Camellia oleifera* Abel as natural colourants for pigment printing of cotton fabric,” *Pigment & Resin Technology*, vol. 46, no. 1, pp. 56–63, 2017.
- [4] L. Zhou, X. Wang, and L. Wang, “Genetic diversity of *Camellia oleifera* germplasm resources revealed by analysis,” *International Journal of Biomathematics*, vol. 8, no. 5, Article ID 150426190942008, 2015.
- [5] S. Jiang and L. Hong, “The first report of anthracnose in *Camellia oleifera*,” *Plant Diseases*, vol. 12, no. 2, 2017.
- [6] L. Deng, Z. Deng, and N. Jiang, “Analysis of physicochemical properties and nutritional components of *Camellia oleifera* seed oil at different refining stages,” *Food Science*, vol. 2015, no. 6, pp. 69–85, 2015.
- [7] H. O. Ahmed, C. M. Wang, A. A. Mariod, and T. A. Hammada, “*Camellia* oil saponins: solid phase extraction and its effect on mice blood and organs,” *Grasas Y Aceites*, vol. 71, no. 2, p. 357, 2020.
- [8] S. Zhong and Luo, “Preparation of tea polyphenol palmitate-stabilized camellia oil-based W/O emulsion: construction of camellia oil as a potential solid fat substitute,” *Food Chemistry*, vol. 2019, no. 3, pp. 68–90, 2019.
- [9] G. Zhu, H. Liu, and W. Li, “Research on storage quality and storage conditions optimization of *Camellia oleifera* seeds,” *Chinese Journal of Agricultural Engineering/Journal of Chinese Agricultural Engineering Society*, vol. 36, no. 2, pp. 301–311, 2020.
- [10] J. Han, R. Sun, X. Zeng et al., “Rapid classification and quantification of camellia (*camellia oleifera* Abel.) oil blended with rapeseed oil using FTIR-ATR spectroscopy,” *Molecules*, vol. 25, no. 9, p. 2036, 2020.
- [11] T. Zhou, Y. Lu, and Inbalajie, “Enhancement of antioxidant activity and cardiovascular protection of hamsters by camellia oil and soybean-camellia mixed oil,” *Nutrition*, vol. 2018, no. 3, pp. 65–78, 2018.
- [12] Y. Xiang, J. Lu, F. Li et al., “[Bactericidal effect of ozonated camellia oil on *Staphylococcus aureus* in vitro],” *Journal of Central South University (Medical Edition)*, vol. 43, no. 2, pp. 139–142, 2018.
- [13] X. Zhou, S. Jiang, D. Zhao et al., “Changes in physicochemical properties and protein structure of surimi fortified with camellia oil,” *LWT - Food Science and Technology*, vol. 84, Article ID S0023643817301718, 2017.
- [14] L. Chun, C. Lin, W. Tao et al., “Potential distribution prediction and evaluation of suitable soil conditions for *Camellia oleifera* in China,” *Forest*, vol. 9, no. 8, p. 487, 2018.
- [15] D. Singhal, S. K. Jena, and S. Tripathy, “Factors influencing consumers’ willingness to purchase remanufactured products: a systematic review and meta-analysis,” *International Journal of Production Research*, vol. 57, pp. 1–11, 2019.
- [16] Q. He, Y. Duan, R. Wang, and Z. Fu, “Factors affecting consumers’ purchase intention of eco-friendly food in China: the evidence from respondents in Beijing,” *International Journal of Consumer Studies*, vol. 43, no. 5, pp. 457–470, 2019.
- [17] X. Wang, F. Pacho, J. Liu, and R. Kajungiro, “Factors influencing organic food purchase intention in developing countries and the moderating role of knowledge,” *Sustainability*, vol. 11, no. 1, p. 209, 2019.
- [18] P. Duarte and S. Silva, “The role of consumer reason identification and attitude in reason-related product intentions,” *International Marketing Review*, vol. 6, 2018.
- [19] K. Zhu, “The mediating effect of attitude on internal and external factors affecting Chinese consumers’ intention to buy organic food,” *Sustainability*, vol. 10, 2018.

Research Article

Financial Shared Services Empower the Real Economy: The Evidence from China

Xue Chen 

School of Accounting, Yunnan University of Finance and Economics, Kunming 650221, China

Correspondence should be addressed to Xue Chen; 201803110020@stu.ynufe.edu.cn

Received 7 July 2022; Revised 19 July 2022; Accepted 5 August 2022; Published 31 August 2022

Academic Editor: Wei Liu

Copyright © 2022 Xue Chen. This is an open access article distributed under the Creative Commons Attribution License, which permits unrestricted use, distribution, and reproduction in any medium, provided the original work is properly cited.

As a product of digital technology, financial shared services can be deeply integrated into enterprise operation and management, which is significant to accelerate the financial transformation of real enterprises and achieve high-quality development. Based on this, this paper examines whether and how financial shared services empower the real economy, using data from listed companies in China from 2008 to 2017 as a sample. The research results show that financial shared services can significantly improve enterprise value and thus empower the real economy, and the optimization of operational efficiency is an important path for financial shared services to empower the real economy. Further research finds that the empowering effect of financial shared services on the real economy mainly exists in enterprises with many subsidiaries, large scale, and high labor intensity. This paper not only bridges the gap between financial shared services and micro-enterprise related research but also provides references and lessons for how to implement financial shared services in the real economy.

1. Introduction

In the current era of digital economy, information technologies such as AI, blockchain, cloud computing, data tech, edge computing, and so on are changing rapidly and continue to create new increment and new space for the real economy. The support and empowerment of science and technology innovation to the real economy will promote the entry of science and technology achievements into the main battlefield of economy and society and further form a powerful “new dynamic energy” for high-quality development. Finance shared service center (FSSC or finance sharing), as an innovative financial management model, is a specific application of information technology in the field of finance [1], which makes finance continuously paperless, online, and automated. It plays an important role in reducing corporate costs [2], strengthening group control [3], refining management in real time [4], improving internal resource allocation [5], and promoting the implementation of corporate strategies [6]. Facing the globalized market with intensified competition and complex and changing business

environment, how to enhance sustainable competitiveness in an uncertain environment has become an important issue of concern for enterprises. Financial shared service, with its stronger resilience [7], faster and more timely response capability [8], more accurate forecasting and risk control capability [9], and self-reinventing management capability [10] to cope with uncertainty, enables enterprises to develop sustainably and with high quality. The research reports on China Huawei and Haier Group show that the shared services have improved the efficiency of these enterprises and promoted the standardization of business processing processes. At the same time, the shared service center has become a data center for these enterprises, enabling financial decisions and business strategies to be more closely aligned with corporate reality and effectively improving operational efficiency [2, 4].

With the continuous adjustment of accounting, taxation, and other related policies in China, such as electronic invoices and electronic files, which prompted the issuance, delivery, and flow of invoices and the management of accounting files to undergo a sea change, more and more large

enterprise groups are implementing financial shared services. By the end of 2020, there were more than 1,000 shared service centers in China [1]. This shows that financial shared services are being accepted or applied by more and more Chinese enterprises, helping them to improve their financial management and achieve financial digital transformation. Can financial shared services truly empower the real economy? And how will it empower the real economy? Existing studies on financial shared services mainly focus on the motivation of its implementation [11–13], key factors [14–16], and impact on company performance [17, 18] but have not yet systematically explored the impact of financial shared services on the operation of the real economy. As financial shared services will have a direct impact on the operation management of the enterprise such as accounts receivable and payable, cash management, cost and expense management, asset turnover, and so on, we chose the perspective of operation management as the entry point of the study, in an attempt to open the black box of how financial shared services empower the real economy, in order to further enrich the research related to financial shared services and microeconomics and to provide possible references and lessons for the high-quality operation of the real economy.

In view of this, this paper takes the data of Shanghai and Shenzhen A-share listed companies from 2008–2017 as a sample and explores the impact of financial shared services on the real economy using operation management as a research perspective. Compared with previous studies, the contributions of this paper are mainly in the following aspects. First, it makes up for the lack of empirical studies related to financial shared services. Existing studies on financial shared services mainly use case studies, questionnaires, and literature induction to construct a framework [16, 18–20]. There are relatively few empirical studies based on credible financial data of listed companies. This paper collects financial shared services data by hand to conduct a large sample test, and the findings are more convincing. Second, studies have shown that the effects of financial shared services may vary among different enterprises and industries [20]. This paper not only enriches the research on the impact of financial shared services but also makes the research on financial shared services more relevant and applicable. Third, it deepens the research on financial shared services and the real economy. Existing studies have not explored the impact of financial shared services on the real economy in depth. This paper analyzes in depth the impact of financial shared services on various aspects of enterprise operation and management from the operational management practices of real enterprises, involving various value chain aspects such as production, operation, inventory, and finance, revealing the black box of the impact of financial shared services on the real economy from the theoretical and practical levels, which is a breakthrough compared with previous studies. The research in this paper not only expands the research related to financial shared services and microeconomics and further enriches the theoretical system of financial shared services but also provides reference for how enterprises can better carry out financial shared services.

2. Literature Review and Research Hypothesis

2.1. Impact of Financial Shared Services on the Real Economy. Based on the resource-based view and the dynamic capability view, from a strategic perspective, a firm is a collection of various resources that are valuable, scarce, difficult to replicate, and difficult to replace, and if the firm has the ability to leverage and develop these resources, it can gain a sustained competitive advantage and create superior performance [21, 22]. While companies need to remain competitive through the constant pursuit of efficiency gains and cost reductions, forward-looking organizations gain competitive advantage by making organizational structures flexible and resilient [23].

Financial shared service is a valuable, scarce, hard-to-replicate, and hard-to-replace strategic resource for enterprises. Some studies have shown that financial shared services have significantly improved the business processing efficiency and financial management capabilities of enterprises through organizational changes and process reengineering and enhanced the market competitiveness of enterprises [5, 7, 20]. Relying on information technology, financial shared services centralize the same and repeatedly set up financial processes among different internal business units to an independent sharing center for processing [12]. The scope of business focuses on financial accounting processes that are less relevant to management decisions, occur frequently, and are easily standardized, mainly including expense reimbursement, purchase to payment, order to receipt, cost accounting, fixed asset accounting, general ledger to report, and so on [2, 13]. The impact of financial shared services on entity enterprises is mainly reflected in the following aspects.

Firstly, financial shared services provide unified, professional, and standardized efficient services for internal customers through the IT system. Through the optimization of business processes and rules, redundant, repetitive, and non-value-added operations are eliminated, and business operations are refined, standardized, or even simplified, realizing a reduction in personnel without an increase in business volume, which is conducive to achieving the purpose of enhancing organizational integration of resources, improving efficiency, and reducing costs [6, 11]. Secondly, through the IT system, the same standard operation process is adopted for all subsidiaries to achieve cross-regional and cross-departmental data integration, which makes data aggregation and analysis no longer time-consuming and laborious and can provide standardized financial analysis reports for each information demander and provide all-round management data for the group's strategic finance and business finance through deep digging of financial data [24] to support management decisions and promote the digitalization of the enterprise [8]. The centralization of finance, human resources, information management, and other functions in the shared service center can help enterprises establish new businesses faster and improve their flexibility in adapting to the market, while the centralization of professional staff can help the shared center establish a knowledge base system that meets its needs and

improve the concentration and efficiency of knowledge utilization [7]. Finally, financial shared services free managers from the complicated non-core business, which helps them focus more on the company's core business and can provide services quickly for the newly established subsidiaries or acquired companies of the enterprise [25], all of which can greatly enhance the integration and analysis capabilities of the enterprise. Based on the above analysis, this paper proposes the following hypothesis.

Hypothesis 1. Financial shared services can enhance enterprise value.

2.2. The Path Mechanism of Financial Shared Services to Empower the Entity. The fundamental goal of the financial shared services model is to reduce the cost and strengthen the management of the enterprise [2, 4], creating more revenue for the enterprise. At the business accounting level, financial shared services drive business and process changes to a certain extent [1], bringing significant changes to the enterprise's settlement management and tax management [9]. In terms of accounts receivable and payable, the integration of business and finance not only enables business and finance to interoperate, making finance staff understand business better and reducing unnecessary troubles in payment and collection, but also facilitates the finance department to analyze business data and provide strong support for business development at the tactical or strategic level. It also enhances the integration and automation of invoicing process, realizes automatic payment according to the billing period, reduces payment links, realizes smooth collection and payment in the unified settlement cycle and capital security, reduces unnecessary occupation of funds, and helps shorten cash and business cycles. In terms of cost and expense, the information system based on the close connection with business scenarios supports the front management of cost and expense, which can track and dynamically respond to all operational activities of the enterprise and eliminate and reduce non-value-added effects, thus achieving the purpose of reducing personnel cost [25] and improving efficiency.

At the level of operation management, through process reengineering and information system integration, the integration of business and finance makes finance extend to the front end of business (including procurement, suppliers, and customers), breaks the boundary between accounting and business and accounting and external stakeholders, makes the enterprise organically integrate with external customers, suppliers, and markets, integrates the enterprise's internal procurement, R&D, production, and sales, and directly generates financial data from production activities. Generate financial data, directly transform material activities in physical form into capital activities in value form, and then realize real-time reflection of logistics, capital flow, work flow, and information flow [7], which can not only provide enterprises with a large amount of information, enable them to effectively control and manage the whole business process, and improve the efficiency of resource

utilization but also realize the sharing, real-time control, and timely collection of internal and external value chain information [26], which is beneficial to strategic decision making of the enterprise. Based on the above analysis, this paper proposes the following hypothesis.

Hypothesis 2. Financial shared services enhance enterprise value by optimizing operational efficiency.

3. Study Design

3.1. Variable Design. The explanatory variable is firm value. This paper uses three indicators, return on total assets (ROA), return on net assets (ROE), and Tobin's Q (Tobin), to measure enterprise value. The explanatory variable is financial shared service, which takes the value of 1 if the listed company has implemented financial shared services and 0 otherwise. In this paper, the following steps were taken to determine whether the listed companies had implemented financial shared services: first, the keywords "shared services" and "financial shared services" were extracted from the annual reports of listed companies in China for screening; second, the relevant text in the annual reports, the reports on the company's website, etc. were carefully read, and the research reports on the sharing sector in China in the past years were combined to check whether the listed companies had established financial shared services service centers.

The intermediate variable is operational efficiency, and since the core business processes of enterprises in production and operation include procurement, production, inventory, sales, and so on, which involve the management of assets, operations, personnel, and other aspects, this paper selects operating cost ratio (Cost), total asset turnover ratio (TATR), current asset turnover ratio (CATR), accounts receivable turnover ratio (ARTR), accounts payable turnover rate (APTR), inventory turnover days (ITD), business cycle (Bcycle), cash cycle (Cash), and personnel efficiency (Tfp) as the measures of operational efficiency.

The control variables mainly include firm size (Size), gearing ratio (Lev), business growth rate (Growth), firm age (FmAge), nature of ownership (Soe), equity concentration (Top1), proportion of independent directors (Ind), dual position (Dual), board size (Board), and Lerner index (Pcm) [16]. In addition, year and industry dummy variables are introduced in this paper to control for year and industry related effects, respectively.

These variables are defined as shown in Table 1.

3.2. Sample Selection and Data Sources. China implemented the shareholding reform in 2006, and relatively few companies implemented financial shared services in 2007 due to the financial crisis. Therefore, the sample of this paper is selected from A-share listed companies from 2008 to 2017, excluding financial and insurance companies and ST and ST* companies, and a total of 422 samples of Chinese listed companies that implemented financial shared services are obtained. Further excluding the samples with incomplete

TABLE 1: Main variables and their specific definitions.

Variable type	Variable name	Variable symbols	Variable values and method descriptions
Explained variables	Total net asset margin	ROA	Net profit/total assets
	Return on net assets	ROE	Net income/net assets
	Tobin's Q value	Tobin	Company market value/book value
Explanatory variables	Financial shared services	FSSC	If the listed company is implementing financial shared services, the value is 1; otherwise, it is 0
Intermediate variables	Operating cost ratio	Cost	Operating costs/operating revenue
	Total assets turnover ratio	TATR	Operating income/average balance of total assets
	Current asset turnover ratio	CATR	Operating income/average balance of current assets
	Accounts receivable turnover ratio	ARTR	Operating income/(net notes receivable + net accounts receivable)
	Accounts payable turnover ratio	APTR	Operating costs/average balance of accounts payable
	Inventory turnover days	ITD	360/(operating cost/average inventory balance)
	Business cycle	Bcycle	Days of turnover of accounts receivable + days of turnover of inventories
	Cash cycle	Cash	Days of turnover of accounts receivable + days of turnover of inventory - days of turnover of accounts payable
	Personnel efficiency	Tfp	Borrowing from Lei Yu and Guo Jianhua's calculation to measure employee efficiency
Control variables	Company size	Size	Natural logarithm of total assets
	Gearing ratio	Lev	Total liabilities/total assets
	Business growth rate	Growth	(Current amount of operating income - previous amount of operating income)/(previous amount of operating income)
	Company age	FmAge	The year in which the company is in minus the year in which it is listed
	Nature of ownership	Soe	The value is 1 if it is state-owned enterprise; otherwise, it is 0
	Shareholding concentration	Top1	Percentage of shareholding of the largest shareholder
	Percentage of independent directors	Ind	Number of independent directors/number of board of directors
	Two jobs in one	Dual	The value is 1 if the board of directors and the general manager are combined; otherwise, it is 0
	Board size	Board	Natural logarithm of the total number of board members
Lerner index	Pcm	Lerner index, measured by (operating revenue - operating costs - selling expenses - administrative expenses)/operating revenue; the smaller the Pcm, the smaller the competitive position of the company	

relevant financial data, a total of 404 samples with financial shared service implementation were obtained. The financial shared services data were mainly obtained from Sina Finance, annual reports of listed companies, China Shared Services Research Report, and the website of International Financial Shared Services Management Association, etc. The financial data were mainly obtained from Wind database and CSMAR database. In this paper, companies that implemented financial shared services were used as the experimental group, and in order to maintain the comparability of samples, companies that did not implement financial shared services were selected as the control group through the PSM one-to-one with put-back matching method, so that the companies in the treatment group and the control group were as similar as possible in terms of total return on assets, company size, growth, industry, corporate governance, etc. A total of 14,865 samples were obtained, including 404 in the experimental group and 14,461 in the control group. Table 2 shows the descriptive statistics of the sample matching results. From the comparison results of the

matched samples, the p values of the two groups of samples in the experimental group and the control group are no longer significant after matching, i.e., no significant differences are achieved in terms of asset size, growth, capital structure, corporate governance, product market competition, etc. This indicates that the two groups of samples are equally likely to implement financial shared services or not, i.e., a rational matching result is achieved.

The distribution of the sample is shown in Table 3. It can be seen that the industries implementing financial shared services are mainly concentrated in manufacturing, wholesale, and retail industries, among which the industry with the most implementation is manufacturing, accounting for 60.19%. The next industry is the wholesale and retail industry, accounting for 11.85%. It can be seen that the companies implementing financial shared services are mainly concentrated in labor-intensive industries. This is mainly due to the fact that the scope of financial shared services business is focused on financial accounting processes that are less relevant to management decisions, occur

TABLE 2: Descriptive statistics of matching results.

Variables	Matching process	Experimental group	Control group	Deviation rate (%)	Deviation reduction (%)	T value	p value
Size	Before matching	23.597	21.983	121.000	97.500	26.40	0.001
	After matching	23.597	23.557	3.000		0.390	0.696
Lev	Before matching	0.504	0.433	35.300	99.000	6.720	0.001
	After matching	0.504	0.505	-0.400		-0.050	0.958
Growth	Before matching	0.203	0.219	-3.200	-113.500	-0.580	0.564
	After matching	0.203	0.236	-6.700		-0.910	0.365
FmAge	Before matching	12.441	9.344	48.500	89.400	9.580	0.001
	After matching	12.441	12.767	-5.100		-0.730	0.465
Soe	Before matching	0.488	0.411	15.400	77.300	3.090	0.002
	After matching	0.488	0.470	3.500		0.490	0.623
Top1	Before matching	39.174	35.370	24.000	90.800	5.060	0.001
	After matching	39.174	38.825	2.200		0.300	0.764
Ind	Before matching	0.384	0.372	21.500	68.300	4.610	0.001
	After matching	0.384	0.388	-6.800		-0.850	0.395
Dual	Before matching	0.171	0.239	-16.900	81.800	-3.180	0.001
	After matching	0.171	0.183	-3.100		-0.460	0.645
Board	Before matching	2.194	2.151	21.800	91.900	4.340	0.001
	After matching	2.194	2.191	1.800		0.240	0.808
Pcm	Before matching	0.103	0.104	-0.300	-7313.600	-0.050	0.963
	After matching	0.103	0.031	23.700		0.650	0.517

TABLE 3: Timing and industry of financial shared service implementation in sample companies.

	2008	2009	2010	2011	2012	2013	2014	2015	2016	2017	Total
Manufacturing	8	12	13	17	18	20	26	29	44	56	243
Wholesale and retail trade	1	1	1	3	5	5	5	6	9	14	50
Information transmission, software, and information technology services	0	1	1	1	2	3	4	6	8	12	38
Construction	0	0	0	0	1	2	2	3	5	7	20
Transportation, storage, and postal services	0	0	0	0	1	1	2	2	3	4	13
Real estate	0	0	0	1	1	1	2	2	2	4	13
Mining	0	0	0	0	0	0	0	0	3	4	7
Electricity, heat, gas, and water production and supply industry	0	0	0	0	0	0	0	1	3	2	6
Culture, sports, and entertainment	0	0	0	0	0	0	0	1	2	2	5
Leasing and business services	0	0	0	0	0	0	1	1	1	1	4
General industry	0	0	0	0	0	0	0	0	1	1	2
Water, environment, and public facilities management industry	0	0	0	0	0	0	0	0	0	1	1
Health and social work	0	0	0	0	0	0	0	0	0	1	1
Agriculture, forestry, animal husbandry, and fishery	0	0	0	0	0	0	0	0	0	1	1
Total	9	14	15	22	28	32	42	51	81	110	404

frequently, and are easily standardized. In terms of implementation time, the number of implemented companies has been increasing year by year since 2014, with an average annual increase of 25%.

3.3. *Model Setting.* In order to investigate the impact of financial shared services on the real economy and the mechanism of the impact, the following regression model is developed:

$$\text{Performance} = \alpha_0 + \alpha_1 \text{FSSC} + \sum \text{Control} + \sum \text{Industry} + \sum \text{Year} + \lambda, \tag{1}$$

$$\text{Operation} = \beta_0 + \beta_1 \text{FSSC} + \sum \text{Control} + \sum \text{Industry} + \sum \text{Year} + \eta, \tag{2}$$

$$\text{Performance} = \lambda_0 + \lambda_1 \text{FSSC} + \lambda_2 \text{Operation} + \sum \text{Control} + \sum \text{Industry} + \sum \text{Year} + \mu. \tag{3}$$

In the model, Control represents the control variable. According to the test procedure recommended by Wen et al. [27], in the first step, model (1) is used to test the effect of the implementation of financial shared services on firm value and examine α_1 . The first step is to examine whether the effect of financial shared services on firm value is significant, and if so, the effect is considered as mediating effect; otherwise, the effect is considered as masking effect. Examine α_1 . If it is significant, the model is based on the mediating effect; otherwise, the model is based on the masking effect. In the second step, test model 2 for β_1 and model 3 for λ_2 in turn. If both of them are significant, then the indirect effect is

TABLE 4: Descriptive statistics for grouping of main variables.

	Average value		Diff	Median		Diff
	FSSC = 1	FSSC = 0		FSSC = 1	FSSC = 0	
ROA	0.06	0.05	0.01	0.05	0.04	0.01
ROE	11.23	8.83	2.40***	9.9	8.4	1.50***
Tobin	1.79	2.37	-0.58***	1.15	1.77	-0.62***
Cost	0.72	0.73	-0.01	0.75	0.76	-0.01
TATR	0.89	0.67	0.22***	0.76	0.56	0.2***
CATR	1.72	1.33	0.39***	1.47	1.06	0.41***
ARTR	37.01	31.87	5.15	4.57	4.71	-0.14
APTR	6.08	8.57	-2.48***	4.76	4.97	-0.21
ITD	132.6	244	-111.40***	76.88	101.8	-24.92***
Bcycle	201.7	322.8	-121.04***	137.8	185.4	-47.6***
Cash	100.64	230.81	-130.17***	59.48	108.91	-49.43***
Tfp	1.17	0.1	1.07***	1.12	0.05	0.07***

Note. After we compared the group differences in asset size between the experimental and control groups, the test results showed that the asset size of the experimental group was significantly larger than that of the non-implemented group at 1% level, thus causing Tobin of the experimental group to be lower than that of the control group. *T* values are in brackets; ***, ** and * indicate $p < 0.001$, $p < 0.01$ and $p < 0.05$, respectively.

significant and go to the third step; if at least one of them is not significant, then use the Bootstrap method to test $H_0: \beta_1\lambda_2 = 0$; if significant, then the indirect effect is significant; otherwise, the indirect effect is not significant; stop the analysis; In the third step, test the model 3 for λ_1 . If it is not significant, it means that there is only a mediating effect; if it is significant, the direct effect is significant, and then compare $\beta_1\lambda_2$ and λ_1 . If the symbols are in the same direction, it indicates a partial mediation effect, and if they are in different directions, it indicates a masking effect.

4. Empirical Results and Analysis

4.1. Descriptive Statistical Analysis. Table 4 shows the results of descriptive statistics for the grouping of the main variables, and the results show that the mean or median of enterprises implementing financial shared services (experimental group) and enterprises not implementing financial shared services (control group) is significantly different from each other, except for ROA, Cost, and ARTR, which are not significantly different, i.e., ROE, TATR, CATR, and Tfp are significantly greater in the experimental group than those in the control group, while ITD, APTR, Bcycle, and Cash are significantly lower than those of the non-implemented group, indicating that the enterprises implementing financial shared services have higher total asset turnover, current asset turnover, accounts receivable turnover, and personnel efficiency, while inventory turnover days, accounts payable turnover, business cycle, and cash cycle are lower. The above indicators initially reflect that the enterprises implementing financial shared services have stronger asset management capability, higher operational efficiency, and thus higher overall value. Thus, the overall value is higher. However, Tobin of the implemented group is lower than that of the unimplemented group, which is inconsistent with our expectation. This is mainly due to the fact that most of the companies implementing financial shared services are large-scale enterprises, and the asset growth ability of large-scale enterprises is often slower than that of small-scale enterprises.

TABLE 5: Impact of financial shared services on the real economy.

	(1) ROA	(2) ROE	(3) Tobin
FSSC	0.605*** (2.66)	1.387*** (3.14)	0.242*** (3.34)
Size	0.802*** (9.58)	1.587*** (10.31)	-0.458*** (-26.17)
Lev	-10.705*** (-18.43)	-6.732*** (-6.39)	-2.902*** (-27.87)
Growth	1.395*** (10.90)	2.911*** (12.43)	0.349*** (9.52)
FmAge	0.011 (1.31)	0.030** (2.01)	-0.001 (-0.21)
Soe	-0.892*** (-8.58)	-1.783*** (-8.77)	-0.319*** (-10.90)
Top1	0.025*** (9.69)	0.046*** (9.26)	0.004*** (4.60)
Ind	-2.803*** (-3.93)	-6.686*** (-4.70)	1.790*** (6.65)
Dual	0.044 (0.50)	0.090 (0.55)	0.140*** (4.13)
Board	0.334* (1.68)	-0.106 (-0.26)	0.147** (1.99)
Pcm	7.463*** (2.75)	12.675*** (2.75)	0.913*** (2.77)
_Cons	-9.879*** (-7.34)	-24.281*** (-9.48)	11.509*** (32.76)
<i>N</i>	14865	14865	14865
Adj. R^2	0.330	0.216	0.484
<i>F</i>	132.414	54.597	259.252

T values are in brackets; ***, ** and * indicate $p < 0.001$, $p < 0.01$ and $p < 0.05$, respectively.

4.2. Impact of Financial Shared Services on the Real Economy

4.2.1. The Impact of Financial Shared Services on the Real Economy. First, this paper examines the impact of financial shared services on the real economy. Columns (1)–(3) in Table 5 are based on model (1), and the effects of financial shared services on total net asset margin, return on net assets, and Tobin's Q are empirically tested. The results show that the coefficients of *FSSC* are all significantly positive at

TABLE 6: Robustness tests.

	Substitution of explanatory variables			Heckman two-stage		PSM without playback
	(1) ROA _{t+1}	(2) ROE _{t+1}	(3) Tobin _{t+1}	(4) FSSC	(5) ROA	(6) ROA
FSSC	1.048*** (3.74)	2.181*** (3.86)	0.352*** (4.11)		0.633*** (2.77)	1.149*** (4.02)
Size	0.475*** (7.70)	1.009*** (8.47)	-0.474*** (-29.24)	0.397*** (15.52)	-0.223 (-0.18)	0.616*** (5.38)
Lev	-8.515*** (-20.60)	-3.035*** (-4.03)	-2.746*** (-28.49)	-0.904*** (-6.31)	-8.650*** (-2.81)	-9.892*** (-8.75)
Growth	0.766*** (7.25)	1.573*** (7.35)	0.213*** (7.43)	-0.036 (-0.76)	1.447*** (15.34)	0.974*** (3.68)
FmAge	0.037*** (4.36)	0.047*** (3.00)	0.006** (2.15)	0.019*** (4.75)	-0.043 (-0.81)	-0.016 (-0.63)
Soe	-0.865*** (-7.90)	-1.793*** (-8.31)	-0.314*** (-10.18)	-0.303*** (-5.27)	-0.131 (-0.14)	0.267 (0.78)
Top1	0.025*** (8.93)	0.044*** (8.24)	0.005*** (5.43)	0.002 (1.51)	0.020** (2.57)	0.015 (1.50)
Ind	-2.208*** (-2.73)	-5.373*** (-3.33)	1.527*** (5.53)	1.117** (2.44)	-5.789* (-1.87)	-1.776 (-0.74)
Dual	0.051 (0.50)	0.187 (0.98)	0.130*** (3.54)	-0.062 (-0.97)	0.199 (1.09)	-0.423 (-1.12)
Board	0.308 (1.34)	-0.022 (-0.05)	0.105 (1.39)	0.077 (0.57)	0.097 (0.32)	0.227 (0.31)
Pcm	9.949*** (5.76)	16.006*** (5.80)	1.198*** (5.17)	-0.222*** (-3.36)	7.704** (2.38)	24.023*** (10.08)
Sons				0.001** (2.12)		
IMR					-2.910 (-0.89)	
_Cons	-4.195*** (-3.50)	-13.631*** (-5.73)	12.932*** (36.34)	-11.303*** (-19.15)	21.181 (0.59)	-7.507*** (-2.75)
N	12152	12149	12152	13994	13993	805
Adj. R ²	0.267	0.161	0.479		0.325	0.482
F	82.147	34.886	211.508		118.255	7.14

T values are in brackets; ***, ** and * indicate $p < 0.001$, $p < 0.01$ and $p < 0.05$, respectively.

1% level, indicating that financial shared service helps to promote the increase of the company’s operating performance and long-term value, i.e., it helps to enhance corporate value, and Hypothesis 1 is verified.

4.2.2. *Robustness Test.* For the reliability of the above regression results, the following robustness tests were conducted in this paper. (1) Replacing the explanatory variables, ROA, ROE, and Tobin in the future period are used to measure the current firm value, and columns (1)–(3) of Table 6 show that the coefficients of FSSC, ROA_{t+1}, ROE_{t+1}, and Tobin_{t+1} are all significantly positive at 1% level, which again verifies Hypothesis 1. (2) Considering the problem of possible sample self-selection bias, this paper adopts the Heckman two-step correction method to correct the estimation bias. In the first stage, based on the control of existing variables, the number of subsidiaries (Sons) of listed companies is introduced, and the probability of implementing financial shared services in listed companies is estimated using the Probit model and the inverse Mills ratio is calculated; in the second stage, the inverse Mills ratio is brought into model (1) to correct the sample selectivity bias. Column (5) test results find that the regression coefficients of

the inverse Mills ratio are not significant, indicating that the endogeneity problem caused by sample self-selection is well controlled, again indicating the robustness of the regression results of Hypothesis 1. (3) This paper also applies the propensity score matching method (PSM) to control for systematic differences between firms implementing financial shared services and those not implementing financial shared services. A total of 805 samples were obtained based on one-to-one no-release nearest neighbor matching of all control variables in the treatment and control groups in this paper. A multiple regression test of the relationship between financial shared services and firm value was conducted using the matched samples, and the results in column (6) show that the coefficient of financial shared services is still significantly positive at 1% level, and Hypothesis 1 is again tested.

4.2.3. *The Path Mechanism of Financial Shared Services to Empower the Real Economy.* Second, this paper tests the path mechanism of financial shared services to empower the real economy. According to model (2), the coefficients of FSSC in columns (1)–(9) in Table 7 are all significantly positive (negative), i.e., financial shared service is significantly positively related to total asset turnover, current asset

TABLE 7: Path mechanisms of financial shared services to empower the real economy (I).

	(1)	(2)	(3)	(4)	(5)	(6)	(7)	(8)	(9)
	Cost	TATR	CATR	ARTR	APTR	ITD	Bcycle	Cash	Tip
FSSC	-0.020*** (-3.09)	0.149*** (6.29)	0.158*** (3.15)	10.615** (1.71)	-2.429*** (-6.70)	-63.709*** (-7.76)	-60.321*** (-6.51)	-64.668*** (-7.51)	0.556*** (7.41)
Size	0.001 (0.22)	0.001 (0.19)	0.084*** (7.82)	-4.750*** (-3.97)	-0.052 (-0.41)	-7.386** (-2.10)	-15.766*** (-4.29)	-12.975*** (-3.78)	0.243*** (17.16)
Lev	0.274*** (12.22)	0.370*** (13.31)	0.603*** (10.38)	27.744*** (4.05)	-6.983*** (-8.57)	82.084*** (3.98)	118.669*** (5.49)	51.097*** (2.60)	0.529*** (6.70)
Growth	-0.002 (-0.40)	0.122*** (13.74)	0.196*** (11.17)	-3.622 (-1.55)	0.626*** (2.69)	-46.882*** (-5.82)	-48.123*** (-5.78)	-44.680*** (-5.89)	0.217*** (7.88)
FmAge	-0.000 (-0.07)	0.001* (1.76)	0.011*** (7.01)	-0.070 (-0.31)	0.130*** (5.80)	2.083*** (3.86)	-0.321 (-0.56)	0.595 (1.11)	-0.001 (-0.55)
Soe	0.031*** (8.79)	0.046*** (5.01)	0.115*** (5.80)	4.372 (1.35)	-1.174*** (-4.44)	-14.773* (-1.83)	-23.141*** (-2.74)	-28.539*** (-3.62)	0.006 (0.19)
Top1	0.000* (1.94)	0.003*** (13.75)	0.006*** (10.73)	0.069 (0.81)	0.035*** (5.06)	0.067 (0.33)	0.067 (0.33)	-0.276 (-1.38)	0.004*** (5.37)
Ind	-0.082*** (-3.64)	-0.212*** (-3.06)	-0.101 (-0.65)	10.824 (0.53)	5.519*** (2.64)	61.657 (1.16)	82.224 (1.45)	73.578 (1.38)	-0.620*** (-2.59)
Dual	-0.015*** (-5.11)	-0.021*** (-2.64)	-0.068*** (-4.14)	-1.591 (-0.74)	-0.063 (-0.25)	32.223*** (5.10)	35.881*** (5.25)	34.349*** (5.43)	0.049* (1.80)
Board	-0.017*** (-2.70)	0.012 (0.59)	0.133*** (2.81)	10.631 (1.42)	-0.313 (-0.53)	-52.763*** (-3.19)	-68.818*** (-3.91)	-68.177*** (-4.13)	-0.201*** (-2.90)
Pcm	-0.312*** (-2.87)	-0.159** (-2.14)	-0.302** (-2.12)	56.617*** (4.72)	-6.442*** (-2.58)	165.841*** (2.58)	152.534** (2.41)	138.218*** (2.62)	0.174 (1.43)
_Cons	0.730*** (15.31)	0.405*** (3.95)	-1.098*** (-4.42)	94.933*** (3.05)	15.181*** (5.20)	450.431*** (5.33)	693.302*** (7.86)	625.085*** (7.49)	-5.662*** (-17.12)
N	14865	14854	14855	14103	14838	14725	14859	14833	14855
Adj. R ²	0.396	0.296	0.285	0.148	0.080	0.570	0.518	0.518	0.316
F	235.001	170.003	175.301	19.806	63.749	113.077	108.888	103.339	157.391

T-values are in brackets; ***, **, and * indicate $p < 0.001$, $p < 0.01$ and $p < 0.05$, respectively. Due to missing data for Cost, TATR, CATR, ARTR, APTR, ITD, Bcycle, and Cash, the number of samples involved in the regression is not consistent with the total sample (same below).

TABLE 8: Path mechanisms of financial shared services to empower the real economy (II).

	(1)	(2)	(3)	(4)	(5)	(6)	(7)	(8)	(9)
	ROA	ROA	ROA	ROA	ROA	ROA	ROA	ROA	ROA
Cost	-8.946***								
TATR		(-7.84) 2.750***	(16.58) 0.703***						
CATR			(10.50) 0.001***						
ARTR				(2.92) 0.003					
APTR					(0.67) -0.001***				
ITD						(-5.18) -0.001***			
Bicycle							(-7.60) -0.001***		
Cash									
Tip									0.734*** (22.83)
FSSC	0.428* (1.92)	0.195 (0.92)	0.495** (2.17)	0.781*** (3.56)	0.685*** (3.09)	0.618*** (2.85)	0.609*** (2.80)	0.595*** (2.72)	0.198 (0.92)
Size	0.808*** (13.06)	0.800*** (9.13)	0.743*** (8.28)	0.646*** (8.84)	0.698*** (9.89)	0.687*** (9.44)	0.675*** (9.25)	0.681*** (9.41)	0.623*** (6.99)
Lev	-8.250*** -9.739***	-9.922*** (-19.57)	-9.843*** (-21.79)	-9.765*** (-20.92)	-9.881*** (-21.18)				-11.723*** -11.096***
Growth	1.379*** (13.70)	1.058*** (7.35)	1.259*** (9.16)	1.199*** (10.57)	1.243*** (11.76)	1.163*** (10.78)	1.186*** (11.00)	1.187*** (11.06)	1.234*** (9.40)
FmAge	0.011 (1.45)	0.007 (0.88)	0.003 (0.41)	0.028** (3.79)	0.016** (1.94)	0.021** (2.47)	0.016* (1.94)	0.018** (2.09)	0.012 (1.46)
Soe	-0.616*** (-7.32)	-1.018*** (-10.24)	-0.973*** (-9.66)	-0.752*** (-7.03)	-0.811*** (-7.89)	-0.820*** (-8.09)	-0.842*** (-8.46)	-0.852*** (-8.55)	-0.899*** (-8.76)
Top1	0.026*** (10.79)	0.016*** (5.87)	0.021*** (7.81)	0.021*** (8.81)	0.023*** (9.40)	0.024*** (9.64)	0.023*** (9.36)	0.023*** (9.46)	0.022*** (8.55)
Ind	-3.535*** (-5.04)	-2.214*** (-3.18)	-2.727*** (-3.86)	-2.500*** (-3.75)	-2.619*** (-3.81)	-2.689*** (-3.94)	-2.445*** (-3.56)	-2.511*** (-3.65)	-2.341*** (-3.37)
Dual	-0.089 (-1.06)	0.097 (1.16)	0.087 (1.02)	-0.016 (-0.20)	0.018 (0.22)	0.051 (0.62)	0.061 (0.74)	0.063 (0.77)	0.005 (0.06)
Board	0.181 (1.60)	0.306 (1.60)	0.246 (1.25)	0.348* (1.74)	0.317 (1.62)	0.293 (1.54)	0.235 (1.21)	0.227 (1.17)	0.488** (2.53)
Pcm	4.674** (2.24)	7.895*** (2.69)	7.669*** (2.72)	14.068*** (5.75)	11.384*** (4.88)	11.645*** (4.71)	11.560*** (4.86)	11.552*** (4.88)	7.337*** (2.63)
_Cons	-3.345*** -8.248***	-8.567*** (-8.27)	-8.035*** (-6.49)	-7.611*** (-7.12)	-7.701*** (-6.24)	-5.721*** (-5.92)			-11.019*** (-9.125)
Intermediary effect	0.177***	0.411***	0.111***	0.010*	-0.007*	0.067***	0.078***	0.083***	0.408***
Direct effect	0.428**	0.195	0.495**	0.781***	0.685***	0.618***	0.609***	0.595***	0.198***
Total effect	0.605***	0.606***	0.606***	0.791***	0.768***	0.685***	0.687***	0.678***	0.606***
N	14865	14854	14855	14103	14838	14725	14859	14833	14855
Adj. R ²	0.386	0.378	0.345	0.405	0.373	0.377	0.380	0.380	0.368
F	175.734	152.539	136.873	147.382	136.412	135.526	139.136	139.893	150.978

T values are in brackets; ***, **, * and * indicate $p < 0.001$, $p < 0.01$ and $p < 0.05$, respectively.

TABLE 9: Further studies.

	Number of subsidiaries		Revenue size		Labor-intensive	
	More	Less	Big	Small	High	Low
	(1)	(2)	(3)	(4)	(5)	(6)
	ROA	ROA	ROA	ROA	ROA	ROA
FSSC	0.878*** (3.60)	0.135 (0.29)	1.039*** (5.00)	-0.063 (-0.10)	0.806*** (3.02)	0.055 (0.13)
Size	0.608*** (6.23)	0.974*** (6.90)	-0.010 (-0.19)	0.388** (2.31)	0.619*** (4.68)	0.836*** (6.05)
Lev	-10.414*** (-12.16)	-10.638*** (-15.13)	-10.515*** (-33.18)	-9.110*** (-17.68)	-11.386*** (-10.65)	-9.336*** (-16.55)
Growth	1.262*** (8.64)	1.444*** (8.45)	1.056*** (11.14)	1.450*** (8.54)	1.500*** (7.73)	1.286*** (9.13)
FmAge	0.041*** (4.80)	-0.027* (-1.95)	0.024*** (3.19)	-0.038*** (-2.76)	0.012 (1.22)	0.001 (0.09)
Soe	-0.682*** (-4.37)	-1.082*** (-7.02)	-0.576*** (-5.99)	-0.674*** (-4.54)	-0.909*** (-4.87)	-0.670*** (-5.12)
Top1	0.020*** (6.55)	0.031*** (7.55)	0.014*** (5.11)	0.032*** (7.61)	0.019*** (5.24)	0.028*** (7.24)
Ind	-2.532*** (-3.03)	-2.486** (-2.11)	-1.523** (-2.01)	-3.010** (-2.58)	-1.396 (-1.62)	-3.570*** (-3.11)
Dual	0.303** (2.53)	-0.223* (-1.82)	0.193* (1.76)	-0.023 (-0.19)	-0.026 (-0.22)	0.124 (1.00)
Board	-0.293 (-1.21)	1.228*** (3.67)	-0.428* (-1.96)	0.787** (2.26)	-0.243 (-0.90)	0.866*** (2.72)
Pcm	12.248*** (2.98)	5.868** (2.14)	23.804*** (35.42)	5.173** (2.37)	13.042** (2.43)	5.557** (2.14)
_Cons	-5.381*** (-3.60)	-15.160*** (-5.55)	8.094*** (7.15)	-2.679 (-0.82)	-5.764*** (-2.58)	-11.327*** (-4.49)
N	7916	6953	7907	6962	7819	7050
Adj. R ²	0.404	0.293	0.547	0.281	0.416	0.282
F	100.490	51.276	160.164	52.429	102.420	56.333

Note. Labor-intensity indicator is obtained by referring to the study of Lu et al. [28], using the logarithm of the number of employees/logarithm of main business revenue; in the grouping of number of subsidiaries, revenue size, and labor intensity, they are grouped according to the sub-year and sub-industry medians of the number of subsidiaries, main business revenue, free cash flow, and labor intensity of listed companies, respectively. *T* values are in brackets; ***, ** and * indicate $p < 0.001$, $p < 0.01$ and $p < 0.05$, respectively.

turnover, accounts receivable turnover, and personnel efficiency and significantly negatively related to operating cost rate, accounts payable turnover, inventory turnover days, operating cycle, and cash cycle, indicating that the implementation of financial shared services can not only speed up the flow of assets, accelerate the speed of fund recovery, and improve personnel output but also reduce operating costs, extend the time of using external funds, shorten inventory turnover days, and optimize the operating cycle and cash cycle, thus improving the overall operational efficiency of the enterprise.

Based on model (3), the coefficients of operating cost ratio (Cost), inventory turnover days (ITD), operating cycle (Bcycle), and cash cycle (Cash) are significantly negative in columns (1) and (6)–(8) of Table 8. The coefficients of total asset turnover ratio (TATR), current asset turnover ratio (CATR), accounts receivable turnover ratio (ARTR), and personnel efficiency (Tfp) are significantly positive, indicating that there is a significant mediating role of the above indicators in the relationship between both financial shared services and enterprise value. Meanwhile, according to the third step of the mediating utility test, the directions of the coefficients of FSSC in model (2) and the product of the coefficients of the above indicators are compared with the

coefficients of FSSC in model (3) in turn, and it is found that the above indicators play only a partial mediating role in the relationship between financial shared services and enterprise value. In column (5), the coefficient of accounts payable turnover ratio (APTR) is insignificant and passes the significance test using Bootstrap method, indicating that accounts payable turnover also plays a mediating utility in the relationship between financial shared services and enterprise value.

It is indicated that financial shared service optimizes operational efficiency by reducing operating costs, improving total asset turnover, accounts receivable turnover, current asset turnover, and personnel efficiency, and reducing inventory turnover days, accounts payable turnover, operating cycle, and cash cycle, thereby improving enterprise value, and operational efficiency plays a mediating variable in the relationship between financial shared services and enterprise value, and Hypothesis 2 is verified.

5. Further Research

Since the companies implementing financial shared services are mainly large enterprise groups with large revenue scale and a large number of subsidiaries as well as those belonging

to labor-intensive industries [2, 13], this paper applied the number of subsidiaries, revenue size, and labor-intensity indicators as grouping variables for the grouping regression of the sample, respectively. The empirical results are shown in Table 9. The regression results in columns (1)–(6) of Table 9 show that the impact of financial shared services on the real economy is significant only in enterprises with many subsidiaries, large revenue scale, abundant free cash flow, and high labor intensity, indicating that financial shared service is more adapted to enterprises with a large number of subsidiaries, large revenue scale, and high labor intensity. This is mainly because, on the one hand, the scope of financial shared services is focused on financial accounting processes that are less relevant to management decisions, occur frequently, and are easily standardized; on the other hand, these enterprises have a more urgent need to improve the efficiency of financial management, so the implementation of financial shared services is more effective in promoting the real economy.

6. Conclusions and Recommendations

This paper investigates the impact of financial shared services on the real economy by using data related to A-share listed companies in Shanghai and Shenzhen from 2008–2017 and concludes the following. Firstly, financial shared services help to enhance enterprise value. Secondly, operational efficiency is the mediating variable in the relationship between financial shared services and enterprise value. Financial shared services empower the real economy by reducing business operating costs, improving total asset turnover, current asset turnover and personnel efficiency, and accounts receivable turnover, and reducing inventory turnover days, accounts payable turnover, operating cycle, and cash cycle. Finally, further research found that the empowering effect of financial shared services on the real economy exists only in enterprises with many subsidiaries, large scale, and high labor intensity.

According to the conclusion of this paper, the following recommendations are made. First, in the era of digital economy, data has become a key production factor and strategic resource, and the digital transformation of finance can empower the real economy and form a “new dynamic energy” for high-quality development of the real economy. Therefore, enterprises should pay attention to the application of financial shared services, accelerate financial digital transformation, use information technology and digital technology to promote business and financial process reengineering, optimize their operation and management capabilities, and achieve “overtaking” in the digital era. Second, financial shared services are not suitable for all enterprises. In large enterprise groups and labor-intensive industries, financial shared services can better play the scale and centralization effects and highlight the improvement of control and service efficiency. Therefore, enterprises should choose and design their financial management models according to their own characteristics and long-term strategies. Third, financial shared services are crucial to improving the operation and management capabilities of

enterprises, and enterprises should make good use of financial shared services to continuously empower their operation and management and transform them into wealth creation capabilities of enterprises, so as to ultimately enhance the contribution and competitiveness of China’s real economy in the world economy.

Data Availability

The data used to support the findings of the study were obtained from the Wind database and CSMAR database.

Conflicts of Interest

The author declares that there are no conflicts of interest.

Acknowledgments

The author would like to thank the National Natural Science Foundation of China (grant nos. 72062033 and 71962035).

References

- [1] H. Chen, “Financial transformation based on shared services,” *Finance and accounting*, no. 21, pp. 23–26, 2016.
- [2] W. Q. Wang, “Practice and exploration of the construction of financial shared service center of central enterprises,” *China General Accountant*, no. 11, pp. 136–137, 2016.
- [3] Q. L. Zhang, “Upcycling financial sharing under digital transformation,” *New Money*, no. 8, pp. 31–34, 2019.
- [4] Y. Guo, Y. N. Zhao, and Y. Q. Liu, “Report on the construction of financial shared services in central enterprises,” *State capital report*, no. 8, pp. 101–105, 2019.
- [5] Y. Yang, Z. Q. Ma, and Y. Li, “Surgical analysis of transnasal frontal sinus balloon dilatation,” *Accounting Research*, vol. 34, no. 1, pp. 23–27, 2020.
- [6] R. J. Zhang, H. Chen, and Y. J. Zhang, “Study on the key factors of process reengineering of financial shared services in enterprise groups--based on the management practice of ZTE Group,” *Accounting Research*, no. 7, pp. 57–64, 2010.
- [7] Q. L. Zhang and Y. B. Zhang, “Research on enterprise treasury management under the perspective of financial transformation,” *Finance and Accounting Monthly*, no. 1, pp. 34–38, 2022.
- [8] Q. L. Zhang, “Study on the upgrading and reengineering of financial shared services in the context of digital transformation,” *China CPA*, no. 1, pp. 102–106, 2020.
- [9] X. R. Zhen, “Based on financial sharing to promote transformation and upgrading,” *Business Watch*, no. 17, pp. 44–47, 2022.
- [10] Q. Zhang, “Reflections on the financial digital transformation of group enterprises,” *Finance and Economics*, no. 17, pp. 110–112, 2022.
- [11] C. Lu, H. Z. Li, and P. Y. Cao, “Information system change under the demand of organizational collaboration--a case study based on the construction of Gome’s shared service center[J],” *Management Accounting Research*, vol. 1, no. 1, pp. 40–47, 2018.
- [12] X. D. Han and H. Y. Yu, “The path of financial sharing in China,” *Finance and Accounting*, no. 12, pp. 73–74, 2017.
- [13] Y. Y. Liu, “Exploring the application of financial sharing center in Chinese enterprises,” *Enterprise Reform and Management*, no. 6, p. 125, 2016.

- [14] M. Janssen, A. Joha, and A. Zuurmond, "Simulation and animation for adopting shared services: evaluating and comparing alternative arrangements," *Government Information Quarterly*, vol. 26, no. 1, pp. 15–24, 2009.
- [15] A. Paagman, M. Tate, E. Furtmueller, and J. de Bloom, "An integrative literature review and empirical validation of motives for introducing shared services in government organizations," *International Journal of Information Management*, vol. 35, no. 1, pp. 110–123, 2015.
- [16] Y. He and X. Zhou, "An empirical study on the key factors of implementing financial shared services in Chinese enterprise groups," *Accounting Research*, no. 4, pp. 59–96, 2013.
- [17] Y. He, "The path and direction of financial process reengineering for enterprise groups based on cloud computing," *Management World*, no. 4, pp. 182–183, 2013.
- [18] H. Y. Xu, Y. L. Jiang, and X. Xu, "Research on the implementation efficiency of financial shared services of China's group companies based on DEA," *Audit and Economic Research*, vol. 32, no. 5, pp. 74–84, 2017.
- [19] D. W. Webster, "Financial management and shared services," *The Journal of Government Financial Management*, vol. 56, no. 2, p. 39, 2007.
- [20] W. Y. Li, Y. Y. Zhu, and M. L. Liu, "Research on service quality of financial shared service center," *Accounting Research*, no. 4, pp. 59–65, 2017.
- [21] J. Barney, "Firm resources and sustained competitive advantage," *Journal of Management*, vol. 17, no. 1, pp. 99–120, 1991.
- [22] S. L. Newbert, "Empirical research on the resource-based view of the firm: an assessment and suggestions for future research," *Strategic Management Journal*, vol. 28, no. 2, pp. 121–146, 2007.
- [23] M. Gottfredson, R. Puryear, and S. Phillips, "Strategic sourcing: from periphery to the core," *Harvard Business Review*, vol. 83, no. 2, p. 132, 2005.
- [24] X. Y. Liu and H. Dong, "New ideas of financial management in the context of artificial intelligence and big data era," *Modern Business*, no. 6, pp. 152–155, 2020.
- [25] Q. L. Zhang, "Realistic problems of financial shared service centers and where to go in the future," *Business Accounting*, no. 19, pp. 6–9, 2017.
- [26] X. Y. Su and J. Gao, "The impact of financial sharing model on the internal control of enterprise groups," *Modern Enterprise*, no. 8, pp. 171–173, 2022.
- [27] Z. L. Wen and B. J. Ye, "Analyses of mediating effects: the development of methods and models," *Advances in Psychological Science*, vol. 22, no. 5, pp. 731–745, 2014.
- [28] C. Lu, S. Y. Tang, and G. M. Liao, "Labor protection, labor intensity and firm investment efficiency," *Accounting Research*, no. 6, pp. 42–47, 2015.

Research Article

The Relationship between Social Entrepreneurship Capability of SOM Neural Network Algorithm and New Enterprise Performance

Tianhua Li 

Department of Management Science and Engineering, School of Economics and Management, University of Science and Technology Beijing, Beijing 100083, China

Correspondence should be addressed to Tianhua Li; b20180402@xs.ustb.edu.cn

Received 21 April 2022; Revised 15 July 2022; Accepted 25 July 2022; Published 28 August 2022

Academic Editor: Wei Liu

Copyright © 2022 Tianhua Li. This is an open access article distributed under the Creative Commons Attribution License, which permits unrestricted use, distribution, and reproduction in any medium, provided the original work is properly cited.

As an important factor in the creation and growth of new enterprises, social entrepreneurship and new enterprise performance have attracted more and more attention from scholars in recent years. This research analyzes the network relationship of new companies on the basis of existing entrepreneurial network research. This paper proposes social entrepreneurial capabilities and new company performance based on the SOM neural network algorithm to solve these problems and then establishes entrepreneurial networks, organizational learning, and new business performance models. The method of this paper is to study the SOM neural network algorithm and then establish the entrepreneurial ability and enterprise performance evaluation system. The function of these methods is to put forward the meaning and research of venture capital. It also defines the meaning and research of innovation capabilities based on innovation theory, ensuring the scientific nature of the evaluation indicators, evaluation standards, and evaluation processes of innovative enterprises. In this survey, this paper conducted a field survey in Shanxi Province, China, and analyzed the internal impact of the network of social entrepreneurship and new companies on corporate performance. The survey results show that the value of the correlation β between entrepreneurial orientation and entrepreneurial environment dynamics is 0.167 ($P < 0.05$). This shows that improving the entrepreneurial environment and enhancing social entrepreneurial capabilities have a positive impact on corporate performance.

1. Introduction

With the acceleration of economic globalization, the knowledge economy is developing rapidly. Countries all over the world are working hard to improve tolerance to adapt to the new trends and requirements of economic development. The spirit of innovation has played a vital role in promoting China's economic growth and development. In recent years, China's entrepreneurial activities have been very active, but the survival rate of new companies is very low. This research is based on the experience of entrepreneurs and knowledge management theory. Its purpose is to make China one of the world's powers at an early date and to enhance its independent innovation capabilities. This paper proposes a conceptual model of the relationship between dual opportunity awareness and new enterprise performance based on learning theory and organizational duality theory, and describes in detail the

differences in the impact of different types of entrepreneurial experience on dual opportunity awareness.

Enterprise innovation has historical significance. Not all technologies in innovation activities mean that they are a single type of innovation, or can they be completed only within the enterprise. The enterprise establishes an enterprise scientific and technological innovation system to improve its independent innovation capability. This is vital to China's future economic and scientific development. This research improves the impact of political connections on corporate performance and provides theoretical support for startups to reduce the negative impact of political connections on companies and exert the beneficial effects of political connections on companies. This research further analyzes the mediating role played by internal knowledge sharing in entrepreneurship and the identification of dual opportunities between different types of entrepreneurial

experiences. This provides some practical guidance for enterprises to avoid innovation risks.

In previous studies, scholars mainly used Chinese listed companies as samples—or industrial, agricultural, tourism, clothing, transportation, and other listed companies as samples—while research on innovative companies hardly existed. This article examines the moderating role of corporate growth, and whether there are significant differences in the relationship between innovation and corporate performance for companies of different growth levels. In this article, innovative companies will be selected for research. This article chooses entrepreneurial companies because there is less research on this type of company, and there is no research on the relationship between innovation and corporate performance. This article fills up the gaps in empirical research in this field through reasonable indicator selection, accurate data screening, and scientific empirical analysis techniques.

2. Related Work

As the trend of innovation and entrepreneurship gradually prevails, people are paying more and more attention to the role of social entrepreneurship, and there are more and more studies on this. Lai et al. conducted a graded waterlogging risk assessment on 56 low-lying spots in Beijing based on the self-organizing map. The results show that SOM-ANN is suitable for automatic quantitative assessment of risks related to waterlogging. It can effectively overcome the interference of subjective factors and produce more objective and accurate classification results [1]. Ni et al. proposed to use GAN-SOM as a new clustering architecture based on deep learning. The SOM-like network is designed to achieve the purpose of encoding and clustering data samples at the same time. The joint training of this network and GAN can optimize the newly defined clustering loss [2]. Suryani and Susilo aim to segment blood vessels using the main method of self-organizing map artificial neural networks. The segmentation method they proposed can effectively improve the test performance of medical machinery and increase the success rate of surgery [3]. Runst et al. proposed a novel classification scheme aimed at improving the identification of entrepreneurial companies in the microcensus. Policy changes are only aimed at entrepreneurial enterprises, and after the complete deregulation of trade, the proportion of enterprises entering the industry has increased significantly, and the innovation and entrepreneurship of enterprises have become stronger and stronger [4]. Hsieh and Wu investigate how entrepreneurs innovate the corporate ecosystem during the entrepreneurial process. He researched and discussed various platform-based enterprise innovations, and also discussed the worries and problems that the ecosystem of innovation platforms may bring to enterprises [5]. Rodriguez et al. aim to further explore the influencing factors of corporate performance through innovative concepts. His research results show that market orientation has a direct impact on organizational performance. He observes the specific ways in which innovation performance structure regulates market orientation [6]. Abushaikh et al. studied the relationship among warehouse operation performance,

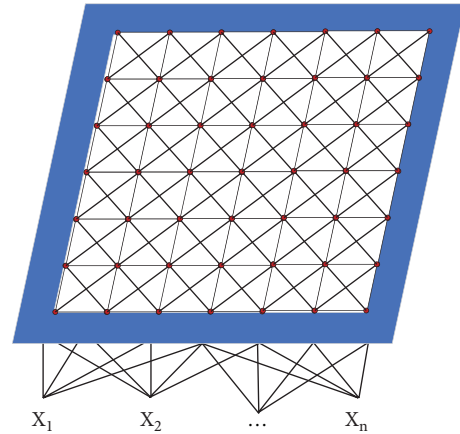


FIGURE 1: SOM neural network topology.

distribution performance, and business performance. He first used Delphi technology to develop relevant questionnaires, then used data to measure the degree of performance improvement in different warehouse activities, and tested his hypotheses. His conclusion is that there is a positive correlation between warehouse operation performance and distribution performance [7].

3. Social Entrepreneurship and Corporate Performance Evaluation Methods

3.1. SOM Neural Network Research. A self-organizing competitive neural network (SOM) was first proposed by Teuvo Kohonen [8]. OM neural network adjusts the weight of the network through self-organizing feature mapping so that the network converges to a stable state. Network learning is self-organized learning under unsupervised conditions. During the learning process, certain neurons are only sensitive to certain types of patterns. Because different neurons have different degrees of sensitivity to different input patterns through unsupervised competitive learning. The operator of the network can detect specific input patterns. Figure 1 shows the network topology of the SOM neural network.

This is a feedforward neural network composed of two layers of neurons. The number of neurons in the input layer is the same as the dimension of the input sample. The output layer, also called the conflict layer, arranges the nodes into a two-dimensional array. The connection between the input layer and the competing layer node is fully connected with variable weight [9].

SOM neural network training steps are as follows:

First, the network is initialized, the network weight is initialized to w_{nm} ($n = 1, 2 \dots n, m = 1, 2 \dots m$), n is the number of neurons in the input layer, and m is the number of neurons in the competition layer. The weights can be initialized randomly. It sets the maximum number of cycles T , inputs training samples, and normalizes them. Then, it calculates the distance D between the normalized input vector $X = (x_1, x_2 \dots x_n)$ and the neuron j of the competition layer as follows:

$$D_j = \sqrt{\sum_{n=1}^m (x_n - w_{mn})^2}. \quad (1)$$

It looks for the winning neuron. The neuron C of the competition layer with the smallest distance from the input vector is selected as the winning neuron. One needs to remember that the class label of the input vector is C_x ; if $C_x = C_i$, then adjust the weight as follows:

$$w_{mn} = w_{mn} + n(x - w_{mn}). \quad (2)$$

Otherwise, adjust as follows:

$$w_{mn} = w_{mn} - n(x - w_{mn}). \quad (3)$$

If neuron i and j belong to different categories, the distance d_i and d_j between neuron i and j and the current input vector satisfy

$$\min \left\{ \frac{d_i}{d_j}, \frac{d_j}{d_i} \right\} > p. \quad (4)$$

Among them, p is the width of the window near the center section of the two vectors that the input vector may contain, usually about two-third. The learning rules of the SOM neural network are derived from the lateral inhibition of neuronal cells. The flowchart is shown in Figure 2.

The adjustment weight, the update formula is as follows:

$$w_{mn} = w_{(m+1)(n+1)} + N(n)h(n)(x_n - w_{mn}). \quad (5)$$

In the formula, $N(n)$ is the learning rate function, and its value range is $0 < N(n) < 1$, and $h(c)$ is the neighborhood function, which gradually decreases with time. Their learning rules are as follows:

$$h(n) = \exp\left(-\frac{d_{cm}^2}{2r^2(n)}\right),$$

$$r(n+1) = \text{INT}\left((r(n) - 1)\left(1 - \frac{n}{T}\right)\right) + 1, \quad (6)$$

$$N(n+1) = N(n) - \frac{N(0)}{T}.$$

In the formula, d_{cm} is the distance between neuron c and neuron m , $r(n)$ is the radius of the neighborhood, INT is the rounding function, and T is the total number of learning times. Let $n = n + 1$, return to perform random initialization processing on the weights until the maximum number of iterations or the learning rate reaches a set value [10].

In order to verify the validity and correctness of the established model, it is necessary to ensure that the sample data provided for fault diagnosis are true and reliable. For multidimensional features, the correlation coefficient method is used for feature extraction. By analyzing the relevant characteristics of different features, the features with lower discrimination are removed and the features with higher discrimination are retained. In the end, only the extracted features are used to train the neural network, and the same feature compression is performed on the test data.

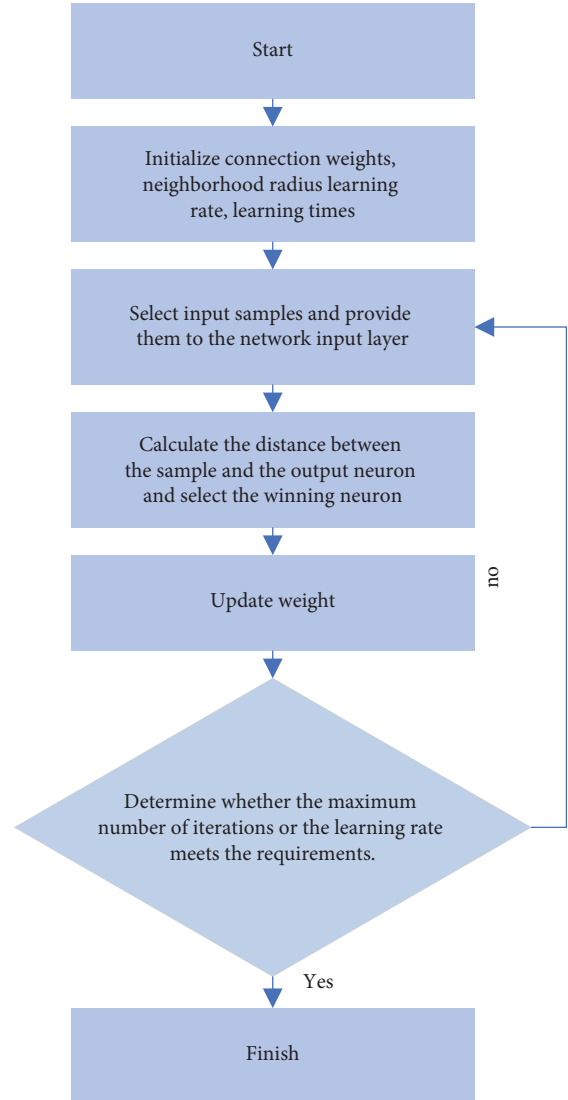


FIGURE 2: SOM neural network algorithm flowchart.

The calculation formula of the correlation coefficient between different features is as follows:

$$p(f, x_m) = \frac{\sum_{n=1}^N (f_n - \bar{f})(x_{nm} - \bar{x}_m)}{\sqrt{\sum_{n=1}^N (f_n - \bar{f})^2 - \sum_{n=1}^N (x_{nm} - \bar{x}_m)^2}} \quad (7)$$

In the formula, f is the target value, x_m is the feature, N is the sample size, and \bar{x}_m is the mean value of the feature. The larger the correlation coefficient, the more obvious this feature distinguishes the failure mode [11].

The SOM network can automatically classify the input mode. It is based on the simultaneous response of multiple neurons to the classification results and does not require a large amount of sample data. Moreover, its network structure is simple, and the algorithm process is relatively easy to implement. However, it also has shortcomings. Before training, the user needs to initialize the number of clusters and the initial weight matrix. That is to say, the number of clusters and the network structure are fixed and

cannot be adjusted during the training process. During the training process, some neurons never win in the competition, forming dead neurons. And some neurons are overused in the learning process, which will affect the training performance of the network. During training, if a new type is added to the training sample, it must be relearned [12].

3.2. Evaluation of Entrepreneurial Ability. There are many indicators to measure enterprise performance. This article will measure the performance of SMEs from two aspects: short-term profitability and long-term growth ability. This article uses the variable return on assets (ROA) used by most scholars to measure the short-term profitability of enterprises.

$$\text{ROA} = \frac{\text{NOPAT}}{\text{TA}}. \quad (8)$$

In the formula, ROA represents the rate of return on total assets, NOPAT represents net operating profit after tax, and TA represents total assets. This article adopts Tobin's Q index used by most scholars to measure the growth performance of SMEs. The calculation formula is as follows:

$$\text{Tobin's Q} = \frac{(\text{EV} + \text{BVL})}{\text{TA}}. \quad (9)$$

In the formula, BVL represents the book value of liabilities, and EV represents the value of equity. Multiple linear regression is a statistical method to study a linear relationship between a dependent variable and multiple independent variables. The basic idea is a statistical method that can estimate the dependent variable and its influence on its variability by using the value of more than one independent variable. Therefore, it is the continuation and promotion of simple regression analysis and correlation analysis [13]. In this study, panel data will be used for multiple regression analysis. The regression formula of panel data is as follows:

$$y_i = b_0 + x_i b_i + z_i r + v_i + E_i. \quad (10)$$

Among them, y_i is the dependent variable, and x_i is the independent variable that varies with the individual and time. z_i is an individual characteristic that does not change over time, such as gender. $v_i + E_i$ constitutes an interference term, v_i is an individual characteristic that is unobservable and does not change with time, E_i is a perturbation term that changes with the individual and time, and hypotheses E_i and v_i are not correlated. The formula (10) is processed, and the two sides are averaged to obtain

$$\bar{y}_i = b_0 + \bar{x}_i b_i + z_i' r + v_i + \bar{E}_i. \quad (11)$$

Performing OLS on formula (11) can get the intergroup estimator, but this requires that it cannot be correlated with all explanatory variables, otherwise the estimation will be invalid. When individuals are related to explanatory variables, this article calls the panel data model a fixed-effects model. At this time, OLS estimates are inconsistent. But this article can be processed to turn it into a consistency estimate [14]. Specifically, it is obtained by formula (10) and formula (11):

$$y_i - \bar{y}_i = x_i - \bar{x}_i b_i + \bar{E}_i - \bar{E}_i. \quad (12)$$

If the errors in the panel data are autocorrelated, then the commonly used standard errors are also incorrect. Because it is derived under the false assumption that autocorrelation does not exist. Furthermore, panel data have potentially nonuniform variance that may be associated with different temporal conditions for a particular individual. This article also uses the Xtgls command to analyze the impact of entrepreneurial social capital (S) on the performance of SMEs. The design of the following multiple regression analysis formulae is as follows:

$$F = A + B_1 S + B_2 L + B_3 G + B_4 Sc + B_5 Ag + \sum_1^t \delta_i Y + \sum_1^t \gamma_k I + E_i. \quad (13)$$

Formula (13) shows the impact of three main aspects of entrepreneurial social capital (S), political connections (POL), industry association relations (BAN), and technology association relations (TAN) on enterprise performance. Due to political relations, trade association relations, and the three technical association relations, there is an important positive relationship. To avoid the problem of multicollinearity, each of the three variables is assigned to the model. In addition, the factors that affect the performance of SMEs (F) are more complex, so this article introduces a set of variables. The debt-to-asset ratio (L) is measured by the company's total debt-to-asset ratio, that is, the company's total liabilities divided by its total assets. Sales growth rate (G) is the company's sales growth rate for the year. Company size (Sc) is measured by the natural logarithm of total assets for the year. The company life (Ag) is calculated from the company registration year as the starting year to the number of years set in the survey sample. In addition, this article adds an industry (I) dummy variable (i.e., $K=20$) and a year (Y) dummy variable (i.e., $I=5$) to the model control. This article hopes to satisfy the assumption that the political relationship between entrepreneurs, the relationship between industry associations, and the relationship between technical associations have a significant positive impact on the performance of SMEs.

In order to intuitively understand the relationship among entrepreneurial political relations, industry group relations, technical group relations, and the performance of SMEs, this paper uses grouping techniques to conduct T -tests. This study tests whether there is a significant difference between the two. For example, does the existence of entrepreneurial social capital have a significant impact on company performance? When testing whether there is a significant difference in the mean of the two groups of variables, it can be distinguished by using the T -test command in Stata.

$$\bar{x}_1 - \bar{x}_2 = u_1 - u_2 + \bar{E}_1 - \bar{E}_2. \quad (14)$$

This article proposes the meaning and research aspects of entrepreneurial social capital by investigating and combining relevant theories, and defines the meaning and

research aspects of innovation ability based on innovation theory.

3.3. Corporate Performance Evaluation. The Herfindahl index (H) is used to measure the degree of diversification of a company. The Herfindahl index was originally used to measure industrial concentration in the theory of industrial organization. It can be used to reflect the relative weight of different business units at a single SIC classification level.

$$H = \sum_{i=1}^n (p_i)^2. \quad (15)$$

Among them, p_i represents the proportion of the operating income of the different industries that the company produces or the industry involved in the business belongs to the total income of the company, and n represents the number of businesses operated by the enterprise. H has an inverse relationship with the degree of corporate diversification. The larger the H , the lower the degree of diversification. In the process of application, many scholars deform H and use the difference of 1 minus H to express the degree of enterprise diversification. This makes H have a positive correlation with the degree of corporate diversification, and the greater the H , the higher the degree of corporate diversification. When the enterprise is a single business, H is equal to 0 [15].

$$H = 1 - \sum_{i=1}^n (p_i)^2. \quad (16)$$

Using entropy measurement to measure the level of diversification:

$$H = \sum_{i=1}^n p_i \ln\left(\frac{1}{p_i}\right). \quad (17)$$

According to the different meanings of p_i and n , the “entropy” index can be used to calculate three indicators of enterprise diversification, that is, the degree of overall diversification, unrelated diversification, and related diversification. When p_i and n represent business indicators belonging to the four-code industry, the “entropy” index calculates overall diversification. When p_i and n represent business indicators belonging to the two-code industry, the entropy index calculates noncorrelated diversification. H is positively correlated with the degree of diversification of the enterprise. The larger the H , the higher the degree of diversification of the enterprise. When H is 0, the enterprise conducts a professional operation.

For an innovative enterprise that integrates technological innovation, brand innovation, system and mechanism innovation, business management innovation, concept and cultural innovation, etc., related performance evaluation theories must also consider social and company benefits.

If there are n decision-making units (DMU), each decision-making unit has m -type input and s -type output. Then, the resource input of the decision-making unit is represented by x as the input of the DMU, and the output of the decision-making unit is represented by y as the output quantity of the

DMU. The weight vectors v and u are allocated, and the efficiency evaluation index of each DMU is as follows:

$$h = \frac{u^T y_i}{w^T x_j} = \frac{\sum_{r=1}^s u_r y_{rj}}{\sum_{i=1}^m w_r x_{rj}}. \quad (18)$$

The weight coefficients w and u can be appropriately obtained, so that $h \leq 1$. Usually, fishbone diagram analysis is used to reflect the formation process of innovative enterprise performance, and to clarify the formation process of innovative enterprise performance. Let us take the decomposition of enterprise performance maximization goal as an example to explain, as shown in Figure 3.

After establishing the strategic goal of maximizing corporate performance, the fishbone diagram can be used to decompose the strategic goals of the enterprise layer by layer in accordance with the method of causality. The scientific nature of the performance evaluation system is the basis for ensuring the accuracy and reasonableness of the performance evaluation results of innovative enterprises. The scientific nature of a performance evaluation activity depends on the scientific nature of various aspects such as evaluation indicators, evaluation standards, and evaluation processes. Compared with the characteristics of traditional enterprise performance evaluation and strategic performance evaluation, the innovation performance evaluation system of innovative enterprises takes into account the actual situation of enterprise strategic innovation. It needs to combine the performance evaluation content of various levels of innovative enterprises to ensure the rationality of the overall structure of the performance evaluation system. In addition, the innovative performance system of innovative enterprises captures the main aspects of the innovation of corporate strategic objectives. Considering the difference between the strategic innovation of innovative enterprises and traditional original enterprise strategies, a certain flexible innovation interval is designed. This can highlight the focus of innovation performance evaluation, and carry out a longitudinal comparison before and after the evaluation of strategic innovation performance of innovative enterprises and at each stage of the innovation process. This will be horizontally compared with similar innovative companies outside, and finally, combined with multilevel performance appraisal content. In this way, it uses a multifaceted performance evaluation system that includes indicators of innovation for innovative enterprises, and finally, forms an efficient and innovative performance evaluation system [16].

4. Experiment and Analysis of the Correlation between Social Entrepreneurship and Corporate Performance

4.1. The Integration of Entrepreneurship Capability. Flexible and efficient knowledge integration represent two completely different combinations of entrepreneurial knowledge integration methods. In the actual entrepreneurial process, new ventures will use these two types of

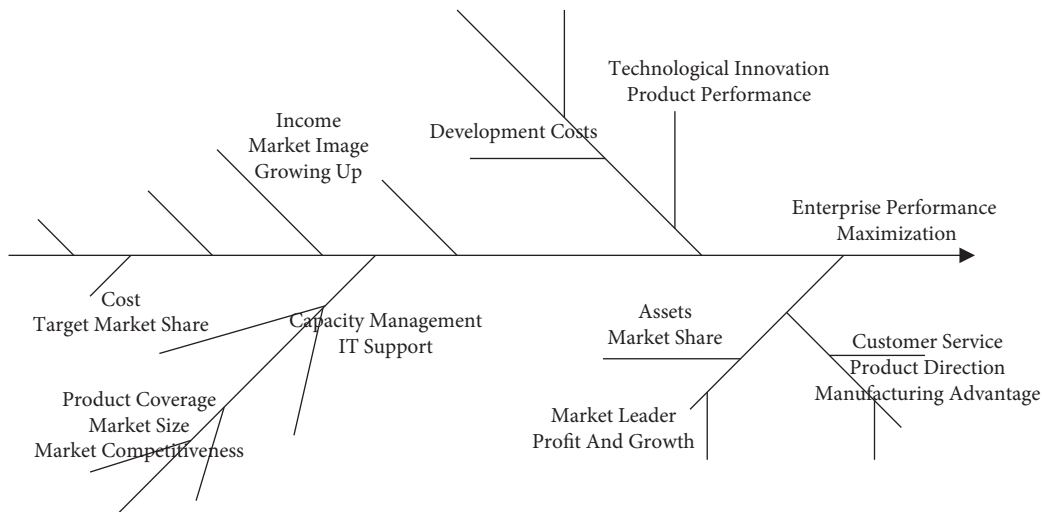


FIGURE 3: The goal decomposition of innovative enterprise performance formation.

TABLE 1: Descriptive statistical analysis of measurement items for flexible knowledge integration.

Item	Mean	Standard deviation
E1 combines market feedback to establish new strategic goals	3.880	0.747
E2 combines new technologies to establish new strategic goals	3.900	0.390
O1 stakeholders promote corporate development	3.400	0.499
O2 cooperate to promote product/service innovation	3.930	0.184
C1 rewards employees for sharing experience	3.300	0.743
C2 provides a resting place for employees	3.850	0.796

entrepreneurial knowledge integration to varying degrees. This helps explain the reasons for the difference in the performance of startups. Based on the above theoretical analysis, this article summarizes the characteristics of the flexible and efficient knowledge integration of the case enterprises.

It assumes that enterprise A has strong performance in both flexible and efficient knowledge integration. It is embodied in the strategic dimension as both emergency and planned knowledge integration. It is embodied in the cultural dimension as both extroverted and introverted knowledge integration. In the institutional dimension, it is embodied as an equal emphasis on coordinated and systematic knowledge integration. Enterprise B focuses on flexible knowledge integration. That is, it is mainly embodied as emergency knowledge integration in the strategic dimension, outward-oriented knowledge integration in the cultural dimension, and coordinated knowledge integration in the institutional dimension. And C enterprise mainly focuses on efficient knowledge integration. That is, in the strategic dimension, it is mainly reflected in planned knowledge integration; in the cultural dimension, it is mainly reflected in introverted knowledge integration; and in the institutional dimension, it is mainly reflected in systematic knowledge integration. As mentioned earlier, it is different from A, B, and C enterprises, and D enterprise has no outstanding performance in strategic, cultural, and institutional knowledge integration. Therefore, the company has weak performance in both flexible and efficient knowledge integration [17]. The average number and

standard deviation of each measurement item of flexible knowledge integration are shown in Table 1.

Factor analysis is an important method to test the validity of the Likert scale, but not all data are suitable for factor analysis. In order to test whether the flexible knowledge integration scale is suitable for factor analysis, this study first performed KMO and Bartlett on the data. The result of the sphere test shows that the KMO coefficient is 0.747, which is much greater than 0.5. The Bartlett sphere test passed ($P < 0.001$), indicating that the scale meets the factor analysis standard, as shown in Table 2.

This paper conducts exploratory factor analysis (EFA) on the scale. The factor load is the value obtained by the orthogonal rotation method. Most of the factor loads on the three common factors exceed 0.7, and are consistent with the dimensions measured in advance. This shows that the scale has high validity, with a cumulative contribution rate of 62.922%. In order to test the reliability of the scale, this study uses Cronbach's alpha coefficient method (abbreviated as "a" coefficient method) to test the reliability of each dimension of the scale and its overall items. The "a" coefficient of each item after deletion is lower than the existing a coefficient, and the "a" coefficient of each dimension is higher than 0.7, and the "a" coefficient of the overall item is 1.353. In summary, the scale has good reliability and validity. This article will use these 10 items to measure flexible knowledge integration.

Entrepreneurship opportunities emerge and entrepreneurial activities also emerge one after another. The process

TABLE 2: Reliability and validity test of the flexible knowledge integration scale.

Dimension	Item	Factor 1	Variance contribution rate (%)	<i>a</i> coefficient after deletion	<i>a</i> coefficient
Emergency	E1	0.749	69.014	0.508	0.608
	E2	0.061		0.146	
Extroverted	O1	0.923	6.586	0.513	0.613
	O2	0.447		0.626	
Coordinated	C1	0.542	87.322	0.031	0.131
	C2	0.092		0.413	
Total table			62.922		1.353

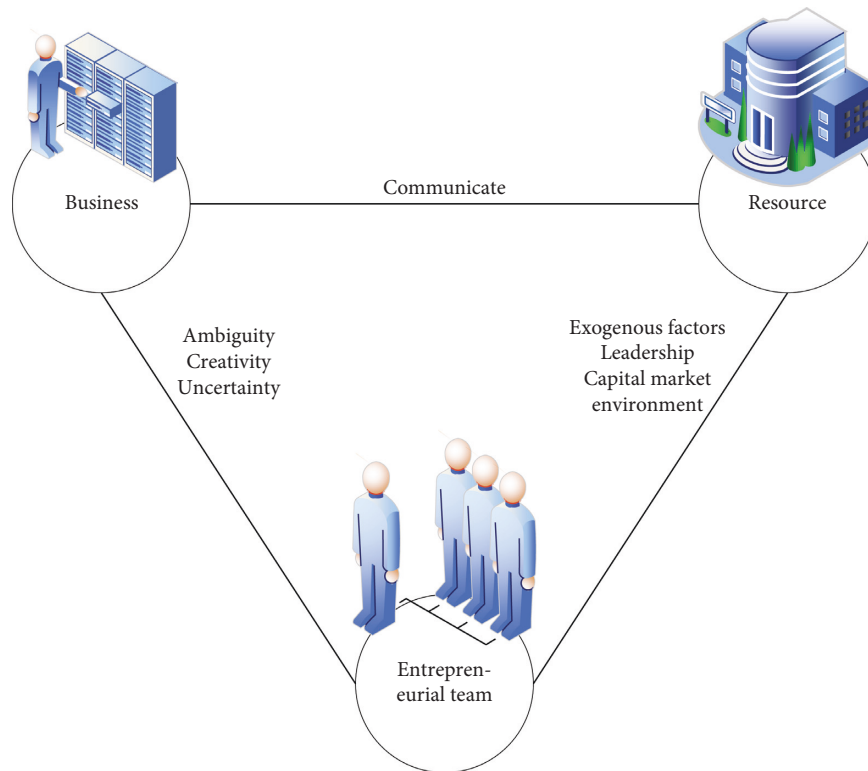


FIGURE 4: Timmons entrepreneurial model.

of continuous integration of entrepreneurial opportunities, entrepreneurial teams, and related entrepreneurial resources is a manifestation of entrepreneurial activities. In this process, various factors in the external environment have an effect on each stage of entrepreneurial activities all the time [18].

The entrepreneurial model is shown in Figure 4. The model is considered that the core position of entrepreneurship should be environmental factors. The model believes that the key elements of entrepreneurship are entrepreneurial resources, entrepreneurial opportunities, entrepreneurial spirit, entrepreneurial transaction behavior, and the external environment of entrepreneurship. The external environment affects and restricts all activities and behaviors involved in the entrepreneurial process.

4.2. Corporate Performance Data Collection. On the basis of the assumptions in Section 4.1, adding a balanced market dual opportunity to construct Model1, the data results show

that the impact of balanced dual opportunities on the performance of the new company is not significant. The Model 1 in Table 3 is used to test the relationship between market duality and new enterprise performance in a sample of non-high-tech industries [19].

The data analysis results in the table show that in non-high-tech industries, only pursuing market exploration and market utilization opportunities will have a significant positive impact on the performance of the new company. The coefficient of influence of market exploration opportunities on business performance is 0.585**, which is higher than the regression coefficient of market utilization opportunities -0.328*. Like nontech companies, the dual opportunities of pursuing a balanced market will have a positive impact on the performance of the new company.

Based on social network theory and organizational learning theory, this paper constructs a research framework for the relationship among entrepreneurial networks, organizational learning, and new corporate performance. The relationship among entrepreneurial networks,

TABLE 3: Regression analysis results of the relationship between the recognition of dual opportunities in the market and the performance of new companies.

Explanatory variables	Explained variable: New enterprise performance			
	High-tech industry		Non-high-tech industries	
	Model 1	Model 2	Model 1	Model 2
Business age	0.145	-0.347	-0.959	0.373**
Enterprise size	0.418**	-0.935	-0.706	-0.561
Education level	-0.213	-0.911	-0.627	0.374
Age of entrepreneur	0.438	-0.955	-0.216	0.160
Gender of entrepreneur	-0.370	-0.761	0.340	0.160
Market exploratory opportunities	0.578	0.934**	0.585**	-0.084
Market exploitable opportunity	-0.809	0.073	-0.328*	0.853
Balanced market dual	0.319	-0.812	0.783	-0.822
R^2	0.822	-0.121	-0.389	0.690
Adjust R^2	-0.350	0.688	-0.973	-0.982
F-value	0.211**	-0.746	0.269**	0.397**

Note. *** indicates the significance level $P < 0.01$ (two-tailed detection), ** indicates the significance level $P < 0.05$ (two-tailed detection), * indicates the significance level $P < 0.1$ (two-tailed detection).

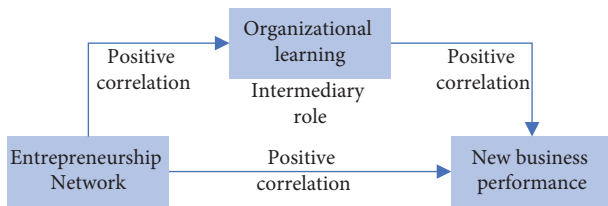


FIGURE 5: The relationship between entrepreneurial networks, organizational learning, and new company performance.

organizational learning, and new company performance is shown in Figure 5.

4.3. Examples of Entrepreneurial Ability and Corporate Performance. Based on theoretical research on knowledge management, experiential learning, organizational duality, entrepreneurial learning, etc., this research constructs a conceptual model of the relationship among entrepreneurial experience, dual opportunity awareness, and new business performance. It further understands the differences in the impact of different types of entrepreneurial experience on the identification of dual opportunities, and the mitigation effect of knowledge sharing between the two. Combining the framework of the technology market, this paper analyzes the difference in the impact of dual opportunity perception on the performance of new companies in the background of different technology-intensive industries [20].

In order to increase the questionnaire response rate, this article will give priority to collecting paper questionnaire data. This article combines the characteristics of Shanxi's small- and medium-sized enterprises based on previous questionnaire surveys in related fields, designed a questionnaire to collect the data needed for the survey, and distributed paper questionnaires.

In this survey, a total of 300 paper questionnaires and online questionnaires were distributed, and 296 paper questionnaires were recovered. Because some survey items were incomplete and could not accurately reflect the actual

situation of the interviewees, 14 invalid surveys were excluded. There were 282 valid paper surveys, the survey recovery rate was 98%, and the survey effective recovery rate was 94%. The specific situation is shown in Figure 6.

The regional distribution of sample data is shown in the figure. Among them, enterprises in the western region accounted for 21%, manufacturing accounted for 25.7%, service industry accounted for 31.9%, and commerce accounted for 12.9%. These three industries accounted for more than 70% of the total sample size, and the remaining industries, including high-tech, finance, and real estate, accounted for less than 20%. This can reflect the concentration and imbalance of Shanxi's small- and medium-sized enterprises in industry selection.

This uneven distribution can reflect to a certain extent the concentration and imbalance of the development of small- and medium-sized enterprises in Shanxi Province. The distribution of the sample data in the industry is shown in Figure 7:

The following are the descriptive statistics of the return on assets, return on net assets, R&D density, engineer ratio, capital investment ratio, patent variables, asset-liability ratio, and company size of the eastern and central western samples. As shown in Figure 8.

In terms of corporate performance, the average corporate performance of the sample of companies in the eastern and western regions is 6.316 and 7.756. The average corporate performance of the sample of enterprises in the central and western regions is 5.770 and 7.296. This can preliminarily judge that enterprises in the eastern region have better corporate performance than those in the central and western regions [21]. According to the clustering results obtained by the P-SOM neural network model, a statistical graph of the results shown in Figure 9 is drawn.

It can be found that among the six management system levels, the first-level company A management system performs well in three aspects: safety performance, social contribution performance, and service performance. All of these have made it difficult for Company A to catch up in

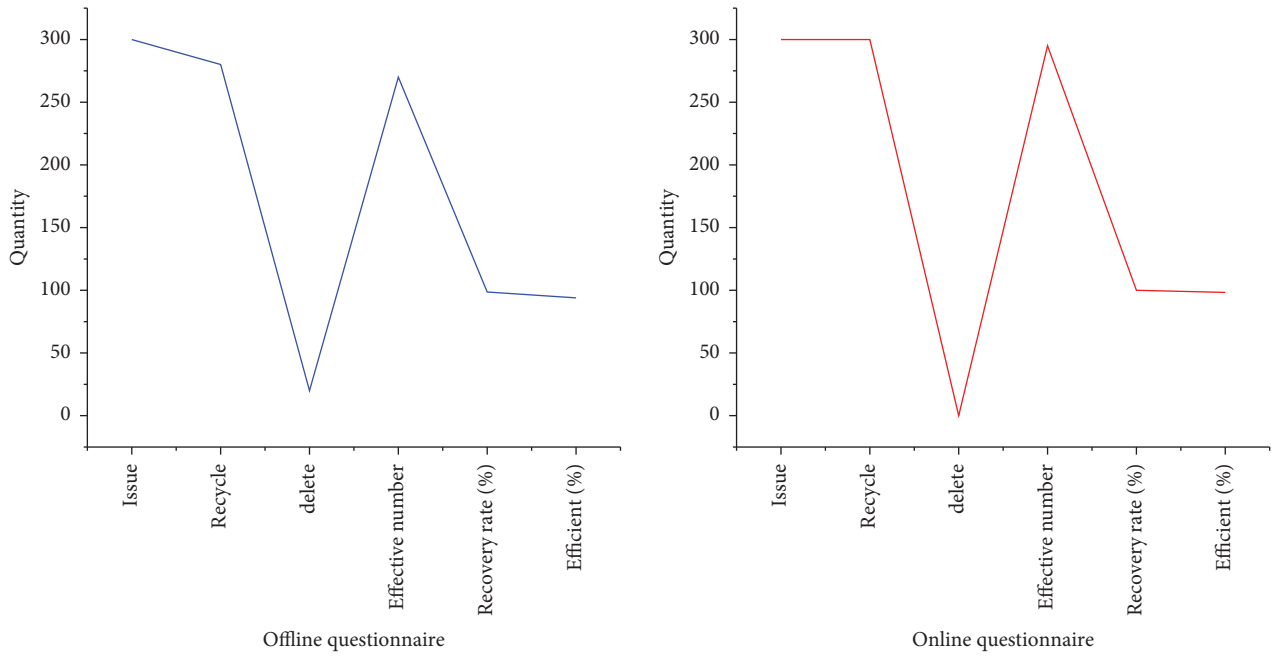


FIGURE 6: Questionnaire distribution and recovery.

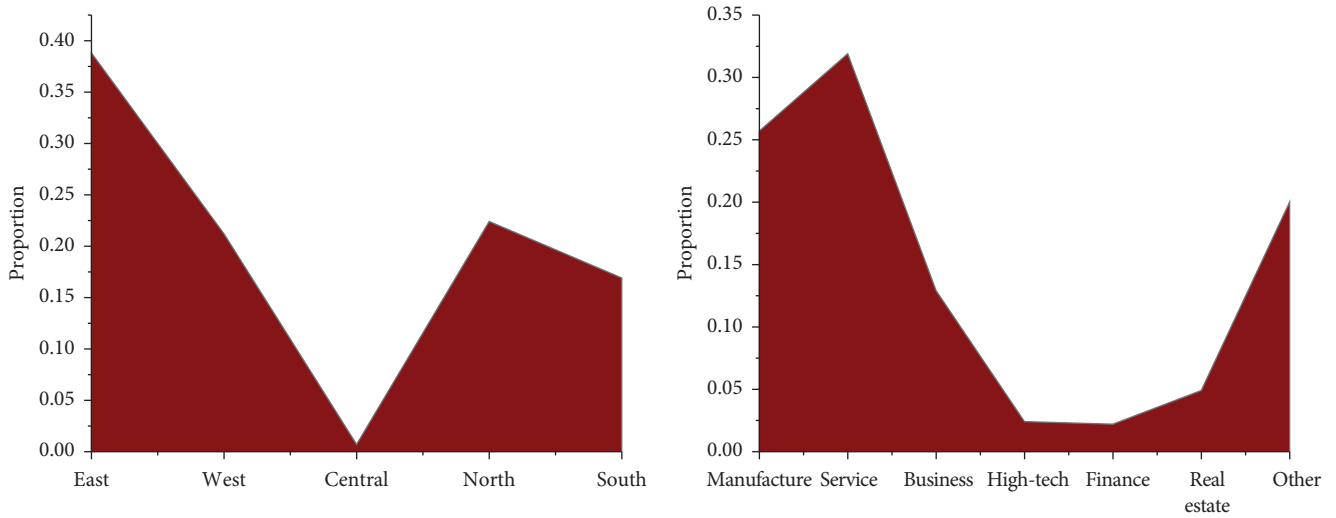


FIGURE 7: Regional distribution and industry category of companies.

financial terms in the following years. In recent years, Company A has actively carried out technological innovation, developed its own ATM system, and sold it. At the same time, it has built a new financing platform, so that its financial performance has a steady and positive trend. On the basis of these studies, if the company’s investment in scientific research and innovation is increased, the changes in the company’s financial performance are shown in Figure 10. This shows that there is a positive correlation between the spirit of social innovation and the performance of new enterprises.

The t value of the interaction term “entrepreneurship orientation \times entrepreneurial environment hostility” is 0.260 ($P > 0.05$). The definition of the entrepreneurial

environment of Shanxi SMEs shows that it does not regulate the relationship between entrepreneurial orientation and corporate performance. Therefore, the hypothesis that “the definition of the entrepreneurial environment of small and medium-sized enterprises in Shanxi Province plays an intermediate role in the relationship between entrepreneurial orientation and corporate performance” does not hold. The t value of the interaction term “entrepreneurship \times entrepreneurial environment dynamics” is 2.698** ($P < 0.05$). The dynamics of the entrepreneurial environment of SMEs in Shanxi Province are entrepreneurial orientation and corporate performance. Therefore, it is assumed that “the dynamics of the entrepreneurial environment of small and medium-sized enterprises in Shanxi Province play a

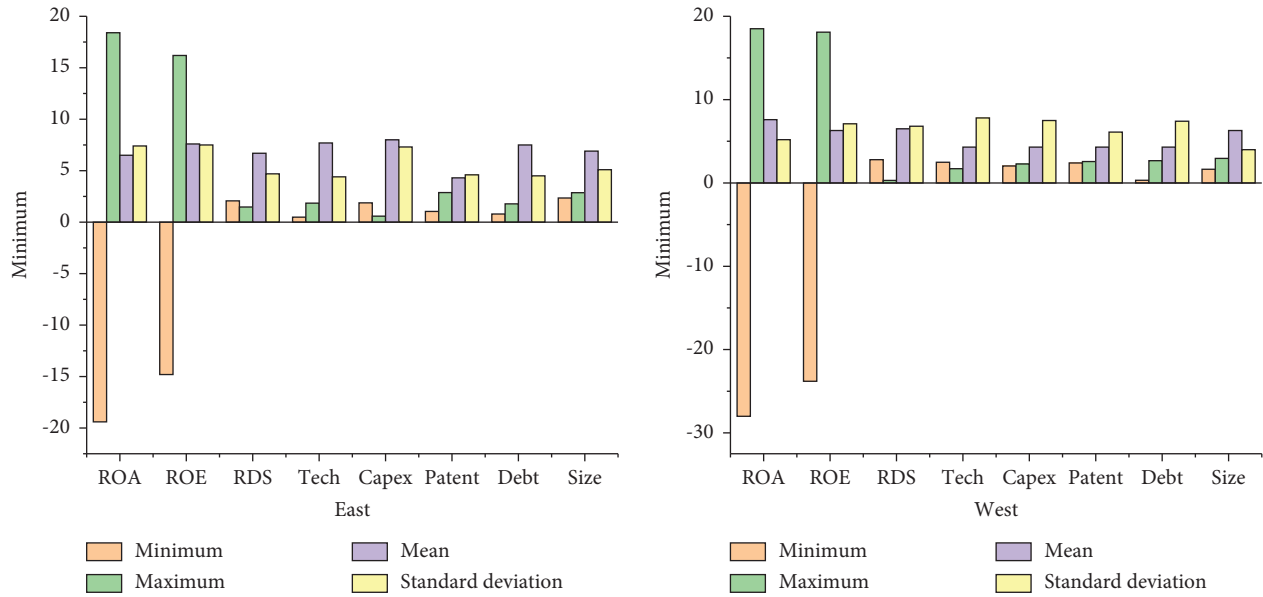


FIGURE 8: Descriptive statistics of samples from east and west regions.

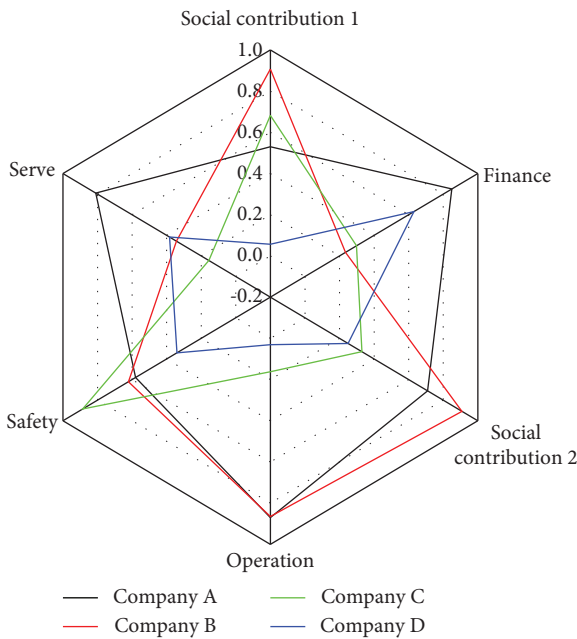


FIGURE 9: Performance factor radar chart.

moderate role in the relationship between entrepreneur-oriented risk-taking and corporate performance.” The specific relationship table is shown in Table 4.

In summary, this survey mainly examines the relationship among the entrepreneurial environment, entrepreneurial orientation, and corporate performance of Shanxi SMEs. However, the unfounded research hypothesis reflects to a certain extent that a large part of the development of small- and medium-sized enterprises in Shanxi Province still relies on the power of the government. The government-led influence on the growth of enterprises is to a certain extent greater than the influence of the market on the growth of

enterprises. This makes certain assumptions fail the verification, but the relationship among the three is basically verified.

This survey examines the impact of the entrepreneurial environment on corporate performance. It also confirmed that the hostility of the entrepreneurial environment of SMEs has a negative impact on corporate performance ($\beta = 0.167, P < 0.05$), and the dynamics of the entrepreneurial environment have a positive impact on corporate performance. This article uses Shanxi Province companies as an alternative sample to study the relationship between technological innovation and corporate performance. Therefore, the research conclusions have certain limitations.

5. Discussion

Based on previous theoretical research and empirical analysis, this paper summarizes the research conclusions on the relationship among entrepreneurial network relationships, technological innovation, and the performance of new ventures as well as research conclusions and the theoretical contributions of entrepreneurs, and proposes future research directions. This article will help entrepreneurs understand the specific role of interpersonal relationships in the performance of new startups and make better use of network resources. With the rapid development of China’s economy, there are more and more business opportunities. With the improvement in social norms and legal systems, the benefits of interpersonal relationships do not appear as quickly or directly as before. However, entrepreneurs need to have some patience and pay attention to the impact that plays a role between network relationships and performance. Due to the characteristics of high risk, small scale, and strong innovation ability of entrepreneurial enterprises, the research results of this paper are only applicable to the

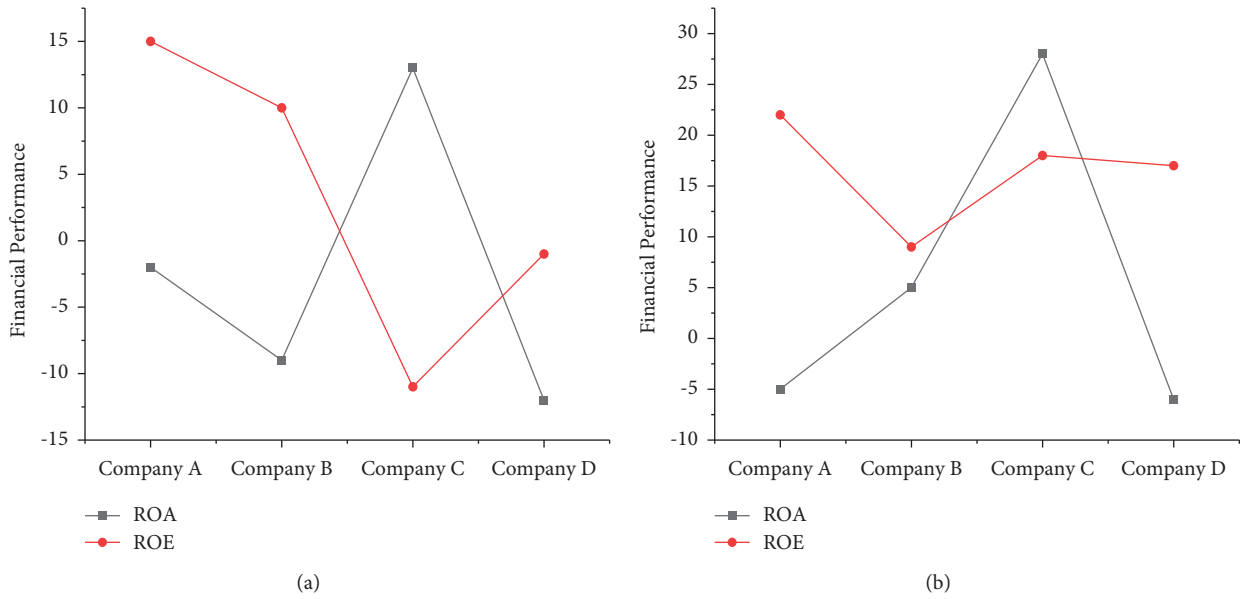


FIGURE 10: Changes in financial performance. (a) Change in financial performance prior to increased investment. (b) Change in financial performance following increased investment.

TABLE 4: The moderating effect of the entrepreneurial environment on the company’s entrepreneurial orientation and corporate performance.

Variable	Model 1 Business performance		Model 2 Business performance	
	β	t	β	t
Independent variable				
A: Entrepreneurial orientation	0.117	6.258	0.621**	8.169**
B: Dynamics of entrepreneurial environment	0.220	0.440	0.738**	3.285**
C: Entrepreneurship hostility	0.023	0.079	0.866	0.124
Interactive item				
A × B			0.167	2.698**
A × C			0.832	0.630
R square	0.545		0.784	
Adj. R square	0.031		0.429	
F	36.569		22.647	
ΔR square	0.530			
Partial F	12.983			
N	99.786			

research of enterprises in this industry. This does not have general applicability, or can it explain the overall technological innovation status of Chinese enterprises taking into account the representativeness of the sample, the comprehensiveness and standardization of information disclosure, and the availability of relevant data.

6. Conclusions

This article is based on industry linkage theory, innovation theory, and core competitiveness theory. It also uses GEM-listed companies as samples to study the relationship between entrepreneurial innovation and corporate performance. It focuses on the research and development efforts and the impact of innovation investment on corporate performance. In addition, this article classified the entire

sample by region and examined the relationship between innovation and corporate performance of sample companies in eastern Shanxi and central and western regions. Finally, in order to investigate the impact of corporate growth on the relationship between innovation and corporate performance, this paper also uses corporate growth as a slow-release variable to perform regression analysis.

Data Availability

No data were used to support this study.

Conflicts of Interest

The author declares that there are no conflicts of interest in this study.

References

- [1] W. L. Lai, H. R. Wang, C. Wang, J. Zhang, and Y. Zhao, "Waterlogging risk assessment based on self-organizing map (SOM) artificial neural networks: a case study of an urban storm in Beijing," *Journal of Mountain Science*, vol. 14, no. 5, pp. 898–905, 2017.
- [2] M. Ni, H. Cheng, and J. Lai, "GAN-SOM: a clustering framework with SOM-similar network based on deep learning," *The Journal of Supercomputing*, vol. 77, no. 5, pp. 4871–4886, 2021.
- [3] E. Suryani and M. Susilo, "The hybrid method of SOM artificial neural network and median thresholding for segmentation of blood vessels in the retina image fundus," *International Journal of Fuzzy Logic and Intelligent Systems*, vol. 19, no. 4, pp. 323–331, 2019.
- [4] P. Runst, J. Thomä, K. Haverkamp, and K. Müller, "A replication of "Entry regulation and entrepreneurship: a natural experiment in German craftsmanship"," *Empirical Economics*, vol. 56, no. 6, pp. 2225–2252, 2019.
- [5] Y. J. Hsieh and Y. J. Wu, "Entrepreneurship through the platform strategy in the digital era: insights and research opportunities," *Computers in Human Behavior*, vol. 95, pp. 315–323, 2019.
- [6] A. L. Leal-Rodríguez, A. J. Ariza-Montes, E. Morales-Fernández, and G. Albort-Morant, "Green innovation, indeed a cornerstone in linking market requests and business performance. Evidence from the Spanish automotive components industry," *Technological Forecasting and Social Change*, vol. 129, pp. 185–193, 2018.
- [7] I. Abushaikha, L. Salhieh, and N. Towers, "Improving distribution and business performance through lean warehousing," *International Journal of Retail & Distribution Management*, vol. 46, no. 8, pp. 780–800, 2018.
- [8] A. Haghighat, S. Farokhi, and E. Ghazaleh, "New replica server placement strategies using clustering algorithms and SOM neural network in CDNs," *The International Arab Journal of Information Technology*, vol. 14, no. 2, pp. 260–266, 2017.
- [9] M. H. Shafiabadi, A. K. Ghafi, D. D. Manshady, and N. Nouri, "New method to improve energy savings in wireless sensor networks by using SOM neural network," *Journal of Service Science Research*, vol. 11, no. 1, pp. 1–16, 2019.
- [10] N. Ghasemi, H. Maddah, M. Mohebbi, and S. AghayariRohani, "Proposing a method for combining monitored multilayered perceptron (MLP) and self-organizing map (SOM) neural networks in prediction of heat transfer parameters in a double pipe heat exchanger with nanofluid," *Heat and Mass Transfer*, vol. 55, no. 8, pp. 2261–2276, 2019.
- [11] S. Bhagavatula, R. Mudambi, and J. P. Murmann, "Management and organization review special issue "the innovation and entrepreneurship ecosystem in India"," *Management and Organization Review*, vol. 13, no. 1, pp. 209–212, 2017.
- [12] L. Wendy and P. De-Costa, "Problematizing enterprise culture in global academic publishing: linguistic entrepreneurship through the lens of two Chinese visiting scholars in a U.S. university," *Multilingua*, vol. 40, no. 2, pp. 225–250, 2021.
- [13] J. Machado, F. Soares, and G. Veiga, "[Lecture notes in electrical engineering] innovation, engineering and entrepreneurship volume 505 || determinants of the well-succeeded crowdfunding projects in brazil: a study of the platform kickante," in *Innovation, engineering and entrepreneurship*-Springer, Berlin/Heidelberg, Germany, 2019.
- [14] F. D. Mas and P. Paoloni, "A relational capital perspective on social sustainability. The case of female entrepreneurship in Italy[J]," *Measuring Business Excellence*, vol. 24, no. 1, pp. 114–130, 2019.
- [15] B. Bhatt, I. Qureshi, and S. Riaz, "Social entrepreneurship in non-munificent institutional environments and implications for institutional work: insights from China," *Journal of Business Ethics*, vol. 154, no. 3, pp. 1–26, 2019.
- [16] P. Demirel, C. L. Qian, F. Rentocchini, and J. Pawan-Tamvada, "Born to be green: new insights into the economics and management of green entrepreneurship," *Small Business Economics*, vol. 52, no. 1, pp. 1–13, 2019.
- [17] B. J. Lo-Bianco, "The discourse of the edge: marginal advantage, positioning and linguistic entrepreneurship," *Multilingua*, vol. 40, no. 2, pp. 261–275, 2021.
- [18] Z. Ye, J. Zheng, and R. Tu, "Network evolution analysis of e-business entrepreneurship: big data analysis based on taobao intelligent information system," *Information Systems and E-Business Management*, vol. 18, no. 4, pp. 665–679, 2020.
- [19] "Business performance," *Acta Universitatis Agriculturae et Silviculturae Mendelianae Brunensis*, vol. 41, no. 3, p. 17, 2017.
- [20] G. Li, S. Shao, and L. Zhang, "Green supply chain behavior and business performance: e," *Technological Forecasting and Social Change*, vol. 144, pp. 445–455, 2019.
- [21] S. P. Kaur, J. Kumar, and R. Kumar, "The relationship between flexibility of manufacturing system components, competitiveness of SMEs and business performance: a study of manufacturing SMEs in northern India," *Global Journal of Flexible Systems Management*, vol. 18, no. 2, pp. 123–137, 2017.

Research Article

One Person Plays Multiple Roles: The Diversified Roles and Functions of Convention Project Hosts by SEM Methods

Jie Zhou ¹, Mengjie Zhao,¹ and Qi Yang²

¹College of Tourism and Service Management, Nankai University, No. 38 Tongyan Road, Haihe Education Park, Jinnan District, Tianjin 300350, China

²School of Public Management, Tianjin University of Commerce, Tianjin University of Commerce School of Public Administration, No. 409, Guangrong Road, Beichen District, Tianjin 300133, China

Correspondence should be addressed to Jie Zhou; zhouj@nankai.edu.cn

Received 28 June 2022; Accepted 8 August 2022; Published 25 August 2022

Academic Editor: Wei Liu

Copyright © 2022 Jie Zhou et al. This is an open access article distributed under the Creative Commons Attribution License, which permits unrestricted use, distribution, and reproduction in any medium, provided the original work is properly cited.

In a convention project, the relationship between the host and professional conference organizers has an important impact on the convention project promotion. However, as an important stakeholder of the convention, the role of hosts in the project is less concerned and studied. Therefore, based on theories of project governance, this paper combines the role of the convention project hosts from the perspective of the project sponsors and formulates the convention hosts' role measuring scale with the project sponsor measuring scale. Then, through content validity analysis and exploratory and confirmatory factor analysis, the scale was optimized and nine items were finally determined. The study found that the hosts of the convention project play three roles in the convention project, the customer role, the controller role, and the supporter role, and verified through the SEM that all three roles have a positive effect on the convention project performance.

1. Introduction

The convention industry has become an important part of the global tourism industry, and the success of the convention project is the micro basis of the healthy and sustainable development of the convention industry. The host and the professional conference organizer (PCOs) are the two core subjects of the convention project, among which the professional conference organizer of the convention project is the main body of the project management and operation, which is responsible for meeting the objectives and improving the satisfaction of the attendees [1]. Therefore, a large number of scholars have explored the motivation of the attendees, to guide the professional conference organizers to improve the performance of the convention projects to the needs of the attendees oriented [2, 3]. In contrast, the host of the convention project, as the initiator of the project, is not the direct subject to meeting the participants, but there is a principal-agent relationship between the host and the professional

conference organizer [4]. Therefore, according to the principal-agent theory, the initiator group for each program should ensure that the governance arrangements are appropriate [5], to reduce the principal-agent conflicts and promote the sustainable satisfaction of the strategic objectives of the project. Undeniably, governance failure has always been considered one of the most prominent reasons for project failure [6]. However, the existing research results rarely excavate the core influencing factors of convention project success from the perspective of project governance subjects (convention project host). Correspondingly, in industry practice, the role of the convention project hosts is usually weakened, and the phenomenon of "emphasizing management, neglecting governance" is more common in the process of project operation [7].

According to the principal-agent theory, as the initiator of the convention project, the host is the owner of the project [8], has the right to claim the residual value of the convention project, and pays more attention to the long-term

stable income of the project. In contrast, the professional conference organizer as the manager pays more attention to the short-term income that can increase his or her own income in the main contract [4]. In the context of the conflict between the interests of the host and the professional conference organizer, the blurry responsibilities can trigger the “internal person” control of the project, and the strategic value of the project is difficult to obtain the correct understanding and implementation [4]. The short-term benefits of management-driven convention projects have been more focused on, while the long-term value of governance-driven convention projects is often ignored. For example, professional conference organizers, driven by short-term interests, only focus on the size of the customer, ignoring the quality of the client; pays attention to the economic value, ignoring the brand value; focus on the satisfaction of the guests and participants and ignore the interests of other stakeholders; pays attention to the direct economic value; ignores the derived social effects; and so on [9]. As the findings of KPMG and PMI in the field of project management, only about 40% of the project results meet the strategic objectives of the initiator or owner [10].

According to the definition of PMBKO, a sponsor refers to “individuals or groups that provide resources and support for projects, project sets, or project combinations responsible for creating conditions for success [11].” To put it simply, a project sponsor is an individual or organization that provides economic or material support for the project [12]. However, relevant research on project governance has consistently shown that the role of sponsors is far from limited to the support of resources [13]. The project sponsor has been conceptualized as a multidimensional structure [14, 15], and a clear definition and active commitment to the sponsor's role is important for optimizing the governance framework [16] and promoting the success of the project [17, 18]. At present, different scholars have discussed the specific work responsibilities that project hosts should undertake or the skills they should have from different perspectives, such as communication with the management teams [19], motivating the management team [20], explanation and assessment of strategic objectives [21], risk prevention and control [22], political and financial support [23], and so on. Therefore, based on the characteristic attributes of the host-organizer relationship of the convention project, this paper will conceptualize the responsibilities of project sponsors formed in the existing research results, form the diversified roles of the convention project host (customer, controller, and supporter) and their core functions, and use factor analysis to verify the proposed three roles. On this basis, the impact of the three roles of the host on the convention project performance is tested by the structural equation model. The research results of this paper are used to clarify the relationship between the host and the professional conference organizer of the convention project. At the same time, it contributes to strengthening the positive role of the host, meeting the needs of the governance of the convention projects, and promoting the realization of the strategic value of the convention projects.

2. Literature Review and Definition of Convention Project Hosts' Roles and Functions

2.1. Customer Role and Information Communication Function. Although the end user of the convention project is the participant, from the perspective of the principal-agent relationship, the direct principal of the professional conference organizer is the host, that is, the host hires the professional conference organizer to perform its duties, to meet the demands of the host. The relationship between the host and the professional conference organizer is a kind of business exchange essentially [24]. Therefore, the host is the project delivery and service object of the organizer, that is, in the convention project governance framework to play the role of the customer.

The matching of demand and supply is the logical basis of service product opening and design. Therefore, the host, as the customer, is necessary to carry out an efficient docking with the management main body of the project (the organizer) [25], which not only needs to effectively transfer the service demand to the management team of the service provider, that is, to clearly define the project's goal, vision, and other information [20], but also needs to timely understand the interests and demands of the project management team through the construction of open relationship [26]. In other words, as the host of the customer role, its core function is “information communication.” Relevant scholars have also pointed out that the high-quality communication skills of the project initiators are critical to the success of the project [19, 27, 28].

According to the core functions of the customer role and drawing on the existing research results on the communication function of the host in project management, from the perspective of “transmitting” and “acquiring” information from the host to the organizer, this research constructed the measurement items of the convention project host's customer role and information communication function as shown in Table 1. The measurement items in Table 1 reflect the specific tasks of the host of the convention project based on the role of the customer, which mainly includes two aspects: first, through communication, to make the organizer clearly understand the host's needs, including the host's strategic intention and goals for initiating the project (C1), the difference in the importance of each work and goal (C2), and the criteria for the success of the project (C3), to form the guidelines for the organizer to promote the project and second, to timely understand the organizers' interests (C4) through communication, with a view to achieving a balance of service supply and demand.

2.2. The Role of the Controller and the Supervisory and Incentive Function. Although the hosts who assume the role of the customer can convey the strategic intention and expected objectives of the project to the organizer, according to the core point of view of principal-agent theory [29], driven by self-interesting, moral hazard of the convention project organizer as an agent will appear [30]. Accordingly, the

TABLE 1: Organizer functions based on customer role and their measurement items.

Role	Core function	Measurement item	Reference
Customer	Information communication	C1: the host's strategic intention and goal to initiate the project	Englund and Bucero [20]
		C2: the host clearly defines the priorities of the work or objectives in the progress of the convention project with the organizer	Bryde [14]
		C3: the host clearly defines criteria or indicators of achievement for the success of the convention project to the organizer	Bryde [14]
		C4: the host is able to understand the interests of the convention project and actively coordinate with the strategic objectives of the convention project	Kloppenborg et al. [8]

TABLE 2: Host's functions based on the role of the controller and measurement items.

Role	Core function	Measurement item	Reference(s)
Controller	Supervision and incentive	M1: to solve the problem of nonprocedural decision-making in boosting convention projects to the organizer, the host can construct strict and formal decision-making procedures for the project	Müller et al. [32], Brunet and Aubry [33]
		M2: the convention host is concerned about the risk and circumvention strategy of the convention project, and the convention project has a formal risk control system	Brunet and Aubry [33]
		M3: the host has the right to terminate the project as a result of environmental changes or expected performance deviations within the progress of the convention project, as specified in the contract	Bryde [14]
		M4: the host of the convention promised and established an incentive system for the professional conference organizer, highlighted the degree of realization of the objectives of the convention projects, and strengthened the close relationship between the interests of the organizer and the management team	Englund and Bucero [20]

“opportunity behavior” that sacrifices the client’s interests to satisfy personal interests will make it difficult for hosts to achieve their goals [4]. Therefore, while assuming the customer identity, the host needs to play the role of a controller, construct a perfect governance mechanism, and ensure that the objectives of the project are consistent with the objectives of the fund supporters [31] so that the direction of the project is consistent with the expectations of the project.

According to the causes and potential behavior deviation of the principal-agent problem, the host of the convention project plays the role of a controller and undertakes the basic function of “supervision and incentive.” On the one hand, prevent the “opportunistic behavior” of professional conference organizers through effective monitoring of project progress and management decisions [32]. On the other hand, through an effective incentive mechanism to promote the interests of professional conference organizers and hosts, thereby reducing principal-agent conflicts [20].

According to the core function of the controller role and the relevant research results of the supervision incentive function of the host in project management, this study constructs the measurement items of the role of the host controller and the supervision incentive function of the convention project, from the perspective of moral hazard avoidance and the compatibility mechanism of the main undertaking interests, as shown in Table 2. The measurement items in Table 2 reflect the specific tasks of the host of the meeting project based on the role of the controller, which mainly includes the question items M1 to M3, which emphasize the supervisory function of the host and prevent and

correct the deviation of the actual progress of the project from the expected objectives; questionnaire item M4 mainly strengthens the scientific design of the incentive mechanism; and contributions to the objectives of the host and the professional conference organizer are tend to be consistent.

2.3. The Role of Supporters and the Function of Resource Supply. The customer role of the host is to make the project organizer understand the expected goal of the project, and the role of the controller is aimed to make the organizer have the willingness to achieve the project goal. However, when the necessary conditions for achieving the project goal are lacking in the process of project promotion, it will be difficult for the organizer to transform the willingness to achieve the goal of the host into reality. Therefore, as the initiator, the host needs to play the role of project supporter [34] to help the professional conference organizer achieve the objectives of the project. Accordingly, the core function of the host, as a supporter, is to provide resource support for the project (tangible and intangible) [23] to create conditions for the success of the project (PMBOK).

According to the core function of the supporter role, taking the existing research results as a reference, and based on the difference between the type and function of the supplied resources, the measurement items of the host’s role as supporter and the resource supply function of the convention project are constructed. As shown in Table 3, the measurement items reflect the specific tasks of the host, that is, the supporter-based convention project in Table 3, which

TABLE 3: Host functions based on the role of supporters and measurement items.

Role	Core function	Measurement item	Reference
Supporter	Resource supply	S1: when the convention project is in financial difficulties, the host can offer the necessary support or help	Crawford and Brett [23]
		S2: the host can provide the professional conference organizer with information or support related to the venue of the convention project	Crawford and Brett [23]
		S3: the host will provide media resources for convention projects with his influence	Bryde [14]
		S4: the host will provide support or help for the invitation and exhibition of investment by the organizer of the convention with his influence	Bryde [14]
		S5: the host will be able to train the convention project staff, if necessary, to ensure the achievement of the project objectives	Bryde [14]
		S6: the host will help the professional conference organizer to provide important environment information and help them to understand the environment and changing trends faced by the convention projects in an accurate and timely manner	Kloppenborg et al. [8]

TABLE 4: Convention project performance measurement items.

Variable	Measurement item	References
Convention project performance	SU1: the convention project can be carried out according to the expected schedule	Bryde [14], Müller et al. [32]
	SU2: the convention project can be completed within budget	
	SU3: the convention project can be advanced in accordance with the expected quality requirements and safety standards	

mainly includes the following: S1 mainly emphasizes the financial support provided by the host for the project; S2–S4 mainly highlight the host’s stakeholders’ resources (social capital) that are provided by the host for its credibility and influence, such as the venues, media resources, and client resources; S5 mainly emphasizes the knowledge resources provided by the host for the project; and S6 mainly emphasizes the information resources provided by the host for the project.

3. Convention Project Performance and Research Hypothesis

Convention performance is the main reference index for judging the success of the convention project. Existing studies have mostly measured the convention project performance from the perspective of participants by measuring the effectiveness of the convention, the degree of communication, and the satisfaction of participants [35, 36]. Few studies have evaluated the performance from the perspective of the organizer. As the organizer of the convention, the host and the organizer jointly serve the convention project. In order to explore the convention project performance from the perspective of the organizer, this article introduces the concept of “project success.”

Among the judging indicators of project success, the project success triangle model has the highest recognition and is the most important factor for measuring project success. Oisen proposed a project triangle model in 1971 and pointed out that the evaluation of project success can start from three dimensions: cost, time, and project quality. Many scholars then evaluated the success of the project with reference to Oisen’s measurement indicators [37]. This article introduces the project success triangle model to

evaluate the convention project performance. Based on the scales of Bryde [14], Müller et al. [32], and the characteristics of convention projects, this paper measures the performance of convention projects from three aspects: time, budget, and quality. The specific measurement items are shown in Table 4.

According to the definition and analysis of the roles and functions of the convention project host, the customer role and its function make sure that the professional conference organizer can accurately understand the convention project performance objectives and requirements, including time, cost, and quality, and the controller role and its function make sure that the professional conference organizer has the willingness to promote the implementation of the project according to the convention host’s performance objectives, and the supporter role and its function make sure that the professional conference organizer has the conditions to promote the project implementation according to the convention host’s performance objectives. The three roles ensure the success of the convention project from different perspectives and play a positive role in improving the convention project performance. According to the above analysis logic, the research hypotheses are as follows:

H1: the commitment level of the convention host’s customer role has a significant positive effect on the convention project performance

H2: the commitment level of the convention host’s controller role has a significant positive effect on the convention project performance

H3: the commitment level of the convention host’s supporter role has a significant positive effect on the convention project performance

4. Methodology

To ensure the efficiency of questionnaire recovery, according to the principle of convenience [8], the research team takes the conference industry employees who have contacted or cooperated with the team members as the research object, and the questionnaires are distributed and collected through the Internet.

4.1. Questionnaire Development Based on the Content Validity Test. In this paper, we will measure the responsibilities of the host perceived by the professional conference organizer through a questionnaire survey, carry out exploratory factor analysis, and obtain three roles of the host before the factor structure examination.

Drawing on the methods of scholars such as Müller et al. [32] and Joslin and Mülle [38], this paper took the project leaders of professional conference organizers (PCOs) of the separated conference project between the host and the organizer in China as the research object; based on the information and perception of the conference project that the respondents were responsible for or participated in recently, the five-point Likert scale (from strongly disagree to strongly agree) was used to evaluate the questions contained in the role of the conference host and the performance level of the conference project.

In this paper, the division of the host's role and the corresponding measurement items constitute the hypothesis of the survey scale and factor structure. According to the summary results of Tables 1–3, based on the literature study of research, the total number of measurement items for the role and function of the host is 14. Although each measurement item is supported by the relevant research results in the field of project management, to a certain extent, it reflects the effectiveness of the questionnaire, but there are some differences in the governance system between the convention project and the general project. To ensure that the related research results of the hosts' responsibilities in the general project are applicable to the convention project, this paper examined the content validity of the preliminary questionnaire proposed above.

Based on the method of Musawir et al. [39], we test the content efficiency of 14 measurement items by the method of Lawshe's content validity ratio (CVR) [40]. First of all, according to the research experience and industry experience, the research team selected 13 experts in the field of convention and exhibition as the object of pre-research, including 4 scholars engaged in convention and exhibition research for a long time and 9 industry experts with many experiences in hosting and organizing the convention project. And 13 experts measured the role of the host in the initial questionnaire and evaluated 14 items related to the specific responsibilities of the host, in which the importance level of each item is divided into "essential," "useful, but not essential," and "not necessary." Finally, according to the proportion of "essential" experts, the content validity of each item is tested according to the calculation method and validity criteria of Ayre and Scally [41].

Based on the above testing methods and steps of content efficiency, questions S2, S5, and S6, out of the 14 initial questions measured in this paper, the host as the supporter, did not pass the content efficiency test, and their CVR was less than 0.538. Therefore, this also shows that the hosts are weak in support of working site selection, management training, and environmental identification, and they are mainly the basic management functions of the convention host.

After deleting the items that failed the content efficiency test, this paper finally retained the 11 final measurement items used to measure the role of the host. Set five-point Likert for each question scale of strongly agree to strongly disagree, which was used to measure the level of responsibility of the participants to evaluate the responsibilities of the most recent convention project.

4.2. Sample Acquisition Process and Results. To guarantee the recovery efficiency of the questionnaire, this paper is based on the principle of convenience [8], and the research team takes the convention practitioners who have contacted or have cooperative relations as the research object and adopts the way of the network as the channel to issue the questionnaire. The total survey lasted for 2 weeks. It added up to 255 copies of the questionnaire; 114 copies of the effective questionnaire were collected; the questionnaire return ratio was 45%; and the proportion of the sample quantity and the potential variable measurement items reached the standard of 5:1.

Although the sample is relatively small compared with the individual-level study, from the perspective of our method, the number of samples meets the proportion requirement between the number of samples and potential variable measurement items proposed by Hair et al. [42]. According to the existing research results, the research samples of Zwikael and Smyrk [43] and Müller et al. [32] project governance are 102 and 121, respectively, which shows that the research sample in this paper basically conforms to the basic rules and quantity of sample acquisition in the field of project management.

5. Results

5.1. Descriptive Statistics Analysis. As shown in Table 5, a total of 114 questionnaires from 34 cities were collected in this study. A total of 98.2% of the respondents had the experience of hosting the convention, and 68% of the respondents had 5 years or more working experience in the convention. In terms of position distribution, 59.6% are middle and senior management personnel, and 40.4% are ordinary members, covering all levels of the organizing team of the convention project hosting team. According to the number of hosts, the convention can be divided into single host and Co-hosted by Multiple hosts, with a ratio of nearly 1:1.

5.2. Exploratory Factor Analysis. The credibility and validity of the questionnaire were measured. The KMO test coefficient of the questionnaire was 0.880 (more than the standard

TABLE 5: Sample basic information.

Variable	Quantity	Proportion
<i>Convention scale</i>		
Small convention (participants < 100)	17	15.79
Medium convention (100 < participants < 1,000)	63	56.14
Large convention (10,000 < participants < 1,000)	19	17.54
Large-scale convention (participants > 10,000)	11	10.53
<i>Number of hosts</i>		
Co-hosted by multiple hosts	64	57.02
Single host	46	42.98
<i>Position</i>		
Other project members	46	40.35
Person liable for project department	32	29.82
Chef person liable for project department	32	29.82
<i>Working years</i>		
0–5 years	36	31.59
5–10 years	30	26.32
10–15 years	29	25.44
15–20 years	11	9.65
More than 20 years	8	7.00

of 0.5), and the significance probability of the chi-square statistical value of the Bartley sphere test was 0.00 (less than 0.05). Therefore, the questionnaire had good structural validity and was suitable for factor analysis. Cronbach’s α coefficient value of the 11 test items used to measure the host’s role was 0.882, indicating that the questionnaire had a high degree of credibility.

An exploratory factor analysis was carried out on each item of the host’s role, and three factors with eigenvalues greater than 1 were extracted, and the cumulative contribution rate was 69.43%. The maximum variance method is used as the rotation method to generate the factor load matrix after rotation (as shown in Table 6). Because item S1 had a double load (the load of the item in both factors is greater than 0.5), the item was deleted. Other items were loaded more than 0.5 in their respective factors, and the items can be retained.

The final factor F1 retained four items, C1, C2, C3, and C4; F2 retained three items, M1, M2, M3, and M4; and F3 retained two items, S3 and S4. According to the meaning of each factor corresponding to the item, the three factors can be named as customer, controller, and supporter. The credibility analysis was carried out on the factors after the deletion of the item; Cronbach’s α coefficient was 0.844; and Cronbach’s α coefficient was 0.766. Cronbach’s α coefficient of the two items in the role of quantity supporter was 0.870, which passed the reliability test, which showed that the consistency of each measurement item was good.

5.3. *Confirmatory Factor Analysis.* The results of the confirmatory factor analysis showed that the fitting degree of the model and the data can be accepted ($\chi^2 = 52.2$, $df = 32$, $\chi^2/df = 1.631$, $NFI = 0.906$, $TLI = 0.944$, $CFI = 0.960$, $RMSEA = 0.075$), but a load of the factor M3 was less than 0.5 and deleted one item, which loading value was

TABLE 6: Factor load matrix rotation.

Factor	1	2	3
C1: the host’s strategic intention and goal to initiate the project	0.808		
C2: the host clearly defines the priorities of the work or objectives in the progress of the convention project to the organizer	0.786		
C3: the host clearly defines the criteria or indicators of achievement for the success of the convention project to the organizer	0.829		
C4: the host is able to understand the interests of the convention project and actively coordinate with the strategic objectives of the convention project	0.571		
M1: to solve the problem of nonprocedural decision-making in boosting convention projects to the organizer, the host can construct strict and formal decision-making procedures for the project		0.663	
M2: the convention host is concerned about the risk and circumvention strategy of the convention project, and the convention project has a formal risk control system		0.580	
M3: the host has the right to terminate the project as a result of environmental changes or expected performance deviations within the progress of the convention project, as specified in the contract		0.795	
M4: the host of the convention promised and established an incentive system for the organizer, highlighted the degree of realization of the objectives of the convention projects, and strengthened the close relationship between the interests of the organizer and the management team		0.678	
S1: when the convention project is in financial difficulties, the host can offer the necessary support or help		0.506	0.554
S3: the host will provide media resources for convention projects with his influence			0.903
S4: the host will provide support or help for the invitation and exhibition of investment by the organizer of the convention with his influence			0.890
Initial eigenvalue	5.173	1.431	1.068
Percentage value of variance	46.704	13.013	9.713
Cumulative percentage value	46.704	59.717	69.430

less than 0.5, and the remaining nine items were retained. The retained items were analyzed again, and the fitting degree of the deleted model with the data was found to be better; the ratio of the chi-square to the degree of freedom was less than 4; the RMSEA was less than 0.08; and the GFI, CFI, NFI, and TLI were all greater than 0.9, as shown in Table 7.

TABLE 7: Overall fitting coefficient table.

χ^2/df	RMSEA	GFI	NFI	IFI	TLI	CFI
1.463	0.064	0.937	0.931	0.977	0.965	0.977

TABLE 8: Verification factor analysis.

Method		AVE	CR	Estimate	SE	CR	P	Cronbach's α
Customer role		0.580	0.846					0.844
C4	<--- F1			0.747				
C3	<--- F1			0.867	0.149	8.880	***	
C2	<--- F1			0.710	0.135	7.330	***	
C1	<--- F1			0.710	0.134	7.329	***	
Controller role		0.549	0.783					0.776
M4	<--- F2			0.663				
M2	<--- F2			0.708	0.163	6.270	***	
M1	<--- F2			0.840	0.173	6.942	***	
Supporter role		0.773	0.872					0.870
S4	<--- F3			0.891				
S3	<--- F3			0.867	0.159	6.561	***	

*** $p < 0.001$.

As shown in Table 8, the results of confirmatory factor analysis showed that Cronbach's α values of each dimension of the host's role were more than 0.7, which indicated that the scale had good credibility. The combination credibility of the three roles was more than 0.7, which indicated that the internal quality of the model was good. After adjusting the model, the load of all indexes in each dimension was more than 0.6, and the average variance extraction of the three dimensions was more than 0.5, which indicated that the data had high convergent validity. The correlation between the factors is shown in Figure 1.

5.4. Impact of the Role of the Host on the Convention Project Performance. The convention host plays multiple roles in the convention project. To explore the impact of different roles on the convention project performance, this article introduces the triangle model of project performance and measures the project performance from three dimensions: time, budget, and quality. This article uses AMOS to build a structural equation model to explore the impact of each role on the performance of the project.

5.4.1. The Impact of Customer Role on Convention Project Performance. The convention host plays the role of the customer and undertakes the function of information communication in the convention project. Through exploratory factor analysis and confirmatory factor analysis, it can be seen that the role of the customer includes four measurement items (C1, C2, C3, and C4), and the convention project performance includes three measurement items (SU1, SU2, and SU3). Based on this, this paper constructs a structural equation model and tests the model. The model is shown in Figure 2.

The path coefficient and model fitness index of the model are shown in Table 9. The results showed that the model and data had a good fit ($\chi^2 = 18.691$, $df = 13$, $\chi^2/df = 1.438$,

$GFI = 0.955$, $NFI = 0.949$, $TLI = 0.973$, $CFI = 0.983$, $RMSEA = 0.062$, $RMR = 0.031$). The path coefficient of the causal relationship between "customer role" and "project performance" was 0.423 and passed the significance test at the 1% level, which indicated that the customer's role assumed by the host had a significant positive impact on convention project performance. H1 is confirmed by the empirical results, which shows that effective communication between the convention host and the professional convention organizer can make the organizer better understand the objectives of the convention project, to improve the convention project performance.

5.4.2. The Impact of Controller Role on Convention Project Performance. The convention host, as the owner of the convention project, has legal responsibility for the project. The host needs to assume the function of supervision and incentives and reduce the agency conflict through effective supervision and incentives to ensure the smooth progress of the convention project. Through exploratory factor analysis and confirmatory factor analysis, it can be known that the role of the controller includes three measures (M1, M2, and M4). To explore the effect of the role of the controller on the performance of the convention project, this paper constructs the structural equation of Figure 3.

The path coefficient and model fitness index of the model are shown in Table 10. The results showed that the fitting degree between the model and the data was acceptable ($\chi^2 = 5.784$, $df = 5$, $\chi^2/df = 0.723$, $GFI = 0.984$, $NFI = 0.978$, $RMR = 0.018$). The path coefficient of the causal relationship between "controller role" and "project performance" was 0.361 ($p < 0.001$), indicating that the hosts assume the role of controller and fulfill the supervision and control responsibility having a significant positive impact on convention project performance. H2 is confirmed by the empirical results, which shows that the effective supervision and

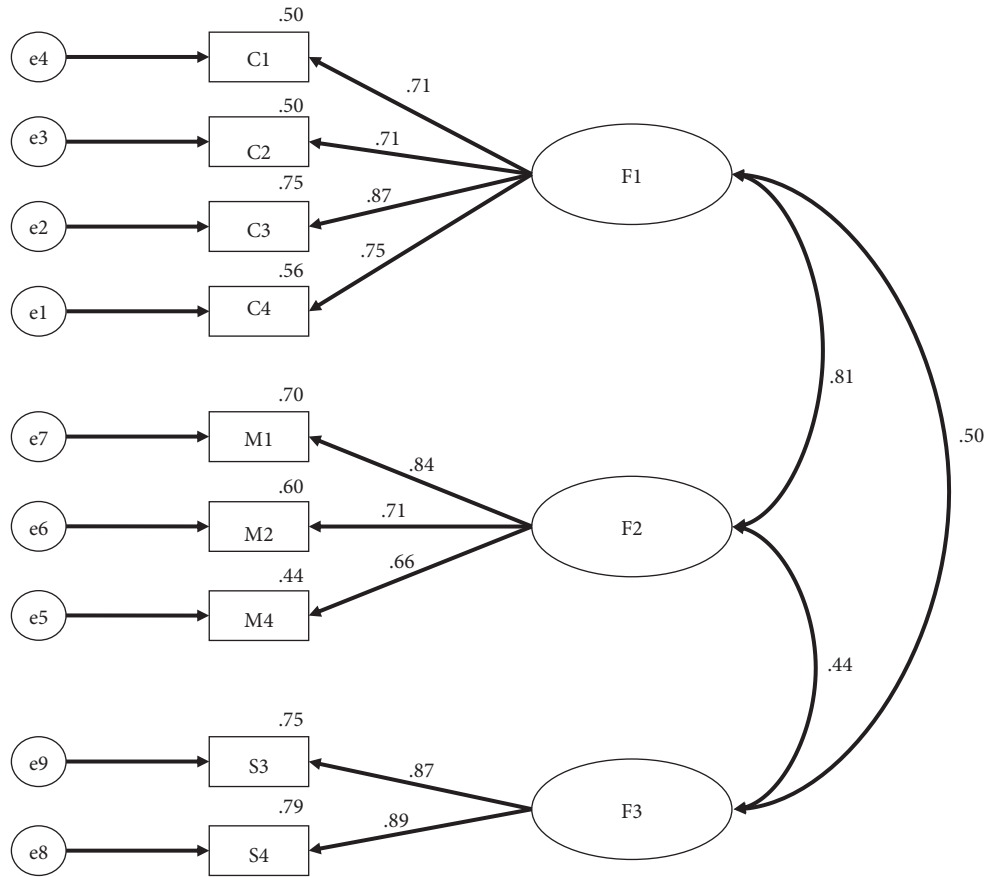


FIGURE 1: Validation factor analysis of convention host's roles.

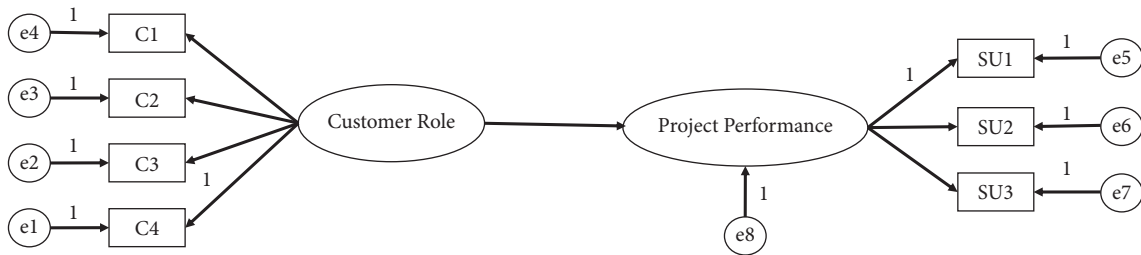


FIGURE 2: Structural equation model of the impact of customer role on convention project performance.

TABLE 9: Structural equation model result.

Hypotheses	Structural path	Path coefficient	SE	CR	P
H1	Project performance <--- Customer role	0.484	0.102	4.165	***

Model fit statistics: CMIN/df = 1.438, NFI = 0.949, CFI = 0.983, GFI = 0.955, IFI = 0.984, TLI = 0.973, RMR = 0.031, RMSEA = 0.062

*** $p < 0.001$.

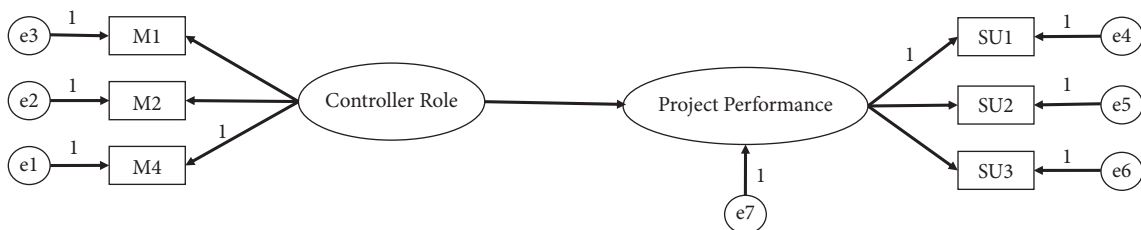


FIGURE 3: Structural equation model of the impact of controller role on convention project performance.

TABLE 10: Structural equation model result.

Hypotheses	Structural path	Path coefficient	SE	CR	P
H2	Project performance <---> Controller role	0.446	0.170	3.653	***
Model fit statistics: CMIN/df = 0.723, NFI = 0.978, GFI = 0.984, IFI = 0.984, RMR = 0.018, RMSEA = 0.000					

*** $p < 0.001$.

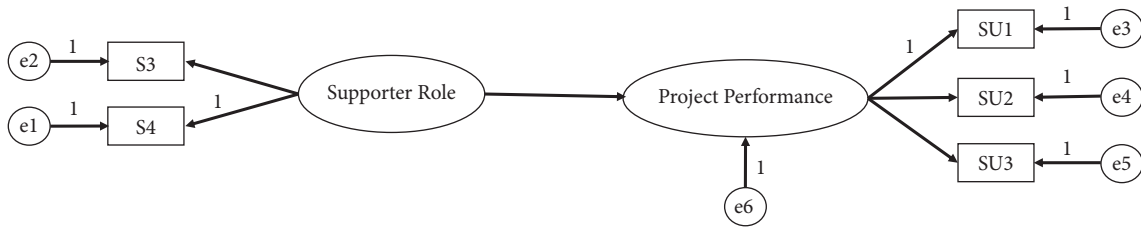


FIGURE 4: Structural equation model of the impact of supporter role on convention project performance.

TABLE 11: Structural equation model result.

Hypotheses	Structural path	Path coefficient	SE	CR	P
H3	Project performance <---> Supporter role	0.374	0.102	3.277	**
Model fit statistics: CMIN/df = 1.061, NFI = 0.984, CFI = 0.999, IFI = 0.999, TLI = 0.998, GFI = 0.986, IFI = 0.984, RMR = 0.011, RMSEA = 0.023					

** $p < 0.01$.

incentive of the professional conference organizer can ensure that the organizers are more willing to act according to the objectives of the convention project, to improve the convention project performance.

5.4.3. The Impact of Supporter Role on Project Performance.

In addition to the customer and controller roles, the convention host also plays the role of supporter in the convention project. The host guarantees the smooth implementation of the convention project by providing the organizer with tangible and intangible resources. Through exploratory factor analysis and confirmatory factor analysis, it can be known that the role of the supporter includes two measures (S3 and S4). Based on this, this paper constructs a structural equation model and tests the model. The model is shown in Figure 4.

The path coefficient and model fitness index of the model are shown in Table 11. The results show that the model and the data had a good fit ($\chi^2 = 4.242$, $df = 4$, $\chi^2/df = 1.061$, $GFI = 0.986$, $NFI = 0.984$, $TLI = 0.998$, $CFI = 0.999$, $RMSEA = 0.023$, $RMR = 0.011$). The path factor of the causal relationship between “supporter role” and “project performance” was 0.334 ($p < 0.01$). It showed that the supporter role of the convention project host had a positive impact on the project performance. H3 is confirmed by the empirical results, which shows that the effective resource support of the professional conference organizer can ensure that the organizer has the ability to achieve the objectives of the convention project, to improve the convention project performance.

Although the research sample in this paper meets the basic requirements, the overall research sample size is relatively small due to the limited number of objects that can be

investigated. Therefore, in the structural equation model, if three latent variables are included in the model at the same time, the degree of freedom estimated by the model will be greatly reduced, and some of the model fitting indicators are relatively poor. In this regard, to ensure the fitting degree of the structure and the validity of the coefficient estimation, latent variables were introduced into the structural equation model in this study. Nonetheless, to maintain a robust structure, this study also introduced three latent variables into the model for the corresponding tests. Although some of the model’s fitting indicators were not ideal, the path coefficients of the three role variables on the performance of exhibition projects were significantly positive, which was consistent with the research conclusion of this paper.

6. Research Conclusions and Implications

6.1. The Conclusions of the Research. This paper makes a conceptual and deconstruction of the responsibility of the project host by combing the existing documents and makes clear the multiroles of the host and the core function of each role. Based on that, the author further explores the role and responsibilities of the host from the perspective of the convention project. The role of the convention project host in the whole project was determined by the exploratory factor analysis and confirmatory factor analysis, and the role measurement scale of the convention project host was constructed. In this paper, the role of the convention host in the convention project is divided into three aspects: the customer role, the controller role, and the supporter role. To further verify the rationality of the identified convention host’s roles, this paper examines the impact of each role on the convention project performance; the results show that

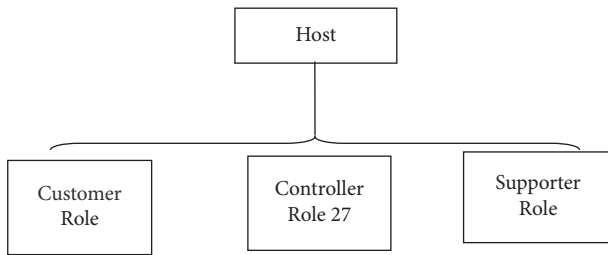


FIGURE 5: Role of the convention host.

the customer role, the controller role, and the supporter role all have a positive impact on the convention project performance. The conclusion shows that in the convention project, the host needs to play multiple roles (as shown in Figure 5) and has an important impact on conference performance.

As the entrusting party in the principal-agent relationship, the host plays the role of the customer in the convention project and is responsible for the demand transfer and information communication [19]. The host needs to define key indicators such as meeting the project target, priorities, and performance standards to the professional conference organizers (PCOs) and to communicate and coordinate with the stakeholders' interests to ensure the success of the convention project.

As the owner of the convention project, the host also plays the role of controller and assumes the responsibility of supervising control and incentives. The host needs to pay attention to the risk identification and control of the convention project and establish an incentive system with the organizer. The convention host needs to follow the progress of the project in real time and provide support for the organizer's decision-making to ensure the smooth progress of the convention project [31, 32].

As the initiator of the convention project and the owner of the resource, the host plays the role of a supporter and has the function of helping the organizer obtain the required resources. In the convention projects, the hosts mainly provide support for the media publicity and investment promotion work. The host utilizes its influence and its own resources to help the convention project enhance its influence and credibility, obtain sponsorship support, improve the brand value, and reduce the pressure of the organizer's convention invitation work [23, 34].

The host of the convention assumes its role in the convention project, can make a positive impact on the convention project performance, and is conducive to the project being held on time and on a budget [15]. The convention host plays the role of customer, controller, and supporter in the convention project and needs to perform the functions of information exchange, supervision and incentive, and resource support. Each role has a positive impact on the realization of project performance. The host should clarify its own role and assume corresponding responsibilities to ensure the smooth running of the convention project and improve the performance of the convention project [13].

6.2. Theoretical and Practical Implications. This paper discussed the role of the host from the perspective of the convention project and clarified the role orientation of the host, an important stakeholder of the convention. This paper introduces the theory of project governance, analyzes the convention project at the governance level, and lays a foundation for future research on the relationship between the main host and the convention governance.

This paper was based on the relevant research results of the project initiators and combined with the related research of the convention project to obtain the measurement questionnaire for the role of the convention project host and optimized questionnaire items with the opinions of experts and scholars in the industry. Through factor analysis, we determined the role of the convention project host and the main functions of each role and formed the role scale of the convention host, to lay the foundation for the follow-up research.

Through the investigation of the professional conference organizers (PCOs), we can understand the current role of the host in the industry. Clarifying the role of the host can make the organizer understand the responsibilities of the host more clearly, define the rights and responsibilities between the host and the organizer, and improve the working efficiency of the host. The role of the host plays an important role in strengthening the positive role of the host and realizing the strategic value and performance of convention projects.

Based on the multiple roles of project sponsors proposed by Crawford and Brett [23], combined with the specific conditions of convention projects and research on project governance, this paper builds a three-role structure of exhibition project sponsors. On this basis, the positive impact of different roles of sponsors on project performance is verified, which is also in line with existing research results on the impact of project sponsor roles [13, 15].

The three roles of the host (customer role, controller role, and supporter role) all have a positive impact on the convention project performance. For the convention host, during the implementation of the convention project, it is necessary to clearly define its own role and actively perform the functions of information exchange, supervision and encouragement, and resource support. For the convention organizers, they need to understand the responsibilities of the hosts, cooperate with the hosts, communicate in a timely manner, and urge them to perform their corresponding duties to ensure the smooth organization of the convention and improve the convention project performance [4, 13].

As a client, the host promotes the information communication between the host and the organizers so that the two parties can reach an agreed goal on a specific convention project, which is the key to promoting the orderly development and success of the project. Compared with the role of supervision and control, the host, as the client role, can effectively guide the project objectives and build an effective relationship between coordination and governance between the sponsors through information communication, which is more important to the success of the project [19].

Lee et al. [4] focused on the convention host's role as a controller and its supervisory and incentive functions in their research on the relationship between convention project hosts and organizers. On this basis, according to the principal-agent theory and project governance research, this paper further expanded its role as a customer and supporter, as well as its functions of information communication and resource supply, and more comprehensively expounded the multiple roles and functional requirements of the host. At the same time, it also verifies the positive impact of the multiple roles and functions of the host on the project performance. Future research will also further analyze the multiple roles and functional utility of the host.

6.3. Research Limitations and Prospects. This paper combs out the role of the convention project hosts through the literature retrieval, optimizes the relevant responsibilities of the host team according to the investigation results, and finally confirms the three roles and the corresponding functions played by the host. There are some limitations in this paper: first, because of the limited number of samples collected in this paper, the results have some limitations. Second, the questionnaire mainly comes from the organizer, the follow-up study can consider the views of more stakeholders. In addition, this study mainly focuses on the role of the host and its impact on convention performance but does not involve the interactive relationship and impact between the host and organizer; the subsequent research can focus on the interactive effect between the host and organizer.

As for the role of the host, there is a large research space in the future. First, in the future, the self-perceived role of the host can be compared with the organizer's feelings, to determine the reason for the difference in perception and strengthen the role orientation of the host. Second, this paper is about the role of the convention host with a summary study. In a follow-up study, it can concentrate on analyzing the different nature of the host and organizer and try to determine the difference in the host's role performance in different situations and to understand the influence of the role of the host in different situations on the performance of the project.

Data Availability

The questionnaire recovery data used to support the findings of this study are available from the corresponding author upon request.

Conflicts of Interest

The authors declare that there are no conflicts of interest.

Acknowledgments

This research was funded by the major social science projects of the Tianjin Municipal Education Commission (2020JWZD23) and the project supported by the Asian Research Center of Nankai University (AS1807).

References

- [1] C.-F. Chen and C.-L. Lee, "Determining the attribute weights of professional conference organizer selection: an application of the fuzzy AHP approach," *Tourism Economics*, vol. 17, no. 5, pp. 1129–1139, 2011.
- [2] S. Jung and S. Tanford, "What contributes to convention attendee satisfaction and loyalty? A meta-analysis," *Journal of Convention & Event Tourism*, vol. 18, no. 2, pp. 118–134, 2017.
- [3] A. Sobitan and P. Vlachos, "Immersive event experience and attendee motivation: a quantitative analysis using sensory, localisation, and participatory factors," *Journal of Policy Research in Tourism, Leisure and Events*, vol. 12, no. 3, pp. 437–456, 2020.
- [4] L. Hye-Rin, B. McKercher, and S. S. Kim, "The relationship between convention hosts and professional conference organizers," *International Journal of Hospitality Management*, vol. 28, no. 4, 2009.
- [5] L. Crawford and T. Cooke-Davies, "Project governance: the role and capabilities of the executive sponsor," *Project Perspectives*, vol. XXXI, no. 2009, pp. 66–74, 2009.
- [6] S. Jenner, "Why do projects 'fail' and more to the point what can we do about it? The case for disciplined, 'fast and frugal' decision-making," *PM World J*, vol. 4, no. 3, 2015.
- [7] S. U. Haq, C. Liang, D. Gu, J. T. Du, and S. Zhao, "Project governance, project performance, and the mediating role of project quality and project management risk: an agency theory perspective," *Engineering Management Journal*, vol. 30, no. 4, pp. 274–292, 2018.
- [8] T. J. Kloppenborg, D. Tesch, and C. Manolis, "Investigation of the sponsor's role in project planning," *Management Research Review*, vol. 34, no. 4, pp. 400–416, 2011.
- [9] B. Panda and N. M. Leepsa, "Agency theory: review of theory and evidence on problems and perspectives," *Indian Journal of Corporate Governance*, vol. 10, no. 1, pp. 74–95, 2017.
- [10] Kpmg, *KPMG New Zealand Project Management Survey 2010*, KPMG, Amstelveen, 2010.
- [11] Pmi (Project Management Institute), *A Guide to the Project Management Body of Knowledge (PMBOK® Guide)*, Project Management Institute Inc, Pennsylvania, 2017.
- [12] Project Management Institute, *A Guide to the Project Management Body of Knowledge (PMBOKw Guide)*, Project Management Institute, Newtown Square, PA, 2004.
- [13] G. Yun, W. J. Yoo, and L. Seungbae, "An impact on project performance by sponsor roles and manager behavioral competencies in ICT projects," *Journal of the Korea Management Engineers Society*, vol. 19, no. 3, pp. 131–145, 2014.
- [14] D. Bryde, "Perceptions of the impact of project sponsorship practices on project success," *International Journal of Project Management*, vol. 26, no. 8, pp. 800–809, 2008.
- [15] R. Breese, O. Couch, and D. Turner, "The project sponsor role and benefits realisation: more than just doing the day job," *International Journal of Project Management*, vol. 38, no. 1, pp. 17–26, 2020.
- [16] S. Sapountzis, K. Yates, M. Kagioglou, and G. Aouad, "Realising benefits in primary healthcare infrastructures," *Facilities*, vol. 27, no. 3/4, pp. 74–87, 2009.
- [17] R. Müller, *Communication of Information Technology Project Sponsors and Managers in Buyer-Seller Relationships*, Unpublished DBA thesis, Henley Management College, Brunel University, UK, 2003.
- [18] Association for Project Management (Apm), *Sponsoring Change: A Guide to the Governance Aspects of Project Sponsorship*, APM, Buckinghamshire, England, 2018.

- [19] R. Müller and J. R. Turner, "Communication between IT project manager and project sponsor in a buyer-seller relationship," in *Proceedings of the Presented at the PMI Research Conference*, Seattle, Washington, July 2002.
- [20] R. L. Englund and A. Bucero, *Project Sponsorship: Achieving Management Commitment for Project Success*, Jossey-Bass, San Francisco, CA, 2006.
- [21] C. Ashurst, N. F. Doherty, and J. Peppard, "Improving the impact of IT development projects: the benefits realization capability model," *European Journal of Information Systems*, vol. 17, no. 4, pp. 352–370, 2008.
- [22] M. P. Abednego and S. O. Ogunlana, "Good project governance for proper risk allocation in public-private partnerships in Indonesia," *International Journal of Project Management*, vol. 24, no. 7, pp. 622–634, 2006.
- [23] L. H. Crawford and C. Brett, "Exploring the role of the project sponsor," in *Proceedings of the Presented at the PMI New Zealand Annual Conference*, Wellington, New Zealand, May 2001.
- [24] A. Sharma, "Professional as agent: knowledge asymmetry in agency exchange," *Academy of Management Review*, vol. 22, no. 3, pp. 758–798, 1997.
- [25] J. Helm and K. Remington, "Effective project sponsorship an evaluation of the role of the executive sponsor in complex infrastructure projects by senior project managers," *Project Management Journal*, vol. 36, no. 3, pp. 51–61, 2005.
- [26] K. Sewchurran and M. Barron, "An investigation into successfully managing and sustaining the project sponsor—project manager relationship using soft systems methodology," *Project Management Journal*, vol. 39, no. 1, pp. S56–S68, 2008.
- [27] M. Hall, R. Holt, and D. Purchase, "Project sponsors under new public management: lessons from the frontline," *International Journal of Project Management*, vol. 21, no. 7, pp. 495–502, 2003.
- [28] F. Hartman and R. A. Ashrafi, "Project management in the information systems and information technologies industries," *Project Management Journal*, vol. 33, no. 3, pp. 5–15, 2002.
- [29] M. C. Jensen and W. H. Meckling, "Theory of the firm: managerial behavior, agency costs and ownership structure," *Journal of Financial Economics*, vol. 3, no. 4, pp. 305–360, 1976.
- [30] M. Bergen, S. Dutta, and O. C. Walker, "Agency relationships in marketing: a review of the implications and applications of agency and related theories," *Journal of Marketing*, vol. 56, no. 3, pp. 1–24, 1992.
- [31] F. Levie, C. M. Burke, and J. Lannon, "Filling the gaps: an investigation of project governance in a non-governmental organisation's response to the Haiti earthquake disaster," *International Journal of Project Management*, vol. 35, no. 5, pp. 875–888, 2017.
- [32] R. Müller, L. Zhai, and A. Wang, "Governance and governmentality in projects: profiles and relationships with success," *International Journal of Project Management*, vol. 35, no. 3, pp. 378–392, 2017.
- [33] M. Brunet and M. Aubry, "The three dimensions of a governance framework for major public projects," *International Journal of Project Management*, vol. 34, no. 8, pp. 1596–1607, 2016.
- [34] L. Crawford, T. Cooke-Davies, B. Hobbs, L. Labuschagne, K. Remington, and P. Chen, "Governance and support in the sponsoring of projects and programs," *Project Management Journal*, vol. 39, no. 1, pp. 43–55, 2008.
- [35] R. Davison, "An instrument for measuring meeting success: revalidation and modification," *Information & Management*, vol. 36, no. 6, pp. 321–328, 1999.
- [36] N. Prenner, J. Klünder, and K. Schneider, "Making meeting success measurable by participants' feedback," *Proceedings of the 3rd International Workshop on Emotion Awareness in Software Engineering*, pp. 25–31, 2018, ACM.
- [37] R. Atkinson, "Project management: cost, time and quality, two best guesses and a phenomenon, its time to accept other success criteria," *International Journal of Project Management*, vol. 17, no. 6, pp. 337–342, 1999.
- [38] R. Joslin and R. Müller, "The relationship between project governance and project success," *International Journal of Project Management*, vol. 34, no. 4, pp. 613–626, 2016.
- [39] A. ul Musawir, C. E. M. Serra, O. Zwikael, and I. Ali, "Project governance, benefit management, and project success: towards a framework for supporting organizational strategy implementation," *International Journal of Project Management*, vol. 35, no. 8, pp. 1658–1672, 2017.
- [40] C. H. Lawshe, "A quantitative approach to content validity," *Personnel Psychology*, vol. 28, no. 4, pp. 563–575, 1975.
- [41] C. Ayre and A. J. Scally, "Critical values for lawshe's content validity ratio: revisiting the original methods of calculation," *Measurement and Evaluation in Counseling and Development*, vol. 47, no. 1, pp. 79–86, 2014.
- [42] J. F. Hair, R. E. Anderson, R. L. Tatham, and W. C. Black, *Multivariate Data Analysis*, Prentice-Hall, New Jersey, 1998.
- [43] O. Zwikael and J. Smyrk, "Project governance: balancing control and trust in dealing with risk," *International Journal of Project Management*, vol. 33, no. 4, pp. 852–862, 2015.

Research Article

An RBF Neural Network Clustering Algorithm Based on K-Nearest Neighbor

Jitao Li ¹, Chugui Xu,¹ Yongquan Liang,² Gengkun Wu ², and Zhao Liang¹

¹Department of Information Science and Technology, Taishan University, Taian 271000, China

²College of Computer Science and Engineering, Shandong University of Science and Technology, Qingdao 266590, China

Correspondence should be addressed to Jitao Li; kisstr@126.com

Received 1 July 2022; Accepted 1 August 2022; Published 24 August 2022

Academic Editor: Wei Liu

Copyright © 2022 Jitao Li et al. This is an open access article distributed under the Creative Commons Attribution License, which permits unrestricted use, distribution, and reproduction in any medium, provided the original work is properly cited.

Neural network is a supervised classification algorithm which can deal with high complexity and nonlinear data analysis. Supervised algorithm needs some known labels in the training process, and then corrects parameters through backpropagation method. However, due to the lack of marked labels, existing literature mostly uses Auto-Encoder to reduce the dimension of data when facing of clustering problems. This paper proposes an RBF (Radial Basis Function) neural network clustering algorithm based on K-nearest neighbors theory, which first uses K-means algorithm for preclassification, and then constructs self-supervised labels based on K-nearest neighbors theory for backpropagation. The algorithm in this paper belongs to a self-supervised neural network clustering algorithm, and it also makes the neural network truly have the ability of self-decision-making and self-optimization. From the experimental results of the artificial data sets and the UCI data sets, it can be proved that the proposed algorithm has excellent adaptability and robustness.

1. Introduction

Cluster analysis is an important method of data mining, whose core idea is to gather high similarity points in the data set into clusters while ensuring that different clusters have significant differences. Clustering can explore hidden patterns and rules in data, which is the embodiment of the decision-making ability of artificial intelligence algorithms, and is now widely used in computer science, information security, and image processing.

In recent years, the sudden development of neural network has shown people its powerful function, which can deal well with the processing of high-dimensional and complex data, and it has achieved successful applications in the fields of image clustering [1, 2], facial recognition [3–5], image segmentation [6, 7], and so on. However, the shortcoming of neural network is also very obvious, the limitation of manual label annotation restrict its self-decision ability. Existing unsupervised learning methods include clustering and dimension reduction, and clustering algorithms are complex and diverse, which can be divided into

clustering methods based on prototype-based, density, hierarchy, and dimension reduction includes Auto-encoders and PCA (Principal Component Analysis) method, whose major for data preprocessing.

From the existing literature, it can be seen that the more common idea is to migrate the loss function of the traditional clustering algorithm to the neural network structure and achieve clustering through global optimization. Yang et al. [8] propose the DCN model, which migrates the loss function of K-means to the feature space of the Auto-encoder, and realize feature learning and clustering through the alternating optimization of network parameters and cluster centers. Yang et al. [9] combine hierarchical clustering algorithm with CNN (Convolutional Neural Networks) and realize feature clustering through global optimization of cluster merging and feature learning. SpectralNet [10] introduces the idea of spectral clustering into deep learning, which first learns the similarity matrix between features through a Siamese Network, then obtain a new feature measure based on the spectral clustering objective function, and finally performs K-means in the feature

space to obtain cluster assignments. VaDE (Variational Deep Embedding) [11] introduces an idea of migrate clustering of GMM (Gaussian Mixture Models) into the Variational Auto-encoder (VAE), which realizes the optimization of feature learning and cluster allocation through the distribution constraints of feature space. Another idea is to directly design a specific cluster loss function based on the desired clustering assumptions [12]. DAC (Deep-adaptive Image Clustering) [13] converts multiclassification problems into binary classification problems instead, continuously generates positive and negative sample pairs with high confidence based on the idea of self-paced learning, which are used as supervised information to guide the training of the model, and finally outputs the clustering result. IMSAT (Information Maximizing Self-Augmented Training) [14] and IIC (Invariant Information Clustering) [15] are based on the same assumption that simple transformations of data do not alter their intrinsic semantic information, and clustering is achieved by maximizing the information entropy of the original sample and its enhanced sample.

In terms of the combination of traditional clustering algorithms and Auto-encoders, Ren et al. [15] propose a deep density clustering framework by combining density clustering with Auto-encoder, which uses the t-SNE (t-distributed stochastic neighbor embedding algorithm) [16] and DPC (density peaking algorithm) [17], which completes the training by alternating or optimization of cluster pseudolabels and feature representations. Mrabah et al. [18] propose a model training method. In the pretraining phase, reliable feature representations are learned in a self-supervised manner by introducing data augmentation and adversarial interpolation techniques [19]. Due to the high dimension of the image, the combination of dimension reduction and traditional clustering algorithms can indeed effectively improve the accuracy of the algorithm, but it does not really use the neural network to classify the data, and it does not make the neural network have the ability of self-decisions.

Unsupervised clustering methods based on deep learning use VAE (Variational Auto-encoder) and GANs (Generative Adversarial Networks) [20, 21], which use existing data to generate data that does not exist in reality, mainly for image generation and sharpening. VaDE is a generative clustering model based on VAE; this algorithm models the process of data generation by introducing a Gaussian hybrid model. GMVAE [22] adopts a strategy similar to VaDE, which imposes a Gaussian mixture distribution constraint on the feature space. By minimizing the information constraints, the model avoids falling into a local solution at the beginning of training. Mukherjee et al. [23] propose a clustering method-based generate adversarial networks. The algorithm utilizes mixed discrete and continuous latent variables to construct new spaces for clustering by interpolating methods.

The existing cluster analysis has less robustness and the self-decision classification ability of neural networks is low. In order to make full use of the advantages of neural network, this paper proposes an RBF neural network clustering algorithm based on KNN graph (RBF-KNN). The core idea of

the algorithm in this paper is to use the K-means algorithm to generate the initial pseudolabels, by using the overall and local information retention ability of the RBF neural network to train the classification network under the pseudolabel, and then use the self-supervision method based on the neighbor to continuously generate the corrected class label, optimize the generated neural network and obtain the clustering results, and finally achieve the purpose of self-optimization and self-decision of the neural network results. The algorithm process in this paper is simple, and while have fewer parameters, it can effectively handle irregular data sets and unbalanced data sets. From the experimental results of the artificial data set and the UCI data set, it can be seen that the proposed algorithm has good robustness and adaptability.

2. Related Works

2.1. RBF Neural Network. In 1985, Powell proposed a Radial Basis Function (RBF) method for multivariate interpolation, which uses a Gaussian kernel function in most cases, and the RBF neural network is a typical three-layer neural network that includes an input layer, a hidden layer, and an output layer. The transformation from input space to hidden space is nonlinear, while the transformation from hidden space to output layer space is linear. The network structure is as Figure 1.

The hidden nodes of BP (Back Propagation) neural network use the input pattern and the inner product of the weight vector as the arguments of the activation function, while the activation function uses the ‘‘Sigmoid’’ function. The parameters have an equally important effect on the output of the BP network, so the BP neural network is a global approximation of the nonlinear map.

Compared to traditional BP neural network, the hidden nodes of RBF neural network use the similarity between the input mode and the central vector (such as Euclidean distance) as the argument of the function, and the radial basis function as the activation function. Farther the input of a neuron is from the center of the radial basis function, the less activated the neuron becomes (Gaussian function). RBF neural network thus carries more local information and have a ‘‘local mapping’’ feature.

2.2. K-Nearest Neighbor and K-Means Algorithms. K-nearest neighbor algorithm is one of the most commonly used algorithms in supervised classification algorithms, which selects K closest sample points to obtain the corresponding class labels through the election method, which have low complexity and high accuracy. The KNN graph is an undirected graph formed by connecting the sample to the adjacent K sample based on the K -neighbor principle.

K-means algorithm is the most commonly used traditional clustering algorithm, which is based on the greedy principle, and selects the global optimal through iterative mode, and its optimization function is

$$y = \min \sum_{i=1}^N \text{dist}(x_i, c_i). \quad (1)$$

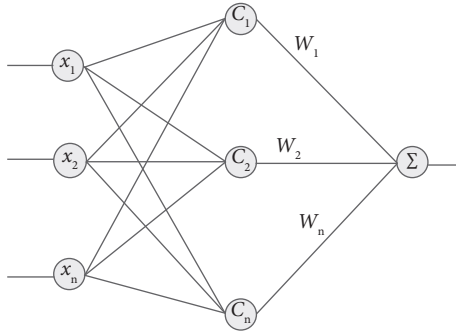


FIGURE 1: Structure of RBF neural network.

The K-means method is simple and practical which can meet most needs, but its problem of sensitivity to noise data and to spherical data has always been a problem that scholars solving, and the existing DPC is a density-based clustering method, but it needs to find a central point, which can also be seen as an improvement of the K-means algorithm.

3. Introduction of Algorithms in This Paper

In this paper, the algorithms need to perform two times K-means clustering and multiple iteration of RBF neural network backpropagation.

3.1. Generate Pre-Trained Pseudo-Labels. Since the training of neural network requires the assistance of class labels, the proposed algorithm first uses the K-means algorithm to cluster the datasets (random labels can also be used, but more iterations are required thus), and the resulting pseudolabels are transformed, as shown in Figure 2.

The resulting pseudolabels are used for the next step of neural network training.

3.2. Full RBF Neural Network Training. The traditional RBF neural network is a locally weighted network, which selects part of the sample set as the center point for the training of the neural network, and its training process is to use RBF as the “base” of the hidden and the input vector is directly mapped to the hidden space. The RBF neural network establishes a mapping relationship around the center point, and the mapping from the implicit layer space to the output space is linear, which means the output of the network is the linear weighted sum of the output of the hidden unit. Among them, the role of the hidden layer is to map the vector from low dimensions to high dimensions through the kernel function, and the situation of linear indivisibility of low dimensions can be mapped to high dimensions to become linearly separable.

The outputs of the RBF network are as follows:

$$y = \sum_{i=1}^n W_i h_i(x), \quad (2)$$

where y is the output of the RBF neural network, n is the number of neurons in the hidden layer, W_i is the connection weight between the i neuron of the hidden layer neuron and

0	[1,0,0]
0	[1,0,0]
1	[0,1,0]
1	[0,1,0]
2	[0,0,1]
2	[0,0,1]

FIGURE 2: Transformation of pseudolabels.

the neuron in the output layer, $h_i(x)$ is the activation function of the neurons of the hidden layer, the activation function usually takes the Gaussian function which is defined as follows:

$$h_i(x) = \exp\left(-\frac{1}{2\sigma_i^2}\|\zeta - \mu_i\|^2\right). \quad (3)$$

$\zeta = (a_1, a_2, \dots, a_m)^T$ is the input matrix, μ_i is the selected center point, σ_i is the width of the neuron, and $\|\zeta - \mu_i\|$ is the Euclidean distance between the input matrix and the radial base center.

Clustering can be seen as a process of optimization of neural network output and weights, the output expression of the radial base network used in this algorithm is as follows, and its objective function can be seen as the process of minimization of the following formula:

$$y = \min \sum_{i=1}^n \sum_{j=1}^n w_{ij} \exp\left(-\frac{1}{2\sigma^2}\|x_i - x_j\|\right). \quad (4)$$

In this paper, the algorithm no longer selects the center point but retains all the samples and uses Gaussian kernel functions to map to high-dimensional space, so that the RBF neural network can retain the information between the data to the greatest extent. Using the pseudolabel to train RBF neural network, the algorithm selects the gradient descent algorithm as the backpropagation method, and finally obtains the appropriate network weights after several iterations of training.

3.3. Generation of Self-Supervised Remediation Labels. Due to the limitations of traditional partition-based clustering algorithms, the class labels obtained by preprocessing are not necessarily correct when facing nonspherical clusters and unbalanced datasets, so the network parameters need to be corrected.

According to the K-nearest neighbor principle, from the microscopic point of view, the data sample must have the same class label as the adjacent data point, so the resulting corrected label is the mean of the neighbor sample class label, the specific formula is as follows:

$$\text{label}_{\text{correction}} = \frac{1}{K} \sum_{n=1}^K \text{label}_{n\text{-nearest}}. \quad (5)$$

The algorithm loss function in this paper uses the MSE (Mean Square Error), and the backpropagation algorithm also uses the gradient descent algorithm, after multiple rounds of iteration, the new measure labels are finally obtained.

3.4. *Clustering Generating Class Labels.* After re-entering the data set X , the new measure labels are obtained, and the K-means clustering algorithm is used again for the resulting output to obtain the final results.

The pseudocode of algorithm in this paper is shown in Table 1.

4. Experimental Results and Analysis

4.1. *Artificial Data Set Verification.* Artificial data set is a human-made set data set with obvious characteristics, which can be easily artificially judged through experience. However, there is a high degree of complexity in artificial data and in terms of data set shape, density, imbalance, or other aspects problems for artificial intelligence algorithms, so it can well test the adaptability of a certain algorithm to a certain class or several types of complex properties.

The manual data sets used in this paper are all two-dimensional data (Table 2), and the used two-dimensional data sets can display more intuitively the quality of the algorithm clustering results and objectively evaluate the performance of the algorithm. The six datasets selected in this paper are typical artificial datasets, and there are problems of density, shape, or complex properties between clusters.

The algorithm in this article first uses the K-means algorithm to do the preprocessing work, and the K-means run the result such as in the left side (Figures 3–8), and the result of the algorithm RBF-KNN in this article is as follows as the right side (Figures 3–8).

The proposed algorithm is a neural network self-supervised clustering method based on partition-based clustering as the basis for preprocessing, so the 6 artificial datasets (ADS) selected in this paper are all datasets that cannot be well processed by the K-means algorithm. It can be seen from the experimental results of RBF-KNN that the processing of the “aggregate,” “long,” “spiral,” and “target” datasets in this paper can achieve an accuracy rate of 100%, and there are still deficiencies in the details of the processing results of the “jain” and “flame” datasets, but the results have been greatly improved compared to the preprocessing results. Although there are still deficiencies in some data sets, it is limited by the functional limitations of neural networks.

The algorithm structure of the RBF-KNN algorithm is simple and has fewer parameters, that is only two parameters (the value of K-nearest neighbor-value is basically 2 or 3), and compared with the traditional clustering algorithm based on division, the results of this algorithm can basically meet the needs of cluster robustness.

4.2. *UCI Data and Validation, and Evaluation Indicators.* In order to verify that the proposed algorithm can achieve a good clustering effect when dealing with practical problems, several UCI datasets are selected to verify the performance of the proposed algorithm (Table 2), all of which are derived from the UCI machine learning library.

UCI data sets come from different types of industries. “Ecoli” is a data set on molecular research and cell biology for the determination and prediction of yeast data. “Iris” is a

TABLE 1: Algorithm process description.

Algorithm1 RBF-KNN clustering
Input: Dataset X , k , K -nearest neighbor-value
Output: Cluster labels c_i of X
(1): Run K-means to pre-divide X int k clusters
(2): Transform pre-divide labels to pseudo-labels
(3): Repeat
(4): Training RBF network by minimizing loss
(5): Repeat
(6): Get correction labels by KNN graph
(7): Update network parameters by minimizing loss
(8): Data_mark = RBF_KNN(X)
(9): Run K-means to divide Data_mark into k clusters

TABLE 2: Attribute description of each data set.

ADS	n	d	k
Aggregate	788	2	7
Jain	373	2	2
Flame	1000	2	2
Spiral	1000	2	2
Target	770	2	6
<i>UCI</i>			
Ecoli	336	7	8
Iris	150	4	3
Seeds	210	7	3
Soybean	47	35	4
Segment	2310	11	7

data set of classification information about iris plants, which is used to distinguish between three types of plants. “Seeds” data set is mainly a coefficient obtained by X-ray technology for three wheat varieties, and a test data set for wheat classification. The “Soybean” data set is Michalski’s famous soybean disease database for predicting the diseases yielded in soybeans, while the “Segment” data set is a data set that classifies image data on higher numerical attributes, which can better test the performance of this algorithm.

The evaluation criteria for the algorithms selected in this paper include the V-measure coefficient, the adjusted rand index (ARI), and the normalized mutual information (NMI), among which ARI requires the use of the Rand index (RI). Because the use of a single evaluation index will lead to the evaluation results being too one-sided, this paper selects multiple evaluation indicators for cross-validation as formulas (6)–(8).

$$v\text{-measure} = \frac{2 * (h * c)}{h + c}, \quad (6)$$

$$RI = \frac{a + b}{C_2^{nsamples}}, \quad (7)$$

$$ARI = \frac{RI - E[RI]}{\max(RI) - E[RI]}, \quad (8)$$

where h denotes homogeneity; c indicates completeness; a and b are the selected categories; C_2^n is the probability of picking 2 classes from all n classes. As an adjustment function of RI, ARI is adjusted using the resulting RI.

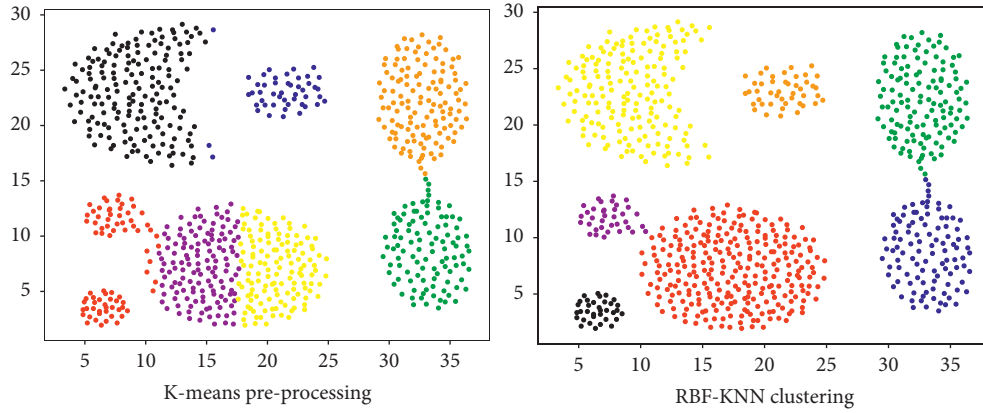


FIGURE 3: Aggregate (K-nearest neighbor-value = 5).

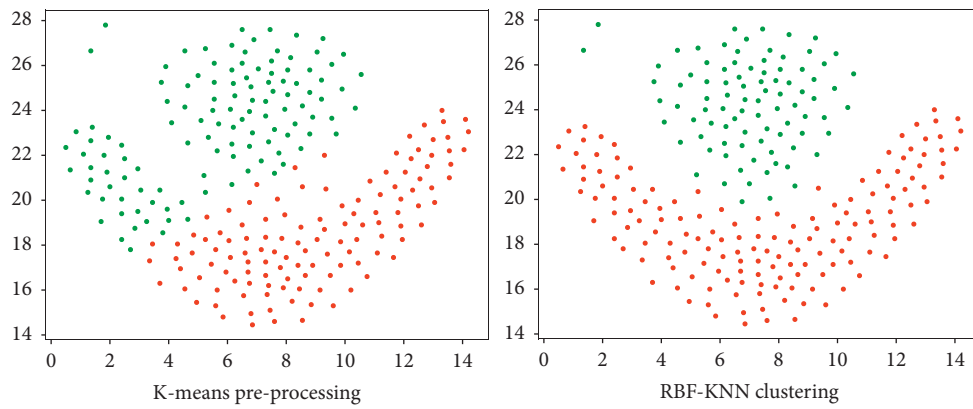


FIGURE 4: Flame (K-nearest neighbor-value = 3).

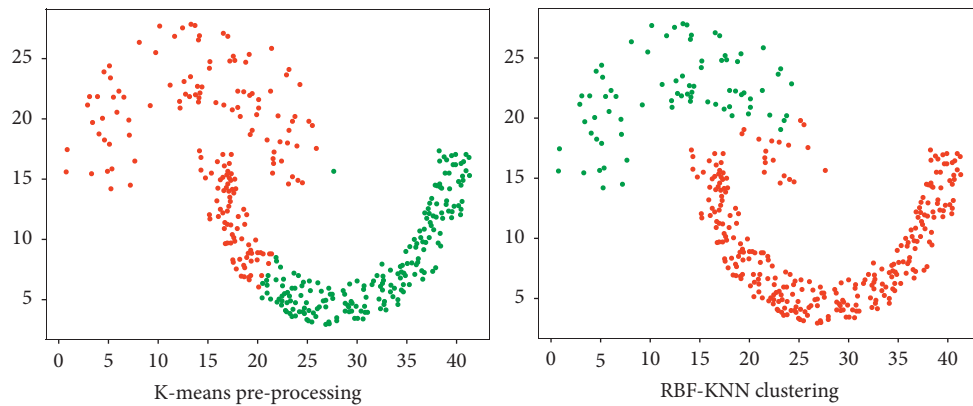


FIGURE 5: Jain (K-nearest neighbor-value = 2).

V-measure represents the harmonized mean of homogeneity and integrity, the value range is [0, 1], and the larger the value, the better the clustering effect. The ARI indicates the degree to which the resulting category information matches the expected category, and the ARI range is [-1, 1], and the larger the value, the higher the coincidence of the clustering result with the real situation.

NMI is defined as the formulas (9) and (10).

$$NMI = \frac{I(X, Y)}{\sqrt{H(X)H(Y)}} \tag{9}$$

$$I(X, Y) = \sum_{h=1}^{k(a)} \sum_{l=1}^{k(b)} n_{h,l} \log \left(\frac{n \cdot n_{h,l}}{n_h^{(a)} n_l^{(b)}} \right) \tag{10}$$

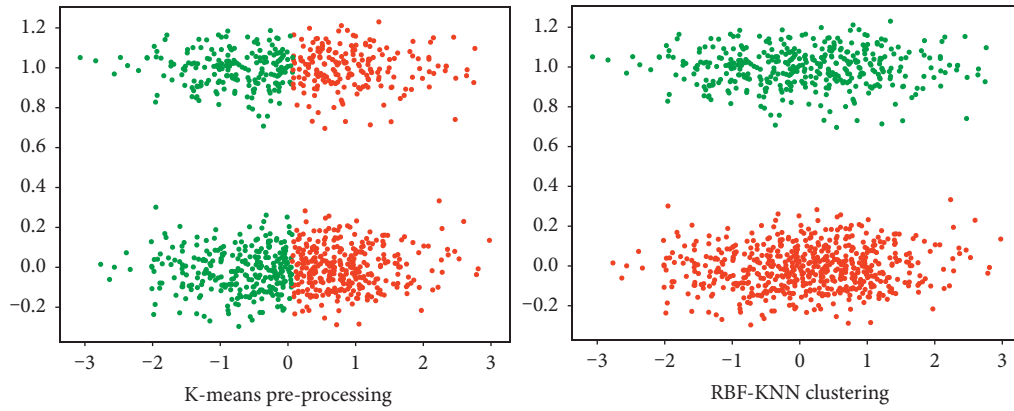


FIGURE 6: Long (K-nearest neighbor-value = 2).

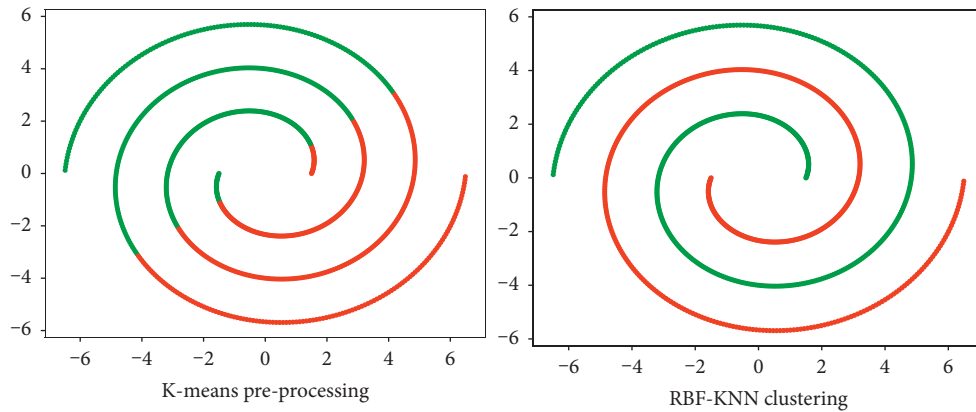


FIGURE 7: Sprial (K-nearest neighbor-value = 2).

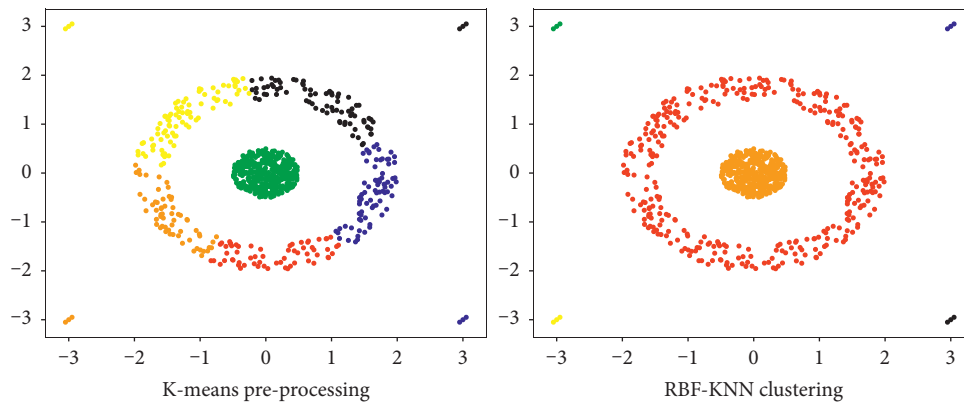


FIGURE 8: Target (K-nearest neighbor-value = 2).

X and Y represent variables, $I(X, Y)$ represents the mutual information of two variables, $H(X)$ and $H(Y)$ represent entropy for the sum of variables.

NMI is a measure of the interdependencies between variables, indicating the strength of the relationship between two variables. The value range of the NMI index is $[0, 1]$, and the closer the value is to 1, the better the clustering effect. On the contrary, the clustering effect is considered to be poor.

Through the above evaluation methods, the processing effect of various algorithms on the data set can be compared more intuitively.

This section selects several types of unsupervised learning methods to compare with the proposed algorithm, including the K-means algorithm based on partitioning, the DPC density clustering algorithm based on K-nearest neighbor, the VaDE clustering algorithm based on VAE and

TABLE 3: Comparison of evaluation indicators V-measure of different algorithms.

	K-means	KNN + DPC	VaDE	DCN	SpectralNet	RBF-KNN
Aggregate	0.4940	1.0	0.5261	0.5620	0.9497	1.0
Jain	0.3690	0.5335	0.2024	0.4587	0.4606	0.7075
Flame	0.3987	0.8865	0.3453	0.4025	0.4595	0.8993
Spiral	0.0268	1.0	0.0406	0.3872	0.3194	1.0
Target	0.2931	0.4655	0.7335	0.4982	0.7917	1.0
Ecoli	0.6409	0.5311	0.2664	0.6130	0.6241	0.6855
Iris	0.7581	0.6182	0.2645	0.7381	0.7660	0.7943
Seeds	0.6992	0.5884	0.2629	0.7200	0.5073	0.7165
Soybean	0.7157	0.7672	0.3872	0.6820	0.2992	0.9457
Segment	0.6040	0.3740	0.2024	0.6135	0.0995	0.6244

TABLE 4: Comparison of evaluation indicators ARI of different algorithms.

	K-means	KNN + DPC	VaDE	DCN	SpectralNet	RBF-KNN
Aggregate	0.3475	1.0	0.3289	0.3625	0.9231	1.0
Jain	0.3241	0.2784	-0.0044	0.4214	0.2165	0.7900
Flame	0.4534	0.6742	0.2895	0.4629	0.2507	0.9502
Spiral	0.0359	1.0	0.0548	0.0115	0.3094	1.0
Target	0.2931	0.4358	0.2192	0.1568	0.8219	1.0
Ecoli	0.6720	0.3884	0.0193	0.6892	0.6552	0.6855
Iris	0.7302	0.5178	0.0192	0.7125	0.7437	0.7566
Seeds	0.7166	0.5521	0.1845	0.7083	0.4134	0.7285
Soybean	0.5452	0.7672	0.3262	0.6726	0.0756	0.9256
Segment	0.4373	0.0346	0.0342	0.3240	0.0012	0.5256

TABLE 5: Comparison of evaluation indicators NMI of different algorithms.

	K-means	KNN + DPC	VaDE	DCN	SpectralNet	RBF-KNN
Aggregate	0.4941	1.0	0.5282	0.3286	0.9498	1.0
Jain	0.3690	0.3034	0.2024	0.4265	0.4607	0.7075
Flame	0.3987	0.7628	0.3454	0.3255	0.4595	0.8993
Spiral	0.0267	1.0	0.0456	0.1153	0.2974	1.0
Target	0.2931	0.4726	0.2098	0.2656	0.8217	1.0
Ecoli	0.6440	0.5312	0.2663	0.5568	0.6307	0.6856
Iris	0.7582	0.6258	0.2657	0.7265	0.7661	0.7857
Seeds	0.6949	0.5884	0.2629	0.7024	0.5079	0.7124
Soybean	0.7158	0.8489	0.3581	0.6526	0.3057	0.9435
Segment	0.6048	0.4000	0.2831	0.5663	0.1427	0.6875

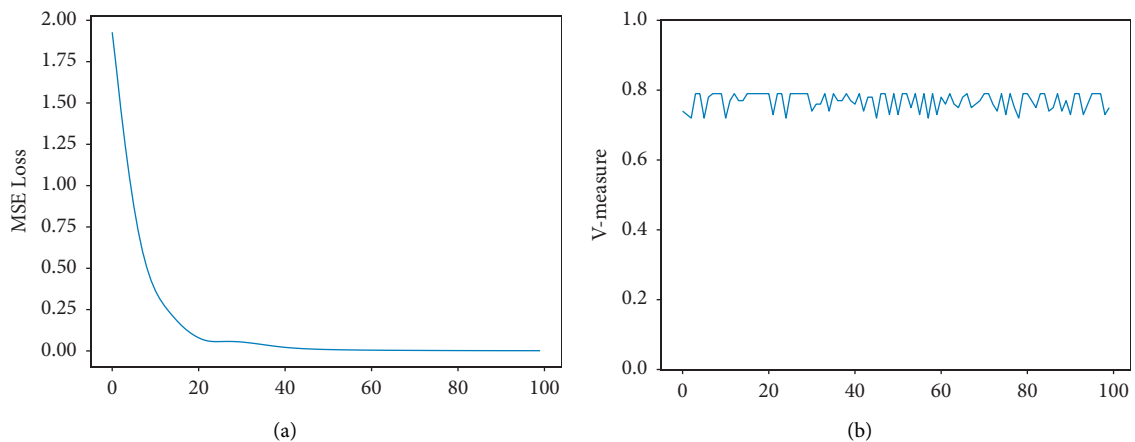


FIGURE 9: Performance of RBF-KNN. (a) Optimization processing. (b) Stability line chart.

GMM clustering algorithms, the DCN clustering algorithm combining Auto-encoder and K-means algorithms, and the semisupervised neural network. SpectralNet clustering algorithm is based on graph theory, of which the SpectralNet algorithm only selects k labeling points in this paper.

It can be seen from the experimental results that compared with the traditional K-means and the DPC algorithm combined with KNN, the algorithm of this paper can obtain better clustering results on each data set, and the comprehensive comparison of the three indicators of V-measure, ARI, and NMI shows the result obtained by the proposed algorithm is more excellent (Tables 3–5).

Compared with the clustering algorithms VaDE and DCN that combine neural networks, both algorithms are clustering algorithms for image processing, and these two algorithms are inefficient in coping with low-dimensional datasets; SpectralNet as a semisupervised clustering algorithm also has poor clustering effect with less prior knowledge. As a self-supervising clustering algorithm, we get better results than the selected 5 algorithms from the three evaluation criteria, which show RBF-KNN has better stability performance and robustness.

4.3. Discussion on RBF-KNN Algorithm Performance and Stability Study. From the V-measure results of the artificial data set, it can be seen that the clustering accuracy of the RBF-KNN algorithm on the Jain data set is low, so the clustering process of the Jain data is selected for analysis in this section, and MSE loss in each iteration is shown in Figure 9(a), and the algorithm can quickly optimized in the 40th iteration. The main step of the algorithm is to map the data set to a Gaussian function and back-propagate, so the algorithm complexity of the RBF-KNN algorithm is $O(n^2 \text{ epochs})$.

In the absence of explicit class label correction, the neural network will cause the clustering process to greatly fluctuate due to initialization problems and missing label problems. In terms of stability, this section still uses the Jain data set and process 100 epochs. The V-measure result is shown in Figure 9(b), and it can be seen from the results that the clustering results of the proposed algorithm do not fluctuate significantly, and the proposed algorithm shows good stability.

5. Conclusion

In this paper, an RBF neural network clustering algorithm based on the K-nearest neighbor principle (RBF-KNN) is proposed, which belongs to a self-supervising clustering algorithm. The central idea is to use the full RBF network to retain global information, and then do back-propagation to self-supervise the resulting neural network based on K-nearest neighbor principle, in order to solve the problem of poor adaptability and lack of robustness of traditional clustering algorithms. From the processing results of the artificial data set and the UCI data set, we can see that the

performance of the proposed algorithm is excellent, and it can handle well with the multitype and unbalanced data.

Based on the above analysis, compared with the lack of versatility of traditional clustering methods and the complex priori conditions of semisupervised clustering, the proposed algorithm can ensure the accuracy of clustering while the process is simple and the simple parameters setting, which shows more obvious advantages than the proposed traditional clustering algorithms and semisupervised neural network clustering algorithms.

Data Availability

The artificial data used to support the findings of this study are included within the article. The UCI data used to support the findings of this study have been deposited in the “<https://archive.ics.uci.edu/ml/index.php>” repository.

Conflicts of Interest

The authors declare that they have no conflicts of interest.

Acknowledgments

This work was supported by Shandong Provincial Natural Science Foundation(ZR2021MF045).

References

- [1] J. L. Chang, Y. W. Guo, L. F. Wang, M. Gaofeng, X. Shiming, and P. Chunhong, “Deep discriminative clustering analysis,” 2019, <https://arxiv.org/abs/1905.01681>.
- [2] J. J. Zhao, D. H. Lu, K. Ma, Y. Zhang, and Y. Zheng, “Deep image clustering with category-style representation,” in *Proceedings of the European Conference on Computer Vision*, pp. 54–70, Springer, Berlin, Germany, August 2020.
- [3] M. Tapaswi, M. T. Law, and S. Fidler, “Video face clustering with unknown number of clusters,” in *Proceedings of the IEEE/CVF International Conference on Computer Vision*, pp. 5027–5036, IEEE, Piscataway, NJ, U.S.A, January 2019.
- [4] M. Wang and W. H. Deng, “Deep face recognition with clustering based domain adaptation,” *Neurocomputing*, vol. 393, pp. 1–14, 2020.
- [5] W. A. Lin, J. C. Chen, C. D. Castillo, and R. Chellappa, “Deep density clustering of unconstrained faces,” in *Proceedings of the IEEE Conference on Computer Vision and Pattern Recognition*, pp. 8128–8137, IEEE, Piscataway, NJ, U.S.A, June 2018.
- [6] Z. Khan and J. Yang, “Bottom-up unsupervised image segmentation using FC-Dense u-net based deep representation clustering and multidimensional feature fusion based region merging,” *Image and Vision Computing*, vol. 94, Article ID 103871, 2020.
- [7] L. Zhou and W. Y. F. Wei, “DIC: deep image clustering for unsupervised image segmentation,” *IEEE Access*, vol. 8, pp. 34481–34491, 2020.
- [8] B. Yang, X. Fu, N. D. Sidiropoulos, and M. Hong, “Towards k-means-friendly spaces: simultaneous deep learning and clustering,” *Proceedings of Machine Learning Research*, vol. 70, pp. 3861–3870, 2017.
- [9] J. Yang, D. Parikh, and D. Batra, “Joint unsupervised learning of deep representations and image clusters,” in *Proceedings of the IEEE Conference on Computer Vision and Pattern*

- Recognition*, pp. 5147–5156, IEEE, Piscataway, NJ, U.S.A., June 2016.
- [10] U. Shaham, K. Stanton, H. Li, B. Nadler, R. Basri, and Y. Kluger, “SpectralNet: spectral clustering using deep neural networks,” in *Proceedings of the International Conference on Learning Representations*, pp. 267–280, IEEE, Piscataway, NJ, U.S.A., January 2018.
 - [11] Z. Jiang, Y. Zheng, H. Tan, B. Tang, and H. Zhou, “Variational deep embedding: an unsupervised and generative approach to clustering,” in *Proceedings of the 26th International Joint Conference on Artificial Intelligence*, pp. 1965–1972, Morgan Kaufmann, San Francisco, CA, U.S.A., January 2017.
 - [12] J. Y. Xie, R. Girshick, and A. Farhadi, “Unsupervised deep embedding for clustering analysis,” in *Proceedings of the International Conference on Machine Learning*, pp. 478–487, ACM, New York, NY, U.S.A., June 2016.
 - [13] J. Chang, L. Wang, G. Meng, S. Xiang, and C. Pan, “Deep adaptive image clustering,” in *Proceedings of the IEEE International Conference on Computer Vision*, pp. 5879–5887, IEEE, Piscataway, NJ, U.S.A., December 2017.
 - [14] W. H. Hu, T. Miyato, S. Tokuis, E. Matsumoto, and M. Sugiyama, “Learning discrete representations via information maximizing self-augmented training,” in *Proceedings of the International Conference on Machine Learning*, ACM, New York, NY, U.S.A., July 2017.
 - [15] Y. Ren, N. Wang, M. Li, and Z. Xu, “Deep density-based image clustering,” *Knowledge-Based Systems*, vol. 197, Article ID 105841, 2020.
 - [16] V. D. M. Laurens and G. E. Hinton, “Visualizing data using t-SNE,” *Journal of Machine Learning Research*, vol. 9, no. 11, pp. 2579–2605, 2008.
 - [17] A. Rodriguez and A. Laio, “Clustering by fast search and find of density peaks,” *Science*, vol. 344, no. 6191, pp. 1492–1496, 2014.
 - [18] N. Mrabah, N. M. Khan, R. Ksantini, and Z. Lachiri, “Deep clustering with a Dynamic Autoencoder: from reconstruction towards centroids construction,” *Neural Networks*, vol. 130, pp. 206–228, 2020.
 - [19] D. Berthelot, C. Raffel, A. Roy, and I. Goodfellow, “Understanding and improving interpolation in autoencoders via an adversarial regularizer,” in *Proceedings of the International Conference on Learning Representations*, pp. 272–284, IEEE, Piscataway, NJ, U.S.A., July 2019.
 - [20] K. L. Lim, X. D. Jiang, and C. Y. Yi, “Deep clustering with variational autoencoder,” *IEEE Signal Processing Letters*, vol. 27, pp. 231–235, 2020.
 - [21] I. J. Goodfellow, A. J. Pouget, M. Mirza et al., “Generative adversarial networks,” *Advances in Neural Information Processing Systems*, vol. 27, no. 3, pp. 2672–2680, 2014.
 - [22] N. Dilokthanakul, P. A. M. Mediano, M. Garnelo et al., “Deep unsupervised clustering with Gaussian mixture variational autoencoders,” 2016, <https://arxiv.org/abs/1611.02648>.
 - [23] S. Mukherjee, H. Asnani, E. Lin, and S. Kannan, “ClusterGAN: latent space clustering in generative adversarial networks,” in *Proceedings of the AAAI Conference on Artificial Intelligence*, pp. 4610–4617, AAAI, Menlo Park, CA, U.S.A., July 2019.

Research Article

Influence of Management Education on Enterprise Scientific and Technological Innovation Based on K-Means Clustering Algorithm

Jun Ma ¹, Zhigang Li,¹ Zichan Liu,¹ Shan Zhang,¹ and Wenling Lai²

¹Guangzhou City Construction College, Guangzhou 510925, Guangdong, China

²Wuchang University of Technology, Wuhan 430223, Hubei, China

Correspondence should be addressed to Jun Ma; marco791@163.com

Received 22 April 2022; Revised 7 July 2022; Accepted 25 July 2022; Published 24 August 2022

Academic Editor: Xuefeng Shao

Copyright © 2022 Jun Ma et al. This is an open access article distributed under the Creative Commons Attribution License, which permits unrestricted use, distribution, and reproduction in any medium, provided the original work is properly cited.

Scientific and technological innovation is the source of the survival and development of enterprises and the key to the realization of the goal of prosperity. In recent years, more and more companies have begun to focus on technological innovation, but the results are not significant, so companies have begun to explore the factors that affect their technological innovation. The management is the helm of the development of the enterprise, the main body of the company's actual production activities, and the direct person in charge of the company's management. Its influence on the innovation of the enterprise is self-evident, and the education level of the management directly determines the manager's ability and vision. However, the current research on management mainly focuses on the position change of management and the rights of management and does not involve the level of education of management. Based on this, this article started from the management education and subdivided it with the K-means clustering algorithm, so as to explore the impact of management education on the technological innovation of enterprises. The experiment showed that there was a significant positive correlation between the educational level of management and the technological innovation ability of enterprises, and the correlation coefficient was 1.521. It fully shows that the management with a higher education background will promote the enterprise to carry out scientific and technological innovation practice and continuously improve the enterprise's innovation ability.

1. Introduction

With the development of science and technology, enterprises pay more and more attention to the integration of technology and products and constantly propose new development plans. However, with the adjustment and upgrading of the industry, there are obvious differences in the investment of enterprises in innovation, which brings challenges to enterprises' innovation planning. Existing researches on the difference of enterprise innovation investment mainly focus on the change of management positions and the rights of management. However, compared with these traditional managers, the level of education of managers can often better reflect the overall quality and ability of managers, so it can also have a greater

impact on the company's innovation decision-making and management.

The long-term development of an enterprise is inseparable from the continuous innovation practice. The management is the leader in the management of the daily affairs of the enterprise, and its education level is often directly reflected in the daily decision-making of the company. Research based on the education level of managers can provide a reference for enterprises to hire relevant management personnel; at the same time, it is helpful for enterprises to assess and motivate management and help to promote the establishment of a more reasonable reward and punishment mechanism. In addition, enterprise scientific and technological innovation is an important part of enterprise management, and it is a key element that determines

the company's development direction, development scale, and development speed. This move can reduce the negative impact of the irrational behavior of company managers on the company and improve the scientific nature of corporate innovation decisions.

After a series of experimental analysis, in the process of clustering division of management education level based on K-means clustering algorithm, when the number of clustering reached 7 times, the clustering result tended to be stable, and the numerical result fluctuated around 2400. At this point, clustering results had the lowest impact on management division. Moreover, the experiment showed that management with higher educational background could approve enterprises to adopt more means to carry out technological innovation, the correlation coefficient was 1.521, and the correlation coefficient between it and the number of patent applications was 1.662. At the same time, the regression coefficient between enterprise innovation input and management with high education background was -0.164 , and the regression coefficient between enterprise innovation input and output and management with higher education was -0.221 , and it was in the horizontal direction of 1%. There was also a significant negative feature at the level, which fully demonstrated the robustness and reliability of the above correlation conclusion. As a result, enterprise management who have experienced higher education will often lead the enterprise to enter the scientific and technological innovation market and continuously improve the enterprise's independent innovation ability.

2. Related Work

With the continuous development of the economy, more and more companies have begun to propose innovation-driven development strategies. At the same time, many experts and scholars have also turned their attention to this area. Yang studied the relationship between work pressure and enterprise innovation cost management. On this basis, he proposed a model to measure the relationship between pressure coefficient and innovation. At the same time, he used the job demand control model to conduct a comprehensive evaluation of employees' mental health, work pressure, engagement, innovation ability, and so on. And then he analyzed the impact of these factors on enterprise technological innovation [1]. Liu took scientific and technological innovation as an intermediate variable and aimed to explore the role of intellectual property protection in the improvement of enterprises' scientific and technological innovation capabilities. In the process, he collected panel data of 80 advanced manufacturing SMEs from 2013 to 2015 and made a detailed analysis of these data [2]. Zhang proposed a plain-text corpus method based on latent Dirichlet assignments, which can automatically construct an ontology in the field of enterprise technology innovation. The method consists of four modules: initial ontology in the field of enterprise technology innovation, preprocessing system, domain-specific terminology mining based on LDA, and related rules defined [3]. Chen aimed to reveal the relationship between firm innovation network and

technological innovation performance from a new perspective. He developed the symbiotic behavior scale and found that symbiotic behavior plays a certain role between the structural characteristics of enterprise innovation network and technological innovation performance. Therefore, he developed the symbiotic behavior measurement scale according to the scale development process and tested the scale using exploratory factor analysis, confirmatory factor analysis methods, and competition models [4].

The above scholars have analyzed the factors that affect the technological innovation of enterprises from different levels, but none of them have studied the impact of management education on technological innovation. K-means clustering algorithm has significant advantages for data classification and mining, so we refer to a series of related literature.

Wang pointed out that disease spot segmentation from crop leaf images is a key prerequisite for disease early warning and diagnosis. In order to improve the accuracy and stability of disease spot segmentation, he proposed an adaptive segmentation method of crop disease images based on K-means clustering [5]. Khan proposed an improved K-means clustering algorithm for intelligent image segmentation, which used an adaptive histogram-based initial parameter estimation process [6]. Li proposed an optimized K-means clustering method and also proposed three optimization principles. At the same time, he pointed out that applying these three principles could minimize the computational cost and improve the computational efficiency of K-means [7]. Allen proposed an improved algorithm for the dependence of the K-means clustering algorithm on the initial cluster center. The algorithm improved the stability and accuracy of the clustering results and sped up the convergence. In the improved K-means algorithm, he selected the initial cluster centers according to the spatial distribution of the data and then sorted the average difference of each sample [8].

The above literature has carried out in-depth research on the K-means clustering algorithm and has carried out relevant optimization and upgrades to the K-means clustering algorithm on the basis of the original algorithm. But for management education, the above scholars have not carried out detailed research. Even if there is, it is a passing area, and the research is not in-depth and detailed enough.

3. Management Education and Enterprise Technological Innovation under K-Means Clustering Algorithm

3.1. Enterprise Technological Innovation. Scientific and technological innovation refers to specific activities used by industrial enterprises in scientific and technological innovation and technology development, including direct expenditures for enterprise research and development activities and all expenditures for indirect research and development activities. Technological innovation is the only way for an enterprise to achieve self-development and innovation. Nowadays, technological innovation capability has increasingly become a key indicator to measure the

comprehensive competitiveness of an enterprise [9]. In the market competition without gunpowder smoke, whoever can first realize technological innovation and technological progress will be the first to seize the market and remain invincible in the fierce competition. Technological innovation is not only the need of a certain region or society, but also the common value pursuit of all mankind. In scientific and technological innovation, the development of science and technology and innovation complement each other. On the one hand, the progress of science and technology will promote the improvement of innovation ability. On the other hand, the improvement of innovation ability will also promote the progress of science and technology to a certain extent [10]. Science and technology not only are used in enterprises, but also cover most fields in society. Figure 1 shows the main application fields of science and technology.

To achieve scientific and technological innovation, enterprises cannot do without the overall innovation in corporate governance thinking. In the process of continuous technological innovation and development, people have gradually summed up several ways of thinking that corporate governance needs to have. These ways of thinking can help us clarify the path and direction of innovation and provide guidance for our scientific and technological innovation experiments.

3.1.1. Innovative Thinking. The innovation of thinking mode is indispensable for enterprises to carry out scientific and technological innovation. Innovative thinking is a kind of thinking gradually formed in the process of scientific and technological innovation, which pays particular attention to the rigour of thinking and usually relies on some specific scientific thinking modes in actual scientific and technological innovation activities [11]. Creative thinking is a pioneering advanced and complex thinking that explores unknown things. It is a kind of original thinking with its own characteristics. Therefore, enterprises can grasp the effective innovative thinking mode in time, which can help enterprises quickly identify the direction of innovation and concentrate all advantages for innovative practice.

3.1.2. Analogical Thinking. Analogical thinking is a way of thinking commonly used in mathematics. Its principle is to compare unfamiliar things with familiar things in order to gain an understanding of new things. However, in the specific innovation practice, enterprises should realize that analogical thinking is only a reasoning method for researching problems, and the cognition provided by it is only a possibility, not a certainty. Therefore, for the final result, the enterprise must conduct a rigorous practice test, so that the result can be adopted. But nonetheless, it is invaluable that the possibilities offered by analogical thinking expand ideas for problem-solving.

3.1.3. Associative Thinking. Associative thinking is a kind of thinking activity produced by the divergent association of the characteristics or attributes of different things [12].

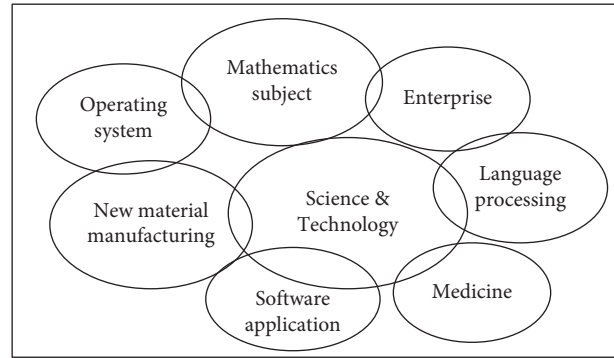


FIGURE 1: Application areas of science and technology.

Associative thinking plays a very important role in daily innovation practice, because associative thinking refreshes the way to see the world and provides us with a reference for innovation. The use of associative thinking by enterprises can fully mobilize their enthusiasm for innovation, provide guidance for other ways of thinking of enterprise innovation, and continuously promote the progress of enterprises' scientific and technological innovation capabilities.

3.1.4. Leap-Forward Thinking. Leap-forward thinking means that after we have thoroughly understood the core concepts and combined them into knowledge ability units, the next thing we need to do is to use the cognition that we can understand better to connect them and memorize them. For example, in business analysis, the marginal benefit, scale effect, and the marginal interpersonal communication field and crowd size in the communication model can be combined and memorized, so as to consolidate the cognition of core concepts and exercise the divergent ability of one's own thinking.

3.2. Enterprise Management. Enterprise managers are the main body of production and operation activities of enterprises [13]. In daily business operation, managers play a leading role in corporate governance and decision-making activities by relying on their own quality and professional knowledge and skills. In the previous corporate structure, the general manager was always the one person in charge of the management, who was responsible for the decision-making and formulation of the company's large and small affairs. Although they mainly manage subordinate employees, they also shoulder specific tasks. However, in modern corporate management activities, the work and functions of the management are artificially subdivided, and the management often completes organizational activities by several managers through coordinating and monitoring the work of others. Figure 2 is a management organization chart of a modern enterprise.

According to the requirements of management, the enterprise management organization divides the production administrative command system of the enterprise according to the principle of division of labor and cooperation, clearly

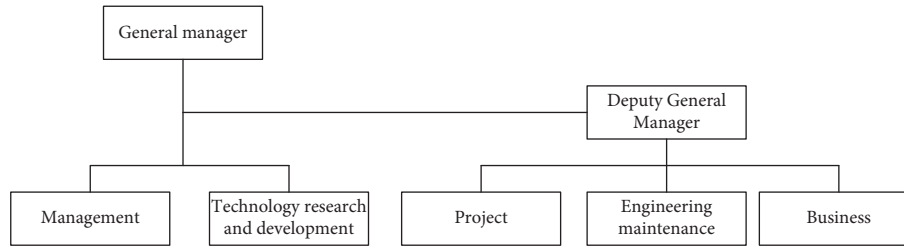


FIGURE 2: Organizational chart of enterprise management.

defines the responsibilities, authority, obligation, and information communication mode of each management level or link, and correspondingly configures a certain number of competent management personnel. Management often has a multilevel structure, which is generally divided into general management, middle management, and senior management. General management is the managers at the lowest level, and they are often managers engaged in production, sales, and other services. General management is the company's grass-roots reserve cadres; they often have the potential to become senior managers. The middle management is the backbone of the company. Their main job is to transmit, that is, to receive tasks from senior management and then assign them to ordinary management. They also oversee the work of ordinary management and accept leadership from senior management. The senior management is at the helm of the enterprise. They formulate the development strategy of the enterprise according to the market environment and use the corporate image to contact the outside world and then adjust the development direction of the enterprise according to the latest changes in the market in real time [14]. They are the core figures of the operation of the enterprise and the executors of accomplishing the goals of the board of directors. An excellent senior manager not only has excellent business ability, but also needs to have a certain financial level.

Because senior management often has extraordinary status and unparalleled power in the company, the object of enterprise management in this paper mainly refers to the management [15]. On the one hand, the senior management decides the direction of the enterprise and has the right to make decisions on all matters of the enterprise. On the other hand, the self-quality and ability of senior managers are the external embodiment of the company, and taking them as the research object can better discover the problems existing in the development process of the enterprise. At the same time, the role of middle management in the enterprise has been a controversial topic. Some researchers believe that the middle management in the company only acts as a transmitter of information and cannot create any value for the enterprise. The other researchers believe that middle management is an indispensable existence in enterprises, because they are responsible for specific tasks and provide technical guidance to ordinary management. Moreover, the middle management can also create an efficient working environment for the enterprise and ensure the integrity of the overall structure of the enterprise.

In the process of researching and discussing management, we found that there is a certain connection between some behaviors and psychology of managers, and the self-quality and ability of managers will be limited by objective conditions. In order to further analyze the factors that affect the behavior and psychology of managers, the following theories are now referred to.

3.2.1. High-Level Echelon Theory. In management, it is generally believed that, due to the complexity and randomness of the external environment, it is impossible for managers to form a comprehensive cognition of things [16]. Even if this thing is something that often occurs around managers, managers cannot observe the whole picture of the thing. In this case, the manager's own ability and quality determine the degree of his understanding of relevant things. In other words, once the development of things exceeds the manager's own cognition, the manager's behavior will have a serious impact on the development of the enterprise. During this process, relevant experts and scholars pointed out that, in order to achieve stable development, enterprises need to rebuild the management structure. The theory developed continuously under the influence of management and economics and was finally summarized as the high-level echelon theory. The high-level echelon theory holds that managers with different experiences and life experiences often have different worldviews and values, and these experiences and experiences will constrain management's decision-making. At the same time, these factors will directly affect their communication and cooperation at work and then indirectly affect the relevant decision-making and strategy formulation of enterprises [17].

3.2.2. Imprint Theory. The imprinting theory was first proposed in the field of biology as an animal cognition theory. With the continuous development of biology, people continue to extend and expand this theory and then introduce it into the field of management [18]. In management, imprinting theory no longer emphasizes simple groups; it begins to focus on individuals with special experiences. The theory holds that things and memories with deep impressions will have a lasting effect on an individual's future development, thereby affecting their future thinking and action. In this theory, the so-called special experience refers to an event that an individual has personally experienced or witnessed, which has the characteristics of a wide range of influence, a significant degree of influence, or a long

time continuation. Moreover, with the in-depth study of this theory, it has been found that the occurrence of individual experiences in the sensitive period is an important condition for the formation of individual imprints [19]. Generally, the academic circle mainly defines the sensitive period from two main aspects: one is certain physiological stages of the individual growth period. The second is a period of great changes in the individual growth environment, which mainly includes the period of education, the period of first work, and the period of marriage.

3.2.3. Managerial Short-Term Orientation. On the basis of the above two theories, another theory was found that affects the decision-making of management. In the process of company management, managers often give up making changes and innovations because of the influence of ready-made interests and then depreciate some innovative strategies. After in-depth research on this phenomenon, people call it managerial short-term orientation [20]. Managerial short-term orientation is a corporate management theory that believes that the problem is that market participants, especially institutional investors, emphasize short-term business results, which leads to undervaluation of companies with long-term investment plans. When companies are undervalued, they become attractive targets for other companies or individual investors with substantial discretionary resources. Management's short-term theory believes that, in the actual company management process, the company's managers will inevitably be involved in the whirlpool of shareholders' interests, so this forces the management to reduce enterprise risk investment and the error rate. However, for the benefit of the enterprise, the management has to carry out some daily investment projects, so the management will purposely crack down on long-term investment projects and try to increase the current profit of the company. At the same time, the manager's short-sighted theory also believes that, in the current market environment, short-term investment will be more in line with managers' psychological expectations. If managers engage in long-term strategic investment, it will expose the enterprise to huge risks, and it will also bring risks to their own employment [21].

3.3. K-Means Clustering Algorithm. The process of classifying and dividing more than three objects according to a specific classification method is called clustering. A cluster generated by clustering is a collection of data objects that are similar to objects in the same cluster and different from objects in other clusters. In the process of clustering, the attributes and characteristics between objects are notable signs to judge their differences from other objects and are also one of the references for clustering. In the natural sciences and social sciences, the commonly used statistical method is the cluster analysis method, which is a common analysis method for studying classification and division problems. From a disciplinary point of view, clustering originally belonged to the category of mathematics, but today's clustering methods are not only used in the field of

mathematics, but also widely used in the fields of statistics and information science. However, clustering is not the same as classification. The difference is that people often do not know the specific number of classifications in advance when performing clustering. In the case of simple classification, the classification standards and categories have already been given. The content of cluster analysis is very rich, including systematic clustering method, ordered sample clustering method, dynamic clustering method, fuzzy clustering method, graph theory clustering method, clustering prediction method, and so on [22]. The general formation process of clusters is shown in Figure 3.

Before clustering, people first need to find a sample center point, which is the cluster center. After the center is determined, the data set is automatically divided into different clusters according to the distance and difference between each data point and the cluster center. In the process of cluster formation, the distance between each data point and the center is the similarity between the data and the cluster center, so the similarity between the data sets can be obtained by calculating the distance.

When studying cluster analysis, people often talk about a concept: similarity, which mainly describes the mutual attributes between objects [23]. The closer two things are, the larger their similarity measure is. The farther away two things are, the smaller their similarity measure is. As can be seen from the above, any data set has a natural structure at the bottom, which constitutes the basis of clustering. When a sample set n is given and the sample set stores several attributes of enterprise managers, such as gender, age, education level, and so on, this sample object is then given a m -dimensional attribute, where E_i represents the education level of the i -th object. Figure 4 is a flowchart of the K -means clustering algorithm.

In the process of calculation, there is a certain Euclidean distance between any two objects, which is defined as

$$d = \frac{1}{m} \sqrt{\sum (x_i - x_j)^2}. \quad (1)$$

Among them, i and j represent the i -th and j -th objects, respectively, and x represents the sample space of the object. The Manhattan distance is expressed as

$$d' = \frac{1}{m} \sum_{k=1}^m |x_i - x_j|. \quad (2)$$

In addition to the above two methods that can represent the relationship between arbitrary objects, there are also some indicators that can also be used as a standard for measuring similarity. But no matter how the way of representation changes, the essence of cluster analysis does not change, that is, to find the inherently similar structure between objects.

K -means clustering in the general sense is an adaptive clustering learning algorithm [24]. The operation process of this algorithm is mainly to set up an objective function and then iterate towards the objective function continuously. The representation of the objective function is generally as shown in the following formula:

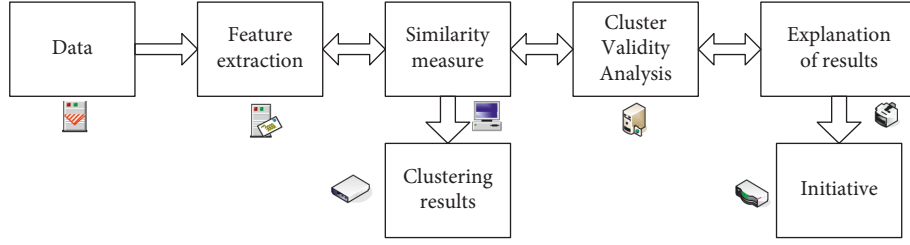


FIGURE 3: Cluster formation process.

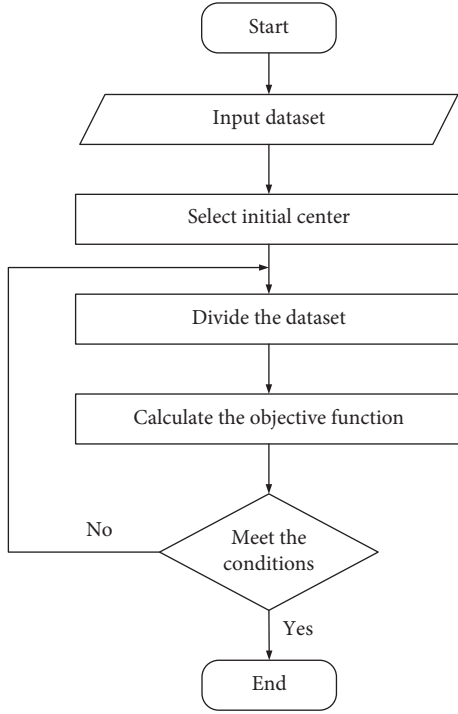


FIGURE 4: Flowchart of K-means clustering algorithm.

$$f = \sum_{j=1}^k \sum_{i=1}^k DIS(X_i, Z_j), \quad (3)$$

$$DIS(X_i, Z_j) = \frac{\left[\sum_{k=1}^n |\omega_i - \omega_j|^2 \right]^{1/2}}{\sqrt{\sum_{k=1}^n (\omega_i - \omega_j)^2}}. \quad (4)$$

Among them, k is the initial cluster center, Z is the cluster center in the adjustment process, and the adjustment operation is as follows:

$$Z_{ij} = \frac{1}{n} \sum_{x_{ij} \in D} x_{ij}. \quad (5)$$

In this formula, x_{ij} represents the j -th value of the sample point at the i -th position, and D is the sample size. However, in many cases, the data is incomplete or the data is too large, which requires us to optimize the above clustering analysis algorithm. On the one hand, characterizing the local similarity between sample data can be done, and on the other hand, the similarity of the data at a certain point needs to be

considered. On this basis, a comprehensive analysis of the sample data can be achieved.

$$\omega_{ij} = F(p_{ij}, q_{ij}), \quad (6)$$

F is the optimized objective function, which in theory we want to decrease as the local similarity increases. In particular, p and q are defined as follows:

$$p_{ij} = p(\Theta_i, \Theta_j) = \left(\frac{\prod_i}{\cos(\theta_t)} \right), \quad (7)$$

$$\cos(\theta_t) = \max_{x_i \in \Theta_i, x_j \in \Theta_j} x_i x_j \cos(\theta_t).$$

In this process, Θ is the tangent space of the sample set, and x_i and x_j express the local structure of the sample points. θ is the angle of the tangent space, which is an adjustable variable.

$$q_{ij} = \prod_{i=1}^d \cos(\theta)^t, \quad (8)$$

$$w_d = \sum_{k=1}^n \cos(\theta)^2 \cdot \prod_{i=1}^k.$$

In the formula, p_{ij} and q_{ij} represent the local similarity and point similarity of the sample data set, respectively. w is the similarity weight derived from the sample tangent space.

Arbitrary similarity weights can form a spectral graph, where the vertices of the graph are formed by the similarity weights of the data. In this case, the aggregation of data is no longer bound by traditional clustering, which can form clusters on arbitrary geometric shapes.

The similarity matrix is constructed as follows:

$$R = \frac{\sum_m \sum_n (A_{mn} - B_{mn})}{\sqrt{\sum_m \sum_n (A_{mn} - B_{mn})^2}},$$

$$A_{mn} = A_{ij} \sum_{i=1, j=1}^n N_{ij}, \quad (9)$$

$$B_{mn} = B_{ij} \sum_{i=1, j=1}^m N_{ij}.$$

In the formula, N is a sample set containing n data nodes, and A_{mn} and B_{mn} are two similarity matrices, respectively.

Similarly, a standardized similarity matrix continues to be constructed to compare its data differences with the general matrix, which is defined as follows:

$$D_{mn} = \sum_j^N W_{ij}. \quad (10)$$

Transform it with a Laplacian matrix to get

$$\begin{aligned} L &= D^{(1/2)} \cdot L \cdot D^{(1/3)}, \\ D &= L - D^{-(1/2)} \cdot W \cdot D^{-(1/2)}, \\ W &= L \cdot L^{-(1/2)} \cdot D^{(1/2)}, \end{aligned} \quad (11)$$

L is a Laplace matrix and W is an identity matrix. After the above process, the maximum eigenvalue of the matrix can be gotten, where D is also called the eigenmatrix.

However, when processing data, problems such as data duplication and inconsistency of attributes are prone to occur in many cases. Therefore, in the actual operation process, the sample data set needs to be modified to delete redundant parts. The modified and normalized definitions of the data are as follows:

$$\begin{aligned} c_i &= \frac{c_i - u}{\sqrt{(1/N) \sum_{i=1}^N (x_i - u)^2}}, \\ u &= \sqrt{c_i \cdot \sum (x_i - \bar{x})^2}. \end{aligned} \quad (12)$$

Among them, the length of the data is N , the normalized value of the data is u , and c_i is any data point in the data set. On the basis of data standardization, the feature matrix needs to continue to be processed to get the following formula:

$$E = D^{(1/2)} \cdot W \cdot L \cdot D^{-(1/2)}. \quad (13)$$

Among them, E is a N -dimensional vector, which describes the basic clustering result of the data, and the matrix W corresponding to the vector is the final clustering result.

Applying the above clustering analysis method can make a simple subdivision of the management of the enterprise. The management division can effectively distinguish which managers can bring long-term benefits and value to the company and which managers can promote enterprise innovation. In the long-term development process of the enterprise, the requirements of the enterprise for the management are gradually transparent. Therefore, after the management is divided, the personal ability and quality of the management will be more prominent. Under the combined effect of the market and economic environment, managers often have some extraordinary skills, so the method of clustering can adapt to different needs.

In the company's internal environment, the management has two purposes, one is to maintain the stability of the company's internal structure, and the other is to ensure the harmony of the company's external environment. The division of the company's management, on the one hand, helps the company's top management to divide the functions of the management, so as to maximize the manager's own

advantages. On the other hand, it can promote the strategic adjustment and personnel adjustment of enterprises. The knowledge and use of the management by the enterprise will magnify the management ability of the manager to continuously meet the needs of enterprise development. When the management repeatedly fails in major decisions, the truth often becomes the target of public criticism. Therefore, managing the management well is more important than managing the employees. Do not let the management be the messenger. From another point of view, the segmentation of enterprise management can be divided into two levels: macrodivision and microdivision. Among them, the macrodivision mainly refers to the subdivision of enterprises according to the business ability of managers and the quality of managers themselves. For example, managers are divided into senior managers, intermediate managers, and general managers according to their educational level. However, this kind of division in the macrosense is mostly the division of a single variable, so on this basis, people put forward microsegmentation. Microdivision also refers to behavioral subdivision. Generally, the results of microdivision are more detailed and complex. For example, managers can be divided into aggressive managers, stable managers, and conservative managers according to their investment behaviors. In the process of this research, not only do the goals need to be set in advance, but also a lot of data need to be analyzed. Figure 5 shows the empirical research process of this paper.

Compared with general research and analysis methods, such as single variable segmentation, behavioral segmentation, or simple macroanalysis, K-means clustering can fit well with the objective function, and the process of dividing does not involve any personal subjective emotions. Therefore, this classification method can more objectively reflect the differences between the target objects. Moreover, when studying the characteristics and application effects of target objects, K-means-based clustering is beneficial to thoroughly understand the segmentation results and to establish a good partition model between objects and targets in advance. In the process of studying the technological innovation of enterprises, the level of education of the company's management is used as the basis for the division, and the management's own ability and literacy are used as the auxiliary division criteria, which can make the research more in-depth and can also fully grasp the company's management quality, personal quality, education level, and innovation ability. On this basis, the company will be able to further clarify the management hiring standards and continue to carry out technological innovation practices under the leadership of the new management.

4. Segmentation of Management Education Based on K-Means Clustering Algorithm

Before the empirical research begins, it is necessary to conduct statistics and analysis on the collected sample data and divide the research objectives according to the K-means clustering algorithm. The statistical results of different variables of the whole sample are shown in Table 1.

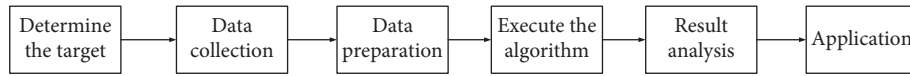


FIGURE 5: Empirical research process.

TABLE 1: Statistical results of different variables in the whole sample.

Variable	Sample size	Mean	Standard deviation	Median
RD	12387	0.030	0.031	0.027
SIZE	12387	21.721	1.152	21.580
LEV	12387	0.410	0.201	0.410
ROA	12387	0.042	0.052	0.049
SEX	12387	0.949	0.223	1
E-HIGH	12387	0.851	0.621	0
E-LOW	12387	0.550	1.382	0.639

TABLE 2: Statistics grouped by managers' education.

Variable	Managers with high education background			Managers without high education background		
	Mean	Standard deviation	Median	Mean	Standard deviation	Median
SIZE	21.334	21.721	21.152	21.591	1.151	21.582
LEV	0.364	0.411	0.201	0.421	0.205	0.404
ROA	0.045	0.048	0.052	0.039	0.055	0.521
SEX	0.897	0.949	0.223	0.952	0.219	1
PATENT	19.111	1.218	0.348	11.210	0.821	0.312
INNOVATION INPUT	12.987	2.314	1.167	9.345	1.213	0.921
INNOVATION OUTPUT	11.321	2.113	0.921	7.611	1.324	0.816

In Table 1, the factors that affect the technological innovation of enterprises are collected, and their impact on the technological innovation of enterprises is calculated. Among them, the variance of the impact of education level on enterprise technological innovation is 0.851, and the variance of the impact of production scale on enterprise technological innovation is 21.721, which indicates that the impact of education level on enterprise technological innovation is relatively stable. However, the educational level of enterprises is not equal to the educational level of managers, so we will analyze the educational level of managers next. The grouping of managers' educational status and their impact on enterprises are shown in Table 2 and 3.

From the above data, it can be known that the manager's educational background coefficient is 0.010, and with the continuous improvement of the manager's educational level, the correlation coefficient is increasing and showing a significant positive feature, with the highest coefficient being 1.76. This shows that the higher the education level of managers, the more likely it will promote enterprises to invest in technological innovation.

In order to explore the influence of the educational background of different levels of management on the technological innovation of enterprises, regression analysis was carried out on the educational background of the general manager and chairman of the board, respectively. Table 4 and 5 are its regression results.

The data shows that different management levels will have different impacts on the technological innovation of

TABLE 3: The impact of higher education background on the investment in scientific and technological innovation of enterprises.

Variable	Correlation coefficient	University	Master	Phd
EDUCATION	0.010	0.004	0.006	0.016
HIGH EDUCATION	1.76	2.92	3.08	3.00
STUDY ABROAD	0.022	0.014	0.201	0.004
RESEARCH INSTITUTE	6.49	7.70	0.052	0.0006
CLUB	0.011	7.89	7.91	7.62
CONSTANT	3.871	2.63	2.66	3.98
ABILITY	-14.82	-5.13	-5.11	-5.05

TABLE 4: The regression results of the influence of the general manager's educational background on the technological innovation of enterprises.

Variable	Company innovation performance			
	Patent	RD	Input	Output
MASTER	0.462	-0.92	1.01	0.70
STUDY ABROAD	0.512	-0.014	1.201	1.004
RESEARCH INSTITUTE	0.351	-0.70	2.052	2.531
UNIVERSITY	0.019	-0.89	1.91	0.62
FAMOUS SCHOOL	1.112	-0.63	1.66	1.98
PHD	4.82	-1.13	6.11	5.05

enterprises. Among them, if the general manager's education level is higher, it will promote the enterprise to implement the innovation-driven strategy, and its highest correlation

TABLE 5: The regression results of the influence of the chairman’s educational background on the technological innovation of enterprises.

Variable	Company innovation performance			
	Patent	RD	Input	Output
MASTER	1.121	-0.11	1.19	1.77
STUDY ABROAD	1.005	-0.914	1.43	1.65
RESEARCH INSTITUTE	0.621	-1.20	2.001	2.901
UNIVERSITY	0.005	-1.50	0.22	0.62
FAMOUS SCHOOL	1.219	-0.23	2.66	3.98
PHD	-3.221	-1.11	3.12	3.05

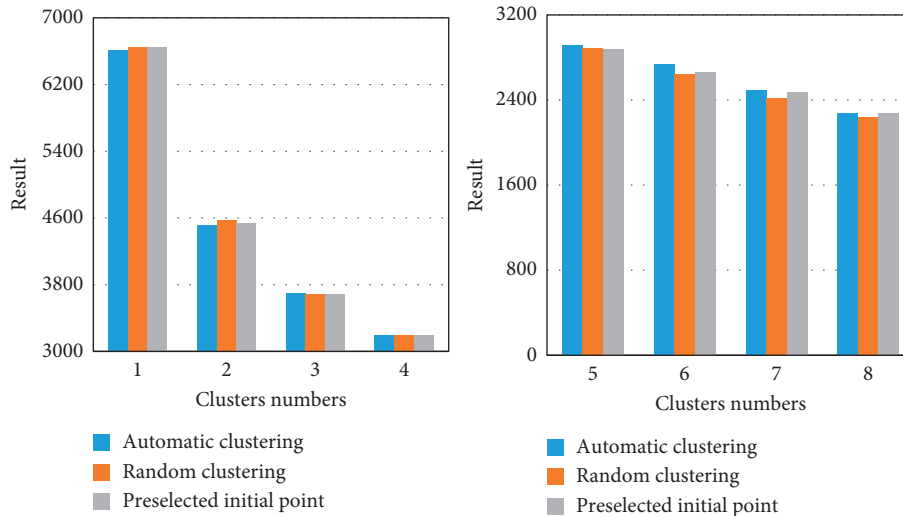


FIGURE 6: Clustering results of different initial points.

coefficient reaches 4.82. The higher education level of the chairman may inhibit the company’s technological innovation, and its highest coefficient is -3.221, which shows that it has a significant negative correlation. The reason is that the chairman of the board is the shareholder of the company and the direct beneficiary of the company’s immediate interests, so it will hinder the company’s innovation to a certain extent. The general manager is generally an external employee of the company, and his income is directly related to the company’s income, so it is in line with his interests to promote innovation.

5. Final Clustering Results

In the actual clustering operation process, different initial points will affect the clustering results. Therefore, for the rationality of the management division, it is necessary to minimize the impact of clustering. Figure 6 shows the clustering results of different initial points.

Figure 6 shows that when the number of clustering is relatively low, there are relatively more clustering results; in particular, after only one clustering, the clustering results are as many as 6300. However, when the number of clustering reaches 7, the clustering results tend to be stable, and the numerical results fluctuate around 2400. At this time, the clustering results have the lowest impact on the management division.

However, within the clusters divided according to the educational level of the management, the gap in the educational level of the management will bring errors to the analysis of the clustering. The intraclass residual is a measure used to describe the clustering error, and the smaller the sum of squares is, the smaller the error is. The intraclass residual sum of squares for different initial points is shown in Figure 7.

As can be seen from Figure 7, as the number of clusters increases, different initial point clusters begin to recombine 10 times. It can be clearly found that the second clustering and the tenth clustering are two obvious watersheds, and the number of clusters in the second watershed has dropped to 4000. In the tenth clustering, the number of clusters decreased from 2200 to about 2000.

After ensuring that the division of management education level will not bring errors and influences to its research, its correlation with corporate technological innovation will be analyzed emphatically. The correlation between management education and corporate technological innovation is shown in Figure 8.

The experiment in Figure 8 shows that managers with higher educational backgrounds approve companies to adopt more means for technological innovation. Among them, the correlation coefficient between technological innovation investment and management with high education background is 1.521, and the correlation coefficient

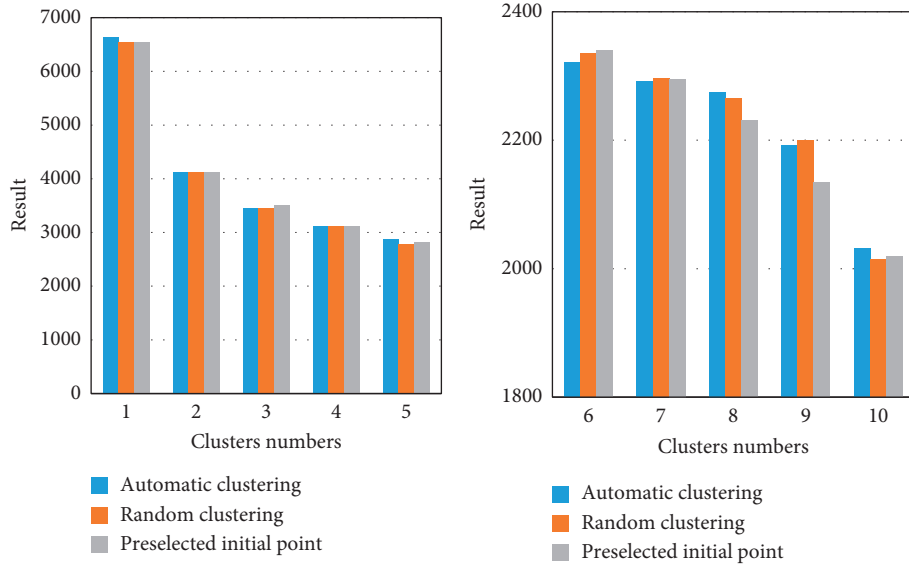


FIGURE 7: Intra-class residual sum of squares for different initial points.

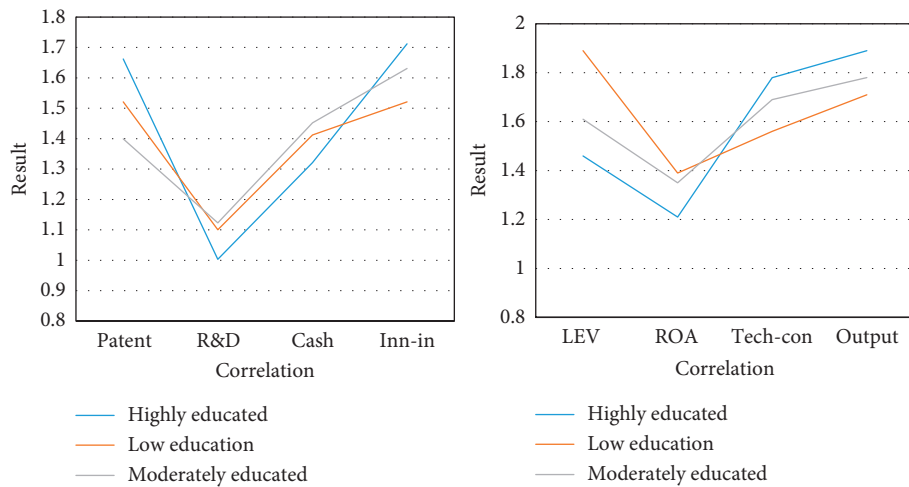


FIGURE 8: Correlation between management education and corporate technological innovation.

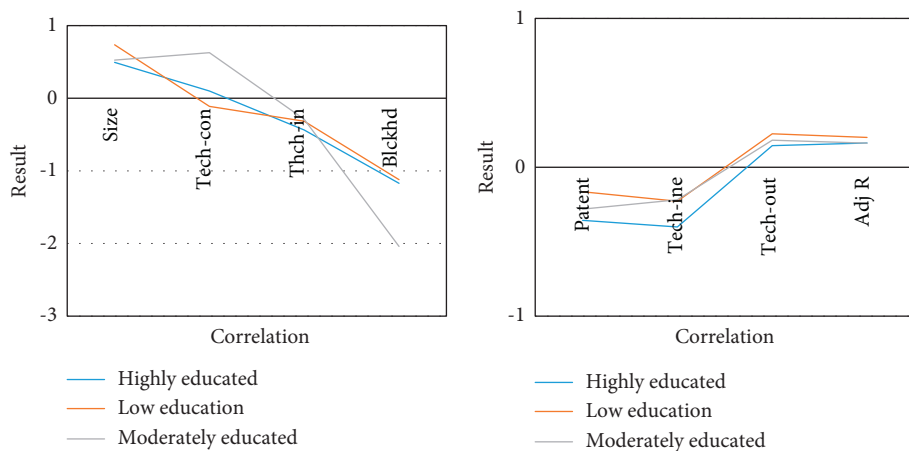


FIGURE 9: Robustness test between management education and corporate technological innovation.

between it and the number of patent applications is 1.662. This fully demonstrates that management with a higher education background will promote technological innovation in enterprises.

Using only the number of patent applications to measure the correlation between a firm's technological innovation and management education can lead to a severe left-biased effect. Therefore, other variables are added to the above correlation test, and the least squares method is used to test the robustness of the correlation. The robustness test results between management education and corporate technological innovation are shown in Figure 9.

It can be seen from Figure 9 that the regression coefficient between corporate innovation input and management with high education background is -0.164 , and the regression coefficient between corporate innovation input and output and management with higher education is -0.221 . And it also exhibits significant negative characteristics at the 1% horizontal level, which fully demonstrates the robustness and reliability of the above correlation conclusion.

6. Conclusions

Starting from the educational level of enterprise management, this paper firstly analyzed the influencing factors of enterprises' technological innovation and the related theories of enterprise management. On this basis, the article then divided the management education level into clusters based on the K-means clustering algorithm and conducted an empirical study on its influence on the technological innovation of enterprises. Experiments showed that management with a high education background tended to promote the practice of scientific and technological innovation in enterprises. However, due to time reasons, the article did not study the education time of enterprise management during the experiment, so the research lacked comprehensiveness. In the future, the paper will comprehensively study the time and current situation of management education and continue to fill in the research gaps.

Data Availability

No data were used to support this study.

Conflicts of Interest

The authors declare that there are no conflicts of interest regarding the publication of this article.

Acknowledgments

This work was supported by Research Project of "13th Five-Year Plan" of Education Bureau of Guangdong, China (Project no. 2020GXJK233); Foundation for Young Innovative Talents of Colleges and Universities of Guangdong, China (Project no. 2020WQNCX244); Research Project of "13th Five-Year Plan" of Education Bureau of Guangdong, China (Project no. 2020GXJK252); and 2020 Key Scientific

Research Platform Project of Higher Education of Guangdong, China (Project no. 2020CJPT029).

References

- [1] J. Yang, Y. Qin, and F. Moulart, "The influence of employee pressure on the management cost of enterprise technological innovation using mental health education," *Work*, vol. 70, no. 4, pp. 1–10, 2021.
- [2] Z. Liu, R. Mu, S. Hu, L. Wang, and S. Wang, "Intellectual property protection, technological innovation and enterprise value-An empirical study on panel data of 80 advanced manufacturing SMEs," *Cognitive Systems Research*, vol. 52, no. 12, pp. 741–746, 2018.
- [3] Q. Zhang, S. Liu, D. Gong, and Q. Tu, "A latent-dirichlet-allocation based extension for domain ontology of enterprise's technological innovation," *International Journal of Computers, Communications & Control*, vol. 14, no. 1, pp. 107–123, 2019.
- [4] J. Chen, S. Lin, and M. Jin, "Learning to use the symbiosis behavior: the mediating effect between enterprise innovation network and technological innovation performance," *Centre Calling*, vol. 42, no. 3, pp. 1222–1229, 2017.
- [5] Z. Wang, K. Wang, S. Pan, and Y. Han, "Segmentation of crop disease images with an improved K-means clustering algorithm," *Applied Engineering in Agriculture*, vol. 34, no. 2, pp. 277–289, 2018.
- [6] Z. Khan, "An improved K-means clustering algorithm based on an adaptive initial parameter estimation procedure for image segmentation," *International journal of innovative computing, information & control: IJICIC*, vol. 13, no. 5, pp. 1509–1525, 2017.
- [7] W. Li, J. Y. Zhao, and T. S. Yan, "Improved K-means clustering algorithm optimizing initial clustering centers based on average difference degree," *Kongzhi yu Juece/Control and Decision*, vol. 32, no. 4, pp. 759–762, 2017.
- [8] S. Allen, A. L. Cunliffe, and M. Easterby-Smith, "Understanding sustainability through the lens of ecocentric radical-reflexivity: implications for management education," *Journal of Business Ethics*, vol. 154, no. 3, pp. 781–795, 2017.
- [9] M. Kolb, L. Fröhlich, and R. Schmidpeter, "Implementing sustainability as the new normal: responsible management education from a private business school's perspective," *International Journal of Management in Education*, vol. 15, no. 2, pp. 280–292, 2017.
- [10] N. Nikolova and L. Andersen, "Creating shared value through service-learning in management education," *Journal of Management Education*, vol. 41, no. 5, pp. 750–780, 2017.
- [11] D. Howell, T. Harth, J. Brown, C. Bennett, and S. Boyko, "Self-management education interventions for patients with cancer: a systematic review," *Supportive Care in Cancer*, vol. 25, no. 4, pp. 1323–1355, 2017.
- [12] S. M. Holliday, C. Hayes, A. J. Dunlop et al., "Does brief chronic pain management education change opioid prescribing rates? A pragmatic trial in Australian early-career general practitioners," *Pain*, vol. 158, no. 2, pp. 278–288, 2017.
- [13] M. Thangamani, R. Vijayalakshmi, M. Ganthimathi, M. Ranjitha, P. Malarkodi, and S. Nallusamu, "Efficient classification of heart disease using KMeans clustering algorithm," *International Journal of Engineering Trends and Technology*, vol. 68, no. 12, pp. 48–53, 2020.
- [14] N. A. Khairani and E. Sutoyo, "Application of K-means clustering algorithm for determination of fire-prone areas utilizing hotspots in west kalimantan province," *International*

- Journal of Advances in Data and Information Systems*, vol. 1, no. 1, pp. 9–16, 2020.
- [15] T. Santoso and F. Saftarina, “Clusterization of paddy field farmers condition in kota metro lampung province Indonesia using K-means clustering algorithm,” *Journal of Agribusiness and Community Empowerment*, vol. 3, no. 1, pp. 37–43, 2020.
- [16] Y. Yang, B. Qian, Q. Xu, and Y. Yang, “Climate regionalization of asphalt pavement based on the K-means clustering algorithm,” *Advances in Civil Engineering*, vol. 2020, no. 4, Article ID 6917243, 13 pages, 2020.
- [17] S. Yin and T. Wang, “An unknown Protocol improved k-means clustering algorithm based on Pearson distance,” *Journal of Intelligent and Fuzzy Systems*, vol. 38, no. 4, pp. 4901–4913, 2020.
- [18] B. Sarada, “Enhanced evolutionary computing assisted K-means clustering algorithm for BigData analytics,” *International Journal of Advanced Trends in Computer Science and Engineering*, vol. 9, no. 4, pp. 6007–6017, 2020.
- [19] X. Lin and J. Xu, “Road network partitioning method based on Canopy-Kmeans clustering algorithm,” *Archives of Transport*, vol. 54, no. 2, pp. 95–106, 2020.
- [20] M. Bhardwaj, “Improved K-means clustering algorithm based on KD-tree approach,” *Bioscience Biotechnology Research Communications*, vol. 13, no. 14, pp. 160–163, 2020.
- [21] X. He, J. Li, B. Wang et al., “Diabetes self-management education reduces risk of all-cause mortality in type 2 diabetes patients: a systematic review and meta-analysis,” *Endocrine*, vol. 55, no. 3, pp. 712–731, 2017.
- [22] U. Srilakshmi, N. Veeraiah, Y. Alotaibi, S. A. Alghamdi, O. I. Khalaf, and B. V. Subbayamma, “An improved hybrid secure multipath routing protocol for MANET,” *IEEE Access*, vol. 9, Article ID 163043, 2021.
- [23] M. Nasir, “A novel fuzzy clustering with metaheuristic based resource provisioning technique in cloud environment,” *Fusion: Practice and Applications*, vol. 6, no. 1, pp. 08–16, 2021.
- [24] M. Shafiabadi, Z. Ahmadi and M. R. Esfandiyari, “Solving the problem of target k-coverage in WSNs using fuzzy clustering algorithm,” *Journal of Intelligent Systems and Internet of Things*, vol. 2, no. 2, pp. 55–76, 2021.

Research Article

Research on Institutional Investors and Executive Compensation Stickiness Based on Fixed Effect Model: A Case Study of Chinese Listed Companies

Yizhao Hong 

University of Science and Technology of China, Hefei, Anhui Province 230000, China

Correspondence should be addressed to Yizhao Hong; hongyizhao00@mail.ustc.edu.cn

Received 6 July 2022; Revised 31 July 2022; Accepted 5 August 2022; Published 24 August 2022

Academic Editor: Wei Liu

Copyright © 2022 Yizhao Hong. This is an open access article distributed under the Creative Commons Attribution License, which permits unrestricted use, distribution, and reproduction in any medium, provided the original work is properly cited.

Based on the relevant data of Chinese A-share listed companies from 2014 to 2018, this paper studies the relationship between institutional investors and executive compensation stickiness by using Excel and Stata15.0 software. By fixed effect model, the results show that the sensitivity of executive compensation to performance of listed companies in China is asymmetric, which means there is a sticky characteristic of executive compensation. With the continuous development of China capital market, institutional investors will significantly inhibit the stickiness of executive compensation; in addition, according to the degree of pressure sensitivity, institutional investors can be divided into bias-pressure-resistant institutional investors and bias-pressure-sensitive institutional investors, and the former has a stronger inhibition effect on executive compensation stickiness than the latter. Therefore, the participation of institutional investors can optimize the executive compensation system, thus further promoting the implementation of contract theory and the development of enterprises.

1. Introduction

In the era of growing economy, all walks of life have made remarkable progress. With the continuous development of China's capital market, institutions' participation in corporate governance as a third party has become a hot topic for scholars, among which how to affect the executive compensation system has attracted much attention. In the early 21st century, the OECD emphasized in its public report that the core of an enterprise is its shareholders and the interests of the shareholders are fundamental. This shows that the old focus on profit maximization has been replaced. However, due to the essential difference of interests between the management and the management, the related behaviors of the management will violate the core and foundation of the enterprise, and both will suffer. Until now, the most authoritative modern theory holds that a company is a set of expectations for the relationship between each stakeholder and the enterprise (Claessens) [1]. Then, no matter whether the ultimate focus of an enterprise is value or stakeholders, it

must balance the interest conflicts among the governance layer, management, and even stakeholders through a certain mechanism (Blair) [2]. Institutional investors have abundant information, resources, management, and professional advantages. They can provide guidance and advice in corporate governance, introduce relevant customers to corporate operations and play a supervisory role in the implementation of executive compensation contracts (Amin et al.,) [3]. Overall, institutional investors are likely to be helpful to corporate governance.

Therefore, this paper uses normative empirical analysis method to explore the mechanism relationship between corporate governance and executive compensation stickiness. According to the domestic and foreign mainstream articles and theories and combined with the actual macro and micro background, the research hypothesis of this paper is given. Then, supported by the data of China's A-share listed companies from 2014 to 2018, appropriate dependent variables, independent variables, and control variables are selected to establish a regression model, and the sample data

are verified by using Stata15.0; finally, the hypothesis is tested one by one and conclusions and suggestions are given accordingly.

2. Literature Review and Research Assumptions

2.1. Literature Review. Institutional investors are generated and active in capital market transactions. They must comply with local laws and regulations and be approved by the government before they can engage in investment activities. They are subject to strict restrictions. Institutional investors are a broad group with certain differences in individual preference, investment philosophy, economic wealth level, and professional level. Therefore, it is difficult to unify the definition of institutional investors. The term “stickiness” is physically used to describe the relationship between fluid stress and its rate of deformation. Then borrowing this idea, “stickiness” is also widely used and explored in management.

Graver [4] first selected the relevant data of 376 companies in 1970–1996 and found that the monetary compensation of chief executive officer is positively correlated with the net profit of the company, and the monetary compensation of chief executive officer will significantly increase when the company’s profit increases, but this will not happen when the profit decreases. Heart [5] through investigation and research, it is found that the proportion of shares held by investors in an organization has a significant positive correlation with their remuneration to senior executives. On this basis, David et al. [6] first proposed the concept of heterogeneity between institutions and investors at the end of the twentieth century and found that the actual shareholding ratio of some radical institutions and investors was significantly negatively correlated with employees’ salaries, while the actual shareholding ratio of some more conservative institutions and investors was not significantly correlated with employees’ salaries. Subsequent Corneet et al. [7] also put forward a similar view: generally speaking, the proportion of shares held by institutional investors is significantly positively correlated with the cash flow and return rate of the enterprise throughout the operation process; in terms of breakdown, institutional investors holding shares that do not have any business relationship with listed companies are positively and closely related to cash flows and return rates in the production and operation of enterprises, while institutional investors that have a potential relationship with companies have no significant impact on cash flow returns in the operation of enterprises.

Chinese scholar Zhihong Yi et al. [8] put forward the view that the existence of institutional investors inhibits the stickiness of executive compensation, and on this basis, the author classified the sensitivity of executive compensation into two types and found that this kind of pressure-resisting type of investors can greatly improve the performance sensitivity of enterprises to compensation. After that, Xiaoshan Chen and Hongduo Liu [9] explored the depth and breadth of institutional investment shareholding on the excess compensation of senior executives and divided the institutions into boosters, supervisors, and bystanders. However, there are also some scholars, who hold opposing

opinions. For example, Chao Li et al. [10] selected listed companies in China from 2004 to 2008 as samples, and used linear probability, probit, and other regression models to show that China institutional investment is not related to executive compensation; Li and Wang [11] believed that under the “one-share-one-vote” system in China, institutional investors, as holders of tradable shares, cannot directly affect corporate governance and executive compensation. Empirical evidence also shows that there is no significant relationship between institutional investors and executive compensation.

To sum up, institutional investors will optimize investment and management by integrating factors such as the scale, industry, culture, strategy, investment, and financing opportunities of the enterprise, so as to improve the internal governance of the enterprise, increase the sensitivity of executive compensation performance, comply with the performance contract system and curb the stickiness of executive compensation. In addition, different types of institutional investors have different degrees of influence on executive compensation, which also lays a foundation for subsequent empirical research.

2.2. Research Assumptions. According to the optimal contract theory and relevant contents of incentive theory, there is a contractual relationship between shareholders and senior management, which maintains and restricts the transaction cooperation between the two parties and seeks the development of the company under the premise of sharing the responsibility risk. At the same time, shareholders are required to pay certain remuneration to senior management as an incentive and warning. According to the incentive theory, executive compensation should be highly positively correlated with the performance they create. When the performance they create rises, the compensation they receive should also rise, which is the combined effect of positive reinforcement and negative reinforcement. However, according to the description of principal-agent theory and information asymmetry theory, in fact, the management is responsible for the real operation, development, and governance of the company, and there is a conflict of interests between the management and shareholders. The dynamic opportunity to pursue short-term interests results in the executive compensation contract not being effectively performed. First, senior managers are generally selected by shareholders themselves. They have professional advantages, management advantages, and information advantages. On the whole, professional managers are definitely beneficial to the long-term development of the company. When the performance of senior executives declines, shareholders will generally have a “failure tolerance” mentality and will not impose too much punishment on senior executives (Lai and Leng) [12]. If the punishment is too high, the management may lose their enthusiasm for work or start their own business with their unique advantages, which is not worth the cost to the company. From a psychological point of view, when the performance of senior executives drops, shareholders will impose a slight punishment or even no

punishment, which will cause the senior executives to feel ashamed and work harder in the next stage, which is actually a kind of reverse incentive. Secondly, shareholders, after all, as the owners of the company, delegate the management of the company to the senior management and enjoy the benefits themselves. For the senior management, there will be an imbalance in their hearts. They think that their efforts do not match the remuneration and most of the company's benefits flow to shareholders. Therefore, Zhu et al. [13] proposed that when the performance of senior executives decreased, the senior executives were dissatisfied with the penalty of salary reduction and even used their power to change their salaries. Third, as a listed company, executive compensation will be disclosed to the public in the annual report. If the executive compensation is reduced too much, it may imply poor management of the enterprise and affect the reputation of the executive. Therefore, companies generally do not significantly reduce executive compensation. Fourthly, Fang (2011) [14] believed that the salary of the company's staff is a health factor, no matter what the salary system is set, the staff should only reach a neutral satisfaction state. On the contrary, when the salary system deteriorates to below the expectations of the staff, a negative attitude will be generated, resulting in a decrease in work efficiency and a consequence of the company's poor development. The economic concept can be introduced from this, that is, salary is a kind of rigid demand. When the company's performance drops, the salary will not drop too fast, which is a gentle curve. To sum up, the company may impose "heavy rewards and light penalties" or even "heavy rewards and zero penalties" on senior executives. Based on this, this paper proposes the hypothesis H1 as follows:

Hypothesis H1: Chinese listed companies have sticky characteristics of executive compensation.

The theory of institutional shareholder activism points out that the scale of institutional investment has expanded rapidly since the 1980s. Many listed companies hold more than half of their shares in institutional investment. Like shareholders, they pay attention to the long-term development of enterprises. The purpose of investment is to return and obtain the maximum benefit with the minimum cost. How to manage the enterprise is the new target of institutional investors in the aspects of fundraising, investment, management, and withdrawal. What's more, for institutional investors, there is also pressure on customers to manage their financial interests. Therefore, it is particularly important to invest correctly and effectively. First, the organization has a very rich and comprehensive investment management team. From the perspective of corporate investment, Liang (2015) [15] pointed out that the management is overconfident. Some radical executives may increase their investment due to performance-based compensation, which will increase their chances of getting compensation and improve their status and reputation. However, in this way, the risk of corporate investment failure will increase significantly, thus infringing on the interests of shareholders and exposing the enterprise to the risk of unsustainable development. Li and Mi [16] believed that when institutional investors enter the enterprise, their rich management

experience can formulate corresponding mechanisms according to specific conditions, so as to prevent this from happening without damaging the interests of the enterprise to seek maximum marginal revenue. Secondly, institutional investors can also play a regulatory role. Institutional investors have the right to remind or reject the radical and unreasonable investment decisions made by senior executives to safeguard the rights and interests of enterprises. Thirdly, the institutional investor team has abundant resources and information. They can bring high-quality customers to the enterprise and set up a more perfect investment system to increase the probability of successful investment and restrain the executives from making aggressive and subjective investment decisions. Finally, Li and Li [17] confirmed through the panel and cross-sectional data that due to the objectivity and completeness of institutional investors and their large shareholding, they are not easy to sell off. Therefore, they pay attention to the long-term development interests of enterprises, and their participation in corporate governance can also reduce the information asymmetry between the governance layer and the management. Compared with corporate executives, institutional investors are more in line with the interests of shareholders. Shareholders can be informed of the company's operation, management, and grasp of market conditions through voting at shareholders' meetings, private negotiations, explanatory letters, and other methods, so as to obtain a more comprehensive understanding of the information. Based on this, this paper proposes the hypothesis H2 as follows:

Hypothesis H2: Institutional investors inhibit the stickiness of executive compensation.

In the previous literature research, institutional investors are a wide range of groups, and their shareholding ratio, shareholding duration, investment philosophy, degree of risk preference, and the degree of state intervention have great differences in corporate governance and executive compensation contracts. If we only consider the impact of institutional investors on the stickiness of executive compensation, there may be certain research errors that affect the judgment of the enterprise. The major institutional investors in China include six categories: securities investment funds, social security funds, qualified foreign institutional investors, securities companies, insurance companies, and trust companies. This paper refers to the classification method of institutional investors by Brickley et al. [18]. See Table 1 for details.

For the pressure-resistant institutional investors, they pay more attention to how to prolong the company's life cycle and stand firm in the competitive industry for a long time (Zhang and Chen) [19]. Coupled with the abundant resources and information advantages of the team, the team will generally actively participate in corporate governance, promote the improvement of corporate organizational structure, enhance the degree of corporate internal governance, enhance the overall reputation of the company and increase the interests of stakeholders. At the same time, the organization will also play the role of supervisor, especially in preventing and negotiating the behaviors of senior executives that are detrimental to the interests of the company.

TABLE 1: Classification of institutional investors.

Classify	Institution name	Investment theme	Investment ratio limit	Relationship with investee
Pressure-resistant institutional investors	Securities investment funds	Risk coexists and marginal revenue is maximized.	Yes	Do not intervene in corporate governance under stringent market supervision conditions
	Social security fund	Responsible investment, safety first	Yes	Active participation in corporate governance with high independence
	Qualified foreign institutional investors	Long-term stable development and multilateral cooperation	Yes	Actively participate in corporate governance, rational investment
Pressure-sensitive institutional investors	Securities company	Capital appreciation, business interests	No	Low independence, often as a stock underwriter
	Insurance company	Seeking profit from stability	Yes	Two-way benefit
	Trust company	Value investment with high liquidity	No	Two-way benefit

They are satisfied with the sense of accomplishment brought by managing and developing the company. Yi et al. [8] found out from the companies that selected the A-shares listed in Shanghai and Shenzhen stock exchanges of China from 2004 to 2006 that this kind of pressure-resistant investors can greatly improve their performance sensitivity to compensation for enterprises, while the relationship between the investors of pressure sensitive institutions and their compensation management performance is not significant, which proves this. For companies, the addition of pressure-resistant institutional investors will make the supervision cost lower than the incremental revenue, thus forming a strategic alliance between shareholders and institutional investors to promote the long-term development of the company. For the pressure-sensitive institutional investors, they have more commercial interests in the company (Jiang and Li) [20]. For example, insurance companies, apart from capital investment to protect their value, are more concerned about insurance coverage and the probability of accidents with customers and will not actively participate in corporate governance. This will not only not be of special help to their own interests but will also increase additional management costs, which will do more harm than good. Based on this, this paper proposes the hypothesis H3 as follows:

Hypothesis H3: Bias-pressure-resistant institutional investors have stronger inhibition on executive compensation stickiness than bias-pressure-sensitive institutional investors.

3. Research Design

3.1. Sample Selection and Data Sources. This paper selects the listed companies in Shanghai and Shenzhen A-share market of China from 2014 to 2018 as the research sample, mainly studying the relationship between corporate governance and executive compensation stickiness. In order to ensure the validity of the data and the empirical results, the following measures are taken to deal with the samples:

- (1) If the enterprises with ST and *ST are excluded, such enterprises may have losses for three consecutive years, and the relevant indicators have abnormal conditions, which may cause large errors in the empirical results, so they are excluded;

- (2) Excluding financial and insurance enterprises, which have different financial statements from general enterprises and lack of universality, so they are excluded;
- (3) The enterprises with incomplete data of relevant variables are excluded, because some enterprises have undisclosed or missing data, which will affect the operation of the model, so they are excluded;
- (4) If the companies with abnormal indicators are excluded, the companies with negative net profit for the current year, asset-liability ratio, and institutional investors holding more than 100% or negative will be excluded. If the companies with abnormal indicators will cause deviation from the empirical results, they will be excluded.

Through the abovementioned processing, a total of 7,670 samples were selected, and the data were mainly from RESSET database. In the empirical part, this paper uses Stata15.0 to conduct comprehensive processing and statistical analysis on the model data.

3.2. Definition of Major Variables

- (1) Executive compensation ($Ln\text{pay}$). In the RESSET database, the total compensation of the top three highest paid executives is selected and the natural logarithm is used to remove the dimension to measure the executive compensation.
- (2) Corporate performance ($Ln\text{perf}$). Referring to the method of Fang [21], the net profit after excluding nonrecurring profit and loss is taken as a measure of the company's performance. In addition, the performance Down of the test variable is defined as: when the company's performance drops year-on-year, the value is 1, and vice versa, 0.
- (3) Institutional investors (IIS). If there is an institutional investor holding 1 in the sample company, otherwise 0.
- (4) Bias-resistant institutional investors ($PRII$). If the actual proportion of total holdings of the pressure-

TABLE 2: Definition of variables.

Variable name	Variable code	Variable definition
Executive compensation	<i>Lnpay</i>	The natural logarithm of the total remuneration of the top three executives
Corporate performance	<i>Lnperf</i>	Natural logarithm of net profit after excluding nonrecurring profit and loss
Decline in performance	<i>Down</i>	If the results of the company decrease year-on-year, 1 will be taken, otherwise, 0 will be taken.
Institutional investor	<i>IIS</i>	If the company has institutional investors holding shares, 1 will be taken; otherwise, 0 will be taken.
Bias-resistant institutional investors	<i>PRII</i>	Bias-resistant institutional investors take 1, otherwise, take 0
Separation of two posts	<i>Dual</i>	If the two positions of chairman and general manager concurrently take 1, otherwise take 0
Holding ratio	<i>Share</i>	Proportion of shares held by the largest shareholder The ultimate controllers are SASAC and finance
Central government control	<i>CG</i>	The ministry and other central institutions and the state-owned enterprises directly under the central government shall take 1, and the contrary shall take 0
Asset-liability ratio	<i>Lev</i>	Ratio of total liabilities to total assets at year-end
Board independence	<i>Indd</i>	Proportion of independent directors to total directors
West	<i>West</i>	If the place of incorporation of the company is in the west, 1 will be taken; otherwise, 0 will be taken.
Central	<i>Central</i>	If the place of incorporation of the company is central, 1 will be taken; otherwise, 0 will be taken.
Company size	<i>Lnsize</i>	Natural logarithm of total assets of a company
Rate of return on common stockholders' equity	<i>ROE</i>	Net profit divided by net assets
Year	<i>Year</i>	Virtual variables that control annual influencing factors
Industry	<i>Industry</i>	Virtual variables, controlling industry influencing factors

resistant institutional investors is greater than the actual proportion of total holdings of the pressure-sensitive institutional investors, it is recorded as 1, otherwise, it is taken as 0.

- (5) See Table 2 for the specific definition of control variables.

3.3. Model Construction

- (1) In order to verify the relevant assumptions proposed by H1, model 1 was constructed with reference to the research method of Junxiong Fang (2009) [21].

$$\begin{aligned}
 \text{Lnpay}_{i,t} = & \alpha_0 + \alpha_1 \text{Lnperf}_{i,t} + \alpha_2 \text{Lnperf}_{i,t} \\
 & \times \text{Down}_{i,t} + \alpha_3 \text{Down}_{i,t} \\
 & + \alpha_4 \text{Dual}_{i,t} + \alpha_5 \text{Share}_{i,t} + \alpha_6 \text{CG}_{i,t} \\
 & + \alpha_7 \text{Lev}_{i,t} + \alpha_8 \text{Indd}_{i,t} + \alpha_9 \text{West}_{i,t} \\
 & + \alpha_{10} \text{Central}_{i,t} + \alpha_{11} \text{Lnsize} + \alpha_{12} \text{ROE} \\
 & + \alpha_{13} \sum \text{Industry}_{i,t} + \alpha_{14} \sum \text{Year}_{i,t} + \varepsilon_{i,t}.
 \end{aligned} \quad (1)$$

In model 1, when the corporate performance (*Lnperf*) rises, *Down* is 0, and the sensitivity of executive compensation (*Lnpay*) to the corporate performance (*Lnperf*) is α_1 ; when the corporate performance (*Lnperf*) drops, *Down* is 1, and the sensitivity of executive compensation (*Lnpay*) to the corporate performance (*Lnperf*) is $(\alpha_1 + \alpha_2)$. If $\alpha_1 > (\alpha_1 + \alpha_2)$, that is $\alpha_2 < 0$, it indicates that there is a sticky characteristic of executive compensation.

- (2) In order to verify the relevant assumptions proposed by H2, model 2 is constructed with reference to the research methods of Lielan Wu and Wen Xu (2019) [22].

$$\begin{aligned}
 \text{Lnpay}_{i,t} = & \beta_0 + \beta_1 \text{Lnperf}_{i,t} + \beta_2 \text{Lnperf}_{i,t} \times \text{Down}_{i,t} \\
 & + \beta_4 \text{Lnperf}_{i,t} \times \text{Down}_{i,t} + \beta_5 \text{Down}_{i,t} \\
 & + \beta_6 \text{IIS}_{i,t} + \beta_7 \text{Dual}_{i,t} + \beta_8 \text{Share}_{i,t} + \beta_9 \text{CG}_{i,t} \\
 & + \beta_{10} \text{Lev}_{i,t} + \beta_{11} \text{Indd}_{i,t} + \beta_{12} \text{West}_{i,t} \\
 & + \beta_{13} \text{Central}_{i,t} + \beta_{14} \text{Lnsize} + \beta_{15} \text{ROE} \\
 & + \beta_{16} \sum \text{Industry}_{i,t} + \beta_{17} \sum \text{Year}_{i,t} + \varepsilon_{i,t}.
 \end{aligned} \quad (2)$$

In model 2, the effect of institutional investors (*IIS*) on the stickiness of executive compensation is studied by adding the triple interaction term (*Lnperf* × *Down* × *IIS*) of institutional investors (*IIS*) with corporate performance (*Lnperf*) and performance decline test variable (*Down*). Referring to the relevant mechanism of model 1, when the coefficient of the interaction between corporate performance (*Lnperf*) and performance decline test variable (*Down*) (*Lnperf* × *Down*) α_2 is significantly negative, the sticky characteristic of executive compensation exists; In model 2, according to the partial derivative and interaction principle, when the triple interaction (*Lnperf* × *Down* × *IIS*) coefficient of an institutional investor (*IIS*), corporate performance (*Lnperf*) and performance decline test variable (*Down*) is opposite

and significant to the interaction ($Lnperf \times Down$) coefficient of corporate performance ($Lnperf$) and performance decline test variable ($Lnperf \times Down$) in the model 1, that is, the triple interaction ($Lnperf \times Down \times IIS$) coefficient of institutional investors (IIS), corporate performance ($Lnperf$) and performance decline test variable ($Down$) β_2 is significantly positive, indicating that institutional investors inhibit the stickiness of executive compensation.

- (3) Model 3 is constructed to verify the relevant assumptions proposed by H3.

$$\begin{aligned} Ln\text{pay}_{i,t} = & \gamma_0 + \gamma_1 Ln\text{perf}_{i,t} + \gamma_2 Ln\text{perf}_{i,t} \times \text{Down}_{i,t} \\ & \times \text{PRII}_{i,t} + \gamma_3 Ln\text{perf}_{i,t} \times \text{PRII}_{i,t} \\ & + \gamma_4 Ln\text{perf}_{i,t} \times \text{Down}_{i,t} + \gamma_5 \text{Down}_{i,t} \\ & + \gamma_6 \text{PRII}_{i,t} + \gamma_7 \text{Dual}_{i,t} + \gamma_8 \text{Share}_{i,t} + \gamma_9 \text{CG}_{i,t} \quad (3) \\ & + \gamma_{10} \text{Lev}_{i,t} + \gamma_{11} \text{Indd}_{i,t} + \gamma_{12} \text{West}_{i,t} \\ & + \gamma_{13} \text{Central}_{i,t} + \gamma_{14} \text{Lnsiz}_{i,t} + \gamma_{15} \text{ROE}_{i,t} \\ & + \gamma_{16} \sum \text{Industry}_{i,t} + \gamma_{17} \sum \text{Year}_{i,t} + \varepsilon_{i,t}. \end{aligned}$$

In model 3, similarly, when institutional investors are biased to resist ($\text{PRII} = 1$) and corporate performance rises ($\text{Down} = 0$), the sensitivity of executive compensation ($Ln\text{pay}$) to corporate performance ($Ln\text{perf}$) is $(\gamma_1 + \gamma_3)$, and the sensitivity of executive compensation ($Ln\text{pay}$) to corporate performance ($Ln\text{perf}$) when corporate performance declines ($\text{Down} = 1$) is $(\gamma_1 + \gamma_2) + (\gamma_3 + \gamma_4)$, which the stickiness of executive compensation is $(\gamma_1 + \gamma_3) / (\gamma_1 + \gamma_2 + \gamma_3 + \gamma_4)$; When institutional investors are biased pressure sensitive ($\text{PRII} = 0$) and corporate performance rises ($\text{Down} = 0$), the sensitivity of executive compensation ($Ln\text{pay}$) to corporate performance ($Ln\text{perf}$) is γ_1 , the sensitivity of executive compensation ($Ln\text{pay}$) to corporate performance ($Ln\text{perf}$) when company performance declines ($\text{Down} = 1$) is $(\gamma_1 + \gamma_4)$, which the stickiness of executive compensation is $(\gamma_1) / (\gamma_1 + \gamma_4)$. If $(\gamma_1) / (\gamma_1 + \gamma_4) > (\gamma_1 + \gamma_3) / (\gamma_1 + \gamma_2 + \gamma_3 + \gamma_4)$, then hypothesis H3 holds.

4. Empirical Analysis

4.1. Descriptive Statistics. According to Table 3, it can be seen that the average value of executive compensation ($Ln\text{pay}$), which is an explanatory variable, is 14.5133, and the standard deviation is 0.6699, indicating that there is little change in executive compensation of listed companies from 2014 to 2018. This also makes sense. For listed companies, executive compensation needs to be disclosed. Moreover, executive compensation also represents the company's strategic planning. If the change is too large, it will have an important impact on both the enthusiasm of the executive and the reputation of the company. Therefore, executive compensation will not change much in five years. The maximum value of corporate performance ($Ln\text{perf}$) as an explanatory variable is 23.2340 and the minimum value is 15.1554. This shows that the performance of listed companies in China

varies greatly due to their different scale, industry, and strategic objectives. The average value of the performance $Down$ variable ($Down$) is 0.3099, which indicates that about 30% of the companies in China experienced a year-on-year decline in performance in the past five years, possibly due to the government's macro control and corporate tightening strategies. The average value of PRII is 0.2912, which indicates that the biased pressure-sensitive institutional investors are dominant. Among the control variables, the average value of $Dual$ is 0.2568, which indicates that about 75% of the listed companies have different governance levels from the most powerful leaders of the management. On the whole, the listed companies in China have good governance in the aspect of dual. The maximum value of the largest shareholder's controlling share is 0.7482, while the minimum value is 0.0903. This shows that the sample companies have a large difference in ownership structure, which also shows that the companies selected in this paper are universal and cover the basic situation. The average value of CG is 0.1246, which indicates that about 12% of enterprises in China are controlled by the central government, and most of them are locally controlled and private enterprises. As for the independence of the board of directors, the minimum value is above 30%, which indicates that the selected samples all meet the basic requirements of modern corporate governance theory for the proportion of independent directors.

From Table 4, it can be seen that in the year of 2014–2018, the manufacturing industry is still the leader of the industry of listed companies in China, accounting for nearly 60% of the total. Information transmission, software and information technology service industry, real estate industry, wholesale and retail industry also reached more than 5%, which is related to China's population base and national conditions of science and technology. Other industries accounted for a relatively fragmented share, thus controlling both annual and industry indicators in this study.

4.2. Correlation Analysis. Table 5 shows that executive compensation ($Ln\text{pay}$) has a significant positive correlation with corporate performance ($Ln\text{perf}$) and a significant negative correlation with performance decline variable ($Down$), which is in line with the relevant content of optimal contract theory and incentive theory. Executive compensation should be highly consistent with corporate performance. However, the difference in the absolute value of the coefficient can also roughly reflect the asymmetry of executive compensation sensitivity to performance. From the perspective of institutional governance, executive compensation ($Ln\text{pay}$) has a significant positive correlation with institutional investors (IIS) and a significant negative correlation with bias-resistance institutional investors (PRII), which indicates that the existence of institutional investors will increase executive compensation to a certain extent. It may be that institutional investors use resources to improve corporate performance and thus increase executive compensation. The existence of biased and resistant institutional investors will reduce executive compensation, which may be

TABLE 3: Descriptive statistics of main variables.

Variable	Observed value	Average/Mean value	Standard deviation	Minimum	Maximum
<i>Ln_{pay}</i>	7670	14.5133	0.6699	13.0303	16.5161
<i>Ln_{perf}</i>	7670	19.0647	1.4781	15.1554	23.2340
<i>Down</i>	7670	0.3099	0.4625	0	One
<i>IIS</i>	7670	0.8318	0.4032	0	One
<i>PRII</i>	6380	0.2912	0.4544	0	One
<i>Dual</i>	7670	0.2568	0.4370	0	One
<i>Share</i>	7670	0.3553	0.1478	0.0903	0.7482
<i>CG</i>	7670	0.1246	0.3303	0	One
<i>Lev</i>	7670	0.4049	0.1928	0.0593	0.8407
<i>In_{dd}</i>	7670	0.3711	0.0507	0.3333	0.5714
<i>West</i>	7670	0.1520	0.3590	0	One
<i>Central</i>	7670	0.1193	0.3242	0	One
<i>Ln_{size}</i>	7670	22.4971	1.2943	20.2191	26.5472
<i>ROE</i>	7670	0.1042	0.0656	0.0090	0.3446

TABLE 4: Sample annual industry distribution.

Industry name	2014	2015	2016	2017	2018	Sum	Specific gravity (%)
Mining industry	21	21	21	21	21	105	1.37
Electricity, heat, gas, and water production and supply industries	57	57	57	57	57	285	3.72
Realty business	81	81	81	81	81	405	5.28
Construction industry	80	80	80	80	80	400	5.22
Transportation, warehousing, and postal services	96	96	96	96	96	480	6.26
Education	2	2	2	2	2	10	0.13
Scientific research and technology services	10	10	10	10	10	50	0.65
Agriculture, forestry, animal husbandry, and fishery	8	8	8	8	8	40	0.52
Wholesale and retail	120	120	120	120	120	600	7.82
Water, environmental, and public facilities management industry	23	23	23	23	23	115	1.50
Health and social work	6	6	6	6	6	30	0.39
Culture, sports, and entertainment	18	18	18	18	18	90	1.17
Information transmission, software, and information technology services	132	132	132	132	132	660	8.60
Manufacturing industry	852	852	852	852	852	4260	55.54
Accommodation and catering	5	5	5	5	5	25	0.33
Comprehensive	5	5	5	5	5	25	0.33
Leasing and business services	18	18	18	18	18	90	1.17
Sum	1534	1534	1534	1534	1534	7670	100.00

due to the fact that institutions such as securities investment funds pay attention to long-term returns, actively participate in corporate governance, and comprehensively supervise the rights of executives, resulting in a decrease in executive compensation. In addition, the correlation coefficients of most variables are below 0.5, which indicates that the probability of multicollinearity among variables in the regression model is very low.

4.3. *Regression Analysis.* According to Table 6, in model 1, the regression coefficient of corporate performance (*Ln_{perf}*) is 0.0688 and significant at 1%, and the regression coefficient of cross term (*Ln_{perf} × Down*) is -0.0278 and significant at 1%. From the abovementioned model construction, it can be seen that the sensitivity degree of executive compensation to performance when the corporate performance increases are 1.6780 times that when the corporate performance decreases. The sticky characteristic of executive compensation exists, assuming H1 is verified. In terms of control variables, the first largest Shareholder’s controlling share, independent

director’s proportion (*In_{dd}*), and the regression coefficient of the company’s place of registration (*West*, *Central*) are significantly negative, indicating that they are significantly negatively correlated with executive compensation, the regression coefficients of performance decline test variable (*Down*), central control (*CG*), company size (*Ln_{size}*), and return on equity (*ROE*) are significantly positive, indicating that they are significantly positively correlated with executive compensation; the *Dual* regression coefficient is positive at the significant level of 10%. The asset-liability ratio (*Lev*) regression coefficient is not significant and has no significant impact on executive compensation. From this, it can be concluded that the existence of the largest shareholder and the independent director with a high proportion will play a role in supervising the senior management to manipulate their own remuneration, which is helpful to the implementation of the senior management remuneration contract; enterprises under central control generally have a sound system with clear rewards and punishments. The larger the company is, the better its operating conditions will be, and the higher the executive compensation will be.

TABLE 5: Correlation coefficient matrix.

	<i>Lnpay</i>	<i>Lnperrf</i>	<i>Down</i>	<i>IIS</i>	<i>PRII</i>	<i>Dual</i>	<i>Share</i>	<i>CG</i>	<i>Lev</i>	<i>Indd</i>	<i>West</i>	<i>Central</i>	<i>Lnsiz</i>	<i>ROE</i>
<i>Lnpay</i>	1.0000													
<i>Lnperrf</i>	0.4717***	1.0000												
<i>Down</i>	-0.0544***	-0.2203***	1.0000											
<i>IIS</i>	0.1653***	0.2170***	-0.0233*	1.0000										
<i>PRII</i>	-0.1404***	-0.1422***	-0.0548***	-0.3821***	1.0000									
<i>Dual</i>	-0.0252**	-0.0986***	-0.0178	-0.1519***	0.1180***	1.0000								
<i>Share</i>	-0.0169	0.1979***	0.0066	0.0271***	-0.0804***	-0.0560***	1.0000							
<i>CG</i>	0.1079***	0.1520***	-0.0110	0.1406***	-0.1023***	-0.1597***	0.1151***	1.0000						
<i>Lev</i>	0.2354***	0.2647***	-0.0148	0.1918***	-0.1302***	-0.0915***	0.1064***	0.1365***	1.0000					
<i>Indd</i>	-0.0012	0.0482***	-0.0150	-0.0390***	0.0366***	0.1538***	0.0791***	0.0078	0.0157	1.0000				
<i>West</i>	-0.1395***	-0.0017	-0.0090	0.0471***	-0.0425***	-0.0279**	-0.0111	-0.0059	-0.0094	-0.0130	1.0000			
<i>Central</i>	-0.0340***	-0.0207*	0.0291**	0.0435***	-0.0394***	-0.0908***	0.0022	0.0883***	0.0551***	-0.1558***	-0.1578***	1.0000		
<i>Lnsiz</i>	0.4604***	0.7683***	-0.0373***	0.3091***	-0.2613***	-0.1527***	0.1906***	0.2211***	0.5983***	0.0080***	-0.0148	0.0128	1.000	
<i>ROE</i>	0.2867***	0.5668***	-0.3361***	-0.0108	0.1009***	0.0488***	0.1222***	-0.0280**	0.0699***	-0.0103	-0.0020	-0.0220*	0.1556***	1.000

Note. **, ***, and **** are significant at 10%, 5%, and 1%, respectively. The same is mentioned below.

TABLE 6: Regression results.

Variable	Model 1	Model 2	Model 3
	Observed value: 7670	Observed value: 7670	Observed value: 6380
<i>Lnperf</i>	0.0688*** (5.25)	0.7166*** (3.94)	0.0622*** (4.97)
<i>Lnperf</i> × <i>Down</i>	-0.0278*** (-2.78)	-0.0278*** (-2.57)	-0.0256*** (-2.94)
<i>Down</i>	0.6026*** (3.19)	0.6101*** (3.14)	0.5507*** (2.88)
<i>Lnperf</i> × <i>Down</i> × <i>IIS</i>		0.0003*** (3.14)	
<i>Lnperf</i> × <i>IIS</i>		0.0037 (0.26)	
<i>Lnperf</i> × <i>Down</i> × <i>PRII</i>			0.0013*** (2.79)
<i>Lnperf</i> × <i>PRII</i>			0.0015* (1.94)
<i>PRII</i>			-0.4557** (-2.15)
<i>Dual</i>	0.0283* (1.78)	0.0328** (2.05)	0.0323** (2.00)
<i>Share</i>	-0.4962*** (-10.32)	-0.4902*** (-10.19)	-0.5346*** (-10.97)
<i>CG</i>	0.1327*** (6.26)	0.1276*** (6.00)	0.1369*** (6.42)
<i>Lev</i>	-0.0533 (-0.99)	-0.0545 (-1.02)	-0.0563 (-1.04)
<i>Indd</i>	-0.3854*** (-2.87)	-0.3715*** (-2.77)	-0.3287** (-2.41)
<i>West</i>	-0.2399*** (-12.61)	-0.2433*** (-12.78)	-0.2421*** (-12.63)
<i>Central</i> (-4.50)	-0.0883*** (-4.17)	-0.0910*** (-4.30)	-0.0957***
<i>Lnsiz</i>	0.1799*** (13.02)	0.1757*** (12.64)	0.1722*** (12.34)
<i>ROE</i>	1.9663*** (12.00)	1.9846*** (12.08)	1.9214*** (13.84)
<i>Cons</i>	9.0816*** (50.58)	9.0695*** (29.94)	9.3545*** (49.13)
<i>Year</i>	Control	Control	Control
<i>Industry</i>	Control	Control	Control
<i>Adj.R²</i>	0.3577	0.3585	0.3595
<i>F</i>	115.48***	106.04***	103.28***

Note. *T* value is shown in brackets. The same below.

In model 2, the regression coefficient of (*Lnperf* × *Down* × *IIS*) is significantly positive, and in model 1, the regression coefficient of (*Lnperf* × *Down*) is significantly negative, indicating that institutional investors significantly inhibit the stickiness of executive compensation, assuming H2 is verified.

In model 3, similarly, when institutional investors are bias-pressure-resistant, the sticky coefficient of executive compensation is 1.6168; when institutional investors are bias-pressure-sensitive, the sticky coefficient of executive compensation is 1.6995. This shows that the former can inhibit the stickiness of executive compensation more than the latter, assuming H3 is verified.

4.4. Robustness Test. In this paper, the operating income is selected to replace the company's results, and the sample data are regressed based on the abovementioned three models. The results are shown in Table 7. It can be concluded from the table that in model 1, the regression coefficient of corporate performance (*Lnperf*) is significantly positive, and the regression coefficient of cross term (*Lnperf* × *Down*) is significantly negative. The sensitivity of executive compensation to performance when corporate performance increases are 1.2469 times that when corporate performance decreases. In model 2, the regression coefficient of triple cross term (*Lnperf* × *Down* × *IIS*) is significantly positive. In model 3, when institutional investors are bias-pressure-

TABLE 7: Results of robustness test.

Variable	Model 1	Model 2	Model 3
	Observed value: 7670	Observed value: 7670	Observed value: 6380
<i>Lnperf</i>	0.1505*** (12.06)	0.1873*** (10.84)	0.0255*** (5.77)
<i>Lnperf</i> × <i>Down</i>	-0.0298*** (-3.13)	-0.0273*** (-2.65)	-0.0090** (-2.15)
<i>Down</i>	0.5652*** (3.15)	0.5596*** (3.03)	0.2587 (1.11)
<i>Lnperf</i> × <i>Down</i> × <i>IIS</i>		0.0026*** (3.29)	
<i>Lnperf</i> × <i>IIS</i>		0.0436*** (3.19)	
<i>Lnperf</i> × <i>Down</i> × <i>PRII</i>		0.8750*** (3.42)	
<i>Lnperf</i> × <i>PRII</i>			0.0010*** (2.82)
<i>PRII</i>			0.0261** (2.24)
<i>Dual</i>			-0.6052** (-2.40)
<i>Share</i>	0.0940*** (6.21)	0.0898*** (5.91)	0.0432*** (2.68)
<i>CG</i>	0.2192*** (4.79)	0.2256*** (4.93)	-0.5576*** (-11.49)
<i>Lev</i>	-1.0832*** (-21.22)	-1.0775*** (-21.12)	-0.2994*** (-6.22)
<i>Indd</i>	-0.2895** (-2.26)	-0.2712** (-2.12)	-0.2898** (-2.14)
<i>West</i>	-0.1109*** (-12.45)	-0.0147*** (-12.81)	-0.2392*** (-12.56)
<i>Central</i>	-0.1563*** (-7.76)	-0.1616*** (-8.02)	-0.0774*** (-3.64)
<i>Lnsize</i>	0.7903*** (60.08)	0.7887*** (59.62)	0.1154*** (8.27)
<i>ROE</i>	0.5649*** (3.62)	0.5632*** (3.60)	1.5692*** (14.03)
<i>Cons</i>	8.9738*** (49.08)	8.3236*** (30.48)	9.1701*** (47.14)
<i>Year</i>	Control	Control	Control
<i>Industry</i>	Control	Control	Control
<i>Adj.R²</i>	0.3663	0.3707	0.3669
<i>F</i>	116.24***	108.38***	106.63***

resistant, the sticky coefficient of executive compensation is 1.1835; when institutional investors are bias-pressure-sensitive, the sticky coefficient of executive compensation is 1.5455. It can be seen that the regression results of the three models are basically consistent with the previous ones, indicating that the empirical results are robust.

5. Conclusions and Enlightenment

This paper takes Chinese A-share listed companies from 2014 to 2018 as the research sample, determines 7,670 observed values after screening, and explores the sticky relationship between corporate governance and executive compensation by establishing three regression models. The conclusions are as follows:

- (1) The executive compensation of listed companies in China has sticky characteristics. Through empirical analysis, the sensitivity of executive compensation to performance when corporate performance increases are greater than that when the corporate performance decreases, so the sensitivity of executive compensation to performance is asymmetric.
- (2) Institutional investors inhabit the stickiness of executive compensation. The organization plays the role of supervising the internal governance of the company and can communicate and negotiate directly with shareholders, which promotes the implementation of executive compensation contracts and increases the sensitivity of executive compensation to performance.

- (3) Compared with the bias-pressure-sensitive institutional investors, the bias-pressure-resistant institutional investors can suppress the stickiness of executive compensation. The former only has a long-term strategic investment partnership with other listed companies, with a high shareholding ratio, and pays attention to the sustainable development of the company and long-term profit return; besides the capital appreciation target, the latter also has a commercial interest relationship with the company and participates in corporate governance passively.

It can be seen that institutional investment has become an indispensable part of the capital market. Then to play the role of institutional investors and optimize executive compensation requires not only internal control but also national government supervision. This paper puts forward the following suggestions:

- (1) Improve relevant laws and regulations. At present, Chinese legislation imposes strict requirements on the shareholding ratio of some fund management companies, which will make institutional investors pay attention to short-term interests and have a negative impact on the capital market. In view of this situation, relevant laws can appropriately relax the policies on the shareholding ratio and duration of institutional investors and can formulate different regulations for different industries, such as putting forward an unlimited policy for some emerging countries to vigorously support industries, and putting forward a high-limit policy for some industries with strong supervision, such as medicine, “teach students in accordance with their aptitude” and “adjust measures to local conditions” to provide a relatively fair competition environment for institutional investors. In addition, regarding the nature, shareholding ratio, and duration of institutional investors, monetary and nonmonetary compensation for executive compensation, the state may require companies to disclose the information completely, which will increase the transparency of market information, be more conducive to the implementation of executive compensation contracts and the choice of institutional investors, and promote the vigorous development of China capital market.
- (2) Optimizing the structure of executive compensation. For senior executives in China, performance bonuses now make up the lion’s share of total compensation. To a certain extent, this can indeed motivate senior executives to work hard, but too large a proportion will often backfire. Executives may manipulate profits for performance rewards and use their power to raise salaries and other illegal and unethical behaviors, which will damage the value and image of the enterprise. In this regard, the corporate governance layer can increase the basic salary of senior executives and appropriately weaken the

performance award. From a psychological point of view, this will make the senior management value the job more, and when their performance does not meet the expectations of the management or the management, holding a high basic salary will cause shame in their hearts, which can also play an incentive effect virtually. Senior executives, as senior management personnel of the company, are excellent both in social experience and work experience. Some studies also show that a high basic salary can promote the enthusiasm of senior executives and enhance the value of the company more than high-performance bonus.

- (3) Improve the performance evaluation method. At present, the company basically uses financial performance as the basis of executive compensation incentives. This is not a comprehensive performance appraisal method, and senior executives can collude with each other to whitewash financial data and even falsify performance awards. The company can adopt a combination of financial and nonfinancial indicators to comprehensively evaluate the performance of senior management, such as increasing customer satisfaction, internal operation indicators, team staff satisfaction, and product performance improvement speed. It can also introduce party and government to promote team development, create a corporate culture, and enhance the company’s core competitiveness. This cannot only reflect the performance of senior management more comprehensively and truly but also increase the unity of staff within the company and improve the internal governance of the company.
- (4) Actively introducing institutional investors. Generally speaking, institutional investors have abundant information, resources, management, and professional advantages, and can play a regulatory role. In addition, they can also negotiate and communicate with the governance and management, which has a positive impact on the sustainable development and value maximization of the company. In this regard, the company should effectively protect the interests of institutional investors, and formulate relevant rules and regulations to attract institutional investors to join in for common development.

This paper also has certain research defects:

- (1) Select the natural logarithm of net profit after excluding nonrecurring profit and loss as the explanatory variable of the company’s results. Since the true number of the logarithm must be greater than zero, the implicit condition is to exclude the sample of companies with negative net profit, which will have a certain impact on the integrity of the sample;
- (2) Directly taking the total remuneration of the top three executives disclosed in the database as the explained variable, without distinguishing the self-

purchase and incentive components in the shares, which will have a certain impact on the explanation strength;

- (3) There are two variables in the selection of the company's place of registration: the western variable and the central variable, which are slightly repetitive;
- (4) There are many classification methods for institutional investors and their heterogeneity. This paper only studies the classification basis of six narrow categories of institutional investors and pressure sensitivity, which has certain limitations.

Future research can go deep into national conditions, and classify and research institutional investors accurately; in the aspect of executive compensation, the aspect of self-purchase of shares can also be excluded, and executive compensation can be considered by adding the proportion and duration of executive shareholding; in terms of studying the stickiness of executive compensation and institutional investors, we can also research on the distraction of investors combined with behavioral finance theory.

Data Availability

This paper selects the listed companies in Shanghai and Shenzhen A-share market of China from 2014 to 2018 as the research sample, mainly studying the relationship between corporate governance and executive compensation stickiness. In order to ensure the validity of the data and the empirical results, the following measures are taken to deal with the samples: (1) if the enterprises with ST and *ST are excluded, such enterprises may have losses for three consecutive years, and the relevant indicators have abnormal conditions, which may cause large errors in the empirical results, so they are excluded, (2) excluding financial and insurance enterprises, which have different financial statements from general enterprises and lack of universality, so they are excluded, (3) the enterprises with incomplete data of relevant variables are excluded because some enterprises have undisclosed or missing data, which will affect the operation of the model, so they are excluded, and (4) if the companies with abnormal indicators are excluded, the companies with negative net profit for the current year, asset-liability ratio, institutional investors holding more than 100% or negative will be excluded. If the companies with abnormal indicators will cause deviation from the empirical results, they will be excluded. Through the abovementioned processing, a total of 7,670 samples were selected, and the data were mainly from the RESSET database. In the empirical part, this paper uses Stata15.0 to conduct comprehensive processing and statistical analysis of the model data.

Conflicts of Interest

The author declares that there are no conflicts of interest.

References

- [1] S. Claessens, "Corporate governance and equity prices," *Quarterly Journal of Economics*, vol. 118, no. 1, pp. 107–155, 1997.
- [2] M. M. Blair, "Closing the theory gap: how the economic theory of property rights can help bring "Stakeholders" back into theories of the firm," *Journal of Management & Governance*, vol. 9, no. 1, pp. 33–40, 2005.
- [3] A. S. Amin, S. Dutta, S. Saadi, and P. P. Vora, "Institutional shareholding and information content of dividend surprises: Re-examining the dynamics in dividend-reappearance era," *Journal of Corporate Finance*, vol. 31, pp. 152–170, 2015.
- [4] J. J. Gaver and K. M. Gaver, "The relation between non-recurring accounting transactions and CEO cash compensation," *The Accounting Review*, vol. 73, no. 2, pp. 235–253, 1998.
- [5] J. E. Heard, "Executive compensation: perspective of the institutional investor," *University of Cincinnati Law Review*, vol. 63, no. 2, pp. 749–767, 1995.
- [6] P. David, R. Kochhar, and E. Levitas, "The effect of institutional investors on the level and mix of ceo compensation," *Academy of Management Journal*, vol. 41, no. 2, pp. 200–208, 1998.
- [7] M. M. Cornett, A. J. Marcus, A. Saunders, and H. Tehrani, "The impact of institutional ownership on corporate operating performance," *Journal of Banking & Finance*, vol. 31, no. 6, pp. 1771–1794, 2007.
- [8] Z. Yi, Y. Li, and W. Gao, "Governance effect of heterogeneous institutional investors: based on the perspective of executive compensation," *Statistics & Decisions*, no. 05, pp. 122–125, 2010.
- [9] X. Chen and H. Liu, "Institutional investor ownership, executive overcompensation and corporate governance," *Journal of Guangdong University of Finance and Economics*, vol. 34, no. 02, pp. 46–59, 2019.
- [10] L. Chao, Q. Cai, and J. Chen, "Can institutional investors improve the remuneration incentives for top executives of listed companies?" *Securities Market Herald*, no. 01, pp. 31–36+68, 2012.
- [11] S. Li and C. Wang, "An empirical study on the relationship between institutional ownership and senior management compensation in listed companies," *Management Review*, no. 01, pp. 41–48+64, 2007.
- [12] D. Lai and J. Leng, "Stickiness of executive compensation, institutional investor holding and innovation investment efficiency," *Friends of Accounting*, no. 08, pp. 121–127, 2021.
- [13] A. Zhu, X. Han, and Z. Hu, "Stickiness of executive compensation, corporate life cycle and innovation investment-based on empirical data of companies listed on GEM," *Friends of Accounting*, no. 09, pp. 84–90, 2021.
- [14] J. Fang, "Asymmetry between executive power and corporate compensation change," *Economic Research*, vol. 46, no. 04, pp. 107–120, 2011.
- [15] S. Liang, "Managerial overconfidence, debt constraints and cost stickiness," *Nankai Business Review*, vol. 18, no. 03, pp. 122–131, 2015.
- [16] Y. Li and M. Jiang, "Family control, institutional investors and executive compensation," *Journal of Chongqing University (Natural Science Edition)*, vol. 22, no. 05, pp. 74–83, 2016.
- [17] W. Li and B. Li, "An empirical study on the effect of institutional investor involvement in corporate governance: an

- empirical study based on CCGI~(NK),” *Nankai Business Review*, no. 01, pp. 4–14, 2008.
- [18] J. A. Brickley, R. C. Lease, and C. W. Smith, “Ownership structure and voting on antitakeover amendments,” *Journal of Financial Economics*, vol. 20, no. 1, pp. 267–291, 1988.
- [19] J. Zhang and S. Chen, “Equity incentive, institutional investor heterogeneity and real earnings management: an empirical study based on A-share listed companies in Shanghai and shenzhen,” *Journal of Lanzhou University*, vol. 49, no. 02, pp. 71–82, 2021.
- [20] H. Jiang and S. Li, “Internal control, heterogeneity of institutional investors and inefficient investment,” *Journal of Finance and Accounting*, no. 06, pp. 109–118, 2019.
- [21] J. Fang, “Is there stickiness in executive compensation of listed companies in China?” *Economic Research*, vol. 44, no. 03, pp. 110–124, 2009.
- [22] L. Wu and X. Wen, “The impact of institutional investor holding on the stickiness of top management compensation in listed companies,” *Southern Finance*, no. 02, pp. 12–20, 2019.

Research Article

Analysis on Vibroacoustic Fatigue Life of Empennage in a Hypersonic Vehicle

Wang Hongxian ¹, Zhang Ming,² and Nie Hong ²

¹Nanjing University of Aeronautics and Astronautics, Nanjing 210016, China

²State Key Laboratory of Mechanics and Control of Mechanical Structures, Nanjing University of Aeronautics and Astronautics, Nanjing 210016, China

Correspondence should be addressed to Wang Hongxian; whx915@nuaa.edu.cn

Received 18 April 2022; Accepted 14 June 2022; Published 23 August 2022

Academic Editor: Wei Liu

Copyright © 2022 Wang Hongxian et al. This is an open access article distributed under the Creative Commons Attribution License, which permits unrestricted use, distribution, and reproduction in any medium, provided the original work is properly cited.

In this study, the fatigue life prediction in hypersonic vehicle noise environment is researched under the structural vibration caused by the engine jet noise and the aerodynamic noise. A finite element analysis model is first established, and then natural frequency and vibration mode are obtained. According to the modal analysis, the vibroacoustic coupling calculation is finished in the dynamic analysis software. Modal participation factor, modal displacement, and the power spectral density of the stress response on the coupled surface are acquired. The finite element, border component, and vibrating stress analytical techniques are also employed in this research to predict the acoustical fatigue performance of the tail fins of a specific type of spacecraft. On the basis of vibration fatigue theory, identified material S-N curve, and linear cumulative damage theory, the Dirlik model in the frequency domain method for vibration fatigue is used to predict the fatigue life of empennage. According to the characteristics of the acoustic load, effects of the load characteristics, and damping ratios on the fatigue conditions, the design of the antifatigue design is put forward.

1. Introduction

Hypersonic aircrafts are subjected to high-frequency vibration loads during flight, and these loads are mainly caused by the jet noise of the engine propulsion system and the aerodynamic noise in the flight mission. The energy of the strong noise in the atmosphere and body of the hypersonic flight engine are far more than those in an ordinary aircraft. The positions near the engine in high strong parts, such as the engine combustion chamber and tail skin, are prone to increasing fatigue problems. When the sound pressure level of the surface of the aircraft exceeds 130 dB, the structural components are subject to high-intensity noise fluctuations that cause the occurrence of resonance or forced vibration, which generates stress brought by structural damage. The sound sensitive equipment in the cabin may also be greatly affected [1]. Hypersonic vehicles move quickly greater than five times the sound speed,

enabling a new category of aircraft vehicles capable of providing quicker space travel, extensive military reaction, and economic airline travel. The body frame, body temperature defense system, fuel storage, and wings layout are the main components. Studying the sonic fatigue of the position at high sound intensity is important. However, the cost of the noise test is often high, the design cycle is long, and the test procedure is complicated. Therefore, research on the acoustic load response and the acoustic fatigue calculation technology of aircrafts must be increasingly conducted [2, 3]. The nonlinear combination between such a high frequencies ultrasound waves and a much shorter wavelength structure motion is used in the Vibroacoustic Modulation technique. The nonlinear surfaces are where this interaction occurs. It monitors fatigue and stress-corrosion damage development in metal using in-plane nonresonance extremely lower frequencies tension vibrations [4].

A novel optimization framework on the basis of a multidisciplinary optimization procedure is applied to the vibroacoustic finite element method (FEM) model of an aircraft fuselage mock-up [4–6]. The current frequency domain methods then simulated the analogue spectrum and selected three materials for comparison in the different frequency domain methods [7, 8]. A random vibration fatigue life estimation of the sample method was proposed through the method with spectral density to describe the characteristics of the wide band random vibration. Several factors of vibration fatigue were also studied. By conducting the time-domain simulation to the power spectral density, the distribution function of loaded rainfall amplitude was obtained, and the vibration fatigue life of the structural was calculated [7, 8]. The modal analysis of the whole state of a certain aircraft in a free state was carried out, and the random vibration response analysis of the structure under aerodynamic noise was performed. Good results were obtained and compared with the experimental results. The fatigue life formula under narrowband random vibration was deduced. Based on the study of differently shaped power spectral density (PSD) correction results and Dirlik, the fatigue life estimation formula for broadband random load was established in 2005 [6, 9]. A Power Spectral Density (PSD) is a metric that compares the power level of a transmission to its wavelength. Broadband randomized events are often described using a PSD. The spectral resolution used to encode the data normalizes the PSD's loudness [10]. Although the sound fatigue problems of the engine and the inlet were widely analyzed in existing literature, research on the sound fatigue of the tail, the fuselage, and the wing in the hypersonic environment is scarce. The vibration fatigue caused by noise load in hypersonic environment was investigated in this study.

2. Main Research Content and Methods

Based on an aerospace plane, this study focuses on the sound–vibration coupling phenomenon of the lightweight V-tail under the engine take-off noise environment; it also estimates the sound fatigue life on the basis of the structural dynamic response obtained from the sound–vibration coupling analysis. On this basis, several influencing factors of acoustic fatigue are proposed, and a set of more complete acoustic fatigue life prediction schemes are summarized. The main research contents of this article include the following:

- (1) Modal analysis based on FEM.
- (2) Acoustic–vibration coupling calculation based on modal.
- (3) Acoustic fatigue calculation based on dynamic response.
- (4) Research on the influencing factors of acoustic fatigue.

The objective of dynamic analysis in structural mechanics would be to identify an object's or structure's inherent dynamic characteristics and energies under simple vibration. A physical object can also be tested to identify its

native frequency and modulus. Acoustic fatigue is a condition that occurs when pipework is subjected to excessive tension as a result of excessive noise. High sound at pressures lowering devices like pressure regulator or limitation holes stimulates downstream pipeline, causes piping shaking, and puts a great deal of stress upon that branches or welded support.

2.1. Method of Fatigue Life under Sound Vibration Judge Coupling. A coupling coefficient (λ_c) can be used to determine whether the coupling action must be considered in the coupling problem [11]. Many unfavorable events can occur from sonic coupling between the components of a microarray transducer. Coupling coefficients are generated through lateral mode creation in the components and also surfaces and lamb waves in the backup and front corresponding levels.

$$\lambda_c = \frac{\rho_0 c}{\rho_t T \omega}, \quad (1)$$

where ρ_0 is the density of the fluid, c is the velocity of the sound in the fluid, ρ_t is the density of the structure, T is the equivalent thickness of the structure, and ω means the angular frequency.

For the acoustic field under the action of random sound field, the range of angular frequency is large, with which the coupling effect is obvious in the data calculation. Therefore, the coupling effect should be considered. The stress response of the structure under the acoustic load is studied. Considering the characteristics of the sound load, the sound field of the model is simulated.

2.2. Definition of the Coupling Surface. For structural and acoustic grids, establishing a data transfer to present a coupling relationship is necessary. Similarly, defining the mapping relationship between both grids is important [12]. Given that nodes and units between different types of grids are not one-to-one, the mapping between grids must be defined. The coupling between the structure and the fluid medium does not exist entirely on the whole structure. In this case, defining a coupling surface is necessary to well simulate the real situation. The process of defining the coupling surface actually implements the transfer process between the grid data. The mapping algorithm includes the node number, maximum distance, element maximum distance, and conservative maximum distance. For the maximum distance algorithm, also defined as the number of influence nodes or maximum distance, the value of the target node is determined by the value of the source node, as in Figure 1. The specific formula is as follows:

$$P_{\text{Target}} = \frac{\sum_{i=1}^N (P_i^{\text{Source}}/d_i)}{\sum_{i=1}^N (1/d_i)}, \quad (2)$$

where P_{Target} refers to the target—the value of the node; d_i is the radius; P_i^{Source} is the value on the source node.

To decouple the kinetic equation represented by the physical coordinates, switching to the modal coordinate

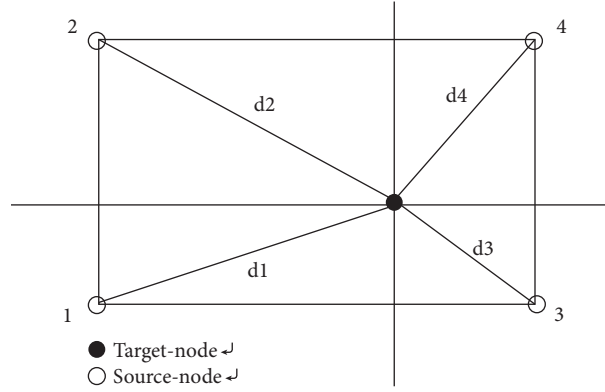


FIGURE 1: Diagram of data transfer.

system is necessary. According to the orthogonality of the eigenvector, the modal matrix, modal mass, modal stiffness, modal damping, and modal coordinates can be defined separately [13]. The vibration displacement can be written as follows:

$$\{u\} = \eta_1\{\phi_1\} + \eta_2\{\phi_2\} + \cdots + \eta_n\{\phi_n\} = \Phi\{\eta\}, \quad (3)$$

where $\{\eta\} = \begin{pmatrix} \eta_1 \\ \eta_2 \\ \vdots \\ \eta_n \end{pmatrix}$ is a vector of modal participation factors η_r .

Through the above transformation, the original coupling of the kinetic equation into the decoupled modal coordinate system under the modal equation is

$$M_r \ddot{\eta}_r + C_r \dot{\eta}_r + K_r \eta_r = F_r, \quad r = 1, 2, \dots, n. \quad (4)$$

By solving the kinetic equation of n independent modal coordinates represented by the above equation, we can obtain the modal participation factor corresponding to the modal coordinates under modal coordinates, including the displacement response of the system in the physical coordinate system. The dynamic response of the system is superimposed by the modal response of each order. The modal participation factor indicates the proportion of the modes in the total response. The participation factor is only related to the system structure parameters and has nothing to do with the disturbance.

2.3. Model of Fatigue Life Estimation. The frequency domain method is used to describe the stress information of the stochastic process with the spectral parameters of the response power spectral density. Then, the S-N curve and fatigue cumulative damage theory are used to calculate the life.

Regarding the random process for various states, a statistical function of the sample function can be used to describe the statistical characteristics of the entire process [13]. In general, the environmental vibration of an aircraft has a steady state of various properties. The first-order amplitude probability density function is defined as

$$p(q_i) = \lim_{\Delta q_i \rightarrow 0} \left[\lim_{T \rightarrow \infty} \frac{1}{T} \sum_{i=1}^{\infty} \Delta t_i \right]. \quad (5)$$

According to Miner linear damage theory, the structure is due to the stress cycle of different stress levels. The total fatigue damage of the structure is

$$D = \sum D_i = \sum \frac{n_i}{N_i}, \quad (6)$$

where the stress level is expressed, indicating the corresponding fatigue life at the stress level. In a certain time T , the stress range in the number of cycles is

$$n_i = \nu T p(S_i) \Delta S_i, \quad (7)$$

where ν is the number of stress cycles per unit time, and $p(S_i)$ is the probability density function of stress amplitude.

The time of fatigue damage can be obtained using the following:

$$D = \nu T \int_0^{\infty} \frac{p(S)}{N(S)} dS. \quad (8)$$

According to the fatigue damage criterion, the structure is destroyed, and the fatigue life is

$$N_T = \frac{1}{\nu \int_0^{\infty} (p(S)/N(S)) dS}. \quad (9)$$

The fatigue life of the structure depends on the stress response density. The broadband distribution method is used to calculate the probability density of the rain flow amplitude.

Dirlik's Monte Carlo time-domain simulation is conducted to study the power spectral density function of different shapes. Four inertia moments are used to describe the amplitude density function. The velocity or path of moving object is controlled by four inertial moments. The ability of items to continue travelling in a single direction at a constant pace when no pressures occur on them would be one example of this feature. Both a translational and a rotating component may be present in the averaged movement [14].

$$p(S) = \frac{(D_1/Q)e^{(-Z/Q)} + (D_2Z/R^2)e^{(-Z^2/2R^2)} + D_3Ze^{(-Z^2/2)}}{2\sqrt{m_0}}, \quad (10)$$

where 0 is the order spectrum moment.

$$\begin{aligned} D_1 &= \frac{2(\chi_m - \gamma^2)}{1 + \gamma^2}, \\ D_2 &= \frac{1 - \gamma^2 - D_1 + D_1^2}{1 - R}, \\ D_3 &= 1 - D_1 - D_2, \\ Z &= \frac{S}{2\sqrt{m_0}}, \\ Q &= \frac{1.25(\gamma - D_3 - D_2R)}{D_1}, \\ R &= \frac{\gamma - \chi_m - D_1^2}{1 - \gamma - D_1 + D_1^2}, \\ \gamma &= \frac{m_2}{\sqrt{m_0 m_4}}, \\ \chi_m &= \frac{m_1}{m_0} \sqrt{\frac{m_2}{m_4}}. \end{aligned} \quad (11)$$

The noise signal of the aircraft is a high-frequency broadband random signal. The Dirlik model is simple, fast, and suitable for wideband signal.

2.4. Average Stress Correction. In different stages of life, the effect of average stress is not the same; for different materials, the effect of average stress is also not the same. To consider the effect of average stress on fatigue life, especially the high-cycle fatigue life, Gerber et al. proposed different correction methods. Meanwhile, Goodman proposed a revised method.

Goodman's mean stress correction equation is as follows:

$$\frac{S_a}{S_e} + \frac{S_m}{S_u} = 1. \quad (12)$$

S_a is the stress amplitude, S_m is the average stress, S_e is the symmetrical cyclic stress, and S_u is the strength limit. Goodman's formula, especially in the fatigue limit, has a small error in processing the average tensile stress.

2.5. Process of Fatigue Life Analysis. Process of fatigue life analysis is shown in Figure 2.

3. Acoustic-Vibration Coupling Analysis Based on Modal

3.1. Modal Analysis Based on FEM

3.1.1. Establishment of FEM. Taking the left side of the tail of a type of spacecraft as the object of study, the CAD diagram of the tail model is established in Figure 3.

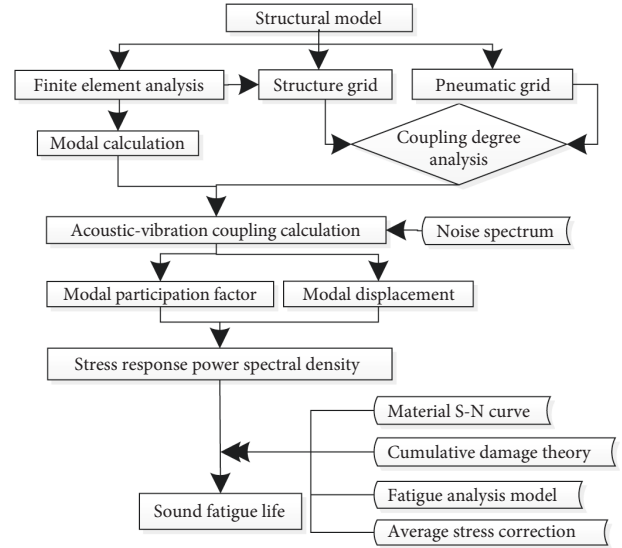


FIGURE 2: Process of fatigue life analysis.

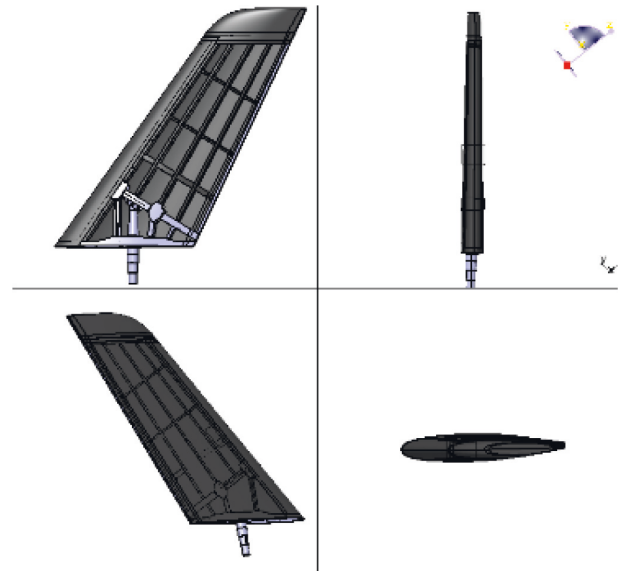


FIGURE 3: CAD diagram of a tail model.

The FEM of the tail fin is also established. With geometric cleanup, geometric simplification, topological restoration, and topological improvement, the resulting simplified FEM is shown below (skin hiding) in Figure 4.

3.1.2. Division of 2D Grid and Boundary Constraints. To facilitate the analysis of sound and vibration, the structural meshing should be consistent with the acoustic grid, that is, to meet the requirements in the acoustic simulation software for grid size. In the analysis of dynamic software, sound reflection and diffraction and refraction effects are considered [15]. The grid size is too large and may lead to a great error in the accuracy of the calculation results. For a linear finite element and a boundary element model, at least six cells in a minimum wavelength and at least three units for

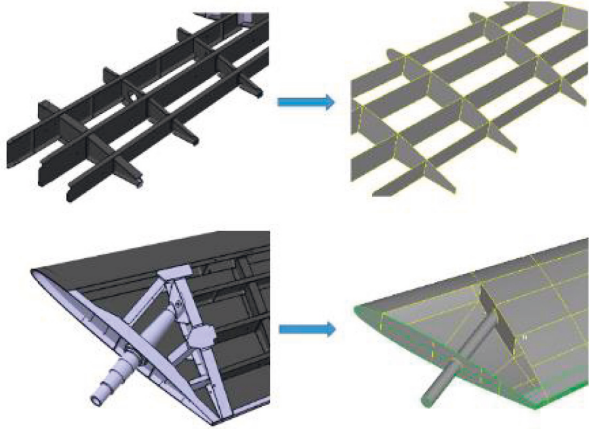


FIGURE 4: Simplified model of geometric relationships.

the quadratic unit are assumed. Given that the linear unit is used here, assuming that the propagation speed of sound is c and the highest frequency is f_{max} , the unit length L which was divided should meet the following conditions [16]:

$$L \leq \frac{c}{6f_{max}}. \tag{13}$$

In this study, the fluid medium is air, the speed of sound is 340 m/s, the maximum frequency calculated is 4000 Hz, and element length $L \leq 14.2$ mm is obtained by substituting the formula. The 14 mm size is selected as the grid standard size to be divided. The divided grid cells are illustrated in Figure 5.

The meshing adopts quadrilateral elements as the main method and triangular elements as the auxiliary method, which not only ensures the calculation accuracy, but also considers the calculation speed. The final divided mesh unit is shown in Figure 5. The full tail model is divided into 19366 meshes and 18037 nodes.

Select the mesh node at the end as the slave node, the master node is automatically obtained through the geometric relationship, constrain the first 5 degrees of freedom of the master node, and release the sixth degree of freedom, that is, the rotation degree of freedom around the rudder axis in Figure 6.

3.1.3. Setting of the Material and Grid Properties. Four main materials are used: T300/603A, T300/603A, TC4, and 30CrMnSiA, as displayed in Figure 7. Thickness of tail wing parts is given in Table 1.

3.1.4. Performance of Modal Analysis. As the maximum external excitation frequency of 4000 Hz, the frequency range of the solution modal control is 1–6000 Hz, the modal solution, to ensure the accuracy of the results and consider the calculation cost at the same time.

3.1.5. Modal Analysis Results. Table 2 shows the natural frequency of the model as a whole. The range of the natural frequency values of the first-order to the 900-

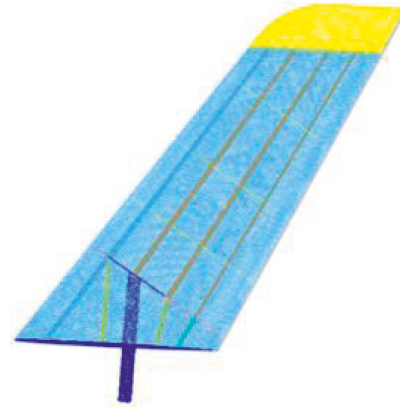


FIGURE 5: Grid division.

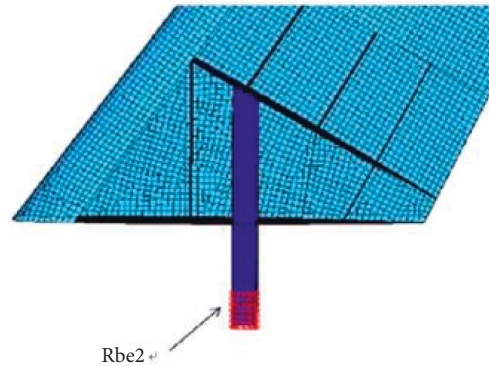


FIGURE 6: Grid division.

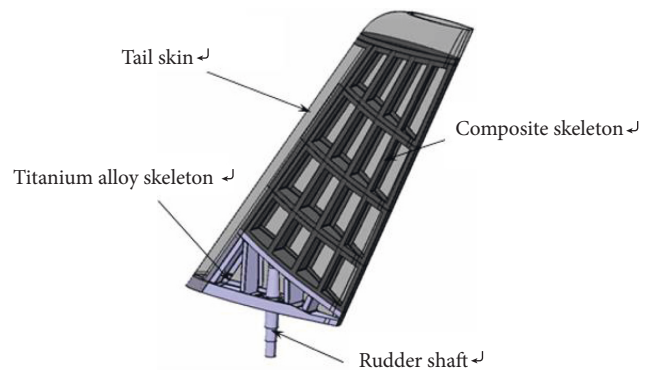


FIGURE 7: Material of the wing components.

TABLE 1: Thickness of tail wing parts.

Numbering	Name	Material	Thickness (mm)
1	Skin	2A14	2.2
2	Rudder shaft	30CrMnSiA	10
3	Ribs	T300/603A	1.5
4	Side ribs	TC4	10
5	Trailing edge	T300/603A	3
6	Wall	T300/603A	3
7	Beam	TC4	4
8	Reinforced ribs	TC4	12

TABLE 2: Natural frequency.

Modal order	Natural frequency (Hz)
1	33.5774
2	36.7333
3	153.0123
4	208.4317
5	397.1541
⋮	⋮
31	1012.5375
⋮	⋮
153	2004.5829
⋮	⋮
495	4005.2000
⋮	⋮
900	6000.4287

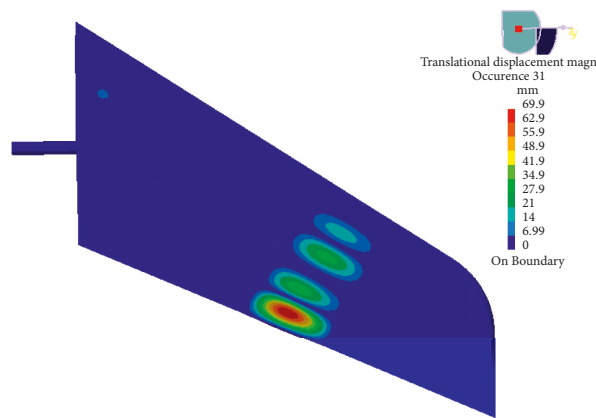


FIGURE 8: Order mode.

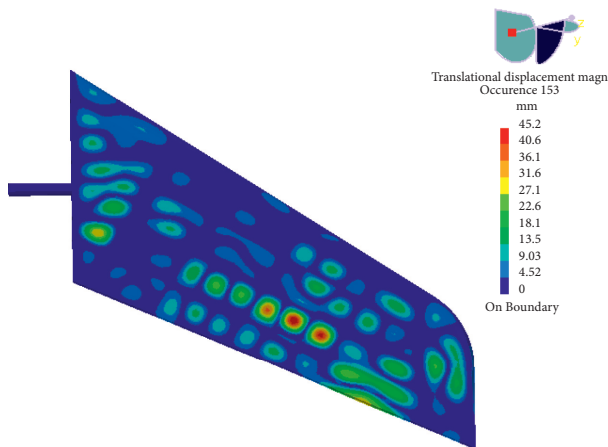


FIGURE 9: 153rd order mode.

order modes of the model is 33.5774–6000.4287 Hz. The table also presents the natural frequency values for several typical orders.

3.1.6. Modal Vibration Mode. In this study, the excitation is the acoustic load, and the frequency is high. Therefore, the high-order mode should be calculated while studying the low-order mode. In Figures 8–11, high-end mode selections

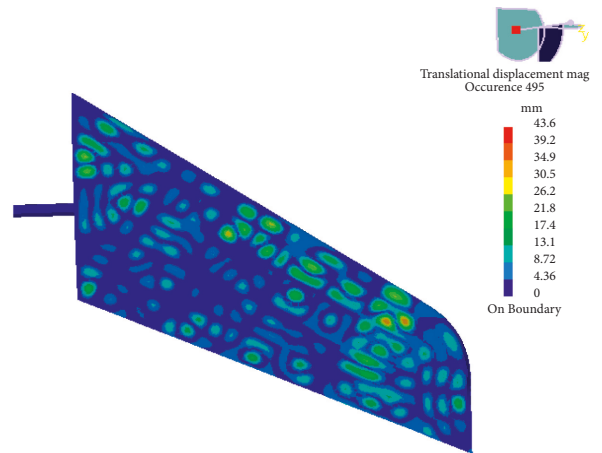


FIGURE 10: 495th order mode.

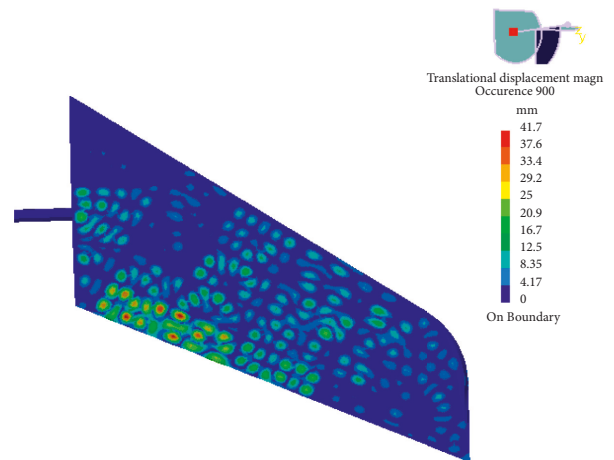


FIGURE 11: 900th order mode.

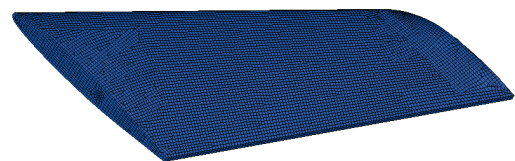


FIGURE 12: Acoustic grid.

31, 153, 495, and 900 correspond to the natural frequency values of 1000, 2000, 4000, and 6000 Hz.

3.2. Acoustic Coupling Calculation. Importation of structure grid, modal, and acoustic grid ware: Acoustic grid involvement is a valuable diagnostic technique for determining which areas of a building contribute considerably to the internal acoustics. Modal analysis aids in determining the vibration signals of a physical building component by displaying the activity of various portions of the building under dynamic loads, including those caused by electrostatic controllers' lateral loads [10]. Grid ware is constantly looking for changes that may affect the grid's overall performance.

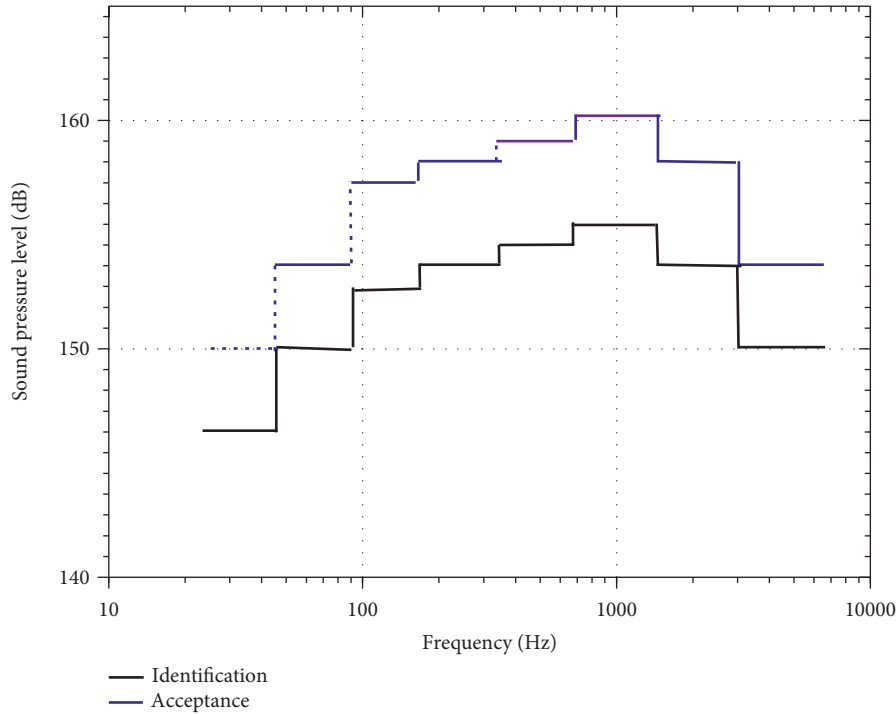


FIGURE 13: Noise spectrum.

The technology identifies defects earlier and in live time, allowing you to arrange rapid adjustments and respond quickly to acoustics emergencies. With the boundary element method used for acoustic numerical calculation, the structure grid, acoustic grid, and structure modal are imported. Acoustic grid panels have a tiling pattern that aids in the absorbing of reflecting waves, allowing audio to be clarified and improved in a space. Because of their size, those screens are good for treating vast areas of a space at the same time. The grid of the analysis structure uses the modal analysis grid. The acoustic grid is divided by a 2D grid. The envelope surface of the structure is first adopted, and then the surface mesh on the envelope surface is divided. To ensure that the structure grid and the acoustic grid have a good correspondence, the standard size is calculated, and the selected acoustic grid size is 14 mm.

Definition of sound load: The external sound load data are obtained from the measured sound pressure level spectrum, as shown in Figure 12. The acceptance test and the identification test sound pressure level spectrum correspond to the solid part and the broken line part in Figure 13. The experiment time is one and three minutes, respectively [16]. The given spectrum is octave, the frequency of each center band is twice the frequency of the center band of the previous band, and the sound pressure level corresponding to each center band is read and tabulated as in Table 3.

Definition of the sound source for the random diffusion of the sound field and the determination of the sound field of the sound pressure distribution by the spectrum [17]: A noise spectrum is the given data in Table 4. Thus, the sound pressure level must be converted to sound pressure to obtain the sound pressure spectrum [18]. The conversion formula is

TABLE 3: Noise acceptance test sound pressure level spectrum.

Center frequency (Hz)	Sound pressure level within octave bandwidth (dB)	
	Acceptance level	Appraisal level
31.5	146	150
63	150	154
125	153	157
250	154	158
500	155	159
1000	156	160
2000	154	158
4000	150	154

TABLE 4: Sound pressure spectrum.

Center frequency (Hz)	Sound pressure level (dB)	Sound pressure effective value (Pa)
31.5	150	632.4
63	154	1002.4
125	157	1415.9
250	158	1588.7
500	159	1782.5
1000	160	2000
2000	158	1588.7
4000	154	1002.4

$$p_e = p_{ref} \times 10^{(L_p/20)}. \tag{14}$$

Definition of the sound load concept and the selection of an idealized distribution of the reverb distribution: In the space where the diffuse sound field is satisfied, the sound

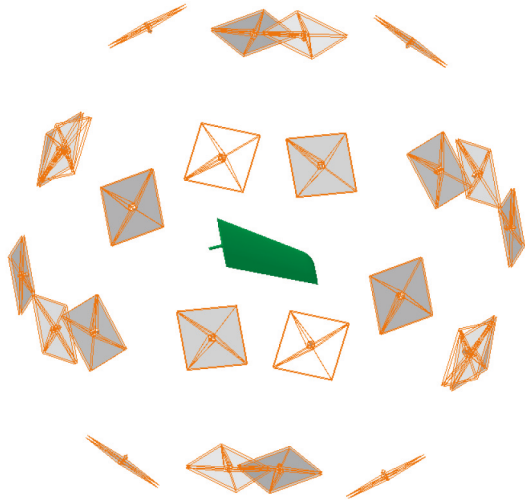


FIGURE 14: Sound pressure distribution.



FIGURE 15: Coupling surface.

field distribution statistics of each point are uniform everywhere, and the acoustic energy probability from each direction is the same. To achieve these conditions, fully reflecting the various walls of sound waves is necessary. The 24 unrelated plane waves, evenly distributed in the structure of the spherical sphere, are defined. The spherical radius is obtained using the algorithm automatically in Figure 14.

3.2.1. Definition of the Coupling Surface. The surface skin of the V-tail is in direct contact with the sound field, and the equivalent thickness of the skin is minimal. Therefore, the contact surface between the skin and the sound field is a strongly coupled region, so that all external skin grids are selected in addition to the control rudder shaft. The corresponding sound field grid is defined as the coupling surface in Figure 15.

3.2.2. Definition of the Coupling Surface. In this study, the acoustic excitation is reduced to 24 plane waves, which are equivalent to 24 irrelevant excitation conditions. Under different operating conditions, the software calculates the participation factors of the modal modes. Here are a few typical equations in the first modal participation factor schematic in Figures 16 to 19.

In contrast to the natural frequency table, all modal participation factors have a maximum value near their corresponding natural frequency. For example, the seventh-order modal participation factor is maximized at a frequency of approximately 500 Hz. The seventh-order mode has the largest proportion of the total response caused by the external excitation at a frequency of 500 Hz.

3.2.3. Displacement Response Result. In this study, the acoustic load spectrum is the octave spectrum; thus, the frequency range is 31.5–4000 Hz, and the incremental step is octave increment; that is, the frequency of the latter step is twice as long as the previous step. This section gives the displacement response under all the calculated frequency excitations under Principal Component 1. As the excitation frequency increases, the displacement response of the structure becomes more complex, and the response amplitude becomes smaller in Figure 20.

3.3. Stress Response. The response of the structure under the action of each plane wave is calculated. In this section, the response of the random response is calculated using the coupling response. Given that the defined plane waves are irrelevant and the coefficient of the participation of Principal Component is 1, it is a unit diagonal matrix. The response of each plane wave is synthesized. A random response of the random field is calculated, and all the nodes on the coupling surface are chosen to calculate the stress response. The stress response can be obtained from the power spectral density. Figures 21 and 22 illustrate the stress and power spectral density of the x and y directions of the mesh cell number 8755; the z -stress in the 2D element is zero. Many peaks can be seen in the stress response power spectral density, which indicates that the structural vibration is caused by multi-mode superposition, and the structural response is expressed as wideband multimodal.

4. Sound Fatigue Calculation

4.1. Stress-Life Curve. The typical stress-life curve (S-N curve) can be divided into three segments: low-cycle fatigue zone, high-cycle fatigue zone, and subfatigue zone. When the external load stress is less than the fatigue limit (i.e., infinite life), in general, take N , which is equal to the corresponding stress value. When the stress is equal to the tensile strength of static tension, the life is a stretching time; in the subfatigue zone, the S-N curve in the logarithmic coordinate system is almost a straight line. In a fatigue analysis, S stands for the stress range that is used to compute the deterioration [19, 20]. It is useful to determine the number of required cycles till a material fails, but it does not tell you how much fatigue damages the materials before the material fails.

Access to information obtained 2A14 aluminum alloy tensile strength $\sigma_b = 440$ MPa; the fatigue limit $S_{ae} = 130$ MPa. Use the power function formula:

$$S^{\alpha} N = C. \quad (15)$$

On both sides of the above pairs of logarithms,

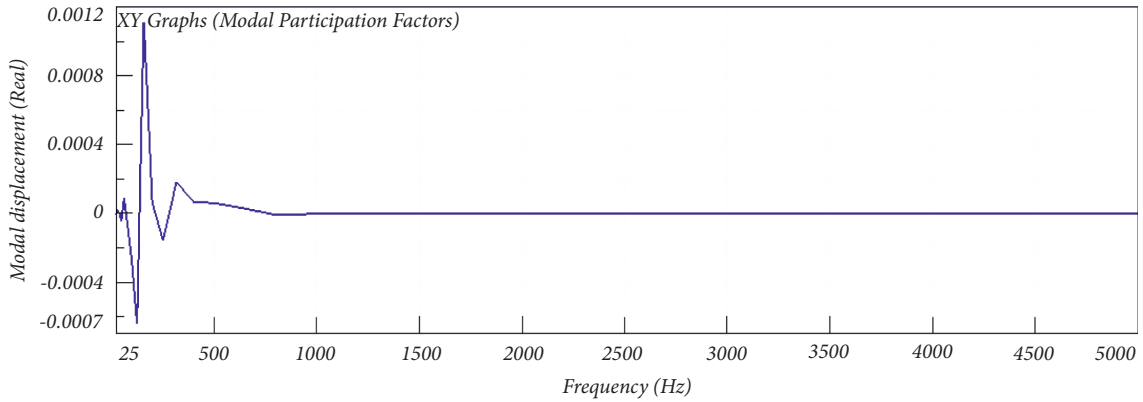


FIGURE 16: Participation factor of the third-step modal.

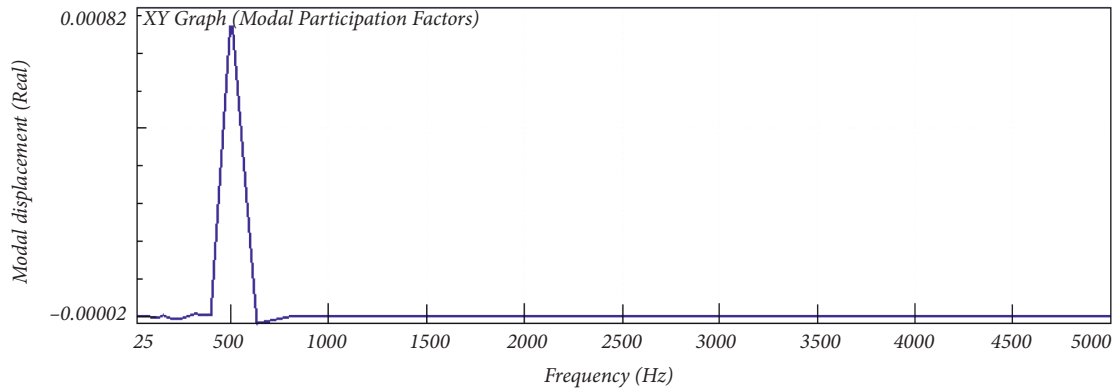


FIGURE 17: Participation factor of the seventh-step modal.

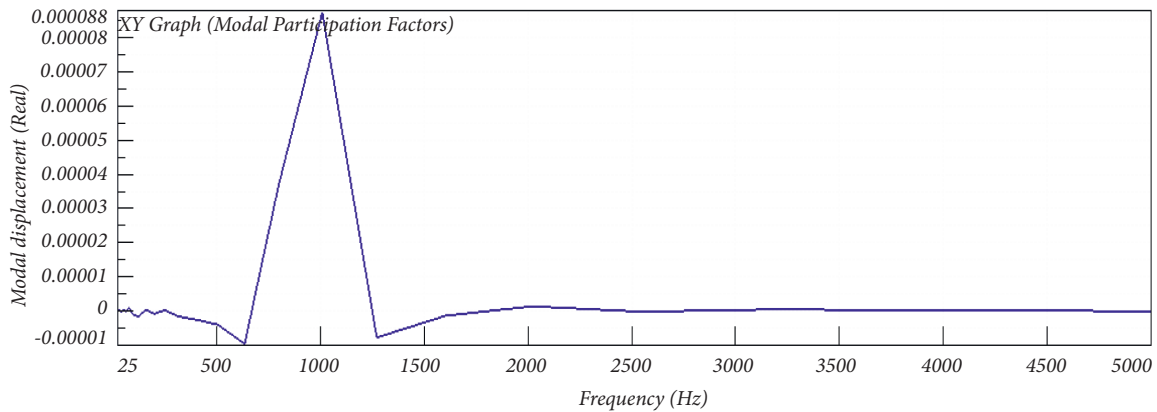


FIGURE 18: Participation factor of the thirty-first-step modal.

$$\lg N = a + b \lg S, \tag{16}$$

where a and b are the material constants, and the empirical formula of the S–N curve of the power function is a straight line on the double logarithmic plot [21].

By studying the effect of loading frequency on the fatigue life curve of metal materials, their loading frequency has little effect on the S–N curve when the metal materials only undergo elastic deformation, as shown in Figure 23. In

this study, the fatigue life curve is calculated by static fatigue.

4.2. Fatigue Life Analysis Theory. This research chooses Miner linear superposition theory.

The fatigue life estimation method of Dirlik model is adopted. The frequency domain method is used to describe the stress information of the stochastic process with the

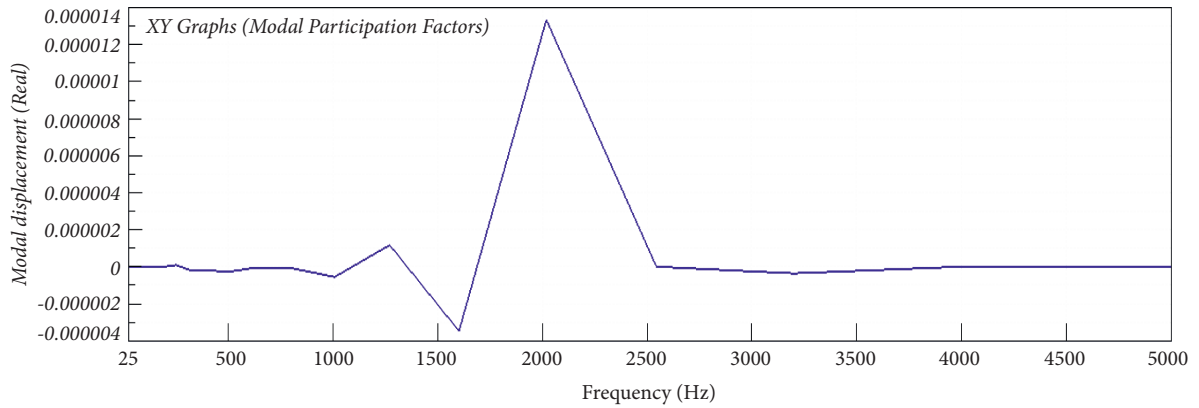


FIGURE 19: Participation factor of the one hundred and fifty-third modal.

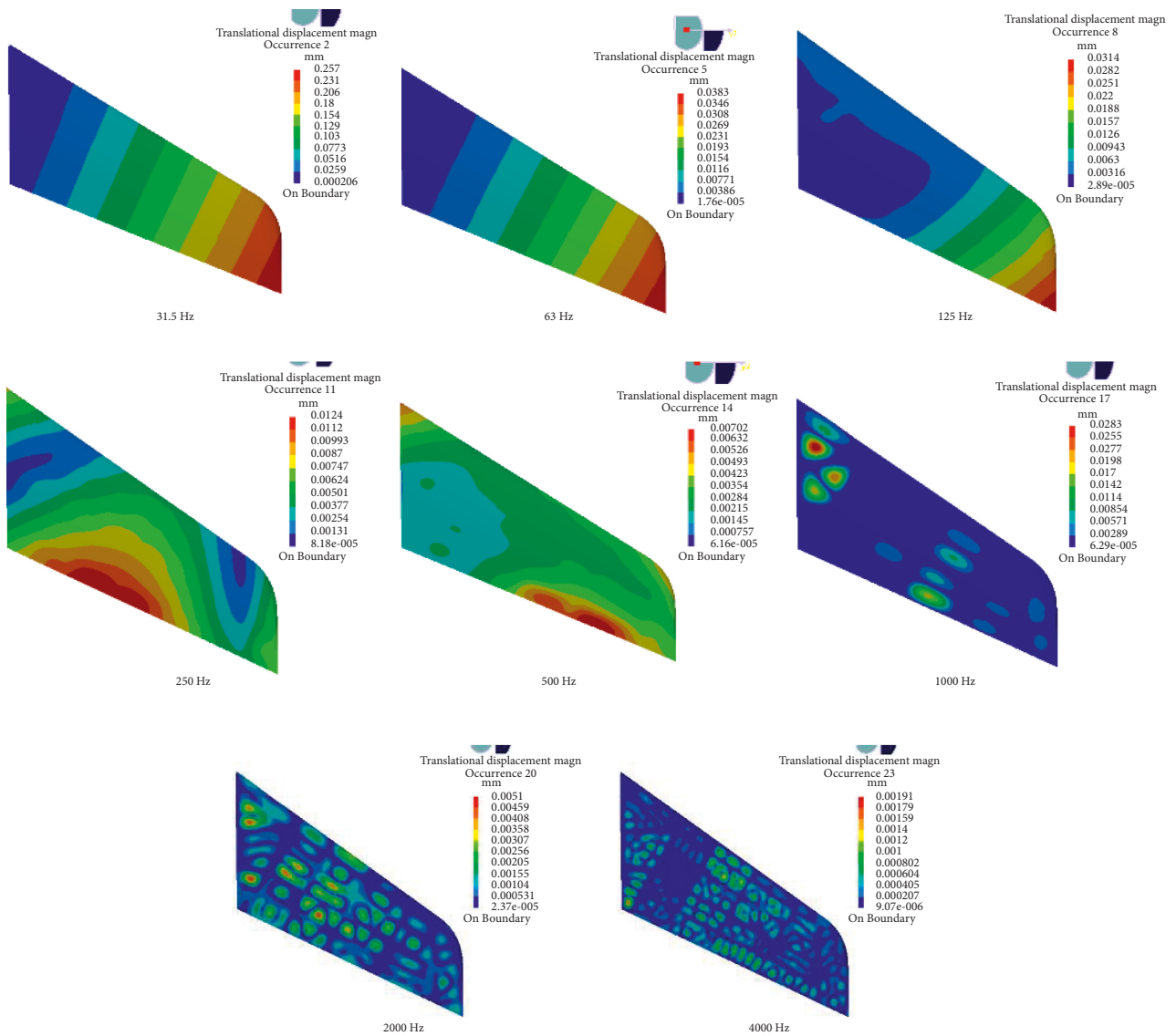


FIGURE 20: Displacement response.

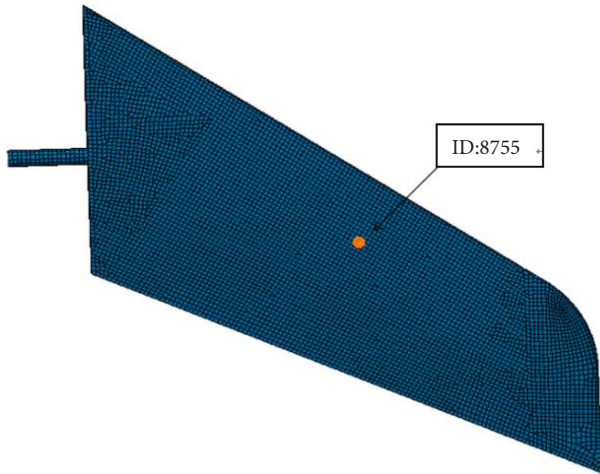


FIGURE 21: Location of ID 8755.

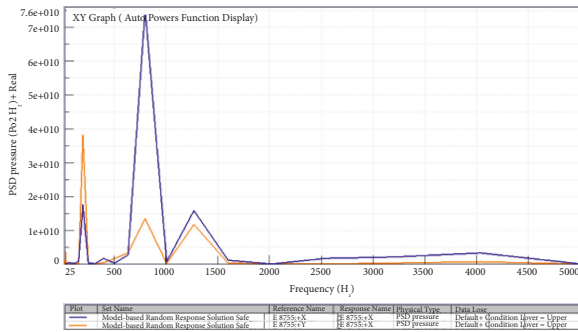


FIGURE 22: Power spectral density of ID 8755.

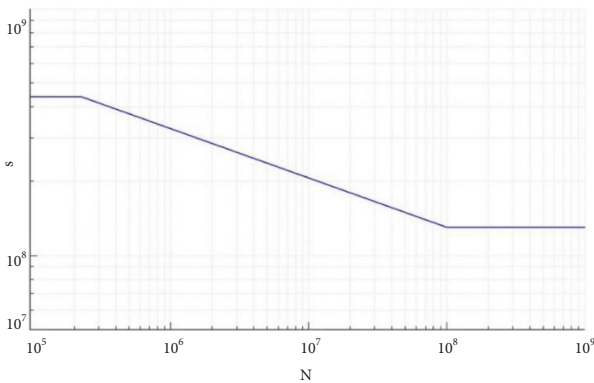


FIGURE 23: 2A14 S-N curve.

spectral parameters of the response power spectral density. Then, the life is calculated by combining the S-N curve and fatigue cumulative damage theory [22].

The noise signal of the aircraft is high-frequency broadband random signal. The Dirlik model is simple, fast, and suitable for wideband signal. In this study, the Dirlik model is selected, and the Goodman linear formula is used to calculate average stress.

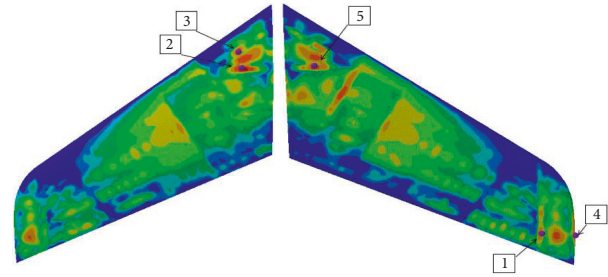


FIGURE 24: Tail hot spots inside and outside the tail.

TABLE 5: Hot damage index and life expectancy.

Hot spot	Grid number	Damage index	Fatigue life (s)
1	1212	-3.26	1.83×10^7
2	6951	-3.43	2.70×10^7
3	6974	-3.46	2.89×10^7
4	1630	-3.47	2.97×10^7
5	6796	-3.54	3.51×10^7

4.3. *Sound Fatigue Life Results.* After determining the stress-life curve of the material, fatigue cumulative damage theory, fatigue life estimation method, and correction method, the external skin of the tail fin is selected as the acoustic fatigue life in Figure 24.

The analysis of Table 5 shows that hot spot 1 is the largest point of damage, and its damage value is $1 \times 10^{-3.26}$ under a standard load. According to the linear fatigue damage accumulation theory, the life under a standard load is $D = 1 \div (1 \times 10^{-3.26}) = 1830$. Since the action time of a standard load is 10000s, the vibration fatigue life of hot spot 1 is 1.83×10^7 s.

The fatigue risk of the tail is the skin at the root of the tail near the rib and the skin at the wing tip.

The research project has not yet been tested at this stage. Therefore, no test data are compared. To discuss the credibility of the results, the findings are compared with those of the present study. In the study of the estimation of random acoustic fatigue life based on the rain flow counting method, the estimated life of open cylindrical shell is calculated at 140 dB of the total sound pressure level. Jin Luanshan and Li Lin stated that the fatigue life of an aeroengine is calculated on the basis of Dirlik's broadband process theory. Zhang Xiuyi studied the properties of the plate, curved plate, stiffened plate, and honeycomb in the design of the acoustic fatigue analysis and the acoustic fatigue design of the aircraft structure. The calculation results are similar. In this research, the thickness of the aluminum skin is 4.4 mm. Hence, although the load is greater, the sound fatigue life is relatively improved.

5. Influencing Factors of Acoustic Fatigue Life

Theoretically, the factors that affect the cycle fatigue life of the structure also affect the vibration fatigue life, in addition to some factors on the vibration fatigue life of a greater impact, especially the dynamic characteristics of the structure, including natural frequency and damping ratio. The problem of the load on sound fatigue is particular that it needs further study.

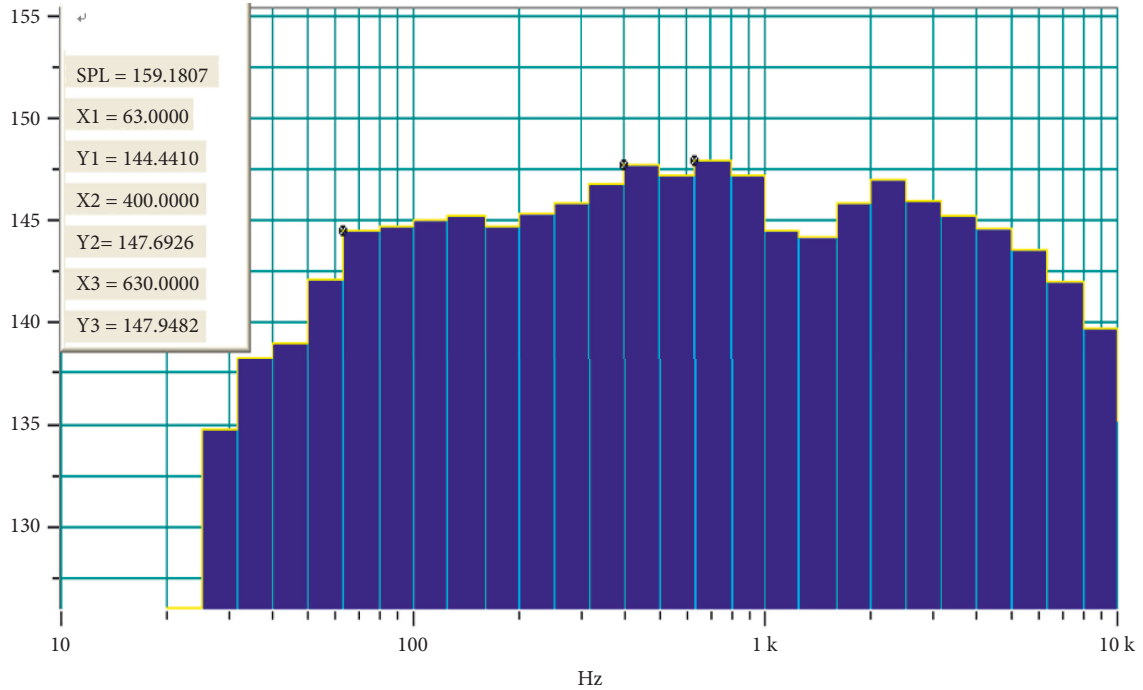


FIGURE 25: Noise spectrum.

TABLE 6: Sound pressure spectrum.

Frequency (Hz)	Sound pressure level L_p	Sound pressure spectrum p_e (Pa)
25	134.8	109.9
31.5	138.1	160.7
40	138.8	174.2
50	142.0	251.8
63	144.4	331.9
80	144.6	339.6
100	144.9	351.6
125	145.1	359.8
160	144.4	331.9
200	145.1	359.8
250	146.0	399.1
315	146.5	422.7
400	147.7	485.3
500	146.8	437.6
630	148.0	502.3
800	146.8	437.6
1000	144.0	317.0
1250	144.0	317.0
1600	146.0	399.1
2000	146.8	437.6
2500	146.0	399.1
3150	145.1	359.8
4000	144.4	331.9

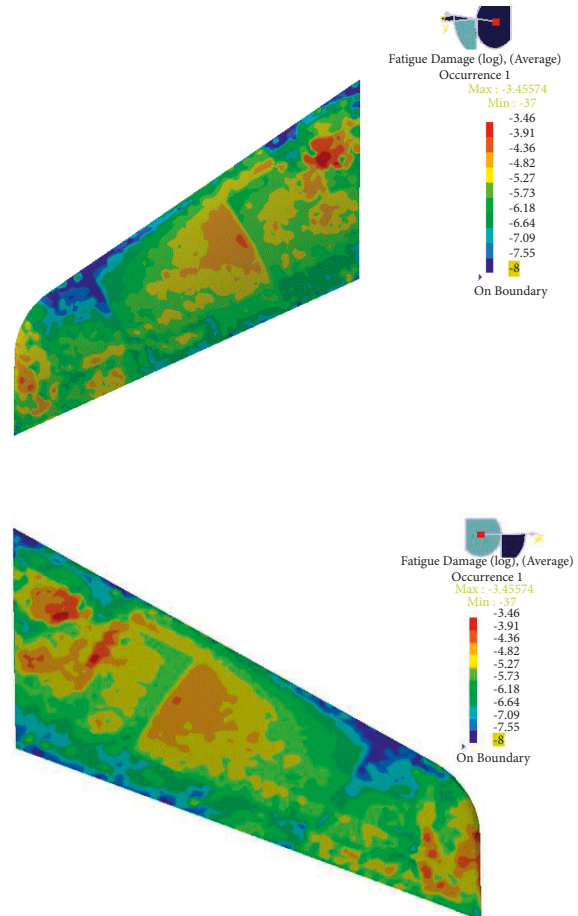


FIGURE 26: Damage index under 1/3 octave conditions inside and outside tail.

5.1. Effects of Load Characteristics. The noise environment of the aircraft at different times varies, and the new noise test data in the new operating conditions are shown in Figure 25. As a result of the use of the 1/3 octave spectrum, the measurement data points likely use the same method in Table 6.

TABLE 7: Sound fatigue life at different sound pressure levels.

Increase or decrease the value	Damage index	Sound fatigue life
-15	-6.22	$1.65 \times 10^{10} s$
-10	-5.41	$2.58 \times 10^9 s$
-5	-4.51	$1.78 \times 10^8 s$
0	-3.26	$1.83 \times 10^7 s$
+5	-2.45	$2.85 \times 10^6 s$
+10	-1.51	$3.21 \times 10^5 s$
+15	-0.33	$2.15 \times 10^4 s$

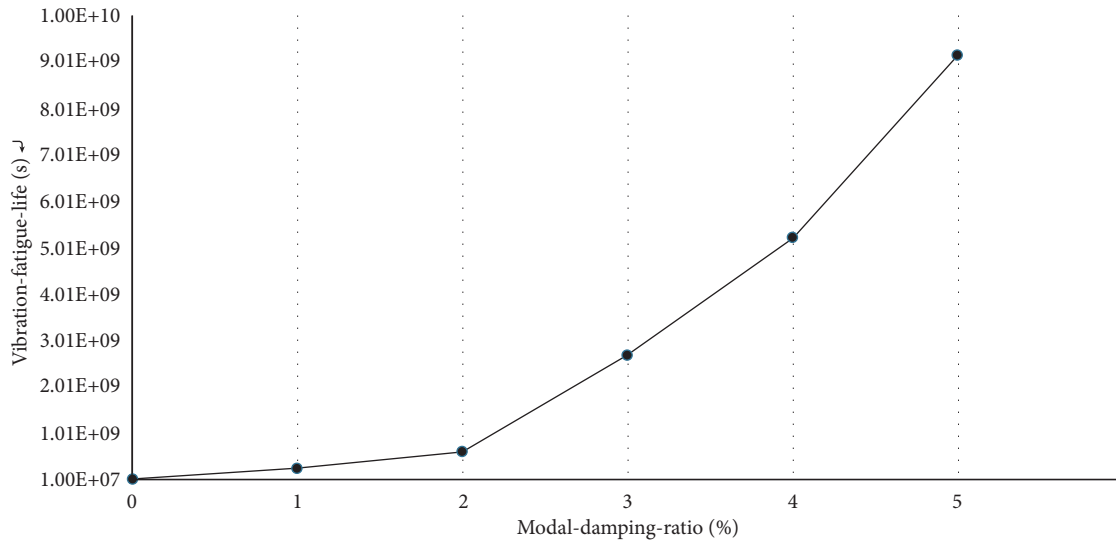


FIGURE 27: Relationship between vibration fatigue life and modal damping ratio.

Comparing damage index under 1/3 octave conditions inside and outside the tail in Figure 26, we find that (1) parts of the fatigue risk are roughly the same, which are the root near the ribs and the wing at the end of the skin. (2) The fatigue life of the new working condition is increased by an order of magnitude compared with that of the initial working condition. The reasons are that the sound pressure level of the frequency band in the new working condition is smaller than the initial working pressure level, and the external load energy is weakened, thereby increasing life expectancy.

5.2. Relationship between Sound Pressure Level and Life. To obtain the relationship between the external excitation pressure level and the acoustic fatigue life, the sound pressure level of each band is increased and decreased on the basis of the sound pressure load of the original octave. The amplitude of increase or decrease is dB. A new sound pressure spectrum is also obtained.

In Table 7, the analysis of the table data reveals the sound pressure level for each additional 5 dB, and the life expectancy is reduced by about an order of magnitude. For each lower 5 dB, the life is increased by about an order of magnitude. Theoretically, the sound pressure level increases by twice as much as the sound pressure level, and the acoustic energy is proportional to the square of the sound pressure. Therefore, the noise level can reduce the sound fatigue life.

5.3. Effect of Structural Damping. For the modal damping ratio of each order, only the important mode of influence is the main mode; hence, only the main modal damping ratio can be obtained. With the increase of the damping ratio, the ability of the structure to dissipate energy is enhanced, and the structural response caused by the external excitation of the same energy is weakened. Therefore, the fatigue life of the structure increases. The relationship between the damping ratio and the fatigue life can be expressed by a certain function by studying the properties of the material.

Taking different modal damping ratios and performing recalculations to obtain the damage index and the fatigue life, the following is summarized in Table 8.

Figure 27 shows that (1) the modal damping ratio has a great influence on the vibration fatigue life of the structure, and the influence coefficient is nonlinearly increased. (2) With the increase of modal damping, the mean square root of the structural response stress decreases, and the acoustic fatigue life is prolonged.

At present, quantitative research on damping is few. The value of engineering application is usually based on empirical data, which lead to the design damping and the actual damping in many structures. Moreover, the prediction accuracy of vibration fatigue life is not high. To improve the acoustic fatigue life, increasing the structural modal damping is of great significance. The damping materials and

TABLE 8: Sound fatigue life under different modal damping ratios.

Modal damping ratio (%)	Damage index	Sound fatigue life (s)
0	-3.26	1.83×10^7
1	-4.39	2.45×10^8
2	-4.77	5.93×10^8
3	-5.43	2.68×10^9
4	-5.72	5.22×10^9
5	-5.96	9.15×10^9

shock absorbers are used in the engineering to achieve the purposes of vibration and noise reduction.

6. Conclusion

In this work, the tail fins of a certain type of spacecraft are studied; the finite element, boundary element, and vibration fatigue analysis method are also used to predict the acoustic fatigue life of the tail fins. On this basis, the influence factors of the acoustic fatigue life are investigated, and some suggestions are put forward for the structural fatigue design.

The damage value of largest point is $1 \times 10^{-3.26}$ under a standard load. According to the linear fatigue damage accumulation theory, the life under a standard load is $D = 1 \div (1 \times 10^{-3.26}) = 1830$. Since the action time of a standard load is 10000 s, the vibration fatigue life of hot spot 1 is 1.83×10^7 s. The fatigue risk of the tail is the skin at the root of the tail near the rib and the skin at the wing tip.

The analysis of the table data reveals the sound pressure level for each additional 5 dB, and the life expectancy is reduced by about an order of magnitude. For each lower 5 dB, the life is increased by about an order of magnitude. Theoretically, the sound pressure level increases by twice as much as the sound pressure level, and the acoustic energy is proportional to the square of the sound pressure. Therefore, the noise level can reduce the sound fatigue life.

The FEM of the tail of a hypersonic aircraft is also performed. The modal parameters within 6000 Hz are calculated, and the natural frequency and mode information are calculated. The acoustic response is given to the acoustic response under the given acoustic load, which includes linear damage accumulation theory, the Dirlik model, and the Goodman linear correction model. The analysis method of vibration fatigue life is studied, combined with the results of dynamic analysis and the stress-life curve of the material; the linear damage accumulation theory, Dirlik model, and Goodman straight line correction model are used to calculate the acoustic fatigue life of the tail wing. In addition, the effects of load characteristics and structural damping on acoustic fatigue life are studied.

Data Availability

The modal data used to support the findings of this study were supplied by Fundamental Scientific Research Business Expenses of Central Universities and access can be obtained from the corresponding author upon request.

Conflicts of Interest

The authors declare that they have no conflicts of interest.

Acknowledgments

This work was supported by Fundamental Scientific Research Business Expenses of Central Universities (NJ2020024).

References

- [1] M. C. Cheng, C. Hsiao, R. J. Shyu, and D. Cheng, "Analysis and test of spacecraft structural response under launch acoustic environment," *12th AIAA/CEAS Aeroacoustics Conference (27th AIAA Aeroacoustics Conference)*, Cambridge, MA, USA, 2006.
- [2] D. Priour, "Finite element method," *Dictionary Geotechnical Engineering/wörterbuch Geotechnik*, vol. 73, pp. 3–13, 2013.
- [3] S. Kong, S. Zhou, Z. Wang, and K. Wang, "The size-dependent natural frequency of Bernoulli-Euler micro-beams," *International Journal of Engineering Science*, vol. 46, no. 5, pp. 427–437, 2008.
- [4] V. Giannella, R. Lombardi, M. M. Pisani, L. Federico, M. Citarella, and R. Citarella, "A novel optimization framework to replicate the vibro-acoustics response of an aircraft fuselage," *Applied Sciences*, vol. 10, no. 7, p. 2473, 2020.
- [5] Ji-li Rong and Bo-chao Fan, "Research on scaling characteristics of sound-vibration environment of rocket fairing," *Journal of Astronautics*, vol. 40, no. 8, 2019.
- [6] F. E. N. G. Jin-long, H.-hong Wang, Y. Zhao, Yi-nan Wang, and D. U. Li-gang, "Finite element-boundary element method simulation for acoustic-vibration problems of spacecraft structures," *Equipment Environmental Engineering*, vol. 15, no. 11, 2018.
- [7] Y. Sha, A. Sise, F. Zhao, and Z. Jiang, "Vibro-acoustic response analysis and fatigue life prediction of thin-walled structures with high speed heat flux," *Acta Aeronautica et Astronautica Sinica*, vol. 41, no. 2, 2020.
- [8] J. Xu, Y. Zhang, Q. Han, J. Lacidogna, and G. Lacidogna, "Research on the scope of spectral width parameter of frequency domain methods in random fatigue," *Applied Sciences*, vol. 10, no. 14, p. 4715, 2020.
- [9] J. Jang and J. W. Park, "Simplified vibration PSD synthesis method for MIL-STD-810," *Applied Sciences*, vol. 10, no. 2, p. 458, 2020.
- [10] A. A. Jaoude and K. El-Tawil, "Analytic and nonlinear prognostic for vehicle suspension systems," *American Journal of Engineering and Applied Sciences*, vol. 6, no. 1, pp. 42–56, 2013.
- [11] A. Portela, M. H. Rooke, and D. P. Rooke, "The dual boundary element method: effective implementation for crack problems," *International Journal for Numerical Methods in Engineering*, vol. 33, no. 6, pp. 1269–1287, 1992.
- [12] J. T. Chen, K. H. Chen, I. L. Chen, and L. W. Liu, "A new concept of modal participation factor for numerical instability in the dual BEM for exterior acoustics," *Mechanics Research Communications*, vol. 30, no. 2, pp. 161–174, 2003.
- [13] P. H. Light and M. C. Light, "Fatigue under wide band random stresses," *Journal of the Structural Division*, vol. 106, no. 7, pp. 1593–1607, 1980.
- [14] G. Manogaran, V. Saravanan, and C. H. Hsu, "Information-centric content management framework for software defined internet of vehicles towards application specific services,"

- IEEE Transactions on Intelligent Transportation Systems*, vol. 22, no. 7, pp. 4541–4549, 2021.
- [15] N. W. M. Bishop, *Vibration Fatigue Analysis in Finite Element Environment*, XVI Encuentro Delgrupo Espanol De Fractura, Torremolinos, Spain, 1999.
- [16] P. A. Kumaraswamy, “A generalized probability density function for double-bounded random processes,” *Journal of Hydrology*, vol. 46, no. 1-2, pp. 79–88, 1980.
- [17] 张. Zhang Lei, 杨. Yang Yang, 高. Gao Jie-chao, and 刘. Liu Xing-yuan, “Study on amplified spontaneous emission properties of EnBOD material,” *Chinese Journal of Luminescence*, vol. 36, no. 6, pp. 661–665, 2015.
- [18] J. Jian Hua and Z. Hong Lun, *The Experimental Research of Goodman Fatigue Diagram of 09V Steel*, Journal of Shanghai Tiedao University, Shanghai, China, 2000.
- [19] O. E. A. Agudelo, C. E. M. Marin, and R. G. Crespo, “Sound measurement and automatic vehicle classification and counting applied to road traffic noise characterization,” *Soft Computing*, vol. 25, no. 18, Article ID 12075, 2021.
- [20] L. Susmel, R. Lazzarin, and P. Lazzarin, “The mean stress effect on the high-cycle fatigue strength from a multiaxial fatigue point of view,” *International Journal of Fatigue*, vol. 27, no. 8, pp. 928–943, 2005.
- [21] N. Nguyen, M. C. Leu, and X. F. Liu, “Real-time Communication for Manufacturing Cyber-Physical Systems,” in *Proceedings of the 2017 IEEE 16th International Symposium on Network Computing and Applications (NCA)*, pp. 1–4, Cambridge, MA, USA, October 2017.
- [22] A. D. Dimarogonas, “Method and apparatus for predicting structural integrity by estimating modal damping factor,” Patent No. 5 US5652386A, 1997.

Research Article

Artificial Intelligence-Based Drug Production Quality Management Data

Chenggong Yu 

Zhejiang Pharmaceutical University, Ningbo 315000, Zhejiang, China

Correspondence should be addressed to Chenggong Yu; yuch1979@163.com

Received 20 May 2022; Revised 20 July 2022; Accepted 3 August 2022; Published 23 August 2022

Academic Editor: Xuefeng Shao

Copyright © 2022 Chenggong Yu. This is an open access article distributed under the Creative Commons Attribution License, which permits unrestricted use, distribution, and reproduction in any medium, provided the original work is properly cited.

As a special commodity, medicine plays a vital role in people's healthy life. The basic effects of drugs are excitation and inhibition. Under the action of drugs, any function that can enhance or increase the function of the body's original tissues and organs is called excitement. On the contrary, any function that can weaken or reduce the function of the original tissues and organs of the body is called inhibition. The nature of action of drugs has three aspects: regulatory function; antipathogen and antitumor; and complementary therapy. If there is a problem with the quality and safety of medicines, it is tantamount to making money and killing people. Based on artificial intelligence, this paper analyzes the current situation and improvement strategies of quality management in pharmaceutical production management enterprises and proposes how to reduce the risk of drug safety with the assistance of artificial intelligence technology. The experimental results in this paper show that the sales of heparin sodium APIs were 2.099 billion yuan, accounting for 91.6% of the operating income in 2015, when company A had not conducted a drug risk assessment in 2015. After the outbreak of drug risks, the sales in 2016 were 1.743 billion yuan, accounting for 77.1% of the operating income in 2016. After the final implementation of the measures, the sales in 2019 were 4.743 billion yuan, accounting for 329.1% of the operating income in 2016. The research method in this paper can improve the hidden safety problems of drugs more efficiently, and it can improve the profit while ensuring the safety.

1. Introduction

As the concept of safe drug use has been deeply rooted in the hearts of the people, this paper puts forward higher standards and requirements for drug quality. It is necessary to achieve rational drug use and to use drugs effectively, safely, appropriately, and economically based on the systematic knowledge and theories of contemporary drugs and diseases. The purpose is to give full play to the efficacy of the drug and minimize the incidence of adverse reactions. These requirements prompt drug manufacturers to pay more attention to the quality management and control of drugs while continuously improving production efficiency. And for a large amount of data, computers have more powerful processing capabilities than humans. Comparing with the subjective judgment of the data, the computer processing will perform an objective data analysis according to the requirements. At the same time, it eliminates the confusion

of the conclusions that the quality assurance personnel can reach due to the results of different degrees of precision caused by different experiences and states. In this way, an analysis report with high accuracy and stable analysis conclusion can be provided for decision makers.

Faced with the challenge of implementing the newly revised drug production quality management standards, the scope of quality assurance work is getting bigger and bigger, and the responsibilities are getting heavier and heavier. This shows that the quality assurance work is facing a huge test. Vigorously promoting the application of computer technology in quality assurance work and continuously improving the knowledge level of relevant practitioners are urgent problems to be solved in the current work. The lack of enterprise quality awareness is also a major hidden danger. First, quality management is a mere formality. It is just to meet the requirements of regulations and does not really understand the essence of GMP management. Second, when

dealing with problematic products, a few pharmaceutical companies still have a fluke mentality and even ignore them directly. It is necessary to make full and effective use of a large amount of production information data generated in production, to mine the laws and associations hidden in these data, and to effectively associate deviation information with various data. This enables quality assurance personnel to find the best solution and analysis results when conducting system analysis.

This article mainly describes a detailed data analysis of the drug management system of company A under the introduction of artificial intelligence algorithms. The innovation is that this paper adopts the most advanced technology when the analysis of the personnel screening system is not clear enough and introduces artificial intelligence technology, which effectively reduces the error. The experimental results are also more realistic, and this article is constantly innovating and growing.

2. Related Work

At present, the management of drug production has attracted much attention, and more and more scholars have carried out research on it. Among them, Selezneva et al.'s study was dedicated to the role of laboratory research in ensuring the quality of domestic medicines. It also reviewed and analyzed regulatory documents and current publications on the subject [1]. The purpose of Kashirina et al.'s study was to study the current industrial practice of drug quality risk management in Russian pharmaceutical companies. This includes assessing the main issues in implementing a risk management system and its compliance with accepted international methodologies [2]. Drugs are elements that inhibit the healthcare system. Logistics management starts with planning the process, purchasing, storing, dispensing, recording, and reporting medications. The purpose of Wulandari et al.'s study was to explore the logistics management of medicines in a pharmacy installation in the work area of the health office in the Kraben district [3]. Drug shortages faced by the US pharmaceutical industry and government in recent years have been a major challenge. Jia and Zhao addressed the problem of drug shortages from a supply chain perspective and a key missing piece in medicine, and he proposed to reduce shortages through drug purchase contracts [4].

Medication and drug optimization play an important role in modifiable physiological risk factors and NCD management. The purpose of Syed et al.'s study was to describe the number of prescriptions for type 2 diabetes (T2DM), hypertension, and hyperlipidemia. The findings of the study will provide the necessary information to inform pharmaceutical policy and practice [5]. Medications should be provided promptly to all patients, whether adults or children. The purpose of Ueyama et al.'s study was to study the current status and characteristics of pediatric drug development in Japan. They used information on the lag in the approval of pediatric directives between Japan and the European Union [6]. In recent years, patient-controlled analgesia (PCA) has been widely used in patients with various pains, with the continuous recognition of pain knowledge, and

the continuous improvement of quality-of-life requirements. The mining technique proposed by Jin and Wu was used to analyze relevant literature. They tried to find out the main drugs of PCA, classify drugs, and mine important drug combination rules [7]. These articles are a good example of the importance of drug quality, but not whether it is based on artificial intelligence. These are not suitable for mainstream technologies in today's society and have certain limitations.

3. Artificial Intelligence Algorithms

3.1. Artificial Intelligence. Artificial intelligence, whose English abbreviation is AI. It is a new technology science that studies and develops theories, methods, techniques, and applied systems for simulating, extending, and expanding human intelligence [8]. Artificial intelligence is a branch of computer science. It tries to understand the nature of intelligence and produce a new kind of intelligent machine. It can respond in a manner similar to human intelligence. Research in this area includes robotics, language recognition, image recognition, natural language processing, and expert systems. From the perspective of research direction, the current research directions in the field of artificial intelligence also include machine learning, knowledge representation, automatic reasoning, computer vision, and robotics. At present, in addition to machine learning (deep learning), natural language processing and computer vision are also hot [9]. Since the birth of artificial intelligence, the theory and technology have become more and more mature, and its application fields have been expanding. It is conceivable that the technological products brought by artificial intelligence in the future will be the "containers" of human intelligence [10]. Artificial intelligence can simulate the information process of human consciousness and thinking [11]. AI is not human intelligence, but it can think like a human and possibly surpass it. The structural framework of one stage is shown in Figure 1.

COM is the abbreviation of Component Object Model. COM is a new software development technology developed by Microsoft for the software production of the computer industry that is more in line with human behavior. This subject uses VC++6.0 to design an artificial intelligence software. At the same time, in order to be compatible with the FaultDoctor2.0 software developed by China Aerospace Measurement and Control Company and avoid troublesome mutual switching, the artificial intelligence software is packaged into a module through COM component technology. It can use data obtained in other ways to diagnose artificial intelligence software or directly use the artificial intelligence module in FaultDoctor 2.0 to diagnose and collect data from the test platform. Both methods incorporate artificial intelligence technologies such as wavelet analysis, information fusion, data mining, and neural networks, and the principles are exactly the same [12]. The schematic diagram of the overall design is shown in Figure 2.

3.2. AI Introduction Algorithm. In nature, flocks of birds, fish, bees, ants, and other social creatures show amazing efficiency in their activities. Their collective intelligence is far greater than the sum of their individual intelligences.

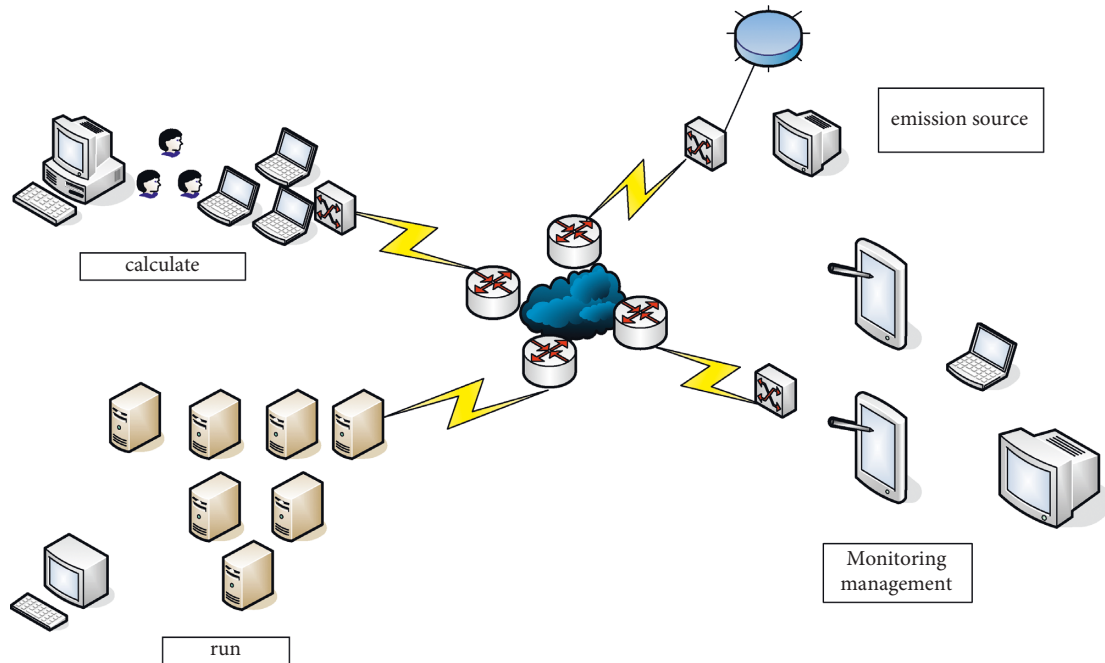


FIGURE 1: Artificial intelligence system framework diagram.

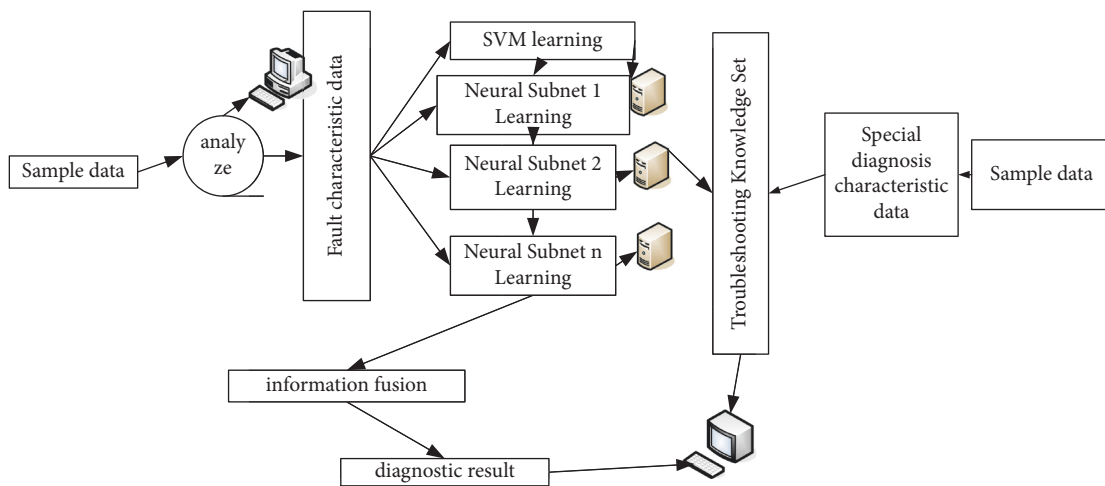


FIGURE 2: Schematic diagram of artificial intelligence software design.

Whether it is a fish, a bird, a bee, or an ant, the probability of wanting to survive alone is extremely low. Therefore, everyone needs to cooperate to complete the more complex work, so that the team can smoothly enter a good state of life.

Particle swarm optimization algorithm is an intelligent algorithm proposed by scientists in 1995 in the process of simulating the foraging process of bird groups, combining human cognition and other social behaviors [13]. Genetic algorithm is a method of searching for optimal solutions by simulating the natural evolution process. The algorithm uses computer simulation operation in a mathematical way. It converts the problem-solving process into a process similar to the crossover and mutation of chromosomal genes in biological evolution. At present, PSO has been used in many fields such as numerical function optimization, acoustic

wave information processing, and antenna array design because of its simple algorithm and easy implementation. However, with the further development of research, various improved algorithms emerge in an endless stream. The improved algorithm broadens the application field of particle swarm optimization. It still attracts the attention and research of a wide range of scholars.

Particle swarm optimization is a random search algorithm. During the search process, a random point in the multidimensional search space is treated as a particle without size and mass, which is also called an individual. In the movement, each individual is guided by the optimal position passed by itself and the optimal position passed by the entire population. But the perturbation scale is randomly assigned in both guiding directions. D represents the

dimension of the search space, and NW is the number of particles. Each particle individual is a D -dimensional vector a_i , and $i = 1, 2, 3, \dots, NP$. $a_i = (a_{i1}, a_{i2}, a_{i3}, \dots, a_{iN})$. The group updates the survey according to the following two formulas [14]:

$$\begin{cases} v_{ji}^{t+1} = v_{ji}^t + p_1 e_1 (w_{ji}^t - a_{ji}^t) + p_2 e_2 (w_{ci}^t - a_{ji}^t), \\ a_{ji}^{t+1} = a_{ji}^t + v_{ji}^{t+1}, \end{cases} \quad (1)$$

$i = 1, 2, 3, \dots, d, j = 1, 2, 3, \dots, nw, t = 1, 2, 3 \dots m$ represents the number of iterations, t is used to record the current generation, $t+1$ is used to record the next generation, $c_1 c_2$ is the acceleration constant, and $c_1 c_2 \in [0, 1]$. In order to prevent overflow, it needs to be bounded, as follows:

$$v_{ji} = \begin{cases} -v_{\max} & \text{if } v_{ji} \leq -v_{\max} \\ v_{\max} & \text{if } v_{ji} \geq v_{\max} \end{cases} \quad (2)$$

Binary encoding refers to the binary code language. It is a language that the computer can directly recognize without any translation. The instructions of each machine, its format, and the meaning represented by the code are rigidly stipulated. This paper studies the algorithm effect of using binary code in PSO and concludes that the particle swarm algorithm after binary code is much faster than genetic algorithm. It is particularly effective in higher-dimensional problems [15]. Velocity updates for elementary particle swarms are too dependent on previous velocities. This makes it easier for particles to fall into the constrained region of the local solution. In order to reduce the dependence on the previous speed, this paper adds an inertia weight factor w to the previous speed, that is, the speed update formula:

$$v_{ji}^{t+1} = w v_{ji}^t + p_1 e_1 (f_{ji}^t - a_{ji}^t) + p_2 e_2 (f_{gi}^t - a_{ji}^t). \quad (3)$$

The velocity update formula based on inertia factor is more in line with the physics inspired model of particle swarm. Through numerical experimental analysis, when $w < 1.2$, the algorithm has weak convergence but strong search performance. When $w < 0.8$, the algorithm has weak search performance but strong convergence. When $w \in (0.8, 1.2)$, the algorithm can achieve a good balance between searchability and convergence. In complex optimization problems, due to the influence of linear descending inertia weights, the global search ability decreases in the later stage of evolution. Such complex problems can be solved by adaptively changing the weight coefficients. It sets the w value to be an adaptive amount that decreases linearly with the evolutionary algebra and achieves good optimization results on four nonlinear functions. The method of shrinking factor is generally used in particle swarm optimization, not neural network. When V_{\max} is small (for Schaffer's f_6 function, $V_{\max} = 3$), it is better to use weight $w = 0.8$. If there is no V_{\max} information, using 0.8 as the weight is also a good choice. When the inertia weight w is small, the local search ability of the particle swarm algorithm is emphasized. When the inertia weight is large, it will focus on exerting the global search ability of the particle swarm algorithm. For complex problems, the method of shrinking factor is introduced in this paper. It ensures the convergence performance of particle swarm optimization by controlling the weight coefficient w and

the control parameter $12cc$ [16]. The update formula of its speed is as follows:

$$v_{ji}^{t+1} = \alpha (v_{ji}^t + p_1 e_1 (f_{ji}^t - a_{ji}^t) + p_2 e_2 (f_{gi}^t - a_{ji}^t)), \quad (4)$$

where α is the shrinkage factor, and the calculation formula is as follows:

$$\alpha = \frac{2\varphi}{|2 - \varepsilon - \sqrt{\chi^2 - 4\chi}|}, \chi = p_1 + p_2, \chi > 4, \varphi \in [0, 1]. \quad (5)$$

Scientists have proposed a new particle swarm algorithm. In order to maintain the diversity of the population, an "attraction" operator and a "repulsion" operator are introduced. The velocity update formula for the "repulsion" phase is as follows:

$$v_{ji}^{t+1} = w v_{ji}^t - p_1 e_1 (f_{ji}^t - a_{ji}^t) - p_2 e_2 (f_{ji}^t - a_{ji}^t). \quad (6)$$

By defining the calculation formula of population diversity, the upper and lower bounds of diversity are calculated, and the local optimization ability and global optimization ability of the algorithm are dynamically adjusted with different speed update formulas [17]. This paper proposes a new speed update formula between the "attraction" operation and the "repulsion" operation as:

$$v_{ji}^{t+1} = w v_{ji}^t + p_1 e_1 (f_{ji}^t - a_{ji}^t) - p_2 e_2 (f_{ji}^t - a_{ji}^t). \quad (7)$$

3.3. Introduction of Artificial Bee Colony Algorithm. Artificial bee colony algorithm (ABC) is another new swarm intelligence algorithm that can effectively solve numerical optimization problems. The excellent performance of artificial bee colony algorithm in high-dimensional numerical optimization problems and continuous problems has attracted much attention from scholars. For a long time, how to use artificial bee colony algorithm to solve discrete problems has become an upsurge in research. With its excellent character, artificial bee colony algorithm has achieved rich research results in the fields of integer programming, multi-objective optimization, neural network training, and so on. In major conferences and academic journals, the algorithm has been used to solve various complex optimization problems.

The artificial bee colony algorithm can be divided into four parts: initializing food source, leading bee mining, following bee mining, and scout bee replacing food source. The way to initialize the food source is as follows:

$$a_{ji} = (a_{ji})_{\min} + \text{rand}(0, 1) \left((a_{ji})_{\max} - (a_{ji})_{\min} \right), \quad (8)$$

where $j = 1, 2, 3 \dots$, $\text{rand}(0, 1)$ is a random number between (0, 1).

Leader bees and follower bees mine according to the following formula:

$$v_{ji} = a_{ji} + q_{ji} (a_{ji} - a_{ki}), \quad (9)$$

where v_{ji} is a new solution generated near a_{ji} . $k \in (1, 2, 3 \dots, NP)$, k, i are all randomly selected. k is a

solution of the neighborhood of i , that is, k cannot be equal to a random number of i . A random number of $q_{ji} \in [-1, 1]$ controls the range of neighborhood generation [18].

The follower bee chooses the food source according to the swing dance of the lead bee. For the optimal minimum problem, the fitness value is generated according to the following formula:

$$wjt_j = \begin{cases} \frac{1}{1+w_j}w_j \geq 0, \\ 1+|w_j|, \end{cases} \quad (10)$$

where w_j is the j th objective function value [19]. The probability of each individual is given by:

$$M_j = \frac{wjt_j}{\sum_{j=1}^{NM} wjt_j}. \quad (11)$$

This paper introduces the best method so far (thebest-so-farmethod). The best way is to introduce an improved version of the artificial bee colony algorithm, which is referred to as BSA. It finds that the best position so far in the method will yield the optimal solution. On this basis, this paper proposes to use this method to update the candidate solutions of the follower bees. This method can not only improve the local search ability of the algorithm but also make it search in the optimal direction and accelerate the convergence speed of the algorithm. The update formula of the solution is as follows:

$$d_{jv} = a_{ji} + \beta p_b (a_{ji} - a_{bi}), \quad (12)$$

where α is a random number on $[-1, 1]$, p_b is the fitness value of the best food source so far, and a_{bi} is the i -th dimension variable value of the best food source so far [20]. However, while speeding up the convergence speed, the algorithm tends to fall into local optimum. Therefore, this paper proposes a method of adaptively adjusting the search radius. It uses the following methods to update candidate solutions during the scout bee search phase:

$$d_{ji} = a_{ji} + \phi_{ji} \left[\varepsilon_{\max} - \frac{t}{W} (\varepsilon_{\max} - \varepsilon_{\min}) \right] a_{ji}, \quad (13)$$

where a_{ji} is the abandoned food source solution, ϕ_{ji} is a random number in $[-1, 1]$, W is the maximum number of iterations, and t is the current number of iterations. ε_{\max} , ε_{\min} represent the maximum and minimum proportions of the position adjustment of the scout bee, and its value is between 0.2–1.

This paper proposes that the initialization of the population has a great influence on the convergence speed of the algorithm and the quality of the final solution, and the random generation strategy is used in the basic algorithm. It has been known before that the initial conditions of the chaotic map have a nonnegligible effect on the chaotic sequence. Therefore, using the chaotic map to generate the initial population can increase the diversity of the population. The formula for improving the performance of the algorithm is as follows:

$$a_{ji} = (a_{ji})_{\min} + \gamma_{ji} \left((a_{ji})_{\max} - (a_{ji})_{\min} \right), \quad (14)$$

where γ_{ji} is a chaotic sequence. In order to further accelerate the convergence speed of the algorithm, it also introduces an antilearning strategy:

$$la_{ji} = (a_{ji})_{\min} + (a_{ji})_{\max} - a_{ji}. \quad (15)$$

Finally, an optimal individual is selected as the initial population.

The population initialization of BSA is the same as the differential evolution algorithm. However, the population initialization of BSA includes the initialization of the population P and the initialization of the historical population oldp, as shown in the following formula:

$$p_{ji} \approx E(\text{low}_i, \text{up}_i), \text{old } q \approx E(\text{low}_i, \text{up}_i), \quad (16)$$

where low_i , up_i denote the upper and lower bounds of the i -th dimension components, respectively, and E denotes the uniform distribution [21].

After the selection I , the individuals in oldq need to be randomly reordered and assigned to oldq. Then, it mutates:

$$\text{Mutant} = Q + F \cdot (\text{old}q - Q). \quad (17)$$

In $F = 3 \times \text{randn}$, randn is a random number that obeys the standard normal distribution. Through standardization, all random variables that obey the general normal distribution become standard normal distributions with a mean of 0 and a standard deviation of 1. For random variables that obey the standard normal distribution, it is specially denoted by z .

During the crossover operation, BSA randomly selects l elements from each individual in the parent population P . It swaps the same-dimensional elements of the collocated individual in the mutated Mutant to generate a new individual, and l is $(0, D)$ in an integer. The crossover lengths are selected as follows:

$$L(i) = [\text{BE} \cdot \text{rand} \cdot D]. \quad (18)$$

BE is the crossover probability and D is the problem dimension.

The two improvements will be described separately below. It also attaches the results of the test functions: Multimodal (M), Non-Separable (N), Unimodal (U), and Separable (S) in Table 1 to illustrate the effect of the improvement.

The BSA variation scale coefficient was set to F . Table 1 is a comparison of the convergence effect of $|F|$ and F on the 30-dimensional Ackley function. When improving the scaling factor, it makes the scaling factor a random number obeying the Maxwell–Boltzmann distribution. It describes the distribution of ideal gas molecular velocities at thermal equilibrium. Extensive numerical experiments have shown that the Maxwell–Boltzmann distribution can perturb the population efficiently, making the mutation process look better in the experimental population [22]. It illustrates that the new varying scale factor has better search performance. The new scaling factor is as follows:

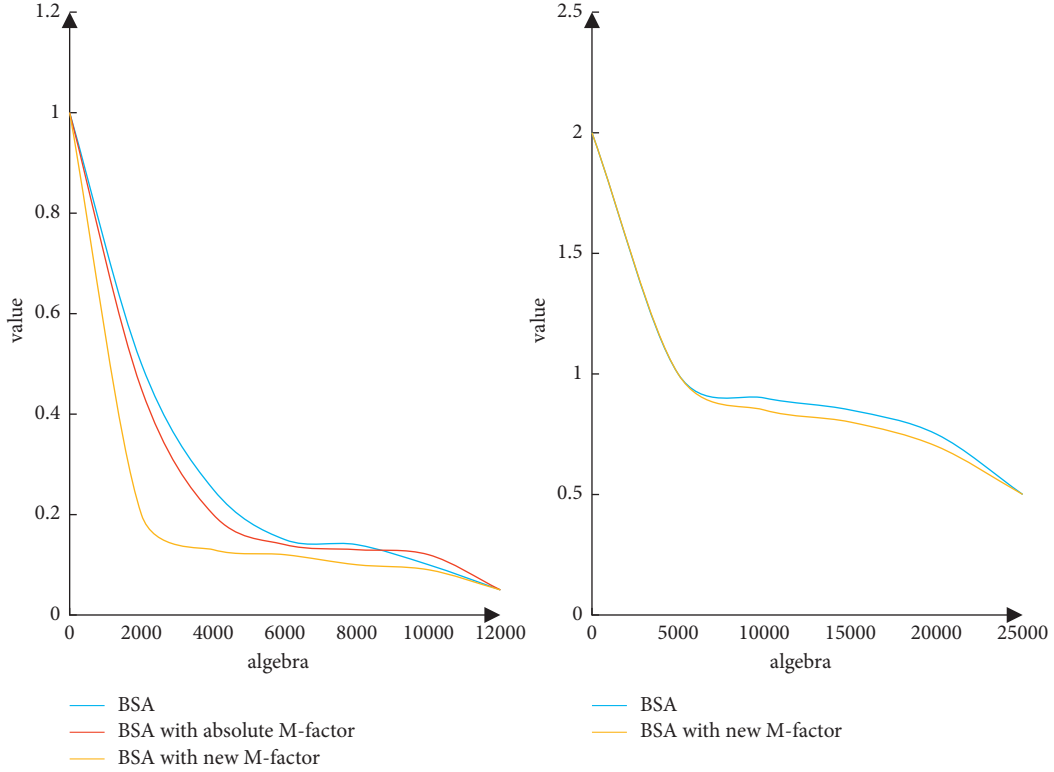


FIGURE 3: F1, F2 convergence curve plot.

TABLE 1: Function to test.

Question	Name	Type	Nether	Upper bound	Dimension	Evolutionary algebra
F1	Rosenbrock	UM	-30	30	50	20000
F2	Ackley	MN	-30	30	50	10000
F3	Griewank	MN	-600	600	50	5000
F4	Rastrigin	MS	-5.12	5.12	50	10000
F5	Foxholes	MS	-65.53	65.53	2	200

$$P = \sqrt{bh3}, bh3 - \varphi^2(3), \quad (19)$$

where $\varphi^2(3)$ is a Chi-square distribution with three degrees of freedom, and $bh3$ is a random number obeying $\varphi^2(3)$, Figure 3 is the normal distribution diagram of its convergence function.

From the convergence curve in Figure 3, it can be seen that the new variation scale coefficient has a fairly good convergence effect in the function test. It is worth noting, however, that the new distribution does not produce a negative scale of variation coefficient. Its magnitude is smaller. The searchability of the algorithm will be improved.

$$\text{newMutant} = q + (1 - e) \cdot F \cdot (\text{old}q - q) + e \cdot (cgq - q) = (1 - e) \cdot \text{Mutant} + cgq, \quad (20)$$

where e is a random number between $[0, 1]$. In order to ensure that the first q individuals can be selected uniformly, this paper designs the following selection strategy to generate cgq [23].

It sets $\text{ind}p$ as the sequence code set of the first p individuals in the whole population. It randomly sorts the elements in $\text{ind}p$ k times, and stores it after each sorting. It finally merges the k sorts into an array ind . The new mutation population function generation is shown in Figure 4:

$$cgQ = Q \text{ind} \left(\frac{1}{nq} \right), \quad (21)$$

In this experiment, eight high-dimensional unimodal functions and eight high-dimensional multimodal functions were selected. The eight limited-dimensional multimodal functions are shown in Table 2.

The comparison results of the convergence time and convergence results of the improved bee colony algorithm, the standard bee colony algorithm, and the backtracking search algorithm are shown in Table 3.

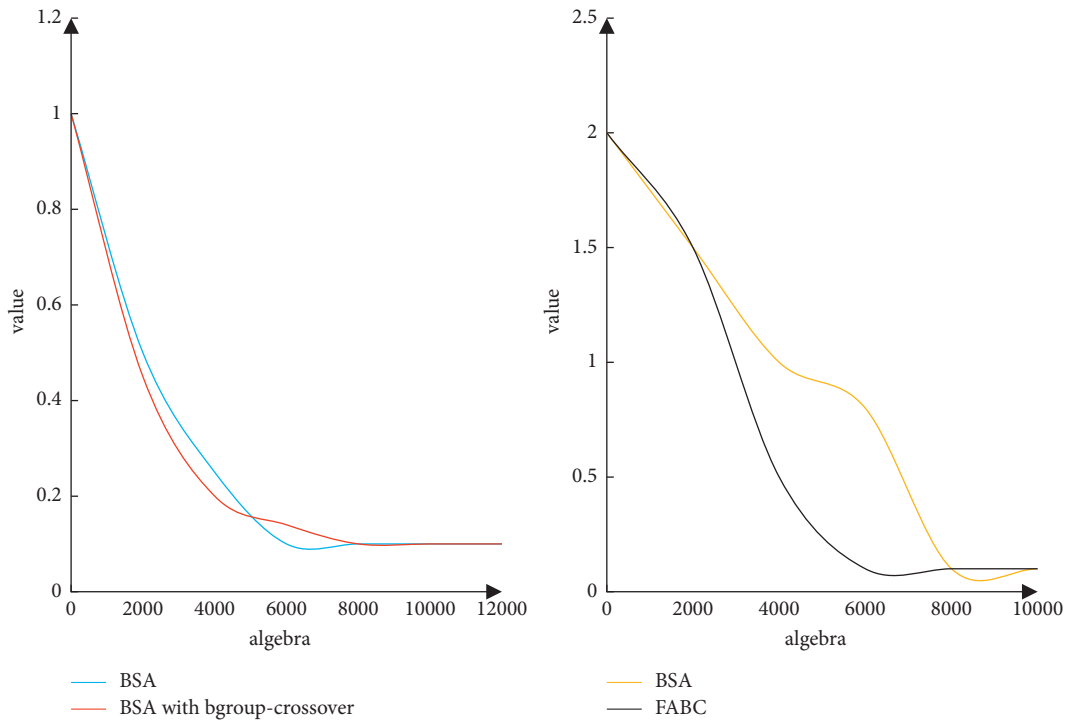


FIGURE 4: F2, F4 test function convergence rate ratio.

From the results of the eight test functions, it can be seen that the convergence effect of IABC is better than that of ABC and BSA. This indicates that the improved hiring stage based on multidimensional and one-dimensional hybrid search strategy can overcome the disadvantage of slow convergence of hiring bees in this one-dimensional search. It shortens the search time and effectively speeds up the convergence speed. Even when solving high-dimensional problems such as griewank, the search efficiency of IABC is much higher than that of ABC and BSA. This is partly due to a more developed search strategy at the hiring bee stage. On the other hand, it is able to follow the effective selection strategy of the bee stage. It fully guarantees the diversity of the population and makes the algorithm less likely to fall into local optimum when the convergence speed is accelerated. The new search strategy and selection strategy not only speed up the convergence speed but also ensure the high stability of the algorithm. Finally, for the accuracy of the experimental data, this paper adopts an improved version of the ABC algorithm for statistical analysis of the data to ensure that the error is reduced to the greatest extent. For the accuracy of the experimental data, we will test the accuracy of these algorithms. In this paper, an improved version of the ABC algorithm is used for statistical analysis of data to ensure that errors are minimized.

4. Data Analysis of Drug Production Quality Management

4.1. Experimental Case. Company A is committed to the research and development, production, and sales of heparin series products. Years of development have enabled the company to gradually achieve a leading position in the field

of domestic heparin APIs and heparin preparations. Not long after the new plant of company A was completed and put into operation, a major adjustment was made to personnel. It is in an initial run-in period in terms of personnel team building. Professional background, age, and work experience vary greatly. Most of the company's personnel have poor quality awareness. Even from the production, warehousing, quality management, and other departments that are closely related to the quality of drugs. In addition, there have been cases where personnel specialists did not wash their hands, did not change clothes, did not wear foot covers and headgear to directly enter the production area to check posts, and workers who borrowed things between different production workshops did not wear clean clothes and entered the clean area without wearing clean clothes, which caused quality risks. The flow of personnel during the break-in period also brings difficulties to the improvement of the quality management system. The company's quality management system is established in accordance with the requirements of international GMP on the basis of drawing lessons from advanced quality management experience at home and abroad. GMP is the abbreviation of good manufacturing practice in English. The World Health Organization defines GMP as regulations that guide the production and quality management of food, pharmaceuticals, and medical products. The file system in the system covers various contents such as verification, hygiene, materials, status identification, plant and facilities, organization, and personnel. There are more than 1,700 files in total, and it is difficult to upgrade the files because of the large number and wide-ranging content. There will also be omissions after the upgrade. The training of a new set of documents will have a

TABLE 2: Restricted dimensional multimodal function.

Question	Name	Type	Nether	Upper bound	Dimension	The optimal value
F2	Powell	UN	-4	4	24	0
F3	Sphere	US	-100	100	30	0
F4	Sum squares	US	-5	5	30	0
F5	Foxholes	UN	-600	600	10	0
F6	Zakharov	MN	-32	32	30	0
F7	Griewank	MN	-5.12	5.12	30	0
F8	Ackley	MS	-10	10	30	0

TABLE 3: Comparison of convergence time and convergence results between improved bee colony algorithm and standard bee colony algorithm.

Question	Evolutionary algebra	Statistics	ABC	BSA	FABC
F1	15000	Mean	0.1314	3.7432	0.4413
		Std	0.2078	12.3765	1.2125
		Best	0.5416	0.8510	0.1526
		Runtime	10.6170	5.9110	6.4740
F2	6000	Mean	2.4695	1.6644	0
		Std	1.3526	9.1161	0
		Best	0	0	0
		Runtime	3.8240	1.1830	1.9860

delay period of learning and assimilation, and then there will be deviations. The file system design is more decentralized. Although it is detailed, there will be repetitions. When training on these written contents, it does not classify people of different qualities well [24].

Figure 5 is the main quality management structure diagram of a pharmaceutical company. A company's quality management implements the general manager responsibility system, and its authorized responsible person is the quality director. It is specifically responsible for all quality management activities by the quality director. It is a separate establishment of the quality department. This is not included in the production department and other departments. The quality director is the deputy general manager of the company, who is in charge of the quality department, production department, laboratory, and other departments. It also incorporates the warehouse into the quality department, dispatches QA personnel to the warehouse to sample and release supplier materials, and supervises and guides warehouse administrators to store finished products. It generally implements the on-site "5S" management system of pharmaceutical production enterprises. The on-site "5S" management system of pharmaceutical production enterprises refers to sorting, rectifying, cleaning, cleaning, and literacy.

Now, the problem of the lack of management ability of some middle and senior leaders has also appeared. Although some of them have been working in the old factory for more than ten years, the accumulation in some aspects needs to be deeper. The quality department is an extremely important department for a manufacturing enterprise. They have the right to supervise and manage all activities and personnel related to product quality. This includes supervising SOP

implementation and supervising the filling of records during production, supplier auditing and management, personnel training, change management, deviation management, CAPA management, QC, warehouse, verification, and so on. But some jobs are really not doing well enough. There are no good managers above, and there are no ordinary employees with higher skill levels and strong consciousness below. As a result, various quality management tasks cannot be carried out smoothly. This will reduce the implementation of GMP and cannot realize the continuous guidance of GMP thought to the work. The problems are particularly prominent in the aspects of change management, deviation management, training management, and supplier management, which cannot keep the product quality at a high level.

In the end, although there are no serious quality and safety accidents that endanger people's lives for a variety of drugs of company A, there will be problems of one kind or another if the management is not standardized. Therefore, it cannot pass the US FDA certification and the European CEP/COS certification. A large part of heparin products is exported to obtain high sales volume. Then company A, which takes heparin as its main drug product, must have suffered huge profit losses. The export value of major heparin exporters is shown in Figure 6:

Hypuri went public in May 2010. The company's main product is heparin sodium API. It is currently the largest manufacturer of heparin APIs in China. The "Hepalink" brand has become an international model for the quality of heparin sodium APIs, which is also the company's core revenue source. In 2015, the company's sales of heparin sodium raw materials were 2.099 billion yuan, accounting for 91.6% of the total operating income in 2015. The sales in 2016 were 1.743 billion yuan, accounting for 77.1% of the operating income in 2016. The sales in 2019 were 4.743 billion yuan, accounting for 99.8% of the operating income in 2019. Jianyou company is the second largest exporter of heparin APIs in China. In recent years, the company's heparin API sales are about 400 million yuan [25]. Moreover, company A's heparin sodium drug varieties have not obtained the US FDA certificate and EU CEP certificate and are not allowed to enter the US market and the European market for sale.

The new version of GMP clarifies the requirements for change control in Articles 241 and 242: it first establishes operating procedures, stipulating the application, evaluation, review, approval, and implementation of changes in packaging materials, production processes, facilities, instruments, workshops, raw and auxiliary materials,

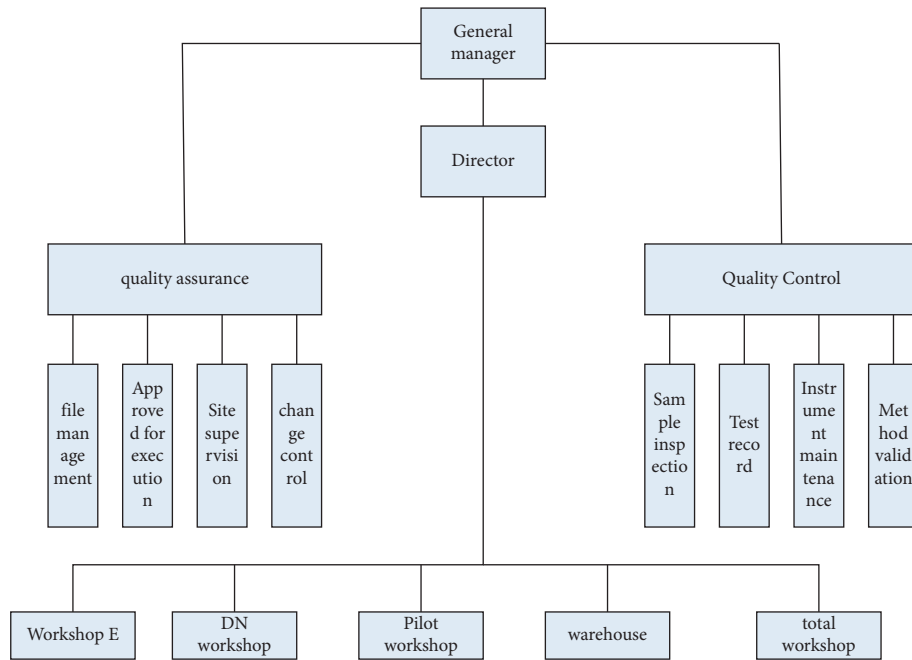


FIGURE 5: A main quality management structure diagram of pharmaceutical company.

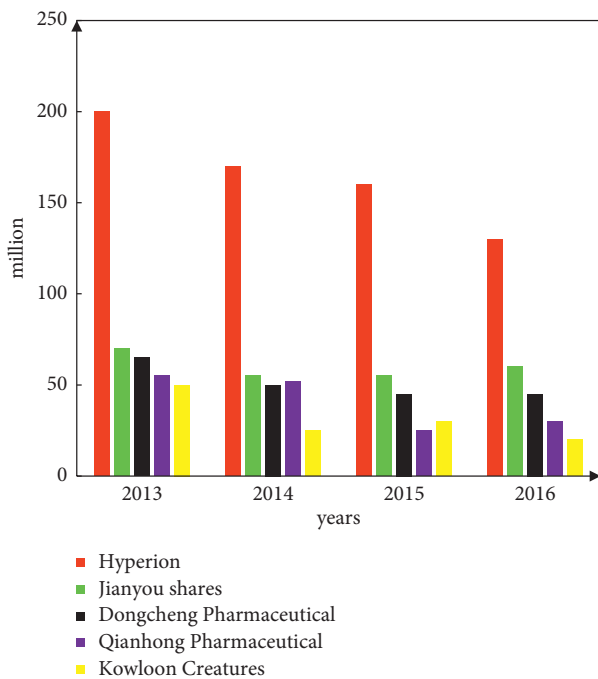


FIGURE 6: The main export value of heparin in 2013–2016.

equipment, quality standards, and inspection methods. It is also designated by the quality department to be responsible for the control of changes. Enterprises should evaluate the potential impact of changes on product quality. It is mainly evaluated according to the scope and nature of the change. It categorizes changes according to the severity of the impact (type I changes, type II changes, and type III changes). Change can be said to be regarded as the main quality management system indicator in pharmaceutical

manufacturing enterprises. The following article makes a horizontal comparison between the number of changes generated by company A from January to December 2015 and the number of changes generated by the other two companies during the same period to better illustrate the situation of company A. It is shown in Figure 7:

Through the comparative analysis of the above charts, it is known that the number of changes of company A in the statistical period has an upward trend. In one year, 98 changes were made, which has exceeded 75 control indicators of the whole plant. Comparing company B with company A, the number of companies in the same period is less than that of company A, which is at a more reasonable level. This shows that company A’s limited change management resources are difficult to effectively manage redundant changes. It believes that there are two problems in the change management of company A at this stage.

- (1) When a new change is proposed, such as the purchase of new production equipment, according to the requirements of GMP, it is necessary to evaluate the impact of the new equipment on the existing equipment and even the system. It requires detailed management procedures as a guide. However, the actual process and method have not been established, and the department that initiated the change does not know how to implement the change. They do not submit normative materials but simply explain the changes on the application form, which will be signed and reviewed by the person in charge of quality, and then easily approved. The whole process is overly reliant on the quality director. Change managers struggle to track the progress of change implementation. This results in the fact that the

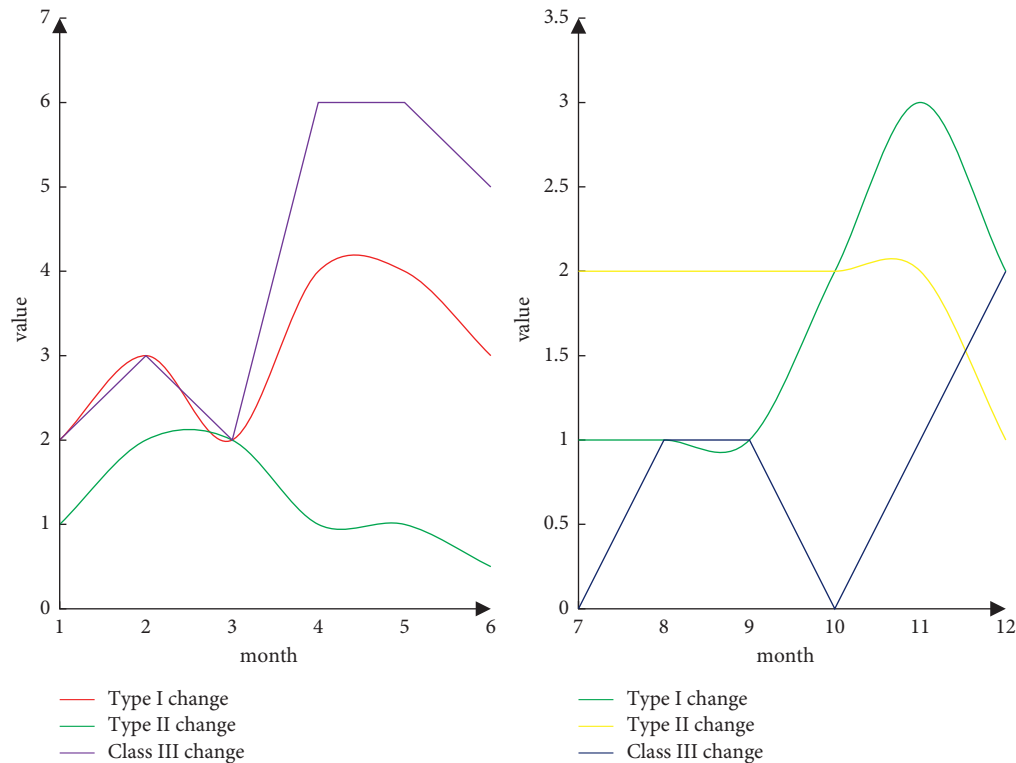


FIGURE 7: The number of changes at all levels of the two companies from June to December 2015.

grasped situation is inconsistent with the actual situation, and there is a certain lag.

- (2) There is no scientific demonstration on what issues should be done when and to what extent. For example, it wants to improve the detection efficiency, save unnecessary work, and reduce the number of detections for intermediates. According to the testing situation in the first half year and the current production arrangement, it is stipulated that every five batches is a sampling testing cycle. For other batches of intermediates, the detection of the content item is omitted. For the five batches in the process of change, without the support of scientific argumentation reports, it is impossible to judge whether the detection frequency is reasonable [26].

4.2. Data Mining

4.2.1. Cluster Analysis Applied to Quality Assurance. Pharmaceutical manufacturers have higher requirements for data. This is directly related to the quality of drug production and more indirectly affects the safety of people's lives. As a means of data mining, cluster analysis plays a vital role in pharmaceutical companies. Cluster analysis is the main task of exploratory data mining and a common technique for statistical data analysis. It is used in many fields including machine learning, pattern recognition, image analysis, information retrieval, bioinformatics, data compression, and computer graphics. Big data in all walks of life or any value discovery at the macro or micro level is the result of cluster analysis with the help of big data.

The experimental data from the laboratory statistics and the production data submitted by the workshop are submitted to the Quality Assurance Department. Quality assurance personnel should analyze these data and provide cluster analysis for linearly coherent data. They look for the invisible correlation between the data and use cluster analysis to classify the experimental data and production, so as to meet the needs of data sorting and risk analysis.

It uses cluster analysis to classify and divide experimental data. In this way, the dense and sparse regions of these experimental data can be identified, and the global distribution pattern of the experimental data can be found. The global distribution pattern of experimental data can provide the analyst with the necessary knowledge. In order to control the measurement error in production and test, it is often used to formulate upper and lower warning values and upper and lower control values according to the density of data distribution.

Taking an infusion enterprise as a simple example, the following figure is a regular chart of pH value and content when deviation occurs, as shown in Figure 8. From the figure, it can be clearly seen that when a certain risk deviation occurs, the data of pH value and content in the laboratory change. Using cluster analysis, this paper can cluster and distinguish the risk deviation data. It finds its central aggregation point and displays the pH value and content of the center. These precious data are directly related to the production situation and the quality of purchased raw and auxiliary materials, so it can be judged that the production situation and the quality of raw and auxiliary materials in this year are stable. It provides important information for

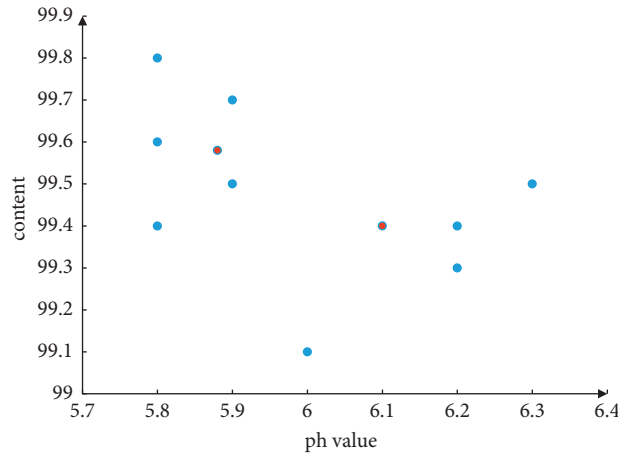


FIGURE 8: Risk deviation PH value content relationship diagram.

redistributing liquid medicine to control its pH value and content.

4.2.2. *Data Selection.* The 188 sets of experimental data are divided according to the gradient. The principle of division is to start from the minimum value, and each 0.1 gradient is set as an interval, so there are 14 intervals from the minimum value of 99.5 to the maximum value of 100.9. It counts how many groups of content experimental data there are in each interval and calculates the percentage of the content data in this interval to the total data, as shown in Table 4.

4.2.3. *Data Analysis.* The statistical pie chart of the annual production situation can give decision makers the most intuitive impression. This plays a vital role for decision makers to grasp the production progress of the production workshop. Decision makers can effectively formulate work priorities and plans for the next year based on the support of production statistics provided by quality assurance personnel. It ensures that the products produced by pharmaceutical companies can meet market needs. It does not have a large backlog of inventory products nor does it make the market in short supply.

First, it analyzes the direct impact of time factors on production. By analyzing the annual production statistics linear statistics in Figure 9, it can be seen that for pharmaceutical manufacturers, the difference in temperature and humidity is an important factor in determining production, and the human body is also obvious for seasonal changes. It will have different seasonal diseases, so the market demand for different products is not the same. Only by grasping the correct production situation, can the production plan for the next year be effectively adjusted.

According to the analysis, the whole infusion workshop produces large quantities of saline 10 and 50 sugar 20. This means that the market popularity of these two products is high. The production of brine 10 is mainly concentrated in April, May, June, and July, while the production of sugar 50 and 20 is mainly concentrated in February, August, and December. The reason for the analysis is that this

TABLE 4: Content data distribution chart.

	Statistical interval	Interval	Percentage (%)
99.5	99.4-99.5	7	2.83
99.6	99.5-99.6	3	1.21
99.7	99.6-99.7	14	5.67
99.8	99.7-99.8	16	6.48
99.9	99.8-99.9	34	13.77
100.0	99.9-100.0	38	15.38

phenomenon occurs due to seasonal reasons. Therefore, decision makers can be advised to adjust the production plan for the increase or decrease of usage caused by seasonal changes.

The occurrence of deviation is directly related to the time factor. Different seasons cause different seasons, and different time periods are not the same for production adjustment. For example, the difference of temperature and humidity affects the spot inspection of production equipment, and the reproduction of insects in different seasons affects the frequency of insect and rodent control work. The quality assurance personnel should analyze the internal relationship between the time factor and the occurrence of deviation.

Analysis of the figure shows that there are many deviations caused by filling equipment each year. Therefore, it is recommended to carry out a comprehensive repair and maintenance of the filling equipment in the next year, thereby reducing the risk of deviation caused by the filling equipment.

At the same time, there were frequent deviations due to personnel errors at the end of the year. The reason for the analysis is due to excessive relaxation of personnel at the end of the year. Therefore, the training and supervision of personnel during this period should be strengthened to minimize or even avoid personnel errors.

According to the analysis, environmental deviation mainly occurred in spring and autumn. Spring is the breeding season for insect recovery, and autumn is also the reserve time for insects to lay eggs and prepare for winter. In these two seasons, the frequency of insect and rodent control

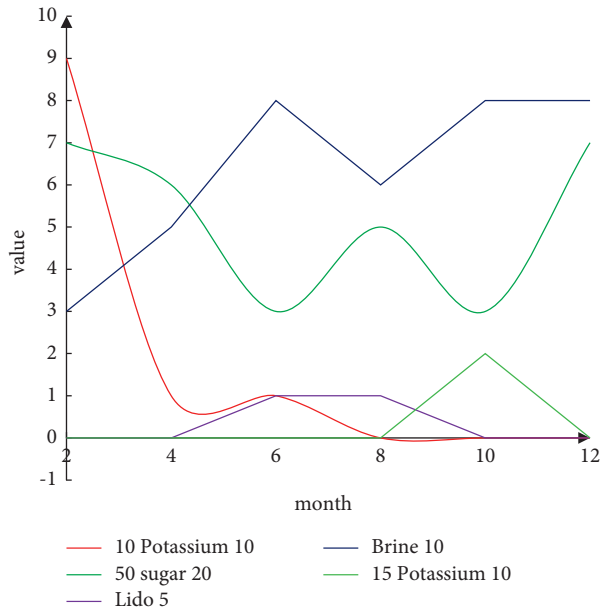


FIGURE 9: Annual production statistics line graph.

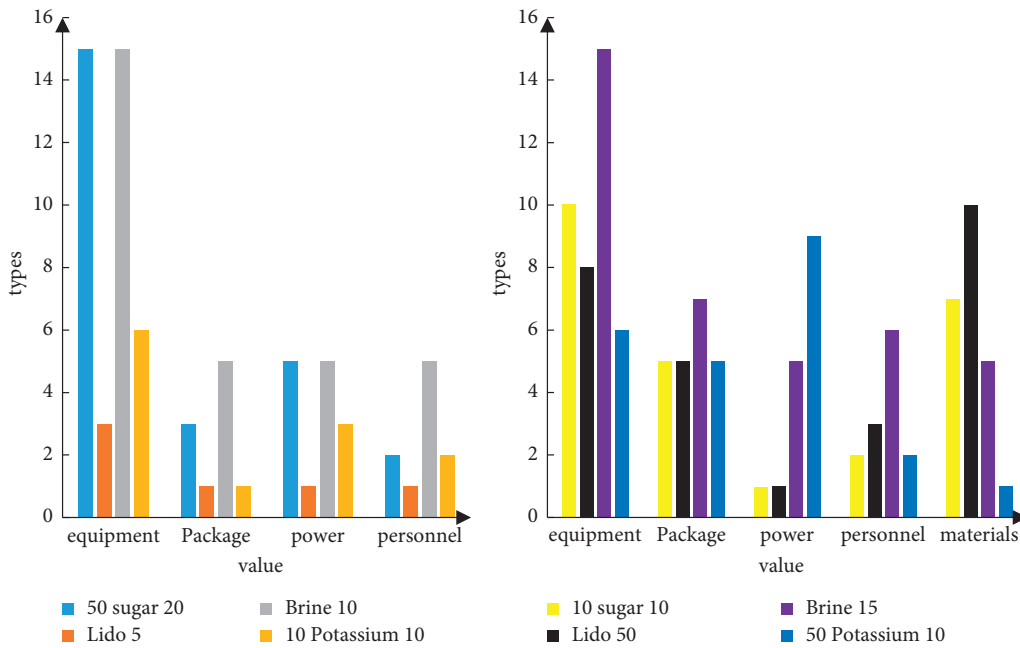


FIGURE 10: Histogram of deviation type and product relationship.

should be strengthened. The hidden danger points that can breed insects in the workshop should be dealt with in time to prevent them from polluting the production products and affecting the product quality.

The histogram of the relationship between deviation types and products is shown in Figure 10.

From the above two histograms, it is not difficult to find that due to the large number of production batches, the deviation of 50 sugar 20 is more frequent than that of brine 10. The reason for this phenomenon is that the viscosity of the 50 sugar 20 product is high, which is a burden to the machine and the production environment. Moreover, the

market demand for this kind of medicine is large, and the production pressure is also large, resulting in the concentrated appearance of deviations. In response to this phenomenon, the management of equipment and environment should be strengthened when producing 50 sugar 20, and a better method to deal with products with higher viscosity should be sought [27].

5. Discussion

The construction and improvement of drug quality management system is a long-term, comprehensive, and systematic project. The unsound and imperfect quality management greatly restricts the development of the enterprise. This paper makes a more detailed summary and analysis of some problems revealed after the comprehensive implementation of the GMP management system by a pharmaceutical company. It drives the change of employees' concept and consciousness, clarifies the object of quality improvement, puts forward specific improvement measures, and completes the improvement plan design. The purpose is to form a practical and effective work system, which is guaranteed to be implemented smoothly, so that the company's current quality management system can be optimized.

6. Conclusions

The improvement of the quality management system is based on the premise that the quality management problems are solved. In the process of checking omissions, filling vacancies, finding problems, and solving them, the research conclusions of this paper are drawn step by step:

- (1) There are commonalities among different quality management concepts
- (2) It is necessary to effectively reduce the deviation problem and deal with the change problem
- (3) It is necessary to efficiently complete production management and quality management work based on internal audit

Of course, the implementation of GMP in pharmaceutical production enterprises is only a basic level of work. Quality management in pharmaceutical production is a complex process. It needs to use the relevant information of the system, product, and process to overcome the weak links of the quality management system; to ensure its continuous improvement; and to obtain the stability and improvement of drug quality. It conducts reasonable analysis on data of different attributes and promotes the utilization of data by enterprises, so as to obtain more knowledge. The author also hopes that the experiment will make the display of the analysis results more perfect and strengthen the visualization effect processing. This enables analysts to get a neat report the first time, rather than a simple postanalysis graph.

Data Availability

No data were used to support this study.

Conflicts of Interest

The author declares that there are no conflicts of interest regarding the publication of this article.

Acknowledgments

This work was supported by 2020 Zhejiang philosophy and social science planning project (20NDJC221YB): Research on Collaborative Governance Path of High-quality Development of Drugs in Zhejiang Province under Big Data Strategy.

References

- [1] A. I. Selezneva, V. A. Smirnov, V. V. Goryachkin et al., "The integrated model of quality management system of laboratory studies of medicines (review)," *Drug Development & Registration*, vol. 10, no. 3, pp. 148–165, 2021.
- [2] A. B. Kashirina, Z. I. Aladys He Va, N. V. Pyatigorskaya, V. V. Belyaev, and V. V. Beregovykh, "Analysis of industrial practice of drug quality risk management in Russian pharmaceutical enterprises," *Pharmacy & Pharmacology*, vol. 8, no. 5, pp. 362–376, 2021.
- [3] L. Wulandari, I. Indasah, and B. M. Suhita, "Analysis of drug logistics management in the pharmacy installation of klaten district health office," *Journal for Quality in Public Health*, vol. 3, no. 2, pp. 334–340, 2020.
- [4] J. Jia and H. Zhao, "Mitigating the U.S. Drug shortages through pareto-improving contracts," *Production and Operations Management*, vol. 26, no. 8, pp. 1463–1480, 2017.
- [5] M. A. Syed, A. S. Al Nuaimi, H. A. A/Qotba, A. A. Zainel, T. Marji, and U. Razaq, "Diabetes, hypertension and dyslipidemia medication prescribing in Qatari primary care settings: a retrospective analysis of electronic medical records," *Journal of Pharmaceutical Policy and Practice*, vol. 14, no. 1, pp. 67–7, 2021.
- [6] E. Ueyama, M. Kaneko, and M. Narukawa, "Analysis of pediatric drug approval lag in Japan," *Therapeutic Innovation & Regulatory Science*, vol. 55, no. 2, pp. 336–345, 2020.
- [7] X. Jin and Y. Wu, "Study on main drugs and drug combinations of patient-controlled analgesia based on text mining," *Pain Research and Management*, vol. 2020, no. 5, pp. 1–7, 2020.
- [8] L. Qiao, Y. Li, D. Chen, S. Serikawa, M. Guizani, and Z. Lv, "A survey on 5G/6G, AI, and Robotics," *Computers & Electrical Engineering*, vol. 95, no. 2021, p. 107372, 2021.
- [9] J. Cao, E. M. van Veen, N. Peek, A. G. Renehan, and S. Ananiadou, "EPICURE: ensemble pretrained models for extracting cancer mutations from literature," in *Proceedings of the 2021 IEEE 34th International Symposium on Computer-Based Medical Systems (CBMS)*, pp. 461–467, IEEE, Aveiro, Portugal, June 7 2021 to June 9 2021.
- [10] F. S. Si and S. M. Berliandaldo, "Mapping of management strategic in improving herbal medicine industry competitiveness," *International Journal of Business Management & Research*, vol. 9, no. 1, pp. 31–37, 2019.
- [11] N. Man, K. Wang, and L. Liu, "Using computer cognitive atlas to improve students' divergent thinking ability," *Journal of Organizational and End User Computing*, vol. 33, no. 6, pp. 1–16, 2021.
- [12] H. Beaujon, "Clichy, FranceQuality and Risk Management Direction, Hôpital Bichat, Paris, France. Risk management in an anticancer drug preparation unit: use of Preliminary Risk

- Analysis method and application to the preparation process,” *Pharmaceutical Technology in Hospital Pharmacy*, vol. 6, no. 1, pp. 901–910, 2021.
- [13] B. Xu, X. Y. Shi, Z. S. Wu, Y. L. Zhang, Y. Wang, and Y. J. Qiao, “Quality by design approaches for pharmaceutical development and manufacturing of Chinese medicine,” *Zhongguo Zhong yao za zhi = Zhongguo zhongyao zazhi = China journal of Chinese materia medica*, vol. 42, no. 6, pp. 1015–1024, 2017.
- [14] I. E. Smekhova, L. V. Shigarova, I. A. Narkevich, E. V. Flisyuk, and V. D. Meteleva, “Documentation of pharmaceutical development. Part 2. Quality system documents,” *Drug Development & Registration*, vol. 10, no. 2, pp. 147–153, 2021.
- [15] D. T. Tran, I. Akpınar, and P. Jacobs, “The costs of industry-sponsored drug trials in Canada,” *PharmacoEconomics - Open*, vol. 4, no. 2, pp. 353–359, 2019.
- [16] R. S. Rana, P. Singh, V. Kandari, R. Singh, R. Dobhal, and S. Gupta, “A review on characterization and bioremediation of pharmaceutical industries’ wastewater: an Indian perspective,” *Applied Water Science*, vol. 7, no. 1, pp. 1–12, 2017.
- [17] M. Schmitt-Egenolf, J. Freilich, N. M. Stelmaszuk-Zadykiewicz, E. Apol, J. B. Hansen, and L. A. Levin, “Drug persistence of biologic treatments in psoriasis: a Swedish national population study,” *Dermatologic Therapy*, vol. 11, no. 6, pp. 2107–2121, 2021.
- [18] J. Ronowicz and N. Piekus-Słomka, “Non-invasive instrumental analytical methods in modern pharmaceutical technology,” *Farmacja Polska*, vol. 76, no. 3, pp. 163–169, 2020.
- [19] C. L. Stokes and J. Schjøtt, “Disproportionality analysis for identification of drug safety signals in a database shared by the Norwegian network of drug information centres (RELIS),” *European Journal of Clinical Pharmacology*, vol. 75, no. 10, pp. 1469–1470, 2019.
- [20] S. J. Semple, J. K. Stockman, D. Goodman-Meza et al., “Correlates of sexual violence among men who have sex with men in tijuana, Mexico,” *Archives of Sexual Behavior*, vol. 46, no. 4, pp. 1011–1023, 2017.
- [21] N. Sabev and D. Trancheva, “Organizational and economic aspects of clinical and laboratory activities - possibilities and perspectives of optimization,” *Knowledge International Journal*, vol. 26, no. 6, pp. 1721–1726, 2019.
- [22] J. Y. Lee, A. S. Y. Ang, N. Mohd Ali, L. M. Ang, and A. Omar, “Incidence of adverse reaction of drugs used in COVID-19 management: a retrospective, observational study,” *Journal of Pharmaceutical Policy and Practice*, vol. 14, no. 1, pp. 84–89, 2021.
- [23] J. Ma and A. Motsinger-Reif, “Prediction of synergistic drug combinations using PCA-initialized deep learning,” *BioData Mining*, vol. 14, no. 1, pp. 46–15, 2021.
- [24] H. K. Bai, J. D. Ahearn, and M. G. Bartlett, “Over-the-Counter drugs: regulatory analysis of warning letters between fiscal years 2015–2019,” *Therapeutic Innovation & Regulatory Science*, vol. 55, no. 2, pp. 426–436, 2020.
- [25] M. E. Eissa, “Drug recall monitoring and trend analysis: a multidimensional study,” *Global Journal on Quality and Safety in Healthcare*, vol. 2, no. 2, pp. 34–39, 2019.
- [26] D. T. Michaeli, S. Stoycheva, S. M. Marcus, W. Zhang, J. C. Michaeli, and T. Michaeli, “Cost-effectiveness of bivalent, quadrivalent, and nonavalent HPV vaccination in South Africa,” *Clinical Drug Investigation*, vol. 42, no. 4, pp. 333–343, 2022.
- [27] J. H. R. Wijegunasekara, “Drug supply management in health care institutions in Sri Lanka: a case study,” *Journal of Drug Delivery and Therapeutics*, vol. 11, no. 1, pp. 3–7, 2021.

Research Article

Research on Optimization of Structural Parameters of Equipment Cabin Bottom Cover

Hua Zou ¹, Qifeng Wu,¹ and Yonggui Zhang²

¹School of Mechanical, Electric and Control Engineering, Beijing Jiaotong University, Beijing 100044, China

²CRRC Qingdao Sifang Co., Ltd., Qingdao 266111, China

Correspondence should be addressed to Hua Zou; hzoubjtu@126.com

Received 23 June 2022; Revised 22 July 2022; Accepted 1 August 2022; Published 22 August 2022

Academic Editor: Wei Liu

Copyright © 2022 Hua Zou et al. This is an open access article distributed under the Creative Commons Attribution License, which permits unrestricted use, distribution, and reproduction in any medium, provided the original work is properly cited.

Since the railway vehicle structure has lots of parameters and several complex constraints, this study establishes a method for structural parameter optimization based on sensitivity analysis and surrogate models. Fatigue crack problem of the equipment cabin bottom cover of the EMU is taken as an example to optimize its structural parameters. First, establish the finite element (FE) model of the bottom cover and compare it with the bench test results to verify the accuracy of the load and restraint conditions. The sensitivity analysis method is used to determine the main parameters. The input samples are obtained by Latin hypercube sampling method, and the output samples are obtained by the method jointly developed by ABAQUS+Python and the surrogate model between the input and output samples is obtained by fitting, and its accuracy is verified. According to the design requirements, the optimization objective function and constraint conditions are established, and the optimization result is obtained by optimization algorithm. The results were substituted into the FE model for verification. The results show that the maximum equivalent stress of the bottom cover is reduced from 126.7 MPa to 78.9 MPa under a cyclic aerodynamic load of ± 4 kPa, which is 37.7% optimized, and the effect is significant. This method avoids the iterative optimization of the FE model and improves the optimization efficiency.

1. Introduction

In the application of large mechanical structural parts, fatigue cracks have always been the main factor leading to their failure [1–3]. Take railway vehicles as an example; fatigue cracks are found on the equipment cabin bottom cover. The reason is that the alternating aerodynamic load under the working conditions when trains enter and exit tunnels is the main factor leading to the initiation and propagation of cracks [4]. Therefore, it is necessary to study the structural optimization design method to reduce the stress level at the crack under alternating aerodynamic loads.

Nowadays, there has been in-depth research on the optimization method of structural parts [5]. The authors in [6–11] separately optimized the structure of energy-absorbing structure, carbody structure, and the subway vehicle air-conditioning suspension. Their weights were reduced while meeting the requirements of strength and modal. But

for the bottom cover, its protection function and manufacturability need to be considered, so the topology optimization results often do not have engineering application value. The authors in [12, 13] optimized the shape of the frame and wheel. But the shape optimization required modification of the floor structure. At the same time, it was also necessary to consider constraints such as installation, connection, and manufacturability, so the space for modification was limited. The size optimization does not require major changes to the floor structure, which is relatively easy to implement and has high engineering value. Therefore, this article uses the size optimization method to optimize the bottom cover.

Now scholars have begun to use a variety of methods to optimize the parameters of the structure [14–16]. Among them, approximate methods have been widely used [17]. For the railway vehicle structure, the structure is complex and the boundary conditions are numerous, which often requires a lot

of time in the simulation calculation. In order to improve the optimization efficiency, many scholars have conducted research on the optimization method of size parameters. Myzrglob and Zielinski [18, 19] studied the optimization method of structural parameters under multi-axial high-cycle fatigue. Sun et al. and Hudson et al. [20, 21] studied the optimization method of carbody parameters considering multiple factors. Sun et al. [22] optimized the modal frequency of the railway vehicle carbody based on SA. Miao et al. [23] used the ant colony algorithm to optimize the composite sandwich structure of the bottom cover. Zhi et al. [24] studied the fuzzy optimization method of bogie frame parameters based on response surface model. Baek et al. [25] optimized the wagon frame structure based on the Chebyshev polynomial model. The authors in [26–28] used surrogate models and multi-objective genetic algorithms to optimize the design of the carbody collision energy absorption structure. The authors in [29–31] optimized the fatigue strength of the welded frame weld by the surrogate model method.

The above research used mathematical models to express the relationship between structural parameters of vehicle components such as carbody, bogie frame, and energy-absorbing structure with modal and strength indicators and optimized them with optimization algorithms to improve optimization efficiency. However, the optimization research on the equipment cabin bottom cover is still lacking at the present stage, and the connection and contact between the various components cannot be ignored for this type of assembly. There are many size parameters and installation parameters of components, and each parameter has a complex nonlinear relationship with the stress response of key points. Establishing a FE model that can reflect the actual components and meet the requirements of optimization accuracy is a prerequisite for optimization design. For this reason, this paper carried out the static strength test of the bottom cover and compared the FE calculation results with the test results to verify the accuracy of the FE model. Considering the complex preprocessing of the FE model and the long calculation time, this paper first extracts the key parameters of the bottom plate according to the sensitivity analysis (SA) method and uses the optimal Latin hypercube sampling to obtain the input sample set of the key parameters. Through the ABAQUS + Python co-simulation method, the FE model under different input parameters is obtained in batches, and the output parameter samples are obtained. Then, the surrogate model is fitted to replace the FE model, and optimization is performed based on the optimization algorithm. This method can effectively improve optimization efficiency.

2. Structural Parameter Optimization Design Method

2.1. Parameter Optimization Process Based on FE Model.

In the FE model, due to the model scale, contact nonlinearity, material nonlinearity, and other issues, it often takes a long time to simulate. At the same time, optimization research needs to modify the parameters multiple times for iterative calculations, so there are many repeated calculations. If the FE model is directly called, it will consume a lot

of time and be inefficient. Therefore, in order to improve the optimization efficiency under the premise of ensuring accuracy, the optimization method shown in Figure 1 can be used for the complicated FE model.

According to Figure 1, firstly, the SA method is used to screen the optimized parameters, and then the optimal Latin hypercube sampling or orthogonal test is used to sample in the range to obtain a uniform and representative parameter sample set. Use the Python program to read the samples in order, modify the parameters of the FE model in ABAQUS, submit calculations, and read the stresses at the key points. Summarize the stress values under different samples and use them as input and output parameters. Use the above input and output parameters as samples and import them into the Isight software to fit the surrogate model and evaluate the goodness of fit. Based on the surrogate model, optimization algorithms such as steepest descent method and genetic algorithm are used for optimization. Then, the optimal solution of the model is obtained and imported into ABAQUS for verification.

2.2. Parameter SA Method. When there are many optimization parameters, the amount of calculation in sampling calculation and optimization calculation is large. The parameter SA method can eliminate the parameters that have little influence on the result. Assuming that there are n parameters, there is the following functional relationship between the i -th parameter p_i and the response r :

$$r = r(p_1, p_2, p_3, \dots, p_n). \quad (1)$$

The sensitivity ε_i of different parameters can be expressed by the following formula:

$$\varepsilon_i = \frac{\partial r(p_1, p_2, p_3, \dots, p_n)}{\partial p_i}, \quad (2)$$

$$i = 1, 2, 3, \dots, n.$$

It is often a discrete variable in engineering applications. Its sensitivity ε_i can be expressed by the finite difference method:

$$\varepsilon_i = \frac{r(p_i + \Delta p_i) - r(p_i)}{\Delta p_i}, \quad (3)$$

$$i = 1, 2, 3, \dots, n.$$

However, when calculating the sensitivity through the above formula, the influence of the parameter scale and the variation range is ignored. When the parameter scale is large, the calculated sensitivity is often small. Therefore, the original parameter value p_{i0} and the original response value r_0 are used as scale factors, and the sensitivity parameters are normalized:

$$\varepsilon_i = \frac{[r(p_i + \Delta p_i) - r(p_i)]/r_0}{\Delta p_i/p_{i0}}, \quad (4)$$

$$i = 1, 2, 3, \dots, n.$$

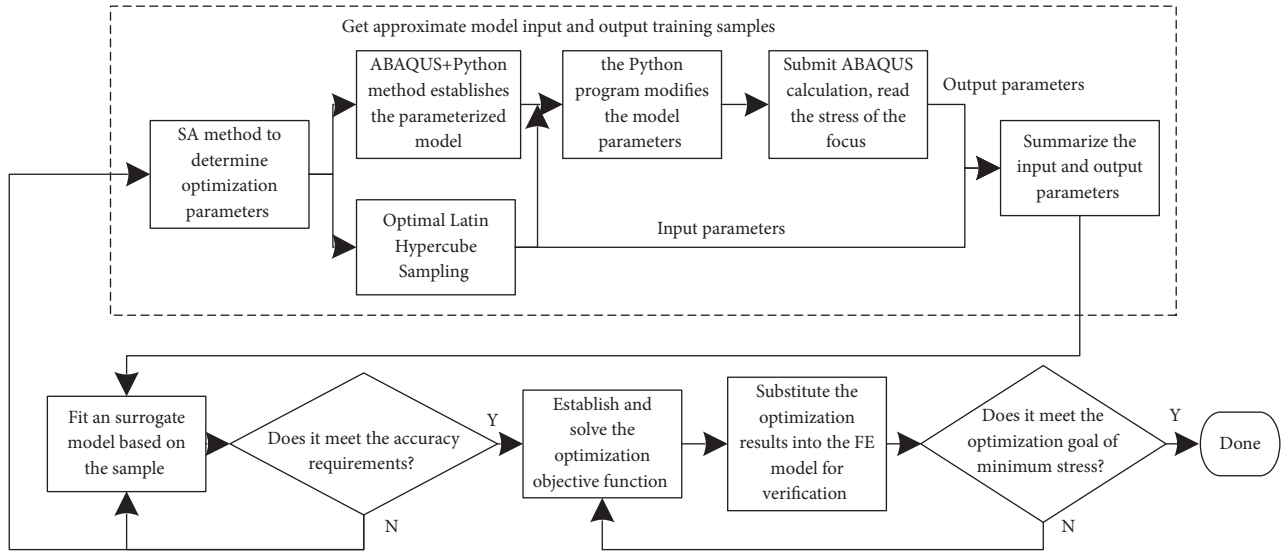


FIGURE 1: Bottom cover optimization method.

In order to improve the accuracy of the sensitivity parameter, take m different difference step size Δp_{ij} ($j = 1, 2, 3, \dots, m$, including the original value, $\Delta p_{i1} = 0$) within the parameter change range. The least square method is used to fit it into a proportional function relationship of $r_i = k_i p_i$, and the absolute value of the slope k_i is taken as the sensitivity parameter:

$$\varepsilon_i = |k_i| = \left| \frac{\sum_{j=1}^m R_{ij} P_{ij}}{\sum_{j=1}^m R_{ij}^2} \right|, \quad (5)$$

$$i = 1, 2, 3, \dots, n,$$

$$j = 1, 2, 3, \dots, m,$$

where

$$R_{ij} = \frac{[r(p_i + \Delta p_{ij}) - r(p_i)]}{r_0}, \quad (6)$$

$$P_{ij} = \frac{\Delta p_{ij}}{p_{i0}}.$$

2.3. Sample Acquisition Method Based on FE Model. According to the optimized parameters and their ranges, a set of representative input parameters needs to be extracted. The optimal Latin hypercube sampling method has strong filling ability, uniform sample distribution, and good representativeness. Assuming that a total of m samples are required, m small hypercubes are randomly selected in the n -dimensional hypercube space composed of n design variables to ensure that each small hypercube is unique in each design variable interval. That is, each design variable will be sampled only once at each level. In this way, a Latin hypercube design matrix with m samples under n design variables is obtained. At the same time, through the optimization algorithm, the Euclidean distance between

different sample points is minimized, and the evenly distributed and representative sampling results are obtained. This paper uses the optimal Latin hypercube method to sample the parameters. Generate the optimal Latin hypercube sampling results in Isight software as input samples.

The FE model is established based on the input parameters, and the output parameters can be obtained through FE simulation. ABAQUS has a powerful secondary development function. Using Python programs, it can perform secondary development on the preprocessing and postprocessing parts of ABAQUS, achieve automatic modeling, automatic submission calculations, and automatic postprocessing batch calculations, which can save simulation time.

Figure 2 shows the parameter flow of using the Python program to obtain the output. First read a set of input parameters from the input parameter set and import the ABAQUS library function into the program, and the ABAQUS library function contains members that can be used for modeling. The members in the Model object under the Mdb object can be used for preprocessing work such as building 3D models, defining material properties, meshing, and defining loads and constraints. The Job object can submit calculations to the model. Each member under the Odb object can read the field output and history output results in the calculated odb result file to obtain the required output parameters. In this loop, the output parameters under different input parameters can be obtained, and the output parameter set can be summarized. The input parameter set and the output parameter set are combined as surrogate model training samples.

2.4. Surrogate Model Establishment Method. Isight software provides a variety of surrogate model fitting algorithms, including response surface model (RSM), radial basis function neural network (RBFNN) model, Kriging model, and so on.

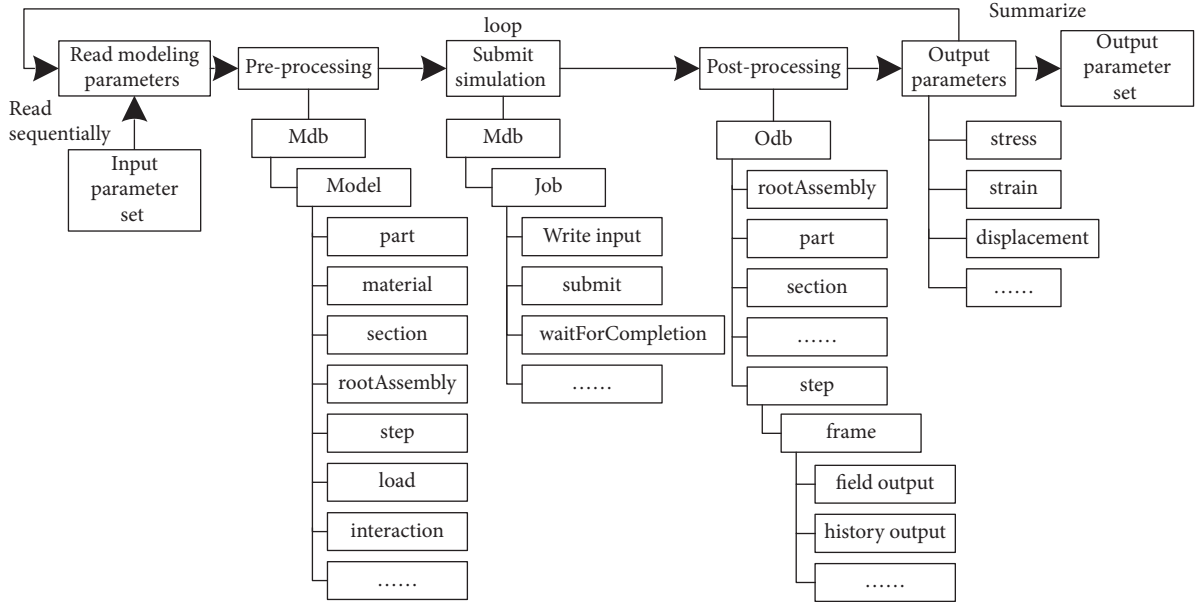


FIGURE 2: Sample acquisition process based on FE parameter model.

2.4.1. *Response Surface Model (RSM)*. Taking the fourth-order response surface model as an example, the surrogate model fitting formula is shown in the following equation:

$$\hat{y} = \beta_0 + \sum_{i=1}^M \beta_i x_i + \sum_{i=1}^M \beta_{M+i} x_i^2 + \sum_{i=1}^M \beta_{2M+i} x_i^3 + \sum_{i=1}^M \beta_{3M+i} x_i^4 + \sum_{i \neq j}^M \beta_{ij} x_i x_j, \quad (7)$$

where M is the number of input variables; x_i represents the input variables; \hat{y} is the output value; and β_i represents the coefficients.

2.4.2. *Kriging Model*. The expression of the Kriging model is shown in the following equation:

$$\hat{y} = f^T(x)\beta + Z(x), \quad (8)$$

where $f^T(x)\beta$ is the global regression model; $Z(x)$ is the random fluctuation; and \hat{y} is the output value.

2.4.3. *Radial Basis Function Neural Network (RBFNN) Model*. In the RBFNN model, the radial function is the basis function of the model, and its independent variable is the Euclidean distance between the measured point and the input point. (3) is the basic form of the radial basis function.

$$\hat{y} = \sum_{j=1}^M H_j(r)w_j = \mathbf{H}^T(r)\mathbf{w}, \quad (9)$$

where w_j is the weight; M is the number of samples; $H_j(r)$ is the radial function; and \hat{y} is the output value. By adjusting the weights, the radial basis function can be used to fit different models.

There are many indicators for evaluating the goodness of fit of a surrogate model. The normalized root mean square error (NRMS) and certainty coefficient (R^2) are commonly used to evaluate the global goodness of fit [32]. The expression of the NRMS is

$$\text{NRMS} = \sqrt{\frac{\sum_{i=1}^N (y_i - \hat{y}_i)^2}{\sum_{i=1}^N y_i^2}}. \quad (10)$$

The value range of NRMS is $[0, 1]$. The closer its value is to 0, the better the goodness of fit is. Its threshold value is 0.1.

The expression of R^2 is

$$R^2 = 1 - \frac{\sum_{i=1}^n (y_i - \hat{y}_i)^2}{\sum_{i=1}^n (y_i - \bar{y})^2}. \quad (11)$$

The value range of R^2 is $[0, 1]$. The closer its value is to 1, the better the goodness of fit is. Its threshold value is 0.9.

y_i is the sample value, \bar{y} is the sample mean, and \hat{y}_i is the surrogate model predicted value.

2.5. *Optimization Method*. The optimization problem with constraints can be expressed as

$$\min_x f(x), x \in \mathbf{R}^n, \quad (12)$$

$$s.t. \begin{cases} g_i(x) \leq 0, \\ h_i(x) = 0. \end{cases} \quad (13)$$

(12) is the optimization objective function. (13) is the optimization constraint, where $g_i(x)$ is an inequality constraint and $h_i(x)$ is an equality constraint. When solving the above two equations, in order to obtain reliable optimization results, it is often necessary to resort to optimization algorithms. Optimization algorithms can be divided into

numerical and exploratory types. Among them, the numerical optimization algorithm has a faster calculation speed and fewer iterations, but it is easy to fall into a local minimum. Representative algorithms include NLPQLP (continuous quadratic programming method), LSGRG (generalized gradient descent method), and so on. Exploratory optimization technology can search the whole world and is not easy to fall into the local minimum, but there are relatively many iterations. Among them, the representative algorithm is genetic algorithm, and the process is shown in Figure 3. Commonly used genetic algorithms include MIGA (multi-island genetic algorithm), NSGA-II (nondominant sorting genetic algorithm), and so on.

3. Establishment and Verification of the Equipment Cabin Bottom Cover FE Model

The equipment cabin bottom cover structure is shown in Figure 4. The main body is a flat plate, which is reinforced by three rectangular tube beams. The plate size is 1144×576 mm. The flat plate and rectangular tube beams are formed by bending 2 mm thick cold-rolled SUS304 stainless steel plates. The bottom cabin is fixed to the side beam of the equipment cabin by a total of eight bolts and backing plates at both ends.

3.1. Static Strength Test of Bottom Cover. The static strength test of the equipment cabin bottom cover is carried out under the conditions of the indoor fatigue test bench, and the stress measurement points are arranged at the key positions of the bottom cover as shown in Figure 5. Vacuum suction cups are uniformly arranged on the surface of the bottom cover to simulate the aerodynamic uniform load. The MTS fatigue testing machine is used to load the aerodynamic load under tension and compression at 4 kPa. The static strength test method and tooling under aerodynamic load are as described in the literature [33]. After the loading force is stable, use TDS-530 static data acquisition instrument to collect strain data. The loading tooling is shown in Figure 6.

3.2. Bottom Cover FE Model. Based on the 3D model of the bottom cover, the FE model of the bottom cover is established in ABAQUS. The flat plate and rectangular tube beam of the bottom cover are extracted from the midsurface and divided into shell elements. Divide the backing plate into solid elements. Both ends simplify the equipment cabin bracket to a discrete rigid body, imitating the fixing of the equipment cabin bracket to the bottom cover. The FE model is shown in Figure 7.

The position of the rivet hole between the flat plate, rectangular tube beam, and backing plate adopts beam element and rigid element to imitate riveting, and the contact pairs are set between each surface as shown in Table 1. A fixed constraint is applied to the equipment cabin bracket and backing plate bolts, and a uniformly distributed aerodynamic load of ± 4 kPa is applied to the surface of the bottom cover. Simulations show that the model can converge reliably.

3.3. Validation of the FE Model. The measurement points with relatively large stress values and relatively small stress gradients are selected to prevent the effect of stress concentration and the zero point error of the strain gauge from affecting the results. The results are compared with the output results of the FE model to verify the FE model. The comparison between the FE simulation results and the test results of some measuring points is shown in Table 2:

In Table 2, measuring points 2, 3, and 4 are the corner positions of the edge of the flat plate, and measurement points 12 to 17 are the process hole edges of the middle rectangular tube beam. In comparison, with the exception of the relatively large gap between measurement point 13 and measurement point 16, the measured stresses of the remaining measuring points are relatively close to the simulated stresses, indicating that the boundary condition settings of the FE model are basically consistent with the actual model. Measuring point 13 and the measuring point 16 are located at the edge of the center process hole rectangular tube beam, where the stress gradient is relatively large due to the stress concentration effect. Therefore, the attachment position of the strain gauge has a greater influence on the final result. The test result is different from the result of the FE model, but the trend is the same, which does not affect the direction and accuracy of the optimization.

Through FE analysis, under aerodynamic loads of ± 4 kPa, the maximum normal stress of the bottom plate appears on the edge of the center process hole rectangular tube beam (its location is marked by the box in Figure 8), and the direction is along the length of the rectangular tube beam. The stress distribution at the edge of the process hole and the maximum nodal stress value are shown in Figure 8.

Under pull working conditions, the maximum nodal stress is -130.7 MPa, and the maximum integration point stress is -138.2 MPa read by Python program; under push working conditions, the maximum nodal stress is 114.1 MPa, and the maximum integration point stress is 119.6 MPa. The nodal stress is obtained by extrapolating the integration point stress. In the following optimization calculations, the integration point stress is used.

In summary, the FE model can imitate the actual model well, and it can converge reliably, ensuring the accuracy of the optimization.

3.4. Calculation of Equivalent Stress under Symmetrical Cycle.

Due to the influence of factors such as contact nonlinearity, when the bottom cover is subjected to a symmetrical cycle of pull and push load, its stress response is not necessarily a symmetrical cycle. The FE method is used to obtain the stress peak-valley value, average stress, and stress amplitude of the bottom cover under ± 4 kPa aerodynamic load. The equivalent stress σ_{-1} under symmetrical cycles can be calculated by the Goodman equation (hereinafter referred to as equivalent stress):

$$\sigma_{-1} = \frac{\sigma_a}{1 - \sigma_m/\sigma_u}, \quad (14)$$

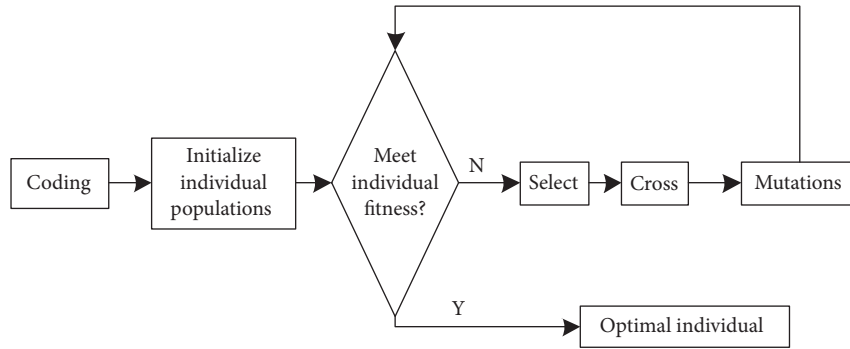


FIGURE 3: The basic process of genetic algorithm.

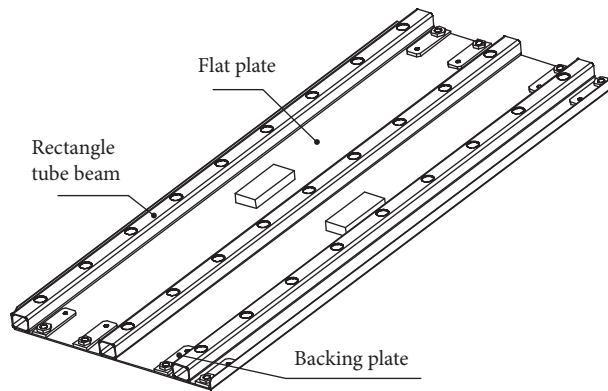


FIGURE 4: Structure of bottom cover.

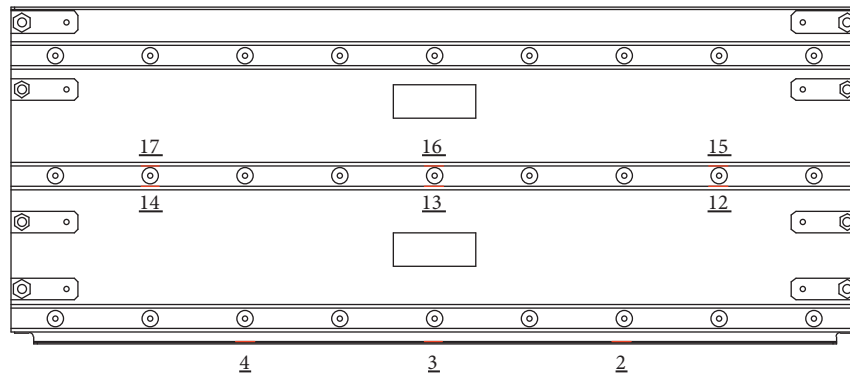


FIGURE 5: Bottom cover measurement point layout.

where σ_a is the stress amplitude, σ_m is the average stress, and σ_u is the ultimate strength of the material. Tensile test is performed on the small sample of the bottom plate on the MTS-810 universal material testing machine, and the mechanical properties are shown in Table 3.

In ABAQUS, the integration point stress of each element under pull and push conditions can be read through the Python program. Then, the equivalent stress of each element at the integration point can be calculated by (14).

4. Structural Parameter Optimization Design of Equipment Cabin Bottom Cover

4.1. Parameter Selection and SA. Combined with the survey results, cracks mostly appeared in the weak points of the hole edge of the rectangular tube beam. After FE analysis and static strength bench test, the edge of the center process hole rectangular tube beam (measurement points 13 and 16 in Figure 5) has relatively high stress, which is likely to be the initiation of cracks. Taking into account factors such as

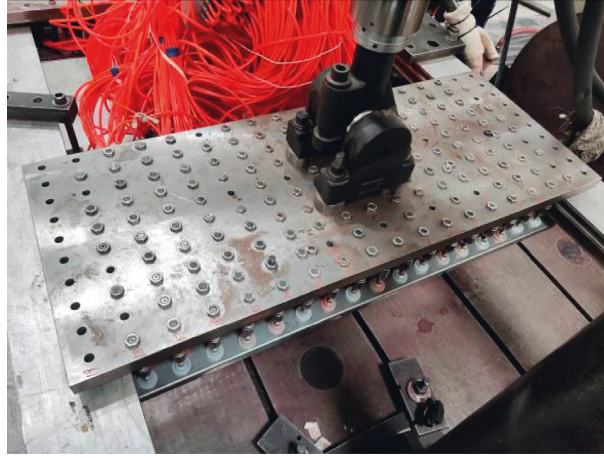


FIGURE 6: Bottom cover loading tool.

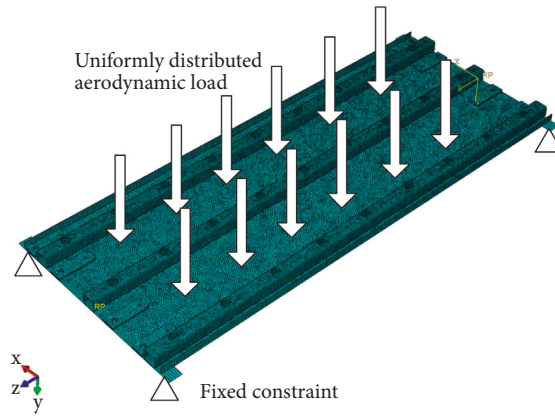


FIGURE 7: FE model of bottom cover.

TABLE 1: Contact attribute settings for each contact pair.

No.	Master surface	Slave surface	Discretization method	Contact property options
1	Flat plate lower surface	Rectangular tube beam upper surface		Hard contact friction coefficient: 0.15
2	Flat plate lower surface	Backing plate upper surface	Surface to surface	
3	Equipment cabin bracket lower surface	Flat plate upper surface		

bottom cover assembly and manufacturability, six parameters are selected as shown in Figure 9.

Among them, d is the distance between the rivet hole and the plate end, d_1 is the lateral hole distance of the rivet hole, p is the longitudinal spacing of the rectangular tube beam, w is the width of the rectangular tube beam midsurface, h is the height of the rectangular tube beam midsurface, and t is the thickness of the rectangular tube beam. The parameters d and d_1 are related to the lateral number of rivets b :

$$d_1 = \frac{(d_c - 2d)}{b}, \quad (15)$$

where d_c is the lateral length of the flat plate, and the original values and value ranges of each parameter are shown in Table 4.

Using the SA method described in Section 2.2, the stress-influence sensitivity of each parameter under the two working conditions of pull and push at 4 kPa aerodynamic loads is shown in Figure 10.

It can be seen from Figure 10 that the sensitivity of the parameters h , t , and w is high, indicating that their changes have the most significant impact on the stress. These three parameters are selected as the optimization parameters, and the other parameters have less impact and are ignored in the optimization.

4.2. *Parameter Sampling and Calculation.* Based on the selected parameters, the range of values is the same as that shown in Table 3, and the optimal Latin hypercube method is

TABLE 2: Comparison of FE simulation and test results of some measuring points.

Measurement point	Pull 4 kPa uniform load		Push 4 kPa uniform load	
	Measured stress/MPa	Simulation stress/MPa	Measured stress/MPa	Simulation stress/MPa
2	-10.4	-9.0	5.7	6.6
3	-14.9	-12.7	12.3	12.2
4	-7.6	-9.0	6.0	6.7
12	-31.8	-37.1	22.4	26.1
13	-55.7	-64.3	40.4	48.9
14	-36.8	-36.8	24.6	27.3
15	-36.0	-36.2	24.0	27.7
16	-58.1	-65.2	41.5	48.0
17	-37.9	-36.7	23.7	27.6

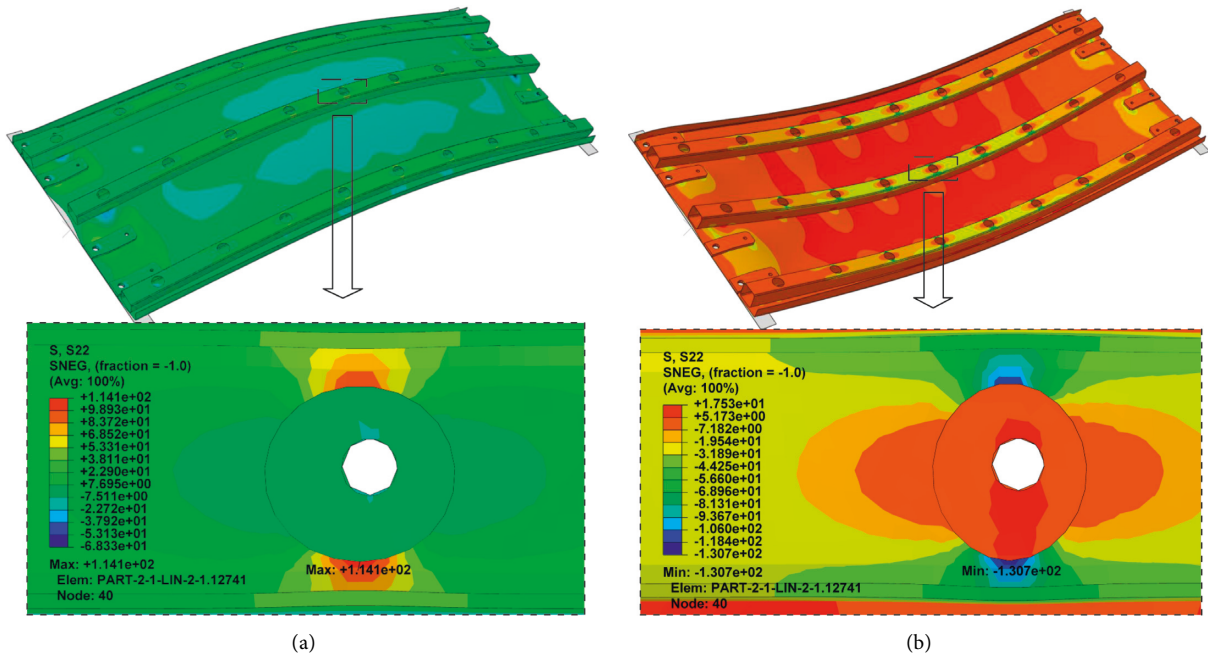


FIGURE 8: Stress distribution on the edge of the center process hole rectangular tube beam. (a) Push working condition. (b) Pull working condition.

TABLE 3: Mechanical properties of SUS304 cold-rolled stainless steel plate.

Material	Yield strength σ_b /MPa	Ultimate strength σ_u /MPa
SUS304	320	660

used to sample them. In order to meet the fitting needs of the surrogate model, the sampled data are initially set to 50 groups. The distribution in the parameter space is shown in Figure 11.

It can be seen from Figure 11 that the distribution of each sample in the parameter space is relatively uniform and representative. Use the Python program to input these 50 groups of samples into ABAQUS to establish a parameter model, complete the preprocessing of the model, and run it in batches. Read the maximum normal stress of the process hole edge of the square tube beam under two different working conditions of the flat plate under push and pull of 4 kPa aerodynamic load and calculate the equivalent stress as

the output parameter in combination with (14). The 50 groups of input and output parameters after all simulations are completed and are shown in Table 5.

The 50 sets of input and output parameters in Table 5 can be used as training samples for the surrogate model and input into Isight for approximate fitting.

4.3. Surrogate Model Fitting. Use different fitting models to fit the training samples in Table 5. Based on the cross-validation method, two indexes of NRMS and R2 are used to evaluate the goodness of fit. The goodness of fit indexes under different models are obtained as shown in Table 6.

From Table 6, the indexes of the RBFNN model are all the best, so the RBFNN model is used as the surrogate model of the original model. The comparison between the predicted value of the output and the original value is shown in Figure 12.

It can be seen from Figure 12 that the distribution of the predicted value and the original value points are all around

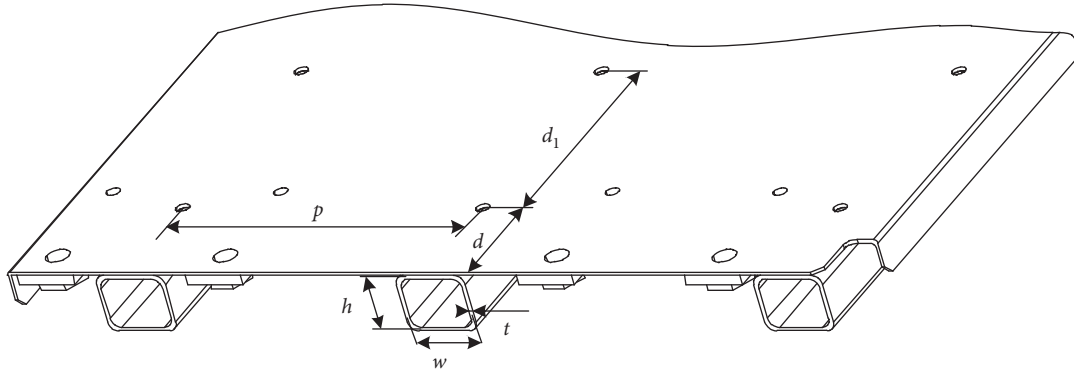


FIGURE 9: Parameter determination.

TABLE 4: The original value of each parameter and its range.

No.	Parameter	Original values	Lower limit	Upper limit
1	d	60 mm	30 mm	100 mm
2	p	193 mm	168 mm	243 mm
3	w	35 mm	35 mm	50 mm
4	h	28 mm	12 mm	50 mm
5	t	2 mm	1 mm	3 mm
6	b	9	7	11

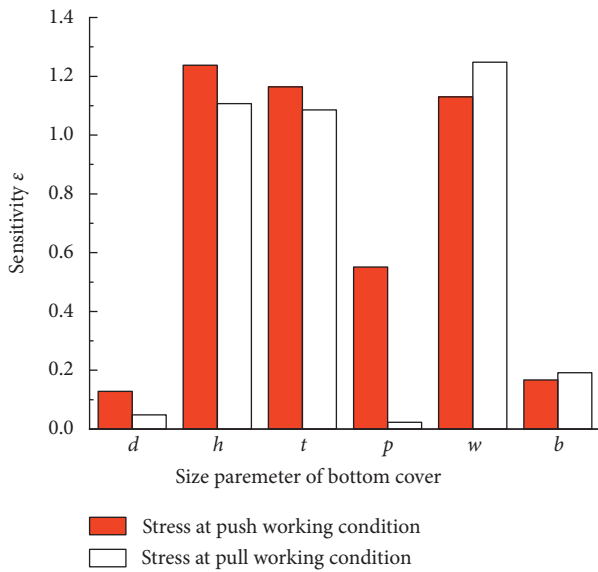


FIGURE 10: Sensitivity index of different parameters.

the straight line $y = x$, indicating that the fitting accuracy is high. The fitted surrogate model can be used as a simplified model to replace the original model for optimization.

4.4. Parameter Optimization Solution and Verification. Based on the above surrogate model, it can be optimized and solved in Isight. The optimized value range of each parameter is shown in Table 4. Determine the optimization goal to minimize the equivalent stress:

$$\min\{\sigma_{-1}\}. \tag{16}$$

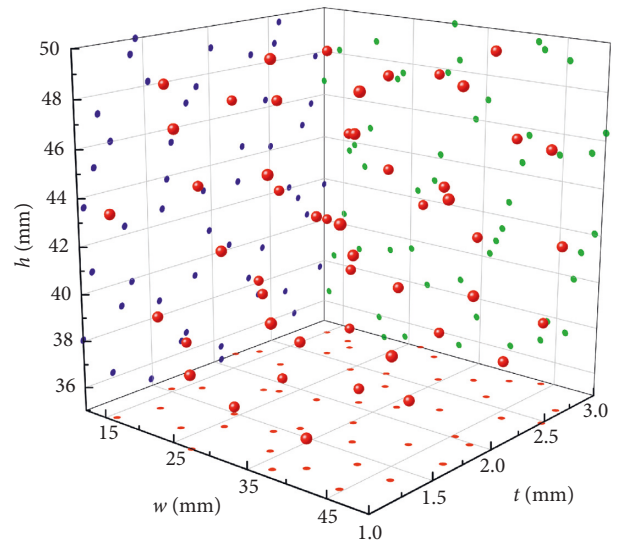


FIGURE 11: Parameter sample space.

In order to control the weight of the optimized bottom cover, corresponding constraint conditions need to be set. Since the above parameters only relate to the cross-sectional area of the rectangular tube beam, the weight of the bottom cover can be controlled by controlling the optimized cross-sectional area of the rectangular tube beam. In the original structure, the square tube beam midsurface height $h = 28$ mm, midsurface width $w = 35$ mm, and thickness $t = 2$ mm; ignoring rounded corners, its area is $S = (35 + 28) \times 2 \times 2 = 252$ mm². Therefore, the optimization constraints can be expressed as

$$s.t. S = 2t(w + h) \leq 252. \tag{17}$$

TABLE 5: Surrogate model training samples.

No.	w/mm	h/mm	t/mm	Equivalent stress/MPa
1	19.76	2.55	48.78	78.0
2	36.04	2.14	40.20	67.2
3	32.16	1.57	38.67	115.6
4	46.90	1.37	39.90	85.9
5	36.82	1.08	40.82	129.0
6	38.37	1.61	42.65	73.9
7	12.78	1.74	36.53	218.2
8	23.63	1.90	47.55	95.8
9	50.00	2.47	46.33	31.3
10	12.00	2.18	46.63	127.8
11	43.80	2.96	37.76	37.4
12	34.49	2.63	37.14	59.9
13	25.18	2.43	39.59	82.4
14	28.29	1.94	42.96	86.5
15	35.27	1.82	46.94	65.8
16	29.06	2.51	44.18	62.2
17	15.10	2.84	40.51	113.2
18	17.43	1.29	38.98	211.3
19	31.39	2.35	48.47	54.1
20	15.88	1.04	43.57	241.2
21	30.61	1.45	50.00	88.7
22	24.41	1.49	35.31	191.9
23	20.53	2.71	35.92	116.2
24	27.51	1.00	38.06	199.8
25	42.24	1.41	49.39	78.0
26	44.57	1.12	45.10	84.9
27	18.20	2.22	42.96	110.1
28	45.35	2.02	49.08	113.2
29	18.98	2.80	44.80	44.9
30	25.96	1.33	42.35	79.3
31	41.47	2.59	49.69	142.5
32	22.86	1.16	47.24	162.8
33	13.55	2.31	38.37	33.2
34	33.71	1.25	46.02	151.5
35	16.65	1.65	43.88	104.0
36	26.73	3.00	41.73	150.8
37	39.92	2.27	44.49	61.3
38	39.14	1.20	36.22	46.4
39	47.67	1.98	41.12	124.5
40	43.02	1.78	36.84	48.1
41	14.33	1.53	48.16	69.8
42	21.31	2.06	35.00	160.3
43	49.22	2.67	42.04	161.0
44	40.69	2.88	45.71	31.8
45	32.16	2.06	35.61	35.5
46	22.08	1.86	39.29	97.5
47	37.59	2.76	41.43	121.4
48	48.45	1.69	45.41	45.3
49	46.12	2.39	37.45	56.2
50	29.84	2.92	47.86	44.5

Using the original parameters as the initial values, after calculation, the iteration times and optimization results of the NLPQLP and MIGA optimization algorithms are obtained as shown in Table 7. It can be seen that the convergence results of the two optimization methods are similar, so the optimization calculation results are credible. Among them, the numerical optimization method is less time-consuming than the exploratory optimization method. The optimization history of the equivalent stress

under the two algorithms is shown in Figure 13 where the red point is the point that does not meet the constraint, the black point is the general point, and the green point is the optimal point.

From the above optimization process, it can be seen that the search speed of the NLPQLP algorithm is faster, but the number of iterations has reached 74. The optimization speed of the MIGA method is slower, but it can perform a global search in the parameter space.

TABLE 6: Goodness of fit under different fitting algorithms.

Fitting model	Goodness of fit	
	NRMS	R^2
Second-order RSM model	0.033	0.982
Third-order RSM model	0.032	0.984
Fourth-order RSM model	0.032	0.984
RBFNN model	0.028	0.988
Kriging model	0.080	0.900
Chebyshev polynomial model	0.032	0.984

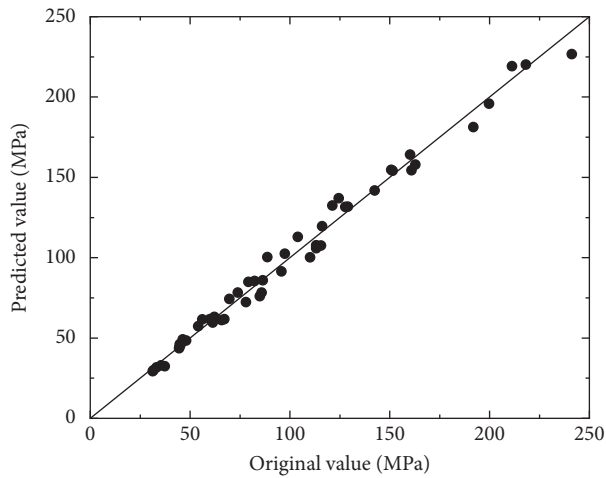
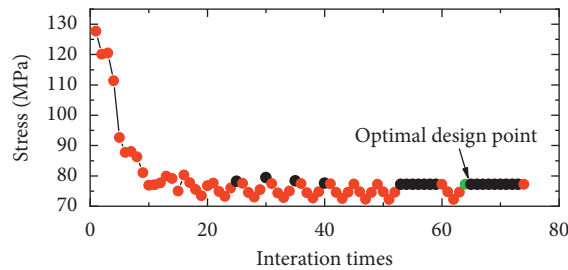


FIGURE 12: Comparison between predicted value and original value.

TABLE 7: Optimization results under different optimization algorithms.

Optimization algorithms	Iteration times	Optimization result		
		w/mm	h/mm	t/mm
NLPQLP	74	43.333	39.151	1.5276
MIGA sub-population size: 40; number of generations: 50; number of islands: 10	20001	44.342	39.308	1.5063



(a)

FIGURE 13: Continued.

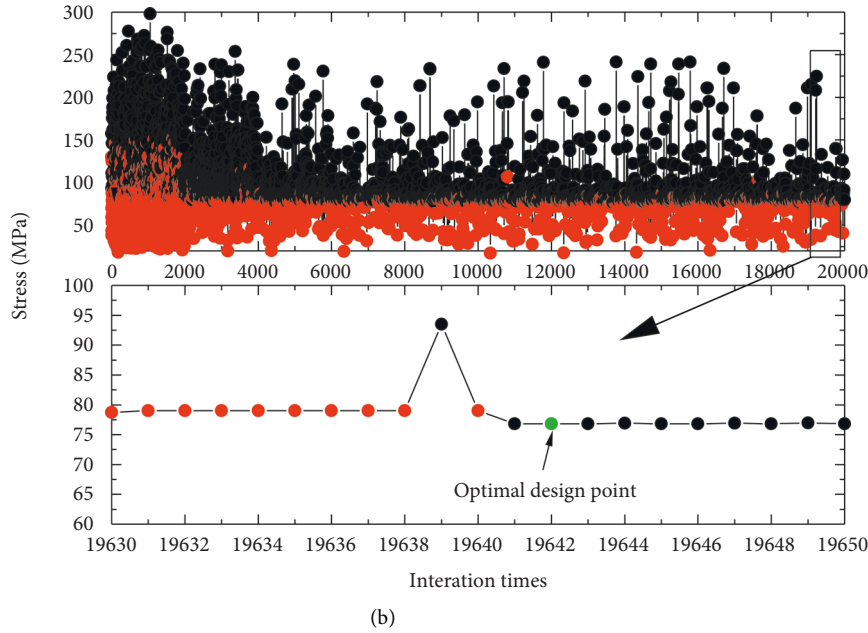


FIGURE 13: Optimization iteration process. (a) NLPQLP. (b) MIGA.

TABLE 8: Comparison between the optimized model and the original model.

	w/mm	h/mm	t/mm	S/mm^2	σ_{-1}/MPa
Original model	35.0	28.0	2.0	252.0	126.7
Optimized model	44.0	39.0	1.5	249.0	78.9
Optimization rate				1.2%	37.7%

Based on the optimization results in Table 7, round the parameters and input them into ABAQUS for FE simulation verification. The output and the original model are shown in Table 8.

It is shown in Table 8 that the equivalent stress of the hole edge of the optimized model is significantly optimized compared with the original model, the optimization rate reaches 37.7%, and its weight is also reduced. The optimization effect is significant.

5. Summary

- (1) Establish the parameterized model of the bottom cover by ABAQUS + Python jointly development method. Obtain the output samples in batches according to the input samples, which eliminates tedious pre and postprocessing and can improve the efficiency of sample acquisition.
- (2) Comparing the FE model with the bench test results of the equipment cabin bottom cover, the stress levels at each measurement point are basically the same, indicating that the boundary conditions and contact conditions of the FE model can basically simulate the actual model. Its accuracy can ensure the subsequent optimization design.

- (3) The bottom cover is optimized based on the SA method and surrogate model. After optimization, the equivalent stress at the edge of the model hole decreased from 126.7 MPa to 78.9 MPa, which was optimized by 37.7%. The optimization effect was significant.
- (4) This study only needs to perform 50 simulations on the FE model to obtain samples, and the surrogate model method can save thousands of repeated optimization calculations on the FE model. Therefore, based on the method in this paper, the optimization efficiency can be improved for complex FE models.

Data Availability

The data used to support the findings of this study are available from the corresponding author upon request.

Conflicts of Interest

The authors declare that they have no conflicts of interest.

Acknowledgments

This study was supported by the National Natural Science Foundation of China (11790281).

References

- [1] A. Vazdirvanidis, S. Papadopoulou, S. Papaefthymiou, G. Pantazopoulos, and D. Skarmoutsos, "Failure investigation of Cu-DHP tubes due to ant-nest corrosion," *International Journal of Structural Integrity*, vol. 10, no. 3, pp. 325–336, 2019.

- [2] M. D. Nor, S. N. Mat Saliah, and A. Ibrahim, "Fatigue damage severity assessment of RC beam[J]," *International Journal of Structural Integrity*, vol. 10, no. 5, pp. 612–620, 2019.
- [3] R. Manouchehry Nya, S. Abdullah, S. Singh Karam Singh, and S. Singh, "Reliability-based fatigue life of vehicle spring under random loading," *International Journal of Structural Integrity*, vol. 10, no. 5, pp. 737–748, 2019.
- [4] W. Zhou, L. Chen, Z. Wang, S. Ding, and Y. Shan, "Aerodynamic load spectrum and fatigue behaviour of high-speed train's equipment cabin," *Fatigue and Fracture of Engineering Materials and Structures*, vol. 42, no. 11, pp. 2579–2595, 2019.
- [5] D. Meng, S. Yang, C. He et al., "Multidisciplinary design optimization of engineering systems under uncertainty: a review," *International Journal of Structural Integrity*, vol. 13, no. 4, pp. 565–593, 2022.
- [6] C. Yang and Q. M. Li, "Structural optimisation for the collapse zone of a railway vehicle," *International Journal of Mechanical Sciences*, vol. 165, 2020.
- [7] H. A. Lee, S. B. Jung, H. H. Jang et al., "Structural-optimization-based design process for the body of a railway vehicle made from extruded aluminum panels," *Proceedings of the Institution of Mechanical Engineers-Part F: Journal of Rail and Rapid Transit*, vol. 230, no. 4, pp. 1283–1296, 2016.
- [8] T. Kuczek, "Application of manufacturing constraints to structural optimization of thin-walled structures," *Engineering Optimization*, vol. 48, no. 2, pp. 351–360, 2016.
- [9] Q. Xiao, W. Guo, L. Yang, S. Zhou, and D. Chen, "Design and topology optimization of air conditioning suspension bracket for metro," *Science Progress*, vol. 103, no. 4, 22 pages, Article ID 003685042098061, 2020.
- [10] D. Wennberg and S. Stichel, "Multi-functional design of a composite high-speed train body structure," *Structural and Multidisciplinary Optimization*, vol. 50, no. 3, pp. 475–488, 2014.
- [11] D. Lang and D. W. Radford, "Design optimization of a composite rail vehicle anchor bracket," *Urban Rail Transit*, vol. 7, no. 2, pp. 84–100, 2021.
- [12] H. S. Kim, C. W. Ahn, and K. H. Choi, "Shape optimization of a bogie frame for the reduction of its weight[J]," *Journal of the Korean Society for Precision Engineering*, vol. 19, no. 9, pp. 186–192, 2002.
- [13] M. Yamamoto, "Non-parametric optimization of railway wheel web shape based on fatigue design criteria," *International Journal of Fatigue*, vol. 134, Article ID 105463, 2020.
- [14] C. Y. Hou, Y. F. Lee, and Y. H. Peng, "Fatigue damage analysis of steel components subjected to earthquake loadings," *International Journal of Structural Integrity*, vol. 10, no. 1, pp. 25–40, 2019.
- [15] A. Takale and N. Chougule, "Optimization of process parameters of wire electro discharge machining for $Ti_{49.4}Ni_{50.6}$ shape memory alloys using the Taguchi technique," *International Journal of Structural Integrity*, vol. 10, no. 4, pp. 548–568, 2019.
- [16] A. H. Makwana and A. A. Shaikh, "Towards hybridization of composite patch in repair of cracked Aluminum panel," *International Journal of Structural Integrity*, vol. 10, no. 6, pp. 868–887, 2019.
- [17] D. Meng, S. Yang, T. Lin, J. Wang, H. Yang, and Z. Lv, "RBMDO using Gaussian mixture model-based second-order mean-value saddlepoint Approximation," *Computer Modeling in Engineering and Sciences*, vol. 132, no. 2, pp. 553–568, 2022.
- [18] M. Mrzyglod and A. P. Zielinski, "Parametric structural optimization with respect to the multiaxial high-cycle fatigue criterion," *Structural and Multidisciplinary Optimization*, vol. 33, no. 2, pp. 161–171, 2006.
- [19] M. Mrzyglod and A. P. Zielinski, "Multiaxial high-cycle fatigue constraints in structural optimization," *International Journal of Fatigue*, vol. 29, no. 9–11, pp. 1920–1926, 2007.
- [20] W. Sun, J. Zhou, D. Gong, and T. You, "Analysis of modal frequency optimization of railway vehicle car body," *Advances in Mechanical Engineering*, vol. 8, no. 4, 12 pages, Article ID 168781401664364, 2016.
- [21] C. W. Hudson, J. J. Carruthers, and A. M. Robinson, "Multiple objective optimisation of composite sandwich structures for rail vehicle floor panels," *Composite Structures*, vol. 92, no. 9, pp. 2077–2082, 2010.
- [22] B. R. Miao, Y. X. Luo, Y. J. Qiu, Q. Peng, C. Jiang, and Z. Yang, "Research on multidisciplinary fatigue optimization design method in structural design of high speed train," *Procedia Structural Integrity*, vol. 22, pp. 102–109, 2019.
- [23] B. Miao, W. Zhang, J. Zhang, and D. Jin, "Evaluation of railway vehicle car body fatigue life and durability using a multi-disciplinary analysis method," *International Journal of Vehicle Structures & Systems*, vol. 1, no. 4, p. 85, 2009.
- [24] P. Zhi, Y. Li, B. Chen, M. Li, and G. Liu, "Fuzzy optimization design-based multi-level response surface of bogie frame," *International Journal of Structural Integrity*, vol. 10, no. 2, pp. 134–148, 2019.
- [25] S. Baek, X. Song, and M. Kim, "Multiobjective optimization of beam structure for bogie frame considering fatigue-life extension[J]," *Journal of Electrical Engineering & Technology*, pp. 1–11, 2021.
- [26] H. Zhang, Y. Peng, L. Hou, G. Tian, and Z. Li, "A hybrid multi-objective optimization approach for energy-absorbing structures in train collisions," *Information Sciences*, vol. 481, pp. 491–506, 2019.
- [27] J. Chen, P. Xu, and S. Yao, "The multi-objective structural optimisation design to improve the crashworthiness of a multi-cell structure for high-speed train[J]," *International Journal of Crashworthiness*, pp. 1–10, 2020.
- [28] J. Li, G. Gao, and H. Dong, "Crushing analysis and multi-objective optimization of a railway vehicle driver's cab," *Thin-Walled Structures*, vol. 107, pp. 554–563, 2016.
- [29] B. Park, N. Kim, and J. Kim, "Optimum design of tilting bogie frame in consideration of fatigue strength and weight[J]," *Vehicle System Dynamics*, vol. 44, no. 12, pp. 887–901, 2006.
- [30] Y. Gao and W. Zhao, "Adaptive optimization with weld fatigue constraints based on surrogate model for railway vehicles," *Mechanics Based Design of Structures and Machines*, vol. 42, no. 2, pp. 244–254, 2014.
- [31] Y. Gao, Q. Liu, and D. Zhao, "Kriging surrogate model based optimisation of welded bogie frame for fatigue improvement [J]," *International Journal of Vehicle Structures & Systems*, vol. 11, no. 4, pp. 349–354, 2019.
- [32] Z. Xia, J. Liu, and Y. Cheng, "Fast prediction of mechanical impedance of an underwater foundation based on surrogate models[J]," *Chinese Journal of Ship Research*, vol. 15, no. 03, pp. 81–87, 2020.
- [33] H. Zou, S. Sun, and L. I. Qiang, "Device for Applying Surface Load: China: CN104677651A[P]," 2015.

Research Article

Design and Implementation of an Interactive English Translation System Based on the Information-Assisted Processing Function of the Internet of Things

Liya Mo 

School of English Language and Culture, Xi'an Fanyi University, Xi'an 710105, Shaanxi, China

Correspondence should be addressed to Liya Mo; moliya@xafyxy.wecom.work

Received 22 April 2022; Revised 18 June 2022; Accepted 6 July 2022; Published 21 August 2022

Academic Editor: Xuefeng Shao

Copyright © 2022 Liya Mo. This is an open access article distributed under the Creative Commons Attribution License, which permits unrestricted use, distribution, and reproduction in any medium, provided the original work is properly cited.

As a new type of language expression, interactive translation is widely used in English, and based on the Internet of Things technology, text harmony and glyphs are combined for information exchange. This design adopts B/S mode to realize the relational query of document content. This paper adopts the B/S architecture mode to design, implement, and test its functional modules and related data analysis to provide a friendly interactive English translation system service to the user group. In this paper, the development of the Internet of Things information-assisted translation system mainly focuses on the semantic embedding and correlation analysis based on the Internet of Things as well as the realization of interactive functions. On this basis, an interactive English translation process based on corpus and text data sets is designed and completed. This method can not only effectively solve the problems of large amount of text and high difficulty of expression but also can make the translation more concise and clear to achieve the required expression effect of the original text. At the same time, the system can automatically perform statistical analysis on the translation results to verify the accuracy and completeness of the translation results, providing reference value for subsequent function implementation. In this paper, we mainly study the realization of interactive functions and propose solutions to its existing problems and deficiencies. The experimental results show that the average BLEU of the system in this paper is 0.985, which indicates that the translation quality of the system is good and the interaction with users is improved.

1. Introduction

In modern Chinese dictionaries, the interpretation of the meaning of words is “meaning.” English literature today defines it as a noun, symbol, or word expressed as a sentence or a work is a meaning. However, due to the semantic characteristics of the language itself and the semantic meaning caused by some human factors, it is difficult to accurately convey the semantic meaning, so people began to seek translation to solve this problem. In modern Chinese dictionaries, the meaning of the word translated is expressed through language, but its essence is not a grammatical meaning but a semantic form. In English, we can understand semantics as “meaning,” so it is also difficult for English translation. The research of this topic has important theoretical significance and practical application value: firstly, the

direct dialogue and real-time communication between the user and the translation can be realized through the development of the Internet of Things information exchange platform; secondly, it can store the mobile phone in the database for easy reading and storage and improve its utilization rate; finally, through the realization of the functions of the system, the user experience can be combined with the translation information to improve interactivity and reduce costs, etc.

The main research direction of this subject is interactive translation system. By combining with traditional text decoding technology, a new and efficient method of language translation based on Internet of Things information is designed. The details are as follows: (1) the key technologies involved in the interactive translation process are systematically described, including language feature extraction,

translation process testing, and text recognition and (2) the system introduces the method of assisting English translation based on Internet of Things technology.

2. Related Work

Regarding the research of the English translation system, many scholars have provided a lot of references. Liu et al. proposed a novel interactive attention mechanism that enables automatic speech recognition and text translation to be performed synchronously and interactively in a single model [1]. Chen and Huang designed an interactive online English teaching system based on Internet of Things technology. He proposed three topologies for building an online English teaching system based on the Internet of Things [2]. Yuan et al. proposed a language analysis research for English translation system based on fuzzy algorithm. He first analyzed English-language features, then used the Gaussian blur algorithm to denoise the images in the translation system, and finally display the image recognition results [3]. Ban and Ning created neural machine translation models using an end-to-end encoder and decoder framework. The machine automatically learns its functions and converts the data into word vectors in a distributed fashion, which can perform the mapping between source and target languages directly through neural networks [4]. Sangeetha and Jothilakshmi proposed a speech-to-speech translation (SST) system that mainly focuses on translation from English to Dravidian (Tamil and Malayalam) [5]. The research of the English translation system is often related to information-assisted processing, so the relevant research results of information-assisted processing are introduced next.

Regarding the research on information-assisted processing, many scholars have provided a lot of references. Muga et al. developed a coupled model of heat and mass transfer to predict the beef temperature and moisture content during briquettes processing using Infrared-Assisted Hot Air Drying (IRHAD) [6]. Tatsuo et al. proposed an information processing method that includes defining a virtual space for the immersion of a user wearing a head-mounted display (HMD) [7]. The data from these studies are not comprehensive, and the results of the studies are open to question. Therefore, it cannot be recognized by the public and thus cannot be popularized and applied. Therefore, this study combines the above two aspects and also solves the pain points of the previous research results.

3. Design and Implementation of Interactive English Translation System

Translation is an important part of English, and it is also considered as a language conversion, which includes many links in this process [8, 9]. As a new discipline and the field of technical science, English-Chinese bilingualism and cognitive linguistics are closely related [10]. As a new emerging language, information-assisted speech recognition based on the Internet of Things network has attracted widespread attention from people from all walks of life and developed rapidly after its emergence [11]. At the same time, due to the

development of network communication technology and the high popularity of the Internet, the development of network communication technology has also brought new challenges to the speech recognition system, making people have more needs for the translation of Internet of Things information [12]. And these demands will provide more extensive, flexible, and diverse and more pertinent, more practical, and more maneuverable texts for interactive English translation based on the Internet. As an emerging technology, the interactive translation system based on the Internet of Things has many advantages in information processing such as rapid retrieval and high accuracy; speech recognition can achieve matching of various types of texts and pictures, etc. [13, 14].

3.1. Theoretical Basis of Related Technologies

3.1.1. Network. The network is the medium of information exchange, which can effectively connect language, data, and other media and realize the mutual communication between voice, text, and other forms [15, 16]. Interactive translation systems are built on the Internet. Text transmission is used when traditional English is used as a carrier of information transmission [17, 18]. With the combination of Internet of Things technology and communication protocol (ICT), there is a new way to complete two-way communication based on Web platform integration network communication function-interactive electronic document translation software (BLOCKP), this translation system has cross-platform features. It transforms text documents in the traditional sense into functions that are highly readable, easy to read and understand, and capable of real-time interaction and control. In the traditional text information processing process, the interactive electronic document translation system needs to go through a large number of paper materials for printing, transmission, and storage [19, 20]. The integrated network communication function based on the Web platform can effectively realize the two-way communication between the user and the translation. At the same time, it also provides readers with a convenient, fast, and efficient service method (PBL) that can provide users with feedback on their reading experience anytime, anywhere. In addition, the interactive electronic document translation system has the characteristics of strong flexibility in the process of traditional text information processing [21]. It can interact on different platforms according to the needs of users and has better flexibility and controllability [22, 23].

3.1.2. Service Platform. The functions of the service platform mainly provide users with text retrieval and voice translation as well as other related auxiliary information [24, 25]. (1) *Text retrieval.* The tool can quickly obtain the required text, pictures, videos, and other resources from the database and generate a document for users to use after the translation is completed. At the same time, you can also search the Internet for topics you want or are interested in to communicate, which facilitates the interaction between readers. In addition, it helps to improve users' interest in English

learning and make them more active in the translation process [26]. (2) *Speech decoding function*. The tool can quickly obtain the required information from the text and process it so that readers can get help in time when they encounter problems in the translation process. (3) *Voice translation*. It can convey the meaning that it needs to express to the translator, and at the same time, it can also realize the functions of direct dialogue with the original author or indirect inquiry of the translator to complete the English word decoding task. The interactive text body developed based on the auxiliary language of the Internet of Things technology has the following characteristics: (1) it facilitates the communication and interaction of users and (2) it is convenient for the defense when encountering problems in the translation process.

3.1.3. The Concept and Calculation Method of Interactive English Translation. Interactive translation is an important English translation method, which has a certain degree of commonality in terms of language ontology and translation methods. In the process of text information extraction and processing, the most basic is to perform a logical and semantic analysis on the translation. Therefore, based on the Internet of Things technology, the research on the relationship between interactive English reading function, word recognition function, and related word reading ability is realized. The interactive translation method based on text information extraction is an effective method to realize the functions of semantic association analysis, sentiment tendency prediction, and reasoning. In the process of English translation processing, the translation of the text is realized through semantic mining and inference of the original content. In this paper, from the process of extracting and processing text information, it is divided into three parts: semantic analysis, sentiment prediction, and related word recognition. Semantic analysis is to extract text information and interpret these different texts as effective and logical relationships according to their content characteristics. In the process of translation, it should be noted that necessary consideration should be given to the sentence structure and expression when connecting words between sentences and chapters. For the same meaning, there may be multiple expressions (such as word order). When a sentence is split into multiple participles for decoding, corresponding processing methods must be made for this situation, which is also an important part of the translation process. In the process of translation, the related words are analyzed to find the relationship between sentences. Based on the above analysis, it is necessary to classify the interactive English translation methods in the translation process so as to facilitate further research on their functions and implementations. Emotional tendency prediction is based on the Internet of Things technology, which builds a bridge between text and sentences to achieve emotional

communication with the original text. This translation method uses language as an intermediary to convey information. Therefore, in the process of translation, language is used as an intermediary to realize the transmission of information. In this process, the translator must express it correctly, which is also the bridge between the text and the user.

3.1.4. Interactive English Translation Algorithm Based on Internet-of-Things Information-Assisted Processing. In the interactive English translation system based on Internet of Things information processing, when translating, it is first necessary to search and analyze the text content. Then, according to the specific vocabulary, discourse, and other data types and attributes input into the database by the user, it is judged whether the original text to be translated is semantic. If it is the same word, it can be classified and stored according to different methods; otherwise, it can be stored again if it does not belong to the next category of the semantic class. Based on the Internet of Things information processing interactive English translation algorithm and according to the specific situation in the translation process, the convolutional neural network algorithm is used to realize the translation of the translated text. The interactive English translation system based on Internet of Things information processing mainly has two methods for semantic analysis of the translated text. The first is to use the word vector as an input variable to describe the relationship between words and sentences; secondly, according to a certain connection between the translation and the original text, an association model is established to identify the author or his location, and what has happened or changed in what he said; finally, the text content is classified and stored in the database based on the text type.

A convolution kernel X of size $\omega * \xi$ performs a convolution operation on the input text S :

$$a = \sum_{\omega=1}^{\omega\xi} x_{\omega} s_{\omega} = X^T S. \quad (1)$$

The generated network is H , the discriminant network is E , and the loss function is given as follows:

$$M^{(E)}(\rho^{(E)}, \rho^{(H)}) = -\frac{1}{2} F_{s-Q_{\text{data}}} \log E(s) - \frac{1}{2} F_{s-Q_a} \log(1 - E(H(a))). \quad (2)$$

Among them, ρ is the neural network parameter variable.

Total loss function:

$$W(\rho^{(E)}, \rho^{(H)}) = F_{s-Q_{\text{data}}} \log E(s) + F_{s-Q_a} \log(1 - E(H(a))) \\ \arg \min_H \max_E W(E, H). \quad (3)$$

Let $H(a) = s$, then we have

$$W = \int q_{\text{data}}(s) \log E(s) + q_h(s) \log(1 - E(s)). \quad (4)$$

Let $g(s) = q_{\text{data}}(s) \log E(s) + q_h(s) \log(1 - E(s))$, and take the derivative of $g(s)$ as follows:

$$\frac{dg(s)}{dE(s)} = \frac{q_{\text{data}}(s)}{E(s)} + \frac{-q_h(s)}{1 - E(s)} = 0. \quad (5)$$

Finally, get $E^*(s)$ as follows:

$$E^*(s) = \frac{q_{\text{data}}(s)}{q_{\text{data}}(s) + q_h(s)},$$

$$W(H, E^*) = \int q_{\text{data}}(s) \log \frac{q_{\text{data}}(s)}{q_{\text{data}}(s) + q_h(s)} ds + \int q_h(s) \log \frac{q_h(s)}{q_{\text{data}}(s) + q_h(s)} ds. \quad (6)$$

KL divergence is given as follows:

$$KL(Q\|R) = \sum Q(s) \log \frac{Q(s)}{R(s)}. \quad (7)$$

JS divergence is given as follows:

$$JS(Q\|R) = \frac{1}{2} KL(Q\|N) + \frac{1}{2} KL(R\|N), \quad (8)$$

where Q and R are two different probability distributions, $N = 1/2(R + Q)$.

$$JS(Q\|R) = \int q(s) \log \frac{q(s)}{q(s) + r(s)/2} ds + \int r(s) \log \frac{q(s)}{q(s) + r(s)/2} ds. \quad (9)$$

The optimal generator should satisfy $q_{\text{data}} = q_h$.

Consistency of recurrent network is given as follows:

$$\begin{aligned} s &\longrightarrow H(s) \longrightarrow G(H(s)) \approx s, \\ z &\longrightarrow G(z) \longrightarrow H(G(z)) \approx z. \end{aligned} \quad (10)$$

A least-squares loss is used instead of the cross-entropy form as follows:

$$\begin{aligned} M_{\text{GAN}}(H, E_Z, S, Z) &= F_{z-Q_{\text{data}(z)}} [\log E_Z(z)] + F_{s-Q_{\text{data}(s)}} [\log(1 - E_Z(H(s)))], \\ M_{\text{GAN}}(G, E_S, S, Z) &= F_{s-Q_{\text{data}(s)}} [\log E_S(s)] + F_{z-Q_{\text{data}(z)}} [\log(1 - E_S(H(z)))]. \end{aligned} \quad (11)$$

In CycleGAN network,

$$\min W_{\text{LSGAN}}(H) = \frac{1}{2} F_{a-Q_a(A)} [(E(H(a)) - 1)^2]. \quad (12)$$

The loss is calculated using the $L1$ norm as follows:

$$M_{\text{cyc}}(H, G) = F_{s-Q_{\text{data}(s)}} [\|G(H(s)) - s\|_1] + F_{z-Q_{\text{data}(z)}} [\|H(G(z)) - z\|_1]. \quad (13)$$

Complete loss function is given as follows:

$$\begin{aligned} L(H, G, E_S, E_Z) &= M_{\text{GAN}}(H, E_Z, S, Z) \\ &+ M_{\text{GAN}}(G, E_S, S, Z) + \eta M_{\text{cyc}}(H, G), \end{aligned} \quad (14)$$

where η is the adjustment weight of the loss.

The final optimized function is given as follows:

$$H^*, G^* = \arg \min_{H, G} \max_{E_S, E_Z} M(H, G, E_S, E_Z). \quad (15)$$

IS Score is given as follows:

$$IS(H) = \exp(F_{s-Q_h} E_{KL}(q(z|s)\|q(z))). \quad (16)$$

FID Score is given as follows:

$$FID(s, h) = \|\sigma_s - \sigma_h\|_2^2 + \zeta(\tau_s + \tau_h - 2(\tau_s \tau_h)^{1/2}). \quad (17)$$

Among them, σ is the mean, ζ is the sum of the diagonal elements of the matrix, τ is the covariance, s is the real sample, and h is the generated sample.

In this paper, the convolutional neural network algorithm is used to systematically learn the words and sentences of the corpus and then translate and output the results according to the input content.

3.2. System Requirements. In the development process of the interactive translation system, requirement analysis is a very important link. First of all, it is necessary to clarify for which functional modules the user needs to have a preliminary understanding, then make a detailed investigation and analysis of this basic information and auxiliary languages, and determine whether the interactive English translation method that needs to be applied can be successfully realized according to the investigation results. Finally, based on the Internet of Things technology, artificial intelligence, and other intelligent technologies, the corresponding interactive software system platform and the hardware connection method of the related interface circuit will be designed to provide convenient conditions for the subsequent development work. In the process of software development, requirement analysis is the most important part of the whole system design and implementation and also provides a basis

for the subsequent programming in the software development stage. It analyzes the system functions, interface circuits, and related data requirements in detail.

3.2.1. System Functions. The main functions of this system include the following points: (1) *the transmission of translation information.* After the user publishes the translation, it is necessary to perform text and speech recognition to determine whether there is a translation. If there is no character or grammar error, you need to return to the Chinese prompt and re-enter; otherwise, the word or sentence is not allowed to use other parts of the Internet of Things directly to realize the interactive translation function. (2) *Conversion of translation information.* After the user publishes the translation, text recognition needs to be performed to determine whether to use the IoT auxiliary language, then convert these words or sentences into RNG words or other natural expressions; finally, convert English words or periods into Chinese words. (3) *Reception of translation information.* After the translation is accepted, the Chinese text needs to be returned and translated into English words or sentences for the user to read, then the Chinese text is converted into RNG words or other natural expressions for the readers to understand and use.

3.2.2. System Data. In the design of the interactive translation system, data storage is very important, and it will provide necessary and accurate, complete, and timely feedback for the translation to readers. This paper mainly provides an overview of the information-assisted language library for the Internet of Things. First, analyze the field structure: the function module consists of two parts. The first part is used to publish information; the second part is to accept instructions and send commands to the server to perform corresponding operations (such as translation) to complete the data that need to be processed in the interactive process, including text types and images. These data will be analyzed in detail here. *Text type.* This function module provides users with an interactive document that can select corresponding attributes according to their needs and can quickly respond to the required information. This classification method belongs to the structure based on graphs and fields, and its characteristics are as follows: first, it defines semantics by simply describing the language and words; secondly, the different objects in the text are interconnected, strongly correlated, and have a high degree of autonomy or predictability features, etc.; finally, it is a graphic-based interactive document, and the text type has obvious interactivity.

3.3. System Design. In the design and implementation of the interactive translation system, it is mainly through the testing and analysis of functions. This article will introduce the process of assisted language translation based on IoT technology. The method consists of two parts: one is to test the user and translation and the other is to operate the user interface, such as the login button, text box single-page

display, and data display module, both use the program control code to automatically complete the task execution to realize the target text recognition and interactive reading process. In addition, it is also necessary to consider the block design of functions and divide different parts into multiple small sections and deal with them separately.

3.3.1. System Architecture. The architecture of the interactive translation system based on the Internet of Things is shown in Figure 1. This program adopts B/S mode (as shown in Figure 2), that is, the translation is completed on a browser, and the result is displayed directly on the page. The B/S mode unifies the client and concentrates the core part of the system function realization on the server, which simplifies the development, maintenance, and use of the system. The algorithm has the characteristics of good fault tolerance and strong practicability; in addition, it can also realize the function of connecting and interoperating with other applications through various interfaces; finally, it has technical support such as powerful and friendly interface and data statistical analysis. (1) *System architecture.* Design based on B/S structure is the most critical link in the development of this translation system. In this translation system, the design of B/S mode is mainly to realize the interactive English translation mechanism based on Internet of Things technology. The method can fully utilize the resources and devices on the network to exchange information. At the same time, the translation results can also be sorted out through the data statistical analysis function. (2) *System function module.* This part mainly implements the interactive translation mechanism based on the Internet of Things technology. In this translation process, users can input different types and corresponding content in the text box and then choose the realization of the translation mechanism according to the required information. Mainly based on the Internet of Things technology, text and picture information are effectively combined in an interactive translation system. The function module can automatically generate corresponding graphics and texts after inputting different types and contents to the user and display them to the relevant interface. (3) *Statistical analysis of data.* The required data and results can be obtained through statistical analysis, and this method can be used when a large number of historical records need to be saved, backed up, or deleted.

3.3.2. The Main Interface of the System. According to the above functions, we can develop the main interface of the interactive translation system, that is, between the user and the administrator, and between the text and the picture. (1) *Registration/login.* After the user completes the construction of the basic module of the IoT information auxiliary language mentioned in this design, the user can register or log in through the mobile app. This part needs to implement two aspects: the first is to provide an input box in the page, and the second function option is “view,” where you can click the button to enter a content under any column to use it directly or exit to the system among; (2) *text classification.* This part needs to realize the automatic recognition of the translated

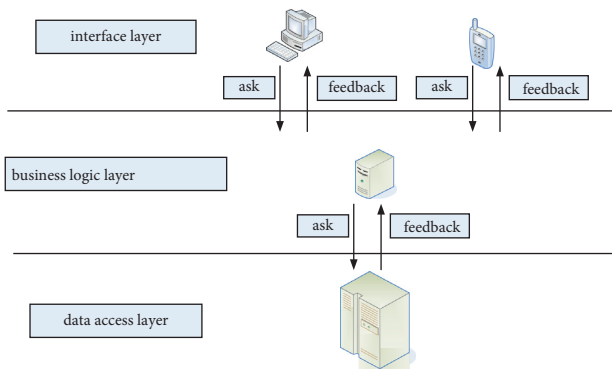


FIGURE 1: The architecture of the interactive translation system based on the Internet of Things.

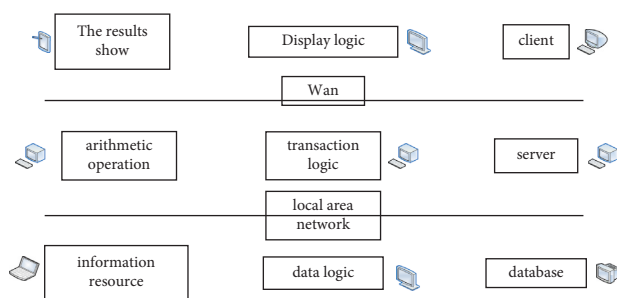


FIGURE 2: B/S three-tier architecture diagram.

text. When translating, the specific meaning can be distinguished by inputting keywords; (3) data storage area; (4) interactive interface; (5) other content such as function options and interface instructions should be included, and detailed records should be made to save the document file, and you can use and query the running results of this translation program and user feedback information and other related issues. According to the above analysis, it can be concluded that the system is an interactive English translation system based on the basic module of the auxiliary language of the Internet of Things, which can realize the recognition, storage, and transmission of the translation.

3.3.3. Collection of System Data. When collecting the data of the interactive English translation system, it is necessary to use a unified Internet of Things technology to collect and store relevant information. In this paper, various forms such as text and images are involved. The information mainly includes the following: (1) text content and (2) multimedia image data such as pictures, audio, video, and animation files. The collection and storage of this information are processed through radio frequency technology. In the interactive English translation system, two functions need to be implemented: one is text and images, that is, users publish to the database, and the other is the speech recognition module. The input data are preprocessed and sent to the neural network, and the word content is recognized by ANN. ANN is an artificial neural network, which abstracts the human brain neuron network from the perspective of information processing, establishes a simple model, and

forms different networks according to different connection methods. The hardware of the speech recognition module is shown in Figure 3.

The STM32F103VET6 chip is a high-performance, 32-bit processor based on the CM3 core, with low power, low voltage, and excellent performance combined with real-time functions. The technical parameters of the STM32F103VET6 chip are shown in Tables 1 and 2.

3.4. Implementation of Interactive English Translation System.

The interactive translation system based on the context of the Internet of Things is a new type of English vocabulary, and its functions mainly include text, voice, and picture information retrieval. In this paper, two different forms of interactive translation are implemented: (1) the combination of semantically related etymology and word templates and (2) online reading auxiliary translation language and automatic decoding are completed to modify the translation and return to the original interface and then judge whether the translation content needs to be supplemented according to the prompt input by the user. Based on the interactive translation method of semantic correlation type etymology and word template, two different forms of text information retrieval are realized, and its functions include voice, picture, and text, and the translation is modified through automatic decoding. In addition, the system needs to be evaluated, and the evaluation adopts the method of manual evaluation (see Figure 4).

3.4.1. System Design Purpose and Implementation Process.

The design of this interactive translation system is to realize the auxiliary processing function of Internet of Things information and to express the corresponding semantics through words with high similarity with the text. In this process, it is necessary to convert the words and sentences into specific vocabulary and then complete the translation according to the specific words. The first thing we need to do is complete all the steps required for a translation task: the first step is to determine the relationship between sentences and words, the second step is to convert these sentences or paragraphs into corresponding semantic forms, the third step is to convert the converted semantics into word forms, and the fourth step is to convert the resulting the corresponding semantic meaning in the text. In this interactive translation system, we need to complete such a task: first, determine whether there are similarities between each sentence; secondly, how to express, it first needs to determine the relationship between sentences; then, we need to convert each sentence into corresponding words; the next step is to connect words between different levels in the same way; finally, the converted text is converted into the characters that need to be used between the corresponding levels, and proofreading is done after the decoding is completed.

3.4.2. The Software System of the Interactive English Translation System. The software system of the interactive translation system is mainly composed of three parts (as

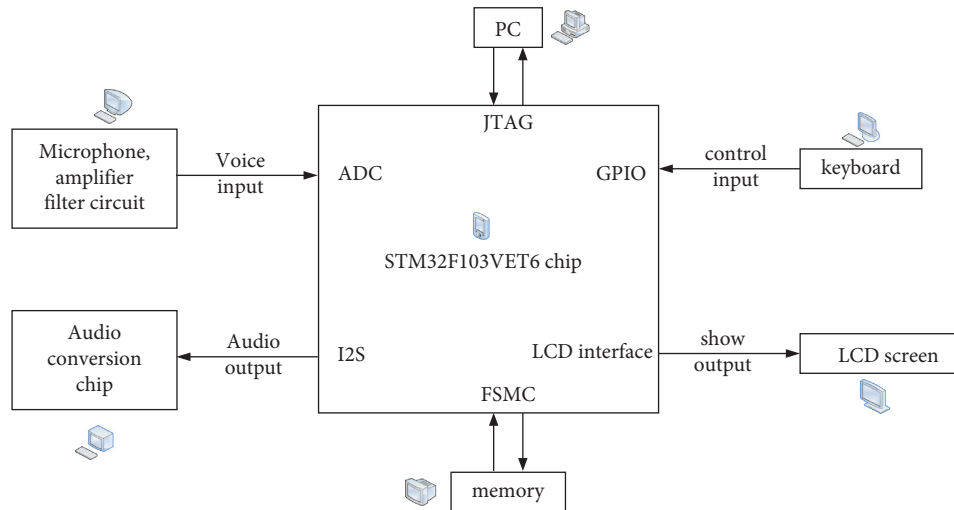


FIGURE 3: Speech recognition module hardware.

TABLE 1: STM32F103VET6 chip technical parameters 1.

Name	Parameter	Name	Parameter
CPU	Arm 32-bit Cortex-M3	Dissipated power (mW)	434
Size (bit)	32	FLASH capacity (B)	524288
Clock frequency (MHz)	72.0	Memory capacity (KB)	512
RAM size (B)	65536	Processor Speed (MHz)	72

TABLE 2: STM32F103VET6 chip technical parameters 2.

Name	Parameter	Name	Parameter
Number of pins	100	GPIO	80
Number of timers	8	Supply voltage range (V)	2~3.6
Number of PWM channels	16	Operating temperature range (°C)	-40~85

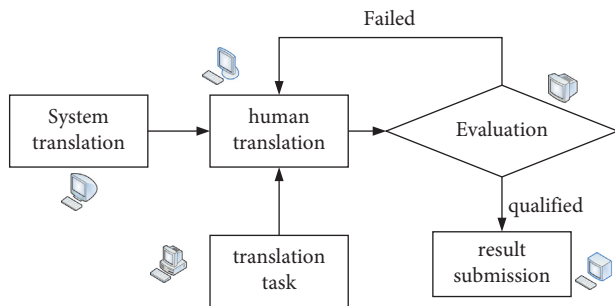


FIGURE 4: Flowchart of manual evaluation.

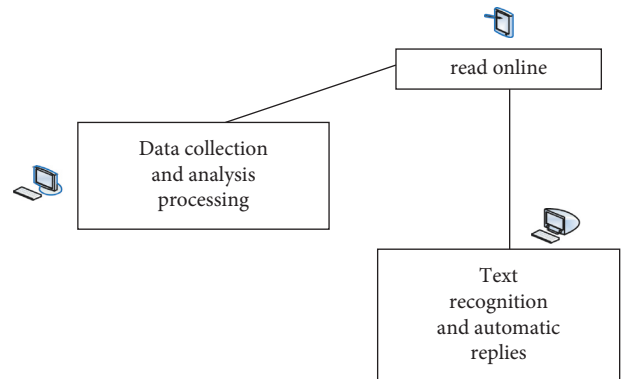


FIGURE 5: System software architecture.

Figure 5): the first module is data acquisition and analysis processing, including text recognition and audio signals. The detailed information is saved in the background database. This module implements the classification of English words. The second subfunction is online reading. This function is to facilitate real-time communication between readers and translation authors, provide assistance, and feedback the original content to the translator team. At the same time, it can also send English translation suggestions to users through the voice interface to guide the translation work of the translation; the last part is used for text recognition and

automatic reply to the original text. When readers encounter problems in translation, the module will automatically reply to the original text.

3.4.3. *Interactive Function.* The interactive function is designed to automatically process the translation during the translation process. Through the conversion between text, pictures, and other information, two-way transmission with

the original text is realized. On this basis, it is also necessary to consider whether the channel capacity and the network environment are compatible (that is, different users can get the same format or content). There are two issues: (1) data transmission speed from the current situation, the development trend of communication technology has been very impressive. But at the same time, we should also see the challenges brought by the high-speed development process—low-speed, low-frequency, and other undesirable phenomena are becoming more and more obvious. Therefore, in order to ensure high efficiency and accuracy, the problem of channel capacity should be considered in the translation process. (2) It is important to think about how to improve the data transmission speed, that is, to realize the fast and efficient transmission of information content by selecting the transmission medium.

Based on the above factors, an interactive English translation system model—RM-test algorithm—is proposed, and the final design and test work are completed on this basis. The basic principle of the RM-test algorithm (see Figure 6) is as follows: first, translation data are given by the translation system, then the text data are transmitted to the decoding layer through the network, the information is matched in the decoding layer, and finally, the original text is returned to the database. The translation system is an interactive English word decoder, which can automatically identify the text data and give the corresponding translation.

3.4.4. Maintenance of Interactive English Translation System.

The maintenance process of the interactive translation system mainly includes the following aspects: (1) it needs to revise the translation to ensure that the translation conforms to the original design specifications. In case of errors, omissions, or inappropriate words used by users when using English, it is necessary to explain to readers in a timely manner. At the same time, it is necessary to strengthen the processing and reply function of user feedback information and the construction of an online message mechanism; (2) for some professional terms, it is necessary to avoid repeated translations to cause semantic confusion. It is necessary to add auxiliary words in the interactive word decoding and make necessary and reasonable modifications before applying them to the translation.

4. Interactive English Translation System Performance

The operating environment of the system is shown in Table 3.

The technical parameters of the translation output machine are shown in Table 4.

The specific situation of the corpus used by the system is shown in Table 5.

300 typical sentences of different lengths were extracted from the corpus analysis database for testing, and the time of pattern feature extraction is shown in Figure 7; this time it includes the time of statement preprocessing and lexical analysis. A support memory bank of 1000 sentences was first

built and tested with another 200 sentences. The system tested the time spent on learning in the following two cases: (1) learning without classification, that is, learning with the simplest memory, and directly storing the input sentences or patterns in the memory bank. (2) It utilizes lazy learning for categorical storage, forming different clusters; Figure 7(b) presents the average time spent in two different cases.

Figure 7(a) shows that the time for feature extraction increases gradually with the number of words in the source pattern. Figure 7(b) shows that as the memory bank increases, so does the time spent on learning. Compared with simple memorization, lazy learning takes about 40% more time. This is the downside of lazy learning, which trades time for improved retrieval speed.

The accuracy of the translation is divided into four levels: A (almost completely correct), B (mostly correct), C (a small part of it is correct), and D (almost completely incorrect). Figure 8 presents the evaluation of translation accuracy for each similarity condition. The examples of the feature index translation failure are concentrated, and then, full-text search is used to realize the translation, and the analysis of the translation results is shown in Figure 8(b).

Figure 8(a) shows that when the similarity of the analogy matches is greater than 80%, most of the translation results retain the meaning of the source text. Only a small fraction (about 24.1%) requires users to make simple modifications based on the analogy-matched reference information to form a more accurate translation. Figure 8(b) shows that although some of these sentences can be retrieved using full-text search to find similar patterns, in most cases, these retrieved patterns are not very helpful for translation of the source text. Not only the similarity is low but also the same part is not enough to provide enough information for the translation of the source text.

In the process of testing the system, in the case of 3000 memorized data, the time of full-text search and translation in the two cases of indexing with abstract features were compared as shown in Figure 9. In addition to the search method, the factor affecting the translation time is the size of the library. For this reason, this paper presents the translation time when the library size is different as shown in Figure 9(b).

It can be seen from Figure 9(a) that the translation time using full-text retrieval is about ten times as long as that using feature indexing, which is enough to show that the abstract feature-constrained retrieval method greatly speeds up the memory search time, thereby significantly improving the translation speed.

The system translation test indicators include BLEU (Bilingual Evaluation Research) and online translation speed. The BLEU value is [0, 1]. The closer the BLEU value is to 1.0, the higher the translation quality, and the more accurate the interaction. Figure 10 is the test result of the BLEU index, and Figure 10(b) is the test result of the online translation speed index.

Figure 10 shows the translation of three test samples using different systems. The BLEU index value of the system in this paper is 0.98 in the Chinese-English system and 0.99 in the English-Chinese system, which is higher than in other

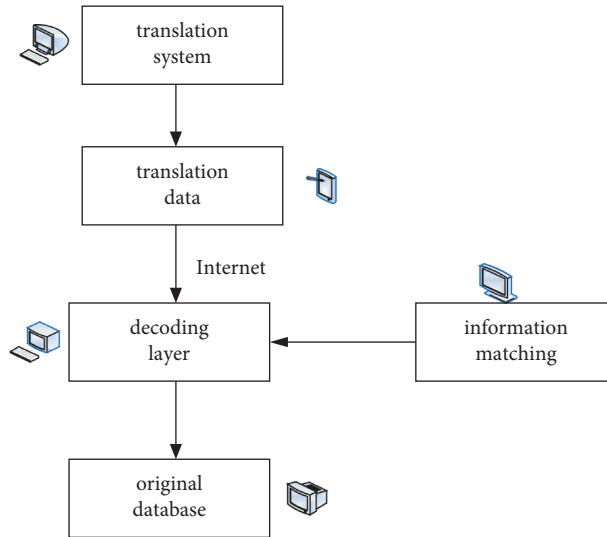


FIGURE 6: Schematic diagram of the RM-test algorithm.

TABLE 3: System operating environment.

Name	Environmental parameters	Name	Environmental parameters
Operating system	Windows 7	RAM	2 GB
Database	Microsoft SQL server 2016	Development language	VRML, HTML, C++
CPU	Pentium ^(R) dual-core CPU E5400 2.70 GHz	Hard drive capacity	320 GB

TABLE 4: Technical parameters of translation output machine.

Name	Parameter	Name	Parameter
Display	3.1-inch retina touchscreen	Power supply	DC 5 V/2 A
Camera	Autofocus HD camera	Battery	2500 mAh
Microphone	12S four-microphone array	Interface	Type-C
System interface	Chinese-English	Flash	LED fill light
Network standard	Mobile/Unicom/Telecom 4G/3G/2G	Processor	8-Core high-speed processor

TABLE 5: Corpus situation.

Numbering	Expected	Numerical value	Types of contextual translations
1	Number of conversations	9452	2
2	Number of sentences	396585	2
3	Total word count	6895698	2
4	Glossary	596694	2

systems. The BLEU index value of the system in this paper is larger and the translation speed is faster, which solves the problem of translation lag and error in the current translation system and improves the interaction with users.

5. Discussion

Through the above test results, we can draw the following conclusions. (1) The assisted translation system based on the Internet of Things can realize the correlation between English words and translations. Due to the large amount of

textual information in interactive online reading, language communication in the traditional sense is many-to-one or one-to-one. Therefore, when translating based on interactive network technology, it is necessary to consider issues such as the relevance between the user and the source word and the channel perception in order to achieve the desired effect. (2) Based on the interactive function of the interactive online translation system, the text information contained in the source language lexicon can be retrieved and matched and stored in the database. Therefore, the software has good real-time performance and accuracy.

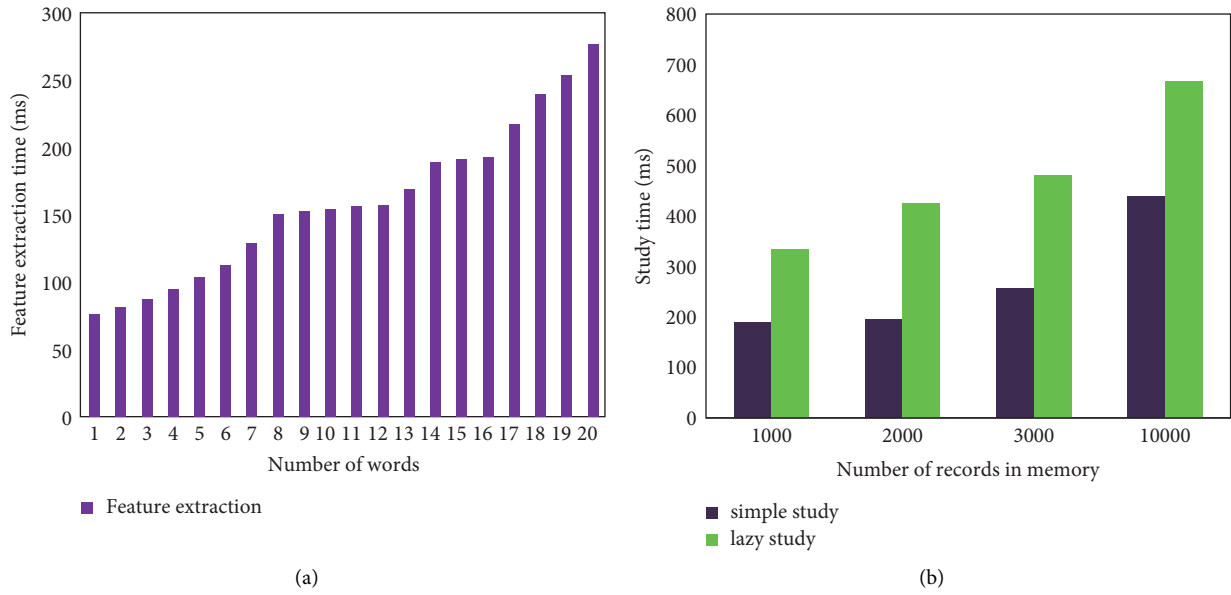


FIGURE 7: Duration of feature extraction and learning.

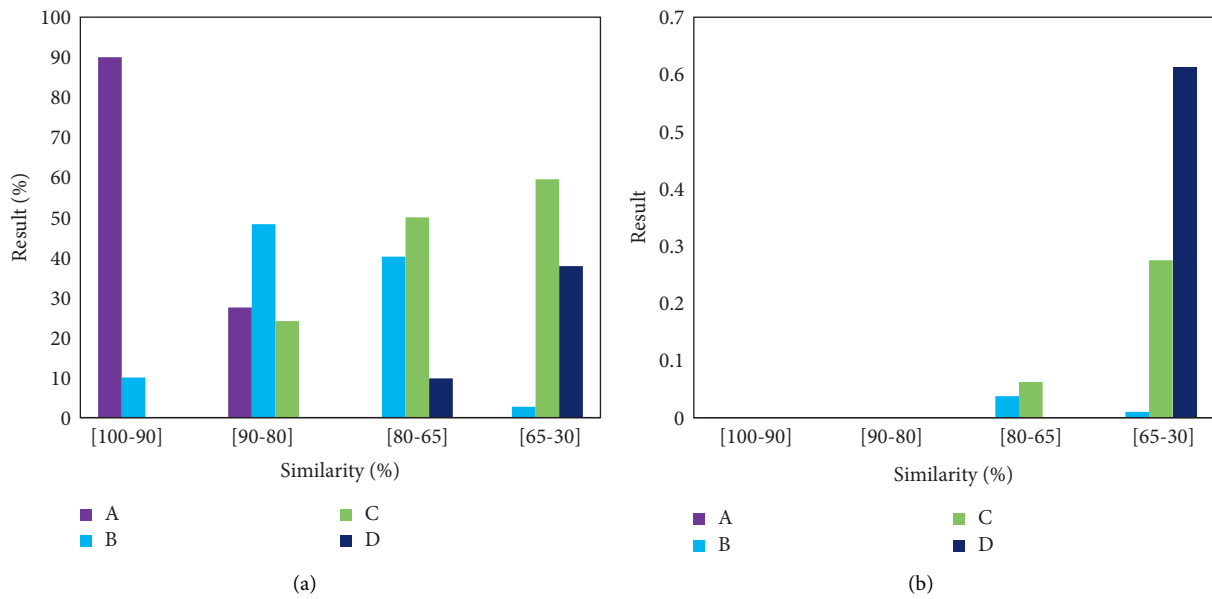


FIGURE 8: Evaluation and translation results.

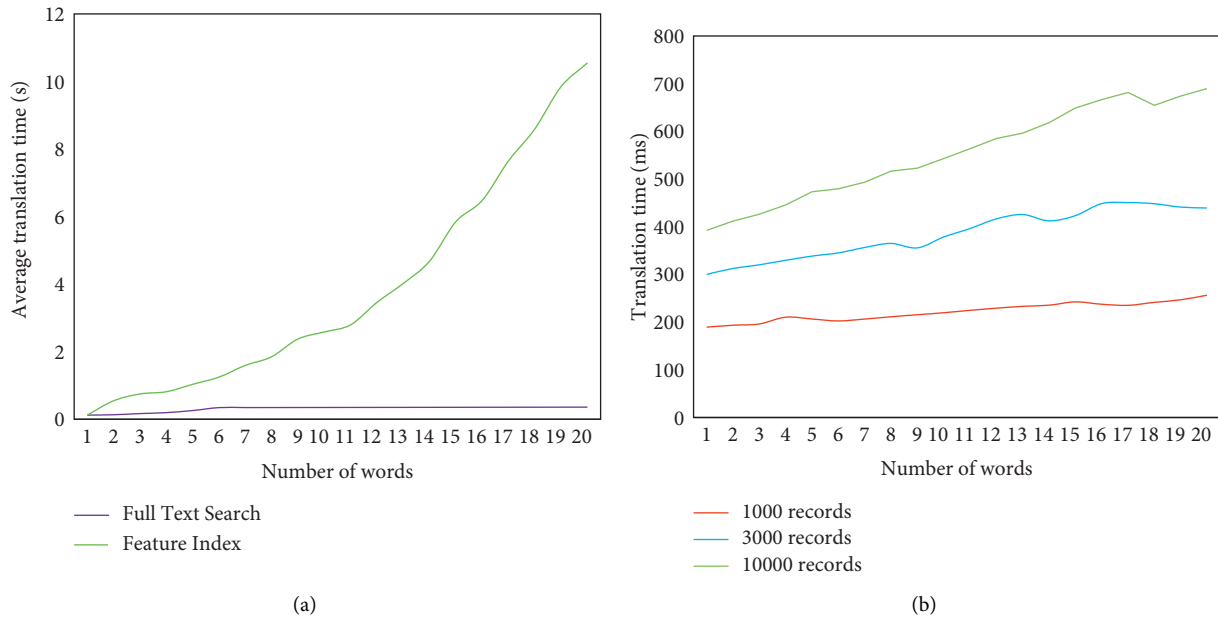


FIGURE 9: Translation duration.

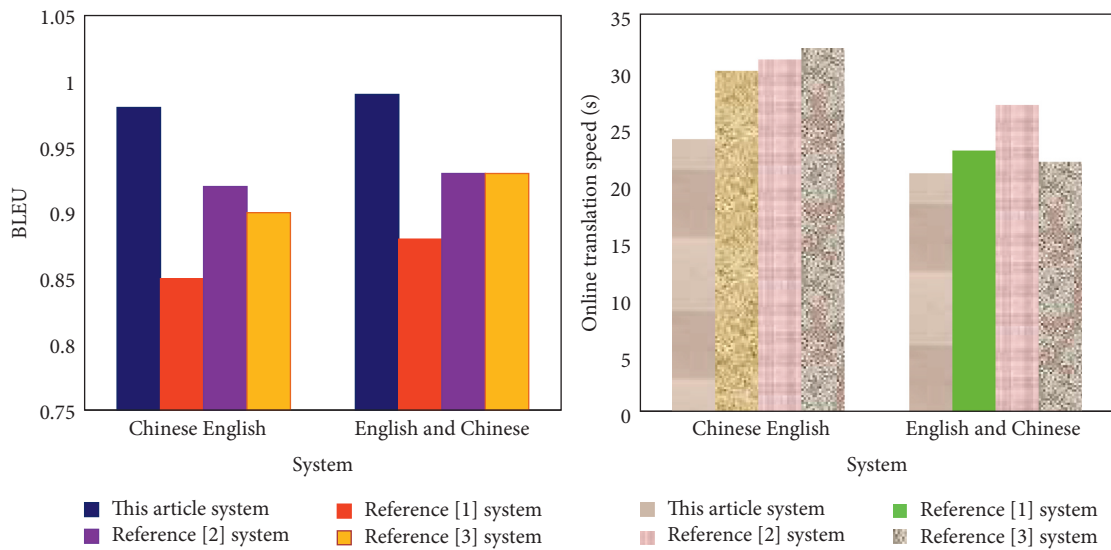


FIGURE 10: System translation performance test results.

6. Conclusion

In order to translate English efficiently and accurately, this research designs an interactive English translation system. The following conclusions are drawn from the work done in this paper: (1) the translation method based on corpus and correlation analysis is an effective, practical, and realistic method, but it cannot be directly applied to the English translation because the method itself is not a huge amount of text. At the same time, because this process requires a lot of data support, we only briefly introduce and verify it in this

paper to achieve related functions. (2) The interactive translation method based on data mining is an efficient and practical translation method. It can effectively retrieve different types of text information such as sentences and parts of speech in the English translation, so this technology has a high research interest value. (3) This translation method can not only solve the problem of huge amount of text and difficult to retrieve but also provide more convenience for English translation. For example, in the process of reading, sentences and parts of speech can be distinguished and relevant information can be extracted. In this paper, we can

find that the interactive translation method based on the Internet of Things can not only achieve text information retrieval but also provide more convenience for English translation. There are still many shortcomings in the paper. For example, due to the consideration of time, energy, and other factors during translation, the original meaning cannot be accurately expressed after the interactive translation is modified. Therefore, the paper focuses on web design based on IoT-assisted languages rather than the study of interaction mechanisms during translation.

Data Availability

The data that support the findings of this study are available from the corresponding author upon reasonable request.

Conflicts of Interest

The author declares that there are no conflicts of interest regarding the publication of this article.

Acknowledgments

This work was supported by Language-Education Collaborative Innovation Research Team in the New Era (XFU21KYTDB01).

References

- [1] Y. Liu, J. Zhang, H. Xiong et al., "Synchronous speech recognition and speech-to-text translation with interactive decoding," *Proceedings of the AAAI Conference on Artificial Intelligence*, vol. 34, no. 05, pp. 8417–8424, 2020.
- [2] H. Chen and J. Huang, "Research and application of the interactive English online teaching system based on the Internet of things," *Scientific Programming*, vol. 2021, no. S1, pp. 1–10, 2021.
- [3] Z. Yuan, C. Jin, and Z. Chen, "Research on language analysis of English translation system based on fuzzy algorithm," *Journal of Intelligent and Fuzzy Systems*, vol. 40, no. 4, pp. 6039–6047, 2021.
- [4] H. Ban and J. Ning, "Design of English automatic translation system based on machine intelligent translation and secure Internet of things," *Mobile Information Systems*, vol. 2021, no. 7639, pp. 1–8, 2021.
- [5] J. Sangeetha and S. Jothilakshmi, "Speech translation system for English to Dravidian languages," *Applied Intelligence*, vol. 46, no. 3, pp. 534–550, 2017.
- [6] F. C. Muga, M. O. Marennya, and T. S. Workneh, "A heat and mass transfer model for predicting the drying of beef during biltong processing using infrared-assisted Hot Air drying," *Journal of Biosystems Engineering*, vol. 46, no. 3, pp. 273–285, 2021.
- [7] K. Tatsuo, M. Takuma, and H. Hiroyuki, "Information processing apparatus, information processing method, and program storage medium," *Iyo Denshi to Seitai Kogaku*, vol. 4, no. 2, pp. 542–545, 2018.
- [8] D. Pandey, B. H. Kim, and H. S. Gang, "Maximizing network utilization in IEEE 802.21 assisted vertical handover over wireless heterogeneous networks," *Journal of Information Processing Systems*, vol. 14, no. 3, pp. 771–789, 2018.
- [9] N. Verma, S. Singh, and D. Prasad, "A review on existing IoT architecture and communication protocols used in healthcare monitoring system," *Journal of the Institution of Engineers: Serie Bibliographique*, vol. 103, no. 1, pp. 245–257, 2022.
- [10] Y. Wu, "Research on interactive model of English translation based on data mining," *International Journal for Engineering Modelling*, vol. 31, no. 1, pp. 273–279, 2018.
- [11] I. E. El-Henawy and M. Abo-Elazm, "Handling within-word and cross-word pronunciation variation for Arabic speech recognition (knowledge-based approach)," *Journal of Intelligent Systems and Internet of Things*, vol. 1, no. 2, pp. 72–79, 2020.
- [12] A. N. A. M. Al-Masri and A. N. A. Al-Masri, "Optimal algorithm for shared network communication bandwidth in IoT applications," *International Journal of Wireless and Ad Hoc Communication*, vol. 2, no. 1, pp. 33–48, 2021.
- [13] N. K. Ambarwati, R. Wiryasaputra, and S. Puspasari, "Pembangunan modul pembelajaran bahasa inggris menggunakan grammar translation method berbasis android," *Jurnal ULTIMATICS*, vol. 8, no. 2, pp. 83–91, 2017.
- [14] H. Anam, M. Sadiq, and H. Jamil, "Development of system usability scale (SUS) for the Urdu language," *International Journal of Computer Science and Information Security*, vol. 18, no. 6 JUN 2020, pp. 73–78, 2020.
- [15] D. Demirkol and C. O. Seneler, "Sistem kullanılabilirlik ölçeğinin türkçeye çevirisi: SUS-tr," *Usak University Journal of Social Sciences*, vol. 11, no. Eylül-2018, pp. 238–253, 2018.
- [16] J. Akbari, H. Heidari Tabrizi, and A. Chalak, "Effectiveness of virtual vs. nonvirtual teaching in improving reading comprehension of Iranian undergraduate EFL students," *The Turkish Online Journal of Distance Education*, vol. 22, no. 2, pp. 272–283, 2021.
- [17] A. Derakhshan and Z. R. Eslami, "The effect of metapragmatic awareness, interactive translation, and discussion through video-enhanced input on EFL learners' comprehension of implicature," *Applied Research in English*, vol. 9, no. 1, pp. 637–664, 2019.
- [18] R. Knowles, M. Sanchez-Torron, and P. Koehn, "A user study of neural interactive translation prediction," *Machine Translation*, vol. 33, no. 1-2, pp. 135–154, 2019.
- [19] A. G. Hapsani, F. Utamingrum, and H. Tolle, "Optical character recognition on English comic digital data for automated language translation," *International Journal of Advances in Soft Computing and Its Applications*, vol. 9, no. 3, pp. 186–198, 2017.
- [20] D. Liu and Y. H. Kim, "The juku online writing system as an interactive college English writing instructional tool in China," *STEM Journal*, vol. 22, no. 2, pp. 58–72, 2021.
- [21] X. Xue, J. Chen, and X. Yao, "Efficient user involvement in semiautomatic ontology matching," *IEEE Transactions on Emerging Topics in Computational Intelligence*, vol. 5, no. 2, pp. 214–224, 2021.
- [22] M. Morales, "Real English interactive level 1 version 2.0," *CALICO Journal*, vol. 18, no. 1, pp. 187–195, 2013.
- [23] L. Jiang, L. Chen, T. Giannetsos, B. Luo, K. Liang, and J. Han, "Toward practical privacy-preserving processing over

- encrypted data in IoT: an assistive healthcare use case,” *IEEE Internet of Things Journal*, vol. 6, no. 6, pp. 10177–10190, 2019.
- [24] N. N. Dao, D. N. Vu, Y. Lee, S. Cho, C. Cho, and H. Kim, “Pattern-identified online task scheduling in multitier edge computing for industrial IoT services,” *Mobile Information Systems*, vol. 2018, no. 1, pp. 1–9, 2018.
- [25] J. Rao, T. Ao, S. Xu, K. Dai, and X. Zou, “Design exploration of SHA-3 ASIP for IoT on a 32-bit RISC-V processor,” *IEICE Transactions on Info and Systems*, vol. E101.D, no. 11, pp. 2698–2705, 2018.
- [26] A. S. Dhanjal and W. Singh, “An automatic machine translation system for multi-lingual speech to Indian sign language,” *Multimedia Tools and Applications*, vol. 81, no. 3, pp. 4283–4321, 2021.

Research Article

Implementation of Creator-Based Virtual Simulation in News Interview

Wen Zhou 

School of New Media and International Communication, South China Business College of Guangdong University of Foreign Studies, Guangzhou 510545, Guangdong, China

Correspondence should be addressed to Wen Zhou; 211032@gwng.edu.cn

Received 8 April 2022; Revised 16 May 2022; Accepted 29 July 2022; Published 21 August 2022

Academic Editor: Xuefeng Shao

Copyright © 2022 Wen Zhou. This is an open access article distributed under the Creative Commons Attribution License, which permits unrestricted use, distribution, and reproduction in any medium, provided the original work is properly cited.

With the development of network information technology, the application of virtual simulation technology in medicine, electromechanical, military, and other fields has changed the traditional field operation mode and achieved good results, but the application of virtual simulation technology in the field of news and communication is very little. This paper takes the construction of virtual simulation news system as an example. Based on the support of 3D modeling technology of Multigen Creator, the functional requirements of virtual simulation news interview system are analyzed, the overall system objectives and architecture are set up, virtual scene database, 3D entity modeling, model optimization, and real-time rendering are established. A virtual simulation system for emergency news interviews is designed and developed, including real-time simulation environment and online operational feedback. This paper discusses the application effect of the system. By means of the questionnaire survey, SPSS23.0 is used to further analyze the feedback data of users. The data show that the expected functions of 3D modeling and real-time simulation of system modules have been realized. The research shows that virtual simulation technology can be successfully applied in the field of news and communication, and can successfully penetrate into the practical dimension of news and communication, change the existing single information interaction mode, and create a new era of real-time simulation.

1. Introduction

The rapid development of computer technology and artificial intelligence technology has brought opportunities for the application of virtual simulation experiment technology in the field of education. Virtual reality, which originated in the late 1960s, has gradually realized the high integration with the depth and breadth of experimental teaching in colleges and universities after decades of maturation. Since the Ministry of Education launched the construction of national virtual simulation experimental teaching center nationwide in 2013, virtual simulation experimental projects of various disciplines have been successively implemented in universities [1]. In October 2018, the Ministry of Education pointed out in the “opinions on accelerating the construction of high-level undergraduate education to comprehensively improve talent cultivation ability,” “to promote the deep integration of modern information technology with

education and teaching, build about 1,000 national virtual simulation experimental teaching projects, and improve the quality and level of experimental teaching” [2]. In the same year, the Ministry of Education announced the first batch of national virtual simulation experimental teaching projects.

However, it cannot be ignored that among the national virtual simulation experimental teaching projects that have been approved, the number of journalism and communication projects is 10, accounting for only 3.4%. In addition, the data obtained from the first simulation teaching competition held by the Chinese simulation society in 2021 showed that journalism and communication accounted for less than 1% of 327 virtual simulation teaching works submitted by 132 colleges and universities across the country. The application of virtual simulation technology is mainly reflected in engineering, medical science, mathematics, physics and chemistry, and other disciplines. Compared with the multi-frequency application of virtual

simulation technology in science and technology, the development of humanities, especially journalism and communication virtual simulation experiment projects, lags behind obviously. Around the world and combining the COVID-19 outbreak, in the construction of emergency news interview fusion virtual simulation experiment platform for practice and theoretical research, related research fields are blank.

The virtual simulation system of emergency news interviews forms powerful support for news interviews with the most intuitive and lifelike experience effect. With its strong immersion and extensive interaction, students can instantly get familiar with the special and strange environment on the “scene,” changing the traditional single information interaction structure, and achieving a good application effect.

Virtual Reality, which can be traced back to the late 1960s, uses advanced technological means to build a virtual simulation system to imitate the real environment of entity existence [3]. This technology relies on the necessary technical guarantee and support brought by the rapid development of electronic technology and digital information technology. The application of VR technology in the early stage is similar to that in the early stage of the development of high-energy computers, with huge volumes and relatively strict requirements for the use of equipment. It is limited to the viewing of secret information in key and special fields, and its single function determines the limited use of this technology.

With the development of digital electronic technology, the well-known head-mounted VR equipment emerged in the 1970s [4], breaking through the limitation of a single functional field of VR equipment, and having abundant involvement and performance in image processing and multimedia technology application field. This emerging technology with the National Aeronautics and Space Administration of the United States of America to the depth of its scope of application, so that VR equipment in a real sense based on optical display for image information interaction, change the existing information interaction structure so that VR technology widely into e-sports, medical, education, and other fields. In the field of e-sports, the application and deep cultivation of VR technology bring a good entertainment experience to players [5].

In the late 1990s, the development and popularization of computer equipment in China laid a solid foundation for the development of information technology in China. The development of Internet market resources has become an important place for the development of China’s information technology industry, and the mainstream direction of Internet market resources development focuses on commercial VR technology. The proliferation of commercial VR technology is driving related fields such as military, medical, and education. The United States and Germany are the first to test VR technology in higher education, accumulating VR technology experience in the field of education. The application of simulation technology in the field of education started in 1989, when professor William Wolf of University of Virginia put forward the concept of virtual experiment for

the first time [6], which became the beginning of virtual simulation experiment research. Subsequently, the iLad remote sharing lab was established at MIT.

Different from foreign virtual simulation technology that entered the field of higher education earlier, domestic virtual simulation technology started late in the field of higher education experiments [7]. Since 2015, China has implemented the “double first-class” education policy, aiming to build China into a higher education country in the middle of the 21st century, enhance international core competitiveness, improve teaching quality, cultivate high-quality talents, accelerate the development of higher education, and realize the modernization of teaching management. Colleges and universities try to carry out virtual simulation experiments teaching by optimizing teaching quality and deepening talent cultivation.

The rise of virtual simulation technology experiment teaching is closely related to the government’s high attention and policy. In August 2013, the Ministry of Education launched the construction of the national virtual simulation experimental teaching center, which fully reflects the important position of virtual simulation teaching in the practical teaching system of colleges and universities [8]. In 2016, 300 national virtual simulation experimental teaching centers have been established in mainland China. In 2017, the Ministry of Education issued the “Notice on the Construction of Demonstration Virtual Simulation Experimental Teaching Project” from 2017 to 2020, advocating universities at all levels to actively build virtual simulation experimental teaching projects combining curriculum systems and training objectives. On October 8, 2018, the Ministry of Education and the Publicity Department of the CPC Central Committee issued opinions on “Improving the Cultivation Ability of Journalism and Communication Talents in Universities and Implementing the Education and Training Plan 2.0 for Outstanding Journalism and Communication Talents,” which clearly pointed out that 50 national virtual simulation experimental teaching projects of journalism and communication should be built [9]. On April 29, 2019, the “six excellent and one top” program 2.0 launch meeting was held, and the virtual simulation gold course was clearly proposed to be included in the first-class course construction “double thousand plan.” According to the “Notice on the Construction of Demonstration Virtual Simulation Experimental Teaching Projects” from 2017 to 2020 issued by the general office of the Ministry of Education, the Ministry of Education will identify about 1000 demonstration virtual simulation experimental teaching projects by 2020 [10].

Under this good opportunity, domestic universities actively respond to the local conditions to carry out virtual simulation experiment technology practice and research in a number of disciplines. At present, the domestic construction of Tsinghua university has a mechanical virtual experiment system, the space remote sensing operation robot research, national university of defense technology of virtual battlefield modeling and simulation technology research, Beijing University of technology in civil engineering national virtual simulation lab, Beijing University of aeronautics and

astronautics build research and development of flight simulator, flight simulation and application of special effects in the scene, The virtual technology and system of vehicle vibration test and vehicle driving dynamics developed by Zhejiang University, and the influential experimental system of human-computer interaction and virtual robot research by Harbin Institute of Technology.

2. Related Work

Since the Ministry of Education launched the construction of national virtual simulation experiment teaching center nationwide in 2013, virtual simulation experiment projects of various disciplines have been successively implemented in colleges and universities. In October 2018, the Ministry of Education announced the first batch of national virtual simulation experimental teaching projects. Among the 296 national virtual simulation experimental teaching projects announced by the Ministry of Education, medicine and pharmacy are 74, accounting for 25%; there are 38 items in engineering, accounting for 12.8%, 29 items in chemistry and chemical engineering, accounting for 9.8%, and 20 items in machinery, accounting for 6.8% [11]. It is not difficult to see that the subject areas of virtual simulation technology have obvious commonalities: the real working environment is a high risk, and there is personal danger in field experiments or investigations; field experiments require expensive equipment, fast wear and depreciation of equipment, short product replacement life cycle, and high experimental costs; in particular, the operation procedure of medical field experiment has irreversibility, and a slight error poses a threat to life and health. The virtual simulation technology is no different from maximizing the experimental teaching effect with a low-cost mimicry environment. On the other hand, only 10, or 3.4%, were approved for journalism and communication. According to the data of the national virtual simulation experiment teaching project sharing platform in 2022, journalism 19 items, radio and television 12 items, communication 7 items, network and new media 5 items, editing and publishing 2 items, and advertising 1 item. At present, digital publishing, fashion communication, international news, and communication have no projects. Compared with the widespread application of virtual simulation technology in science and technology, the development of virtual simulation experiment projects in humanities is still lagging behind [12]. This is related to the traditional humanities paradigm. The traditional liberal arts education emphasizes the self-sufficiency of the subject knowledge system, and the humanistic theory is elaborated more than the technology or technical thinking. With the penetration and development of new technologies, humanities should shift from a self-sufficiency knowledge system to social demand orientation under the guidance of new technologies. Supported by the global new scientific and technological revolution and based on the new economic development model, the new humanistic thinking of interdisciplinary integration has not yet become a consensus. It can be seen that most universities in China have not taken advantage of the existing geographical resources and

teaching resources to develop virtual simulation experiment projects but it also brings great development potential and space in the application of simulation experiment teaching.

According to the names of the projects that have been established, the subjects of the successful journalism experiment projects are mainly news gathering and reporting in the traditional media environment. For example, Wuhan University's "Data News Writing Process Simulation Experiment Teaching Project," Renmin University of China's "Virtual simulation Experiment Teaching Project of Integration of Major Themes in Media Reporting and Public Decision support." The topics of communication programs include "Virtual Simulation Experiment of Mobile News Client Development" of Huazhong University of Science and Technology, "Virtual Simulation Experiment of Integrated News Reporting of Science and Technology Powerful Country" of Shanghai Jiao Tong University, and "Virtual Simulation Experiment of Quantitative Empirical Research Ability Test" of Beijing Foreign Studies University. Web and new media topics, such as Zhejiang University's "Online Video Production and Publishing Virtual Simulation Major Experimental Teaching." Current project themes focus primarily on traditional information operations. Lack of new media digital product production, creative communication, and writing topics; the applicants are mainly from China's top-notch universities with strong comprehensive strength. The virtual simulation projects of journalism and communication in nondouble first-class universities are still blank. Investigate its reason, the equipment used for VR 360 panoramic shooting mainly includes SLR camera, fisheye lens, tripod, panoramic head, spare battery, camera bag, SD card, etc. The hardware cost is not low. In addition to the cost of conventional equipment and hardware, it needs a lot of production time and technical support to make the virtual news and communication platform. However, the lack of compound talents restricts the construction of virtual simulation platforms of nondouble first-class universities. Application talents of virtual simulation technology not only need strong professional knowledge structure, accurate grasp of platform theme direction and innovative media thinking but also need to be able to skillfully apply virtual simulation technology. Due to the limitation of capital, equipment, technology, and talent demand, virtual simulation project is difficult to put into practice in nondouble-first-class universities.

There are many kinds of research on the application and efficiency of virtual simulation technology at home and abroad. Chasson et al. pointed out that the internal motivation for learning comes from students' sense of acquisition and self-identification of learning activities. Virtual simulation technology enhances learners' learning motivation by providing learners with personalized services, colorful presentation forms, and timely feedback [13]. Andreev et al. hold a similar view that virtual simulation can bring positive emotions such as relaxation, pleasure, and satisfaction to students. Thus, students' internal motivation for learning can be stimulated [14]. Putz et al. focused on the study of factors influencing the learning effect of virtual simulation systems [15]. Some domestic scholars focus their research on

virtual simulation technology in fields closely related to social life, such as Li's research and design of a subway driving simulator based on simulation technology [16], Lu and Dong pointed out that the construction and practice of virtual simulation experiment teaching center for materials majors [17], Yao et al. pointed out that application of virtual simulation experiment teaching in molecular biology experiment teaching [18]. There are few studies on the application of virtual simulation in the field of news and communication. Liu proposed to build a "hierarchical + gradient" virtual simulation experimental teaching system and a "multi-platform + collaborative" virtual simulation experimental teaching matrix with the goal of gold course construction [19]. Taking journalism and communication majors as an example, Fan explored the application effects and influencing factors of virtual simulation experiment teaching projects in cloud environments through empirical methods [20]. Yang and Sun put forward measures to construct the sustainable development model of "VR + Journalism education" on the basis of analyzing the application status of virtual reality technology in journalism and communication practical teaching [21]. The research at home and abroad focuses on the application of virtual simulation technology in the field of science and technology, but the application research in journalism and communication is few. In cnKI.COM, the comprehensive search of "virtual simulation news and communication" in the categories of works, conference papers, journals, master and doctoral papers shows only 161 relevant literature, and 11 literature related to the virtual simulation platform of journalism and communication involving nondouble first-class universities, accounting for 6.83%. Continue to discuss and study, help to fill the theory of the deficiency and lack.

3. The Architecture of Virtual Simulation News Interview Platform Based on Creator

News interview is a basic skill for journalists. As a professional basic course for undergraduate students of journalism, news interview is the main course for students of journalism and communication to understand and master the knowledge of news interview, and it is also an indispensable compulsory course for journalists. The teaching of this course focuses on enabling students to master the internal laws and methods of news acquisition, learn to use the basic principles of news acquisition, and lay a solid foundation for news acquisition in the future. The classroom teaching of journalism interviews focuses on cultivating and training students' professional skills and creativity.

Theory should be put into practice. However, at present, the practical teaching of this subject is limited to the lack of social resources, and most of it is merely theoretical teaching in class. There are few practical forms for students to go out of school and truly understand and master the skills of interviews. Therefore, the reform of education and teaching is imperative. Especially in the news interview of emergency that cannot reach the interview site due to objective factors, it is an important part of the teaching content of news interview. In view of this, the author and her team built a

virtual simulation experimental teaching platform for the integration of emergency news interviews and reporting, and simulated the real environment through VR virtual simulation teaching experiment, making a positive attempt and discussion for the virtual simulation experimental teaching of news and communication in independent colleges.

3.1. Construction Purpose. According to the definition of the concept of emergency defined in The Law of the People's Republic of China on Emergency Response (2019.08.30), an emergency is a natural and accidental disaster, public health and social security event that occurs suddenly, causes, or produces serious harm to the society and requires immediate management measures. From SARS, which first broke out in Guangdong in 2003, to COVID-19, which is now raging around the world, people's lives and health have been endangered and society has been greatly affected in many aspects. From SARS, which first broke out in Guangdong in 2003, to COVID-19, which has now affected 210 countries, territories, and regions around the world, endangering people's lives and health and causing a huge impact on many aspects of society. Public health emergencies are characterized by abruptness, difficulty in approaching, inability to reproduce the scene, and inability for journalists to arrive at the scene for the first time. In actual teaching, it is difficult for teachers to restore the news scene through traditional teaching methods such as pictures and texts, and it is difficult to leave an intuitive impression on students. In view of the fact that students have little real interview experience and the innovative thinking advocated by the school, the author makes a preliminary attempt to build a virtual simulation news interview platform based on creator. Before the teaching of the news interview course, students have learned "Integrated journalism," "Network Journalism Practice," "Introduction to Media science," "Media Development History," "Network Public Opinion Monitoring and Research," "Web design and Production" and other related courses, and have certain media literacy and technical operation ability. On the basis of students' full understanding of news events and knowledge of relevant news points, through the experimental mode that teachers combine virtual simulation technology with news interview teaching, students can have an immersive and interactive experience and master the methods and skills of news interview of emergencies represented by public health emergencies. This project aims to cultivate students' news sensitivity, news information acquisition ability, emergency response ability, humanistic care, and journalism professionalism in public health emergencies.

3.2. Construction Roadmap. Combined with the outbreak of the public health crisis of COVID-19, a virtual simulation environment is set for interviews of Novel Coronavirus infected patients in Wuhan Jinyintan Hospital. The new model of "virtual simulation experience—evaluation and feedback of experimental results—effect improvement" is adopted to allow users to enter the virtual scene independently. Immersive and interactive experience of all links of on-site interview,

exercise users' ability of information collection, writing, and verification, and cultivate news sensitivity, professional ethics, and self-protection awareness.

This system restores the specific situation that the reporter interviews in the crisis scene of public health events for the students. Here, users can not only enter the hospital hall, doctors' offices, and nurses' stations, observe the surrounding environment and equipment and facilities, but also learn various information about medical staff and patients, such as the psychological status of medical staff, epidemic control situation, patient admission rate, and discharge rate. At the same time, users need to select appropriate clothing equipment for protection before entering the hospital, so as to ensure personal safety.

Traditional emergency news is confined to the classroom teaching, teaching mode because of breaking news events immediacy, the scene is difficult to reproduce, the reporter to the first arrival event scene, this system set the interview situation simulation reduction, task-driven, project management. The three stages strengthen the immersive virtual simulation technology, interactive and idea. In the interview situation reduction key link, is meticulous divided into background knowledge, news, online testing, test results, feedback, etc., and set in each link of different tasks, such as according to the field observation information check, what problem can carry, interview the purpose, to encourage students to actively explore, to complete the corresponding task. This project adopts the gamification setting mechanism, which will give immediate feedback according to the completion of the task of the virtual reporter. The correct operation will be encouraged, and the improper operation will be reminded accordingly, which can effectively motivate the experimenter, continuously increase the difficulty of the challenge and stimulate the interest in participation.

3.3. Technical Support. High-speed network exists, high-performance server, large capacity storage, network firewall, virtual simulation experiment management platform, and other equipment and facilities are used for virtual simulation experiment project operation. Network the system deployed on a LAN server must have a broadband speed greater than 50 MBIT/s and can support 100 concurrent online users. Users can use computers, mobile phones, tablet computers, and other devices to log in to the virtual simulation experiment platform to complete the experience under the broadband network environment.

The opening and operation of the virtual simulation project of emergency news interview rely on the support of the open virtual simulation experiment teaching management platform, and the two are connected seamlessly through the data interface. Based on computer simulation technology, multimedia technology, and network technology, the platform adopts service-oriented software architecture development and integrates physical simulation, intelligent guidance, automatic correction of virtual experiment results, and teaching management. The construction target is a virtual experiment platform with good autonomy, interactivity, and extensibility.

At present, the representative development tools for virtual simulation experiment projects include Unity, 3D Max, Maya, Nibiru Creator, MuGeDa, Pr, Animator, Captivate, Flash, etc. Multigen Creator is a real-time visualization 3D software system, which is a professional software for real-time visual simulation. Multigen Creator features powerful polygon modeling, vector modeling, and accurate generation of large area terrain. Built-in Vega Prime-based previews, the users can browse the processing modeling (RPM) wizard tool to quickly create buildings and other objects, and create wySIWYG 3D modeling environment. Its various plug-ins can efficiently and optimally generate real-time 3D (RT3D) database, which can be connected to the real-time simulation software. Multigen Creator features polygon modeling and modification tools such as construction points, extrusion, subdivision, and T-vertex elimination. Viewing volume and clipping planes can be set, and functional nodes such as DOF (degree of joint freedom), LOD (level of detail), and Switch (logic Switch) can greatly meet the requirements of virtual simulation system for a news interview. Based on this, the system uses Multigen Creator 3D modeling software and Vega Prime real-time driver software as technical support and adopts distributed virtual reality system (DVR), that is, virtual reality systems scattered in different geographical locations are connected together through the Internet. The unified structure, standards, protocols, and databases are adopted internally to form a synthetic virtual environment that is coupled with each other in time and space. To satisfy multiple participants to simultaneously participate in a virtual space and freely interact and work collaboratively. The most typical examples of such systems are multi-user virtual environments that are widely used abroad, such as Second Life, Active World, Whyville, and Kitley platforms [22].

The design idea of the system is shown in Figure 1. 3D software modeling and processing, 3D engine driving, and the virtual simulation system is constructed and completed. The basic process of the system is mainly divided into 6 links, including construction objectives, field investigation, overall design, test and verification, interactive roaming, and practical application, as shown in Figure 2. Among them, database construction, modeling, texture mapping, and integrated rendering are the key links of actual construction.

4. Design and Implementation of Virtual Simulation Emergency News Interview Platform

4.1. 3D Visualization Modeling Technology. The system needs 3D visualization modeling of protective equipment and interview equipment room, hospital office area, and hospital outpatient building. Protective equipment and interview equipment room area set up equipment racks, protective clothing, masks, cameras, microphones, and other object models; the office area includes a desk, computer, file cabinet, screen, and other models; it is shown in Figure 3. In the modeling of Wuhan Jinyintan Hospital, the outpatient

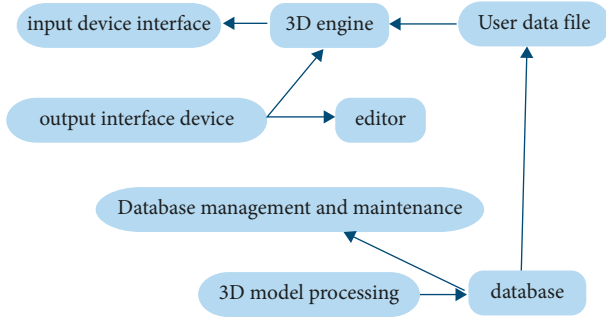


FIGURE 1: Construction idea of virtual simulation system.

building hall, doctor's office, and nurse's office were mainly created.

4.1.1. Examples of Technology. The instance technique in Multigen Creator minimizes the repetition of building the same model, greatly save and free up memory space. When multiple models with the same physical structure are required to construct simulation scenes, the data of one model can be shared and its position can be changed through matrix transformation to improve the rendering performance of the system. Through matrix conversion, the shared model can be rotated, translated, zoomed in, and zoomed out in virtual space to complete the construction of multiple models. Assume that the geometric transformation matrix of the 3D model is T_{3D} , and its expression is as follows:

From the perspective of a transformation function,

$$T_{3D} = \begin{bmatrix} a_{11} & a_{12} & a_{13} & a_{14} \\ a_{21} & a_{22} & a_{23} & a_{24} \\ a_{31} & a_{32} & a_{33} & a_{34} \\ a_{41} & a_{42} & a_{43} & a_{44} \end{bmatrix} \text{ it can be divided into four:}$$

$$T_{3D1} = \begin{bmatrix} a_{11} & a_{12} & a_{13} \\ a_{21} & a_{22} & a_{23} \\ a_{31} & a_{32} & a_{33} \end{bmatrix} T_{3D2} = \begin{bmatrix} a_{14} \\ a_{24} \\ a_{34} \end{bmatrix} T_{3D3} = [a_{41} \ a_{42} \ a_{43}]$$

$$T_{3D4} = [a_{44}]$$

Among them, T_{3D1} produces geometric transformations such as proportion and rotation; T_{3D2} produces projection transformation; T_{3D3} produces translation transformation; T_{3D4} produces a global scale transformation. For example, to translate the model from point $A(x, y, z)$ to point $B(l_x, l_y, l_z)$, the translation equation is mentioned below:

In order to scale the model relative to the origin of coordinates, the scaling ratio is (t_x, t_y, t_z) , and the transformation matrix equation is: $[x' \ y' \ z' \ 1] = [x \ y \ z \ 1]$

$$\begin{bmatrix} t_x & 0 & 0 & 0 \\ 0 & t_y & 0 & 0 \\ 0 & 0 & t_z & 0 \\ 0 & 0 & 0 & 1 \end{bmatrix}$$

If the rotation operation is to be carried out, it is assumed that β Angle is rotated around the coordinate axis relative to the origin of the coordinate system, the transformation equation of its rotation around the three coordinate axes is:

We rotate it around the x -axis $[x' \ y' \ z' \ 1] =$

$$[x \ y \ z \ 1] \begin{bmatrix} 1 & 0 & 0 & 0 \\ 0 & \cos\beta & \sin\beta & 0 \\ 0 & -\sin\beta & \cos\beta & 0 \\ 0 & 0 & 0 & 1 \end{bmatrix}$$

We rotate it around the y -axis $[x' \ y' \ z' \ 1] =$

$$[x \ y \ z \ 1] \begin{bmatrix} \cos\beta & 0 & -\sin\beta & 0 \\ 0 & 1 & 0 & 0 \\ \sin\beta & 0 & \cos\beta & 0 \\ 0 & 0 & 0 & 1 \end{bmatrix}$$

We rotate it around the z -axis $[x' \ y' \ z' \ 1] =$

$$[x \ y \ z \ 1] \begin{bmatrix} \cos\beta & 0 & \sin\beta & 0 \\ -\sin\beta & 1 & \cos\beta & 0 \\ 0 & 0 & 1 & 0 \\ 0 & 0 & 0 & 1 \end{bmatrix}$$

4.1.2. Texture Mapping. Texture mapping refers to mapping 2d images to corresponding points of 3D models without increasing the number of polygons, so as to enhance the realistic visual effect of the model and improve its truthfulness of the model. After the basic modeling is completed, texture mapping can be further combined with material and light and shadow fusion to enhance the fidelity of the model. Texture can provide the best 3D line elements due to the full use of perspective transformation. In addition, texture can reduce the number of polygons in the virtual environment, and speed up the transformation and refresh frequency of the graphics display.

The basic modules for texture mapping are texture toolbox, texture palette, and MoD texture. After the basic modeling of the main geometric model construction, material, and light source is completed, texture production is started to complete the preparation of texture. After that, texture import-setting the current texture-selecting target geometry-applying texture, texture mapping is completed, and the model effect is checked by window preview/LynX preview/Vega preview.

In the process of texture preparation, image processing tools such as photoshop can be used to process images. When the model texture is in JPG format, it cannot be displayed in the real-time operating environment of Vega. Thus, when the texture is prepared, the texture can be saved to the graphics output formats acceptable to openflight, such as 8-bit grayscale format, 8-bit grayscale and 8-bit alpha channel format, 24-bit tricolor format, 32-bit tricolor, and 8-bit alpha channel format. Multigen Creator supports a variety of general standard image formats, commonly used mainly INT, INTA, RGB, and RGBA, when mapping texture using RGB and RGBA two formats, its purpose can be better compatible with Vega. When rendering texture, the real-time system requires that the size of the texture image in the horizontal and vertical directions must be 2 to the power of n , such as $32 * 64$, $128 * 256$, and other ways conducive to system reading, otherwise, it will not be displayed normally or distorted. Second, it is recommended to use the corresponding path of the texture. Use the List Texture tool to change the path, otherwise, the texture will not be displayed.

Texture space is a coordinate space with U and V as horizontal and vertical axes, respectively. The minimum unit of a two-dimensional texture image in the texture space is the grain element. After the texture image is loaded into the texture memory, the real-time system can call texture resources in the model database at run time. Calculation formula of texture memory for: X direction texels size

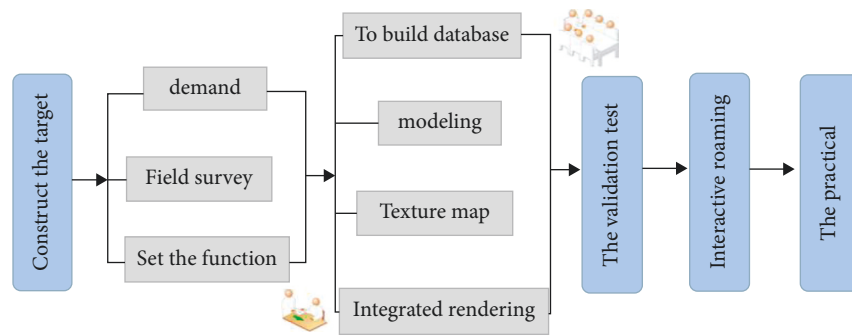


FIGURE 2: Development flow of virtual simulation system.

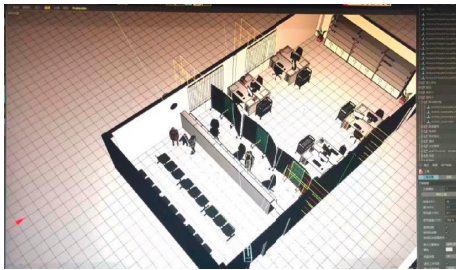


FIGURE 3: Outpatient hall of Wuhan Jinyintan Hospital.



FIGURE 4: Modeling equipment room.

multiplied by the Y direction texels size multiplied by the number of color channels. The X- and y-direction pixel size represents the length and width of the texture image respectively. After importing the texture image into MultiGen Creator, select the geometric model object to be pasted with the texture, and then use the texture mapping tool to map the texture image to the polygon surface of the model. Three-point mapping, four-point mapping, surface mapping, and column mapping are the main mapping methods. According to different mapping objects, select the corresponding mapping mode; according to the production requirements, the flexible use of texture mapping tools to complete texture mapping. Texture mapping can preview the mapping effect in LynX. Based on the consistency of MultiGen series software products, as long as the built model can see a good mapping effect in LynX, it can be normally applied in the simulation system developed based on Vega.

Specific to the construction of a single model, such as a female doctor, basic modeling, batch processing rendering tools, texture mapping, etc., can be used to make the prototype of the model concrete and vivid step by step. Figures 3 and 4, respectively, show the interview equipment room for modeling protective equipment and the outpatient hall of Wuhan Jinyintan Hospital. Figures 5 and 6 show the process of a female doctor from prototype to finished product. The system for model construction, model optimization, texture mapping, model rendering maximum quality production, and original scene plot, reflect the required model scene or object high fidelity, and improve the user's sense of immersion.

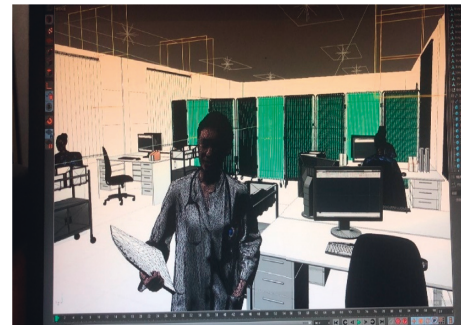


FIGURE 5: Model the female doctor prototype.

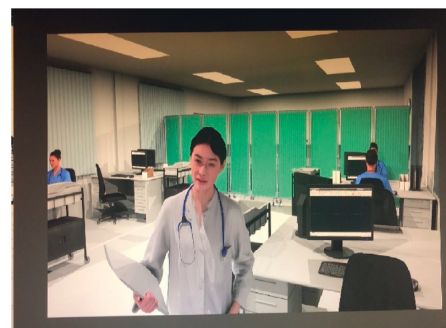


FIGURE 6: Modeling a female doctor.

4.2. System Application. The model of this project adopts classroom teaching integrated with virtual simulation experimental platform teaching, task-driven and online testing, and experimental result evaluation.

4.2.1. Virtual Simulation Experiment Platform Classroom Teaching. Teachers adopt the problem-oriented PBL (Problem-based Learning) teaching mode to conduct theoretical teaching from four dimensions: brief introduction of emergency, basic requirements of emergency interview, virtual simulation experiment, and humanistic care of emergency interview.

In the brief introduction of emergencies, teachers can focus on four types of emergencies, such as natural disasters, accidents, public health, and social security, with high pixels and strong impact images to enhance students' memory of the types of emergencies. With a positive attitude, the transmission mechanism should continue to explore the value determination, theme selection, and interview perspective of emergencies, enrich the interview strategies of catastrophic events, and find their own role and space. Therefore, the basic requirements of the emergency interview are to do a good job in planning the report and determine the report scheme; second, to prepare for the interview, make interview plan, make necessary material preparations, and interview outline in advance; when teaching interview preparation, students should clarify the latest background of COVID-19, policy requirements for epidemic prevention and control, information points to be obtained. The necessary material preparation can be carried out on the virtual simulation news interview platform. The teacher is required to introduce the functional modules in the virtual simulation system and their use methods, and explain the experimental requirements, experimental content, and experimental process. After mastering the types of emergencies and interview requirements, students entered the interview simulation scenario of COVID-19, a public health crisis.

The experiment project reproduced the specific situation of the all-media journalists entering Wuhan Jinyintan Hospital for interviews in 2020 when the COVID-19 epidemic was raging around the world and Wuhan was completely shut down, as shown in Figure 7. The first step is in the interview equipment and protective equipment room. All media reporters need to select appropriate interview equipment and protective equipment. If they make a wrong choice, they will be prompted accordingly. All media reporter has entered the hospital clinic, the doctor's office, the nurse station, experiential observation interview hospital treated patients, patients can open information, control epidemic situation, pay attention to health care workers and patients' psychological status, interview questions reveal of humanistic care, manifests the journalist's occupational morality and comprehensive quality.

4.2.2. Task-Driven and Online Testing. This project mainly evaluates the ability of all-media journalists to obtain information, interview information, and check information, as well as their awareness of self-protection. In the task-driven aspect, the abilities and skills to be assessed are divided into preparation before the interview, background acquisition, obtaining news clues, interview plan, interview outline, interview questions, news writing, news release, and other links. Different tasks and tests are set up in each link. For example, when interviewing doctors, appropriate questions can be asked about what aspects of the event. After the selection of all-media reporters, warm tips will be given for attention. Human-computer interaction friendly interface, not only promotes the exploration desire of all media journalists, at the same time but also strengthens the adhesion of virtual simulation experiment platform users.

4.2.3. Evaluation of Experimental Results. The evaluation of experimental results takes students as a group to evaluate the virtual simulation experiment platform experience, and students can share their experimental experience or summarize the shortcomings of the experiment. The teacher comments and summarizes the practical operation of each group. Through continuous review between teachers and students, students can understand the significance of news interviews about public health emergencies and relevant policy requirements, master the methods and skills of news interviews of public health emergencies, and master various methods and skills of acquiring information in news interview of public health emergencies.

However, due to the difference in personal subjective evaluation, the evaluation of experimental results will be different, which becomes the most prominent problem encountered in the construction and application of the system. It is suggested to adopt the control method of process evaluation. Through the student's experimental data acquisition and data analysis of the process, teachers can maximize the student's acquire the cognition of experiment content, based on the quantitative evaluation of the data to reduce the subjective deviation of a single teacher evaluation, provide students with more diverse, more objective, more comprehensive evaluation, stimulate students to raise their ability of practice better. The feedback mechanism of the system needs to be further improved.

Virtual simulation technology breaks through the original traditional classroom teaching method in the emergency news interview system, successfully infiltrates into the practical dimension that news and communication are particularly missing, changes the existing information interaction structure, and combines online and offline innovative modes. A new ecological development environment of practical education was established by using various experimental teaching methods such as scene virtual restoration, task-driven, and online testing.

4.3. System Application Effect. Six months after the operation of the system, the author issued questionnaires to 498 students who had used or had contact with the platform. A total of 498 users were undergraduate students majoring in journalism and communication who had graduated or were in the first, second, and third grades. A total of 317 valid questionnaires were recovered after excluding irrelevant invalid samples. SPSS23.0 was used to analyze the data in this paper. In the dimension of frequency analysis, response percentage = number of response cases/total number of responses, and case percentage = number of response cases/number of effective cases are taken as the benchmark, and the data results are shown in Table 1.

In order to test the application effect of virtual simulation news interview platform, six response variables are set. As can be seen from Figure 8, 84.8% chose "improved ability of cooperation, expression, and communication"; 79.9% of the students chose "deepen the understanding and memory of knowledge"; 76.4% of the students thought they have solved practical problems in practice. Nearly 70% of the



FIGURE 7: Enter the virtual simulation experiment platform.

TABLE 1: Application effect of virtual simulation news interview platform based on creator.

	The response		Percentage of cases (%)	
	The case number	The percentage (%)		
The application effect of virtual simulation news interview platform ^a	Deepen the understanding and memory of knowledge	247	18.5	79.9
	The ability of cooperation, expression and communication has been improved	262	19.7	84.8
	Know how to use what I've learned to solve problems	236	17.7	76.4
	The ability of knowledge acquisition and utilization has been improved	216	16.2	69.9
	Improve the ability to analyze and solve problems	215	16.1	69.6
	The ability of autonomous learning has been improved	157	11.8	50.8
Total sum	1333	100.0	431.4	

^aBinary groups are tabulated with a value of 1.

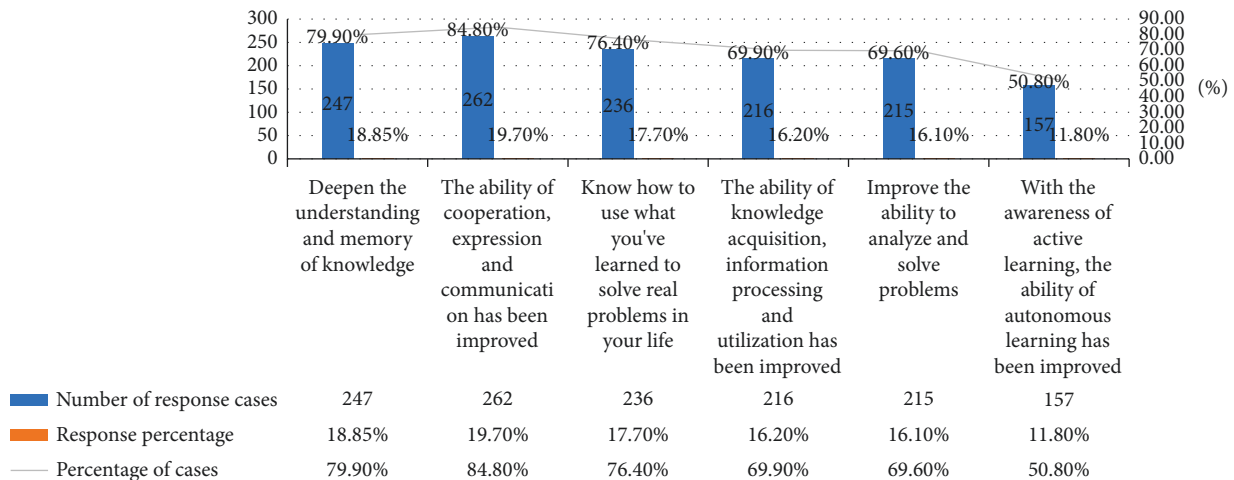


FIGURE 8: Response variables of virtual simulation news platform application effects.

students believe that their abilities in knowledge acquisition, information processing and utilization, problem analysis, and problem-solving have been improved. In addition, about 50.0% of the students believe that their active awareness of learning has been enhanced and their ability to do independent learning has been improved. Data show that the application of the virtual simulation emergency news interview platform based on Creator improves students' teamwork, knowledge understanding, analysis and solution of practical problems, autonomous learning, and other aspects to varying degrees.

5. Conclusion

This paper describes the architecture and design ideas of the virtual simulation emergency news interview system, and mainly studies the key technical issues such as important instance technology and texture mapping of 3D interactive simulation. Taking the COVID-19 public health event as the carrier of virtual environment, in the virtual simulation system, Design and realize the construction of the whole three-dimensional interactive simulation system can be stable in real-time operation. First of all, in the process of system implementation, the problem of how to interact and optimize the model in the system, the modeling technology of 3D model, and how to create the simulation effect of the real environment are solved. Secondly, this paper stated the application method of the system, through the questionnaire investigation, using SPSS23.0 feedback data to make further analysis to the users, set up six response variables, test and application effect of virtual simulation platform of news interview, case percentage points more than 50%, the function of show that the system has good scalability, The expected functions of system module 3D modeling and real-time simulation have been realized. The research shows that virtual simulation technology can be successfully applied in the field of news and communication, changing the current single information interaction mode.

The design of this system has been directly applied in practice and has been piloted in the major of network and new media. The simulation system and traditional classroom teaching of news interviews complement each other and are recognized by teachers and students majoring in journalism and communication. After the system becomes more mature, the category of news events on the platform will expand to a broader category of natural emergencies and social emergencies. The innovative construction of the experimental system opens up the first step for the application of virtual simulation technology in the field of journalism and communication and provides the research foundation and certain practical experience for further expanding the application effect of virtual simulation technology in the field of journalism and communication.

Data Availability

The data used to support the findings of this study are available from the author upon request.

Conflicts of Interest

The author declares that she has no conflicts of interest or personal relationships that could have appeared to influence the work reported in this paper.

Acknowledgments

The work was supported by the Guangdong Provincial Department of Education. The final research result of Guangdong Quality Engineering Construction Project is "Exploration on the Application of PBL Mode based on innovation Ability Cultivation in News Interview teaching in independent Colleges and Universities" (GDJG201907).

References

- [1] J. Yang, "Research status and development of virtual reality technology at home and abroad," *Information/Communication*, vol. 1, pp. 50–56, 2020.
- [2] D. Yang, "The new normal of virtual simulation teaching under the vision of internet +," *Journal of tianjin association of vocational colleges*, vol. 20, no. 8, pp. 47–50, 2018.
- [3] H. Liu, Y. Song, and L. T. Ma, "Development status of virtual simulation teaching," *Education Teaching Forum*, vol. 17, pp. 124–126, 2020.
- [4] F. Wang, "Analysis of the construction of the teaching project of news communication class virtual simulation experiment teaching projects," *Satellite TV and Broadband Multimedia*, vol. 17, no. 8, pp. 8–13, 2020.
- [5] Y. Wang and T. Zhang, "Research on virtual simulation test teaching of computer network courses based on university data analysis," *Science and Technology Vision*, vol. 12, pp. 124–132, 2019.
- [6] X. P. Sun and L. Chen, "Design framework of computer network virtual experiments under large data," *Laboratory Research and Exploration*, vol. 36, no. 12, pp. 113–124, 2018.
- [7] L. Q. Feng, W. H. Zhang, and Z. Ren, "Research on virtual experimental teaching design for constructivism," *China Education Technique and Equipment*, vol. 15, pp. 119–127, 2018.
- [8] L. Chen, "Research on Architecture of High School Information Technology Virtual Simulation Experiment Platform Based on VRP", Ningbo: Ningbo University, 2017.
- [9] G. M. Deng and T. Yan, "Cross-media learning styles, theories and resource Environment for the Intelligent Age- Inspiration from international multimedia learning research," *The Journal of Distance Education*, vol. 15, pp. 61–69, 2019.
- [10] Q. Yao, "Discussion on the application of virtual simulation technology in the construction of news communication laboratory," vol. 2pp. 139–152, New West, 2019.
- [11] M. Wu and L. Chen, "Research on teaching application of Media major based on Virtual simulation technology," *Journal of Beijing University*, vol. 6, pp. 57–67, 2018.
- [12] Z. Q. Wei and Y. J., "Discussion on application strategy of national demonstration virtual simulation experiment teaching project," *Experimental Technology and Management*, vol. 35, no. 9, pp. 236–238, 2018.
- [13] G. S. Chasson, C. Elizabeth Hamilton, A. M. Luxon, A. J. De Leonardis, S. Bates, and N. Jagannathan, "Rendering promise: enhancing motivation for change in hoarding disorder using virtual reality," *Journal of Obsessive-Compulsive and Related Disorders*, vol. 25, Article ID 100519, 2020.

- [14] V. V. Andreev, L. N. Vasilieva, V. I. Gorbunov, O. K. Evdokimova, and N. Timofeeva, "Creating a psychologically comfortable educational environment as a factor of successful academic program acquisition by technical university students," *Universal Journal of Educational Research*, vol. 8, no. 10, pp. 4707–4715, 2020.
- [15] L. M. Putz, F. Hofbauer, and H. Treiblmaier, "Can gamification help to improve education? Findings from a longitudinal study," *Computers in Human Behavior*, vol. 110, Article ID 106392, 2020.
- [16] D. X. Li, "Research and design of subway driving Simulator based on computer simulation technology," *Electronic test*, vol. 15, pp. 20–25, 2016.
- [17] Y. L. lu and W. Q. Dong, "Construction and practice of virtual simulation experiment Teaching center for material specialty," *Laboratory research and exploration*, vol. 37, no. 11, pp. 153–157, 2018.
- [18] Q. S. Yao, J. Y. Qin, and X. H. Zhang, "Thinking on the application of virtual simulation experiment teaching in molecular biology experiment teaching," *Health vocational education*, vol. 38, no. 5, pp. 82–83, 2020.
- [19] Z. Y. Liu, "Research on virtual simulation experiment teaching reform of journalism and communication specialty," *Guide to journalism studies*, vol. 12, no. 3, pp. 36–39, 2021.
- [20] Y. L. Fan, "Research on the Influencing factors of virtual simulation experiment teaching project sharing application," *Interview and editing*, vol. 8, pp. 140–145, 2021.
- [21] F. Yang and X. W. Sun, "Research on practical teaching of journalism communication based on virtual reality Technology," *Media education*, vol. 21, pp. 104–110, 2021.
- [22] A. A. Boniello and A. A. Conti, *Minecraft Our City, an Erasmus Project in Virtual World: Building Competences Using a Virtual World*, pp. 293–315, IGI Global, Pennsylvania, 2021.

Research Article

Human Capital Digital Incentive Mechanism Construction Based on Deep Learning

Jie He¹ and Jianhua Zhang² 

¹College of Economics and Management, Pingdingshan University, Pingdingshan 467000, Henan, China

²School of Japanese Studies, Shanghai International Studies University, Shanghai 200083, China

Correspondence should be addressed to Jianhua Zhang; 1896@shisu.edu.cn

Received 14 April 2022; Revised 5 July 2022; Accepted 15 July 2022; Published 17 August 2022

Academic Editor: Xuefeng Shao

Copyright © 2022 Jie He and Jianhua Zhang. This is an open access article distributed under the Creative Commons Attribution License, which permits unrestricted use, distribution, and reproduction in any medium, provided the original work is properly cited.

The introduction of human capital can be traced back to the ancient Greek period, emphasizing the important role of knowledge and skills in the production and life process. Human capital reward mechanism promotes modern social and economic development and is an important part of social and economic growth. The core management of the enterprise is the management of human capital, and the central work of human capital management is the incentive of human capital. Many enterprises are now facing difficulties in industrial operation, serious brain drain, and lack of core competitiveness in the market. As a result, enterprises cannot adapt to the speed and requirements of today's social and economic development. One of the important reasons is that the enterprise lacks attention to the value of the human capital incentive system, or the human capital incentive system of the enterprise is unreasonable, which leads to a series of problems such as poor employee enthusiasm and low enterprise performance. How to establish a reasonable and effective incentive mechanism to mobilize the enthusiasm and creativity of employees has become a problem that enterprises must pay attention to. Taking the technical managers and general technicians of a high-tech enterprise as an example, combined with the deep learning method, the article made a detailed analysis of the four major incentive factors of enterprise human capital. It made employees' satisfaction with corporate cultural incentives reaching 56.1%, which showed that emotional motivation was also one of the key factors for employees to be satisfied with the corporate incentive system.

1. Introduction

With the rapid development of science and technology and the advent of the digital age, the human capital incentive mechanism closely follows the pace of the times and changes the original traditional model. At the same time, deep learning has achieved great success in a series of fields such as computer vision, image processing, natural language processing, and semantic recognition in recent years. However, the application of deep learning in the construction of human capital incentive mechanism is still limited. In the digital age, applying deep learning to the human resources incentive mechanism can create a new creative method for enterprises, which can improve the effectiveness of the incentive mechanism. The construction of a reasonable and effective corporate incentive mechanism

is based on a fair and just, employee-centered principle and center. It must meet the differentiated needs of employees and pay attention to the material and spiritual needs of employees, and can arouse the enthusiasm of employees with long-term generous material rewards, a good working environment, and corporate organizational culture. While retaining talents for the enterprise, it can also bring the economic development of the enterprise.

This paper conducted a systematic analysis and research on deep learning algorithms and explored the role of deep learning methods in the establishment of human capital incentive mechanisms, and on this basis, it found out what digital incentives mean for businesses and employees. From the analysis of the four motivational factors of human capital, it was found that material incentives and spiritual incentives were more valued in the hearts of employees.

Employees needed not only real salary incentives to meet material needs but also respect and care to meet certain spiritual needs. This finding had guiding significance for mobilizing employees' enthusiasm and creativity. In addition, a good corporate culture and corporate environment were also an effective way to retain talents.

With the wide application of deep learning, there are more and more research studies on deep learning in the construction of human capital incentive mechanism. Shen et al. provided an overview of computer-aided image analysis in the field of medical imaging. Recent advances in machine learning, particularly deep learning, facilitate the recognition, classification, and quantification of patterns in medical images. Central to these advances is the provision of hierarchical feature representations learned only from data rather than artificially designed features based on domain-specific knowledge. Deep learning is rapidly becoming a state-of-the-art technique that improves the performance of a wide range of medical applications and so on. Finally, research questions were discussed and future directions for further improvements were proposed [1]. Dong and Li summarized recent advances in deep learning-based acoustic models and examined the motivations and insights behind these techniques [2]. Ravi et al. provided a comprehensive and up-to-date review of research on the adoption of deep learning in health informatics, critically analyzing the relative merits, potential pitfalls, and future prospects of this technology [3]. In the study of Schirrmeyer et al., convolutional neural networks (ConvNets) were applied to the EEG anomaly corpus at Temple University Hospital for the task of differentiating pathological from normal EEG recordings. Two basic architectures, surface and deep convNets, and algorithms developed for this purpose were used to decode task-relevant information from the EEG. When decoding EEG pathology, both ConvNets achieved much higher accuracy than the only published results on this dataset (85% and 79% improvement in accuracy, respectively, compared to 6% accuracy). In addition, both ConvNets maintained high accuracy when trained on one-minute recordings and when tested on six-second recordings. An automatic method was then used to optimize the hyperparameters of the architectures, and interestingly, different ConvNet architectures were found. After viewing additional features using spectral power variations in the delta (0–4 Hz) and theta (4–8 Hz) bands, the visualization of ConvNet decoding behavior was consistent with that expected from the spectral analysis of EEG and textual diagnostic data. The text analysis of diagnostic reports also showed that accuracy could be improved by including background information (e.g., subject's age) [4]. Hou et al. investigated the visual quality of images assessed blindly by learning the rules of linguistic descriptions and proposed several learning-based IQA models by analyzing the mappings from images to numerical scores. However, the accuracy of the learned mappings is not sufficient because some information is lost due to the irreversible transformation from linguistic descriptions to numerical scores. Therefore, we propose a blind IQA model that learns qualitative scores directly and outputs numerical scores for

general use and fair comparison. Images are represented by statistical features of natural scenes. Images are represented by statistical features of natural scenes, and a discriminative depth model is trained to classify these features into five levels corresponding to five explicit psychological concepts: excellent, good, fair, poor, and very poor. These qualitative labels were then converted into scores by applying a newly designed quality library. This classification framework is not only more natural than the regression-based model but also more robust to small batch problems. To validate the effectiveness, efficiency, and robustness of the model, exhaustive experiments were conducted on a common database [5]. The study of Grimpe et al. concluded that the ability of innovative firms to create and capture values depends on the rapid and widespread adoption of innovations. However, stakeholder concerns may be a significant barrier to diffusion; Grimpe et al. examined the human capital challenge and investigated whether innovative firms pay a wage premium to new employees who have worked for advocacy organizations such as Transparency International. Human capital and stakeholder theory are also combined to discuss the experience of advocacy groups and their transfer of innovation from the perspective of stakeholder knowledge. Valuable human capital signals were created in terms of legitimacy transfer. Using matched data from 3,562 Danish employees, it is found that new recruits with advocacy team experience enjoy higher wage premiums in technologically superior companies, in occupations with direct stakeholder interaction, and in the top management of advocacy teams [6]. Saeed et al. found that the success of an organization's program for environmental sustainability depended on employees' environmental behavior. One of the important contemporary challenges faced by HR professionals was ensuring that environmental sustainability was properly integrated into HR policies. Green HRM was developed from organizations working on issues related to environmental protection and maintaining ecological balance. The purpose of their study is to examine the effects of green HRM practices (green recruitment and selection, green training and development, green performance management and evaluation, green rewards and compensation, and green empowerment) on employees' green behaviors. In addition, the mediating effects of pre-environmental psychological capital and environmental knowledge on the pre-environmental behavior of green HRM practices will be examined. The results show that green HRM practices positively influence employees' pro-environmental behaviors, and pro-environmental psychological capital mediates this association. The moderating role of employees' environmental knowledge on the effect of green HRM practices on pro-environmental behavior [7]. These literatures were very detailed in the introduction of deep learning and human resource theory incentive system and had a constructive role in the research of this article.

Based on the restricted Boltzmann machine, autoencoder, and multilabel classification method of convolutional neural networks and recurrent neural networks in deep learning, this paper analyzed and compared the satisfaction degree of an enterprise's technical management personnel

and general technical personnel to the enterprise's incentive mechanism. It found out the psychological tendency characteristics of these employees in the incentive mechanism, summarized these characteristics, and then constructed a reasonable and effective incentive mechanism based on these characteristics.

2. Human Capital Digital Incentive Mechanism Construction Method Based on Deep Learning

2.1. Restricted Boltzmann Machine. Restricted Boltzmann Machine (RBM) is developed from the Boltzmann machine, which is a two-layer undirected graph model [8, 9]. Figure 1 is a structural model diagram of a restricted Boltzmann machine. According to different tasks, the restricted Boltzmann machine can be trained by supervised learning or unsupervised learning.

The energy function $F(w, b)$ of a restricted Boltzmann machine can be expressed as

$$F(w, b) = - \sum_i w_i h_i - \sum_j b_j c_j - \sum_{i,j} w_{ij} b_j L_{ij} \quad (1)$$

Both i and j represent nodes, w and b represent the value and bias of the node, and L_{ij} represents the connection weight between the visible layer and the hidden layer.

In 2007, some experts used the restricted Boltzmann machine model for the first time to construct the digital incentive mechanism of human capital, as shown in Figure 2 [10]. The restricted Boltzmann machine model made two changes on the traditional model. The first was that the visible layer used a 0-1 vector unit of length K to represent employee performance data. Second, because employees generally could not be rewarded every day, employees without reward records were represented by a special unit (No reward), and the special unit and the hidden layer unit were not connected. In the restricted Boltzmann machine, the visible layer usually represents the original input data, while the hidden layer represents the data generated through learning, expressing the implicit characteristics of the original data. Each rewarded employee was represented by a separate restricted Boltzmann machine, all of which corresponded to a common hidden layer. The weight and bias parameters were shared between all RBMs, so if two employees had the same reward record and were rewarded at the same time, the same weight was used for the calculation [11].

Compared with the traditional restricted Boltzmann machine model, the weight value between the hidden layer and the visible layer of the changed model is S times that of the previous model. v represents the reward matrix, which is a multidimensional matrix; Z_i is a normalized item, which is used to ensure that the sum of the probabilities of all user scores on item i is 1; and the updated energy function is obtained:

$$F(w, b) = - \sum_i v_i^s h_i^s - \sum_j b_j c_j - \sum_{i,j} v_i^s w_j L_{ij}^s + \sum_i i \log Z_i \quad (2)$$

After the above training is completed, set the known employee reward as T , and the reward corresponding to the

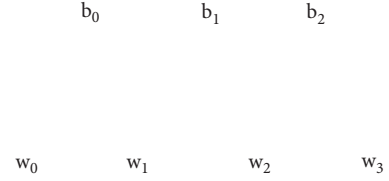


FIGURE 1: Structure model diagram of the restricted Boltzmann machine.

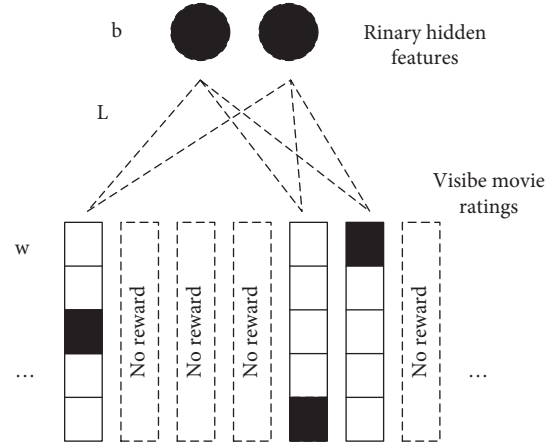


FIGURE 2: RBM collaborative filtering model.

employee reward record according to the employee's work performance data is

$$\chi = F(w_y) = \sum s * P\left(w_y^s = \frac{1}{T}\right) \quad (3)$$

When the restricted Boltzmann machine model is applied to the employee reward mechanism, the employee reward mechanism is effectively improved and optimized, and the reward algorithm process is simplified [12, 13]. The restricted Boltzmann machine model has been successfully applied to collaborative filtering, classification, dimensionality reduction, image retrieval, information retrieval, language processing, automatic speech recognition, time series modeling, document classification, nonlinear embedding learning, transient data model learning, and signal and information processing.

2.2. Autoencoder. Autoencoder is a kind of neural network related to deep learning. The main role of an autoencoder is to train between input values and output values, also known as unsupervised learning models [14]. The structure of the autoencoder is shown in Figure 3. This model includes three parts: encoder, decoder, and hidden layer. The working process of the automatic encoder includes two parts: encoding and decoding. In the encoding stage, the input data is mapped to the feature space, while in the decoding stage, the encoded data is mapped back to the original sample space.

When the decoder activation function is an identity function, the resulting even variance formula is

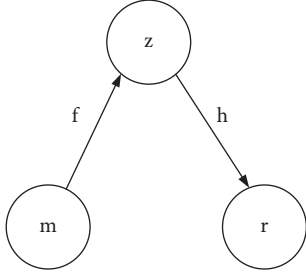


FIGURE 3: Schematic diagram of the structure of the autoencoder.

$$L(m, n) = m - n^2. \quad (4)$$

When the decoder activation function is a sigmoid function, the cross entropy function is obtained:

$$L(m, n) = - \sum_{i=1}^x [m_i \log(n_i) + (1 - m_i) \log(1 - n_i)]. \quad (5)$$

According to the reconstruction error function, the overall loss function is obtained:

$$Y_{AE}(\partial) = \sum_{m \in S} L(m, h(f(m))). \quad (6)$$

S is the training set, and minimizing the function can get the required parameters.

In an autoencoder, the hidden layer represents the input, and the goal of the hidden layer is to keep the information of the input layer stable [15]. In order to improve the availability of the data, the original data cannot be completely copied. Some experts propose denoising autoencoders to better represent features, improving the ability of the autoencoder to capture key information features by adding robustness and noise to the original input data to destruct the original input data [16, 17]. The calculation process of the denoising autoencoder is as shown in Figure 4.

Assuming that the input data is w , and the randomly corrupted input data is w' , this mapping process is represented by function $f_\theta(w)$:

$$h = f_\theta(w) = s(Pw' + b). \quad (7)$$

$\theta = \{P, b\}$ represents the entire set of maps, s represents a nonlinear function like sigmoid, and b represents the bias vector.

When $\theta = \{P', b'\}$ represents the set of reconstructed mappings, the decoder remaps the implicit feature m to the reconstructed data n , the value range of implicit feature m is $m \in [0, 1]^d$, and we obtain the formula

$$n = k_\theta(m) = s(P'm + b'). \quad (8)$$

When the input data in the denoising autoencoder represents $w^{(i)}$, the hidden layer feature represents $m^{(i)}$, and the reconstructed original data represents $n^{(i)}$, the minimum reconstruction error is obtained by continuously adjusting and optimizing the parameters in the model:

$$L(m, n) = \|m - z\|^2. \quad (9)$$

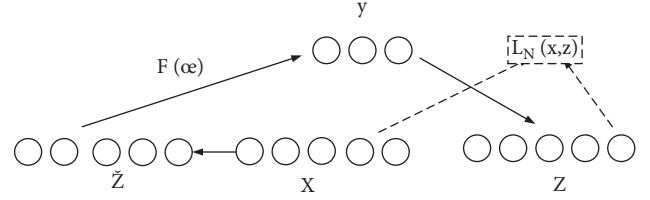


FIGURE 4: Calculation process of denoising autoencoder.

At the same time, in order to prevent the model from overfitting due to too much weights, it is necessary to set a weight decay term for the model

$$D = \frac{1}{2} \|P\|^2. \quad (10)$$

We get the objective function:

$$z = \frac{1}{2v} \sum_{i=1}^v L(m^{(i)}, n^{(i)}) + \beta D. \quad (11)$$

β is the weight parameter after decay. Z is the optimization parameter. The denoising autoencoder will get a low-dimensional representation of the input data.

2.3. Multilabel Classification Method of Convolutional Neural Network. To build a mature human capital incentive mechanism, it is inseparable from the classification of the characteristics of each employee's work performance. It is crucial for an enterprise to establish a more accurate reward system based on the classification of each characteristic of employees' work performance [18]. The convolutional neural network is a relatively simple deep learning structure with excellent classification and recognition capabilities. It is mainly composed of four layers: convolution layer, pooling layer, fully connected layer, and output layer. Each layer has the same weight as the previous layer, which can simplify the training parameters and accurately extract key data features [19].

A method commonly used in convolutional neural networks for multiclassification tasks is the Softmax regression model. The Softmax function is often used as the final classifier, which is an extension of the logical classifier only applicable to binary classification problems. Softmax maps the outputs of multiple neurons to the (0, 1) interval, and the sum of all output values is 1. In the classification process, each performance feature is classified, and each feature is classified into a class and represented by a label. After completing the training, multilabel classification can automatically assign one or more category labels to the samples, which can better adapt. In addition, compared with the single label learning framework in which each sample is only associated with one category label, each sample in the multilabel learning framework can be associated with multiple category labels. Its purpose is to effectively predict the label set of unknown samples by learning a given multilabel training set. In addition, multilabel classification faces problems such as higher algorithm complexity and uncertain number of related labels.

Suppose there is a training set $\{(m^{(1)}, n^{(2)}), \dots, (m^{(s)}, n^{(s)})\}$ of s samples, and the feature vector m is $t + 1$ dimension. Therefore, for the input m samples, the probability $r(w = k|m)$ of each category of work data category k is obtained. The number of class labels v in Softmax regression is greater than 2, and the probability formula for outputting a v -dimensional vector representing each class is

$$h_{\alpha}(m^{(i)}) = \begin{bmatrix} r(w^{(i)} = 1|m^{(i)}; \alpha) \\ r(w^{(i)} = 2|m^{(i)}; \alpha) \\ \vdots \\ r(w^{(i)} = v|m^{(i)}; \alpha) \end{bmatrix} = \frac{1}{\sum_{j=1}^v e^{\alpha_j^p m^{(i)}}} \begin{bmatrix} e^{\alpha_1^p m^{(i)}} \\ e^{\alpha_2^p m^{(i)}} \\ \vdots \\ e^{\alpha_v^p m^{(i)}} \end{bmatrix}, \quad (12)$$

$\alpha_1, \alpha_2, \dots, \alpha_v$ is the model parameter [20], and then the cost function definition formula is

$$\nabla_{\alpha_j} K(\alpha) = -\frac{1}{x} \sum_{i=1}^x [m^{(i)}(1\{w^{(i)} = k\} - r(w^{(i)} = k|m^{(i)}; \alpha))]. \quad (13)$$

Using iterative optimization such as gradient descent, the solution parameters need to be minimized to $K(\alpha)$, and the gradient formula after derivation is

$$K_{(\alpha)} = -\frac{1}{x} \left[\sum_{i=1}^x \sum_{j=1}^v 1\{w^{(i)} = k\} \log \frac{e^{\alpha_j^p m^{(i)}}}{\sum_{l=1}^v e^{\alpha_l^p m^{(i)}}} \right]. \quad (14)$$

After the gradient is calculated, it is brought into the gradient descent algorithm and the parameters are updated iteratively. After the parameter training is completed, the output feature m is classified as the probability of category k , and the formula used is

$$r(w^{(i)} = k|m^{(i)}; \alpha) = \frac{e^{\alpha_k^p m^{(i)}}}{\sum_{l=1}^v e^{\alpha_l^p m^{(i)}}}. \quad (15)$$

2.4. Recurrent Neural Network. Recurrent Neural Network (RNN) solves the problem of knowledge reserve to a certain extent and is a kind of neural network with memory function. The memory function is mainly realized by the feedback neural network between the input data and output data of the regret layer, which is the biggest difference from the traditional neural network. The shared weights of all recurrent neural networks can be expanded according to time nodes, and it is a deep feedforward neural network with the weight shared by all layers, which feeds back the output of the hidden layer to the input of the hidden layer. The connection structure of this feedback neural network makes RNN have the corresponding memory ability, as shown in Figure 5.

The parameters of the recurrent neural network mainly include three parts. At each time point, the same parameters were used for the calculation of the input information. Input the information in chronological order and get an output and hidden state information at each moment, and input the hidden state information together with the next time point

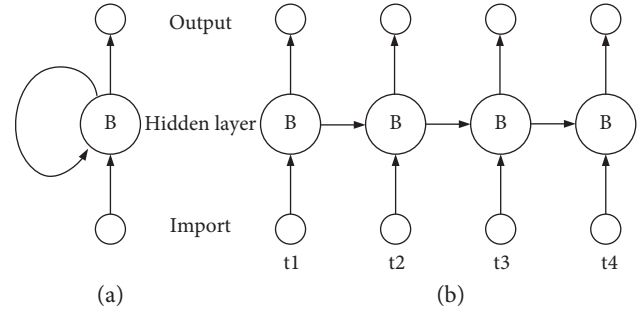


FIGURE 5: Schematic diagram of the recurrent neural network mechanism. (a) Single layer recurrent neural network and (b) recurrent neural network expanded by time nodes.

into the network for the calculation of the next time point [20, 21].

Like traditional neural networks, RNN can be trained using the backpropagation algorithm, which is also known as backpropagation through time [22]. In the forward propagation, the information is calculated in sequence according to the experimental order. Similarly, the backpropagation is to define a loss function and then transfer the accumulated residual at each time point from the last time point to the first time point. The traditional recurrent neural network has memory function but also has some drawbacks. Since some information is lost with each feedback, the initial memory will gradually fade or even disappear over time. Each iteration of the derivative is a multiplicative relationship since backpropagation needs to be accumulated over time points. If the conduction value is less than 1, the residual transmitted to the first time point after multiple multiplication tends to be close to 0, resulting in the disappearance of the gradient, so that the network cannot converge. On the contrary, if the conduction value is greater than 0, a large number will be obtained after multiple multiplication, which will also lead to non-convergence and become gradient explosion [23]. In response to these problems, an improved recurrent neural network, called Long Short-Term Memory (LSTM), was first proposed in 1997, which has been continuously improved and developed. This kind of long and short memory recurrent neural network can solve the problem of nonconvergence very well so that the nervous system can preserve long-term “memory.”

Figure 6 is a schematic diagram of the basic functional unit gate structure of the long-short-term memory model. The gate structure diagram of the long-short memory model includes four parts: the input gate, the cellular memory unit, the forgetting gate, and the output gate. The gate structure is a vector with an operation output value between 0 and 1 that allows information to selectively pass through. Its main function is to record, add, or erase memories. The proportion of information passing through the model is determined by the Sigmoid function. When other parts of the model are discarded, the calculation formula is obtained:

$$h_t = \varepsilon(m_h \cdot [x_{t-1}, r_t] + n_h). \quad (16)$$

Among them, h_t represents the proportion of information retention, t represents the variable of the time node,

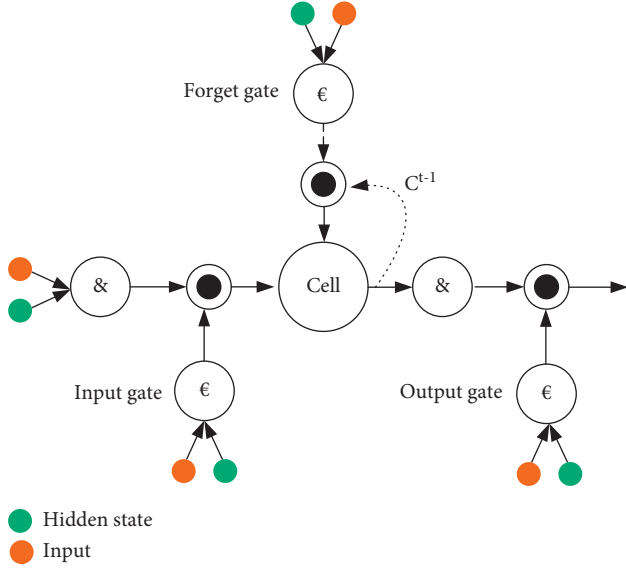


FIGURE 6: Schematic diagram of the basic functional unit gate structure of the long-short-term memory model.

m_h represents the parameters of each gate, and r_t represents the hidden state of the cell.

When the calculation determines that the cell should retain information, the input gate information and the input cell information are used for calculation, and the formula is obtained:

$$i_t = \varepsilon(m_h \cdot [x_{t-1}, r_t] + n_h). \quad (17)$$

Multiply the state value of the cell at the previous time point by the forget gate, and add it to the new candidate value vector generated by the tanh function to obtain the new cell state. The updated formula is

$$\begin{aligned} \tilde{e}_t &= \tanh(m_e \cdot [x_{t-1}, r_t] + n_e), \\ e_t &= h_t \times e_{t-1} + i_t \times \tilde{e}_t. \end{aligned} \quad (18)$$

Finally, the output of the cell is determined by the state of the cell, and the formula can be obtained:

$$\begin{aligned} y_t &= \varepsilon(m_y \cdot [x_{t-1}, r_t] + n_y), \\ x_t &= y_t \times \tanh(e_t). \end{aligned} \quad (19)$$

3. Human Capital Digital Incentive Mechanism Experiment

The so-called incentive mechanism is a way to reflect the interaction between the incentive subject and incentive object through a set of rational systems. It is also the sum of the internal operation structure and development and evolution law of enterprise incentive employees. It is an institutional system established and implemented to make the personal behavior of enterprise employees consistent with the enterprise objectives, realize the win-win strategy of enterprise and employees, and give full play to the personal ability of each employee [24]. The establishment of the incentive mechanism is inseparable from the

interpretation of incentive theory. The traditional motivation theory is mainly divided into two categories: process type and content type. Content type includes Maslow's hierarchy of needs theory, two-factor theory, ERG theory, etc. They focus on researching the starting point and source basis of incentives, meeting the basic needs of employees, and mobilizing the enthusiasm of employees through incentive systems. Process motivation theory mainly includes Locke's goal setting theory, Froome expectation theory, etc. They impress the psychology of employees through the incentive process, including what kind of goal needs to be achieved and what kind of reward can be obtained after a big wish, both material rewards and spiritual rewards, and then stimulate the enthusiasm of employees and strength. This paper took a high-tech enterprise as an example to discuss the current situation and problems of human capital in the company.

3.1. The Status Quo of the Company's Human Capital.

The current situation of the human capital of the company is shown in Figure 7 and Table 1, which is the company's personnel distribution in 2021 and the distribution of employees' technical grades and educational levels. With the development of the company, the number of employees continues to grow. The company's front-line employees account for 64% of the company's employees, and the technical employees account for 26%. From the technical level and educational level of the company's employees, it can be seen that the educational level is 32.4% of technical secondary school and high school staff, 52.98% of junior high school and below employees, and 86.8% of the total number of people without professional titles, indicating that in the company, general technical personnel account for a large number of the total number, and the proportion is unbalanced.

Although the company had achieved some operating results, there were still many problems in human capital incentives. The unreasonable salary structure of employees and the low salary level led to a serious loss of manpower in the company. The company's incentive mechanism did not play an effective role, the salary level did not meet the expectations of employees, and some excellent technical talents chose to change jobs.

Table 2 shows the company's technical talent loss in 2018. Over a four-year period, the attrition rate of technical managers was greater than that of general technical personnel. From 2018 to 2021, the company lost one technical manager per year, with a maximum turnover rate of 50%. The turnover rate of general technicians had increased year by year, rising from 12% in 2018 to 17% in 2019, as high as 21% in 2020, and 25% in 2021. It can be seen from the data that the ratio of technical personnel turnover has reached a quarter in the past four years. There are many reasons for general employees to leave, but salary is a very important factor. Coupled with the increase of external competitive pressure, many employees will choose rival companies with more reasonable salary structure and in line with their expectations. Therefore, establishing a reasonable and perfect salary system is the basic method to retain talents.

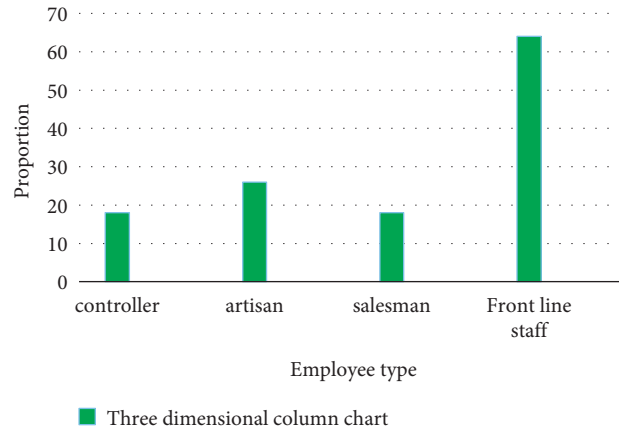


FIGURE 7: Company personnel distribution in 2021.

TABLE 1: Distribution of technical grades and educational levels of employees in 2021.

Educational level	Number of people	Proportion in total (%)	Technical grade	Number of people	Proportion in total (%)
Graduate student	4	2	Senior title	3	1.4
Undergraduate	24	5.68	Intermediate title	8	3.4
Specialty	36	8.32	Primary title	36	8.4
Technical secondary school and senior high school	64	32.4	No title	155	86.8
Junior high school and below	72	52.98			

TABLE 2: Technical staff turnover from 2018 to 2021.

Loss type number of people lost	2018		2019		2020		2021	
	Loss number	Loss rate (%)	Loss number	Loss rate (%)	Loss number	Loss rate (%)	Loss number	Loss rate (%)
Supervisory engineering staff	1	25	2	50	2	50	1	25
General technical personnel	11	12	14	17	17	21	20	25

3.2. Comparative Analysis of the Weights of Human Capital Incentives. As shown in Figure 8, it is the vertical plane coordinate axis of the analysis of the combined characteristics of human capital material and spiritual incentives. The points on the coordinate axis correspond to the corresponding combination of excitation types, including the indifference curve and the ability growth curve. The indifference curve represents the combined preference for the two incentives, and the ability growth curve represents the preference for a certain incentive. It is found that whether it is material incentive or spiritual incentive, the two complement each other and form the characteristics of mixed cross-demand. Material incentives provide material conditions for employees to survive and develop, followed by spiritual needs.

Starting from the four factors of human capital’s material incentive, emotional incentive, cultural incentive, and work incentive, the satisfaction performance of the company’s incentive system on the four levels of

technical managers and general technical personnel is obtained by collecting the satisfaction of the company’s employees.

Material incentive is the basis of the incentive mechanism. Its core is to link the interests of the enterprise with the personal interests of employees so that the objectives of the enterprise can become the consistent objectives of employees’ work. As can be seen from Figure 9, technical managers are more satisfied with the company’s material incentive system than the general technical staff. The satisfaction of general technicians is relatively low, and the satisfaction with the proportion of various incentive elements is also relatively low. For general technicians, the satisfaction of vocational training at the beginning of entry is higher. It reflects the unreasonable salary structure of technical management personnel and general technical personnel, and the proportion of performance appraisal elements is relatively large. Therefore, when establishing a digital incentive

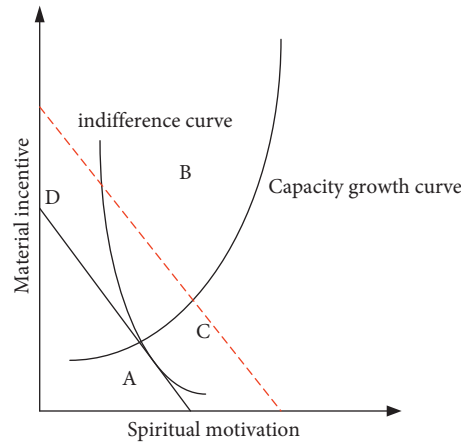


FIGURE 8: The combination of the human capital material and spiritual incentives.

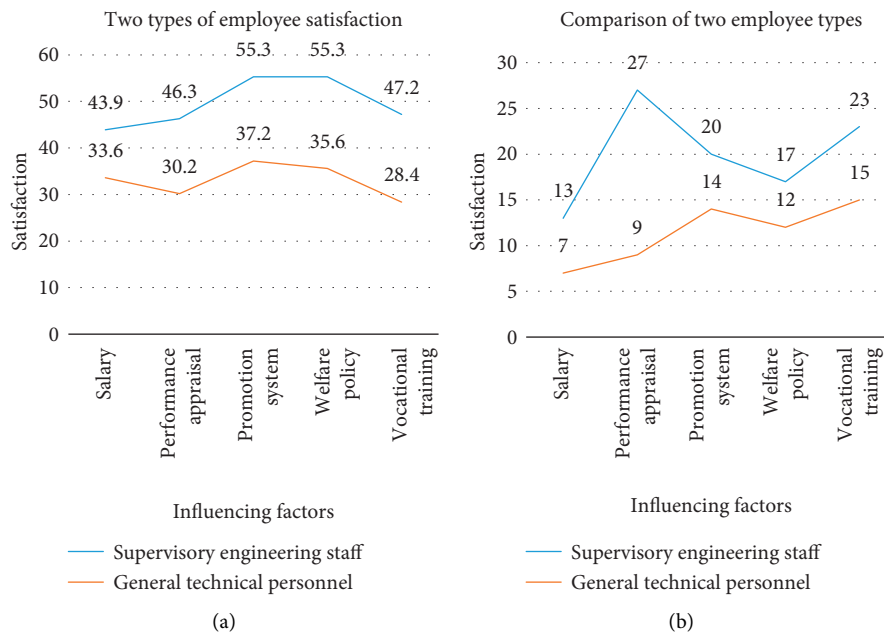


FIGURE 9: Employee satisfaction with material incentives. (a) Two types of employee satisfaction and (b) comparison of two employee types.

system, it is necessary to strengthen the optimal combination of salary treatment and performance appraisal and take into account other factors.

The most commonly used incentive methods in enterprise emotional incentive are integration incentive, questioning incentive, authorization incentive, participation incentive, and tolerance incentive. From Figure 10, it can be seen that emotional incentive satisfaction and paying attention to employees' emotional needs are also key parts of establishing a mature incentive system. The above data shows that the two types of employees are less satisfied with caring for employees and honoring them, and the emotional needs of employees are not met. Therefore, when establishing a digital incentive system, it is necessary to focus on the concern and praise of

employees in terms of emotional incentive factors and to take into account other emotional factors.

Cultural incentives are an invisible force emanating from an enterprise's corporate culture. According to Figure 11, the two groups of technicians are highly satisfied with the communication rapport, especially the technical management staff's satisfaction with the communication rapport reaches 56.1%. Two groups of employees are less satisfied with the organizational culture and work environment. Therefore, when building a new digital incentive system, more consideration should be given to enhancing the fun of organizational activities, relieving employees' pressure, and at the same time creating a good working environment and atmosphere so that employees can work better.

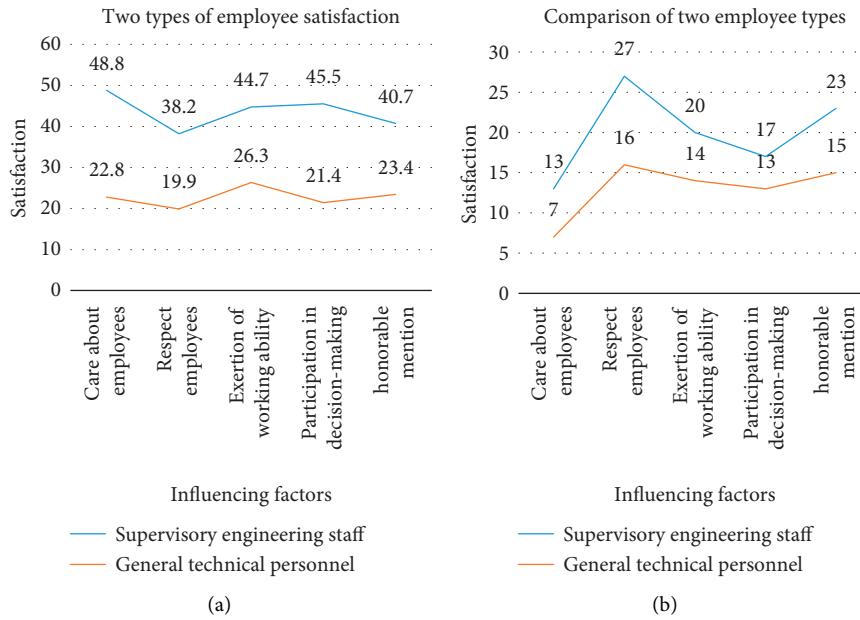


FIGURE 10: Employee satisfaction with emotional motivators. (a) Two types of employee satisfaction and (b) comparison of two employee types.

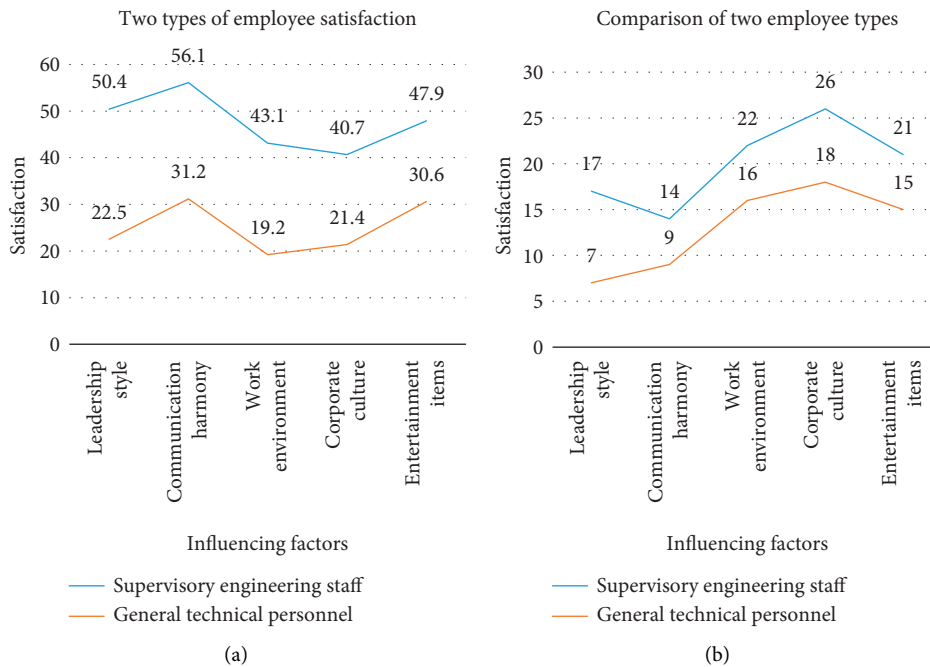


FIGURE 11: Employee satisfaction with cultural incentives. (a) Two types of employee satisfaction and (b) comparison of two employee types.

From Figure 12, technical managers and general technical staff have the highest satisfaction with technical collaboration among members. The data results show that it is necessary to improve the challenge and autonomy of employees in their work. The low satisfaction of employees in this area also indicates that employees have higher requirements for themselves. Therefore, in the design of the digital incentive system, the challenge and autonomy of

work should be strengthened so that employees can realize their maximum value.

As can be seen from Table 3, a mature and effective incentive system can be constructed according to the proportion of each element. Material incentives are the foundation of all incentives, and spiritual incentives are the core. Only by combining the two can achieve the effectiveness of the incentive system.

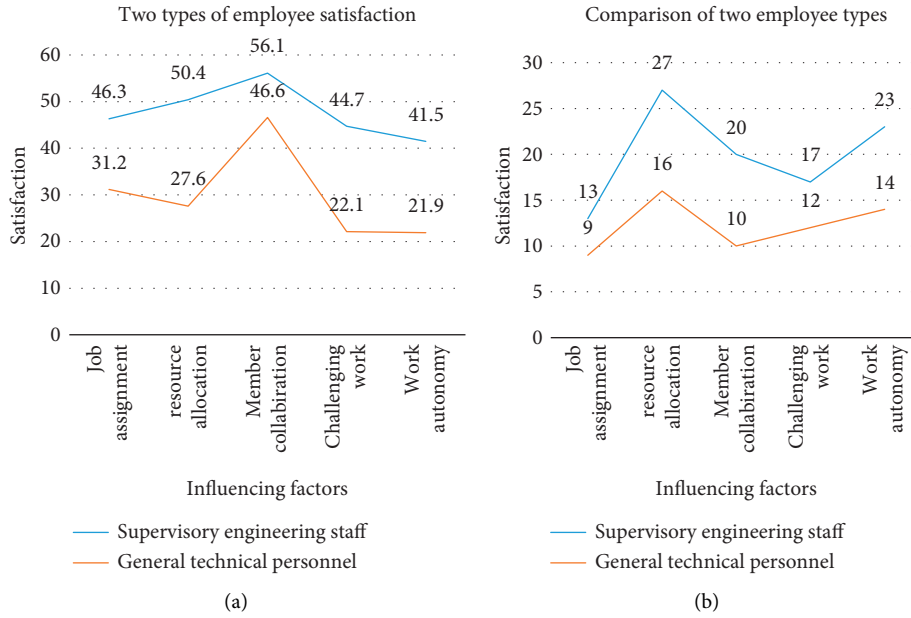


FIGURE 12: Employee satisfaction with job motivators. (a) Two types of employee satisfaction and (b) comparison of two employee types.

TABLE 3: Analysis of the four motivating factors of human capital.

Factor satisfaction	Very satisfied	Satisfied	Commonly	Dissatisfied	Very dissatisfied	Satisfaction (%)	Proportion of each factor
Material incentive factors	10	40	51	12	10	40.7	0.21
Emotional incentives	8	38	60	9	8	37.4	0.34
Cultural incentives	9	40	59	9	6	39.8	0.24
Job incentives	8	42	55	10	8	40.7	0.21

3.3. Incentive Mechanism Model Construction. The establishment of a reasonable incentive system for enterprises is conducive to the common development of enterprises and employees. In the incentive mechanism model in Figure 13, the company provides employees with a favorable working environment and a good corporate culture. By striving to achieve goals at work, the material and spiritual needs of employees are met. Increasing the challenge and innovation of work can stimulate the internal potential of employees. At the same time, a reasonable and effective incentive system can retain excellent talents for enterprises, create a benign competitive environment for employees, mobilize employees' enthusiasm, and attract excellent talents for the company to a certain extent.

4. Discussion

In this paper, various deep learning algorithms were applied to the human capital incentive system, and the characteristics of employees' satisfaction with the incentive mechanism were summarized and analyzed, and then an incentive mechanism that meets the needs of most employees was constructed according to the satisfaction characteristics. From the comparative analysis of the weights of human capital incentive factors, it could be seen that the company's

technical personnel strongly required the company to meet their needs in material and spiritual rewards among the four categories of incentive factors. Under these circumstances, the company's incentive mechanism should be optimized and integrated to maximize the interests of the company and employees.

5. Conclusions

The success of an enterprise is inseparable from the reasonable human resources incentives of the enterprise. Building a reasonable and effective incentive mechanism and using effective incentives to maximize corporate profits and enable enterprises and employees to obtain the most optimal and most satisfactory benefits are the result of their joint efforts. Based on various methods of deep learning, in order to protect the basic needs and rights of employees at work, the company must establish basic incentive methods, incentive directions, and incentive time, and adjust the salary structure. The company must optimize the combination of company systems, improve the market structure, provide employees with a better working environment and organizational culture, and enhance their enthusiasm based on the principles of fairness, justice, and efficiency [25].

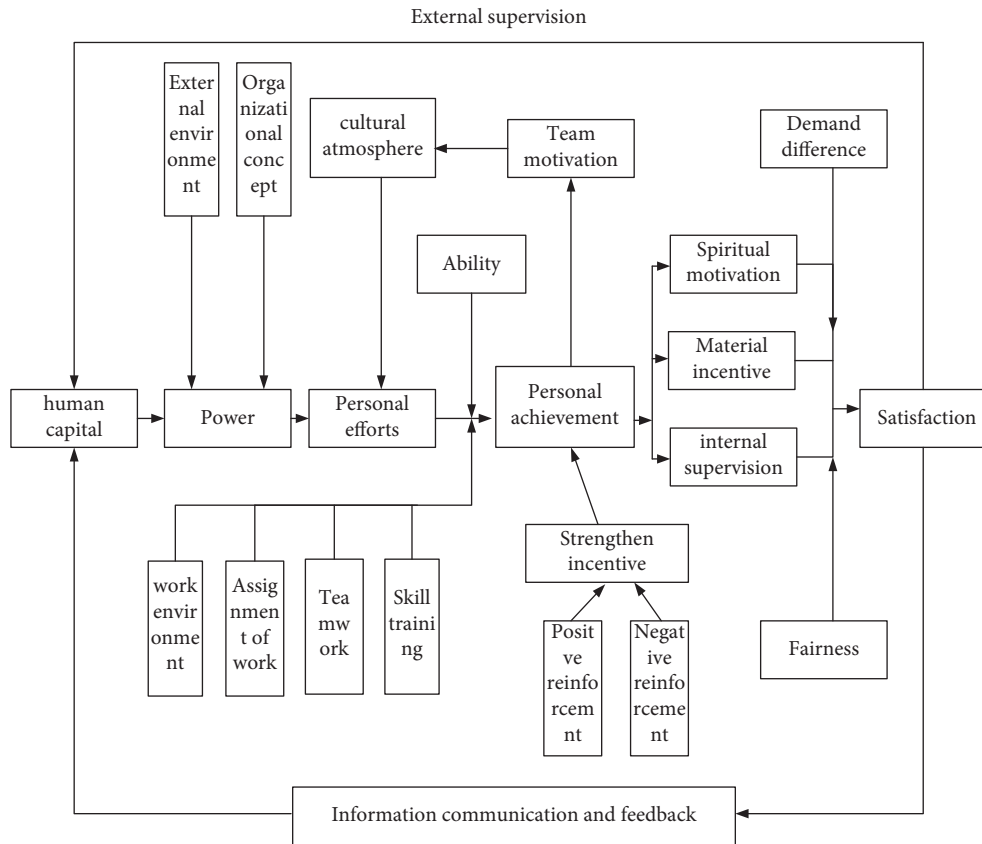


FIGURE 13: Incentive mechanism model.

Data Availability

No data were used to support this study.

Conflicts of Interest

The authors declare that they have no conflicts of interest.

Acknowledgments

This work was supported by the Soft science project of Henan Science and Technology Department “Research on internal mechanism and realization path of digital economy enabling high-quality development of Henan Manufacturing Industry” (222400410531) and the Young Teachers Key Project of Henan Education Department “Study on Modern Logistics Development Mode of Nylon City in Pingdingshan” (2019).

References

[1] D. Shen, G. Wu, and H. I. Suk, “Deep learning in medical image analysis,” *Annual review of biomedical engineering*, vol. 19, no. 1, pp. 221–248, 2017.
 [2] Y. Dong and J. Li, “Recent progresses in deep learning based acoustic models,” *IEEE/CAA Journal of Automatica Sinica*, vol. 4, no. 03, pp. 396–409, 2017.
 [3] D. Ravi, C. Wong, and F. Deligianni, “Deep learning for health informatics,” *IEEE Journal of Biomedical & Health Informatics*, vol. 21, no. 1, pp. 4–21, 2017.

[4] R. T. Schirrmeister, L. Gemein, and K. Eggenesperger, “Deep learning with convolutional neural networks for decoding and visualization of EEG pathology,” *Human Brain Mapping*, vol. 38, no. 11, pp. 5391–5420, 2017.
 [5] W. Hou, X. Gao, and D. Tao, “Blind image quality assessment via deep learning,” *IEEE Transactions on Neural Networks and Learning Systems*, vol. 26, no. 6, pp. 1275–1286, 2017.
 [6] C. Grimpe, U. Kaiser, and W. Sofka, “Signaling valuable human capital: advocacy group work experience and its effect on employee pay in innovative firms,” *Strategic Management Journal*, vol. 40, no. 4, pp. 685–710, 2019.
 [7] B. B. Saeed, B. Afsar, and S. Hafeez, “Promoting employee’s proenvironmental behavior through green human resource management practices,” *Corporate Social Responsibility and Environmental Management*, vol. 26, no. 2, pp. 424–438, 2019.
 [8] A. M. Obeidat, S. H. Abualoush, and H. J. Irtaimah, “The role of organisational culture in enhancing the human capital applied study on the social security corporation,” *International Journal of Learning and Intellectual Capital*, vol. 15, no. 3, pp. 258–276, 2018.
 [9] I. Rahim and T. Fatayh, “Reward and recognition with employee motivation: a study on a Malaysian private sector,” *Advanced Science Letters*, vol. 23, no. 8, pp. 7338–7341, 2017.
 [10] D. O. Walker and J. Yip, “Paying it forward? The mixed effects of organizational inducements on executive mentoring,” *Human Resource Management*, vol. 57, no. 5, pp. 1189–1203, 2018.
 [11] C. C. Orga, C. O. Odo, and D. C. Okeke, “Evaluating the relationship between leadership development and human capital condition of non-metallic product manufacturing

- firms in south east, Nigeria,” *Archives of Business Research*, vol. 9, no. 3, pp. 52–71, 2021.
- [12] A. Aurellia, “Pengaruh komponen human capital terhadap disiplin kerja karyawan di rumah sakit bedah surabaya,” *Medical Technology and Public Health Journal*, vol. 5, no. 1, pp. 1–7, 2021.
- [13] A. Wikumurti, M. R. Luddin, and T. Suyatno, “Human resource architecture transformation case study in construction company,” *IJHCM (International Journal of Human Capital Management)*, vol. 3, no. 2, pp. 27–40, 2019.
- [14] B. Jlassi, L. Ren, and S. Chen, “Stabilize IoT blockchain using smart rewarding mechanism: incremental block reward,” *IJARCCCE*, vol. 8, no. 8, pp. 5–10, 2019.
- [15] R. Matthew, “Marvel.Human capital and search-based discovery: a study of high-tech entrepreneurship,” *Entrepreneurship: Theory and Practice*, vol. 37, no. 2, pp. 403–419, 2017.
- [16] H. Li, P. Loyalka, and S. Rozelle, “Human capital and China’s future growth,” *The Journal of Economic Perspectives*, vol. 31, no. 1, pp. 25–48, 2017.
- [17] F. Ochsensfeld, “Why do women’s fields of study pay less? A test of devaluation, human capital, and gender role theory,” *European Sociological Review*, vol. 30, no. 4, pp. 536–548, 2017.
- [18] A. Bhattacharya and D. De, “SigSense: mobile crowdsensing based incentive aware geospatial signal monitoring for base station installation recommendation using mixed reality game,” *Wireless Personal Communications*, vol. 123, no. 3, pp. 2863–2894, 2021.
- [19] L. Kening and S. Huaming, “School of Economics. Contract and incentive mechanism in low-carbon R&D cooperation,” *Supply Chain Management: International Journal*, vol. 22, no. 3, pp. 270–283, 2017.
- [20] B. Matthias and R. Claudia, “Escaping Europe: health and human capital of Holocaust refugees1,” *European Review of Economic History*, vol. 22, no. 1, pp. 1–27, 2018.
- [21] A. Xg, Q. A. Qi, and G. B. Xin, “Economy supervision mode of electricity market and its incentive mechanism - Science-Direct,” *Global Energy Interconnection*, vol. 3, no. 5, pp. 504–510, 2020.
- [22] J. D. Savage and J. D. Caverley, “When human capital threatens the Capitol: foreign aid in the form of military training and coups,” *Journal of Peace Research*, vol. 54, no. 4, pp. 542–557, 2017.
- [23] L. Li and J. Zhang, “Research and analysis of an enterprise E-commerce marketing system under the big data environment,” *Journal of Organizational and End User Computing*, vol. 33, no. 6, pp. 1–19, 2021.
- [24] G. He, “Enterprise E-commerce marketing system based on big data methods of maintaining social relations in the process of E-commerce environmental commodity,” *Journal of Organizational and End User Computing*, vol. 33, no. 6, pp. 1–16, 2021.
- [25] R. molina masegosa and J. gozalvez, “lte-V for sidelink 5G V2X vehicular communications: a new 5G technology for short-range vehicle-to-everything communications,” *IEEE Vehicular Technology Magazine*, vol. 12, no. 4, pp. 30–39, 2017.

Research Article

Mathematics Deep Learning Teaching Based on Analytic Hierarchy Process

Yonghua Duan 

School of Information Engineering, Xi'an University, Xi'an 710065, Shaanxi, China

Correspondence should be addressed to Yonghua Duan; dyhua_0_0@xawl.edu.cn

Received 28 April 2022; Revised 5 July 2022; Accepted 15 July 2022; Published 10 August 2022

Academic Editor: Wei Liu

Copyright © 2022 Yonghua Duan. This is an open access article distributed under the Creative Commons Attribution License, which permits unrestricted use, distribution, and reproduction in any medium, provided the original work is properly cited.

Deep learning is an important concept introduced into modern learning science. It is different from the surface learning of mechanically and passively acquiring knowledge and storing individual information but emphasizes learners' active and critical learning. It wants them to understand the full meaning of what they have learned. By establishing a link between existing knowledge and new knowledge, it transfers existing knowledge to a new environment, makes decisions, and solves problems. Deep learning plays an important role in students' learning. Deep learning ability is the key factor affecting the quality of learning and the development of students' academic ability. The quality of in-depth teaching is difficult to guarantee, which requires a complete, comprehensive, and evaluation system to evaluate it. This paper introduces the analytic hierarchy process to weight the indexes in mathematics deep learning and puts forward some suggestions on creating an environment for deep learning. The experimental results show that teachers' teaching accounts for the highest proportion of primary indicators, reaching 67%. Multimedia resources account for the highest proportion of secondary indicators, reaching 73.01%. This paper then puts forward some suggestions for indicators with large weights.

1. Introduction

A common problem with school curricula today is that they are not comprehensive and are still quite superficial. In class, the information received by students is often only superficial understanding, mechanically printed in their memory; they are only application, and the information they master is only superficial. Restricted by many factors such as examination, there are still many problems in classroom teaching. There are still a considerable number of teachers who take the "spoon feeding" and "indoctrination" teaching methods as the leading teaching methods, regard students as a container for receiving knowledge, and do not regard students as a complete "person." It lacks humanized education; of course, it cannot promote people's long-term and all-round development, and teaching is a lack of innovative consciousness.

Deep learning is more than just teaching superficial knowledge. Instead, it makes teaching adapt to students' cognitive styles and individual differences, which enables

them to study deeply. Deep learning aims to greatly change students' learning process and results through teachers' deep learning. The goal of positive deep learning is to find ways to teach less and learn more. It makes the school happy and peaceful and reduces the unpleasant burden. The innovations of this paper are as follows: (1) this paper uses analytic hierarchy process to analyze the data, constructs the model of in-depth teaching quality evaluation system, and determines the weight of single ranking index of in-depth teaching quality evaluation. (2) On the basis of establishing the model of evaluation information collection and processing, this paper divides the evaluation information into indirect and direct evaluation information according to whether it can directly reflect the evaluation results.

2. Related Work

Relevant scientists have done the following research on deep learning teaching. Hossain D. proposed a method based on a deep belief neural network for target detection. A robot took

an object of the user's choice and placed it at the desired location. The three developed learning systems are easy to use for nonempirical experts and give different results in terms of time and accuracy to complete the task. The proposed method can simplify the use of a robot manipulator and help inexperienced users in various assembly tasks. It applies it to object detection and implements three intuitive schemes for learning robot manipulators [1]. Li discussed the characteristics of university music education in relation to other cultural subjects, the potential of multimedia technology in school music education, and the complementary role of music education. It proposed intelligent functions of deep learning algorithms to monitor the teaching and learning process of music and analyze its quality. He presented a multimedia teaching plan with theoretical guidelines and references for the application of multimedia technology in music education in Chinese high schools and universities [2]. Long and Zhao used particle swarm image recognition and deep learning technology to process intelligent classroom video, extract features for classroom tasks in real time, and send them to the teacher. To overcome the early convergence of the conventional optimization algorithm, it proposed an improved strategy for multiparticle swarm optimization algorithm. To improve the search efficiency of the PSO algorithm and solve the problem of early convergence of the algorithm, he combined useful features from other algorithms into the algorithm. This increases the particle diversity of the algorithm and improves the overall particle search performance. As a result, efficient feature extraction is achieved [3]. Considering the analytical hierarchical process, the participating researchers have conducted the following studies. Jagtap and Bewoor introduced an application of the analytical hierarchical process to the identification of key equipment in a thermal power plant. In this analysis, based on the analytical hierarchical process, four criteria are considered in the critical analysis, namely, the impact of the faulty equipment on power generation, environment and safety, the frequency of faults, and maintenance cost. The study considers the main equipment of thermal power plants, namely, steam turbine, generator, induction fan, forced draft fan, primary pressure fan, boiler feed pump, cooling water pump, condenser water pump, and HV motor for mills [4].

Student evaluation of teaching can improve the quality of higher education. Emmanuel proposed a holistic method for assessing higher education that combines a hierarchical analytic process and data-driven analysis. The hierarchical analytic process allows for varying the importance of different standards for teaching performance, while the data-driven analysis compares teachers' opinions about students and determines the degree of improvement for each teacher. He used data from Greek universities to illustrate the proposed method for evaluating teaching [5]. Timiryanova aimed to link the geographical level with the order of reproduction. He tried to decompose the observed changes in transportation volume with a hierarchical linear model according to the hierarchical structure of economic space. The results show that the analytic hierarchy process can be used to analyze the relationship between production,

distribution, and consumption. In the territory under consideration, transport volumes were mainly affected by domestic consumption, while the impact of wholesale trade was much smaller. The application of analytic hierarchy processes strengthens the analysis of reproduction [6]. Supplier selection has been addressed in the supply chain management literature. It is very important because it affects the composition, strategy, and performance of the whole supply chain. Santis R proposed a decision model based on the hierarchical analytical fuzzy process (AHP) and applied it to the practical case of selecting a maintenance supplier for a large Brazilian railroad company. He used eight criteria to evaluate five potential suppliers [7]. In the above study, deep learning and the application of the analytic hierarchy process are analyzed in detail. It is undeniable that these studies have contributed significantly to the development of these fields. We can learn a lot about methods and data analysis. However, the analytic hierarchy process has been relatively studied in the teaching of deep learning, and it is necessary to fully apply these techniques to research in this area.

3. Teaching Methods of Mathematics Deep Learning

3.1. Deep Learning Teaching. Deep learning is a form of learning based on understanding. Learners can critically absorb new knowledge and ideas, integrate new knowledge and ideas into existing cognitive structures, establish connections between multiple ideas, and transfer existing knowledge to new situations to make decisions and solve problems. Deep learning refers to the process of learning and the situation of learners' learning. The focus is on learners' deeper understanding of the basic concepts and principles of knowledge and their own joint construction of learning content and knowledge [8].

In deep learning, learners can connect new ideas and concepts with previous knowledge and explore basic principles and models. By actively evaluating new ideas and conclusions, they integrate learning into the relevant conceptual framework and understand the dialogue process of knowledge construction. It critically examines the logic of its claims and consciously reflects on its own learning and knowledge. Deep learning is a learning process, which selects challenging and stimulating topics under the guidance of competent teachers. Students can actively and wholeheartedly participate in it, experience the richness of the process, and acquire relevant development skills [9]. Deep learning not only focuses on the knowledge and skills eventually acquired by individuals but also focuses on understanding the nature of learning, unique interests, and valuable needs formed in the process. Deep learning is not passive learning but an intensive process and space of active exploration, active construction, and rational application under the guidance of teachers. The process of deep learning can also be said to be a deliberate learning process. It pays more attention to exploring the essence of learning, discovering the significance of students' learning, and cultivating students' habit of independent learning through active exploration [10].

In the classroom learning under traditional pedagogy, learners regard the course content as the content that has nothing to do with their existing knowledge and experience. Learners regard the course content as irrelevant knowledge fragments or modules. Learners cannot understand why and how to do it, just memorize facts and imitate operating procedures. Learners have great difficulties in understanding concepts different from the contents of this book. The learner always regards static knowledge as the authority. Learners cannot consciously reflect on their learning intentions and their own learning strategies.

It analyzes the key and difficult points in the theme of teaching and looks for teaching methods that are more conducive to students' cognition. Only when teachers are familiar with the key and difficult points in the teaching process can they have targeted teaching. At the same time, the key and difficult points of knowledge also run through the main line of the whole teaching process. It is also the direction for teachers and students to overcome together. Teachers should carry out corresponding situational teaching from students' existing cognitive structure and improve students' cognitive structure and learning transfer ability on the basis of students' familiarity. Its carefully designed key and difficult teaching process can effectively promote the construction of students' knowledge structure and form correct mathematical ideas and values. At the same time, it also increases students' desire to explore knowledge and expand their horizons.

The effectiveness of teaching depends not only on teachers' teaching methods but also on students' learning level. Teachers' teaching does not match students' learning. The teachers of intensive teaching are different from the students of intensive learning. Therefore, teaching should focus on students' learning and be based on observing and analyzing students' learning. Contemporary learning theory holds that students' learning is multidimensional and holistic, and the formation of knowledge and meaning, the development of skills, and the acquisition of emotional and behavioral values form a whole in deep learning [11]. At present, teacher-centered learning is contrary to the basic learning law that determines students' learning style. Chinese textbooks have been in the process of reform. The connection between disciplines and between grades is becoming more and more obvious. However, it cannot effectively understand the teaching materials and knowledge system. Teachers ignore the links between chapters and disciplines in the process of teaching. It is often a lesson, a topic, and a unit. This makes many students not aware of the connections between various knowledge points, and they are often unable to apply flexibly, change, and adapt, let alone learning transfer. The cohesion of teaching materials and teachers' own cultural cultivation and knowledge reserve have a great relationship with whether students can learn effectively [12].

Theme teaching is one of the effective teaching modes to promote students' in-depth learning. It can not only let teachers guide students around a certain knowledge theme, make students change and improve their cognitive structure, and improve their learning transfer ability. It can also

integrate the three-dimensional goals of students' knowledge, skills, emotional attitudes, and values. At the same time, it can also enable students to actively participate in teaching, feel its rich process, and obtain corresponding development ability. It enables students to understand the essence of learning, unique high-level emotion, positive and optimistic attitude, and correct value orientation formed in this process [13]. As shown in Figure 1, it is the framework diagram of theme teaching research design.

The theme is the link between all things and one or more characteristics, such as the concept of integrity in the first section of the first chapter of middle school mathematics. Thematic teaching is a way of planning and teaching information in a specific context or in a common or similar learning style. Special subject teaching is to guide people to learn interdependent knowledge modules through various research and teaching methods. It is a way to change and strengthen people's cognitive structure. Topic teaching is actually a form of learning. Teachers guide students to find their own way of learning and thinking about a topic. Its purpose is not to acquire knowledge but to pay attention to imparting knowledge, improving skills, strengthening emotional experience, and cultivating correct values in the learning process. Figure 2 shows the schematic diagram of the theme teaching design.

In terms of computer artificial intelligence, deep learning actually refers to algorithmic thinking. Its core is that the computer simulates the deep thinking of the human brain, so as to realize the complex operation of data [14]. In the field of artificial intelligence, computer processing information is a process of automatic coding and automatic decoding. It is a process from data extraction, abstract cognition to optimal selection. The human brain processes information layer by layer. Computer artificial intelligence simulates the cognitive structure of the human brain to process complex information. Artificial intelligence does not rely solely on data models. The process of artificial intelligence simulation from symbol reception, decoding, and connection establishment to optimal selection is also structured [15].

It is a great advantage for learners to use rich curriculum resources and Internet resources for learning. To show learners' learning process and meaning construction process, what is more effective is the amount of data downloaded by learners. The resources here include the resources of the course itself (usually provided by teachers) and Internet resources. The former includes the use of resources in the in-depth teaching platform (such as problem resources and e-library). We can determine the online learning time of learners by recording the time when they log in and log out of the system. It provides learners' learning range, learning progress, and other information through the browsing range and times of the course content page. It uses the browsing of problem resources and e-library materials to understand the depth and breadth of learners' learning. It uses learners' statements in the discussion area or chat room to collect learners' learning attitude, understanding of learning topics, problem solving, adjustment of learning strategies, and meaning construction.

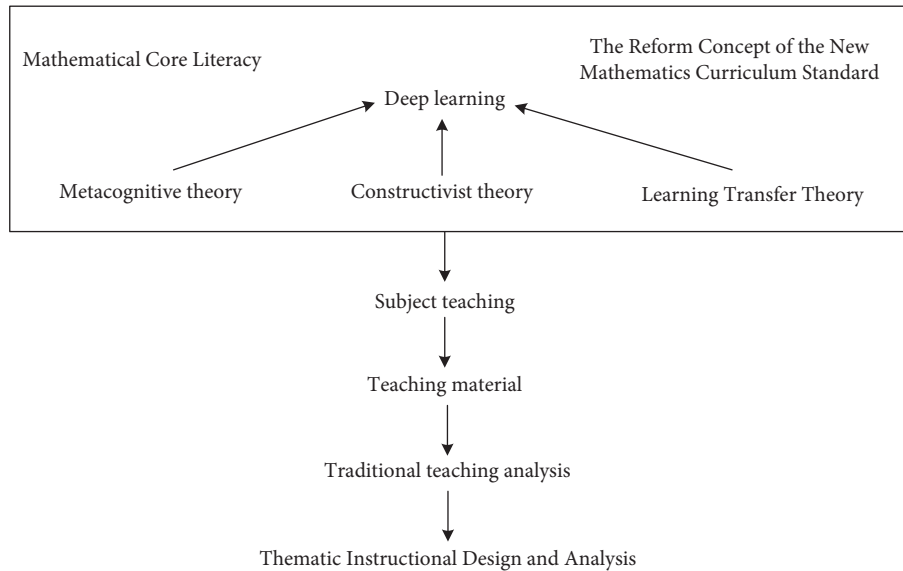


FIGURE 1: Framework diagram of theme teaching research design.

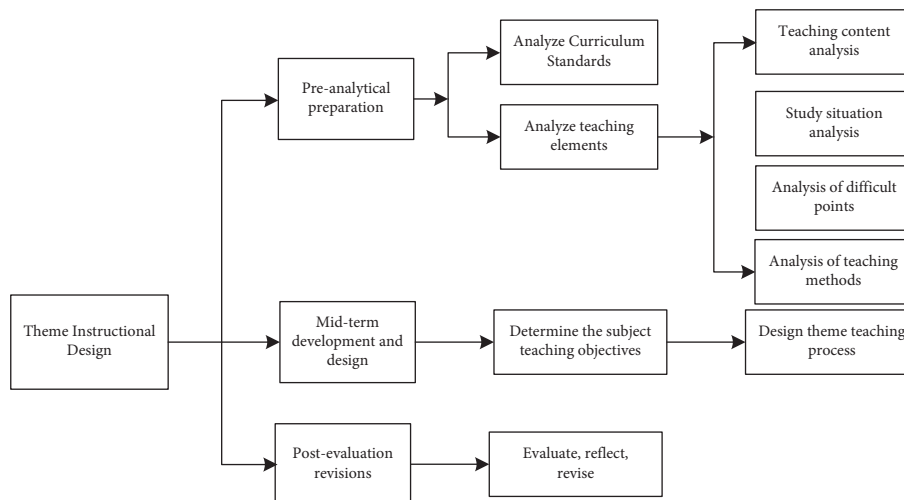


FIGURE 2: Schematic diagram of theme teaching design.

The depth of teaching is the real meaning of teaching. It goes beyond superficial symbol communication and develops from superficial symbol teaching to the teaching with real logical significance. The depth of teaching does not mean deepening the teaching content or increasing the teaching difficulty. It is not to increase the difficulty of knowledge and infinitely expand the number of knowledge but to guide students to comprehensively deal with knowledge and information. It helps them deepen their mastery of knowledge and achieve real understanding. It is learning in context, meaningful learning, developmental learning, interactive learning, and the development of attitudes and emotional values in a special sense [16]. The depth of learning refers to the degree of explanation and development of students' knowledge. Deep learning does not rely on technology and procedures to guide the teaching process, and increasing students' knowledge is the only purpose of teaching, but focuses on the essence of teaching.

It pays attention to the teaching situation and process and the value and significance of teaching. It emphasizes that students learn to change from superficial symbolic knowledge to the symbol of knowledge, real thought, method system, general logical structure, and real in-depth understanding. The general logical structure and corresponding value and significance transform traditional symbolic learning into deep and meaningful learning in the general sense, making students' learning full of happiness, significance, and humanistic interest [17].

It forms a relationship of listening to each other attentively. They are good at appreciating each other's feelings, understanding each other's meaning, opening up, and accepting each other. If the atmosphere of listening to each other flows in the classroom, the knowledge and information expressed by teachers and students will have their own emotional factors and the temperature of their own lives. The teacher's classroom discourse is not just to convey

knowledge but a sense of skin-cutting flowing from the depths of his heart. What students say is not only the correct answer the teacher wants but the real idea in his heart. Such teaching provides students with the opportunity to give birth to wonderful ideas.

Deep learning does not mean a specific teaching method, tool, or strategy but a real teaching concept. The process of in-depth teaching is aimed at students' growth and development, developing their internal rich emotions, caring for the consistency of students' life development, and looking for guidance for the quality development of teaching in the future. Structuralists pay attention to the basic structure of the discipline, while teachers pay attention to students' understanding and mastery of the basic structure of the discipline. Constructivism emphasizes foundationalism, which means that concepts must be both broad and adaptive. On the other hand, structure refers to the relationship between the basic concepts, principles, and laws of various disciplines. In the context of a specific field, it refers to the concepts, principles, and legal system that are crucial to the field [18].

3.2. Analytic Hierarchy Process. Analytic hierarchy process is mainly used in dealing with multiobjective factor optimization problems, resolving complex problems into several level problems, and making comparative judgment based on experience. By calculating the proportion of each level index to the total target weight, the greater the weight proportion, the best the scheme. It implements relevant strategies for the scheme according to the modeling results [19]. The steps of analytic hierarchy process are as follows: (1) It establishes a hierarchical index model. Through the combination of literature search and actual situation, the research problem of decision-making is divided into several levels, including general goal, subgoal of each level, evaluation criteria, and scheme level. (2) The construction of the judgment matrix is to find out the key factors in the same level of indicators according to experience, compare the two factors according to subjective opinions, and determine the weight of the upper level goal, so as to construct the judgment matrix. Through the comparison of quantitative figures, it transforms the research object from qualitative problems to quantitative problems, which can better describe the objective reality. It provides a mathematically accurate description for practice. (3) It solves the judgment matrix by calculating the maximum eigenvalue of the determinant of the judgment matrix. It calculates the corresponding feature vector according to the maximum feature root and uses normalization processing to obtain that each feature vector is the weight of each index, which determines the quality of the scheme according to the weight [20]. (4) The rationality test of its judgment matrix is a judgment matrix constructed according to subjective factors, which is the ranking result between indicators. These indexes are not completely transitive. The eigenvectors are calculated according to the matrix, and the weights represented by these eigenvectors may not be combined with reality. At this time, the weight needs to be tested at one time, and the pairwise comparison matrix is constantly modified according to the test until it passes the test. (5) The consistency test of overall

objective ranking calculates the maximum eigenvalue of the matrix by constructing the pairwise comparison judgment matrix. It calculates the feature vector according to the feature root and obtains the weight of each index. It sorts the proportion of the total target weight according to the weight of each index to determine the importance of each factor. At this time, the results are not necessarily accurate, and a one-time inspection is still needed. If the inspection fails, it needs to be adjusted until the inspection passes.

Hierarchical single ranking refers to the relative weight of each factor of all judgment matrices according to its criteria. In essence, it is to calculate the weight vector. Each column of the consistency judgment matrix is normalized and calculated by using the principle to obtain the corresponding weight. It normalizes and calculates each column of the inconsistency judgment matrix to obtain the approximate corresponding weight.

$$\sigma_u = \frac{1}{b} \sum_{v=1}^b \frac{i_{uv}}{\sum_{k=1}^b i_{kv}}, \quad (1)$$

$$U_I(m) = \exp \left[\frac{-(m-a)^2}{\omega^2} \right],$$

where b is the number of column vectors and σ_u is the arithmetic mean of column vectors.

$$\begin{aligned} CI &= \frac{\phi_{\max} - b}{b - 1}, \\ \bar{I}_u &= \sqrt[b]{\prod_{v=1}^b i_{uv}} \end{aligned} \quad (2)$$

where CI is the consistency indicators.

$$\begin{aligned} \sigma^{(k)} &= (\sigma_1^{(k)}, \sigma_2^{(k)}, \dots, \sigma_b^{(k)})^T = v^{(k)} \sigma^{(k-1)}, \\ \sigma_u^{(k)} &= \sum_{v=1}^a \phi_{uv}^{(k)} \sigma_v^{(k-1)}, \end{aligned} \quad (3)$$

where a is the number of elements and kk is the number of layers of element sorting.

$$\begin{aligned} CR &= \frac{\sum_{v=1}^b \sigma_v CI_v}{\sum_{v=1}^b \sigma_v RI_v}, \\ I_u &= \frac{\bar{I}_u}{\sum_{u=1}^b \sqrt[b]{\prod_{v=1}^b i_{uv}}}, \end{aligned} \quad (4)$$

where CI_v is the consistency of single sorting and $RI_v RI_v$ is the mean random consistency.

$$\begin{aligned} \phi_{\max} &= \frac{1}{b} \sum_{u=1}^b \frac{i_{uv} I_u}{I_u}, \\ C.I. &= \frac{\phi_{\max} - b}{b - 1}, \end{aligned} \quad (5)$$

where ϕ_{\max} is the maximum eigenvalue and b is the order.

$$D_k = \sum_{u=1}^b r_{ku}, \quad (6)$$

where D_k is the sum of all times or times and b is the total number of students.

$$\text{avg}_k = \frac{D_k}{b}, \quad (7)$$

where avg_k is the average time or times in the index.

$$x_1 = \sum_{u=1}^b (I_u \times Pu), \quad (8)$$

where x_1 is the assessment of learning activities.

Analytic hierarchy process is a systematic and hierarchical analysis method, which combines the qualitative and quantitative analysis of nonqualitative events. It is mainly used for decision-making problems under uncertainty with only a few analysis criteria. In this method, a complex problem is decomposed into various factors, which are grouped in a dominant relationship to form an orderly level. The importance of each factor is determined by two comparisons, which then combines human factors to determine the order of possibilities. Analytic hierarchy process aims to simplify complex problems. It divides it into different levels by establishing an interactive level. Through detailed quantification and evaluation, it helps decision makers make appropriate decisions and reduce the risk of wrong decisions. It ensures the scientificity of qualitative analysis, the accuracy of quantitative analysis, and the consistency of the overall evaluation of qualitative and quantitative indicators. It is a simple, flexible, and practical multistandard decision-making method. Since its introduction, analytic hierarchy process has been widely used to solve the problems of various industries.

The basic principle of analytic hierarchy process is to decompose all levels of complex problems into orderly levels and connect them together. Elements at each level have roughly the same status. Each level has a specific relationship with its previous and subsequent levels, and an orderly hierarchical model is formed on the basis of mutual relationship. Hierarchical model usually consists of some key levels, such as goal level, standard level, and decision level. In a recursive hierarchical model, the importance of each level is quantified through the evaluation of some objective facts, that is, the level. Through two comparisons and quantification, the relative importance of each layer of facts is determined and an evaluation matrix is formed. Then, the relative importance weight of each index in the evaluation matrix is calculated by mathematical method. Finally, by combining the relative weights of the importance of each layer, it calculates the relative importance weights of the indicators of each layer in the recursive hierarchy model to calculate the weights of all indicators. Figure 3 shows the technical roadmap of analytic hierarchy process.

Analytic hierarchy process takes the research object as a system and makes decisions according to the thinking mode

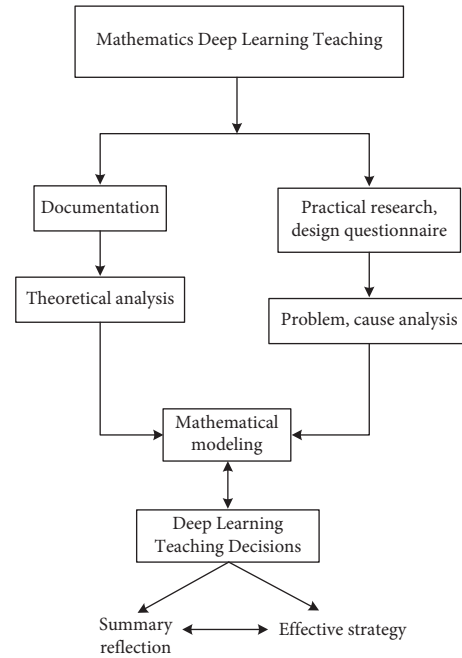


FIGURE 3: AHP technology roadmap.

of decomposition, comparative judgment, and synthesis. It has become an important tool of system analysis developed after mechanism analysis and statistical analysis. The idea of the system is not to cut off the influence of various factors on the results, and the weight setting of each layer in the analytic hierarchy process will directly or indirectly affect the results. Moreover, the degree of influence of each factor in each level on the results is quantified and very clear. This method can especially be used for the systematic evaluation of unstructured characteristics and the systematic evaluation of multiobjective, multicriteria, and multiperiod. The function of analytic hierarchy process is to select the best one from the alternatives. When applying the analytic hierarchy process, there may be a situation where our own creativity is not enough, resulting in the fact that although we choose the best of many schemes we think of, the effect is still not good enough for the enterprise. Then, it points out the shortcomings of the known scheme or even puts forward the improvement scheme; this analysis tool is more perfect. But obviously, analytic hierarchy process has not been able to do this.

Analytic hierarchy process regards a subject as a system and decomposes and compares the influence of various factors on the evaluation results of the whole system. The contribution of each level in the analytic hierarchy process has a direct or indirect impact on the final evaluation results, and the impact of factors at each level on the final evaluation results can be quantified in a very clear way. This method is very suitable for multiobjective, multicriteria, and multiphase systems. Hierarchical analysis is easy for decision makers to understand and use. The foundation and steps are very simple and easy to calculate, and the results are not complex. The evaluation of the relative importance of each level of reasoning is transformed into the analysis of the

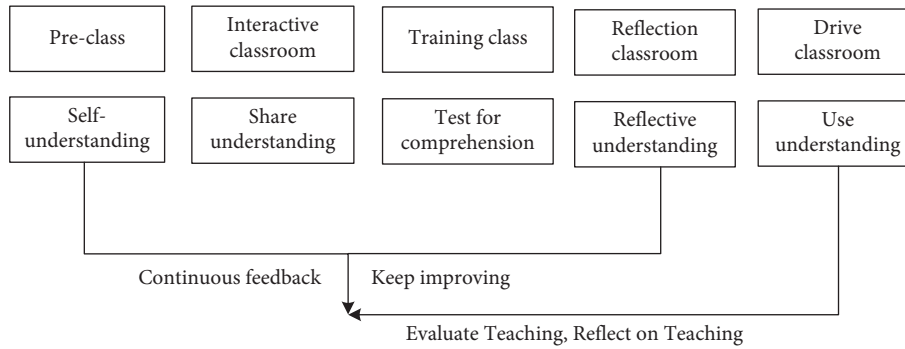


FIGURE 4: In-depth teaching classroom design process.

relative importance of the human decision maker, and the evaluation of the component of each level of reasoning is based on the calculation. Analytic hierarchy process is most suitable for the hierarchical system with interrelated evaluation indexes and decision-making problems whose target value is difficult to quantify. This paper uses the analytic hierarchy process, which is widely used in system evaluation, system design, and decision-making. It examines the evaluation standards of deep learning quality from three different perspectives and analyzes the quality of deep learning. It identifies five of the many factors that affect the quality of education: educational services, educational management, teachers, students' learning, and social reputation.

Analytic hierarchy process is mainly used in the fields of safety science and environmental science. In the aspect of safety production science and technology, the main applications include coal mine safety research, hazardous chemicals evaluation, oil depot safety evaluation, urban disaster emergency response capacity research, and traffic safety evaluation. The application in environmental protection research mainly includes water safety assessment, water quality indicators and environmental protection measures, eco-environmental quality assessment index system, and determination of pollution sources in aquatic wildlife reserves. In addition, analytic hierarchy process can be more used to guide and solve the problems encountered in personal life, such as professional choice, job choice, and house purchase choice. It can clarify the level of work ideas and thinking problems by establishing hierarchical structure and measurement indicators.

4. Teaching Experiment of Mathematics Deep Learning

In this paper, through the design of in-depth teaching program applied to the actual classroom, we can understand what problems exist in the application of in-depth teaching in the actual classroom. Figure 4 shows the classroom design process of in-depth teaching.

In order to better understand the concept of students' learning, we randomly select students for learning behavior survey, and let students answer questions from multiple perspectives, such as listening habits and attitudes,

questions, answering questions, group discussion, and so on. Tables 1 and 2 show the students' answers.

This problem needs to consider the factors affecting the teaching quality of deep learning. In this paper, the analytic hierarchy process is used to determine the subjective weight of each factor, and then the weighted sum is carried out, so as to construct the model of distance teaching quality evaluation system based on analytic hierarchy process. The model is divided into the following three layers. The top layer of distance learning quality evaluation based on analytic hierarchy process is the target layer; the middle layer corresponds to the primary index layer, and the bottom layer is the criterion layer, which corresponds to the secondary index layer. Figure 5 shows the quality evaluation of distance teaching based on analytic hierarchy process.

In practice, a consistency test is needed to judge whether the matrix meets the general consistency requirements. Only when the general consistency is satisfied can the logical rationality of the judgment matrix be confirmed, and then the results need to be continuously analyzed. As shown in Table 3, it is the average random consistency index.

According to the questionnaire survey, the proportion of indicators obtained through statistics is shown in Figure 6. As can be seen from the figure, teachers' teaching accounts for the highest proportion of primary indicators, reaching 67%. Multimedia resources account for the highest proportion of secondary indicators, reaching 73.01%.

To sum up, it determines the index weight of hierarchical single ranking of deep learning teaching quality evaluation based on analytic hierarchy process as shown in Figures 7 and 8.

In order of importance, teachers' teaching accounts for 40.89%, teaching management 21.96%, students' learning 21.96%, facilities and services 7.59%, and social reputation 7.59%.

Deep learning must consider creating an atmosphere of daily dialogue in the classroom, so as to truly connect the classroom with life and re-establish the classroom life situation. Teachers should treat students as friends and learning partners. Listening and responding are the proper performance in class. It conducts in-depth learning in a natural and cohesive dialogue environment, collects knowledge, and concentrates culture and spirit. The teachers are full of true feelings and guided by good manners.

TABLE 1: Questions in class and difficulties encountered in learning.

Take the initiative to ask the teacher	Discuss with classmates	Solve by looking up data	Nothing more
8%	36%	34%	22%
Actively raise your hand to speak	Selective question and answer	Only care about the part that interests you	Only care about the part that interests you
16%	44%	34%	6%

TABLE 2: Group discussions in classroom learning and what kind of lessons do you like.

Often discussed	According to the actual situation, occasionally discuss	Little opportunity for discussion	Do not know what to discuss
12%	38%	32%	18%
The teacher explains directly	Teacher asks questions, students think	Group discussion	Carry out various forms of activities and small competitions
6%	30%	9%	55%

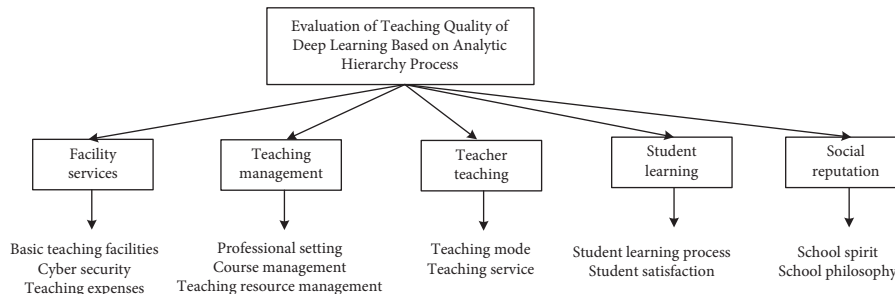


FIGURE 5: The quality evaluation of distance teaching based on analytic hierarchy process.

TABLE 3: Mean stochastic consistency indicator.

Matrix order	1	2	3	4	5
RL	0	0	0.52	0.88	1.12
Matrix order	6	7	8	9	10
RL	1.25	1.36	1.42	1.46	1.49

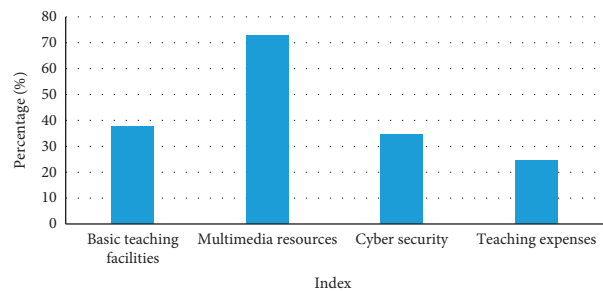
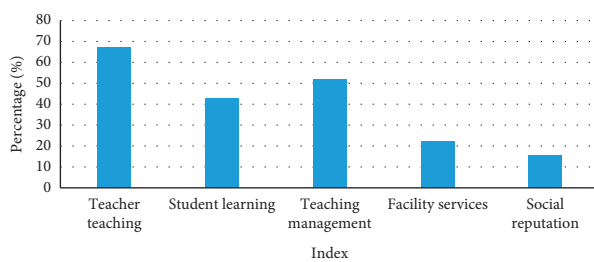


FIGURE 6: Percentage of indicators.

Teachers and students realize opposite wisdom, mutual arousal of emotions, mutual integration of souls, familiar language forms, grammar between people, and affectionate understanding, and learning becomes a seemingly simple and pleasant dialogue. To build a learning community, we should build a platform for communication. To establish a community, we should create more opportunities for mutual cooperation and learning. It has study report meeting, reading exchange meeting, online blog forum, community

activities, and other projects, which are good communication platforms. In this process, teachers should play a guiding role as the chief in equality. It includes how to choose topics, find students' potential in the process of activities, give vivid guidance, guide the selection of materials and methods, reduce the blindness of learning, pay attention to emotional communication, timely coordinate and resolve contradictions, and promote the effective implementation of learning activities.

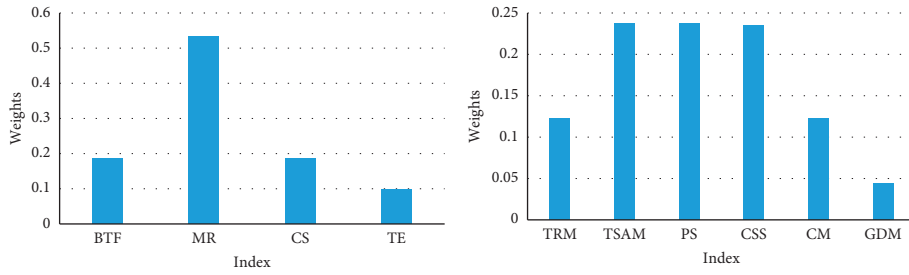


FIGURE 7: Facility service and teaching management weight.

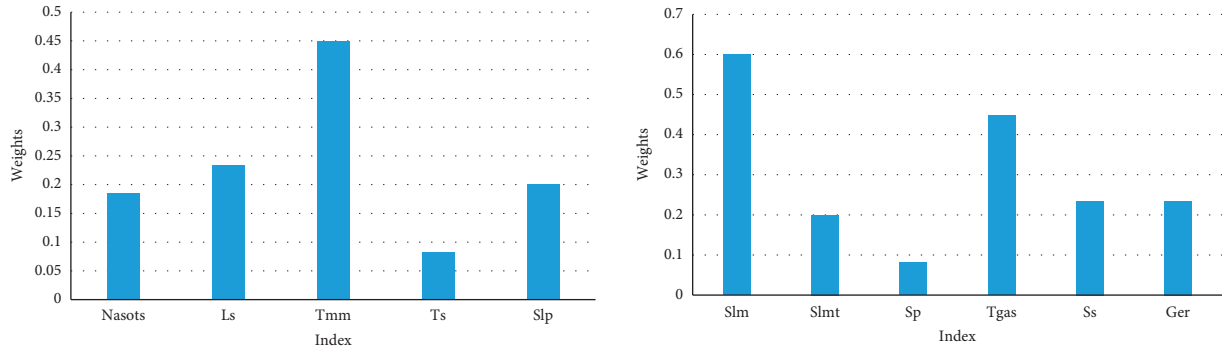


FIGURE 8: Teachers' teaching and teachers' teaching weights.

To build a learning community, we must first have a common vision of mutual recognition. A common vision is the development of desire and vision established by the community for teams and individuals based on the present and pointing to the future. It has a strong driving force. In the process of realizing the common vision, learners will inspire great strength to pursue learning goals and the meaning of life. It will integrate the personal vision into the common vision and make the personal vision in harmony with the common vision. It integrates individual wisdom into the collective, learns in communication, and communicates in learning. Through the impact of different thinking and wisdom, it forms collective wisdom and realizes in-depth learning in a democratic and harmonious atmosphere.

5. Conclusion

In the educational reform, different teaching methods have appeared, but these teaching methods have the same effect on students. Those teaching methods are similar, and there is no systematic teaching method to cultivate the educational objectives and abilities of all students. Deep learning is a model of science learning, which is different from the traditional classroom tolerance, strict attendance, and poor teaching methods. After the improvement of curriculum standards, teachers supervise in the classroom, and the student-centered classroom teaching method can be continued. This paper introduces the analytic hierarchy process, constructs the deep learning teaching quality evaluation system, and weights the indexes in the system. It puts forward corresponding suggestions for different weights. According to the results of mathematical modeling by

analytic hierarchy process, whether it is feasible in practice is demonstrated, and the theoretical model is constantly revised according to practical problems to guide teaching practice.

Data Availability

No data were used to support this study.

Conflicts of Interest

The author declares that there are no conflicts of interest regarding the publication of this article.

References

- [1] D. Hossain, G. Capi, M. Jindai, and S. I Kaneko, "Pick-place of dynamic objects by robot manipulator based on deep learning and easy user interface teaching systems," *Industrial Robot: International Journal*, vol. 44, no. 1, pp. 11–20, 2017.
- [2] W. Li, "Multimedia teaching of college musical education based on deep learning," *Mobile Information Systems*, vol. 2021, Article ID 5545470, 10 pages, 2021.
- [3] S. Long and X. Zhao, "Smart teaching mode based on particle swarm image recognition and human-computer interaction deep learning," *Journal of Intelligent and Fuzzy Systems*, vol. 39, no. 4, pp. 5699–5711, 2020.
- [4] H. P. Jagtap and A. K. Bewoor, "Use of analytic hierarchy process methodology for criticality analysis of thermal power plant equipments," *Materials Today Proceedings*, vol. 4, no. 2, pp. 1927–1936, 2017.
- [5] T. Thanassoulis, P. K. Dey, K. Petridis, I. Goniadis, and A. C. Georgiou, "Evaluating higher education teaching performance using combined analytic hierarchy process and data

- envelopment analysis,” *Journal of the Operational Research Society*, vol. 68, no. 4, pp. 431–445, 2017.
- [6] V. M. Timiryanova, “Examining the relationship between production, trade and consumption using hierarchical analysis methods,” *Economy of Region*, vol. 17, no. 1, pp. 145–157, 2021.
- [7] R. B. d. Santis, L. Golliat, and E. P. d. Aguiar, “Multi-criteria supplier selection using fuzzy analytic hierarchy process: case study from a Brazilian railway operator,” *Brazilian Journal of Operations & Production Management*, vol. 14, no. 3, pp. 428–437, 2017.
- [8] X. Du, A. Slipinski, Z. Liu, and H. Pang, “Description of a new species of *esc.*,” *ZooKeys*, vol. 982, no. 2, pp. 1–9, 2020.
- [9] E. Kimberly and N. Anderson, “Teaching note - bring class concepts to life: implementing intensive interview projects for deep learning,” *Bridgewater Review*, vol. 36, no. 2, pp. 29–32, 2017.
- [10] A. Zureck, “Achieving active learning and deep learning with media using the example of teaching finance,” *Problems of Education in the 21st Century*, vol. 79, no. 3, pp. 485–504, 2021.
- [11] Ş. Gür, M. Hamurcu, and T. Eren, “Selecting of Monorail projects with analytic hierarchy process and 0-1 goal programming methods in Ankara,” *Pamukkale University Journal of Engineering Sciences*, vol. 23, no. 4, pp. 437–443, 2017.
- [12] D. Marion, V. Vera, H. Micka, S. Fauser, C. Gross, and S. Stock, “comparing analytic hierarchy process and discrete-choice experiment to elicit patient preferences for treatment characteristics in age-related macular degeneration,” *Value in Health*, vol. 20, no. 8, pp. 1166–1173, 2017.
- [13] S. Ahmed and P. Vedagiri, K. V. Krishna Rao, Prioritization of pavement maintenance sections using objective based Analytic Hierarchy Process,” *International Journal of Pavement Research and Technology*, vol. 10, no. 2, pp. 158–170, 2017.
- [14] M. Chi, D. Zhang, G. Fan, W. Zhang, and H. Liu, “Prediction of top-coal caving and drawing characteristics by the analytic hierarchy process-fuzzy discrimination method in extra-thick coal seams,” *Journal of Intelligent and Fuzzy Systems*, vol. 33, no. 4, pp. 2533–2545, 2017.
- [15] A. M. Yusoff, S. Salam, S. N. M. Mohamad, and R. Daud, “Gamification element through massive open online courses in TVET: an analysis using analytic hierarchy process,” *Advanced Science Letters*, vol. 23, no. 9, pp. 8713–8717, 2017.
- [16] J. S. Hurley, “Quantifying decision making in the critical infrastructure via the analytic hierarchy process (AHP),” *International Journal of Cyber Warfare & Terrorism*, vol. 7, no. 4, pp. 23–34, 2017.
- [17] H. Y. Chen, “Development of perfume bottle visual design model using fuzzy analytic hierarchy process,” *Art and Design Review*, vol. 05, pp. 13–25, 2017.
- [18] A. M. Abudeif and A. A. Abdelmoneim, A. F. Farrag, GIS-based multi-criteria earthquake hazards evaluation using analytic hierarchy process for a nuclear power plant site, west Alexandria, Egypt,” *Environmental Earth Sciences*, vol. 76, no. 23, pp. 796–801, 2017.
- [19] M. Ivanco, G. Hou, and J. Michaeli, “Sensitivity analysis method to address user disparities in the analytic hierarchy process,” *Expert Systems with Applications*, vol. 90, pp. 111–126, 2017.
- [20] X. Jiang and Y. Zhang, “The development of public health sports in colleges and universities based on the analytic hierarchy process,” *Revista Brasileira de Medicina do Esporte*, vol. 27, no. spe, pp. 73–75, 2021.

Research Article

Monetary Policy, Fiscal Policy, and Capital Structure Dynamic Adjustment: Evidence from Chinese Listed Companies

Liangwei Wan 

School of Finance, Jiangxi University of Finance and Economics, Nanchang 330013, Jiangxi, China

Correspondence should be addressed to Liangwei Wan; wanlongway@126.com

Received 22 May 2022; Accepted 6 July 2022; Published 8 August 2022

Academic Editor: Wei Liu

Copyright © 2022 Liangwei Wan. This is an open access article distributed under the Creative Commons Attribution License, which permits unrestricted use, distribution, and reproduction in any medium, provided the original work is properly cited.

Monetary and fiscal policies are important means of macroeconomic regulation by the Chinese government, and their combination is an important guarantee for the stable development of economy. We analyze the impact of monetary and fiscal policies on capital structure adjustment and empirically test the data of Chinese nonfinancial listed companies in A-share market from 2000 to 2020. The research shows that, under the loose monetary policy and expansionary fiscal policy, enterprises will adjust their capital structure upward, improve their asset-liability ratio, and speed up their capital structure adjustment. In addition, the speed of capital structure adjustment of enterprises with low financing constraints is faster than that of enterprises with high financing constraints.

1. Introduction

Monetary and fiscal policies are important means for the Chinese government to carry out macroeconomic regulation and control. The combination of monetary and fiscal policies is an important guarantee for the stable development of economy in China. According to the instructions of the Central Economic Work Conference, the Chinese government has continued to implement a prudent monetary policy and a proactive fiscal policy since 2019.

Judging from the actual operation of the People's Bank of China (PBC), the Chinese central bank adopted a moderately loose monetary policy in 2019. In 2019, central banks around the world entered the easing mode and began to slash interest rates. From January 2018 to August 2019, the real interest rate of Chinese enterprises rose from 1.4% to 4.8% after the PPI adjustment, and the PBC lowered the required reserves ratio three times to release liquidity in the market. Monetary policy has been adjusted many times since 2004 in China. In 2004, China implemented a tight monetary policy to curb economic overheating. From 2005 to 2006, the Chinese government adopted a prudent monetary policy. In 2007, the PBC raised the required reserves ratio 10 times. What is more, China implemented a moderately loose

monetary policy in response to the financial crisis in 2008 and maintained a prudent monetary policy from 2011 to 2013. In addition, in 2019, China continued to implement a proactive fiscal policy and began to cut taxes and fees on a large scale. China's fiscal policy mainly goes through the following stages: first, the proactive fiscal policy aimed at expanding demand implemented in the early 21st century, second, the relatively prudent fiscal policy period from 2005 to 2007, which was aimed at preventing the economy from overheating, and third, the active fiscal policy since 2008, which mainly includes expanding government public investment, promoting tax and fee reform, expanding domestic demand and consumption, and optimizing the structure of fiscal expenditure.

Adjustment of monetary policy and fiscal policy is closely related to the development of national economy. Monetary policy and fiscal policy will have a significant impact on the macroeconomic outlook, enterprise financing environment, financing constraints, and the cost of financing and then affect the behavior of enterprises, financial decision-making, and financing strategy and finally affect the enterprise's capital structure. How will the monetary policy, fiscal policy, and other macroeconomic policies affect the adjustment of enterprise capital structure? What is the

relationship between the adjustment of monetary policy and fiscal policy and the adjustment speed of enterprise capital structure? Are there differences in the impact of monetary policy and fiscal policy on the capital structure of enterprises with different financing constraints? All these problems are worth studying.

To answer the above questions, we take the data of nonfinancial listed companies in China's A-share market from 2000 to 2020 as samples, introduce macroeconomic policy factors such as monetary policy and fiscal policy into the partial adjustment model of capital structure, and systematically study the relationship between monetary policy, fiscal policy, and capital structure dynamic adjustment. We may have the following marginal contributions: First, it discusses the impact of China's monetary and fiscal policies on the capital structure of enterprises from the perspective of the relationship between macroeconomic policies and enterprises' microbehavior. Second, the heterogeneity analysis of monetary and fiscal policies on the speed of capital structure adjustment is studied from the perspective of financing constraints.

2. Literature Review

As Keynesian theory universally accepted by western governments, national economy is developing from the era of laissez-faire capitalism into the era of state capitalism. More and more governments take intervention to economy through macroeconomic policy. Chinese and other scholars have studied macroeconomic policies and the relationship of the capital structure adjustment. Huang and Jiang [1] found a correlation between product market competition and the speed of capital structure adjustment. Killi et al. [2]; Gu and Zhou [3]; and Li and Pei [4] found that economic policy uncertainty is correlated with dynamic adjustment of capital structure. Liu et al. [5] systematically investigated the influence of macroeconomic environment on corporate leverage ratio. Levy and Hennessy [6]; Su and Zeng [7]; Jiang and Huang [8]; Liu et al. [9] verified the significant impact of macroeconomic environment on capital structure adjustment through empirical research.

Many Scholars pay attention to the research on the relationship between monetary policy and capital structure. Gertle and Gilchris [10] found that monetary policy would have an impact on the financing constraints of enterprises and then affect the financing decisions of enterprises and lead to changes in capital structure. Oliner and Rudebusch [11] studied the classification of enterprise credit grades and found that monetary policies have different influences on the financing decisions of enterprises with different credit grades. When monetary policies were tightened, enterprises with high credit grades tended to borrow money by issuing commercial paper while those enterprises with low credit grades tended to borrow money from banks. After the 21st century, the dynamic model of capital structure was established, and empirical analysis became a research hotspot. Banerjee et al. [12] established the dynamic adjustment model of capital structure for the first time and empirically analyzed the relationship between currency supply and the

dynamic adjustment speed of domestic enterprises' capital structure in the United States and the United Kingdom. The empirical results show that the capital structure adjustment speed of companies in American is faster than those in British. Cooley and Quadrini [13] studied the impact of monetary policy shocks on corporate financing decisions and found that different enterprise sizes would have different impacts in the face of monetary policy shocks, and the impact of monetary policy shocks on small companies was more significant. Cook and Tang [14] conducted an empirical study on the relationship between macroeconomic policies and the speed of capital structure adjustment and found that the speed of capital structure adjustment was faster in economic prosperity than in economic depression. After 2010, more and more Chinese scholars began to pay attention to the relationship between the changes of China's monetary policy and the capital structure of enterprises. Ma and Hu [15] realized the connection between monetary policy and credit channel; the study found that monetary policy directly affects the supply of credit and the financing constraint degree was closely related to the supply of credit, which also proved that the capital structure of enterprises with high degree of financing constraint is more significantly affected by monetary policy. Nie and Luo [16] found that increasing currency supply and lowering real interest rate would speed up capital structure adjustment. Wu et al. [17] took monetary policy tools as a starting point and found that different monetary policy tools had different impacts on the speed of capital structure adjustment. Song 'et al. [18] found that monetary policies have different effects on the speed of capital structure adjustment due to different growth characteristics of enterprises. Yuan and Guo [19] found that easy monetary policy would accelerate the speed of capital structure adjustment, while monetary tightening policy would slow it down. Most scholars in the study of relationship between monetary policy and capital structure are given priority to theoretical analysis, analyzing the difference of the degree of financing constraints which caused by the microcharacteristics of companies such as enterprise scale, enterprise growth, and credit rating.

On the relationship between fiscal policy and capital structure, many scholars have also carried out many researches. Choe et al. [20] and Boyer [21] discussed the influence of fiscal expenditure on macroeconomic aggregate demand, consumption, and enterprise investment. He [22] investigated the impact of fiscal policies on the capital structure of Chinese listed companies for the first time in China and found that the looser the national fiscal expenditure, the lower the target capital structure of enterprises, and the tighter the national financial expenditure, the higher the target capital structure of enterprises. Luo and Nie [16] believed that expansionary fiscal policy would speed up the adjustment of capital structure. Wang et al. [23] found that local fiscal expenditure had a positive impact on the target leverage ratio of enterprises, while central fiscal expenditure had a negative impact on the target leverage ratio. The papers directly researching relationship between the fiscal policy and the capital structure are not universal, and the Chinese scholars began to study the relationship between fiscal policy

and capital structure in 2010, while the fiscal policy measured by dummy variables instead of quantitative indicators was lack of continuity.

Gulen and Ion [24] point out that there are various forms of external environment uncertainty, and economic policy uncertainty is an important uncertainty faced by enterprises in developing economies. Policy uncertainty mainly consists of policy expectation, implementation, and policy stance change. Many scholars at home and abroad have shown that the uncertainty of economic policies will have an important impact on enterprise financing decisions and then affect the change of enterprise capital structure, which is mainly reflected in the following two aspects: On the one hand, at the level of capital demand, enterprise management will adjust its expectation of the government's policy implementation according to changes in the uncertainty of economic policy. Rao et al. [25] and Fabian [26] found that the uncertainty of product demand is positively correlated with the uncertainty of economic policy. If the uncertainty of economic policy increases, Gulen and Ion [24] believe that corporate managers are risk-averse, and the increase of economic policy uncertainty will weaken their investment willingness, while the decrease of investment scale will reduce financing demand and thus promote downward adjustment of capital structure. In addition, Wang et al. [27] found that as the degree of economic uncertainty increases, the uncertainty of corporate cash flow will also increase, and the risk of corporate bankruptcy will also increase accordingly. Enterprises will reduce debt financing to reduce corporate leverage ratio. Julio and Yook [28] adopted the year of political election as a proxy variable of policy uncertainty and found that corporate investment decreased by 4.8% on average in presidential election years compared with nonelection years. On the other hand, the increase of economic policy uncertainty will have a negative impact on the external financing environment of enterprises. Cao [29] found that the increase of the uncertainty of economic policies would increase the market's expectation of the uncertainty of monetary or credit policies and increase the risk of financial market. Pastor and Veronesi [30] pointed out that the increase in the uncertainty of economic policies would lead to drastic fluctuations in corporate cash flow and increase the information asymmetry between enterprises and creditors. Creditors' estimation of the net present value of enterprise projects would also be more inaccurate, and the increase in the probability of default risk would lead to the reduction of capital supply by banks and other creditors. Francis et al. [31] showed that increased economic policy uncertainty would increase the nonperforming ratio of bank debt and lead to tighter credit policies. With the increase of financing costs and loan requirements of enterprises, banks would reduce capital supply in a disguised way. Finally, the change of economic policy uncertainty will have a significant impact on corporate leverage and capital structure. Gong Rukai et al. [32] found that economic policy uncertainty has a significant negative impact on corporate leverage, and this negative effect is more obvious in short-term debt ratio, private, small-scale, and manufacturing enterprises. Wang et al. [33] found that the uncertainty of economic policies

hindered the dynamic adjustment of capital structure through the channel of uncertainty avoidance, and the difference in sensitivity of policy changes in different industries affected the capital structure adjustment of enterprises in the industry. Gu and Zhou [3] found that, with the increase of policy uncertainty, capital structure decisions tend to be more and more conservative, and the value of financial flexibility plays an important role in this process. The increase of policy uncertainty leads to the increase of financial flexibility value, thus accelerating the speed of capital structure adjustment of enterprises.

Harrod [34] proved that capital structure is always in the process of dynamic adjustment. The macroeconomic policy is only one of the many factors that affect the adjustment of enterprise capital structure. Fischer et al. [35] pointed out that enterprises generally consider the adjusted income and adjustment cost when deciding whether to adjust capital structure, and enterprises will adjust only when the adjusted income is greater than the adjustment cost. Tong [36] verified the relationship between the speed and extent of capital structure adjustment and the adjustment cost. The adjustment cost is related to the adjustment speed; the higher the adjustment cost, the slower the capital structure adjustment speed; on the contrary, the lower the adjustment cost, the faster the capital structure adjustment speed. An et al. [37] found that bankruptcy risk and information disclosure are closely related to capital structure adjustment.

3. Theoretical Analysis and Hypothesis

Monetary policy refers to the control and adjustment of the currency supply in circulation by the central bank through monetary tools such as interest rate, exchange rate, open-market operations, and required reserve ratio. First of all, the interest rate is not only the most important index of capital cost, but also the direct determinant of corporate debt financing cost. The interest rate will have an important impact on corporate capital structure. Under normal circumstances, when the interest rate is high, the PBC will carry out tight monetary policy. At this time, the cost of direct debt financing of enterprises increases, and the cost of capital structure adjustment of enterprises also increases correspondingly. Then the capital structure will be adjusted downward, leading to the decreasing of the speed of capital structure adjustment. On the contrary, when the interest rate is low, the PBC will carry out loose monetary policy, which would decrease the cost of enterprise capital structure adjustment. Then the capital structure will be adjusted upward and the speed of capital structure adjustment will be accelerated. Secondly, considering the credit transmission mechanism, the changes of monetary policy will affect bank credit scale through the credit transmission mechanism. In general, when the tight monetary policy is executed by the PBC, the banks will quickly reduce controllable credit scale through the credit transmission mechanism. It will be more difficult for the companies to get external financing, leading to the rise of the cost of capital structure adjustment. Thus, the capital structure will be adjusted downward and the speed of capital structure adjustment will be lowered. On the

contrary, when the central bank implements loose monetary policy, the controllable credit scale of banks will increase. It will be easier for the companies to get external financing, leading to the decrease of the cost of capital structure adjustment. Thus, the capital structure will be adjusted upward and the speed of capital structure adjustment will be accelerated. Finally, considering the relationship between the monetary policy and financial ecological environment, Xie et al. [38] pointed out that the loose monetary policy will optimize the financial ecological environment, alleviate the financing pressure, and reduce the degree of financing constraints of the enterprise. To a certain extent, these will reduce the cost of capital structure adjustment and help to adjust capital structure upward and speed up the capital structure adjustment. In summary, the following hypotheses are proposed:

H1: Tight monetary policy promotes the downward adjustment of enterprises' capital structure, while loose monetary policy promotes the upward adjustment of enterprises' capital structure.

H2: Tight monetary policy will slow down the speed of enterprises' capital structure adjustment; loose monetary policy will speed up the enterprises' capital structure adjustment.

Fiscal policy means that the government adjusts the total social demand through the allocation of fiscal expenditure and the adjustment of tax policy. Chen and Yang [39] pointed out that the government increased investment and reduced tax rate, which indicated that the government carried out the fiscal policy of expansion. With the macroeconomic situation getting better and better, enterprises could obtain more investing opportunities and have more growing space. First of all, from the perspectives of macroeconomic situation, the authorities carry out expansionary fiscal policy, referring to the positive macroeconomic situation, the improving of enterprises growth, and the optimizing of enterprise management. With the improvement of enterprise profitability and the expansion of production, the fixed assets are also increasing and the degree of financing constraints is decreasing. With the increasing of credit scale obtained from banks, the capital structure will be adjusted upward. At the same time, the financing barriers of enterprises are reduced and the financing cost is reduced, so the cost of capital structure adjustment is reduced and the speed of capital structure adjustment is accelerated. Second, according to the western finance theory, treasury bonds influence the price of capital in the market through the nature of the benchmark interest rates. When suffering the economic depression, the authorities tend to implement expansionary fiscal policy to stimulate the economy by reducing national bond rate to promote lower interest rates in financial markets. So the enterprise external financing cost is reduced; the capital structure is adjusted upward. The decline of financial market interest rate directly reduces the cost of capital structure adjustment and accelerates the speed of capital structure adjustment. Finally, considering the perspective of industrial support, the financial support to enterprises from Chinese government is a characteristic feature. In order to

support industrial development, the authorities will provide financial capital to relevant enterprises by direct investment and financial subsidies. Wu et al. [40] pointed out that government supports including direct intervention means such as financial support, technology regulation, and market access, as well as indirect guidance means such as financial subsidies, tax incentives, and financial policies. When the government implements the fiscal policy of expansion, the direct financial support for enterprises will increase. Meanwhile, the increase of government expenditure will also indirectly improve the business environment and expand the capital source of enterprises. What is more, the government support policies for relevant industries will guide the investment of bank credit funds and adjust the capital structure upward. The decrease of capital structure adjustment cost accelerates the speed of capital structure adjustment. In summary, the following hypotheses are proposed:

H3: Expanding fiscal policy promotes the capital structure adjusted upward, while tightening fiscal policy promotes the capital structure adjusted downward.

H4: Tightening fiscal policy will slow down the speed of capital structure adjustment, while expanding fiscal policy will increase the speed of capital structure adjustment.

4. Methods and Variables

4.1. Model Construction. In order to study the relationship between corporate capital structure and monetary and fiscal policies, based on the practice of Faulkender et al. [41], we select a series of corporate characteristic variables to construct equation (1) to fit the target capital structure and deduce the capital structure adjustment speed of the enterprise:

$$\text{debrate}_{i,t} = \gamma + \beta X_{i,t-1} + \eta M_t, \quad (1)$$

$\text{debrate}_{i,t}$ means the enterprise capital structure; the vector $X_{i,t-1}$ means the microcontrol variables influencing the enterprise capital structure, the vector $X_{i,t-1}$ refers to a series of $(t-1)$ year characteristic variables of enterprises, including company size, uniqueness, nondebt tax shields, profitability, business growth, liquidity, and degree of financing constraints. The β means the coefficient of characteristic variables of enterprises. The vector M_t means the macroeconomic factors affecting the capital structure. The vector M_t refers to the macroeconomic variables in t year, including economic growth, monetary policy, fiscal policy, and financial structure.

In order to study the relationship between capital structure adjustment speed and monetary policy and fiscal policy, we constructed the following model by referring to Huang and Jiang [1]:

$$\text{debrate}_{i,t}^* = \gamma + \beta X_{i,t-1} + \eta M_t, \quad (2)$$

$\text{debrate}_{i,t}^*$ means the optimal capital structure of enterprises i in the year of t . Other variables have the same meanings as described above. We use the partial adjustment model to estimate and calculate the capital structure adjustment speed

of enterprises. The standard partial adjustment model is established as follows:

$$\text{debrate}_{i,t} - \text{debrate}_{i,t-1} = \theta (\text{debrate}_{i,t}^* - \text{debrate}_{i,t-1}), \quad (3)$$

$\text{debrate}_{i,t}$ represents the capital structure of enterprise i at the end of year t , $\text{debrate}_{i,t-1}$ represents the capital structure of enterprise i at the beginning of year t , the capital structure is represented by the asset-liability ratio, and θ represents the speed of capital structure adjustment¹. $\theta=0$ means the capital structure of enterprises has not been adjusted, and the asset-liability ratio remains unchanged; $\theta<0$ represents that the capital structure adjustment of the enterprise deviates from the target capital structure; $0<\theta<1$ means the direction of enterprise adjustment is consistent with the target capital structure and has been partially adjusted; $\theta > 1$ means the enterprise has excess adjustment on the target capital structure.

In order to study the influence of macroeconomic policy on the speed of capital structure adjustment, we regard θ as a linear function of monetary policy and fiscal policy as shown in

$$\theta = \alpha_0 + \alpha_1 \text{Mac}_t, \quad (4)$$

where Mac_t is the monetary policy (fiscal policy) in t year. Substitute equation (2) and equation (4) into equation (3), and get equation (5) after sorting.

$$\begin{aligned} \text{debrate}_{i,t} = & \alpha_0 \gamma + (1 - \alpha_0) \text{debrate}_{i,t-1} - \alpha_1 \text{debrate}_{i,t-1} \\ & \times \text{Mac}_t + \alpha_0 \beta X_{i,t-1} + \alpha_0 \eta M_t + \alpha_1 \beta X_{i,t-1} \\ & \times \text{Mac}_t + \alpha_0 \eta M_t \times \text{Mac}_t + \mu_i + \lambda_t + \varepsilon_{i,t}. \end{aligned} \quad (5)$$

So the impact of monetary policy (fiscal policy) on the speed of capital structure adjustment can be examined through α_0 and α_1 . In formula (4), the second part on the right side of the equation is the first-order lag term of asset-liability ratio, the third part is the cross term of monetary policy or fiscal policy and the first-order lag term of asset-liability ratio, the fourth part is the microfactors controlled, the fifth part is the macroeconomic factors controlled (excluding monetary policy and fiscal policy), the sixth part is the cross term of monetary policy (fiscal policy) and microcontrol variables, and the seventh part is the cross term of monetary policy (fiscal policy) and macrocontrol variables. μ_i and λ_t are time and individual effects, respectively, and $\varepsilon_{i,t}$ are random interference terms. We mainly focus on $(1-\alpha_0)$ and $-\alpha_1$, which need to be converted into α_0 and α_1 to measure the impact of monetary policy (fiscal policy) on the speed of capital structure adjustment in equation (4).

4.2. Description of Variables. Monetary policy [18] used 1-year loan interest rate (calculated by monthly weighted average method) and annual year-on-year growth rate of broad monetary aggregates M2, respectively, to measure the degree of monetary policy tightness. If the interest rate is

higher, the authorities will carry out tight monetary policy. If the interest rate is lower, the authorities will carry out loose monetary policy. If the growth rate of monetary supply is fast, it indicates that the authorities carry out relatively loose monetary policy. And a slower pace of monetary supply growth indicates a tightening of monetary policy.

Fiscal policy [16] used the annual growth rate of fiscal expenditure to measure the tightness of fiscal policy. The high growth rate of fiscal expenditure indicates that the government is pursuing an expansionary fiscal policy. The low growth rate of fiscal spending indicates tightening fiscal policy.

Asset-liability ratio [42] is widely used to measure capital structure, that is, the ratio of total liabilities to total assets of an enterprise.

Since the enterprise's own characteristics and the macroeconomic factors will affect the capital structure, we draw on the experience of most scholars to selected microcharacteristic factors such as the company size, nondebt tax shields, profitability, business growth, tangible assets, and macrofactors such as economic growth and financial structure as control variables. The specific definitions are shown in Table 1.

- (1) Firm size [43] is measured by the natural logarithm of total assets. In general, the larger the size of the company, the stronger the operation capacity of the company. And the probability of financial distress is smaller with the higher asset-liability ratio.
- (2) Nondebt tax shield [14] is measured by the proportion of accumulated depreciation, deferred expenses, and deferred assets in total assets. The larger the scale of the company, the more significant the tax shield effect. Increasing the credit ratio will further enhance the value of the enterprise.
- (3) Profitability [44] is measured by the ratio of net profit to total assets. The higher profitability indicates the more stable cash flow, the less bankruptcy risk, and the stronger antirisk ability. So the enterprise operators tend to increase the asset-liability ratio.
- (4) Growth [45] is measured by the growth rate of sales revenue. The better the growth of an enterprise is, the more inclined it is to increase financial leverage to expand its scale to increase market value.
- (5) Tangible assets [46] are measured by the ratio of fixed assets to total assets. Generally, the more fixed assets an enterprise has, the greater the probability of obtaining mortgage loans from financial institutions, and the company operators are more willing to increase the asset-liability ratio.
- (6) Economic growth rate [14] is measured by GDP growth rate. The higher the economic growth rate is, the better the macroeconomic environment is, and the enterprises will increase the asset-liability ratio.
- (7) Financial structure [6] is measured by the ratio of total stock market value to the total loans from financial institutions. When the market financial

TABLE 1: Variable declarations.

Type	Name	Code	Explanation
Explained variable	Capital structure	debrate	Total liability/ Total asset
Explaining variables	Monetary policy	Mon1 Mon2	1-year loan rate year-on-year growth rate of M2
	Fiscal policy	Fin	Growth rate of fiscal expenditure
Control variables	Firm size	lnasset	The natural log of total assets
	Nondebt tax shield	nontax	(Accumulated depreciation + Deferred expenses + Deferred assets)/Total asset
	Profitability	profit	Net profit/Total asset
	Growth	grow	Sales growth rate
	Tangible assets	tang	Fixed assets/Total assets
	Economic growth rate	GDPgrow	GDP growth rate
	Financial structure	stru	Total stock market value/ Total loans from financial institutions

structure is dominated by capital market, enterprises are more willing to increase the asset-liability ratio. When the financial structure is dominated by banks, enterprises will decrease the asset-liability ratio.

5. Data and Results

5.1. Data and Statistic. The data comes from Wind database. We select the annual data of nonfinancial enterprises listed in China's A-share market from 2000 to 2020 as the research object and perform the following screening procedures: (1) excluding the samples of financial listed companies; (2) excluding samples of B shares or H shares issued at the same time; (3) excluding the samples treated with special treatment (ST or PT); (4) eliminating samples with negative owner's equity; (5) deleting missing data. Finally, a total of 41569 data samples were obtained. In order to eliminate the possible influence of outliers on the robustness of regression results, Winsorize the upper and lower 1% of all continuous variables.

Figure 1 reflects the trend of monetary and fiscal policies in recent years in China. The monetary policy gradually showed a trend of easing from 1998 and reached its peak around 2008. When the financial crisis broke out in 2008, the PBC released RMB 300 billion liquidity to rescue the market and the degree of monetary policy easing reached its peak. Then the PBC began to tighten the monetary policy. Since 1998, fiscal policy began to show a trend of gradual expansion, and the expansionary fiscal policy in China reached its peak around 2009. Subsequently, Chinese government implemented a prudent fiscal policy, and the degree of fiscal expansion gradually decreased and reached its lowest point in 2018.

Table 2 presents descriptive statistical results for the main variables. The average asset-liability ratio is 45%, which is at a medium level worldwide, so there is considerable room for adjustment. Macrofactors: (1) average 1-year loan interest rate is 4.64%, average M2 year-on-year growth rate (monetary policy) is 14.6%, and maximum is 26.5%, indicating that monetary policy is relatively loose; (2) average year-on-year growth rate of fiscal expenditure (fiscal policy) is 14.3%, indicating that fiscal policy is also in an expansionary state; (3) the average financial structure is 68.5% and the type is still bank-dominated in China, meaning indirect financing of bank loans occupies the mainstream of social

financing. Microfactors: (1) the profitability is not outstanding with the average level being 3.14%, (2) the average proportion of tangible assets (fixed assets) to total assets is 23.9%; the lower ratio indicates that financing difficulties still exist to some extent since bank loans need to be secured by fixed assets.

5.2. Correlation Analysis. In order to test whether multicollinearity exists between explanatory variables and control variables, correlation test is conducted before regression analysis. The results are shown in Table 3. The correlations between monetary policy fiscal policy and economic growth rate are 0.644 and 0.750, that between monetary policy and fiscal policy also reaches 0.684, and the correlation between loan interest rate and M2 growth rate is -0.723. Correlations between other variables are weak. In addition, it is understandable that monetary policies and fiscal policies are strongly correlated with GDP growth rate. Macroeconomic policies are adjusted according to macroeconomic development, and fiscal policies and monetary policies are often used together to regulate the macroeconomy. Therefore, multicollinearity of the model can be ruled out on the whole.

5.3. Regression Results

5.3.1. Monetary Policy, Fiscal Policy, and Capital Structure. In order to verify the relationship between monetary policy, fiscal policy, and capital structure, linear regression is performed on equation (1), and the actual capital structure of an enterprise is used to replace the optimal capital structure to discuss the correlation between capital structure, fiscal policy, and monetary policy. The regression results are shown in Table 4.

Table 4 shows the results of the fixed effects regression. The columns (1), (2), and (3) are the regression results of monetary policy, fiscal policy, and enterprise capital structure without control variables, showing that Mon1 is significantly negative at 10% level and the M2 growth rate (*Mon2*) and fiscal expenditure growth rate (*Fin*) are significantly positive at 1% level. Columns (4), (5), and (6), respectively, represent the regression results with control variables. Mon1 is significantly negative at the level of 5%, and the M2 growth rate (*Mon2*) and fiscal expenditure



FIGURE 1: Trends of monetary policy (M2 growth rate) and fiscal policy (fiscal expenditure growth rate) in China.

TABLE 2: Descriptive statistical results for the main variables.

Variable	Obs	Mean	Std.Dev.	Min	Max
debrate	41,569	0.450	0.205	0.0821	0.873
lnasset	41,569	21.55	1.405	12.31	28.52
nontax	41,569	0.0331	0.01342	0.00183	0.09451
profit	41,569	0.0314	0.0684	-0.367	0.219
grow	41,569	-0.293	3.345	-23.50	7.750
tang	41,569	0.239	0.174	0	0.971
Mon1	41,569	0.0464	0.0216	0.0496	0.0743
Mon2	41,569	0.146	0.0438	0.0828	0.265
Fin	41,569	0.143	0.0592	0.0630	0.257
stru	41,569	0.685	0.212	0.223	1.421
GDPgrow	41,569	0.0853	0.0198	0.0660	0.142

growth rate (*Fin*) are significantly positive at the level of 1%. Columns (7) and (8) include fiscal policy, monetary policy, and control variables in the regression model. The regression results show that *Mon1* is significantly negative at the level of 10%, and the M2 growth rate (*Mon2*) and fiscal expenditure growth rate (*Fin*) are significantly positive at the level of 1%. To sum up, loose monetary policy and expansionary fiscal policy will promote the upward adjustment of capital structure of enterprises and increase the asset-liability ratio of enterprises. When monetary and fiscal policies are tightened, companies will adjust capital structure downward and reduce their debt to asset ratios. Hypothesis H1 and hypothesis H3 are verified.

5.3.2. Monetary Policy, Fiscal Policy, and the Speed of Capital Structure Adjustment. In order to verify the relationship between monetary policies, fiscal policies, and the speed of capital structure adjustment, linear regression is performed on equation (5). Firstly, regression is made on the relationship between monetary policy and the speed of capital structure adjustment. And the whole sample is divided into subsamples for discussion according to the degree of financing constraint. Here, tangible assets are taken as the measurement index of financing constraint degree. Generally, if tangible assets (fixed assets) account for a large proportion in enterprises, the probability of obtaining financial support from banks and other external financial

institutions is relatively high, and the degree of external financing constraint is relatively low. So the tangible assets can be used as an index to measure the degree of financing constraint of enterprises. The higher the proportion of tangible assets in total assets, the lower the degree of financing constraints. The results are shown in Table 5.

Table 5 shows the results of fixed-effect regression on equation (5). Under the total samples (1) and (2), the speed of capital structure adjustment can be deduced: $\theta = 0.528 - 0.371 * Mon1$ and $\theta = 0.481 + 0.775 * Mon2$, indicating that if the *Mon1* increases by 1%, the speed of capital adjustment will decrease by 0.37%; if the M2 growth rate (*Mon2*) increases by 1%, the speed of capital adjustment will increase by 0.775%. The above analysis shows that loose monetary policy will accelerate the speed of capital structure adjustment, while tight monetary policy will slow down the speed of capital structure adjustment. In addition, we divide the total sample into two subsamples with high degree and low degree according to the mean value of financing constraint. It can be found that, under the impetus of loose monetary policy, enterprises with low degree of financing constraint adjust their capital structure faster than those with high degree, which verifies hypothesis H2 to some extent.

Then, regression is made on the relationship between fiscal policy and the speed of capital structure adjustment. The whole sample is also divided into subsamples for discussion according to the degree of financing constraint. The results are shown in Table 6.

Table 6 shows the results of fixed-effect regression on equation (5); under the total sample column, we can get $\theta = 0.429 + 0.474 * Fin$, indicating that if fiscal expenditure increases by 1%, the speed of capital structure adjustment will increase by 0.474%. The expansionary fiscal policy will accelerate the speed of capital structure adjustment. In addition, we also divide the total sample into two subsamples with high degree and low degree of financing constraint according to the mean value. It can be found that, under the impetus of expansionary fiscal policy, enterprises with low degree of financing constraint adjust their capital structure faster than those with high degree. The hypothesis H4 is verified.

5.3.3. Robustness Test. Different robustness test methods were used to test the relevant results. (1) Replace variables. Because the measurements of monetary policy and fiscal policy measure are not unified, different macroeconomic policy measures may lead to the different research conclusion. So we use M3 year-on-year growth rate (*Mon3*) and the ratio of fiscal expenditure to fiscal revenue (*Fin2*) to measure the monetary policy and fiscal policy. The higher M3 year-on-year growth rate indicates the loose monetary policy. The larger ratio of fiscal expenditure to fiscal revenue indicates that the government carries out the expansionary fiscal policy. The estimated results are consistent with the above. (2) Different models are used to estimate the target capital structure. The fixed-effect model (FE) (Anet al., 2015) is used to estimate equation (5) as showed in previous part. GMM model is also used to estimate equation (5) here, and the conclusions are consistent. The specific results are shown in

TABLE 3: Correlation coefficient matrix of variables.

	Debrate	Lnasset	Nontax	Profit	Grow	Tang	Mon1	Mon2	Fin	Stru	GDPgrow
Debrate	1										
Lnasset	0.279	1									
Nontax	0.0604	0.0216	1								
Profit	-0.291	-0.147	-0.0196	1							
Epsgrow	-0.118	0.0110	-0.0573	0.333	1						
Tang	0.112	0.0733	0.0778	-0.0440	-0.0576	1					
Mon1	-0.115	0.0246	0.1025	0.0139	-0.0014	0.1072	1				
Mon2	0.121	-0.228	0.101	0.0692	0.0279	0.117	-0.723*	1			
Fin	0.130	-0.227	0.101	0.0520	-0.00490	0.121	0.0821	0.684**	1		
Stru	-0.0441	0.0721	-0.0522	0.0708	0.0491	-0.0966	0.0776	-0.0881	0.143	1	
GDPgrow	0.155	-0.217	0.125	0.0308	0.0188	0.155	-0.426	0.644*	0.750*	-0.0567	1

***, **, and * represent significance at 1%, 5%, and 10% levels, respectively.

TABLE 4: Regression results of capital structure, monetary policy, and fiscal policy.

Variables	(1) Debrate	(2) Debrate	(3) Debrate	(4) Debrate	(5) Debrate	(6) Debratet	(7) Debrate	(8) Debrate
Mon1	-0.072* (0.0413)			-0.061** (0.0298)			-0.067* (0.0385)	
Mon2		0.185*** (0.0120)			0.358*** (0.0197)			0.230*** (0.0209)
Fin			0.271*** (0.0159)			0.410*** (0.0179)	0.403*** (0.0224)	0.337*** (0.0191)
Stru				0.0172*** (0.00298)	0.0137*** (0.00302)	0.0405*** (0.00324)	0.0417*** (0.00585)	0.0361*** (0.00326)
GDPgrow				0.658*** (0.0375)	0.739*** (0.0459)	0.363*** (0.0521)	0.271*** (0.0514)	0.282*** (0.0525)
Inasset_lag				0.0410*** (0.00245)	0.0307*** (0.00105)	0.0316*** (0.00104)	0.0417*** (0.00103)	0.0343*** (0.00106)
Nontax_lag				-0.744*** (0.0872)	-0.766*** (0.0957)	-0.719*** (0.0954)	-0.689*** (0.1025)	-0.728*** (0.0953)
Profit_lag				-0.512*** (0.0142)	-0.457*** (0.0128)	-0.472*** (0.0128)	-0.394*** (0.0174)	-0.482*** (0.0128)
Grow_lag				-0.0017*** (0.00021)	-0.00163*** (0.000204)	-0.00178*** (0.000203)	-0.00157*** (0.000194)	-0.00165*** (0.000203)
Tang_lag				-0.0172** (0.00924)	-0.0191** (0.00851)	-0.0193** (0.00849)	-0.0199** (0.00960)	-0.0201** (0.00847)
Constant	0.416*** (0.00204)	0.425*** (0.00183)	0.412*** (0.00241)	-0.319*** (0.0278)	-0.204*** (0.0252)	-0.176*** (0.0244)	-0.249*** (0.0266)	-0.252*** (0.0253)
Observations	41,569	41,569	41,569	37,774	37,774	37,774	37,774	37,774
R-squared	0.006	0.006	0.008	0.182	0.189	0.194	0.189	0.197

***, **, and * in the table represent significance at 1%, 5%, and 10% levels, respectively, and the values in brackets represent standard deviations.

TABLE 5: Regression results of speed of capital structure adjustment and monetary policy.

Variables	Total sample	Total sample	High financing constraints	High financing constraints	Low financing constraints	Low financing constraints
Debrate_lag	0.472*** (0.0157)	0.519*** (0.0129)	0.565*** (0.0197)	0.560*** (0.0206)	0.463*** (0.0182)	0.445*** (0.0174)
Debrate_lag × Mon1	0.371* (0.205)		0.428* (0.252)		0.527* (0.314)	
Debrate_lag × Mon2		-0.775*** (0.0814)		-0.441*** (0.127)		-0.947*** (0.112)
Constant	-0.286*** (0.0223)	-0.247*** (0.0206)	0.104*** (0.0214)	-0.169*** (0.0341)	0.117*** (0.0305)	-0.226*** (0.0288)
Control variables	Control	Control	Control	Control	Control	Control
Observations	37,774	37,774	15,966	15,966	21,808	21,808
R-squared	0.467	0.496	0.448	0.521	0.431	0.420

***, **, and * in the table represent significance at 1%, 5%, and 10% levels, respectively, and the values in brackets represent standard deviations.

TABLE 6: Regression results of speed of capital structure adjustment and fiscal policy.

Variables	Total sample	High financing constraints	Low financing constraints
Debrate_lag	0.571*** (0.00896)	0.642*** (0.0161)	0.512*** (0.0128)
Debrate_lag × Fin	-0.474*** (0.0584)	-0.0722 (0.0895)	-0.435*** (0.0965)
Constant	-0.314*** (0.0228)	-0.185*** (0.0298)	-0.157*** (0.0321)
Control variables	Control	Control	Control
Observations	37,774	15,966	21,808
R-squared	0.485	0.507	0.422

***, **, and * in the table represent significance at 1%, 5%, and 10% levels, respectively, and the values in brackets represent standard deviations.

TABLE 7: Robustness test of the relationship between monetary policy, fiscal policy, and capital structure (substitution variables).

Variables	(1) Debrate	(2) Debrate	(3) Debratet	(4) Debratet	(5) Debratet
Mon3	0.154*** (0.0132)		0.277*** (0.0193)		0.231*** (0.0207)
Fin2		0.187*** (0.0168)		0.353*** (0.0215)	0.342*** (0.0147)
Constant	0.465*** (0.00186)	0.359*** (0.00172)	-0.216*** (0.0175)	-0.157*** (0.0242)	-0.198*** (0.0354)
Control variables	Not control	Not control	Control	Control	Control
Observations	41,569	41,569	37,774	37,774	37,774
R-squared	0.008	0.010	0.152	0.171	0.182

TABLE 8: Robustness test of the relationship between monetary policy, fiscal policy, and the speed of capital structure adjustment (substitution variables).

Variables	Monetary policy			Fiscal policy		
	Total sample	High Financing Constraints	Low financing constraints	Total sample	High financing constraints	Low financing constraints
Debrate_lag	0.428*** (0.0129)	0.567*** (0.0374)	0.426*** (0.0208)	0.497*** (0.01024)	0.624*** (0.0342)	0.523*** (0.0185)
Debrate_lag × Mon3	-0.672*** (0.0937)	-0.467*** (0.117)	-0.935*** (0.114)			
Debrate_lag × Fin2				-0.565*** (0.0734)	-0.0778 (0.0850)	-0.624*** (0.0935)
Constant	-0.445*** (0.0375)	-0.184*** (0.0307)	-0.227*** (0.0214)	-0.275*** (0.0475)	-0.247*** (0.0354)	-0.175*** (0.0317)
Control variables	Control	Control	Control	Control	Control	Control
Observations	37,774	15,966	21,808	37,774	15,966	21,808
R-squared	0.421	0.504	0.463	0.497	0.512	0.424

the following tables. Tables 7 and 8 use M3 year-on-year growth rate and ratio of fiscal expenditure to fiscal revenue to measure the changes and adjustments of monetary and fiscal policies. Tables 9 and 10 use GMM model to estimate

equation (5) and get consistent results (***, **, and * in the tables represent significance at 1%, 5%, and 10% levels, respectively, and values in brackets represent standard deviations).

TABLE 9: Robustness test of the relationship between monetary policy, fiscal policy, and capital structure (GMM model).

Variables	(1) Debrate	(2) Debrate	(3) Debrate	(4) Debrate	(5) Debratet	(6) Debratet	(7) Debrate	(8) Debratet
Mon1	-0.069* (0.0411)			-0.075** (0.0312)			-0.072* (0.0399)	
Mon2		0.176*** (0.0142)			0.360*** (0.0199)			0.216*** (0.0218)
Fin			0.282*** (0.0175)			0.431*** (0.0185)	0.417*** (0.0231)	0.342*** (0.0196)
Control variables	Not control	Not control	Not control	Control	Control	Control	Control	Control
Constant	0.422*** (0.00218)	0.421*** (0.00175)	0.418*** (0.00255)	-0.325*** (0.0296)	-0.234*** (0.0356)	-0.175*** (0.0243)	-0.252*** (0.0275)	-0.249*** (0.0287)
Observations	41,569	41,569	41,569	37,774	37,774	37,774	37,774	37,774
R-squared	0.007	0.007	0.008	0.179	0.172	0.191	0.186	0.192

TABLE 10: Robustness test of the relationship between monetary policy, fiscal policy, and the speed of capital structure adjustment (GMM model).

Variables	Monetary policy						Fiscal policy		
	Total sample	Total sample	High financing constraints	High financing constraints	Low financing constraints	Low financing constraints	Total sample	High financing constraints	Low financing constraints
Debrate_lag	0.475*** (0.0165)	0.502*** (0.0134)	0.593*** (0.0259)	0.561*** (0.0207)	0.467*** (0.0196)	0.468*** (0.0198)	0.583*** (0.0125)	0.671*** (0.0254)	0.441*** (0.0147)
Debrate_lag × Mon1	0.381* (0.216)		0.431* (0.256)		0.529* (0.321)				
Debrate_lag × Mon2		-0.763*** (0.0925)		-0.442*** (0.123)		-0.987*** (0.156)			
Debrate_lag × Fin							-0.463*** (0.06741)	-0.0773 (0.0944)	-0.576*** (0.0752)
Constant	-0.279*** (0.0235)	-0.258*** (0.0213)	0.113*** (0.0285)	-0.165*** (0.0371)	0.120*** (0.0317)	-0.234*** (0.0321)	-0.245*** (0.02324)	-0.125*** (0.0332)	-0.221*** (0.0476)
Control variables	Control	Control	Control	Control	Control	Control	Control	Control	Control
Observations	37,774	37,774	15,966	15,966	21,808	21,808	37,774	15,966	21,808
R-squared	0.452	0.442	0.475	0.523	0.442	0.421	0.472	0.501	0.439

6. Conclusion and Suggestions

6.1. Conclusion. We analyze the impact of monetary policy and fiscal policy on capital structure and the speed of capital structure adjustment and empirically test the data of non-financial listed companies in A-share market from 2000 to 2020 in China. After empirical research, the following conclusions are drawn: (1) Under the loose monetary policy, enterprises will adjust the capital structure upward, improve the asset-liability ratio, and accelerate the speed of capital structure adjustment. In addition, the speed of capital structure adjustment of enterprises with low financing constraints is faster than that with high financing constraints. (2) Under the expansionary fiscal policy, enterprises will also adjust their capital structure upward, improve their asset-liability ratio, and accelerate the speed of capital structure adjustment. During the adjustment process, enterprises with low financing constraints adjust their capital structure faster than those with high financing constraints.

6.2. Suggestions. Based on the conclusions drawn from the research, we put forward corresponding policy suggestions from both macro- and microaspects.

Macroaspects. (1) In the implementation of monetary policy and fiscal policy, the government should pay sufficient attention to the enterprise's capital structure change and take some fine-tuning of policy according to the macroeconomic environment. When the macroeconomic is in downturn, expansionary fiscal policy and loose monetary policy will reduce the enterprise's financing cost and speed up the enterprise to the optimal capital structure adjustment. When the economy is overheated, the reverse macropolicy operation will curb the excessive adjustment of the capital structure of enterprises. (2) Monetary policies and fiscal policies should be used in a correct and scientific way. The market's expectation of macropolicies will have an impact on the entire financial environment, which is closely related to the financing cost and operating conditions of enterprises. (3) The government should establish an enterprise credit

management system and collect enterprise credit files to strengthen the relationship between financial institutions and enterprises and further improve the capital market and financing environment. Establishing a platform to help small-scale enterprises raise external funds and giving more policy support to small-scale enterprises deeply constrained by financing are effective measures to relieve the pressure of financing constraints faced by small-scale enterprises, but also enable them to broaden financing channels and obtain external funds they need. (4) The adjustment of monetary policy and fiscal policy has different impact on enterprises with different degree of financing constraint, and the capital structure adjustment speed of enterprises with different degree of financing constraint has different sensitivity to the same type of economic policy adjustment. Therefore, the microtransmission mechanism of macroeconomic policy should be fully considered. Differentiated monetary and fiscal policies and corresponding credit policies should be formulated to provide favorable conditions for optimizing the capital structure of enterprises. (5) Government departments should disclose information about changes in fiscal and monetary policies through various channels, improve the transparency of government policies, and help improve marketization to promote the capital structure adjustment of enterprises.

Microaspects. (1) Different degrees of financing constraints cause differences in the impact of macroeconomic policies on capital structure of enterprises. Enterprises should expand internal financing and improve the operation to reduce their dependence on bank credit capital. (2) Enterprises should make a correct judgement of macroeconomic policies and adjust their financing decisions according to the changes of policies. (3) Enterprises should adjust their capital structure in time according to the changes of policies and make timely measures to deal with various risk factors brought by policy changes to enterprise financing. In this way, enterprises can effectively respond to the impact of policy adjustment on their capital structure. At the same time, enterprises should expand the breadth and depth of information disclosure and improve the quality of information disclosure to reduce the degree of information asymmetry with financial institutions, which help reduce the degree of financing constraints. Therefore, we can optimize the capital structure of enterprises, promote the speed of capital structure adjustment, and promote the sustainable and healthy development of enterprises. (4) Enterprises should establish a policy analysis department which help establish a regular policy analysis mechanism, so that it can timely grasp the changes of monetary and fiscal policies and then provide an important basis for enterprise capital structure adjustment and change decisions.

Data Availability

The data used to support the findings are from Wind database.

Conflicts of Interest

The author declares that there are no conflicts of interest.

References

- [1] J. Huang and F. Jiang, "Product market competition and the speed of capital structure adjustment," *The Journal of World Economy*, no. 7, pp. 99–119, 2015.
- [2] A. Killi, M. S. Rapp, and T. Schmid, "Can financial flexibility explain the debt conservation puzzle? Cross-county evidence from listed firms," TechnischeUniversitaetMunchen working paper, 2011.
- [3] Y. Gu and Q. Zhou, "Policy uncertainty, value of financial flexibility and dynamic adjustment of capital structure," *The Journal of World Economy*, no. 6, pp. 102–126, 2018.
- [4] S. Li and C. Pei, "Economic policy uncertainty and the nonlinear dynamic adjustments of capital structure," *Collected Essays on Finance and Economics*, no. 1, pp. 43–51, 2019.
- [5] G. Liu, J. Zhang, and Y. Liu, "Financial asset Allocation, Macroeconomic conditions and firm's leverage," *The Journal of World Economy*, no. 6, pp. 148–173, 2018.
- [6] A. Levy and C. Hennessy, "Why does capital structure choice vary with macroeconomic conditions?" *Journal of Monetary Economics*, vol. 54, no. 6, pp. 1545–1564, 2007.
- [7] D. Su and H. Zeng, "Macroeconomic factors and corporate capital structure changes," *Economic Research Journal*, no. 12, pp. 52–65, 2009.
- [8] F. Jiang and J. Huang, "Marketization Process and Capital Structure Dynamic adjustment," *Management World*, no. 3, pp. 124–134, 2011.
- [9] G. Liu, Y. Liu, and M. Min, "Financialization and dynamic adjustment of capital structure: evidence from China," *Journal of Management Sciences in China*, no. 3, pp. 71–89, 2019.
- [10] M. Gertle and S. Gilchris, "The role of credit market imperfections in the monetary transmission mechanism: arguments and evidence," *Scandinavian Journal of Financial Economics*, vol. 95, no. 1, pp. 43–64, 1993.
- [11] S. D. Oliner and G. D. Rudebusch, "Is there a broad credit channel of monetary policy?" *FRBSF Economic Review*, vol. 1, no. 1, pp. 3–13, 1996.
- [12] S. Banerjee, H. Almas, and W. Clas, "The Dynamics of Capital structure," *SSE/EFI Working Paper Series In Economics and Finance*, p. 333, 2000.
- [13] T. F. Cooley and V. Quadrini, "Monetary policy and the financial decisions of firms," *Economic Theory*, vol. 27, no. 1, pp. 243–270, 2006.
- [14] D. O. Cook and T. Tang, "Macroeconomic conditions and capital structure adjustment speed," *Journal of Corporate Finance*, vol. 16, no. 1, pp. 73–87, 2010.
- [15] W. Ma and S. Hu, "Monetary policy, credit channel and capital structure," *Accounting Research*, no. 11, pp. 39–48, 2012.
- [16] W. Nie and M. Luo, "Fiscal policy, monetary policy and dynamic adjustment of capital structure: empirical evidence from Chinese listed companies," *Economic Science*, no. 5, pp. 18–32, 2012.
- [17] Z. Wu, Ya Zhang, and W. Zhang, "Credit policy and capital structure of corporation—evidence from listed firms in China," *Accounting Research*, no. 3, pp. 51–58, 2013.
- [18] X. Song, Y. Wu, and J. Ning, "Monetary policy, enterprise growth and capital structure dynamic adjustment," *Studies of International Finance*, no. 11, pp. 46–55, 2014.
- [19] C. Yuan and J. Guo, "Research on the influence of monetary policy change on dynamic adjustment of enterprise capital structure," *Macroeconomics*, no. 7, pp. 19–32, 2018.
- [20] H. Choe, R. W. Masulis, V. Nanda, and K. Vikram, "Common stock offerings across the business cycle: Theory and

- evidence,” *Journal of Empirical Finance*, vol. 1, no. 1, pp. 3–31, 1993.
- [21] R. Boyer, “Is a finance-led growth regime a viable alternative to Fordism? A preliminary analysis,” *Economy and Society*, vol. 29, no. 1, pp. 111–145, 2000.
- [22] J. He, “Do macroeconomic conditions affect capital structure adjustment speed?—evidence from Chinese listed companies,” *South China Journal of Economics*, no. 12, pp. 3–16, 2010.
- [23] C. Wang, C. Wang, and L. Zeng, “Fiscal policy, enterprise property and dynamic adjustment of capital structure—empirical research based on listed firms in A shares market,” *Public Finance Research*, no. 9, pp. 52–63, 2016.
- [24] H. Gulen and M. Ion, “Policy uncertainty and corporate investment,” *Review of Financial Studies*, vol. 29, no. 3, pp. 523–564, 2016.
- [25] P. Rao, H. Yue, and G. Jiang, “Research on economic policy uncertainty and firm investment Behavior,” *The World Economy*, no. 2, p. 27–51, 2017.
- [26] V. Fabian, “Aggregate uncertainty and the supply of credit,” *Journal of Banking and Finance*, no. 88, pp. 150–165, 2017.
- [27] H. J. Wang, L. I. Qing-Yuan, and F. Xing, “Economic policy uncertainty, cash holding level and market value,” *Journal of Financial Research*, vol. 110, no. 7, pp. 53–68, 2017.
- [28] B. Julio and Y. Yook, “Political uncertainty and corporate investment cycles,” *Management World*, no. 1, pp. 143–156, 2013.
- [29] C.-F. Cao, “Political power shifting and corporate investment,” *Journal of Banking and Finance*, no. 88, pp. 150–165, 2017.
- [30] L. Pastor and P. Veronesi, “Political uncertainty and risk premia,” *Journal of Financial Economics*, vol. 110, no. 3, pp. 520–545, 2013.
- [31] B. B. Francis, I. Hasan, and Y. Zhu, “Political uncertainty and book loan contracting,” *Journal of Empirical Finance*, vol. 12, no. 29, pp. 281–286, 2014.
- [32] R.-K. Gong, Y.-X. Xu, and D.-Z. Wang, “Economic policy uncertainty and corporate leverage,” *Journal of Financial Research*, no. 10, pp. 59–78, 2019.
- [33] H.-jian Wang, L. I. Qing-yuan, and F. Xing, “Economic Policy uncertainty, cash holding level and market value,” *Journal of Financial Research*, no. 7, p. 53–68, 2017.
- [34] R. F. Harrod, “An essay in dynamic theory,” *The Economic Journal*, vol. 49, no. 193, pp. 14–33, 1939.
- [35] E. O. Fischer, R. Heinkel, and J. Zechner, “Dynamic capital structure choice: theory and tests,” *The Journal of Finance*, no. 1, pp. 19–40, 1989.
- [36] Y. Tong, “Dynamic adjustment of capital structure and the determinants,” *Journal of Finance and Economics*, no. 10, pp. 96–104, 2004.
- [37] Z. An, D. Li, and J. Yu, “Firm crash risk, information environment, and speed of leverage adjustment,” *Journal of Corporate Finance*, no. 31, pp. 132–151, 2015.
- [38] J. Xie, Z. Huang, and C. He, “Macro monetary policy and corporate financial ecologic environment: micro evidence from corporate financing constraint,” *Economic Review*, no. 4, pp. 116–123, 2013.
- [39] Z. Chen and J. Liu, “Approach to policy effect on corporate cash flow under the background of financial crisis,” *Accounting Research*, no. 4, pp. 42–49, 2010.
- [40] C. Wu, W. Li, and Q. Tang, “Industrial policy and the speed of leverage adjustment,” *Journal of Financial Research*, no. 4, pp. 92–110, 2019.
- [41] M. Faulkender, M. J. Flannery, K. W. Hankins, and J. M. Smith, “Cash flows and leverage adjustments,” *Journal of Financial Economics*, vol. 103, no. 3, pp. 632–646, 2012.
- [42] F. Jiang, Z. Yin, F. Su, and L. Huang, “Characteristics of Managerial Background and Corporate Overinvestment behavior,” *Management World*, no. 1, pp. 130–139, 2009.
- [43] M. J. Flannery and K. P. Rangan, “Partial adjustment toward target capital structures,” *Journal of Financial Economics*, vol. 79, no. 3, pp. 469–506, 2006.
- [44] W. Yu, X. Jin, and Y. Qian, “Macro shocks, financing constraints and dynamic adjustment of corporate capital structure,” *The Journal of World Economy*, no. 3, pp. 24–47, 2012.
- [45] A. Miguel and J. Pindado, “Determinants of capital structure: new evidence from Spanish panel data,” *Journal of Corporate Finance*, vol. 7, no. 1, pp. 77–99, 2001.
- [46] F. Jiang, Y. Qu, Z. Lu, and Li Yan, “Product market competition and dynamic capital structure adjustment,” *Economic Research Journal*, no. 4, pp. 99–110, 2008.

Research Article

Development and Application of an Expert Decision-Making System for Personalized Exercise Prescriptions for Children with Special Physiques

Li-Fang Zhang, Chun-Long Fang, and Liang Zhou 

Women and Children Research Center, Changsha Normal University, Changsha, China

Correspondence should be addressed to Liang Zhou; zhouliang@csnu.edu.cn

Received 18 May 2022; Revised 21 June 2022; Accepted 5 July 2022; Published 8 August 2022

Academic Editor: Xuefeng Shao

Copyright © 2022 Li-Fang Zhang et al. This is an open access article distributed under the Creative Commons Attribution License, which permits unrestricted use, distribution, and reproduction in any medium, provided the original work is properly cited.

The expert decision-making system is developed to provide a scientific and reasonable exercise solution management platform for primary and middle school students, especially children with special physiques, such as obesity and thinness, to improve the universality and compliance of exercise prescriptions for children with special physiques. The system provides personal information management, exercise management, exercise solution formulation, data statistics, and image management functions, enables self-selection, and free combination of children exercise prescriptions, and can improve the effectiveness of such prescriptions through personalized design. The system first divides exercise prescriptions into three bigger sections: the warm-up section, the main exercise section, and the cool-down section, then subdivides them into 15 smaller sections, further chooses, matches, verifies, and revises the components of the exercise prescription according to the object's basic demographic information and body mass index and finally formulates a personalized and reasonable exercise prescription. It also can track and manage the exercise solution formulated and dynamically adjust the exercise solution according to the change of the object's body index, thus strengthening the degree of freedom and personalized characteristics of the exercise prescription.

1. Introduction

The material civilization in modern society is highly developed. Since the last century, the incidence of childhood obesity in developed countries has continued to rise, many chronic diseases have become prevalent at a younger age [1], and health service for obese children has become an important social issue [2]. Exercise and nutrition intervention is considered to be the main means to improve body metabolism, control body weight, and promote healthy development of the body [3]. For example, Dias et al. [4] studied and compared the effects of different intensity of exercise on myocardial function of children with obesity. Carrel et al. [5] adopted lifestyle intervention measures combining exercise and nutrition education to reduce the risk of type 2 diabetes in high-risk children. Unlike the high attention paid to obese children, there are few studies on thin children. However, we cannot ignore the impact of thinness

on children's health. At present, the exercise intervention of children with special physiques still depends on school physical education, with general group intervention as the main means [6]. As personalized exercise solutions or prescriptions for children with special physiques require a lot of human and intellectual resources, it is very difficult to implement personalized exercise prescriptions [7]. At present, the existing research is mainly for the development of exercise prescription and the construction of an exercise prescription resource pool. Most of these resource pool provides only relatively fixed and limited exercise prescription, which are inadequate in the face of various individual needs. We adopt innovative research ideas to build sports project resources and manage those sports project by category, different users freely choose different modules of movement content. Users can freely make up optional exercise prescription according to their choice, so as to improve the pertinence and effectiveness of special physical

children health intervention, this is of important practical significance. This paper will report our study from several parts, including the overall design of the expert decision system for special body children, system database construction, main functions, and its implementation, system testing, and future prospects.

2. Overall Design Thinking of the Software

The purpose of the software design is to develop a web-based intelligent expert decision-making system providing self-selected and personalized exercise prescriptions for children with special physiques, so as to improve the pertinence, universality, and compliance of children exercise prescriptions and improve the health promotion benefits of exercise intervention for this group. In the application of the software, the user first should input basic personal information, demographic characteristics, and basic physical test data and then choose the built-in exercise, intensity, duration, and frequency in the warm-up section, the main exercise section, and the cool-down section of the system's exercise center. Based on the combination, the system verifies and generates an exercise prescription according to the user's basic personal information (mainly the BMI). The system also provides addition and revision functions and finally generates a scientific and reasonable personalized exercise prescription through continuous human-computer interaction, so as to improve its pertinence and compliance. The general design thinking of the software is shown in Figure 1.

The exercise center is the core of the software, mainly stores and adds the data of exercises suitable for the ages and metabolic characteristics of children with special physiques, and divides the data into three major categories for management: the warm-up section, the main exercise section, and the cool-down section. The warm-up and cool-down sections are restricted in four aspects: exercise method, exercise essentials, exercise requirements, and exercise memo, while the main exercise section is restricted from seven aspects: exercise method, exercise essentials, exercise requirements, exercise definition, exercise posture, exercise advice, and exercise memo, to form a repository enabling limited expansion and an unlimited combination of exercise prescriptions. The specific design thinking of the exercise center is shown in Figure 2.

3. Introduction of Main Functional Modules of the System

The system first sets the basic information functional module. The module mainly completes the collection and management of the service object's personal information and enables fuzzy multicondition query. By inputting information such as the name, the user can quickly access the object's profile and exercise file. The built-in user information collection table includes the name, height, age, weight, gender, exercise intensity, grade, body mass index (BMI), basic metabolism (BMR), collection time, and physique type. In addition to the user information module,

the system mainly includes the following four major functional modules:

3.1. Exercise Management Function. The exercise management function stores the information about the exercise items and exercise types suitable for children exercise prescriptions in the exercise center electronically, provides fast and simple management function, as well as a fuzzy multicondition query function. By inputting information such as the name of the exercise, the user can quickly access the specific information of the exercise.

3.2. Exercise Prescription Formulation Function. The exercise solution formulation refers to the formulation of exercise prescriptions according to the object's body mass index collected by the system and the exercise information in the exercise center (the warm-up section, main exercise section, and cool-down section), and their management. Meanwhile, the system can form the individual body mass index that can be dynamically followed according to the dynamic change of the object's information, adjust and formulate dynamically changed exercise solutions accordingly.

3.3. Exercise Data Statistics Function. The data statistics function refers to the statistical analysis of the data information stored in the exercise center divided by warm-up section, main exercise section and cool-down section, the matching exercise prescription, and the display of the composition of the exercise prescription with a bar chart. The children exercise prescription data are intuitively displayed so that children and parents can have a clear understanding of the structure of exercise prescription.

3.4. Image Management Function. The image management function refers to the intuitive definition of the exercise items of the warm-up section, main exercise section, and cool-down section of the exercise prescription, including the management and display of the images related to exercise posture, exercise essentials, to facilitate children to learn and ensure the effect and safety of exercise.

4. Database Table Structure of the System

The system adopts MySQL relational database management system and adopts JDBC to connect MySQL database. The relational database stores data in different tables instead of one big repository, which increases speed and flexibility. The SQL language used by MySQL is the most commonly used standardized language for accessing databases. The MySQL software adopts the dual licensing policy, including the community version and commercial version. Because of its small size, high speed, and low total cost of ownership, especially open source, MySQL has generally been chosen as the website database in the development of small and medium-sized websites. The data tables designed in the exercise prescription formulation module mainly include the exercise method table, exercise definition table, exercise

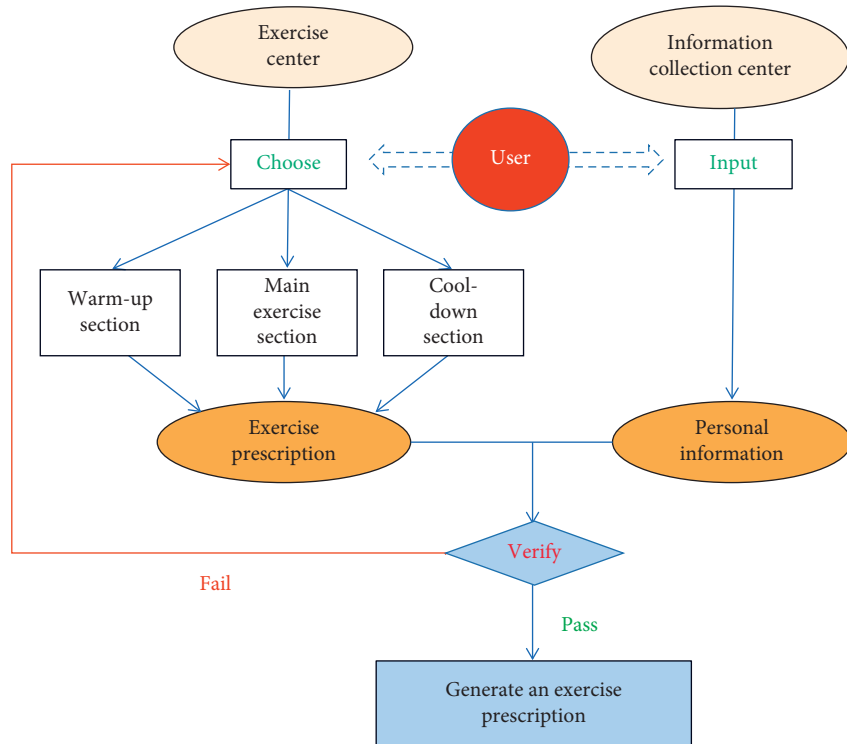


FIGURE 1: Overall design thinking of the software.

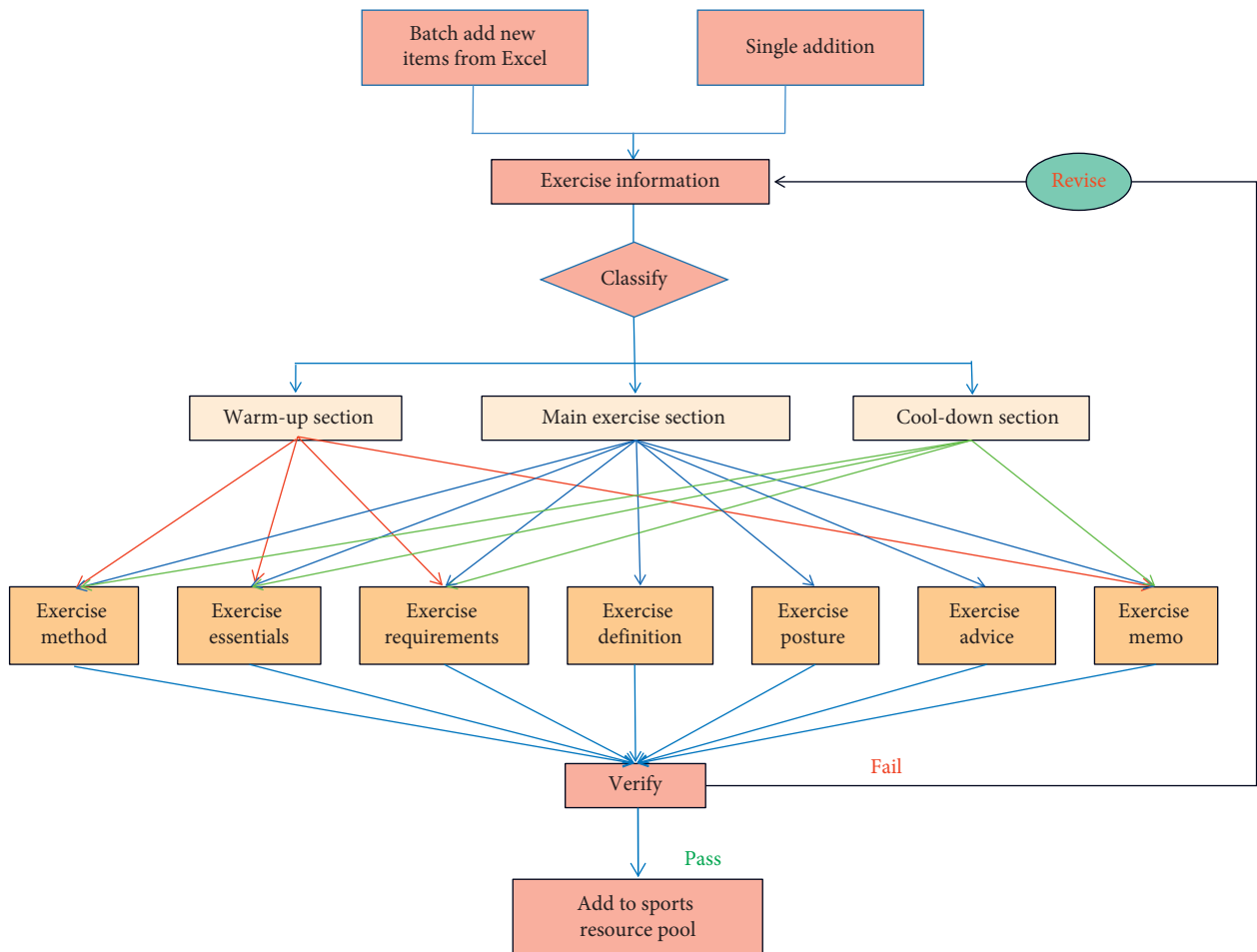


FIGURE 2: Design thinking of the exercise center.

TABLE 1: Data table structure of the system.

Data table classification	Function and role	Content and item
Exercise method table	Store exercise method data	Serial number, method name, method description, etc.
Exercise definition table	Store exercise definition data	Method serial number, definition content, image information, etc.
Exercise essentials table	Store exercise essentials data	Method serial number, essentials content, image information, etc.
Exercise posture table	Store exercise posture data	Method serial number, posture content, image information, etc.
Exercise requirements table	Store exercise requirements data	Method serial number, exercise requirements, etc.
Exercise advice table	Store exercise advice data	Method serial number, exercise advice, etc.
Exercise memo table	Store exercise memo data	Method serial number, exercise venue, exercise equipment, exercise interval, exercise intensity, exercise time, etc.
Image management table	Store exercise images	Image type, image name, image path, etc.

essentials table, exercise posture table, exercise requirements table, exercise advice table, exercise memo table, and image management table. The specific data table structure is shown in Table 1.

5. Implementation of System Functions

5.1. Implementation of Exercise Management Functions

5.1.1. Concept of Hierarchical Management. The exercise management function first divides the exercise items into two levels for management, the first level includes the exercise items in the warm-up, main exercise, and cool-down sections. Then, the exercise items in the warm-up section are divided into four smaller sections for management: exercise method, exercise essentials, exercise requirements, and exercise memo; the exercise items of the main exercise section are divided into seven smaller sections: exercise method, exercise definition, exercise essentials, exercise posture, exercise requirements, exercise advice, and exercise memo. The exercise items of the cool-down section are divided into four smaller sections: exercise method, exercise essentials, exercise requirements, and exercise memo.

The system divides the children exercise prescriptions into two levels and 15 small sections for management. When the user chooses the exercise information, he first chooses the exercise method section, then chooses other exercise information related to the exercise method, highlighting the hierarchy of the exercise information. Each small section of the management function has the basic functions of adding, deleting, and modifying. The exercise information is hierarchical, rich, and diversified and includes the use information of most of the everyday exercise items; the exercise-related information will participate in the subsequent exercise prescription formulation. The import of exercise-related information includes two modes: single addition, and batch import and collection. The system also has a complete fuzzy multi-condition query function, including advanced fuzzy query and multicondition mixed query. The advanced fuzzy query can quickly access multiple corresponding exercise item information, and multicondition mixed query can accurately access the specific item information. The system also sets an Excel export function to facilitate the verification and utilization of exercise item information at any time.

5.1.2. Operation Flow. In the specific operation process, the exercise method, exercise definition, exercise essentials, exercise posture, exercise requirements, exercise advice, and exercise memo operations all have the functions of single addition, excel batch addition, single deletion, batch deletion, modification, excel export, and so on. A single new addition process is shown in Figure 3, and an excel batch addition process is shown in Figure 4.

5.1.3. Input Items. To add a new exercise method, the user should input the method name, method description, and memo; to add a new exercise definition, the user should input the definition content, image information, memo, and choose the serial number of the method; to add new exercise essential, the user should input the content of the essentials, the image information, memo, and choose the serial number of the method; to add new exercise posture, the user should input the content of the posture, image information, memo and choose the serial number of the method; to add new exercise requirement, the user should input the content of the requirement, memo and choose the serial number of the method; to add new exercise advice, the user should input the content of the advice, memo and choose the serial number of the method; to add new exercise memo, the user should input the exercise venue, exercise equipment, exercise interval, exercise intensity, exercise time, memo and choose the serial number of the method.

5.2. Implementation of Exercise Prescription Formulation Functions

5.2.1. Implementation Thinking of Exercise Prescription Formulation. The exercise prescription formulation function formulates the exercise solution mainly based on the user's body mass index and the built-in basal metabolic rate according to the age characteristics, chooses and scientifically matches the exercise items and content of the warm-up section, main exercise section, and cool-down section. With respect to the function of selecting a specific exercise, a flexible 2-level linkage query is adopted to accurately locate the required exercise item number, and export the exercise method, exercise definition, exercise essentials, exercise posture, exercise requirements, exercise advice, exercise

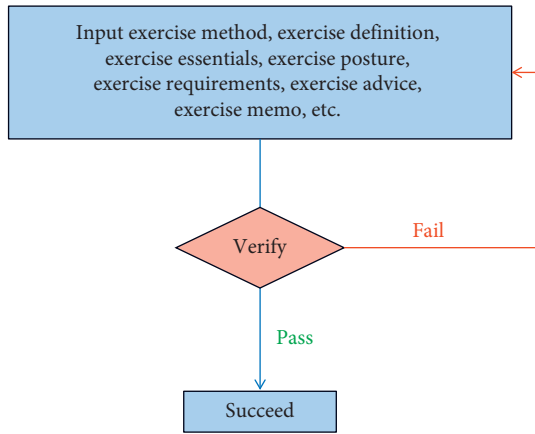


FIGURE 3: Single new addition flow.

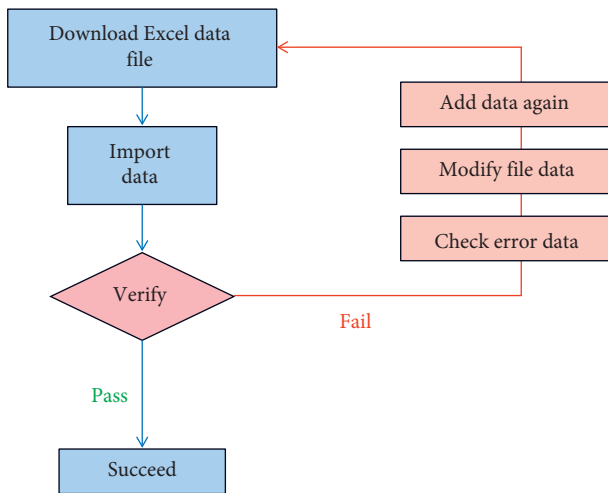


FIGURE 4: Excel batch addition flow.

memo, and other information to form a complete exercise prescription, verify it and provide it to the user.

Verification mainly includes the verification of key information such as the total exercise duration, total exercise amount, and total energy consumption. If the verification fails, it is necessary to reselect the matching solution of the exercise prescription and verify it again until it is passed.

The user also can add or delete some exercise item content according to his own preferences and can realize exercise content query and addition through the comprehensive fuzzy multicondition query function. The query includes an advanced fuzzy query and a multicondition mixed query.

The advanced fuzzy query can quickly access the corresponding exercise item information, and the multicondition mixed query can access the needed information more accurately. The exercise prescription formulation function enables basic addition, deletion, modification, and excel export, facilitating the use of information in many aspects.

5.2.2. *Operation and Implementation.* The generation of exercise prescriptions adopts a typical 2-level linkage query; that is, the exercise method is queried first, and then other exercise-related details are queried. This function is flexible and convenient, and the operation rhythm is strong. The specific process of exercise prescription formulation is shown in Figure 1.

5.3. *Implementation of Data Statistics Function.* The data statistics function enables basic data statistics and displays the exercise quantity and matching exercise solution quantity of the warm-up section, main exercise section, and cool-down section stored in the exercise center in the form of a bar chart. With the bar chart, the data can be presented intuitively.

5.4. *Image Management Function.* The image management function refers to the management of the images related to the exercise definition, exercise posture, and exercise essential modules of the warm-up section, main exercise section, and cool-down section of the system. The image management function enables basic new uploading, deleting and modifying, and comprehensive fuzzy multicondition query. The image management enables preview and downloading, more convenient view of the image effect, and guides users to complete the exercise safely and effectively.

6. System Test and Operation

6.1. *Black Box Testing.* Black box testing, also known as functional testing, is to test whether each functional module of the software can be used properly through computer testing. The black box testing regards the program as a black box that cannot be opened. Without considering the internal structure and internal characteristics of the program, it only checks whether the program function is used normally in accordance with the requirement specification and whether the program can properly receive input data and produce correct output information.

Black box testing focuses on the external structure of the program, does not consider the internal logical structure, and mainly tests software interfaces and functions. From the point of view of the user, the black box testing starts from the corresponding relationship between the input data and the output data. It does not need to know how the program works and only pays attention to the test results, so it is more suitable for this system. Some of its functional test cases are shown in Table 2.

6.2. *Test Analysis Report.* The black box test finds that: (1) the system successfully realizes some basic service functions of the physical health management of primary and middle school students; (2) after a series of tests, the system errors are roughly within the allowable range and will not affect the operation and effect of system. (3) There is room for further improvement of the interface typesetting, such as improving the visual effect, beautifying the interface, and improving the

TABLE 2: Black box test case table.

Test item	Precondition	Test procedure and user case	Results
Role-based authorization management	The administrator or authorized user successfully logs in	First click system management and then click authorization management. Enter the authorization page, input role names according to the conditions, and click save. Select the corresponding information to carry out modification, deletion, and other operations in turn. Authorize corresponding roles to add, delete, change, and query the menu	Display the results corresponding to the conditions you inputted on the results display page. (1) Display the new role information; (2) display the information after modification; (3) display the information after deletion; (4) corresponding roles are authorized
Information collection	The administrator or authorized user successfully logs in	First click collection center and then click information collection. Enter the collection page, input the name, height, age, weight, gender, exercise intensity, grade, memo, and other information according to the conditions and then click save. Select the corresponding information to carry out modification, deletion, and other operations in turn. Click export to excel	Display the results corresponding to the conditions you inputted on the results display page. (1) Display the newly collected information of the object; (2) display the information after modification; (3) display the information after deletion; (4) get the excel file
Exercise management	The administrator or authorized user successfully logs in	First click exercise center, exercise management, warm-up exercise/Main exercise/Cool-down exercise, and then click exercise method/Exercise definition/Exercise essentials/Exercise posture/Exercise requirements/Exercise advice/Exercise memo, enter the corresponding page, input related information according to the conditions, and then click save. Choose corresponding information to carry out modification, deletion and other operations. Click export to excel	Display the results corresponding to the conditions you inputted on the results display page. (1) Display the new exercise method/exercise definition/exercise essentials/exercise posture/exercise requirements/exercise advice/exercise memo; (2) display the information after modification; (3) display the information after deletion; (4) get the excel file
Exercise prescription formulation	The administrator or authorized user successfully logs in	First click exercise nutrition center, and then click exercise nutrition solution formulation. Enter the information display page, click exercise solution formulation, enter the exercise solution formulation page, and then click new exercise solution. Add the warm-up section, main exercise section, and cool-down section of the exercise solution. Click save	Display the results corresponding to the conditions you inputted on the results display page. (1) Display the exercise solution formulated
Image management	The administrator or authorized user successfully logs in	First click exercise center, then click exercise management, image management, and finally click exercise solution image, enter the corresponding page, input the relevant information according to the conditions, and then click save. Select the corresponding information to carry out modification, deletion, downloading, and other operations	Display the results corresponding to the conditions you inputted on the results display page. (1) Display the new image information; (2) display the information after modification; (3) display the information after deletion; (4) get the downloaded file
Data statistics	The administrator or authorized user successfully logs in	Click the data statistics menu in the menu bar	Display the results corresponding to the conditions you inputted on the results display page. (1) Display the corresponding data statistics

human-computer interaction; (4) when inputting conditions for query, the system can return error information corresponding to inappropriate data input, the operation

feasibility is greatly improved, so is the human-computer interaction; (5) the running speed of the system is affected by batch data collection.

7. Key Technical Specification for the Development of the Expert Decision-Making System

The system development platform is MyEclipse, follows the MVC (Model View Controller) three-layer design mode, and the server side adopts JSP + JavaBean + Servlet development mode to separate the view layer, model layer, and controller layer. Users use B/S (Browser/Server) mode to access Apache server through a browser, the system accesses SQL Server 2008 database through ADO.NET technology and is compiled in the object-oriented programming language Java.

8. Discussion

Childhood obesity is one of the most serious public health challenges in the 21st century. The prevalence of childhood obesity is a global problem. It first occurs in developed countries and is steadily affecting many low-and middle-income countries, especially children living in urban environments [8]. The weight gain of most overweight children is not caused by endocrine disorders or genetic diseases, the most common cause is the positive energy balance caused by calorie intake exceeding calorie consumption [9]. Reduced physical activity, sedentariness, long screen time, and food desert are common sociological factors leading to childhood obesity [10, 11]. Therefore, increasing physical activity and reducing energy intake are the main means to prevent and control the prevalence of childhood obesity.

Of course, we should also pay attention to another aspect; that is, children's lack of physical exercise may lead to muscle loss, muscle weakness, and physical weakness. A survey of 425 children by Tanaka and Tanaka [12] found that thin children spend less time participating in moderate-intensity and above exercise than normal children. Tanaka claims that high-intensity exercise is a necessary means to increase muscle mass in thin children. Compared with childhood obesity, childhood thinness has not been given enough attention. Narchi et al. [13] investigated the prevalence of thinness and its effect on height velocity among school-age children in the United Arab Emirates (UAE). 1/4 of children aged 4–6 and 1/3 of children aged 7–9 have a thin body ($BMI \leq 18.5 \text{ kg/m}^2$), and the peak height velocity of thin children was delayed by 1–3 years on average. According to the World Health Organization, 3.3% of children are severely thin, 6.9% are thin, 8.7% are overweight and 6.7% are obese [14]. Scientific exercise prescription is of great significance to the health promotion of special children groups such as obesity and thinness [15]. Children of different physiques may need different exercise interventions. For example, obese children should participate in longer aerobic exercises to consume excess energy, while thin children may need high-intensity exercise or resistance training to stimulate muscle growth [16].

Although a large number of studies have shown that exercise has great significance to the health promotion for children with special body types [17, 18], the long-term health benefits of exercise are often questioned [19]. The

reason may be that the exact dose-response effect of exercise intervention is difficult to determine [20] because the actual health status (physical condition, diseases, and medications) of the patients can be so diverse that its additional effects for health show too much variance [21]. Therefore, in order to consolidate the health intervention effect of exercise training on obese or thin children, personalized exercise prescription and sustainable exercise guidance are very important. In other words, personalized exercise prescription means not only personalized guidance during the experimental intervention but also constantly adjusted personalized exercise prescription by continuously matching the changes of individual health status, exercise habits, living environment, etc., [22]. In recent years, studies on personalized exercise interventions in obese and lean children have also been commonly reported [23]. However, this personalized intervention is usually limited to the duration of the experiment, and it is difficult to guarantee the long-term intervention after the end of the experiment. Normally, centralized and unified school physical education cannot provide targeted exercise solutions for children with different physiques, therefore, personalized exercise prescriptions can be used as a supplement to school physical education, which is of great significance for children with special physiques, such as obesity and thinness.

With the development of modern information technology, the construction of an information-based exercise prescription database has become a common option to provide a wide range of exercise prescription options [22]. Especially after the outbreak of COVID-19, telemedicine and mobile health services have been identified as effective means to respond to the increased sedentary behaviour and screen time [24]. For example, Johnson et al. [15] used online exercise prescriptions (such as exercise videos) to guide exercise in children with neuro developmental disorders to compare the compliance differences between online exercise prescriptions and traditional paper exercise prescriptions. However, the experimental results show that the exercise effect of the online guidance has no significant advantage compared with the traditional paper exercise prescription, that is to say, the online guidance and supervision do not improve the children's compliance with the exercise prescription. From this experiment, we found that merely changing the implementation of the exercise prescription and without changing the content of the exercise prescription does not necessarily improve its adherence. Traditional closed exercise prescriptions have poor compliance and universality for the health promotion of large groups of obese and thin children and require a lot of human and intellectual resources. Although the exercise prescription database have improved the universality of exercise prescription, the degree of personalization still can not meet the requirements, so the compliance of children is still low. Personalized exercise prescription is necessary to improve the pertinence and compliance of exercise intervention for an information-based exercise prescription database [25]. Therefore, we designed an exercise item database based on children's age and metabolic characteristics and developed an expert decision-making system to help users freely select

and combine sports content to form personalized sports prescription. The expert decision-making system can not only improve the universality of children exercise prescriptions but also effectively improve children's compliance with exercise prescriptions.

In recent years, there are many research studies on the expert system of exercise prescription for children's health. For example, Jiang et al. [26] studied the expert system of adolescent weight loss exercise prescription, and Patadia et al. [27] studied the generation of exercise prescription based on data mining. However, the generation mode of exercise prescription in its core is still the traditional limited generation, so the personalization and pertinence of exercise prescription are still limited. Our expert decision-making system of children exercise prescription first constructs the exercise resource database, and then constructs three sub-databases of warm-up, main exercise, and cool-down exercises. Different exercise items are arranged in terms of exercise method, exercise definition, exercise essentials, exercise posture, exercise requirements, exercise advice, and exercise memo. It is convenient for users to choose the content of personalized exercise prescription and guide children to do exercise. The test finds that our expert decision-making system of children exercise prescription can effectively improve the pertinence and compliance of children's participation in physical exercise.

The choice of web page development framework is the most important thing in the development of an expert decision-making system for children exercise prescriptions based on network information technology. A good development framework can improve the development efficiency, reduce the development cycle and cost, and support the rapid expansion and migration of the system in the future [28]. SSM framework (Spring + SpringMVC + MyBatis) is a typical monolithic lightweight framework and can divide the system into four layers in terms of responsibility: presentation layer, service layer, persistence layer, and view layer, which can help developers build strongly reusable and easy-to-maintain programs in a short time [29]. Our project chooses the SSM framework to design and implement the physical health management system of primary and secondary school students and strives to achieve scientific and convenient effective management of the physical health of primary and secondary school students.

9. Conclusion and Outlook

Exercise intervention has important significance for the health promotion of special children such as obesity and emaciated, and personalized exercise prescription is more conducive to improving the compliance and persistence effect of children. Given that the formulation of personalized exercise prescription requires a lot of human and material resources, we study how to achieve self-help exercise prescription generation with information technology (Internet, cloud technology, etc.). First of all, we constructed a pool of sports items that can be extended and accordingly provided sports requirements, movement methods, movement essentials, movement posture, sports suggestions, and remarks

information for children, some sports items were also matched with sports pictures. Secondly, we classified and managed the above-given sports project resources according to the preparation activity, the subject part, and the relaxation part, and users can freely choose the sports content in different modules to form their own personalized exercise prescription. Through the black box testing and a small range of use, we prove that our expert decision system is convenient to use, the exercise prescription is rich and popular with users and has a certain promotion value.

With the development of modern information technology, especially after the outbreak of COVID-19, mobile health services have become an explosive growth in demand [30, 31]. Although obese or thin children are of a special body shape, sports contraindications are not common, so mobile health services in this field are relatively safe. Although our study addresses the issue of adherence and universality of exercise interventions in this group. Looking forward to future studies, we believe that at least in the following aspects: first, the use of wearable devices for exercise load monitoring to help the children continue to participate in sports; second, we should establish comparable exercise and health records and give timely feedback to improve the enthusiasm of children to participate; third, using mobile terminals to strengthen school-child-family-community cooperation to inspire more subjects to participate in children's health promotion; fourth, how to improve the macrolevel policy support to form an atmosphere and environment suitable for children's exercise; fifth, how to accumulate big data on children's health management and sports participation in order to improve the environment, product research and development, policy formulation, and other data support.

Data Availability

Data sharing is not applicable to this article as no new data were created or analyzed in this study.

Disclosure

The sponsors have not been involved in study design, data collection, analysis, or decision-making related to the publication or preparation of the study.

Conflicts of Interest

The authors declare that they have no conflicts of interest.

Authors' Contributions

The software design was conducted by Li-fang Zhang and Chun-long Fang, under the guidance of Liang Zhou. The manuscript writing was done by Li-fang Zhang. Liang Zhou provided editorial review and research mentorship. All the authors provided critical revisions of the manuscript for important intellectual content.

Acknowledgments

The research was done under the support of the Young Scholars' Social Science Research Fund of the Ministry of Education (Grant no. 21YJC890045), the Natural Science Foundation of Hunan Province (Grant no. 2019jj40317), and the Hunan Philosophy and Social Science Research Foundation (Grant no. 19YBA034).

References

- [1] L. J. Apperley, J. Blackburn, K. Erlandson-Parry, L. Gait, P. Laing, and S. Senniappan, "Childhood obesity: a review of current and future management options," *Clinical Endocrinology*, vol. 96, no. 3, pp. 288–301, 2022.
- [2] H. Jebeile, A. S. Kelly, G. O'Malley, and L. A. Baur, "Obesity in children and adolescents: epidemiology, causes, assessment, and management," *Lancet Diabetes & Endocrinology*, vol. 10, no. 5, pp. 351–365, 2022.
- [3] H. L. Mayr, F. Cohen, E. Isenring, S. Soenen, and S. Marshall, "Multidisciplinary lifestyle intervention in children and adolescents - results of the project GRIT (Growth, Resilience, Insights, Thrive) pilot study," *BMC Pediatrics*, vol. 20, no. 1, p. 174, 2020.
- [4] K. A. Dias, J. S. Coombes, D. J. Green et al., "Effects of exercise intensity and nutrition advice on myocardial function in obese children and adolescents: a multicentre randomised controlled trial study protocol," *BMJ Open*, vol. 6, no. 4, Article ID e010929, 2016.
- [5] A. Carrel, A. Meinen, C. Garry, and R. Storaardt, "Effects of nutrition education and exercise in obese children: the Ho-Chunk Youth Fitness Program," *Wisconsin Medical Journal*, vol. 104, no. 5, pp. 44–47, 2005.
- [6] V. Calcaterra and G. Zuccotti, "Prevention and treatment of cardiometabolic diseases in children with overweight and obesity: the future of healthcare," *Children*, vol. 9, no. 2, p. 176, 2022.
- [7] L. Stoner, D. Rowlands, A. Morrison et al., "Efficacy of exercise intervention for weight loss in overweight and obese adolescents: meta-analysis and implications," *Sports Medicine*, vol. 46, no. 11, pp. 1737–1751, 2016.
- [8] A. J. Negrete Cortés, A. Vite Sierra, and C. A. Cavita Castro, "Promoting self-control in overweight and obese children," *Nutricion Hospitalaria*, vol. 37, no. 2, pp. 251–259, 2020.
- [9] S. Kumar and A. S. Kelly, "Review of childhood obesity: from epidemiology, etiology, and comorbidities to clinical assessment and treatment," *Mayo Clinic Proceedings*, vol. 92, no. 2, pp. 251–265, 2017.
- [10] F. C. Bull, S. S. Al-Ansari, S. Biddle et al., "World Health Organization 2020 guidelines on physical activity and sedentary behaviour," *British Journal of Sports Medicine*, vol. 54, no. 24, pp. 1451–1462, 2020.
- [11] P. S. Tandon, T. Sasser, E. S. Gonzalez, K. B. Whitlock, D. A. Christakis, and M. A. Stein, "Physical activity, screen time, and sleep in children with ADHD," *Journal of Physical Activity and Health*, vol. 16, no. 6, pp. 416–422, 2019.
- [12] C. Tanaka and S. Tanaka, "Objectively-measured physical activity and body weight in Japanese pre-schoolers," *Annals of Human Biology*, vol. 40, no. 6, pp. 541–546, 2013.
- [13] H. Narchi, A. Alblooshi, M. Altunajji et al., "Prevalence of thinness and its effect on height velocity in schoolchildren," *BMC Research Notes*, vol. 14, no. 1, p. 98, 2021.
- [14] E. E. Elrayah, S. A. Balla, and H. A. Ahmed, "Anthropometric assessment of school children in khartoum locality, khartoum state, Sudan - 2014/2015," *Anthropologischer Anzeiger*, vol. 74, no. 5, pp. 393–401, 2018.
- [15] R. W. Johnson, S. A. Williams, D. F. Gucciardi, N. Bear, and N. Gibson, "Can an online exercise prescription tool improve adherence to home exercise programmes in children with cerebral palsy and other neurodevelopmental disabilities? A randomised controlled trial," *BMJ Open*, vol. 10, no. 12, Article ID e040108, 2020.
- [16] R. J. Sigal, A. S. Alberga, G. S. Goldfield et al., "Effects of aerobic training, resistance training, or both on percentage body fat and cardiometabolic risk markers in obese adolescents: the healthy eating aerobic and resistance training in youth randomized clinical trial," *JAMA Pediatrics*, vol. 168, no. 11, p. 1006, 2014.
- [17] F. Cosentino, P. J. Grant, V. Aboyans et al., "2019 ESC Guidelines on diabetes, pre-diabetes, and cardiovascular diseases developed in collaboration with the EASD," *European Heart Journal*, vol. 41, no. 2, pp. 255–323, 2019.
- [18] M. Zhao, S. P. Veeranki, S. Li, L. M. Steffen, and B. Xi, "Beneficial associations of low and large doses of leisure time physical activity with all-cause, cardiovascular disease and cancer mortality: a national cohort study of 88, 140 US adults," *British Journal of Sports Medicine*, vol. 53, no. 22, pp. 1405–1411, 2019.
- [19] L. S. Pescatello, "Exercise measures up to medication as antihypertensive therapy: its value has long been underestimated," *British Journal of Sports Medicine*, vol. 53, no. 14, pp. 849–852, 2019.
- [20] M. S. Emery, "Long term strenuous exercise: is there a dose effect?" *Journal of the South Carolina Medical Association*, vol. 112, no. 2, pp. 197–199, 2016.
- [21] R. Ross, B. H. Goodpaster, L. G. Koch et al., "Precision exercise medicine: understanding exercise response variability," *British Journal of Sports Medicine*, vol. 53, no. 18, pp. 1141–1153, 2019.
- [22] M. Dvorák, M. Tóth, and P. Ács, "The role of individualized exercise prescription in obesity management-case study," *International Journal of Environmental Research and Public Health*, vol. 18, no. 22, Article ID 12028, 2021.
- [23] V. Vasankari, J. Halonen, T. Vasankari et al., "Physical activity and sedentary behaviour in secondary prevention of coronary artery disease: a review," *American Journal of Preventive Cardiology*, vol. 5, Article ID 100146, 2021.
- [24] V. Calcaterra, E. Verduci, M. Vandoni et al., "Telehealth: a useful tool for the management of nutrition and exercise programs in pediatric obesity in the COVID-19 era," *Nutrients*, vol. 13, no. 11, p. 3689, 2021.
- [25] G. O'Donoghue, C. Blake, C. Cunningham, O. Lennon, and C. Perrotta, "What exercise prescription is optimal to improve body composition and cardiorespiratory fitness in adults living with obesity? A network meta-analysis," *Obesity Reviews: An Official Journal of the International Association for the Study of Obesity*, vol. 22, no. 2, Article ID e13137, 2021.
- [26] L. Jiang, P. Xie, and M. Wang, "Research on expert system of personalized adolescent weight loss exercise prescription based on performance monitoring," *Journal of South China Normal University (Social Science Edition)*, vol. 39, no. 04, pp. 181–186, 2014.
- [27] V. K. Patadia, M. J. Schuemie, P. M. Coloma et al., "Can electronic health records databases complement spontaneous reporting system databases? A historical-reconstruction of the association of rofecoxib and acute myocardial infarction," *Frontiers in Pharmacology*, vol. 9, p. 594, 2018.

- [28] F. Ke and Z. Liu, "Research on web application security mechanism based on SSM framework," *Wireless Internet Technology*, vol. 16, no. 24, pp. 19-20, 2019.
- [29] Li. Qin and Q. Ai, "Design and implementation of student life service platform based on SSM framework," *Computer Knowledge and Technology*, vol. 17, no. 13, pp. 80-82, 2021.
- [30] R. S. H. Istepanian, "Mobile health (m-Health) in retrospect: the known unknowns," *International Journal of Environmental Research and Public Health*, vol. 19, no. 7, p. 3747, 2022.
- [31] S. Sujarwoto, T. Augia, H. Dahlan, R. A. M. Sahputri, H. Holipah, and A. Maharani, "COVID-19 mobile health apps: an overview of mobile applications in Indonesia," *Frontiers in Public Health*, vol. 10, Article ID 879695, 2022.

Research Article

Brainwave Acquisition Terminal Based on IoT Smart Sensor for English Listening Test

Juan Bi 

Hefei Preschool Education College, Hefei 230013, Anhui, China

Correspondence should be addressed to Juan Bi; bijuan512799@163.com

Received 20 April 2022; Revised 21 June 2022; Accepted 11 July 2022; Published 8 August 2022

Academic Editor: Xuefeng Shao

Copyright © 2022 Juan Bi. This is an open access article distributed under the Creative Commons Attribution License, which permits unrestricted use, distribution, and reproduction in any medium, provided the original work is properly cited.

In our teaching, teachers cannot understand students' learning situation deeply, they can only judge students' mastery of English through usual homework situation and test scores, but this is not an accurate way of judging. In addition, the combination of the Internet of Things and sensors and their application in the teaching field has made preliminary progress, and the phenomenon of Internet of Things smart sensors being used in teaching is becoming more and more common. For this reason, this article proposes that the brainwaves of the students' learning process can be sent to a remote server for persistent transmission through the Internet of Things. It also collects brainwave data to match the learning structure in the student management system and finally establishes a machine learning model for analyzing the student's learning process to analyze the student's learning situation. This article discusses and constructs a brain wave collection terminal based on the intelligent sensor of the Internet of Things for English listening test. Experiments have shown that the brainwave collection terminal in this article has achieved an accurate grasp of how students learn in the English listening test. Its accuracy is as high as 89.34%. It pays more and more attention to the education of their children. However, the understanding of the students' learning situation only stays on the surface, and it is impossible to have a deep understanding of the students' specific learning situation. In addition, the development of science and technology has become more and more mature. The Internet of Things and smart sensors are gradually being used in the teaching field. Although they provide convenience for daily teaching activities, their research and development in this area is not very mature, and there are still many problems. In addition, products used in the field of brainwave sensors for teaching have appeared. However, the data cannot be obtained and the computer wave model cannot be established or modified. Therefore, the technology for applying brain wave sensors to teaching is not mature. Therefore, this article needs to study the brainwave collection terminal of English listening test, and provide technical support for more accurate grasp of students' learning situation.

1. Significance

The brainwave acquisition terminal for the English listening test studied in this article can solve the problem of immature technology in the current teaching field and provide a set of practical brainwave data acquisition devices for the market. Second, the brainwave acquisition device studied in this article can assist schools in completing daily teaching activities and can also provide the collection of student learning data for scientific research institutions or teaching institutions. In addition, the device can better model the learning data of students and provide better scientific and technical support for accurately grasping the learning situation of students, and this article still has a great

breakthrough in the setting of brain wave collection terminal, which provides a good reference value for the subsequent replacement of brain wave devices.

2. Related Work

With the rapid development of science and technology, mankind has made major breakthroughs in intelligent technology, especially in language learning. Researchers spend a lot of time to intelligentize the process of language learning and improve the efficiency of human language learning. Among them, Ockey and French has done a series of studies on the need to assess multilingual listening skills in a global context, which is becoming more and more

common. His research is aimed to determine the degree of influence of accent intensity and familiarity on listening comprehension, and developed an accent intensity scale in this regard [1]. Green focuses his research on different types of listening behaviors, including a series of sound files that reflect different types of discourse, themes, target audiences, and purposes. He first describes the test population, instructions, and sound files, and then gives the task. What follows is a discussion of each task, according to the type of listening behavior that the test developer wants to measure, according to the applicability of the reflection-sound file [2]. Lee et al. has studied the machine to understand the content of spoken language and developed a machine that can understand the content of spoken language. He passed the TOEFL listening test, showing that the model uses the hierarchical structure of natural language and the ability to select attention mechanisms, which is better than the original method and other neural network-based models [3]. Lee and Young described two prototype studies before a new English listening test can be used in practical applications. One of the prototype studies collected evidence to support domain description inference, that is, whether the test task appropriately sampled the examinee's general English listening comprehension ability [4]. Wang studied the holding of listening test-training courses in Beijing Science District. The course is held in the "AES Engineer Training Camp" of Aisin Jufu, and is aimed at domestic and foreign sound and sound engineers. His research purpose is to cultivate the subjective and objective listening of young sound engineers to achieve the most accurate [5]. In order to prove the difference in semantics, Dal Palu et al. rolled office chairs to make sounds and asked 90 participants to take a hearing test, and described the moving sounds of two high-quality and low-quality office chairs. He then presented the recorded stimulus information to the listeners through headphones, and found that the difference in chair sound was related to calm and rough surfaces, happy and annoying moods [6]. These studies have made good elaboration on human hearing, but they have not stated in the study that sound entering the brain may still be transmitted to the world outside the brain in another form. How to record the form of sound after entering the brain is rarely mentioned in the research of English listening. Most of these studies focus on the study of humans receiving sound, no one has studied the changes and manifestations of sound after it enters the brain.

3. Innovation

This article has the following innovations in the study of brainwave acquisition devices for English listening tests: (1) the research device in this article is based on the production process of English listening audio and the students' English listening test. It will be more in line with the actual learning situation of students, and at the same time, it will be able to more accurately grasp the impact of changes in English audio on brain waves. (2) It combines the Internet of Things and sensors to form an Internet of Things smart sensor, which can remotely obtain and integrate the information and data of the Internet of Things storage server. (3) On the

basis of the original English listening test brain wave collection terminal, it combines the science and technology of the intelligent sensor of the Internet of Things. This makes it possible to model the collected student learning data and better provide technical support for daily teaching activities. (4) In the process of English listening, brain waves are not only stimulated by external audio but also affected by inevitable physiological signals. Therefore, this article uses IoT smart sensors to reduce the brain waves generated by the influence of the signal, so that the student's learning data is more accurate.

4. Design Method of Brainwave Acquisition Terminal for English Listening Test

4.1. Audio Signal Collection and Output. In daily life, the songs we hear, as well as the current audio television and audio movies, require some recording equipment and sound output equipment in the production process. These include high-sensitivity condenser microphones, audio and tone modulators, and control equipment. It is shown in Figure 1.

As shown in Figure 1, there are various devices in the audio recording process, and the technologies and principles involved are also different. For example, the principles of audio sensors and speakers are also different. In addition, when we do the English listening test, the most basic material is the listening audio, and then the paper or electronic manuscript test questions. But how is the English listening audio produced, and how is it played and output synchronously in different classrooms? Figure 2 shows the floor plan of the simultaneous English listening test in different classrooms.

In Figure 2, to play synchronized English listening in different teaching buildings requires network transmission. In this process, the network plays a key role, so the network is indispensable in the English listening test. Of course, we need to trace back to the collection of English listening audio. If it needs to make English listening audio, it needs to collect audio signals. The collection of audio signals requires the use of some recording equipment, as well as a sound source. This sound requires someone to read a piece of English to our recording equipment, but cannot use other equipment to play the voice for recording, because in this way, the source of the sound cannot be obtained. The audio obtained then needs to be analyzed and modulated on the recorded spectrum before it can be output. The analysis of the frequency spectrum requires the application of related principles, and the principles are as follows:

$$\begin{aligned}
 E_{(f)} &= \sum_{z=1}^N t(s) g_N^{(s-1)(f-1)}, \\
 t(z) &= (2/N) \sum_{k=1}^N E_{(f)} g_N^{(s-1)(f-1)}, \\
 g_{(N)} &= f^{(\pi z)/N}.
 \end{aligned} \tag{1}$$

In processing the frequency spectrum, we use the FFT function in the audio signal-processing tool. In formula (1),

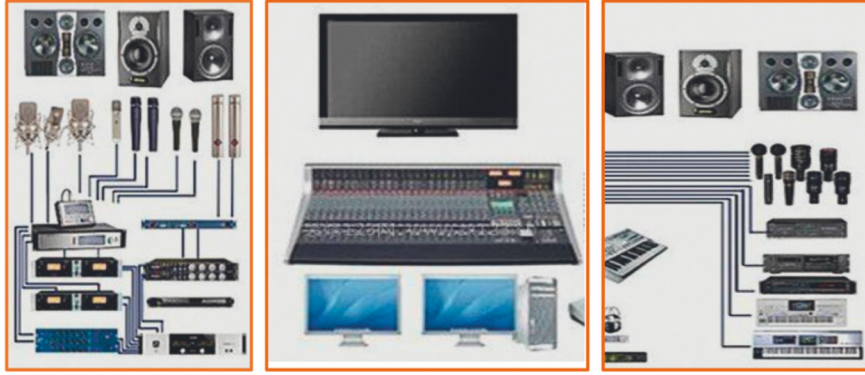


FIGURE 1: Audio capture device diagram.

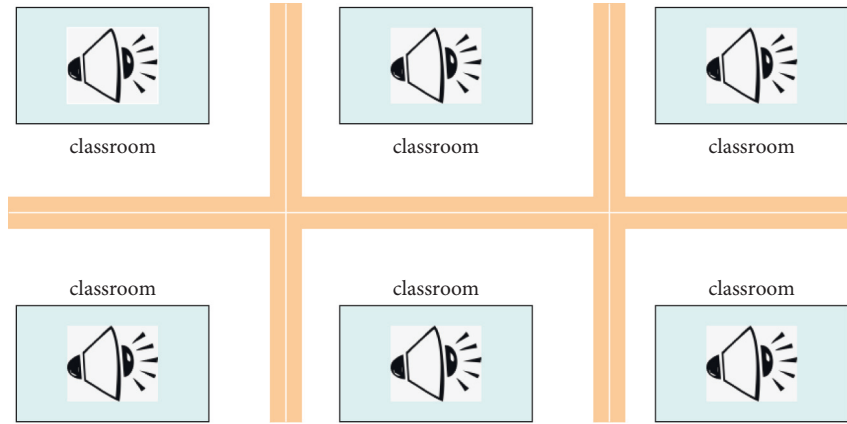


FIGURE 2: Plan of simultaneous English listening test in different classrooms.

E is the serial number, S is the audio duration, t is the highest value of the audio amplitude, g is the lowest value of the audio amplitude, f is the average of all audio amplitudes, and z is the amplitude of the audio duration. After analyzing the frequency spectrum, we need to modulate and demodulate the audio model, and the final piece of audio is considered complete. The principle of modulation and demodulation is as follows:

$$g(s) = E(t) * ins(g_N * f),$$

$$E = \frac{1}{2} \left\{ E_{(g+g_N)} + E_{f(g+g_N)} \right\}, \quad (2)$$

$$E_0(f) = g(f) * ins(g_N * t).$$

The audio modulation process needs to add Gaussian white noise for demodulation. The Gaussian in the so-called “White Gaussian Noise” means that the probability distribution is a normal function, while the white noise means that its second-order moments are uncorrelated. The first moment is a constant, which refers to the correlation of successive signals in time. Gaussian white noise is an ideal model for analyzing channel additive noise. So the above formula E_0 represents the sequence of Gaussian white noise. Finally, after filtering the modulated and demodulated audio signals, they can be put into the audio player for playback, which is the process of our audio output [7]. In fact, the

collection and production of audio signals is relatively cumbersome, but the development of technology nowadays has provided a more convenient device for audio production, that is, a recorder. Although there are many principles involved in the recorder, it is possible to automate the processing of the collected audio signals during the audio production process. The output method only needs to transmit the finished audio to the designated device through the network for output [8]. The entire audio production process is shown in Figure 3.

The production process of English audio is basically the same. In English listening, sound is transmitted to the brain through our ears to generate brain waves, and when the sound passes through the ear, our eardrum is equivalent to a sensor. When receiving audio signals, the central nervous system will feed back to the brain, and the brain will produce brain waves in response. This research is to design a terminal to collect these brain waves.

4.2. The Perception of English Listening Audio by IoT Smart Sensors

4.2.1. IoT Smart Sensors. Since the development of sensors, there are more and more types of them [9], and with the development of communication technology, sensors can sense some information from a long distance. For example,

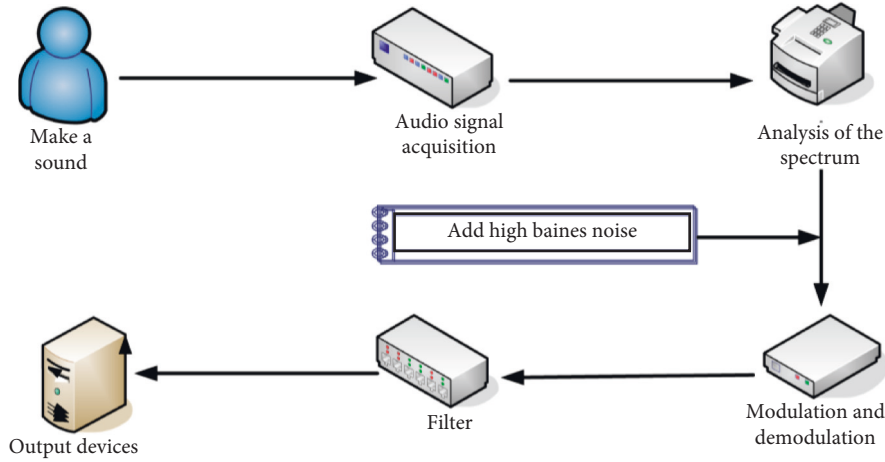


FIGURE 3: Flow chart of the audio production process.

the use of electrical appliances in our smart home can be remotely controlled through the Internet of Things [10]. The Internet of Things unites people, machines, and things. It combines it with the sensor, making the sensor more intelligent. The Internet of Things smart sensor is more similar to the Internet of Things architecture [11], and affected by the principle of the Internet of Things, the Internet of Things smart sensor can also be seen as a combination of collecting signals and controlling and processing signals [12]. For example, if the Internet of Things is used in our audio sensors, it can be more clearly transferred to the mind, and the sensor is blessed by the Internet of Things, the signal is more stable, and the tone will be clearer. The combination diagram of the Internet of Things and audio sensors is shown in Figure 4.

As shown in the figure, the Internet of Things connects sensors with sensors through network signals. Moreover, among the audio collected by each sensor, it will be transmitted to a general sensor service device through the network signal, and then passed into the human ear through the sound output device to enter the brain. In addition, IoT smart sensors can reduce noise according to the noise in different audio, and make the audio we want to hear clearer. The principle of noise reduction is as follows:

When the volume and loudness of this section of noise is h and the duration of the accompanying section of audio is X , there will be changes in the audio frequency during this process. Therefore, it is necessary to control the audio frequency M , and the time X_0 when the noise starts to appear and the time when the noise ends are X_3 . Then we first need to reduce the volume of the noise, then:

$$h = \frac{M}{E} * |X_0 - X_3| * ins(x). \quad (3)$$

Then the internal modulator of the sensor reduces the tone of the noisy audio, and the principle is to add Gaussian white noise for demodulation as mentioned above. There are many types of ground principles involved in IoT smart sensors. But in this article, the combination of smart audio sensors and the Internet of Things is mentioned, so the principle is to collect various audios. The principle involved

and the principle of the Internet of Things have been added to the previous audio sensors. Of course, in order to prevent the confusion of language types, we can set the language type that it needs to record to English. The setting principle is as follows:

$$E = \sqrt[M]{M} * \cap_t S * g. \quad (4)$$

In the above formula, E represents the number of language conversions, and X is the duration of the metaphorical audio mentioned above, and M is the frequency of English audio, S is the duration of English audio, t is the highest value of English audio amplitude, and g is the lowest value of English audio change amplitude. In the process of intelligent language conversion, the perception layer inside the smart sensor will completely preserve the English audio, and can use the Internet of Things to transmit it to a device dedicated to broadcasting.

4.2.2. Perception of English Listening Audio. Perception of English speech audio is closely related to listening level [13]. Just as we have taken a lot of English tests, basically, every English test cannot be separated from the English listening test. The ability to perceive English speech includes learners' perception and recognition of English segments, supersegments, and changes in continuous speech [14]. Therefore, when English speech is introduced into our ears, each person's different perception abilities will have different effects on the brain, and also have different effects on brain waves. Because whether people can hear English voice clearly, their brain waves are generated and the brain waves can be converted into English through sensors. In other words, when we are doing English listening, the brain waves generated can also be restored through the collection terminal. When our brain is full of alpha waves, the brain's attention is highly concentrated, and the perception of listening to English audio is also clearer. At this time, the human body has the least energy consumption, the right brain is powerful, the memory of English audio is the best, and the perception ability is the strongest. However, when the brain is full of beta waves, the brain is in a state of high

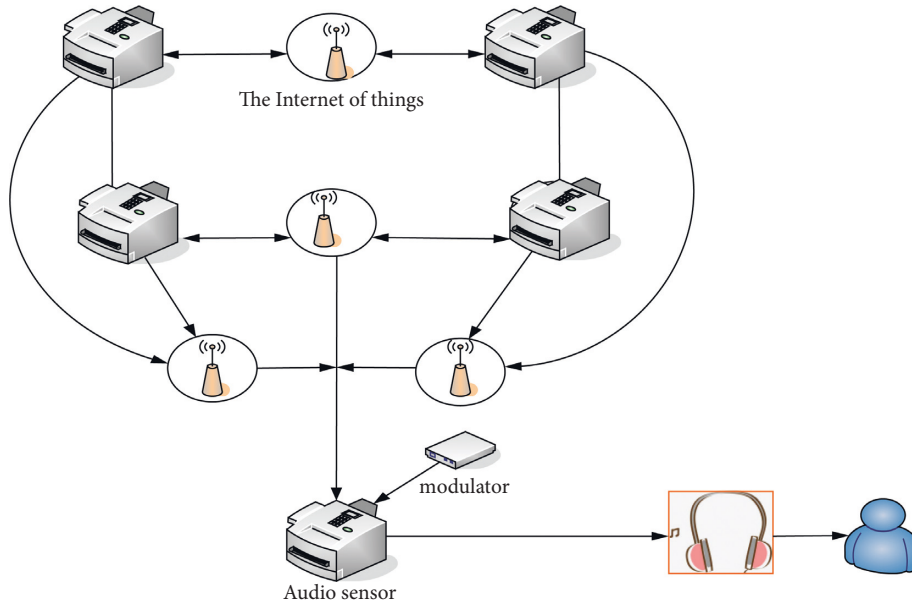


FIGURE 4: The combination of the Internet of Things and audio sensors.

tension and consumes the greatest energy to the human body. It is in a state of avoiding English listening all the time, that is, the brain will become sleepy in English and its ability to perceive English listening audio is weakened; when English listening audio stops, the human body will be in a relaxed state, the brain is full of gamma waves, the brain is in a resting state, and the ability to perceive English listening audio disappears [15].

Therefore, the ability to perceive English listening audio has an impact on the brain waves inside the brain. When the English listening audio enters the brain, the sound of the English listening audio will change the brain waves of the human brain. This brain wave can be collected and analyzed with the help of a terminal to restore the original English listening, and because of our different learning abilities, our familiarity with English will be different, and our perception of English listening audio is different [16].

4.2.3. The Perception of English Listening Audio by IoT Smart Sensors. When we have hearing audio, we need to get the text of the hearing audio, then we can use some sensor equipment, such as our mobile phone. Downloading a Baidu translation software or other translation software in your mobile phone, and then turn on the voice translation function of this software. When it aligns with the English audio playback source, it can be seen that the perceived English listening audio in the mobile phone is converted into text form and is being translated [17]. In this process, we need to open the network to use this function with our mobile phone. When the sensor setting in the mobile phone hears hearing audio, it will quickly search on the storage server of the Internet of Things through the communication network and display the audio text form before us. The process diagram of voice conversion is shown in Figure 5.

Of course, smart sensors will lag behind the network due to the speed of audio speech, so sometimes what they hear

may not be completely correct, and there may be some minor errors, but this can be judged by sentence meaning. Among the smart sensors of the Internet of Things, the principle of its design is shown in Figure 6.

As shown in Figure 6, the Internet of Things is like an interconnected network, and when smart sensors receive English listening audio, the sensors will quickly integrate data and information stored in various places in the Internet of Things through the communication network. The principle of information integration is as follows:

$$Inf_1 = \frac{1}{2} \sum_t^g (X + T) * v, \quad (5)$$

$$Inf_2 = \frac{1}{2} \sum_t^g (S + N) * v. \quad (6)$$

Formulas (5) and (6) are the principle of the intersection and integration of four far-distant information in the Internet of Things. Where g is a weight value in the smart sensor, t represents the network speed, which is the speed of the network speed, and v is a matrix in the process of integrating the information of the Internet of Things memory with 4 storages that are far apart, as shown:

$$v = \begin{Bmatrix} g & Y & g \\ H & g & R \\ g & M & g \end{Bmatrix}. \quad (7)$$

In the same way, the information integration principle of other storage servers can be obtained as follows:

$$Inf_3 = \frac{1}{4} \sum_t^g \frac{|H - R|}{|Y - M|} * \eta. \quad (8)$$

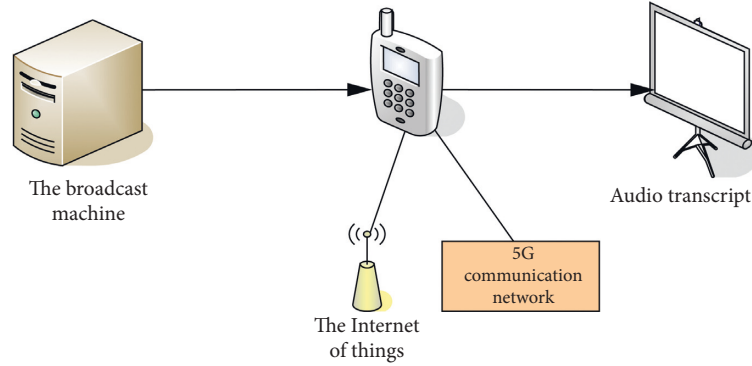


FIGURE 5: Process diagram of voice conversion.

In formula (8), because the four storage distances are similar, the network speed will be faster. Converge in four directions at the same time, and then quickly integrate and output in the smart sensor, and a matrix that maintains the balance of information will be generated in the above process. Its form is as follows:

$$\eta = \begin{Bmatrix} X & S \\ N & T \end{Bmatrix}. \quad (9)$$

Then it is integrated with the information of the other four storage servers. The principle is as follows:

$$Inf_4 = \frac{(Inf_1)}{(Inf_2)} * g * \frac{Inf_3}{k} * t. \quad (10)$$

In formula (10), κ is an information integration matrix, and its form is as follows:

$$k = \frac{1}{\begin{Bmatrix} X & Y & S \\ H & t & R \\ N & M & T \end{Bmatrix}}. \quad (11)$$

Finally, the principle of the complete English audio converted in the mobile phone is as follows:

$$Inf = Inf_4 * g * \frac{1}{k}. \quad (12)$$

In this way, the entire process of the IoT smart sensor for English audio needs to be completed. If it wants to collect the brain waves of the English listening test, it needs to use the Internet of Things smart sensors to perceive and convert the brain waves, and perhaps use smart sensors to perceive them.

4.3. The Design of Brainwave Acquisition Terminal for English Listening Test. Brain waves are the rhythmic discharge effect of the human brain in the physiological process. It is formed by receiving stimuli or spontaneous reactions to human body functions, and the brain electricity is the result of the comprehensive discharge of neurons. In our daily life, the brain generates EEG signals due to external stimuli. In the

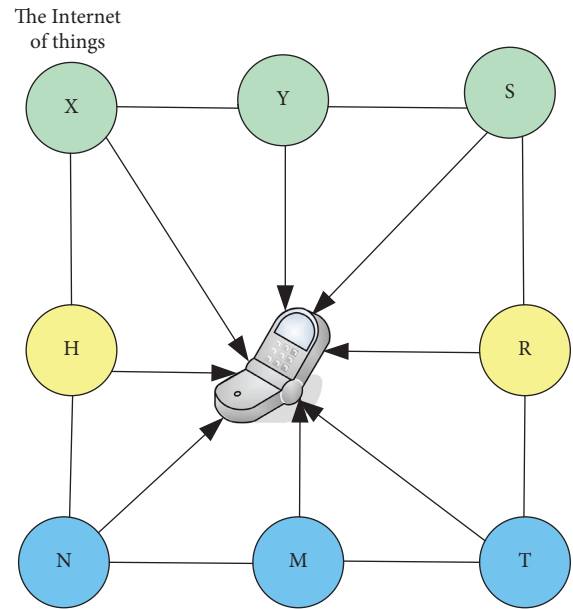


FIGURE 6: Schematic of the design.

English listening test, our brain is stimulated by audio to produce brain wave signals about English listening. The schematic diagram of the EEG signal acquisition equipment is shown in Figure 7.

What this article needs to design is the brain wave collection terminal based on the smart sensor of the Internet of Things, which is susceptible to interference in the English listening test, so the brain wave signal will also be interfered. There are two main sources of interference. The first is our own interference, and while we are collecting EEG signals for English listening tests, we will also collect bioelectric signals such as ECG, EOG, and EMG. These signals are difficult to distinguish and remove in the process of our collection, so we need to use IoT smart sensors to reduce or even eliminate the generation of these signals [18]. Another interference is the interference of the surrounding environment during the English listening test, and our surroundings are full of electromagnetic fields. These electromagnetic fields can easily enter the EEG signal through electromagnetic induction, so signal interference is a problem that we should fully consider in the design process.



FIGURE 7: Schematic diagram of EEG signal acquisition equipment.

Therefore, in the process involved, we need to reduce the noise of the audio before the sound enters the human brain so that the impact on the EEG signal of our English listening test will be reduced [19]. In addition, blinking must be avoided as much as possible during the hearing process to reduce the interference of biological signals on brain electrical signals. Of course, it is best to reduce noise, because biological signals are unavoidable. The EEG signal acquisition terminal design of this article is shown in Figure 8.

In the schematic diagram in Figure 8, it is obvious that when the English audio is played, the audio will enter the modem first. This modem will eliminate the noise generated during the hearing test, so that the interference from the external environment is excluded in the first step. Then enter the Internet of Things smart sensor to improve the quality of timbre and other aspects. After entering the human body to stimulate the brain to generate brain waves, a round of process has been completed here. After entering the brain, it is necessary to use equipment to collect the brain waves during the English listening test. First, the Internet of Things smart sensor is added to the brainwave acquisition equipment, and then the brainwave output from the brain will first pass the Internet of Things smart sensor to identify the brainwave generated by the biological signal and reduce the effect of its influence. Then it enters the brain wave collection terminal, and finally enters the brain wave display.

In the brain wave collection of the English listening test, the brain electrode is the medium connecting the brain wave and the collection terminal, and the high-performance brain electrode can reduce the introduction of interference. However, polarization voltage and electrode artifacts still exist, and these appear as DC signals in the circuit, as long as the DC blocking is used. In addition, because the resistance of brain waves and brain electrodes is very large, the acquisition circuit of brain waves needs to have a large input impedance capability [20]. In addition, coupled with the blessing of IoT smart sensors, it is possible to minimize the interference signal to the brain waves in the English listening test. From this it can refer to the circuit diagram of the brain wave acquisition equipment, as shown in Figure 9.

In Figure 9, in our brainwave acquisition device, direct current is used, so we need to convert our alternating current to direct current. There are more prominent resistors, which can play a certain impedance role on the brain waves and the resistance of the brain electrodes.

5. Experiment and Analysis of Brainwave Collection Terminal for English Listening Test

5.1. Test of English Listening and Audio Perception. In the teaching process, we can only check the student's learning situation through the English test, which can check the student's perception of English listening audio [21]. Therefore, in this experiment, we will select ten students with the same level of English and similar learning abilities to take the English listening test, and have tested their perception of English audio. The perceptual ability of English audio is designed to test the ten students' perception of English segments, supersegments, and sound changes in continuous speech [22], and record the test results of these ten students. The test content and scores are shown in Table 1.

Table 1 shows the content of the test required for this experiment. It finds these ten students in a quiet classroom and conducts English listening tests on them, and uses the results to judge their English perception and English listening proficiency. Then their test scores are shown in Figure 10.

From the overall score in Figure 10, it is undoubtedly that the English listening level of student No. 2 is higher. His English listening learning situation is the best because his listening test score reached 52 points, and his ability to perceive English listening is the strongest. But from the analysis of the accuracy of the question type, student No. 4 has the best learning situation for the question type sound change test, and has the strongest ability to perceive sound change; however, from the segment test, students No. 1, No. 2 and No. 7 tied for the first place, all scored 18 points, and these three students have the strongest perception of the sound segment; from the question-type supersegment test, student No. 6 scored 18 points. This student has the strongest ability to perceive English supersegment. If it is judged from the performance of each question type to judge the student's learning situation, it is difficult to distinguish which of them has the best learning situation. But judging from the overall results, such a judgment is too general. Because every student has his own strengths and weaknesses, it is difficult to make accurate judgments about the student's learning situation. In addition, it is easy to fall into a misunderstanding by using grades to judge students' learning. That is, he will consider which part of the student has the

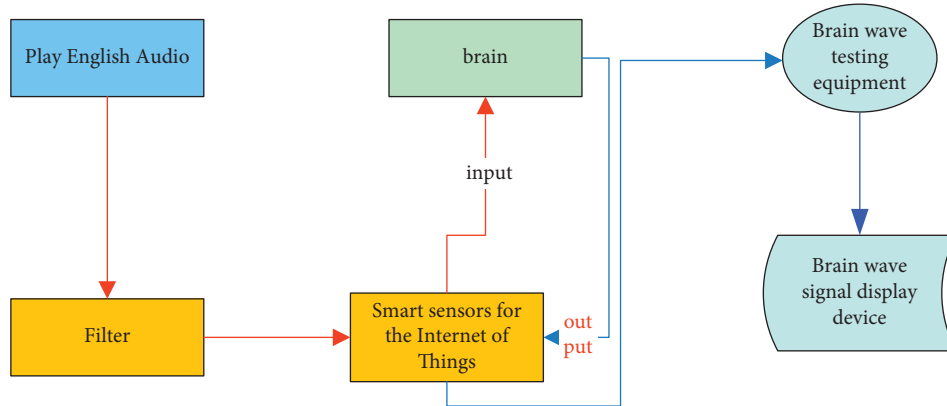


FIGURE 8: The EEG signal acquisition terminal design in this article.

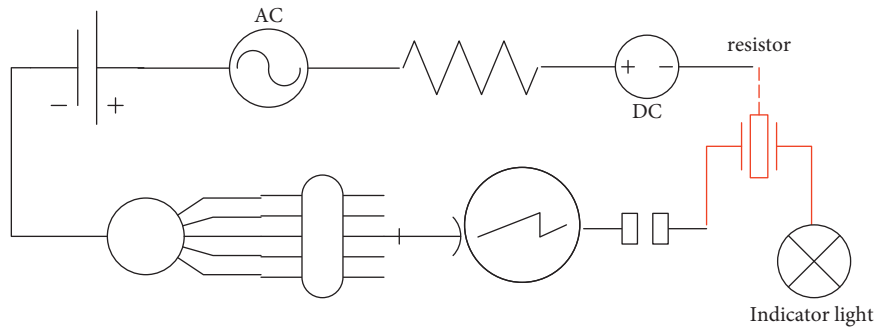


FIGURE 9: Circuit diagram of brainwave acquisition equipment.

TABLE 1: Test content and score.

Testing content	Question type	Number of question	Subject score
Segment test	Objective question	20	20
Ultrasonic section test	Subjective question	20	20
English sound change test	Objective question	20	20

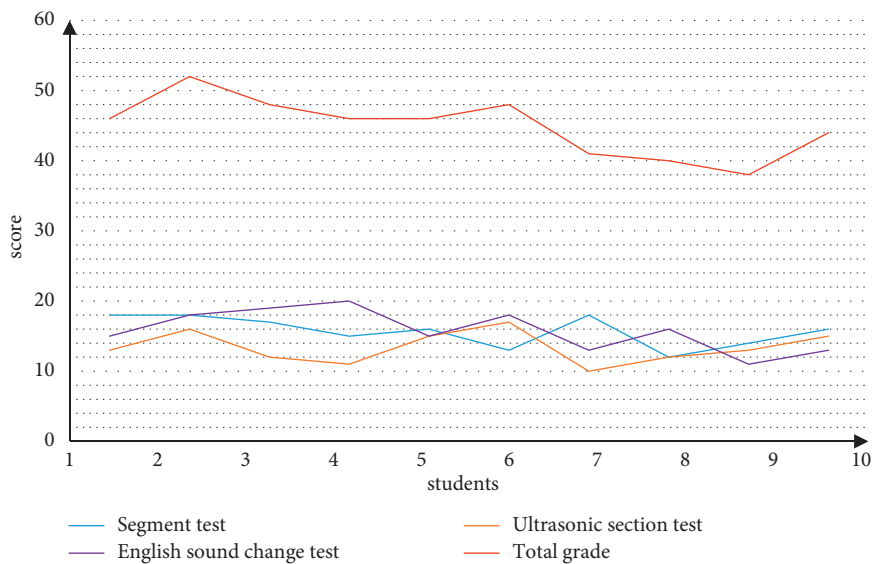


FIGURE 10: The score chart of the student test.

lowest score, and he should fill up which part of the question type. We understand that the grades of the supersegment question type of student No. 1 are the lowest among the three question types, so we generally recommend him to make up for this aspect of listening. But this kind of judgment is only superficial, so it is not accurate enough to judge the student's learning situation through grades. Judging from the analysis of the chart, it is rather one-sided to judge the student's learning by grades. Because every student will have some parts that he is good at, and some parts that he is not good at, and there may be factors that do not perform well in the test.

5.2. Experiments on Brainwave Acquisition Terminal Pairing and Learning. We all know that brain waves are divided into four types, of which the brain is most easily "opened up" in the alpha wave state, the mind is concentrated, and the thinking is clear [23]. So when the α wave generated in the mind in the English listening test, the learning situation is the best; when β waves dominate the brain waves, it has a key benefit for positive attention enhancement and the development of cognitive behavior; when the θ wave is the dominant brain wave, the human consciousness is interrupted and the body is deeply relaxed [24]; the last type of brain wave is generated during deep sleep, so this is unlikely to be generated in the English listening test site, so it is impossible to collect δ wave in this experiment [25]. For this reason, we still add the brain waves of these ten students during the English listening test on the basis of the previous experiment. The collection device is the computer wave collection terminal based on the intelligent sensing of the Internet of Things that we study in this article, and its accuracy will be higher. The test situation is shown in Table 2.

The results of their listening test are shown in Table 3.

According to the descriptions in Tables 2 and 3, it can be seen that in the English listening test, the first and fifth students have the best mental state, and both of them scored 50 points. The brainwaves collected by the second and fourth classmates are the same, and their mental state is the same. However, the test score of the second student was 41, and the score of the fourth student was 52. Obviously, the fourth student's learning situation is better; the last 3 students in the table may be drowsy during the test, so their grades are not very satisfactory. In addition, the collected brain waves are basically dominated by theta waves. Therefore, it is necessary to maintain a good mental state during the learning process, and the learning effect will be better.

5.3. Experimental Summary of This Article. Two experiments were designed this time. One is to analyze the students' learning ability from the English listening test scores, and the second is to analyze the students' learning situation from the brainwave signals of the students during the test combined with the test scores. Judging from the comparison of the two experiments and the data, in the first experiment, it is not comprehensive enough to judge the students' learning by their grades. Especially in each of the different types of tests, the level is uneven, and the learning situation is only on the

TABLE 2: Brain waves collected in English listening test.

Student	Dominant brain wave	Subdominant brain waves
1	B	α
2	A	θ
3	B	θ
4	A	θ
5	B	α
6	B	θ
7	\ominus	β
8	B	θ
9	\ominus	β
10	\ominus	β

TABLE 3: Listening test score sheet.

Student	Segment test	Ultrasonic section test	English sound change test	Total score
1	18	16	16	50
2	17	16	18	41
3	15	13	16	44
4	16	16	20	52
5	19	14	17	50
6	15	16	14	45
7	12	14	13	39
8	14	13	12	39
9	11	12	11	32
10	10	11	15	36

surface through the total score. In the second experiment, brain waves were collected during the test, which can deeply analyze the mental state of the students during the listening process. Looking at their learning situation in combination with their grades is completely different from the results analyzed in Experiment 1. The learning situation of students from the English listening test is only a small part, but it is necessary to complete the modeling through this data and analyze their comprehensive learning situation again [26].

6. Discussion on Brainwave Acquisition Terminal for English Listening Test

When designing the brainwave collection terminal for English listening test, this article discusses the entire production process of English listening audio and has a deep understanding of the audio changes of English listening audio after it is played. In order to ensure the stimulation of the human brain by the sound volume of the audio during the production process, the principle of noise reduction is used to adjust and demodulate the audio. In addition, the smart sensor of the Internet of Things protects the played audio from the influence of the space and the surrounding environment, ensuring that the sound coming into the brain is consistent. In addition, brainwave signal memory is affected by the external environment and physiological signals. Therefore, this article uses the intelligent sensors of the Internet of Things to distinguish and weaken the brain waves affected by the

external environment and physiological signals to achieve the accuracy of the brain wave signals. This article studies devices based on IoT smart sensors, which are more sensitive to brainwave collection. At the same time, the smart sensors of the Internet of Things can also be set up so that they can intelligently identify various types of brain waves. And it displays the brainwave signals we need in the display screen, so that it can be better used in our English listening test [27]. On the basis of smart sensors and previous brainwave devices, adding the Internet of Things and combining the two to invest in the field of education will be of great help to the completion of daily teaching content. This article has verified through experiments that the brainwave acquisition device studied in this article can collect brainwaves during the English test, and it helps teachers to deeply understand the test status of students in the listening test and can combine the test results to analyze the learning situation of the test. If the brainwave acquisition signal studied in this article is applied to the students' usual learning process, the students' usual learning data can be obtained, and the teacher can have a more specific and intuitive experience of analyzing the student's learning situation and help teachers improve teaching methods [28].

7. Conclusions

The brainwave acquisition terminal for English listening test based on the intelligent sensor of the Internet of Things studied in this paper has great reference significance for the application of science and technology in the education field. This article discusses the production process of English listening audio and the application of the Internet of Things in its production process. It combines the Internet of Things and smart sensors and studies the ability of the Internet of Things and sensors to perceive English audio and voice conversion capabilities, which lays the foundation for the subsequent brainwave collection terminal design. In this paper, IoT sensors are applied to the brainwave acquisition equipment for English listening test, and the accurate acquisition of English brainwaves is realized. It provides technical support for in-depth understanding of students' learning conditions, and to a large extent can help complete daily teaching tasks and promotes the maturity of brain wave acquisition device technology in the field of education. Of course, the brainwave acquisition terminal studied in this article is still in the preliminary development stage and is not very mature. This article hopes that it can be further improved in future research.

Data Availability

No data were used to support this study.

Conflicts of Interest

The authors declare that there are no conflicts of interest regarding the publication of this article.

Acknowledgments

This work is a Research and Innovation Team Project; project name: English Education Innovation Research Team (Project No. KCTD202006).

References

- [1] G. J. Ockey and R. French, "From one to multiple accents on a test of L2 listening comprehension," *Applied Linguistics*, vol. 37, no. 5, pp. 693–715, 2016.
- [2] R. Green, "Designing listening tests," *What makes a good listening task?*, pp. 115–143, 2017, (Chapter 5).
- [3] C. H. Lee, H. Y. Lee, S. L. Wu et al., "Machine comprehension of spoken content: TOEFL listening test and spoken SQuAD," *IEEE/ACM Transactions on Audio, Speech, and Language Processing*, vol. 27, no. 9, pp. 1469–1480, 2019.
- [4] B. Lee and J. Young, "Evidence supporting a validity argument for an English listening comprehension test," *The Journal of Mirae English Language and Literature*, vol. 21, no. 4, pp. 311–342, 2016.
- [5] S. Wang, "Listening test training in Beijing," *Journal of the Audio Engineering Society*, vol. 67, no. 5, p. 340, 2019.
- [6] D. Dal Palu, E. Buiatti, G. E. Puglisi et al., "The use of semantic differential scales in listening tests: a comparison between context and laboratory test conditions for the rolling sounds of office chairs," *Applied Acoustics*, vol. 127, no. dec, pp. 270–283, 2017.
- [7] K. Hiratsuka, "A question-answering inferencing system based on definition and acquisition of knowledge in written English text," *International Journal of Digital Information and Wireless Communications*, vol. 6, no. 4, pp. 292–298, 2016.
- [8] H. Wei, Y. Long, and H. Mao, "Improvements on self-adaptive voice activity detector for telephone data," *International Journal of Speech Technology*, vol. 19, no. 3, pp. 623–630, 2016.
- [9] I. Butun, P. Österberg, and H. Song, "Security of the Internet of Things: vulnerabilities, attacks, and countermeasures," *IEEE Communications Surveys & Tutorials*, vol. 22, no. 1, pp. 616–644, 2020.
- [10] J. Jun and L. Lee, "English-speaking children's acquisition of derivational morphology based on the affix level in the affix ordering hierarchy: analyses of the CHILDES database," *Korean Journal of Linguistics*, vol. 41, no. 3, pp. 521–543, 2016.
- [11] K. Lee, "The effects of controlled writing on English grammar acquisition of EFL College students," *English21*, vol. 30, no. 2, pp. 227–246, 2017.
- [12] R. S. Bhadoria and N. S. Chaudhari, "Pragmatic sensory data semantics with service-oriented computing," *Journal of Organizational and End User Computing*, vol. 31, no. 2, pp. 22–36, 2019.
- [13] S. Phoocharoensil, "Noun phrase accessibility hierarchy: a corpus-driven quest for order of difficulty in L2 English relative clause acquisition," *The International Journal of Communication and Linguistic Studies*, vol. 15, no. 3, pp. 17–29, 2017.
- [14] A. Sivieri, L. Mottola, and G. Cugola, "Building Internet of Things software with ELIoT," *Computer Communications*, vol. 89–90, no. 2, pp. 141–153, 2016.
- [15] N. Alhakbani, M. M. Hassan, M. Ykhlef, and G. Fortino, "An efficient event matching system for semantic smart data in the Internet of Things (IoT) environment," *Future Generation Computer Systems*, vol. 95, no. JUN, pp. 163–174, 2019.

- [16] Y. Seon and D. Hat, "Connectivity frameworks for smart devices: the Internet of Things from a distributed computing perspective," *Computing Reviews*, vol. 58, no. 7, pp. 386-387, 2017.
- [17] T. Wang, H. Luo, W. Jia, A. Liu, and M. Xie, "MTES: an intelligent trust evaluation scheme in sensor-cloud-enabled industrial Internet of Things," *IEEE Transactions on Industrial Informatics*, vol. 16, no. 3, pp. 2054-2062, 2020.
- [18] R. Dan, "Inside the Internet of Things. Water efficiency," *The journal for water conservation professionals*, vol. 13, no. 3, pp. 22-30, 2018.
- [19] K. P. Thomas and A. P. Vinod, "Toward EEG-based biometric systems: the great potential of brain-wave-based biometrics," *IEEE Systems, Man, and Cybernetics Magazine*, vol. 3, no. 4, pp. 6-15, 2017.
- [20] R. C. Aguilera, M. P. Ortiz, J. P. Ortiz, and A. A. Banda, "Internet of things expert system for smart cities using the blockchain technology," *Fractals*, vol. 29, no. 01, pp. 2150036-2150060, 2021.
- [21] B. George, J. K. Roy, and V. J. Kumar, "Interfaces for autarkic wireless sensors and actuators in the Internet of Things," *[Smart Sensors, Measurement and Instrumentation] Advanced Interfacing Techniques for Sensors Volume*, vol. 25, pp. 167-189, 2017, Chapter 5.
- [22] M. Antonini, M. Vecchio, F. Antonelli, P. Ducange, and C. Perera, "Smart audio sensors in the Internet of Things edge for anomaly detection," *IEEE Access*, vol. 6, no. 99, pp. 67594-67610, 2018.
- [23] V. Angelakis and E. Tragos, "Security and privacy for the Internet of Things communication in the SmartCity," *Springer International Publishing*, pp. 109-137, 2017, Chapter 7.
- [24] I. Ubhayaratne, M. P. Pereira, Y. Xiang, and B. F. Rolfe, "Audio signal analysis for tool wear monitoring in sheet metal stamping," *Mechanical Systems and Signal Processing*, vol. 85, no. feb, pp. 809-826, 2017.
- [25] T. Tang and A. T. K. Ho, "A path-dependence perspective on the adoption of Internet of Things: evidence from early adopters of smart and connected sensors in the United States," *Government Information Quarterly*, vol. 36, no. 2, pp. 321-332, 2019.
- [26] K. F. Tsang and V. Huang, "Conference on sensors and Internet of Things standard for smart city and inauguration of IEEE P2668 Internet of Things maturity index [chapter news]," *IEEE Industrial Electronics Magazine*, vol. 13, no. 4, pp. 130-131, 2019.
- [27] P. Xu, D. Flandre, and D. Bol, "Analysis, modeling, and design of a 2.45-GHz RF energy harvester for SWIPT IoT smart sensors," *IEEE Journal of Solid-State Circuits*, vol. 54, no. 10, pp. 2717-2729, 2019.
- [28] R. A. Potyrailo, "Correction to multivariable sensors for ubiquitous monitoring of gases in the era of Internet of Things and industrial Internet," *Chemical Reviews*, vol. 116, no. 23, p. 14918, 2016.

Research Article

New Technological Measures of Sustainable Buildings in Triple Bottom-Line Analysis

Yi Ding 

Department of Civil Engineering, The University of Melbourne, Melbourne 3000, Australia

Correspondence should be addressed to Yi Ding; yddin1@student.unimelb.edu.au

Received 18 May 2022; Revised 6 July 2022; Accepted 14 July 2022; Published 4 August 2022

Academic Editor: Xuefeng Shao

Copyright © 2022 Yi Ding. This is an open access article distributed under the Creative Commons Attribution License, which permits unrestricted use, distribution, and reproduction in any medium, provided the original work is properly cited.

At present, China is in a period of rapid urbanization, and the concept of green structure is getting more and more attention. Green structures can solve asset utilization and ecological problems brought about by rapid urbanization. Therefore, green structure has become the only way for the development of China's construction industry. This paper aims to study the feasibility analysis of new green building technology measures. The related concepts of green building, the analytic hierarchy process, and the meaning of life cycle cost are proposed. The main assessment bottom lines include engineering, environmental, social, and economic bottom lines. From the application examples of green building technology in the starting area of Guangzhou International Financial City, it can be seen that, based on the green building technology proposed in this paper, it is necessary to sort out specific technologies and practices suitable for the actual application of the project in a specific project. Then, the applicability and incremental cost of each technology can be analyzed, and finally, a green building technology system suitable for specific project applications is formed. The experimental results show that compared with residential buildings, the increase of public buildings is 338 million yuan, and the increase of nonassigned parts is about 9.84 million yuan.

1. Introduction

As cities continue to grow in size and overall populations, interest in energy and assets in urban communities continue to expand, and so does disease in urban communities. With people's in-depth thinking on urban issues, the concepts of "sustainability" and "green" have gradually become a consensus around the world. In the context of large-scale urbanization, the construction industry has entered an era of relatively rapid development. Large-scale building demolition makes large buildings occupy a lot of land resources, consume a lot of water resources, and have a great negative impact on urban air quality and microenvironment. The waste generated from the construction to the demolition process of the building will have a huge load on the ecological environment.

The optimization and integration of green building comprehensive evaluation system is an important research direction in the current green building field. The research on the evaluation system is conducive to the development of the evaluation and comparison of green buildings and helps to

formulate evaluation standards for green buildings. It also contributes to the design, construction, operation, and management of green buildings. The concept of green building includes not only the quality of the indoor environment but also the impact of the building on the external environment. The innovation of this paper is to discuss the feasibility analysis of new green building technology measures, which has certain innovation and practicability, and is conducive to the sustainable development of economy and society.

2. Related Work

With the escalation of the logical inconsistency between monetary turn of events and ecological security, the basic and broad plan strategies for the customary development industry have been not able to meet the necessities of practical turn of events, green structure energy preservation, and natural assurance, which will definitely turn into the prerequisites of future structures. Accordingly, the improvement of the development business has turned into an

examination area of interest. Shi and Song started from the green building theory, which combines the characteristics of life cycle cost and takes sustainable development as the guide. The green building cost is divided into five stages: decision making, design, construction and commissioning, operation and maintenance, and recovery [1]. Blanco et al. accepted that a manageable innovation for further developing energy effectiveness in structures is the utilization of metropolitan vegetation, and found that building indoor air temperature relies upon a few distinct boundaries. These boundaries are connected with the environment of the area, the actual structure, and its motivation [2]. Liu established a virtual building model using building information modeling (BIM) and used this model to analyze and simulate the annual energy consumption [3]. Gogoi expounded the characteristics of green buildings and tried to find out the factors that affect the satisfaction of occupants in purchasing or recommending green buildings [4]. However, the shortcoming of these studies is that they are too one-sided.

With the development of social economy, more and more scholars have conducted research on AHP. Jagtap and Bewoor introduced the application of analytic hierarchy process (AHP) in the identification of key equipment in thermal power plants [5]. Emmanuel proposed a higher education teaching evaluation method combining analytic hierarchy process (AHP) and data envelope analysis (DEA) [6]. Ahmed et al. proposed a goal-based AHP method. The method assigns pairwise comparison values based on field data collected from the Mumbai city road network (consisting of 28 road segments) [7]. For exact testing utilizing well-being administrations research instruments, Agapova et al. met a false ACR AC board of crisis division radiologists and nonradiologists. The general propriety of imaging studies to analyze thought a ruptured appendix was evaluated by multistandard choice examination [8]. However, the shortcoming of these studies is that the model is not scientific enough and needs to be further improved.

3. Relevant Methods for the Feasibility Deconstruction of New Green Building Technical Measures

3.1. Green Building Technology

3.1.1. Green Building Technology Development Process. As per the turn of events and activity of green structure innovation, the existence pattern of green structure innovation improvement is isolated into five phases and three periods [9]. The specific stages are shown in Figure 1.

In the generation stage, in the process of conception and gestation of green building technology, the main work includes the initial conception of technology and the generation of technology prototype. The second stage of green building technology development is the technical review stage. At this stage, a specific analysis is carried out to generate the technology of the stage, and a feasibility study report of the technology is formed. The technical design stage is the third stage of technical development, and the

work in this stage includes preliminary design and construction drawing design. In the fourth stage of technical construction, green building technology is put into operation, and the main work includes technical preparation, technical construction, and technical completion acceptance. As the last stage of green building technology development, the use feedback stage often requires a longer feedback time and, at the same time, can best reflect the technical operation effect, also known as the posttechnical evaluation stage [10].

3.1.2. Material Selection and Construction of Green Buildings. Building materials are an integral part of buildings, and green building materials are the basis for green buildings. At present, one of the reasons why the concept of sustainable building development in China is not implemented in place is that building materials consume high resources and energy in the production process and use process, causing serious environmental pollution [11–13]. Trying to use environmentally friendly and pollution-free green building materials and vigorously building green buildings is one of the effective ways to save energy and protect the environment.

In recent years, green building materials used in buildings include ecological cement, green ecological concrete, green paint, green glass, and other green materials (as shown in Table 1).

The basic mineral composition and performance of ecological cement are similar to ordinary cement, but the quality is high and the cost is low. There are many types of green ecological concrete. Permeable concrete has water permeability and is mainly used for road and ground pavement, with great application potential. At present, 7%–15% of urban roads in China are covered by concrete. Sound-absorbing concrete can significantly reduce noise, mainly used in airports, highways, subways, and other places where constant noise is generated [14, 15]. Green HPC extends the life of buildings and is cost-effective. Green paint has the characteristics of strong adhesion, long service life, and harmless to people. It is a high-performance paint. Low-E glass is a kind of green glass, which can greatly reduce the dissipation and radiation of indoor heat to outdoor spaces [16].

3.1.3. Theoretical Basis for Economic Analysis of Green Buildings

(1) The Principle of Correlation Analysis. Statistical analysis of correlation is one of the commonly used methods in economics. The calculation principle of the correlation coefficient is as follows: in the first place, the covariate of the two factors is determined, and afterward partitioned by the different scattering and standard deviation of the two factors to normalize to acquire a normalized score with a unit eliminated [17]. The calculation formula of the correlation coefficient is as follows:

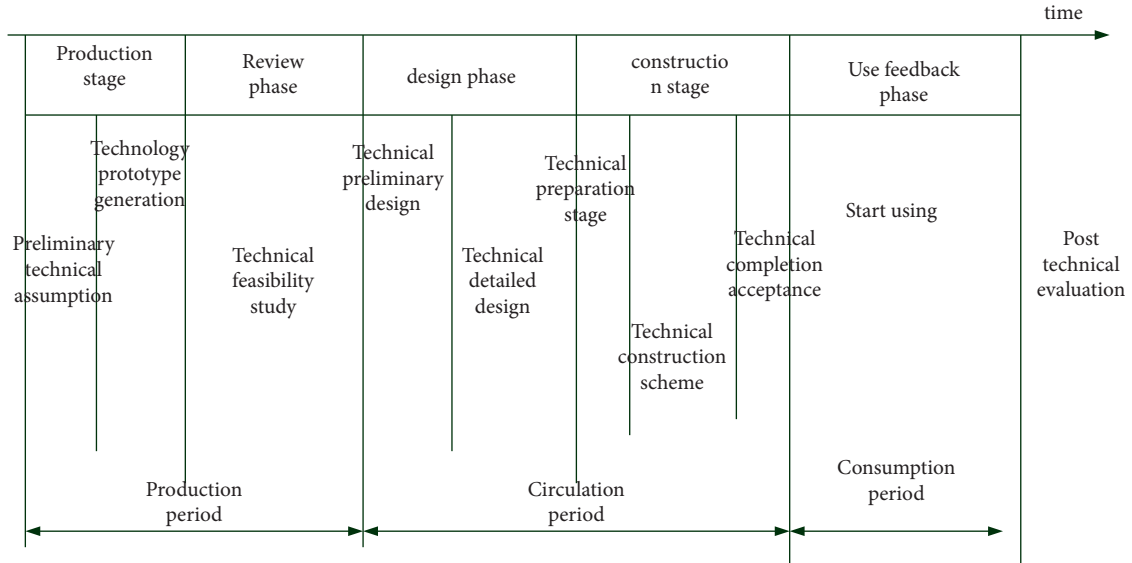


FIGURE 1: Development process of green building technology in the whole life cycle.

TABLE 1: Classification statistics of green building materials.

Serial number	First-class classification of green building materials	Secondary classification of green building materials
1	Green cement	
2	Green concrete	Permeable concrete; sound-absorbing concrete; radiation proof concrete; keywords green high-performance concrete; recycled concrete; plant compatible concrete
3	Green paint	Waterborne coatings; solvent-free coating; solvent-based coatings with high solid content; powder coating
4	Green glass	Hollow glass; vacuum glass; low radiation glass; smart glass
5	Other green materials	Thermal insulation materials; waterproof materials; green chemical building materials; other new products of green building materials

$$r = \frac{\text{cov}(a, b)}{S_a S_b},$$

$$= \frac{\sum(A - \bar{A})(B - \bar{B})}{\sqrt{\sum(A - \bar{A})^2 \sum(B - \bar{B})^2}}$$

(1)

$$T = \frac{P}{\sqrt{1 - p^2/n - 2}}$$

$$= \frac{p\sqrt{n-2}}{\sqrt{1 - p^2}}$$

(2)

The correlation coefficient r is between -1 and 1 . A positive value indicates a positive correlation between the variables, and a negative value indicates a negative correlation between the variables. The degree of correlation between variables is proportional to the absolute value of the r coefficient. A and B are the independent variable and dependent variable in the sample point, respectively. \bar{X}, \bar{Y} are the mean of the independent variable and the mean of the dependent variable in the sample points, respectively. Since the correlation coefficient is a t-distribution, the test of the correlation coefficient is as follows:

- (a) Make assumptions: $H_0: R=0; H_1: R \neq 0$;
- (b) Calculate the value of the statistic based on the data of the research sample:

Among them, n is the number of samples.

- (c) Carry out inspection and judgment:

When the significance level is ∂ , we check the T distribution table, the degree of freedom is $n-2$, and the corresponding critical value is $T_{\partial/2}(n-2)$. If there is $|T| > T_{\partial/2}(n-2)$, the null hypothesis should be rejected, which means that at the significance level of ∂ , the two variables are significantly related. Otherwise, the null hypothesis should be accepted that at significance level ∂ , the two variables are not correlated [18].

(2) *The Principle of Linear Regression Analysis.* The main purpose of regression analysis is to build a regression model with the help of independent variables; according to the

measured data, the parameters of each index in the model are solved. The reliability of the model is judged by the degree of fit between the predicted data and the measured data, so that the model can be used to predict the relative dependent variables.

Generalized mathematical model for multiple linear regression analysis. Let the predictable variable be B , which is affected by m variables A_1, A_2, \dots, A_m and unpredictable random factors, the general multiple linear regression model is expressed as follows:

$$B = \beta_0 + \beta_1 A_1 + \beta_2 A_2 + \dots + \beta_m A_m + \varepsilon. \quad (3)$$

Among them, $\beta_1, \beta_2, \dots, \beta_m$ is the regression coefficient. For the existing n sets of sample data, it can be expressed as follows:

$$\begin{bmatrix} B_1 \\ B_2 \\ \dots \\ B_n \end{bmatrix} = \begin{bmatrix} 1 & a_{11} & \dots & a_{m1} \\ 1 & a_{12} & \dots & a_{m2} \\ \dots & \dots & \dots & \dots \\ 1 & a_{1n} & \dots & a_{mn} \end{bmatrix} \cdot \begin{bmatrix} \beta_0 \\ \beta_1 \\ \dots \\ \beta_m \end{bmatrix} + \begin{bmatrix} \varepsilon_1 \\ \varepsilon_2 \\ \dots \\ \varepsilon_n \end{bmatrix}. \quad (4)$$

This matrix can be rewritten as $B = A \cdot \beta + \varepsilon$. The least square method is used to calculate the value of the model regression coefficient β . First, the sum of squares of errors (SSE) must be minimized so that the minimum sum of squares of errors can be obtained through the partial differentiation of formula (5) to β .

$$SSE = (B - X\beta)' \cdot (B - X\beta). \quad (5)$$

Among them, ε' is the transpose matrix of ε . The normal formula to obtain the least squares theory is $(A' A)\beta = AB$.

Therefore, the regression coefficient matrix can be obtained as follows:

$$\beta = (A' A)^{-1} AB. \quad (6)$$

Tests of regression mathematical models. After the model is established, it is also necessary to test the model and calculate the prediction error. Tests of regression mathematical models include the following: fit degree test, overall model significance test, regression coefficient significance test, collinearity diagnosis, and homogeneity of variance test [19]. In the fit test, the coefficient of determination R^2 represents the fit and explanatory power of the linear regression model established by the independent and dependent variables. The value of R^2 is between 0 and 1, and the closer to 1, the higher the degree of fit. The formula for calculating R^2 is as follows:

$$R^2 = \left(\frac{\sum (A - \bar{A})(B - \bar{B})}{\sqrt{\sum (A - \bar{A})^2} \sqrt{\sum (B - \bar{B})^2}} \right)^2. \quad (7)$$

The F test was used to determine whether the overall regression model was significant. The variance is decomposed to calculate the value of the F statistic. When the F

value is larger, the significance level is higher. The formula for calculating F is as follows:

$$F = \frac{\sum (\hat{B} - \bar{B})^2 / m}{\sum (B - \hat{B})^2 / (n - m - 1)}. \quad (8)$$

Among them, SSR refers to the variance between the sample point and the average point; SSE refers to the variance of the distance from the sample point to the regression point. F obeys $F(m, n - m - 1)$ distribution. When the significance level is ∂ , if F is greater than $F_{\partial}(m, n - m - 1)$, it indicates that the overall regression model is significant and can be used for prediction; otherwise, it is not significant.

The T test was used to judge whether the regression coefficient of the regression model was significant. The formula for calculating the T statistic is as follows:

$$T_u = \frac{\hat{\beta}_u}{\hat{\sigma} / \sqrt{\sum_{v=1}^n (A_{uv} - \bar{A}_u)^2}}. \quad (9)$$

Among them,

$$\hat{\sigma} = \sqrt{\frac{\sum_{u=1}^n (B_u - \hat{B}_u)^2}{n - m - 1}}. \quad (10)$$

The statistic T obeys the $T(n - m - 1)$ distribution. When the significant level is ∂ , if there is a T greater than $T_{\partial}(n - m - 1)$, the regression coefficient reaches the significant level. Otherwise, it is not significant. In addition to the insignificant correlation between the independent variable and the dependent variable, there are other reasons for the insignificant regression coefficient. For example, the number of samples or variables is too small, and a certain independent variable and other independent variables have complex collinearity [20].

In order to avoid the correlation between independent variables being too high, affecting the stability and significance of the regression coefficient, and making the analysis results of the regression model difficult to interpret, a complex collinearity analysis should be carried out on the independent variables. We use tolerance or variance inflation factor (VIF) to assess the degree of collinearity of independent variables. Tolerance is calculated as follows:

$$\text{Tolerance} = 1 - R_u^2. \quad (11)$$

Among them, R_u^2 is the square of the complex correlation coefficient between the i th independent variable and other independent variables.

Tolerance and VIF are reciprocals of each other. The value of tolerance is between 0 and 1. The closer to 0, the stronger the collinearity is; the closer to 1, the weaker the collinearity. Similarly, the larger the VIF, the higher the degree of collinearity between variables. When the VIF is greater than or equal to 10, it means that there is a serious multicollinearity between the variables.

Self-correlation analysis. After the model is established, the error between the regression value and the actual value should not only show a random normal distribution but also

the errors generated between the variables should be independent of each other without self-correlation [21]. The DW statistic is used to determine whether the error terms are independent, and the calculation formula is as follows:

$$DW = \frac{\sum_{u=2}^n (\varepsilon_u - \varepsilon_{u-1})^2}{\sum_{u=2}^n \varepsilon_u^2}. \quad (12)$$

The value of DW is between 0 and 4. When DW is 0, it means complete positive autocorrelation; when DW is between 0 and 2, it means that there is positive autocorrelation; when DW is 2, it means no autocorrelation. DW between 2 and 4 indicates that there is a negative autocorrelation; DW of 4 indicates a complete negative autocorrelation. Generally, when the DW value is between 1.5 and 2.5, it can be considered that there is no self-correlation phenomenon. The test of the significant relationship and correlation of the regression model is based on the assumption of the regression model. If the assumption of the model does not hold, the regression model cannot be used, so the regression hypothesis should be tested.

3.2. Hierarchical Deconstruction Process

3.2.1. The Concept of AHP. AHP is a hierarchical weighted decision analysis method proposed in the early 1970s. As analytic hierarchy process (AHP) can be seen from the name, this method is that when using AHP to analyze problems, it is necessary to first concretize and stratify the layers. Then, a hierarchical organization model is established [22–24]. Through the hierarchical model, the research question will be composed of several elements, which form a hierarchy according to the logical relationship, which can generally be divided into three categories: the highest layer, the middle layer, and the lowest layer. Analytic hierarchy process is divided into four steps, namely, the creation of the ladder hierarchical structure model, the establishment of each judgment matrix in each layer, the single-level sorting and the total sorting, and their respective consistency checks. The specific operation process can be seen in Figure 2 [25].

AHP is a systematic analysis method, and it is concise and practical. We effectively combine qualitative and quantitative methods, decompose complex problems, and make it easier to grasp and understand. At the same time, AHP requires less data and information, and focuses more on qualitative analysis and judgment than the general quantitative method, and finally realizes qualitative and quantitative optimization problem decision analysis.

3.2.2. The Basic Steps of AHP. The first premise of establishing a hierarchical model is to fully understand the problem that needs to be solved. On the basis of fully understanding the problem, it is necessary to grasp the scope and factors contained in the problem, and to understand the mutual relationship and subordination of these factors. Only after having a clear understanding of the above content can we classify the factors involved in the problem to be analyzed. We construct a hierarchical model diagram with interconnected elements as shown in Figure 3.

- (1) The highest level (target level) represents the problem that needs to be solved; that is, the overall goal is to be achieved by the analytic hierarchy process.
- (2) The middle layer (criteria layer) represents the intermediate link to achieve the overall goal, such as the criteria and indicators for measuring the overall goal.
- (3) The bottom layer (the solution layer) represents various solutions and measures selected to solve the problem.

3.2.3. Weight Vector of the Judgment Matrix $A = (x_{uv})_{n \times n}$

- (1) Calculate the product of all elements of each row of the matrix, that is:

$$y_u = \prod_{v=1}^n x_{uv} \quad (u = 1, 2, \dots, n). \quad (13)$$

- (2) Find the n th root of y_u , that is:

$$W_u = \sqrt[n]{y_u} \quad (u = 1, 2, \dots, n). \quad (14)$$

- (3) Normalize the vector W , that is:

$$Q = \frac{W_u}{\sum_{k=1}^n W_k} \quad (u = 1, 2, \dots, n). \quad (15)$$

Then $Q = (Q_1, Q_2, \dots, Q_n)^T$ is the required weight vector, which indicates that for the overall target M , the weight of each criterion Z_u is Q_1, Q_2, \dots, Q_n , and Z_1, Z_2, \dots, Z_n can be sorted in a hierarchical order with a value of Q_u .

3.2.4. Consistency Test of Judgment Matrix. When the compared elements are ambiguous and complex, in general, the constructed judgment matrix cannot be completely guaranteed to be completely consistent. At this time, the largest eigenroot λ_{\max} of the judgment matrix A will be greater than the order n of the matrix, and there are other eigenvalues that are not 0. If we make the largest eigenroot λ_{\max} of the judgment matrix close to n and make other eigenvalues close to 0, we can make the judgment matrix have a satisfactory consistency. This further ensures that reasonable results are obtained. Then, in order to judge whether the consistency of a matrix meets the satisfactory requirements, it is necessary to carry out the consistency test.

First, we need to obtain λ_{\max} (maximum eigenroot) of the judgment matrix A according to the following formula:

$$\lambda_{\max} = \sum_{u=1}^n \frac{(AQ)_u}{nQ_u} \quad (u = 1, 2, \dots, n). \quad (16)$$

Among them, AW is the product of the judgment matrix A and the eigenvector Q , and $(AQ)_u$ is the u th component of AQ .

Next, we calculate the consistency index (C.I.)

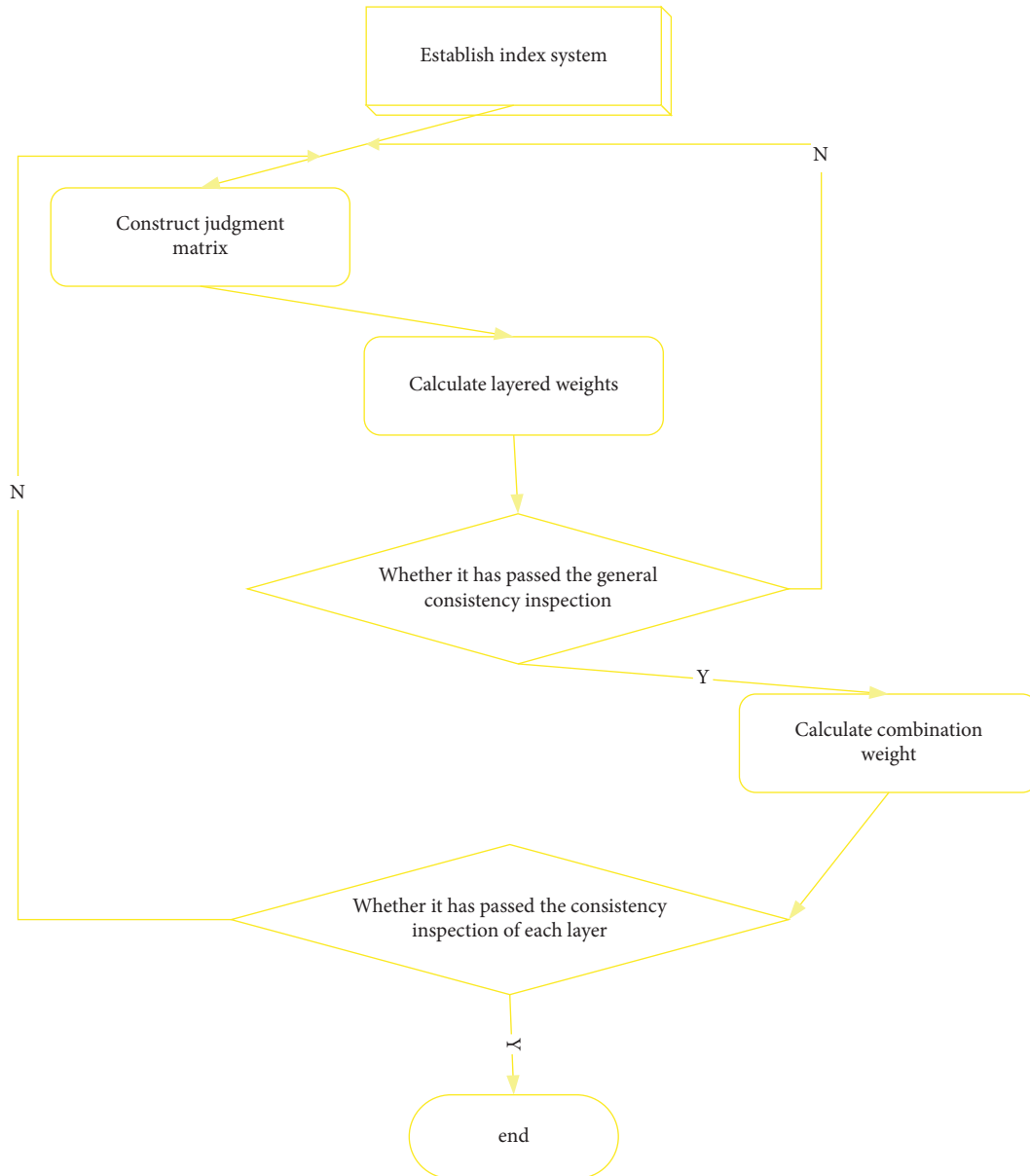


FIGURE 2: Step diagram of AHP.

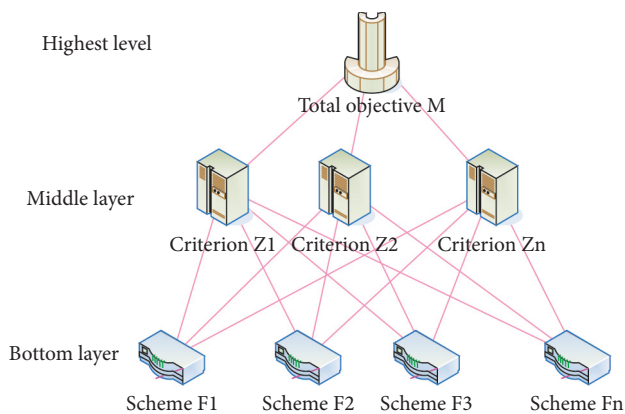


FIGURE 3: Analytic hierarchy structure model diagram.

$$C.I. = \frac{(\lambda_{\max} - n)}{(n - 1)} \tag{17}$$

Furthermore, C.R. is obtained by the following formula:

$$C.R. = \frac{C.I.}{R.I.} \tag{18}$$

In the formula, C.R. is the consistency ratio, and R.I. is the average random consistency index.

3.3. Life Cycle Costs

3.3.1. *Definition of Life Cycle Cost Analysis.* Life cycle cost (LCC) was first proposed by the US Department of Defense, and this theory was applied to the procurement of military equipment. The U.S. Department of Defense originally

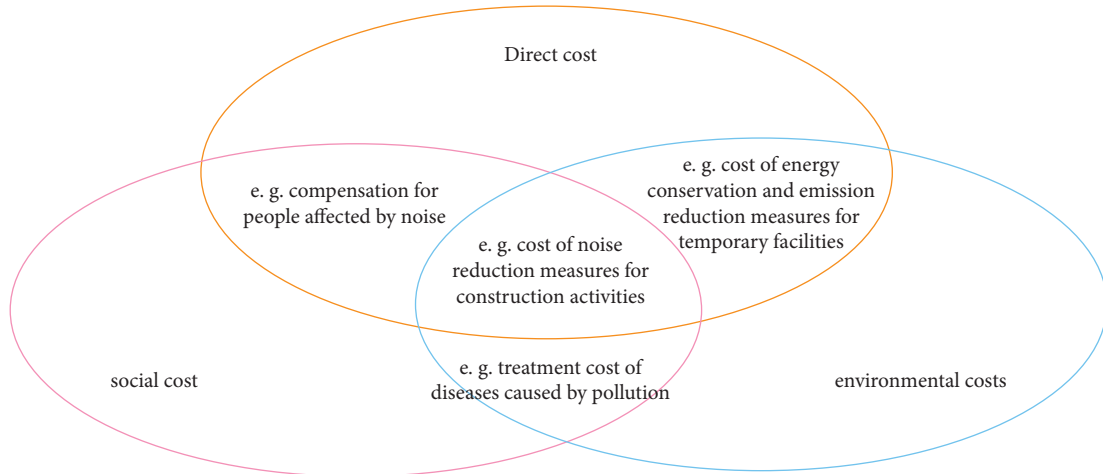


FIGURE 4: Schematic diagram of generalized life cycle cost.

defined LCC as the total cost to the government to set up and acquire the system and the life cycle of the system, which includes development, setup, use, logistical support, and decommissioning. Life cycle costs calculated earlier are static costs and do not take into account the time value of money. Its schematic figure is shown in Figure 4.

Life cycle cost refers to the sum of costs throughout the entire life process of a product. Generally speaking, it includes various costs from the research, design, production, use of the product to the research, design, production, use, maintenance, and the final disposal stage of the waste life process [26].

Based on different perspectives and classification methods, the life cycle cost of a product can be divided into different parts. Generally speaking, the life cycle cost of a product can be divided into external cost and internal cost. External cost refers to the synthesis of all environmental costs in the life cycle process, while internal cost refers to the cost of raw materials and basic engineering invested by the enterprise in the production process of the product.

3.3.2. *Technical Framework of Life Cycle Cost Analysis.* Unlike LCA, LCC currently does not have internationally accepted implementation methods and steps. Based on the comprehensive analysis of previous research results, this paper summarizes the implementation steps of LCC with reference to the technical framework of life cycle assessment, which is also based on the idea of life cycle. It can be summarized as the following steps, and the details are shown in Figure 5.

Step 1: the determination of the evaluation scope. Similar to a life cycle assessment, the first step in an LCC study is to define the scope of the study, which generally covers the entire life cycle of the product or process, but also depends on the actual situation. This step determines the scope of application of LCC and the size of the subsequent workload.

Step 2: Identify the costs of each stage. We divide the life cycle stages of the product according to the determined evaluation scope, track the energy flow and

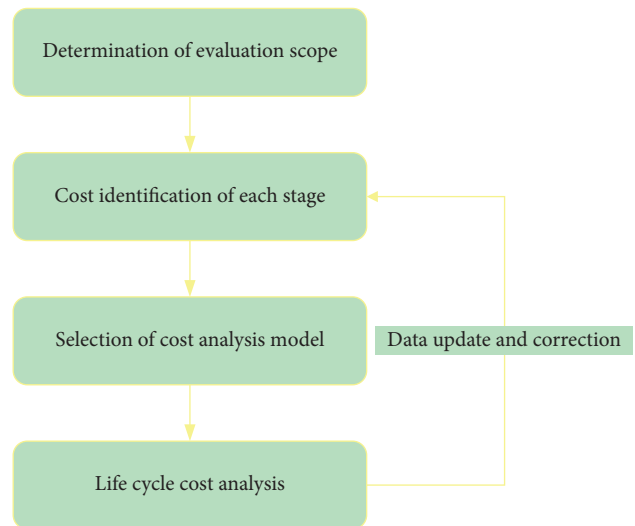


FIGURE 5: Life cycle cost analysis technology roadmap.

material flow of each stage, conduct inventory analysis, and obtain the cost list of different stages.

Step 3: the choice of cost analysis model. On the basis of the above steps, the possible costs of each stage are summarized, an appropriate cost analysis model is selected, and a reasonable cost structure is constructed so that each cost has a clear cost relationship.

Step 4: life cycle cost analysis. We choose an appropriate analysis method to analyze each element in the life cycle cost model. Commonly used analysis methods include linear regression, correlation analysis, and sensitivity analysis.

4. Experiment Deconstruction with Suitable Green Building Technology in the New Urban Area of Guangzhou

4.1. *Deconstruction of the Status Quo of Green Building Development in China.* Since the first application for the green

building label in 2008, from the deployment of various central documents to the implementation of corresponding local laws, the management system related to green buildings has been gradually improved, which has laid a good social environment for the vigorous development of green buildings in China (Figure 6). As of December 31, 2014, a total of 2,538 green building project labels have been applied for and evaluated (including design labels and operation labels) nationwide, covering an area of 290 million square meters. Among them, there are 2,379 design and identification projects (with an area of 21.118 million square meters), accounting for 93.7% of the total number of applications. There were 159 operating identification projects (with an area of 19.547 million square meters), accounting for 6.3% of the total number of applications. Compared with 2008, the total number of applications for green building labels has increased by 109 times. It can be seen that the social consensus on the development of green buildings in China has gradually formed.

The projects applying for the green building evaluation label are mainly one-star and two-star levels, and three-star level is lower than the former two [27]. Taking the data from 2008 to 2014 as an example (as shown in Figure 6(a)), there are 966 one-star projects (126.328 million square meters), 1054 two-star projects (118.505 million square meters), and 518 three-star projects (45.868 million square meters).

Guangzhou's green building work has been developed from point to face to ecological city construction, and a local green building policy, technology, and management system has been initially established. At present, Guangzhou is creating a green eco-city area, hoping to effectively control the quality of Guangzhou's development and become an advanced area of national green buildings. At the same time, in order to implement the new requirements put forward by the central government since the 18th National Congress of the Communist Party of China, the special green building work in Guangzhou urgently needs to start the research work on the implementation of the green technology system and form a green building technology application system that can guide the planning and design [28].

For the types of buildings applying for label certification, the 51% rate for residential buildings is slightly higher than 48% for public buildings and only 0.9% for industrial buildings. The participation of residential buildings and public buildings in green building evaluation already has a certain social cognition foundation, but the participation of industrial buildings in the evaluation of green building labels started late and developed slowly. Up to now, China has evaluated 28 green industrial building projects, including 3 three-star operation logos. The identification projects are distributed in 8 provinces and cities, 5 of which are coastal provinces. Guangdong and Jiangsu provinces, which are ranked high in terms of GDP, are particularly advanced in the number of applications for green industrial building labels. It can be seen that the local high economic level and the development level of civil green buildings also affect the degree of local industrial building development (Figure 7).

4.2. Four Bottom Lines of Deconstructing Architecture

4.2.1. nBL Evaluation Overview. This report uses the nBL assessment method. The nBL is a consistent structure that distinguishes and integrates significant elements into the strategy pursuing cycle and choice settling on process by guaranteeing that choices follow manageability standards. The report evaluates four bottom lines. The first bottom line is the engineering bottom line, which mainly includes fire resistance, seismic resistance, life, and main functions of the structure. The second bottom line is the environmental bottom line, which mainly includes environmental bottom line, mercury emissions, energy emissions, and recyclability. The third bottom line is the social bottom line, which mainly includes volume control, noise control, competition, community, and stress relief. The last bottom line is the economic bottom line, which mainly includes material cost, energy consumption rate, and saving of recyclable materials [29].

There are six stages from choosing markers, gathering significant information to changing information into ultimate conclusion values, which can be utilized to assess BAU and the first-level marks of options. To begin with, we pick a pointer. Second, gather logical information for tertiary markers. This information should be in a similar unit for additional correlation. Then, the information is standardized, weighted, and totaled. At long last, we analyze BAU and elective arrangements. These issues will be talked about exhaustively beneath.

4.2.2. Selection and Description of Indicators. In the first place, we pick a proper marker in view of the reason for the pointer, the spatial size of the undertaking, and the time span. The reason for these measurements is to think about the manageability of BAU and elective arrangements really. The spatial size of the task is situated at the University of Melbourne's Parkville grounds. The time span is from the material to the development handling stage. Based on these three factors, secondary and tertiary indicators were selected. A detailed description of each indicator is discussed in Figure 8.

4.2.3. Normalization, Weighting, and Aggregation. Subsequent to gathering BAU values and choices for each level-3 pointer, the information was standardized utilizing formula (19). Then, markers were emotionally weighted by the strength of significance utilizing the analytic hierarchy process (AHP) Saaty's pairwise rating scale. We standardize the segments by isolating the heaviness of every section by the complete load of every segment. After this, the amount of every segment ought to be one, and the last weight is the normal of each column. The measurements are then collected utilizing the added substance accumulation technique (formula (20)). The result of the standardized file and the weight is the collected measurement, which is the worth of each level 2 measurement. Therefore, the values of the level 3 indicators are aggregated into the values of the level 2 indicators. We repeat the same steps to aggregate the values of

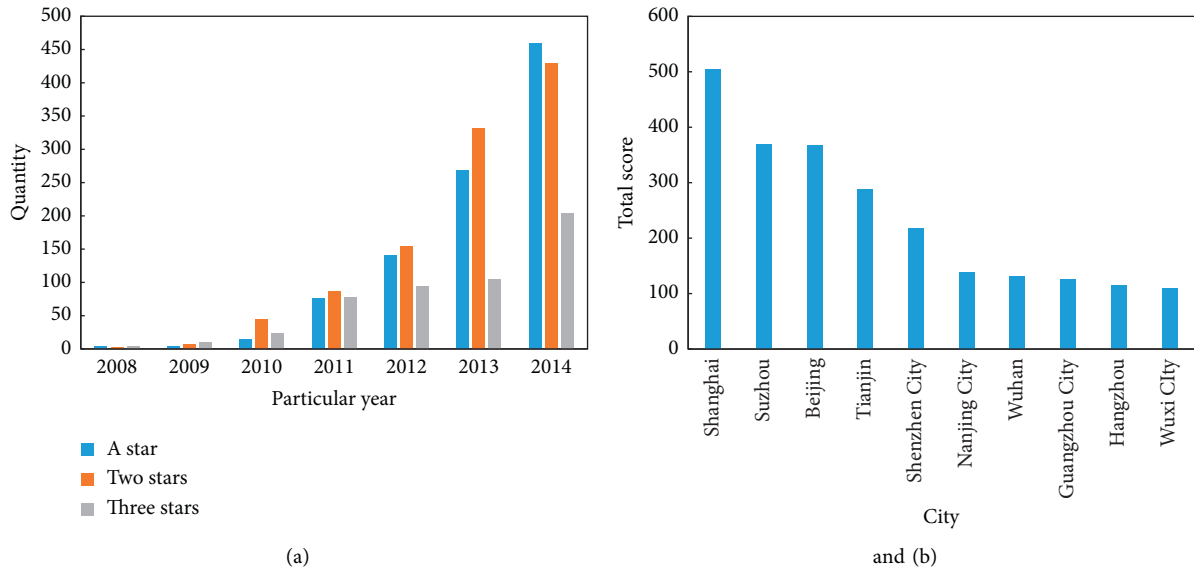


FIGURE 6: Status and ranking of green building development in China: (a) Status Quo of Green Building Development (2008–2014) and (b) ranking by the total score of urban green buildings in the “Green Building Map” website database.

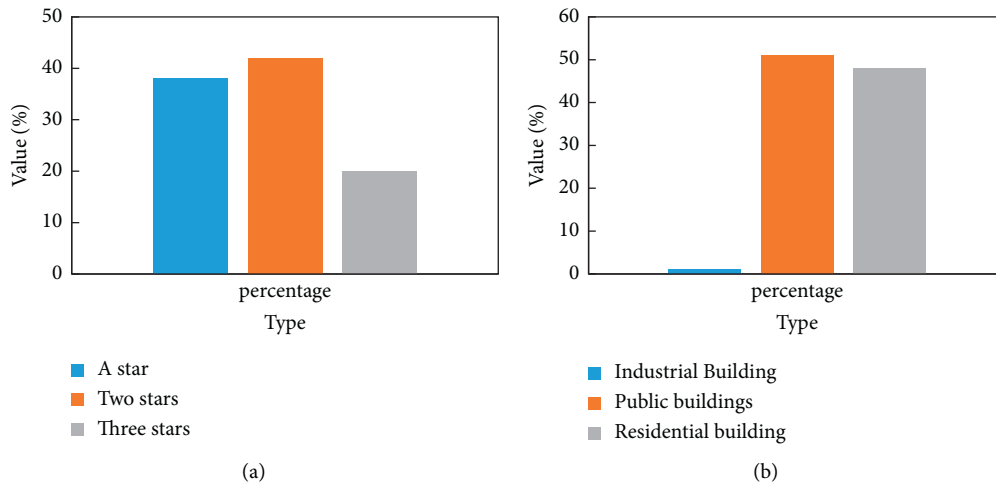


FIGURE 7: The distribution of stars and types of buildings with green building evaluation labels from 2008 to 2014: (a) star distribution of green building evaluation signs and (b) building type distribution of green building evaluation signs.

the level 2 metrics into the values of the level 1 metrics. First, level 2 indicators are subjectively measured according to the strength of their importance. We standardize the sections so every segment totals to one. Then, the result of the weight and the standardized record is the totaled incentive for each level 1 pointer.

$$\text{Normalized Index} = \frac{\text{Indicator value} - \text{worst value}}{\text{best value} - \text{worst value}}, \quad (19)$$

$$\text{Aggregated Indicator} = \sum (\text{Weight} * \text{Normalized Index}). \quad (20)$$

The loads of the four button lines (designing, financial, social, and natural) are emotional. The designing primary

concern includes fire and seismic tremor opposition and the life span of the structure, with an accentuation on the wellbeing of the structure. Simply by guaranteeing the wellbeing of the structure and individuals inside will the remainder of the conversation be significant. Along these lines, indeed, designing is the main model. This report expects that proprietors have serious areas of strength for a natural manageability.

4.2.4. *Weights and Results of Economic Indicators.* Its weight distribution is shown in Table 2 and Figure 9.

4.2.5. *Comprehensive Evaluation Results.* The weights of the four button rows (engineering, economic, social, and

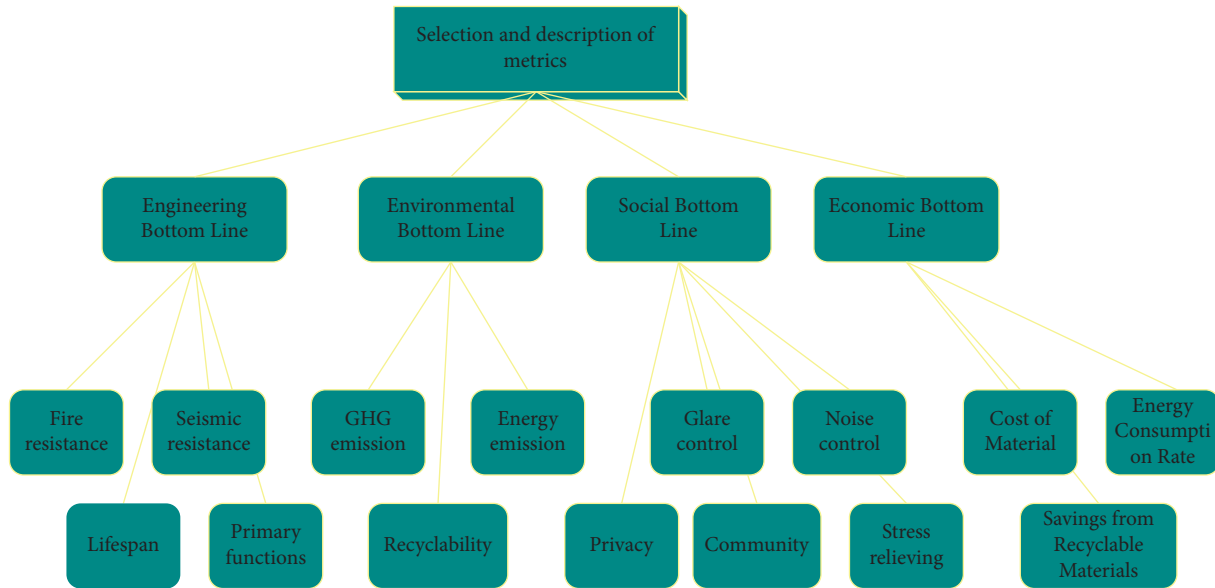


FIGURE 8: Metric selection and description.

TABLE 2: Weight distribution.

Level 1 aggregated	BAU	Economic BL		
	ALT		0.661	
			0.444	
Level 2 aggregated		Life cycle costs		Benefits
	BAU	0.791		0.400
	ALT	0.432		0.466
	Weights	0.667		0.333
Level 3 aggregated		Cost of material	Energy consumption rate	Savings from recycling of external wall
	BAU	0.787	0.800	0.400
	ALT	0.214	0.869	0.466
	Weights	0.667	0.333	1.000

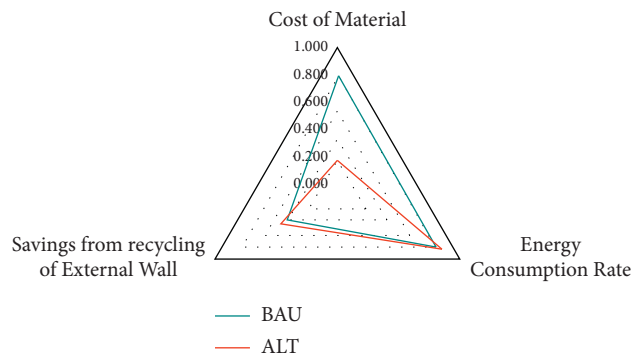


FIGURE 9: Economic indicator scores.

environmental) are subjective [30]. This report accepts that proprietors have major areas of strength for an ecological maintainability. Understudies of Architecture will concentrate on the design, materials, and soul of this structure. Sightseers can visit this famous structure and get a shallow impression of the college or the city. It has the obligation to

communicate and direct certain social qualities—ecological assurance. Accordingly, the ecological properties have the most noteworthy weight. As per the authority site, the University of Melbourne is a public government assistance establishment that makes special commitments to society. Its monetary properties are not huge. Social and engineering

TABLE 3: Level 1 indicator scores.

	Score of level metrics		Weight (%)
	BAU	ALT	
Social BL	0.504	0.751	42.31
Environmental BL	0.691	0.803	12.25
Economic BL	0.661	0.444	22.72
Engineering BL	0.736	0.666	22.72
Total	0.664	0.689	

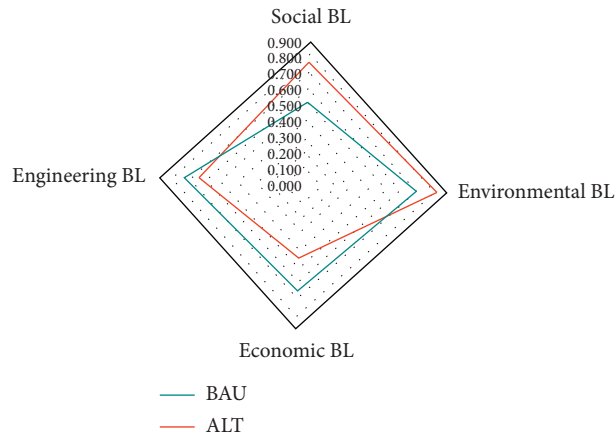


FIGURE 10: Level 1 indicator score.

TABLE 4: Green technologies used in typical green stormwater infrastructures.

Control measures	Green technology
Decentralized control measures at source	Tree pond, green roof, rainwater tank/bucket, sunken green space, rainwater garden, infiltration pavement, etc. (as shown in Figure 11(a))
Conveying measures	Grass planting ditch, ecological ditch, etc. (as shown in Figure 11(b))
Terminal centralized control measures	Landscape water body, rainwater pond, rainwater wetland, multifunctional regulation, and storage facilities (as shown in Figure 11(c))



FIGURE 11: Typical green stormwater infrastructure. (a) is the decentralized control measures at the source—concave green space; (b) is the transportation measure—shallow ditch with vegetation; (c) is the centralized control measure at the end—ecological pool.

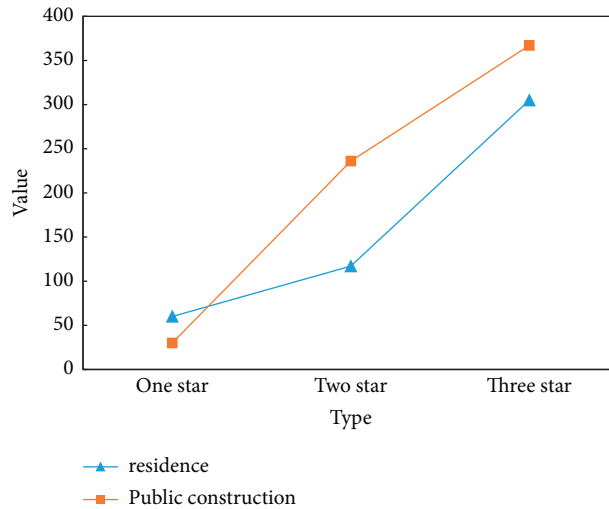


FIGURE 12: Schematic diagram of incremental costs of green buildings.

have no specific inclination, so they have a similar weight. That said, the environment matters, and the economy is the bottom line. Pairwise comparisons were performed based on Saaty's rating scale (Table 3, Figure 10).

4.3. Application Strategies of Water Saving and Water Resource Utilization Technology

4.3.1. Green Rainwater Infrastructure and Rainwater Utilization. Green stormwater infrastructure and rainwater utilization green stormwater infrastructure (GSI) mainly refer to a type of green infrastructure for urban stormwater control and utilization. Typical green rainwater infrastructures are divided into decentralized control measures at the source, transmission measures, and centralized control measures at the end, as shown in Table 4 (Figure11).

4.3.2. Promote High-Efficiency Water-Saving Sanitary Ware. We promote the use of water-saving appliances with higher water-efficiency grades, which can improve water-use efficiency at the source and reduce building water supply and sewage production. It can also reduce the scale of sewage treatment facilities and the energy consumed by sewage treatment, thereby achieving significant economic and environmental benefits. Since the technology is not limited by the nature of the building, the cost is low, and the incremental cost is low, it should be preferentially promoted in the new urban area of Guangzhou.

Nontraditional water sources mainly include reclaimed water, rainwater, and seawater. However, due to the abundant rainfall in Guangzhou, the use of river water as miscellaneous water also belongs to rainwater utilization in a broad sense. The rainy season in Guangzhou is from April to September every year, with an average monthly rainfall of 190 mm. The cooling water consumption period is basically the same as the peak rainfall period in Guangzhou. Due to the lower cost of rainwater treatment, it is more cost-effective.

4.4. Pre-Assessment of the Application of Green Building Technology in the Starting Area of Guangzhou International Financial City. According to the statistics of relevant institutions, the incremental cost of green building technology can generally be controlled at 2.7~9.3% of the overall construction cost. The incremental cost of a one-star green public building is only about 30 yuan/square meter, a two-star level is about 236 yuan/square meter, and a three-star level is about 367 yuan/square meter. From the perspective of the entire life cycle of buildings, vigorously promoting green buildings is an inevitable choice for building a low-carbon eco-city (Figure 12).

Compared with the national level, the investment cost of green building construction in the starting area of the Financial City has certain advantages. There are already supporting regional centralized resource utilization facilities such as overall development of underground space, municipal reclaimed water reuse system, regional centralized cooling, green transportation, and other supporting facilities in the starting area. *Requirements for the use of passive design techniques.* Therefore, the incremental cost of green buildings in the starting area of the Financial City can be estimated by the following amounts: according to the potential distribution map of green building grades in the starting area, the incremental cost of public buildings is 20 yuan per square meter for one-star green buildings, 100 yuan per square meter for two-star grades, and 200 yuan per square meter for three-star grades. Residential buildings are calculated based on the incremental cost of one-star green buildings of 10 yuan per square meter, and the total incremental cost of one-, two-, and three-star green buildings is about 348 million yuan. Among them, the increase in the transfer part is 338 million yuan, and the increase in the nontransfer part is about 9.84 million yuan.

5. Conclusions

The use of green structure innovation is a perplexing and orderly issue. This paper mostly concentrates on the

advocacy and utilization of the innovation through the examination of the versatility of the innovation and plans the innovation application procedure. In order to further optimize and promote the application of green building technology in the new urban area of Guangzhou, future research on the application of green building technology needs to focus on the social aspects of technology promotion, which are management issues. It is also necessary to conduct more in-depth and comprehensive research on the existing problems, realization paths, and mechanism research of green building promotion in Guangzhou. These issues need to be deepened and improved in future research and study.

Data Availability

The data that support the findings of this study are available from the author upon reasonable request.

Conflicts of Interest

The author declares no potential conflicts of interest with respect to the research, authorship, and/or publication of this article.

References

- [1] Y. Shi and P. Song, "Life cycle cost of green building based on BIM Technology," *Revista de la Facultad de Ingenieria*, vol. 32, no. 11, pp. 789–792, 2017.
- [2] I. Blanco, E. Schettini, and G. Vox, "Effects of vertical green technology on building surface temperature," *International Journal of Design & Nature and Ecodynamics*, vol. 13, no. 4, pp. 384–394, 2018.
- [3] Y. Liu, "Green building design based on building information modeling technology," *Agro Food Industry Hi-Tech*, vol. 28, no. 1, pp. 1307–1311, 2017.
- [4] B. J. Gogoi, "Green building features and factors affecting the consumer choice for green building recommendation," *International Journal of Civil Engineering & Technology*, vol. 9, no. 6, pp. 127–136, 2018.
- [5] H. P. Jagtap and A. K. Bewoor, "Use of analytic hierarchy process methodology for criticality analysis of thermal power plant equipments," *Materials Today Proceedings*, vol. 4, no. 2, pp. 1927–1936, 2017.
- [6] E. Thanassoulis, P. K. Dey, K. Petridis, I. Goniadis, and A. C. Georgiou, "Evaluating higher education teaching performance using combined analytic hierarchy process and data envelopment analysis," *Journal of the Operational Research Society*, vol. 68, no. 4, pp. 431–445, 2017.
- [7] S. Ahmed, P. Vedagiri, and K. Krishna Rao, "Prioritization of pavement maintenance sections using objective based Analytic Hierarchy Process," *International Journal of Pavement Research and Technology*, vol. 10, no. 2, pp. 158–170, 2017.
- [8] M. Agapova, B. W. Bresnahan, K. F. Linnau et al., "Using the analytic hierarchy process for prioritizing imaging tests in diagnosis of suspected appendicitis," *Academic Radiology*, vol. 24, no. 5, pp. 530–537, 2017.
- [9] U. Nadiyah Nor Ali, N. Mohd Daud, N. Mohamad Nor, M. Alias Yusuf, and M. Azani Yahya, "Enhancement in green building technology including life cycle cost," *The Social Sciences*, vol. 14, no. 4, pp. 148–154, 2019.
- [10] V. D. Sekerin, M. Dudin, A. E. Gorokhova, E. A. Shibanihin, and M. H. Balkizov, "Green building: technologies, prospects, investment attractiveness/international journal of civil engineering and technology (IJCIET)," *International Journal of Civil Engineering & Technology*, vol. 9, no. 1, pp. 657–666, 2018.
- [11] N. A. Yusof, S. S. M. Ishak, and R. Doheim, "An exploratory study of building information modelling maturity in the construction industry," *International Journal of BIM and Engineering Science*, vol. 1, no. 1, pp. 06–19, 2018.
- [12] C. Ahiable, "A comparative review of building information modeling frameworks," *International Journal of BIM and Engineering Science*, vol. 2, no. 2, pp. 23–48, 2019.
- [13] B. A. Alnoor, "BIM model for railway intermediate station: transportation perspective," *International Journal of BIM and Engineering Science*, vol. 4, no. 2, pp. 33–48, 2021.
- [14] T. Yunchao, C. Zheng, F. Wanhui, N. Yumei, L. Cong, and C. Jieming, "Combined effects of nano-silica and silica fume on the mechanical behavior of recycled aggregate concrete," *Nanotechnology Reviews*, vol. 10, no. 1, pp. 819–838, 2021.
- [15] Y. Tang, W. Feng, Z. Chen, Y. Nong, S. Guan, and J. Sun, "Fracture behavior of a sustainable material: recycled concrete with waste crumb rubber subjected to elevated temperatures," *Journal of Cleaner Production*, vol. 318, Article ID 128553, 2021.
- [16] W. Tushar, N. Wijerathne, W. T. Li et al., "Internet of things for green building management: disruptive innovations through low-cost sensor technology and artificial intelligence," *IEEE Signal Processing Magazine*, vol. 35, no. 5, pp. 100–110, 2018.
- [17] J. Ding, S. Chao, H. Wu, Z. He, and J. Li, "Key technology of green building in the Shanghai Tower structural design," *Jianzhu Jiegou Xuebao/journal of Building Structures*, vol. 38, no. 3, pp. 134–140, 2017.
- [18] M. F. . Hossain, "Green science: advanced building design technology to mitigate energy and environment," *Renewable and Sustainable Energy Reviews*, vol. 81, no. 2, pp. 3051–3060, 2018.
- [19] D. Green, H. Soller, Y. Oreg, and V. Galitski, "How to profit from quantum technology without building quantum computers," *Nature Reviews Physics*, vol. 3, no. 3, pp. 150–152, 2021.
- [20] V. D. Sekerin, M. N. Dudin, A. E. Gorokhova, E. A. Shibanihin, and M. H. Balkizov, "Green Building: technologies, prospects, investment attractiveness," *International Journal of Civil Engineering & Technology*, vol. 9, no. 1, pp. 657–666, 2018.
- [21] Y. Zhou and G. Jian, "Application of parametric building information modeling (BIM) technology in green building design," *Revista de la Facultad de Ingenieria*, vol. 32, no. 11, pp. 241–246, 2017.
- [22] S. W. Park, L. Mesicek, J. Shin, K. Bae, K. An, and H. Ko, "Customizing intelligent recommendation study with multiple advisors based on hierarchy structured fuzzy analytic hierarchy process," *Concurrency and Computation: Practice and Experience*, vol. 33, no. 1, 2020.
- [23] M. Lee, L. Mesicek, and K. Bae, "AI Advisor Platform for Disaster Response Based on Big Data," *CONCURRENCY AND COMPUTATION-PRACTICE & EXPERIENCE*, Article ID e6215, 2021, <https://doi.org/10.1002/cpe.6215>.
- [24] K. Sharma, A. Shankar, and P. Singh, "Information security assessment in big data environment using fuzzy logic," *Journal of Cybersecurity and Information Management*, vol. 5, no. 1, pp. 29–42, 2021.

- [25] R. Janani, P. Chakravarthy, and R. R. Raj, "A study on value engineering & green building in residential construction," *International Journal of Civil Engineering & Technology*, vol. 9, no. 1, pp. 900–907, 2018.
- [26] L. Gao, L. Zhu, H. Zhou, L. Zhou, and Q. Liu, "The energy-saving potential analysis of green universities building on operating data," *Journal of Xi'an University of Architecture and Technology*, vol. 49, no. 3, pp. 422–426, 2017.
- [27] Z. Liu and A. Guo, "Application of green building materials and multi-objective energy-saving optimization design," *International Journal of Heat and Technology*, vol. 39, no. 1, pp. 299–308, 2021.
- [28] W. O. Collinge, H. J. Rickenbacker, A. E. Landis, C. L. Thiel, and M. M. Bilec, "Dynamic life cycle assessments of a conventional green building and a net zero energy building: exploration of static, dynamic, attributional, and consequential electricity grid models," *Environmental Science & Technology*, vol. 52, no. 19, pp. 11429–11438, 2018.
- [29] P. Pal and M. Nandi, "Model house of green building," *International Journal of Engineering and Technology*, vol. 5, no. 6, pp. 2501–2503, 2019.
- [30] D. Manna and S. Banerjee, "A review on green building movement in India," *International Journal of Scientific & Technology Research*, vol. 8, no. 10, pp. 1980–1986, 2019.

Retraction

Retracted: Application of Boiler Optimization Monitoring System Based on Embedded Internet of Things

Mathematical Problems in Engineering

Received 1 August 2023; Accepted 1 August 2023; Published 2 August 2023

Copyright © 2023 Mathematical Problems in Engineering. This is an open access article distributed under the Creative Commons Attribution License, which permits unrestricted use, distribution, and reproduction in any medium, provided the original work is properly cited.

This article has been retracted by Hindawi following an investigation undertaken by the publisher [1]. This investigation has uncovered evidence of one or more of the following indicators of systematic manipulation of the publication process:

- (1) Discrepancies in scope
- (2) Discrepancies in the description of the research reported
- (3) Discrepancies between the availability of data and the research described
- (4) Inappropriate citations
- (5) Incoherent, meaningless and/or irrelevant content included in the article
- (6) Peer-review manipulation

The presence of these indicators undermines our confidence in the integrity of the article's content and we cannot, therefore, vouch for its reliability. Please note that this notice is intended solely to alert readers that the content of this article is unreliable. We have not investigated whether authors were aware of or involved in the systematic manipulation of the publication process.

Wiley and Hindawi regrets that the usual quality checks did not identify these issues before publication and have since put additional measures in place to safeguard research integrity.

We wish to credit our own Research Integrity and Research Publishing teams and anonymous and named external researchers and research integrity experts for contributing to this investigation.

The corresponding author, as the representative of all authors, has been given the opportunity to register their agreement or disagreement to this retraction. We have kept a record of any response received.

References

- [1] H. Zhang, M. Qiu, X. Yu, Y. Wu, and Y. Ma, "Application of Boiler Optimization Monitoring System Based on Embedded Internet of Things," *Mathematical Problems in Engineering*, vol. 2022, Article ID 9974393, 12 pages, 2022.

Research Article

Application of Boiler Optimization Monitoring System Based on Embedded Internet of Things

Haiqing Zhang ¹, Mingxiang Qiu,² Xingjiang Yu,² Yujiao Wu,¹ and Yinhong Ma¹

¹SIPPR Engineering Group Co., Ltd., Zhengzhou 450007, China

²Hangzhou Cigarette Factory of China Tobacco Zhejiang Industrial Co., Ltd., Hangzhou 310024, China

Correspondence should be addressed to Haiqing Zhang; 2020050016@stu.cdut.edu.cn

Received 26 May 2022; Revised 26 June 2022; Accepted 2 July 2022; Published 1 August 2022

Academic Editor: Xuefeng Shao

Copyright © 2022 Haiqing Zhang et al. This is an open access article distributed under the Creative Commons Attribution License, which permits unrestricted use, distribution, and reproduction in any medium, provided the original work is properly cited.

In order to study the deficiency of tuning PID controller in traditional boiler combustion air system, this paper proposes an embedded Internet of things monitoring system and puts forward a method of fuzzy PID controller with the help of nonlinear optimization algorithm to reasonably set the initial value of control parameters. Through the simulation comparison with the traditional engineering tuning PID controller, it is found that when the simulation process is $t = 2000$ s, the step disturbance with amplitude of 0.1 is added to the system input, and there will be slight disturbance in the combustion process. Through fuzzy PID and strong robustness support, the modeling error of the monitoring system model can be controlled between 10%~25%, which proves that the nonlinear optimized PID has strong anti-interference and can meet the process requirements of the system.

1. Introduction

Boiler is the most common heating equipment and the most widely used heating device in human production and life [1]. However, if the combustion process of boiler is not effectively controlled, it will inevitably lead to the decline of boiler combustion efficiency, which will not only produce large economic losses, but also discharge fuel gas with high carbon content, causing varying degrees of damage to the ecological environment. If the boiler combustion process is not reasonably controlled, even danger will occur [2]. At present, most of the boiler combustion control systems used are basically engineering adjusted PID controllers, which have great shortcomings. Based on this problem, this research proposes a fuzzy PID controller based on the nonlinear optimization method and further optimizes the boiler monitoring system with the help of embedded Internet of Things monitoring system.

2. Literature Review

The most common problem encountered in video surveillance is the recognition of surveillance targets, also known as motion detection. The current research methods are mainly

divided into static scene and dynamic scene. In recent years, morphological filtering has been gradually applied to the analysis of video images. For static analysis, there are two kinds of analysis methods: background difference and streamer field [3]. At present, the research on the background difference method has been very mature, and its principle is relatively easy to understand. Therefore, the research results for it are relatively rich. The background subtraction method of Gaussian mixture model was proposed by foreign scholars; these research results are based on the background subtraction method. It can be seen that this method is universal. Similarly, some researchers have also studied the results of using background feature modeling [4]. Some scholars proposed a deep understanding of the background subtraction method and a sequential kernel density approximation method. When using the background difference method, it can not only form its own theory, but also be combined with other methods, such as the new concept of double threshold adopted by the W4 system; in the knight intelligent monitoring system, the combination of the Gaussian mixture model and gradient detection is used to improve the target acquisition; SAKBOT system can effectively analyze various shadows in the monitoring image.

In traditional control problems, people hope to optimize the control effect by improving the accuracy of the system dynamic model. However, in the actual production and life, the problems that people want to solve are becoming more and more complex [5]. The simple and accurate system model is too ideal and has no practical application value. It is difficult to describe the dynamics of complex systems correctly. With the development of modern science, scientists and engineers try to simplify the system to achieve the purpose of control, but the effect is not ideal. In short, traditional control methods have strong control ability for simple and clear systems. However, for complex or difficult to accurately describe the system, it cannot achieve a good control effect, and even cannot meet the requirements of the process. Therefore, in the face of such control problems, the idea of fuzzy mathematics came into being [6].

The research on Fuzzy Mathematics in China began in the early stage of reform and opening up. In the following decades, fuzzy mathematics has made a lot of achievements in theory and application [7]. In 1988, a university professor and his scientific research team successfully developed the fuzzy inference engine, that is, the prototype of discrete component machine, and used it to carry out the inverted pendulum control experiment [8]. The controller shows good results for all kinds of controlled objects with different shapes and even soft objects, and has the advantages of fast and real-time. Its operation speed can reach 1.5 million times/s. Such a high operation speed indicates that China has made great progress in fuzzy information processing.

3. Design of Monitoring System for Embedded Internet of Things

3.1. System Architecture. According to the environmental requirements of the site, the system uses ARM9 series microprocessor as the hardware core, embedded Linux as the operating system, and constructs an embedded system as the server to manage the webcam, collect the image data of the webcam, and provide users with the functions of real-time viewing, monitoring, and historical playback through the built-in Apache Web server [9]. The whole system is of B/S structure, and the system composition is shown in Figure 1.

The main hardware modules of the system include ARM920T series processor based on ARMv4T architecture, FLASH, SDRAM, power module, Ethernet controller, and RS232C. The specific hardware structure is shown in Figure 2.

S3C2410 processor is a 32 bit RISC microcontroller with ARM920T processor core and 0.18um manufacturing process. It is a low-power and highly integrated microprocessor specially designed for embedded devices. It supports thumb and arm instruction sets, has MMU and Cache, and integrates rich peripherals in the chip, which greatly reduces the cost of the whole system. Its instruction execution efficiency has been greatly improved [10]. The processor has AMBA BUS and Harvard cache architecture. LCD controller supporting TFT, starting from nandflash, with 4 DMA with external request pins, 3 UART, 2 SPI, etc. The operating frequency of S3C2410 processor can reach

203MHz. This running frequency can run embedded Linux and other systems well. The microprocessor divides the storage space into eight blocks, each with a size of 128 MB and a capacity of 1 G. The memory controller supports the storage formats of Big Endian and Little Endian. Bank0 is 16/32 bit addressing, others are 8/16/32 bit addressing, and Bank0 to Bank5 are used for ROM and SRAM. Bank6 and Bank7 are used for ROM, SRAM, or SDRAM. The starting address of Bank6 is fixed and the starting address of Bank7 is changed [11].

3.2. Software Design of the System. The embedded network monitoring system adopts B/S structure, constructs the embedded system as the server, and uses the web browser as the user interface of the system. The system adopts the idea of component design, applies object technology to system design, and further abstracts the implementation process of object-oriented programming. The functions of the system can be expanded through continuous functional components to meet the growing and changing needs of users [12]. Therefore, the system has strong scalability and the ability of secondary development and continuous development. The overall architecture of the system is shown in Figure 3.

The components of embedded monitoring system belong to interprocess communication and data acquisition through files. Because the communication modes between components are different, the interprocess communication is provided by each component to hide the communication mode. The specific software communication interface is shown in Table 1.

The main processing part of the webcam management module includes initialization processing at startup, end processing at the end of the process, and sending/receiving processing of external API messages. See Figure 4 for details.

Initialization processing during process startup includes application and initialization of shared memory, application and initialization of FIFO, application and initialization of semaphore, application and initialization of socket, updating shared memory according to configuration file, opening FIFO for management, initializing shared memory allocated for the latest image, and generating network camera monitoring thread [13]. The initialized resources need to be released at the end of the process; otherwise, it will cause memory leakage or system crash (because the end processing in case of power failure cannot be executed, and the end processing of the process will not be executed). See Figure 5 for details.

Message processing process of webcam management process: when receiving a message sent by an external API, judge the type of received message, make corresponding processing according to the message type, and then return data to the corresponding external. The specific types and processing of messages sent from external APIs are shown in Table 2.

The main work of this chapter is to provide a feasible implementation scheme, which combines embedded technology, network communication technology, and intelligent monitoring technology to build a practical, low-cost,

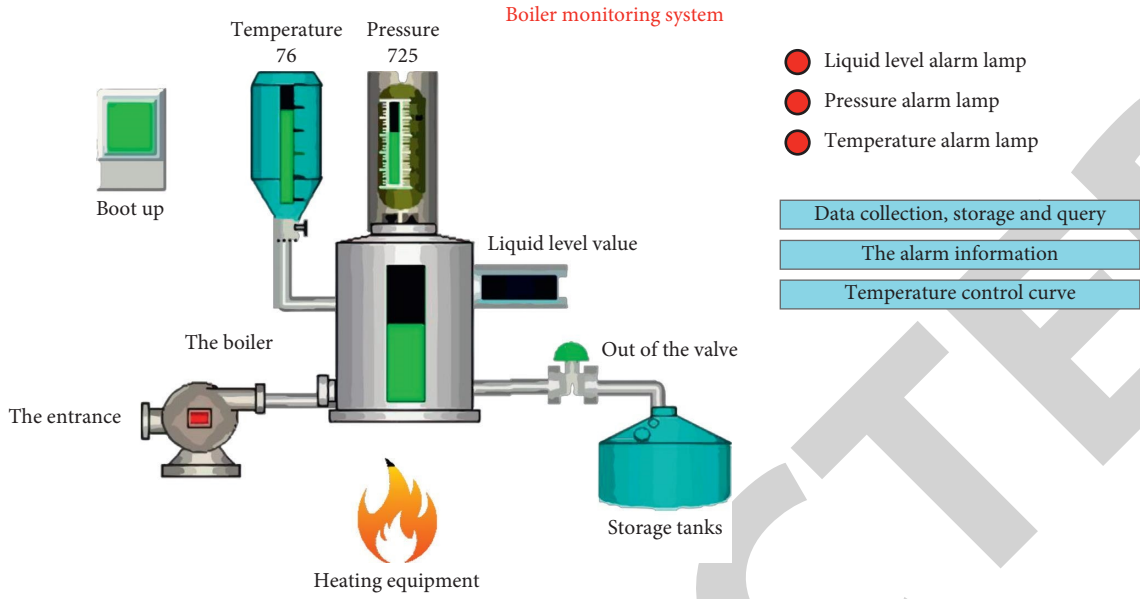


FIGURE 1: System composition.

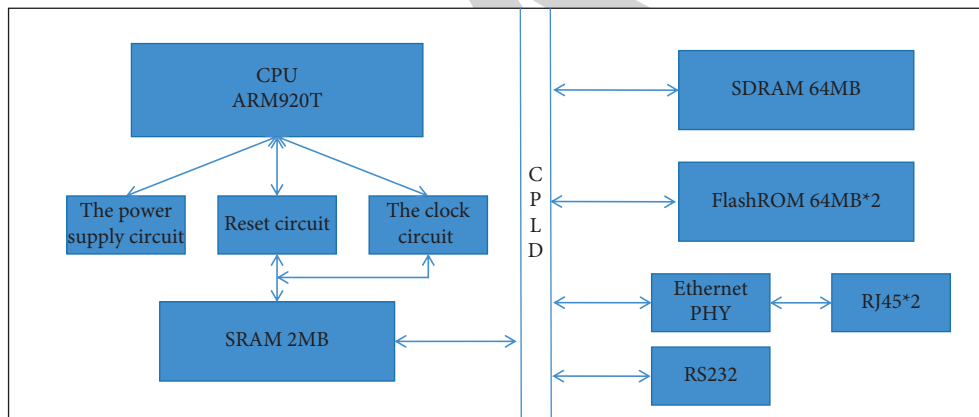


FIGURE 2: Physical structure of hardware.

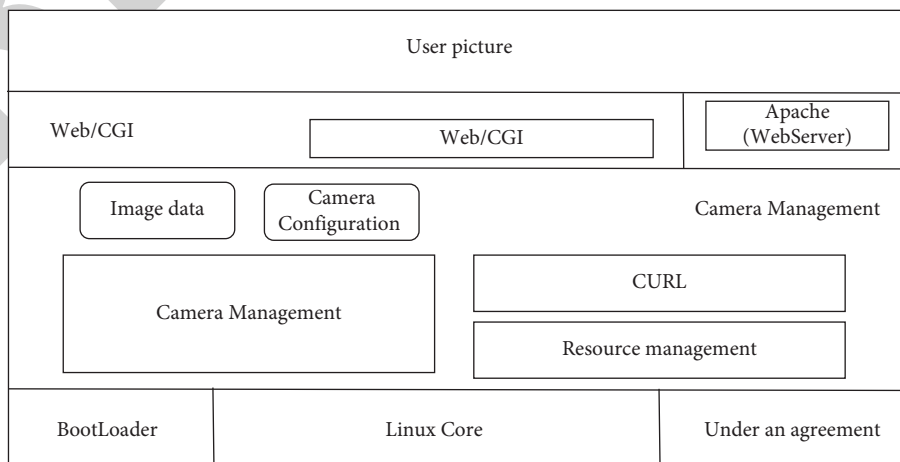


FIGURE 3: Software structure.

TABLE 1: List of communication modes between components.

Serial number	Communication mode between components	Explanation
1	FIFO	The interface is provided in the form of dynamic library, which is mainly used for interprocess message passing.
2	Socket	The interface is provided in the form of dynamic library, which is mainly used for communication with network camera.
3	Shared memory	The interface is provided in the form of dynamic library, which is mainly used for communication with CG I.
4	File	The interface is basically provided in the form of dynamic library. When the dynamic library cannot be used, it can be accessed directly.

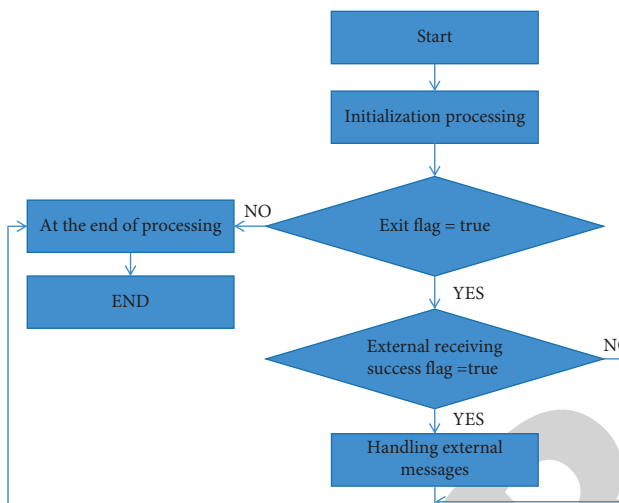
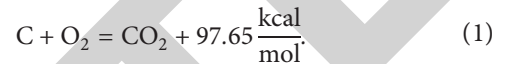


FIGURE 4: Main processing of network camera management.

scalable, flexible, and efficient embedded network monitoring system [14]. This paper systematically analyzes the current situation of video surveillance and puts forward a video surveillance scheme based on S3C2410 according to the specific requirements of the application of video surveillance in the family field. The network camera image acquisition, network transmission, and local storage are realized. In the process of image acquisition and data transmission, most of the technologies of interprocess communication such as pipeline and socket are used. At the same time, multithread technology is used to manage the network camera, which improves the execution efficiency of the system [15]. The whole system adopts modular design to ensure the balance between closure and openness and efficiency. Through the selection and combination of modules, it can meet the customized needs of different users and is also conducive to the reuse and upgrading of the system.

4. Design of Combustion Process Monitoring Scheme for Coal-Fired Chain Boiler

4.1. Composition of Boiler Combustion Control System. Fuel combustion is a chemical reaction with oxygen in the air at a certain temperature, in which chemical energy will be released. Taking standard coal combustion as an example, the reaction equation is



In order to ensure that the heat released in the combustion process reaches the theoretical value, the fuel and air must maintain a certain proportion in order to achieve full combustion and improve combustion efficiency. The control system mainly controls the coal feed, furnace negative pressure, and air supply volume to achieve the best combustion effect. The control system includes two loop controls, namely, coal feeding control and furnace negative skin control, as well as a proportional control system and “air supply coal feeding” ratio control system. For the hot water boiler, the coal feeding quantity control is to detect the water supply temperature, calculate the deviation from the set value, and adjust the grate motor speed to change the coal feeding quantity, and then realize the water temperature control [16]. For the steam boiler, the coal feeding amount is adjusted by detecting the steam pressure of the output pipeline so as to realize the control of the boiling effect of the heat energy generated by combustion on the water in the boiler and then realize the control of the steam pressure. The air supply volume is controlled in proportion to the coal supply according to the reactant ratio of the combustion reaction equation. Table 3 lists each measurement variable, its measurement device, and its role in the control system.

The controlled variables and control equipment of boiler combustion process are given in Table 4.

4.2. Boiler Combustion System Control Scheme

4.2.1. Coal Feeding Control System. The structure diagram of coal feeding control system is shown in Figure 6. That is, a simple feedback control system compares the water temperature at the outlet of the boiler with the set value by detecting the water temperature and transmits the deviation to the PID controller [17]. In this project, the PID controller is realized by the lower computer PLC. The controller will output 4–20 mA current and control the motor driving the grate to rotate.

The lower computer PID control program is a part of the lower computer PLC control program, which is skillfully developed in the configuration software. When programming PLC control program, it is necessary to configure and variable configuration in the software first. The program flowchart of PID part is shown in Figure 7.



FIGURE 5: End processing of webcam.

TABLE 2: Message types and processing.

Classification	Message type	Message code	Processing summary	Return data
Real time image request	GET	OXO1	(1) Check the range of webcam ID value. (2) Obtain the real-time image of the webcam, store it in the common memory and return it to the CGI caller.	Real-time image
Webcam action notification	GET	OXO2	(1) Find the ID of the webcam in the configuration information according to the IP address of the webcam. (2) Generate the action processing thread of the webcam with the corresponding ID	OK

TABLE 3: Boiler combustion process detection transformer and its detection equipment.

Controlled variable	Testing equipment	Control function
Boiler outlet supply/return water temperature	Supply/return water temperature measuring instrument	Reaction boiler load
Steam pressure at drum outlet	Steam pressure detector	Output steam pressure of reaction boiler
Furnace negative pressure	Furnace pressure sensor	Negative pressure of reaction furnace and flue gas emission

TABLE 4: Controlled variables and their actuators in boiler combustion process.

Controlled variable	Executing agency	Control function
Coal feed	Grate motor	Adjust coal feed
Air supply volume	Blower	Adjust the air supply volume
Induced air volume	Induced draft fan	Adjust furnace negative pressure

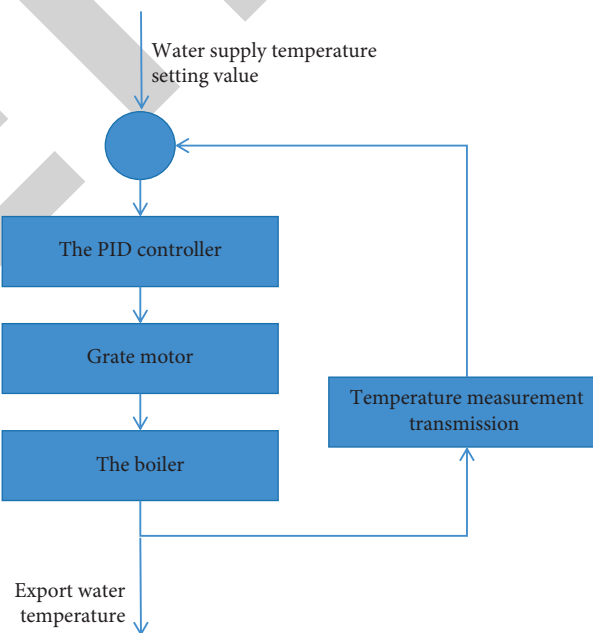


FIGURE 6: Block diagram of coal feeding control system.

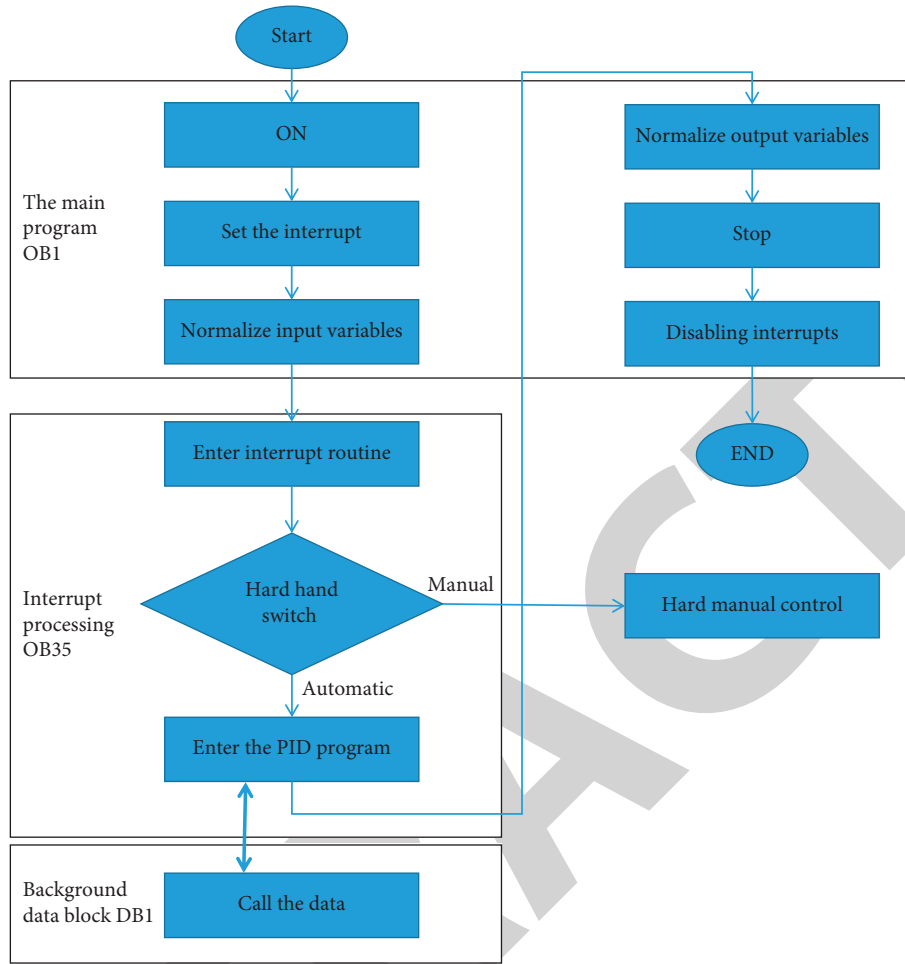


FIGURE 7: Calling part of PID module control program.

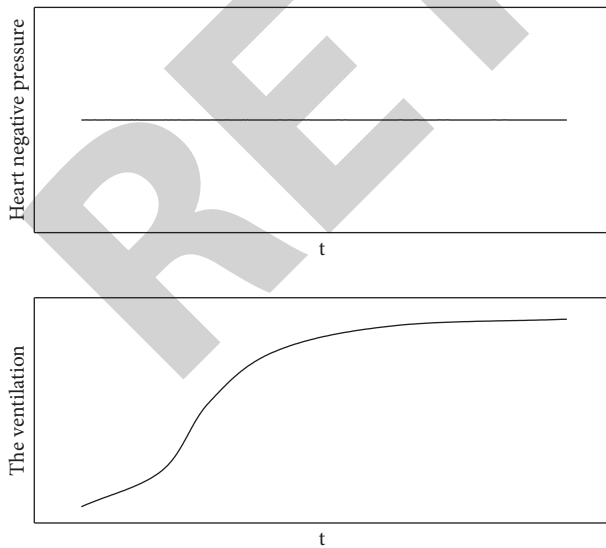


FIGURE 8: Step response curve of furnace negative pressure to induced air volume.

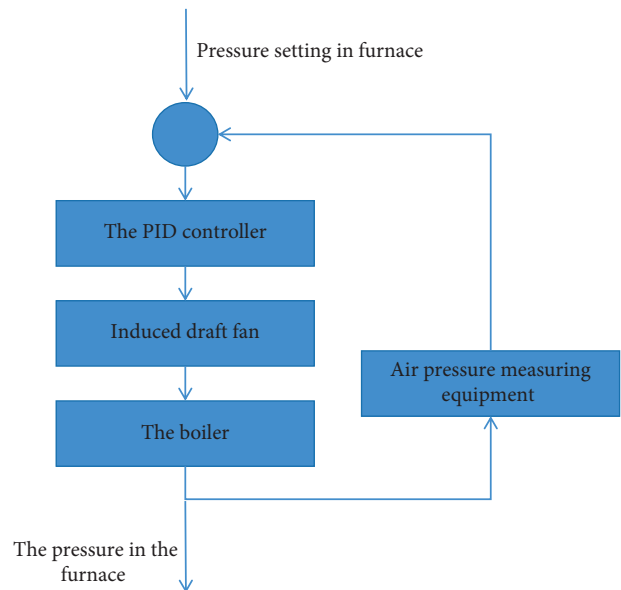


FIGURE 9: Structure diagram of furnace negative pressure control system.

For the “soft manual” control of the upper computer, its priority is lower than the “hard manual” control on-site. When the “hard manual” switch is set to “1,” the system is in manual control state, and the upper computer cannot switch to manual control mode. This part of logic is realized in the upper computer [18].

4.2.2. Induced Air Volume Control System. Controlling the furnace cavity in a micronegative pressure state is an important condition to ensure the safety of on-site staff and the on-site equipment from damage. Furnace negative pressure is mainly controlled by adjusting the air pressure in the furnace through induced draft fan. Of course, factors such as forced draft fan and furnace air leakage will also affect the control of furnace negative pressure. The characteristic curve of the step change of furnace negative pressure with induced air volume is given in Figure 8. It can be seen from the curve that the negative pressure of the furnace reacts quickly to the induced air volume, the delay is small, and it is easy to control [17].

The structure diagram of furnace negative pressure control system is shown in Figure 9. It is the same as the implicit principle of coal feed control. It is also a single loop feedback control system. The negative pressure of the furnace is greatly affected by the air supply volume, so the control system needs to have good robustness. The optimization of the control system will be described in detail below [19].

4.3. Development of Monitoring System

4.3.1. Design Ideas. Before developing the boiler group combustion process monitoring operating system, the framework of the monitoring system needs to be structured in combination with the functions and advantages of WINCC.

- (1) Type of project. The project types provided by WINCC include single user, multiuser and client. The project type selected by the boiler group combustion process monitoring operating system is single user [20].
- (2) Definition of variables. Before creating the project, count the variables to be controlled, monitored, and collected variables and alarm variables in combination with the PLC control program of the lower computer. WINCC provides users with two types of variables: internal variables and process variables. The use of internal variables can make the development W and application of the monitoring system more flexible. It is created for some operation and display status of the monitoring system without connecting the variable address of PLC program. The process variable needs to be connected with the variable address in the PLC program. Through the process variable, it can not only operate the field equipment but also collect the field real-time data in time. The number of process variables allowed by

WINCC is directly related to the purchased WINCC authorization.

- (3) The use of scripts. WINCC’s script function is divided into global script and action script. It supports ANSI-C and VBS editing languages. The action script can also be directly connected.

4.3.2. Monitoring System Architecture. The most important principle of developing the monitoring system is to be able to monitor the working state of the site in real time and inform the operators of the problems on the site at the first time. Therefore, on the premise that the monitoring screen can reflect the status of field equipment, we must strive to be concise, give the operator the most intuitive feeling, and facilitate its operation. The startup interface of the monitoring system is “boiler group monitoring main interface.” In the main interface, you can see the operation status of each boiler of the boiler group and provide some public parameter data and status ideas. Through the main interface, you can enter the monitoring subsystem of each boiler, and the monitoring system interface of each boiler is basically similar [21]. Taking the monitoring screen of boiler No. as an example, the picture structure of boiler monitoring system is shown in Figure 10.

4.3.3. Monitoring Process Variable Record. The configuration process variables are archived in the “WinCC Explorer” interface. Select “variable record” to open the variable record editor. The variable record editor can set the sampling period timer of W data and add w record to the data for archiving. The system automatically provides five timers: 500 ms, 1s, 1 min, 1 H, and 1 day to trigger the archiving of variables in the system. You can also customize the new archiving cycle. You only need to create a new timer in “variable record” and set it. The archiving of system variables can be created according to the “archiving Wizard” provided by WinCC software. After that, select the variable to be recorded and configure its properties. The variables to be archived in this project are given in Table 5.

4.3.4. Alarm Record. In the combustion process control system of boiler group, in order to avoid the wrong operation or negligence of on-site personnel, resulting in dangerous shade or affecting the operation of heating pipe network. In the design of the monitoring system, the alarm information is recorded and displayed, and W timely reminds the operator to deal with it.

- (1) For alarm record configuration, select “alarm record” under the directory in the “WinCC Explorer” interface, and select “system Wizard” in “alarm Wizard.” Follow the prompts to configure various information and display attributes required. After setting the display properties of the alarm record, add the alarm signal. Double click the position of “1” under the window to open the variable window, select “NO.1dig” → “NO1_GLCSpress_L” under the

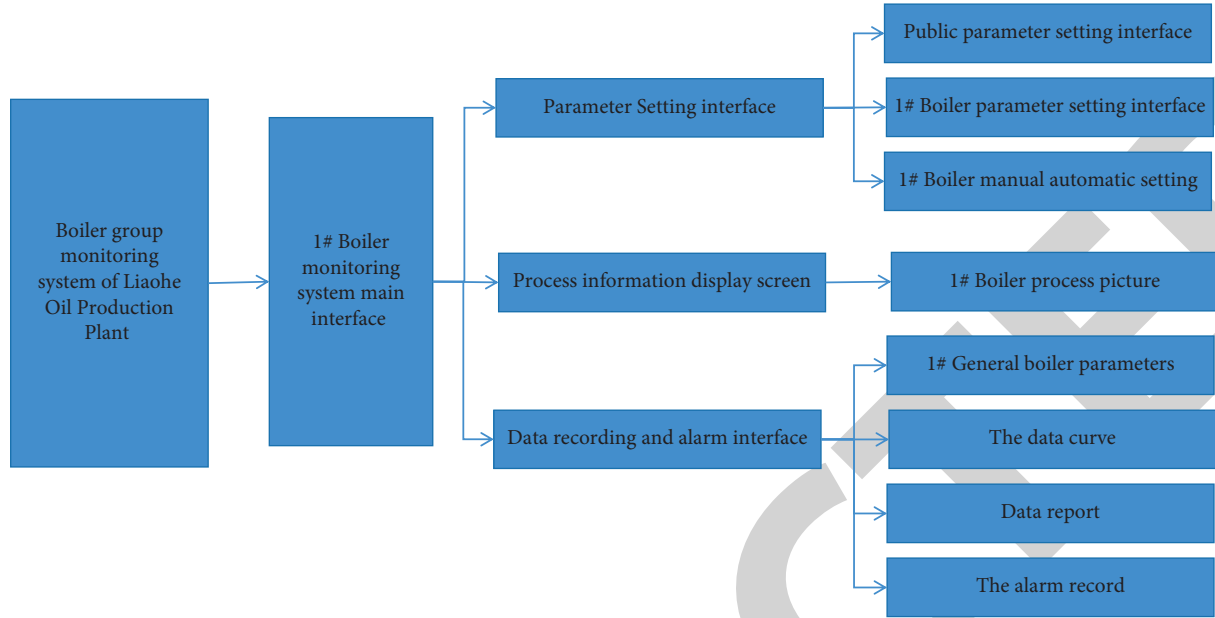


FIGURE 10: Picture structure of boiler monitoring system.

TABLE 5: Partial archive variables.

Variable name	Variable type	Acquisition cycle	Archive/display cycle
Water supply header pressure	Analog quantity	1 second	1 second
Return header pressure	Analog quantity	1 second	1 second
Outlet water temperature of 1# boiler	Analog quantity	1 second	1 second
1# boiler blast speed	Analog quantity	1 second	1 second
1# boiler grate speed	Analog quantity	1 second	1 second
1# boiler house negative pressure	Analog quantity	1 second	1 second
1# boiler induced draft speed	Analog quantity	1 second	1 second

internal variable directory, fill in “boiler outlet pressure is too low” under “message text,” and enter “1 boiler” at “error point” to complete the alarm record setting caused by the signal of too low pressure at the boiler outlet. Set other alarm signals in the same way [22].

- (2) Display alarm record, create a new graphical interface, and name it “alarm record.” Add a control named “WinCC Alarm Control” using the method described earlier. Set control ownership. In the message list tab, add text message and error point to display the contents of text message and error point.

4.4. Research on Optimization Algorithm of Boiler Combustion Control System

4.4.1. Nonlinear Optimization Method with Constraints. The general nonlinear programming problem has the following form:

Binding issues:

$$\min f(x). \quad (2)$$

With constraints:

$$G_i = 0 \quad i = 1, \dots, m_e, \quad (3)$$

$$G_i \leq 0 \quad i = m_e + 1, \dots, m, \quad (4)$$

$$x = [x_1, x_2, \dots, x_n], \quad (5)$$

$$G_x = [g_1(x), g_2(x), \dots, g_m(x)]. \quad (6)$$

Formula (5) is the design parameter vector and formula (6) is the function vector. Where $f(x)$ is the objective function, m_e is the boundary value of equality or inequality constraints, and $f(x)$ and $g(x)$ can be nonlinear functions at the same time.

SQP algorithm is a sequential optimization method for solving general nonlinear programming problems. Firstly, the following Lagrange functions are approximately quadratic;

$$L(x, \lambda) = f(x) + \sum_{i=1}^m \lambda_i g_i(x), \quad (7)$$

where λ is the Lagrange factor, and then the QP subproblem is solved. After linearizing the nonlinear constraints, the following problems can be obtained:

Its objective function is

$$\min \frac{1}{2}d^T H_k d + \nabla f(x_k)^T d. \quad (8)$$

The constraints are

$$\begin{aligned} \nabla g_i(x)^T d + g_i(x) &= 0, i = 1, \dots, m_e \\ \nabla g_i(x)^T d + g_i(x) &\leq 0, i = m_e + 1, \dots, m, \end{aligned} \quad (9)$$

where d is the search direction of all variables, ∇ is the gradient, and matrix H is the positive definite quasi-Newton approximation of Hessian matrix of Lagrange function.

In the problem of PID parameter tuning, some performance criteria can be used as the optimization objective function and some performance indexes of expected output can be used as constraints. In the programming simulation, the constraints composed of the system simulation output and performance indexes are taken as the input variables of the optimization process.

These constraints can be regarded as piecewise linear boundary, and a segment n linear boundary y_{bnd} can be expressed as

$$y_{bnd}(t) = \begin{cases} y_1(t) & t_1 \leq t \leq t_2 \\ y_2(t) & t_2 \leq t \leq t_3 \\ \dots & \dots \\ y_n(t) & t_n \leq t \leq t_{n+1}. \end{cases} \quad (10)$$

Then, the distance between the simulation output and the boundary is calculated. For the lower boundary, this signed distance value can be expressed as

$$c = \begin{cases} \max_{t_1 \leq t \leq t_2} y_{bnd} - y_{sim} \\ \max_{t_2 \leq t \leq t_3} y_{bnd} - y_{sim} \\ \dots \\ \max_{t_n \leq t \leq t_{n+1}} y_{bnd} - y_{sim} \end{cases}, \quad (11)$$

where y_{sim} is the simulation output, that is, the function with the parameters to be optimized as variables. For the upper boundary, the distance value can be expressed as

$$c = \begin{cases} \max_{t_1 \leq t \leq t_2} y_{sim} - y_{bnd} \\ \max_{t_2 \leq t \leq t_3} y_{sim} - y_{bnd} \\ \dots \\ \max_{t_n \leq t \leq t_{n+1}} y_{sim} - y_{bnd}. \end{cases} \quad (12)$$

The nonlinear programming problem with constraints can be solved by using `fmincon` function in MATLAB. `fmincon` function requires the nonlinear constraint inequality to have the following form:

$$C(x) \leq 0. \quad (13)$$

Transfer the simulation output and the boundary value of each segment to `fmincon` function. By constantly calling `fmincon` function to optimize the three control parameters of PID to meet the output performance index, the problem of initial value setting of PID parameters can be solved [23].

4.4.2. Design of Fuzzy PID Controller. In fuzzy control, the real range of input and output signals is defined as the basic domain. In this paper, the input variables are temperature deviation e and deviation change rate ec . According to the characteristics of boiler combustion system, the basic domain of e is $[-80,80]$, and the basic domain of ec is $[-10,10]$. Let the universe of deviation e fuzzy set be

$$X = \{-n, -n + 1, \dots, 0, 1, \dots, n - 1, n\}. \quad (14)$$

The fuzzy set domain of deviation change rate ec is

$$Y = \{-m, -m + 1, \dots, 0, 1, \dots, m - 1, m\}. \quad (15)$$

For quantization factors K_e and K_{ec} :

$$\begin{aligned} K_e &= \frac{n}{e} \\ K_{ec} &= \frac{m}{ec}. \end{aligned} \quad (16)$$

If $n = m = 6$ is selected in this paper, there are

$$X = Y = \{-6, -5, -4, -3, -2, -1, 0, 1, 2, 3, 4, 5, 6\}. \quad (17)$$

That is, the fuzzy universe of input variables E and EC , so it is concluded that

$$\begin{aligned} K_e &= \frac{n}{e} = \frac{6}{80} = 0.075 \\ K_{ec} &= \frac{m}{ec} = \frac{6}{10} = 0.6. \end{aligned} \quad (18)$$

According to the concept of quantization factor of input variable fuzzification, the scale factor of antifuzzification of input variable is defined as

$$G_u = \frac{u}{l}, \quad (19)$$

where u is the basic universe of control quantity and l is the number of quantization files of the basic universe of control quantity. Similarly, the scale factor $G_p = 0.13, G_I = 0.02, G_D = 1$ is obtained.

After designing the fuzzification and defuzzification part of the fuzzy controller, it is necessary to establish the fuzzy control rule base. For the boiler combustion process, it is mainly to control the heat output of the combustion system by adjusting the grate speed, air supply, and other variables to make the outlet water temperature meet the control requirements. In this paper, the output $\Delta K_p, \Delta K_I, \Delta K_D$ of fuzzy controller is the increment of PID control parameter K_p, K_I, K_D .

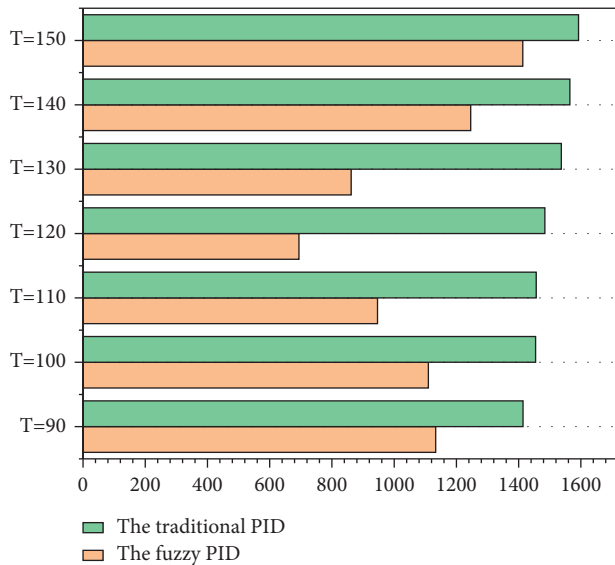


FIGURE 11: Histogram of adjustment time comparison.

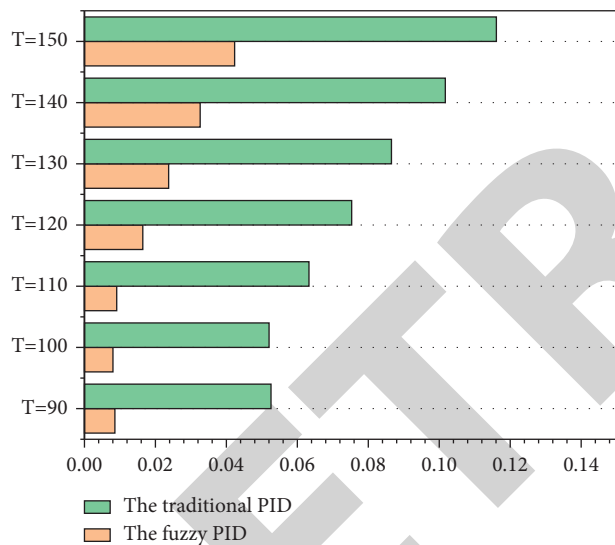


FIGURE 12: Comparison histogram of relative percentage overshoot.

4.4.3. Algorithm Simulation Research. As the control group, the traditional PID adopts the parameter setting method based on IST^2E criterion, that is the time square error square integral criterion. This paper makes a simulation analysis when the expected performance index of the system is Rise Time $t_r \leq 600s$ (90%), adjustment time $t_s \leq 1000s$ (2%), and percentage overshoot $\sigma\% \leq 5\%$. In order to explore the influence of nonlinear optimization fuzzy PID controller on system robustness, a comparative analysis is made when the inertia time τ of the controlled object model changes by -25% – $+25\%$ and the delay time τ changes by -17% – $+17\%$. The simulation results show that when the inertia time constant of the controlled object changes to -25% , the nonlinear optimization fuzzy PID is less affected, and the overall performance is better than the traditional PID. Moreover, the cost of fuzzy PID control is also less than that

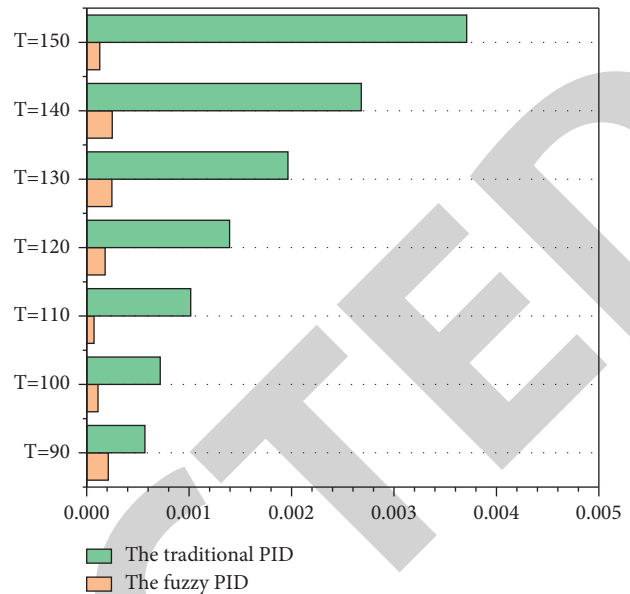


FIGURE 13: Comparison histogram of steady state error.

of traditional PID. Next, the simulation experiment is carried out when the inertia time coefficient increases by 25%. It can be seen that when the inertia time constant increases to 25%, the traditional PID control system has a large overshoot, needs a long time to converge, and there is a certain steady-state error.

For some specific performance indicators, such as adjustment time, relative percentage overshoot quantization, and steady-state error, fuzzy PID shows good robustness and control effect. This paper uses the data of several main performance indexes of the two kinds of PID to make a histogram for analysis and comparison, as shown in Figures 11, 12, and 13.

Through the histogram, we can clearly see that the nonlinear optimized fuzzy PID can still meet the process requirements to a certain extent when the model parameters of the controlled object change to a certain extent, so that the system has a certain robustness and maintains a good control effect.

Through the above experiments, it can be concluded that the nonlinear optimization fuzzy PID has better adaptability to the change of model and improves the robustness of the system compared with the traditional PID. Fuzzy PID has short response time, small relative overshoot, small steady-state error, and its ability to suppress interference is also stronger than traditional PID. Therefore, nonlinear optimization fuzzy PID has strong practical significance in the boiler combustion process with nonlinearity, time variability, and frequent interference. Its strong robustness can ignore about 10% to 25% of the modeling error of the controlled model. Moreover, it can also play a good control effect on the dynamic change of the model in the combustion process. Under the disturbance of boiler system heat supply network load or the disturbance caused by the change of external environment, the anti-interference of nonlinear optimization fuzzy PID can still make the system meet the process requirements.

In this chapter, the nonlinear fuzzy PID is expounded and analyzed from theory to practice. Firstly, the nonlinear programming theory and its application in tuning the initial value of PID control parameters are described. Then, the fuzzy control theory and the working principle of fuzzy controller are introduced. On this basis, a fuzzy PID controller based on nonlinear programming method to adjust the initial value of control parameters is proposed. MATLAB software is used to simulate and compare the nonlinear optimization fuzzy PID and traditional PID. It is concluded that the nonlinear optimization fuzzy PID still has a good control effect when the model parameters of the controlled object change to a certain extent, can still meet the process requirements in a certain range of parameter changes, improves the robustness of the system, and has a strong suppression effect on interference. It shows that it has strong practical value in boiler control system.

5. Conclusion

After understanding the process flow, equipment, functions, and control requirements of the boiler combustion control system, this study gives the general control scheme of the boiler combustion process control system. This set of distributed control system for combustion process of boiler group with redundant function is developed. Firstly, this paper introduces the hardware configuration and network configuration of the control level lower computer of the control system, as well as the development process of the monitoring interface of the monitoring level upper computer, and designs the functions of data recording, alarm recording, and historical curve. Then, this paper studies the application of advanced control method in boiler combustion process. Based on the previous use of fuzzy PID controller for water temperature control of hot water boiler, air pressure control of steam boiler, and furnace negative pressure control, a method based on nonlinear programming algorithm to optimize the initial value of fuzzy PID is proposed to make the controller have better control effect. The simulation experiment is carried out in the Simulink environment of MATLAB software. It is roughly estimated that the mathematical model of combustion process is a first-order large inertia and large time delay model. Through the comparative analysis of inertia time constant change, delay time change, and step disturbance experiment, it is verified that the fuzzy PID controller based on nonlinear optimization proposed in this paper has better robustness and anti-interference than the traditional PID controller based on error integral criterion. Therefore, in the project implementation, the approximate parameters of the model can be obtained by means of system identification or manual rough identification, and the initial value of the optimized control parameters can be obtained by calculus in the Simulink environment. The implementation of the algorithm can be completed by using the PLC program of the lower computer to realize the function of the fuzzy p-melon controller. Through the simulation comparison experiment with the traditional engineering tuning PID controller, it is found that when the simulation process is =2000 s, the step

disturbance with amplitude of 0.1 is added to the system input, and there will be slight disturbance in the combustion process. Through the support of fuzzy PID and strong robustness, the modeling error of the monitoring system model can be controlled between 10%~25%, which proves that the nonlinear optimized PID has strong anti-interference and can meet the process requirements of the system.

As the project is in the implementation stage, there will be some problems in the process of on-site commissioning in the future. This needs to be a control system with high safety and economy. Our designers and constructors should treat each step and process carefully to prevent accidents and accidents.

Data Availability

The data used to support the findings of this study are included within the article.

Conflicts of Interest

The authors declare that they have no conflicts of interest.

References

- [1] X. Lv and M. Li, "Application and research of the intelligent management system based on internet of things technology in the era of big data," *Mobile Information Systems*, vol. 2021, no. 16, pp. 1–6, 2021.
- [2] H. Fan, H. Zhan, S. Cheng, and B. Mi, "Research and application of multi-objective particle swarm optimization algorithm based on α -stable distribution," *Xibeigongye Daxue Xuebao/Journal of Northwestern Polytechnical University*, vol. 37, no. 2, pp. 232–241, 2019.
- [3] Q. Chen, "The application of adaptive operation decision technology and optimization algorithm model of smart supply chain oriented to the internet of things [J]," *IETE Journal of Research*, no. 2, pp. 1–12, 2021.
- [4] A. K. Sangaiah, A. A. R. Hosseinabadi, M. B. SharehShareh, S. Y. Bozorgi Rad, A. Zolfagharian, and N. Chilamkurti, "Tot resource allocation and optimization based on heuristic algorithm," *Sensors*, vol. 20, no. 2, p. 539, 2020.
- [5] N. Kashyap, A. C. KumariKumari, and R. Chhikara, "Service discovery and selection in internet of things - a review," *Recent Patents on Engineering*, vol. 14, no. 1, pp. 4–11, 2020.
- [6] F. Li and Q. Xi, "Research and implementation of a fabric printing detection system based on a field programmable gate array and deep neural network," *Textile Research Journal*, vol. 92, no. 7-8, pp. 1060–1078, 2022.
- [7] Y. Mao and L. Zhang, "Optimization of the medical service consultation system based on the artificial intelligence of the internet of things," *IEEE Access*, vol. 9, p. 1, 2021.
- [8] B. Cao, Y. Zhang, J. Zhao, X. Liu, L. SkoniecznySkonieczny, and Z. Lv, "Recommendation based on large-scale many-objective optimization for the intelligent internet of things system [J]," *IEEE Internet of Things Journal*, p. 1, 2021.
- [9] Y. Feng and Z. Pan, "Optimization of remote public medical emergency management system with low delay based on internet of things," *Journal of Healthcare Engineering*, vol. 2021, no. 1, 10 pages, Article ID 5570500, 2021.
- [10] B. Cao, X. Wang, W. Zhang, H. Song, and Z. Lv, "A many-objective optimization model of industrial internet of things

Research Article

Construction of Rural Governance Digital Driven by Artificial Intelligence and Big Data

Ruolan Huang 

Faculty of Business, Economics and Law, The University of Queensland, Brisbane 4072, Queensland, Australia

Correspondence should be addressed to Ruolan Huang; ruolan.huang@uqconnect.edu.au

Received 7 June 2022; Revised 30 June 2022; Accepted 6 July 2022; Published 31 July 2022

Academic Editor: Wei Liu

Copyright © 2022 Ruolan Huang. This is an open access article distributed under the Creative Commons Attribution License, which permits unrestricted use, distribution, and reproduction in any medium, provided the original work is properly cited.

Rural governance relies on distinct geographical, population, and fundamental service attributes for deploying digital construction and operation modes. The digital platform for rural governance includes surveying, identifying, and fulfilling the demands through application-specific user interactions. This article discloses a Modular Data Representation Method (MDRM) for improving the data semantics in digital platforms. The proposed method improves the presentation, analysis, and interaction in the governance process through requirements-based intelligent processing. The processing is performed based on the data organization as recommended by the regression learning paradigm. In this paradigm, the forward regression for data representation and service delegations are linearly analyzed. Based on the processing, the service requirement is met with big data availability. Therefore, the representation recommendations and data-driven analysis are provided through digital platform implications, improving the service availability. This is consistently provided based on the regressive outputs for data analysis. Therefore, the proposed method's performance is analyzed using the metrics analysis time, data processing rate, and unavailability.

1. Introduction

Rural governance is a process that provides various strategies and methods to improve the productivity, economic rate, and political and social development of the rural region. Rural governance introduces many methodologies to facilitate people and improves the lifestyle of village people [1]. Rural governance influences both local and administrative processes to provide better solutions for the people. Digital platform plays a vital role in constructing rural governance system. The digital platform increases the literacy level of rural people that improves their problem-facing capabilities of people [2]. The digital platform provides various helps for farmers, students, and other people in the rural region. Nowadays, various fields are digitalized by using certain technologies and methodologies that reduce unwanted problems in rural areas. Banks provide loans, policies, and schemes via digital platforms [3]. Farmers search for necessary information regarding seeds, plants, and weather conditions using a digital system. Digital-related services are

widely available in rural areas that provide necessary services to citizens using an Internet connection. Digital technologies ensure the safety of products that occurred via the traceable system and detection process in the rural governance system [4, 5].

Big data analysis is a process that uses certain analytic techniques to find out particular information from a large amount of data. The big data analysis process identifies the data that is necessary for performing a particular task in a system [6]. The big data analysis process is widely used in various fields that improve the performance and reliability of an application and systems. Rural governance system uses big data analysis process to enhance the accuracy rate in providing services for people [7]. Big data analysis provides comprehensive information services for various processes in the rural governance system. Services such as data collection, analysis, processing, and storage are provided using big data analysis. The big data analysis process is an important thing that is needed in the rural governance system [8]. A big data analysis platform allows rural governance to access a huge

amount of data that are needed to perform a particular operation. The big data analysis process reduces the latency rate and energy consumption rate in the identification process which improves the effectiveness of the rural governance system [9]. In rural governance systems, the big data analysis process reduces the complexity rate in accessing and processing huge amounts of data. Hidden patterns, features, and details are identified by a big data analysis process that provides actual information for performing a task [10].

Artificial intelligence (AI) is a process that uses human intelligence to perform tasks. AI is a subset of machine learning (ML) techniques that use ML to identify the patterns and features of data. AI is mostly used in computer-based applications to improve the efficiency and effectiveness of the system [11]. AI is widely used for data analysis processes that provide several ways to capture and process information. The data analysis process plays a vital role in various fields that enhance the performance and feasibility of the system. In rural governance, an AI-based data analysis process is used to provide necessary services for the citizens [12]. AI uses ML models to perform data analysis processes in the rural governance system. AI-based data analysis process performs a process such as modeling, preparing, producing, and identifying the necessary set of data [13]. Data analysis based on AI is used to find out the particular detail about the data that are presented in the storage. The convolutional neural network (CNN) model is mostly used in a rural governance system that improves the accuracy rate in the data analysis process. CNN improves the prediction rate that increases the development and construction process of the rural governance system. Bidirectional long short-term memory (BLSTM) is also used in the data analysis process that identifies the necessary information from the database and produces a feasible set of data [14, 15]. The main contribution of MDRM is shown below.

- (i) The solution under consideration enhances the governance process's display, analysis, and engagement by utilising requirements-based intelligent processing.
- (ii) As part of this paradigm, data representation and service delegation are both subject to a linear analysis of forward regression.
- (iii) Therefore, the representation recommendations and data-driven analysis are offered through digital platform implications, which improve service availability.
- (iv) Consequently, criteria like analysis time, data processing rate, and unavailability are used to enhance the effectiveness of the proposed technique

2. Related Works

Serrano and Zorrilla [16] introduced a reference framework for the fourth industrial revolution. A data governance system is implemented in the proposed framework to get an appropriate set of data for the analysis and accessing process. Data governance systems use big data analysis processes to find out the requirements for the identification process. The

big data analysis process reduces the latency rate in the searching process. The proposed reference framework improves the performance and reliability of industry 4.0.

Castro et al. [17] proposed a new ontology-based data governance model for the big data analysis process. Distributed component-based autonomous system is presented for data governance. An ontology represents all information that is related to data governance. The proposed method improves the accuracy rate in the decision-making process. Certain semantic techniques are used here to provide automatic ontology services. The proposed model also reduces the complexity rate in the management process which enhances the feasibility of the system.

Xu et al. [18] introduced a system dynamic analysis method for data governance. The proposed method measures the container port congestion and provides an actual set of data for the further analysis process. The main of the proposed method is to check the port congestion of containers and produce necessary information for the data governance process. Experimental results show that the proposed method increases the accuracy rate in the congestion evaluation process.

Zorrilla and Yebenes [19] proposed a reference framework for a data governance system in the fourth industrial revolution. The proposed reference framework identifies the key features and patterns of industry 4.0 that provide necessary information for the analysis process. Both cloud and edge computing systems are used in reference frameworks to perform governance processes. The proposed method improves the performance and effectiveness of the data governance system.

Xiao and Xie [20] introduced big data-based rational planning for smart cities. The proposed method improves the lifestyle of people in both rural and urban areas. The rural planning process provides appropriate ideas and techniques to improve the life quality of people in rural areas. Urban governance is implemented here to improve the construction capabilities of industries. When compared with other methods, the proposed method increases the effectiveness and efficiency rate of urban enterprises and industries.

Fürstenau et al. [21] proposed a platform management framework for digital health care systems. The proposed framework captures every detail about the patients and produces a final set of data for analysis and detection process. An evaluation process is performed here to find out the exact scaling and positioning of users in the health care system. The proposed platform management framework improves the efficiency and reliability of the system by reducing the complexity rate in the management process.

Jnr [22] introduced a new governance model for distributed ledger technology (DLT) in organizations. The governance model provides an appropriate set of details for the decision-making process. The proposed model improves the understanding of the organization that enhances the efficiency of the system. DLT identifies the key issues and problems in an organization that reduces unwanted problems. The governance model enhances the adoption of DLT which accelerates the digitalization process in an organization.

Liu et al. [23] proposed a decentralized service computing paradigm using a blockchain approach for a data governance system. The blockchain approach provides the necessary set of information for a data governance system that reduces the complexity rate. The big data analysis process is used here to manage a huge amount of data in the data governance system. The proposed governance system identifies the key instruction and issues using the computing paradigm.

Bosua et al. [24] introduced a data governance framework to measure the gender diversity rate in computer science. Public data is used here to get a relevant set of information for the identification and analysis process. The proposed data governance system analyses every detail of people and produces a final set of data for the measuring process. Public data is a collection of gender information that plays a vital role in the governance system. The proposed method increases the accuracy rate in the identification process which improves the efficiency of the system.

Petersen [25] proposed blockchain-based automatic governance for business networks. The blockchain approach identifies both traditional and conceptual functions in the governance process. The proposed method performs as interorganizational governance that improves the accuracy rate in the evaluation process. Blockchain finds out the important coordinates in the governance system that enhances the safety of the organization from the attackers. Experimental results show that the proposed method improves the performance and effectiveness of the system.

König [26] introduced a new data governance system for smart cities. Both legitimacy and ethical problems are identified by the data governance system. The proposed method provides appropriate solutions to solve problems. A data governance system improves the security level of both organizations and industries that enhance the reliability and feasibility of the system. The proposed method increases the accuracy rate in the decision-making process which provides better services for the users.

Malekpour et al. [27] proposed collaborative governance for urban areas. Key principles and features are first identified by using the collaborative method. Nature-based solutions are provided by a governance method that reduces the issues and error rate in the urbanization process. Preference and influence rate of people are identified and that is used for the decision-making process. The proposed method reduces the complexity level of the data governance process which improves the effectiveness and efficiency of the system.

Sagi et al. [28] proposed a data analytic process for data governance in smart urban areas. Machine learning (ML) techniques are used in the proposed method to improve the accuracy rate in the identification process. The artificial neural network (ANN) approach is used to find out the key issues and features of the governance system. The neighborhood shapes and levels are identified by the proposed method that improves the lifestyles of urban areas. The summary of related work is discussed in Table 1.

The big data analysis process reduces the latency rate in the searching process. The identification and the

development of data processing have less accuracy and produce less feasible data. Less development and construction process of the rural governance system are obtained from all classification methods. The proposed method enhances the performance and reliability of the system.

3. Modular Data Representation Method (MDRM)

Construction and operation modes of rural governance based on AI and big data analysis are becoming a continuous representation due to the growing population and fundamental service attributes on the digital platform. Amid the challenges in rural household perceptions such as living, production, and ecological spaces are the appropriate service requirements to satisfy people's wellbeing and solve social problems (loneliness, isolation, etc.) for rural place-based development. The community, regions, bottom-up, and place-based approaches are used to incorporate local people's needs, commitments, initiatives, and meanings are often regarded as precise meaning to improve rural development. Due to differences in living, development, and production between regions, the endowment factors between the regions also vary. The unequal distribution of needs, production, and means has decreased the growth of the agricultural economy and increased social problems. However, the average distribution of needs, commitments, and means of production does not in line with the actual development means and needs; therefore the solution is the rational distribution of needs and productions between the regions. The equality and adjustment of industrial structure through digital rural governance are mainly reflected in the investment in agricultural productions through the big data analysis. The proposed method is illustrated in Figure 1.

The big data analysis accurately predicts the demand of productions and needs based on the different regions. The big data in MDRM is linearity checked with data availability and data processing with few services and demands. The data processing and the data availability in the digital platform mainly depend on the users and the services. Based on the identification of the mobile population in previous statistical surveys, the digital platforms include surveying, identifying, and fulfilling the needs, productions, and demands through application-specific user interactions that require diverse services. Therefore, regardless of the needs and demands of the users/people, reliability in data representation and distribution is a prominent consideration. The proposed MDRM method is focusing on this consideration by artificial intelligence and big data information through available digital rural governance. In this proposal, service availability is administrable for people and their services with the available digital platforms.

The AI and big data users access their services through data representation and distribution using digital rural governance. MDRM method operates between the applications and users. In this method, availability and processing for the available services and linearity check are easily able to achieve data semantics for the different users and services. Further, this method aims to provide unavailability-less data

TABLE 1: Summary of related work.

Author	Finding	Limitation
Sagi et al. [28]	The paper's contribution to urban government is the recommendation of a smart and adaptive system targeted at designating the most suitable areas for urban administration given a certain period and circumstance.	The proposed method cannot be implemented to the ever-changing conditions of urban areas.
Malekpour et al. [27]	The framework further underlines that all of those factors must be taken into account with an eye toward their intended impact degree. We will utilise real-world examples from significant Australian urban development projects to demonstrate how our approach may be put into practise.	In addition, a bridge from experimental forums to continuous collaboration structures must be provided when necessary. Policy design and large institutional reform efforts are typically used to attain this goal.
König [26]	Ethics are translated into a set of governance procedures that are at the same time grounded in the conception of democratic oversight, which is at the heart of the framework	In addition, a bridge from experimental forums to continuous collaboration structures must be provided when necessary. Policy design and large institutional reform efforts are typically used to attain this goal.
Petersen [25]	Blockchain technology now gives the capacity to automate the formulation, verification, and implementation of private ordering among exchange parties. This should drive a re-evaluation of existing theories of interorganizational administration, according to the article's conclusion.	The framework built may be empirically validated, as well as prospects for further theoretical research, and investigates the practical implications of blockchain-based governance for practitioners.

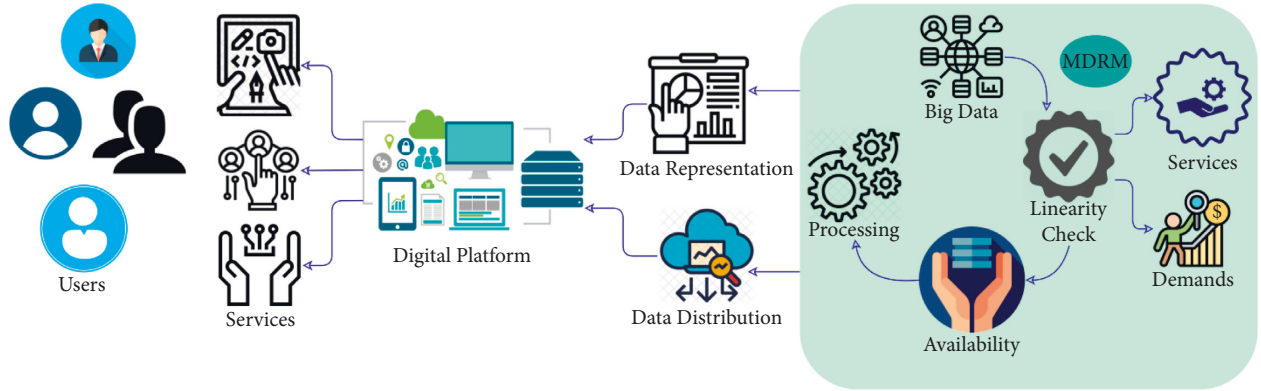


FIGURE 1: MDRM illustration.

processing and to maximize the available data distribution. The proposing method operates in two forms for data availability and processing concurrently. The data representation is different for service and delegations based on forwarding regression analysis, to check the big data availability of the users. The introducing function of the construction of digital rural governance is kept as in equations (1a) and (1b).

$$\left. \begin{aligned} & \max_{i \in t} \text{imize } u_s \forall D_r = D_d \\ & \text{and} \\ & \text{minimize } at_i \forall D_r \end{aligned} \right\} \quad (1a)$$

where

$$\left. \begin{aligned} & at_i = t_{D_d} - t_{D_r} \\ & \text{and} \\ & \text{minimize } P_r \forall i \in D_r \end{aligned} \right\} \quad (1b)$$

In the above equations (1a) and (1b), the variables s, u, D_r, D_d denote the digital platform for rural governance

relies on i^{th} service, users, data representation, and distribution at different time intervals, respectively. The data are represented in the form of different services for rural governance D_r and the data availability D_d . The data processing D_r in the form of operation helps to achieve data semantics for the different users and services. In the next continuous representation, the variables $at_i, at_{D_r},$ and at_{D_d} are used to represent analysis time, data representation time, and distributing time, respectively. The big data analysis of minimizing the processing is represented using the variable $P_r \forall i \in D_r$. Let $u = \{1, 2, \dots, u\}$ represents the set of users in the digital rural governance platform, then the number of services in the analysis time at is $D_r \times t$, whereas its data representation is $u \times D_r$. Based on the overall data representation, $u \times D_r$ and $t \times D_r$ are admissible services for data analysis. The data processing and availability are performed using presentation, analysis, and user interaction in the governance process through service requirements-based intelligent processing of the upcoming rural governance data processing. In this instance, the performance of data representation and pending services is important to identify big data information. The demanding service requirement is the

availability (A_n) of the n rural governance users; the remaining time needed for data processing is the assisting factor for improving data representation. The data distribution of the service assigned for the available n is performed based on the data organization as recommended using logical regression learning. Later, depending upon the data distribution, the service requirement processing is the augmenting factor. For the data organization, big data analysis is the requirement-based intelligent processing instance for defining different data processing. The big data analysis-based services and the available data processing is important in the following session.

Case 1. Continuous representation of services.

Analysis 1. In this continuous representation, the data distribution of $(D_r \times t)$ for all n based on A_n is considering big data analysis. The probability of surveying, identifying, and fulfilling the demands (ρ_d) through application-specific user interactions in a continuous manner is given as

$$\left. \begin{aligned} \rho_d &= (1 - \rho_{cr})^{i-1}, n \in t \\ \text{where} \\ \rho_{cr} &= \left(1 - \frac{D_r \in n}{D_r \in t}\right) \end{aligned} \right\} \quad (2)$$

In equation (2), the variables ρ_d and ρ_{cr} represent user demands and the continuous data representation follows the probability of n such that there are no pending services in the digital rural governance; hence the data distribution is computed in the above equation (1a) and 1b. Therefore, the distribution of data for ρ_d follows:

$$\text{Distribution}(n) = \frac{1}{|D_d - D_r + 1|} (\rho_d)^i, \text{ if } \forall n \in t. \quad (3)$$

However, the data distribution for n as in equation (3) is valid in both the condition of $(u \times D_r)$ and $(t \times D_d)$ ensuring the data semantics in digital platforms. Figure 2 presents the data processing for continuous representation.

The data from different real-time sources (e.g. population, land, buildings, etc.) are surveyed yearly and updated. Based on the availability/update from the governance platform, the data is split into linear and nonlinear. The linear data is used for demand satisfaction and distribution. This is used for providing a complete data representation. Contrarily, the nonlinear data is further validated for its availability and assessment (Figure 2). The big data processing of rural governance information is based on user demands and needs to reduce the problem of the unequal distribution condition $(u \times D_r) > (t \times D_d)$, and the service requirement-based intelligent processing is descriptive using the representation. Therefore, the recommended conditions $u > t$ and ρ_{cr} are less to satisfy equation (1a) and (1b). Hence, the contrary output of Case 1 is the prolonging continuous representation and therefore the analysis time, resulting in unavailability.

Case 2. Linearity analysis for data representation

Analysis 2. In the linearity check for data representation, the unbalancing condition of $u > t$ is high, and therefore the distribution of services in the digital platform is time-invariant based on the data organization. Along with the idle time of n , the big data analysis and pending services are the considering factors. The probability of linearity analysis (ρ_{L_a}) is given as

$$\rho_{L_a} = \frac{\rho_d \cdot \text{Distribution}(n) \cdot [(D_d - D_r) * \rho_{cr} - (D_d - D_r/n)u_s/t_{D_r}]}{f(d) \times n} \quad (4a)$$

where

$$f(d) \in \text{Distribution}(n) = \int_1^{D_r} at^{i-1} \cdot \frac{\rho_{cr}}{t_{D_r}} (1 - \rho_d)^{t-1} n(D_r). \quad (4b)$$

From equations (4a) and (4b), the variable $f(d)$ denotes the data distribution function for services. For all the data distribution processing, the data availability in accessing services based on n is an unavailability issue. The distribution as in equations (4a) and (4b) requires high analysis time and thereby increases the data processing rate and service delay. Figure 3 illustrates the data representation based on linear validation.

The accumulated (surveyed) data (linear and nonlinear) is distributed using $f(d)$. This relies on $f(d, S_d)$ differentiation for fetching previous data representation, and the nonlinear data is managed. After the representation, linear validation is performed for preventing unavailability (refer to Figure 3). As per the above big data analysis of Case 1 and Case 2, the differentiation of availabilities based on $u > t$ in Case 1 and n overloading and analysis time are the considering factors. These factors are addressable using logical regression learning to mitigate the problems through regression analysis; the following section illustrates the data representation for the processing to mitigate the above determining issues.

3.1. Availability and Processing Analysis Based on the Service Requirements Using Linearity Check. The decisions for performing the availability process rely on logical regression learning. It aids availability for both continuous and discrete data instances. In Case 1 (Linear/continuous) and Case 2 (nonlinear/discrete), data processing is met with the big data availability using regression learning. The data representation process depends on different service requirements and attributes for analyzing the demands and service delegations probabilities at the time of data distribution. Hence, the cases for data distribution are different from the representation process, which follows the availability procedure through representation. The data representation is prescribed in Case1 and 2 by calculating the n available probability and representation of data for analyzing time.

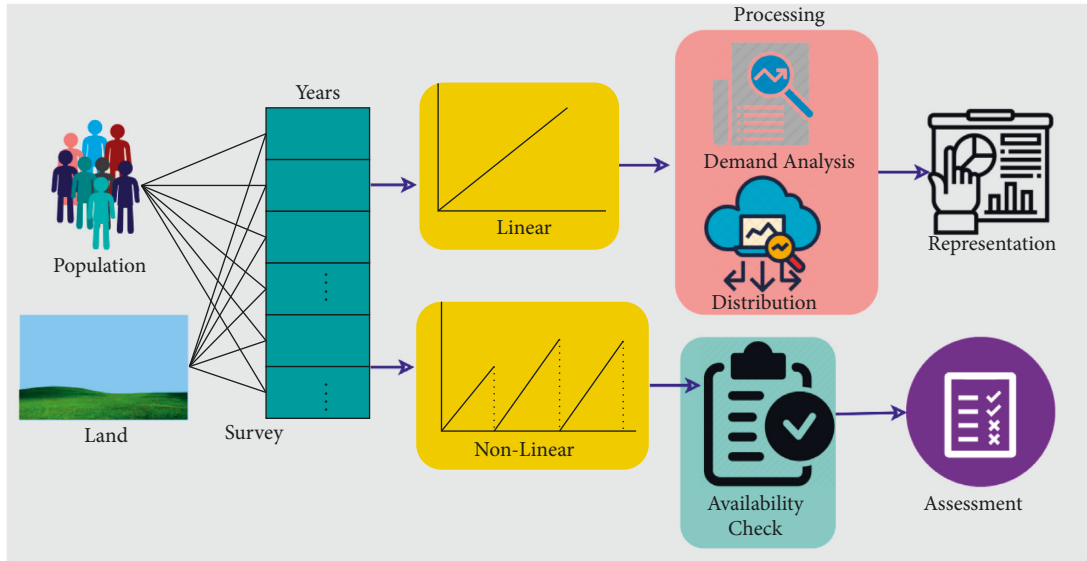


FIGURE 2: Data processing for continuous representation.

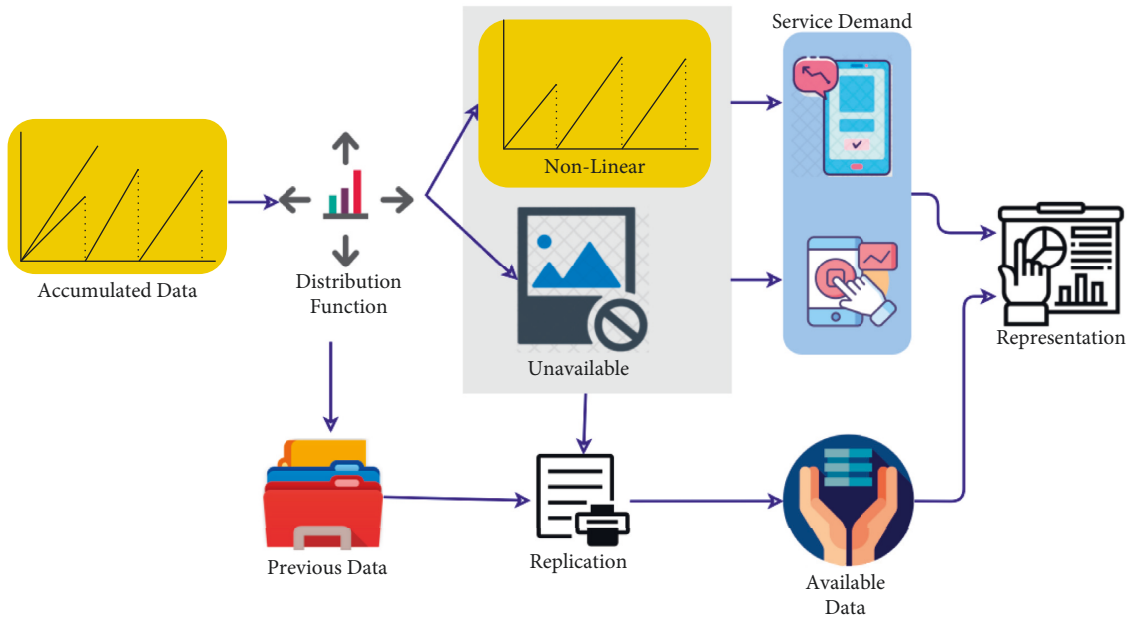


FIGURE 3: Data representation using linear validation.

The first data representation relies on maximum service delegations (S_d) and $f(d)$ as

$$\left. \begin{aligned}
 f(d, S_d) &= \left[D_d - \left(\frac{at}{t_{D_r}} \right) + \frac{1}{n} \right] - Di \text{ stribution } (n) + 1 \\
 \text{such that,} \\
 n &= \sum_{i \in s} Di \text{ stribution } (n) - (\rho_{L_a})
 \end{aligned} \right\} \quad (5)$$

In the above equation (5), the forward regression for data representation and service delegations are linearly analyzed

depending on the distribution of the services in the digital platform for Case 1 as in ρ_d and Distribution (n). Here, the chances of achieving continuous services are

$$\left. \begin{aligned}
 \rho_{L_a} \left(\frac{s}{d} \right) &= \frac{1}{\sqrt{2Nt^2}} \text{experssion} \left[\frac{D_r - \rho_{cr}}{A} \right] \\
 \text{where} \\
 A &= \frac{D_r - \rho_{cr}}{n}
 \end{aligned} \right\} \quad (6)$$

In equation (6), the aim is to balance the users and services to reduce the analysis time, and hence, the actual data distribution is given as

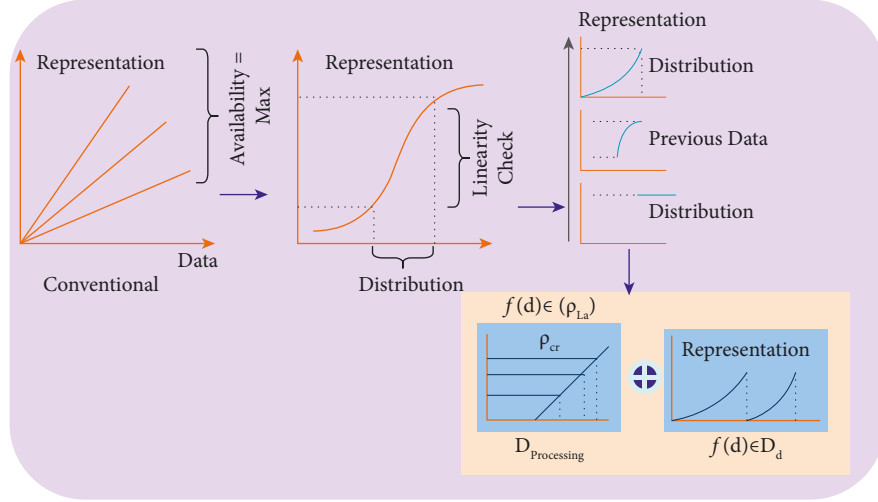


FIGURE 4: Regressive representation for distribution.

$$D_d = \max \left[\frac{\rho_d \times D_r}{D_i \text{ distribution } (n) - \rho_{cr}} \right]. \quad (7)$$

Therefore, the availability is $[1 - (\rho_d \times D_r / \text{Distribution } (n) - \rho_{cr})]$ and this availability based on the analysis time with the data processing instances of D_r . The excluding D_r is $[D_r * f(a, S_d)]$ is the P_r instances and therefore the analysis time is demandingly high. The bounds of analysis time based on demanding services (as per the distribution) in the rural governance are either of service (or) delegations, in both instances, if $\rho_{cr} = 0$, then $A = D_r = D_d$ is the maximum availability condition and if $\rho_{cr} = 1$, $D_r = D_d - n$ or $D_r = D_d$. Hence, the occurrence of $D_r = D_d$ is a regressive output. The analysis time for all the data representation (without processing) is given in equation (7). The regressive representation for distribution is depicted in Figure 4.

The data representation using logical regression is presented in Figure 4. The initial classification is based on linearity and distribution checks. In this process, the $f(d) \in \rho(L_a)$ and $f(d) \in D_d$ are classified for further analysis. Based on the analysis, data processing and augmentation are determined. In this scenario, the available users and services in the digital platform and the data representation and distribution are processed, hence the analysis time is consistent as in equation (1a) and 1b. The process of availability is $(D_r - \rho_{cr} * n)$ and $\sqrt{2\pi} (t)^2$, this analysis determines the representation and analysis time along with the data processing rate for the processing D_r . The availability process of $(D_r - \rho_{cr} * n)$ and $\sqrt{2\pi} (t)^2$ from the available services is illustrated, respectively. The availability process of big data information is based on a linearity check for data representation and service delegations of (D_r, D_d) and (D_{rs-1}, D_{ds-1}) based on available services from the data representation. The probability of ρ_{cr} and ρ_d and ρ_{L_a} is the considering factor for both types of availability processing as given in the above equation. The availability occurrences for (D_r, D_d) and (D_{rs-1}, D_{ds-1}) is linearly analyzed based on S_d for $f(d)$ is given as

$$\text{Availability } (n) = \begin{cases} \frac{n - (\rho_{cr} \times D_r)}{n + (\rho_d) D_r} \forall D_r = D_d. \\ \frac{n - (\rho_{cr} \times D_r)}{n + (\rho_d + \rho_{L_a} - \rho_{cr}) D_r} \forall D_r < D_d, \end{cases} \quad (8)$$

In this case of availability, n (or) $(n - (D_r/A))$ is the data distribution irrespective of the users and services. In the next section of data representation, minimizing $P_r = \{1, 2, \dots, D_r\}$ as from equation (8) is discussed to reduce unavailability and service delays.

3.2. Processing. The data representation recommendation and data-driven analysis follow either of the distribution as in equation (8). It is different for both the data representation and distribution as the first instance requires no more users and services, whereas the second instance requires distribution as $(n - D_r)$ is the retaining data representation. As per the sequence in the previous section, the representation of data for $P_r \in D_d = (n + 1) D_r / n$ is regressive and it does not require additional analysis time for processing. In the data processing ($D_{\text{Processing}}$) of a service requirement in this data, distribution is the considering factor and it differs for each n depending on the availability of processing (n_p). This analysis time is computed using equation (9) for both instances in equation (7)

$$D_{\text{Processing}} = \frac{n_p}{\text{Distribution } (n)} + \frac{f(a, S_d)(\rho_{cr} + \rho_{L_a} - \rho_d)}{\text{Distribution } (n)}, \forall D_d < D_r. \quad (9)$$

In equation (9), $D_{\text{Processing}} \in [D_d, D_r]$ and the last of data processing (i.e.) $(D_{\text{Processing}} * D_r)$ are the maximum analysis time and data processing rate (increase) for handling $(n - D_r)$ representations. Therefore, the distribution of data for all $s \in D_r$ increases both P_r and $a_i \forall i \in D_r$. This data

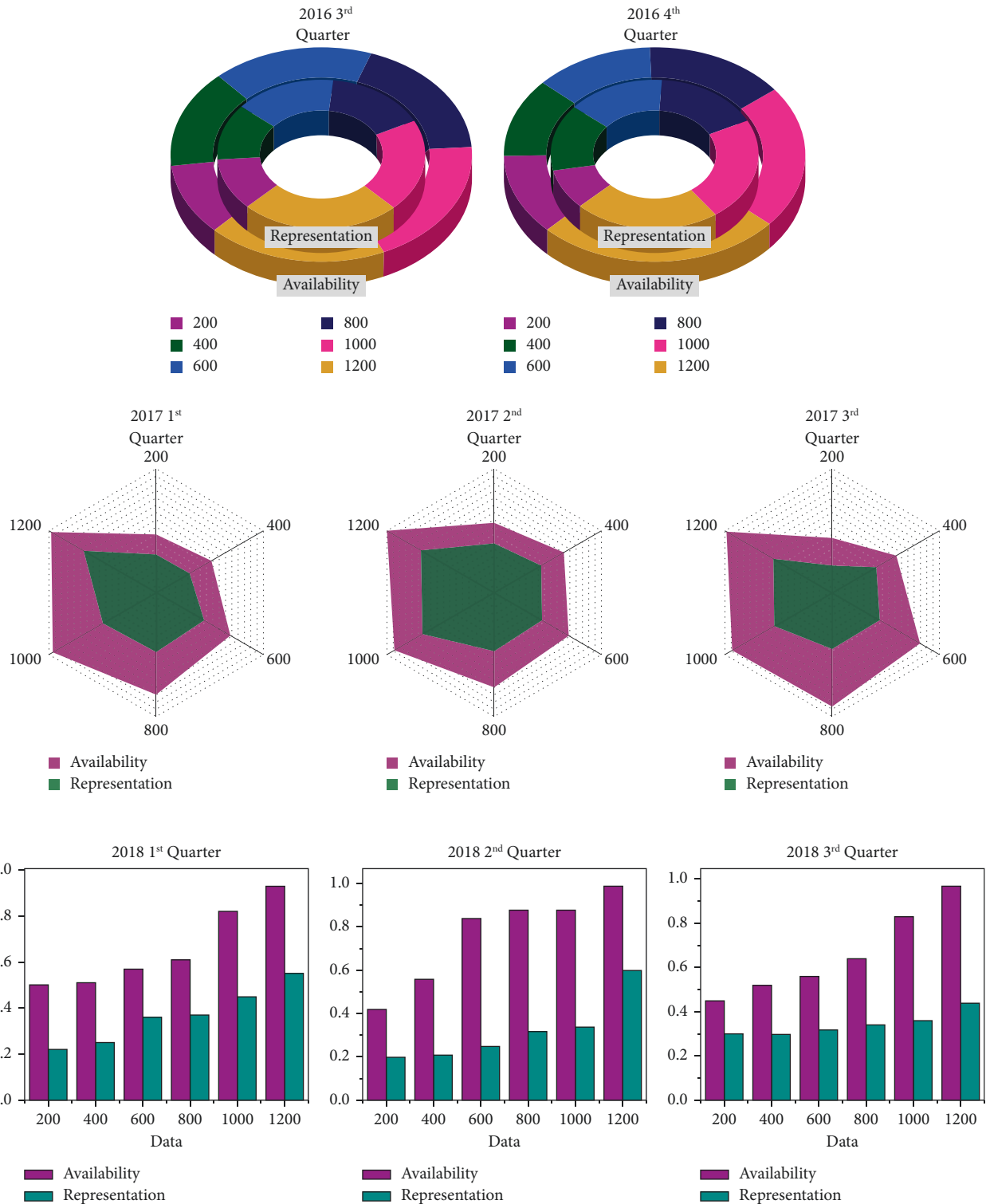


FIGURE 5: Availability and representation.

distribution process as mentioned above depends on available n users and services without requiring additional processing and relies on two instances of S distribution. The services in the digital platform performed under $0 < \rho_A < 1$ in the previous service availability. The data distribution follows the condition $0 < \rho_A < 1$ and $\rho_A = 1$ of n services such

that the representation recommendation and data-driven analysis are performed. Here, the analysis time of service requirements is the sum of service delegations in two or more n that do not augment $n \in \rho_r$. Therefore, the unavailability is identified between processes of $0 < \rho_A < 1$ and $P_r = 1$ processing without increasing the availability and

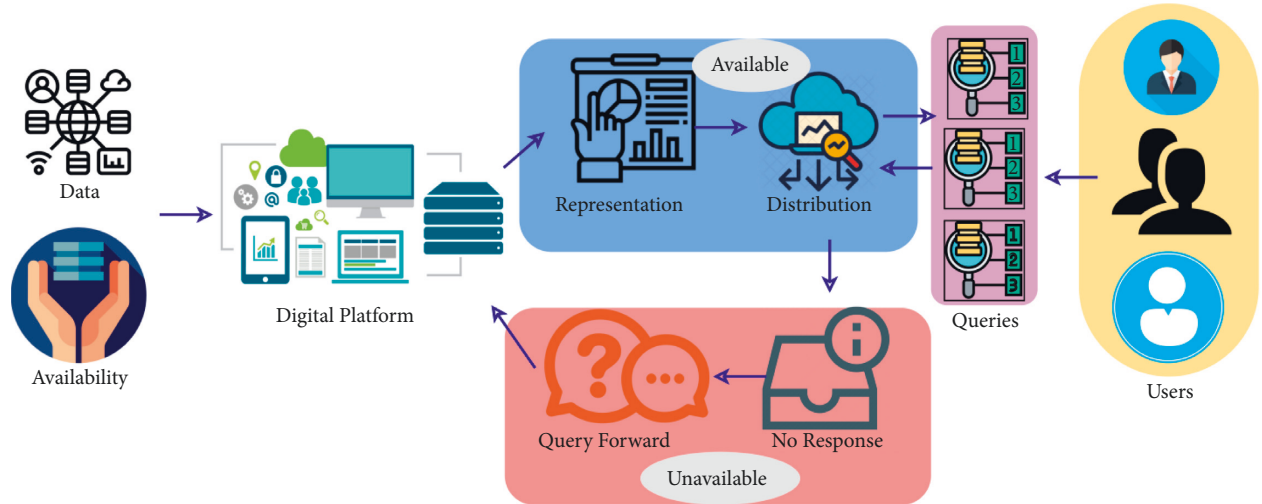


FIGURE 6: Available and unavailable data illustration.

reducing unavailability other than linearly analyzing the services. The pending service in the rural governance is served in this continuous manner, reducing the unavailability. The data between 2016 and 2018 is analyzed for availability and representation as in Figure 5.

The above representation is provided before regressive implication for identifying missing input data. The representation is provided for the data available for the service queries. A formal illustration for differentiating available and unavailable data is presented in Figure 6.

Depending upon the queries and responses, the available and unavailable data are linked to digital platform. The user requests for services are forwarded based on availability and analysis. If the unavailable data is accessed, then the query is forwarded to the service provider. Depending on the availability, the representation is modified due to which the availability chances are high. For the unavailable data, filling from the previous instances is performed for meeting the user demands. The filling is performed using regressive learning, as a sample illustration of data between 2016 and 2018 in Table 2.

The available data is marked as 1 else 0 based on the data set information. The unavailable data is regressed linearly for preventing unnecessary lag in data distribution. Based on Availability (n), the regression model is estimated as in Figure 7.

The regressive analysis relies on ρ_{L_q} and $f(d)$ for precise data distribution, representation, and analysis. This is required for preventing unavailability based on $D_{\text{processing}}$; it is improved for improving the data availability. The failing regressive processes are recused for cumulative data representations, preventing failures. After the regressive process, the data-related attributes are tabulated in Table 3.

4. Results and Discussion

The performance of the proposed method is analyzed using a test case for data representation obtained from [29]. This data source provides food outlets opened between 2016 and

TABLE 2: Data availability between 2016 and 2018.

Year	Name	Services	Human resource	Values	Profit	Loss	Variables
2016	0	1	1	0	0	1	1
2017	0	1	1	0	0	0	1
2018	1	1	1	0	0	1	0

2018 in rural regions of Mississippi. The data representations are projected based on available services; distinguishing distribution and previous data. The dataset contains 8 fields based on installation, commissioning, and running details. With this information, the data analysis and representation are analyzed.

4.1. Discussion on Comparative Analysis

4.1.1. Analysis Time. In Figure 8, the rural governance depends on population, distinct geographical and fundamental service attributes in digital platform based on artificial intelligence, and big data analysis for deploying operation modes and digital construction are the consideration factor that does not provide continuous data representation at different intervals. The forward regression for data representation and service delegations based on data semantics for the available services and linearity checking for the availability considered for further application-specific user interactions based on service requirements for both the instance $u \times D_r$ and $t \times D_r$ in a consecutive analysis of data processing. This availability monitoring analysis is addressed by linearity analysis based on rural governance construction $P_r \forall i \in D_r$ in the previous survey-based on analysis time and processing, preventing unavailability. Rural governance includes surveying, identifying, and fulfilling the demands that are analyzed based on the user interactions depending on the logical regression analysis that provides data distribution for service requirements and data organization in the digital platform. Based on the unavailability and processing

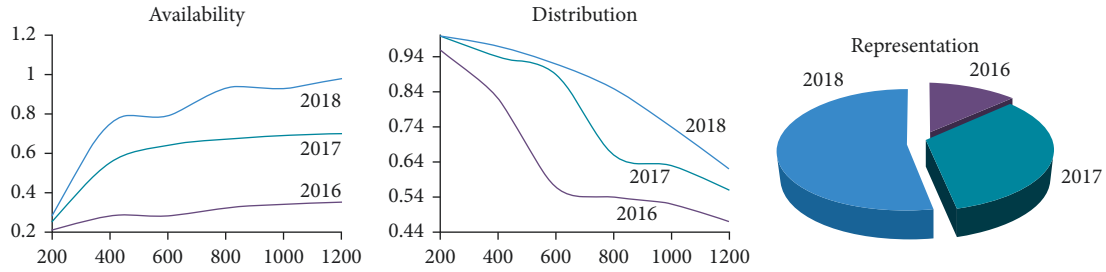


FIGURE 7: Regression model outputs.

TABLE 3: Postregression data features.

Metric	Before			After		
	Availability	Representation	Distribution	Availability	Representation	Distribution
Name	0.3	0.21	0.4	0.58	0.41	0.6
Services	0.32	0.31	0.51	0.62	0.48	0.74
HR	0.41	0.39	0.59	0.59	0.52	0.68
Values	0.52	0.43	0.63	0.65	0.74	0.76
Profit	1	0.74	0.74	1	0.87	0.97
Loss	0.65	0.35	0.89	0.74	0.75	0.84
Variable	0.82	0.69	0.92	0.98	0.82	0.89

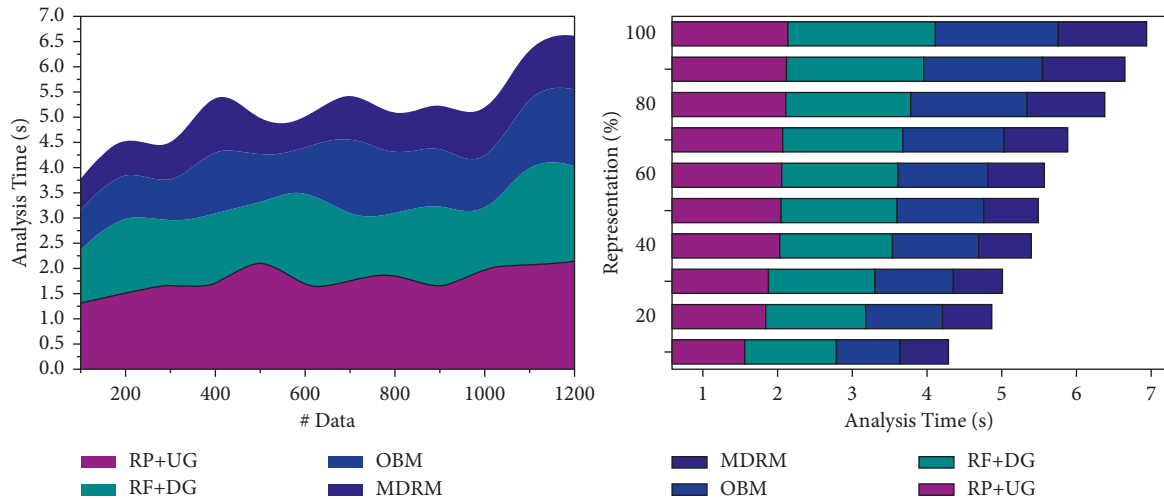


FIGURE 8: Analysis time.

rate in the rural governance, the proposed method satisfies less analysis time.

4.1.2. Data Processing Rate. The availability and processing analysis for digital rural governance in big data analysis are represented in Figure 9. This proposed method satisfies fewer data processing rates by computing the service requirements based on application-specific user interactions and fundamental service attributes in the digital platform at different time intervals and fulfilling the user demands and needs. In this unavailability and processing based on discrete data representation, such that $(1 - D_r \in n/D_r \in t)$ is performed and reduces the need for additional representation. The proposed method identifies the digital platform implications for mitigating service availability depending upon the data representation and

distribution in a digital platform, wherein the services in rural governance digital platform based on analysis time are preceded using equations (4a)–(7) estimation. This continuous representation processing prevents linearity analysis to forward regression through regression learning based on the unavailability, service-based attributes and requirements and analyzed through regression learning. Based on this consecutive manner of data representation, the analysis time of service delegations is computed at different time intervals.

4.1.3. Unavailability. This proposed method augments the analysis, presentation, and interaction in the governance process through requirements-based intelligent processing between analysis time intervals and does not provide data semantics during processing in the digital platform. The computation of

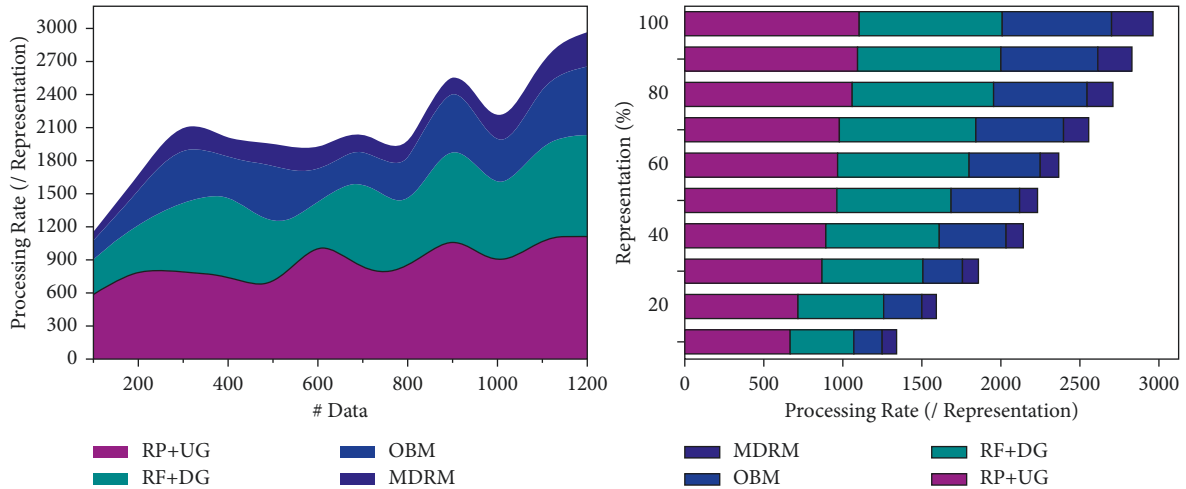


FIGURE 9: Processing rate.

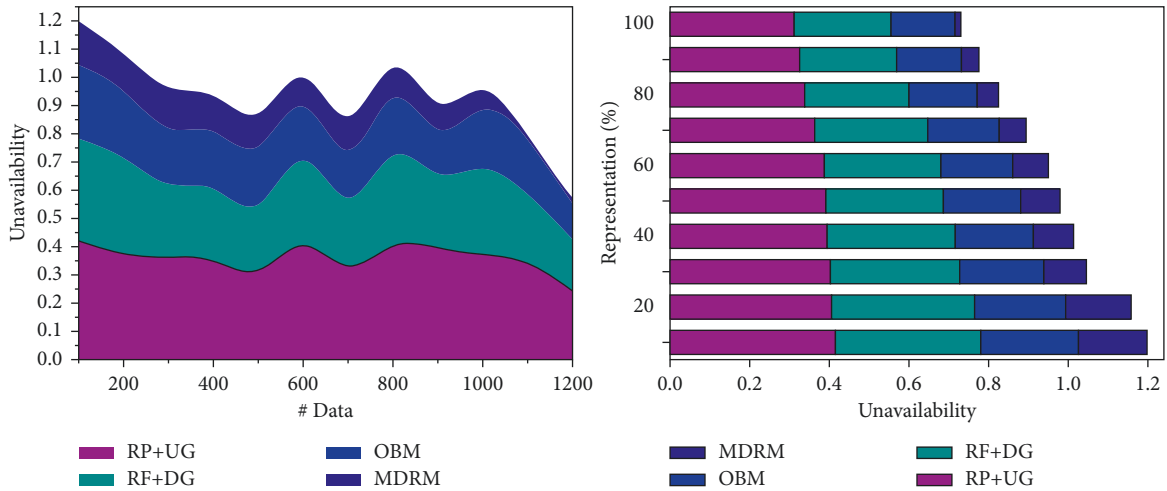


FIGURE 10: Unavailability.

the fundamental service attribute is considering factors based on the data organization and linearity checking based on data representation. Distribution (n) is computed using unavailability identification and service delegations for analysis time and data distribution analysis sequence of users and services-based linear and nonlinear data processing can be analyzed for the above condition in the digital platform. Based on the unavailability and service-based attributes, requirements are analyzed through regression learning. The analysis of data representation can be processed in two conditions, namely processing and availability analysis are performed based on the service distribution at a different time interval and then previous regressive output without increasing the analysis time. The proposed method provides linearity analysis based on the service requirements and attributes for which digital rural governance achieves less unavailability as presented in Figure 10.

4.1.4. Service Delegation. This proposed method achieves high service delegations for rural governance and the unavailability of big data monitoring based on data

representation at different intervals is aided in identifying the service requirements (refer to Figure 11). The continuous representation analysis and linearity checking are mitigated based on $u > t$ the rural governance users, and services for analyzing the big data information due to representation recommendation and data-driven analysis in the digital platform through logical regression learning. The service unavailability is due to data representation and service delegations in rural governance applications based on AI and Big Data analysis in a different interval for service unavailability identification for reducing the data processing rate based on the fundamental service attributes observed from the services in both the instances $D_r = D_d - n$ and $D_r = D_d$ for available users and services of processing require the previous survey about the services in the rural governance. Therefore, the linearity checking based on Big Data for increasing the data processing rate for verifying linearity depends on considering factors in the digital platform, and therefore, the service delegation is high and service availability also increases. The above comparative analysis is summarized in Tables 4 and 5 for the varying # Data and Representation %

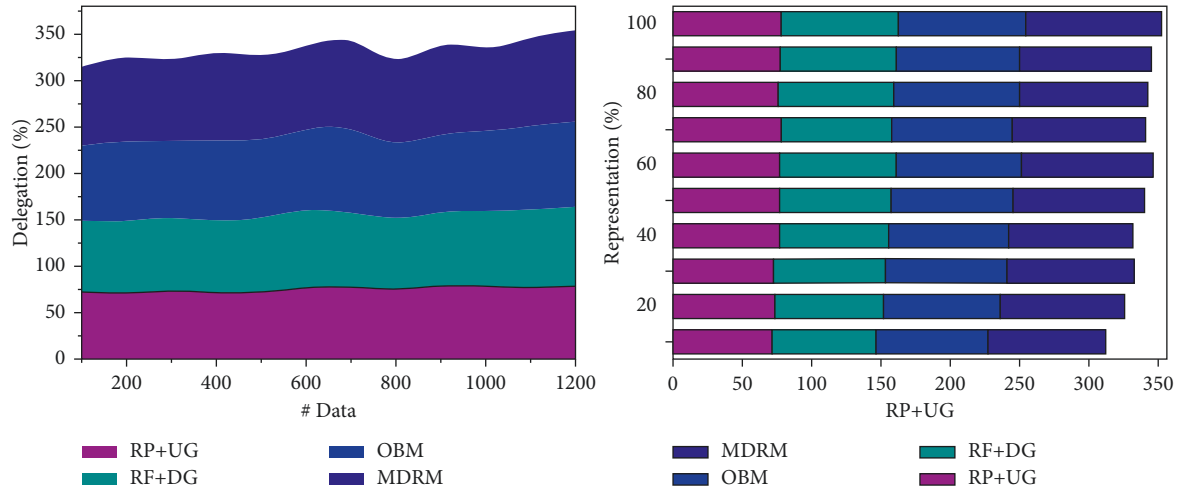


FIGURE 11: Delegation %.

TABLE 4: Comparative analysis summary (varying data).

Metrics	RP + UG	RF + DG	OBM	MDRM	Findings
Analysis time (s)	2.14	1.89	1.52	1.074	6.9% less
Processing rate (/representaion)	1106	921	626	311	10.81% less
Unavailability	0.242	0.182	0.122	0.024	15.8% less
Delegation %	78.52	84.71	92.38	98.508	13.3% high

TABLE 5: Comparative analysis summary (varying representation %).

Metrics	RP + UG	RF + DG	OBM	MDRM	Findings
Analysis time (s)	2.14	1.97	1.64	1.191	6.3% less
Processing rate (/representation)	1103	904	687	270	11.65% less
Unavailability	0.312	0.243	0.161	0.0149	11.19% less
Delegation %	78.28	84.63	91.32	98.044	13.3% high

5. Conclusion

This article introduced a modular data representation method for improving the service availability of rural governance on digital platforms. The semantics-based data analysis, distribution, and representation are performed using this method aided by artificial intelligence and digital scenarios. The preprocessed data organization, availability, and linear analysis are aided by regression learning. Based on the availability, the continuous and processing distributions are analyzed for preventing retardations in service delegations. The service requirements are satisfied using diverse representations as deserved from the regressive output. The service distribution is planned based on previous delegations and current data available for ensuring maximum service delegations. This induces improvements in data processing with limited time for different services. For the varying representation ratios, the proposed method achieves 6.3% less analysis time, 11.65% less processing rate per representation, 11.19% less unavailability, and 13.3% high service delegation.

Data Availability

Data sharing is not applicable to this article as no datasets were generated or analyzed during the current study.

Conflicts of Interest

The authors declare that there are no conflicts of interest with any financial organizations regarding the material reported in this article.

References

- [1] C. Georgios and H. Barraí, "Social innovation in rural governance: a comparative case study across the marginalised rural EU," *Journal of Rural Studies*, 2021.
- [2] K. Kosec and L. Wantchekon, "Can information improve rural governance and service delivery?" *World Development*, vol. 125, Article ID 104376, 2020.
- [3] Q. Li, L. Lan, N. Zeng et al., "A framework for big data governance to advance RHINs: a case study of China," *IEEE Access*, vol. 7, pp. 50330–50338, 2019.
- [4] I. Merrell, *Blockchain for Decentralised Rural Development and Governance*, p. 100086, Blockchain, NE1 7RU, UK, 2022.
- [5] M. Al-Ruithe, E. Benkhelifa, and K. Hameed, "A systematic literature review of data governance and cloud data governance," *Personal and Ubiquitous Computing*, vol. 23, no. 5-6, pp. 839–859, 2019.
- [6] M. C. Iban and O. Aksu, "A model for big spatial rural data infrastructure in Turkey: sensor-driven and integrative approach," *Land Use Policy*, vol. 91, Article ID 104376, 2020.

- [7] L. Yang, J. Li, N. Elisa, T. Prickett, and F. Chao, "Towards big data governance in cybersecurity," *Data-Enabled Discovery and Applications*, vol. 3, no. 1, p. 10, 2019.
- [8] T. Deng, K. Zhang, and Z. J. M. Shen, "A systematic review of a digital twin city: a new pattern of urban governance toward smart cities," *Journal of Management Science and Engineering*, vol. 6, no. 2, pp. 125–134, 2021.
- [9] R. Wei, X. Wang, and Y. Chang, "The effects of platform governance mechanisms on customer participation in supplier new product development," *Journal of Business Research*, vol. 137, pp. 475–487, 2021.
- [10] B. Carballa Smichowski, "Alternative data governance models: moving beyond one-size-fits-all solutions," *Inter-economics*, vol. 54, no. 4, pp. 222–227, 2019.
- [11] A. Zuiderwijk, Y. C. Chen, and F. Salem, "Implications of the use of artificial intelligence in public governance: a systematic literature review and a research agenda," *Government Information Quarterly*, vol. 38, no. 3, Article ID 101577, 2021.
- [12] D. M. F. Saldanha, C. N. Dias, and S. Guillaumon, "Transparency and accountability in digital public services: learning from the Brazilian cases," *Government Information Quarterly*, vol. 39, no. 2, Article ID 101680, 2022.
- [13] M. Solvak, T. Unt, D. Rozgonjuk, A. Vörk, M. Veskimäe, and K. Vassil, "E-governance diffusion: population level e-service adoption rates and usage patterns," *Telematics and Informatics*, vol. 36, pp. 39–54, 2019.
- [14] L. Lepore, L. Landriani, S. Pisano, G. D'Amore, and S. Pozzoli, "Corporate governance in the digital age: the role of social media and board independence in CSR disclosure. Evidence from Italian listed companies," *Journal of Management & Governance*, pp. 1–37, 2022.
- [15] B. Engels, "Data governance as the enabler of the data economy," *Inter-economics*, vol. 54, no. 4, pp. 216–222, 2019.
- [16] J. Serrano and M. Zorrilla, "A data governance framework for Industry 4.0," *IEEE Latin America Transactions*, vol. 19, no. 12, pp. 2130–2138, 2021.
- [17] A. Castro, V. A. Villagra, P. Garcia, D. Rivera, and D. Toledo, "An ontological-based model to data governance for big data," *IEEE Access*, vol. 9, pp. 109943–109959, 2021.
- [18] B. Xu, J. Li, X. Liu, and Y. Yang, "System dynamics analysis for the governance measures against container port congestion," *IEEE Access*, vol. 9, pp. 13612–13623, 2021.
- [19] M. Zorrilla and J. Yebenes, "A reference framework for the implementation of data governance systems for industry 4.0," *Computer Standards & Interfaces*, vol. 81, Article ID 103595, 2022.
- [20] X. Xiao and C. Xie, "Rational planning and urban governance based on smart cities and big data," *Environmental Technology & Innovation*, vol. 21, Article ID 101381, 2021.
- [21] D. Fürstenu, C. Auschra, S. Klein, and M. Gersch, "A process perspective on platform design and management: evidence from a digital platform in health care," *Electronic Markets*, vol. 29, no. 4, pp. 581–596, 2019.
- [22] B. A. Jnr, "Toward a collaborative governance model for distributed ledger technology adoption in organizations," *Environment Systems and Decisions*, vol. 42, pp. 276–294, 2022.
- [23] X. Liu, S. X. Sun, and G. Huang, "Decentralized services computing paradigm for blockchain-based data governance: programmability, interoperability, and intelligence," *IEEE Transactions on Services Computing*, vol. 13, no. 2, pp. 343–355, 2019.
- [24] R. Bosua, M. Cheong, K. Clark et al., "Using public data to measure diversity in computer science research communities: a critical data governance perspective," *Computer Law & Security Report*, vol. 44, Article ID 105655, 2022.
- [25] D. Petersen, "Automating governance: blockchain delivered governance for business networks," *Industrial Marketing Management*, vol. 102, pp. 177–189, 2022.
- [26] P. D. König, "Citizen-centered data governance in the smart city: from ethics to accountability," *Sustainable Cities and Society*, vol. 75, Article ID 103308, 2021.
- [27] S. Malekpour, S. Tawfik, and C. Chesterfield, "Designing collaborative governance for nature-based solutions," *Urban Forestry and Urban Greening*, vol. 62, Article ID 127177, 2021.
- [28] A. Sagi, A. Gal, D. Czamanski, and D. Broitman, "Uncovering the shape of neighborhoods: harnessing data analytics for a smart governance of urban areas," *Journal of Urban Management*, vol. 11, no. 2, pp. 178–187, 2022.
- [29] "Delta Food Outlets Study," 2020, <https://data.world/us-usdago/296e839e-e659-45d6-be6c-7970d988e9f7>.

Research Article

Deep Collaborative Filtering: A Recommendation Method for Crowdfunding Project Based on the Integration of Deep Neural Network and Collaborative Filtering

Pei Yin , Jing Wang, Jun Zhao, Huan Wang, and Hongcheng Gan

Business School, University of Shanghai for Science and Technology, 516 Jungong Road, Shanghai 200093, China

Correspondence should be addressed to Pei Yin; pyin@usst.edu.cn

Received 13 April 2022; Revised 1 June 2022; Accepted 29 June 2022; Published 21 July 2022

Academic Editor: Wei Liu

Copyright © 2022 Pei Yin et al. This is an open access article distributed under the Creative Commons Attribution License, which permits unrestricted use, distribution, and reproduction in any medium, provided the original work is properly cited.

In real recommendation systems, implicit feedback data is more common and easier to obtain, and recommendation algorithms based on such data will be more applicable. However, implicit feedback data cannot directly express user preferences. Meanwhile, data sparsity caused by massive data is still an urgent problem to be solved in recommendation system. In response to this phenomenon, this paper proposes a deep collaborative filtering algorithm. In the perspective of implicit feedback, this method uses the advantages of convolutional neural network for effective learning of the nonlinear interaction of users and items and the characteristics of collaborative filtering algorithm for modeling the linear interaction of users and items and combines the two methods for recommendation. Finally, the baseline method is set up and the comparative experiment and parameter adjustment is carried out. The experimental results show that the proposed algorithm has significantly improved the recommendation accuracy on public dataset (Yahoo! Movie). The parameter adjustment results show that, under the condition of uniformly collecting negative feedback data and setting a certain number of convolution layers, the sparser the data is, the better the recommendation performs. As a result, this paper has made some progress in solving the problem of data sparsity and enriching the research of recommendation system.

1. Introduction

Crowdfunding is a new financing method that emerged with the rise of the Internet [1]. So far, Kickstarter1, the world's largest crowdfunding platform, has successfully raised \$4,384,962,222 for 165,564 projects and the famous European crowdfunding platform Ulule2 has more than 2.6 million users and has successfully funded 28,294 projects, with a total financing amount of €143,381,350. However, Kickstarter's funding success rate is only 37%, and Ulule's is only 65%. Project creativity, project advertising exposure, and project duration may affect the success rate of project financing [2]. However, the biggest reason is that there are so many projects on the platform that it is difficult for investors to browse the projects that they are really interested in. Therefore, crowdfunding project recommendation, matching investors' preferences, is conducive to improving the platform's financing success rate.

The survey shows that the sparsity of user behavior on most crowdfunding platforms is higher than 99%. Too sparse data makes common collaborative filtering algorithms invalid, such as user-based collaborative filtering. Due to the lack of a large amount of data, similarity between users cannot be calculated effectively. In addition, the public datasets commonly used in recommender system research are user ratings, such as Movie-lens, Netflix Prize, etc. These datasets can directly judge the level of interest of users according to the score, so as to determine positive and negative feedback data. However, the user investment behavior data of crowdfunding websites does not have a clear score, which belongs to the implicit feedback data.

For the sake of reducing the impact of sparse data on recommendation, the matrix decomposition technology represented by Singular Value Decomposition (SVD) decomposed the user's rating of the item into the eigenvector

matrix of the user and the item and utilized the potential relationship between the user and the item to obtain the predicted value, so as to achieve the dimension reduction of high-dimensional sparse matrix. Then, after dimensionality reduction [3], matrix decomposition uses low-dimensional space to estimate high-dimensional user-item interaction, affecting the accuracy of recommendation.

For the past few years, the deep learning technology developed by artificial neural network has achieved remarkable results in the fields of natural language understanding, speech recognition [4], and image processing. Deep neural network in deep learning has brought new ideas to the research of recommendation system. Therefore, by combining deep learning technology, it can make up for the simple linear combination of traditional collaborative filtering when learning complex user-item interactions.

Therefore, this paper proposes a deep collaborative filtering algorithm based on matrix factorization (CNNMF). The algorithm uses the Kronecker product to calculate the relationship between users and items to construct a relationship graph and then uses a convolutional neural network to perform nonlinear learning on the relationship graph. Finally, through comparative experiments, the influence of linear and nonlinear relationship on recommendation accuracy is investigated. The experimental data in this paper are extremely sparse implicit feedback data with little feature information.

The contributions of this paper are summarized as follows:

- (1) Take Internet financial projects as the object, by designing recommendation algorithms, quantifying investors' preferences, and realizing accurate project recommendation, thereby improving the success rate of project financing.
- (2) Define a new model called "deep collaborative filtering algorithm based on matrix factorization." The algorithm calculates the relationship between users and items by Kronecker product, constructs a relationship graph, and then uses the advantage of convolutional neural network to effectively learn local features to perform nonlinear learning on the relationship graph.
- (3) The experimental data is extremely sparse implicit feedback data with little feature information. Combined with the characteristics of crowdfunding websites and recommendation algorithms, we conduct in-depth research to solve the problem of sparse implicit feedback data, which has certain practical significance and enriches the research on recommendation systems of crowdfunding platforms.

The rest of the paper is organized as follows. The second part of this paper will introduce the research status of collaborative filtering recommendation in detail and fully understand the main content, existing problems, and current research trends of collaborative filtering recommendation. In the third part, combined with the characteristics of collaborative filtering algorithm to model user-item

interaction information and the advantages of convolutional neural network to extract features, the implementation process of deep collaborative filtering algorithm based on matrix decomposition is described in detail. In the fourth and fifth parts, experiments and analysis are carried out. First of all, this paper is a research on the data of crowdfunding websites, so the data of crowdfunding websites are collected, processed, and analyzed. Then, the evaluation method and experimental design are proposed. Furthermore, the experiment is carried out with the user-item implicit feedback data of crowdfunding websites as the object, and the influences of the number of hidden factors in the hidden layer, the number of convolution layers, and different negative feedback data collection methods on the recommendation effect are compared. And compare and analyze the performance of the algorithm proposed in this paper with the baseline method. Finally, a summary and outlook are given, and the research work and experimental results of this paper are summarized. On this basis, the shortcomings of the work are discussed, and the future research direction of the algorithm combining deep neural network and collaborative filtering is prospected.

2. Related Works

2.1. Recommendation in Crowdfunding Platforms. Recently, researchers have begun to focus on designing recommender systems for crowdfunding platforms, with the aim of increasing the success rate of projects getting fully funded. The research of the researchers mainly focuses on two aspects. On the one hand, the recommendation algorithm is constructed based on the mathematical model. For example, Vineeth et al. [5] proposed a probabilistic recommendation model called CrowdRec, which recommends projects to investors by combining the ongoing state of the project, the individual preferences of individual members, and the collective preferences of groups. Song et al. [6] proposed a recommender system based on a structural econometric model to match returning donors with fundraising activities on charitable crowdfunding platforms. Maximize the utility of altruism (from the welfare of others) and egoism (from personal motivation). Zhang and Zhang [7] proposed a personalized crowdfunding platform recommendation system, which is based on a multiobjective evolutionary algorithm. Consider the profit and variety of recommendations while capturing investor preferences. However, it is not very effective for crowdfunding platforms with a lot of data, on the other hand, building a crowdfunding platform personalized recommendation algorithm based on machine learning. For example, Benin [8] compared the application of various machine learning algorithms in crowdfunding platforms, such as gradient boosting tree, Bayesian belief nets collaborative filtering, latent semantic collaborative filtering etc. Wang and Chen [9] proposed a bipartite graph-based collaborative filtering model by combining collaborative filtering and personal rank. The model divides the nodes into user nodes and market activity nodes, calculates the global similarity by

personal rank, and finally generates a recommendation list for any node through the collaborative filtering algorithm.

Although some scholars have found that collaborative filtering alleviates the problem of data sparseness, it is far from deep learning. Deep learning technology can extract more complex and abstract features from historical user-item interaction data and has a strong ability to represent large-scale data, but few scholars have applied it to crowdfunding platform recommendation.

2.2. Recommender Systems. Collaborative filtering algorithms have been widely used in recommender systems. Hu et al. [10] divided collaborative filtering recommendation algorithms into two main categories: one is memory-based collaborative filtering recommendation, and the other is model-based collaborative filtering recommendation. For the past few years, with the rapid rise of artificial intelligence research, deep learning technology is gradually applied to collaborative filtering recommendation. Since it mainly constructs models to learn user preferences, it is also a model-based collaborative filtering recommendation.

2.2.1. Memory-Based Collaborative Filtering. Memory-based collaborative filtering recommendations usually load data into memory for operations and generate recommendations based on similarity. These include user-based CF and item-based CF collaborative recommendation. For example, Zhan and Hong [11] proposed the ternary interaction between consumers, items, and producers. By using the collaborative filtering recommendation based on adversarial learning, disturbances were added to the parameters of the ternary model to solve the binary interaction problem and improve the accuracy. Zhu et al. [12] proposed an algorithm that fuses time weighting factors and item attributes based on user rating preferences. The algorithm considers the user's preference for items is time-sensitive and the impact of item attributes on similarity to improve the calculation of item similarity. However, it is difficult for both user-based and item-based algorithms to solve the problem of data sparsity effectively, so many scholars have conducted improvement research on this problem in recent years. For example, Hong and Yu [13] proposed a collaborative filtering recommendation algorithm based on correlation coefficient. This algorithm is founded on item-based collaborative filtering algorithm, fills unrated items in accordance with the correlation coefficient, and introduces semantic similarity to improve the calculation of item similarity to deal with data sparsity. Logesh et al. [14] proposed a collaborative filtering recommendation system based on bio-inspired clustering ensemble, which finds the closest neighborhood for users by clustering method and generates similarity matrix for recommendation.

2.2.2. Model-Based Collaborative Filtering. Model-based collaborative filtering is to build a model in the light of the user's historical ratings to predict scores. Such methods usually employ dimensionality reduction to extract latent

features of users and items. For example, Wang et al. [15] proposed an algorithm that combines the Singular Value Decomposition (SVD) technology with the trust model, which reduces the dimension of a high-dimensional sparse matrix and then improves the prediction accuracy by introducing a trust factor. However, SVD is too slow when decomposing data with dimensions above 1000, and it has certain limitations in the calculation of up to tens of millions of dimensions in real systems.

In recommender system research, implicit feedback data is more common than explicit feedback data (such as ratings), including user clicks, purchases, and searches, etc., which has attracted more and more scholars' attention. For example, Hu et al. [16] model the implicit feedback data based on matrix factorization. They believe that explicit feedback represents the user's preference for items, while implicit feedback represents the confidence of the preference, so that the user behavior data is decomposed into preference and confidence. And then they use the objective function of matrix decomposition to solve it; Koren and Bell [17] proposed a matrix factorization model supporting implicit feedback (SVD++), which is an improved algorithm on the basis of SVD. The introduction of implicit feedback information increases the prediction accuracy. Bi-yi et al. [18] proposed an EIFCF algorithm combined with explicit and implicit feedback, which makes the most of the implicit feedback data to reflect the user's hidden preference and the explicit feedback to reflect the user's preference. Besides, weighted matrix factorization is used to overcome the problem of lack of negative samples in implicit feedback data, thereby alleviating the impact of data sparsity.

2.2.3. Deep Learning-Based Collaborative Filtering. With the continuous research and application of deep learning technology, collaborative filtering based on deep learning has developed into a hot research trend, which not only improves the accuracy of recommendation and broadens application scenarios, but also enriches model-based collaborative filtering recommendations.

Deep learning can use deep neural networks to learn the raw data, so as to find the more abstract feature representation relationships between users and items in a finer-grained manner. For instance, Yi et al. [19] proposed a deep matrix factorization model embedded with implicit feedback. This model constructs a deep network pool to extract latent factors from the input of user and item information and uses them to predict user ratings. Wu et al. [20] proposed a collaborative denoising autoencoder model (CDAE). By adding noise to the user's rating vector, the robustness of this model is improved, and the low-dimensional user implicit vector is obtained. And then it is used to predict the missing score.

Convolutional neural network has application in recommender systems to better address data sparsity issues. At present, convolutional neural networks are primarily planed on modeling auxiliary information of users or items (such as item descriptions, reviews, etc.), while matrix factorization techniques are still utilized to model user-item interactions

(such as user-item ratings). For example, Kim et al. [21] proposed a convolutional matrix factorization model that associates convolutional neural network with matrix factorization. In this model, the convolutional neural network is used to extract the features in the context information and the auxiliary information of the item is used to address the sparsity issues and enhance the accuracy of rating prediction. Zheng et al. [22] constructed a convolutional neural network to learn features from using user and item reviews. And then user-item interaction information is obtained through matrix decomposition to predict ratings. Finally, the impact of data sparsity on recommendation results is reduced. Zhang et al. [23] proposed a collaborative knowledge base embedding learning model (CKE), which mines implicit feedback information through the knowledge base and obtains the implicit vectors of users and items to predict ratings.

2.3. Literature Review. Existing research has proposed many solutions to the problem of data sparseness. However, there is still room for improvement.

First: Memory-based collaborative filtering mainly reduces the sparsity of data by fusing features such as user and item attributes or clustering users. However, it is oriented towards explicit feedback data and collected auxiliary information of users and items, which is highly dependent on data and not scalable.

Second: Model-based collaborative filtering conducts research on implicit feedback information, and matrix decomposition technology also alleviates the problem caused by data sparsity to some extent. However, matrix factorization mainly uses a simple and fixed inner product for linear modeling, which is not conducive to estimating the complex characteristic relationship between users and items.

Third: Collaborative filtering based on deep learning handles the problem of sparse data through the learning of auxiliary information and extracts features to obtain deeper relationships between users and items. However, although these methods use auxiliary information to replace the construction of linear models, the sparsity problem of user-item interaction data in collaborative filtering recommendation still remains unsolved.

Therefore, in view of the above shortcomings, a recommendation algorithm based on deep learning and collaborative filtering is proposed in this paper. For the implicit feedback data set of crowdfunding projects, this model exploits the advantages of convolutional neural networks to learn local features effectively and the characteristics of collaborative filtering algorithm to model user-item interaction information to reduce the impact of user-item interaction information sparsity on recommendation accuracy.

3. Our Proposed CNNMF Method

3.1. Deep Collaborative Filtering Model. The deep collaborative filtering model in this paper combines matrix decomposition with deep neural network. The basic idea is shown in Figure 1. This model uses investors' investment behavior data and negative feedback data to perform the linear learning of matrix decomposition and nonlinear learning of deep neural network, respectively, and finally outputs the recommendation list.

The collaborative filtering recommendation algorithm firstly uses the user's preference for the item to form the user-item interaction matrix and models this interaction matrix to learn the interaction between users and items. Then the predictive value or recommendation list is obtained.

The model of deep collaborative filtering is shown in Figure 2. Each layer is implemented as follows.

Input layer. The input layer includes user ID and country, as well as item ID and category, and uses one-hot encoding to convert them into binary sparse vectors represented by v_d, v_c, v_a, v_g .

This paper analyzes the collection of negative feedback data in the implicit feedback data of crowdfunding websites. In the label data, the user behavior data with project investment behavior is marked as 1 in the implicit feedback matrix, and the uninvested project is marked as 0, as shown in

$$z_{uv} = \begin{cases} 1, & \text{invested,} \\ 0, & \text{uninvested.} \end{cases} \quad (1)$$

Since the implicit feedback data does not have the characteristics of negative feedback, 0 here does not represent the user's negative feedback intention. Therefore, in the experimental part, the negative feedback data will be uniformly collected and non-uniformly collected, and different negative feedback collections will have different effects on the model recommendation results.

Embedding layer. The embedding layer reduces the dimension of the sparse vector obtained by the input layer to obtain the feature matrix of the user, p_d, p_c , and the feature matrix of the item, q_d, q_g . As shown in formulas (2)–(5), the embedding matrix $P_{m \times k}, P_{t \times k}, P_{n \times k}$, and $p_{h \times k}$ is K -dimensional weight matrix. K represents the number of hidden factors set by the embedding layer, that is, the dimension of users and items after dimension reduction. The dense vector obtained by the linear transformation of the embedding layer not only represents the corresponding relationship of a single user or item, but also represents the internal relationship of all users or all items. During the training of the model, the embedding matrix updates the weights according to the user-to-user, item-to-item relationship.

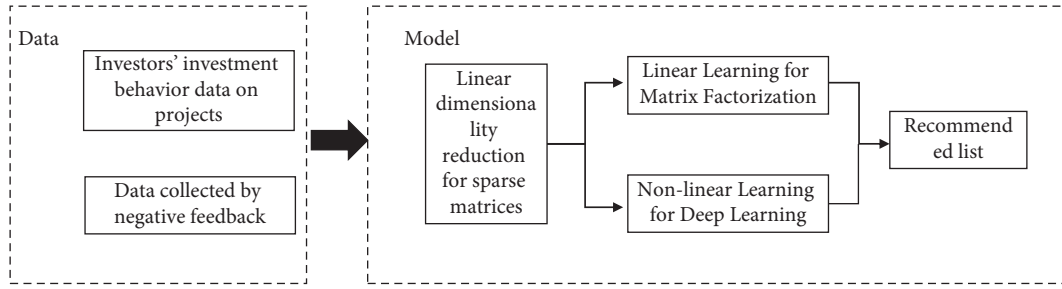


FIGURE 1: The basic idea of deep collaborative filtering algorithm.

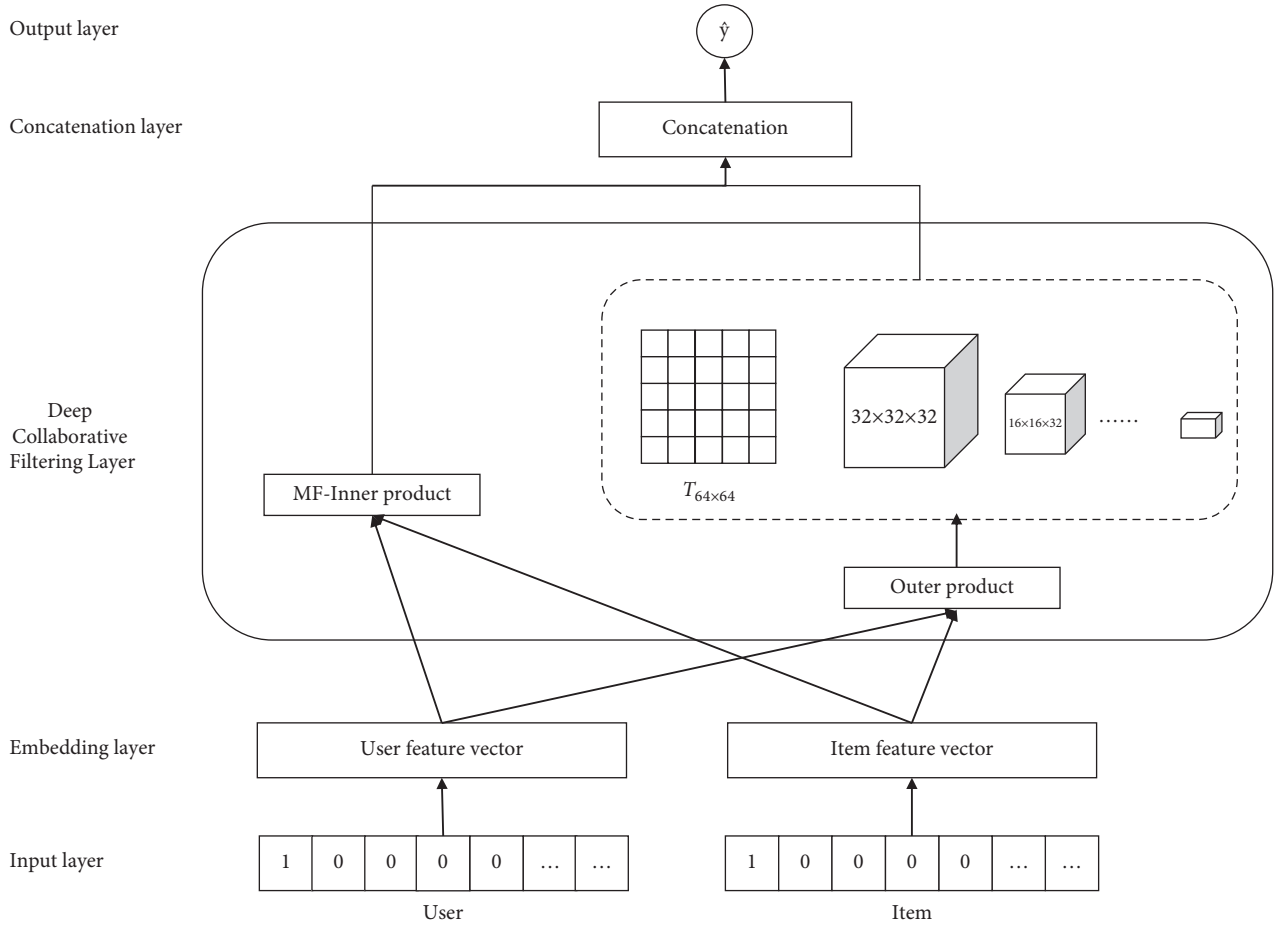


FIGURE 2: Deep collaborative filtering model.

$$p_d = P_{m \times k} v_d, \quad (2)$$

$$p_u = p_d + p_c, \quad (6)$$

$$p_c = P_{t \times k} v_c, \quad (3)$$

$$q_i = q_d + q_g. \quad (7)$$

$$q_d = P_{n \times k} v_d, \quad (4)$$

$$q_g = P_{h \times k} v_g. \quad (5)$$

After the output of the embedding layer, the user-related features are fused, and the item-related features are fused to form the user feature matrix and the item feature matrix, respectively, as shown in the following equations:

Deep Collaborative Filtering Layer. Perform linear learning for matrix factorization and nonlinear learning for deep neural network, respectively. The details are as follows.

Matrix Decomposition Layer. Matrix factorization linearly decomposes the Interaction matrix of users and items into two matrices multiplied together, and the obtained predicted score is the result of the interaction between the potential features of users and items. The

operation of the matrix factorization layer is to perform a Hadamard product operation on the latent feature matrices of users and items, as shown in

$$f_1(p_u, q_i) = p_u \odot q_i. \quad (8)$$

Convolutional Neural Network Layer. The premise of the convolutional neural network layer is that the feature matrices of users and items perform Kronecker product operations. Kronecker product is the interaction of one element of a matrix with each element of another matrix, that is, learning its relationship with elements in other dimensions. Because there may be a correlation between each dimension of the features of users and items, the Kronecker product operation is used to generate the relationship feature matrix $T_{k \times k}$. Use \otimes to denote the Kronecker product calculation. K is the number of hidden factors set by the embedding layer, as shown in equation (9). In the nonlinear learning of convolutional neural networks, the relationship matrix of users and items constitutes an interaction graph, and through the advantages of convolutional neural networks processing graphs, the interaction between users and items in the latent space is learned.

$$p_u \otimes q_i = T_{k \times k}. \quad (9)$$

In the nonlinear learning of convolutional neural networks, the relationship matrix of users and items constitutes an interaction graph, and through the advantages of convolutional neural networks processing graphs, the interaction between users and items in the latent space is learned, as shown in Figure 3.

The output of the last layer is the latent feature vector of users and items. Therefore, the overall calculation of the convolutional neural network layers is shown in

$$f_2(p_u, q_i) = \Phi_x(\dots \Phi_2(\Phi_1(p_u \otimes q_i))). \quad (10)$$

The deep collaborative filtering layer combines the advantages of matrix decomposition and deep neural network to train recommendation models. Mapping the relationship between user and item to potential space by linear matrix factorization to obtain f_1 , simultaneously, the deep neural network is leveraged to learn the hidden layer characteristics of users and items to obtain f_2 . Such a combination of linear and nonlinear learning methods enables more precise matching between users and items.

Concatenation Layer. Concatenate the latent feature vectors f_1 and f_2 learned by matrix factorization and deep neural network.

Output Layer. The predicted value \hat{y} is obtained by linear calculation, as shown in

$$\hat{y} = w \begin{bmatrix} f_1 \\ f_2 \end{bmatrix} + b, \quad (11)$$

where m is the number of users, n is the number of items, f_1 is the inner product function of matrix decomposition, f_2 is the nonlinear function of deep learning, and Φ_x is the nonlinear learning of the x layer of deep neural network.

3.2. Deep Collaborative Filtering Algorithm. Firstly, in the embedding layer, the algorithm uses matrix decomposition to obtain the feature dense vectors p_u and q_i of users and items. Matrix factorization can reduce the dimensionality of high-dimensional sparse data and predict ratings by calculating the inner product of the eigenvectors of users and items. However, the user's historical rating data is sparse, resulting in a large number of vacancies in the rating matrix. And matrix decomposition uses a simple linear combination to learn user-item interactions, which makes it difficult to fill the vacancies. Therefore, this paper introduces a convolutional neural network to calculate the potential nonlinear function of the user or item and then learns the potential relationship between users and items they interact with, so as to supplement the missing data.

Secondly, the algorithm learns the relationship of each dimension of the feature vector through the outer product and obtains the relationship feature matrix $T_{k \times k}$ of the users and the items.

Finally, the relationship feature matrix $T_{k \times k}$ is input into the convolutional neural network, local connectivity is extracted in the convolutional layer of each layer, and the convolutional kernel is used to convolve the relational matrix to extract the potential interaction of users and items.

The activation function of each layer is ReLU, which iterates, and the input of the next layer is the output of the upper layer. The convolutional kernel of each layer is a 2×2 matrix, and each convolution layer generates K channels $\Phi_1^1, \Phi_1^2, \dots, \Phi_1^l$; that is, the number of channels is compared to the dimension of the embedding layer with the same number ($l=K$). The algorithm learns K features in the convolutional kernel, and the first convolution of the l th convolution kernel obtains $c_{1,1}^l$; Φ_1^l represents the feature matrix extracted by the l th convolutional kernel of the first layer after performing $s/2^l$ convolution operations, as shown in equations (12)–(14).

$$c_1^l = \text{ReLU} \left(\sum_{i=0}^1 \sum_{j=0}^1 t_{i,j} \cdot w_{i,j} + b \right), \quad (12)$$

$$\Phi_1^l = \begin{bmatrix} c_{1,1}^l & \dots & c_{1,s}^l \\ \vdots & \ddots & \vdots \\ c_{s,1}^l & \dots & c_{s,s}^l \end{bmatrix}, \quad (13)$$

$$\Phi_1 = [\Phi_1^1, \Phi_1^2, \dots, \Phi_1^l]. \quad (14)$$

The nonlinear activation functions include sigmoid, tanh, or ReLU. In this paper, the ReLU function is selected, which is

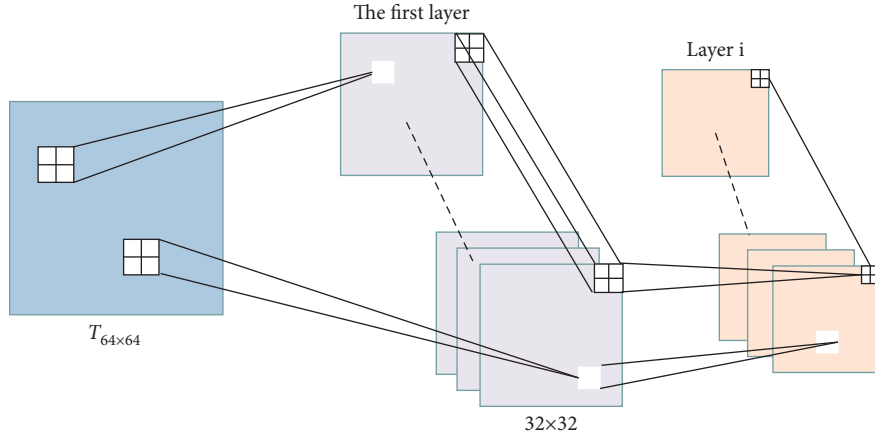


FIGURE 3: Structural diagram of convolutional neural network.

similar to the activation response of brain neurons to information. The ReLU function only activates the accepted information, while other information is filtered, so it is more suitable for sparse dataset calculation. Both the sigmoid and tanh functions have the problem of gradient disappearance, and overfitting will occur during the training process. The final results of the experiment also show that the performance of the ReLU function is better than the other two.

3.3. Deep Collaborative Filtering Model Training. Crowdfunding data in this paper are implicit feedback data with values of 1 or 0.1 meaning that the user has invested in the project; that is, the user is interested in the project. 0 may indicate that the user is not interested in the project or the user is unaware of the project's existence. Explicit feedback data (such as ratings) directly reflect the user's preference for an item, while the implicit feedback data cannot indicate the user's preference, but can only measure the confidence of the user's preference. Therefore, the final output of this model is not a prediction of ratings, but a personalized list of recommendations for the target user.

The ranking of items in the recommendation list is directly related to the user's satisfaction with the recommendation results. Therefore, the model adopts the Bayesian Personalized Ranking loss function [24] to learn the ranking of positive and negative feedback samples in pairs, as shown in equation (16).

In rating prediction, the goal of pointwise learning is to minimize the mean squared error between the predicted value and the label. When paired learning samples rank in the recommendation list, the positive feedback sample i should be ranked higher than the negative feedback j . And make the difference between the two predictions as large as possible. \hat{y}_{ui} is the predicted value of the positive feedback, and \hat{y}_{uj} is the predicted value of negative feedback, as

$$\hat{y}_{uij} = \hat{y}_{ui} - \hat{y}_{uj}, \quad (15)$$

$$L = \sum_{(u,i,j) \in D} \ln \sigma(\hat{y}_{uij}) - \lambda_{\Theta} \|\Theta\|^2, \quad (16)$$

where λ_{Θ} is the regularization parameter. D means $D = \{(u, i, j) | i \in y_{ui} \wedge j \notin y_{ui}\}$; that is, user u interacts with item i .

In model training, Adaptive Moment Estimation (Adam) [25] is used. In stochastic gradient descent (SGD), the learning rate is kept constant during the training process. It uses a single learning rate to correct the weights, which takes a long time to train. However, Adam computes different adaptive learning rates for different parameters, which dynamically adjusts the learning rate of each parameter by using the first and second moment estimates of the gradient. Experimental results also show that Adam converges faster than SGD on our model.

4. Performance Analysis

4.1. Experimental Design. This paper takes the investment of users in projects on Ulule, the largest crowdfunding platform in Europe, as the research object. And then collect data and design experiments to measure the recommendation performance of this algorithm. The experimental process is divided into three parts: model, training, and experiment, as shown in Figure 4.

Model part: We analyze the user behavior data of the crowdfunding website, learn user and item feature information through the deep collaborative filtering layer to generate a feature matrix, and then output it through the fully connected layer.

Training part: We train the deep collaborative filtering model on the training set, output the predicted score of the item, and generate the recommendation list. Then, the model iterates, updates the weights and parameters iteratively based on the Adam training process, and saves the best recommendation list after 100 times, along with the weights and parameters at this time.

Experimental part: We conduct experiments to verify the effects of data with different sparsity, the number of layers of convolutional neural networks, and implicit feedback data collection methods on recommendation performance and select the baseline method and design

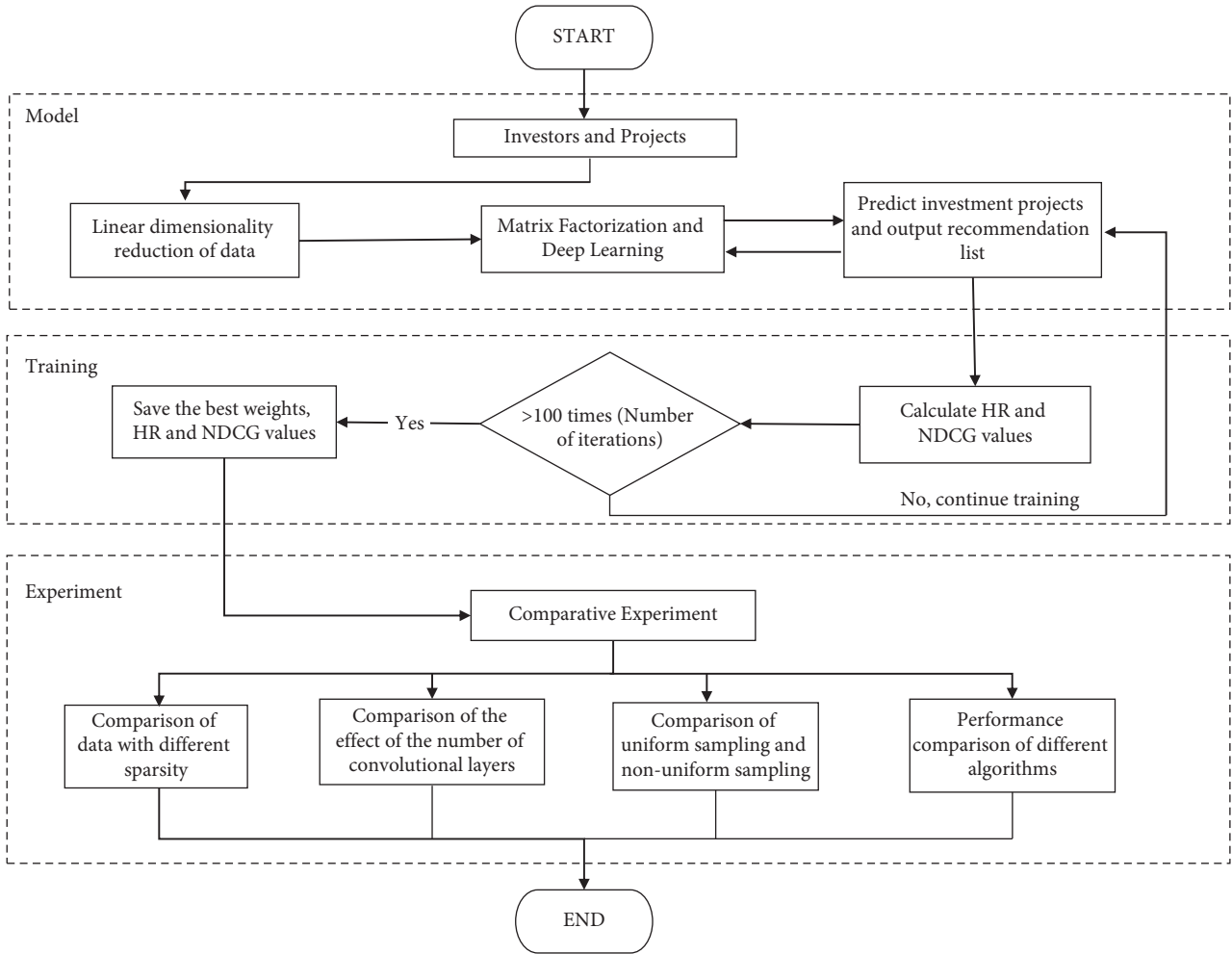


FIGURE 4: Experimental procedure.

comparative experiments to verify the superiority of the proposed algorithm.

4.2. Experimental Data Collection. The homepage of the crowdfunding platform Ulule displays the number of users, the number of successful projects, and the success rate of the platform in real time. The website is open to everyone, and all data can be crawled through their API. Although the crowdfunding projects that have expired cannot be crawled, the website has collected statistics, including the number of successful financing projects each year, the financing success rate, the number of projects being funded, and the number of website user registrations, etc., as shown in Table 1.

In this paper, web crawler technology is used to obtain experimental data. In terms of projects, it obtains key information such as project codes and classification labels; in terms of users, key information such as the codes of users and the codes of each invested project is crawled. The collected data includes the following: (i) In terms of projects, crawl the list of all successful financing and in-progress projects, where the content of the project list includes the project home page, whether the financing has been completed, the total amount of financing, the country of the

TABLE 1: Ulule website related data.

Ulule website related data	Year			
	2019	2018	2017	2016
Number of financings	705,350	640,523	577,985	520,777
Number of project startups	6,042	8,049	7,452	7,045
Number of successful crowdfunding	4,398	5,152	4,856	4,804
Financing success rate	73%	64%	65%	68%

publisher, the project code, and the classification label of the project. (ii) According to all the invested projects, crawl the projects that the user has invested in, including projects that are still in progress, where the content of the user list includes the user code, user homepage, user country, language, and time zone. Iterate in this way until the dataset has a certain size.

4.3. Experimental Data Description. This article crawled data from the Ulule crowdfunding website in April 2019. The data obtained is in Jason's data format. After cleaning the data, a total of 363,608 users' project investment behavior data were

obtained. After statistics, there were 274,292 users and 41,894 projects where users participated in financing. Among them, 27,241 projects were successfully financed, with a success rate of 65%. As shown in Figure 5, most users invest less than 5 times, among which users who invest once are the most (this crawling does not include users with 0 investment), which is about 82.5%. Therefore, the data sparsity of the computing website is 99.98%.

The data sparsity influences the recommendation accuracy, which is one of the main research issues in this paper. Therefore, datasets with different sparsity are collected by us to observe the performance of the proposed model. And the data is processed according to the number of times users invest in crowdfunding projects. According to the degree of sparseness [26], it is divided into low-sparse data (9 or more investment times per capita), moderately sparse data (5 times or more per capita investment), and extremely sparse data (3 times or more per capita investment), as shown in Table 2. After statistics, the more investment times, the fewer users, the fewer projects, and the lower data sparsity.

4.4. Training Set and Test Set. In this paper, the leave-one-out method is used to divide the training set and test set. The data set of n samples is divided into the training set of $n - 1$ samples and the test set of 1 sample. Firstly, 99 projects are randomly matched from the projects that the user has not invested in, and then the last invested project is taken out of the projects that the user has invested in to form a test set of 100 uninvested projects. Excluding one item extracted in the test set, the remnant items invested by users are the training set.

4.5. Collection of Negative Feedback Data. For the collection of negative feedback data, this paper conducts two experiments of uniform sampling and nonuniform sampling.

- (i) **Uniform sampling:** Uniform sampling is to collect all uninvested projects of users as negative feedback data in each iteration or flexibly controls the ratio of positive feedback to negative feedback according to the experimental situation.
- (ii) **Nonuniform sampling:** Nonuniform sampling is mainly to set a standard for the selection of items, such as high popularity, many exposure opportunities, etc., because users have a high probability of finding these items in a great volume of items. Therefore, if users do not invest, it is more likely that they are not interested in it.

We perform uniform and nonuniform sampling on extremely sparse datasets, respectively. Using the uniform sampling method, 4 negative feedbacks are randomly collected for each user, and the obtained negative feedbacks are evenly distributed among the 230 items, as shown in Figure 6.

Nonuniform sampling collects items according to their popularity, and the negative feedback obtained is concentrated on 7 items, while other items only get a small amount of collection, as shown in Figure 7.

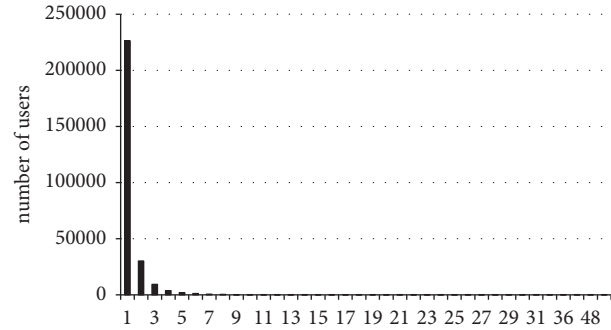


FIGURE 5: Statistics on the number of user investment projects.

In the collection of negative feedback in the data set, the fluctuation of randomly obtained negative feedback samples is small, and the degree of data dispersion is small, while the degree of dispersion of samples obtained by nonuniform collection is large.

4.6. Metrics. We employ two evaluation methods to measure the performance of the recommendation algorithm.

- (i) **Hit ratio (HR):** in top- K recommendation, HR is a commonly used metric to measure recall. It calculates the ratio of fundraising items in the top- K recommendation list that belong to the test set, as shown in equation

$$HR = \frac{n}{N}, \quad (17)$$

where n represents the number of items in the test set in the recommendation list, and N is the total number of items in the test set.

- (ii) **Normalized discount cumulative gain (NDCG):** NDCG is an evaluation index used to measure the quality of the $TOP-K$ ranking. It not only reflects whether the predicted $TOP-K$ results are really relevant, but also reflects the relative ranking of the $TOP-K$ results. Putting an item that users are not interested in at the top of the recommendation list will have a higher error rate, as shown in equations (18) and (19)

$$DCG = \sum_{i=1}^{10} \frac{2^{rel_i} - 1}{\log_2(i + 1)}, \quad (18)$$

$$NDCG = \frac{DCG}{IDCG}, \quad (19)$$

where rel_i represents the correlation between the item and the user at position i in the recommendation list. Equation (18) shows that DCG combines recommendation accuracy with ranking position. In order to have comparability between different recommendation lists, normalization processing is performed, as shown equation (19). The value of DCG is between $(0, IDCG]$ and the value of NDCG is between $(0, 1]$.

TABLE 2: Data sets with different sparsity.

Dataset	Investments per capita	Sparsity (%)	Number of investors	Number of items	Total number of investments
Low-sparse data	9 times or more	94.36	639	220	7922
Moderately sparse data	5 times or more	96.81	2986	229	21847
Extremely sparse data	3 times or more	97.95	8598	230	40542

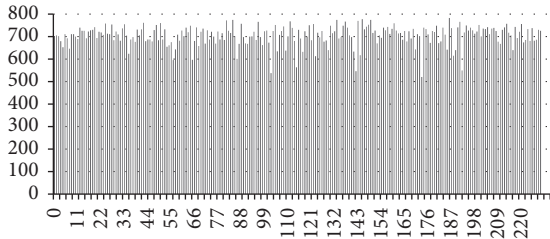


FIGURE 6: The distribution of negative feedback obtained by balanced collection method.

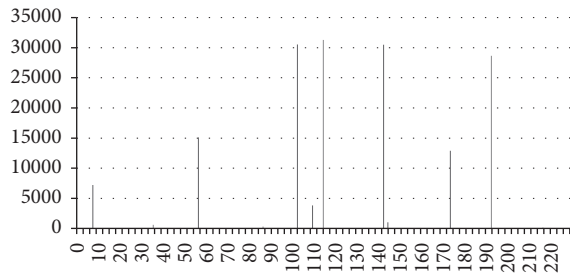


FIGURE 7: The distribution of negative feedback obtained by imbalanced collection method.

5. Experimental Results

5.1. Performance of Data with Different Sparsity on Recommendation Results. For the purpose of eliminating the impact of the number of convolutional layers on the experimental considerations result, the number of convolutional layers is set to 4, 5, and 6 layers for experiments, respectively. The obtained results are shown in Tables 3 and 4. The deep collaborative filtering model achieves the best recommendation effect on extremely sparse datasets when taking different convolutional layers. Under the circumstances of extremely sparse data and a large amount of data, the majority of memory-based collaborative filtering algorithms will be limited in the recommendation performance. This is because the similarity between users (items) will be difficult to calculate accurately as the data is sparse and the dimension increases, which will affect the recommendation effect. However, deep learning methods can break through this limitation and achieve better recommendation results on extremely sparse datasets. In addition, on the crowdfunding platform Ulule, the data sparsity is much larger than the extremely sparse dataset selected in this paper. Therefore, the proposed model is suitable for the Ulule platform with large and sparse data.

TABLE 3: The maximum value of HR of recommendation on datasets of different sparsity.

Layer	Dataset		
	Low-sparse	Moderately sparse	Extremely sparse
4	0.43348	0.47857	0.53920
5	0.46478	0.50569	0.54268
6	0.45696	0.49062	0.53512

TABLE 4: The maximum value of NDCG of recommendation on datasets of different sparsity.

Layer	Dataset		
	Low-sparse	Moderately sparse	Extremely sparse
4	0.23946	0.27741	0.31798
5	0.26223	0.29240	0.33299
6	0.26287	0.29350	0.32186

5.2. Performance of Convolutional Layers of Convolutional Neural Network on Recommendation Results. The number of the convolution layers of convolutional neural network will have a noticeable impact on the extraction of user and project features, which in turn affects the recommendation effect. Therefore, the effects of different convolutional layers on the recommendation results are compared through experiments.

Since the previous experimental results have proved that the proposed model can produce the best recommendation effect on extremely sparse datasets, this experiment will select extremely sparse datasets to construe the effect of the number of convolution layers. Moreover, similar algorithm is applied for the optimization of the parameter tuning process during the convolutional neural network training [27].

Figure 8 shows that as the number of convolutional layers increases, the HR value and the initial value of NDCG also increase, and when the convolutional layers increase to 6, the HR and NDCG values begin to decrease. It can be seen that the number of convolutional layers of the convolutional neural network has a significant impact on the recommendation results. And when the number of convolutional layers increases to a critical point, the optimal recommendation effect will be achieved. Continuing to increase the number of layers will reduce the accuracy of feature extraction of convolutional neural networks.

5.3. Performance of Negative Feedback Data Sampling Methods on Recommendation Results. The extremely sparse data set is also used as the experimental data. For each user,

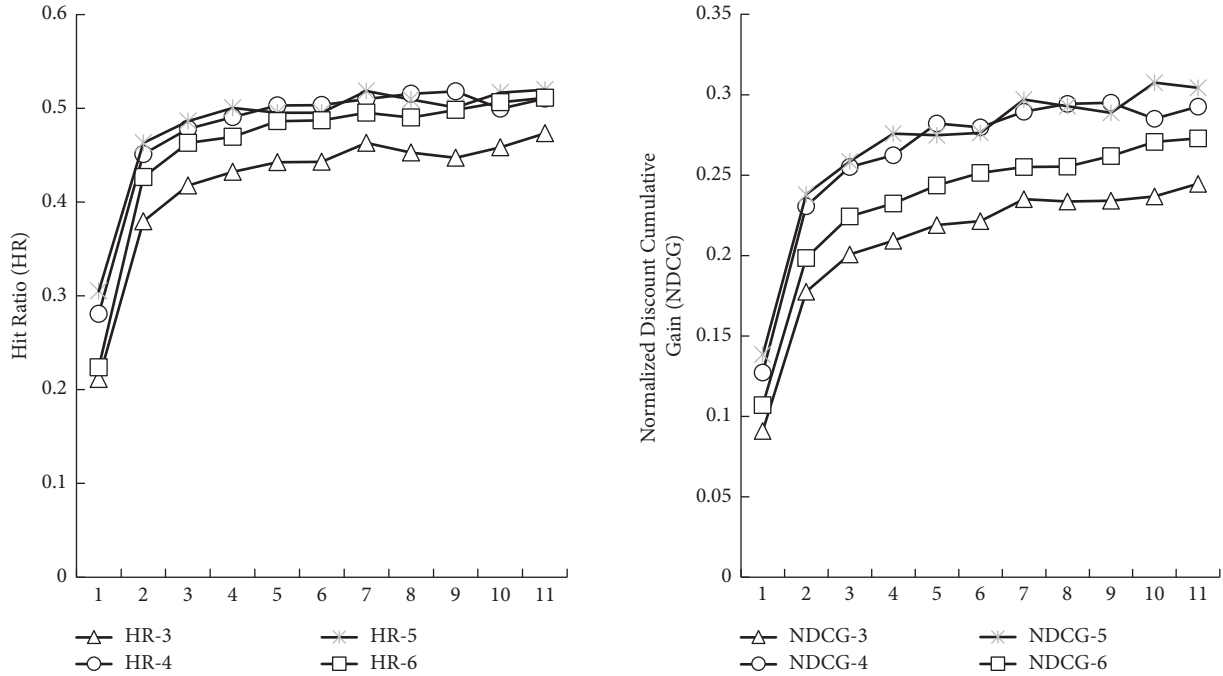


FIGURE 8: The HR and NDCG of recommendation based on the model with different convolution layers on extremely sparse dataset.

1~4 negative feedbacks are collected, respectively. The effects of the negative feedback data collection methods of uniform sampling and nonuniform sampling on recommendation are compared, and the results are shown in Tables 5 and 6.

Tables 5 and 6 show that the recommended effect of the uniform sampling method is better, and the best recommendation effect can be obtained when the number of collections is 1.

Figure 9 shows the iterative process of 4 negative feedbacks for uniform and nonuniform sampling [28]. The abscissa represents the interval of the number of iterations, and the ordinate represents the average value of HR and NDCG corresponding to each interval. In the iterative process, the convergence speed of the two methods is close, but the effect of uniform acquisition is obviously superior to that of nonuniform acquisition. Additionally, the peak values of HR are all in the third interval; that is, the best results are obtained when the iteration is about 20 times, indicating that increasing the number of experiments will limit the results. Different parameter settings have different convergence speeds of iterations.

The reason for the poor experimental results of non-uniformly sampled negative feedback data is probably that, in the data set constructed in this paper, users are not sensitive to the popularity of the project, and the negative feedback data set is highly discrete. The negative feedback sample collection based on the popularity of the items only focuses on the 7 most popular items, and the negative feedback repeatedly selects these 7 items, resulting in extremely poor results.

5.4. Comparative Experiments. This paper selects the five algorithms as baseline method and a deep collaborative filtering algorithm to design comparative experiments. The

TABLE 5: The HR of recommendation with different negative feedback collection methods on extremely sparse dataset.

Number of negative feedback	HR uniform	HR nonuniform
1	0.50524	0.10329
2	0.52366	0.19405
3	0.53311	0.24883
4	0.54268	0.28936

TABLE 6: The NDCG of recommendation with different negative feedback collection methods on extremely sparse dataset.

Number of negative feedback	NDCG uniform	NDCG nonuniform
1	0.25393	0.05372
2	0.27859	0.0856
3	0.30628	0.09459
4	0.33299	0.11475

six baseline methods include classic recommendation algorithms and cutting-edge algorithms, so as to comprehensively examine the performance and effects of our algorithms.

Most Popular. The recommendation list of this method is sorted according to the popularity of the items, which is a nonpersonalized recommendation. All users get the same recommendation result. This algorithm is often used to compare recommendation results.

eALS. He et al. [29] proposed a matrix factorization model based on implicit feedback. The model weights the unrated parts according to the popularity of the item. Simultaneously, for the purpose of improving the

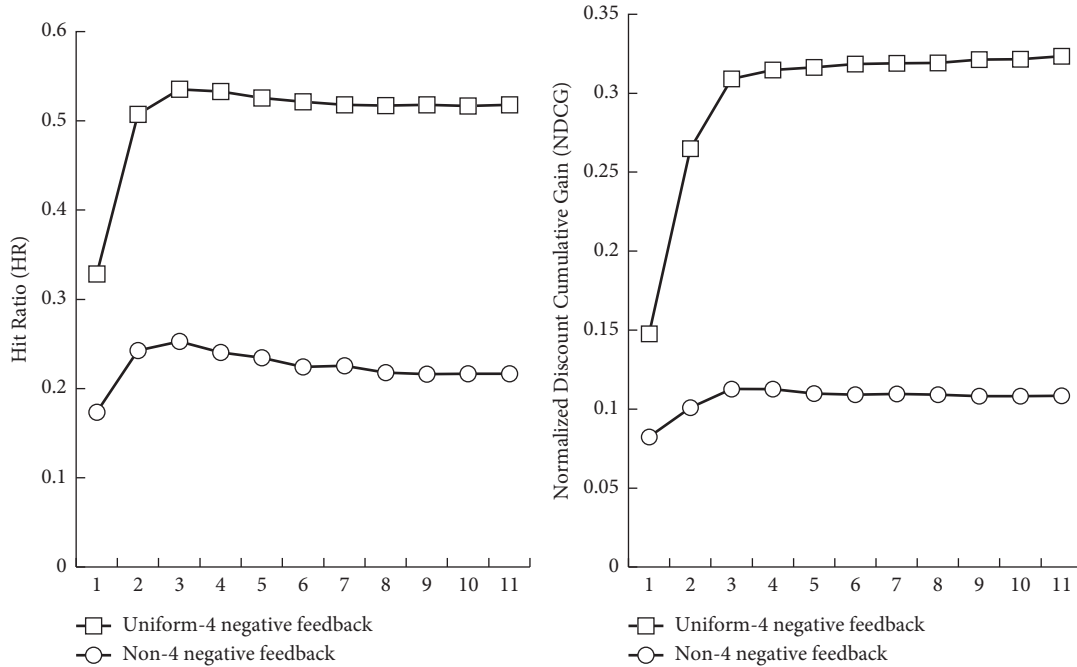


FIGURE 9: Uniform and nonuniform sampling of 4 negative feedback HR and NDCG values.

computational efficiency of model parameters, an eALS learning algorithm is designed, and an online update strategy suitable for dynamic data is established on this basis to capture users' short-term preferences. Moreover, the online scene enables the implicit feedback-based matrix factorization to be applied in large-scale practical environments.

BPR. A personalized ranking algorithm based on Bayesian theory has been proposed by Rendle et al. [24]. The algorithm sorts and optimizes the personalized recommendation list generated by the matrix decomposition or nearest neighbor method according to the implicit feedback data, so as to improve the user's satisfaction with the recommendation list. Using the partial order relationship between the purchased and unpurchased products, the maximum a posteriori estimate is derived by Bayesian analysis, and then the model is trained. Finally, the optimized item ranking is generated.

CM-RIMDCF. A two-stage deep collaborative filtering model has been proposed by Fu et al. [30]. In the first stage, users and items are learned separately through local and global models to obtain feature information representing user-user and item-item, and this is input into the second stage. Then, the second stage uses neural networks to learn information about user and item interactions, resulting in predictive scores.

Multicriteria DCF. Nassar et al. [31] proposed a multicriteria deep collaborative filtering model. The model divides user preferences into overall ratings and multicriteria ratings to quantify users' interest in different features of items. On this basis, a two-stage deep neural network model is designed. The first stage first predicts

the multicriteria score and then feeds it into the next stage of the deep neural network to predict the overall score.

Deep Collaborative Filtering Algorithm (FMMLP). Inspired by the effective combination of deep learning technology and recommendation system in recent years, we combine the advantages of factorization machine second-order interaction with multilayer perceptron to fully learn the information of each dimension in user behavior. In this way, the recommendation effect of the model can be improved.

Comparative experiments use public datasets. Yahoo! Movies user rating dataset: Users rate movies on a scale of A+ to F. Since this dataset is an explicit feedback dataset, it needs to be preprocessed as implicit feedback data. The behavior of "rating" (regardless of the size of the score) is regarded as 1, indicating that there is an interactive behavior and 0 otherwise. In this dataset, users rated more than 10 movies, and each movie has at least one user rating. Therefore, with a total of 7,642 users and 11,915 movies, the rating (number of interactions) is 211,231 and the sparsity is 99.77%.

The recommendation results of our algorithm and the other method are shown in Table 7. According to the experimental results, both HR and NDCG values of CNNMF are significantly better than the other six methods. Therefore, the CNNMF algorithm can competently enhance the performance of recommendation.

Further analysis of the reasons is as follows:

- (i) In the extremely sparse dataset (40,542 total investment times), the investment times of the top 10 most popular items accounted for 37.97% of the

TABLE 7: The comparison between the proposed algorithm and the baselines.

Recommendation algorithm	HR	NDCG
Most popular	0.492	0.388
eALS	0.563	0.444
BPR	0.520	0.410
CM-RIMDCF	0.422	0.327
MulticriteriaDCF	0.830	0.655
FMMLP	0.496	0.403
CNNMF	0.886	0.699

total investment times, but the top 10 items accounted for only 4.35% of the total number of items. It can be seen that the top 10 popular items have already received more attention from users, and it cannot provide users with personalized items. Therefore, the recommendation effect of the most popular algorithm is also the worst.

- (ii) BPR and Eals algorithms propose different optimization methods for implicit feedback data but still build models based on traditional matrix factorization. Their processing of sparse data has certain limitations, which affects both model training and recommendation results.
- (iii) The CM-RIMDCF algorithm learns the interaction of users and items based on the correlation between users and items. However, the local and global representation model proposed by this method, which uses explicit scoring for learning, is not suitable for implicit feedback. This affects the predictions of the second-stage neural network. In addition, the neural network in this method has only one fully connected hidden layer, which has certain limitations in learning the relationship between users and items.
- (iv) The multicriteria scoring proposed by multicriteria DCF can explain the reasons for user preferences. However, in practical application scenarios, this type of data is limited, most of which are single overall scores. In addition, this method only uses deep neural networks to calculate multicriteria scores and overall scores, which is still insufficient in the fusion of deep neural networks and collaborative filtering.
- (v) The effect of the algorithm FMMLP in this paper is also poor, including two reasons: One is that the Yahoo! Movies dataset has no feature information, so the factorization machine layer does not play a role in the algorithm. The second is that the algorithm is a serial structure. The second-order linear learning of the factorization machine is the input of the nonlinear learning. The feature learning of the factorization machine affects the nonlinear learning of the multilayer perceptron. The sparser the data, the greater the impact. So the algorithm performs worse on sparser data. The experimental results also

show that it is the worst among the six personalized recommendation algorithms in this paper.

Therefore, the deep collaborative filtering model learns the potential relationship between user and item feature information more accurately by better integrating deep neural network and collaborative filtering, so as to obtain better recommendation effect.

6. Conclusion

In view of the extremely sparse data of crowdfunding platform Ulule, and the investment behavior of platform users with implicit feedback data without negative feedback, this paper integrates deep neural network and collaborative filtering recommendation algorithms to generate personalized crowdfunding project recommendations list for investors. In this way, the matching degree between investors and projects is improved, thereby improving the overall financing success rate of the crowdfunding platform.

For the recommendation problem of crowdfunding platform, the proposed algorithm has been enhanced in the following aspects:

- (i) Extract the feature data of users and items, as well as the actual interaction information, and train the model.
- (ii) Combine matrix factorization and convolutional neural network to learn feature information, respectively, to extract the potential relationship between user and item feature information. The complementary advantages of the two methods are used to improve the accuracy of feature extraction.
- (iii) Sampling and analyzing the implicit feedback data of the crowdfunding platform through uniform and nonuniform negative feedback sample sampling methods.

For the purpose of verifying the effectiveness of the algorithm, five baseline methods are selected for comparative experiments. The final experimental results show that the recommendation effect of the deep collaborative filtering model on the dataset is significantly improved compared with the baseline model. At the same time, it is proved that integrating deep neural network to learn the nonlinear interaction between investors and projects can effectively address the issue of data sparsity. And for the problem of larger and sparser data, the best recommendation performance can be obtained by adjusting the number of convolutional layers of the convolutional neural network. In addition, for the collection of negative feedback data, the characteristics of the project need to be considered. Although nonuniform collection has a better interpretation effect, it is not necessarily suitable for the training of this model.

This study not only helps to enhance the financing success rate of crowdfunding platforms, but also enriches the research on recommender systems. In future research, the following aspects are worth exploring in depth:

- (i) Consider contextual information, including industry developments, macroeconomics, and timing effects. Taking these factors into consideration will help to predict user preference.
- (ii) Experiments can be carried out on the user and project data of different Internet financial platforms to further explore the generality of the method proposed in this paper.
- (iii) Add auxiliary information as experimental data, such as user comments, item description information and item type, etc., to enrich the feature information of users and items.
- (iv) Further explore the application of other deep learning methods in recommender systems.

Data Availability

No data were used to support this study.

Conflicts of Interest

The authors declare that there are no conflicts of interest with any financial organizations regarding the material reported in this manuscript.

Acknowledgments

This work was supported by the National Natural Science Foundation of China (nos. 71771177 and 71871143). This financial support is gratefully acknowledged by the authors.

References

- [1] A. Agrawal, C. Catalini, and A. Goldfarb, "Some simple economics of crowdfunding," *Innovation Policy and the Economy*, vol. 14, no. 1, pp. 63–97, 2014.
- [2] M. H. Por, S. B. Yang, and T. Kim, "Successful crowdfunding: the effects of founder and project factors," in *Proceedings of the 18th Annual International Conference on Electronic Commerce: e-Commerce in Smart connected World*, pp. 1–7, Suwon, Republic of Korea, 2016.
- [3] B. M. Sarwar, G. Karypis, J. A. Konstan, and J. T. Riedl, "Application of dimensionality reduction in recommender system—a case study," in *Proceedings of the KDD Workshop on Web Mining for e-Commerce: Challenges and Opportunities*, Boston, MA, USA, 2000.
- [4] Y. LeCun, Y. Bengio, and G. Hinton, "Deep learning," *Nature*, vol. 521, no. 7553, pp. 436–444, 2015.
- [5] R. Vineeth, C. L. Wang, and K. R. Chandan, "Probabilistic group recommendation model for crowdfunding domains," in *Proceedings of the Ninth ACM International Conference on Web Search and Data Mining*, pp. 257–266, San Francisco, CA, USA, 2016.
- [6] Y. Song, Z. Li, and N. Sahoo, "Matching returning donors to projects on philanthropic crowdfunding platforms," *Management Science*, vol. 68, no. 1, pp. 355–375, 2021.
- [7] L. Zhang, X. Zhang, F. Cheng, X. Y. Sun, and H. K. Zhao, "Personalized recommendation for crowdfunding platform: a multi-objective approach," in *Proceedings of the IEEE Congress on Evolutionary Computation (CEC)*, Wellington, New Zealand, pp. 3316–3324, 2019.
- [8] A. C. Benin, "A comparison of recommender systems for crowdfunding projects," *Universidade Federal do Rio Grande do Sul*, Porto Alegre, Brazil, 2018.
- [9] H. Wang and S. Chen, "A bipartite graph-based recommender for crowdfunding with sparse data," *Banking and Finance*, IntechOpen, London, UK, 2020.
- [10] Y. Hu, Q. Peng, X. Hu, and R. Yang, "Time aware and data sparsity tolerant web service recommendation based on improved collaborative filtering," *IEEE Transactions on Services Computing*, vol. 8, no. 5, pp. 782–794, 2015.
- [11] W. Zhan, Z. Hong, L. Fang, Z. Wu, and Y. Lyu, "Collaborative filtering recommendation algorithm based on adversarial learning," *Computer Science*, vol. 48, no. 7, pp. 172–177, 2021.
- [12] L. Zhu, Q. Hu, L. Zhao, and J. Yang, "Collaborative filtering algorithm based on rating preference and item attributes," *Computer Science*, vol. 47, no. 04, pp. 67–73, 2020.
- [13] B. Hong and M. Yu, "A collaborative filtering algorithm based on correlation coefficient," *Neural Computing & Applications*, vol. 31, no. 12, pp. 8317–8326, 2019.
- [14] R. Logesh, V. Subramaniaswamy, D. Malathi, N. Sivaramakrishnan, and V. Vijayakumar, "Enhancing recommendation stability of collaborative filtering recommender system through bio-inspired clustering ensemble method," *Neural Computing & Applications*, vol. 32, no. 10, pp. 2141–2164, 2020.
- [15] J.-F. Wang, X. Li, W.-Q. Wu, and Y. Liu, "An algorithm of collaborative filtering based on SVD and trust factors," *Journal of Chinese Computer Systems*, vol. 38, no. 06, pp. 1290–1293, 2017.
- [16] Y. Hu, Y. Koren, and C. Volinsky, "Collaborative filtering for implicit feedback datasets," in *Proceedings of the 9th IEEE International Conference on Data Mining*, pp. 263–272, Miami, FL, USA, 2009.
- [17] Y. Koren and R. Bell, "Advances in collaborative filtering, recommender systems handbook," in *Recommender Systems Handbook*, F. Ricci, L. Rokach, and B. Shapira, Eds., Springer, Boston, MA, pp. 77–118, 2015.
- [18] C. Bi-yi, L. Huang, C.-D. Wang, and L. Jing, "Explicit and implicit feedback based collaborative filtering algorithm," *Journal of Software*, vol. 31, no. 3, pp. 794–805, 2020.
- [19] B. Yi, S. Shen, H. Liu et al., "Deep matrix factorization with implicit feedback embedding for recommendation system," *IEEE Transactions on Industrial Informatics*, vol. 15, no. 8, pp. 4591–4601, 2019.
- [20] Y. Wu, C. DuBois, A. X. Zheng, and M. Ester, "Collaborative denoising auto-encoders for top-n recommender systems," in *Proceedings of the Ninth ACM International Conference on Web Search and Data Mining*, pp. 153–162, San Francisco, CA, USA, 2016.
- [21] D. Kim, C. Park, J. Oh, S. Lee, and H. Yu, "Convolutional matrix factorization for document context-aware recommendation," in *Proceedings of the 10th ACM Conference on Recommender Systems*, pp. 233–240, MA, USA, 2016.
- [22] L. Zheng, V. Noroozi, and P. S. Yu, "Joint deep modeling of users and items using reviews for recommendation," in *Proceedings of the Tenth ACM International Conference on Web Search and Data Mining*, pp. 425–434, Cambridge, UK, 2017.
- [23] F. Zhang, N. J. Yuan, D. Lian, X. Xing, and M. Wei-Ying, "Collaborative knowledge base embedding for recommender systems," in *Proceedings of the 22nd ACM SIGKDD International Conference*, pp. 353–362, San Francisco, CA, USA, 2016.

- [24] S. Rendle, C. Freudenthaler, Z. Gantner, and S. T. Lars, "BPR: Bayesian personalized ranking from implicit feedback," in *Proceedings of the 25th Conference on Uncertainty in Artificial Intelligence*, pp. 452–461, Montreal, Canada, 2009.
- [25] D. Kingma and J. Ba, "Adam: a method for stochastic optimization," in *Proceedings of the 3rd International Conference for Learning Representations*, pp. 1–15, San Diego, CA, USA, 2015.
- [26] Z. Chen and J. Yan, "Collaborative filtering recommendation algorithm based on sparse data preprocessing," *Computer Technology and Development*, vol. 26, no. 7, p. 6, 2016.
- [27] Y. Jiang, G. Tong, H. Yin, and N. Xiong, "A pedestrian detection method based on genetic algorithm for optimize XGBoost training parameters," *IEEE Access*, vol. 7, pp. 118310–118321, 2019.
- [28] J. Ding, Y. Quan, Q. Yao, Y. Li, and D. Jin, "Simplify and robustify negative sampling for implicit collaborative filtering," *NeurIPS*, 2020.
- [29] X. He, H. Zhang, M. Y. Kan, and C. Tat-Seng, "Fast matrix factorization for online recommendation with implicit feedback," in *Proceedings of the 39th International ACM SIGIR conference on Research and Development in Information Retrieval*, pp. 549–558, Italy, 2016.
- [30] M. Fu, H. Qu, Z. Yi, L. Lu, and Y. Liu, "A novel deep learning-based collaborative filtering model for recommendation system," *IEEE Transactions on Cybernetics*, vol. 49, no. 3, pp. 1084–1096, 2019.
- [31] N. Nassar, A. Jafar, and Y. Rahhal, "A novel deep multi-criteria collaborative filtering model for recommendation system," *Knowledge-Based Systems*, vol. 187, Article ID 104811, 2020.

Research Article

Special-Purpose English Teaching Reform and Model Design in the Era of Artificial Intelligence

Yali Ruan 

School of Humanities and International Education, Xi'an Peihua University, Xi'an 710000, Shaanxi, China

Correspondence should be addressed to Yali Ruan; 150832@peihua.edu.cn

Received 21 April 2022; Revised 9 June 2022; Accepted 30 June 2022; Published 20 July 2022

Academic Editor: Xuefeng Shao

Copyright © 2022 Yali Ruan. This is an open access article distributed under the Creative Commons Attribution License, which permits unrestricted use, distribution, and reproduction in any medium, provided the original work is properly cited.

Research on English teaching reform and model design is the focus of the current society. It is a novel idea to use artificial intelligence algorithm to design an English teaching platform, which combines the current field of English teaching reform with the field of artificial intelligence network. The current method is to use the sincent algorithm in artificial intelligence to design the model. Its defect is that the single network education learning makes the learners feel boring. In order to solve these problems, this paper proposes an English blended education method based on artificial intelligence, which aims to study the integration of the network teaching platform and traditional education. This paper uses the artificial intelligence sincent algorithm to establish a teaching platform framework and simulate application strategies for the development of blended education. Through the investigation process of blended English teaching, the results show that the proportion of students who are generally satisfied with English teaching has reached 53.67% and the proportion of students who feel generally satisfied has reached 27.83%. The results of this survey indicate that the majority of students approve of this type of English blended education method.

1. Introduction

With the continuous integration and development of “Internet + education,” great changes have taken place in the way of information organization, the way of knowledge transmission, and the way of school teaching. Personalized development and customized teaching needs are an inevitable trend. In this context, blended teaching has flourished in recent years. The integration and development of knowledge in the information age requires matching advanced learning models and innovative thinking. We are in the “Internet +” era of innovation and development. New technologies bring huge space for innovation, and the key to innovation is talents. Talents pay more attention to soft skills, among which soft skills include courage to innovate, cross-border compounding, multidirectional thinking, and comprehensive quality. However, in the actual English teaching, the ninth grade faces the pressure of further education. Teachers pay attention to “filling the classroom” with language and often ignore students’ classroom experience and ability to use

language in practice, which will be detrimental to students’ sustainable development.

This research starts from the teaching practice of this paper, takes students’ weak points of English learning as a breakthrough point, and explores the innovative practice of English teaching based on blended teaching under the guidance of constructivist learning theory, situational learning theory, and microlearning theory. Specifically, the following studies were carried out: first, by systematically combing the relevant literature of blended teaching at home and abroad, the concept of blended teaching is defined, and the relevant research studies on blended teaching design, development, application, and evaluation are reviewed, which provides a theoretical and practical basis for the overall design of this study. Secondly, by analyzing the relevant literature and cases of English teaching at home and abroad, this paper explores the logical basis for blended teaching to support the innovative practice of English teaching and constructs a cooperative classroom teaching model based on blended teaching. On the basis of this model, focusing on the characteristics of primary school English,

blended teaching of primary school grammar, vocabulary, and discourse is designed and produced, so as to improve classroom teaching and enhance students' autonomous learning ability.

This paper has a novel idea and a rigorous framework. Starting from the constructivist learning theory, situational learning theory, and microlearning theory, a cooperative classroom teaching model based on blended teaching is constructed. The cooperative classroom teaching mode based on blended teaching is applied to actual teaching, and classroom teaching reform is carried out around junior high school English grammar, vocabulary, and discourse, which effectively improves students' comprehensive ability to use English in junior high school. It further deepens the theoretical research on the teaching mode of blended teaching, explores the application practice in the reteaching of blended teaching, and promotes the normalization and sustainable development of teaching applications.

2. Related Work

English teaching has become a top priority area at present, and from a global perspective, many scholars are conducting research in this area. Richards aimed to outline the role of language proficiency issues in the ELT literature. He described the professional language skills required to teach English through English, exploring the relationship between language ability and teaching ability [1]. Alhassan suggested that in the past two decades, there has been a surge in TESOL/applied languages calling for English as an international teaching [2]. Polat aims to design a scale to test teachers' attitudes towards the role of grammar in the English teaching process and to find out the reliability and validity of the designed scale and other psychometric qualities [3]. Rozhina and Baklashkova introduced the main methods that help to cultivate the highest communicative competence of young children, the problems and solutions in children's English teaching [4]. Ayçiçek and Yankar Yelpan proposed that flipped classrooms are commonly applied in higher education, including providing lecture materials outside of classroom contact, setting aside face-to-face classroom time for more interactive learning, discussion, integration, and application of content [5]. However, the above research is still only in the theoretical part and cannot be fully practiced.

For artificial intelligence, it has penetrated into all fields of life. The following are the opinions and research of many experts on artificial intelligence. Zhao et al. research discusses the basic situation of robot global path planning, the application, advantages, and improvement measures of the ant colony algorithm in robot path planning, which provides help for further research [6]. Payedimarrri et al. study findings suggest that quarantine should be the best strategy to contain COVID-19. Nationwide lockdowns have also shown positive effects, while social distancing is only considered effective when combined with other interventions, including closing schools and businesses and restricting public transport [7]. Dolezel et al. introduced a specific neural network-based decision procedure that can be

considered for any traffic-characteristic-based network traffic processing controller. This decision-making process is based on a convolutional neural network that processes input stream features and provides decisions and it can be understood as firewall rules [8]. Maham studied the mechanical properties of two different types of recycled concrete (using wood and rubber) relative to pure concrete in terms of maximum load and natural frequency [9]. Visaggi et al. researched several options. Blood biomarkers offer an inexpensive, noninvasive screening strategy for cancer, and new technologies have allowed the identification of candidate markers for EC. The esophagus is easily examined by endoscopy, and endoscopic imaging represents the gold standard for cancer surveillance [10]. However, the current research on English education reform and model design in the era of artificial intelligence is still not based on traditional educational thinking, and there is a lack of in-depth analysis and exploration of the functionality of artificial intelligence. At present, only a hybrid English education method that combines the English education platform under artificial intelligence with traditional education can be achieved. This also hinders the high integration and advantages of artificial skills technology and education. The accuracy and data analysis of artificial intelligence cannot be brought into play, which also hinders the high integration and advantage of artificial skills technology and education. Therefore, further discussion is needed to tap the potential of artificial intelligence, improve the teaching ecology, and improve the level of education.

3. Algorithm of Artificial Intelligence

3.1. Sincnet Network Structure. Sincnet is an interpretable convolutional neural network proposed. Different from traditional CNN, Sincnet improves the first layer of the network and introduces the sinc function to learn more effective filters for audio data [11]. In digital signal processing, the normalized sinc function is usually defined as

$$\sin c(x) = \frac{\sin(\pi x)}{\pi x}. \quad (1)$$

The purpose of introducing the sinc function is to obtain a rectangular pulse with an amplitude of 1 after the Fourier transform of the sinc function. When extracting the original speech signal, it is often combined with time domain and frequency domain information for analysis [12]. For frequency domain signals, filtering methods are often used to obtain characteristic information contained in different frequency bands. Therefore, when performing feature extraction on speech signals, narrowband information is extracted by selecting rectangular bandpass filters in the frequency domain. On the premise of reducing noise interference, the feature information in each frequency band can be extracted more efficiently as shown in Figure 1.

The Fourier transform can realize the conversion of information in the time domain and the frequency domain. According to the properties of the Fourier transform, the

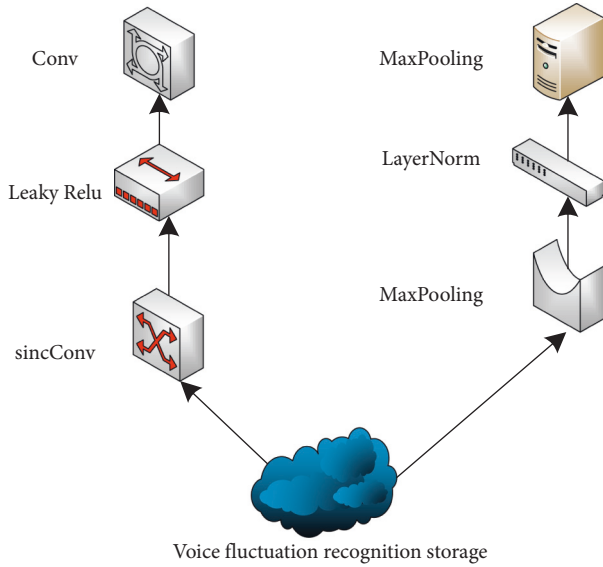


FIGURE 1: Sincnet network structure diagram.

multiplication in the frequency domain corresponds to the phase convolution operation in the time domain.

Among them, L represents the length of the filter. For speech recognition tasks, the input speech data is usually sampled at a specific frequency, so the original speech waveform data has high dimensionality. If the CNN network is used for the construction of the speech recognition model, the design of the first layer network is very important. If the selected filter is too small, the amount of calculation will increase, which will bring inconvenience to the training of the model. If the selected filter is too large, it will affect the feature extraction effect of the model on the input data, which is not conducive to the analysis of high-dimensional features.

The sincnet algorithm is novel in the application of the English education platform because it can process the speech signal so that the oral language part of the English teaching platform is also built.

3.2. Connectionist Temporal Classification (CTC). The speech recognition problem is essentially a sequence-to-sequence mapping problem. In the traditional speech recognition model, the mixed model method is often used. It obtains the mapping from input features to states through the acoustic model, uses a dictionary lookup method to achieve the mapping from phonemes to words, and then processes the language model to output the final audio recognition result [13]. The entire speech recognition model is composed of multiple modules, which need to be trained separately, so the learning of the entire speech recognition model becomes decentralized, which is not conducive to the overall tuning of the model.

After the input speech signal is processed by feature extraction and the sequence information of the LSTM network, the output layer contains each transcription label of the acoustic modeling unit (such as phoneme, note, or word) and a blank extra label, which represents an empty

launch. For a given input sequence x of length T , the output vector y is normalized by the softmax function to obtain the probability of the label corresponding to the k th index at time t , which can be expressed by as

$$p(k, t|x) = \frac{\exp(y_t^k)}{\sum_{k'=1}^k \exp(y_t^{k'})}. \quad (2)$$

It can be seen from the above, y_t^k represents the k th element of the output sequence y_t at time t . For a transcribed sequence ϕ , it is a sequence of length T composed of units in the transcribed tag set and blank tags.

CTC solves the problem of strict alignment from input to output by increasing the many-to-one mapping between output sequences and actual labels. The essence of the CTC loss function is a maximum likelihood function, which trains a speech time series classifier end-to-end to maximize the probability of outputting target 1 when the input is x [14].

3.3. Speech Decoding Algorithm. In communication systems, speech decoding is quite important because, to a large extent, speech decoding determines the received speech quality and system capacity. In mobile communication systems, broadband is very precious. Low bit rate speech decoding provides a solution to this problem. On the premise that the decoder can transmit high-quality voice, if the bitbook is lower, more high-quality voice can be transmitted within a certain bandwidth.

The decoding process based on the CTC speech recognition model is actually a spatial search process. Like the search space used in model training, the decoding process selects the optimal path as the output within a limited time [15]. Commonly used decoding algorithms include Prefix Search and Beam Search. In this paper, Beam Search is used for model decoding output. The schematic diagram of the algorithm is shown in Figure 2.

The expansion probability of a node is defined as $p(W, t)$, that is, the probability that the label corresponding to the output sequence at time t is W .

4. Design of English Teaching Model

4.1. Teaching Mode Construction. In the early stage of model construction, this paper mainly refers to the published "Personalized Online Learning Plan." The report clearly pointed out that, with the support of information technology, teachers rely on online resource platforms to teach online specifically as shown in Figure 3.

4.2. Preliminary Model. The model of this study is to be gradually improved through continuous revision on the premise that the preliminary model designed based on the existing research on individualized teaching and the teaching experience of this paper. Later, it was further modified and improved in practice, and finally an initial blended teaching model was designed, as shown in Figure 4. However, this model is only a preliminary idea, and the

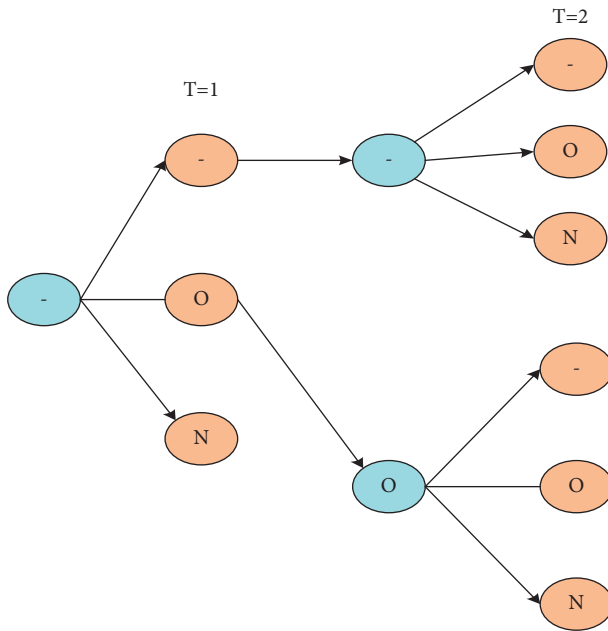


FIGURE 2: Schematic diagram of the improved algorithm.

model will be adjusted and improved in the future to form the final model.

Now we briefly introduce the preliminary model of the blended teaching mode of network resources. As shown in the figure, this model divides the teaching process into pre-class, in-class, and after class [16]. First of all, before class, mainly relying on the network platform, teachers select videos suitable for teaching tasks on the teaching platform and inform students to watch them independently, or students can arrange learning tasks independently according to their own learning progress, select suitable videos to watch, as long as they finally complete the learning tasks assigned by teachers. Secondly, in the classroom, teachers should divide into corresponding study groups according to the characteristics of students, or students should divide study groups independently according to their own interests [17]. Then the teachers organize corresponding teaching activities according to the teaching tasks. Before the teaching activity, the teacher first asked the corresponding questions according to the teaching objectives and arranged for the students to watch the video and the corresponding PPT again. After the end, the students showed their learning results. The form of learning outcomes is not limited to students' answers to questions, and students are responsible for their own speeches on topics. Finally, after class, according to the different performances of the students, a teaching evaluation is formed. The results of teaching evaluation not only have a certain impact on teachers' teaching but also can adjust students' learning goals according to the teaching evaluation. However, the setting of tasks should not be too complicated to avoid students losing interest in learning, resulting in an unsatisfactory teaching effect.

4.3. Model Adjustment and Final Design. In the adjustment stage of the model, this paper considers that the design of the initial model is still insufficient by consulting the relevant

literature. The Design and Practice of "Flip Classroom" Teaching Mode Based on Blended Teaching has an important guiding role in the design of this model [18]. Based on this literature, this paper modifies the model according to the definition of blended teaching. The teaching model design of this paper adopts the combination of online students' autonomous learning and offline teachers' classroom teaching. At the same time, the teaching stage is divided into before class, during class, and after class, as shown in Figure 5.

Primary school English is a basic subject, and the emphasis is on the cultivation of students' English application ability. Therefore, the main role of students must be more reflected in the model design. On the one hand, in the process of pre-class learning or small-class learning, teachers must let students learn with a purpose with problems, and learning without clues and goals may lead to poor learning results; on the other hand, for primary school students, this stage is in the stage of rapid development of language ability, their imitation ability and memorization ability develop rapidly. For blended teaching, it should focus on cultivating students' autonomous learning ability, let students develop the habit of independent learning in the classroom who be the master of the classroom, and make the English classroom more lively and lively, so that students fall in love with the English classroom.

In the pre-class stage, it is mainly advocated to focus on students' autonomous learning, using the form of problem-based learning to allow students to carry out pre-class learning with tasks. Teachers assign teaching tasks before class, which will make students think actively and stimulate students' learning motivation. However, the setting of tasks should not be too complicated to avoid students losing interest in learning, resulting in an unsatisfactory teaching effect. The theory of multiple intelligences states that each student has different intellectual strengths, and therefore different degrees of mastery of what they have learned. In this mode, teachers can guide students to formulate their own learning goals and learning plans according to their different foundations without exceeding the existing teaching goals. The tasks at this stage of the students' pre-class are completely carried out by the students themselves, and the teachers only provide learning resources and collect the difficulties encountered by the students when watching the video. Therefore, students in this stage of learning behavior can choose their own learning location, just watch the video.

4.4. Implementation Process of Primary School English Teaching Mode. As a new product in today's information age, online network resources have attracted a large number of learners and researchers. The emergence of online resources not only enables learners to obtain more learning resources and changes the original learning methods, but also further expands the teaching methods of teachers. Referring to the applied research on blended teaching, it can be roughly divided into three types: before class, during class, and after class. The teaching mode of

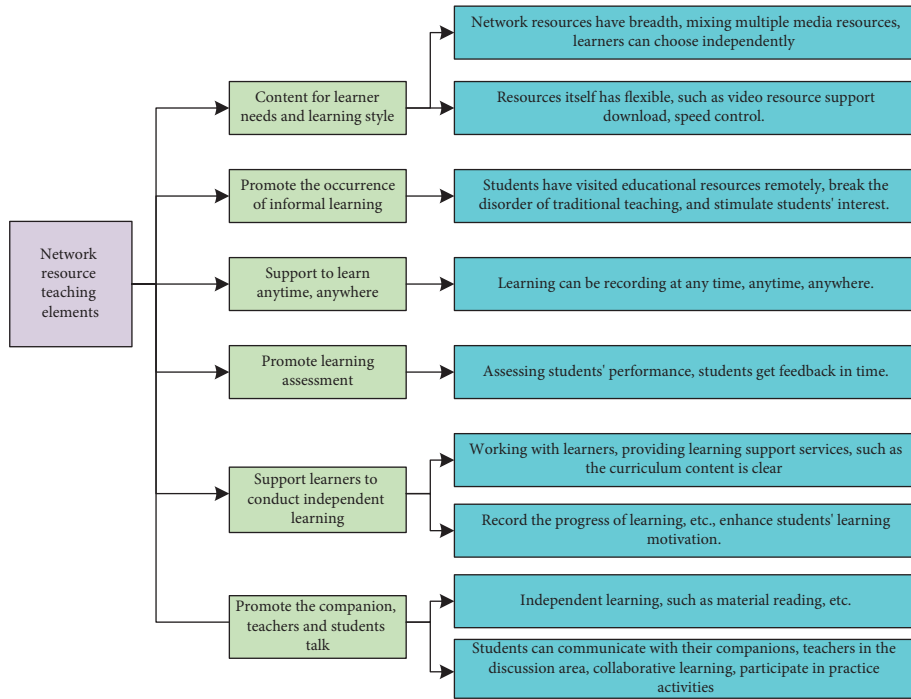


FIGURE 3: 6 elements of teacher network resource teaching in the network environment.

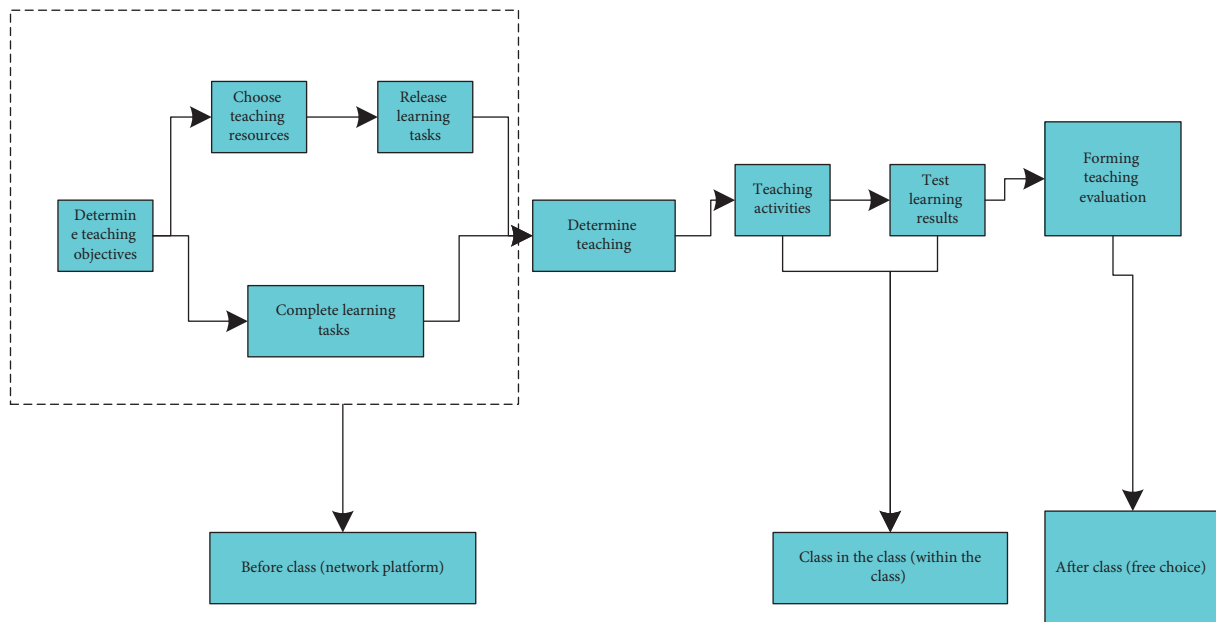


FIGURE 4: Preliminary model of blended teaching.

this research is under the premise of continuous modification and gradual improvement based on the existing research on blended teaching and further modification and improvement in three rounds of teaching practice. Finally, the mixed teaching mode of English for the upper grades of primary school is constructed, and the process is shown in Figure 6.

5. Discussion on the Current Situation of English Teaching Reform

5.1. Students' English Learning Attitude and Difficulties. The student's learning attitude is the key factor that determines the student's learning result, and it is the performance of the learning motivation in the student's overall

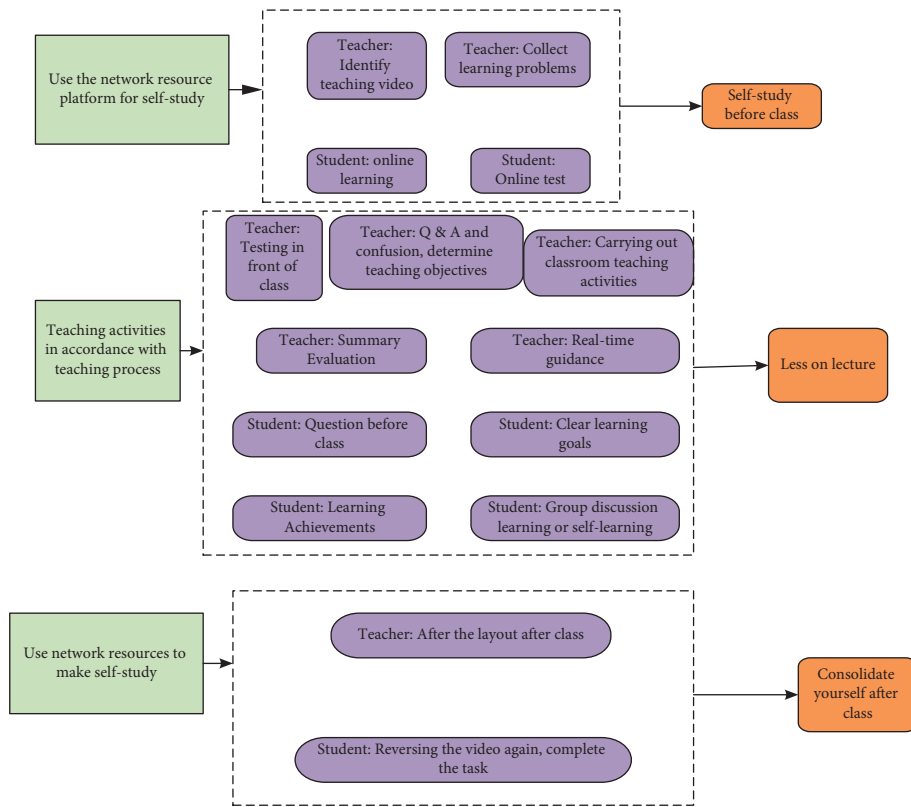


FIGURE 5: Teaching flowchart.

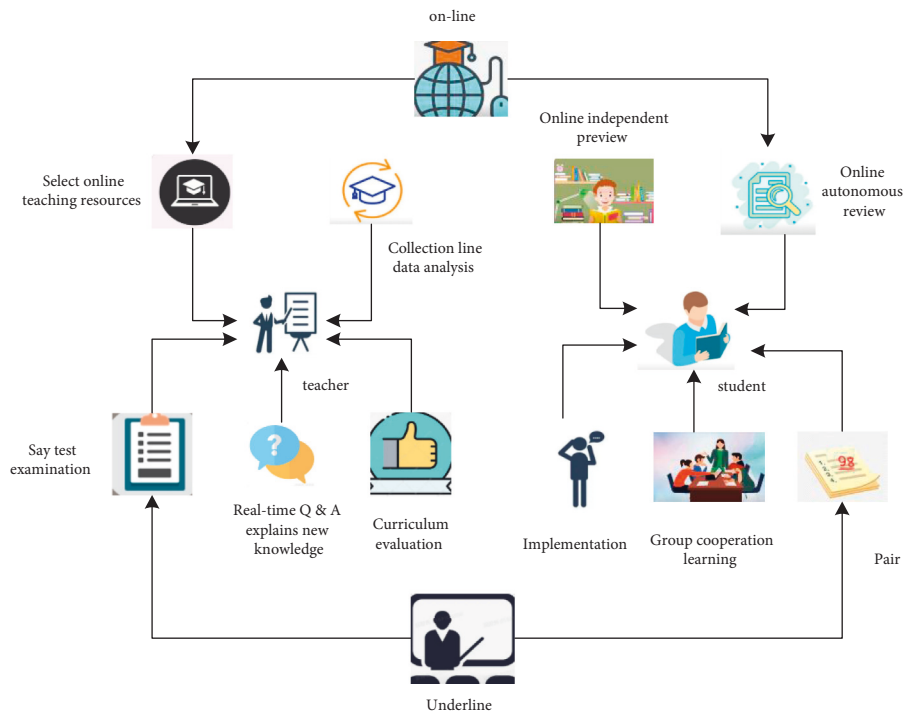


FIGURE 6: Flowchart of blended teaching mode.

learning activities. Therefore, this paper uses the network resources in artificial intelligence and artificial intelligence algorithm technology to conduct a survey and research on all students in a certain school. When students are interested in teachers' English courses and can actively and seriously engage in learning, students' own learning efficiency and learning results can achieve good results. However, when students learn English, they will inevitably encounter many difficulties, which requires teachers to carry out targeted teaching according to students' learning difficulties so that students' English learning can achieve good results [19]. The current goal of English teaching is to enable students to develop in an all-round way in listening, speaking, reading, and writing. However, when students are currently studying English, due to the large amount of course content and limited course time, students will encounter many difficulties in the process of English learning. In this survey, in order to have a clearer understanding of the current students' English learning difficulties, this paper has also conducted a survey on the biggest difficulties students think of English learning at present. All the survey results are shown in Figure 7.

In the survey, 29.7% of the students believed that their current difficulty in English learning lies in oral expression. Students believe that the main reasons for the difficulty of oral language learning are that teachers seldom create an oral language environment, and students do not use it well after class. 9.39% of students think that listening is the biggest obstacle, which is mainly reflected in listening, which accounts for less in daily exams. Teachers use Chinese in their daily teaching and other factors, and students do not understand because they do not listen enough. The proportion of students who think that grammar learning is difficult is 13.33%. The difficulty of grammar learning is mainly reflected in the understanding of grammar knowledge, and they do not know the various forms and flexible application of grammar knowledge. Word learning difficulties reached 12.73%, and this part of the students believed that the memory of words was an obstacle to English. Most of them use the way of marking the pronunciation of words to memorize words. This method not only makes English pronunciation inaccurate but also cannot achieve good memory effect. Only 4.85% of the students thought that there were difficulties in vocabulary, grammar, speaking, and listening. At present, most students believe that listening and speaking are the major obstacles in English learning. How to improve the listening and speaking skills of primary school students at this stage and further improve students' interest in learning is particularly critical [20].

5.2. Student Questionnaire

5.2.1. Students' Views on the Curriculum Design of the Teaching Platform. As shown in Figure 8, 62% of the students believe that the online "learning resource pack" provided in teaching practice is sufficient and helpful for self-learning new knowledge, but 18% of the students still think that the learning materials still need to be expanded,

indicating that there is still much room for improvement in resource construction. 80% of students believe that the "learning resource pack" is helpful for self-study in English and can improve their learning effect. 62% of students believe that the amount of tasks posted on the SPOC platform before class is suitable, and 12% of students believe that the amount of tasks can be increased. Therefore, in the pre-class learning on the network platform, it is necessary to pay attention to matching the personal situation of most students and then add personalized teaching modules and set up basic modules and expansion modules for different students to learn by division. More than 80% of the learners of the after-school homework assigned on the sPOC platform believe that the difficulty and quantity are reasonable, which is conducive to improving and consolidating the classroom learning effect [21].

The data surveyed in this paper reflects students' views on the SPOC platform and curriculum design. The evaluation grades are divided into five categories: A is very helpful, B is helpful, C is average, D is not helpful at all, and E is not helpful. More than two-thirds of the students believe that ten minutes of "English speaking" in the flipped classroom creates a full-English situation and enables them to quickly enter the learning state. Nearly three-quarters of the students recognized the role of the five-minute summary session in deepening knowledge learning in classroom teaching. Students think that situational teaching activities such as problem analysis and discussion in the classroom are very helpful for the mastery of English professional knowledge, and the proportion is 80%. The results are shown in Table 1.

5.2.2. Analysis of Students' Satisfaction with the Teaching Platform Model. The following survey is an analysis of students' satisfaction with the learning results. The evaluation grades are divided into five categories: A means very helpful, B means helpful, C means average, D means not helpful at all, and E means no help, as shown in the Table 2.

5.3. Investigation on the Current Situation of English Teaching. Understanding the current state of English teaching is one of the keys to this research. This paper conducts a questionnaire survey on students, and makes a relevant understanding of the current situation of English teaching in a primary school. It carried out statistics and analysis of the survey results and found some problems in teachers' teaching and students' learning as shown in Table 3.

It can be seen from the above table that 4.24% of the students think that it is very consistent with the current English teaching status, and teachers have used the form of blended teaching in teaching. 15.76% of the students believe that it is in line with the current English teaching status; 16.97% of the students think that the degree of teachers' use of blended teaching is relatively general, while 24.24% of the students and 38.79% of the students think that teachers use the blended teaching in English teaching does not meet or is very inconsistent with the current English teaching status. It can be seen that in the current English teaching process,

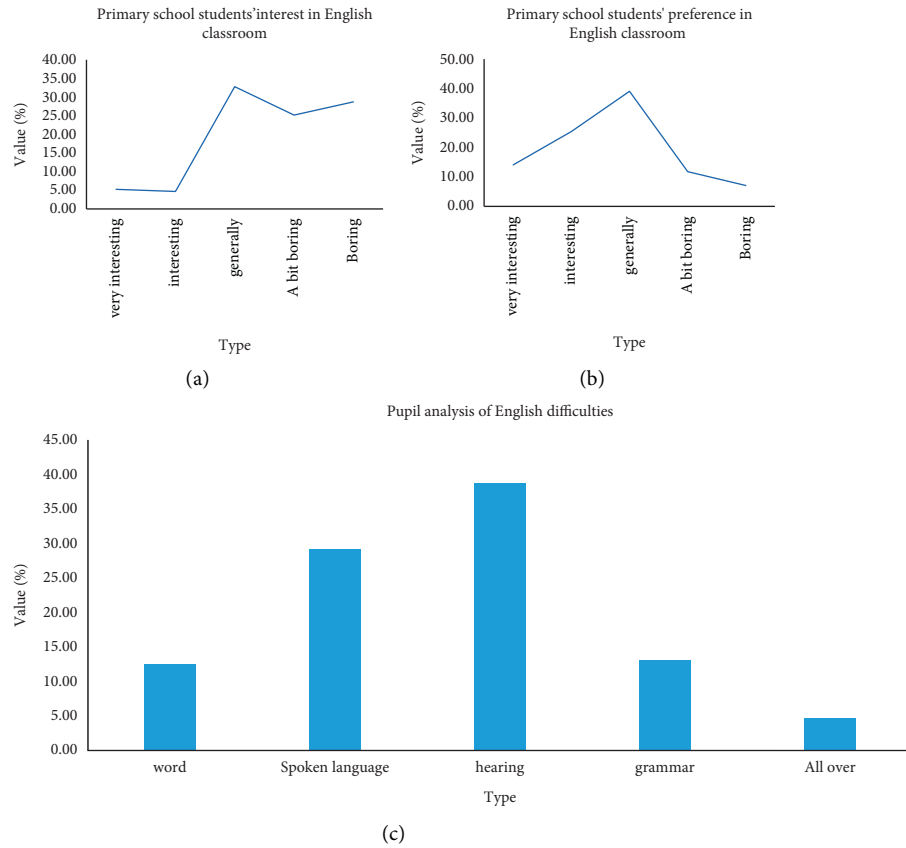


FIGURE 7: A survey of primary school students on English education classrooms. (a) Primary school students' interest in English classroom; (b) primary school students' preference in English classroom; (c) pupil analysis of English difficulties.

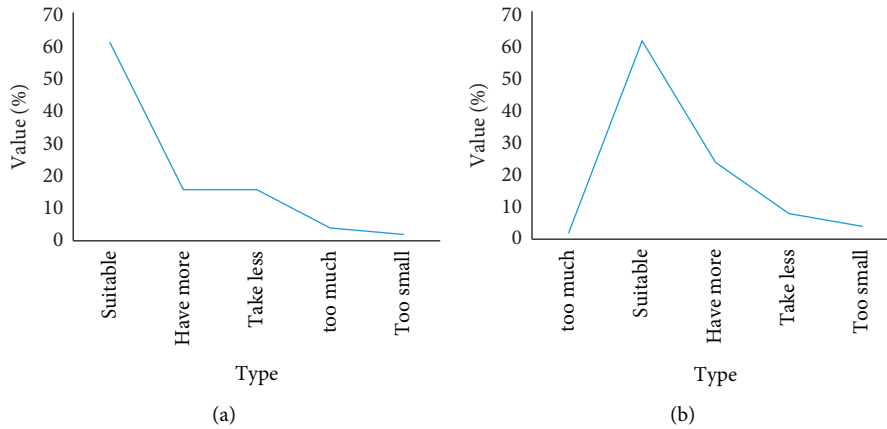


FIGURE 8: Survey of students' attitudes towards teaching platforms. (a) Data on students' attitude towards teaching resources. (b) Data on students' attitude towards pre-class tasks.

TABLE 1: Survey of students' attitudes towards teaching platforms.

Evaluation indicator	Evaluation results				
	A (%)	B (%)	C (%)	D (%)	E (%)
Ten minutes "English said"	7/14	30/60	9/18	4/8	0/0
Five minutes summary	15/30	28/56	7/14	0/0	0/0
Group mutual evaluation	9/18	27/54	14/28	0/0	0/0
Forum	11/22	26/52	12/24	1/2	0/0

TABLE 2: Analysis of student satisfaction with learning outcomes.

Evaluation indicator	Evaluation results				
	A (%)	B (%)	C (%)	D (%)	E (%)
Improve learning efficiency	12/24	30/60	7/14	1/2	0/0
In-depth grasp of full English knowledge	11/22	30/60	9/18	0/0	0/0
Improve operational skills	9/18	28/5%	13/26	0/0	0/0
Improve problem-solving ability	10/20	30/60	10/20	0/0	0/0
Improve independent learning skills	9/18	34/68	7/14	0/0	0/0

TABLE 3: Questionnaire about the current situation of English teaching.

Question	Option	Percentage
At present, English teachers use the way of mixed teaching	Consistent	4.24
	Meets the	15.76
	Generally	16.97
	Incompatible	24.24
	Unqualified	38.79
You think the teaching resources provided by English teachers are lacking	Consistent	27.12
	Meets the	32.42
	Generally	18.97
	Incompatible	11.18
	Unqualified	10.3
In English class, teachers often use multimedia to teach	Consistent	23.64
	Meets the	32.73
	Generally	26.06
	Incompatible	9.09
	Unqualified	8.08

teachers seldom or hardly adopt the method of blended teaching. In the teaching, the traditional classroom teaching mode is still adopted in which teachers teach in the classroom and students listen to the lectures below. This kind of teaching method makes the students' participation in the classroom not high, and the teacher's indoctrination is more, which seriously reduces the teaching quality [22].

Through the analysis of the results of the questionnaire, it can be seen that 78.51% of the students believe that the teaching resources provided by English teachers are lacking or the teaching resources are relatively general. Only 21.48% of the students believed that the teaching resources provided by English teachers were rich or very rich. The lack of teaching resources provided by teachers is still one of the problems existing in English teaching at present. Providing abundant teaching resources is the key to ensure the learning effect of students and the teaching effect of teachers.

5.4. Network Resource Requirements. Blended teaching is the combination of online learning and classroom teaching, and it is extremely important to know what kind of teaching form students expect teachers to use in the teaching process. In addition, the experimental subjects selected in this study are primary school students. Whether the type of network resources selected by teachers before class can stimulate students' interest in learning is also one of the issues to be paid attention to in this investigation and research [23, 24]. At the same time, the duration of online resources and videos expected by students is the focus of this

questionnaire. Therefore, this paper investigates the above questions and presents the survey results as shown in Figure 9.

5.5. Survey of Primary School English Teaching Based on Artificial Intelligence

5.5.1. Analysis of Student Questionnaires. Teachers' classroom teaching and students' autonomous learning after class are mutually integrated and mutually supportive. The teaching video provided by the network platform is the extension of teachers' classroom teaching knowledge after class, and the teacher's classroom teaching also provides directional guidance for students to learn network resources independently after class. In this section, this paper investigates the effect of the teaching experiment, using two methods of questionnaire survey and interview, to discuss and analyze the survey results [25, 26]. First, a questionnaire survey was carried out on whether primary school students were satisfied with the teaching resources provided by teachers, whether they were autonomous in their learning, and whether they could improve students' interest in English learning. The results of the survey are shown in Table 4.

It can be seen from the table that 23.18% and 50.86% of the students believe that the network resources selected by the teacher have played a certain role in their English learning; 6.84% and 3.71% of students believe that the online resources selected by teachers are not helpful to their English learning, which shows that most of the students are satisfied

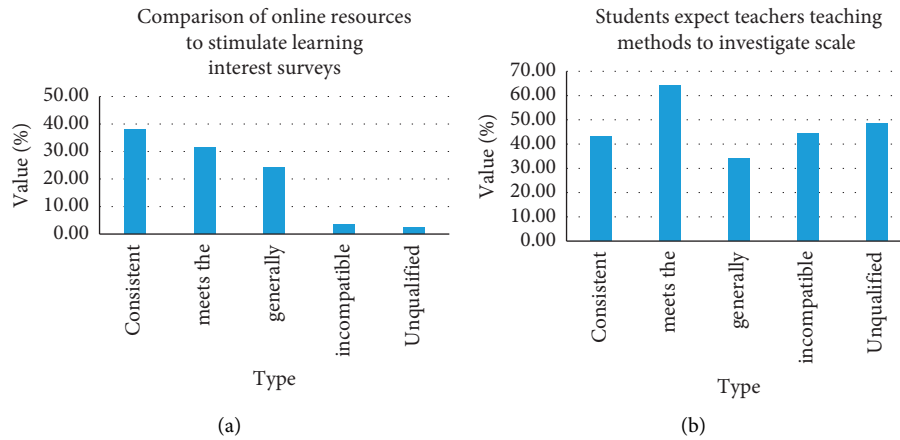


FIGURE 9: Statistical chart for the analysis and comparison of network resources for students’ needs. (a) Comparison of online resources to stimulate learning interest surveys. (b) Students expect teachers teaching methods to investigate scale.

TABLE 4: Student questionnaire posttest results questionnaire.

Question number	Title statement	Consistent (%)	Meets the (%)	Generally (%)	Not in line with (%)	Incompatible (%)
1	Teachers choose network resources play a certain help to my English learning	23.18	50.86	15.41	6.84	3.71
2	Teacher’s mixed teaching model has stimulated my English learning interest	53.67	27.83	10.42	5.69	2.40
3	Compared with traditional teaching modes. I prefer mixed teaching models	23.67	32.74	19.52	16.80	7.37
4	I will watch the network platform video in accordance with the teacher’s request before class	24.31	34.41	20.72	5.41	15.15
5	For questions you do not understand, I will watch teaching videos after the class	6.30	16.08	17.99	27.15	32.48

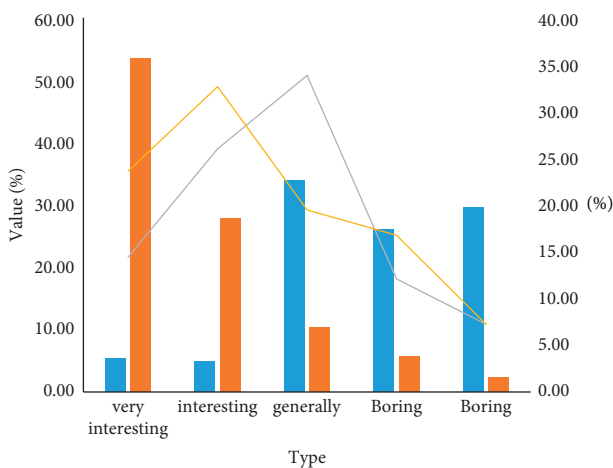


FIGURE 10: Comparative analysis of the degree of interest and love of the course before and after.

with the resources selected by teachers, which has played a certain role in promoting their English learning. The teaching mode of teachers has stimulated my interest in English learning. 53.67% of the students chose to be very consistent, 27.83% of the students chose to be in line, 10.42% of the students chose to be average, 8.09% of the students

chose not to be in line with very inconsistent, which shows that most of the students believe that the current teaching method can stimulate their interest in learning English. Figure 10 shows a statistical chart of the comparison and analysis before and after the interest and love of English courses.

It can be seen from Figure 10 that in the later stage, most of the students’ preference for English courses has increased significantly compared with the pre-test, but there are still some students who do not like English courses, but their dislike of the teaching mode adopted by teachers has increased compared with the pretest.

6. Conclusions

The blended teaching based on artificial intelligence not only improves the students’ interest in English learning, but also improves the students’ learning enthusiasm, and the teaching experiment effect is remarkable. This study believes that under the guidance of the blended teaching model, teachers’ teaching atmosphere has also undergone relatively obvious changes, students’ participation in the classroom is higher, and classroom communication is significantly improved. Although the blended teaching model based on artificial intelligence can effectively improve students’

interest in English learning and academic performance, it has higher requirements on students' autonomous learning ability and is not suitable for students with poor autonomous learning ability, which is the blended of this teaching method. The quality of blended teaching depends not only on teachers' classroom teaching, but also on students' autonomous learning after class. As an online course, network resources have the advantages of openness, breadth and immediacy of teaching content far more than traditional classrooms, but at the same time, it puts forward high requirements for students' autonomous learning and self-control. Although the teaching forms of network resources are rich and colorful, the teaching forms are relatively simple and all teaching is presented to learners in the form of videos. For learners, the learning process lacks the supervision of teachers and parents, and the learning effect is difficult to guarantee. Therefore, in the future, traditional teaching and online teaching should be mixed to ensure the learning effect of students [27].

Data Availability

Data sharing is not applicable to this article as no new data were created or analyzed in this study.

Conflicts of Interest

The author states that this article has no conflicts of interest.

Acknowledgments

This work was supported by General Special Scientific Research Projects of Education Department of Shaanxi Province (no. 21JK0275).

References

- [1] J. C. Richards, "Teaching English through English: proficiency, pedagogy and performance," *RELC Journal*, vol. 48, no. 1, pp. 7–30, 2017.
- [2] A. Alhassan, "Teaching English as an international/lingua franca or mainstream standard language? Unheard voices from the classroom," *Arab World English Journal*, vol. 8, no. 3, pp. 448–458, 2017.
- [3] M. Polat, "Teachers' attitudes towards teaching English grammar: a scale development study," *International Journal of Instruction*, vol. 10, no. 4, pp. 379–398, 2017.
- [4] V. A. Rozhina and T. A. Baklashova, "Teaching English language to young school-age children while making projects, playing games and using robotics," *XLinguae*, vol. 11, no. 1, pp. 102–113, 2018.
- [5] B. Ayçiçek and T. Yanpar Yelken, "The effect of flipped classroom model on students' classroom engagement in teaching English," *International Journal of Instruction*, vol. 11, no. 2, pp. 385–398, 2018.
- [6] H. Zhao, H. Zhou, and G. Yang, "Research on global path planning of artificial intelligence robot based on improved ant colony algorithm," *Journal of Physics: Conference Series*, vol. 1744, no. 2, p. 022032, 2021.
- [7] A. B. Payedimarri, D. Concina, L. Portinale et al., "Prediction models for public health containment measures on COVID-19 using artificial intelligence and machine learning: a systematic review," *International Journal of Environmental Research and Public Health*, vol. 18, no. 9, p. 4499, 2021.
- [8] P. Dolezel, F. Holik, J. Merta, and D. Stursa, "Optimization of a depiction procedure for an artificial intelligence-based network protection system using a genetic algorithm," *Applied Sciences*, vol. 11, no. 5, p. 2012, 2021.
- [9] maham, "using artificial intelligence for optimizing natural frequency of recycled concrete for mechanical machine foundation," *Recycling*, vol. 6, no. 3, pp. 43–44, 2021.
- [10] P. Visaggi, B. Barberio, M. Ghisa et al., "Modern diagnosis of early esophageal cancer: from blood biomarkers to advanced endoscopy and artificial intelligence," *Cancers*, vol. 13, no. 13, p. 3162, 2021.
- [11] Y. Liu, "Artificial intelligence-assisted endoscopic detection of esophageal neoplasia in early stage: the next step?" *World Journal of Gastroenterology*, vol. 27, no. 14, pp. 1392–1405, 2021.
- [12] S. Dewitte, J. P. Cornelis, R. Müller, and A. Munteanu, "Artificial intelligence revolutionises weather forecast, climate monitoring and decadal prediction," *Remote Sensing*, vol. 13, no. 16, p. 3209, 2021.
- [13] C. Berg, A. Geissinger, and N. R. . Managers, "Minds and machines in the age of artificial intelligence," *Academy of Management Annual Meeting Proceedings*, vol. 2021, no. 1, pp. 13120–13121, 2021.
- [14] J. Ye, "Research on enterprise value management of emerging industries in the age of artificial intelligence," *Journal of Physics: Conference Series*, vol. 1861, no. 1, p. 012037, 2021.
- [15] J. S. Suri, S. Agarwal, R. Pathak et al., "Covlias 1.0: lung segmentation in COVID-19 computed tomography scans using hybrid deep learning artificial intelligence models," *Diagnostics*, vol. 11, no. 8, p. 1405, 2021.
- [16] M. D. O. Fornasier, "The regulation of the use of artificial intelligence (ai) in warfare: between international humanitarian law (ihl) and meaningful human control," *Revista Jurídica da Presidência*, vol. 23, no. 129, p. 67, 2021.
- [17] R. Palomino, K. B. Low, C. Ji, I. Petrovic, F. Waltz, and T. Schmitz, "Micro computed tomography analysis of four-way conversion catalysts using artificial intelligence-enabled image processing," *Microscopy and Microanalysis*, vol. 27, no. S1, pp. 1028–1029, 2021.
- [18] P. Swpu, "Recent progress and new developments of applications of artificial intelligence (AI), knowledge-based systems (KBS), and Machine Learning (ML) in the petroleum industry," *Petroleum*, vol. 6, no. 4, pp. 319–320, 2021.
- [19] G. Dilip, R. Guttula, S. Rajeyyagari et al., "Artificial intelligence-based smart comrade robot for elders healthcare with strait rescue system," *Journal of Healthcare Engineering*, vol. 2022, no. 5, p. 9904870, 2022.
- [20] C. Wang, C. Yao, P. Chen, J. Shi, Z. Gu, and Z. Zhou, "Artificial intelligence algorithm with ICD coding technology guided by the embedded electronic medical record system in medical record information management," *Journal of Healthcare Engineering*, vol. 2021, no. 4, pp. 1–9, 2021.
- [21] Y. Su, G. Chen, M. Li, T. Shi, and D. Fang, "Design and implementation of web multimedia teaching evaluation system based on artificial intelligence and jQuery," *Mobile Information Systems*, vol. 2021, no. 12, pp. 1–11, 2021.
- [22] D. Hassabis, D. Kumaran, C. Summerfield, and M. Botvinick, "Neuroscience-inspired artificial intelligence," *Neuron*, vol. 95, no. 2, pp. 245–258, 2017.
- [23] A. F. A. Mentis, I. Garcia, J. Jiménez et al., "Artificial intelligence in differential diagnostics of meningitis: a nationwide study," *Diagnostics*, vol. 11, no. 4, p. 602, 2021.

- [24] Z. Lv, H. Song, P. Basanta-Val, A. Steed, and M. Jo, "Next-generation big data analytics: state of the art, challenges, and future research topics," *IEEE Transactions on Industrial Informatics*, vol. 13, no. 4, pp. 1891–1899, 2017.
- [25] G. M. Abdulsahib and O. I. Khalaf, "Comparison and evaluation of cloud processing models in cloud-based networks," *International Journal of Simulation. Systems, Science and Technology*, vol. 19, no. 5, 2019.
- [26] R. S. Bhadoria and N. S. Chaudhari, "Pragmatic sensory data semantics with service-oriented computing," *Journal of Organizational and End User Computing*, vol. 31, no. 2, pp. 22–36, 2019.
- [27] R. Fusco, R. Grassi, V. Granata et al., "Artificial intelligence and COVID-19 using chest CT scan and chest X-ray images: machine learning and deep learning approaches for diagnosis and treatment," *Journal of Personalized Medicine*, vol. 11, no. 10, p. 993, 2021.

Research Article

Statistics and Analysis of Effective Data on Online Teaching of College English Audiovisual Teaching

Kerong Wang 

Basic Department, Yantai Vocational College, Yantai 264670, Shandong, China

Correspondence should be addressed to Kerong Wang; 20170530@ytvc.edu.cn

Received 31 March 2022; Revised 23 May 2022; Accepted 2 June 2022; Published 19 July 2022

Academic Editor: Wei Liu

Copyright © 2022 Kerong Wang. This is an open access article distributed under the Creative Commons Attribution License, which permits unrestricted use, distribution, and reproduction in any medium, provided the original work is properly cited.

Since the end of 2020, the COVID-19 outbreak has partly changed the way people live and the way schools across the country teach. In order to solve the impact of the new coronavirus pneumonia pandemic on the opening of universities and classroom teaching, it is particularly important to study how universities implement and ensure the development of online foreign language teaching. This article aims to study the effectiveness of online teaching of college English audiovisual listening. We actively carry out teaching activities such as online teaching and online learning of English audiovisual teaching and perform statistical analysis of progress and the quality of college English teaching in online teaching. This article aims to combine these two paradigms, collect data and conduct qualitative and quantitative analysis, and analyze the accuracy of effective data in English audiovisual online teaching. This survey uses two survey methods: questionnaire survey and structured interview. In order to understand the interviewee's feelings and obtain more detailed feedback information, interviews about learning strategies were organized. The conclusion is that under the background of the "COVID-19 pandemic," college English courses based on various online learning platforms (such as MOOC) are very valuable learning experiences for students. In order to adapt the online learning, students need to use appropriate learning strategies. This kind of learning experience also provides valuable opportunities for students, enabling them to develop their independent learning abilities and review their learning achievements. College English course teaching based on multiple online learning platforms such as MOOC provides inspiration and experience for future college English teaching. Teachers become instructors for students to master and use learning strategies. Only teachers and students work together to ensure the quality of online teaching.

1. Introduction

1.1. Background. Affected by the new coronavirus pneumonia pandemic, the provincial education department has formulated guidelines to promote online teaching in all types of schools, that is, relying on existing platforms to open online learning channels to ensure that courses are not suspended. The goal of the policy is to ensure that students' can maintain the same learning effect by online learning. Therefore, online teaching and online learning must be carried out. According to the characteristics of foreign language teaching, we discuss how teachers can carry out online teaching activities during this pandemic period to ensure the progress and quality of foreign language teaching in colleges and universities.

1.2. Significance. As one of the factors affecting the effective teaching of college English, the design and realization of audio-visual course objectives are very important. College English can mainly cultivate students' English application ability, so it is necessary to use audition courses to cultivate students' speaking and listening. Therefore, it has far-reaching significance to conduct research from the perspective of objectives to observe the effectiveness of English listening and speaking teaching in universities. Theoretically speaking, on the one hand, research is conducted from a different perspective to explore the purpose of effective teaching, which expands the scope of effective teaching and learning. On the other hand, the survey can enrich the connotation of college English goals and provide references for further research. In practice, the research is beneficial to

teachers, school leaders, and students. This research from the perspective of teachers can awaken teachers' sense of goal and allow them to reflect on their own teaching in college English teaching. In other words, this research can provide positive feedback for teachers' education and self-reflection, so that teachers can form a systematic and overall view of the goal. Looking at leaders from the school's point of view, research can provide clues for promoting the professionalization of English teachers and, at the same time, provide references for managers to formulate education policies and plans.

1.3. Related Work. In this era of rapid development of Internet Plus, the reform of college English teaching keeps up with the pace of the times, and online education models have begun to emerge in the reform of English teaching, and they are becoming more and more popular. Leire C put forward the idea that the Massive Open Online Course (MOOC) aims to provide barrier-free education. The MOOC "Green Economy: Lessons from Scandinavia" was launched in 2015. MOOC learning activities are different from traditional online courses. To meet the expectations of stakeholders on the MOOC, teachers' continuous learning and adaptation are essential to e-learning, and learners' motivation may affect the success of the course. But at the beginning, when the online courses were opened, the teaching quality and effects presented in actual teaching were not as good as expected [1]. Jorg Mussig studied that during the COVID-19 pandemic, many educators were asked to provide courses online. A particular challenge is to implement practical laboratory experiments in the field of science and engineering. The main questions are as follows: How do students conduct laboratory experiments at home? In this case, how can applications on mobile devices provide help? How to organize experiments so that students can learn this topic in a self-motivating and exciting way [2]? Kim's research seeks to enhance the method of blending general English learning in online and offline English classes. Students can visit the class homepage in their spare time for online learning and communication, no matter where they are. This method is called the reverse learning model. The research compares the reverse learning model with the more traditional hybrid learning model to study the difference in effect. After the experiment, the comparative *t*-test of the two groups showed that the statistical reliability of 99.9% had a statistically significant difference [3].

1.4. Main Content. In order to understand the implementation status of teachers' online teaching and the effectiveness of students' learning at home and to further adjust and improve the school's online teaching management measures, the school used a questionnaire to survey the teachers and students of the whole school. The results show that under the premise of preventing and controlling the pandemic, teachers have found an effective teaching path for online teaching, which ensures the effectiveness and practicability of online teaching. On this basis, the school should strengthen the management of online teaching, improve the

teaching quality of online teaching, strengthen the guidance to students and parents, and not disturb the mental health education of students [4].

2. Effective Statistical Methods for Online Teaching

2.1. Effective Data Statistical Methods

2.1.1. Interview Method. After the open questionnaire were distributed, subjects were randomly selected to conduct interviews to explore the understanding of blended learning and English learning, to determine important themes of online English learning or issues that need to be further explored, and to understand the importance of online college English teaching through the Internet Influencing factors to interview the students and teachers in the later stage to improve the conclusion of the paper [5, 6].

2.1.2. Investigation Method. The use of convenient sampling methods to formally issue questionnaires to explore college students' English language concepts, English classroom learning satisfaction, online English learning students' satisfaction, and present corresponding teaching strategies based on the survey results [7] to investigate and verify the suggestions made.

2.2. Statistical Learning Theory. The learning process of the basic knowledge of this course is relatively flexible. The basic knowledge of English courses includes four aspects: listening, speaking, reading, and writing. The introduction explains why the theory in this section is used. Students can choose when and where to learn this part of knowledge according to their own characteristics, and they can learn repeatedly, which greatly improves the flexibility of learning and improves the efficiency of learning [8]. In this way, the specific composition of the function is expressed as (a_1, b_1) and (a_n, b_n) , and statistical learning needs to find the best dependence relationship between the above independent training sample $\{f(a, c)\}$ function set $f(a, C_0)$. When estimating the optimal result, the expected risk $R(c)$ should also be considered, as shown in

$$R(c) = \int L(b, f(a, c))dF(a, b). \quad (1)$$

The expression $L(b, f(a, c))$ shows that the prediction function learns to predict the loss of y .

$$L(b, f(a, c)) = (b - f(a, c))^2. \quad (2)$$

When we study the expected hazard function (2), we need to get the details of the joint probability density function $F(a, b)$ [1, 9]. In the context of similar algorithms, it is necessary to introduce the theorem of large numbers and introduce relevant empirical risk functions. The formula is as follows:

$$R_{\text{emp}}(c) = \frac{1}{n} \sum_{i=1}^n L(b_i, f(a_i, c)). \quad (3)$$

In the MOOC teaching process, there is a lack of control links and students learn at will, resulting in serious loss of students [10]. The MOOC course activity process is an autonomous learning process. Students need to have a strong sense of autonomy to complete the entire learning process, but for most students, this is not realistic. In addition, students' learning motivation may be of temporary interest and three-minute enthusiasm [11, 12]. Learning motivation is not firm enough, and it is destined that the investment of learning energy cannot be guaranteed. When learning interest is lost or the learning process is disturbed, students are easy to abandon the course and lose their way. Judging from the current study-tracking survey of MOOC students, the situation is basically the same [13]. Many courses have a considerable number of students, but there are absolutely very few students who complete the course from start to finish. This situation is due to the lack of management and control over the learning process [14]. Statistical learning theory summarizes a series of problems and limitations and proposes a new solution, that is, the probability of real risk and empirical risk meets the following conditions:

$$R(c) \leq R_{\text{emp}}(c) + h \left(\frac{\ln(2n/h) + 1}{n} \right) - \ln \left(\frac{n}{4} \right). \quad (4)$$

On the basis of meeting the classroom teaching reform of our school, we transfer the system platform to local or national application-oriented universities, aiming to lower the threshold of online teaching in similar universities, speed up the promotion of online classroom teaching mode, and give full play to the platform in a wider range. This will help us to improve the quality of higher education teaching [15]. According to (4), the risk components of statistical learning theory are empirical risk and risk confidence interval, which are related to the risk capital dimension h and the training sample set n .

$$R(c) \leq R_{\text{emp}}(c) + \Phi \left(\frac{h}{n} \right). \quad (5)$$

According to the characteristics of linearly separable problems, the optimal classification surface satisfies the following formula, which is not only suitable for multi-input and multioutput production departments but also can be applied to public departments such as schools for performance evaluation. The model does not need to set estimated parameters and can also simplify calculations. Secondly, it can compare its own development process vertically according to the relative efficiency of different time periods, or horizontally compare the relative efficiency of various departments, then find out the reasons, and propose measures to improve. According to (5), if the H value gradually increases, the model complexity and learning ability of statistical learning will also increase correspondingly [16]. According to the characteristics of the linearly separable problem, the optimal classification surface satisfies the following:

$$c \cdot a + e = 0. \quad (6)$$

Taking into account the influence of different values of different parameters on the model results, the normalization method is used to obtain the optimal classification surface parameters, which satisfies the restriction of

$$b_i [(c \cdot a_i) + e] - 1 \geq 0, \quad i = 1, 2, \dots, n. \quad (7)$$

3. Data Statistics Experiment

3.1. Online Teaching Technology. Ensuring the normal operation of the network is the basic prerequisite for ensuring online teaching. Due to a large number of students, the basic network conditions vary greatly from place to place, and using the same software to broadcast courses at the same time will definitely cause pauses, connection interruptions, sound transmission failures, and video signal instability [17]. This requires strengthening the coordination between the industry and the information department and the network operating company, actively cooperating and supporting, starting from the actual situation, and guiding students to "interleaved" log-in learning based on the local network situation. The interaction between students for local learning is helpful for their cultural exchange and oral communication. All network operating companies and software developers also provide teacher training for teachers at the beginning of the school year to ensure online foreign language teaching in colleges and universities [18, 19]. The training content will be expanded from the aspects of teacher literacy, course skills, and the use of related software. Teachers should learn and use online classroom teaching platforms, such as Yu Class, MO Class, and Tencent Class, to enhance the feasibility of online teaching in the Internet era [20].

3.2. Effective Data Statistics Steps. The content of the questionnaire used in the research includes two parts: basic information and latent variable information. The number of preliminary surveys was planned to be 850, and 800 questionnaires were returned. The recovery rate is 94%. This was mainly used to investigate the English learning concepts of college students. Among them, the sample size of students from grade one to grade four is 800 and were surveyed from two aspects of college English classroom learning satisfaction and online learning platform satisfaction [21]. Finally, after sorting out the collected questionnaire data, the validity analysis, standard deviation, T -test, and significance test are carried out. The use of questionnaires can better reflect the real thoughts of students, which is conducive to feedback on learning effects.

4. Online Teaching Survey Results

4.1. Survey and Research Results

4.1.1. Investigation and Research Results of College English Audiovisual Online Teaching. It can be seen from Table 1 that the study subjects were planned as 850 copies, but 800 questionnaires were actually returned. The ratio of men to

TABLE 1: Basic situation of survey subjects.

Gender	Number of people	Percentage
Male	600	75
Female	200	25

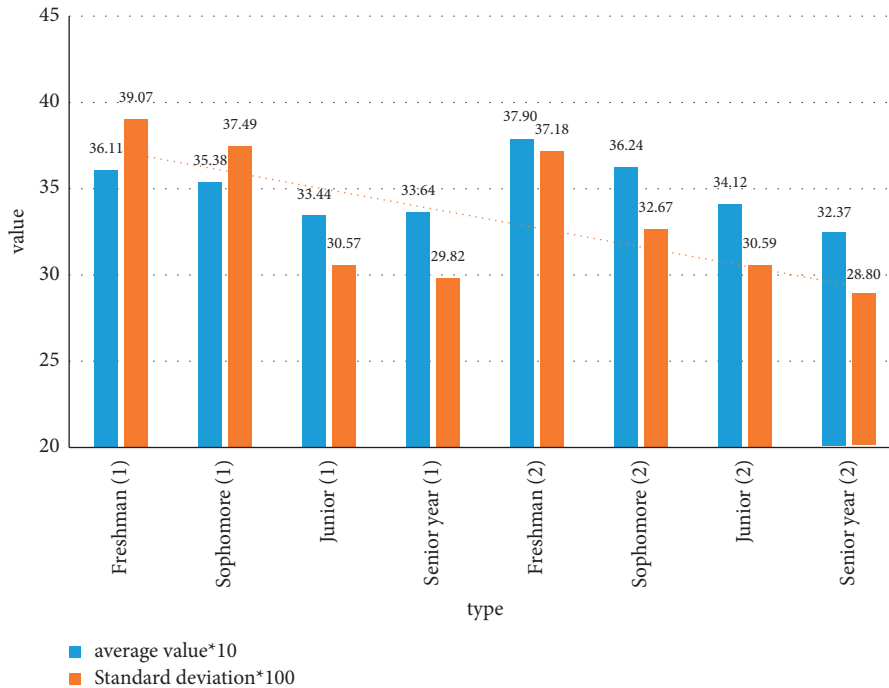


FIGURE 1: Overall satisfaction analysis table of Questionnaire Two and Questionnaire Three completed by different grades.

women is quite different. This study designed two questionnaires, namely, the College English Online Learning Student Satisfaction Survey (Questionnaire 2) and the College English Class Satisfaction Survey (Questionnaire 3), and 800 valid questionnaires were collected. The statistical analysis of the results mainly analyzes the following two aspects: first, the analysis of the overall satisfaction of college online learning and college English classroom students and second, the analysis of the difference between the college online learning and the college English classroom student satisfaction.

Figure 1 shows the satisfaction of Questionnaire 2 and Questionnaire 3, respectively. Regardless of online learning or classroom teaching, the degree of satisfaction from high to low is in the order of freshman, sophomore, junior, and senior. The reason for the highest satisfaction in freshmen may be that college English learning is easier than in high school. In the learning process, freshmen are more likely to meet their expectations and are more satisfied with their learning results.

As shown in Figure 1, students' satisfaction with online learning and classroom teaching is basically the same. No matter from which dimension, the satisfaction of Questionnaires 2 and 3 is above 3, indicating that students are

basically satisfied with English learning. In addition to the factor of personal operation network learning, the content of network learning has become a crucial factor for the evaluation of network learning satisfaction. In order to have a good effect of online learning, teachers of colleges and universities must change their consciousness and jointly improve the quality of online teaching content. They can purchase relevant high-quality teaching resources through special funds.

We carry out a statistical analysis of the different dimensions of the overall satisfaction analysis table of Questionnaire 2 and then the overall satisfaction analysis table of the different dimensions of the three questionnaires, and the results are shown in Figures 2 and 3.

From the data analysis in Figures 2 and 3, which show the overall satisfaction analysis of the three different dimensions of the questionnaire, we can find that the teacher's satisfaction exceeds 80%, so the teacher has the highest satisfaction. It can be seen that teachers and teaching facilities are also crucial factors, which indirectly shows that in traditional classroom English teaching, teachers play an important role, mainly based on the traditional teaching of teachers and students. The educational model puts higher demands on English teachers

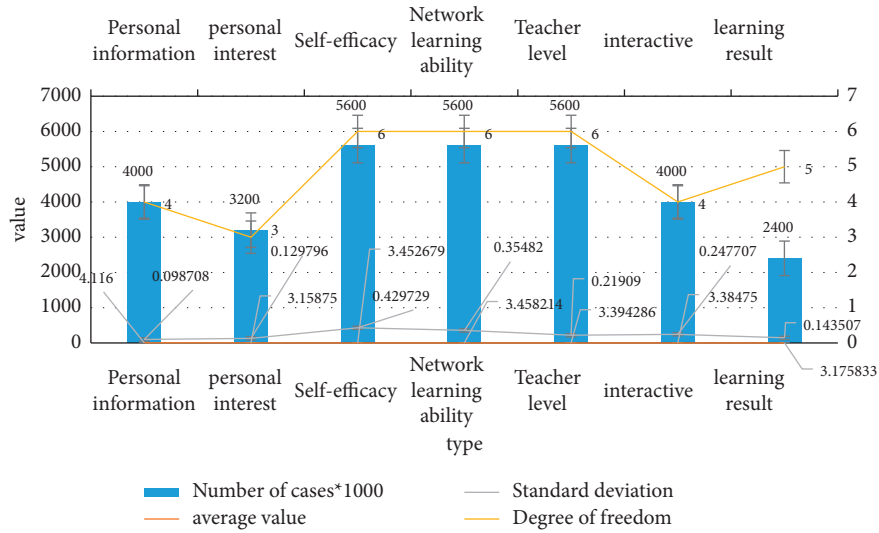


FIGURE 2: Different dimensions of overall satisfaction analysis table of Questionnaire 2.

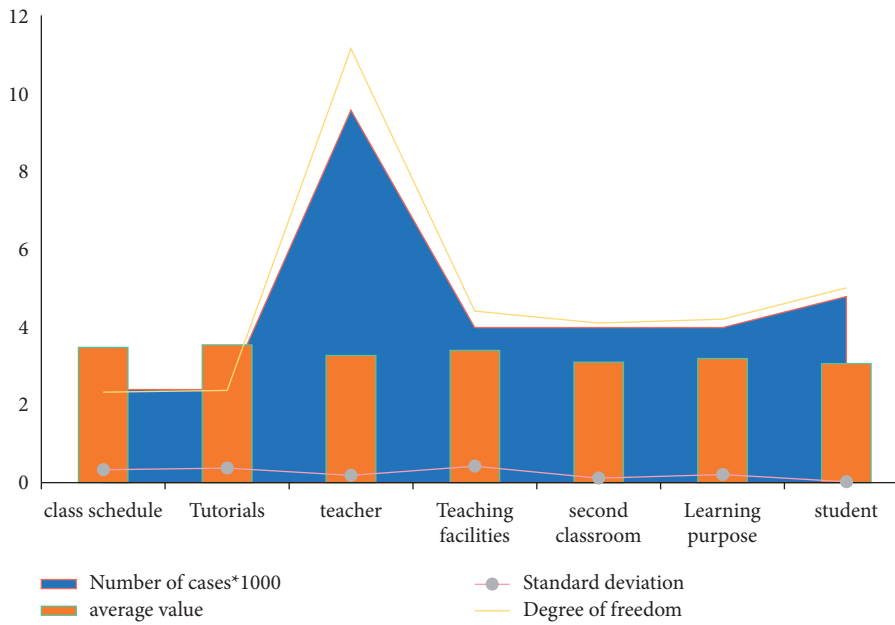


FIGURE 3: The overall satisfaction analysis table of the three different dimensions of the questionnaire.

TABLE 2: System building modules of the English online learning platform.

Module function	Effect
Course selection module	Choosing your favourite courses and teachers, and canceling the ones you do not like
Online course modules	The live and recorded courses can be interchanged in the study
Class practice module	Divided into preclass and postclass exercises
Evaluation module	Teacher evaluation, student mutual evaluation and self-evaluation, focus on process evaluation and summative evaluation
AC module	Convenient for teachers and students to communicate and learn

and also illustrates the necessity and urgency of online English teaching.

4.2. Validity Test. In this study, a questionnaire about online courses was used. According to the methods of searching and reading the relevant literature, expert evaluation, and personal interviews, the scale was revised several times before it was formally distributed. Therefore, the content of the questionnaire is highly effective. After testing, the correlation coefficients between each item in the questionnaire and its dimensions are higher than other factors. Other factors refer to factors that are related to the teacher's teaching and are not related to the classroom. These indicate that the internal consistency and validity of the scales in this study are relatively high.

According to Table 2, it can be seen that the online learning of English audiovisual listening and speaking is becoming more and more popular. Summarizing the abovementioned learning theories and social development trends, English learning has developed towards informatization, diversification, and ability. Students should occupy the dominant position in the learning process, but there are still large deviations in the actual learning life.

5. Conclusions

5.1. Survey Results. There are differences in the status quo of teaching in online courses. The results of gender differences show that boys' total scores, classroom participation, technology application, and awareness of the Internet are significantly lower than girls'. The curriculum design should consider how to mobilize boys' learning enthusiasm and grade differences. The results show the total score of the freshman. The curriculum design should consider the grade difference, and the learning process design should be more abundant. In online teaching based on network courses, digital courses can use digital processing technology and communication platform to complement offline teaching. Online courses break through the limitations of the traditional face-to-face teaching mode in terms of content and presentation form. By analyzing the standard requirements for reading, listening, and speaking of English courses, online teaching provides more alternative knowledge for teachers and students in teaching and learning. Wide range of content, broader time and space, and more convenient interactive channels have brought a new integration model and broad innovation space for foreign language education in colleges and universities. The deficiencies of this research focus on the following aspects: First of all, there are still relatively few related studies linking learning input research and online teaching. The author designed an online teaching model based on learning input based on previous experiences. Because the author's personal research is limited, omissions or fallacies will inevitably occur in the process of model design and application research. Secondly, the sample size of this experimental design is relatively small, so if the model is fully applicable to large-volume learners in other domestic colleges, there are certain problems.

Data Availability

No data were used to support this study.

Conflicts of Interest

The author declares no conflicts of interest regarding the publication of this article.

Acknowledgments

This work was supported by the project of Shandong Vocational and Technical Education Society, "The Research and Practice of Information-Based Teaching Mode of Public English Course in Higher Vocational Colleges under the Background of "Double High" (Serial Number: ZJXH2020Z13).

References

- [1] C. Leire, K. McCormick, J. L. Richter, P. Arnfalk, and H. Rodhe, "Online teaching going massive: input and outcomes," *Journal of Cleaner Production*, vol. 123, no. Jun.1, pp. 230–233, 2016.
- [2] J. Müssig, A. Clark, S. Hoermann, G. Loporcaro, C. Loporcaro, and T. Huber, "Imparting materials science knowledge in the field of the crystal structure of metals in times of online teaching: a novel online laboratory teaching concept with an augmented reality application," *Journal of Chemical Education*, vol. 97, no. 9, pp. 2643–2650, 2020.
- [3] Y. Kim, "Developing inverted blended model of integrated class teaching college English," *The Journal of Mirae English Language and Literature*, vol. 21, no. 3, pp. 151–173, 2016.
- [4] N. Martin, R. Priya, and F. Smarandache, "Decision making on teachers' adaptation to cybergogy in saturated interval-valued refined neutrosophic overset/underset/offset environment," *International Journal of Neutrosophic Science*, vol. 12, no. 2, pp. 58–70, 2020.
- [5] V. Slyck, "Responding to xenophobia: politics, populisms and our teaching," *English Studies in Africa*, vol. 63, no. 1, pp. 104–118, 2020.
- [6] D. He, "Theoretical analysis of college English online teaching mode," *Agro Food Industry Hi-Tech*, vol. 28, no. 1, pp. 2834–2836, 2017.
- [7] Z. Biqian, "Blended teaching of college English based on online teaching software," *Boletin Tecnico/Technical Bulletin*, vol. 55, no. 14, pp. 482–487, 2017.
- [8] J. Yin and Y. Na, "Path analysis of college English teaching ability improvement based on MOOC and multimedia systems," *Boletin Tecnico/Technical Bulletin*, vol. 55, no. 8, pp. 427–433, 2017.
- [9] C. Fang, "Intelligent online teaching system based on SVM algorithm and complex network," *Journal of Intelligent and Fuzzy Systems*, vol. 40, no. 5, pp. 1–11, 2020.
- [10] L. Tian, L. Hibbard, T. Franklin, and R. David, "Preparing teacher candidates for virtual field placements via an exposure to K-12 online teaching," *Journal of Information Technology Education: Research*, vol. 16, no. 16, pp. 1–14, 2016.
- [11] J. Rhode, S. Richter, and T. Miller, "Designing personalized online teaching professional development through self-assessment," *TechTrends*, vol. 61, no. 5, pp. 1–8, 2017.
- [12] M. Adnan, F. Kalelioglu, and Y. Gulbahar, "Assessment of a multinational online faculty development program on online

- teaching: reflections of candidate E-tutors,” *The Turkish Online Journal of Distance Education*, vol. 18, no. 1, p. 22, 2017.
- [13] A. R. Abas, I. El-Henawy, A. Amr, and H. Mohamed, “Survey on deep learning approaches for aspect level opinion mining,” *Journal of Cybersecurity and Information Management*, vol. 4, no. 1, pp. 46–66, 2020.
- [14] S. I. Lei and A. S. I. So, “Online teaching and learning experiences during the COVID-19 pandemic – a comparison of teacher and student perceptions,” *Journal of Hospitality and Tourism Education*, no. 2, pp. 1–15, 2021.
- [15] K. Salih, C. A. Rashid, H. A. Salih, and B. Taylan, “The role of online teaching tools on the perception of the students during the lockdown of covid-19,” *International Journal of Social Sciences and Educational Studies*, vol. 7, no. 3, pp. 178–190, 2020.
- [16] C. Z. Javid, N. S. Althobaiti, and E. A. Al-Malki, “A comparative investigation of the impact of effective online teaching strategies practiced during corona pandemic in ensuring sustainable pedagogy,” *Universal Journal of Educational Research*, vol. 9, no. 1, pp. 17–31, 2021.
- [17] H. Liu, Y. Liu, and J. Feng, “The realistic dilemma and breakthrough ways of improving the quality of online teaching resources of physical education in colleges and universities,” *Advances in Physical Education*, vol. 11, no. 1, pp. 1–11, 2021.
- [18] P. González-Vera and A. Hornero Corisco, “Audiovisual materials: a way to reinforce listening skills in primary school teacher education,” *Language Value*, vol. 8, no. 1, pp. 1–25, 2016.
- [19] B.-D. Oh, Y. So, and Y. So, “Exploring English online research and comprehension strategies of Korean college students,” *English teaching*, vol. 73, no. 3, pp. 53–76, 2018.
- [20] K. Y. Chau, K. M. Y. Law, and Y. M. Tang, “Impact of self-directed learning and educational technology readiness on synchronous E-learning,” *Journal of Organizational and End User Computing*, vol. 33, no. 6, pp. 1–20, 2021.
- [21] R. S. M. Permana, L. Puspitasari, and S. S. Indriani, “Pelatihan post-produksi (Audio-Visual editing) film indie di Armidale English college soreang, bandung,” *Jurnal Pengabdian Pada Masyarakat*, vol. 4, no. 1, pp. 19–28, 2019.

Research Article

Research on Optimization of the AGV Shortest-Path Model and Obstacle Avoidance Planning in Dynamic Environments

Ruixi Liu 

Chongqing Police College, No. 666 Jing Zheng Road, Chongqing, China

Correspondence should be addressed to Ruixi Liu; dianqi206@outlook.com

Received 17 May 2022; Revised 8 June 2022; Accepted 20 June 2022; Published 19 July 2022

Academic Editor: Xuefeng Shao

Copyright © 2022 Ruixi Liu. This is an open access article distributed under the Creative Commons Attribution License, which permits unrestricted use, distribution, and reproduction in any medium, provided the original work is properly cited.

This paper proposes a support vector machine (SVM)-based AGV scheduling strategy that enhances the scheduling efficiency of automated guided vehicles (AGVs) in intelligent factories. The developed scheme optimizes the task area division process to endow the AGVs with the ability to avoid obstacles in complex dynamic environments. Specifically, given the two AGV motion cases, i.e., towards a single target point and multiple target points, the optimal path was determined utilizing the exhaustive and the Q-learning methods, while path optimization was realized by utilizing different schemes. Based on the shortest path obtained, a nonlinear programming model with the shortest time as the objective was built, and the AGV's turning path was proved to be optimal by the non-dominated sorting genetic algorithm (NSGA-II). Several simulation tests and calculation results validated the proposed method's effectiveness, highlighting that the developed scheme is a rational solution to the obstacle congestion and deadlock problems. Moreover, the experimental results demonstrated the proposed method's superiority in path planning accuracy and its ability to respond well in complex dynamic environments. Overall, this research provides a reference for developing and applying AGV cluster scheduling in real operational scenarios.

1. Introduction

Traditionally, warehouses have been mostly managed manually. With the rise of e-commerce [1], AGVs, shuttles, and Delta sorting robots [2] are playing an essential role in automated warehouse logistics systems. Therefore, to ensure proper automated warehouse logistics system management, achieving reasonable obstacle avoidance of AGVs in complex smart warehouses is necessary to reach optimal scheduling. Some scholars have tried solving the scheduling of AGVs using path planning algorithms, such as Dijkstra's algorithm [3], A* algorithm [4], and ant colony algorithm [5]. However, as the task dimensionality increases, the solution takes more time and becomes more complicated. Moreover, these algorithms have drawbacks, such as slow convergence and a tendency to fall into locally optimal solutions. Besides, the methods only focus on avoiding obstacles and do not consider the impact of local obstacle avoidance planning on subsequent operations. Consequently, the trajectory should

be adjusted after obstacle avoidance to bring the AGVs back to the global path [6], reducing operational efficiency.

AGV assignment in scheduling problems has been studied by some researchers. To minimize the makespan and intercellular motions of components, Azadeh et al. [7] developed a nonlinear CFP which included intra-cell scheduling and material handling using AGVs. However, on the other hand, nonlinear CFP is only suited for small-scale AGV systems since it cannot adjust dynamically to the transportation environment. Chu et al. [8] used an adaptive memetic differential search method to tackle the problems, which included cross-training with a learning/forgetting impact that improves the flexibility of routing. However, the method cannot quickly determine the optimal solutions of multiple objective functions, limiting instantaneity and global optimality in large-scale transportation. To address the work assignment issue of AGVs, Radhia et al. [9] presented a hybrid method based on the Dijkstra algorithm, genetic algorithm, and heuristic algorithm, which can

ensure conflict-free control of a large fleet on any layout, and that permits optimized routing for all AGVs' schedules. For AGV collision and deadlock complications, Malopolski [10] devised a novel approach to determine one-way, two-way, or multilane flow fields, which can adapt AGV control techniques in real time to the mobility environment. However, this method cannot motivate AGVs to arrive at destinations as rapidly as possible. In the meantime, it does not completely overcome the restrictions of the disadvantages in AGV control. Through the framework of a time-windows graph, Kim and Jin [11] used Dijkstra's shortest-path method to design AGV's course. The vehicle agent optimizes the distribution of transportation for AGVs and improves efficiency. A multi-AGV A* algorithm based on a collision-free dynamic route planning approach was described by Chunbao Wang et al. [12]. The method categorized probable conflicts in order to find the shortest route that is conflict-free. The method classified potential conflicts in order to find the shortest conflict-free route. Similarly, Tai et al. [13] introduced a priority route planning method and achieved coordinated management of multi-AGVs based on time frames, which contributes to the conflict-free routing and shorter completion time, which contributes to the conflict-free routing and shorter completion time.

Considering the characteristics of existing AGV systems, this paper develops an AGV scheduling strategy based on the nonlinear programming model and the non-dominated sorting genetic algorithm NSGA-II [14]. Furthermore, obstacle avoidance simulations were conducted to minimize the total AGV moving path by optimizing the model so that the sorting stations reached a reasonable balance. Our trials concluded that the AGV path was optimal for the minimum radius and the circle center located at the obstacle's vertex (the circular obstacle was located at the circle's center), thereby avoiding obstacle congestion and deadlock in the current AGV scheduling [3].

The main work of this paper are as follows:

- (1) Proposing an SVM-based AGV scheduling strategy that enhances the scheduling efficiency of AGVs in intelligent factories,
- (2) Optimizing the division process to endow the AGVs with the ability to avoid obstacles,
- (3) Determining the optimal path by utilizing the exhaustive and the Q-learning methods,
- (4) Proving the optimal path by the non-dominated sorting genetic algorithm (NSGA-II),
- (5) Providing a reference for developing and applying AGV cluster scheduling in real operational scenarios.

The structure of the remaining sections is as follows. Section 2 includes the problem statement. Section 3 describes the considered models and computational results of the study. Section 4 provides a discussion of the results and validation analyses. The concluding remarks and further research directions are provided in Section 5.

2. Problem Description and Hypotheses

2.1. Warehouse Information and Problem Description. The goal of scheduling is to assign handling tasks to s (AGVs) in different locations so that the total handling time is minimized without collision or deadlock. The unmanned warehouse discussed in this paper is a 32×22 rectangular area, simplified in Figure 1.

The node types are as follows.

- (1) Path node (gray): AGV can pass freely.
- (2) Storage node (green): Place pallets or ordinary shelves.
- (3) Reserved node (yellow): Reserved position.
- (4) Column node (black): Obstacle.
- (5) Work station node (blue): AGVs pack the goods at the work station and exit from the conveyor belt.
- (6) Replenishment node (purple): the placement point of replenished goods.
- (7) Empty pallet recovery node (red): empty pallet recovery place.

The map used in Figure 1 is simplified to a dotted map as follows (Figure 2).

It is assumed that the AGV can only move within the limits of this plane scene. The region representation is shown in Table 1.

2.2. Condition Hypotheses. To simplify the calculations, the following reasonable assumptions are given.

- (1) The AGV can turn accurately along a circular arc.
- (2) The initial speed of the AGV is 5 units per second.
- (3) The speed of the AGV will not be affected when it cuts from a straight line to an arc.
- (4) AGVs do not stop accidentally.
- (5) Ignore the factors that affect the non-minimum turning radius and minimum safety distance of AGV travel.

2.3. Illustration of Symbols. The symbols are specified as follows (Table 2).

Idling: A continuous process in which an AGV stops moving but runs at its lowest possible speed.

Acceleration: A continuous process in which the acceleration of an AGV is greater than 0.1 ms^{-2} .

Deceleration: A continuous process in which the acceleration of an AGV is less than -0.1 ms^{-2} .

Constant speed: A continuous process in which the absolute value of the acceleration of an AGV is less than 0.1 ms^{-2} , a nonidling speed.

Average speed: The arithmetic mean of the speed of an AGV over a period.

Average driving speed: The arithmetic mean of the speed of an AGV when it is driven, excluding idling.

Idling time ratio: The percentage of total idling time in the total running time of an AGV.

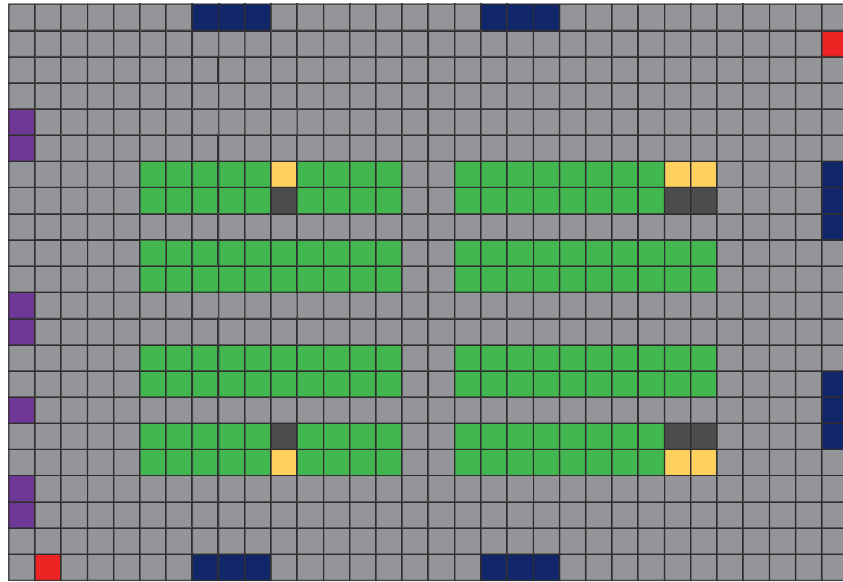


FIGURE 1: Unmanned warehouse map.

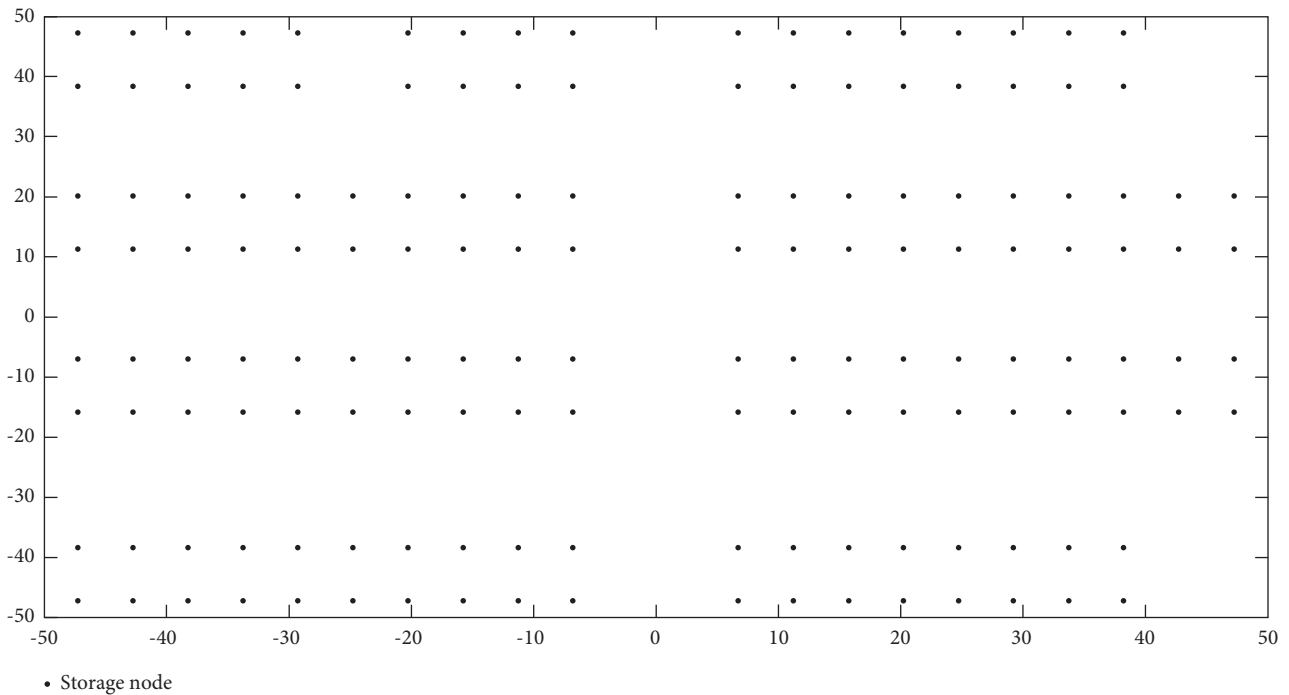


FIGURE 2: Simplified dot plot of unmanned warehouse distribution.

Average acceleration: The arithmetic mean of acceleration per unit time (second) of an accelerating AGV.

Average deceleration: The arithmetic mean of deceleration per unit time (second) of a decelerating AGV.

Acceleration time ratio: The percentage of accumulated time in acceleration in the total time of a period.

Deceleration time ratio: The percentage of accumulated time in deceleration in the total time of a period.

Speed standard deviation: The standard deviation of the speed of an AGV over a period, including idling.

Acceleration standard deviation: The standard deviation of the acceleration of an AGV that is accelerating over a period.

3. Modeling and Solution Finding

3.1. Minimization of Walking Path. Given the ignorance of possible collisions caused by AGVs during task implementation, we designed appropriate for an unmanned warehouse scenario. The possible shortest path from the starting point to the target

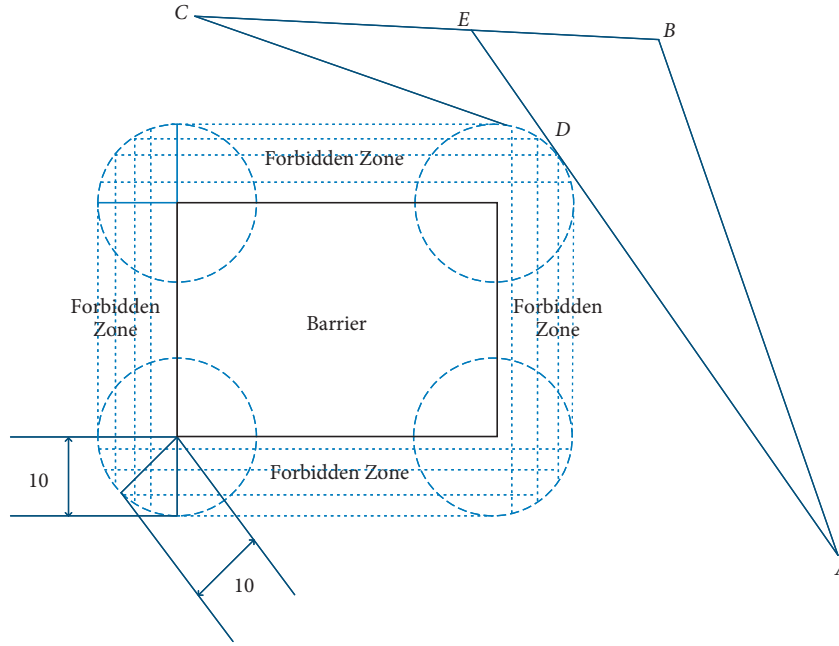


FIGURE 4: Change of direction at the top of the penalty area.

Adding the two equations yields:

$$AB + BE + EC + DE > AD + DE + DC. \quad (4)$$

Simplifying gives:

$$AB + BC > AD + DC. \quad (5)$$

In the process of $A > B$, the AGV chooses the shortest path when turning at D .

3.1.4. Shortest Path in the Case of the Minimum Turning Radius. For an AGV to move from point A to point B , it should bypass the prohibited area and turn near its vertex. The smaller the turn radius is, the shorter the path is. As depicted in Figure 5, the path from point A to point B is regarded as a stretchable rope and is assumed to naturally stretch (line segment AB) when the two points connect. The rope is stretched as the AGV needs to steer clear of the prohibited area. Additionally, the minimum turning radius of the AGV and the diameter of the prohibited area are 10. Thus, the rope can pass directly around the edge of the prohibited area.

$$E_p = \frac{1}{2}k\Delta L^2. \quad (6)$$

According to the principle of minimum potential energy, the systems' potential energy reaches its minimum value when the elastic body is in equilibrium. Here, the circle was considered elastic in the initial state illustrated in the above figure. Under the forces illustrated in the figure, the system gradually reaches equilibrium as the circle tends to shrink, ultimately obtaining the minimum potential energy of the elastic rope, which decreases as the circle radius reduces, i.e., the shortest path goes down. This finding proves that the

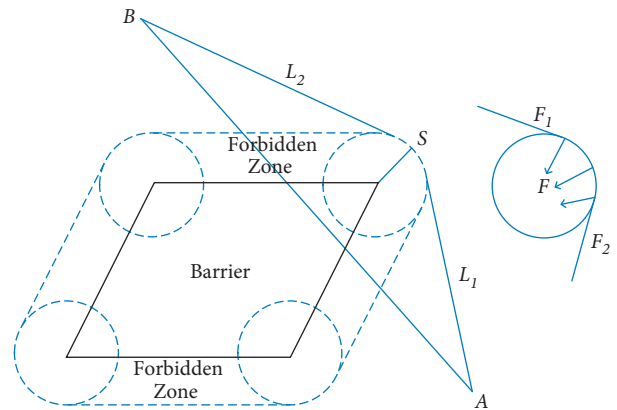


FIGURE 5: AGV obstacle turning radius.

path is the shortest in the case of the minimum turning radius.

3.1.5. Shortest Path in the Case of the Center of the Turning Arc Located at the Vertex. When the AGV turns near the vertex of the prohibited area, the path is the shortest if the center of the turning arc is at the vertex. As illustrated in Figure 6, both circles O and O' with a radius of R and R' , respectively, bypass the farthest point D . Notably, the center of circle O falls on the vertical line. L_1, S, L_2 , and L_1', S', L_2' are the lengths of the tangent segments from points A and B to the circles O and O' and the arcs contained, respectively.

$$L_1 + S + L_2 < L_1' + S' + L_2'. \quad (7)$$

Point D and circle center O fall on the vertical line (passing D) of the line segment AB , while the circle center O' is located beyond this vertical line. Therefore, the two circles

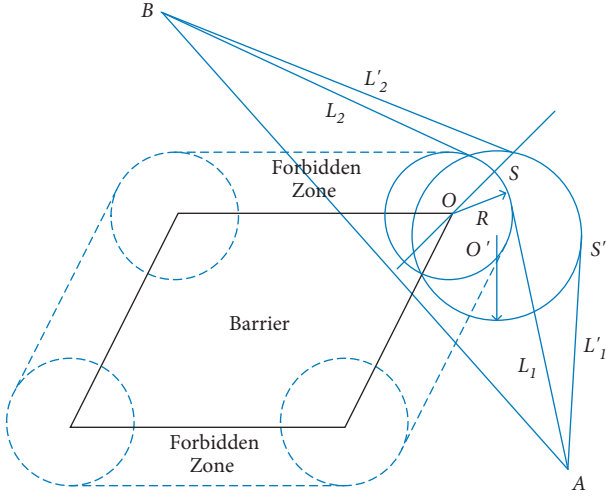


FIGURE 6: Obstacle avoidance turning circle center position.

are only intersected rather than tangent. To pass point D , the maximum distance from the point on circle O' to the straight-line AB must be greater than that from the point on circle O to the straight-line AB . Based on the conclusions proved above, the result below was generated:

$$L_1 + S + L_2 < L_1' + S' + L_2'. \quad (8)$$

When the AGV bypasses an obstacle with a vertex, the shortest path is the arc turning with the vertex as the center and the minimum turning radius so that the minimum turning radius is the same as the minimum safe distance between the AGV and the obstacle. In other words, the path is the shortest when the AGV makes a turn along the edge of the prohibited area.

3.1.6. Modeling. Based on the above conclusions, the shortest path is always constituted by several tangents and arcs, regardless of the number of obstacles between the starting and target points. As proved previously, the path is the shortest when the AGV passes through all obstacles by turning along the edge of the prohibited area, where the radius of the turning arc is that of the hazardous area. Therefore, in the model below, when passing through obstacles, the AGV turns at the obstacle's vertex with the minimum turning radius r placed at the obstacle's center.

Given that the AGV aims to move from starting point A (x_1, y_1) to target point B (x_2, y_2), while turning on the arc centered at vertex D (x_3, y_3) with radius r , and C and E are the tangency points, the point C and E coordinates and the length of $ACEB$ should be calculated:

$$AB = \sqrt{(x_1 - x_2)^2 + (y_1 - y_2)^2}, \quad (9)$$

$$AD = \sqrt{(x_1 - x_3)^2 + (y_1 - y_3)^2}, \quad (10)$$

$$BD = \sqrt{(x_3 - x_2)^2 + (y_3 - y_2)^2}, \quad (11)$$

$$DE + BEDC + AC \quad (12)$$

$$\begin{aligned} BE &= \sqrt{BD^2 - r} \\ &= \sqrt{(x_3 - x_2)^2 + (y_3 - y_2)^2 - r}, \end{aligned} \quad (13)$$

$$\begin{aligned} AC &= \sqrt{AD^2 - r} \\ &= \sqrt{(x_1 - x_3)^2 + (y_1 - y_3)^2 - r}. \end{aligned} \quad (14)$$

Setting the coordinates of points C and E as (x_i, y_i) and (x_j, y_j) , respectively, provides the following formulae:

$$\begin{cases} BE = \sqrt{(x_2 - x_j)^2 + (y_2 - y_j)^2}, \\ DE = \sqrt{(x_3 - x_j)^2 + (y_3 - y_j)^2}, \end{cases} \quad (15)$$

$$\begin{cases} AC = \sqrt{(x_1 - x_i)^2 + (y_1 - y_i)^2}, \\ DC = \sqrt{(x_3 - x_i)^2 + (y_3 - y_i)^2}. \end{cases} \quad (16)$$

Moreover, the coordinates of point E are expressed as:

$$\begin{cases} \sqrt{(x_3 - x_2)^2 + (y_3 - y_2)^2 - r} = \sqrt{(x_2 - x_j)^2 + (y_2 - y_j)^2}, \\ \sqrt{(x_3 - x_j)^2 + (y_3 - y_j)^2} = r. \end{cases} \quad (17)$$

and the coordinates of point C :

$$\begin{cases} \sqrt{(x_1 - x_3)^2 + (y_1 - y_3)^2 - r} = \sqrt{(x_1 - x_i)^2 + (y_1 - y_i)^2}, \\ \sqrt{(x_3 - x_i)^2 + (y_3 - y_i)^2} = r. \end{cases} \quad (18)$$

(17) and (18) can be connected to the coordinates of C and E .

$$\angle ADC = \arccos \frac{AD^2 + BD^2 - AB^2}{2AD \times BD}, \quad (19)$$

$$\angle ADC = \arccos \frac{r}{AD}, \quad (20)$$

$$\angle BDE = \arccos \frac{r}{BD}, \quad (21)$$

$$\angle CDE = 2\pi - \angle ADC - \angle BDE - \angle ADB. \quad (22)$$

The length of arc is

$$\widehat{CE} = r \times \angle CDE. \quad (23)$$

The path length for the AGV turning once on the way was calculated as:

$$S = AC + BE + \widehat{CE}. \quad (24)$$

Furthermore, the traveling time was:

$$T = \frac{AC}{v_0} + \frac{BE}{v_0} + \frac{\widehat{CE}}{v_\rho} \quad (25)$$

3.1.7. *Model Calculation.* It was assumed that on the path from the starting point to the target point, there were m straight lines with a length of d_m and n arcs with a length of u_n . Thus, the total distance for the AGV moving from the starting point to the target point was expressed as:

$$s = \sum_{m=1}^m d_m + \sum_{n=1}^n u_n \quad (26)$$

Moreover, the traveling time was:

$$T = \frac{\sum_{m=1}^m d_m}{v_0} + \frac{\sum_{n=1}^n u_n}{v_\rho} \quad (27)$$

where $v_\rho = (v_0/1 + e^{10 \cdot 0.1\rho^2})$ and ρ is the turning radius.

Figure 7 illustrates the possible optimal paths, as proved in the above sections.

The two paths having a basic line-circle structure could be directly solved by model 1, obtaining 471.032 and 505.9835 units, respectively, through MATLAB. Therefore, the optimal total distance of the AGV passing from the upper left of obstacle 5 was $S = 471.0372$ units, the total traveling time was $T = 96.0178$ s, containing two straight-line segments and one arc line segment (at center (80, 210) and radius $r = 10$). The specific conditions of the path are listed in Table 3:

Through the calculations performed by MATLAB, the optimal total distance of the AGV was $S = 3,812.52$ units. The traveling time was $T = 585.6712$ s, involving 16 straight-line segments and 15 arcs. Further details are reported in Tables 4 and 5.

3.2. *Task Equalization.* This section presents the hardware conditions of the experiment in order to validate the performance of the proposed methodology. The algorithm was coded in MATLAB 2021 software using a computer with the following specifications: Intel (R) Core (TM) i9-10885H CPU @ 2.40 GHz.

To better balance the sorting stations' load and prevent local AGV handling congestion, we proposed a SVM-based AGV scheduling strategy. According to the experimental results of dividing the equilibrium task area, the proposed SVM method outperformed the single-attribute AGV scheduling rules. In the suggested scheme, first, we set a sorting station for each pallet, thus realizing the pairing optimization. On this basis, the model of problem 1 was rebuilt to:

$$X_{ij} = \begin{cases} 1, & \text{Pallet } i \text{ assigns picking station } j, \\ 0, & \text{Others,} \end{cases} \quad (28)$$

where X_{ij} represents the j^{th} picking station specified for the i^{th} pallet.

Generating the training sample involves the following steps. As a supervised learning technique, SVM can output

a maximum-boundary hyperplane to perfectly separate two types of training samples [17]. The training samples in the supervised learning comprise features and labels, which refer to the current system state and optimal scheduling rules in the case of AGV scheduling, respectively. This rule can be dynamically chosen based on the current system state.

The training sample set is not linearly separable, i.e., it cannot be well separated by a linear hyperplane. In this case, the kernel function ($\Phi: f \rightarrow H$) will map the feature vector (f) into a higher-dimension Hilbert space (H). Here, the Hilbert space was reproduced by a Gaussian kernel (or radial basis function, RBF), where the RBF parameters were defined by candidate scheduling rules selected via an SVM scheduler [18]. Thus, the scheduling rules were taken as the SVM labels. The AGV scheduling rules considering the order due date were also the candidate scheduling rules since the average work delay was taken as the performance indicator.

Partitioning rules for the candidate scheduling area:

- (1) Shortest travel time (STT): select the task closest to the AGV.
- (2) First come, first served (FCFS): select more urgent tasks.
- (3) Minimum remaining output queue space (MROQS): select tasks in the output queue with the remaining space.
- (4) Earliest due date (EDD): select the task with the closest due date.
- (5) Critical ratio (CR): select tasks with the lowest critical ratio [$CR = (\text{due date} - \text{this date}) / (\text{remaining operation time})$].
- (6) Dynamic slack (DS): select tasks with the shortest slack time (remaining slack time = remaining operation time).
- (7) Nearest vehicle (NV): select the AGV closest to the task location.
- (8) Longest idle AGV (LIV): select the AGV with the longest idle time.
- (9) Lowest utilization AGV (LU): select the AGV with the lowest utilization ratio.

The division distribution of the ten regions was determined by the division rules as shown in Figure 8.

In machine learning, every system attribute potentially influencing the system's performance should be considered an environmental state. Given the environment of this research, we chose the system attributes relative to the AGV, which empirically are nine, utilized as the training samples. Moreover, the average delay rate was recorded at the end of scheduling and was employed as a performance indicator. After performing N simulations with a fixed random seed, the performance of N scheduling rules was recorded, and the scheduling rule with the highest performance was used as the label of the training sample.

The error diagrams of the SVM scheduling after training in each division are provided in Table 6:

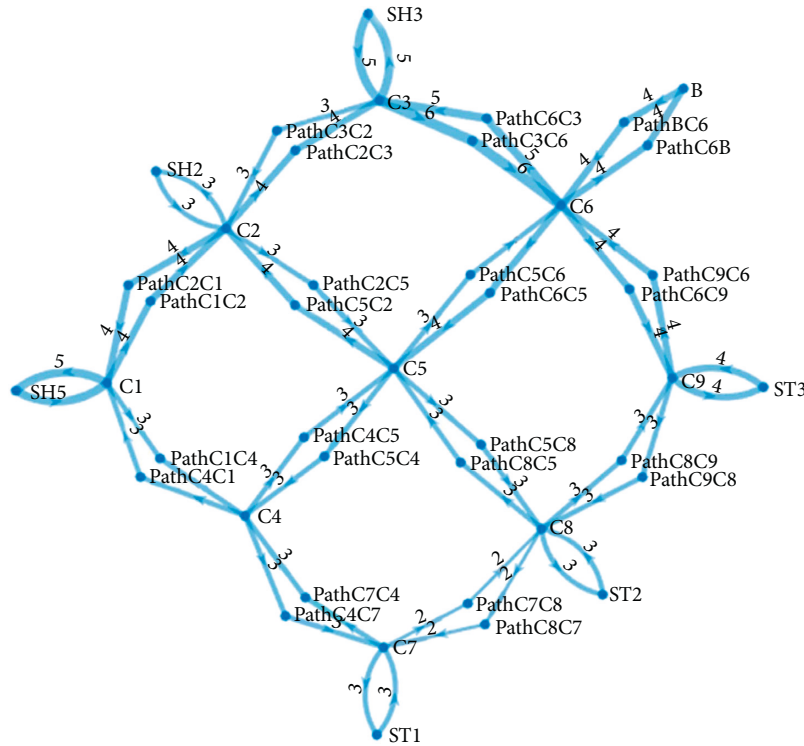


FIGURE 7: Diagram of possible optimal paths.

TABLE 3: Shortest path situation.

	Start point coordinates	Endpoint coordinates	Turning arc center	Distance	Time
Straight 1	(0, 0)	(70.50595, 213.1405)	—	224.4994	44.9
Arc 1	(70.50595, 213.1405)	(76.60645, 219.4066)	(80,210)	9.051	3.7402
Straight 2	(76.60645, 219.4066)	(300,300)	—	237.4868	47.4974
Sum	—	—	—	471.0372	96.1376

TABLE 4: Partial shortest paths for multiple target points.

	Start point coordinates	Endpoint coordinates	Turning arc center	Distance	Time
Straight 1	(0,0)	(70.5059, 213.1405)	—	224.4994	44.8999
Arc 1	(70.5059, 213.1405)	(76.6064, 219.4066)	(80,210)	9.25	3.7
Straight 2	(76.6064, 219.4066)	(294.1547, 294.6636)	—	229.98	45.996
Arc 2	(294.1547, 294.6636)	(281.3443, 301.7553)	(290.8855 304.1141)	15.3589	6.1436
...
Straight14	(727.9377, 513.9178)	(492.0623, 206.0822)	-	387.81	77.562
Arc length14	(492.0623, 206.0822)	(491.6552, 205.5103)	(500,200)	0.6981	0.2792
Straight15	(491.6552, 205.5103)	(412.1387, 90.2314)	-	133.04	26.608
Arc15	(412.1387, 90.2314)	(418.3348, 94.4085)	(410,100)	7.6794	3.0718
Straight16	(418.3348, 94.4085)	(0,0)	—	421.84	84.368
Sum				2812.52	585.6712

The error of the trained SVM scheduling division results is shown in Figure 9. The single-attribute scheduling rule shows a slow convergence and weak stability. Obviously, the SVM scheduler significantly outperformed most of the single-attribute scheduling rules.

Different combinations of single-attribute scheduling rules and SVM scheduling methods were tested and simulated. For each scheduling method, 30 tests were conducted using a typical random number (CRN) technique.

Specifically, the comparison value was expressed as the average delay value of a single scheduling rule divided by that of the SVM scheduler, thereby comparing the performance of the single scheduling rule and the SVM scheduler. A statistical analysis of the results was carried out to determine whether the SVM scheduling rule was superior to the single-attribute scheduling rule [19]. Obviously, the SVM scheduler significantly outperformed most of the single-attribute scheduling rules.

TABLE 5: Shortest path through multiple target points on-the-way to the specific situation.

	Start point coordinates	Endpoint coordinates	Turning arc center	Distance	Time
Straight 1	(0, 0)	(70.5059, 213.1405)	—	224.4994	44.8999
Arc 1	(70.5059, 213.1405)	(76.6064, 219.4066)	(80, 210)	9.25	3.7
Straight 2	(76.6064, 219.4066)	(294.1547, 294.6636)	—	229.98	45.996
Arc 2	(294.1547, 294.6636)	(281.3443, 301.7553)	(290.8855, 304.1141)	15.3589	6.1436
Straight 3	(281.3443, 301.7553)	(229.8206, 531.8855)	—	236.83	47.366
Arc length 3	(229.8206, 531.8855)	(225.4967, 537.6459)	(220, 530)	6.8068	2.7228
Straight 4	(225.4967, 537.6459)	(144.5033, 591.6462)	—	96.95	19.39
Arc length 4	(144.5033, 591.6462)	(140.8565, 595.9507)	(150, 600)	5.7596	2.3038
Straight 5	(140.8565, 595.9507)	(99.08612, 690.2698)	—	103.16	20.632
Arc 5	(99.08612, 690.2698)	(109.113, 704.2802)	(108.296, 694.3191)	20.7694	8.3078
Straight 6	(109.113, 704.2802)	(270.8817, 689.9611)	—	162.4	32.48
Arc length 6	(270.8817, 689.9611)	(272, 689.7980)	(270, 680)	1.0472	0.4188
Straight 7	(272, 689.7980)	(368, 670.282)	—	97.98	19.596
Arc 7	(368, 670.282)	(370, 670)	(370, 680)	2.0944	0.8378
Straight 8	(370, 670)	(430, 670)	—	60	12
Arc length 8	(430, 670)	(435.5878, 671.7068)	(420, 680)	5.9341	2.3736
Straight 9	(435.5878, 671.7068)	(534.4115, 738.2932)	—	119.16	23.832
Arc 9	(534.4115, 738.2932)	(540, 740)	(540, 730)	5.9341	2.3736
Straight 10	(540, 740)	(670, 740)	—	130	26
Arc length 10	(670, 740)	(679.9126, 731.3196)	(670, 730)	14.3846	5.7538
Straight 11	(679.9126, 731.3196)	(690.9183, 648.6458)	—	83.403	16.6806
Arc 11	(690.9183, 648.6458)	(693.5095, 643.1538)	(709.7933, 642.0227)	6.17	2.468
Straight 12	(693.5095, 643.1538)	(727.3214, 606.8116)	—	129.6305	25.9261
Arc length 12	(727.3214, 606.8116)	(730, 600)	(720, 600)	7.4928	2.997
Straight 13	(730, 600)	(730, 520)	—	80	16
Arc 13	(730, 520)	(727.9377, 513.9178)	(720, 520)	6.4577	2.583
Straight 14	(727.9377, 513.9178)	(492.0623, 206.0822)	—	387.81	77.562
Arc length 14	(492.0623, 206.0822)	(491.6552, 205.5103)	(500, 200)	0.6981	0.2792
Straight 15	(491.6552, 205.5103)	(412.1387, 90.2314)	—	133.04	26.608
Arc 15	(412.1387, 90.2314)	(418.3348, 94.4085)	(410, 100)	7.6794	3.0718
Straight 16	(418.3348, 94.4085)	(0, 0)	—	421.84	84.368
Sum		—		2812.52	585.6712

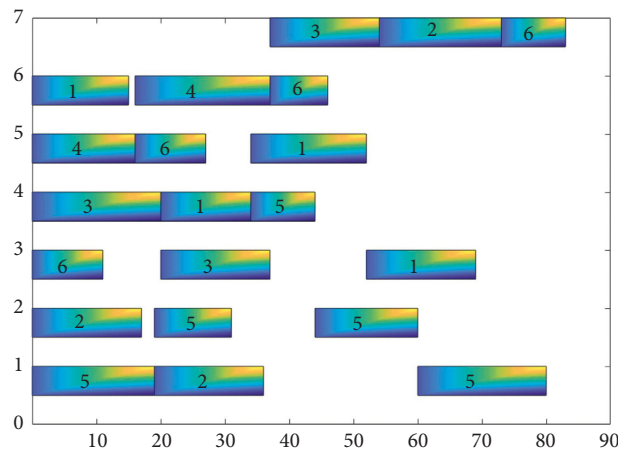


FIGURE 8: The division of the distribution map.

4. Results and Evaluation

4.1. *Simulation and Validation.* According to the relationship between the turning radius and speed, path optimization was realized based on the model for calculating the shortest path. Then, a nonlinear programming model for the shortest time was constructed. Utilizing

NSGA-II provided the shortest time of 94.22825 s, the turning radius of 12.9886 units, and the circle center coordinates of the turning were 82.1414 and 207.1387 [20]. The obstacles were classified into two categories: having vertices and having no vertices. Next, the path proved to be optimal when the AGV made a turn with the minimum radius and the circle center was located at the obstacle's

TABLE 6: Scheduling rule performance.

Scheduling area division mode	NV	LIV	LU	SVM
STT	275.02	278.05	279.27	—
MROQS	655.87	727.90	657.08	—
FCFS	1237.31	1235.06	1243.26	—
EDD	746.85	734.53	735.35	—
DS	671.71	671.90	674.12	—
CR	600.33	602.18	602.29	—
SVM	—	—	—	253.99

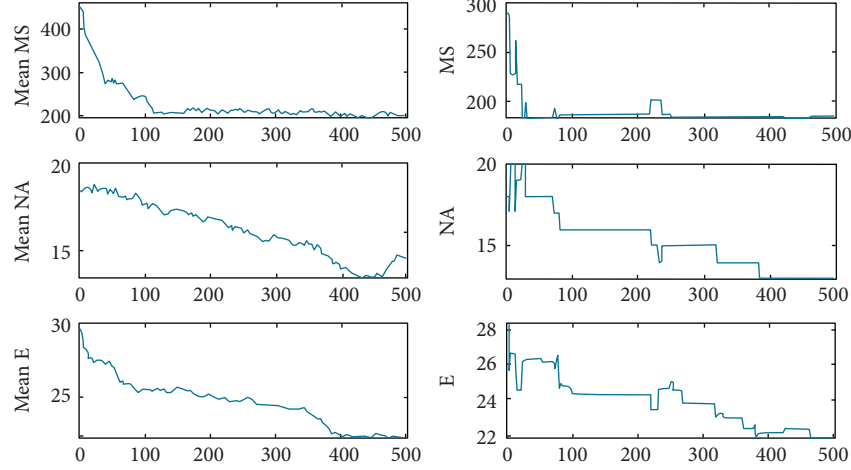


FIGURE 9: Error diagram.

vertex (the circular obstacle was located at the circle center), thus reasonably solving the problems of obstacle congestion and deadlock.

The problem here was the shortest time spent by the AGV traveling from point O to point A and bypassing obstacle 5. According to the shortest path calculated, the time was also the shortest when the AGV passed from the upper left of obstacle 5. The total time spent by the AGV comprised the time on the straight line and arc line segments. The paths with the shortest time and the shortest distance were different, so the path with the shortest time should be calculated first. Since the closest distance between the AGV and the obstacle must not be less than 10 units, the traveling range of the AGV was determined by the obstacles to be avoided on its path and the range influencing its action.

The maximum turning speed of the AGV was expressed as:

$$v = v(\rho) = \frac{v_0}{1 + e^{10-0.1\rho^2}} \quad (29)$$

The time spent by the AGV in passing the arc was:

$$t = \frac{\alpha\rho}{v_\rho} \quad (30)$$

Based on the above formulae, decreasing the turning radius slows the AGV, and the arc it followed became

shorter. When the turning radius of the AGV increased, both the AGV's turning speed and the arc's length increased. Thus, we did not identify any direct linear relationship between the turning time t and the turning radius ρ . Hence, the turning radius ρ change was limited. In practice, an excessively large ρ may cause collisions, while the AGV may roll over for a very small ρ (less than 10).

Then, a nonlinear programming model for the minimum time was built based on the variation range of ρ , thereby obtaining ρ at the minimum t . Here, $O(x_1, y_1)$ was set as the starting point, $A(x_2, y_2)$ was the target point, and $P(x_3, y_3)$ was the upper left vertex of obstacle 5. It was assumed that the AGV made a turn at point $C(x_c, y_c)$, with $N(x, y)$ as the center and r as the radius, passed arc \widehat{BC} , and then turned at point $B(x_b, y_b)$, to ultimately obtain the path with the shortest time spent. Points B and C were connected to generate line segment BC , perpendicular to segment ND . The length of ON , AN , tangent OC , and tangent AB is denoted as a , b , s_1 , and s_2 , respectively.

Let $BD = d$. Since both point B and point C are tangent points, the following results were obtained:

$$\angle DNB = \frac{1}{2}\theta, \quad (31)$$

$$BD = \frac{1}{2}BC. \quad (32)$$

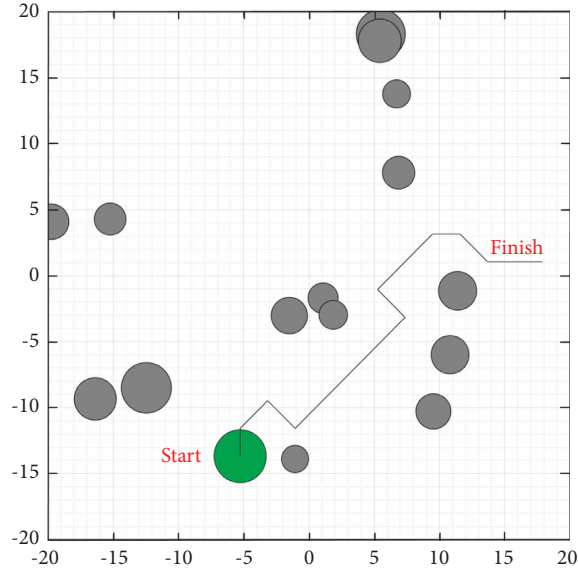


FIGURE 10: Diagram of AGV obstacle avoidance simulation (a).

The radius of the circle in which B and C are located is

$$a = \sqrt{(x - x_1)^2 + (y - y_1)^2}, \quad (33)$$

$$b = \sqrt{(x - x_2)^2 + (y - y_2)^2}, \quad (34)$$

$$\sqrt{(x_c - x)^2 + (y_c - y)^2} = r, \quad (35)$$

$$\sqrt{(x_b - x)^2 + (y_b - y)^2} = r, \quad (36)$$

$$s_1 = \sqrt{a^2 - r^2}, \quad (37)$$

$$s_2 = \sqrt{b^2 - r^2}, \quad (38)$$

$$BC = \sqrt{(x_b - x_c)^2 + (y_b - y_c)^2}, \quad (39)$$

$$\sin\left(\frac{\theta}{2}\right) = \frac{\sqrt{(x_b - x_c)^2 + (y_b - y_c)^2}}{2 \times r}, \quad (40)$$

$$l = 2r \times \arcsin\left(\frac{\sqrt{(x_b - x_c)^2 + (y_b - y_c)^2}}{2r}\right). \quad (41)$$

The objective of the shortest time was formulated based on the straight-line distance, speed of AGV, the arc length, and the AGV's speed while passing the arc:

$$\text{Min} = \frac{s_1 + s_2}{v_o} + \frac{l}{v_p}. \quad (42)$$

Given that the distance between the AGV and the obstacle must be more than 10 units, the radius r was also constrained, i.e., the arc-obstacle distance must be over 10 units:

$$r - \sqrt{(x - x_3)^2 + (y - y_3)^2} \geq 10. \quad (43)$$

The range of the two tangent points is

$$\begin{aligned} x_c &< 80, \\ y_b &> 210. \end{aligned} \quad (44)$$

The constraints that the circle center had the shortest distance from the obstacle were expressed as follows:

$$80 \leq x \leq 230, \quad (45)$$

$$0 < y \leq 210. \quad (46)$$

The AGV obstacle avoidance simulated through MATLAB programming is illustrated in Figures 10 and 11:

The turning path of an AGV must include an arc tangent to the straight-line path. Points C and B are on a circle with a radius r .

$$\sqrt{(x_c - x)^2 + (y_c - y)^2} = r, \quad (47)$$

$$\sqrt{(x_b - x)^2 + (y_b - y)^2} = r, \quad (48)$$

$$s_1 = \sqrt{a^2 - r^2}, \quad (49)$$

$$s_2 = \sqrt{b^2 - r^2}. \quad (50)$$

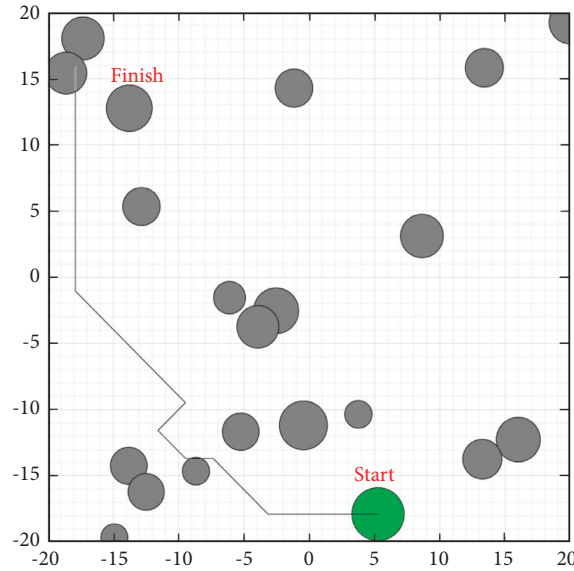


FIGURE 11: Diagram of AGV obstacle avoidance simulation (b).

TABLE 7: Shortest path.

	Start point coordinates	Endpoint coordinates	Turning arc center	Distance	Time
Straight 1	(0,0)	(69.8045, 211.9779)	—	223.1755	44.6351
Arc 1	(69.8045, 211.9779)	(77.74918, 220.1387)	(82.1414, 207.9153)	11.7899	2.360433
Straight 2	(77.74918, 220.1387)	(0,0)	—	236.1636	47.23272
Sum	—	471.129	94.22825		

Based on the conditions above, the optimization model for the shortest time was built:

$$\text{Min} = \frac{s_1 + s_2}{v_o} + \frac{l}{v_p}, \quad (51)$$

$$\begin{cases} r - \sqrt{(x - x_3)^2 + (y - y_3)^2} \geq 10, \\ r = \sqrt{(x_b - x)^2 + (y_b - y)^2}, \\ r = \sqrt{(x_c - x)^2 + (y_c - y)^2}, \\ s_2 = \sqrt{(x - x_2)^2 + (y - y_2)^2} - r^2, \\ s_1 = \sqrt{(x - x_1)^2 + (y - y_1)^2} - r^2, \\ 80 < x < 230, \\ y_b > \end{cases} \quad \begin{matrix} s \\ t \end{matrix} \quad \begin{matrix} 210, x_c < 80, 0 < y < 210. \end{matrix} \quad (52)$$

Utilizing Lingo and NSGA-II software, the shortest time of 94.22825 s and the turning radius of $r=12.9886$ were obtained. The results are reported in Table 7 and the resulting diagram Figure 12:

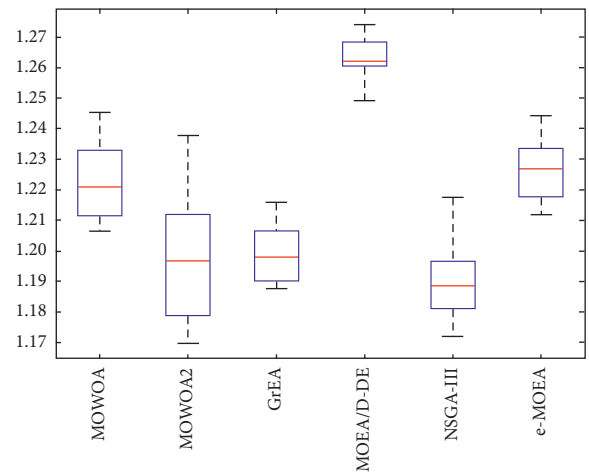


FIGURE 12: Comparison diagram of AGV obstacle avoidance results obtained by NSGA-II.

4.2. Model Promotion. In this paper, the problem of deadlock was simplified. Nevertheless, further model optimization is required when the actual deadlock situation is more complicated. This work assumed that the AGV moved from the starting point R to the target point M_0 ,

where the path comprised linear segments and arcs, set as m and n , respectively. Thus, the objective function was expressed as:

$$\begin{aligned} \text{Min} &= \sum_{i=1}^m d_i + \sum_{j=1}^n l_j, \\ &\begin{cases} r \geq 1, \\ k \geq 1. \end{cases} \end{aligned} \quad (53)$$

Computer software such as MATLAB or Lingo can be used to solve the optimal path between the start point and the target point.

5. Conclusion

According to the features of existing AGV cluster systems, an SVM-based AGV scheduling strategy was developed by determining the shortest possible path between the starting point and the target point. Then, the optimal path was determined by the exhaustive method and the Q-learning method and was optimized by several schemes, through which the optimal path in the relative optimization was obtained. A nonlinear programming model for the shortest time was built based on the relationship between the turning radius and speed based on the shortest path. The calculation with NSGA-II proved that the AGV path was optimal when the AGV turned with the minimum radius, and the circle center was located at the obstacle's vertex (the circular obstacle was located at the circle center). Several simulation tests and calculation results validated the proposed method, which rationally solved the problem of obstacle congestion and deadlock. After optimization, the constructed model was solved with high accuracy via analytical geometry. However, the processing burden increased, resulting in low utilization efficiency. Hence, the proposed method is inefficient for complicated deadlock situations.

Future research will consider the minimum spanning tree, and the shortest path of the AGV combined the dynamic monitoring and real-time data of AGV cluster systems.

Data Availability

The data used to support the findings of the study can be obtained from the author upon request.

Conflicts of Interest

The author declares that there are no conflicts of interest regarding the publication of this paper.

Acknowledgments

The author would like to express his gratitude to EditSprings (<https://www.editsprings.cn>) for the expert linguistic services provided and Zhi Dong Li for experimental assistance. This

research was supported by the 2021 Innovation Training Program for University Students (nos. 202112757001, 202112757005, 202112757006, and 202112757016) and the Chongqing Police College Studies Research Project Program.

References

- [1] S. Vinoth, H. L. Vemula, B. Haralayya, P. Mamgain, M. F. Hasan, and M. Naved, "Application of cloud computing in banking and e-commerce and related security threats," *Materials Today Proceedings*, vol. 51, pp. 2172–2175, 2022.
- [2] P. Giridharan, R. G. Chittawadigi, and G. Udupa, "Intuitive manipulation of delta robot using leap motion," in *Mechanism and Robotics: In Machines* Springer, Singapore, 2022.
- [3] J. Chen, X. Zhang, X. Peng, D. Xu, and J. Peng, "Efficient routing for multi-AGV based on optimized Ant-agent," *Computers & Industrial Engineering*, vol. 167, Article ID 108042, 2022.
- [4] Y. Zhou and N. Huang, "Airport AGV path optimization model based on ant colony algorithm to optimize Dijkstra algorithm in urban systems," *Sustainable Computing: Informatics and Systems*, vol. 35, Article ID 100716, 2022.
- [5] A. Meysami, J. C. Cuillière, V. François, and S. Kelouwani, "Investigating the impact of triangle and quadrangle mesh representations on AGV path planning for various indoor environments: with or without inflation," *Robotics*, vol. 11, no. 2, 2022.
- [6] C. Liang, X. Hu, L. Shi, H. Fu, and D. Xu, "Joint Dispatch of Shipment Equipment Considering Underground Container Logistics," *Computers & Industrial Engineering*, vol. 165, Article ID 107874, 2022.
- [7] A. Azadeh, M. Ravanbakhsh, M. Rezaei-Malek, and A. Taheri-Moghaddam, "Unique NSGA-II and MOPSO algorithms for improved dynamic cellular manufacturing systems considering human factors," *Applied Mathematical Modelling*, vol. 48, pp. 655–672, 2017.
- [8] X. Chu, D. Gao, S. Cheng, L. Wu, J. Chen, and Q. Qin, "Worker assignment with learning-forgetting effect in cellular manufacturing system using adaptive memetic differential search algorithm," *Computers & Industrial Engineering*, vol. 136, pp. 381–396, 2019.
- [9] R. Zaghdoud, K. Mesghouni, S. C. Dutilleul, and K. Ghedira, "A hybrid method for assigning containers to AGVs in the dynamic environment of container terminals," *Studies in Informatics and Control*, vol. 24, no. 1, pp. 43–50, 2015.
- [10] W. Malopolski, "A sustainable and conflict-free operation of AGVs in a square topology," *Computers & Industrial Engineering*, vol. 126, pp. 472–481, 2018.
- [11] S. Kim, H. Jin, M. Seo, and D. Har, "Optimal path planning of automated guided vehicle using dijkstra algorithm under dynamic conditions," in *Proceedings of the 2019 7th International Conference on Robot Intelligence Technology and Applications*, pp. 231–236, Daejeon, Korea, November 2019.
- [12] C. Wang, L. Wang, J. Qin et al., "Path planning of automated guided vehicles based on improved A-Star algorithm," in *Proceedings of the 2015 IEEE International Conference on Information and Automation*, pp. 2071–2076, Lijiang, China, August 2015.
- [13] R. Tai, J. Wang, and W. Chen, "A prioritized planning algorithm of trajectory coordination based on time windows for

- multiple AGVs with delay disturbance,” *Assembly Automation*, vol. 39, no. 5, pp. 753–768, 2019.
- [14] N. Singh, Q. V. Dang, A. Akcay, I. Adan, and T. Martagan, “A matheuristic for AGV scheduling with battery constraints,” *European Journal of Operational Research*, vol. 298, no. 3, pp. 855–873, 2022.
- [15] Y. Li, W. Gu, M. Yuan, and Y. Tang, “Real-time data-driven dynamic scheduling for flexible job shop with insufficient transportation resources using hybrid deep Q network,” *Robotics and Computer-Integrated Manufacturing*, vol. 74, Article ID 102283, 2022.
- [16] Q. Zhu, S. Su, T. Tang, W. Liu, Z. Zhang, and Q. Tian, “An eco-driving algorithm for trains through distributing energy: a Q-Learning approach,” *ISA Transactions*, vol. 122, pp. 24–37, 2022.
- [17] J. S. Nisha, V. P. Gopi, and P. Palanisamy, “Classification of informative frames in colonoscopy video based on image enhancement and phog feature extraction,” *Biomedical Engineering: Applications, Basis and Communications*, vol. 34, no. 2, Article ID 2250015, 2022.
- [18] R. Hu, J. Gan, X. Zhu, T. Liu, and X. Shi, “Multi-task multi-modality SVM for early COVID-19 Diagnosis using chest CT data,” *Information Processing & Management*, vol. 59, no. 1, Article ID 102782, 2022.
- [19] M. A. Djeziri, O. Djedidi, N. Morati, J. L. Seguin, M. Bendahan, and T. Contaret, “A temporal-based SVM approach for the detection and identification of pollutant gases in a gas mixture,” *Applied Intelligence*, vol. 52, no. 6, pp. 6065–6078, 2022.
- [20] G. K. Suman, J. M. Guerrero, and O. P. Roy, “Stability of microgrid cluster with Diverse Energy Sources: a multi-objective solution using NSGA-II based controller,” *Sustainable Energy Technologies and Assessments*, vol. 50, Article ID 101834, 2022.

Research Article

Economic Policy Uncertainty, Investor Sentiment, and Stock Price Synchronisation: Evidence from China

Jing Wu ^{1,2}

¹Graduate Business School, UCSI University, Kuala Lumpur 560000, Malaysia

²School of Economics and Management, Huangshan University, Huangshan 245041, Anhui, China

Correspondence should be addressed to Jing Wu; 1001957222@ucsiuniversity.edu.my

Received 19 May 2022; Accepted 29 June 2022; Published 12 July 2022

Academic Editor: Wei Liu

Copyright © 2022 Jing Wu. This is an open access article distributed under the Creative Commons Attribution License, which permits unrestricted use, distribution, and reproduction in any medium, provided the original work is properly cited.

This paper explores the general decision mechanism of stock price synchronicity through in-depth research on the two main viewpoints of information efficiency view and irrational behaviour view. On this basis, we explore the effect of China's economic policy uncertainty gradually on the synchronisation of stock prices and provide a reasonable explanation for it. Based on the China Economic Policy Uncertainty Index developed by Baker et al., this paper takes China's A-share listed firms from 2010 to 2019 as the primary sample and tests the effect of China's economic policy uncertainty on the synchronicity of stock prices by constructing a comprehensive mediation effect test procedure. The fundamental effect and its internal mechanism of action have been supplemented and verified from investor sentiment. Strengthening the research on economic policy uncertainty and stock price synchronisation may deeply explore the internal mechanism of the listed firms' stock price changes, help in improving the information production function and information transmission function of the securities market, help in improving the resource allocation capacity of the entire capital market, and then promote the long-term healthy development of China's capital market. The main findings of this paper are as follows: (1) in China's stock market, which is driven by noise, the increase of economic policy uncertainty will significantly reduce the synchronisation of stock prices; (2) increased uncertainty about China's economic policy will fuel the investor sentiment and reduce stock price synchronicity, with investor sentiment playing an intermediary role.

1. Introduction

With an unpredictable macroeconomic environment, the economic policy is fraught with uncertainty, while the stock market's movement can reflect the investor sentiment and the economic performance of real businesses in real time. Thus, the microeconomic effect of uncertain economic policies may be studied through the lens of the stock market. The capital market's principal role is to maximise resource allocation through the stock signal mechanism. Stock prices can optimise resource allocation by steering resources through an extremely efficient capital market. The capacity of a stock price which represents a company's operational circumstances accurately may influence the degree to which the resource allocation is led by the stock price, which is also an essential indicator of a country's capital market's operating efficiency and maturity. While the stock price in a

mature capital market may properly represent a firm's qualities, the stock price in an emerging capital market is further affected by market forces and cannot accurately reflect a firm's features. Due to the aforementioned issues, stock price synchronisation has been a popular topic in the field of stock market research in recent years, thus garnering considerable interest from academic and practical sectors.

Stock price synchronisation refers to the degree to which the stock prices of firms increase or decrease in lockstep over time, that is, the phenomenon of "simultaneous rise and fall." Due to the synchronicity of stock prices, investors cannot incorporate a large amount of corporate personality information into the value evaluation of listed firms when utilising the capital asset pricing model (CAPM) to conduct investment decision analyses, resulting in the low investment value of such firms. To some extent, this destroys the specific functions of stock prices in incorporating value

evaluation (such as screening and evaluation), which hinders the information transmission mechanism of firms and reduces the effectiveness of stock prices in resource allocation. Excessive stock price synchronisation will reduce the efficiency of asset pricing and economical operation, interfere with the operation of security market screening mechanism, affect the economic growth, and bring negative economic consequences [1–4].

Further interpretation of the connotation of stock price synchronisation needs to focus on the formation mechanism of stock price synchronisation, which is separated approximately into two schools: first, the view of information efficiency (also known as information interpretation), represented by Morck et al. [1], believes that the stock price synchronicity reflects the degree to which the personal or private information of a firm is included in the stock price and measures the degree of information efficiency. Lower stock price synchronisation meant a richer idiosyncratic information content, thus reflecting a higher efficiency. Secondly, the view of irrational behaviour (also known as noise explanation), represented by West [5], believes that a firm's fundamentals cannot explain the abnormal fluctuations of stock prices. Stock prices are significantly affected by irrational factors, while the synchronicity of stock prices measures the number of irrational factors, such as market noise and investor sentiment. Low stock price synchronicity results from abnormal volatility caused by investors' irrational behaviour and thus reflects high noise bias. On the premise of an efficient market, the stock price can fully reflect all relevant information, any change of stock price is caused by information flow, noise is only a random disturbance term with an average of zero, in which the synchronisation of stock price reflects information efficiency. However, when the market is not efficient, the stock price is greatly affected by the market noise, and the stock price is mainly driven by noise, wherein the synchronicity of the stock price reflects the noise deviation. In reality, market efficiency is often a problem of degree and period, in which stock price synchronicity is the information and noise. Jin and Myers [6] argued that stock price synchronicity may differ in various countries, the reason is that each country's stock market is at different stages of development, the stock market in the emerging world is not mature enough, often caused by information asymmetry herding effect and speculation, and medium and small investors in such an environment cannot be efficient to collect information and make rational decisions. Most of the investment is based on the overall situation of the market and industry, wherein the price synchronisation is high. Therefore, the variables of stock price synchronisation have gained academic interest to avoid the harmful effect of simultaneous increase and fall of stock prices. For the influence of policy system on stock price synchronisation, existing studies have obtained a large number of theoretical and empirical results, but mainly from the protection level of property rights, the legal system, accounting system, and other aspects of the study, not involving economic policies, especially economic policy uncertainty [7–11].

The policy market phenomenon is quite apparent in China's stock market. Thus, what effect will the uncertainty

of economic policy have on the synchronicity of Chinese stock prices? Investor sentiment research focuses on both individual and institutional investor sentiment in relation to stock price synchronisation. When the investor group is evaluated, the relationship between investor emotion and stock price synchronisation is macroscopically significant. As a result, this article focuses primarily on the link among economic policy uncertainty, investor sentiment, and stock price synchronisation in China.

2. Literature Review and Hypothesis Development

2.1. Relationship between Economic Policy Uncertainty and Stock Price Synchronisation. Economic policy uncertainty (EPU) may arise from the government's failure to describe the direction and magnitude of economic policy expectations, policy implementation, and policy attitude changes. The principal symptom is that economists are unable to forecast with certainty whether, when, or how the government will alter present economic policies in the future [12, 13]. According to Williamson [14], human-limited rationality and future uncertainty are impossible to forecast completely. Precisely foreseeing the contents of policies prior to their implementation is difficult for listed firms. After the policies are implemented, there are several options for their intensity and effect, while economic subjects are frequently confronted with the uncertainty of economic policies throughout the real decision-making process [15]. Economic policy uncertainty will have a substantial effect on the capital market's stock price reaction and even on the capital market's overall stock price volatility. Pastor and Veronesi [16] discovered that when policy changes are announced, stock prices decrease, and the higher the uncertainty, the larger the decline in stock prices. As a result, increased economic policy uncertainty reduces the stock returns and increases the overall stock price volatility. Brogaard and Detzel [17] used text analysis to examine the influence of policy uncertainty on stock returns and volatility in 21 nations and discovered that economic policy uncertainty increased the individual stock volatility considerably. The volatility of individual stocks and market prices is an essential determinant of stock price synchronisation. Therefore, the uncertainty of China's economic policies may also affect stock price synchronisation. At the same time, compared with the volatility of individual stocks, the market volatility and the beta coefficient of individual stocks remain relatively stable, in which China's economic policy uncertainty is anticipated to diminish stock price synchronisation by raising each stock's relative volatility.

H1: The higher the level of economic policy uncertainty, the lower the synchronicity of stock prices would be.

2.2. Economic Policy Uncertainty, Investor Sentiment, and Stock Price Synchronisation. Investor sentiment is a perception held by investors about the future cash flow and investment risk of assets, although it cannot fully reflect the underlying facts [18]. Due to future uncertainty, investors

can only establish an expectation or belief about the quantity and risk of future cash flows provided by assets at the moment. This expectation or belief is related not only to the asset's fundamentals, but also to the investor's own education, investment experience and knowledge, social background, information, personality, and preference, all of which contribute to a "subjective and objective" comprehensive assessment of the asset's future worth. As a result, various individuals would have varying opinions regarding the same asset, which are referred to as "sentiments." Numerous studies have demonstrated that sentiment has an effect on investors' decision-making, particularly when the sentiment is highly social. Under the social interaction mechanism, people's behaviours tend to be consistent, resulting in repeated errors and market mispricing.

Behavioural finance theory determined that the investors' cognition is limited, and they will show irrational characteristics such as overconfidence, loss avoidance, and psychological accounts, and often make irrational investment behaviours. This type of irrational behaviour plays an essential role in the economic system. According to the investor demand hypothesis, investors often think that a particular market event conveys a specific message; thus, they overreact under the influence of irrational factors such as preferences and sentiments. Scholars have also conducted many studies on the effect of investor sentiment on stock price synchronisation. West [5] believed that the irrational behaviour caused by investors' psychological deviation resulted in low stock price synchronisation. Barberis et al. [19] studied the influence of investor sentiment on stock price synchronisation using behavioural finance theory. They found that the irrational investors' particular preference for a firm would trigger irrational investment behaviour, thus affecting the stock price synchronisation of the firm. Barberis et al. [19]; Greenwood and Sosner [20]; Greenwood [21]; and Li [22] et al. also found that investor sentiment would affect the level of stock price synchronisation. Frijns et al. [23] decomposed stock returns into fundamental and nonfundamental components and found that nonfundamental components were strongly correlated with stock returns. Changes in stock returns were driven by investor sentiment, which would exacerbate the stock prices' volatility.

When investors tend to pursue policies, the uncertainty of economic policies will cause the volatility of investors' sentiment, which would lead to their inappropriate response to stock prices and aggravate the volatility of individual stocks. If EPU represents the continuous release of policy dividends, investors will form a consistent optimistic expectation. Economic policy uncertainty will increase the investors' risk appetite and make them overly optimistic about stock prices. Economic policy uncertainty can cause investors to overreact to stock prices by influencing their attitude to risk. At the same time, due to the investors' limited attention and overconfidence, economic policy uncertainty is likely to increase the cognitive bias of investors, leading to their overreaction to stock prices. Psychological accounts would hinder such inappropriate reactions, resulting in persistent systemic overvaluation or

undervaluation of asset prices. Skaife et al. [24] believed that in semi-strong or weak efficient markets, the noise would often drown corporate trait information and play a dominant role in stock prices, which meant that stock price fluctuations in emerging markets are mainly affected by market noise. Considering the actual situation, although China's capital market has achieved rapid development in recent years, its effectiveness and maturity are still insufficient, while various institutional facilities and related support services are imperfect, investor protection is insufficient, and supervision is relatively lagging behind. The investor group with retail investors as the main body cannot make professional judgments and act rationally. Phenomena such as "policy market," "theme stocks," and "outlet theory" indicate that a high speculative atmosphere in China was observed [25]. The "stock market crash" of 2015 to 2016 provides direct evidence. The aforementioned analysis shows that China's stock market prices were mainly driven by noise in the past for quite an extended period.

The uncertainty of China's economic policy will lead to investor sentiment changes and inappropriate reactions to stock prices, thus enhancing noise trading in the market. In addition to improving the level of noise trading by affecting the investors' risk attitude and cognitive bias, the information processing dilemma brought by economic policy uncertainty would damage the effectiveness of information arbitrage by limiting the investors' rational assessment of intrinsic enterprise value and lead to the increase of irrational noise trading level. When adverse selection caused by information asymmetry leads to "bad money (irrational investors) driving out good money (rational investors)" and forms a "lemon market" dominated by irrational investors, noisy transactions related to policy uncertainty would flood the whole market and aggravate abnormal fluctuations of individual stocks. Therefore, from the perspective of investor sentiment and the restriction of economic policy uncertainty on rational arbitrage, the rise of economic policy uncertainty would reduce stock price synchronisation by boosting investor sentiment.

H2: The level of economic policy uncertainty increases, investor sentiment increases, and stock price synchronicity decreases. Investor sentiment plays a mediating role in the relationship between economic policy uncertainty and stock price synchronisation.

3. Data, Variables, and Methodology

3.1. Sample Selection and Data Sources. This paper selects China's Shanghai and Shenzhen A-share listed firms as the research sample, while the sample period is from 2010 to 2019. This study's economic policy uncertainty data come from <http://www.policyuncertainty.com>, while other data come from the Wind and CSMAR databases. Steps to preprocess selected samples are as follows:

- (1) Delete the sample of enterprises whose industry is the financial industry.
- (2) Delete enterprise samples that are ST, *ST.
- (3) Delete samples of companies with missing data.

- (4) To ensure the reliability of measuring stock price indicators, the sample of companies with annual trading weeks of less than 30 weeks will be deleted.

This paper treats extreme values with 1% upper and lower extreme values to eliminate extreme values' influence on multiple regression results. This article uses STATA16.0 for data processing and operation.

3.2. Variable Definitions

3.2.1. Economic Policy Uncertainty (EPU). The EPU composite index can measure economic policy uncertainty. This index is constructed and calculated by Baker et al. and is mainly used to reflect the economic and policy uncertainties of the world's major economies. The EPU composite index mainly comprises the news index, tax law expiration date index, and economic forecast difference index. The China EPU index is calculated by using the news index in the EPU composite index, taking The South China Morning Post as the analysis object, identifying the monthly articles on the uncertainty of China's economic policy, and dividing the identification results by the total number of articles published in that month to obtain the China EPU index of that month (<http://www.policyuncertainty.com>). Although China's EPU index is only a news index, Baker et al. [15] determined through verification that it has a strong correlation with the general index, wherein it is still representative.

3.2.2. Investor Sentiment (CICSI). The key of investor sentiment research lies in the measurement of sentiment. In the past, single indicators such as the discount of closed-end funds were mainly used to measure changes in investor sentiment (Lee, 1991; Swaminathan, 1996); [26]. However, these methods have problems of excessively single measurement index and impure measurement results. To address these issues, He et al. (2017) introduced variables which may indicate changes in investor mood in the local stock market by upgrading the Baker and Wurgler index's building process, that is, the discount on closed-end funds, trading volume, the number of initial public offerings and their first-day earnings, the consumer confidence index, and the number of newly established investor accounts. Simultaneously, they regulate the consumer price index, the industrial producer price index, industrial added value, macroeconomic climate index, and a variety of other macroeconomic factors. The Chinese Stock Market Investor Sentiment Composite Index (CICSI) is calculated annually.

3.2.3. Stock Price Synchronisation (SYN). Stock price synchronisation represents the correlation between the volatility of enterprise stock price and the average volatility of stock price in the securities market. Stock price synchronisation first appeared in finance, which is mainly used to analyse the explanatory power of market return index in capital asset pricing model (CAPM) to individual company return index. Morck, and Yeung and Yu [1] first proposed

this concept, who conceptualised the R^2 studied by Roll [27]. On this basis, this paper constructs the annual index of stock price synchronisation and designs the following estimation model by using the daily return rate of stocks in a trading year and the corresponding market daily return rate:

$$r_{i,t,w} = \beta_0 + \beta_1 r_{m,t,w} + \varepsilon_{i,t,w},$$

$$SYN_{i,t} = \ln\left(\frac{R_{i,t}^2}{1 - R_{i,t}^2}\right). \quad (1)$$

3.2.4. Control Variables. To enhance the explanatory capacity of core explanatory factors and the model's stability, this article used previous literature to pick numerous control variables to participate in the model's parameter estimation. Specific factors include the size of the firm (Size), the asset-liability ratio (Lev), the return on assets (ROA), the years since listing (ListAge), if the chairman and general manager positions are merged (Dual), and the sales growth rate (Growth). Additionally, it has control over industry (Ind) and year (Year).

3.2.5. Model Design. Firstly, to explore the effect of China's economic policy uncertainty on stock price synchronisation, the hypothesis H1 is tested and the following model is constructed:

$$SYN_{i,t} = \alpha_0 + \alpha_1 EPU_t + \sum \alpha \text{Controls} + \lambda_t + \lambda_{\text{int}} + \varepsilon_{i,t}. \quad (2)$$

The subscripts i , t , and int represent the individual, time, and industry of the listed firm, respectively.

To investigate the mediating influence of China's economic policy uncertainty on stock price synchronisation further, we tested hypothesis H2 and built the following models:

$$\begin{aligned} CICSI_{i,t} &= \beta_0 + \beta_1 EPU_t + \sum \beta \text{Controls} + \lambda_t + \lambda_{\text{int}} + \varepsilon_{i,t}, \\ SYN_{i,t} &= \gamma_0 + \gamma_1 EPU_t + \sum \gamma \text{Controls} + \lambda_t + \lambda_{\text{int}} + \varepsilon_{i,t}. \end{aligned} \quad (3)$$

4. Analysis

4.1. Descriptive Statistics. Table 1 reports the descriptive statistical results for the primary variables: the variable name, sample size, minimum, maximum, mean, median, and standard deviation from left to right.

The median of stock price synchronicity SYN is -0.415, which is an absolute value higher than those of Morck et al. [1] and Eun et al. [28]. Most of the countries reported corroborating the high stock price synchronisation in China. The EPU averaged 3.290, while the standard deviation was 2.179, reflecting China's higher economic policy uncertainty. The reported results of other variables are consistent with the existing studies. They are typically within a tolerable range, indicating that the calculated values for the pertinent

TABLE 1: Result of descriptive statistics.

Variable	N	min	max	mean	p50	sd
SYN	24500	-9.322	10.56	-0.491	-0.415	0.962
EPU	24500	0.989	7.919	3.290	2.444	2.179
CICSI	24500	0.321	0.474	0.409	0.413	0.0421
Lev	24500	0.0278	0.925	0.431	0.423	0.209
Size	24500	19.50	26.37	22.15	21.98	1.280
ROA	24500	-0.452	0.226	0.0398	0.0381	0.0651
ListAge	24500	0	3.332	2.136	2.303	0.801
Dual	24500	0	1	0.264	0	0.441
Growth	24500	-0.632	4.806	0.190	0.114	0.463

TABLE 2: Result of correlation analysis.

	SYN	EPU	CICSI	Lev	Size	ROA	ListAge	Dual	Growth
SYN	1								
EPU	-0.053 ^a	1							
CICSI	0.064 ^a	0.598 ^a	1						
Lev	0.016 ^a	-0.020 ^a	-0.030 ^a	1					
Size	0.150 ^a	0.112 ^a	0.082 ^a	0.519 ^a	1				
ROA	0.028 ^a	-0.070 ^a	0.008	-0.383 ^a	-0.039 ^a	1			
ListAge	0.039 ^a	0.058 ^a	-0.006	0.415 ^a	0.406 ^a	-0.283 ^a	1		
Dual	-0.048 ^a	0.055 ^a	0.044 ^a	-0.156 ^a	-0.187 ^a	0.056 ^a	-0.247 ^a	1	
Growth	-0.050 ^a	-0.055 ^a	0.045 ^a	0.027 ^a	0.042 ^a	0.211 ^a	-0.044 ^a	0.020 ^a	1

Note:^a $p < 0.01$.

variables in this study are correct and dependable, thus allowing for additional investigation.

4.2. Correlation Analysis. The correlation test results for the main variables are reported in Table 2. Firstly, a significant (at the 1% level) and negative correlation between the explanatory variable stock price synchronisation (SYN) and the explanatory variable economic policy uncertainty (EPU) was observed, which indicates that the uncertainty of China’s economic policy will have a negative effect on the stock price synchronisation, thus supporting H1. Secondly, there is a substantial connection between the interpreted variable and the mediating variable CICSI (at the 1% level), as well as a significant association between the explanatory variable (EPU) and the mediating variable CICSI (at the 1% level). This indicates a possible mode of mediation. Thirdly, there is a substantial link between EPU and all other variables (at the 1% level), indicating the wide effect of China’s economic policy uncertainty. Fourthly, all control variables are substantially associated with stock prices at the 1% level. Fifthly, the absolute value of the variable correlation coefficient is frequently less than 0.4.

4.3. OLS Regression Analysis. The step-by-step test method is used to verify whether the uncertainty of China’s economic policy is verified by investor sentiment affecting stock price synchronisation, which is as follows:

First, test whether the coefficient of EPU in the model (3–1) is significant. If it is insignificant, it indicates that the uncertainty surrounding China’s economic policies has had no effect on the synchronisation of stock prices, while the test is therefore concluded; if it is significant, the follow-up

TABLE 3: Result of OLS regression analysis 1.

	(1) SYN	(2) SYN
EPU	-0.0223*** (-7.90)	-0.0705*** (-18.19)
Lev		-0.453*** (-12.99)
Size		0.162*** (29.88)
ROA		0.201** (2.12)
ListAge		0.0356*** (4.49)
Dual		-0.0205 (-1.63)
Growth		-0.135*** (-11.27)
Ind	Yes	Yes
Year	Yes	Yes
_cons	-0.418*** (-37.55)	-3.527*** (-30.12)
N	24466	24466
R ²	0.003	0.255

Note: t statistics in parentheses; ** $p < 0.1$, * $p < 0.05$, *** $p < 0.01$.

inspection procedure is conducted. Table 3 reports the corresponding regression results where column (1) is a direct regression result that does not consider the control variable, while column (2) is a regression result which considers all control variables. The coefficient of the explanatory variable (EPU) is negative and significant at the 1% level, indicating that China’s economic policy uncertainty will have a significant and adverse effect on stock price synchronisation,

TABLE 4: Result of OLS regression analysis 2.

	(1) CICSI	(2) SYN
EPU	0.0119*** (118.35)	-0.0556*** (-8.61)
CICSI		-4.382*** (-3.46)
Lev	-0.00343** (-2.48)	-0.453*** (-12.99)
Size	0.00134*** (6.26)	0.162*** (29.88)
ROA	0.0101*** (2.69)	0.201** (2.12)
ListAge	0.00128*** (4.07)	0.0356*** (4.49)
Dual	0.000365 (0.73)	-0.0205 (-1.63)
Growth	0.00694*** (14.58)	-0.135*** (-11.27)
Ind	Yes	Yes
Year	Yes	Yes
_cons	0.337*** (73.05)	-1.676*** (-3.08)
N	24466	24466
R ²	0.385	0.255

Note: *t* statistics in parentheses; ** $p < 0.1$, * $p < 0.05$, *** $p < 0.01$.

TABLE 5: Result of robustness test 1.

	(1) adj_SYN	(2) adj_SYN
EPU	-0.0233*** (-7.63)	-0.0356*** (-11.63)
Lev		-0.442*** (-10.78)
Size		0.160*** (25.03)
ROA		0.120 (1.04)
ListAge		0.0196** (2.10)
Dual		-0.0300* (-1.95)
Growth		-0.133*** (-9.05)
Ind	Yes	Yes
Year	Yes	Yes
_cons	-0.534*** (-44.32)	-3.872*** (-30.00)
N	24027	24027
R ²	0.002	0.037

Note: *t* statistics in parentheses; ** $p < 0.1$, * $p < 0.05$, *** $p < 0.01$.

supporting H1; that is, leaving other factors unchanged, the increase in uncertainty in the country's economic policy would generally reduce the synchronisation of stock prices.

Second, column (1) of the table below shows the CICSI's regression results to the EPU and other control variables. As

TABLE 6: Result of robustness test 2.

	(1) SYN	(2) SYN
EPU	-0.0122*** (-4.16)	-0.00928** (-2.26)
Lev		-0.291*** (-4.23)
Size		0.130*** (8.23)
ROA		-0.183 (-1.37)
ListAge		-0.169*** (-6.91)
Dual		-0.0148 (-0.65)
Growth		-0.0646*** (-4.51)
Ind	Yes	Yes
Year	Yes	Yes
_cons	-0.451*** (-40.10)	-2.838*** (-8.78)
N	24466	24466
R ²	0.001	0.006

Note: *t* statistics in parentheses; ** $p < 0.1$, * $p < 0.05$, *** $p < 0.01$.

TABLE 7: Result of robustness test 3.

	(1) SYN	(2) SYN
EPU	-0.0223*** (-7.90)	-0.0364*** (-12.75)
Lev		-0.409*** (-10.71)
Size		0.143*** (21.54)
ROA		0.248** (2.27)
ListAge		0.00610 (0.61)
Dual		-0.0369** (-2.56)
Growth		-0.132*** (-9.64)
TobinQ		-0.0288*** (-5.88)
Top1		-0.136*** (-3.15)
Ind	Yes	Yes
Year	Yes	Yes
_cons	-0.418*** (-37.55)	-3.233*** (-23.52)
N	24466	23504
R ²	0.003	0.041

Note: *t* statistics in parentheses; ** $p < 0.1$, * $p < 0.05$, *** $p < 0.01$.

shown in Table 4, the coefficient of the explanatory variable EPU is positive and significant at the 1% level, showing that China's economic policy uncertainty would considerably

enhance investor sentiment, which is consistent with earlier estimates.

Column (2) is the regression result of the stock price synchronisation SYN to the explanatory variable EPU, the intermediary variable CICSII, and other control variables. The CICSII coefficient is negative and significant at the 1% level, indicating that increased investor sentiment significantly reduces stock price synchronisation. According to the general rules of the intermediary effect test, the intermediary effect of investor sentiment has been established. The uncertainty of China's economic policy would reduce the synchronisation of stock prices by encouraging investor sentiment, thereby providing direct support for the noise interpretation mechanism of China's economic policy uncertainty to reduce stock price synchronisation, thus supporting H2.

4.4. Robustness Test. This paper mainly tests the robustness of the primary conclusions by changing the weighing method of market and industry returns, which was previously weighed by circulating market capitalisation, and is now recalculated by equal weight and total market capitalisation; second, it is tested by a fixed-effect model; third, control variables are added for testing. Tables 5, 6, and 7 reported the results of each of the three robustness tests.

Thus, all three robustness tests have passed, and the previous conclusions are still valid.

5. Conclusions

Based on the current research results and theoretical analysis, this paper examined the Chinese A-share nonfinancial listed firms from 2010 to 2019 and the essential effect of national economic policy uncertainty on stock price synchronisation and its internal mechanism. Overall, the results are consistent with the theoretical analysis expectations, while the main conclusions are as follows: (1) in the Chinese stock market, which is more clearly driven by noise, the increase in economic policy uncertainty would significantly reduce the synchronisation of stock prices; (2) economic policy uncertainty in China can reduce stock price synchronisation overall by fuelling investor sentiment. Investor sentiment has mediated and equally supported noise interpretation.

On the basis of the foregoing results and pertinent findings, this study concludes as follows: (1) because the stock price is determined by private information and noise, and because the level of stock price synchronisation is affected by the expected influence of private information integration and noise trading, the market efficiency cannot be determined solely by the level of stock price synchronisation, and when more noise was observed in the market and it has a significant effect, stock price synchronisation is likely to be insufficient as a proxy for capital market efficiency. The issue is not so much with the nominal level of stock price synchronisation as it is with its creation method and mechanism of operation. (2) While the evidence supports the effect of uncertainty in China's economic policies

on stock price synchronisation, the information efficiency notion retains a unique explanatory capacity when other control variables are considered. Thus, while analysing the process of stock price synchronisation in various conditions, the notion of information efficiency and irrational behaviour may apply, and the organic combination of the two may be more favourable to providing a fair explanation for the real situation. (3) There is much noise in the Chinese stock market and a substantial effect, reflecting the low information quality environment and immature investor literacy in the Chinese capital market, in which a large room exists for improving the information environment of the capital market and improving the quality of investors. Firstly, because China's economic policy uncertainty affects investor sentiment, reducing policy uncertainty is a viable path to improve the market information environment and keep the capital market running smoothly. The government should strengthen communication with the market and reduce the interference of policy uncertainty on the market. Secondly, due to the long-term investor structure of the Chinese stock market dominated by retail investors, the atmosphere of following the trend is intense. The policy-chasing tendency is evident, resulting in excessive market noise. The regulatory authorities should cooperate with industry associations and relevant financial institutions to increase investor education, cultivate the concept of value investing, promote the construction of institutional investors, and promote the transformation of the market structure from retail to institutional.

The shortcoming of this paper is that it fails to subdivide economic policies, and it is difficult to distinguish which economic policies are more sensitive to investor sentiment. The following research can consider subdividing economic policies, further analyse the differences in investor sentiment caused by different economic policies, and then examine the impact on the synchronisation of stock prices [29, 30].

Data Availability

This study's economic policy uncertainty data come from <http://www.policyuncertainty.com>, while other data come from the Wind and CSMAR databases.

Conflicts of Interest

The author declares that there are no conflicts of interest.

References

- [1] R. Morck, B. Yeung, and W. Yu, "The information content of stock markets: why do emerging markets have synchronous stock price movements?" *Journal of Financial Economics*, vol. 58, no. 1-2, pp. 215-260, 2000.
- [2] A. Durnev, R. MorckMorck, and B. Yeung, "Value-enhancing capital budgeting and firm-specific stock return variation," *The Journal of Finance*, vol. 59, no. 1, pp. 65-105, 2004.
- [3] Q. ChenChen, I. Goldstein, and W. JiangJiang, "Price informativeness and investment sensitivity to stock price," *Review of Financial Studies*, vol. 20, no. 3, pp. 619-650, 2007.

- [4] H. Chun, J. W. Kim, R. Morck, and B. J. J. o. F. E. Yeung, "Creative destruction and firm-specific performance heterogeneity," *Journal of Financial Economics*, vol. 89, 2008.
- [5] K. D. West, "Dividend innovations and stock price volatility," *Econometrica*, vol. 56, no. 1, p. 37, 1988.
- [6] L. Jin and S. Myers, "R2 around the world: new theory and new tests," *Journal of Financial Economics*, vol. 79, no. 2, pp. 257–292, 2006.
- [7] V. Colombo, "Economic policy uncertainty in the US: does it matter for the Euro area?" *Economics Letters*, vol. 121, no. 1, pp. 39–42, 2013.
- [8] W. Kang, K. Lee, and R. A. Ratti, "Economic policy uncertainty and firm-level investment," *Journal of Macroeconomics*, vol. 39, pp. 42–53, 2014.
- [9] Z. Su, M. Lu, and L. Yin, "Chinese stock returns and the role of news-based uncertainty," *Emerging Markets Finance and Trade*, vol. 55, no. 13, pp. 2949–2969, 2019.
- [10] S. Y. Choi, "Industry volatility and economic uncertainty due to the COVID-19 pandemic: evidence from wavelet coherence analysis," *Finance Research Letters*, vol. 37, no. 11, Article ID 101783, 2020.
- [11] W. Q. Huang and P. Liu, "Asymmetric effects of economic policy uncertainty on stock returns under different market conditions: evidence from G7 stock markets," *Applied Economics Letters*, vol. 29, no. 9, pp. 780–784, 2021.
- [12] H. I. Gulen and M. Ion, "Political uncertainty and corporate investment," *SSRN Electronic Journal*, vol. 29, pp. 523–564, 2015.
- [13] B. Julio and Y. J. J. o. F. Yook, "Political uncertainty and corporate investment cycles," *The Journal of Finance*, vol. 67, no. 1, pp. 45–83, 2012.
- [14] O. E. Williamson, *Markets and Hierarchies: Analysis and Antitrust Implications*, Free Press, New York, NY, USA, 1975.
- [15] S. R. Baker, N. Bloom, and S. J. Davis, "Measuring economic policy uncertainty," *Quarterly Journal of Economics*, vol. 131, no. 4, pp. 1593–1636, 2016.
- [16] L. Pastor and P. J. J. o. F. Veronesi, "Uncertainty about Government Policy and Stock Prices," 2012, https://papers.ssrn.com/sol3/papers.cfm?abstract_id=1625845.
- [17] J. BrogaardBrogaard and A. Detzel, "The asset-pricing implications of government economic policy uncertainty," *Management Science*, vol. 61, no. 1, pp. 3–18, 2015.
- [18] M. Baker and J. Wurgler, "Investor sentiment and the cross-section of stock returns," *The Journal of Finance*, vol. 61, no. 4, pp. 1645–1680, 2006.
- [19] N. Barberis, A. Shleifer, and J. Wurgler, "Comovement," *Journal of Financial Economics*, vol. 75, no. 2, pp. 283–317, 2005.
- [20] R. M. GreenwoodGreenwood and N. Sosner, "Trading patterns and excess comovement of stock returns," *Financial Analysts Journal*, vol. 63, no. 5, pp. 69–81, 2007.
- [21] R. M. J. R. o. F. S. Greenwood, "Trading restrictions and stock prices," *Review of Financial Studies*, vol. 22, no. 2, pp. 509–539, 2009.
- [22] J. Li, "Multi-period sentiment asset pricing model with information," *International Review of Economics & Finance*, vol. 34, no. nov, pp. 118–130, 2014.
- [23] B. Frijns, W. F. VerschoorVerschoor, and R. C. ZwinkelsZwinkels, "Excess stock return comovements and the role of investor sentiment," *Journal of International Financial Markets, Institutions and Money*, vol. 49, pp. 74–87, 2017.
- [24] H. Ashbaugh-SkaifeAshbaugh-Skaife, D. W. Collins, and W. R. Kinney, "The discovery and reporting of internal control deficiencies prior to SOX-mandated audits," *Journal of Accounting and Economics*, vol. 44, no. 1-2, pp. 166–192, 2007.
- [25] S. Dasgupta, J. Gan, and N. Gao, "Transparency, price informativeness, and stock return synchronicity: theory and evidence," *Journal of Financial and Quantitative Analysis*, vol. 45, no. 5, pp. 1189–1220, 2010.
- [26] R. Neal and S. Wheatley, "Adverse selection and bid-ask spreads: evidence from closed-end funds," *Journal of Financial Markets*, vol. 1, no. 1, pp. 121–149, 1998.
- [27] "R2," *The Journal of Finance*, vol. 43, no. 3, pp. 541–566, 1988.
- [28] C. S. Eun, L. Wang, and S. C. Xiao, "Culture and R2," *Journal of Financial Economics*, vol. 115, no. 2, pp. 283–303, 2015.
- [29] H. G. Huang, W. C. Tsai, P. S. Weng, and M. H. Wu, "Volatility of order imbalance of institutional traders and expected asset returns: evidence from Taiwan," *Journal of Financial Markets*, vol. 52, Article ID 100546, 2021.
- [30] Z. Yi and N. Mao, "Measurement study of China's stock market investor sentiment- construction of CICS1," *Finance Research*, vol. 11, pp. 174–184, 2009.

Research Article

Lightweight Fall Detection Algorithm Based on AlphaPose Optimization Model and ST-GCN

Hongtao Zheng and Yan Liu 

School of Information and Electrical Engineering, Zhejiang University City College, Hangzhou 310000, China

Correspondence should be addressed to Yan Liu; liuy@zucc.edu.cn

Received 9 May 2022; Accepted 9 June 2022; Published 11 July 2022

Academic Editor: Xuefeng Shao

Copyright © 2022 Hongtao Zheng and Yan Liu. This is an open access article distributed under the Creative Commons Attribution License, which permits unrestricted use, distribution, and reproduction in any medium, provided the original work is properly cited.

Falls cause great harm to people, and the current, more mature fall detection algorithms cannot be well-migrated to the embedded platform because of the huge amount of calculation. Hence, they do not have a good application. A lightweight fall detection algorithm based on the AlphaPose optimization model and ST-GCN was proposed. Firstly, based on YOLOv4, the structure of GhostNet is used to replace the Darknet53 backbone network of the YOLOv4 network structure, the path convergence network is converted into BiFPN (bidirectional feature pyramid network), and DSC (deep separable convolution) is used to replace the standard volume of spatial pyramid pool, BiFPN, and YOLO head network product. Then, the TensorRt acceleration engine is used to accelerate the improved and optimized YOLO algorithm. In addition, a new type of Mosaic data enhancement algorithm is used to enhance the pedestrian detection algorithm, improving the effect of training. Secondly, use the TensorRt acceleration engine to optimize attitude estimation AlphaPose model, speeding up the inference speed of the attitude joint points. Finally, the spatiotemporal graph convolution (ST-GCN) is applied to detect and recognize actions such as falls, which meets the effective fall in different scenarios. The experimental results show that, on the embedded platform Jeston nano, when the image resolution is 416×416 , the detection frame rate of this method is stable at about 8.33. At the same time, the accuracy of the algorithm in this paper on the UR dataset and the Le2i dataset has reached 97.28% and 96.86%, respectively. The proposed method has good real-time performance and reliable accuracy. It can be applied in the embedded platform to detect the fall state of people in real time.

1. Introduction

Falls can cause all kinds of trauma, which can be life-threatening in severe cases. Studies also show that nearly half of all falls worldwide lead to medical attention, decreased functioning, impaired social or physical activity, and even death [1, 2]. Medical surveys have shown that if timely treatment can be performed after a fall, the risk of death can be reduced by 80% and the survival rate can be significantly improved. However, all actions taken after a fall are less important than detecting a person's posture before they fall. Therefore, it is of great significance to quickly detect the occurrence of falls [3].

At present, the research on fall detection can be divided into three main categories: (1) detection methods based on environmental equipment [4–6], which are detected

according to the environmental noise formed when the human body falls, e.g., sensing the object's pressure and sound changes, are used to detect falls, however, this method has a higher false positive rate and is less likely to be adopted. (2) Detection methods based on wearable sensors [7–10], e.g., using accelerometers and gyroscopes, to detect falls, however, wearing sensors for a long time will affect people's comfort and increase the physical burden. The false positive rate is also higher for complex activities. (3) Detection methods based on visual recognition [11–15] can be divided into two categories: one is the traditional machine vision method to extract effective fall features. It requires low hardware requirements for the running platform, however, the robustness is not strong, and it is easily disturbed. The other type is artificial intelligence method, which uses the image captured by the image sensor for the training and

reasoning of the convolutional neural network, and the recognition accuracy can reach a high level. However, at the same time, this method also requires a high training environment configuration, which greatly limits the application and promotion of this method. At the same time, in recent years, many embedded devices have appeared, such as Jeston nano, Jeston NX, Jeston TX2. Relatively cheap and small embedded devices also have considerable computing power, which provides the possibility for the migration and deployment of artificial intelligence algorithms. Most of the methods currently on the market cannot run well on embedded devices. Hence, this paper proposes a fall detection algorithm to solve this problem.

The specific improvement of the algorithm in this paper is as follows:

- (1) In the early stage, to enhance the generalization ability of the dataset, the original mosaic data enhancement algorithm was improved and optimized, and a new mosaic data enhancement method was proposed.
- (2) To reduce the structural complexity of the target detection algorithm, and at the same time, ensure a better recognition accuracy for people at different levels of complexity, this paper improves the structure of YOLOv4 and proposes a structure of a novel object detection algorithm.
- (3) To improve the YOLO algorithm to a greater extent, this paper uses the TensorRt acceleration engine to accelerate.
- (4) To ensure the accuracy of the detection algorithm, the joint detection algorithm selected in this paper is AlphaPose, and at the same time, considering the need to migrate AlphaPose to embedded devices, this paper proposes an optimization method for the detection model of AlphaPose.
- (5) Introduce a spatiotemporal graph convolution algorithm as the actual detection of the fall state.

2. Related Work

At present, the most common and generally effective fall detection algorithm is the vision-based detection algorithm. Generally speaking, the overall operation logic of the vision-based detection algorithm is to first use the target detection algorithm to detect the pedestrians in the image and input the detection results into the joint point detection algorithms, such as AlphaPose and openpose, and finally according to the specific parameters of the joint points, the coordinates are combined with the behavioral state at the time of the fall to determine whether to fall.

2.1. Object Detection Algorithm Based on Pedestrian Detection. Traditional pedestrian detection methods mainly extract features manually. Tian et al. [16] propose a novel multiplex classifier model, which is composed of two multiplex cascades parts: Haar-like cascade classifier and shapelet cascade classifier. [17] proposed a histogram of oriented gradients

(HOG), which exploits the directionality of edges to describe the overall appearance of pedestrians. However, the extraction steps of this extraction method are cumbersome, and the calculation of the recognition algorithm is complicated, resulting in poor real-time performance.

Pedestrian detection has achieved rapid progress because of recent developments in deep learning research. At present, target detection algorithms based on deep learning can be roughly divided into two categories: (1) two-stage detection algorithms represented by R-FCN (region-based fully convolutional neural network) [18] and (2) YOLO as the representative single-stage detection method (you only look once) [19]. The two-stage detection method has high accuracy and poor real-time performance. The single-stage detection method has slightly lower accuracy but has good real-time performance and fast detection speed.

The two-stage detection method realizes the cascade structure, the network calculation amount increases, and the accuracy is correspondingly improved, however, the detection speed is sacrificed accordingly, and the real-time requirements cannot be met. The problem has not been fixed well since then, although it has worked hard to make up for this shortcoming. Regarding the single-stage detection method, Redmon et al. proposed YOLO (you only look once) [19] in 2016, which is the first single-stage detection method based on deep learning. It creatively combines candidate regions with target recognition, which solves the problem of low efficiency of two-stage target detection algorithms. Redmon and Farhadi then went on to propose YOLOv2 [20] and YOLOv3 [21], which significantly improved the detection performance and enabled the YOLO family of methods to be widely used in various tasks. In 2020, Bochkovskiy improved the network structure of YOLOv3 and proposed YOLOv4. YOLOv4 greatly improves detection accuracy while ensuring speed. More recently, Jocher proposed YOLOv5, which brings together other state-of-the-art technologies. Compared with YOLOv4, although the performance of YOLOv5 is slightly worse, it is more flexible and faster than Yolov4 and has certain advantages in rapidly deploying models.

2.2. Development of Joint Detection Algorithms. In human pose detection, there are two main methods of joint point detection: bottom-up and top-down. The bottom-up approach is represented by Openpose [22], which is an end-to-end detection algorithm based on convolutional neural networks, supervised learning, and an open-source library developed with caffe as the framework. It can realize pose estimation, such as human motion, facial expression, movement, and so on. It has excellent robustness for single and multiplayer. The algorithm, firstly, detects all human body joint points in the image and then distinguishes which human body the joint points belong to through the relationship between the joint points. Although this method has a faster operation speed, it is easily disturbed by nonhuman bodies. The top-down method is represented by AlphaPose [23], which is a multistage detection method. Firstly, target detection is performed to identify the human target in the

image and mark each human body area rectangle to exclude nonhuman interference, the detection of joint points for each human body area is very accurate, and the calculation speed is also fast.

2.3. Other Recommendations. Reference [24] proposed a multilayer dual LSTM network-based framework for multimodal sensor fusion to perceive and classify patterns of daily activities and highly shared events. Reference [25] proposed an optically anonymous image sensing system, which uses convolutional neural networks and autoencoders for feature extraction and classification to detect abnormal behaviors, which largely protects the privacy of the elderly. Reference [26] uses the two-dimensional image data to extract an effective image background through the frame difference method, Kalman filter, etc., and uses it as the input of KNN (K-nearest neighbor) classifier, which achieves an accuracy rate of 96%, and it is susceptible to variable factors. Reference [27] uses the two-dimensional image data to calculate optical flow information and sends it to VGG (visual geometry group) for feature extraction and classification of optical flow information to detect falls. In the literature [28], the feature information extracted by the CNN convolutional layer and the fully connected layer is sent to the long short-term memory (LSTM) network to train to extract the temporal correlation of human spatial actions and identify human behavior. LSTM needs to dynamically store and update data with limited real-time performance.

3. Materials and Methods

The basic flow of the fall detection algorithm in this paper is as follows: (1) regarding the training of the front weight file, the pedestrian dataset is collected by ordinary cameras and the new mosaic data enhancement method is used for data enhancement, and the target detection algorithm and the joint point detection algorithm are carried out, respectively. (2) Regarding the running process of the overall algorithm, the camera connected to Jeston nano captures real-time pedestrian images, uses the improved new YOLOv4 algorithm to accelerate the TensorRt engine to detect the target, and then converts the detection result to the tensor data structure to serialize the target image, invests in the Alphapose joint point detection algorithm optimized by the model, and finally, the spatiotemporal graph convolutional neural network ST-GCN uses the coordinates of the key points of the human skeleton extracted by AlphaPose as the model input and constructs a joint as the graph node. The temporal relationship of the same joint is the spatiotemporal graph of the graph edge, taking the natural connection of human bones and the time relationship of the same joint as the time-space diagram of the edge of the graph, so that the information is integrated in the spatiotemporal and spatial domains. The final result is obtained by combining the motion analysis research. The specific algorithm structure flow chart is shown in Figure 1.

3.1. Object Detection Algorithm Based on Pedestrian Detection. The mosaic method was first proposed in the YOLOv4 paper. This method is based on the CutMix (cutting and mixing) [29] method to expand the generated data enhancement algorithm. The two blue paths in Figure 2 are mentioned in the YOLOv4 paper. m_1 represents the original image input, m_4 represents the image four-in-one input, and the innovation of the mosaic algorithm in this paper is that an input form m_9 is added under these two paths, which represents the image nine-in-one input. Once input, the specific generation flow chart is shown in Figure 3. Compared with m_4 , m_9 greatly enriches the background of detected objects. In BN calculation, the data of 9 pictures can be calculated at a time, which makes the hardware resource requirements lower during training and can save more hardware resources.

The specific operation is as follows: the first step is to take the length and width (w, h) of the input image as a boundary value. Then, scale the image, where the x -axis and y -axis are, respectively, scaled to a certain multiple of k_x and k_y , whose formulas are as follows:

$$k_x = \text{Rand}(k_w, k_w + \Delta k_w), \quad (1)$$

$$k_y = \text{Rand}(k_h, k_h + \Delta k_h). \quad (2)$$

Among them, k_x and k_y are the minimum values of the length and width scaling multiples, respectively, and Δk_w and Δk_h are the lengths of the random size of the length-width scaling multiples, which are the hyperparameters. The Rand function is a random function.

The coordinates of the upper left corner and the lower right corner of the image after scaling are (A_i, B_i) and (a_i, b_i) , and these four unknowns are obtained by the following formulas:

$$A_i = \begin{cases} 0, & i = 1, 2, 3, \\ w \times k_1, & i = 4, 5, 6, \\ w \times k_2, & i = 7, 8, 9, \end{cases} \quad (3)$$

$$B_i = \begin{cases} 0, & i = 1, 4, 7, \\ h \times k_3, & i = 2, 5, 8, \\ h \times k_4, & i = 3, 6, 9, \end{cases}$$

$$c_i = A_i + w \times k_w,$$

$$d_i = B_i + h \times k_h.$$

Among them, k_1 and k_2 are the ratios of the distance between the upper left coordinate point and the 0 point of the two sets of images on the x -axis, except for the 0 point to the total width. Similarly, k_3 and k_4 are in the y -axis, except for the 0 point. k_3 and k_4 are the distance between the upper left coordinate point and the 0 point of the two sets of images and the total length ratio. The vertical dotted line in the figure is the picture width scale, accounting for one-tenth of the picture width, and the horizontal small dotted line is the picture length scale, accounting for one-tenth of the picture length. The first photo is of the same scale as the other eight photos, and the width and length are k_w and k_h times the original.

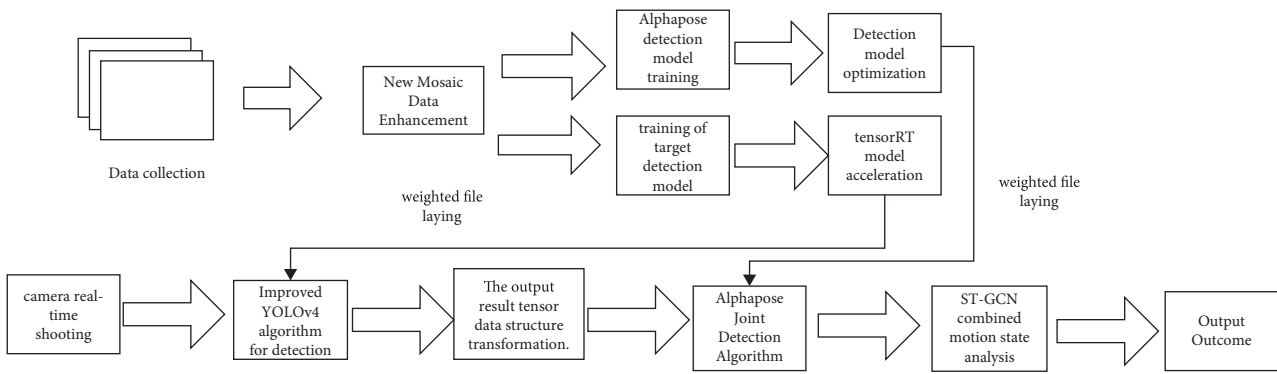


FIGURE 1: Magnetization as a function of the applied field. Note. “Fig.” is abbreviated.

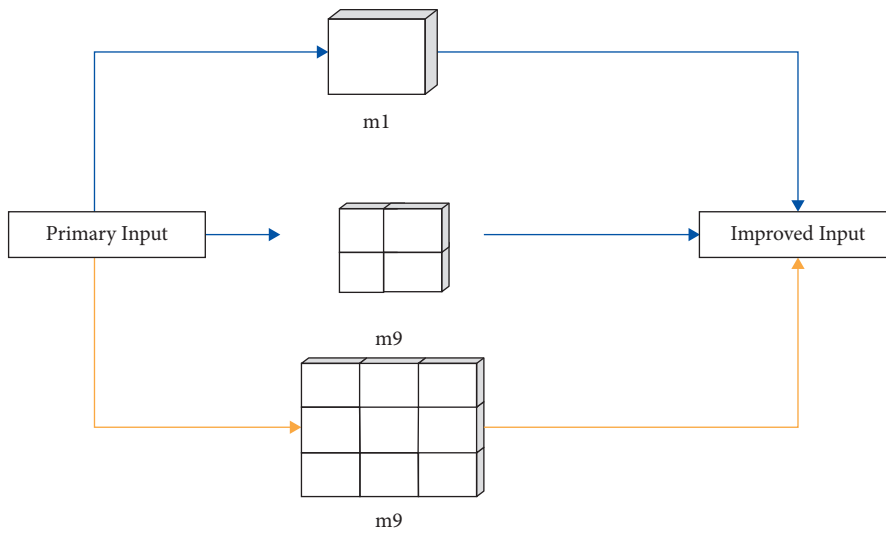


FIGURE 2: Improved mosaic data enhancement method.

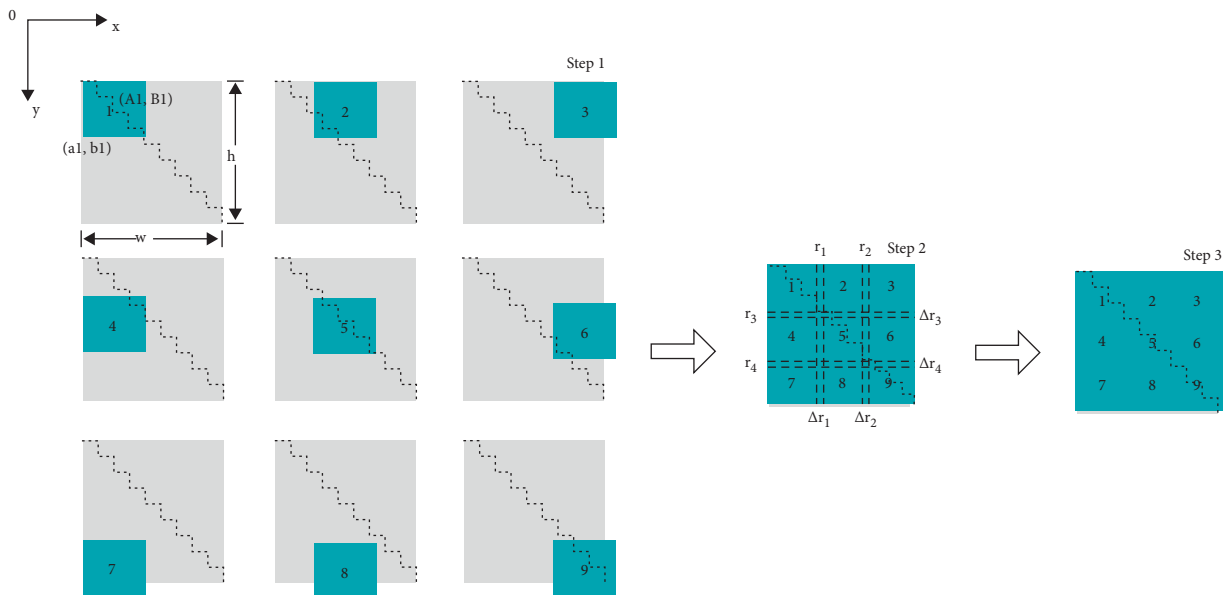


FIGURE 3: Mosaic nine-in-one data enhancement flowchart.

In step 2, flip, color gamut, and stitch the 9 photos cropped in the previous stage. Rely on the bounding box to limit the size of the stitched pictures, and crop the excess. There will be overlapping images. According to the schematic diagram of step 1 in Figure 3, the position of the small area needs to be reassigned, as shown in the following formula:

$$\begin{aligned} C'_i &= \begin{cases} C_i, & C_1 < w, \\ w, & C_1 \geq w, \end{cases} \\ D'_i &= \begin{cases} D_i, & D_1 < w, \\ h, & D_1 \geq w. \end{cases} \end{aligned} \quad (4)$$

After the edge is cropped, use eight parallel dashed lines (as shown in step 2) to enclose four square areas, and use them as a random area for segmentation; $k_1, k_2, k_3,$ and k_4 are the ratios of the coordinates of the segmentation line to the distance from the origin and the boundary. In the third stage, the inner overlapping part is to be cut for the second time, and the coordinate S_i of the dividing line can be obtained by the following formula:

$$S_i = \text{Rand}(k_i, k_i + \Delta k_i) \quad i = 1, 2, 3, 4. \quad (5)$$

After cropping, the m_9 image stitching is completed. Since there will be some missing content in scaling and splicing, the edge targets of the original image may be cropped. Hence, the real boxes of these targets need to be cropped to meet the needs of target detection.

3.2. Structure Optimization of Human Object Detection Algorithm. The original AlphaPose human target detection algorithm uses YOLOv3, however, YOLOv4 proposed in recent years has significantly surpassed YOLOv3 in terms of detection accuracy and detection speed. It can cope with more complex detection environments (such as complex light and occlusion). However, because of the large amount of calculation, it is not suitable to migrate to embedded devices. Therefore, the human target detection algorithm in this paper is improved on the basis of the YOLOv4 algorithm structure, which ensures high pedestrian detection accuracy and faster recognition of frames.

The improvement of the specific structure is as follows: (1) the structure of GhostNet [29] is adopted to replace the CSPDarknet53 backbone network in the YOLOv4 network structure, which realizes the simplification of the network while maintaining the accuracy. (2) Convert the path aggregation network into BiFPN (bidirectional feature pyramid network) [30] to shorten the path from low-level information to high-level information and build the residual structure of the feature pyramid network to integrate richer semantic features and save spatial information. (3) DSC (deep separable convolution) [31] is adopted to replace the standard convolution of spatial pyramid pooling. BiFPN and YOLO head the network, which greatly reduces the amount of computation and improves network performance. The improved YOLOv4 algorithm structure is shown in Figure 4.

3.2.1. Human Feature Extraction Based on Ghostnet. Since the CSPDarknet53 structure in YOLOv4 requires a large amount of computation while efficiently extracting image features, this paper chooses a lightweight network structure like the GhostNet. The core idea of GhostNet is to use some operations with lower computational cost to generate the same features. There are many similarities between the network feature layers, and the redundant part in the feature layer may be an important part. Hence, GhostNet saves redundant information and obtains feature information with a lower computational cost.

The convolution block of GhostNet is the Ghost Module. Its function is to replace ordinary convolution. It divides ordinary convolution into two parts. Firstly, a 1×1 ordinary convolution is performed. For example, the convolution of 32×32 channels is normally used. But the GhostNet network uses 16-channel convolutions, the function of this 1×1 convolution is similar to feature integration, generating the feature concentration of the input feature layer. Then, we perform a depthwise separable convolution, which is a layer-by-layer convolution that uses the previous step to perform features. Condensation generates ghost feature maps.

The network structure combined with the GhostNet is shown in Figure 1, in which GBN is represented as GhostNetBottleNeck, which is a component of GhostNet. The GhostNetBottleNeck bottleneck layer consists of two GhostModules. The first is used to expand the number of channels, and the second is used to reduce the number of channels, matching the number of channels connected to the input. When the input is 416×416 , the construction method of the GhostNet is shown in Table 1. When a picture is input into the GhostNet, we perform a 16-channel ordinary 1×1 convolution block (convolution + normalization + activation function). After that, the stacking of the ghost bottlenecks began. Using ghost bottlenecks, a $7 \times 7 \times 160$ feature layer was finally obtained (when the input was $224 \times 224 \times 3$). Then, a 1×1 convolution block is used to adjust the number of channels, and a $7 \times 7 \times 960$ feature layer can be obtained at this time. After that, a global average pooling is performed, and then a 1×1 convolution block is used to adjust the number of channels to obtain a $1 \times 1 \times 1280$ feature layer. Then, after tiling, the full connection can be performed for classification.

The operation of generating n feature images for any convolutional layer can be expressed as follows:

$$Y_0 = XO + b, \quad (6)$$

where $X \in R^{h \times c \times w}$, and $f \in R^{c \times k \times k \times m}$ is the convolution kernel of this layer. O represents the convolution operation, and b is the bias term. At this time, the feature map is as follows:

$$Y_0 \in R^{h' \times w' \times m'}. \quad (7)$$

The required floating-point number is $n \times h' \times w' \times c \times k \times k$. Assume that the ghost module contains an intrinsic feature map and $m \times (s - 1) = n/s \times (s - 1)$ linear transformation operations. The size of each operation kernel and the theoretical speedup of the ghost module upgrading the ordinary convolution are as follows:

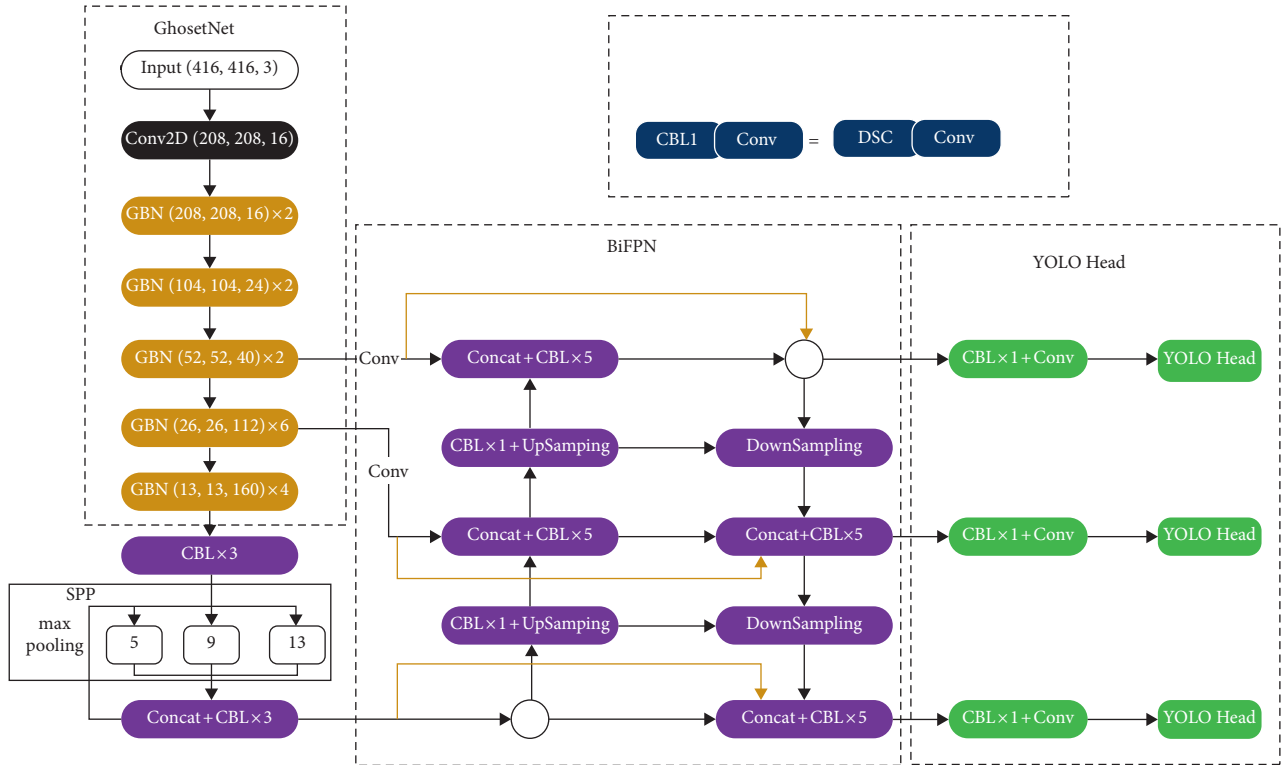


FIGURE 4: Improved structure of YOLOv4 algorithm.

TABLE 1: GhostNet construction method diagram.

Input	Operator	#exp	Out	SE	Stride
$416^2 \times 3$	Conv2d 3×3	—	16	—	2
$208^2 \times 16$	GBN	16	16	—	1
$208^2 \times 16$	GBN	48	24	—	2
$104^2 \times 24$	GBN	72	24	—	1
$104^2 \times 24$	GBN	72	40	1	2
$52^2 \times 40$	GBN	120	40	1	1
$52^2 \times 40$	GBN	240	80	—	2
$26^2 \times 80$	GBN	200	80	—	1
$26^2 \times 80$	GBN	184	80	—	1
$26^2 \times 80$	GBN	184	80	—	1
$26^2 \times 80$	GBN	480	112	1	1
$26^2 \times 112$	GBN	672	112	1	1
$26^2 \times 112$	GBN	672	160	1	2
$13^2 \times 160$	GBN	960	160	—	1
$13^2 \times 160$	GBN	960	160	1	1
$13^2 \times 160$	GBN	960	160	—	1
$13^2 \times 160$	GBN	960	160	1	1
$13^2 \times 160$	Conv2d 1×1	—	960	—	1
$13^2 \times 960$	AvgPool 7×7	—	—	—	—
$1^2 \times 960$	Conv2d 1×1	—	1280	—	1
$1^2 \times 1280$	FC	—	1000	—	—

$$\begin{aligned}
 r_c &= \frac{n \times h' \times w' \times c \times k \times k}{(n/s) \times h' \times w' \times c \times k \times k + (s-1) \times (n/s) \times h' \times w' \times d \times d} \\
 &= \frac{c \times k \times k}{(1/s) \times c \times k \times k + ((s-1)/s) \times d \times d} \approx \frac{s \times c}{s + c - 1} \approx s,
 \end{aligned} \tag{8}$$

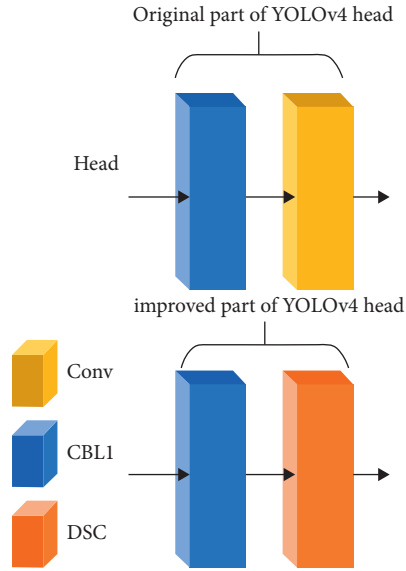


FIGURE 5: The modified part of CBL1 on the head of small-YOLOv4.

where $d \times d$ and $k \times k$ are similar. The theoretical parameter compression ratio is as follows:

$$r_c = \frac{n \times c \times k \times k}{n/s \times c \times k \times k + (s-1)/s \times n \times d \times d} \approx \frac{s \times c}{s + c - 1} \approx s. \quad (9)$$

The theoretical parameter compression ratio of replacing ordinary convolution with the ghost module is approximately equal to the theoretical speedup ratio.

3.2.2. Improving Panet with reference to BIFPN. BiFPN (bidirectional feature pyramid network) was first proposed in the paper of EffientDet [31], and the author proposed that its purpose was to pursue a more efficient multiscale fusion method.

YOLOV4's original PANet adds a bottom-up channel based on FPN, and its CNN backbone provides a long path from the bottom to the top through more than 100 layers. In BiFPN, the input nodes and output nodes of the same layer can be connected across layers to ensure that more features are incorporated without increasing the loss. This algorithm performs cross-layer connections on the same level of PANet (the three orange lines in Figure 4). In this way, the path from low-level information to high-level information can be shortened, and their semantic features can be combined together. In BiFPN, adjacent layers can be merged in series. In this paper, the adjacent layers of PANet are merged in series (the two blue lines in Figure 4).

The improved PANet has the characteristics of bidirectional cross-scale connection and weighted feature fusion, which improves the feature fusion ability and further increases the feature extraction ability.

3.2.3. DSC Replaces Standard Convolution. In the algorithm of this paper, the 1×1 standard convolutional network in the CBL1 module of the YOLOv4 head is replaced with DSC

(deep separable convolution), which further reduces the network computing cost in practical applications. The modified part of CBL1 is shown in Figure 5. The standard convolutional network calculation uses a weight matrix to realize the joint mapping of spatial dimension features and channel dimension features at the cost of high computational complexity, high memory overhead, and many weight coefficients.

DSC specifically divides the traditional convolution operation into two steps. Assuming that the original convolution is 3×3 , DSC is to first convolve M feature maps of M 3×3 convolution kernels one-to-one. M results are generated directly without summing. Then, the M results previously generated are normally convolved with N 1×1 convolution kernels, summed, and finally, N results are generated. Therefore, the literature [17] divides DSC into two steps, as shown in Figure 6 below. One step is called depthwise convolution, which is B in the figure below, and the other step is pointwise convolution, which is C in the figure below.

Assuming that the size of our input feature map is $D_F \times D_F$, the dimension is M , the size of the filter is $D_k \times D_k$, the dimension is N , and assuming that the padding is 1, the stride is 1. Hence, the original convolution operation requires the following number of matrix operations: $D_k \times D_k \times M \times N \times D_F \times D_F$. The parameter of the convolution kernel is $D_k \times D_k \times M \times N$, and the number of matrix operations that DSC needs to perform is $D_k \times D_k \times M \times D_F \times D_F + M \times N \times D_F \times D_F$. The parameter of the convolution kernel is $D_k \times D_k \times M + N \times M$. Since the convolution process is mainly a process of reducing spatial dimension and increasing channel dimensions, namely $N > M$, the convolution kernel parameter of standard convolution is larger than that of DSC. At the same time, the ratio of the parameter quantity of DSC to the standard convolution parameter quantity is as shown in equation (4).

From equation (4), we can get a convolution kernel with a size of 3×3 , which reduces the computation to 11.1% of the standard convolution.

3.3. Structure Optimization of Human Object Detection Algorithm. Commonly used model compression methods are as follows: network pruning, knowledge distillation, model quantization, etc. Since the network structure used in this paper is replaced by the lightweight GhostNet network, if the network continues to be pruned, it is very likely to destroy the integrity of the model and have a greater impact on the accuracy. Therefore, this paper uses model quantization to further reduce the number of parameters and model size.

The quantization method is further divided into quantization-aware training and post-training quantization. The post-training quantization method is divided into hybrid quantization, 8-bit integer quantization, and half-precision floating-point quantization. Post-training quantization directly quantizes the model after ordinary training. The process is simple, and there is no need to consider the quantization problem during the training process. The

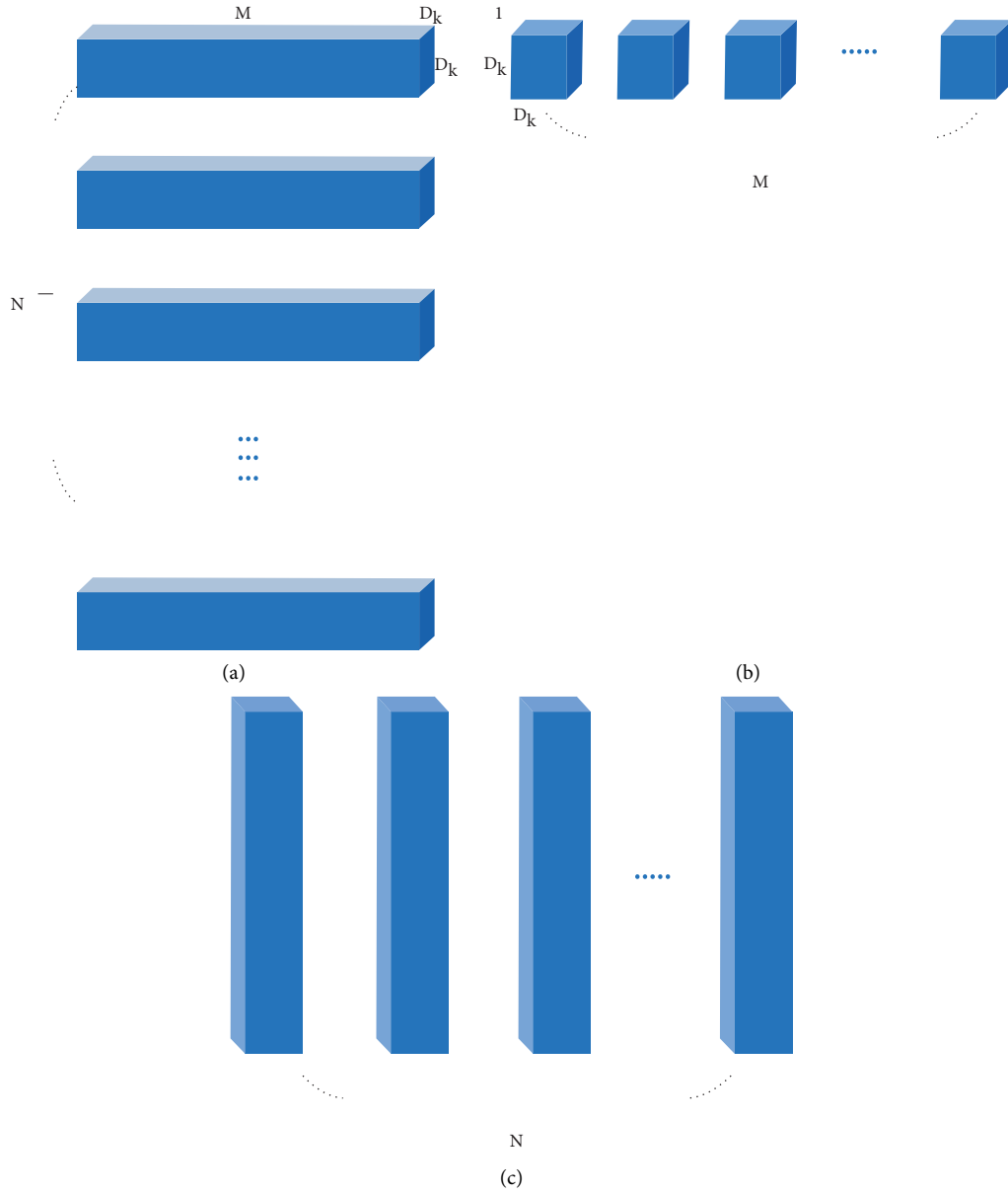


FIGURE 6: Structure diagram of DSC. (a) Stand convolution filters. (b) Depthwise convolution filters. (c) Depthwise separable convolution.

accuracy of the model with a large amount of parameter redundancy is lost.

This paper uses the TensorRT acceleration engine to convert the model weight file into an int8 type trt file using the post-training quantization method and performs overall optimization through a series of operations, such as tensor fusion, kernel adjustment, and multistream execution. Figure 7 is a schematic diagram of the overall optimization of TensorRT.

3.4. Structure Optimization of Human Object Detection Algorithm. After the detection result is obtained through the target detection algorithm, the detection result is converted into a 2-dimensional tensor data structure, and the specific data structure form is shown in equation (9).

$$T_d = [[x_1, y_1, w_1, h_1, c_1], [x_2, y_2, w_2, h_2, c_2], \dots, [x_i, y_i, w_i, h_i, c_i]], \quad (10)$$

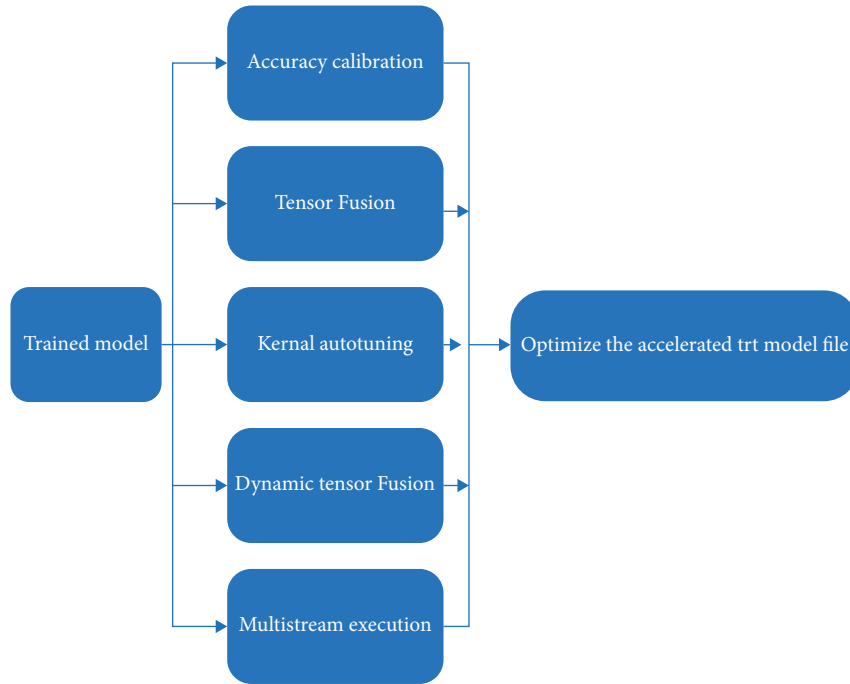


FIGURE 7: Schematic diagram of TensorRT optimization.

where $[x_i, y_i, w_i, h_i, c_i]$ represents the structured data of the i^{th} pedestrian, and x represents the upper left corner of the prediction box.

The original image T_m is transformed into a floating-point 32-bit tensor type data T_t . Hence, formula (1) represents a normalization operation on Im_t , where $T_t[0]$ is the R channel data of Im_t , G channel data of $T_t[1]$, and B channel data for $T_t[2]$.

$$\begin{cases} T_t[0]+ = -0.416, \\ T_t[1]+ = -0.461, \\ T_t[2]+ = -0.479. \end{cases} \quad (11)$$

According to T_d , the human body area images are cut out from the original images, and they are arranged in the descending order of confidence to obtain a serialized image list, which realizes the serialization of human body images and improved data interaction efficiency between the target detection model and the human joint point detection model.

3.5. Optimization of Algorithm Model for Pose Joint Point Detection. The algorithm of AlphaPose in the original text uses the Fast_Reset50-based network, and the optimization method is shown in Figure 8.

The pose joint point detection model inputs dummy network layer dimension initialization, and the dummy network layer input dimension is set to tensor type $(1, 3, H_{\text{dummy}}, W_{\text{dummy}})$, where 1 means that the batchsize is 1, 3 means the number of image channels, and $W_{\text{dummy}}, H_{\text{dummy}}$ indicates the network layer input image normalization scale. In this paper, $W_{\text{dummy}} = 160$ and $H_{\text{dummy}} = 224$. Customize the design for the input and output network layers of the dimensionally initialized model. The input layer

is set to input, and the output layer is set to output. Create a target detection model calculation graph, set the input dimension of the calculation graph to $(1, 3, W_d, H_d)$, where 1 means the batchsize is 1, 3 means the number of image channels, and W_d, H_d means the network layer input image normalization scale. $W_d = 160, H_d = 224$ in this paper. Load the model conversion optimizer to generate the pose joint detection optimization model AlphaPose-trt.

3.6. Spatial Temporal Graph Convolutional Networks for Skeleton-Based Action Recognition. Using the spatio-temporal graph convolutional network ST-GCN [32], using the coordinates of human skeleton key points output by the AlphaPose algorithm as model input, construct a graph node with joint points as the natural connection of the human skeleton and the same joints. The temporal relationship is a spatiotemporal graph of graph edges, so that information is integrated in the temporal and spatial domains.

The spatiotemporal graph convolutional neural network is divided into a spatial graph convolution and temporal graph convolution. Spatial graph convolution is to construct spatial graph convolution within frames based on the natural connectivity of human joints. Spatial graph convolution is to construct spatial graph convolution within the frame according to the natural connectivity of human joint points, which can be recorded as $G_s = (V_s, E_s)$, where $V_s = \{v_{ti} | i = 1, 2, \dots, N_s\}$ represents all the joint points in a skeleton, and $E_s = \{v_{ij} v_{ij} / (i, j) \in H\}$ represents the connection between the joint points. Each node is described by a feature vector $F(V_i)$ to describe the spatial feature, which is represented by the spatial graph convolution which is obtained. Temporal graph convolution connects the same nodes in consecutive multiframe images on the spatial graph to form

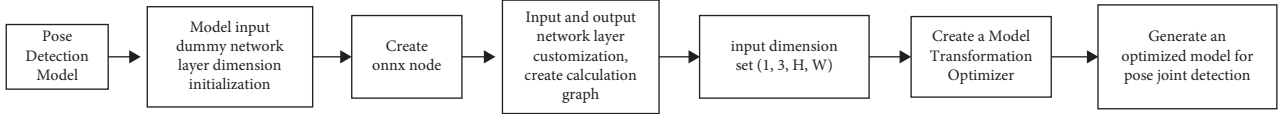


FIGURE 8: Optimization steps of AlphaPose detection model.

the spatial-temporal graph of the skeleton sequence, denoted as $G_T = (V_T, E_T)$. $V_T = \{v_{ij} | t = 1, 2, \dots, N_{ij}\}$ represents the joint point sequence of the same part, and $E_T = \{v_{ij}v_{(t+1)}\}$ represents the connection between them, as shown in Figure 9.

The spatiotemporal graph convolution algorithm combines the motion analysis research to divide the spatial graph into three subsets, which represent the features of centripetal motion, eccentric motion, and rest, respectively. The root node is the selected skeleton joint point itself, including static features. Connecting the neighbor nodes closer to the center of gravity of the skeleton than the root node includes centripetal motion features. Connecting the neighbor nodes farther from the root node than the center of gravity of the skeleton includes centrifugal motion features. The three subset convolution results express action features at different scales, respectively.

The spatiotemporal graph convolutional neural network model takes the joint coordinate vector of the graph node as input and extracts deeper features through the 9-layer ST-GCN convolution module. The feature dimension of each node is 256, and the key frame dimension is 38. Then, the obtained tensors are globally pooled, and backpropagation is used to train the model end-to-end. Finally, the SoftMax classifier obtains the corresponding action category probability and outputs the action with the highest probability. Each ST-GCN layer adopts the Resnet structure to enhance the gradient propagation and adds a dropout strategy to the ST-GCN layer to solve the gradient explosion problem. The overall flow of the model is shown in Figure 10.

4. Experiments and Analysis

4.1. Dataset Analysis. The datasets used for training in this experiment mainly include 20 categories of VOC2007 and VOC2012, and 10,000 datasets of people that the author randomly collected. Through the program, VOC2012 and VOC2007 only retain the label information of this category. The dataset of 10,000 people collected by the author is divided into the training set, validation set, and test set according to the ratio of 6:2:2. The final number of images is shown in Table 2.

4.2. Anchor Box. To be more suitable for the category of person, the prior frame in the improved target detection algorithm in this paper is obtained by the K-means clustering dataset method. The image input in this paper adopts 416×416 , and the clustering iteration reaches 73 times. The union ratio of the box and the prior box reaches 78.91%, and nine a priori boxes are obtained, as shown in Table 3.

4.3. Training and Operation Environment. The model training platform in our laboratory is RTX 3090, video memory 24G, etc. The specific parameters are shown in Table 4. The network model is trained on the deep learning framework of Tensorflow2.5 based on GhostNet and CSPDarknet53. All input images are of size 416×416 . The follow-up effect verification and testing platform of the experiment is with Jeston nano.

4.4. Evaluation Criteria. We use FPS, precision, mAP, accuracy, F-score, sensitivity, specificity, and other indicators to evaluate our proposed method. The test set is divided into two categories, one is positive samples and the other is negative samples. TP is the number of positive samples predicted as positive samples. FP is the number of negative samples predicted as positive samples. FN is the number of predicted positive samples as negative samples. TN is the number of predicted negative samples as negative.

4.4.1. FPS (Frames per Second). The evaluation standard of detection speed used in this paper is FPS, which refers to the number of frames per second. The larger the FPS, the more frame rates the American Standard transmits, and the smoother the displayed image. To meet the real-time requirements of human body detection, the larger the FPS value, the smoother the picture seen, and the better the effect.

4.4.2. mAP (Mean Average Precision). The definition of the mAP is shown in equation (12), which represents the average value of the average precision APi of n types of targets, and $n = 1$ in this experiment.

$$\text{mAP} = \frac{\sum AP}{N(\text{Class})} = \sum AP. \quad (12)$$

4.4.3. Accuracy. Accuracy is a commonly used evaluation index. Generally speaking, the higher the accuracy rate, the better the classifier.

$$\text{Accuracy} = \frac{TP + TN}{TP + TN + FP + FN}. \quad (13)$$

4.4.4. Precision. Precision can measure the accuracy of object detection, specifically defined as shown in equation (14) below.

$$\text{precision} = \frac{TP}{TP + FP}. \quad (14)$$

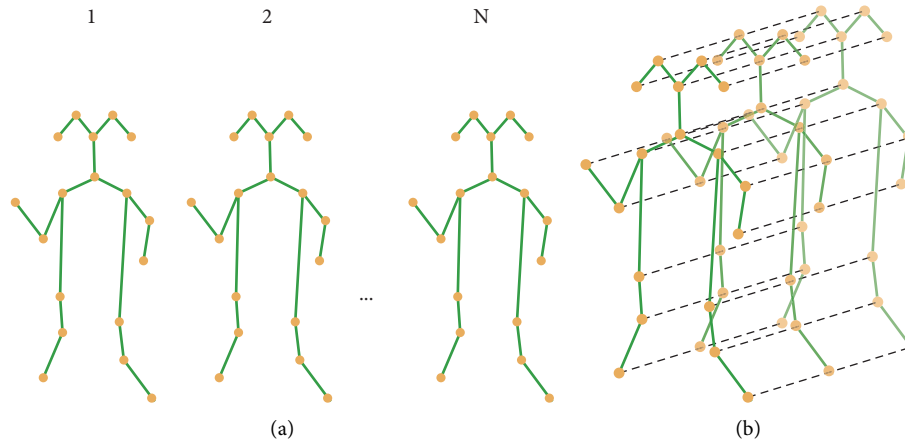


FIGURE 9: Construction of the spatio-temporal map of human joint points. (a) Bone space map sequence of N frames. (b) Skeleton space time-diagram (arrows indicate time series edges).

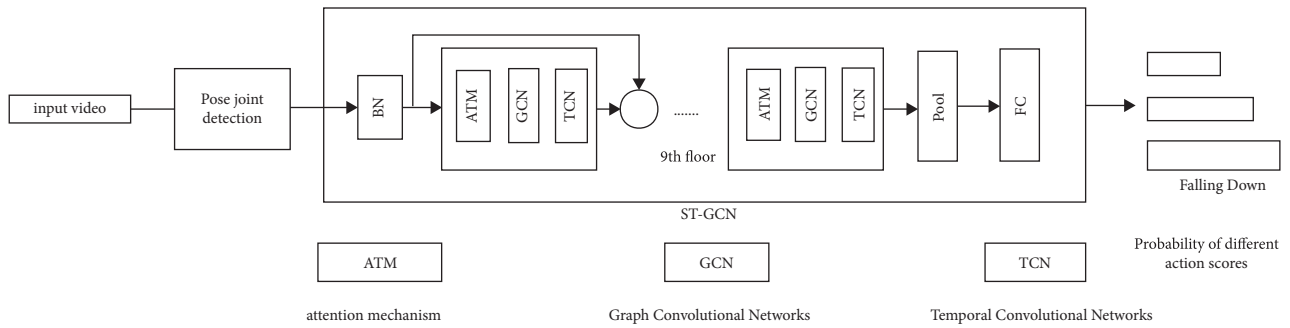


FIGURE 10: The overall framework of ST-GCN.

TABLE 2: The number of various data sets.

Types of data sets	Total number
Training sets	14265
Test sets	4765
Validation set	4755

TABLE 3: A priori frame size.

Size	Anchor box
13×13	(234, 280), (260, 379), (377, 354)
26×26	(107, 270), (135, 351), (171, 190)
52×52	(27, 44), (60, 121), (75, 230)

TABLE 4: Software and hardware configuration.

Component	Configuration
Operating system	Ubuntu 18.04
Memory	64
GPU	Nvidia GeForce RTX 3090
GPU acceleration library	CUDA 11.2 cuDNN v8.2.1
Deep learning framework	Tensorflow2.5
Programming language	Python3.9

4.4.5. *F-Score*. The *F-Score* indicator combines the results of precision and recall outputs. The value of *F-Score* ranges from 0 to 1, where 1 represents the best output result of the model, which is specifically defined as shown in equation (15) below.

$$F - \text{score} = \frac{2TP}{2TP + FP + FN} \quad (15)$$

4.4.6. *Sensitivity*. Sensitivity represents the sensitivity, which represents the predictive ability of positive examples (the higher, the better), and it is numerically equal to the recall rate, which is specifically defined as shown in equation (16) below.

$$\text{Sensitivity} = \frac{TP}{TP + FN} \quad (16)$$

4.4.7. *Specificity*. Sensitivity represents the predictive power of positive examples (higher is better), and the specific definition is shown in equation (17) below.

TABLE 5: The influence of mosaic data enhancement method on target recognition accuracy under different proportions.

Algorithm type	$m_1 : m_4 : m_9$	Dim light (%)	Chaotic environment mAP (%)	Human body occlusion mAP (%)
Algorithm in this paper	1 : 0 : 0	72.28	71.54	75.55
	0 : 1 : 0	60.11	65.58	66.18
	0 : 0 : 1	41.74	50.69	50.10
	1 : 1 : 0	72.45	71.99	75.10
	1 : 0 : 1	70.71	70.24	73.56
	1 : 1 : 1	72.19	71.58	76.01
	2 : 2 : 1	76.28	76.68	78.10
	2 : 1 : 1	72.27	70.44	73.56
	3 : 2 : 1	72.78	72.57	76.15
	4 : 2 : 1	73.35	72.16	74.20
	4 : 3 : 2	72.80	72.01	75.98
	5 : 3 : 2	74.01	74.48	77.52
	YOLOv4	1 : 1 : 0	75.90	75.56

$$\text{Specificity} = \frac{\text{TN}}{\text{TN} + \text{FP}} \quad (17)$$

4.5. Evaluation Criteria

4.5.1. A Novel Mosaic Data Augmentation Method. The new Mosaic data enhancement method in this paper is used to enhance the dataset, and the image input ratio of the three paths of m_1 , m_4 , and m_9 in Figure 2 that can maximize the accuracy of identifying complex situations is a problem that needs to be discussed. Table 5 below shows the influence of different input ratios of m_1 , m_4 , and m_9 on the accuracy of human recognition in three complex situations of dim light, chaotic environment, and human occlusion in the dataset. It can be seen from this table that when m_1 , m_4 , and m_9 ratio is 2 : 2 : 1, the effect of data enhancement is most obvious.

4.5.2. Target Detection Algorithm Network Improvement Effectiveness. To verify the impact of the improvement of the target detection algorithm on the performance of the YOLOv4 model, the above three improved methods were designed for ablation experiments on Jeston nano for more adequate comparison, thus proving the necessity and effectiveness of the proposed method. Among them, “+” indicates that the improved method is used in the experiment, “-” indicates that the method is not used, and the test indicators in this table refer to the detection effect of the human body in the test set of this paper. As can be seen from Table 6, after replacing the backbone network with the GhostNet, although the mAP value for the identification of person categories has been slightly reduced, the running frame rate has been significantly improved. After the introduction of BiFPN, the running frame rate has basically not changed, however, the mAP value has been greatly improved. Using the depthwise separable convolution to replace the ordinary convolution in the original YOLOv4 head, the running frame rate is significantly improved while the mAP value is slightly reduced. Compared with YOLOv4, the improved network structure has a slight decrease in the mAP value for the detection effect of Person, however, at the same time, the running frame rate has been significantly

improved, which meets the basic ability of running on embedded devices. Finally, we chose to use the TensorRt framework to accelerate, and after using the TensorRt framework, the runnable frame rate was greatly improved, while the mAP value remained basically unchanged.

4.5.3. Comparison of Optimization Effectiveness of AlphaPose Algorithm Model. To verify the effectiveness of the AlphaPose algorithm model optimization method in this paper, this paper chooses to compare the effects of three models, including openpose, AlphaPose, and AlphaPose-trt. The mAP value in this paper is the human detection effect for the test set of this paper. The results of running on Jeston nano are shown in Table 7 below. It can be seen from Table 7 that the frame rate of openpose is lower than that of AlphaPose, while the mAP value is also lower than that of AlphaPose. Compared with the original model (AlphaPose), the optimized model (AlphaPose-trt) has a stable mAP value and greatly improves the running frame rate.

4.5.4. Comparison of Effectiveness of Fall Detection Algorithms. Because of the need to further demonstrate the overall advantages of the algorithm in this paper in detection accuracy and running frame rate, we need to compare the algorithm in this paper with other computer vision algorithms of the same type, however, considering that many of the more popular algorithms are not open source, it is impossible to migrate to Jeston nano to run. Hence, the selected comparison algorithms cannot have an accurate running frame rate, however, after analyzing the structure of these algorithms, it can be concluded that these algorithms are computationally complex and require a large number of calculations, and they do not have the ability to migrate to embedded devices. The final results are shown in Table 8. The data in this table is analyzed, and various evaluation data for human fall detection are tested in the Le2i fall and UR fall datasets, respectively. Compared with this paper, the literature [33] has achieved better results. The reason for the F1-score is because they employ a two-pass ensemble, using two classifiers, including random forest (RF) and multilayer perceptron (MLP), to identify falls, however, it leads to more

TABLE 6: Ablation study on the people dataset.

	GhostNet	Bi-FPN	DSC	TensorRt	mAP (%)	FPS
YOLOv4	-	-	-	—	87.27	2.35
	+	-	-	—	86.38	6.32
	-	+	-	—	87.40	2.23
	-	-	+	—	86.51	3.12
	+	+	-	—	87.08	6.13
	+	+	+	—	86.81	8.02
Our method	+	+	+	+	86.81	24.33

TABLE 7: The report posture detection model performance comparisons.

Pose estimation model	Frame rate	mAP (%)	Resolution of the image
Openpose	3.66	71.11	416 × 416
AlphaPose	7.72	82.12	416 × 416
AlphaPose-trt	13.13	82.05	416 × 416

TABLE 8: Comparison of different fall detection algorithms.

Algorithm type	Dataset	Accuracy (%)	Precision (%)	Sensitivity (%)	Specificity (%)	F-score	FPS
Wang et al. [33]	Le2i fall	96.91	97.65	96.51	97.37	97.08	—
Chamle et al. [35]	Le2i fall	79.31	79.41	83.47	73.07	81.39	—
Our method	Le2i fall	96.86	97.01	96.71	96.81	96.77	8.33
Wang et al. [33]	UR fall	97.33	97.78	97.78	96.67	97.78	—
Harrou et al. [34]	UR fall	96.66	94	100	94.93	96.91	—
Our method	UR fall	97.28	97.15	97.43	97.30	97.29	8.33

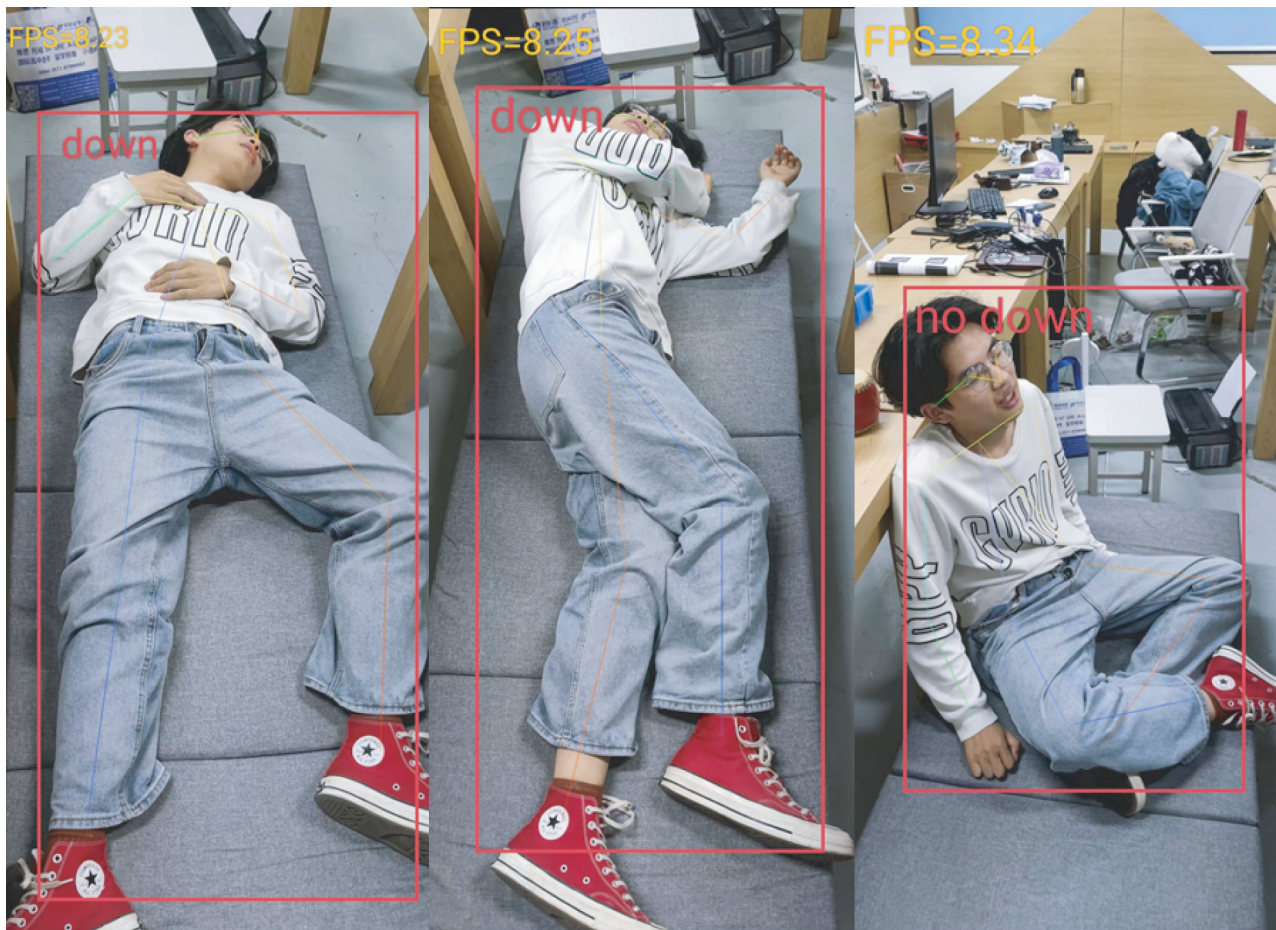


FIGURE 11: Effect diagram of experimental results.

computational complexity. It may also take more time from the classifier to the ensemble result, which leads to the poor real-time and transferability of the detection method. In contrast, the F1-score of the algorithm in this paper is slightly lower than that of [33]. At the same time, the real-time performance and migration are excellent. Compared with the methods of [34, 35] under the same dataset, the algorithm in this paper also has advantages in migration and real-time performance, and it also achieves a better balance in the two indicators of sensitivity and specificity. The results of analyzing the two validation datasets are similar, which further proves the stability of the algorithm in this paper. Figure 11 shows the detection results of the fall detection algorithm in this paper.

5. Conclusions and Future Work

This paper mainly studies the fall detection method based on computer vision technology. This method combines YOLO, AlphaPose, and ST-GCN. Through YOLO and AlphaPose, the key points and position information of the human body are obtained then output the recognition result through the spatiotemporal graph convolutional network. ST-GCN takes the output coordinates of the key points of human skeleton as a model input and constructs a spatiotemporal graph with joint points as graph nodes, natural connections of human skeletons, and the temporal relationship of the same joints as graph edges, so that the information is in the time and space domains that are integrated together.

The experimental results show that the method is transferable. In this paper, the improvement and optimization of the YOLOv4 algorithm and the effectiveness of the detection model optimization of AlphaPose are obtained under the running test of VOC07 + 12 and the self-made dataset. In addition, through the more popular fall detection algorithm in recent years and the test and verification of the algorithm in this paper in the UR Fall dataset, it is concluded that the algorithm in this paper has a high running frame rate on the basis of the detection accuracy, which is not much different from other algorithms, and it has better mobility and better adaptability in embedded devices.

In the future, we will focus more on complex fall detection and multiperson detection, such as outdoor fall detection and crowd trampling. At the same time, combined with the high applicability of embedded devices, we will integrate algorithms into real life, such as fall detection algorithms and monitoring systems. At the same time, there are many details that need to be improved for the operation effect of the algorithm in this paper, and we will continue to work hard.

Data Availability

The datasets used to support the findings of this study are available from the authors upon reasonable request.

Conflicts of Interest

The authors declare that they have no conflicts of interest.

Acknowledgments

This work received support from the Industry University Research Innovation Fund of Science and Technology Development Center of the Ministry of Education (No. 2021JQR004), Public Welfare Projects in Zhejiang Province (No. LGF20F030002), Project of Hangzhou Science and Technology Bureau (No. 20201203B96), 2021 National Innovation Training Project for College Students (No. 202113021008), The Ministry of Education Industry-University Cooperation Collaborative Education Project (202102019039), and Zhejiang University City College Scientific Research Cultivation Fund Project (J-202223). It is supported by the Zhejiang University Student Science and Technology Innovation Activity Plan (Xinmiao Talent Plan), project number: 2021R437010.

References

- [1] J. Gutiérrez, V. Rodríguez, and S. Martin, "Comprehensive review of vision-based fall detection systems," *Sensors*, vol. 21, no. 3, p. 947, 2021.
- [2] M. Mubashir, L. Shao, and L. Seed, "A survey on fall detection: principles and approaches," *Neurocomputing*, vol. 100, pp. 144–152, 2013.
- [3] P. Pierleoni, A. Belli, L. Palma, M. Pellegrini, L. Pernini, and S. Valenti, "A high reliability wearable device for elderly fall detection," *IEEE Sensors Journal*, vol. 15, no. 8, pp. 4544–4553, 2015.
- [4] M. Alwan, P. J. Rajendran, and S. Kell, "A smart and passive floor-vibration based fall detector for elderly," in *Proceedings of the Information & Communication Technologies*, Ictta. IEEE, Berkeley, CA, USA, May 2006.
- [5] Y. Zigel, D. Litvak, and I. Gannot, "A method for automatic fall detection of elderly people using floor vibrations and sound-proof of concept on human mimicking doll falls," *IEEE Transactions on Biomedical Engineering*, vol. 56, no. 12, pp. 2858–2867, 2009.
- [6] S. M. Khan, M. Yu, P. Feng, L. Wang, and J. Chambers, "An unsupervised acoustic fall detection system using source separation for sound interference suppression," *Signal Processing: The Official Publication of the European Association for Signal Processing (EURASIP)*, vol. 110, 2015.
- [7] J.-S. Lee and H.-H. Tseng, "Development of an enhanced threshold-based fall detection system using smartphones with built-in accelerometers," *IEEE Sensors Journal*, vol. 19, no. 18, pp. 8293–8302, 2019.
- [8] X. Xi, W. Jiang, and L. ü Zhong, "Daily activity monitoring and fall detection based on surface electromyography and plantar pressure," *Complexity*, vol. 2020, Article ID 9532067, 12 pages, 2020.
- [9] O. Kerdjidi, N. Ramzan, and K. Ghanem, "Fall detection and human activity classification using wearable sensors and compressed sensing," *Journal of Ambient Intelligence and Humanized Computing*, vol. 11, 2019.
- [10] S. Angela and J. José Vargas-Bonilla, "Real-life/real-time elderly fall detection with a triaxial accelerometer[J]," *Sensors*, vol. 18, no. 4, p. 1101, 2018.
- [11] S. G. Miaou, P. H. Sung, and C. Y. Huang, "A customized human fall detection system using omni-camera images and personal information," in *Proceedings of the Conference on Distributed Diagnosis & Home Healthcare*, IEEE, Arlington, Virginia, April 2006.

- [12] F. Merrouche and N. Baha, "Depth camera based fall detection using human shape and movement," in *Proceedings of the IEEE International Conference on Signal & Image Processing*, IEEE, Beijing, China, September 2017.
- [13] K. H. Chen, Y. W. Hsu, and J. J. Yang, "Enhanced characterization of an accelerometer-based fall detection algorithm using a repository," *Instrumentation Science & Technology: Designs and applications for chemistry, biotechnology, and environmental science*, vol. 45, 2017.
- [14] W. N. Lie, A. T. Le, and G. H. Lin, "Human fall-down event detection based on 2D skeletons and deep learning approach," in *Proceedings of the 2018 International Workshop on Advanced Image Technology (IWAIT)*, IEEE, Chiang Mai, Thailand, January 2018.
- [15] A. Lotfi, S. Albawendi, H. Powell, K. Appiah, and C. Langensiepen, "Supporting independent living for older adults; employing a visual based fall detection through analysing the motion and shape of the human body," *IEEE Access*, vol. 6, pp. 70272–70282, 2018.
- [16] H. Tian, Z. Duan, and A. Abraham, "A novel multiplex cascade classifier for pedestrian detection," *Pattern Recognition Letters*, vol. 34, no. 14, pp. 1687–1693, 2013.
- [17] N. Dalal and B. Triggs, "Histograms of oriented gradients for human detection," in *Proceedings of the 2005 IEEE Computer Society Conference on Computer Vision and Pattern Recognition (CVPR'05)*, pp. 886–893, IEEE, San Diego, CA, USA, June 2005.
- [18] J. Dai, Y. Li, and K. He, "Object detection via region-based fully convolutional networks," *Advances in Neural Information Processing System*, vol. 29, 2016.
- [19] J. Redmon, S. Divvala, R. Girshick, and A. Farhadi, "You only look once: unified, real-time object detection," in *Proceedings of the 2016 IEEE Conference on Computer Vision and Pattern Recognition*, pp. 779–788, IEEE, Las Vegas, NV, USA, June 2016.
- [20] J. Redmon and A. Farhadi, "Yolo9000: better, faster, stronger," in *Proceedings of the IEEE conference on computer vision and pattern recognition*, pp. 7263–7271, Honolulu, HI, USA, July 2017.
- [21] J. Redmon and A. Farhadi, "Yolov3: an incremental improvement," 2018, <https://arxiv.org/abs/1804.02767>.
- [22] H.-S. Fang, S. Xie, Y.-W. Tai, and C. Lu, "RMPE: regional multi-person pose estimation," in *Proceedings of the 2017 IEEE International Conference on Computer Vision (ICCV)*, pp. 2353–2362, Venice, Italy, October 2017.
- [23] Z. Cao, T. Simon, S. Wei, and Y. Sheikh, "Realtime multi-person 2D pose estimation using Part Affinity fields," in *Proceedings of the 2017 IEEE Conference on Computer Vision and Pattern Recognition (CVPR)*, pp. 1302–1310, Honolulu, HI, USA, July 2017.
- [24] H. Li, A. Shrestha, and H. Heidari, "Bi-LSTM network for multimodal continuous human activity recognition and fall detection," *IEEE Sensors Journal*, vol. 20, no. 3, pp. 1191–1201, 2019.
- [25] C. Ma, A. Shimada, H. Uchiyama, H. Nagahara, and R.-i. Taniguchi, "Fall detection using optical level anonymous image sensing system," *Optics & Laser Technology*, vol. 110, pp. 44–61, 2019.
- [26] K. De Miguel, A. Brunete, M. Hernando, and E. Gamba, "Home camera-based fall detection system for the elderly," *Sensors*, vol. 17, no. 12, p. 2864, 2017.
- [27] A. Núñez-Marcos, G. Azkune, and I. Arganda-Carreras, "Vision-based fall detection with convolutional neural networks," *Wireless Communications and Mobile Computing*, vol. 2017, no. 1, pp. 1–16, 2017.
- [28] H. Gammulle, S. Denman, and S. Sridharan, "Two stream LSTM: a deep fusion framework for human action recognition," in *Proceedings of the 2017 IEEE Winter Conference on Applications of Computer Vision*, pp. 24–31, Piscataway: IEEE, Honolulu, HI, USA, July 2017.
- [29] Y. Yang, G. Xie, and Y. Qu, "Real-time detection of aircraft objects in remote sensing images based on improved YOLOv4," in *Proceedings of the 2021 IEEE 5th Advanced Information Technology, Electronic and Automation Control Conference (IAEAC)*, vol. 5, pp. 1156–1164, Chongqing, China, March 2021.
- [30] M. Tan, R. Pang, and Q. V. Le, "EfficientDet: scalable and efficient object detection," in *Proceedings of the 2020 IEEE/CVF Conference on Computer Vision and Pattern Recognition (CVPR)*, pp. 10778–10787, Seattle, Washington, USA, June 2020.
- [31] F. Chollet, "Xception: deep learning with depthwise separable convolutions," in *Proceedings of the IEEE conference on computer vision and pattern recognition*, pp. 1251–1258, Honolulu, HI, USA, July 2017.
- [32] S. Yan, Y. Xiong, and D. Lin, "Spatial temporal graph convolutional networks for skeleton-based action recognition," 2018, <https://arxiv.org/abs/1801.07455>.
- [33] B.-H. Wang, J. Yu, K. Wang, X.-Y. Bao, and K.-M. Mao, "Fall detection based on dual-channel feature integration," *IEEE Access*, vol. 8, pp. 103443–103453, 2020.
- [34] F. Harrou, N. Zerrouki, Y. Sun, and A. Houacine, "An integrated vision-based approach for efficient human fall detection in a home environment," *IEEE Access*, vol. 7, pp. 114966–114974, 2019.
- [35] M. Chamle, K. G. Gunale, and K. K. Warhade, "Automated unusual event detection in video surveillance," in *Proceedings of the International Conference on Inventive Computation Technologies. (ICICT)*, pp. 1–4, IEEE, Bangkok, Thailand, August 2016.

Research Article

Improvement and Optimization of a 3D Reconstruction Algorithm for SEM Images of Porous Materials

Cheng Cheng ¹, Ning Dai,² and Tao Tang¹

¹College of Aeronautical Engineering, Nanjing Vocational University of Industry Technology, Nanjing 210046, China

²College of Mechanical and Electrical Engineering, Nanjing University of Aeronautics and Astronautics, Nanjing 210016, China

Correspondence should be addressed to Cheng Cheng; 2018100891@niit.edu.cn

Received 5 May 2022; Accepted 17 June 2022; Published 11 July 2022

Academic Editor: Xuefeng Shao

Copyright © 2022 Cheng Cheng et al. This is an open access article distributed under the Creative Commons Attribution License, which permits unrestricted use, distribution, and reproduction in any medium, provided the original work is properly cited.

Porous materials have become increasingly common in people's daily lives as the industry has advanced. Porous materials have numerous applications in the petroleum and chemical industries, as well as in everyday life. The study of diffusion, thermal conductivity, and percolation properties of porous materials has an important engineering application background and scientific value. The microstructure of materials affects their properties and attributes, so the description and visualization of the microstructure of porous materials is of great importance in the study of materials science. Due to the specificity of the internal structure of porous materials, many scenarios require 3-dimensional reconstruction of porous materials in practical engineering. In order to improve the effect of 3-dimensional reconstruction of porous materials, a 3D reconstruction method based on the improved generative adversarial neural network (GAN) is proposed in this paper for SEM images of porous materials. First, scanning electron microscope (SEM) images of porous materials are acquired, and then the acquired SEM images are pre-processed, including denoising and determining the boundary. Second, an improved GAN-based image super-resolution reconstruction model (ISRGAN) is used, and then the preprocessed images are fed into the ISRGAN model for training. Thus, multiple intermediate layer images are generated. Third, the 3D reconstruction of the intermediate layer images is performed using the slice combination method. The relationship between the unit cell pixels and the porosity is analyzed in the experiments to verify the effectiveness of the 3D reconstruction method used in this paper, and it is concluded that the porosity tends to be stable when the unit cell pixels converge to 110 and converge to the porosity of the real sample. The experimental results validate the feasibility and effectiveness of the method presented in this paper in the 3D reconstruction process.

1. Introduction

Porous materials are commonly found all around us, and the material plays a significant role in structure, cushioning, vibration damping, insulation, sound dissipation, and filtration. High porosity solids have low rigidity and high density, so naturally porous solids are often used as structural bodies, such as wood and bone. Humans have also developed many functional uses for porous material use. The study of porous materials began with zeolites. Zeolite is an ore that was first discovered in 1756. Cronstedt, a Swedish mineralogist, discovered a class of natural silica-aluminate ores that boil when burned. Molecular sieves have a homogeneous microporous structure and have a preferential adsorption capacity for polar and saturated molecules. As a

result, molecules with different degrees of polarity, saturation, molecular size, and boiling point can be separated. The relative pore content of porous materials is variable. According to the pore size, below 2 nm is called microporous, 2 nm–50 nm is mesoporous, and above 50 nm is called macroporous. It can also be divided into porous metal, porous ceramic, porous plastic, etc. based on the material. Also, based on the size of porosity, it can be divided into low and medium porosity materials and high porosity materials. The former is mostly closed type, and the latter will present three types, which are honeycomb material, open cell foam material, and closed cell foam material. Porous material is a composite composed of solid phase, and pores are formed through the solid phase, and the most distinctive feature that distinguishes it from ordinary dense solid materials is the

presence of useful pores. The most basic parameters of porous materials are the indicators that directly characterize their pore properties, such as porosity, pore size, and specific surface area. In addition, the properties of porous materials also depend heavily on the pore morphology, pore size, and its distribution.

The microstructure of porous materials is very important for engineering analysis as well as practical engineering applications, and traditional two-dimensional images cannot meet the engineering needs. Therefore, 3D reconstruction techniques based on porous materials are widely studied. Three-dimensional reconstruction is the process of recovering three-dimensional space from a two-dimensional image using a primitive map, that is, studying the relationship between the three-dimensional coordinates of points, lines, and surfaces in three-dimensional space and the two-dimensional coordinates of corresponding points, lines, and surfaces in two-dimensional image in order to achieve quantitative analysis of the object's size and the fold mutual position relation. Currently, the main imaging techniques are computed tomography (CT) technology [1, 2], SEM [3, 4], focused ion beam-scanning electron microscopy (FIB-SEM) [5, 6], and nuclear magnetic imaging (MRI) [7, 8]. Compared to the images produced by other imaging techniques, SEM images have several advantages: first, it has high resolution. The resolution of the SEM secondary electron image can reach 3 nm, the resolution of the ultrahigh resolution SEM secondary electron image is up to 1 nm, which is two orders of magnitude higher than the limiting resolution of optical microscopy of 200 nm. Second, the depth of field is large. At a magnification of 100 \times , the depth of field of an optical microscope is 1 μm , while a SEM can reach 1 mm. But even when the magnification reaches 40,000 times, the scanning electron microscope can still have a depth of field of about 1 μm . Third, the magnification is continuously adjustable in a wide range, and the image has sufficient signal brightness at high magnification. Fourth, the sample is relatively easy to produce. Fifth, dynamic observation is possible. SEM techniques are widely used for microscopic morphology and structure of solid samples, microregional elemental composition, line distribution, and surface distribution of samples, which are widely used in nanotechnology, materials, physics, chemistry, and environmental science [9, 10].

At present, three-dimensional reconstruction technology has been very mature. The current methods of 3D reconstruction modeling are mainly the following three: (1) direct model construction using traditional geometric modeling techniques, that is, the use of modeling software to construct 3D models [11, 12]; (2) dynamic reconstruction using 3D scanning equipment to scan real objects to directly get the information of object space points, and then reconstruct the model [13, 14]; (3) static reconstruction, based on digital pictures of 3D reconstruction, using images to recover the geometric shape of the object, that is, reconstructing the model using two or more images of the real object taken by cameras and digital cameras from various viewpoints [15, 16]. Reference [17] developed a system for picture-based 3D reconstruction. Reference [18] developed

an enhanced 3D modeling system using algorithms such as an uncalibrated structure from motion and camera self-calibration. Reference [19] proposed a 3D reconstruction system for buildings. Reference [20] created a human-computer interactive reconstruction system that employs a series of panoramic views of an object, that is, n pictures of the object from all angles, and then processes these images to reconstruct its 3D solid. Reference [21] used a self-calibration method of the camera to reconstruct the building's morphology. From these studies, it can be seen that 3D reconstruction techniques have been maturely applied in various industries. For 3D reconstruction of porous materials, reference [22] proposed an improved convolutional neural network for 3D reconstruction of porous materials for 3D reconstruction of porous materials. Reference [23] compares the performance of several algorithms for 3-dimensional reconstruction of porous materials, including the genetic algorithm, particle swarm optimization, differential evolution, firefly algorithm, artificial bee colony, and gravitational search algorithm. The experimental structure shows that the genetic algorithm gives the best results. Reference [24] proposed the ST-CGAN network based on the GAN network to extract effective information from 2D images to construct 3D effects. Reference [25] proposed a 3D reconstruction of CT images of rocks using GAN networks with good results. Since the SEM images of porous materials have the advantages of high resolution and the magnification of the images are continuously adjustable in a wide range, this paper focuses on the SEM images of porous materials and uses an improved GAN network for 3D reconstruction of porous materials. Similar techniques are widely used [26].

2. Related Knowledge

2.1. Introduction to Porous Materials. There are many porous materials, such as porous metals and porous ceramics. Compared with dense metal materials, porous metals have a lot of good characteristics, such as low thermal conductivity, high heat transfer and heat dissipation capacity, sound absorption and good sound insulation, excellent wave transmission, good electromagnetic wave absorption, fire resistance, and thermal shock resistance. Commonly used porous metal materials are bronze, nickel, titanium, aluminum, stainless steel, and other metals and alloys. Porous ceramic is a new type of ceramic material, and the manufacture of its use began in the late 1950s. Initially, it was used only as a bacterial filter material. Porous ceramic materials have good permeability, low density, high hardness, large surface area, and small thermal conductivity, so they are widely used in metallurgy, chemical industry, environmental protection, energy, biology, food, medicine, and other fields. The most widely used porous ceramic preparation process is organic foam immersion slurry replication technology, which produces a mesh ceramic which is a porous material consisting of ceramic network surrounded by connected voids.

A porous material is a collection of units of solid matter that are combined in some way. These units have pores between them, and these pores allow the circulation of

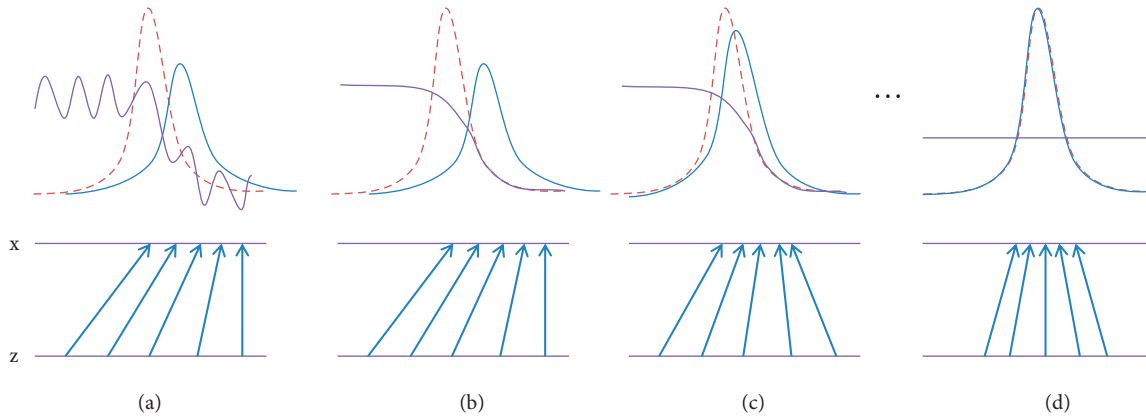


FIGURE 1: GAN training process.

substances such as gases and liquids. The most important characteristic of porous materials is that they have many pores compared to other materials with a tighter structure, and the size and shape of the pores vary from one porous material to another. The appearance of porous materials that people see with the naked eye is actually the appearance of all the units gathered together. Porous materials rely on solid material units to maintain their shape and properties, so the sum of interconnected units in porous materials is usually called the solid skeleton. From the above analysis, it is clear that porous material is a material form composed of solid skeleton and pore space together. The space between the units in a porous material is called the pore of the porous material. The shape of the units is very irregular and thus the pore shape is extremely complex; it is so complex that it is difficult to describe the geometry precisely by mathematical means. The pores are homogeneous at the macroscopic level and randomly distributed in the porous material at the microscopic level. Some pores are interconnected and they play a major role in the permeability of the medium. Some pores are isolated and closed by the solid skeleton and become dead-pores, while some pores are partially isolated and only one end is connected to other pores and are called dead-end-pores, which can store fluids but contribute little to the permeability of the medium. Some pores are located between units and are called intergranular pores in geoscience. Some pores are located inside the unit and are referred to as intragrain pores in geoscience. The larger scale pores in the medium are often in the form of fissures, cuttings, cracks, or cavities. Regardless of the type, pores are interwoven in porous materials to form a complex network, and it is not meaningful to study individual pores in isolation.

2.2. Generating Adversarial Neural Network (GAN). GAN was proposed 8 years ago [27]. The principle of GAN is similar to copying a painting in people's daily life. When copying more and more times, the more similar the painting becomes at the end. At the highest level, the copied painting is exactly the same as the copied painting. In the GAN network, the operation of drawing is replaced by model training. The GAN network is used to learn data distribution

patterns and generate data that are similar to the original data distribution. The GAN network structure consists of two parts, a generator and a discriminator, and the GAN training process is depicted in Figure 1.

The GAN is trained alternately with the generator and discriminator during the training process. The red dashed line indicates the distribution of the real data, the blue solid line indicates the generator output distribution, and the purple solid line indicates the recognition curve of the discriminator. The horizontal line is a uniformly sampled region, the horizontal line x is a partial region of the real data, and the upward-facing arrow represents the mapping $x = B(z)$. B shrinks in the high-density region and spreads in the low-density region. To train the GAN network, the discriminator is trained by first fixing the generator parameters. When the discriminator has been trained, adjust the parameters and train the generator. After the generator is trained, the discriminator is trained again. The generator and discriminator are trained alternately and finally reach the equilibrium state. The data distribution generated by the generator is consistent with the real data distribution in the equilibrium state. GAN's mathematical expression is as follows:

$$\min_B \max_A V(A, B) = E_{y \sim O(y)} [\log A(y)] + E_{z \sim N(z)} [\log (1 - A(B(z)))], \quad (1)$$

where $E(*)$ is the expected value of the distribution function, y is the true data, $O(y)$ is the true sample distribution, z is the noise input to the G-network, $B(z)$ is the data generated by the G-network, $N(z)$ is the noise distribution defined in the lower dimension, and $A(y)$ is the probability of whether the data is true, with closer to 1 indicating more realistic data. $A(B(z))$ is the likelihood of the D-network determining whether the data generated by the G-network is correct. The generating network wants to generate a more realistic picture, that is, the larger the $A(B(z))$, the better, when $V(A, B)$ is smaller. For the discriminative network, the stronger the discriminative ability is, that is, the larger the $A(y)$ is, the larger the $V(A, B)$ will be at this time. Fix B first and find the optimal solution A :

$$\begin{aligned}
V(A, B) &= E_{y \sim O(y)}[\log A(y)] + E_{y \sim p_B(y)}[\log(1 - A(y))] \\
&= \int_y O(y) \log A(y) dy + \int_y p_B(y) \log(1 - A(y)) dy \\
&= \int_y [O(y) \log A(y) + p_B(y) \log(1 - A(y))] dy \\
A^*(y) &= \frac{O(y)}{O(y) + p_B(y)}.
\end{aligned} \tag{2}$$

The optimal A is obtained by bringing the optimal A to $\max_A V(B, A)$:

$$\begin{aligned}
\max_A V(B, A) &= V(B, A^*) = E_{y \sim O} \left[\log \frac{O(y)}{O(y) + p_B(y)} \right] \\
&\quad + E_{y \sim p_B} \left[\log \frac{p_B(y)}{O(y) + p_B(y)} \right] \\
&= \int_y O(y) \log \frac{O(y)}{O(y) + p_B(y)} dy \\
&\quad + \int_y p_B(y) \log \frac{O(y)}{O(y) + p_B(y)} dy \\
&= -2 \log 2 + \int_y O(y) \log \frac{O(y)}{(O(y) + p_B(y))/2} dy \\
&\quad + \int_y p_B(y) \log \frac{p_B(y)}{(O(y) + p_B(y))/2} dy \\
&= -2 \log 2 + K \left(O(y) \left\| \frac{O(y) + p_B(y)}{2} \right\| \right) \\
&\quad + K \left(p_B(y) \left\| \frac{O(y) + p_B(y)}{2} \right\| \right) \\
&= -2 \log 2 + 2J(O(y) \| p_B(y)),
\end{aligned}$$

$$K(a \| b) = \sum a \log \frac{a}{b},$$

$$J(a \| b) = \frac{1}{2} K \left(a \left\| \frac{a+b}{2} \right\| \right) + \frac{1}{2} K \left(b \left\| \frac{a+b}{2} \right\| \right), \tag{3}$$

where K represents the Kullback–Leibler divergence and J represents the Jensen–Shannon divergence. $\max_A V(B, A)$ denotes the difference between the two distributions with a minimum value of $-2 \log 2$ and a maximum value of 0. B is optimal when $p_B(y) = O(y)$.

2.3. SRGAN Model. When the magnification of the image is relatively low, the image super-resolution reconstruction algorithm incorporating traditional deep learning convolutional neural networks is advantageous. When the

magnification of the image is more than four times the size of the image itself, the image processed by this technique will be blurred or lack of image details. The reason for this is that this algorithm mostly uses two techniques, interpolation convolution or interpolation padding convolution. On the other hand, since traditional neural networks usually use mean squared difference MSE as the loss function during model training, a high peak signal-to-noise ratio can be achieved, but the disadvantage is that the images generated using this technique tend to lose high-frequency details, causing the images to become smooth, thus affecting one's visual experience. In view of this, an image super-resolution reconstruction model based GAN (SRGAN) based on generative adversarial networks is introduced in the literature [28]. In the model training process, the new method employs a perceptual loss function, and then achieves image super-resolution through upsampling and convolution. The experimental results show that the recovered image with the SRGAN model has more high-frequency details, ensuring the image's quality. Figure 2 depicts the SRGAN model.

As shown in the SRGAN model in Figure 2, the model mainly consists of several core components, including the generator, discriminator, VGG network, and loss function. It has been shown that the amount of feature information extracted by the network is closely related to the depth of the network structure. In other words, a deeper network structure has to be constructed in order to extract more feature information. However, the cost of doing so is that the problem of gradient dispersion or gradient explosion will occur. The use of residual blocks, on the other hand, can solve the problem and thus ensure the effective transfer of gradient information. In view of this, first, we further develop the optimization of the generator based on ResNet. It has several residual blocks, and each residual block has two 3×3 convolutional layers. Then, the batch normalization (BN) layer is located behind the convolution layer, which utilizes Relu as the activation function, while the two $2 \times$ subpixel convolutional layer are used to expand the feature information inch. Finally, the output 3-channel image is generated by using a 3×3 convolution layer. In this way, with this model, super-resolution images can be obtained even with the input low-resolution images. Second, the discriminator contains eight convolutional layers, and any one of them is connected with a batch normalization layer BN. Along with the deeper and deeper layers of the network, the number of features becomes more and more, and the size of the features keeps getting smaller, so LeakyRelu is utilized as the activation function. Finally, the batch normalization layer BN is followed by two fully connected layers, with a sigmoid activation function that is used to determine the likelihood that the judgment is a natural image. The role of the VGG network is that it outputs the super-resolution image SR generated at the end of the generator to the already trained network on ImageNet. The loss function of the SRGAN model refers to the loss function D_Loss for training the discriminator and the loss function G_Loss for training the generator, respectively, where the latter includes content loss and adversarial loss.

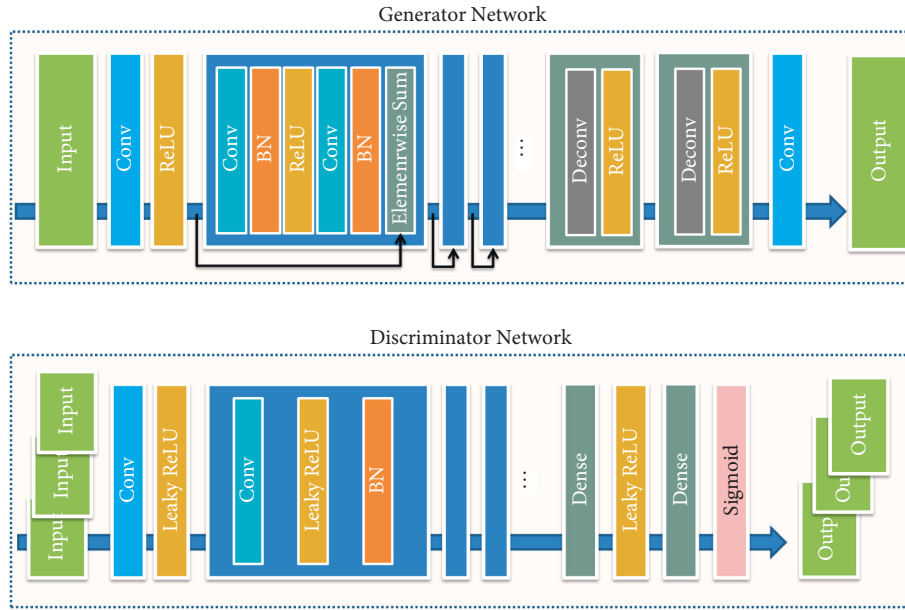


FIGURE 2: SRGAN model.

3. 3D Reconstruction Method for SEM Images of Porous Materials

3.1. *Execution Flow of the 3D Reconstruction Method.* The execution flow of this paper with the 3D reconstruction method is shown in Figure 3. First, the SEM images of the porous material are acquired. It is important to note that the acquired SEM images show the entire porous material as much as possible and are continuous. Second, the initial SEM images are often noisy and have unclear boundaries. Therefore, the initial SEM images need to be preprocessed. The common means of preprocessing is binarization or filtering techniques. Third, for 3D reconstruction, the intermediate layer images are very important. In this paper, an improved SRGAN model (ISRGAN) is used to generate the middle layer image. The middle layer image is characterized by a high similarity to the actual acquired SEM image. It is reflected by its void feature distribution which is the same as the acquired SEM image. Fourth, 3D reconstruction is performed using the generated intermediate layer images. The reconstruction is done by using layer-by-layer extraction and stacking in this way.

3.2. *ISRGAN Model.* The SRGAN model is characterized by a very large number of residual convolution layers. This characteristic, although the final result obtained is better, is very time-consuming to train and requires high performance of the hardware. The authors of [29] proposed a convolution-deconvolution network structure that can effectively approach the image super-resolution reconstruction problem. The convolution-deconvolution network structure is shown in Figure 4.

The network structure shown in Figure 4 is completely symmetric. The figure shows that the convolution layer is followed by downsampling and the deconvolution layer is

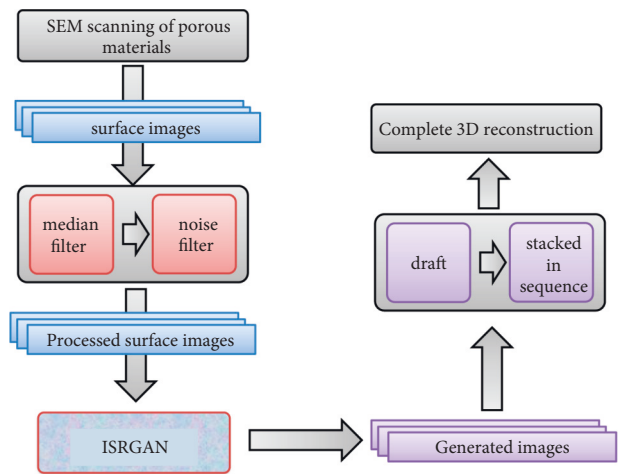


FIGURE 3: 3D reconstruction process.

followed by upsampling. The convolution operation is multiple inputs and one output. The deconvolution operation is the opposite, with one input and multiple outputs. The deconvolution is actually the process of expansion, so the operation can get more comprehensive information and thus obtain more detailed information of the image. In this paper, the ISRGAN model is obtained by introducing the convolution-deconvolution structure on the basis of the SRGAN model. The structure of the model is shown in Figure 5.

The generator of the ISRGAN model contains seven convolutional and seven deconvolutional layers each. The parameters of the generator are set as shown in Table 1.

In addition to the improved generator of the model, the discriminator is also improved in this paper. The discriminator is mainly used to determine the generated forged image and the real image to calculate the minimum variance

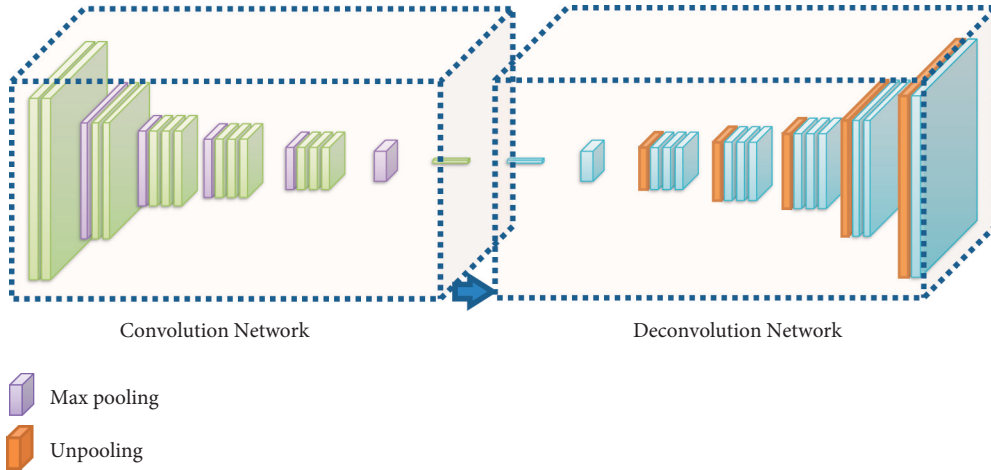


FIGURE 4: Convolutional-deconvolutional network structure.

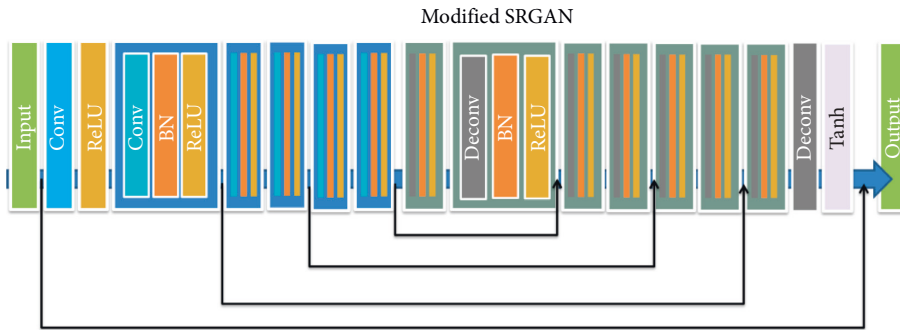


FIGURE 5: ISRGAN model structure.

TABLE 1: Parameter details.

Conv layer	Size of the kernel	Number of kernels
Conv1	3 × 3	256
Conv2	3 × 3	256
Conv3	3 × 3	256
Conv4	3 × 3	128
Conv5	3 × 3	64
Conv6	3 × 3	32
Conv7	3 × 3	1
Deconv1	3 × 3	32
Deconv2	3 × 3	64
Deconv3	3 × 3	128
Deconv4	3 × 3	256
Deconv5	3 × 3	256
Deconv6	3 × 3	256
Deconv7	3 × 3	1

of the pixel space between them. In order to recover better image information, this paper assists in extracting image features by training the VGG19 network, and its structure is given in Figure 6.

The feature map of a layer is extracted from a previously trained VGG19, and the generated fake image FEATURE MAP is compared to the real image MAP to determine the Euclidean distance between the generated image and the real image feature representations. L_M calculates the degree of

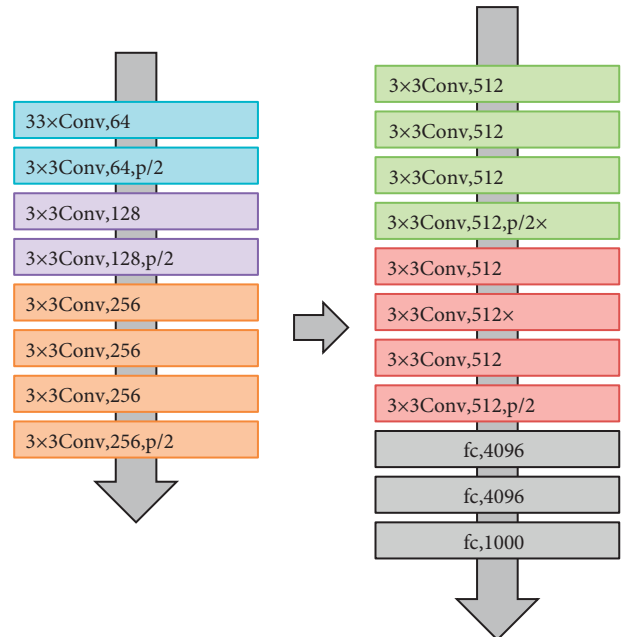


FIGURE 6: VGG19 network structure.

matching between pixels and the loss function and L_v expression of the degree of matching of a certain feature layer is as follows:

$$L_V = \frac{1}{L_{i,j} D_{i,j}} \sum_{x=1}^{L_{i,j}} \sum_{y=1}^{D_{i,j}} \left(\lambda_{i,j} (M^T)_{x,y} - \phi_{i,j} (G_{\theta_G} (M^T))_{x,y} \right)^2, \quad (4)$$

where $L_{i,j}$, $D_{i,j}$ is the feature map size, $\lambda_{i,j}$ is the feature map obtained by the j th convolution before the i -th maximum pooling layer, and M^T is the real image. Equation (5) shows the discriminator's loss function in the GAN:

$$D(y) = \begin{cases} \text{sigmoid}(C(y) - E_{y_f \sim Q} C(y_f)), & \text{if } y \text{ is real,} \\ \text{sigmoid}(C(y) - E_{y_r \sim P} C(y_r)), & \text{if } y \text{ is fake.} \end{cases} \quad (5)$$

When y is real data, the result is the output of the real data minus the average of the output of all the fake data, and then the sigmoid is taken over the result. When y is fake data, the result is the output of the fake data minus the average of the output of all the real data, and then the sigmoid is taken over the result.

The loss functions of the SRGAN discriminator and generator are modified as shown in equations (6) and (7), respectively:

$$L_D = -E_{y_r} [\log(D(y_r))] - E_{y_f} [\log(1 - D(y_f))], \quad (6)$$

$$L_G = -E_{y_f} [\log(D(y_f))] - E_{y_r} [\log(1 - D(y_r))]. \quad (7)$$

Finally, the generator's loss function is depicted as follows:

$$L_G = L_V + \beta L_G, \quad (8)$$

where β is the balancing factor, whose role is to balance the loss values of the loss function.

3.3. 3D Model Reconstruction. According to the 3D model construction process given in this paper, once the ISRGAN model generates all the intermediate layer images, then the intermediate layer images are overlapped from the top to the bottom according to the stacking method, as shown in Figure 7.

The 3D model reconstruction method used here is the slice-combination method. The operation schematic of the slice-combination method is shown in Figure 8.

It should be noted here that the boundaries of 3D models constructed by overlapping multiple intermediate layer images are usually rough and can be seen to overlap multiple layers; therefore, smoothing is essential. Commonly used smoothing techniques include weight smoothing, mean filtering, median filtering, Gaussian filtering, and bilateral filtering. Mean filtering is highly efficient and simple in thought. Therefore, in this paper, the mean filter is chosen to smooth the boundary.

4. Experimental Results and Analysis

Image size affects the performance of the training model. An image that is too large will consume memory, while the one

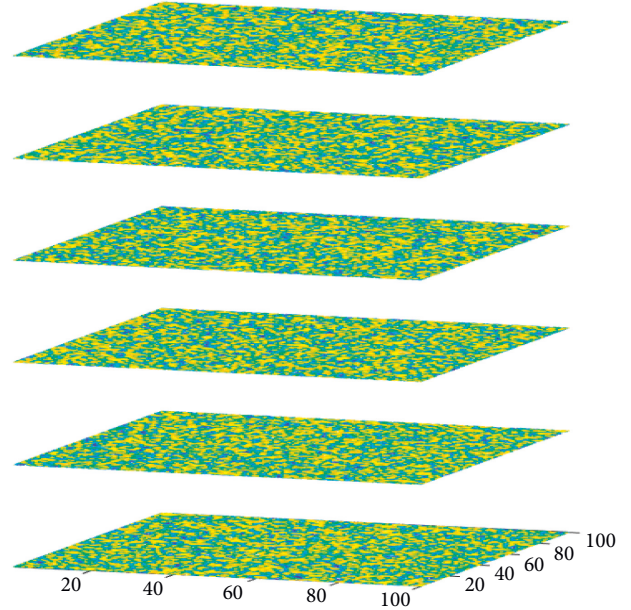


FIGURE 7: Stacking method.

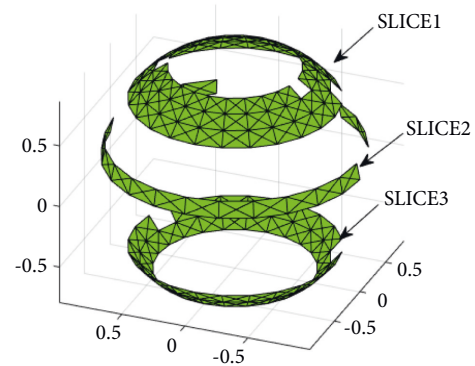


FIGURE 8: Schematic diagram of the slicing combination method.

that is too small will not be able to characterize the internal information. To quantify the size of the dataset used in this paper, the relationship between different image sizes and the running time of the algorithm was experimentally compared. The settings of each parameter of the model in this paper are shown in Table 2.

In this paper, SEM scanned images of coal-based porous carbon are selected as the input data for 3D reconstruction. The 3D reconstruction algorithm's performance is measured by whether the porosity approximates the real porosity of the sample. Different cell sizes have different effects on porosity. Based on the Avizo software, the cell sizes on the whole 3D model are extracted and the cell porosity is calculated. Experiments were conducted on three samples with different cell edge lengths, and the porosity comparison for each sample was obtained by calculation as shown in Table 3 as well as Figure 9.

In the porosity variation curves of the three samples shown in Figure 9, all three samples have a large variation in porosity until the cell size is 100. Samples 1 and 3 have a

TABLE 2: Parameter settings.

Parameters	Value
Epoch	16
Learning rate	0.0002
Number of iterations	2000

TABLE 3: Porosity of each sample at different unit body sizes.

Unit length (pixels)	Sample 1	Sample 2	Sample 3
12	0.95971	0.72774	0.42106
24	0.94117	0.63002	0.35040
36	0.84414	0.52746	0.32491
48	0.73488	0.45411	0.31143
60	0.52119	0.38342	0.22431
72	0.44802	0.34614	0.22388
84	0.40205	0.31535	0.23450
96	0.37209	0.30007	0.23158
108	0.35407	0.29256	0.21633
120	0.34615	0.28357	0.20914
132	0.34600	0.27362	0.20133
144	0.34305	0.26655	0.19302
156	0.34154	0.25846	0.18960
168	0.34154	0.25846	0.18923
180	0.33715	0.25487	0.18197

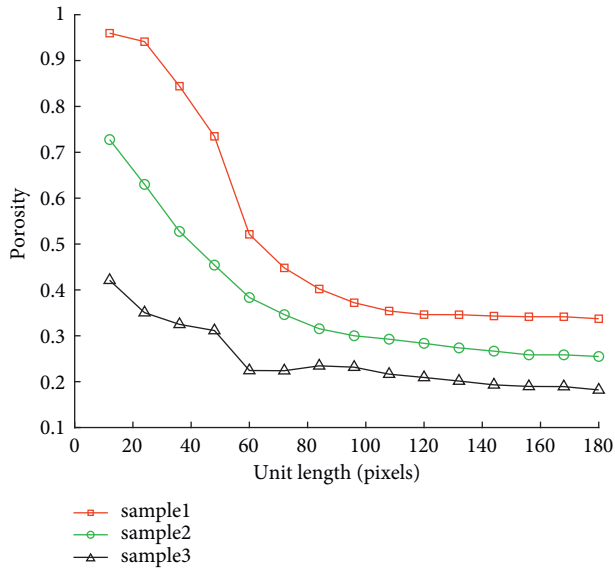


FIGURE 9: Porosity of each sample at different unit body sizes.

stable porosity region at a unit size of 100, and sample 2 has a stable porosity region at a unit size of 110. This indicates that the optimal unit cell size is different for different coal-based porous carbon samples. In this paper, a $180 \times 180 \times 180$ pixel unit cell was finally used as the study object. The experimental results show that the 3D reconstruction model used in this paper is capable of obtaining the closest porosity to the real object. The reason for the good results of 3-dimensional reconstruction based on SEM images of porous materials in this paper is the perfect simulation generation of the intermediate layer images of the 3D model using the

ISRGAN model. The experimental results show that the generation of the middle layer image is effective, and the information of the void part in the middle layer image can be generated as much as possible and close to the real image. The experimental results show that the ISRGAN model used in this paper is very effective and superior. The method can also be applied to other porous materials for 3D reconstruction in the future.

5. Conclusion

The pore structure of porous materials is very complex, and its representation has been a difficult problem in this research area. Adequate analysis is needed before modeling to derive a suitable stochastic model expression; otherwise, the reconstructed model will not truly reflect the geometric characteristics of porous materials. In this paper, we have conducted an in-depth study on the selection of scanning images, preprocessing, 3D mathematical modeling, and model validation in the modeling process and also implemented the corresponding algorithms mainly in the following aspects. First, by analyzing and comparing the advantages and disadvantages of various scanning images, we finally determined that using SEM images is the most beneficial for 3D reconstruction. The reason is that SEM images have higher resolution, large depth of field, continuously adjustable magnification in a wide range, relatively easy specimen preparation, and dynamic observation. The SEM images of porous materials were acquired, and the acquired SEM images are pre-processed, including noise removal and determination of boundaries. Second, for the generation process of the intermediate layer images, an improved deep learning model for image super-resolution reconstruction is used in this paper. This model is an improvement of the SRGAN model, which has 16 layers of residual convolution in the generator, and although the deeper network can extract more details of the characteristics, the large network structure is not conducive to training, the requirements for hardware and other experimental environments are relatively high, and the stability of the training process is difficult to be guaranteed. The ISRGAN model, on the other hand, circumvents these problems. The preprocessed images are fed into the ISRGAN model for training. Thus, multiple intermediate layer images are generated. Third, the 3D reconstruction of the middle layer images is performed using the slice combination method. In order to validate the efficacy of the 3D reconstruction method used in this paper, the experiments examine the relationship between unit cell pixels and porosity. It is concluded that the porosity tends to be stable when the unit cell pixels is over 110, and it is converged to the real porosity of the sample. The experimental results validate the feasibility and efficacy of the method presented in this paper in the process of 3D reconstruction. However, the samples reconstructed in 3D based on image processing techniques will have information loss and addition, and how to extract the desired information features without loss is the direction of our next stage of research.

Data Availability

The labeled dataset used to support the findings of this study are available from the corresponding author upon request.

Conflicts of Interest

The authors declare no competing interests.

Acknowledgments

This work was supported by the Natural Science Foundation of the Jiangsu Higher Education Institutions of China (20KJB410005) and the Scientific Research Foundation of Nanjing Vocational University of Industry Technology (YK18-03-03).

References

- [1] M. Alodat, "Analyzing CT scan images using deep transfer learning for patients with covid-19 disease," *Lecture Notes in Electrical Engineering*, vol. 784, pp. 71–78, 2022.
- [2] S. Jafari, S. Kaffashan, S. Saeedi-Moghadam, P. Iranpour, and B. Zeinali-Rafsanjani, "Assessment of the hallmarks of wilson disease in CT scan imaging," *Journal of Medical Imaging and Radiation Sciences*, vol. 51, no. 1, pp. 145–153, 2020.
- [3] S. Hailstone and R. K. Hailstone, "SEM nano: an electron wave optical simulation for the scanning electron microscope," *Microscopy and Microanalysis*, vol. 28, no. 2, pp. 441–453, 2022.
- [4] R. Huber, J. E. Edwards, C. R. Dragnevski, G. Edwards, Ed Williamson-Brown, and K. Dragnevski, "An investigation into experimental in situ scanning electron microscope (SEM) imaging at high temperature," *The Review of scientific instruments*, vol. 91, no. 6, Article ID 063702, 2020.
- [5] A. V. Maltsev, B. Caffrey, M. Gonzalez-Freire, L. Hartnell, S. Subramaniam, and L. Ferrucci, "Semi-automated 3D segmentation of human skeletal muscle using focused ion beam-scanning electron microscopic images reveals network of mitochondria," *Biophysical Journal*, vol. 118, no. 3Suppl1, pp. 292a-293a, 2020.
- [6] J. Heinen-Weiler, M. Hasenberg, M. Heisler, S. Settelmeier, and A.-L. Beerlage, "Superiority of focused ion beam-scanning electron microscope tomography of cardiomyocytes over standard 2D analyses highlighted by unmasking mitochondrial heterogeneity," *Journal of Cachexia, Sarcopenia and Muscle*, vol. 12, no. 4, pp. 933–954, 2021.
- [7] K. A. Harrington, P. Paudyal, and R. K. G. Do, "MRI of the pancreas," *Journal of Magnetic Resonance Imaging*, vol. 53, no. 2, pp. 347–359, 2020.
- [8] F. Allen and C. Allen, "Progress in prostate MRI quality," *Academic Radiology*, vol. 29, no. 1, pp. 15–16, 2022.
- [9] E. Vesseur, "Live color SEM imaging," *Microscopy and Microanalysis*, vol. 25, no. S2, pp. 562–563, 2019.
- [10] E. Pajorová and L. Hluchý, "3D SEM based functional nanostructure for medical imaging," *Lecture Notes in Networks and Systems*, vol. 263, pp. 173–179, 2021.
- [11] M. Di Nützmänn and H.-W. Nützmänn, "Modeling the 3D genome of plants," *Nucleus*, vol. 12, no. 1, pp. 65–81, 2021.
- [12] M. Elçin, A. Elçin, and Y. Murat Elçin, "Biomimetic 3D-bone tissue model," *Methods in Molecular Biology*, vol. 2273, pp. 239–250, 2021.
- [13] D. Thuy, N. T. T. Ngoc, N. C. Trung, and N. T. Le, "Mannequin modeling from 3D scanning data," *Intelligent Systems and Networks*, vol. 243, pp. 362–372, 2021.
- [14] B. Bebeskko, K. Khorolska, N. Kottenko et al., "3D modelling by means of artificial intelligence," *Journal of Theoretical and Applied Information Technology*, vol. 99, no. 6, pp. 1296–1308, 2021.
- [15] A. E. D. Barioni and M. A. M. de Aguiar, "Complexity reduction in the 3D Kuramoto model," *Chaos, Solitons & Fractals*, vol. 149, Article ID 111090, 2021.
- [16] B. Telesiński, "Between 3D models and 3D printers. Human- and AI-based methods used in additive manufacturing suitability evaluations," *Lecture Notes in Networks and Systems*, vol. 319, pp. 556–562, 2022.
- [17] C. Tomasi and T. Kanade, "Shape and motion from image streams under orthography: a factorization method," *International Journal of Computer Vision*, vol. 9, no. 2, pp. 137–154, 1992.
- [18] P. Jeanne, J. Rutqvist, D. Vasco et al., "A 3D hydrogeological and geomechanical model of an enhanced geothermal system at the geysers, California," *Geothermics*, vol. 51, no. 1, pp. 240–252, 2014.
- [19] S. Simon, R. Dewil, and K. Allacker, "Circularity of building stocks: modelling building joints and their disassembly in a 3D city model," *Procedia CIRP*, vol. 105, pp. 712–720, 2022.
- [20] S. Kin, T. Doke, Y. Yamashita et al., "Development of integrated 3-dimensional computer graphics human head model," *Operative Neurosurgery*, vol. 20, no. 6, pp. 565–574, 2021.
- [21] J. García, B. Quintana, A. Adán, V. Pérez, and F. J. Castilla, "3D-TTA: a software tool for analyzing 3D temporal thermal models of buildings," *Remote Sensing*, vol. 12, no. 14, p. 2250, 2020.
- [22] T. Xia, P. Lu, and F. Lu, "3D stochastic reconstruction of porous media based on attention mechanisms and residual networks," *Stochastic Environmental Research and Risk Assessment*, vol. 36, no. 4, pp. 1063–1081, 2022.
- [23] G. A. Papakostas, J. W. Nolan, and A. Mitropoulos, "Nature-inspired optimization algorithms for the 3D reconstruction of porous media," *Algorithms*, vol. 13, no. 3, p. 65, 2020.
- [24] R. Shams, M. Masihi, R. B. Boozarjomehry, and M. J. Blunt, "A hybrid of statistical and conditional generative adversarial neural network approaches for reconstruction of 3D porous media (ST-CGAN)," *Advances in Water Resources*, vol. 158, Article ID 104064, 2021.
- [25] A. Damas, S. Arechalde, C. Tubilleja, and J. Arechalde, "Stochastic reconstruction of 3D porous media from 2D images using generative adversarial networks," *Neurocomputing*, vol. 399, pp. 227–236, 2020.
- [26] X. Zhang, E. Jaman, A. Habib et al., "A Novel 5-Amino-levulinic Acid-Enabled Surgical Loupe System-A Consecutive Brain Tumor Series of 11 Cases," *Operative Neurosurgery*, vol. 22, no. 5, pp. 298–304, 2022.
- [27] G. Baykal, F. Ozcelik, and G. Unal, "Exploring deshuffle GANs in self-supervised generative adversarial networks," *Pattern Recognition*, vol. 122, Article ID 108244, 2022.
- [28] C. Ledig, Z. Wang, and W. Shi, "Photo-realistic single image super-resolution using a generative adversarial network," in *Proceedings of the 2017 IEEE Conference on Computer Vision and Pattern Recognition (CVPR)*, pp. 105–114, Honolulu, HI, USA, July 2016.
- [29] H. Noh, S. Hong, and B. Han, "Learning deconvolution network for semantic segmentation," in *Proceedings of the IEEE International Conference on Computer Vision*, pp. 1520–1528, Santiago, Chile, December 2015.

Research Article

Understanding the Impact of Rural Returnees' Hometown Identity on Their Successful Entrepreneurship with the Operations Research Framework

Feihan Sun ¹, Xumei Miao ², Xiaoyan Feng ³, and Chongliang Ye ¹

¹Zhejiang College of Security Technology, Wenzhou 325016, China

²Shenzhen MSU-BIT University, Shenzhen 518172, China

³Wenzhou University, Wenzhou 325035, China

Correspondence should be addressed to Xiaoyan Feng; sun2019vlad@gmail.com and Chongliang Ye; daogu1979@126.com

Received 25 May 2022; Revised 4 June 2022; Accepted 10 June 2022; Published 29 June 2022

Academic Editor: Xuefeng Shao

Copyright © 2022 Feihan Sun et al. This is an open access article distributed under the Creative Commons Attribution License, which permits unrestricted use, distribution, and reproduction in any medium, provided the original work is properly cited.

In the past ten years, China's rapid urbanization has hollowed out the rural population considerably. Although returnee entrepreneurship has become a catalyst for retaining people and revitalizing the countryside, most disenfranchised Chinese villages struggle to retain their returnees, owing to their lack of infrastructure and low quality of life. However, many e-commerce villages and live broadcast villages have emerged in the eastern coastal plains of China. Returnees, inspired with a strong hometown identity, have become the driving force in the development of these villages. This study investigates the relationship between the hometown identity of returnees and their entrepreneurial success with the operations research framework. We explored the mediating role of the agglomeration of knowledge to illustrate the mechanism between the hometown identity and entrepreneurial success, while testing the moderating effect and conditional indirect effects of the returnees' creativity through moderated mediation analysis. Using the time lag research method, we collected field data from villages in the northern plains of Jiangsu Province. The research results showed a positive correlation between the hometown identity and entrepreneurial success, with agglomerated knowledge production as an important intermediary. Returnees with a stronger sense of a hometown identity and higher creativity are more likely to enjoy entrepreneurial success. This research has important reference significance for all levels of government concerned with rural development, and returnees who desire to start their own businesses.

1. Introduction

"Arrival City" has become the development trend of cities and villages around the world [1]. Chinese society has a long-standing dual structure, with urban and rural antagonisms and large gaps between the rich and the poor [2]. Hindered by low income and the lack of employment opportunities other than agriculture, rural residents suffer a low economic growth rate, exacerbated by the relative lack of government support, and a shortage of long-term delivery services for labor materials for urban construction [3]. In addition to the explicit economic differences, there are also implicit differences in living habits and cultural practices between urban and rural areas. The custom of patronizing sons over daughters has long been the basic pattern of opportunity distribution for children

among rural families in China [4]. The countryside is also a typical acquaintance society. Nowadays, with more alienated human relationships, the metropolis has become an acquaintance society without subjects [5], with a noticeable disparity in the ideology and ideals of the older and younger generations [6]. In addition, rural fragmentation, disorder, and passivity of rural subjects are the biggest obstacles to the realization and enhancement of the activism, rights, and identity of Chinese rural subjects [7]. The explicit and implicit challenges have become a source of discomfort for the returnee's contrasting urbanization and modernization on one hand, and the ideals of idyllic Chinese countryside on the other. How to exert the enthusiasm, motivation, and creativity of the subjects of rural development has obviously become the main challenge of rural development.

Well-built villages, however, still cannot attract young people, and this is a bottleneck for the development of countries around the world [8, 9]. In order to solve this conundrum, the Chinese government continues to implement exploratory adjustment of development strategies, and constantly strives to narrow the gap between urban and rural areas in all aspects and in multiple fields. At the end of 2005, for example, the state required local governments to develop a new socialist countryside in accordance with the requirements of “production development, ample life, civilized rural customs, clean villages, and democratic management.”

Another example was the college student village official plan from October 2008, which intended to “guide college graduates to work in the village, and implement the goal of ensuring ‘one college student per village,’” and the focus on training health professionals engaged in general medicine at the level of township hospitals and below, also complemented that effort. In 2014, the Ministry of Agriculture launched the promotion of China’s leisure villages, which drove development projects in the countryside, culminating in a rural revitalization strategy whose goal was to realize rural modernization. Another effort to narrow the gap between urban and rural areas was the 2018 stipulation by the Ministry of Education that publicly funded normal students who graduated must teach in rural compulsory education schools for at least one year. In addition, the government also supports policies in environmental assessment, land use, financial credit, etc., to achieve sustainable agriculture and rural development [10].

In recent years, rural entrepreneurship is increasing, and it mainly consists of returning to the countryside and entering the countryside [11]. In rural areas, laborers transfer to coastal areas and large and medium-sized cities to work and accumulate entrepreneurial skills, who then return to their hometowns to allocate entrepreneurial resources to benefit their neighbors [12]. Science and technology, management talents, and entrepreneurs with the ability and desire to start a business in the city generally enter the countryside because of its natural resources and labor resources endowment, and gradually increase with the in-depth implementation of the rural revitalization strategy [13]. Meanwhile, with China’s regional economic growth, improved Internet infrastructure, more convenient transportation, gentrification of the living environment, new ruralism, and new lifestyles (people in the city who choose to live in the countryside) have gradually emerged [14]. Coupled with the national policy of “mass entrepreneurship and innovation,” there has been a marked increase in returnees starting businesses in their rural hometowns, especially in the developed eastern coastal areas of China, most notably in Jiangsu Province, where the economic development is most balanced [15]. In the context of top-down national development, those returning to their rural hometowns have used their capital, experience, skills, and wisdom to transform their hometowns, and numerous entrepreneurial stars and models have emerged. To a certain extent, it has alleviated the “shortcomings” of the lack of rural talents by introducing new technologies and new information, thus becoming the backbone of rural reform,

development, and revitalization [16]. These talents in rural Chinese society have greatly increased in entrepreneurial fields, such as self-build entrepreneurial opportunities, e-commerce, and product sales on live broadcast platforms [17, 18].

The hometown identity of the Chinese is a part of inherited tradition and has become the cultural capital for the revitalization of rural areas and the sustainable development of communities in modern China [19]. China was formerly a provincial agricultural society, where people depended on the same land for generations to survive. Even when they migrated to other countries, “falling leaves returned to their roots” [20, 21]. However, since ancient times, rural society has relied on local wise men to build their hometowns, and they have become an extremely important force in rural management. They actively participate in local affairs, maintain order, and have made great contributions to grassroots governance [22]. The characteristics of the differential pattern of rural society [23] firmly consolidate the identity of the Chinese countryside and still affect the cognition, social evaluation, and behavioral decision-making of returnees to this day [24]. The hometown identity can stimulate entrepreneurs’ internal power resources and has the greatest impact on villagers’ willingness to participate in rural revitalization [25]. Therefore, due to their hometown identification, returnees tend to actively perform and gather in the acquaintance society for knowledge sharing to rejuvenate the village. In other words, the hometown identity of returnees is the soul of rural revitalization and the key to resolving the crisis of contemporary rural development. Specifically, it is an emotional mechanism of the security-trust-expression-identity that is oriented to nostalgia, sentiment, and rural culture, with perception, conflict, integration, and interaction as paths [26]. Based on the above arguments, we can attribute the successful entrepreneurship of returnees to the role of hometown identification from the perspective of operations research.

First, we focus on enhancing the contribution of the hometown identity to entrepreneurial success. Most returnee entrepreneurs are troubled by the vitality of the rural market, the system of support services, and psychological quality [27]. This inherent rural stereotype has become a key factor in the success or failure of entrepreneurship. Therefore, successful entrepreneurship requires enhancement of the hometown identity, which has been the focus of China’s current social development, addressing policies, funds, and improving rural infrastructure, leading to the establishment of the National Rural Revitalization Bureau at the end of February 2021.

Second, agglomeration strategy as an intermediate variable in this study frames the link between the hometown identity and entrepreneurial success. Since the state’s top-down consolidation of the hometown identity has received more policy support and guidance, returnees are more likely to share entrepreneurial knowledge with villagers. This comes as a result of their deeper understanding of the urban market, while independently believing that agglomeration development is meaningful and positively impacts rural development. This kind of agglomeration strategy can be

used to solve difficult entrepreneurial challenges, which will have a positive impact on the execution and completion of entrepreneurial goals. Third, we analyzed the moderating effect of the creativity of returnees. Creativity is tested as a boundary condition that influences the connection between the hometown identity and entrepreneurial success because the literature shows that returnees with professional creativity are critical to agglomeration practice and performance [28]. Our research was confined to the coastal plains of China. We determined survey points to collect data from the list of rural industrial clusters announced by the Ministry of Agriculture and Rural Affairs and the Ministry of Finance, as well as the villages where many returnees consolidated. Judging from the existing literature, there is a lack of research on the recognition of the successful entrepreneurship of Chinese returnees. Therefore, we have also addressed an important academic gap.

2. Theory and Hypothesis

2.1. Hometown Identity and Entrepreneurial Success. Hometown identity can be defined as “explaining the individual’s internal emotional attachment, attitude tendency, and explicit behavior, and explaining the connection between values and behavior” [29]. In the past few decades, the research of identity and the success of entrepreneurship have aroused great interest in academia. Many subfields of pedagogy, history of science and technology, applied economics, sociology, and psychology, including professional identity, leadership, team performance, task performance, motivation, decision-making, and creativity, are all included in the study of identity. It is closely related to the attitudes and behaviors of individuals, groups, and communities [30, 31].

The concept of the hometown identity is composed of four cognitions: meaning, decision-making, confidence, and sense of accomplishment. Specifically, meaning refers to the degree to which homecoming entrepreneurship itself is meaningful to the construction of the concept of returnees. Decision-making refers to the sense of motivation and autonomy that returnees have in entrepreneurial decision-making. Confidence refers to the degree to which returnees are confident in their own ventures, and able to cope with entrepreneurial challenges and have a sense of accomplishment, which involves the feeling that their personal achievements have made a significant contribution to the development and revitalization of themselves and the countryside.

Similar to the psychological identity of practitioners in various industries, returnees also face psychological challenges brought about by returning to their villages to start a business. Although returnees can freely pursue their dreams, they will always face various difficulties in the complex and evolving entrepreneurial process. They often experience more negative emotions than their employees do, such as isolation, stress, fear of failure, loneliness, mental stress, and sadness [32]. Do the returnees face it positively or negatively? Would one insist on starting a business or reenter the city to choose salaried employment? This partly depends on

whether returnees truly believe in economic activities in their hometowns and whether they regard returning as a lifelong career pursuit and ideal employment setting. The hometown identity is a core element of entrepreneurial drive, and there are significant differences among the different types of entrepreneur. Of the “true believer,” “clueless,” “practical,” and “reluctant” types of entrepreneurs, there are three characteristics that differentiate them, namely: achievement needs, risk-taking propensity, and commitment.

Among them, true believer entrepreneurs have the highest entrepreneurial commitment [33] because they firmly believe in the value of their identity, having a higher degree of conviction concerning their return to their home to start a business. For them, the construction of the hometown identity is more meaningful and influential for entrepreneurial success, leading to internal motivation.

Returnees, having specific knowledge and skills, would have high employment expectations in their hometown. Meanwhile, they have made a decision to transition from urban to rural employment after consideration of factors, such as the hometown’s policy environment [25]. The decision-making process makes returnees more confident, believing that their entrepreneurial ideas can actually help villages develop economically and rise out of poverty. The returnees’ sense of identity is transformed into power, decision-making, information, autonomy, initiative and creativity, knowledge, skills, and sense of responsibility in entrepreneurship, which becomes the internal driving force for their successful entrepreneurship. They persevere and perform well [34].

The identity self-construction model can explain the connection between the hometown identity and entrepreneurial success [35]. The individual internalizes the value of self-employment and transforms this meaning into self-definition, thus forming their hometown identity. Identity-based motivation is about “whether the individual wants to do something,” so that the value of this identity guides and drives goal-oriented behavior, often transforming possibilities into realities [36].

Moreover, the multiple identities possessed by returnees enable them to manage emotions more effectively [37]. Entrepreneurship is “a life of nine deaths.” The self-concept mainly focuses on the identity of the entrepreneur, and when setbacks and failures arise, it challenges their self-verification and self-esteem, possibly reducing their enthusiasm. However, maintaining multiple identities can not only better exert the positive effects of returnees’ self-verification [38] but they can pay more attention to identity management, which in turn bolsters their abilities [39].

Many scholars believe that hometown identification has greatly improved overall productivity, especially in entrepreneurial projects [29]. Returnees who have a stronger sense of belonging tend to believe that their entrepreneurship has far-reaching significance and influence [25]. Hence, with increased passion, they lead innovations to accomplish their entrepreneurial goals. Therefore, we assume the following:

Hypothesis 1. Hometown identity is directly proportional to the entrepreneurial success of returnees.

2.2. The Mediating Role of Agglomeration Strategies. Agglomeration strategy plays the role of knowledge production and sharing, which can be defined as “the act of providing information to others in the organization” ([40], p. 341), it aims to solve the problems encountered by the returnee group in starting a business, the exchange of market information, and the mutual consultation of opinions. In an agglomeration environment, knowledge production and sharing are a crucial team process because if knowledge resources are not shared, they cannot be fully utilized [41]. Knowledge-intensive business activities are the staple of entrepreneurship. In this knowledge-driven environment, team development and management agglomeration strategies become imperative [42].

With specific goals, the entrepreneurial ecosystem adopts open cooperation and innovation, seeking resource complementation, division of labor and collaboration, value sharing, and coexistence [43]. The concept and the relationship network that the hometown identity constructs are key factors that enhance the dissemination of knowledge among members of agglomeration [44]. The hometown identity enhances interpersonal trust, which becomes an agglomeration of knowledge production and sharing [45].

Agglomeration strategy forms an ecosystem with diverse internal roles [46]. There can be more efficient division of labor and coordination according to specific resource endowments, including “producers,” “consumers,” “disintegrators,” and “catalysts” (including lawyers, accountants, and intellectual property experts) [47]. There can be a free sharing of strategic knowledge, technical knowledge, and training and services for villagers in preparation for returnees, forming an agglomeration ecosystem for the rural industry.

- (1) Strategic entrepreneurial knowledge. Returnees who have started their own businesses are in the growth and exploration stage of their knowledge of entrepreneurial strategic planning and the business model design. The creative team that agglomeration strategy forms provides returnees with wisdom, vision, market information, and entrepreneurial experience, which greatly improves the success rate of agglomeration strategy [48].
- (2) Technical entrepreneurial knowledge. This mainly comprises knowledge and experience in core technology research and development, product development, business operations, and management. For example, returnees in the technology sector and professionals with various knowledge and skills can solve difficult problems in technology, business models, and business operations in entrepreneurial projects.
- (3) Entrepreneurship training and services for villagers. Returnees use the Internet to live broadcast goods to help villagers sell agricultural products and other

wares while opening up new markets for these products, allowing villagers to become self-sufficient [49]. Innovative guidance services through the network, video, and other media provide policy consultation, technical guidance, marketing, brand cultivation, and other services for potential entrepreneurs in rural areas.

Returnees form a cluster space, which is a key resource for realizing rural economic development and entrepreneurial ecological sustainability [50]. Through the collective knowledge sharing, knowledge can be exchanged and spread among themselves and with the villagers to form a network. This has led to an increase in the success rate of entrepreneurship. Since knowledge sharing in turn produces a very small probability of errors, it is more possible to experience relatively error-free entrepreneurial project execution [51]. Based on the above findings, we assume the following:

Hypothesis 2. Agglomeration strategies can adjust and add value the relationship between the hometown identity and entrepreneurial success.

2.3. The Moderating Role of Returnees’ Creativity. In the context of rural revitalization, returning to the hometown is a new way for youth development, as opposed to the metropolitan environment [52]. This requires returnees to have a degree of creativity and to improve the possibly outdated production methods in their villages of origin. Increasingly, returnee entrepreneurs are using the skills, personal connections, insights into market rules, and accumulated funds that they have acquired over the years to upgrade rural industries, develop rural areas, and change traditional development into innovative development [29, 53]. Thus, innovative thinking and creativity are the main characteristics of returnees [54]. In recent years, China’s rural e-commerce has developed rapidly, and some returnees have discovered various niches of novelty products that have become popular online, even though many returnees are still engaged in traditional industries, such as agriculture, vegetables, flower-plant industry, and livestock and aquaculture. However, although they have been conceived from the traditional production model, they have begun to approach a new model of standardization, intensification, and clustering [55].

The creativity of returnees is a way to generate new and useful ideas and solve problems. People are paying more attention to the research on how returnees influence and enhance each other’s creativity [56]. The challenges become more demanding for returnees who start their own businesses, and they usually have to accomplish their entrepreneurial goals creatively. Every process when running a business needs creativity, and business owners need to embrace this creative thinking to establish a conducive business environment. Creativity is an important component of individual cognitive processing. It is the ability to generate novel and innovative ideas through the recombination and matching of information and knowledge [57]. In the field of entrepreneurship, individual creativity refers to

the process by which entrepreneurs can combine existing ideas and resources to generate new and feasible ideas or resources, thereby starting a new business [58]. For entrepreneurial activities, creativity is particularly important, because creating a new business is itself a creative activity. Maintaining creativity is a quality that successful entrepreneurs must possess [47].

A high level of creativity can help returnees to better understand the connections between objects, identify business opportunities, and rationally allocate entrepreneurial resources to create value efficiently. Difficulties in the entrepreneurial process, such as shortages of resources and inability to enter the market, require creative individuals who are able to generate more ideas about products or services [59]. A successful returnee is more confident in transforming creativity into self-performance, that is, high creativity is an asset to their entrepreneurship. Some scholars have pointed out that the study of entrepreneurial goals should include creativity as an important alternative predictor [49]. With the continuous advancement of the strategy of “popular entrepreneurship, mass innovation,” entrepreneurship has gradually become a new driving force for sustainable economic development. Entrepreneurship itself is a highly creative value-creation activity, and active innovative thinking is a distinctive feature of entrepreneurs. In Schumpeter’s theory of innovation, the view of “creative destruction” essentially predicts the creativity of entrepreneurs [60]. Creativity from the entrepreneurial perspective is embodied in the process of developing novel and useful products or services [61].

Therefore, we expect the creativity of returnees to have a positive moderating effect between hometown identification and agglomeration strategies, and predict the following:

Hypothesis 3. The creativity of returnees will rely on agglomeration strategies to enhance the indirect influence of the hometown identity on entrepreneurial success. Specifically, more creative employees have a greater indirect impact.

The conceptual framework is presented in Figure 1.

3. Method

3.1. Study Context: Creative Villages of the Jiangsu Coastal Plain in China. We aimed this study at returnees from the coastal plains of Jiangsu, China, where creative villages have sprouted [53]. We chose them for two main reasons. First, these villages do not have any innate resource endowments, such as impressive natural resources for tourism. Traditional agriculture has long been the principal economic activity. With the advent of the Internet age, these villages which are close to the Yangtze River Delta economic circle in China have seen the budding development of creative villages, which has changed the traditional path of rural development and achieved substantial economic benefits. There are many returnees who have started businesses in this plain area and achieved remarkable success. Second, the careers of returnees are innovation-oriented. Hence, our selected sample comprises returnees who personify our research topic.

3.2. Sample and Procedure. Our sample comprises returnee entrepreneurs from several villages in the coastal plain of Jiangsu, China (mainly concentrated in Donghai and Guanyun counties in Lianyungang City and Shuyang and Siyang counties in Suqian; as shown in Figure 2). Before data collection, we conducted a prestudy of 12 college students who planned to return to their hometowns to start a business in order to revise and adjust items in this study while expanding the generality of the results. Prior to this data collection process, we conducted several field surveys and semi-structured interviews at the survey sites in 2018 and 2019 to obtain preliminary data and establish good relationships with some returnees. We formed a working relationship with other returnees through the introduction of key informants, which established a good foundation for the credibility of investigation. This research topic hinged on previous data and used online questionnaires to obtain research data (using the “Wenjuanxing” survey questionnaire platform).

Initially, we contacted 28 entrepreneurial teams (197 people in total), and the key informants of each entrepreneurial team led the members in completing the questionnaire voluntarily. Respondents are either self-employed or entrepreneurial partners. They are engaged in e-commerce, logistics, design, creativity industry, livestreaming, marketing, sound and vision, video editing, research and development, education and training, short videos, etc. In order to reduce potential general method bias [62], we adopted a time lag design and independent measures (self and supervisory reporting). At time 1, we distributed links for the online questionnaire to key informants from the returnee team. We asked them to provide their job status, demographics (gender, age, educational background, and entrepreneurial experience), opinions on the hometown identity, agglomeration strategies, entrepreneurial expectations, and entrepreneurial success.

In the questionnaire’s introduction, we explained to them the purpose of the research and stated that their participation in the questionnaire was voluntary, and that we guaranteed them anonymity and confidentiality because the respondents did not need to mention their names in the answer. A total of 192 returnees completed the questionnaire, and the feedback rate was 97.46%. The survey lasted for a four-week interval (time 2) from October to November 2019. We used the scores of 28 key informants in the entrepreneurial teams to evaluate the creativity of team members. In order to match the answers of returnees, the key informant identified them through the job identities we obtained at time 1. We received 116 complete matching responses (key reporters rated returnees who participated in the survey). On average, key reporters rated the creativity of four returnees, and the participation rating accounted for 58.88%.

Most of the participants (72.58%) were men, with 51.77% having a higher vocational education degree (after three years of vocational education after graduating from high school), and 41.62% with a bachelor’s degree. By age category, 52.28% of the respondents were between 27 and 34 years old, and most of them (46.7%) had been running their hometown business for 5–9 years.

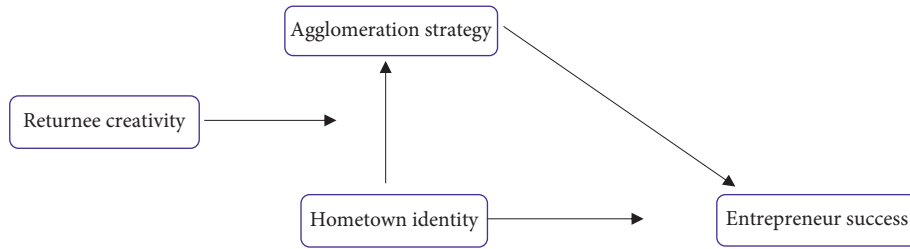


FIGURE 1: Proposed research model: The HIDENCESS model.

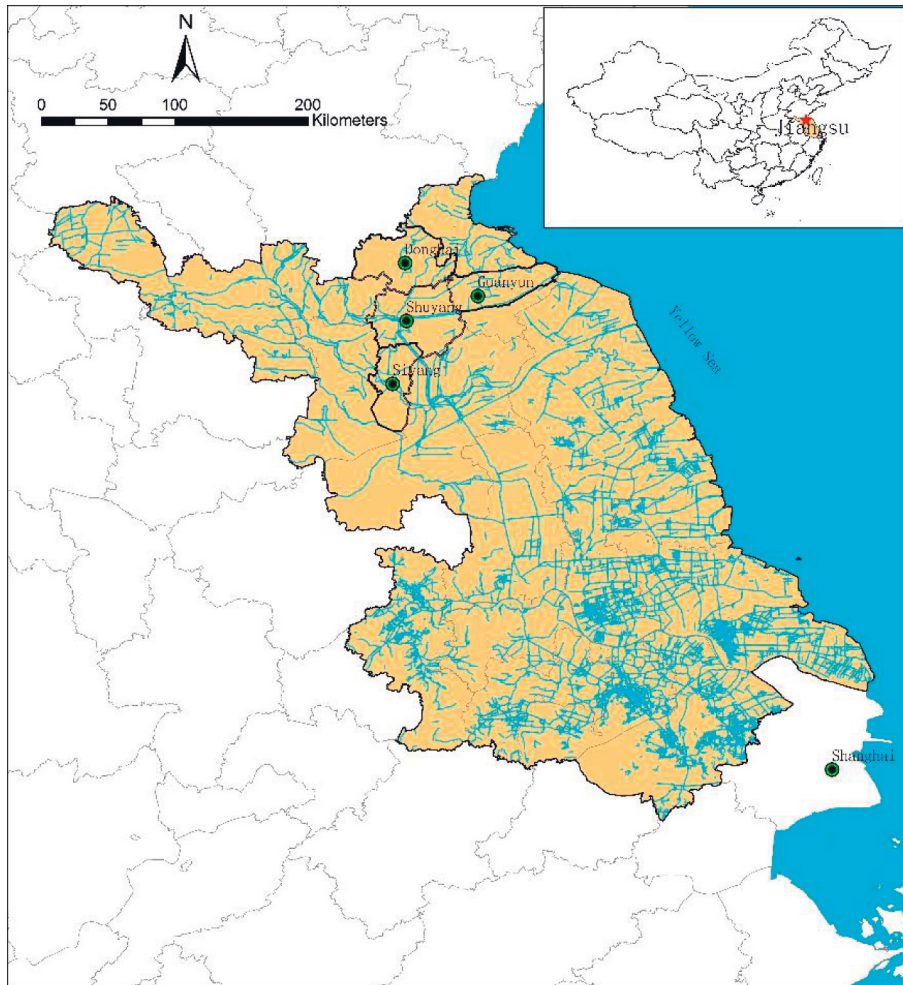


FIGURE 2: Map of sites.

3.3. Measures. The measurement tools used in this research are all scales that have been used in Anglophone research. We translated and back-translated each item of the scale to improve the accuracy of language expression. We referred to the 11-item scale developed by Spreitzer [63] to measure the hometown identity. Examples of topics included: “It makes sense for me to return to my hometown to start a business” and “Hometown is a good platform for entrepreneurship.” We referred to Cummings’ 5-item scale [64] to measure agglomeration strategy; examples include: “How often do you share your experience during the entrepreneurial period?” We also referred to Zhou and George [65] and used the 5-point

Likert scale to study the creativity of returnees. We modified the scale in the context of entrepreneurship in China to obtain the opinions of key informants from the team of returnees. Examples of these points included “the returnee often has novel ideas for entrepreneurial development projects.” For the measurement of entrepreneurial success, we referred to the research of Liñán and Chen [66] with items, such as “I have completed the entrepreneurial goals.”

In the above scale, the item’s measurement scores used a 5-level judgment matrix, from 1 to 5 representing completely disagree to completely agree, never to many, and exceptionally low to very high. Using Cronbach’s α

TABLE 1: Factor analysis.

Variable	Minimum factor loading	Cronbach's α	KMO	Total variance explained (%)
Home identity	0.79	0.85	0.89	67.11
Returnee creativity	0.63	0.77	0.82	58.73
Agglomeration strategy	0.71	0.76	0.78	59.41
Entrepreneur success	0.82	0.91	0.91	74.31

coefficient as the criterion of reliability, the obtained hometown identity, agglomeration strategy, the creativity of returnees, and the success or failure of entrepreneur were 0.85, 0.77, 0.76, and 0.91, respectively.

4. Empirical Results

4.1. Reliability and Validity Test. In this study, we used Cronbach's α coefficient as the reliability criterion, and Table 1 displays the results. The alpha value of each variable was higher than 0.7, and the KMO value was also higher than 0.7. The minimum value of the total variance contribution rate was 58.73%, and the minimum factor loading was 0.63, which is higher than the acceptable critical value.

Table 2 lists the mean (Mean), standard deviation (SD), and correlation coefficient of each variable. It is evident from Table 2 that the composite reliability of each concept is relatively high, with a minimum value of 0.86. In the test of discriminative validity, we used the AVE value for judgment. Combining with Table 3, the AVE values are visibly all higher than 0.5, and the square root of AVE is greater than the correlation coefficient between the variable itself and other variables, showing that each variable has a higher discriminative validity. Meanwhile, using AMOS17.0 to perform confirmatory factor analysis on variables, the results show that the basic model of this study has a good fit ($\chi^2/df = 2.508$, CFI = 0.936, GFI = 0.882, TLI = 0.927, IFI = 0.937, NFI = 0.901, RMSEA = 0.059); each index basically meets the standard, and the discrimination validity is good.

4.2. Common Method Variance (CMV). Since the survey data acquisition method is mainly through the self-report method of the online questionnaire, the common method deviation may be abnormal. However, several targeted measures have been taken in our survey design process to avoid this deviation. First, we used a time-lag survey design to establish time intervals between the measurement results of the main variables [62]. Second, by using the feedback of key informants from the returnees' cluster team to measure the creativity of other returnees, we limited self-reporting bias. Third, we ensured the anonymity and confidentiality of their answers and established good social relationships in the preliminary investigation. Through this, we urged them to answer questions as honestly as possible, thus reducing research bias.

Finally, we used the Harman single factor test to ascertain the common method deviation. The analysis results show that all items were automatically aggregated into four factors with eigenvalues greater than 1, with the total variance contribution rate at 64.89%. Among them, the first factor explained 32.79% of the variance of all items, which

did not account for half of the total variance explained, indicating that we had successfully controlled the common method deviation of the data in this paper.

4.3. Tests of Hypotheses

4.3.1. Test of the Relationship between Hometown Identity, Agglomeration Strategy, and Entrepreneurial Success. Controlling for the gender, age, and education level of interviewees, this study performed multiple regression analysis on the relationships among the core variables studied, as shown in Table 3. M3 examined the influence of control variables on dependent variables, and the results show that gender is a factor that affects entrepreneurial success, while age and the education level did not significantly affect individual entrepreneurial success. In order to verify the main effect, we introduced independent variables on the basis of M3. It can be seen from M4 that the influence of the hometown identity on entrepreneurial success reached significance ($\beta = 0.58$, $P < 0.01$). The hometown identity could explain 36% of the total variation of entrepreneurial success, indicating that it had a significant impact on entrepreneurial success. Therefore, Hypothesis 1 is verified.

M2 uses agglomeration strategy as the dependent variable and the hometown identity as the independent variable for regression. The results show that the hometown identity had a significant positive effect on agglomeration strategy ($\beta = 0.63$, $P < 0.01$), and the hometown identity explained 40% of the total variance of agglomeration strategy. M5 examines the relationship between agglomeration strategy and entrepreneurial success. The results show that agglomeration strategy has a significant positive impact on entrepreneurial success ($\beta = 0.59$, $P < 0.01$), thus supporting Hypothesis 2.

4.3.2. The Mediation Test of Agglomeration Strategy. The Baron and Kenny's mediating effect test method (1986) [67] was used to verify the mediating effect of agglomeration strategy. The first step is to test whether the independent variable has a significant influence on the dependent variable. It can be seen from M4 that the hometown identity has a significant positive effect on entrepreneurial success ($\beta = 0.58$, $P < 0.01$); the second step is to test whether the independent variable, hometown identity, has a significant effect on intermediary variable agglomeration strategy. The results of M2 show that the hometown identity has a significant positive effect on agglomeration strategy ($\beta = 0.63$, $P < 0.01$); the third step is to perform the regression of the dependent variable on the independent variable and the intermediate variable, and apply the independent variable's

TABLE 2: Descriptive statistics and correlations.

Variables	Mean	SD	1	2	3	4	5	6	7
1. Gender	1.47	0.51							
2. Age	1.81	0.58	-0.132**						
3. Education level	1.74	0.43	0.016	0.036					
4. Home identity (T1)	3.22	0.67	-0.202**	-0.008	-0.064	0.773			
5. Returnee creativity (T2)	3.33	0.64	-0.118*	0.025	-0.119*	0.625**	0.771		
6. Agglomeration strategy (T1)	3.14	0.72	0.081	-0.081	-0.043	-0.071	-0.011	0.756	
7. Entrepreneur success (T1)	3.21	0.78	-0.199**	0.049	-0.002	0.598**	0.594**	-0.461**	0.83
AVE						0.61	0.59	0.57	0.72
CR						0.91	0.87	0.86	0.93

Note. ** $P < 0.01$, * $P < 0.05$; The diagonal is the square root of AVE; T = TIME.

TABLE 3: Multiple regression analysis results.

	Agglomeration strategy			Entrepreneur success				
	M1	M2	M3	M4	M5	M6	M7	M8
Gender	0.116*	-0.014	0.198**	0.075	0.129**	0.081*	0.099**	0.092**
Age	0.016	0.038	0.024	0.044	0.014	0.030	-0.015	-0.024
Education level	0.110*	0.072	0	-0.036	-0.065	-0.062	-0.047	-0.030
Home identity		0.63**		0.58**		0.36**		
Agglomeration strategy					0.58**	0.37**	0.58**	0.53**
Returnee creativity							0.42**	0.41**
Agglomeration strategy × returnee creativity								0.18**

Note. ** $P < 0.01$, * $P < 0.05$, $M = \text{Model}$.

hometown identification and intermediate variable agglomeration strategy into regression equation simultaneously. As M6 shows, agglomeration strategy has a significant impact on entrepreneurial success ($\beta = 0.37$, $P < 0.01$). The influence of the hometown identity on entrepreneurial success is also significant ($\beta = 0.36$, $P < 0.01$), but its regression coefficient has declined ($0.36 < 0.58$). This shows that agglomeration strategy has a partial mediating effect between hometown identification and entrepreneurial success. Thus, Hypothesis 2 is verified.

4.3.3. The Moderating Effect Test of Returnees' Creativity. In testing Hypothesis 3, that is, the influence of returnees' creativity on the relationship between the hometown identity and entrepreneurial success, we first set entrepreneurial success as the dependent variable. We gradually add the control variables, agglomeration strategy, and returnees' creativity, as well as the product of agglomeration strategy and returnees' creativity, namely M3, M7, and M8 in Table 3. In order to eliminate the problem of collinearity, we processed agglomeration strategy and returnees' creativity separately, and then constructed the product term of the two. As M8 shows, the product term of agglomeration strategy and the creativity of returnees has a significant positive impact on entrepreneurial success ($\beta = 0.18$, $P < 0.01$). This shows that the positive impact of agglomeration strategies on entrepreneurial success strengthens when returnees' creativity increases. This verifies Hypothesis 3.

5. Discussion and Conclusion

This article focuses on the relationship between the hometown identity of rural returnees and their entrepreneurial success with the operations research framework. It discusses the relationship between the hometown identity, agglomeration strategy, entrepreneurial success, and the creativity of returnees. Through qualitative and quantitative surveys of 197 entrepreneurs returning to their rural hometowns in the coastal plains of Jiangsu Province, the study verifies the following: (1) The hometown identity of returnees has a significant positive impact on entrepreneurial success; (2) Agglomeration strategy can adjust and complement the relationship between the hometown identity and entrepreneurial success; and (3) Creativity coupled with agglomeration strategies enhances the indirect influence of the hometown identity on entrepreneurial success.

In this study, we proved that the hometown identity of returnees can be beneficial to entrepreneurial success. Our results are consistent with previous research hypotheses, indicating that since the strong hometown identity of returnees provides motivation for success, the willingness to venture into entrepreneurship will increase [68]. According to Bandura's self-efficacy theory [69], the identity of the entrepreneurial subject (individual or team) plays a fundamental role in the self-efficacy of returnees. The hometown identity can not only provide them with the resource support they need for entrepreneurship but also enhance the

entrepreneur's self-efficacy by replacing role models, verbal persuasion, and awakening. This level of performance translates into returnees' success.

In addition, agglomeration strategy significantly moderated this relationship because returnees drew great intrinsic motivation from it. Participating in the knowledge-sharing of the agglomeration space improved their performance and ultimately increased the success rate of entrepreneurship [70]. In addition, we discovered the moderating effect of returnees' creativity on the hometown identity and entrepreneurial success. Highly creative returnees achieved success by implementing ideas to achieve a competitive advantage [71]. Therefore, returnees with higher creativity were more likely to participate in entrepreneurial knowledge-sharing activities.

5.1. Theoretical Implications. This research advances the literature on the hometown identity, agglomeration strategy, and returnees' creativity from four important aspects. First, through research hypothesis testing to study the relationship between variables, it provides theoretical enlightenment for our research. We hypothesize that the hometown identity and creativity significantly affect the entrepreneurial success of returnees. We supplement the literature through our examination of the indirect effects of returnees' creativity and agglomeration strategies. Our results show that the hometown identity and creativity of returnees can solve the difficulties and challenges encountered in entrepreneurship, such as isolation, through the cooperative nature of agglomeration strategy and by inspiring them to achieve better results. In most cases, these strategies can enable returnees to make better decisions through coping strategies, such as cooperation and collusion and knowledge complementation. Second, by incorporating agglomeration strategy as an intermediary mechanism into this research, we have increased and deepened the research on the hometown identity and entrepreneurial success. Third, this article highlights the role of the creativity of returnees and uses appropriate mediation methods to determine the relationship between the hometown identity and the success of returnee entrepreneurship, thereby deepening our understanding and supplementing the literature.

Our research emphasizes that creative returnees will exert their motivation for themselves and their hometowns, and drive the rural economy and the common development of the villagers. Because of their hometown identity, the returnees nurture a strong cohesion within their group, which promotes the formation of clusters to encourage more fluid knowledge complementation. Logically, the quality of knowledge shared among agglomeration groups is a direct result of the scale of the entrepreneurs' creativity. Finally, through empirical research, we analyzed the relationship between the hometown identity, agglomeration strategy, returnees' creativity, and returnees' entrepreneurial success. This contributes to the development of rural areas in Chinese cases and literature supplements, and verifies that the

China's rural revitalization model is effective in non-developed countries.

5.2. Managerial Implications. This research has practical reference significance for the top-down management of the village. Since there is a direct connection between the hometown identity of returnees and their entrepreneurial success, this study suggests that government personnel should establish the policy mechanism, financial support, and social security mechanism for the formation, maintenance, and consolidation of the hometown identity from the perspective of operations research. Government can also play a part in consolidating and enhancing the observable factors (such as rural environmental governance and improvement of transportation facilities) and intangible factors that affect the formation of the hometown identity in all directions (developing beneficial cultural concepts and eliminating patriarchal customs), and prioritizing the empowerment of returnees. The local residents and returnees can learn from agglomeration strategy to form a creative space for rural development, and provide professional knowledge support for the development of rural industries and the improvement of villagers' livelihoods. Entrepreneurial partners face challenges often, and these measures would help them persevere and support their creativity in the face of such adversity.

Returning entrepreneurs need to consider many factors, such as the self-efficacy of their creativity, internal motivation, and satisfaction, that are closely related to personal entrepreneurial values. The factors are interrelated, and the lack of any one factor may have an adverse effect on their creativity and consequent success. In order to improve the creativity of returnees, the policy support and efficiency of the local government are crucial to the success of returnees' entrepreneurship. Local government managers should establish supportive measures to develop the assembly of returnees in order to spread knowledge and share entrepreneurial insights to support rural development. Local governments, where conditions permit, can also use incentive measures to encourage rural areas to form a good entrepreneurial atmosphere for industrial agglomeration and development.

5.3. Limitations and Directions for Future Research. Although this article has certain theoretical and practical significance for the study of rural decline and development from the perspective of the hometown identity and returnee entrepreneurship, there are still some limitations. First, this article used a self-assessment questionnaire to measure the relationship between the hometown identity and entrepreneurial success, which can be susceptible to various biases. In future research, especially when the epidemic is over, it will be necessary to conduct a return survey of questionnaire participants in the field to obtain a more objective measurement of this relationship. Second, this research focuses on the impact of the hometown identity on the success of returnees' entrepreneurship. We can explore the impact of returnees' creativity on entrepreneurial performance,

entrepreneurial growth, and rural industry development. Third, constrained by the epidemic, the samples in this study are concentrated in the rural areas of the Yangtze River Delta in China.

Also, we can further expand the scope of investigation and increase the number of samples to improve the external validity of research conclusions in future. Furthermore, the emergence of an entrepreneurship model by hometown returnees will be a good catalyst and input for future research on rural revitalization and sustainable development. The following research areas will be stimulated: (1) how to formulate policies to attract returnees; (2) how returnees can harness their creativity to build entrepreneurial advantages; and (3) how to construct the returnee identity. Along with the accumulation and exploration of these studies, the paradigm of rural development will become more and more scientific and perfect.

Data Availability

The data used to support the findings of this study are available from the corresponding author upon request.

Disclosure

The authors Chongliang Ye, Xumei Miao and Xiaoyan Feng contributed equally to this work and should be considered co-first authors.

Conflicts of Interest

The authors declare that they have no conflicts of interest.

Acknowledgments

The authors would like to thank all members who were involved in the research upon which this paper is based and the two referees for their helpful improvement.

References

- [1] D. Saunders, *Arrival City: How the Largest Migration in History Is Reshaping Our World* Random House, New York, NY, U.S.A, 2011.
- [2] F. Gao, "The "miracle" of China's poverty reduction from the perspective of urban-rural dual structure transformation," *Academic Monthly*, vol. 4, pp. 54–66, 2020.
- [3] E. Jie, "Urbanisation and poverty reduction in rural China," *Economic Science*, vol. 03, pp. 5–16, 2020.
- [4] J. Guo and Q. Liu, "Declining fertility rates and the anti-discriminatory growth of girl education in rural China," *Ideological Front*, vol. 4, pp. 34–39, 2013.
- [5] C. Wu, "From an acquaintance society to a "no subject acquaintance society," *Reading*, vol. 01, pp. 19–25, 2011.
- [6] H. Zhang, X. Lin, R. Liang, and J. Lan, "Urban ecological civilisation construction and a new generation of labor mobility: a new perspective of labor resource competition," *China Industrial Economy*, vol. 4, pp. 81–97, 2019.
- [7] B. Liu and G. Wang, "Research on farmers' subjectivity in rural revitalization in the new era," *Explorations*, vol. 05, pp. 116–123, 2019.

- [8] L. H. Berckmoes and B. White, "Youth, farming, and precarity in rural Burundi," in *Generationing Development*, pp. 291–312, Palgrave Macmillan, London, U.K, 2016.
- [9] B. White, "Agriculture and the generation problem: rural youth, employment and the future of farming," *IDS Bulletin*, vol. 43, no. 6, pp. 9–19, 2012.
- [10] J. Chen, H. Zhu, and C. Weng, "Targeted poverty alleviation policies and relative poverty in rural areas: based on the analysis of poor villages and establishment of files," *Journal of Jiangsu University (Natural Science Edition)*, vol. 5, pp. 39–51, 2020.
- [11] M. Qi, J. Liang, and H. Wang, "The sustainable path of rural entrepreneurship under the rural revitalization strategy," *Journal of Northwest University for Nationalities (Philosophy and Social Sciences Edition)*, vol. 02, pp. 105–114, 2022.
- [12] F. Zhao and Y. Wang, "A study on the impact of market-oriented credit and non-market-oriented credit on the performance of returning entrepreneurial enterprises—evidence based on the questionnaire of China's returning entrepreneurial enterprises," *Economics*, vol. 04, pp. 67–81, 2022.
- [13] S. Chen and C. Li, "Monitoring and analysis of migrant workers returning to hometown pioneer parks based on mobile phone signaling," *China Agricultural Resources and Zoning*, vol. 12, pp. 154–159, 2021.
- [14] R. Garber, "Coming full circle: new ruralism," *Architectural Design*, vol. 87, no. 3, pp. 104–113, 2017.
- [15] S. Zhang, "Suqian: implementing the "Returning Hometown and Establishing Business Plan" to create a green channel for young people to return to their hometowns to start businesses," *Chinese Communist Youth League*, vol. 21, pp. 16–17, 2020.
- [16] C. Liu and G. Huang, "Theoretical perspective, realistic opportunities and development challenges of migrant workers returning to their hometowns to start a business," *Economic Circle*, vol. 6, pp. 83–87, 2016.
- [17] M. Liu, Q. Zhang, S. Gao, and J. Huang, "The spatial aggregation of rural e-commerce in China: an empirical investigation into Taobao Villages," *Journal of Rural Studies*, vol. 80, pp. 403–417, 2020.
- [18] Y. D. Wei, J. Lin, and L. Zhang, "E-commerce, taobao villages and regional development in China," *Geographical Review*, vol. 110, no. 3, pp. 380–405, 2020.
- [19] B. Chen, "Rural complex and rural revitalisation: the approach and prospect of Chinese rural anthropology research," *Guangxi Ethnic Studies*, vol. 6, pp. 94–102, 2020.
- [20] A. Louie, *Chineseness across Borders: Renegotiating Chinese Identities in China and the United States*, Duke University Press, Durham, NC, U.S.A, 2004.
- [21] S. Model, "Falling leaves return to their roots': Taiwanese-Americans consider return migration," *Population, Space and Place*, vol. 22, no. 8, pp. 781–806, 2016.
- [22] B. Hu, "Cultivating contemporary rural sages and rebuilding rural society," *Social Governance*, vol. 2, pp. 103–108, 2016.
- [23] X. Fei, *Fertility System in Rural China*, Peking University Press, Beijing, China, 1998.
- [24] R. Ma, "The pattern of differences" —an interpretation of Chinese traditional social structure and Chinese behaviour," *Journal of Peking University*, vol. 2, pp. 131–142, 2007.
- [25] M. Luo and B. Chen, "Research on the influencing factors and effects of villagers' willingness to participate in rural revitalisation," *Hunan Social Sciences*, vol. 6, pp. 69–78, 2020.
- [26] Y. Shen, "The cultural crisis in rural revitalization and the reconstruction of cultural confidence—based on the perspective of cultural sociology," *Academics*, vol. 245, no. 10, pp. 56–66, 2018.
- [27] C. Tan, "Analysis of the plight and countermeasures of rural youth returning to start a business under the background of rural revitalisation," *Hubei Agricultural Sciences*, vol. 19, pp. 178–182, 2020.
- [28] F. Jin, *Research on the Application Strategy of Collaborative Design in the Promotion of Rural Food Value*, Master's Thesis, Jiangnan University, Wuxi, China, 2017.
- [29] F. Sun, "Research on the sustainable development of traditional cultural space tourism from the perspective of experience," *Journal of Sichuan Tourism University*, vol. 1, pp. 27–31, 2021.
- [30] R. Gill and G. S. Larson, "Making the ideal (local) entrepreneur: place and the regional development of high-tech entrepreneurial identity," *Human Relations*, vol. 67, no. 5, pp. 519–542, 2014.
- [31] X. Su, J. Xiao, and J. Chen, "Entrepreneur's social identity recognition and new venture innovation," *Southern Economics*, vol. 10, pp. 108–124, 2020.
- [32] H. Patzelt, T. A. Williams, and D. A. Shepherd, "Overcoming the walls that constrain us: the role of entrepreneurship education programs in prison," *The Academy of Management Learning and Education*, vol. 13, no. 4, pp. 587–620, 2014.
- [33] J. Tang, Z. Tang, and F. T. Lohrke, "Developing an entrepreneurial typology: the roles of entrepreneurial alertness and attributional style," *The International Entrepreneurship and Management Journal*, vol. 4, no. 3, pp. 273–294, 2008.
- [34] K. Baird, S. Su, and R. Munir, "The relationship between the enabling use of controls, employee empowerment, and performance," *Personnel Review*, vol. 47, no. 1, pp. 257–274, 2018.
- [35] J. Guichard, "Self-constructing," *Journal of Vocational Behavior*, vol. 75, no. 3, pp. 251–258, 2009.
- [36] H. Hoang and J. Gimeno, "Becoming a founder: how founder role identity affects entrepreneurial transitions and persistence in founding," *Journal of Business Venturing*, vol. 25, no. 1, pp. 41–53, 2010.
- [37] S. Stryker, "Integrating emotion into identity theory," in *Theory and Research on Human Emotions* Emerald Group Publishing Limited, Bingley, U.K, 2004.
- [38] S. Stryker and P. J. Burke, "The past, present, and future of an identity theory," *Social Psychology Quarterly*, vol. 63, no. 4, pp. 284–297, 2000.
- [39] G. Charness, E. Karni, and D. Levin, "Individual and group decision making under risk: an experimental study of Bayesian updating and violations of first-order stochastic dominance," *Journal of Risk and Uncertainty*, vol. 35, no. 2, pp. 129–148, 2005.
- [40] M. Ipe, "Knowledge sharing in organizations: a conceptual framework," *Human Resource Development Review*, vol. 2, no. 4, pp. 337–359, 2003.
- [41] L. Argote, "Organisational Learning: Creating, Retaining, and Transferring Knowledge," Springer, New York, U.S.A, 1999.
- [42] W. T. Wang, Y. S. Wang, and W. T. Chang, "Investigating the effects of psychological empowerment and interpersonal conflicts on employees' knowledge sharing intentions," *Journal of Knowledge Management*, vol. 23, no. 6, pp. 1039–1076, 2019.
- [43] J. A. Peerally and C. D. Fuentes, "Typifying latecomer social enterprises by ownership structure: learning and building knowledge from innovation systems," in *Entrepreneurial Ecosystems Meet Innovation Systems* Edward Elgar Publishing, Cheltenham, U.K, 2020.

- [44] Y. Wang, *Research on the Internal Mechanism of Organisational Knowledge Construction*, Ph.D. Thesis, Nanjing University, Nanjing, China, 2013.
- [45] H. Zhang, "Triple-driven interpersonal trust mechanism," *Journal of Xi'an Jiaotong University*, vol. 3, pp. 29–33, 2006.
- [46] R. Xiao, X. Liu, and Z. Liu, "Co-evolution mechanism and equilibrium analysis among populations within the ecosystem of agricultural industrial clusters," *Jiangsu Agricultural Sciences*, vol. 24, pp. 298–301, 2017.
- [47] X. Liu, "Research on the Entrepreneurial Ecosystem of College Students in Jiangsu Based on Ecology," Master's thesis, Nanjing Forestry University, Nanjing, China, 2020.
- [48] R. D. Wadhvani, D. Kirsch, F. Welter, W. B. Gartner, and G. G. Jones, "Context, time, and change: historical approaches to entrepreneurship research," *Strategic Entrepreneurship Journal*, vol. 14, no. 1, pp. 3–19, 2020.
- [49] Z. Wang, "How 'live broadcast+ e-commerce' can help rural revitalisation," *People's Forum*, vol. 15, pp. 98–99, 2020.
- [50] Y. Jiang, "Research on the Mechanism and Effects of Rural E-Commerce Industry Agglomeration and Regional Economic Synergistic Development," Master's thesis, Hangzhou Dianzi University, Hangzhou, China, 2020.
- [51] W. Sun, "The mechanism analysis of entrepreneurial vigilance, psychological capital, and knowledge sharing on college students' entrepreneurial decision-making," *Journal of Yangzhou University (Agricultural and Life Science Edition)*, vol. 1, pp. 72–75, 2016.
- [52] Y. Mao, "The basis, types and functions of young people returning to their hometowns to start a business under the background of rural revitalisation," *Journal of Agricultural and Forestry Economics and Management*, vol. 1, pp. 1–9, 2021.
- [53] S. Feihan, D. Haidong, Y. Chongliang, and M. Xumei, "The counter-urbanization creative class and the sprout of the creative countryside: case studies on China's coastal plain villages," *Journal of Economy Culture and Society*, vol. 63, pp. 1–19, 2021.
- [54] Y. Zheng and C. Lu, "The path to attracting college students to return to their hometowns to start their own businesses: taking Dazhangzhuang Town, Yiyuan County as an example," *Rural Science and Technology*, vol. 27, pp. 24–25, 2020.
- [55] X. Li and X. Zhao, "Live broadcast to help farmers: a new model of rural e-commerce that integrates rural revitalisation and network poverty alleviation," *Business and Economic Research*, vol. 19, pp. 131–134, 2020.
- [56] F. Ma and W. Li, "The influence of the new rural culture on the entrepreneurial behaviour of young people returning home," *Science and Technology of Energetic Materials*, vol. 1, pp. 18–20, 2021.
- [57] M. Entrialgo and V. Iglesias, "Entrepreneurial intentions among university students: the moderating role of creativity," *European Management Review*, vol. 17, no. 2, pp. 529–542, 2020.
- [58] S. S. Metwaly, B. F. Castilla, E. Kyndt, and W. V. D. Noortgate, "Testing conditions and creative performance: meta-analyses of the impact of time limits and instructions," *Psychology of Aesthetics, Creativity, and the Arts*, vol. 14, no. 1, pp. 15–38, 2020.
- [59] X. Zhang and K. Zhang, "The relationship between creativity and entrepreneurial intention: a moderated mediating effect model," *Foreign Economics and Management*, vol. 40, no. 3, pp. 67–78, 2018.
- [60] J. L. Xing and N. Sharif, "From creative destruction to creative appropriation: a comprehensive framework," *Research Policy*, vol. 49, no. 7, Article ID 104060, 2020.
- [61] T. M. Amabile, "The social psychology of creativity: a componential conceptualization," *Journal of Personality and Social Psychology*, vol. 45, no. 2, pp. 357–376, 1983.
- [62] P. M. Podsakoff, S. B. MacKenzie, J. Y. Lee, and N. P. Podsakoff, "Common method biases in behavioral research: a critical review of the literature and recommended remedies," *Journal of Applied Psychology*, vol. 88, no. 5, pp. 879–903, 2003.
- [63] G. M. Spreitzer, "Psychological, empowerment in the workplace: dimensions, measurement and validation," *Academy of Management Journal*, vol. 38, no. 5, pp. 1442–1465, 1995.
- [64] J. N. Cummings, "Work groups, structural diversity, and knowledge sharing in a global organization," *Management Science*, vol. 50, no. 3, pp. 352–364, 2004.
- [65] J. Zhou and J. M. George, "When job dissatisfaction leads to creativity: encouraging the expression of voice," *Academy of Management Journal*, vol. 44, no. 4, pp. 682–696, 2001.
- [66] F. Liñán and Y. W. Chen, "Development and cross-cultural application of a specific instrument to measure entrepreneurial intentions," *Entrepreneurship: Theory and Practice*, vol. 33, no. 3, pp. 593–617, 2009.
- [67] R. M. Baron and D. A. Kenny, "The moderator-mediator variable distinction in social psychological research: conceptual, strategic, and statistical considerations," *Journal of Personality and Social Psychology*, vol. 51, no. 6, pp. 1173–1182, 1986.
- [68] S. B. Dust, C. J. Resick, J. A. Margolis, M. B. Mawritz, and R. L. Greenbaum, "Ethical leadership and employee success: examining the roles of psychological empowerment and emotional exhaustion," *The Leadership Quarterly*, vol. 29, no. 5, pp. 570–583, 2018.
- [69] A. Bandura, "Self-efficacy," *The Corsini Encyclopedia of Psychology*, John Wiley & Sons, Hoboken, NJ, U.S.A., pp. 1–3, 2010.
- [70] C. Law and E. Ngai, "An empirical study of the effects of knowledge sharing and learning behaviors on firm performance," *Expert Systems with Applications*, vol. 34, no. 4, pp. 2342–2349, 2008.
- [71] H. Kremer, I. Villamor, and H. Aguinis, "Innovation leadership: best-practice recommendations for promoting employee creativity, voice, and knowledge sharing," *Business Horizons*, vol. 62, no. 1, pp. 65–74, 2019.

Research Article

Application of Computer 3D Modeling Technology in the Simulation Design of Modern Garden Ecological Landscape

Zhiyong Tian 

College of Arts, Henan University of Animal Husbandry and Economy, Zhengzhou 450000, Henan, China

Correspondence should be addressed to Zhiyong Tian; 81413@hnuah.edu.cn

Received 29 March 2022; Accepted 16 May 2022; Published 25 June 2022

Academic Editor: Wei Liu

Copyright © 2022 Zhiyong Tian. This is an open access article distributed under the Creative Commons Attribution License, which permits unrestricted use, distribution, and reproduction in any medium, provided the original work is properly cited.

Modern landscape design not only needs creativity but also needs auxiliary tools that can predict the design effect, so as to ensure that the deficiencies can be found through the renderings before the landscape is completed, and targeted rectification can be carried out. At present, the research of landscape planning and design assisted by virtual reality technology in China is basically in its infancy. The rapid development of information-based computer technology, powerful 3D modeling, and solid rendering and animation functions have created a good environment for landscape design, so landscape design is inseparable from the help of computer-aided design technology. However, the conventional method to model and simulate the landscape is rather time-consuming. Based on the research on the application of computer-aided design technology in landscape design, the computer-aided design technology is briefly explained, and the application of computer-aided landscape design is explored step by step.

1. Introduction

The garden landscape is relatively long such as the palace garden landscape in the West and the classical garden in China. More often, only some limited thoughts can be expressed, and they cannot be fully conveyed and expressed to others. On the one hand, with the progress and development of science and technology, landscape architects are gradually liberated from primitive and inefficient tools and labor, especially the rapid development of computer technology, the efficiency of hardware, and the rapid update and iteration of software, garden landscape engineering design is also gradually getting rid of the shackles of paper and pen, especially with the emergence of drawing software technology, a fundamental breakthrough has been made in the working methods and efficiency of designers, and they are freed from heavy drawing tasks. On the other hand, with the rapid development of the economy and society, environmental problems have become more and more prominent [1–3]. Whether for a country or for an individual, the expectations and attention to garden landscapes have reached an unprecedented height. The country has successively formulated garden cities and gardens. The standard of the

county seat has now been upgraded to require the construction of an ecological garden city and encourage and support the construction of urban garden landscape belts, green corridors, and greenways across the country to meet people's demands for green, green mountains, and clear waters. These have laid a solid foundation for the great development of the garden landscape. In recent years, computer-aided technology has made great progress, the existing assistive technologies and platforms have been optimized, and some of them have become special technologies for landscape design, such as sketch masters [4–6].

The application of computers to engineering design is called CAD technology. At present, the application of CAD technology in landscape design is mainly in drawing pictures and is a part of auxiliary calculation [7, 8]. Among them, AutoCAD is the most popular computer-aided design software used at home and abroad. With its colorful drawing functions, smart editing functions, and superior user interface, AutoCAD enjoys a good reputation among engineers and technicians and is generally welcomed by everyone. In particular, AutoCAD software also provides a variety of editing tools and interfaces, making it convenient for users to complete secondary development and

manufacturing on the basis of this software. In addition, AutoCAD software enhances the functions of 3D modeling and image processing, and also has a powerful set of additional tools, supports ActiveX automation programming interface, has powerful network drawing functions, supports a variety of image access formats, and is compatible with different CAD systems. Graphics can be transferred further [9–11]. Computer-aided technology has a good application in all aspects, especially in the field of landscape planning and design, there is a broader prospect, and landscape designers need to strengthen the study and application of this aspect.

With the popularization of the internet and the advent of the electronic information age, virtual technology has been applied to all walks of life. However, with the continuous development of virtual technology, its drawbacks are gradually discovered by people [12]. The purpose of people applying this technology is only to meet their own needs, to have a more detailed and comprehensive observation of the real environment, and to avoid some omissions in the observation of the environment caused by some objective factors, rather than to use the virtual environment to replace it. The real environment place, but due to some technical problems, such as the running speed of the equipment and the quality of modeling, not only can it not restore the real scene but also distort the image and cause information loss, resulting in an unsatisfactory user experience [13–15]. Therefore, in order to improve this problem, people have invented a new technology-augmented reality technology. As a kind of virtual technology, augmented reality technology combines computer technology with real situations to generate a very realistic 3D virtual environment, so that users can experience it through various sensing devices. Today, this technology has been used in technology, entertainment, medical, and military industries, and has good developmental prospects [16, 17].

In the past, the frame of the garden design was expressed by hand-drawing. With the progress of the times and the development of computer software and hardware technology, the new technology of 3D drawing became more and more popular. This does not mean that 3D drawings can completely replace traditional manual drawings, but they are better applied to garden design separately. That is, we use manual drawing in the early stage of design and use 3D drawing when drawing high-quality drawings. The 3D has made technical improvements to Editable Poly with almost every upgrade, so its capabilities go beyond editing meshes to become the primary tool for polygon modeling [18–20]. It takes a brand-new perspective to do landscape planning and design, modeling, virtual tour, and other technologies that can be combined with the real landscape, complement each other, better express its design ideas, and design intentions.

The requirement for designers is to be proficient in 3D drafting-related software, as shown in Figure 1. At present, the overall requirements for designers are getting higher and higher, and the use of software to express design intentions is far from meeting the design requirements. It is also necessary to coordinate various related software to exert their respective functions and characteristics. With the rapid

development of the times, the requirements for design and drawing personnel in various fields are also getting higher and higher. Designers themselves are also dissatisfied with only relying on 3D drawing software to achieve depapering operations. They are more inclined to use 3D software to improve their work quality and devote their energy to more meaningful work [21, 22].

Driven by the development of information technology, the efficiency of landscape design has been improved. In order to more accurately express the intention of landscape design, the field of landscape design has already entered a new era. The application of CAD technology to assist landscape design has long been the general trend. Therefore, as a landscape designer, you need to dare to try and apply more, and you need to master the functions and characteristics of CAD, so as to ensure that this technology becomes a good tool for expressing your design intentions [23, 24]. At the same time, in the development of science and technology, all kinds of software are constantly innovating, and this part of the software has many shortcut commands, so designers also need to strengthen the mastery of shortcut commands to improve work efficiency. Landscape engineering design is the science and art of the analysis, planning, layout, design, transformation, management, protection, and restoration of landscape engineering. Built on the basis of artistic esthetics and natural science, it is the product of their combination. The use of land according to local conditions is the key to garden landscape planning and design. Scientific and artistic esthetic planning, utilization, and analysis of land, topography, landforms, etc. are carried out, and perfect solutions are obtained to create more in line with people's esthetic needs and ecology. This study focuses on computer-aided technology, introduces the contemporary mainstream computer-aided software and platforms, and also expounds on the application in the planning and design process of landscape engineering. First of all, it gives an overview of the developmental history of garden landscape design and also introduces the process of the gradual combination and application of computer-aided technology in landscape planning and design. The basic concepts of modern garden landscape planning and design can include the scheme of garden planning and design and the computer-aided technology garden design technology [25, 26]. Therefore, first of all, it gives an overview of the development history of garden landscape design and also introduces the process of the gradual combination and application of computer-aided technology in landscape planning and design, the basic concepts of modern garden landscape planning and design, including the introduction of garden planning and design thinking, and the current situation of designers using computer-aided technology and related design software.

2. Mathematical Modeling of Garden Landscape

Due to its complexity and diversity, garden landscape design has not had a relatively unified and authoritative definition in the academic world. The landscape itself has dual attributes of geography and ecological type. From the perspective

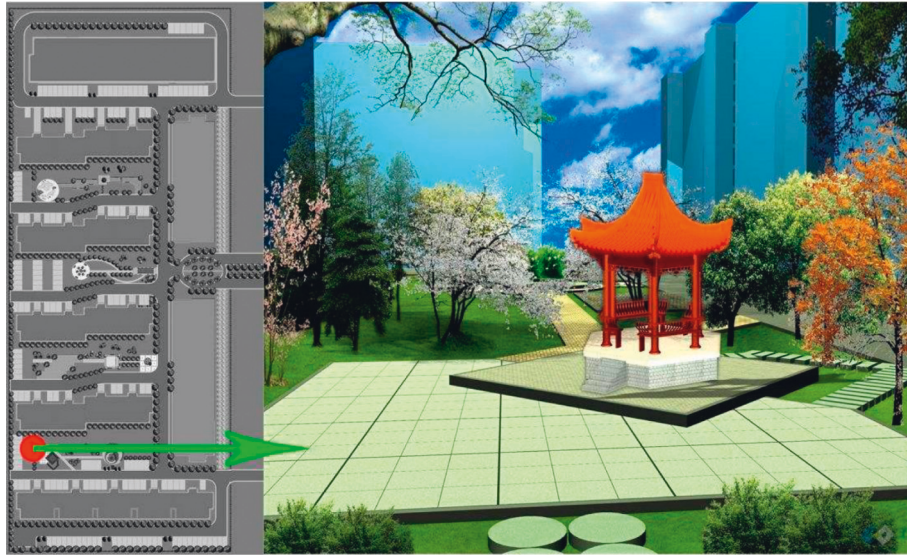


FIGURE 1: 3D-assisted garden drafting.

of geography, more attention is paid to the entire landscape such as topography and landforms. From an ecological point of view, more attention is paid to the collocation and relationship between plants and nonplants in the landscape, and it is more willing to treat the landscape as a self-circulating ecological system; on this basis, garden landscape planning and design are considered to be “complex objects on the land. It is a complex natural process and the imprint of human activities on the earth; garden landscape engineering is the carrier of various functions (processes), so it can be understood and expressed as follows: landscape, the object of the visual esthetic process; habitat, the space and environment in which humans live; ecosystem, an organic system with structure and function, with internal and external connections; and a record of the human past, the expression of hopes and ideals, the language, and spiritual space on which identification and sustenance are based.” Garden landscape reflects the meaning of visual esthetics, which has the same meaning as “landscape.” This meaning is also recognized by the literary and art circles and the vast number of landscape architects.

It is this cross-cutting and multidimensional characteristics that make landscape architecture rich in connotation and more extension. This study focuses on computer-aided technology, introduces the contemporary mainstream computer-aided software and platforms, and also expounds on the application in the planning and design process of landscape engineering.

This study takes the plants in the garden landscape as an example to carry out mathematical modeling. It can be seen from the concept of string replacement that the initials and productions in the Lindenmayer system (L -system) are described by strings. It boils down because L -systems are a formal language. To connect the L -system with the plant simulation, so that it can represent the structure of real plant branches, it is necessary to assign a specific geometrical meaning to each letter in the L -system. In order to vividly illustrate it, the concept of turtle shape can be introduced.

Postprocessing usually uses PS software and finally uses a color laser printer to print out the renderings.

We can extend the turtle-shaped interpretation of the L -system from 2D to 3D. First, three vectors H , L , and U that describe the current direction of the turtle shape are given. They represent the forward, left, and upward directions of the turtle shape, respectively. They are all unit lengths and are perpendicular to each other, and satisfy the following equation:

$$H \times L = U. \quad (1)$$

The rotating turtle shape can be represented by the equation as follows:

$$[H', L', U'] = [H, L, U] \times R, \quad (2)$$

where R is the 3×3 rotation matrix. The matrix representation of the rotation angle a with respect to the vectors H , L , and U is as follows:

$$R_H(a) = \begin{bmatrix} \cos a & \sin a & 0 \\ -\sin a & \cos a & 0 \\ 0 & 0 & 1 \end{bmatrix}, \quad (3)$$

where a is the variable.

$$R_L(a) = \begin{bmatrix} \cos a & 0 & -\sin a \\ 0 & 1 & 0 \\ \sin a & 0 & \cos a \end{bmatrix}, \quad (4)$$

$$R_U(a) = \begin{bmatrix} 1 & 0 & 0 \\ 0 & \cos a & -\sin a \\ 0 & \sin a & \cos a \end{bmatrix}. \quad (5)$$

The plant images generated by the determined L -system are relatively simple, and the plants generated according to the same L -system are very similar. If we put these plants in

the same picture (producing a picture of a forest), there would be significant, artificial regularity. In order to avoid this, it is necessary to introduce differential changes between different species, which can change some details of the plant on the basis of maintaining the overall structure of the plant. These changes can be accomplished by randomizing the turtle interpretation or engineering system. Simply randomizing the turtle interpretation would have limited effect because it only changed the external geometry of the plant's morphology, such as the length of the stem and the angle of the branches, but not the underlying topology of the plant. Correspondingly, if this randomness is applied to the production, it can not only affect the geometric appearance of the plant but also change the topology of the plant. We have also made great strides in the development of computer-aided technology in recent years.

A random L -system is an ordered quaternion as follows:

$$G = \langle V, \omega, P, \pi \rangle. \quad (6)$$

An example of a simple random L -system is as follows:

$$\begin{aligned} \omega: F \\ p_1: F \xrightarrow{0} .33 F [+F] F [-F] F. \end{aligned} \quad (7)$$

Although L -systems with turtle-shaped interpretations can produce a range of objects, from abstract fractals to plant-like branching structures, their modeling capabilities are limited. A major problem is that all line segments are integer multiples of unit steps. This leads to some simple figures, such as right-angled isosceles triangles, and cannot be drawn correctly because the slope of its hypotenuse and right-angled sides is an irrational number $\sqrt{2}$. Taking a rational number approximation provides only a limited solution, since the unit step size must be the common denominator of all line segments in the model. Thus, even a simple internode model of a plant requires a large number of symbols. In order to solve this problem, a method combining mathematical parameters and L -system notation—parameter L -system—is introduced. In the process of postprocessing, the artistic effect should be comprehensively considered, so various special filter functions in the computer-aided design software can be used to correct the artistic effect in time.

The parameter L -system extends the most basic concept of parallel rewriting, from words consisting of only characters to words with parameters. The parameter L -system operates on parameter words, which are module strings consisting of characters with parameters. Characters belong to character set V , and arguments belong to the real number set R . It consists of characters AEV and parameters as follows:

$$a_1, a_2, \dots, a_n \in R. \quad (8)$$

The module composed of the above formula is denoted as follows:

$$A(a_1, a_2, \dots, a_n). \quad (9)$$

Every module belongs to a collection as follows:

$$M = V \times R^*, \quad (10)$$

where R^* is the set of all finite parameter sequences, and the set of all module strings and nonempty strings is denoted as follows:

$$M^* = (V \times R^*)^*, \quad (11)$$

$$M^+ = (V \times R^*)^+. \quad (12)$$

Therefore, according to the above model, the probability can be obtained and is shown in Figure 2.

3. Computer-Aided Garden Landscape Design

Landscape architects can absorb and introduce more intentions and understand different landscape configurations through the human-computer interaction function of the virtual reality system, so as to modify and improve their own design schemes. In specific operations, designers can break through the limitation of two-dimensional plane thinking, observe landscape works from plane to 3D, multidimensional, multiperspective, better grasp the space, and achieve a more intuitive understanding of the design scheme. More importantly, based on the support of technology, landscape architects can break through the limitations of traditional design methods and expressions, and make garden landscapes more artistically pursued. The description of landscape details and the perfect presentation of effects by virtual reality technology further stimulate the designer's inspiration and intention, and enhance the originality of the landscape design scheme. Of course, the landscape design is not limited to the places where the surface can be viewed.

In addition, there is a rich spatial environment design and expression, and the multidimensional composition of landscape architecture. These characteristics are reflected in the combination of factors such as culture, space, time, nature, and society, and provide conditions and foundations for creating the overall atmosphere and special artistic conception of the garden landscape space environment. The 3D scene formed by virtual reality technology can fully express the multidimensional spatial form of the garden landscape. Compared with traditional computer-aided animation production, virtual reality is more powerful in real-time sculpting and interactive functions. Landscape designers can more easily control scene elements, such as weather, season, morning, and evening backgrounds, and can create virtual spaces that cannot be achieved using traditional expressions. In the virtual reality landscape space, different scenes can be switched in real time, and different observation angles or different observation sequences will produce different scenes and experiences.

The prerequisite for realizing virtual reality technology is to have a 3D model, and the construction of virtual space and landscape is based on a large number of 3D models. Therefore, the models are required to be of various types, with realistic effects and easy operation. In this way, a virtual scene with rich content and smooth operation can be established. The reason why the requirements for virtual

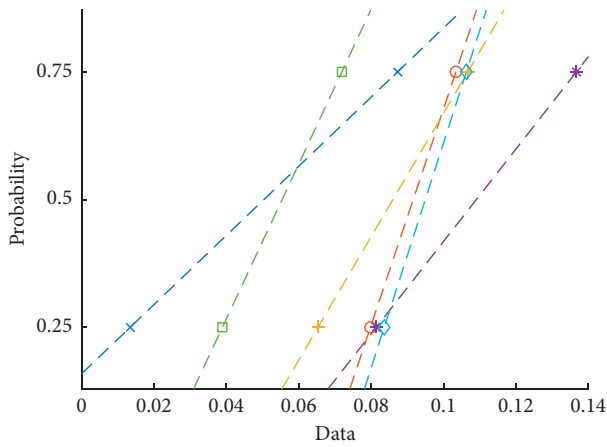


FIGURE 2: The probability calculated by the proposed method.

tours are high is because the audience can choose any viewing angle to watch by themselves, which requires the quality of the virtual rendering model to be very high, any small surface must be handled without flaws, and even the difference between the front and back of a leaf must be one side with veins and the other side not. In order to achieve a real-level virtual effect, when modeling, special attention should be paid to the processing of light and dark effects, to enhance the 3D sense of the 3D model, and to highlight the content of the environment in which the landscape modeling is located. The data predicted by the proposed method are plotted in Figure 3, which shows the validation of the proposed method. It is also necessary to consider the adjustment of the temperature, humidity, and other elements in the local area through CAD technology, so as to achieve the purpose of noise reduction and pollution reduction, and ensure the perfect landscape design.

Immersion, that is, experience, is the advantage of virtual reality technology compared with traditional graphic image creation. In order to allow users to have a good experience as immersive, it is necessary to integrate people's vision, hearing, and touch into virtual reality. From the very beginning, simple display screens and headsets initially solved the problems of vision and hearing. Later, the emergence of VR-specific headsets strengthened the above two sensory experiences. Recently, the use of finger nerves has appeared in Europe to bring part of the tactile sense into the virtual world. With the replacement of technology, the virtual modeling of the garden landscape will bring users an experience that is indistinguishable from the real one.

3.1. Application of Construction Drawing Production.

When we carry out landscape planning, we generally formulate corresponding construction drawings and renderings, which reflect a certain design concept. Its objects are generally buildings and landscapes in the city, including residential areas, squares, pedestrian streets, parks and natural landscapes, and other spatial forms. Here are some applications of the corresponding computer image

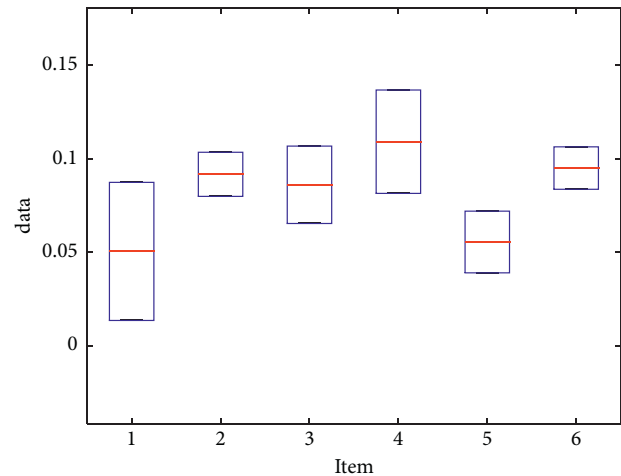


FIGURE 3: Data evaluated by the proposed method.

production technology for construction drawings. Hence, in order to verify the drawing production, the predicted value vs item is shown in Figure 4.

The previous construction drawings were all hand-painted by design engineers. The process was tedious and tedious, requiring a lot of calculations, and wasting time, and the accuracy of the final product was also flawed. During the construction process, it was also necessary to confirm and repeatedly modify it. CAD developed by Autodesk company has been widely used all over the world; due to its simple operation and professional design, designers can fully control it in a short time. Designers communicate with customers in advance, conceive products, and complete them in the shortest time, which improves work efficiency and is now a necessary computer software tool in the industry. At present, software widely used in landscape planning and design includes CAD, sketch master, and geographic information system. They are simple operation, easy to use, low cost, and good effect to improve the quality and efficiency of landscape planning and design.

3.2. Rendering and Application of Renderings. The renderings are the final architectural effects that will be presented in the production of landscape gardens. In the process of production, designers must first consider the overall color matching, the structure is complete, and it can give people a good feeling. When designing, different drawing software should be used for various terrain buildings in order to better complete the whole work.

- (1) Modeling of basic terrain building design. The $3d_{max}$ is the basic terrain of landscape design and the software of choice for architectural modeling. Every year, some new designs are added according to the user's experience, and the functions are becoming more and more perfect. The best product we have experienced is MAX2014. The newly added graphite modeling tool can basically meet the production of complex models. When applied to landscape design terrain, we only need to use two-dimensional images

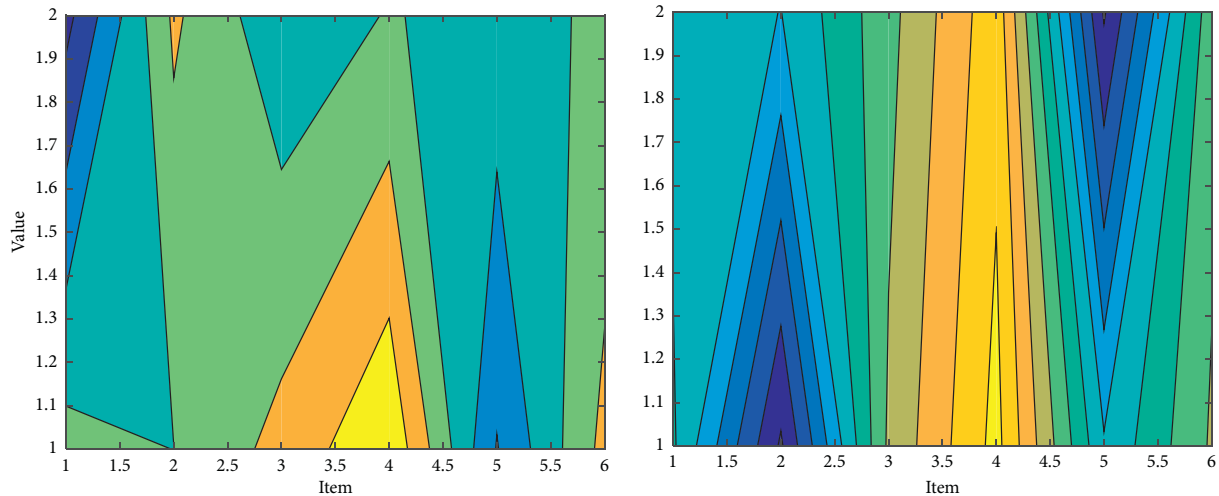


FIGURE 4: Value vs item.

and basic commands to achieve Conception, the effect is perfectly presented, and the operation is simple.

The English name of Sketch Master is SketchUp. In recent years, there is a trend of catching up and surpassing $3d_{max}$. At present, some designers are using it, especially in the field of landscape garden design, which is favored by a large number of designers. Its advantage lies in the display and production of landscape terrain. There is an independent interface, and the production and rendering can be independently completed.

- (2) Mountains and slope terrain. Terrain with slopes is a part of our design that we often have to make, and making it in software is a bit cumbersome. What we commonly use now is a terrain production tool using the max synthesis panel, which can draw terrain slopes of different heights, which is difficult to use. But the controllability is poor.
- (3) Green plants. What we often use in this regard is a forest plugin called Forest, which is used to create distant landscape trees for buildings. It can instantly create up to 10,000 trees and control their heights while optimizing the rendering of the scene. The latest version of the update now adds 3D functionality. Similar in function to it is a plugin called V-Ray.
- (4) Building auxiliary facilities. The auxiliary facilities of the building include bridges, characters, vehicles, etc., which can be directly imported into the existing model in a relatively simple way, saving time. The later stage plays an irreplaceable role in the entire landscape design. The commonly used software is Photoshop, which has a relatively powerful color correction function, and some less frequently used ones, such as fusion and nuke, will be used in the postproduction of some film and television dramas. In order to explain the modeling method, the prediction is shown in Figure 5.

Landscape designers use computer-aided rendering technology to present realistic visual effects and visual experience, so that both the owner and the designer can better feel the advantages and disadvantages of the design, so as to facilitate mutual communication and improvement. Computer-aided rendering technology has provided assistance in all aspects of landscape planning and design, and also brought some realistic and obvious role design demonstrations, providing users with a sensory visual sense, which is used in the design, procurement, approval, management, etc. Intuitive information is used to help designers and managers understand designs more easily. Taking the rainwater collection system of garden landscape design in Xinghua Park as an example, from the performance diagrams and examples, it is easy to see the materials used, the process of rainwater collection, and even the latest concept of garden landscape design, sponge city, in specific design and application. First of all, it can be seen that the ecological permeable ground is laid, the permeable bricks are laid on the roads in the park, and the reasonable sidewalk slope is set; although it is only a design scene, we can also feel the comfort of someone stepping on it. Collection of road rainwater-green space is obviously three to five centimeters lower than roads, and rainwater is more likely to penetrate into drains; road pavement is made of flat teeth, so it is easier for rainwater to flow into roadside drains when it rains; sidewalks paved with pebbles or stone blocks form a permeable surface; pipes for collecting rainwater are laid under the park according to the terrain, and underground cisterns are constructed; and after a series of rainwater collection and storage measures, it is finally connected with the municipal pipe network to form a large sponge patch. The predicted value is shown in Figure 6.

Virtual reality simulation landscape technology is the mainstream technology of computer-aided landscape performance, and its main features are multiperception, experience, interaction, and imagination. Through the rendering of the virtual reality platform such as Lumion, and the modeling software such as Sketch Master, the landscape effect of our design can be simulated. The use of virtual reality

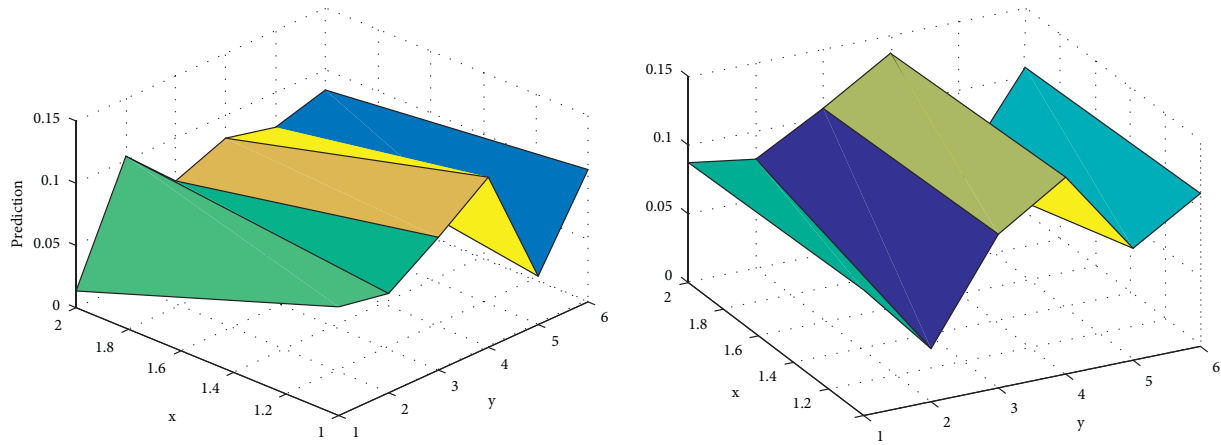


FIGURE 5: Prediction.

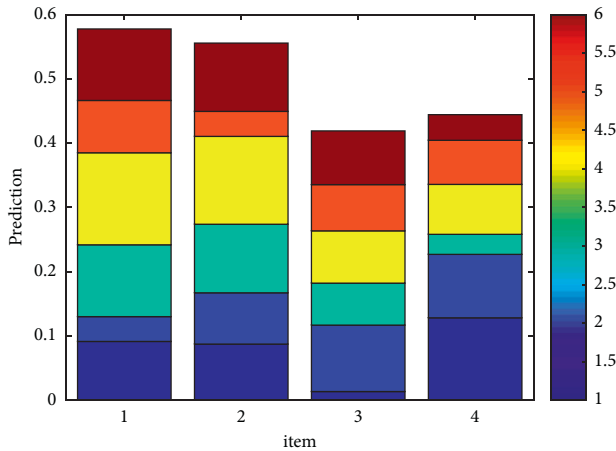


FIGURE 6: Predicted value.

technology can quickly establish the intended high-quality landscape of the design plan, and express it to users and landscape designers in a timely manner through hardware equipment, improve the owner’s participation and sense of creation in the design, and help designers discover their own designs in time. Whether it conforms to your own design ideas, you can use the virtual landscape platform to interact with the owner in time, so that the final design result is also conducive to the owner’s acceptance. We avoid the large-scale modification and rework of the past, resulting in a waste of time and resources. Using rendering technology to achieve “photo-level” renderings, we fully express the positioning of the landscape architect for the park and also interpret to people what is new Chinese classical in a 3D, intuitive, and vivid way, as shown in Figure 7 below. In the landscaping of virtual gardens, flowers and plants are mainly arranged at the edge of the entire layout to reflect the naturalness. In the current landscape design, special attention is paid to the collocation of flowers and plants with other plants. Taking the landscape engineering design of Xinghua Park as an example, there are basically no particularly large and gorgeous flowers, but in harmony with vine plants, the choice of coreopsis, iris,

purple gold flowers, etc. form a local large-scale “flower sea” effect. In rendering production and expression, we should pay attention to layering, medium and long-term perspective, and light and shadow effects.

As an important landscape element in landscape design, plants occupy an important proportion in landscape shaping. In landscape design blueprints, they play the role of creating atmosphere and improving quality. In the design process, the addition of plants is performed later. According to the overall positioning of the park and the zoning planning and layout, the conventional practice is to separately plant trees, shrubs, and grasses. Sometimes, in order to obtain a comprehensive landscape effect, they are also mixed and planted, and the advantages of using computer-aided technology for layout can be clearly reflected here, because the software can easily carry out the matching of regions and the increase or decrease in the number of plants, and the continuous correction is scientific and reasonable. Through the real-time imaging capability of the virtual reality platform, landscape designers can get the effect of plant configuration for the first time and achieve their design intentions through changes in species, arrangement of locations, increase or decrease in quantity, etc. Of course, as a garden landscape design, teachers cannot completely rely on the computing technology to assist the platform, but also need to be familiar with the local tree species in the area, and understand the biological collocation of trees and shrubs. For example, it is very good in terms of computers and aesthetics, but in actual construction, it is difficult to survive, or this kind of plant configuration cannot show the landscape effect of virtual reality in the local climate environment. Therefore, the requirements for landscape planners are very comprehensive, and they can be skilled in operating mainstream computer-aided platforms, Sketch Master, Lumion virtual rendering platform, and large-scale landscape planning geographic information system and other technologies and platforms, and have enough esthetic ability and ecological knowledge to meet the sensory experience demands of owners and audiences, and plants, soil, climate, and other natural properties and configurations are very familiar. The predicted fluctuation is shown in Figure 8.



FIGURE 7: Simulated landscape.

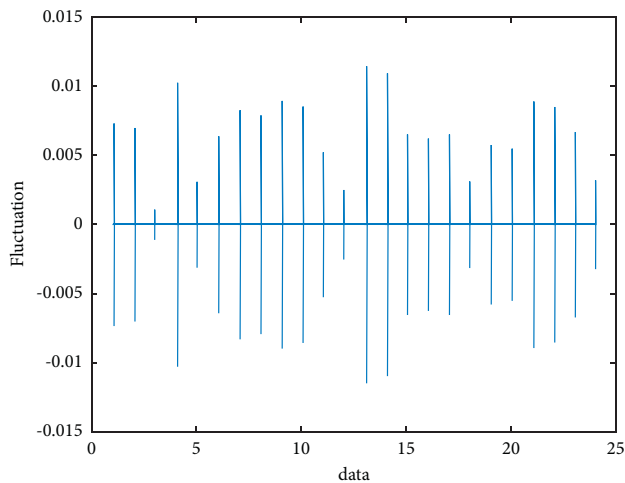


FIGURE 8: Predicted fluctuation.

4. Conclusions

Computer-aided technology, especially the virtual reality platform, can provide users with a beautiful virtual landscape and an immersive experience. In the process of interacting with the virtual scene, landscape architects can discover their own works. If there are any defects or inconsistencies with their own design intentions, they should be changed and improved in a timely manner. The computer-aided plane software can accurately draw the landscape construction drawings. In the actual project construction, the landscape can be constructed according to the drawings and standards, so as to ensure that the actual results are consistent with the design effects and improve the quality of the landscape.

The research on the realistic graphic rendering of the virtual plant model, the intelligent modeling of various plants, and the various natural factors affecting the growth of plants is not deep enough, and the established system is still far from the actual plant growth process.

Data Availability

The data used to support the findings of this study are available from the corresponding author upon request.

Conflicts of Interest

The authors declare that they have no conflicts of interest or personal relationships that could have appeared to influence the work reported in this paper.

Acknowledgments

This work was supported by the 2019 Young Backbone Teachers Training Plan of Henan Colleges and Universities by Henan Education Department: Research on the Living Protection and Inheritance of the Regional Culture of Traditional Villages in Central China under the Rural Revitalization Strategy (No. 2019GGJS261); and General Project of Philosophy and Social Sciences Planning of Henan Province in 2020: Research on the Protection and Development of Traditional Village Cultural Landscape in Henan Province (No. 2020BYS012).

References

- [1] E. Mikhail and A. Dimitris, "Computer-assisted structure elucidation (CASE): current and future perspectives," *Magnetic Resonance in Chemistry*, vol. 59, no. 7, pp. 667–668, 2021.
- [2] U. Jozef and K. Tibor, "Roadmap for computer-aided modeling of theranostics and related nanosystems," *EPJ Web of Conferences*, vol. 173, p. 05017, 2018.
- [3] F. Guo and Q. Zhang, "Computer aided modeling design of external gear pump," *IOP Conference Series: Earth and Environmental Science*, vol. 769, no. 4, pp. 1–9, 2021.
- [4] Xi. Han, "Artificial intelligent based energy scheduling of steel mill gas utilization system towards carbon neutrality," *Applied Energy*, vol. 295, pp. 765–778, 2021.
- [5] L. Manzoni, D. M. Papetti, P. Cazzaniga et al., "Surfing on fitness landscapes: a boost on optimization by fourier surrogate modeling," *Entropy*, vol. 22, no. 3, p. 285, 2020.

- [6] Q. Zhang, "Virtual reality modelling of garden geography and geology based on 3D modelling technology," *Journal of Physics: Conference Series*, vol. 1952, no. 2, pp. 23–34, 2021.
- [7] V. P. Bhange, U. V. Bhivgade, and A. N. Vaidya, "Artificial neural network modeling in pretreatment of garden biomass for lignocellulose degradation," *Waste and Biomass Valorization*, vol. 10, no. 6, pp. 1571–1583, 2019.
- [8] B. Yu, Z. Zhao, G. Zhao et al., "Provincial renewable energy dispatch optimization in line with Renewable Portfolio Standard policy in China," *Renewable Energy*, vol. 174, pp. 236–252, 2021.
- [9] P. Daniele, B. Riccardo, and K. Lado, "Subsidisation cost analysis of renewable energy deployment: a case study on the Italian feed-in tariff programme for photovoltaics," *Energy Policy*, vol. 154, pp. 1–9, 2021.
- [10] H. Liang, W. Li, and Q. Zhang, "Semantic-based 3D information modelling and documentation of rockeries in Chinese classical gardens: a case study on the rockery at Huanxiu Shanzhuang, Suzhou, China," *Journal of Cultural Heritage*, vol. 37, pp. 247–258, 2019.
- [11] H. Liang, W. Li, S. Lai, W. Jiang, L. Zhu, and Q. Zhang, "How to survey, model, and measure rockeries in a Chinese classical garden: a case study for Huanxiu Shanzhuang, Suzhou, China," *Landscape Research*, vol. 45, no. 3, pp. 377–391, 2020.
- [12] W. Beavers Alyssa et al., "Garden characteristics and types of program involvement associated with sustained garden membership in an urban gardening support program," *Urban Forestry and Urban Greening*, vol. 59, pp. 232–242, 2021.
- [13] H. I. Hanson, E. Eckberg, M. Widenberg, and J. Alkan Olsson, "Gardens' contribution to people and urban green space," *Urban Forestry and Urban Greening*, vol. 63, p. 127198, 2021.
- [14] E. Hoyle Helen, "Climate-adapted, traditional or cottage-garden planting? Public perceptions, values and socio-cultural drivers in a designed garden setting," *Urban Forestry and Urban Greening*, vol. 65, pp. 1–9, 2021.
- [15] M. E. Menconi, L. Heland, and D. Grohmann, "Learning from the gardeners of the oldest community garden in Seattle: resilience explained through ecosystem services analysis," *Urban Forestry and Urban Greening*, vol. 56, p. 126878, 2020.
- [16] S. Bell et al., "Spending time in the garden is positively associated with health and wellbeing: results from a national survey in England," *Landscape and Urban Planning*, vol. 200, no. 1, pp. 23–34, 2020.
- [17] J. Jiang, F. Peng, and B. Zhao, "Mutual exclusion algorithm for real-time traffic dispatching based on game theory," *IOP Conference Series: Materials Science and Engineering*, vol. 782, no. 3, p. 032058, 2020.
- [18] L. Sun, Q. Xu, X. Chen, and Y. Fan, "Day-ahead economic dispatch of microgrid based on game theory," *Energy Reports*, vol. 6, no. Supl.2, pp. 633–638, 2020.
- [19] A. M. Dixon Lee, "Collectively planting garden vegetation for biodiversity: are hard surfaced gardens and householder unwillingness a constraint?" *Urban Forestry and Urban Greening*, vol. 68, pp. 1–8, 2022.
- [20] J. Mou, J. Cohen, Y. Dou, and B. Zhang, "International buyers' repurchase intentions in a Chinese cross-border e-commerce platform," *Internet Research*, vol. 30, no. 2, pp. 403–437, 2019.
- [21] Z. Sun, J. Xie, Y. Zhang, and Y. Cao, "As-built BIM for a fifteenth-century Chinese brick structure at various LoDs," *ISPRS International Journal of Geo-Information*, vol. 8, no. 12, p. 577, 2019.
- [22] J. R. Sky and H. G. Momm, "An index for quantifying geometric point disorder in geospatial applications," *Computers & Geosciences*, vol. 151, pp. 1–7, 2021.
- [23] S. D'Oro, L. Galluccio, S. Palazzo, and G. Schembra, "A game theoretic approach for distributed resource allocation and orchestration of softwarized networks," *IEEE Journal on Selected Areas in Communications*, vol. 35, no. 3, pp. 721–735, 2017.
- [24] M. Schwaborn and N. Aschenbruck, "On modeling and impact of geographic restrictions for human mobility in opportunistic networks," *Performance Evaluation*, vol. 130, pp. 17–31, 2018.
- [25] S. Simon, "Geo-analytical question-answering with GIS," *International Journal of Digital Earth*, vol. 14, no. 1, pp. 1–14, 2021.
- [26] Z. Huangfu, H. Hu, N. Xie, Y.-Q. Zhu, H. Chen, and Y. Wang, "The heterogeneous influence of economic growth on environmental pollution: evidence from municipal data of China," *Petroleum Science*, vol. 17, no. 4, pp. 1180–1193, 2020.

Research Article

Color Matching in Children's Room Based on Computer Interactive Experience

Jia Huang 

Hunan International Economics University, Changsha 410205, China

Correspondence should be addressed to Jia Huang; huangjia1204@163.com

Received 12 April 2022; Accepted 27 May 2022; Published 25 June 2022

Academic Editor: Wei Liu

Copyright © 2022 Jia Huang. This is an open access article distributed under the Creative Commons Attribution License, which permits unrestricted use, distribution, and reproduction in any medium, provided the original work is properly cited.

In order to improve the effect of color matching in children's room, this paper studies the color matching of children's room combined with computer interactive experience technology. Moreover, this paper analyzes the basic knowledge of colorimetry, the principle of color measurement equipment, the basic concepts and mathematical models of color conversion, equipment color characteristic correction, and color gamut matching used in color management research and analyzes the color perception in the process of computer interaction experience. The color design method based on hue harmony is a color harmony design method extracted on the basis of the basic color system and Chevreul's theory of color harmony. The experimental research shows that the indoor color matching system for children's room based on computer interactive experience proposed in this paper has a good color matching effect.

1. Introduction

With the improvement of people's living standards, people's requirements for the indoor environment are also getting higher and higher, and the requirements for the growth environment of the only child in the family are placed in the highest position. Having a healthy environment for children to grow up is a common concern of every parent and child-loving person. The color in the children's room is closely related to the physical and mental health of children. From birth, the color in the room will affect the physical and psychological growth and development of children all the time. Therefore, people must pay enough attention to it.

The children's room is the place where children's dreams begin, and it is also the place that has the deepest impact on their life. It is our responsibility to create a good environment for children to grow up. Moreover, it is our goal to make a beautiful living environment affect and nurture children's beautiful personality. The current family model makes parents pay more and more attention to the growth environment of children, and the design of children's room has become an important part of interior design. As the most important part of interior design, color design is particularly

important. At present, modern scientific experiments have proved that color plays an important role in stimulating children's visual development, regulating children's psychological emotions, promoting children's right brain development, and cultivating children's imagination.

People's sense of beauty mainly comes from vision. Only through the visual system can we see rich colors and beautiful things. Thirty one-year-old children are full of curiosity about everything in this world. They like bright and highly saturated colors. During this period, they should consciously cultivate and emphasize their color perception ability and help children establish correct aesthetics, improve their appreciation level of beauty, and gain the enjoyment of beauty, thereby improving children's comprehensive aesthetic quality. However, in the current home improvement market, the color design of children's rooms is often based on the subjective wishes of parents, and it is often a matching case that is taken for granted or an adult version of the children's room. Without scientific theories and mature cases to guide, wrong color matching will seriously affect the physical and mental health of children, and the formation of unsound characters also makes parents and even children experts find no reason.

There are no particularly successful and representative cases in the scientific research and application of indoor colors in children's rooms in China. Therefore, this subject has great research value.

Being in a similar environment for a long time will keep the nerves of children in a state of tension and excitement, which will lead to a lack of security in the long run and even violent intrusion in severe cases. Conversely, blue is a cool color that can make people calm, thoughtful, and peaceful. When children are in such an environment for a short time, it is conducive to thinking about problems and maintaining a quiet and peaceful state of mind. However, too long and too much contact may cause children to suppress their introverted and inarticulate characters. Therefore, color will have various effects on children's growth, both positive and negative. Only through scientific color design to promote strengths and avoid weaknesses, seek advantages and avoid disadvantages, and effectively play the positive aspects of color in children's growth environment can we achieve our ultimate goal.

This paper studies the color matching of children's rooms combined with computer interactive experience technology and builds a computerized intelligent children's room interior color matching system to promote the healthy development of children's physical and mental health.

2. Related Work

Under normal circumstances, the family's understanding of the importance of children's room design can be divided into three situations. The first one is too much emphasis on functionality, and there is no difference in the choice of colors on furniture walls, ignoring the impact of colors on children [1]. The second is to consciously consider the color of the children's room while satisfying the functionality, but lacking understanding of color matching knowledge; the effect is naturally not ideal [2]; the third is to pay attention to the design of the children's room, query, and understand the relevant knowledge, to create a children's room suitable for children to live and grow [3].

Color matching is very important for children in the growth process, and choosing a rich and reasonable color matching will have a great impact on them. First of all, matching according to the personality characteristics of each child is more conducive to the healthy growth of children's body and mind [4]. Light tones, natural and soft color systems, such as beige, light brown, and light khaki, can give people a simple and natural feeling, can relieve anxiety and tension, and feel relaxed; the second is slightly bright, positive, calm, and excitement colors, such as vibrant red and yellow, which are conducive to mobilizing children's enthusiasm and cultivating positive thinking ability; followed by the fresh and natural plant light and color system, giving people a calm and stable atmosphere, based on green colors. It can relieve fatigue [5]; the other is the warm color system, which is too bright in the eyes of adults, but for children, orange and yellow can make them feel energetic and happy, and it is very important for children's cultivation.

An open, pure, and lively character is helpful. However, orange and yellow are not suitable for large-scale use, which will cause visual impact and easily affect emotional instability. It can be used as an embellishment on the overall tone [6]. Secondly, children grow and learn in a "bright" space for a long time, which can better promote children's development in a subtle way. If the brightness and purity of the color selected in the children's room are relatively high, it will be more suitable for children's lively psychology and stimulate children's intellectual growth [7]. Through the measurement of children's IQ, the study found that when children were tested in a room with bright colors such as light blue, yellow, yellow-green, and orange, their IQ increased by an average of 12 points, while in white, black, and brown, when tested in a dark room, the average IQ is reduced by 14 points [8], and rich colors can improve children's IQ. Therefore, the children's room is not only a place for children to rest but also a place for children to learn and play [9]. While satisfying the spatial functionality, the collocation and use of colors, from safety to individualization, affects children's personality and mood and plays an important role in their growth [10].

Indoor color is mainly divided into indoor environment color, indoor intermediate color, and indoor environment decorative color, which are mainly manifested in shape, material, and space wall [11]. The environmental color mainly refers to the color of the wall, the ground, and the top surface. The overall tone of the environmental color should be used harmoniously; the intermediate color mainly refers to the color of large furniture such as indoor cabinets, beds, and sofas. The choice of furniture color should echo the space environment. Decorative color mainly refers to the color of indoor furniture, accessories, green plants, and other small decorative objects, which play a harmonious role in the overall color tone of the space [12].

Ambient colors, intermediate colors, and decorative colors should be used harmoniously: first, the ambient color in the indoor color should occupy a larger area of the color tone in the space, followed by the intermediate color; the decorative color is the smallest, and the area occupied by the three indoor colors should be separated. There is a relationship between the golden ratio; the second is that the three colors cannot be the same; otherwise, it will easily cause the monotony of the space color and even produce a blurred feeling of the surface painting; third, the environment color and the intermediate color should maintain a harmonious relationship; decoration color and ambient color should have both contrast and coordination in color relationship [13].

In the color selection of children's room, proceed from the character of the child. Children's rooms should choose brighter, more relaxed, and cheerful colors, and the beating colors can stimulate children's strong thinking interest and imagination. In many cases, the correct use of color matching can also help to compensate for the defects of children's personality [14]. The combination of bright red and beautiful blue is contrasting which is suitable for introverted children; light blue is an elegant and gentle color suitable for children with more lively personality; the combination of pink and purple gives a romantic feeling. The

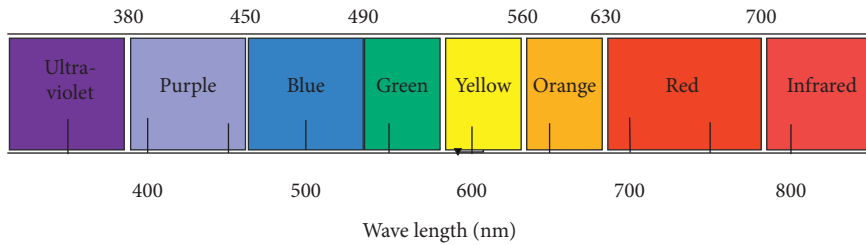


FIGURE 1: Schematic diagram of colors corresponding to different wavelength spectra.

warm visual experience is suitable for some withdrawn children; the green color is more suitable for children with poor eyesight [15].

When choosing a color combination, some colors should also be avoided and have a negative impact on the child’s psychology. For example, the use of a large area of black will make people feel depressed, resulting in unfavorable negative psychology. The combination of very bright yellow and orange indicates danger and is easy to generate tension [16]; a large area of white will make people feel monotonous and lack of vitality and fun, resulting in negative and hopeless emotions; although blue is widely used, it is a lonely tone, and large areas of blue are easy to produce lonely and contemplative emotions; large areas of red and excessive red decorative colors can easily lead to emotional instability and excitement of people [17]. Under normal circumstances, the space color matching should not exceed three. For the matching of colors and materials, the suitability of children should be fully considered, and materials with different materials but with the same color system should not be put together [18]. To maintain the principle of moderation, the overall interior tone is too full or unsuitable for space, white and black cannot be used as the main tone, and gold and silver can be used as a foil color; by fine-tuning the relationship between tone, lightness, and purity, the primary and secondary tones can be achieved. Secondary distribution, reasonable collocation of colors, and unification of primary and secondary colors contribute to harmony [19].

3. Visual Model of Color

Color can be defined as the human eye’s perception of light, and it is fundamentally a subjective sensation that exists only in the human brain. The color of any object is the result of the action of the following three basic elements: the light source, the object, and the observer.

When there is no light, there is no color, and the color of a fixed object seen by the observer changes as the lighting changes. The scientific understanding of color originated from Newton, who used a prism to divide white light into sequential colored lights, explaining that white light is composed of a series of colored lights. Modern science interprets visible light as a small part of the electron spectrum, and it is generally believed that radiation in the wavelength range of 380 nm–780 nm can cause a visual response in the human eye, called visible light. The wavelength of visible light is different, which causes the human eye to perceive different colors. The wavelength of

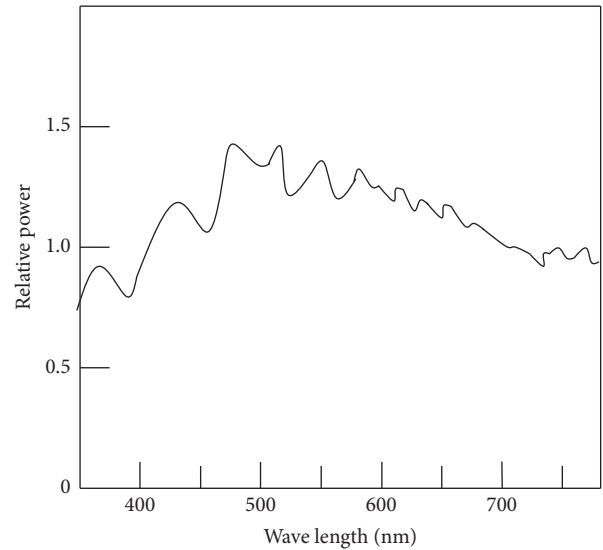


FIGURE 2: Schematic diagram of solar spectral power distribution.

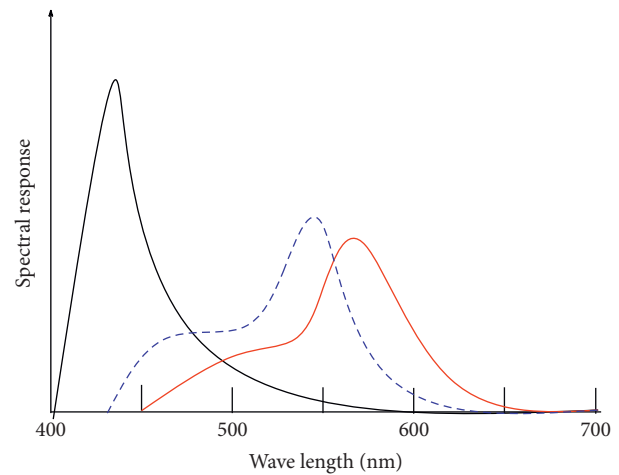


FIGURE 3: Corresponding graph of the spectrum of pyramidal cells.

monochromatic light is from long to short, corresponding to the perceived color from red to purple, as shown in Figure 1.

According to the above conclusions, any visible light is composed of radiation of a certain wavelength and intensity, and the function of radiation power and corresponding wavelength can quantitatively and accurately describe all light sources, which is called spectral power distribution. The spectral power distribution of perceived white light is

approximated as a straight line, and Figure 2 shows a typical daytime daylight spectral power distribution.

The decomposition of incident light into three independent stimuli by pyramidal cells is important for color reproduction (as shown in Figure 3). Another very important phenomenon is that two types of light with different spectral power distributions may produce the same tristimulation signal in pyramidal cells. The significance is that if we want to replicate the visual effect of a color, we do not necessarily have to create the same spectral power distribution, but only need to have three pyramidal cells produce the same stimulus signal as the source color. This phenomenon is called “metamefism.”

When two identical colors are each added and mixed with two other identical colors, the color remains the same. The formula is expressed as

$$\begin{aligned} &\text{if } A = B, C = D, \\ &\text{be } A + C = B + C, \end{aligned} \quad (1)$$

where “=” indicates that the colors match each other.

For two identical colors, each correspondingly subtracts the same color, and the remainder remains the same. The formula is expressed as

$$\begin{aligned} &\text{if } A = B, C = D, \\ &\text{be } A - C = B - C. \end{aligned} \quad (2)$$

If the color of one unit is the same as the color of another unit, then the two colors are enlarged or reduced by the same multiple at the same time, and the two colors are still the same. The formula is expressed as

$$\begin{aligned} &f A = B, \\ &\text{be } nA = nB. \end{aligned} \quad (3)$$

According to the law of substitution, colors that feel the same can be substituted for each other to obtain the same visual effect.

A color matching equation is an algebraic expression for color matching. If (C) represents the unit of the matched color, (R) , (G) , and (B) represents the unit of the three primary colors of red, green, and blue that produce the mixed color. R , G , B , and C represent the number of red, green, blue, and matched colors, respectively. When the two halves of the field of view are matched in the experiment, this result can be expressed by the following equation:

$$C(C) = R(R) + G(G) + B(B). \quad (4)$$

In the formula, “=” means visual equality, that is, color matching; R , G , and B are the number of generations, which can be negative.

In the color matching experiment, the color light to be measured can also be a monochromatic light of a certain wavelength (also known as spectral color). When a series of similar matching experiments are performed for monochromatic light of one wavelength, the tristimulus values corresponding to monochromatic light of various wavelengths can be obtained. If the radiant energy value of each

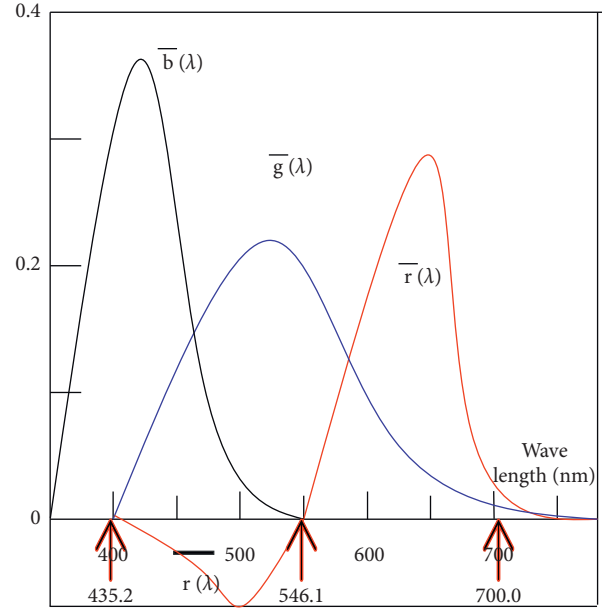


FIGURE 4: Color matching function of RGB chromaticity system.

monochromatic light is kept the same (such a spectral distribution is called iso-energy spectrum) to carry out the above experiment, the obtained tristimulus value is the spectral tristimulus value, that is, the number of three primary colors that match the spectral color of equal energy. It can be denoted by the symbol \bar{r} , \bar{g} , \bar{b} . The spectral tristimulus value is also called the color matching function, and its value only depends on the visual characteristics of the human eye. The matching process is expressed as [20]

$$C_\lambda(C) = \bar{r}(R) + \bar{g}(G) + \bar{b}(B). \quad (5)$$

Any color light is composed of monochromatic light. If the spectral tristimulus value of each monochromatic light is measured in advance, the tristimulus value of the color light can be calculated according to the principle of color mixing. The calculation method is to use the spectral distribution function $\varphi(\lambda)$ of the light to be measured, weight the spectral tristimulus value of each wavelength to obtain the tristimulus value of each wavelength, and then integrate it to obtain the tristimulus value of the light to be measured as follows:

$$\begin{aligned} \dot{R} &= \int_{vis} k\varphi(\lambda)\bar{r}(\lambda)d\lambda, \\ G &= \int_{vis} k\varphi(\lambda)\bar{g}(\lambda)d\lambda, \\ B &= \int_{vis} k\varphi(\lambda)\bar{b}(\lambda)d\lambda. \end{aligned} \quad (6)$$

The integration range is visible light band, generally from 380 nm to 780 nm.

Figure 4 is a graph of spectral tristimulus values drawn with the tristimulus value as the ordinate and the wavelength as the abscissa.

It can be seen from Figure 4 that a large part of the \bar{r} , \bar{g} , \bar{b} -spectral tristimulus values and the chromaticity coordinates of the spectral locus have negative values.

The conversion relationship between the tristimulus values of the XYZ system and the RGB system is as follows [21]:

$$\begin{bmatrix} X \\ Y \\ Z \end{bmatrix} = \begin{bmatrix} 2.7689 & 1.7517 & 1.1302 \\ 1.0000 & 4.5907 & 0.0601 \\ 0.0000 & 0.0565 & 5.5943 \end{bmatrix} \begin{bmatrix} R \\ G \\ B \end{bmatrix}, \quad (7)$$

$$\begin{bmatrix} R \\ G \\ B \end{bmatrix} = \begin{bmatrix} 0.41844 & -0.15866 & -0.08283 \\ -0.09117 & 0.252422 & 0.01570 \\ 0.00092 & -0.00255 & 0.17858 \end{bmatrix} \begin{bmatrix} X \\ Y \\ Z \end{bmatrix}. \quad (8)$$

By formula (7), the tristimulus color matching function of the CIE standard chromaticity system can be calculated according to the CIE-RGB system, as shown in Figure 5. Since it is considered that only the Y value represents both magenta and brightness when XYZ selects the primary color, while X and Z only represent magenta, the $\bar{y}(\lambda)$ function curve is consistent with the photopic spectral luminous efficiency $V(\lambda)$, that is, $\bar{y}(\lambda) = V(\lambda)$.

The CIELab space adopts the following three-dimensional rectangular coordinate color space:

$$\begin{cases} L = 116f\left(\frac{Y}{Y_n}\right) - 16, \\ a = 500\left\{f\left(\frac{X}{X_n}\right) - f\left(\frac{Y}{Y_n}\right)\right\}, \\ b = 200\left\{f\left(\frac{Y}{Y_n}\right) - f\left(\frac{Z}{Z_n}\right)\right\}. \end{cases} \quad (9)$$

Among them, the function $f(x)$ is expressed as follows [22]:

$$f(x) = \begin{cases} x^{1/3}, & x > 0.008856, \\ 7.787x + 16/116, & x \leq 0.008856. \end{cases} \quad (10)$$

Among them, X , Y , and Z are the tristimulus values of the object, X_n , Y_n , and Z_n are the tristimulus values of the completely diffuse reflection surface and are normalized to $Y_n = 100$.

The color difference in the CIELab color space and the correlation quantities (lightness, chroma, and hue angle) approximately corresponding to the psychological correlation quantities can be obtained by the following methods:

- (1) Color difference: the color difference between two chromaticity values (L_1, a_1, b_1) , (L_2, a_2, b_2) in the CIE color space.

ΔE_{ab} is determined by

$$\Delta E_{ab} = \left((\Delta L)^2 + (\Delta a)^2 + (\Delta b)^2 \right)^{1/2}, \quad (11)$$

where

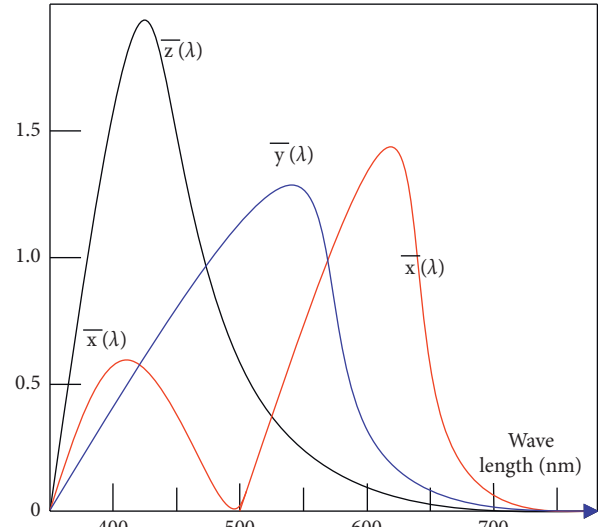


FIGURE 5: Color matching function of XYZ color system.

$$\begin{aligned} \Delta L &= L_1 - L_2, \\ \Delta a &= a_1 - a_2, \\ \Delta b &= b_1 - b_2. \end{aligned} \quad (12)$$

- (2) Brightness:

$$L = 116f\left(\frac{Y}{Y_n}\right) - 16. \quad (13)$$

- (3) Chroma:

$$C_{ab} = (a^2 + b^2)^{1/2}. \quad (14)$$

- (4) Hue angle:

$$H_{ab} = \text{tg}^{-1}\left(\frac{b}{a}\right). \quad (15)$$

The establishment of the CIE standard chromaticity system lays the foundation for people to objectively measure the color of an object, and the color can be determined by measuring the color tristimulus value of the object. The purpose of color management is to achieve consistent color reproduction across devices, which is enough to accurately reproduce CIE chromaticity values on various devices. One of the prerequisites for color management is to obtain the accurate CIE chromaticity value of the color. Through the corresponding relationship between the CIE chromaticity value of the color sample and the device driver value, the output model of the device is established to achieve accurate reproduction of any CIE chromaticity value. We know that the formula for calculating the tristimulus value is

$$\begin{aligned} X &= K \int_{\text{vis}} S(\lambda) \beta(\lambda) \bar{x}(\lambda) d\lambda, \\ Y &= K \int_{\text{vis}} S(\lambda) \beta(\lambda) \bar{y}(\lambda) d\lambda, \\ Z &= K \int_{\text{vis}} S(\lambda) \beta(\lambda) \bar{z}(\lambda) d\lambda, \end{aligned} \quad (16)$$

where $S(\lambda)$ is the spectral distribution of the light source, $\beta(\lambda)$ is the spectral radiance parameter of the object, and $\bar{x}(\lambda)$, $\bar{y}(\lambda)$, and $\bar{z}(\lambda)$ are the color matching functions of the standard observer. The spectral distribution $S(\lambda)$ of the light source, the spectral radiance parameter $\beta(\lambda)$ of the object, and the standard observer spectral tristimulus value $\bar{x}(\lambda)$, $\bar{y}(\lambda)$, and $\bar{z}(\lambda)$ are all necessary to obtain the color tristimulus value. A color measuring instrument is a tool to obtain the color tristimulus value through a certain way. According to the different ways of obtaining the three laser values, color measuring instruments can be mainly divided into two categories: spectrophotometers and colorimeters.

One of the main contents of this study is how to get the mapping relationship F_{device} and F_{device} between the device-dependent color space and the CIE color space.

The process by which a scanner scans a color image and records its chromaticity values can be expressed as

$$\mathbf{c}_i = H(\mathbf{M}^T \mathbf{r}_i), \quad (17)$$

where the matrix M represents the three-channel spectral stimulus response parameters including the scanner illumination, \mathbf{r}_i represents the spectral reflection of the i th point in the image space, H represents the nonlinear correction model of the scanner (reversible within the scanner recognition range), and \mathbf{c}_i represents the vector of the color recorded by the scanner, that is, the digital drive value of the scanner, usually a vector in the RGB space, which can be expressed as $\mathbf{c} = [RGB]^T$.

The ideal scanner is colorimetric. That is, colors that look different to a standard observer will be scanned and recorded as different device-dependent color values. For all $\mathbf{r}_k, \mathbf{r}_j \in \Omega_r, k \neq j$, we have

$$\mathbf{A}^T \mathbf{L}_v \mathbf{r}_k \neq \mathbf{A}^T \mathbf{L}_v \mathbf{r}_j \Rightarrow \mathbf{M}^T \mathbf{r}_k \neq \mathbf{M}^T \mathbf{r}_j, \quad (18)$$

where $\dot{\Omega}_r$ represents the set of reflectance spectra of the oscillating medium that can appear, the column vector of matrix A contains the CIEXYZ color matching function, and the diagonal matrix L_v represents the lighting conditions of the observation environment. In other words, a colorimetric scanner scans an image just as a standard observer would observe the image under light L_v . For such scanners, the calibration problem is to determine a continuous mapping $F_{\text{scanner}}(\cdot)$ to convert the scanned color values into the CIE color space. For all $\mathbf{r} \in \Omega_r$, the chromaticity value t in the device-independent color space can be obtained as

$$\mathbf{t} = \mathbf{A}^T \mathbf{L}_v \mathbf{r} = F_{\text{scanner}}(\mathbf{z}). \quad (19)$$

For the scanner, there is always a set of reflection spectra B_{scan} of the scanned medium, such that the conversion $F_{\text{scanner}}(\cdot)$ from the scan value to the CIEXYZ chromaticity value exists. The color of the output images, photos, and other media of the decoration simulation platform is always produced by the combination of colorants within a certain range, so the reflection spectrum that can be produced is also limited to a set B_{media} . Generally, in such a set, a transformation is ubiquitous such that (18) is satisfied, for all $r \in B_{\text{scanner}}$.

Therefore, in all calibration methods, the first step is to select a set of calibration samples whose reflectance spectrum belongs to set B_{scanner} , to ensure that the scan value of this set of samples has a one-to-one mapping relationship with the device-independent color space. The reflectance spectrum of this set of M_q samples is $\{\mathbf{q}_k\}, 1 \leq k \leq M_q$. The device-independent color space colorimetric values of these samples are measured by a spectrophotometer or other type of colorimeter according to the following relationship:

$$\{\mathbf{t}_k = \mathbf{A}^T \mathbf{L}_v \mathbf{q}_k\}, 1 \leq k \leq M_q. \quad (20)$$

In order not to lose generality, $\{\mathbf{t}_k\}$ denotes the chromaticity value of any device-independent color space, such as CIEXYZ. In this case, $\{\mathbf{t}_k = L(\mathbf{A}^T \mathbf{L}_v \mathbf{q}_k)\}$, where $L(\cdot)$ stands for CIEXYZCIElab and CIELuv.

At the same time, scan these samples with a scanner to obtain the scan value $\mathbf{c}_k = H(\mathbf{M}^T \mathbf{q}_k), 1 \leq k \leq M_q$. Accordingly, the scanner calibration problem can be described as finding a transformation $F_{\text{scanner}}(\cdot)$ that satisfies

$$F_{\text{gsmer}} = \arg \left(\min_F \sum_{i=1}^{M_q} \|F(\mathbf{c}_i) - \mathbf{t}_i\|^2 \right), \quad (21)$$

where $\|\cdot\|^2$ is the second norm in the CIE color space, which represents the color difference in the CIE space.

The CMY value output by the decoration simulation platform is c (three-dimensional coordinates), and the measured CIE chromaticity value is t (three-dimensional coordinates), and $F_{\text{printer}}(\cdot)$ represents the nonlinear mapping relationship from the decoration simulation platform color space (CMY space) to the CIE color space. Then, there are

$$\mathbf{t} = F_{\text{printer}}(\mathbf{c}), \mathbf{c} \in \Omega_{\text{printer}}, \quad (22)$$

where Ω_{printer} represents the set of all CMY values of the decoration simulation platform. Correspondingly, for each CIE chromaticity value in the color gamut of the decoration simulation platform, the chromaticity value can always be converted into a CMY value output by transforming $F_{\text{printer}}^{-1}(\cdot)$, namely,

$$\begin{aligned} \mathbf{c} &= F_{\text{printer}}^{-1}(\mathbf{t}), \\ \mathbf{t} &\in G_{\text{printer}}. \end{aligned} \quad (23)$$

The color gamut G_{printer} of the decoration simulation platform is defined as

$$G_{\text{printer}} = \{\mathbf{t} \in \Omega_{\text{cie}} | \exists \mathbf{c} \in \Omega_{\text{device}}, r_{\text{device}}(\mathbf{c}) = \mathbf{t}\}. \quad (24)$$

In essence, the color correction of the decoration simulation platform is to find out the mapping relationship $F_{\text{printer}}^{-1}(\cdot)$, so as to complete the accurate conversion from the CIE chromaticity value to the CMY value of the decoration simulation platform.

The process of calibrating the decoration simulation platform is as follows. First, the platform selects a set of calibration samples distributed in the color space of the entire decoration simulation platform, namely, the device

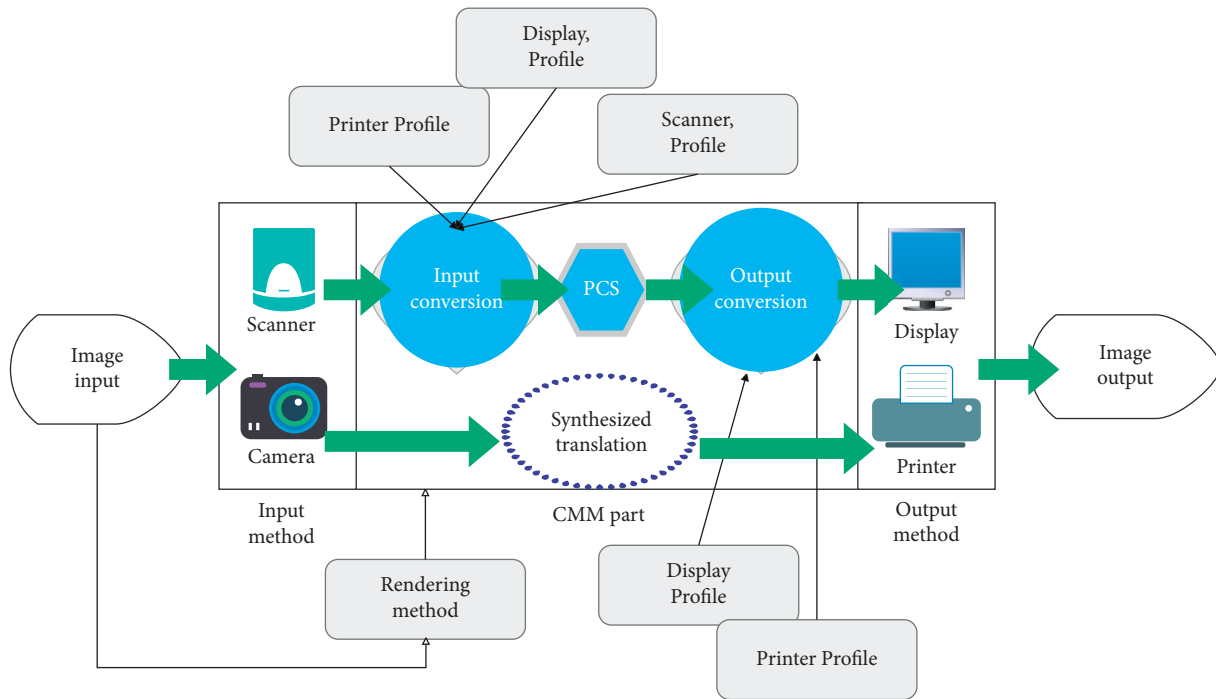


FIGURE 6: CMM color conversion process.

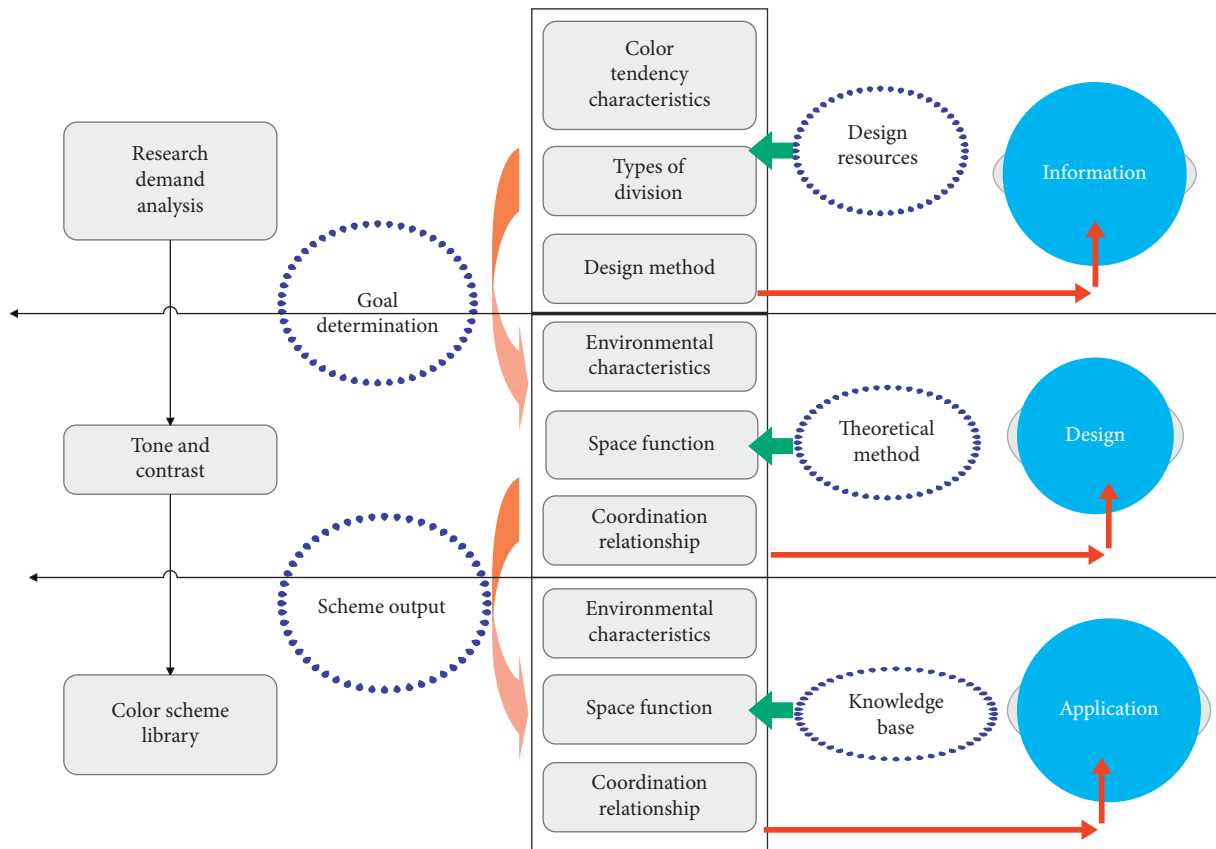


FIGURE 7: Color matching system in children’s room based on computer interactive experience.

drive value, which is defined as $\{c_k\}, 1 \leq k \leq M_q$. After the platform result is output, the spectral reflectance $\{p_k\}, 1 \leq k \leq M_q$ of the calibrated color target is obtained.

Using a colorimeter, the CIE chromaticity value $\{t_k\}, 1 \leq k \leq M_q$ of the corresponding color sample can be measured and has the following relationship:

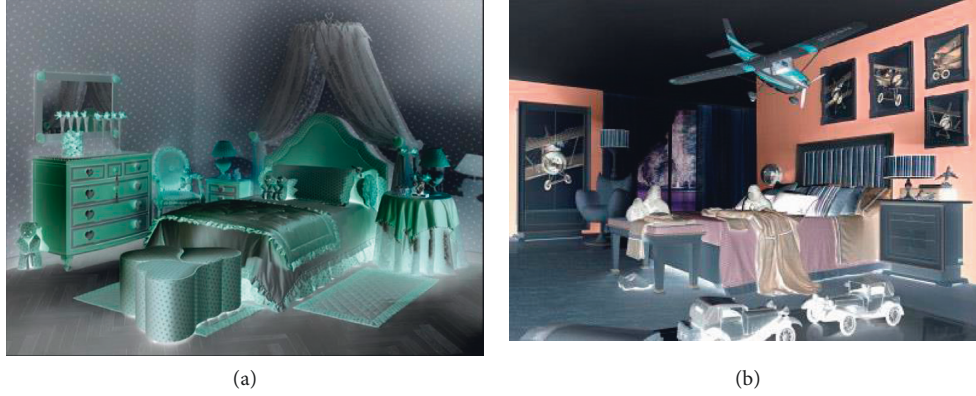


FIGURE 8: Simulation of female children's room and male children's room. (a) Indoor color matching for girls. (b) Indoor color matching for boys.

$$\{\mathbf{t}_k = \mathbf{A}^T \mathbf{L}_v \mathbf{q}_k\}, 1 \leq k \leq M_q, \quad (25)$$

where \mathbf{t}_k represents the CIE chromaticity value, which is generally the Lab value. Therefore, the correction of the decoration simulation platform needs to first find the mapping $F_{\text{printer}}(\cdot)$ to meet the following optimization conditions:

$$F_{\text{printer}} = \arg \left(\min_F \sum_{i=1}^{M_p} \|F(\mathbf{c}_i) - \mathbf{t}_i\|^2 \right). \quad (26)$$

The color correction of the decoration simulation platform is generally carried out with the help of CIELab space. This space is a visually uniform space, that is, the Euclidean distance between two points in the space is proportional to the visual difference. In addition, the Euclidean distance has an isoscopic color space, that is, the Euclidean distance of two points in the space is proportional to the visual difference so that the color gamut matching problem can be solved by an intuitive geometric method.

All output devices, such as decoration simulation platforms and monitors, have their own color reproduction capabilities and can only output colors within a certain range, which is defined as color gamut. Ω_{cie} is the chromaticity value range of the CIE color space and Ω_{printer} is the output device color space, that is, the digital drive value range of the device; then, the device color gamut can be defined as follows:

$$G = \{\mathbf{t} \in \Omega_{\text{cie}} | \exists \mathbf{c} \in \Omega_{\text{device}} \text{ where } F_{\text{device}}(\mathbf{c}) = \mathbf{t}\}. \quad (27)$$

Out-of-gamut is defined as

$$G^c = \{\mathbf{t} \in \Omega_{\text{cie}} | \exists \mathbf{t} \notin G\}. \quad (28)$$

When a color image is transmitted between different devices, ICCM will use the information provided by the device profile to convert the color data of the image from the color space of the source device to the color space of the destination device. The conversion process is as follows: first, the color data of the image is converted from the source device color space to the PCS space and

then from the PCS space to the destination device space. The algorithm and related information used in the conversion are provided by the device Profile. For example, when the image on the display is output through the decoration simulation platform, the CMM first uses the profile of the display to convert the color data of the image from the ROB space to the Lab space and then converts the color data from the Lab space to the CMYK space according to the Profile of the decoration simulation platform. The decoration simulation platform uses the CMYK data obtained at this time to output the image. Through two conversions, the color of the output image of the decoration simulation platform can be more consistent with the color displayed on the monitor, that is, the color can be accurately transmitted between different image devices. Figure 6 shows the general workflow of the CMM.

4. Color Matching in Children's Room Based on Computer Interactive Experience

The color design method based on hue harmony is a color harmony design method extracted on the basis of the basic color system and Chevreul's theory of color harmony. It uses the color matching relationship between the main environment and the background and the application of color management to generate a user interface for visual circulation operation in the CAD environment and obtains the basic color modeling scheme of the indoor environment. This paper designs an indoor color matching system for children's room based on computer interactive experience, as shown in Figure 7.

Figure 8 shows the simulation diagram of the female children's room and the male children's room designed by the color matching system in the children's room based on the computer interactive experience.

On the basis of the above research, the effect verification of the indoor color matching system in children's room based on computer interactive experience proposed in this paper is carried out. The color matching effect is verified by multiple sets of simulation experiments, and the results are shown in Table 1.

TABLE 1: Effect verification of color matching system in children's room based on computer interactive experience.

Number	Color matching	Number	Color matching	Number	Color matching
1	84.29	21	79.05	41	86.25
2	80.11	22	90.46	42	88.61
3	89.06	23	80.51	43	91.43
4	86.22	24	86.29	44	87.41
5	81.78	25	88.44	45	91.74
6	81.53	26	89.26	46	85.60
7	81.75	27	87.75	47	82.35
8	89.80	28	84.56	48	83.20
9	80.65	29	87.82	49	82.15
10	87.96	30	88.33	50	85.64
11	79.27	31	85.70	51	88.28
12	90.67	32	85.87	52	86.79
13	89.22	33	81.08	53	91.21
14	80.85	34	81.17	54	82.10
15	85.39	35	81.86	55	88.12
16	83.56	36	86.25	56	86.94
17	91.74	37	86.56	57	88.48
18	91.56	38	83.44	58	88.14
19	84.10	39	86.49	59	80.47
20	86.92	40	79.12	60	89.09

From the above experimental research, it can be seen that the color matching system in children's room based on computer interactive experience proposed in this paper has a good color matching effect.

5. Conclusion

The effect of color on children's psychology and physiology not only is the stimulation effect in the general sense of color psychology but also has the unique group nature of children. High-saturation colors such as big red and bright orange can quickly stimulate children to be in a state of excitement, quickly and effectively improve children's creativity and sensitivity to things, and even improve children's IQ by 8% to 10%. However, it is absolutely impossible to stay in such an environment for a long time. This study uses computer interactive experience technology to study the color matching of children's rooms and builds a computer-intelligent color matching system in children's rooms. The experimental results show that the indoor color matching system in children's room based on computer interactive experience proposed in this study has a good color matching effect.

Data Availability

The labeled dataset used to support the findings of this study are available from the author upon request.

Conflicts of Interest

The author declares no conflicts of interest.

Acknowledgments

This work was supported by Hunan International Economics University.

References

- [1] A. I. Martyshkin, "Motion planning algorithm for a mobile robot with a smart machine vision system," *Nexo Revista Cientifica*, vol. 33, no. 02, pp. 651–671, 2020.
- [2] A. Chaudhury, C. Ward, A. Talasaz et al., "Machine vision system for 3D plant phenotyping," *IEEE/ACM Transactions on Computational Biology and Bioinformatics*, vol. 16, no. 6, pp. 2009–2022, 2018.
- [3] D. Wang, H. Song, and D. He, "Research advance on vision system of apple picking robot," *Transactions of the Chinese Society of Agricultural Engineering*, vol. 33, no. 10, pp. 59–69, 2017.
- [4] L. Cheng, B. Song, Y. Dai, H. Wu, and Y. Chen, "Mobile robot indoor dual Kalman filter localisation based on inertial measurement and stereo vision," *CAAI Transactions on Intelligence Technology*, vol. 2, no. 4, pp. 173–181, 2019.
- [5] V. N. Ganesh, S. G. Acharya, S. Bhat, and S. V. Yashas, "Machine vision robot with real time sensing," *Journal of Advancements in Robotics*, vol. 1, no. 3, pp. 30–34, 2020.
- [6] H.-H. Chu and Z.-Y. Wang, "A study on welding quality inspection system for shell-tube heat exchanger based on machine vision," *International Journal of Precision Engineering and Manufacturing*, vol. 18, no. 6, pp. 825–834, 2017.
- [7] N. Noguchi, "Agricultural vehicle robot," *Journal of Robotics and Mechatronics*, vol. 30, no. 2, pp. 165–172, 2018.
- [8] V. Villani, F. Pini, F. Leali, C. Secchi, and C. Fantuzzi, "Survey on human-robot interaction for robot programming in industrial applications," *IFAC-PapersOnLine*, vol. 51, no. 11, pp. 66–71, 2018.
- [9] S. Huang, K. Shinya, N. Bergström, Y. Yamakawa, T. Yamazaki, and M. Ishikawa, "Dynamic compensation robot with a new high-speed vision system for flexible manufacturing," *International Journal of Advanced Manufacturing Technology*, vol. 95, no. 9-12, pp. 4523–4533, 2018.
- [10] H. Zhang, M. Li, S. Ma, H. Jiang, and H. Wang, "Recent advances on robot visual servo control methods," *Recent Patents on Mechanical Engineering*, vol. 14, no. 3, pp. 298–312, 2021.

- [11] S. S and R. G, "Robot assisted sensing, control and manufacture in automobile industry," *Journal of ISMAC*, vol. 01, no. 03, pp. 180–187, 2019.
- [12] S. Papanastasiou, N. Kousi, P. Karagiannis et al., "Towards seamless human robot collaboration: integrating multimodal interaction," *International Journal of Advanced Manufacturing Technology*, vol. 105, no. 9, pp. 3881–3897, 2019.
- [13] J. Li, J. Yin, and L. Deng, "A robot vision navigation method using deep learning in edge computing environment," *EURASIP Journal on Applied Signal Processing*, vol. 2021, no. 1, pp. 1–20, 2021.
- [14] Y. Onishi, T. Yoshida, H. Kurita, T. Fukao, H. Arihara, and A. Iwai, "An automated fruit harvesting robot by using deep learning," *Robomech Journal*, vol. 6, no. 1, pp. 1–8, 2019.
- [15] Y. Xiong, Y. Ge, L. Grimstad, and P. J. From, "An autonomous strawberry-harvesting robot: design, development, integration, and field evaluation," *Journal of Field Robotics*, vol. 37, no. 2, pp. 202–224, 2020.
- [16] Y. Wang, "On theoretical foundations of human and robot vision," *Learning*, vol. 4, no. 1, pp. 61–86, 2022.
- [17] Y. Cho, J. Jeong, and A. Kim, "Model-assisted multiband fusion for single image enhancement and applications to robot vision," *IEEE Robotics and Automation Letters*, vol. 3, no. 4, pp. 2822–2829, 2018.
- [18] A. Tabb and K. M. A. Yousef, "Solving the robot-world hand-eye (s) calibration problem with iterative methods," *Machine Vision and Applications*, vol. 28, no. 5, pp. 569–590, 2017.
- [19] M. M. Al-Isawi and J. Z. Sasiadek, "Guidance and control of a robot capturing an uncooperative space target," *Journal of Intelligent and Robotic Systems*, vol. 93, no. 3, pp. 713–721, 2019.
- [20] S. Ali, Y. Jonmohamadi, Y. Takeda, J. Roberts, R. Crawford, and A. K. Pandey, "Supervised scene illumination control in stereo arthroscopes for robot assisted minimally invasive surgery," *IEEE Sensors Journal*, vol. 21, no. 10, pp. 11577–11587, 2020.
- [21] X. Xu, "Research on teaching reform of mechanical and electronic specialty based on robot education," *Open Access Library Journal*, vol. 8, no. 8, pp. 1–9, 2021.
- [22] A. G. Pour, A. Taheri, M. Alemi, and A. Meghdari, "Human–robot facial expression reciprocal interaction platform: case studies on children with autism," *International Journal of Social Robotics*, vol. 10, no. 2, pp. 179–198, 2018.

Research Article

Smart Mobile Information Systems on the Key Systems of Blockchain Privacy Protection

Xiaobo Wei 

School of Business, Xijing University, Xi'an 710123, Shaanxi, China

Correspondence should be addressed to Xiaobo Wei; 20060041@xijing.edu.cn

Received 18 April 2022; Revised 25 May 2022; Accepted 6 June 2022; Published 25 June 2022

Academic Editor: Wei Liu

Copyright © 2022 Xiaobo Wei. This is an open access article distributed under the Creative Commons Attribution License, which permits unrestricted use, distribution, and reproduction in any medium, provided the original work is properly cited.

In the process of data collaboration, the data source copyright, equity boundaries, and other issues must be ensured to ensure the data owner's income rights. The data on the blockchain are transaction data. After the data are verified, they are added to the block by the node that has the right to keep accounts. Once the data are added to the blockchain, they cannot be deleted or changed, and only authorized query operations can be performed. The transaction records on the blockchain are completely public, and the fund transactions between accounts can reflect a lot of valuable information, especially some special accounts track the IP of transaction users through methods such as address reuse, taint analysis, and cluster analysis. At the same time, a credit contribution certification mechanism is established to ensure that the contributions are directly proportional to the rewards, and finally, a credit mechanism for data fraud is established. This paper mainly analyzes the key systems of privacy protection through research data and blockchain. The research results show that different companies conduct the Pailler homomorphic encryption of data and use the secure multiparty calculation to obtain the results. The execution of the whole process is controlled by a specific intelligent contract, and the records of the execution process are stored in the blockchain. It can be seen that the blockchain-based data distribution system changes the traditional data distribution mode so that the data source and the data user can interact directly, which promotes the maintenance of the system's security and stability.

1. Introduction

The data privacy of users in the cloud computing environment is secret data, which is information that others do not want to know. From the perspective of privacy owners, privacy data can be divided into personal privacy data and common privacy data. Personal privacy data include information that can be used to identify or locate individual and sensitive information. The privacy and accessibility of data can ensure the user's control over the information and make access to unrestricted information [1, 2]. The conflict between data privacy and accessibility occurs naturally [3, 4], and data in the urban traffic is closely related to these two characteristics [5, 6].

Big data has become China's national strategy. China needs to speed up. "Big data" requires new processing modes to have stronger decision-making power, insight

discovery power, and process optimization ability to adapt massive, high growth rate and diversified information assets.

Each node has the same rights, and data updates and transaction validation are done through circulated hubs that follow an agreement system [7, 8]. Specifically, what is put away on the blockchain is not simply the exchange, yet the hash of the exchange [9, 10], which is stored in the form of Merkle trees in blocks that form chained data structures in chronological order and longest chain criteria [11]. Therefore, the construction of a unified, open, and diversified "chain network" blockchain infrastructure is important [12]. The important significance of building a blockchain framework is to ensure that data of different formats and sources can be integrated and that different applications can be perfectly integrated into the blockchain hotspot [13, 14].

2. Experimental Procedure

Blockchain is a distributed database technology developed on the basis of the application of digital encryption currency. The blockchain system has the characteristics of decentralization, immutability, distributed consensus, traceability, and eventual consistency, which makes it suitable for solving data management problems in untrusted environments. The unique data management function of blockchain has become the key to exerting the value of blockchain in applications in various fields. Blockchain technology is becoming more and more popular [15, 16]. Blockchain is a new type of distributed protocol, which can be realized without the mutual trust of nodes, thus effectively reducing the trust cost in the real economy [17, 18]. At present, the biggest application of blockchain technology is digital currency, and it is also one of the ten typical judicial technology applications of the Internet. Although blockchain significantly improves data security and reliability, the storage scalability of blockchain is poor [19, 20]. For example, bitcoin currently has a total capacity of more than 160 GB. The current bitcoin system uses nearly 1600 PB of storage space, only for about 160 GB of data, which greatly wastes storage space. In addition, as time goes by, the blockchain will increasingly occupy a large amount of node storage space. The function introduction of each part of the block header is shown in Table 1.

In this context, a scheme for implementing scalable is proposed and the extended blockchain storage is studied to realize the privacy protection of multiparty shared data:

$$c = E_{pk}(m) = g^m r^n \text{mod} n^2. \quad (1)$$

As shown in Figure 1, according to the homomorphic nature of the encryption system,

$$\begin{aligned} E_{pk}(m_1 + m_2) &= E_{pk}(m_1) + E_{pk}(m_2) \\ &= g^{m_1+m_2} (r_1 r_2)^n \text{mod} n^2, \\ E_{pk}(a \cdot m_1) &= E_{pk}(m_1)^a = g^{am_1} r_1^{an} m \text{mod} n^2, \\ C &= E_{pk}\left(\sum_{k=1}^K v_k\right) = \prod_{k=1}^K E_{pk}(v_k). \end{aligned} \quad (2)$$

The protocol presented in this study also supports partial anonymity. Imagine Alice wants to send some money to Bob, but he does not want anyone to know that these currencies are for Bob. Table 2 shows the roles assigned to users, the permissions each role has, and the relationship between user-role-permission-device.

Assuming n of account are chosen. Then, the $n-1$ address from the anonymous set is randomly selected. Finally, she performs the transfer, sending the ciphertext of the currency to a blind feature of $n-1$ addresses that are randomly selected.

In order to encrypt the message, an integer is randomly selected, and then, calculate the ciphertext:

$$E_{pk}(m, r) = (N + 1)^m \cdot r^N \text{mod} N^2. \quad (3)$$

TABLE 1: The function introduction of each part of the block header.

Module	Size	Function
Version	4	Record the version number of the block header
Prev Block Hash	32	Record the hash worth of the past square
Merkle Root	32	Record the root value of the Merkle tree hash of the transaction contained in the current block
Timestamp	4	Record the creation timestamp of the current block
Difficulty Target	4	Record the computational difficulty of the current block
Nonce	4	Random number generated with the block

For decryption,

$$m = \frac{(E_{pk}(m, r)^\lambda \text{mod} N^2) - 1}{N} \cdot \lambda^{-1} \text{mod} N. \quad (4)$$

The given scheme can also use the consensus to recover the random number in a given ciphertext:

$$\begin{aligned} r &= c^{N-1 \text{mod} \lambda} \text{mod} N, \\ c &= E_{pk}(m, r) \cdot (N + 1)^{-m} \text{mod} N. \end{aligned} \quad (5)$$

From the nature of the encryption system, the following equations can be obtained:

$$\begin{aligned} E_{pk}(m_1, r_1) \cdot E_{pk}(m_2, r_2) &= E_{pk}(m_1 + m_2, r_1 \cdot r_2), \\ E_{pk}(m, r)^k &= E_{pk}(k \cdot m, r^k). \end{aligned} \quad (6)$$

The Paillier encryption system also has a blind feature, which is the ability to change a ciphertext without changing the corresponding plaintext:

$$E_{pk}(m, r_1 \cdot r_2) = E_{pk}(m, r_1) \cdot E_{pk}(o, r_2). \quad (7)$$

Assuming different values (i.e., $x_m^{k_1} \neq x_m^{k_2}$), in the next place, in the payment privacy, if Alice is transferring money to n of accounts during the transfer, then only the probability of selecting Bob's account is $1/n$. The equipment information used in the mechanism simulation experiment in this paper is shown in Table 3.

By hiding each transaction with a different anonymous set, the rate of increase is gradually increased, as shown in Figure 2.

3. Results and Discussion

3.1. Blockchain-Based Enterprise Data Collaboration and Sharing Solution. The blockchain-based undertaking information cooperation and sharing plans are given in Figure 3. The main roles of the scheme are the homomorphic encryption scheme, the contribution proof protocol, and the smart contract technology. It solved the problems existing in the current contribution of enterprise data collaboration.

Multiple enterprises participating in the collaboration encrypt the data to be shared homomorphic output the

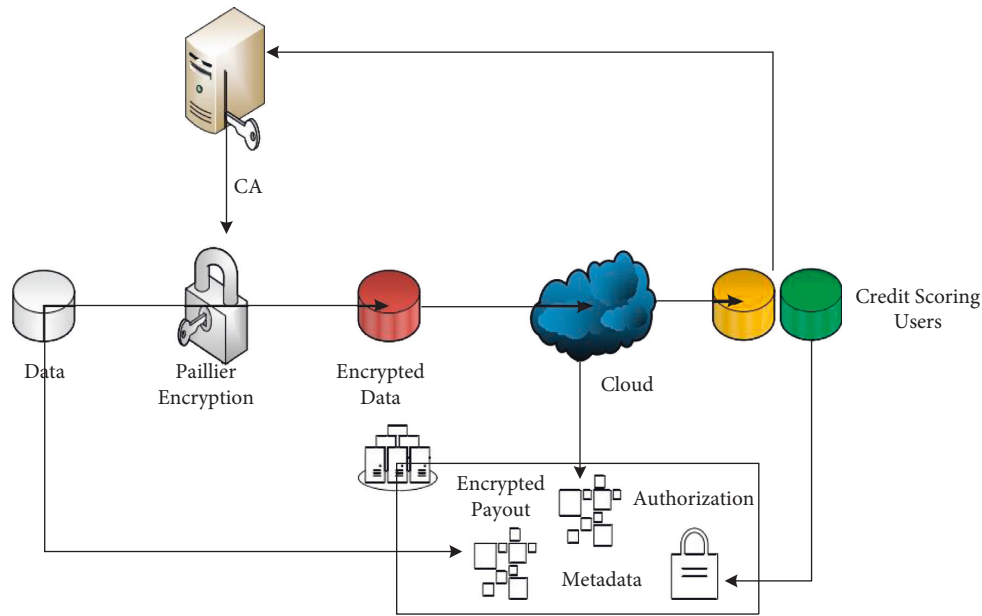


FIGURE 1: System model.

TABLE 2: Roles assigned to users, the permissions each role has, and the relationship between user-role-permission-device.

Module	Size	Function
Version	4	Record the version number of the block header
Prev Block Hash	32	Record the hash value of the previous block
Merkle Root	32	Record the root value of the Merkle tree hash of the transaction contained in the current block
Timestamp	4	Record the creation timestamp of the current block
Difficulty Target	4	Record the computational difficulty of the current block
Nonce	4	Random number generated with the block

TABLE 3: The equipment information used in the mechanism simulation experiment in this paper.

Equipment	CPU	Working	Memory (GB)	Hard disk
Lenovo Think Station P910	Intel Xeon E5-2640 v4, 2 4 GHz	Window 10(64 bit)	64	2 TB
Lenovo 10N9CTO1 WW	Intel Core i7-7700, 3.6 GHz	Window 7(64 bit)	8	2 TB
Lenovo N50	Intel Core i5-4210, 1.7 GHz	Window 7(64 bit)	4	500 GB
Raspberry model B	Contex A53, 1.2 GHz	Raspbian GNU/Linux 8	1	16 GB

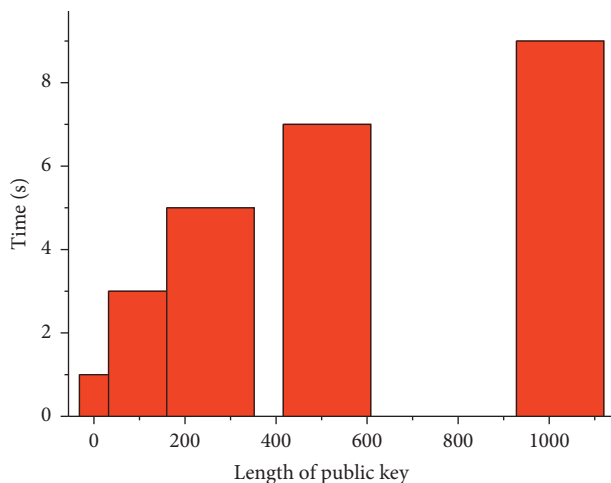


FIGURE 2: Paillier key generation time.

encrypted data, and use the secure multiparty computing technology to merge the previously designed algorithms together for collaborative computing. After the result of the safe multiparty calculation comes out, demander utilizes the Paillier homomorphic decoding calculation to unscramble the result and acquire the information that they really want. Each data provider and the collaborative data result calculation party distribute the predesigned total reward according to the score obtained, and under the control of another smart contract, the rewards that each party should receive are sent to the accounts of these users. Whatever the transmitted data, the process of data transfer, the process of collaborative data operations, the process of returning data results, the process of contributing proof calculations, the process of reward distribution, and the results are recorded in blockchain by smart contracts. This article records the results of multiple visits, as shown in Table 4.

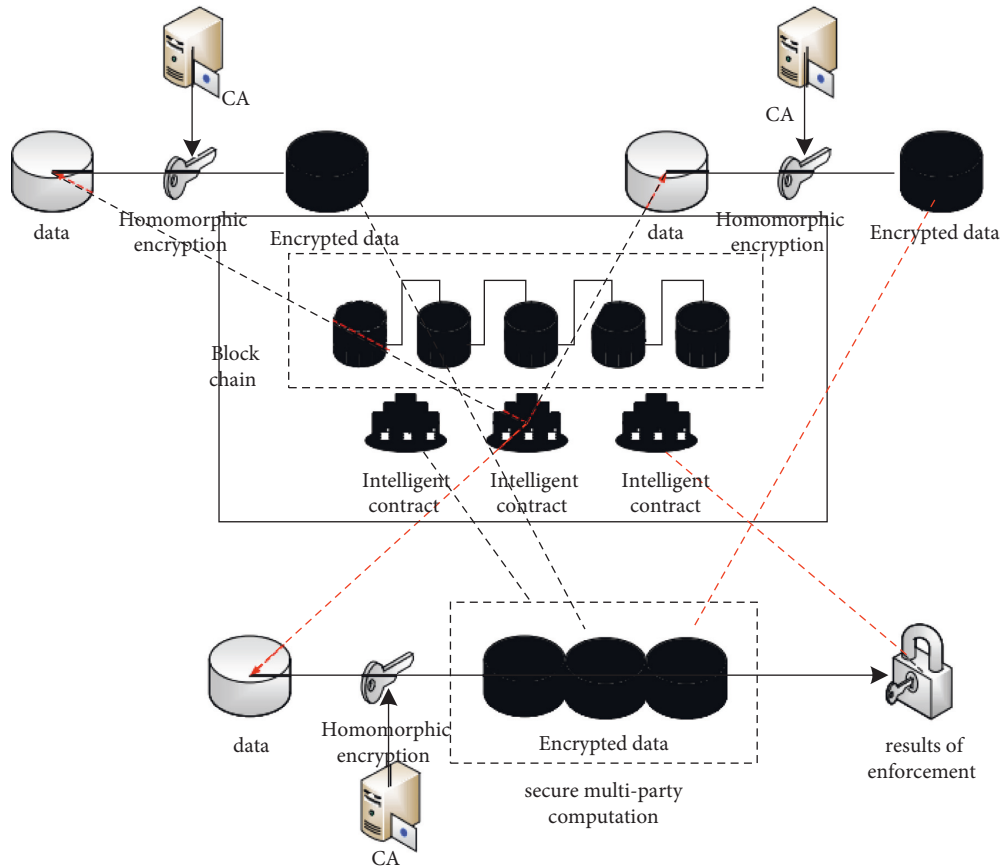


FIGURE 3: Execution process of enterprise data collaboration.

TABLE 4: Results of multiple visits.

User	Role	Operate	Results	Time
PK 1	Manager	Execute	Allow	2019.6.6 9:43
PK 2	Supervisor	Write	Allow	2019.6.6 15:35
PK 3	Partner	Storage	Deny	2019.6.7 10:15
PK 4	Client	Read	Allow	2019.6.7 15:42

3.2. *Implementation Steps of Enterprise Data Collaboration and Sharing Based on Blockchain.* Users participating in enterprise data sharing requirements, the data are prepared to be transmitted through the encrypted secure channel. It passes the data through a secret channel to a secure computing container. The relevant data are automatically encrypted, automatically decrypted, and ready to perform related operations, as shown in Figure 4.

Received data are manipulated using a secure multiparty computing algorithm that implements the determination, as shown in Figure 5.

Under the strong supervision through the reverse one-way secure channel, the collaborative data result is immediately eliminated after being delivered to the collaborative data requester and is not backed up, as shown in Figure 6.

Without leaving a backup, raw original is also done, as shown in Figure 7.

Due to the huge number of IoT devices, in order to satisfy as many access requests of IoT devices as possible, local

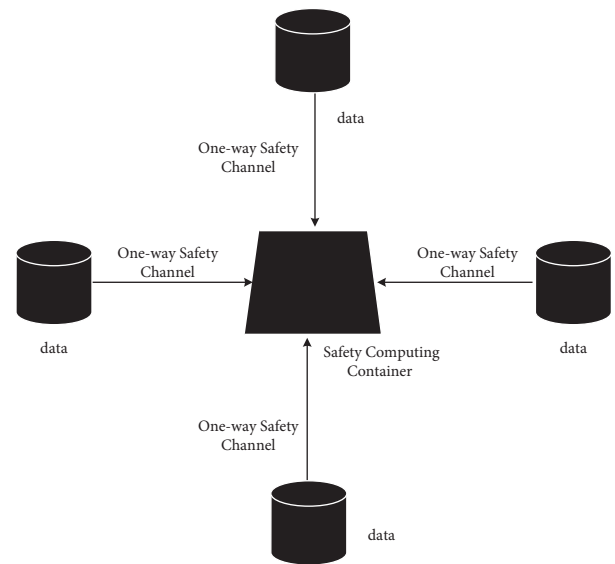


FIGURE 4: Collaborative data transmission.

gateways need high-performance features. Therefore, this article tried the throughput and data transmission of the neighborhood door, and the experimental outcomes are displayed in Figure 8.

The initiator information stored by the verification node is shown in Table 5.

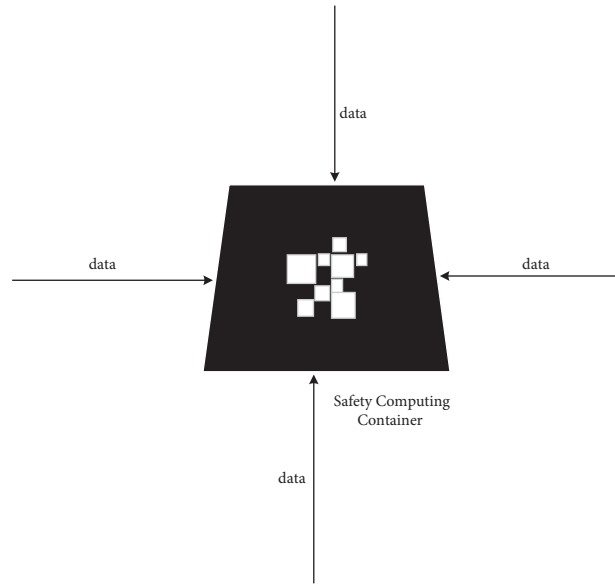


FIGURE 5: Collaborative data operation.

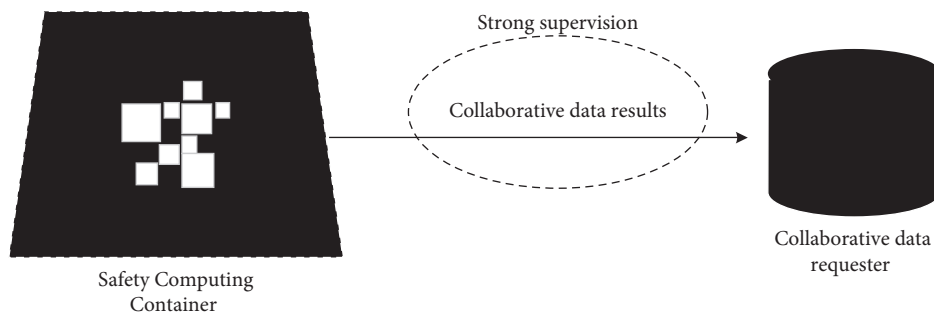


FIGURE 6: Collaboration data return.

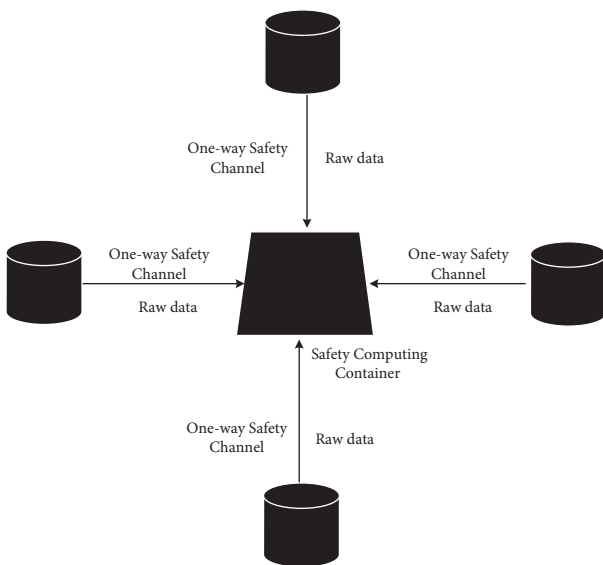


FIGURE 7: Raw data return.

Taking into account the network delays in real transactions, this experiment introduces network delays when simulating the transaction process, taking random numbers

as 0.21587, 0.76817, 0.16967, 0.57892, 0.82071, 0.68045, 1.26064, 0.77601, 0.55335, and 0.34181. The transaction delay value of each round of simulation is displayed in Table 6.

Users with high permissions can check the statistics of these health data at any time through the authorized homomorphic public key. However, since the private key signature is added during cannot be spied on before the permission of the SP is obtained. User privacy data are shown in Table 7.

3.3. Blockchain-Based Government Data Collaboration and Sharing Solution. In this study, through the decentralized blockchain technology, an innovative data distribution system is constructed. Blockchain technology is mainly proposed for the trust problem of the centralized accounting system of existing financial institutions. It is composed of distributed storage, P2P network, encryption algorithm, consensus mechanism, and other technologies. In the system proposed in this study, there are six different roles, namely information source, media, information buyer, system maintainer, content distributor, and advertisers.

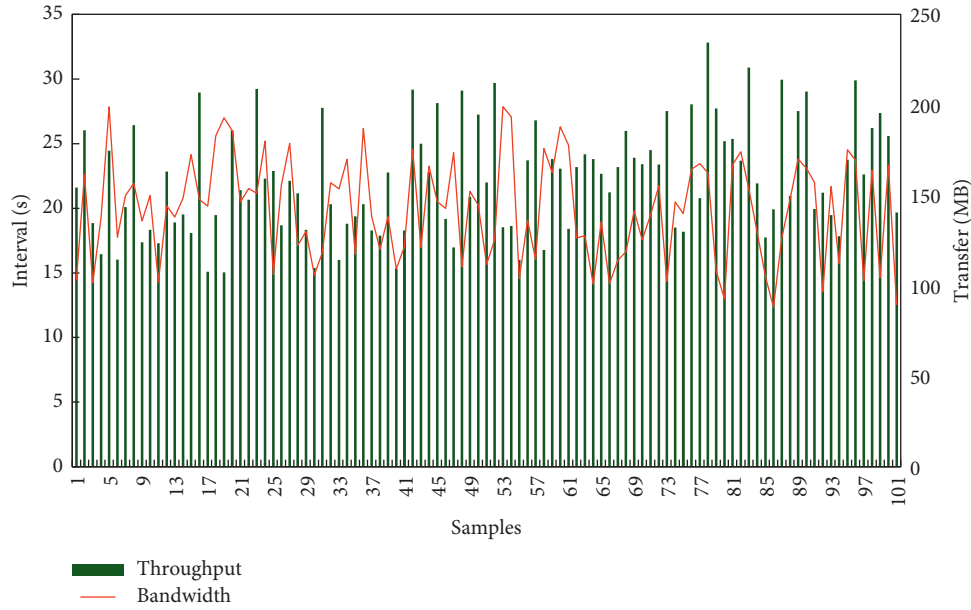


FIGURE 8: The test results.

TABLE 5: The initiator information stored by the verification node.

Rounds	Alice	Bill	Mark	Joan
Round1	354414	7.80769	6.92872	3.57067
Round2	6.86712	4.72692	5.68037	4.99165
Round3	0.37410	7 35849	6.30477	3.64614
Round4	4.43557	6.27414	5.70371	3.88766

TABLE 6: The transaction delay value of each round of simulation.

Numbers	Alice	Bill	Mark	Joan
1	254454	7.70725	2.52772	2.57027
2	2.72752	4.72252	5.27027	4.55525
3	0.27450	7 25745	2.20477	2.24254
4	4.42557	2.27454	5.70275	2.77722

TABLE 7: User privacy data.

Index	User ID			
	1	2	3	4
HR	88	76	90	77
BP	107	124	110	101
RR	16	13	18	12

The information source uploads the created information to a given blockchain system, while doing this, the information source needs to provide a certain commission to the system. The source of information generally refers to the information transmitted through a certain substance; that is, the origin/source of the information (including the place of production and occurrence of information resources, the source, and the base). The information source can use built-in smart contract module in the system to initiate content crowdfunding and set the revenue share portion and investment deadline for the transfer. Within the limited time,

the information buyers can invest the content by share, and the content producer can obtain the lump sum basis at first, and the content will be automatically allocated in portions by the smart contract to the information source and the investor in information purchaser after the lock-up period. The media is the medium, in which information buyers contact information published by information sources, and is also the channel through which advertisers place advertisement [21, 22]. The media enjoys the advertising share in proportion to the prearranged smart contract, which encourages the media to expand the user base and improve the user experience. Information sources can be divided according to the storability of information, the time sequence of production, the form of existence, the production process, and the content of the generated information.

3.4. Research on Blockchain Data Distribution System.

The data purchasers are require to pay a specific measure of cost to the data source and the fundamental asset supplier while buying the data in the framework. The information buyers can participate in the crowdfunding initiated by the information source; that is, the users are allowed to invest in the excellent content generated by other users and obtain the part of the revenue share, while the information buyers can also share the content, the sharing action is recorded by the smart contract on the blockchain, and profit share can be obtained from the advertising revenue of the shared content [23]. Framework maintainers come to a settlement on an agreement system to finish the information on the blockchain. System maintainers have high requirements for computing and communication resources. The main sources of revenue for system maintainers are consensus incentives and transaction fees charged.

Multimedia information dissemination and sharing have high requirements on the network, including storage and

streaming media forwarding cost, which can account for more than 40% of operating costs. In a blockchain-based information distribution system, users with idle resources and eco-partners can voluntarily join nodes to provide bandwidth and storage capacity services for blockchain-based information distribution system users and obtain corresponding commission incentives; thereby, the operating costs in the ecosystem have been significantly reduced. Advertisers are able to pay for advertising based on the data because the clicks, downloads, or page views of the content on the blockchain-based information distribution system are publicly transparent.

Information sources can upload, categorize, fill brief introduction, and fix a price of their own work. Consumers can search the platform for their favorite content and authors, browse content by category, view content profiles and user reviews, purchase content, and rate and comment on purchased content.

Considering that the blockchain-based data distribution system needs to store a lot of photos, videos, texts, and other information. The nodes in the blockchain-based data distribution system are divided into data storage nodes, system maintenance nodes, and common nodes. The data storage nodes are used to maintain the system's data resources. According to the incentive model of the blockchain-based data distribution system, choosing the right data resource for storage, as a data storage node of the system, first needs to have enough storage capacity. The system maintenance node is used to "mining," in this way to maintain the blockchain ledger of the blockchain-based data distribution system. A system maintenance node is not only be in a position of a certain amount of storage capacity and be suitable for the global ledger of storage system but also sufficient computing power is required to complete the proof of work. Ordinary nodes can also be light nodes. Such nodes have the lowest requirements on the nodes themselves. Under normal circumstances, only the account books and data related to themselves need to be stored.

4. Conclusion

In the context of big data, the inherent or potential value of data makes it an important asset. Common data in daily life generally undergoes a series of processing. Due to the lack of necessary transparency in the intermediate process, it is difficult for users to judge its source and reliability. Through the combination of blockchain technology and other scenarios and technologies, many tasks that were previously considered difficult to accomplish can be accomplished. Digital cities will inevitably require digitization of production factors and holographic economic activities to form a scalable economy. Blockchains can replace the original "face-to-face trust" relationship with "back-to-back trust," reducing the cost of transactions and exchanges. In the meantime, the "chain network" is used to unitize the blockchains of different architectures and different scenarios, realize the digitalization of the production factors, and completely record the whole process of the flow, connection, and equity distribution of social production materials. The

blockchain system provides limited identity privacy and data privacy protection capabilities. This article analyzes the identity privacy and data privacy leakage problems of the blockchain system in-depth and combines privacy protection mechanisms and cryptographic algorithms to propose solutions and protections to enhance user identity privacy. The public key of data privacy can search for the blockchain data privacy protection scheme, which improves the privacy protection mechanism of the blockchain system. Based on the ecological environment of the blockchain system, using the distributed data storage function of the blockchain system can bring new application modes to a large number of field application systems. At present, various application fields have formed a preliminary accumulation in blockchain technology, gradually combining the functions of the blockchain system with the original business system, using the characteristics of the blockchain to solve the drawbacks of the business system, and at the same time, improving the blockchain system itself has shortcomings and limitations. Now, applications in various fields have presented more new challenges to the blockchain system.

This study merged the blockchain and big data together, and the big data privacy protection and scalability issues are deeply studied and analyzed based on the existing blockchain system architecture, and some research results are obtained, but there are still many works that can be further studied. According to the viewpoint of tackling the security assurance and versatility of large information sharing, this study proposes a shared data privacy protection and scalability solution. This solution solves the data storage problem to some extent, but the recorded data are still stored in the cloud. There may still be the possibility of centralization failure. The next step will be to expand the solution based on the existing research results to further solve the problem of centralization failure.

Data Availability

No data were used to support this study.

Conflicts of Interest

The author declares that there are no conflicts of interest with any financial organizations regarding the material reported in this manuscript.

Acknowledgments

This work was supported by the scientific research project of the Shaanxi Provincial Education Department in 2018 (project no. 18JK1189).

References

- [1] L. Liu and B. Xu, "Research on Information Security Technology Based on Blockchain," in *Proceedings of the 2018 IEEE 3rd International Conference on Cloud Computing and Big Data Analysis (ICCCBDA)*, pp. 380–384, Chengdu, China, April 2018.

- [2] H.-T. Wu and C.-W. Tsai, "Toward blockchains for health-care systems: applying the bilinear pairing technology to ensure privacy protection and accuracy in data sharing," *IEEE Consumer Electronics Magazine*, vol. 7, no. 4, pp. 65–71, 2018.
- [3] H. Zhao, P. Bai, Y. Peng, and R. Xu, "Efficient key management scheme for health blockchain," *Caai Transactions on Intelligence Technology*, vol. 3, no. 2, pp. 114–118, 2018.
- [4] S. Prasad, R. Shankar, R. Gupta, and S. Roy, "A TISM modeling of critical success factors of blockchain based cloud services," *Journal of Advances in Management Research*, vol. 15, no. 4, pp. 434–456, 2018.
- [5] R. Qin, Y. Yuan, and F.-Y. Wang, "Research on the selection strategies of blockchain mining pools," *IEEE Transactions on Computational Social Systems*, vol. 5, no. 3, pp. 748–757, 2018.
- [6] B.-K. Zheng, L.-H. Zhu, M. Shen et al., "Scalable and privacy-preserving data sharing based on blockchain," *Journal of Computer Science and Technology*, vol. 33, no. 3, pp. 557–567, 2018.
- [7] P. Mamoshina, L. Ojomoko, Y. Yanovich et al., "Converging blockchain and next-generation artificial intelligence technologies to decentralize and accelerate biomedical research and healthcare," *Oncotarget*, vol. 9, no. 5, pp. 5665–5690, 2018.
- [8] L. Li, J. Liu, L. Cheng et al., "CreditCoin: a privacy-preserving blockchain-based incentive announcement network for communications of smart vehicles," *IEEE Transactions on Intelligent Transportation Systems*, vol. 19, no. 7, pp. 2204–2220, 2018.
- [9] M. N. Kamel Boulos, J. T. Wilson, and K. A. Clauson, "Geospatial blockchain: promises, challenges, and scenarios in health and healthcare," *International Journal of Health Geographics*, vol. 17, no. 1, p. 25, 2018.
- [10] A. Zhang and X. Lin, "Towards secure and privacy-preserving data sharing in e-health systems via consortium blockchain," *Journal of Medical Systems*, vol. 42, no. 8, p. 140, 2018.
- [11] M. Benchoufi and P. Ravaud, "Blockchain technology for improving clinical research quality," *Trials*, vol. 18, no. 1, p. 335, 2017.
- [12] K. Fan, Y. Ren, Y. Wang, H. Li, and Y. Yang, "Blockchain-based efficient privacy preserving and data sharing scheme of content-centric network in 5G," *IET Communications*, vol. 12, no. 5, pp. 527–532, 2018.
- [13] B. D. Trump, M.-V. Florin, H. S. Matthews, D. Sicker, and I. Linkov, "Governing the use of blockchain and distributed ledger technologies: not one-size-fits-all," *IEEE Engineering Management Review*, vol. 46, no. 3, pp. 56–62, 2018.
- [14] T. T. A. Dinh, R. Liu, M. Zhang, G. Chen, B. C. Ooi, and J. Wang, "Untangling blockchain: a data processing view of blockchain systems," *IEEE Transactions on Knowledge and Data Engineering*, vol. 30, no. 7, pp. 1366–1385, 2018.
- [15] A. Panarello, N. Tapas, G. Merlino, F. Longo, and A. Puliafito, "Blockchain and IoT integration: a systematic survey," *Sensors*, vol. 18, no. 8, p. 2575, 2018.
- [16] B. Yu, J. Wright, S. Nepal, L. Zhu, J. Liu, and R. Ranjan, "IoTChain: establishing trust in the internet of things ecosystem using blockchain," *IEEE Cloud Computing*, vol. 5, no. 4, pp. 12–23, 2018.
- [17] C. Kuner, F. Cate, O. Lynskey, C. Millard, N. Ni Loideain, and D. Svantesson, "Blockchain versus data protection," *International Data Privacy Law*, vol. 8, no. 2, pp. 103–104, 2018.
- [18] M. Zhaofeng, H. Weihua, and G. Hongmin, "A new blockchain-based trusted DRM scheme for built-in content protection," *EURASIP Journal on Image and Video Processing*, vol. 2018, no. 1, p. 91, 2018.
- [19] M. Yang, A. Margheri, R. Hu, and V. Sassone, "Differentially private data sharing in a cloud federation with blockchain," *IEEE Cloud Computing*, vol. 5, no. 6, pp. 69–79, 2018.
- [20] Y. Chen, S. Ding, Z. Xu, H. Zheng, and S. Yang, "Blockchain-based medical records secure storage and medical service framework," *Journal of Medical Systems*, vol. 43, no. 1, p. 5, 2018.
- [21] R. Zinko, H. de Burgh-Woodman, Z. Z. Furner, and S. J. Kim, "Seeing is believing," *Journal of Organizational and End User Computing*, vol. 33, no. 2, pp. 85–104, 2021.
- [22] M. Shemeis, T. Asad, T. Asad, and S. Attia, "The effect of big five factors of personality on compulsive buying: the mediating role of consumer negative emotions," *American Journal of Business and Operations Research*, vol. 2, no. 1, pp. 5–23, 2021.
- [23] A. Sharma, Y. Sharma, R. Bansal et al., "Implementation of crowd sale using ERC-20 tokens," *Journal of Cybersecurity and Information Management*, vol. 2, no. 1, pp. 05–12, 2020.

Research Article

Application of Conditional Random Field Model Based on Machine Learning in Online and Offline Integrated Educational Resource Recommendation

Erqi Zeng 

School of Foreign Languages, Xuchang University, Xuchang, Henan 461000, China

Correspondence should be addressed to Erqi Zeng; zeq1977@163.com

Received 20 February 2022; Revised 2 April 2022; Accepted 22 April 2022; Published 24 June 2022

Academic Editor: Xuefeng Shao

Copyright © 2022 Erqi Zeng. This is an open access article distributed under the Creative Commons Attribution License, which permits unrestricted use, distribution, and reproduction in any medium, provided the original work is properly cited.

It is of great significance to mine the learning resources that learners are interested in from massive data and recommend appropriate educational resources to them according to the characteristics of students. To improve the accuracy of educational resource recommendation, this paper proposes an educational resource recommendation system based on a graph attention network and conditional random field fusion model. It builds all comments for each student and educational resource into a comment graph. Through the graph's topological structure to capture the network and the dependency between words in the commentary text, the adjacency information of each node is aggregated by the graph attention network based on connection relation. After the graph attention network layer, the conditional random field inference layer is added. The label sequence with the highest probability is output by the dependent random field inference layer, which is taken as the final recommendation result of the model. Experimental results show that the proposed algorithm has better performance in accuracy and diversity than the traditional recommendation algorithm.

1. Introduction

With the development of social science and technology, many online learning resources have grown. Learners cannot find the learning content from the massive and complicated data. In the process of searching, learners will be interfered with by a lot of irrelevant information, thus wasting their time and continuously decreasing their learning efficiency and interest [1]. Therefore, how to recommend learning resources that users are interested in has become the primary research content of this subject [2]. By combining personalized recommendation with learning, learners can obtain more targeted learning resources in the learning resource recommendation system more accurately and quickly [3].

As important auxiliary information in the recommendation system, comment text can describe users' interests and hobbies in different aspects of the project [4]. Recommendation methods, based on comment text, mainly include topic modeling methods and deep learning methods (such as convolutional neural networks and cyclic neural

networks) [5]. Although these methods have achieved specific performance improvements, they still have limitations. Topic-based modeling methods can only capture the semantic information of the text at the global level and ignore the critical word order and word context information in the text [6]. Based on the deep learning method, we can effectively capture the adjacent word context information, in the long-term, global capture between word and the word, and the continued dependence of [7] has some limitations. However, this kind of method only considers the single static preferences of the user or the project side and fails to capture the preference characteristics at the interaction level [8].

In the recommendation field, foreign literature [9] adopts a collaborative filtering algorithm to recommend interested and appropriate online learning resources for different learners according to their other goals and interest directions. Literature [10], through studying learners' characteristic preferences and activity behaviors, improved the shortcomings in the modeling process and established a dynamic preference model for further recommendation. Regarding

domestic recommendation technology, literature [11] proposed associating learning resource tree with user access records, establishing a user preference matrix and making calculations in a comprehensive way of collaborative filtering and popular recommendation. Literature [12] presented a new technology, namely, the calculation method of assigning information entropy and changing it according to the attribute value change, finally obtaining the weight of user preference. Experimental results show that the recommended result is more accurate. Literature [13] mines and analyzes data from multiple perspectives, which is embodied in constructing a multiassociated data warehouse for the data in user system logs. Literature [14] proposed the long-short Time Memory (LSTM) network by enhancing the traditional recurrent neural network. Literature [15] established a recommendation model of online learning resources and provided personalized learning resource sequences for learners by solving the learning resources with the most negligible differences with learners' characteristics through binary particle swarm optimization. Literature [16] constructed a learning resource recommendation system from the perspective of semantic Web ontology and mapped learner features and learning resource features into the ontology for matching recommendations. Literature [17] proposed using ontology integration to learn resource relationship features and then carry out recommendation calculations through a genetic algorithm. Literature [18] proposed a new e-learning intelligent recommendation system, which can evolve itself. The system realizes the self-adaptation of learners and the self-adaptation of an open network environment. Literature [19] introduces semantic Web technology into personalized recommendation services in the network learning system and proposes an intelligent recommendation system based on semantic discovery and learning preference.

In view of the above problems, this paper proposes an educational resource recommendation system based on a graph attention network and conditional random field fusion model. The recommendation algorithm RGP is used to construct a review graph from all the review sets of each user or project. The graph topology captures long-term, global, and discontinuous dependencies between words in the commentary text. The adjacency information of each node is aggregated using a graph attention network based on connection. The word order relation is considered. Conditional random field (CRF) inference layer is added after the BiLSTM network layer. CRF limits the previous model's output by considering the relationship between adjacent labels to ensure the rationality of prediction labels. Finally, the embedded representation of the user and item ID and their comment graph represents the coupled input, and a Factorization Machine (FM) is used to predict the score.

2. The Proposed Educational Resource Recommendation System

2.1. Recommendation Model for Learning Representation Based on Comment Text Graph. In this paper, $S_p = \{s_p^1, s_p^2, \dots, s_p^{W_p}\}$ represents the comment set generated by user p . $N_x = \{n_x^1, n_x^2, \dots, n_x^{T_x}\}$ represents the set of

comments received by education resources x , where W_p and T_x represent the total number of comments contained by user p and education resources x , respectively. The score of user p on education resources x is defined as j_{px} , and all the score datasets are represented as D .

The RGP network structure of the recommendation algorithm based on comment text graph representation learning is shown in Figure 1. It contains three modules: the user module (the left two columns of Figure 1). Education resources modules (the right two columns of Figure 1). Prediction module based on FM [20]. The user module has the same network architecture as the education resources module, which users learn. Education resources modules are used to represent projects. The prediction module takes the user and the education resources representation as input and calculates the user's rating of the education resources.

The user (education resources) module consists of three parts: The section that builds the comment text graph builds the comment text set for each user's education resources) into a graph. In graph representation learning, the connection-based graph attention network and the interaction-based attention mechanism are used to extract the representation of the whole graph. The representation fusion part coupled the embedded representation of user (item) ID and its graph representation to obtain the indication of end-user (item). The network architecture of the user module is the same as that of the education resources module. The details of each part of the user module are described below.

2.2. Comment Text Graph Construction. This paper uses the method of reference [20] to construct a review text graph. In the comment text, if two words appear together in a window of size ω (i.e., the distance between the two words is less than ω), then the two words are connected. This paper saves the word order information on this basis. For user p 's comment text set S_p , first, keywords of each comment in S_p are selected using text preprocessing techniques such as sentence segmentation and preposition clearing. Then, all comments are constructed into a directed graph, in which the nodes are the keywords of the comment text, and the edges in the graph describe the cooccurrence relationship between words in a sliding window of fixed size ω . The word order relationship of critical text is significant in reflecting the semantic meaning of the text. For example, "not very good" and "very bad" convey different levels of negative emotion. To preserve the word order information in the graph, this paper defines three types of connection relation: forward relation e_f , backward relation e_h , and self-connection relation e_s . Take a comment s_p^n from the comment set S_p . If the selected keyword (node) i_2 appears before the keyword i_1 in s_p^n and the distance between i_2 and i_1 is less than ω in the original comment, an edge $E(i_2, i_1)$ from i_2 to i_1 is established in the graph. The connection of this edge is e_f . At the same time, an edge $E(i_1, i_2)$ from i_1 to i_2 is established, and the connection of this edge is e_h . If i_2 appears both before and after i_1 (which is rare), the edge connection is randomly set to e_f or e_h . In addition, to consider the information of the word itself, each node in the graph adds an edge connected to itself

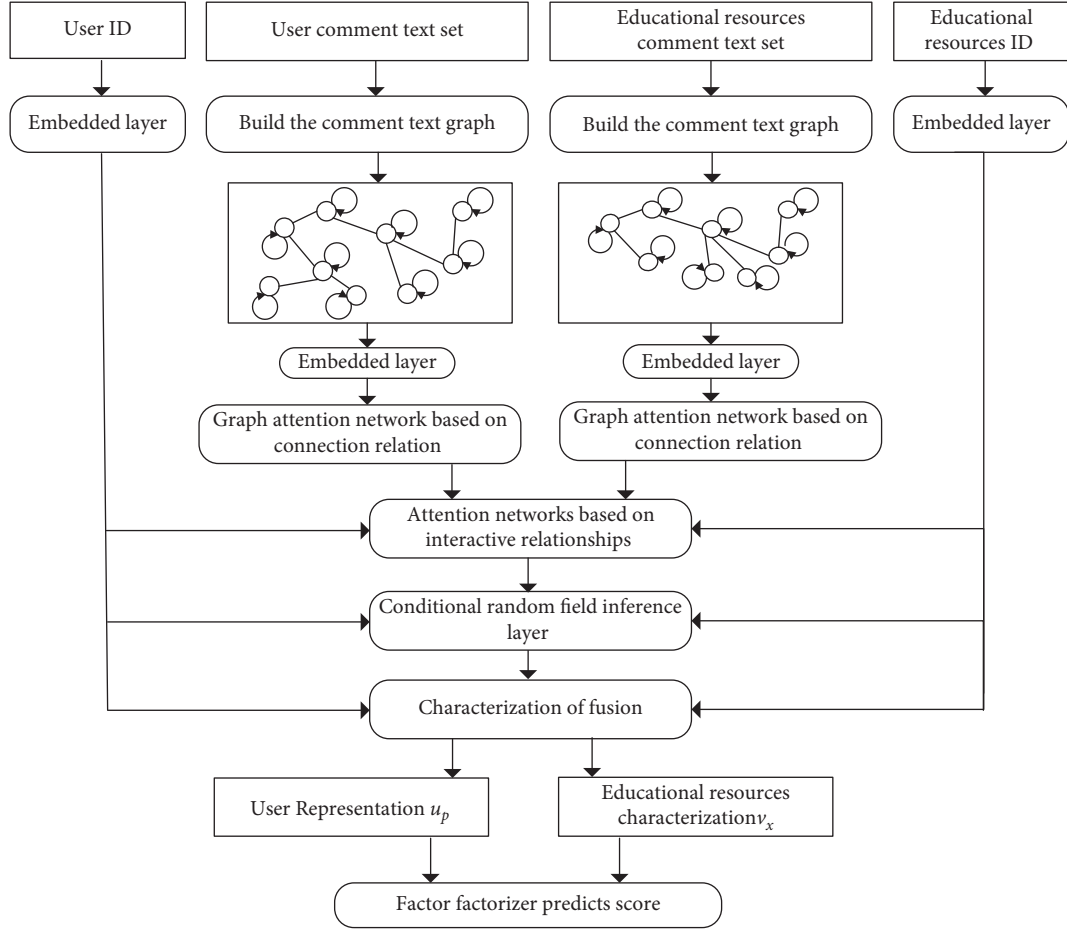


FIGURE 1: RGP algorithm neural network structure.

(for example $E(i_1, i_1)$) and defines its connection as e_s . Figure 2 shows an example of structuring the comment, “Friends love this nice durable mouse.” “Friends,” “like,” “good-looking,” “durable,” and “mouse” were all selected as keywords in the comments. The word “this” is removed, and the window size ω is set to 3. If the distance between the keyword “good-looking” and the three keywords (“like,” “durable,” and “mouse”) in the comment is less than 3, 3 bidirectional edges are established, and edge types are defined according to word order. And so on, build the comment text graph.

For user p , $\mathcal{G}_p = \{\mathcal{X}_p, \mathcal{E}_p\}$ is used to represent its corresponding comment text graph. \mathcal{X}_p is the set of nodes (i.e., keywords), \mathcal{E}_p is the triplet set of node-edge-to-node (i_h, r, i_n) , and r is the connection relation between nodes i_h and i_n (one of the above three relations). A comment text graph of project x , $\mathcal{G}_x = \{\mathcal{X}_x, \mathcal{E}_x\}$ can be built in the same way.

2.3. Figure Represents Learning

2.3.1. Embedded Layer. The input of the embedding layer, user ID, comment text ID, word ID, and connection relation ID is mapped to different embedding spaces to obtain the corresponding low-dimensional embedding features. In this paper, $e_p, e_x, i, e_r \in \mathbb{R}^{1 \times d_0}$ are, respectively, used to represent

the low-dimensional embedding features of user p , comment text x , word i , and connection relation r , where d_0 is the vector dimension of the embedding space.

2.3.2. Graph Attention Network Based on Connection Relation. The information of words in the commentary text is not independent, and the semantic information of a word can be enriched by the words around it. A graph attention network based on connection relation is proposed to aggregate adjacency information. Assume that the input in $\mathcal{G}_p = \{\mathcal{X}_p, \mathcal{E}_p\}$, for the nodes in the graph i_h , uses $\mathcal{N}_h = \{i_n | (i_h, r, i_n) \in \mathcal{E}_p\}$ says i_h adjacent points, \mathcal{N}_h contains i_h itself. Assuming that it is currently at layer l of the graph attention network, the importance weight of the adjacent point i_n can be calculated as follows:

$$\alpha^l(i_h, r, i_n) = \frac{\exp[\pi^l(i_h r, i_n)]}{\sum_{i_n \in \mathcal{N}_h} \exp[\pi^l(i_h \bar{r}, i_n)]}, \quad (1)$$

$$\pi^l(i_h, r, i_n) = \sigma \left[(i_h^l M_1^l) (i_n^l M_1^l + e_r^l M_2^l)^N \right], \quad (2)$$

where $M_1^l, M_2^l \in \mathbb{R}^{d_0 \times d_1}$ are transformation weight matrices of corresponding nodes and connection relations, respectively. $i_h^l, e_r^l, i_n^l \in \mathbb{R}^{1 \times d_0}$ are the vector representations of i_h, r

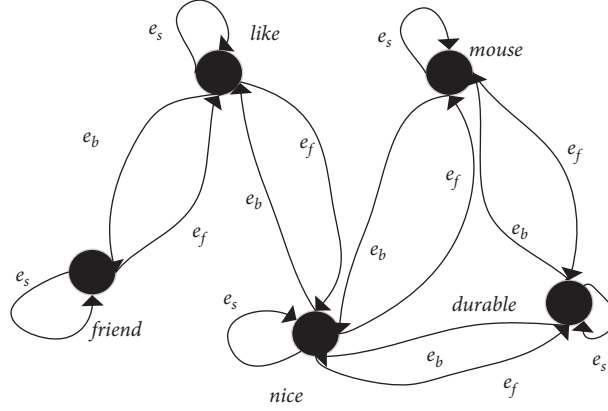


FIGURE 2: Review text graph example.

and i_n at the l layer, respectively, and the initial l layer representation is the low-dimensional embedding characteristics of the output of the corresponding embedding layer. σ is the LeakyRelu activation function. d_1 is the vector dimension of the representation space. $d_* = d_0$ at the first layer and $d_* = d_1$ at other layers.

The importance weight describes the importance degree of adjacency. According to this weight, the vector representation of the adjacency is integrated, and the output vector representation of i_h is obtained as follows:

$$i_h^{l+1} = \text{Tanh} \left(\sum_{i_n \in \mathcal{N}} \alpha^l(i_h, r, i_n) i_n^l M_1^l \right), \quad (3)$$

where Tanh is the activation function. The long-term dependence of words in the commentary text is captured by stacking multilayer graph attention networks. Assuming the number of stacking layers is l , the corresponding output vectors of l i_h can be represented as $\{i_h^2, i_h^3, \dots, i_h^{l+1}\}$.

2.3.3. Attention Mechanism Based on Interactive Relationship. When all nodes of graph \mathcal{G}_p pass through the l layer graph attention network based on connection relation, a graph attention mechanism based on interaction relation is proposed in this paper. The aggregation node representation gives the representation of the whole graph. The attention mechanism assigns importance weights to the interaction level to each node in the graph based on information from user p and comment text x . Assuming that the representation of output nodes of the graph attention network at the above layer l is aggregated, the weight of node i_h can be calculated as follows:

$$\beta_h^l = \frac{\exp[\rho(i_h p, x)]}{\sum_{i_h \in \mathcal{X}_p} \exp[\rho(i_h p, x)]}, \quad (4)$$

$$\rho^l(i_h, p, x) = \sigma \left(i_h^{l+1} \left(\text{Tanh} \left(\left[e_p \| e_x \right] M_3^l \right) \right)^N \right), \quad (5)$$

where $M_3^l \in R^{2d_0 \times d_1}$ is the transformation weight matrix. $\|$ for vector concatenation operation. According to the weighted

sum of node representation of output, the output representation of layer l of graph \mathcal{G}_p can be obtained as follows:

$$a_p^{l+1} = \sum_{i_h \in \mathcal{X}_p} \beta_h^l i_h^{l+1}. \quad (6)$$

2.3.4. Representation Fusion. To improve the expression ability of the model, a layer of nonlinear transformation is applied to the low-dimensional embedding feature e_p based on user ID.

$$w_p = \text{Tanh}(e_p M_4), \quad (7)$$

where $M_4 \in R^{d_0 \times d_1}$ is the transformation weight matrix. The final representation of the user is the concatenation of w_p and the graph representation output above at all levels.

$$u_p = w_p a_p^2 a_p^3 \dots \| a_p^{L+1}. \quad (8)$$

Following the same process, the final representation of comment text x , v_x can be obtained.

2.4. CRF Inference Layer. CRF inference layer is added after the BiLSTM network layer to make the model learn the constraint information between tags. CRF limits the output results of the previous model by considering the relationship between adjacent labels to ensure the rationality of predicted labels. The steps of the CRF algorithm are as follows:

- (1) For the input sequence $i = (i_1, i_2, \dots, i_t)$, for a given tag sequence $(j = j_1, j_2, \dots, j_t)$, the score is shown in the following equation:

$$S(i, j) = \sum_{x=0}^t G_{j_x, j_{x+1}} + \sum_{x=1}^t U_{x, j_x}, \quad (9)$$

- (2) where G represents the transition score matrix and $G \in R^{(z+2) \times (z+2)}$, and G_{xy} represents the transition score from label x to label y . j_0 and j_{t+1} represent the start and end tags in a sentence. The matrix U is the output of the BiLSTM layer and $U \in R^{t \times z}$. U_{xy} represents the output score of the x word under the y

tag. t represents the length of the sequence, and z represents the number of tags.

- (3) Softmax function is used to normalize and obtain the maximum probability of sequence j label, as shown in equation as follows:

$$U\left(\frac{j}{i}\right) = \frac{e^{S(i,j)}}{\sum_{\bar{j} \in J_i} e^{S(i,\bar{j})}}, \quad (10)$$

- (4) where \bar{J} represents the actual value. J_i represents the set of all possible tags. During training, the likelihood probability of the correct tag sequence is maximized as shown in the following:

$$\log_g U\left(\frac{j}{i}\right) = S(i, j) - \sum_{\bar{j} \in J_i} S(i, \bar{j}), \quad (11)$$

- (5) The sequence with the highest predicted total score among all the sequences is regarded as the optimal sequence, that is, the final text recognition result of educational resources as shown in the following equation:

$$j^* = \underset{j \in Y_x}{\operatorname{argmax}} S(i, \bar{j}). \quad (12)$$

2.5. Score Prediction. In this paper, a FM calculates users' ratings of educational resources. First, the final representation of users and educational resources is combined as follows:

$$k = u_p \parallel v_x. \quad (13)$$

The scoring is calculated as follows:

$$\hat{j}_{px} = h_0 + h_p + h_x + km^N + \sum_{t=1}^d \sum_{w=t+1}^d \langle q_t, q_w \rangle k_t k_w, \quad (14)$$

where h_0 , h_p , and h_x are the global deviation, user deviation, and project deviation, respectively. $m \in R^{1 \times d}$ is a weight vector, and $d = 2(L+1)d_1$; $q_t, q_w \in R^{1 \times z}$ are the potential factor vectors corresponding to the elements of the t th and W th dimension of k . k_t is the value of the element in the t -dimension of k . $\langle \cdot \rangle$ is an inner product operation.

To learn the parameter Θ of the whole model, this paper defines the loss function of the model as follows:

$$\min_{\Theta} \sum_{(p,x) \in \mathcal{D}} (j_{px} - \hat{j}_{px})^2 + \lambda \|\Theta\|_F^2, \quad (15)$$

where λ is the regularization coefficient. The whole model can be trained efficiently by an end-to-end backward propagation algorithm.

2.6. Algorithm Flow. The RGP algorithm flow is as follows (Algorithm 1).

2.7. System Module Design. A college education information recommendation system based on the fuzzy algorithm of

multiple mixed criteria is an education information recommendation system with a retrieval engine. The system consists of a retrieval module, database module, and recommendation display module. The web retrieval engine is set in the retrieval module, which is used for educational information retrieval and efficient transmission of educational data. The block diagram is shown in Figure 3.

- (1) Retrieval module: After the user logs into the system and enters the retrieval module, he/she selects the corresponding language according to the language he/she knows. The retrieval module supports Mongolian, Chinese, and English. Users use three languages to input the types of educational resources, keywords, and subject information in the search interface.
- (2) Database module: This module has various management modes for educational information and corresponding management for system and user information. Users can be classified as registered users, common users, and management users. Registered users can retrieve educational information for browsing. General users can search for educational information and download educational information. Management Users have the right to manage the overall functions of the database.
- (3) Recommendation display module: The recommendation display module mainly presents the education information with the highest recommendation degree to users. The recommended display module has three main panels: The first is the list of learning resources. The second is the list of recommended resources. The third is the neighbor list. Click the names of lists in the recommended display module panel to activate the corresponding functions. The downloaded learning resources are displayed in the learning resource list. The list of recommended resources shows that the database module extracts the education information with the highest recommendation degree according to the user's retrieval information. The neighbor list lists all educational information similar to that retrieved by the user.

3. Experiment

3.1. The Data Set. To verify the effectiveness of the proposed algorithm, public datasets Citeulike-c and Citeulike-h were used in the experiment. Table 1 shows the statistical information of nodes and the relationship between users' nodes, educational resources, and labels in the two datasets. The sparsity of interactive data in the two datasets is 0.23% and 0.08%, respectively.

3.2. Experimental Methods. The model implements the recommendation model based on comment text graph representation learning. After the dataset is divided, the last interaction is reserved as a positive sample for testing for each user in the dataset. The remaining interactions are

- (i) Enter the user's rating data D for educational resources, the text set of comments by users, and educational resources
- (ii) Output RGP prediction model $F(p, x|\Theta) = \hat{j}_{px}$
- (1) Randomly initialize all parameters of the model θ
- (2) For p , item x , j_{px} in score data D .
- (3) Construct the comment text map A_p and A_x of user p and educational resource x .
- (4) Assume \hat{j}_{px} based on equations (1) to (8) and equations (13) to (14).
- (5) According to equation (15), the backward propagation algorithm is used to calculate the gradient of all parameters θ .
- (6) Gradient descent method (Adam) is used to update parameters
- (7) end for
- (8) return $F(p, x|\Theta)$

ALGORITHM 1: RGP algorithm.

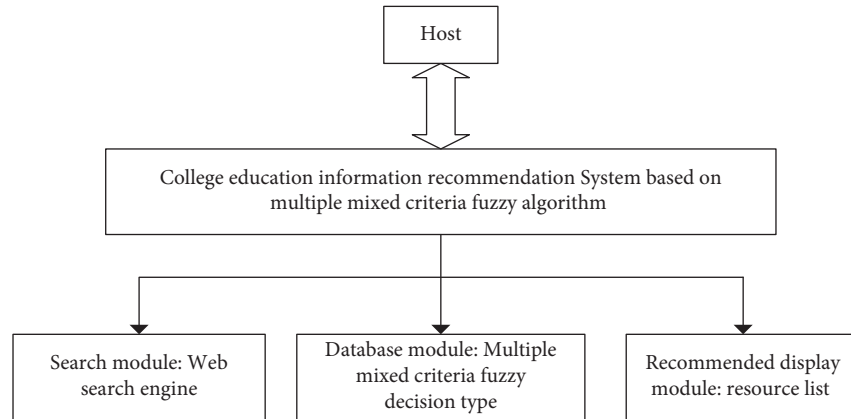


FIGURE 3: Composition block diagram of college education information recommendation system based on multivariate mixed criteria fuzzy algorithm.

TABLE 1: Dataset statistics.

	Dataset	CiteULike-c	CiteULike-h
Node	User	5551	7947
	Educational resources	16980	25975
	Label	46391	52946
Relation	User - educational resources	204987	134860
	Educational resources - educational resources	89418	32565
	User - label	239253	290830

positive samples for training. 1000 comments with no previous interaction were randomly selected for each user as a negative test sample. The feature dimension is 64, the word vector is a pretraining model, and the output dimension is 768. The autoencoder adopts a three-layer neural network structure, and the dimension of the middle layer is 64. Feature random zero ratio 0.3.

3.3. Evaluation Indicators. This paper evaluates the performance of the model from two aspects: accuracy and diversity. In terms of accuracy, choose HR@K and NDCG@K. The recommended length is K. HR@K is the hit rate, which measures the proportion of users' test positive sample educational resources in educational resources in the recommendation list. NDCG@K is the normalized impairment cumulative gain that measures the ranking quality of the recommendation list. The higher the user's test positive

sample educational resources, the greater its value. The accuracy of the model is directly proportional to the size of the two values.

In terms of diversity, choice ILS@K and HD@K, K is the length of the recommended list. ILS is the internal list similarity, which measures the similarity of a single user's recommendation list. The larger the ILS value, the higher the similarity and the lower the diversity of a single user's recommendation list. This paper uses the cooccurrence vector of educational resources and tags to calculate the similarity of ILS. HD is the Hamming distance. In information theory, the Hamming distance between two equal-length strings is the number of different characters in the corresponding position of the two strings. Measure the similarity of recommendation lists between different users. The larger the HD value, the lower the similarity between different users and the higher the diversity.

3.4. Experimental Results and Analysis. The experiment compares the evaluation indexes of the proposed algorithm and the traditional recommendation algorithm. To unify variables, K in the recommendation list Top-K is set to 10. The experimental results on the two datasets are shown in Table 2 and 3, respectively. It can be seen from the experimental results:

- (i) The performance of the proposed algorithm is superior to that of other models in both datasets. Compared with [25], in the experimental results of CiteULike-c dataset, the algorithm in this paper improves by 4.62% on NDCG and 0.29% on ILS. In the experimental results of the CiteULike-h dataset, the algorithm in this paper improved by 3.53% on NDCG and 1.17% on ILS. This is due to multi-semantic feature extraction, 3d convolution high-order feature mining, and diversity loss function.
- (ii) Compared with literature [21], literature [22] and literature [23] increased by 1.61% and 0.98% in HR. In NDCG, the results improved by 6.64% and 6.06%, indicating that text and heterogeneous information networks can effectively alleviate the problem of data sparsity and improve the accuracy of recommendation. It shows that semantic features of heterogeneous information networks can effectively enhance the diversity of recommendations.
- (iii) The evaluation index of the accuracy of the deep learning model is improved by 10%–14% compared with the method based on matrix decomposition, indicating the advantage of neural networks in fitting high-order interaction relations. In the deep learning model, HR indexes of literature [24] and literature [25] were compared, and the latter improved by 2.21%, indicating that the fusion method of cross-product could obtain more accurate recommendation results.

3.5. System Effect Test. The system is applied in a school library for 70 days. The experimental users were 1500 teachers and students, and the system was used to search books. The experiment shows that the system in this paper can recommend related books according to user search terms, and the recommendation degree of recommended books is 99%. Note the system in this paper can realize book recommendations according to the user preference and the optimal recommendation degree. To deeply test the application effect of the system in this paper, the user discovery accuracy and recommendation recall rate are taken as test indexes, and the performance comparison experiment is conducted by using the system in this paper, the recommendation system in literature [26], and the recommendation system in literature [27].

- (1) User discovery accuracy: the ratio of the number of educational information recommended by the system selected by users to the total number of recommendations.

TABLE 2: Results of experiments on CiteULike-c.

Model	HR	NDCG	ILS	HD
Literature [21]	52.79	32.51	20.46	98.86
Literature [22]	53.64	34.67	21.44	99.57
Literature [23]	53.31	34.48	20.36	99.65
Literature [24]	58.28	38.84	20.46	99.59
Literature [25]	59.57	39.15	20.38	99.58
Proposed	60.38	40.96	20.32	99.65

The results of the proposed method.

TABLE 3: Results of experiments on CiteULike-h.

Model	HR	NDCG	ILS	HD
Literature [21]	50.21	31.05	17.94	98.81
Literature [22]	51.03	33.27	18.22	99.15
Literature [23]	50.36	32.51	17.86	99.52
Literature [24]	51.32	34.95	18.03	99.54
Literature [25]	52.95	35.62	18.04	99.56
Proposed	54.27	36.88	17.83	99.58

TABLE 4: Comparison results of user discovery accuracy of recommendation education information of the three systems.

Number of users	Proposed	[26]	Literature
100	0.98	0.91	0.94
200	0.96	0.84	0.82
300	0.97	0.86	0.85
400	0.94	0.81	0.75
500	0.94	0.87	0.78

- (2) Five hundred teachers and students were randomly selected as users from 1500 teachers and students in the school. When the number of users increased, the three systems' user discovery accuracy was tested. The results are shown in Table 4. According to the data in Table 4, as the number of users increases, the three systems' user discovery accuracy begins to decrease. However, the user discovery accuracy of the system in this paper decreases in a small extent and at a slow speed. When the number of users increased from 400 to 500, the system users found that the accuracy was stable at 0.94. When the number of users increases from 400 to 500, the discovery accuracy of the users of the two systems is less than 0.88.
- (2) Recommended recall rate: the ratio between the amount of recommended educational information selected by users and the total amount of educational information applied by users.

Based on the above experimental settings, the recommended recall rates of the three algorithmic recommendation systems were tested, and the comparison results are shown in Figure 4.

By comparing the fluctuation trend of the recommendation recall rate of the three algorithmic recommendation systems in Figure 4, the peak value of the recommendation recall rate of the proposed algorithmic recommendation system is greater than 0.92, showing significant advantages.

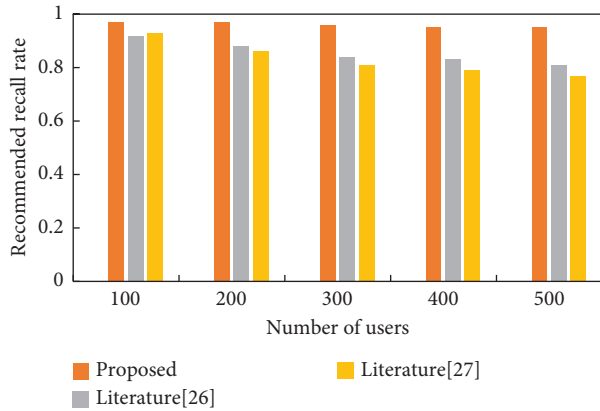


FIGURE 4: Comparison results of recommended recall rates of three systems.

As the number of users increases, it always ranks above the other two algorithmic recommendation systems with minimal fluctuation. The lowest recommendation recall rate of the other two algorithmic recommendation systems falls below 0.81, so most of the educational recommendation information of the algorithm system in this paper is adopted by users.

4. Conclusion

This paper proposes an educational resource recommendation system based on the review text graph representation learning recommendation algorithm RGP combined with a CRF fusion model. The system effectively combines the performance advantages of comment text and graph representation learning. By introducing the graph attention network based on connection relation and the attention mechanism based on interaction relation, the relevant information between word and word, interaction behavior, and comment text can be more fully captured. The label sequence with the maximum probability is output by the CRF inference layer and taken as the final recommendation result of the model. Experimental results on datasets show that the proposed algorithm can effectively improve the recommendation accuracy compared with the traditional recommendation algorithms. The resource recommendation system proposed in this paper has significant advantages in recommendation recall rate and high discovery accuracy from the system effect test. The next step will be to introduce more nonscoring auxiliary information to establish a more accurate distribution of user preferences and item features to improve recommendation accuracy. [27].

Data Availability

The labeled dataset used to support the findings of this study is available from the author upon request.

Conflicts of Interest

The author declares no conflicts of interest.

Authors' Contributions

Erqi Zeng contributed to the writing of the manuscript and data analysis. Dalei Jiang supervised the work and designed the study. All the authors have read and agreed with the final version to be published.

Acknowledgments

This work was supported by Henan Educational Science Planning Project: Research on the construction of a three-dimensional foreign language teaching model in Colleges and Universities under the background of educational informatization (2019-JKGHYB-0182).

References

- [1] J. Maldonado-Mahauad, M. Pérez-Sanagustín, R. F. Kizilcec, N. Morales, and J. Muñoz-Gama, "Mining theory-based patterns from big data: identifying self-regulated learning strategies in massive open online courses," *Computers in Human Behavior*, vol. 80, pp. 179–196, 2018.
- [2] S. Wan and Z. Niu, "A hybrid E-learning recommendation approach based on learners influence propagation," *IEEE Transactions on Knowledge and Data Engineering*, vol. 32, no. 5, pp. 827–840, 2020.
- [3] J. Shu, X. Shen, H. Liu, B. Yi, and Z. Zhang, "A content-based recommendation algorithm for learning resources," *Multi-media Systems*, vol. 24, no. 2, pp. 163–173, 2018.
- [4] Q. Li, S. Li, S. Zhang, J. Hu, and J. Hu, "A review of text corpus-based tourism big data mining," *Applied Sciences*, vol. 9, no. 16, p. 3300, 2019.
- [5] H. Jelodar, Y. Wang, R. Orji, and S. Huang, "Deep sentiment classification and topic discovery on novel coronavirus or COVID-19 online discussions: NLP using LSTM recurrent neural network approach," *IEEE Journal of Biomedical and Health Informatics*, vol. 24, no. 10, pp. 2733–2742, 2020.
- [6] M. Han, X. Zhang, X. Yuan, J. Jiang, W. Yun, and C. Gao, "A survey on the techniques, applications, and performance of short text semantic similarity," *Concurrency and Computation: Practice and Experience*, vol. 33, no. 5, p. e5971, 2021.
- [7] W. Wei, Z. Wang, X. Mao, G. Zhou, P. Zhou, and S. Jiang, "Position-aware self-attention based neural sequence labeling," *Pattern Recognition*, vol. 110, p. 107636, 2021.
- [8] T. Pradhan, P. Kumar, and S. Pal, "CLAVER: an integrated framework of convolutional layer, bidirectional LSTM with attention mechanism based scholarly venue recommendation," *Information Sciences*, vol. 559, pp. 212–235, 2021.
- [9] X. Yu, Q. Peng, L. Xu, F. Jiang, J. Du, and D. Gong, "A selective ensemble learning based two-sided cross-domain collaborative filtering algorithm," *Information Processing & Management*, vol. 58, no. 6, p. 102691, 2021.
- [10] C. Zheng and D. Tao, "Attention-based dynamic preference model for next point-of-interest recommendation," in *Proceedings of the International Conference on Wireless Algorithms, Systems, and Applications*, pp. 768–780, Springer, Qingdao, China, September 2020.
- [11] E. Crocker, B. Condon, A. Almsaeed et al., "TreeSnap: a citizen science app connecting tree enthusiasts and forest scientists," *Plants, People, Planet*, vol. 2, no. 1, pp. 47–52, 2020.
- [12] P. Chen, "Effects of normalization on the entropy-based TOPSIS method," *Expert Systems with Applications*, vol. 136, pp. 33–41, 2019.

- [13] J. Wang, L. Yue-xin, and W. Chun-ying, "Survey of recommendation based on collaborative filtering," *Journal of Physics: Conference Series*, vol. 1314, no. 1, Article ID 012078, 2019.
- [14] Y. Peng, N. Kondo, T. Fujiura, T. Suzuki, H. Wulandari, and E. Itoyama, "Classification of multiple cattle behavior patterns using a recurrent neural network with long short-term memory and inertial measurement units," *Computers and Electronics in Agriculture*, vol. 157, pp. 247–253, 2019.
- [15] D. Juan and Y. Hong Wei, "Particle swarm optimization neural network for research on artificial intelligence college English classroom teaching framework," *Journal of Intelligent and Fuzzy Systems*, vol. 40, no. 4, pp. 1–13, 2021.
- [16] O. El Aissaoui and L. Oughdir, "A learning style-based Ontology Matching to enhance learning resources recommendation," in *Proceedings of the 2020 1st International Conference on Innovative Research in Applied Science, Engineering and Technology (IRASET)*, pp. 1–7, IEEE, Meknes, Morocco, April 2020.
- [17] G. George and A. M. Lal, "Review of ontology-based recommender systems in e-learning," *Computers & Education*, vol. 142, Article ID 103642, 2019.
- [18] S. Pariserum Perumal, G. Sannasi, and K. Arputharaj, "An intelligent fuzzy rule-based e-learning recommendation system for dynamic user interests," *The Journal of Supercomputing*, vol. 75, no. 8, pp. 5145–5160, 2019.
- [19] Q. Yang, "A novel recommendation system based on semantics and context awareness," *Computing*, vol. 100, no. 8, pp. 809–823, 2018.
- [20] R. Mihalcea and P. Tarau, "TextRank: bringing order into text," in *Proceedings of the 2004 Conference on Empirical Methods in Natural Language Processing*, pp. 404–411, Association for Computational Linguistics, Barcelona, Spain, July 2004.
- [21] B. Loni, R. Pagano, and M. Larson, "Bayesian personalized ranking with multi-channel user feedback," in *Proceedings of the 10th ACM Conference on Recommender Systems*, pp. 361–364, ACM, Boston, MA, USA, September 2016.
- [22] L. Shen and Y. C. D. L. Feng, "Curriculum dual learning for emotion-controllable response generation," 2020, <http://arxiv.org/abs/2005.00329>.
- [23] C. Shi, B. Hu, W. X. Zhao, and P. S. Yu, "Heterogeneous information network embedding for recommendation," *IEEE Transactions on Knowledge and Data Engineering*, vol. 31, no. 2, pp. 357–370, 2019.
- [24] Y. Peng, R. Hu, and Y. Wen, "CA-NCF: a category Assisted neural collaborative filtering approach for personalized recommendation," in *Proceedings of the 2021 IEEE International Conference on Progress in Informatics and Computing (PIC)*, pp. 241–247, IEEE, Shanghai, China, December 2021.
- [25] F. Yuan, L. Yao, and B. Benatallah, "Exploring missing interactions: a convolutional generative adversarial network for collaborative filtering," in *Proceedings of the 29th ACM International Conference on Information & Knowledge Management*, pp. 1773–1782, Dublin, Ireland, October 2020.
- [26] Y. Cheng and X. Bu, "Research on key technologies of personalized education resource recommendation system based on big data environment," *Journal of Physics: Conference Series*, vol. 1437, no. 1, Article ID 012024, 2020.
- [27] I. Balush, V. Vysotska, and S. Albota, "Recommendation system development based on intelligent search NLP and machine learning methods," in *Proceedings of the CEUR Workshop*, vol. 2917, pp. 584–617, Kyiv (Kiev), Ukraine, September 2021.

Research Article

Brand Preference Prediction Method of Cross-Border E-Commerce Consumers Based on Potential Tag Mining

Xujie Qin 

School of Management, Anhui Business and Technology College, Hefei 231131, Anhui, China

Correspondence should be addressed to Xujie Qin; qinxj@ahbvc.edu.cn

Received 13 April 2022; Revised 21 May 2022; Accepted 30 May 2022; Published 24 June 2022

Academic Editor: Wei Liu

Copyright © 2022 Xujie Qin. This is an open access article distributed under the Creative Commons Attribution License, which permits unrestricted use, distribution, and reproduction in any medium, provided the original work is properly cited.

There are many brands in cross-border e-commerce platforms. Obtaining consumers' preference for brands will help promote the development of cross-border e-commerce industry. A brand preference prediction method of cross-border e-commerce consumers based on potential tag mining is proposed. Preprocess the cross-border e-commerce brand comment information obtained, build a HowNet emotion dictionary, and calculate consumers' emotional tendency towards the brand on this basis. The projection pursuit regression model is optimized by differential evolution algorithm to reduce the dimension of the obtained consumer brand emotion information. Mining the potential labels of the information after dimensionality reduction, combined with Bayesian personalized sorting method and paired interaction tensor decomposition method, this paper constructs a brand preference's prediction model to predict the brand preference of cross-border e-commerce consumers. The experimental results show that the proposed method has high accuracy of brand tendency calculation results, small average absolute error of prediction results, and high model accuracy.

1. Introduction

Under the background of the rapid development of Internet technology, cross-border e-commerce has been more restricted in the international market. With the fierce trend of mutual suppression, e-commerce not only has the problem of product infringement, but also reduces profits [1, 2]. In the international mainstream market, international big brands occupy an important position, so domestic e-commerce businesses mainly focus on nonmainstream products. The low degree of consumers' satisfaction and preference for domestic brands is mainly due to a series of problems in China's cross-border e-commerce, including low internationalization level, low market position, and poor innovation ability [3]. In order to improve the position of China's cross-border e-commerce in the international market, it is necessary to obtain consumers' preference for brands.

Li and Maomao [4] and others designed a consumer preference questionnaire to obtain the current situation information of consumer brand preference, extracted brand

features from four aspects of society, brand, service, and price perceived value through in-depth learning model, and established a consumer brand preference prediction model according to the feature extraction results. However, this method cannot accurately calculate consumer brand preference, which has the problem of large average absolute error of prediction results. Sun et al. [5] and others obtained online text and consumer keyword index data and used sliding time window technology to complete the above data screening. At the same time, combined with a variety of machine learning methods, the prediction model of consumer information index is established, to obtain the consumer information index of different brands and realize the prediction of consumer brand preference. The disadvantage is that the accuracy is low.

In order to solve the problems in the above methods based on the calculation of brand preference emotional tendency, this paper realizes the prediction of cross-border e-commerce consumers' brand preference by mining potential tags.

2. Calculation of Brand Preference and Emotional Tendency

2.1. Comment Pretreatment. One of the main tasks to predict the brand preference of cross-border e-commerce consumers is comment preprocessing. The specific process is as follows in Figure 1.

Reprocess the comment data according to the process in Figure 1 to ensure the accuracy of brand preference and emotional tendency prediction. Obtain brand comment data from the Internet or other websites through web crawler technology. The comment data is segmented by means of annotation text, word segmentation, and annotation, which is divided into clauses with the smallest unit to ensure the integrity of its semantic expression.

Compared with English writing methods, Chinese writing methods are usually quite different. In Chinese writing rules, words in sentences are not divided by display separators such as spaces. The smallest semantic unit in the text is words, which is of great significance for emotion analysis about consumer brand. As the most basic step, word segmentation has many research results in the practical problems of Chinese natural language processing [6, 7]. The function of words in sentences can be described by part of speech. Therefore, part of speech tagging is an important link in the process of comment preprocessing. The commonly used open source tools for part of speech tagging and Chinese word segmentation are shown in Table 1.

In natural language processing, the word segmentation package in the tool library is usually used to complete data segmentation, and then the weight of different data is given according to the unused work and emotional needs to build the final comment database and emotion table. So far, comment data preprocessing is realized.

2.2. Construction of Emotional Dictionary. In terms of natural language processing, most countries have built knowledge bases, such as HowNet in China, Korean WordNet in Korea, and mindnet in Microsoft. HowNet has a high position in Chinese emotional dictionary. HowNet contains the relationships between ideas. It is a semantic web based on world knowledge. Its content is more detailed. The main relationships in HowNet are shown in Figure 2.

The concept in HowNet shown in Figure 2 includes many semantic relationships such as synonymy and antonymy. Among them, the most important relationship is the synonymous and antisense relationship of words. According to the relationship between different words, the word attributes of corresponding words can be decomposed.

Decompose concepts in HowNet to obtain multiple semaphores. The similarity $S(w_1, w_2)$ between words can be calculated through the distance $d(w_1, w_2)$ value in the semaphore tree, as shown in formula (1):

$$S(w_1, w_2) = \frac{\beta}{\beta + d(w_1, w_2)}, \quad (1)$$

where β represents the change parameter, which represents the polarity value of this type of emotion, and this parameter

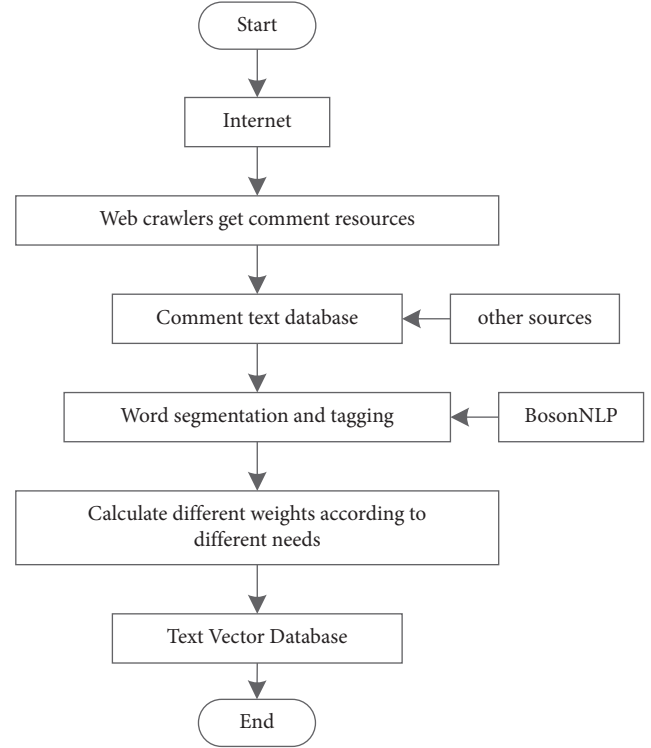


FIGURE 1: Comment preprocessing.

is greater than zero. The calculation results of the above formula are prone to errors. Therefore, the proposed method calculates the similarity between words according to the correlation between the word and the negative word reference word b_1 and the positive word reference word b_2 , that is, the semantic tendency value $t(w)$, as shown in formula (2):

$$t(w) = \frac{\sum_{i=1}^n s(w_i, b_1)}{n} - \frac{\sum_{j=1}^m s(w_j, b_2)}{m}, \quad (2)$$

where n and m represent the number of positive and negative reference words, respectively. When the semantic propensity value $t(w)$ of a word is positive, it belongs to a negative word. When the semantic propensity value $t(w)$ of a word is negative, it belongs to a positive word. Specific subjects based on brand preference classification fill the existing affective polarity dictionary, and the cross-border e-commerce prediction method of the consumer brand preference based on potential tag mining describes the attributes of words through binary W , as shown in formula (3):

$$W = (D, V), \quad (3)$$

where D represents the emotional polarity corresponding to the word, and its value is 1 or -1 . When the value is -1 , it belongs to negative words, and when the value is 1, it belongs to positive words. The nouns and adjectives of B and V are as shown in formula (4):

$$V = (B, S, M). \quad (4)$$

According to the attributes of two tuple descriptors, the emotion dictionary is constructed, which is used to judge the emotional bias in brand comments.

TABLE 1: The commonly used open source tools for part of speech tagging and Chinese word segmentation.

Analysis tools	Part of speech tagging	Analysis granularity	Accuracy	Interface	Website
Pao ding-analysis	None	Multiple choice	—	Jar package	https://code.google.com/p/paoding/
BosonNLP	Having	Multiple choice	0.947	REST API	https://bosonnlp.com/dev/center
IK analyzer	None	Large	0.748	Jar package	https://www.oschina.net/p/ikanalyzer
Pan gu segment	None	Multiple choice	0.803	None	https://pangusegment.codeplex.com/
NLPIR	Having	Minor	0.913	Jar package	https://ictclas.nlpir.org/docs

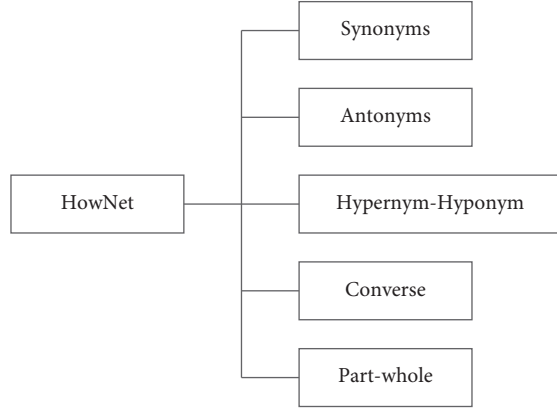


FIGURE 2: Main relationship diagram.

2.3. Calculation of Brand Emotional Tendency. The proposed method transforms the text content into vector operation in vector space through vector space model [8, 9], and the semantic similarity is measured by vector similarity.

In the process of text processing, vector space model uses multidimensional feature vectors to represent each document. When the number of documents in the data set is m , $m \times n$ dimensional vector space is used to represent the whole data set and abstract the text into vectors. The prediction method about brand preference of cross-border e-commerce consumers based on potential tag mining obtains text features through linear combination feature algorithm.

2.3.1. Word Frequency Method. The importance of features can be measured by word frequency [10, 11]. Count the frequency $G(t)$ corresponding to all words after word segmentation, delete the entries with $G(t)$ value of 1, and sort the remaining entries according to word frequency in order from large to small. The importance of words is directly proportional to word frequency.

2.3.2. Mutual Information Method. Mutual information describes the amount of information generated by mutual influence when two things happen at the same time [12, 13]. From the granularity of emotional analysis, the initial emotional analysis is to analyze the words with emotional color; that is, the words with emotional color are divided into positive and negative aspects, because the function of emotional dictionary is mainly to judge whether there are emotional words in the constructed emotional dictionary after word segmentation of a brand comment. \dot{D} represents the dictionary of emotional polarity, and its expression is as follows in formula (5):

$$\dot{D} = PF \cup NF, \quad (5)$$

where set NF is composed of negative words, set PF is composed of positive words, and set F is composed of words with frequency higher than one. The candidate word set J is obtained through the above process, as shown in formula (6):

$$J = \dot{D} \cap F. \quad (6)$$

There are n words in set J where the cross-border e-commerce consumer brand preference prediction method based on potential tag mining selects features through the mutual information method [14, 15] and obtains the mutual information $O(y, v)$ between category v and entry y through the following formula, as shown in formula (7):

$$O(y, v) = \log_2 \frac{P(y|v)}{P(y)}, \quad (7)$$

where $P(y)$ represents the probability of the number of documents to which entry y belongs in the total number of documents; $P(y|v)$ represents the probability that the entry y appears in the data of category C , and the calculation results are sorted in the order from large to small. For features, the average value $O(y)$ corresponding to the entry is calculated by the following formula:

$$o(y) = \sum_{i=1}^k O(v_i)O(y, v_i), \quad (8)$$

where k represents the number of categories; $O(v_i)$ represents the probability corresponding to category v_i .

2.3.3. Linear Combination Feature Selection. The proposed method combines word frequency and mutual information to calculate the feature score of consumer brand emotion, as shown in formula (9):

$$\text{Score} = (1 - \mu)O(y_i) + \mu \text{Freq}(y_i), \quad (9)$$

where μ represents the regulating factor; $\text{Freq}(y_i)$ represents the word frequency corresponding to the entry y_i . According to the brand emotion characteristics extracted in the above process, the brand emotion tendency is obtained.

3. Cross-Border E-Commerce Consumer Brand Preference Prediction Regression Algorithm

3.1. Projection Pursuit Regression. Projection pursuit combines computer science, modern statistics, and applied mathematics. It is a high-tech and can complete nonlinear,

nonnormal, and high-dimensional data processing and analysis [16, 17]. The proposed method constructs a projection pursuit regression model to process the brand emotional tendency data obtained in the above process, to realize the prediction of consumer brand preference.

3.2. Differential Evolution Algorithm. Different from evolutionary strategy, evolutionary programming, and genetic algorithm, differential evolutionary algorithm [18, 19] has many advantages. The algorithm obtains mutation operator according to the difference vector between parent individuals, sets probability, cross processes mutation individuals, and parent individuals, generates new individuals, that is, test individuals, and selects the optimal individual between test individuals and parent individuals according to the fitness. The prediction method about brand preference of cross-border e-commerce consumers based on potential tag mining adopts differential evolution algorithm to optimize the prediction method about brand preference to complete the dimensionality reduction processing of brand emotional tendency data. The processing process is as follows.

Considering that the brand affective tendency data obtained by projection pursuit regression has certain pertinence, scale, and representativeness, in order to obtain the optimal brand affective tendency data that meets the requirements, this paper uses differential evolution algorithm to reduce its dimension. Initialize the population in the feasible solution space, and a new population will be generated after the cross mutation operation of the current population. Then, the selection operation based on greedy idea is used to select the two populations one-to-one, so as to obtain a new generation of population. The specific process is to perform mutation operation on individual x_i^t in each t time through formula (9) to obtain the corresponding mutant individual v_i^{t+1} , as shown in formula (10):

$$v_i^{t+1} = x_{r_1}^t + K(x_{r_2}^t - x_{r_3}^t), \quad (10)$$

where $x_{r_1}^t$ is the parent basis vector, $(x_{r_2}^t - x_{r_3}^t)$ is the parent difference vector, and K is the scaling factor. Then, x_i^t and v_i^{t+1} were processed by cross operation to obtain test individual u_i^{t+1} . The objective functions of individuals u_i^{t+1} and x_i^t are constructed, and the individuals with lower function values are selected as the individuals of the new species group, as shown in formula (11).

$$x_i^{t+1} = \begin{cases} u_i^{t+1} & f(u_i^{t+1}) < f(x_i^t) \\ x_i^t & \text{else} \end{cases}, \quad (11)$$

where $f(\cdot)$ is the objective function. In order to reduce the complexity of the algorithm, the feasible set scale is N_1 , the infeasible group scale is N_2 , and the maximum scale is N_3 . The total complexity of the diversity group is $M = (N_1, N_3)$. Then the complexity of the difference algorithm after one iteration can be expressed as formula (12):

$$M = K + O(v_i) \lg(N_1 + N_3). \quad (12)$$

If the search scope is $N = N_1 + N_2 + N_3$, it indicates that the data dimension of brand emotional tendency is effectively reduced.

3.3. Regression Algorithm of Brand Preference Prediction Based on Potential Tag Mining. Based on potential tag mining, the proposed method combines Bayesian personalized ranking method BPR and paired interaction tensor decomposition method (PITF) to build a brand preference prediction model.

Tag addition belongs to the user's information release behavior, which often includes the user's understanding of the content characteristics and themes of the brand they are browsing or the expression of the content themes they are interested in, which more clearly implies that the user is very interested in the content themes involved in the brand. So, according to the contextual relationship between brands and users, the proposed method mines high-value label samples to obtain the following labels:

- (1) Negative class label: $T_B = \{t_B | (u, i, t_B) \notin D \cap (u, i, t_B) \notin D_p\}$.
- (2) Potential label: $T_P = \{t_P | (u, i, t_P) \in D_p\}$.
- (3) Positive label: $T_A = \{t_A | (u, i, t_A) \in D\}$.

On the basis of the above labels, make word frequency statistics on the brand preferred words of cross-border e-commerce consumers, arrange the word frequency in descending order, select the first 100 words, and draw the word cloud diagram using word cloud in word cloud module, as shown in Figure 3.

Based on the above labels, we can predict the brand preference of cross-border e-commerce consumers. Bayesian personalized ranking method (BPR) obtains the correct ranking of brands based on Bayesian theory [20], as shown in formula (13):

$$a(\Gamma | \chi_{u,i}) \propto a(\chi_{u,i} | \Gamma) a(\Gamma), \quad (13)$$

where $a(\Gamma)$ represents a priori probability function; Γ represent the parameters of the interactive tensor decomposition model; $a(x, u, i | \Gamma)$ represents the likelihood function. Assuming that all preferences (u, i) are independent of each other, the maximum a posteriori probability can be described by the following formula:

$$\max \prod_{(u,i) \in D} a(y_A \chi_{u,i} y_B | \Gamma) a(\Gamma), \quad (14)$$

where y_A represents the observation label; D represents the triple set of $\langle \text{user } u, \text{brand } i, \text{label } y_A \rangle$, and its expression is as follows in formula (15):

$$D = \{(u, i, y_A) | u \in U, i \in I, y_A \in Y\}, \quad (15)$$

$a(y_A \chi_{u,i} y_B | \Gamma)$ represents the probability of partial order relationship. The proposed method describes the above probability through sigmoid function, as shown in formula (16):

$$a(y_A \chi_{u,i} y_B | \Gamma) = \varsigma [G_A(\Gamma) - G_B(\Gamma)]. \quad (16)$$

In the formula, G_A and G_B represent the prediction score, and the parameters ς to be obtained can be calculated by the following formula:

$$\varsigma = \frac{1}{1 + \exp(-x)}. \quad (17)$$

According to the relationship among users, brands, and labels, the proposed method models the preference through the paired interaction tensor decomposition method to obtain the preference value of preference (u, i) for label y_A , as shown in formula (18):

$$G(\Gamma) = U_i V_i + U_u T_{y_A}^U + V_i T_{y_A}^V. \quad (18)$$

Among them, $U_i, V_i, U_u, T_{y_A}^U$, and $T_{y_A}^V$ all represent the implicit factor matrix.

Based on the above calculation results, build a prediction model of cross-border e-commerce consumer brand preference, as shown in formula (19):

$$\min_{\Gamma} Z_1 = \sum_D \ln \varsigma [G_A(\Gamma) - G_B(\Gamma)] + \frac{\varsigma}{2} \|\Gamma\|_2^2. \quad (19)$$

According to the solution results of the prediction model, the brand preference prediction of cross-border e-commerce consumers based on potential tag mining is completed.

4. Experimental Analysis

In order to verify the effectiveness of the brand preference prediction method of cross-border e-commerce consumers based on potential tag mining, the brand preference prediction method of cross-border e-commerce consumers based on potential tag mining, literature [4] method, and literature [5] method are used to predict their brand preference.

4.1. Data Analysis. This paper selects the shopping comment information of 200 consumers on Amazon's cross-border e-commerce platform as the data source and uses Python web crawler technology to capture the comment data of different brands. The 200 consumers, including college students and company employees, have a certain understanding of cross-border e-commerce brands. The specific situation of 200 users is shown in Tables 2 and 3.

4.2. Analysis of Dimensionality Reduction Effect of Brand Emotional Tendency Data. The dimensionality reduction effect of brand affective tendency data is related to the response speed of the final prediction model. Therefore, through the response speed index analysis, this paper uses differential evolution algorithm to reduce the dimensionality of brand affective tendency data. The test results are shown in Figure 4.

It can be seen from the analysis of Figure 4 that the response speed of this method is always lower than 60 ms,

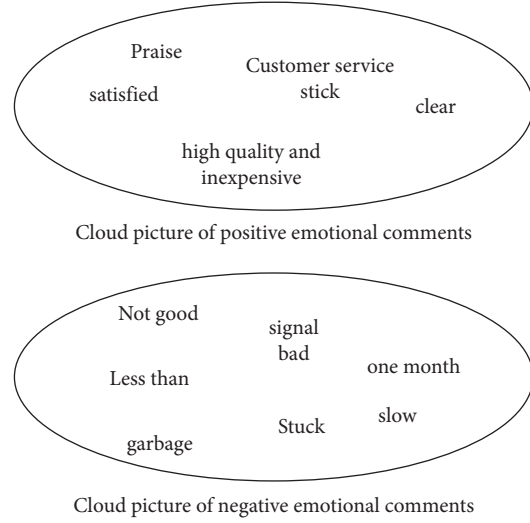


FIGURE 3: Cloud picture of words.

TABLE 2: Age distribution of consumers.

Age distribution	Number/person	Percentage/%
Under 20	58	29.0
21-30 years old	46	23.0
31-40 years old	69	34.5
41-50 years old	27	13.5
Over 50	0	0.0
Total	200	100.0

TABLE 3: Gender distribution of consumers.

Gender	Number/person	Percentage/%
Male	77	38.5
Female	123	61.5
Total	200	100.0

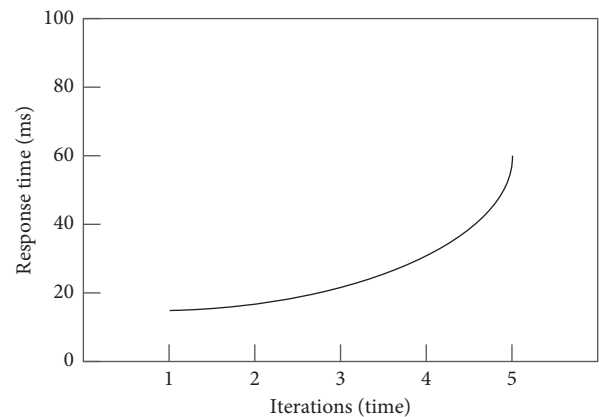


FIGURE 4: Response speed of this method.

which has a faster prediction effect of brand emotional tendency. The main reason is that this method uses differential evolution algorithm to reduce the dimension of the data on the basis of constructing the brand emotional tendency data analysis model based on projection pursuit

TABLE 4: Calculation results of consumers' emotional tendency.

Iterations/ time	Male consumers/%			Female consumers/%		
	Literature [4] methods	Literature [5] methods	The method of this paper	Literature [4] methods	Literature [5] methods	The method of this paper
1	60	50	86	58	60	94
2	50	76	89	60	59	92
3	70	80	87	70	69	93
4	64	40	86	68	59	92
5	42	68	88	59	56	90

regression, reduces the complexity and dimension of the data through multiple iterations, and improves the prediction response speed.

4.3. Calculation of Brand Emotional Tendency. The proposed method, literature [4] method, and literature [5] method are used to calculate the brand emotion tendency of the above consumers, and the calculation accuracy of different methods is compared, as shown in formula (20):

$$\text{Accuracy} = \frac{N_Z}{N_{\text{all}}}, \quad (20)$$

where N_Z represents the number of correctly calculated samples; N_{all} represents the total number of samples. According to formula (19), the calculation results of consumers' emotional tendency under the application of the proposed method, literature [4] method, and literature [5] method are obtained, as shown in Table 4.

In order to better display the calculation results of emotional tendency of male and female consumers, Table 4 is drawn into Figure 5. The following figure fully shows the changes.

Figure 5 is comparison chart of calculation of consumer sentiment propensity; it can be seen from Figure 5 that the accuracy of the three methods in calculating the brand sentiment propensity of male consumers is lower than that of female consumers. The main reason may be that male consumers publish less shopping comments, and the brand sentiment propensity data obtained by the corresponding methods are relatively less. At the same time, male consumers are more rational than female consumers and more rational for comments, Therefore, it is difficult to distinguish their emotional tendencies, resulting in low accuracy. For male consumers, the accuracy of the proposed method is 89% and that of female consumers is 94%, while the accuracy of literature [4] method and literature [5] method is 70% and 70%, 80% and 69%, respectively. From a comprehensive point of view, whether male or female consumers, the calculation results of brand emotion tendency of the proposed method are better than those of [4] and [5], because the proposed method constructs a HowNet emotion dictionary, which is used to calculate consumers' brand emotion tendency and improve the accuracy of the calculation results.

It can be seen from Figures 6 and 7 that the calculation results of brand emotion tendency of both male and female consumers by the proposed method are better than those in

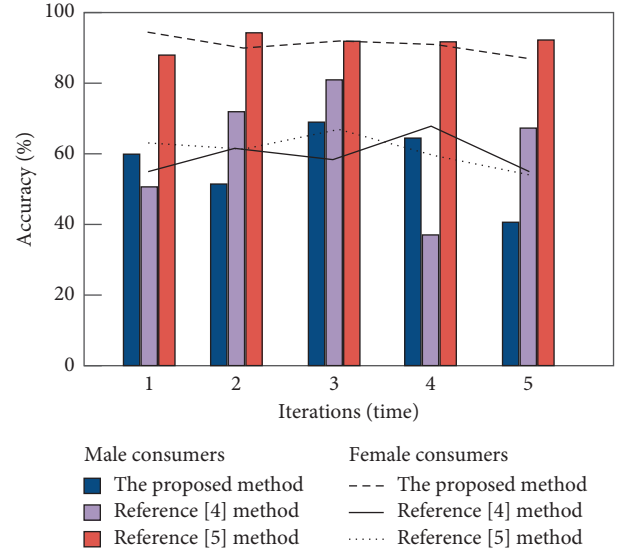


FIGURE 5: Comparison chart of calculation of consumers' emotional tendency.

[4] and [5], because the proposed method constructs a HowNet emotion dictionary to calculate consumers' brand emotion tendency on this basis, which improves the accuracy of the calculation results.

4.4. Prediction Results. The average absolute error MAE is used as an index to test the brand preference prediction results of the proposed method, the method in [4], and the method in [5], as shown in formula (21).

$$MAE = \frac{\sum_{i=1}^k |a_i - t_i|}{k}, \quad (21)$$

where a_i represents the prediction result; t_i represents the actual results; k represents the number of brands.

As can be seen from Figure 8, the average absolute error obtained by the proposed method when predicting consumers' brand preference for cross-border e-commerce consumers of different ages is low, with the highest error of 0.2%, which is lower than 0.6% of the method in [4] and 0.5% of the method in [5]. The main reason is that the proposed method obtains more accurate input data from the consumer comment data in the cross-border e-commerce platform through preprocessing and dimensionality reduction before prediction, the average absolute error of prediction is reduced, and the effectiveness of the proposed

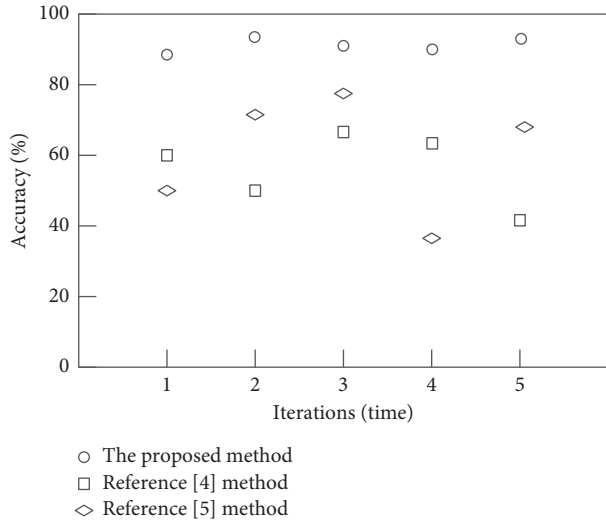


FIGURE 6: Calculation results of brand emotional tendency of male consumers.

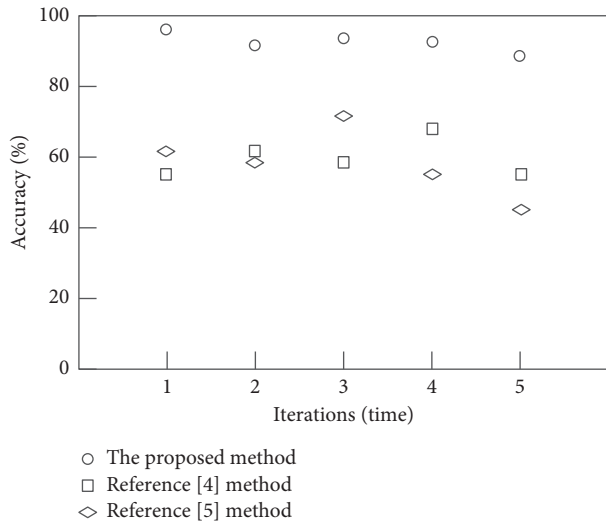


FIGURE 7: Calculation results of brand emotional tendency of female consumers.

method is verified. At the same time, according to Figure 7, the average absolute error of the prediction of the three methods is relatively high in the age group of 21 ~ 30. The main reason may be that the brands concerned by this group are more likely to buy goods for the parent group in addition to the acceptable brands in their own age group. At the same time, this group involves young couples with children, so their brands cover a wide range, resulting in a relatively high average absolute error of prediction.

4.5. Model Evaluation. Using the ROC curve, the farther the ROC curve from the pure opportunity line, the stronger the discrimination of the subjects, and test the accuracy of the model constructed by the proposed method, the method in [4], and the method in [5]. The test results are shown in Figure 9.

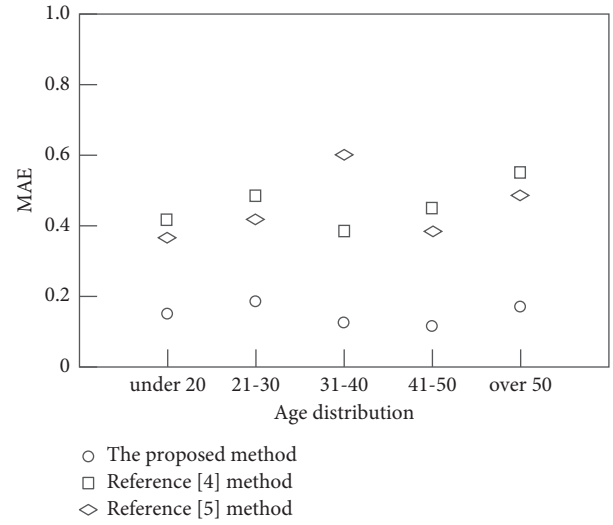


FIGURE 8: Prediction results of different methods.

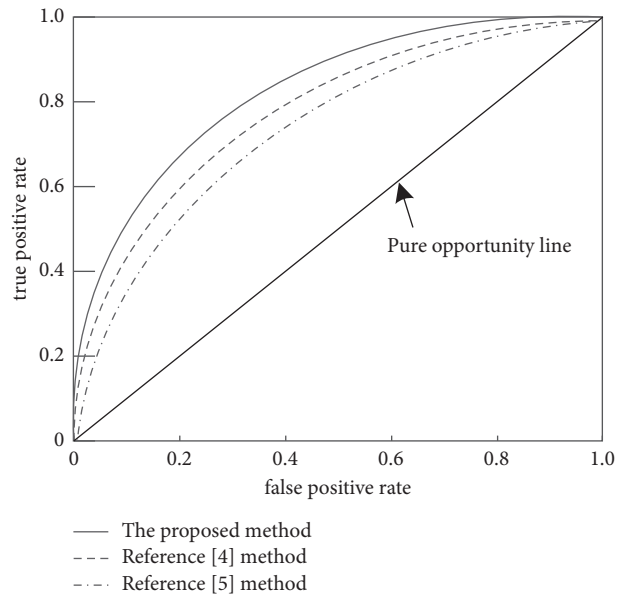


FIGURE 9: ROC curves of different methods.

The abscissa in Figure 9 is the false positive rate and the ordinate is the true positive rate. The model constructed by the proposed method is farther from the pure opportunity line, indicating that the accuracy of the model constructed by the proposed method is higher. The main reason is that the proposed method optimizes the model input and improves the prediction accuracy of the model by mining the potential labels of brand preference of cross-border e-commerce consumers.

5. Conclusions and Prospects

Aiming at the problems of low accuracy of brand tendency calculation results, large average absolute error of prediction results, and low model accuracy caused by many cross-border e-commerce brands, a cross-border e-commerce

consumer brand preference prediction method based on potential tag mining is proposed. Based on the calculation of cross-border e-commerce brand emotional tendency, this paper uses differential evolution algorithm to optimize the projection pursuit regression model, reduces the dimension of the obtained consumer brand emotional data, and realizes the prediction of brand preference based on Bayesian method. The experimental results show that this method has high accuracy for the calculation results of consumer brand tendency of different genders and different ages and improves the accuracy of the prediction model, It can provide data reference for the development of cross-border e-commerce industry, but the research on the prediction efficiency of the proposed method is insufficient, and improving the prediction efficiency will be taken as the research direction in future work.

Data Availability

The datasets generated for this study are included within the article.

Conflicts of Interest

The authors declare that there are no conflicts of interest regarding the publication of this paper.

Acknowledgments

This work was supported by the Key Research Project of Humanities and Social Sciences in Colleges and Universities of Anhui Province: Research on the Strategies of Transforming Cross-Border E-Commerce for Anhui Traditional Foreign Trade Enterprises from the Perspective of the "Belt and Road" Initiative (Project no. SK2018A0915), and Major Research Project of Humanities and Social Sciences in Colleges and Universities of Anhui Province: Research on the Policy and Path Of Low Carbon Economy Development in Anhui Province (Project no. SK2018ZD060).

References

- [1] X. Zhang and S. Liu, "Action mechanism and model of cross-border E-commerce green supply chain based on customer behavior," *Mathematical Problems in Engineering*, vol. 2021, no. 3, 11 pages, Article ID 6670308, 2021.
- [2] X. Zhang and Y. Shi, "Trade Facilitation and the Development of Cross-Border E-Commerce in China -- an Empirical Analysis Based on Double Difference Method," *East China Economic Management*, vol. 34, no. 2, pp. 94–103, 2020.
- [3] W. Su and Y. Wang, "Zhang Chonghui Economic effect of tax impact of foreign cross-border e-commerce: a study based on tso-dsge model," *Statistical research*, vol. 37, no. 1, pp. 17–32, 2020.
- [4] W. Li and C. Maomao, "Wang Weijun Research on online consumer preference prediction based on perceived value," *Journal of management*, vol. 18, no. 6, pp. 912–918, 2021.
- [5] J. Sun, J. Zhu, and H. Li, "Gao Zhe Research on rolling prediction of consumer confidence index based on Internet data," *Journal of Xi'an Jiaotong University (SOCIAL SCIENCE EDITION)*, vol. 41, no. 6, pp. 68–77, 2021.
- [6] Z. Cui, E. Zhao, and W. Luo, "Chinese word segmentation model of multi head attention for professional fields -- taking animal husbandry in Tibet as an example," *Chinese Journal of information technology*, vol. 35, no. 7, pp. 72–80, 2021.
- [7] F. Lizhou, G. Yang, and Xu Xue, "Two way matching Chinese word segmentation method based on n-gram," *Mathematical statistics and management*, vol. 39, no. 4, pp. 633–643, 2020.
- [8] Y. Wang and P. Wang, "Zhang Yu Research on technology information user portrait and scenario Service push based on vector space model," *Modern intelligence*, vol. 40, no. 2, pp. 3–10, 2020, + 25.
- [9] B. Xie, yuerun Dong, and L. pan, "Text emotion classification based on multi feature LSTM self attention," *Computer simulation*, vol. 38, no. 11, pp. 479–484, 2021.
- [10] X. Chen and D. Meurers, "Word frequency and readability: predicting the text-level readability with a lexical-level attribute," *Journal of Research in Reading*, vol. 41, no. 3, pp. 486–510, 2018.
- [11] W. Lu, S. Huang, J. Yang, Y. Bu, Q. Cheng, and Y. Huang, "Detecting research topic trends by author-defined keyword frequency," *Information Processing & Management*, vol. 58, no. 4, Article ID 102594, 2021.
- [12] M. Riahi-Madvar, A. Akbari Azirani, B. Nasersharif, and B. Raahemi, "A new density-based subspace selection method using mutual information for high dimensional outlier detection," *Knowledge-Based Systems*, vol. 216, no. 2, Article ID 106733, 2021.
- [13] J. Lewandowsky, S. J. Dongare, R. Martín Lima, M. Adrat, M. Schrammen, and P. Jax, "Genetic algorithms to maximize the relevant mutual information in communication receivers," *Electronics*, vol. 10, no. 12, p. 1434, 2021.
- [14] Q. Li, Y. Mou, and C. Zhanqi, "Defect Location Method Based on Mutual Information," *Design and Computer Engineering*, 2022.
- [15] F. Runze, X. Luo, and Z. Zhang, "Cigarette formula maintenance method based on mutual information of single cigarette," *Tobacco science and technology*, vol. 54, no. 3, pp. 65–71, 2021.
- [16] J. Yang and Q. Li, "Xie Jieyi Evaluation index system of regional scientific and technological Financial Development -- Analysis Based on projection pursuit model," *Research on science and technology management*, vol. 40, no. 6, pp. 69–74, 2020.
- [17] Y. Liu, "Shengxi Evaluation of urban high-quality development based on projection pursuit model weight optimization and its influencing factors," *Practice and understanding of mathematics*, vol. 51, no. 24, pp. 53–63, 2021.
- [18] C. Van Kien, H. P. H. Anh, and N. N. Son, "Adaptive inverse multilayer fuzzy control for uncertain nonlinear system optimizing with differential evolution algorithm," *Applied Intelligence*, vol. 51, no. 1, pp. 527–548, 2021.
- [19] Z. Pan, S. Fang, and H. Wang, "LightGBM technique and differential evolution algorithm-based multi-objective optimization design of DS-APMM," *IEEE Transactions on Energy Conversion*, vol. 36, no. 1, pp. 441–455, 2021.
- [20] C. Su, F. Ye, T. Liu, Y. Tian, and Z. Han, "Computation offloading in hierarchical multi-access edge computing based on contract theory and bayesian matching game," *IEEE Transactions on Vehicular Technology*, vol. 69, no. 11, pp. 13686–13701, 2020.

Research Article

Data Mining and Economic Application in the Age of Financial Big Data: A Case Study of Shadow Banking and Interest Rate Liberalization in China

Shi Liang 

School of Economics and Business Administration, Central China Normal University, Wuhan 430073, Hubei, China

Correspondence should be addressed to Shi Liang; liangshi@mails.ccn.edu.cn

Received 11 March 2022; Revised 21 April 2022; Accepted 22 May 2022; Published 20 June 2022

Academic Editor: Xuefeng Shao

Copyright © 2022 Shi Liang. This is an open access article distributed under the Creative Commons Attribution License, which permits unrestricted use, distribution, and reproduction in any medium, provided the original work is properly cited.

With the booming of big data in finance, data mining technologies, as a new method of data statistics, have made superior economic applications available to researchers. Based on the relationship between shadow banking and interest rate liberalization, this paper intended to analyze the bidirectional relationship between shadow banking and interest rate liberalization using big data mining technologies. The relationship between data mining and the economic application of shadow banking was proven using data from 2014 to 2021. On this basis, this paper identified the bidirectional influence between shadow banking and interest rate liberalization. The findings show that shadow banking has positive contributions to the liberalization of interest rate, and the interest rate distortion resulting from interest rate control also drives the development of shadow banking. Moreover, feasible suggestions have been proposed for supervision on policies.

1. Introduction

Technologies represented by 5G, big data, artificial intelligence (AI), blockchain, and cloud computing have become the main players in today's financial technology development, and among them, big data technology with its wide-ranging implications is the top priority. Data mining technology, as a new method of data statistics, can achieve in-depth data mining horizontally, thus meeting the needs for the accuracy of economic statistical data as well as scientific analysis and decision-making. Focusing on the relationship between shadow banks and interest rate liberalization, by analyzing large data mining technology out of the traditional economic statistics to the observation of the shadow banking representative data and interest rate marketization, before it is different from the theoretical analysis of scholars, this article, from the perspective of empirical based on shadow banking and interest rate marketization of the bidirectional relationship, proposed the new application of data mining, and for later related scholars, the study provides a reference basis.

The currency creation mechanism has shifted to the complex model of “central bank-commercial bank-off-balance-sheet-shadow banks” from the previous simple model of “central bank-commercial bank.” Also, the Central Bank, the Banking Regulatory Commission, the Insurance Regulatory Commission, and the Securities Regulatory Commission have formulated new regulations to control the leverage rate of shadow banks. As a result, the leverage ratio will be uniformly applied to products launched by all types of financial institutions in an attempt to eliminate regulatory arbitrage and embark on the regulation of shadow banks in China. The relationship between shadow banking supervision and financial marketization has become the focus of government, industry, and academia.

1.1. Connotation of Shadow Banks. Discussions on the specific definition and connotation of shadow banks can be found in a great deal of literature at home and abroad. From a global point of view, the term was first proposed by McCulley, the executive director of PIMCO, at the annual meeting of Jackson Hole held by the Federal Reserve in 2017,

drawing extensive attention and leading to profound research in the financial community. According to McCulley, unlike traditional commercial banks, shadow banks, specialized in businesses similar to traditional commercial banks, are outside the traditional commercial banking system for their leveraged financial products are launched through non-bank investment channels. In consequence, some level of concern has been aroused in the financial innovation means of shadow banks. With reference to the definition of shadow banks by IMF, regarding whether shadow banks should be supervised by the corresponding department, Bill Gross (2007) held that shadow banks are complex financial instruments formed by multilayer packaging on the basis of basic financial derivatives, lacking supervision. Secondly, concerning whether it corresponds to traditional banks and exerts an impact on the real economy, Gorton et al. (2010) suggested that non-bank financial institutions make profits from complex financial instruments, being significantly different from those of traditional commercial banks. Regarding whether it plays the role of credit intermediary, Paul Tucher (2010) stated that shadow banks, featuring term mismatch and increased leverage rate, can partially substitute the business of commercial banks via institutions that are independent or cooperated with traditional banks.

In terms of supervision and business, as for scholars worldwide, whether it is a credit intermediary or financial intermediary existing outside the banking system with engagement in asset securitization and independence of relevant departments is a criterion for shadow banks. Concerning the Chinese market, shadow banks in China have a significant degree of localization since the financial market development, social and economic development structure, and related regulatory measures in China are significantly different from those in major Western economies. In China's shadow banking, the definition of shadow banking is different in some aspects, and the specific features of China's shadow banking are shown in Table 1.

Chinese experts focus more on the scale and boundary of shadow banks. Ba [1] defined that shadow banks in China are composed of bank wealth financing, trust, and financial companies. As for Li (2012), shadow banks in China consist of Off-Balance Sheet Activities (OBS) of commercial banks as well as businesses and institutions that can function as a credit intermediary outside the banking system. Shadow banking funds mainly come from wholesale financing, lack stable sources of funds such as core deposits, and engage in a large number of over-the-counter transactions, and information is not transparent, and the leverage ratio is usually high. Based on the previous description, the Criteria for Differentiating Shadow Banks in China are shown in Table 2.

1.2. Connotation of Interest Rate Liberalization. Interest rate liberalization means that the pricing interest rate that financial institutions depend on is determined by market supply and demand. In his study on the U.S. banking industry from 1970 to 1986, de Rezende [2] found that financial innovation and reform of the interest rate

liberalization in the U.S. were triggered by the choice of capital investment outside the bank channel, as the low deposit interest rate of banks is not appealing under the restraint of Q treaty. Xiao [3] believed that the pricing mechanism of shadow banks can better reflect the supply and demand of market funds, contributing to the marketization of RMB interest rates. Ba [1] held that shadow banks can break interest rate control in disguised form and meet market financing needs via the regulation of market funds using the market-based pricing mechanism, thereby enhancing interest rate liberalization. Dang et al. (2014) believed that individual investors who gain fewer earnings from investment under the long-standing dual-track interest rate system and strict deposit and loan interest rates in China tend to invest in financial products with a high rate of return, further stimulating the development of bank financial products. Barth et al. (2015) held that the development of shadow banks in China is driven by the long-term control over interest rate upon analyzing China's empirical data.

Compared with previous studies, this study presents the following marginal contributions: (a) we studied the problems of shadow banks and market interest rate from status analysis based on the latest monthly data from 2014 to 2021; (b) we find evidence for the bidirectional relationship between shadow banks and liberalized interest rates. (c) We proposed opinions based on independent thinking in the general background that "the financial management departments shall quickly carry out countermeasures on shadow banks in an attempt to eliminate systemic financial risks under the leadership and deployment of the Party Central Committee and the State Council of China."

2. Research Hypothesis

Theoretically, a bidirectional relationship can be observed between shadow banks and interest rate liberalization. The shadow banking system in developed countries is to make greater profits using innovative financial tools with interest rate liberalization as the foundation and asset securitization as the main business. However, shadow banks in China have been developed under long-term financial repression, that is, born and developed from interest rate control. To some extent, the financing demands of enterprises in urgent needs of loans cannot be met under the extremely low interest rate liberalization caused by interest rate control, hampering the emergence and development of shadow banks.

2.1. Influence of Interest Rate Liberalization on the Development of Shadow Banks. The American economist E. J. Kane proposed the theory of circumvented regulation in 1984 and believed that financial innovation is caused by the behavior of banks making profits through circumventing regulation of government agencies. Financial institutions actively innovate to circumvent restrictive measures imposed by the administrative control of government agencies over certain profitable activities, making them unable to maximize profits.

TABLE 1: Features of shadow banking in China.

Features	Implications
Centralization	With the bank as a core, it is manifested as the “shadow of the bank”
Arbitrage	Targeted regulatory arbitrage, violations of laws and regulations are commonly seen.
Rigid payment	There is a rigid payment or an expectation of rigid payment
Channel charge	The profit model of channel charge is widely seen
Credit risk	It is dominated by quasi-loans with prominent credit risks

TABLE 2: Criteria for differentiating shadow banks in China.

Standards	Implications
Supervisory circumvention	Financial credit intermediary activities are not part of the banking supervision system
High leverage	Complicated business structure, nested layers and excessive leverage.
Non-transparent information	Incomplete disclosure and low transparency
Highly contagious	High pressure on centralized cash as well as high association and risk contagion in the financial system

Interest rate control policies are formulated by the government to manage the interest rate of the financial market for adjusting economic operations. As an essential part of the interest rate policy, it plays an important role in the performance of economic leverage by interest rate. Interest rate is critical in maintaining financial stability, and its changes may affect the direction and efficiency of resource allocation.

Interest rate control will increase financing costs at a low level of interest rate liberalization, leading to disruption in the normal competition among financial institutions. The rapid development of shadow banks is ultimately driven by the demands of circumventing interest rate controls.

2.2. Influence of Shadow Banking System on Interest Rate Liberalization. Luo and Feng [4] believe that the rapid development of shadow banking has changed China’s traditional monetary policy transmission mechanism. The investment and financing business of shadow banks, as products of financial innovation, can partly serve as a substitution for the deposit and loan business of traditional commercial banks. The interest rate of shadow banks is priced to the market under the negotiation of the supply and demand ends of capital, which can press ahead with the reform in commercial banks to relax the restrictions on deposit and loan interest rates. In this way, it can enhance interest rate liberalization.

2.2.1. Role of Shadow Banking Innovation in Financing Channels. As China’s shadow banking system is developed under the special financial environment in China, its influence on the real economy is also complex. In the positive aspect, it can broaden the financing channels of the real economy and optimize the investment structure of the real economy [5]. The loan interest rate of bank credit is determined by the banking system. On the contrary, in the shadow banking market, borrowers are allowed to choose from capital prices and sources, which not only broadens the financing channels of enterprises, but also makes up for the deficiencies of traditional financing channels and intensifies

competition in the banking industry. This can partly ease the overcontrol of interest rates, so that the loan interest rate can be floated to the market equilibrium interest rate, that is, improving the liberalization of loan interest rates.

2.2.2. Role of Shadow Banking Innovation in Investment Channels. Regarding investment channels, shadow banks launch products that are significantly different from traditional investment channels and consistent with the needs of investors under continuous innovation, making a variety of products available to investors. At the same time, investors can choose between risks and returns of the two investment channels and play games with financial institutions, which can promote the liberalization of deposit interest rates to a certain extent.

2.2.3. Role of Shadow Banking Innovation in the Pricing Mechanism. Concerning the pricing mechanism, different from the traditional pricing model of deposit and loan interest rates anchored by benchmark interest rates, a quantitative pricing model is adopted in the interest rates of shadow banks business such as trust products and interbank payment, better reflecting the real supply and demand relationship of capitals in the financial market. The formation of the shadow banking pricing mechanism can promote the further development of the financial market and the reform in interest rate liberalization.

At the same time, the interest rate control causes the low degree of marketization of interest rate, and capital price distortions may also promote the development of the scale of the shadow banking. Huang Yi’s (2012) study, such as trust, asset management plan channel bank docking shadow banking businesses such as financial capital, is the financial repression and monetary tightening policy taken by the folk interest rate marketization; accordingly, This paper proposes the following two hypotheses:

Hypothesis 1. Low liberalization level of interest rate and the distortion of capital prices caused by interest rate control contribute to the scale development of shadow banks, and

the liberalization level of interest rate is negatively associated with the growth rate of shadow banks; that is, the lower the liberalization of interest rate is, the faster the scale development of shadow banks will be.

Hypothesis 2. Shadow banks accelerate the interest rate liberalization, and the liberalization level of interest rate is positively related to the growth rate of shadow banks; that is, the faster the scale development of shadow banks in China is, the higher the liberalization of interest rate will be.

3. Sample and Research Design

3.1. Sample Selection and Data Sources. The monthly data from 2014 to 2021 obtained through big data mining, together with data from the CSMAR database and the website of the People's Bank of China, are used as research samples. Two indicators were selected. One is Sbank. According to the "Report on Shadow Banks in China" compiled by the research group of the China Banking and Insurance Regulatory Commission (CBIRC), as well as research by related scholars [6], it is found that entrusted loans, trust loans, and the sum of undiscounted bank acceptances have high proportions of the current scale of shadow banks in China. The scale of shadow banks in China was measured using the sum of entrusted loans, trust loans, and the sum of undiscounted bank acceptances, and its development was measured using the growth rate of the scale. The second indicator is variables related to interest rate liberalization. Interest rate liberalization was divided into loan interest rate liberalization and deposit interest rate liberalization according to the previous study [7–9]. DRD, LRD, DRG, and LRG were selected as indicators for measuring the liberalization level of interest rate, with detailed implications shown in Table 3. All variables in Table 3 are seasonally adjusted except for the benchmark interest rate.

The liberalization level of interest rates is represented by the distorted degree of interest rates. Since interest rate control is manifested in overestimation of loan and loan interest rate as well as underestimation of deposit interest rate, LRD is normally positive, presenting that the larger the value, the lower the liberalization level of interest rate. The distorted degree of deposit interest rate is usually negative, presenting that the greater the value, the lower the liberalization level of interest rate. Similarly, the excessively high variation in the loan interest rate or the excessively low variation in the deposit interest rate also indicates the low liberalization level of interest rates.

3.2. Model Design. In order to prove Hypothesis 1, this paper refers to the study of Zhao, [7, 10]; and on this basis, the regression model is set as

$$\text{Sbank}_t = \alpha + \beta_1 \text{LRD}_t + \beta_2 \text{DRD}_t + \beta_3 \text{LRG}_t + \beta_4 \text{DRG}_t + \epsilon_t. \quad (1)$$

Using the simplified OLS model, the influence of liberalized interest rates on the expansion of Sbank (Sbank_t) can be observed through the results of β_1 and β_2

To prove Hypothesis 2, the regression model was set as

$$\text{LRD}_t = \alpha + \beta_1 \text{Sbank}_t + \beta_2 \text{DRD}_t + \beta_3 \text{LRG}_t + \beta_4 \text{DRG}_t + \epsilon_t, \quad (2)$$

$$\text{DRD}_t = \alpha + \beta_1 \text{Sbank}_t + \beta_2 \text{LRD}_t + \beta_3 \text{LRG}_t + \beta_4 \text{DRG}_t + \epsilon_t. \quad (3)$$

The simplified OLS model was also adopted. This model can further judge the two-way influence relationship between Shadow banking and interest rate liberalization in China. To be specific, the influencing level of the expansion of Sbank (Sbank_t) on liberalization of deposit interest rate and liberalization of loan interest rate can be elementally proven together with the results of β_1 coefficient of (2) and (3). To obtain robust results, regression is performed on LRD_t after taking the absolute value (Abs_LRD_t) with consideration that DRD is normally negative. Moreover, regressions with and without control variables are also performed on (2) and (3) as whether DRG and LRG have impacts on DRD and LRD is inclusive.

4. Analysis of Empirical Results

4.1. Descriptive Statistical Analysis. Descriptive statistical results of the main research variables are shown in Table 4. As the results indicate, shadow banks have been expanded on a large scale in recent years. But less information can be observed for time series variables. Thus, a time trend of main research variables is also plotted.

Figure 1 shows the expansion of shadow banking. As it shows, shadow banks before 2017 are expanded drastically, since the Central Economic Work Conference called for greater importance to be placed on the prevention and resolution of financial risks at the end of 2016. The 15th meeting of the Central Financial and Economic Leading Group, held at the beginning of 2017, emphasized that it is of great necessity to timely compensate for the deficiencies of supervision and resolutely control market chaos. The drastic and irregular growth of shadow banks was effectively curbed upon three-year efforts in special governance.

We can also see that the marketization level of interest rate also presents a significant watershed around 2017. While the savage growth of shadow banking is being regulated, the actual marketization level of interest rate also presents a downward trend, which indicates that the expansion trend of silver banks is strongly correlated with the market interest rate. When the interest rate control intensity is greater, the shadow banking system in China will develop faster. The price of market funds is not the cause of shadow banking.

4.2. Main Empirical Regression Results. Benchmark regression was performed according to the above-mentioned hypotheses, with results shown in Table 5.

Column (1) shows that Sbank is significantly positively correlated to LRD and significantly negatively associated with DRD, proving Hypothesis 1 that the low liberalization level of interest rate and the distortion of capital price caused by interest rate control have advanced the scale development of shadow banks. To further verify Hypothesis 1, the author

TABLE 3: Measurable indicators for liberalization level of interest rates and scale expansion of shadow banks.

Variable type	Variable name	Implications
Explained variables	Sbank	Year-on-year growth rate of entrusted loans, trust loans, and the sum of undiscounted bank acceptances
	DRD	Benchmark deposit rate - market interest rate
Explaining variables	LRD	Benchmark loan rate - market interest rate
	DRG	Benchmark loan rate - inflation rate
	LRG	Benchmark deposit rate - inflation rate

TABLE 4: Statistical description of variables to Be studied.

Variables	Observation	Average	Median	Standard deviation	Minimum	Maximum
Sbank	69	0.177	-4.200	26.65	-36	55.50
LRD	63	1.295	1.577	0.810	-2.787	2.408
DRD	63	-1.510	-1.278	0.594	-2.631	-0.570
LRG	63	-96.92	-96.75	1.326	-102.7	-94.80
DRG	63	-99.77	-99.61	1.068	-102.8	-98

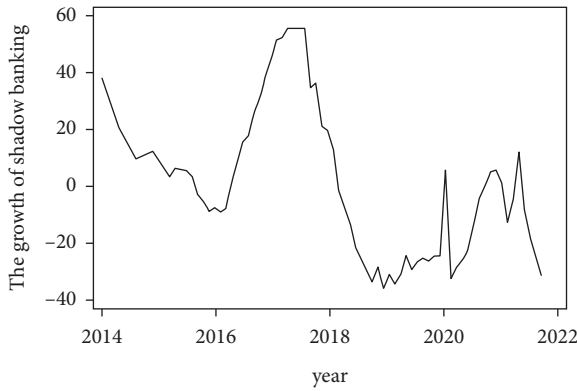


FIGURE 1: The expansion of shadow banking.

proves that the correlation coefficient between LRD and DRD and Sbank at faster Sbank is significantly greater than that at slow Sbank, and the latter has an insignificant correlation coefficient. Then, the second half of Hypothesis 1 is proved: the liberalization level of interest rates is positively related to the growth rate of shadow banks. In other words, the lower the liberalization level of interest rates, the faster the scale development of shadow banks in China. Evidently, the interest rate control system that distorts capital price is the main factor facilitating the emergence of the shadow banking system.

By regressing the OLS models of equation (2) and (3), the following results were obtained in Table 6:

Data given in the table show that Abs_LRD_t and DRR are remarkably inhibited by Sbank with or without control variable, proving Hypothesis 2 that the interest rate liberalization can be promoted by shadow banks to some extent. Similarly, Hypothesis 2 was verified through group regression.

The regression results in Table 7 show that LRD and DRD can only be suppressed when Sbank is high, leading to a higher level of interest rate liberalization. Besides, as the interest rate level begins to distort when Sbank stands low,

the higher level of interest rate liberalization cannot be achieved by the reduction in market control and Sbank supervision.

The liberalization level of interest rate is positively related to the growth rate of shadow banks; that is, the faster the scale development of shadow banks in China is, the higher the liberalization level of interest rate will be.

4.3. Robust Regression Results. To achieve robust results, the data was further verified using the quantile regression model (as shown below) with reference to the research of some scholars [6,7]. For the multiple linear regression model $y_q = X'\beta + u_q$, solving the coefficient $\hat{\beta}^q$ of the regression equation for the qth quantile is to minimize the following objective function:

$$Q = \sum_{i: y_i < X'\hat{\beta}^q} q|y_i - X'\hat{\beta}^q| - \sum_{i: y_i < X'\hat{\beta}^q} (1 - q)|y_i - X'\hat{\beta}^q|, \quad (4)$$

where $y_i - X'\hat{\beta}^q$ is the residual of the regression equation at the qth quantile.

Quantile regression was performed following the above-mentioned hypotheses, with the results shown in Table 8.

The impacts of LRD and DRD are insignificant at low quantile. It is probably because the shadow banks have no significant advantage in comparison with the on-balance sheet business of traditional banks when the interest rate and the official benchmark interest rate of shadow banks are low in quantile, thereby restraining the rapid development of shadow banks. At high quantile (Quantile ≥ 0.5), on the other hand, the impacts of LRD and DRD on the scale of shadow banks are significantly positive and negative, respectively. Also, Table 5 shows that the estimated parameter of DRD in the absolute value is greater than that of LRD in this quantile no matter what the quantile is.

It indicates that the impacts of interest rate control on shadow banks in China over deposits and loans are asymmetric. The impacts of the distortion of deposit interest rate

TABLE 5: Main empirical regression results.

Variable	(1) Complete sample	(2) High expansion trend Sbank	(3) Low expansion trend
LRD	17.224 * (8.947)	26.961 *** (3.915)	6.201 (6.351)
DRD	-51.001 *** (9.648)	0.000 (.)	-12.243 (8.990)
LRG	-13.617 * (7.364)	-9.487 (23.720)	-5.458 (5.192)
DRG	21.136 *** (7.509)	12.284 (25.112)	10.821 ** (5.222)
<i>N</i>	63.000	30.000	33.000
<i>R</i> ²	0.701	0.652	0.318

(standard error in parentheses) * $p < 0.1$, ** $p < 0.05$, *** $p < 0.01$.

TABLE 6: Main empirical regression results 2.

Variable	(1)	(2)	(3)	(4)
	No control variable		With control variables	
	Abs_LRD _{<i>t</i>}	DRD	Abs_LRD _{<i>t</i>}	DRD
Sbank	-0.015 *** (0.003)	-0.017 *** (0.002)	-0.018 *** (0.002)	-0.019 *** (0.002)
LRG			0.743 *** (0.090)	-0.014 (0.070)
DRG			-0.590 *** (0.113)	0.156 * (0.089)
<i>N</i>	63.000	63.000	63.000	63.000
<i>R</i> ²	0.251	0.583	0.686	0.639

TABLE 7: Group regression results.

Variable	(1)	(2)	(3)	(4)
	High expansion trend		Low expansion trend	
	Abs_LRD _{<i>t</i>}	DRD	Abs_LRD _{<i>t</i>}	DRD
Sbank	-0.025 *** (0.004)	-0.025 *** (0.004)	0.002 (0.014)	-0.003 (0.006)
<i>N</i>	30.000	30.000	33.000	33.000
<i>R</i> ²	0.637	0.637	0.001	0.009

on the scale of shadow banks in China are stronger than those of the distortion of loan interest rate. The possible reason may be that the market-oriented reform of RMB loan interest rate has been faster than the liberalization level of RMB deposits, leading to a liberalization level of loan interest rate higher than that of deposit interest rate. Relatively, the more stringent control over deposit interest rate is more conducive to shadow banks to obtain more capital at low cost, thereby enabling investment inviting banks to grow increasingly larger in scale.

Hypothesis 1 is further proved to be robust and correct according to the empirical results of robust regression. When the liberalized level of interest rate is insufficient, a distortion of deposit and loan interest rates will be caused by the deviation between the official

benchmark interest rate and the benchmark interest rate of the market. This is the condition for the birth of shadow banks. The greater the distorted degree is, and the lower the liberalized level is, the greater the development scale of shadow banks will be. Moreover, it is also found that the distortion of deposit interest rate is more conducive to the development of shadow banks than the distortion of loan interest rate.

The results of Table 9 show that Sbank can significantly enhance the liberalization level of loan interest rates under various quantiles, and the faster growth of Sbank at high quantile (≥ 0.5) can better contribute to the decline in the degree of LRD, thereby enhancing a higher level of deposit and loan interest rates in China. High consistency is presented in the same conclusion when it comes to the distorted

TABLE 8: Quantile regression results 1.

Variable	(1) Quantile0.2	(2) Quantile0.4	(3) Quantile0.6	(4) Quantile0.8
			Sbank	
LRD	6.575 (19.090)	14.425 (9.750)	20.680 * (12.171)	29.602 ** (12.921)
DRD	-34.932 * (20.585)	-45.687 *** (10.513)	-55.059 *** (13.124)	-67.095 *** (13.933)
LRG	-6.213 (15.713)	-11.758 (8.025)	-16.142 (10.018)	-22.609 ** (10.635)
DRG	15.767 (16.023)	19.694 ** (8.183)	22.339 ** (10.215)	28.991 *** (10.845)
<i>N</i>	63.000	63.000	63.000	63.000
<i>R</i> ²	0.251	0.583	0.686	0.639

TABLE 9: LRD quantile regression results.

Variable	(1) Quantile 0.2	(2) Quantile 0.4	(3) Quantile 0.6	(4) Quantile 0.8
			Abs.LRD _{<i>t</i>}	
Sbank	-0.016 *** (0.005)	-0.019 *** (0.003)	-0.019 *** (0.003)	-0.023 *** (0.003)
DRD	0.939 *** (0.185)	1.022 *** (0.109)	1.090 *** (0.108)	*** (0.128)
LRG	-0.771 *** (0.234)	-0.850 ** (0.137)	-0.968 *** (0.137)	-0.964 *** (0.162)
<i>N</i>	63.000	63.000	63.000	63.000
<i>R</i> ²	0.251	0.583	0.637	0.657

degree of deposit interest rates; please refer to the appendix for details.

5. Conclusions and Inspiration

5.1. *Conclusions.* This paper found that, first, low liberalization level of interest rate and the distortion of capital prices caused by interest rate control contribute to the scale development of shadow banks, and the liberalization level of interest rate is negatively associated with the growth rate of shadow banks; that is, the lower the liberalization of interest rate is, the faster the scale development of shadow banks will be. Second, shadow banks can propel the interest rate liberalization, and the liberalization level of interest rate is positively related to the growth rate of shadow banks; that is, the faster the scale development of shadow banks in China is, the higher the liberalized degree of interest rate will be.

Shadow banks have pushed up the leverage level and elevated the financial and systemic risks in China together with associated contagion risks. There is no doubt that shadow banks should be regulated and tracked. But what CBIRC practices are absolutely right? Although it has clamped down on a variety of vicious shadow banks, CBIRC has implemented too many “one-size-fits-all” approaches to the supervision of shadow banks. The scales of investment inviting banks that can promote interest rate liberalization and even financial innovation in China have been directly reduced. It can be also found that the level of interest rate

liberalization in China has been lowered with the declined scale of shadow banks. This paper believed that there must be an inevitable connection between the two. Efforts should be made to strengthen supervision over vicious shadow banks, and shadow banks that can promote financial innovation should also be protected. Only in this way can the financial market-based transformation in China be performed in a more comprehensive manner.

The author believes that various innovations in shadow banks have significantly elevated the market-oriented reform of RMB interest rates. More precisely, innovations in financing channels have improved the liberalization level of loan interest rates; innovations in investment channels have accelerated the market-oriented reform of deposit interest rates; innovations in the pricing mechanism have contributed to the establishment and improvement of the market-oriented formation mechanism of RMB interest rate in China; and innovations in supervision have propelled innovation and built a stable reform environment for interest rate liberalization.

5.2. Policy Suggestions

5.2.1. *The Information Disclosure Mechanism Should Be Strengthened and Improved.* In view of the conclusion that the low degree of interest rate liberalization caused by interest rate regulation and the distortion of capital price promote the scale development of shadow banking, this

paper suggests to strengthen the full disclosure of financial market information, which is conducive to the prevention and resolution of risks in the financial market apart from enhancing the operational efficiency of the financial market. The information disclosure mechanism of shadow banks can be strengthened in the following aspects. First, it is imperative to improve the regulatory transparency of the supervision departments, innovate risk indicators, and conduct regular assessments on risks and risk levels. Second, a statistical information disclosure mechanism for shadow banks and research on information disclosure and accounting methods for innovative financial products should be established to discover and resolve existing problems in a timely manner as well as to improve the quality and effectiveness of major information disclosure. Third, the overall quality of supervisors should be enhanced through regular training and assessment to improve their sensitivities to market changes and capabilities of risk early warning.

5.2.2. The Process of Interest Rate Liberalization Should Be Promoted in an Orderly Manner. In view of the conclusion that shadow banking promotes interest rate liberalization to a certain extent and that the degree of interest rate liberalization is positively related to the growth rate of shadow banking, this paper holds that gradually promoting interest rate liberalization is an important way to promote the sunshine development of shadow banking in China. Accelerating the interest rate liberalization is beneficial to reasonably determining the interest rate level, contributing to truly and accurately reflecting the relationship between market supply and demand, and lowering interest rate risks. More than that, it can also create an active trading environment and promote fair competition between traditional banks and shadow banks, improving the financial structure in China and advancing the healthy and stable development of the financial system.

5.2.3. The Self-Regulation of Relevant Subjects Should Be Improved. The presence of shadow banking has increased the level of leverage, financial and systemic risk in China, and the associated risk of contagion. Shadow banks should also improve and enhance their internal control mechanism while accepting external supervision. It is imperative to improve the internal control system of shadow banks, complete their risk monitoring mechanism, regulate their operation and management, and establish an effective and reasonable monitoring scheme. In this way, systemic risks can be prevented, offering a supporting mechanism for the effectiveness of external supervision.

5.2.4. International Regulatory Cooperation Should Be Enhanced. Domestic supervision is insufficient to deal with the problem of cross-border supervision over shadow banks. The global and the cross-border characteristics of shadow banks call for cross-border cooperation over their supervision. To this end, countries around the world should conduct cross-border cooperation and formulate regulations

and policy agreements with cross-regional impacts, such as international agreements on minimum margin to limit the amount of leveraged financing used by financial institutions. In this way, cooperation in the supervision of shadow banks can be implemented regionally and even globally.[8–13].

Data Availability

No data were used to support this study.

Conflicts of Interest

There are no potential conflicts of interest in this study.

References

- [1] S. Ba, "On strengthened supervision of shadow banking system," *China Financialyst*, vol. 49, no. 14, pp. 24-25, 2009.
- [2] F. C. D. Rezende, "The structure and the evolution of the U.S. Financial system, 1945-1986," *International Journal of Political Economy*, vol. 40, no. 2, pp. 21-44, 2011.
- [3] K. Xiao, *Monetary Transmission in Shadow banks* Columbia Business School, New York, USA, 2018.
- [4] Z. Luo and Ke Feng, "Shadow banking and monetary policy transmission in China," *Wuhan Finance*, vol. 24, no. 04, pp. 19-22, 2012.
- [5] C. Li and D. Yang, "Shadow banking's influence on the real economy in our country and the countermeasures," *Journal of economic aspect*, vol. 19, no. 03, pp. 106-111, 2017.
- [6] A. Feng, L. Wang, X. Chen et al., "Developmental Origins of Health and Disease (DOHaD): implications for health and nutritional issues among rural children in China," *Bioscience trends*, vol. 9, no. 2, pp. 82-87, 2015.
- [7] J. Zhao, "Reforms in Shadow banks, interest rate control and interest rate liberalization," *Shanghai Finance*, vol. 34, no. 06, pp. 50-55, 2019.
- [8] Z. Mao and Y. Wan, "Research on the stable threshold effect of shadow banks and banking system in China," *International Finance Research*, vol. 35, no. 11, pp. 65-73, 2012.
- [9] G. Dai and P. Fang, "Interest rate liberalization and bank risks: a study from the perspective of shadow banks and Internet finance," *Financial Forum*, vol. 19, no. 08, pp. 13-19+74, 2014.
- [10] J. Li and X. Han, "Shadow banking and operational risks of non-financial enterprises," *Economic Research*, vol. 54, no. 08, pp. 21-35, 2019.

Research Article

Construction of Data Mining Analysis Model in English Teaching Based on Apriori Association Rule Algorithm

Shufei Wang 

Department of Foreign Language, Harbin University of Commerce, Harbin, Heilongjiang 150028, China

Correspondence should be addressed to Shufei Wang; 15104504977@163.com

Received 23 March 2022; Revised 19 April 2022; Accepted 27 April 2022; Published 15 June 2022

Academic Editor: Wei Liu

Copyright © 2022 Shufei Wang. This is an open access article distributed under the Creative Commons Attribution License, which permits unrestricted use, distribution, and reproduction in any medium, provided the original work is properly cited.

How to create an English data mining analysis model based on prior association strategy algorithm is learned. First, the basic principles of data mining and organizational strategy are investigated, and the cooperative strategy algorithm in data mining technology is studied. This document makes a comprehensive analysis of the classical Apriori algorithm and studies the extension of organizational strategy and the technique of deleting participation strategy after decision-making. Then, the application of Apriori algorithm in instruction management is analyzed. There is often a lot of information in command management. We need to collect the data, then sort, and review it. Finally, taking the two adults' classes, class (39) and class (40) as the research objects, of which class (39) has 41 people and class (40) has 43 people. The two classes were brought to the board of directors. The results showed that over the course of 4 months, the students scored better on the mixed tests in the lab than those in the control room. The average score of the subjects before the experiment was 17.6, the average score of the subjects after the experiment was 20.1, and the significant P value of the corresponding t -test was $p \leq 0.001$, less than 0.05, indicating significant differences between the two groups of data. After studying data using writing styles in class, students focused more on complex patterns, concepts, technical expressions, and line patterns. Dynamic assessment of student writing is an effort to improve student writing by using interactive assessment techniques.

1. Introduction

With the development of data information, database technology is more and more mature, and data are used more and more widely. The data information accumulated by the world is also developing at an exponential growth rate. In the 1990s, with the advent and rapid development of the Internet, the whole world was penetrated a small global village by the Internet. People in different places can exchange data and information between each other across time and space and provide help to each other through the Internet. After using the Internet, people are not only facing their own departments, their own units, or their own specific industry databases but also facing the whole ocean of information, covering all fields. From the appearance, there is not much correlation between these data, but if we carefully analyze them, we can find a large amount of technical knowledge

information hidden in them. Until the mid-1980s, most databases can only simply perform data entry, data query, and data statistics. Data mining is the process of finding interesting knowledge from many data information stored in databases, data warehouses, or other information bases. The steps and process are shown in Figure 1. The application of this technology can not only enable people to experience and query the previously saved data but also find out the all-in-one relationship between these data, to speed up the transmission of information. In recent years, with the progress of science and technology, people gradually began to widely study rule association mining technology, which has also become an important topic in the direction of data mining. In data mining, association rule is one of the main technologies, which reflects the correlation and dependence between the events. It is also the most common form of mining local patterns in unsupervised learning system. If

there is a correlation between two or more things, we can use other related things to predict the occurrence of something [1].

With the diversification of college English courses and methods, improving college English courses attracts more and more attention. Since 1990, English classes in many Chinese universities have completed certification procedures. Its main purpose is to improve the measurement of teaching and promote the improvement of teaching quality through regular monitoring of teaching process [2]. The measurement of good teaching is the important foundation of good teaching. Existing measuring instruments are often given a wide measuring range, which is usually based on multiple measuring levels. For example, the primary level measurement criteria include teacher teaching, syllabus, teaching, teaching results, etc., while the secondary level measurement criteria are the focus of the primary level. According to the role and direction of these indicators in good classroom teaching, different weights are used as a complete measurement standard. There are two main types of assessment: peer assessment and student assessment. This teaching method of quality evaluation has been widely used in colleges and universities and has achieved certain results. However, there are still some differences in the quality assessment process [3].

Based on this, this study argues that the objectives and findings of the key groups that affect English proficiency teaching in colleges and universities are the basis and basis for appropriate evaluation and improvement of teaching. This study presents a method to determine the best use of data mining techniques. Through the analysis of teaching materials, this study tries to find out the advantages of teaching strategies, situations, and environments, in order to provide new ideas and approaches for reviewing and improving teaching quality. Data mining (DM) is an approach to providing data that uses statistical techniques to find certain rules and identities of the data. It is a great way to get knowledge out of big data and is widely used in industrial decision-making and management practice. This study uses data mining to identify the characteristics of good teaching and acquire knowledge of teaching data storage [4].

2. Literature Review

Li and Yu believe that data mining can not only bring huge competitive advantages to enterprises and institutions but also create huge economic benefits for the society. Under such temptation, many famous companies in the world have also entered the ranks of data mining, using data mining systems to develop software and tools related to the company's future development [5]. Cui et al. argue that the composition of quality standards is largely based on the experience of manufacturers. There are a lot of details and attributes in the measurement, and the weight of the measurement is usually based on previous experience, or even the same. Many different disciplines accept the same teaching methods [6]. Wei believe that college English teaching has its own characteristics (such as teacher-student interaction and differences in teaching and events), and

many factors that affect good teaching are often hidden. The curriculum, environment, and conditions were not easy to find. Only by demonstrating these situations can an effective teaching model be formed, which should not only be based on the characteristics of college English teaching but also study, appropriate, and exempt education [7]. Kong et al. conducted an empirical study on the characteristics affecting students' evaluation results and found that six characteristics can explain 25.8% of the variation of students' evaluation results. Students' evaluation of teachers' teaching has certain limitations, which can only be used as a reference for teachers to improve teaching [8]. On the other hand, the evaluation of students' performance can be greatly influenced by the way of Glanbock, but on the other hand, it has no influence on the evaluation of students' performance. Therefore, this quality evaluation method is a "result" evaluation method, which can only answer the question of "how" the teaching effect but cannot answer the questions of "why" and "how to improve" the teaching effect [9]. Tseng et al. use data mining technology to learn online English learning platform, college English listening, teaching, test scores, evaluation scores, and administration. For online English learning, assessment panels are used to group students. For English proficiency, the participatory algorithm is used to identify the relationship between output and input skills, and genetic algorithm is used to develop automated English language [10]. In terms of college English listening, Nes and See, based on the understanding of college English listening and research data on the Internet, used information such as gender, teaching, educational objectives, experiment, and language teaching, and found that the first influence was satisfactory in listening test, and the second influence was teaching [11]. Liu et al. believed that compared with other countries, in the field of Chinese companies and organizations, the use of data mining technology to help enterprises and organizations' commercial activities is still in its infancy. There are some good examples of data mining technology in Chinese industry and its application, so there is still a lot of room for improvement in data mining industry, mining technology, industry scientists, and project developers [12].

3. Method

3.1. Data Mining Foundation and Association Rules

3.1.1. Data Mining. With the development of computer technology, the database has evolved from the early file processing to a more powerful database system and further evolved into the current commonly used relational database system. Users can easily access the database through structural query language. With the increasing amount of information, some new problems arise. These fast-growing data are stored in many databases. The traditional database processing technology cannot effectively analyze and apply these massive data and provide users with valuable analysis results. In this context, data mining technology came into being. The operation of extracting useful, implicit, potential, and unknown information from a large amount of data with random interference, noise, errors, missing, and incomplete

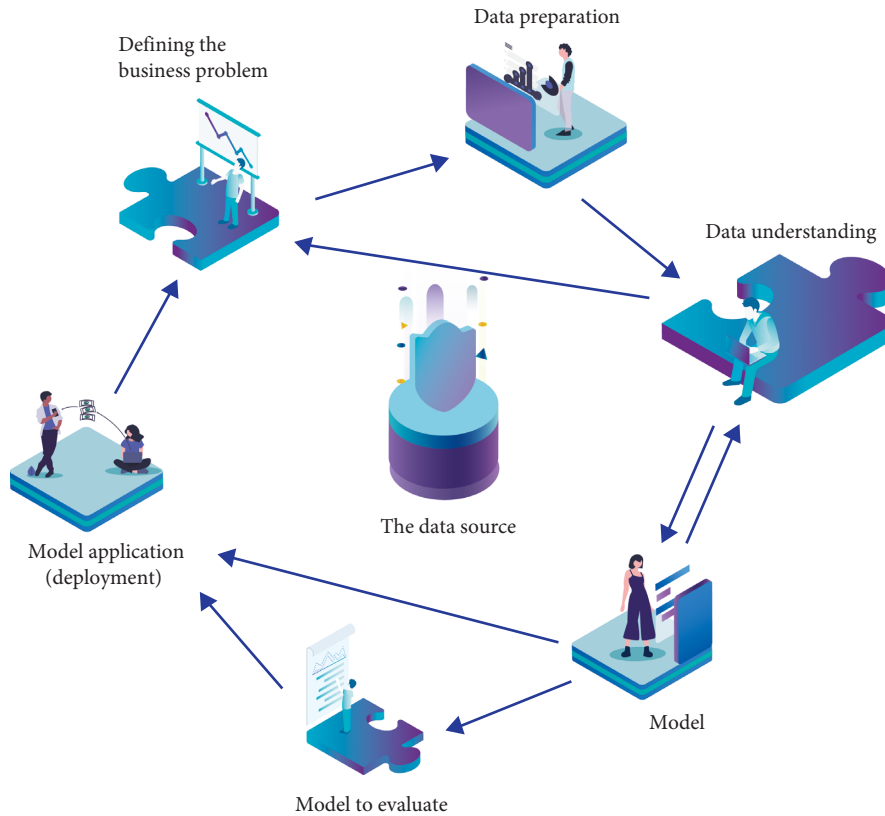


FIGURE 1: Data mining.

is called data mining. Based on potential knowledge and useful information, data mining technology extracts it from a large amount of data. It is the key link of knowledge discovery data (KDD). Its process is listed in Table 1 [13].

Typical data mining includes user interfaces, measurement models, mining engines, data warehouse servers, and data source text (such as databases, data warehouses, the World Wide Web, and other data). Its structure is shown in Figure 2. The knowledge discovery request put forward by the user is interpreted and converted into a specific pattern through the user interface, submitted to the data mining engine, and mined the cleaned data set through the database or data warehouse server [14]. The patterns found in the mining stage need to be further analyzed and evaluated. If there are redundant or irrelevant patterns, they need to be deleted to generate valuable knowledge and modify the knowledge base through the user. The data mining engine also updates accordingly with the update of the knowledge base.

The process of data mining can be described by three stages: data preparation, mining, and result description and evaluation. Constantly repeating the above three operations is the process of knowledge discovery data (KDD). The data mining process is shown in Figure 3.

(1) *Data Preparation Stage.* In the data mining process, the time-consuming stage is usually the data preparation stage, accounting for 50% of the whole process. The data preparation process can be divided into three parts: data selection, data preprocessing, and data transmission. The activities for each level are listed in Table 2.

(2) *Data Mining Stage.* The most concerned problem of scholars and experts in the field of data mining is the data mining stage. This stage really carries out the mining work, which shows the essence of data mining technology. The first is algorithm planning, such as data summary, classification, clustering, association rule discovery, or sequential pattern discovery, that is, to decide what type of data mining method to use. The second is to select an algorithm for the mining method. This directly affects the quality of the mining patterns. The application of data mining algorithm is carried out after the preparation is completed.

(3) *Result Expression and Interpretation Stage.* According to the different value of information, the extracted information is analyzed and studied, and the analysis results are described based on the user's decision-making objectives. The main tasks of this stage are as follows: deleting redundant and irrelevant information and analyzing and evaluating the data information found in the data mining stage [15]. If the results do not meet the needs of users, then it means that the mining results are inaccurate, and it is necessary to carry out mining calculation again, adjust the parameter value, change the data transformation mode, reselect the data, and even select a new data mining algorithm. In order to intuitively show the results of data mining to people, we should visually process the mining results, for example, "if...then..." rules describe the classification decision tree, which simplifies the difficulty of data analysis.

TABLE 1: Knowledge discovery process of database.

Step	Name	Operation
Step 1	Data cleaning	Clear noise or inconsistent data
Step 2	Data integration	Many files can be merged. Along with cleansing the data, this is considered the first step to storing the data in a data warehouse
Step 3	Data selection	Retrieve data related to the analysis task from the database
Step 4	Data transformation	Transform or share data through content or assembly into a format suitable for mining
Step 5	Data mining	Use intelligent methods to extract data patterns

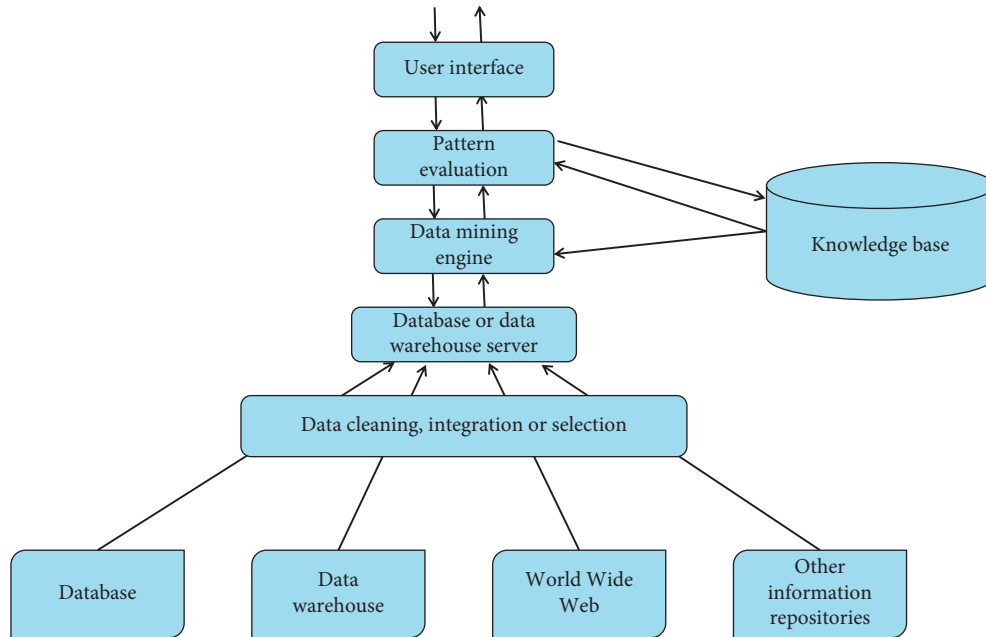


FIGURE 2: Structure of typical data mining system.

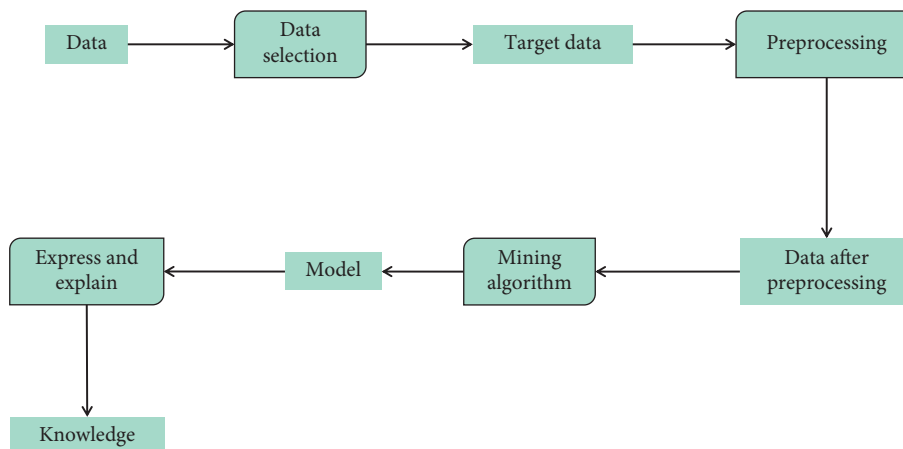


FIGURE 3: Data mining process.

3.1.2. *Association Rules.* The association discovery policy identifies associations interested in or affiliated with products in various forms. It is a major of data mining and has been widely studied in the industry in recent years.

At present, there are many different types of cultural organizations. Because of the grouping changes to the code, they can be divided into Boolean and numeric associations;

according to the analysis of the data in the rule, it can be divided into a set of rules and a set of rules; depending on the size of the file involved in the code, it can also be divided into rule combinations and multiple consortiums [16].

(1) *Principle of Association Rule Algorithm.* Association rules are ruling whose support and trust meet the threshold given

TABLE 2: Three substages of data preparation.

Data preparation	Explain
Data selection	Selecting a file usually involves deleting data affected by an existing file or database to create a target file
Data preprocessing	Data preprocessing process extracts data to meet the requirements of data mining
Data transformation	The main purpose of exchanging data is to reduce the width of the data, that is, to find the main features of the first feature in order to reduce the number of features or differences in data mining

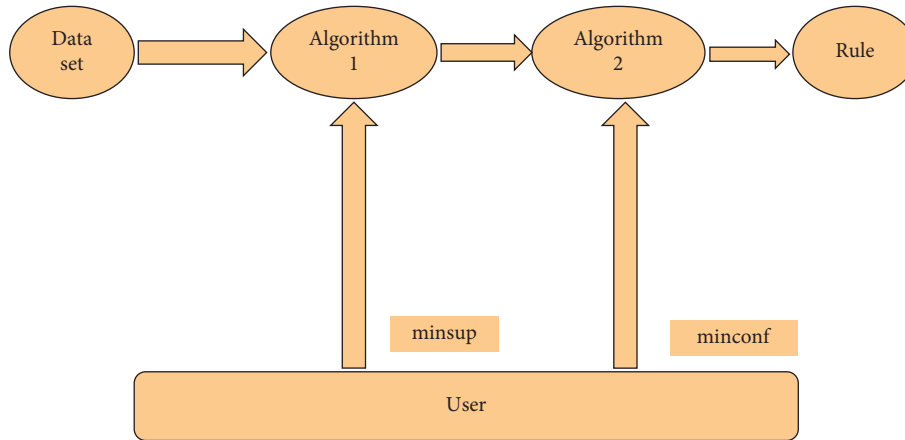


FIGURE 4: Basic model of association rule mining.

TABLE 3: Association rule mining steps.

Step	Operate
Find out the frequent item set	Find all frequent items, whose support is no less than a given threshold
Generate strong association rules	Find out the set of frequent items, namely, support and confidence, respectively

by users respectively, that is, strong rules. The data sample set corresponding to strong rules must appear frequently in the sample training set. We can deduce the confidence of the corresponding association rules according to the support of these frequent sample sets. In other words, the whole process of association rules is divided into two stages.

First, the frequent item set in the sample training set is determined by the preset minimum support threshold. This step is the central problem of the whole mining process, and it is also an important index to determine the efficiency of the algorithm. All association rules are generated according to the obtained frequent item set and the minimum confidence threshold. The implementation process of this process is as follows: for each element in the frequent item set, that is, each frequent item generates all nonempty subsets and calculates the confidence for each nonempty subset. If the confidence is greater than or equal to the minimum confidence, then the strong rule is output. The basic model is shown in Figure 4.

The basic steps of association rule mining are listed in Table 3.

In the process of mining association rules, the first step is the focus and key. The performance and effect of mining association rules directly depend on the execution results of the first step. Therefore, the first step is the main starting point of mining association rules algorithm. Compared with

the first step, the second step is much simpler. All association rules of frequent itemsets are listed, and these association rules are evaluated and measured. Based on the confidence and support threshold, valuable association rules must meet the requirements of confidence and support threshold. In fact, all association rules generated by frequent itemsets must meet the requirements of support threshold. Therefore, there is no need to judge the support threshold of association rules, if the association rules are measured according to the requirements of confidence threshold, which simplifies the evaluation process.

Usually, users specify minimum support (min SUP) and minimum confidence (min CONF) according to mining needs. Support and confidence are two important concepts to describe association rules. The specific definitions are as follows:

(1) Support:

$$\text{support}(AB) = P(A \cup B) = \frac{NH_{A-B}}{N} \times 100\%. \quad (1)$$

That is, the probability that two itemsets A and B appear simultaneously in transaction set D , which is used to measure the statistical importance of association rules in the whole data set.

(2) Confidence:

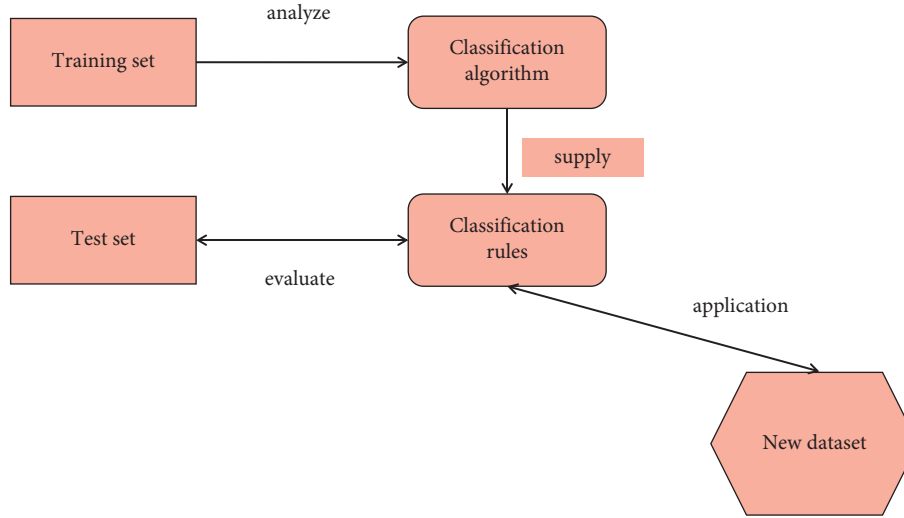


FIGURE 5: Data classification process.

$$\text{confidence}(AB) = P(A \cup B) = \frac{NH_{A-B}}{N} \times 100\%. \quad (2)$$

That is, in the transaction set D of itemset A , the probability that itemset B also appears at the same time [17].

The task of data analysis is classification and prediction. The classification task is to map each attribute set X to a predefined class label y by learning or obtaining an objective function F . Classification is mainly used to predict the category of data objects. First, according to the samples in the given training sample set, an appropriate classification model, that is, classifier, is constructed. In the process of classification, the classifier is used to specify the most appropriate class mark for the sample instances that have not determined the class mark in the data set.

The whole classification process can be divided into two stages: learning and classification. First, the classification algorithm is used to analyze the training data set and obtain the classification rules, which is the so-called learning stage; The second stage is the classification stage, which tests the accuracy of the classification rules obtained by the data set evaluation. If the accuracy is within the allowable range, the rule will be used in the new classification process. Otherwise, the classification rule will be abandoned. The whole process is shown in Figure 5.

We briefly describe the classification as follows: if a specific instance form can represent $(a_1, a_2, \dots, a_n, c)$, where $a_i (i = 1, 2, \dots, n)$ identifies the attribute field value and C represents the class mark. We briefly describe the classification as follows: given the training data sample set $D = \{x_1, x_2, \dots, x_n\}$, the goal of the classification task is to analyze the data set D and determine a mapping function gate $f(A_1, A_2, \dots, A_n) \rightarrow C$, so that the instance $xi = (a_1, a_2, \dots, a_n)$ of any unknown category can be identified by the appropriate class label C .

The amount of information can only reflect the uncertainty of the symbol, and the information entropy can be used to measure the overall uncertainty of the whole source X . Let something have n mutually independent possible

results (or states), the probability of each result is $P(X_1), P(X_2), \dots, P(X_n)$, and there are

$$\sum_{i=1}^n P(X_i) = 1. \quad (3)$$

Then, the uncertainty $H(X)$ of the thing is as follows:

$$H(X) = \sum_{i=1}^n P(X_i) \log_2 P(X_i). \quad (4)$$

Information gain is used to measure the expected reduction of the direct line, which can help us to ask the least questions when classifying the sample set. Suppose that the training set of tuples marked with class D has m different values of class label attribute [18], then it is recorded as $C_i (i = 1, 2, \dots, m)$. $|D|$ and $|C_{1,D}|$ respectively represent the number of tuples in D and the number of principles of class C_1 in D . If P_i is the probability value that a tuple in D belongs to class C_1 , then the direct $Info(D)$ of D is described as the expected information for the classification of tuples in D , and the formula is written as follows:

$$\ln fo(D) = \sum_{i=1}^m \log_2(P_i). \quad (5)$$

Information gain is defined as the difference between the original classified information demand and the new classified information demand, which is as follows:

$$\text{gain}(D, A) = \ln fo(D) - \ln fo_A(D). \quad (6)$$

Therefore, the obtained information gain $\text{gain}(D, A)$ can also be defined as follows:

$$\text{gain}(D, A) = \ln fo(D) - \sum_{j=1}^v \frac{|D_v|}{|D|} \times \ln fo(D_j), \quad (7)$$

$\text{gain}(D, A)$ indicates the expected compression of the lineage caused by clarifying attribute A . The larger $\text{gain}(D, A)$

is, the more information the test attribute A provides for classification. Therefore, for each attribute, it is sorted according to its information gain, and the attribute that obtains the maximum information gain is selected as the branch attribute. ID3 algorithm uses information gain as the splitting basis [19].

3.2. Apriori Algorithm. Apriori algorithm to realize association rule mining includes two basic steps: the first is to mine frequent itemsets from the transaction database and then generate association rules based on frequent itemsets.

Finding frequent itemsets layer by layer iteratively is the key and core of Apriori algorithm, which can be completed by pruning and connecting itemset. Generating a set C_k of candidate k -item sets for the k -item frequent itemset L is the key to the connection step, which is realized by connecting the k -item frequent itemset L_{k-1} with itself. The whole transaction data set is scanned and compared with the transaction items with the preset minimum support threshold, and the events with support lower than this threshold are deleted, which is called the pruning step.

Taking the generation of L_k through L_{k-1} as an example, this study explains how to use the Apriori algorithm when mining frequent items. The purpose of generating L_k through L_{k-1} can be realized by connecting and deleting.

3.2.1. Connection Steps. The two itemsets are connected in L_{k-1} and the candidate set C_k of L_k is calculated to find L_k . Suppose L_{k-1} contains two itemsets l_i and l_j right, and the j th item in l_i and the penultimate item in l_i are represented by $l_i[j]$ and $l_i[k-2]$ respectively. In order to simplify the analysis process, it is assumed that the records in the database are stored in dictionary order. $L_{k-1} \oplus L_{k-1}$ is used to represent L_{k-1} -connection operation, which means that if l_1 and l_2 have the same first $(k-2)$ items, and l_1 and l_2 in L_{k-1} can be connected. In order to ensure the uniqueness of itemset, the constraint condition of $l_1[k-1] < l_2[k-1]$ must be satisfied.

3.3. Implementation of Apriori Algorithm in Teaching Management. The purpose of the joint venture is to find relationships between products in the database, which is a shopping basket analysis. The most famous example is the "Butt and Beer" story. The organizational policy has many uses. In sales, organizational rules can be applied to sales to make more money; as far as the insurance industry is concerned, if there is a difference in demand, then it could be fraudulent and needs further investigation. In terms of treatment, we can see combination therapy, talk about marketing, identify customers, and approve services of interest. The Apriori algorithm is one of the most classical algorithms in the custom organization [20].

Teaching management is very informative. This information provides flexibility for our ordinary business, but how does the information generated by these industries affect our management? Can we find some social organizations that can play a role in improving our day-

to-day governance and decision-making? This concept is still rare in our approach to teaching management. The purpose of the system is to identify the relevance of the data generated during the course, draw final conclusions, and send them to management as a basis for supporting decision-making.

Command management often has a lot of data. We must first compile the data, then review and analyze the data, and store it in an archive. Then, the improved Apriori algorithm is used to eliminate the influence of these data in data mining technology, produce negative results, identify results, then make some adjustments, and finally produce the desired results from the support decision, presented in a computer. Therefore, the system can be divided into data acquisition data, collision data and analysis, operation data, collision, and presentation modules.

The design model of improved Apriori algorithm in instruction management is shown in Figure 6.

(1) *Information Received and Received in Advance.* This module is used to identify and compile all kinds of data in the management system, identify the data useful to the system, and extract and modify the format of these data for the system to use.

(2) *Filter and Clean Files.* Cleaning data in a data store is used to generate data. It can clean data, select subdevices, remove inaccurate data and duplicate data, and view important information in the process. Preliminary data can improve the quality of discovery data. After selecting the features of the former data, the research and exploration are completed by using analytical analysis, system analysis, classification, and clustering algorithms [21].

(3) *The Improved Apriori Algorithm Was Used to Analyze the Data.* The improved Apriori algorithm is used to create shared files that filter and clean up the data to get the results we used.

(4) *Edit Information.* Results may differ slightly due to different data storage and analysis algorithms. Therefore, the deviation case is processed and the second result is obtained. If the results are not satisfactory, then the archive is edited and finally, the results we want are obtained.

Main functional modules are as follows:

(1) *Data Received Before the Module Runs.* The module is designed by receiving data and predata. Data retrieval is typically based on data collected from each business report in the daily command management system. It is only extracted from the database. The business process data need to be analyzed into what we know and then converted into system files. Database processes are typically handled by SQL server: Windows databases.

(2) *Data Filtering Module.* This module uses data extraction to generate data for analysis. Due to the separation of different characteristics, the requirements for data are also different. Therefore, the main purpose of this module is to filter out the data that

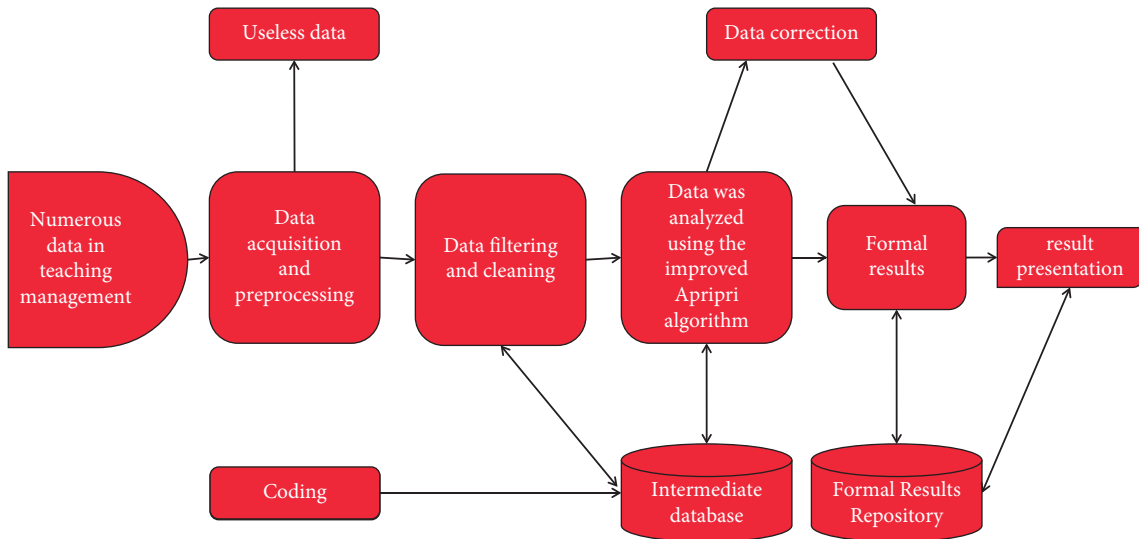


FIGURE 6: Application structure design of improved Apriori algorithm in teaching management.

does not conform to this specification, find the data we need, and remove the features and weak data recovered from data. The final analysis results are stored in the mean data, and these important data are separated to achieve the effect of data cleaning.

- (3) *Data Analysis Module.* Data analysis is an important part of system operation. Its job is to use data from a central database as a data source. These data are then analyzed one or more times using the improved Apriori algorithm in order to get the relationship hidden in the data and make it useful to us [22].
- (4) *Modification of Module Files.* Since the effectiveness of Apriori algorithm in data mining is unpredictable, we cannot be sure whether it will perform well after being tested. These models are used to edit and reevaluate the initial data of the results, resulting in multiple conclusions. If the conclusions are the same, then we consider the conclusions to be valid. The data editing process is shown in Figure 7.
- (5) *Result Presentation Module.* The final result of data mining needs to be presented to the managers of the unit for decision analysis, so the first thing is to ensure the accuracy and reliability of the data. At the same time, it is also easy to understand the results, so the result presentation module generally adopts intuitive reports and icons, which are very common in common office software.

4. Experimental Analyses

4.1. Subjects. To answer the research questions, two adults from class 39 and class 40 were selected as research materials, with 41 students from class 39 as the laboratory and 43 students from class 40 as the administration room. Before the experiment, the composition of the final examination of the next semester of high school was selected as a pretest to determine the writing differences between the two classes.

The reasons for choosing these two classes as experimental classes are as follows: first, they are taught by the author, which excludes the influence of teachers' characteristics on the research; second, the two classes use the same textbooks and the same writing style, eliminating the interference of different courses difficulty; finally, the average writing score was 17.6 in the test room and 18.8 in the control room, based on measurements obtained before the experiment.

4.2. Experimental Method

4.2.1. Questionnaire Survey Method. The questions were divided before and after the experiment. The main purpose of the questionnaire is to understand the current situation of students' writing, that is, students' English writing behavior, students' assessment of their writing ability, and the current situation of students' writing ability. The purpose of the post-test is to measure whether the improvement of DA standard and its application in English writing can improve students' writing skills and abilities [23].

4.2.2. Quantitative Analysis. This study uses the quantitative analysis method and SPSS 22.0 social science statistical software to statistically analyze the experimental data obtained in the process of teaching. The analysis and comparison of students' English composition scores before and after the experiment can be done by providing the data support; thus, the reliability of this study can be increased.

4.2.3. Interview Method. To better understand how students feel about the DA standard being used in high school English writing, the course also uses interviews. It is an additional source of information after the questionnaire and written test. This interview will help teachers better understand the changes in students' writing behavior after the experiment, whether their writing ability has improved, and whether they

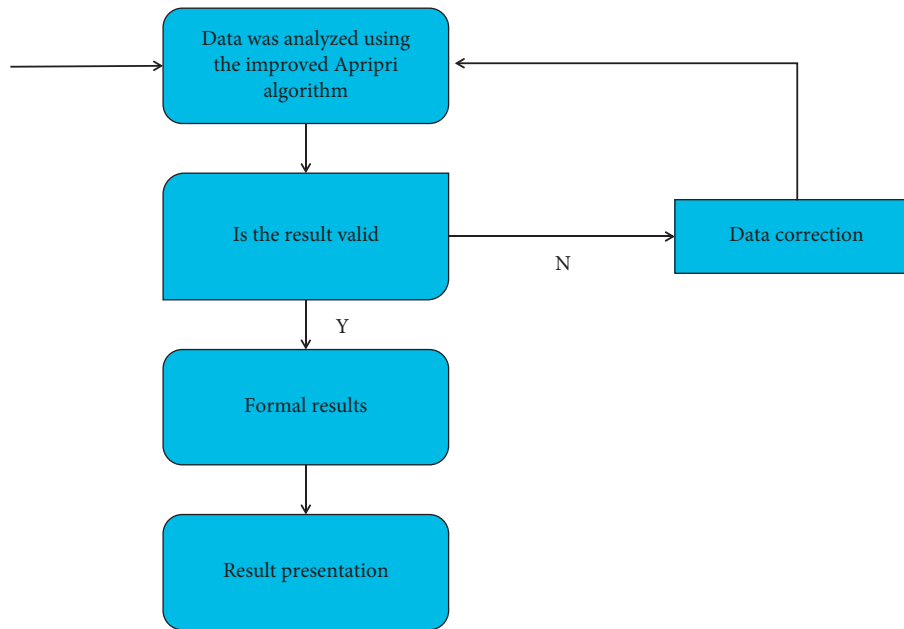


FIGURE 7: Flow chart of data correction.

are interested in the design and applied teaching of English writing classroom.

4.3. Research Process. This study consists of three stages: in the first stage, the students of the two classes fill in the preexperiment questionnaire in order to understand the students' current English writing attitude. When filling in the questionnaire, students should truthfully fill in the questionnaire in combination with their own personal experiences.

4.3.1. Construction of Writing Teaching Process Based on Dynamic Evaluation Model. In the experimental class, according to the characteristics of intrusive and interactive dynamic assessment introduced in Section 2, combined with the specific characteristics of English writing teaching, the author intends to apply the constructed.

DA model to the teaching practice of 4 months. The experimental process of DA mode is mainly divided into the following five stages: prewriting stage, mutual evaluation stage, modification stage, teacher evaluation stage, and final draft stage.

4.3.2. Specific Operation of Writing Teaching in Dynamic Evaluation Mode. Mainly through the use of the constructed DA model for teaching, one of the composition lessons is selected to show how the DA model is applied to the English writing class in senior high school [24].

4.3.3. Control Class Teaching Process. In the English writing class of the control class, the teachers still use the traditional teaching method; that is, according to the process of "teachers assign writing tasks, students write independently, then students hand in their compositions, teachers evaluate

and teachers comment on the model composition." After the teacher assigns the writing task, he does not give any tips and help to the students. In the writing process, the middle school students are not allowed to use reference books or communicate with the students. They are handed in after completing the writing in class within the specified 30 minutes. The students' composition is a one-time manuscript, which is directly handed over to the teacher for evaluation and scoring without modifying the first and second drafts. Teachers only give a comprehensive score in the scoring link, rather than scoring separately. Students pay more attention to the scores assessed by teachers, not to the writing process and the help obtained in the process. Finally, the teacher leads the whole class to appreciate the standard model essay, analyzes the vocabulary and advanced sentence patterns used in the model essay, and then asks the students to imitate and apply them to the next composition writing.

4.4. Data Collection and Analysis. The data used in the experiment were one adult's final English test and two adults' writing scores in the final English test. The scores of the composition examinations are given independently. The concept of composition is close to college and students' life in the entrance examination, which is very difficult. Test scores are based on high school English standards. Therefore, the reliability of test data is very reliable. By observing the changes in test scores after the laboratory and control room, whether the standard of achievement is suitable for improving students' writing ability is determined. By observing changes in test scores before and after laboratory tests, this study determines whether Da applied standards in English teaching can support students' writing resources [25].

In order to understand the validity of this experiment, questions and interviews were also used in this study. The

TABLE 4: Questionnaire of students' writing status before the experiment.

Question number	Percentage (%)				
	①	②	③	④	⑤
1	0	2.4	7.3	23.3	58
2	7.2	14.6	30.5	24.4	16.3
3	12.4	19.5	34.2	23.2	10.3
4	8.2	27.2	8.2	35.4	17
5	6.1	15.9	47.5	21.6	8.9
6	6.1	17.1	58.5	15.3	3.7
7	19.8	24.4	42.7	7.6	2.8
8	28.1	30.5	32.9	7.3	0
9	12.3	28	39.1	14.5	2.5
10	0	1.2	7.8	22.1	69.5

questionnaire is divided into pretest questionnaire and post-test questionnaire. The pretest questionnaire consists of 10 questions and usually examines the current situation of English writing students. The post-test also contains 10 questions designed to explore the benefits of using the Da model for English teaching.

In this experiment, SPSS 22.0 social science statistical software is used to statistically analyze the experimental data.

4.5. Experimental Analysis. Before the experiment, 85 questionnaires were distributed to the laboratory and control room. The author asks the students of both classes to answer at the same time and brings them back to the scene. All 85 questionnaires were returned and all 85 questionnaires were valid. The pre-experiment questionnaire consisted of 11 small questions. The first two questions are designed to assess students' current writing behavior. Questions 3 to 6 are students' assessment of their own content, questions 7 to 8 are students' assessment of their current writing level, and the last two questions are students' assessment of the writing process. After collecting the data query, the author analyzed the research data from various angles. The evaluation results are listed in Table 4.

Questions 1–2 of this questionnaire are intended to investigate the current students' attitude towards writing. According to the data in the table above, 65% of the students in question 1 agree very much, 21.2% agree that English writing is very important, and no students disagree very much that English writing is very important. Therefore, up to 89.9% of the students agree on the importance of English writing. Question 2 talks about whether students like English writing class. About 30.5% of students have a vague attitude, 15.3% of students say they do not like English writing class, and 7.1% of students do not like English writing class very much, suggesting that students' current English writing attitude needs to be changed.

After the 4-month writing teaching experiment in the experimental class, the author issued a second questionnaire to the experimental class. This time, the author wants to investigate the effect of students' application of dynamic assessment model in English writing teaching after the experiment. There are 40 people in this experimental class.

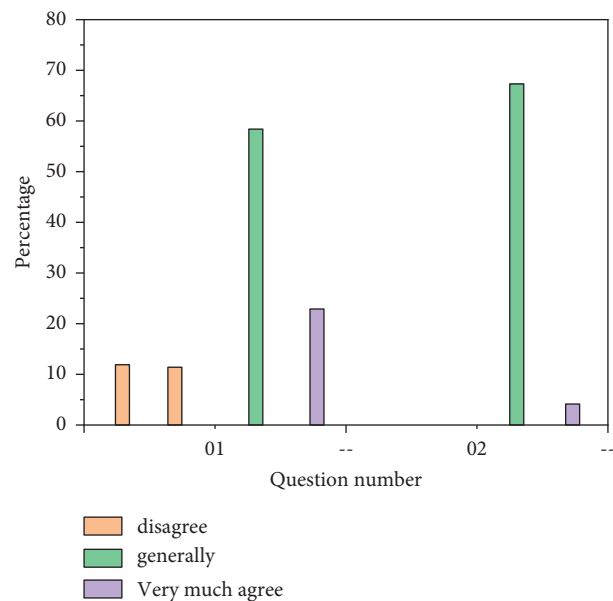


FIGURE 8: The influence of DA mode on students' writing confidence and habits.

About 40 questionnaires are distributed, 40 are recovered, and 40 valid questionnaires are available. Students are allowed to answer and hand them in within a unified time. The questionnaire contains 10 subquestions in total. Now, the percentage of people corresponding to each subquestion and each option is displayed in the form of column chart, as shown in Figure 8:

Questions 1 and 2 are to understand whether the students' writing confidence and writing habits have changed after the experiment compared with those before the experiment. After 4 months of dynamic evaluation teaching experiment, the author again investigated whether the students in the experimental class are confident in writing English compositions and whether they are used to making sketches and making outlines and revising them for many times. It can be clearly seen from Figure 8 that 57% of the students are confident in writing English compositions and 23% of the students are very confident in writing English compositions. Nearly half of the students in the first two

classes had vague attitudes when asked whether they were confident of writing well, which shows that the dynamic assessment model is conducive to increasing students' confidence in English writing; as for question 2, the chart data show that 72% of the students have formed the habit of writing and revising their compositions for many times after the experiment, while the survey results of the same questions in the two classes before the experiment show that only 12% of the students will do so, which shows that the dynamic evaluation model has a good impact on students' writing habits.

In Figure 9, the author mainly investigates the students' recognition of DA mode and each process in the experimental class. Questions 3–6 of this questionnaire are to investigate the feelings of students in each link of DA mode writing. In question 3, none of the students in the class dislikes brainstorming very much. The proportion of students who like this link very much is as high as 70%. In the peer evaluation link of question 4, more than half of the students like this link. Students have slowly begun to adapt to the idea that teachers are no longer the only composition evaluators, and students can also help each other evaluate compositions [26].

Questions 7 and 8 in Figure 10 mainly investigate the impact of DA mode on students' writing interest and writing ability. As can be seen from question 7 in the figure, 55% of the students agree that DA mode improves students' interest in writing, and 20% of the students agree very much with the impact of DA mode on students' interest in writing. In question 8, none of the students strongly disagreed that DA mode can improve writing ability, and 65% of the students agreed that DA mode can improve writing ability. DA mode has a great impact on students' writing interest and writing ability.

To prove that there was no significant difference in English writing scores between the laboratory and the control room, the authors had students from both classes take the predictive test scores. The current SPSS 22.0 identification data are listed in Table 5:

Table 5 lists 40 students in the lab and 42 students in the control room. The standard deviation of the test class was about 1.37, and that of the control class was about 1.57. The average pretest score before the class was about 16.7, and that before the control class was about 18.9. There was a 0.2 difference between the pre-experimental class and the control class.

Four months later, in order to check the application of dynamic measurement standards in high school English classes and to see whether there is any difference in the scores of English writing test between the examination room and the control room, the city unified English test was taken. At the end of the last semester of the senior year, it is based on the follow-up exam section. The results of target analysis are listed in Table 6.

In Table 6, the scores between the test room and the control room in the later tests were higher than in the previous tests. The average score of the subjects in the pretest increased from 17.6 to 20.1, and the average score of the control class in the pretest increased from 18.9 to 20.6. After

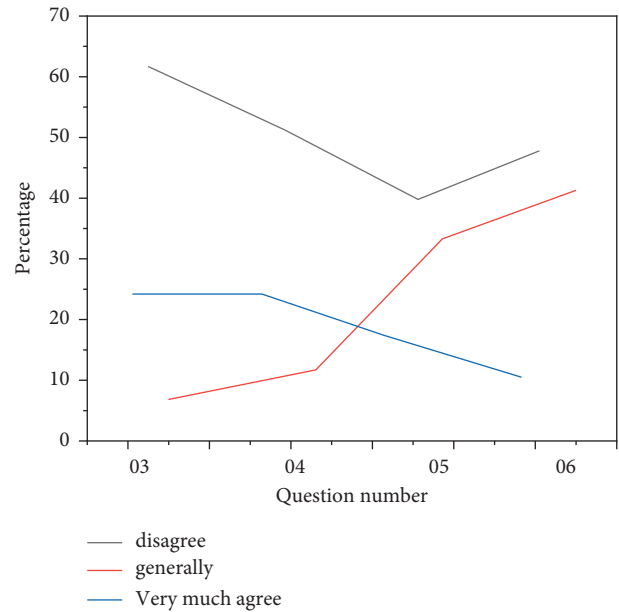


FIGURE 9: Students' recognition of each process of DA mode.

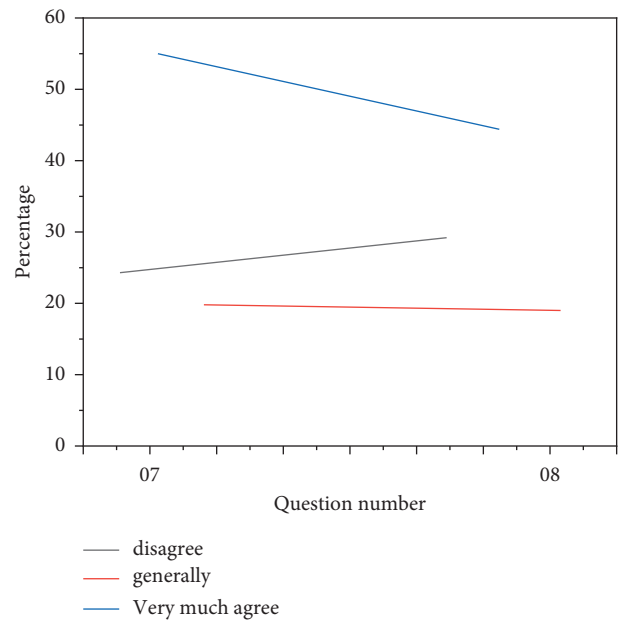


FIGURE 10: The influence of DA mode on students' writing.

4 months of English writing study, the result of the composition was good. Both classes have improved. The difference is that the results of the experimental class and the control class differ greatly in the post-test. At the same time, due to the use of variables, the experimental class achieved faster results, and the average score of the experimental class was 1.3 points higher than the control class.

Finally, students' scores on all types of questions have the greatest impact on students' passing exams and making responsible decisions, depending on where they study. The main model used in the experiment was students who had taken multiple English language courses or English tests.

TABLE 5: Description and statistics of pretest groups in experimental class and control class.

	Front side grouping	Figure	Average value (E)	Standard deviations	Standard error mean value
Class	Control class	41	17.8532	1.53742	24233
	Experimental class	43	17.5000	1.57165	25106

TABLE 6: Grouping description and statistics of post-test composition scores in experimental class and control class.

	Backside grouping	Figure	Average value (E)	Standard deviations	Standard error mean value
Backside	Control class	41	20.1340	1.19872	19543
	Experimental class	43	18.5554	1.30254	18792

When students have no special weakness in listening, speaking, reading, and writing, the probability of passing the exam is high; when students can complete the previous level through all types of questions, students are more likely to pass the final exam; in addition, students who pass CET 4 and 6 with high scores also have a higher chance of passing the exams. It can be seen from the data that the scores of multiple-choice questions, final level, CET 4, and CET 6 will all affect boys' basic English, and there are reasons for girls' learning. Therefore, students' basic English level is conducive to passing the exam.

5. Conclusion

To determine the teaching benefits of developing quality measurement standards and organizational policy algorithms and apply them to high school English teaching, the author conducted equivalent experiments in two classes and examined questionnaires and tests before and after exams. The material is discussed. The results show that the research problem has been successfully solved; that is, the use of dynamic measurement model in high school English class can improve students' satisfaction and grades. According to the characteristics of data processing and response behavior developed by the system, this study understands the theory and technology of data mining and machine learning. Using the logistic regression model, the improved decision tree model, and the model after integrating the logistic regression model and the improved decision tree model, the students' previous estimation can be completed. In classification problems, the logistic regression model is the most used algorithm in the industry, such as the media click pass value problem, while the improved logarithmic model decision is a powerful performance algorithm with multiple decision tree models. The prediction results are more accurate than the one-to-one decision model, which confirms the application of data mining technology in the problem classification of college English.

The systematic collection of body shape data is insufficient, especially the behavior data of students in English practice or test. All kinds of information are needed, both from the point of view of creating a student user profile and from the point of view of predicting a student's English proficiency in the past. There are many factors that can affect a student's ability to pass an exam later; for example, there

are many factors that can affect a student's ability to pass an exam. In addition, there are many factors to consider in subsequent studies, such as not taking the test.

Data Availability

The labeled datasets used to support the findings of this study are available from the corresponding author upon request.

Conflicts of Interest

The author declares that there are no conflicts of interest.

Acknowledgments

This study was supported by 2021 Harbin University of Commerce Teacher's "Innovation" Project, The Practical Research of Cultivating the Compound Foreign Language Teachers in Heilongjiang Province from the Perspective View of ESP (20YYD218).

References

- [1] P. H. Lu, J. L. Keng, F. M. Tsai, P. H. Lu, and C. Y. Kuo, "An apriori algorithm-based association rule analysis to identify acupoint combinations for treating diabetic gastroparesis," *Evidence-based Complementary and Alternative Medicine*, vol. 2021, no. 17, pp. 1–9, Article ID 6649331, 2021.
- [2] G. Liu, "Information platform for classroom teaching quality evaluation and monitoring based on artificial intelligence technology," *Big Data Analytics for Cyber-Physical System in Smart City*, Springer, Singapore, pp. 149–155, 2020.
- [3] T. S. Murthy, M. S. Roy, and M. K. Varma, "Improving the performance of association rules hiding using hybrid optimization algorithm," *Journal of Applied Security Research*, vol. 15, no. 3, pp. 423–437, 2020.
- [4] W. S. Leite and R. C. D. Lamare, "List-based omp and an enhanced model for doa estimation with non-uniform arrays," *IEEE Transactions on Aerospace and Electronic Systems*, vol. 57, no. 6, pp. 4457–4464, 2021.
- [5] J. Li and K. Yu, "An alternative to the bathe algorithm," *Applied Mathematical Modelling*, vol. 69, pp. 255–272, 2019.
- [6] J. Cui, L. Kan, F. Cheng et al., "Construction of bifunctional electrochemical biosensors for the sensitive detection of the sars-cov-2 n-gene based on porphyrin porous organic polymers," *Dalton Transactions*, vol. 51, no. 5, pp. 2094–2104, 2022.

- [7] L. Wei, "Study on the application of cloud computing and speech recognition technology in English teaching," *Cluster Computing*, vol. 22, no. S4, pp. 9241–9249, 2019.
- [8] X. Kong, Y. M. Wang, X. Wang et al., "Monitoring damage evolution in a titanium matrix composite shaft under torsion loading using acoustic emission," *Acta Metallurgica Sinica*, vol. 32, no. 10, pp. 1244–1252, 2019.
- [9] K. Glanbock, "Donaldo macedo (ed.) decolonizing foreign language education—the misteaching of English and other colonial languages," *Language Policy*, vol. 20, no. 1, pp. 135–137, 2021.
- [10] J. J. Tseng, Y. S. Cheng, and H. N. Yeh, "How pre-service English teachers enact tpack in the context of web-conferencing teaching: a design thinking approach," *Computers & Education*, vol. 128, pp. 171–182, 2019.
- [11] A. Nes and B. H. See, "Does explicit teaching of critical thinking improve critical thinking skills of English language learners in higher education? a critical review of causal evidence," *Studies In Educational Evaluation*, vol. 60, pp. 140–162, 2019.
- [12] Y. Liu, Z. Yu, and Y. Yang, "Diabetes risk data mining method based on electronic medical record analysis," *Journal of Healthcare Engineering*, vol. 2021, no. 6, 11 pages, Article ID 6678526, 2021.
- [13] R. Zhou, H. Chen, H. Chen, E. Liu, and S. Jiang, "Research on Traffic Situation Analysis for Urban Road Network through Spatiotemporal Data Mining: A Case Study of Xi'an, china," *IEEE Access*, vol. 9, no. 99, p. 1, 2021.
- [14] N. A. Fauzi, N. Ali, P. J. Ker, V. A. Thiviyathan, and L. H. Mun, "Fault Prediction for Power Transformer Using Optical Spectrum of Transformer Oil and Data Mining Analysis," *IEEE Access*, vol. 8, no. 99, p. 1, 2020.
- [15] J. Hu, J. Fang, Y. Du, Z. Liu, and P. Ji, "Application of pls algorithm in discriminant analysis in multidimensional data mining," *The Journal of Supercomputing*, vol. 75, no. 9, pp. 6004–6020, 2019.
- [16] J. Xu and Y. Liu, "Cet-4 score analysis based on data mining technology," *Cluster Computing*, vol. 22, no. S2, pp. 3583–3593, 2019.
- [17] R. Aaij, S. Benson, M. D. Cian et al., "A comprehensive real-time analysis model at the lhcb experiment," *Journal of Instrumentation*, vol. 14, no. 04, 2019.
- [18] X. Zhu and Y. Liu, "An efficient frequent pattern mining algorithm using a highly compressed prefix tree," *Intelligent Data Analysis*, vol. 23, pp. S153–S173, 2019.
- [19] M. S. Akhtar, P. Sawant, S. Sen, A. Ekbal, and P. Bhattacharyya, "Improving word embedding coverage in less-resourced languages through multi-linguality and cross-linguality: a case study with aspect-based sentiment analysis," *ACM Transactions on Asian and Low-Resource Language Information Processing*, vol. 18, no. 2, pp. 15.1–15, 2019.
- [20] U. Khadam, M. M. Iqbal, M. A. Azam, S. Khalid, and N. Chilamkurti, "Digital watermarking technique for text document protection using data mining analysis," *IEEE Access*, vol. 7, no. 99, p. 1, 2019.
- [21] Y. Wang, H. Ye, T. Zhang, and H. Zhang, "A data mining method based on unsupervised learning and spatiotemporal analysis for sheath current monitoring," *Neurocomputing*, vol. 352, pp. 54–63, 2019.
- [22] Y. Shi, T. Yu, Q. Liu, H. Zhu, and Y. Wu, "An approach of electrical load profile analysis based on time series data mining," *IEEE Access*, vol. 8, no. 99, p. 1, 2020.
- [23] C. H. Chen, J. S. He, T. P. Hong, and S. R. Kannan, "Post-analysis framework for mining actionable patterns using clustering and genetic algorithms," *IEEE Access*, vol. 7, no. 99, p. 1, 2019.
- [24] H. Zou, "Clustering algorithm and its application in data mining," *Wireless Personal Communications*, vol. 110, no. 1, pp. 21–30, 2020.
- [25] N. Fatima, L. Li, S. Hong, and H. Ahmed, "Prediction of breast cancer, comparative review of machine learning techniques and their analysis," *IEEE Access*, vol. 8, no. 99, p. 1, 2020.
- [26] J. Zhang, L. Chu, C. Guo, Z. Fu, and D. Zhao, "A novel energy management strategy design methodology of a phev based on data-driven approach and online signal analysis," *IEEE Access*, vol. 9, no. 99, p. 1, 2021.

Retraction

Retracted: Mathematical Model of Quantitative Evaluation of Financial Investment Risk Management System

Mathematical Problems in Engineering

Received 13 September 2023; Accepted 13 September 2023; Published 14 September 2023

Copyright © 2023 Mathematical Problems in Engineering. This is an open access article distributed under the Creative Commons Attribution License, which permits unrestricted use, distribution, and reproduction in any medium, provided the original work is properly cited.

This article has been retracted by Hindawi following an investigation undertaken by the publisher [1]. This investigation has uncovered evidence of one or more of the following indicators of systematic manipulation of the publication process:

- (1) Discrepancies in scope
- (2) Discrepancies in the description of the research reported
- (3) Discrepancies between the availability of data and the research described
- (4) Inappropriate citations
- (5) Incoherent, meaningless and/or irrelevant content included in the article
- (6) Peer-review manipulation

The presence of these indicators undermines our confidence in the integrity of the article's content and we cannot, therefore, vouch for its reliability. Please note that this notice is intended solely to alert readers that the content of this article is unreliable. We have not investigated whether authors were aware of or involved in the systematic manipulation of the publication process.

Wiley and Hindawi regrets that the usual quality checks did not identify these issues before publication and have since put additional measures in place to safeguard research integrity.

We wish to credit our own Research Integrity and Research Publishing teams and anonymous and named external researchers and research integrity experts for contributing to this investigation.

The corresponding author, as the representative of all authors, has been given the opportunity to register their agreement or disagreement to this retraction. We have kept a record of any response received.

References

- [1] X. Wang, "Mathematical Model of Quantitative Evaluation of Financial Investment Risk Management System," *Mathematical Problems in Engineering*, vol. 2022, Article ID 2439549, 14 pages, 2022.

Research Article

Mathematical Model of Quantitative Evaluation of Financial Investment Risk Management System

Xiaoling Wang ^{1,2}

¹College of Finance, Heilongjiang University of Finance and Economics, Harbin 150500, Heilongjiang, China

²International College, Krirk University, Bangkok 10220, Thailand

Correspondence should be addressed to Xiaoling Wang; jfwangmath@hrbnu.edu.cn

Received 22 April 2022; Revised 16 May 2022; Accepted 23 May 2022; Published 10 June 2022

Academic Editor: Xuefeng Shao

Copyright © 2022 Xiaoling Wang. This is an open access article distributed under the Creative Commons Attribution License, which permits unrestricted use, distribution, and reproduction in any medium, provided the original work is properly cited.

The financial investment risk management system refers to an analysis and control of the intelligent system to invest in the lower financial situation so that investors quickly understand the situation in the financial industry. The purpose of this article is to use a digital model to evaluate financial investment risk management system. The investment risk value can be better evaluated by building a digital model. This paper first introduces financial investment risks and then elaborates the evaluation system and related digital models. The standards of the evaluation system are also given. The GARCH model is established to analyze the LME copper and LME aluminum case selected by this paper by investigation and analysis of the current status of corporate financial investment risks. The experimental results show that the evaluation results are often close to the reality when using the GARCH model evaluation of financial investment risk management system, and the accuracy is quite high. In addition to the EGARCH-N model, the established model is more accurate at 90% confidence level, which is more accurate and is relatively close to a given significance level.

1. Introduction

With the development of the economy, the rapid development of the national economy and the urbanization process have promoted the rapid development of financial investment. Meanwhile, China's financial investment projects continue to maturity. In order to improve the competitiveness of financial investment and reduce financial investment risks, most people choose evaluation through financial investment risk management systems. Financial risks refer to financial related risks, such as financial market risks, financial product risks, financial institutions, etc. The financial investment risk management system refers to an analysis and control of the intelligent system to invest in the lower financial situation so that investors quickly understand the situation in the financial industry. The analysis of the underlying financial industry is a nice choice for the analysis of the financial investment risk management system.

Today, in the development of financial investment and multiproject investment development, how investors

control financial investment risks in multiproject decisions and how they use financial investment opportunities to obtain investors and society's largest investment benefits for development and growing financial markets have far-reaching significance. Financial investment risk management systems have small restrictions on problems, and their application range is very wide. In recent years, scholars have studied this system which is used to solve the problem of real investment, but the mathematical model of quantitative analysis in financial investment risk management system is relatively small. Therefore, this paper studies the mathematical model of quantitative analysis of financial investment risk management system, which has certain theoretical significance and a certain practical significance.

With the depth research of financial investment, more and more scholars have studied financial investment risk management systems. S Jirásková analyzed fiscal risk management earlier, defining the basic terms related to risk management. He also explained the negative consequences of risk and pointed out the importance of financial risk

management [1]. However, he did not write very comprehensively in the end of the article. Later, Korzh N studied the essence and nature of financial risks. He classified them and also discussed the characteristics and main management methods of financial risk management [2]. However, he did not use the latest data in the text. Later, Nikitina et al. [3] determined the essence of investment projects by analyzing concepts. In order to determine the investment project, theory and system provided the possibility of clearing the basic characteristics of the investment project, ensuring effective interaction with internal and external dynamic environments [3]. But they did not deal with the calculation of the effective interactive part of the inner and outer parts. Gunjan et al. [4] used descriptive statistics and variance analysis to invest in three types of investors, namely, commercial, paid class, and professional class investors, which explained the preference style and their investment model in investment decisions [4]. But they did not use the most suitable model to study in the empirical analysis phase.

After the study of other scholars, Hmyria et al. [5] studied the financial risk assessment of Irish iron and steel company and its impact on enterprise economic security. They found that financial risks and the operation mode of today's enterprises were closely related [5]. But they did not perform a detailed analysis discussion on the operation mode of the company in the article. However, Kotova et al. [6] had proposed a method of forming a natural monopoly subject investment plan to establish a monitoring system to perform long-term investment projects of natural monopoly before them [6]. However, the concept of monitoring system in writing did not take into account reality influencing factors. In contrast, Tang et al. [7] used descriptive statistics and variance analysis to invest in three types of investors, namely, commercial, paid class, and professional class investors, which explained the preference style and their investment model in the investment decision [7]. But they did not make a more detailed explanation of investment models.

The innovation of this article is as follows: (1) In terms of financial investment decisions, digital models to evaluate financial investment risks can firstly be used. Then financial investment can be achieved, which has greatly reduced the risk of investors. (2) The GARCH model is applied to the quantitative analysis of the evaluation of financial investment risk management system and made a survey on the status quo of financial enterprises' living conditions. In other applications, GARCH is often an algorithm model. However, this article is committed to in-depth characteristics and advantages within GARCH, applying the algorithm itself to assess financial investment risks, thereby giving a risk predictive value.

2. Evaluation of Financial Investment Risk Management System

2.1. Features and Risk Assessment of Financial Venture Investment

2.1.1. *Risk Investment Has a Distinctive Feature Difference from Other Investment Methods.* It has specific investment

objects and methods. The field of venture capital is quite broad, such as logistics, gold, medical facilities, liquor, etc., covering almost all possible, high-quality, high-efficiency, low-cost products or services and high investment returns. The way and timing of risk capital entering into the company also have speciality.

Risk investment itself is a business behavior. It is determined that the subject of venture capital can only be a business behavior. The competitive characteristics of high-tech products or projects determine that this investment can only be carried out by private investment mains outside the country.

It also has a basis for different investment decisions. The most important question of venture capitalists in investing in business is the ability of investment object management and whether the market is large enough or whether it has development potential, as well as the market competition environment faced by the company.

It has unique investment management and profitable channels. The entry of venture capital is not based on the control of the company, but through the operation of the equity investment income and the transfer of the shareholding in the capital market [8].

Risk investment is a high risk investment method. Risk investment has a huge risk from its operation beginning. The financing, project screening, evaluation, and decision-making stages, or investment in project management, and even final profitability have a lot of variables [9, 10]. It can be said that the operation of venture capital is the process of risk identification, evaluation, and management [11].

2.1.2. *Investors' Goals and the Risk of Every Stage of Venture Capital Operations Are Different.* The entry risk of funds in the seed period will be extremely high, and the products and operations of the company are only in a concept and plan. Therefore, at this stage of venture capitalists, it will be cautiously invested in a small amount of funds, and more enterprises will be required to ensure higher expected yields [6].

Foundation period (start period): At this stage, the enterprise starts production operation, but the investment risk is still very high. Venture capitalists usually enter with preferred stocks, and the funds invested are mainly used for planning marketing and testing market competition. But investors will also demand a higher expected rate of return of 40%–60% [4].

Growth period (development period): At this stage, the product starts to be sold, from not yet profitable to beginning to generate profit, but the net cash flow of the enterprise is very small at this time, and the investment risk is still high. At this stage, venture capital funds are mainly used to increase market share, purchase more equipment, expand productivity to achieve economies of scale, strengthen marketing, upgrade products, and maintain a stable profit growth rate. Investors will require 25%–50% of higher expected yields [7].

Mature period (exit period): At this stage, the enterprise grows rapidly, which is close to saturation, and the

investment risk is low, but there may still be internal risks such as loss of managers, improper financial control, and external risks such as reduced market growth rates and hindered company listings. The funds entered at this stage are to maintain profitability, wait for the opportunity to prepare for listing or resell to other investors or allow other companies to merge, or partially realize the previous investment in order to adjust the equity structure and the manager's shares. For venture investors, it is mainly the risk of exit [12].

Classification can also be classified in financial investment project risk recognition, as shown in Figure 1. It can be seen from the figure that financial investment risks can be divided into seven categories. In the financial world, investors or companies often pay more attention to credit risk.

For example, the new fusion warehouse model at home and abroad is used as an example, and the risk of each link is analyzed [13]. The integration class business model is one of the main modes of logistics finance. Its operational basis is a delegate agency theory, referring to one or more objects to specify other objects in economic activities in economic activities in economic activities [14]. In most cases, the one with insufficient information and disadvantage in cooperation is often the principal, and the party with sufficient information is often the agent. Therefore, under this theory, due to the information asymmetry between subjects, it will lead to the situation of moral hazard and adverse selection to some extent. It can be seen from Figure 2 that, in this model, the main body of the financial warehouse model is a two-party principal-agent model, and the third-party logistics, as an agent, plays a role in the communication and connection between the bank and the small and medium-sized enterprises [15].

2.2. Processing of the Indicator System of Financial Risk. Financial risk refers to the possibility that financial market entities will suffer losses in the process of currency, capital, and credit transactions. As an economic phenomenon, financial risk will lead to financial crisis if it is not prevented and resolved. The so-called financial risk early warning is mainly to analyze and forecast the possibility of financial asset loss and financial system damage that may occur in the process of financial operation and to provide countermeasures and suggestions for financial security operation. The indicator of financial risk involves many aspects, and it has five monitoring subsystems. If the financial investment risk status is divided into safety (S1), basic safety (S2), risk (S3), and greater risk (S4) [12], then the financial risk detection index system is as follows.

2.2.1. Macroenvironment (Y1). The indicators of the macroenvironment are shown in Table 1. It can be seen that, in the GDP growth rate, when the financial risk is high, the growth rate is in a polarized state, which may be <3.5 or >12.5 . It shows that different companies have different states when facing financial risks.

2.2.2. Inside the Bank (Y2). As shown in Table 2, within the bank, when the financial risk is relatively high, the non-performing loan ratio of wholly state-owned commercial banks increases significantly to >22 , indicating that financial risk has a great impact on the nonperforming loan ratio.

2.2.3. National Debt (Y3). As shown in Table 3, it can be found that treasury bonds are relatively stable under different risk conditions.

2.2.4. Foam Type (Y4). As shown in Table 4, when the financial risk is high, the total stock market value of the bubble type exceeds 91, which shows that financial risk has a deep influence on it.

2.2.5. Foreign Trade (Y5). As shown in Table 5, when the financial risk is high, the external debt is greater than 31, while the short-term external debt is greater than 36, which shows that the impact of financial risk on the foreign trade industry is very large.

2.3. Overview of Digital Models Related to Investment Risks. It first obtains the influencing factors that represent the credit situation of the enterprise, which is the measurement method of credit risk, then puts these influencing factors into the digital model to calculate, and finally obtains the probability of corporate credit risk and the degree of corporate loss [16].

(1) Z and ZETA scoring models

$$Z = 1.2Y_1 + 1.4Y_2 + 3.3Y_3 + 0.6Y_4 + 0.999Y_5. \quad (1)$$

In this formula, Y_1 refers to the current asset rate, Y_2 represents the undistributed profit rate, Y_3 is the net profit rate, Y_4 is the interest market value debt rate, and Y_5 refers to the income rate.

When $Z < 1.8$, the enterprise bears great risk; when $Z > 2.99$, the enterprise bears less risk [17].

(2) Logit model

Logit regression method is a model that uses some financial indicators and then evaluates the probability of default risk of enterprises. Q_L means financial situation, $Q_L = 0$ means no investment risk, and $Q_L = 1$ means risk may occur. The formula for the probability of default risk is as follows:

$$Q_L = Q\left(\frac{1}{C_L}\right). \quad (2)$$

(3) Credit Portfolio View Model

This model is a corporate credit risk measurement model researched by McKinsey Company based on econometric theory. It analyzes the credit risk level in different production environments through a lot of extensive big data [18]. Based on extensive big data analysis, the Credit Portfolio View model can give

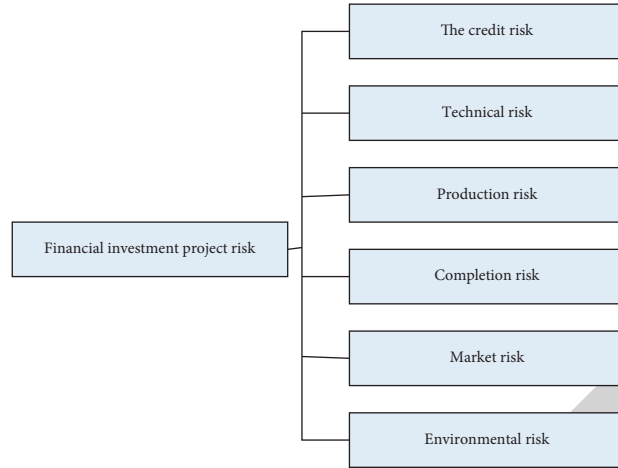


FIGURE 1: Financial investment project risk identification.

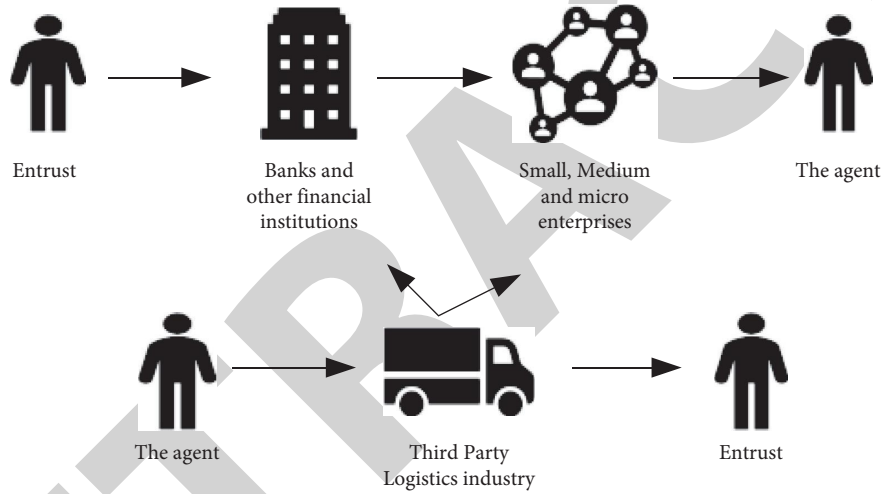


FIGURE 2: Financial warehouse business model.

investors a more accurate risk assessment in the current environment with a high accuracy rate. But some macroeconomics in the model are hard to come by and it is not very stable [19].

(4) GARCH (p, q) model

GARCH models are often used to analyze the interactions among many financial markets, such as volatility spillovers and correlations. The economic meaning of this model is better, but because of the large number of parameters of this model, it limits its wider application. In general, it is more common to use its simplified form [20].

As shown below, in this model, E is a $(M(M+1)/2) \times 1$ -dimensional vector, and S_L, N_L are both $M(M+1)/2$ -dimensional square matrices.

$$\begin{aligned} \text{VECH}(J_Y) = E + \sum_{L=1}^W S_L \text{VECH}(\vartheta_{Y-1} - \vartheta_{Y-1}^Y) \\ + \sum_{K=1}^Q N_K \text{VECH}(J_Y - K). \end{aligned} \quad (3)$$

The general formulation of the GARCH (p, q) model includes the mean and variance equations, which are expressed as

$$\begin{aligned} T_Y = \vartheta_Y + S_1 T_{Y-1} + \dots + S_Q T_{Y-Q} + \vartheta_Y, \\ \vartheta_Y | O_{Y-1} \sim \prod (0, j_y), \\ J_Y = \rho + \sum_{l=1}^w \sigma_l \tau_{Y-1}^2 + \sum_{k=1}^q \mu_k j_{Y-1}, \end{aligned} \quad (4)$$

ϑ_Y represents the interference item, T_Y is the corresponding return value of the financial asset in the Y period, and μ_k is the variance parameter, which reflects the influence of the variance lag period of the residual item on the variance of the current period [21]. This model can analyze things in combination with the whitening weight function. The commonly used whitening weight functions are upper limit measure whitening weight function, lower limit measure whitening weight function, and moderate measure whitening weight function. Among them, the moderate measure whitening weight function is also called the triangular whitening weight function [21]. The basic functional forms of these three whitening weight functions are shown in Figure 3.

Assuming that this function is used to describe the classification degree to which the risk factors of financial investment belong, Figure 4 can be obtained. It can be seen that the classification degree of risk factors basically presents a stepped span.

3. Experiment of Quantitative of Financial Investment Risk Management System Evaluation

3.1. Formulate Evaluation Indicators. The establishment of the evaluation index system is the precondition and the core of the risk evaluation model of financial investment projects. Whether the establishment of the evaluation index system is scientific and perfect determines whether the evaluation model is effective. It also determines the accuracy of the entire financial investment risk assessment. Principles for the establishment of the index system are very important for the evaluation of the risk of financial investment projects. Therefore, in order to ensure the scientificity and rationality of the establishment of the index system, the following principles should be followed when constructing the risk evaluation index system of financial investment projects [22].

- (1) The principle of purpose. The construction of risk evaluation index system of financial investment projects is the indefinite foundation for the construction of risk evaluation model. Therefore, when constructing the evaluation index system, it should be guided by the purpose of construction and focus on the principle of purpose.
- (2) Scientific principles. The selection of the index system must be based on recognized scientific theories. At the same time, it must be combined with the analysis of the current situation of the financial industry. The concept of the selected risk index of financial investment projects should be clear, with precise connotation and extension, and the index system should reflect the nature of the risk as reasonably as possible.
- (3) Comprehensiveness principle. The construction of the risk evaluation index system of financial investment projects should fully and completely reflect

the risk situation of high-tech projects at all levels and aspects. At the same time, investors' current preferences and interests in investment should also be considered. And fully consider the various risks faced by the project to ensure the comprehensiveness of the construction of the risk evaluation index system.

- (4) Systematic principles. When constructing the risk evaluation index system of financial investment projects, each index factor should be interrelated and mutually restrictive. Among them, the horizontal relationship reflects the mutual restriction relationship between different risk factors, and the vertical relationship reflects the inclusive relationship between different risk factors.
- (5) Principle of independence. When constructing the risk evaluation index system of financial investment projects, the index factors in the system should be independent of each other, and the overlapping area between each index should be minimized. There cannot be any relationship between inclusion and inclusion between the indicators at the same level, so that the indicator system can reflect the risk dynamics of high-tech project financing from all aspects.
- (6) The principle of universality and the construction of risk rating index system for financial investment projects are the premise and foundation of risk evaluation and management. Therefore, the constructed system must have broad applicability; that is, it can reflect the needs of risk assessment of financial investment projects in different industries. In addition, the constructed system should also be flexible; that is, it can be adjusted and used flexibly according to different high-tech projects of different industries and enterprises.
- (7) Operability principle. When constructing the risk evaluation index system of financial investment projects, the difficulty and reliability of the index quantification and data acquisition involved in the system should be considered. It should construct a reasonable index system with as few indexes as possible to achieve the goal of optimizing the overall function of the index system. In this way, it is more convenient and effective for investors to analyze financial investment risks.

3.2. Investigation on Status Quo of Existence of Financial Enterprises. The questionnaire on "The Survival Predicament of Small and Medium-Sized Enterprises" truly reflects the current living conditions of small and medium-sized enterprises and their attitudes towards future prospects. The subjects of the questionnaire were 143 small and medium-sized enterprises from all over the country. Most of them come from the Yangtze River Delta and the Pearl River Delta, and some companies come from Sichuan, Beijing, Shanxi, Hunan, and other places, covering a wide range. The

TABLE 1: Macroeconomic stability subsystems.

Index	The risk status			
	S1	S2	S3	S4
Y1(1): GDP growth rate	5.5–8.5	5–6.5 or 9.5–11	3.5–5 or 11–12.5	<3.5 or >12.5
Y1(2): growth rate of fixed asset investment	14–18	10–13 or 19–22	7–10 or 22–25	<7 or >25
Y1(3): inflation rate	<4	4–7	7–10 or (–2)–0	<(–2) or >10
Y1(4): M2 growth rate	5–16	15–20	0–5 or 20–25	<0 or >25
Y1(5): Enterprise asset-liability ratio	<46	45–65	65–85	>85

TABLE 2: Bank internal stability subsystem.

Index	The risk status			
	S1	S2	S3	S4
Y2(1): nonperforming loan ratio of wholly state-owned commercial banks	<12	12–17	17–22	>22
Y2(2): capital adequacy ratio of wholly state-owned commercial banks	>12	8–12	4–8	<4
Y2(3): capital gains of wholly state-owned commercial banks	0.4	0.2–0.4	0–0.2	<0

TABLE 3: Treasury shock risk subsystem.

Index	The risk status			
	S1	S2	S3	S4
Y3(1): debt dependence	<11	10–21	21–31	>31
Y3(2): negative yield of treasury bonds	>14	16–21	21–26	<26
Y3(3): ratio of fiscal revenue to GDP	>23	21–25	16–21	<15

TABLE 4: Bubble risk subsystem.

Index	The risk status			
	S1	S2	S3	S4
Y4(1): stock price/earnings ratio	<41	41–61	61–81	>81
Y4(2): total market value of stocks/GDP	<31	31–61	61–91	<91

TABLE 5: Foreign trade shock risk subsystem.

Index	The risk status			
	S1	S2	S3	S4
Y5(1): external debt/GDP	<21	21–24	26–31	>31
Y5(2): short-term external debt/total external debt	<16	14–24	26–36	>36
Y5(3): time of import supported by foreign exchange reserves (month)	>7	5–7	16–213–4	<4
Y5(4): current account balance/GDP	0–4	3–4.5	4.5–5	<0 or >5

distribution industries are food, textile, electromechanical, steel, Internet, etc. We divided this survey into two parts .

- (1) The first part of the investigation: Whether a new round of financial crisis will recur and what the biggest difficulty facing small and medium-sized enterprises is.

As shown in Figure 5, 51% of companies believe that financing is difficult. Even if they think that the capital turnover is good, they still admit that “financing difficulty” is the biggest problem facing small and medium-sized enterprises, followed by too high labor costs, high taxes, and high production costs. 50% of SMEs believe that a new round of financial crisis will appear. Recently, the world’s major economies have faced many problems such as slow economic

recovery, stagnant development, and sovereign debt crisis, while emerging economies are also faced with the dilemma of weak growth and high inflation. Therefore, there is a view that a new round of financial crisis will reappear. 51% of companies find financing difficult. Even if they think that the capital turnover is good, they still admit that “financing difficulty” is the biggest problem facing small and medium-sized enterprises, followed by too high labor costs, high taxes, and high production costs.

- (2) The second part: changes in the current overall operation of the enterprise compared with the previous year and whether the enterprise will expand capital and equipment investment in the coming year.

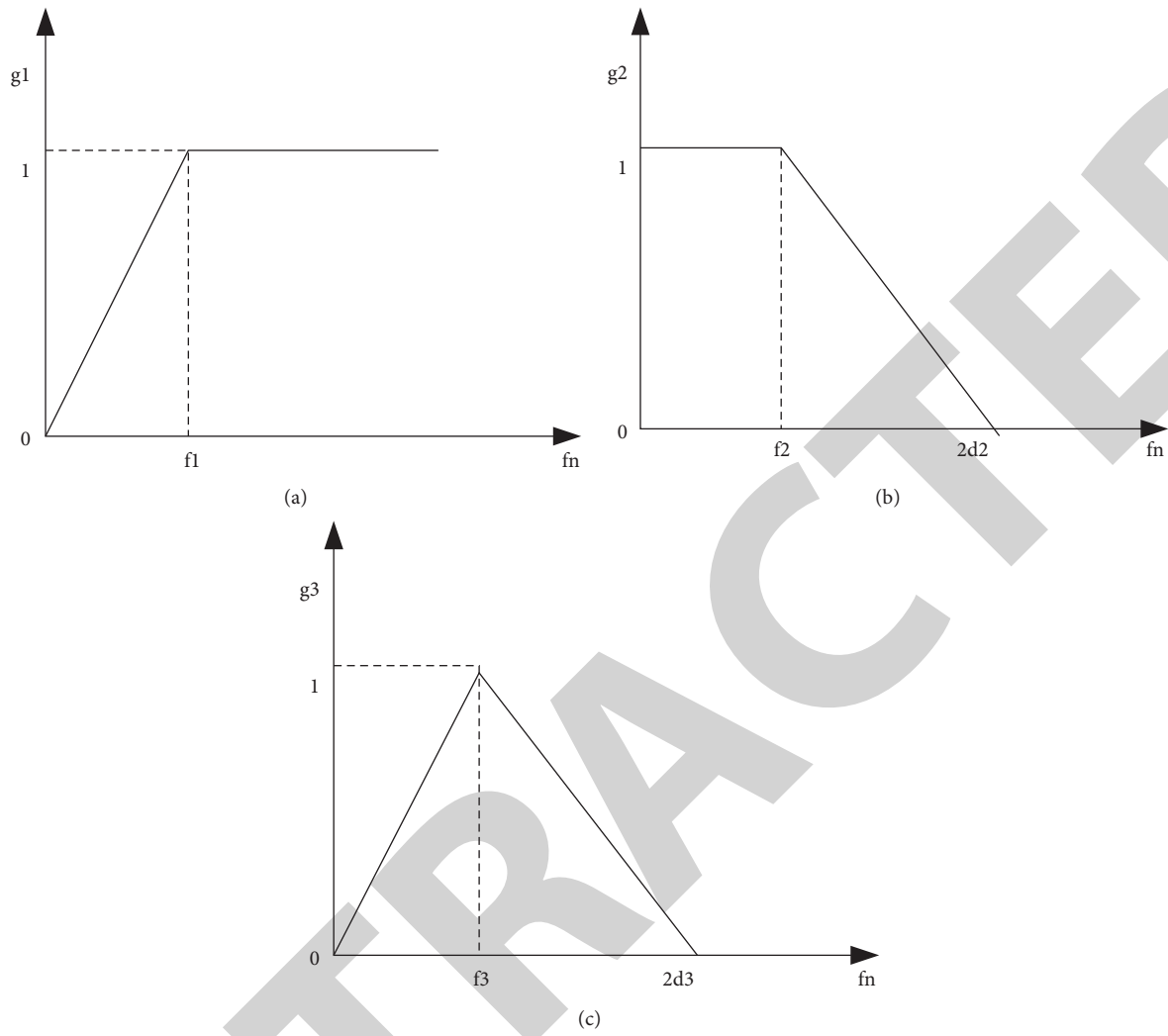


FIGURE 3: Basic functional form of whitening weight function. (a) Upper measure whitening weight function, (b) lower bound measure whitening weight function, (c) moderate measure whitening weight function.

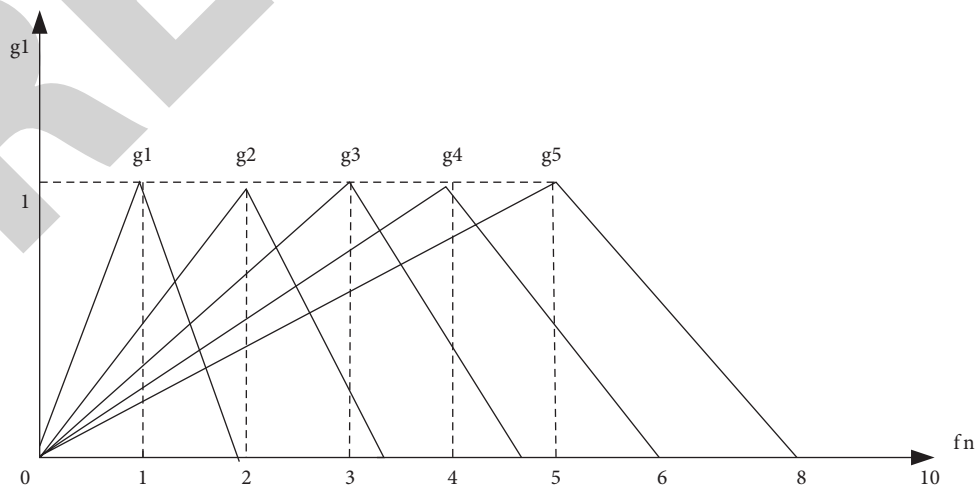


FIGURE 4: Whitening weight function for risk evaluation of financial investment projects.

As shown in Figure 6, 36% of companies reported that their operating conditions were worse than the previous year. The main reason is that the current small and medium-sized enterprises are facing an unprecedented survival dilemma, such as difficulty in financing, labor shortage, and high cost, which continue to squeeze the living space of small and medium-sized enterprises. 57.3% of enterprises will expand capital investment in the next year. At the same time, 27.3% of corporate decision makers indicated that they would not expand capital and equipment investment. This shows that the survival status of each enterprise basically belongs to a state of vigorous and upward development.

3.3. Quantitative Digital Model of Financial Investment Risk Management System Evaluation. Timely and accurate evaluation of the risk level of financial investment projects is of great significance to the management and implementation of financial investment projects. A quantitative evaluation result is more conducive to the sponsors of financial investment projects to make scientific decisions. It takes reasonable risk aversion measures to raise the funds needed for the project construction. This chapter comprehensively applies the theory of financial investment risk management system. It builds the GARCH digital model for risk assessment of financial investment items and applies it.

3.3.1. Data Extraction. This paper selects the daily closing price of copper and aluminum as the research object. In the calculation process, the GARCH formula will be widely used for auxiliary calculation. The market return takes the form of logarithmic daily return, which is defined as

$$T_{O,Y} = \ln(Q_{O,Y-1}), \quad L = 1, 2, 3. \quad (5)$$

$T_{O,Y}$ represents the yield on day Y in the L -th market, and $Q_{O,Y}$ represents the price on the Y -day in the L market. The yield sequence chart of the three markets is shown in Figure 7. It can be seen that there are volatility agglomeration and explosiveness in all of them, and it can be considered that the two return sequences are random.

3.3.2. Parameter Estimation. The estimated results of the three-variable DCC model are as follows.

When $L = 1, 2, 3$, and $S_{LK}, N_{LK} (L \neq K)$ in the variance formula is obviously not equal to 0, it means that the market $K(L)$ has volatility overflow to the market $L(K)$. Then the mean formula can be obtained as

$$\begin{aligned} T_{1,Y} &= 0.000226 - 0.03978^* T_{1,Y-1} \\ &\quad - 0.013515 T_{L,Y-1} + \varphi_{1,Y}, \\ T_{2,Y} &= -0.000313 + \delta_{2,Y}, \\ T_{3,Y} &= -0.000166 + \sigma_{3,Y}, \\ \begin{pmatrix} J_{11,Y} \\ J_{22,Y} \\ J_{33,Y} \end{pmatrix} &= \begin{pmatrix} 0.00000638 \\ 0.00000055 \\ 0.00000027 \end{pmatrix} \\ &\quad + \begin{pmatrix} 0.096578 & -0.066408^* & 0.118344 \\ -0.004912 & 0.040377^{***} & 0.045218 \\ -0.000298 & -0.01514^{***} & -0.010334 \end{pmatrix} \begin{pmatrix} \beta_{1,Y-1}^2 \\ \beta_{2,Y-1}^2 \\ \beta_{3,Y-1}^2 \end{pmatrix}. \end{aligned} \quad (6)$$

Variance formula:

$$\begin{pmatrix} 0.883276^{***} & 0.052306 & -0.290724 \\ 0.027268 & 0.898716^{***} & -0.331348^{**} \\ -0.014273^* & 0.081532^{***} & 1.0461216^{***} \end{pmatrix} \begin{pmatrix} J_{11,Y-1} \\ J_{22,Y-1} \\ J_{33,Y-1} \end{pmatrix}, \quad (7)$$

$$\begin{aligned} W_Y = (W_{OK,Y}) &= (1 - 0.0074 - 0.7564)\theta \\ &\quad + 0.0074\gamma_{Y-1}\gamma_{Y-1} + 0.7564W_{Y-1}, \end{aligned}$$

* means obvious at 10%; ** means obvious at 5%; *** means obvious at 1%. According to the variance formula, we can see that the change of the LME aluminum residual series in the previous period will affect the variance fluctuation of the LME copper and the dollar. According to an OVA, there is a two-way volatility spillover effect between LME aluminum and USD index. The price fluctuations of LME copper and LME aluminum will affect the price fluctuations of the US dollar index, and the price fluctuations of LME copper are not significantly affected by the US dollar index.

3.3.3. The Dynamic Correlation of the Three. According to Figure 8, it can be seen that there is a high positive correlation between LME copper and LME aluminum, and the correlation coefficient is mainly concentrated between [0.69 0.71]. There is a negative correlation between LME copper and LME aluminum and the US dollar index, respectively, and the correlation interval is concentrated between [-0.40 -0.35]. Their correlations with each other were significantly strengthened during the financial crisis.

3.3.4. Parameter Estimation Results. The parameter estimation of the three-variable BEKK model is based on the assumption that the residuals follow the Student Y distribution, and it is done with the help of external software. The algorithm is the BHHH algorithm. The estimated results are as follows:

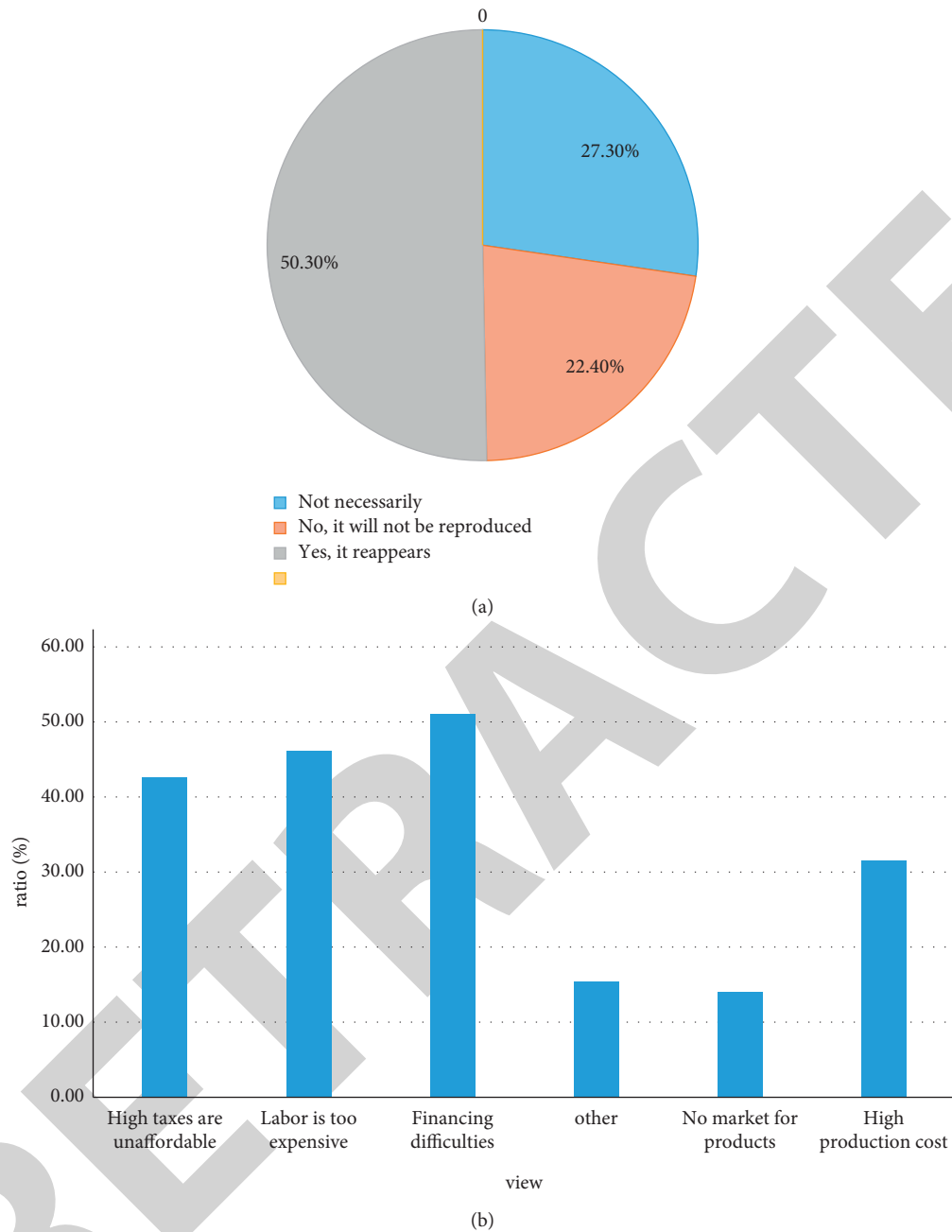


FIGURE 5: Part 1 survey results: (a) views on whether a new round of financial crisis will recur, (b) views on the greatest difficulties the business is currently facing.

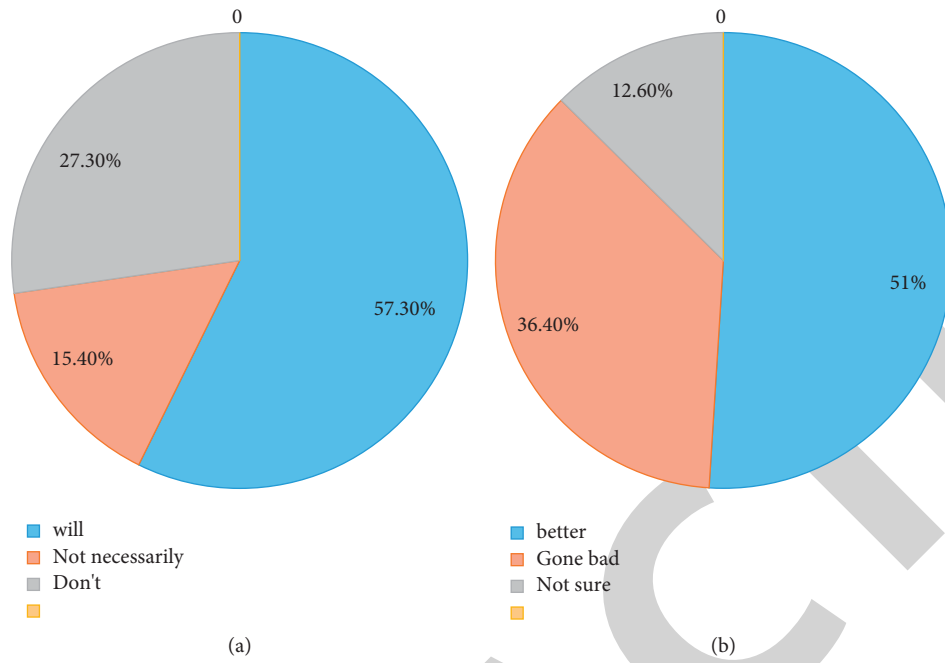


FIGURE 6: Part 2 survey results: (a) opinions on whether the company will expand capital and equipment investment in the next year, (b) views on how the current overall operation of the enterprise has changed compared to the previous year.

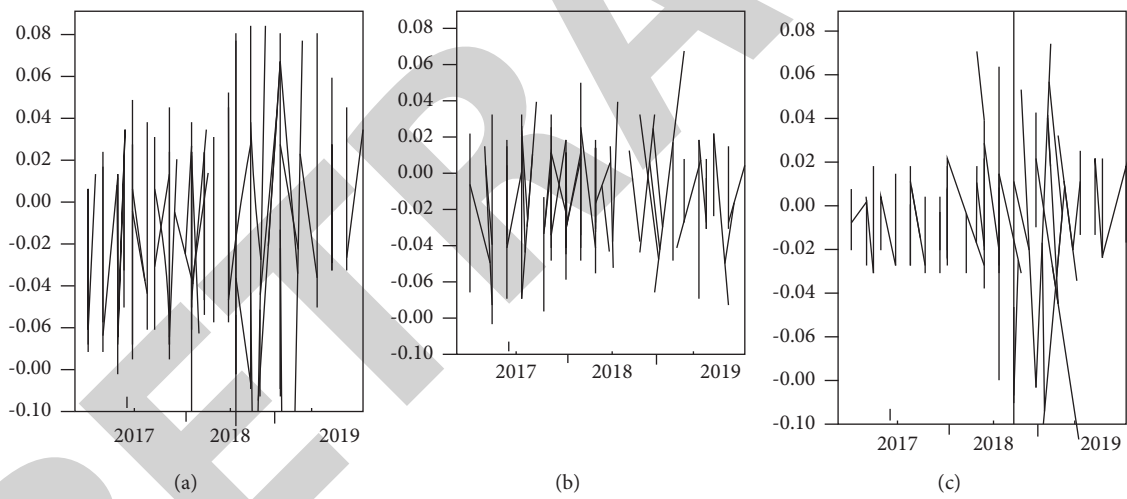


FIGURE 7: The yield sequence diagram of the three: (a) LME copper, (b) LME aluminum, (c) US dollar index UDI.

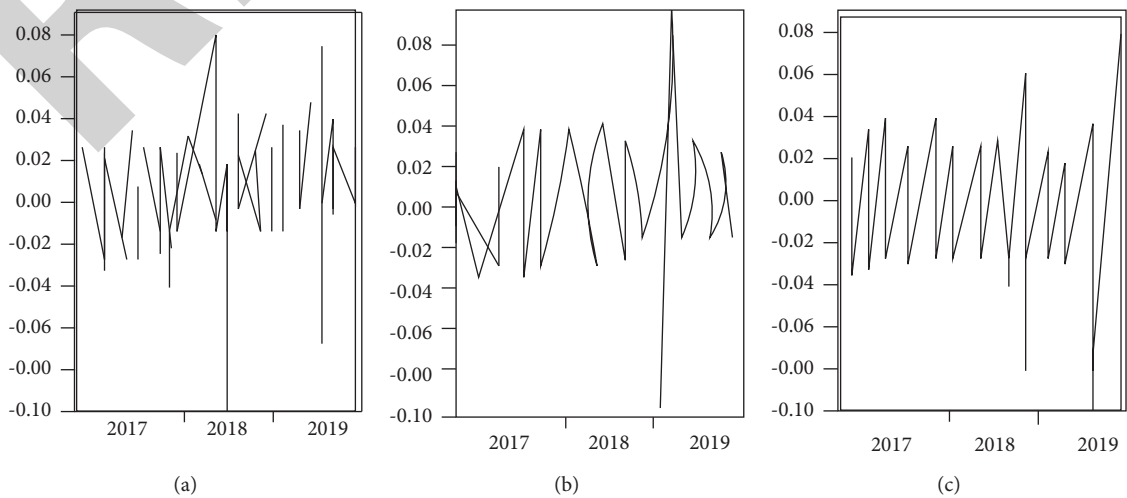


FIGURE 8: Dynamic correlation coefficient diagram under DCC model: (a) LEM Cu and LV dynamic correlation coefficient 12, (b) KME Cu and UDI dynamic correlation coefficient 12, (c) LME LV and UDI dynamic correlation coefficient 12.

Mean formula:

$$\begin{aligned} T_{1,Y} &= 0.00065 - 0.03635T_{1,Y-1} - 0.01267T_{1,Y-3} + \varepsilon_{1,Y}, \\ T_{2,Y} &= -0.00006894 + \varepsilon_{2,Y}, \\ T_{3,Y} &= -0.00023116 + \varepsilon_{3,Y}. \end{aligned} \tag{8}$$

Variance formula coefficient matrix estimates

$$\begin{aligned} V &= \begin{pmatrix} 0.003143^{***} & 0 & 0 \\ 0.00087 & 0.00128^{***} & 0 \\ -0.000014 & -0.00013 & 0 \end{pmatrix}, \\ S &= \begin{pmatrix} 0.298431^{***} & 0.006082 & -0.012908 \\ -0.0837498 & 0.1102728^{***} & -0.014008 \\ 0.351747^{**} & 0.143898 & 0.1497217^{***} \end{pmatrix}, \\ N &= \begin{pmatrix} 0.950187^{***} & 0.011703 & 0.0064179 \\ -0.0029019 & 0.9694506^{***} & 0.0016893 \\ -0.1274555^{***} & -0.0636107^{***} & 0.9928174^{***} \end{pmatrix}, \end{aligned} \tag{9}$$

* means obvious at 10%; ** is significant at 5%; *** is significant at 1%; when $S_{LK}, S_{LK} (l \neq k)$ is obviously not equal to zero in the variance formula, it means that market K(L) has volatility overflow to market L(K).

3.3.5. *VaR Prediction and Effect Evaluation Based on Multivariate GARCH Model.* As shown in Figure 9, it can be seen from the dynamic combined weight map under the two models that the two models are basically not very different. But UDI and UDL obviously have the highest weight values, both floating around 0.8.

It can be known from the above that a comprehensive market risk evaluation of multiple financial assets can be realized through the multivariate GARCH family model. At the same time, it is also possible to evaluate the market risk of one of the assets. The key difference between this evaluation and the univariate GARCH family model is that the multivariate GARCH family model can introduce the shock of exogenous variables or the previous fluctuations of exogenous variables into the financial asset under study. It reflects the indirect impact of the shock of the exogenous variable innovation on it and the degree of the indirect impact of the fluctuation of the exogenous variable. For example, the variance formula for the conditional variance J of LME copper at time Y in the three-variable BEKK model is as follows:

$$IN(J_{11,Y}) = \omega + \alpha \left[\frac{\vartheta - L}{\sigma - L} \right] + \gamma \left[\left[\frac{\vartheta - L}{\sigma - L} \right] - \mu \right] + \beta J_{11,Y}. \tag{10}$$

3.3.6. *VaR Evaluation of LME Copper under Different Models.* Confidence levels of 90%, 95%, and 99% are selected accordingly and then compared with the actual portfolio returns. The specific situation is shown in Figure 10. It can be seen that the higher the confidence level is,

the greater the absolute value of dynamic risk is, and the less the portfolio return exceeds the risk value, that is to say, the lower the failure rate of evaluation is. These models are suitable for evaluating VaR of financial investment risk.

On the whole, these models are more suitable for evaluating financial investment risk. Considering the obtained data, the evaluation effect of EGARCH-T is the best in general, the evaluation effect of DCC-T model is second, and the evaluation effect of EGARCH-N is the worst. In the process of evaluating financial investment risks, the models we have established show that the evaluation results of the models cover actual losses. It is too small for the partial value compared with it, indicating that the estimated result is too conservative. In addition to the EGARCH-N model, the established model is more accurate in evaluating financial investment risk at the 90% confidence level. It is relatively close to the given significance level. This shows that the use of digital models to study the evaluation of financial investment risk management systems can indeed make the evaluation results closer to the actual risk evaluation and improve the accuracy of investment.

4. Discussion

This paper is devoted to researching and designing a mathematical model for quantitative analysis of financial investment risk management system evaluation. This paper applies it to the complex analysis and treatment of investment risks in LME copper and LME aluminum. It not only expands the application scope of digital models, but also is a new attempt to evaluate the complexity of financial investment risk management systems. Through qualitative analysis of LME copper and LME aluminum investment risks, digital models are mined as an important tool to study system complexity. It has a certain potential in the study of the complexity of financial markets. In addition, on the basis of in-depth research on many models in China, the most suitable model is selected in this paper, combined with the survey of enterprise survival status. Combined with the special environment in which the Chinese financial market is located, it makes the model suitable for the investment environment of the Chinese financial market. For the research on the evaluation of financial investment risk management system, this paper starts from the most basic introduction of financial investment risk, analyzes the evaluation system, and introduces a variety of digital models. It successfully combines the GARCH digital model and the financial investment risk management system evaluation and draws conclusions. In the stage of empirical analysis, the GARCH model is used to obtain effective chart data, and this paper analyzes the data in many aspects. The results show that the obtained results are in line with the actual situation.

Through the analysis of this case, it shows that the use of the financial investment risk management system to evaluate the quantitative analysis of the mathematical model is more effective than a single type of investment. Investors can use the model to assess risk. This can greatly reduce financial investment risks and make decisions on multiproject portfolios. In the specific practical investment portfolio

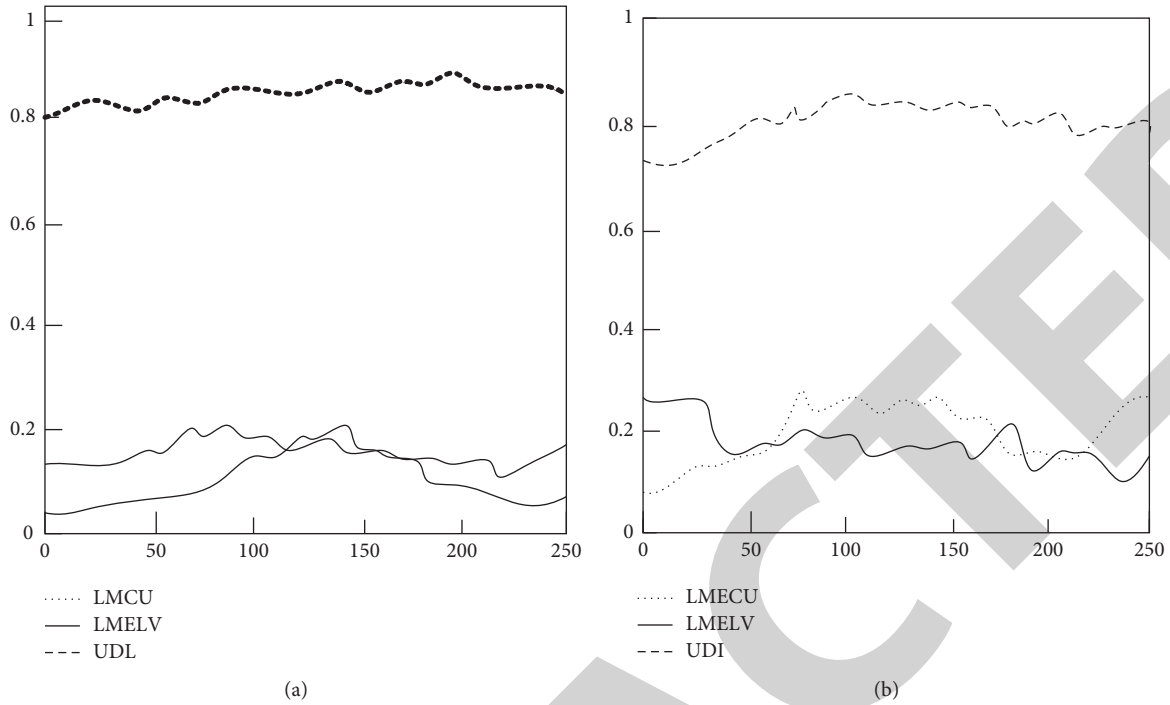


FIGURE 9: Dynamic combination weights graph: (a) dynamic combination weights under the DCC model; (b) dynamic combination weights under the BEKK model.

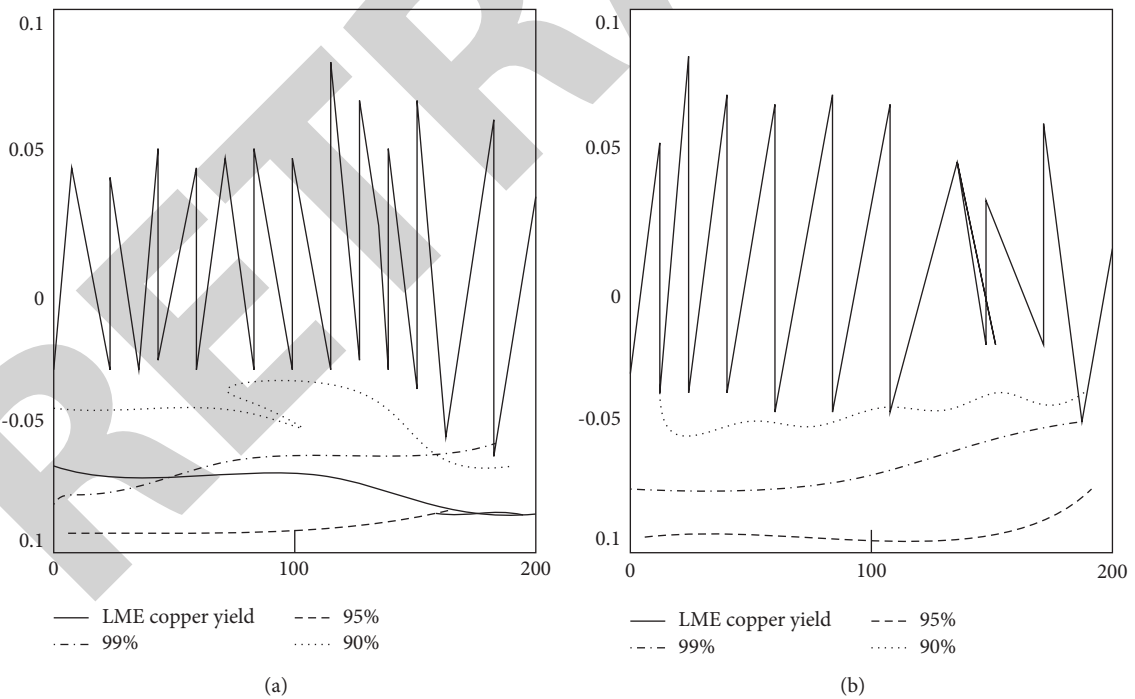


FIGURE 10: Continued.

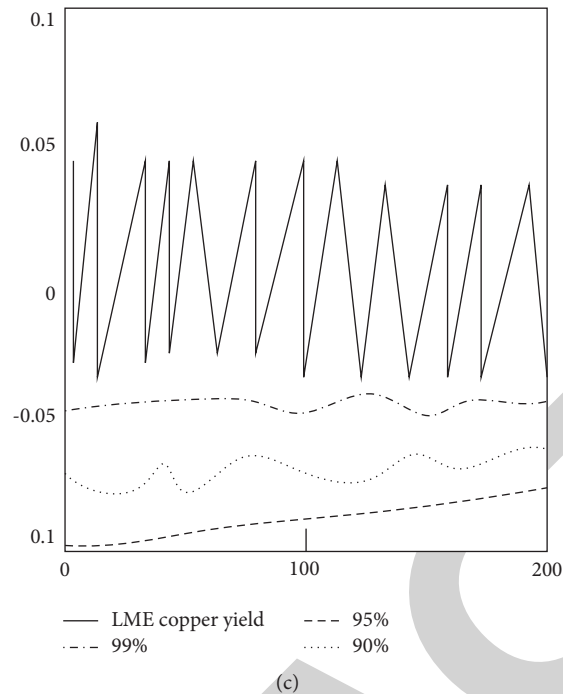


FIGURE 10: LME copper VaR at different levels of significance. (a) GARCH-N, (b) GARCH-T, (c) EGARCH-N.

decision-making, enterprises or investors expect to formulate different investment strategies according to their own risk preferences and investment goals and choose the risk value and return goals of the project reasonably and flexibly. It substitutes the risk and return target value into the investment portfolio decision for calculation and analysis, selects the optimal investment portfolio plan, and makes the most effective investment decision.

This paper takes LME copper and LME aluminum investment risks as a case study. First, through the investigation and qualitative analysis of enterprise investment risk status, the investment risk data is determined. And it uses the GARCH model to evaluate the investment portfolio according to the investor's risk level. Through the analysis of the data, it is concluded that the digital model applied in this paper is still very accurate for financial investment risk prediction. Through the analysis of the data, it is concluded that the GARCH model applied in this paper is very suitable for quantitative analysis of the evaluation of financial investment risk management system.

5. Conclusion

Through the case study, the important conclusions are drawn: In general, the quantitative analysis of the financial investment risk management system evaluation using the GARCH model is very close to the reality. This means that the model has a very high degree of accuracy in evaluating financial investment risks. However, this is not absolute. It does not rule out the arrival of a special period, and some financial investment risks may have extremely unstable factors, such as the research project in this case. This requires

investors to conduct more detailed research and quantitative analysis of the program. It can determine a more effective investment risk value. The project discussed in this paper is to use a digital model to conduct a quantitative analysis of the evaluation of financial investment risk management systems to determine the investment risk value. However, the selection of projects is relatively limited, and the realistic financial investment risk evaluation will often face more combination choices. And real investment should also be combined with a variety of irresistible factors for investment analysis; the analysis of investment risk will have greater value. Of course it will also be more difficult. But it is undeniable that, with the progress of society and the rapid development of the financial world, there are more and more studies related to text topics. There can also be better solutions to the problem of financial investment risk assessment. The future of the financial industry is still promising. At the same time, we also believe that the risk factors considered in the study of financial investment risk evaluation by the digital model will be more comprehensive and specific, and more detailed issues that have not been considered in this article can also be taken into account, making this financial investment risk management system more scientific.

Data Availability

No data were used to support this study.

Conflicts of Interest

The authors declare that there are no conflicts of interest in the paper.

Research Article

A Semantic Model of Internet of Things for Intelligent Translation and Learning

Nan Wei 

Henan Polytechnic Institute, Nanyang, Henan 473000, China

Correspondence should be addressed to Nan Wei; 2008050@hnpi.edu.cn

Received 14 April 2022; Accepted 13 May 2022; Published 8 June 2022

Academic Editor: Xuefeng Shao

Copyright © 2022 Nan Wei. This is an open access article distributed under the Creative Commons Attribution License, which permits unrestricted use, distribution, and reproduction in any medium, provided the original work is properly cited.

There were a lot of multisource data and heterogeneous devices in the intelligent system of the Internet of things, and the existing methods were difficult to meet the service needs of users for intelligent entities. Therefore, this paper proposed a semantic model construction method of the Internet of things based on intelligent translation and learning. Firstly, on the basis of summarizing the relevant theories of semantic Internet of things, this paper analyzed the semantic data and its characteristics, and expounded the common ontology matching methods. Secondly, according to the characteristics of service ontology and user ontology in intelligent Internet of things system, a method of matching two different ontologies based on string and semantic relationship was proposed, and the cyclic neural network method was used to organically integrate the semantic data of ontology. Finally, in order to realize the perception and representation of the context information of the Internet of things, a semantic model of the Internet of things based on intelligent translation and learning was constructed. Through experimental comparative analysis, the results showed that compared with the traditional methods based on semantic similarity and semantic distance, the semantic model of the Internet of things proposed in this paper had better performance in accuracy and recall, and can achieve better application effect of the Internet of things system. The model proposed in this paper will provide a theoretical reference for further exploring the sharing and service of heterogeneous devices and data in the intelligent Internet of things system.

1. Introduction

As the application extension of the Internet, the Internet of things is a product driven by a variety of technologies such as computer and communication. Internet of things is a network that connects various sensing devices and intelligent objects through the Internet. It uses intelligent devices to perceive the objective world and realize the interconnection of different objects. The nodes of the Internet of things use the data perception method to identify the physical world, use the network to establish the information transmission channel, and realize the interactive operation between people and things through the calculation and processing of a large amount of data, so as to effectively control and manage the objective world [1]. With the continuous development of electronic and communication technology, intelligent application system based on Internet of things has also developed rapidly. However, due to the multisource and

heterogeneity of data perception of intelligent devices related to the Internet of things, there are many problems in information interaction, logical reasoning, and knowledge representation of different intelligent platforms, which affect the normal use of the intelligent system of the Internet of things. For example, in the smart home IOT system, not only there are multisource data generated by indoor lighting, television, light intensity sensors, temperature sensors, and other equipment, but also they are related to relevant IOT systems such as intelligent medical system, intelligent security system, and intelligent power system. These different systems also have differences in equipment connection mode, data transmission format, and so on. Therefore, in view of the heterogeneity and multisource of data perception of the Internet of things, how to interconnect and integrate different data has attracted extensive attention of relevant scholars [2].

Different from other networks, the application of Internet of things system involves many fields and requires

different types of intelligent equipment. In addition to general sensors, it also includes intelligent instruments, intelligent appliances, and machinery [3]. In the Internet of things system, not only new nodes can be added at any time, but also new data types or protocols that need to be processed or supported by the system can appear at any time. Therefore, the Internet of things is a dynamic system. In addition, the Internet of things system is limited by space-time and other conditions, in which the impact of intelligent devices on the system is diverse and complex, which adds difficulties to the semantic modeling of the Internet of things system [4]. Although properly adding semantic information to the Internet of things system can solve the problem of data heterogeneity, it cannot solve the problems of interaction mode and behavior response of intelligent objects. In order to realize the semantic interoperability and data interaction between heterogeneous systems of the Internet of things, this paper proposed a semantic model construction method of the Internet of things based on intelligent translation and learning. By summarizing the data characteristics and semantic collaboration methods of semantic Internet of things, this paper used ontology matching technology to describe the semantics of intelligent devices and interaction behavior, and constructed the semantic translation and learning model of Internet of things by using cyclic neural network method. This paper will provide theoretical support for the realization of intelligent interaction and operation of Internet of things.

2. Related Works

In order to solve the problem of interoperability and collaboration between heterogeneous devices and cross systems in the application field of Internet of things, some researchers propose to realize semantic unification between heterogeneous devices through sharing environment and service components based on semantic web and agent technology, which provides a foundation for the development of semantic Internet of things [5]. Subsequently, some people proposed to use a different middleware to provide adaptive processing systems for the Internet of things environment. By classifying and labeling the intelligent devices of the Internet of things, the operating components are connected with network services, users, and objects, so as to solve the problems of heterogeneous information and sharing and reuse of intelligent devices [6]. Aiming at the diversity and dynamics of Internet of things data types, some people put forward semantic technology based on machine recognition and expression, and apply it to the description of intelligent devices, data sharing, and knowledge reasoning, which provides a theoretical basis for further research on semantic annotation and semantic understanding based on Internet of things ontology.

In the field of artificial intelligence, the introduction of ontology concept is mainly used for knowledge representation and knowledge organization [7]. With the continuous application and development of the Internet of things, the meaning of the concept of ontology and its elements have also changed. In the application field of Internet of things,

the relationship between entity objects is mainly described by ontology. Therefore, the description of object concepts and their relationships in different application fields can be transformed into the same or similar ontology, so as to provide semantic basis for the interaction between heterogeneous devices and things. Establishing the corresponding ontology model according to different Internet of things application systems is very important to realize the data perception, semantic association, and fusion of Internet of things [8]. Although different Internet of things application systems have differences in the construction of ontology model, there may be a certain degree of data and semantic relevance between different systems. Therefore, its universality and matching should be considered when constructing the Internet of things ontology model.

Because the ontology model of Internet of things is usually related to the application field, these ontologies not only are limited to describing the concepts in this field, but also need to redefine the existing ontology model when adding new concepts, so the scalability of ontology is poor. In addition, when an Internet of things application system needs to add new relationships between concepts, it needs to traverse the existing element relationships in all ontologies, which undoubtedly increases the additional time overhead [9]. Although the use of semantic technology can enable the application system to publish a large amount of domain-related information through the semantic web, due to the data transmitted to the Internet from different devices or systems, and the lack of semantic relevance between a large amount of data, the machine cannot achieve the expected effect when interpreting and responding to the data.

In recent years, some scholars have proposed a semantic interaction model based on ontology technology, which provides a basis for entity interaction between different systems or heterogeneous devices [10]. Because the model includes the association relationship between service entities in the ontology, it can meet the actual needs of users by semantic annotation and knowledge reasoning, so as to avoid the impact of multisource data or heterogeneous devices on semantic interaction. Semantic interaction includes not only the interaction between intelligent devices or entities in the Internet of things, but also the interaction process between users and intelligent entities [11]. Using ontology theory and semantic technology to study the interaction between users and intelligent entities not only needs to identify the actual needs of users from a large number of perceptual data, but also needs to establish a common interaction channel between different users and intelligent devices, so as to effectively provide users with the required services.

3. Semantic Technology Foundation of Internet of Things

3.1. Semantic Internet of Things. With the rapid development of Internet of things technology and its application, various devices related to Internet of things are gradually increasing, and the perception and control requirements for Internet of things devices are also gradually improving. Due to the

heterogeneity of different devices, the access and use of Internet of things resources are not ideal. The semantic technology based on machine recognition solves the resource description, data sharing, and information integration of Internet of things [12]. Using semantic technology in the Internet of things and making full use of the characteristics of semantic knowledge representation and data sharing to build the semantic Internet of things can provide a technical basis for the interaction of Internet of things resources.

As a method or model to solve the internal contradiction of the Internet of things, semantic Internet of things mainly constructs an intelligent service system that can cooperate with each other on the basis of the existing Internet of things, Internet, and communication network from the perspective of the interactive relationship between the elements constituting the information ecosystem. Semantic Internet of things effectively integrates different software and hardware resources and systems, organizes various heterogeneous objects, and realizes the intelligent interaction between people and things through semantic collaboration.

Semantic Internet of things integrates the relevant functions of semantic web, wireless sensor network, and Internet. Semantic technology is applied to the Internet of things. Through semantic annotation of the information of Internet of things devices, people, things, and devices in the Internet of things can have a unified recognition language [13]. Through the devices in the Internet of things and the semantic method based on ontology, we can accurately find the information on the network and make further reasoning on the information according to the existing knowledge, so as to effectively realize the network intelligence. As shown in Figure 1, the relationship between semantic Internet of things, wireless sensor network, Internet, and Internet of things is described.

Although the traditional Internet of things has the characteristics of openness and flexibility, due to the diversity of information forms of Internet of things devices and the inconsistent understanding and description of information by different users and devices, the resulting information diversity makes the data analysis inaccurate and then affects the application effect of Internet of things.

3.2. Semantic Data and Features. Semantic data are stored in ontology, which is not only the premise of the realization of semantic Internet of things, but also the condition of information sharing and exchange on the Internet [14]. Semantic Internet of things has the basic functions of semantic web and Internet of things at the same time. As shown in Figure 2, it is a schematic diagram of the working process of semantic Internet of things.

The article information provided by the producer needs to be standardized through coding, and then, the encoded information is saved in the electronic label. Then, the intelligent device and decoder are used to extract the target information. Because the information of objects is an ontology marked with semantics, it provides information for sharers and completes further reasoning through ontology

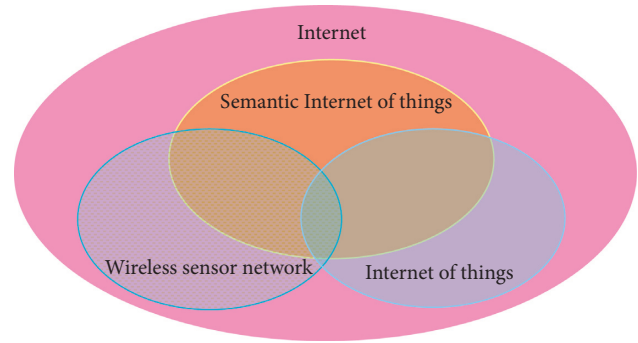


FIGURE 1: Relationship between semantic Internet of things and other different networks.

and partial order relationship. At the same time, the information of the extracted object is released to the Internet through the machine reading device, and the information of the object can be shared.

From the working process of semantic Internet of things, ontology not only is a form of semantic annotation of the information of things, but also can provide specific information of things for sharers through partial order relationship. Therefore, ontology is very important in semantic Internet of things [15]. As shown in Figure 3, it reflects the role of ontology in different application scenarios.

As a knowledge base, ontology uses semantic annotation to reflect the things and their relationship in different fields. By combining the specific field characteristics, it can establish the corresponding knowledge system for the field. In recent years, ontology technology has been well applied to the Internet of things, e-commerce, and other related fields. Using ontology technology can effectively solve the heterogeneity problem in different Internet of things applications. As shown in Figure 3, due to the different regions and application fields of smart city and smart medical, the data provided by the two Internet of things platforms cannot be directly used for the development of remote service applications.

Ontology mainly includes objects, instances, relationships, attributes, and other related elements. Among them, the object is mainly used to describe something, and the object can contain one or more sub-objects to describe a specific thing. Examples are mainly used to describe the specific things contained in a certain class of objects. Relationship is used to represent the ownership relationship between things and attributes [16]. Property is used to describe the properties of objects and sub-objects.

In order to facilitate the description of things and their internal relations in ontology, directed graph can be used to describe the relationship between various elements of ontology. As shown in Figure 4, an example of an ontology is reflected through a directed graph.

3.3. Intelligent Application and Semantic Collaboration of Internet of Things. The intelligent application platform established by the Internet of things is usually a system of human-computer interaction and cooperation. The system

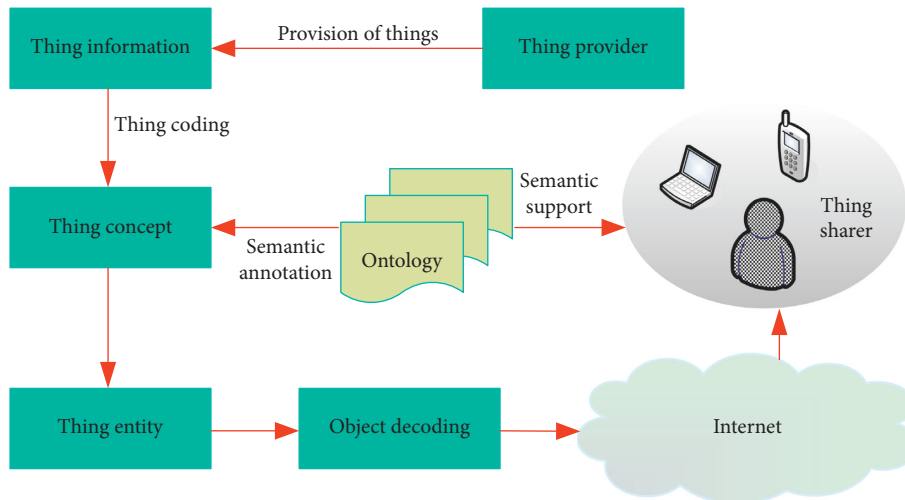


FIGURE 2: Schematic diagram of the working process of semantic Internet of things.

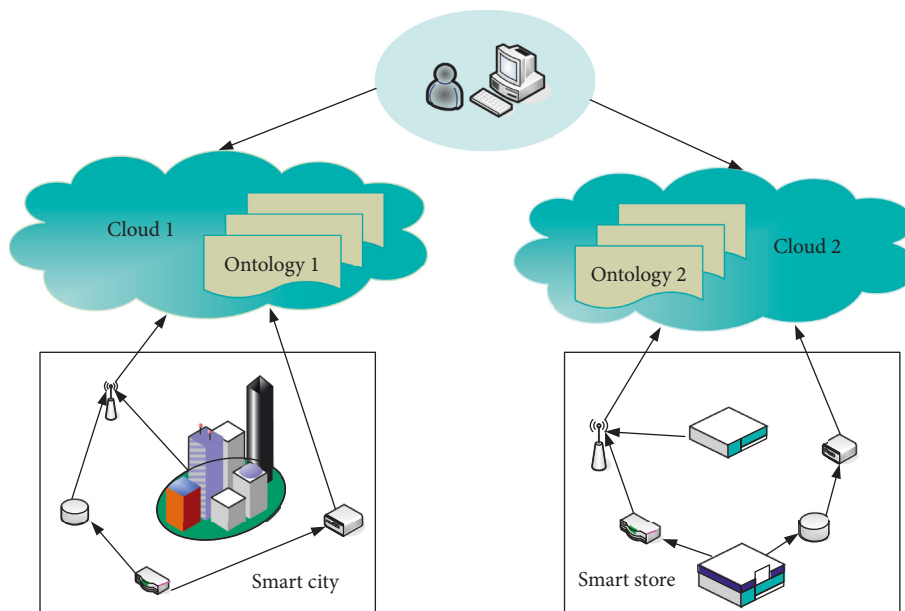
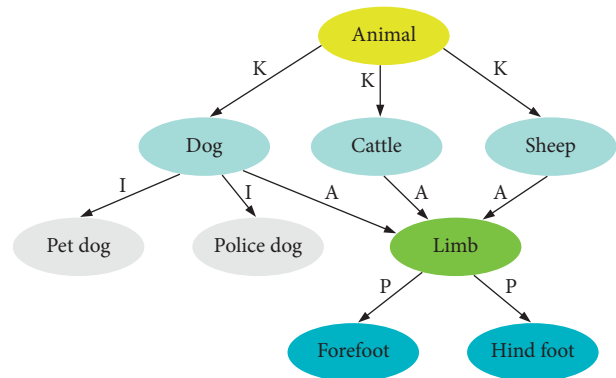


FIGURE 3: The role of ontology in different application scenarios.

organizes a large number of sensors, embedded computers, and information devices into a network structure through universal network in order to meet different application requirements [17]. As shown in Figure 5, it is a schematic diagram of intelligent application mesh space established based on the Internet of things.

Users can use various intelligent terminal devices to interact with the intelligent application platform, so as to meet the specific needs of users. By automatically monitoring the dynamic information about intelligent devices, the intelligent application platform can not only provide various control and management functions for different users, but also put forward effective countermeasures for events in the intelligent system [18]. Because the intelligent application system has good dynamics, the user's terminal equipment can interoperate with the intelligent system at any time. Due to the deployment of a large number of



K: kind of
 P: part of
 A: attribute of
 I: instance of

FIGURE 4: Directed graph representation example of ontology.

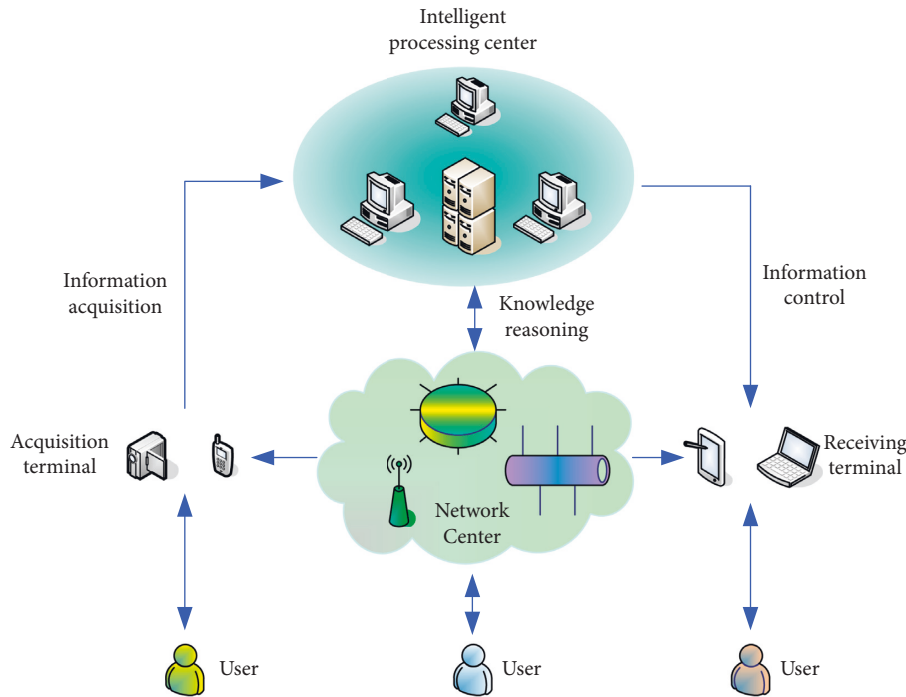


FIGURE 5: Architecture diagram of intelligent Internet of things application platform.

wireless sensors in the intelligent application system, it can process the information perceived by users in real time and feed back the processing results to users in time.

Because the intelligent application platform integrates a variety of devices and network systems, it not only has a large amount of data computing tasks and heavy work of digital fusion processing, but also affects the cooperation between heterogeneous devices. Because different devices may adopt different operation standards, it is necessary to realize the collaborative work of different devices with the help of an interoperability framework, semantic web. Providing different devices with semantic information that is helpful for Internet understanding through semantic web can not only realize the automatic operation of tasks, but also avoid the shortcomings caused by manual operation.

In order to give full play to various service functions provided by intelligent application platform, semantic collaboration is usually adopted to solve the problem of heterogeneity between devices. Semantic collaboration mainly regulates the information interaction process between different entities in the Internet of things environment, so as to ensure the smooth realization of the Internet of things. Semantic collaboration realizes the information sharing between different things in the Internet of things by solving the problem of semantic heterogeneity. Semantic collaboration mainly uses semantic correlation analysis and semantic mapping to deal with semantic heterogeneity in the Internet of things [19]. On the basis of judging the correlation between heterogeneous semantics, semantic mapping is used to transform unrelated semantics, and a mapping relationship is established.

Because the heterogeneity of ontologies in different fields affects the service function of intelligent application

platform, it is necessary to standardize the processing of different ontologies through semantic collaboration. As a common method of semantic collaboration, ontology matching can effectively solve ontology heterogeneity, information sharing, and interoperability. Ontology matching mainly uses the semantic relationship between two different ontologies to find their matching elements, so as to obtain knowledge that can be shared by different entities.

Ontology matching can not only establish the corresponding relationship or semantic mapping between different ontology concepts, but also calculate the similarity between different ontologies. At present, common ontology matching methods include ontology methods based on morphology or semantics, and matching methods based on rules or statistics. Different matching methods have their own characteristics in practical application. We need to combine specific objects and adopt a variety of methods to realize ontology matching.

4. Semantic Model of Internet of Things Based on Intelligent Translation and Learning

4.1. Intelligent Translation Architecture. The common ontologies in intelligent application platform are various service ontologies and user ontologies. Due to the heterogeneity and mismatch of different ontologies, it is difficult for users to obtain the services provided by the intelligent system. In order to solve the problem of interoperability between heterogeneous devices in the Internet of things environment, it is necessary to match the user data with the data stored in the intelligent Internet of things system.

For different ontologies in the intelligent Internet of things system, in order to realize the interoperability between ontologies, it is necessary to match the user ontology and system ontology, so as to realize the interoperability between users and systems through intelligent translation. According to different matching objects, ontology matching can be divided into ontology element matching and ontology structure matching.

For two different ontologies, we need to compare the similarity of all elements in the two ontologies according to the synonyms of the two ontologies. If the similarity value range of two ontologies is 0–1, when the similarity of two elements is 1, it means that the two elements are exactly the same [20]. When comparing all elements of two ontologies, the comparison result can be expressed as matrix H based on similarity, which is shown as follows:

$$H = \begin{pmatrix} a_{11} & a_{12} & \cdots & a_{1n} \\ a_{21} & a_{22} & \cdots & a_{2n} \\ \vdots & \vdots & \vdots & \vdots \\ a_{m1} & a_{m2} & & a_{mn} \end{pmatrix}, \quad (1)$$

where H denotes a matrix with m rows and n columns. m is the number of elements contained in ontology 1, and n is the number of elements contained in ontology 2. The element value of matrix H represents the similarity based on fuzzy string comparison.

Semantic distance query method can realize semantic similarity matching. As shown in Figure 6, it shows the flowchart of matching two ontologies.

Ontology matching for strings is mainly to match all elements contained in different ontologies. It is mainly to compare the similarity of strings contained in ontologies, which has nothing to do with the semantic information of ontologies. This method mainly determines the similarity between two ontologies from the perspective of the similarity of two strings. If the similarity of two strings reaches a certain value, it can be considered that the two strings are similar.

In string-based ontology matching, the similarity of two ontologies can be calculated by editing times similarity method. The number of edits is the minimum number of edits required to convert one string to another [21]. For example, when editing a string, you can convert one string to another by replacing, inserting, or deleting it. The calculation formula of editing times similarity is as follows:

$$SIM_t(e_1, e_2) = 1 - \frac{\text{times}(e_1, e_2)}{\max(|e_1|, |e_2|)}, \quad (2)$$

where SIM_t represents the editing times similarity between the two ontologies, and e_1 and e_2 are strings in two ontologies, respectively. $\text{times}(e_1, e_2)$ is the number of edits of two strings. $\max(|e_1|, |e_2|)$ is the maximum length of two strings.

String-based ontology matching is to match the ontology from the perspective of the font of ontology elements, without considering the semantic content between different ontologies. In order to match the similarity of different

ontologies from the semantic perspective of ontology elements, a matching method based on linguistics needs to be adopted. Therefore, the semantic similarity of different ontologies can be calculated with the help of WordNet. WordNet can use the semantic relationship of ontology to construct vocabulary. The semantic relationship of ontology mainly includes synonym relationship, upper and lower relationship, antonym relationship, part and whole relationship, etc.

WordNet organizes the semantic units of ontology in a tree way. Nodes refer to the collection of ontology units with the same semantics, and edges refer to the correlation between different nodes. As shown in Figure 7, the tree structure composed of different semantic units in the ontology described by WordNet is adopted.

The semantic similarity between two ontologies can be expressed by their distance in the tree. The calculation formula of semantic similarity of different ontologies is as follows:

$$SIM_s(e_1, e_2) = \frac{1}{2} \left(\frac{\text{Len}(s_1, s_2)}{\text{Len}(s_1, s_r)} + \frac{\text{Len}(s_1, s_f)}{\text{Len}(s_2, s_r)} \right), \quad (3)$$

where s_1 and $\text{Len}(s_1, s_2)$ represent the meanings of lexical units e_1 and e_2 in their respective ontologies, s_f is their parent node, and s_r is the root node of the tree. $\text{Len}(s_1, s_2)$ denotes their distance in the tree.

The distance calculation formula between semantic units of two ontologies is as follows:

$$\text{Len}(s_i, s_j) = \frac{1}{\sum_P \sum_{k=P_i}^{P_j} w_k}, \quad (4)$$

where s_i and s_j are ontology semantic units, w is the weight of semantic relationship between s_i and s_j , and P represents the path set from s_i to s_j , which contains all paths connecting s_i and s_j nodes. According to the above calculation formula, the semantic similarity between different ontologies is inversely proportional to the distance between them.

4.2. Semantic Learning Method Based on Cyclic Neural Network. Since the string after ontology matching is mainly a serialized information string, in order to obtain the complete information of ontology, these serialized data need to be further used for modeling to generate the required specific text information. The general neural network method is usually used to process a single input information. Because it is unable to distinguish the internal relationship between continuous input information, it is not suitable for processing sequential data. Therefore, the method of recurrent neural network (RNN) can be used to learn and train the serialized data and generate the corresponding text [14]. Because the memory and parameter sharing of RNN are very beneficial to the nonlinear feature learning and processing of sequence data, RNN is widely used in natural language processing fields such as machine translation and language modeling.

The hidden state of RNN model is mainly used to store information. Therefore, the model has a certain memory

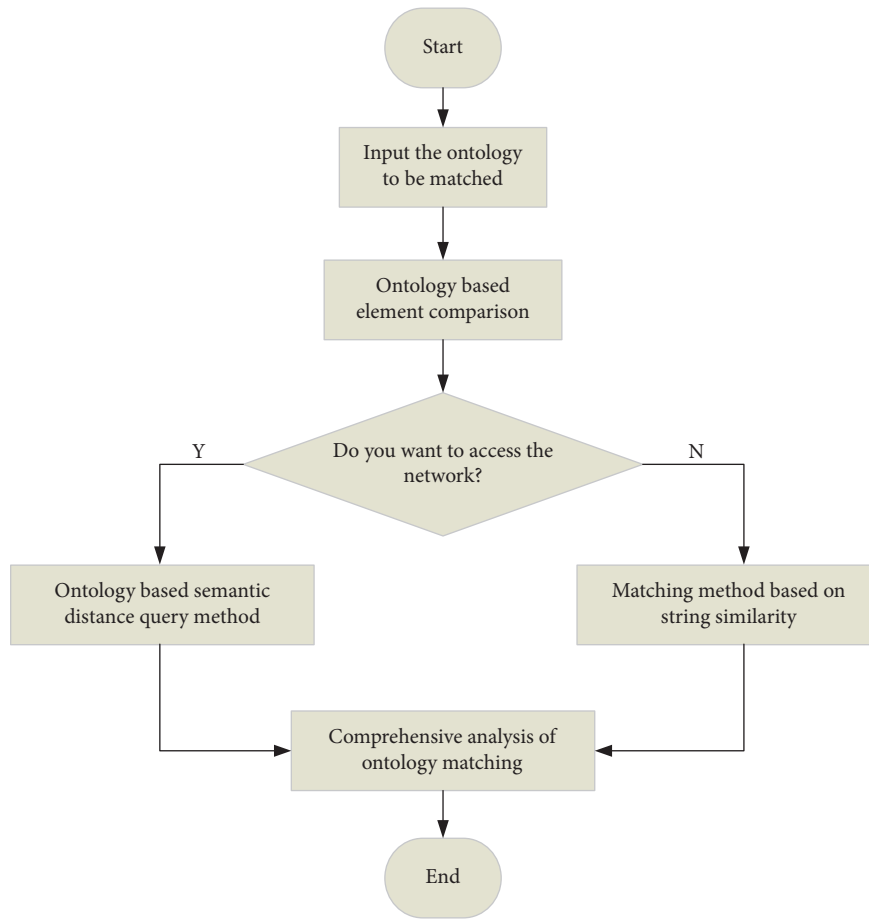


FIGURE 6: Schematic diagram of ontology matching process.

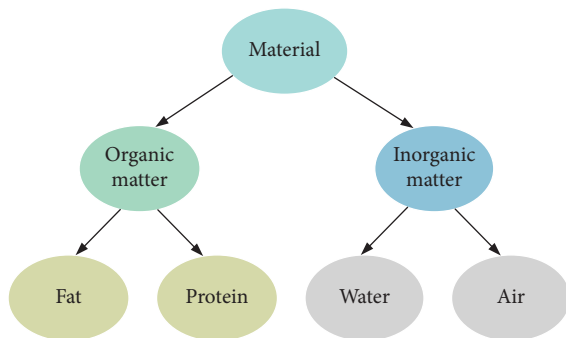


FIGURE 7: Tree structure of ontology elements based on WordNet.

function. The input object of RNN is usually a set of vector sequences, and the network model can use the last output value to generate the current output result. The model uses one input object at a time to generate an output result, which depends on the last data sequence.

As shown in Figure 8, the composition of the cyclic neural network model is shown. On the left is the unexpanded part of the RNN, and on the right is the successively expanded part of the RNN after processing the sequence input values.

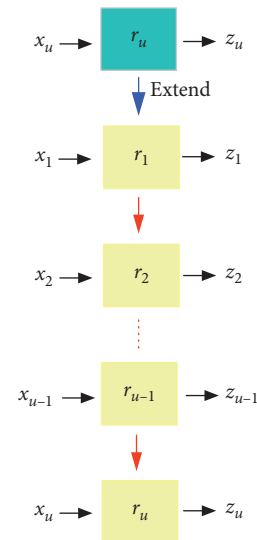


FIGURE 8: Composition diagram of cyclic neural network model.

In Figure 8, x_u represents the input part of the model, r_u is the hidden layer, and z_u is the output result of the model. The above relationship can be expressed as follows:

$$\begin{aligned} r_u &= g(r_{u-1}, x_u), \\ r_u &= g(W_{xr}x_u + W_{rr}r_{u-1} + c), \end{aligned} \quad (5)$$

where W is the weight matrix and c is the offset coefficient. The output result can be expressed by the following formula:

$$z_u = f(W_0r_u + c_0). \quad (6)$$

According to Figure 8 and the above calculation formula, the value of r_u is determined by r_{u-1} and x_u . r_{u-1} indicates that RNN has certain memory function, and its value is determined by r_{u-2} and x_{u-1} . Therefore, the value of r_u is determined by x_1, x_2, \dots, x_{u-1} ; that is, RNN memorizes the previously input sequence information. Since the result of RNN is output successively from left to right, and the weight matrix W_{rr} corresponding to each sequence information is unchanged, it can not only reduce the complexity of model parameters, but also remember the previous sequence information.

4.3. Semantic Model of Internet of Things. In order to realize the perception and representation of the context information of the Internet of things, this paper constructs a semantic model of the Internet of things based on intelligent translation and learning. As shown in Figure 9, it shows the construction process of the semantic model of the Internet of things.

Firstly, we need to collect data, extract the processing functions required by things or services, such as turning on the air conditioner, and closing doors and windows, and map them to the corresponding item layer. The processing functions of these different services can be combined and interacted with each other.

Then, several function sequences are created according to user needs and specific Internet of things application scenarios. Related semantic tags are included in functions, such as semantic text descriptions of functions. The specific interaction between different functions is determined by user requirements and service providers. In the context-aware layer of the Internet of things, a set of function sequences are composed of different functions.

For the semantic tags contained in the function sequence, the semantic measurement method can be used to establish the corresponding semantic relationship diagram. Because users need different services, the meanings of edges and weights in different semantic graphs are also different. Therefore, ontology semantic matching method needs to be used to integrate different types of semantic maps, so as to obtain the context map of the Internet of things. Through the learning and representation of the context map of the Internet of things, the interactive operation of users, things, and information can be realized, for example, various service recommendations and intelligent interactive process in Internet of things applications.

In order to objectively and accurately evaluate the text generated by the semantic model of the Internet of things, Bleu (bilingual evaluation understudy) can be used to effectively evaluate the fluency, accuracy, and coherence of the text content of the output result of the model.

Bleu is mainly used to evaluate the results of machine translation. High-quality machine translation usually

overlaps with the reference translation. When there are more similar parts with the reference translation, the greater the value obtained by Bleu. Therefore, the similarity between the generated text and the reference text of the semantic model of the Internet of things can be obtained according to the similar parts of the semantic model of the Internet of things. The calculation formula is as follows:

$$\begin{aligned} \text{Bleu} &= \eta \times \exp\left(\sum_{i=1}^M w_i \log p_i\right), \\ \eta &= \begin{cases} e^{(1-l_s/l_r)} & l_s \leq l_r, \\ 1 & l_s > l_r \end{cases}, \end{aligned} \quad (7)$$

where p_i represents the accuracy rate of the translated text, w_i is the weight of the corresponding text, M denotes the number of words, η is the penalty factor, l_s is the length of the translation generated by the model, and l_r is the length of the reference translation.

5. Experiment and Analysis

5.1. Experimental Design and Evaluation Index. In order to verify the semantic model of Internet of things based on intelligent translation and learning, this paper designs an application scenario of Internet of things. When the user enters a commodity intelligent purchase platform of the Internet of things application system, and the user uses the mobile terminal with knowledge intelligent processing module to send the commodity purchase service request to the purchase platform, the Internet of things application system will respond to the service request put forward by the user in time. Then, the real-time ontology matching and processing are carried out through the commodity intelligent purchase platform, and the commodity purchase results are fed back to users through the Internet of things equipment, so as to complete the whole interactive operation. The ontology of commodity purchase description in the ontology of Internet of things application system is adopted. Select 100 knowledge intelligent processing devices to represent the application devices in the commodity intelligent purchase platform. After sending the purchase service request to the knowledge intelligent processing equipment, the matching results of the purchase service are analyzed.

Experiments were carried out on the query and matching of 20 groups of commodity purchase services by grouping. The number of intelligent device services selected by each group was 10, 20, 30, 40, 50, 60, 70, 80, 90, 100 in turn. In order to facilitate the comparison with the model proposed in this paper, the ontology matching method based on semantic similarity and the ontology matching method based on WordNet semantic distance are used for comparative experiments. The experimental results obtained by different methods are counted, the precision and recall of each group of experiments are calculated, and then the different methods are evaluated and analyzed.

When evaluating the performance of the semantic model of the Internet of things based on intelligent translation and learning proposed in this paper, we first need to evaluate the

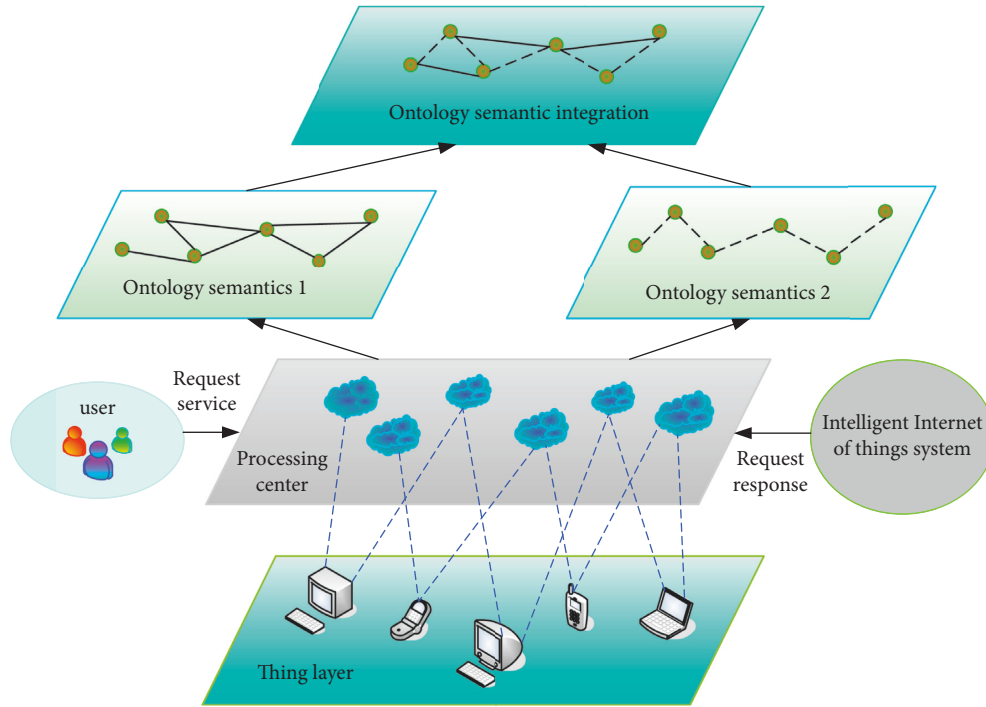


FIGURE 9: Workflow diagram of semantic model of Internet of things.

accuracy of the results of goods purchase services requested by users through the Internet of things application system, that is, the accuracy (ACC) [22]. The calculation formula is as follows:

$$ACC = \frac{C_q}{C_r} \times 100\%, \quad (8)$$

where C_r represents the result returned by the intelligent system of the Internet of things after service response to the user's demand and C_q denotes the requested service required by the user.

In addition, it is necessary to evaluate the integrity of the services provided by the Internet of things application system after the user makes a request, that is, the recall rate (REC). The calculation formula is as follows:

$$REC = \frac{C_1 \cup C_2 \cup \dots \cup C_{k-1} \cup C_k}{C_q} \times 100\%, \quad (9)$$

where $C = \{C_1, C_2, \dots, C_{k-1}, C_k\}$ represents the set of required results obtained by the intelligent system of the Internet of things after responding to the user's needs and C_q is the set of requests required by the user.

Through the accuracy and recall, we can evaluate the service results provided by the Internet of things application system and satisfy users. They can intuitively reflect the function and efficiency of the intelligent Internet of things service system.

6. Results and Analysis

Under the same conditions, different methods are adopted and the service request is sent to the intelligent system of the

Internet of things according to the user service request ontology, and then the service results are compared. In this paper, the following experimental statistical results are obtained by averaging 10 experiments. As shown in Figure 10, it shows the number of system return results obtained by different methods.

It can be seen from Figure 10 that the model proposed in this paper obtains fewer results than other methods when realizing ontology matching, which reduces the redundancy of the results. At the same time, more results are obtained than the traditional ontology matching method, which ensures the completeness of query results to a certain extent, so as to ensure that all results that meet the needs of users are obtained.

As shown in Figure 11, the comparison results of service precision obtained by different methods are shown.

According to the comparison results reflected in Figure 11, the service precision obtained by the ontology matching method based on semantic similarity is low, while the service precision obtained by the ontology matching method based on WordNet semantic distance is relatively high. The service precision obtained by this method is higher than that of other methods.

As shown in Figure 12, the comparison results of service recall obtained by different methods are shown.

According to the comparison results reflected in Figure 12, the recall rate obtained by using the ontology matching method based on semantic similarity is relatively low, while the recall rate obtained by using the ontology matching method based on WordNet semantic distance is similar to the method proposed in this paper and is significantly higher than that by using the ontology matching method based on semantic similarity. This shows that the

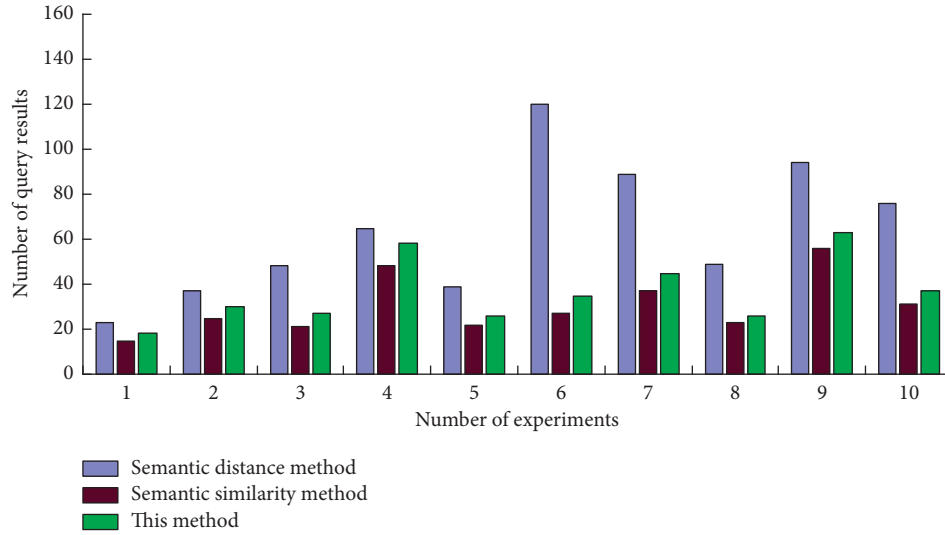


FIGURE 10: Number of query results obtained by different methods.

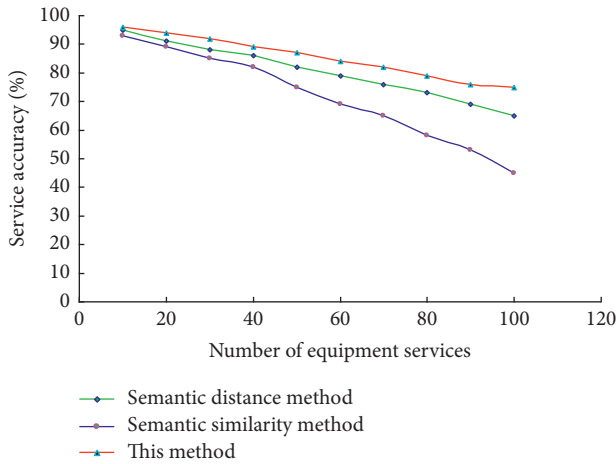


FIGURE 11: Comparison results of service accuracy obtained by different methods.

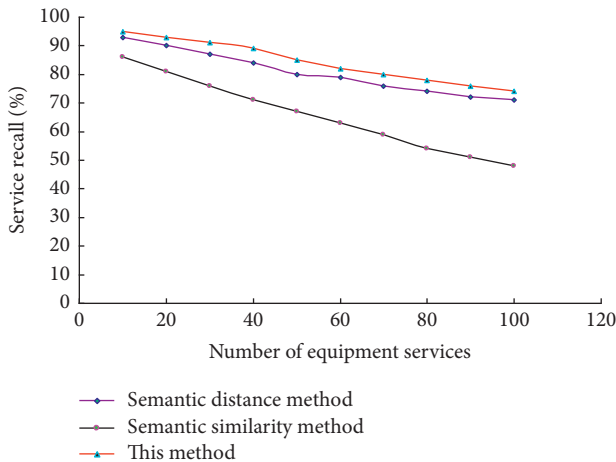


FIGURE 12: Comparison results of service recall rate obtained by different methods.

semantic model of Internet of things proposed in this paper can better meet the recall requirements of Internet of things intelligent system for user services.

7. Conclusion

Aiming at the problem that the existing methods were difficult to solve the semantic interoperability and data interaction between heterogeneous systems of the Internet of things, this paper proposed a semantic model of the Internet of things based on intelligent translation and learning. Based on the analysis of the theory of semantic Internet of things, this paper summarized the semantic data and its characteristics, as well as the common methods of semantic collaboration and ontology matching of Internet of things. According to the characteristics of service ontology and user ontology contained in the intelligent system of Internet of things, an ontology matching method based on string and semantic relationship was proposed. The organic integration of ontology semantic data information was realized through the cyclic neural network method, and a semantic model of Internet of things based on intelligent translation and learning was constructed to realize the perception and representation of the context information of Internet of things. The experimental results showed that the semantic model of the Internet of things proposed in this paper was better than the traditional ontology semantic matching method in accuracy and recall, and had achieved good system application results. This research can provide theoretical support and technical reference for the in-depth study of intelligent device interaction and multisource data sharing in the Internet of things.

Data Availability

The labeled dataset used to support the findings of this study is available from the corresponding author upon request.

Conflicts of Interest

The author declares that there are no conflicts of interest.

Acknowledgments

This study was supported by Henan Polytechnic Institute.

References

- [1] A. D. Wade and K. Wang, "The rise of the machines: artificial intelligence meets scholarly content," *Learned Publishing*, vol. 29, no. 3, pp. 201–205, 2016.
- [2] A. Shaban, F. Almasalha, and M. H. Qutqut, "Hybrid user action prediction system for automated home using association rules and ontology," *IET Wireless Sensor Systems*, vol. 9, no. 2, pp. 85–93, 2019.
- [3] H. M. Kim and M. Laskowski, "Toward an ontology-driven blockchain design for supply-chain provenance," *Intelligent Systems in Accounting, Finance and Management*, vol. 25, no. 1, pp. 18–27, 2018.
- [4] C. J. Matheus, A. Boran, D. Carr et al., "Semantic network management for next-generation networks," *Computational Intelligence*, vol. 35, no. 2, pp. 285–309, 2019.
- [5] M. Safyan, Z. Ul Qayyum, S. Sarwar, M. Iqbal, R. Garcia Castro, and A. Al-Dulaimi, "Ontology evolution for personalised and adaptive activity recognition," *IET Wireless Sensor Systems*, vol. 9, no. 4, pp. 193–200, 2019.
- [6] M. Haghgoo, I. Sychev, A. Monti, F. H. P. Fitzek, and P. Fitzek, "Sargon - smart energy domain ontology," *IET Smart Cities*, vol. 2, no. 4, pp. 191–198, 2020.
- [7] H. Hamidi and K. Fazeli, "Using Internet of Things and biosensors technology for health applications," *IET Wireless Sensor Systems*, vol. 8, no. 6, pp. 260–267, 2018.
- [8] H. Rahman and M. I. Hussain, "Fog-based semantic model for supporting interoperability in IoT," *IET Communications*, vol. 13, no. 11, pp. 1651–1661, 2019.
- [9] L. Leydesdorff and A. Nerghe, "Co-word maps and topic modeling: a comparison using small and medium-sized corpora ($N < 1,000$)," *Journal of the Association for Information Science and Technology*, vol. 68, no. 4, pp. 1024–1035, 2017.
- [10] D. Liu, M. Zhao, H. Xu, and M. Mehrgan, "A new model to investigate the impact of innovative IT services on smart urban growth: the mediating role of urban planners' knowledge," *Growth and Change*, vol. 52, no. 2, pp. 1040–1061, 2021.
- [11] X. Yu, C. Han, J. Guo, and Y. Chen, "The role of superior image composition in children's analogical reasoning," *Software: Practice and Experience*, vol. 50, no. 11, pp. 2082–2094, 2019.
- [12] Y. Liu, J. Wu, J. Li, W. Yang, H. Chen, and G. Li, "ISRF: interest semantic reasoning based fog firewall for information-centric Internet of Vehicles," *IET Intelligent Transport Systems*, vol. 13, no. 6, pp. 975–982, 2019.
- [13] M. Jarrah, B. Al-khatieb, N. Mahasneh, B. Al-khateeb, and Y. Jararweh, "GDBApex: a graph-based system to enable efficient transformation of enterprise infrastructures," *Software: Practice and Experience*, vol. 51, no. 3, pp. 517–531, 2020.
- [14] M. Yuan, K. Deng, and W. A. Chaovallitwongse, "Manufacturing resource modeling for cm," *International Journal of Intelligent Systems*, vol. 32, no. 4, pp. 414–436, 2017.
- [15] H. Cheng, L. Yan, Z. Ma, and S. Ribarić, "Fuzzy spatio-temporal ontologies and formal construction based on fuzzy Petri nets," *Computational Intelligence*, vol. 35, no. 1, pp. 204–239, 2019.
- [16] H. Nouredine, C. Ray, and C. Claramunt, "A hierarchical indoor and outdoor model for semantic trajectories," *Transactions in GIS*, vol. 26, no. 1, pp. 214–235, 2022.
- [17] L. Yin, Y. Guo, H. Zhang, W. Huang, and B. Fang, "Threat-based declassification and endorsement for mobile computing," *Chinese Journal of Electronics*, vol. 28, no. 5, pp. 1041–1052, 2019.
- [18] C. Sirichanya and K. Kraissak, "Semantic data mining in the information age: a systematic review," *International Journal of Intelligent Systems*, vol. 36, no. 8, pp. 3880–3916, 2021.
- [19] P. Araújo-de-Oliveira, F. Durán, and E. Pimentel, "A procedural and flexible approach for specification, modeling, definition, and analysis for self-adaptive systems," *Software: Practice and Experience*, vol. 51, no. 6, pp. 1387–1415, 2021.
- [20] C. Liu, Z. Lu, L. Ma, L. Wang, X. Jin, and W. Si, "A modality conversion approach to MV-DRs and KV-DRRs registration using information bottlenecked conditional generative adversarial network," *Medical Physics*, vol. 46, no. 10, pp. 4575–4587, 2019.
- [21] J. S. Mboli, D. Thakker, J. L. Mishra, and L. Jyoti, "An Internet of Things-enabled decision support system for circular economy business model," *Software: Practice and Experience*, vol. 52, no. 3, pp. 772–787, 2020.
- [22] J. K. Arnulf, A. Dysvik, and K. R. Larsen, "Measuring semantic components in training and motivation: a methodological introduction to the semantic theory of survey response," *Human Resource Development Quarterly*, vol. 30, no. 1, pp. 17–38, 2019.

Research Article

Regional Financial Economic Data Processing Based on Distributed Decoding Technology

HuiLi Zhang 

Yellow River Conservancy Technical Institute, Kaifeng 475000, China

Correspondence should be addressed to HuiLi Zhang; zhanghuili@yrcti.edu.cn

Received 18 April 2022; Accepted 17 May 2022; Published 8 June 2022

Academic Editor: Wei Liu

Copyright © 2022 HuiLi Zhang. This is an open access article distributed under the Creative Commons Attribution License, which permits unrestricted use, distribution, and reproduction in any medium, provided the original work is properly cited.

To improve the effect of regional financial and economic data processing, this study combines the distributed decoding technology to construct the regional financial data processing system. Furthermore, this study combines the technical characteristics of cooperative communication and unitary space-time codes to design a non-differential distributed space-time code based on cyclic unitary matrix groups. In addition, this study uses the particularity of trigonometric functions to design a non-differential distributed space-time code based on trigonometric functions. Finally, according to the characteristics of the distributed space-time code of trigonometric functions, this study obtains a decoding algorithm with low decoding complexity and uses MATLAB to conduct simulation experiments to verify the financial data processing and economic analysis effect of the system in this study. The experimental analysis results show that the regional financial and economic data processing system based on distributed decoding technology proposed in this study can play an important role in the analysis of financial and economic data.

1. Introduction

The Internet financial data mining system obtains the required financial data from a specific financial website and then performs a series of extraction processing on these financial data to form structured financial data, which are stored in the database of the target server for query and use by users dealing with financial services. In the current complex economic situation at home and abroad, people need to use the open network to obtain real-time and effective financial data. The Internet financial data collection and analysis system can provide enterprises or individual users with real-time and accurate financial data through the Internet, so that users can observe the data changes in various financial information in real time and obtain the most humanized information recommendation, and it provides a data basis for users to carry out various financial business activities. At the same time, under the current complex economic situation at home and abroad, people need to obtain a large amount of data to realize accurate mining of financial data. Therefore, it is very necessary to design an efficient, simple, and accurate Internet financial data mining system.

How to obtain the required information on a specific website, store the useful information, and display it in a certain form is beneficial to the financial data research, which makes the Web financial data mining technology a hot spot of current research. Since the establishment of China's security market for more than ten years, with the continuous development of computer technology, informatization, and networking, various financial institutions in the financial industry have stored and accumulated a large amount of original financial data. How to continuously improve financial data mining management has also become a problem. It has become a hot topic. At present, multidimensional data are ubiquitous, especially in the economic field. The cumbersome multidimensional financial data bring great difficulties to users' analysis and understanding. With the increasing capacity and complexity of financial data, traditional visualization technology is difficult to meet the needs of users. Fast and convenient visualization and analysis of multidimensional information data have become a research hotspot in the financial field.

To effectively improve the cognitive law of parallel coordinates and reduce visual clutter, clustering is widely used

in various fields, and most of the clustering methods are based on single data or based on visual space. Data-based clustering is to preprocess and classify the data before drawing, but due to the large range of the dataset, the results drawn in parallel coordinates after clustering may still be very messy, and it is difficult to identify the data characteristics of each classification and trends. The clustering method based on visual space transforms and classifies by analyzing the geometric relationship between line segments in parallel coordinates, which often leads to the clustering results without considering the actual meaning of the data itself, which affects the accuracy of clustering. Since the single visual space-based clustering method simply relies on the results of the visualization of parallel coordinates, clustering by analyzing the geometric relationship between line segments does not integrate the meaning represented by the data itself, which reduces the accuracy of classification to a certain extent and affects the application and promotion of parallel coordinate technology in the financial field.

This study combines distributed decoding technology to construct a regional financial data processing system to improve the effect of regional financial data processing and promote the reliability of financial analysis.

2. Related Work

Traditional financial data analysis methods mainly use mathematical statistics to establish corresponding mathematical-statistical models for analysis and prediction [1]. The proposed multivariate discriminant analysis model for financial data is also known as the Z score model [2]. The multiple discriminant analysis model is to select one or two most representative indicators from the indicators such as asset liquidity, profitability, solvency, and operating capacity. The coefficients in the model are relative to each indicator obtained according to the statistical results. Measure of importance: a large number of empirical studies have shown that the model has a good early warning function for corporate financial crisis [3]. However, its prediction effect is also different due to the length of time. The shorter the prediction period, the stronger the prediction ability. Therefore, this model is more suitable for the judgment of short-term risks of enterprises. According to Altman's financial ratio discriminant analysis model to expand and improve, the financial ratio discriminant analysis and logit regression method are used to establish and estimate the early warning model, and a good prediction effect has been achieved [4]; the component financial early warning model, because the principal component analysis method in the field of artificial intelligence is introduced into the judgment model, improves the rationality of the selection of indicators, thus greatly improving the accuracy of financial early warning [5]. For financial time-series data, commonly used statistical analysis methods include autoregressive moving average model, correlation coefficient analysis, asset pricing portfolio analysis, and ARCH model analysis. Among them, the ARCH model is considered to be the most concentrated model that reflects the characteristics of variance changes and is widely used in the time-series analysis of financial data. It is the most important innovation in the development of financial econometrics [6].

Among all volatility models, ARCH models are unique in terms of the depth of theoretical research and the breadth of empirical application. These analysis methods play an objective and quantitative analysis role in the study of financial markets and corporate financial status, so they have been widely used [7]. Usually, the method of data statistics is used to establish a mathematical model. It must be assumed in advance that the observed data satisfy a certain type of model, and then, statistical tests are used to determine whether the assumed model conforms to the actual situation of the data. If it does not conform, the model must be adjusted until predictive analysis can only be performed if the assumptions are met [8]. Every mathematical model is established under certain constraints and only applies to a specific range. The financial market is a complex dynamic system, so a statistical model determined only by limited parameters cannot be comprehensive and accurate. To describe the real situation of the market, it cannot effectively predict the future development trend of the market [9]. In recent years, machine learning methods, data mining methods, and related dynamic methods in the field of artificial intelligence have been unprecedentedly developed, and data analysis methods based on artificial intelligence have also been effectively and widely used in the financial field [10].

On the basis of the original industrial theoretical model, the relationship between financial agglomeration and the industrial structure formed by financial development is studied [11]; the combination of financial big data and algorithms provides an ideal technical foundation for the transformation and upgrading of traditional financial services. The perspective of different types of financial structures to study their impact on the industry [12]. The combination of the two provides an ideal technological foundation for the transformation and upgrading of traditional financial services. In the field of banking and finance, big data financial algorithms are widely used in customer marketing, product innovation, risk control, operation optimization, etc. [13]; through the algorithmic processing of customer financial information, a panoramic portrait of customers is obtained and the acquisition rate of new customers is improved. The marketing model of financial business is improved through cross-marketing algorithm analysis, precision marketing algorithm analysis, personalized recommendation algorithm analysis, etc.; through financial market risk algorithm analysis, SME risk assessment algorithm analysis, real-time fraud transaction algorithm analysis, anti-money laundering activity algorithm analysis, etc., to improve financial risk management and control capabilities [14]; and through channel optimization algorithm analysis, market hotspot algorithm analysis, and other big data methods to optimize the quality of financial operations. In the field of securities, the widespread application of artificial intelligence investment advisors driven by big data financial algorithms has become an important business model for modern security trading [15]. In the insurance industry, big data financial algorithms play an important role in insurance innovation, customer marketing, effective use of insurance funds, and risk control. In traditional financial fields such as the trust industry, financial leasing industry, and guarantee industry, big data financial algorithms are also constantly optimizing and reconstructing the business

model of traditional finance. The field has gained a broad application space [16].

3. Distributed Decoding Technology

A non-differential distributed unitary space-time coding based on a cyclic unitary matrix group is proposed, and a partially coherent distributed differential code under the multi-hop model is constructed. The performance comparison of two-hop and multi-hop modes is analyzed and compared, and it is concluded that the system performance in multi-hop mode is better at a high signal-to-noise ratio.

Definition 1. we assume that a is an element of group G , and the smallest positive integer n that makes $a^n = e$ (identity element of group G) is called the order of element a . The order of an element a is usually represented by $|a|$.

Definition 2. we assume that G is a group and H is a non-empty subset of G . If the multiplication of G by H itself also acts as a group, it is called a subgroup of G .

Definition 3. if a group G can be generated by an element a , that is, $G = \langle a \rangle$, then G is called a cyclic group generated by a , and this process is called a generator of G [17].

Definition 4. we assume that $\langle a^n \rangle$ is a cyclic group of finite order then the power of the element with base a is called the element index of the cyclic group.

Lemma 1. we assume that the order of the element a in the group G is n , and then, $a^m = e \Leftrightarrow n|m$.

Lemma 2. if the order of element a in the group is n , then $|a^k| = n / (k, n)$, where k is any integer.

Lemma 3. a subgroup of a cyclic group is also a cyclic group.

We assume that Ω is the set of L different west matrices; that is, $\Omega = \{\mathbf{u}_1, \mathbf{u}_2, \dots, \mathbf{u}_{L-1}\}$.

The easiest way to construct a commutative group with L elements is to construct a cyclic group; that is,

$$\mathbf{u}_l = \mathbf{u}_1^l, \quad (1)$$

where \mathbf{u}_1 is the generator matrix of the cyclic group, and it is a diagonal matrix, which can be expressed as follows:

$$\mathbf{u}_1 = \begin{bmatrix} e^{j\frac{2\pi}{L}u_1} & 0 & \dots & 0 \\ 0 & e^{j\frac{2\pi}{L}u_2} & \dots & 0 \\ \vdots & \vdots & \ddots & \vdots \\ 0 & 0 & \dots & e^{j\frac{2\pi}{L}u_k} \end{bmatrix}. \quad (2)$$

In the formula, $u_k \in \{0, 1, \dots, L-1\}, k = 1, 2, \dots, m$.

Then, any element in the cyclic group can be expressed as follows:

$$\mathbf{u}_l = \begin{bmatrix} e^{j\frac{2\pi}{L}u_1 l} & 0 & \dots & 0 \\ 0 & e^{j\frac{2\pi}{L}u_2 l} & \dots & 0 \\ \vdots & \vdots & \ddots & \vdots \\ 0 & 0 & \dots & e^{j\frac{2\pi}{L}u_k l} \end{bmatrix}, l = 1, 2, \dots, L-1. \quad (3)$$

The source node maps $\log_2 L$ bits of information to a certain matrix of the Ω set. Without loss of generality, we apply the following formula when constructing a circulant matrix [18]:

$$\Phi_l = \Theta' \Phi_0. \quad (4)$$

In this study, $\Theta = \mathbf{u}_1$, and then, $\Theta' = \mathbf{u}_l = \mathbf{u}_1^l$. Because the system models built in this section have only one source node, we assume that Φ_0 is a column vector, which can be expressed as $\Phi_0 = 1/\sqrt{m} [1 \ 1 \ \dots \ 1]^T$.

Then, the transmission matrix can be expressed as follows:

$$\Phi_l = \frac{1}{\sqrt{m}} \begin{bmatrix} e^{j\frac{2\pi}{L}u_1 l} & e^{j\frac{2\pi}{L}u_2 l} & \dots & e^{j\frac{2\pi}{L}u_k l} \end{bmatrix}^T. \quad (5)$$

To get better system performance, we need to obtain the optimal parameters u_1, u_2, \dots, u_k and obtain the optimal constellation, and the constellation parameter group is denoted as the vector \mathbf{v} .

Without loss of generality, $0 \leq u_1, u_2, \dots, u_k \leq L-1$ is set, which is chosen in this study according to the following criteria:

$$\begin{aligned} \min_{0 \leq u_1, \dots, u_k \leq L-1} \max_k \frac{1}{k} \sum_{i=1}^k \exp \left[j \frac{2\pi}{L} u_i l \right] \\ = \min_{0 \leq u_1, \dots, u_k \leq L-1} \delta. \end{aligned} \quad (6)$$

In the formula, $\delta \triangleq \frac{2}{1 \leq l \leq L} \|\Phi_0^H \Phi_k\|$. To associate δ with the singular value $\|\Phi_0^H \Phi_k\|$, we assume that μ is the mean of the squares of these singular values; that is, $\mu = (1/N_t) \sum_{i=1}^{N_t} v_i^2 = \|\Phi_0^H \Phi_k\|^2$, so that $\delta = \sqrt{\mu}$. For a given fixed mean μ , the error probability is minimized when the singular values are equal (i.e., uniformly distributed). Therefore, if two groups have the same δ , the group of parameters with more agreement should be selected.

As shown in Figure 1, in the first stage of cooperative communication, the source node P_1 transmits the code words in the codebook $S = \{\mathbf{s}_1, \mathbf{s}_2, \mathbf{s}_3, \dots, \mathbf{s}_L\}$ with transmit power, where $E[\mathbf{s}_i^H \mathbf{s}_j] = 1$. The signal received by the i th relay node can be expressed as follows:

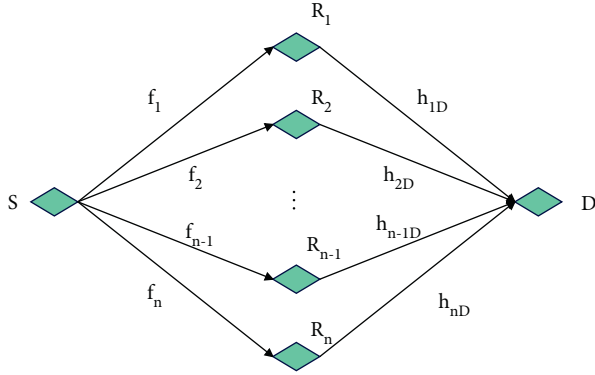


FIGURE 1: Multi-relay two-hop cooperative system model.

$$\mathbf{y}_{s,r_i} = \sqrt{P_1} f_i \mathbf{s} + \mathbf{v}_i, i = 1, 2, \dots, n. \quad (7)$$

In the second stage, the information obtained after the relay node performs linear processing on the received information can be expressed as $t_i = \sqrt{P_2/N_0 + \delta_{s,r_i}^2} P_1 \mathbf{y}_{s,r_i} \mathbf{A}_i$, and then, all n relay nodes simultaneously forward the processed information t_i to the destination node D with power P_2 . Among them, \mathbf{A}_i is the west matrix constructed according to the Hadamard matrix criterion.

The signal received by destination node D can be expressed as [19] follows:

$$\mathbf{y}_D = \sum_{i=1}^n h_{iD} \mathbf{t}_i + \mathbf{w} = \sqrt{\frac{P_1 P_2}{N_0 + \delta_{s,r_i}^2} P_1} \mathbf{S} \mathbf{h} + \mathbf{w}, i = 1, 2, \dots, n. \quad (8)$$

In the formula, \mathbf{w} is additive white Gaussian noise, which obeys a cyclic symmetric Gaussian distribution with mean 0 and variance δ^2 . The equivalent channel coefficient \mathbf{h} can be expressed as $\mathbf{h} = [f_1 h_1 \ f_2 h_2 \ \dots \ f_n h_n]^T$. The code word sent by the relay end is expressed as $\mathbf{S} = [\mathbf{A}_1 \mathbf{s} \ \mathbf{A}_2 \mathbf{s} \ \dots \ \mathbf{A}_n \mathbf{s}]$.

The signal matrix decoded by the maximum-likelihood decoding algorithm can be expressed as follows:

$$P(\mathbf{Y}|\mathbf{S}) = \frac{\exp\left(-tr\left\{\left(\mathbf{I}_T + \mathbf{S}\mathbf{S}^H\right)^{-1} \mathbf{Y}\mathbf{Y}^H\right\}\right)}{\pi \left|\mathbf{I}_T + \mathbf{S}\mathbf{S}^H\right|}. \quad (9)$$

The signal matrix decoded by the maximum-likelihood decoding algorithm can be expressed as follows:

$$\hat{\mathbf{S}} = \arg \max P(\mathbf{y}|\mathbf{S}, h_i). \quad (10)$$

According to formula (5) and formula (6), formula (10) is simplified, and the maximum-likelihood decoding in the partially coherent two-hop network is obtained, as follows:

$$\hat{\mathbf{S}} = \arg \max(\mathbf{y}^H \mathbf{S} \mathbf{A} \mathbf{K} \mathbf{S}^H \mathbf{y}). \quad (11)$$

In the formula, $\Lambda = \text{diag}(\eta_1, \eta_2, \dots, \eta_n)$, $\eta_i = |h_i|^2 (|h_i|^2 + \alpha\beta^{-1})^{-1}$, $\alpha = (1 + (P_2/1 + P_1) \sum_{i=1}^n |h_i|^2) \mathbf{I}_T$, $\beta = (P_1 P_2 T / 1 + P_1)$.

According to formula (11), it can be equivalent to as follows:

$$\arg \max_{k \in \{1, 2, \dots, L\}} (\mathbf{y}_1^H \Lambda_1 \mathbf{y}_1 + \text{Re}\{\mathbf{y}_1^H \Lambda_2 \mathbf{y}_2\} + \mathbf{y}_2^H \Lambda_3 \mathbf{y}_2). \quad (12)$$

Among them, $\mathbf{y}_1 = [y_1 \ y_2 \ \dots \ y_R]^T$, $\mathbf{y}_2 = [y_{R+1} \ y_{R+2} \ \dots \ y_{2R}]^T$, $\Lambda_1 = \gamma_1 \odot \Omega$, $\Lambda_2 = \gamma_2 \odot \Omega$, $\Lambda_3 = \gamma_3 \odot \Omega$, $[\gamma_1]_{i,j} = \omega^{(u_i - u_j)k}$, $[\gamma_2]_{i,j} = \omega^{(u_i - u_{R+j})k}$, and $[\gamma_3]_{i,j} = \omega^{(u_{R+i} - u_{R+j})k}$, Ω is a Hermitian matrix of $n \times n$, and the i th row j column in the matrix is $\Omega_{i,j} = \sum_{\lambda=1}^n (\eta_\lambda m_{i\lambda} m_{j\lambda}^*)$, $i, j = 1, \dots, n$, $\eta_i = |h_i|^2 (|h_i|^2 + \alpha\beta^{-1})^{-1}$, $j = 1, \dots, R$.

To verify that the selection of the parameter matrix has a certain influence on the performance of the west space-time coding, $L = 16$ is selected. The channel coefficient and noise are both independent and identically distributed complex Gaussian random variables with mean 0 and variance 1. Both the source node and the destination node are one antenna, and there are four antennas at the relay to participate in the cooperation. Five groups of different parameter matrices were selected, $\mathbf{v} = [5 \ 5 \ 5 \ 5]$, $\mathbf{v} = [1 \ 3 \ 5 \ 7]$, $\mathbf{v} = [1 \ 11 \ 13 \ 15]$, $\mathbf{v} = [5 \ 5 \ 11 \ 13]$, $\mathbf{v} = [7 \ 11 \ 13 \ 15]$. The performance simulation results are shown in Figure 2.

Comparing the non-differential cyclic unitary matrix group code with the differential cyclic group code, the simulation result of the bit error rate is shown in Figure 3. The results show that the differential coding does not require channel estimation in the decoding process, which saves the time and power of sending training sequences, but its performance is about 3 dB worse than that of coherent distributed space-time coding.

In the actual communication environment, sometimes the two communication devices do not have the conditions for direct communication, and the communication between the source node and the destination node must rely on multiple relay nodes to be forwarded many times before it can be realized. This is the multi-hop relay in cooperative communication. The multi-hop relay cooperative communication model is shown in Figure 4.

A multi-hop non-differential distributed space-time code based on unitary group code is proposed, and the three-hop communication system model is shown in Figure 5.

In this model, we assume that the wireless communication system has $m + n + 2$ nodes, one of which is the source node and the other is the destination node, and $m + n$ relay nodes assist the source node to communicate. Among them, m is the number of first-hop relay nodes and n is the number of second-hop relay nodes. The whole communication process can be divided into three stages. In the first stage, the source node transmits the signal to the relay node R_{1i} . The signal received at the i th relay node is represented as follows:

$$\mathbf{y}_{s,r_{1i}} = \sqrt{P_1} f_i \mathbf{s} + \mathbf{v}_i, i = 1, 2, \dots, m. \quad (13)$$

In the formula, \mathbf{s} is an $L \times 1$ -dimensional transmission data vector under the power constraint condition $\|\mathbf{s}\|_F^2 \leq L$, where $L = n$, and $\|\cdot\|_F^2$ represents the Frobenius norm. Without loss of generality, we assume that the channel of the relay node is symmetric; that is, for $\forall i$, $f_i \sim \text{CN}(0, \delta_{s,r_i}^2)$ represents the channel gain between the source node and the R_{1i} th relay node.

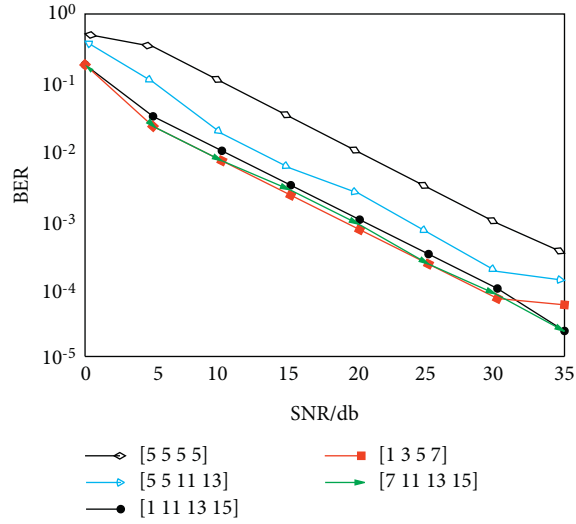


FIGURE 2: In the two-hop cooperative communication, $L = 16$, the performance comparison of different parameter matrices.

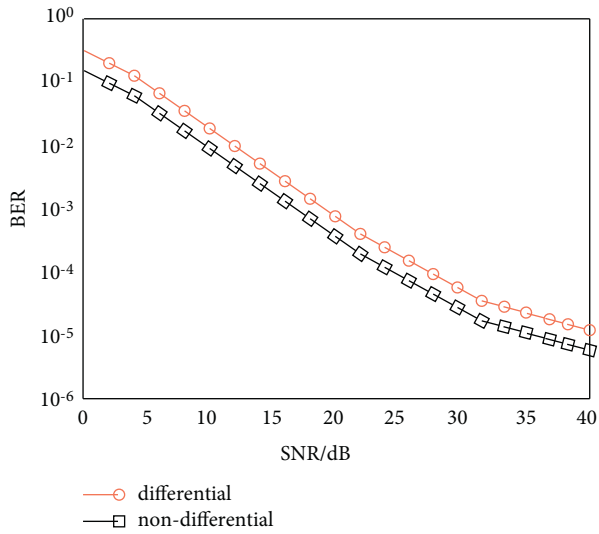


FIGURE 3: In the two-hop cooperative communication, $L = 16$, the performance comparison of differential and non-differential coding.

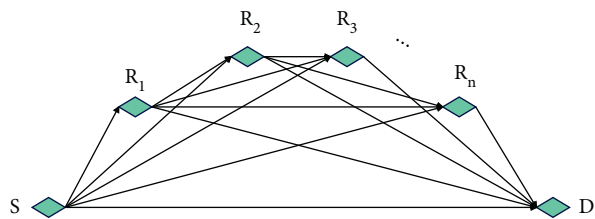


FIGURE 4: Cooperative communication model under multi-hop and multi-relay.

In the second stage, the relay node R_{1i} sends the received signal to the relay node R_{2j} after linear processing. This uses \mathbf{A}_i to represent the west transformation matrix at the i th

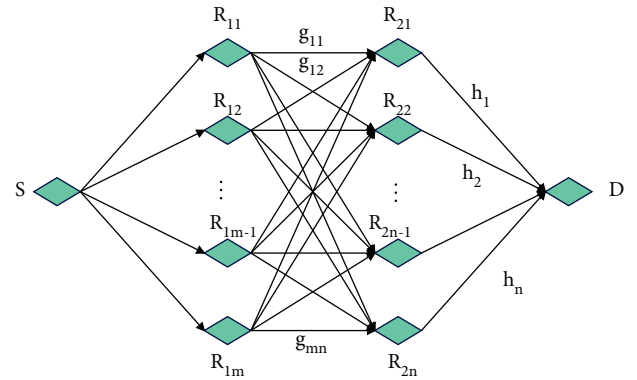


FIGURE 5: System model of a three-hop communication network.

relay node. In addition, the power of the received signal needs to be normalized to ensure that the signal sent from the relay node can meet the power limit condition. Normalizing this ensures that the average transmit power per symbol is $P = P_1 + P_2$. The signal after linear processing is $\mathbf{t}_i = \sqrt{P_2/N_0 + \delta_{s,r_i}^2 P_1} \mathbf{y}_{s,r_i} \mathbf{A}_i$, where P_2 is the average transmit power of each relay, and the processed signal is sent to R_{2j} .

The signal received at relay node R_{2j} is as follows:

$$y_{r_{2j}} = \sum_{i=1}^m g_{ij} \mathbf{t}_i + \mathbf{w}_j = \sqrt{\frac{P_1 P_2}{N_0 + \delta_{s,r_i}^2 P_1}} \mathbf{S}_1 \mathbf{h}_j + \mathbf{w}, j = 1, 2, \dots, n. \quad (14)$$

In the formula, the equivalent channel is $\mathbf{h}_j = [f_1 g_{1j} \ f_2 g_{2j} \ \dots \ f_m g_{mj}]^T$, $\mathbf{w} = \sqrt{P_2/N_0 + \delta_{s,r_i}^2 P_1} (\sum_{i=1}^m g_{ij} \mathbf{v}_i \mathbf{A}_i) + \mathbf{w}_j$, \mathbf{w}_j is the noise vector at the relay node R_{2j} , and \mathbf{w} is the additive white Gaussian noise at the node, which includes the noise forwarded from the relay node R_{1i} and the noise at the node itself. Therefore, the linear transformation at the relay node is finally selected

as the west linear transformation to ensure that the noises w are independent of each other. The code word matrix $S_1 = [A_1s \ A_2s \ \dots \ A_ms]$ in the formula reflects the role of distributed space-time code here.

In the third stage, the relay node R_{2j} sends the received signal through the west linear transformation again, and B_j represents the west transformation matrix at the j th relay node. The signal after the western linear transformation is as follows:

$$\tilde{y}_{r_{2j}} = \sqrt{\frac{P_3}{N_0 + \delta_{s,r_{1i}}^2 P_1 + m\delta_{r_i,r_{2j}}^2 P_2}} \mathbf{y}_{r_{r_j}} \mathbf{B}_j. \quad (15)$$

In the formula, P_3 is the average transmit power of each relay in the relay node, and the processed signal is sent to the destination node D .

Then, the signal received by destination node D is as follows:

$$\begin{aligned} \mathbf{y}_D &= \sum_{j=1}^n \tilde{y}_{r_{2j}} h_j + \mathbf{v}_d \\ &= \sqrt{abP_1} [f_1 A_1s \ f_2 A_2s \ \dots \ f_m A_ms] \begin{bmatrix} g_{11} & g_{12} & \dots & g_{1n} \\ g_{21} & g_{22} & \dots & g_{2n} \\ \dots & \dots & \dots & \dots \\ g_{m1} & g_{m2} & \dots & g_{mn} \end{bmatrix} \\ &\quad \cdot [\mathbf{B}_1 h_1 \ \mathbf{B}_2 h_2 \ \dots \ \mathbf{B}_n h_n]^T + \mathbf{n}, j = 1, 2, \dots, n. \end{aligned} \quad (16)$$

According to the equivalent transformation of the matrix, the above formula can be transformed into

$$\begin{aligned} \mathbf{y}_D &= \sqrt{abP_1} [A_1s \ A_2s \ \dots \ A_ms] \begin{bmatrix} f_1 \\ f_2 \\ \dots \\ f_m \end{bmatrix} \begin{bmatrix} g_{11} & g_{12} & \dots & g_{1n} \\ g_{21} & g_{22} & \dots & g_{2n} \\ \dots & \dots & \dots & \dots \\ g_{m1} & g_{m2} & \dots & g_{mn} \end{bmatrix} \begin{bmatrix} \mathbf{B}_1 \\ \mathbf{B}_2 \\ \dots \\ \mathbf{B}_n \end{bmatrix} \begin{bmatrix} h_1 \\ h_2 \\ \vdots \\ h_n \end{bmatrix} + \mathbf{n} \\ &= \sqrt{abP_1} [A_1s \ A_2s \ \dots \ A_ms] [\Lambda_1 \ \Lambda_2 \ \dots \ \Lambda_i] \begin{bmatrix} \Psi_1 \\ \Psi_2 \\ \dots \\ \Psi_i \end{bmatrix} \begin{bmatrix} h_1 \\ h_2 \\ \vdots \\ h_n \end{bmatrix} + \mathbf{n} \\ &= \sqrt{abP_1} \mathbf{S} \mathbf{H} + \mathbf{n}, i = 1, 2, \dots, n. \end{aligned} \quad (17)$$

In the formula, there are

$$a = \frac{P_2}{N_0 + \delta_{s,r_{1i}}^2 P_1}, b = \frac{P_3}{N_0 + \delta_{s,r_{1i}}^2 P_1 + m\delta_{r_i,r_{2j}}^2 P_2}, \Lambda_i = \text{diag} \left[\underbrace{\mathbf{B}_i \mathbf{B}_i \dots \mathbf{B}_i}_{m \text{ individual}} \right], \quad (18)$$

$$\Psi_i = [f_1 g_{1i} \ f_2 g_{2i} \ \dots \ f_m g_{mi}]^T, \mathbf{n} = \sqrt{ab} \sum_{j=1}^n \sum_{i=1}^m g_{ij} \mathbf{v}_i \mathbf{A}_i \mathbf{B}_j h_j + \sqrt{b} \sum_{j=1}^n w_j \mathbf{B}_j h_j + \mathbf{v}_d,$$

$$\mathbf{S} = [\mathbf{s}_1 \ \mathbf{s}_2 \ \dots \ \mathbf{s}_n], \mathbf{s}_i = [\mathbf{A}_1 \mathbf{B}_i s \ \mathbf{A}_2 \mathbf{B}_i s \ \dots \ \mathbf{A}_m \mathbf{B}_i s], \quad (19)$$

$$\mathbf{H} = [\mathbf{h}_1 \ \mathbf{h}_2 \ \dots \ \mathbf{h}_i]^T, \mathbf{h}_i = [f_1 g_{1i} h_i \ f_2 g_{2i} h_i \ \dots \ f_m g_{mi} h_i]^T, i = 1, 2, \dots, n. \quad (20)$$

For the generalized Butson–Hadamard matrices, $\mathbf{M} \mathbf{M}^H = \mathbf{M}^H \mathbf{M} = \gamma \mathbf{I}_T$ must be satisfied, where \mathbf{M} is a $\gamma \times \gamma$ -dimensional matrix whose elements satisfy $m_{ij}^* = m_{ij}^{-1}$.

In this section, we assume that D is a generalized Butson–Hadamard matrix of $m \times m$, and matrix D is used to construct a diagonal west matrix A_i , such that

$A_i = \text{diag}(\mathbf{D}_{1i} \mathbf{D}_{2i} \dots \mathbf{D}_{mi}), i = 1, 2, \dots, m$. Each of the diagonal elements \mathbf{D}_{ij} is the element of the i th row and the j th column of the matrix D .

The first-hop relay node sends the vector $A_i \Phi_k$ of $m \times 1$ to the second-hop relay node, that is, S_1 in formula (14), which is recorded as follows:

$$\mathbf{S}_{k1} = [\mathbf{A}_1 \Phi_k \quad \mathbf{A}_2 \Phi_k \quad \cdots \quad \mathbf{A}_m \Phi_k] = \frac{1}{\sqrt{m}} \Theta^k \mathbf{D}, k = 1, 2, \dots, L. \quad (21)$$

In the formula, \mathbf{S}_{k1} satisfies $\mathbf{S}_{k1}^H \mathbf{S}_{k1} = \mathbf{I}_m$.

In the same way, the second-hop relay matrix \mathbf{B}_j is designed. We assume that \mathbf{G} is a generalized Butson–Hadamard matrix of $m \times m$ dimension, and the matrix \mathbf{G} is used to construct the diagonal west matrix \mathbf{B}_j , so that $\mathbf{B}_j = \text{diag}(\mathbf{G}_{1j} \quad \mathbf{G}_{2j} \quad \cdots \quad \mathbf{G}_{mj})$, $j = 1, 2, \dots, m$, where each diagonal element \mathbf{G}_{ij} is the element in the i th row and the j th column of the matrix \mathbf{G} . Then, the second-hop relay node sends $\mathbf{B}_j \mathbf{S}_{k1}$ to the destination node; that is, \mathbf{S} in formula (17) is obtained, as shown as follows:

$$\mathbf{S}_k = [\mathbf{B}_1 \mathbf{S}_{k1} \quad \mathbf{B}_2 \mathbf{S}_{k1} \quad \cdots \quad \mathbf{B}_m \mathbf{S}_{k1}] = [\Psi_{k1} \quad \Psi_{k2} \quad \cdots \quad \Psi_{kn}]. \quad (22)$$

In the formula, $\Psi_{kj} = [\mathbf{A}_1 \mathbf{B}_j \Phi_k \quad \mathbf{A}_2 \mathbf{B}_j \Phi_k \quad \cdots \quad \mathbf{A}_n \mathbf{B}_j \Phi_k]$, $j = 1, 2, \dots, n$.

The relay matrices $\mathbf{A}_i, \mathbf{B}_j$ in formula (16) are west matrices, and the random vectors $\mathbf{v}_i, \mathbf{w}_j$, and \mathbf{v}_d all obey the Gaussian distribution, and they are independent of each other. We assume that the number of relay nodes in the first hop is the same as the number of relay points in the second hop; that is, $m = n = R$.

Then, the covariance matrix of additive noise is as follows:

$$E[\mathbf{n}] = \mathbf{0}_T, \\ E[\mathbf{nn}^H] = \left(ab \sum_{i=1}^m \sum_{j=1}^n |g_{ij} h_j|^2 + b \sum_{j=1}^n |h_j|^2 + 1 \right) \mathbf{I}_T = \xi \mathbf{I}_T. \quad (23)$$

Since this study is based on a partially coherent network, we assume that the destination node only knows about g_{ij} and h_j but not f_i . From this, it can be concluded that

$$E[\mathbf{y}|\mathbf{S}, g_i, h_i] = \mathbf{0}_T, \\ E[\mathbf{y}\mathbf{y}^H|\mathbf{S}, g_i, h_i] = E[abP_1 \mathbf{S}\mathbf{H}\mathbf{H}^H \mathbf{S}^H + \mathbf{nn}^H]. \quad (24)$$

Since $m = n = R$, we have

$$E[\mathbf{H}\mathbf{H}^H|g_i, h_i] = \text{diag}(\beta_1 \quad \beta_2 \quad \cdots \quad \beta_i). \quad (25)$$

In the formula, $\beta_i = \text{diag}(|g_{1i} h_i|^2 |g_{2i} h_i|^2 \cdots |g_{Ri} h_i|^2)$, $i = 1, 2, \dots, R$.

$E[\mathbf{H}\mathbf{H}^H|g_i, h_i] = \mathbf{K}$ is set, and formula (23) and formula (25) are substituted into formula (24), and the covariance matrix of the received signal is expressed as follows:

$$E[\mathbf{y}\mathbf{y}^H|\mathbf{S}, g_i, h_i] = \rho \mathbf{S}\mathbf{K}\mathbf{S}^H + \xi \mathbf{I}_T = \Gamma_y. \quad (26)$$

In the formula, $\rho = abP_1$ and it satisfies $\mathbf{S}\mathbf{S}^H = t\mathbf{I}$.

Finally, the conditional probability density function under the partially coherent network can be obtained, which is expressed as follows:

$$P(\mathbf{y}|\mathbf{S}, g_i, h_i) = \frac{1}{\pi^{|\Gamma_y|}} \exp[-(\mathbf{y}^H \Gamma_y^{-1} \mathbf{y})]. \quad (27)$$

At the receiving end, the maximum likelihood is used for decoding, and the decoding decision information of the partially coherent distributed space-time code is obtained.

$$\hat{\mathbf{S}} = \arg \max P(\mathbf{y}|\mathbf{S}, g_i, h_i). \quad (28)$$

According to the matrix inversion lemma, if the matrices $\mathbf{A} \in \mathbb{C}^{N \times N}$, $\mathbf{C} \in \mathbb{C}^{N \times N}$ are non-singular matrices, and the matrices are $\mathbf{B} \in \mathbb{C}^{N \times N}$, $\mathbf{D} \in \mathbb{C}^{N \times N}$, then the matrix $\mathbf{A} + \mathbf{B}\mathbf{C}\mathbf{D}$ has the inverse matrix $(\mathbf{A} + \mathbf{B}\mathbf{C}\mathbf{D})^{-1} = \mathbf{A}^{-1} - \mathbf{A}^{-1}\mathbf{B}(\mathbf{D}\mathbf{A}^{-1}\mathbf{B} + \mathbf{C}^{-1})^{-1}\mathbf{D}\mathbf{A}^{-1}$, and the equivalent formula $|\mathbf{I} + \mathbf{A}\mathbf{B}| = |\mathbf{I} + \mathbf{B}\mathbf{A}|$. We get

$$\Gamma_y^{-1} = \xi^{-1} (\mathbf{I} - \mathbf{S}(\rho^{-1} \xi \mathbf{I} - \mathbf{K})^{-1} \mathbf{K}\mathbf{S}^H). \quad (29)$$

Formula (28) simplifies to

$$\hat{\mathbf{S}} = \arg \max (\mathbf{y}^H \mathbf{S}(\rho^{-1} \xi \mathbf{I} - \mathbf{K})^{-1} \mathbf{K}\mathbf{S}^H \mathbf{y}). \quad (30)$$

Now, the simulation and comparison of the bit error rate performance of the partially coherent distributed space-time code under the multi-hop multi-relay cooperative communication system are carried out. The channel fading coefficient and noise are both independent and identically distributed complex Gaussian random variables with mean 0 and variance 1.

We assume that the unitary matrix selects 4 sets of different parameter matrices, which are, respectively, $\nu = [5555]$, $\nu = [1357]$, $\nu = [1111315]$, and $\nu = [551113]$. The simulation results are shown in Figure 6. It can be seen from the figure that under the same system model and the same L , the performance obtained by the selection of the unitary matrix parameters will also be different, and the selection of the parameter matrix has a greater impact on the system performance. To optimize the system performance, it is necessary to select an appropriate parameter matrix according to the actual situation during encoding.

The bit error rate performance of the proposed three-hop multi-relay distributed space-time code and the two-hop multi-relay system is simulated and compared. In the simulation, L16, the parameter matrix used is $\nu 551113$. Comparison of bit error rate performance under multi-hop multi-relay and two-hop relay networks is shown in Figure 7, and the simulation results are shown in Figure 8. The simulation results show that the bit error rate of the two-hop communication system model is slightly better than that of the three-hop model under the condition of a low signal-to-noise ratio. However, the three-hop communication model is better than the two-hop under a high signal-to-noise ratio. When the bit error rate is 10⁻⁵, the difference between the two is about 3 dB.

We assume that the wireless communication system model is shown in Figure 9, which is a multisource two-hop distributed space-time code system with a total of $M + N + 1$ nodes. Among them, M source nodes are denoted as S_i , $i = 1, 2, \dots, m$, N relay nodes are denoted as R_j , $j = 1, 2, \dots, n$ respectively, and a destination node is denoted as D . There is no direct link between source node S and destination node D . The channel coefficient from source node S_i to relay node R_j is denoted as f_{ij} , and the channel coefficient from relay

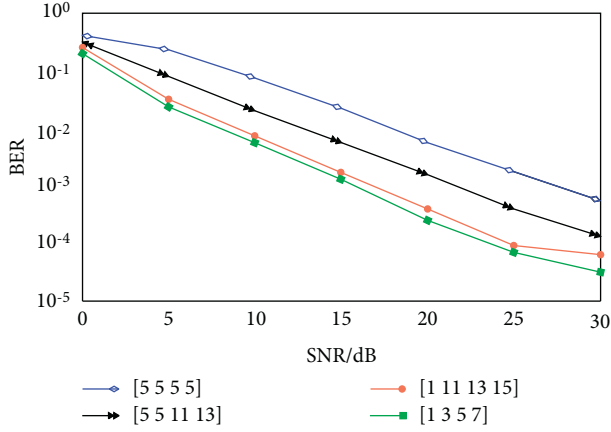


FIGURE 6: In the multi-hop multi-relay network, $L=16$, the performance comparison under different parameter matrices.

node R_j to destination node D is denoted as h_{jD} . We assume that the channel is a flat Rayleigh channel, all nodes are half-duplex, and they are synchronized at the symbol level, the channel coefficients f_{ij} and h_{jD} are independent of each other, and they obey a complex Gaussian distribution with mean 0 and variance 1.

The structure of the designed $2m \times m$ western space-time constellation diagram based on trigonometric functions is expressed as follows:

$$\mathbf{S}_l = \begin{bmatrix} \mathbf{S}_m \\ \mathbf{C}_m \end{bmatrix} = \begin{bmatrix} \sin\left(\frac{\pi l}{L}\right) \cdot \mathbf{I}_m \\ \cos\left(\frac{\pi l}{L}\right) \cdot \mathbf{I}_m \end{bmatrix}. \quad (31)$$

In the formula, $l = 0, 1, \dots, L-1$, \mathbf{S}_l represents the $l+1$ th constellation matrix in the constellation diagram. Both $\mathbf{S}_m = \sin(\pi l/L) \cdot \mathbf{I}_m$ and $\mathbf{C}_m = \cos(\pi l/L) \cdot \mathbf{I}_m$ are diagonal matrices of $m \times m$, and the diagonal elements are $\sin(\pi l/L)$ and $\cos(\pi l/L)$, respectively.

The matrix in formula (31) satisfies the following formula:

$$\mathbf{S}_l^H \mathbf{S}_l = \mathbf{S}_m^2 + \mathbf{C}_m^2 = \sin^2\left(\frac{\pi l}{L}\right) \cdot \mathbf{I}_m^2 + \cos^2\left(\frac{\pi l}{L}\right) \cdot \mathbf{I}_m^2 = \mathbf{I}_m. \quad (32)$$

Therefore, the matrix is a west space-time matrix based on trigonometric functions.

In the relay phase, the signal received at the j th relay node R_j is as follows:

$$\begin{aligned} \mathbf{y}_{R_j} &= \mathbf{s}_1 f_{1j} + \mathbf{n}_{1j} + \mathbf{s}_2 f_{2j} + \mathbf{n}_{2j} + \dots + \mathbf{s}_i f_{ij} + \mathbf{n}_{ij} \\ &= \mathbf{S} \cdot [f_{1j} \ f_{2j} \ \dots \ f_{ij}]^T + \mathbf{n}_j, i = 1, 2, \dots, m, j = 1, 2, \dots, n. \end{aligned} \quad (33)$$

In the formula, $\mathbf{S} = [\mathbf{s}_1 \ \mathbf{s}_2 \ \dots \ \mathbf{s}_i]$ represents the signal code word matrix sent by the source node, and \mathbf{s}_i is the column vector, which represents the element to be sent by each antenna of the source node.

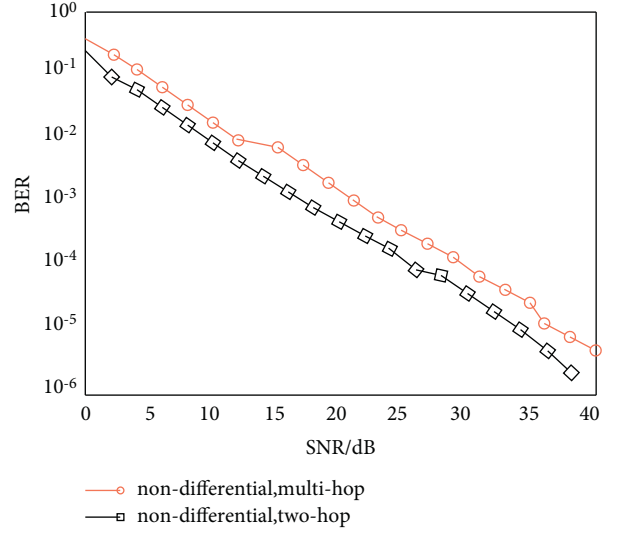


FIGURE 7: Comparison of bit error rate performance under multi-hop multi-relay and two-hop relay networks.

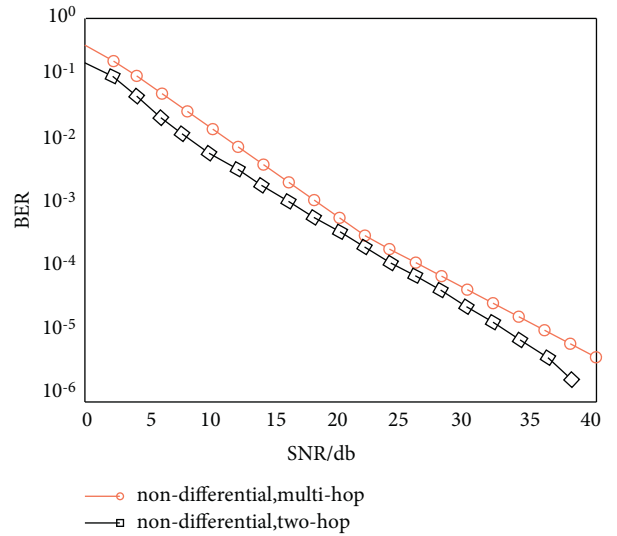


FIGURE 8: Performance simulation comparison of differential and non-differential coding under multi-hop and multi-relay.

The relay node firstly performs maximum-likelihood decoding on the received signal \mathbf{y}_{R_j} and decodes to obtain the signal \mathbf{S}'_{ij} . If the decoding is correct, the decoded information is re-encoded to obtain a new code word matrix $\tilde{\mathbf{S}}'_{ij}$ and then forwarded. If the decoding is wrong, it will not be forwarded.

No matter what kind of relay processing method is used, the signal processed by the relay node is uniformly expressed as follows:

$$\mathbf{Y} = [\mathbf{A}_{m \times n} \ \mathbf{B}_{m \times n}]^T. \quad (34)$$

The system block diagram of the destination receiver firstly combines the signal code words sent by the relay node using the maximum ratio combining method and then performs west space-time demodulation, and finally, it inversely maps the corresponding bit sequence. The signal

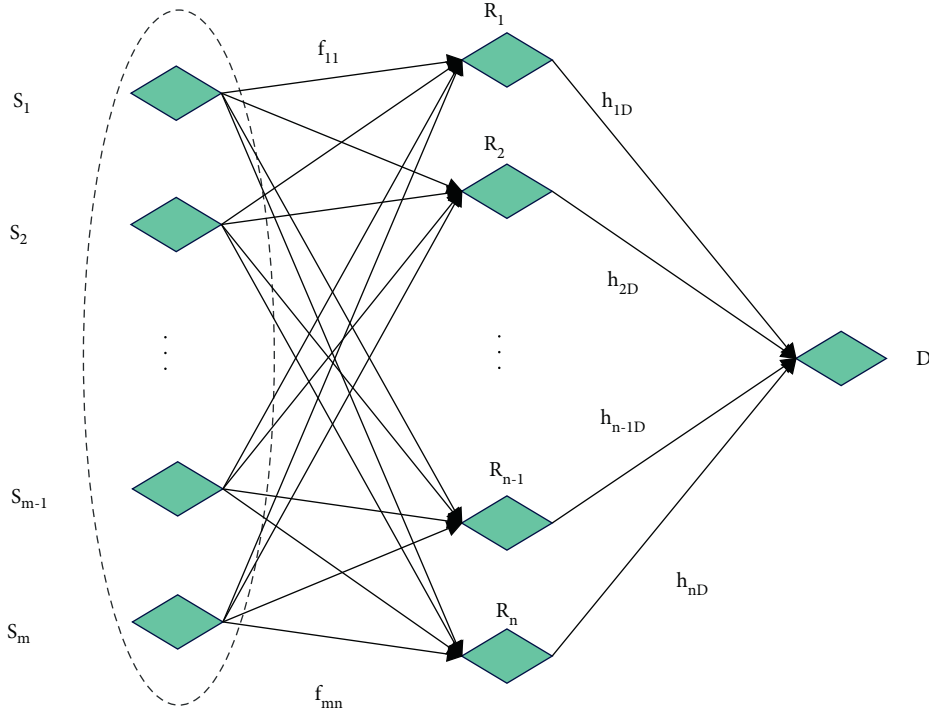


FIGURE 9: Multisource two-hop distributed space-time code system model.

information received by the receiver under the two cooperation modes will be different, which are as follows:

- (1) In AF cooperation mode, the signal received by the destination receiver is as follows:

$$\mathbf{Y}_D = \sum_{j=1}^n h_{jD} \mathbf{Y}'_{R_j} + \mathbf{w}_D. \quad (35)$$

In the formula, \mathbf{w}_D is the additive white Gaussian noise at the destination receiver.

- (2) In DF cooperation mode, the signal received by the receiver is as follows:

$$\mathbf{Y}_D = \sum_{j=1}^n h_{jD} \tilde{\mathbf{S}}'_{ij} + \mathbf{w}_D. \quad (36)$$

In the formula, \mathbf{w}_D is the additive white Gaussian noise at the destination receiving end.

When the transmitted signal is \mathbf{S} , the conditional probability density of the received signal is shown in formula (39). Therefore, when the channel fading factor is unknown, the destination node adopts the maximum-likelihood decoding:

$$\hat{\mathbf{S}} = \arg \max p(\mathbf{Y}|\mathbf{S}) = \arg \max \frac{\exp(-\text{tr}\{\Lambda^{-1} \mathbf{Y} \mathbf{Y}^H\})}{\pi^{|\Lambda|}}. \quad (37)$$

In the formula, $p(\mathbf{Y}|\mathbf{S})$ is the conditional probability that the receiving matrix is \mathbf{Y} when the transmitting signal is \mathbf{S} . tr represents the trace of the matrix, $\Lambda = \mathbf{I}_T + \mathbf{S} \mathbf{S}^H$.

Formula (37) describes the maximum-likelihood decoding algorithm for western space-time modulation. Because of the special structure of the constellation diagram proposed in this study, its ML demodulation algorithm can be simplified.

We assume that the transmitted signal matrix is \mathbf{S}_l , \mathbf{Y} is the corresponding receiving matrix, and formula (37) can be simplified to obtain the decision signal of the WST modulation:

$$\hat{\mathbf{S}}_{ML} = \arg \max_{\mathbf{S}_l \in \{s_0, \dots, s_{L-1}\}} \text{tr}\{\mathbf{Y}^H \mathbf{S}_l \mathbf{S}_l^H \mathbf{Y}\}. \quad (38)$$

To facilitate the calculation, at the destination node, the receiving matrix \mathbf{Y} is written as follows:

$$\mathbf{Y} = [\Phi_s \quad \Phi_c]^T. \quad (39)$$

In the formula, Φ_s and Φ_c are both $m \times 1$ matrices, because there is only one antenna in the design of the receiving node in the system model. The maximum-likelihood demodulation algorithm can be obtained by substituting formula (31) and formula (39) into formula (38), and the derivation process is as follows:

$$\arg \max_{\mathbf{S}_l \in \{s_0, \dots, s_{L-1}\}} \text{tr}\{\mathbf{Y}^H \mathbf{S}_l \mathbf{S}_l^H \mathbf{Y}\} = \arg \max_{l \in \{0, \dots, L-1\}} \text{tr}\left\{|\Phi_s| \sin\left(\frac{\pi l}{L}\right) + |\Phi_c| \cos\left(\frac{\pi l}{L}\right)\right\}^2. \quad (40)$$

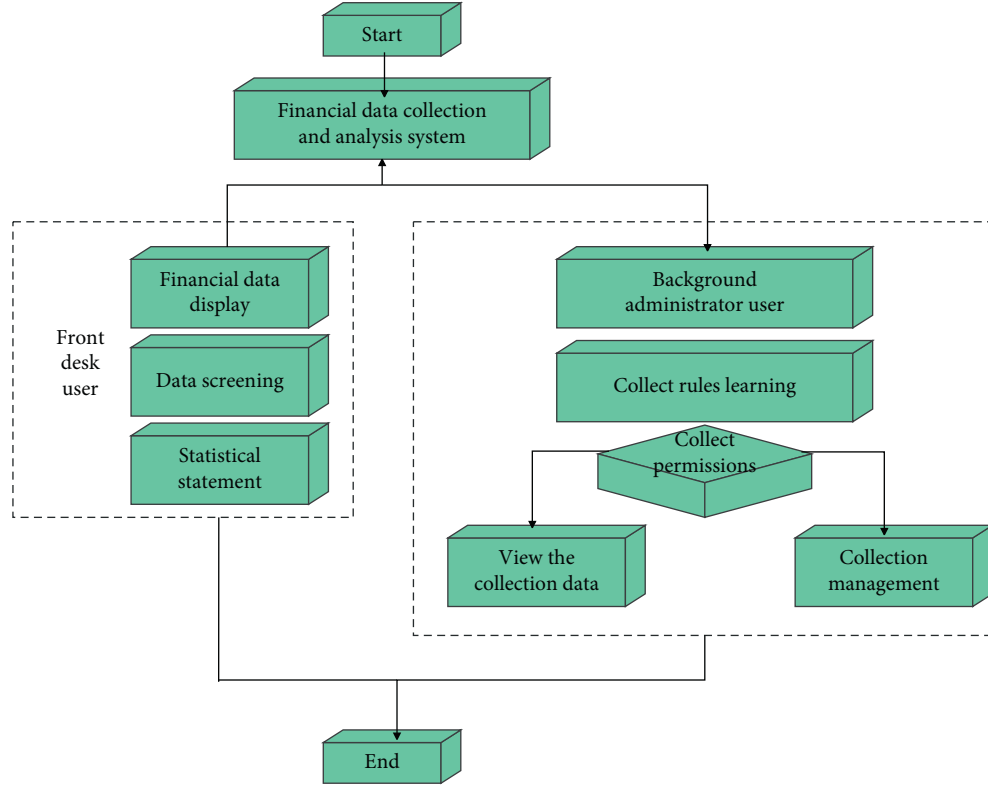


FIGURE 10: System business flow chart.

Therefore, the following formula (41) can obtain the $l \in [0, \dots, L-1]$ search of the maximum value, as follows:

$$tr \left\{ \left| \Phi_s \right| \sin \left(\frac{\pi l}{L} \right) + \left| \Phi_c \right| \cos \left(\frac{\pi l}{L} \right) \right\}^2. \quad (41)$$

According to the transformation relationship of trigonometric functions, there are as follows:

$$(A \sin \alpha + B \cos \alpha)^2 = \frac{A^2 + B^2}{2} + \frac{B^2 - A^2}{2} \cos 2\alpha + AB \sin 2\alpha. \quad (42)$$

Formula (41) can be written as follows:

$$\begin{aligned} & tr \left\{ \left| \Phi_s \right| \sin \left(\frac{\pi l}{L} \right) + \left| \Phi_c \right| \cos \left(\frac{\pi l}{L} \right) \right\} \\ &= tr \left\{ \frac{\left| \Phi_s \right|^2 + \left| \Phi_c \right|^2}{2} + \frac{\left| \Phi_s \right|^2 - \left| \Phi_c \right|^2}{2} \cos \left(\frac{2\pi l}{L} \right) + \operatorname{Re} \left(\Phi_c \Phi_s^H \right) \sin \left(\frac{2\pi l}{L} \right) \right\}. \end{aligned} \quad (43)$$

After further simplification, formula (38) can be expressed as follows:

$$\begin{aligned} \hat{\mathbf{S}}_{ML} &= \operatorname{argmax}_{S_l \in (s_0, \dots, s_{L-1})} tr \{ \mathbf{Y}^H \mathbf{S}_l \mathbf{S}_l^H \mathbf{Y} \} \\ &= \operatorname{argmax}_{l \in [0, \dots, L-1]} \left[a \cos \left(\frac{2\pi l}{L} \right) + b \sin \left(\frac{2\pi l}{L} \right) \right] \\ &= \operatorname{argmax}_{l \in [0, \dots, L-1]} \left(\xi \cos \left(\frac{\varphi - 2\pi l}{L} \right) \right). \end{aligned} \quad (44)$$

In the formula, $\xi = \sqrt{b^2 + a^2}$, $\varphi = \arctan(b/a)$, $a = \sum_{i=0}^{m-1} |\Phi_{ci}|^2 - |\Phi_{si}|^2 / 2$, $b = \operatorname{Re}(\sum_{i=0}^{m-1} \Phi_{ci} \Phi_{si}^H)$, and Φ_{si} and Φ_{ci} , respectively, represent the i th row element in the receiving matrix, where $i = 1, 2, \dots, m$. Therefore, formula (44) can be understood as finding $l \in [0, \dots, L-1]$ to make the following function achieve the maximum value:

$$f(l) = \xi \cos \left(\frac{\varphi - 2\pi l}{L} \right). \quad (45)$$

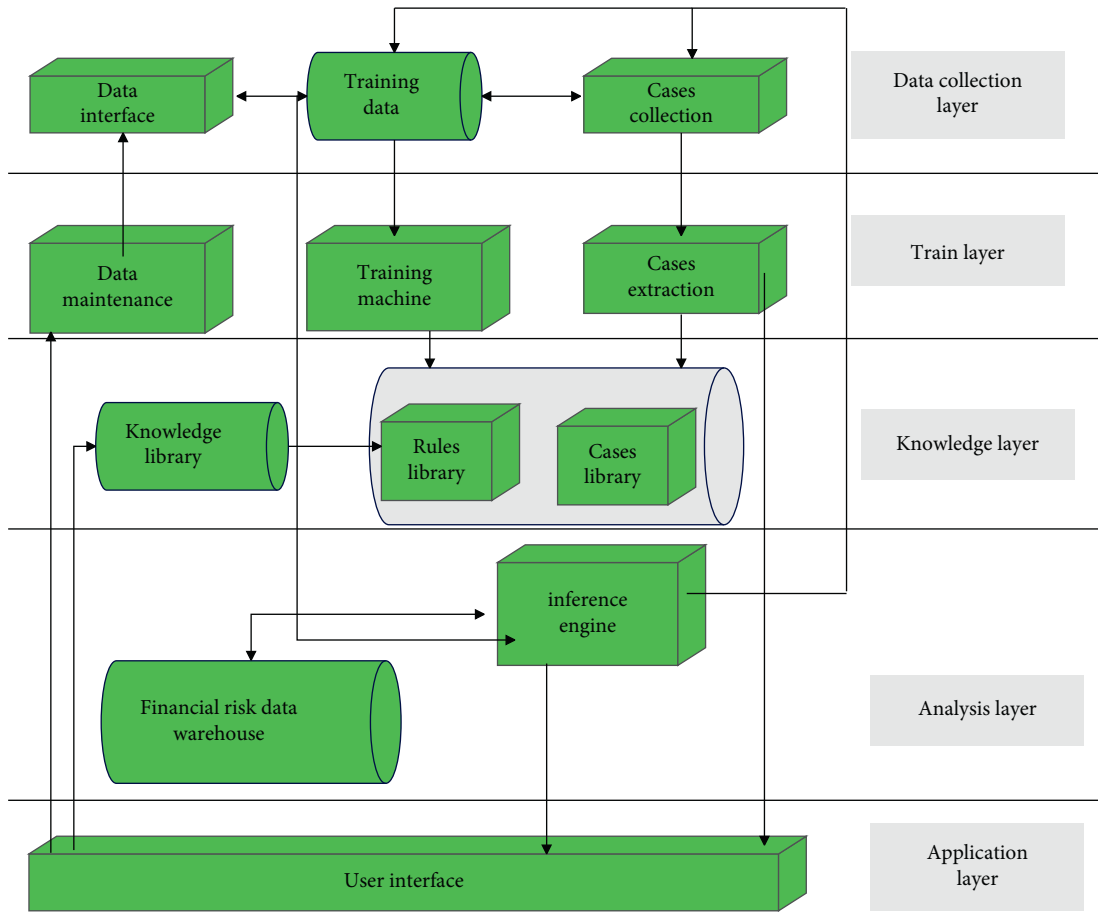


FIGURE 11: Overall system model.

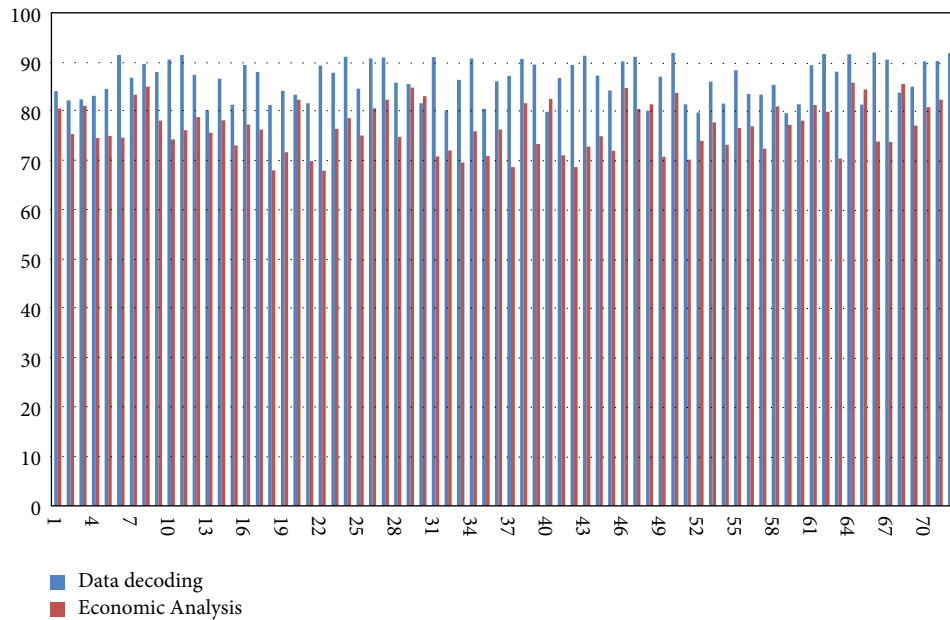


FIGURE 12: Experimental verification of regional financial and economic data processing system based on distributed decoding technology.

Observing formula (45), it can be seen that to make the function $f(l)$ achieve the maximum value, only $\cos(\varphi - 2\pi l/L) = 1$; that is, $l = \varphi L/2\pi$. Therefore, the decoding algorithm only needs to know the value of l to determine the signal to be sent.

4. Regional Financial Economic Data Processing Based on Distributed Decoding Technology

The whole mining query system is composed of two parts, the client module and the server module, and adopts the typical B/S mode. The system administrator directly logs in to the background of the financial data mining system through the URL address for data mining management. Moreover, ordinary users in the foreground view the mined data through the data display page. The business flow chart of the system is shown in Figure 10.

Financial data analysis includes two levels of individual analysis and regional analysis. Among them, the individual analysis obtains the potential financial risk factors for a single financial institution by analyzing the operational data and external environment of the individual financial institution. Regional analysis analyzes the operation data and external environment of all financial institutions in a certain region and combines the results of individual analysis to obtain regional financial risk assessment in a certain region. This study focuses on individual risk analysis and introduces external environmental data of financial institutions into individual risk analysis. The overall model design of the system is shown in Figure 11.

The model proposed in this study uses the distributed decoding technique described above for data processing. Through the simulation test of MATLAB, the financial data processing and economic analysis effect of the system in this study are verified, and the results shown in Figure 12 are obtained.

It can be seen from the experimental analysis that the regional financial and economic data processing system based on distributed decoding technology proposed in this study can play an important role in the analysis of financial and economic data.

5. Conclusion

Due to the specific economic meaning contained in the data itself in financial data, a single data-based clustering method can effectively classify the data, thereby effectively assisting domain experts to observe and analyze the initial data. However, due to the large scale of financial data, the results of clustered parallel coordinates are still messy and difficult to distinguish, which brings great challenges to further identifying the characteristics and trends of each classification. This study combines distributed decoding technology to construct a regional financial data processing system to improve the effect of regional financial data processing. The experimental analysis shows that the regional financial and economic data processing system based on distributed decoding technology proposed in this study can play an

important role in the analysis of financial and economic data.

Data Availability

The labeled dataset used to support the findings of this study is available from the author upon request.

Conflicts of Interest

The author declares no conflicts of interest.

Acknowledgments

This study was sponsored by the Yellow River Conservancy Technical Institute.

References

- [1] T. Abou-Chadi and T. Kurer, "Economic risk within the household and voting for the radical right," *World Politics*, vol. 73, no. 3, pp. 482–511, 2021.
- [2] T. R. Chowdhury, S. Chakrabarty, M. Rakib, S. Saltmarsh, and K. A. Davis, "Socio-economic risk factors for early childhood underweight in Bangladesh," *Globalization and Health*, vol. 14, no. 1, pp. 54–12, 2018.
- [3] E. Asare, A. K. Hoshide, F. A. Drummond, G. K. Criner, and X. Chen, "Economic risk of bee pollination in Maine wild blueberry, *Vaccinium angustifolium*," *Journal of Economic Entomology*, vol. 110, no. 5, pp. 1980–1992, 2017.
- [4] F. Rodriguez, T. Toulkeridis, W. Sandoval, O. Padilla, and F. Mato, "Economic risk assessment of Cotopaxi volcano, Ecuador, in case of a future lahar emplacement," *Natural Hazards*, vol. 85, no. 1, pp. 605–618, 2017.
- [5] B. J. Galli and G. Battiloro, "Economic decision-making and the impact of risk management: how they relate to each other," *International Journal of Service Science, Management, Engineering, and Technology*, vol. 10, no. 3, pp. 1–13, 2019.
- [6] J. Belás, L. Smrcka, B. Gavurova, and J. Dvorsky, "The impact of social and economic factors in the credit risk management of SME," *Technological and Economic Development of Economy*, vol. 24, no. 3, pp. 1215–1230, 2018.
- [7] S. Chakrabarti, M. T. Khan, A. Kishore, D. Roy, and S. P. Scott, "Risk of acute respiratory infection from crop burning in India: estimating disease burden and economic welfare from satellite and national health survey data for 250 000 persons," *International Journal of Epidemiology*, vol. 48, no. 4, pp. 1113–1124, 2019.
- [8] K. Peng, M. Tian, M. Andersen et al., "Incidence, risk factors and economic burden of fall-related injuries in older Chinese people: a systematic review," *Injury Prevention: Journal of the International Society for Child and Adolescent Injury Prevention*, vol. 25, no. 1, pp. 4–12, 2019.
- [9] J. E. Laine, V. T. Baltar, S. Stringhini et al., "Reducing socio-economic inequalities in all-cause mortality: a counterfactual mediation approach," *International Journal of Epidemiology*, vol. 49, no. 2, pp. 497–510, 2020.
- [10] C. O'Connell, M. Motallebi, D. L. Osmond, and D. L. Hoag, "Trading on risk: the moral logics and economic reasoning of North Carolina farmers in water quality trading markets," *Economic Anthropology*, vol. 4, no. 2, pp. 225–238, 2017.

- [11] J. Odehnal and J. Neubauer, "Economic, security, and political determinants of military spending in NATO countries," *Defence and Peace Economics*, vol. 31, no. 5, pp. 517–531, 2020.
- [12] K. Broekhuizen, D. Simmons, R. Devlieger et al., "Cost-effectiveness of healthy eating and/or physical activity promotion in pregnant women at increased risk of gestational diabetes mellitus: economic evaluation alongside the DALI study, a European multicenter randomized controlled trial," *International Journal of Behavioral Nutrition and Physical Activity*, vol. 15, no. 1, pp. 23–12, 2018.
- [13] N. R. Mosteanu, "The influence of financial markets on countries' economic life," *Economics World*, vol. 5, no. 3, pp. 268–280, 2017.
- [14] A. Qiu, M. Shen, C. Buss et al., "Effects of antenatal maternal depressive symptoms and socio-economic status on neonatal brain development are modulated by genetic risk," *Cerebral Cortex*, vol. 27, no. 5, pp. 3080–3092, 2017.
- [15] T. Haer, W. W. Botzen, J. Zavala-Hidalgo, C. Cusell, and P. J. Ward, "Economic evaluation of climate risk adaptation strategies: cost-benefit analysis of flood protection in Tabasco, Mexico," *Atmósfera*, vol. 30, no. 2, pp. 101–120, 2017.
- [16] P. Pan, D. Chao, and Q. Yu, "Economic policy uncertainty, bank risk-taking and firm investment," *Journal of Finance and Economics*, vol. 46, no. 02, pp. 67–81, 2020.
- [17] J. B. Carr, C. V. Hawkins, and D. E. Westberg, "An exploration of collaboration risk in joint ventures: perceptions of risk by local economic development officials," *Economic Development Quarterly*, vol. 31, no. 3, pp. 210–227, 2017.
- [18] S. S. Mirza and T. Ahsan, "Corporates' strategic responses to economic policy uncertainty in China," *Business Strategy and the Environment*, vol. 29, no. 2, pp. 375–389, 2020.
- [19] T. D. van der Pol, E. C. van Ierland, and S. Gabbert, "Economic analysis of adaptive strategies for flood risk management under climate change," *Mitigation and Adaptation Strategies for Global Change*, vol. 22, no. 2, pp. 267–285, 2017.

Research Article

Effects and Appraisal of Grain Subsidy Policy Based on Statistical Analysis

Xiaoya Hu 

Institute of Food Economics, Nanjing University of Finance and Economics, Nanjing 210000, China

Correspondence should be addressed to Xiaoya Hu; xiaoyahu1011@163.com

Received 18 March 2022; Revised 1 May 2022; Accepted 13 May 2022; Published 7 June 2022

Academic Editor: Wei Liu

Copyright © 2022 Xiaoya Hu. This is an open access article distributed under the Creative Commons Attribution License, which permits unrestricted use, distribution, and reproduction in any medium, provided the original work is properly cited.

At present, the grain subsidies in China are mainly in forms of technical subsidies, like subsidies for superior seed varieties and general subsidies for agricultural production supplies and grain purchase prices. However, the purpose of the paper focuses on whether these subsidy policies can cause good effects and encourage farmers to grow grains and what impact these subsidy policies have on farmers' income. The paper takes a specific area as a research object and sorts the data using the statistical analysis put in the paper. Considering the current agricultural production conditions, the paper studies the content and structure of grain subsidy policy and the changes in grain growing acreage, farmers' income, and agricultural power machinery under the implementation of grain subsidy policy. In the end, the paper makes a research into the effect of implementing the grain subsidy policy, uses the statistical analysis to empirically analyze the impact the grain subsidy policy has on grain growing acreage, and draws a conclusion.

1. Introduction

It is a major decision-making issue facing the Chinese government to improve my country's agricultural subsidy policy under the WTO framework, improve the performance of agricultural subsidy policy, and improve the agricultural subsidy policy system, thereby ensuring national food security, increasing farmers' income, and promoting the comprehensive, stable, and sustainable development of my country's agriculture.

Agriculture is a fundamental production department in national economy for a nation of which other departments can exist and develop on the premise and a base of social development and human progress. Grain production is the base of agricultural production. Compared with other agricultural products, grain has become an important competitive capital among countries due to its special significance and function in national political economy [1]. China is the most populous country in the world, so the grain problem obviously matters a lot. However, such an important fundamental department is quite fragile in our national economy and still restricts the weak link of our

national economic development. The grain production in our country still remains in a comparatively tight balanced state of supply and demand [2].

Grain, being not only the foundation of national economic development but also the source of life for a nation, is one of the important material goods of nation's economy and people's livelihood as well as national defense capabilities [3]. China, the most populous country on Earth, must guarantee the grain safety so as to allow the people to have meals and stay away from being hungry. Since the foundation, agricultural problem, agricultural development, agricultural production, and output value changes have attracted the government's and people's attention. Grain subsidy policy has mainly gone through three stages, that is, monopoly on the purchase and marketing, coexistence of three prices, and subsidies for producers. With the development of social economy, grain subsidy policy should be suitable for present economic development, and rational subsidy program should be made. The state chose Anhui and Jilin as pilot cities to implement the subsidy policy, and then other cities followed. A series of agricultural benefit policies including state's cancellation of agricultural tax and fee

institution have positive influence on grain stable increment, comprehensive development of rural economy, and deep revolution in the villages.

With the development of social economy and the increasingly prominent industrial development, the growth of agricultural benefits has been in a relatively slow state. In addition, the problem of urban-rural development gap has become more and more prominent, and the impact of various factors such as unbalanced social and economic development has affected the country. The food security issues, agricultural development, and even harmony and stability of the entire society have brought certain impacts. How to adopt agricultural subsidy policies to ensure national food security, realize the benefits of food planting, and increase farmers' income from planting is an important issue that my country needs to solve at present. Food is the material basis on which people live. Only by ensuring and meeting the people's most basic food needs can a series of economic activities be better carried out.

Based on the actual development of agricultural production today, this paper analyzes the implementation content of the grain subsidy policy; the structure of the policy; and the changes in the grain sown area, farmers' income, and total power of agricultural machinery under the implementation of the grain subsidy policy. Researching and improving the analysis effect of grain subsidy policy is the main object.

2. Related Works

The nonagricultural employment of farmers has always been the focus of international academic circles. Literature [4] proposes to use a standard labor-leisure model to study the distribution of labor time for farm managers. Literature [5] studies the nonagricultural employment decision-making issues of rural households from two aspects: nonagricultural labor participation decision-making based on the individual level and nonagricultural labor time based on the family level. With the increase in subsidies, farmers' labor time allocation decisions have changed, and researchers have begun to pay attention to the impact of subsidy policies on farmers' labor time allocation decisions. Literature [6] theoretically studies the mechanism of the impact of subsidy policies on farmers' labor time decision-making and believes that subsidy policies can affect their labor time allocation decisions through three ways: increasing the marginal value of labor, increasing family wealth, and weakening farmers' income fluctuations. Literature [7] concludes through empirical research that the subsidy policy has a negative impact on farmers' nonagricultural labor and a positive impact on agricultural labor. In contrast, literature [8] believes that decoupling subsidies will prompt farmers to reduce agricultural working hours and increase nonagricultural employment time. Domestic research on nonagricultural employment issues of rural households mainly focuses on the discussion of factors that affect rural households' nonagricultural employment decision-making. Literature [9] studies the impact of individual characteristic variables of farmers, especially human capital variables, on farmers' participation in nonagricultural employment in poverty-

stricken areas in the west. Literature [10] mainly examines the influence of factors such as the status of farm households' family management, the characteristics of the family's labor force, and the relationship between the family and the outside world on the allocation of farm households' labor time. Literature [11] takes farmers as the research object; selects dummy variables such as family characteristic variables, social environment, and geographical characteristics; studies the factors that affect farmers' nonagricultural employment decision-making; and concludes that family characteristic variables are the main factors affecting the allocation of nonagricultural labor time of farmers. Literature [12] explores the choice mode of nonagricultural employment for farmer couples through individual characteristic variables of farmer households and family characteristic variables. Literature [13] examines the gender differences in nonagricultural employment decision-making of farmers. Literature [14] incorporates rural infrastructure into the nonagricultural employment decision analysis system of farmers.

Whether the agricultural subsidy policy promotes or inhibits the production input of farmers, foreign scholars pay close attention to this issue, but the research conclusions are still controversial. Some scholars have discovered through research that subsidy policies can encourage farmers to increase their agricultural production input levels in a variety of ways. Literature [15] believes that the subsidy policy encourages farmers to increase production input by reducing farmers' risks. Literature [16] finds that subsidy policies can influence farmers' credit constraints and encourage farmers to increase their production input levels. Literature [17] indicates that subsidy policies directly promoting the increase of farmers' income level will help them increase their agricultural investment. Literature [18] believes that the subsidy policy has little effect on the production input of farmers. At present, domestic scholars' research on farmers' input behavior mainly focuses on the mechanism of farmers' input behavior and the factors that affect farmers' input. Regarding the mechanism of farmer household input behavior, scholars mainly inquire into whether farmer household behavior is rational or not. From the perspective of farmers themselves, literature [19] believes that farmers are rational, and the behaviors used to prove farmers' irrational behaviors just show farmers' rational performance under external conditions. Literature [20] believes that the premise of analyzing the behavior mechanism of farmers' farmland investment is farmers' rationality.

The above research focuses on agricultural subsidy policy from an international macro perspective, and the research on agricultural support policy still needs to be filled and perfected. It is necessary to innovate, considering the actual national conditions while absorbing the international advanced theories, experiences, and methods to study agricultural subsidy policy issues.

3. Statistics of Grain Subsidy Data

This paper considers that agricultural subsidies include market price support measures and government financial

subsidies to agricultural producers or agricultural sectors, and on this basis, the relevant research on food subsidies is carried out.

Stratification theory is first applied in the field of social science. It is one of the important basic theories in the research of sociology of science abroad in recent years. Western scholars have widely used it as a powerful tool to study the internal structure of science. In social science, its data structure is often hierarchical in the following sense: we have variables to describe individuals, but individuals form a large group, and each group is composed of a certain number of individuals. For larger groups, there are a series of variables to describe.

Through the application in various disciplines, the concept of stratification is given in mathematics.

3.1. Hierarchical Definition. Let X and Y be two topological spaces and $f: X \rightarrow Y$ be a continuous correspondence. The so-called “ Y layered by f ” refers to the decomposition of Y into the sum of several disjoint subspaces, as follows:

$$Y = Y_0 \cup Y_1 \cup Y_2 \cdots, \quad (1)$$

where Y_0, Y_1, \dots is defined as follows.

Y_0 is the largest open set of Y and makes

$$\left(f^{-1}(Y_0), Y_0, f|_{f^{-1}(Y_0)} \right), \quad (2)$$

a local space of Y .

Y_1 is the largest open set of $Y - Y_0$ and makes

$$\left(f^{-1}(Y_1), Y_1, f|_{f^{-1}(Y_1)} \right), \quad (3)$$

a local space of Y_0 . By analogy, we can get the following.

Y_i is the largest open set of $Y_i - Y_{i-1}$ and makes

$$\left(f^{-1}(Y_{i-1}), Y_{i-1}, f|_{f^{-1}(Y_{i-1})} \right) (i = 1, 2, 3 \dots), \quad (4)$$

a local space of Y_{i-1} .

The idea of layering theorem is based on the layering concept. According to the maximum system granularity, divide the system space into two parts and so on, and finally obtains the layering subsystem.

3.2. Layering Theorem. Let $E(X_k)$ be a space composed of k variables and ρ_k represent the maximum rank up to which the space $E(X_k)$ can be divided, and then the layering theorem can be expressed as follows:

$$\begin{aligned} E(X_n): \cdots \rightarrow E(X_{k+1}) \rightarrow E(X_k) \rightarrow \cdots \rightarrow E(X_1), \\ \downarrow \rho_1 \downarrow \rho_{k+1} \downarrow \rho_k \downarrow \rho_n \\ W(X_n): \cdots \rightarrow W(X_{k+1}) \rightarrow W(X_k) \rightarrow \cdots \rightarrow W(X_1). \end{aligned} \quad (5)$$

The finally obtained $W(X_i)$ is a set of layered subspaces and meets the requirement that any subsystem cannot be subdivided.

According to the layering theorem, which describes the idea of solving complex information problems, we can

describe the emergency information resources hierarchically. The hierarchical description of emergency information resources is based on the hierarchical theorem. According to the previous description of the characteristics and classification of emergency information resources, emergency information resource space $E(X_n)$ is divided into knowledge resource $W(X_n)$ and auxiliary response information resource $E(X_{n-1})$ and then further layered according to the different properties of the two spaces. Applying the hierarchical theory to the field of emergency management can layer the complex and diverse emergency information resources according to certain laws, which is conducive to the extraction of emergency decision knowledge and the construction of metadata structure.

With people’s understanding of things deepening, they have a better grasp of the factors affecting the occurrence and development of events. People prefer a structured representation operation method to express the known development laws and rules. This way can solve similar problems more systematically. We call this method modeling method. The key to the success or failure of modeling method is the representation of model.

According to the analysis and classification principles of emergency information resources, based on system engineering, the representation of emergency information resources is modeled and abstracted from the perspective of knowledge and according to the general law of people’s understanding of the world.

It is shown as follows:

M_O represents the basic concept attribute set of emergency information resources; M_I represents emergency information resource data and information set; M_S represents emergency information resource structure and knowledge set; M_P represents the set of emergency information problems; M_M represents the mathematical model set of emergency information; M_D represents emergency decision or optimization model set.

In general, according to the breadth or comprehensiveness of the model’s described things, there are the following relationships:

$$M_O > M_I > M_S > M_P > M_M > M_D. \quad (6)$$

However, according to the depth or logic of the model’s described things, there are the following advantages:

$$M_O < M_I < M_S < M_P < M_M < M_D. \quad (7)$$

In the modern computing environment, in addition to performing complex mathematical analysis and calculation, computer and its network can also carry out complex set of operations such as membership, intersection, or association of massive datasets. Therefore, many decision-making models in emergency management are not limited to M_M and M_D ; more and more people have considered the description of things for which it is difficult to apply mathematical models and analyzed them directly at the data or information level, that is, made full use of the analysis and processing ability of computer to M_O , M_I , M_S , and M_S models. Therefore, from the perspective of modern

computing environment and management, the new model concept should be a hybrid model of knowledge, data, information, rules, and mathematics. This kind of model is set as

$$M = M_O \cup M_I \cup M_S \cup M_P \cup M_M \cup M_D. \quad (8)$$

This kind of model is also one, or metamodel. Metadata and metamodel are essentially knowledge; the research of model management is to reveal and apply this knowledge. There are differences and limitations in the perspective of knowledge domain in the understanding of model management. From the perspective of mathematical analysis, it focuses on the mathematical logic mechanism and deduction of the model, and the management of M_M and M_D . The knowledge perspective focuses on the research and management of unstructured M_I , M_S , and M_S models. The management decision-making perspective pays more attention to the model accuracy and practicability, while the information technology perspective pays more attention to the system implementation of the representation, storage, and operation of the existing model. Obviously, a single application of knowledge in a knowledge domain cannot well realize the model scientific management; that is, there are limitations in the knowledge domain. Therefore, it is necessary to apply the ideas and methods of system science, comprehensively apply the knowledge of various disciplines, and explore the systematic model management method.

Metadata management in data management is a very important core part. It provides a hierarchical way to construct metadata according to the classification of metadata of emergency information resources. From the bottom layer, core metadata management provides a front-end support for users to access storage resources. Through core metadata management, the connection between users and the underlying storage resources are established. From the high level of the business domain, application metadata integrates the management process to define application metadata from the practical perspective of emergencies and completes the release, sharing, and management of application metadata.

The knowledge system of model is a more extensive knowledge model, which is the basis of model formalization and model management. In the field of emergency management, the dependence on knowledge model is more extensive. Therefore, we make model emergency information resources from the commonness of emergency knowledge model to obtain knowledge description, abstract the basis for the establishment of a metaknowledge model, and provide theoretical support for the further division of emergency information resources.

The common knowledge feature of the model is the basis of general model management and model integration; it mainly comes from the generalized concept of the model, as the basic concept and attribute feature of the model objective thing. Corresponding to a specific model $m (m \in M)$, set N_m as the concept and attribute name of the corresponding thing; let A_m represent its corresponding attribute state set and R_m represent the mapping relationship set on $A_m \times A_m$

to describe the attribute state change and interaction relationship. Then, the common knowledge described by the corresponding model can be expressed as the following triple:

$$K_m = (N_m, A_m, R_m) \quad \forall m \in M. \quad (9)$$

Generally, for a recognized thing, there are $N_m \neq \phi$, $A_m \neq \phi$, $R_m \neq \phi$ contrast to $\forall m \in M$. When $\forall m \in M_O \cup M_I \cup M_S$, generally, A_m is the state set described qualitatively, and R_m is the attribute state change relationship set described by structural relationship and rule or knowledge. When $\forall m \in M_P \cup M_M \cup M_D$, generally, A_m is the measurable state set described quantitatively, and R_m is the attribute state change relationship set described by mathematical logic relationship and function.

Set $a \in A_m (m \in M)$; if the change of the corresponding attribute state itself at different time points is comparable, it is said to be descriptive. If the corresponding attribute state is measurable, it is said to be measurable and has measure dimension d_a . If the attribute state changes randomly, d_a represents the probability distribution. If the attribute state is fuzzy measurable, d_a represents the corresponding fuzzy number. If the attribute state is measurable and the change of state value with time is identified, there is a function $a_t = f_a(a_{t-1}, t)$, where the attribute state value at time t . In this way, there are knowledge elements corresponding to attributes

$$K_a = (p_a, d_a, f_a) \quad \forall a \in A_m \quad (\forall m \in M), \quad (10)$$

where p_a is the measurable feature description. When $p_a = 0$, it indicates that the attribute state is indescribable; when $p_a = 1$, it can be described; when $p_a = 2$, it is conventionally measurable; when $p_a = 4$, it is random and measurable; when $p_a = 4$, it is fuzzy and measurable; etc. Obviously, there is $p_a > 0$, $d_a \neq \phi$, but f_a may be empty.

Set $r \in R_m (m \in M)$ as a mapping relation on $A_m \times A_m$; in general, r has mapping attribute description p_r , such as structure, membership, linear, nonlinear, fuzzy, random, and specific mapping functions. At the same time, there are $r: A_r^I \rightarrow A_r^O (A_r^I \subseteq A_m \text{ and } A_r^O \subseteq A_m, \forall m \in M)$, where A_r^I is called the input attribute state set and A_r^O is called the output attribute state set. There is a specific mapping function $A_r^O = f_r(A_r^I)$, where the attribute state value at time t . There is a knowledge element corresponding to the change relationship as follows:

$$K_r = (p_r, A_r^I, A_r^O, f_r) \quad \forall r \in R_m (\forall m \in M), \quad (11)$$

where p_r can not only describe the attribute characteristics of f_r , but also expand the method characteristics of how to identify the formula. Here, $p_r \neq \phi$, $A_r^I \neq \phi$, $A_r^O \neq \phi$, $f_r \neq \phi$.

In this way, the common knowledge or basic knowledge K of the model can be comprehensively described as follows:

$$K_b = \bigcup_{m \in M} \left(K_m \cup \left(\bigcup_{a \in A_m} K_a \cup \bigcup_{r \in R_m} K_r \right) \right). \quad (12)$$

Therefore, the further division of emergency information resources can be described in three parts: conceptual

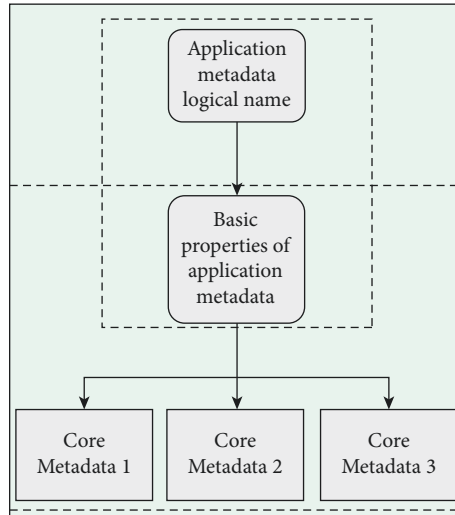


FIGURE 1: Application metadata hierarchical naming method.

attributes, states, and mapping relationships according to the above formula.

In the emergency information resource management environment, there are different application metadata according to different emergency information requirements. How to store and manage application metadata has become an important issue that needs to be considered in emergency information resource management. The application layer of emergency information resource management provides a kind of tree-shaped metadata management, and the sharing mechanism of data resources and storage resources can be formulated on this management layer.

The core metadata is in the middle layer of the metadata management model. It is a bridge connecting storage resources and application metadata. It is used to describe the information associated with the metadata and storage, as well as the basic information that can describe the core of the emergency. For the underlying storage resources, the core metadata only provides information that identifies and describes the physical aspects of the metadata, such as titles and identifiers. For the application layer of the upper level, the core metadata provides basic information about the core of the emergency, such as the location, latitude, and longitude. The core metadata is abstracted from the previous accumulation of business work in the form of emergency information resources. We have extracted 10 core metadata elements in the field of emergency response: data table, picture, text, hypertext, database table, text library table, GIS attribute table, external database table, database view, and xml information object.

The middle layer of metadata management is similar to the human brain and is used to govern the fundamental knowledge of the entire system model. The basic information of each subcategory of the four major categories of public emergencies is stored in the middle layer. This information is stored according to the structure, state, and mapping relationship defined on the metadata base. Complete the classification, naming, and library table organization of core metadata in related fields, and complete the mapping relationship according to the organization provided by the organization layer.

Application metadata is integrated by the organization strategy of the organization layer and the core metadata resources of the middle layer. It belongs to a higher-level metadata application. Therefore, it not only has the elements of metadata itself, but also inherits some basic attributes of core metadata. In order to meet these two requirements, we adopt a hierarchical naming method, as shown in Figure 1.

This naming structure can adopt loose coupling relationship between core metadata and application metadata. This loose coupling can make metadata management more flexible and quickly solve problems according to different needs. At the same time, this naming structure can better solve the metadata structure problem of the index system.

At the application layer, it is the high-level management level of the metadata management model. It mainly integrates the metadata of emergency information resources from the perspective of emergencies.

In order to unify the access mode of data, metadata management should define the information resources in emergencies in a unified standard format. The core includes data resources, image resources, and text resources. All resources can be broadly understood as a “file” stored in data management, and its metadata must include one of the core metadata elements that can be marked in the system.

Each application metadata element records its own basic attributes, and the basic attributes of calling the core metadata, mark whether it is the root node or the id value of the child node in the library table stored of the attribute structure, and the data structure is defined as follows:

$$\begin{aligned}
 &\langle ?xml\ version = "1.0" encoding = "GB2312" \rangle? \\
 &\quad \langle IDTOE \rangle \\
 &\quad \langle ID \rangle \\
 &\quad \langle NAME \rangle \quad (13) \\
 &\quad \langle PID \rangle \\
 &\quad \langle DPTYPE \rangle \\
 &\quad \langle CHTLD \rangle.
 \end{aligned}$$

The application metadata closely related to the application can create new application metadata according to different requirements from different organizational strategies proposed by the organization layer and different core metadata in the middle layer.

According to its metadata classification, emergency information resources can be divided into two domains, which can be defined as physical domain and virtual domain. Each physical domain provides the emergency information description and auxiliary decision information description of emergency information resources. At the same time, the resources in this domain can integrate the metadata structure of emergency information resources through the integration template component called by the organization layer. In a single domain, the metadata organization structure can be defined as a binary tree; between multiple physical domains, the root metadata node of each domain constructs a common tree for interconnection to describe an application metadata. The structure is shown in Figure 2.

All business processes are controlled by metadata, and different application metadata is established according to different businesses. Therefore, the business components we implement in emergency management are flexible and changeable models based on metadata.

According to the previous description of the characteristics of emergency information resources, we can know that there will be entry and exit of some metadata in emergency decision-making management. In view of the above situation, this section adopts a dynamic management method to meet the needs of emergency management.

In data processing and analysis, how to discover predictable data in massive data and predict the future based on data processing is an important function of data warehouse. It is necessary to display the development trend of data processing and business process in front of users in an intuitive way.

For the general situation in emergency decision management, the metadata management platform has provided a series of available application metadata domains for management activities. The fields and subdomains included in the domain can meet the requirements of basic transactional work in emergency decision-making. However, for some unconventional emergencies, the general application metadata may not meet the requirements of describing events; therefore, the function of dynamically adding and deleting basic metadata is provided in this model. The specific workflow is shown in Figure 3.

It can be classified into two main functions: data information maintenance and data presentation, which together constitute user interaction management components. Data information maintenance includes data entry, data addition, data deletion, and data query functions, and data presentation includes graphic display function and table display function.

After a user enters the system and establishes an access right, the metadata management model establishes metadata access and operation policies in the middle layer. After the user sends a request to add application metadata, the

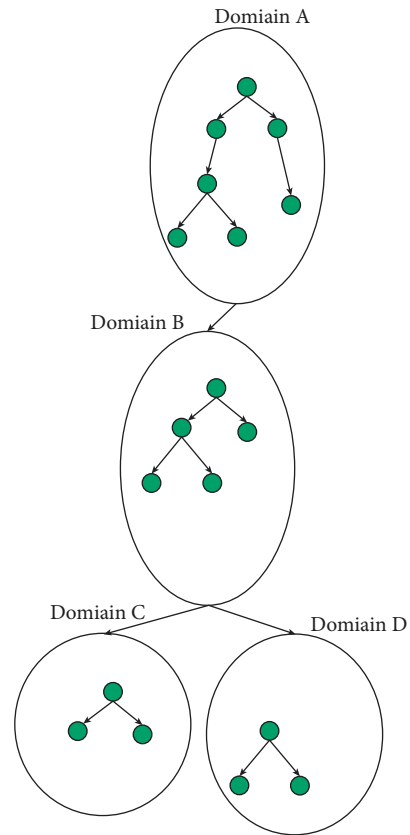


FIGURE 2: Application metadata tree structures.

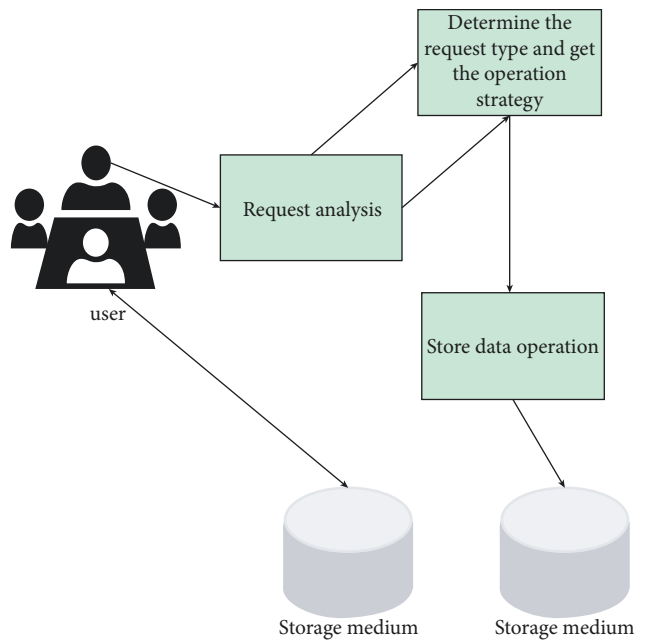


FIGURE 3: Workflow of dynamic management.

metadata management model is based on the following two situations.

Case 1: add the metadata as a node in the emergency domain. Case 2: add the metadata as a single domain for its

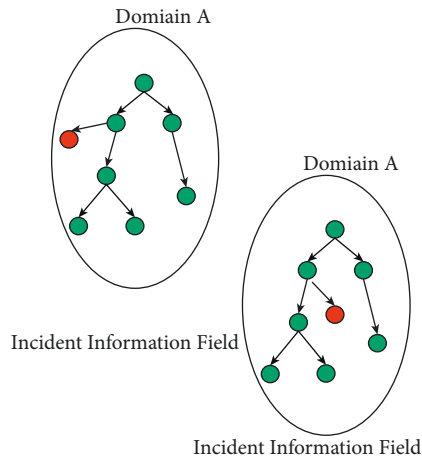


FIGURE 4: Root node change in emergency domain node.

node, and request that it becomes any node in the auxiliary information domain. In a single physical domain, you can request that the new application metadata be inserted into any position in the tree structure of the domain, which can be divided into two cases: being added as a leaf node and a root node in the emergency domain. The system processes the request. The dynamic nodes joining in the emergency domain involve the structural adjustment of different trees in the two domains. In the emergency domain, the added node is the common tree leaf nodes addition and deletion of the metadata in the physical domain. From the whole application metadata tree domain, the emergency domain is the root node domain of the whole domain, as shown in Figures 4 and 5.

In general, components encapsulate the details of design and implementation. Only one interface is provided externally. In this way, the component can realize the clear identification of the function through the interface.

When it comes to the domain group combination of multiple application metadata, for the security of metadata management, only allow the domain to join the whole application metadata domain as a leaf node; at this time, only add one leaf node to the parent node of the domain, which will not affect the established tree structure, as shown in Figure 6.

4. Evaluation of the Effect of Grain Subsidy Policy Based on Mathematical Statistical Analysis

The components used to control business flow and user interaction are called presentation components. The system presentation component expresses a complete user interaction scene by assembling logical components and user interface through a component-oriented graphical development environment.

Take a certain area as an example for research, combined with the physical structure of data statistics proposed in this article for data processing. According to the purpose of this empirical study, the object of the study, and the

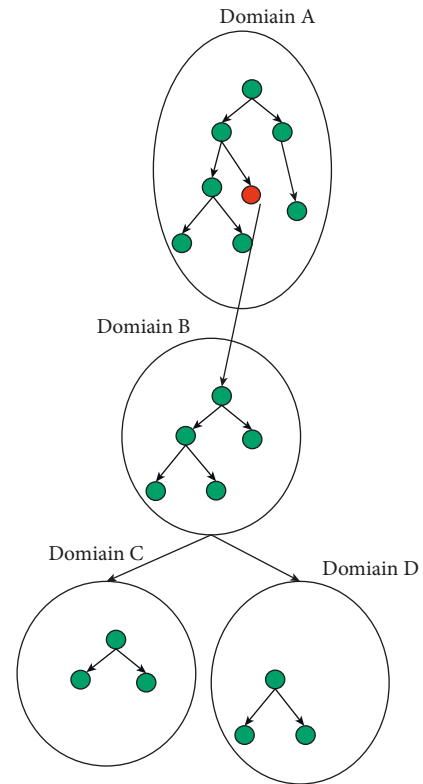


FIGURE 5: Added root node applied to metadata.

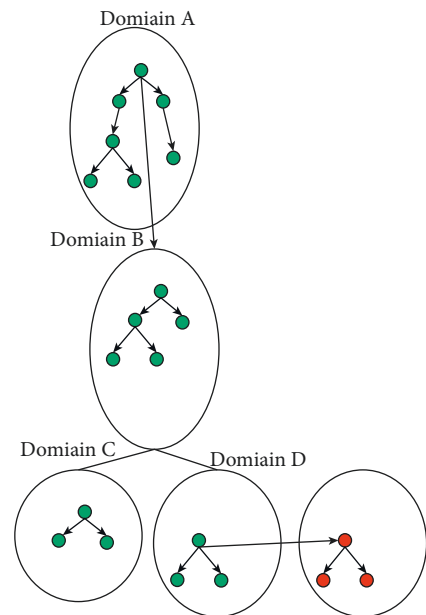


FIGURE 6: Single physical domain joining tree structure.

characteristics of operability, the main data selected is to sort out and calculate the amount of food subsidies in a certain area from 2011 to 2020. In the past ten years, the grain sown area for the ten years' period from 2011 to 2020 is mainly increased. The time span of the research data is ten years, and the consumer price index will be different every year. The difference in the consumer price index will influence the

TABLE 1: Changes in grain sown area and grain subsidies.

Years	Sown area (thousand hectares)	Direct food subsidies (100 million yuan)	Subsidies for improved varieties (100 million yuan)	Comprehensive subsidies for agricultural materials (100 million yuan)	Agricultural machinery purchase subsidy (100 million yuan)
2011	6261.0	7.6	0.0	19.0	2.7
2012	6158.0	7.7	6.9	20.9	3.3
2013	6219.6	7.8	0.0	31.4	4.7
2014	6279.2	7.8	12.4	35.8	5.8
2015	6344.8	7.8	14.6	45.4	6.6
2016	6349.5	7.9	14.8	51.6	6.6
2017	6365.4	8.4	15.5	52.8	7.4
2018	6379.1	8.8	15.9	58.0	9.5
2019	6395.3	9.4	16.4	60.9	10.4
2020	6456.3	9.8	16.3	63.7	11.4

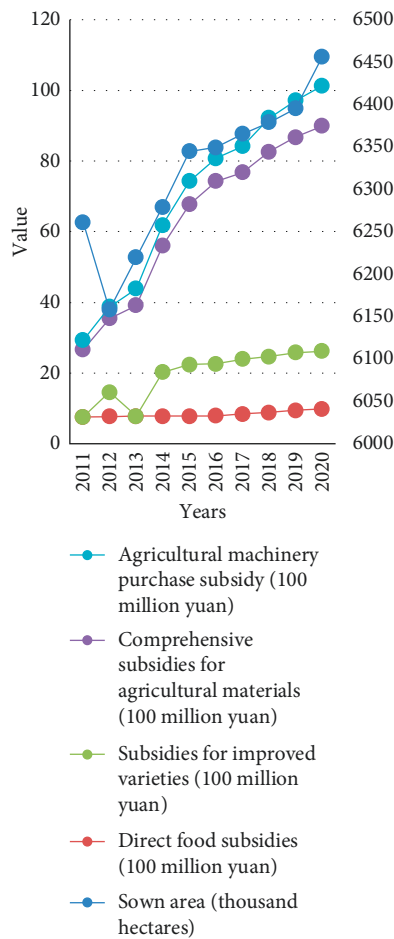


FIGURE 7: Data change line plot.

effect of the amount of grain subsidies on the sown area of grain. In order to avoid the impact on the results after the measurement analysis is carried out, the price of each year will be adjusted before the measurement analysis is carried out. The factors are eliminated and then analyzed to ensure the correctness and scientificity of the results.

The data of the empirical analysis in this paper mainly includes the grain sown area from 2011 to 2020 and the annual specific direct grain subsidies, subsidies for improved

varieties, comprehensive subsidies for agricultural materials, and subsidies for the purchase of agricultural machinery. Among them, the specific amount of various political subsidies is obtained through detailed calculation and collation. See Table 1 and Figure 7.

If the original initial data is directly regressed, it may be affected by the price factor every year, and the final result will be wrong. Therefore, the annual price factor should be eliminated before the regression analysis to ensure the

TABLE 2: Grain sown area and changes in food subsidies after excluding the price index.

Years	Sown area (thousand hectares)	Consumer price index (%)	Direct food subsidies (100 million yuan)	Subsidies for improved varieties (100 million yuan)	Comprehensive subsidies for agricultural materials (100 million yuan)	Agricultural machinery purchase subsidy (100 million yuan)
2011	6260.99	101.00	7.58	0.00	19.00	2.68
2012	6157.97	106.15	7.30	6.60	19.87	3.11
2013	6219.58	109.18	7.19	0.00	29.04	4.36
2014	6279.17	101.30	7.80	12.34	35.71	5.79
2015	6344.82	104.64	7.52	14.09	43.79	6.33
2016	6349.47	107.57	7.39	13.87	48.46	6.16
2017	6365.42	103.53	8.20	15.15	51.53	7.24
2018	6379.06	104.54	8.48	15.36	56.02	9.18
2019	6395.32	102.82	9.26	16.10	59.84	10.24
2020	6456.33	101.51	9.80	16.23	63.42	11.33

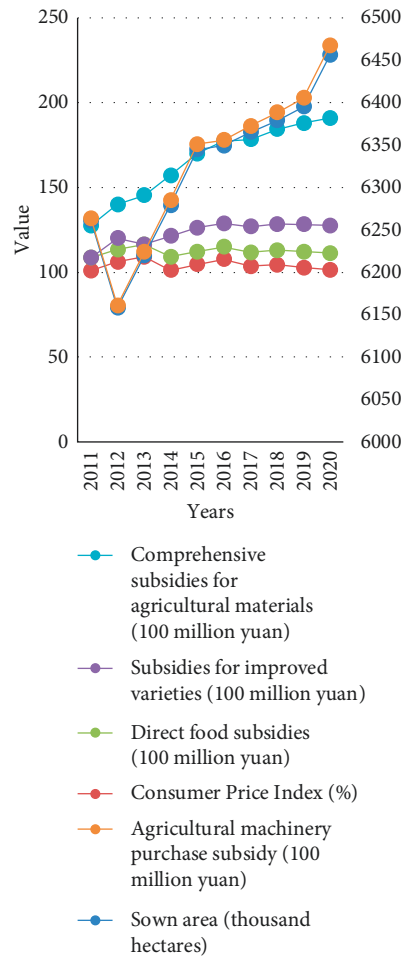


FIGURE 8: Line plot after data analysis.

accuracy of the analysis result. Among the results, 2011 is the initial year as the base period, and the price index is 100. The data after deflation is shown in Table 2 and Figure 8.

Through the above analysis, we can see that the method proposed in this paper can realize the effective evaluation of food subsidy policy.

5. Conclusion

After a long period of continuous optimization and adjustment, the food subsidy policy has achieved certain results while still having shortcomings. This article first summarizes and organizes the effects of food subsidy policies in detail

through the study of relevant literature and previous studies on the effects of grain subsidy policies. Considering the actual development of agricultural production today, it analyzes the implementation content of the grain subsidy policy; the structure of the policy; and the changes in the grain sown area, farmers' income, and total power of agricultural machinery under the implementation of the grain subsidy policy. Finally, the effect of the implementation of the grain subsidy policy is studied, and a mathematical statistical model is used to empirically analyze the impact of the grain subsidy policy and the grain sown area and draw conclusions. Through research and analysis, we can see that the method proposed in this paper can realize the effective evaluation of food subsidy policy.

Data Availability

The labeled dataset used to support the findings of this study is available from the author upon request.

Conflicts of Interest

The author declares that there are no conflicts of interest.

Acknowledgments

This study was sponsored by Nanjing University of Finance and Economics.

References

- [1] A. Ruane, J. Antle, J. Elliott et al., "Biophysical and economic implications for agriculture of +1.5° and +2.0°C global warming using AgMIP Coordinated Global and Regional Assessments," *Climate Research*, vol. 76, no. 1, pp. 17–39, 2018.
- [2] W. Khan and S. A. Ansari, "Does agriculture matter for economic growth of Uttar Pradesh (India)?" *Economy of Region*, vol. 14, no. 3, pp. 1029–1037, 2018.
- [3] M. Paul, "Community-supported agriculture in the United States: social, ecological, and economic benefits to farming," *Journal of Agrarian Change*, vol. 19, no. 1, pp. 162–180, 2019.
- [4] I. Pattanaik, K. Lahiri-Dutt, S. Lockie, and B. Pritchard, "The feminization of agriculture or the feminization of agrarian distress? Tracking the trajectory of women in agriculture in India," *Journal of the Asia Pacific Economy*, vol. 23, no. 1, pp. 138–155, 2018.
- [5] G. Salmoral, D. Rey, A. Rudd, P. Margon, and I. Holman, "A probabilistic risk assessment of the national economic impacts of regulatory drought management on irrigated agriculture," *Earth's Future*, vol. 7, no. 2, pp. 178–196, 2019.
- [6] B. Lanz, S. Dietz, and T. Swanson, "Global economic growth and agricultural land conversion under uncertain productivity improvements in agriculture," *American Journal of Agricultural Economics*, vol. 100, no. 2, pp. 545–569, 2018.
- [7] J. Cai, J. Luo, S. Wang, and S. Yang, "Feature selection in machine learning: a new perspective," *Neurocomputing*, vol. 300, pp. 70–79, 2018.
- [8] J. N. Goetz, A. Brenning, H. Petschko, and P. Leopold, "Evaluating machine learning and statistical prediction techniques for landslide susceptibility modeling," *Computers & Geosciences*, vol. 81, pp. 1–11, 2015.
- [9] H. Darabi, B. Choubin, O. Rahmati, A. Torabi Haghighi, B. Pradhan, and B. Kløve, "Urban flood risk mapping using the GARP and QUEST models: a comparative study of machine learning techniques," *Journal of Hydrology*, vol. 569, pp. 142–154, 2019.
- [10] N. M. Trendov, "Index of circular agriculture development in the republic of Macedonia," *Visegrad Journal on Bioeconomy and Sustainable Development*, vol. 6, no. 1, pp. 35–38, 2017.
- [11] M. Carus and L. Dammer, "The circular bioeconomy-concepts, opportunities, and limitations," *Industrial Biotechnology*, vol. 14, no. 2, pp. 83–91, 2018.
- [12] N. Gontard, U. Sonesson, M. Birkved et al., "A research challenge vision regarding management of agricultural waste in a circular bio-based economy," *Critical Reviews in Environmental Science and Technology*, vol. 48, no. 6, pp. 614–654, 2018.
- [13] W. Peng and A. Pivato, "Sustainable management of digestate from the organic fraction of municipal solid waste and food waste under the concepts of back to earth alternatives and circular economy," *Waste and biomass valorization*, vol. 10, no. 2, pp. 465–481, 2019.
- [14] B. Garske, J. Stubenrauch, and F. Ekardt, "Sustainable phosphorus management in European agricultural and environmental law," *Review of European, Comparative & International Environmental Law*, vol. 29, no. 1, pp. 107–117, 2020.
- [15] D. Fytili and A. Zabaniotou, "Circular economy synergistic opportunities of decentralized thermochemical systems for bioenergy and biochar production fueled with agro-industrial wastes with environmental sustainability and social acceptance: a review," *Current Sustainable/Renewable Energy Reports*, vol. 5, no. 2, pp. 150–155, 2018.
- [16] M. Kouhizadeh, Q. Zhu, and J. Sarkis, "Blockchain and the circular economy: potential tensions and critical reflections from practice," *Production Planning & Control*, vol. 31, no. 11–12, pp. 950–966, 2020.
- [17] K. R. Skene, "Circles, spirals, pyramids and cubes: why the circular economy cannot work," *Sustainability Science*, vol. 13, no. 2, pp. 479–492, 2018.
- [18] A. Heshmati, "A review of the circular economy and its implementation," *International Journal of Green Economics*, vol. 11, no. 3/4, pp. 251–288, 2017.
- [19] S. Lee, "Role of social and solidarity economy in localizing the sustainable development goals," *The International Journal of Sustainable Development and World Ecology*, vol. 27, no. 1, pp. 65–71, 2020.
- [20] K. Govindan and M. Hasanagic, "A systematic review on drivers, barriers, and practices towards circular economy: a supply chain perspective," *International Journal of Production Research*, vol. 56, no. 1–2, pp. 278–311, 2018.

Retraction

Retracted: Embedded Demand, Policy Supply, and the Urban Spatial Effect of the Transformation of the New Generation of Migrant Workers into Citizens

Mathematical Problems in Engineering

Received 13 September 2023; Accepted 13 September 2023; Published 14 September 2023

Copyright © 2023 Mathematical Problems in Engineering. This is an open access article distributed under the Creative Commons Attribution License, which permits unrestricted use, distribution, and reproduction in any medium, provided the original work is properly cited.

This article has been retracted by Hindawi following an investigation undertaken by the publisher [1]. This investigation has uncovered evidence of one or more of the following indicators of systematic manipulation of the publication process:

- (1) Discrepancies in scope
- (2) Discrepancies in the description of the research reported
- (3) Discrepancies between the availability of data and the research described
- (4) Inappropriate citations
- (5) Incoherent, meaningless and/or irrelevant content included in the article
- (6) Peer-review manipulation

The presence of these indicators undermines our confidence in the integrity of the article's content and we cannot, therefore, vouch for its reliability. Please note that this notice is intended solely to alert readers that the content of this article is unreliable. We have not investigated whether authors were aware of or involved in the systematic manipulation of the publication process.

In addition, our investigation has also shown that one or more of the following human-subject reporting requirements has not been met in this article: ethical approval by an Institutional Review Board (IRB) committee or equivalent, patient/participant consent to participate, and/or agreement to publish patient/participant details (where relevant).

Wiley and Hindawi regrets that the usual quality checks did not identify these issues before publication and have since put additional measures in place to safeguard research integrity.

We wish to credit our own Research Integrity and Research Publishing teams and anonymous and named external

researchers and research integrity experts for contributing to this investigation.

The corresponding author, as the representative of all authors, has been given the opportunity to register their agreement or disagreement to this retraction. We have kept a record of any response received.

References

- [1] L. Yu, J. Yin, and W. Qiao, "Embedded Demand, Policy Supply, and the Urban Spatial Effect of the Transformation of the New Generation of Migrant Workers into Citizens," *Mathematical Problems in Engineering*, vol. 2022, Article ID 4323308, 13 pages, 2022.

Research Article

Embedded Demand, Policy Supply, and the Urban Spatial Effect of the Transformation of the New Generation of Migrant Workers into Citizens

Lin Yu ¹, Jianbing Yin,² and Wei Qiao¹

¹School of Management, Wuxi Institute of Technology, Wuxi 214121, Jiangsu, China

²School of Finance and Economics, Wuxi Institute of Technology, Wuxi 214121, Jiangsu, China

Correspondence should be addressed to Lin Yu; yul@wxit.edu.cn

Received 3 April 2022; Accepted 13 May 2022; Published 7 June 2022

Academic Editor: Wei Liu

Copyright © 2022 Lin Yu et al. This is an open access article distributed under the Creative Commons Attribution License, which permits unrestricted use, distribution, and reproduction in any medium, provided the original work is properly cited.

Drawing on the urban space theory, based on the interaction between policy supply and right demand, this paper constructs a theoretical model of the spatial fit and inhibition effect of the urban transformation of the new generation of migrant workers from the perspective of right demand and policy supply, to explore the urban space fit and restraining effect caused by the policy supply on the new generation of migrant workers. For that reason, under the guidance of the theoretical model, this paper makes an investigation and empirical analysis on the transformation of some new-generation migrant workers in the Yangtze River Delta, and the conclusion is as follows: the basic rights demand of the new generation of migrant workers embedded in urban space has a positive effect on the realization of their citizens' transformation will, but the supply policy of citizens' transformation has a restraining effect.

1. Introduction

In recent years, with the continuous deepening of new-type urbanization in China, the level of urbanization in the country has been constantly raised. The rate of increase of both registered and permanent residents has increased by a large margin, especially in the Yangtze River Delta, Pearl River Delta, and other developed provinces, and the degree of urbanization is far higher than the national average. In 2017, in the report to the 19th National Congress of the CPC, General Secretary Xi Jinping further stressed that "Urban agglomerations should be the main body to construct the urban pattern of coordinated development of large, medium, and small cities and towns, and speed up the citizenization of the population transferred from agriculture" [1]. According to the research of literature, it is generally believed that the providing household registration and residence for migrant workers is the basic condition to ensure their transformation into citizens. According to the 2019 National Bureau of Statistics of the People's Republic of China statistics, there are still more than 200 million migrant workers in China

who have not solved the problem of transforming into citizens. And more than half of them are the new generation of migrant workers (mainly refers to the 80s and 90s after the rural Hukou Youth). Most of the new generation of migrant workers are generally better educated. On the one hand, the new generation of migrant workers has become the new force of China's new urbanization and rural revitalization. On the other hand, most of them were born or grew up in cities, which have a greater influence on them in general. They move frequently between cities. That is different from the pendulum movement between urban and rural areas of the old generation of migrant workers, which is not conducive to economic development and social stability [2].

For a long time, the household registration system has been the most important system to affect China's population mobility [3]. With the deepening of urbanization, the household registration system has been regarded as an important means to implement the new urbanization strategy and promote the transformation of citizens. However, in recent years, the urbanization rate of household registration in China is far lower than that of the resident

population, and the rate of growth is gradually slowing down [4]. In response to this paradox, Tian Ming and other scholars believe that the market-oriented reform in other fields related to household registration has gradually stripped away the social welfare attached to the household registration and weakened the role of household registration as a whole. The rate of “Household registration” cannot be regarded as the only index to evaluate the reform of household registration system. The reason is that the social benefits related to household registration are the important factors that affect the rural-to-urban migration. Thus, while the traditional household registration system has been carefully loosened, just how much room does the government have for migrant workers in cities, so as to make them integrate effectively into the city by providing citizenization policies and gradually turn them into citizens?

With the deepening of urbanization, household registration system has been used as an important means to implement the new urbanization strategy and promote the citizenization of migrant workers. However, in recent years, the urbanization rate of household registration is far lower than that of permanent population, and the growth rate slows down. The “settlement” rate cannot be the only evaluation index of household registration system reform, and the social benefits matching with household registration are the important obstacles for the settlement in the city. In view of this, based on the theory of urban space and the interaction between policy supply and right demand, this paper constructs a theoretical model of spatial fit and inhibition effect of the new generation of migrant workers’ citizens’ transformation and discusses the fit and inhibition effect of policy supply on the new generation of migrant workers’ citizens’ transformation of urban space. Through the investigation and empirical research on the transformation of the new generation of migrant workers in the “Yangtze River Delta,” the results show that the basic rights demand embedded in the urban space of the new generation of migrant workers has a positive impact on the realization of their citizens’ transformation willingness. The higher the education level, the more they like the living city, the longer the living years are, and so on, the more urgent the housing, occupation, and life needs of the new generation of migrant workers in the city. The supply of housing, occupation, and life policies has an important impact on the transformation willingness of the new generation of migrant workers and has a positive impact on the satisfaction of their basic rights embedded in the urban space. The research conclusions are expected to provide theoretical support for the country to promote the urbanization process and the citizenization of migrant workers.

The urban space provided by the citizenization policy in different cities certainly presents different characteristics. In view of this, compared with the current literature, this paper has the following marginal innovation effect:

- (1) Based on the theory of urban space, this paper designs a conceptual model of urban spatial fit and spatial inhibition effect on the new generation of migrant workers and citizens from the perspective of policy supply.

- (2) By using the method of positive and negative evaluation, this paper compares and analyzes the adaptability and inhibition of the urban space transformation of the new generation of migrant workers. Therefore, the empirical study of this paper can further explain the “Paradox” phenomenon and provide policy enlightenment for the realization of the basic rights of the new generation of migrant workers embedded in urban space.

The rest of this paper is organized as follows: Section 2 makes an analysis of the theory of urban space and the influence mechanism of the policy supply of citizenization. Section 3 makes an explanation about the conceptual model of urban spatial embeddedness demand, policy supply, and the transformation effect of the new generation of migrant workers. Section 4 shows the measure of the transformation effect of the new generation of migrant workers, urban spatial embeddedness demand, and policy supply. Section 5 provides implications for policy management. Finally, Section 6 draws the research conclusions.

2. An Analysis of the Theory of Urban Space and the Influence Mechanism of the Policy Supply of Citizenization

2.1. Theory of Urban Space. Space is an important concept in sociology. Promoted by Henri Lefebvre, Georg Simmel, Michel Foucault, Pierre Bourdieu, and other sociologists, urban space has become a core issue in western mainstream sociology [5]. Marxism regards “Space” as a physical situation, a field in which people carry out various social and economic activities, which can be understood as objective environmental conditions [6]. Durkheim developed the theory of space from the perspective of social determinism and revealed the social differences in the division of space [7]. Georg Simmel and Georg reconstructed the theory of Space Division from the perspective of mind and interaction, arguing that space is formed naturally in the course of individual interaction [8]. The founder of the urban sociology theory, Henri Lefebvre, developed the theory of social space. In his book “the right of the city,” he distinguished effectively between industrialization and urbanization and proposed to realize “Daily life” by realizing “The right of the city” and “The right of difference,” thus endowing the legitimacy of the new social space practice [9]. Henri Lefebvre argues that social space (Urbanization) has great significant effect on the reconstruction of daily life in modern cities and that the effective distribution of social productive rights is a prerequisite for the transfer of residents’ location. Thus, both Marxism’s concept of physical situation space and urban sociology’s theory of social space emphasize that the realization of urban rights, residential space, production space, and the corresponding living space decides the basic space for urban residents to realize the location transfer.

Migrant workers are urban migrants and are not natural urban residents. Although they have been separated from rural space for some time, they cannot be compared with urban residents in terms of equal urban rights, and there is a

big difference in equity between them. There are many literatures about the comparison between migrant workers and urban residents. Some scholars, such as Qi diming, put forward the idea of reducing the isolation of living space, occupation space, and community space between migrant workers and urban residents and promoted urban integration through spatial integration. There is not only a “Natural spatial isolation” between migrant workers and urban residents, but also an “Artificial spatial isolation” due to the dual system. The traditional urban and rural household registration system caused by historical reasons is generally regarded as rigid segregation, while the existing citizenization policies in different cities or regions are regarded as flexible segregation. The Chicago School, based on a deep study of the urban sociology, concluded that urban spatial segregation can be divided into active and passive segregation. On the basis of previous studies, we believe that, under the general trend of the gradual disappearance of the urban-rural dual system, especially under the premise of the gradual looseness of the household registration system, the active citizenization policy provided by the government is helpful in eliminating the passive spatial segregation of migrant workers, thus eliminating the “Natural spatial segregation”(active segregation) between migrant workers and local residents.

2.2. The Impact Mechanism of the Policy Supply of Citizenization on the Transformation of the New Generation of Migrant Workers into Citizens. As early as 1989, from the perspective of occupation and residence, Huang Zuhui considered that the shift of agricultural population was firstly to shift surplus labor force from agricultural production to nonagricultural production, then gradually to be permanent population, and then eventually to become urban residents [10]. Later, scholars explored the transformation of migrant workers into citizens from different perspectives and formed different understandings. Liu and Cheng [11] put forward four aspects of transformation: firstly, occupational transformation: migrant workers from the subsidiary, informal labor market into the primary, formal labor market; the second one is the transformation of social status, from peasant workers to citizens; the third is the transformation of ideology, from peasant workers to citizens; and last but not least, the transformation of daily life of peasant workers, including consumption, behaviors, and other means of urbanization [11].

According to the space theory, Qi and Zhang think that obtaining the right of residence, the right of production, and the corresponding right of life are the basic conditions to help the migrant workers realize the location transfer [12]. These three “City rights” are closely related to the citizenization policies of different cities, which determine the living space of migrant workers and play an important role in their realization of the transformation of citizens. Firstly, the citizenization policy guarantees the basic living space of migrant workers in the city and reduces the space isolation with the local residents. For example, completely eliminating the phenomenon of “Work sheds,” “Villages in cities,” and

“Collective dormitories” in which migrant workers live together, and bringing migrant workers into the same community management as local residents, will help migrant workers eliminate the sense of living space isolation. Secondly, the citizenization policy provides equal space for the employment market, provides equal jobs and employment opportunities with the local residents, and shares the same occupational space with the local residents, which is conducive to acquire occupational information and enhance learning ability and professional ability by migrant workers. Thirdly, the citizenization policy provides the same living space public service facilities, basic medical care, unemployment insurance, etc. as local residents. For migrant workers, particularly poor migrant workers, providing the same hardship allowance and unemployment relief as local residents can help them improve personal efficacy and enhance the ability to adapt to city life.

Compared with the old generation, the new generation of migrant workers has a stronger sense of belonging to the city and eagerly desire to be citizens [13]. If the government adopts an active citizenization policy. The new generation of migrant workers should, in theory, response strongly. Because the old generation of migrant workers roots in the countryside, the vast majority have land, homestead, or they preserve some kind of rural complex. The desire to convert citizens is not so strong as the new generation of migrant workers. Most of the new generation of migrant workers were born or grew up in cities, and the desire to take root in cities is stronger. But because most young migrant workers do not enjoy the same welfare treatments as local residents, the original urban and rural dual social spatial structure gradually transformed into urban and rural three-dimensional social spatial structure [14]. In order to eliminate the urban dual social spatial structure, it is imperative to meet the needs of the new generation of migrant workers. Although there are many complicated factors affecting the willingness of the new generation of migrant workers to convert, there are many literatures about this in the academic circle. Based on the viewpoint of living space in space theory, policy supply must firstly meet the basic needs of migrant workers city life and help them manage production practice, interpersonal communication skills, and other aspects.

3. Conceptual Model of Urban Spatial Embedded Demand, Policy Supply, and the Transformation Effect of the New Generation of Migrant Workers

In view of the increasing social distance between migrant workers and urban residents, even the emergence of class antagonism, the State Council’s “Opinions on deepening the construction of a new type of urbanization” (No. 8[2016] of the State Council) clearly puts forward the priority of settling down the new generation of migrant workers. However, overall, the proportion of the rural-to-urban migrants who are both capable of and willing to settle in cities and towns is relatively small, and the total number of those who do settle

in cities and towns is limited. The urbanization rate of registered permanent residents has been far lower than the urbanization rate of permanent residents [15]. The theory of urban space explains the level and stage of social space in the city and also explains the process of citizenization of the new generation of migrant workers, that is, from embedding into the city to gradually integrating into the city [16]. Until the dual system of urban and rural areas is truly broken down, the citizenization policy adopted by any city is like a double-edged sword. On the one hand, the policy of urbanization promotes the transformation of the new generation of migrant workers from being embedded in urban space to being integrated with urban space, so that they can obtain equal urban social rights and realize equity and justice in urban space; on the other hand, due to the limitation of urban capacity, the policy of citizenization restrains migrant workers from transforming into citizens and also prevents them from fitting in with urban space [17]. This is a dilemma that China's new-type urbanization is facing. As the urban space theory points out, there must be a "Boundary factor" embedded in urban space for a new class to realize location transfer. So, what "Boundary factors" are the new generation of migrant workers facing in the unfamiliar city? Based on the situation of the new generation of migrant workers entering the city, this paper constructs the urban space fit and inhibition effect model, which can reflect the citizens' transformation will, in order to express the "Boundary factors" clearly [18]. Figure 1 is the conceptual model of urban spatial embedded demand, policy supply, and the transformation effect of the new generation of migrant workers.

As shown in Figure 1, the so-called border factors, from a psychological point of view, refers to the extent to which migrant workers are willing to transform into urban citizens. Because of the influence of the material factors on the transformation will of the peasant workers, we should understand the demand of the new generation peasant workers' urban space embedding and the policy supply of the city's urbanization in the sense of "Material" in the model, focusing on "Living," "Occupation," and "Life." For the convenience of research, the boundary factors that reflect the transformation will of the new generation of migrant workers are simplified into three aspects: living, occupation, and life [19]. A balance can be found between the demand for rights embedded in urban space and the supply of citizenization policies. In the economic sense, there are three conditions between supply and demand. They are equilibrium state, supply exceeding demand, and demand exceeding supply. In the sociological sense, there is no difference between the first two states. But the insufficient supply state illustrates the obvious distance boundary factor between the urban space demand and the citizenization policy supply. The shadow part of the figure represents the "Boundary factors" that affect the transition intention of the new generation of migrant workers, which can be considered as the most basic conditions to realize the transition. In view of this, eliminating "boundary factors" has positive significant effect to promote the transformation of the new generation of migrant workers into citizens.

4. Measure of the Transformation Effect of the New Generation of Migrant Workers, Urban Spatial Embeddedness Demand, and Policy Supply

4.1. Construction of the Transformation Effect Model of the New Generation of Migrant Workers, Urban Spatial Embeddedness Demand, and Policy Supply

4.1.1. Construction of the Model to Measure the Fit Effect of the Urban Spatial Embeddedness of the New Generation of Migrant Workers

(1) *Model Building.* The Biprobit model is constructed from the policy supply of urban citizenization to measure the fit effect of urban spatial embeddedness of the new generation of migrant workers. Based on the space theory [20], the basic space demand of residence, production, and life has evolved into three basic policies: "urban housing," "employment promotion," and "insurance guarantee" [21], and the expression for the measure model is constructed as follows (expression 1):

$$\begin{cases} y_1^* = x_1\beta_1 + \varepsilon_1, & \text{if } y_1^* > 0, y_1 = 1; y_1^* \leq 0, y_1 = 0, \\ y_2^* = x_2\beta_2 + \varepsilon_2, & \text{if } y_2^* > 0, y_2 = 1; y_2^* \leq 0, y_2 = 0. \end{cases} \quad (1)$$

In formula (1), y_1^* represents the implicit variable, namely, the basic rights demand of the new generation of migrant workers embedded in urban space. y_1 is used as a control variable to measure the basic rights demand of the new generation of migrant workers embedded in urban space, x_1 as an explanatory variable, to measure the influence factors of the new generation of migrant workers on the demand of citizen transformation policy, and y_2^* as an implicit variable, to measure the supply of citizenization policy. y_2 stands for the control or decision variables of the supply of the citizenization policy and the explanatory variables that affect the supply of the citizenization policy. The perturbation term $(\varepsilon_1, \varepsilon_2)$ should obey the two-dimensional joint normal distribution according to the relevant requirement, from which we can know that its expectation is 0, variance is 1, and correlation coefficient is ρ .

And when y_1, y_2 all take 1, we can use formula (2) to distinguish the embeddedness fit effect of the new generation peasant workers transforming in the urban space. Its concrete expression is as follows:

$$y = \begin{cases} 1, & \text{if } y_1 = 1, y_2 = 1, \\ 0. & \end{cases} \quad (2)$$

(2) *Variable Selection.* Variable selection is divided into demand variables and supply variables. The demand variable is described as "The right demand of the new generation of migrant workers to integrate into the urban space," which is mainly reflected in the desire of the new generation of migrant workers in the city to realize the transformation of citizens. The right demand can be reflected by two indexes: the sense of city belonging and the length of residence. The

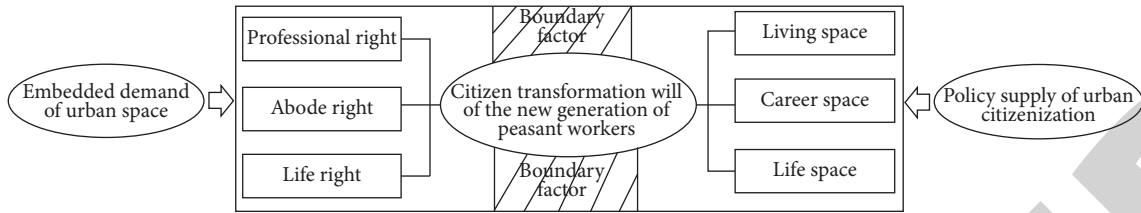


FIGURE 1: The conceptual model of urban spatial embedded demand, policy supply, and the transformation effect of the new generation of migrant workers.

supply variable is described as “The evaluation of the urbanization policy supply of the new generation of migrant workers,” which is reflected by the observation indexes of the supply variable from three aspects: the housing policy, the employment policy, and the insurance guarantee policy.

Variable selection is divided into demand variables and supply variables. The demand variable of basic rights embedded in the urban space of the new generation of migrant workers is named as “demand variable.” Using the questionnaire “Are you willing to settle down under the condition that the current policy of urbanization remains unchanged?” y_1 represents whether the new generation of migrant workers has the will to realize the transformation of citizens in their cities if you choose to be assigned a value of $y_1 = 1$; otherwise, assign a value of 0. The basic rights demand embedded in urban space of the new generation of migrant workers can also choose the observation indexes of demand variables from two aspects: the sense of city belonging and the length of residence; the sense of city belonging is divided into two aspects: cultural level and city preference. In view of the cultural level of the transferred population, it is generally believed that the longer the educational time, and the higher the educational level of the urban integration population, the easier it is to accept the corresponding culture of the town. In other words, the higher the education, the easier it is to integrate into the citizen class, the more easily the citizen quality is reflected in the higher education group of migrant workers [22]. In the process of variable setting, we take the “compulsory education” as the cut-off point and set it as a virtual variable; that is, those who have higher education than junior middle school are assigned a value of 1, that is, $edu = 1$, and those with other degrees are assigned a value of 0. In view of the preference of the transferred population for the town, we think that the more they like the living city, the stronger the spatial demand is for realizing the right. In the course of field research, we used 5-level Likert scale in the questionnaire design, and the preference of the respondents to the city was gradually divided into five levels: “very like, more like, general like, dislike, and strange.” We set the overall preference as a virtual variable; that is, we set “like = 1” for the first two items and “like = 0” for the last three items, and set “years of residence” as the virtual variable; that is, more than three years of residence is assigned a value of 1, otherwise, 0.

The supply dimension of urban citizenization policy is named “supply variable,” and the setting “How do you evaluate the supply of urban citizenization policy in your city?” indicates the overall judgment of the new generation

of migrant workers on the policy space they enjoy. We also used a 5-level Likert scale, which gradually divided the respondents’ overall judgment on the enjoyment of policy space from high to low into five levels: “very satisfied, satisfied, basically satisfied, uncertain, and dissatisfied.” We set respondent satisfaction as the dummy variable. If the participant chooses one of the first three, we set $y_2 = 1$, and if the participant chooses the second two, we set $y_2 = 2$ to 0. In addition, we choose the supply variables from three aspects: housing policy, employment policy, and insurance policy. “Housing policy” mainly includes the urban housing security rights and interests (hous) such as affordable housing, subsidized rental housing, collective housing resettlement, urban and rural self-built housing, and their own housing, not enjoying any subsidies or preferential policies. When setting up the model, we assign any one of the first three types of housing 1, and assign the values of “self-built housing in urban and rural areas” and “self-seeking housing without any subsidies or preferential policies” 0. This is because the latter two types are not associated with the urban migration of migrant workers. “Employment Policy” is mainly concerned with access to employment guidance and training. The “insurance security policy” is mainly concerned with the social security rights on an equal footing with urban residents of the same age, including health care, unemployment, and old-age insurance (safe). The overall judgment of the insurance policy is divided into “very satisfied, satisfied, basically satisfied, uncertain, and dissatisfied.” We set the variable according to the satisfaction of respondents. If the interviewees choose one of the first three, we set “safe = 1,” and if they choose the second two, we set “safe = 0.” The average value and standard deviation of the supply-demand equation of the willing fit state are shown in Table 1. Table 1 is the data relating to mean and standard deviation, which divides the new generation of migrant workers into “Post-80” and “Post-90,” according to the situation of our country.

4.1.2. Construction of the Model to Measure the Inhibition Effect of the Urban Spatial Embeddedness of the New Generation of Migrant Workers. The dependent variable of the model is the degree of the urban embeddedness of the new generation of migrant workers [23]. In order to examine the relationship between the spatial distance and the urban embeddedness of the new generation of migrant workers, we choose the Logit Model. In addition, to better ensure the robustness of the test results, we assign values of 1 and 0 to

TABLE 1: Data relating to mean and standard deviation.

	Totality		"Post-80"		"Post-90"	
	Mean value	Standard deviation	Mean value	Standard deviation	Mean value	Standard deviation
y1	0.57	0.56	0.59	0.54	0.64	0.55
y2	0.28	0.34	0.39	0.33	0.21	0.48
Edu	0.41	0.58	0.42	0.46	0.37	0.68
Like	0.38	0.52	0.65	0.43	0.55	0.38
Year	5.39	0.63	6.35	0.61	4.52	0.57
Hous	2.34	2.63	2.18	1.47	2.36	1.77
Guide	1.27	0.38	0.77	0.32	1.18	0.43
Train	0.82	0.66	0.73	0.58	0.82	0.53
Safe	0.53	0.46	0.71	0.65	0.67	0.64

identity and settlement intention, respectively. If the interviewee considers himself or herself to be a city dweller or an equivalent city dweller, the answer is 1. If the interviewee considers himself or herself a country dweller, the answer is 0. A value of 1 is assigned if the interviewee is willing to settle permanently in the city, and 0 is assigned if he or she considers himself or herself an alien. Simultaneously satisfying those who consider themselves urbanites or equivalent urbanites and who are willing to settle in a city is defined as "Already embedded in the urban space," and the rest are the three dependent variables, which cannot be embedded into the urban space. According to the above definition, the explanatory variable, that is, the spatial boundary factor, is divided into Habitable space, professional space, and life space, and the dimension variables such as housing, rate of migrant workers, and whether or not to participate in social insurance (safe) are used to express the boundary distance. In addition, the age (age), marital status (marri), educational background (edu), time spent in the city (year), and income in the city (incom) of the new generation of migrant workers are used as control variables in the model test. Build a measurement model as follows:

$$pr(\text{distance} = 1 \mid \text{factor}, X, \varepsilon_i) = \frac{\exp(\alpha + \beta \text{factor} + \sum_i k_i X_i + \varepsilon_i)}{1 + \exp(\alpha + \beta \text{factor} + \sum_i k_i X_i + \varepsilon_i)} \quad (3)$$

In formula (3), "distance" refers to the core variable to be examined, namely, the boundary distance, and "factor" refers to the boundary factor, which mainly includes three aspects of living, occupation, and life, and X is the control variable, including age, marital status, education, time in town, and income. ε_i is a random perturbation of the model [24]. In this paper, the definition of model variables, as well as the relevant descriptive statistics of the variables, is shown in Table 2. Table 2 is the definition and description of variables.

4.2. Measurement of the Transformation Effect Model of the New Generation of Migrant Workers, Urban Spatial Embedded Demand, and Policy Supply

4.2.1. Data Sources, Uptake, Reliability, and Validity. In the course of the empirical study, the sample data were

collected from the questionnaire of the National Social Science Foundation. The questionnaire was designed through the literature review, expert interview, and small sample preinvestigation and large sample formal investigation [25]. The questionnaire was designed with a five-level Likert scale. In the second half of 2018, the research group hired researchers to go to the relevant provinces and cities of Yangtze River Delta Economic Zone for the on-the-spot research and network research [26]. The network and on-the-spot method was easily adopted to carry out the survey, on the one hand, because the overall cultural level of the new generation of migrant workers is relatively high, and, on the other hand, the new generation of migrant workers use the modern information technology conveniently. The survey team distributed 600 questionnaires and collected 562 questionnaires by means of Internet survey. Through the field investigation, 400 questionnaires were distributed, 374 questionnaires were collected, and a total of 936 questionnaires were collected. After sorting and summarizing, the incomplete or incorrect questionnaires were eliminated, and finally 900 valid questionnaires were collected, with an efficiency of 90%. Before the formal large sample survey, we first selected 100 new generation migrant workers in Suzhou, Wuxi, Changzhou, and other cities in Jiangsu Province to carry out a small sample presurvey and used SPSS21.0 software to calculate the survey data, it was found that the overall reliability and validity of the questionnaire, as well as the reliability and validity of each dimension scale, reached the minimum standard of 0.7. On this basis, we tested the reliability and validity of the large sample survey, which also met the requirements of the study. In order to better understand the transformation of the new generation of migrant workers into citizens, so as to carry out comparative analysis, we have to distinguish the new generation of migrant workers between the "Post-80s" and "Post-90s" by combining experts' opinions and adopt the method of hierarchical classification statistics. This paper is to observe the differences of the spatial survival of the new generation of migrant workers in different ages. The descriptive statistics of this research sample are shown in Table 3. Table 3 is the descriptive statistics of large sample survey data. See Figures 2 to 6 for details. Figure 2 is the distribution of educational levels. Figure 3 is the gender distribution. Figure 4 is the occupational

TABLE 2: Definition and description of variables.

Variable name	Definitions and values	Mean value	Standard deviation
Age	Age	34.21	11.36
Hous	Length of residence: 1 = stable residence; 0 = temporary residence	0.55	0.47
Rate	Number of migrant workers in the unit: %	74.46	23.63
Safe	Whether migrant workers participate in social insurance: 1 = yes; 0 = No	0.07	0.25
Marri	Marital status: 1 = married, 0 = unmarried	0.63	0.46
Edu	Education level (years)	7.48	2.15
Year	Various years in the city (years)	8.45	6.70
Incom	Last month's salary: Yuan	2684.37	1578.78

TABLE 3: Descriptive statistics of large sample survey data.

Indicators	Categories	%
Age	"Post-80"	51.35
	"Post-90"	48.65
Sex	Male	55.32
	Female	44.68
Level of education	0~6 year	13.36
	7~9 year	49.52
	10~12 year	37.12
Marital status	Single	33.71
	Married	66.29
Occupation	Handyman	22.15
	Low-skilled workers	23.57
	High-skilled workers	16.68
	Business services	26.31
	Small business manager	11.29

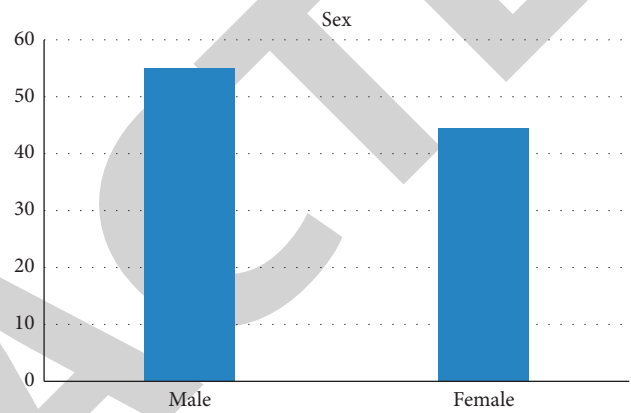


FIGURE 3: Gender (sex) distribution.

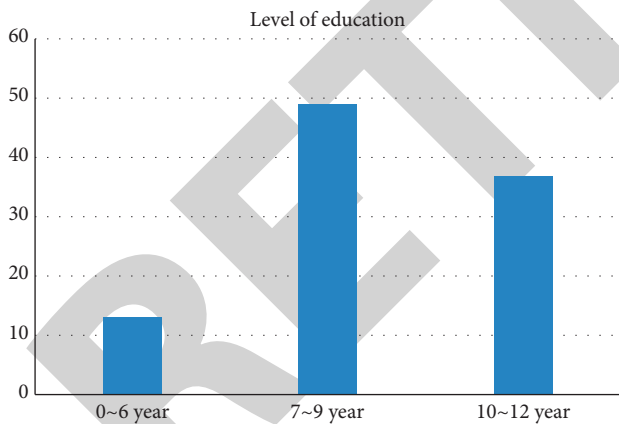


FIGURE 2: Distribution of educational levels.

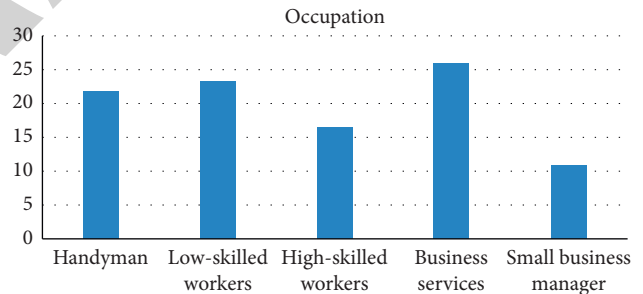


FIGURE 4: Occupational distribution.

distribution. Figure 5 is the marital status distribution. Figure 6 is the age distribution.

4.2.2. Empirical Study on the Urban Spatial Fit Effect in the Process of the Transformation of the New Generation of Migrant Workers into Urban Residents. In order to better test the effect of urban spatial integration in the process of the transformation of the new generation of migrant workers, we propose to construct a Biprobit model to study the effect. But before the model is built, it is necessary to

calculate the correlation between the variables to ensure that there is no collinearity. Through the calculation, we found that the correlation between the sample variables is less than 0.7 standard, so we can conclude that there is no serious collinearity among the variables. Based on correlation analysis, we use Biprobit model to test the fit effect of urban space in the process of the transformation of the new generation of migrant workers. In Wald test of Rho, T model for measuring the fit effect of urban spatial embeddedness of the new generation of migrant workers, its P value is 0.001, which can be used to judge the two equations of the new generation of migrant workers. There are some correlations between their perturbation terms, which are suitable for running the model. The specific estimated values of the model are shown in Table 4. Table 4 is the Biprobit model estimate.

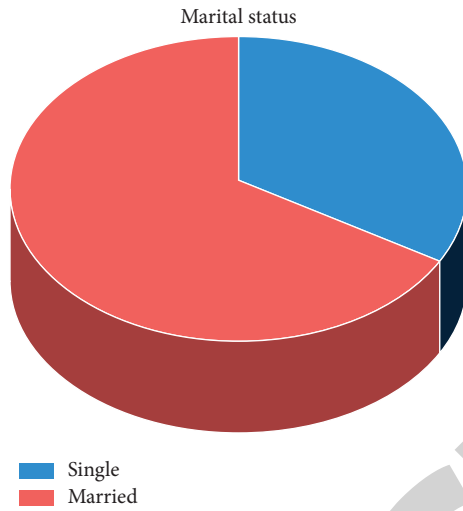


FIGURE 5: Marital status distribution.

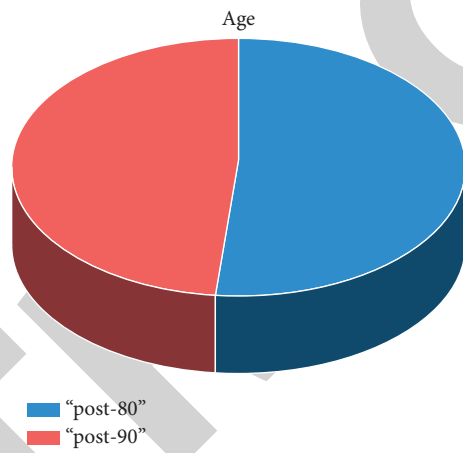


FIGURE 6: Age distribution.

TABLE 4: Biprobit model estimate.

	Totality		"Post-80"		"Post-90"	
	Right demand	Policy supply	Right demand	Policy supply	Right demand	Policy supply
Edu	0.247*** (3.24)		0.241*** (3.61)		0.376*** (2.07)	
Like	0.215*** (5.50)		0.238*** (4.64)		0.157*** (5.31)	
Year	0.351*** (6.11)		0.246*** (4.53)		0.176*** (6.15)	
Hous	0.164*** (4.46)	0.018*** (7.37)	0.235*** (7.53)	0.107* (7.15)	0.144*** (3.47)	0.027*** (3.18)
Guide	0.458*** (6.36)	0.373*** (4.46)	0.405*** (5.05)	0.271*** (5.61)	0.234*** (4.11)	0.133*** (4.37)
Train	0.205*** (4.03)	0.057*** (7.13)	0.262*** (3.17)	0.175*** (3.12)	0.428*** (2.75)	0.113*** (5.44)
Safe	0.246*** (1.77)	0.126*** (2.38)	0.214** (2.41)	0.152*** (3.31)	0.117* (1.86)	0.081*** (2.17)
Cons	-4.635*** (-10.57)	-4.181** (-15.06)	-5.561** (-7.76)	-4.384** (-11.16)	-4.420** (-6.16)	-3.242** (-10.76)
Wald test of rho	0		0.004		0.001	
N	900		436		464	

Note. (1) *T* value in parentheses, *, ** and *** are significant at the levels of 10%, 5%, and 1%, respectively. (2) The result of Wald test of Rho is *p*.

(1) *Urban Spatial Embedded Needs of the New Generation of Migrant Workers.* From the perspective of the basic rights demand embedded in the urban space of the new generation of migrant workers (Table 4 is the Biprobit model estimate), the influence of the education level, the degree of preferences to the living city, and the length of residence on the basic rights demand of the new generation of migrant workers in the city are all positive and significant at the 1% level. In other words, the basic rights demand embedded in urban space of the new generation of migrant workers has a positive impact on the realization of their citizens' will to transform. The educational level of the "Post-90s" migrant workers is higher than that of the "Post-80s", and the demand for vocational guidance and training is stronger. About liking the current city, "Post-90s" are not as strong as "Post-80s," with a correlation value of 0.157. The "Post-80s" migrant workers, because of the relative stability of family structure, mature professional skills, relatively high salary, and so on, show the relative stability of living in the city. In terms of length of residence, the "Post-80s" migrant workers generally live longer in cities than the "Post-90s." Therefore, the "Post-80s" demanding living quality is significantly higher than the "Post-90s." The "Post-90s" have high expectation for their career, which is reflected in career guidance and vocational training, at the significance of 99%. As the "Post-90s" have just entered the city for work and are unfamiliar with the urban environment, they are more concerned about their career stability, career income, and postcompetency, for the purpose of "pursuing freshness and curiosity" in different cities. The results of the study confirm the research point of view that the lack of job stability of the new generation of migrant workers is the most direct cause of their frequent urban mobility.

(2) *Supply of the Policy of Citizenization.* From the perspective of the supply of citizenization policy (Table 4), the supply of housing, occupation, and life-related citizenization policy have a positive effect on the demand of basic rights of the new generation of migrant workers embedded in urban space, and most of the observed indexes are significant at the level of 1%. In other words, housing, occupation, and life-related citizenship policies have a significant impact on their desire to achieve civic transformation. First of all, from the urban housing policy supply, the obvious imbalance occurs between the new generation of migrant workers' housing demand and supply; especially, the "Post-90s" migrant workers' housing policy space is more limited; the coefficient is only 0.027. From the employment guidance and training policy, overall, the government attaches importance to employment guidance, but not enough to vocational training. The vocational training of the "Post-90s" is much lower than that of the "Post-80s" (0.113). From the insurance policy supply, the new generation of migrant workers' overall insurance rate is not high. The "Post-90s" migrant workers enjoy more limited policy space. Thus, there is a significant imbalance between the demand and policy supply.

4.2.3. *The Inhibitive Effect of Urban Spatial Embeddedness of the New Generation of Migrant Workers in the Process of Urban Transformation Is Examined.* According to the value of likelihood chi-square statistics, the model has a strong explanatory power to the urban spatial embedding of the new generation of migrant workers and passes the test at the level of 1% significance. The new generation of migrant workers embedded in the city is set up as the settlement will of the city, the identity of the city people, or the settlement will of both the city and the identity of the city people. In this process, the control variables are firstly regressed, and the boundary variables between the citizens' willingness to transform and the actual distance are gradually added. The value of R_2 increases, and it shows that the model is well explained overall.

(1) *Boundary Variables.* The factor of residential boundary passed the test of significance at the level of 1%, and its coefficient sign is positive, which indicates that the factor of residential boundary can obviously prevent the new generation of migrant workers from embedding into urban space. The probability of spatial embeddedness of the new generation of migrant workers with stable living conditions may increase by 10.24%. The reason is obvious. If the new generation of migrant workers have more stable homes and have time to help them find more suitable jobs, they will also pay attention to the quality of life and raise their awareness of risks in life, occupation, health, etc. Then, they can promote their interaction with the city and eventually enhance the adaptability and self-security of the city. The occupational boundary factor has also passed the significance test at the level of 1%, and its coefficient is negative, indicating that the higher the proportion of migrant workers in the unit, the lower the probability of urban spatial embeddedness, and for every 1 percentage point increase in the proportion of new generation migrant workers in the same unit, the probability of their urban spatial embeddedness may decrease by 0.09%, because, on the one hand, it shows that most of them are in informal employment and concentrate in labor-intensive industries such as manufacturing and construction. On the other hand, it also shows that their occupational space is narrow, and they lack opportunities for vocational training and promotion and also lack high-level occupational mobility. Only the influence of life boundary factors on the social insurance of the new generation of migrant workers passes the significant test, and its coefficient sign is positive, which shows that the insurance of migrant workers is helpful for their settlement in the city but has no significant influence on the identity of the urban people. Because most of the new generation of migrant workers do not enjoy a comprehensive basic insurance system, the effects such as job instability, urban mobility, and other urban policy benefits cannot be excluded.

(2) *Control Variables.* The age, education, length of time in the city, income, and marital status of the new generation of migrant workers have all passed the significant test at the level of 1%, and the influence coefficient is positive.

These factors also have certain explanation function to their urban spatial embeddedness and promote their urban spatial embeddedness remarkably. Among them, the income factor is more obvious, because the new generation of migrant workers just start or just live in the city. Income increase is conducive to the stability of their living. It is also conducive to eliminate the instability of residence and the adverse factors from occupation and life. Table 5 is the statistical table of logit model regression analysis results.

(3) *The Spatial Embeddedness of the New Generation of Migrant Workers and the Difference of Urban Scale.* In order to investigate the differences between the urban spatial embedded groups of the new generation of migrant workers and cities, the regression analysis was made according to the groups after “80s” and “90s” and the size of cities, and the results of the “Urban spatial inhibition effect” on the urban embeddedness of the new generation of migrant workers are shown in Table 6. From the living boundary factor, whether after “80s” or “90s”, the variable is significant at the level of 1%, and the coefficient is positive. The factors of living boundary are unfavorable to the spatial embeddedness of the new generation of migrant workers. From the view of urban space inhibition effect, the impact on the “Post-90s” is greater than that of the “Post-80s,” because the “Post-80s” have a longer time in the city, a better base, and a richer social capital accumulation. From the view of city scale, the factors of living boundary can restrain the spatial embeddedness of the new generation of migrant workers, but the degree of inhibition is relatively small in small- and medium-sized cities. The occupation boundary factor has a significant effect on the urban spatial embeddedness of the “Post-90s” group but has no significant effect on the post-80s group. There are two possible reasons for this: first, some labor-intensive industries have gradually taken “Post-90s” migrant workers as the main body, and second, with the promotion of rural revitalization strategy, returning home to start a business has promoted the “Post-80s” return tide. Table 6 is the groups and urban differences of inhibition effect of spatial embeddedness of the new generation of migrant workers.

5. Policy Implications and Management Implications

5.1. Policy Implications. This paper takes the transformation of the basic rights needs of the new generation of migrant workers into urban space as the starting point. Based on the theory of urban space, this paper constructs the conceptual model of fit and restraint for the transformation of urban space embeddedness of the new generation of migrant workers and citizens around the basic point of “living, production, and life.” Through the empirical research, it is revealed that “Housing, occupation, and living security” is the basic starting point for the new generation of migrant workers from embedded into urban space to integrated into urban space. When the city adopts the corresponding

citizenization policy, it should take the basic rights demand of the new generation of migrant workers into account.

5.2. Management Inspiration. In order to push forward the new-type urbanization, we need to push forward the transformation of the new generation of migrant workers into urban residents. In order to effectively transform the new generation of migrant workers into citizens, it is necessary for the government to take measures and formulate policies from the aspects of salary treatment, employment, children’s school enrollment, social security, and housing household registration and establish and improve the employment security system for migrant workers. In order to better promote the transformation of the new generation of migrant workers into citizens, the government and enterprises should set up a reasonable employment security system, including market access, labor relations, and system design, provide equal opportunities for the new generation of migrant workers to find employment in cities, and ensure their effective access to public resources and services, so as to make it possible for their stable employment in cities. First, urban development policies should be in line with the urban employment policy of migrant workers. Policies for the economic development of urban industries should be adjusted according to the employment of migrant workers. The government should pay more attention to this group’s demand of job changes caused by the upgrading of technology-intensive and labor-intensive industries. Timely clarify and release professional ability standards to the society. Encourage migrant workers to update their technical skills in a timely manner. Increase employment opportunities in cities, and enhance their employability. Second, vocational skills training should be organized through multiple channels, and multimeasures mechanism should be set up in administrative enterprises and schools to enhance employability. The Labor Department should, in accordance with the needs of different positions, organize vocational skills training activities in a timely manner and bring the vocational training of the rural transferred labor force into the urban development system. Last but not least, it is important to construct a fair, reasonable attractive salary incentive system. The urban government shall timely adjust the wage and benefits level in accordance with the urban minimum wage standards, so as to guarantee the survival of migrant workers in urban employment. It is necessary to encourage Labor Union to play an active role in forming a dialogue mechanism that can represent the rights and interests of migrant workers, enhance their voice, and form a new type of labor-capital relations so as to effectively protect their legitimate rights and interests.

Expand the service scope of the public service system. To effectively promote the transformation of the new generation of migrant workers into urban residents and integrate them into cities and towns, the important link is to ensure that urban public services can be equal and fair. The pluralistic and dualistic public service systems are not beneficial for the integration of the transferred labor force into the cities and towns and do not reflect the original intention of

TABLE 5: Statistical table of logit model regression analysis results.

	Urban identity		Intention to settle in the city		Into the space of the city	
	Regression 1	Regression 1	Regression 1	Regression 1	Regression 1	Regression 1
Age	0.0005*** (0.0016)	0.0004 (0.0014)	0.0059*** (0.0019)	-0.0049*** (0.0069)	0.0109*** (0.0015)	-0.0059 (0.0059)
Marri	0.0425*** (0.0316)	-0.0016 (0.0316)	0.0157*** (0.0416)	-0.0396*** (0.0464)	0.0633*** (0.0267)	0.0519 (0.0615)
Edu	0.0271*** (0.0058)	0.0226*** (0.0066)	0.0228*** (0.0076)	0.0996*** (0.0316)	0.1646*** (0.0367)	0.0593 (0.0453)
Year	0.0037*** (0.0031)	0.0076 (0.0016)	0.0051*** (0.0016)	0.0067* (0.0064)	0.0047*** (0.0087)	0.0037*** (0.0054)
Incom	0.0003*** (0.0001)	-0.001*** (0.0001)	0.0005*** (0.0006)	-0.001*** (0.0004)	0.0001*** (0.0001)	-0.0003*** (0.0004)
Hous		0.1066*** (0.0273)		0.2166*** (0.0273)		0.1024*** (0.0273)
Rate		-0.0051*** (0.0006)		-0.0020*** (0.0004)		-0.0009*** (0.0007)
Safe		-0.0951** (0.0006)		0.0762** (0.0004)		-0.0824** (0.0005)
Prob > chi ²	0.0000	0.0000	0.0000	0.0000	0.0000	0.0000
Sample size	900		436		464	

Note. T value in parentheses, *, ** and *** are significant at the levels of 10%, 5%, and 1%, respectively.

TABLE 6: The groups and urban differences of inhibition effect of spatial embeddedness of the new generation of migrant workers.

Variable	Group	Inhibitory effect	Standard error	Group	Inhibitory effect	Standard error
Living	“Post-90”	0.1516*	0.0257	Big city	0.1073*	0.0316
	“Post-80”	0.1054	0.0336	Small and medium cities	0.1590	0.0368
Profession	“Post-90”	-0.0a110*	0.0005	Big city	-0.0007	0.0005
	“Post-80”	-0.0016	0.0006	Small and medium cities	-0.0002	0.0006
Life	“Post-90”	0.0471	0.0823	Big city	0.0067	0.0476
	“Post-80”	-0.0504	0.0307	Small and medium cities	-0.0525	0.0505

equality and fairness as well. The government should provide reasonable public service for the employment of rural migrant workers in cities and towns, expand the scope of urban public service, and effectively attract rural migrant workers to integrate into cities and towns from the aspects of children’s school enrollment, health care, and culture. The first one is to guarantee the children of migrant workers to attend school. The government should formulate policies to ensure that the children of migrant workers enjoy the same rights in education as urban residents. The government should increase financial input to ensure compulsory education, vocational education, and higher education for the children of migrant workers and give them appropriate educational subsidies. It is fine to formulate a reward system to encourage urban schools to admit migrant workers’ children to school and implement a free system for migrant workers’ children to receive vocational education. Secondly, it must ensure that migrant workers and their families enjoy the same medical treatment. The government should encourage the community to build a medical care system including migrant workers’ medical care, help them solve the medical problems in the city, and make sure that they can devote themselves to the urban construction healthily. The

government should provide the children of migrant workers equal medical and epidemic prevention treatment and so other social services for free. Then, migrant workers will be satisfied with public services in urban areas. Thirdly, encourage migrant workers to actively participate in community activities, requesting communities to eliminate discrimination, actively absorbing migrant workers to participate in community cultural activities, and ensuring that migrant workers enjoy equal cultural rights and interests in cities, so as to gradually integrate into urban life. Establish urban household registration, housing, and social security systems for migrant workers. Housing and social security are the main obstacles for the new generation of migrant workers to be urban residents. Therefore, the government should set up the urban housing and social security system to speed up the process. Firstly, the government should start from the supply side to provide housing security for the new generation of migrant workers in urban. The government should increase the construction of public rental housing, low-cost housing, affordable housing, and price-restricted housing in response to the demand of migrant workers and encourage them to purchase housing in cities and towns. At the same time, the

government should encourage employers to provide migrant workers with dormitories that meet the needs of modern life or provide them with rental subsidies, so as to effectively break one of the bottlenecks of migrant workers integration. Secondly, the government should conduct top-level design and construct the support policy, which is helpful for migrant workers to buy their own house. The local government may, according to the whole working life cycle, encourage the employers to pay a certain proportion of housing subsidies for the migrant workers and help the migrant workers establish a corresponding public reserve fund system, thereby helping the migrant workers to buy houses in cities and towns. The government should formulate policies to reduce or exempt relevant taxes and encourage migrant workers to purchase limited-price urban housing or affordable housing. Financial institutions shall be encouraged to provide long-term and low-interest loans for rural migrant workers to purchase houses in cities and towns. Thirdly, the government should establish the urban employment medical system and the industrial injury medical insurance system for rural migrant workers, so as to ensure that rural migrant workers, if they encounter industrial injury or other occupational diseases, can be treated in time and receive corresponding compensation. The fourth is to encourage employers to pay endowment insurance according to a certain proportion for migrant workers, so as to build a minimum foundation for transformation. At the same time, the government should provide necessary relief for migrant workers during their employment in cities and towns, as well as social relief for families or individuals in special circumstances.

6. Conclusion

Based on the perspective of urban space theory, this paper constructs the conceptual model and measures the model of spatial embeddedness fit and inhibition. Through a questionnaire survey on the transformation of the new generation of migrant workers in some cities in the “Yangtze River Delta” region, from the perspective of right demand and policy supply, this paper investigates the degree of integration and inhibition of the transformation of urban spatial embeddedness by the “Post-80s” and “Post-90s” migrant workers, as well as the differences between groups and cities in the process of new urbanization.

The measurement of the fit effect of the new generation of migrant workers’ urban spatial embeddedness shows that the basic rights demand of the new generation of migrant workers’ urban spatial embeddedness has a positive impact on the realization of their citizens’ transformation will. The higher the education level is, the more they like living in the city. The longer they live in city, the more urgent they are eager for house, occupation, and other needs. From the perspective of the supply of citizenization policy, the effect of the supply of housing, occupation and life-related citizenization policy on the demand of basic rights of the new generation of migrant workers embedded in urban space is positive, and it has an important influence on the realization of citizens’ will to transform. However, there is an obvious

imbalance between the demand and policy supply of the three basic rights. The empirical test on the spatial inhibition effect of the new generation of migrant workers in the process of urban transformation shows that the age, education, length of urban residence, income, and marital status of the new generation of migrant workers have some influence on their spatial embeddedness in the city. From the perspective of “urban spatial inhibition effect,” the current policy of urbanization is a double-edged sword, and it also has a certain degree of inhibition to the new generation of migrant workers.

“Post-90s” and “Post-80s” migrant workers have obvious difference in the fit effect of urban spatial embeddedness. First, the “Post-90s” and “Post-80s” need to focus on their own. The second is that the “Post-80s” are better than the “Post-90s” in terms of the policy universality they enjoy. Therefore, the above results of the new generation of migrant workers urban transformation of the spatial inhibition show that the policy inhibition effect of the “post-90s” is more obvious. From the view of city scale, the restraining effect of citizen transformation policy is different in different cities. Overall, the restraining effect is smaller in medium and small cities than that of big cities. In other words, if the new generation of migrant workers want to settle down in small- and medium-sized cities, the cost of transforming citizens is relatively small.

Data Availability

The simulation experiment data used to support the findings of this study are available from the corresponding author upon request.

Conflicts of Interest

The authors declare that there are no conflicts of interest regarding the publication of this paper.

Acknowledgments

The work was supported by National Social Science Foundation Project (16BRK009), Jiangsu Province “333 High-level Talent Training Project” Funding Project (Su Talent [2022] No.2), and Key project of the Wuxi Vocational Education Innovation and Development Program (2020 Zjzd02).

References

- [1] F. Zhang, “Research on the urban settlement decision of the new generation of migrant workers in China,” *IOSR Journal of Research & Method in Education*, vol. 11, no. 5, pp. 46–48.
- [2] China Federation of Trade Unions and L. Day, “Research report on the new generation of migrant workers,” *Employee Education in China*, vol. 5, no. 14, pp. 18–20, 2010.
- [3] F. Cai, Y. Du, and M. Wang, “Household Registration System and labor market protection,” *Economic Research*, vol. 12, no. 20, pp. 41–49, 2001.
- [4] M. Tian, C. Li, and D. Lai, “Reform of household registration system and settlement of agricultural transfer population:

Research Article

Increase in Suspended Sediment Contents by a Storm Surge in Southern Bohai Sea, China

Yongqiang Zhang,¹ Yongfu Sun ,² Zejian Hu,³ Shuhua Bian,³ Congbo Xiong,³ Jianqiang Liu,³ Wanqing Chi,³ and Wanjun Zhang³

¹College of Earth Science and Engineering, Shandong University of Science and Technology, First Institute of Oceanography, Ministry of Natural Resources, Qingdao, Shandong 266590, China

²College of Earth Science and Engineering, Shandong University of Science and Technology, National Deep Sea Center, Qingdao, Shandong 266590, China

³First Institute of Oceanography, Ministry of Natural Resources, Qingdao, Shandong 266061, China

Correspondence should be addressed to Yongfu Sun; sunyongfu8003@163.com

Received 22 March 2022; Revised 10 May 2022; Accepted 16 May 2022; Published 7 June 2022

Academic Editor: Wei Liu

Copyright © 2022 Yongqiang Zhang et al. This is an open access article distributed under the Creative Commons Attribution License, which permits unrestricted use, distribution, and reproduction in any medium, provided the original work is properly cited.

Most of the existing results were related to the impact of land storms on sediment, and few explained the impact of storms on sediment movement and its formation law from the mechanism. At present, the research on the impact of storm on sediment suspension on the North Bank of Longkou City in the south of Bohai Sea was not clear. Therefore, this study aimed to explore the formation and mechanism of storm on suspended sediment from the perspective of hydrodynamic characteristics and sediment distribution by monitoring the impact of storm on sediment suspension in the south of Bohai Sea. A storm with wind speeds of 4.5–13.5 m/s occurred in the coastal area of the north side of Longkou City located in Southern Bohai Sea in April, 2015. Suspended sediment samples were obtained using automatic samplers, and the results showed that the suspended sediment content was 7.8 mg/L under normal weather conditions, which reached 121.2 mg/L at the highest during the storm event. Waves and tides were synchronously observed by acoustic Doppler current meter. Wave height was more closely correlated with wind speed when the wind veered to north, and the maximum wave height was 243 cm. The reciprocating motion of the current at the sampling site was strong, with the maximum current speed of 43.8 cm/s and a water depth of 10 m. The results of laser analysis showed that the bottom sediments were composed of 92% sand and 8% silt, with a medium diameter of 0.102 mm. From the experimental observation and result analysis, it was known that the strong dynamic process during storm surge led to the movement of sediment surface and the resuspension of sediment.

1. Introduction

For a long time, the plateau sediment around the Yellow River Basin has been flowing into the Bohai Sea, and the Yellow River Delta of more than 5000 square kilometers has been formed. The long-term interaction between marine geological and biological resources is the main channel for the formation of different geological and chemical deltas. As the intersection area of logistics and energy flow, the delta is affected by different spheres of the Earth, which makes the land and ocean interact with each other,

resulting in a certain impact on the ecology and environment. The delta region is greatly affected by human life and climate change.

Storms have a large effect on sediment movement [1]. Strong cyclonic wind stress accelerates sediment resuspension, and the concentration of suspended particles in the seawater column might be increased by dozens of times during and after storms [2, 3]. Under wind speeds of 5–15 m/s and wave heights of 50–150 cm, the suspended content in the Yellow River Delta reached 5.7–49.6 kg/m³, which is 10–100 times higher than that under normal weather

conditions [2]. Sediment resuspension may cause various problems to ocean engineering. For example, scour around piles and pipelines and deposition in harbors and channels occurred in the Yellow River Delta during storms. In October 2006, 1.2 m of sediment was deposited in a test channel with a depth of 2.5 m in only 10 days during a storm after it had been dredged for 1 month [4].

The Bohai Sea belongs to a semiclosed inland sea zone, which has been affected by gale climate for a long time. Storms in the Bohai Sea generally occur in winter every year and last about half a year. On average, there are about 6 storms above grade 8 every year [5]. The waves generated by storms in the Bohai Sea can reach about 7 m. The research shows that the marine dynamic seasonality is obvious. The average water depth in the Bohai Sea area is about 18 m. The sediments are more vulnerable to the impact of waves than other sea areas. The sediment suspension is the result of the impact of storms on the sediments, which leads to certain changes in the structure of sediments in the Yellow River Delta and Bohai Sea. Storm surges in the southwest Bohai Sea are larger than those in the north [6]. Longkou Port, sea embankments, and the intake of Longkou Power Plant were all located in coastal area of the north side of Longkou City, Southern Bohai Sea, China. Erosion and collapse of embankments, siltation of navigable waterways, and abrasion of the inner wall of the circulating water pipeline may be caused by sediment resuspension. According to the statistical data of Longkou Ocean Station, the annual average of wind speed in this area is 6.4 m/s, and the maximum wind speed is 28 m/s. The occurrence frequency of strong wind of force six or above (the speed is more than 10.8 m/s) is 8.44%, and the occurrence frequency of gale-force wind (the speed is more than 13.9 m/s) is 4.54%. Thus, sediment movement during storms is the key question in marine science research in this area. However, to date, it is still unclear how much sediment can be suspended into water column of the north side of Longkou City, and how the suspended sediments are distributed temporally and spatially during storms in this area. Therefore, the research on the diffusion of suspended sediment and its effect on the formation of surrounding landform has important theoretical significance and application value.

At present, there are few studies on the impact of storms on sediments in the Delta and Bohai Sea and the law of sediment suspension movement. In this study, the effects of storm on sediment suspension in coastal area of the north side of Longkou City located in Southern Bohai Sea and the possible mechanisms were researched. First, the suspended sediment contents during and after a storm event in April 2015 were detected and compared with that during normal weather conditions. Then, winds, waves, and tides were synchronously observed and correlation analyses between those indexes were carried out, to explore the possible mechanisms of sediment resuspension from the perspectives of hydrodynamic characteristics. Last, source, composition, and particle size of sediment were discussed, to further explore the possible mechanisms of sediment resuspension from the perspectives of sediment characteristics.

2. Materials and Methods

2.1. Sampling Time and Sampling Site. In order to explore the influence of storm, wave, and other factors on the change of suspended sediment content, the experiment is mainly carried out under the adverse weather conditions in the coastal area north of Longkou City in the south of Bohai Sea, and different stations are selected to observe the relevant indicators in this area. According to the hydrological and meteorological forecast, the coastal area of the north side of Longkou City, Southern Bohai Sea, was expected to experience strong winds on April 11–14, 2015. Therefore, the wind, wave, tide, and suspended sediment were observed from 20:00 on April 11, 2015 to 02:00 on April 14, 2015. During the test, the observation indexes mainly include suspended sediment, wind speed and direction. Among them, the samples for sediment sampling are mainly suspended sediment, and the sampling point is the same as that of wave and tide observation station (station 1), while the wind speed and direction data are from Longkou hydro-meteorological station (station 2), which is located about 8 km west of station 1. To study the suspended sediment characteristics under normal weather conditions and make comparisons to those during storms, suspended sediment sampling was carried out at 09:00 on April 10 (before the storm) and 9:00 on April 15 (after the storm), and suspended sediment data were also collected and analyzed from four nearby stations (station 3–6) set up by our team during good weather conditions in June 2004. Bottom sediment was sampled from seven stations (No. 7–13) along a cross section of the suspended sediment sampling station (station 1) during normal weather conditions in April 2015 for analysis of sediment composition and particle size. As shown in Figure 1, this is the basic distribution of the sampling station map. Table 1 shows the basic geographic information of the sampling station.

Figure 2 shows the process diagram of water exchange in the Bohai Sea and other sea areas.

The experiment is mainly completed by outdoor sampling and indoor analysis. Outdoor sampling mainly measures the flow velocity and direction of water meter, water and underwater at each station. The direct reading current meter is used to observe the flow velocity and direction. The measurement range of flow velocity is 0.05–3.5 m/s, the accuracy is +2.5%, the measurement range of flow direction is 0–360°, and the accuracy is +5°. At the same time, water samples are collected at different water levels for indoor measurement of suspended sediment content and salinity. Among them, the salinity is measured by a salinometer with a measurement range of 2.5–45.5 psu and a measurement accuracy of 0.01 psu. The suspended sediment content is treated by suction filtration, drying, and weighing. The diameter of the filter membrane is 45 mm and the pore diameter is 0.55 μm fiber double filter membrane, the lower filter membrane is used for correction, and the weighing is carried out on the balance. The water depth is measured by single frequency sounder. Suspended sediment samples were obtained using an improved MULTI-LIMNOS automatic sampler (Hydro-bios, German). The samples were filtered

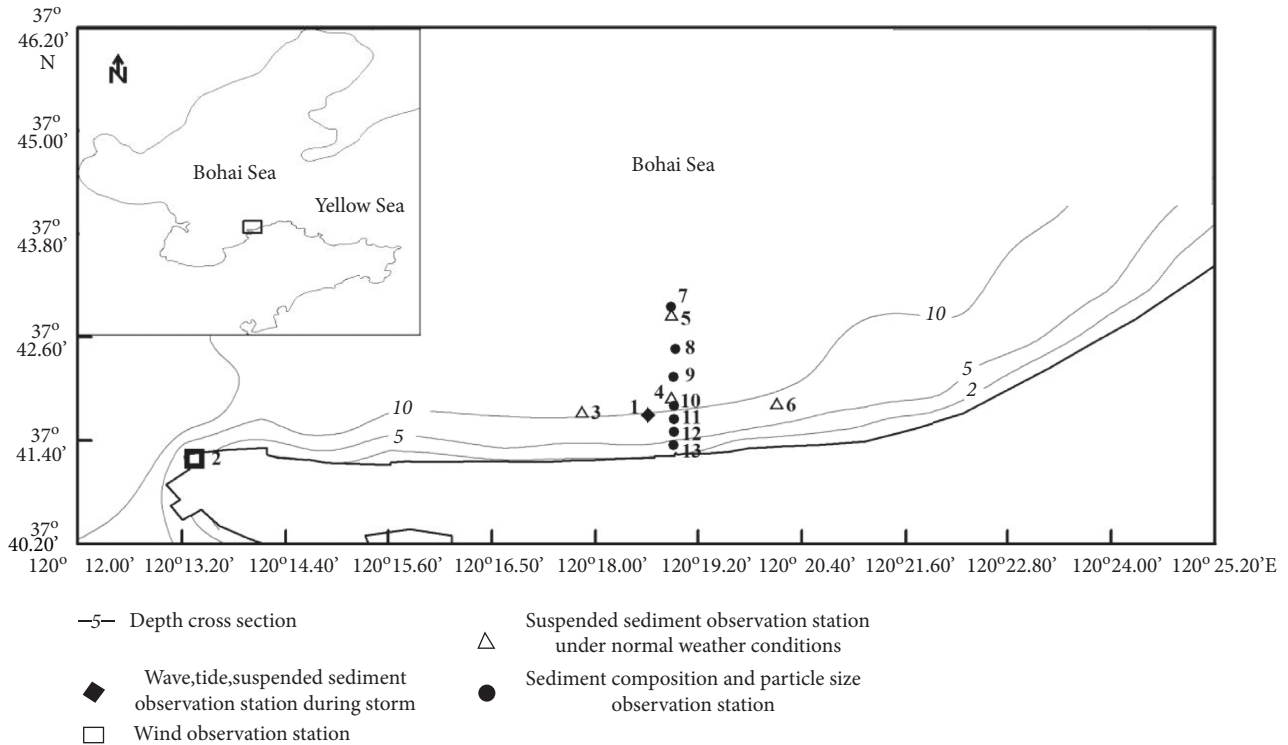


FIGURE 1: Map of sampling stations.

TABLE 1: Geographical information of sampling stations.

Station	East longitude	North latitude
1*	120°18.645'	37°41.696'
2#	120°13.300'	37°41.200'
3&	120°17.862'	37°41.719'
4&	120°18.934'	37°41.866'
5&	120°18.909'	37°42.859'
6&	120°20.127'	37°41.824'
7□	120°18.924'	37°42.947'
8□	120°18.957'	37°42.466'
9□	120°18.945'	37°42.142'
10□	120°18.947'	37°41.834'
11□	120°18.938'	37°41.648'
12□	120°18.939'	37°41.500'
13□	120°18.933'	37°41.345'

*Collected data: wave, tide, and suspended sediment during storm. #Collected data: wind. &Collected data: suspended sediment under normal weather conditions. □Collected data: average sediment concentration, sediment composition, and particle size.

with the filter membrane of $0.45 \mu\text{m}$ pore size and dried in the laboratory to calculate the suspended content. The automatic water samplers are easy to be damaged under bad weather conditions. Especially, the sample bottles may fall off from the sampler due to the strong current. Thus, the automatic sampler was reinforced with antiwave grid structure (patent of China: 201320886378.7) and set up using an anchor system at approximately 1.5 m above the seabed to ensure the collection of suspended samples during storms.

The automatic water sampler was equipped with ten sampler bottoms, each with a volume of 1 L. Two rubber tubes were installed in the mouth of the sampler bottom, one of which was water inlet and the other was exhaust tube.

Before the water sample was collected, the two tubes both were bent and fixed in bow-shaped knot to ensure that the sampler bottom was closed. When the predetermined time was coming, the tubes opened to collect water sample and exhaust the air. The process for each bottle to obtain enough water sample was about 10 minutes, and the ball valve floated to block the inlet when the bottle was full-filled. The sampling interval during the storm event was 6 hours. The sampling of the suspended sediment in normal weather conditions in a spring tide lasted for 25 hours with a sampling interval of 1 hour, and the average suspended sediment content was calculated to represent the baseline under normal weather conditions.

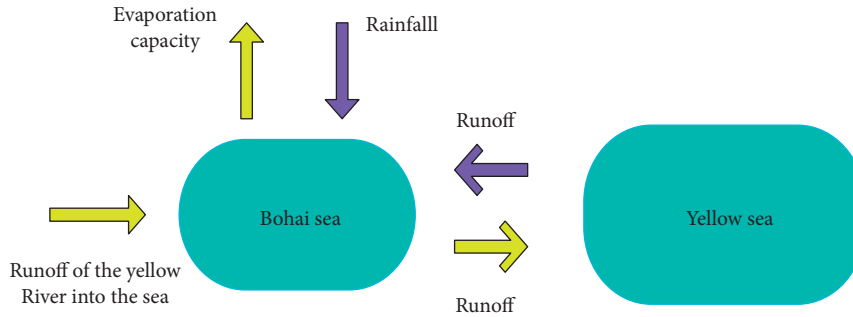


FIGURE 2: The observed wind direction and speed during the observation under the storm.

2.2. Collection and Observation of Wind and Hydrodynamics Data. In addition, wind speed, wind direction, and other important indicators affecting suspended sediment content were observed during the experiment. Wave direction, wave height ($H1/10$), current velocity, and current direction were obtained by a WHS600-1-UG57 acoustic Doppler current profiler (ADCP, RDI, USA) placed at the bottom of the seabed, with the sampling frequency of 2 Hz and the observing frequency of 1 h. Water level was observed by a TGR-2050 self-capacitance tide gauge (RBR, Canada) placed at the bottom of the seabed, with the observing frequency of 10 min.

2.3. Analysis of Bottom Sediment Composition and Particle Size. A total of seven bottom sediment samples were obtained with a grab sampler along the cross section. The sediment composition and particle size was analyzed in the laboratory by a laser analyzer (GSL-101Bi).

3. Results and Discussion

In order to facilitate analysis and comparison, the observation data of some stations with the same location of continuous stations during sampling in summer 2010 and winter 2015 are selected for comparison, and the average sediment concentration and its changes of these stations are selected for comparative study. The comparison results are shown in Table 2.

According to the observation and statistics results in Table 2, the concentration of suspended sediment in Bohai Sea area in winter is significantly higher than that in summer. The results of sampling data from different observation stations show that the average sediment concentration in winter in the inlet area is about 25 times higher than that in summer, while that in other observation stations is about 15 times higher than that in summer.

During the period of water and sediment regulation in the surrounding waters of the Bohai Sea in summer, the diffusion range of sediment into the sea is small. In the sediment content of the surface and middle water body of the sea, except that the sediment content near the coast is greater than 15 mg/L, the sediment content in most other areas is less than 3 mg/L. Although the bottom sediment concentration of the seabed is mostly greater than 3 mg/L, the range of water areas with sediment concentration greater

than 15 mg/L is basically the same as that of the surface and middle layers. However, in winter, the sediment concentration of the experimental observation station is greater than 15 mg/L in all layers of the water body, and the water area with sediment concentration greater than 80 mg/L near the coast is significantly greater than the water area with sediment concentration of 15 mg/L in summer.

In order to observe the movement law of suspended sediment in different seasons, the changes of sediment flux at different stations in summer and winter are compared in the experiment, as shown in Table 3.

According to the observation results of sediment flux changes at different stations, during the water and sediment regulation in summer, except that the sediment flux at the observation station near the sea inlet is less than that in summer, the sediment flux at other stations in winter is 3–120 times that in summer, as shown in Table 3. The observation results show that the suspended sediment flux increases significantly at stations with shallow water depth, which is more than 8 times that in summer and up to 120 times. Meanwhile, during the period of water and sediment regulation, the suspended sediment flux is affected by the flow velocity and direction, and the suspended sediment mainly moves from nearshore to offshore.

3.1. Wind. Based on the data from Longkou hydrometeorology station, there were 3 stages of storms during the observation period, as shown in Figure 3. During stage 1 (from 20:00 on April 11 to 08:00 on April 12), the wind speed was increased abruptly with a maximum value of 13.5 m/s at the end. A steering effect was observed as the wind changed from partial southern direction at stage 1 to partial northern direction at stage 2 (from 08:00 on April 12 to 02:00 on April 13) and stage 3 (from 02:00 on April 13 to 02:00 on April 14). The velocity was kept on a high plane ranging from 11.0 m/s to 13.5 m/s at stage 2, and then the wind speed was decreased gradually to 4.5 m/s at stage 3.

3.2. Suspended Sediment Content. In order to explore the suspended sediment content and its variation law, the suspended sediment concentration at different observation stations was tested. According to the experimental sampling results, the low concentration suspended sediment waters on the surface of the station occupy most of the Bohai Sea area,

TABLE 2: Comparison of sediment concentration between summer 2010 and winter 2015.

Station	Average sediment concentration in summer of 2010 (mg/L)	Average sediment concentration in winter of 2015 (mg/L)
7	16.1	342.6
8	13.5	241.8
9	23.7	586.4
10	9.3	143.7
11	8.5	119.4
12	16.3	303.6
13	12.8	218.5

TABLE 3: Comparison of sediment flux between summer 2010 and winter 2015.

Station	Sediment flux in summer 2010 (mg/L)		Sediment flux in summer 2015 (mg/L)	
	Size (kg/m/s)	Direction (°)	Size (kg/m/s)	Direction (°)
7	0.18	158.4	5.64	167.2
8	0.43	238.7	8.39	135.6
9	0.27	196.5	5.17	179.5
10	0.14	214.3	6.28	95.3
11	0.06	318.6	5.14	126.5
12	0.07	194.5	6.46	135.9
13	0.06	316.7	5.27	103.6

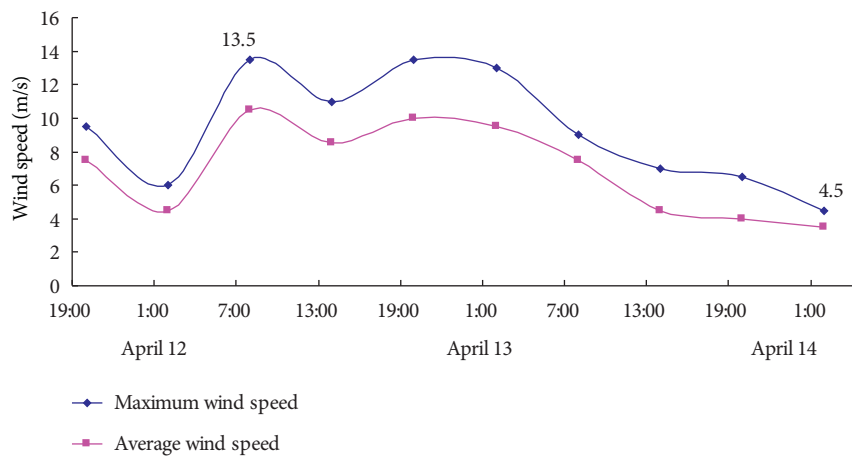


FIGURE 3: The observed wind direction and speed during the observation under the storm.

and the areas with high sediment concentration are mainly concentrated near the coast and the estuary. The high concentration sediment at the sea inlet is mainly distributed in the sea and its north and south sides. The sediment concentration near the sea inlet is the highest, but the distribution is limited. Medium concentration sediment is mainly distributed within 10–20 km from the shore, and the sea area with sediment concentration less than 5 mg/L is generally beyond 20 km, especially in the area of washed fresh water, with relatively low sediment content. The experimental results show that the distribution characteristics of sediment concentration in the middle water area are basically consistent with that in the surface. The sediment concentration in the bottom water area is significantly higher than that in the surface and middle water areas. The sediment concentration in some areas of the estuary can reach 6500 mg/L, while the water area with sediment concentration >5 mg/L has a large distribution range.

According to the data sampled from different stations, the suspended sediment content during the storm is significantly higher than that under normal weather conditions, as shown in Table 4. The suspended sediment content before the storm (April 10) was determined to be 7.8 mg/L, which was consistent with the results from the four nearby stations during good weather conditions in June 2004 (7.3 mg/L–27.6 mg/L), as shown in Table 5. During the storm event, the suspended sediment content varied from 17.6 mg/L to 121.2 mg/L, as shown in Table 4. To be specific, on the first two days of the storm occurrence (April 11 and 12), the suspended sediment content was around 20 mg/L, slightly increased compared with that before the storm, but it was still in the range of suspended sediment content during good weather conditions according to the observation of June 2004. Conversely, on the last two days of the storm occurrence (April 13 and 14), the suspended sediment content was increased markedly to at least 54.4 mg/L,

TABLE 4: Suspended sediment content before, during, and after the storm surge in April, 2015.

Period	Sampling time		Sampling water depth (m)	Suspended sediment content (mg/L)
	Day	Hour		
Before the storm	April 10, 2015	09:00	9.1	7.8
	April 11, 2015	20:00	8.8	26.8
		02:00	9.4	20.0
	April 12, 2015	08:00	9.1	17.6
14:00		9.2	21.2	
20:00		9.1	20.8	
During the storm	April 13, 2015	02:00	9.7	98.8
		08:00	*	
	April 13, 2015	14:00	9.5	60.0
		20:00	9.2	121.2
After the storm	April 14, 2015	02:00	9.4	54.4
	April 15, 2015	09:00	9.3	28.0

*Data at 08:00 in April 13, 2015, were not used in the analysis because the bottle did not open during the observation period.

TABLE 5: Suspended sediment content in normal weather conditions in June 2004.

Station	Average suspended sediment content (mg/L)	
	Spring tide	Neap tide
3	14.1	7.3
4	15.1	11.7
5	15.6	14.0
6	21.4	27.6

and the maximum value of 121.2 mg/L appeared at 20:00 on April 13.

Combined with the influence of storm factors and seasons on the variation of suspended sediment content, the results show that the sediment content in winter is significantly higher than that in summer. Among them, the suspended sediment at the entrance observation station in winter is 15 times higher than that in summer. The sediment in winter is greatly affected by the change of wind direction and wind force, while the sediment in summer is also affected by wind direction and wind force, but it is smaller than that in winter. Therefore, winter is the main season for sediment transport in the Bohai Sea area, and the transport of suspended sediment to the southern sea area mainly occurs in winter, which is basically consistent with the variation law of sediment in the east coast of China.

3.3. Wave, Current, and Water Level. According to the sediment concentration in the corresponding layer of each observation station and the influence of sediment content on water body density [7–9], the water body density of the observation station can be calculated, and the calculation formula is as follows:

$$\rho_w = \rho_z + s_c \left(1 - \frac{\rho_z}{\rho_0} \right), \quad (1)$$

where ρ_w denotes the density of water body and ρ_z is the seawater density calculated according to the parameters such as temperature, salinity, and pressure, using the international seawater equation of state. s_c is the sediment content and ρ_0 is the sediment density constant.

Consistent with the wind, there were 3 stages of wave process during the observation period, as shown in Figure 4. During stage 1 (from 20:00 on April 11 to 02:00 on April 13), the wave height was increased significantly with a maximum value of 1.82 m at the end. The wave height was kept on a high plane ranging from 1.68 m to 2.43 m at stage 2 (from 02:00 on April 13 to 14:00 on April 13), with the maximum appearing when the wave direction was north-north-east, and then it was decreased gradually at stage 3. Statistics showed that the wave lasted for approximately 21 hours with a significant wave height of more than 100 cm.

The reciprocating motion of the current at the sampling site was strong. Normally, the direction of flood current was north-west and the direction of ebb current was north-east. The effects of storm on flow direction and velocity was significant on the last two days of the storm occurrence (April 13 and 14). Specifically, under the influence of partially north wind, the flow direction in April 13 is eastern-biased, and the current speed was accelerated, with the maximum current speed of approximately 43.8 cm/s appearing at 17:00 on April 13.

Under normal weather conditions, depth of water changed between 9.3 m and 10.0 m. During the storm, there was a clear additional water level increase apart from the tidal level change. For example, the storm caused the low tide level at 20:00 on April 12 to be increased by approximately 30 cm, and the subsequent high tide level in the small hours of April 13 also rose by approximately 40 cm. As shown in Figure 5, the observed current direction, current speed, and water level during the observation under the storm are described.

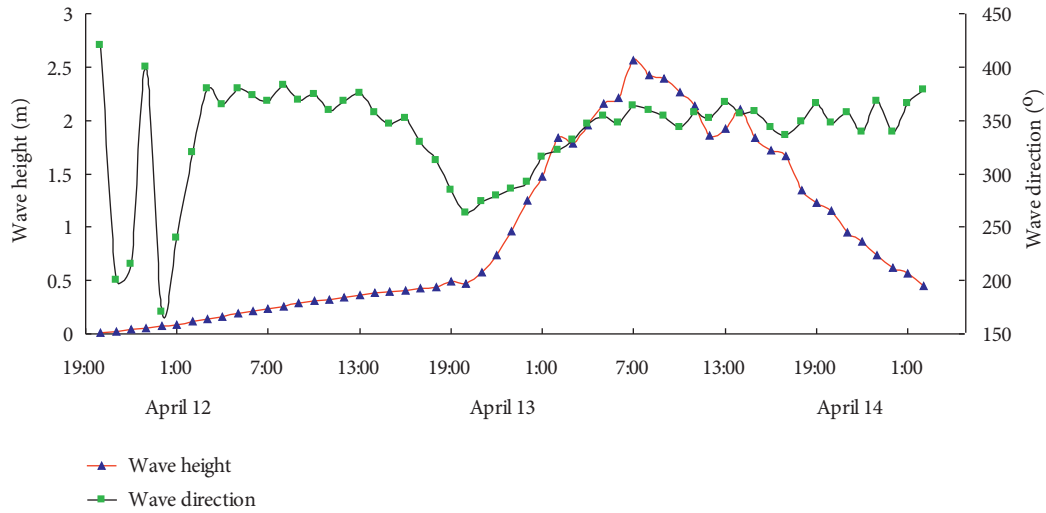


FIGURE 4: The observed wave direction and height during the observation under the storm.

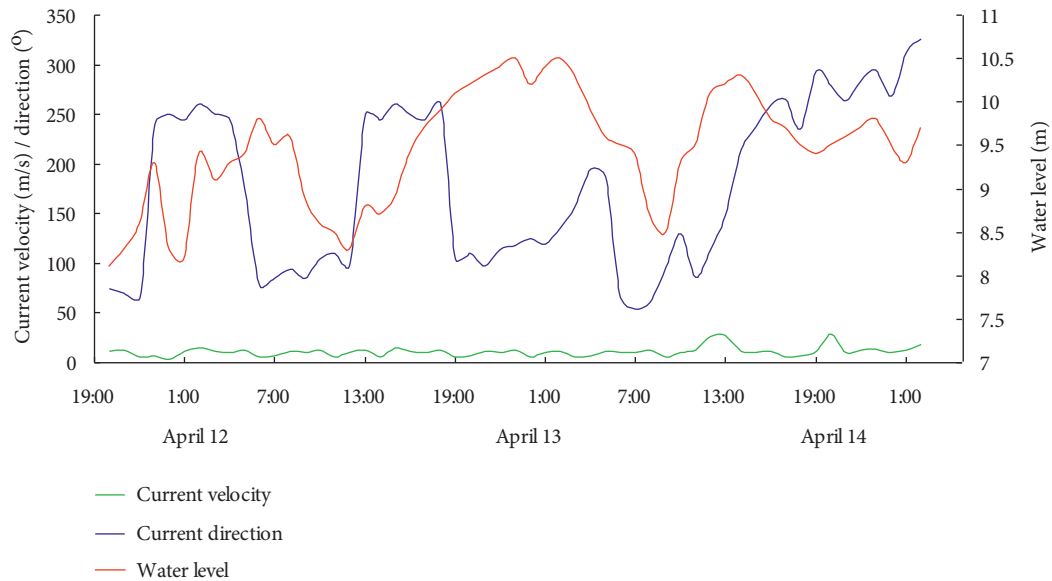


FIGURE 5: The observed current direction, current speed, and water level during the observation under the storm.

According to the experimental results and existing studies, there is a positive correlation between the force causing sediment movement and wave height. In other words, the higher the waves, the greater the sediment incipient motion and the higher the suspended sediment content [10]. It can be seen that hydrodynamics was closely correlated with wind especially when the wind veered to north, with lag phases of about 6 h for wave and 12 h for current. Then, the seafloor particles were carried by storm-driven wave and current and resuspended in the seawater, resulting in an order-of-magnitude increase in suspended sediment content [11, 12].

It is known from the existing research that during the period of water and sediment regulation, the runoff in the Bohai Sea is large. In the process of ebb tide, the runoff into the sea enters the relevant observation stations due to factors such as high temperature, low salt, and high sediment

concentration. As the runoff from the Bohai Sea mainly diffuses on the surface of the water body, there is an obvious density difference between the low-density water body with high temperature and low salt on the surface of the observation station and the high-density seawater with high salt and low temperature on the lower layer, and a density thermocline is formed in a certain water depth [13]. The sediment entering the sea is gradually deposited during diffusion. When the sediment settles to the pycnocline, due to the difference of water density, the suspended sediment cannot continue to settle due to the reverse action of the pycnocline and then form a suspended state near the pycnocline. The research shows that the shear front usually causes a large amount of sedimentation of suspended sediment in the water body, which leads to the rapid sedimentation of surface sediment, the destruction of layered structure, the continuous downward diffusion of upper

water body, the continuous increase of temperature and sediment content of lower water body, and the gradual decrease of salinity [14]. It can be seen that the sediment content of the water body after being affected by the shear front shows a downward trend. In the process of diffusion to the sea, due to the capture effect of the circulation, most of the sediment entering the sea is deposited in the area about 15 km away from the estuary. At the same time, because the high concentration of suspended sediment generally cannot reach the surface of the water body, these sediments are mainly distributed in the water area below the thermocline [15, 16].

From the density distribution of water body and the vertical distribution law of velocity, in order to reflect the vertical structure difference of water body, the vertical coefficient of water body V_w can be calculated according to the following formula:

$$V_w = -\frac{(g/\rho_w)(d\rho_w/du)}{(dy/du)^2}, \quad (2)$$

where ρ_w indicates the density of water body, y is the horizontal velocity of water body, and u is positive upward. The denominator reflects the sediment flow caused by the flow velocity of the water body, and the numerator reflects the stratification structure strength caused by the change of water density. When $V_w > 0.3$, it means that the intensity of water body stratification structure is greater than the sediment flow caused by the action of water velocity; at this time, it is mainly stratified structure. While $V_w \leq 0.3$ means that the water body is mainly sediment flow.

3.4. Bottom Sediment Composition and Particle Size. According to Shepard's ternary diagrams, S (sand), TS (silty sand), and ST (sandy silt) were successively distributed along the measured section [17]. The sand content decreased, while the silt, which can be suspended, increased with the offshore distance and the water depth along the section. Station 9, the nearest bottom sediment sampling site to the suspended sediment sampling site (station 1), was located in shallow sea area around the 10 m depth contour, where the bottom sediments were composed of a large amount of sand (92%) and a small amount of silt (8%).

The particle size of the bottom sediments in the study area became finer from the coast to the sea. Station 9, the nearest bottom sediment sampling site to the suspended sediment sampling site (station 1), was located in shallow sea area around the 10 m depth contour, where the medium diameter (Md) was about 3.3ϕ (0.102 mm). As shown in Figure 6, the composition and medium diameter of the bottom sediment along the cross-section are described.

According to the Misaki Sato's empirical formula [18, 19], 2.0 m-high wave can cause sediment surface movement with a particle size of 0.1 mm under a water depth of 10 m, and intense movement of sediment with a particle size of 0.1 mm under a water depth of 10 m will be induced by wave with a height of 2.8 m, as shown in Table 6.

The water depth of sediment surface movement is calculated as

$$\frac{H_0}{L_0} = 1.35 \left(\frac{d_m}{L_0} \right)^{1/3} \sinh \left(\frac{2\pi D_C}{L} \right) \cdot \frac{H_0}{H}. \quad (3)$$

The water depth of sediment intense movement is calculated as

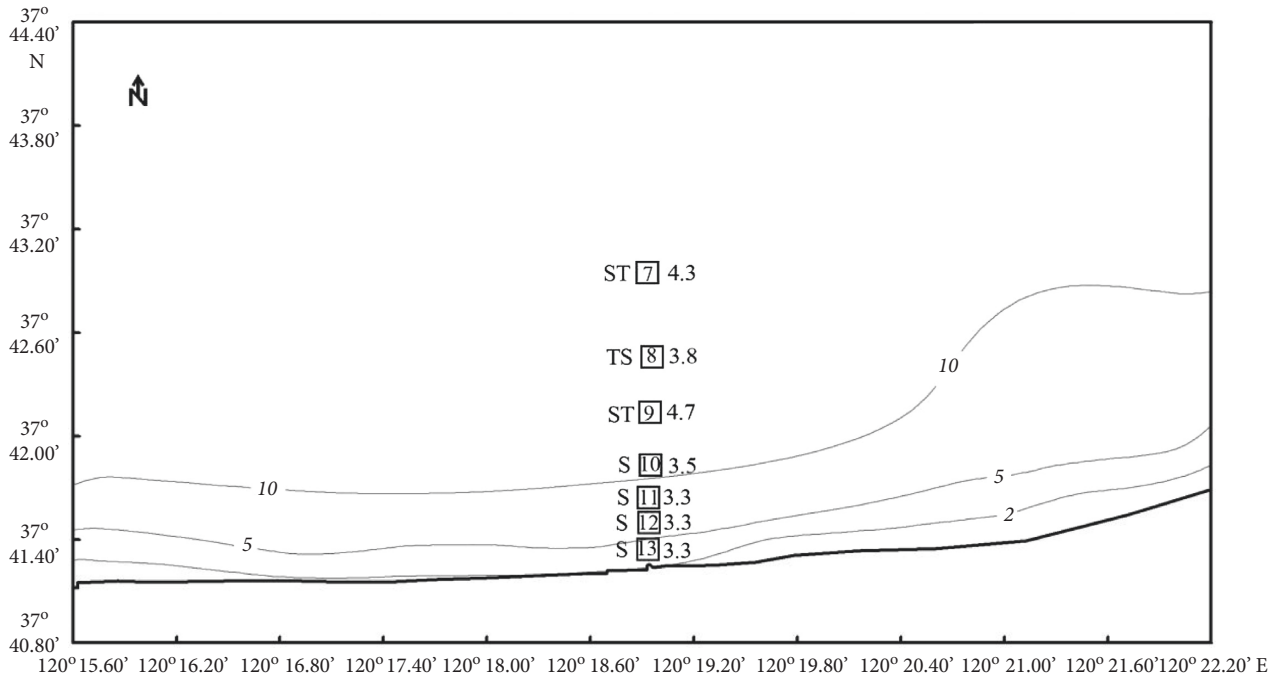
$$\frac{H_0}{L_0} = 2.40 \left(\frac{d_m}{L_0} \right)^{1/3} \sinh \left(\frac{2\pi D_C}{L} \right) \cdot \frac{H_0}{H}, \quad (4)$$

where H_0 denotes the deep-water wave height, L_0 is the deep-water wave length, H represents the wave height at the calculation point, L shows water depth at the calculation point, D_C indicates the water depth of sediment movement, and d_m expresses the medium diameter of bottom sediment.

During the observation period in this study, the maximum wind speed was 13.5 m/s, and the maximum wave height was 2.43 m, leading to the sediment surface movement of station 1. This is just a representative of wind and wave with moderate intensity in coastal area of the north side of Longkou City. According to the statistical data of Longkou Ocean Station, the occurrence frequency of wind with the speed of more than 10.8 m/s is 8.44%, the occurrence frequency of wave with the height of more than 2 m is 8.7%, and the maximum wave height is 7.2 m, as shown in Table 7. Thus, it is reasonable to suspect that the suspended sediment content measured in April 2015 is far from the maximum for the study area, and more seabed sediments will be suspended under stronger storm events, especially when sediment intense movement is caused by wave ranging from 2.8 m to 7.2 m.

According to the sediment content measured by some scholars in summer and the estimated water outflow from the Bohai Sea, the sediment flux from the Bohai Sea to the Yellow Sea can be calculated, which is basically consistent with the observation results in this paper. This shows that although the observation stations selected in this experiment are different from previous studies, the observation results are basically consistent.

Although the amount of sediment entering the sea of the Yellow River is decreasing, its impact on the sediment content in the Bohai Sea is not significant [20, 21]. The predecessors did not consider the seasonal variation of suspended sediment content and flow in the study area, which makes the calculation of sediment content inaccurate. In addition, the material transported from the Bohai Sea to the Yellow Sea is mainly the suspended sediment from the Yellow River into the sea caused by storms in winter [22]. In addition to the newly deposited sediment, it also includes the sediment from the Yellow River Delta into the sea. Compared with the previous research results, this paper considers the seasonal variation, but the experiment is mainly based on the measured data in winter, and the continuous observation stations selected are limited. Therefore, the calculation of suspended sediment content and its variation affected by storms in the Bohai Sea is also rough [23]. If we want to obtain more accurate results, we need to observe at multiple continuous stations in different seasons over a long period of time in the future. Nevertheless, the observation results



—5— Depth cross section
 Sediment types | Observation station | Particle size
 (S:dand, (Unit:φ,
 TS:silty sand 1φ = 2^{-φ}mm)
 ST:sandy silt)

FIGURE 6: Composition and medium diameter of the bottom sediment along the cross section.

TABLE 6: Water depth of sediment movement with a particle size of 0.1 mm according to wave with different heights.

$H_{1/10}$ (m)	Water depth of sediment surface movement (m)	Water depth of sediment intense movement (m)
2.0	10.07	6.97
2.8	14.57	10.01

TABLE 7: Occurrence frequencies of wave with different heights in Longkou ocean station.

Wave height	Occurrence frequency
$H_{1/10} \leq 0.9$ m	71.66
$1.0 \text{ m} \leq H_{1/10} < 2.0$ m	19.74
$2.0 \text{ m} \leq H_{1/10} < 3.0$ m	5.76
$H_{1/10} \geq 3.0$ m	2.90
Total	100.00

obtained in this experiment have been greatly improved compared with previous studies, and the change of suspended sediment content is obtained under the influence of storms in winter and spring [24]. If the effects of other seasonal storms or geological factors on the suspended sediment content and its changes are considered, the sediment content formed in the Bohai Strait may be doubled higher than the results obtained in this paper, which is also a problem that needs to be verified by experimental observation in the future [25–27].

4. Conclusion

Most of the existing achievements were based on the impact of storms on land sediment, but there was a lack of research on the impact mechanism of storms on suspended sediment. Therefore, this paper took the sediment suspension on the North Bank of Longkou City in the south of Bohai Sea as the research object. By monitoring the impact of storm on sediment suspension in the south of Bohai Sea, this paper explored the formation and action law of storm on suspended sediment from the perspective of hydrodynamic characteristics and sediment distribution. Through the test sampling and analysis of different observation stations, the results showed that under normal weather conditions, the suspended sediment content was 7.8 mg/L, reaching the highest value of 121.2 mg/L during the storm. When a storm surge occurred in the coastal area on the north side of Longkou City in the south of the Bohai Sea, the maximum wind speed was 13.5 m/s and the maximum wave height was 2.43 m. At a water depth of 10 m, the surface movement of

seabed sediments was caused, and the content of suspended sediment increased to 121.2 mg/L. The test results showed that the strong dynamic process during storm surge led to the movement of sediment surface and the resuspension of sediment. The research results of the impact of storm on the sediment suspension on the North Bank of Longkou City in the south of Bohai Sea will have certain guiding significance for exploring the diffusion of suspended sediment and its impact on the formation of surrounding landform.

Data Availability

The labeled dataset used to support the findings of this study are available from the corresponding author upon request.

Conflicts of Interest

The authors declare no conflicts of interest.

Authors' Contributions

Yongqiang Zhang wrote the manuscript. Yongfu Sun and Yongfu Sun designed the experiment. Wanqing Chi and Shuhua Bian undertook the experimental tasks and data processing work. Jianqiang Liu and Bingzhi Huang prepared the figures. All authors reviewed the manuscript.

References

- [1] J. A. Goff, M. A. Allison, and S. P. S. Gulick, "Offshore transport of sediment during cyclonic storms: hurricane ike (2008), Texas gulf coast, USA," *Geology*, vol. 38, no. 4, pp. 351–354, 2010.
- [2] S. Bian, Z. Hu, J. Liu, and Z. Zhu, "Sediment suspension and the dynamic mechanism during storms in the yellow river delta," *Environmental Monitoring and Assessment*, vol. 189, no. 1, p. 3, 2016.
- [3] Y. Li, H. Li, L. Qiao, Y. Xu, X. Yin, and J. He, "Storm deposition layer on the Fujian coast generated by Typhoon Saola (2012)," *Scientific Reports*, vol. 5, Article ID 14904, 2015.
- [4] R. Liu, Z. Han, and T. Liu, "Bottom sediment characteristics and feasibility of proposed deepwater channel of Dongying port," *J. Waterw. Harb.* vol. 34, pp. 118–122, 2013.
- [5] J. M. Martin, J. Zhang, M. C. Shi, and Q. Zhou, "Actual flux of the huanghe (Yellow River) sediment to the western pacific ocean," *Netherlands Journal of Sea Research*, vol. 31, no. 3, pp. 243–254, 1993.
- [6] J. Feng, D. Li, Y. Li, Q. Liu, and A. Wang, "Storm surge variation along the coast of the Bohai Sea," *Scientific Reports*, vol. 8, Article ID 11309, 2018.
- [7] Q. S. Liu, G. H. Liu, C. Huang, and H. Li, "Soil physico-chemical properties associated with quasi-circular vegetation patches in the Yellow River Delta, China," *Geoderma*, vol. 337, pp. 202–214, 2019.
- [8] F. Oliva, M. C. Peros, A. E. Viau, E. G. Reinhardt, F. C. Nixon, and A. Morin, "A multi-proxy reconstruction of tropical cyclone variability during the past 800 years from Robinson Lake, Nova Scotia, Canada," *Marine Geology*, vol. 406, pp. 84–97, 2018.
- [9] E. R. Eisemann, D. J. Wallace, M. C. Buijsman, and T. Pierce, "Response of a vulnerable barrier island to multi-year storm impacts: LiDAR-data-inferred morphodynamic changes on Ship Island, Mississippi, USA," *Geomorphology*, vol. 313, pp. 58–71, 2018.
- [10] Y. C. Zhou, X. Y. Yao, Y. Q. Gu et al., "Biological effects on incipient motion behavior of sediments with different organic matter content," *Journal of Soils and Sediments*, vol. 21, no. 1, pp. 627–640, 2021.
- [11] B. Ferré, K. Guizien, X. Durrieu de Madron, A. Palanques, J. Guillén, and A. Grémare, "Fine-grained sediment dynamics during a strong storm event in the inner-shelf of the Gulf of Lion (NW Mediterranean)," *Continental Shelf Research*, vol. 25, no. 19–20, pp. 2410–2427, 2005.
- [12] L. Cheng and F. Li, "Modelling of local scour below a sagging pipeline," *Coastal Engineering Journal*, vol. 45, no. 2, pp. 189–210, 2003.
- [13] P. W. Miller, A. Kumar, T. L. Mote, F. D. S. Moraes, and D. R. Mishra, "Persistent hydrological consequences of hurricane maria in Puerto Rico," *Geophysical Research Letters*, vol. 46, no. 3, pp. 1413–1422, 2019.
- [14] J. B. Zambon, R. Y. He, and J. C. Warner, "Tropical to extratropical: marine environmental changes associated with Superstorm Sandy prior to its landfall," *Geophysical Research Letters*, vol. 41, no. 24, pp. 8935–8943, 2014.
- [15] J. A. Keller, K. Wilson Grimes, A. S. Reeve, and R. Platenberg, "Mangroves buffer marine protected area from impacts of Bovoni Landfill, St. Thomas, United States Virgin Islands," *Wetlands Ecology and Management*, vol. 25, no. 5, pp. 563–582, 2017.
- [16] X. H. Ma, Z. Z. Han, Y. Zhang et al., "Heavy minerals in shelf sediments off fujian-zhejiang coast of the east China sea: their provenance and geological application," *Journal of Ocean University of China*, vol. 17, no. 6, pp. 1369–1381, 2018.
- [17] F. P. Shepard, "Nomenclature based on sand-silt-clay ratios," *Journal of Sedimentary Petrology*, vol. 24, pp. 151–158, 1954.
- [18] G. C. Chang, T. D. Dickey, and A. J. Williams III, "Sediment resuspension over a continental shelf during hurricanes edouard and hortense," *Journal of Geophysical Research: Oceans*, vol. 106, no. C5, pp. 9517–9531, 2001.
- [19] H. D. Smith and D. L. Foster, "Modeling of flow around a cylinder over a scoured bed," *Journal of Waterway, Port, Coastal, and Ocean Engineering*, vol. 131, no. 1, pp. 14–24, 2005.
- [20] B. Tansel and S. Rafiuddin, "Heavy metal content in relation to particle size and organic content of surficial sediments in Miami River and transport potential," *International Journal of Sediment Research*, vol. 31, no. 4, pp. 324–329, 2016.
- [21] J. L. Breithaupt, N. Hurst, H. E. Steinmuller et al., "Comparing the biogeochemistry of storm surge sediments and pre-storm soils in coastal wetlands: hurricane irma and the Florida everglades," *Estuaries and Coasts*, vol. 43, no. 5, pp. 1090–1103, 2020.
- [22] J. Hodge and H. Williams, "Deriving spatial and temporal patterns of coastal marsh aggradation from hurricane storm surge marker beds," *Geomorphology*, vol. 274, pp. 50–63, 2016.
- [23] J. C. Bregy, D. J. Wallace, R. T. Minzoni, and V. J. Cruz, "2500-year paleotempestological record of intense storms for the northern Gulf of Mexico, United States," *Marine Geology*, vol. 396, pp. 26–42, 2018.

- [24] J. D. Naquin, K. B. Liu, and T. A. McCloskey, "Storm deposition induced by hurricanes in a rapidly subsiding coastal zone," *Journal of Coastal Research*, vol. 70, pp. 308–313, 2014.
- [25] A. W. Tweel and R. E. Turner, "Contribution of tropical cyclones to the sediment budget for coastal wetlands in Louisiana, USA," *Landscape Ecology*, vol. 29, no. 6, pp. 1083–1094, 2014.
- [26] D. T. Pham, C. Gouramanis, A. D. Switzer et al., "Reprint of 'Elemental and mineralogical analysis of marine and coastal sediments from Phra Thong Island, Thailand: i,'" *Marine Geology*, vol. 396, pp. 79–99, 2018.
- [27] H. F. L. Williams, "Contrasting styles of hurricane irene washover sedimentation on three east coast barrier islands: cape lookout, North Carolina; assateague island, Virginia; and fire island, New York," *Geomorphology*, vol. 231, pp. 182–192, 2015.

Research Article

Construction of a Multimedia Education Resource Security Model Based on Multistage Integration

Lina Yuan 

Changchun Humanities and Sciences College, Changchun 130117, China

Correspondence should be addressed to Lina Yuan; yuanlina@ccrw.edu.cn

Received 14 April 2022; Accepted 13 May 2022; Published 3 June 2022

Academic Editor: Xuefeng Shao

Copyright © 2022 Lina Yuan. This is an open access article distributed under the Creative Commons Attribution License, which permits unrestricted use, distribution, and reproduction in any medium, provided the original work is properly cited.

A security model of multimedia education resource fusion based on multistage integration of multimedia educational resources is constructed in this paper in the context of smart education. First, the teaching model of multimedia education resource fusion is analyzed and the IoT communication evolution model and functional architecture model are constructed accordingly, based on which the realization path of IoT intelligent sensing, intelligent management, emotional computing, device sharing, and vision simulation functions for smart education are discussed. The security model uses a decentralized cryptographic data security sharing method based on blockchain for protection and supports blockchain to record user attributes to ensure the confidentiality and integrity of data. The experimental and analytical results indicate that the scheme can effectively reduce the computational overhead of smart devices while ensuring the security of data sharing. Moreover, the proposed model in the paper achieves better performance than other methods in terms of security strength, encryption, and decryption time.

1. Introduction

In the current context of the gradual improvement of China's science and technology level, both the way of life and the content of work have seen certain changes. The application of information technology can not only guide the stable development of China's social economy but also create good conditions for the healthy development of education. In the Internet environment, various multimedia technologies are applied in school teaching activities. The integration of multimedia teaching resources can lead to the reform and innovation of information-based teaching methods. This can cater to the development needs of the times and set a perfect teaching system [1, 2]. Information-based teaching is not only a single teaching technology but also a reflection of modern teaching methods and concepts [3]. This not only promotes the integration of multimedia educational resources and classroom teaching resources but also broadens the transmission channels of professional subject knowledge and expands the horizons of students' professional subject knowledge. Emphasis on the development of the teaching model with the integration of

multimedia educational resources can enrich the educational resources of professional disciplines and achieve the effectiveness of the development of the teaching model [4].

Smart education is formed by drawing on the core of the concept of "wisdom", integrating it closely with culture, and extending it to the field of education. Smart education relies on technology integration, which upholds the principle of optimal collaboration, pursues the creation of thinking with precision and personalization, and facilitates teachers to effectively broaden their teaching paths. At the same time, it uses efficient and flexible teaching methods to provide learners with personalized teaching services that enhance their learning experience and stimulate their learning and creative potential, while it implicitly guides learners to form correct values and refine their thinking quality [5]. Smart education is a new form of education that emerges from the integration of new-generation information technologies such as cloud computing, big data, social networks, wireless communication, and the Internet of Things under the guidance of advanced educational ideas [6, 7]. The development of smart education has set off the fourth wave after digital education, mobile education, and ubiquitous

education and has become one of the current hot spots with the highest attention in the international education field. The key technologies of smart education are mainly composed of multimedia, radio frequency identification (RFID), sensors, network communication, data processing and fusion, etc. Through the use of RFID, sensors, infrared sensors, laser scanners, global positioning systems, and other information collection devices, any item information is connected to the Internet for communication and interaction to achieve intelligent perception, identification, calculation, display, monitoring, positioning, tracking, and management [8, 9].

The development of smart education environment depends on the development process and strength of smart education Internet of Things (IoT), which has developed rapidly in China in the last decade [10]. Especially after National Leaders inspected R&D Center, smart education IoT has received wide attention and related research has shown explosive growth [11]. Between 2015 and 2021, keywords such as multimedia education resource integration, affective computing, visual simulation, smart classroom [12], and education informatization 2.0 became the buzzwords of smart education [13]. This indicates the development trend of smart education IoT on the one hand and the era of mature application of smart education IoT on the other hand. However, there are fewer studies to study the functional model of IoT with the entry point of smart education centered on the integration of multimedia educational resources. Also, for the security of IoT education data, in-depth research is needed [14].

Facing the security problem of IoT in a cloud computing environment, many solutions have been proposed [15]. The literature [16] addresses the problem of IoT resource management in cloud computing services. Literature [17] distributed a fog resource management framework for IoT services using dynamic resource configuration in the fog framework to handle user requests. There are also cryptographic-based security privacy frameworks for IoT [18]. The literature [19] uses blockchain combined with keyword-based searchable attribute-based encryption (KSABE) to achieve IoT security and privacy protection. Literature [20] proposed a blockchain data access control scheme based on a ciphertext-policy attribute-based encryption (CP-ABE) algorithm. A blockchain-based secure verifiable data sharing scheme for in-vehicle social networks is proposed in literature [21]. This scheme relies on traditional trusted third-party AA servers to manage user attributes and a cloud service provider (CSP) to keep the attribute private keys. Therefore, it has the risk of data leakage due to single point of failure of the third party and malicious impersonation of legitimate cloud service providers by attackers. Literature [22] uses blockchain technology to ensure the integrity and tamper-evidence of data in the CP-ABE searchable encryption scheme. The abovementioned schemes effectively improve the security of IoT, but they are not able to resist the problem of user impersonation attribute attacks and the encryption of data is single algorithm or less identity authentication.

Based on the above research, in order to improve the security performance of the smart education IoT model

centered on the integration of multimedia educational resources, this paper proposes a multistage IoT security model based on multimedia education resource fusion. The model constructs the IoT communication evolution model and functional architecture model for smart education, in which a blockchain-based multistage decentralized cryptographic data security sharing scheme is designed for the model, which can effectively ensure the security of education IoT in a cloud computing environment.

Section 2 of the paper is the state of the art, which is an introduction to the multimedia educational resources integration features and the IoT model for smart education. Section 3 is the methodology, which is about the security scheme of the IoT model. Section 4 is the result analysis and discussion. Section 5 is the conclusion.

2. State of the Art

Smart education relies on network technology and multimedia technology to carry out intelligent teaching with digital characteristics. It upholds the concept of “learner-centered”, relies on an open teaching platform, realizes intelligent teaching, and instantly achieves a high level of sharing of teaching information. Relying on large-scale digital and networked teaching, smart education realizes in-depth teaching interaction and highlights the differentiated features and personalized advantages of ubiquitous learning. Through innovative information technology, smart education can widely acquire and precisely find teaching resources and complete the comprehensive production of teaching resources according to teaching needs. Moreover, in the process of building the teaching environment, it relies on cloud technology, various types of smart terminals, and flexibly uses diversified teaching methods to promote the teaching effect to achieve significant enhancement.

The important value of IoT for smart education in the process of promoting qualitative changes in smart education is mainly reflected in two aspects. (1) The frontier technology of IoT for smart education has triggered changes in education management mode and teaching mode, profoundly changed the learning and lifestyle of teachers and students, and can promote the cultivation of students’ innovation ability. (2) The IoT for smart education has a great application potential, which helps to better promote students’ growth, improve teaching quality and efficiency, and create a new future for education development.

2.1. Characteristics of Multimedia Education Resource Integration

2.1.1. Multiple Teaching Modes in Conjunction. The smart education model of multimedia educational resources is a task-driven model with teaching objectives as a guide for exploration, leading students, and teachers to move toward the goals in the process of learning and education implementation, thus achieving the goal of good education according to the material. The smart education mode, relying on multimedia educational resources, promotes the diversification of professional subject education. Through

the cooperation of various teaching modes, including group cooperative learning mode and contextual teaching mode, the mode of knowledge transfers and instillation is changed, thus driving students' learning enthusiasm, promoting students' acquisition, absorption and perception of knowledge, and thus promoting students' effective mastery of subject knowledge.

2.1.2. Changes in the Role. In the traditional teaching mode, the teacher is the leader, delivering professional course knowledge to students. In contrast, the wisdom education mode of multimedia education resources' integration is different from the previous education form, which attaches more importance to students' subjective learning status. In this mode of education, teachers are the organizers and leaders of teaching, organizing teaching activities for students, and carrying out effective theoretical and practical teaching modes. This allows students to rely on multimedia educational resources to carry out effective learning mode, so that students can continue to improve their own abilities and qualities in independent learning.

2.1.3. Enriching Educational Resources. Multimedia educational resources are rich, innovative, comprehensive, mobile, diverse, miniaturized, and of high quality. This can provide rich educational resources for the implementation of intelligent education mode, so as to realize the effectiveness of professional subject education and teaching. With the further development of information technology, multimedia education resources are also constantly being broadened and improved. For example, the generation of thinking and the amount of information of network data are unimaginable. After further research of educators, the richness and comprehensiveness of multimedia educational resources will be further optimized.

2.2. IoT Communication Evolution Model and Functional Architecture Model. The evolution of smart education IoT communication includes functional evolution and field evolution. The Internet and mobile Internet provide conditions for intelligent interaction in smart education. The IoT communication evolution model for smart education is shown in Figure 1.

Smart education communication is rapidly developing based on the underlying communication protocols of computer and communication technology. The information is sensed and identified through IoT PADs, RFID of smart devices, sensors, global positioning system (GPS), programmable logic controller (PLC), etc., to obtain audio, video, images, and other information. The acquired information is then proximity-propagated by Zigbee, near field communication (NFC), and Bluetooth to the ubiquitous sensor network (USN). Smart education IoT communication evolution has gone through three stages: first, the Machine-Machine (M2M) phase, i.e., the computer education era. This phase saw its sensing information evolve rapidly toward IP-based (field evolution) and intelligent (functional

evolution) directions, respectively. Then, it enters the human-object communication stage, i.e., the network education era. This stage realizes communication for all Human-Human (H2H) through telegraphic telephones, mobile telephones, and leveraging mobile Internet and Internet, and its perceived information continues to evolve toward broadbandization (field evolution) and mobility (functional evolution). Finally, it enters the education communication stage, in which advanced teaching interaction is realized through IPV6, educational cloud computing, and educational big data technology, and its perceived information develops rapidly in the direction of ubiquitination and wisdom. This stage is also the "artificial intelligence + education" era of intelligent education.

The evolution of the communication of smart education IoT shows the recurrence of its structural functions. The smart education IoT is characterized by intelligence, perception, interconnection, automation, and its polymorphic interaction function. According to the smart education IoT evolution, the development trend of itself and the smart education environment has been evolved. And from the analysis of the conceptual model of IoT, the model of IoT architecture level (sensing layer, transmission layer, and application layer) and the social IoT architecture model. Starting from the analysis of smart education applications (smart campus, smart classroom, smart laboratory, and smart library, etc.) and smart education development architecture, a smart education IoT functional architecture model is constructed as shown in Figure 2.

Perception technology and wireless sensor networks (WSN) for smart education IoT are the foundation of smart education communication. Internet and mobile networks are the key to human-computer interaction. Smart chips, sensors, and GPS sense the information of smart education environment. Zigbee, Bluetooth, WiFi, NFC, etc. transmit information and carry out network identification, positioning, tracking, monitoring, display, and management through "Human-Thing" (H2T), "Human-Machine" (H2M), "Thing-Machine" (T2M), "Human-Human" (H2H), "Thing- Thing" (T2T), and "Machine-Machine" (M2M). M2M interactions provide services for smart learning and meet the requirements of interactive experiences for learners. Humanized multistate interaction often depends on the "Human-Thing" communication equipment "intelligence" and multimodal "human-computer" interaction design. Smart education IoT provides support for natural, convenient, and efficient interactions between people, machines, and things to achieve intelligent perception, intelligent management, emotional computing, device sharing, and vision simulation.

2.3. Function Implementation. From the smart education IoT functional architecture model, it is found that the functional realization paths are mainly as follows.

2.3.1. Intelligent Sensing. Intelligent sensing is the most essential feature of smart education. Smart perception includes accurate location, comprehensive sensing, and

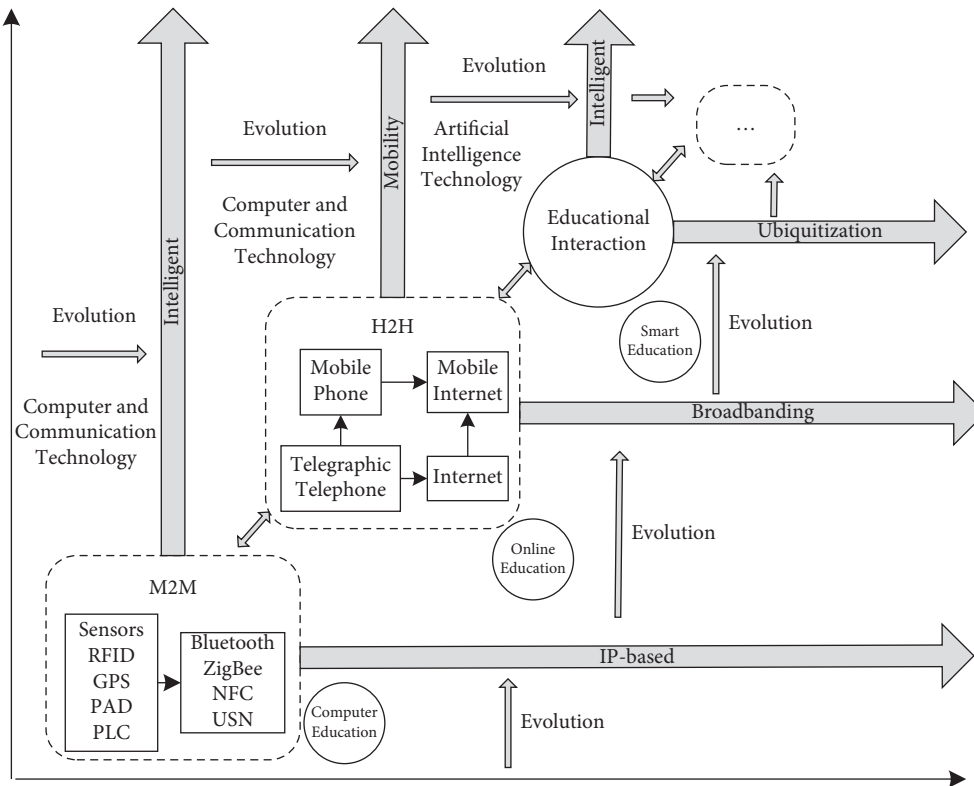


FIGURE 1: IoT communication evolution model.

reliable transmission. Smart perception senses information about students through sensor nodes and provides students with autonomous, personalized, and adaptive learning services. Smart perception in smart education is mainly manifested in three aspects: First, the smart perception of the learning environment. Second, intelligent perception of learning contents. The third is the intelligent perception of the learning context. The three aspects are processed in batches. The inconsistency, incompleteness, and imprecision in each batch of information can be cleared up before its inference, so that the uncertainty of high-level information can be limited to a specific degree.

2.3.2. Smart Management. The IoT for smart education can be built with functions such as teacher and student identification and positioning, teaching and learning process management, learning and teaching information inquiry, and early warning. The intelligent management process with the theme of teacher-student communication, teaching evaluation, learning test, and information tracking is shown in Figure 3.

The mechanism of smart management is to read and write information through RFID sensor chips, then exchange information with information database through reader, and finally query, release, and present information and management through the IOT “PC management terminal” for smart education. We use sensors, RFID, and Zigbee to integrate teachers, teaching, evaluation, communication, students, learning, testing, tracking, and other information to a card or a smart bracelet for smart

management. At present, the common management functions of IoT for smart education include the following: location management, access management, dormitory management, attendance management, and meeting management, etc.

2.3.3. Emotional Computing. Emotional computing collects data and extracts information through high-precision sensor interfaces, performs emotion computing based on the information (including face emotion recognition, gesture action recognition, human posture recognition, voice emotion recognition, smell emotion recognition, and touch emotion recognition of students in universal learning activities), and finally provides emotion computing information to the intelligent education service platform. The platform is established with students’ expression database, posture database, subject knowledge database, subject test database, students’ knowledge level database, and students’ knowledge structure database. Through intelligent emotion computing and emotion-aware computing, it realizes emotional interaction and personalized homework. Emotion computing for intelligent education IoT includes emotion computing of sensory channel and emotion computing of the text channel.

2.3.4. Equipment Sharing. With big data as the core, mobile Internet as the nerve network, education sensing network as the nerve endings, adaptive and personalized user interaction as the means, and smart education application services

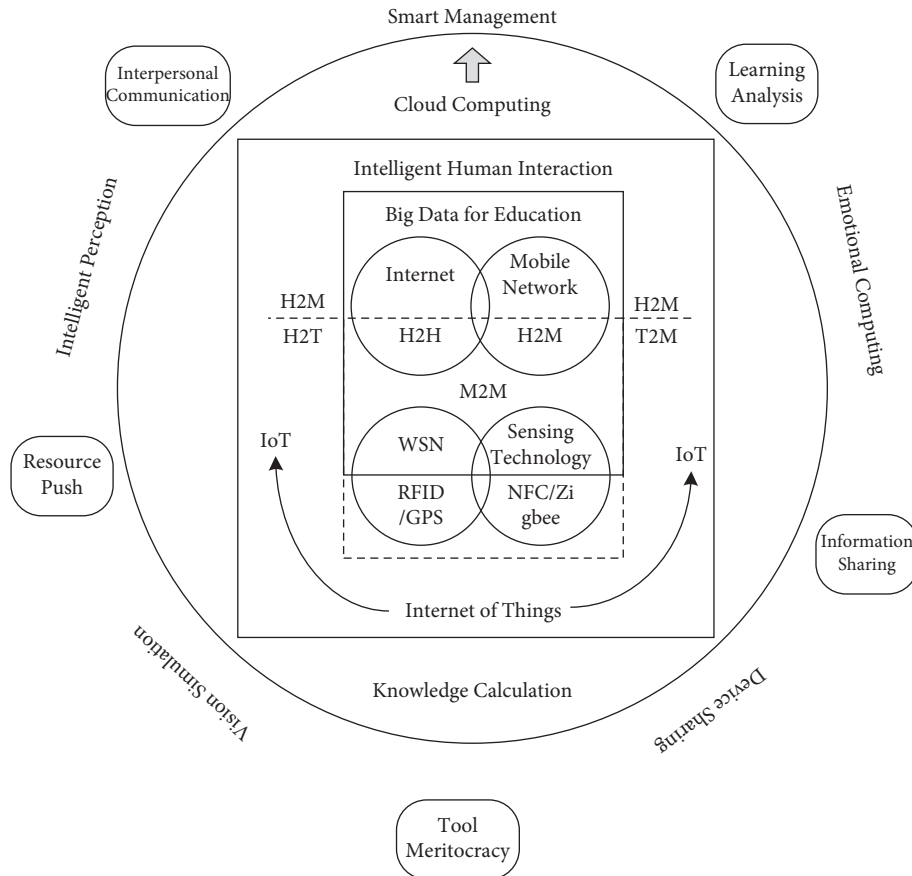


FIGURE 2: Smart education IoT functional architecture model.

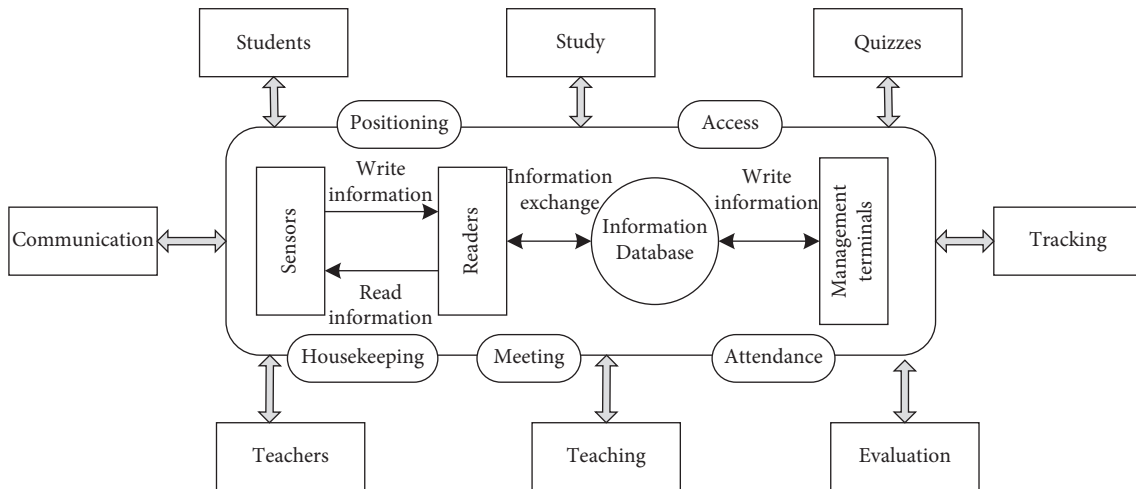


FIGURE 3: Intelligent management process.

as the goal, device data computing completes the transmission, analysis, storage, and display of its information.

3. Methodology

With the massive amount of data and information carried by the Internet of Things for smart education, coupled with its open architecture, there are undoubtedly potential new

security and privacy issues in addition to the security issues of traditional networks. Issues such as data confidentiality for perceptual interactions with students and the inability to identify and track without authorization are particularly salient in education. Illegal users may forge RFID tags to send information to readers, resulting in confusion in the processing of school information systems and posing a serious threat to the information security of teachers and

students. Therefore, the smart education data center server in the background must maintain a strict ban on unauthorized access routes and must prevent illegal access and tampering of information to avoid illegal profitability of educational information or loss of data information.

3.1. Decentralized Ciphertext Data Secure Sharing Framework. For the security and privacy issues of smart education IoT, this paper proposes a decentralized data security framework.

To address the needs of decentralized data sharing, resistance to user attribute forgery and tampering attacks, frequent state changes in smart education environments, and to achieve secure sharing effects without trusted third parties and with low node computation, this paper constructs a decentralized cryptographic data sharing framework for smart education models based on federal blockchain, CP-ABE, and outsourced decryption. The details are shown in Figure 4. The framework shown in Figure 4 contains three entities, namely, data owners (DO), data user (DU), attribute authorities (AAs), and the identity-attribute chain (IAC) with the file block (FIC).

3.1.1. Property Authority. AAs are groups of nodes that make up the blockchain network and are also participants and maintainers of the federated chain, consisting of a set of high-performance servers.

$$AAs = \{\text{Server}_x | 4 \leq x \leq t\}, \quad (1)$$

where t is the number of servers. AAs are responsible for managing user attributes and forwarding data between users and the smart contracts deployed locally on them.

AAs assign the corresponding attributes according to the user's identity and calculate and distribute the attribute private keys through smart contracts to record the identity and attributes in the form of transactions on the IAC. In addition, AAs integrate the user's uploaded file information and file key cipher text through smart contracts to form transactions for uploading to FIC.

3.1.2. Data Owners (DO). DO is the data provider and has the control of the data. DO makes the access policy N for the files. DOs can access the data when the attribute set S satisfies $N_i(S) = 1$. DO is a set of smart devices that share data in the smart home. DO has limited computing and storage capacity. DO can encrypt the shared files and upload them to the cloud storage system. Considering the mobility of smart devices, DO can dynamically join or exit the access control system.

3.1.3. Data Users (DU). DU is a data consumer and obtains the corresponding file by initiating a data access request. DU owns the attribute set S . In practice, both DO and DU are possible in an IoT model.

3.1.4. Identity Attribute Chain (IAC). Each transaction on the IAC corresponds to a set of user's identity attribute pairs.

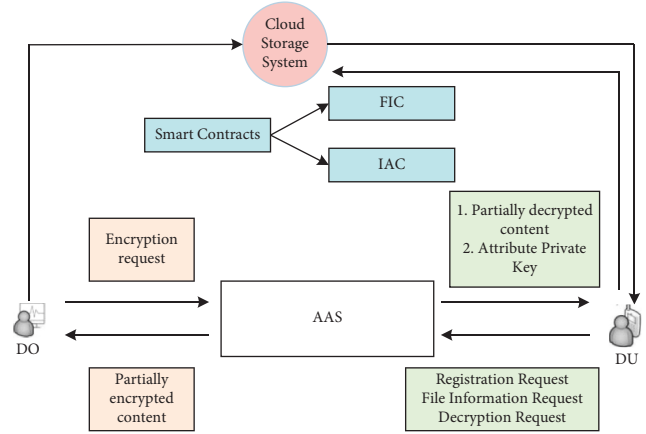


FIGURE 4: Decentralized ciphertext data secure sharing framework.

The federation chain uses a node access management mechanism and the feature that only smart contracts can access the identity attribute pair information to effectively protect user privacy. In this framework, each new member needs to register with AAs to get its own attribute private key. The registration process is done autonomously by AAs invoking a smart contract, which constructs a transaction to record the user's identity, attribute set, and other information and stores it on the IAC after encryption.

In addition to some information such as the generic transaction ID, signature key, etc., the transaction information on the IAC block contains the following.

- (1) Device identifier (DID, device identity): $ID = \{0, 1\}^{16}$, a unique identifier for each user.
- (2) Attribute set (ATTRS, attribute set): the set of attributes corresponding to the user's identity, $ATTRS \subseteq S$. When ATTRS changes, the user's access rights also change.

3.1.5. File Information Chain (FIC). FIC maintains the meta-information about the user's uploaded files $\text{File Info} = \{\text{FileAddr}, \text{Keywords}, \text{hash}, \text{CN}_Z\}$.

In addition to some information such as the generic transaction ID and signature key, the transaction information on the FIC contains the following.

FileAddr: The address of the file on the cloud storage system. The user requests the corresponding encrypted file based on this address.

A collection of document keywords, which is used to quickly retrieve and match user request documents. $\text{Keywords} = \{\text{Keyword1}, \text{Keyword2}, \dots\}$.

hash: hash of the encrypted file, which is used to ensure the integrity of the file and avoid missing data due to the network. $\text{hash} = \text{SHA256}(\text{digest}(\text{file}))$.

CN_Z : the ciphertext of the symmetric encryption key Z used by the user to encrypt the file.

3.2. Multistage Decentralized Ciphertext Data Security Protection. The blockchain-based decentralized ciphertext data secure sharing method supports blockchain to record

user attributes, ensures data confidentiality and integrity, and improves the efficiency of data sharing. In order to better describe the proposed method, the conventional encryption and decryption operations involved are defined.

Definition 1. $\text{Encopt}(\bullet)$, where $\text{opt} \in \{\text{AES}, \text{PPK}\}$. AES denotes the symmetric encryption AES (advanced encryption standard) algorithm and PPK denotes the execution of the RSA encryption algorithm using the public key PPK.

Definition 2. $\text{Decopt}(\bullet)$, where $\text{opt} \in \{\text{AES}, \text{PSK}\}$. PSK denotes the execution of the RSA decryption algorithm using the private key PSK.

The proposed method consists of four phases: setup phase, register phase, upload phase, and secure sharing phase.

3.2.1. Setup Phase. The initialization process is mainly completed to deploy smart contracts and generate system master key pairs. The initialization and registration process is shown in Figure 5.

In the initialization phase, first the smart contracts SC_{XG} , SC_{FX} on AAs, subsequently SC_{XG} constructs the bilinear cyclic group A_0 of order prime p and its generating element g and the bilinear pair mapping $e: A_0 * A_0 \rightarrow A_1$ with randomly chosen $g, h \in K_u$ and computes

$$b = a^h, \quad (2)$$

$$e(a, a)^g. \quad (3)$$

The master key pair ($MSK = \{h, a^g\}$, $PK = \{A_0, a, b, e(a, a)^g\}$) is generated. MSK is the system master key and PK is the system public key.

3.2.2. Register Phase. When a new user joins the system, it first sends a registration request to the AAs with its device identifier DID, and the AAs verify the user's identity based on the DID. The AAs assign the corresponding attribute set S and public-private key pair $\langle \text{PPK}, \text{PSK} \rangle$ to the user and forward $\langle \text{DID}, S \rangle$ to the smart contract SC_{XG} , which selects a random number $r \in K_u$ and calculates

$$SZ_r = a^{g+r/h}. \quad (4)$$

For each attribute y within S , choose a random number $r_y \in K_u$ and compute

$$SZ_s = \{\forall y \in S, D_y = a^{r_y} \cdot B(y)^{r_y}, D'_y = a^{r_y}\}. \quad (5)$$

The attribute private key $SK = \{SZ_r, SZ_s\}$ is obtained. Finally, SC_{XG} returns $\langle \text{SK}, \text{PPK}, \text{PSK} \rangle$ to the user via AAs and uploads $\langle \text{DID}, S \rangle$ to IAC in the form of transactions.

3.2.3. Upload Phase. Data sharing is the process of user uploading data. In this phase, DO first selects the key Z , calculates $C_f = \text{Enc}_{\text{AES}}(Z, \text{file})$, and uploads C_f to IPFS. Subsequently, DO encrypts Z to get CN_Z .

DO choose a random number $s \in K_u$ and compute

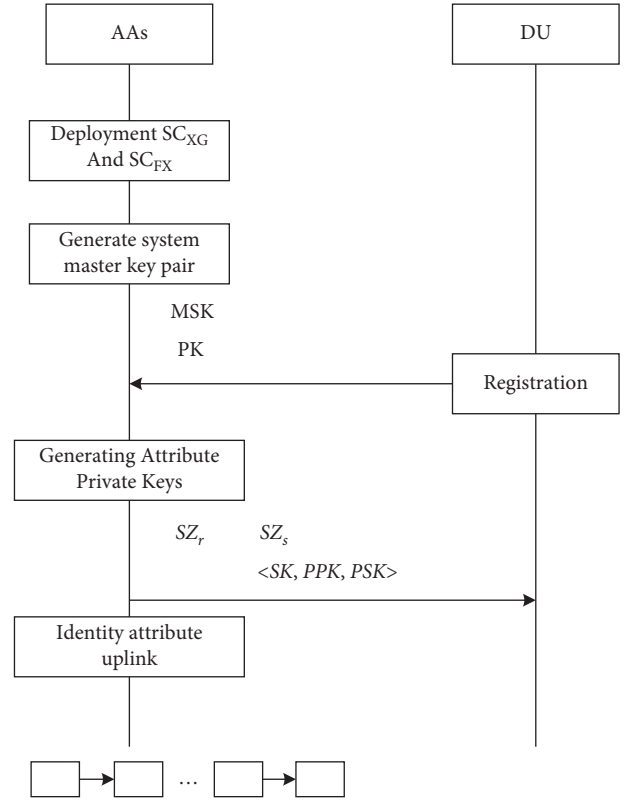


FIGURE 5: System initialization and user registration process.

$$\tilde{C} = Ze(a, a)^{gs}, \quad (6)$$

$$C = b^s, \quad (7)$$

$$CN_g = \{\tilde{C}, C\}.$$

At the set J of leaf nodes of N , compute for $\forall j \in J$

$$C_j = a^{v_j(0)}, \quad (8)$$

$$C'_j = B(\text{attr}(j))^{v_j(0)},$$

where $\text{attr}(j)$ means to obtain the attribute corresponding to j . Let $CN_s = \{C_j, C'_j\}$, DO generates the ciphertext $CN_Z = \{CN_g, CN_s\}$, and the file information FileInfo , where $\text{FileInfo} = \{\text{FileAddr}, \text{Keywords}, \text{hash}, CN_Z\}$.

In the calculation of CN_s , $v_i(\cdot)$ is constructed as follows.

- (1) Starting from the root node R , choose a polynomial $v_i(\cdot)$ from top down for each node i of N . The number of times d_i of $v_i(\cdot)$ is 1 smaller than its threshold value z_i , i.e., $d_i = z_i - 1$.
- (2) Starting from the root node R , choose a random number, $v_R(0) = S$, and randomly choose d_R points of $v_R(\cdot)$ to perfect $\delta v_R(\cdot)$.
- (3) For other nodes i , let $v_i(0) = v_{\text{parent}(i)}(\text{index}(i))$ and randomly choose d_i points to perfect $v_i(\cdot)$.

Finally, DO signs the FileInfo and forwards $\langle \text{FileInfo}, \delta \text{DO}(\text{FileInfo}) \rangle$ to SC_{XG} via AAs. SC_{FX} verifies the signature and uploads the FileInfo to FIC.

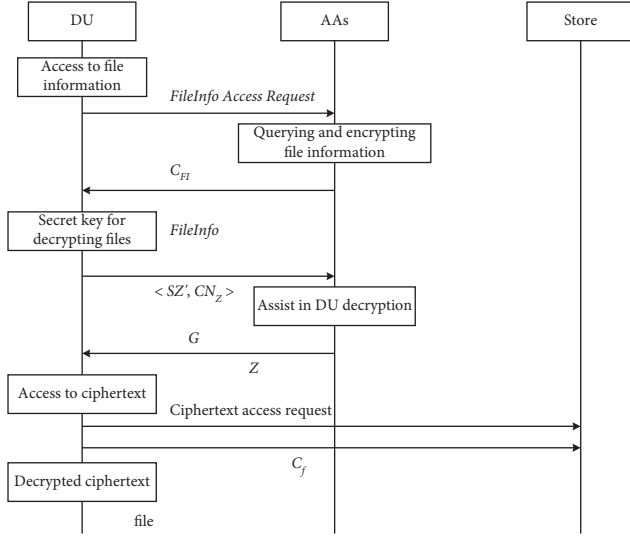


FIGURE 6: Secure sharing process.

3.2.4. Secure Sharing Phase. Secure sharing is the process of user access to data, the flow is as shown in Figure 6. In this phase, DU initiates access request $\langle \text{DID}, \text{Keywords} \rangle$ to the contract through the attribute server cluster AAs. The SC_{XG} determines whether the user is registered according to the DID. the SC_{FX} gets the corresponding FileInfo according to the Keywords, calculates $C_{FI} = \text{Enc}(\text{File Info})$, and returns it to DU.

DU downloads C_f via FileAddr and obtains FileInfo. To recover Z , DU chooses a random number $n \in K_u$ and converts the attribute private key

$$SZ' = \{SZ_g^n, SZ_s\}. \quad (9)$$

Send $\langle SZ', CN_z \rangle$ to AAs.

AAs act as a decryption outsourcing server provider (DSP) to perform decryption calculations for each leaf node i in N

$$\text{Decrypt Leaf}(CN_z, SZ', i) = e(a, a)^{rv_i(0)}. \quad (10)$$

Then, the result is returned to DU.

$$\begin{aligned} Z &= \frac{\tilde{C}}{e(C, D'^{1/n})/G} \\ &= \frac{\tilde{C}}{e(b^s, a^{g+r/h})/e(a, a)^{rs}}, \end{aligned} \quad (11)$$

where $G = e(a, a)^{rv}(0) = e(a, a)^{rs}$ and $D' = SZ_r^n$.

Finally, DU obtains the plain text of the file.

Decrypt Leaf (CN_z, SZ', i) is computed as follows: for each node i in N , if i is a leaf node, let $x = \text{attr}(i)$, then when $x \in S$

$$\begin{aligned} \text{Decrypt Leaf} &= \frac{e(D_x, C_i)}{e(D'_x, C'_i)} = \frac{e(a^r \cdot B(x)^{r_x}, b^{y_i(0)})}{e(a^{r_x, B(x)^{y_i(0)}})} \\ &= e(a, a)^{rv_i(0)}. \end{aligned} \quad (12)$$

If i is a nonleaf node, compute $F_k = \text{Decrypt Leaf}(N_z, SZ', k)$ for all subnodes k of i .

Let S_i be the set of subnodes of x and S_i of size z_i with $F_k \neq \perp$. If S_i does not exist, the function returns \perp .

4. Result Analysis and Discussion

In this paper, experiments are conducted on the basis of PBC library and CP-ABE base development kit using an elliptic curve as $y^2 = x^3 + x$. The experimental environment is a dual-core CPU with 4.0 GHz, 64 GB RAM, and Ubuntu 18.04 64 bit operating system. In addition, AAs are used as blockchain nodes to build a blockchain network based on the Hyperledger-Fabric system with the use of the Byzantine fault-tolerant consensus mechanism. The simulation parameters for IoT are set as shown in Table 1.

4.1. Security Analysis. This section mainly analyzes the security of the proposed scheme in terms of data confidentiality, data integrity, complicity attacks, and attribute tampering and impersonation attacks, and finally compares it with other schemes as shown in Table 2.

It can be seen that the performance of this paper's scheme outperforms other schemes in several aspects such as data confidentiality, data integrity, complicity attacks, and attribute tampering and impersonation attacks, indicating the effectiveness of this paper's scheme. This is because literature [20, 22] have no AA to manage user attributes and lack protection against user attribute tampering and impersonation attacks. Literature [21] is based on a traditional trusted third-party AA server. Its security threshold against attribute impersonation attacks is 100%, but it is powerless against user attribute tampering attacks. Literature [23] is weak against attribute impersonation attacks. Literature [24] has a security threshold of 75% against attribute tampering attacks but is unable to resist attribute impersonation attacks due to the absence of attribute management features. It shows that the model security scheme in this paper can improve the security of data access and provide a reliable guarantee for secure data sharing under smart education.

4.2. Performance Analysis. The experimental performance is evaluated in terms of user encryption and decryption and the total overhead time of the scheme for comparison, and the experiments are conducted using a gradual increase in the number of policy attributes.

As can be seen from Figure 7 to 9, with the increase in the number of access policies or attributes, the time overhead on all aspects of the proposed scheme in this paper is significantly reduced compared to the blockchain trusted data sharing based scheme [23] and the CP-ABE based blockchain data access control scheme [20]. It can be seen that, in comparison with the distributed computing-based data sharing scheme, the scheme proposed in this paper effectively reduces the computation and time cost of the sharing process while ensuring the security of all aspects of data sharing. Compared with blockchain-based onboard data sharing schemes using CSP proxy computing [21, 22], the

TABLE 1: Simulation parameter settings.

Parameters	Settings
Simulation area	1,000 m × 1,000 m
Number of users	50
Number of educational IoT devices	50
Number of trusted institutions	1
Number of cloud servers	2
Number of gateways	2

TABLE 2: Safety comparison.

Programs	Data confidentiality protection	Anti-conspiracy attack	Anti-attribute tampering attack	Data integrity protection	Anti-attribute counterfeit attack
[20]	✓	✓	✗	✓	✓
[21]	✓	✓	✗	✓	✓
[22]	✓	✓	✗	✓	✓
[23]	✓	✓	✓	✓	✗
[24]	✓	✓	✗	✓	✗
Proposed	✓	✓	✓	✓	✓

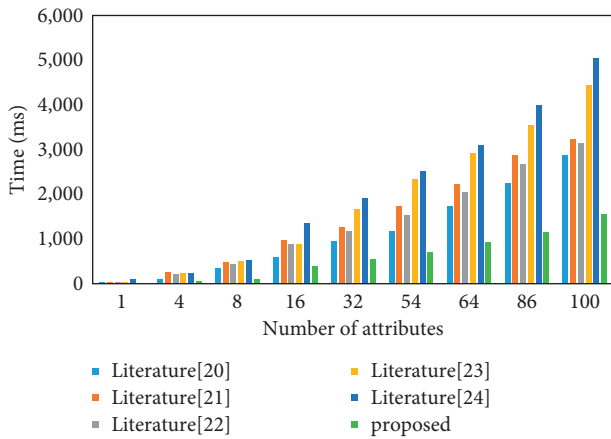


FIGURE 7: User encryption time.

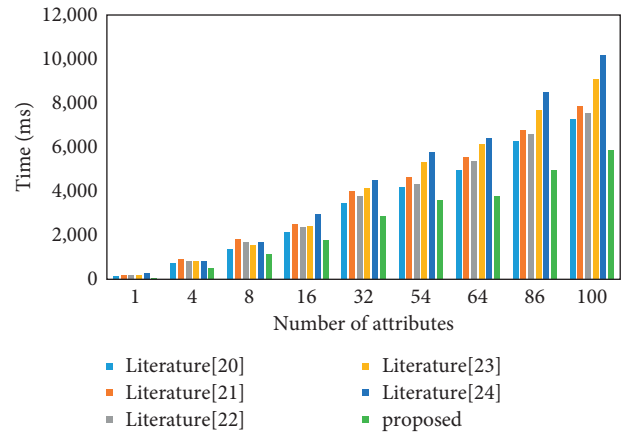


FIGURE 9: Shared program time.

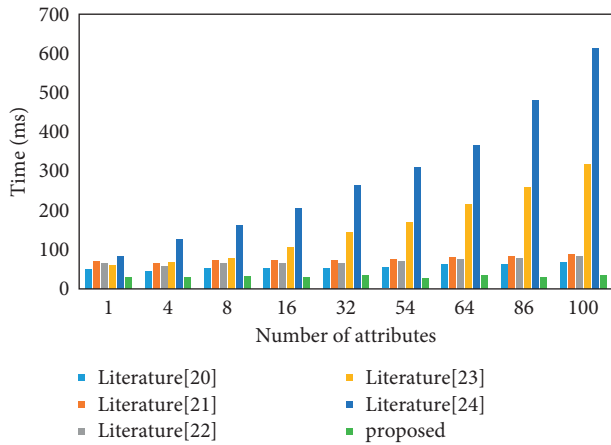


FIGURE 8: User decryption time.

scheme proposed in this paper reduces user decryption time delay based on outsourced decryption technology, which can effectively resist the threat of data leakage due to attribute tampering by users and malicious users stealing CSP attribute private keys while ensuring data sharing efficiency. Compared with the blockchain-based trusted data sharing scheme [23] and the CP-ABE-based blockchain data access control scheme [24], the scheme proposed in this paper achieves better security against user attribute counterfeiting and tampering, etc., and improves the reliability of data sharing while reducing the time overhead of data sharing.

In addition, literature [24] has the computational overhead of user access to the network since the user is used as a blockchain network node, which first needs to access the blockchain network for the user with the deployment of smart contracts before the access control occurs.

The proposed scheme uses AAs as blockchain network nodes and users only need to interact with AAs without becoming blockchain system nodes, thus reducing the overall latency of the scheme and improving the efficiency of data sharing in the smart education environment. Therefore, the author's proposed scheme effectively improves the efficiency in the smart education environment while ensuring security.

5. Conclusion

With the arrival of 5G era and the rapid advancement of education informatization 2.0, the development and application of smart education IoT for the integration of multimedia education resources has attracted great attention from the education community at home and abroad, and smart education will become the main development direction of future education. In this paper, the evolution model and functional architecture model of smart education IoT are constructed and the path of functional realization of smart education IoT is given. In the IoT model, a decentralized ciphertext data security sharing scheme based on multistage technology is designed. The security model and scheme ensure the confidentiality and integrity of data and improve the efficiency of data sharing. The experimental and analytical results illustrate that the security model in this paper can meet the requirements of secure data sharing in the smart education environment. The future work is to improve the encryption methods in the security model to further enhance the efficiency of security protection.

Data Availability

The labeled datasets used to support the findings of this study are available from the corresponding author upon request.

Conflicts of Interest

The authors declare that they have no conflicts of interest.

Acknowledgments

This study was supported by Jilin Province Higher Education Association Higher Education Research Project "Research on the Practice Path of Internet Culture to Enhance College Students' Values" (No. JGJX2021B28).

References

- [1] D. Xia, "English multimedia teaching resources integration system based on big data technology," in *Proceedings of the 2020 International Conference on Computers, Information Processing and Advanced Education (CIPAE)*, pp. 22–25, Ottawa, ON, Canada, October 2020.
- [2] W. Fu, "The Integration Mechanism of Multimedia Computer Technology and College English Education," *ACM*, in *Proceedings of the 2021 2nd International Conference on Computers, Information Processing and Advanced Education*, pp. 1165–1169, Ottawa, ON, Canada, May 2021.
- [3] J. Leem and E. Sung, "Teachers' beliefs and technology acceptance concerning smart mobile devices for SMART education in South Korea," *British Journal of Educational Technology*, vol. 50, no. 2, pp. 601–613, 2019.
- [4] H. Singh and S. J. Miah, "Smart education literature: a theoretical analysis," *Education and Information Technologies*, vol. 25, no. 4, pp. 3299–3328, 2020.
- [5] N.-S. Chen, C. Yin, P. Isaias, and J. Psotka, "Educational big data: extracting meaning from data for smart education," *Interactive Learning Environments*, vol. 28, no. 2, pp. 142–147, 2020.
- [6] A. Z. Faroukhi, I. El Alaoui, Y. Gahi, and A. Amine, "Big data monetization throughout big data value chain: a comprehensive review," *Journal of Big Data*, vol. 7, no. 1, pp. 1–22, 2020.
- [7] M. Mohammed Sadeeq, N. M. Abdulkareem, S. R. M. Zeebaree, D. Mikaeel Ahmed, A. Saifullah Sami, and R. R. Zebari, "IoT and cloud computing issues, challenges and opportunities: a review," *Qubahan Academic Journal*, vol. 1, no. 2, pp. 1–7, 2021.
- [8] M. Stoyanova, Y. Nikoloudakis, S. Panagiotakis, E. Pallis, and E. K. Markakis, "A survey on the internet of things (IoT) forensics: challenges, approaches, and open issues," *IEEE Communications Surveys & Tutorials*, vol. 22, no. 2, pp. 1191–1221, 2020.
- [9] A. Khanna and S. Kaur, "Internet of things (IoT), applications and challenges: a comprehensive review," *Wireless Personal Communications*, vol. 114, no. 2, pp. 1687–1762, 2020.
- [10] M. Kassab, J. DeFranco, and P. Laplante, "A systematic literature review on Internet of things in education: benefits and challenges," *Journal of Computer Assisted Learning*, vol. 36, no. 2, pp. 115–127, 2020.
- [11] D. K. A. R. Al-Malah, H. H. K. Jinah, and H. T. S. ALRikabi, "Enhancement of educational services by using the internet of things applications for talent and intelligent schools," *Periodicals of Engineering and Natural Sciences*, vol. 8, no. 4, pp. 2358–2366, 2020.
- [12] M. K. Saini and N. Goel, "How smart are smart classrooms? A review of smart classroom technologies," *ACM Computing Surveys*, vol. 52, no. 6, pp. 1–28, 2019.
- [13] D. Sulistiyarini and F. Sabirin, "21st century literacy skill of information technology and computer education students," *JPI (Jurnal Pendidikan Indonesia)*, vol. 9, no. 4, pp. 576–585, 2020.
- [14] S. Dhawan and R. Gupta, "Analysis of various data security techniques of steganography: a survey," *Information Security Journal: A Global Perspective*, vol. 30, no. 2, pp. 63–87, 2021.
- [15] S. P. Mohanty, V. P. Yanambaka, E. Kougiannos, and D. Puthal, "PUFchain: a hardware-assisted blockchain for sustainable simultaneous device and data security in the internet of everything (IoE)," *IEEE Consumer Electronics Magazine*, vol. 9, no. 2, pp. 8–16, 2020.
- [16] A. Javadpour, G. Wang, and S. Rezaei, "Resource management in a peer to peer cloud network for IoT," *Wireless Personal Communications*, vol. 115, no. 3, pp. 2471–2488, 2020.
- [17] A. W. Malik, T. Qayyum, A. U. Rahman, M. A. Khan, O. Khalid, and S. U. Khan, "XFogSim: a distributed fog resource management framework for sustainable IoT services," *IEEE Transactions on Sustainable Computing*, vol. 6, no. 4, pp. 691–702, 2020.
- [18] M. Elhoseny, K. Shankar, S. K. Lakshmanaprabu, A. Maselena, and N. Arunkumar, "Hybrid optimization with cryptography encryption for medical image security in

- Internet of Things,” *Neural Computing & Applications*, vol. 32, no. 15, pp. 10979–10993, 2020.
- [19] S. Liu, J. Yu, Y. Xiao, Z. Wan, S. Wang, and B. Yan, “BC-SABE: blockchain-aided searchable attribute-based encryption for cloud-IoT,” *IEEE Internet of Things Journal*, vol. 7, no. 9, pp. 7851–7867, 2020.
- [20] Y. Qiu, H. Zhang, Q. Cao, Z. Jiancong, C. Xingshu, and J. Hongjian, “Blockchain data access control scheme based on CP-ABE algorithm,” *Chinese Journal of Network and Information Security*, vol. 6, no. 3, pp. 88–98, 2020.
- [21] K. Fan, Q. Pan, K. Zhang et al., “A secure and verifiable data sharing scheme based on blockchain in vehicular social networks,” *IEEE Transactions on Vehicular Technology*, vol. 69, no. 6, pp. 5826–5835, 2020.
- [22] S. Niu, P. Yang, Y. Xie, and D. U. Xiaoni, “Cloud-assisted ciphertext policy attribute based encryption data sharing encryption scheme based on Blockchain,” *Journal of Electronics and Information Technology*, vol. 43, no. 7, pp. 1864–1871, 2021.
- [23] M. Shen, J. Duan, L. Zhu, J. Zhang, X. Du, and M. Guizani, “Blockchain-based incentives for secure and collaborative data sharing in Multiple clouds,” *IEEE Journal on Selected Areas in Communications*, vol. 38, no. 6, pp. 1229–1241, 2020.
- [24] S. Gao, G. Piao, J. Zhu, X. Ma, and J. Ma, “TrustAccess: a trustworthy secure ciphertext-policy and attribute hiding access control scheme based on blockchain,” *IEEE Transactions on Vehicular Technology*, vol. 69, no. 6, pp. 5784–5798, 2020.

Research Article

A Two-Level Integrated Scheduling Strategy for Vehicle-Network Synergy considering New Energy Consumption

Yifei Gao 

Logistics Engineering College, Shanghai Maritime University, Shanghai, China

Correspondence should be addressed to Yifei Gao; 201910230037@stu.shmtu.edu.cn

Received 6 April 2022; Accepted 6 May 2022; Published 31 May 2022

Academic Editor: Xuefeng Shao

Copyright © 2022 Yifei Gao. This is an open access article distributed under the Creative Commons Attribution License, which permits unrestricted use, distribution, and reproduction in any medium, provided the original work is properly cited.

With the substantial increase in the number of electric vehicles, the charging of electric vehicles without regulation and scale control will bring about problems, such as overloading of distribution transformers; the proportion of new energy power generation is also increasing year by year, and the access of new energy to the power grid will cause volatility. In order to solve the problems above, this paper proposed a coordinated and orderly scheduling strategy considering new energy consumption, which protects the interests of both users and the integrated power grid. First, a two-level vehicle-network interaction model considering both supply and demand sides was established. The upper-level model optimized the indicators on the distribution grid side, and a term of charge-discharge margin as well as grid-side load variance model was proposed. The lower-level optimization model was set based on the users' condition. The average discharge rate index was defined to evaluate the battery loss satisfaction in the scheduling strategy, which fully considered users' charging and discharging cost, and finally achieved a win-win situation between the power grid and the user. Secondly, the fast nondominated sorting genetic algorithm (NSGA-II) was used to figure out the effect of the strategy proposed in this paper, and a community is taken as an example for simulation. The results confirmed the economy and rationality of the above strategy, by rationally scheduling the charging and discharging behavior of electric vehicles, consuming new energy, restraining the fluctuation of the remaining new energy power generation, realizing the dynamic balance between the charging and discharging load and the output of new energy in a certain area, and finally effectively suppressing the fluctuation of the power grid load while improving the availability of clean energy.

1. Introduction

Electric vehicle (EV), as a new generation of green transportation, shows unique advantages and broad application prospects compared with traditional vehicles in terms of changing the energy structure, saving energy, reducing emissions, curbing global warming, and so on. As an important contributor of “peak” and “carbon neutrality,” EV has been widely valued and promoted by automobile manufacturers, relevant departments, and energy companies. The load growth caused by the disorderly charging of electric vehicles, especially during the peak period, will further increase the peak-to-valley difference of the grid load, which may lead to a series of problems like voltage drop, increased network loss, overloading of the distribution network lines, and overloaded distribution of transformers [1, 2].

The traditional control method uses power generation to track load fluctuations and adjust the system operating state. The controllable load characteristics of electric vehicles will provide new solutions to this problem. Managing the load of electric vehicles to shave peaks and fill valleys can effectively reduce network losses, reducing grid operation risks, and alleviate grid peak regulation pressure. The grid-side energy storage-based dispatch strategy and the user side incentives such as time-of-use electricity prices can well solve the problem of excessive load peak-to-valley difference. Load scheduling [3] is to use load to track the change of renewable energy output. As a supplement to power generation scheduling, it helps adjust the operating state of the system. The time-of-use power price (TOU) [4] is another significant way to realize peak shaving and valley filling, which can alleviate the contradiction between supply and demand, bringing benefits in many aspects.

Through proper scheduling of electric vehicle charging, together with taking full use of its characteristics (distributed energy storage and flexible scheduling), it is possible to coordinate and optimize the scheduling of electric vehicles and new energy sources, such as wind and solar [5], and to further achieve the dynamic equilibrium between the charging load and the output of new energy in a certain area. Leveraging the advantages of flexible and adjustable electric vehicles and huge energy storage can not only restrain the fluctuation of the remaining new energy power generation, but also reduce its impact on the power grid system. It can effectively stabilize the load fluctuation of the power grid while improving the utilization of clean energy and reducing the negative impact of the two when they are connected to the grid.

2. Literature Review

In terms of orderly charging and discharging scheduling of electric vehicles, Liu [6] established a minimum model strategy for user charging and discharging costs that takes into account battery loss, but it is mainly based on the user side and lacks consideration of the demand on the grid side. Xu and Li [7] proposed an optimization strategy aiming at minimizing the peak-to-valley difference rate of power grid load, but in the optimization process, only the user's response to the peak-valley electricity price policy was analyzed, and the user's response to the scheduling strategy was not considered. Zhang et al. [8] employed the central limit theorem to calculate the distribution of the charging load of all vehicles with the goal of reducing the centralized charging under the electricity price during the valley period as much as possible and proposed a charging load calculation method based on the time-of-use electricity price. Wang [9], on the basis of user charging satisfaction and distribution network security constraints, and with the goal of optimizing operational economy, built a two-level optimization model of distribution network-charging station based on hierarchical management. Wang [10] analyzed the charging and discharging characteristics of electric vehicles from the perspective of mathematical modeling and considered the output of wind and solar power generation. However, his scheduling optimization of electric vehicles only involved the grid level and failed to notice the impact of the scheduling strategy on users and the economic analysis. Bao [11] proposed a model that achieved the mutually friendly interaction of power between electric vehicles and the power grid, which can calibrate the real-time active power demand of electric vehicles and protect the stability of power grid operation. Su et al. [12] proposed a multiobjective optimization model of dynamic TOU power price with the introduction of wind and solar, which facilitates the orderly charging of electric vehicles to achieve local consumption of new energy.

According to the above research, this paper raised a two-level vehicle-network interaction model that considers the consumption of new energy sources on both supply side and demand side comprehensively and conducted an economic research on peak shaving and valley filling and users'

charging and discharging. The upper-level optimization model focused on the distribution network and was evaluated from the aspects of charge and discharge margin and load variance on the grid side so as to improve the stability of the grid operation. The lower-level optimization model fully considered the users' demand, defined the battery loss satisfaction to evaluate the battery loss cost in the V2G response process, and realized the optimal charging and discharging cost on the user side.

In addition, the coordinated optimal scheduling of electric vehicles and wind-solar, that is, the proper scheduling of the charging and discharging behavior of electric vehicles to absorb new energy and restrain the fluctuation of the remaining new energy power generation, will achieve a dynamic equilibrium between the charging and discharging load and the output of new energy in a certain area. The dynamic balance between the power grid not only effectively stabilizes the fluctuation of the grid load, but also improves the utilization of clean energy. The fast nondominated sorting genetic algorithm (NSGA-II) with elite strategy is adopted to optimize multiple objectives at the same time and find the global optimal solution. The strategy proposed in this paper is analyzed and verified by numerical example simulation, which proves that the strategy proposed in this paper can realize peak shaving and valley filling, absorbing wind, and solar power grid connection, effectively reducing the pressure on the grid. Scheduling charging and discharging behaviors also reduces user charging costs.

3. Mathematical Models (Electric Vehicle Model and New Energy Model)

3.1. Electric Vehicle Load Model. The charging behavior of electric vehicles is mainly determined by the travel needs of users and is also affected by factors such as device attributes and user habits. As far as the regional power system is concerned, it is also affected by the number and scale of electric vehicles and the perfection of charging facilities. The uncertainty and difference of user needs and behaviors will inevitably lead to randomness and dispersion of charging loads. Through the data statistics of the travel time distribution law of electric vehicles in residential areas in real life, and by normalizing the statistical graph data, the electric vehicle travel time distribution curve is fitted, and the electric vehicle load model is established. The Monte Carlo method is used to simulate the conventional load curve of the residential area [13–15], while the electric vehicle information and trip plan are obtained from the electric vehicle travel distribution model and the return distribution model.

- (1) The travel distribution density function of electric vehicles is

$$f_{\mu_1, \sigma_1}(td) = \frac{1}{\sqrt{2\pi}\sigma_1} e^{-\frac{(t - \mu_1)^2}{2\sigma_1^2}}. \quad (1)$$

- (2) The probability density function of the regression distribution is

$$f_{\mu_2, \sigma_2}(ta) = \frac{1}{\sqrt{2\pi}\sigma_2} e^{-\frac{(t - \mu_2)^2}{2\sigma_2^2}}. \quad (2)$$

In the formula, td is the travel time of the user, ta is the return time of the user, μ_1 and μ_2 are the expected values, and σ_1 and σ_2 are the standard deviations.

In the travel distribution, $\mu_1 = 8$, $\sigma_1 = 1.33$, while the return distribution parameter is $\mu_2 = 18.5$, $\sigma_2 = 1.99$. Whether to go out is randomly generated, and it is assumed that the total travel probability of residents is 0.8.

(3) Daily mileage

Daily mileage [16] is an important parameter of the behavior characteristics of car owners in residential areas. The daily mileage of electric vehicles is log-normal distributed, and its probability density function is shown in the following formula:

$$f_s(x) = \frac{1}{x\sigma_s\sqrt{2\pi}} e^{-\frac{(\ln x - \mu_s)^2}{2\sigma_s^2}}. \quad (3)$$

In the formula, x is the daily mileage of the electric vehicle, μ_s is the expected value, and σ_s is the standard deviation; among them, $\mu_s = 3.2$, $\sigma_s = 0.88$.

(4) Initial state of charge

According to the daily mileage of the car and the battery parameters, the initial state of charge when the vehicle starts to charge can be obtained [16], as shown in the following formula:

$$\text{SOC}_{s,i} = \left(\text{SOC}_{e,i} - \frac{x}{100} \times \frac{E_{100}}{B} \right) \times 100\%. \quad (4)$$

In the formula, $\text{SOC}_{e,i}$ denotes the state of charge of the i th electric vehicle at the end of charging. If the power expectation is constant, the battery power of the electric vehicle when the user leaves home is the same as the user's charging expectation; $\text{SOC}_{s,i}$ is the initial state of charge of the i th electric vehicle; E_{100} is the power consumption of electric vehicles per 100 kilometers, in units of kWh; B is battery capacity, in units of kWh; and x is daily mileage.

The calculation of the time required by the user to charge is shown in the following formula:

$$T_{c,i} = \frac{(\text{SOC}_{s,i} - \text{SOC}_{b,i})B}{P_c}. \quad (5)$$

In the formula, $T_{c,i}$ is the time required for charging; the unit is h ; P_c is the charging power for electric vehicles, in units of kW.

3.2. New Energy Model

3.2.1. Wind Power Model. The relationship between the output characteristics of the wind power generation system and the wind speed is as follows [17]:

$$P_{WT} = \begin{cases} 0 & v \leq v_i \text{ or } v \geq v_o \\ P_N \frac{v - v_i}{v_N - v_i} & v_i \leq v \leq v_N \\ P_N & v_N \leq v \leq v_o \end{cases}, \quad (6)$$

P_{WT} is the actual output power, P_N is the rated output power, v is the actual wind speed, v_i is the cut-in wind speed, v_N is the rated wind speed, and v_o is the cut-out wind speed.

3.2.2. Photovoltaic Power Generation Mathematical Model. Photovoltaic cells [17] are obviously characterized by their volatility, which is directly related to the light intensity and operating temperature. Its output power is expressed as follows:

$$P_{pv} = P_{STC} \frac{G_{ING}}{G_{STC}} (1 + k(T_c - T_r)). \quad (7)$$

P_{pv} is the actual output power; P_{STC} is the maximum output power of STC (standard test environment: irradiation intensity 1000 W/m, ambient temperature 25°C); G_{ING} is the irradiation intensity under STC, G_{STC} is the actual irradiation intensity; k is the power temperature coefficient; T_c is the actual battery temperature; and T_r is the reference temperature.

Among them, the surface temperature of photovoltaic cell modules is not easy to measure directly, but can be estimated by empirical formula:

$$T_c = T_{et} + 0.0138 \times (1 + 0.0138T_{et}) \times (1 - 0.042v) \times G_{ING}. \quad (8)$$

In the formula, T_{et} is the ambient temperature; v is the current wind speed.

4. Vehicle-Network Interaction Optimization Model

In order to realize the distributed management of large-scale electric vehicles and guide users to charge and discharge in an orderly manner, this paper established a vehicle-network interaction optimization model. This model is composed of an upper-level optimization model of the distribution network and a lower-level optimization model of the user side. The upper one considered the charge and discharge margin and load fluctuation to optimize the safety and stability of the distribution network, while the lower layer one considered the charge and discharge of users' side. The battery loss and user costs in the process are optimized out of economic issues.

4.1. Upper-Level Optimization Model of Distribution Network

4.1.1. Charge and Discharge Margin Model. The charging margin represents the maximum charging load capacity that the grid allows the electric vehicle to bear in a certain period of time, which is represented by the optimized charging load; the discharge margin represents the maximum load absorbing capacity of the electric vehicle discharging to the grid in a certain period of time, which is represented by the optimized charging load. The discharge during the peak load period offsets the power difference between the predicted demand and the optimal load [18]. Therefore, the discharge margin model is shown in

$$P_{\text{dis}}(i) = \begin{cases} \int_{t_i}^{t_{i+1}} (P^*(t) - P(t))dt, & P^*(i) \geq P(i) \\ 0, & P^*(i) < P(i) \end{cases}, \quad (9)$$

$P_{\text{dis}}(i)$ represents the discharge margin of the i period, $P(t)$ represents the charging load after optimization at time t , $P^*(i)$ is the predicted load value of the power grid in period i . The charging margin $P(i)$ in the period i is the optimized charging load. When the predicted charging load in period i is greater than the optimized charging load, $P_{\text{dis}}(i)$ is equal to the difference integral of the two in the period ti to $ti + 1$; otherwise, it is equals 0.

4.1.2. Grid-Side Load Fluctuation Model. The grid-side load consists of two parts: the basic load of the grid and the electric vehicle charging and discharging load, so it can be expressed as

$$Fc = \min \frac{1}{T} \sum [(P(t+1) + EV_{\text{load},t} + 1) - (P(t) + EV_{\text{load},t})]^2. \quad (10)$$

In the formula, $P(t+1)$ and $P(t)$ represent the basic load during $t+1$ and t , respectively. $EV_{\text{load},t} + 1$ and $EV_{\text{load},t}$ represent the load of the electric vehicle in the period t .

4.1.3. Restrictions

- (1) Fast charging and slow charging cannot be performed at the same time during the charging behavior of electric vehicles

$$\lambda_k(\theta_1) + \lambda_k(\theta_2) \leq 1. \quad (11)$$

- (2) Grid-side discharge decision factor constraints

$$\omega_{ch} = \begin{cases} 1, & T_{ch} \geq \Delta T_{ch} \\ 0, & T_{ch} \leq \Delta T_{ch} \end{cases}. \quad (12)$$

In the formula, T_{ch} represents the total time for the user to connect to the grid for continuous charging and discharging, and ΔT_{ch} represents the minimum stay time for the grid company to allow electric vehicles to take discharge measures. The car interacts with the distribution network, and the SOC of the

electric vehicle can still ensure the normal travel of the user when it is off the grid.

- (3) Safety constraints of battery operation

$$\text{SOC}_{\text{min}} \leq \text{SOC}_{n,t} \leq \text{SOC}_{\text{max}}. \quad (13)$$

Among them, SOC_{min} and SOC_{max} represent the maximum and minimum values of the state of charge of the electric vehicle, respectively.

4.2. User-Side Lower-Level Optimization Model

4.2.1. Battery Depletion Model. In the actual scheduling process, users' concern about the impact of frequent charging and discharging on the battery will affect the development and promotion of the V2G project. Therefore, in order to evaluate the battery response cost in the process of implementing V2G for electric vehicles, the battery loss cost in the V2G response process needs to be fully considered, and the average discharge rate index [19] is proposed to quantify the discharge frequency:

$$\bar{\sigma} = \frac{\sum_{i=1}^N \sum_{k=1}^{24} |L_{d,k+1}^i - L_{d,k}^i|}{N}. \quad (14)$$

In formula (14), σ represents the average discharge rate index, which can reflect the average degree of dispatchable electric vehicles participating in the discharge. It is defined as the ratio of the discharge times in the electric vehicles participating in the dispatch strategy to the number of dispatched electric vehicles, which can intuitively express the discharge frequency.

In the application process, the excessively frequent charging and discharging behaviors in the V2G process will cause battery loss of EVs, thus affecting the interests of users. In order to improve user-side requirements and achieve optimization, this paper proposes a definition called battery loss satisfaction [20, 21]:

$$\omega = 1 - \frac{\bar{\sigma}_k}{\bar{\sigma}_{k,\text{max}}}. \quad (15)$$

In formula (15), is battery loss satisfaction; the larger the value, the less the discharge times of electric vehicles participating in V2G, and the smaller the battery loss is, the more satisfied the user is with the battery loss; is the average discharge rate index in the k period.

4.2.2. Charge and Discharge Cost. The orderly charging and discharging strategy of electric vehicles is not only related to the optimization of user side costs, but also involves practical problems, such as power distribution network loss and load balance. Simply controlling the variance coefficient of peak shaving and valley-filling cannot achieve the expected efficient operation mode of the power grid. Formulate the lower-level optimization model that optimizes the user's charging and discharging cost.

Considering that the user side requires more options of charging modes due to different travel purposes and travel

frequencies, the power grid company can formulate various charging modes and charging prices that meet the needs of users. At the same time, as a mobile load, electric vehicles have the dual characteristics of charging and discharging and can also be used as random distributed power sources to transmit electric energy to the distribution network so that users can obtain discharge benefits and help the distribution network system run stably. The user's discharge benefits B_u can be expressed as

$$B_u = w_{u,s}(\theta) p_{EV} \eta_{u,c}(t). \quad (16)$$

In the formula, p_{EV} represents the discharge capacity of electric vehicles in residential quarters or parking lots, and its value depends on the user's expectation of electric vehicles to transmit electric power to the distribution network system; $w_{u,s}(\theta)$ is the user-side discharge decision factor, and its value is determined by whether the user chooses to allow electric vehicle charging decision; and $\eta_{u,c}(t)$ represents the time-of-use electricity price (yuan/kWh) set by the power grid company according to the system operation and revenue cost.

Combining the above factors, the charging and discharging cost of electric vehicles C_{uc} can be expressed as

$$C_{uc} = \omega_{ch} \sum_{i=1}^N B_u - \sum_{i=1}^N \sum_{j=i+1}^J \lambda_k(\theta_1) P_{EV,t} \rho_{v1}(t) (t_{end} - t_{start}). \quad (17)$$

$$\omega_{u,s}(\theta) = \begin{cases} 1, & \text{Electric vehicles are involved in discharging electricity to the grid} \\ 0, & \text{Electric vehicles do not participate in discharging to the grid} \end{cases}. \quad (18)$$

- (2) Electric vehicle charging and discharging power constraints in adjacent periods

$$|EV_{load,t+1} - EV_{load,t}| \leq \Delta EV_{p \min}. \quad (19)$$

Among them, $\Delta EV_{p \min}$ represents the maximum allowable charging power in adjacent time periods under the charging state of the electric vehicle.

- (3) Electric vehicle charge and discharge capacity limitation

$$SOC_{N,t+1} = \begin{cases} SOC_{N,t} + \frac{\mu_{ch} P_{N,t} (t_{end} - t_{start})}{SOC_m}, & w_{u,s}(\theta) = 0 \\ SOC_{N,t} - \frac{\mu_{sp} P_{N,t} (t_{end} - t_{start})}{SOC_m}, & w_{u,s}(\theta) = 1 \end{cases}. \quad (20)$$

In the formula, $SOC_{N,t}$ represents the state of charge at the end of time; μ_{ch} and μ_{sp} represent the charging and discharging efficiency of charging piles in residential areas or parking lots; $P_{N,t}$ represents the charging and discharging power provided by the user's choice of connecting to the grid mode; and

In the formula, ω_{ch} represents the grid-side discharge decision factor, and its value depends on the charging and discharging time of the electric vehicle connected to the grid; $\lambda_k(\theta)$ is the charging and discharging decision variable; if the user chooses fast charging according to his travel situation, then $\lambda_k(\theta) = 1$; otherwise, $\lambda_k(\theta) = 0$; $\rho_v(t)$ is the time-of-use electricity price (yuan/kWh), which is based on the change of grid load in a day, divides a day into multiple periods such as peak period, low peak period, and peak period, and formulates different electricity prices according to the characteristics of load curves in different periods. Encourage users to choose the charging mode and charging time reasonably, which will cause the curve to cut peaks and fill valleys; $P_{EV,t}$ indicates the total charging power of the electric vehicle in the t period; and t_{start} and t_{end} represent the starting time and the leaving time of the electric vehicle user accessing the charging pile, respectively.

4.2.3. Restrictions

- (1) Discharge decision factor constraints on the user side

SOC_m represents the battery capacity in the user's electric vehicle.

- (4) Unscheduled time period constraints

$$\begin{cases} w_{u,s}(\theta) = 0 \\ \lambda_k(\theta_1) = 0, \forall N, t < t_{start} \text{ or } t_{end} \\ \lambda_k(\theta_2) = 0 \end{cases}. \quad (21)$$

5. Optimization

The paper adopted one of the multiobjective optimization algorithms; NSGA-II [22] is a fast nondominated sorting genetic algorithm with elite strategy. It not only excels in simultaneously optimizing multiple objectives by using service decision variables and constraints, but also can find the global optimal solution.

NSGA-II algorithm uses a fast nondominant sorting procedure [23], an elite retention method and a parameter-free localization operator. The fast nondominant sorting process divides the target solution to generate the Pareto frontier, and the Pareto frontier level optimal solution composes the Pareto solution set. This allows the optimal

solution set to find a better Pareto-optimal front; the obtained nondominant front converges better and maintains a better solution expansion.

The selection operator is achieved by combining the parental and progeny populations, while selecting the best (with regard to fitness and spread) solutions and creating mating pools. The algorithm generates a set of Pareto-optimal solutions through continuous iteration, mutation, cross selection, and other operations.

As for the fast crowded distance estimation, it makes the optimal solution set distribute in sound order. Crowding distance represents the degree of crowding among individuals and is used to calculate the distance between a unit and other units in the front end. The crowding degree distance calculation is based on the former, calculating the crowding distance of the adjacent solutions on the Pareto frontier of each level. The solution with a larger crowding distance is used as the child population and enters the cycle again so as to ensure the diversity and convergence. The specific flow of the algorithm [22] is shown in Figure 1.

6. Case Simulation

6.1. Example Description. Here is the scenario: there are 780 households in an old community, and each household owns a car. If the penetration rate of electric vehicles is 50%, the number of electric vehicles in the community will be 390, and if each electric vehicle parking space is equipped with a charging pile, there will be 390 electric vehicles correspond to 390 charging piles. The battery capacity of the electric vehicle is 40 kWh; the charging and discharging power is 7 kW.

Among them, the optimal front-end individual coefficient set by the algorithm parameters is 0.3, the population size is 100, the maximum evolutionary algebra is 200, the stopping algebra is also 200, and the fitness function value deviation is $1e-100$.

The TOU power price is shown in Table 1.

Through the simulation calculation, the total charging load of electric vehicles in residential areas and the total load in residential areas can be obtained [23]. The load data of the power grid is shown in Figure 2.

6.2. Analysis of Simulation Results. The disordered charging mode refers to the mode before optimization. After optimization, the following three aspects should be considered: economic scheduling (minimum cost), stability scheduling (minimum variance), and integrated scheduling (integrated economy and grid stability and optimal). It can be seen from the algorithm convergence diagram that the Pareto front is uniformly distributed, which proves that the simulation results have good convergence.

The calculation formula of load rate is shown in the following formula:

$$g = \frac{P_{av}}{P_{max}}. \quad (22)$$

6.2.1. Analysis of Scheduling Strategy under 50% Penetration Rate. From the simulation results and Figure 3, it can be seen that the orderly scheduling strategy is generally better than the disordered charging. The reason is that it can reduce the load peaks caused by the disordered charging, fill the load valleys, and will not cause new peaks and valleys. The cost of economic scheduling is the smallest, which is 359.1 yuan, and its variance is 49575.44. The variance is the smallest during smooth scheduling, which is 1369.2, and the cost is 12329.59 yuan at this time. The scheduling results are normalized by the minimum variance and the minimum cost to obtain the optimal charge-discharge load curve. The smaller the value, the higher the satisfaction. Among them, the variance of the optimal charge-discharge curve is 21302.27, which is more obvious than the peak-cutting and valley-filling effect of the minimum-cost load curve; its corresponding cost is 785.4 yuan, which is lower than that of the minimum-variance curve. Therefore, the overall effect is the best.

From Table 2, it can be seen that in the case of 50% penetration rate (i.e., 195 vehicles are connected to the power grid), compared with disordered charging, the two-level vehicle-network interaction model on both sides of the comprehensive supply and demand is used to compare with disordered charging:

- (a) . The peak value is reduced by 563.90, and the change rate is 20%; the valley value is increased by 425.40, while the change rate is -37% ; the peak-valley difference is reduced by 989.30, and the change rate is 59%. It is proved that orderly charging has a sound effect on shaving peaks and filling valleys, effectively solving the problem of “adding peaks to peaks” on the grid caused by disordered charging of electric vehicles.
- (b) . The standard deviation is reduced by 305.42, while the change rate is 61%, indicating that orderly charging can improve the smoothness and stability of system operation.
- (c) The load rate is increased by 16%, and the change rate is -22% , which helps to reduce the network loss and improve the utilization rate of power generation equipment and the economic benefits of system operation.

6.2.2. Scheduling Strategy Analysis in the Case of Wind and Solar Access at 50% Penetration Rate. From the simulation results and Figure 4, it is known that the cost of economic scheduling is the smallest, which is 512.4 yuan, and the variance is 43055.98; the variance of stable scheduling is the smallest, which is 20086.56, and the cost is 1192.8 yuan at this time; the scheduling results are normalized by the minimum variance and the minimum cost process to obtain the optimal charge-discharge load curve. The variance of the optimal charge-discharge curve is 26318.54, which is more obvious than the peak-cutting and valley-filling effect of the minimum-cost load curve, and the system runs more smoothly; the corresponding cost is 747.6 yuan, which is

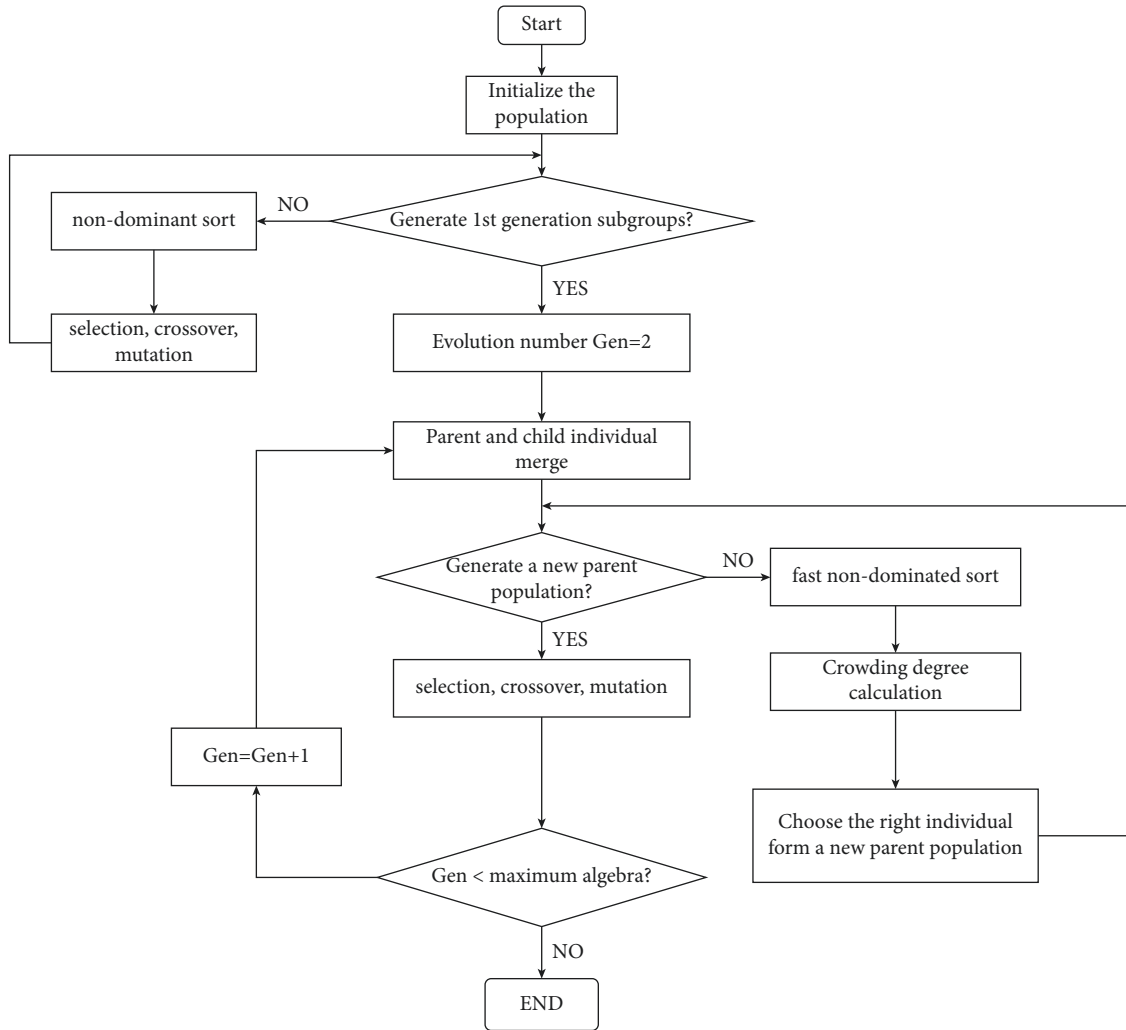


FIGURE 1: NSGA-II algorithm flowchart.

TABLE 1: Time-of-use power price parameter settings for charging and discharging.

Period	Charge and discharge electricity price (yuan·(kW·h) ⁻¹)
Valley time (0:00–3:00, 22:00–24:00)	0.30
(3:00–7:00, 15:00–17:00)	0.60
Peak hours (7:00–15:00, 17:00–22:00)	0.90

more economical than the minimum-variance curve. Therefore, the overall effect is the best. In addition, it can be found that under the same 50% penetration rate, the introduction of new energy will increase the curve volatility, and the orderly scheduling of electric vehicles can reduce the volatility of the load curve and stabilize the load.

It can be seen from Table 3 that when the penetration rate is 50%, and when the wind and solar is introduced, the double-layer vehicle-network interaction model on both sides of the comprehensive supply and demand is compared with the disordered charging:

- (a) The peak is cut by 563.90, and the rate of it was 23%; the valley is increased by 259.00, and the rate of change is -29%; peak-to-valley difference is cut by

822.00, which shows a change rate of 52%. It is proved that orderly charging can effectively reduce load peaks and fill load valleys.

- (b) The standard deviation is reduced by 485.46, the change rate is 59%, and the stability of the system operation is greatly improved.
- (c) The load rate is increased by 17%, and the change rate is -27%, which helps to improve the utilization rate of power resources and the operation efficiency of power distribution equipment.

6.2.3. Analysis of Scheduling Strategy under 100% Penetration Rate. As is shown in Figure 5, it can be judged that the

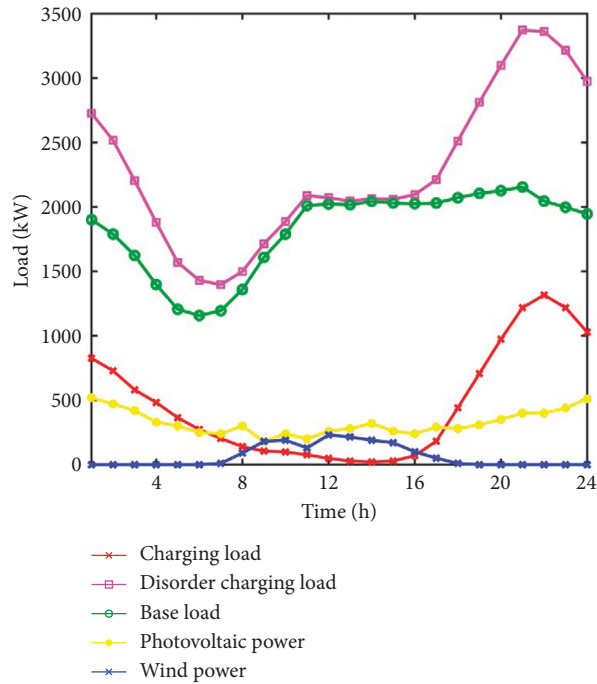


FIGURE 2: Microgrid base load curve.

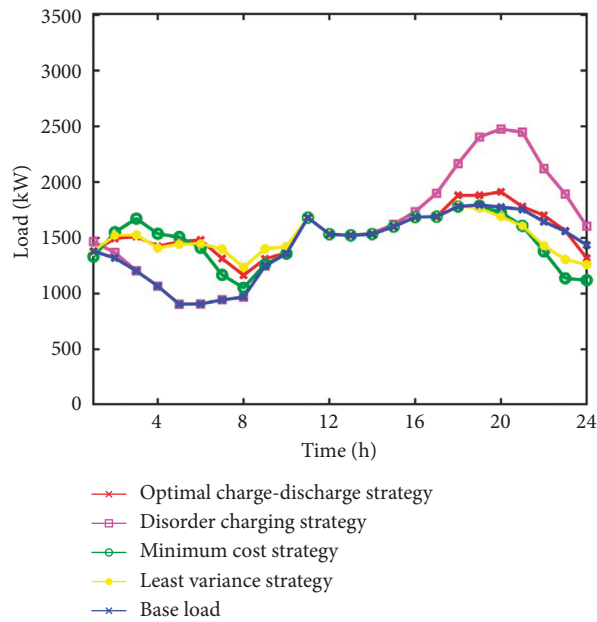


FIGURE 3: Load curve under the condition of 50% permeability.

TABLE 2: Comprehensive scheduling results of 50% penetration rate.

	Disorder charging	Comprehensive scheduling	Difference before and after optimization	Rate of change before and after optimization (%)
Peak (kW)	2847.60	2283.70	563.90	20
Valley value (kW)	1157.30	1582.70	-425.40	-37
Peak-to-valley difference (kW)	1690.30	701.00	989.30	59
Load standard deviation (kW)	497.87	192.45	305.42	61
Load average (kW)	1976.50	1940.30	36.20	2
Load rate	69%	85%	-16%	-22

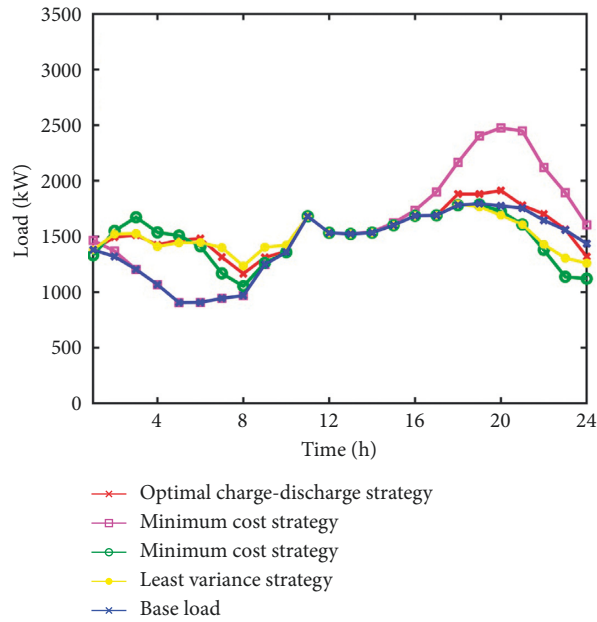


FIGURE 4: Load curve under the condition of new energy access (50% penetration rate).

TABLE 3: 50% penetration rate wind-solar access integrated scheduling results.

	Disorder charging	Comprehensive scheduling	Difference before and after optimization	Rate of change before and after optimization (%)
Peak (kW)	2475.70	1912.70	563.90	23
Valley value (kW)	905.70	1164.70	-259.00	-29
Peak-to-valley difference (kW)	1570.00	748.00	822.00	52
Load standard deviation (kW)	485.46	197.26	288.20	59
Load average (kW)	1586.70	1550.00	36.70	2
Load rate	64%	81%	-17%	-27

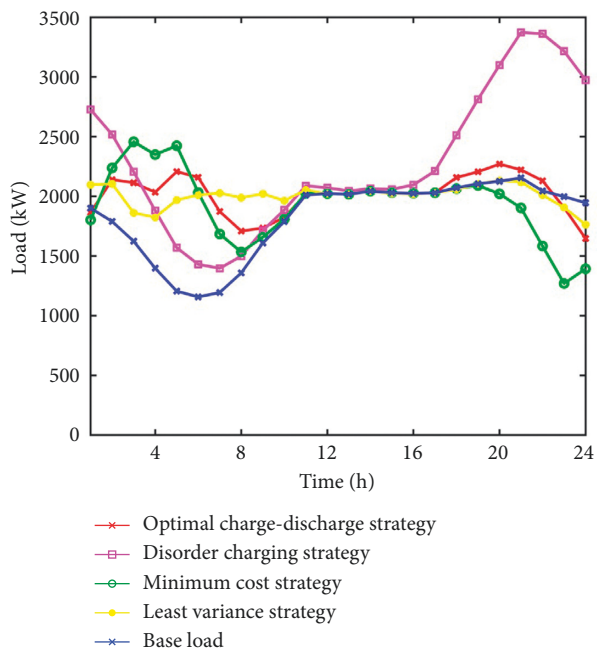


FIGURE 5: Load curve under the condition of 100% penetration rate.

TABLE 4: Comprehensive scheduling results of 100% penetration rate.

	Disorder charging	Comprehensive scheduling	Difference before and after optimization	Rate of change before and after optimization (%)
Peak (kW)	3372.60	2140.60	1232.00	37
Valley value (kW)	1397.10	1526.70	-129.60	-9
Peak-to-valley difference (kW)	1975.50	613.90	1361.60	69
Load standard deviation (kW)	608.30	164.67	443.63	73
Load average (kW)	2283.60	1940.90	342.70	15
Load factor	68%	91%	-23%	-34

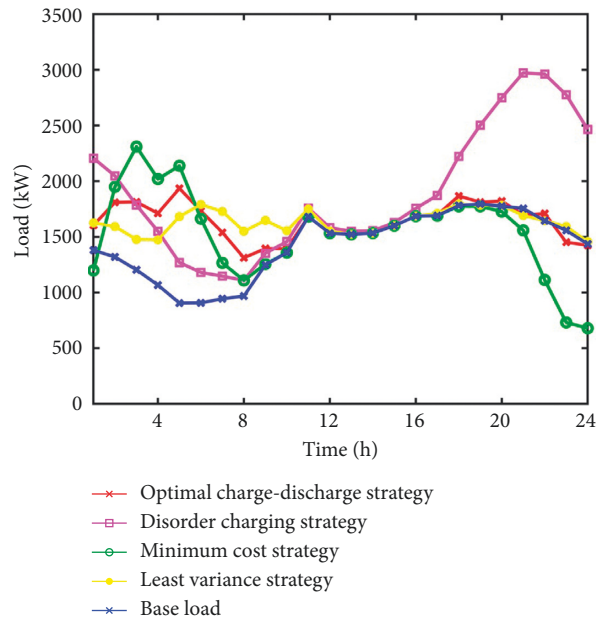


FIGURE 6: Load curve under the condition of new energy access (100% penetration rate).

TABLE 5: 100% penetration rate wind-solar access integrated scheduling results.

	Disorder charging	Comprehensive scheduling	Difference before and after optimization	Rate of change before and after optimization (%)
Peak (kW)	2972.60	1934.70	1037.90	35
Valley value (kW)	1108.73	1311.70	-202.97	-18
Peak-to-valley difference (kW)	1863.90	623.00	1240.90	67
Load standard deviation (kW)	584.63	167.85	416.79	71
Load average (kW)	1893.80	1636.60	257.20	14
Load rate	64%	85%	-21%	-33

charging cost is the smallest, which is 1354.5 yuan during economic scheduling; the variance is 144574.5 at this time; the variance is the smallest in smooth scheduling, which is 20040.4, and the cost is 3301.2 yuan at this time; the scheduling results are normalized by the minimum variance and the minimum cost process to obtain the optimal charge-discharge load curve. The variance of the optimal charge-discharge curve is 52779.85, which is more obvious than the

peak-shaving and valley-filling effect of the minimum-cost load curve, and the system runs more smoothly; the corresponding cost is 2030.7 yuan, which is more economical than the minimum-variance curve. Therefore, the overall effect is the best. In addition, it can be found that the higher the penetration rate, the better the smoothness.

From Table 4, it can be seen that in the case of 100% penetration rate, compared with disordered charging, the

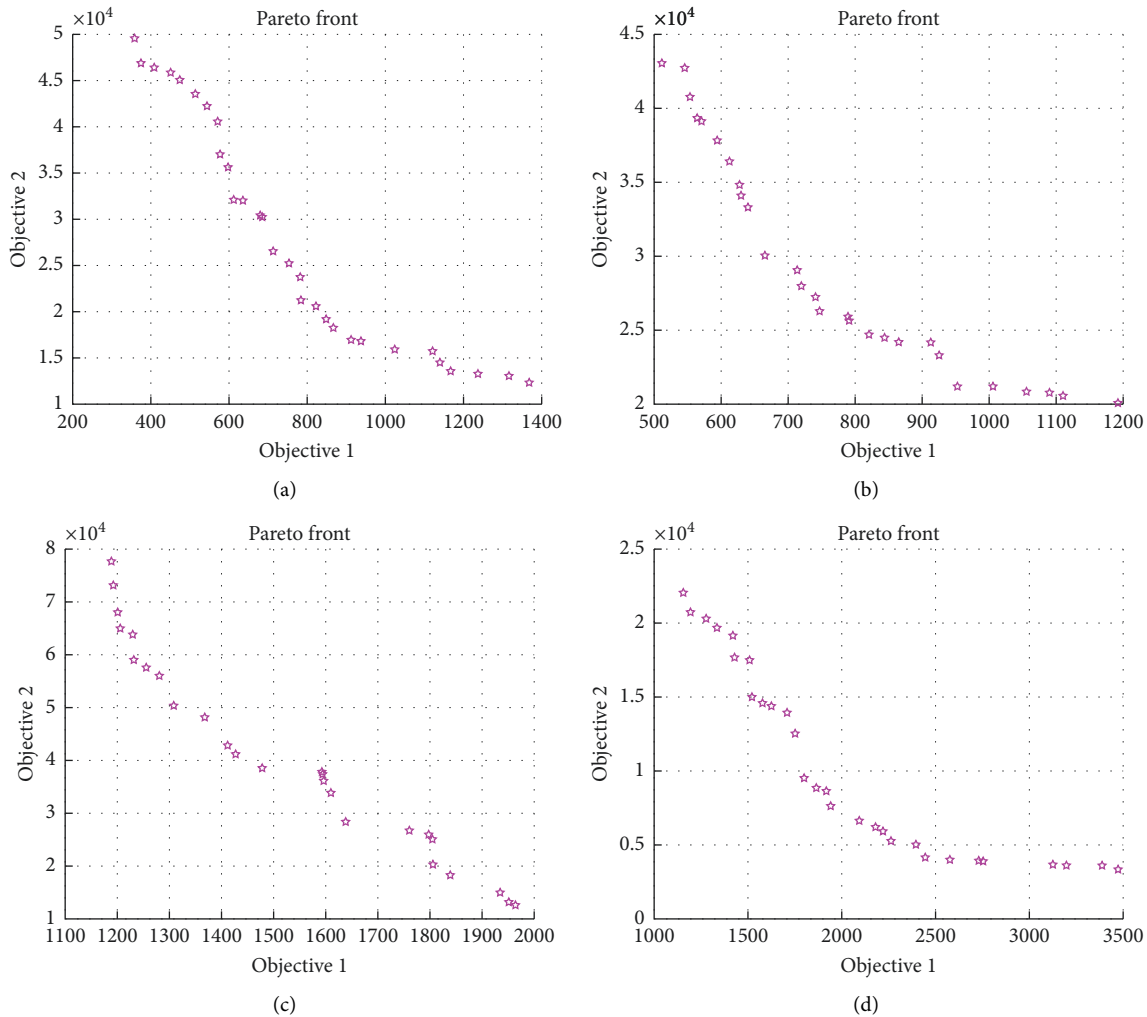


FIGURE 7: Algorithm convergence graph. (a) 50% penetration Pareto frontier. (b) Introducing the scenery, 50% penetration Pareto frontier. (c) 100% permeability Pareto frontier. (d) Introducing the scenery, 50% penetration Pareto frontier.

double-layer vehicle-network interaction model on both sides of the comprehensive supply and demand is compared with disordered charging:

- (a) The peak value is reduced by 1232.00, and the rate of change is 37%; the valley value is increased by 129.60, whose change rate is -9%; the difference between peak and valley is reduced by 1361.60, and its rate of change is 69%. It is proved that orderly charging has a good effect of shaving peaks and filling valleys and effectively solves the problem of “adding peaks to peaks” on the grid caused by disordered charging of electric vehicles.
- (b) The standard deviation is reduced by 443.63, and the change rate is 73%, indicating that orderly charging can improve the smoothness and stability of system operation.
- (c) The load rate is increased by 23%, and the change rate is -34%, which helps to reduce network losses and improve the utilization rate of power generation equipment and the economic benefits of system operation.

6.2.4. *Scheduling Strategy Analysis in the Case of Wind and Solar Access with 100% Penetration Rate.* As is shown in Figure 6, compared with the disordered charging curve, the ordered charging curve can effectively cut peaks and fill valleys. The cost of economic dispatch is the smallest, which is 1150.8 yuan, and its variance is 221197.6; variance is the smallest during smooth scheduling, which is 33799.68, and its cost is 3473.4 yuan. The scheduling results are normalized by the minimum variance and the minimum cost, and the optimal charge-discharge load curve is obtained. The variance of the optimal charge-discharge curve is 76823.1, which is more obvious than the peak-cutting and valley-filling effect of the minimum cost load curve, and the system runs more smoothly at this time. Its corresponding cost is 1938.3 yuan, which is more economical than the minimum variance curve. Therefore, the overall effect is the best. In addition, it can be found that the introduction of new energy sources such as wind and solar will bring volatility, but stability will improve as the penetration rate increases.

From Table 5, it can be seen that in the case of 100% penetration rate (introducing scenery), compared with

disordered charging, the double-layer vehicle-network interaction model on both sides of the comprehensive supply and demand is adopted.

- (a) The peak value is reduced by 1037.90, and the change rate is 35%; the valley value is increased by 202.97, and the change rate is -18% ; the peak-valley difference is reduced by 1240.90, and the change rate is 67%. It is proved that orderly charging has a good effect of shaving peaks and filling valleys and effectively solves the problem of “adding peaks to peaks” on the grid caused by disordered charging of electric vehicles.
- (b) The standard deviation is reduced by 416.79, and the change rate is 71%, indicating that orderly charging can improve the smoothness and stability of system operation.
- (c) The load rate is increased by 21%, and the change rate is -33% , which helps to improve the utilization rate of power generation equipment and the economic benefits of system operation.

6.2.5. Results' Comparison and Analysis. By comparing the optimization results under different permeability conditions, we can find in Figure 7 that the comprehensive scheduling mode after optimization is compared with that before optimization:

- (a) The load rate has been significantly improved, which not only helps to reduce network losses, but also improves the economic benefits of system operation.
- (b) The introduction of new energy will bring volatility; that is to say, the load variance will become larger when the penetration rate is the same.
- (c) The cost is reduced, and the economy of the system operation is improved.
- (d) The system peak-valley difference is reduced, giving full play to the peak-shaving and valley-filling effect of the electric vehicle charging load, effectively solving the problem of “peaks over peaks” of the grid caused by disordered charging of electric vehicles, and the utilization and distribution of power resources. The operating efficiency of electrical equipment is significantly increased.
- (e) The peak level of the system is significantly reduced, and the valley value has greatly improved, which is conducive to reducing the times of starts and stops, improving the safety of system operation, and saving costs.
- (f) The load variance is reduced, and the stability of the system operation is greatly improved. The reduced load variance of the distribution network also means that the degree of stability is improved. With the improvement of the responsiveness, it is more and more stable, and economy grows better as well.

7. Conclusion

Under the background of the large-scale application of electric vehicles and the increase of new energy power generation year by year, this paper proposed a coordinated optimal scheduling strategy for electric vehicles and wind-solar synergy. By rationally scheduling the charging and discharging behavior of electric vehicles, the dynamic balance between the charging and discharging load and the output of new energy in a certain area can be achieved, and the intermittent load of renewable energy can be effectively stabilized, while the load fluctuation can be stabilized, and the peaks and valleys can be cut. This paper also built a two-level vehicle-network interaction optimization model that takes into account the interests of both the user side and the grid side so as to achieve a win-win situation. Since there are multiple optimization objectives in the analysis process, the fast nondominant sorting genetic algorithm NSGA-II with elite strategy was adopted, and a series of “approximate optimal solutions” were obtained by weighing each objective function to generate the Pareto solution set. Finally, the strategy proposed in this paper was analyzed and affirmed by numerical example simulation, which proved that orderly charging of electric vehicles can cut peaks and fill valleys, improve the utilization rate of power generation equipment, increase the reliability of power supply, and improve the efficiency and reliability of power grid operation.

This paper only considers the time-disordered scheduling of private vehicles and does not discuss the long-term scheduling strategy of electric vehicles. In reality, the charging rules of EVs vary greatly with factors such as seasons, weather, and policies, and it is difficult to ensure the accuracy of load forecasting. Therefore, the analysis and prediction of the actual charging behavior of electric vehicles in combination with the actual scene still need further research.

Data Availability

The data used to support the findings of this study are available from the corresponding author upon request.

Conflicts of Interest

The author declares no conflicts of interest regarding the publication of this paper.

References

- [1] L. Tang, F. Wang, and X. Y. Liu, “Research on the influence of electric vehicle charging load on the life loss of distribution transformers,” *Electrotechnical Application*, vol. 37, no. 12, pp. 80–88, 2018.
- [2] X. Y. Duan, C. Yan, G. Zizhen, C. Xi, D. Ning, and Z. Yang, “Optimal charging and discharging strategy for electric vehicles in large timescales,” *Power Technology*, vol. 42, no. 12, pp. 4037–4044, 2018.

- [3] S. Y. Kuai, "EV charging load dispatching benefit and potential research," *Electronic Measurement Technology*, vol. 42, no. 14, pp. 37–42, 2019.
- [4] G. H. Yu, "Order charging method research of electrical vehicle based on dynamic distributed time electricity cost need answer," *Rural Electrification*, vol. 08, pp. 57–60, 2021.
- [5] J. D. Duan, "Coordinated charging control for EV charging stations considering wind power accommodation," *Energy Storage Science and Technology*, vol. 10, no. 2, pp. 630–637, 2021.
- [6] L. B. Liu, "Orderly charging and discharging strategy optimization for electric vehicles considering dynamic battery-wear model," *Automation of Electric Power Systems*, vol. 40, no. 5, pp. 83–90, 2016.
- [7] S. Xu and Y. Li, "An optimization model of peak-valley price time interval for guiding the orderly charging and discharging of electric vehicles," *Power Demand Side Management*, vol. 20, no. 5, pp. 11–15, 2018.
- [8] Z. Zhang, X. Huang, Y. Cao, H. Yang, and B. Xiao, "Charging load calculation considering TOU for electric vehicles," *Electric Power Automation Equipment*, vol. 34, no. 2, pp. 24–29, 2014.
- [9] X. X. Wang, "Multi-objective Bi-level electric vehicle charging optimization considering user satisfaction degree and distribution grid security," *Power System Technology*, vol. 41, no. 7, pp. 2165–2172, 2017.
- [10] X. Wang, "Research on Optimal Scheduling Strategy of Electric Vehicle Charging and Discharging in V2G mode," Master Dissertation, North China Electric Power University, Beijing, China, 2021.
- [11] Z. D. Bao, "Research on Charging and Discharge Technology Control Method of Electric Vehicles Based on V2G mode," Master Dissertation, Ningxia University, Ningxia, China, Ningxia University, 2021 .
- [12] S. W. Su, "Research on coordinated charging for electric vehicles considering new energy accommodation," *Journal of China Three Gorges University*, vol. 41, no. 5, pp. 84–89, 2019.
- [13] S. N. Wang and S. B. Yang, "Strategies for orderly control of electric vehicle charging load in residential areas," *Automation of Electric Power Systems*, vol. 40, no. 4, pp. 71–77, 2016.
- [14] Z. W. Xu, Z. Hu, Y. Song, H. Zhang, and X. Chen, "Coordinated charging strategy for PEV charging stations based on dynamic time-of-use tariffs," *Proceedings of the CSEE*, vol. 34, no. 22, pp. 3638–3646, 2014.
- [15] P. Chen, Q. H. Meng, and Y. J. Zhao, "The electric vehicle charging load calculation based on the Monte Carlo method," *Journal of Electrical Engineering*, vol. 11, no. 11, pp. 40–46, 2016.
- [16] Y. Ao, "Research on orderly control strategy of electric vehicle charging in residential areas," Nanchang University, Master Dissertation, 2021.
- [17] J. Y. Zhu, "Research on Microgrid Economic Dispatch Considering the Response of Electronic Users," Master Dissertation, Hebei University of Technology, Tianjin, China, 2017.
- [18] Y. Wang, "Sequential charge-discharge guidance strategy for electric vehicles based on time-sharing charging-discharging margin," *Power System Technology*, vol. 43, no. 12, pp. 4353–4361, 2019.
- [19] Y. R. Li, "Charging and discharging scheduling strategy of EVs considering demands of supply side and demand side under V2G mode," *Electric Power Automation Equipment*, vol. 41, no. 03, pp. 129–135+143, 2021.
- [20] K. Deb, A. Pratap, S. Agarwal, and T. Meyarivan, "A fast and elitist multiobjective genetic algorithm: nsga-II," *IEEE Transactions on Evolutionary Computation*, vol. 6, no. 2, pp. 182–197, 2002.
- [21] M. Wang, "Three-dimensional MultiUAV cooperative path planning based on an improved NSGAI algorithm," *Machinery & Electronics*, vol. 39, no. 11, pp. 73–80, 2021.
- [22] X. Jin, H. Tang, X. Wang, G. Qi, X. Jin, and D. Li, "Design of nuclear reactor power LQG controller based on NSGA-II algorithm," *Atomic Energy Science and Technology*, pp. 1–11, 2022, <http://kns.cnki.net/kcms/detail/11.2044.TL.20220218.1150.006.html>.
- [23] R. F. Shi, Z. H. Liang, and Y. Ma, "TOPSIS method based orderly charging strategy for electric vehicles in residential area," *Automation of Electric Power Systems*, vol. 42, no. 21, pp. 104–110+159, 2018.

Retraction

Retracted: Promotion Strategy of Low-Carbon Consumption of Fresh Food Based on Willingness Behavior

Mathematical Problems in Engineering

Received 13 September 2023; Accepted 13 September 2023; Published 14 September 2023

Copyright © 2023 Mathematical Problems in Engineering. This is an open access article distributed under the Creative Commons Attribution License, which permits unrestricted use, distribution, and reproduction in any medium, provided the original work is properly cited.

This article has been retracted by Hindawi following an investigation undertaken by the publisher [1]. This investigation has uncovered evidence of one or more of the following indicators of systematic manipulation of the publication process:

- (1) Discrepancies in scope
- (2) Discrepancies in the description of the research reported
- (3) Discrepancies between the availability of data and the research described
- (4) Inappropriate citations
- (5) Incoherent, meaningless and/or irrelevant content included in the article
- (6) Peer-review manipulation

The presence of these indicators undermines our confidence in the integrity of the article's content and we cannot, therefore, vouch for its reliability. Please note that this notice is intended solely to alert readers that the content of this article is unreliable. We have not investigated whether authors were aware of or involved in the systematic manipulation of the publication process.

In addition, our investigation has also shown that one or more of the following human-subject reporting requirements has not been met in this article: ethical approval by an Institutional Review Board (IRB) committee or equivalent, patient/participant consent to participate, and/or agreement to publish patient/participant details (where relevant).

Wiley and Hindawi regrets that the usual quality checks did not identify these issues before publication and have since put additional measures in place to safeguard research integrity.

We wish to credit our own Research Integrity and Research Publishing teams and anonymous and named external researchers and research integrity experts for contributing to this investigation.

The corresponding author, as the representative of all authors, has been given the opportunity to register their agreement or disagreement to this retraction. We have kept a record of any response received.

References

- [1] Z. Zhao, X. Zhong, and Y. Zhu, "Promotion Strategy of Low-Carbon Consumption of Fresh Food Based on Willingness Behavior," *Mathematical Problems in Engineering*, vol. 2022, Article ID 9571424, 10 pages, 2022.

Research Article

Promotion Strategy of Low-Carbon Consumption of Fresh Food Based on Willingness Behavior

Zhao Zhao,^{1,2} Xiaqing Zhong ,¹ and Yuqing Zhu³

¹School of Management, Shanghai University of Engineering Science, Shanghai 201620, China

²Odette School of Business, University of Windsor, N9B 3P4, Windsor, Canada

³Information Center, Ministry of Science and Technology, B15 Fuxing Road, Beijing 100862, China

Correspondence should be addressed to Xiaqing Zhong; m330121268@sues.edu.cn

Received 21 April 2022; Revised 9 May 2022; Accepted 13 May 2022; Published 28 May 2022

Academic Editor: Wei Liu

Copyright © 2022 Zhao Zhao et al. This is an open access article distributed under the Creative Commons Attribution License, which permits unrestricted use, distribution, and reproduction in any medium, provided the original work is properly cited.

The research on the influencing factors of residents' low-carbon consumption willingness and low-carbon consumption behavior of fresh food has certain practical guiding significance. Existing studies have analyzed the low-carbon consumption willingness, but the factors considered are not comprehensive and the degree of fit needs to be improved. Therefore, this paper starts with 37 variables from six aspects: demographic factors, psychological factors, low-carbon related knowledge, external factors, policy norms, and product factors. The binary logistic model is used to carry out regression analysis on low-carbon consumption willingness and low-carbon consumption behavior, and the fitting degree is higher and reaches about 90%. The regression results show that sense of responsibility, government tax, low-carbon product quality, and low-carbon product price have a significant impact on residents' low-carbon consumption willingness. Whether there are fake and shoddy products in the market and whether the products are really of low carbon have a significant impact on low-carbon consumption behavior. Finally, starting from the three subjects of government, enterprises, and residents, this paper puts forward targeted suggestions to improve residents' low-carbon consumption willingness and promote residents' low-carbon consumption behavior, in order to promote low-carbon consumption.

1. Introduction

Environmental problems have become a serious problem faced by the world in the 21st century; in particular the increase of carbon emissions year by year leads to the acceleration of global warming but also has an adverse impact on people's life and social and economic development. COVID-19 is the main reason for this problem, which is the large amount of carbon emissions produced by human beings in production and life. According to the statistics of world energy statistics yearbook, the global carbon emissions reached 343.6 billion tons in 2019. In 2020, the carbon emissions of various regions in the world were generally reduced, and the global carbon emissions dropped to 322.8 billion tons, down 6.3% from the same period last year. As shown in Figure 1, although the quantity has decreased compared with previous years, there is still much room to control its emission. Low-carbon

consumption, with carbon emission reduction in consumption as the main content, will become an important part of the "double carbon" goal. In the field of consumption, residents are the main body of consumption, and fresh products are the necessities of their daily life. Fresh products refer to the primary products sold without deep processing such as cooking and production, which are only kept fresh and simply sorted on the shelves, as well as the commodities of on-site processing categories such as bread and cooked food. Fresh products are mainly circulated through the cold chain, but the high cost of cold chain logistics and easy disconnection in transportation will lead to the increase of carbon emissions [1]. The overall demand is large. However, due to the characteristics of being perishable and difficult to preserve, as well as the diversified, personalized, and high-quality needs of consumers, the carbon emission increases in the whole consumption process. Therefore, exploring the influencing factors of

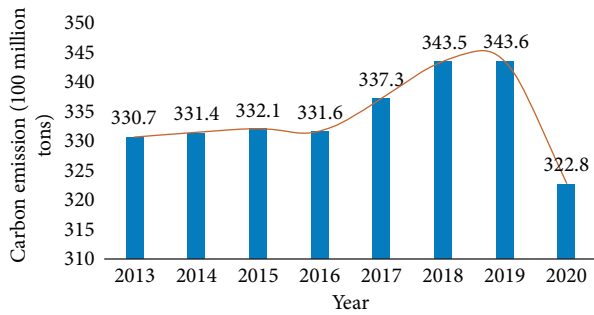


FIGURE 1: Change trend of global total carbon emissions from 2013 to 2020.

residents' willingness and behavior to consume fresh products is of great significance to reduce carbon emissions.

At present, urban residents are the main body of low-carbon consumption. The products produced by residents' consumption enterprises are also affected by relevant government policies. However, the consumption demand of urban residents for fresh products presents diversified and personalized characteristics. Therefore, to effectively control carbon emissions, it is necessary to effectively identify, influence, and guide residents' consumption patterns. The key is to fully grasp the influencing factors in the process of residents' low-carbon consumption. At present, the academic research results on low-carbon consumption are relatively rich. Looking at the existing literature, we can find that they are mainly concentrated in three aspects: "low-carbon consumption cognition," "low-carbon consumption factors," and "low-carbon consumption countermeasures."

1.1. Research on Low-Carbon Consumption Cognition.

The low-carbon behavior and cognitive level of users' families can be measured from three aspects: family energy consumption, daily travel, and living consumption [2]. Low-carbon knowledge is divided into system knowledge, action knowledge, and effectiveness knowledge. By establishing a double intermediary model of the action mechanism of different low-carbon knowledge on low-carbon behavior, it can be found that publicity and education need to reduce the cognitive imbalance of residents' low-carbon behavior according to the action mechanism of different knowledge [3]. Socialist construction needs to build a smart city, and the key is to save energy and reduce emissions [4]. Most employees have a low level of low-carbon cognition, showing the law of gradual transition from low-carbon cognitive defects to one-sided, low-carbon negative employees and low-carbon advocates and employees [5]. Through the field investigation and tourist sampling questionnaire survey of Zhangjiajie National Forest Park, it is found that Zhangjiajie tourists have relatively high awareness and willingness of low-carbon tourism [6]. The carbon emission reduction action of tourism transportation and accommodation in Wutai Mountain is the most convenient to carry out, but tourists' low-carbon tourism cognition is still in the primary stage, so it is

difficult to implement low-carbon tourism [7]. The overall level of emission reduction behavior of urban residents in China is low, and environmental awareness and environmental responsibility can significantly improve the public's emission reduction behavior [8]. The increasingly diversified needs of consumers have intensified the competition of network service providers in providing products [9].

1.2. Research on Low-Carbon Consumption Factors.

Publicity and education had the greatest impact on low-carbon consumption behavior, followed by the degree of implementation convenience, the impact of low-carbon behavior knowledge was weak, and the impact of low-carbon psychological awareness and social reference norms on low-carbon consumption behavior was not obvious [10]. Low-carbon cognition, energy-saving behavior, and waste disposal behavior have a significant positive impact on low-carbon consumption intention, while marginal carbon crisis awareness has a significant impact [11]. Demographic characteristics, personal cognition, environmental scenarios, and other factors have an impact on residents' low-carbon consumption willingness and behavior, and corresponding policy suggestions are put forward accordingly [12]. Technological constraints, market risks, and policy risks will restrict low-carbon production of industrial enterprises, while low-carbon life attitudes, government policies, social norms, and the quality and price of low-carbon products will affect residents' low-carbon consumption [13]. Financial technology can promote the development of green finance, so effective measures can be taken from three aspects: top-level design, technology research, and supervision [14]. Conformity psychology and ecological value perception have a positive impact on low-carbon consumption intention, and age and monthly income have a negative impact on low-carbon consumption behavior [15]. The government performance appraisal system, the attitude of enterprise executives, and consumers' consumption will affect the decision-making of the three subjects. Suggestions to promote low-carbon consumption can be put forward from the above aspects [16]. There is a significant positive correlation between ecological personality and low-carbon consumption behavior, in which ecological agreeableness and ecological responsibility are the main influencing factors, and urban residents' ecological personality shaping policies and low-carbon consumption behavior guidance policies are put forward, in order to promote low-carbon consumption behavior [17]. Low-carbon awareness, low-carbon knowledge, personal norms, social norms, and situational factors have an impact on residents' low-carbon behavior, and situational factors have an inhibitory effect on private and public low-carbon behavior [18]. Psychological factors, demographic factors, family factors, and situational factors will affect residents' low-carbon consumption behavior [19]. Attitudes, subjective norms, and perceived behavior control have a significant positive impact on low-carbon consumption behavior intention, and collectivist values have a significant direct positive impact on low-carbon consumption behavior intention [20]. Attitudes, situations,

habits, policies and regulations, economic costs, and social norms will affect their low-carbon consumption behavior and put forward suggestions to guide college students' low-carbon consumption from the government and school levels [21].

1.3. Research on Low-Carbon Consumption Countermeasures.

Taking measures from participants, product specifications, market cultivation, publicity and education, consumption scenes and other aspects can effectively solve the problem of imperfect low-carbon consumption market [22]. We should guide the green transformation of consumption mode and promote the realization of carbon peak and carbon neutralization from the consumer side by improving consumer awareness, optimizing consumption policy design, tapping the potential of cities as key areas of emission reduction, paying attention to informal institutional factors, and encouraging low-carbon consumption in key areas of emission reduction such as transportation and construction [23]. The implementation of carbon tax policy can reduce carbon emissions to a certain extent. The strategy of combining repurchase and subsidy can reduce emissions and improve economic benefits at the same time [24]. The theoretical model of system situation behavior can be used for reference to promote the development of residents' low-carbon consumption behavior from the aspects of establishing low-carbon consumption values, establishing low-carbon consumption ethics, abandoning high-carbon consumption habits, and creating a low-carbon consumption atmosphere [25]. Comprehensive fitness can promote people to participate in leisure fitness, enhance physique, and achieve physical fitness [26]. The introduction of "boosting" policies such as energy labels, reconstruction of information presentation, provision of normative information feedback, and improvement of personal education and energy literacy can effectively reduce the energy efficiency gap and cultivate low-carbon consumption habits [27]. In order to reduce the environmental pollution caused by abandoned household medical devices, the government can take dynamic punishment and dynamic subsidy measures [28]. Through the concept of low-carbon consumption, guide consumers from meeting their desires to meeting their needs, so as to curb their excessive consumption behavior [29]. The development of industry can promote economic development, but it will also produce a lot of carbon emissions, which will harm the environment [30]. There is a balance point of game among consumers, enterprises, and the government, which can build a low-carbon consumption guidance mechanism with enterprises as leverage [31]. Increasing the intensity of supervision and punishment can affect the "free riding" behavior of enterprises and promote green emission reduction [32, 33].

To sum up, it can be found that the factors affecting the low-carbon consumption of fresh products mainly include policies, products, cognition, and values. The countermeasures and suggestions put forward by the above researchers mainly include improving the awareness of low-carbon

consumption and issuing relevant policies. However, with the continuous development of economy and society, with the improvement of the education level of the whole people and other factors, residents' cognition and consumption concept will also change. The existing studies do not consider low-carbon consumption comprehensively and do not integrate the consideration of fresh products. Therefore, this study combines reality, combs the existing literature, carries out division again comprehensively, considers various factors, analyzes the influencing factors affecting residents' low-carbon consumption willingness and low-carbon consumption behavior of fresh food, and puts forward corresponding countermeasures and suggestions.

2. Research Methods and Variable Design

2.1. Research Method. Low-carbon consumption means green consumption and sustainable consumption. Low-carbon consumption intention is people's idea of low-carbon consumption, and low-carbon consumption behavior is people's behavior of low-carbon consumption. Because the explanatory variable of this paper is residents' "low-carbon consumption willingness," it can be divided into "willing" and "unwilling". Residents' "low-carbon consumption behavior" can be divided into "yes" and "no." Both "low-carbon consumption willingness" and "low-carbon consumption behavior" are binary variables, which cannot meet the preconditions and assumptions of general regression analysis and the value requirements of explained variables in general linear regression analysis. Therefore, it cannot be analyzed with general linear regression model. Combined with the actual situation and considering various factors, the explanatory variables designed in this paper include both numerical variables and subtype variables. Therefore, this paper selects the binary logistic model to conduct regression analysis on the residents' low-carbon consumption willingness and low-carbon consumption behavior of fresh food, set as the probability of occurrence of residents' low-carbon consumption intention (behavior) of fresh products, and the value range is $[0, 1]$; then $P/(1 - P)$ represents the probability of occurrence of low-carbon consumption intention (behavior) of fresh products and the probability of nonoccurrence of low-carbon consumption intention (behavior) of fresh products; $\ln(P/(1 - P))$ can be obtained by taking logarithm; then we can get $P = 1/(1 + e^{-(w_0 + w_1x_1 + w_2x_2 + \dots + w_nx_n)})$; it is logistic regression model. Among them, w_0 is a constant, x_1, x_2, \dots, x_n is the explanatory variable, there are n explanatory variables, which are n influencing factors of low-carbon consumption intention (behavior) of fresh food, and w_1, w_2, \dots, w_n is the regression coefficient. Combined with the reality of this paper, the explanatory variable is set to $y_i (i = 1, 2)$, y_1 indicates low-carbon consumption willingness, y_2 indicates low-carbon consumption behavior, and $y_i = \begin{cases} 0, & \text{yes} \\ 1, & \text{no} \end{cases}$. Set the explanatory variable to $x_{ij} (i = 1, 2, \dots, 5; j = 1, 2, \dots, 8)$, representing the j -th variable of the i -th dimension.

2.2. Variable Design. According to the research theme, combined with the existing relevant literature, this paper uses the questionnaire survey method to carry out the research, sets up two explanatory variables of “low-carbon consumption intention” and “low-carbon consumption behavior” of fresh products, and sets the explanatory variables into six aspects: demographic factors, psychological factors, low-carbon related knowledge of fresh products, external factors, policy norms, and product factors, with a total of 35 variables. Among them, demographic factors include gender, age, education level, and monthly income; psychological factors include trying new products, the influence of people around, recommending products, improving the quality of life, paying attention to global warming, saving energy, making contributions, and working together; the low-carbon knowledge of fresh food includes seven variables: understanding low-carbon, paying attention to low-carbon related issues, sharing low-carbon knowledge, understanding the importance of low-carbon, knowing how to reduce carbon emission, giving practice, and encouraging others to reduce carbon; external factors include six variables: practical publicity content, effective educational activities, convenient purchase of products, fake and shoddy products, many types of products, and smooth purchase channels; policy norms include four factors: government subsidies, government taxation, ignoring incentives, and avoiding punishment; product factors include six factors: low-carbon fresh product quality, cost performance. Among them, psychological factors, fresh low-carbon related knowledge, external factors, policy norms, and product factors are investigated in the form of Likert five-level scale. Each question is set with five options of “very disagree,” “relatively disagree,” “general,” “relatively agree,” and “very agree,” which are recorded as 1, 2, 3, 4, and 5, respectively.

3. Results Analysis

The research and analysis data came from the research group from January 2022 to March 2022. Due to the epidemic situation, we adopted the method of random sampling and conducted an online survey on Shanghai residents by using the method of questionnaire; 190 questionnaires were collected this time. After reviewing and proofreading the collected questionnaires, it was found that the contents of 4 questionnaires were incomplete, so they were eliminated as invalid questionnaires. A total of 186 valid questionnaires were formed, and the effective recovery rate of the final questionnaire reached 97.89%. There were 37 variables in this questionnaire, and the number of valid questionnaires recovered was more than five times the number of variables. Therefore, questionnaire analysis can be carried out.

This paper uses SPSS25 to analyze the collected data. Firstly, it makes a descriptive statistical analysis on the collected samples to check whether the samples are well representative. Secondly, it tests the reliability and validity of the collected questionnaire data and then centralizes the questionnaire data to facilitate more effective regression analysis; centralization means that the explanatory variable and the explained variable subtract their own average value,

respectively. Finally, the “low-carbon consumption intention” and “low-carbon consumption behavior” are analyzed by binary logistic regression from five aspects: psychological factors, low-carbon related knowledge of fresh products, external factors, policy norms, and product factors, to explore the factors and influence degree of residents’ low-carbon consumption intention and behavior of fresh products and then put forward targeted countermeasures and suggestions.

3.1. Descriptive Analysis. Figure 2 reveals that the numerical characteristics of demographic factors reflect the distribution of the respondents. The basic characteristics of the sample are as follows: there are 78 males, accounting for 41.94%, and 108 females, accounting for 58.06%. In terms of age distribution, it is mainly concentrated in the youth group aged 21–30, with the number reaching 101, accounting for 54.30%. The overall proportion distribution is in the shape of olive. In terms of education level, there are 110 college or undergraduate students, accounting for 59.14% of the total; there are 45 graduate students and above, accounting for 24.19% of the total; there are 31 people in senior high school and below, accounting for 16.67% of the total. It can be seen that the education is mainly concentrated in junior college or undergraduate, and the residents of other education levels are evenly distributed. From the perspective of monthly income, it is mainly distributed at 5000 yuan and below, followed by 5000–8000 yuan. The samples of other monthly income levels also account for a certain proportion. Overall, the distribution of the demographic data of the survey sample is reasonable and representative, which is suitable for the data analysis of this study.

3.2. Reliability and Validity Analysis

3.2.1. Reliability Analysis. The value range of reliability coefficient is 0-1. The closer it is to 1, the higher the reliability. SPSS is used to analyze the reliability of each dimension and the whole. From Table 1, we can find that, in terms of psychological factors, the overall standardized reliability coefficient is 0.914; in terms of low-carbon related knowledge of fresh products, the overall standardized reliability coefficient is 0.923; in terms of external factors, the overall standardized reliability coefficient is 0.909; in terms of policy norms, the overall standardized reliability coefficient is 0.869; in terms of product factors, the overall standardized reliability coefficient is 0.916. At the same time, the reliability coefficients of specific factors of psychological factors were 0.906, 0.906, 0.902, 0.898, 0.905, 0.899, 0.906, and 0.898, respectively; the reliability coefficients of specific factors of low-carbon related knowledge were 0.914, 0.909, 0.913, 0.911, 0.909, 0.913, and 0.911, respectively; the detailed reliability coefficients of external factors were 0.887, 0.896, 0.886, 0.901, 0.888, and 0.891, respectively; the reliability coefficients of specific factors of policy norms are 0.846, 0.821, 0.828, and 0.837, respectively; the reliability coefficients of specific factors of product factors

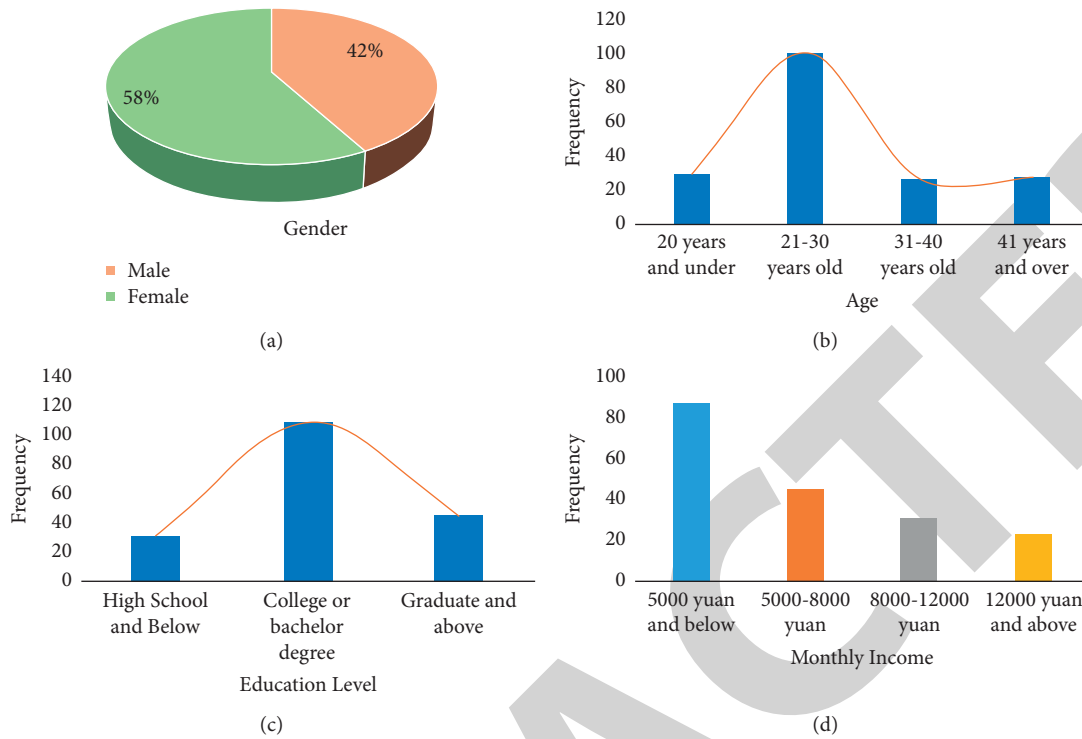


FIGURE 2: Descriptive analysis of demographic factors.

TABLE 1: Analysis results of each dimension and overall reliability.

Analysis results of each dimension and overall questionnaire	
Option	Standardized reliability coefficient
Psychological factor	0.914
Low-carbon related knowledge of fresh products	0.923
External factors	0.909
Policy norms	0.869
Product factors	0.916
Totally	0.978

are 0.903, 0.9, 0.905, and 0.895, respectively. We can find that the reliability coefficient after deleting the items of the above dimensions is less than the overall standardized reliability coefficient. Therefore, the dimensions of psychological factors, low-carbon related knowledge of fresh products, external factors, policy norms, and product factors have high reliability, and the internal consistency of each dimension is good. The title does not need to be adjusted. Finally, the overall reliability is analyzed, and the standardized Cronbach coefficient is 0.978, indicating that the overall reliability of the questionnaire is very high.

3.2.2. Validity Analysis. The coefficient of KMO test ranges from 0 to 1. The closer it is to 1, the better the validity of the questionnaire. According to the results of exploratory factor analysis above, the coefficient result of this KMO

test is 0.975, indicating that the validity of the questionnaire is relatively good.

Through the above analysis, it can be seen that the reliability and validity of the questionnaire data are relatively high, and the next regression analysis can be carried out on the questionnaire data.

3.3. Binary Logistic Regression Analysis. Binary logistic regression analysis was conducted with “low-carbon consumption intention” and “low-carbon consumption behavior” of fresh products as explanatory variables, respectively. Tables 2 and 3 depict the regression results of low-carbon consumption intention after deleting insignificant variables.

The regression results show the following:

- (1) Low-carbon consumption intention: the significance of being willing to try new fresh products is 0.002, which is less than the given significance level of 0.05, indicating that trying new fresh products has a significant positive impact on residents’ low-carbon consumption intention, and the influence coefficient is 1.646, indicating that residents’ low-carbon consumption intention is closely related to new products. The significance of recommending fresh products to others is 0.021, which is less than the given significance level of 0.05, indicating that recommending fresh products to others has a significant positive impact on residents’ low-carbon consumption intention, and the influence coefficient is 1.331, indicating that the more the residents are

TABLE 2: Logistic regression results of low-carbon consumption intention.

Logistic model regression results			
Variable options	Low-carbon consumption willingness		
	Coefficient	Significance	Exp(B)
I am willing to try new products	1.646	0.002	0.193
I will recommend my products to others	1.331	0.021	3.784
I should make a contribution to reducing carbon emissions	1.460	0.009	0.232
I understand the importance of low-carbon behavior	1.206	0.027	0.299
Government taxation contributes to low-carbon consumption	1.260	0.039	3.526
I will consider the cost performance of the product	-1.257	0.013	0.285
Reducing the price of low-carbon products will help China's low-carbon consumption	1.975	0.007	7.205
Constant		-1.723	

TABLE 3: Logistic regression results of low-carbon consumption behavior.

Logistic model regression results			
Variable options	Low-carbon consumption behavior		
	Coefficient	Significance	Exp(B)
There are fake and shoddy products in the market	-0.882	0.049	0.414
In order to avoid punishment, I will take the initiative of low-carbon consumption	1.527	0.013	4.604
I'm not sure if some fresh products are really low-carbon	-1.325	0.048	0.266
Constant		-1.695	

willing to recommend fresh products, the higher their low-carbon consumption intention of fresh products is. The significance of the contribution that should be made to carbon emission reduction is 0.009, which is less than the given significance level of 0.05, indicating that the contribution that should be made has a significant positive impact on the willingness of low-carbon consumption, and the influence coefficient is 1.460, indicating that residents have a strong sense of responsibility in low-carbon consumption. The significance of understanding the importance of low-carbon behavior is 0.027, which is less than the given significance level of 0.05, indicating that understanding the importance of low-carbon behavior has a significant positive impact on low-carbon consumption intention, and the influence coefficient is 1.206, indicating that residents' understanding of low-carbon

consumption is conducive to their willingness to produce low-carbon consumption. The significance that government taxation contributes to low-carbon consumption is 0.039, which is less than the given significance level of 0.05, indicating that government taxation has a significant positive impact on low-carbon consumption intention, and the influence coefficient is 1.260, indicating that taxation can enhance residents' low-carbon consumption intention. Considering that the significance of the cost performance of products is 0.013, it shows that the cost performance of fresh products has a significant negative impact on low-carbon consumption intention, and the influence coefficient is 1.257. The significance of reducing the price of low-carbon fresh products to low-carbon consumption is 0.007, which is less than the given significance level of 0.05, indicating that reducing the price of carbon fresh products has a significant positive impact on the willingness of low-carbon consumption, and the influence coefficient is 1.975, indicating that residents pay more attention to the quality and price of low-carbon fresh products, which provides development space for enterprises to launch high-quality and low-cost low-carbon fresh products and also puts forward new requirements. Through the above analysis, we can get the regression model of low-carbon consumption intention of fresh products:

$$P(y_1 = 1|x_{ij}) = \frac{1}{1 + e^{-x_1}},$$

$$\begin{aligned} X_1 = & -1.723 + 1.646x_{21} + 1.331x_{23} \\ & + 1.460x_{27} + 1.206x_{34} + 1.260x_{52} \\ & - 1.257x_{62} + 1.975x_{66}. \end{aligned} \quad (1)$$

The regression results show the following:

- (2) Low-carbon consumption behavior: the significance of fake and shoddy products in the market is 0.049, which is less than the given significance level of 0.05, indicating that the existence of fake and shoddy products in the market has a significant negative impact on residents' low-carbon consumption behavior, and the influence coefficient is 0.882, indicating that the less fake and shoddy products in the market, the more conducive to more residents' low-carbon consumption behavior. The significance of active low-carbon consumption to avoid punishment is 0.013, which is less than the given significance level of 0.05, indicating that active low-carbon consumption to avoid punishment has a significant positive impact on residents' low-carbon consumption behavior, and the influence coefficient is 1.527, indicating that appropriate mandatory measures can help to improve residents' low-carbon consumption behavior. It is

impossible to determine whether some fresh products are really low-carbon. The significance is 0.048, which is less than the given significance level of 0.05, indicating that whether fresh products are really low-carbon has a significant negative impact on residents' low-carbon consumption behavior, and the influence coefficient is 1.325, indicating that, in order to promote residents' low-carbon consumption behavior, it is very necessary to supervise and popularize the low-carbon nature of fresh products and how to identify whether fresh products are low-carbon. Through the above analysis, it can be concluded that the regression model of low-carbon consumption behavior is

$$P(y_2 = 1|x_{ij}) = \frac{1}{1 + e^{-X_2}},$$

$$X_2 = -1.695 - 0.882x_{44} + 1.527x_{54} - 1.325x_{63}. \quad (2)$$

3.4. Model Check. Firstly, the Hosmer-Lemeshow test table of the binary logistic model based on low-carbon consumption intention is 0.986, which is greater than the given significance level of 0.05, indicating that the difference between the observed value and the expected value is not significant, indicating that the model has a good fit. At the same time, the overall prediction accuracy of the binary logistic model established with "low-carbon consumption intention" as the explanatory variable has reached 90.3%, indicating that the prediction effect is good and the accuracy is high. Secondly, the significance of the Hosmer-Lemeshow test table of the binary logistic model based on low-carbon consumption behavior is 0.436, which is greater than the given significance level of 0.05, indicating that the difference between the distribution of the observed value and the expected value is not significant, indicating that the fitting degree of the model is good. Finally, the overall prediction accuracy of the binary logistic model established with "low-carbon consumption behavior" as the explanatory variable reached 92.5%, indicating that the prediction effect is good and the accuracy is high. In summary, the model established in this paper has practical significance.

4. Conclusions and Recommendations

4.1. Conclusion. Through the research, it can be found that the main factors affecting residents' low-carbon consumption intention are whether residents are willing to try new fresh products, whether residents are willing to recommend their purchased fresh products to others, residents' sense of responsibility to contribute to carbon emission reduction, awareness of the importance of low-carbon behavior, government taxes, the quality of fresh products, and the price of fresh products. The main factors affecting residents' low-carbon consumption behavior are

whether there are fake and shoddy products in the market, whether residents will consume low-carbon in order to avoid punishment, and whether fresh products are really low-carbon. Through the binary logistic regression model, the factors affecting the low-carbon consumption of fresh products are found out. The fitting degree of the model in this paper is higher than that in the past, reaching more than 90%. Next, this paper considers further optimizing the model to improve the fitting effect and fit the actual situation more closely.

4.2. Recommendations. Through the above research, we can draw the main factors affecting residents' willingness and behavior of low-carbon consumption of fresh food. Because the government plays a guiding role in low-carbon consumption, enterprises, as suppliers of low-carbon consumption products, build a bridge between the government and residents and play an intermediary role. Residents, as practitioners of low-carbon consumption, can test the effectiveness of government guidance and products supplied by enterprises. As the main body of low-carbon consumption, Figure 3 reveals the role of them in low-carbon consumption. It can be seen that, in order to better improve residents' low-carbon consumption willingness and promote residents' low-carbon consumption behavior, the joint efforts of the government, enterprises, and residents are needed.

4.2.1. Government. Firstly, take necessary mandatory measures to guide and regulate residents' low-carbon consumption willingness, introduce relevant laws and regulations that help residents to carry out low-carbon consumption of fresh products, give certain rewards to residents who take the initiative to implement low-carbon consumption, and take certain punitive measures for those who violate relevant regulations.

Secondly, give full play to the regulatory role of tax. Because the price of low-carbon fresh products has a certain impact on consumer demand, the government can provide financial subsidies for the purchase of low-carbon fresh products and appropriately adjust the consumption tax of low-carbon fresh products, and effective material incentives can enhance residents' low-carbon consumption willingness. At the same time, for enterprises providing low-carbon products, based on a certain tax preference, it can reduce the operating cost of enterprises, indirectly reduce the price of low-carbon fresh products, and then effectively attract residents to buy low-carbon fresh products.

Thirdly, encourage the innovation and R&D of low-carbon technologies, provide infrastructure conditions for R&D, award corresponding awards and bonuses to individuals and teams who make achievements, and improve the corresponding intellectual property law to protect R&D achievements. At the same time, it can also give full play to the economic value of intellectual property and give impetus to individual and team R&D.

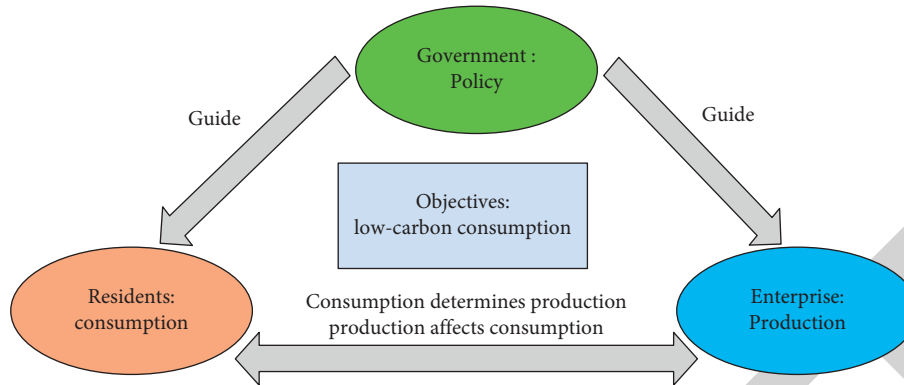


FIGURE 3: Role relationship of low-carbon actors.

Fourth, strengthen publicity and education, publicize low-carbon consumption in schools, communities, shopping malls, and other places, quantify the benefits of low-carbon consumption to residents, improve residents' attention to low-carbon consumption, and enhance residents' sense of responsibility for low-carbon consumption.

4.2.2. Enterprise. Firstly, with the improvement of residents' lives, the trend of increasing consumption in the market is gradually emerging. Enterprises should strengthen the research and development of low-carbon environmental protection technology, energy-saving technology, and energy technology. At the same time, enterprises can also cooperate with colleges and universities and introduce talents from colleges and universities to promote the research and development of low-carbon fresh product technology, so as to produce more kinds of low-carbon fresh products.

Secondly, based on the needs of consumers, carry out market segmentation of low-carbon fresh products, develop appropriate low-carbon fresh products, make classification marks in the sales and circulation of products, guide consumers to use low-carbon fresh products, and improve consumers' selection space and discrimination ability of low-carbon fresh products.

Thirdly, pay attention to improving the performance of low-carbon fresh products. In the process of product circulation, enterprises should take the initiative to bear social responsibility to avoid flooding the market with fake and shoddy products and affecting residents' confidence in low-carbon fresh products. At the same time, enterprises should abide by market rules, moderately reduce the price of low-carbon fresh products, and provide more high-quality low-carbon fresh products and low-carbon services.

4.2.3. Residents. Firstly, as the main body of market consumption, while safeguarding their own rights and interests, residents should also actively assume social responsibility, consciously establish and cultivate the values of low-carbon consumption, actively participate in public welfare low-carbon activities organized by the government and social media, constantly learn the

knowledge of low-carbon consumption, and distinguish the authenticity and quality of low-carbon fresh products.

Secondly, residents should implement low-carbon consumption and effectively achieve low-carbon consumption in their lives, such as consuming low-carbon fresh products as much as possible and reducing the consumption of fresh products with high-carbon emissions.

Thirdly, as a main body of society, residents cannot only receive the publicity and education of low-carbon knowledge, but also spread the correct low-carbon consumption concept and knowledge to the surrounding people, which will help to form a good social atmosphere in which low-carbon consumption is everyone's responsibility and low-carbon consumption starts from me.

5. Conclusion

Based on the binary logistic regression model, this paper analyzes the influencing factors of residents' willingness and behavior of low-carbon consumption of fresh food. Firstly, the descriptive analysis of the data is carried out, followed by the reliability and validity test, and then the willingness and behavior are regressed, respectively, to explore the factors affecting residents' low-carbon consumption. Finally, the relevant suggestions are given from the three aspects of government, enterprises, and residents. This paper attempts to use the quantitative model method to study the influencing factors of residents' low-carbon consumption, which is a good supplement to a large number of qualitative research and has strong practical significance.

Data Availability

The simulation experiment data used to support the findings of this study are available from the corresponding author upon request.

Conflicts of Interest

The authors declare that there are no conflicts of interest regarding the publication of this paper.

Acknowledgments

This work was supported by the Soft Science Research Project of Shanghai Science and Technology Committee (Grant no. 22692104000), the Key Lab of Information Network Security of Ministry of Public Security (Grant no. C20609), Municipal Key Curriculum Construction Project of University in Shanghai (Grant no. S202003002), and Shanghai Philosophy and Social Science Planning Project (Grant no. 2020BGL007).

References

- [1] Z. Liu, H. Guo, H. Guo et al., “on the optimized route of cold chain logistics transportation of fresh products in context of energy-saving and emission reduction,” *Mathematical Biosciences and Engineering*, vol. 18, no. 2, pp. 1926–1940, 2021.
- [2] J. Zhang, L. Zhang, Y. Qin, X. Wang, Y. Sun, and P. Rong, “Study on Influencing Factors of low carbon behavior of residents in Zhengzhou from the perspective of separation of knowledge and practice,” *Progress in geographical science*, vol. 39, no. 2, pp. 265–275, 2020.
- [3] L. Mi, J. Cong, C. Ding, L. Qiao, and T. Xu, “Causes of cognitive imbalance of low-carbon behavior of urban residents—a double intermediary model of knowledge behavior,” *Resource science*, vol. 41, no. 5, pp. 908–918, 2019.
- [4] Z. Liu, B. Hu, B. Huang, L. Lang, H. Guo, and Y. Zhao, “Decision optimization of low-carbon dual-channel supply chain of auto parts based on smart city architecture,” *Complexity*, vol. 2020, Article ID 2145951, 14 pages, 2020.
- [5] Z. Cheng, L. Wen, T. Liu, and L. Niu, “Research on low carbon cognition level of Wutaishan Hotel practitioners,” *Resources and environment in arid areas*, vol. 33, no. 7, pp. 37–42, 2019.
- [6] C. Tang, Y. Yu, C. Yang, L. Zhong, and H. Li, “Analysis on low carbon cognition, willingness and behavior of tourists in Zhangjiajie National Forest Park,” *Resources and Environment in Arid Areas*, vol. 32, no. 4, pp. 43–48, 2018.
- [7] Z. Cheng, J. Cheng, and A. Zhang, “Study on tourists’ cognition and influencing factors of low-carbon tourism in Wutai Mountain scenic spot,” *Journal of Tourism*, vol. 33, no. 3, pp. 50–60, 2018.
- [8] W. Nie, “Environmental cognition, environmental responsibility and low-carbon emission reduction behavior of urban and rural residents,” *Research on science and technology management*, vol. 36, no. 15, pp. 252–256, 2016.
- [9] Z. Liu, H. Guo, Y. Zhao et al., “Optimal pricing decision of composite service offered by network providers in E-commerce environment,” *Electronic Commerce Research*, vol. 22, no. 1, pp. 177–193, 2022.
- [10] Q. Li, Z. Wang, and X. Mao, “Quantitative analysis of influencing factors of low-carbon consumption behavior of urban residents—a case study of Beijing,” *Ecological Economy*, vol. 35, no. 12, pp. 139–146, 2019.
- [11] W. Liu and R. Ji, “The impact of low-carbon awareness and low-carbon lifestyle on low-carbon consumption intention,” *Ecological Economy*, vol. 35, no. 8, pp. 40–45, 2019.
- [12] X. Tan, “Analysis on Influencing Factors of residents’ low carbon consumption from the perspective of public choice theory,” *Business economics research*, vol. 11, pp. 51–53, 2019.
- [13] Y. Zhong, Z. Wang, and H. Zhang, “Influencing factors of low-carbon production and consumption of actors: based on the survey of Jiangsu Province,” *Statistics and decision making*, vol. 34, no. 24, pp. 147–150, 2018.
- [14] Z. Liu, J. Song, H. Wu et al., “Impact of financial technology on regional green finance,” *Computer Systems Science and Engineering*, vol. 39, no. 3, pp. 391–401, 2021.
- [15] H. Shi, “Hongjing Low carbon consumption promotion strategy based on the perspective of “will behavior” gap repair,” *Resource development and market*, vol. 34, no. 9, pp. 1304–1309, 2018.
- [16] Y. Fang, “Analysis on Influencing Factors of low-carbon consumption from multi-agent perspective,” *Business economics research*, no. 7, pp. 56–58, 2017.
- [17] J. Wei, H. Chen, and R. Long, “Ecological personality and its impact on low-carbon consumption behavior of urban residents,” *Journal of Beijing University of Technology*, vol. 19, no. 2, pp. 45–54, 2017.
- [18] W. Chen and J. Li, “Who are the low-carbon activists? Analysis of the influence mechanism and group characteristics of low-carbon behavior in Tianjin, China,” *The Science of the Total Environment*, vol. 683, pp. 729–736, 2019.
- [19] Z. Ding, X. Jiang, Z. Liu, R. Long, Z. Xu, and Q. Cao, “Factors affecting low-carbon consumption behavior of urban residents: a comprehensive review,” *Resources, Conservation and Recycling*, vol. 132, pp. 3–15, 2018.
- [20] X. Jiang, Z. Ding, and R. Liu, “Can Chinese residential low-carbon consumption behavior intention be better explained? The role of cultural values,” *Natural Hazards*, vol. 95, no. 1, pp. 155–171, 2019.
- [21] Y. Liu, R. Liu, and X. Jiang, “What drives low-carbon consumption behavior of Chinese college students? The regulation of situational factors,” *Natural Hazards*, vol. 95, no. 1, pp. 173–191, 2018.
- [22] F. Bo and G. Zhuang, “Action mechanism and promotion policy of low-carbon consumption under the goal of “double carbon”,” *Journal of Beijing University of Technology*, vol. 22, no. 1, pp. 70–82, 2022.
- [23] G. Zhuang, “Consumption responsibility and policy suggestions under the guidance of carbon neutralization target,” *People’s forum academic frontier*, vol. 14, pp. 62–68, 2021.
- [24] Z. Liu, B. Hu, Y. Zhao et al., “Research on intelligent decision of low carbon supply chain based on carbon tax constraints in human-driven edge computing,” *IEEE Access*, vol. 8, pp. 48264–48273, 2020.
- [25] M. Liu and Z. Zeng, “Informal institutional research on Residents’ low-carbon consumption behavior from the perspective of scenario structure,” *Journal of Xiangtan University*, vol. 44, no. 2, pp. 80–85, 2020.
- [26] Z. Liu, S. Zhang, L. Li et al., “Research on the construction and prediction of China’s national fitness development index system under social reform,” *Frontiers in Public Health*, vol. 783, Article ID 878515, 2022.
- [27] H. Deng and H. Wang, “New progress in household low carbon consumption research from the perspective of behavioral economics,” *Economic Trends*, vol. 1, pp. 128–141, 2020.
- [28] Z. Liu, L. Lang, L. Li, Y. Zhao, and L. Shi, “Evolutionary game analysis on the recycling strategy of household medical device enterprises under government dynamic rewards and punishments,” *Mathematical Biosciences and Engineering*, vol. 18, no. 5, pp. 6434–6451, 2021.
- [29] S. Xue and H. Xue, “Low carbon behavior style guidance in product design,” *Packaging Engineering*, vol. 39, no. 22, pp. 230–234, 2018.
- [30] Z. Liu, L. Lang, B. Hu, L. Shi, B. Huang, and Y. Zhao, “Emission reduction decision of agricultural supply chain considering carbon tax and investment cooperation,” *Journal of Cleaner Production*, vol. 294, Article ID 126305, 2021.

Retraction

Retracted: An Accurate Method of Determining Attribute Weights in Distance-Based Classification Algorithms

Mathematical Problems in Engineering

Received 13 September 2023; Accepted 13 September 2023; Published 14 September 2023

Copyright © 2023 Mathematical Problems in Engineering. This is an open access article distributed under the Creative Commons Attribution License, which permits unrestricted use, distribution, and reproduction in any medium, provided the original work is properly cited.

This article has been retracted by Hindawi following an investigation undertaken by the publisher [1]. This investigation has uncovered evidence of one or more of the following indicators of systematic manipulation of the publication process:

- (1) Discrepancies in scope
- (2) Discrepancies in the description of the research reported
- (3) Discrepancies between the availability of data and the research described
- (4) Inappropriate citations
- (5) Incoherent, meaningless and/or irrelevant content included in the article
- (6) Peer-review manipulation

The presence of these indicators undermines our confidence in the integrity of the article's content and we cannot, therefore, vouch for its reliability. Please note that this notice is intended solely to alert readers that the content of this article is unreliable. We have not investigated whether authors were aware of or involved in the systematic manipulation of the publication process.

Wiley and Hindawi regrets that the usual quality checks did not identify these issues before publication and have since put additional measures in place to safeguard research integrity.

We wish to credit our own Research Integrity and Research Publishing teams and anonymous and named external researchers and research integrity experts for contributing to this investigation.

The corresponding author, as the representative of all authors, has been given the opportunity to register their agreement or disagreement to this retraction. We have kept a record of any response received.

References

- [1] F. Liu and J. Wang, "An Accurate Method of Determining Attribute Weights in Distance-Based Classification Algorithms," *Mathematical Problems in Engineering*, vol. 2022, Article ID 6936335, 15 pages, 2022.

Research Article

An Accurate Method of Determining Attribute Weights in Distance-Based Classification Algorithms

Fengtao Liu  and Jialei Wang

Glorious Sun School of Business & Management, Donghua University, Shanghai 200051, China

Correspondence should be addressed to Fengtao Liu; lft@dhu.edu.cn

Received 6 April 2022; Revised 8 May 2022; Accepted 11 May 2022; Published 27 May 2022

Academic Editor: Xuefeng Shao

Copyright © 2022 Fengtao Liu and Jialei Wang. This is an open access article distributed under the Creative Commons Attribution License, which permits unrestricted use, distribution, and reproduction in any medium, provided the original work is properly cited.

Weight determination aims to determine the importance of different attributes; determining accurate weights can significantly improve the accuracy of classification and clustering. This paper proposes an accurate method for attribute weight determination. The method uses the distance from the sample point of each class to the class center point. It can minimize the weights and determines the attribute weights of the constraints through the objective function. In this paper, the attribute weights obtained by the exact solution are applied to the K-means clustering algorithm; three classic machine learning data sets, the iris data set, the wine data set, and the wheat seed data set, are clustered. Using the normalized mutual information as the evaluation index, a confusion matrix was established. Finally, the clustering results are visualized and compared with other methods to verify the effectiveness of the proposed method. The results show that this method improves the normalized mutual information by 0.11 and 0.08, respectively, compared with the unweighted and entropy weighted methods for iris clustering results. Furthermore, the performance on the wine data set is improved by 0.1, and the performance on the wheat seed data set is improved by 0.15 and 0.05.

1. Introduction

Weights reflect the importance of different attributes, and the influence of different attribute weights on algorithm results is sometimes very different. It is necessary to determine accurate attribute weights. Let us take K-means as an example. K-means clustering is a typical distance-based clustering algorithm. K-means is widely used due to its fast-running speed, simplicity, and ease of understanding. However, traditional K-means does not consider the importance of features, resulting in poor clustering effects with traditional K-means in some problems. The distance class algorithm uses the distance between sample attributes to classify and cluster [1, 2]. Generally, the sample cluster is divided by clustering birds of a feather [3, 4] to achieve the effect of high similarity within the cluster and low similarity outside the cluster [5]. The distance between sample attributes is a “distance measure” [6, 7]. The similarity measure defined by us means that the larger the distance, the smaller the

similarity [8, 9]. Differences between different attributes may not be obvious or even wrong in some distance performance, which can be achieved through “distance metric learning.” In other words, assigning different weights to sample attributes improves learning effects [10].

At present, the problem of weight determination can be divided into two methods: subjective weight determination and objective weight determination. Domain experts compare the importance degree of each attribute with fuzzy language to determine the weight. The methods of subjective weight determination by experts include the analytic hierarchy process (AHP), sequence diagram method, simple weighting, etc. The analytic hierarchy process is a widely used method at present. Pourghasemi et al. used fuzzy logic and an analytic hierarchy process (AHP) model to make a landslide sensitivity map of Iran’s landslide-prone area (Haraz) for land planning and disaster reduction [11]. Lin and Kou [12], based on the multiplication AHP model, proposed a heuristic method, and priority vectors were derived from the PCM in the whole hierarchy.

Although the subjective weight determination method has achieved good results in some conditions, it is limited by the shortcomings of artificial judgment, inability to find experts, and so on. Therefore, the objective weight determination method is used in many cases. The methods of objective weight mainly include the entropy weight method, principal component analysis method, and factor analysis. Meimei et al. proposed two methods to determine the optimal weight of attributes based on entropy and measure [13]. Chen combined the entropy weight method with Topsis to determine the weight of Topsis attributes and analyzed the influence of electronic warfare on Topsis [14]. Amaya et al. proposed a proposal on collaborative cross entropy to solve combinatorial optimization problems [15]. In addition to the above method, Lu et al. used a KNN combination of distance thresholds to determine the weight [16]. And other scholars used algorithm combinations to determine the weight [17–20]. In recent years, ensemble learning has become a research hotspot, and some scholars have determined the contribution degree of attributes to classification results through ensemble learning algorithms, for example, random forest [21], XGBoost, etc. Random forest determines the weight by calculating the attribute contribution, which is a way of calculating the weight value developed with the development of ensemble learning [22]. And Liu et al. constructed multiple mixed 0–1 linear programming models (MLPMs) to obtain the classification range of alternatives and weights of policy attributes applied in maldistributed decision-making problems [23].

In this paper, a distance-based classification algorithm is proposed to find the minimum distance between the midpoint of the category to which the data belong and the attribute vector. The distance between data points in the same category is closer and the distance between data points in different categories is farther to achieve the effect of improving the classification. In this paper, Lingo is used to solve the weights, and the solved weights are applied to the K-means clustering iris data set, wine data set, and wheat seed data set. Compared with the weights determined by the class and entropy weight method, the method proposed in this paper has different degrees of improvement in the clustering effect.

The key contributions of this work are as follows: (1) The algorithm accurately determines the attribute weights and identifies the solution from the data set itself. (2) This method overcomes the shortcomings of AHP and other methods. (3) It is less subjective and does not need to calculate entropy [24, 25]. (4) There is no need to use formulas such as variance to obtain attribute weights. There is no need for many trial and error steps, and there is no need for integrated learning to build models.

The rest of this paper is organized as follows: Section 2 explains the idea of solving the weights in this paper. Section 3 describes the K-means clustering process and evaluation indicators. Section 4 describes the experimental procedure. Section 5 is a summary of the full text.

2. Determining Weights

2.1. The Solution Idea. The purpose of clustering and classification is to obtain groups such that objects within a group

are more similar than objects in different groups [26]. The weights are determined by minimizing the distances between attribute vectors within the same group and the center vector to maximize the distance between the different groups, thus effectively separating the different clusters. When the distance between the attribute vectors of each group and the center of the group reaches the minimum value, the distance between the different groups is maximized. The weight determined is the optimal attribute weight. The weight of the solution is applied to a known or unknown data set to improve the learning effect. The solution idea comes from the KNN algorithm [27].

2.1.1. KNN Algorithm. The KNN algorithm is a relatively mature and simple machine learning algorithm in theory. The idea of KNN is that if a sample has a high probability of belonging to a certain category among the k nearest samples in the feature space, and most of them belong to a certain category, then the sample is also classified in this category. KNN is classified by measuring the distance between different characteristic values, generally using the Euclidean distance. In classification decisions, this method only determines the category of the samples to be classified according to the category of the nearest sample or several samples. The KNN solution process is as follows:

Step 1: Calculate distances. The distance between characteristic values is calculated, the distance between the test data and each training data value. Generally, the Euclidean distance is used for calculation, and the Manhattan distance and Mahalanobis distance can also be used. Table 1 shows some distance formulas.

Step 2: Sort by increasing distance.

Step 3: Classify samples according to distance. Select k data points with the smallest distance from the sample point to determine the type of data with the highest frequency among the K sample points.

Step 4: Identify categories. The category with the highest frequency in the first K points is used as the predictive classification of the test data. Classification methods are divided into simple and weighted voting methods.

2.1.2. Weight Solution Idea. The idea of solving weights comes from the reverse solution method of KNN. KNN makes classification judgments according to the occurrence frequency of categories, and the purpose of determining the weight is to improve the learning effect. In the KNN algorithm, we aim to make all k surrounding sample points belong to a certain category. The distance between samples of the same category should be small, and the distance between samples of different categories should be large. The minimum distance between the sample vector of a category and the center point is reflected in the sample vector of the category. The steps of determining the weights are as follows:

Step 1: Identify categories. Classify sample data of different categories according to the known data.

TABLE 1: Several commonly used distance formulas.

Distance name	Brief explanation	Distance formula
Euclidean distance	The straight-line distance between two points	$d = \sqrt{\sum_{k=1}^n (x_{1k} - x_{2k})^2}$
Manhattan distance	The sum of the absolute wheelbases of two points in standard coordinates	$d = \sum_{k=1}^n x_{1k} - x_{2k} $
Chebyshev distance	The maximum value of the difference between coordinates	$d = \max_i (x_{1i} - x_{2i})$
Markov distance	The covariance distance of data	$d = \sqrt{(X - \mu)^T S^{-1} (X - \mu)}$. The covariance matrix is denoted as S, and the mean is denoted as μ

Step 2: Choose K . The sample number of each category is calculated after classification, and the value K is the sample number of the category.

Step 3: Calculate the distance. Calculate the distance between the sample of the category and the center point vector, carry out the weighting calculation, and obtain the weight when the distance is the smallest.

2.2. *Solution Process.* The goal of this method is to minimize the distance between a classification sample of the data set and the center point of the category to which it belongs. In this experiment, the Euclidean distance is adopted. In addition to the Euclidean distance, other distance functions, such as the Mahalanobis distance, Manhattan distance, and Chebyshev distance, can be adopted. This paper presents an accurate analytical method for weighted attribute distance functions.

Sample classification $C = \begin{pmatrix} c_1 \\ \vdots \\ c_i \\ \vdots \\ c_n \end{pmatrix}$. The attribute vector of each sample is $x_i = \begin{pmatrix} r_1^i \\ \vdots \\ r_p^i \\ \vdots \\ r_k^i \end{pmatrix}$. The attribute vector values of the center point under the label are

$s^i = \begin{pmatrix} s_1^i \\ \vdots \\ s_p^i \\ \vdots \\ s_k^i \end{pmatrix}$ ($i = 1, 2, 3, \dots, n$), where λ_p ($p = 1, 2, \dots, k$) is

the weight of each attribute. The constraint conditions are $0 \leq \lambda_p \leq 1$, $\sum_{p=1}^k \lambda_p = 1$, and $n = n_1 + n_2 + \dots + n_i + \dots + n_n$.

Let us define the objective function as

$$sd = \arg \min \sum_{m=1}^n \left[\sum_{i=1}^{n_i} \sqrt{\sum_{p=1}^k \lambda_p^2 (r_p^i - s_p^i)^2} \right], \quad (1)$$

where n_i is the number of samples under each category and n is the total number of samples. By solving the attribute vector of the center point of each label, the minimum value λ_p of the objective function is obtained by taking the partial derivative or using the gradient descent method. When sd is the minimum value, the weight λ_p of each attribute is obtained. Namely, the sum of the distance between the sample

point of each category and the center point of each category is the smallest. Table 2 shows the meanings of the other parameters. In this experiment, the Euclidean distance is used to determine the weight; other distances can also be used for the calculation.

3. K-Means Algorithm

3.1. *K-Means Algorithm Process.* The K-means algorithm is an unsupervised learning algorithm that has become one of the most widely used clustering algorithms [28, 29]. It is a distance-based clustering algorithm that uses the distance between objects as an evaluation index of similarity.

The traditional K-means Algorithm 1 process is as follows:

3.2. *Evaluation Indicators.* In this experiment, the normalized mutual information [30, 31] (NMI) is used as the evaluation index of clustering quality. NMI is commonly used in clustering to measure the similarity of two clustering results. It can objectively evaluate the accuracy of an algorithm partition compared with the standard partition. The range of NMI is 0 to 1, and the higher it is, the greater the accuracy is. The concept of NMI comes from relative entropy, namely, KL divergence and mutual information.

Relative entropy is an asymmetrical measure of the difference between two probability distributions, and in the discrete case, it is defined as

$$KL(p||q) = \sum p(x) \log \frac{p(x)}{q(x)}, \quad (2)$$

where $p(x)$ and $q(x)$ are the two probability distributions of the random variable x .

Mutual information [32] is a useful information measure in information theory. It can be regarded as the amount of information contained in a random variable about another random variable. Mutual information is the relative entropy of the joint probability distribution and edge probability product distribution of two random variables X and Y , which is defined as

$$I(X; Y) = \sum_x \sum_y p(x, y) \log \frac{p(x, y)}{p(x)p(y)}. \quad (3)$$

Normalized mutual information is the result of the normalization of mutual information and is defined as

TABLE 2: Brief explanations of various parameters.

Parameter name	Parameter meaning
C	Sample classification
x_i	Sample attribute vector
s^i	Vector of the center point under each class
λ_p	Weight value
n_i	Number of samples under the category
n	Total number of samples
k	Number of attributes
sd	Objective function value

Input: number of clusters K , data set D

Output: K clusters.

Algorithm steps:

Step 1: Take K , which means we will divide the data set into K groups.

Step 2: Randomly select K points from the data set as the initial clustering centers.

Step 3: Calculate the distances between all points and the K cluster centers and put the samples into the class with the center with the shortest distance.

Step 4: Calculate the average coordinates of the data points in each class cluster to update the center of the cluster.

Step 5: Repeat steps (3) and (4) until the cluster center remains unchanged.

ALGORITHM 1: K-means clustering process.

$$NMI(X; Y) = 2 \frac{I(X; Y)}{H(X) + H(Y)}, \quad (4)$$

where $H(X)$ and $H(Y)$ are the information entropy of the random variables X and Y and $I(X; Y)$ is the mutual information of X and Y .

3.3. K-Means with the Accurate Weight Determination Method. The traditional K-means algorithm does not consider the importance degree of attributes, so the distance weights from each attribute to the center point of the cluster are equal. However, in many cases, the importance of different attributes may not be equal. Application of traditional K-means to these scenarios will inevitably lead to inaccurate clustering results. In this paper, the exact solution process of feature weights is carried out before the K-means algorithm is applied. The obtained weights are weighted by the distance between each attribute and the center point to obtain the final distance between the sample point and the center of the cluster. Figure 1 shows the flowchart of the k-means algorithm using the exact weight solution method.

4. Experimental Process

4.1. Introduction to the Data Sets

4.1.1. Iris Data Set. The iris data set is a commonly used machine learning data set [33]. It includes four attributes, the length of the calyx (Sepal Length), the width of the calyx (Sepal Width), the length of the petal (Petal Length), and the width of the petal (Petal Width). The unit of the four attributes is CM, which is a numerical variable, and there are no missing values. Figure 2 shows a scatter plot of iris data

attributes. Figure 3 shows the histogram of iris data attributes. The mountain iris, chameleon iris, and Virginia iris are the three categories. Each category collects 50 sample records, for a total of 150 irises.

4.1.2. Wine Data Set. The wine data set is a publicly available data set from the University of California Irvine (UCI). It is the result of a chemical analysis of wines grown in the same region of Italy from three different varieties. The analysis determined the values of 13 attributes of each of the three wines. The attributes are class identifiers, represented by categories 1, 2, and 3. Figure 4 shows the distribution of wine attributes. There are 59 samples in category 1, 71 samples in category 2, and 48 samples in category 3. There are no missing values in this data set.

4.1.3. Wheat Seed Data Set. The wheat seed data set is commonly used in classification and clustering tasks. There are 210 records, 7 features, and 1 label in the data set. Figure 5 shows the distribution of wheat seed attributes. The labels are divided into 3 categories with 70 samples in each category, and there are no missing values.

4.2. Determining Attribute Weights

4.2.1. Determining the Attribute Weights of the Iris Data Set. The category number of the iris data set is 3, so the objective function used to determine the weights of the four attributes according to formula (1) is

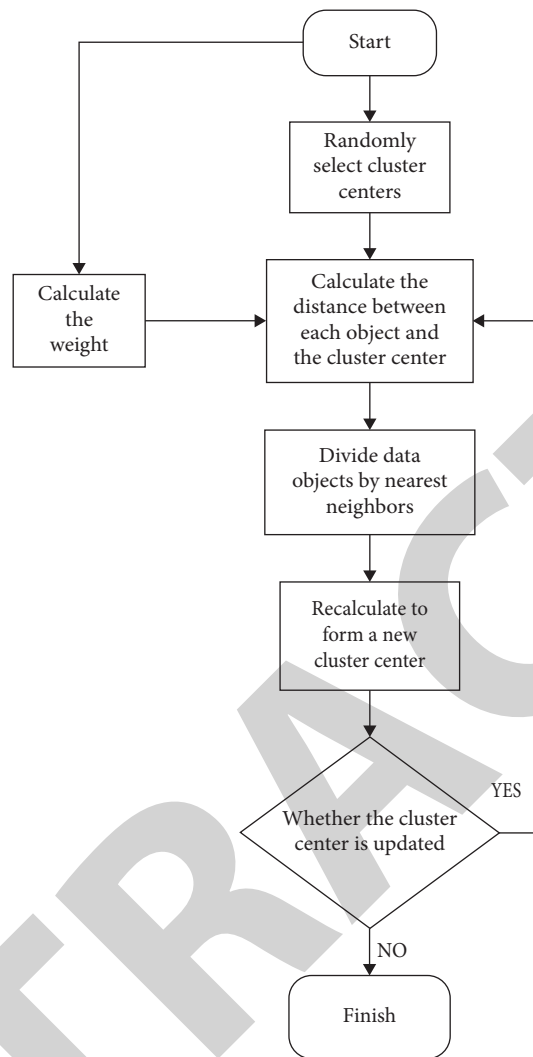


FIGURE 1: Flowchart of applying the exact weight determination method to the K-means algorithm.

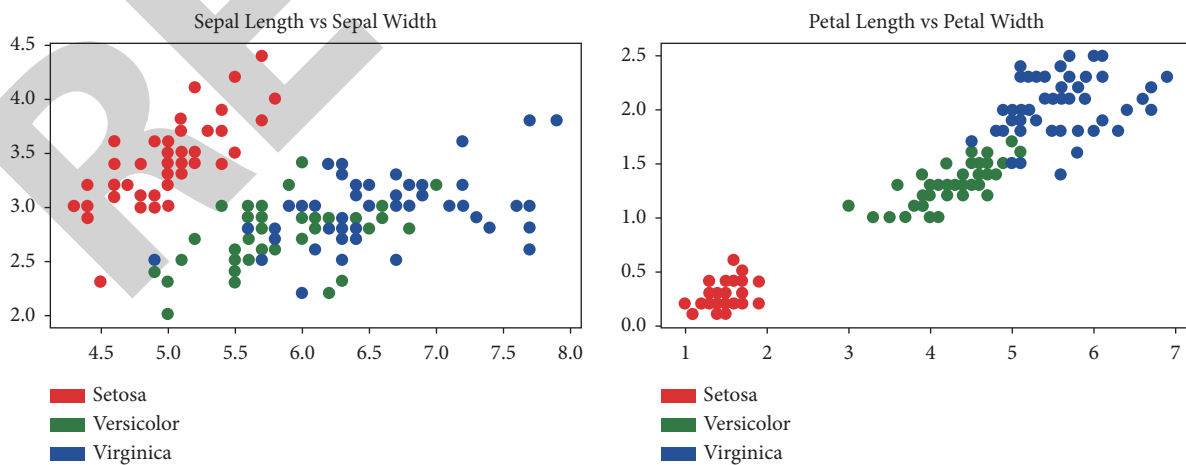


FIGURE 2: Scatter plot of calyx length and width and petal length and width in the iris data set.

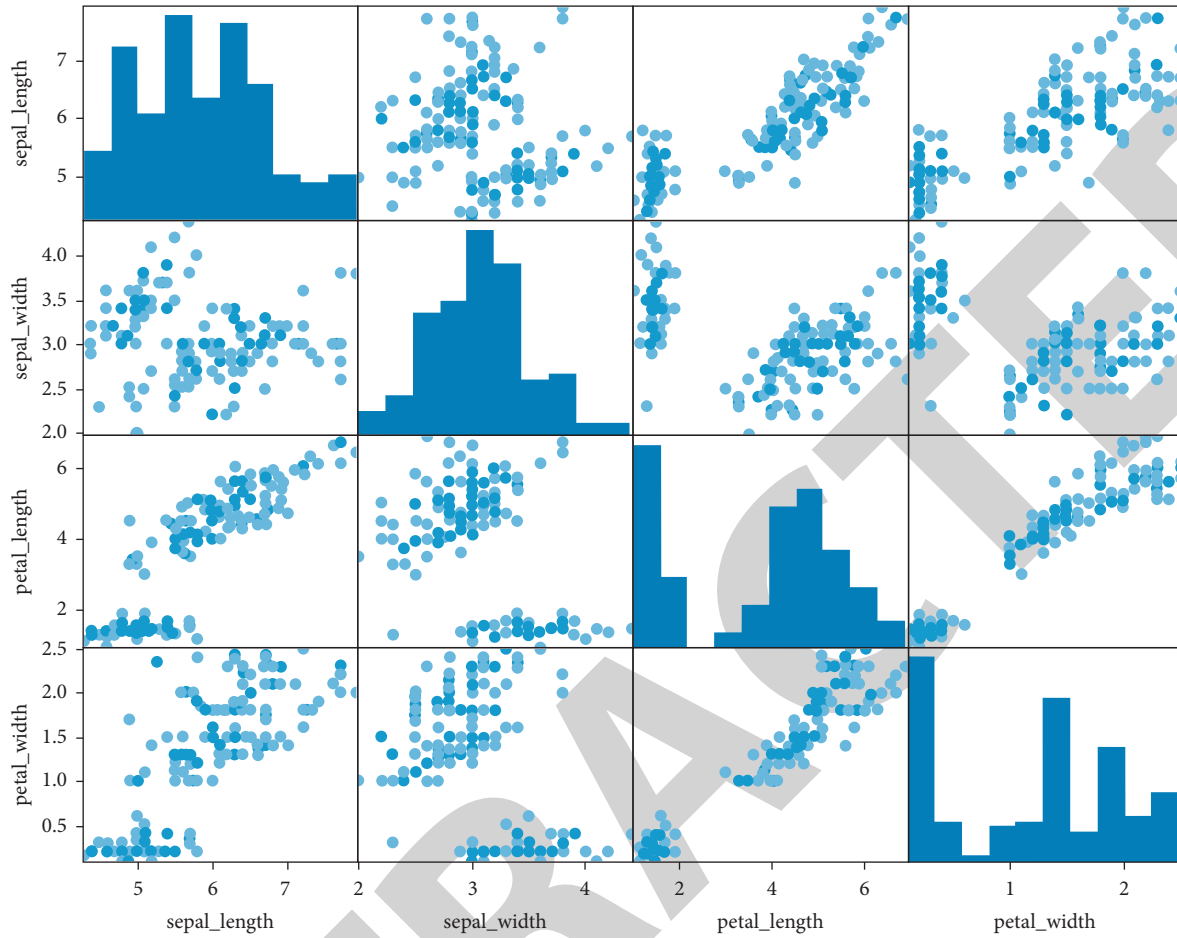


FIGURE 3: Histogram and scatter diagram of each attribute in the iris data set.

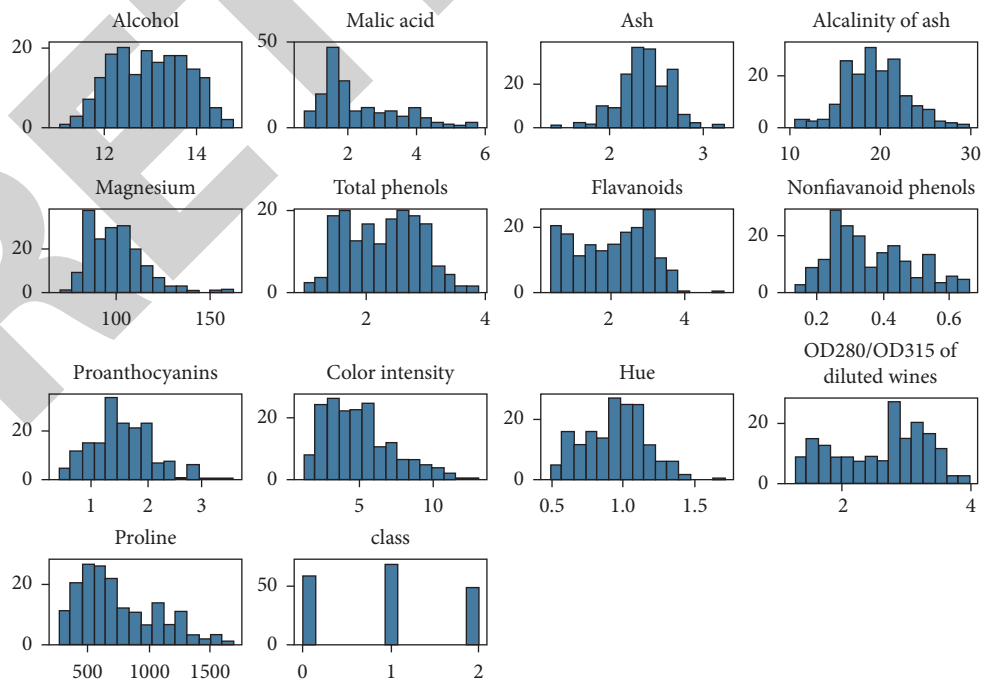


FIGURE 4: Wine data set.

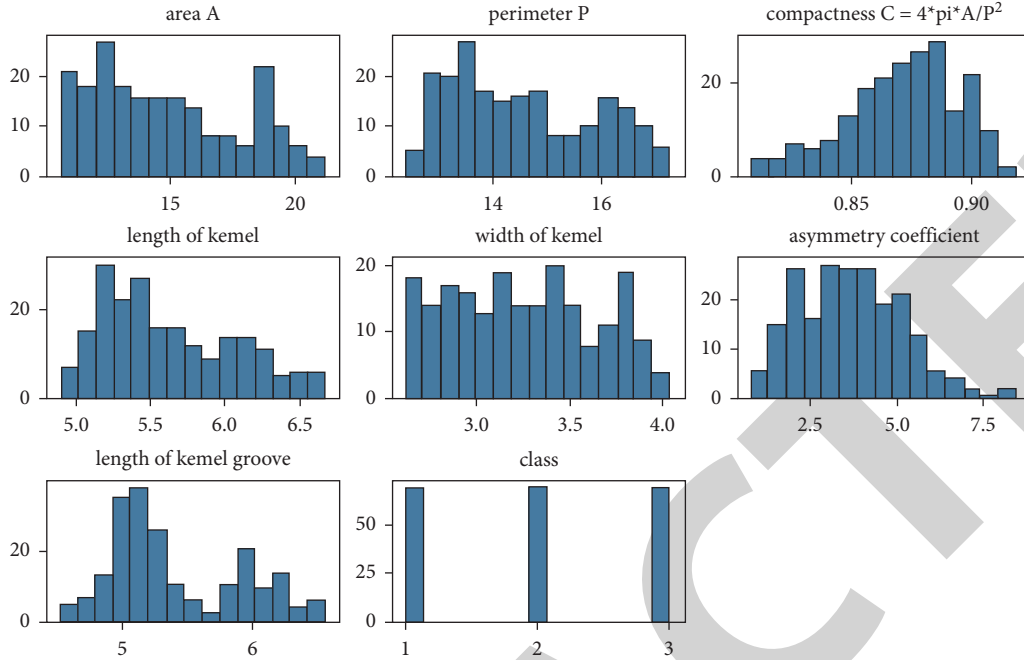


FIGURE 5: Wheat seed data set.

$$sd = \arg \min \left\{ \left[\sum_{i=1}^{n_1} \sqrt{\sum_{p=1}^k \lambda_p^2 (r_p^i - s_p^h)^2} \right] + \left[\sum_{j=1}^{n_2} \sqrt{\sum_{p=1}^k \lambda_p^2 (r_p^j - s_p^l)^2} \right] + \left[\sum_{r=1}^{n_3} \sqrt{\sum_{p=1}^k \lambda_p^2 (r_p^r - s_p^m)^2} \right] \right\}, \quad (5)$$

where n_1, n_2, n_3 are the numbers of samples of mountain iris, chameleon iris, and Virginia iris, respectively; n is the total number of samples; k is the number of attributes; the iris has four attributes of calyx length, calyx width, petal length, and petal width (so $k = 4$); and the meanings of the other parameters are given below. Table 3 illustrates the number of irises and the k value for each category, and Table 4 shows the center vectors and parameter meanings of various types of flowers.

We separate the three categories of the data set and calculate the attribute vector values of the center points under

the three tags $s^h = \begin{pmatrix} 5.006 \\ 3.428 \\ 1.462 \\ 0.246 \end{pmatrix}$, $s^l = \begin{pmatrix} 5.936 \\ 2.77 \\ 4.26 \\ 1.326 \end{pmatrix}$, and $s^m =$

$\begin{pmatrix} 6.588 \\ 2.974 \\ 5.552 \\ 2.026 \end{pmatrix}$. In the experiment, LINGO12.0 is used to solve, and

the values are rounded to $\lambda_k (k = 1, 2, 3, 4)$ in Table 5.

4.2.2. Determining the Wine Data Set Attribute Weights.

The number of sample categories in the wine data set is 3. The objective function is established according to formula (5). Data set is divided by the mean of the attributes for dimensionless processing, where n_1, n_2, n_3 are the numbers of samples under different sample categories, n is the total number of samples, and K is the number of attributes. The meaning of each parameter is given below. Table 6 lists the

number and parameter significance of the three categories of the wine data set. Table 7 illustrates the three categories of wine center vector parameters.

The vector values of the attributes of the center points under the three labels are $s^h = (1.057, 0.860, 1.037, 0.873, 1.066, 1.237, 1.469, 0.801, 1.193, 1.092, 1.109, 1.209, 1.493)^T$, $s^l = (0.9444, 0.827, 0.948, 1.038, 0.947, 0.984, 1.025, 1.004, 1.024, 0.610, 1.103, 1.066, 0.695)^T$, and $s^m = (1.011, 1.426, 1.029, 1.098, 0.995, 0.731, 0.385, 1.236, 0.725, 1.462, 0.713, 0.644, 0.843)^T$.

The rounded results $\lambda_3 \lambda_k (k = 1, 2, \dots, 13)$ are given below. Table 8 shows the weight values.

4.2.3. Determining the Attribute Weights of the Wheat and Wheat Seed Data Set.

The number of sample categories in the wheat seed data set is 3. The objective function is established according to formula (5). Data set is divided by the mean of the attributes for dimensionless processing, where n_1, n_2, n_3 are the numbers of samples under different sample categories, n is the total number of samples, k is the number of attributes, and the meanings of each parameter are as given below. Table 9 shows the parameter values needed to calculate the weight of wheat seeds.

The meanings of the other attributes are the same as in Table 7. The vector values of the attributes of the center point under the three labels are $s^h = (0.965, 0.981, 1.010, 0.978, 0.995, 0.720, 0.940)^T$, $s^l = (1.234, 1.108, 1.014, 1.092, 1.128, 0.985, 1.113)^T$, and $s^m = (0.799, 0.909, 0.975, 0.929,$

TABLE 3: Main parameter explanation and the determined values of the objective functions of the iris attribute weights.

Symbol	Brief explanation	Numerical value
n_1	Number of mountain iris samples	50
n_2	Number of chameleon iris samples	50
n_3	Number of Virginia iris samples	50
k	Number of data set attributes	4

TABLE 4: Explanation of other parameters used in solving the objective function of iris attribute weights.

Symbol	Brief explanation
s^h	Center vector of mountain iris samples
s^l	Center vector of chameleon iris samples
s^m	Center vector of Virginia iris samples
x_i	Sample attribute vector of the category

TABLE 5: The weight values of the iris characteristic attributes are accurately determined.

Weight	Value
λ_1	0.053
λ_2	0.117
λ_3	0.107
λ_4	0.722

TABLE 6: Main parameters and values of the objective functions of wine attribute weights.

Symbol	Brief explanation	Numerical value
n_1	Samples with a category of 1	59
n_2	Samples with a category of 2	71
n_3	Samples with a category of 3	48
k	Number of data set attributes	13

TABLE 7: Explanation of the other parameters of the objective functions of wine attribute weights.

Symbol	Brief explanation
s^h	The sample category has 1 center vector
s^l	The sample category has 2 center vectors
s^m	The sample category has 3 center vectors
x_i	The sample attribute vector of the category

0.875, 1.294, 0.946)^T. The rounded λ_k ($k = 1, 2, \dots, 7$) results are given below. Table 10 shows the calculated weights of wheat seed attributes.

4.3. Analysis of the Experimental Results. The methods of K-means with accurately determined weights, traditional K-means, and K-means with entropy weights are used to cluster the iris, wine, and wheat seed data sets. The normalized mutual information and the confusion matrix [34] are used as evaluation criteria to evaluate the three methods.

4.3.1. Weight Entropy Method. The basic idea of the entropy weight method [35, 36] used to determine the objective weight is the index variability. Weight is determined

TABLE 8: The weight values of the wine characteristic attributes are accurately obtained.

Weight	Value
λ_1	0.745
λ_2	0.0043
λ_3	0.065
λ_4	0.036
λ_5	0.036
λ_6	0.017
λ_7	0.01
λ_8	0.0068
λ_9	0.0077
λ_{10}	0.0069
λ_{11}	0.023
λ_{12}	0.026
λ_{13}	0.011

TABLE 9: Main parameter explanation and value of the objective functions in determining wheat seed attribute weights.

Symbol	Brief explanation	Numerical value
n_1	Samples with a category of 1	70
n_2	Samples with a category of 2	70
n_3	Samples with a category of 3	70
k	Number of data set attributes	7

TABLE 10: Weight values of wheat seed characteristic attributes obtained by the accurate solution method.

Weight	Value
λ_1	0.0328
λ_2	0.151
λ_3	0.504
λ_4	0.133
λ_5	0.071
λ_6	0.0012
λ_7	0.104

according to the information entropy [37], which is the expectation of information content. The probability of the occurrence of a data value is negatively correlated with it. The higher the information entropy of an attribute is, the less information it can provide, the smaller the role it plays in evaluation, and the smaller its weight is. Table 11 shows the weight values of iris attributes obtained by the exact solution method. Table 12 shows the weight values of the attributes of the wine data set obtained by the exact solution method. Table 13 shows the weight values of the attributes of the wheat seed data set obtained by the exact solution method.

4.3.2. Iris Data Clustering Results. The experiment is implemented in the Python 3.8.5 environment, and the maximum number of K-means iterations after inputting the attribute weight is 200. The normalized mutual information is selected as the evaluation criterion, and the confusion matrix is established. The normalized mutual information

TABLE 11: Weight values of iris attributes obtained by the entropy weight method.

Weight	Value
λ_1	0.193
λ_2	0.112
λ_3	0.318
λ_4	0.376

TABLE 12: Weight values of wine characteristic attributes obtained by the entropy weight method.

Weight	Value
λ_1	0.049
λ_2	0.123
λ_3	0.022
λ_4	0.041
λ_5	0.059
λ_6	0.066
λ_7	0.109
λ_8	0.080
λ_9	0.067
λ_{10}	0.099
λ_{11}	0.069
λ_{12}	0.091
λ_{13}	0.120

TABLE 13: Weight values of wheat seed characteristic attributes obtained by the entropy weight method.

Weight	Value
λ_1	0.205
λ_2	0.158
λ_3	0.07
λ_4	0.155
λ_5	0.168
λ_6	0.115
λ_7	0.126

can make the clustering results to 0-1 so that the clustering accuracy of the two methods can be seen intuitively [38]. The effect of clustering on a certain category can be obtained through a confusion matrix [39]. Clustering results can be visualized to make the results more intuitive [40]. The above methods are used to compare the results of the K-means algorithm with weights, K-means without weights, and K-means with weights determined by the entropy weight method. Table 14 shows the NMI of the iris data set after clustering by the three methods.

NMI is an external evaluation standard method for clustering [41]. By calculating the normalized mutual information of the real labels and the labels after clustering, the accuracy of clustering can be seen [42, 43]. The NMI of the three methods after clustering the iris data set is shown in Table 14. First, it can be concluded from the table that the NMI after clustering by K-means with weights is approximately 0.11 higher than that after clustering without weights. The clustering effect of K-means after determining the attribute weights is better, which confirms the feasibility of this method. Second, when the results obtained by the entropy

TABLE 14: NMI of the iris data set after clustering by the three methods.

Normalized mutual information (NMI)	
K-means with the exact weight	0.864
K-means without weight	0.758
K-means with the entropy weight	0.785

weight method are put into the K-means algorithm, the NMI after clustering is 0.785. It is 0.03 higher than that of traditional K-means without weights. However, the NMI after clustering of the algorithm proposed in this paper for accurately determining the weights is 0.08 higher than that of the entropy weight method. Finally, although the weight determined by the entropy weight method improves the accuracy of the iris data clustering class to a certain extent compared with clustering without weights, it is far from the improvement achieved by the weight determination method proposed in this paper. The confusion matrix after clustering is given below. Table 15 shows the confusion matrix of the effect of the three methods on iris clustering.

The confusion matrix is an effective tool for evaluating classifications and clustering criteria [44], as it can be used to clearly see in which categories the model does not perform well [45]. The confusion matrix [46, 47] after the three methods of clustering is shown in Table 15. First, it can be seen from the table that the clustering effect of the three methods is equally good for the mountain iris. These samples can be clustered accurately. All three methods are largely accurate in the category of the chameleon iris, but there is a large difference among the three in the category of the Virginia iris. K-means without weights incorrectly clustered 14 samples of Virginia iris into the category of chameleon iris. Compared with K-means clustering without weights, the improvement of K-means clustering after weight determination by the entropy weight method is not very large. Second, for the clustering of Virginia iris, the weight clustering results are almost the same as those of all attributes after weight determination by the entropy weight method. After the weights are determined by the entropy weight method, 13 Virginia irises are incorrectly clustered into the chameleon iris category, while only 14 samples are incorrectly classified even with uncertain weights. Neither method could accurately cluster Virginia irises, and it was more difficult to cluster Virginia irises than the other two iris categories. Figure 2 shows that the calyx and petal lengths and widths of the Virginia iris and chameleon iris are similar. The data are mixed and difficult to distinguish, which means that the two methods cannot distinguish the two flower categories well. The difference in the properties of the mountain iris and the other two flowers is relatively large. The weight obtained by the algorithm with the accurate solution is applied to K-means, which can distinguish the two categories well, proving the accuracy and efficiency of the method. Finally, the effect of K-means clustering determined by the entropy weight method is visualized.

Figure 6 shows the results of clustering the iris data set with the weights obtained by our method. Figure 7 shows the clustering results without attribute weights. Figure 8

TABLE 15: Confusion matrix of the three methods for clustering the iris data set.

Confusion matrix		Mountain iris	Chameleon iris	Virginia iris
Accurate method	Mountain iris	50	0	0
	Chameleon iris	0	48	2
	Virginia iris	0	4	46
Without weight	Real category y	Mountain iris	0	0
	Chameleon iris	0	48	2
	Virginia iris	0	14	36
Entropy weights	Mountain iris	50	0	0
	Chameleon iris	0	49	1
	Virginia iris	0	13	37

shows the clustering results of the weights determined by the entropy weight method. The effect diagram after clustering shows more intuitively that some sample points are still mixed in the clustering results of chameleon iris and Virginia iris by K-means without weights. These points are not effectively divided into different clusters. However, K-means with accurately determined weights has a better effect on the clustering of the two types. Points of different categories are effectively clustered into different clusters.

4.3.3. Wine Data Clustering Results. The wine data set has more attributes than the iris data set. The results of the following three methods are compared: the K-means algorithm for calculating the weights by the exact solution method, K-means without weights, and K-means with weights determined by the entropy method. Table 16 shows the NMI values of the three methods for clustering the wine data set, and Table 17 shows the confusion matrix of the three methods for clustering the wine data set.

According to the NMI after clustering by the three methods, the method for solving the weight proposed in this paper improves the results by approximately 0.1 compared with those of the other two methods. The entropy weight method does not improve the results much in the wine data clustering class, so different weight solving methods apply to different situations. According to the confusion matrix after clustering by the three methods, the exact solution method performs better than the other two methods on the three sample categories. There is little difference between the entropy weight method and K-means without weights. Figure 9 shows the clustering results of the wine data set by the method in this paper, Figure 10 shows the clustering results without attribute weights, and Figure 11 shows the entropy weighting method clustering results.

4.3.4. Cluster Results on Wheat Seed Data. The number of attributes in the wheat seed data set is between those of the iris data set and the wine data set. The results of the weighted K-means algorithm, the K-means package in SKLearn, and weighted K-means with weights determined by the entropy weight method are compared below. Table 18 shows the NMI results of the three methods for clustering wheat seeds,

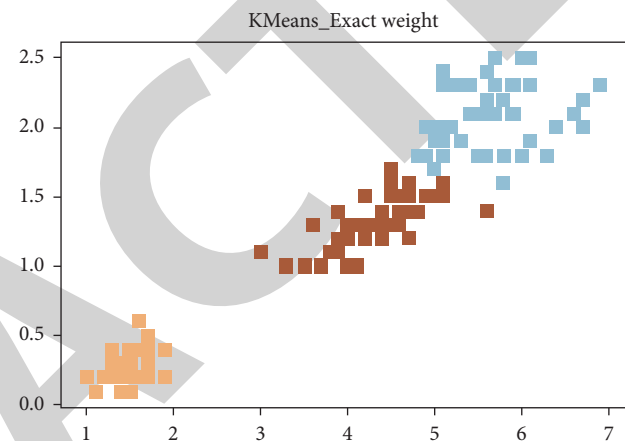


FIGURE 6: K-means clustering effect diagram of the iris data after the exact solution method is used to determine the weights.

and Table 19 shows the confusion matrix results after clustering.

The attribute importance of the wheat seed data set varies. Compared with the K-means clustering results without weights, the normalized mutual information after K-means clustering with weights is greatly improved. The normalized mutual information after applying the exact solution method and the entropy weight method of determining the weights is improved by 0.15 and 0.1, respectively. However, compared with the entropy weight method, the weight method proposed in this paper improves the normalized mutual information by 0.05, and the clustering effect is better.

It can be seen from the confusion matrix after clustering by the three methods that the improvement of weighted K-means compared with unweighted K-means is mainly in the data set of categories 3. The number of correct samples in the clustering of the precise solution method and entropy weight method is increased by 19 and 15, respectively, compared with that of traditional K-means. Compared with the entropy weight method, the exact solution method performs better in the clustering of category 3. Figure 12 represents the clustering result of wheat seed data by the method in this paper, while Figure 13 shows the clustering results of the unweighted data set. Figure 14 shows the clustering results of the wheat seed data set by the entropy weight method. As seen from the

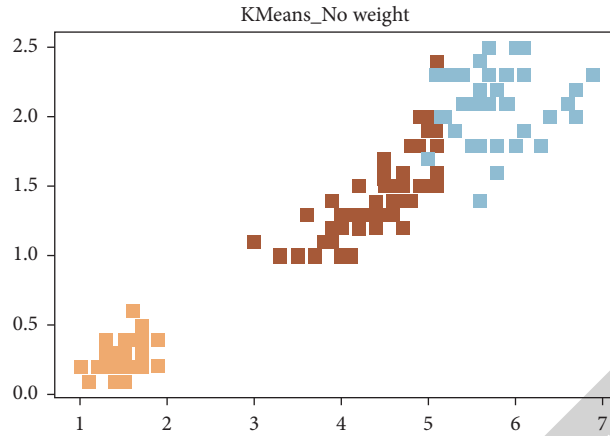


FIGURE 7: Effect diagram of K-means without weights on iris data clustering.

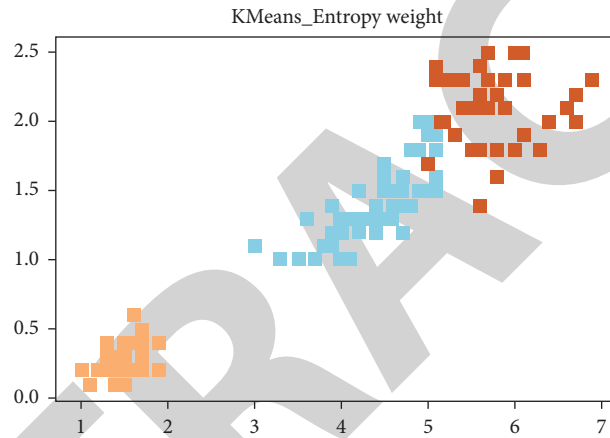


FIGURE 8: K-means clustering effect diagram of iris data after the entropy weight method is used to determine the weights.

TABLE 16: NMI aggregated by the three methods for wine data.

Normalized mutual information (NMI)	
K-means with the exact weight	0.865
K-means without weights	0.765
K-means with entropy weight	0.765

TABLE 17: Confusion matrix of the three methods for clustering the wine data set.

Confusion matrix		Category y_pred after K-means clustering with the exact solution method		
		Category 1	Category 2	Category 3
Accurate method	Category 1	59	0	0
	Category 2	5	64	2
	Category 3	0	0	48
Without weight	Category 1	58	0	1
	Category 2	2	60	9
	Category 3	1	0	47
Entropy weights	Category 1	58	1	0
	Category 2	2	60	9
	Category 3	0	1	47

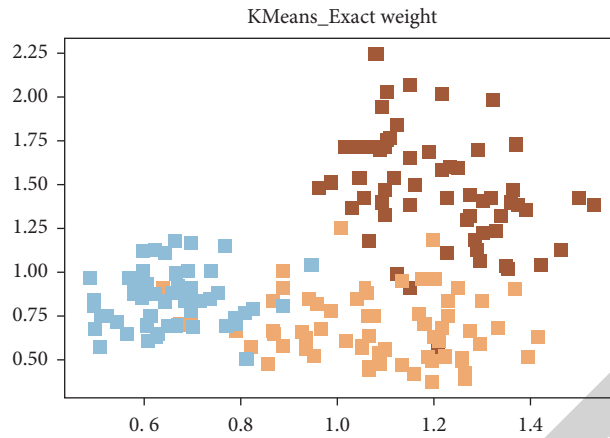


FIGURE 9: Effect diagram of K-means clustering of the wine data after the exact solution method is used to determine the weights.

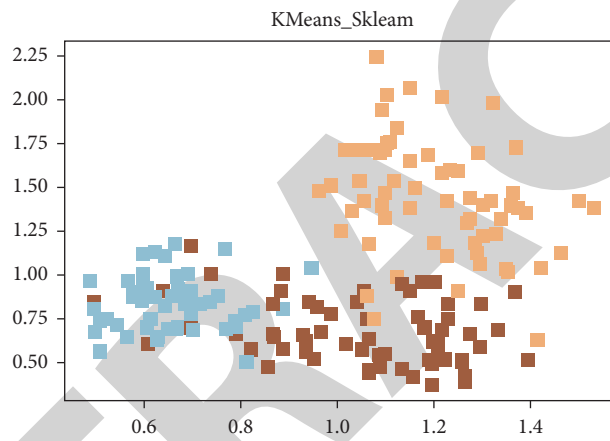


FIGURE 10: Effect diagram of K-means without weights on wine data clustering.

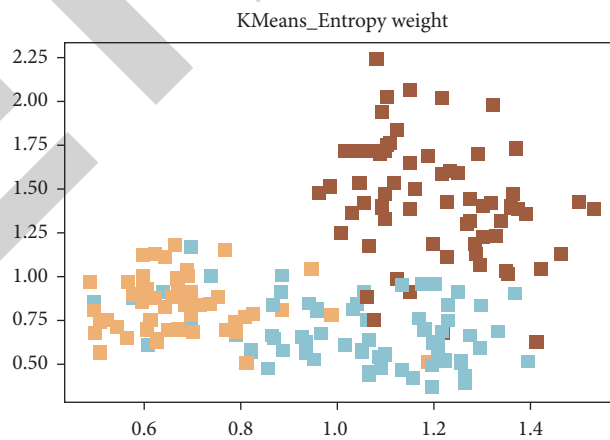


FIGURE 11: Effect diagram of K-means clustering of the wine data after the entropy weight method is used to determine the weights.

TABLE 18: NMI of wheat seed data aggregated by the three methods after classification.

Normalized mutual information (NMI)	
K-means with the exact weight	0.673
K-means without weights	0.524
K-means with entropy weight	0.621

TABLE 19: Confusion matrix of the three methods for clustering the wheat seed data set.

Confusion matrix		Category 1	Category 2	Category 3	
Accurate method	Category 1	55	2	13	
	Category 2	9	61	0	
	Category 3	1	0	69	
Without weight	Real category y	Category 1	58	11	1
	Category 2	10	60	0	
	Category 3	20	0	50	
Entropy weights	Category 1	60	10	0	
	Category 2	12	57	9	
	Category 3	3	2	65	

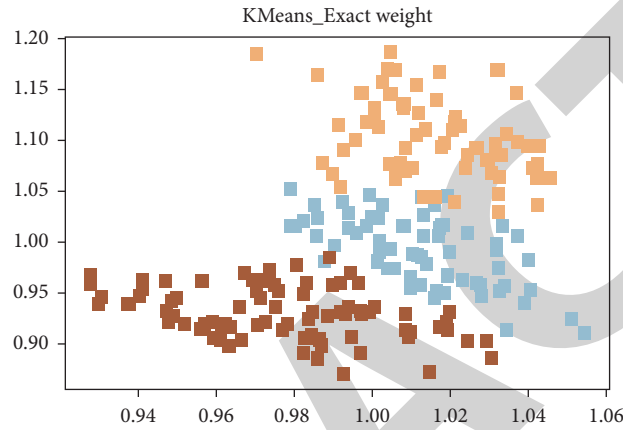


FIGURE 12: K-means clustering effect diagram of wheat seed data after the exact solution method is used to determine the weights.

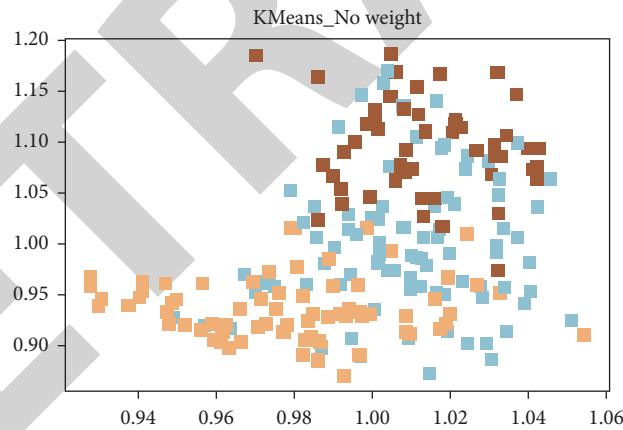


FIGURE 13: Effect diagram of K-means without weights on wheat seed data clustering.

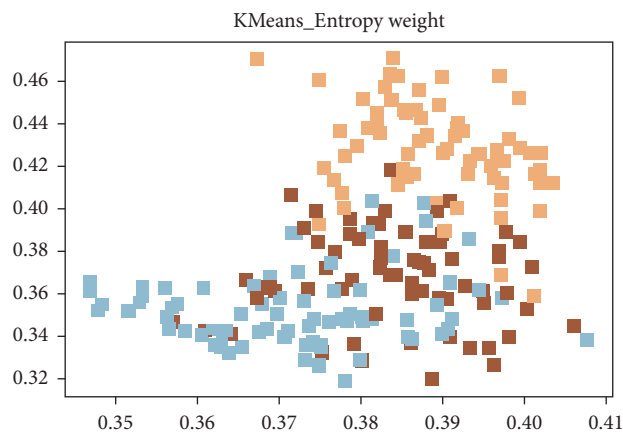


FIGURE 14: The K-means clustering effect of wheat seed data after the entropy weight method is used to determine the weights.

visualization, the clustering effects of the accurate solution method and entropy weight method are significantly better than that of traditional K-means. Samples of different categories are divided into different clusters.

5. Discussion and Conclusions

Class distance-based data classification algorithms are used to deal with different scenarios, where determining weights is an important and difficult problem. Based on the data value itself, this paper proposes a precisely determined distance weight, which makes the method more objective. The weight is determined only by solving the minimum function, and methods such as the entropy weight method and principal component analysis (PCA) are not needed. After determining the minimum Euclidean distance between the attribute vector of each category and the center point vector of the category to determine the weight, the obtained result is applied to the K-means clustering algorithm. Experiments were conducted using normalized mutual information as an evaluation criterion and a confusion matrix to evaluate clustering details. In this paper, we cluster the iris data set, wine data set, and wheat seed data set. The results show that, using the weight determination method proposed in this paper, confusion matrix and normalized mutual information results are better than the other two methods. Based on entropy and traditional K-means, the solution method is proven to be effective. Finally, the method is compared with the entropy weight method, to compare clustering results. The effect of the entropy weight method in determining class weight is not as good as that of the method proposed in this paper, which proves the accuracy and efficiency of this method. However, this paper only uses Euclidean distance as a distance function to measure each sample point and the center point to which it belongs. There are other distance functions in addition to Euclidean distance. Validating this approach with other distance functions is our next step. In addition, three classic machine learning data sets are taken as examples to demonstrate the effectiveness and efficiency of this method for determining weights. However, different weight determination methods are suitable for different data sets, and more verification is required for different scenarios and different data sets. For other methods, such as neural networks, further verification is required in future work. The distance-based weight determination method proposed in this paper still needs to be improved in the future, but the distance-based weight determination method is different from the subjective, entropy, and variance methods and provides a new idea for future weight determination.

Data Availability

The simulation experiment data used to support the findings of this study are available from the corresponding author upon request.

Conflicts of Interest

The authors have no conflicts of interest to declare.

Acknowledgments

This work was supported by the General Topics of Shanghai Philosophy and Social Science Planning (2020BGL007) and the National Natural Science Foundation of China (71832001).

References

- [1] S. Zeraatkar and F. Afsari, "Interval-valued fuzzy and intuitionistic fuzzy-KNN for imbalanced data classification," *Expert Systems with Applications*, vol. 184, Article ID 115510, 2021.
- [2] S. Rengasamy and P. Murugesan, "K-means-laplacian clustering revisited," *Engineering Applications of Artificial Intelligence*, vol. 107, Article ID 104535, 2022.
- [3] S. Huang, Z. Kang, Z. Xu, and Q. Liu, "Robust deep K-means: an effective and simple method for data clustering," *Pattern Recognition*, vol. 117, Article ID 107996, 2021.
- [4] F. D. Bortoloti, E. D. Oliveira, and P. M. Ciarelli, "Supervised kernel density estimation K-means," *Expert Systems with Applications*, vol. 168, Article ID 114350, 2021.
- [5] K. S. Gyamfi, J. Brusey, A. Hunt, and E. Gaura, "A dynamic linear model for heteroscedastic LDA under class imbalance," *Neurocomputing*, vol. 343, pp. 65–75, 2019.
- [6] Y. Donyatalab, F. Kutlu Gündoğdu, F. Farid, S. A. Seyfi-Shishavan, E. Farrokhzadeh, and C. Kahraman, "Novel spherical fuzzy distance and similarity measures and their applications to medical diagnosis," *Expert Systems with Applications*, vol. 191, Article ID 116330, 2021.
- [7] G. Kovács, B. Nagy, and B. Vizvári, "Weighted distances on the truncated hexagonal grid," *Pattern Recognition Letters*, vol. 152, pp. 26–33, 2021.
- [8] A. Panda, R. B. Pachori, and N. D. Sinnappah-Kang, "Classification of chronic myeloid leukemia neutrophils by hyperspectral imaging using Euclidean and Mahalanobis distances," *Biomedical Signal Processing and Control*, vol. 70, Article ID 103025, 2021.
- [9] E. Azhir, N. Jafari Navimipour, M. Hosseinzadeh, A. Sharifi, and A. Darwesh, "An efficient automated incremental density-based algorithm for clustering and classification," *Future Generation Computer Systems*, vol. 114, pp. 665–678, 2021.
- [10] Y.-L. Xu, S. Chen, and B. Luo, "A weighted locally linear KNN model for image recognition," *Communications in Computer and Information Science*, Springer, Singapore, pp. 567–578, 2017.
- [11] H. R. Pourghasemi, B. Pradhan, and C. Gokceoglu, "Application of fuzzy logic and analytical hierarchy process (AHP) to landslide susceptibility mapping at Haraz watershed, Iran," *Natural Hazards*, vol. 63, no. 2, pp. 965–996, 2012.
- [12] C. Lin and G. Kou, "A heuristic method to rank the alternatives in the AHP synthesis," *Applied Soft Computing*, vol. 100, Article ID 106916, 2021.
- [13] M. Xia and Z. Xu, "Entropy/cross entropy-based group decision making under intuitionistic fuzzy environment," *Information Fusion*, vol. 13, no. 1, pp. 31–47, 2012.
- [14] P. Chen, "Effects of the entropy weight on TOPSIS," *Expert Systems with Applications*, vol. 168, Article ID 114186, 2021.
- [15] J. E. Amaya, E. Camargo, J. Aguilar, and M. Tarazona, "A proposal for a cooperative cross-entropy method to tackle the unit commitment problem," *Computers & Industrial Engineering*, vol. 162, Article ID 107764, 2021.
- [16] C. Lu, D. Liang, S. Wang, L. Zeng, and Y. Zhao, "Pre-cut KNN algorithm based on threshold of distance," in *Proceedings of*

Research Article

The Network Transmission Path Risk Assessment and Application of Chemical Substances in Toys

Sainan Zhang  and Yuncai Ning

School of Management, China University of Mining & Technology (Beijing), Beijing 100083, China

Correspondence should be addressed to Sainan Zhang; bqt1700501022@student.cumtb.edu.cn

Received 28 March 2022; Revised 25 April 2022; Accepted 7 May 2022; Published 26 May 2022

Academic Editor: Wei Liu

Copyright © 2022 Sainan Zhang and Yuncai Ning. This is an open access article distributed under the Creative Commons Attribution License, which permits unrestricted use, distribution, and reproduction in any medium, provided the original work is properly cited.

Through the analysis of the risk transmission mechanism of chemical substances in toys, this paper identifies risk sources, transmission carriers, key nodes, and risk recipients, and draws a risk transmission path diagram. Taking the risk factors in the supply chain system as the research subject, this paper constructs a risk index system for chemical substances' limit in toys, and calculates the probability of risk and the degree of influence by the fuzzy evaluation method. Based on the Bayesian network model, this paper analyzes the causality of risk transmission effects. Through the comprehensive use of fuzzy evaluation and Bayesian network methods, a relatively complete chemical substance risk transmission path assessment system has been established using China's Guangdong toy companies as the data store to provide a feasible basis for responding to the risk control measures of toxic and hazardous chemical substances in toys.

1. Introduction

Along with the vigorous development of the global economy, people's living standards have gradually improved; as a result, toys have become an indispensable entertainment good for infants and young children. However, it has been reported that children face the hidden hazards of "toxic toys" in recent years [1], and the chemical substances contained in them cause serious harm to the healthy growth of infants and young children when come in contact or suck them. In order to protect the health and safety of children, various countries have put forward strict standards for restricting the use of toxic and hazardous chemical substances in toys (e.g., European standard EN 71 and ASTM F963 by U.S.). These standards put forward a severe test on how to control the content of chemical substances in the manufacturing process of toys. For China, as a major producer of toys, in order to better face this challenge, it is particularly important to master the risk transmission mechanism and risk assessment methods of chemical substances added to toys from raw materials, semi-finished products to finished toy goods. Based on the risk transmission mechanism of the chemical

substance supply chain in toys, this paper identifies the risk factor index system, and applies the fuzzy evaluation method to quantify the probability of risk occurrence and the consequences for the sake of effectively controlling the risk events caused by the content of chemical substances. Based on the Bayesian network model, the causality of risk factor transmission is calibrated so as to provide technical support for enterprises to take targeted risk prevention and control measures.

2. Research on the Risk Assessment of the Supply Chain Transmission Path

Supply chain risk has received wide-ranging attention from the academic and practice circles. Scholars at home and abroad have accumulated rich research experience on supply chain risk management (SCRM), risk identification, and risk assessment, which can effectively mitigate and avoid uncertain factors. Hudnurkar et al. (2017) mention that the common definition of supply chain risk is the degree of potential economic loss caused by the unexpected deviation of expected performance indicators or results in the supply

chain caused by the triggering of interference events by enterprises in the supply chain [2]. Aven (2008) points out that the uncertain risk and loss results in the supply chain are quantifiable [3]. Harland et al. (2003) believe that with the development of globalization, supply chain networks have become more complex and risk impacts have become more dynamic [4]. Heckmann et al. (2015) describe that risk spreads along the supply chain network and exacerbates it. If a single risk is partially isolated, it will not affect the normal operation of other links in the supply chain [5]. Swierczek (2018) indicates that a variety of risk factors caused by emergencies spread in the supply chain in a forward or reverse manner [6]. These views reflect that supply chain risks are quantifiable, additive, dynamic, and directional. Compared with foreign research, there are many research results on the risk transmission mechanism and modeling analysis of the supply chain in China. Shi (2006) discusses that risk transmission requires four elements, risk source, transmission carrier, transmission node, and risk receiver [7]. Cheng and Liu (2009) [8] discuss the accumulation and release process of risk flow, the path selection, and the orderly path transmission mechanism of transmission direction. The dynamic diffusion of risk transmission is directly related to the relevance and anti-risk ability of enterprises. Zhang (2011) refines the risk transmission process of supply chain and added the dynamic elements of trigger, transmission valve, and transmission path [9]. Wan et al. (2011) [10] state that risk can be blocked or weakened by internally adjusting the node enterprises. However, when internal adjustment cannot digest the risk, the risk will spread to the upstream- and downstream-related enterprises, forming a risk accumulation and leading to a vicious circle.

In order to effectively control and reduce the risk, many researchers have developed different risk assessment methods of supply chain transmission. In recent years, domestic and foreign research on supply chain transmission risk assessment focuses more on finance and food safety. Wang et al. (2021) use the epidemic model to study the mechanism and evolution of the complex supply chain network risk transmission, and gain important management enlightenment [11]. Hernadewita and Saleh (2020) conducted a systematic analysis of 35 construction supply chain risk identification and assessment frameworks, and found that the combination of supply chain operation reference model (SCOR) and failure mode and effect analysis (FMEA) is an effective method to identify and evaluate construction supply chain risk [12]. Handayani and Prihatiningsih (2019) take small and medium-sized enterprises that produce fish balls as the research subject, identify the production risk factors based on the traceability system, and use the gray theory method to evaluate the impact of hazardous substances in halal food [13]. Zhang et al. (2018) used structural equation modeling to explore the transmission of supplier's disruption risk along the supply network in Chinese automotive-related companies, and revealed that the disruption risk affects its manufacturers, who conduct direct business trades with it [14]. Guritno and Khuriyati (2018) conducted in-depth interviews with 19 subjects at different levels in the

fresh vegetable supply chain to determine the internal and external risks, and evaluated the risk management ability of each level using the expected loss ranking matrix; they analyzed the risk transfer to consumers, and farmers and traders reduced the expected loss of risk [15]. Lei and Liu (2017) use game theory to analyze the transmission mechanism of moral hazard in the supply chain of agricultural products, and find that risk entities, especially responsible entities with high correlation, can prevent and control risks to the greatest extent possible to prevent risks from occurring [16]. Liu (2015) applies the method of system dynamics to establish a risk transmission model for the vegetable supply chain in Baoding, identifies the risk factors in the system, and proposes that the risk transmission should be suppressed from quality, inventory, purchase, price, and information transmission [17]. Wang (2015) analyzes the internal and external influencing factors of the quality risk of Chinese pharmaceutical manufacturers, constructs a quality risk transmission causality diagram, analyzes the transmission influence of risk factors through system dynamics simulation, and concludes that blocking the transmission of risk transmission paths is the most significant prevention and control effect [18]. Zhang (2012) [19] used the expert scoring method and entropy method to quantitatively analyze the correlation degree and the risk threshold of supply chain node enterprises in the automobile manufacturing industry. The risk transfer coefficient is introduced to construct a selective mechanism model of supply chain risk transfer, and it is found that the correlation degree of node enterprises is positively correlated with the amount of risk transfer.

From all of the aforementioned studies, although different risk assessment methods have been applied in the fields of manufacturing, food, and medicine, the research on the identification or assessment of the transmission risk of hazardous chemical substances in toys is almost blank. At the same time, the risk transmission analysis lacks systematic risk identification, transmission effect, and comprehensive quantitative analysis of influence degree. This paper combines the Bayesian network and the fuzzy judgment analysis method to improve the transmission effect evaluation system of the risk path.

3. The Mechanism of Risk Transmission Path of Chemical Substances in Toys

3.1. Overview of the Risk Transmission Path of Chemical Substances in Toys. With reference to the concepts of corporate risk transmission in the supply chain [20] and food quality risk transmission [21], the risk transmission of chemical substances in toys refers to that in the whole supply chain system network of raw materials production, processing and manufacturing, quality inspection, storage, and transportation and distribution, the content of toxic and harmful chemicals in products exceeds the standard due to the influence of uncertain risk factors, and the transmission effect is produced along the chain network structure in production-related enterprises. The risk assessment of the chemical substances' transmission path in toys is the

measurement and analysis of the uncertainty of the factors influencing the content of chemical substances in the toy supply chain to determine the possibility of the occurrence of risk factors and the degree of risk hazard, and to evaluate the risks of stakeholders in the supply chain influences.

3.2. Risk Transmission Elements of Chemical Substances in Toys

3.2.1. Risk Sources. As the origin of risk events, risk sources are a set of internal and external uncertain risk factors. The effective identification of risk sources is the first step to prevent and control the internal and external transmission of risks. The reason for the excessive content of trigger chemicals in toy products comes from the production of raw materials, processing and manufacturing of semi-finished products/finished products, and packaging and transportation. From the perspective of production and manufacturing, it involves demand design risks and manufacturing risks. The purpose of adding hazardous chemicals to toys is to change certain characteristics of the product (for example, hexavalent chromium in metal toys can improve the corrosion resistance of the product) in order to meet the performance requirements of product design, resulting in the addition of chemical substances that do not meet the standard requirements. In addition to design risks, a series of problems in the manufacturing process, such as equipment failure, backward process technology, and even manual operation errors and environmental pollution (such as polycyclic aromatic hydrocarbon chemicals in toys that are susceptible to air pollution), can increase the possibility of excessive content. From the perspective of inspection and supervision, inspection technology and equipment accuracy are the prerequisites for management and control, and effective inspection methods can reduce or prevent the business risk of purchasing or producing substandard raw and auxiliary materials. Because toys have industry standards, national standards, and national export standards, the inconsistency or lack of standard standards leads to testing difficulties. Therefore, system management has also become a necessary measure and means to control risks. From the perspective of transportation and storage, the storage, packaging, and transportation of chemical materials in toys triggers problems such as chemical pollution and causes changes in substance content.

3.2.2. Transmission Carrier. In the supply chain, risks need to be transmitted dynamically by means of carrying media such as material, technology, manpower, capital, and information. Among them, the material carrier includes raw and auxiliary materials and machinery and equipment required for toy production. The technology carrier includes R&D capabilities and production processes. R&D capabilities determine whether there are new substitute substances or processes that can be optimized to meet content requirements and achieve the characteristics of original chemical substances. The human carrier is mainly based on

purchasers, inspectors, producers, technicians, and managers, and the ability to control risks among the subjects. The information carrier plays a decisive role in promoting the standardization of stakeholders. Effective information flow transmission in business can quickly respond to risk control decisions. The financial carrier is the driving force for the sustainable development of the enterprise, and the R&D and the introduction of precision equipment and instruments require a large amount of financial support.

3.2.3. Key Nodes. Key nodes refer to single or multiple risk gathering points from internal processes and external business. The node can derive, amplify, or block the harm brought by emergency events in the spatial dimension, and can transform the risk from static node to dynamic "critical point" that diffuses to another node. According to the on-the-spot investigation of toy manufacturing enterprises, through summarizing the internal processes of different toy productions (plastic toys as shown in Figure 1 and metal toys as shown in Figure 2), it can be seen that the key internal nodes of chemical content risk in products are mainly spray/paint, pad printing, and electroplating. It is reported that the content standard of chemical substances in paint raw materials is the key point of prevention and control, and the problems of process dosage, sticky pollution, and qualified sampling inspection determine the important links of reaching the standard of chemical substances in finished products. The key points of external business mainly focus on three business links, i.e., raw and auxiliary material suppliers, product manufacturers, and quality inspection institutions.

3.2.4. Risk Recipient. The recipient of the risk can also be the sender of the risk, with the characteristics of risk retention, absorption and digestion, continued transmission, and resistance [22]. The main bodies of risk recipients are chemical material suppliers, toy processing manufacturers, and quality inspection supervisors, and ultimately circulate to consumer risk recipients. If the risk recipient takes effective early warning and control measures, the risk will be digested and blocked at this node. Otherwise, it will continue to be passed on to other key links in a way of buffering degradation. At this time, the role of the receiver becomes a risk sender.

3.2.5. Transmission Path. As the name implies, transmission path is the route that risks spread to the terminal in an orderly direction. The transmission direction can be divided into chain-type forward or reverse, central radiation, network concentration, or interactive network transmission [23]. According to the analysis of the inventory status of chemical substances, the raw and auxiliary materials, semi-finished products, and finished products of toys adopt three transmission modes, chain forward, radiation, or centralized. The chain-type forward transmission path uses a unidirectional flow from upstream to downstream in the supply chain, i.e., raw and auxiliary material procurement

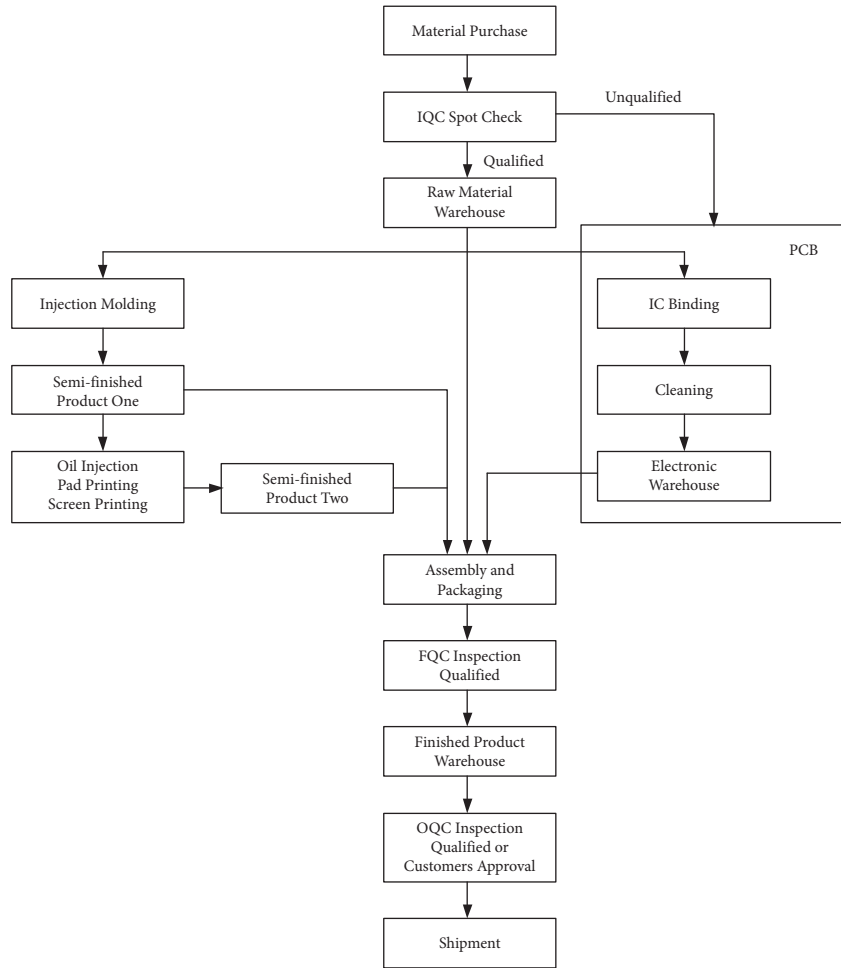


FIGURE 1: Production process of plastic toys.

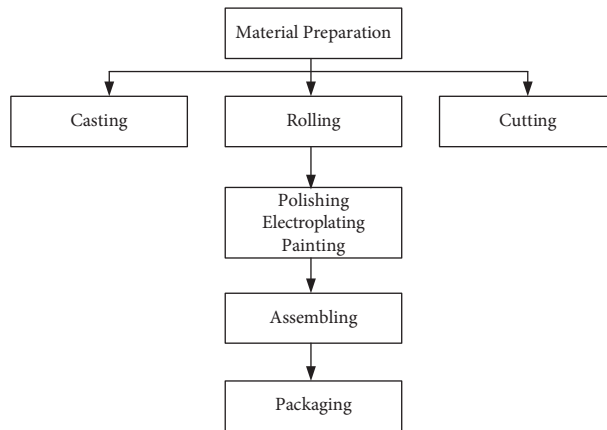


FIGURE 2: Production process of metal toys.

→ semi-finished product processing → finished product manufacturing → packaging, storage, and transportation, and finally circulation to consumers. The radial transmission path transmits risks from the upstream of the supply chain to the same level or downstream levels. The risk of multiple enterprises in a centralized transmission path is all to the same enterprise. The next-level network node is enterprise

transfers, and it gradually transfers to the risk recipient, namely the consumer.

Based on the research of the risk transmission mechanism of chemical substances in toys, the process of chemical substance transmission path is the process that the risk of excessive chemical content of products is transmitted to similar enterprises or downstream risk-accepting enterprises

along the chain positive or network divergent mode in the toy supply chain system network. The excessive content of toxic and harmful chemical substances directly or indirectly affects the related enterprises such as raw materials, semi-finished products, and finished products. As a risk source, the excessive content relies on various risk transmission carriers such as production and processing, transportation, and products. Through the risk accumulation or coupling of related businesses, the risk will spread to the downstream key node enterprises. The risk sender is also the risk receiver in the supply chain system. Each node enterprise is a risk subsystem. The change of risk flow is related to the risk early warning, prevention and control mechanism, and the adaptive regulation mechanism of the risk subsystem. Risk receivers with strong prevention and control ability can reduce or block the risk by taking effective measures. From this, we can draw the risk transmission path map of the supply chain of chemicals in toys, which is composed of four levels (as shown in Figure 3).

4. Risk Assessment Method of Chemical Substance Transmission Path in Toys

Based on the study of chemical substance transmission mechanism in toys, it is found that the influence of risk sources on parameters in various key links is uncertain or fuzzy. The Bayesian network can solve the uncertainty of related links by means of probability reasoning. Combined with the risk transmission path map, the Bayesian network, also known as the directed acyclic graph model, is constructed to identify the risk index system. The prior probability and conditional probability of the risk event factor set are evaluated by expert experience, and then the posterior probability of other links along the directed edge is calculated. According to the obtained joint probability propagation network of risk factors, the causal relationship among the key nodes in the risk transmission path is explained.

4.1. Fuzzy Evaluation of Risk Probability and Influence Consequence

4.1.1. *Establish the Risk Index System (as Shown in Table 1).* Chemical substances in toys take supply and manufacturing enterprises as the key nodes. According to the risk sources identified by the transmission path, a set of risk factors $R = \{R_i | i = 1, 2, \dots, 5\} = \{\text{procurement risk, production risk, R\&D risk, quality inspection risk, and management risk}\}$ are established, in which the risk subset is $R_t = \{R_{it} | t = 1, 2, \dots, n\}$. Table 1.

4.1.2. *Determine the Comment Set and Weight.* Experts judge the probability and degree of impact of risks based on the actual situation of the enterprise, and assign values using the center of gravity method. Occurrence rating $I = \{I_j | j = 1, 2, 3, 4\} = \{\text{occur rarely, occur occasionally, occur frequently, and occur inevitably}\} = \{0.1, 0.3, 0.6, 1\}$; the impact degree comment set and the assignment situation are shown in Table 2.

In order to reduce the impact of subjective assessment, determine the first-level indicator risk factor weight set $W = \{\omega_i\}$, which satisfies $\sum_{i=1}^5 \omega_i = 1$ and $\sum_{i=1}^5 \omega_i \geq 0$, set up the secondary index weight set $\tilde{W} = \{\omega_{it}\}$, and normalize the weights separately, such as $\omega_i = \omega'_{i'} / \sum_{i=1}^k \omega'_{i'}$.

4.1.3. *Fuzzy Evaluation.* The paper establishes the membership vector matrix $\tilde{D} = (d_{ij})_{m \times n}$ of the risk factor set R and rating I , where d_{ij} denotes the fuzzy mapping of each risk factor R_i corresponding to I_j . In this paper, the fuzzy transformation of the risk factors in the first-level fuzzy evaluation is carried out, and $\tilde{P} = \tilde{W}$. $\tilde{D} = V_{i=1}^n (\omega_{it} \wedge d_{ij}) = (P_s | s = 1, 2, \dots, m)$. According to the first-level fuzzy operation principle, the fuzzy evaluation of the second-level index and the weight matrix of the first-level index are multiplied by the fuzzy matrix to obtain the fuzzy vector of the index.

$$P' = W \circ \tilde{P} = W \circ \begin{bmatrix} P_1 \\ P \\ P_3 \\ P_4 \\ P_5 \end{bmatrix} = (P_r | r = 1, 2, \dots, m). \quad (1)$$

4.1.4. *Comprehensive Evaluation.* The weighted average principle is used to evaluate the probability of risk occurrence.

$$P = \frac{\sum_{i=1}^m I_j P_r}{\sum_{j=1}^m P_r}. \quad (2)$$

Among them, P_r is the membership degree of risk factor R_i to the evaluation grade I_j , and I_j is the rating assignment of the evaluation set.

4.2. *Build the Bayesian Network Model.* Bayesian network (BN) is a directed acyclic probability graph $G = \langle R, E, \Theta \rangle$ composed of multiple nodes, in which each node represents the corresponding risk factor variable $R = \{R_i\}$, the directed edge set E represents the dependence among variables, and the parameter Θ represents the conditional probability table (CPT) among node states. Based on the Bayesian statistical theory, the Bayesian network can calculate the joint probability distribution $P(R_1, R_2, \dots, R_n)$ of risk events caused by excessive chemical substances, which is written by chain rules

$$\begin{aligned} P(R_1, R_2, \dots, R_n) &= P(R_1)P(R_2|R_1)P(R_3|R_1, R_2) \dots \\ &P(R_n|R_1, R_2, \dots, R_{n-1}), \\ &= \prod_{i=1}^n P(R_i|R_1, R_2, \dots, R_{i-1}). \end{aligned} \quad (3)$$

Taking toy product manufacturing and purchasing as an example, a simple Bayesian network of chemical risk events is constructed, as shown in Figure 4, where nodes

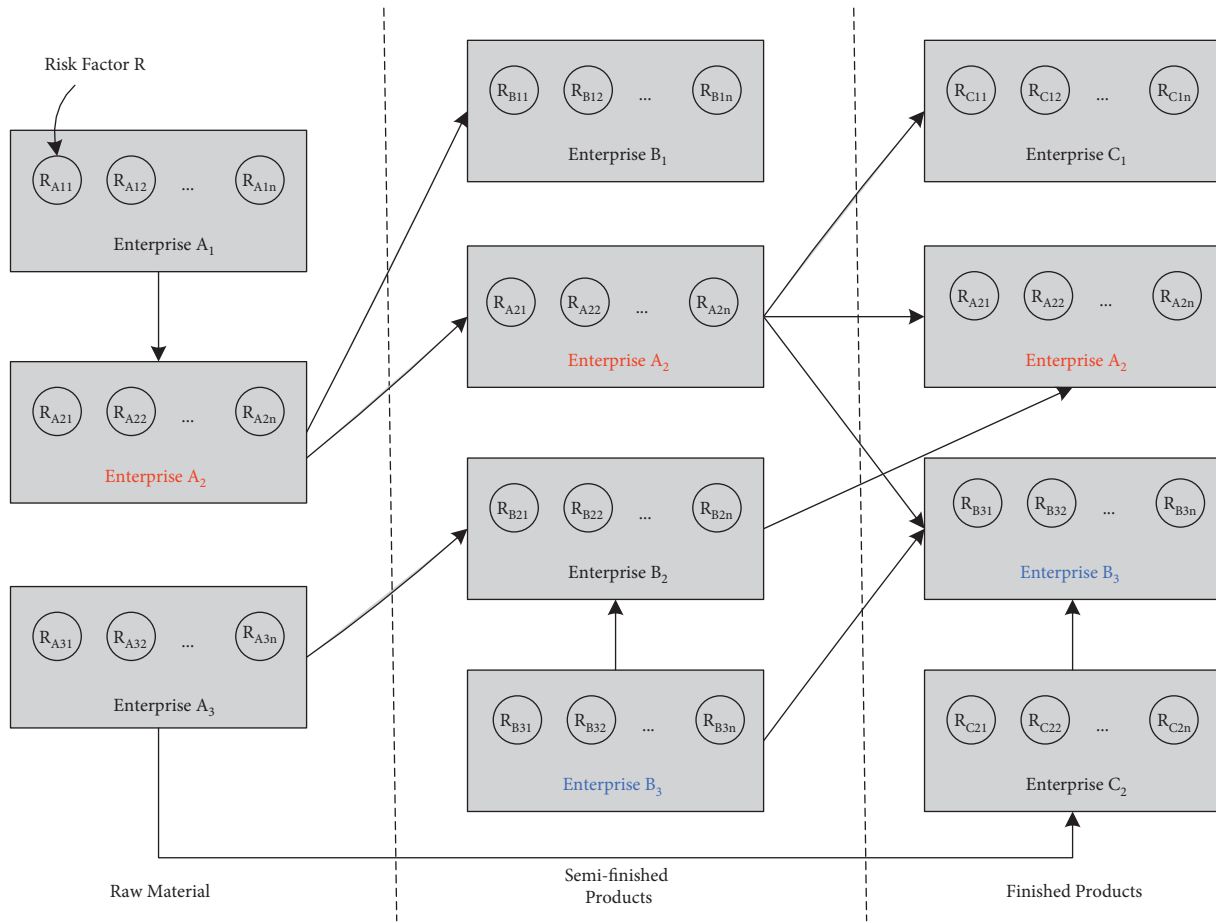


FIGURE 3: Risk transmission path of chemical substance supply chain in toys.

TABLE 1: Risk factors of toy chemical supply chain identification.

Primary indicators	Secondary indicators	Description
Procurement risk R_1	Supplier selection risk R_{11}	Supplier qualification review
	Raw material review risk R_{12}	Storage of unqualified raw and auxiliary materials
Production risk R_2	Technology risk R_{21}	Risks of painting and coating links and equipment
	Production environment risk R_{22}	Environmental pollution triggers risk
	Staff operation risk R_{23}	Misuse by employees
	Packaging, storage, and transportation risk R_{24}	Pollution or deterioration of packaging, storage, and transportation
R&D risk R_3	Product design risk R_{31}	Designer's ability to recognize standards
	R&D capability risk R_{32}	Lack of alternative products or new technologies
Quality inspection risk R_4	Detection process risk R_{41}	Detection technology and equipment accuracy level
	Testing skills risk R_{42}	Technical level of inspectors
Management risk R_5	Information sharing risk R_{51}	Information/standard delivery delayed or inconsistent
	Regulatory system risk R_{52}	Comprehensive rationality of the management system
	Regulatory enforcement risk R_{53}	Management execution ability level
	Recall product disposal risk R_{54}	Recall product recycling and utilization

TABLE 2: Rating table of risk impact consequences.

Risk degree	Degree of loss caused (1000 yuan)	Evaluation (1000 yuan)
Negligible	$0 \leq I_j < 10$	5
Slight	$10 \leq I_j < 100$	55
Common	$100 \leq I_j < 500$	300
Serious	$500 \leq I_j < 1000$	750
Disastrous	$I_j \geq 1000$	1000

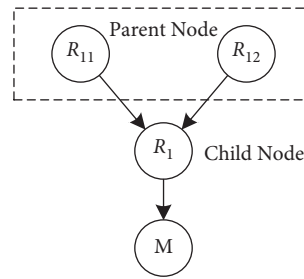


FIGURE 4: Bayesian network in procurement link of toy manufacturer M.

R_{11} and R_1 have a directed edge, and call R_{11} is the parent node of R_1 . On the contrary, R_1 is the child node of R_{11} . For any child node with a parent node $Pa(R_i)$, it satisfies the joint probability distribution $P(R_1, R_2, \dots, R_n) = \prod_{i=1}^n P(R_i | Pa(R_i))$; if $Pa(R_i) = \emptyset$, i.e., the probability of node R_{11} is estimated as edge distribution $P(R_{11})$. Therefore, the risk joint probability of M procurement link of finished product manufacturer $P(R_1, R_{11}, R_{12}, M) = P(R_1 | R_{11}, R_{12}) \cdot P(M | R_1) \cdot P(R_{11}) \cdot P(R_{12})$. Among them.

5. Application of the Risk Assessment Method for Chemical Substance Transmission in Toys

5.1. Data Sources. This paper selects a large toy enterprise and its raw and auxiliary material suppliers in Shantou City, Guangdong Province as the research subject (as shown in Table 3). Through the open questionnaire survey and expert forum, the prior probability of risk factors is investigated by 48 professionals, and the evaluation vector is weighted by the survey results.

5.2. Fuzzy Comprehensive Evaluation

5.2.1. Determine Weight. Use the Analytic Hierarchy Process (AHP) and MATLAB software to get the weight set (as shown in Table 4) and fuzzy evaluation grade of chemical substances exceeding the standard risk $W = [0.041, 0.533, 0.093, 0.242, 0.091]$ $CR = CI/RI = 0.097/1.12 < 0.10$, pass the consistency test.

5.2.2. Probability of Occurrence and Impact Assessment. According to the fuzzy evaluation and comprehensive evaluation methods, the risk probability (P) and risk impact consequences (c) are calculated.

Through the data analysis in Table 5, it can be concluded that the risk of excessive chemical substances of domestic raw material suppliers is lower, even negligible. However, the possibility of risk caused by the finished product manufacturers in domestic and foreign trade sales markets is higher, accounting for 32.3%, but the loss caused is lower than that of raw material suppliers.

5.3. Construct a Bayesian Network Simulation Experiment. Based on the relationship between the internal and external risk factors and the supply chain production, this paper establishes

the node relationship diagram between the second-level risk factors and the corresponding first-level indicators. Then, all the risk factors are gathered into the chemical risk events triggered by the enterprise. According to the prior probability and conditional probability distribution of variable parameters of each node, the posterior probability of the target node is calculated by formula (3). Then, the Bayesian network of risk of chemical substance transmission in toys is established by Netica software (as shown in Figure 5).

5.4. Risk Effect of the Chemical Substance Transmission Path in Toys. Through the demonstration data of Bayesian reasoning in Figure 5, it can be seen that when the risk occurs in the raw material node enterprise (SUPL_DOM), the associated production manufacturer enterprise (MFR_IN_DOM) will produce a transmission effect. From the Bayesian inference probability, it can be found that from the perspective of external risk, the risk has an amplified cumulative effect in the transmission process of the supply chain of the two companies. From the perspective of enterprise internal risk, due to the prevention and control measures taken by the finished product manufacturers, the risk occurrence of the node enterprises triggered by internal risk factors is inhibited or reduced. Besides, due to the constraints of the regulatory agencies or the government, the possibility of risk occurrence is further hindered.

The probability loss model $RS = PB \times C$ (RS stands for risk value) proposed by Mitchell (1995) [24] is used to measure the impact effect of risk events, which can better measure the risk level of chemical substances. Combined with the fuzzy evaluation of risk consequence C and Bayesian probability PB parameter values, the risk impact effect of the supply chain network is ranked: $RS(\text{SUPL_DOM}) > RS(\text{MFR_IN_DOM})$; obviously, the risk events caused by domestic raw material supply enterprises have a greater impact. This is because the regulations or standards of toy products have not yet formed global integration, and enterprises need to meet the requirements of technical regulations and standards of different countries to enter the international sales market. Compared with foreign standards, the regulation of toy chemical safety standards in China is more relaxed. Through investigation, it is found that in order to meet the requirements of different standards, China's foreign trade enterprises have implemented the production mode of "the same standard, the same quality, and the same line," so as to avoid serious losses caused by confused production.

TABLE 3: Overview of toy chemical substances research enterprises.

Enterprise type	Enterprise scale	Enterprise area	Sales market
Toy products manufacturer (MID)	Large	Shantou city, Guangdong province	Integration of domestic and foreign markets
Raw material supplier (SD)	Small	Shantou city, Guangdong province	Domestic market

TABLE 4: Weights of risk factors in the supply chain of toy chemical substances.

Primary indicators	Weights	Secondary indicators	Weights
Procurement risk R_1	0.041	Supplier selection risk R_{11}	0.667
		Raw material review risk R_{12}	0.333
Production risk R_2	0.533	Technology risk R_{21}	0.255
		Production environment risk R_{22}	0.083
		Staff operation risk R_{23}	0.427
		Packaging, storage, and transportation risk R_{24}	0.235
R&D risk R_3	0.093	Product design risk R_{31}	0.750
		R&D capability risk R_{32}	0.250
Quality inspection risk R_4	0.242	Detection process risk R_{41}	0.200
		Testing skills risk R_{42}	0.800
Management risk R_5	0.091	Information sharing risk R_{51}	0.406
		Regulatory system risk R_{52}	0.182
		Regulatory enforcement risk R_{53}	0.351
		Recall product disposal risk R_{54}	0.061

TABLE 5: Results of fuzzy comprehensive evaluation.

Enterprise type	Fuzzy evaluation set of occurrence possibility	Fuzzy evaluation of occurrence possibility	Fuzzy evaluation set of influence consequence	Fuzzy evaluation grade of influence consequence
Domestic and foreign manufacturers of finished Products (MFR_INT_DOM)	(0.299, 0.398, 0.267, 0.014)	0.323	(1, 0, 0, 0)	5
Raw material supplier (SUPL_DOM)	(0.423, 0, 0, 0)	0.042	(0.77, 0.23, 0, 0)	16.49

Through the comparison between the Chinese toy safety standard GB6675-2014 and the European Union toy standard EN 71-3, it is obvious that in the limit range of transferable elements in toy products, China imposes restrictions on 8 chemical elements, while the EU imposes strict restrictions on 19 chemical elements. In the future, if China formulates toy standards with international standards, increases the category of chemical elements, and reduces the threshold value of substance content, the domestic trade-oriented small and medium-sized enterprises will face a severe test. According to the Bayesian probability results in Figure 5, it is found that the raw material supply enterprises and the finished product manufacturing enterprises are in a low-level state. Among them, the most influential factor of raw material supply in

the supply chain is the production link. According to the Bayesian risk probability level, the $P(SD-R_2) > P(SD-R_4) > P(SD-R_1) > P(SD-R_5) > P(SD-R_3)$ is ranked. The factor that triggers the risk of chemical substance exceeding the standard in the finished product manufacturing enterprise is the procurement link, and the risk occurrence level is ranked as $P(MID-R_1) > P(MID-R_3) > P(MID-R_4) > P(MID-R_2) > P(MID-R_5)$. Therefore, the raw material enterprises should adopt advanced production technology and substitute new technology to replace the previous production process, while the finished product manufacturing enterprises should strictly control the upstream suppliers, so as to ensure that the raw materials and auxiliary materials meet the supply standards.

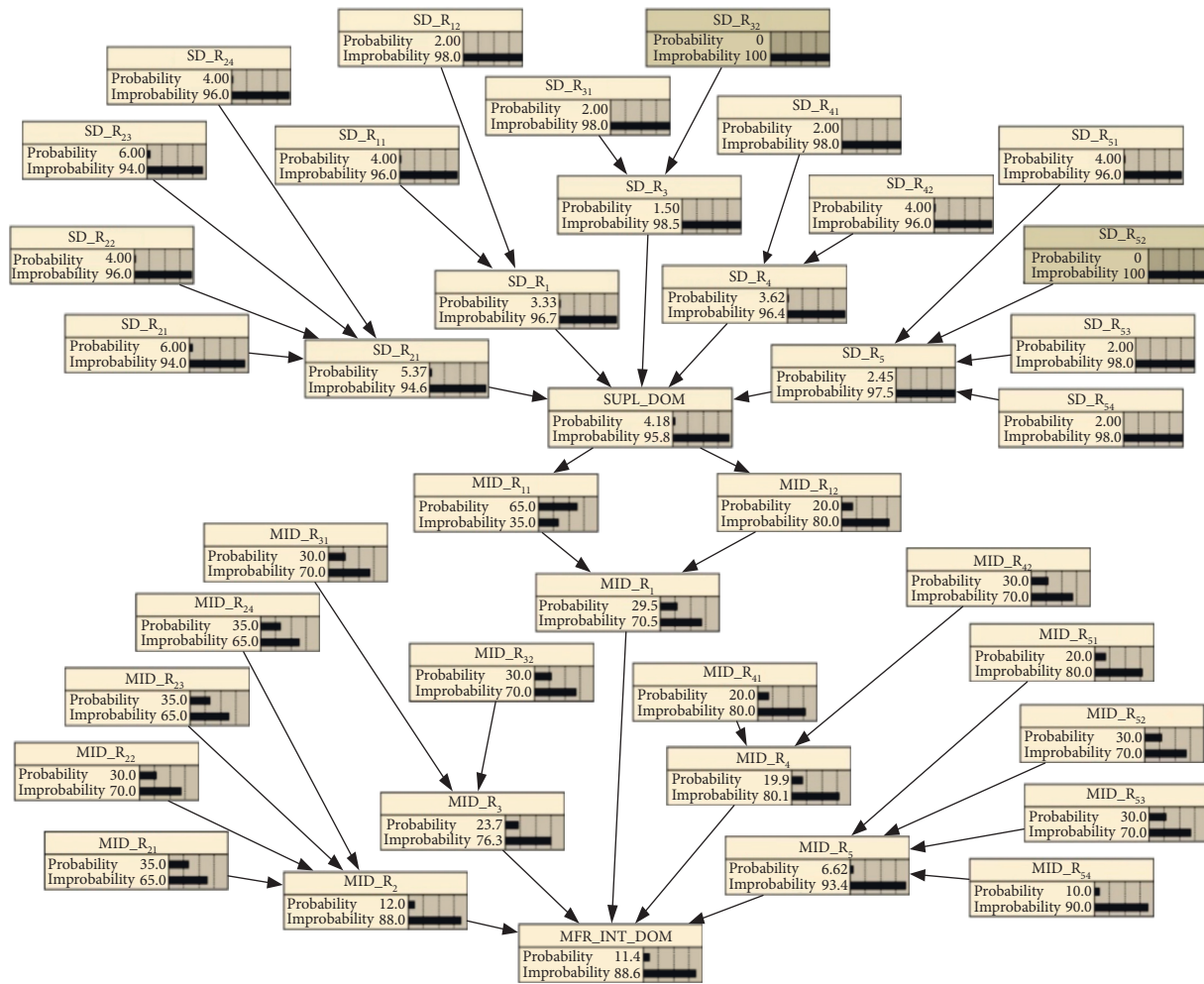


FIGURE 5: Bayesian network of risk of chemical substance transmission in toys.

6. Conclusion

Taking the upstream and downstream manufacturers of toy supply chain as the research subject, this paper analyzes the transmission mechanism of supply chain leading to the excessive risk of chemical substances, identifies risk factors, and establishes an index system. In this paper, fuzzy language is used to evaluate the risk probability and loss consequence, which solves the uncertainty and subjectivity of the assessment. Based on the Bayesian network probabilistic reasoning system, this paper clearly shows the conduction effect between key nodes in the supply chain. Through the comprehensive application of fuzzy evaluation and the Bayesian network evaluation method system, this paper can achieve objective evaluation, simplify the calculation complexity, and clearly infer the causal relationship, which is more scientific and reasonable.

Data Availability

The datasets generated during the current study are not publicly available due to privacy restrictions but are available from the corresponding author on reasonable request.

Conflicts of Interest

The authors declare that there are no conflicts of interest regarding the publication of this paper.

Acknowledgments

This work was supported by the Major National Key R&D Program of China, 2018YFF0214804.

References

- [1] P. Song, "The colorful toys damaged to baby," *The Family Education of China*, vol. 2020, no. 3, pp. 28-29, 2020.
- [2] M. Hudnurkar, S. Deshpande, U. Rathod, and S. K. Jakhar, "Supply chain risk classification schemes: a literature review," *Operations and Supply Chain Management: International Journal*, vol. 10, no. 4, pp. 182-199, 2017.
- [3] T. Aven, *Risk Analysis: Assessing Uncertainties beyond Expected Values and Probabilities*, John Wiley & Sons, Hoboken, NJ, USA, 2008.
- [4] C. Harland, R. Brenchley, and H. Walker, "Risk in supply networks," *Journal of Purchasing and Supply Management*, vol. 9, no. 2, pp. 51-62, 2003.

- [5] I. Heckmann, T. Comes, and S. Nickel, "A critical review on supply chain risk - definition, measure and modeling," *Omega*, vol. 52, pp. 119–132, 2015.
- [6] A. Swierczek, "Supply chain risk management in the transmission and amplification of disruptions," *Supply Chain Risk Management*, Springer, Berlin, Germany, pp. 155–178, 2018.
- [7] Y. Y. Shi, "Theoretical research on risk conduction mechanism and risk energy," *Journal of Wuhan University of Technology*, vol. 9, pp. 48–51, 2006.
- [8] G. P. Cheng and Q. Liu, "To study on changing for transmitting path of the supply chain risk," *Value Engineering*, vol. 28, no. 4, pp. 1–3, 2009.
- [9] J. G. Zhang, "Research on the elements and process of supply chain risk conduction," *Logistics Engineering and Management*, vol. 33, no. 11, pp. 139–151, 2011.
- [10] C. D. Wan, J. C. Bai, and C. J. Chen, "Discussion on risk conduction mechanism of supply chain based on the perspective of risk consequences," *Logistics Sci-Tech*, vol. 34, no. 3, pp. 45–48, 2011.
- [11] J. Wang, H. Zhou, and X. Jin, "Risk transmission in complex supply chain network with multi-drivers," *Chaos, Solitons & Fractals*, vol. 143, Article ID 110259, 2021.
- [12] H. Hernadewita and B. I. Saleh, "Identifying tools and methods for risk identification and assessment in construction supply chain," *International Journal of Engineering*, vol. 33, no. 7, pp. 1311–1320, 2020.
- [13] D. Handayani and T. Prihatiningsih, "Application of grey theory method for halal food risk assessment based on the traceability system in food supply chain," in *Proceedings of the 2019 1st International Conference on Engineering and Management in Industrial System (ICOEMIS 2019)*, pp. 426–434, Atlantis Press, Malang, Indonesia, August 2019.
- [14] J. Zhang, X. Chen, and C. Fang, "Transmission of a supplier's disruption risk along the supply chain: a further investigation of the Chinese automotive industry," *Production Planning & Control*, vol. 29, no. 9, pp. 773–789, 2018.
- [15] A. D. Guritno and N. Khuriyati, "An application of RapAgRisk (rapid agricultural supply chain risk assessment) method on fresh vegetables for identifying and reducing damage during delivery to consumers," *KnE Life Sciences*, vol. 4, no. 2, pp. 1–8, 2018.
- [16] X. P. Lei and R. Qiu, "Supply chain-based risk transmission mechanism of agricultural product quality and safety," *Jiangsu Agricultural Sciences*, vol. 45, no. 13, pp. 242–249, 2017.
- [17] A. Q. Liu, *Study on the Vegetable Supply Chain Risk Conduction Problems and Suggestions of Baoding City*, Hebei Agricultural University, Baoding, China, 2015.
- [18] Z. J. Wang, *Research on Management and Control of Quality Risk and Their Conduction of Pharmaceutical Manufacturers in China*, Wuhan University of Technology, 2015.
- [19] Z. Y. Zhang, *Research on Selective Mechanism in the Supply Chain Risk Transmission Based on the Manufacturing*, Nanjing University of Aeronautics and Astronautics, Nanjing, China, 2012.
- [20] J. H. Chen and L. Q. Xu, "Application of elasticity coefficient in study about supply chain risk conduction," *Journal of Anhui Agricultural Sciences*, vol. 1, pp. 313–314, 2007.
- [21] C. D. Wan and Z. B. Qin, "Research on food quality safety risk conduction system in food supply chain," *Journal of Harbin Institute of Technology*, vol. 1, no. 22, pp. 131–134, 2016.
- [22] S. L. Dai, *Research on Mechanism and Empirical Analysis of Enterprises' Marketing Risks Conduction*, Wuhan University of Technology, Wuhan, China, 2009.
- [23] G. P. Cheng and Y. G. Qiu, "Research on the mode of the supply chain risk conduction," *Journal of Wuhan University of Technology*, vol. 22, no. 2, pp. 36–41, 2009.
- [24] V. W. Mitehell, "Organisation risk perception and reduction: a literature review," *British Journal of Management*, vol. 6, no. 2, pp. 115–133, 1995.

Research Article

Computer Digital Technology Combined with Dynamic Visual Communication Sensors in Target Tracking with Big Data

Zhihui Han ¹ and Jianhua Zhao²

¹Intelligence Manufacture Department, Changchun Sci-Tech University, ChangChun 130000, JiLin, China

²NetWork Center, ChangChun Normal University, ChangChun 130000, JiLin, China

Correspondence should be addressed to Zhihui Han; 100186@cstu.edu.cn

Received 19 January 2022; Accepted 1 March 2022; Published 25 May 2022

Academic Editor: Wei Liu

Copyright © 2022 Zhihui Han and Jianhua Zhao. This is an open access article distributed under the Creative Commons Attribution License, which permits unrestricted use, distribution, and reproduction in any medium, provided the original work is properly cited.

The detection algorithm is explored to improve the dynamic visual sensors (DVS) combined with computer digital technology, build a DVS network, and complete the monitoring and tracking of the target. Ultimately, the problem that needs to be solved is the poor quality of traditional communication sensor data transmission, which needs to be improved by DVS. Firstly, the structure and function of the network are described through dynamic visual perception requirements analysis. Secondly, by introducing a target tracking algorithm that combines event flow and grayscale images, two methods are proposed, namely, the event flow noise reduction method based on event density and the optical flow detection feature tracking algorithm. Finally, through experiments, the tracking and detection effect of the optical flow detection algorithm on the target object in the dark environment is verified in the high-speed motion scene and the reflection environment. The results show that the average error of target object detection and tracking is 3.2 pixels in a dark environment. The average error of target tracking in high-speed motion scenes and reflective environments is 4.86 pixels and 2.88 pixels, respectively. This research has practical reference value for the digital and intelligent development of digital video surveillance systems.

1. Introduction

As the most influential technological change in the new century, sensor networks [1–3] have provided strong technical support for the completion of target detection and tracking tasks since their inception. In a specific and complex environment, it is difficult to use human resources to track specific targets. A large amount of manpower and material and financial resources are needed for coordination and deployment. Appropriate sensor nodes are used in the target environment, and the location information of each sensor node is coordinated and controlled by the overall network. Through the coordinate information of each sensor, tasks such as monitoring and tracking of the target are completed. Therefore, in the sensor network, the basic function of the network system is achieved through appropriate measurement methods. Even in a complex environment with severe occlusion, it can also realize the sensory positioning of visual nodes in the visual sensor network.

The construction of the dynamic visual sensor (DVS) network requires the addition of vision sensor nodes (VSN) [4–6] to the general sensor network to meet the high-speed monitoring requirements of the sensor network. The sensor network contains intelligent sensors that can perceive a variety of physical quantities. It can collect target-related information in a complex and high-risk environment. It can monitor and track environmental data information through visual sensor nodes, realize the detection of the designated area, and then transmit the data to the data center through the transmission channel [7]. Additionally, the traditional vision sensor has the problem of motion blur when collecting high-speed moving targets, and it does not perform well for the data collection effect in the reflective environment and the dark environment. DVS can solve these problems due to their high dynamic range. Therefore, it has great potential in target tracking. DVS performs tracking and detection by the shape of the target, which can not only realize feature tracking and monitoring in multiple scenarios

but also transfer and forward each sensor node, reducing the burden of data access in the data center.

However, the traditional sensor network has an uncertain scale, and the detection and tracking range of a sensor network that is too small is insufficient to achieve large-scale regional environmental data monitoring [8]. Excessively large sensor networks are often limited by factors such as cost, power consumption, and flexibility. Some nodes may lack global positioning devices and cannot achieve real-time positioning of all nodes, which in turn affects the effect of target monitoring and tracking [9, 10]. Therefore, based on the analysis of the requirement of DVS, the event stream noise reduction method and the event density-based optical flow detection feature tracking algorithm are proposed to study the detection algorithm by introducing the target tracking algorithm combining event stream and grayscale image. The research realizes the tracking and detection of target objects in dark environments, high-speed object motion scenes, and reflective environments. The research results have an important reference value for the intelligent application of vision sensors and the improvement of the accuracy of target detection algorithms.

2. Recent Related Work

After years of development, the types of sensors have become more and more diverse, and the target monitoring and recognition algorithms used by the sensors have attracted more attention. Sensors using traditional recognition algorithms have poor performance in monitoring and data transmission. The use of deep learning algorithms has achieved good results in the application of sensor target monitoring and target tracking and recognition. Therefore, in the field of sensor vision, deep-learning-related algorithms are widely used. Quaid and Jalal [11] have studied human behavior pattern recognition algorithms for wearable smart sensors. A new idea with a variant of the genetic algorithm was proposed, to solve the problem of complex feature selection and classification using sensor data. The proposed system is by the statistical dependence between the behavior and the corresponding signal data, which can maximize the possibility of obtaining the best feature value. Jalal et al. [12] used depth sensors to identify human interaction by the maximum entropy Markov model. Through extensive experiments, the average accuracy of the proposed feature extraction algorithm and cross-entropy optimization model reached 91.25%. Ma et al. [13] used support vector machines (SVM) to study human activity recognition. The experimental results verify the reliability of the proposed tensor-based feature representation model and the weighted support tensor machine algorithm for human activity recognition. Cheng-Bing and Xi-hao [14] proposed the use of a fuzzy C-means clustering algorithm (FCM) and adaptive neuro-fuzzy inference system (ANFIS) algorithm for array pattern recognition of the sensor. The calculation speed and convergence speed of the adaptive neuro-fuzzy inference system are greatly improved. Khomami and Shamekhi [15] used a sign language recognition sensor system to study

Persian sign language recognition. The research results show that the average recognition accuracy rate reaches 96.13%. This can provide satisfactory results for 20 gestures. There have been many studies on the application of sensors in the field of target monitoring and target tracking and recognition, but there are relatively few studies on the use of bionic smart sensors to construct DVS. Therefore, combining computer digital technology and DVS, DVS is constructed to carry out application research on target monitoring and tracking. This provides a certain reference for the digital and intelligent development of vision sensors.

3. Feature Tracking Algorithm by Optical Flow Detection

3.1. Dynamic Vision Sensing Demand Analysis. With the advancement of semiconductor technology, photoelectric imaging devices [16–18] have significantly improved their performance indicators and imaging quality in recent years. Compared with the existing photoelectric imaging device's working mode of fixed frequency exposure and frame-by-frame output of grayscale images, the DVS is an intelligent camera inspired by biology. It can capture the vitality of the scene, thereby reducing data redundancy and delay. In modern cities, the increase in population and vehicles puts tremendous pressure on road traffic. Intelligent sensor interaction technology is used to collect road vehicle information, and the data collection system is used to collect and forward the information to the user terminal. On this basis, the Internet of Things (IoT) is used to digitize all the information elements of the system vehicles, and the virtual intelligent road traffic service platform is reconstructed in the network space to form a situation of coexistence and virtual integration of the road system in the physical dimension and the digital traffic control center in the information dimension. Therefore, physical systems and digital systems coexist and merge in the information dimension. During vehicle detection and identification, the system can provide vehicle historical data query function. It will also display road traffic information and traffic flow in real time, query statistical historical status data, and the stability and scalability of data storage. After the data are collected by the DVS, the data need to be transmitted to the data storage center through the central node. The overall network structure is shown in Figure 1.

3.2. Target Tracking Algorithm Combining Event Stream and Grayscale Image. In DVS, the edge of a moving object generates an event. In a short period of time Δt , the increase in logarithmic brightness can be recorded as $\Delta L(u(t), t)$, which is calculated as

$$\Delta L(u(t), t) = L(u, t) - L(u, t - \Delta t), \quad (1)$$

where $L(u, t)$ represents the event flow function. Assuming that the brightness is a constant, deriving the equation (1) to obtain the following equation:

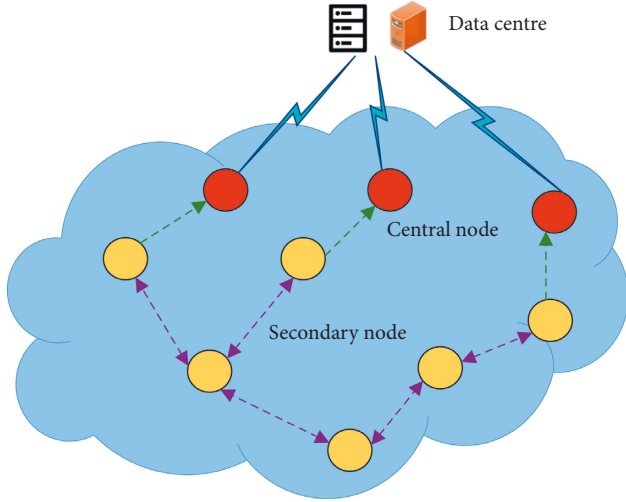


FIGURE 1: The architecture of DVS.

$$\frac{\partial L(u(t), t)}{\partial t} + \nabla L(u(t), t) \cdot \dot{u}(t) = 0. \quad (2)$$

Meanwhile, through Taylor Formula, the increment of logarithmic brightness can be expressed as the following equation:

$$\Delta L(u(t), t) \approx \frac{\partial L(u(t), t)}{\partial t} \Delta t. \quad (3)$$

By combining the above equations, $u(t)$ represents the speed, which can also be denoted as v . Solve by the way of obtaining the gradient of the grey image, the increment of the logarithmic brightness is shown in the following equation:

$$\Delta L(u(t), t) \approx -\nabla L(u(t), t) \cdot v \cdot \Delta t. \quad (4)$$

After calculating the brightness increment model, the target tracking algorithm is designed using the relationship between the event flow and the brightness increment calculated by the grayscale image. The overall process framework of the algorithm is shown in Figure 2.

In a period Δt , the events are integrated pixel by pixel to obtain the integral graph I_e . Let p_k be the number of events that need to be integrated in this period, and the generation principle of the integral graph is shown in the following equation:

$$I_e = \sum_{t_k \in \Delta t} p_k C \delta(u, u_k), \quad (5)$$

where $\delta(u, u_k)$ represents the Kronecker delta. According to the principle of DVS, in a short time Δt , the optical flow can be regarded as a constant v . The brightness increment value I_p produced by the optical flow in the time Δt calculated by the grey image is shown in the following equation:

$$I_p = -\nabla L(u(t), t) \cdot v \cdot \Delta t. \quad (6)$$

In the process of tracking the target feature points, in order to simplify the calculation, the translation transformation and rotation transformation of the target image will be mainly considered. The calculation matrix of the transformed image is written as w . The integral map is changed by affine to obtain the prediction map $I_p(u; w, v)$, and the calculation is shown in the following equation:

$$I_p(u; w, v) = -\nabla L(u, w)v(u)\Delta t. \quad (7)$$

3.3. Research on Event Flow Noise Reduction Method by Event Density. During the use of the sensor, the thermal noise of the reset switch transistor will generate background activity noise. Noise will have a certain impact on the stability of sensor data transmission [19]. The event flow information of the fixed scene is collected. After statistical analysis, the background activity noise can be calculated by the Poisson distribution, as shown in the following equation:

$$P\{N(t) = n\} = \frac{(\lambda t)^n}{n!} e^{-\lambda t}, \quad (8)$$

where n represents the number of background activity noise events, t represents the accumulation time of the events, λ represents the average value of noise events generated on average, and $P\{N(t) = n\}$ represents the probability of n noise events generated in the time period t . Through the analysis of the generation mechanism of noise and the temporal and spatial characteristics of the event stream, the event stream noise reduction method of event density is adopted. For newly arrived events, set the time neighbourhood to $\Omega_{\Delta t}^L$ and the spatial neighbourhood size to $L * L$, and accumulate the number of $L * L$ pixel output events within $\Omega_{\Delta t}^L$ to obtain the density matrix D . The calculation of matrix element $D_{i,j}$ is shown in the following equation:

$$D_{i,j} = \sum_{t=t_0-\Delta t}^{t_0} \gamma\left(x_0 - \frac{L-1}{2} - 1 + i, y_0 - \frac{L-1}{2} - 1 + j, t\right) 1 \leq i, j \leq L, \quad (9)$$

where (x_0, y_0, t) is the space coordinates of the newly arrived event, and $\gamma(x, y, t)$ is a binary function, calculated as shown in the following equation:

$$\gamma(x, y, t) = \begin{cases} 1 & \text{if there is an event } e(x, y, t), \\ 0 & \text{otherwise.} \end{cases} \quad (10)$$

In a fixed time interval T , the more the amount of background noise generated by a nonhot pixel, the lower the probability. In a fixed time and space, the amount of background activity noise will be less than a certain threshold, and the number of events generated by the real target will likely be greater than the threshold; that is, the equation (11) is satisfied.

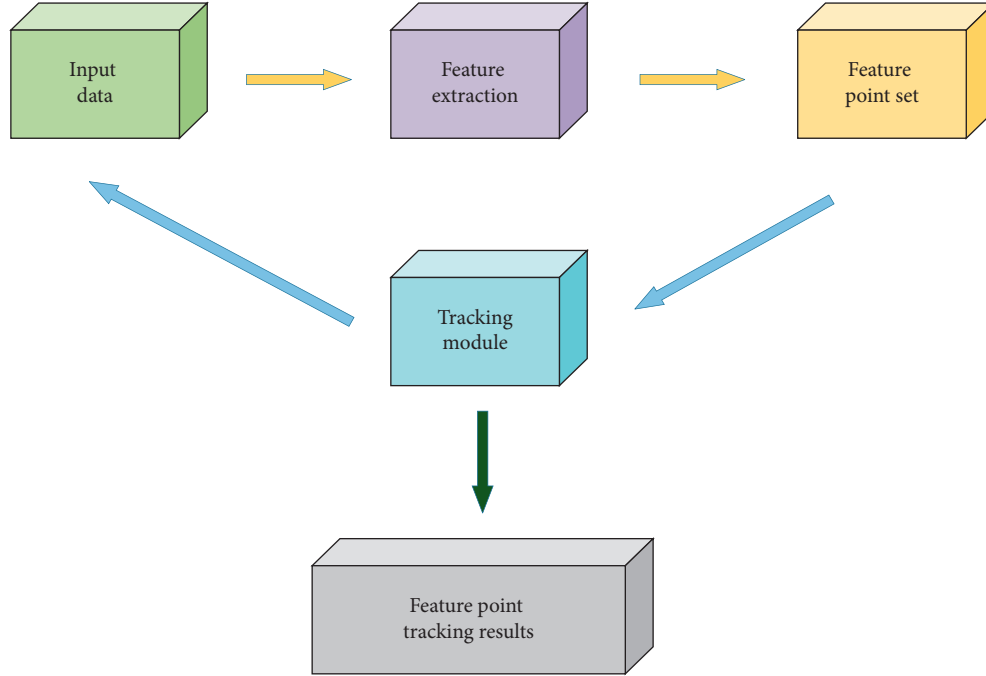


FIGURE 2: Framework diagram of target tracking algorithm flow.

$$\iiint_{x_i, y_i, t_i \in \Omega_{\Delta t}^L} \delta(x - x_i, y - y_i, t - t_i) dx dy dt \begin{cases} < \Psi \text{ if there are BASin } \Omega_{\Delta t}^L \\ \Psi \text{ if there are Objects in } \Omega_{\Delta t}^L \end{cases}, \quad (11)$$

where Ψ is the threshold of the number of events. The threshold is related to the threshold of the switch comparator of the DVS and the target size.

Since the hot pixel noise occurs at a high frequency at a fixed position, the result after the event density threshold filtering is further refined. After the filtering, the noise reduction effect of the event stream by the probability of the real event is evaluated, and the event stream evaluation result generated by the periodic movement of the target is used to determine whether the event is a real event or noise. The probability of a real event is calculated as shown in the following equation:

$$P(e_i) = \sum_j \frac{1}{\sigma \sqrt{2\pi}} e^{-\min|l_i - t_j - kL|/2\sigma^2}, \quad (12)$$

where L is the turntable period of the sensor motor, j represents the number of noise events and $0 < j < n$, n is the total number of events generated by the pixel. When the event is related to the degree of temporal and spatial correlation of other events, the probability that the event is a target can be quantified to produce a true event, as expressed by the following equation:

$$P_{RE}(e_0) = \sum_i \frac{1}{2\pi\sigma_1\sigma_2} e^{-(d_i/2\sigma_1^2 + \tau_i/2\sigma_2^2)}, \quad (13)$$

where $P_{RE}(e_0)$ represents the probability that the event e_0 is a true event. When this probability is greater than a certain threshold, the event is recognized as a true event. The determination of this threshold requires statistics on the area of noise events. The average true event probability of noise events is shown in the following equation:

$$P_{ARE} = \frac{\sum \sum_i 1/2\pi\sigma_1\sigma_2 e^{-(d_i/2\sigma_1^2 + \tau_i/2\sigma_2^2)}}{N}, \quad (14)$$

where P_{ARE} is the threshold for judging noise, N is the total number of statistical noise events, and σ_1, σ_2 are all constants. If the correlation degree of the event in the event stream is higher than P_{ARE} , the event is deemed to be a real event. Otherwise, the event is judged to be a noise event, and the noise reduction is performed to eliminate the event data [20].

3.4. Feature Tracking Algorithm of Optical Flow Detection. In high-speed motion scenes [21], reflective scenes [22], and dark environments [23], it is difficult for traditional visual sensors to achieve timely and effective tracking of feature points. The feature tracking algorithm by optical flow is used to realize the feature point extraction in the integral map by the event flow integral map. The optical flow constraint equation [24–26] uses the brightness change of the pixel

during the movement of the target to calculate the following equations:

$$I(x, y, t) = I(x + dx, y + dy, t + dt), \quad (15)$$

$$I(x + dx, y + dy, t + dt) = I(x, y, t) + \frac{\partial I}{\partial x} dx + \frac{\partial I}{\partial y} dy + \frac{\partial I}{\partial t} dt + \varepsilon, \quad (16)$$

where $I(x, y, t)$ represents the brightness of the pixel at the position s in the image at time t . $(x + dx, y + dy)$ represents the position of the pixel after the time interval of dt .

Assume that the speed of the target along the horizontal direction is $u = dx/dt$. The velocity along the vertical direction is $v = dy/dt$, and then, $\partial I/\partial x$ and $\partial I/\partial y$ represent the partial derivatives of the image in two directions. The optical flow constraint equation is shown in the following equation:

$$\frac{\partial I}{\partial x} \frac{dx}{dt} + \frac{\partial I}{\partial y} \frac{dy}{dt} + \frac{\partial I}{\partial t} \frac{dt}{dt} = 0. \quad (17)$$

Among the data collected by the sensor, the optical flow constraint equation of the image collected by the traditional sensor cannot be used for optical flow calculation. The constraint equation for the event flow requires the DVS to perform discrete data collection [27, 28]. In three-dimensional coordinates, the position transformation of the event stream over a period can be mapped to the coordinate change of the initial plane. The event mapping generated at the same point is the same. According to the time interval when the optical flow mapping is generated at different points, the detection of the position movement of the detection object can be realized. The flow chart of the feature tracking algorithm by the optical flow detection method is shown in Figure 3.

Additionally, an image window $B_s = \{u \in R^2 \mid \|u - f\| < s\}$ is established with the pixel point of the optical flow to be determined as the center. If the time of the initial plane is 0, the events in the space-time

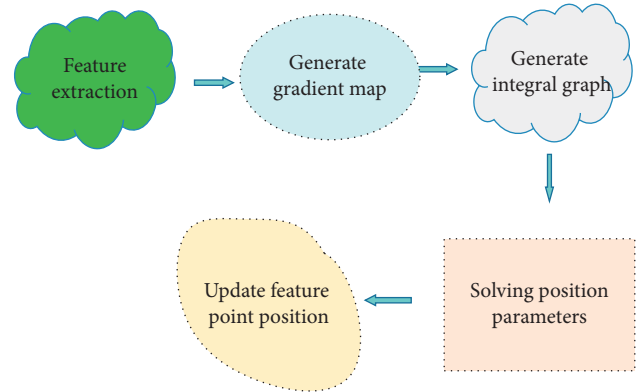


FIGURE 3: Flow chart of feature tracking algorithm by optical flow detection method.

window centered on the pixel can be regarded as a set. The optical flow in the window is a constant. For many events in the window, the probability model cannot be used to make simple judgments of the corresponding relationship between the events, and further connections between the data need to be established.

For any two events in the time-space window, there must be a relationship shown in the following equation:

$$\left(\sum_{j=1}^m r_{ij} r_{kj} \right) (u_i - t_i v) - (u_k - t_k v)^2 = 0. \quad (18)$$

Assuming there are n events in the window, the optical flow in the window is calculated as the following equation:

$$\min_v \sum_{i=1}^n \sum_{k=1}^n \left(\sum_{j=1}^m r_{ij} r_{kj} \right) (u_i - t_i v) - (u_k - t_k v)^2. \quad (19)$$

According to the principle of the least square method, the simplified optical flow calculation after the constant iterative solution is as shown in the following equation:

$$Y = (UD^T)(DD^T)^{-1} = \frac{\sum_{i=1}^n \sum_{k=1}^n w_{ik} (u_i - u_k) (t_i - t_k)}{\sum_{i=1}^n \sum_{k=1}^n w_{ik} (t_i - t_k)^2}, \quad (20)$$

$$Y = v^T D = \left[\sqrt{w_{12}} (t_1 - t_2), \dots, \sqrt{w_{1n}} (t_1 - t_n), \dots, \sqrt{w_{n(n-1)}} (t_n - t_{n-1}) \right],$$

$$\text{Among them, } U = \left[\sqrt{w_{12}} (u_1 - u_2), \dots, \sqrt{w_{1n}} (u_1 - u_n), \dots, \sqrt{w_{n(n-1)}} (u_n - u_{n-1}) \right], \quad (21)$$

$$w_{ik} = \sum_{j=1}^m r_{ij} r_{kj}.$$

4. Results and Discussion

4.1. The Target Tracking Result of Event Stream Combined with Grey Image. When the optical flow tracking algorithm is used to track and recognize the target, the sensor should first accurately detect the feature points according to the

event flow and collect effective object information from the grayscale images in different environments. The target tracking detection results are shown in Figure 4.

The DVS is used to track and detect the target object. The result of tracking and detecting the target object in a high-speed motion scene is shown in Figure 4(a). Figure 4(b)

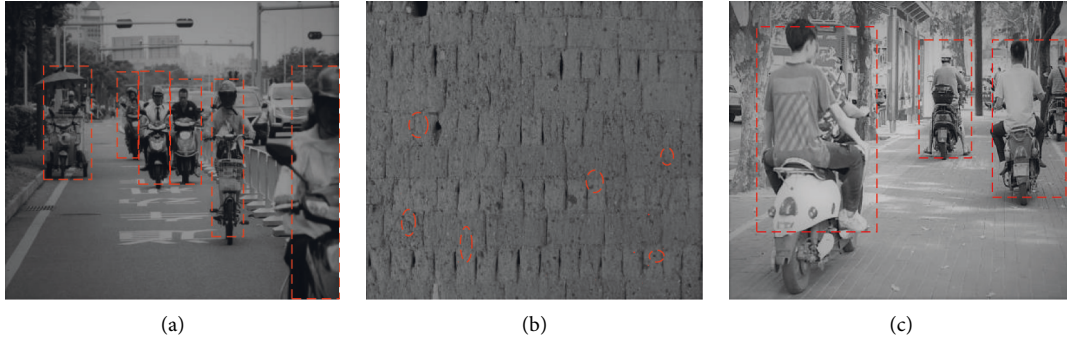


FIGURE 4: Grayscale image of target tracking detection results. (a) Target object tracking and detection in high-speed motion scenes. (b) Static object tracking and detection in dark environments. (c) Static object tracking and detection in reflective environments.

shows the result of static object detection in a dark environment. Large black areas in the grayscale image cannot be detected and identified by the event stream. Figure 4(c) shows the result of tracking and detecting static objects in a reflective environment. The optical flow detection algorithm can effectively extract the feature points of dynamic objects and can be accurately identified even in a dark environment.

4.2. Data Processing Results of Event Stream Noise Reduction Method. The data results after noise reduction processing using the event stream method are evaluated, and the original event stream is time-sliced. Each time slice is 10 ms in length and is divided into 286 time slices in total. The average true rate P_{ARE} is calculated from the number of noise events, as shown in Figure 5. Additionally, the number of noise events in the real events (NIR) and the number of real events in the filtered events (NIF) are evaluated with two parameter values, as shown in Figures 6 and 7.

From the average true rate change curve of the results of each event stream slice in Figure 5, although the average true rate of each segment fluctuates, the average true rate of each event, in general, is basically maintained at about 1.2. This shows that the event stream slices the authenticity and reliability of the method.

Figures 6 and 7 show that the event density-based method and the background activity filter processing method are used. The average NIF values of these two methods are 171.355 and 158.222, respectively. The noise reduction method by event density is more effective than the background activity filtering method. Because the event density method is by the event density to make judgments, the accuracy rate is higher.

Additionally, the spatiotemporal filter is used to process the experimental data collected by the sensor. The sampling factors of the spatiotemporal filter are, respectively, set to 2, 4, and 6. The experimental data processing results are shown in Figures 8–10.

Figures 8–10 show that the sampling factor settings of the spatiotemporal filter are different, and the NIR and NIF values of the processed data will have large differences. There are higher NIF values under different sampling factors. This is since the time is stored in different groups due to different sampling. When the sampling factor is 2, the maximum NIR

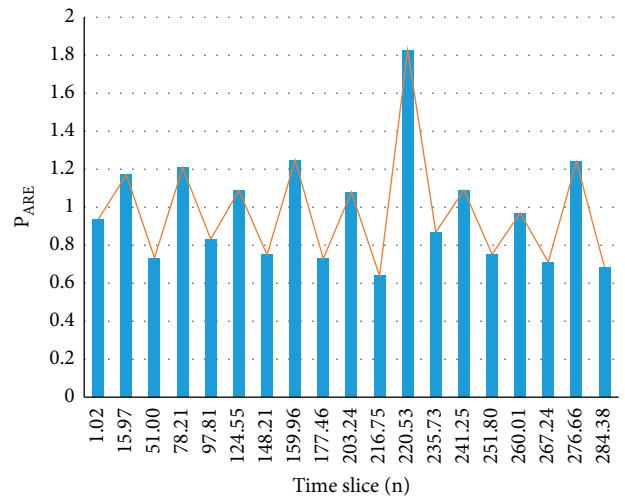


FIGURE 5: The average true rate change curve of each event stream slice.

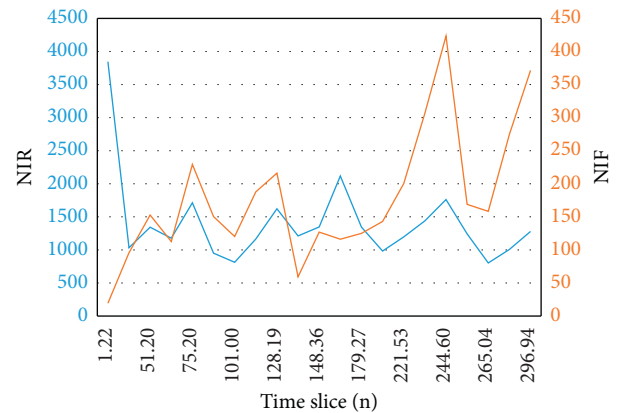


FIGURE 6: The value of NIR and NIF in each time slice after event density noise reduction processing.

value after filtering can reach above 8000, and the maximum NIF value is about 1200. As the sampling factor increases, both the NIR value and the NIF value will decrease. When the sampling factor is 6, the highest value of NIR value can only reach about 2500, and the highest value of NIF value can only reach about 500. At the peak of NIR and the trough

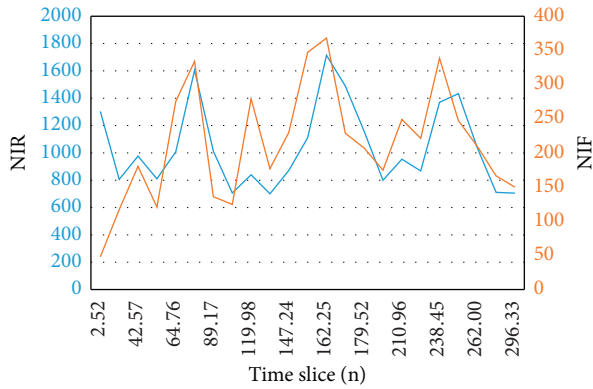


FIGURE 7: After background activity filtering, the values of NIR and NIF in each time slice.

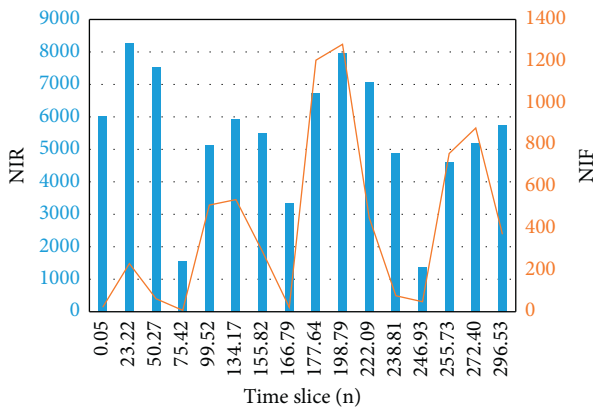


FIGURE 8: The values of NIR and NIF in each time slice after processing by the spatiotemporal filter with a sampling factor of 2.

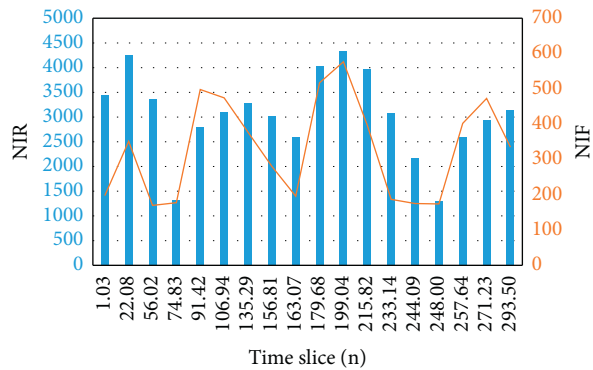


FIGURE 9: The values of NIR and NIF in each time slice after processing by the spatiotemporal filter with a sampling factor of 4.

of NIF, the number of real events will decrease due to the increase in noise. This is because the latest events are judged. The number of support events is insufficient.

4.3. Performance Analysis Results of Optical Flow Detection and Feature Tracking Algorithms. In order to verify the performance advantages of the optical flow detection method compared with the traditional algorithm, the optical

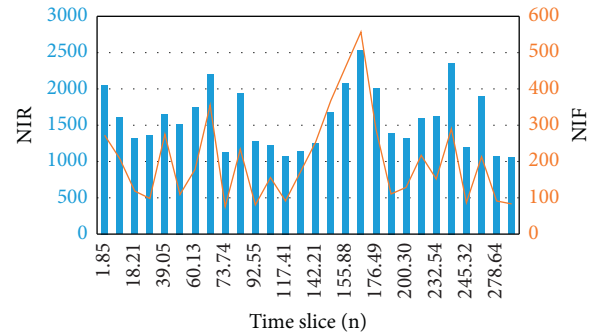


FIGURE 10: The values of NIR and NIF in each time slice after processing by the spatiotemporal filter with a sampling factor of 6.

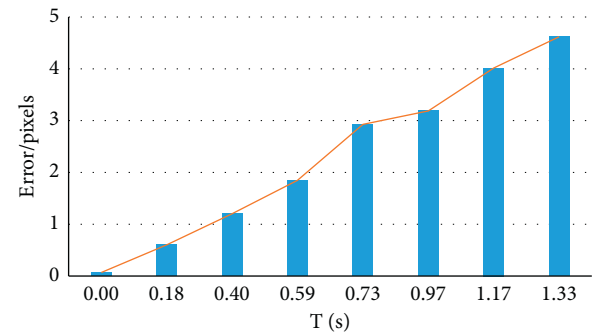


FIGURE 11: Target feature tracking in a dark environment.

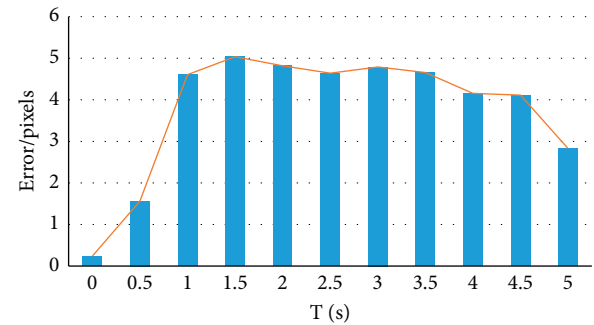


FIGURE 12: Target tracking and recognition under high-speed object motion scenes.

flow detection method is used to track and detect the target object in the dark environment, the high-speed motion scene of the object, and the reflective environment. The average error result of the detection and tracking is shown in Figures 11–13:

Figures 11–13 show that the average error of target object detection and tracking in a dark environment is 3.2 pixels. The average error of object tracking in high-speed motion scenes is 4.86 pixels. The average error of target tracking in a reflective environment is 2.88 pixels. Experimental description: the proposed optical flow detection method is applied to the tracking and detection of target objects, which can effectively extract the feature points of the image and can achieve good tracking and detection effects even in a dark environment.

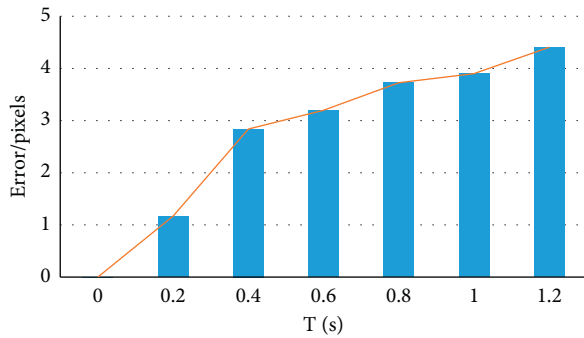


FIGURE 13: Tracking and detection of target objects in a reflective environment.

5. Conclusion

The accuracy and speed with which sensors are used to detect target objects are gradually improving. However, the detection effect of traditional sensors is not good in high-speed motion scenes, reflective scenes, and dark environments. Firstly, through DVS technology, the computer digitization technology is used to study and improve sensor target detection and recognition algorithms. Subsequently, event flow target detection algorithms and optical flow target tracking algorithms are proposed. The proposal of these algorithms has an important reference value for the intelligent application of vision sensors. However, some disadvantages are unavoidable. Firstly, the target detection algorithm based on event flow can build a deeper detection network to further improve the detection accuracy. Secondly, if a sensor device with higher precision is added, the accuracy of the experimental data obtained will be higher. In the future, more real-world event datasets can be added. The addition of these datasets will make object detection and validation more general.

Data Availability

The data used to support the findings of this study are included within the article.

Conflicts of Interest

The authors declare that they have no conflicts of interest.

Acknowledgments

This work was supported by the research on the Training Model of Computer Professionals in Higher Vocational Colleges under the certificate system of “1 + X” (project no. 2020XH223).

References

- [1] C. Zhan, Y. Zeng, and R. Zhang, “Energy-efficient data collection in UAV enabled wireless sensor network,” *IEEE Wireless Communications Letters*, vol. 7, no. 3, pp. 328–331, 2018.
- [2] A. D. Salman, O. I. Khalaf, and G. M. Abdulsahab, “An adaptive intelligent alarm system for wireless sensor network,” *Indonesian Journal of Electrical Engineering and Computer Science*, vol. 15, no. 1, pp. 142–147, 2019.
- [3] S. Otoum, B. Kantarci, and H. T. Mouftah, “On the feasibility of deep learning in sensor network intrusion detection,” *IEEE Networking Letters*, vol. 1, no. 2, pp. 68–71, 2019.
- [4] E. Stromatias, M. Soto, T. Serrano-Gotarredona, and B. Linares-Barranco, “An event-driven classifier for spiking neural networks fed with synthetic or dynamic vision sensor data,” *Frontiers in Neuroscience*, vol. 11, p. 350, 2017.
- [5] Z. Liu, E. Ren, F. Qiao et al., “NS-CIM: a current-mode computation-in-memory architecture enabling near-sensor processing for intelligent IoT vision nodes,” *IEEE Transactions on Circuits and Systems I: Regular Papers*, vol. 67, no. 9, pp. 2909–2922, 2020.
- [6] P. Bhowmik, M. J. H. Pantho, and C. Bobda, “HARP: hierarchical attention oriented region-based processing for high-performance computation in vision sensor,” *Sensors*, vol. 21, no. 5, p. 1757, 2021.
- [7] Y. Berezovskaya, C. W. Yang, A. Mousavi, V. Vyatkin, and T. B. Minde, “Modular model of a data centre as a tool for improving its energy efficiency,” *IEEE Access*, vol. 8, pp. 46559–46573, 2020.
- [8] S. Ali, R. P. Singh, M. Javaid et al., “A review of the role of smart wireless medical sensor network in COVID-19,” *Journal of Industrial Integration and Management*, vol. 05, no. 04, pp. 413–425, 2020.
- [9] O. I. Khalaf, G. M. Abdulsahab, and B. M. Sabbar, “Optimization of wireless sensor network coverage using the Bee Algorithm,” *Journal of Information Science and Engineering*, vol. 36, no. 2, pp. 377–386, 2020.
- [10] D. Li, R. Wang, C. Xie et al., “A recognition method for rice plant diseases and pests video detection based on deep convolutional neural network,” *Sensors*, vol. 20, no. 3, p. 578, 2020.
- [11] M. A. K. Quaid and A. Jalal, “Wearable sensors based human behavioral pattern recognition using statistical features and reweighted genetic algorithm,” *Multimedia Tools and Applications*, vol. 79, no. 9–10, pp. 6061–6083, 2020.
- [12] A. Jalal, N. Khalid, and K. Kim, “Automatic recognition of human interaction via hybrid descriptors and maximum entropy Markov model using depth sensors,” *Entropy*, vol. 22, no. 8, p. 817, 2020.
- [13] N. Ahmed, J. I. Rafiq, and M. R. Islam, “Enhanced human activity recognition based on smartphone sensor data using hybrid feature selection model,” *Sensors*, vol. 20, no. 1, p. 317, 2020.
- [14] L. Cheng-Bing and M. Xi-hao, “Array sensors online pattern recognition based on FCM and ANFIS,” *International Journal of Computers and Applications*, vol. 43, no. 4, pp. 352–359, 2021.
- [15] S. A. Khomami and S. Shamekhi, “Persian sign language recognition using IMU and surface EMG sensors,” *Measurement*, vol. 168, Article ID 108471, 2021.
- [16] A. Bercegol, G. El-Hajje, D. Ory, and L. Lombez, “Determination of transport properties in optoelectronic devices by time-resolved fluorescence imaging,” *Journal of Applied Physics*, vol. 122, no. 20, Article ID 203102, 2017.
- [17] C. Choi, M. K. Choi, S. Liu et al., “Human eye-inspired soft optoelectronic device using high-density MoS₂-graphene curved image sensor array,” *Nature Communications*, vol. 8, no. 1, pp. 1664–1711, 2017.

- [18] J. Xu and M. Shalom, "Conjugated carbon nitride as an emerging luminescent material: quantum dots, thin films and their applications in imaging, sensing, optoelectronic devices and photoelectrochemistry," *ChemPhotoChem*, vol. 3, no. 4, pp. 170–179, 2019.
- [19] I. Kwon, "Self-reset switching preamplifier for improvement of counting rate," *Journal of Radiation Industry*, vol. 14, no. 1, pp. 9–12, 2020.
- [20] R. I. Alfian, A. Ma'arif, and S. Sunardi, "Noise reduction in the accelerometer and gyroscope sensor with the kalman filter algorithm," *Journal of Robotics and Control (JRC)*, vol. 2, no. 3, pp. 180–189, 2021.
- [21] H. Akolkar, S. H. Ieng, and R. Benosman, "Real-time High Speed Motion Prediction Using Fast Aperture-Robust Event-Driven Visual Flow," *IEEE Transactions on Pattern Analysis and Machine Intelligence*, vol. 44, 2020.
- [22] S. A. U. Hasan, H. Lee, G. Lee, and S. Lee, "Photorealistic ray-traced visualization of manufacturing tolerances of freeform vehicle side mirror," *Current Optics and Photonics*, vol. 4, no. 6, pp. 516–523, 2020.
- [23] A. Al-Naji, K. Gibson, S. H. Lee, and J. Chahl, "Real time apnoea monitoring of children using the Microsoft Kinect sensor: a pilot study," *Sensors*, vol. 17, no. 2, p. 286, 2017.
- [24] Z. Huang and A. Pan, "Non-local weighted regularization for optical flow estimation," *Optik*, vol. 208, Article ID 164069, 2020.
- [25] R. Shi, X. Leng, and H. Chanson, "On optical flow techniques applied to breaking surges," *Flow Measurement and Instrumentation*, vol. 72, Article ID 101710, 2020.
- [26] J. Zhou, W. Yang, Y. Yin et al., "Improved two-color LIF thermometry for gas-liquid system by optical flow algorithm," *Experiments in Fluids*, vol. 62, no. 6, pp. 125–212, 2021.
- [27] G. Deng, Z. Zhou, S. Shao, X. Chu, and C. Jian, "A novel dense full-field displacement monitoring method based on image sequences and optical flow algorithm," *Applied Sciences*, vol. 10, no. 6, p. 2118, 2020.
- [28] D. Gorjup, J. Slavič, A. Babnik, and M. Boltezar, "Still-camera multiview spectral optical flow imaging for 3D operating-deflection-shape identification," *Mechanical Systems and Signal Processing*, vol. 152, p. 107456, 2021.

Research Article

Improvement of English Teaching Process Management Based on Intelligent Data Sampling

Jin Cheng 

School of Foreign Languages, Luoyang Normal University, Luoyang 471934, China

Correspondence should be addressed to Jin Cheng; jincheng@lynu.edu.cn

Received 14 March 2022; Revised 18 April 2022; Accepted 27 April 2022; Published 24 May 2022

Academic Editor: Wei Liu

Copyright © 2022 Jin Cheng. This is an open access article distributed under the Creative Commons Attribution License, which permits unrestricted use, distribution, and reproduction in any medium, provided the original work is properly cited.

In order to improve the management effect of English teaching process, this paper combines intelligent data to use technology to improve the management of English teaching process, improve the effect of English teaching, and construct an intelligent English teaching process management system. Moreover, this paper considers the interpolation problem of time series data in the metric space defined by dynamic time warping, and proposes an oversampling method for unbalanced time series data. In addition, this paper chooses to classify the Gaussian process model that is sensitive to unbalanced time series data to test the effect of the model. The experimental research results show that the English teaching process management system based on intelligent data sampling proposed in this paper can play an important role in English teaching management and can effectively improve the efficiency of English teaching.

1. Introduction

Inquiry-based English teaching is an important achievement in the development and reform of modern western science education and is known as a new milestone in the innovation and development of modern science education. With the development of science, people's accumulation of knowledge continues to increase, and the contradiction between tradition and innovation has become increasingly prominent in the process of moving towards the Frontier of knowledge. In particular, the traditional English teaching, which is mainly based on knowledge transfer in educational English teaching, has to focus on the teacher in order to pursue the coherence, system, and integrity of knowledge. In this way, it is easy to evolve into a cramming education, and it is difficult to improve the subjectivity and innovation ability of students.

The new curriculum encourages students to experience the methods and processes of scientific inquiry. At the same time, in order to effectively construct the chemical inquiry classroom and improve the quality of chemical inquiry English teaching, we should also pay attention to improving the effectiveness of the implementation of chemical inquiry English teaching [1]. The effectiveness of the current inquiry-

based English teaching needs to be improved, and there are many obstacles, which should be improved from many aspects. Through the investigation and analysis of the current influence of various obstacles, suggestions for improvement can be put forward. At the same time, by combining the design of inquiry-based English teaching cases and the implementation of improvement strategies, the effectiveness of inquiry-based English teaching can be effectively improved [2]. In addition, with the development of information technology and the popularization of Internet, the development of online office management has become more and more rapid, and more and more people are adapting to this type of office mode. The standardized and scientific management system design is not only conducive to the improvement of office efficiency, but also brings about the emergence of a more scientific and fair management model. For school management, the most important thing is to improve the quality of English teaching in schools, so designing a complete and scientific management system for the English teaching process plays a pivotal role in improving the quality of English teaching [3].

English teaching process management is the management of the entire English teaching process, including the

management and maintenance of the course, the supervision and management of the English teaching process, the evaluation and management of English teaching, and other complete course management systems. With the development of ELearning (e-learning), the teaching and learning of teachers and students on the network platform has become more adaptable to the interaction between teachers and students, and it also reduces the burden on the management of educational administrators. At the same time, the sharing of English teaching resources for teachers, the creation of course forums, and the design of students' communication environment have become more prominent; online examinations, online Q&A, online attendance, etc., can be incorporated into the English teaching process with the development of network learning. In the management system, the improvement of teachers' English teaching ability requirements is also accompanied by comprehensive evaluation of teachers in various aspects such as breadth and depth, and the realization of a complete English teaching evaluation system can also better reflect the advantages of informatization development. The systematic and scientific statistical analysis and evaluation results can also play a great role in various aspects such as teachers' English teaching level and teachers' English teaching ability. Therefore, based on the existing design and implementation and the existing technical support, the design of a complete English teaching process management system can promote the development of informatization, improve the educational administration management system, and improve the scientific nature of educational administration management.

This paper combines intelligent data and technology to improve the English teaching process management, improve the English teaching effect, and construct an intelligent English teaching process management system, which provides a reference for the further improvement of the quality of English teaching in the future.

2. Related Work

Teaching quality monitoring is a process of purposefully monitoring, evaluating, and applying effectiveness to the teaching quality system in order to achieve the intended purpose of teaching quality [4]. Teaching quality monitoring is a management process of detecting, measuring, judging, and improving the deviation of predetermined teaching quality goals in the process of teaching quality management and teaching implementation to ensure the effectiveness of teaching goals. The formulation of professional training objectives is usually based on [5]. Teaching quality monitoring is to ensure that the quality of personnel training can achieve the predetermined goals and that school leaders and teaching quality management departments can timely regulate teaching work, correct deviations, coordinate relationships and fully stimulate the full potential of all aspects [6]. Teaching quality monitoring is a process of monitoring and regulating the teaching process according to the expected quality standards in order to meet the needs of

customers and ensure that all the teaching process and the quality of student training can achieve the predetermined purpose and develop continuously [7]. Reference [8] defines teaching quality monitoring as follows: The teaching quality monitoring system in colleges and universities refers to a series of teaching quality management work systems and monitoring operation mechanisms that are used to ensure the teaching quality in the teaching operation process of colleges and universities. The monitoring organization uses certain methods and means to carry out detailed planning, inspection, evaluation, feedback, and adjustment of various influencing factors of teaching quality and each link of the teaching process, so as to improve the quality of teaching and personnel training. Teaching quality monitoring can be divided into two monitoring forms: external quality monitoring and internal quality monitoring according to the monitoring subject and scope. The practical activities or management behaviors that the organization or department outside the school (usually refers to the education administrative department, social group, etc.) supervises and evaluates the teaching quality of the school as a whole is the external monitoring of the teaching quality [8]. The monitoring and control practice activities or management behaviors carried out by the school's teaching quality management department and teachers and students on teaching quality are called internal monitoring of teaching quality [9]. Teaching quality monitoring is an important means and link of teaching quality management in colleges and universities.

The teaching quality monitoring system refers to the use of corresponding methods and means by colleges and universities to ensure and improve their own teaching quality and to achieve the expected teaching quality goals under the guidance of scientific teaching concepts [10]. A stable and effective quality management mechanism and system is established by effective monitoring and regulation to ensure and improve teaching quality [11]. The teaching quality monitoring system is mainly composed of six elements: subject, object, purpose, standard, method, and system of teaching quality monitoring [12]. The links of teaching quality monitoring mainly include the following: establishing quality standards for teaching links, monitoring information on teaching process, sorting and analysis of relevant data, evaluation, feedback information, and regulation and rectification. Through the effective operation of the teaching quality monitoring system, various information can be fed back in a timely and accurate manner, and the problems and causes that deviate from the predetermined goals in the process of teaching and teaching management can be analyzed by sorting out various information the goal of [13].

In the existing educational administration system, there is no detailed design and implementation of the management of the entire teaching process in terms of architecture, course notifications, online exams, online Q&A, etc., designed for teaching tasks, and at the same time, there is no management record of each link in the teaching process. It

can achieve real-time and scientific teaching evaluation feedback for teachers and does not involve objective records in the teaching process and complete systematic analysis of student-teacher evaluation results [14]. Similarly, each university has its own teaching process management in its own educational administration system, but it is designed for the different teaching characteristics and school-running styles of each school. Most of the systems have evaluation systems that are not perfect and have no systematic details. Design and statistical analysis are not scientific enough to apply to the university's established process management normative requirements. Therefore, proposing a feasible teaching process management scheme can play a huge role in the educational administration system [15].

3. Smart Data Sampling

In this paper, the interpolation problem of time series data is considered in the metric space defined by dynamic time wrapping (DTW). It proposes an oversampling method for unbalanced time series data and selects a Gaussian process model sensitive to unbalanced time series data for classification to test the effect of the model.

DTW uses the time warping function that satisfies the boundary, continuity, and monotonicity conditions, calculates the minimum distance between two sequences, and solves the time warping function corresponding to the minimum distance.

We are given two sequences $A = (a_1, a_2, \dots, a_i, \dots, a_m)$ and $B = (b_1, b_2, \dots, b_j, \dots, b_n)$, and we first define the dynamic warping path as [16]

$$W = (w_1, w_2, \dots, w_K), \max(m, n) \leq K \leq m + n - 1. \quad (1)$$

Among them, w_k corresponds to the synchronization point $(i, j)_k$ ($k = 1, 2, \dots, K$), i represents the index of the element on the sequence A, j represents the index of the element on the sequence B, and the indexes of all the elements of the sequences A and B must appear on the regular path, and $w_1 = (1, 1)$, $w_K = (m, n)$. If it is known that the path has passed the synchronization point (i, j) , the next synchronization point to pass through is only $(i + 1, j)$, $(i, j + 1)$, $(i + 1, j + 1)$, and the number of paths that satisfies the condition is exponential, the goal of dynamic time warping is to find the path that minimizes the cost of warping, and the mathematical expression is

$$\text{DTW}(A, B) = \min_W \sum_{k=1}^K d(w_k). \quad (2)$$

The minimum cost path can be calculated by accumulating distance, and the accumulative distance is defined as [17]

$$\gamma(i, j) = d(i, j) + \min\{\gamma(i - 1, j - 1), \gamma(i - 1, j), \gamma(i, j - 1)\}. \quad (3)$$

Among them, $d(i, j)$ is the distance between a_i and b_j . Different distance calculation methods can be used for distance, such as Euclidean distance and Manhattan distance. The most commonly used Euclidean distance is used

in this paper. In order to find a regular path that satisfies the minimum cumulative distance, the cumulative distance corresponding to this path is the DTW distance of the two sequences.

Figure 1 shows the cost matrices of the two sequences and the path with the least normalized cost. DTW needs to calculate the value of each element in the cost matrix, and then search for the path with the least regular cost. The regular path in the figure is $W = \{(1,1), (2,2), (3,3), (3,4), (3,5), (4,5), (5,6), (6,7), (7,7), (7,8), (8,8)\}$, there are vertical lines and horizontal lines on the path, that is, there are vertical lines and horizontal lines on the path; that is, there are one-to-many and many-to-one, which originate from the stretch and offset of the sequence on the time axis.

Figure 2 is a schematic diagram of the two sequences. Sequence A and sequence B have position offset and scale scaling. Using DTW calculation, it is concluded that the distance between the two is extremely small and the similarity is high.

DTW can effectively measure the similarity between time series data. The time and space complexity is $O(N^2)$, and it is usually used on small-scale time series datasets. Because of the high time and space complexity, it reduces the computational efficiency when applied to large-scale datasets.

FastDTW combines two methods of restriction and data abstraction to speed up the calculation of DTW (as shown in Figure 3), while avoiding the shortcomings of both methods. The specific algorithm is as follows:

- ① Coarse-grained: the algorithm abstracts the original time series data to obtain a coarse-grained dataset. Each coarse-grained data point represents multiple fine-grained data points (each coarse-grained data point can be an average of multiple fine-grained data points). The coarse-grained process can be performed iteratively multiple times, sequentially from $1/2^k \rightarrow 1/2^{k-1} \rightarrow \dots \rightarrow 1/2 \rightarrow 1/1$.
- ② Projection: the algorithm uses the standard DTW algorithm to calculate the regular path on the coarse-grained dataset after data abstraction.
- ③ Fine-grained: the algorithm adjusts the regular path obtained on the coarse-grained dataset in step ② to a finer-grained space through local adjustment. That is, on the neighbor cost matrix unit of the regular path in the coarse-grained space, the optimal path of the finer-grained space is found, and the size of the neighbor can be adjusted by the radius (similar to the window width of the restriction method) parameter.

In this paper, FastDTW is used to calculate the DTW distance and regular path, and the efficiency of this method is improved under the condition of ensuring the accuracy.

This paper considers the characteristics of time series data, draws on the interpolation idea and the adaptive advantage, and proposes an unbalanced time series data processing method based on DTW. For the convenience of description, the oversampling method proposed in this paper is abbreviated as SDTW, that is, sampler with dynamic time warping.

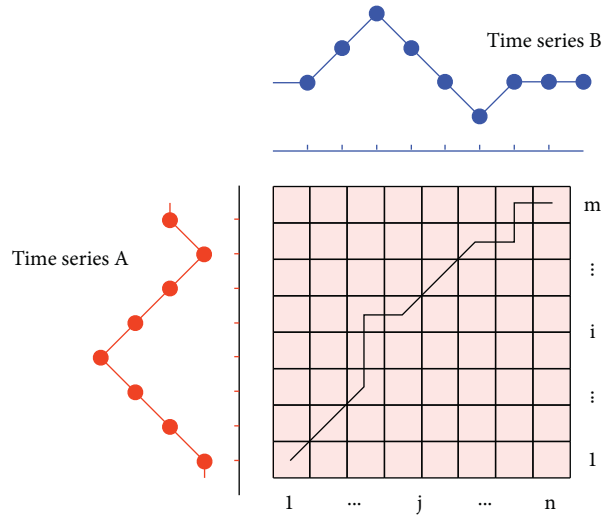


FIGURE 1: Schematic diagram of cost matrix and minimum cost path.

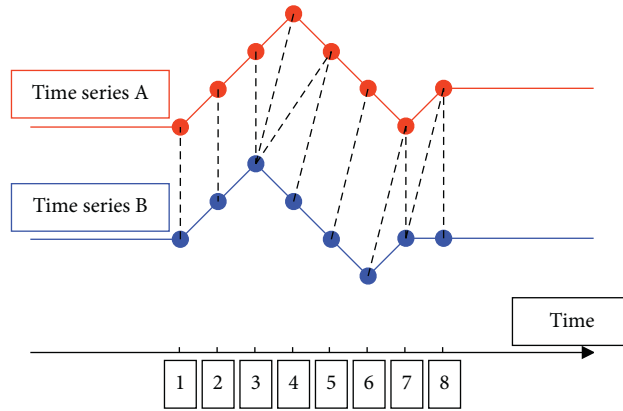


FIGURE 2: Schematic diagram of the regularity of the two sequences.

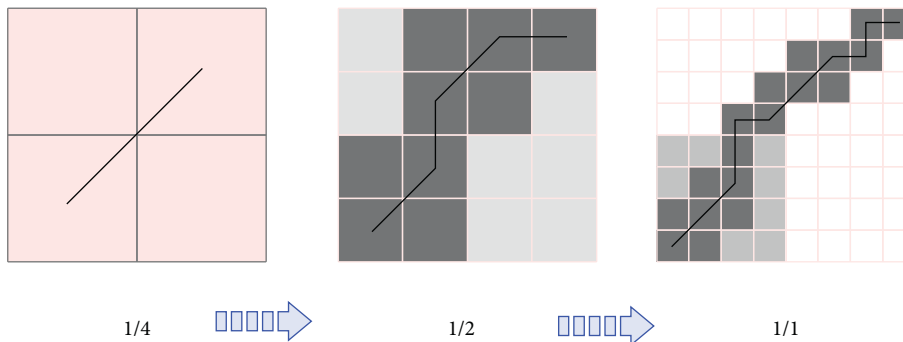


FIGURE 3: Schematic diagram of FastDTW algorithm.

① First, the total number of minority class samples to be generated is determined as follows [18]:

$$G = (N_- - N_+) \times a. \tag{4}$$

Among them, N_+ and N_- represent the number of minority class and majority class samples in the

original data, respectively, and $\alpha (0 < \alpha \leq 1)$ is the adjustment degree, which is usually taken as 1.

② For each minority class sample x_{i+} , the DTW distance and regular path between it and other samples are calculated. According to the DTW distance ordering, the k nearest neighbors of the sample are

found. Then, we calculate the ratio using the following formula:

$$r_i = \frac{k_{i+}}{k}, \quad (5)$$

$$i = 1, 2, \dots, N_+.$$

Among them, k_{i+} is the number of samples belonging to the minority class among the k nearest neighbor samples.

- ③ The threshold $\theta (0 < \theta \leq 1)$ is set. The ratio r_i is divided into two numerical sets according to the threshold, corresponding to two different regions of the sample set: the noise set $\chi_{\text{noise}} (r_i \in [0, \theta))$ and the safe set $\chi_{\text{safe}} (r_i \in [\theta, 1])$. Considering that the noise set contains wrong sensitive information, it is not conducive to the learning process of the model. Therefore, the minority class samples belonging to the noise set do not participate in the artificial sample synthesis process.
- ④ The ratio distribution of the samples of the normalized security set χ_{safe} is obtained \hat{r}_i . Considering that the sample is over-ignored because the ratio is too small, the exponential function is used for smoothing correction:

$$\hat{r}_i = \frac{\exp(r_i)}{\sum_{l=1}^{N_+} \left[1_{\{x_l \in \chi_{\text{safe}}\}} \cdot \exp(r_l) \right]}, \quad (6)$$

$$\sum_i \hat{r}_i = 1.$$

Among them, 1_A is an indicative function. If A is true, the indicator function takes the value 1, otherwise, it is 0.

- ⑤ The number of sampling samples is determined: for each minority class sample x_{i+} in the security set, the number of sampling samples is

$$g_i = \lceil G \cdot \hat{r}_i \rceil. \quad (7)$$

Among them, $\lceil \cdot \rceil$ means round up. It is worth noting that if the total number of samples obtained by sampling exceeds the set number of samples G , the method of simple random sampling is used to eliminate the excess samples sampled.

- ⑥ The sampling process is as follows: for each minority class sample x_{i+} in the safe set, a minority class sample x_k among its k nearest neighbor samples is randomly selected. We assume that the dynamic time warping path of sample sequences x_{i+} and x_k is (w_1, w_2, \dots, w_L) . Among them, the synchronization point $w_l = (w_{il}, w_{kl})$, $l = 1, 2, \dots, L$, $n \leq L \leq 2n - 1$, n is the sample sequence length (because the lengths of time series data samples in the UCR dataset used in this paper are all the same, for the convenience of understanding, it is assumed that the time series

samples used are of equal length, and the case where the sample sequences are not of equal length is similar, that is, $\max(m, n) \leq L \leq m + n - 1$). The specific steps (as shown in Figure 4) are as follows:

Step 1: counting between synchronization points of the regularized path, new sample points are generated. However, due to the existence of one-to-one, one-to-many, and many-to-one situations in the regular path, when calculating the sample value of the sampling point, it is necessary to perform the same interpolation operation on the sampling time point for subsequent adjustment, that is,

$$x_P = x_{W_i} + \lambda_0 (x_{W_k} - x_{W_i}), \quad (8)$$

$$P = W_i + \lambda_0 (W_k - W_i).$$

Among them, x_P is the new sample sequence $x_P = (x_{p_1}, x_{p_2}, \dots, x_{p_L})$ obtained by path interpolation, P is the sampling time point corresponding to the new sample sequence $P = (P_1, P_2, \dots, P_L)$, λ_0 is a random number ($0, \lambda \leq 1$) between $(0, \lambda)$, and $x_{w_i} = (x_{w_{i1}}, x_{w_{i2}}, \dots, x_{w_{iL}})$ and $x_{w_k} = (x_{w_{k1}}, x_{w_{k2}}, \dots, x_{w_{kL}})$ are the sample value sequences of the minority class sample x_{i+} corresponding to the synchronization point on the DTW path and its nearest neighbor minority class sample x_k , respectively. $W_i = (w_{i1}, w_{i2}, \dots, w_{iL})$ and $W_k = (w_{k1}, w_{k2}, \dots, w_{kL})$ are the sequences composed of the points of the minority class samples x_{i+} and x_k corresponding to the synchronization points on the DTW path, respectively.

Step 2: the sampling time point is adjusted. Due to the existence of one-to-one, one-to-many, and many-to-one situations in the regular path, this may lead to the situation that the sampling interval of the interpolation sample points is unequal and inconsistent with the sampling interval of the original sequence. Therefore, the sampling time point $P = (p_1, p_2, \dots, p_L)$ of the new sample sequence needs to be adjusted to be consistent with the sampling time point $T = (t_1, t_2, \dots, t_n)$ of the original data, and the adjusted sample value sequence $x_{a dj} = (x_{t_1}, x_{t_2}, \dots, x_{t_n})$ is given. For each $t_j \in T$, then we have the following:

- (1) If there is $p_l \in P$ such that $p_l = t_j$, then the sample value corresponding to t_j is

$$x_{t_j} = x_{p_l}. \quad (9)$$

Among them, $x_{p_l} \in x_P$.

- (2) If there is no $p_l \in P$ such that $p_l = t_j$, then $\underline{p} = \max\{p_l: p_l < t_j\}$ and $\bar{p} = \min\{p_l: p_l > t_j\}$ are solved first, that is, $\underline{p} < t_j < \bar{p}$. In this paper, the linear interpolation method is used (other interpolation methods such as square interpolation and cubic interpolation can also be used, but the

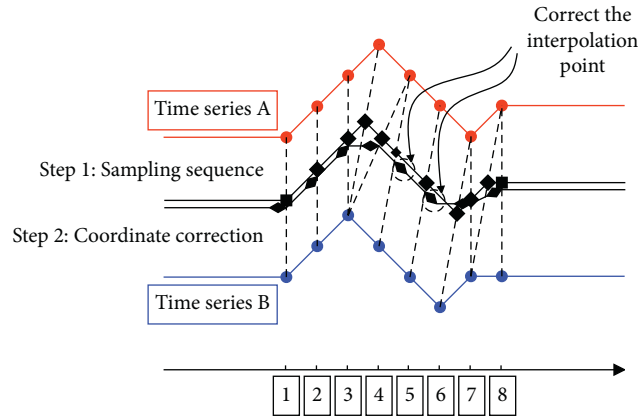


FIGURE 4: Schematic diagram of sample generation process.

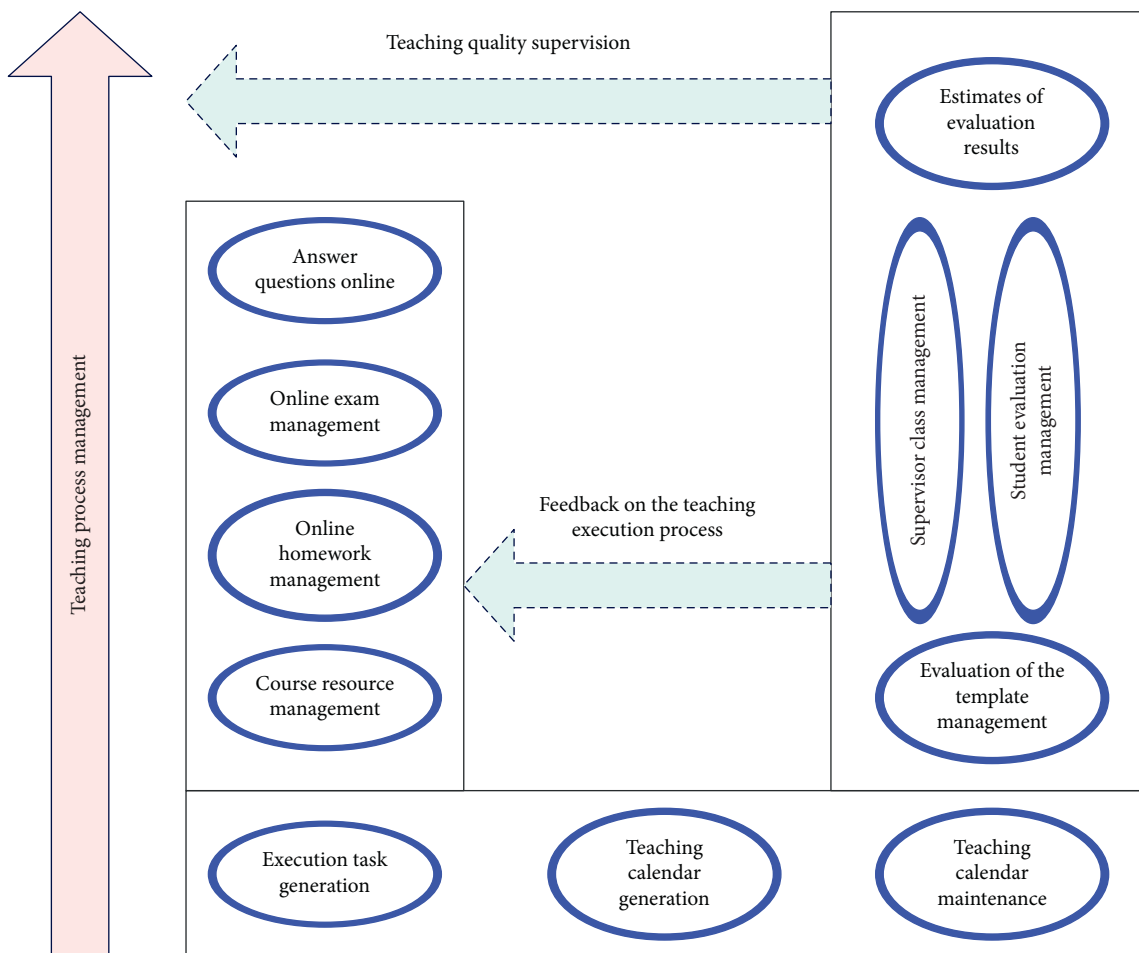


FIGURE 5: Overall demand diagram of English teaching process management.

linear interpolation method is simpler and more efficient after trying), and the sample value corresponding to t_j the calculation is

$$x_{t_j} = \frac{(t_j - \underline{p})}{(\bar{p} - \underline{p})} (x_{\bar{p}} - x_{\underline{p}}) + x_{\underline{p}}. \quad (10)$$

Among them, $x_{\underline{p}}, x_{\bar{p}} \in x_P$.

Step 3: We repeat the first and second steps until g_i samples are generated.

- ⑦ The algorithm repeats step ⑥ until a specified number of samples are generated around each minority class sample in the safe set.

The Bayesian method is introduced into the Gaussian process model, which can accurately calculate the

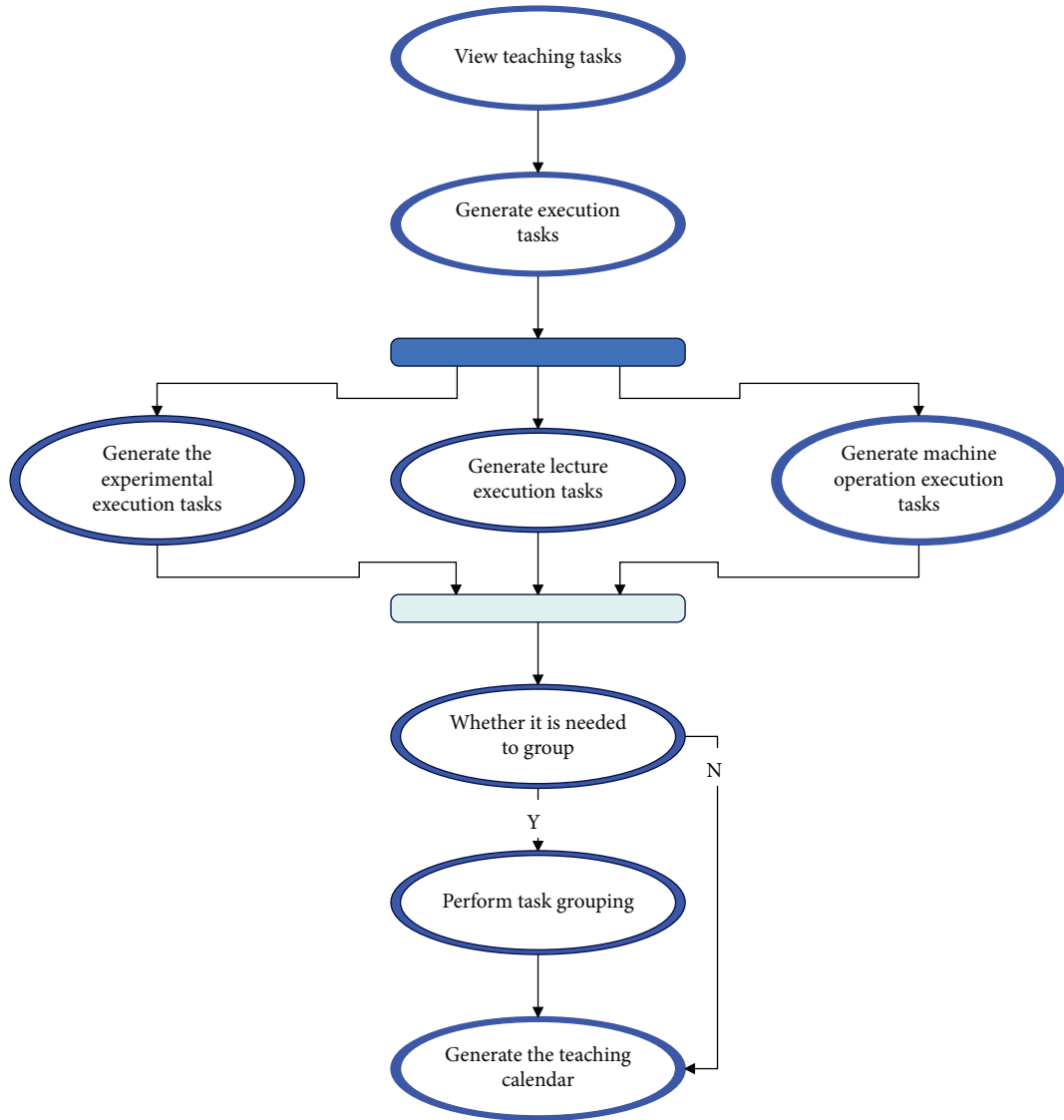


FIGURE 6: Activity diagram of English teaching calendar generation.

posterior probability value, and the results are easy to interpret. It has the characteristics of adaptive acquisition of hyperparameters and flexible nonparametric inference. Moreover, the kernel function is adopted, so that the model can be used in nonlinear and high-dimensional problem processing. In the case of unbalanced data, the model is more inclined to the majority class, and the ability to identify the minority class decreases, that is, it is sensitive to unbalanced time series data. In this paper, GPC is used to classify the unbalanced time series data before and after sampling to test the effectiveness of the sampling method.

A Gaussian process refers to a set of random variables, and any finite number of random variables in the set obeys a joint Gaussian distribution. Any Gaussian process can be determined by the mean function $m(x)$ and the covariance function $k(x, x')$ of a random process $f(x)$:

$$f \sim GP(m(x), k(x, x')). \quad (11)$$

Among them, $m(x) = E(f(x)), k(x, x') = E((f(x) - m(x))(f(x') - m(x'))^T)$. The idea of the Gaussian process classification model is to replace the non-Gaussian real posterior distribution by a Gaussian approximate posterior distribution, and then we use the approximate posterior distribution to give test data to approximate the predicted distribution.

We give the training set $S = \{(x_i, y_i), i = 1, 2, \dots, n\}$, x_i is the input, and y_i is the output. Given x , the conditional probability of y is $p(y, x) = \Phi(f(x))$. Among them, $f(x)$ defines the mapping relationship between input data and output. When x is given, $f(x)$ is the implicit function obeying the Gaussian process $f(x, \theta) \sim GP(0, K(\theta))$, θ is the parameter of the covariance function $K(\theta)$, and $\Phi(\cdot)$ is the cumulative probability density function of the standard normal distribution.

We give $f = [f_1, \dots, f_n]^T, f_i = f(x_i)$, and we set $Y = [y_1, \dots, y_n]^T, X = [x_1, \dots, x_n]^T$. Since the observed data are independent of each other, there is a likelihood

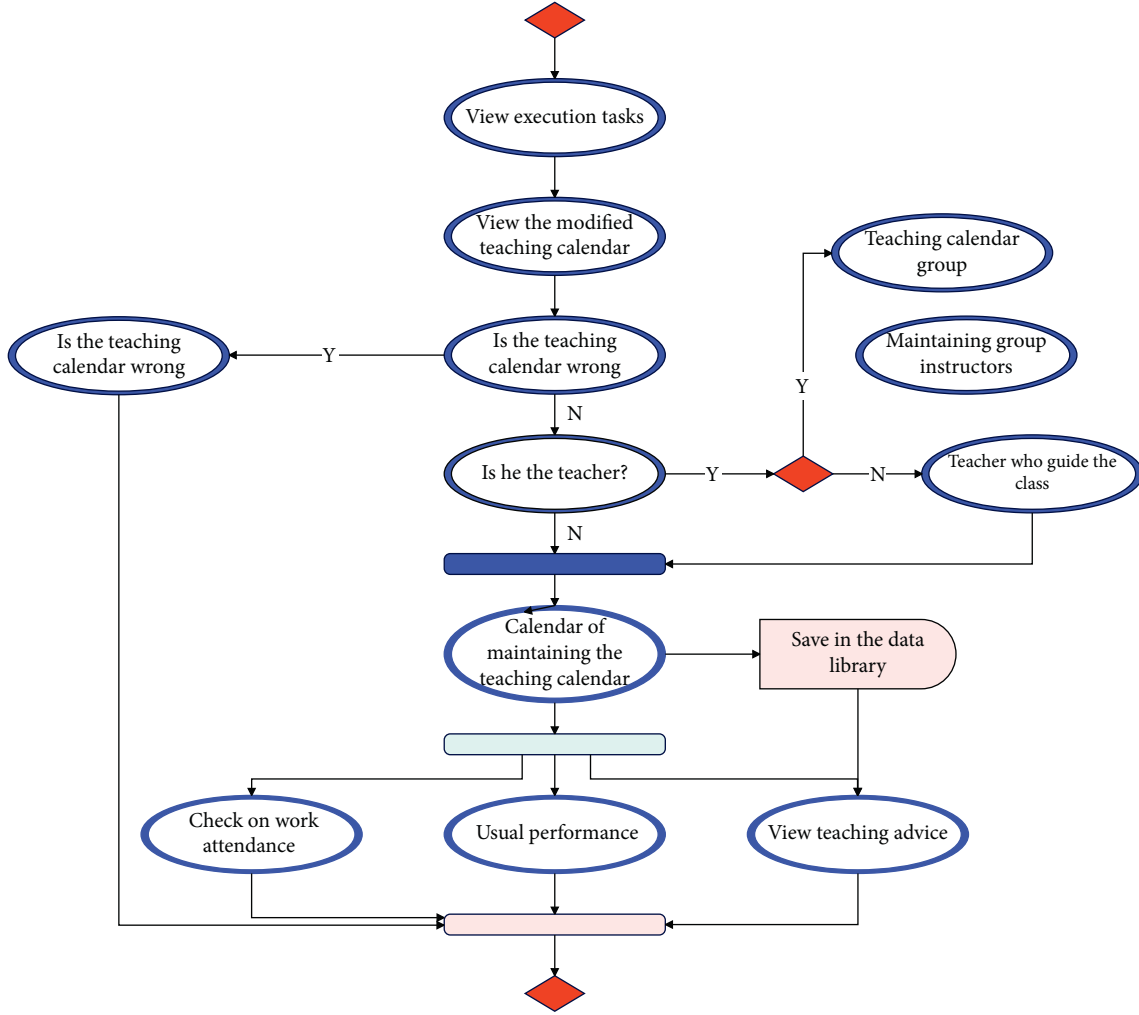


FIGURE 7: Activity diagram of English teaching calendar maintenance and management.

function $p(Y, f) = \prod_{i=1}^n p(y_i, f_i) = \prod_{i=1}^n \Phi(y_i, f_i)$, the prior distribution of the implicit function f is $p(f, X, \theta) = N(0, K, k_{ij} = k(x_i, x_j, \theta), k(\cdot)$ is the covariance function. The Gaussian kernel function is commonly used as the covariance function ($k(\|x - x_c\|) = \sigma_f^2 \exp\{-1/(2d^2)(x - x_c)^2\}$), x_c is the center of the kernel function, the parameter is $\theta = \{\sigma_f, d\}$, d is the window width. The posterior distribution of the implicit function f can be expressed as

$$p(f, S, \theta) = \frac{p(Y, f)p(f, X, \theta)}{p(S, \theta)}, \quad (12)$$

$$= \frac{N(0, K)}{p(S, \theta)} \prod_{i=1}^n \Phi(y_i, f_i).$$

It is worth noting that the posterior distribution is non-Gaussian.

We predict the class y_* given the sample x_* to be classified. First, the conditional probability of its implicit function f_* is calculated:

$$p(f_*, S, \theta, x_*) = \int p(y_*, f, X, \theta, x_*)p(f, S, \theta)df. \quad (13)$$

Using the conditional probability distribution of this implicit function f_* , the probability distribution of class labels y_* is obtained as follows:

$$p(y_*, S, \theta, x_*) = \int p(y_*, f_*)p(f_*, S, \theta, x_*)df. \quad (14)$$

The conditional probability of f_* is not a Gaussian likelihood. Therefore, it cannot be calculated directly using the integral. An alternative approach is to use a Gaussian-like approximate posterior distribution $q(f, S, \theta) = N(f, (\mu, \Sigma))$ to approximate the true posterior distribution $p(f, S, \theta)$. We substitute this approximate posterior distribution into the conditional probability calculation formula of the implicit function f_* , and after obtaining the approximate Gaussian test of the implicit function f_* , we finally verify it, as follows:

$$q(f_*, S, \theta, x_*) = N(f_*, (\mu_*, \sigma_*^2)). \quad (15)$$

Among them, $\mu_* = k_*^T K^{-1} \mu$, $\sigma_*^2 = k(x_*, x_*) - k_*^T (K^{-1} - K^{-1} A K^{-1}) k_*$, $k_* = [k(x_1, x_*), \dots, k(x_n, x_*)]^T$ is the prior covariance function between the sample x_* to be classified

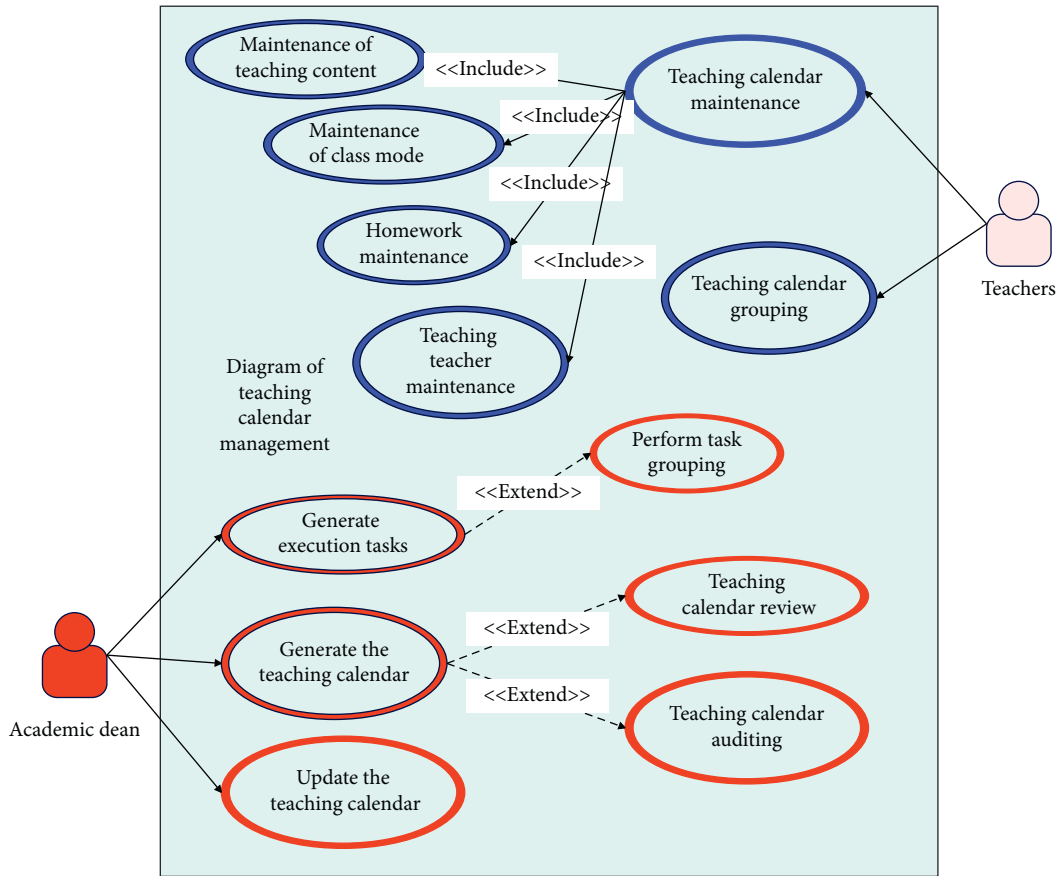


FIGURE 8: Use case diagram of English teaching calendar maintenance management.

and the training set X. Thus, the approximate prediction distribution of the samples to be classified is

$$\begin{aligned}
 q(y_* = 1, S, \theta, x_*) &= \int \Phi(f_*)N(f_*, (\mu_*, \sigma_*^2))df \\
 &= \Phi\left(\frac{\mu_*}{\sqrt{1 + \sigma_*^2}}\right).
 \end{aligned}
 \tag{16}$$

Therefore, the parameter $\theta_* = \{\mu_*, \sigma_*^2\}$ of the approximate Gaussian posterior distribution can be solved by approximation algorithms such as maximum likelihood method and Laplace approximation.

4. Improvement of English Teaching Process Management Based on Intelligent Data Sampling

The overall design of the system starts from the stage of English teaching process management, improves the English teaching process management, optimizes the management mode, and improves the quality of English teaching. It mainly includes three aspects of demand analysis. The overall system demand analysis is shown in the overall demand diagram of English teaching process management in Figure 5.

At present, for the courses of theory plus experiment or theory plus computer in the system, when the execution task is generated, the experimental or computer part is stripped, and the execution task is set up separately, and then the English teaching calendar is generated. The main activity diagram of English teaching calendar generation is shown in the activity diagram of English teaching calendar generation in Figure 6.

In the management of the whole English teaching process, the maintenance and management of the English teaching calendar is a key step, and the good design and management of the English teaching calendar can have a direct impact on the management of the English teaching process. The maintenance of the English teaching calendar plays a paving role in the management of the subsequent English teaching process. The overall description of the maintenance and management of the English teaching calendar is shown in the activity diagram of the maintenance and management of the English teaching calendar in Figure 7.

The system use case analysis diagram of teaching staff and teachers is shown in Figure 8, the English teaching calendar maintenance and management use case diagram.

Figure 8 can visually show the main participants of the system in the maintenance of the English teaching calendar. Among them, the main role of each role can be clearly

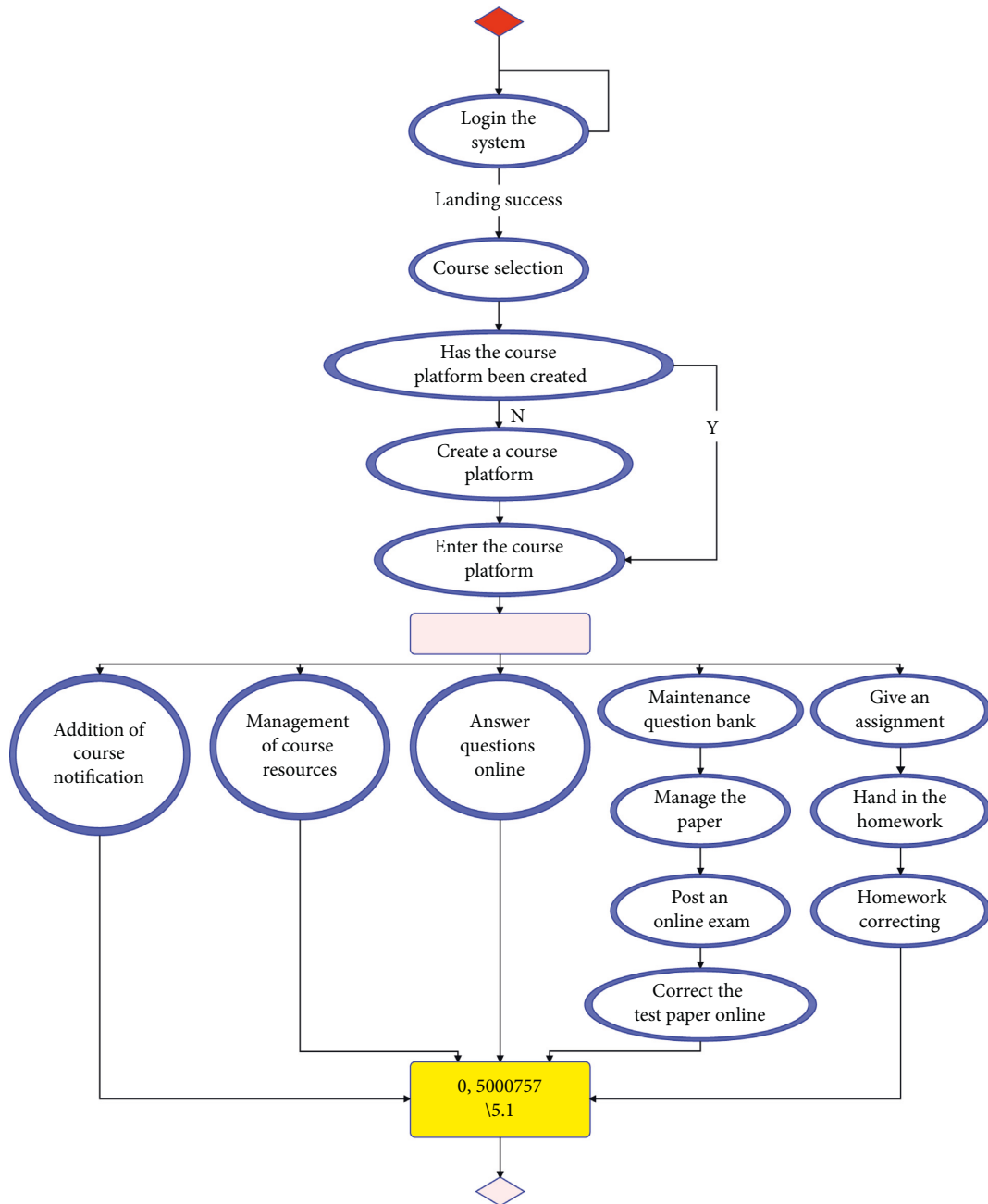


FIGURE 9: Teacher activity diagram of course learning platform.

defined through the description of the use case. The main use case for teaching staff includes generating executive tasks, generating English teaching calendars, and English teaching calendar updates. The main use case scenarios for teachers include the maintenance of the English teaching calendar and the grouping of the English teaching calendar. By analyzing the use cases of teachers and educational administrators, the main operating rights of system users are given according to their roles. Through the analysis of the above use case diagram, the main participants and the main demand use cases in the process of English teaching calendar maintenance and management can be clarified. In a word, the generation of the

English teaching calendar is the foundation of the English teaching process management. Through the generation and maintenance of the English teaching calendar, it has laid the cornerstone for the realization of other main functions of the system. On the basis of performing tasks, the English teaching execution process is supervised, and an online management learning platform is established. On the basis of the English teaching calendar, the course evaluation is open, and the English teaching process is fed back through real-time evaluation conclusions.

Based on the demand analysis of the above online learning platform, the activity diagram of teachers in the platform is shown in Figure 9.

TABLE 1: The effect of English teaching process management system based on intelligent data sampling.

Number	Teaching management	Number	Teaching management	Number	Teaching management
1	83.38	23	71.87	45	74.03
2	79.56	24	82.55	46	82.22
3	74.85	25	82.02	47	84.91
4	83.55	26	77.16	48	71.39
5	79.91	27	83.36	49	76.73
6	84.99	28	81.12	50	84.70
7	71.62	29	86.60	51	83.28
8	78.27	30	78.64	52	83.35
9	81.59	31	69.59	53	82.39
10	86.43	32	72.16	54	76.73
11	85.73	33	72.80	55	75.10
12	74.42	34	74.04	56	82.13
13	74.33	35	75.19	57	71.89
14	77.94	36	73.17	58	74.50
15	81.33	37	80.82	59	71.28
16	71.41	38	75.91	60	75.05
17	73.63	39	79.05	61	77.57
18	72.10	40	70.70	62	71.47
19	85.66	41	83.78	63	83.93
20	71.61	42	79.22	64	79.55
21	84.38	43	86.48	65	86.62
22	82.30	44	75.16		

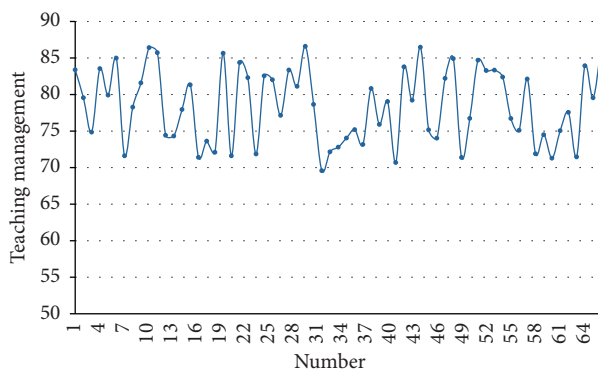


FIGURE 10: Statistical diagram of the effect of the English teaching process management system based on intelligent data sampling.

On the basis of the above research, this paper evaluates the English teaching process management system based on intelligent data sampling proposed in this paper, and explores its effect on the English teaching process management. The test results are shown in Table 1 and Figure 10.

It can be seen from the above research that the English teaching process management system based on intelligent data sampling proposed in this paper can play an important role in English teaching management and can effectively improve the efficiency of English teaching.

5. Conclusion

The study found that there are a series of factors hindering the effectiveness of inquiry-based English teaching. It is embodied in the factors of teachers, students and policy

environment. Teachers are mainly influenced by their own educational beliefs and evaluation views. The second is the impact of technology, including teachers' lack of effective English teaching strategies, insufficient knowledge and insufficient English teaching skills. The main factor of students is the lack of knowledge reserve and ability of students. The environmental aspects are mainly the lack of English teaching conditions, English teaching time and the level of attention of leaders. This paper combines intelligent data sampling technology to improve the English teaching process management, improve the English teaching effect, and construct an intelligent English teaching process management system. The research shows that the English teaching process management system based on intelligent data sampling proposed in this paper can play an important role in English teaching management and can effectively improve the efficiency of English teaching.

Data Availability

The labeled dataset used to support the findings of this study are available from the corresponding author upon request.

Conflicts of Interest

The author declares no conflicts of interests.

Acknowledgments

This work was sponsored in part by Henan Research Project on Teacher Education Curriculum Reform (2021-JSJYZD-016).

References

- [1] B. S. M. Abdelshaheed, "Using flipped learning model in teaching English language among female English majors in majmaah university," *English Language Teaching*, vol. 10, no. 11, pp. 96–110, 2017.
- [2] A. S. N. Agung, "Current challenges in teaching English in least-developed region in Indonesia," *SOSHUM: Jurnal Sosial dan Humaniora*, vol. 9, no. 3, pp. 266–271, 2019.
- [3] T. Ara Ashraf, "Teaching English as a foreign language in Saudi Arabia: struggles and strategies," *International Journal of English Language Education*, vol. 6, no. 1, pp. 133–154, 2018.
- [4] B. Ayçiçek and T. Yanpar Yelken, "The effect of flipped classroom model on students' classroom engagement in teaching English," *International Journal of Instruction*, vol. 11, no. 2, pp. 385–398, 2018.
- [5] A. Coşkun, "The application of lesson study in teaching English as a foreign language," *İnönü Üniversitesi Eğitim Fakültesi Dergisi*, vol. 18, no. 1, pp. 151–162, 2017.
- [6] A. Gupta, "Principles and practices of teaching English language learners," *International Education Studies*, vol. 12, no. 7, pp. 49–57, 2019.
- [7] N. Guzachchova, "Zoom technology as an effective tool for distance learning in teaching English to medical students," *Бюллетень науки и Црактики*, vol. 6, no. 5, pp. 457–460, 2020.
- [8] M. S. Hadi, "The use of song in teaching English for junior high school student," *English Language in Focus (ELIF)*, vol. 1, no. 2, pp. 107–112, 2019.
- [9] L. B. Kelly, "Preservice teachers' developing conceptions of teaching English learners," *Tesol Quarterly*, vol. 52, no. 1, pp. 110–136, 2018.
- [10] A. Mahboob, "Beyond global Englishes: teaching English as a dynamic language," *RELC Journal*, vol. 49, no. 1, pp. 36–57, 2018.
- [11] D. A. W. Nurhayati, "Students' perspective on innovative teaching model using edmodo in teaching English phonology: "A virtual class development," *Dinamika Ilmu*, vol. 19, no. 1, pp. 13–35, 2019.
- [12] A. B. Rinekso and A. B. Muslim, "Synchronous online discussion: teaching English in higher education amidst the covid-19 pandemic," *JEE*, vol. 5, no. 2, pp. 155–162, 2020.
- [13] N. Sadat-Tehrani, "Teaching English stress: a case study," *TESOL Journal*, vol. 8, no. 4, pp. 943–968, 2017.
- [14] N. I. Sayakhan and D. H. Bradley, "A nursery rhymes as a vehicle for teaching English as a foreign language," *Journal of University of Raparin*, vol. 6, no. 1, pp. 44–55, 2019.
- [15] M. A. Saydaliyeva, E. B. Atamirzayeva, and F. X. Dadaboyeva, "Modern methods of teaching English in Namangan state university," *International Journal on Integrated Education*, vol. 3, no. 1, pp. 8–9, 2020.
- [16] M. Siregar, "The use of pedagogical translation in teaching English by scientific approach," *Budapest International Research and Criticsin Linguistics and Education (BirLE) Journal*, vol. 2, no. 4, pp. 111–119, 2019.
- [17] H. Sundari, "Classroom interaction in teaching English as foreign language at lower secondary schools in Indonesia," *Advances in Language and Literary Studies*, vol. 8, no. 6, pp. 147–154, 2017.
- [18] O. Tarnopolsky, "Principled pragmatism, or well-grounded eclecticism: a new paradigm in teaching English as a foreign language at Ukrainian tertiary schools?" *Advanced Education*, no. 10, pp. 5–11, 2018.

Research Article

Analysis of Public Mental Health Status and Exploration of Social Anxiety in the Context of Epidemic

Yuanxin Lu 

Xinyang Vocational and Technical College, Xinyang 464000, China

Correspondence should be addressed to Yuanxin Lu; luyuanxin2022@xyvtc.edu.cn

Received 11 March 2022; Revised 15 April 2022; Accepted 4 May 2022; Published 24 May 2022

Academic Editor: Wei Liu

Copyright © 2022 Yuanxin Lu. This is an open access article distributed under the Creative Commons Attribution License, which permits unrestricted use, distribution, and reproduction in any medium, provided the original work is properly cited.

To explore the mental health and social anxiety of the public in the context of the epidemic, this article combines intelligent analysis methods to explore social anxiety. In this article, the digital voltage signal output by the processor chip interface is converted into an analog voltage signal. Moreover, this article changes the changing law of duty cycle with the program designed to achieve the purpose of outputting a variety of mental health waveforms that is composed of the sine wave, triangular wave, and square wave. In addition, this article constructs an intelligent hardware system. The research shows that the system proposed in this article can play an important role in the analysis of mental health and social anxiety in the context of the epidemic and has a certain supporting role in the psychological counseling of the social masses in the context of the epidemic.

1. Introduction

COVID-19 is highly contagious and people are generally susceptible [1]. The World Health Organization pointed out that when community transmission of major infectious diseases occurs, providing timely information to the public to take action (such as symptom identification and medical consultation guidelines) is one of the important public health measures [2]. Moreover, providing information to the public is an important part of epidemic prevention and control [3]. At the same time, providing sufficient and in-depth information can effectively mobilize the enthusiasm of the public to take self-protection measures and participate and cooperate with the epidemic prevention and control measures. Governments, at all levels in China, have launched a press conference system since January 2020 to report information on the epidemic daily and release scientific information on prevention and control. In addition, the National Health and Health Commission uses new media channels such as the official WeChat of “Healthy China” to carry out public health communication and health education on time. In addition to reprinting the press conference, major media also conducted in-depth interviews with relevant experts and reported the latest relevant research progress.

Health literacy is an important factor affecting health. Improving health literacy can strengthen the grasp of correct health knowledge, establish correct health concepts, and develop correct healthy behaviors and habits of the public. Moreover, psychological factors are also crucial to healthy behavior. For example, different levels of anxiety can cause sleep disturbances, adverse reactions to the body, and even suicidal tendencies in severe cases. Therefore, improving public health literacy can effectively improve the existing medical and health services, and is conducive to solving the imbalance and insufficiency of health resources of a country in terms of regions, population, and other factors. The health literacy of residents is affected by factors such as national political and economic level, regional education and medical level, and population characteristics, among them, occupational type also has a greater impact.

This article analyzes the mental health status of the public in the context of the epidemic and combines intelligent analysis methods to explore social anxiety, to improve its effectiveness.

2. Related Work

Literature [4] systematically discusses psychological crisis, arguing that each of us is striving to maintain a stable state of

our own, to balance and coordinate ourselves with the environment, and when major social problems or stressful events occur, individuals feel difficult to cope with. When the time comes, the balance will be broken, the normal lifestyle will be disturbed, the inner tension will continue to accumulate, there will be a loss or even disordered thinking and behavior, and will enter a state of psychological crisis. The research of disaster psychology shows that both individuals and the public have different psychological and behavioral response characteristics in the face of natural disasters at different stages. Therefore, different psychological intervention strategies and contents should be formulated at different stages [5]. Some studies summarize the different stages of people's psychological reactions when natural disasters occur. First, the acute stress stage generally develops within 1–2 days after the disaster, when people experience negative emotions such as shock, numbness, anxiety, worry, fear, guilt, and sadness. At this stage, the affected population may fall into a state of uncontrollable and panic-stricken psychological imbalance, and generally do not seek help from others. Psychological assistance at this stage focuses on stabilizing emotions, eliminating anxiety and fear, and providing psychological services based on psychological support and companionship. Second, the chronic stress stage generally develops from the second day to the third month after the disaster, where the psychological symptoms of the affected population may show different characteristics according to the degree of trauma exposure of the disaster-affected people [6]. Disaster survivors often have symptoms such as flashbacks and hypersensitivity, and their emotions are mainly characterized by anxiety, fear, sadness, helplessness, anger, and guilt. People affected by disasters will experience anxiety, fear, helplessness, and other emotions. They often have a strong motivation to seek help during the chronic stress stage, so this stage is a critical period for psychological assistance. Emotional counseling and psychological education should be the main focus to deal with various emotions and find resources to solve problems [7]. Third, the psychological rehabilitation stage (also known as the psychological recovery and reconstruction stage) generally develops within 3 months to several years after the disaster. For most people, the direct impact of the disaster is not obvious, the corresponding stress symptoms have also eased over time, and life has slowly returned to the right track; however, some people may experience posttraumatic stress disorder syndrome, depression, anxiety disorders, etc. [8]. The focus of psychological assistance at this stage is to strengthen the identification, assessment, and treatment of mental disorders, to continue to pay attention to psychological distress, and to prevent symptoms from worsening. Major public health emergencies will have an important impact on the psychological behavior of people, and this impact has different development and changes in different stages of the event. Emotional problems are the most prominent experiences and feelings of the public in the face of public health emergencies, and the common manifestations include psychological symptoms such as panic, anxiety, hypochondriasis, depression, and obsessive-compulsive reactions [9]. Literature [10] divides the development of the

epidemic into the high-incidence period, decline period, and subsidence period. The study found that during the epidemic, the most sought help from the psychological hotline was for emotional problems. The issue is getting more and more attention. The panic period is the first 1–2 weeks after the hotline is opened. The seekers are generally in an emotional state of anxiety, tension, and panic, and are prone to irrational behaviors such as panic buying and hypochondriasis. The depression period is the 3rd to 4th week, when the people are in the stable or problem-solving stage in response to the crisis, the panic gradually subsides and the depression begins to highlight. As the normal pace of study, life, and work is disrupted, and it is difficult to predict when the epidemic will end, people are easily psychologically uncertain or insecure, which induces depression, anxiety, irritability, and other emotions; anxiety intensified. The recovery period began in the 5th week. With the gradual improvement of the epidemic and the gradual recovery of the pace of study, work, and life, the mentality of the people became normal, and the amount of help from the psychological hotline also decreased [11].

In the face of public health emergencies, people will have different degrees of psychological crisis, among which emotional problems are the most prominent. With the progress of time and the intervention of government departments, people will gradually recover from the psychological crisis brought about by public health events [12]. However, what are the characteristics of changes in people's psychological symptoms in different periods of the epidemic? What role does the time course play in the gradual reduction of people's psychological symptoms? Research on these issues is still very lacking. In the face of major public health emergencies such as the new crown pneumonia, it is necessary to accurately grasp and analyze the psychological crisis response and characteristics of the people in the event and to dynamically monitor and track the psychological changes of the people in different stages of the epidemic. The department provides important information such as the psychological trend and risk characteristics of the people so that they can take different psychological interventions, according to the psychological characteristics of different stages, and builds a psychological crisis intervention model for public health emergencies [13]. Continuous monitoring of the psychological reactions of the people under the new crown pneumonia epidemic can not only grasp the psychological changes of the people in time and make psychological interventions more targeted but also help to build a social and psychological early warning system for public health emergencies, which is beneficial to Government departments make decisions and improve their response capabilities during the epidemic [14].

3. Hardware System of Social Anxiety and Mental Health Detection System

According to the aforementioned overall demand analysis, to realize the various functions of the instrument, this article adopts the modular concept to design the instrument. This

design uses the microprocessor ATmega128 as the main control core chip to control the peripheral chips and circuits to complete the task. Moreover, this article uses the following hardware circuit design framework diagram to implement the concrete representation (Figure 1):

This design divides all circuits into five modules to better distinguish the functions of each hardware circuit: stimulation main circuit, power circuit, music playback circuit, low-pass filter, and peripheral circuit. The stimulation main circuit module is the core of the hardware part. This module can generate output that meets the requirements and is composed of the main control chip, H bridge circuit, and current limiting circuit. The power circuit module is used to generate 100 V to ensure that the output of the instrument can effectively form a conduction current on the acupoints. At the same time, a step-down chip is also configured in the power supply circuit module to provide the 5 V power supply voltage required by the microcontroller and peripheral circuit chips. The core of the music playback module is the audio decoding circuit, which decodes the audio files to be played, so that patients can listen to soft antianxiety music while receiving physical therapy. The function of the low-pass filter module is to filter out the high-order harmonics in the SPWM output waveform to ensure that the output waveform is not distorted. The peripheral circuit module includes circuits such as D/A conversion circuit, temperature monitoring circuit, LCD liquid crystal display circuit, and key circuit. While realizing the auxiliary functions of the instrument, this module can also help the user to input commands and obtain the working status of the instrument to complete the human-computer interaction. This article will describe the design ideas and working principles of each module of the hardware circuit in detail from the next section.

The common boost circuit is designed to obtain a 100 V AC input with the help of transformer boost, and then realize AC to DC conversion and ripple and noise suppression through bridge full-wave rectifier circuit and large-capacity filter capacitor. Although this circuit is relatively mature, the transformer used is large in size, large in heat dissipation, high in price, and has obvious defects. This design uses the BOOST boost chopper circuit as the boost scheme, which has the advantages of lightness, simplicity, and high conversion efficiency.

In the BOOST boost circuit, the control of the boost multiple depends on the value of the duty cycle. The formula is [15]:

$$D = \frac{(V_0 - V_i)}{V_0} \quad (1)$$

In engineering design, when the duty cycle reaches 0.9, the boost limit of about 10 times can be reached. Therefore, if you want to get 100 V through the BOOST circuit, you need to use an external power supply above 10 V. In order to facilitate the use of the instrument and no longer increase the number of instrument power lines in the operating room, the external power supply of this design uses a 12 V battery for power supply. The boost circuit inside the device uses a BOOST boost chopper circuit to achieve a boost from 12 to

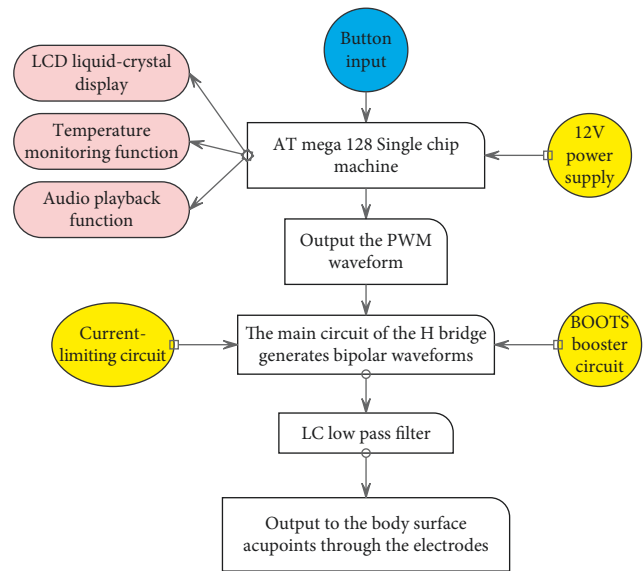


FIGURE 1: Hardware circuit frame diagram.

100 V DC. Substituting 12 and 100 V into the formula as V_i and V_o , respectively, we get a duty cycle of 88%.

Based on this, the design requires a PWM boost control chip that can achieve a high duty cycle of about 90% to complete the design of the boost circuit. This design selects UC3843, which is a high-performance fixed-frequency current-mode control chip with a fine-tuning oscillator and a maximum duty cycle of more than 90%. Moreover, it can perform accurate duty cycle control, temperature compensated reference, equipped with high gain error amplifier, current sampling comparator, and high current totem pole output, which is an ideal device for driving power MOSFET. Its internal principle block diagram is shown in Figure 2.

By combining the working principle of the BOOST boost circuit and the UC3843 chip data, the boost circuit is designed. The circuit diagram is shown in Figure 3.

The switch Q_2 periodically turns on and off according to the frequency of the UC3843 chip oscillator to guide the charging and discharging of the inductance L_3 . When Q_2 is on, the power supply charges L_3 at a speed of V_i/L . After Q_2 is turned off, L_3 releases reverse voltage to act as a power supply, and its stored energy is absorbed by output capacitor C_{11} after passing through diode D_6 at a speed of $(V_i - V_o)/L$. The capacitor ability to store energy determines the output voltage, and the peak value of the inductor current determines the efficiency of energy transfer to the capacitor.

In theory, the designed circuit output voltage is 100 V, but since the load is human skin, the resistance value varies greatly when it is dry, wet, or diseased. Moreover, the skin resistance value of different parts of the human body is also different, and the resistance value between two points on the skin can range from several hundred to tens of thousands of ohms. At the same time, the output voltage stability will be affected due to load changes. To ensure the stability of the output voltage, two closed-loop feedbacks are designed in the circuit for control [16].

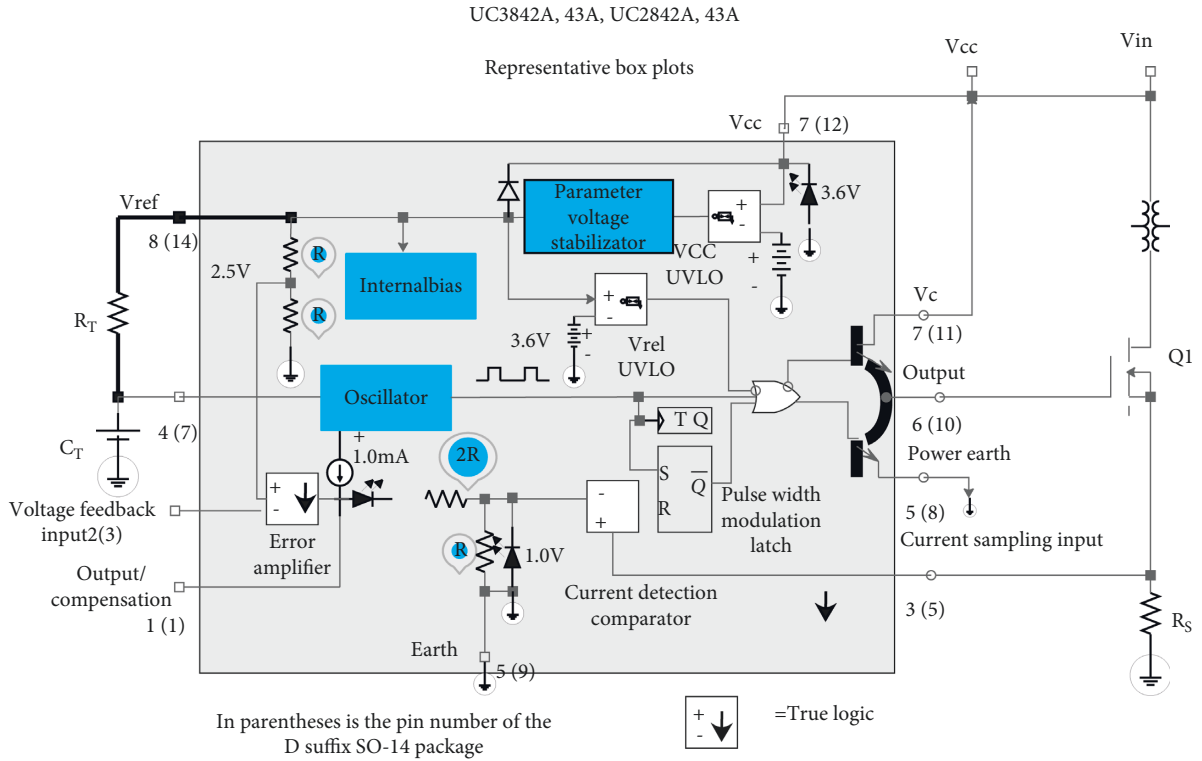


FIGURE 2: UC3843 principle block diagram.

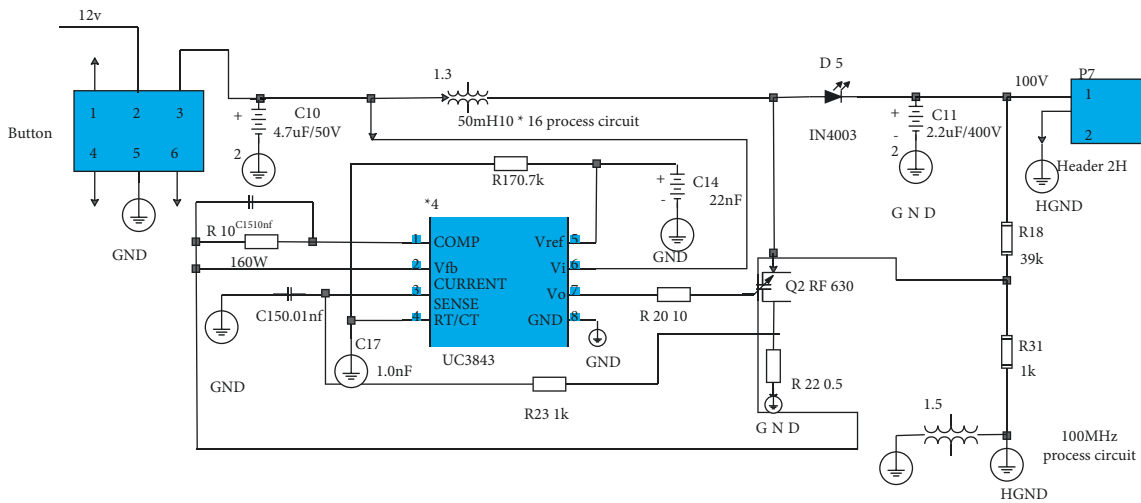


FIGURE 3: BOOST boost module circuit diagram.

In closed-loop 1, after the output voltage of 100 V is divided by R_{18} and R_{21} , a feedback voltage V_{fb} of 2.5 V is obtained, which is fed back to the boost chip through pin 2. There is a 2.5 V reference voltage obtained by dividing the 5 V inside the chip. V_{fb} is compared with the reference voltage, and the generated error is amplified by the error amplifier (Error AMP) and then enters the post-stage, modulates the pulse width of the PWM signal, changes its duty cycle, and changes the output voltage. In closed-loop 2, pin 3 of the UC3843 chip is a current detection terminal. The current flowing through the source of the switch tube generates a voltage-type signal through R_{22} to enter the non-inverting

terminal of the PWM comparator and compares it with the output signal of the error amplifier. The comparison result will be input to the PWM pulse width modulator (PWM latch) to control the change of the duty cycle of the PWM output signal, thereby adjusting the output voltage. In addition, when the source current of the switch tube is too large, the chip will stop working, and the switch tube will enter the off state, which plays the role of overcurrent protection.

The combined action of the two closed-loop feedback circuits ensures the stability of the output voltage and peak current. The following will calculate the important parameters of the boost circuit and select the components.

3.1. Chip Oscillator Frequency. The frequency of the oscillator is determined by the desired maximum duty cycle of the PWM signal, which can be up to 500 kHz. According to the definition of duty cycle, the formula is as follows:

$$D_{\max} = 1 - \left(\frac{t_{\text{dead}}}{t_{\text{period}}} \right). \quad (2)$$

The duty cycle required for this design is approximately 88%. The relationship between oscillator frequency $F_{\text{oscillator}}$ and t_{period} is as follows [17]:

$$t_{\text{period}} = \frac{1}{F_{\text{oscillator}}}. \quad (3)$$

R_T is connected to the V_{ref} terminal, the output current is through this pin, and R_T is charged by C_T . The desired frequency can be generated by adjusting the values of the resistor R_T and the capacitor C_T . Looking at the chip data, it can be found that when C_T is a fixed value, the ratio of R_T and frequency f is close to linear, and the relationship diagram is shown in Figures 4 and 5):

It can be seen that under the condition that R_T is greater than 5 k Ω and the capacitance takes a fixed value, R_T is linearly proportional to the frequency f . For the convenience of type selection and calculation, the value of C_T is set as 10 nf, and it is substituted into the above formula and Figure 5 to calculate and obtain $t_{\text{dead}} = 3 \mu\text{s}$, $t_{\text{period}} = 30 \mu\text{s}$, $F_{\text{osc}} = 33.33 \text{ kHz}$. We take F_{osc} as 30 kHz and substitute it into the formula [18]:

$$F_{\text{oscillator}} (\text{kHz}) = \frac{1.72}{(R_T (\text{K}) \times C_T (\mu\text{f}))}. \quad (4)$$

R_T is obtained as 5.7 k Ω . Therefore, $C_{17} = 10 \text{ nf}$, $R_{17} = 5.7 \text{ k}\Omega$.

3.2. Calculation and Selection of Energy Storage Inductance. We make the power supply circuit work in continuous operation mode to ensure the continuity of the charging of the inductor to the capacitor, and the critical conditions are as follows:

$$I_{L(\text{avr})} \geq \frac{\Delta I_L}{2}. \quad (5)$$

That is, the average current value of the inductor must be at least half of the ripple current.

According to the definition of duty cycle and the conservation, the input power of the inductor is equal to the output power, the formula for the average current of the inductor can be deduced as:

$$I_{L(\text{avr})} = \frac{I_0}{1-D} = 41.67 \text{ mA}. \quad (6)$$

The formula for calculating the ripple current of the inductor is:

$$\Delta I_L = \frac{(V_I - V_S)t_{\text{on}}}{L} = \frac{(V_I - V_S)D}{Lf}. \quad (7)$$

In this operating state, the minimum value of the inductance is:

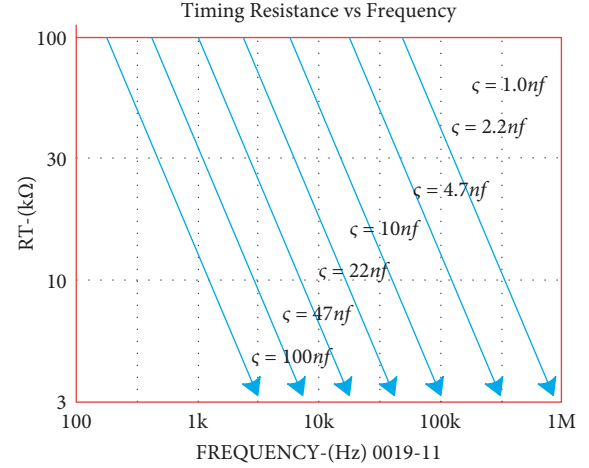


FIGURE 4: Relationship between resistance R_T and frequency f .

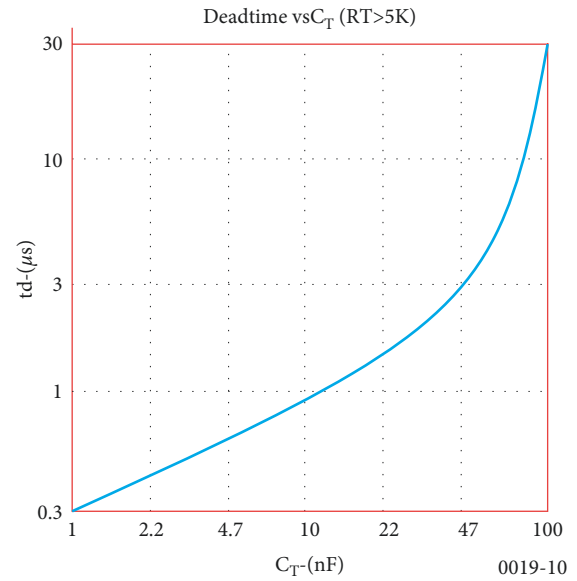


FIGURE 5: Relationship between capacitance C_T and dead time.

$$L \geq \frac{2(V_I - V_S)D(1-D)}{I_0 f} = 15.6 \text{ mH}. \quad (8)$$

In actual work, underrated output conditions, the ripple current of the inductor is usually 20% to 30% of the average current, and 20% is taken in the design to obtain: $\Delta I_L = 20\% \times I_{L(\text{avr})} = 8.34 \text{ mA}$.

Therefore, the peak current of the inductor is $I_{LP} = I_{L(\text{avr})} + \Delta I_L/2 = 45.83 \text{ mA}$, which is also the peak current of the switch. By substituting the data into formula (7), $L = (V_L - V_S)D/\Delta I_L f = 39.0 \text{ mH}$ is obtained.

Considering the margin and the convenience of winding, we take $L_3 = 50 \text{ mH}$.

3.3. Calculation and Selection of Capacitors. In continuous operation mode, the selection of capacitors must meet the following conditions [19]:

$$C \geq \frac{I_0 \times D}{f \times \Delta V} \quad (9)$$

In the formula, ΔV is the ripple voltage of the capacitor, because the output is 100 V, considering that the output voltage will directly act on the human body, the output ripple noise is best controlled within $\Delta V = 1\%$. By plugging the relevant data into the formula, we calculate and derive $C \geq 1.37 \mu\text{F}$.

The equivalent series resistance (ESR) of the capacitor is calculated as shown in formula.

$$\text{ESR} \leq \frac{\Delta V_0}{(I/1 - D) + (\Delta I_L/2)} = 1.2. \quad (10)$$

According to the ESR and the calculated minimum value of the capacitor, the capacitor is selected. Finally, the capacitor C_{11} is selected as $2.2 \mu\text{F}$, and the withstand voltage value is 400 V, so that the peak voltage is within the withstand voltage range to ensure the safety of the circuit.

3.4. Selection of Switches and Diodes. After the above calculation, the peak current of the switch tube is 45.83 mA. Considering other factors such as withstand voltage, IRF640 is selected as the boost switch. The drain and source withstand voltage of this type of switch is as high as 200 V, the on-state resistance (R_{ds}) is only 0.4Ω , the drain current I_d can reach 9.2 A, and the on-time is 170 ns, which can fully meet the requirements of this design.

When selecting a diode, it is necessary to consider whether its hardware parameters such as withstand voltage, maximum current, conduction time, and maximum frequency meet the design requirements. After research, 1N4003 is selected as the diode in the power supply part. Its maximum withstand voltage value of 200 V and the maximum allowable current value of 1 A can meet the design requirements and prevent reverse breakdown.

3.5. Calculation of Voltage Divider Resistance. When the load resistance changes, the 100 V output voltage is likely to be changed. The chip needs to adjust the pulse width and change the duty cycle to restore the output voltage to the normal value. Therefore, it is necessary to design the resistors R_{18} and R_{21} to divide the voltage, so that the $2.5 \text{ V } V_{fb}$ can be fed back to the UC3843 and compared with the reference voltage. We take R_{21} as $1 \text{ k}\Omega$. According to the formula:

$$\frac{R_{21}}{R_{21} + R_{18}} = \frac{V_{fb}}{V_0} \quad (11)$$

We can get R_{18} to be $39 \text{ k}\Omega$.

3.6. Design of PI Adjustment Compensation Circuit. To make the value of the feedback voltage more accurately and also to allow UC3843 to more accurately adjust the pulse width and duty cycle, so that the switch G pole of the switching power supply circuit can generate the required on-off waveform, this design designs a proportional-integral

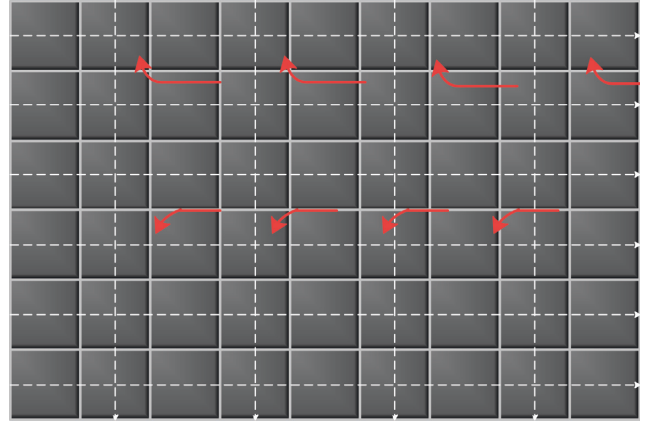


FIGURE 6: Waveform of G pole of switch tube.

adjustment circuit (PI adjustment circuit) around pin 1 of the chip. It consists of resistance R_{19} and capacitance C_{15} . According to the design experience of similar circuits, the value of C_{15} is 10 nF, and repeated experiments are carried out by inserting a sliding varistor, and the resistance value of R_{19} is determined when the G pole generates an on-off waveform to meet the requirements. The final value of R_{19} is $160 \text{ k}\Omega$, and the output of the G pole of the switch tube measured by the oscilloscope is shown in Figure 6.

To supply the 5 V power of the microcontroller and peripheral circuit chips, a step-down circuit needs to be designed to convert the 12 V input voltage to 5 V. This design uses the LM2596S chip to design a step-down circuit. As shown in Figure 7, the circuit is composed of four peripheral devices such as general inductors and diodes in conjunction with the chip. The structure is simple and the cost is low.

Before designing the low-pass filter, the principle of sine wave pulse width modulation (SPWM) is introduced. The positive half cycle of a full sine waveform is divided into n equal parts. If each aliquot is considered a pulse, it will have a pulse width of π/n , but its amplitudes will vary sinusoidally. However, pulses with equal and unequal shapes have the same effect when loaded on the same object with inertia. Therefore, if the n equal pulses of the positive half cycle of the sine wave are replaced by rectangular pulses, the center lines corresponding to the two pulses are kept coincident, and the amplitude of the rectangular pulse is specified as a fixed value, allowing the pulse width to change. Under the above conditions, ensuring that each rectangular pulse has the same area as the corresponding sinusoidal pulse within the response interval, a set of PWM waveforms with sinusoidal pulse widths can be obtained, as shown in Figure 8. Such PWM waveforms are called SPWM waveforms. For the negative half cycle of the sine wave, the negative SPWM can also be generated according to the above principle, to obtain a bipolar SPWM waveform. It can be seen that the essence of the SPWM waveform is still a PWM waveform. The amplitude of each pulse is equal but the pulse width is unequal, and the pulse width keeps changing according to the sinusoidal law. It overcomes the shortcomings of pulse width waveforms such as PWM and

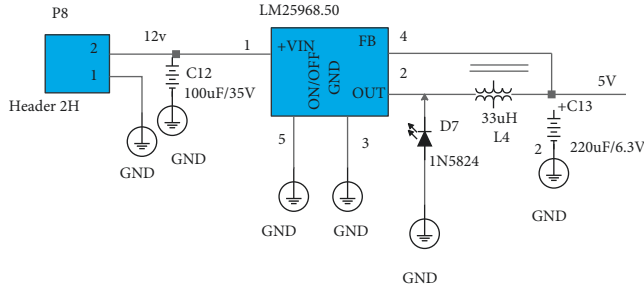


FIGURE 7: Schematic diagram of 5 V step-down circuit.

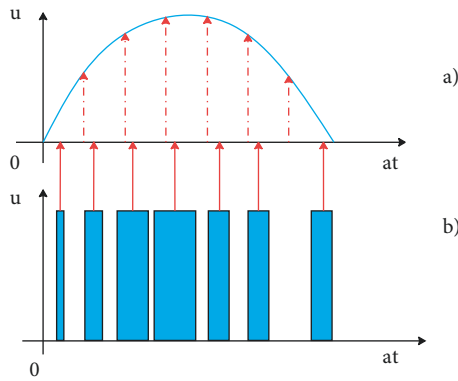


FIGURE 8: Schematic diagram of the principle of implementing SPWM by the equal area method.

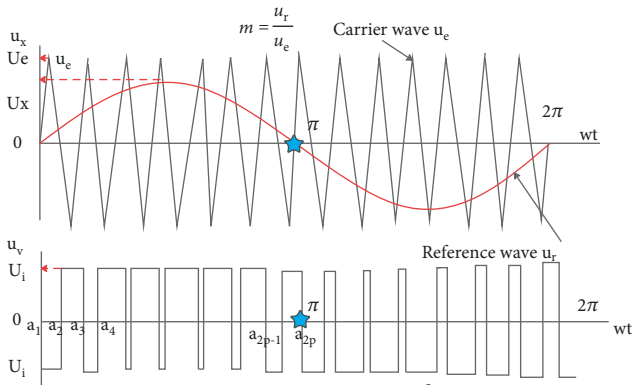


FIGURE 9: Schematic diagram of bipolar SPWM control.

achieves frequency adjustability. Therefore, it has been widely and maturely used in the field of inverter and single-chip design.

The PWM triangular wave generated by the single-chip microcomputer is used as the carrier wave U_c , and the sine wave whose frequency is much lower than the triangular wave is used as the reference wave U_r . By modulating the sine wave to make the two intersect, the duty cycle of the obtained output pulse also has the law of sinusoidal variation, as shown in Figure 9.

It can be seen that the output voltage U_0 is centrosymmetric in the 2π period and axisymmetric in the half period. Therefore, the Fourier expansion of the output voltage is:

$$U_0(t) = \sum_{n=1,3,5,\dots}^{\infty} A_n \sin n\omega t, \quad (12)$$

$$A_n = \frac{2}{\pi} \int_0^{\pi} U_0(t) \sin n\omega t d(\omega t).$$

Due to the symmetry of the graph, the output voltage U_0 can be regarded as the combination of two square waves with amplitude U_i and frequency f on the positive and negative half cycles. The first negative-going pulse starts at a_1 and ends at a_2 , and subsequent positive-going pulses start at a_2 and end at a_3 . Therefore,

$$\begin{aligned} A_n = & \frac{2}{\pi} \left[\int_0^{\pi} U_i \sin n\omega t d(\omega t) - \int_{a_1}^{a_2} U_i \sin n\omega t d(\omega t) \right. \\ & \left. - \int_{a_3}^{a_4} U_i \sin n\omega t d(\omega t) - \dots - \int_{a_{2p-1}}^{a_{2p}} U_i \sin n\omega t d(\omega t) \right] \\ = & \frac{2U_i}{n\pi} \left[1 - \sum_{k=1}^{\infty} (\cos na_{2k-1} - \cos na_{2k}) \right]. \end{aligned} \quad (13)$$

Substituting into formula (12), we get:

$$U_0(t) = \sum_{n=1,3,5,\dots}^{\infty} \frac{2U_i}{n\pi} \left[1 - \sum_{k=1}^{\infty} (\cos na_{2k-1} - \cos na_{2k}) \right] \sin n\omega t. \quad (14)$$

It can be seen that the obtained output U_0 has a large number of high-order harmonic components, and these high-order harmonics will seriously distort the sinusoidal waveform. Therefore, a low-pass filter (LPF) needs to be designed to filter out the high-order harmonics in the output.

The normalization method is a parameter calculation method commonly used in the design of LPF. The so-called normalized LPF refers to the calculation of the parameters of the target filter based on the LPF of the characteristic impedance of 1Ω and the cutoff frequency of 1 rad/s ($\approx 0.159 \text{ Hz}$). First, it determines the parameters of the normalization method. According to the demand, the highest frequency of SPWM in the treatment mode is 100 Hz . In this design, the output loss is expected to be 3 dB in the state of 300 Hz , that is, the response amplitude at 300 Hz is attenuated to 0.707 times the amplitude of the output at 100 Hz . However, the loss is 20 dB at the extreme maximum frequency of 1000 Hz of low-frequency physiotherapy, that is, the response amplitude is attenuated to $1/10$ of the original value. At this point, the normalized angular frequency is $\omega' = 1000/300 = 10/3$, and the loss is $x = 20 \text{ dB}$, which is substituted into the formula:

$$n = \frac{\log(10^{0.1x} - 1)}{2 \log \omega'}. \quad (15)$$

We get $n = 1.908$. Here n represents the number of reactive components required, so a second-order LC filter

TABLE 1: Analysis of the effect of public mental health status.

Num	Analysis of mental health	Num	Analysis of mental health	Num	Analysis of mental health
1	83.16	23	84.46	45	87.95
2	87.62	24	81.83	46	82.22
3	81.06	25	82.02	47	90.69
4	82.13	26	90.72	48	89.74
5	80.02	27	85.29	49	90.08
6	82.13	28	90.29	50	80.98
7	84.85	29	83.34	51	88.42
8	84.56	30	81.23	52	85.39
9	89.65	31	86.76	53	86.67
10	87.19	32	90.84	54	88.96
11	89.76	33	90.47	55	83.22
12	88.18	34	81.66	56	86.34
13	88.42	35	82.95	57	81.11
14	85.75	36	84.49	58	88.42
15	89.74	37	85.54	59	79.81
16	84.35	38	79.05	60	83.02
17	84.59	39	81.49	61	90.45
18	89.16	40	82.93	62	88.67
19	83.22	41	81.32	63	85.39
20	83.19	42	88.32	64	87.53
21	80.46	43	90.06	65	81.95
22	86.81	44	84.88	66	81.14

TABLE 2: Analysis of social anxiety in the context of the epidemic.

Num	Social anxiety analysis	Num	Social anxiety analysis	Num	Social anxiety analysis
1	75.51	23	81.77	45	76.43
2	77.83	24	72.45	46	80.76
3	76.05	25	73.81	47	74.03
4	83.47	26	74.56	48	76.23
5	74.24	27	81.03	49	83.73
6	83.06	28	83.72	50	80.36
7	74.65	29	72.55	51	81.60
8	79.20	30	79.72	52	78.26
9	79.67	31	78.92	53	72.13
10	83.15	32	73.44	54	76.84
11	80.62	33	83.28	55	73.06
12	78.07	34	81.86	56	72.59
13	73.57	35	80.48	57	80.54
14	74.13	36	81.49	58	78.60
15	81.73	37	74.32	59	81.46
16	81.27	38	77.15	60	72.16
17	78.77	39	83.64	61	78.63
18	81.01	40	82.72	62	80.07
19	78.32	41	74.81	63	80.34
20	82.46	42	78.43	64	72.69
21	77.94	43	80.81	65	83.35
22	81.76	44	74.14	66	80.62

consisting of an inductor and a capacitor can meet the design requirements. The characteristic impedance of the LC filter generally needs to be determined according to several factors such as the internal resistance of the output source, the load resistance, and the characteristic impedance of the reference filter. In this design, to improve the input resistance and load capacity, an emitter follower is added to the filter, and the output is connected to the acupoints on the surface of the human body. According to the above, the output resistance can be determined to be

about 10k Ω . Considering it comprehensively, take K as 200, L_{base} and C_{base} as 1H and 1F. According to the above data, substitute the relevant formula of the normalization method for calculation.

$$M = \frac{f_1}{f_2} = \frac{300}{1/2\pi} = 1883.24. \quad (16)$$

In the formula, f_1 is the cutoff frequency of the filter to be designed (Hz); f_2 is the cutoff frequency (Hz) of the reference filter.

$$L_{\text{new}} = \frac{K \times L_{\text{base}}}{M} = 106.2 \text{ mH},$$

$$C_{\text{new}} = \frac{C_{\text{base}}}{M \times K} = 2.65 \mu\text{F}.$$
(17)

To facilitate the selection of common standard parts to build the circuit, the value of the inductance in the LC filter is 100 mH, and the value of the capacitor is 2.2 μF . Since the output current is only up to 5 mA, the inductors can be made by winding thin 0.1 mm diameter copper wires on manganese, zinc, and ferrite alloys. The fabricated inductor has the advantages of high magnetic permeability, high magnetic flux density, and high efficiency. In addition, customized inductors can also be used directly. The output waveform filtered by LPF will directly act on the human body and will no longer be specially grounded. Therefore, it is necessary to choose a capacitor type that can withstand frequent polarity changes. Therefore, this design uses a CBB capacitor commonly used as a starting capacitor for AC motors.

4. Analysis of Public Mental Health Status and Exploration of Social Anxiety in the Context of Epidemic

After constructing the above hardware system, the analysis of the mental health of the public and social anxiety in the context of the epidemic is carried out to explore the effectiveness of this system. First of all, this article studies the effect of the system in the analysis of public mental health status, obtains data from the survey, processes the data through the system, and obtains the results shown in Table 1.

It can be seen from the above research that the system proposed in this article can play a certain role in the analysis of public mental health under the background of the epidemic. On this basis, this article conducts analyzes social anxiety in the context of the epidemic and obtains the results shown in Table 2.

It can be seen from the above research that the system proposed in this article can play an important role in the analysis of social anxiety in the context of the epidemic and has a certain supporting role in the psychological counseling of the social masses in the epidemic.

5. Conclusion

The public awareness of the basic knowledge of COVID-19 and how to deal with it need to be further improved, but they still lack the ability to convert knowledge into active preventive behaviors, and the anxiety of the public is relatively serious. For the whole society, large-scale anxiety and stress will cause panic, leading to the emergence of unhealthy behaviors, that have a negative effect on the development of the disease and the outcome of the disease, and even cause social security turmoil. Therefore, improving public health awareness, preventive behavior, and psychological state are conducive to curbing the spread of public health emergencies and infectious diseases in my country, and at the same time slowing down the occurrence and development of

the high incidence of chronic noncommunicable diseases. This article analyzes the mental health status of the public under the background of the epidemic and explores social anxiety by combining intelligent analysis methods. The research results show that the system proposed in this article can play an important role in the analysis of mental health and social anxiety in the context of the epidemic and has a certain supporting role in the psychological counseling of the social masses in the epidemic.

Data Availability

The labeled dataset used to support the findings of this study is available from the author upon request.

Conflicts of Interest

The author declares no conflicts of interest.

Acknowledgments

This work was supported by Xinyang Vocational and Technical College.

References

- [1] J. Park, U. G. Kang, and Y. Lee, "Big data decision analysis of stress on adolescent mental health," *Journal of The Korea Society of Computer and Information*, vol. 22, no. 11, pp. 89–96, 2017.
- [2] J. Deckro, T. Phillips, A. Davis, A. T. Hehr, and S. Ochylski, "Big data in the veterans health administration: a nursing informatics perspective," *Journal of Nursing Scholarship*, vol. 53, no. 3, pp. 288–295, 2021.
- [3] F. F. Nastro, D. Croce, S. Schmidt, R. Basili, and F. Schultze-Lutter, "Insideout project: using big data and machine learning for prevention in psychiatry," *European Psychiatry*, vol. 64, no. S1, p. S343, 2021.
- [4] H. Jung and K. Chung, "Social mining-based clustering process for big-data integration," *Journal of Ambient Intelligence and Humanized Computing*, vol. 12, no. 1, pp. 589–600, 2021.
- [5] M. Gonçalves-Pinho, J. P. Ribeiro, and A. Freitas, "Schizophrenia related hospitalizations - a big data analysis of a national hospitalization database," *Psychiatric Quarterly*, vol. 92, no. 1, pp. 239–248, 2021.
- [6] M. Gonçalves-Pinho, J. P. Ribeiro, A. Freitas, and P. Mota, "The use of big data in psychiatry - the role of pharmacy registries," *European Psychiatry*, vol. 64, no. S1, p. S793, 2021.
- [7] M. V. Rudorfer, "Psychopharmacology in the age of "big data": the promises and limitations of electronic prescription records," *CNS Drugs*, vol. 31, no. 5, pp. 417–419, 2017.
- [8] A. B. R. Shatte, D. M. Hutchinson, and S. J. Teague, "Machine learning in mental health: a scoping review of methods and applications," *Psychological Medicine*, vol. 49, no. 09, pp. 1426–1448, 2019.
- [9] W. N. Price and I. G. Cohen, "Privacy in the age of medical big data," *Nature Medicine*, vol. 25, no. 1, pp. 37–43, 2019.
- [10] J. Liu, X. Zhai, and X. Liao, "Bibliometric analysis on cardiovascular disease treated by traditional Chinese medicines based on big data," *International Journal of Parallel, Emergent and Distributed Systems*, vol. 35, no. 3, pp. 323–339, 2020.

- [11] D. Wilfling, A. Hinz, and J. Steinhäuser, "Big data analysis techniques to address polypharmacy in patients - a scoping review," *BMC Family Practice*, vol. 21, no. 1, pp. 180–187, 2020.
- [12] Y. Wang, L. Kung, W. Y. C. Wang, and C. G. Cegielski, "An integrated big data analytics-enabled transformation model: application to health care," *Information & Management*, vol. 55, no. 1, pp. 64–79, 2018.
- [13] A. Hong, B. Kim, and M. Widener, "Noise and the city: leveraging crowdsourced big data to examine the spatio-temporal relationship between urban development and noise annoyance," *Environment and Planning B: Urban Analytics and City Science*, vol. 47, no. 7, pp. 1201–1218, 2020.
- [14] X. Cheng, L. Fang, X. Hong, and L. Yang, "Exploiting mobile big data: sources, features, and applications," *IEEE Network*, vol. 31, no. 1, pp. 72–79, 2017.
- [15] M. Moessner, J. Feldhege, M. Wolf, and S. Bauer, "Analyzing big data in social media: text and network analyses of an eating disorder forum," *International Journal of Eating Disorders*, vol. 51, no. 7, pp. 656–667, 2018.
- [16] J. Miller, R. Atala, D. Sarangarm et al., "Methamphetamine abuse trends in psychiatric emergency services: a retrospective analysis using big data," *Community Mental Health Journal*, vol. 56, no. 5, pp. 959–962, 2020.
- [17] M. Gonçalves-Pinho, J. P. Ribeiro, and A. Freitas, "Schizophrenia hospitalizations - a big data approach," *European Psychiatry*, vol. 64, no. S1, pp. S157–S158, 2021.
- [18] R. T. Perdue, J. Hawdon, and K. M. Thames, "Can big data predict the rise of novel drug abuse?" *Journal of Drug Issues*, vol. 48, no. 4, pp. 508–518, 2018.
- [19] S. Graham, C. Depp, E. E. Lee et al., "Artificial intelligence for mental health and mental illnesses: an overview," *Current Psychiatry Reports*, vol. 21, no. 11, pp. 116–118, 2019.

Research Article

Enterprise Financing Risk Analysis and Internal Accounting Management Based on BP Neural Network Model

Haojie Liao ^{1,2,3}, Huabo Yue ¹, Yibin Lin,² Dong Li,³ and Lei Zhang⁴

¹College of Graduate Studies, Master of Management Program in Management (International Program) WALAILAK University, 222 Thaiburi, Thasala, Nakhon Si Thammarat 80160, Thailand

²Chakrabongse Bhuvanath International Institute for Interdisciplinary Studies, Rajamangala University of Technology, Tawan-Ok 10600, Thailand

³Accounting and Audit School, Guangxi University of Finance and Economics, Nanning, Guangxi 530003, China

⁴College of Graduate Studies, Bansomdejchaopraya Rajabhat University, Bangkok 10600, Thailand

Correspondence should be addressed to Huabo Yue; yuehuabo1990@163.com

Received 22 February 2022; Revised 8 April 2022; Accepted 22 April 2022; Published 20 May 2022

Academic Editor: Wei Liu

Copyright © 2022 Haojie Liao et al. This is an open access article distributed under the Creative Commons Attribution License, which permits unrestricted use, distribution, and reproduction in any medium, provided the original work is properly cited.

A BP neural network-based model is proposed to study corporate financial risk analysis and internal accounting management. Using MATLAB software and the BP neural network model, it is possible to obtain enterprise financing risk situations over a period by simulating and predicting enterprise financing risks by creating an early warning model for enterprise financing risks. Finally, from the point of view of the company's internal and external operations, the company's financial risk prevention measures and proposals are proposed to improve the financing efficiency of the companies and to prevent financial risks. This study predicts the financing risk of companies listed on the Mongolian Stock Exchange and analyzes the causes of the risk status. According to the test results, the learning speeds for successive substitutions are as follows: 0.005, 0.01, 0.02, 0.03, and 0.04. Finally, it was found that the error was minimal and the stability was best when the learning speed was exactly 0.01. The error is 0.0031011, and the step size is 157, which is only slightly lower than the target error value, which indicates that the learning speed is good. In addition, the novelty of this study is the use of the BP neural network model to conduct an early warning study of corporate financial risks. The BP neural network assessment model for corporate lending risk in this document is highly accurate. In addition to providing theoretical insights to researchers, it can be a good tool for banks to realistically assess the credit risk of SME supply chain financing.

1. Introduction

The SMEs are a product of economic reform and have contributed to economic development and social progress. However, traditional small- and medium-sized enterprises have been overwhelmed and unable to resist the external environment and fierce market competition that has become increasingly complex during development. In addition, their enterprises lack viability and are poorly managed [1]. During this period, small and medium enterprises have collapsed one after another, and several negative cases and adverse effects have occurred. It should be noted that the driving force behind the transition of enterprises is no

longer simple elements but soft forces such as technological innovation. In contrast, China's traditional economic path of high consumption and low energy not only wastes a lot of manpower and material resources but also misses out on good development opportunities. With China's accession to the WTO, it must face the general pattern of globalization, improve its national strength, and prioritize technological innovation to further improve the living standards of its people. The development of an innovative economy and the creation of an innovative social system have become a priority. As the backbone of small and medium enterprises, it is clear that innovative small and medium enterprises play a positive role. In this context,

modern small and medium enterprises have emerged, joined the economic wave, and walked the forefront of the time [2].

The influx of international champions, the fierce competition of domestic companies under the middle bag, and the lack of funding for the development of innovative small- and medium-sized enterprises have not been resolved. Although foreign scholars have contributed to the challenges and proposals for financing SMEs, there are very few analytical studies using the financing capacity of the new era of SMEs, especially the BP neural network method. The laws of a market economy are unstable. The allocation of scientifically sound and efficient resources depends on the development prospects of enterprises. Therefore, it is necessary to be closely related to the current basic conditions of development of the market economy, to direct private capital to local conditions, and to implement legal and rational capital operations (Figure 1). These issues are the theoretical basis for the system for assessing the financing capacity of innovative small and medium enterprises, and the requirements for multi-channel and innovative financing of enterprises. At present, technological research and industrial innovation are the main content of research in innovative enterprises, but the financing capacity of innovative enterprises is rarely considered in terms of financing structure. This study examines innovative financing for small and medium enterprises as an integrated system. This document, which is at the peak of the sustainable development strategy of enterprises, systematically proposes a comprehensive evaluation index system appropriate to the financing capacity of innovative small and medium enterprises, which is important to guide innovation small and medium enterprises' financial risk assessment and program optimization [3].

2. Literature Review

Lan and Li pointed out, in the process of organizational cooperation or alliance cooperation, that mutual trust among members can effectively reduce the risk of failure, which is very important for the whole cooperative enterprise [4]. Aiqun et al. specially studied the important impact of trust on R & D through empirical experiments and pointed out that the higher the degree of trust between members, the easier it is to promote R & D. On the contrary, the lower the degree of trust, the easier it is to bring risks to cooperation [5]. Li et al. believe that a cooperation lacking trust cannot last for a long time. To establish a long-term cooperative relationship, members must strengthen mutual trust [6]. Zhao and Lv believe that the intellectual property risk caused by bad credit has become a shackle hindering cooperative R & D, explore the causes of such risks, and give corresponding prevention and control measures [7]. Li and Quan take fast trust as the research perspective and believe that fast trust plays a positive role in solving intellectual property risks and forming performance of innovation alliance [8]. For example, Wu and Lu established a conceptual model of

risk transmission among enterprises participating in cooperative innovation and pointed out that inhibiting risk transmission should be carried out from the two dimensions of prevention and process control to weaken the negative effect of risk transmission. They also believe that building a corresponding risk early warning system, improving the enterprise's understanding of risk transmission, and the ability to deal with risks are the three aspects of enterprise prevention and control; the three aspects of process control are to monitor the interaction of risks, reduce the speed of risk transmission among enterprises, and hinder the transmission path of risks [9]. Xuesong et al. calculated the index risk value of each partner in the cooperative alliance from the perspective of the third party, constructed the early warning system of information sharing risk, and gave different early warning information according to different degrees of risk, so as to curb the risk caused by information sharing [10]. Nayak et al. constructed a technological innovation risk early warning model integrating functions, early warning index system, and risk response strategies, which pointed out the direction for the response and strategy research of enterprise technological innovation risks [11]. Shen et al. established a risk early warning system for enterprise technological innovation projects using a rough neural network, which is both effective and feasible, pointing out the direction for the risk early warning management of enterprise technological innovation projects [12]. Zou analyzed the characteristics of risks in the process of joint innovation from the perspective of financial management and constructed a new financial early warning system. The system has the functions of monitoring, early warning, incentive, and reward and can effectively avoid the risks [13].

Based on the current research, a BP neural network model is proposed. Using the MATLAB software and the BP neural network model to build the enterprise financing risk early warning model, the enterprise financing risk simulation forecast gets a certain period in the future enterprise financing risk status. Finally, for the company's internal activities and external activities, to ensure that enterprises achieve the purpose of improving financing efficiency and preventing financing risk, this must be considered from the two perspectives of corporate financing risk prevention countermeasures and suggestions. This study predicts the financing risk of listed companies and analyzes the causes of the risk.

3. Financing Risk Analysis Based on BP Neural Network

3.1. Establishment of 1bp Neural Network Model. The establishment of the BP neural network model is divided into six stages. The first stage is to find and process the financing risk early warning index data required by the BP network model. The second stage is to determine the training input data, training target data, test input data, test target data, and prediction input data of the BP network model. The third stage is to divide the early warning and warning

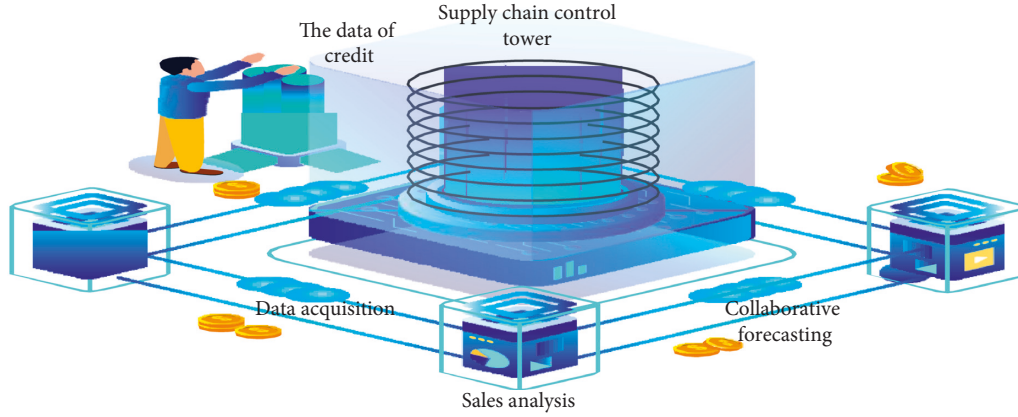


FIGURE 1: Enterprise financing risk analysis.

interval of financing risk. In the fourth stage, the training input data and training target data of the BP network model are input, the parameters of the model are set, and sample training is conducted. In the fifth stage, the test input data and test target data selected by the early warning model are input for the sample test. In the sixth stage, the prediction input data selected by the early warning model are input for sample prediction.

The algorithm flow of the BP neural network model is shown in Figure 2, including starting, determining data, calculating the node output value of the hidden layer and output layer, calculating the deviation value, comparing and meeting the deviation, adjusting parameters, and obtaining the model.

The algorithm flow of the BP neural network model is shown in Figure 2. The flow is simple, including starting, determining the input data and target data, calculating the node output value of the hidden layer and output layer, calculating the deviation value between the target value and actual output, comparing and meeting the deviation, adjusting parameters, and obtaining the model [14].

First, the input data and target data of the model are determined, and then, the output values of each hidden layer and output layer node of the model are obtained. Through the comparison of the target value and output value, the deviation between the target value and the actual output is obtained. When the error fluctuation is within a certain range, the algorithm is ended, so as to obtain the established BP network model; if the error fluctuation exceeds the limited range, the error of hidden layer nodes should be calculated, the error gradient should be calculated, then, the parameters of the number of hidden layers and nodes should be set, and then, the target value and actual output error are calculated until the obtained error meets the set error range, so as to establish the BP network model and obtain the parameters, threshold, and weight of the model.

The learning process of the BP neural network model is to minimize the error. The training process of the model needs to provide input vectors.

X and target vector y can adjust the weight and threshold of the network according to the error performance of the adjustment model, with the purpose of making the model achieve the process of learning and imitation.

Let the model have n layers of the neural network, the input independent variable of the model is x , and let the sum of the input information of the i -th neuron of the m -th layer of the BP network model be S_i^m and R_i^m as the output information of the i -th neural node, A_{ij} is the connection weight between the i -th neural node of this layer and the j -th neural element output of the upper layer, and f is the functional relationship between the input data and the output data. The relationship between input and output is shown as follows:

$$\begin{aligned} R_i^m &= f(S_i^m), \\ S_i^m &= \sum A_{ij}R^{m-1}. \end{aligned} \quad (1)$$

The C_j is set as the target output value of the model. R_i^n is the actual output result calculated by the system network. It is a function obtained by connecting weight and input mode [15]. The error function is represented by error E , which is the sum of squares of the difference between the actual output value and the target output value, and its expression is as follows:

$$e = \frac{1}{2} \sum (R_i^n - c_j)^2. \quad (2)$$

The meaning of this function is to make the actual output value close to the target output value by calculating the minimum value of the error function. In order to achieve the purpose of error, nonlinear programming method can be used to reduce the error function along the gradient direction. The updated amount ΔA_{ij} of its weight A_{ij} can be expressed by the following formula:

$$\Delta A_{ij} \propto -\varepsilon \frac{\partial d}{\partial A_{ij}}. \quad (3)$$

Therefore, the following formula can be listed:

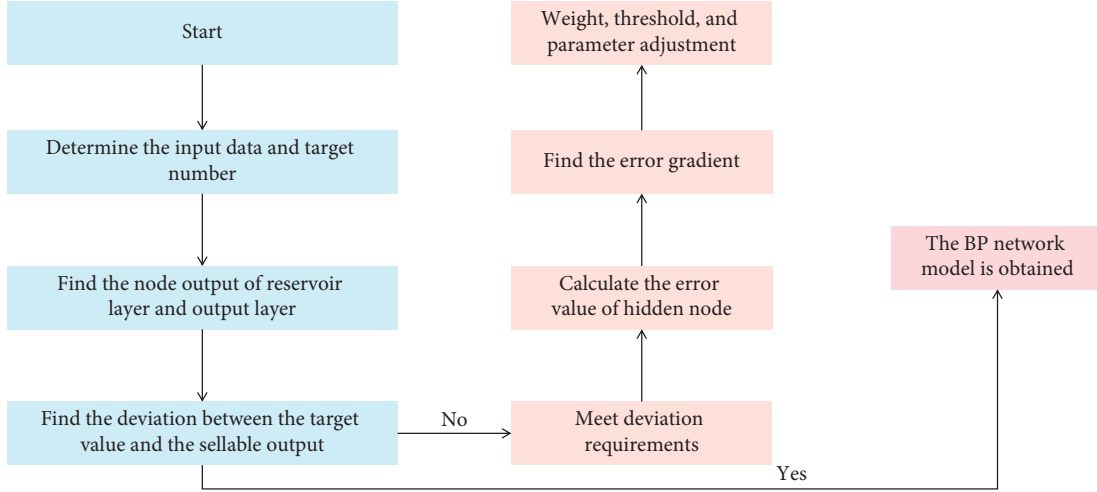


FIGURE 2: Flowchart of the BP network model.

$$\frac{\partial S_i^m}{\partial A_{ij}} = \frac{\partial}{\partial A_{ij}} (A_{ij} R_j^{m-1}) = R_j^{m-1},$$

$$\frac{\partial e}{\partial A_{ij}} = \frac{\partial e}{\partial S_j^m} \frac{\partial S_j^m}{\partial A_{ij}} = \frac{\partial e}{\partial S_j^m} R_j^{m-1},$$

$$\Delta A_{ij} = -\varepsilon \frac{\partial e}{\partial S_j^m} R_j^{m-1}, \quad (4)$$

$$d_j^m = \frac{\partial e}{\partial S_j^m},$$

$$\Delta A_{ij} = -\varepsilon d_j^m R_j^m.$$

In equation (2), ε represents the parameter of learning rate.

$$R_i^m = f(S_i^m),$$

$$\frac{\partial R_i^m}{\partial S_j^m} = f'(S_j^m). \quad (5)$$

If $f(S_j^m)$ is a nonlinear sigmoid function,

$$f(S_j^m) = \frac{1}{1 + \exp(-S_j^m)},$$

$$f'(S_j^m) = R_j^m (1 - R_j^m). \quad (6)$$

If I is the node in the output layer, then, $M = n$, and then, C_j is the target ax value preset by the system.

Then, the formula $(\partial e / \partial x)$ is found; if i is a node in the output layer, then, $m = n$, and then, C_j is the target ax value preset by the system, that is,

$$\frac{\partial e}{\partial S_j^m} (R_j^n - c_j),$$

$$d_j^n = R_j^n (1 - R_j^n). \quad (7)$$

If i is not the node of the output layer, but the node of the hidden layer, then,

$$\frac{\partial e}{\partial R_j^m} = \sum_i \frac{\partial e}{\partial S_i^{m+1}} \frac{\partial S_i^{m+1}}{\partial R_j^m}$$

$$= \sum A_{ij} d_i^{m+1}, \quad (8)$$

$$d_j^m = R_j^m (1 - R_j^m) \sum A_{ij} d_i^{m+1}.$$

Through the repeated operation of the model, it can be concluded that the error signal d_j^m of layer m is directly proportional to the error signal of layer $m-1$, and it can be adjusted according to the direction of consistency. In addition, the above calculation processes can prove that the principle of signal transmission of the BP neural network is the error function obtained by comparing the actual output value R_j obtained from the forward transmission of the input data of independent variables with the target output value and finally reducing the error value to a certain range through a series of parameter adjustments such as weight and threshold.

The weight adjustment can be reflected by the following formula:

$$\Delta A_{ij} = -\varepsilon \frac{\partial e}{\partial S_j^m} R_j^{m-1},$$

$$d_j^n = R_j^n (1 - R_j^n) (R_j^n - C_j), \quad (9)$$

$$d_j^m = R_j^m (1 - R_j^m) \sum A_{ij} d_i^{m+1}.$$

The above formula proves that the error signal d_j^m of m layer has strong correlation with the error signal d_i^{m+1} of $m+1$ and proves that the error signal is transmitted from the input layer to the output layer. After adjusting the weight, threshold, and other parameters of the BP neural network system for many times, the output value within the error range is finally reached. At this time, the system will

automatically stop learning and complete the construction of the BP network model [16].

3.2. Selection of Relevant Indicators. The early warning indicators of this study include 17 indicators in two aspects: capital integration and capital financing. The integration of funds includes financing scale, financing cost, financing structure, fund availability, and so on. In particular, as shown in Table 1, the financing scale selects two indicators: asset equity ratio and debt financing ratio; the financing cost includes debt financing cost and equity financing cost; the financing structure is reflected by the equity debt ratio, and the degree of funds in place is reflected by the speed of financing. The ability of financing includes profitability, operation ability, solvency, and growth ability. It is an important reference to measure the financing status of enterprises and analyze financing risks.

Profitability includes return on total assets and return on equity; operational capacity is assessed by three indicators: total capital turnover, inventory turnover, and receivables turnover; solvency is reflected in the following two indicators: current ratio, capital turnover, debt ratio, and growth capacity. Four financial indicators are as follows: total capital turnover ratio, fixed asset growth rate, operating income growth rate, and earnings per share growth rate.

Asset-to-equity ratio. The ratio of assets to equity is the ratio of owners' equity to total assets. This ratio reflects the share of the owner's investment, liabilities, and the relative amount of total equity in the firm's financing. In general, the higher the capital-to-capital ratio, the lower the financing risk and the lower the financing risk for the entity. The index formula is as follows:

$$\text{Asset equity ratio} = \frac{\text{owner's equity}}{\text{total assets}}. \quad (10)$$

Debt financing ratio. The debt financing ratio refers to the ratio of debt financing through short-term borrowing, long-term borrowing, issuance of bonds, and other debt financing to the total financing of the company. The greater the value of debt financing cost, the greater the financing risk, and the greater the possibility of financing risk. On the contrary, the smaller the financing risk, the less likely the enterprise will have financing risk. The enterprise occurrence index formula is as follows:

$$\text{Debt financing ratio} = \frac{\text{total debt financing}}{\text{total assets}}. \quad (11)$$

Debt financing costs. Debt financing cost refers to the proportion of expenses incurred in the process of raising funds by listed coal companies through short-term loans, long-term loans, issuance of bonds, and other loan relationships. In particular, this expense is the financial expense on the balance sheet of each enterprise. The greater the value of debt financing cost, the greater the financing risk, and the greater the possibility of financing risk. On the contrary, the smaller the debt financing cost, the smaller the financing risk, and the smaller the possibility of financing risk [17]. The index formula is as follows:

TABLE 1: Financing early warning indicators' table.

Index selection	Financing ability	Indicators
Money into	Financing scale	Asset equity ratio Debt financing ratio
	The cost of financing	Debt financing cost Equity financing cost
	Financing structure	Equity to debt ratio
	Degree of funding	Raising speed Return on total assets
	Profitability	Return on equity Total asset turnover Inventory turnover
	Ability to operate	Accounts receivable turnover Current ratio
Money RongChu	Debt paying ability	Asset-liability ratio Growth rate of total assets Growth rate of fixed assets Growth rate of operating income
	Growth ability	Growth rate of earnings per share

Debt financing cost

$$= \frac{\text{financial expense}}{(\text{short-term loan} + \text{long-term loan} + \text{bonds payable})}. \quad (12)$$

Equity financing cost refers to the proportion of expenses incurred by enterprises through equity financing channels such as IPO, share allotment, and additional issuance. In this study, the equity financing cost is estimated by calculating the sum of the risk return rate and risk-free return rate through the capital asset pricing method (CAPM). The greater the value of equity financing cost, the greater the financing risk, and the greater the possibility of financing risk. The smaller the value of equity financing cost, the smaller the financing risk, and the smaller the possibility of financing risk of the enterprise. The index formula is as follows:

$$\text{CAPM} = R_F + \beta(R_M + R_F). \quad (13)$$

In the formula, R_f is the risk-free rate of return, and the interest rate of the three-year treasury bill is selected, which is about 6%. R_f is the average profit margin of the coal listed company industry.

Equity debt ratio. The equity debt ratio is an indicator that reflects the financing structure of a company and is the ratio of the company's total liabilities to total shareholders' equity. The greater the value ratio of equity to liabilities, the greater the financing risk of the enterprise, and the greater the possibility of financing risk of the enterprise. Conversely, the smaller the financing risk of the enterprise, the smaller the possibility of financing risk. The index formula is as follows:

$$\text{Equity to debt ratio} = \frac{\text{total debt}}{\text{total shareholders' equity}} \quad (14)$$

Financing speed. The financing rate is an index of an entity's capital adequacy, which is the ratio of the entity's core business income to its total cash flow from financing activities. In general, the faster the financing rate, the lower the financing risk, and the lower the financing risk for the entity. Conversely, the larger the scope of enterprise financing, the greater the opportunity to finance risk. The index formula is as follows:

$$\text{Financing rate} = \frac{\text{total cash flow from business income}}{\text{financing activities}} \quad (15)$$

Return on total assets. Return on total assets is an important indicator of the profitability of the formula and an important reference in choosing whether to conduct debt financing activities. This is equal to the ratio of the firm's average net profit to total assets. In general, the higher the financing value of the total return on an asset, the lower the financing risk, and the lower the probability that the entity will be exposed to the financing risk. Conversely, the higher the risk of corporate financing, the greater the opportunity to finance the risk. The index formula is as follows:

$$\text{Return on total assets} = \frac{\text{net profit}}{\text{average of total assets}} \quad (16)$$

$$\text{Total capital turnover} = \frac{\text{sales revenue}}{\text{average total assets}} \quad (18)$$

$$\text{Average total assets} = \frac{(\text{total assets at the end of the period} + \text{total assets at the beginning of the period})}{2}$$

Inventory turnover. Inventory turnover rates are an important basis for reflecting an entity's operational capacity at the same rate as total asset turnover. It also compensates for the turnover ratio of current assets. In particular, the inventory turnover ratio reflects the management of the enterprise in the three stages of sales of goods purchased, put

ROE. Return on equity, or the return on equity, also known as ROE, is an important indicator of the ratio of a company's profitability and net profit to the average shareholder's equity. In general, the higher the return on equity, the higher the profitability of mining companies, the better the operating efficiency, the lower the financing risk, and the lower the risk of financing. Conversely, the higher the financing risk, the higher the probability that the entity will be at financial risk. The index formula is as follows:

$$\text{Return on net assets} = \frac{\text{net profit}}{\text{total average shareholders' equity}} \quad (17)$$

Total capital turnover. The ratio of total assets to turnover is an important basis for assessing the operational capacity of an enterprise. It can measure the distribution between the extent of an enterprise's capital investment and the level of activity. It represents the ratio of average sales to total assets. In general, the higher the share of total capital turnover, the higher the return on assets, the higher the level of asset management of the entity, the lower the financing risk, and the lower the financing risk. Conversely, the higher the risk of financing an entity, the higher the risk of financing that entity. The index formula is as follows:

into production, and recycled, and the cost of sales is equal to the ratio of average inventory. In general, the higher the inventory turnover rate, the faster the entity's inventory disposal rate, the stronger its liquidity, and the lower its financing risk. Conversely, the higher the risk of financing an entity, the higher the risk of financing that entity. The index formula is as follows:

$$\text{Inventory turnover} = \frac{\text{Sales costs}}{\text{Average inventory}} \quad (19)$$

$$\text{Average inventory size} = \frac{(\text{Starting Inventory} + \text{Ending Inventory})}{2}$$

Accounts receivable turnover rate. The turnover rate of accounts receivable reflects the turnover rate of accounts

receivable and the financial management efficiency of the enterprise and reflects the operation ability of the enterprise. It is the ratio of net sales revenue to the average

balance of accounts receivable. The higher the turnover rate of accounts receivable, the faster the recovery rate of accounts receivable, which means that the average collection period is shorter, and this shows that the listed coal companies have strong asset liquidity and short-term

solvency. The smaller the financing risk of the enterprise, the less likely it is to have a financing crisis. On the contrary, the financing risk of the enterprise is greater, and the possibility of a financing crisis is greater [18]. The specific formula is as follows:

$$\text{Turnover rate of accounts receivable} = \frac{\text{net sales revenue}}{\text{average balance of accounts receivable}}$$

Average balance of accounts receivable

$$= \frac{(\text{balance of accounts receivable at the beginning of the period} + \text{balance of accounts receivable at the end of the period})}{2} \quad (20)$$

Current ratio. The current ratio can explain and explain the liquidity of enterprise assets and the solvency of enterprises. It is the ratio of current assets to current liabilities. The larger the current ratio, the stronger the short-term solvency of the enterprise, and the less likely the enterprise a financing crisis is. On the contrary, the weaker the solvency of enterprises, the greater the possibility of financing crisis. The specific formula is as follows:

$$\text{Turnover ratio} = \frac{\text{current assets}}{\text{current liabilities}} \quad (21)$$

Gear ratio. The ratio of assets to liabilities may reflect the liquidity of the entity's current assets before the maturity of short-term liabilities and is equal to the ratio of total liabilities to total assets. In general, the lower the capital-to-debt ratio, the stronger the long-term solvency of an entity and the less likely it is to enter a financial crisis, and conversely, the lower the solvency of an entity,

the higher the probability of a financial crisis. The specific formula is as follows:

$$\text{Debt ratio} = \frac{\text{total liabilities}}{\text{total assets}} \quad (22)$$

Gross asset growth rate. The growth rate of total assets is an important indicator of an enterprise's ability to accumulate and develop capital, and it is a measure of the ability to protect against changes in the scale of total assets. This is the ratio of value added to total assets at the beginning of the reporting period. In general, a growth rate in total assets indicates that the business is expanding. The higher the growth rate of total assets, the faster the amount of capital will grow, and the lower the risk of financing of enterprises, the higher the financing risk will be. If the growth rate of a company's assets is negative, there is a very high probability that the company will face a financial crisis. The specific formula is as follows:

$$\text{Asset growth rate} = \frac{(\text{total assets at the end of the period} - \text{total assets at the beginning of the period})}{\text{total assets at the beginning of the period}} \quad (23)$$

The growth rate of fixed assets. The growth rate of fixed assets reflects the growth of fixed assets of enterprises. This is an important indicator of an enterprise's ability to develop and protect against risk. This is the ratio of the value added of fixed assets to total fixed assets at the beginning of the period. In general, the growth rate of fixed assets is positive and the scope of enterprise development is expanding. The higher the rate of growth of fixed assets, the faster the size of the enterprise's assets, and the lower the rate of financing, the lower the rate of growth of fixed assets. If the growth rate of fixed assets is negative, the probability of a financial crisis is very high. The specific formula is as follows:

Growth rate of fixed assets

$$= \frac{(\text{end - time fixed assets} - \text{early fixed assets})}{\text{early fixed assets}} \quad (24)$$

Operating income growth rate. The rate of growth of operating income is an important indicator of the growth and development of an enterprise. This is a key indicator of enterprise development. This is the ratio of operating income growth to operating income. In general, the growth rate of operating income is positive and the scope of enterprise development is expanding. If operating income growth is negative, the company is more likely to finance the crisis. The specific formula is as follows:

$$\text{Operating growth rate} = \frac{(\text{current operating income} - \text{operating income at the beginning of the period})}{\text{operating income at the beginning of the period}} \quad (25)$$

Percentage growth rate per share. The rate of increase in earnings per share can be expressed as the ratio of a company's performance growth and development capacity, i.e., the rate of earnings per share, to earnings per share at the beginning of the period. In general, the higher the growth rate of EPS, the lower the risk of corporate financing and the

higher the probability of a financial crisis; conversely, the lower the EPS growth rate, the higher the financing risk and opportunity. opportunity, and the smaller the financing risk. If the increase in earnings per share is negative, the company will have a great opportunity to finance the crisis. The specific formula is as follows:

$$\begin{aligned} & \text{Percentage increase in earnings per share} \\ & = \frac{(\text{earnings per share at the end of the period, earnings per share at the beginning of the reporting period})}{\text{earnings per share at the beginning of the period}} \end{aligned} \quad (26)$$

3.3. Strategies for Improving the Internal Accounting Management System of Enterprises

3.3.1. Establishing Internal Accounting Management System. Managers are fully responsible for the accounting work of the enterprise and improving the accounting management system. Enterprises shall supervise and supervise the behavior of accounting staff, accounting institutions, and other personnel. Reward accountants are loyal to their duties and make remarkable achievements. Enterprise staff shall strictly implement accounting rules and laws, ensure that accounting materials are legal, true, accurate, and complete, and implement enterprise accounting management rules and regulations. An internal accounting management system is built, and supervision and assessment are improved. According to the actual situation of the enterprise, reasonable planning is made and the responsibilities of the accounting supervisor and the person in charge of the accounting organization are clarified. The working relationship and responsibilities of enterprise accounting are clarified, and it is ensured that accounting staff exercise their functions and powers according to the law.

3.3.2. Establishing a High-Quality Accounting Team. Accountants are managers and supervisors of enterprise business activities. The quality of accounting managers is closely related to the level of financial management. After the implementation of the new accounting system, higher requirements are put forward for the overall quality of enterprise financial accounting managers. Business management and accounting work need a group of

qualified accountants. Accountants should constantly learn advanced financial management methods and new financial professional skills, master professional knowledge and financial system, and ensure the standardization of enterprise financial accounting work. At the same time, we should fully understand the actual development requirements of the market economy, constantly improve our ability, and skillfully apply the knowledge of financial management. At present, the quality of the enterprise accounting team is generally low. Enterprises should strengthen training and optimize the accounting team. Through formal training and learning, the professional quality of enterprise accounting staff should be improved, and the knowledge structure should be constantly improved, so that the staff can adhere to the principles, strictly exercise self-discipline, and be loyal to their duties. The quality of accountants has a direct impact on the quality of accounting work and is related to the implementation of the accounting management system. Enterprise accountants must have a strong ability to analyze and solve problems, a high-quality professional level, extensive knowledge, and good adaptability. Enterprise accountants should actively learn the contents of the new accounting system and relevant knowledge of financial accounting to improve their ability [19].

3.3.3. Establishing the Internal Management System of Accounting Computerization. Computerized accounting is conducive to the formulation of modern enterprise system and the improvement of accounting work quality. It is of great significance to the improvement of financial work efficiency and work quality. It is an important development direction of accounting. Full-time personnel should be used to manage accounting

TABLE 2: Relationship between hidden layer unit number and training step number.

Number of nodes in hidden layer	4	5	6	7	8	9	10	11	12	13	14	15	16
The training steps	167	268	163	255	152	233	241	255	156	230	179	236	160

computerization and carry out relevant training. The internal management system of accounting computerization should be established, given a full play to the role of accounting computerization, and improve the efficiency and quality of accounting work. Enterprises should regularly check the implementation of financial and accounting indicators, conduct financial and accounting analysis, find problems in time actively and improve, and improve the internal accounting management level of enterprises.

3.3.4. *Establishing Internal Containment System.* The establishment of a long-term and effective internal containment system in enterprises can strengthen the supervision and restraint of internal personnel, prevent favoritism, fraud, and serious mistakes and ensure the quality of accounting management. Reasonable division of labor and full implementation of the internal accounting system of enterprises need to build an internal containment system. The establishment of an internal containment system is conducive to the implementation of a modern enterprise internal accounting system. During the period of asset reorganization and a major investment, the enthusiasm of accountants should be brought into full play to ensure the stable operation of various economic activities. Enterprise managers should pay attention to correction, control, inspection, supervision, and other methods, carry out targeted enterprise management, and adhere to legal compliance. Internal control is of great value to ensure the safety of assets, the legitimate rights and interests of investors, and the quality of accounting information. Based on internal containment, the system should be constantly adjusted, and the internal control of the enterprise should be strengthened. Accounting control should be standardized, and the work of each link within the constraints of laws and regulations should be carried out. It should be insisted on stopping and exposing noncompliance, illegality, and other accounting to ensure the legitimacy and quality of accounting work.

4. Experimental Results and Analysis

An analysis of the structure of the BP neural network shows that the number of latent nodes in the BP neural network model for risk assessment of SME credit for supply network financing should be between 5 and 14. In the case of setting the same parameters in this chapter, the number of nodes in the hidden layer should be alternated, the systematic errors of the model should be compared, a complete comparison should be made, and the most appropriate number of nodes in the hidden layer should

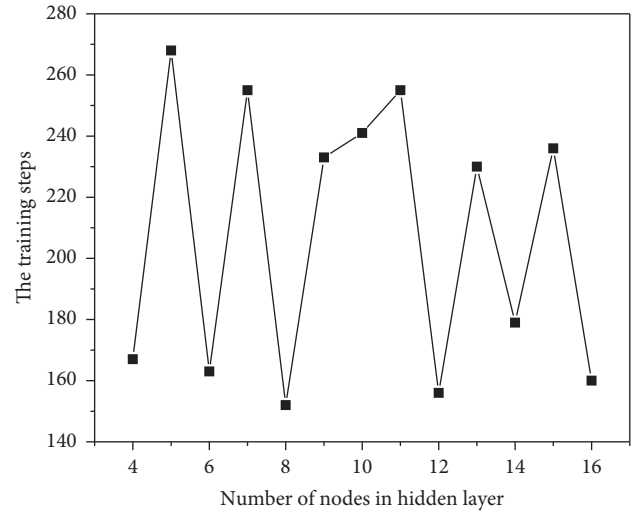


FIGURE 3: Relationship between the number of hidden layer units and the number of training steps.

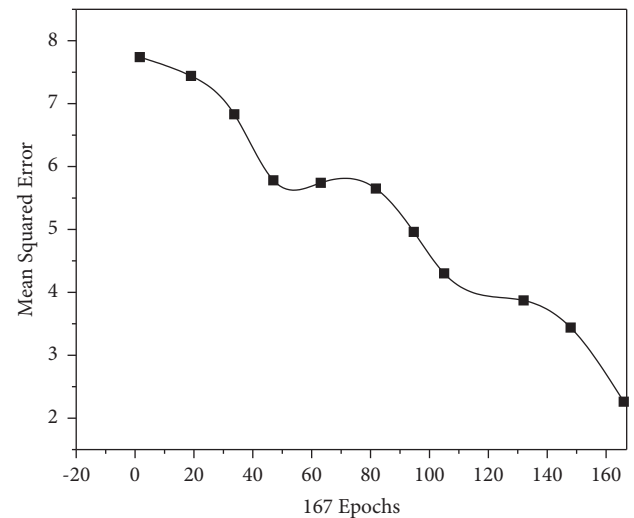


FIGURE 4: Error curve when hidden layer node is 4.

be selected. In the BP neural network model, the latent layer excitation function is tansig, the output layer excitation function is the logsig function, and the training function is the traindm. The network learning era is defined as 2000, and the default value for the model learning speed is 0.01. The target error was set to 0.005 according to the actual output requirement. The number of nodes in the hidden layer is 4–16 each, and the size and convergence of the model errors are observed in the different nodes. By varying the number of nodes in the hidden layer, it is possible to obtain the relationship between the number of units in the hidden layer and the

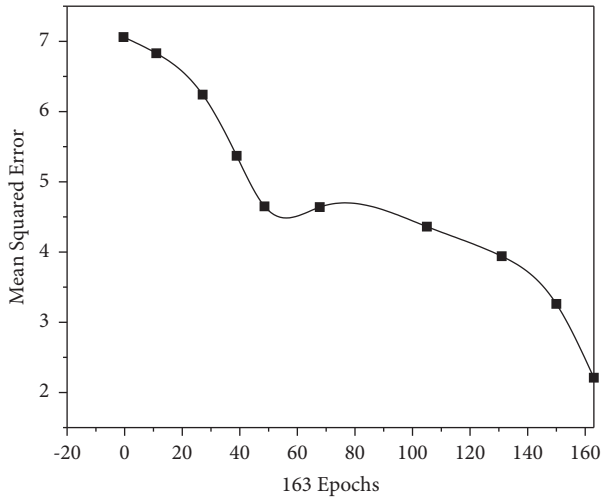


FIGURE 5: Error curve when hidden layer node is 6.

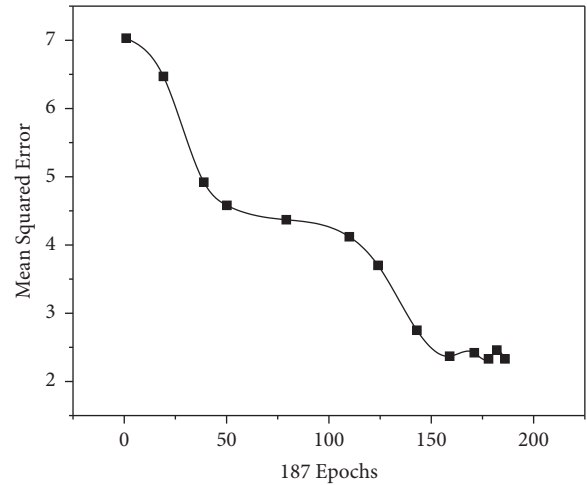


FIGURE 8: Error curve when hidden layer node is 14.

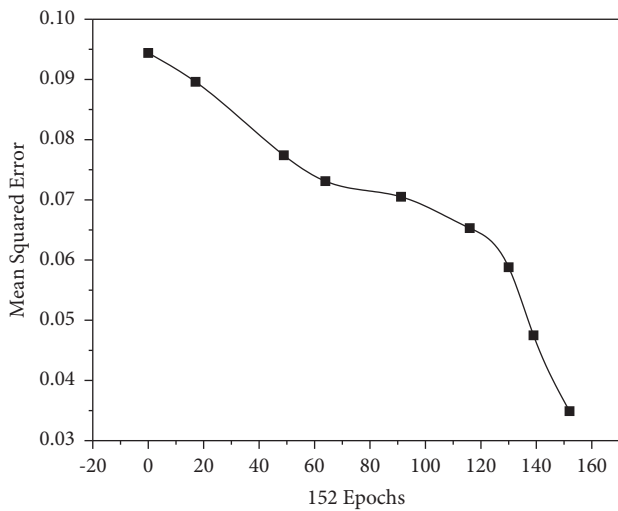


FIGURE 6: Error curve when hidden layer node is 8.

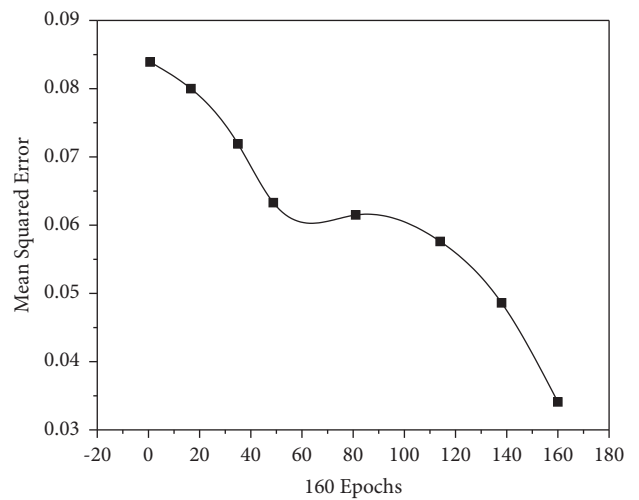


FIGURE 9: Error curve when hidden layer node is 16.

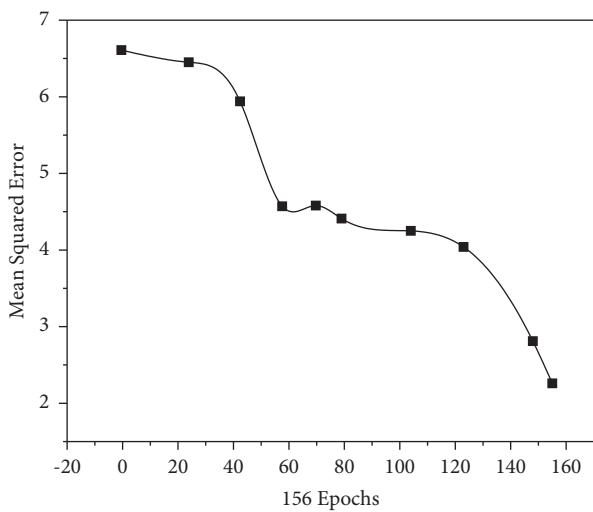


FIGURE 7: Error curve when hidden layer node is 12.

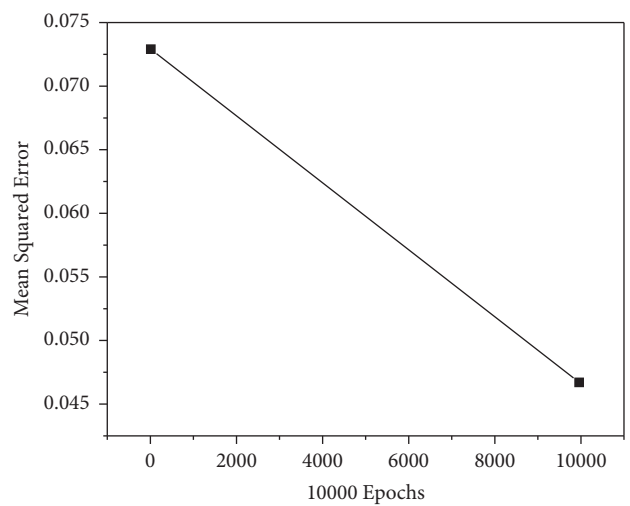


FIGURE 10: Training function error curve.

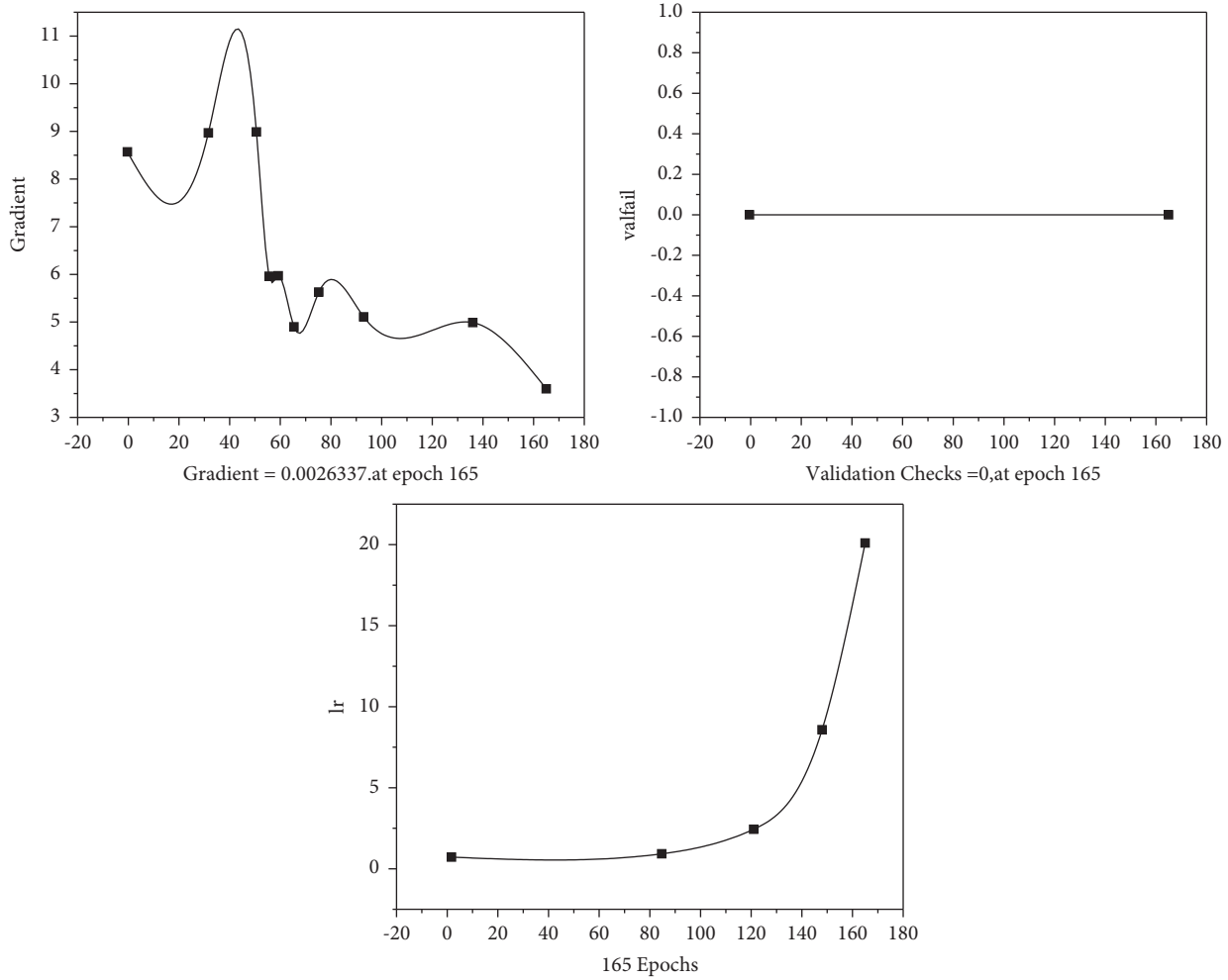


FIGURE 11: Traingdx is the error curve of the training function.

number of training steps when there are 4–16 nodes, Table 2 and Figure 3.

It can be seen from the above table that when the number of hidden layer nodes is 4, 6, 8, 12, 14, and 16, the number of training steps required for network training to reach the preset error is less. The error curve circle of the above node model is shown in Figures 4–9.

As can be seen from the above table and system error diagram, the number of hidden layer nodes is small, and the network performance is poor. The hidden layer has 8 nodes. Although it meets the requirements after 156 times of training, the number of nodes is small and the neural network is unstable. When the number of hidden layer nodes is 12, 14, and 16, the training steps are 156, 187, and 160 times, respectively, and meet the target error requirements of the research. When the number of hidden layer neurons is larger than 12, the error requirements can be met, but the increase in the number of neurons leads to the increase in network burden and the increase in training times, and cannot significantly improve the network performance. Therefore, the hidden layer of the BP neural network model constructed in this study selects 12 neuron nodes [20].

This study has analyzed in detail that the BP neural network model of the credit risk of small- and medium-sized enterprises in supply chain financing should select a new training function. The new training functions of the BP neural network are traingdm and traingdx. When the number of hidden layer nodes and other parameters is the same, the two functions are used to train, respectively, and then, the optimal training function is determined according to the error. When traingdm is selected as the training function, it does not converge to the preset target error value within 10000 steps w (see Figure 10 below). Therefore, this study constructs the BP neural network model and selects traingdx as the training function (Figures 11 and 12).

The learning rate has a great influence on the stability and convergence of the neural network model. According to Figure 12, in the above training process, the learning rate is 0.01 by default. Therefore, this study replaces the following learning rates in turn: 0.005, 0.01, 0.02, 0.03, and 0.04. Finally, it is found that when the learning rate is exactly the default 0.01, the error is the smallest and the stability is the best. The error is 0.0031011, and the step size is 157, which is

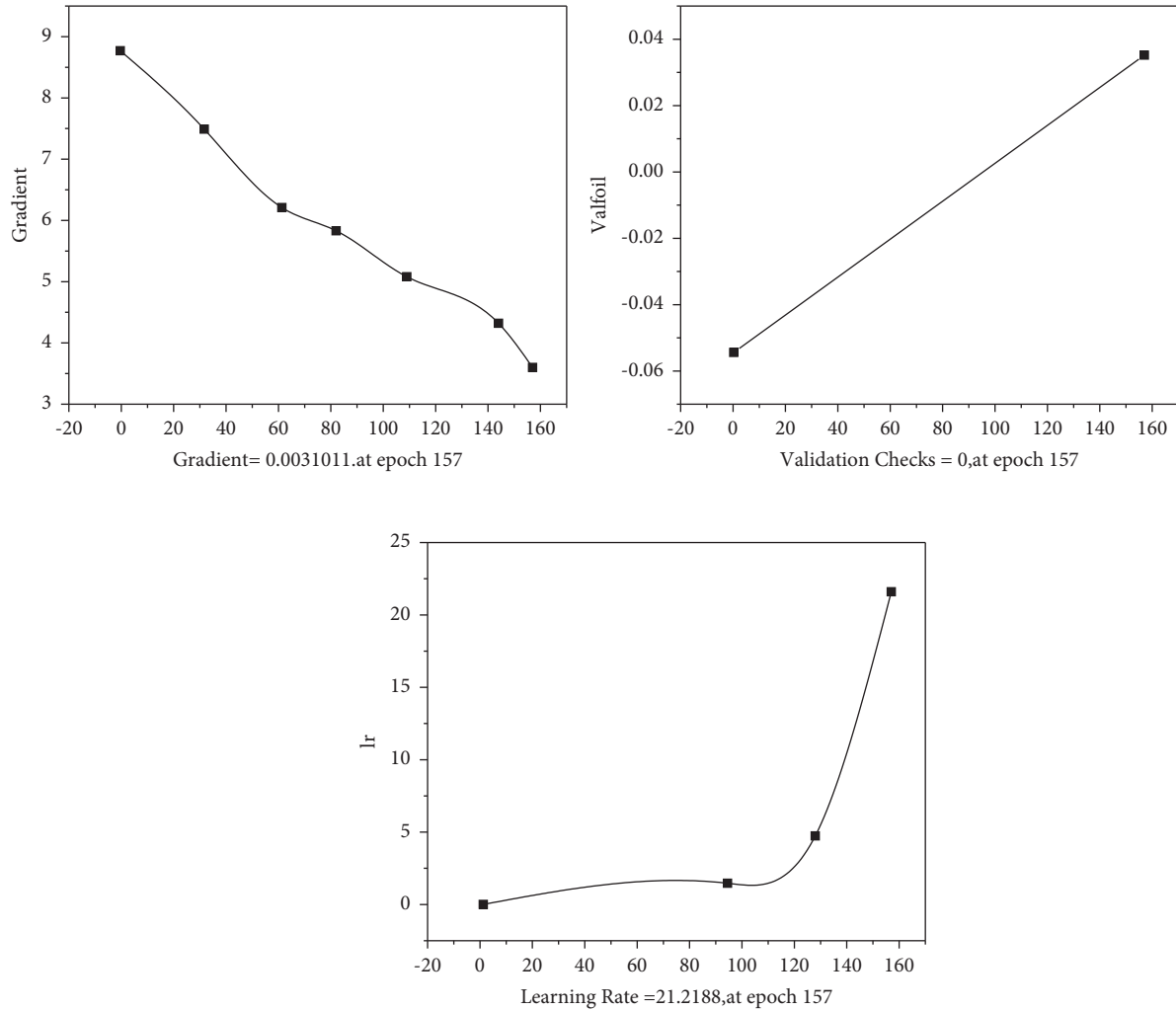


FIGURE 12: Systematic error diagram at a learning rate of 0.01.

just less than the target error value, indicating that the learning rate is better [21, 22].

5. Conclusions

This study discusses in detail the possibility of using the BP neural network model in the corporate financial risk assessment process. As far as we know, the BP neural network model has been very well researched in the financial sector. Finally, this study selects 19 indicators and provides a concise, scientific, and effective system of indicators. The BP has developed a credit risk assessment model for banking-based banking institutions based on the MATLAB software platform. With the help of wind databases and sample data collected from questionnaires, network design is trained and model accuracy is verified. The BP neural network assessment model for corporate lending risk in this document is highly accurate. In addition to providing theoretical insights to researchers, it can be a good tool for banks to realistically assess the credit risk of SME supply chain financing.

Data Availability

The labeled dataset used to support the findings of this study is available from the corresponding author upon request.

Conflicts of Interest

The authors declare no conflicts of interest.

Acknowledgments

This work was supported by the Key Project of Guangxi Higher Education Undergraduate Teaching Reform Project in 2019 (no. 2019JGZ145), part of the Guangxi University of Finance and Economics High-level Talent Introduction Project in 2017 (no. BS2019010) or the National Social Science Foundation of China in 2018 (no. 18BJY015), the Integration Innovation Project of Accounting Undergraduate Major of Guangxi University for Nationalities in 2020 (no. 2020JGA166), and/or the Guangxi Education science Planning Funding Key Project in 2021 (no. 2021A038).

References

- [1] W. Xie, "Spatial aggregation analysis and systemic risk prevention of internet finance based on neural network model," *Journal of Physics: Conference Series*, vol. 1744, no. 4, Article ID 042176, 2021.
- [2] D. Liu, H. Yu, and C. Zhang, "Analysis and forecast of special car market based on bp neural network," *Journal of Physics: Conference Series*, vol. 1345, no. 4, Article ID 042073, 2019.
- [3] Y. Wang, X. Wang, W. Zhang, K. Zheng, and X. Fu, "Comprehensive analysis of risk factors in internet agricultural finance based on neural network model," *Journal of Intelligent and Fuzzy Systems*, vol. 40, no. 4, pp. 6593–6604, 2021.
- [4] Y. Lan and X. Li, "A brief analysis of the application of enterprise's internal accounting and financial management in computer," *E3S Web of Conferences*, vol. 235, no. 24, 03087 pages, 2021.
- [5] W. Aiqun, H. Zicong, and W. Yilin, "Risk assessment of logistics finance enterprises based on bp neural network and fuzzy mathematical model," *Journal of Intelligent and Fuzzy Systems*, vol. 39, no. 4, pp. 5915–5925, 2020.
- [6] W. Li, "Research on project knowledge management risk early warning based on bp neural network," *Journal of Physics: Conference Series*, vol. 1744, no. 3, Article ID 032250, 2021.
- [7] S. Zhao and N. Lv, "Pgpermaking enterprise financing and the mechanism of financial risk transmission based on cluster model," *Paper Asia*, vol. 35, no. 2, pp. 40–44, 2019.
- [8] S. Li and Y. Quan, "Financial risk prediction for listed companies using ipso-bp neural network," *International Journal of Performability Engineering*, vol. 15, no. 4, pp. 1209–1219, 2019.
- [9] X. Wu and Q. Lu, "Financial asset yield series forecasting based on risk-neutral fuzzy bilinear regression and probabilistic neural network," *Journal of Intelligent and Fuzzy Systems*, vol. 40, no. 6, pp. 11829–11844, 2021.
- [10] T. Xuesong, W. Bin, Y. Guangming, F. Fulai, Q. Jinyu, and D. W. Hongjiang, "The risk quantification evaluation strategy for the distribution line based on emlr," *E3S Web of Conferences*, vol. 236, no. 10, Article ID 01005, 2021.
- [11] M. Nayak, T. Abdullah, and T. Abdullah, "Short term predication of risk management integrating artificial neural network ANN," *International Journal of Engineering and Advanced Technology*, vol. 9, no. 3, pp. 2828–2833, 2020.
- [12] T. Shen, J. Chang, J. Xie, and L. Huang, "Analysis of microchannel resistance factor based on automated simulation framework and bp neural network," *Soft Computing*, vol. 24, no. 5, pp. 3379–3391, 2020.
- [13] X. Zou, "Analysis of consumer online resale behavior measurement based on machine learning and bp neural network," *Journal of Intelligent and Fuzzy Systems*, vol. 40, no. 2, pp. 2121–2132, 2021.
- [14] M. L. Ling, L. Yuan, and C. Y. Wei, "Risk analysis of the real estate financial market based on risk energy theory," *International Journal of Corporate Finance and Accounting*, vol. 8, no. 1, pp. 15–26, 2021.
- [15] X. L. Fan and J. D. P. Bezerra, "Cytospora diaporthales in China," *Persoonia - Molecular Phylogeny and Evolution of Fungi*, vol. 45, no. 1, pp. 1–45, 2020.
- [16] F. Xu, X. Zhang, Z. Xin, and A. Yang, "Investigation on the Chinese text sentiment analysis based on convolutional neural networks in deep learning," *Computers, Materials & Continua*, vol. 58, no. 3, pp. 697–709, 2019.
- [17] F. Tao, "Performance analysis of real estate management entities based on dea model and bp neural network model," *Journal of Physics: Conference Series*, vol. 1744, no. 2, Article ID 022025, 2021.
- [18] G. Wei and Y. Jin, "Human resource management model based on three-layer bp neural network and machine learning," *Journal of Intelligent and Fuzzy Systems*, vol. 40, no. 2, pp. 2289–2300, 2021.
- [19] Z. Qin, P. Luo, W. Zhang, X. Liu, and J. Zhou, "Artificial core matching design model based on bp neural network," *Oilfield Chemistry*, vol. 36, no. 1, pp. 174–180, 2019.
- [20] X. Fan, Y. He, P. Cheng, and M. Fang, "Identification of pressure control model in a solenoid valve based on ga-bp neural network," *Journal of Physics: Conference Series*, vol. 1345, no. 2, Article ID 022050, 2019.
- [21] Y. Zhang, X. Xiong, X. Wu, Z. Song, and Z. Xue, "Optimization of sofc stack gas distribution structure based on bp neural network and cfd," *E3S Web of Conferences*, vol. 245, no. 7, Article ID 03007, 2021.
- [22] Y. Liu, "Incomplete big data imputation mining algorithm based on bp neural network," *Journal of Intelligent and Fuzzy Systems*, vol. 37, no. 4, pp. 4457–4466, 2019.

Research Article

Analysis of Music Teaching in Basic Education Integrating Scientific Computing Visualization and Computer Music Technology

Yanyan Zhao 

Department of Music and Dance, Anhui University of Arts, Hefei 230011, China

Correspondence should be addressed to Yanyan Zhao; 114034@ahua.edu.cn

Received 14 March 2022; Revised 14 April 2022; Accepted 27 April 2022; Published 19 May 2022

Academic Editor: Wei Liu

Copyright © 2022 Yanyan Zhao. This is an open access article distributed under the Creative Commons Attribution License, which permits unrestricted use, distribution, and reproduction in any medium, provided the original work is properly cited.

In the current music education, the music teaching method is too simple, boring, relatively backward, unable to attract the attention of the students, and the students gradually lose their interest in music courses. In basic education, music, as a highly practical subject, must create a good classroom atmosphere, make the classroom active, and enable students to better experience music, enjoy music, and like music. Therefore, in order to change this situation, this paper, based on scientific computing visualization, studies the application of computer music technology in basic education music teaching, and proposes a related computing method based on scientific computing visualization-image segmentation method. This review compares the spectrum extraction accuracy between the improved algorithm and the two traditional algorithms and finds that the average accuracy of the improved algorithm is 90.88%. It can be seen that the method proposed in this review is more suitable for the study of computer music technology in basic education music teaching. Applied research and most students are more interested in music teaching combined with computer music technology, so learning music teaching combined with computer music technology is very necessary. The development of computer music technology is closely related to the development of modern information technology.

1. Introduction

Scientific computing visualization, also known as visualization, is defined as follows: "Visualization is a computational method that converts symbols or data into intuitive geometric figures that allow researchers to observe their simulations and computational processes." Visualization includes image synthesis. Today, Chinese science and technology has achieved unprecedented development, and the role of computers has become greater and greater, penetrating into various music fields including music education. Computer music education is a new education model based on computer software and hardware, which realizes the learning and creation of music. Now, China is paying more and more attention to the development of high-quality education, especially in the field of basic education. As a part of high-quality

education, music education is receiving more and more attention. The correct and interesting way to understand music knowledge in the classroom is a problem that needs to be solved as soon as possible, and the introduction of computer music technology can help improve the efficiency of education. The visualization of scientific computing is a new research field proposed in the second half of the 1980s. In this article, we will study its application to music education in basic education.

The teaching method of music subject should be different from other subjects, and the teaching method should be richer. The use of computer music technology can greatly improve the existing teaching mode, and students will also have a huge impact on the teaching concept of music. The use of computer music technology can explore new methods and approaches for improving the traditional music-teaching mode. The core of scientific

computing visualization is the visualization of three-dimensional data fields, and it is believed that its use in music teaching can increase the visual impact, improve the interest of teaching, and make students' classroom experience better. The combination of computer music technology and scientific computing visualization is believed to make the classroom more colorful.

Since computer music technology was invented, it has been widely accepted by people and applied to various music fields. Since the introduction of computer music technology, many scholars have conducted research on it. In the middle of the twentieth century, the invention of software was a huge breakthrough for modern humans, and it is unique for computer musicians to predict the future through creation and coding. Scaletti combines the artist's imagination and courage with the technology that can make fictional things become reality, which is innovative [1]. Mcpherson and Tahiroğlu studied the ways in which computer music language may also affect the aesthetic decision-making of digital music practitioners, with particular attention to the concept of habituation. Then, he communicated with developers of several major music-programming languages, and conducted surveys on creators of digital musical instruments, examining the relationship between idiomatic patterns of the language and the characteristics of the generated instruments and music, but the research lacks data support [2]. In this article, Hayes introduces the large-scale project of sound, electronics, and music. The themes of the project include collective electroacoustic synthesis, live recording, and improvisation. Particular emphasis is placed on providing a form of music education that should enable everyone to practice creatively, regardless of their musical ability and background. The findings and results of the project indicate that people should not limit the discussion of how to continue the practical education of computer music to the next generation at the university level [3]. El-Shimy and Cooperstock provide a set of key principles for the design and evaluation of new user-driven interactive music systems and investigate the evaluation techniques provided by the new directions of HCI, linguistics, interactive arts and social sciences. His goal is to lay the foundation for designers of new music interfaces to develop and customize their own methods, but there are few survey categories in this study [4]. Combining traditional art with advanced technology is a challenging task, and Park's task is to instill tradition into technology, so as to protect and develop tradition at different levels. He believes that the future of Korean music education is to learn Korean music. As for the production materials and new works, it depends on how many materials and works are produced. The shortcoming of this research is that no specific countermeasures are proposed [5]. The purpose of Haning's research is to investigate the type, quantity, and effect of technical teaching currently provided to undergraduates majoring in music education. The survey involved 46 undergraduates who received technical guidance during their undergraduate degree courses and their plans to implement technology in the classroom in the future. The results showed that 43% of the participants were not prepared for

effective use of technology in future teaching positions, and it would be better if the study gave suggestions to enhance undergraduates' use of technology for music education [6]. The term "music technology" defined by Chakraborty refers to electromagnetic and mechanical equipment, including musical instruments, electric sound generators, and related computer technology. Chakraborty started writing in the form of dialogue, introducing the ontology of music (where, why, and how) and the ontology of music (facts, processes, and gestures) [7].

The innovation of this article is (1) combining scientific computing visualization and computer music technology and applying it to music teaching in basic education, and introduces its related methods, which is a methodological innovation. (2) A teaching experiment was designed based on scientific computing visualization and computer music technology, which proved the superiority of this new teaching method, which is an innovation in experiment.

2. Application Methods

2.1. Visualization of Scientific Computing. Scientific computing visualization refers to the use of computer graphics and image processing technology to convert data into graphics and images in the process of scientific computing [8]. The realization of scientific computing visualization can greatly speed up the data processing process so that the huge data generated every day can be effectively used; it can realize image communication between people and data, and between people, instead of text communication or communication. Digital communication allows scientists to understand what is happening in the computing process and can change parameters, observe their effects, and guide and control the computing process. In short, the tools and environment for scientific computing can be further modernized.

2.1.1. Classification and Process of Visual Chemistry Subjects in Scientific Computing. There are many fields of scientific computing visualization design. Figure 1 shows the subjects covered by the visualization of scientific computing.

The basic process of scientific computing visualization is to first preprocess the data, then use the mapping algorithm to map the application data to obtain geometric data, then draw the geometric data to obtain image data, and finally output to the terminal device and display [9]. The details are shown in Figure 2.

2.1.2. Visualization Methods of Scientific Computing

(1) 3D Surface Editing Method Based on Sampling Points. Direct editing is parameter-free modeling, that is, you do not need to modify the parameters and features of the parts one by one, but directly modify the model and preview the modified model directly. First, the model needs to be embedded in the scalar field, and then the scalar value is calculated at each vertex of the embedded part. In the process of free deformation, each vertex is always restricted by the level

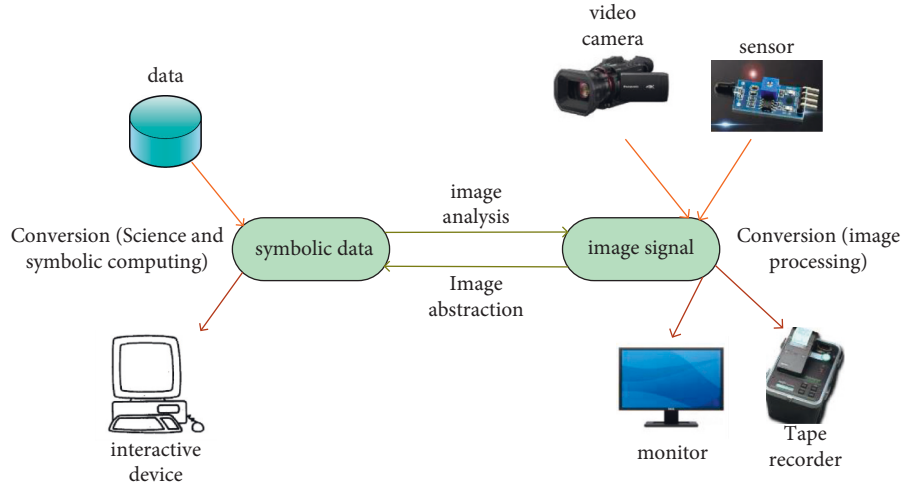


FIGURE 1: Visual classification of scientific computing.

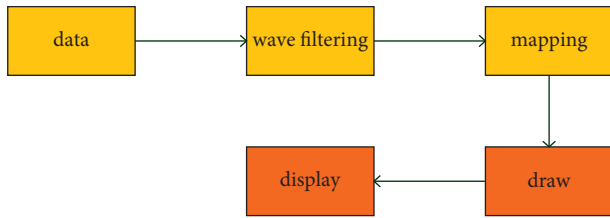


FIGURE 2: Visualization flow chart.

set, and the level set is initialized with the vertex stream. When the user modifies the scalar field, the vertices will move according to the free deformation of the embedded object. After the scalar field is deformed in space, since there is no scalar deformation technology, the reconfigured vertices in the deformed object remain in the same level set [10] and get the derivative of $f(X(t), t)$:

$$\frac{df(X(t), t)}{dX} = \frac{\partial f(X(t), t)}{\partial X} \cdot \frac{dX(t)}{dt} + \frac{\partial f(X(t), t)}{\partial t} = 0. \quad (1)$$

In equation (1), $df(X(t), t)/dX$ represents the gradient of X , and velocity $dX(t)/dt$ is regarded as the velocity value along the three coordinate axes of x , y and Z in the three-dimensional space, adding smoothness constraints to the model to minimize the change of vertex velocity in a local area. Smoothness is an index for evaluating the degree of convexity and concavity on the surface of paper or cardboard, which is very important for printing paper. ∇f represents the gradient and replace $f(X(t), t)$ with f to obtain the following minimum objective function:

$$P = \int \left(\frac{\partial f}{\partial t} + v \cdot \nabla f \right) + \theta \cdot \nabla v^2 dX. \quad (2)$$

In the formula, P represents the smoothing coefficient, θ represents the Lagrangian coefficient, and X represents the vertex. Discretizing this formula, let k represent a voxel mesh vertex, and Q_k represents adjacent mesh vertices. The approximate error of the vulnerability constraint is

$$E(k) = \left[\frac{\partial f}{\partial t} + \frac{\partial f}{\partial x} v_x k + \frac{\partial f}{\partial y} v_y k + \frac{\partial f}{\partial z} v_z k \right]^2. \quad (3)$$

According to the speed difference between vertex k and its neighboring points, the smoothness of local area motion can be calculated [11]:

$$P(k) = \frac{1}{Q_k} \sum_{j \in Q_k} \left[(v_x(k) - v_x(j))^2 + (v_y(k) - v_y(j))^2 + (v_z(k) - v_z(j))^2 \right]. \quad (4)$$

S represents the smoothing coefficient, Q_k represents the number of vertices of the voxel mesh in Q_k , then

$$G = \sum_k (E(k) + \theta P(k)). \quad (5)$$

The previous level set algorithms have only a single velocity function, in the evolution process of the zero-level set, the minimization of the energy function is a very complicated process, and there are many problems with a single velocity function. Although the velocity field of the associated voxel, grid can be obtained according to the change of the scalar field, and their position cannot be changed. As an alternative, through the velocity function defined in the following level set method [12], use H to represent the velocity function of the curved surface scalar field, and use the velocity field v obtained above to update the curved surface scalar field:

$$H = \frac{\nabla S \cdot v}{|\nabla S|}. \quad (6)$$

(2) *Surface Update and Resampling Method.* Since the scalar free deformation technology requires that the relocation of the vertex $X(t)$ should assume that the implicit function is a zero-level set, the reciprocal of $f(X(t), t)$ can be expressed as follows:

$$\frac{dS(X(t), t)}{dX} = \frac{\partial S(X(t), t)}{\partial X} \cdot \frac{dX(t)}{dt} + \frac{\partial S(X(t), t)}{\partial t}. \quad (7)$$

When the density of points on the surface becomes low, new sampling points need to be inserted so that the points on the surface remain uniform. The basic idea of the method is to calculate the Voronoi histogram of adjacent points on the tangent plane [13]. A histogram is a statistical chart that uses rectangular bars to compare numerical values of different categories. Use the length of vertical or horizontal columns to compare the magnitude of numerical values, where one axis represents the categorical dimension that needs to be compared, and the other axis represents the corresponding numerical value.

(3) *Level Set Method*. Another advantage of the level set method is that it can easily track the topological changes of objects. For example, when the shape of the object is divided into two, creating a hole, or vice versa. The level set method is a numerical calculation method to solve the deformation evolution of implicit curves and curved surfaces [14], as shown in Figure 3. By moving the level set function, that is, through the rise, fall, and expansion of the level set function, the contours of the closed curve at different times can be obtained. The evolution result of the level set function surface must be related to the evolution result of the closed curve.

2.1.3. *Visualization Algorithms for Scientific Computing*. In the early days of computer visualization, the visualization system only provided the functions of drawing and printing one-dimensional curves and two-dimensional contours and surface views. Three-dimensional visualization technology is the separation between the initial stage of computer visualization and the new era of scientific computing visualization [15]. Compared with the initial computer visualization system, the main feature of the scientific computing visualization technology is the three-dimensional visualization technology. The visualization algorithm is shown in Table 1.

2.2. *Teaching Technology Based on Computer Music Technology*. Music is divided into two parts: visual scores and auditory songs, and its teaching targets are usually young people. Therefore, the practical process often needs some methods that highlight the characteristics of music and art that can directly allow learners to see and hear than traditional theoretical teaching [16]. The spectrum recognition is to help music teachers to realize visual score recognition and auditory music recognition. Among them, “spectrum” refers to the recognition of graphic music scores using computer image processing, and “tone” refers to music recognition using computer signal processing, audio processing, and other knowledge. In general, it is necessary to realize both visual score recognition and auditory music recognition. Therefore, in order to explain the educational technology of computer music technology, this chapter is

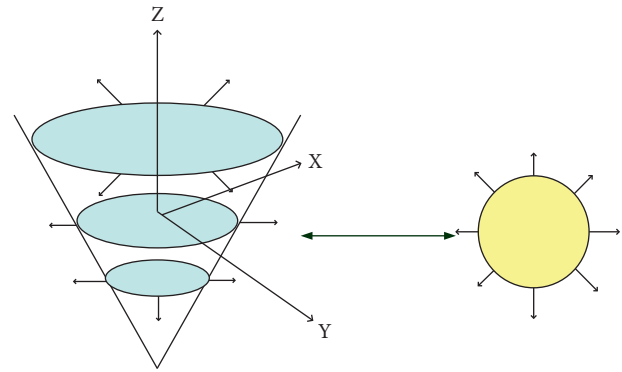


FIGURE 3: Circle and its level function.

divided into two parts: score recognition and music recognition [17].

2.2.1. *Numbered Musical Notation Recognition*. This section uses basic image processing techniques to study and identify the musical theory symbols in the numbered musical notation pictures, hoping to bring some convenience to the teaching of numbered musical notation. The numbered musical notation recognition is generally divided into image preprocessing, inclination correction, and bar line recognition.

(1) *Image Preprocessing*. Preprocessing is basically the first step of all image recognition technologies, and the quality of preprocessing sometimes has a decisive impact on the recognition accuracy. The basic steps are as follows: the main purpose of image preprocessing is to eliminate irrelevant information in images, recover useful real information, enhance the detectability of relevant information, and simplify data to the greatest extent, thereby improving the reliability of feature extraction, image segmentation, matching, and recognition:

Gray conversion:

Before starting the score recognition, grayscale conversion can be performed. The RGB three-dimensional information of the image is converted into one-dimensional, which greatly reduces the amount of calculation and improves the efficiency of subsequent symbol recognition. The current gray conversion methods mainly include the maximum value method, the average value method, and the weighted average method. Through the image conversion of the image captured by the camera, the format of the image is converted to RGB565 first, then the grayscale conversion is performed, and finally the binarization process is performed. Different weights are assigned to RGB according to the sensitivity of human eyes to colors, and the grayscale calculation uses the weighting formula [18]:

$$y = 0.299R + 0.587G + 0.114B. \quad (8)$$

TABLE 1: Typical visualization techniques.

Dimension	Scalar	Tensor	Fitness vector
1D	Line drawing, histogram, bar chart	—	—
2D	Contour line, surface view, image display	—	2D arrow
3D	Isosurface, 3D point cloud surface	Tensor ellipse	3D arrow, particle system, 3D streamline

The weights of the red, green, and blue channels are measured according to the sensitivity of the human eye to color, and the above formula can be used to obtain a more ideal grayscale image.

Denoising:

This step is used to remove image noise and distortion. Methods to remove noise include Gaussian blur, bilateral filtering, median filtering, and so on. Under normal circumstances, the background of the music score is mainly bright colors, and the music score is mainly dark, because the noise in the form of isolated noise is the most, so if the Gaussian filter is used, the image itself can be restored most accurately. While maintaining the signal of the score itself, it reduces noise.

Sharpen:

Although Gaussian Blur can reduce noise, it blurs the key part of the image—the music score, so it needs to further sharpen the picture to highlight the characteristics of the music score. Laplace transform is an integral transform commonly used in engineering mathematics, also known as Laplace transform. The Laplace transform is a linear transform. Laplacian is the operation that can highlight the details of the image and enhance the region of the image with sudden grayscale changes. The Laplace transform of a two-dimensional image is defined as the formula:

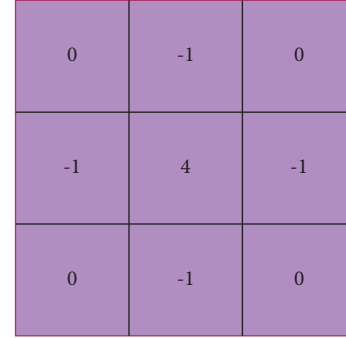
$$\text{Laplace}(f) = \frac{\partial^2 f}{\partial x^2} + \frac{\partial^2 f}{\partial y^2}. \quad (9)$$

Edge detection is a fundamental problem in image processing and computer vision. The purpose of edge detection is to identify points in digital images with obvious changes in brightness. Significant changes in image properties often reflect significant events and changes in properties. The Laplacian operator is very useful in edge detection, and its representation as a template is shown in Figure 4:

Binarization:

Binarization is a simple form of thresholding. It selects the threshold t and extreme values a , b for the entire image, and for any pixel $f(x, y)$ at the coordinate (x, y) in the source image, if the pixel value at the target image coordinates (x, y) is $g(x, y)$, then

$$\begin{cases} g(x, y) = a, & f(x, y) < t, \\ g(x, y) = b, & f(x, y) \geq t. \end{cases} \quad (10)$$



0	-1	0
-1	4	-1
0	-1	0

FIGURE 4: Laplacian operator template.

The local threshold segmentation rule is not the case. It divides the original image into multiple smaller sub-images and selects the corresponding threshold for each subimage, and then performs local threshold segmentation [19]. Due to the influence of illumination, the gray level of the image may be unevenly distributed, and the segmentation effect of the single threshold method is not good. Therefore, the local threshold segmentation method should be used.

(2) *Inclination Correction.* This step is to try to eliminate the influence of the inclination of the score caused by the angle error in the shooting process and make the spectrum line parallel to the axis of the image coordinate system [20].

Angle extraction:

To correct the angle of the sheet music, the most important thing is to extract the inclination of the sheet music. No matter how the notation is slanted, every line of the musical notation ends with a bar line at the end, and the bar lines between the lines are aligned. This means that as long as a straight line can be found from the image, and this straight line crosses the last bar of each line of the numbered musical notation, its inclination also represents the inclination of the musical score. It can be imagined that in the image coordinates, all the infinite straight lines passing through (i, j) correspond to infinite points in the (ρ, θ) coordinates, and these points constitute a characteristic curve.

$$\rho = x \cos \theta + y \sin \theta. \quad (11)$$

Image rotation:

After extracting the inclination of the score, you only need to perform a simple rotation operation on the binarized image to get the horizontal score image. An arbitrary affine transformation can be expressed in the

form of multiplying by a matrix and adding a vector, which is defined as follows [21]:

$$\begin{aligned} A \cdot X + B &= X' \cdot t \\ &= \begin{bmatrix} a_{00} & a_{01} & b_0 \\ a_{10} & a_{11} & b_1 \end{bmatrix}. \end{aligned} \quad (12)$$

By changing the value of t , the mapping from any parallelogram to another parallelogram can be achieved. For a two-dimensional image with width w and height h , the 2×3 rotation matrix based on the counterclockwise rotation of the center in radians is as follows:

$$\begin{aligned} t &= [A \ B] \\ &= \begin{bmatrix} \cos \theta & \sin \theta & 0.5w \\ -\sin \theta & \cos \theta & 0.5h \end{bmatrix}. \end{aligned} \quad (13)$$

2.2.2. Music Recognition. Music recognition refers to the digital recognition process of recorded human voice or musical instrument audio files. It involves physical acoustics, music art, computer science, and other interdisciplinary subjects and has very large application development prospects [22].

(1) *Basic Knowledge of Signal Processing.* The human ear hears music directly in a perceptual way, but computers do not. The computer sound card converts the continuous waveform signal of the sampled sound wave into a digital signal, and then stores the music information in the form of a file after sampling according to the Nyquist sampling theorem. In practical applications, the human vocal frequency range is 85–1100 Hz, and the sampling rate of a general sound card can reach 44100 Hz, which is much higher than the human voice frequency, so its sound wave information can be completely preserved, laying the foundation for further fundamental frequency extraction.

(2) *Fundamental Frequency Extraction.* There are many methods of fundamental frequency extraction, here are a few to introduce.

Harmonic peak method:

Harmonic peak method is a typical algorithm based on fast Fourier transform, which reflects the relationship between signal frequency and amplitude, so it is widely used to calculate the frequency spectrum of the signal.

$$\begin{aligned} F(x) &= F[f(t)] \\ &= \int_{-\infty}^{+\infty} f(t)e^{-txt} dt. \end{aligned} \quad (14)$$

The harmonic peak method considers that the peak with the highest amplitude in the spectrogram corresponds to the fundamental wave of the audio signal and takes its frequency value as the fundamental frequency

value, that is, set the fundamental frequency value to m , then

$$m = F^{-1}[\max(F(x))]. \quad (15)$$

The biggest advantage of this method is that it is simple enough, and the time complexity and space complexity are very low. Now, the fast Fourier transform is performed on the C1 key tone recorded in an environment without background noise, and the resulting spectrum is shown in Figure 5 [23]. The function of Fourier transform is mainly to convert the function into the form of multiple sine combinations. In essence, the signal after the transformation is still the original signal, just a different way of expression.

Confidence method:

In this method, a factor of 1 to 5 can be obtained for the maximum peak frequency as the candidate fundamental frequency, and then the amplitude of the n th harmonic of each candidate fundamental frequency is summed. The candidate fundamental frequency with the largest sum has the greatest confidence and the greater the likelihood of being the fundamental frequency. Its confidence is as follows:

$$\begin{cases} L(N) = \frac{f}{N}, & 1 \leq n \leq 5, \\ R(N) = \sum_{i=1}^n p(i). \end{cases} \quad (16)$$

$L(N)$ is the candidate fundamental frequency, f is the maximum peak frequency, $R(N)$ is the confidence level, $p(i)$ is the amplitude of a certain order of harmonics, and n is the number of harmonics.

(3) *Semantic Understanding.* So far, the time value and pitch of all the notes have been identified. To understand the semantics of the notes and restore them to notes, the reverse formula is needed as follows:

$$\begin{cases} x = \min(r - r, 1 + r - r), \\ r = 12 \log_2 \frac{f}{440} + 49, \end{cases} \quad 1 \leq x \leq 88. \quad (17)$$

In the formula, x represents the key number, and f is the pitch, which is the fundamental frequency value. Then it is further converted into the number num of numbered musical notation and the number of high and low points t , as shown in the following formula:

$$\text{num} = \begin{cases} \frac{(x - 12t - k + 2)}{2} & \text{num} = 1, 2, 3, \\ \frac{(x - 12t - k + 3)}{2} & \text{num} = 4, 5, 6, 7, \end{cases} \quad t = \frac{(x - k)}{12}. \quad (18)$$

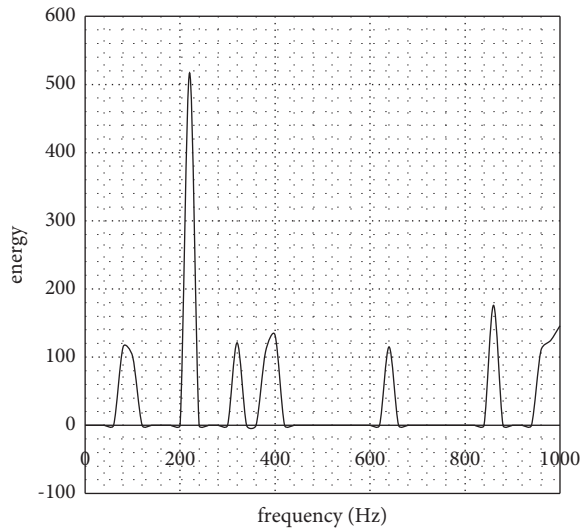


FIGURE 5: Spectrum of C1 button.

As for the time value part, suppose the time signature is m/n , the speed is s , the duration of a note is t seconds, and the note is a z -quaver, and there is the following:

$$z = \frac{60n}{ts}. \quad (19)$$

In this way, the frequency can be expressed as numbered musical notation and high and low points, and the duration can be converted into a time value.

3. The Teaching Application Method of Computer Music Technology

In today's music classrooms, most of them are still teacher-oriented. Teachers teach music theory, teach singing, and let students enjoy music. The modern education theory believes that students are the main body of the classroom and should be based on students. At this time, the application of computer music technology can bring new development to music teaching [24].

3.1. The Application of Computer Music Technology in the Teaching of Music Theory. The guiding method of music theory is relatively traditional, and it is no longer suitable for this fast-developing society. Teachers can use computer music technology to play the songs they want to teach at any time. In addition, teachers can also input music scores on the computer when preparing lessons. This can greatly save the time of copying the blackboard, and students can have a new perspective on music. Music theory is no longer an intangible thing, but a subject that can be understood face to face. Many schools have limited musical instruments, so all the musical instruments cannot be displayed in the classroom. According to computer technology, it is possible to combine the image of the musical instrument and the sound of the musical instrument to achieve the effect of unifying the eyes and ears of students. Through the combination of vision and hearing, the difficulty of music

theory knowledge can be reduced, and the learning efficiency of students can be improved.

3.2. The Application of Computer Music Technology in the Teaching of Music Appreciation. Music appreciation covers a wide range of fields and requires a wide range of knowledge. If only traditional teaching methods and CDs or tapes are used, such courses will lose vitality. The application of computer music technology in appreciation courses can expand students' knowledge fields and improve educational efficiency. Through the application of computer music technology, knowledge can be clearly conveyed to students. Just like appreciating an opera, if you use computer technology, the whole course will become more beautiful and get better results. Through the use of computer technology, the theoretical knowledge of music appreciation can be made more intuitive, and the score and the lyrics of the music can be completely combined, which greatly improves the enthusiasm and initiative of students in learning. In the music appreciation classroom, teachers can use computer music technology to set various performance methods according to the guidance needs so that students can start playing at any time, so as to concentrate on learning.

3.3. The Application of Computer Music Technology in the Teaching of Music Composition. The curriculum standards of primary and secondary schools require students to cultivate and cultivate creativity. The students are young and their music knowledge is relatively weak, unable to reach the level that can create works [25], so it is enough to cultivate students' creative spirit. Using computer technology, text, audio, video, etc., can be integrated to arouse the enthusiasm of students from a visual and auditory perspective. In this way, the efficiency of teaching will also be improved. In addition, through the use of computer technology, students can also hear the sounds of musical instruments other than the piano, and then try to create on musical instruments.

To sum up, as an interdisciplinary subject, computer music education must be combined with actual conditions to find a practical and feasible path for the development of computer music education. From the perspective of building a computer music curriculum system and practice system, a set of teaching system construction plans suitable for the actual situation of the college are formulated, as shown in Figure 6. Establish a more systematic and scientific education and teaching quality assurance system that reflects the concept of total quality management, highlights process control, and achieves the satisfaction of the government and society.

4. Experimental Analysis and Results

4.1. Music Teaching Experiment Based on Computer Music Technology

4.1.1. Numbered Musical Notation Recognition Experiment

(1) Experimental Design. The platform of this experiment is Visual Studio, and the test of numbered musical notation recognition is carried out on this platform. This experiment

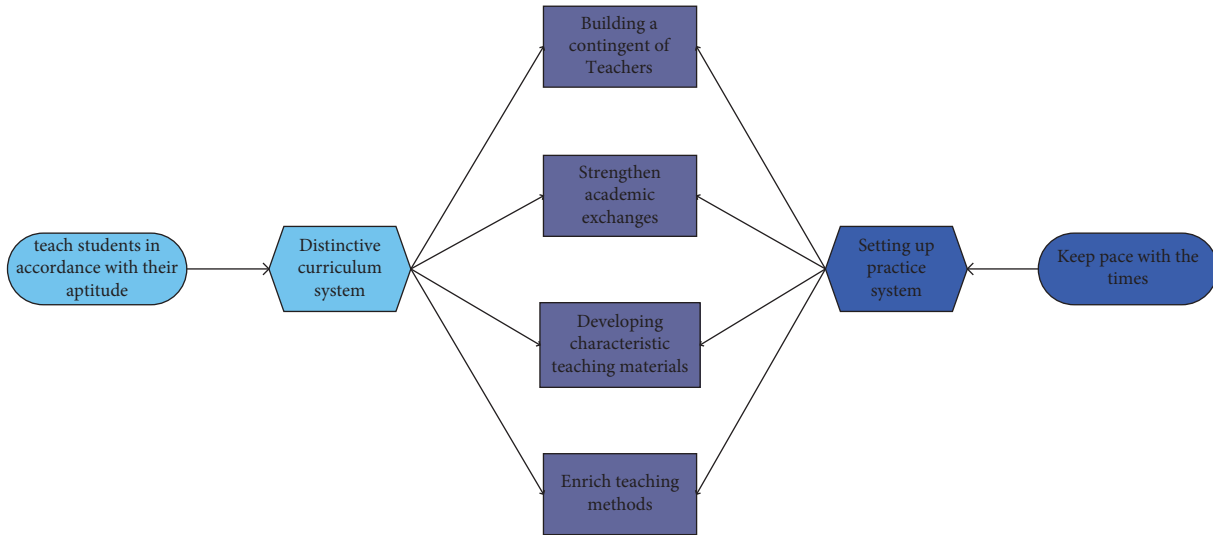


FIGURE 6: Teaching system construction.

studies music teaching in basic education, so the numbered musical notation of several songs in the textbooks of elementary and middle schools is selected for experiment. The selected songs include the song of selling newspapers, two tigers, the song of the seven sons, and the song of the fishing boat. The resolution of the numbered musical notation of these songs is increased in turn, and the accuracy of the numbered musical notation recognition algorithm for each numbered musical notation element is tested to explore the relationship between the resolution and the recognition accuracy of the numbered musical notation. It needs to number the numbered musical notation of several songs first, as shown in Table 2.

(2) *Experimental Results and Analysis.* Statistics on the identification results of each element are obtained, and Table 3 is obtained.

It can be seen from the table that the experiment counts the number of tuplets, digital notes, underscores, dashes, and dots in each numbered musical notation, and the true and recognized values of these numbers in the numbered musical notation. We calculated the total amount of these values to solve the accuracy of numbered musical notation recognition, and the results obtained were 98.4, 98.0, 98.4, and 95.7%. It proves that there is no significant difference between the recognition accuracy and the resolution of the numbered musical notation. Looking at the recognition time again, it can be seen from the table that the higher the resolution of the picture, the longer the recognition time.

4.1.2. Music Recognition Experiment

(1) *Algorithm Design.* There are many ways to extract the fundamental frequency mentioned above. This experiment proposes an improved fundamental frequency extraction method, and this algorithm is designed based on the harmonic peak method and the confidence method introduced above.

The steps of the algorithm are as follows: the frequency range needs to be found first, and then the spectrum function is obtained. The expression of the spectrum function is

$$f(x) = |\text{FFT}(y)|, \quad (20)$$

where x is in the frequency range; then the first n extreme points of $f(x)$ need to be calculated, and these extreme points are set as candidate frequency bases; each candidate frequency base is calculated using a confidence function; finally, it is calculated according to the following formula:

$$x = \max_i [h(x_i)]. \quad (21)$$

The following compares the performance of the improved method with the traditional harmonic peak method and confidence method.

(2) *Experimental Design.* The music recognition experiment platform is also Visual Studio, and the object of this experiment is a 5 s piano recording in a noise-free environment. The applied algorithm of this experiment is the harmonic peak method and the confidence method mentioned above, as well as the improved algorithm involved in this experiment. In order to test the accuracy of different algorithms in different situations, this study designed several sets of different signal-to-noise ratio environments, and designed the signal-to-noise ratio from 30 dB to 100 dB to test the accuracy of the algorithm for fundamental frequency extraction.

(3) *Experimental Results and Analysis.* Figure 7 shows the fundamental frequency extraction accuracy results of the three algorithms at different signal-to-noise ratios.

It can be seen from the figure that, regardless of the signal-to-noise ratio, the accuracy of the fundamental frequency extraction of the improved algorithm is always the highest. The accuracy curve is hovering around 90%, and

TABLE 2: Numbering table.

	A	B	C	D
Name	Selling newspaper songs	Two tigers	Song of seven sons	Fishing boat singing night
Resolving power	857×784	991×619	1586×2242	2481×3508
Time-consuming (ms)	569	1127	3257	10294

TABLE 3: Numbered musical notation recognition results.

	A		B		C		D	
	True value	Identification value	True value	Identification value	True value	Identification value	True value	Identification value
Continuous note	10	10	6	6	9	8	3	3
Digital note	75	76	24	24	48	48	179	168
Underline	27	29	45	45	67	65	23	23
Short horizontal line	12	12	33	31	56	55	37	37
Attachment point	3	3	19	17	6	6	12	12
Gross value	127	129	197	193	186	183	254	243
Accuracy	98.4%		98.0%		98.4%		95.7%	
Time-consuming (ms)	569		1127		3257		10294	

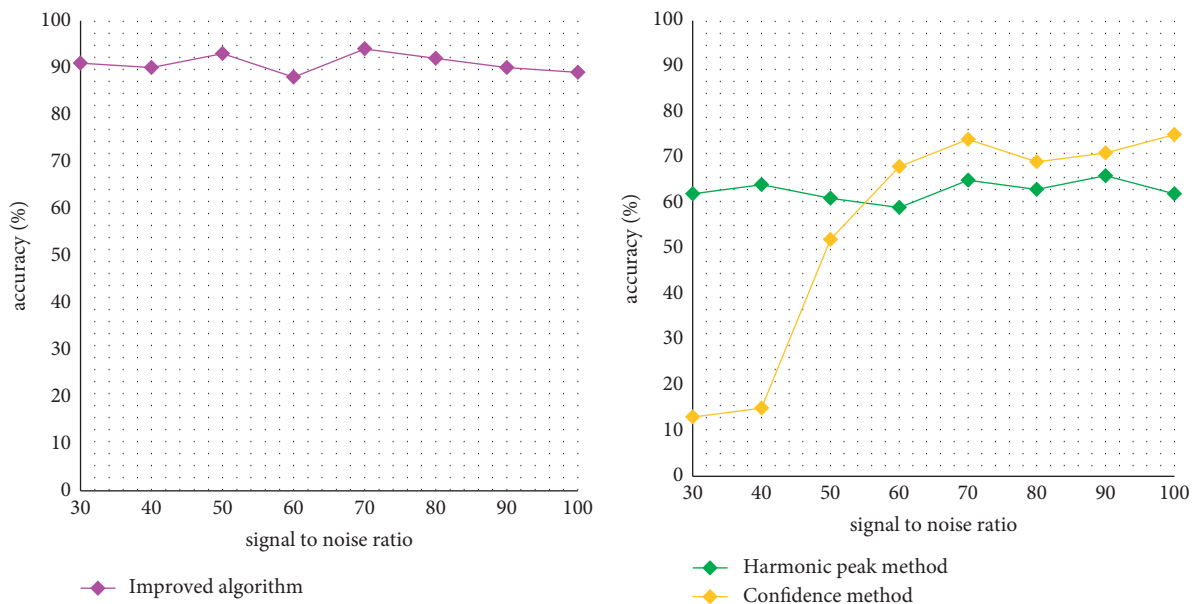


FIGURE 7: Fundamental frequency extraction accuracy.

after calculation, the average accuracy of the improved algorithm is 90.88% during the period when the signal-to-noise ratio is 30–100 dB. This value is relatively high, and even if the signal-to-noise ratio increases, the accuracy of the improved algorithm does not decrease significantly, indicating that the algorithm is not interfered by noise. The accuracy of the harmonic peak method is stable at about 62% during the period when the signal-to-noise ratio is 30–100 dB, and it is not interfered by noise. In the confidence method, when the signal-to-noise ratio is 30–60 dB, the accuracy rate increases with the increase of the signal-to-noise ratio. After 60 dB, it stabilizes at about 70%, and its accuracy is greater than that of the harmonic peak method.

In addition to accuracy, the execution time of the fundamental frequency extraction is also an important evidence to measure the algorithm. Figure 8 shows the average time of processing all samples and the average time of processing 1s samples for the three algorithms.

It can be seen from the figure that among all the algorithms, the harmonic peak method has the shortest average processing time for all samples or 1s samples. The improved algorithm has the longest processing time, and the improved algorithm has 18.6% longer average time for processing all samples than the harmonic peak method, and 11.2% longer average time for processing 1s samples.

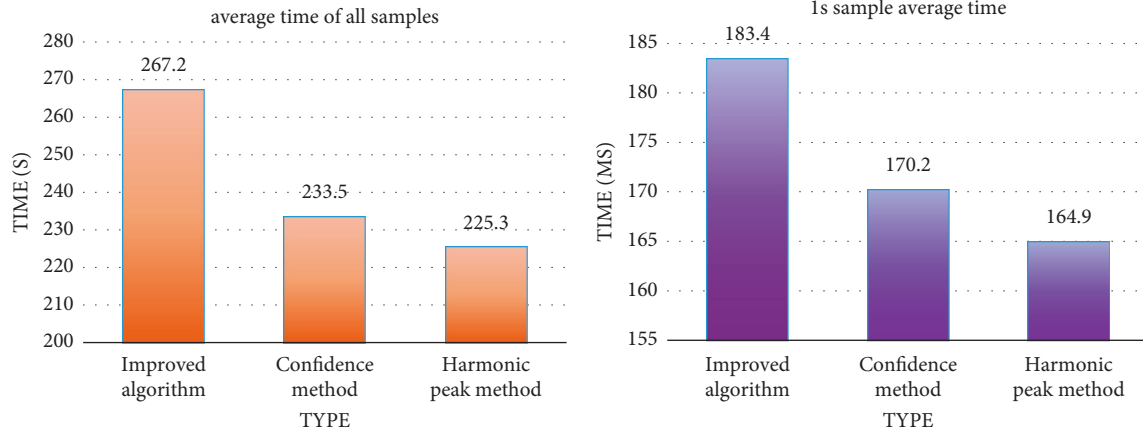


FIGURE 8: Sample processing time.

In summary, although the traditional harmonic peak method has low accuracy, it has strong noise immunity and takes less time; the accuracy rate of the confidence method is slightly higher than that of the harmonic peak method, but it also takes slightly more time than the harmonic peak method. The accuracy of the improved algorithm proposed in this paper is much higher than the other two algorithms. Although it takes more time, it is only more than 10% more than the harmonic peak method, which is within the acceptable range.

4.2. Student Satisfaction Survey Experiment

4.2.1. Experimental Design. In order to have a thorough and accurate understanding of the effects of scientific computing visualization and computer music technology on music teaching in basic education, we will conduct a questionnaire survey for elementary and middle school students and divide these students into two groups. One group is an experimental group, accepting the computer technology-based music teaching described in Section 2.3, which we call the new type of teaching. The other group is the control group, still receiving traditional music teaching. The number of students in both groups is 80, and both are middle-school students and elementary-school students each with 40 students. After a month of teaching, a questionnaire survey was conducted among these students.

4.2.2. Experimental Results and Analysis. This experiment conducted a satisfaction survey on students and asked them to score music lessons. Figure 9 shows the scoring results of the two groups.

It can be seen from the figure that whether it is the experimental group or the control group, the number of people with a score between 91 and 100 is the largest, and as the score interval increases, the number of people selected is increasing. It can be seen that students have a natural interest in music classes and generally prefer music classes. Comparing the two groups, it was found that 49 people in the experimental group scored between 91 and 100, while 35

people in the control group had a 40% increase in the number of people in the experimental group compared to the control group, proving that new music teaching methods can greatly improve students' interest. In order to explore the difference between the influence of new music teaching methods on junior high school students and elementary school students, this experiment separated the junior high school students from the elementary school students and made a statistics. The result is shown in Figure 10.

It can be seen from the figure that for the control group, the number of pupils in the 91–100 interval is higher than that of junior high school students. It can be seen that primary school students are more interested in music lessons than junior high school students, which is related to the characteristics of primary school students. Among elementary school students, for the 91–100 scoring area, the number of people in the experimental group is 26 and the number in the control group is 21, an increase of 23.8%. Among junior high school students, for the 91–100 scoring area, the number of people in the experimental group was 23 and the number in the control group was 14, which increased by 50%. It can be seen that the new teaching method has a greater impact on junior high school students and is more popular with junior high school students.

5. Discussion

This article believes that computer music technology and scientific computing visualization technology entering the basic education music classroom will have very good results and powerful implementation possibilities. With the application of computer music technology, demonstrations under the guidance of teachers will become more intuitive, reducing the difficulty of learning for students and improving the plasticity of work. Computer music technology has many advantages in music education. Computer music technology is becoming more and more perfect, and its functions are not only suitable for music production but also for music education. Visualization of scientific computing can visually present students with more beautiful and intuitive music content. With the reform of the music

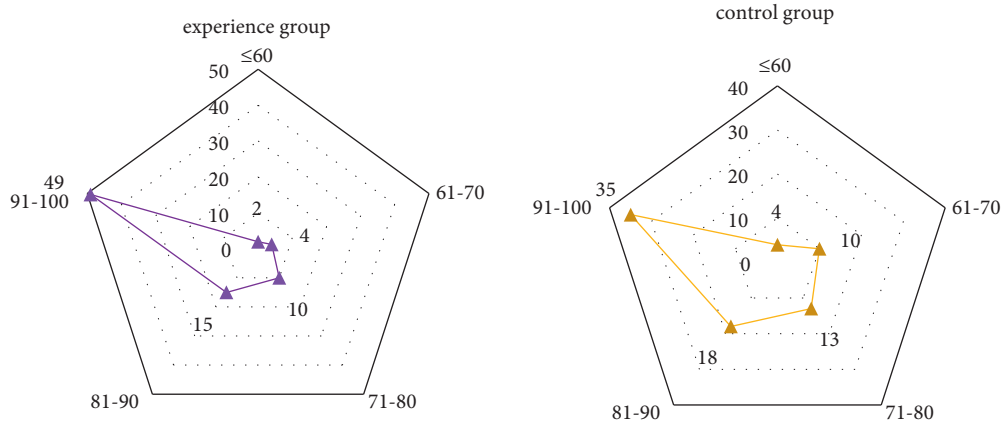


FIGURE 9: Satisfaction score results.

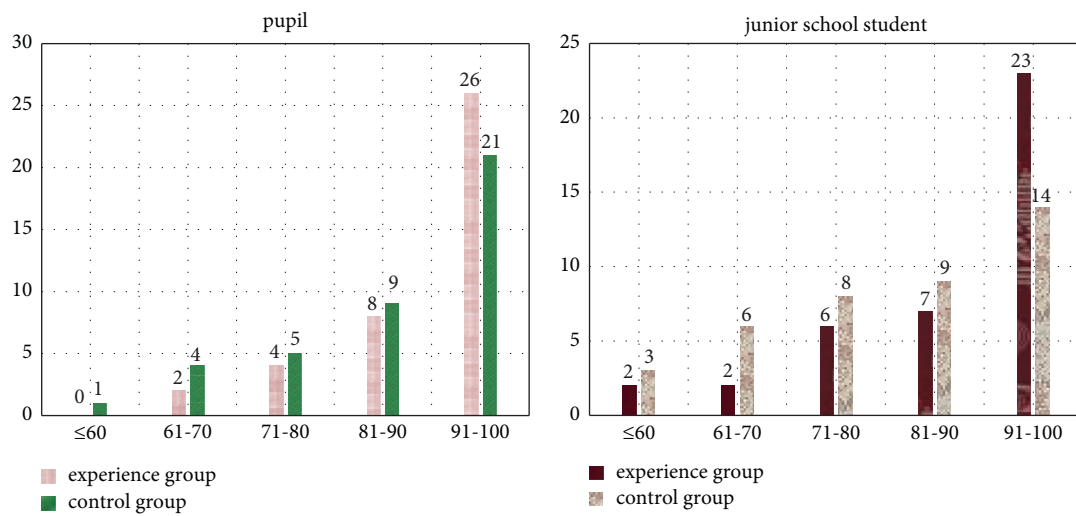


FIGURE 10: Satisfaction results for different age groups.

education system and the pursuit of music teaching methods by all parties, the combination of computer music technology, scientific computing visualization, and music education will become a trend, and its advantages such as intuitive teaching demonstration and easy learning process will gradually appear.

6. Conclusion

This article introduces the related methods of scientific computing visualization and computer music technology, and introduces their application methods in music teaching. It also designed experiments based on scientific computing visualization and computer music technology. The first experiment is to test the accuracy of numbered musical notation recognition and the accuracy of music recognition, and the results are as follows: (1) The average recognition rate of numbered musical notation is higher than 95%, and there is no obvious change with the increase of the resolution of numbered musical notation pictures. (2) Comparing the accuracy of music recognition between the improved algorithm in this paper and the two traditional algorithms, it is

found that the average accuracy of the improved algorithm is 90.88%, which is the highest. However, the identification time is the longest, but it is within an acceptable range. The second experiment divided students into a control group who studied in traditional music classes and an experimental group who learned in new teaching based on scientific computing visualization and computer music technology. Comparing students' satisfaction with music lessons, the experiment found that (1) in the 91–100 interval, the number of people in the experimental group increased by 40% compared to the control group, proving that the new music teaching method can greatly increase the interest of students. (2) The analysis of elementary school students and junior high school students separately proves that the new teaching method has a greater impact on junior high school students and is more popular with junior high school students.

Data Availability

The data used to support the findings of this study are available from the author upon request.

Conflicts of Interest

The author declares no conflicts of interest.

Acknowledgments

This study was sponsored by Anhui University of Arts.

References

- [1] C. Scaletti, "Looking back, looking forward: a keynote address for the 2015 international computer music conference," *Computer Music Journal*, vol. 40, no. 1, pp. 10–24, 2016.
- [2] A. Mcpherson and K. Tahiroğlu, "Idiomatic patterns and aesthetic influence in computer music languages," *Organised Sound*, vol. 25, no. 1, pp. 53–63, 2020.
- [3] L. Hayes, "Sound, electronics, and music: a radical and hopeful experiment in early music education," *Computer Music Journal*, vol. 41, no. 3, pp. 36–49, 2017.
- [4] D. El-Shimy and J. R. Cooperstock, "User-driven techniques for the design and evaluation of new musical interfaces," *Computer Music Journal*, vol. 40, no. 2, pp. 35–46, 2016.
- [5] J. B. Park, "A study on development of virtual Korean musical instruments and its application method," *The Journal of Korean Music Education Research*, vol. 10, no. 2, pp. 123–143, 2016.
- [6] M. Haning, "Are they ready to teach with technology? An investigation of technology instruction in music teacher education programs," *Journal of Music Teacher Education*, vol. 25, no. 3, pp. 77–86, 2016.
- [7] S. . Chakraborty, "Basic music technology: an introduction," *Computing Reviews*, vol. 60, no. 12, 456 pages, 2019.
- [8] A. Holzapfel, B. L. Sturm, and M. Coeckelbergh, "Ethical dimensions of music information retrieval technology," *Transactions of the International Society for Music Information Retrieval*, vol. 1, no. 1, pp. 44–55, 2018.
- [9] M. J. Cook, "Augmented Reality: examining its value in a music technology classroom. Practice and potential," *Waikato Journal of Education*, vol. 24, no. 2, pp. 23–38, 2019.
- [10] J. Navarro, "Machine learning in music generation," *Oriental Journal of Computer Science and Technology*, vol. 11, no. 2, pp. 75–77, 2018.
- [11] W. Yan, "Research on the making technology of virtual orchestral instrument," *Journal of the Korea Society of Computer and Information*, vol. 22, no. 1, pp. 77–87, 2017.
- [12] J. Powell and K. Chesky, "Reducing risk of noise-induced hearing loss in collegiate music ensembles using ambient technology," *Medical Problems of Performing Artists*, vol. 32, no. 3, pp. 132–138, 2017.
- [13] M. Toro, "Current trends and future research directions for interactive music," *Journal of Theoretical and Applied Information Technology*, vol. 96, no. 16, pp. 5569–5606, 2018.
- [14] R. Boa, K. S. Hyo, S. M. Shin, "Applying the technology acceptance model to the digital exhibition - a case study on <van gogh inside: festival of light and music> ," *Journal of the Korea Society of Computer and Information*, vol. 21, no. 10, pp. 21–28, 2016.
- [15] S. L. Burton and A. Pearsall, "Music-based iPad app preferences of young children," *Research Studies in Music Education*, vol. 38, no. 1, pp. 75–91, 2016.
- [16] L. Dunbar, "Music for mstts," *General Music Today*, vol. 30, no. 1, pp. 38–40, 2016.
- [17] B. C. K. Deniz, "Examining music teachers self-confidence levels in using information and communication technologies for education based on measurable variables," *Educational Research and Reviews*, vol. 12, no. 3, pp. 101–107, 2017.
- [18] C. K. Ting, C. L. Wu, and C. H. Liu, "A novel automatic composition system using evolutionary algorithm and phrase imitation," *IEEE Systems Journal*, vol. 11, no. 3, pp. 1284–1295, 2017.
- [19] P. Saari, G. Fazekas, T. Eerola, M. Barthelet, O. Lartillot, and M. Sandler, "Genre-adaptive semantic computing and audio-based modelling for music mood annotation," *IEEE Transactions on Affective Computing*, vol. 7, no. 2, pp. 122–135, 2016.
- [20] S. M. Jit, "Clickstream analysis methods and systems," *Asian Journal of Management Sciences & Education*, vol. 1, no. 3, pp. 57–65, 2017.
- [21] J. Kim, J. Urbano, C. C. S. Liem, and A. Hanjalic, "One deep music representation to rule them all? A comparative analysis of different representation learning strategies," *Neural Computing & Applications*, vol. 32, no. 4, pp. 1067–1093, 2020.
- [22] H. C. Eren and E. K. Ztu, "The implementation of virtual choir recordings during distance learning," *Cypriot Journal of Educational Sciences*, vol. 15, no. 5, pp. 1129–1139, 2020.
- [23] R. Sundberg and W. Cardoso, "Learning French through music: the development of the Bande à Part app," *Computer Assisted Language Learning*, vol. 32, no. 1-2, pp. 49–70, 2019.
- [24] M. Goto and R. B. Dannenberg, "Music interfaces based on automatic music signal analysis: new ways to create and listen to music," *IEEE Signal Processing Magazine*, vol. 36, no. 1, pp. 74–81, 2019.
- [25] J. Nonaka, . InacioOno, . Kawashima, . Kawanabe, and . Shoji, "Data I/O management approach for the post-hoc visualization of big simulation data results," *International journal of modeling, simulation and scientific computing*, vol. 9, no. 3, Article ID 1840006.16, 2018.

Research Article

Modeling and Analysis of the Impact of Information and Communication Technology on Household Consumption Expenditure in Different Regions

Chaozhi Fan , Siong Hook Law, Saifuzzaman Ibrahim, and N. A. M. Naseem

School of Business and Economics, Universiti Putra Malaysia, Serdang, Selangor 43400, Malaysia

Correspondence should be addressed to Chaozhi Fan; gs57155@student.upm.edu.my

Received 30 March 2022; Accepted 29 April 2022; Published 19 May 2022

Academic Editor: Wei Liu

Copyright © 2022 Chaozhi Fan et al. This is an open access article distributed under the Creative Commons Attribution License, which permits unrestricted use, distribution, and reproduction in any medium, provided the original work is properly cited.

Based on the panel data of cities and towns in China, by using the generalized estimation method of a dynamic panel, through the construction of regional household consumption expenditure evaluation models, optimize the impact evaluation algorithm of household consumption expenditure in different regions, standardize critic indicators, and build the impact modeling of household consumption expenditure in combination with relevant algorithms such as the Engel coefficient. Finally, it is verified by experiments that the impact model of ICT on household consumption expenditure in different regions has high practicability and fully meets the research requirements.

1. Introduction

With the rapid development of mobile businesses, broadband services, and broadcast television businesses in China, the “three-network convergence” is deepening. Broadband, radio, and television entered the era of information and communication technology marked by Internet Plus [1]. At the same time, the penetration, driving, and multiplication of the information and communication technology industry into the national economy are becoming more and more significant, becoming a driver of economic development, and further promoting and accelerating the transformation and upgrading of the national economy [2]. Therefore, this paper studies ICT innovation diffusion and its influencing factors from industrial integration, and the results provide a reference for 5G operation and Internet integration development. The study of literature found that the research on Internet consumer finance and consumer behavior mainly focuses on the influencing factors of residents’ consumer behavior and the relationship between Internet consumer finance and residents’ consumer demand [3]. Scholars generally believe that consumers’ lasting and instantaneous income, unexpected income, income change, consumption

habits, and other factors will affect residents’ consumption behaviors. The modern consumption theory starts with the precautionary theory and the liquidity hypothesis. They study the optimal choice of consumers under the condition of uncertainty.

2. Modeling the Impact of Household Consumption Expenditure in Different Regions

2.1. Evaluation Model of Regional Household Consumption Expenditure. To better study the changes and influencing factors of communication consumption of urban residents, this paper attempts to put forward countermeasures and suggestions for the government and enterprises to promote the consumption of urban residents [4]. Therefore, this paper studies the changing structure of information and communication consumption expenditure, as shown in Figure 1.

With the rapid development and renewal of information and communication technology and the continuous penetration in the field of consumption, communication consumption has become one of the important contents of daily

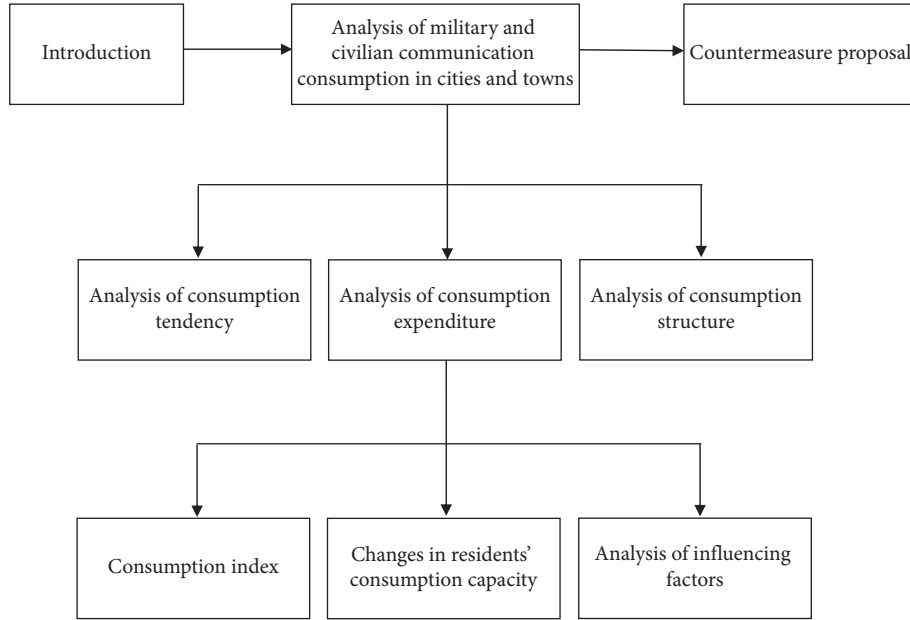


FIGURE 1: Change structure of information and communication consumption expenditure.

consumption [5]. It is one of the indicators to improve people's quality of life and promote economic and social development. From the proportion of urban per capita communication consumption in per capita income, it also shows an inverted U-shaped change trend, as shown in Figure 2.

This series of data reflects the current development status of China's communication industry: compared with residents' income and other consumption, communication consumption has a relatively downward trend [6]. Furthermore, from the perspective of each region, with the increase of income and consumption, although residents' communication consumption is also increasing, the communication consumption coefficient and the proportion of communication consumption in per capita income also show a downward trend [7]. Many factors affect the communication consumption of urban residents. To study these influencing factors more scientifically, the following panel data model is constructed, and the specific form is shown in the equation.

$$Comm_{i,t} = C + \beta' X_{i,t} + \lambda_i + \varepsilon_{i,t}. \quad (1)$$

Advantages of panel data: individual heterogeneity can be controlled. The degree of freedom is increased and the collinearity between explanatory variables is reduced. It is more suitable to study the dynamic adjustment process [8], where i and t represent region and year, respectively; $Comm_{i,t}$ refers to the per capita communication consumption of urban residents in region i in year t (yuan), that is, the per capita communication consumption calculated according to the permanent resident population of each province and city; $X_{i,t}$ and $x_{i,t}$ are the factors that may affect the communication consumption of urban residents; λ_i is the unobservable provincial and municipal effect, which is used to control the provincial and municipal fixed effect; $\varepsilon_{i,t}$

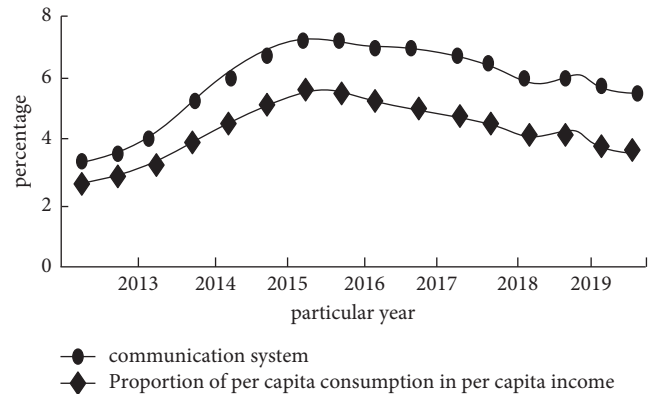


FIGURE 2: Change trend of "communication consumption coefficient" and "per capita communication consumption as a proportion of per capita income" of urban residents.

is the residual term; C is a constant term; β' is the coefficient corresponding to each variable. According to the consumption function theory, consumption has inertia [9]. As a kind of consumer goods, communication consumption also has inertia; that is, the current consumption will be affected by the inertia of the previous consumption. The introduction of lag dependent variable is more in line with theory and reality. Therefore, the lag term of communication consumption can be introduced into the model to build a dynamic panel data model. The specific form is as follows:

$$Comm_{i,t} = \alpha comm_{i,t-1} + \beta' X_{i,t} + \lambda_i + \varepsilon_{i,t}. \quad (2)$$

To make the data of each year more comparable, the relevant data for these three variables is reduced with 2020 as the benchmark period [10]. At the same time, to reduce the heteroscedasticity of model fitting, take the natural logarithm of these three variables, respectively, and the

TABLE 1: Statistical description of variables (2015–2020).

Variable	Symbol	Mean value	Standard deviation	Minimum value	Maximum	Observed value
Per capita income of urban residents	Inincome	9.28	0.35	8.69	10.36	377
Per capita communication consumption of urban residents	Incomm	6.20	0.35	5.26	6.98	377
Engel coefficient of residents	Ee	37.56	4.25	12.68	52.25	377
Per capita income tax of working age	Intax	4.36	0.98	2.85	7.23	377
Real interest rate	r	0.02	1.98	-6.15	4.62	377
Child support index	Edr	22.58	5.56	9.36	42.06	377
Average family model	Family	3.20	0.36	2.65	4.68	377

corresponding coefficient of the index after taking the logarithm represents the concept of elasticity [11]. The statistical description of each variable is shown in Table 1.

According to the life cycle theory, under limited income constraints, consumers will reasonably distribute all their income among the consumption of various goods to obtain the maximum utility. Compared with the absolute income theory, it emphasizes consumption analysis at all stages of life [12]. Consumers will choose between current consumption and expected consumption and advance future consumption to current consumption, which provides a theoretical basis for the research of Internet consumer finance [13]. Based on the traditional theory, Cox and Ludwigson [14] bring consumer credit into the equation of consumers' intertemporal consumption optimization choice and expound the relationship between consumer credit conditions and residents' consumption. It is assumed that the consumer credit constraints of current consumers are as follows:

$$D_{t+1} = (1 + r)(D_t + C_t - Y_t). \quad (3)$$

In the formula, D_{t+1} represents the consumer credit in the current period, r represents the established rate of return, D_t represents the consumer credit in the previous period, C_t represents the consumer's consumption status in the previous period, and Y_t represents the consumer's income level in the previous period. The current consumer credit D_{t+1} meets the constraints.

$$D_{t+1} \leq \bar{D}_{t+1} = \frac{1}{\omega} Y_t \exp(\xi_t). \quad (4)$$

In the above algorithm, $\xi_{t+1} = \varphi \xi_t + v_{t+1}$. Among them, ω represents a set of determined coefficients, ξ_t represents the impact of external conditions on the current consumer credit constraints, and the basic formula is assumed to obey autoregressive model. D_{t+1} represents the current borrowing limit of consumers. The relationship in the formula shows that residents' personal income and external impact determine the current consumer credit ceiling [15]. The goal of consumers' intertemporal choice is to reasonably distribute income to maximize the utility in their life cycle. Therefore, the utility maximization equation of consumers is as follows:

$$\text{Max}U = E_t \sum_{j=0}^T (1 + \varepsilon)^{-j} u(C_{t+j}). \quad (5)$$

Select the simple model for quantitative analysis and construct the relationship model between consumer finance and residents' consumption level. Its advantage is that the model is not limited by specific theories and special environments and can more objectively reflect the actual impact of the Internet on consumer finance and consumer demand [16]. The explanatory variables in the model are divided into three categories: basic variable y , core variable x , and control variable K , where x represents each province on the section, T represents each time, and P represents the individual effect of the region, and ε represents a random error term. (C_{t+j}) indicates the explanatory variable, i.e., consumption level [17]. J represents the consumption category, which is basic survival expenditure and development enjoyment expenditure, respectively. u represents the change of consumption level. u represents the basic explanatory variable, i.e., income level. E_t is the coefficient of promoting consumption for income reflecting the impact of income on residents' consumption. X represents the core explanatory variable, i.e., Δy and Δ [18]. It represents the change of income level and the change of Internet consumer finance level, respectively. β represents control variables, that is, other potential variables that may have an impact on urban residents' consumption. These variables include residents' savings rate Con_{it-1} , the social security level Icr_{it} , the urbanization level Inc_{it-1} , and other macro variables.

$$\begin{aligned} \Delta \text{Con}_{j,it} = & \beta_0 \Delta \text{Con}_{it-1} + \beta_1 \Delta \text{Inc}_{it-1} + \beta_2 \Delta \text{Icr}_{it} + \beta_3 \Delta \text{Inc}_{it} \\ & + \beta_4 \Delta K_{it} + \mu_i + \varepsilon_i. \end{aligned} \quad (6)$$

The Bass model is used to study and analyze innovation diffusion. Bass uses probability theory and calculus theory to set up and deduce the innovation diffusion model of durable electronic products, namely, the Bass model [19]. The differential expression of the classical Bass model is

$$n(t) = \frac{dN(t)}{dt} = p[m - N(t)] + \frac{q}{m} N(t)[m - N(t)], \quad (7)$$

where d is the number of noncumulative adopters; $N(t)$ is the cumulative number of adopters; m is the maximum value of cumulative adopters in the whole life cycle; p is the innovation coefficient, and $p > 0$; q is the imitation coefficient, and $q > 0$. The new adopter or noncumulative adopter model at time t is

$$n(t) = m \frac{(p+q)^2}{p} \frac{e^{-(p+q)t}}{\left[\frac{q}{p} e^{-(p+q)t} + 1 \right]^2}. \quad (8)$$

The maximum value of adopter (s^*) and the time to reach the maximum value (t^*) during $(0, t)$ are obtained by derivation, and their expressions are

$$S^* = m \frac{(p+q)^2}{4q}, \quad (9)$$

$$T^* = -\frac{1}{p+q} \ln \frac{p}{q}.$$

The parameter estimation of the Bass model mostly adopts the “hybrid” method of the least square method, nonlinear least square method, least square method, and nonlinear least square method. With the development of computer technology, modern intelligent algorithms are more and more used in Bass model parameter estimation [20]. With the deep application of computer technology in econometric analysis, quantitative modeling gradually evolves from section modeling and panel modeling to dynamic spatial panel modeling. Dynamic spatial panel models have stronger explanatory power than reality and better fitting effects. Panel data spatial econometric models are divided into fixed effects and random effects [21]. Compared with the random effect model, the fixed effect model is more applicable than the random effect model, with more robust

estimation results and simpler calculation. In recent years, many scholars at home and abroad have used panel data with a fixed effect dynamic spatial autoregressive model for spatial econometric analysis.

$$Y_t = \mu + \tau Y_{t-1} + \delta WY_t + \eta WY_{t-1} + X_i \beta + \xi_t + \varepsilon_t. \quad (10)$$

The individual effect term μ in the formula does not vary over time and satisfies the requirement that the individual effect μ is related to the variable matrix X , consistent with a spatial fixed effect model. The time effect term ξ_t is consistent in the time dimension and does not vary with individuals, while satisfying the individual effect ξ_t that is related to the variable matrix X and is consistent with the time fixed effect model. If it satisfies both individual effect and time effect, the model is consistent with a spatiotemporal fixed effect model. The spatial econometric model partial differential is used to explain the influence of variable changes in the model, and the main diagonal element in the partial derivative matrix is used to represent the direct effect, and the nondiagonal element is used to represent the indirect effect. A spatial dynamic general econometric model of panel data is proposed. At a specific time point, from the partial derivative matrix of Y expected value corresponding to the K explanatory variable in X of spatial units $1 \sim n$, the expressions of short-term effect and long-term effect are as follows:

$$\left[\frac{\partial E(\mathbf{Y})}{\partial E(x_{1k})} \cdots \frac{\partial E(\mathbf{Y})}{\partial E(x_{Nk})} \right]_i = (\mathbf{I}_N - \delta \mathbf{W})^{-1} [\beta_{1k} \mathbf{I}_N + \beta_{2k} \mathbf{W}], \quad (11)$$

$$\left[\frac{\partial E(\mathbf{Y})}{\partial E(x_{1k})} \cdots \frac{\partial E(\mathbf{Y})}{\partial E(x_{Nk})} \right] = [(1 - \tau) \mathbf{I}_N - (\delta + \eta) \mathbf{W}]^{-1} [\beta_{1k} \mathbf{I}_N + \beta_{2k} \mathbf{W}].$$

The maximum likelihood method (ML) is used to estimate the spatial and temporal static fixed effect spatial model. The quasi-maximum likelihood method is proposed to effectively estimate the spatial dynamic panel SAR model. Using the annual data of 144 countries, the spatial static and dynamic models of panel data are used to study the influencing factors and spatial spillover effects of national defense expenditure. These research results provide a valuable reference for this study. Noncumulative Bass model is used to fit the “bell” classic line of innovation diffusion. City i noncumulative Bass model (Extended) expression is

$$n(t)_i = k + m \frac{(p+q)^2}{p} \frac{e^{-(p+q)t}}{\left[\frac{q}{p} e^{-(p+q)t} + 1 \right]^2}, \quad (12)$$

where $n(t)_i$ represents the year-end arrival number of ICT adopters in the city, and K is the intercept term. It is necessary to estimate the parameters k , m , p , and q in the formula. Model parameter estimation method: this paper uses simulated annealing method to estimate the parameters of ICT innovation diffusion Bass model in 288 prefecture

level cities in China, to improve the accuracy of modeling impact analysis.

2.2. Characteristics of ICT Consumption Structure. To reflect the impact of the application of information and communication technology on cost location factors, it is assumed that the transportation cost in economic activities is 0, and all geospatial units are homogeneous and symmetrically distributed on both sides of the equator. At this time, projecting the three-dimensional Earth from the north pole to the south pole onto the two-dimensional plane will form a circular map symmetrical about the equator. It is assumed that the mapping of the Earth g in the Gaussian plane 2 is a unit circle; see Figure 3.

Figure 4 is the fitted scatter diagram of China cities’ “rank scale.” The y -axis is the logarithm of China’s urban population-scale ranking, and the x -axis is the logarithm of the corresponding urban population. The fitted straight-line slope is -1.176437 , and its absolute value is the 10-year average Ziff coefficient of China’s urban spatial structure.

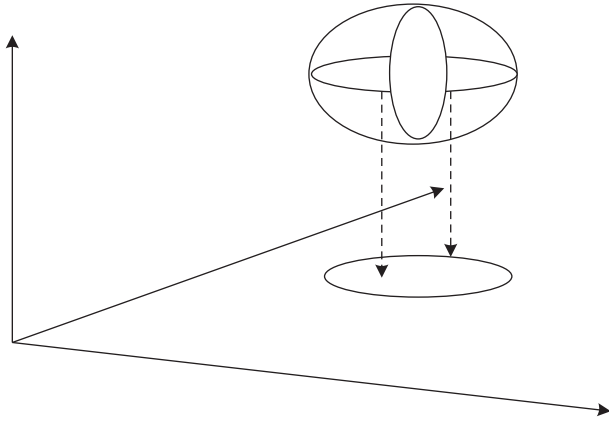


FIGURE 3: Mapping of three-dimensional information communication in Gaussian plane.

As China’s basic industry, the telecommunications industry was the first to implement the government regulation reform. The overall route of the reform is to break the monopoly and encourage competition. Relevant policies and regulatory mechanisms guide the changes in telecom operation patterns. Figure 5 shows the evolution of the consumption market structure of China’s telecom industry.

At present, state space model is widely recognized and used in econometric literature. Economists often use this model to estimate unobservable factors, such as unobservable time series, measurement errors, rational expectations, and long-term income. Many financial time series models such as simple linear model and ARIMA model can be written as special cases into state equations and estimate their parameters. The advantage of state space model is that state variables, i.e., unobservable factors, can be incorporated into the observable model to obtain the estimation results together. Kalman filter has a strong iterative algorithm, and the state space model uses Kalman filter to estimate the parameters. The following is the state space form of the variable parameter model.

$$\begin{aligned} y_t &= x_t\beta + Z_t\alpha_t + \varepsilon_t, \\ \alpha_t &= \varphi\alpha_{t-1} + \gamma. \end{aligned} \tag{13}$$

The process of deriving the best estimate of the state vector in the state space model by using Kalman filter is considering the conditional distribution of the state vector at time and defining the variance matrix and mean value of the conditional distribution.

2.3. Implementation of Impact Analysis of Household Consumption Expenditure. When defining the concept of network information consumption, the author includes the network tools to realize consumption behavior. Therefore, when dividing the types of information products, the electronic information products, including network tools, are also included. In addition to electronic products, another necessary type of information product is literature information resources, which can be divided into printed and nonprinted versions from the carrier’s perspective, as shown

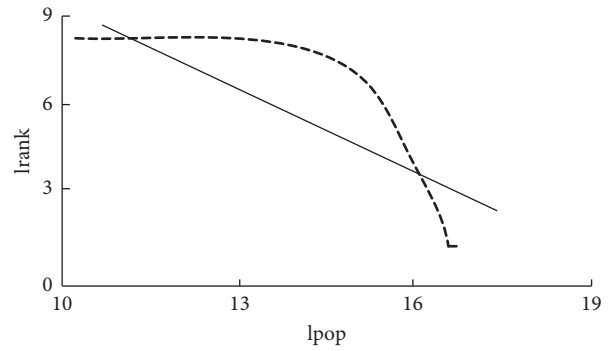


FIGURE 4: Overall urban rank scale fitting in China.

in the figure. Information products mainly refer to electronic products and network versions of nonprinting information products for in-network information consumption. Figure 6 shows the consumption categories and grade classification of information products.

Information service is mainly an information value-added activity where the information service subject studies the needs of users, organizes services, transmits valuable and effective information to users, and solves the needs of users. In the network environment, the network information service business is more extensive and powerful, which can provide users with full knowledge coverage and high-quality information, and the carrier forms of information products are more diversified, so that the information needs of different users can be solved efficiently and with high quality. In the network information service, according to the paid meter, it can be divided into paid and free information services. The former mainly includes paid online classrooms, paid online consultations, paid audio-visual resource downloads, etc.; free information services include e-mail, instant messaging, information search, and other services. It is also the most widely consumed network information consumption content among network users. It can also be divided into information acquisition, leisure and entertainment, e-commerce, life service, etc. With the deepening and refinement of user needs, the forms of network information services are becoming more and more diverse. According to different classification standards, they can be divided into different types. It is worth mentioning that, under the network environment, the library’s information service has also been enriched and developed and has become an important provider of network information service. The information behavior of network users refers to the activities that network users use network tools to search, select, absorb, utilize, communicate, and publish network information under the control of information demand and ideological motivation. According to the process from the generation of information demand to the absorption and utilization of information, Yan Hai [22] divided it into information demand behavior, information search behavior, information browsing behavior, information selection behavior, and information utilization behavior. Ren LiXiao [23] divides users’ network information behavior into information release behavior, information search behavior, information selection behavior, information exchange

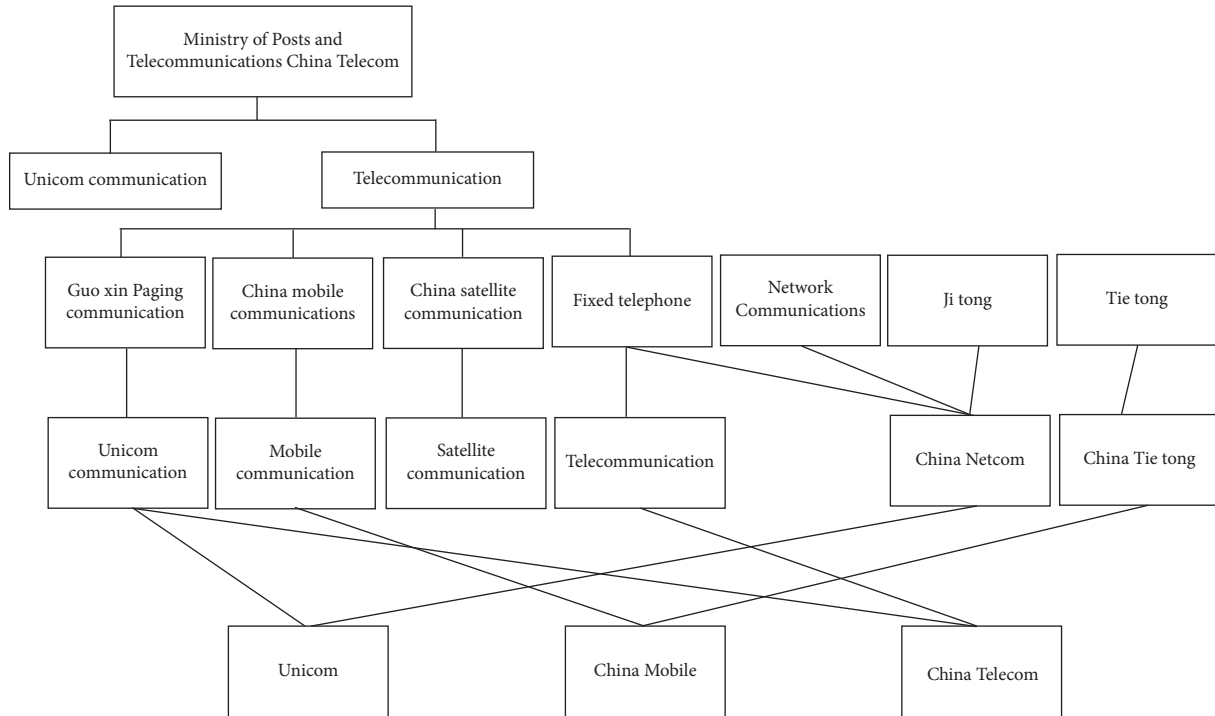


FIGURE 5: Evolution process of consumption market structure of China's telecom industry.

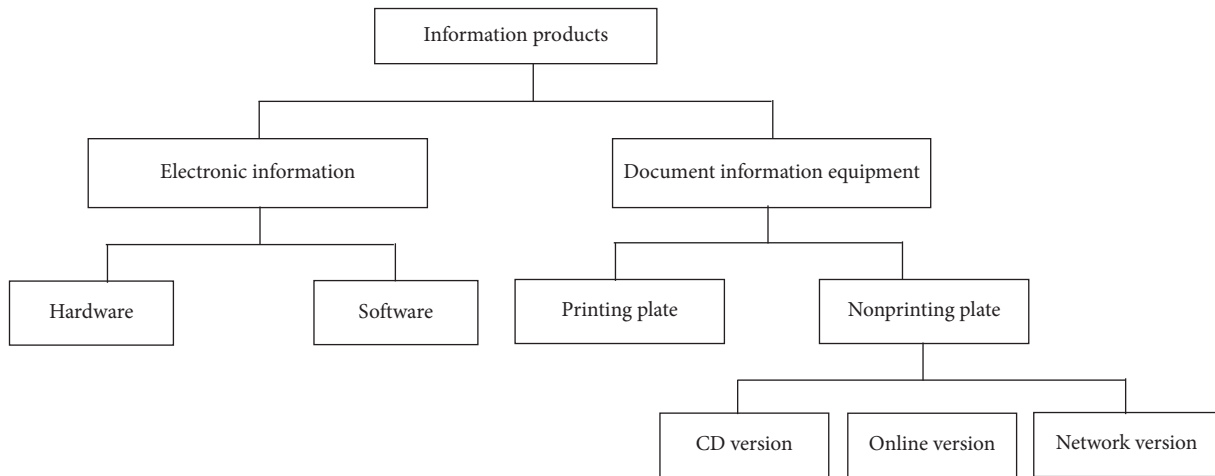


FIGURE 6: Classification of consumption categories and grades of information products.

behavior, information download behavior, information absorption and utilization behavior, etc. From this perspective, information related behaviors completed through network devices (including desktop computers, notebooks, mobile phones, tablet computers) belong to network information behaviors. The difference between network information consumption behavior and network information behavior lies in the word “consumption,” which makes the network information consumption behavior not only have all the behavior modes of network information behavior, but also have some characteristics of network consumption behavior, that is, postconsumption satisfaction evaluation, which promotes the emergence of information release

behavior. Figure 7 shows the network information consumption behavior and the relationship between network information consumption behavior and network information behavior.

It is believed that different people will have different sequences of information search behavior, or the same person may have different sequences at different times. Therefore, EIS compares and analyzes the individual information search modes of various social scientists and summarizes the strategic model of information search behavior (Figure 8), which is divided into eight strategies: start, connection, browsing, discrimination, tracking, collection, confirmation, and end [24].

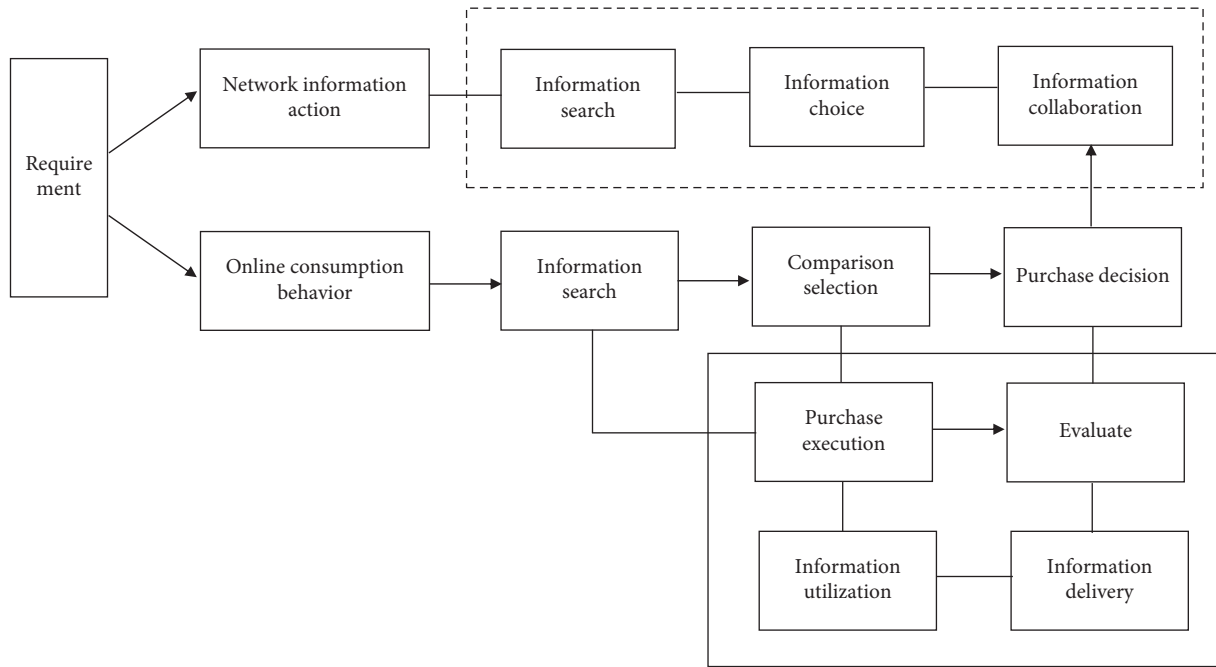


FIGURE 7: Relationship between network information consumption behavior, network consumption behavior, and network information behavior.

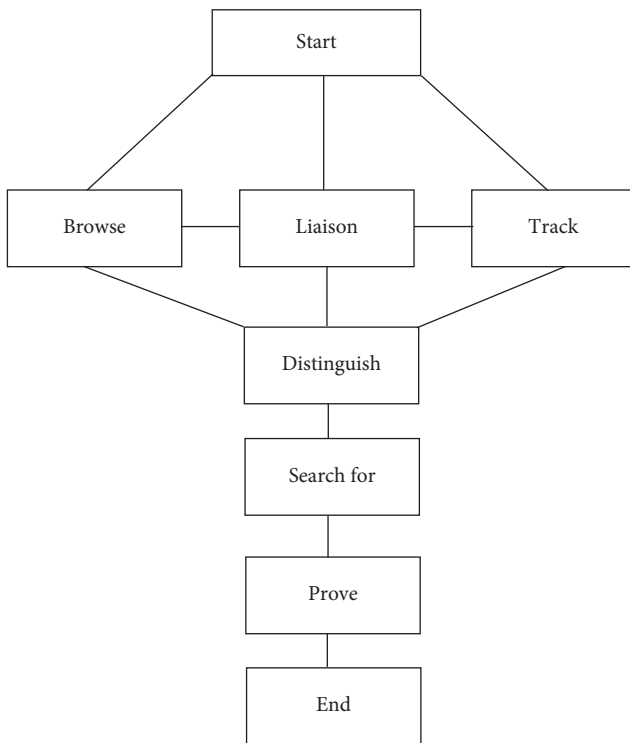


FIGURE 8: Search and identification strategy model of information consumption behavior.

In the traditional environment, scholars use different research methods to explore the construction of information behavior model from different perspectives, which provides an important reference for later scholars. Although network information behavior is still a new research field, the

research perspective is focused on the construction of network information search behavior model to ensure the accuracy and effectiveness of modeling and analysis.

3. Analysis of Experimental Results

To avoid the phenomenon of “pseudo regression,” it is necessary to test the stationarity of relevant data before regression. Considering that there may be differences in unit roots of panel data, LLC and PP Fisher test methods will be used to test the balance of variables. The test results are shown in Table 2.

The above table shows that when each variable is in the horizontal sequence, each test statistic significantly rejects the original hypothesis of “existence of unit root” at the level of 5%, obeys the zero-order single integer I (0), and can directly enter the model for regression analysis. Due to the lag of dependent variables, the dynamic panel model has an endogenous problem, which can be solved by the generalized moment estimation method. Therefore, the generalized moment estimation method is used to empirically study the influencing factors of communication consumption of urban residents. The research results are shown in Table 3.

From the measurement results, according to the standard deviation corresponding to the estimated coefficient, Sargan test and residual sequence correlation test, the two-step estimation of difference GMM and System GMM is better than one-step estimation. The joint significance Wald test results of two-step estimation of differential GMM and System GMM show that the model is very significant in general. The *P* values of Sargan test are greater than 0.05, indicating that the instrumental variables are effective as a whole. The results of AR (1) test and AR (2) test show that

TABLE 2: Balance test of variables.

Variable symbol	Inspection form	LLC inspection		PP Fisher test	
		Statistic	Probability value	Statistic	Probability value
Inincome	(c,t,o)	-5.351283	0.0000	75.3652	0.0359
Incomm	(c,t,o)	-9.521436	0.0000	236.058	0.0000
Ee	(c,t,o)	-19.3568	0.0000	105.684	0.0000
Intax	(c,t,o)	-3.254786	-0.0004	276.378	0.0000
r	(c,t,o)	-22.8135	0.0000	265.365	0.0000
Cdr	(c,t,o)	-8.05868	0.0000	152.365	0.0000
Family	(c,t,o)	-7.36586	0.0000	118.982	0.0000

TABLE 3: Generalized moment estimation results of dynamic panel of communication consumption of urban residents.

Dependent variable = incomm	Differential GMM		System GMM	
	One-step prediction	Two-step prediction	One-step prediction	Two-step prediction
Inincome	0.262*** (0.047)	0.265*** (0.021)	0.162*** (0.052)	0.168*** (0.031)
Incomm	0.523*** (0.052)	0.532*** (0.035)	0.587*** (0.052)	0.562*** (0.033)
Ee	-0.012*** (0.002)	-0.021*** (0.003)	-0.012*** (0.001)	-0.016*** (0.005)
Intax	-0.052** (0.021)	-0.053*** (0.012)	-0.049*** (0.018)	-0.035*** (0.010)
R	0.008** (0.002)	0.008*** (0.003)	0.012*** (0.004)	0.011*** (0.001)
Cdr	-0.002 (0.002)	-0.002 (0.003)	-0.007** (0.002)	0.007*** (0.001)
Family	-0.066** (0.032)	-0.055*** (0.015)	0.009*** (0.029)	0.013 (0.013)
Obs.	315	315	352	352

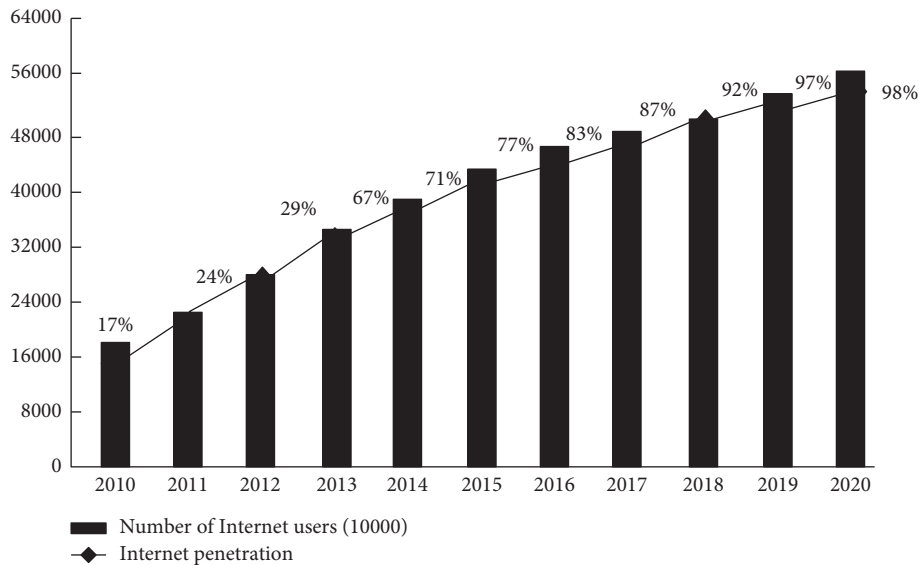


FIGURE 9: Scale of Internet users and Internet consumption in China.

there is only first-order sequence correlation, but no second-order sequence correlation. The greater the p value of Sargan test is, the more it can explain the effectiveness of instrumental variables. From the estimation results, the System GMM two-step estimation is better than the differential GMM two-step estimation. Therefore, take the System GMM two-step estimation as an example for analysis. Figure 9 shows the scale of Internet users and Internet consumption in China and Figure 10 shows the consumption scale and proportion of mobile Internet users in China is used for further analysis.

The System GMM two-step estimation shows that the per capita communication consumption of urban residents is affected by many factors. Among them, the lag of the logarithm of per capita communication consumption of urban residents in the first period has a significant impact on the current period, and the estimation coefficient is 0.561, indicating that the per capita communication consumption of urban residents will be affected by the previous period, reflecting that communication consumption is an aspect of residents' consumption; it also has strong consumption inertia. The logarithm of per capita income of urban

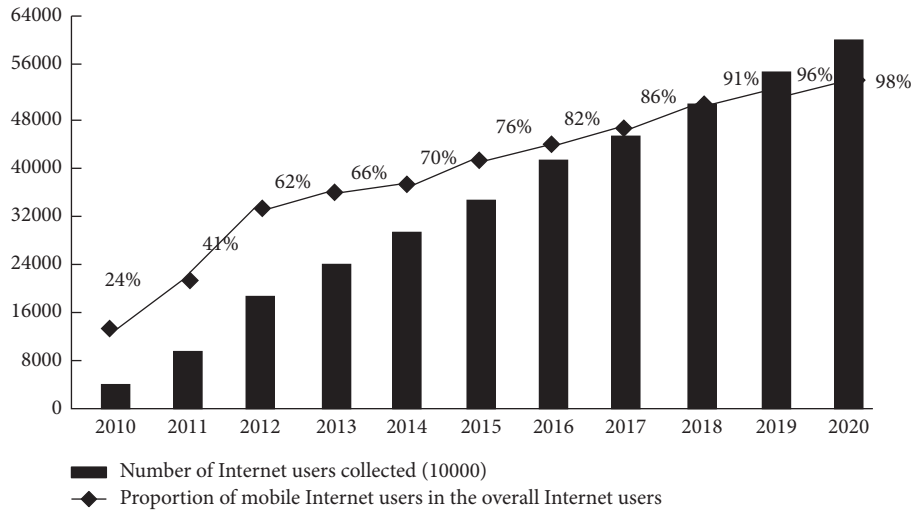


FIGURE 10: Consumption scale and proportion of mobile Internet users in China.

TABLE 4: Per capita communication expenses of urban residents of different income levels.

Particular year	Total average	Lowest income household	Low income household	Lower middle households	Middle income household	Upper middle households	High income household	Highest income household
2017	543.25	123.25	206.68	435.65	523.658	632.58	985.35	2038.56
2018	598.26	139.68	235.85	468.68	612.58	698.25	1052.32	2186.32
2019	623.57	148.68	278.65	583.65	682.58	766.35	1352.32	2535.65
2020	657.97	152.38	216.35	583.65	723.35	865.95	1585.36	2238.95

residents also has a positive and significant impact on the logarithm of per capita communication consumption. For every 1% increase in per capita income of urban residents, per capita communication consumption will increase by 0.158%. This also confirms Keynesian consumption theory that income is a function of consumption and income is the main factor affecting consumption demand. As an indispensable kind of consumption in contemporary life, communication consumption is naturally affected by income. The logarithm of the per capita personal income tax of the working age population has a significant negative impact on the logarithm of the per capita communication consumption of the residents. For every 1% increase in the per capita personal income tax of the working age population, the per capita communication consumption of the residents will decrease by 0.034%, which shows that the increase in the per capita personal income tax will hinder the communication consumption of the residents. This is also in line with the reality. When the individual income tax of residents increases, the disposable income naturally decreases, which affects the communication consumption. Different consumer groups have different income levels, so their consumption ability and consumption tendency will be different, which makes their consumption expenditure on communication services very different. According to the statistical norms of the National Bureau of statistics, all survey households are ranked from low to high according to their per capita disposable income and are divided into seven levels: lowest income households, low income households,

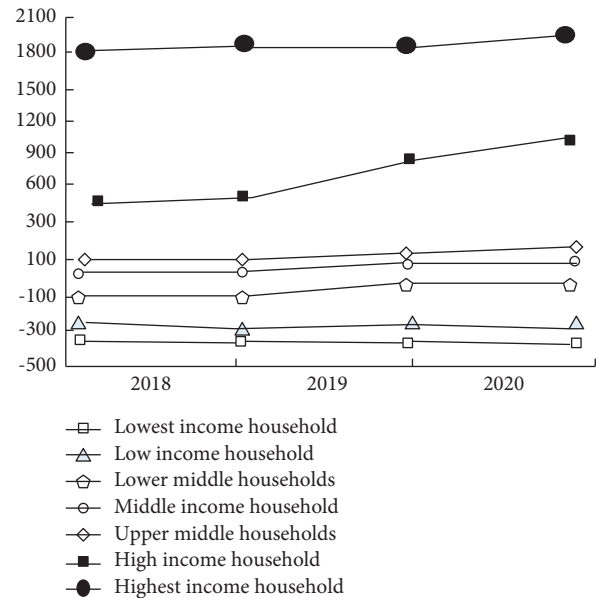


FIGURE 11: Comparison of per capita communication cost difference among residents of different income levels.

lower middle income households, middle income households, upper middle income households, high income households, and highest income households. Table 4 shows the per capita communication consumption of urban residents in China by level.

From the “total average” in the second column to the “highest income households” in the last column, the per capita communication consumption expenditure of urban residents and communication consumption expenditure at all levels in China show an increasing trend, and the “total average” annual growth rate is about 17%. Further analyze and record the expenditure of communication consumption of residents at all income levels, as in Figure 11.

It can be found that there are great differences in the communication level and growth range of different income classes. Taking the difference of per capita communication fee between low income households and high income households as an example, this paper makes a comparative analysis. In terms of consumption level, there is a great gap between low income households and high income households. The consumption expenditure of the highest income households is 15 times that of the lowest income households. In terms of growth rate, high income households are 8 percentage points higher than low income households. To observe and compare the per capita communication expenses of urban residents of different income levels in China, the figure can be used for comparative analysis more intuitively.

4. Conclusion

The communication consumer price index is one of the important factors affecting the change in communication consumption of urban residents in China, which shows that the pricing mode of the telecom business is bound to have a substantial impact on residents’ communication consumption. Due to the fierce competition in the telecom market, major telecom operators launch new services and fight a price war at the same time. Therefore, disorderly competition may be the biggest threat to the sustainable development of the telecom industry. The telecom service pricing model is not only related to the profits of telecom enterprises, but also related to the development prospects of the whole telecom industry. With the relevant government departments gradually paying attention to the supervision of telecom prices, there are still unreasonable standards in the service pricing of the telecom market, which is a problem that communication enterprises must solve. Therefore, telecom operators must actively adopt more scientific telecom service pricing models and methods. Firstly, we should follow the principle of classified pricing for different telecom services. For example, for new business pricing, the operator should independently determine the tariff according to the market: The basic telecommunications industry has the typical nature of a natural monopoly. Various basic telecommunications services have accumulated a large amount of funds for the competition and development of other services. Its pricing can adopt the government’s guidance price or government pricing based on cost accounting. The second is to comprehensively consider market and user factors. Facing the complex and changeable situation of the telecom market, a single pricing model cannot meet the changing needs, nor is it conducive to enterprises’ giving full play to their respective business advantages. Therefore, the

tariff for the same service can also consider the different needs of different customers in the market as much as possible, provide customers with a variety of tariff schemes, subdivide the user group, and increase the selectivity of the telecom tariff. Finally, operators should strengthen the research on pricing methods to ensure the enforceability of the pricing model and make the pricing model more competitive.

Data Availability

The labeled dataset used to support the findings of this study is available from the corresponding author upon request.

Conflicts of Interest

The authors declare no conflicts of interest.

Acknowledgments

This study was sponsored by Universiti Putra Malaysia.

References

- [1] N. Abolhassani, B. Santos-Eggimann, A. Chiolero, V. Santschi, and Y. Henchoz, “Readiness to accept health information and communication technologies: a population-based survey of community-dwelling older adults,” *International Journal of Medical Informatics*, vol. 130, Article ID 103950, 2019.
- [2] W. Liu, X.-F. Shao, C.-H. Wu, and P. Qiao, “A systematic literature review on applications of information and communication technologies and blockchain technologies for precision agriculture development,” *Journal of Cleaner Production*, vol. 298, Article ID 126763, 2021.
- [3] T. D. P. Perera, D. N. K. Jayakody, I. Pitas, and S. Garg, “Age of information in swipt-enabled wireless communication system for 5g,” *IEEE Wireless Communications*, vol. 27, no. 5, pp. 162–167, 2020.
- [4] Z. D. Grève, J. Bottieau, D. Vangulick et al., “Machine learning techniques for improving self-consumption in renewable communities,” *Energies*, vol. 13, no. 18, p. 4892, 2020.
- [5] H. Fujii, A. Shinozaki, S. Kagawa, and S. Managi, “How does information and communication technology capital affect productivity in the energy sector? New evidence from 14 countries, considering the transition to renewable energy systems,” *Energies*, vol. 12, no. 9, p. 1786, 2019.
- [6] M. Salo, H. Savolainen, S. Karhinen, and A. Nissinen, “Drivers of household consumption expenditure and carbon footprints in Finland,” *Journal of Cleaner Production*, vol. 289, Article ID 125607, 2021.
- [7] H. Kumagai, H. Sakurauchi, S. Koitabashi et al., “Development of resilient information and communications technology for relief against natural disasters,” *Journal of Disaster Research*, vol. 14, no. 2, pp. 348–362, 2019.
- [8] Z. Chu, W. Wang, A. Zhou, and W.-C. Huang, “Charging for municipal solid waste disposal in Beijing,” *Waste Management*, vol. 94, pp. 85–94, 2019.
- [9] O. F. Beyca, B. C. Ervural, E. Tatoglu, P. G. Ozuyar, and S. Zaim, “Using machine learning tools for forecasting natural gas consumption in the province of Istanbul,” *Energy Economics*, vol. 80, pp. 937–949, 2019.

- [10] D. S. Ehiakpor, G. Danso-Abbeam, G. Dagunga, and S. N. Ayambila, "Impact of Zai technology on farmers' welfare: evidence from northern Ghana," *Technology in Society*, vol. 59, Article ID 101189, 2019.
- [11] O. S. Odhiambo, S. W. Wanyonyi, D. M. Marangu, I. J. Nguli, and M. M. Mwitii, "Analysis of Household Electricity Consumption in Nonresident Rent Halls Using Linear Regression Analysis Model," *Asian Journal of Probability and Statistics*, vol. 2, 2018.
- [12] Q. Wang, B. Zhou, C. Zhang, and D. Zhou, "Do energy subsidies reduce fiscal and household non-energy expenditures? A regional heterogeneity assessment on coal-to-gas program in China," *Energy Policy*, vol. 155, Article ID 112341, 2021.
- [13] X. Wang and S. Chen, "Urban-rural carbon footprint disparity across China from essential household expenditure: survey-based analysis, 2010-2014," *Journal of Environmental Management*, vol. 267, Article ID 110570, 2020.
- [14] J. Cox and S. C. Ludvigson, "Drivers of the great housing boom-bust: credit conditions, beliefs, or both?" *Real Estate Economics*, vol. 49, no. 3, pp. 843–875, 2021.
- [15] D. Fischer, J.-L. Reinermann, G. Guillen Mandujano, C. T. DesRoches, S. Diddi, and P. J. Vergragt, "Sustainable consumption communication: a review of an emerging field of research," *Journal of Cleaner Production*, vol. 300, Article ID 126880, 2021.
- [16] B. Zhang, C. Dou, D. Yue, Z. Zhang, and T. Zhang, "Consensus-based economic hierarchical control strategy for islanded MG considering communication path reconstruction," *Journal of the Franklin Institute*, vol. 356, no. 16, pp. 9043–9075, 2019.
- [17] M. Haseeb, S. Kot, H. I. Hussain, and K. Jermisittiparsert, "Impact of economic growth, environmental pollution, and energy consumption on health expenditure and R&D expenditure of ASEAN countries," *Energies*, vol. 12, no. 19, p. 3598, 2019.
- [18] S. A. Sarkodie, "Causal effect of environmental factors, economic indicators and domestic material consumption using frequency domain causality test," *The Science of the Total Environment*, vol. 736, Article ID 139602, 2020.
- [19] D. C. Jain, "Diffusion of Innovations: Modeling, Estimation, and Normative Developments," Doctoral dissertation, China Europe International Business School, 2020.
- [20] A. L. Proque, G. F. dos Santos, A. A. Betarelli Junior, and W. D. Larson, "Effects of land use and transportation policies on the spatial distribution of urban energy consumption in Brazil," *Energy Economics*, vol. 90, Article ID 104864, 2020.
- [21] J. Millward-Hopkins and Y. Oswald, "'Fair' inequality, consumption and climate mitigation," *Environmental Research Letters*, vol. 16, no. 3, Article ID 034007, 2021.
- [22] H. Yan, "Discussion on the changes and laws of user information demands in the network environment," *Journal of Intelligence*, vol. 1, pp. 44–46, 2002.
- [23] L. Ren, "Research on Information Behavior Measurement of Internet Users," Master's Thesis, Lanzhou University, 2006.
- [24] C. Urquhart, A. Light, R. Thomas et al., "Critical incident technique and explicitation interviewing in studies of information behavior," *Library & Information Science Research*, vol. 25, no. 1, pp. 63–88, 2003.

Research Article

Research on the Development Path of Manufacturing Industry and Its Economic Effect Based on Computational Visualization

Shiyuan Zhou ¹, Zhixiong Liao,² and Xiaoqin Yang³

¹*Institute of Business Administration, Henan University, Kaifeng 475001, China*

²*Xinxiang Institute of Engineering, Xinxiang 453700, China*

³*School of Business Administration, Yellow River Conservancy Technical Institute, Kaifeng 457004, China*

Correspondence should be addressed to Shiyuan Zhou; 10090098@vip.henu.edu.cn

Received 7 March 2022; Revised 6 April 2022; Accepted 27 April 2022; Published 17 May 2022

Academic Editor: Wei Liu

Copyright © 2022 Shiyuan Zhou et al. This is an open access article distributed under the Creative Commons Attribution License, which permits unrestricted use, distribution, and reproduction in any medium, provided the original work is properly cited.

In order to improve the analysis effect of the manufacturing development path and improve the economic benefits of the manufacturing industry, this paper combines the computer visualization technology to analyze the manufacturing development path and its economic effect. Moreover, this paper introduces the minimum ill-posedness criterion in the optimal placement criteria of time-domain sensors and the modal guarantee criterion in the optimal placement criteria for frequency-domain sensors. In addition, in this paper, the optimal arrangement of sensors is carried out based on the above two criteria, and the improved monkey swarm algorithm is applied to the optimization problem of the sensor of the visual system, and an intelligent computer visualization system is constructed. The experimental research results show that the research model of the manufacturing development path and its economic effects based on computational visualization proposed in this paper has certain practical effects.

1. Introduction

At present, China is actively participating in the development path of returning to the manufacturing industry and has put forward the strategic plan of “Made in China 2025” of great significance and hopes to change the status quo that China’s manufacturing industry is large but not strong before 2025 and upgrade from a large manufacturing country to a manufacturing power.

In recent years, countries around the world has adopted a series of policy measures such as the establishment of special economic zones, export processing zones, coastal development zones along the river, customs bonded zones, and free trade zones and the adoption of various tariff concessions and exemptions, export tax rebates, and foreign direct investment to penetrate into the international industrial cooperation and economic division system on a large scale and in an all-round way [1]. In particular, manufacturing has become an important part of the world industrial cycle system. The international trade volume,

especially the manufacturing processing trade volume, has grown rapidly and has gradually formed a processing trade model with “the three-plus-one trading-mix” as the main form and “both-ends-abroad” as the dominant feature [2]. In this way, manufacturing enterprises are embedded in labor-intensive production links such as processing and assembly in the division of labor in the global value chain by virtue of sufficient labor factors and cheap labor costs and become “world factories.” Although the world-renowned East Asian Miracle has been achieved through high-input and high-output import and export trade, the growth of macro and industrial total factor productivity is an important support for maintaining medium-to-high-speed economic growth and improving the quality of economic growth in the future. Judging from the current situation, it is an undeniable fact that China and developed countries have obvious differences in the international division of labor, and the international division of labor of products further solidifies the status of China and developed countries in the international division of labor. Manufacturing industries in

developed countries are generally at the high end of the value chain engaged in high value-added activities such as upstream R&D and downstream brand marketing. However, China's manufacturing industry is generally "locked" in the low value-added middle- and low-end links in the value chain division of labor, mainly manufacturing and processing [3]. Therefore, how to help local manufacturing companies get rid of the "low-end lock" and "capture" effects of the value chain, change the overall low total factor productivity of the manufacturing industry, and realize the task of climbing from low-end manufacturing and export to medium- and high-end value chain is imminent.

This paper combines computer visualization technology to analyze the development path of manufacturing industry and its economic effect, which provides a theoretical reference for the subsequent development of manufacturing industry.

2. Related Work

Manufacturing is an important part of industry, an important force driving the development of the national economy, and an important guarantee for the country's comprehensive national strength. As we all know, the quality of German products is well known all over the world, and the important guarantee for winning these products comes from the long-term prosperity of the German manufacturing industry. The quality of German manufacturing has always maintained a world-leading level [4]. With the support of the government, Japan's manufacturing industry has maintained a steady growth in the total amount of Japan's manufacturing industry through a series of measures such as reducing energy consumption, strengthening technological innovation and foreign investment, continuing Japan's manufacturing industry continued prosperity [5]. Literature [6] pointed out the disparity in the status of developing countries and developed countries in the value chain. When developing countries rely on low-level elements such as resources to embed into the value chain, developed countries will dominate the global value chain with advanced elements such as technology and brand. From the perspective of the integrated development of manufacturing and service industries, literature [7] makes a quantitative analysis of the two using the relevant data of manufacturing and service industries in the United States and points out that the servitization of manufacturing is essentially the integration of manufacturing and service industries developing. Literature [8] believes that there are two ways for multinational enterprises to integrate into the global value chain. Only by embedding the global value chain from the high end of the value chain can the international competitiveness of the enterprise be improved. If it is embedded from the low end of the value chain, the enterprise will face the danger of falling into a poverty-stricken growth trap. Reference [9] analyzes the impact of global value chains on the international division of labor in the manufacturing industry by using the method of export technical complexity. Literature [10] believes that the import of intermediate products is

beneficial to the improvement of domestic manufacturing production efficiency.

Literature [11] believes that technological progress is an important driving force for the upgrading of manufacturing industries in developing countries. Literature [12] emphasizes the focus on dynamic capabilities, which is the ability of enterprises to develop and innovate by learning new knowledge and mastering new technologies in the long-term learning process. Literature [13] pointed out that enterprises should pay attention to the core competitiveness and the ability to create value for consumers through the research on the transformation and upgrading of the manufacturing industry. Reference [14] pointed out that the essence of the manufacturing upgrade process is the process of manufacturing enterprises from low value-added to high value-added and from labor-intensive to capital-intensive, and in this process, enterprises realize the promotion of their status in the division of labor and trade. Under the pattern of the division of labor in the value chain, technological innovation is the basis for realizing the upgrading of the manufacturing industry. Reference [15] pointed out that when developing countries try to upgrade high value-added links in the value chain division of labor, they will be hindered and controlled by developed countries. Literature [16] found through research on China that although the development of the processing and manufacturing industry has promoted a substantial increase in China's trade level to a certain extent, this export-oriented and highly competitive industry based on imported technology and foreign-funded enterprises has limited local trade, production, and technological diffusion in China's domestic industry.

Literature [17] conducted a general research and exploration on the dynamic mechanism and governance structure in the theory of global value chain, aiming to explore how manufacturing enterprises can make use of their strengths and avoid weaknesses to realize industrial transformation and upgrading from the perspective of value chain under the background of economic globalization and deepening competition. Literature [18] measured the cost of each link in the enterprise value chain from the perspective of cost and proposed countermeasures and suggestions to improve the competitiveness of enterprises by reducing costs. Literature [19] conducted an empirical analysis and research on the factors affecting the transformation and upgrading of manufacturing enterprises at the microlevel and pointed out that industrial agglomeration, external supporting services, and exports have a significant impact on the transformation and upgrading of the manufacturing industry. Reference [20] starts from the value chain theory and studies the upgrading of the processing and manufacturing industry from the positive and negative effects of the value chain on the processing and manufacturing industry. Literature [21] analyzed the correlation between the processing manufacturing industry and the logistics industry and pointed out that there is a close connection between the logistics industry and the upgrading of the processing manufacturing industry. The development of the modern logistics industry has accelerated the upgrading of the technological structure of the processing manufacturing

industry to a certain extent. It is of great significance to the transformation and upgrading of the processing and manufacturing industry.

3. The Construction of Computer Visualization Network Based on the Internet of Things

There are many sensor points to be selected for large-scale structures. In order to better reflect the dynamic characteristics of the structure and obtain more sufficient structural information, a good sensor layout scheme is required. The development of sensor optimal layout criteria provides a basis for sensor layout, and different sensor optimal layout criteria enable the structural health monitoring system to obtain different recognition effects. In order to better monitor the health of the structure, this paper selects the minimum ill-posedness criterion and the modal assurance criterion to optimize the arrangement of sensors.

3.1. Minimum Ill-Posedness Criterion for a Single Type of Sensor. Any multi-degree-of-freedom linear elastic finite element equation of motion can be expressed by the following formula:

$$\mathbf{M}\ddot{\mathbf{x}} + \mathbf{C}\dot{\mathbf{x}} + \mathbf{K}\mathbf{x} = \mathbf{F}(t). \quad (1)$$

Among them, \mathbf{M} is the mass matrix, \mathbf{C} is the damping matrix, and the Rayleigh damping model is used. \mathbf{K} is the stiffness matrix, $\mathbf{F}(t)$ is the external load, and $\ddot{\mathbf{x}}$ is the acceleration response.

When a structure is damaged, stiffness usually decreases. α_i is the local stiffness change rate of the i -th element of the structure, $-1 \leq \alpha_i \leq 0$. When $\alpha_i = -1$, it means that the structural stiffness at this time is 0; that is, complete damage has occurred. When $\alpha_i = 0$, it means that the stiffness of the structure has not changed. When $-1 < \alpha_i < 0$, it means that the structure has been damaged to a certain extent, and the stiffness of the structure is reduced. Taking the partial derivative of the local stiffness change rate on both sides of the equation of motion, we can get

$$\mathbf{M} \frac{\partial \ddot{\mathbf{x}}}{\partial \alpha_i} + \frac{\partial \mathbf{M}}{\partial \alpha_i} \ddot{\mathbf{x}} + \mathbf{C} \frac{\partial \dot{\mathbf{x}}}{\partial \alpha_i} + \frac{\partial \mathbf{C}}{\partial \alpha_i} \dot{\mathbf{x}} + \mathbf{K} \frac{\partial \mathbf{x}}{\partial \alpha_i} + \frac{\partial \mathbf{K}}{\partial \alpha_i} \mathbf{x} = \frac{\partial \mathbf{F}}{\partial \alpha_i}. \quad (2)$$

Among them, the mass matrix is \mathbf{M} , and the external load \mathbf{F} is independent of the local stiffness change rate. Therefore, its partial derivative to the local stiffness change rate is 0, and (3) can be obtained after arranging (2):

$$\mathbf{M} \frac{\partial \ddot{\mathbf{x}}}{\partial \alpha_i} + \mathbf{C} \frac{\partial \dot{\mathbf{x}}}{\partial \alpha_i} + \mathbf{K} \frac{\partial \mathbf{x}}{\partial \alpha_i} = -\frac{\partial \mathbf{K}}{\partial \alpha_i} \mathbf{x} - a \frac{\partial \mathbf{K}}{\partial \alpha_i} \dot{\mathbf{x}}. \quad (3)$$

Among them, $\partial \ddot{\mathbf{x}}/\partial \alpha_i$, $\partial \dot{\mathbf{x}}/\partial \alpha_i$, $\partial \mathbf{x}/\partial \alpha_i$ is the sensitivity vector of acceleration, velocity, and displacement, respectively.

The form of (3) at this time is exactly the same as that of equation of motion (1), and the sensitivity vectors of acceleration, velocity, and displacement can be solved by the explicit Newmark - β -direct integration method.

If it is assumed that the structure has N units and g is the response of the i -th sensor to be measured, the functional relationship between γ_i and the local rate of change of all units can be established, as shown in the following formula:

$$\gamma_i = f_i(\alpha_1, \alpha_2, \dots, \alpha_N). \quad (4)$$

At this time, taking the response of the measuring point as the acceleration, and expanding it according to the multivariate Taylor series, the formula about the acceleration signal can be obtained:

$$S_a \alpha + o(\alpha^2) = \Delta \ddot{\mathbf{X}}. \quad (5)$$

Among them, S_a is the total acceleration sensitivity matrix, α is the stiffness change rate vector, and $\Delta \mathbf{X}$ is the difference between the measured acceleration and the calculated acceleration. Then, the total acceleration sensitivity matrix can be expressed as

$$S_a = [S_{a_1}, S_{a_2}, \dots, S_{a_N}]. \quad (6)$$

When the damage identification (5) is obtained, the multivariate Taylor series method is used, and the second-order and higher-order terms are ignored, there is an error between the stiffness change rate vector α and the real value, and the error needs to be eliminated by an iterative method. After each iteration, the stiffness will be corrected once, and a new stiffness change rate vector α will be obtained. The iteration termination condition is

$$\frac{\|\alpha_{k+1} - \alpha_k\|}{\alpha_{k+1}} < T. \quad (7)$$

Among them, m is a minimum value close to 0, and the final stiffness change rate vector α is obtained by adding the stiffness change rate vectors obtained in each iteration.

The correlation coefficient between each column vector of the acceleration sensitivity matrix S_a is calculated by the following formula:

$$e_{a_{i,j}} = \begin{cases} 0, & i = j, \\ \frac{|s_{a_i}(S_{a_j})^T|}{\sqrt{|S_{a_i}(S_{a_i})^T|} \cdot \sqrt{|S_{a_j}(S_{a_j})^T|}}, & i \neq j. \end{cases} \quad (8)$$

By assembling the correlation coefficients, the acceleration correlation coefficient matrix e_a can be obtained:

$$e_a = \begin{pmatrix} e_{a_{1,1}} & \cdots & e_{a_{1,i}} & \cdots & e_{a_{1,N}} \\ \vdots & \ddots & \vdots & \ddots & \vdots \\ e_{a_{i,1}} & \cdots & e_{a_{i,i}} & \cdots & e_{a_{i,N}} \\ \vdots & \ddots & \vdots & \ddots & \vdots \\ e_{a_{N,1}} & \cdots & e_{a_{N,i}} & \cdots & e_{a_{N,N}} \end{pmatrix}_{N \times N}. \quad (9)$$

There are as many sensor layout schemes as there are acceleration correlation coefficient matrices e_a . The

acceleration arrangement index β_a can be obtained by summing all the correlation coefficients in each acceleration correlation coefficient matrix e_a . The smaller the acceleration placement index β_a is, the smaller the correlation between the column vectors of different elements of the structure is and the better the placement position of the sensor is.

$$\beta_a = \sum_{i=1, j=1}^N e_{a_{ij}}. \quad (10)$$

3.2. Minimum Ill-Posedness Criterion for Two Types of Sensors. In (3), the displacement sensitivity vector can be solved by the direct integration method of Newmark – β , and then the displacement sensitivity matrix S_d can be solved by the same method. Strain sensitivity and displacement sensitivity are the partial derivatives of strain and displacement with respect to the local rate of stiffness change, respectively. In finite element theory, the strain at a point on the structure can be obtained from the displacement of the nodes at both ends of the element through the transformation matrix. Therefore, the strain sensitivity matrix S_ε can also be obtained from the displacement sensitivity matrix S_d , and the calculation formula is as follows:

$$S_\varepsilon = BRS_d. \quad (11)$$

Among them, B is the unit strain transformation matrix, R is the unit rotation axis matrix, and the same strain sensitivity matrix can be divided into N strain sensitivity vectors:

$$S_\varepsilon = [S_{\varepsilon_1}, S_{\varepsilon_2}, \dots, S_{\varepsilon_N}]. \quad (12)$$

By assembling the obtained acceleration sensitivity matrix S_a and strain sensitivity matrix S_ε , the dual-signal sensitivity matrix can be obtained. However, the magnitudes of the acceleration sensitivity matrix S_a and the strain sensitivity matrix S_ε are inconsistent. If it is directly assembled, it will inevitably cause the calculation information of the smaller order of magnitude to be masked. Therefore, the order of magnitude of the two types of sensitivity matrices can be made consistent with the help of the standardization method. The standardization process is as follows:

$$\frac{1}{\|\ddot{X}_c^j\|} S_a^j \alpha = \frac{1}{\|\ddot{X}_c^j\|} (\ddot{X}_m^j - \ddot{X}_c^j) \Rightarrow S_a^{j*} \alpha = \ddot{X}_m^{j*} - \ddot{X}_c^{j*}. \quad (13)$$

In the formula, \ddot{X}_m^j is the measured acceleration response at the j th sensor position; \ddot{X}_c^j is the calculated acceleration response at the j th sensor position; \ddot{X}_m^{j*} is the normalized measured acceleration response at the j th sensor position; \ddot{X}_c^{j*} is the normalized calculated acceleration response at the j th sensor placement.

$$S_a^* = \begin{pmatrix} S_{a_1}^{1*} & \dots & S_{a_i}^{1*} & \dots & S_{a_N}^{1*} \\ \vdots & \ddots & \vdots & \ddots & \vdots \\ S_{a_1}^{j*} & \dots & S_{a_i}^{j*} & \dots & S_{a_N}^{j*} \\ \vdots & \ddots & \vdots & \ddots & \vdots \\ S_{a_1}^{Na*} & \dots & S_{a_i}^{Na*} & \dots & S_{a_N}^{Na*} \end{pmatrix}. \quad (14)$$

In the formula, Na is the number of acceleration sensors; S_a^* is the normalized acceleration sensitivity matrix; N is the number of units of the structure.

$$\frac{1}{\|\varepsilon_c^j\|} S_\varepsilon^j \alpha = \frac{1}{\|\varepsilon_c^j\|} (\varepsilon_m^j - \varepsilon_c^j) \Rightarrow S_\varepsilon^{j*} \alpha = \varepsilon_m^{j*} - \varepsilon_c^{j*}. \quad (15)$$

In the formula, ε_m^j is the measured strain response at the j th sensor position; ε_c^j is the calculated strain response at the j th sensor position; ε_m^{j*} is the normalized measured strain response at the j th sensor location; ε_c^{j*} is the normalized calculated strain response at the j th deployed sensor location.

$$S_\varepsilon^* = \begin{pmatrix} S_{\varepsilon_1}^{1*} & \dots & S_{\varepsilon_i}^{1*} & \dots & S_{\varepsilon_N}^{1*} \\ \vdots & \ddots & \vdots & \ddots & \vdots \\ S_{\varepsilon_1}^{j*} & \dots & S_{\varepsilon_i}^{j*} & \dots & S_{\varepsilon_N}^{j*} \\ \vdots & \ddots & \vdots & \ddots & \vdots \\ S_{\varepsilon_1}^{N\varepsilon*} & \dots & S_{\varepsilon_i}^{N\varepsilon*} & \dots & S_{\varepsilon_N}^{N\varepsilon*} \end{pmatrix}. \quad (16)$$

In the formula, $N\varepsilon$ is the number of strain sensors; S_ε^* is the normalized strain sensitivity matrix.

By assembling the normalized acceleration sensitivity matrix S_a^* and the normalized strain sensitivity matrix S_ε^* , the dual-signal sensitivity matrix S^* can be obtained:

$$S^* = \begin{bmatrix} S_{a_1}^* & \dots & S_{a_i}^* & \dots & S_{a_N}^* \\ S_{\varepsilon_1}^* & \dots & S_{\varepsilon_i}^* & \dots & S_{\varepsilon_N}^* \end{bmatrix} = [S_1^* \dots S_i^* \dots S_N^*]. \quad (17)$$

By assembling the standardized measured acceleration response \ddot{X}_m^* , the standardized calculated acceleration response \ddot{X}_c^* , the standardized measured strain response ε_m^* , and the standardized calculated strain response ε_c^* in the same way, the dual-signal damage identification equation can be obtained:

$$S^* \alpha + o(\alpha^2) = \Delta y^*. \quad (18)$$

Among them, Δy^* is the difference between the measured response and the calculated response of the dual signal. Similarly, the ill-posedness of the dual-signal damage identification equation is judged by the arrangement index method.

The correlation coefficient between each column vector of the dual-signal sensitivity matrix S^* is calculated by formula (19):

$$\begin{cases} e_{i,j} = 0, & i = j, \\ e_{i,j} = \frac{|s_{a_i}(\mathbf{S}_{a_j})^T|}{\sqrt{|s_{a_i}(\mathbf{S}_{a_i})^T|} \cdot \sqrt{|s_{a_j}(\mathbf{S}_{a_j})^T|}}, & i \neq j, \end{cases} \quad (19)$$

$$\mathbf{e} = \begin{pmatrix} e_{1,1} & \cdots & e_{1,i} & \cdots & e_{1,N} \\ \vdots & \ddots & \vdots & \ddots & \vdots \\ e_{i,1} & \cdots & e_{i,i} & \cdots & e_{i,N} \\ \vdots & \ddots & \vdots & \ddots & \vdots \\ e_{N,1} & \cdots & e_{N,i} & \cdots & e_{N,N} \end{pmatrix}_{N \times N}. \quad (20)$$

The two-signal arrangement index e can be obtained by summing all the correlation coefficients in each two-signal correlation coefficient matrix β . The smaller the dual-signal arrangement index β , the smaller the correlation between the column vectors of different elements of the structure, the smaller the ill-posedness of the dual-signal damage identification equation, and the more reasonable the sensor arrangement position.

$$\beta = \sum_{i=1, j=1}^N e_{i,j}. \quad (21)$$

The modal guarantee criterion can be used to monitor the magnitude of the angle between two vectors and then evaluate the magnitude of the linear independence between the two vectors. The formula of the modal guarantee criterion is shown in the following formula:

$$\text{MAC}_{ij} = \frac{(\varphi_i^T \varphi_j)^2}{(\varphi_i^T \varphi_i)(\varphi_j^T \varphi_j)}. \quad (22)$$

The off-diagonal elements in the MAC matrix represent the size of the space angle between the two vectors, that is, the size of the correlation between the two vectors. MAC_{ij} is an element in the modal guarantee matrix, and the value of MAC_{ij} have magnitudes between 0 and 1. When MAC_{ij} is equal to 1, it means that the angle between the two vectors is 0, and the two vectors are completely related. When MAC_{ij} is equal to 0, it means that the two vectors are orthogonal to each other, and the vectors are independent of each other. Among them, φ_i, φ_j denotes a vector of order i and order j .

The traditional monkey swarm algorithm is introduced first, and then an improved monkey swarm algorithm is proposed.

Algorithm parameters: population size, climbing step length, viewing field width, jumping interval length, number of climbing, looking, and jumping processes, number of iterative cycles, and dimension of the solution problem.

Algorithm termination condition:

- (1) The algorithm reaches the specified number of iterations.
- (2) The optimal solution of the fitness function value reaches a certain limit range.

- (3) After the specified number of consecutive iterations, the optimal solution of the fitness function value does not change.

The monkey swarm algorithm defines the feasible region of the optimization problem as the overall activity range of the monkey swarm. The specific search process is as follows.

3.2.1. Climbing Process. Each monkey searches in a small local area of its own location, and if it finds a better location, it moves to the better location until it reaches the specified number of climbs. The position of each monkey is $\mathbf{x}_i = (x_{i1}, x_{i2}, \dots, x_{ig})$, where g is the number of elements each monkey contains. The climbing step length is p , and the column vector $d\mathbf{x}_i = (dx_{i1}, dx_{i2}, \dots, dx_{ig})$ is generated in a random manner. The generation rule is shown in the following formula:

$$d\mathbf{x}_{ij} = \begin{cases} p, & \text{Probability is 0.5} \\ -p, & \text{Probability is 0.5} \end{cases}, \quad (j = 1, 2, \dots, g). \quad (23)$$

Each monkey moves according to the pseudogradient direction at its own position to reach the next position \mathbf{y}_i . If \mathbf{y}_i exceeds the value range of the monkey group, \mathbf{y}_i takes the boundary value, and the objective function value at \mathbf{y}_i is compared. If the objective function value at \mathbf{y}_i is better, then \mathbf{y}_i is replaced by \mathbf{x}_i ; otherwise, climbing is not performed. The above process is repeated until the specified number of climbs is reached, or the value of the objective function basically does not change. The pseudogradient calculation formula is shown in

$$f'_{ij}(\mathbf{x}_i) = \frac{f(\mathbf{x}_i + d\mathbf{x}_i) - f(\mathbf{x}_i - d\mathbf{x}_i)}{2 d\mathbf{x}_{ij}}. \quad (24)$$

The position reached along the pseudogradient is $\mathbf{y}_i = (y_{i1}, y_{i2}, \dots, y_{ig})$, and the calculation formula of \mathbf{y}_i is shown in

$$\mathbf{y}_j = \mathbf{x}_{ij} + p \cdot \text{sign}(f'_{ij}(\mathbf{x}_i)). \quad (25)$$

3.2.2. Looking Process. After the climbing process, the monkeys stood on their local highest peaks and looked around to see if there were higher peaks. If there is, it jumps to the higher peak; otherwise it does not move on the original peak. We set the visual field width to be s , which is the furthest distance the monkey can observe at its own position. At this time, the position of each monkey is $\mathbf{x}_i = (x_{i1}, x_{i2}, \dots, x_{ig})$, and the position of the foothold of the field of vision is $\mathbf{y}_i = (y_{i1}, y_{i2}, \dots, y_{ig})$, where the calculation formula of r is shown in

$$y_{ix} = \text{rand}(0, 1) \times (x_{ix} - s, x_{ix} + s). \quad (26)$$

If \mathbf{y}_i exceeds the value range of the monkey group, then \mathbf{y}_i takes the boundary value. The objective function value at \mathbf{y}_i is computed. If the objective function value at \mathbf{y}_i is better, then \mathbf{x}_i is replaced by \mathbf{y}_i ; otherwise, the position remains unchanged. The above process is repeated until the desired

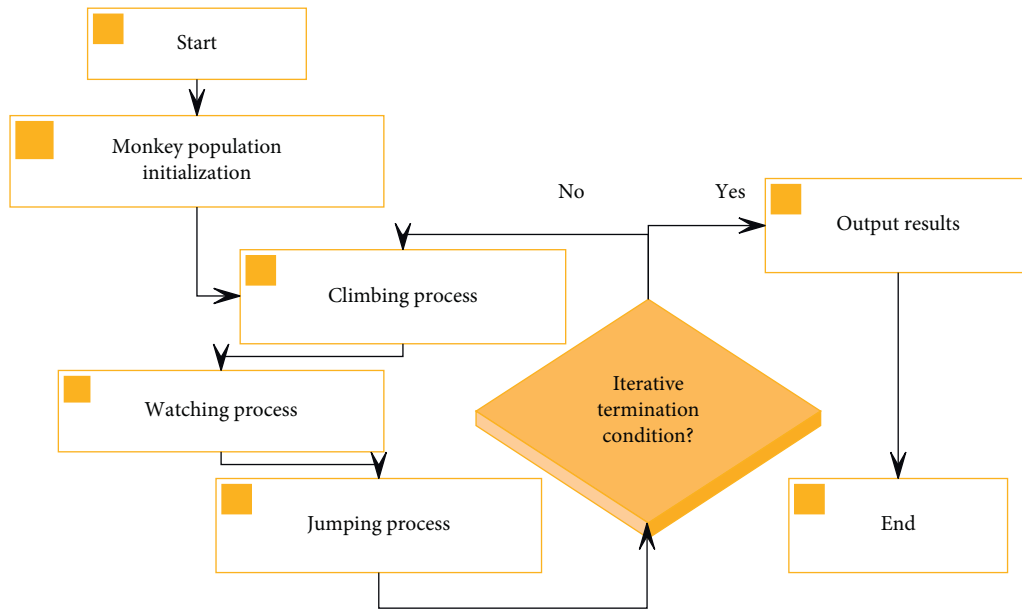


FIGURE 1: Flow chart of traditional monkey swarm algorithm.

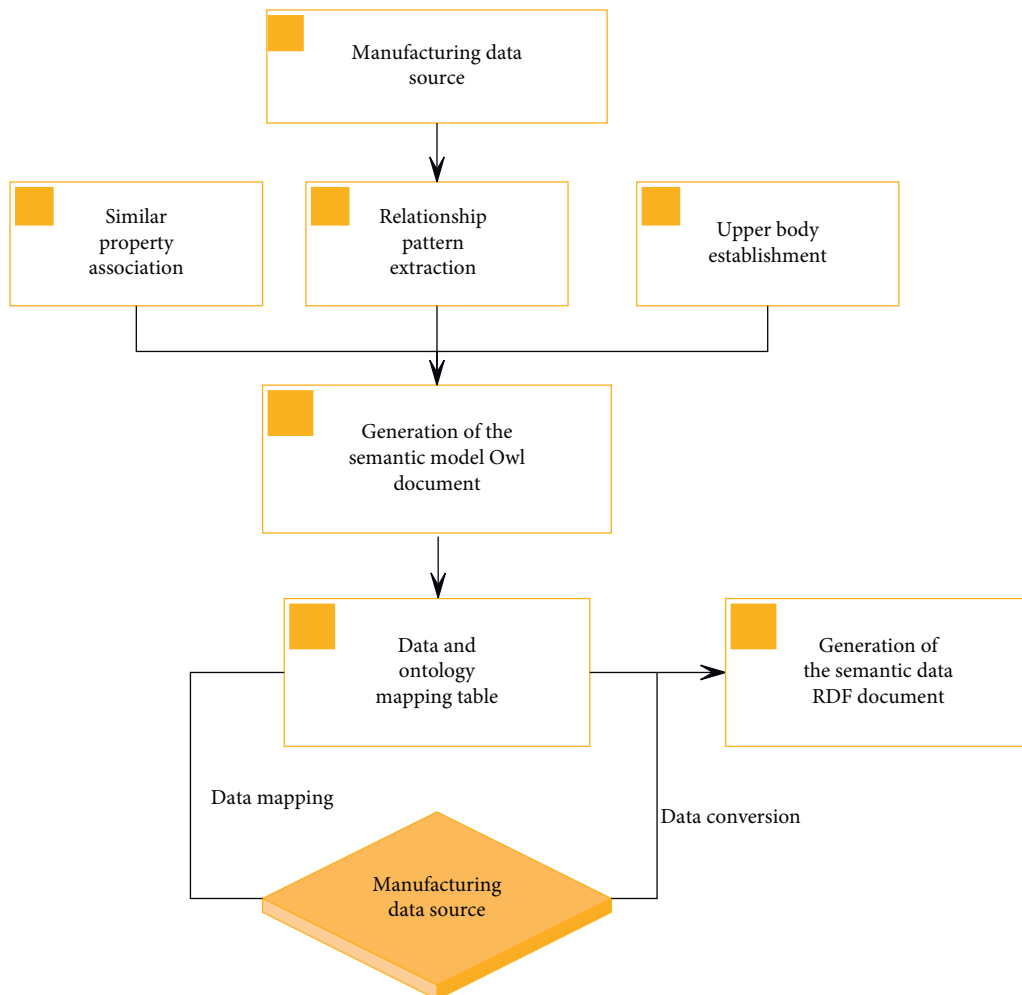


FIGURE 2: Semantic modeling flowchart.

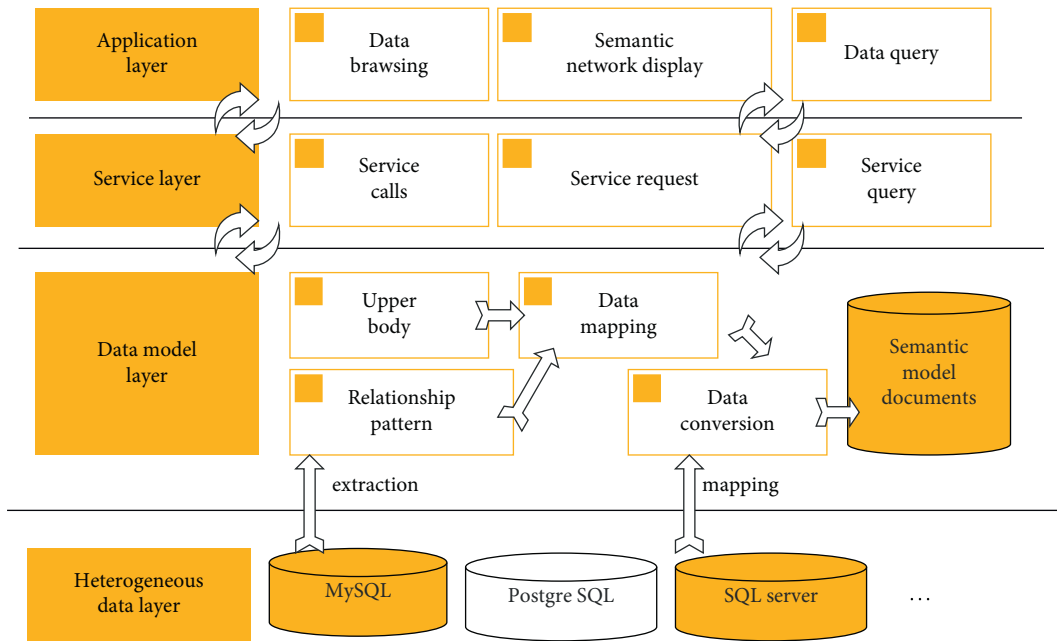


FIGURE 3: Visualization system architecture diagram.

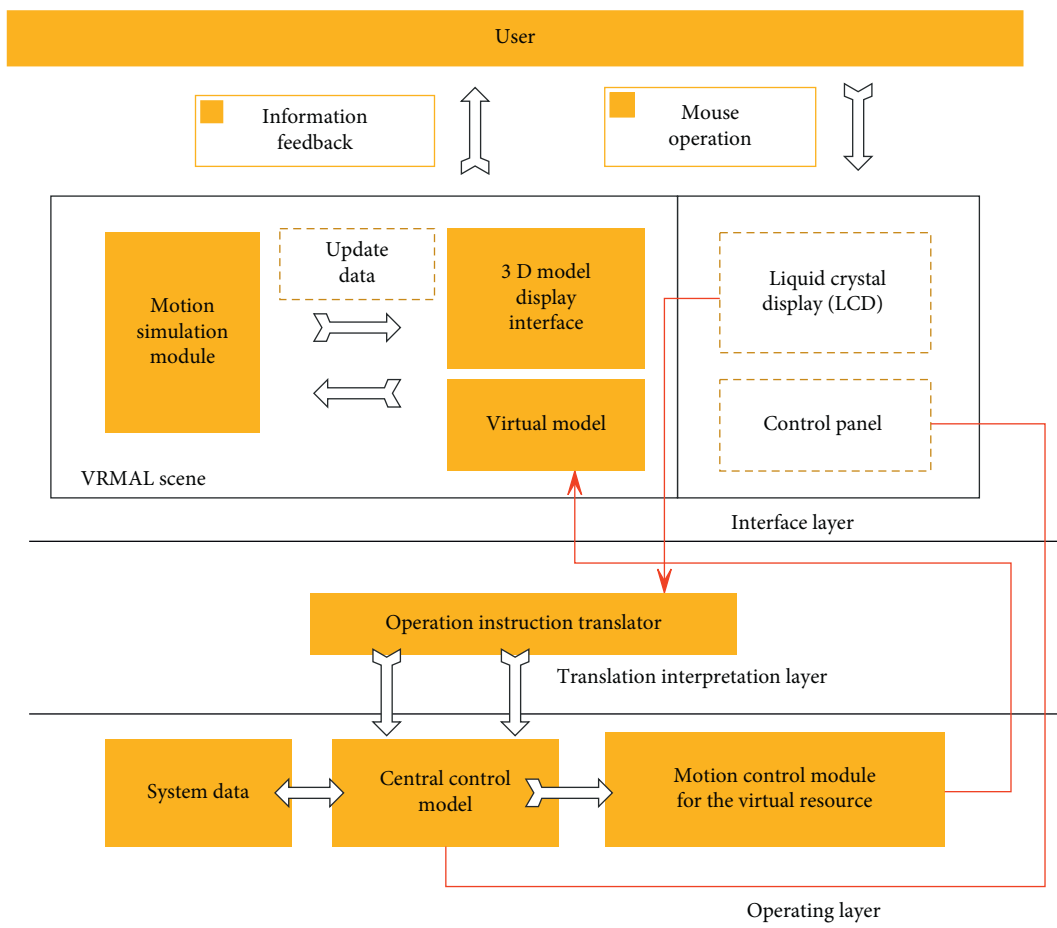


FIGURE 4: System structure of the simulation platform.

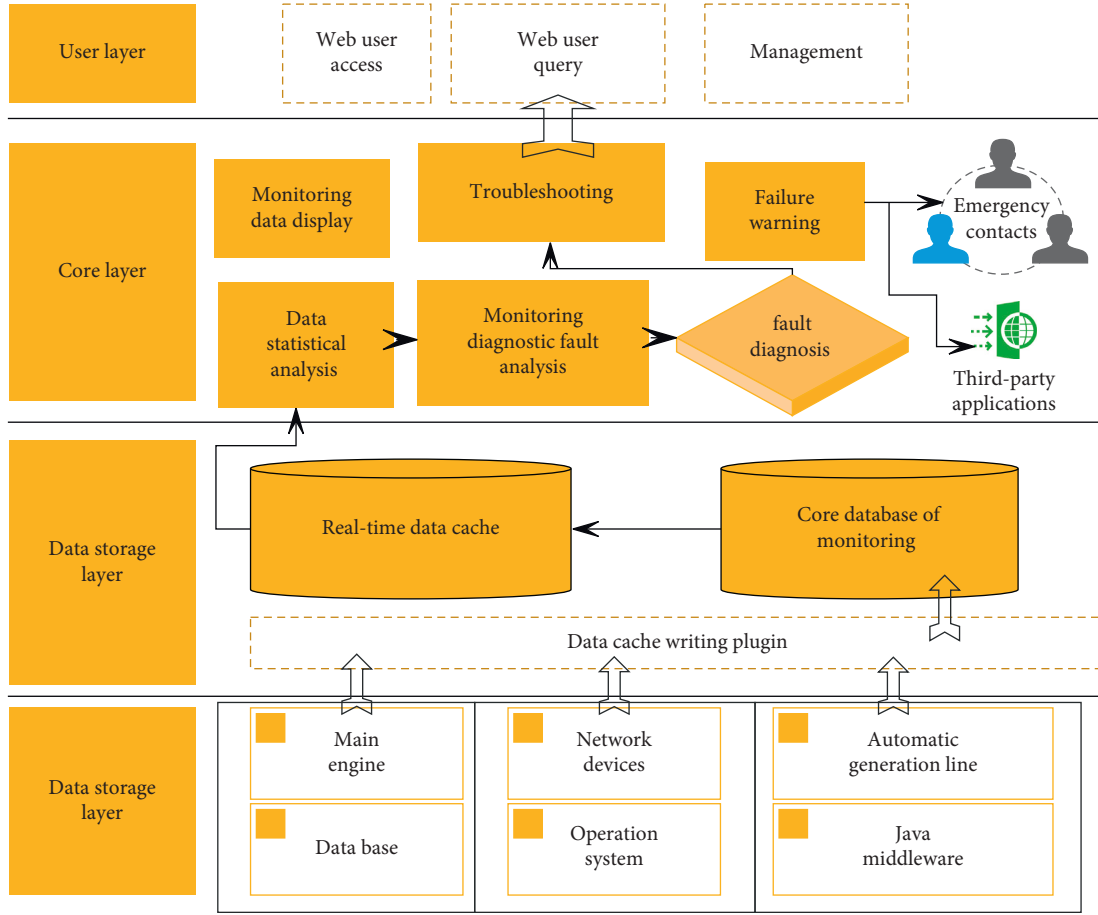


FIGURE 5: Architecture design of monitoring management platform.

number of times is reached, or the value of the objective function basically does not change.

3.2.3. Jump Process. After the monkey finds the local optimal solution, it goes to find the global optimal solution. It uses a certain position as a support point, jumps at a certain distance, reaches a new area, realizes the escape behavior, and then continues the process of climbing, looking, and jumping in the new area. The length of the jump interval is $[b, c]$, and the length of the flip radius f is any value in the jump interval $[b, c]$. The calculation formula is shown in

$$f = \text{rand}(0, 1) \times [b, c]. \quad (27)$$

The support point is the center of gravity $P = (p_1, p_2, \dots, p_g)$ of the monkey group, the population size is N , and the calculation formula of the position of the center of gravity is shown in

$$p_j = \frac{1}{N} \sum_{i=1}^N x_{ij}, \quad j = 1, 2, \dots, g. \quad (28)$$

The new position after the jump is $y_i = (y_{i1}, y_{i2}, \dots, y_{ig})$, and the calculation formula is shown in

$$y_{ij} = x_{ij} + f(p_j - x_{ij}). \quad (29)$$

If y_i exceeds the value range of the monkey group, y_i takes the boundary value. The objective function value at y_i is calculated; if the objective function value at y_i is better, x_i is replaced with y_i ; otherwise, the monkey does not jump. The above process is repeated until the specified number of hops is reached, or the value of the objective function basically does not change.

The traditional monkey swarm algorithm has three detailed processes of climbing, looking, and jumping, and the specific process of the traditional monkey swarm algorithm can be obtained as shown in Figure 1.

3.2.4. Accumulation Rule of Sensor Layout. The study found that there is an accumulation rule for the sensor layout scheme, that is, the layout scheme of $n + 1$ sensors; in order to search on the basis of the original n sensor layout schemes, the n sensor layout schemes are a subset of $n + 1$ sensor layout schemes. For example, the optimal layout plan for 2 sensors is $\{5, 8\}$, the optimal solution for 3 sensors is $\{5, 8, 10\}$, the optimal solution for 4 sensors is $\{5, 8, 10, 12\}$, and so on. This accumulation law can effectively overcome the shortcomings of the traditional optimal arrangement of

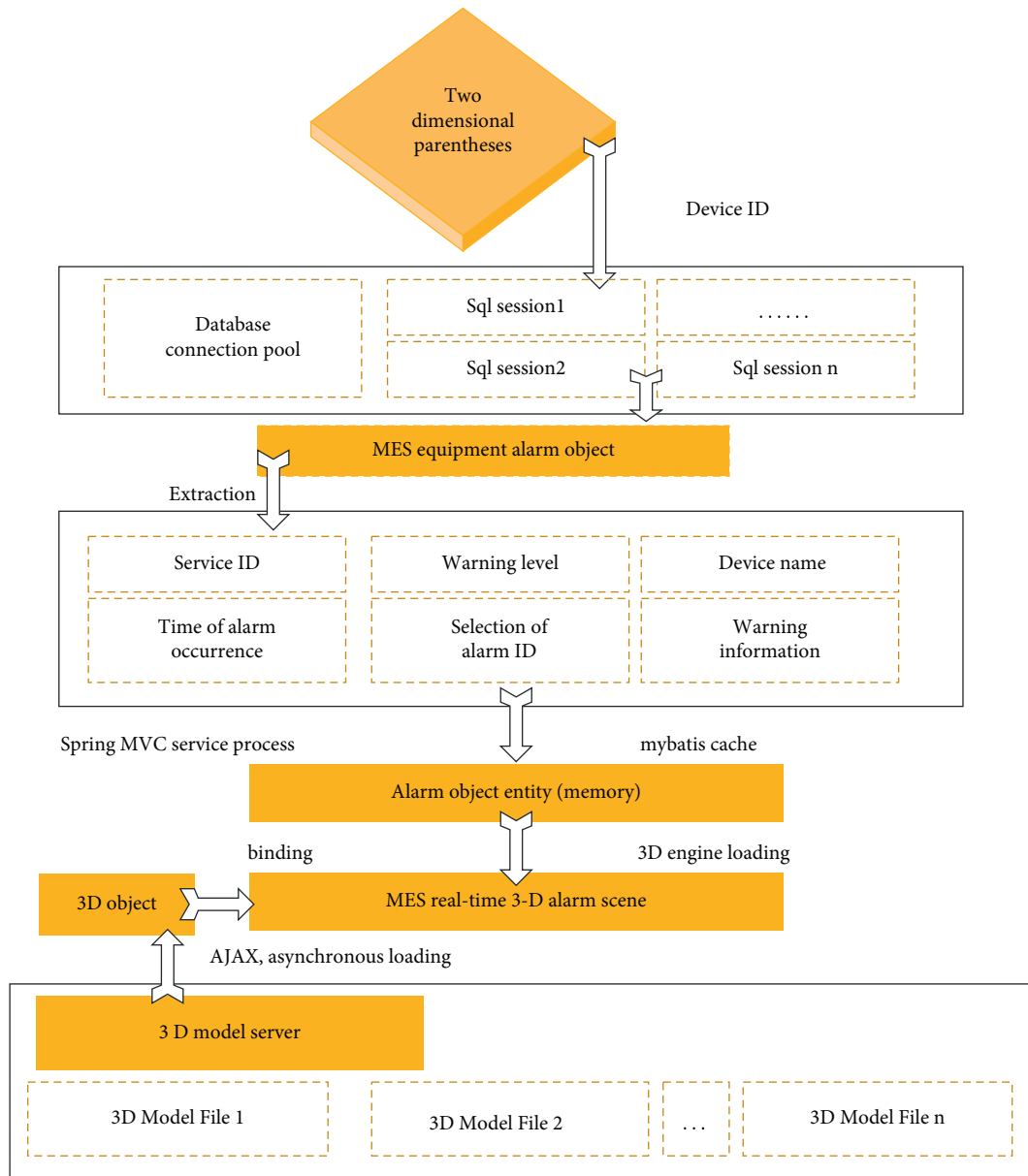


FIGURE 6: System data analysis and processing.

sensors, which greatly increases the calculation time with the increase of the number of sensors. The accumulation law is combined with the traditional monkey group algorithm, which is the cumulative monkey group algorithm. It can significantly improve the computational efficiency of determining the optimal arrangement of sensors of different numbers.

4. Research on the Development Path and Economic Effect of Manufacturing Industry Based on Computer Visualization

The modeling in this paper has the following points: upper-level ontology establishment, relational schema extraction, schema mapping, and data transformation, as shown in Figure 2.

Based on the semantic model, this paper establishes a visualization platform to visualize the semantic model established above and, at the same time, browse the instance data of the semantic model. On the one hand, it is convenient for users to view the semantic model to further improve the modeling. On the other hand, as a prototype system of data management system, it provides data browsing and data query, which provides strong support for cross-platform data integration and cross-enterprise data sharing. The platform adopts B/S mode and J2EE technology development framework, and its structure is shown in Figure 3.

The visual simulation platform is designed in the form of a browser/server (B/S) structure and consists of three parts: the interface layer, the compilation and interpretation layer, and the control layer, as shown in Figure 4.

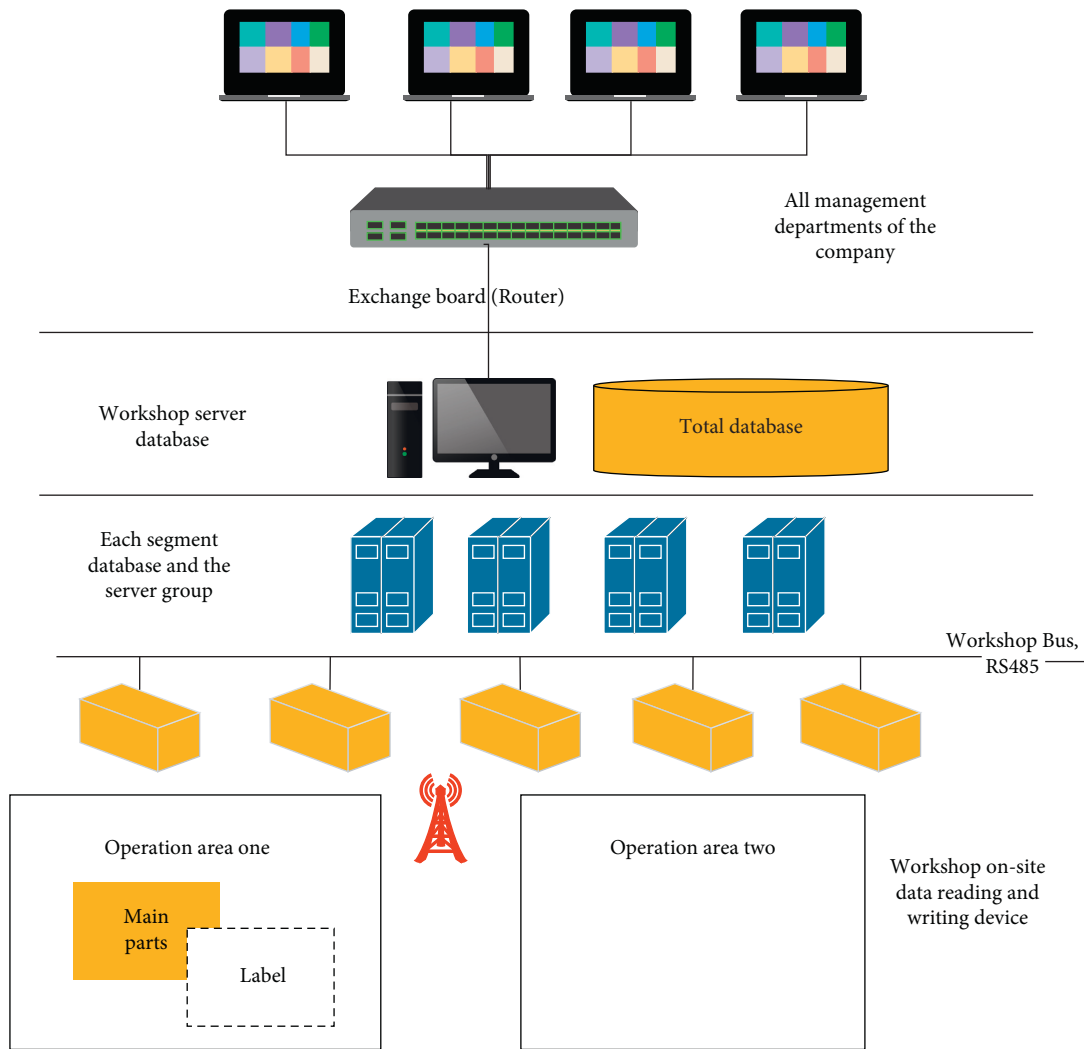


FIGURE 7: Physical architecture diagram of RFID data acquisition system.

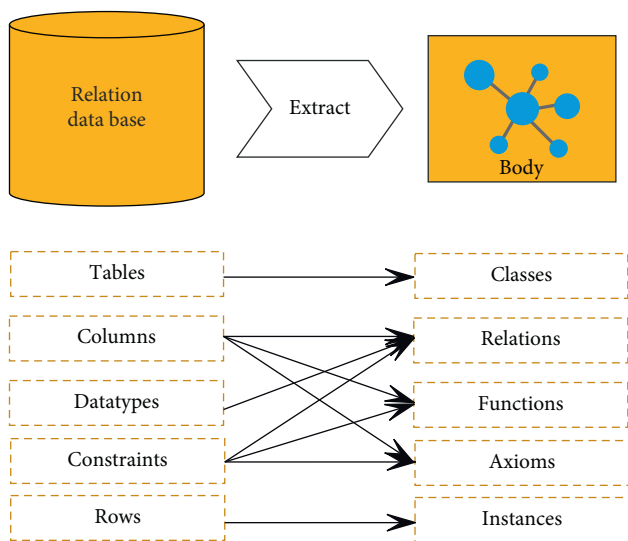


FIGURE 8: Mapping relationship from relational database to ontology.

The overall structure of the integrated monitoring and management system platform is shown in Figure 5.

Different monitoring platforms correspond to different 3D scene files and only need to replace the corresponding scene files. After the program is packaged, a page link is added to the main page of the monitoring platform. As long as the user clicks on the page, the browser will jump to the 3D visualization platform page. The data analysis and processing of the 3D visual alarm system is shown in Figure 6.

It is also possible to introduce RFID technology to realize the physical structure of the actual collection of data, as shown in Figure 7:

The mapping relationship of the ontology extracted from the relational database can be determined, as shown in Figure 8.

On the basis of the above research, this paper analyzes the development path of the manufacturing industry based on computer visualization and its economic effect, counts the research effect of the model in this paper, and obtains the

TABLE 1: Model evaluation data.

Number	Model effect	Number	Model effect	Number	Model effect
1	84.68	26	86.85	51	89.28
2	86.48	27	80.12	52	82.44
3	82.78	28	81.78	53	82.60
4	85.47	29	84.70	54	82.20
5	85.26	30	88.17	55	81.49
6	88.64	31	89.91	56	88.40
7	85.21	32	88.70	57	79.07
8	84.15	33	85.44	58	79.78
9	79.64	34	85.45	59	85.85
10	85.60	35	83.15	60	79.34
11	81.90	36	81.79	61	83.84
12	89.47	37	80.14	62	79.20
13	80.04	38	85.81	63	79.06
14	83.68	39	79.14	64	79.84
15	79.99	40	85.66	65	88.10
16	81.36	41	83.25	66	82.55
17	84.23	42	89.68	67	83.21
18	82.65	43	89.07	68	82.66
19	87.41	44	84.22	69	80.33
20	79.62	45	84.29	70	90.50
21	87.60	46	79.39	71	80.16
22	81.32	47	87.02	72	89.95
23	90.08	48	82.72	73	89.36
24	79.80	49	89.77	74	87.36
25	85.36	50	86.66	75	85.32

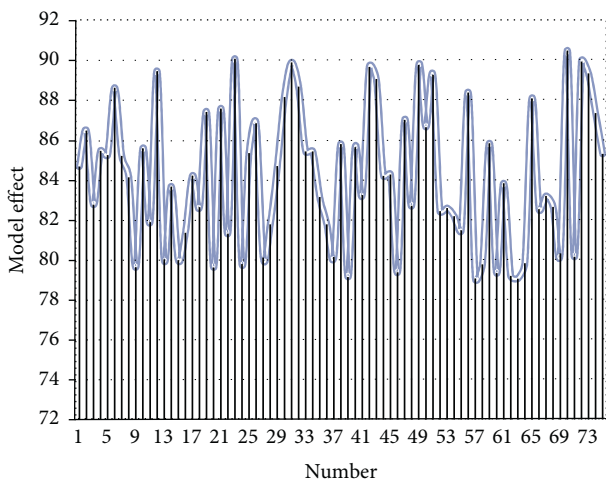


FIGURE 9: Statistical results of model evaluation.

model effect evaluation results shown in Table 1 and Figure 9.

From the above research, it can be seen that the research model of the manufacturing development path and its economic effects based on computational visualization proposed in this paper has certain practical effects.

From the perspective of the enterprise, the level of cost management directly affects the performance of the enterprise, which in turn affects the level of service-oriented development. Therefore, enterprises should strive to improve the management level of cost control and cost

optimization and continuously optimize their capital structure according to market changes, so as to serve the manufacturing industry and provide a good development environment. In addition, it is necessary to improve the internal governance mechanism of the enterprise and properly solve the problems of talents and funds in the process of servitization. From the government’s point of view, first, the government should provide an environment for integrated development of manufacturing services and support corresponding development strategies. In terms of investment and financing environment, tax environment, and policy environment, it will facilitate the manufacturing service-oriented development. At the same time, efforts will be made to build a manufacturing service-oriented demonstration zone, build an information platform for manufacturing service-oriented development, and conduct a nationwide strategy from the level of manufacturing development strategy and regional strategic planning. Second, the government should further improve the regulatory policy system for the servitization of the manufacturing industry and strive to promote the transformation and upgrading of the manufacturing industry to high-end servitization. In terms of policy regulation, the government should carry out the top-level design of the servitization of the manufacturing industry, create a series of supporting frameworks for the selection of the servitization direction of the manufacturing industry, formulate models and optimize development, and promote the upgrading of the servitization of the manufacturing industry. From a social point of view, it should be committed to cultivating manufacturing service-oriented talents with professional service level. The healthy development of manufacturing servitization is inseparable from professional service talents. All walks of life, especially various intermediary training institutions and human resource management institutions, should consciously cultivate specialized talents for manufacturing servitization, so as to provide services for the process of manufacturing servitization—the right talent team.

5. Conclusion

At present, China’s labor-intensive manufacturing industry accounts for a large proportion. With the gradual deepening of economic globalization and the increasingly refined international division of labor, the development of international division of labor has been refined from the division of labor between industries to the division of labor for different production processes on the same product. At the same time, countries around the world are actively integrating into the global value chain to make efforts to realize the value-added of different production links in the value chain. For many years, China’s manufacturing industry has mainly undertaken the transfer of low-end links in the value chain of developed countries and carried out production processes such as processing and assembly with low technical content. This paper combines computer visualization technology to analyze the development path of manufacturing industry and its economic effects. The experimental research results show that the research model of the manufacturing

development path and its economic effects based on computational visualization proposed in this paper has certain practical effects.

Data Availability

The labeled dataset used to support the findings of this study is available from the corresponding author upon request.

Conflicts of Interest

The authors declare no conflicts of interest.

Acknowledgments

The study was supported by Henan Provincial Soft Science Program, Henan (Grant no. 212400410107), and Henan Philosophy and Social Science Planning Project, Henan Province, Henan (Grant no. 2020BJJ015), and Key Scientific Research Projects of Colleges and Universities in Henan Province, Henan (Grant no. 21A790003).

References

- [1] R. C. Basole, A. Srinivasan, H. Park, and S. Patel, "ecoxight: Discovery, exploration, and analysis of business ecosystems using interactive visualization," *ACM Transactions on Management Information Systems*, vol. 9, no. 2, pp. 1–26, 2018.
- [2] M. Daradkeh, "Critical success factors of enterprise data analytics and visualization ecosystem: An interview study," *International Journal of Information Technology Project Management*, vol. 10, no. 3, pp. 34–55, 2019.
- [3] B. M. Drake and A. Walz, "Evolving business intelligence and data analytics in higher education," *New Directions for Institutional Research*, vol. 2018, no. 178, pp. 39–52, 2018.
- [4] M. Golfarelli and S. Rizzi, "A model-driven approach to automate data visualization in big data analytics," *Information Visualization*, vol. 19, no. 1, pp. 24–47, 2020.
- [5] H. Gubler, N. Clare, L. Galafassi, U. Geissler, M. Girod, and G. Herr, "Helios: History and anatomy of a successful in-house enterprise high-throughput screening and profiling data analysis system," *SLAS Discovery*, vol. 23, no. 5, pp. 474–488, 2018.
- [6] M. Hilario, D. Esenarro, H. Vega, and C. Rodriguez, "Integration of the enterprise information to facilitate decision making," *Journal of contemporary issues in business and government*, vol. 27, no. 1, pp. 1042–1054, 2021.
- [7] T. C. Huber, A. Krishnaraj, D. Monaghan, and C. M. Gaskin, "Developing an interactive data visualization tool to assess the impact of decision support on clinical operations," *Journal of Digital Imaging*, vol. 31, no. 5, pp. 640–645, 2018.
- [8] M. Jayakrishnan, A. K. Mohamad, and A. Abdullah, "Journey of an enterprise architecture development approach in Malaysian transportation industry," *International Journal of Engineering and Advanced Technology*, vol. 8, no. 4, pp. 765–774, 2019.
- [9] K. Kasemsap, "Knowledge discovery and data visualization: Theories and perspectives," *International Journal of Organizational and Collective Intelligence*, vol. 7, no. 3, pp. 56–69, 2017.
- [10] A. M. P. Milani, F. V. Paulovich, and I. H. Manssour, "Visualization in the preprocessing phase: Getting insights from enterprise professionals," *Information Visualization*, vol. 19, no. 4, pp. 273–287, 2020.
- [11] K. Palanivel, "Modern network analytics architecture stack to enterprise networks," *International Journal for Research in Applied Science and Engineering Technology*, vol. 7, no. 4, pp. 263–280, 2019.
- [12] D. A. Pashentsev, A. I. Abramova, N. D. Eriashvili et al., "Digital software of industrial enterprise environmental monitoring," *Ekoloji*, vol. 28, no. 107, pp. 243–251, 2019.
- [13] L. Po, N. Bikakis, F. Desimoni, and G. Papastefanatos, "Linked data visualization: Techniques, tools, and big data," *Synthesis Lectures on the Semantic Web: Theory and Technology*, vol. 10, no. 1, pp. 1–157, 2020.
- [14] D. H. Rhodes and A. M. Ross, "A vision for human-model interaction in interactive model-centric systems engineering," *Insight*, vol. 20, no. 3, pp. 39–46, 2017.
- [15] R. O. Valdiserri and P. S. Sullivan, "Data visualization promotes sound public health practice: The AIDSvu example," *AIDS Education and Prevention*, vol. 30, no. 1, pp. 26–34, 2018.
- [16] J. Walny, C. Frisson, M. West et al., "Data changes everything: Challenges and opportunities in data visualization design handoff," *IEEE Transactions on Visualization and Computer Graphics*, vol. 26, no. 1, pp. 12–22, 2019.
- [17] X. Wang, Y. Dong, M. Chen, F. Su, and L. Ling, "Research on real-time temperature control method for multi-visualization of hot runner system based on internet of things," *Journal of Applied Science and Engineering*, vol. 22, no. 4, pp. 683–690, 2019.
- [18] J. W. Windsor, F. E. Underwood, E. Brenner et al., "Data visualization in the era of COVID-19: An interactive map of the SECURE-IBD registry," *American Journal of Gastroenterology*, vol. 115, no. 11, pp. 1923–1924, 2020.
- [19] D. T. Y. Wu, S. Vennemeyer, K. Brown et al., "Usability testing of an interactive dashboard for surgical quality improvement in a large congenital heart center," *Applied Clinical Informatics*, vol. 10, no. 05, pp. 859–869, 2019.
- [20] T. Xu, G. Song, Y. Yang, P.-X. Ge, and L.-X. Tang, "Visualization and simulation of steel metallurgy processes," *International Journal of Minerals, Metallurgy and Materials*, vol. 28, no. 8, pp. 1387–1396, 2021.
- [21] K. Zhao, R. Sun, C. Deng, L. Li, Q. Wu, and S. Li, "Visual analysis system for market sales data of agricultural products," *IFAC-Papers OnLine*, vol. 51, no. 17, pp. 741–746, 2018.

Research Article

Optimization of the Index System of the Sports Social Organization Development Ability Relying on Image Optimization, Recognition, and Simulation

Wei Sun 

Sports and Military Education Department, Zhejiang University of Water Resources and Electric Power, Hangzhou 310018, China

Correspondence should be addressed to Wei Sun; sunwei@zjweu.edu.cn

Received 8 March 2022; Revised 7 April 2022; Accepted 22 April 2022; Published 13 May 2022

Academic Editor: Xuefeng Shao

Copyright © 2022 Wei Sun. This is an open access article distributed under the Creative Commons Attribution License, which permits unrestricted use, distribution, and reproduction in any medium, provided the original work is properly cited.

Sports social organizations refer to nonprofit, nongovernmental, and group organizations that achieve specific service goals and common aspirations and spontaneously form various sports and fitness activities in accordance with the rules. This article aims to study how to optimize the index system of the capacity developments by relying on image optimization and recognition simulation. This article puts forward the relevant theoretical knowledge of image optimization and recognition and capacity developments and proposes two algorithms based on image optimization and recognition. In 2019, the percentage of growth of sports social organizations rose from 6.7% to the final 27%; in 2020, the growth rate of sports social organizations is getting higher and higher, from 9% at the beginning to 34% at the end. It can be seen that people's love for sports activities is getting higher and higher, and the state is paying more and more attention to sports social organizations. The factors that affect the development ability of sports social organizations include the quality, education, and management capabilities of the members of the organization, and the country and the government should also take corresponding measures. The improvement of the development ability of sports social organizations is of great significance to the development of sports social organizations.

1. Introduction

At this stage, China has entered a social transformation period of innovation and comprehensive reform. As one of the main lines of the reform and development of the social field, social organization has a certain social necessity to deeply explore its modern organizational development model with Chinese characteristics. As the intermediary and hub connecting the sports power of the nation and the nationwide fitness program, the importance of its existence and development is self-evident. The development of sports social organizations is inseparable from the social environment, in which they are located, and the guidance of national policies and regulations plays a vital role in the growth and development of the organization.

The capacity developments refer to the correct control of the actual ability of sports social organizations, and related sports activities are shown by the interaction of political, economic, social, and regional environments related to themselves. It has the conditions for internal management functions, service functions, and social influence. Image recognition technology is an important technology in the information age, and its purpose is to allow computers to replace humans to process a large amount of physical information. With the development of computer technology, human beings have a deeper and deeper understanding of image recognition technology. The process of image recognition technology is divided into information acquisition, preprocessing, feature extraction and selection, classifier design, and classification decision-making.

With the development of society, the field of sports has attracted more and more attention. Chouksey and Jha found that image segmentation can generally be used for object recognition and detection. In the field of image segmentation, the multilevel threshold method is one of the leading methods. However, the computational cost of this method is high. They proposed a new algorithm, which is the quasi-inverse multiverse optimization algorithm. It can perform image segmentation by finding the optimal threshold. The disadvantage of this experiment is that the advantages and disadvantages of the two methods are not compared, and the new algorithm is not prominent [1]. Quan et al. found that face recognition is very important in computer vision. In order to solve some of the problems in traditional face recognition, they proposed a new optimization method for face recognition. This method allows people to match the best state of the energy function more quickly and accurately. But the disadvantage is that they did not propose how to use this method specifically, and the reliability of the method has not been proven [2]. Gupta et al. found that it is a difficult task to make image recognition the lowest cost and highest efficiency. In order to reduce the cost of identification and improve efficiency, they proposed a new multiobjective optimization framework. In this work, they proposed a better harmony search algorithm than traditional algorithms. But they did not mention the advantages of the algorithm in comparison, so the authenticity is still uncertain [3]. Schubert et al. found that embedded image retrieval problems in robotic tasks provide additional structures that can be utilized, so they proposed a graph-based framework to systematically utilize different types of additional structures and information. They believed that this method can also quickly collect other knowledge about database image poses, but this method has not designed an experiment to prove it, so there are still many doubtful places [4]. Song et al. found that deep learning is widely used in the field of machine vision. To obtain effective image recognition, a large amount of data must be collected; otherwise, it is easy to make mistakes. The neural network in deep learning can rely on the improved network to generate a highly diversified balanced image dataset. Simulation results show that the algorithm's image recognition speed is faster and more efficient. However, no specific examples are used to complete the analysis, so this is a shortcoming of the experiment [5]. Gurevich and Yashina discussed the modern development of descriptive image analysis and its development potential. Descriptive image analysis is one of the leading and intensive development areas of modern mathematical image analysis theory. Their research is dedicated to standardizing descriptive algorithm image analysis and the generation of recognition schemes. However, their research has not been supported by related experiments. A variety of experimental comparisons should be carried out to get the best method [6]. Long and Ning found that in computer vision, it becomes difficult to identify objects from rotated and zoomed images. The log-polar coordinate transformation is a mapping method that is invariant to rotation and scale. However, this method has many problems, so they proposed a new template matching

algorithm based on global LPT. They were also inspired by pigeons to optimize the search strategy to complete the object recognition of drones with varying target rotations and scales. However, this method has not been proved to be effective through experiments, and the two methods have not been compared [7]. Revina and Sam Emmanuel are very interested in facial expression recognition. They think it is very interesting because it enables people to recognize facial expressions in daily life. However, most traditional methods cannot accurately recognize facial expressions because facial expressions are based on the movement of the human face. The facial recognition method they proposed improves the accuracy of face recognition. The experiment of the algorithm they proposed is carried out using a database, but there are many face recognition methods, and there is no specific description of which method is not good [8]. Through the experimental analysis of the scholars, we can know the following: they agree that relying on image optimization and recognition for simulation in various fields has been widely used. For image recognition and various facial recognition, it is of great significance to society. However, the experiment did not mention the comparison of the algorithms before and after the improvement, so it is impossible to determine which method is the best.

The innovations of this paper are as follows. (1) It introduces the relevant theoretical knowledge of image optimization recognition simulation and the capacity development and using the target detection and recognition technology algorithm to analyze how to study the optimization of the index system of the capacity developments. (2) It conducts experiments and analysis on the capacity developments based on target detection and recognition technology algorithms. Through investigation and analysis, it is found that if the capacity developments are improved, it will be beneficial to the development of society.

2. Target Detection and Recognition Technology Algorithm Based on Image Optimization and Recognition

With the widespread application of artificial intelligence technology, especially deep learning algorithms in the field of computer vision, the accuracy and real-time performance of target detection and recognition technology in images and videos are getting higher and higher. More and more relevant research results have been published in various top journals and conferences on artificial intelligence, computer vision, and pattern recognition, and more and more computer vision start-up companies are applying this technology to real scenes. On various public datasets, the level of target detection and recognition algorithms continues to rise, and the performance of algorithms is constantly approaching or even surpassing humans.

Optical information processing refers to the generation, transmission, detection, and processing of optical images. Necessary images are called signals, and unnecessary noise may be generated during processing. The input information of optical information processing is optical information

converted from optical information such as images, electrical information, or sound information. Compared with digital image processing, optical processing system has strong information processing ability and fast calculation speed, especially parallel processing, which is especially suitable for high-speed, real-time processing of images [9]. As the main branch of optical information processing, the optical image recognition technology developed based on Fourier optics fully inherits the previously mentioned characteristics. It performs parallel processing on all sampling points and performs Fourier transform at the speed of light [10]. The simulation process is shown in Figure 1:

As shown in Figure 1, optimizing the recognition of complex targets in the image can effectively improve the speed and accuracy of target recognition in the human-machine interface. Image target recognition needs to extract the color and texture characteristics of image information, which is completed through decision-making fusion processing [11].

2.1. Target Monitoring and Recognition Technology Algorithm. The interframe difference method is a method of obtaining the contour of a moving target by performing a difference operation on two adjacent frames in a video image sequence. It can be well adapted to the situation where there are multiple moving targets and camera movement. The interframe difference method is a method that uses the relationship between the prestate and poststate in the image sequence to detect the moving area. It is shown in Figure 2.

As shown in Figure 2, when there is abnormal object movement in the surveillance scene, there will be more obvious differences between frames. The two frames are subtracted to obtain the absolute value of the brightness difference of the two frames. It judges whether it is greater than the threshold to analyze the motion characteristics of the video or image sequence and determines whether there is any object movement in the image sequence. The frame-by-frame difference of the image sequence is equivalent to high-pass filtering of the image sequence in the time domain. Discrimination of motion area or background is as follows:

$$\text{Mask}_1(a, b) = \begin{cases} 1, & |I_t(a, b)| > T_d, \\ 0, & \text{otherwise.} \end{cases} \quad (1)$$

In the formula, T_d is the discrimination threshold.

2.1.1. HOG Features. The calculation formula of gradient strength and direction is as follows:

$$h = \sqrt{I_x^2 + I_y^2}. \quad (2)$$

Finally, it creates a direction histogram with each cell in the image as a unit.

2.1.2. Decision Area and Decision Function. In the field of machine learning, the goal of classification is to gather objects with similar characteristics. A linear classifier makes

classification decisions through linear combinations of features to achieve this goal. The characteristics of objects are usually described as eigenvalues, and in vectors, they are described as eigenvectors. The classifier has been applied in many ways. The main tasks of the classifier are shown in Figure 3.

As shown in Figure 3, circles and triangles are used to represent the first type of sample and the second type of sample. Each type of sample is represented by a vector, and the category boundary is represented by an ellipse in the figure [12].

In addition, there is a straight line connecting the two categories in the graph. The parameters of the equation include coordinates x, x_2 , which are as follows:

$$d(x) = w_1x_1 + w_2x_2 + w_0 = 0, \quad (3)$$

$d(x)$ can divide the space into two different decision-making regions, which is called a linear decision function.

The weight vector can be set to $w = [w_1 \dots w_d]^t$, and the generalized linear decision function of the d -dimensional feature space can be obtained as follows:

$$d(x) = w^* x^* = w^1 x + w_0. \quad (4)$$

2.1.3. SVM Classifier. SVM is also a support vector machine, which is a two-classification model. It maps the feature vector of the instance to some points in the space. The purpose of SVM is to draw a line to distinguish these two types of points "best." Even if there are new points in the future, this line can also make a good classification. SVM is suitable for small and medium-sized data samples and nonlinear, high-dimensional classification problems. The goal of SVM operation is to find a more reasonable method to obtain a more suitable classification hyperplane in the high-dimensional feature space. Hyperplane classification can optimize the generalization of understanding of the world. Optimization theory can provide an important mathematical method for hyperplane optimization [13].

Assuming that the nonlinear mapping is $x \rightarrow \phi(x)$, then the objective function of the dual form is as follows:

$$Q(\alpha) = \sum_{k=1}^n \alpha_k - \frac{1}{2} \sum_{j=1}^n \sum_{i=1}^n \alpha_i \alpha_j b_i b_j. \quad (5)$$

It is proposed to replace the inner product operation with a kernel function that satisfies the condition $s \sum_{k=1}^n \alpha_k$. The optimal discriminant function $Q(\alpha)$ of the kernel form is as follows:

$$f(a) = \text{sgn} \left(\sum_{x_i \in SV} \alpha_i^* b_i k(a * a_i) + b^* \right). \quad (6)$$

2.2. SAR Image Simulation

2.2.1. The Basic Algorithm of SAR Image Simulation. An important way of SAR image processing is to perform edge extraction and image segmentation after coherent speckle



FIGURE 1: Image simulation process.

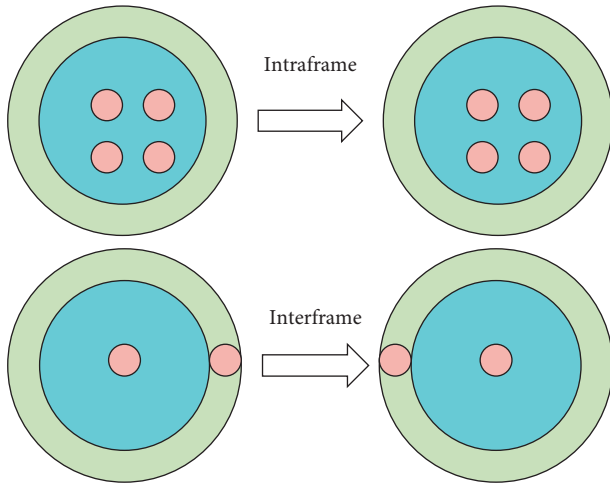


FIGURE 2: Motion between frame differences.

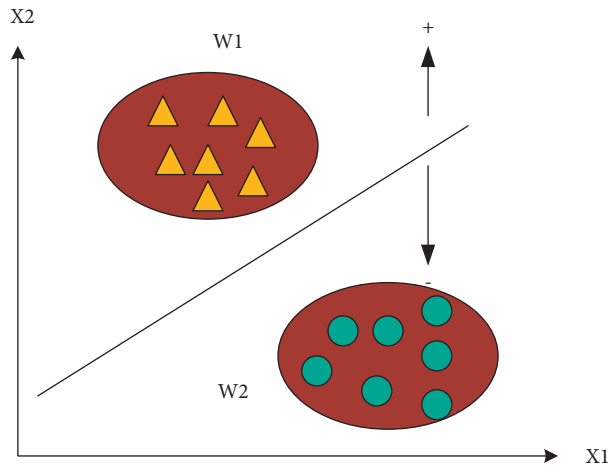


FIGURE 3: The main tasks of the classifier.

noise filtering. The commonly used filtering methods are low-pass filtering, which better keeps the speckle noise and blurs the image at the same time. This includes mean filtering, Gaussian filtering, and so on. SAR target recognition refers to the use of SAR to detect a single target or target group, analyze the information obtained, and determine the target type, model, and other attributes [14]. The target recognition process is shown in Figure 4.

As shown in Figure 4, this layered method makes the amount of calculation more and more large, while the amount of data that needs to be processed is gradually reduced, which is greatly reduced, thereby improving the target recognition system.

Compared with matched filter correlator, joint transform correlator has many advantages, such as high spatial bandwidth product, no filtering synthesis, and easy real-time operation. So, in recent years, it has attracted more research interest. The joint transform correlator has a plane that forms a joint input, and the flowchart of joint transform correlation recognition by a computer [15] is shown in Figure 5.

As shown in Figure 5, the Fourier transform spectrum realized by the function is located in the upper left corner of the image, so it is also necessary to pay attention during the simulation process. In order to obtain the simulated optical Fourier, in the case of the image center leaf transform, a function that moves the zero frequency component to the center of the spectrum must be called [16].

2.2.2. Coherent Speckle Noise. The coherent speckle noise of synthetic aperture radar (SAR) images seriously reduces the interpretability of the image and affects the subsequent target detection, classification, and recognition applications. The coherent speckle noise of SAR images is a principle defect in the imaging process. Because of the coherent speckle noise, it will have a certain impact on the synthetic aperture radar image. In order to process and image the echo data faster and to identify the target more accurately, multiview processing is usually used to remove [17]. Multiview processing mainly researches the use of geometric methods and restores three-dimensional objects through several multiview geometric two-dimensional images. In short, it is the study of three-dimensional reconstruction, which is mainly used in computer vision. Then, the speckle noise is as follows:

$$a_i = \delta_i \times n_i. \quad (7)$$

Among them, the mean of q is n_i , and σ^2 is a measure of spot intensity. The additive noise model related to the signal is equivalent to the following:

$$\begin{cases} a_i = \delta_i + n_i^*, \\ \delta_i (n_i - 1). \end{cases} \quad (8)$$

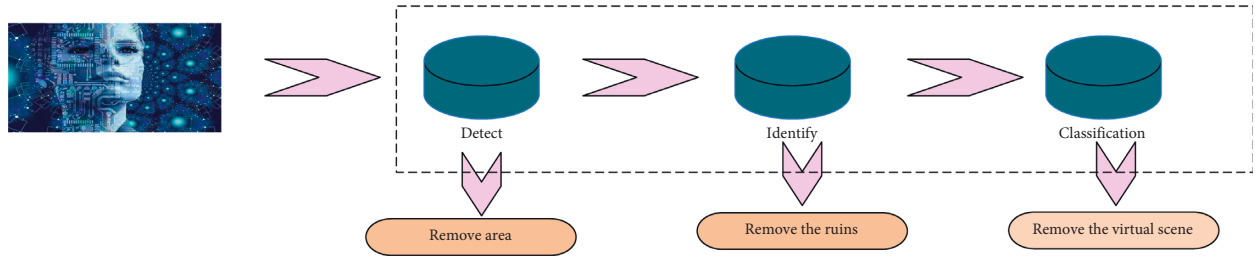


FIGURE 4: Schematic diagram of a typical SAR target recognition system.

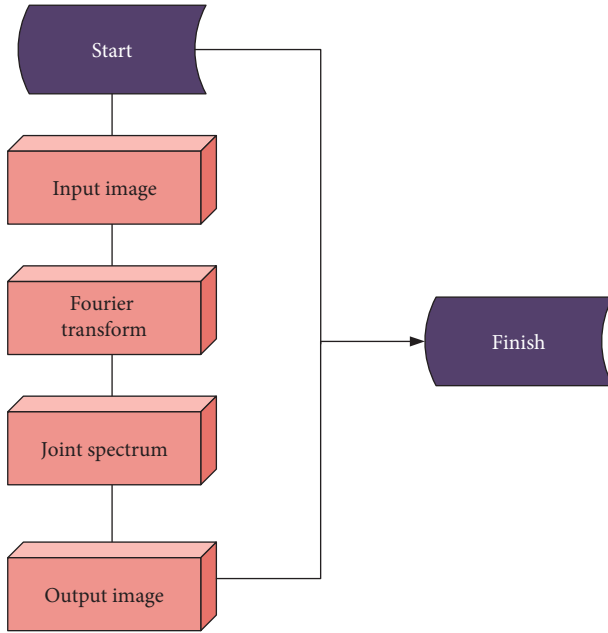


FIGURE 5: Flowchart of the related process of joint transformation.

Among them, n_i^* is additive noise, and the variance is as follows:

$$\text{var}(n^*) = E\{(n_i^* - 0)^2\} = E(a_i^2) \cdot \frac{\sigma_i^2}{(1 + \sigma_i^2)}. \quad (9)$$

For the same image, $\sigma_i^2 / (1 + \sigma_i^2)$ can be considered as a constant, especially in homogeneous regions. According to the multiplicative model of noise, the noise and the image data are independent of each other and the mean value is 1. As a result, a set of random numbers with a mean value of 1 according to the Rayleigh distribution are generated. Multiplying the random number with the image data can get a SAR simulation image with coherent speckle noise [18].

2.2.3. Multiview Processing. Using $H_L(R)$ to represent the average of L independent images at position R , the following is obtained:

$$H_L = \left(\frac{1}{L}\right) \sum_{i=1}^L H_i. \quad (10)$$

The variance $(H_L - H_0)^2$ is reduced to the original $1/L$ as follows:

$$\text{var}(H_L) = E\{(H_L - H_0)^2\} = \frac{1}{L^2 \times E} \left[\left(\sum_{i=1}^L (H_L - H_0)^2 \right) \right]. \quad (11)$$

2.3. Fourier Transform Based on Optical Imaging

2.3.1. Fourier Transform Algorithm. In different research fields, Fourier transform has many different variant forms, such as continuous Fourier transform and discrete Fourier transform. At first, Fourier analysis was proposed as a tool for analytical analysis of thermal processes. The most important theory in information processing is the Fourier transform [19]. It is as follows:

$$\begin{cases} G(f) = \int_{-\infty}^{\infty} g(a) \exp(-j2\pi fa) da, \\ g(a) = \int_{-\infty}^{\infty} G(f) \exp(-j2\pi fa) df, \end{cases} \quad (12)$$

$G(f)$ is called the Fourier transform of $g(a)$, or frequency spectrum. When $G(f)$ is a complex function, it can be expressed as follows:

$$G(f) = A(f) \exp[-j\varphi(f)], \quad (13)$$

where $A(f) = |G(f)|$ is the amplitude spectrum of $g(a)$ [20].

The inverse Fourier transforms $g(a)$ and $\varphi(f)$ called $g(a)$ as $G(f)$ constitute the Fourier transform. It is generalized to the following:

$$G(u, v) = \int_{-\infty}^{\infty} \int_{-\infty}^{\infty} g(a, b) \exp[-j2\pi(ua + vb)] da db, \quad (14)$$

where $\sqrt{u^2 + v^2}$ represents the spatial frequency after Fourier transform.

2.3.2. Histogram Equalization Enhancement. Histogram equalization is a method in the field of image processing that uses image histograms to adjust contrast. This method is usually used to increase the global contrast of many images, especially when the contrast of the useful data of the image is quite close. In this way, the brightness can be better distributed on the histogram. The histogram equalization refers to the process of converting an image into different histograms using the equalization of gray-scale mapping conversion as follows:

$$P_r(d_i) = \frac{m_i}{m}, \quad (15)$$

where m is the total number of pixels, and d_i satisfies the normalization condition [21].

The image transformation function expression is as follows:

$$S_i = T(d_i) = \sum_{i=0}^{k-1} p_d(d_i) = \sum_{i=0}^{k-1} \frac{m_i}{m}. \quad (16)$$

Among them, k is the number of gray levels.

This is the histogram before and after the histogram equalization (Figure 6).

As shown in Figure 6, it can be seen from the figure that after the histogram is equalized and corrected, the gray interval of the image histogram is enlarged. This helps the analysis and recognition of the image and the use of the equalized histogram to correct the image [22].

2.3.3. Smoothing Filter Enhancement. The following briefly introduces the basic principles of linear smoothing filters [23]. The gray value is $F(j, k)$, and the output corresponding to pixel $F(j, k)$ is as follows:

$$G(j, k) = \frac{1}{H} \sum_{(a,b)=L} F(a, b). \quad (17)$$

That is, the average gray value of the window pixels is used to replace the original gray value of $F(j, k)$.

If the contrast between the object and the background is clear, the object boundary is located at the highest point of the image gradient. Like the differential emphasis method, the gradient emphasis method is easily affected by noise and deviates from the object boundary [24]. Usually, it needs to smooth the gradation image $G[f(i, j)]$ before emphasizing. For digital images, it is defined as follows:

$$G[f(i, j)] = [f_a(i, j)^2 + (f_b(i, j))^2]^{1/2}. \quad (18)$$

The energy of the image is mainly concentrated in the low and middle frequencies of the amplitude spectrum, while the edges and noise of the image correspond to the high frequency part. The function of the low-pass filter is to remove these high-frequency components through the filter, maintain low-frequency components, and smooth the image information [25]. The low-pass filter is as follows:

$$G(u, v) = F(u, v)H(u, v). \quad (19)$$

In formula (19), $F(u, v)$ is the Fourier transform of the original image $F(a, b)$ with noise; $G(u, v)$ is the Fourier transform of the image output by the low-pass filter.

In area D_0 of a Fourier plane, the transfer function of an ideal low-pass filter is as follows:

$$H(u, v) = \begin{cases} 1, & D(u, v) \in D_0, \\ 0, & D(u, v) \notin D_0. \end{cases} \quad (20)$$

From a theoretical analysis, the frequency band in area D_0 passes through without loss, while the high-frequency

signal outside the area is filtered out; if a large amount of edge information contained in the high-frequency signal is also filtered out, the phenomenon of image blur will occur.

3. Experiment and Analysis of the Investigation of the Capacity Developments

3.1. Investigation and Analysis of the Capacity Development Trend. Capacity development index system not only needs to meet theoretical requirements but also needs to be verified through actual data. Therefore, this article takes sports social organizations as an example to test the scientific nature of the index system. This reflects the current situation and problems of the development capabilities of sports social organizations and puts forward relevant policy recommendations. The continuous advancement of the reform and opening policy has greatly promoted the further development of the national economy and at the same time has created a good environment and conditions for the development of sports social organizations. After 1979, sports associations were established in various places and basically every province and city established sports associations. China has always been a benchmark in the development of sports. After the establishment of various associations, it has actively promoted the growth and development of social organizations to more comprehensively and effectively meet the needs of the people to participate in physical exercise. This article investigates the development trend of Chinese sports organizations from 2015 to 2018, as shown in Table 1.

As shown in Table 1, from 2015 to 2018, the development of sports social organizations increased with the increase of the year, but the magnitude was not high. By 2016, sports social groups have been unable to keep up with the increase in the number of sports nongroups.

That is because there is no effective use of the media and holding events to conduct better social publicity, increase the social influence of sports social organizations, attract more people to participate, and improve the active role of sports social organizations in promoting mass fitness.

This article investigates the development trend of Chinese sports social organizations from 2019 to 2020, as shown in Figure 7.

As shown in Figure 7, the development trend of sports social organizations from 2019 to 2020 is getting better and better, and the growth rate is getting higher and higher. At the same time, with the continuous economic development and the improvement of people's living standards, people's demands for health are getting higher and higher. They have sufficient economic strength and willingness to participate in certain sports associations, participate in corresponding sports activities, and enjoy relevant sports services. This has promoted the development of sports activities, sports performances, sports events, and the development of sports social organizations and the sports industry. The good development of sports social organizations has provided better and better sports services to the public, thus achieving a virtuous circle.

This article also conducted a survey on the social organization of sports in other countries, as shown in Table 2.

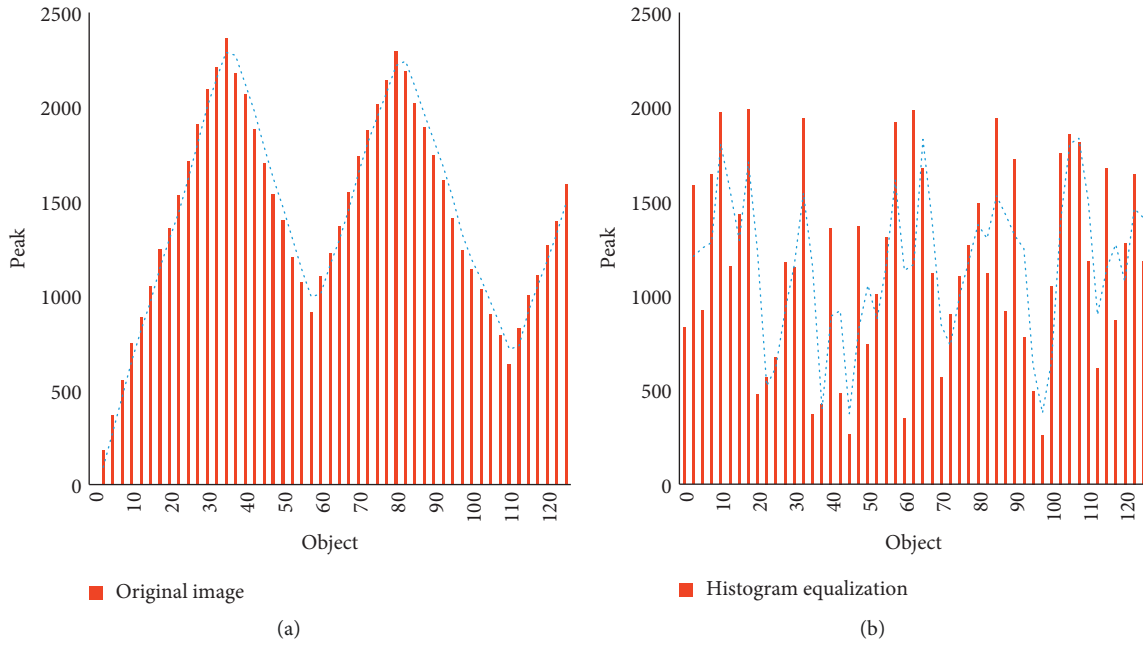


FIGURE 6: Histogram before and after histogram equalization. (a) Histogram before histogram equalization. (b) Histogram after histogram equalization.

TABLE 1: Trends in the development of Chinese sports organizations from 2015 to 2018.

Year	Sports social groups	Sports civil nonorganization	Sports foundation
2015	789	43	56
2016	875	3212	67
2017	1234	4532	78
2018	1343	5422	93

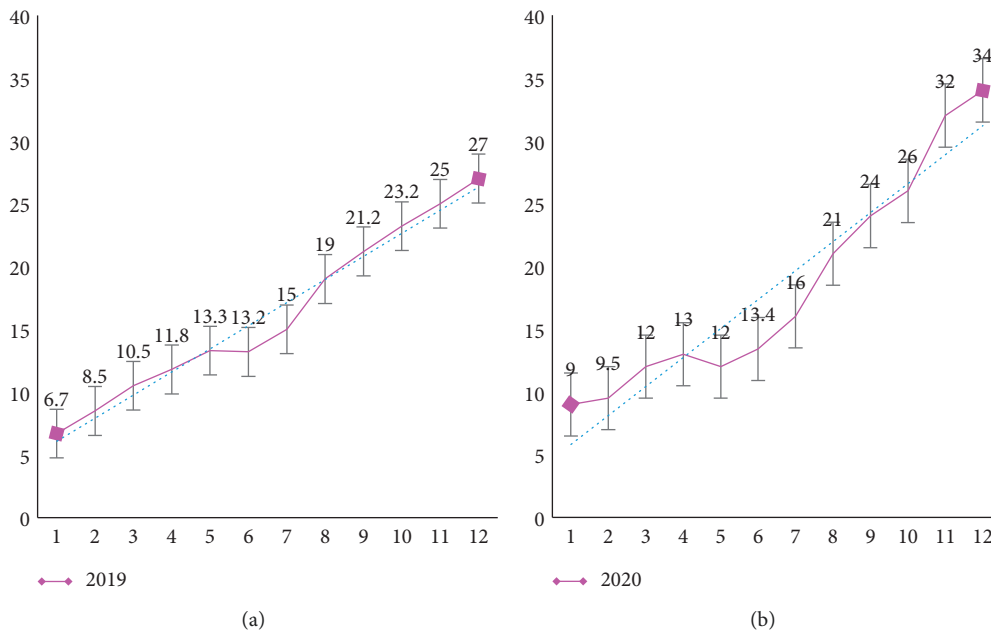


FIGURE 7: The development trend of Chinese sports social organizations from 2019 to 2020. (a) The development trend of Chinese sports social organization in 2019. (b) The development trend of Chinese sports social organization in 2020.

TABLE 2: Sports social organizations in other countries.

Year	Sports social groups	Sports civil nonorganization	Sports foundation
Country A	4321	742	121
Country B	4214	656	132
Country C	3873	564	89
Country D	3768	486	97
Country E	3453	365	67

As shown in Table 2, country A is the most important in terms of sports organizations, reaching 4321 organizations. In developed countries such as Europe and the United States, sports activities are emphasized and integration into daily life has become a way of life. The health consciousness of the masses is very strong, and the most basic requirement for people to participate in sports activities is to improve the quality of their health. Meeting this demand is based on the premise of continuous and regular participation in sports activities. Therefore, various social sports organizations came into being and developed rapidly.

This article also investigated the situation of the main personnel of a certain sports organization, as shown in Table 3.

As shown in Table 3, the age of the personnel of this sports organization is generally within the age of 18–66, and the number of participants between the ages of 30–42 is the largest, accounting for 42.6%. It can be seen that middle-aged people are more likely to refer to sports organizations, and they pay more attention to sports than other ages.

This article conducted a rough survey of the members of the five sports organizations surveyed, as shown in Table 4.

As shown in Table 4, the members of the five sports organizations have a high school education or above, and two organizations have a bachelor's degree or above; the overall age range is between 15 and 65 years old, and the degree of interest in sports is more than 70%. It can be seen that the differences between the five sports organizations are not significant.

Running was the most important activity type among the five sports social organizations that were randomly selected and investigated. It is shown in Table 5.

As shown in Table 5, people usually like to organize activities such as running, badminton, martial arts, and table tennis. Among them, running is the most popular among sports organizations, and the average number of runs selected by the five sports organizations is about 55 times.

This question investigates the factors that affect the development of sports social organizations, as shown in Figure 8.

As shown in Figure 8, the main factors affecting are age, income, whether it love sports, personality, education, and physical fitness. Among them, experts believe that the most influential factor in the development of sports social organizations is whether they love sports, because talents who love sports will actively organize activities to participate in activities.

In summary, the factors affecting the development of sports organizations are as follows.

3.1.1. Income. People between the ages of 18–45 are the pillars of social development, and they are the most stressful part of social life. These people most need a strong body to face life but also need to release life and work stress through exercise. However, people with high monthly incomes need to pursue spiritual life and healthy body after solving the food and clothing in life. Therefore, more people will choose to exercise their bodies through sports to strengthen their physique and release stress, while also expanding their social spheres and delighting the body and mind.

3.1.2. The Quality of the Person in Charge of the Organization. The management system of more than half of sports social organizations adopts the responsibility system of the person in charge of the organization, and the person in charge of the organization determines the organization's decision-making and the arrangement of the activity plan. A correct organizational decision or a perfect event arrangement is not only responsible for the organization itself but also responsible for the members of the organization. Persons in charge with higher quality are often able to make correct organizational decisions or arrangements for activities. Therefore, high-quality responsible persons with good management capabilities are essential to the development of sports social organizations.

3.1.3. The Enthusiasm of the Organization Members to Exercise. The rapid development of sports social organizations is rooted in people's extensive fitness needs; the promotion of national fitness policies especially in recent years has set off an upsurge of national fitness. This makes various sports and fitness organizations emerge in endlessly while meeting the huge fitness needs of the people. In the past two years, people's fitness demand has shown a rapid upward trend, and the rapid growth of people's demand for sports fitness has also brought various sports social organizations into a period of rapid development. People's enthusiasm for physical exercise is soaring, which has given birth to more sports social organizations.

3.2. Measures to Promote the Development of Sports Organizations

- (1) It is necessary to promote a strong national awareness of fitness and willingness to participate in sports activities. It needs to promote the development of sports social organizations. The development of sports social organizations has promoted the development of nationwide fitness activities and

TABLE 3: The situation of the main personnel of a sports organization.

Age	Under 18	18–30 years old	30–42 years old	42–54 years old	54–66 years old
Quantity	6	432	567	64	76
Percentage (%)	1	32.4	42.6	11	13

TABLE 4: Five memberships of sports organizations.

Survey object	1	2	3	4	5
Education	Undergraduate	Junior college	Undergraduate	Junior college	High school
Age	18–60	18–60	15–65	17–64	18–65
Hobby (%)	70	75	73	74	72

TABLE 5: Main types of activities of sports social organizations.

Sports social organization	Running	Badminton	Martial arts	Pingpong
1	56	46	32	27
2	54	45	32	25
3	57	47	34	24
4	53	43	35	27
5	55	46	31	28

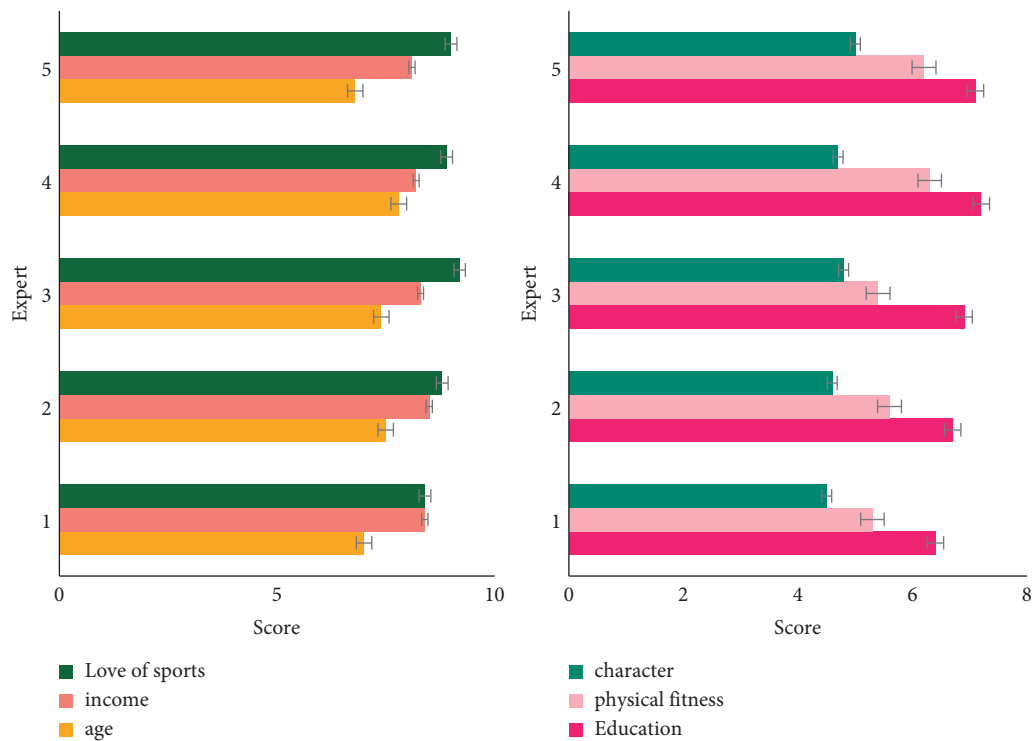


FIGURE 8: Factors affecting the capacity developments.

provided people with better and more comprehensive sports public services.

- (2) The degree of socialization is relatively high. Various sports organizations in some economically developed countries have achieved a certain degree of development without government funds. These are generally funds provided by enterprises or benefit from the development of mass sports. Various sports

associations, clubs, and other sports organizations provide individuals with various sports opportunities to meet individual needs. This improves people's sports ability and interest in sports and ultimately makes sports activities a part of life.

- (3) Mass sports promotes the development of the sports industry. In Europe and the United States and other countries, private clubs based on profit give mass

sports activities a strong vitality. These clubs vary in size and are widely distributed. Through sports activities, the physical fitness of the masses has been enhanced, and many people have voluntarily joined the ranks of “spending money for health.” People attach importance to healthy life, actively join various sports associations and sports clubs, and participate in various sports and fitness activities, which greatly promotes the development of sports service industry, sports goods industry, and other related sports industries.

4. Discussion

This paper analyzes how to optimize the research on the development ability index system of sports social organizations based on image optimization and recognition simulation. The related concepts of image optimization recognition and the capacity developments are expounded, and the relevant theories based on image optimization recognition and the capacity developments are studied. It explores the method of optimizing the index system of the capacity developments and discusses the influencing factors of the capacity developments through investigating method cases. In the end, it takes the optimization of the index system of the capacity developments and the integration of image optimization recognition simulation technology as an example to explore the correlation between the two.

This paper also makes reasonable use of the target detection and recognition technology algorithm based on image optimization and recognition simulation and the basic algorithm of SAR image simulation. With the wider application of the two algorithms, people are paying more and more attention to them, and many scholars have begun to apply these two algorithms to their lives.

This article concluded through experiments the following. With the development of society, people pay more and more attention to sports, and the capacity developments also need to be improved. Although there are many factors that affect the capacity developments, the research on optimizing the index system of the capacity developments is very important for sports.

5. Conclusions

The focus of this article is the optimization of the index system of the capacity developments that rely on image optimization and recognition simulation. The description is based on the two keywords of image optimization and recognition and the capacity developments. In the method part, this paper proposes the target detection and recognition technology algorithm and the basic algorithm of SAR image simulation based on image optimization and recognition simulation. It uses these two methods to illustrate the simulation of image recognition. The experiment part analyzes the development trend of sports organizations and finds that the demand for sports organizations has been increasing in recent years. This also means that the capacity

developments should be correspondingly improved develop sports ability. The main factors that affect the development of sports organizations are the age, quality, educational background, and income of the members of the organization. It must adopt an inclusive and encouraging attitude towards sports social groups and actively participate in national fitness service activities. The research on the optimization of the index system of the capacity developments involves many fields, but the author’s knowledge is limited to the analysis of this article. Research on the optimization of the index system of the capacity developments is very meaningful.

Data Availability

The data used to support the findings of this study are available from the author upon request.

Conflicts of Interest

The author declares no conflicts of interest.


References

- [1] M. Chouksey and R. K. Jha, “A joint entropy for image segmentation based on quasi opposite multiverse optimization,” *Multimedia Tools and Applications*, vol. 80, no. 6, pp. 1–38, 2021.
- [2] Z. Quan, Z. Cheng, W. Yu et al., “Face recognition via fast dense correspondence,” *Multimedia Tools and Applications*, vol. 77, no. 12, pp. 1–19, 2018.
- [3] A. Gupta, R. Sarkhel, N. Das, and M. Kundu, “Multiobjective optimization for recognition of isolated handwritten Indic scripts,” *Pattern Recognition Letters*, vol. 128, no. Dec, pp. 318–325, 2019.
- [4] S. Schubert, P. Neubert, and P. Protzel, “Graph-based nonlinear least squares optimization for visual place recognition in changing environments,” *IEEE Robotics and Automation Letters*, vol. 6, no. 2, pp. 811–818, 2021.
- [5] X. Song, S. Gao, X. Liu, and C. Chen, “An outdoor fire recognition algorithm for small unbalanced samples,” *Alexandria Engineering Journal*, vol. 60, no. 3, pp. 2801–2809, 2021.
- [6] I. B. Gurevich and V. V. Yashina, “Descriptive image analysis: Part IV. Information structure for generating descriptive algorithmic schemes for image recognition,” *Pattern Recognition and Image Analysis*, vol. 30, no. 4, pp. 638–654, 2020.
- [7] X. Long and X. Ning, “Biological object recognition approach using space variant resolution and pigeon-inspired optimization for UAV,” *Science China*, vol. 60, no. 010, pp. 1577–1584, 2017.
- [8] I. M. Revina and W. R. Sam Emmanuel, “Face expression recognition with the optimization based multi-SVNN classifier and the modified LDP features,” *Journal of Visual Communication and Image Representation*, vol. 62, no. JUL, pp. 43–55, 2019.
- [9] C. P. Kleweno, W. K. Bryant, A. M. Jacir, W. N. Levine, and C. S. Ahmad, “Discrepancies and rates of publication in orthopaedic sports medicine abstracts,” *The American Journal of Sports Medicine*, vol. 36, no. 10, pp. 1875–1879, 2017.
- [10] L. Shuai and J. G. Malins, “Encoding lexical tones in jTRACE: a simulation of monosyllabic spoken word recognition in Mandarin Chinese,” *Behavior Research Methods*, vol. 49, no. 1, pp. 1–12, 2017.

- [11] H. Kindl, A. Martin, K. Spade, F. Williams, and K. Clarke, "Improving rapid response recognition," *Journal for nurses in professional development*, vol. 33, no. 4, pp. 217-218, 2017.
- [12] H. Chen, Z. Li, X. Wang, and B. Lin, "A graph- and feature-based building space recognition algorithm for performance simulation in the early design stage," *Building Simulation*, vol. 11, no. 2, pp. 1-12, 2018.
- [13] N. Ahalawat and J. Mondal, "An appraisal of computer simulation approaches in elucidating biomolecular recognition pathways," *Journal of Physical Chemistry Letters*, vol. 12, no. 1, pp. 633-641, 2020.
- [14] T. N. Tamati, L. Sijp, and D. Bařkent, "Talker variability in word recognition under cochlear implant simulation: does talker gender matter?" *Journal of the Acoustical Society of America*, vol. 147, no. 4, pp. EL370-EL376, 2020.
- [15] V. M. Arora, J. M. Farnan, and V. M. Arora, "Use of simulation to assess incoming interns' recognition of opportunities to choose wisely," *Journal of Hospital Medicine*, vol. 12, no. 7, pp. 493-497, 2017.
- [16] Y. Hu and T. Wan, "Efficient wideband MRCS simulation for radar HRRP target recognition based on MSIB and PCA," *Applied Computational Electromagnetics Society Journal*, vol. 34, no. 12, pp. 1804-1813, 2019.
- [17] J. Sun, M. Liu, and N. Yang, "Insight into the origin of SARS-CoV-2 through structural analysis of receptor recognition: a molecular simulation study," *RSC Advances*, vol. 11, no. 15, pp. 8718-8729, 2021.
- [18] B. R. Dandekar and J. Mondal, "Capturing protein-ligand recognition pathways in coarse-grained simulation," *Journal of Physical Chemistry Letters*, vol. 11, no. 13, pp. 5302-5311, 2020.
- [19] A. Ahmadi, E. Mitchell, C. Richter et al., "Toward automatic activity classification and movement assessment during a sports training session," *IEEE Internet of Things Journal*, vol. 2, no. 1, pp. 23-32, 2017.
- [20] D. S. Fick, "Management of concussion in collision sports," *Postgraduate Medicine*, vol. 97, no. 2, pp. 53-60, 2017.
- [21] J. Vanrenterghem, N. J. Nedergaard, M. A. Robinson, and B. Drust, "Training load monitoring in team sports: a novel framework separating physiological and biomechanical load-adaptation pathways," *Sports Medicine*, vol. 47, no. 5, pp. 2135-2142, 2017.
- [22] M. J. Ellis, D. M. Cordingley, S. Vis, K. M. Reimer, J. Leiter, and K. Russell, "Clinical predictors of vestibulo-ocular dysfunction in pediatric sports-related concussion," *Journal of Neurosurgery: Pediatrics*, vol. 19, no. 1, pp. 38-45, 2017.
- [23] E. Brymer and R. D. Schweitzer, "Evoking the ineffable: the phenomenology of extreme sports," *Psychology of Consciousness: Theory, Research, and Practice*, vol. 4, no. 1, pp. 63-74, 2017.
- [24] Y. Li, B. Wu, Y. Zhao, H. Yao, and Q. Ji, "Handling missing labels and class imbalance challenges simultaneously for facial action unit recognition," *Multimedia Tools and Applications*, vol. 78, no. 14, pp. 1-24, 2019.
- [25] Y. Dong, M. Wu, and J. Zhang, "Recognition of pneumonia image based on improved quantum neural network," *IEEE Access*, vol. 8, no. 99, p. 1, 2020.

Research Article

Construction of Enterprise Financial Early Warning Model Based on Intelligent Mathematical Model

Jing Cheng,¹ Xiaofan Lu,² and Xionggang Zhang ³

¹Wuhan City Polytechnic, Wuhan 430064, China

²University of Chinese Academy of Sciences, Beijing Zhongguancun High School, Beijing 100086, China

³Hubei University, Wuhan 430062, China

Correspondence should be addressed to Xionggang Zhang; 20041895@hubu.edu.cn

Received 14 March 2022; Revised 13 April 2022; Accepted 28 April 2022; Published 13 May 2022

Academic Editor: Wei Liu

Copyright © 2022 Jing Cheng et al. This is an open access article distributed under the Creative Commons Attribution License, which permits unrestricted use, distribution, and reproduction in any medium, provided the original work is properly cited.

In order to improve the ability of enterprises to cope with financial risks, this paper analyzes the financial early warning of enterprises combined with intelligent mathematical models and builds an intelligent financial early warning model to assist in analyzing the financial status of enterprises. Moreover, this paper combines the existing information technology and expenditure business scenarios to construct an intelligent early warning frame for enterprise financial control based on an intelligent mathematical model. In addition, this paper combines the K-means clustering algorithm to design a financial approval process integrity control early warning method to warn the integrity of the financial approval process. Finally, this paper presents the early warning of financial standard compliance control based on the C4.5 decision tree algorithm. The experimental research shows that the enterprise financial early warning model based on the intelligent mathematical model proposed in this paper can play an important role in the enterprise financial management and effectively improve the ability of the enterprise to cope with financial risks.

1. Introduction

Financial risk corresponds to business risk in a relatively narrow sense. It refers to a risk situation in which investors' expected returns are reduced due to unreasonable corporate financial status and improper financing, and, at the same time, the company may lose its solvency. The financial early warning system we discuss and build here does not only refer to the company's financial debt crisis but is a financial concentrated manifestation of various internal contradictions and external risks that exist and are latent in the company's operation process.

The generation of financial risks is the result of internal and external contradictions, and these changes in financial early warning and its unfavorable influencing factors are called "warning sources." "Alert source" is divided into endogenous "alarm source" and exogenous "alarm source." To a certain extent, the endogenous alarm source is controllable, because this kind of problem is not directly related

to the production management of the company, while the exogenous alarm source is on the contrary; this kind of problem is beyond the control of the company, so it is more harmful. It is manifested as the uncertainty of the political environment, the uncertainty of the natural environment, the uncertainty of the industry competition environment, and the uncertainty of the economic environment. Because the company's operation is to pursue the maximization of profits, but high returns are often accompanied by high risks, and financial risks are everywhere in the company's production and operation process, if it is allowed to continue to develop beyond the company's risk tolerance, then there will be financial crises such as bankruptcy. Financial risks are not out of control from the beginning. According to medical terms, they can be divided into incubation period, development period, and deterioration period. Each stage has a relatively obvious and unique appearance, which is called "warning sign." Therefore, if you want to effectively prevent and control financial risks, you must pay close attention to

the warning signs in the company's operation, management, and finance. The company's goal is to maximize profits, but profits and risks are always in direct proportion to each other, and the normal operation of the company will face various crises. Therefore, with the emergence of warning signs at different stages, the company also needs to take various effective measures in a timely manner to prevent the further development and deterioration of the warning situation. In the early stage, warning signs are usually single, with only a little hidden change in one aspect of financial indicators, and it is usually difficult to attract the attention of the company's top management at this stage. The production and operation and financial status of the company have been greatly impacted, and the financial risk has further deteriorated; in the end, the crisis is severe, and the company can only face bankruptcy.

This paper combines the intelligent mathematical model to analyze the financial early warning of the enterprise and constructs an intelligent financial early warning model to assist in the analysis of the financial situation of the enterprise and improve the ability of the enterprise to deal with the financial crisis.

2. Related Work

Literature [1] believes that the poor effect of enterprise risk management is due to the lack of strong risk awareness of executives, and there is no appropriate method to manage enterprise risk. After the emergence of the term risk management, the related theories have officially become popular in academia. Literature [2] further defines risk management as the use of economic or technical means to reduce enterprise risks to the lowest level under the premise of analyzing the risk factors existing in each business link. In this definition, the purpose of enterprise risk management is clearly stated, that is, to reduce enterprise risk. With the popularity of risk management, scholars have gradually linked risk management with corporate financial activities, and the importance of financial risk management has been paid attention to. Literature [3] puts forward the theory of enterprise adversity management, expounds the causes and laws of business failure, management fluctuation, management behavior mistakes, and other phenomena, and conducts theoretical analysis on how to prevent and deal with enterprise adversity. Based on the theory of enterprise adversity management, literature [4] proposes an early warning and precontrol management model to deal with the adverse effects of business failure or management errors. The early warning and precontrol management model provides a literature for the theoretical study of financial risk early warning. Literature [5] believes that financial risk early warning is not only the identification of enterprises with high financial risks but also the early warning of enterprises whose financial risks may increase. Literature [6] believes that financial risk early warning is a process of using the risk early warning value and the actual value to measure the financial risk level of the enterprise and return the early warning results based on the financial status of the enterprise and the internal and external environment.

As an important way of financial risk management, financial risk early warning has received attention, and there have been a large number of studies on early warning indicators, and some scholars have integrated cross-disciplinary research methods into financial risk early warning models, further enriching the types of models. Literature [7] uses a single financial indicator to predict financial risk and designs a univariate early warning model. Literature [8] uses the financial data of 79 companies to compare and analyze two types of companies that fail to operate and operate normally based on 30 financial ratios. It is found that the most accurate prediction is the debt coverage ratio indicator, followed by the asset-liability ratio indicator, and prediction success rates improve as bankruptcy day approaches. This study still does not use indicators with higher prediction accuracy to construct an early warning model that can be used for a long time but analyzes the relationship between the prediction accuracy of indicators and the time of financial crisis outbreak. Literature [9] studies off-balance sheet indicators, and the results show that company size, capital structure, and asset realization ability can make financial risks change significantly. This study shows that nonfinancial indicators with a high degree of correlation with corporate financial risks can be considered when selecting early warning indicators. Literature [10] uses the catastrophe theory to carry out financial risk early warning and proves that it has certain applicability. Literature [11] uses the BCC model of data envelopment analysis for index analysis and risk prediction and compares it with the Z-score model, which proves that the data envelopment analysis method is suitable for financial risk early warning and has higher accuracy. Literature [12] divides the deterioration process of enterprise risk into latent, onset, and deterioration periods and explores the omens of financial risks from the perspectives of internal control and external environment and proposes that enterprises should set up an alert monitoring system. The discussion of warning signs in this study provides ideas for the selection of early warning indicators, emphasizing the impact of external factors on corporate financial risks. Literature [13] conducts text sentiment analysis on the information related to listed companies on the Internet through web crawler, forms sentiment indicators, and constructs a financial risk early warning model incorporating sentiment indicators. This study takes sentiment indicators into consideration and provides ideas for indicator selection from different perspectives. Literature [14] proposes using partial least squares method to screen early warning indicators, which proves that this method can effectively improve the accuracy of model prediction, and provides a new indicator screening method. Literature [15] quantifies the emotional description in management discussion and analysis to form sentiment index and finds that the model that introduces this sentiment index has a higher classification accuracy, which proves that some effective information in the management discussion and analysis can predict the future performance level of the enterprise to a certain extent. This study takes into account the effect of management discussion and analysis on early warning, which enriches the perspective of indicator selection.

Literature [16] draws the conclusion that property rights ratio and equity net interest rate are two financial indicators with strong early warning ability. Using the single financial indicators of 19 companies to analyze, research on enterprise financial risk early warning is conducted. The early warning research at this time is based on the direct corresponding relationship between a single indicator and the financial risk of the enterprise, and the relationship of each indicator is relatively independent. Literature [17] is one of the intelligent models of univariate financial risk early warning model established by using 30 financial indicators. Literature [18] uses statistical methods to build a financial risk early warning model. Literature [19] researches and analyzes 66 companies from the perspectives of profitability, solvency, and current ratio, establishes a Z-score model, uses financial indicators and combines statistical methods, and uses multivariate linear discrimination in financial risk early warning method. The model uses multiple variables for analysis, which overcomes the shortcomings of the single-variable model to a certain extent and is more comprehensive.

3. Enterprise Financial Early Warning Process Based on Intelligent Mathematical Model

The integrity control of the approval process is reflected in the three levels of control over the unit business, relevant departments and positions, and approval efficiency and approval quality. On the basis of constructing the pre-warning indicators for the integrity of the administrative expenditure approval process under the financial cloud platform, after sorting out the corresponding indicator data, scientific methods are needed to classify the data reasonably, to decide the target process that requires early warning, and to achieve the division of early warning levels.

K-means algorithm is a classic, simple, and fast clustering algorithm and is often used in evaluation analysis. According to the designed warning level, the sample data is given for training and learning, so as to achieve a reasonable classification of the sample data. The classification of enterprise expenditure approval process integrity warning needs to be given training data for unsupervised learning. After that, the early warning indicators of various types of data are analyzed and clustered, and the early warning levels are divided.

In the early warning of the integrity of the enterprise expenditure approval process, it is not necessary to know the warning level of each sample data in advance but only the number of categories that the data is finally divided into. In this chapter, the early warning is set to four levels, namely, level 1 early warning, level 2 early warning, level 3 early warning, and complete, that is, $K=4$. The idea of K-means clustering is roughly to randomly select K data from the sample as the initial "cluster center." It then calculates the distances of the remaining samples to the "cluster centers," assigns them to the closest clusters, and finally recalculates the "cluster centers" for each cluster. The algorithm itself has the function of optimization and iteration. It iteratively corrects and prunes the existing clusters to determine the

clustering of the samples and finally classifies all the sample data according to the similarity, which overcomes the uncertainty of the clustering of a small number of samples.

The samples are $x^{(i)} = \{x_1^{(i)}, x_2^{(i)}, \dots, x_n^{(i)}\}$ and $x^{(j)} = \{x_1^{(j)}, x_2^{(j)}, \dots, x_n^{(j)}\}$, where $i, j = 1, 2, \dots, m$ represents the number of samples and n represents the number of features. There are three main methods for calculating the distance from the sample to the "cluster center."

3.1. The Ordered Attribute Distance Is Used to Measure the Minkowski Distance.

$$\text{dist}_{\text{mk}}(x^{(i)}, x^{(j)}) = \left(\sum_{u=1}^n |x_u^{(i)} - x_u^{(j)}|^p \right)^{1/p}. \quad (1)$$

Euclidean distance is the Minkowski distance at $p = 2$:

$$\text{dist}_{\text{ed}}(x^{(i)}, x^{(j)}) = \|x^{(i)} - x^{(j)}\|_2 = \sqrt{\sum_{u=1}^n |x_u^{(i)} - x_u^{(j)}|^2}. \quad (2)$$

Manhattan distance is the Minkowski distance at $p = 1$:

$$\text{dist}_{\text{man}}(x^{(i)}, x^{(j)}) = \|x^{(i)} - x^{(j)}\|_1 = \sum_{u=1}^n |x_u^{(i)} - x_u^{(j)}|. \quad (3)$$

Most of the datasets in this paper are continuous attributes, so the Euclidean distance is used for calculation in the algorithm.

3.2. Disordered Attribute Distance Metric VDM (Value Difference Metric).

$$\text{VDM}_p(x_u^{(i)}, x_u^{(j)}) = \sum_{z=1}^k \left| \frac{m_{u,x_u}^{(i),z}}{m_{u,x_u}^{(i)}} - \frac{m_{u,x_u}^{(j),z}}{m_{u,x_u}^{(j)}} \right|^{1/p}. \quad (4)$$

In the above formula, $m_{u,x_u}^{(i)}$ represents the number of samples whose value is $x_u^{(i)}$ on attribute u , and $m_{u,x_u}^{(i),z}$ represents the number of samples whose value is $x_u^{(i)}$ on attribute u in the z -th sample cluster. $\text{VDM}_p(x_u^{(i)} - x_u^{(j)})$ represents the VDM distance between two discrete values $x_u^{(i)}$ and $x_u^{(j)}$ on attribute u .

3.3. The Mixed Attribute Distance Measure Is the Combination of Order and Disorder.

$$\text{MinkovDM}_p(x^{(i)}, x^{(j)}) = \left(\sum_{u=1}^{n_c} |x_u^{(i)} - x_u^{(j)}|^p + \sum_{u=n_c+1}^n \text{VDM}_p(x_u^{(i)}, x_u^{(j)})^{1/p} \right)^{1/p}. \quad (5)$$

It contains n_c ordered attributes and $n - n_c$ unordered attributes.

Based on the steps of the K-means clustering algorithm, this paper combines the characteristics of the enterprise expenditure approval process integrity control early warning process to construct the expenditure approval process integrity control early warning process, as shown in Figure 1.

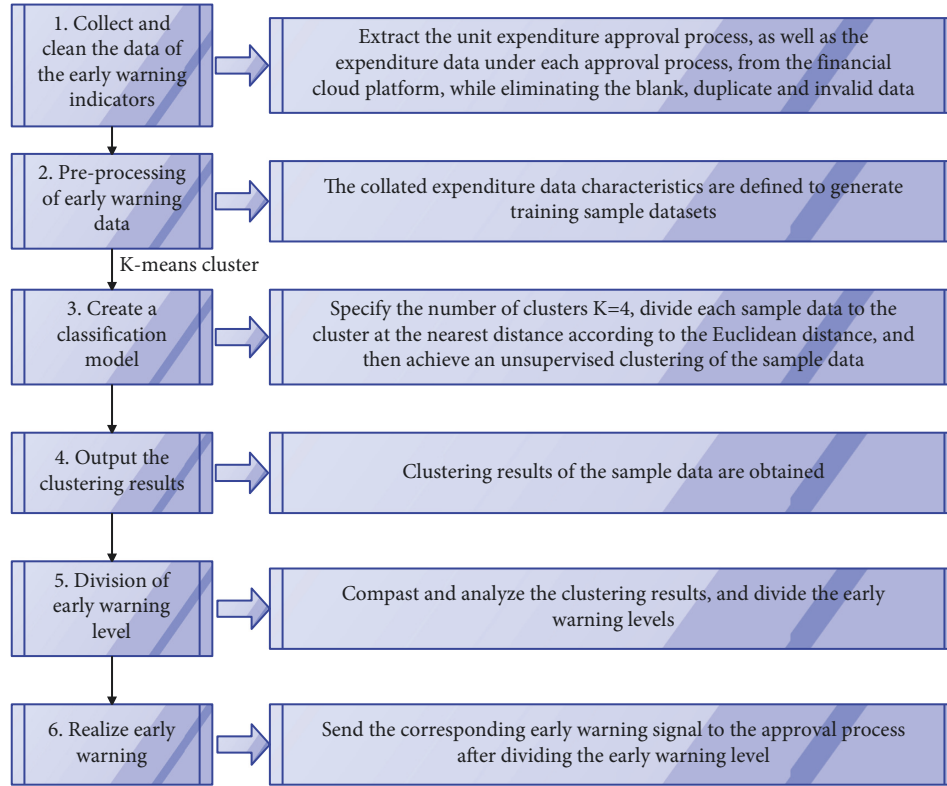


FIGURE 1: Integrity control and early warning process of expenditure approval process based on K-means clustering algorithm.

After extracting the early warning indicators of the integrity control of the enterprise expenditure approval process, it is necessary to collect data according to the characteristics of the samples. In order to fully reflect the integrity control of the enterprise expenditure approval process, the coverage of the approval process, the efficiency of the approval process, and the quality of the approval process are included in the scope of the sample characteristics. In order to meet the needs of early warning data for the integrity control of the expenditure approval process, it is necessary to collect portal information, fund approval, financial accounting, payment inquiry, expense reimbursement, expenditure economic classification, and other module data related to expenditure approval records, process settings, expenditure business classification, and expenditure audit post information from the expenditure management database of the unit's financial cloud platform.

The basic principle of the K-means clustering algorithm is to set the clustering parameter K , randomly select K data samples as the "cluster center," and then calculate the distance between the remaining sample data and each "cluster center" by the Euclidean formula. Finally, it assigns all the data to the nearest cluster to achieve classification. At the same time, the algorithm will iteratively correct and prune the clustering of the data samples on the basis of the existing clustering and optimize the unreasonable parts of the initial unsupervised learning sample classification. The specific process is shown in Figure 2.

3.3.1. The Algorithm Defines the Sample Dataset X . The approval process integrity control early warning dataset after cleaning and conversion is defined as sample $x^{(i)} = \{x_1^{(i)}, x_2^{(i)}, \dots, x_n^{(i)}\}$, where $i = 1, 2, \dots, m$ represents the number of samples and n represents the number of features.

3.3.2. The Algorithm Sets the Clustering Parameter K . The first step for K-means to implement clustering is to set the clustering parameters. Since this chapter divides the expenditure approval process integrity control early warning into four levels, process integrity, level 3 early warning, level 2 early warning, and level 1 early warning, the clustering parameter $K = 4$ is set.

3.3.3. The Algorithm Specifies the "Cluster Center". The number of clusters is 4, so 4 "cluster centers" need to be specified. There are two ways to select "cluster centers": random method and longest distance method. Among them, the longest distance method is to randomly designate a sample in the sample dataset as the first "cluster center." Then, the algorithm calculates the distance between the remaining samples and the sample, selects the sample with the farthest distance as the second "cluster center," and so on, until four "cluster centers" are selected, and the "cluster center" is set to C ; that is,

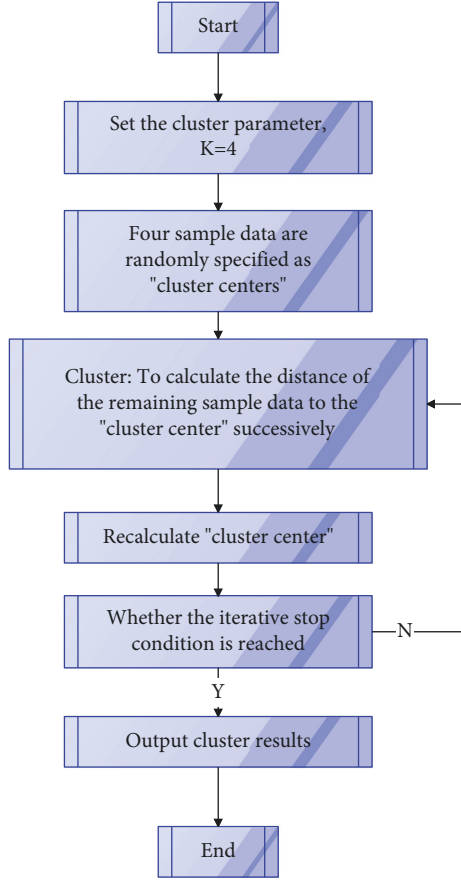


FIGURE 2: K-means algorithm's clustering process.

$$C^i = \{C_1^i, C_2^i, \dots, C_n^i\}, \quad i = 1, 2, 3, 4. \quad (6)$$

The algorithm uses the Euclidean distance formula to calculate the distances from each data sample to the four "cluster centers" in turn and assigns them to the nearest cluster. The calculation formula is as follows:

$$\text{dist}_{\text{ed}}(x^{(i)}, x^{(j)}) = \|x^{(i)} - x^{(j)}\|_2 = \sqrt{\sum_{u=1}^n |x_u^{(i)} - x_u^{(j)}|^2}. \quad (7)$$

3.4. The Algorithm Updates the "Cluster Center". After all the sample data are allocated, it is necessary to recalculate the "cluster center" of the four types of data and calculate the mean value of the sample data in each cluster. The calculation formula is

$$C^i = \frac{1}{n^i} \sum_{x \in C^i} x, \quad i = 1, 2, 3, 4. \quad (8)$$

3.5. The Algorithm Stops Iterating. In order to ensure the quality of classification, K-means clustering generally needs to go through several iterations before the cluster center will not change. It can be judged whether to stop the iteration by specifying the number of iterations and setting the range of cluster center variation. When specifying the number of

iterations, it stops when the number reaches the specified value. When setting the variation range ε of the cluster center, when the distance between the new "cluster center" and the old "center" is less than ε , it will stop running.

An important step in implementing C4.5 is to discretize continuously valued data features. The given expenditure data training sample set is D , and the continuous feature C_i in the expenditure data has a different value on the sample set D . The C4.5 algorithm will deduplicate the value of feature C_i and sort it in ascending order, marked as $\{C_i^1, C_i^2, \dots, C_i^n\}$. Taking the dividing point t in the value of feature C_i , the training set D is divided into subsets D_t^- and D_t^+ . D_t^- contains data samples whose value of feature C_i is less than t , and D_t^+ contains data samples whose value of feature C_i is greater than t . The division result is the same when the division point t takes any value in the adjacent eigenvalue interval $[C_i^m, C_i^{m+1})$. Therefore, a set of candidate division points contains $n - 1$ elements in a continuous feature C_i in the expenditure data; the calculation formula is

$$T_{C_i} = \left\{ \frac{C_i^m + C_i^{m+1}}{2} \mid 1 \leq m \leq n - 1 \right\}. \quad (9)$$

The partition node t is the midpoint of the adjacent eigenvalue interval $[C_i^m, C_i^{m+1})$.

The information gain of all the division points is calculated, and the maximum value of the information gain is selected as the best division point. The information gain of this division point is the information gain of the node, thus completing the discretization process. The information gain calculation formula is

$$\begin{aligned} \text{Gain}(D, C_i) &= \max_{t \in T_{C_i}} \text{Gain}(D, C_i, t) = \max_{t \in T_{C_i}} \text{Info}(D) \\ &\quad - \sum_{\lambda \in \{-, +\}} \frac{|D_t^\lambda|}{|D|} \text{Info}(D_t^\lambda). \end{aligned} \quad (10)$$

The data feature information gain calculation formula for discrete values is the same as above.

After discretizing the features with continuous values, the information entropy of all nodes needs to be calculated. In the training set D , the information entropy calculation formula of feature a is as follows:

$$\text{Split Info}_a(D) = - \sum_{j=1}^n \left(\frac{|D_j|}{|D|} \log_2 \frac{|D_j|}{|D|} \right). \quad (11)$$

In the above formula, n is the number of values of feature C_i , which can be expressed as $\{C_{i,1}, C_{i,2}, \dots, C_{i,n}\}$, and D_j is the set of sample data in the dataset D where the value of feature C_i is $C_{i,j}$.

The information gain rate is defined. The information gain rate formula can be obtained as follows:

$$\text{Gain Ratio}(D, a) = \frac{\text{Gain}(D, a)}{\text{SplitInfo}_a(D)}. \quad (12)$$

The information gain rates of all nodes are compared, and the node with the largest information gain rate will

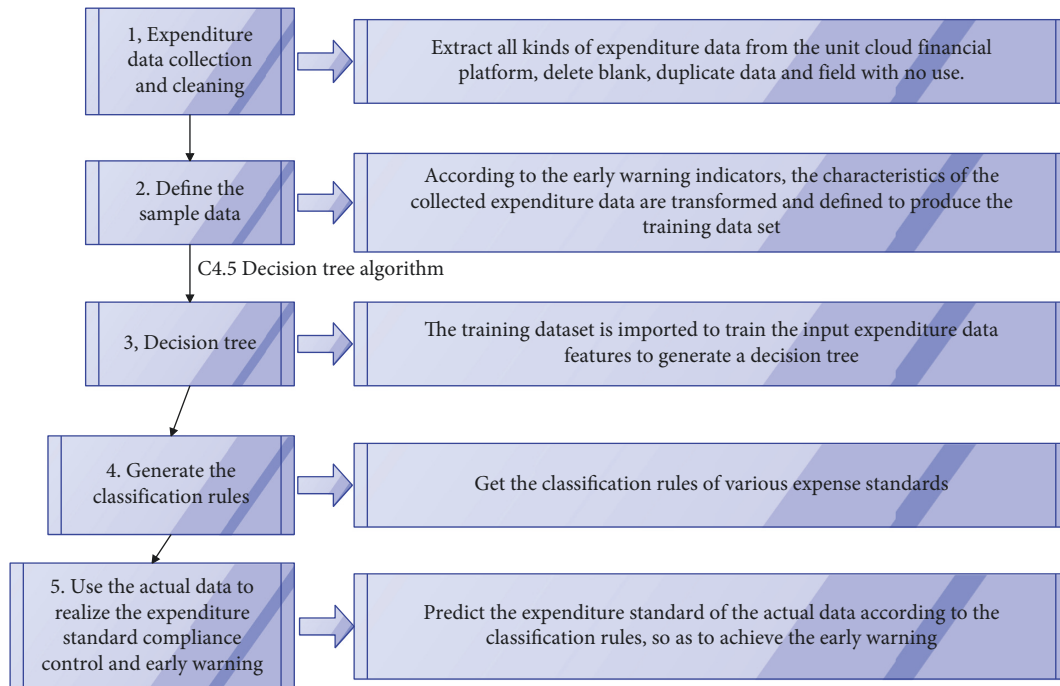


FIGURE 3: Expenditure standard compliance control early warning process based on C4.5 decision tree algorithm.

become the root node to divide the data feature. Then, based on the left and right branches of the root node, the information gain rate is calculated for the remaining data features, and the node with the largest gain rate is selected as the next classification node, thus recursing until all the datasets are classified.

Based on the steps of the C4.5 decision tree algorithm, combined with the formulation basis of the enterprise expenditure standard and the characteristics of the data, an early warning process for the compliance control of the expenditure standard is constructed, as shown in Figure 3.

This paper extracts various types of expenditure data from the financial cloud platform of the unit, such as travel expense schedule, conference fee schedule, and training fee schedule. Moreover, this paper uses SQL statements to process the extracted detailed data of various expenditures and removes duplicates, missing values, and other data that will affect the classification results. At the same time, this article deletes irrelevant fields, such as bank account number, entry time, reviewer, and other related fields.

Discrete features such as expenditure category, expenditure details, personnel rank/activity category, and other data feature values cannot be recognized by the algorithm and need to be converted in advance and replaced with ordered numbers like 1, 2, 3, and so on. For standard compliance as the target attribute, 1 means compliance and 0 means noncompliance.

After the defined training sample set is connected to the C4.5 algorithm, the algorithm first discretizes the continuous data features in the expenditure data and realizes the continuous feature discretization by calculating the optimal splitting point. The algorithm then calculates the

information gain rate of each feature, selects the classification node by the information gain rate, and generates a decision tree iteratively. At the same time, the algorithm generates various types of expenditure standards to follow the classification rules for situation prediction. The specific process is shown in Figure 4.

The trained C4.5 decision tree algorithm can predict the compliance with the expenditure standard of the actual expenditure data of the unit. The early warning system will issue early warning signals for data that do not meet the expenditure standards and remind financial personnel to check the relevant expenditure details, thereby strengthening the compliance control of corporate expenditure standards.

On the basis of constructing early warning indicators for rationality control of enterprise expenditures, after sorting out the data of each early warning indicator, it is necessary to use scientific methods to classify the rationality control data of expenditures and divide the early warning levels.

Self-organizing feature map network, also known as Kohonen network, is an unsupervised, competitive learning clustering algorithm. Kohonen uses feature mapping to achieve dimensionality reduction of data and reduces high-dimensional data to low-dimensional space for display through geometric relationships. Compared with the non-neural network clustering algorithm, Kohonen has better robustness, high efficiency, and good clustering effect. The Kohonen neural network is used to perform unsupervised clustering on the data of the rationality control of basic expenditures of various institutions and secondary units within the enterprise. According to the clustering results, the data characteristics of each cluster are analyzed, the warning

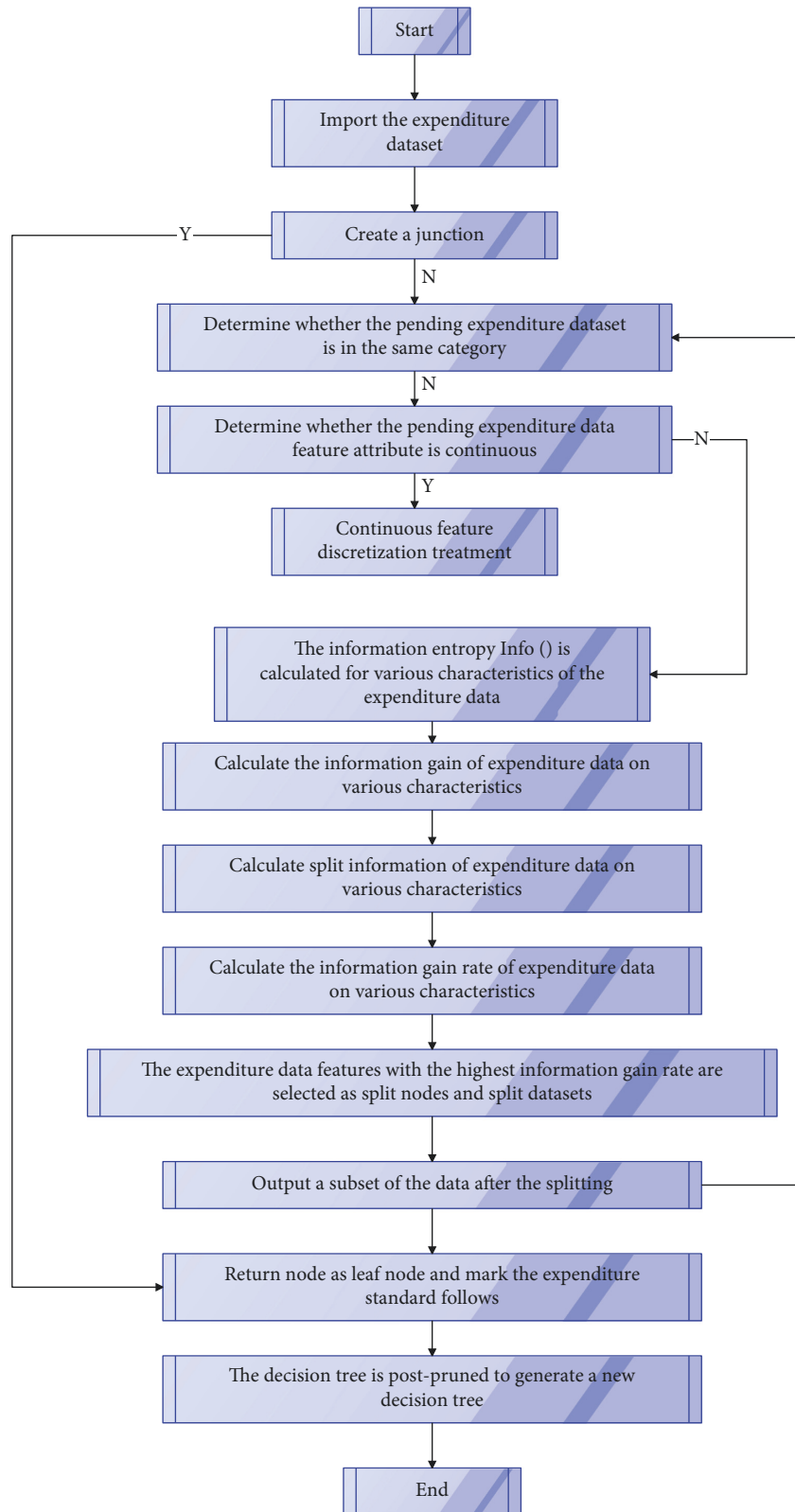


FIGURE 4: Classification process of expenditure standard compliance based on C4.5 algorithm.

levels are divided, and the warning labels are marked on the clustering results. The Kohonen algorithm's steps are summarized as follows:

- (1) The algorithm initializes the network, neighborhood radius r_0 , learning rate lr , and other parameters and randomly initializes the connection weight w_{ij} ($i =$

$1, 2, \dots, n; j = 1, 2, \dots, m$) between the input layer node and the competition layer node.

- (2) The algorithm inputs training samples and assumes that the input data is an n -dimensional vector, $X = (x_1, x_2, \dots, x_n)$ has m output nodes, and the total competition layer is g . The algorithm uses the Euclidean distance calculation method to calculate the distance d_j from the sample to each output node and selects the node corresponding to the minimum distance as the winning node v . The distance calculation formula is

$$d_j = \|X - W_{ij}\| = \sqrt{\sum_{i=1}^n (x_i - w_{ij})^2}, \quad (i = 1, 2, \dots, n; j = 1, 2, \dots, m). \quad (13)$$

Through steps (1) and (2), the winning neuron can be obtained, that is, the central position of the topological field in the competition layer.

- (3) The algorithm determines the neighborhood of neuron V :

$$N_v(j) = \{j \mid \text{find}(\text{norm}(\text{pos}_j, \text{pos}_v) < r)\}; \quad j = 1, 2, \dots, m. \quad (14)$$

In the above formula, $\text{pos}_j, \text{pos}_v$ are the locations of neurons V and j , respectively, and r is the neighborhood radius. The ownership values in the neighborhood are corrected according to the obtained neighborhood.

- (4) The algorithm modifies the weights according to the weight learning rules, and the change of the weights is

$$d_w = \text{lr}^* a_2^* (x - w). \quad (15)$$

In the above formula, lr represents the learning rate, and function a_2 is determined by the neuron spacing d , the output a , and the learning neighborhood size r :

$$a_2(i, q) = \begin{cases} 1, & a(i, q) = 1 \\ 0.5, & a(j, q) = 1 \text{ And } D(i, j) \leq r \\ 0, & \text{other} \end{cases} \quad (16)$$

- (5) The algorithm performs reinput and repeats steps (2), (3), and (4) until the end of training.

On the basis of raw data training, experience can be accumulated, so as to realize the rapid classification of expenditure rationality control data. After the clustering is completed, the data characteristics of the clustering results are analyzed and the warning level is calibrated.

After the clustering is completed, it is necessary to identify and train the calibrated expenditure rationality control data and finally realize the early warning of basic expenditure rationality control. SVM, also known as Support Vector Machine, is a supervised learning algorithm commonly used for linear regression and classification.

Moreover, the SVM algorithm uses the kernel function to realize high-dimensional space mapping and maximizes the interval between the sample and the decision surface, and the classification idea is simple and effective. In addition, the SVM algorithm has strong generalization ability and can be trained and learned based on a small amount of data. The steps to implement the SVM algorithm are as follows:

- (1) The algorithm inputs training samples:

$$X = \{(x_1, y_1), (x_2, y_2), \dots, (x_n, y_n)\}. \quad (17)$$

In the above formula, x_i represents the training sample point, y_i represents the category of the sample, and $i = 1, 2, \dots, n, n$ is the number of samples in the training set.

- (2) The algorithm selects the applicable kernel function and parameters.
 (3) The algorithm constructs the convex quadratic programming problem and solves it.

$$\text{s.t. } \sum_{i=1}^n y_i a_i = 0. \quad (18)$$

In the above formula, $0 \leq a_i \leq C, i = 1, 2, \dots, n$, and the final solution is $a^* = (a_1^*, a_1^*, a_2^*, \dots, a_n^*)^T$.

- (4) The algorithm calculates b^* , where a_i^* is the component of a^* in interval $(0, C)$.
 (5) Decision function is constructed:

$$f(x) = \text{sgn}(g(x)), \quad (19)$$

$$g(x) = \sum_{i=1}^n y_i a_i^* k(x_i, x) + b^*$$

and, on the basis of verifying the sample data, the algorithm judges the category of x by the value of $f(x)$.

- (6) The algorithm judges whether the classification error meets the expectation. If it is satisfied, then the algorithm outputs the result and the algorithm ends. However, if it is not satisfied, the algorithm returns to step (2) to repeat the above process.

Based on the characteristics of enterprise basic expenditure rationality control early warning data, the expenditure rationality control early warning process based on Kohonen-SVM combined classifier is shown in Figure 5.

Through the analysis of the rational control of the basic expenditure of the enterprise, this paper sorts out eight early warning indicators: the size of the unit's jurisdiction, the number of employees in the unit, the type of expenditure, the amount of expenditure, the proportion of expenditure in the same period, the historical growth rate in the same period, the expenditure per capita, and the rate of incomplete/excess expenditure. After that, this paper assigns the early warning indicators and normalizes them. The

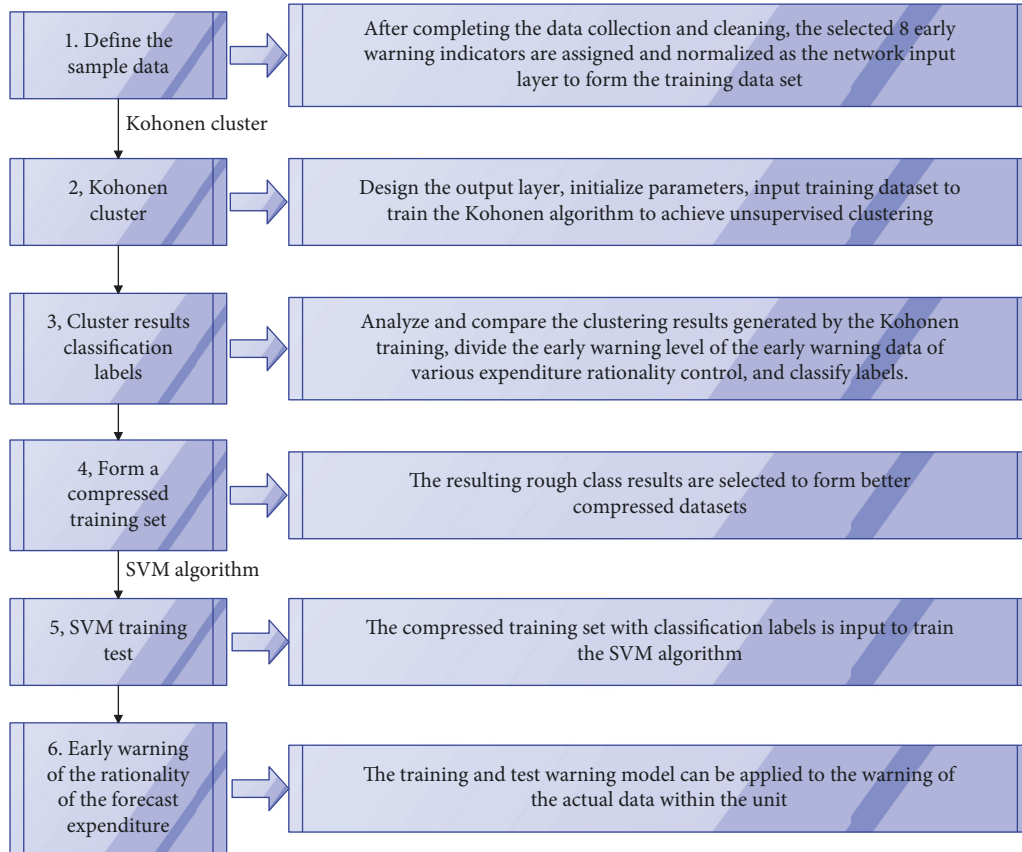


FIGURE 5: Early warning process of enterprise expenditure rationality control based on Kohonen-SVM combination classifier.

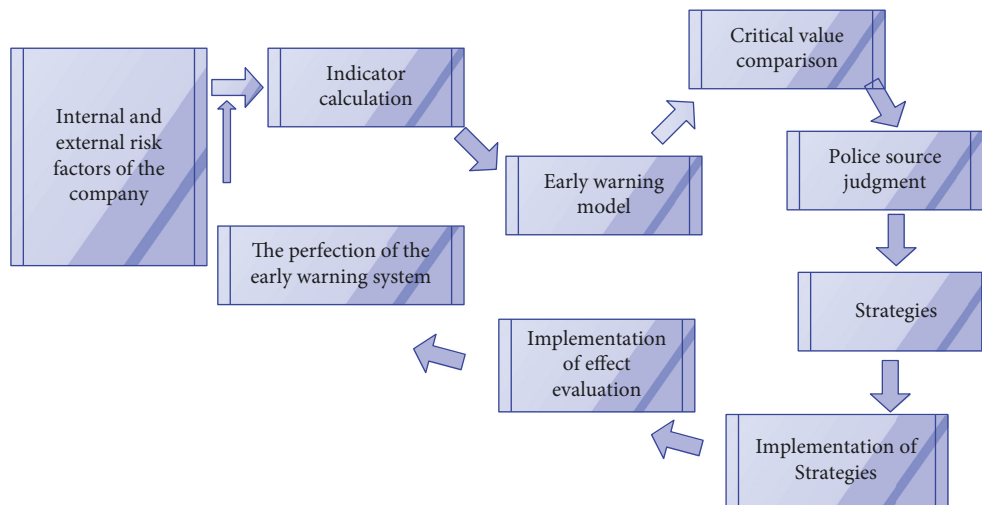


FIGURE 6: Internal principle of financial early warning.

eigenvalues of early warning indicators such as the size of the unit’s jurisdiction, the number of employees in the unit, and the amount of expenditure are processed as decimals between (0, 1). The processing formula is

$$x_i = \frac{x_i - x_{\min}}{x_{\max} - x_{\min}} \quad (20)$$

4. Intelligent Enterprise Financial Early Warning Model

The financial crisis of a company generally goes through three stages: the latent stage, the development stage, and the deterioration stage. The purpose of constructing financial early warning is to remind the company that it should take

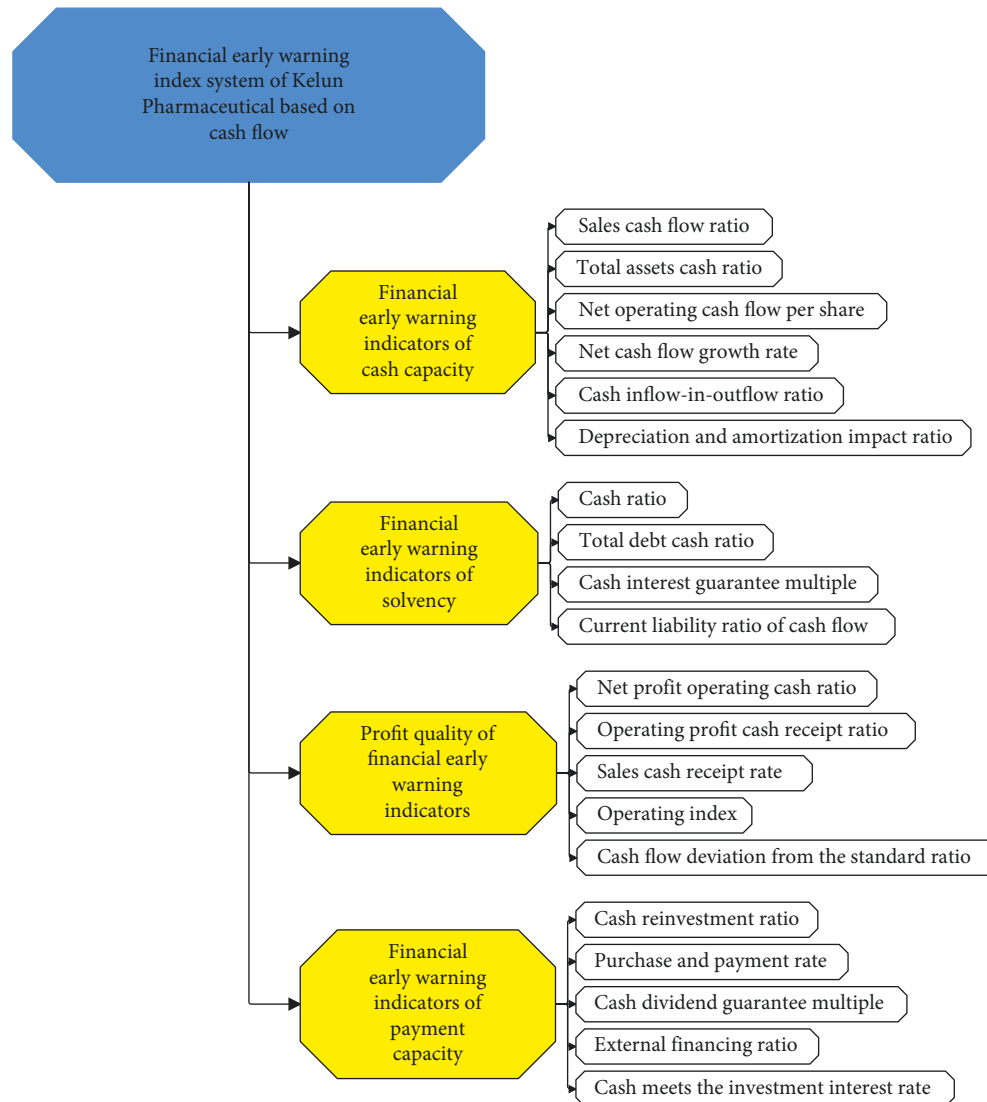


FIGURE 7: Financial early warning indicator system.

corresponding measures to prevent it before the company has a crisis. The process of the company's financial crisis is as follows: the warning source causes the warning situation, the warning situation evolves and deteriorates, and the warning signs appear. Therefore, the financial early warning system constructed in this paper will reverse the mentioned process. Its internal principle is shown in Figure 6.

In order to assess whether a company has the ability to adapt to the changing economic environment and seize good investment opportunities, early warning on affordability meets this requirement. Affordability refers to the degree of matching between the cash generated by the various activities of the enterprise and the cash required by the enterprise. If the enterprise's ability to pay is stronger, that is, the cash generated by the enterprise can meet its own needs, it does not need to borrow money from banks or take other ways to raise funds. When a good investment opportunity arises, the company has enough cash to seize the opportunity and gain income. On the contrary, when an enterprise needs

cash, it can only raise funds from the outside, which is called weak ability to pay. If this is the case for a long time, the enterprise will face a large amount of debt, and the pressure to repay the debt will gradually increase, which will ultimately affect the viability of the enterprise. The financial early warning indicator system based on cash flow is shown in Figure 7.

This paper uses the enterprise financial early warning model based on the intelligent mathematical model for simulation research and evaluates the financial data processing and financial early warning effect of the model in this paper, and the results shown in Table 1 and 2 are obtained, respectively.

From the above research, it can be seen that the enterprise financial early warning model based on the intelligent mathematical model proposed in this paper can play an important role in the financial management of enterprises and effectively improve the ability to cope with financial risks of enterprises.

TABLE 1: Data processing effect of enterprise financial early warning model based on intelligent mathematical model.

No.	Financial treatment	No.	Financial treatment	No.	Financial treatment
1	93.6	23	92.3	45	92.9
2	92.3	24	84.8	46	88.8
3	87.2	25	90.8	47	92.7
4	84.2	26	91.5	48	90.3
5	91.8	27	90.4	49	87.7
6	91.0	28	86.2	50	90.5
7	83.8	29	84.9	51	88.4
8	88.4	30	84.2	52	91.8
9	89.5	31	83.1	53	83.4
10	85.1	32	90.9	54	89.5
11	91.5	33	83.0	55	84.0
12	91.9	34	85.0	56	89.9
13	83.2	35	90.9	57	91.7
14	83.5	36	92.0	58	93.2
15	91.0	37	91.5	59	88.8
16	92.3	38	93.6	60	84.2
17	87.7	39	90.7	61	91.1
18	87.2	40	85.2	62	85.8
19	88.2	41	87.2	63	91.9
20	91.4	42	92.5	64	86.6
21	85.2	43	91.9	65	92.4
22	85.4	44	86.2		

TABLE 2: Financial early warning effect of enterprise financial early warning model based on intelligent mathematical model.

No.	Financial warning	No.	Financial warning	No.	Financial warning
1	82.5	23	67.8	45	76.6
2	73.2	24	82.7	46	69.9
3	77.1	25	62.0	47	74.8
4	66.6	26	63.8	48	81.8
5	65.7	27	74.6	49	63.2
6	66.4	28	78.1	50	71.4
7	63.5	29	69.5	51	68.4
8	74.7	30	73.4	52	79.9
9	73.0	31	70.7	53	73.8
10	62.4	32	72.4	54	67.3
11	78.1	33	67.7	55	73.0
12	73.4	34	66.0	56	73.8
13	61.7	35	72.8	57	70.6
14	65.5	36	64.2	58	71.1
15	65.7	37	61.9	59	83.2
16	66.7	38	69.3	60	70.7
17	79.7	39	80.7	61	83.0
18	81.2	40	75.1	62	83.0
19	80.5	41	83.3	63	77.7
20	63.9	42	64.0	64	66.7
21	69.1	43	69.6	65	77.7
22	80.6	44	82.7		

5. Conclusion

If an enterprise has a financial crisis, it will not only cause serious economic and reputation losses to the enterprise itself but also cause more serious harm to investors, creditors, and shareholders. Moreover, it leads to losses in industries related to the benefit chain and even negatively affects the entire industry in which the stock is located. In the

face of such a huge securities market, how to effectively control these listed companies and maintain the normal operation of the market has become an arduous and important task. At present, most listed companies are mainly manifested by poor cash flow liquidity, unreasonable capital structure, flooding of related-party transactions in the industry, and ineffective company management systems. This paper analyzes the enterprise financial early warning combined with the intelligent mathematical model and constructs an intelligent financial early warning model. The experimental research results show that the enterprise financial early warning model based on the intelligent mathematical model proposed in this paper can play an important role in the enterprise financial management and effectively improve the ability of the enterprise to cope with financial risks.

Data Availability

The labeled datasets used to support the findings of this study are available from the corresponding author upon request.

Conflicts of Interest

The authors declare no conflicts of interest.

References

- [1] K. S. Kumar, "Factors affecting the adoption of computerized accounting system (CAS) among smes in Jaffna District," *SAARJ Journal on Banking & Insurance Research*, vol. 8, no. 6, pp. 11–15, 2019.
- [2] B. L. Handoko, A. N. Mulyawan, J. Tanuwijaya, and F. Tanciady, "Big data in auditing for the future of data driven

- fraud detection,” *International Journal of Innovative Technology and Exploring Engineering*, vol. 9, no. 3, pp. 2902–2907, 2020.
- [3] Z. Rezaee, A. Dorestani, and S. Aliabadi, “Application of time series analyses in big data: practical, research, and education implications,” *Journal of Emerging Technologies in Accounting*, vol. 15, no. 1, pp. 183–197, 2018.
- [4] E. Huerta and S. Jensen, “An accounting information systems perspective on data analytics and Big Data,” *Journal of Information Systems*, vol. 31, no. 3, pp. 101–114, 2017.
- [5] S. Balne, “Analysis on research methods in bigdata applications,” *International Journal of Innovative Research in Computer and Communication Engineering*, vol. 8, no. 10, pp. 4059–4063, 2020.
- [6] P. B. De Laat, “Algorithmic decision-making based on machine learning from Big Data: can transparency restore accountability?” *Philosophy & technology*, vol. 31, no. 4, pp. 525–541, 2018.
- [7] G. Tucker, “Sustainable product lifecycle management, industrial big data, and Internet of things sensing networks in cyber-physical system-based smart factories,” *Journal of Self-Governance and Management Economics*, vol. 9, no. 1, pp. 9–19, 2021.
- [8] P. B. de Laat, “Big data and algorithmic decision-making: can transparency restore accountability?” *ACM SIGCAS - Computers and Society*, vol. 47, no. 3, pp. 39–53, 2017.
- [9] T. E. Marshall and S. L. Lambert, “Cloud-based intelligent accounting applications: accounting task automation using IBM watson cognitive computing,” *Journal of Emerging Technologies in Accounting*, vol. 15, no. 1, pp. 199–215, 2018.
- [10] D. Chessell and O. Neguriță, “Smart industrial value creation, cyber-physical production networks, and real-time big data analytics in sustainable Internet of Things-based manufacturing systems,” *Journal of Self-Governance and Management Economics*, vol. 8, no. 4, pp. 49–58, 2020.
- [11] B. Abdualgalil and S. Abraham, “Efficient machine learning algorithms for knowledge discovery in big data: a literature review,” *Database*, vol. 29, no. 5, pp. 3880–3889, 2020.
- [12] O. Throne and G. Lăzăroiu, “Internet of Things-enabled sustainability, industrial big data analytics, and deep learning-assisted smart process planning in cyber-physical manufacturing systems,” *Economics, Management, and Financial Markets*, vol. 15, no. 4, pp. 49–58, 2020.
- [13] E. Nica, C. I. Stan, A. G. Luțan, and R. Ș. Oa, “Internet of things-based real-time production logistics, sustainable industrial value creation, and artificial intelligence-driven big data analytics in cyber-physical smart manufacturing systems,” *Economics, Management, and Financial Markets*, vol. 16, no. 1, pp. 52–63, 2021.
- [14] D. B. L. Shallal Almutairi, “Impact OF COVID19 ON accounting profession from the perspective OF a sample OF head OF accounting departments within KUWAITI manufacturing sector,” *Psychology and Education Journal*, vol. 58, no. 2, pp. 4758–4768, 2021.
- [15] V. Q. Thong, “Factors defining the effectiveness of integrated accounting information system in ERP environment—Evidence from Vietnam’s enterprises,” *ECONOMICS AND BUSINESS ADMINISTRATION*, vol. 7, no. 2, pp. 96–110, 2020.
- [16] J. R. A. Q. Al Natour, “The impact of information technology on the quality of accounting information (SFAC NO 8, 2010),” *Turkish Journal of Computer and Mathematics Education (TURCOMAT)*, vol. 12, no. 13, pp. 885–903, 2021.
- [17] A. P. Aaron, M. L. Kohlstrand, L. V. Welborn, and S. T. Curvey, “Maintaining medical record confidentiality and client privacy in the era of big data: ethical and legal responsibilities,” *Journal of the American Veterinary Medical Association*, vol. 255, no. 3, pp. 282–288, 2019.
- [18] B. J. Ali and M. S. Oudat, “Accounting information system And financial sustainability OF commercial and islamic banks: a review OF the literature,” *Journal of Management Information and Decision Sciences*, vol. 24, no. 5, pp. 1–17, 2021.
- [19] V. Brock and H. U. Khan, “Big data analytics: does organizational factor matters impact technology acceptance?” *Journal of Big Data*, vol. 4, no. 1, pp. 21–28, 2017.

Research Article

Evaluation of Multimedia Classroom Teaching Effectiveness Based on RS-BP Neural Network

Nan Xie 

Liaoning Urban Construction Technical College, Shenyang 110000, China

Correspondence should be addressed to Nan Xie; xienan0301@163.com

Received 3 March 2022; Revised 31 March 2022; Accepted 28 April 2022; Published 13 May 2022

Academic Editor: Xuefeng Shao

Copyright © 2022 Nan Xie. This is an open access article distributed under the Creative Commons Attribution License, which permits unrestricted use, distribution, and reproduction in any medium, provided the original work is properly cited.

With the popularization of information technology, multimedia teaching has been widely used in universities as a new form of classroom teaching. In this paper, based on the classroom process, 12 evaluation indexes are initially obtained from three dimensions of “courseware, classroom teaching, and classroom effect,” which are reduced to 7 core indexes and evaluated comprehensively by using the rough set theory (RS), and the evaluation results are used as input data for simulation training of the BP neural network. The RS-BP neural evaluation model of multimedia classroom teaching effect (MCTE) is successfully trained, and finally five nonuniversities are selected for empirical research. The empirical study shows that this model has certain applicability when MCTE is such a nonlinear problem and can provide reference for the quality evaluation and improvement of multimedia teaching. The model in this study has certain practical value, but the index system is not comprehensive enough, the training data is insufficient, and the model maturity still needs further improvement.

1. Introduction

With the advent of the information age, the rapid development of science and technology has accelerated the updating of knowledge in the field of education, and the traditional teaching mode and teaching methods have failed to meet the needs of modern teaching and the requirements of current social, economic, and cultural development [1]. Multimedia classroom teaching (MCT), as a product of the combination of computer technology and current education technology, can be rich in teaching content and vivid teaching forms applied in teaching. The application of modern education technology can fully reveal the subjectivity of students, through contextual design and writing learning, and promote students’ active thinking and exploration, so that students become the main body of information processing in the learning process. Practice has proved that multimedia teaching has the characteristics of image, diversity, and intuition, which can stimulate students’ interest in learning and play a fairly important role in deepening classroom teaching reform, improving teaching quality and comprehensively improving students’ comprehensive quality.

Most of the current studies on MCT stay on partial improvement, lacking holistic research, and are not distinguished from traditional classroom teaching evaluation in terms of evaluation [2]. Compared with traditional classroom teaching, MCT pays more attention to and emphasizes the process of students’ independent participation and self-learning, while teachers provide students with a self-learning environment through multimedia teaching means, so that students can rise from perceptual to rational understanding and realize the unity of educational regularity and purpose [3]. The teaching evaluation system is a comprehensive examination of teaching quality, and the evaluation of teaching activities is a correct evaluation derived from the teaching objectives and through technical analysis methods [4]. Therefore, it is necessary to establish a scientific and reasonable evaluation system of MCT.

The evaluation of teaching quality is one of the most important aspects of teaching and learning, and Caballero (2017) states that online resources as a new vehicle for knowledge fragmentation and contextualization reform can be very useful for optimizing teaching and learning [5]. The multimedia classroom allows for “self-directed learning

strategies,” motivating students with a variety of learning strategies that allow them to discover the teaching context [6]. In this environment, online teaching is a key information resource for students’ independent learning. In recent years, the development of information processing technologies has accelerated the expansion of online instructional databases, bringing a wealth of information to students and teachers [7]. To address the main problems of application in multimedia teaching, Yong (2020) proposed an online classroom visual data tracking system combined with an advanced data mining-based tracking quality evaluation method [8]. Representing, analyzing, interpreting, and teaching evaluation results can make evaluation play a more important role in teaching level evaluation activities [9]. Ke (2021) pointed out that building a multimedia classroom evaluation index system for universities should be combined with the era of 5G multimedia network, and the evaluation process should include steps such as data collection, analysis, result output, and result feedback [10].

In terms of evaluation index system construction, Hiary used hierarchical analysis to construct an importance matrix and then determined the teaching quality evaluation index system [11]. Liu pointed out that teaching quality evaluation indexes should include teaching goal evaluation, teaching program evaluation, teaching process evaluation, and teaching effect evaluation [12]. Khedif et al. used a fuzzy mathematical mining algorithm to analyze the satisfaction of teaching quality and derived key indicators affecting teaching evaluation [13]. Liu proposed a hybrid intelligent algorithm based on the genetic algorithm and back-propagation neural network to evaluate teaching quality and proved that this evaluation method is effective and reasonable [14]. Kuriakose introduced feature selection based on certain evaluation criteria to preprocess the initial data and optimize from the original feature set to the low-Witt levy set to reduce data redundancy [15]. Ji et al. pointed out the role of functional selection of rough set neural networks that can be effectively applied to the solution of evaluation models [16]. Considering the advantages of rough sets and neural networks in evaluation [17], this study uses RS-BP neural networks to analyze MCTE evaluation indexes in order to establish a better MCTE evaluation index system and provide more accurate evaluation.

2. Evaluation Index System of MCTE

Multimedia classroom teaching evaluation should be guided by modern education theory and modern education evaluation theory, and on the basis of determining evaluation subjects and evaluation methods, the evaluation index system should be finally formed after repeated discussion and modifications using the Delphi method.

In the evaluation index system designed in this paper, the evaluation subjects should have a close relationship with teaching quality, including students, peer teachers, experts, and teachers themselves. Students’ evaluation refers to students’ effective value evaluation through their participation in classroom teaching practice. The effectiveness of teaching in terms of meeting classroom teaching objectives,

the demand for teaching contents, students’ classroom participation, students’ adaptation to learning, and students’ adaptation to learning can be reflected in students’ evaluation results. Peer teachers, on the other hand, are able to consider the effectiveness of teachers’ teaching in terms of the subject characteristics of their teaching, mastery of new knowledge, teaching style, and teaching ideology. Expert evaluation means that the school hires connoisseurs to assess the level and quality of teachers’ teaching, to evaluate the quality of teachers’ teaching by listening to classes with them, and to make a rational evaluation of teachers’ teaching from the perspective of subject development and overall training of students’ quality. Teacher self-evaluation is to ask the evaluated teachers to evaluate their own performance according to the evaluation principles and against the evaluation standards, so as to fully mobilize teachers’ enthusiasm and initiative and then to play the functions of teacher evaluation such as motivation, development, and management.

The multimedia teaching evaluation index system is to make various kinds of indicators specific and behavioral, so that teaching evaluation is measurable. Teaching evaluation is not a single-factor judgment work; it is multidimensional and is a process of multiple factors interacting and influencing each other. After the initial determination of the evaluation indexes, through several times using the Delphi method for revision and improvement, it is clear that the first-level indicators of multimedia classroom teaching evaluation include multimedia courseware, classroom teaching process, and classroom teaching effect, and the specific evaluation indexes are shown in Table 1. Multimedia courseware in the classroom teaching process is an inseparable whole, which embodies the teaching ideas, classroom teaching design, and teaching content and belongs to the static multimedia classroom presentation. Multimedia classroom teaching is a dynamic organizational process, using courseware to achieve multimedia teaching.

The evaluation criteria of multimedia courseware should reflect teaching meaning, logic, and operability and make use of the interactivity, control, and nonlinearity of multimedia computers to diversify and three-dimension Alize the teaching process. The quality of multimedia courseware is an important aspect to measure the actual teaching value and teaching effect, which is not only designed to the teaching design idea, teaching content, teaching plan design intention, and other pedagogical issues but also involves the technicality and artistry of courseware design and use. In addition, the economy of the courseware production is also a factor that must be verified in teaching evaluation. The pedagogical nature of the courseware should be reflected in the delivery of the teaching content specified in the syllabus and the unique teaching function of the multimedia courseware on the basis of achieving the expected teaching objectives. Technicality is mainly reflected in the maintainability and stability of the courseware and its ease of use in operation. Artistic is to the beauty and coordination of pictures, text, sound, and images of the courseware, that is, the relevant elements of multimedia courseware need to conform to the laws of aesthetics, to make the presentation

TABLE 1: Explanation of Cantonese teaching evaluation index.

Index	Explanation
A_{11}	Pedagogical: the delivery of the teaching content specified in the syllabus
A_{12}	Technical: the maintainability and stability of the courseware and its ease of use in operation
A_{13}	Artistic: the beauty and coordination of pictures, text, sound and images of the courseware
A_{14}	Economic: the production should follow the principle of minimum cost or the law of maximum value
A_{21}	Teaching attitude: the teacher's enthusiasm for lesson preparation and lessons, etc.
A_{22}	Teaching content: whether the teaching content is adequate and relevant to reality
A_{23}	Teaching ability: teachers' teaching experience and teaching of important and difficult points
A_{24}	Teaching organization: the teacher's familiarity with the course content and how it is delivered before, during, and after the class
A_{25}	Multimedia operation: teachers' proficiency in the operation of multimedia-related machines and technologies
A_{31}	Student attendance: calculate the number of students in the class divided by the total number of students by means of a random classroom check
A_{32}	Classroom teacher-student interaction: classroom activity, teacher-student question, and answer situation
A_{33}	Teaching effectiveness: students' scores and overall quality improvement

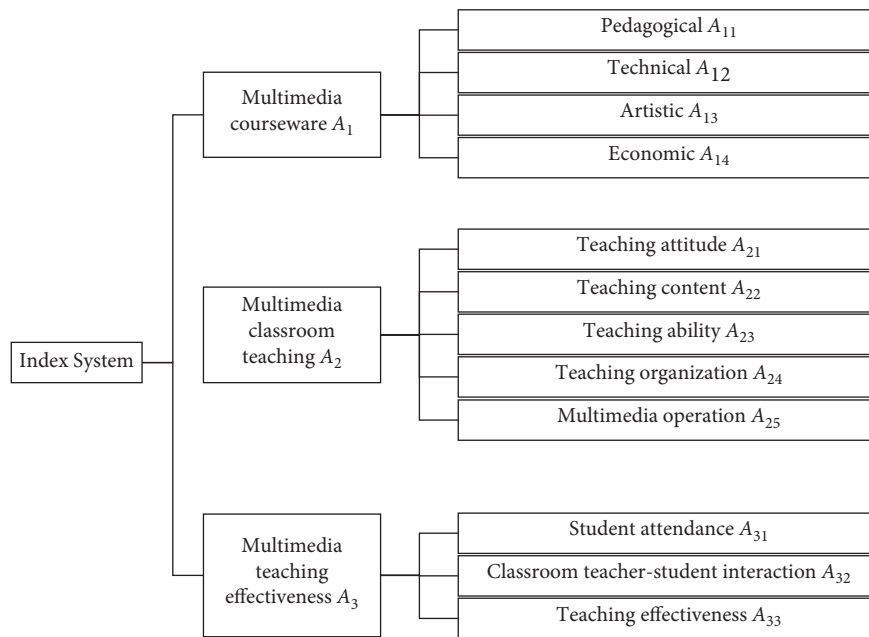


FIGURE 1: Evaluation index system of multimedia classroom teaching.

of content with artistic expression and infectious power without violating the premise of science and education. Economy means that the production of courseware should follow the principle of minimum cost or the law of maximum value. Specific indicators include pedagogical A_{11} , technical A_{12} , artistic A_{13} , and economic A_{14} .

Multimedia classroom teaching is a dynamic process of implementing classroom programs using multimedia courseware. Although it differs from the traditional classroom, there are still commonalities in the basic objectives, basic rules, and basic requirements of classroom teaching. Therefore, in the evaluation of multimedia classroom teaching process, it is necessary to emphasize the coordination of classroom teaching and the use of various media and the openness of information sources and the evaluation of creative ability and comprehensive application ability, so that teachers can grasp the systematic and holistic nature of teaching. The specific indicators include five aspects: teaching attitude A_{21} , teaching content A_{22} , teaching ability

A_{23} , teaching organization A_{24} , and multimedia operation A_{25} .

The evaluation of multimedia teaching effectiveness needs to consider the determination of comprehensive qualitative indicators and requires direct feedback from learners on relevant information. The overall effectiveness of instruction includes student classroom interactions, student work completion, and value judgments on quantified results based on instructional goals. Learning evaluation is an important part of teaching design, which can measure the behavioral changes of students at different stages of teaching, and teachers understand the learning status of students by evaluating them. Multimedia teaching effectiveness evaluation indexes mainly include student attendance A_{31} , classroom teacher-student interaction A_{32} , and teaching effectiveness A_{33} (Figure 1).

The above evaluation index system can summarize the actual situation of multimedia classroom teaching in a more comprehensive way. Using the data of multimedia teaching

effect evaluation indexes as the input samples of the evaluation model, the evaluation of multimedia classroom teaching effect can be realized.

3. Evaluation Model of MCTE

3.1. Rough Set Theory (RS). RS theory is able to analyze and reason about some incomplete information, discover the implied knowledge, and reveal the potential patterns among the data. Since the rough set method does not require any a priori information when dealing with uncertain information. The theory is able to analyze and infer some incomplete information based only on the observed data, discover the implied knowledge, and reveal the potential patterns among the data. Therefore, it is more objective than conventional methods in the description and treatment of uncertainty problems.

Due to the advantages of RS such as attribute simplification, objectivity, and reduction of computational pressure, the research on optimization and evaluation of index system based on RS has gradually becomes one of the hot spots in academia and is widely used in many fields such as management, sociology, and economics. The working principle of rough set theory for multi-indicator evaluation is based on data mining: first, removing the redundant indicators by combining the attribute simplification principle to obtain the core indicators, then calculating the objective weight of each indicator according to the importance of each core indicator, and then obtaining the comprehensive score of each evaluation object.

Generally, the core of RS is the approximation of unclear, or undefined, knowledge based on existing knowledge [18]. In RS theory, an information system can be represented by a quadruple $S = (U, A, V, f)$, where U is the universe of discourse, that is, the nonempty finite set of evaluation objects; A is the attribute set, containing the condition attribute C and the decision attribute D ; V is the value range of the attribute set; f is the mapping relationship. The calculation process of the importance of C to D is

$$\begin{aligned} sig(c, C, D) &= r_c(D) - r_{c-(C)}(D) \\ &= \frac{|Pos_C(D)| - |Pos_{C-(C)}(D)|}{|U|}, \end{aligned} \quad (1)$$

where $C = (c_1, c_2, \dots, c_n)$ stands for conditional attribute set; $sig(c, C, D)$ stands for importance; and Pos stands for the positive region of the variable. The weight of the condition attribute is

$$w_n^c = \frac{sig(c, C, D)}{\sum_{i=1}^z sig(c_i, C, D)}. \quad (2)$$

The dependence of D on C is calculated:

$$r_c(D) = \frac{\sum |Pos_C(y)_n|}{|U|}. \quad (3)$$

Similarly, the dependence of D on the remaining c is achieved by decreasing:

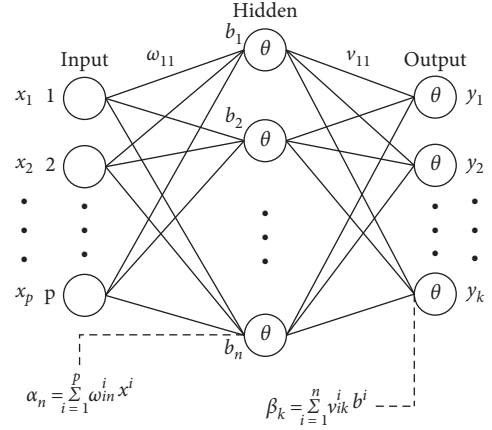


FIGURE 2: Description of the neural network structure.

$$r_{c-c_k}(D) = \frac{\sum |Pos_{c-c_k}(y)_n|}{|U|}. \quad (4)$$

From this, the final importance of each conditional attribute can be obtained:

$$I_D(c_k) = r_D(D) - r_{c-c_k}(D). \quad (5)$$

The weight of the conditional attribute can be obtained by normalization: $\omega_i = (I_{D_i} / \sum I_{D_i})$. In the process of determining the index weight, the introduction of RS to improve the content with greater interference and noise and weaken the influence of subjective experience factors can objectively solve the problems caused by some uncertain factors.

3.2. BP Neural Network. A typical BP neural network consists of three layers: input, hidden, and output. During forward propagation, the learning samples enter from the input layer and are calculated layer by layer through the hidden layer to reach the output layer. If the output layer does not get the expected output, it will be back-propagated; back-propagation is from the output layer back through the hidden layer. In the process of the input layer, during the training process, the output error is reduced by continuously modifying the neuron weights of each layer until the desired output target value is reached.

Give a training set $D = \{(x_1, y_1), (x_2, y_2), \dots, (x_n, y_n)\}$, $x_i \in R^d$, $y_i \in R^l$. In order to facilitate the derivation of equations, Figure 2 is given for illustration. The weight between input layer i and hidden layer h is ω_{ih} , and the weight between hidden layer h and output layer j is v_{hj} . The input received by the h -th hidden layer neuron is α_h . The input received by the j -th output layer neuron is β_j . All activation functions θ are sigmoid. The underlying index information in the evaluation index system is used as the input vector of the BP neural network, and the corresponding desired output value is used as the output vector. The network is trained with the sample data, different input vectors get different output values, and the output values are compared with the expected values, when the error is less

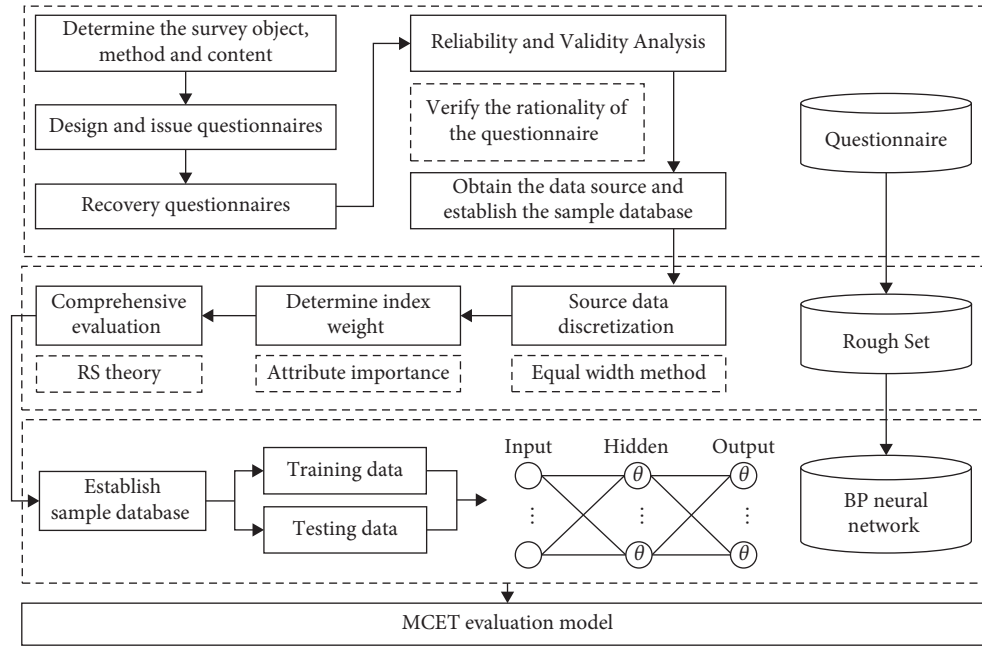


FIGURE 3: Evaluation model generation process.

than a set value, the neural network model training is completed.

3.3. *MCTE Evaluation Model Based on the RS-BP Method.* Combined with the RS theory and the principle of BP neural network, the steps of the MCTE evaluation model constructed in this paper are shown in Figure 3:

- (1) Obtain the source data by means of a questionnaire and conduct reliability and validity tests on the data to ensure the rationality of the questionnaire design and the data
- (2) Discrete preprocessing of the source data by the equal width method
- (3) Apply the principle of attribute importance to determine the weights of each core evaluation index
- (4) Conduct comprehensive evaluation of MCTE quality based on RS
- (5) According to the comprehensive evaluation results, constitute learning samples to input into the BP neural network for learning training and generate the RS-BP neural network evaluation model of MCTE after the training is completed and then use the evaluation model to evaluate other multimedia classes

4. Experimental Results

4.1. *Data Preprocessing.* In order to obtain qualified qualitative data, this study selects students and teachers from five different universities (HU, HE, HN, HP, and ST) in Hebei Province as the research object. In order to improve the professionalism and participation of the questionnaire, we conducted a visit survey. A total of 350 questionnaires were

TABLE 2: Internal consistency test results.

	HU	HE	HN	HP	ST
Cronbach's α	0.944	0.938	0.932	0.921	0.917

TABLE 3: Tests of KMO and Bartlett.

Kaiser–Meyer–Olkin measure of sampling adequacy	0.935	
Bartlett sphericity test	Approximate chi-square	10142.46
	df	498
	Sig.	.000

distributed, and 314 questionnaires were recovered. After dealing with outliers through SPSS, 309 valid questionnaires were obtained, with an effective rate of 88.29%.

The reliability and validity test results of the questionnaire are shown in Tables 2 and 3. The Cronbach's α of each questionnaire is above 0.9, the KMO coefficient is 0.935, and the P value is 0.000. This shows that the internal consistency of each questionnaire is good, the structural design is reasonable and can better reflect the content of the required survey, and the questionnaire has high reliability in the above universities. In this paper, the equal width method is used to discretize all data. Let the interval number $n = 3$, the maximum value of data is Max, the minimum value of data is Min, and then the width of each interval is $(\text{Max} - \text{Min})/n$. Therefore, the value of the first interval is 0, the second is 1, and the third is 2.

4.2. *Comprehensive Evaluation Based on RS.* Attribute reduction based on the importance of attributes is the core concept in rough set theory. Redundant information that has no value in the original data and can be deleted through

TABLE 4: Weight of core indicators.

Index	A_{11}	A_{13}	A_{22}	A_{23}	A_{25}	A_{32}	A_{33}
Weight	0.1273	0.1514	0.1511	0.1514	0.1447	0.1522	0.1219

TABLE 5: Comprehensive score of MCTE.

Evaluation object	HU	HE	HN	HP	ST
Score	2.7368	3.7547	3.5731	3.6561	2.8694
Grade	II	III	III	III	II

reduction, so as to simplify the indicators and obtain the core evaluation indicators. The genetic algorithm provided by MATLAB is used for reduction to remove redundant index attributes, and the reduced results are shown in Table 4; using the core evaluation index to evaluate has the same effect as the original evaluation index.

Based on the RS theory and method, the MCTE of the above five colleges are evaluated. The weight of the core evaluation index is calculated by the RS theory and method, as shown in Table 4.

The comprehensive score of MCTE of each school is shown in Table 5. This paper uses the equal width method to divide the comprehensive score. The lowest comprehensive score is 1, the highest comprehensive score is 5, the number of intervals is 4 (4-5, 3-4, 2-3, 1-2), and the evaluation grades are IV, III, II, and I. The comprehensive scores of HE, HN, and HP are 3.7547, 3.5731, and 3.6561, respectively, belonging to grade III; while the score of HU and ST are 2.7368 and 2.8694, respectively, belonging to grade II.

4.3. Training and Evaluation of the BP Neural Network.

In the five schools, 15 evaluation data (60 in total) are selected to form the BP neural network test and evaluation sample database, and the remaining evaluation data (249 in total) form the learning and training sample database. The proportion of training set and verification set is 8:2.

Firstly, MATLAB is used to program and construct a $7 \times 3 \times 1$ neural network. For the three-layer BP neural network model, the tansig function is selected as the neuron transfer function in the middle hidden layer, the logsig function is selected as the neuron in the output layer, the trainlm function with the largest memory demand and the fastest convergence speed is selected as the network training function, the maximum number of iterations is set to 10000 times, the display step size is 50, the learning efficiency is 0.05, and the target error is set to be less than 0.0001. The initial weights and thresholds are random numbers. Then, 249 training samples are input into the BP neural network model for training and learning, and the error target is achieved after 56 iterations. The BP neural network model after training is called MCTE evaluation model based on the RS-BP neural network in this paper.

In order to verify the rationality and advantages of this model, we choose two other common machine learning methods: support vector machine (SVM) and random forest (RF) to compare and analyze the accuracy of the model. The

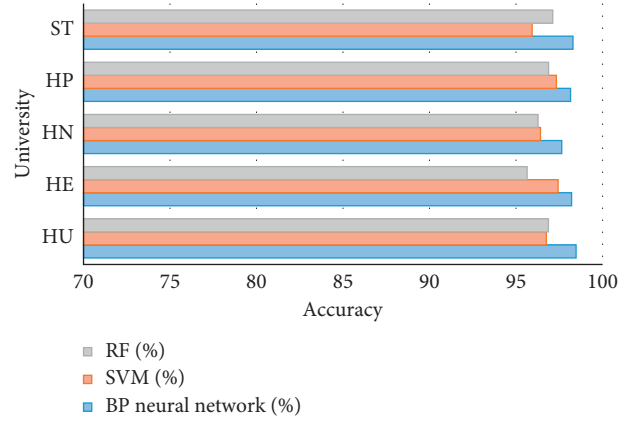


FIGURE 4: Accuracy comparison in the training set.

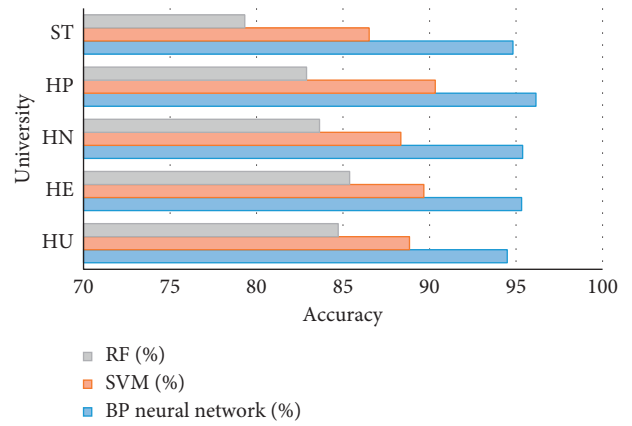


FIGURE 5: Accuracy comparison in the testing set.

accuracy comparison between the model training set and the verification set is shown in Figure 4 and 5. In general, the statistical data in this paper have strong discrimination, which also shows that MCTE is suitable for machine learning evaluation. The accuracy of the BP neural network, SVM and RF methods in the training set is very high, reaching 98.12%, 96.77%, and 96.56%, respectively. However, the average accuracy on the validation set is 95.23% and 88.74% And, 83.19%, which shows that SVM and RF have different degrees of over fitting and also reflects the advantages of BP neural network when the sample data increase. The accuracy of the model shows that, under the BP neural network method, the MCTE score of each school is almost the same as the comprehensive evaluation score, which has certain accuracy and feasibility. It is proved that the RS-BP neural network model can be used in the evaluation of MCTE in other universities.

The MCTE core evaluation index and comprehensive evaluation model constructed in this paper provide a reference for university managers and teachers to improve the efficiency of multimedia teaching. In the multimedia classroom, the communication between teachers and students, teaching ability, and the artistry of courseware have the highest weight, which should also be the focus of universities. With the development of automatic speech

recognition and other technologies, teachers can combine courseware with emerging technologies, which can not only enhance their interest but also improve the effective communication between teachers and students.

MCTE evaluation is a means of teaching quality monitoring. Its purpose is to help teachers find out the advantages and disadvantages in teaching, make them develop their strengths and avoid their weaknesses in teaching, and constantly improve teaching, so as to achieve the goal of teaching and educating people. Teachers can analyze the current shortcomings through the evaluation results, adjust their knowledge structure and ability structure, and constantly improve their teaching methods and teaching quality. The ideal feedback time should be before the end of the final exam of the semester and the holiday, so that teachers can adjust and improve their teaching with reference to the feedback results when preparing the course of the next semester, so as to achieve an immediate effect. The school will adjust the training mode with the change of social needs for talents. Similarly, MCTE evaluation indicators should also comply with the development of the times and monitor and guide teachers' teaching quality.

5. Conclusion

The evaluation of multimedia teaching is a systematic and complex project. We should pay attention to the accuracy of content and the effectiveness and guidance of teaching, so as to scientifically and reasonably control the teaching progress and finally promote the construction of students' knowledge.

Based on the use process of multimedia in efficient classroom, this paper obtains 12 evaluation indexes suitable for MECT from the five dimensions of courseware, classroom, and teaching effect. After attribute reduction by RS theory, it is 7 core indexes, which reduces the input dimension of the BP neural network, saves training time, and has higher network convergence.

RS does not need a priori data, so it is used to determine the weight of core evaluation indexes, which effectively overcomes the problem of relying too much on the subjective weight of expert experience and knowledge in traditional evaluation methods. After RS evaluation, Hu and ST are rated as II. It is necessary to take improvement measures from the above seven evaluation indexes.

The practical application of the RS-BP neural network evaluation model in five typical colleges and universities in Hebei Province shows that the model has certain feasibility. The model can be applied to MCTE evaluation of other colleges and universities, help teachers obtain classroom performance, and play a guiding role in improving the overall effect of the course and students' achievement.

Due to the limitations of time, energy, and conditions, the research done in this paper still needs to be improved. In the future research, it is also necessary to conduct large-scale empirical research, modify, and improve the index system to make it more scientific, reasonable, and more suitable for teaching practice. Based on this research, we can also improve the multimedia technology combined with the

intelligent voice system, so as to improve the overall level of MCTE in universities.

Data Availability

The labeled datasets used to support the findings of this study are available from the corresponding author upon request.

Conflicts of Interest

The author declares no conflicts of interest.

Acknowledgments

This work was supported by the Liaoning Urban Construction Technical College.

References

- [1] X. Zhang and Q. Zhu, "Information-centric virtualization for software-defined statistical QoS provisioning over 5G multimedia big data wireless networks [J]," *IEEE Journal on Selected Areas in Communications*, no. 99, p. 1, 2019.
- [2] S. Zhao, M. Hu, Z. Cai, Z. Zhang, T. Zhou, and F. Liu, "Enhancing Chinese character representation with lattice-aligned attention," *IEEE Transactions on Neural Networks and Learning Systems*, pp. 1–10, 2021.
- [3] J. Akbarian, Sadraie, and M. Forozandeh, "Evaluation of Giardia lamblia genetic differences in Khorramabad city and surrounding villages by use of PCR and sequencing," *Mol. Liquids*, vol. 252, pp. 83–96, 2018.
- [4] J. Preparing, "Students for class: a clinical trial testing the efficacy between multimedia pre-lectures and textbooks in an economics course [J]," *Journal of College Teaching & Learning*, vol. 13, no. 2, p. 37, 2016.
- [5] D. Caballero, A. Caro, M. d M. Avila, P. Garcia Rodriguez, T. Antequera, and T. Perez Palacios, "New fractal features and data mining to determine food quality based on MRI," *IEEE Latin America Transactions*, vol. 15, no. 9, pp. 1777–1784, 2017.
- [6] L. Tao and M. Zhang, "Understanding an online classroom system: design and implementation based on a model blending pedagogy and HCI," *IEEE TRANSACTIONS ON HUMAN-MACHINE SYSTEMS*, vol. 43, no. 5, pp. 465–478, 2013.
- [7] M. Edwards, A. Rashid, and P. Rayson, "A systematic survey of online data mining technology intended for law enforcement," *ACM Computing Surveys*, vol. 48, no. 1, pp. 1–54, 2015.
- [8] N. Yang, "On-line classroom visual tracking and quality evaluation by an advanced feature mining technique [J]," *Signal Processing: Image Communication*, vol. 84, p. 115817, 2020.
- [9] G. Zhao, X. Qian, X. Lei, and T. Mei, "Service quality evaluation by exploring social users' contextual information," *IEEE Transactions on Knowledge and Data Engineering*, p. 1, 2016.
- [10] K. Li and S. B. Tsai, "An empirical study on the countermeasures of implementing 5G multimedia network technology in college education [J]," *Mobile Information Systems*, vol. 13, p. 2547648, 2021.
- [11] S. Hiary, I. Jafar, and H. Hiary, "An efficient multi-predictor reversible data hiding algorithm based on performance

- evaluation of different prediction schemes,” *Multimedia Tools and Applications*, vol. 76, no. 2, pp. 2131–2157, 2017.
- [12] X. Liu, H. Zhou, J. Xiang et al., “Energy and delay optimization of heterogeneous multicore wireless multimedia sensor nodes by adaptive genetic-simulated annealing algorithm,” *Wireless Communications and Mobile Computing*, vol. 2018, Article ID 7494829, 13 pages, 2018.
- [13] L. Y. B. Khedif, A. Engkamat, and S. Jack, “The evaluation of users’ satisfaction towards the multimedia elements in a courseware,” *Procedia - Social and Behavioral Sciences*, vol. 123, pp. 249–255, 2014.
- [14] T. Liu and S. Yin, “An improved particle swarm optimization algorithm used for BP neural network and multimedia courseware evaluation,” *Multimedia Tools and Applications*, vol. 76, no. 9, pp. 11961–11974, 2017.
- [15] T. K. Sheeja and A. S. Kuriakose, “A novel feature selection method using fuzzy rough sets,” *Computers in Industry*, vol. 97, pp. 111–116, 2018.
- [16] W. T. Ji, Y. Pang, and X. Y. Jia, “Fuzzy rough sets and fuzzy rough neural networks for feature selection: a review [J],” *Wiley Interdisciplinary Reviews- Data Mining and Knowledge Discovery*, vol. 11, no. 3, pp. 1–15, 2021.
- [17] X. Zhang, C. Mei, D. Chen, and Y. Yang, “A fuzzy rough set-based feature selection method using representative instances,” *Knowledge-Based Systems*, vol. 151, pp. 216–229, 2018.
- [18] S. Zhao, M. Hu, Z. Cai, and F. Liu, “Dynamic modeling cross-modal interactions in two-phase prediction for entity-relation extraction,” *IEEE Transactions on Neural Networks and Learning Systems*, pp. 1–10, 2021.

Research Article

The Construction of College Sports Culture Based on Intelligent Information Management Technology

Baihua Luo 

Henan Police College, Zhengzhou 450046, China

Correspondence should be addressed to Baihua Luo; lbh@hnp.edu.cn

Received 10 March 2022; Revised 13 April 2022; Accepted 27 April 2022; Published 11 May 2022

Academic Editor: Wei Liu

Copyright © 2022 Baihua Luo. This is an open access article distributed under the Creative Commons Attribution License, which permits unrestricted use, distribution, and reproduction in any medium, provided the original work is properly cited.

In order to improve the effect of sports culture construction in colleges and universities, this study combines intelligent information management technology to analyze the path of sports culture construction in colleges and universities and builds an intelligent system to assist the construction of sports culture in colleges and universities. Moreover, this study describes the oversampling SMOTE algorithm for imbalanced datasets, proposes specific problems that need to be solved to optimize the SMOTE algorithm, and provides a unified classification model for the classification of imbalanced datasets. In addition, this study constructs a college sports culture construction platform based on intelligent information management technology. According to the simulation research results, it can be seen that the college sports culture construction platform based on intelligent information management technology proposed in this study has a good sports culture construction effect.

1. Introduction

College sports culture has broad and narrow meanings. In a broad sense, college body culture refers to the sum of sports material and sports spirit created by students and teachers in the process of learning and living in the specific environment of colleges and universities. In a narrow sense, college sports culture is the sports wealth, sports value, sports essence, sports ability, and sports behavior jointly created by college teachers and students in practice [1]. College sports culture has formed a unique value in college culture, which has an irreplaceable role for college students to develop a correct concept of fitness and establish a lifelong awareness of physical exercise. Moreover, it has become a bright window for colleges and universities to disseminate college information, render college brands, and improve college functions and play an increasingly important role in the inheritance and development of college culture [2].

Information environment is information behavior, which usually refers to the sum of all natural and social factors related to human information activities. It mainly means that it occurs in the information environment and is influenced and restricted by the information environment

and, at the same time, affects and changes the information environment through its own initiative and creativity. There are many aspects to sports information. It mainly includes sports management and decision-making, sports teaching and training, sports competition and training, sports science and technology, sports economic industry, sports venue equipment, and sports spiritual civilization construction and many other aspects of information, as well as various sports news and other aspects [3].

The dissemination of college sports information promotes the formation of college sports culture by forming an information environment that relies on the participants in college sports activities. In this process, the influence of sports information environment on sports culture is manifested through its role in the cycle of campus sports culture. The information environment of college sports culture is an environment system composed of sports related information, language, and meaning. In the study of cultural representation by western scholars, “cultural circulation” is regarded as the main practice method of producing culture. This cycle has a regular effect on both the social cultural system and the subcultural system based on a specific group. The cycle of culture includes the identification of groups in a

specific culture, the rules of value, the production of culture, and group behavior, as well as the representation process of the abstract concept of culture in a specific way. The construction of the information environment in the sports culture of colleges and universities is the basic problem of how the meaning expression, the value norm, and the sports culture are represented at the behavioral level among the sports culture groups.

This study analyzes the path of college sports culture construction based on intelligent information management technology, constructs an intelligent system to assist the construction of college sports culture, and promotes the dissemination and development of college sports culture.

2. Related Work

Although there are many definitions of the concept of sports culture, it is still in the stage of a hundred schools of thought contending and a hundred flowers blooming. Different scholars and experts have their own opinions and views [4]. Thành et al. [5] explain campus sports culture as follows: “campus sports culture is based on the campus as the space, with the participation of students and teachers as the main body, with physical exercises as the means, and a variety of physical exercise programs as the main content, with unique performance, a form of group culture.” Petrov et al. [6] believe that campus sports culture can be expressed in various forms, including morning exercises, interclass exercises, after-school group activities, training of high-level sports teams, and small and diverse sports competitions, distinctive sports lectures and reports, sports skills performances, and school sports festivals. Hua et al. [7] put forward its own point of view on campus sports culture: “the real connotation of campus sports culture is to pursue the combination of sports and humanistic spirit, through participating in various sports activities, to have a healthy physique and sports ethics, and to form a harmonious social value. Concept: achieve the coordination and unity of spirit, ideal, morality, knowledge, personality, and body and guide students to become complete people in the true sense.” Aso et al. [8] believe that campus sports culture should be understood from four aspects. First is campus sports culture ideological. It contains the spirit of sports, that is, the spirit of struggle in life, the spirit of unity and cooperation, the spirit of mutual help and friendship, etc. Second is the materiality of campus sports culture. It contains various sports facilities and equipment on campus, students’ own sports equipment and clothing, etc. Third is the behavior (practice) of campus sports culture. It includes students’ various fitness activities, physical education, and sports competitions. Fourth is the dissemination of sports culture on campus which is inspirational, including the visual stimulation of students and the content of conversation. Campus sports culture is explained in the literature [9] as “campus sports culture is developed by the mutual influence, integration, penetration, and promotion of campus culture and sports culture and certain social politics, economy, culture, education, sports, etc. It is based on its conditions. It is the sum of sportsmanship and wealth jointly created by all

teachers, students, and employees in practice. It has profound connotations and rich denotations.” All definitions are only conditional and relative meanings and can never include connections to all aspects of a fully developed phenomenon. The above scholars have different definitions and expressions of the concept of campus sports culture, which to a certain extent shows that the definition of campus sports culture is still in the stage of improvement [10]. We can understand campus sports culture as follows: campus sports culture is the general goal of teachers, students, and employees in the specific environment of the school to complete the school’s teaching and training tasks. It takes physical exercise as the basic means and is manifested in various forms [11]. Sports culture is mainly based on the sports values of school teachers and students, as well as the material form, institutional form, and thinking form revealed by the implementation of these values. Campus sports culture is an important part of social culture. It is the product of mutual influence, fusion, penetration, and promotion of sports culture and campus culture. It belongs to a special and complex subculture form [12].

With the in-depth advancement of quality education and people’s new understanding of physical education, the school sports culture festival has been given a new historical mission, that is, to replace the traditional school sports meeting. As we all know, school sports meet is the best carrier to spread values and an effective means to stimulate students’ interest in sports. However, traditional school sports meet is influenced by the idea of competition-centered and only focuses on exploring human’s biological potential and pursuing human’s physiological limit. Catching less and releasing more, ignoring all students, thus depriving the majority of students the right to participate equally, obliterating the essential difference between competitive sports and school sports, and resulting in a misalignment of the school sports meeting so that a few people do and many people see, there is a strange phenomenon that most people have nothing to do. Therefore, there are misunderstandings in understanding and misunderstandings in operation in the traditional school sports meeting [13].

Zarkeshev and Csiszár [14] believe that the reason why sports is a culture is that sports culture is a unique way for human beings to grasp the world, a compound condition for the existence of human society, and an intermediary system for human self-relatedness. The most basic means of sports is to recreate human body functions through physical activities, thereby improving human beings themselves. Secondly, sports create dual conditions for people’s survival and development needs by improving people’s physical and mental development and improving people’s ability to control nature. McNally et al. [15] believe that sports culture not only is the core of sports, the fundamental way, and the method of physical and mental exercise and entertainment but also accompanied by the way of economic activities and business operations, political and diplomatic activities, sports literature and art activities, media communication and news, sports venues and equipment and other cultural phenomena, and prominent and unique human culture. Sports culture can be summarized through the origin,

development, and inheritance of sports culture. Hwang and Choi [16] emphasize that sports culture is a set of the normative system and the value system established on the basis of various social sports activities. The content of people's needs for sports, ideas, theoretical methods, and other ideological forms and various sports activities externalized in the real world, as well as the organizational forms of activities, the norms of activities, and the facilities are composed, including a variety of complex spiritual and material factors. Overall, Korniyenko and Galata [17] wrote sports activities usually serve people for a long time in the form of direct feelings and deep impressions. It belongs to the dynamic mode of sports venue construction and other forms. It is a static way to covertly transmits sports cultural information to teachers and students, which contains great ability and continues to influence the sports behavior of teachers and students.

3. Intelligent Information Management Technology

When processing an imbalanced dataset, the oversampling method balances the dataset by increasing the number of samples in the minority class dataset to improve the processing effect of the imbalanced dataset. The SMOTE algorithm conducts data-level research on imbalanced datasets and achieves very good conclusions. Its theoretical framework and main points are introduced in the following.

We assume that a dataset (training sample) has two types of data (the reality is far more complicated than this; we only take the simplest case as an example). If the numbers between the two types of data are basically similar and the boundaries are clear, it is called a balanced dataset. A plot of the balanced dataset represented by a 2D plane is shown in Figure 1(a).

From Figure 1(a), we can see that the number of a type of data represented by a circle is basically similar to that of a type of data represented by a five-pointed star, and the boundaries between the two are clear and easy to distinguish. Such datasets are called balanced datasets.

If the number of one type of data in the dataset is much more than the number of another type of data, we call the type of data with a larger number of data as the majority class sample (generally also called the negative class sample). However, a class of data with a small number of data is called a minority class sample (generally can also be called a positive class sample). It can be seen that the imbalanced dataset is that the number of a certain type of data in the dataset is far less than the number of data contained in other types of data. The two-dimensional representation of this association for an imbalanced dataset is shown in Figure 1(b).

From Figure 1(b), we can see that, in the imbalanced dataset, there is a large gap in the amount of data between the two types of data. The data of the minority class are far less than the data of the majority class, and the boundaries between the data classes are often unclear (as shown in Figure 1(b), the two types of data in the square have

intersection), which increases the difficulty of data classification.

The main purpose of the SMOTE algorithm is to balance the dataset by increasing the number of minority class samples. The basic idea is described as follows.

We assume an imbalanced dataset, and for each data sample X in the minority class sample, search its nearest neighbor K samples (the K nearest neighbor samples belong to the minority class sample). We assume that the upsampling ratio of the dataset is n ; then, randomly select n samples from the K nearest neighbor samples (there must be $K > n$) and record these n samples as y_1, y_2, \dots, y_n . The associated data samples X and y_i are subjected to the corresponding random interpolation operation through the association formula between X and y_i ($i = 1, 2, \dots, n$), and the interpolation sample p_i is obtained. In this way, for each data sample, n corresponding minority class samples are constructed.

The interpolation formula is shown as follows [18]:

$$p_i = X + \text{rand}(0, 1) * (y_i - X), \quad i = 1, 2, \dots, n, \quad (1)$$

where X represents the data sample in the minority class, $\text{rand}(0, 1)$ represents a random number in the interval $(0, 1)$, and y_i represents the i th of the n nearest neighbors of the data sample X .

The sampling ratio n depends on the imbalance degree of the dataset, which calculates the imbalance level (IL) between the majority class and the minority class of the dataset. The calculation formula of sampling ratio n is shown as

$$n = \text{round}(\text{IL}), \quad (2)$$

where $\text{round}(\text{IL})$ represents the value obtained by rounding IL. Through the above interpolation operation, the majority class samples and minority class samples can be effectively balanced, thereby improving the classification accuracy of imbalanced datasets.

Formula (1) can be interpreted with a simple example, which has appeared in many literature studies. We assume a two-dimensional dataset and take one of the data sample points X ; its coordinate point is $(9, 5)$, the random value of $\text{rand}(0, 1)$ is set to 0.6, and the coordinate value of a nearest neighbor sample point y_3 of X is set to $(3, 7)$. The representation of the data sample X and its K nearest neighbors is shown in Figure 2.

From Figure 2, we know that the 5 nearest neighbor data samples of the data sample $X(9, 5)$ are $(y_1, y_2, y_3, y_4, y_5)$, and now, the sampling operation is performed between X and the nearest neighbor y_3 .

Then, according to formulas (1) and (2), we can obtain [19]

$$\begin{aligned} p_3 &= X + \text{rand}(0, 1) * (y_3 - X), \\ &= (9, 5) + 0.6 * ((3, 7) - (9, 5)), \\ &= (9, 5) + (-3.6, 1.2), \\ &= (5.4, 6.2). \end{aligned} \quad (3)$$

That is, our constructed interpolation is $P_3(5.4, 6.2)$.

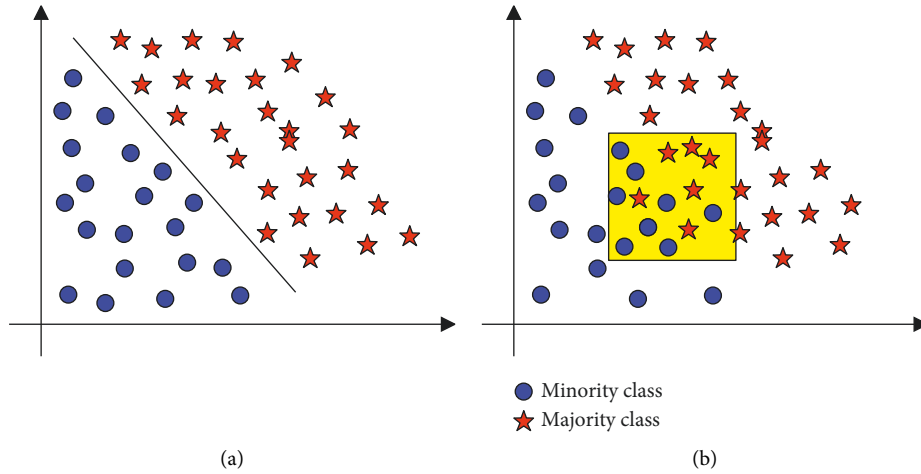


FIGURE 1: Representation of the dataset. (a) Representation diagram of the balanced dataset. (b) Representation diagram of imbalanced dataset.

The entire interpolation process of constructing new data is represented on the two-dimensional coordinate axis, as shown in Figure 3.

From Figure 3, we can see that the sampling of the SMOTE algorithm is to perform random interpolation on the connection between the data sample point X and its nearest neighbor data sample. This approach can be thought of as linear interpolation, but is a huge improvement over simply duplicating the original data samples.

We go on to introduce a more obviously imbalanced dataset. We assume that there are 25 samples in the majority class and 7 samples in the minority class in this dataset. The data distribution of the dataset is shown in Figure 4(a) [20].

As can be seen from Figure 4(a), in the imbalanced dataset, there is a large gap between the majority class samples and the minority class samples. If data classification is performed in this case, it will seriously reduce the accuracy of data classification. Therefore, we need to use the SMOTE algorithm to oversample the unbalanced data. According to the basic principle of the SMOTE algorithm and formula (2), we know that the sampling ratio of the algorithm is 4 so that the minority class samples can reach the same number of data as the majority class samples. We take one of the points as an example, and the result after processing by the SMOTE algorithm is shown in Figure 4(b).

In Figure 4(b), circles represent minority classes, squares represent majority classes, and triangles represent synthetic data. From the figure, we can see that if an original data sample is selected for the interpolation operation of its nearest neighbors, all the interpolations are on a certain connection line between the original sample and its nearest neighbor.

Figure 4(c) shows the result after the entire minority class dataset is processed. It can be seen from Figure 4(c) that the minority class and the majority class basically reach a balance. Due to the sampling ratio, the minority class has more data samples than the majority class, which means that, after the minority class is oversampled, the

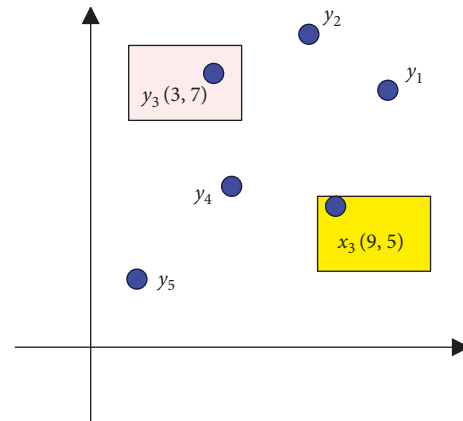


FIGURE 2: Representation of data sample X and its K nearest neighbors.

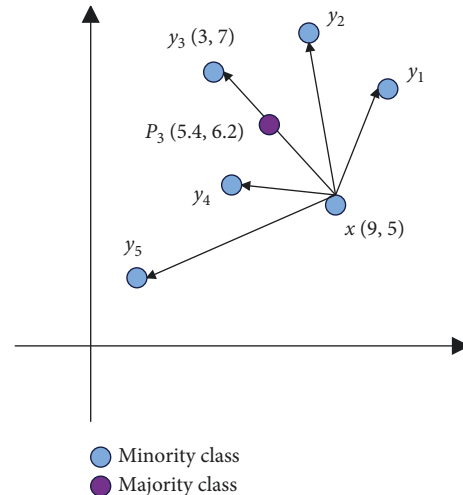


FIGURE 3: Interpolation principle of SMOTE algorithm.

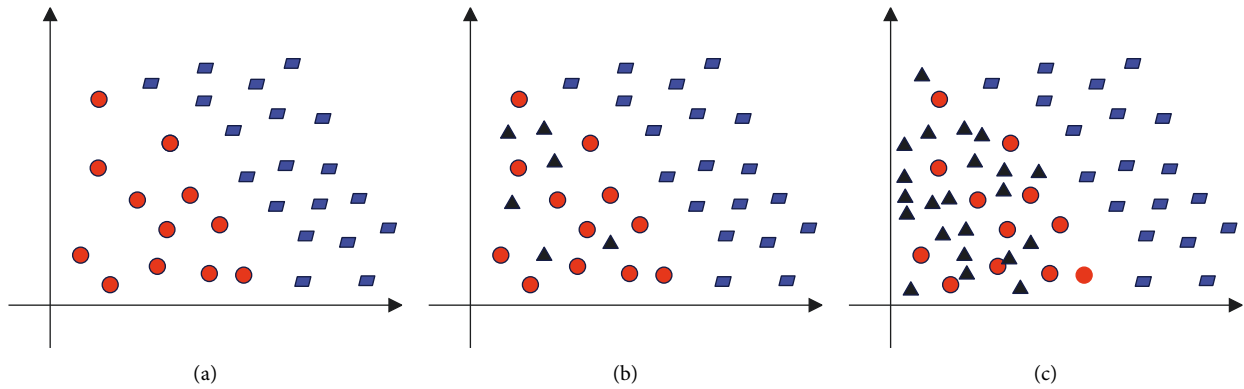


FIGURE 4: Example of a dataset. (a) Example of imbalanced dataset. (b) Oversampling of a data. (c) Complete oversampling.

oversampled dataset needs to be processed to make the dataset reasonable.

Through the basic theory of the SMOTE algorithm and the analysis of the imbalanced dataset before oversampling, it can be seen that the SMOTE imbalanced data oversampling algorithm is mainly improved from the following two points:

- (1) It reduces the limitations and blindness of the SMOTE unbalanced data oversampling algorithm in the sampling process. The previous sampling method of the SMOTE algorithm was a random upsampling method, which can balance the dataset, but due to the serious lack of principles of random sampling, the sampling effect is not ideal. The SMOTE unbalanced data oversampling algorithm uses the basic mathematical theory of linear interpolation. For the data sample x , it selects the K samples of its nearest neighbors and then constructs the data purposefully according to certain mathematical rules, which can effectively avoid blindness and limitations.
- (2) The phenomenon of overfitting is effectively reduced. The traditional oversampling technique adopts the method of duplicating data, which leads to overfitting due to the reduction of the decision domain during the sampling process. The SMOTE algorithm can effectively avoid this defect.

However, although the SMOTE algorithm has been greatly improved over the previous oversampling method, there are still some shortcomings to be improved, which are embodied in the following three aspects:

(1) The validity of interpolation: considering the criticality of the K nearest neighbor samples of the SMOTE algorithm, if there are some sample hash points, the interpolated sample will appear in the middle of the hash points. This calls into question the validity of the interpolated samples, as shown in Figure 5.

It can be seen from Figure 5 that, among the synthetic samples p_1 and p_2 , p_1 is a relatively reasonable synthetic sample, but the validity of p_2 is still open to question. p_2 is in the data range of most classes; this kind of synthetic data will

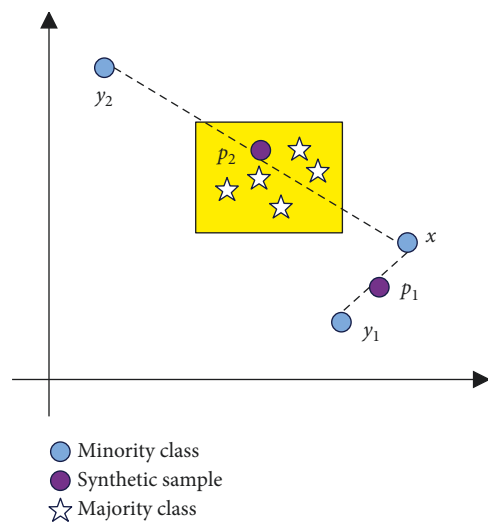


FIGURE 5: Effectiveness of interpolation.

not only fail to improve the classification accuracy of the data but also will become the noise of the dataset, which will seriously affect the classification of the dataset.

(2) Fuzzy positive and negative class boundaries: if a negative class sample is on the edge of a minority class dataset, performing SMOTE interpolation may result in a nearby “artificial” sample that is also on the edge. Moreover, due to the randomness of K nearest neighbor interpolation, this marginalization will gradually increase, thereby blurring the positive and negative class boundaries, as shown in Figure 6(a).

From Figure 6(a), we can see that because a minority class sample is an edge sample, with the increase of synthetic data, this edge data become more and more, and finally, the boundary between the minority class and the majority class is gradually blurred.

(3) The distribution of minority class data is affected. For some minority data, there is a certain distribution pattern, and the SMOTE algorithm will gradually blur this distribution, causing the distribution pattern of the dataset to be changed. The SMOTE algorithm operates on all minority class samples. When there is an outlier problem, if this

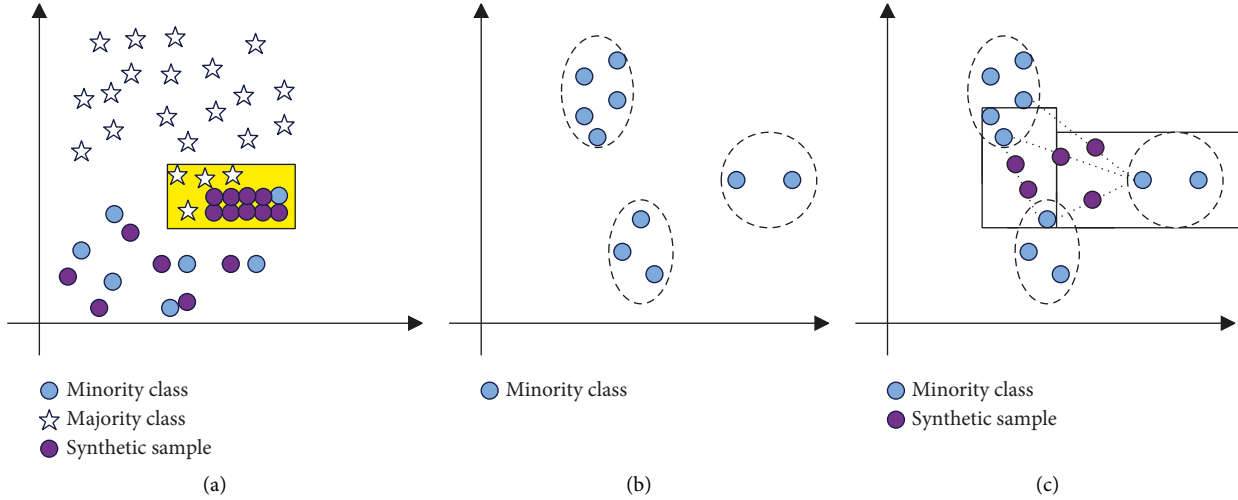


FIGURE 6: Data sample distribution. (a) Fuzzy positive and negative class boundaries. (b) Minority class samples. (c) Data distribution after oversampling.

particularity is not considered, it is difficult to avoid the influence of noise on the minority class classification effect, as shown in Figure 6(b).

From Figure 6(b), we can see that the minority class forms an obvious data distribution pattern. If the SMOTE algorithm is used to oversample it, the situation shown in Figure 6(c) may occur.

From Figure 6(c), we can see that the obvious distribution pattern of the data that existed before is gradually blurred by the synthetic data, which will lead to deviations in the distribution pattern of the minority data, or even be completely changed, and ultimately affect the classification effect of the data.

The above is a brief overview and analysis of the SMOTE algorithm. The following will focus on clustering and random forest. Euclidean distance, is a commonly used definition of distance. The calculation formula of Euclidean distance is as follows.

The Euclidean distance between two points $a(x_1, y_1)$ and $b(x_2, y_2)$ on a two-dimensional plane is shown as

$$d_{ab} = \sqrt{(x_1 - x_2)^2 + (y_1 - y_2)^2}. \quad (4)$$

The Euclidean distance between two points $a(x_1, y_1, z_1)$ and $b(x_2, y_2, z_2)$ in three-dimensional space is shown as

$$d_{ab} = \sqrt{(x_1 - x_2)^2 + (y_1 - y_2)^2 + (z_1 - z_2)^2}. \quad (5)$$

The Euclidean distance between two n -dimensional vectors $a(x_{11}, x_{12}, \dots, x_{1n})$ and $b(x_{21}, x_{22}, \dots, x_{2n})$ is shown as

$$d_{ab} = \sqrt{\sum_{k=1}^n (x_{1k} - x_{2k})^2}. \quad (6)$$

In this study, the K-means algorithm combined with the SMOTE algorithm is selected among many clustering algorithms to preprocess the imbalanced dataset. Studies have

shown that this combination can effectively make up for the shortcomings of the SMOTE algorithm and improve the classification accuracy of unbalanced data. Next, we will briefly introduce and analyze the K-means clustering algorithm.

For a set of test datasets $\{x_1, x_2, \dots, x_n\}$, each test data is an h -dimensional vector. If k data are taken from the dataset by a specific method as the starting cluster center, each data point represents a cluster; there are k clusters $\{c_1, c_2, \dots, c_k\}$ in total. The degree of relationship between other arbitrary test data $p \in c_i$, ($i = 1, 2, \dots, k$) and the cluster is represented by Euclidean distance so that the classification process satisfies $\min_c \sum_{i=1}^k \sum_{x_j \in c_i} \|x_j - u_i\|^2$, where u_i is the cluster center of c_i .

After obtaining the complete k clusters, it recalculates the cluster center and replaces the original cluster center with it and repeats the above process until the maximum number of iterations is reached or the difference between the two Euclidean distances is less than a given threshold.

There are two points worth paying attention to in this algorithm: one is the selection of the k value and the other is the placement of random cluster centers.

Random forests are learning models used to solve prediction problems. Based on G decision trees, a random forest is generated using an ensemble learning model, and each decision tree is a basic classifier. The entire classification result will be voted based on the classification results of different decision trees and then will be output by random forest.

The description of G decision trees is shown as

$$\{h(X, \theta_k), \quad k = 1, 2, \dots, G\}, \quad (7)$$

where G is the number of decision trees contained in the random forest and $\{\theta_k\}$ represents an independent and identically distributed random vector. For the white variable X , G decision trees will be classified, and then, the optimal classification result will be selected. The classification result is shown as

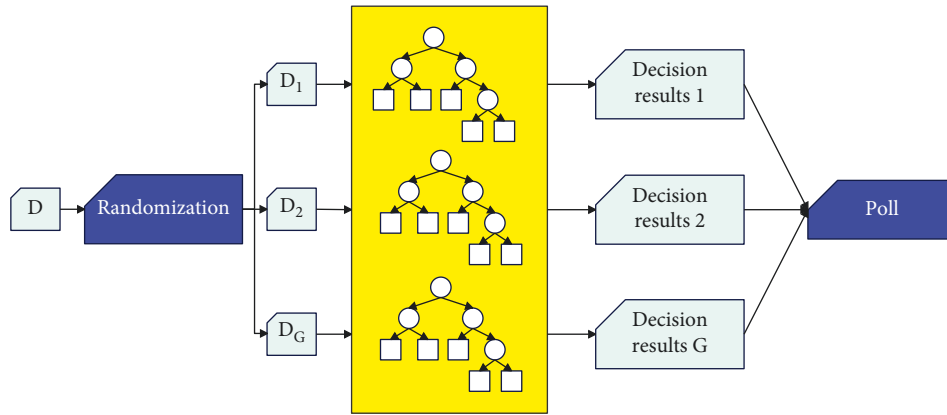
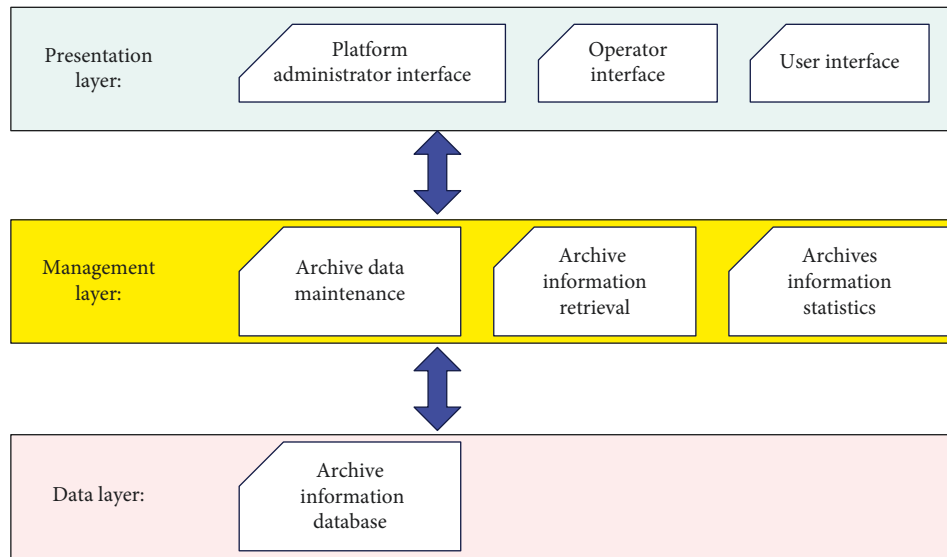
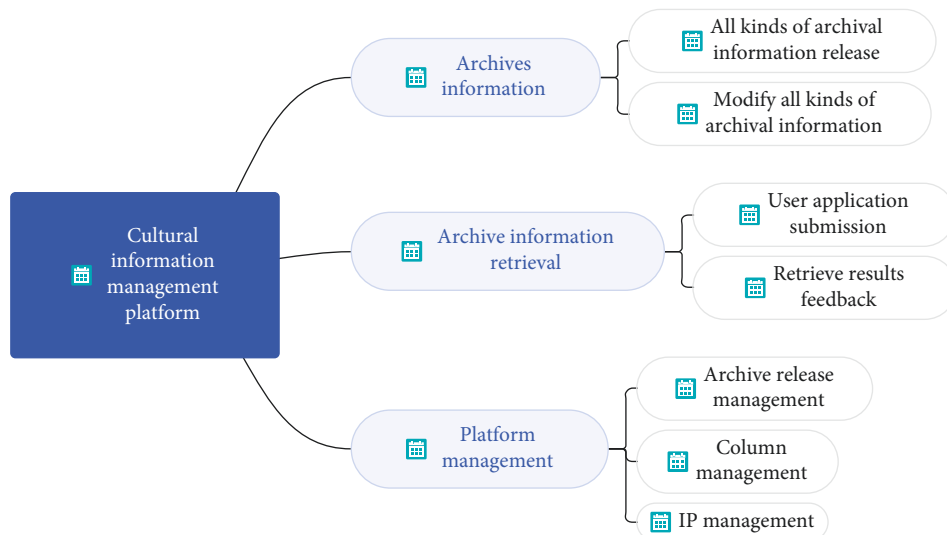


FIGURE 7: Classification structure diagram of random forest.



(a)



(b)

FIGURE 8: College sports culture construction platform based on intelligent information management technology. (a) System structure construction diagram. (b) Functional module structure diagram.

TABLE 1: The effect of intelligent information management of sports culture.

Number	Cultural management	Number	Cultural management	Number	Cultural management
1	78.28	24	76.11	47	74.25
2	75.81	25	66.42	48	78.25
3	67.50	26	75.96	49	73.22
4	68.88	27	71.61	50	72.89
5	71.59	28	74.32	51	76.02
6	76.45	29	69.03	52	76.89
7	77.10	30	74.28	53	71.40
8	78.40	31	69.07	54	71.82
9	69.91	32	74.26	55	69.21
10	76.44	33	66.84	56	69.85
11	74.30	34	78.25	57	66.56
12	68.93	35	73.15	58	78.94
13	77.59	36	69.35	59	75.77
14	68.57	37	67.40	60	77.79
15	78.10	38	69.28	61	73.06
16	68.63	39	76.91	62	73.09
17	69.07	40	69.30	63	77.78
18	71.82	41	75.34	64	73.02
19	66.20	42	73.65	65	75.13
20	70.83	43	76.06	66	71.71
21	77.72	44	71.41	67	71.14
22	72.53	45	68.41	68	77.27
23	73.00	46	72.18		

$$G(x) = \operatorname{argmax}_Y \sum_{i=1}^k I(h_i(x) = Y), \quad (8)$$

where $G(x)$ represents the overall random forest model, and the final result is given by voting, and $I(*)$ is the indicative function of the classifier. The overall classification model represents a single classification model of a decision tree through an indicative function. h_i represents a single classification model, and Y is the output variable of the decision tree classification result.

For random forest, its training and classification process can be regarded as a collection of multiple decision tree training and classification. In the process of training and classification, it can be said that the decision trees are independent of each other, so their training and classification are also independent of each other, which enables parallel design to reduce program time. The decision diagram of random forest is shown in Figure 7.

From Figure 7, we can see that the random forest randomly samples the training data and finally establishes the relevant decision tree model. Moreover, it classifies the test data by establishing G decision tree models, obtains G decision results, and votes the G decision results to obtain the final classification result.

4. The Construction of College Sports Culture Based on Intelligent Information Management Technology

The platform design includes a three-layer framework of presentation layer, management layer, and data layer. The presentation layer includes administrators, operators, and ordinary users to meet the different requirements of various

users. The management layer includes archive data maintenance, archive information retrieval, and archive information statistics, which is the technical core of the platform, responsible for managing and maintaining the data security of various archive information of sports culture and reviewing user identities and retrieval access rights. The data layer refers to the database of various archives' information of sports culture, which is the core of the data information of the platform. The three-layer frame structure relies on each other to form an organically connected whole, which promotes the benign operation and sustainable development of the platform, as shown in Figure 8(a).

The platform management module is mainly used for system maintenance of various functions of the platform. It mainly includes file publisher management, column management, and IP management. Among them, file publisher management refers to the setting and maintenance of the file publisher's file information publishing authority. Column management is mainly used for the management, maintenance, and statistics of the file information of each column section of the platform. IP management is mainly responsible for reviewing the eligibility review and screening of readers and users to visit the platform to check and submit messages to ensure the security of the platform (Figure 8(b)).

After constructing the above system platform, this study evaluates the effect of the college sports culture construction platform based on intelligent information management technology and counts the effect of intelligent information management of sports culture and the effect of sports culture construction. The results shown in Tables 1 and 2 are obtained.

From the above research, we can see that the college sports culture construction platform based on intelligent

TABLE 2: The effect of sports culture construction.

Number	Cultural construction	Number	Cultural construction	Number	Cultural construction
1	74.40	24	74.52	47	78.24
2	75.92	25	74.18	48	75.99
3	81.29	26	77.56	49	77.09
4	81.72	27	77.11	50	77.49
5	74.89	28	74.95	51	75.50
6	80.34	29	81.47	52	80.92
7	80.84	30	81.80	53	76.10
8	81.51	31	79.00	54	79.02
9	79.32	32	78.40	55	75.33
10	80.22	33	79.06	56	77.02
11	81.55	34	80.99	57	78.35
12	80.32	35	80.39	58	81.38
13	80.38	36	77.29	59	76.66
14	74.53	37	75.32	60	75.86
15	80.76	38	75.92	61	74.29
16	77.25	39	79.48	62	77.83
17	75.63	40	75.05	63	81.12
18	80.68	41	79.68	64	77.78
19	78.39	42	76.47	65	81.63
20	76.01	43	81.01	66	80.42
21	76.10	44	80.35	67	77.09
22	79.81	45	80.24	68	78.63
23	76.01	46	79.93		

information management technology proposed in this study has a good sports culture construction effect.

5. Conclusion

Good college sports communication channels will play a positive role in promoting the construction of college sports culture. Moreover, good publicity and promotion is an important carrier for inheriting college sports culture. Through multichannel, multiperspective, three-dimensional, and all-round systematic publicity, it is more conducive to promote the integration of college sports and culture, so as to form a rapid and effective communication of college sports culture. At the same time, college sports culture has a special environment. It takes teachers and students as the main body and physical exercises as the main means. Only by continuously promoting the selection and reconstruction between campus sports and campus culture, it can continuously build itself and gather the “intersection point” of the integration of the two. This intersection should not only show the manifestation of campus culture but also reflect the important content of college sports culture. This study analyzes the path of college sports culture construction based on intelligent information management technology and builds an intelligent system to assist the construction of college sports culture. The research results show that the college sports culture construction platform based on intelligent information management technology proposed in this study has a good sports culture construction effect.

Data Availability

The labeled dataset used to support the findings of this study are available from the corresponding author upon request.

Conflicts of Interest

The author declares that they have no conflicts of interest.

Acknowledgments

This study was sponsored by Henan Police College.

References

- [1] J. Xu, K. Tasaka, and M. Yamaguchi, “[Invited paper] fast and accurate whole-body pose estimation in the wild and its applications,” *ITE Transactions on Media Technology and Applications*, vol. 9, no. 1, pp. 63–70, 2021.
- [2] G. Szűcs and B. Tamás, “Body part extraction and pose estimation method in rowing videos,” *Journal of Computing and Information Technology*, vol. 26, no. 1, pp. 29–43, 2018.
- [3] R. Gu, G. Wang, Z. Jiang, and J.-N. Hwang, “Multi-person hierarchical 3d pose estimation in natural videos,” *IEEE Transactions on Circuits and Systems for Video Technology*, vol. 30, no. 11, pp. 4245–4257, 2020.
- [4] M. Nasr, R. Osama, H. Ayman, N. Mosaad, N. Ebrahim, and A. Mounir, “Realtime multi-person 2D pose estimation,” *International Journal of Advanced Networking and Applications*, vol. 11, no. 06, pp. 4501–4508, 2020.
- [5] N. T. Thành, L. V. Hùng, and P. T. Công, “An evaluation of pose estimation in video of traditional martial arts presentation,” *Journal of Research and Development on Information and Communication Technology*, vol. 2019, no. 2, pp. 114–126, 2019.
- [6] I. Petrov, V. Shakhuro, and A. Konushin, “Deep probabilistic human pose estimation,” *IET Computer Vision*, vol. 12, no. 5, pp. 578–585, 2018.
- [7] G. Hua, L. Li, and S. Liu, “Multipath affinity stacked-hourglass networks for human pose estimation,” *Frontiers of Computer Science*, vol. 14, no. 4, pp. 144701–144712, 2020.

- [8] K. Aso, D. H. Hwang, and H. Koike, "Portable 3D human pose estimation for human-human interaction using a chest-mounted fisheye camera," in *Proceedings of the Augmented Humans Conference 2021*, pp. 116–120, Finland, February 2021.
- [9] D. Mehta, S. Sridhar, O. Sotnychenko et al., "VNect," *ACM Transactions on Graphics*, vol. 36, no. 4, pp. 1–14, 2017.
- [10] S. Liu, Y. Li, and G. Hua, "Human pose estimation in video via structured space learning and halfway temporal evaluation," *IEEE Transactions on Circuits and Systems for Video Technology*, vol. 29, no. 7, pp. 2029–2038, 2019.
- [11] S. Ershadi-Nasab, E. Noury, S. Kasaei, and E. Sanaei, "Multiple human 3d pose estimation from multiview images," *Multimedia Tools and Applications*, vol. 77, no. 12, pp. 15573–15601, 2018.
- [12] X. Nie, J. Feng, J. Xing, S. Xiao, and S. Yan, "Hierarchical contextual refinement networks for human pose estimation," *IEEE Transactions on Image Processing*, vol. 28, no. 2, pp. 924–936, 2019.
- [13] Y. Nie, J. Lee, S. Yoon, and D. S. Park, "A multi-stage convolution machine with scaling and dilation for human pose estimation," *KSII Transactions on Internet and Information Systems (TIIS)*, vol. 13, no. 6, pp. 3182–3198, 2019.
- [14] A. Zarkeshev and C. Csiszár, "Rescue method based on V2X communication and human pose estimation," *Periodica Polytechnica: Civil Engineering*, vol. 63, no. 4, pp. 1139–1146, 2019.
- [15] W. McNally, A. Wong, and J. McPhee, "Action recognition using deep convolutional neural networks and compressed spatio-temporal pose encodings," *Journal of Computational Vision and Imaging Systems*, vol. 4, no. 1, p. 3, 2018.
- [16] K. Hwang and M. Choi, "Effects of innovation-supportive culture and organizational citizenship behavior on e-government information system security stemming from mimetic isomorphism," *Government Information Quarterly*, vol. 34, no. 2, pp. 183–198, 2017.
- [17] B. Y. Korniyenko and L. P. Galata, "Design and research of mathematical model for information security system in computer network," *Наукоемні технології*, no. 2, pp. 114–118, 2017.
- [18] X. Tan, S. Su, Z. Huang et al., "Wireless sensor networks intrusion detection based on smote and the random forest algorithm," *Sensors*, vol. 19, no. 1, p. 203, 2019.
- [19] A. Blagorzumov, P. Chernikov, G. Glukhov, A. Karapetyan, V. Shapkin, and L. Elisov, "The background to the development of the information system for aviation security oversight in Russia," *International Journal of Mechanical Engineering & Technology*, vol. 9, no. 11, pp. 341–350, 2018.
- [20] M. K. Özlen and I. Djedovic, "Online banking acceptance: the influence of perceived system security on perceived system quality," *Journal of Accounting and Management Information Systems*, vol. 16, no. 1, pp. 164–178, 2017.

Research Article

Evaluation of Urban Park Landscape Satisfaction Based on the Fuzzy-IPA Model: A Case Study of the Zhengzhou People's Park

Lei Feng  and Jie Zhao

Department of Architecture, Henan Technical College of Construction, Zhengzhou 45000, Henan, China

Correspondence should be addressed to Lei Feng; felix2009@126.com

Received 5 March 2022; Revised 16 April 2022; Accepted 26 April 2022; Published 10 May 2022

Academic Editor: Xuefeng Shao

Copyright © 2022 Lei Feng and Jie Zhao. This is an open access article distributed under the Creative Commons Attribution License, which permits unrestricted use, distribution, and reproduction in any medium, provided the original work is properly cited.

Based on the fuzzy comprehensive evaluation theory, a continuous triangular fuzzy quantitative landscape satisfaction evaluation index is used to comprehensively evaluate the landscape satisfaction of Zhengzhou People's Park. By using the factor analysis method to determine the weight of the evaluation index, an index system of urban park landscape satisfaction evaluation is constructed. And the important expression performance quadrant analysis of the landscape satisfaction evaluation index is combined with the IPA analysis method to propose the improvement of urban park landscape satisfaction. The fuzzy-IPA combination model provides a new way for the satisfaction evaluation of urban park landscape.

1. Introduction

Greenland of urban park is an important part of the urban green space system and ecological infrastructure, as well as an important place for public leisure and recreation [1]. The current sustained and rapid economic growth has accelerated the urbanization process and the construction of urban parks which have developed rapidly. As an important indicator to measure the level of landscape quality in urban parks, landscape satisfaction directly reflects the public's recognition of the park landscape [2]. At present, foreign research on satisfaction evaluation mainly constructs evaluation models to measure through expectation differences, service quality and performance, and nondifferential scores [3]; the quantitative research on satisfaction evaluation in China mainly uses methods, such as hierarchical analysis [4], grey correlation analysis [5], neural network analysis [6], and factor analysis. Satisfaction evaluation of urban park landscape is a comprehensive evaluation combining qualitative and quantitative aspects. As the evaluation index of park landscape is featured with multiobjective and compound attributes, the objectivity of landscape and the subjectivity of landscape cognition [7–9] shall be considered during the evaluation process. A scientific and reasonable

satisfaction evaluation of urban park landscape can help to improve the overall landscape quality of urban parks.

Fuzzy comprehensive evaluation uses fuzzy mathematics theory to make an overall evaluation of things or objects that are affected by multiple factors [10]. The fuzzy mathematical algorithm is used for quantitative evaluation to provide a basis for correct decision-making, and it is suitable for solving various nondeterministic problems [11]. There is subjectivity, randomness, and fuzziness in the perception of evaluation indicators by respondents in the process of landscape satisfaction evaluation, while the change levels of evaluation indicators are usually expressed by discrete values, such as the Likert attitude scale, ignoring the continuity between changes [12]. In the fuzzy comprehensive evaluation, the rating of evaluation indicators is nondiscrete; there is a continuous buffer area and the evaluation scores show “ambiguous” in the fuzzy region [13, 14]. Proposed by Martilla and James in 1977 [15], importance-performance analysis (IPA) is a simple, intuitive, and easy-to-use method that is widely used in quality assessment in various services and will be more widely used in the development and application of tourism field. The IPA analysis method simply compares the importance of each impact factor with the actual satisfaction of the audience and analyzes the real evaluation results of these impact factors.

This study uses continuous triangular fuzzy numerical values to quantify comments based on the triangular fuzzy evaluation theory, converts the triangular fuzzy evaluation values of landscape satisfaction indicators into logical values based on the de-fuzzy rule, constructs the evaluation index system of urban park landscape satisfaction with factor analysis, determines the weights of evaluation indicators, and derives quadrant analysis of the satisfaction value and the weight value of evaluation indicators by combining with importance-performance analysis (IPA), the optimization, management, and sustainability of urban park landscape in the future provides scientific guidance that combines quantitative and qualitative.

2. Overview of the Study Area

Zhengzhou People's Park is located on the west of North Erqi Road in the center of the city, and it is built after liberation on the basis of Peng Gong Ancestral Hall and Hu Gong Ancestral Hall, with an advantageous geographical location and convenient transportation around. The park covers an area of 30.14 hectares, including 3.37 hectares of water bodies and 25.41 hectares of green space, with a green space ratio of 83.2% and a green coverage rate of 92.5%. It consists of 11 scenic spots, such as the Bonsai Garden, Magnolia Garden, *Begonia* Garden, Peony Garden, European Garden, Cherry Garden, and Bamboo Garden, and is the largest comprehensive park in the downtown area of Zhengzhou. The park is rich in vegetation and has a natural environment, a large area of garden landscapes. Its planning and design focus on the inheritance of history and culture and the use of Chinese gardening techniques, with a reasonable layout and complete functions, making it an important place for public leisure and entertainment.

3. Research Methodology and Data Source

3.1. Questionnaire Design and Sample Analysis. The design of the questionnaire mainly includes three parts: the first part is the basic information of the respondents, including gender, age, education, occupation; the second part is the evaluation variable survey based on triangular fuzzy judgment; the third part is the urban park landscape satisfaction evaluation index system and overall satisfaction. Satisfaction evaluation indicators and overall satisfaction were measured using 5-level comment variables: very satisfied (VS), satisfied (S), fair (F), unsatisfied (US), and very unsatisfied (VUS).

After designing, the questionnaire was distributed on the online platforms. Fifty questionnaires were randomly selected from the returned questionnaires for pre-survey, and the results were fed back into the detailed design of the questionnaire and the revision and improvement of the questions to form the final questionnaire. The questionnaire was distributed at the east, west, and south gates of Zhengzhou People's Park to the public who came to the park from 5 to 8 December 2020. A total of 230 questionnaires were distributed and 203 were returned, of which 186 were valid, with an efficiency rate of 91.6%. The

statistical analysis showed that 47.3% of the respondents were male and 52.7% were female, mainly young- and middle-aged people with relatively high education level, and 62.4% of the respondents had obtained college education or above.

3.2. Fuzzy Comprehensive Evaluation of Questionnaire Rubric Variables. The triangular fuzzy values were used in the questionnaire to describe the rubric variables and classified the rubric variables into five evaluation levels [16]: very satisfied (VS), satisfied (S), fair (F), unsatisfied (US), and very unsatisfied (VUS) (Figure 1).

Due to the variability of the respondents in terms of gender, age, occupation, and education, their perceived judgments of the comment variables were not exactly the same. The law of fuzzification (equation 1) was applied to calculate the mean triangular fuzzy values of the respondents' descriptions of the comment variables in the valid questionnaire as the respondents' perceived levels of the comment variables (Table 1):

$$\begin{aligned}\widetilde{A}_k &= \frac{\sum_{i=1}^n \widetilde{A}_k^i}{n} \\ &= \frac{(\sum_{i=1}^n a_{k1}^{(i)}, a_{k2}^{(i)}, a_{k3}^{(i)})}{n}, \quad i = 1, 2, 3, \dots, n; k = 1, 2, 3, 4, 5,\end{aligned}\quad (1)$$

where \widetilde{A}_k denotes the triangular fuzzy value of the k th variable, \widetilde{A}_k^i denotes the perceived level of the k th variable by the i th respondent, $a_{k1}^{(i)}$, $a_{k2}^{(i)}$, and $a_{k3}^{(i)}$ denote the low, medium, and high values of the triangular fuzzy value, respectively, n denotes the number of respondents, and k denotes the number of comment variables.

3.3. Evaluation of Evaluation Indicators and Overall Satisfaction. Based on the triangular fuzzification of the comment variables, the law of fuzzification (Eq. 2 and Eq. 3) was applied to make overall evaluation to the evaluation indicators and overall landscape satisfaction in combination with the results of the valid questionnaire, whose triangular fuzzy values were defuzzified (Eq. 4), and the weighted average method was applied to calculate the triangular fuzzy values and logical values of the item layer (Table 2):

$$\begin{aligned}\widetilde{A}_j &= \frac{\sum_{i=1}^n \widetilde{A}_j^i}{n} = \frac{(\sum_{i=1}^n a_{j1}^{(i)}, a_{j2}^{(i)}, a_{j3}^{(i)})}{n}, \quad i = 1, 2, 3, \dots, n; \\ & \quad j = 1, 2, 3, 4, 5,\end{aligned}\quad (2)$$

where \widetilde{A}_j denotes the triangular fuzzy value of the j th evaluation indicator, \widetilde{A}_j^i denotes the i th respondent's perception of the j th evaluation indicator, $a_{j1}^{(i)}$, $a_{j2}^{(i)}$, and $a_{j3}^{(i)}$ denote the low, medium, and high values of the triangular fuzzy value of \widetilde{A}_j^i , respectively, n denotes the number of respondents, and m denotes the number of landscape satisfaction evaluation indicators.

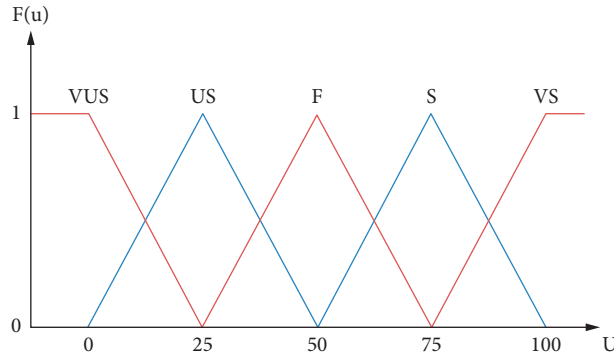


FIGURE 1: The cognitive levels of the i th respondent on the evaluation variables.

TABLE 1: The triangle fuzzy variables.

Comment variables	Low value	Medium value	High value
VUS	0	6.05	23.04
US	6.72	24.14	47.23
F	27.83	49.09	69.81
S	52.58	75.59	93.01
VS	78.44	92.72	100

TABLE 2: Fuzzy value and logic value of urban park landscape satisfaction.

Item level	Triangle fuzzy value of item level	Item-level logical value	Evaluation index level	Triangular fuzzy value of evaluation index	Logical value of evaluation index
Environmental satisfaction	(57.24, 76.75, 90.60)	75.33	Environmental coordination	(57.30, 76.91, 90.82)	75.48
			Visual aesthetics of the environment	(57.53, 77.13, 90.98)	75.69
			Ecological suitability	(56.88, 76.21, 90.02)	74.83
Facility satisfaction	(29.36, 47.51, 66.20)	47.64	Recreational facilities	(33.70, 52.89, 71.36)	52.71
			Guide facility	(29.92, 47.95, 66.42)	48.06
			Publicity service facilities	(24.45, 41.70, 60.81)	42.17
Traffic satisfaction	(35.05, 53.91, 71.88)	53.69	Road paving design	(30.11, 48.45, 67.15)	48.54
			Barrier-free design	(36.47, 55.30, 72.97)	55.01
			Traffic organization rationality	(38.58, 57.97, 75.53)	57.51
Site satisfaction	(47.46, 66.94, 82.80)	66.03	Location rationality	(47.95, 67.26, 82.91)	66.35
			Functional diversity	(41.59, 61.16, 78.30)	60.55
			Site participation	(52.83, 72.39, 87.19)	71.20
Space satisfaction	(40.25, 59.23, 76.23)	58.74	Scale rationality	(41.65, 60.33, 76.84)	59.79
			Spatial variability	(35.03, 54.12, 72.28)	53.89
			Sense of space security	(44.07, 63.25, 79.57)	62.53
Overall satisfaction	(51.22, 71.34, 86.85)	70.19			

$$\widetilde{TS} = \frac{\sum_{i=1}^n \widetilde{TS}^i}{n} = \frac{(\sum_{i=1}^n TS_1^{(i)}, TS_2^{(i)}, TS_3^{(i)})}{n}, \quad (3)$$

where \widetilde{TS} denotes the respondents' perception of overall landscape satisfaction, \widetilde{TS}^i denotes the i th respondent's perception of overall landscape satisfaction, $TS_1^{(i)}$, $TS_2^{(i)}$, and $TS_3^{(i)}$ denote the low, medium, and high values of the triangular fuzzy value of \widetilde{TS}^i , respectively, and n denotes the number of respondents.

$$V_A = \frac{(a_1 + 2a_2 + a_3)}{4}, \quad (4)$$

where V_A denotes the logical value of the fuzzy value $\widetilde{A}(a_1, a_2, a_3)$.

3.4. Construction of Satisfaction Evaluation System of Urban Park Landscape. In order to ensure the reliability of the index data and reduce the influence of subjective judgment on the evaluation results, during constructing the satisfaction evaluation system of urban park landscape, the factor analysis method is used to test the reliability and validity of the evaluation data.

The test to the evaluation indicators of satisfaction of urban park landscape by reliability analysis in SPSS 22.0 showed that Cronbach's alpha reliability value was 0.931, indicating the reliability of the questionnaire was good [17]. The test to the survey data by KMO and Bartlett's spherical test showed that the KMO value was 0.902, which was greater than 0.7, indicating that the structural validity of the questionnaire was good. Bartlett's Sig. was 0.000, indicating that the null hypothesis of the spherical test was rejected and suitable for factor analysis [18]. In the indicator validity analysis, 0.4 was selected as the critical value for factor loading, and indicators with factor loading less than 0.4 were excluded and 15 evaluation indicators were obtained. The factor analysis was carried out on the data to get the factor load matrix after rotation (Table 3), and the cumulative variance contribution of the first five common factors extracted was 78.602% (>60%), which indicated that the five common factors extracted were reasonable. Based on the attributes of the indicators, the extracted common factors were classified into five evaluation aspects, including "environmental satisfaction," "facility satisfaction," "traffic satisfaction," "site satisfaction," "space satisfaction," and "space satisfaction."

Extraction method: principal component analysis method; rotation method is the maximum variance method.

In order to test the rationality of the urban park landscape satisfaction evaluation index weight determined by the factor analysis method, the evaluation index weight was verified by the analytic hierarchy process. Firstly, the evaluation indicators are classified according to their relationship, and an evaluation system with a hierarchical structure is established. Then, 10 experts from Henan Agricultural University, Henan University of Science and Technology, Central South University of Forestry and Technology, and Henan Institute of Science and Technology were invited to compare each level of indicators according to the AHP calibration series and then score them to obtain a judgment matrix. After processing, the weight of the evaluation index to the superior index is obtained. After comparative analysis, the weights of the evaluation indicators determined by the AHP and the evaluation indicators determined by the factor analysis method are basically the same in order, which proves that the evaluation indicators' weights of the urban park landscape satisfaction determined by the factor analysis method are scientific and reasonable and can reflect contribution of evaluation indicators to landscape satisfaction.

3.5. Determination of the Weights of Satisfaction Evaluation Indicators of Urban Park Landscape. In order to reduce the errors of subjective judgments, factor analysis was applied to determine the weights of the satisfaction evaluation indicators of urban park landscape (Table 4). Firstly, the variance contribution rate of the five-aspect indicators of the item level was standardized, and the proportion of the variance contribution rate of each indicator to the total variance contribution rate was the weight of each item-level indicator. The weights of the five item-level indicators on the target level landscape satisfaction were calculated as 0.185, 0.200,

0.208, 0.209, and 0.198, respectively. Secondly, the maximum factor loading coefficient of each evaluation indicator was normalized to derive the contribution of the evaluation indicator to the item level, which is the weight of the evaluation indicator. Finally, the weight of each evaluation indicator to the item level was calculated by the weighting method.

4. Analysis of Evaluation Results

4.1. Analysis of the Satisfaction Evaluation of the Urban Park Landscape. Table 2 shows that the overall satisfaction score of Zhengzhou People's Park is 70.19, which is satisfactory, and it indicates that the public is satisfied with the overall satisfaction level of Zhengzhou People's Park. The score of "environmental satisfaction" (75.33) is greater than that of overall satisfaction (70.19), which indicates that the ecological environment in the park is more suitable, the landscape is in harmony with the park environment, the perception of environmental beauty is higher, and the natural environment as a whole is satisfactory. The scores of "site satisfaction" (66.03), "space satisfaction" (58.74), and "traffic satisfaction" (53.69) are lower than that of overall satisfaction (70.19), which is between average and satisfactory, indicating that the public's perception of satisfaction is relatively low and further improvement is required, which indicates that the level of public satisfaction is low and needs to be improved.

In terms of the overall scores of the evaluation indicators, the scores for "environmental coordination," "visual aesthetics of the environment," "ecological suitability," and "site participation" are higher than that of overall satisfaction, which indicates that these four evaluation indicators are in a good state of perception and shall be maintained and strengthened as appropriate.

The scores for "recreational facilities," "barrier-free design," "traffic organization rationality," "location rationality," "functional diversity," "spatial variability," and "sense of spatial security" are lower than the overall satisfaction scores, and the satisfaction level is between average and satisfactory, which indicates that these eight evaluation indicators are important factors affecting the satisfaction evaluation of the park landscape and need to be further optimized and improved. The scores of "road paving design," "orientation indication facilities," and "publicity service facilities" are smaller than the overall satisfaction score, and the satisfaction level is fair, which indicates that there are more problems with these three evaluation indicators and are less well accepted by the public, and it shall be improved and focused on.

4.2. Analysis of the Weights of the Evaluation Indicators of Satisfaction with the Urban Park Landscape. Table 4 shows that the weight values of the evaluation indicators at all levels are relatively balanced. In the item level, the weight values of "site satisfaction" and "traffic satisfaction" are relatively high, accounting for 20.9% and 20.8% of the total weight, respectively, indicating that the public is more concerned

TABLE 3: Rotated factor loading and variance contribution rate.

Evaluation index	Environmental satisfaction	Facility satisfaction	Traffic satisfaction	Site satisfaction	Space satisfaction
Environmental coordination	0.748				
Visual aesthetics of the environment	0.771				
Ecological suitability	0.707				
Recreational facilities		0.786			
Guide facility		0.802			
Publicity service facilities		0.746			
Road paving design			0.761		
Barrier-free design			0.750		
Traffic organization rationality			0.850		
Location rationality				0.689	
Functional diversity				0.779	
Site participation				0.857	
Scale rationality					0.731
Spatial variability					0.703
Sense of space security					0.831
Variance contribution rate	14.522	15.756	16.368	16.412	15.544
Cumulative variance contribution rate	14.522	30.278	46.646	63.058	78.602

TABLE 4: The judgment result of evaluation index weight about landscape satisfaction of urban parks in Zhengzhou.

Target level	Item level	Item-level weight	Index level	Index level weight	Total weight
A city park landscape satisfaction	B1 environmental satisfaction	0.185	C11 environmental coordination	0.336	0.062
			C12 environmental visual beauty	0.346	0.064
			C13 ecological suitability	0.318	0.059
	B2 facility satisfaction	0.200	C21 recreational facilities	0.337	0.067
			C22 guide facilities	0.344	0.069
			C23 publicity service facilities	0.319	0.064
			C31 road paving design	0.322	0.067
	B3 traffic satisfaction	0.208	C32 barrier-free design	0.318	0.066
			C33 traffic organization rationality	0.36	0.075
			C41 location rationality	0.296	0.062
			C42 functional diversity	0.335	0.070
	B4 site satisfaction	0.209	C43 site participation	0.369	0.077
			C51 scale rationality	0.323	0.064
			C52 space variability	0.31	0.061
	B5 space satisfaction	0.198	C53 space security	0.367	0.073
Average				0.066	

about both site and traffic in park recreation activities. Improving the functionality and participatory nature of the landscape and optimizing the traffic organization and road layout are important measures to improve park satisfaction. The weighting of “facility satisfaction” and “spatial satisfaction” is slightly lower than that of the first two indicators, accounting for 20% and 19.8% of the total weighting, respectively, indicating that the spatial perception of recreational facilities and activity places in parks is an important factor in park landscape satisfaction. The setting up of facilities with human care and practical functions, and the shaping of activity spaces with appropriate scale and orderly changes and a sense of security play an important role in

improving park satisfaction. “Environmental satisfaction” is the lowest ranked indicator, accounting for 18.5% of the total weighting, but its weighting is not significantly lower than that of the previous indicators; therefore, the coordination, ecology, and visual aesthetics of the landscape environment in parks shall not be ignored.

The weighted average value of the 15 evaluation indicators is 0.066. The evaluation indicators that are greater than the weighted average value include seven items, such as site participation, traffic organization rationality, sense of spatial security, functional diversity, guide facilities, recreational facilities, and road paving design; the evaluation indicators that are less than the weighted average value

include seven items, such as visual aesthetics of the environment, environmental coordination, ecological suitability, publicity service facilities, location rationality, scale rationality, and spatial variability. The weight value of barrier-free design is equal to the average value of the weights.

4.3. IPA Analysis of the Factors Influencing Satisfaction of the Urban Park Landscape. The IPA evaluation model was used to analyze the factors affecting the satisfaction of the landscape of Zhengzhou People's Park, the quadrant distribution of satisfaction evaluation indicators (Figure 2) was drawn with the mean value of the weights of the 15 evaluation indicators (0.066), and the comprehensive score of the overall satisfaction evaluation of the landscape of Zhengzhou People's Park (70.19) is drawn as the boundary.

From Figure 2, the first quadrant is the area of high weighting and high satisfaction, i.e., the "advantage area," which includes C43 site participation, indicating that the participatory and experiential nature of park open space places has a significant impact on landscape satisfaction and public perceptions of satisfaction, and the public's perception of satisfaction is also higher. Therefore, on the basis of maintaining the strengths, the participatory design of park activity areas shall be further optimized to meet the public's requirements for the landscape of places.

The second quadrant is the area of high satisfaction and low weighting, i.e., the "maintenance area," which includes the evaluation indicators, such as C11 environmental coordination, C12 visual aesthetics of the environment, and C13 ecological suitability. The corresponding item-level indicator is "environmental satisfaction," which is a fundamental factor affecting the satisfaction of the park landscape. Although the weighting of the evaluation index is not too high, the satisfaction value from the public is high, which indicates that the ecological and natural environment has a high landscape value. The evaluation indicators for the "maintenance area" shall be further improved while maintaining their strengths so that the level of public satisfaction will be kept.

The third quadrant is the low satisfaction and low weighting area, i.e., the "nonconcern area," which includes indicators such as C23 publicity service facilities, C41 location rationality, C51 scale rationality, and C52 spatial variability. Although the satisfaction scores and weightings of these indicators are relatively low, their impact on the quality of the park landscape shall not be ignored.

The fourth quadrant is the area of low satisfaction and high weighting, i.e., the "area of concern," which includes C21 recreational facilities, C22 guide facilities, C31 road paving design, C32 barrier-free design, C33 traffic organization rationality, C42 functional diversity, and C53 sense of space security, and the evaluation indicators mainly focus on the level of "facility satisfaction" and "traffic satisfaction." This shows that the design of park recreational facilities and road traffic has an important influence on the overall satisfaction of the landscape, while the public's perception of their actual experience is very low. In the construction of the park landscape, we shall strengthen the improvement and optimization of the indication of "area of concern,"

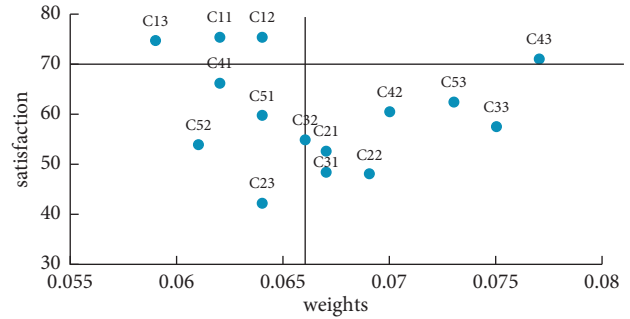


FIGURE 2: The IPA analysis of urban park landscape satisfaction evaluation.

reasonably set up recreational service facilities, improve the road traffic organization, and create activity places with reasonable spatial layout and various functions, so as to improve the level of satisfaction of the park landscape.

5. Conclusions and Recommendations

Based on the triangular fuzzy evaluation theory, the traditional discrete numerical comment variable description method is changed in the study, and continuous triangular fuzzy comment variables are used to describe the urban park landscape satisfaction evaluation indicator, and a fuzzy comprehensive evaluation of the Zhengzhou People's Park landscape satisfaction is carried out. Through the exploratory factor analysis of the survey data of Zhengzhou People's Park, it is concluded that there are 5 evaluation dimensions and 15 evaluation indicators in the landscape satisfaction evaluation system, and the weight of the evaluation indicators is determined. After analysis to the landscape satisfaction evaluation indicators with the IPA analysis method, it is concluded that it is in the "advantage area" if the satisfaction score and weight value of the "site participation" in the evaluation indicators are both high, which requires attention and maintenance of its advantages; the evaluation indicators of the two aspects of "facilities satisfaction" and "traffic satisfaction" are mainly located in the "concern area," which are the main factors affecting the landscape quality of urban parks. The improvement of its quality is conducive to the improvement of landscape satisfaction and shall be focused and optimized; the "environmental satisfaction" dimension indicators are in the "maintenance area." Although the weight of the evaluation indicators to the landscape satisfaction is low, the satisfaction scores are high, and their advantages shall be kept; although indicators such as "publicity service facilities," "location rationality," "scale rationality," and "spatial variability" are in "nonconcern area" with a low weight and low satisfaction, their impact on landscape quality shall not be ignored. During the construction of the urban park landscape in the future, we shall focus on the indicators of "advantage area" and "concern area," take into account the indicator of "maintenance area," and coordinate the indicator of "nonconcern area" so that the level of park landscape satisfaction can be effectively improved.

The study attempts to evaluate urban park landscape satisfaction by the fuzzy-IPA model, which provides a quantitative reference and basis for the construction of urban park landscape, the continuous fuzzy comment variable can more truly reflect the evaluation subject's cognitive level of the landscape object and reduce the subjective error of evaluation; the weight of the evaluation index determined by the factor analysis method is used to obtain the importance of the evaluation index to the landscape satisfaction; the importance-performance analysis method obtains the quadrant analysis chart of the satisfaction value of the evaluation index and the importance of the evaluation index and divides and proposes the evaluation index into different categories; but there are still some shortcomings: the selection of indicators for the questionnaire of the urban park landscape satisfaction is relatively simple, the number of questionnaires distributed is limited, and the error handling of the survey results is insufficient, which fails to fully reflect the public's perception of urban park landscape satisfaction, and it shall be further improved and adjusted in future research.

Data Availability

No data were used to support this study.

Conflicts of Interest

The authors declare that there are no conflicts of interest with any financial organizations regarding the material reported in this manuscript.

Acknowledgments

This work was supported by Science and Technology Project Plan of Henan Province (212102310230).

References

- [1] L. Feng and J. Zhao, "Research on landscape quality evaluation of urban parks based on AHP-TOPSIS combination model," *Journal of Shandong Agricultural University (Natural Science Edition)*, vol. 49, no. 5, pp. 777–781, 2018.
- [2] L. I. Yan, *Study on Park Satisfaction of Orange Island in Changsha City, Hunan Province*, Central South University of Forestry and Technology, Changsha, China, 2010.
- [3] Q. Y. Xia and C. H. Wang, "On mountainous scenic spot tourist satisfaction by fuzzy-IPA--A case study of Mt. Huangshan scenic spot," *Journal of Anhui Normal University*, vol. 35, no. 5, pp. 471–476, 2012.
- [4] X. Z. Xu and J. H. Xue, "Aesthetic evaluation for plant landscape of wetland park based on AHP," *Journal of Northwest Forestry University*, vol. 27, no. 2, pp. 213–216, 2012.
- [5] E. X. Wang and C. Y. Wu, "A study on the satisfaction of inbound tourism service quality based on grey correlation analysis," *Tourism Tribune*, vol. 23, no. 11, pp. 30–34, 2008.
- [6] F. Z. Zeng and Y. H. Wang, "The application of NNT in measuring customer satisfaction degree," *Journal of Beijing Institute of Technology (Social Sciences Edition)*, vol. 7, no. 1, pp. 45–47, 2005.
- [7] J. Zhao, S. B. Bai, L. Feng, and Y. Zhang, "Research on the appraise system of city square landscape architect adaptability," *Sichuan Building Science*, vol. 35, no. 5, pp. 255–257, 2009.
- [8] L. Feng, X. J. Hu, X. L. Jin, J. Zhao, and Y. C. Zhang, "An evaluation system of landscape environment adaptability in residential area--analysis on newly-built residential area of Xinxiang," *Journal of Northwest Forestry University*, vol. 23, no. 1, pp. 190–194, 2008.
- [9] Y. LI, "plant landscape evaluation of park green space in Zhengzhou city," *Journal of Fujian Forestry Science and Technology*, vol. 4, no. 1, pp. 143–147, 2013.
- [10] J. D. Li, X. H. Chen, D. Y. Zheng et al., "Application of AHP--Fuzzy Comprehensive Evaluation Model in the Post Evaluation for Water-Saving Society Establishment," *Pearl River*, vol. 40, no. 1, pp. 12–19, 2019.
- [11] L. Qin, "Research on index system of scientific achievement assessment," *Information and Communications Technology and Policy*, vol. 45, no. 1, pp. 14–17, 2019.
- [12] S. Armanda and D. Gopal, "The impact of job satisfaction, adaptive selling behaviors and customer orientation on Salesperson's performance: exploring the moderating role of selling experience," *Journal of Business & Industrial Marketing*, vol. 28, no. 7, pp. 554–564, 2013.
- [13] K. Y. Tian, Y. W. Zhu, and C. L. Huang, "Fuzzy comprehensive evaluation of the theme park tourist satisfaction based on AHP," *Journal of Anhui Normal University*, vol. 33, no. 5, pp. 490–493, 2010.
- [14] K. Y. Tian, "An empirical study of factors that affect tourist satisfaction in scenic areas based on fuzzy-IPA," *Tourism Tribune*, vol. 25, no. 5, pp. 61–65, 2010.
- [15] G. F. Zhang, "Investigation and research of college landscape satisfaction based on IPA," *Journal of Chaohu University*, vol. 18, no. 5, pp. 61–66, 2016.
- [16] H. H. Lin and S. K. Mo, "Empirical research on influencing factors of community education satisfaction in western rural areas--micro survey data from 557 farmers," *Vocational and Technical Education*, vol. 39, no. 30, pp. 52–56, 2018.
- [17] X. Y. Wang and H. Qin, "A fuzzy-IPA-based satisfaction evaluation model of campus plant landscape in southwestern university," *Journal of Southwest University(Natural Science Edition)*, vol. 40, no. 3, pp. 174–180, 2018.
- [18] L. Y. Jia and Q. Du, *SPSS Statistical Analysis Standard Course*, Posts and Telecom Press, Beijing, China, 2010.

Retraction

Retracted: The Influence of the Network Evolutionary Game Model of User Information Behavior on Enterprise Innovation Product Promotion Based on Mobile Social Network Marketing Perspective

Mathematical Problems in Engineering

Received 13 September 2023; Accepted 13 September 2023; Published 14 September 2023

Copyright © 2023 Mathematical Problems in Engineering. This is an open access article distributed under the Creative Commons Attribution License, which permits unrestricted use, distribution, and reproduction in any medium, provided the original work is properly cited.

This article has been retracted by Hindawi following an investigation undertaken by the publisher [1]. This investigation has uncovered evidence of one or more of the following indicators of systematic manipulation of the publication process:

- (1) Discrepancies in scope
- (2) Discrepancies in the description of the research reported
- (3) Discrepancies between the availability of data and the research described
- (4) Inappropriate citations
- (5) Incoherent, meaningless and/or irrelevant content included in the article
- (6) Peer-review manipulation

The presence of these indicators undermines our confidence in the integrity of the article's content and we cannot, therefore, vouch for its reliability. Please note that this notice is intended solely to alert readers that the content of this article is unreliable. We have not investigated whether authors were aware of or involved in the systematic manipulation of the publication process.

Wiley and Hindawi regrets that the usual quality checks did not identify these issues before publication and have since put additional measures in place to safeguard research integrity.

We wish to credit our own Research Integrity and Research Publishing teams and anonymous and named external researchers and research integrity experts for contributing to this investigation.

The corresponding author, as the representative of all authors, has been given the opportunity to register their

agreement or disagreement to this retraction. We have kept a record of any response received.

References

- [1] T. Liu, X. He, X. Guo, and Y. Zhao, "The Influence of the Network Evolutionary Game Model of User Information Behavior on Enterprise Innovation Product Promotion Based on Mobile Social Network Marketing Perspective," *Mathematical Problems in Engineering*, vol. 2022, Article ID 1416488, 12 pages, 2022.

Research Article

The Influence of the Network Evolutionary Game Model of User Information Behavior on Enterprise Innovation Product Promotion Based on Mobile Social Network Marketing Perspective

Tingting Liu ¹, Xiaofei He ², Xin Guo ¹, and Yi Zhao ²

¹School of International Trade and Economics, Shanghai Lixin University of Accounting and Finance, Shanghai 200030, China

²School of Management, Shanghai University of Engineering Science, Shanghai 201620, China

Correspondence should be addressed to Xiaofei He; m030120514@sues.edu.cn

Received 28 March 2022; Accepted 18 April 2022; Published 2 May 2022

Academic Editor: Wei Liu

Copyright © 2022 Tingting Liu et al. This is an open access article distributed under the Creative Commons Attribution License, which permits unrestricted use, distribution, and reproduction in any medium, provided the original work is properly cited.

User information behavior is an important factor affecting the promotion effect of enterprises' innovative products on mobile social networks. To provide insights as to how enterprises can better promote innovative products, this paper conducts a quantitative study of its internal function. We introduce a network evolutionary game model based on the Bass model, first to describe the background of the mobile social network, then to simulate the diffusion process of the social network and the user's decision-making game behavior during promotion of enterprises' innovative products, and finally to simulate the promotion effect on innovative products and solve for the conditions for the best innovative product marketing effect and the model are simulated from multiple angles. Our simulation results show that mobile social network marketing in the initial stage of product promotion has a significant impact on the promotion effect of innovative products. When user feedback is poor, advertisement diffusion has an obvious effect on product promotion. In mobile social networks, the proportion of positive feedback from users has a greater impact on the product promotion effect, while the proportion of negative feedback has a smaller impact on the product promotion effect. The impact of negative reviews is time sensitive. According to the simulation results, we propose several suggestions to improve the promotion effect of enterprises' innovative products on mobile social networks.

1. Introduction

According to the 48th Statistical Report on Internet Development in China, the total number of Internet users in China reached 1.01 billion in June 2021, and mobile social networks such as Weibo and WeChat are becoming the main platforms through which the public spreads information and shares resources. The multiple attributes that allow mobile social networks to spread information and share resources has brought public attention to mobile social network marketing. Therefore, product marketing using mobile social networks triggers the participation of many users and provides the public with multiple dimensions for evaluating related products. The dissemination and influence of mobile social networks have gradually increased, and mobile social

network platforms have gradually become the earliest accepted platforms for emerging things, so using mobile social networks to publicize innovative products has gradually become more mainstream. User information behavior has a significant impact on the promotion effect of enterprises' innovative products [1]. User information behavior in mobile social networks mainly includes information acquisition, creation, interaction, and utilization. The public will comment or provide positive feedback on innovative products promoted by enterprises, and other users will learn from these reactions and change their attitude towards the products, which affects the promotion and marketing effect [1]. Under the influence of a strong network, user-generated content, especially negative content, will have a negative impact on innovative products and even on the innovation

of enterprises [2–4]. Therefore, there is a need to study the relevant mechanisms of user information behavior and their effect on enterprise innovative product promotion, as well as to identify the influence of changes in user information behavior on enterprise product promotion and product innovation promotion [5–8].

In recent years, the influence of economic globalization has continued to increase, China's economic development has accelerated, market competition has grown stronger, and companies have introduced new products to increase innovation and research and development. In the face of fierce market competition, enterprises must effectively promote their innovative products in order to convert them into economic benefits. At a time when mobile social networks have become the main force of advertising communication, the trend of public opinion on innovative products expressed on mobile social networks will have a significant impact on product promotion. Therefore, it is extremely important for enterprises to understand how to address public opinion or negative feedback on mobile social networks, as well as how to promote innovative products more effectively on mobile social network platforms and convert them into economic benefits.

In order to further study the influence of user information behavior on the promotion effect of enterprises' innovative products, it is necessary to simulate different user information behaviors using control variable methods. Existing studies mostly focus on the impact of negative user information behavior on enterprise product promotion: the number [3], intensity [2], and release time [9] of negative comments all affect users' purchase intentions. Negative evaluations will also change the emotional utility of users and thus change their information behavior, which will have a negative impact on the effect of product promotion [10–12] and increase the negative impact of product promotion. From the perspective of user information behavior, users' willingness to share will also have an impact on the product promotion effect of enterprises. Sharing advertising information helps to strengthen communication and contact; moreover, users can get satisfaction from such sharing, thereby generating positive feedback and enhancing the product promotion effect [13]. In summary, we assume that user information behavior will be found to have different degrees of influence on the promotion effect of enterprises' innovative products when considered from multiple perspectives.

From the perspective of research methods, most existing studies have considered the promotion effect of innovative products by selecting a single variable of user information behavior, such as comments' sentiment polarity [14], users share for [15–17], or mobile social network use time [18–20]. There are few studies on the synergistic effect of multiple user information behaviors on the product promotion effect. In addition, most existing studies use questionnaire surveys, qualitative studies, or case studies. Quantitative analysis of scientific systems is relatively lacking; its complex evolutionary process has not been well-depicted and -described, so it is difficult for corporate marketing planners to evaluate the effect of social advertising and take corresponding

measures. At the same time, some scholars used evolutionary game model to describe the complex evolutionary system of abandoned medical supply chain [21] and green supply chain [22] under the condition of decision-maker's bounded rationality and provided some enlightenment. Based on the above discussion, this paper establishes a Bass model-based network evolutionary game model that is suitable for examining the promotion and diffusion characteristics of enterprises' innovative products under the influence of user information behaviors. This paper also simulates the influence of different user information behaviors on the promotion of enterprises' innovative products against the background of mobile social networks, as well as conducting simulation analysis. Using a formula to describe the promotion effect, this paper conducts a quantitative study of how user information behavior affects the promotion effect of enterprises' innovative products. In this way, we are able to provide strategic suggestions for the marketing of innovative products and for improving enterprises' reputation. These suggestions are made with reference to the diffusion effect of innovative products and can be used to convert innovative products into economic benefits to promote the innovation and development of enterprises.

2. Model Construction: The Influence of User Information Behavior on the Promotion Effect of Enterprises' Innovative Products

2.1. User Information Behavior in the Promotion of Innovative Products of Enterprises. User information behavior refers to mobile social network users' information acquisition, creation, interaction, and utilization via mobile social networks. Mobile social networks are used as a medium for promoting enterprises' innovative products. The generation of user information behavior in the promotion of mobile social networks is a result of the mutual influence and interaction of many individual users, which is called "group behavior" in this context. According to group dynamics, group behavior will be affected by environmental changes and group member behavior changes. The formation of group behavior is a game process and is affected by the psychological state and motivation of group members. Group members will compare their own behaviors with group behaviors and update their own strategies accordingly [23].

When mobile social networks promote enterprises' innovative products, users' positive actions and comments will make enterprises' innovative products seem more favorable to other users. However, unanimous praise can generate doubts and resistance among users, as this seems inconsistent with reality [24, 25]. Therefore, negative comments are typical on most social platforms. In the face of both positive and negative comments, users will form a game in their hearts. At this time, users will seek more information to determine their final decision scheme and create information connections with other users around them [26]. The users' final behavioral decision is formed by considering the information offered by one or more users; under the

influence of these users, they may subsequently update their own policy according to the information update obtained. Users will then comment or take positive action according to a certain probability, which will affect the subsequent information behavior of other users. For example, it affects the number of likes and positive and negative comments in the advertisements of enterprise innovative products in mobile social networks, which in turn affects the promotion effect of mobile social networks. The formation process of group behavior under mobile social network promotion advertising influences the impact of user information behavior on the mobile social network promotion effect. If users are regarded as different nodes and the influence of information behavior between users is regarded as the line connecting these nodes, then network evolutionary game theory can fully examine the influence of surrounding nodes on the central node. Based on the above discussion, this paper builds a network evolutionary game model to describe the impact of user information behavior on enterprise innovative product promotion from the perspective of mobile social network marketing.

2.2. Theoretical Basis of a Network Evolutionary Game.

The essential elements of a network evolutionary game are the participants, the strategies adopted by each participant, the benefit functions of the participants, and the strategy renewal rules of the participants' actions. The factors affecting population change have a certain degree of randomness and a disturbance phenomenon. A network evolutionary game entails a process of studying the constant changes among different strategies in a network structure. Ohtsuki et al. [27] studied three different updating rules for the replication dynamic equations in the network evolutionary game: BD updating, DB updating, and IM updating mechanisms. The BD updating mechanism involves selecting an individual in an appropriate proportion in the network, so that the individual's offspring replaces its random neighbor nodes. The DB updating mechanism involves randomly selecting a dead individual in the network, after which the neighbor nodes of the dead individual compete for the vacant node, replacing the individual according to the appropriate proportion. The IM updating mechanism selected in this paper involves randomly selecting an individual in the network to update its strategy. It can choose to maintain its current strategy or imitate a neighbor's strategy with proportionality, which is in line with the formation process of group behavior in mobile social network advertising. An $n * n$ matrix $B = [b_{ij}]$, Matrix B, can be created for the above three updating mechanisms as follows:

$$\begin{aligned} \text{BD: } b_{ij} &= \frac{a_{ii} + a_{ij} - a_{ji} - a_{jj}}{k - 2}, \\ \text{DB: } b_{ij} &= \frac{(k + 1)a_{ii} + a_{ij} - a_{ji} - (k + 1)a_{jj}}{(k + 1)(k - 2)}, \\ \text{IM: } b_{ij} &= \frac{(k + 3)a_{ii} + 3a_{ij} - 3a_{ji} - (k + 3)a_{jj}}{(k + 3)(k - 2)}. \end{aligned} \quad (1)$$

Set $g_i = \sum_{j=1}^n x_j a_{ij}$ represents the local competition between different strategies, $f_i = \sum_{j=1}^n x_j a_{ij}$ represents the

average fitness of strategies i , which is derived from the interaction of all strategies in the whole network, and $\sum_{i=1}^n x_i g_i = 0$.

Set $x_i(t)$ as the expected ratio of strategy i at time t and degree k , and the replication dynamic equation in the network is

$$\frac{dx_i}{dt} = x_i (f_i + g_i - \phi), i = 1, 2, \dots, n. \quad (2)$$

The average fitness in the network is

$$\phi = \sum_{i=1}^n x_i (f_i + g_i) = \sum_{i=1}^n x_i g_i = \sum_{i,j=1}^n a_{ij} x_i x_j. \quad (3)$$

Then, substitute f_i, g_i, ϕ into (2) to obtain

$$\frac{dx_i}{dt} = x_i \left[\sum_{j=1}^n x_j (a_{ij} + b_{ij}) - \phi \right], i = 1, 2, \dots, n, \quad (4)$$

where a_{ij} is the payoff of strategy i versus strategy j . Therefore, the complete graph in evolutionary game dynamics is transformed into a regular graph with degree k , and the corresponding return matrix becomes $[a_{ij}] \rightarrow [a_{ij} + b_{ij}]$.

2.3. Establishment of the Network Evolutionary Game Model.

Product innovation is a source of enterprise competitiveness, and the promotion of innovative products is an important step to establishing a company's reputation. According to the theory of innovation diffusion, the distribution of a product's diffusion velocity over time when enterprises promote their innovative products on mobile social network platforms is consistent with the normal distribution. At the early stage of diffusion, the diffusion rate is very slow. When the number of adopters expands to between roughly 10% and 25% of the residents, the diffusion rate will accelerate suddenly, and both the diffusion rate and the number of adopters will increase rapidly, a trend that will be maintained in the future. Progress slows as the number of adopters approaches the saturation point. The change process of the number of innovative product adopters over time is similar to an S-shaped curve. According to the diffusion theory of innovation and the Bass model, early adopters act as "lobbyists" to encourage opinion leaders to accept innovative products. The Bass model divides the crowd into the potential consumer group and the actual consumer group, and the purchasing decision of the innovation group is independent of those of other members of the social system. The time at which the imitation group buys new products is affected by the social system [28–32], so the innovation group plays a significant role in enterprise promotion. Therefore, enterprises should fully consider the role of initial adopters when promoting relevant innovative products [33–35]. Thus, the Bass model is added in the establishment of the product promotion model according to the "innovative" characteristics of enterprises' innovative products, which fully considers the diffusion characteristics of innovative products.

When innovative products are advertised via a mobile social network, positive feedback and negative feedback will be

generated from users [36–38]. Because advertising itself is time sensitive and users are constantly changing, the Bass model describes the dynamic proportion of positive-feedback and negative-feedback users. In this paper, the potential consumer group and actual consumer group in the Bass model are regarded as the group that provides positive feedback to the advertisement, and the remaining users are regarded as the group that provides negative feedback to the promotion advertisement. The Bass model entails an innovation effect and an imitation effect. The innovation effect refers to the positive emotions spontaneously generated from mass media, and in this the innovation population generated by the innovation index of the advertisement is made up of the initial adopters following the promotion of innovative products. The imitation effect refers to the positive emotions generated by individuals who are influenced by users that express positive emotions, namely, consumers who are influenced by initial adopters to accept new products after the promotion of innovative products. The basic formula of the Bass model is as follows:

$$\frac{dN(t)}{dt} = p[m - N(t)] + q \frac{N(t)}{m} [m - N(t)]. \quad (5)$$

Here, $N(t) = mF(t)$, where $N(t)$ represents the number of users who have positive feedback on product promotion. $p[m - N(t)]$ in the formula represents users who provide positive feedback on the product promotion; that is, the users who become innovative product adopters. $qN(t)/m[m - N(t)]$ represents users who generate positive feedback under the influence of other users. In the formula, p represents the innovation coefficient, q represents the imitation coefficient, and p, q range from $[0, 1]$. $F(t)$ represents the cumulative proportion of users who give positive feedback on the product's promotion, and $f(t)$ is the proportion of users who generate positive feedback on the product's promotion. $F(t)$ and $f(t)$ can be obtained by solving the differential equations as follows:

$$F(t) = \frac{1 - e^{-(p+q)t}}{1 + (q/p)e^{-(p+q)t}}, \quad (6)$$

$$f(t) = \frac{(p+q)^2 e^{-(p+q)t}}{p[1 + (q/p)e^{-(p+q)t}]^2}.$$

Here, $\bar{F} = 1 - F$ is defined as the proportion of users that have a negative impact on product promotion.

In this paper, the proportion of positive feedback generated from variable advertisement communication is briefly denoted as APF, and the proportion of negative feedback generated from advertisement communication is abbreviated as ANPF. Based on the above Bass model, the expressions of APF and ANPF can be obtained as $APF = F(t)$, $ANPF = \bar{F}(t) = 1 - F(t)$.

When users come into contact with advertisements for innovative products on mobile social networks, they usually choose one of three strategies: favoring, disliking, or ignoring the advertisement. When the advertisement is favorable to the user, the user's information behavior may include giving a "thumbs up" to it, or leaving positive comments. When users feel negatively about the advertisement, the user's information behavior may include commenting on the negative content and

TABLE 1: Variables impacting the effect of innovative product promotions on mobile social networks.

Variable	Meaning
Likes number (LN)	Percentage of users who like an ad
Advertisement positive feedback (APF)	Proportion of positive feedback groups in advertising communication
Advertisement nonpositive feedback (ANPF)	Proportion of nonpositive feedback groups in advertising communication
Ratio of positive reviews (RPR)	Proportion of positive sentiment in online comments
Ratio of negative reviews (RNR)	Proportion of negative sentiment in online comments
Possibility of ignoring the advertisement (PI)	Likelihood that users ignore the ad

giving negative feedback to the advertisement itself. When the user ignores the advertisement, they take no action other than ignoring it entirely. Based on the above reasoning, variables impacting the effect of innovative product promotions on mobile social networks are identified, as shown in Table 1.

The parameters in the income matrix are simplified into three variables as follows:

$$\begin{aligned} V_P &= APF + LN + RPR, \\ V_R &= ANPF + RNR, \\ V_I &= PI. \end{aligned} \quad (7)$$

Then, the payoff matrix of the network evolutionary game model can be obtained as follows:

$$\begin{array}{c} P \quad R \quad I \\ \begin{array}{c} P \\ R \\ I \end{array} \begin{pmatrix} 0 & a_{12} & a_{13} \\ a_{21} & 0 & a_{23} \\ 0 & 0 & 0 \end{pmatrix}. \end{array} \quad (8)$$

Therefore,

$$\begin{aligned} a_{12} &= \frac{V_P - V_R}{3}, \\ a_{21} &= \frac{V_R - V_P}{3}, \\ a_{13} &= \frac{V_P - V_I}{3}, \\ a_{23} &= \frac{V_R - V_I}{3}, \end{aligned} \quad (9)$$

where a_{ij} represents the probability that the user who chooses strategy i will persuade the user who originally chose strategy j to choose strategy i , which can be identified from the above equation $a_{ij} = -a_{ji}$. Users who generate positive or negative feedback will not be persuaded to adopt the "ignore" attribute, and users who adopt the "ignore" strategy will only be persuaded to adopt a positive or a negative feedback strategy. In addition, users who adopt the same

strategy do not need to convince each other, so the diagonals of the revenue matrix are all 0. Finally, the data in the matrix have been standardized in this paper, and their absolute value is [0, 1].

3. Solution to, and Analysis of, the Network Evolutionary Game Model

3.1. *Solving the Evolutionary Game Model.* There should be no deleted nodes in the entire network of the mobile social network's advertising users, so the IM model is applied, and the formula is as follows:

$$B = \begin{pmatrix} 0 & \frac{6a_{12}}{(k+3)(k-2)} & \frac{3a_{13}}{(k+3)(k-2)} \\ \frac{6a_{21}}{(k+3)(k-2)} & 0 & \frac{3a_{23}}{(k+3)(k-2)} \\ \frac{-3a_{13}}{(k+3)(k-2)} & \frac{-3a_{23}}{(k+3)(k-2)} & 0 \end{pmatrix}. \quad (10)$$

The average fitness of the whole population is expressed as follows:

$$\phi = x_1x_3a_{13} + x_2x_3a_{23}. \quad (11)$$

According to the dynamic equation of network replication, the positive feedback, negative feedback, and replication dynamic equation for ignoring three behaviors of the promotion advertisement can be obtained as follows:

$$\begin{cases} \frac{dx_1}{dt} = x_1 \left[\frac{k^2+k}{(k+3)(k-2)}x_2a_{12} + \frac{k^2+k-3}{(k+3)(k-2)}x_3a_{13} - x_1x_3a_{13} - x_2x_3a_{23} \right], \\ \frac{dx_2}{dt} = x_2 \left[\frac{k^2+k}{(k+3)(k-2)}x_1a_{21} + \frac{k^2+k-3}{(k+3)(k-2)}x_3a_{23} - x_1x_3a_{13} - x_2x_3a_{23} \right], \\ \frac{dx_3}{dt} = x_3 \left[\frac{3}{(k+3)(k-2)}x_1a_{13} + \frac{3}{(k+3)(k-2)}x_2a_{23} - x_1x_3a_{13} - x_2x_3a_{23} \right]. \end{cases} \quad (12)$$

3.2. *Stability Analysis of the Game Model.* The revenue matrix after transformation is as follows:

$$[a_{ij} + b_{ij}] = \begin{pmatrix} 0 & a_{12} + \frac{6a_{12}}{(k+3)(k-2)} & a_{13} + \frac{3a_{13}}{(k+3)(k-2)} \\ a_{21} + \frac{6a_{21}}{(k+3)(k-2)} & 0 & a_{23} + \frac{3a_{23}}{(k+3)(k-2)} \\ \frac{-3a_{13}}{(k+3)(k-2)} & \frac{-3a_{23}}{(k+3)(k-2)} & 0 \end{pmatrix}, \quad (13)$$

$$P_P = x_2 \left[a_{12} + \frac{6a_{12}}{(k+3)(k-2)} \right] + x_3 \left[a_{13} + \frac{3a_{13}}{(k+3)(k-2)} \right]$$

$$P_R = x_1 \left[a_{21} + \frac{6a_{21}}{(k+3)(k-2)} \right] + x_3 \left[a_{23} + \frac{3a_{23}}{(k+3)(k-2)} \right]$$

$$P_I = x_1 \left[\frac{-3a_{13}}{(k+3)(k-2)} \right] + x_2 \left[\frac{-3a_{23}}{(k+3)(k-2)} \right].$$

To achieve the best effect of advertising promotion, $P_p > P_R, P_p > P_I$ should be satisfied at the same time. The following is the income analysis of the two cases.

Case 1. $P_p > P_R$; that is, when promoting innovative products, the revenue generated by users who give positive

$$\varepsilon \left[a_{12} + \frac{6a_{12}}{(k+3)(k-2)} + a_{13} + \frac{3a_{13}}{(k+3)(k-2)} - a_{23} - \frac{3a_{23}}{(k+3)(k-2)} \right] - (1-2\varepsilon) \left[a_{21} + \frac{6a_{21}}{(k+3)(k-2)} \right] > 0, \varepsilon \rightarrow 0. \quad (14)$$

If the above formula is true, it is satisfied by $a_{21} + 6a_{21}/(k+3)(k-2) < 0$. If $a_{12} > 0$, then

$$\begin{aligned} V_p - V_R &= APF + LN + RPR - ANPF - RNR > 0, \\ APF + LN + RPR &> ANPF + RNR. \end{aligned} \quad (15)$$

feedback on advertisements is greater than that generated by users who give negative feedback. Moreover, supposing $x_2 = \varepsilon_1, x_3 = \varepsilon_2, x_1 = 1 - \varepsilon_1 - \varepsilon_2$, this formula can be simplified as $\varepsilon_1 = \varepsilon_2 = \varepsilon, x_1 = x_3 = \varepsilon, x_2 = 1 - 2\varepsilon$.

If $a_{21} + 6a_{21}/(k+3)(k-2) = 0$, the following formula shall be satisfied:

$$\begin{aligned} a_{12} + \frac{6a_{12}}{(k+3)(k-2)} + a_{13} + \frac{3a_{13}}{(k+3)(k-2)} - a_{23} - \frac{3a_{23}}{(k+3)(k-2)} &> 0 \\ \Rightarrow (APF + LN + RPR)(2k^2 + 2k - 3) &> (ANPF + RNR)(2k^2 + 2k - 3) + PI \\ \Rightarrow PI &< 0. \end{aligned} \quad (16)$$

However, $PI \geq 0$, so the above inequality is not true.

Case 2. $P_p > P_I$, that is, when the enterprise promotes innovative products, the revenue generated by satisfying users

who express negative reactions to the advertisement is greater than the revenue generated by satisfying users who ignore the advertisement. We still assume that $x_2 = \varepsilon_1, x_3 = \varepsilon_2, x_1 = 1 - \varepsilon_1 - \varepsilon_2$.

$$\varepsilon \left(a_{12} + \frac{6a_{12}}{(k+3)(k-2)} + a_{13} + \frac{3a_{13}}{(k+3)(k-2)} + \frac{3a_{23}}{(k+3)(k-2)} \right) - (1-2\varepsilon) \left(\frac{-3a_{13}}{(k+3)(k-2)} \right) > 0, \varepsilon \rightarrow 0. \quad (17)$$

If the above formula is true, then $3a_{13}/(k+3)(k-2) > 0, a_{13} > 0$ must be satisfied. Then, the following formula shall be satisfied:

$$\begin{aligned} V_p - V_I &= APF + LN + RPR - PI > 0, \\ APF + LN + RPR &> PI. \end{aligned} \quad (18)$$

If $3a_{13}/(k+3)(k-2) = 0$, then the following formula must be satisfied:

$$a_{12} + \frac{6a_{12}}{(k+3)(k-2)} + a_{13} + \frac{3a_{13}}{(k+3)(k-2)} + \frac{3a_{23}}{(k+3)(k-2)} > 0. \quad (19)$$

After reduction, the formula is as follows:

$$\begin{aligned} (2k^2 + 2k - 3)(APF + LN + RPR) &> (k^2 + k - 3)(ANPF + RNR) \\ &+ (k^2 + k)PI \\ \Rightarrow APF + LN + RPR &> ANPF + RNR. \end{aligned} \quad (20)$$

Based on the above three situations, we can get the best conditions for promoting and disseminating innovative products when

$$\begin{aligned} &''APF + LN + RPR > ANPF + RNR'' \text{ and} \\ &''APF + LN + RPR > PI'' \text{ or} \\ &APF + LN + RPR = PI \text{ and } APF + LN + RPR > ANPF + RNR''. \end{aligned} \quad (21)$$

4. Simulation Results and Analysis

According to the constraint conditions, replication dynamic equation, and Bass model outlined in the previous section, in order to further simulate the influence of user information behavior on the promotion effect of innovative products of enterprises in mobile social networks, as well as to intuitively identify the influence of various parameter changes on the promotion effect, the revenue matrix parameters should be set as $k = 3, p = 0.4, q = 0.8, LN = 0.3, RPR = 0.3, RNR = 0.3, PI = 0.6$. Additionally, the initial policy proportions of the three kinds of user information behaviors are, respectively, $P = 0.25, R = 0.15, I = 0.6$. According to the replication dynamic model (17), MATLAB tools are used to simulate the changing trends of user information behaviors for giving positive feedback, giving negative feedback, and ignoring the advertisement, as shown in Figure 1.

Through the test, the set initial value satisfies the constraint condition, and the promotion effect achieves the best state. As can be seen in Figure 1, as time goes on, users who give positive feedback on promotion advertisements in mobile social networks continue to increase and reach the optimal state when they are stable. Conversely, the proportion of users who ignore the advertisement or generate negative feedback declines and stabilizes at 0 over time. In order to further study the influence of each parameter of the revenue matrix on the promotion effect of enterprises' innovative products, MATLAB is used to simulate the change assignment of each parameter. Under the condition that the linkage reaction satisfies the constraint conditions without considering parameters, we observe the influence of the simulation results of each group on the promotion effect.

When measuring the advertising promotion effect on mobile social networks, the number of positive feedback comments on advertisements is N_P , the number of negative feedback comments is N_R , and the total number of users is N . The product promotion effect index (PPEI) is introduced as follows:

$$PPEI = \frac{N_P - N_R}{N} \quad (22)$$

4.1. Influence of the Initial Diffusion of Enterprises' Innovative Products on the Promotion Effect. We change the values in the Bass model when other parameter values remain unchanged and show the simulation results in Figure 2. The results reveal that the higher the value of the innovation effect coefficient and imitation effect coefficient, the stronger the advertising effect of the innovation product promotion and the sooner it reaches a stable value. However, when p and q reach a certain threshold, they have little positive impact on the promotion effect. When the innovation effect is very low but the imitation effect is high, the positive effect of advertising will reach the optimal state and become stable. Figure 3 shows that the advertisement itself then spreads faster, and when the t value reaches 5, the advertisement spread reaches a stable value. As shown in Figure 2, in the case of setting $p = 0.4, q = 0.8$, when the t value reaches 30, the advertising diffusion will reach a stable level. Therefore, the advertising itself plays a significant role in the effect of

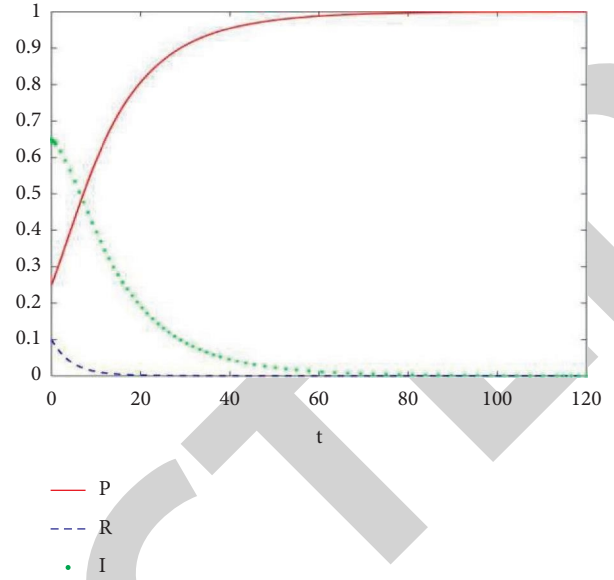


FIGURE 1: Variation trend of different information strategy selection ratio.

mobile social network advertising in the early stage, whereas it has little effect in the later stage. We find that enterprises must plan advertising effectively in the early stage of product promotion to improve the innovative effect of advertising, as this will expand the scope of the enterprises' innovative products and develop a better reputation for the innovative products. We also find that the initial advertising planning of product promotion plays an important role in the effect of product promotion, as shown in Figures 2 and 3.

4.2. Influence of the Number of Likes on the Promotion Effect.

When other parameters remain unchanged, changing the value of the proportion of likes (LN) that users give to mobile social network advertisements will influence the effect of advertisement promotion, as shown in Figure 4. The figure shows that in extreme cases, such as when the proportion of likes is extremely low (for example, $LN = 0$), keeping other parameters unchanged will cause a short-term decrease in the advertising effect, and the promotion effect will reach the optimal value and become stable. The value of the time will be extended accordingly, but the diffusion effect will ultimately remain optimally stable. Furthermore, by varying the LN values, we find that the higher the number of likes for advertisements on a mobile social network platform, the better the effect of product promotion.

4.3. Influence of the Proportion of Emotional Polarity of Product Promotion Advertising Comments on the Product Promotion Effect.

When other parameters remain unchanged, changing the proportion of the emotional polarity of comments on the product advertisement on mobile social networks influences the product promotion effect, as shown in Figure 5. Figure 5(a) shows that the more positively biased the comments, the more beneficial the product promotion effect. Figure 5(b) further shows

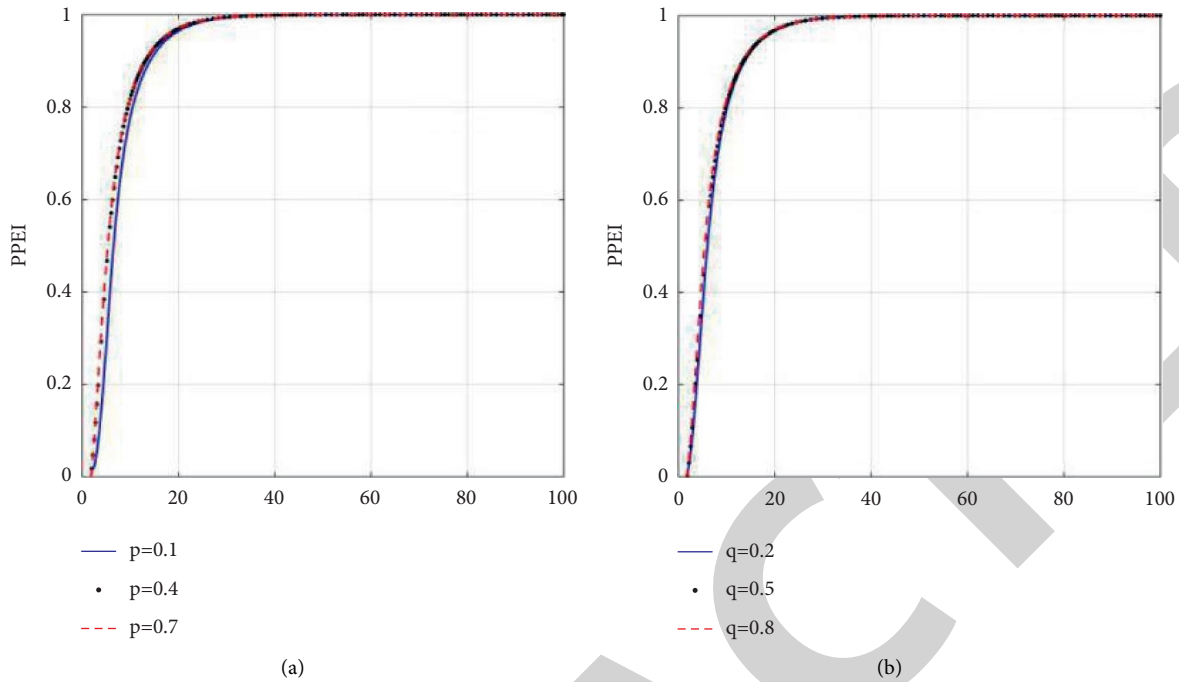


FIGURE 2: The influence of innovation effect coefficient P (a) and imitation effect coefficient Q (b) on the product promotion effect of product advertising on mobile social networks.

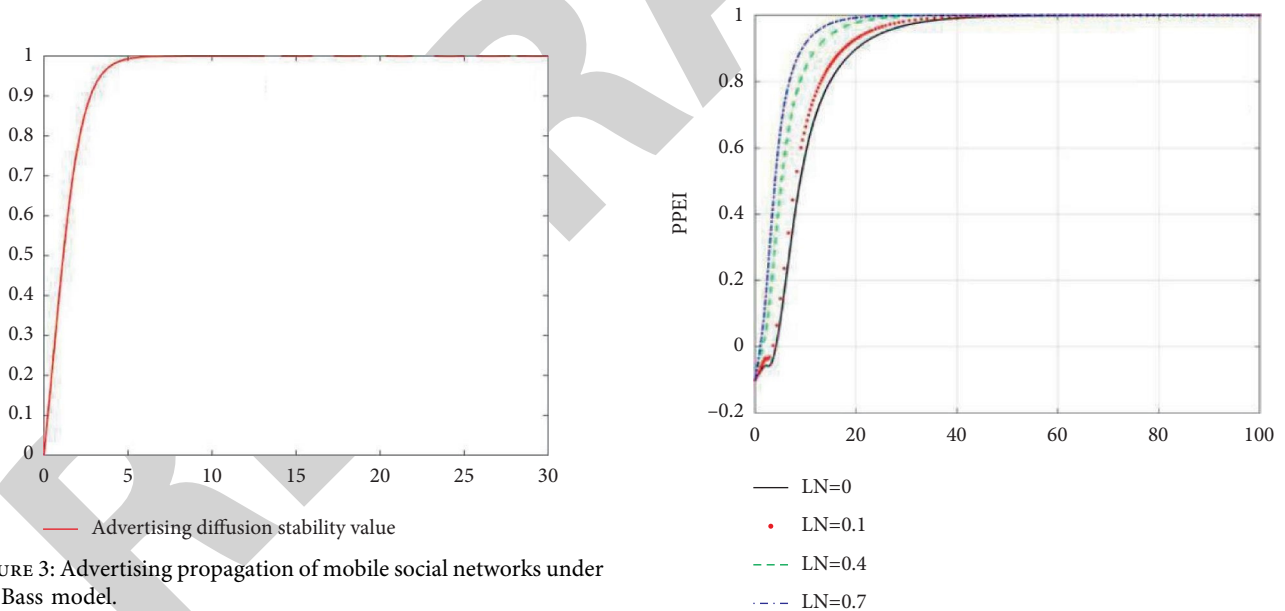


FIGURE 3: Advertising propagation of mobile social networks under the Bass model.

FIGURE 4: Influence of proportion of users' likes on the product promotion effect.

that if there are many negative comments, the time it takes for product promotion to reach the optimal effect will slow down. In extreme cases, the effect of product promotion will be negatively affected, so that the proportion of users with negative reactions to product advertisements on mobile social networks will be larger than that of users with positive reactions. When there are more negative comments than positive ones, it becomes vital to implement successful promotion strategies to influence public opinion of the products.

4.4. Influence of the Proportion of Users following the Ignore Strategy on the Product Promotion Effect. Changing the proportion of users who adopt the ignore strategy influences the product promotion effect, as shown in Figure 6 (assuming that other parameters remain unchanged). Figure 6 shows that the higher the proportion of users who adopt the ignore strategy, the longer it will take for the promotion effect to reach the optimal state. Therefore, enterprises

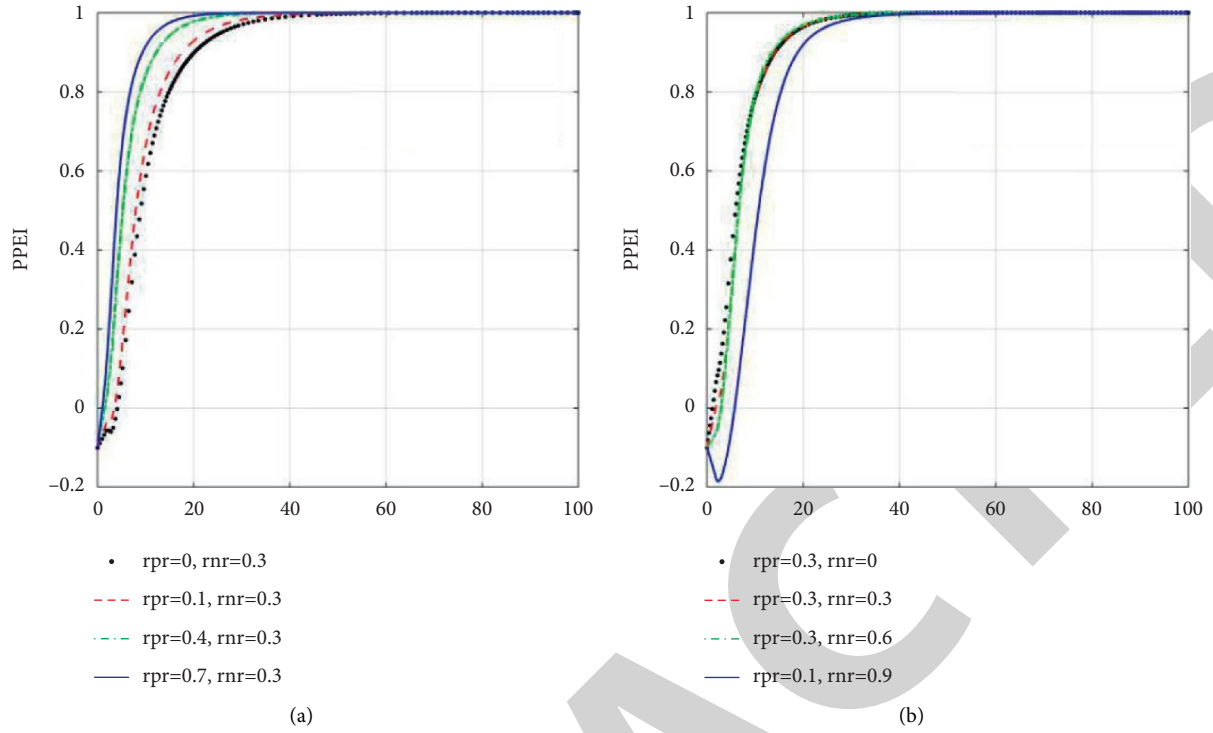


FIGURE 5: Influence of the proportion of positively biased comments (a) and negatively biased comments (b) on mobile social network advertisements on the effect of product promotion.

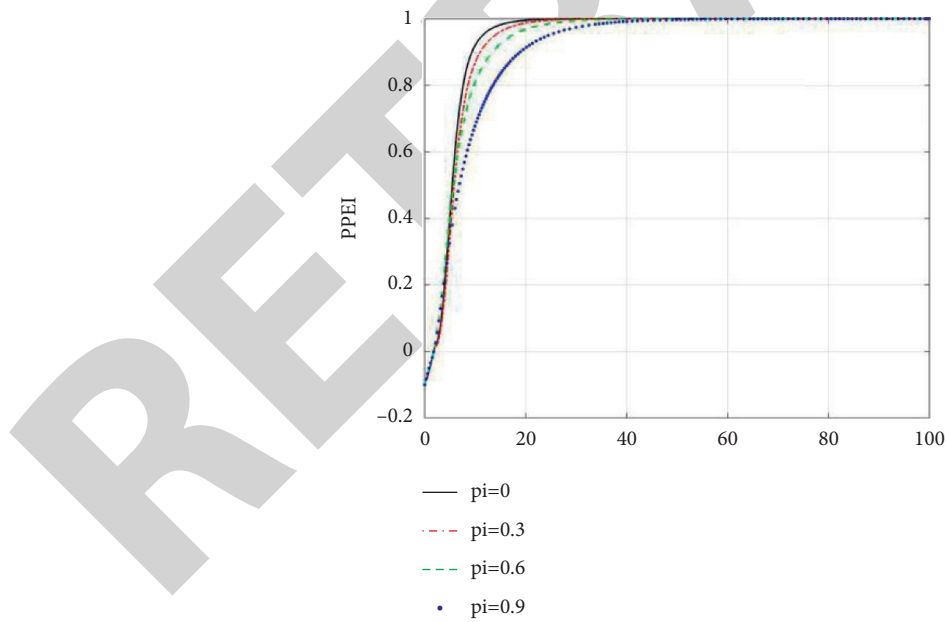


FIGURE 6: Influence of the proportion of users using the ignore strategy on product promotion effect.

should ensure successful product publicity in the early stage of promotion, so that more target users are exposed to their advertisements and the effect of promotion will reach the best state this morning.

5. Conclusions and Recommendations

According to the model constructed in this paper, and the simulation depicted, mobile social network marketing has a significant impact on the promotion effect of innovative products in the initial stage of product promotion, and user information behavior on mobile social network platforms will impact the promotion effect of innovative products from multiple perspectives. First, the diffusion of enterprises' innovative products in the initial stage of promotion has a significant impact on the promotion effect, while the later stage has little impact. Second, when user feedback is poor, advertisement diffusion has an obvious effect on product promotion. Third, on mobile social networks, the proportion of positive user feedback has a greater impact on the product promotion effect, while the proportion of negative feedback has a smaller impact on the product promotion effect. Fourth, the impact of negative comments is time sensitive. Combined with the above conclusions, and based on mobile social networks, we propose the following suggestions for the promotion of enterprises' innovative products.

- (1) When promoting innovative products, enterprises should pay attention to initial adopters of the product following its promotion and should strive to improve the innovation effect so as to drive the imitation effect. Enterprises can effectively plan, compare, and screen out their product use paths by studying consumers' use scenarios, finding consumers' pain points and comfort points, and locking in early adopters of innovative products. Moreover, by establishing an emotional connection with initial adopters of the product, enterprises can improve their positive impact on other potential consumer groups.
- (2) Enterprises should reduce the display of negative comments on their innovative product advertisements on mobile social networks and increase the display of "likes." When choosing an innovative product promotion platform, enterprises can choose to reduce the RNR in the model and increase the proportion of LN to accelerate the product promotion effect and reach the optimal value. For example, an advertisement can display not only the number of "likes" but also the number of "favorites," "reposts," and "shares." This will generate positive psychological hints when users watch the advertisements of the company's innovative products, so that the promotion effect will continue to improve.
- (3) By promoting innovative products on mobile social network platforms, enterprises can prolong the dividend period of advertising diffusion; that is, increasing LN and RPR in the model can improve the

diffusion effect when users perform poorly in promoting mobile social network platforms. The effectiveness of the advertising lasts through the initial stage of advertising dissemination, but by creating an overall positive public opinion on the platform, enterprises can prolong the duration of the positive effect of advertising diffusion. Official media can facilitate interesting interactions on online platform advertisements. When enterprises promote innovative products, they can effectively carry out promotional activities and interactions on the platform, which can prolong the "bonus" period of advertising diffusion, allowing the promotion effect of innovative products to reach an optimal and stable state as soon as possible and thereby improving the effect of product promotion.

- (4) Through the online comments function, mobile social network advertisements increase the amount of information that users have access to; however, some users may post unwarranted negative feedback on products to confuse people. When encountering these negative comments, the enterprise should maintain the diffusion speed of advertising and ensure product quality, as well as continuing to encourage positive comments and likes. After a short period of decline, the product promotion effect will naturally recover.

6. Conclusion

Based on the network evolutionary game model, this paper studies the influence of user information behavior on mobile social network platforms on the promotion effect for enterprises' innovative products. Based on bounded rationality, we construct a game model based on the group's choice of strategy in mobile social network marketing communication, obtain the corresponding mean field equation, and solve this equation for the group's choice of strategy under different conditions. We use a MATLAB tool for the numerical simulation of the model, and we provide a visual presentation of how the user's choice of strategy affects the promotion effect of enterprises' innovative products. Finally, we provide relevant suggestions based on our findings. This paper uses quantitative model methods to study the influence of user information behaviors on the promotion effect of enterprises' innovative products, which augments extant qualitative research. In future research, real data could be used to verify this model.

Data Availability

The simulation experiment data used to support the findings of this study are available from the corresponding author upon request.

Conflicts of Interest

The authors declare that there are no conflicts of interest regarding the publication of this paper.

Acknowledgments

This research was funded by the Shanghai Sailing Program, grant number (20YF1433800).

References

- [1] Y. Liu, "Word of mouth for movies: its dynamics and impact on box office revenue," *Journal of Marketing*, vol. 70, no. 3, pp. 74–89, 2006.
- [2] T. Chen, L. Peng, J. Yang, and G. Cong, "Analysis of user needs on downloading behavior of English vocabulary APPs based on data mining for online comments," *Mathematics*, vol. 9, no. 12, Article ID 1341, 2021.
- [3] D. Chen, "How the service recovery of negative online reviews affect customers' purchase intention-based on the platform of taobao," in *Proceedings of the China Marketing International Conference*, pp. 679–693, Xi'an, China, 2015.
- [4] M.-L. Chung, H.-J. Jhan, M.-Y. Liou, J.-S. Li, and Y.-S. Hou, "An investigation of innovation imitation products and consumer purchases situational attribute," *Procedia - Social and Behavioral Sciences*, vol. 40, pp. 689–694, 2012.
- [5] Z. Li, F. Li, J. Xiao, and Z. Yang, "Effects of negative customer reviews on sales: evidence based on text data mining," in *Proceedings of the IEEE International Conference on Data Mining Workshops*, pp. 838–847, Singapore, November 2018.
- [6] J. Ren, W. Yeoh, M. Shan Ee, and A. Popovič, "Online consumer reviews and sales: examining the chicken-egg relationships," *Journal of the Association for Information Science and Technology*, vol. 69, no. 3, pp. 449–460, 2017.
- [7] Z. Zhao, J. Wang, H. Sun, Y. Liu, Z. Fan, and F. Xuan, "What factors influence online product sales? Online reviews, review system curation, online promotional marketing and seller guarantees analysis," *IEEE Access*, vol. 8, pp. 3920–3931, 2020.
- [8] Z. Zhou, G. Zhan, and N. Zhou, "How does negative experience sharing influence happiness in online brand community? A dual-path model," *Internet Research*, vol. 30, no. 2, pp. 575–590, 2019.
- [9] C. Dellarocas, "The digitization of word of mouth: promise and challenges of online feedback mechanisms," *Management Science*, vol. 49, no. 10, pp. 1407–1424, 2003.
- [10] R. R. Mukkamala, J. I. Sørensen, A. Hussain, and R. Vatrpu, "Detecting corporate social media crises on facebook using social set analysis," in *Proceedings of the IEEE International Congress on Big Data*, pp. 745–748, New York, NY, USA, July 2015.
- [11] M. U. Nazir, S. Tharanidharan, M. S. Mian et al., "Social media competitive analysis - a case study in the pizza industry of Pakistan," *Communications in Computer and Information Science*, vol. 932, pp. 313–325, 2019.
- [12] P. Li, X. Yang, L.-X. Yang, Q. Xiong, Y. Wu, and Y. Y. Tang, "The modeling and analysis of the word-of-mouth marketing," *Physica A: Statistical Mechanics and Its Applications*, vol. 493, pp. 1–16, 2018.
- [13] C. Peters, C. H. Amato, and C. R. Hollenbeck, "An exploratory investigation of consumers' perceptions of wireless advertising," *Journal of Advertising*, vol. 36, no. 4, pp. 129–145, 2007.
- [14] Q. Shen and J. Miguel Villas-Boas, "Behavior-based advertising," *Management Science*, vol. 64, no. 5, pp. 2047–2064, 2018.
- [15] L.-J. Kao and Y.-P. Huang, "An effective social network sentiment mining model for healthcare product sales analysis," in *Proceedings of the 2018 IEEE International Conference on Systems, Man, and Cybernetics (SMC)*, pp. 2152–2157, Miyazaki, Japan, October 2018.
- [16] I. C. Juanatas, R. R. Fajardo, E. T. Manansala, A. A. Pasilan, J. R. Tabor, and H. D. A. Balmeo, "Sentiment analysis platform of customer product reviews," in *Proceedings of the International Conference on Computational Intelligence and Knowledge Economy*, pp. 230–234, Dubai, UAE, December 2019.
- [17] F. Li and T. C. Du, "The effectiveness of word of mouth in offline and online social networks," *Expert Systems with Applications*, vol. 88, pp. 338–351, 2017.
- [18] M. A. A. Dewi, N. N. Annisa, P. Kareen, A. Edwita, and D. I. Sensuse, "Analysing the critical factors influencing consumers' knowledge sharing intention in online communities and its impact on consumer product involvement, product knowledge and purchase intention," in *Proceedings of the 2017 International Conference on Advanced Computer Science and Information Systems (ICACSIS)*, pp. 149–158, Bali, Indonesia, October 2017.
- [19] M. Jianjun, "Research on collaborative filtering recommendation algorithm based on user behavior characteristics," in *Proceedings of the International Conference on Big Data & Artificial Intelligence & Software Engineering*, pp. 425–428, Bangkok, Thailand, November 2020.
- [20] C. H. Tsai, Z. G. Zhu, T. Ku, and W. F. Chien, "Personal APP behavior analysis based on mobile device networks," in *Proceedings of the 2016 Eleventh International Conference on Computer Science & Education (ICCSE)*, pp. 405–412, Nagoya, Japan, August 2016.
- [21] Z. Liu, L. Lang, L. Li, Y. Zhao, and L. Shi, "Evolutionary game analysis on the recycling strategy of household medical device enterprises under government dynamic rewards and punishments," *Mathematical Biosciences and Engineering: MBE*, vol. 18, no. 5, pp. 6434–6451, 2021.
- [22] Z. Liu, Q. Qian, B. Hu et al., "Government regulation to promote coordinated emission reduction among enterprises in the green supply chain based on evolutionary game analysis," *Resources, Conservation and Recycling*, vol. 182, Article ID 106290, 2022.
- [23] X. Li, L. Cheng, X. Niu, S. Li, C. Liu, and P. Zhu, "Highly cooperative individuals' clustering property in myopic strategy groups," *The European Physical Journal B*, vol. 94, no. 6, p. 126, 2021.
- [24] C. Li, H. Xu, and S. Fan, "Synergistic effects of self-optimization and imitation rules on the evolution of cooperation in the investor sharing game," *Applied Mathematics and Computation*, vol. 370, Article ID 124922, 2020.
- [25] Y. A. Argyris, A. Muqaddam, and Y. Liang, "The role of flow in dissemination of recommendations for hedonic products in user-generated review websites," *International Journal of Human-Computer Interaction*, vol. 36, no. 3, pp. 271–284, 2020.
- [26] T. Klaus and C. Changchit, "Toward an understanding of consumer attitudes on online review usage," *Journal of Computer Information Systems*, vol. 59, no. 3, pp. 277–286, 2019.
- [27] H. Ohtsuki and M. A. Nowak, "The replicator equation on graphs," *Journal of Theoretical Biology*, vol. 243, no. 1, pp. 86–97, 2006.
- [28] J. D. Bohlmann, R. J. Calantone, and M. Zhao, "The effects of market network heterogeneity on innovation diffusion: an agent-based modeling approach," *Journal of Product Innovation Management*, vol. 27, no. 5, pp. 741–760, 2010.

Research Article

PLS-SEM Model of Integrated Stem Education Concept and Network Teaching Model of Architectural Engineering Course

Ping Wang 

Department of Architectural Engineering, Handan Polytechnic College, Handan 056001, China

Correspondence should be addressed to Ping Wang; wangping0074@163.com

Received 15 March 2022; Revised 4 April 2022; Accepted 15 April 2022; Published 2 May 2022

Academic Editor: Wei Liu

Copyright © 2022 Ping Wang. This is an open access article distributed under the Creative Commons Attribution License, which permits unrestricted use, distribution, and reproduction in any medium, provided the original work is properly cited.

In order to cultivate talents more effectively in construction engineering and cultivate students' critical thinking, creative thinking, high-level thinking, as well as students' perseverance, learning ability, global competence, and responsibility, combined with the integrated stem education concept, this paper makes an in-depth study on the online teaching model of construction engineering course in PLS-SEM mode. This paper mainly discusses how to apply stem education concept in architectural engineering teaching through literature analysis and the design of architectural engineering teaching cases. Take the integrated stem education concept as the guiding ideology, design research as the methodological guidance, and learn from the research model of design research in the field of curriculum and teaching "formative research." After the prototype of the teaching mode is put forward, with three rounds of iterative implementation and revision, a feasible and effective mathematics teaching mode in Engineering Higher Vocational Colleges under the concept of stem education (hereinafter referred to as "stem-HVE teaching mode") is finally obtained. It provides a new way for engineering teaching and opens a new chapter of integrated stem education in the field of engineering teaching.

1. Introduction

Stem is the abbreviation of science, technology, engineering, and mathematics, as shown in Figure 1. The integrated stem education concept aims to place the core content of stem field in a real and attractive problem situation, adopt a problem-solving driven student-centered teaching method, support students' learning of mathematics and/or science content, and help students acquire engineering design and/or technical means. At the same time, by emphasizing the integration between middle schools and disciplines in the process of displaying problem-solving, it helps students understand the close relationship between disciplines, experience the value of disciplines, and cultivate new skills in the 21st century, positive attitude towards stem disciplines, and enthusiasm for stem career [1]. Integrated stem education can help engineering higher vocational education achieve the goal of talent training. When applied to the

discipline of construction engineering, the integrated stem education concept not only supports students' learning of construction engineering, but also improves students' learning attitude and promotes their understanding of construction engineering, to make education truly serve the engineering specialty. Under the new normal of China's economy, the driving force of growth is changing from factor driven and investment driven to innovation driven. This transformation is in line with the development of economic, natural, and social laws and also reflects the country's urgent demand for high-level human resources. To develop an innovative country and improve the level of human capital, education reform is the "first chess." Only first-class education can have first-class talents and build a first-class country [2]. As a new direction of education reform in the 21st century, stem education has attracted extensive attention all over the world and is recognized as an effective way to enhance innovation and competitiveness.

TABLE 1: Level of discipline integration.

Integration level	Characteristic
Discipline integration	Acquire skills and concepts by learning a subject alone
Multidisciplinary integration	Learn from one project and master the concepts and skills of different disciplines
Interdisciplinary integration	Deepen the skills and concepts of each discipline through the study of two or more disciplines
Interdisciplinary integration	Through the study of two or more disciplines, acquire interrelated concepts and skills, match with practical activities, and strengthen the application of skills

2. Literature Review

Plessis A. and others believe that, with the continuous advancement of stem education, many educators in the world have recognized its teaching methods. Stem education should run through the whole learning stage of learners, carry out all-round training through formal in-school learning, and then polish it through informal out-of-school learning, so that mathematics, science, technology, and engineering are gradually integrated [3]. Plutynski A. and others said that, in the process of discipline integration, enterprises and business circles pay more attention to the practical ability of workers, while many theoretical knowledge and practical work are in contradiction. Therefore, in the view of integration, some scholars also issued a questionnaire, as shown in Table 1 [4].

Dewsbury and others believe that, in the integrated learning of stem education, more attention is paid to the connection between disciplines and knowledge. Through dynamic learning methods, learners can better master the application skills of acquiring abilities and skills in practice, apply the learned knowledge, alleviate the contradiction between theoretical knowledge and practical work in society, and further improve the application value of learning in society [2]. Jones and others said that, in the new era, structural equation model, namely, PLS-SEM, is an analysis method widely used in the field of statistics in recent years. It can flexibly deal with various complex variables and is widely used in statistics, economics, management, sociology, and other fields [5]. Woodford and others believe that, in order to widely apply it to the network education of current architecture courses, it should be modified to deal with the design of each section of architecture network courses flexibly [6]. Dolighan and Owen believe that, with the continuous promotion and application of SEM, the commonly used SEM software at present includes Amos, smartplis, LISREL, and so on. Most of LISREL and Amos use the maximum likelihood method to estimate the variables through estimation, which has high requirements. If the number to be counted is no more than 200, it is difficult to obtain a more stable solution. However, it is difficult to collect more than 200 kinds of variables in relevant fields, especially in the field of education. Therefore, it is difficult to ensure its stability by using the maximum likelihood method [7]. Verma A. and others believe that the model can be set through PLS-SEM through the least square method, which is different from other algorithms. This PLS-SEM model is easier to establish in the network teaching of architectural

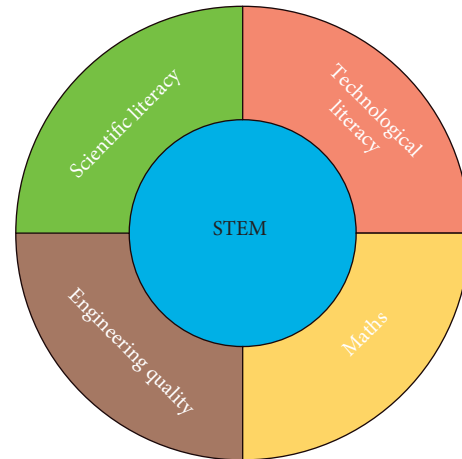


FIGURE 1: Stem concept diagram.

engineering courses [8]. Rodic and Rodic said that the online teaching of architectural engineering courses should have the education and learning contents of organization, tracking, evaluation, sending, and management, promote the interaction between learners and the network, and master various concepts and skills in the field of architecture in the process of continuous interaction. In the process of model design, it can be designed mainly through learning resource database, management system, content system, and general network [9]. Zhao et al. and others said that, in the process of practice, previous designs also exposed many problems, which hindered the effective development of construction engineering online education curriculum, lacked the cognition of practical teaching, and generally existed the educational concept of emphasizing theory and neglecting practice [10]. However, Hermans et al. and others said that, in the current era, all sectors of society pay more attention to learners' practical ability in the process of employment. Many learners' basic cultural level is relatively weak, and it is difficult to achieve effective practical effect if the teaching method is mainly lecture [11].

3. Method

3.1. Solutions to Research Problems

3.1.1. Principles of Stem Education. In stem education, education and teaching need to be closely connected with each other, cultivate learners' further skills through integration, and teach learners the ability to solve practical problems through theoretical knowledge.

First, we should follow its interdisciplinary principle in education. From the perspective of stem, we should subdivide various disciplines, including the main educational disciplines, make reasonable planning, deeply study the interrelated places between various disciplines, strengthen the links between disciplines, and strengthen learners' learning effect and absorption ability. Stem represents the fields of science, technology, engineering, and mathematics, which are closely related to each other. In stem education, we should not only focus on a single discipline, but also emphasize the communication and connection between disciplines, to cross the boundaries between disciplines and cultivate learners' ability of comprehensive thinking, so that learners can think from multiple angles to solve problems [12], as shown in Figure 2.

Second, the principle of interest should be followed. Stem's new educational concept is an educational policy born in the new era, and in the new era, all sectors of society also put forward different requirements for the education industry. Many scholars believe that education in the new era should break the traditional constraints, strengthen learners' learning motivation and enthusiasm through flexible and interesting education methods, stimulate learners' sense of achievement, and let learners experience happiness in the learning process. Therefore, in the process of education, teachers should pay attention to integrating the concepts of various disciplines into different situations to stimulate learners' skills and enable learners to have more initiative in the learning process [13].

Third, we should follow the principle of experience. In the process of education, stem education should actively cultivate learners' practical ability and enable learners to participate in the learning process by means of hands-on and brain use. Learners should also skillfully use their theoretical knowledge to solve various problems, so that learners can skillfully use more skills in the process of practice, experience more learning and practice methods, and strengthen learners' adaptability to various fields of society.

Fourth, the principle of cooperation should be followed. In stem education, in order to strengthen the learning effect in an all-round way, when designing teaching, teachers should emphasize the cultivation of the cooperative ability of learners, let learners help and inspire each other in the learning process, and build a learning community in a new era. At the same time, we can also strengthen the communication between teachers and experts through community, so that learners can actively participate in communication and discussion, and combine learning with the environment. In this way, learners can also collect learning materials in the community, ask more questions, and discuss with each other how to better complete learning tasks and strengthen learners' cooperation, which will be of great help to their work and life in the future [14].

3.1.2. PLS-SEM Mode Architectural Engineering Course Design Scheme from the Perspective of Stem. In PLS-SEM mode, the course design of architectural engineering should follow the structural equation model, which is divided into

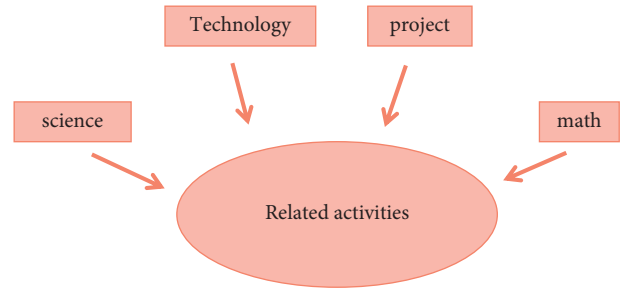


FIGURE 2: Curriculum integration of stem education.

measurement model and structural model. Since the measurement model represents the correlation between observation variables and latent variables, the measured model can also become an external model, while the structural model can also become an internal structure due to the correlation between internal variables [15]. During the establishment of external model, the relationship between each variable and potential variable should be observed, as shown in formulas (1) and (2):

$$x = A'_x \xi + \eta_x, \quad (1)$$

$$y = A'_y \eta + \eta_y. \quad (2)$$

The vector composed of exogenous indicators is set as x , the vector composed of endogenous indicators is set as y , the exogenous latent variable is set as ξ , while the endogenous latent variable is set as η , A'_x is the factor load of exogenous indicators on exogenous latent variables, and A'_y is also the factor load of endogenous indicators on endogenous latent variables. The relationship between exogenous indicators and exogenous variables can also be shown through the formula. At the same time, the relationship between endogenous indicators and endogenous variables can also be investigated. The nonerror between them can be expressed by η_x and η_y . Therefore, the weight relationship equation between them can also be obtained, as shown in equations (3) and (4):

$$\xi_1 = \sum_h w_{th} x_{th}. \quad (3)$$

$$\eta = \sum_k w_{th} y_{th}. \quad (4)$$

w_{th} is the h -th weight of the estimated latent variable ξ_1 and x_{th} is the h -th observation value of the estimated latent variable ξ_1 . At the same time, the estimated variables can also be shown by the right equation, and the weight coefficients and weight observations between each other can also be expressed by $\sum_k w_{th}$, etc. The method adopted in this paper is based on in-depth study of architectural engineering design, combined with stem education concept and PLS-SEM, designed the online education course of architectural engineering through various design modes, and finally designed several education stages for the overall online learning course [16].

First, the participation stage: The design should adhere to the basic goal of stimulating learners' enthusiasm and paying attention to improving learners' participation. Teachers should give a certain degree of advance notice of the course content in the process of teaching, so that learners can preview before class, to produce the initial concept and understanding of the classroom teaching content and guide the learners through questions to explain their self-understanding of the course, to evaluate the learners' understanding ability and design level. Learners should also strengthen their mastery of learning objectives and be familiar with the learning contents to a certain extent through review.

Second, the exploration stage: In the design of this stage, we should also pay attention to providing more opportunities for learners to build themselves, so that learners can build their own value system and understanding ability through the exploration stage, strengthen the training of practical ability, and let learners ask questions according to the problems generated in the process of practice and exploration. Teachers should also guide learners, so that learners have the desire to actively explore and ask questions, and provide learners with learning materials to guide learners to think further [17]. Teachers should establish the concept of modeling in teaching, put forward the guidance of various problems to learners, judge learners in the process of exploration, and then promote learners' understanding of learning content and participate in class learning together through group data collection and brainstorming.

Third, the interpretation stage should be carried out. In the interpretation stage, learners should be given the ability to reflect. Teachers should also deeply modify and refine various knowledge in this stage. Learners should also actively use various concepts and do a good job in the production process of design scheme. Teachers take this opportunity to explain the principles of various theoretical knowledge to learners and let them master it. Among them, they should also pay attention to communication and exchange, let learners restate the summarized knowledge, let learners have in-depth communication and cooperation, promote the connection with each other, and let learners establish correct concepts through guidance [18].

Fourth, the engineering stage should also be combined with the design of PLS-SEM. It should focus on enabling learners to apply the knowledge they have learned in practical engineering examples and enable learners to grasp the practical application of various concepts and skills more deeply, focusing on cultivating learners' practical ability. For example, the devices in the construction are used in the aspects of test and verification, construction principle, construction technology, etc., and the teaching concepts designed by teachers are restated to enable learners to learn in exploration, monitor and manage learners' production process, and improve various design schemes [19].

Fifth, in the deepening stage, learners should strengthen their ability to apply various knowledge and skills and deepen learners' application of various complex engineering concepts. At the same time, we should also strengthen

learners' knowledge understanding in the learning process. Teachers can provide learners with new material resources and let learners use what they have learned before and integrate into the new field of knowledge. It can not only strengthen the integration ability, but also give play to the characteristics of rich resources in online education, guide learners to further communicate and discuss, and then combine it with new situations to try and explore, so that learners can master more new technologies, new devices, and new methods. In the final evaluation stage, teachers need to test the learning effect of learners and promote teachers' mastery of learners' ability through the test work, to flexibly master targeted educational methods in the teaching process of the next stage, and strengthen the interaction between teachers and learners [20]. Through the feedback platform, learners can also feedback teachers' opinions in the learning process or communicate with teachers' deficiencies in the teaching process, so as to reduce the adverse phenomena that it was difficult for both sides to communicate effectively in the past and strengthen the effectiveness of construction engineering network education courses.

3.2. Integrated Stem Education Concept and Teaching Process.

Under the concept of integrated stem education, teachers play the role of organizer, guide, and helper in the biology teaching process of junior middle school. The flowchart is shown in Figure 3 [21]. Teachers' work contents include the following:

- (1) Create engineering or scientific situations close to students' personal experience
- (2) Explain the core concepts of biology and interdisciplinary concepts
- (3) Through situational analysis, questioning and inspiration, demonstration experiment, sharing information, providing examples, and other teaching supports, we can help students explore and practice and help students solve problems or complete projects and observe students' performance and give performance evaluation
- (4) Listen to group communication and arrange intensive exercises according to the results of different groups
- (5) After solving the problem or completing the project, give a summary evaluation according to the results and performance of the group

As the explorer, builder, and finisher of stem project, students mainly work as follows:

- (1) Clarify the theme of interdisciplinary projects according to the engineering or scientific situation created by teachers.
- (2) Construct the core concepts of biology and interdisciplinary concepts in combination with teachers' lectures and materials consulted before class.
- (3) After the division of labor is clear, the group will carry out orderly coordination and cooperation.

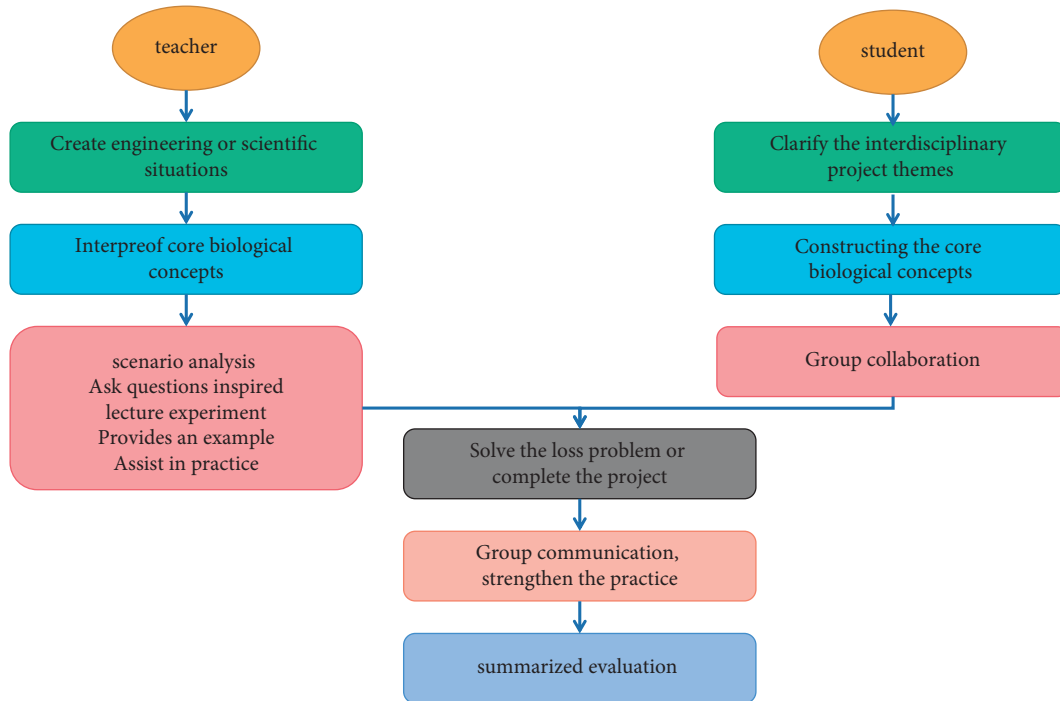


FIGURE 3: Teaching flowchart of integrated stem education concept.

- (4) Jointly complete the practical exploration driven by the project or problem, including expressing the problem, summarizing the specific requirements, evaluating the scheme, and communicating the problem. This is a multiround and dynamic revision and improvement process. And finally solve the problem or complete the project.

The group will conduct intragroup and intergroup communication on the results obtained and complete the intensive exercises arranged by the teacher.

The teaching process includes five links: creating engineering or scientific situations and clarifying the theme; clarifying the core concepts of biology; team work to revise and improve repeatedly, solve problems, or complete projects; reporting results; intensive exercise. The key to the implementation of teaching process lies in the creation of engineering and scientific situations. Different ways of putting forward teaching topics will lead to different students' enthusiasm and participation. Before integrated stem teaching, teachers must complete more detailed and sufficient preclass preparation than conventional teaching in order to ensure the smooth progress of teaching [22]. According to the stem interdisciplinary project design pattern, extract the preclass preparation that teachers need to complete, as shown in Figure 4.

Teaching analysis is mainly a detailed analysis of teaching objectives, interdisciplinary learning content in teaching, and learner characteristics from the perspective of integrated stem education concept [5]. The learning task design of integrated stem teaching with "project or problem" as the core mainly includes the design of tools and resources, learning support, activity process, and evaluation scale.

3.3. *General Steps of Engineering Design Process.* Using engineering practice or design as the realistic situation of integrated stem education, it is necessary for us to understand the steps that engineers generally experience when doing engineering design or practice, that is, the core of engineering practice: engineering design process [23]. The engineering design process is generally carried out in seven stages, as shown in Figure 5.

Stage 1: identify problems and constraints. When engineers face engineering tasks or projects, they first need to identify problems for three purposes: first, determine work objectives; second, analyze the views of stakeholders of the project and find ways to integrate them into the design; third, clarify all restrictions (such as objective or subjective constraints such as time and supply) and standards (the characteristics to be met by the final product, such as beauty and energy conservation) [24]. This step is very important. At this stage, each participant needs to reach a consensus on the design objectives and limits.

Stage 2: basic research. Facing a certain engineering task or project, the engineer will first do some background and basic research, to get the necessary information for drafting the preliminary design scheme. For example, understand the background knowledge and supplement the domain knowledge; investigate the previous work related to the design theme to avoid repeated work; be familiar with design evaluation standards; and even be familiar with rules, customs, laws, environmental problems caused by investigation, and design [25].

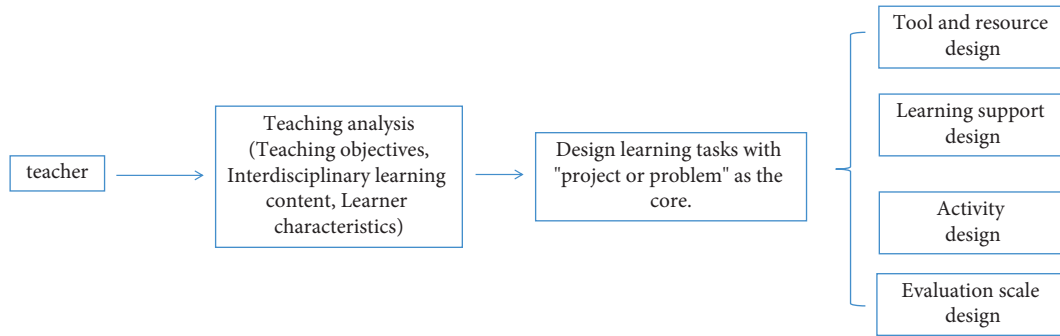


FIGURE 4: Preparation for integrated stem teaching.

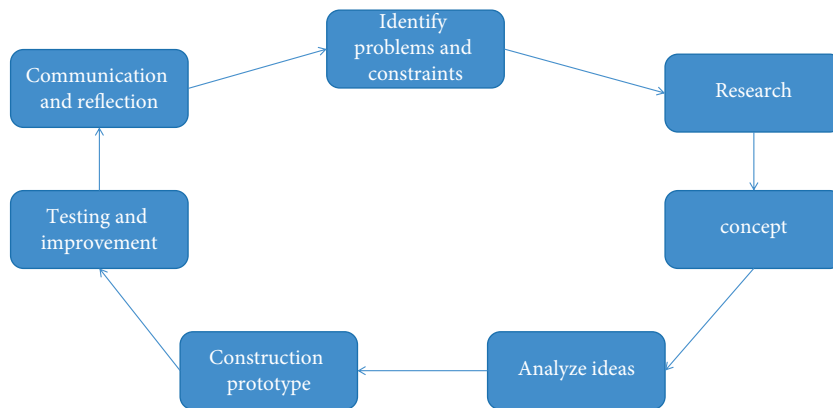


FIGURE 5: Engineering design process 7 stages.

Stage 3: conceive. Engineers usually need to conceive several different solutions first and then further analyze them to get the optimal solution. “Creation” is the focus of this stage. In order to stimulate inspiration, engineers usually use “brainstorming.” This method is very effective in solving a specific problem and can produce a series of new high-quality ideas.

Stage 4: analyze ideas. At this stage, engineers will use mathematical and scientific knowledge and principles to refine and improve the scheme initially constructed in the previous stage and select the best feasible scheme according to customer needs and situational constraints. For example, establish mathematical models to predict the performance of different schemes. In this process, engineers will make extensive use of mathematics, comprehensively consider the conflict between standards and constraints, and critically evaluate and exchange the advantages and disadvantages of each design scheme. If there are problems in the analysis, the engineer needs to reflect and return to a previous stage.

Stage 5: build the prototype. After establishing the best design scheme, the engineer needs to construct a full-scale working model or sample. It should be noted that the products of the project are not always materialized. The goal of a project can be a new design process, scheme, etc.

Stage 6: test and refine. Engineers use technical means to empirically test and evaluate the prototype and

establish a comprehensive evaluation file, including test conditions, observation results, etc. If there are problems in the test, the engineer needs to reflect and return to the previous stages.

Stage 7: communicate and reflect. The era of engineers working alone in a small attic has ended. Modern engineering design needs effective communication. There are at least four forms of communication: face-to-face, oral, visual, and written communication.

The above seven stages are a cyclic and iterative process, and iteration is an important feature of the engineering design process. Through this process, engineers gradually develop engineering thinking and the ability to analyze and solve problems by using mathematical tools and scientific knowledge.

4. Conclusion and Analysis

4.1. Experimental Method to Verify the Scheme. In course design, PLS-SEM is generally used to discuss the analysis method of the relationship between latent variable and manifest variable. In structural equation model, the relationship between variables is the most important to be analyzed. In curriculum design, learners’ satisfaction with class, course time, teachers’ teaching quality, and the rationality of curriculum design can be regarded as different variables and latent variables. According to the characteristics of these variables, in the process of classification and

integration, we should also clearly know the abstraction of the variables themselves. Many variables that are difficult to measure directly can only be estimated. However, the advantage of PLS-SEM is that it can carry out regression analysis between many variables where it is difficult to obtain accurate values and multiple dependent variables. When setting the regression path, it is calculated by analyzing each dependent variable separately. Although the measurement error is difficult to avoid, it can be assumed that there is no error in the independent variables, and the variables of the structural equation in the analysis process contain measurement error [26].

The least square path based on PLS-SEM can be constructed through new multivariate analysis technology, regression path, and modeling. The structural equation model also has two kinds of variables. We strive to build the model by taking the minimum variable value and then stabilize it through iterative parameters such as formulas (5) and (6):

$$\eta = \pi_{\eta}y + \partial_{\eta}. \quad (5)$$

$$\xi = \pi_{\xi}x + \partial_{\xi}. \quad (6)$$

η and ξ are endogenous variable vectors, x and y decibels represent the explicit variable vectors of endogenous and exogenous variables, π_{η} and π_{ξ} are coefficient matrices, and ∂_{η} and ∂_{ξ} are residual vectors. The reaction model is constructed, as shown in Figure 6. It also includes various variables such as x_{11} .

In the network curriculum design of construction engineering, stem education should represent the way of curriculum organization, reduce the impact caused by the neglect of the relevance between various disciplines and subjects in traditional education, and let learners make adaptive groundwork for future work planning and career development, to help learners have a deeper understanding of the discipline. For example, in architecture curriculum, it can relate to psychological curriculum and artistic aesthetic curriculum. Through detailed curriculum arrangement and careful coordination plan, it can carry out common learning among various disciplines, which also requires teachers of various disciplines to negotiate and communicate together, to strive for the rationality and effectiveness of curriculum design and strengthen the learning effect of learners. In the process of integration, when integrating knowledge, teachers should focus on more complex or valuable problem situations and let learners understand and construct the knowledge system in the way of cooperation, to form the ability to use their own knowledge and skills to solve various problems in the current practical life and strengthen the application ability of knowledge, make full use of the relevance between the situation and the problem, and give full play to the effectiveness of the situation and learning. In addition, in the process of learning, we should also pay attention to the integration with life, which is also to build the main framework of learning for learners through lifestyle and further deepen that learner can solve various problems in life through knowledge. Through academic knowledge, the problems in life can be transformed, so that learners can

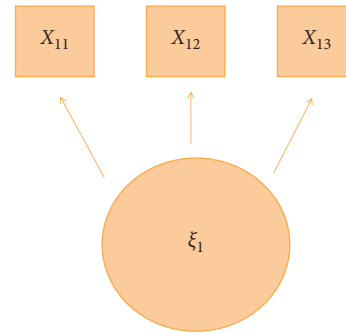


FIGURE 6: Schematic diagram of reaction model.

experience the practical application of knowledge from life or work and strengthen their enthusiasm for learning.

4.2. Analysis of Students' Learning Experience. After the implementation of teaching activities, in order to understand the students' learning experience in this teaching activity, a questionnaire is adopted for investigation. A total of 10 questions were compiled around the three dimensions of learning interest, teaching design, and teaching implementation, including 3 learning interests, 3 teaching designs, and 4 teaching implementations. A total of 85 test papers were distributed, 85 were recovered, and 85 valid questionnaires were received, with a recovery rate of 100%.

4.2.1. Reliability Analysis of Questionnaire. Cronbach's alpha is used to analyze the reliability of the three dimensions of teaching effect questionnaire, learning interest, teaching design, and teaching implementation. The reliability of each dimension is shown in Table 2.

According to the research, the reliability coefficients of the questionnaire are 0.782, 0.757, and 0.746, respectively, and the coefficients are between 0.7 and 0.8, indicating that the questionnaire has high reliability and can be studied.

4.2.2. Questionnaire Validity Analysis. This paper analyzes the questionnaire from three dimensions: learning interest, teaching design, and teaching implementation. Questions 1–3 are the investigation of learning interest, including practical ability, cooperation and exploration ability, and technical and cultural understanding.

As shown in Figure 7, the analysis and survey results show that, in the process of this teaching activity, more than 87% of students have high interest in learning this teaching activity and think that their practical ability can be greatly improved, and less than 13% of students are uncertain. However, more than 87% of the students said they were very satisfied with the teaching activity and 13% of the students maintained an uncertain attitude. Therefore, according to the overall teaching effect, the satisfaction is very high.

As shown in Figure 8, the survey results show that more than 88% of the students agree with this teaching activity and think that they have completed the teaching task perfectly in the activity, and their cooperation ability and independent inquiry ability have been improved to a certain extent. Only

TABLE 2: Reliability test of each dimension.

Reliability index	Reliability coefficient	Number of problems
Learning interest	0.782	3
Instructional design	0.757	3
Teaching implementation	0.746	4

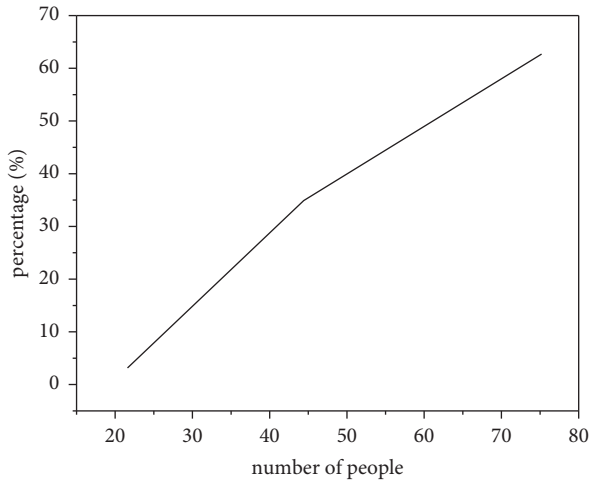


FIGURE 7: Survey of practical ability.

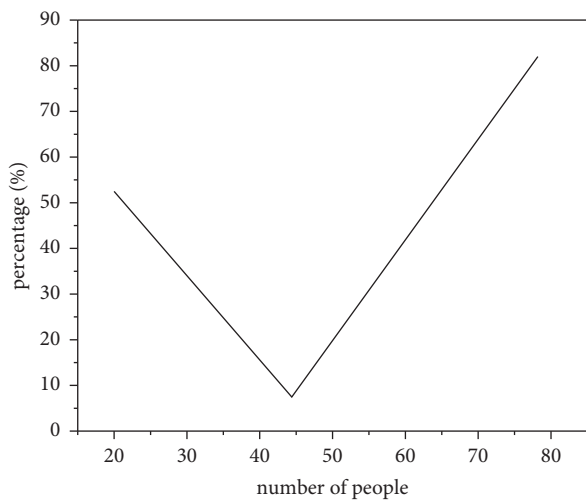


FIGURE 8: Survey of cooperation and inquiry ability.

12% of the students are uncertain about whether to acquire the ability. However, more than 88% of the students agree with the ability acquired in their activities, and 12% of the students maintain an uncertain attitude. Therefore, according to the overall teaching effect, the degree of recognition is very high.

As shown in Figure 9, the survey found that more than 90% of the students said that the teaching theme and activities made them full of interest in general technology courses, and less than 10% said that their interest in learning was average. The content of this teaching activity involves students' understanding of folk traditional crafts. In the

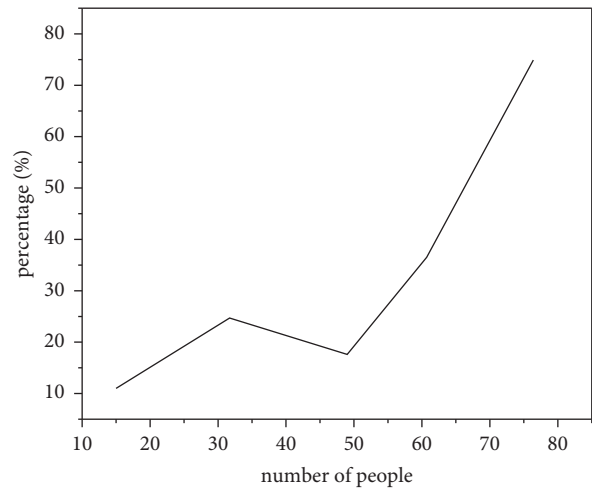


FIGURE 9: Technical culture understanding survey.

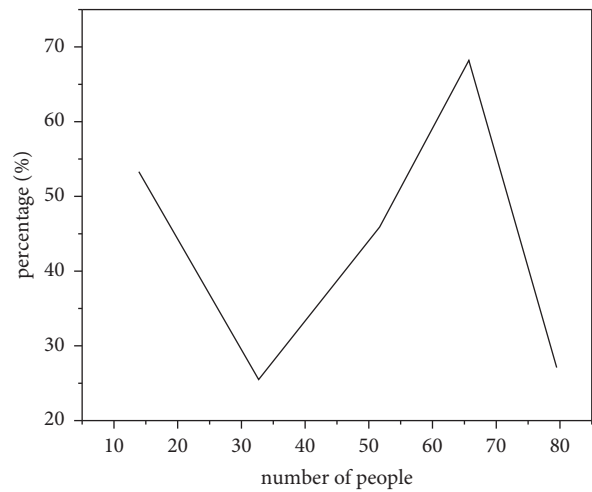


FIGURE 10: Survey of teaching topics.

form of interview, students' spare time is selected for investigation. It is found that they show great interest in traditional culture, which virtually gives good encouragement and recognition to the teaching and research at this stage. It shows that this teaching activity has a good effect on students' in-depth understanding of technical culture and deepening their love of traditional culture.

Questions 4–6 mainly investigate the students' recognition of this traditional folk culture teaching activity. According to the statistical results, it is found that the teaching theme content and learning objectives meet the students' learning needs for general technology courses to a certain extent, and the students have a high degree of recognition, as shown in Figure 10, indicating that the teaching is relatively successful.

Questions 7–10 are a survey of the teaching implementation stage, including teachers' explanation of cases, division of labor within the group, improvement of learning skills, and evaluation of self-learning and group cooperative learning. The students' satisfaction with the teacher's case explanation is shown in Figure 11. The survey results show

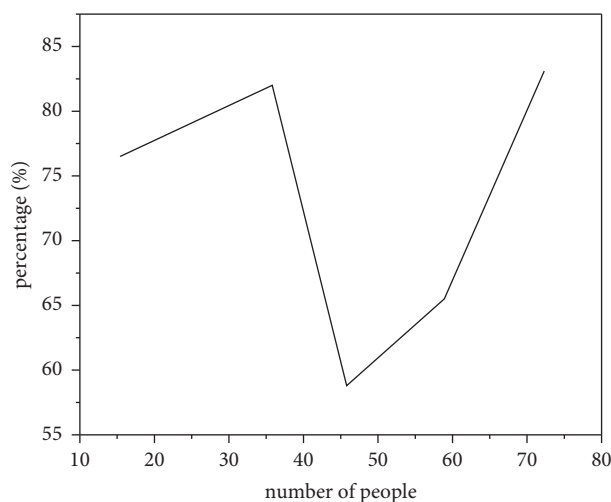


FIGURE 11: Case explanation and investigation.

that more than 85% of the students think that the teacher's explanation of the case task is very clear in this teaching activity, and 15% of the students maintain an uncertain attitude. The students who think that the teacher's explanation is clear account for 6/7 of the whole class, which shows that the teacher's explanation of this teaching activity is relatively clear, but the teacher should communicate more with the students after class to understand the real ideas of the students.

5. Conclusion

Through the integrated teaching of stem, the construction engineering network education course built in PLS-SEM mode has the mechanism of teaching content display, teaching material expansion, self-test, learning and communication among students, feedback, and evaluation. Students can complete various learning tasks through online education, which is more effective than the systematic learning in the classroom of colleges and universities. They can also learn regardless of time and place, providing more possibilities for learning. This learning method can also fully improve learners' initiative. Through the learning of network platform, students can break the limitations of traditional learning process and make use of diversified network forms and the integration of educational resources. It reduces the bottleneck of education and learning caused by the lack of teachers in the past curriculum teaching, liberates learners from single and monotonous learning, and further improves learners' acceptance and curriculum communication in the learning process. And adopt diversified and multidisciplinary integration to study, strengthen the personalization of the classroom, create a richer learning atmosphere and classroom atmosphere for learners, and strengthen learners' love and participation in the construction engineering course. In addition, in the learning process, it also plays a role in the integration and classification of educational resources by designing the curriculum into different stages. In this way, it improves learners' initiative, cultivates their abilities of independent exploration, independent research,

cooperation, and communication, gives full play to the advantages and value of online classroom, promotes the deepening development of stem education model in China, and improves the effectiveness of education curriculum.

Data Availability

The labeled datasets used to support the findings of this study are available from the corresponding author upon request.

Conflicts of Interest

The authors declare no competing interests.

Acknowledgments

This work was supported by the Handan Polytechnic College.



References

- [1] S. M. Letourneau, D. Bennett, K. McMillan Culp, P. Mohabir, D. Schloss, and C. J. Liu, "A shift in authority: applying transformational and distributed leadership models to create inclusive informal stem learning environments," *Curator: The Museum Journal*, vol. 64, no. 2, pp. 363–382, 2021.
- [2] B. M. Dewsbury, "Deep teaching in a college stem classroom," *Cultural Studies of Science Education*, vol. 15, no. 1, pp. 169–191, 2020.
- [3] A. E. Du Plessis, "The lived experience of out-of-field stem teachers: a quandary for strategising quality teaching in stem?" *Research in Science Education*, vol. 50, no. 4, pp. 1465–1499, 2020.
- [4] S. Zhao, M. Hu, Z. Cai, Z. Zhang, T. Zhou, and F. Liu, "Enhancing Chinese character representation with lattice-aligned attention," *IEEE Transactions on Neural Networks and Learning Systems*, pp. 1–10, 2021.
- [5] A. H. Jones, "What is an educational good? theorising education as degrowth," *Journal of Philosophy of Education*, vol. 55, no. 1, pp. 5–24, 2021.
- [6] P. J. Woodford, "Philosophy in the science classroom: how should biology teachers explain the relationship between science and religion to students?" *Cultural Studies of Science Education*, vol. 15, no. 4, pp. 937–950, 2020.
- [7] T. Dolighan and M. Owen, "Teacher efficacy for online teaching during the covid-19 pandemic," *Brock Education Journal*, vol. 30, no. 1, pp. 95–116, 2021.
- [8] A. Verma, S. Verma, P. Garg, and R. Godara, "Online teaching during covid-19: perception of medical undergraduate students," *Indian Journal of Surgery*, vol. 82, no. 3, pp. 299–300, 2020.
- [9] M. V. Rodic and D. D. Rodic, "Plans vs reality: reflections on chemical crystallography online teaching during covid-19," *Journal of Chemical Education*, vol. 97, no. 9, pp. 3038–3041, 2020.
- [10] S. Zhao, M. Hu, Z. Cai, and F. Liu, "Dynamic modeling cross-modal interactions in two-phase prediction for entity-relation extraction," *IEEE Transactions on Neural Networks and Learning Systems*, pp. 1–10, 2021.
- [11] J. Hermanns, B. Schmidt, I. Glowinski, and D. Keller, "Online teaching in the course "organic chemistry" for nonmajor

- chemistry students: from necessity to opportunity,” *Journal of Chemical Education*, vol. 97, no. 9, pp. 3140–3146, 2020.
- [12] J. Huang, “Successes and challenges: online teaching and learning of chemistry in higher education in China in the time of covid-19,” *Journal of Chemical Education*, vol. 97, no. 9, pp. 2810–2814, 2020.
- [13] Y. H. Hu, “Effects of the covid-19 pandemic on the online learning behaviors of university students in taiwan,” *Education and Information Technologies*, vol. 27, no. 1, pp. 469–491, 2021.
- [14] J. Dancy, “Honing practical judgement,” *Journal of Philosophy of Education*, vol. 54, no. 2, pp. 410–424, 2020.
- [15] W. Small, “Practical knowledge and habits of mind,” *Journal of Philosophy of Education*, vol. 54, no. 2, pp. 377–397, 2020.
- [16] R. Bell, “Underpinning the entrepreneurship educator’s toolkit: conceptualising the influence of educational philosophies and theory,” *Entrepreneurship Education*, vol. 4, no. 1, pp. 1–18, 2021.
- [17] R. Curren, “Peters redux: the motivational power of inherently valuable learning,” *Journal of Philosophy of Education*, vol. 54, no. 3, pp. 731–743, 2020.
- [18] K. Takayama, “Engaging with the more-than-human and decolonial turns in the land of shinto cosmologies: “negative” comparative education in practice,” *ECNU Review of Education*, vol. 3, no. 1, pp. 46–65, 2020.
- [19] M. D. Burbank, M. M. Goldsmith, J. Spikner, and K. Park, “Montessori education and a neighborhood school: a case study of two early childhood education classrooms,” *Journal of Montessori Research*, vol. 6, no. 1, pp. 1–18, 2020.
- [20] V. Giannakakis, “Neoliberalism and culture in higher education: on the loss of the humanistic character of the university and the possibility of its reconstitution,” *Studies in Philosophy and Education*, vol. 39, no. 4, pp. 365–382, 2020.
- [21] S. Sturm, S. Ceder, *Towards a posthuman theory of educational relationality*. abingdon; New York, ny: routledge, *Studies in Philosophy and Education*, vol. 39, no. 4, pp. 447–451, 2020.
- [22] S. Goodchild, “Book review: the philosophy of mathematics education today,” in *Educational Studies in Mathematics*, Paul Ernest, Ed., vol. 103, no. 1, pp. 109–119, 2020.
- [23] C. Martin, “Educational justice and the value of knowledge,” *Journal of Philosophy of Education*, vol. 54, no. 1, pp. 164–182, 2020.
- [24] S. Laugier, “Film as moral education,” *Journal of Philosophy of Education*, vol. 55, no. 1, pp. 263–281, 2021.
- [25] C. Robertson, Z. Al-Moasseb, Z. Noonan, and J. G. Boyle, “The 3-d skills model: a randomised controlled pilot study comparing a novel 1–1 near-peer teaching model to a formative osce with self-regulated practice,” *Medical Science Educator*, vol. 31, no. 6, pp. 1789–1801, 2021.
- [26] H. Bardesi, A. Al-Mashaikhi, A. Basahel, and M. Yamin, “Covid-19 compliant and cost effective teaching model for king abdulaziz university,” *International Journal of Information Technology*, vol. 13, no. 4, pp. 1343–1356, 2021.

Research Article

Mathematical Problems in Engineering Landscape Ecological Security Assessment and Ecological Pattern Optimization of Inland River Basins in Arid Regions: A Case Study in Tarim River Basin

Yuanrui Mu ^{1,2} and Wei Shen ¹

¹School of Earth Sciences and Resources, China University of Geosciences, Beijing 100083, China

²No. 11 Geological Party, Xinjiang Bureau of Geology and Mineral Resources, Changji, Xinjiang 831100, China

Correspondence should be addressed to Yuanrui Mu; 3001180140@cugb.edu.cn

Received 10 March 2022; Revised 2 April 2022; Accepted 7 April 2022; Published 2 May 2022

Academic Editor: Xuefeng Shao

Copyright © 2022 Yuanrui Mu and Wei Shen. This is an open access article distributed under the Creative Commons Attribution License, which permits unrestricted use, distribution, and reproduction in any medium, provided the original work is properly cited.

Tarim River Basin (TRB), located at the Eurasia center, is a typical arid inland basin. It is critical to maintain the ecological security of TRB for the sustainable development of oases. With the inputs of four period land use data, the landscape ecological risk assessment model, the minimum cumulative resistance model, and network analysis were applied to analyze the landscape ecological security pattern and to optimize the landscape pattern. The results show that, during the period 1990–2020, (1) landscape ecological risks of TRB increased by 1.76%; (2) landscape ecological risks tend to agglomerate in space in each period. The clusters of high-high risk are mainly distributed in the central and eastern desert areas, while low-low risk clusters are mainly distributed in watersheds Oasis and mountains. (3) Ecological security pattern network of the basin becomes more complex and better. The optimized pattern, called Oasis Corridor Functional Area with one ring, two screens, two belts, ten corridors, and multicenter, is expected to provide reference for the ecological environment management and restoration.

1. Introduction

As an essential part of national security [1–5], ecological security is equally essential to political security, homeland security, military security, and economic security [6]. It has a strategic position and great significance, and it is also the key to achieving sustainable development [7, 8]. The concept of ecological security pattern and optimization originates from the West. In 1967, Mac Arthur and Wilson put forward the theory of island biogeography and “ecological network model” [9]. At present, based on different perspectives such as land use, landscape pattern, and ecological infrastructure construction, scholars have gradually developed from simple qualitative and quantitative pattern and planning analysis to more complex space research such as static pattern optimization, dynamic pattern simulation, and ecological state trend analysis [10]. The research methods mainly include

multi-index comprehensive evaluation, minimum cumulative resistance model, scenario simulation, and landscape ecological index. Taken together, the index construction and methods of ecological security pattern research are still in further exploring. Most studies use the framework of “source-resistance surface-corridor” to construct the regional ecological security pattern [11]. In addition, most researchers regard the identification of ecological sources and ecological corridors as an important part of the construction of ecological security pattern, but the identification of strategic points is ignored.

Compared with other regional ecological risks, watershed ecological risk assessment has unique watershed characteristics [12]. In the current study, landscape analysis method is mainly used to analyze watershed ecological risk [13]. For example, Craig et al. [14] combined land use with landscape structure and used ecological threat index to

evaluate the ecological risk status of Colorado River Basin; Yan et al. [15] constructed a watershed ecological risk assessment model according to the three indexes of landscape risk, vulnerability, and loss to evaluate the ecological risk of Taihu Lake Basin; Xu et al. [16] analyzed the temporal and spatial pattern of ecological security of coastal wetlands in Jiangsu by using landscape interference index and vulnerability index; Xie et al. [17] constructed an ecological risk assessment system based on landscape vulnerability, landscape structure index, and landscape component area to evaluate the ecological risk of Taihu Lake; Ma et al. [18] selected landscape indicators to quantitatively characterize the landscape pattern in medium and downstream of Shule River according to the degradation situation of the ecosystem; Ran et al. [19] applied an ecological risk assessment framework integrating landscape pattern characteristics and landscape vulnerability dynamics to analyze the spatio-temporal variations of landscape ecological risk in the Yangtze River Delta from 2000 to 2018. The above achievements provide the theoretical basis for watershed ecological planning, landscape structure adjustment and optimization, and social and economic sustainable development at home and abroad.

The Tarim River Basin (TRB) is the fifth largest in the world, and also the largest inland river basin in China. Its watershed runs around the Taklimakan Desert from west to east and through the Tarim Basin. It is a hybrid system with natural and social attributes, which compose of forests, grasslands, wetlands, deserts, and people living in the basin. It has typical characteristics such as good primitiveness and naturalness. The TRB is an essential part of the ecological barrier in northwest China in regulating the climate, conserving water sources, preventing desertification, protecting biodiversity, and maintaining the ecological balance. Due to the vulnerability of the ecological environment in arid areas and the sensitivity to external interference [20], the TRB has become one of the key areas for global change researches. Over the decades, global climate change and human activities have had a great impact on the ecological environment of the TRB. For example, the changes of Land Cover and landscape pattern, and drastic desertification, the shrinkage of wetland area, grassland degradation, reduction in biodiversity, and the ecological risks have attracted more and more attention. At present, the research on ecological risk assessment mainly focuses on some key areas in TRB [21–26], while the large-scale research on the whole TRB is still lacking. At the same time, for the optimization of landscape pattern, many studies focus on models and methods but lack the combination of landscape ecological security and pattern optimization and lack the evolution analysis on time series. This study grasps the watershed ecosystem pattern and ecological risk changes from a macro perspective. Taking the whole TRB as the research object, the paper uses the landscape ecological risk evaluation model to quantitatively evaluate the temporal and spatial distribution and change characteristics of landscape ecological risk and then designs the optimal layout scheme of ecological spatial structure in the TRB. It is expected to provide scientific reference for optimizing the ecological spatial structure of

TRB, ensuring regional ecological security and promoting regional sustainable development.

2. Study Area and Data Source

2.1. Study Area. The TRB (71°39′–93°45′E, 34°20′–43°39′N) is located in the center of Eurasian continent and the south of Xinjiang. It borders the Pamir Plateau in the west, the Kunlun Mountains and Altun Mountains in the south, and Kuruktag Mountain in the east. The Taklimakan Desert is located in the middle of the basin. The area of TRB is about $1.02 \times 10^6 \text{ km}^2$ [27], and it is the largest inland river basin in China (Figure 1). It has abundant natural resources but a fragile ecological environment [27–29]. The total length of the Tarim River is 2179 km. At present, only the Aksu River, Hotan River, Yarkant River, and Kaidu-Peacock River have surface hydraulic connections with the mainstream of the Tarim River [27]. Its runoff mainly comes from its source and snowmelt and glacial meltwater in the Tianshan and Kunlun Mountains [30, 31]. The basin is located in the hinterland of the Eurasian continent at mid-latitudes. The terrain of the basin is low in the middle and high around, inclined from west to East. TRB situates the inland with dry climate, scarce precipitation, and high evaporation. The average annual precipitation of TRB is 17.4–42.8 mm, and the annual average temperature is 10.6–11.5°C. And the climate type of TRB is a temperate arid continental climate [26]. The land use types are mainly sandy land, unused land, and grassland, and the ecological environment is extremely sensitive and fragile.

2.2. Data. The land use/land cover change data in 1990, 2000, 2010, and 2020 are from the Resource and Environmental Science Data Center of the Chinese Academy of Sciences (<https://www.resdc.cn>), with a spatial resolution of $30\text{m} \times 30\text{m}$. With ArcGIS 10.2, the secondary land types were reclassified into nine land-use types: cropland, forest, grassland, waterbody, sandy land, saline-alkali land, Gobi, and construction and unused land. The GDEM V2 digital elevation data was used, with a spatial resolution of $30\text{m} \times 30\text{m}$. It is collected from the Geospatial Data Cloud Platform of the Computer Network Information Center of the Chinese Academy of Sciences (<https://www.gscloud.cn/>). This study uses the Albers_Conic_Equal_Area projected coordinate system.

3. Method

The framework of this study is mainly divided into three parts (Figure 2) Firstly, the landscape indexes are used to dynamically evaluate the landscape ecological risk of TRB. The ecological sources are determined according to the InVEST model and landscape connectivity indexes, and the cumulative resistance surface is constructed combined with the results of landscape ecological risk assessment. Then, the ecological corridors are extracted through MCR model and circuit theory, the ecological nodes and ecological obstacles are identified, and the watershed ecological security pattern is constructed. Finally, according to the above research

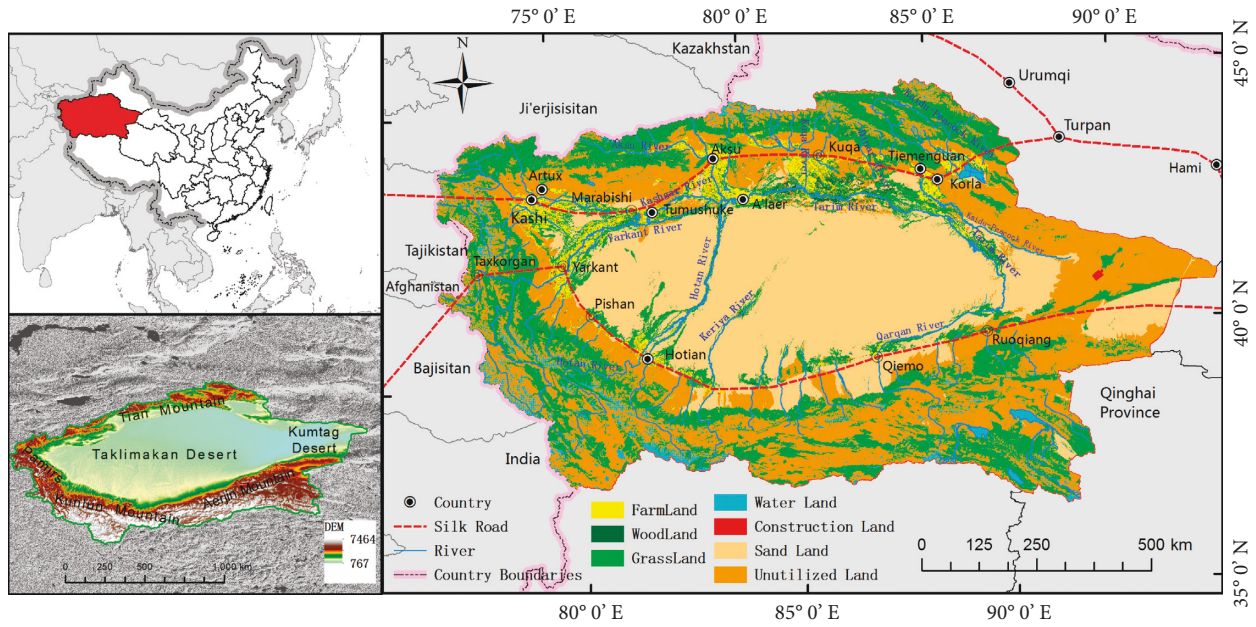


FIGURE 1: The location and land use/land cover of Tarim River Basin.

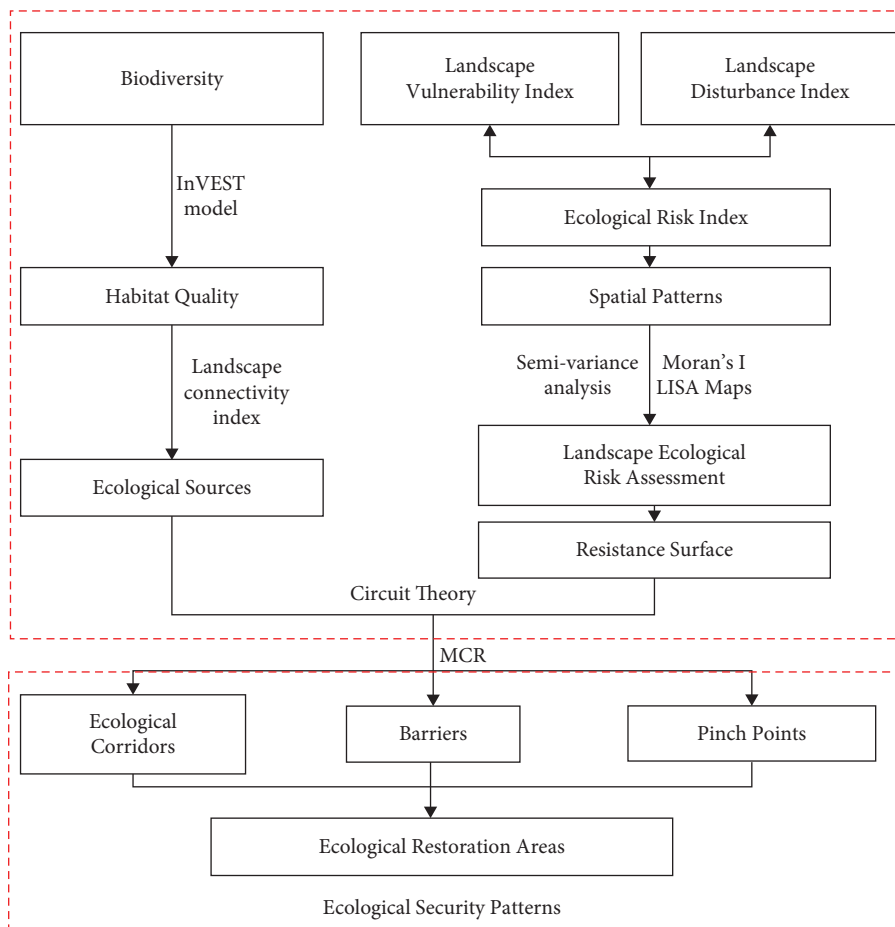


FIGURE 2: Framework of this study.

results, the measures and suggestions for the optimization of ecological security pattern are put forward. The specific framework is shown in Figure 2.

3.1. Construction of Landscape Ecological Risk Assessment Index System. The landscape pattern index highly condenses the information and is a simple quantitative index that expresses some aspects of its structural composition and spatial configuration. Based on previous research results [32, 33] and according to the relationship between the ecosystem landscape pattern and ecological risk, the landscape interference index, landscape fragmentation index, landscape separation index, landscape dominance index, landscape fragility index, and landscape loss index were used to establish the model of ecological risk index (Table 1). In order to spatially express the regional heterogeneity of landscape ecological risk [34, 35], a square grid of 10 km × 10 km was selected to divide the study area. The total number of risk areas is 5522. The ecological risk of each grid was calculated as the landscape ecological risk at the center point of each sample area.

3.2. Specialization of Landscape Ecological Risk. This study used ArcGIS10.2, GS + 9.0, spatial autocorrelation analysis, and semivariance analysis to represent the landscape ecological risk in the TRB spatially. Through the calculation of spatial weight and Moran's I index, the spatial autocorrelation of ecological risk in the study area is obtained, which reflects the distribution of adjacent ecological risk values in space. Spatial autocorrelation analysis can be divided into global correlation and local correlation [38, 39]. The best-fitting model was obtained by fitting the semivariogram to the point data through the geostatistical analysis module of ArcGIS [40–42]. We used the ordinary kriging interpolation method to get the spatial distribution map of ecological risk in four different periods.

- (1) Global spatial autocorrelation (Moran's I). Global spatial autocorrelation is used to study the spatial correlation and regularity of variable attributes. The formula is as follows:

$$Moran's I = \frac{N \sum_{i=1}^n \sum_{j=1}^n W_{ij} (x_i - \bar{x})(x_j - \bar{x})}{\sum_{i=1}^n (x_i - \bar{x})^2 (\sum_{i=1}^n \sum_{j=1}^n W_{ij})}, \quad (1)$$

where N is the total number of sample areas in the study area; x_i and x_j , respectively, represent the observation value of a characteristic attribute x on the spatial unit ($i \neq j$) \bar{x} is the mean value of x ; W_{ij} is the spatial weight matrix.

- (2) Local spatial autocorrelation. Local spatial autocorrelation can better show the spatial aggregation of ecological risk. It can show the spatial aggregation of ecological risk in the form of graphics, which can be divided into High-High, High-Low, Low-Low, and Low-High aggregation [43, 44]. The calculation formula is

$$I_i = \left(\frac{x_i - \bar{x}}{m} \right) \sum_{j=1}^n W_{ij} (x_j - \bar{x}), \quad (2)$$

where if the I_i value is positive, it indicates the spatial agglomeration of similar values (high or low values) around the regional unit, and if it is negative, it indicates the spatial agglomeration between dissimilar values.

- (3) Semivariogram analysis method. In this paper, GS + 9.0 software is used to fit the semivariogram, establish the fitting model, and carry out the spatial analysis of eco-environmental security to reflect the changes of observed values at different distances [33, 45]. Then, the semivariogram can be expressed as

$$\gamma(h) = \frac{1}{2N(h)} \sum_{i=1}^{N(h)} [z(x_i) - z(x_i + h)]^2, \quad (3)$$

where $\gamma(h)$ represents the semivariogram, h is the step size, $N(h)$ represents the number of samples with interval h , and $z(x_i)$ and $z(x_i + h)$ represent the measured values at $z(x_i)$ and $z(x_i + h)$, respectively.

3.3. Habitat Quality Model. InVEST model was developed by Stanford University and the World Wide Fund for Nature in the United States. The original intention is to weigh the relationship between regional development and conservation. "Habitat Quality" in the model can be used as a reflection of habitat quality. It is a quantitative evaluation of habitat quality from the perspective of biodiversity [46, 47]. According to the InVEST model guide [48, 49] and the natural conditions of the TRB, this study set wetlands, woodlands, grasslands, and waters as habitats, and other lands as nonhabitats. Residential sites, roads, railways, and rural roads are considered threat sources for habitats. Based on reference values in the InVEST model guide and related literature [49–51], we set the various parameters. The habitat quality calculation formula is as follows:

$$Q_{xj} = H_j \left[1 - \left(\frac{D_{xj}^z}{D_{xj}^z + k^z} \right) \right], \quad (4)$$

where Q is the habitat quality of the grid x of land use type j , H is the habitat suitability of the land type j , D is the habitat degradation degree of the grid x of the land type j , k is the half-saturation constant, which is generally 0.50, and z is the default parameter, generally 2.50 [48, 52, 53].

3.4. Construction and Optimization of Ecological Security Pattern. In this study, the cumulative resistance surface of the landscape pattern was constructed according to the results of ecological source and landscape ecological risk assessment, and the minimum cumulative resistance model (MCR) and network analysis were used to establish ecological corridors, identify ecological nodes, and optimize the landscape pattern. The formula is as follows [26]:

TABLE 1: The methods of landscape pattern indices.

Index	Formula	Ecological meaning of landscape pattern index
Landscape fragment, C_i	$C_i = n_i/A_i$	C_i represents the fragmentation degree to which the landscape is segmented at a given time and nature, with higher values representing higher fragmentation of the landscape and greater human disturbance to the landscape. n_i is the number of patches of landscape type i , A_i is the total area of landscape type i .
Landscape separation, N_i	$N_i = A/2A_i\sqrt{n_i/A}$	N_i represents the degree of separation of patch distribution in the same landscape type, and the larger the value, the more complex the corresponding landscape spatial distribution and the higher the degree of fragmentation [36]. A is the total landscape area.
Landscape fractal dimension, F_i	$F_i = 2 \ln(p_i/4)/\ln A_i$	F_i is a noninteger dimension value representing the geometric complexity of the patch or landscape mosaic. The value ranges from 1 to 2. The larger the value, the more complex the structure and change of the landscape patch. P_i is the perimeter of landscape type i .
Landscape interference, E_i	$E_i = aC_i + bN_i + cF_i$	E_i represents the effect of human interference on the area. The smaller the value, the better the survival of the creature. a , b , and c are the weights of the corresponding landscape indices, and $a + b + c = 1$, assign a , b , and c to 0.5, 0.3, and 0.2, respectively [37, 38].
Landscape fragility, V_i	Expert consultation and normalization	V_i represents the sensitivity of different landscape types to external disturbances, and the larger the value, the higher the ecological risk. According to the actual situation of the study area, the desert and Gobi are assigned a value of 7. The saline-alkali land is assigned a value of 6. The water area is assigned a value of 5. The cropland land is assigned a value of 4. The grassland is assigned a value of 3. The forest is assigned a value of 2. The urban land in the oasis in the arid area is the main area of human activities, the most stable, and is assigned a value of 1. Then, the landscape fragility is calculated using normalization.
Landscape loss degree, R_i	$R_i = E_i \times V_i$	R_i expresses the difference in the ecological loss suffered by various types of landscapes when disturbed, that is, the degree of loss of natural attributes. Through the comprehensive reflection of landscape disturbance index and landscape vulnerability index
Ecological risk index, ERI	$ERI = \sum_{i=1}^N A_{xi}/A_x \times R_i$	Based on the landscape disturbance index and vulnerability index, the spatial pattern was transformed into ecological risk variables by sampling method, and the ecological risk index of land use was constructed. N is the number of landscape types, A_{xi} is the area of the i -th type of landscape component in the x -th risk area, and A_x is the total area of the x -th risk area

$$MCR = f_{\min} \sum_{i=1}^m \sum_{j=1}^n D_{ij} W_i, \quad (5)$$

where MCR represents the cumulative value of the minimum resistance between ecological source j and any grid i ; D_{ij} represents the distance from the i -th grid to the j -th ecological source on the landscape pattern resistance; W_i represents the resistance value of the first grid on the surface of landscape pattern resistance to the operation of ecological flows. This study used the Linkage Mapper module to build ecological corridors. We use the Linkage Mapper toolbox to construct ecological corridors in ArcGIS10.2 software.

- (1) Identification of “ecological source” and the generation of resistance surface. In this study, the habitat quality model was used to identify the comprehensive ecological source of the TRB. Firstly, the patches with an area greater than 100 km were imported into Conefor Sensinode 2.6 Software. The threshold is set to 2000, and the connectivity probability is set to 0.5. Then, the three landscape indexes, including landscape coincidence probability (LCP), Integral index of connectivity (IIC), and Probability of connectivity (PC), could be calculated. Finally, the patches with patch importance of higher than 1 in the core area are identified as the

ecological source. With the inputs of landscape ecological risk and the selected ecological sources, the cumulative resistance surface of the TRB was calculated by the cost distance tool. Using the natural breakpoint method, the ecological land in the study area is divided into five levels: ecological core area, ecological buffer area, ecological transition area, ecological optimization area, and ecological governance area.

- (2) The establishment of ecological corridors. With the input of the selected “ecological source” and the cumulative resistance surface of the landscape pattern, this study mainly used the Linkage Mapper tool to calculate the minimum cost path between each ecological source and the rest of the ecological source. The minimum cost path is the ecological corridor. The ratio of the cost-weighted distance of the least-cost path to the path length is used to describe the relative resistance of moving along the path [54]. And the ratio of each corridor is divided into small resistance, medium resistance, and high resistance according to the natural breakpoint method.
- (3) Identify ecological “pinch points” and ecological barrier points. Ecological “pinch points” refer to areas that play an important role in ecological

protection. The identification of ecological “pinch points” is to ground one node (ecological source ground), input the same current electrical to other nodes (ecological source ground), and obtain the cumulative current electrical of each pixel through the iterative operation. The point with the high value of cumulative current electrical is the ecological “pinch point” [54, 55]. Ecological “pinch points” have high current electrical density and irreplaceability [56]. This study identifies “pinch points” in ecological corridors through the Pinchpoint Mapper module in Linkage Mapper toolbox. Ecological barrier points refer to areas where the movement of species between habitat patches is hindered. Removing these areas can increase the connectivity between ecological sources [57], and ecological restoration should be carried out in these areas. We use the Barrier Mapper module of Linkage Mapper toolbox to identify the barrier points in the ecological corridor.

- (4) Optimizing the layout of ecological spatial structure in the TRB. According to the construction of the ecological security pattern in the TRB, identify the main components of the ecological security pattern and analyze their spatial and temporal distribution characteristics. Based on reference to the “green-heart corridor group network” ecological space structure optimization combination mode proposed by Yang Tianrong et al. [58] and the “corridor group network” ecological space structure optimization combination mode proposed by Guo Rongchao et al. [59], this study optimizes and reorganizes the ecological security pattern of the TRB. Based on the identified ecological source areas, relying on topographical features to build an ecological safety protection zone and dividing the ecological function zones of the TRB, we use central river systems, roads, and intersource corridors to connect functional areas to build a regional ecological corridor network system. Through the optimization and reorganization of “point-line-surface” ecological spatial structural elements such as oasis areas, ecological pinch points, and corridor networks [60], an ecological spatial structure system with multilevel and complex “oasis corridor group network” is constructed in the arid inland river basin.

4. Results

4.1. The Spatial-Temporal Evolution of Landscape Ecological Risk in the TRB. This study used the index model to fit the ecological risk and generated a four-phase landscape ecological risk distribution map (Figure 3). Using the natural breakpoint method, the ecological risk value is divided into five grades: low risk ($ERI < 0.028$), relatively low risk ($0.028 \leq ERI < 0.032$), medium risk ($0.032 \leq ERI < 0.036$), relatively high risk ($0.036 \leq ERI < 0.040$), and high risk ($ERI \geq 0.040$). The results showed that the landscape ecological risks at the four phrase in the TRB had similar

structure and distribution characteristics. In the composition of risk levels, high-risk areas occupy the highest proportion of area, followed by relatively high-risk areas, and the ratio of the low-risk areas is the smallest. The spatial distribution of risk levels generally follows a pattern of high in the central and eastern regions and low in the surrounding areas.

Spatially, high-risk areas are mainly distributed in the central and eastern parts of the Tarim Basin and the transition zone between mountains and oases. These regions are sandy land, Gobi, and saline-alkali land with high landscape sensitivity and vulnerability. The landscape type is single, and the external world’s resistance is weak, resulting in a high landscape ecological risk. The relatively low-risk areas are distributed in the southern slope of the Tianshan Mountains, the Pamir-Kunlun Mountains-Aljin Mountains, and the alluvial plains in the middle and lower reaches of the river. The landscape in this area is mostly grassland, cultivated land, and swampy land. The low-risk areas are distributed in the southern slope of the Tianshan Mountains, the Pamir-Kunlun Mountains, and the Altun Mountains. This area is rich in water resources and has diverse landscape types, mainly grasslands, waters, and woodlands. And there is little human disturbance, so the landscape ecological risk level is low.

As the trend of ecological risk, the statistics of the area of each ecological risk level in the four periods (Table 2) show that the degree of ecological risk overall increases. The ecological risk of TRB is mainly of a high ecological risk level, accounting for more than 30%. The trend of ecological risk area in the four periods is as follows: the area of high and relatively high-risk levels has increased at the cost of decreasing the areas of the low, relatively low, and medium risk level. Among them, the areas of high-risk areas and relatively high-risk areas increased by 3.77% and 0.22%, respectively. The high areas were mainly distributed in the transition zone of desert margins, cities, and oasis margins. The interweaving changes of cropland, construction land, grassland, saline-alkali land, and sandy land reduce the landscape continuity and increase the landscape fragmentation, resulting in an increasing trend of landscape ecological risks. From 2010 to 2020, the areas of relatively low, medium, and high ecological risk levels increased, and the areas of low and high-risk levels decreased significantly. And the share of the low ecological risk level decreased from 9.37% to 8.24%. The area of low and high-risk levels is mainly transferred to the relatively low and relatively high-risk areas. With the implementation of environmental protection policies and policies in the Tianshan Mountains, Pamir-Kunlun Mountains, and Altun Mountains, many mines have been shut down, the forest and grassland areas have increased significantly, and the ecological risk has been reduced. The oasis area around the Tarim River continues to develop with urbanization, increasing ecological level. In the future, we should focus on strengthening the ecological protection, planning, and construction of the oasis area around the Tarim River and the transition zone at the edge of the desert with medium and above ecological risk levels.

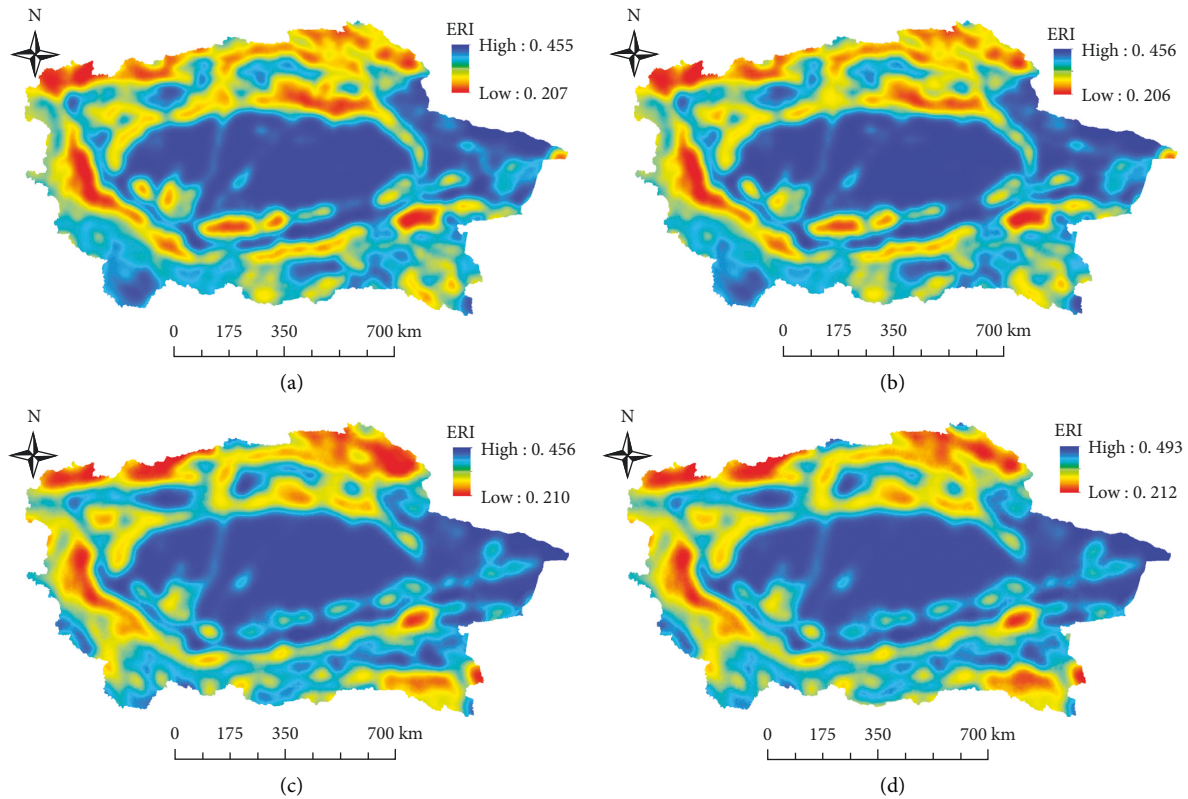


FIGURE 3: The spatial distribution of landscape ecological risks in the Tarim River Basin in four periods. (a) 1990, (b) 2000, (c) 2010, (d) 2020.

TABLE 2: The ratio of each ecological risk level in TRB in four periods.

Risk level	Area/km ²				Change ratio/%		
	1990	2000	2010	2020	1990–2000	2000–2010	2010–2020
Low risk	105490.74	102003.28	96890.42	85162.72	−3.42	−5.28	−13.77
Relatively low risk	153342.37	151718.48	142635.10	144424.86	−1.07	−6.37	1.24
Medium risk	204713.05	206221.62	180941.32	192709.24	0.73	−13.97	6.11
Relatively high risk	231268.06	229987.72	229288.61	233568.51	−0.56	−0.30	1.83
High risk	338523.99	343407.11	383582.75	377472.88	1.42	10.47	−1.62

4.2. *Spatial Autocorrelation of Landscape Ecological Risk in the TRB.* Figure 4 shows that the distribution of landscape ecological risks in the TRB is highly coupled with the regional geographical environment, and the degree of agglomeration of human activities corresponds to the degree of spatial agglomeration of risks. The landscape ecological risk in the TRB is dominated by High-High (H-H) and Low-Low (L-L) clustering patterns, showing significantly spatial clustering characteristics. The areas with H-H in the TRB are mainly concentrated in the central part of the study area (Taklimakan Desert), the eastern part (Kumtage Desert), and the transition zone between mountains and oases. The related landscape types are mainly sandy land, saline-alkali land, and the Gobi. The L-L agglomeration areas are mainly distributed in the southern Tianshan Mountains, Kunlun Mountains, Altun Mountains, and oasis areas in the TRB, and the landscape types are dominated by grasslands, waters, and woodlands. From 1990 to 2010, the distribution of H-H areas in the southern and eastern part of the watershed in the contact zone between desert and Oasis gradually expanded.

The area of L-L gradually shrank and the change of the L-L are mainly in oases such as Korla City and Hotan County. This is mainly due to the expansion of human activities and the small-scale land reclamation in the Oasis middle-agricultural area, which results in the increase of landscape fragmentation and the reduction of the L-L area. From 2010 to 2020, the H-H areas gradually shrunk, and the L-L areas gradually expanded.

4.3. Optimization of Landscape Ecological Pattern

4.3.1. *Spatial-Temporal Dynamic of Habitat Quality in the TRB.* Figure 5 showed that industrial and mining construction land, desert, saline-alkali land, Gobi, and bare land are the main distribution areas with low habitat quality in the study area. The Taklimakan Desert in the middle and the Kumtag Desert in the east have the largest low habitat quality. At the same time, there is an excellent correlation between the distribution of habitat quality and topographic

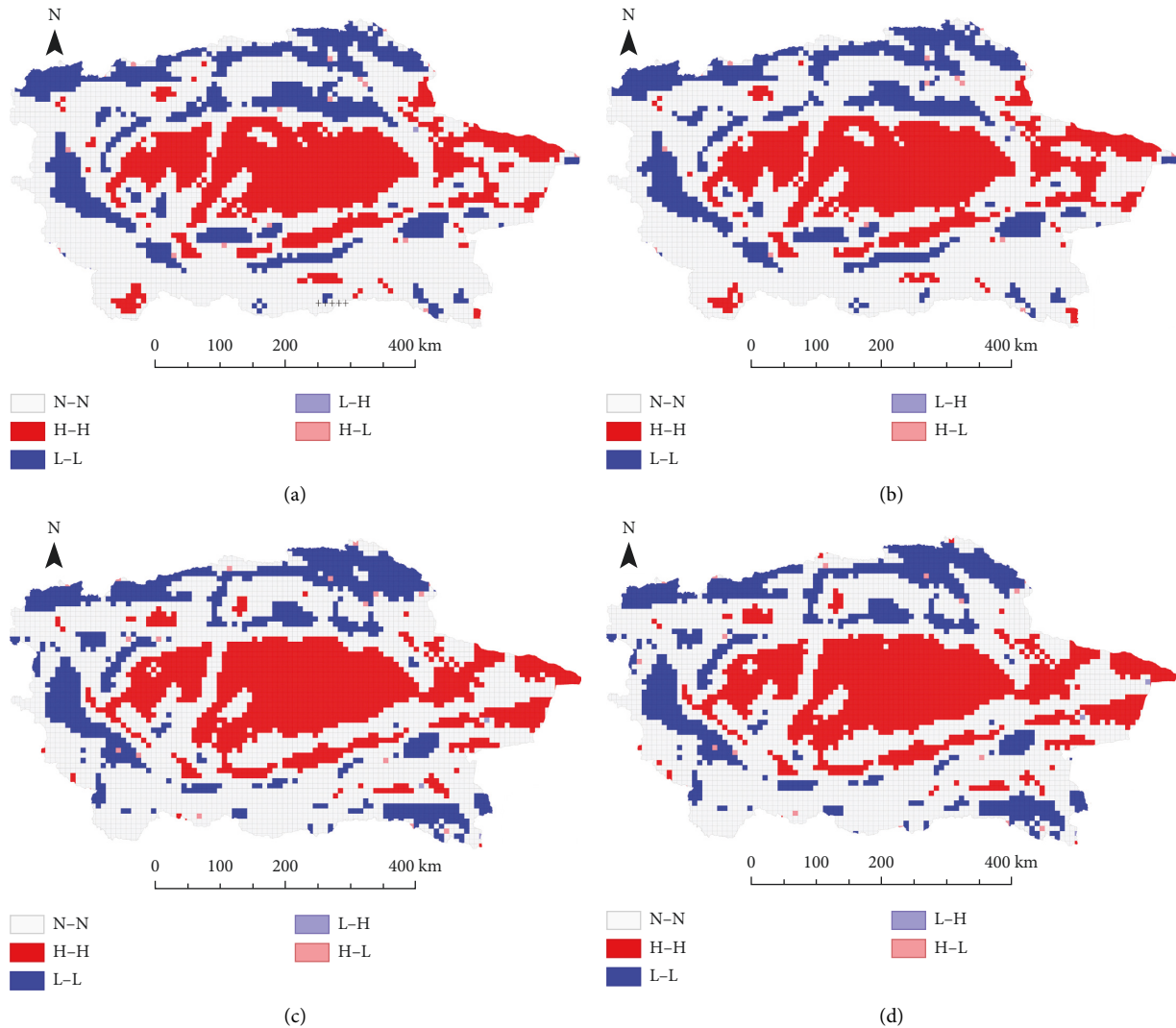


FIGURE 4: Local spatial autocorrelation clustering map of landscape ecological risks in the Tarim River Basin in four periods. (a) 1990, (b) 2000, (c) 2010, (d) 2020.

conditions. The areas with low habitat quality mostly have low altitudes, where desert areas are widely distributed. And the mountains and oasis areas with high altitudes and high vegetation coverage are mostly the areas with suitable habitat quality. Spatially, Figure 4 shows that the areas with high habitat quality in the four periods are distributed in the oases and mountainous areas, and the landscape types are mainly grasslands, oases, and shelter forests on the edge of the desert. The areas with low habitat quality are concentrated in the sandy land and saline-alkali land in the central and eastern parts, construction land such as towns and villages in the oases, and the Gobi area in the transition zone between the oases and the piedmont, which is largely different from the areas with high habitat quality.

In terms of trend, the average habitat quality of the TRB was 0.3751, 0.3736, 0.3686, and 0.3694 in the four periods, respectively. And the habitat quality overall decreased. From 1990 to 2000, many croplands was reclaimed, resulting in a gradual reduction in the area of wetlands and grasslands, and the patches became more and more fragmented. During the

period 2000–2010, with the rapid urban development, construction land expanded significantly, and the extension of urban outlines took up a large amount of cropland, grassland, and woodland. In addition, grasslands were degraded to unused land on the edge of deserts, resulting in a sharp drop in habitat quality. In mountainous areas such as the Tianshan Mountains and the Kunlun Mountains, the habitat quality level is greatly affected by natural factors, and the change of habitat quality in this area was small. From 2010 to 2020, the habitat quality increased slightly. During this period, the water body area increased from 27970.69 km² to 27213.10 km². The reduction rate of forest and grassland areas decreased from 2.21% in 2010 to 1.40% in 2020. The area converted from cropland land to forest and grassland is 2282.94 km². These indicate that the continuous popularization of the water-saving drip irrigation model in the Oasis, the transformation of the land use pattern, and the implementation of the “ecological water delivery” and “returning farmland to forests and grasslands” has improved the ecological environment of the TRB.

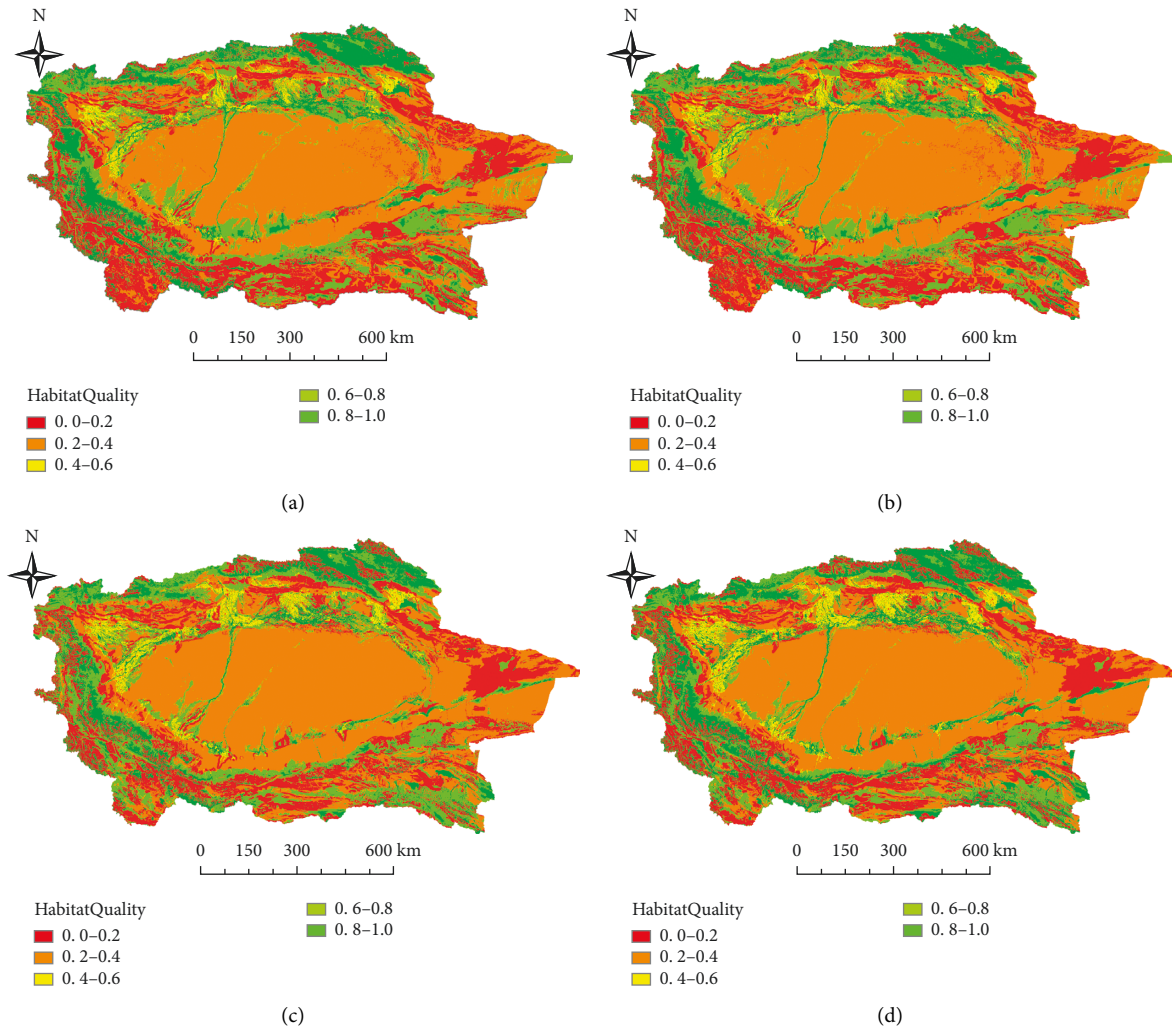


FIGURE 5: The spatial distribution of habitat quality in the Tarim River Basin in the four periods. (a) 1990, (b) 2000, (c) 2010, (d) 2020.

4.3.2. *Spatial-Temporal Characteristics of Ecological Sources.*

The ecological source area is generally an area with high habitat quality, which positively affects the ecological environment. Based on the evaluation results of the habitat quality of the TRB, the distribution of ecological sources was identified (Figure 6). From 1990 to 2020, the area of ecological sources in the TRB increased overall. The ecological sources are mainly distributed in the southern slope of the Tianshan Mountains, the Pamir-Kunlun Mountains- Altun Mountains, and the watershed oasis area. The Tianshan Mountains and the Pamir-Kunlun Mountains-Altun Mountains water conservation areas are the primary areas for ecological security in the TRB and the ecological bottom line for urbanization development and resource and environmental development and construction. Development and construction activities must be strictly prohibited in the above regions. From 1990 to 2000, the ecological source areas of the mainstream of the Tarim River, the Kashgar River, and the Yarkant River decreased, which was related to the unreasonable use of water resources in the middle and lower reaches of the basin, which resulted in the cut-off of the river. By 2010, the area of ecological sources increased

significantly, and the source area accounted for 10.86% of the study area, which was related to the policies of ecological water delivery and returning farmland to forests and grasslands in the middle reaches. By 2020, the areas of ecological sources increase significantly, accounting for 11.32% of the study area. Under a series of environmental management measures, the connectivity of green landscape patches continues to increase, and the degree of aggregation between patches increases.

4.3.3. *Construction of Comprehensive Ecological Security Pattern.*

Based on the establishment of the cumulative resistance surface of the landscape pattern in the TRB, the ecological corridors and ecological nodes were identified, respectively, and they were superimposed and combined to construct the ecological security pattern of the TRB (Figures 7–9). Overall, from 1990 to 2020, the area of ecological land in the TRB increased, the ecological quality gradually began to improve, and the ecological security pattern network system became more complex and better.

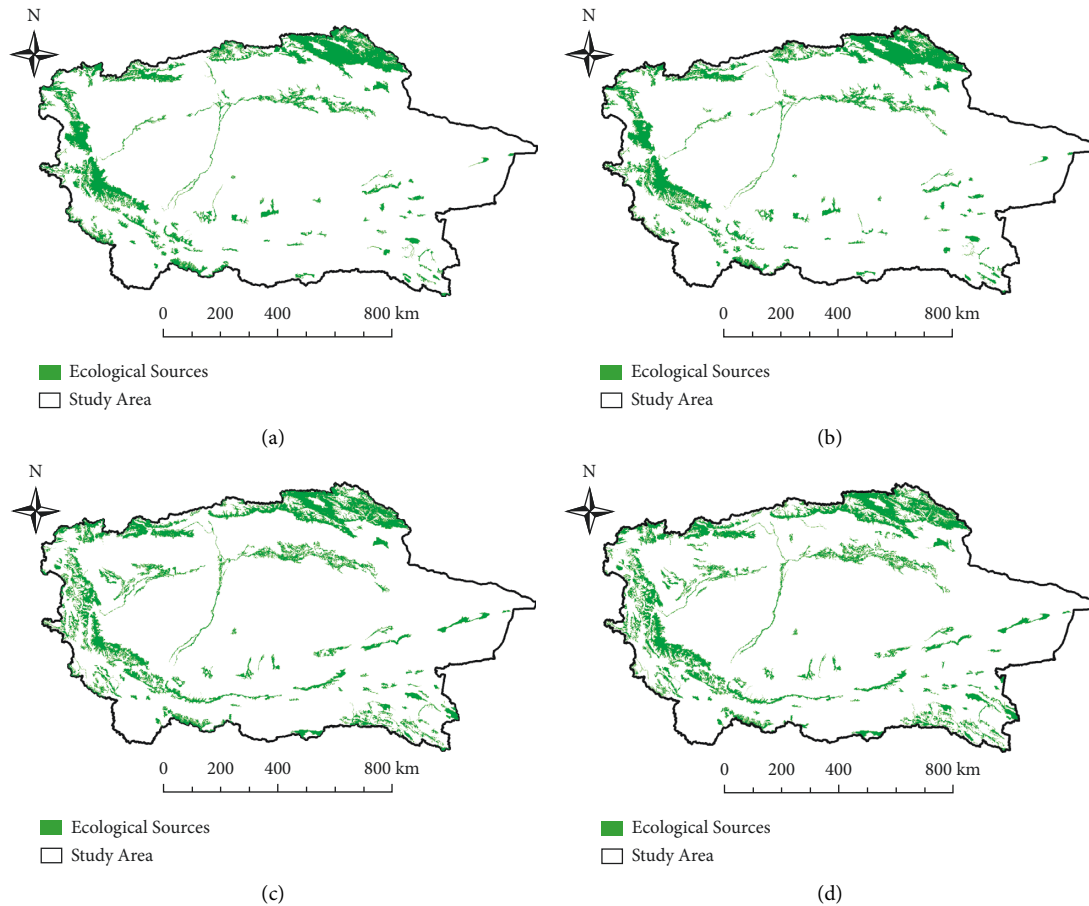


FIGURE 6: The spatial and temporal distribution of ecological sources in Tarim River Basin in four periods. (a) 1990, (b) 2000, (c) 2010, (d) 2020.

In 1990, the ecological security pattern identified 58 ecological strategic nodes, 18 ecological barrier points, and 240 corridors (21 large resistance corridors, 142 medium resistance corridors, and 77 small resistance corridors). The ecological strategic nodes are mainly distributed at the intersection of corridors, the ecological barrier points are mainly distributed in the transition zone between oases and mountains, and the ecological corridors surround the entire TRB. In 2000, there were 56 ecological strategic nodes, 20 ecological barrier points, and 241 ecological corridors (23 large resistance corridors, 126 medium resistance corridors, and 92 small resistance corridors). The ecological corridor mainly has two rings connecting the primary “source” areas. The middle ring is distributed along the mainstream of the Tarim River, and the outer ring is distributed along the Tianshan Mountains-Pamirs -Kunlun Mountains-Altun Mountains. The medium-resistance corridors are longitudinally connected to the transverse corridors, and some of the transverse corridors are connected to a small part of the source and intersect with the corridors. In 2010, the ecological security pattern had 53 ecological strategic nodes, 18 ecological barrier points, and 292 ecological corridors (26 large resistance corridors, 138 medium resistance corridors, and 128 small resistance corridors). Compared with 2000, the number of corridors increases, the connectivity and

network connection between sources are stronger, and the horizontal and vertical corridors in the watershed’s middle and lower reaches are intertwined, strengthening the connection between regions. In 2020, 70 ecological nodes, 21 ecological barrier points, and 337 ecological corridors (40 high-resistance corridors, 179 medium-resistance corridors, and 118 low-resistance corridors) were extracted. The main line of the corridor is still along with the distribution of the mainstream of the Tarim River and its tributaries, and the ecological source area has increased. And the number of ecological corridors between the Kashgar River in the west and the Qarqan River in the east has increased significantly.

Figure 9 also showed that the spatial distribution of corridors in the TRB is significantly different. The central and eastern deserts of the basin lack ecological sources and are not connected by corridors. And the number of corridors between patches around the Tarim River is large, the network density is high, and the connectivity is strong. The ecological sources in the northern Tianshan Mountains, the western Pamir Plateau, the southern Kunlun Mountains-Altun Mountains, and the Oasis have small resistance and a large number of low-resistance corridors, but the ecological sources are separated by deserts and Gobi, and the resistance is relative. And the distribution of small-area ecological sources acts as a “stepping stone,” connecting the various

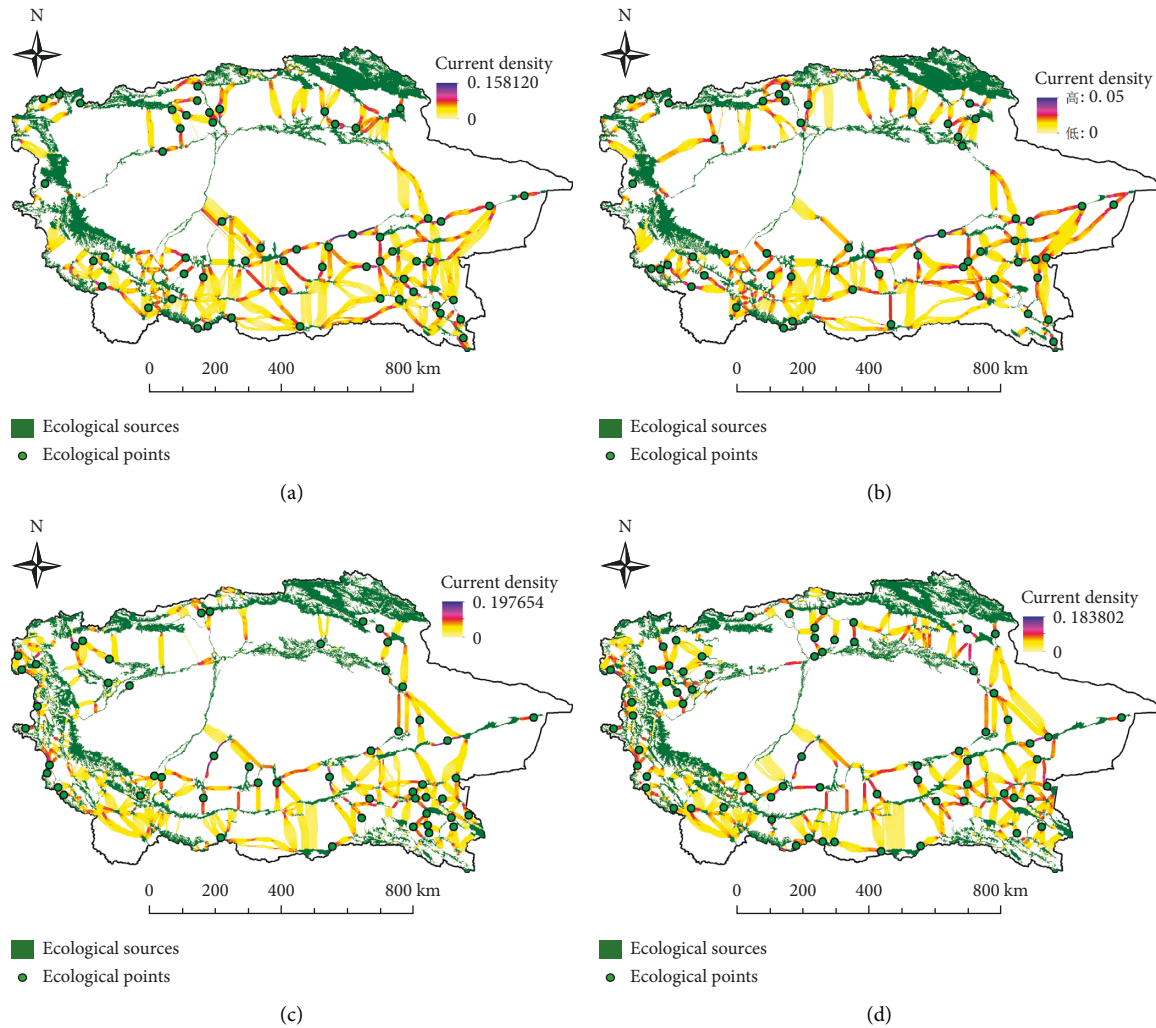


FIGURE 7: The spatial distribution of ecological nodes in four periods. (a) 1990, (b) 2000, (c) 2010, (d) 2020.

ecological sources to generate multiple high-resistance ecological corridors, which together constitute the optimal corridor network in the TRB. From 2010 to 2020, the number of ecological nodes and corridors increased significantly, especially the high-resistance corridors, which are mainly concentrated in the transitional areas between the upper and middle, and lower reaches of the Tarim River, and are the key areas for soil and water conservation. The obstacle points in the study area are mostly distributed in the high-resistance ecological corridor. From the comparison with Figure 8, it can be found that most of the barrier points are construction land and road land, and they all appear in the area where natural and artificial ecosystems blend. A few barrier points appear in areas with frequent human activities, which are mostly urban residential land. The ecological corridors in these areas are relatively short and narrow, and as the resistance value of the obstacle points increases, the ecological corridors may be directly cut off. Therefore, the improvement and restoration of obstacle points are the focus of ecological pattern network optimization and promote the complexity of the ecological security pattern network system.

4.3.4. Optimal Layout Design of the Ecological Spatial Structure. Based on the analysis of the background characteristics of ecological security in the TRB and related policy orientations, the elements of the TRB are optimized and reorganized. The oasis ecological source through the watershed is the ecological green center; other land uses are the matrix elements. The corridor is the ecological low resistance area between the main ecological source areas. The ecological high resistance area is the restoration zone, and the transition zone between the Oasis and mountainous areas is the key ecological restoration belt. The areas between the Oasis and desert (Gobi) are ecological protection belts, and the area outside the ecological protection belt is the main governance area. And the Tianshan Mountains and Kunlun Mountains-Altun Mountain ecological barriers are the ecological functional area, which is mainly for water conservation and ecological diversity maintenance. These will eventually form an oasis ecological ring in the Tarim Basin with green hearts embellishing the matrix, connecting five major water system corridors in each functional area. And a compound ecological spatial structure optimization system with “one ecological ring, two ecological barriers, two

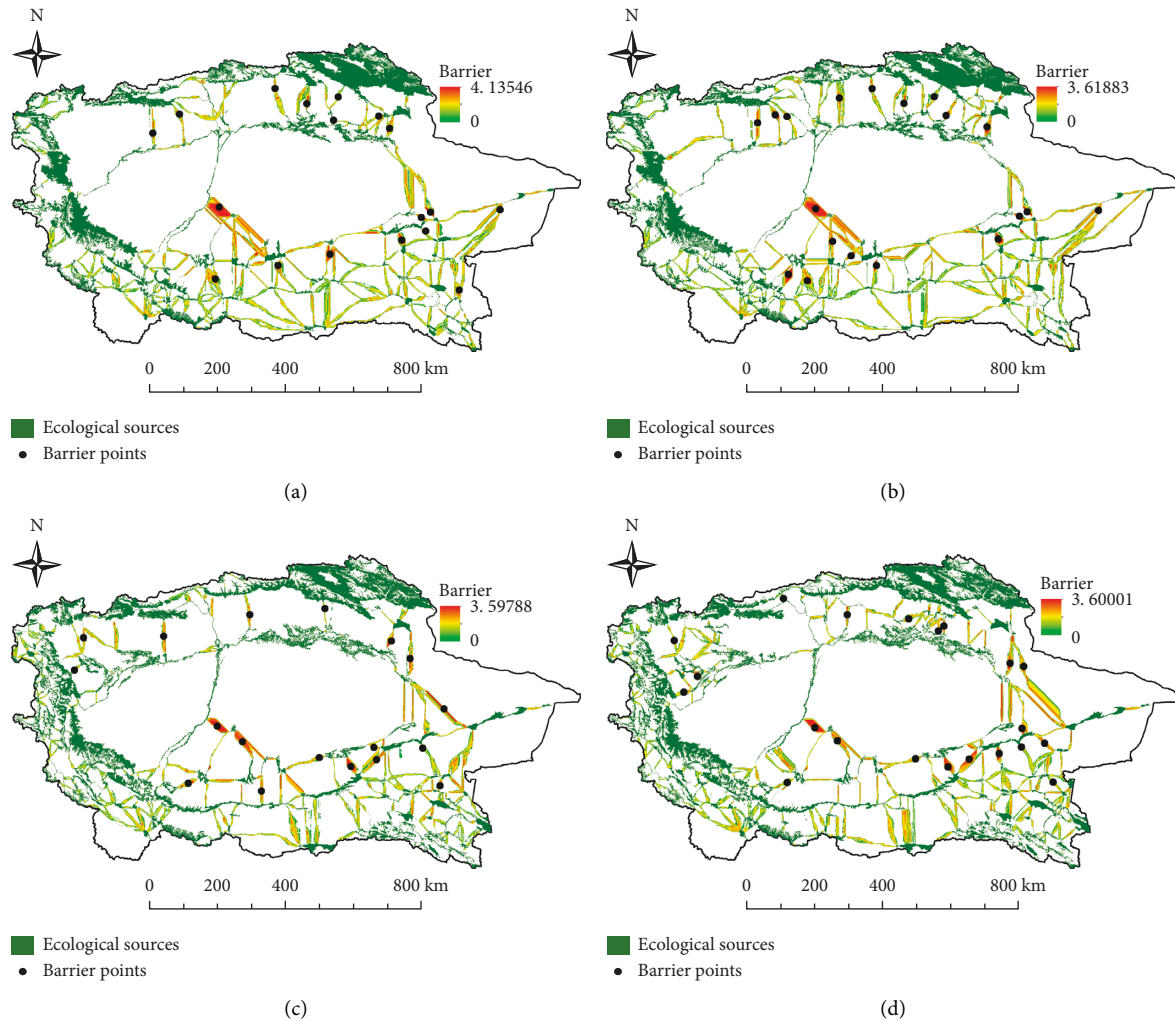


FIGURE 8: The spatial distribution of barrier points in Tarim River Basin in four periods. (a) 1990, (b) 2000, (c) 2010, (d) 2020.

restoration belts, and ten ecological corridors” will be conducted (Figure 10).

5. Discussion

5.1. Suggestions for Ecological Space Structure Optimization in the TRB

- (1) Build an oasis ecological restoration belt and a windbreak and sand fixation protective belt to strengthen the ecological environment quality of the “two districts.” To ensure the orderly development of the nine oasis areas and prevent sandstorms and soil erosion, protective belts are constructed in highly vulnerable areas between desert areas and oasis areas, mountain areas, and oasis areas to prevent desertification, salinization, and grassland degradation. The Kunlun-Altun Mountain North Slope Restoration Zone and the Tianshan South Slope Ecological Restoration Zone are located in the transition zone between the mountainous area and the oasis area, which are of great importance for soil and water conservation. The governance optimization area in

the desert area in the central TRB and the water source conservation ecological functional area in Tianshan Mountain and Pamir-Kunlun-Altun Mountain are two critical areas in the ecological optimization layout. The water conservation areas in the north and south are the water sources of the entire TRB. To ensure the normal development of the oasis area, enclosure protection should be strengthened to ensure water conservation. The optimized management area is mainly in deserts with the worst habitat quality, which is the biggest threat to the development of the oasis area. The management measures include adopting ecological measures to fix the sand, implementing water-saving irrigation measures, and planting desert vegetation.

- (2) Coordinate the relationship between “oases” and build a water systems and road corridors network. The oasis ecological ring along the Tarim Basin connects the nine oases (Akesu Oasis, Kuqa Oasis, Kashgar Oasis, Yarkant Oasis, Korla Oasis, Hotan Oasis, Yanqi Oasis, Ruoqiang Oasis, and Qiemo Oasis), which is an essential corridor for preventing

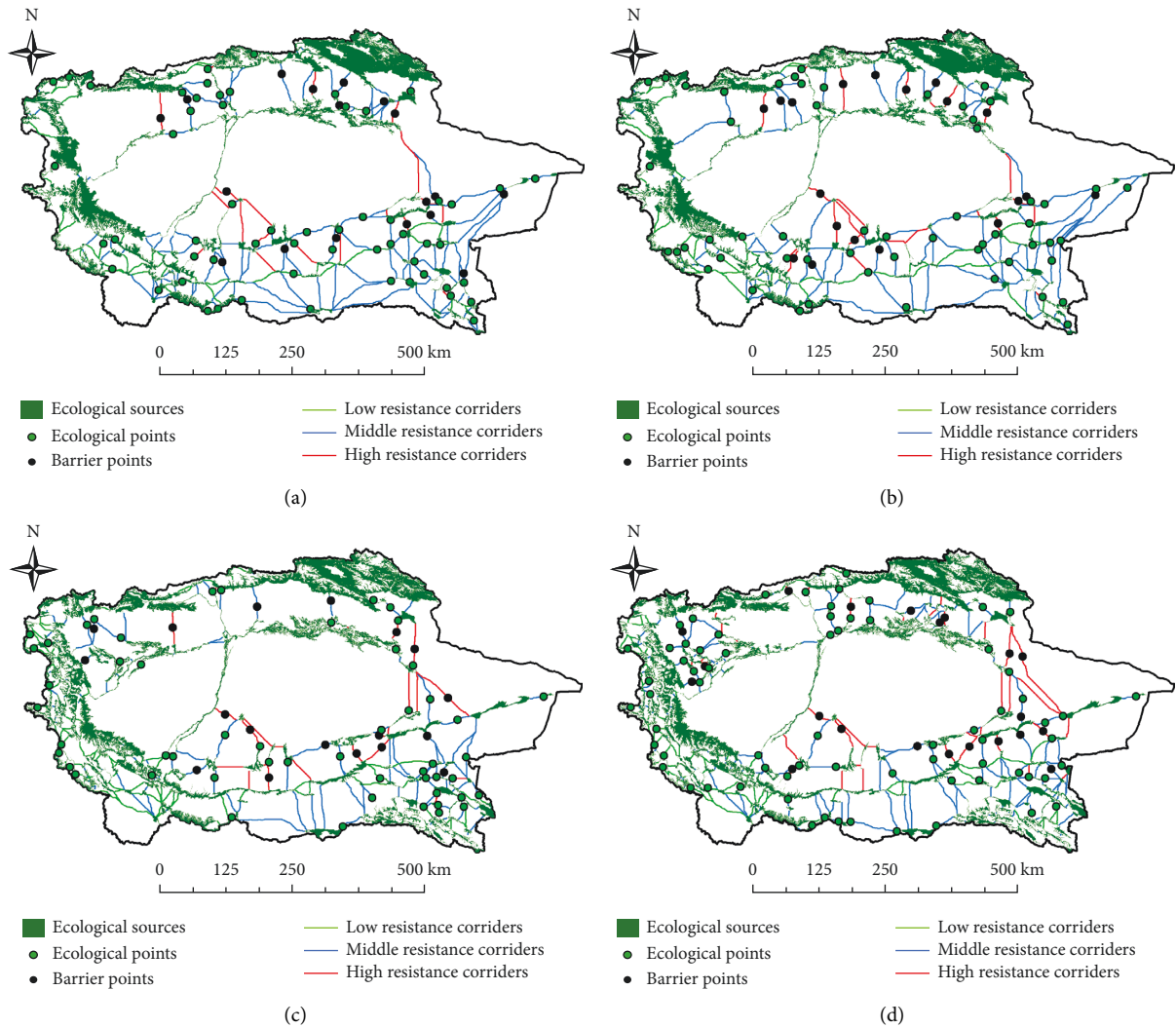


FIGURE 9: Comprehensive ecological security pattern changes in spatial and temporal in Tarim River Basin in four periods. (a) 1990, (b) 2000, (c) 2010, (d) 2020.

and controlling desert expansion and maintaining the stability and security of Oasis. Based on the oasis ecological ring of the Tarim Basin, the main ecological corridor consists of water systems (Aksu River, Weigan River, Kashgar River, Qarqan River, Kaidu-Peacock River, Hotan River, Yarkant River, and the mainstream of Tarim River) and the main roads. Increase the connectivity between oasis areas through a ring and ecological corridor, which is more conducive to oasis development. The complementarity of the ring and ecological corridor will jointly promote the development of the ecological environment in the TRB and build a more complete ecological security pattern network system. Strengthen the protection of ecological nodes and water sources, maintain critical ecological areas, and promote energy flow, ecological flow, and diffusion between species. Further, conserve water resources, maintain biodiversity, and optimize and adjust the relationship between humans and land in the oasis area.

- (3) Create a “one-ring, multipoint” urban agglomeration to coordinate ecological and economically sustainable development. The Tarim Basin Oasis Ecological Ring is the core area of the “Belt and Road” initiative, the China-Pakistan Economic Corridor (CPEC), and an important Silk Road passage. Therefore, it is also the economic circle of the Tarim Basin. Build four major urban agglomerations (Kashgar, Hetian, Korla, and Aksu) along the economic circle of Tarim Basin, play the radiation and driving role of the oasis city group, build a green ecological security barrier, and form a more secure, stable, and green sustainable national space.
- (4) Actively respond to government planning and optimize ecological space structure. The overall layout of Xinjiang’s space plan (2021–2035) proposes that the upstream areas need to strengthen enclosure protection and continue building the Tianshan Mountains and Pamir-Kunlun-Altun Mountains water conservation forest. And in the middle and

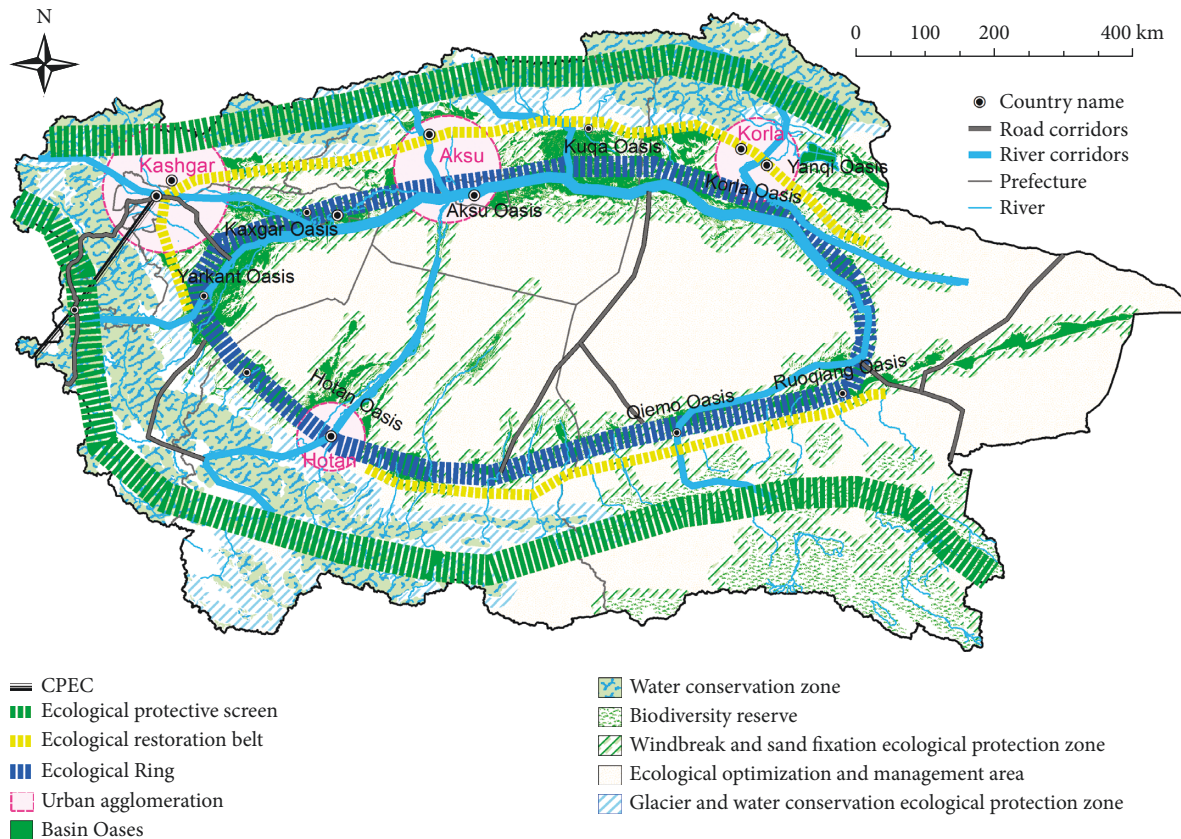


FIGURE 10: The design of the optimized layout of ecological space structure.

lower reaches, we should strengthen water conservation, renovate the water-saving system, and conduct the oasis shelter forest system. These are all for constructing the water conservation area in the Tianshan Mountains and Pamir-Kunlun Mountains, corridor basin oasis functional area, the interactive functional area between desert and Oasis, and desert area. Based on the relevant policies and planning, this study reconstructs the spatial boundary in the form of space, realizes the spatial governance from the perspective of space, scientifically and rationally divides the spatial structure of the watershed, and promotes the sustainable development of the region.

5.2. The Uncertainty of the Methods. Uncertainty analysis of landscape ecological risk assessment: the choice of indexes, the determination of the relationship between indexes and ecological risk, and the combination of indexes to obtain the comprehensive results of ecological risk may lead to the uncertainty of the results. For example, the assignment of vulnerability in landscape ecological risk reflects the relative vulnerability of landscape types in the study area. The differences in landscape ecological classification also lead to the low general applicability of vulnerability assignment. Therefore, how to improve the accuracy of vulnerability index assignment or construct new vulnerability index and adopt more scientific methods to study landscape ecological security needs to be further improved. In addition, this study

uses the landscape index to construct the ecological security evaluation model. From the perspective of landscape spatial structure to analyze the temporal and spatial changes of watershed ecological security, there is a lack of consideration of watershed socio-economic factors, and the results are relative.

The selection of ecological sources may affect the results of ecological corridors identification. Some small or scattered ecological sources may be ignored in the analysis, but they may play an important role in regulating the regional environment. Therefore, we should pay attention to the uncertainty in landscape ecological risk assessment, so as to provide accurate scientific basis for relevant ecological environment decision-making.

6. Conclusion

As a typical watershed of Inland Arid area, TRB has a fragile Desert-Oasis ecosystem, which is highly sensitive to human activities. Watershed landscape management is a major challenge for the government. How to realize the sustainable development of the watershed? In this study, the temporal and spatial dynamic changes of ecological security are analyzed by constructing a landscape ecological risk assessment model in TRB from 1990 to 2020. Secondly, the spatial autocorrelation analysis of landscape ecological risk is carried out to determine its spatial clustering characteristics. Using the MCR model and circuit theory, this paper constructs the landscape ecological security pattern of TRB from

1990 to 2020, defines the ecological function areas, ecological corridors, and ecological points, and realizes the combination of spatiotemporal dynamic evaluation and optimization of regional ecological security. The main research results are summarized as follows: the landscape ecological risk shows an upward trend from 1990 to 2020. The areas with high ecological risk are the desert areas in the middle and east of the study area, the transition zone between piedmont area and oasis. There is a significant aggregation phenomenon of landscape ecological risk in TRB. Taking the results of landscape ecological risk assessment and the ecological sources selected through Habitat Quality and landscape connectivity as the basis for the generation of landscape pattern resistance surface, this paper constructs the landscape ecological security pattern of the basin and optimizes the ecological spatial structure of arid inland rivers. The distribution pattern is “one ring, two screens, two belts, ten corridors, and multiple centers,” so as to ensure the continuity of ecological processes in the study area. The corresponding optimization suggestions are put forward: the key corridors connecting the nine oases around the TRB. Urban development should consider the current ecological resources and corridors to prevent landscape fragmentation, strengthen the improvement and restoration of ecological obstacles, and formulate the spatial planning of the Kunlun-Altun Mountain North Slope Restoration Zone and the Tianshan South Slope Ecological Restoration Zone. This study can provide a scientific basis for the Ecological Planning and Urban Master Planning of inland basins in arid area in the future. With future research, human factors should be added to the dynamic change of landscape security pattern, especially in the analysis of the relationship between national policies, watershed planning, socioeconomic statistics, and land use. In addition, according to the research on the contradiction between water resources protection and economic development in arid areas, it needs to be further explored to build a practical ecological security model to realize ecological and economic development.

Data Availability

The data used to support the findings of this study are included within the article.

Conflicts of Interest

The authors declare that there are no conflicts of interest regarding the publication of this paper.

References

- [1] J. X. Gao, “Ecological security is an important part of national security,” *Qiushi*, vol. 24, pp. 43–44, 2015.
- [2] D. Geneletti, E. Beinart, C. F. Chung, A. G. Fabbri, and H. J. Scholten, “Accounting for uncertainty factors in biodiversity impact assessment: lessons from a case study,” *Environmental Impact Assessment Review*, vol. 23, no. 4, pp. 471–487, 2003.
- [3] Q. Huang, R. Wang, Z. Ren, J. Li, and H. Zhang, “Regional ecological security assessment based on long periods of ecological footprint analysis,” *Resources, Conservation and Recycling*, vol. 51, no. 1, pp. 24–41, 2007.
- [4] 叶. Ye Xin, 邹. Zou Changxin, 刘. Liu Guohua, 林. Lin Naifeng, and 徐. Xu Mengjia, “Main research contents and advances in the ecological security pattern,” *Acta Ecologica Sinica*, vol. 38, no. 10, pp. 3382–3392, 2018.
- [5] C. Bingshuai, D. L. Xu, H. S. Dou et al., “Index system of ecological security of inland lakes in cold arid region: a case study of Hulun Lake, China,” *Acta Ecologica Sinica*, vol. 41, no. 8, pp. 2996–3006, 2021.
- [6] N. Bonheur and B. D. Lane, “Natural resources management for human security in Cambodia’s Tonle Sap Biosphere Reserve,” *Environmental Science & Policy*, vol. 5, no. 1, pp. 33–41, 2002.
- [7] C. X. Zou and W. S. Shen, “Research progress of ecological security Rural,” *Eco-Environment*, vol. 19, no. 1, pp. 56–59, 2003.
- [8] X. Chen and C. H. Zhou, “Review of the studies on ecological security,” *Progress in Geography*, vol. 24, no. 6, pp. 8–20, 2005.
- [9] R. H. Mac Arthur and E. O. Wilson, *The Theory of Island Biogeography*, Princeton University Press, Princeton, 1967.
- [10] J. Peng, H. J. Zhao, Y. X. Liu, and J. S. Wu, “Research progress and prospect on regional ecological security pattern construction,” *Geographical Research*, vol. 36, no. 3, pp. 407–419, 2017.
- [11] J. H. Pan and Y. Wang, “Ecological security evaluation and ecological pattern optimization in Taolai River Basin based on CVOR and circuit theory,” *Acta Ecologica Sinica*, vol. 41, no. 7, pp. 2582–2595, 2021.
- [12] W. Q. Zhao, Z. H. Yang, W. C. Su, and K. Li, “Ecological risk assessment and management of watershed based on landscape pattern change—a case study of the Chishui river basin in Guizhou,” *Resources and Environment in the Yangtze Basin*, vol. 26, no. 8, pp. 1218–1227, 2017.
- [13] R. F. Wang and Z. R. Nan, “Applied research on the risk assessment of the Heihe River Basin based on the theory of landscape ecology,” *Journal of Safety and Environment*, vol. 13, no. 6, pp. 133–137, 2013.
- [14] P. Craig P, P. Kristen L, W. Joanna B, and D. Julian, “Development and assessment of a landscape-scale ecological threat index for the Lower Colorado River Basin,” *Ecological Indicators*, vol. 11, no. 2, pp. 304–310, 2011.
- [15] 许. Xu Yan, 高. Gao Junfeng, and 郭. Guo Jianke, “The ecological risk assessment of Taihu Lake watershed,” *Acta Ecologica Sinica*, vol. 33, no. 9, pp. 2896–2906, 2013.
- [16] C. Xu, L. Pu, M. Zhu et al., “Ecological security and ecosystem services in response to land use change in the coastal area of Jiangsu, China,” *Sustainability*, vol. 8, no. 8, p. 816, 2016.
- [17] X. P. Xie, Z. C. Chen, F. Wang, M. W. Bai, and W. Y. Xu, “Ecological risk assessment of Taihu Lake basin based on landscape pattern,” *Chinese Journal of Applied Ecology*, vol. 28, no. 10, pp. 3369–3377, 2017.
- [18] L. Ma, J. Bo, X. Li, F. Fang, and W. Cheng, “Identifying key landscape pattern indices influencing the ecological security of inland river basin: the middle and lower reaches of Shule River Basin as an example,” *The Science of the Total Environment*, vol. 674, pp. 424–438, 2019.
- [19] P. Ran, S. Hu, A. E. Frazier, S. Qu, D. Yu, and L. Tong, “Exploring changes in landscape ecological risk in the Yangtze River Economic Belt from a spatiotemporal perspective,” *Ecological Indicators*, vol. 137, Article ID 108744, 2022.

- [20] Y. J. Wang, *Study on the Influence of the Change of Water Resources and its Impact on Ecological Security in the Arid: An Example of Ebinur Lake Basin in Xinjiang*, Xinjiang University, Ürümqi, China, 2018.
- [21] Y. N. Chen, W. C. Cui, W. H. Li, Y. P. Chen, and H. F. Zhang, "Utilization of water resources and ecological protection in the Tarim River," *Acta Geographica Sinica*, vol. 58, no. 2, pp. 215–177, 2003.
- [22] Z. J. Kong, M. J. Deng, H. B. Ling, G. Y. Wang, S. W. Xu, and Z. R. Wang, "Ecological security assessment and ecological restoration countermeasures in the dry-up area of the lower Tarim River," *Arid Zone Research*, vol. 38, no. 4, pp. 1128–1139, 2021.
- [23] Z. M. Yang and X. P. Liu, "Ecological carrying capacity monitoring and security pattern construction in the Aksu River Basin, Xinjiang," *Arid Land Geography*, vol. 44, no. 5, pp. 1489–1499, 2021.
- [24] J. H. Qi, *The Research on Oasis Ecological Evolution of Shule River Basin*, Zhenzhou University, Zhengzhou, China, 2014.
- [25] Z. Z. He, H. W. Wang, S. T. Yang, B. Fang, Z. Y. Zhang, and X. Y. Liu, "Spatial-temporal differentiation and pattern optimization of landscape ecological security in the Ugan-Kuqa river oasis," *Acta Ecologica Sinica*, vol. 39, no. 15, pp. 5473–5482, 2019.
- [26] N. N. Shi, Y. Han, Q. Wang et al., "Risk assessment of sandstorm diffusion and landscape pattern optimization in southern Xinjiang," *Acta Geographica Sinica*, vol. 76, no. 1, pp. 73–86, 2021.
- [27] P. Zhang, "Research on the Coupling System of Society, e-coenvironment and Water in Tarim River basin," China Institute of Water Resources and Hydropower Research, PHD Thesis, 2019.
- [28] X. Y. Zhang, "Study on Computing Methods and its Application of Dynamic Carrying Capacity of Water Resources under the Climate Change," Zhengzhou University, PHD Thesis, 2015.
- [29] M. J. Deng, Z. L. Fan, H. L. Xu, and H. Y. Zhou, "Ecological function regionalization of Tarim River basin," *Arid Land Geography*, vol. 40, no. 4, pp. 705–717, 2017.
- [30] L. Q. Xue, J. Wang, and G. H. Wei, "Dynamic evaluation of the ecological vulnerability based on PSR modeling for the Tarim River Basin in Xinjiang," *Journal of Hohai University(Natural Sciences)*, vol. 47, no. 1, pp. 13–19, 2019.
- [31] 楚. 徐. 罗. 孙. Chu Zhi, C. C. Xu, Y. X. Luo, and Q. Sun, "Land use simulation and ecological benefit evaluation in the Tarim River basin based on ecological protection red line management," *Acta Ecologica Sinica*, vol. 41, no. 18, pp. 1–13, 2021.
- [32] X. B. Zhang, P. J. Shi, J. Luo, H. L. Liu, and W. Wei, "The ecological risk assessment of arid inland river basin at the landscape scale: A case study on shiyang river basin," *Journal of Natural Resources*, vol. 29, no. 3, pp. 410–419, 2014.
- [33] Y. Zhao, Z. J. Luo, Y. T. Li, J. Y. Guo, X. H. Lai, and J. Song, "Study of the spatial-temporal variation of landscape ecological risk in the upper reaches of the Ganjiang River Basin based on the "production-living-ecological space"," *Acta Ecologica Sinica*, vol. 39, no. 13, pp. 4676–4686, 2019.
- [34] N. Rangel-Buitrago, W. J. Neal, and V. N. de Jonge, "Risk assessment as tool for coastal erosion management," *Ocean & Coastal Management*, vol. 186, Article ID 105099, 2020.
- [35] X. Y. Chen Xinyi, G. Z. Xie, and J. P. Zhang, "Landscape ecological risk assessment of land use changes in the coastal area of Haikou City in the past 30 years," *Acta Ecologica Sinica*, vol. 41, no. 3, pp. 975–986, 2021.
- [36] J. Peng, Y. Wang, Y. Zhang, J. Wu, W. Li, and Y. Li, "Evaluating the effectiveness of landscape metrics in quantifying spatial patterns," *Ecological Indicators*, vol. 10, no. 2, pp. 217–223, 2010.
- [37] W. Zhang, W. J. Chang, Z. C. Zhu, and Z. Hui, "Landscape ecological risk assessment of Chinese coastal cities based on land use change," *Applied Geography*, vol. 117, Article ID 102174, 2020.
- [38] Y. Xiong, M. Wang, H. P. Yuan, C. Y. Du, and H. P. Wu, "Landscape ecological risk assessment and its spatio-temporal evolution in Dongting Lake area," *Ecology and Environmental Sciences*, vol. 29, no. 7, pp. 1292–1301, 2020.
- [39] L. Xue, B. Zhu, Y. Wu et al., "Dynamic projection of ecological risk in the Manas River basin based on terrain gradients," *The Science of the Total Environment*, vol. 653, pp. 283–293, 2019.
- [40] X. Jin, Y. Jin, and X. Mao, "Ecological risk assessment of cities on the Tibetan Plateau based on land use/land cover changes - case study of Delingha City," *Ecological Indicators*, vol. 101, pp. 185–191, 2019.
- [41] J. Wang, W. Bai, and G. Tian, "Spatiotemporal characteristics of landscape ecological risks on the Tibetan Plateau," *资源科学*, vol. 42, no. 9, pp. 1739–1749, 2020.
- [42] J. Wang, X. L. Zhang, and H. R. Du, "Spatial pattern evolution and characteristics of the economy in Xinjiang at the county level," *Progress in Geography*, vol. 30, no. 4, pp. 471–478, 2011.
- [43] C. S. Ye and Y. F. Feng, "Ecological risk assessment for Pearl River Delta based on land use change," *Transactions of the Chinese Society of Agricultural Engineering*, vol. 19, pp. 224–232, 2013.
- [44] H. Shi, Z. P. Yang, F. Han, T. G. Shi, and F. M. Luan, "Characteristics of temporal-spatial differences in landscape ecological security and the driving mechanism in Tianchi scenic zone of Xinjiang," *Progress in Geography*, vol. 32, no. 3, pp. 475–485, 2013.
- [45] R. J. Yao, J. S. Yang, and G. M. Liu, "Spatial variability of soil salinity and moisture and their estimations by cokriging method: a case study in characteristic field of Yellow River Delta," *Journal of Soil and Water Conservation*, vol. 20, no. 5, pp. 133–138, 2006.
- [46] X. Zhang, J. Zhou, G. Li, C. Chen, M. Li, and J. Luo, "Spatial pattern reconstruction of regional habitat quality based on the simulation of land use changes from 1975 to 2010," *Journal of Geographical Sciences*, vol. 30, no. 4, pp. 601–620, 2020.
- [47] L. Rahimi, B. Malekmohammadi, and A. R. Yavari, "Assessing and modeling the impacts of wetland land cover changes on water provision and habitat quality ecosystem services," *Natural Resources Research*, vol. 29, no. 6, pp. 3701–3718, 2020.
- [48] H. T. Tallis, T. Ricketts, and A. Guerry, *InVEST 2.5.6 User's Guide*, The Natural Capital Project, Stanford, 2013.
- [49] J. Gong, Y. Xie, E. Cao, Q. Huang, and H. Li, "Integration of InVEST-habitat quality model with landscape pattern indexes to assess mountain plant biodiversity change: a case study of Bailongjiang watershed in Gansu Province," *Journal of Geographical Sciences*, vol. 29, no. 7, pp. 1193–1210, 2019.
- [50] Y. Wang, J. X. Gao, Y. Jin et al., "Habitat quality of farming-pastoral ecotone in bairin right banner, inner Mongolia based on land use change and InVEST model from 2005 to 2015," *Journal of Ecology and Rural Environment*, vol. 36, no. 5, pp. 654–662, 2020.
- [51] Y. Y. Gu, X. F. Huang, C. X. Zou, X. Ye, N. F. Lin, and W. M. Zhang, "Monitoring habitat quality changes in yuanjiangyuan nature reserve based on landsat images,"

- Journal of Ecology and Rural Environment*, vol. 35, no. 6, pp. 764–772, 2019.
- [52] Y. J. Liang and L. J. Liu, “Simulating land-use change and its effect on biodiversity conservation in a watershed in north-west China,” *Ecosystem Health and Sustainability*, vol. 3, no. 5, pp. 13–23, 2017.
- [53] Q. Sun, L. Zhang, X. L. Ding, J. Hu, Z. W. Li, and J. J. Zhu, “Slope deformation prior to Zhouqu, China landslide from InSAR time series analysis,” *Remote Sensing of Environment*, vol. 156, pp. 45–57, 2015.
- [54] L. L. Song and M. Z. Qin, “Identification of ecological corridors and its importance by integrating circuit theory,” *Chinese Journal of Applied Ecology*, vol. 27, no. 10, pp. 3344–3352, 2016.
- [55] 付. 刘. 刘. Fu Fengjie, Z. H. Liu, and H. Liu, “Identifying key areas of ecosystem restoration for territorial space based on ecological security pattern: a case study in Hezhou City,” *Acta Ecologica Sinica*, vol. 41, no. 9, pp. 3406–3414, 2021.
- [56] L. Y. Huang, S. H. Liu, Y. Fang, and L. Zou, “Construction of Wuhan’s ecological security pattern under the quality-risk-requirement framework,” *Chinese Journal of Applied Ecology*, vol. 30, no. 2, pp. 615–626, 2019.
- [57] B. H. McRae, S. A. Hall, P. Beier, and D. M. Theobald, “Where to restore ecological connectivity? Detecting barriers and quantifying restoration benefits,” *Plos One*, vol. 7, no. 12, Article ID e52604, 2012.
- [58] T. R. Yang, W. H. Kuang, W. D. Liu, A. L. Liu, and T. Pan, “Optimizing the layout of eco-spatial structure in Guanzhong urban agglomeration based on the ecological security pattern,” *Geographical Research*, vol. 36, no. 3, pp. 441–452, 2017.
- [59] R. C. Guo, S. H. Song, and C. H. Miao, “Optimizing and upgrading of structure and function in urban agglomerations region: a case study of zhongyuan urban agglomeration,” *Scientia Geographica Sinica*, vol. 31, no. 3, pp. 322–328, 2011.
- [60] 杨. 王. 魏. 杨. 郭. Yang Liangjie, J. Wang, W. Wei, Y. C. Yang, and Z. C. Guo, “Ecological security pattern construction and optimization in arid inland river basin: a case study of shiyang river basin,” *Acta Ecologica Sinica*, vol. 40, no. 17, pp. 5915–5927, 2020.

Research Article

Correction of Chinese Dance Training Movements Based on Digital Feature Recognition Technology

LinJuan Zhang 

Hangzhou Normal University, Qianjiang College, HangZhou, Zhejiang 310018, China

Correspondence should be addressed to LinJuan Zhang; q0060127@hznu.edu.cn

Received 28 February 2022; Revised 22 March 2022; Accepted 4 April 2022; Published 30 April 2022

Academic Editor: Xuefeng Shao

Copyright © 2022 LinJuan Zhang. This is an open access article distributed under the Creative Commons Attribution License, which permits unrestricted use, distribution, and reproduction in any medium, provided the original work is properly cited.

In order to improve the effect of Chinese dance training, this paper combines digital feature recognition technology to correct and analyze Chinese dance training movements and constructs an intelligent auxiliary training system. In order to solve the travel time problem at the computationally complex interface and ensure its computational accuracy, a local adaptive triangulation technique is used in the fast-advance algorithm. Moreover, this paper designs the function of the system according to the user's needs, transforms the design concept into a figurative visual representation through the interactive prototype according to the function, carries out the visual design of the interface according to the interactive prototype, and uses the interactive technology to realize the development of the system. From the test analysis results, it can be seen that the Chinese dance training action correction system based on the digital feature recognition technology proposed in this paper has a good effect and can effectively promote the improvement of the Chinese dance training effect.

1. Introduction

As one of the important components of Chinese culture and art, Chinese classical dance has a very long and splendid development history. At present, under the general trend of carrying forward the history of the Chinese nation and advocating the inheritance of traditional Chinese cultural heritage, Chinese classical dance has received attention and has been widely disseminated and carried forward. Moreover, beautiful performances of Chinese classical dance are often seen in important celebrations and diplomatic ceremonies. In addition to performing tasks on major occasions, more tasks of Chinese classical dance are to popularize cultural and artistic performance tasks across the country and around the world and have a large number of audiences and performance participants in the folk. It is the common wish of every teacher and student engaged in this work to improve and enhance the basic training and teaching of Chinese classical dance. The teaching and scientific research work of Chinese classical dance thus carried out can not only provide urgent basic training in dance teaching but also promote the popularization of Chinese classical dance

among the people, thus benefiting the majority of dance lovers in the society. Therefore, this research work has profound social significance and broad application prospects.

The existence of a digital society puts forward new requirements for dance teaching and also provides us with good development opportunities. Teachers who are responsible for dance education should face the following issues directly: (1) update dance education and teaching concepts as soon as possible, absorb new knowledge structures, broaden knowledge fields, and become learners of digital technology; (2) adapt to teachers in accordance with the shifting changes of students in the new teaching process, students are the center, and a variety of teaching methods are provided; (3) learn to apply digital tools and technologies for curriculum design and skillfully use digital tools to serve dance teaching. Digital dance teaching helps to update knowledge. With the help of a digital high-speed dissemination system and digital technology, knowledge updates will be accelerated. Various media and mobile devices provide audiences with learning conditions that are not limited by space and time, especially for students'

“fragmented” learning, which provides convenience. The ubiquitous computing and display devices, in the study of audiovisual arts, help to strengthen the interconnection of theoretical learning and practical links. Whether at school, in the dormitory, at home, or on the road, dance learning will combine theoretical knowledge with diverse practical opportunities. All in all, the constant updating of knowledge and the constant changes of new things urge us to continue to learn for a long time and adapt to the development rhythm of the digital society. As the inner force of dance teaching reform, teachers should take on the conscious of digital teaching reform and regard digital dance teaching as an important development opportunity.

This paper combines the digital feature recognition technology to carry out the correction and analysis of Chinese dance training movements and constructs an intelligent auxiliary training system to improve the correction effect of Chinese dance training movements.

2. Related Work

Today, with the explosive growth of multimedia data, various forms of multimedia information such as text, images, voice, and video are rapidly expanding. Multimedia information has become an urgent desire of people [1]. In multimedia information, video data have the most complex structure and richest information, but, due to the lack of expression means, it is also the most difficult to store, organize, and retrieve. How to effectively solve the problem of video data organization and retrieval has also become a research hotspot [2]. Traditional video retrieval methods rely on human memory to recall video content and then describe it in words. This method is often subjective and slow and has a high error rate [3]. The content-based image query and video retrieval method proposed in [4] has made a breakthrough in the research in this field. This method only needs to analyze the sequence structure of the video and distinguish the changes of the video according to the change degree of the content of the frame. Video retrieval requires finding the desired video clips in a large amount of video data, but because of the large and complex video content, video retrieval is very difficult, which is largely different from image retrieval [5]. Video is currently the most informative data, so the retrieval of video has become a prominent problem in real life. In the past ten years, after people’s unremitting efforts, content-based video retrieval technology has been continuously developed and achieved exciting results [6]. The expression of video content can be divided into three levels: raw data (awdata), low-level visual content (low-levelvisualeontent), and semantic content (semantientent). The original data are composed of basic video units, data format, frame frequency (framearet), etc.; the low-level visual content is composed of visual features such as color, shape, and texture; the semantic content includes high-level concepts such as object (object)t, event (veen)t. [7]. In the field of video retrieval, most of the work is still in the use of low-level visual content, and the retrieval of semantic level is only carried out in specific fields [8]. Reference [9] proposes a method for automatic video

annotation using human behavior analysis and domain-specific knowledge of specialized tennis matches. At the semantic level, the support of a knowledge base is generally required. Because of its complexity, progress has not been satisfactory. Video analysis is carried out on the basis of image analysis, so the visual features of images such as color, shape, and texture are naturally introduced into the video and have been widely used. In addition, in order to better express the video and solve the unsatisfactory video analysis results caused by the discontinuity of the visual features of the video in the spatiotemporal expression, people have introduced features that can reflect the continuity of the video, such as motion features (including objectmotion and canreramotion), or comprehensively use the correlation of different media, such as the recognition of sound and text in the video to assist the semantic recognition of the video [10]. Because visual features are intuitive, simple, and effective, they have been widely used in video retrieval. Even in today’s increasingly in-depth research, using video’s color, texture, shape, motion, and other low-level visual features to retrieve videos is still difficult and is the main method for video retrieval [11]. Video retrieval combined with traditional database technology can easily store and manage massive video data; combined with traditional Web search engine technology, it can be used to retrieve rich video information in HTML pages. In the foreseeable future, content-based video retrieval technology will be widely used in the following fields: multimedia database, intellectual property protection, digital library, network multimedia search engine, interactive television, art collection and museum management, telemedicine and military command system, etc. [12]. Although content-based video retrieval has received extensive attention and some applications, its real application is still in its infancy. At present, the main retrieval goals of video retrieval are retrieving similar videos, locating similar video segments in a video, and retrieving similar shots. [13]. Based on the characteristics of dance video, the composition and characteristics of digital video, video analysis, scene switching detection, and key frame selection are analyzed. A variety of methods are used, and on this basis, the content-by-content retrieval of video data is analyzed [14].

Dance is an art of human movement, which is human movement transformed into dance. The general human movement has the characteristics of nonstop flow and change and exists in a certain time and space while dance generally needs to be accompanied by music, wear specific costumes, and some have various props. On the other hand, there are also lighting and scenery, so dance is a spatial, temporal, and comprehensive dynamic plastic art [15]. Human movements are the activities of the whole body or part of the body, which are used to express the needs of emotion, thought, and life. According to the role of aesthetics, human body movements can be divided into two types: daily life movements and artistic movements. The former refers to various movements in ordinary life, and the latter refers to the movements that have been processed, organized, refined, and beautified, generally referring to dance movements [16]. Therefore, dance movements are

derived from the movements of the natural form of the human body and must be refined, added, and beautified artistically. From the movement of the human body's natural form to dance movement, it must be processed and developed in two aspects: one is to go through regular development, and the other is to go through purposeful development. Regular development refers to organizing Bai Ranyouxu's life movements into orderly movements, making life movements rhythmic; purposeful development means that each dance movement has a clear motive and expresses certain characteristics. These emotions and thoughts reflect the bamboo play and the strength of the dance [17]. The movement of the dance is to move and fit together. Any dance must move, but it cannot be a dance if it does not move. The dance moves are dynamic. From the perspective of form, the movements of the human body can be divided into three categories, namely shape, quality, and potential. Shape: there are size, square, height, length, straight, straight, and oblique; quality: there are rigid and soft, thickness, strength, and severity; momentum: there are rapidity, movement, gathering and dispersing, advancing and retreating, and sinking and rising. These opposing factors are properly unified in dance art, forming a harmonious dance beauty [18].

3. Digital Feature Technology Algorithm

The definition of the B-spline function is that for a given $n+1$ control point $P_i (i = 0, 1, \dots, n)$, the following p -th degree B-spline function is defined:

$$C_p(u) = \sum_{i=0}^n N_{i,p}(u)P_i, \quad (1)$$

where $N_{i,p}(u)$ is the p -order B-spline basis function, and $u = [u_0, u_1, \dots, u_n]$ is the nondecreasing node vector set. In this paper, $P_i (i = 0, 1, \dots, n)$ is connected in sequence with polyline segments to form a polygon, which is called a B-spline control polygon.

Then, the basis function of a B-spline of degree p can be defined as follows:

$$\left\{ \begin{array}{l} N_{i,0}(u) = \begin{cases} 1, u \in [u_i, u_{i+1}), \\ 0, \text{other}, \end{cases} \\ N_{i,p}(u) = \frac{u - u_i}{u_{i+p} - u_i} N_{i,p-1}(u) + \frac{u_{i+p+1} - u}{u_{i+p+1} - u_{i+1}} N_{i+1,p-1}(u), p \geq 2, \\ \text{regulations } \frac{0}{0} = 0. \end{array} \right. \quad (2)$$

Then, the B-spline basis function $N_{i,0}(u)$ of degree 0 is a step function, which is 0 everywhere outside the half-open interval $[u_i, u_{i+1})$.

From the definition of the basis function in formula (2), it can be obtained that adjusting the node vector of the B-spline function will cause the change of the curve shape, and how to calculate the node vector will directly determine its value effect. According to formula (2) and the two zero-order B-spline basis functions $N_{i,0}(u)$ and $N_{i+1,0}(u)$, then, this paper combines the two linearly to obtain the first-order B-spline basis function, and its expression is

$$\begin{aligned} N_{i,1}(u) &= \frac{u - u_i}{u_{i+1} - u_i} N_{i,0}(u) + \frac{u_{i+2} - u}{u_{i+2} - u_{i+1}} N_{i+1,0}(u) \\ &= \begin{cases} \frac{u - u_i}{u_{i+1} - u_i}, & u \in [u_i, u_{i+1}), \\ \frac{u_{i+2} - u}{u_{i+2} - u_{i+1}}, & u \in [u_{i+1}, u_{i+2}), \\ 0, & \text{other}. \end{cases} \end{aligned} \quad (3)$$

The subscript i of $N_{i,1}(u)$ in formula (3) is replaced by $i+1$, and the expression of $N_{i+1,1}(u)$ can be obtained, as follows:

$$N_{i+1,1}(u) = \begin{cases} \frac{u - u_{i+1}}{u_{i+2} - u_{i+1}}, & u \in [u_{i+1}, u_{i+2}), \\ \frac{u_{i+3} - u}{u_{i+3} - u_{i+2}}, & u \in [u_{i+2}, u_{i+3}), \\ 0, & \text{other}. \end{cases} \quad (4)$$

Formulas (2) and (4) can express the basis function of the quadratic B-spline as follows:

$$\begin{aligned} N_{i,2}(u) &= \frac{u - u_i}{u_{i+2} - u_i} N_{i,0}(u) + \frac{u_{i+3} - u}{u_{i+3} - u_{i+1}} N_{i+1,1}(u) \\ &= \begin{cases} \frac{(u - u_i)^2}{(u_{i+1} - u_i)(u_{i+2} - u_i)}, & u \in [u_i, u_{i+1}), \\ \frac{(u - u_i)(u_{i+2} - u)}{(u_{i+2} - u_i)(u_{i+2} - u_{i+1})} + \frac{(u - u_{i+1})(u_{i+3} - u)}{(u_{i+3} - u_{i+1})(u_{i+2} - u_{i+1})}, & u \in [u_{i+1}, u_{i+2}), \\ \frac{(u_{i+3} - u)^2}{(u_{i+3} - u_{i+2})(u_{i+3} - u_{i+1})}, & u \in [u_{i+2}, u_{i+3}). \end{cases} \end{aligned} \quad (5)$$

Similarly, other quadratic B-spline basis functions can be obtained by "translation" of the subscript i . P -th degree B-spline functions can be derived through the above transformation and equation (2). I will not go into details here. At the same time, the function value on each node can also be obtained according to the basis function derived above.

The cubic B-spline value used in the fast-forwarding algorithm introduced in this paper uses the uniform cubic B-spline value after the "translation" of the basis function. For example, the node vector u in the interval $[0,1]$ can obtain the function value of the function in the interval $[-3,-2],[-2,-1],[-1,0]$, and the process is deduced as follows.

If we assume $u_i = i (i = L, -1, 0, 1, L)$, after bringing the node vector u into formula (2), according to the "translation" property of the uniform B-spline basis function, we have

$$N_{0,1(u)} = \begin{cases} u, u \in [0, 1), \\ 2 - u, u \in [1, 2), \\ 0, \text{other}, \end{cases}$$

$$N_{i,1(u)} = N_{0,1(u-i)}, i = L, -1, 0, 1, L,$$

$$N_{0,2(u)} = \begin{cases} \frac{1}{2}u^2, u \in [0, 1), \\ \frac{1}{2}(-3 + 6u - 2u^2), u \in [1, 2), \\ \frac{1}{2}(3 - u)^2, u \in [2, 3), \\ 0, \text{other}, \end{cases} \quad (6)$$

$$N_{i,2(u)} = N_{0,2(u-i)}, i = L, -1, 0, 1, L,$$

$$N_{0,3(u)} = \begin{cases} \frac{1}{6}u^3, u \in [0, 1), \\ \frac{1}{6}(4 - 12u + 12u^2 - 3u^3), u \in [1, 2), \\ \frac{1}{6}(-44 + 60u - 24u^2 + 3u^3), u \in [2, 3), \\ \frac{1}{6}(4 - u)^3, u \in [3, 4), \\ 0, \text{other}, \end{cases}$$

$$N_{i,3(u)} = N_{0,3(u-i)}, i = L, -1, 0, 1, L.$$

Considering the basis function of a uniform B-spline in the interval $[0, 1]$, the nonzero polynomial function in other intervals can be calculated in the interval $[0, 1]$, and its expression is as follows:

$$\begin{cases} N_{-1,1(u)} = 1 - u, \\ N_{0,1(u)} = u, \end{cases} u \in [0, 1], \quad (7)$$

$$\begin{cases} N_{-2,2(u)} = \frac{1}{2}(1 - u)^2, \\ N_{-2,2(u)} = \frac{1}{2}(1 - u)^2, \\ N_{-2,2(u)} = \frac{1}{2}(1 - u)^2, \\ N_{-1,2(u)} = \frac{1}{2}(1 + 2u - 2u^2), u \in [0, 1], \\ N_{0,2(u)} = \frac{1}{2}u^2, \end{cases} \quad (8)$$

$$\begin{cases} N_{-3,3(u)} = \frac{1}{6}(1 - u)^3, \\ N_{-2,3(u)} = \frac{1}{6}(4 - 6u^2 + 3u^3), \\ N_{-1,3(u)} = \frac{1}{6}(1 + 3u + 3u^2 - 3u^3), \\ N_{0,3(u)} = \frac{1}{6}u^3. \end{cases} \quad (9)$$

Equation (9) used in this papershowsthe B-spline interpolation calculation formula.

Because the digital light field is in a nonuniform layered medium, the interface changes with the depth and the regular grid nodes cannot describe the velocity nodes on the interface in detail, so the accuracy of the algorithm cannot be guaranteed. To this end, in order to calculate the travel time problem at complex interfaces and at the same time ensure its calculation accuracy, the fast forward algorithm adopts a local adaptive triangulation technique. The detailed schematic diagram of its principle is shown in Figure 1. In the study area, the adaptive triangular mesh is locally used to stitch the mesh nodes near the interface; that is, the triangulation algorithm is used to calculate and update the node travel time in the local study area, while the regular grid algorithm is still used for the grid nodes in other areas. Figure 2 shows an enlarged schematic diagram to demonstrate the technique. This detail characterization algorithm, which is only used in a specific area, can effectively save computing costs, improve efficiency, and ensure the accuracy of the fast-advance algorithm in ray-tracing calculations.

The following will describe in detail how the technology uses the triangular mesh to calculate the travel time value of the nodes on the interface. Figure 3 shows a schematic diagram of the triangular grid computing node travel time.

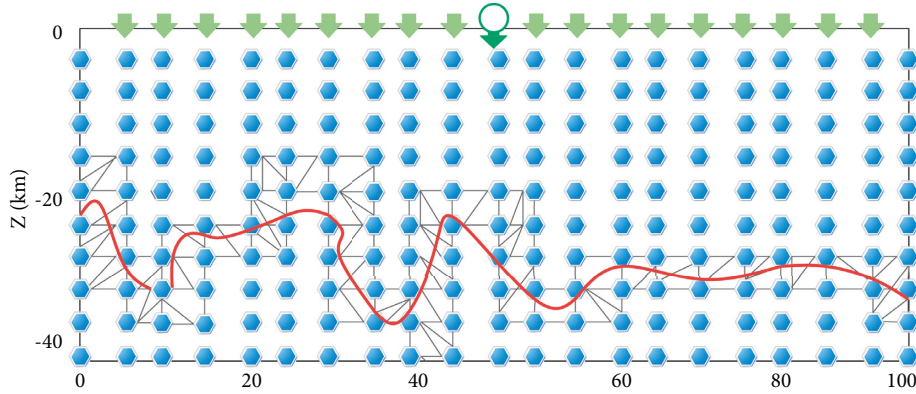


FIGURE 1: Schematic diagram of interface adaptive triangulation mesh.

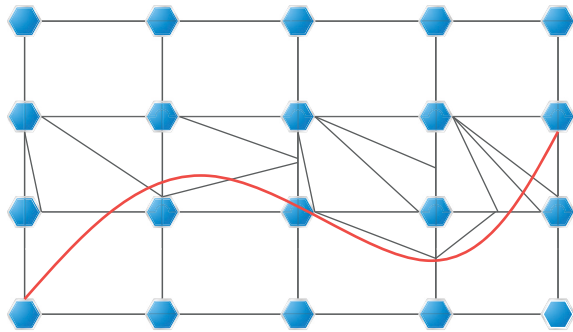


FIGURE 2: Schematic diagram of the enlarged view of the triangular mesh of the interface.

We assume that the travel-time values T_A and T_B of the fixed points A and B are known, and the first-order difference operator is used to solve the program function equation, and the travel-time value T_O at the point O can be obtained. If the travel time from T_A to T_O is t and $T_B > T_A$, the following quadratic equation can be obtained:

$$(a^2 + b^2 - 2ab)t^2 + 2u(a \cdot b - b^2)t + (b^2u^2 - s_o^2[a^2b^2 - (a \cdot b)^2]) = 0, \quad (10)$$

where S_o is the slowness of point O, $u = T_B - T_A$, a and b are distance vectors, and $a = |a|$, $b = |b|$. In order to satisfy the propagation law of seismic waves, the viscous solution of formula (10) is solved, as shown in Figure 3(b). The direction of ∇T_O must be between points A and B and $u < t$; that is, it satisfies the following formula:

$$\frac{a \cdot b}{b} < \frac{b(t - u)}{t} < \frac{a^2b}{a \cdot b}. \quad (11)$$

Equation (10) is calculated under the condition that equation (11) is satisfied, and the travel time value at point O is obtained as $T_O = t + T_A$; in addition, $T_O = \min\{bs_o + T_A, as_o + T_B\}$, and the smaller value of the two is selected to locate the travel time of point O in area 4. As shown in Figure 3(a), in order to update the travel time at point O, it is necessary to calculate the travel time of point O of the four

triangular mesh regions, respectively; that is, the same operation as above is used to obtain the travel time of point O corresponding to the triangular mesh regions 1, 2, and 3, and finally, the travel time with the smallest value and greater than zero among these four values is selected as the actual travel time value of the final point O.

It should be pointed out here that when calculating the travel time at point O, the triangular mesh must be an acute triangle. When encountering obtuse-angle triangular meshes, this calculation process does not hold, and the problem will be explained in detail below, and a reasonable explanation will be given. In order to calculate the travel time at point O, Figure 4 shows three situations that will be faced during the calculation, and in these three cases, the wavefront must propagate in the direction of point O.

- (1) The triangular meshes in Figure 4(a) are all acute angles. The angles of the five nodes that diverge from the center to the point O are all 72° ; that is, no matter from which angle the wavefront propagates to the point O, it will inevitably pass through two adjacent points, so the travel time at point O can be directly calculated by equation (11).
- (2) The triangular meshes in Figure 4(b) are all right-angled triangles. The angles of the four nodes radiating from the center to the point O are all right angles. When the wavefront propagates to the point O, only in the four vertical directions, other angles are the same as in the first case. Figure 4(b) just shows the special case where the wavefront is incident from point A at a normal angle. Therefore, the travel time at point O in this case can be calculated by $T_O = T_A + S_o \cdot AO$.
- (3) The triangular meshes in Figure 4(c) are all pin-angled triangles. Point O is the center, and the angles of the three nodes radiating from the center are all 120° . Here, the author only takes the obtuse triangle A O B as an example.

When the wavefront propagates to the point O, within the θ angle, that is, in the area of the dashed lines that are perpendicular to each other, the wavefront passes through

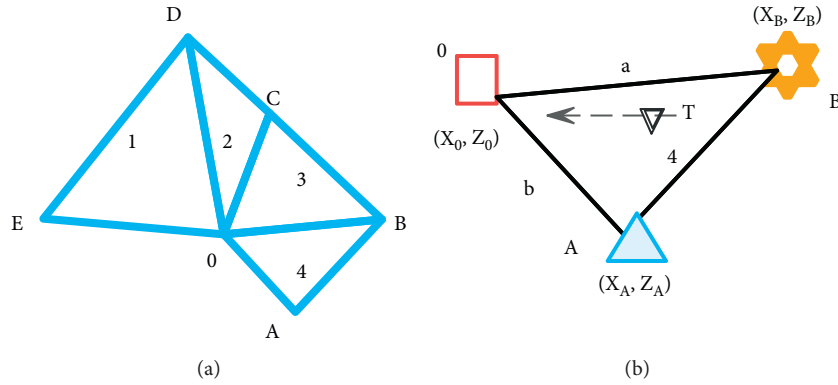


FIGURE 3: Schematic diagram of updating travel time in the triangle area.

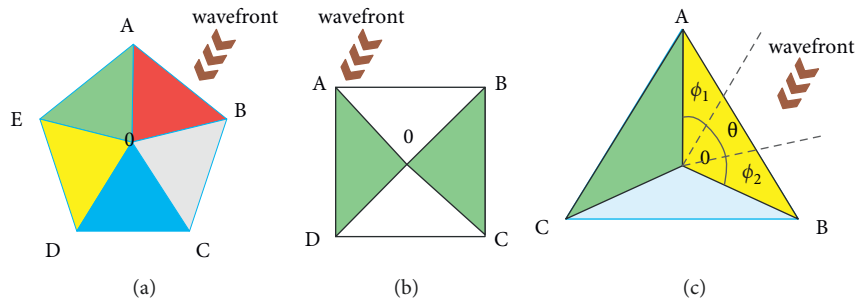


FIGURE 4: (a) Incident wavefront of acute triangle mesh. (b) Incident wavefront of right triangle mesh. (c) Incident wavefront of obtuse triangle mesh.

the point A and the point B. In other areas, the wavefront only passes through the point A or the point B. If the obtuse angle in Figure 4(c) is encountered, the travel time at point O is approximately calculated by $T_O = T_A + S_{OAO}$, and its proportion to the first-order accuracy can be specifically expressed by the following formula:

$$r = 100 \left(\frac{2\psi - \pi}{\psi} \right), \quad (12)$$

where ψ is $\angle AOB$, and its size range is $\pi/2 \leq \psi \leq \pi$.

After the above analysis, it can be concluded that when the triangulation is obtuse angle, the calculation of the interface travel time is lower than the first-order accuracy, and the travel time calculation does not hold when encountering an obtuse triangle. However, in the actual algorithm division, the needle-angle triangle is an unavoidable problem. Therefore, Figure 5 shows a split coping strategy that is different from the previous division when facing obtuse triangles. As shown in Figure 5, (b) O is replaced by A C, and the obtuse triangle problem can be transformed into the above two situations that can be dealt with.

In this paper, a new mesh refinement strategy is adopted, which also takes into account the accuracy and computational efficiency and successfully reduces the error near the source point. Figure 6 shows the whole process of mesh refinement near the source point of the algorithm, that is, using the double mesh technique. Among them, the red solid

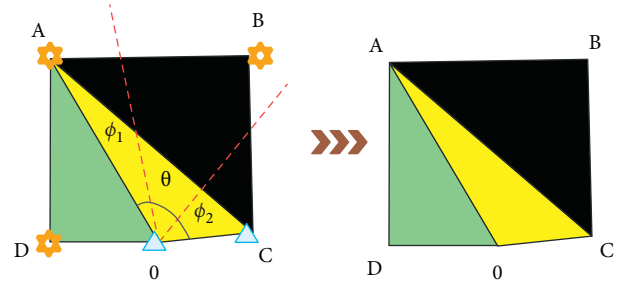


FIGURE 5: Alternative splitting strategy for obtuse triangles.

point is the source point, the black thick line is the narrow band, and a finer grid is used around the source point. These meshes help to characterize the narrowband in finer detail, allowing it to approximate the expansion of the simulated wavefront in a finer manner. Subsequently, the narrow band continued to expand around. When the narrow band is about to reach the boundary of the fine mesh, the mesh in this area will be instantly changed from the fine mesh to the coarse mesh. Under the premise that the computational time cost increases by an extremely small order, this refinement operation can greatly improve the computational accuracy of the fast-advance algorithm.

A heap is a completely binary tree-shaped data structure; that is, it is a sequence $\{a_1, a_2, \dots, a_n\}$ composed of n elements, where the elements need to satisfy $a_i \leq a_{2i}, a_i \leq a_{2i+1}$

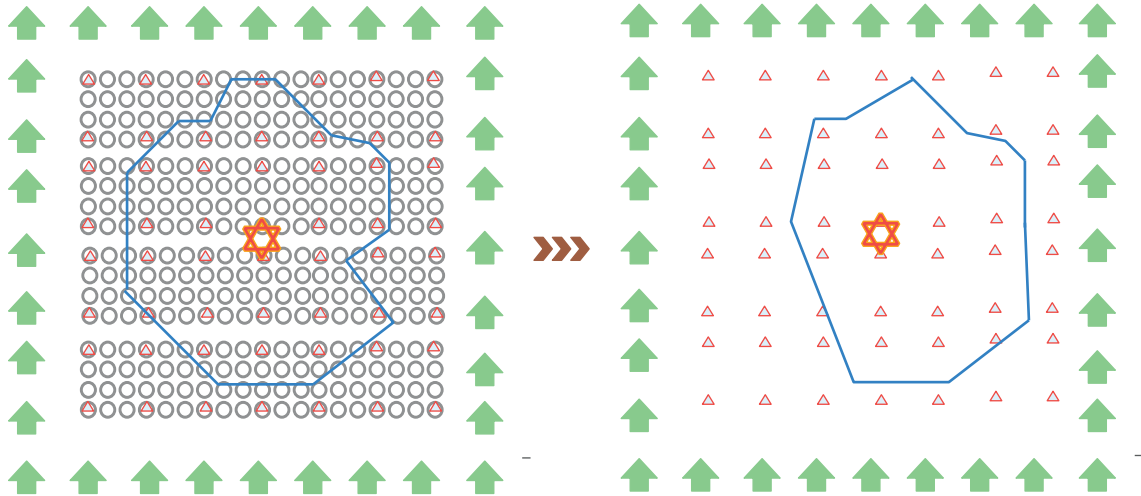
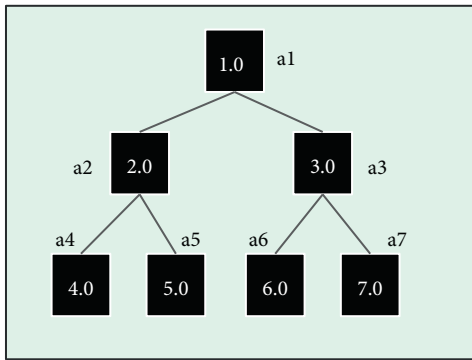


FIGURE 6: Mesh refinement implementation process near the source.



a1	a2	a3	a4	a5	a6	a7
1.0	2.0	3.0	4.0	5.0	6.0	7.0

FIGURE 7: The correspondence between the complete binary tree heap and each element.

or $a_i \geq a_{2i}, a_i \geq a_{2i+1}, (i = 1, 2, 3\Lambda, n/2)$. Then, the sequence is called a heap. The top node of the heap is called the root node. However, as a binary tree structure, each parent node has two corresponding child nodes. The minimum heap is used in the fast forward algorithm; that is, in the binary tree heap structure, the value of each parent node is smaller than its corresponding two child nodes. In a complete binary tree heap, the corresponding relationship between its data structure and its elements is shown in Figure 7. The traditional heap sorting operation process for data structure includes two aspects: one is to initialize the heap, and the other is to rebuild the heap. The time complexity of its algorithm operation is $T(n) = 2n \log_2 n + o(n)$, and the size of the complexity depends on the number of comparisons between elements in the process of heap reconstruction.

We assume that there are n nodes in the narrowband at a certain moment in the process of calculating the travel time of the fast forward algorithm, and the corresponding minimum heap has n elements, and then, the structure depth

of the heap is $h = [\log_2 n] + 1$. When the narrowband is expanded again, it corresponds to the operations of heap initialization and heap reconstruction. The process of performing this operation in a conventional heap is shown in Figure 8(a), which can be roughly divided into the following three steps:

- (1) The algorithm removes the root element and moves the last element at the bottom of the heap to the top of the heap
- (2) The algorithm takes the new root element as the parent node, compares it with the smallest child node in turn, and adjusts it downward in turn to complete the heap reconstruction
- (3) The algorithm puts the newly added element into the position of the last element at the bottom of the heap, and compares and adjusts the position upward in sequence, and stops the above operations when the new minimum heap data structure is completed.

When the operations of the above three steps are continuously performed, the maximum number of comparisons between the root element and the data under the heap is $2(h - 1)$. However, when the last element at the bottom of the heap is compared and adjusted upward, the maximum number of comparisons is $(h - 1)$. In the process of rebuilding the heap, the maximum number of comparisons of conventional heap sorting is $3h$, and the time complexity of its algorithm is $T_1(n) = 3[\log_2 n]$. Figure 8 shows the heap operation flow of deleting 1 and adding 8.

Through the above implementation process of traditional heap sorting and combining the characteristics of narrowband expansion, it is possible to try to improve the conventional heap sorting technology. The improved heap sorting adopts the vacancy sinking method. Compared with the traditional method, the improved heap sorting using the vacancy sinking method mainly improves the details of its contrast adjustment for the newly added elements. The improved heap sort operation can be divided into the following two steps:

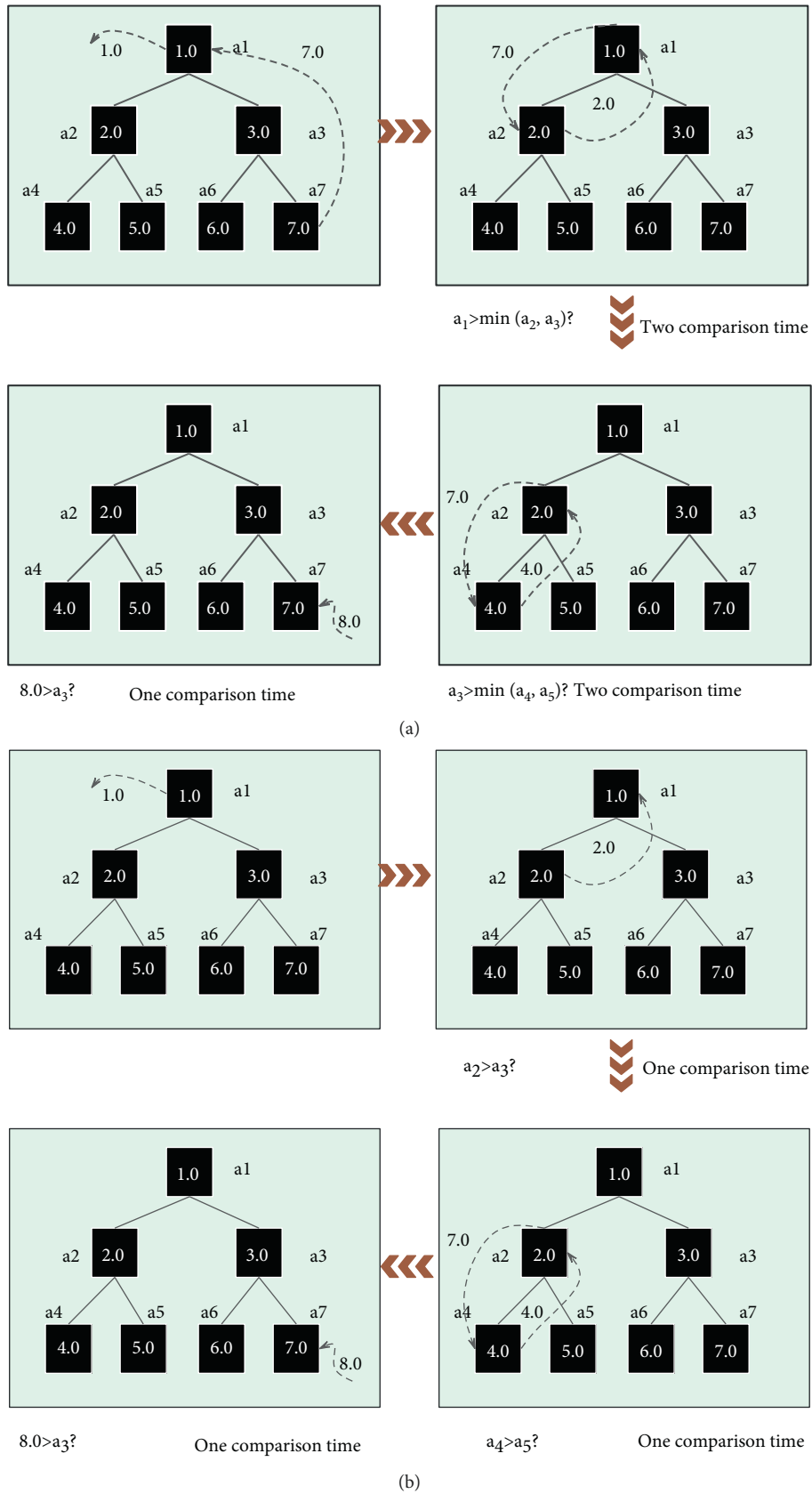


FIGURE 8: Flowchart of normal and improved heap sort rebuilding heap operations. (a) Regular heap sort. (b) Improve heap sort.

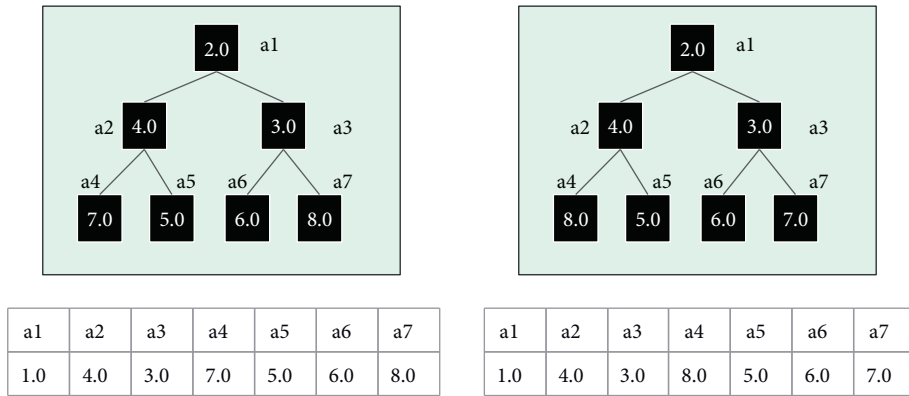


FIGURE 9: Data structure after regular and improved heap reconstruction.

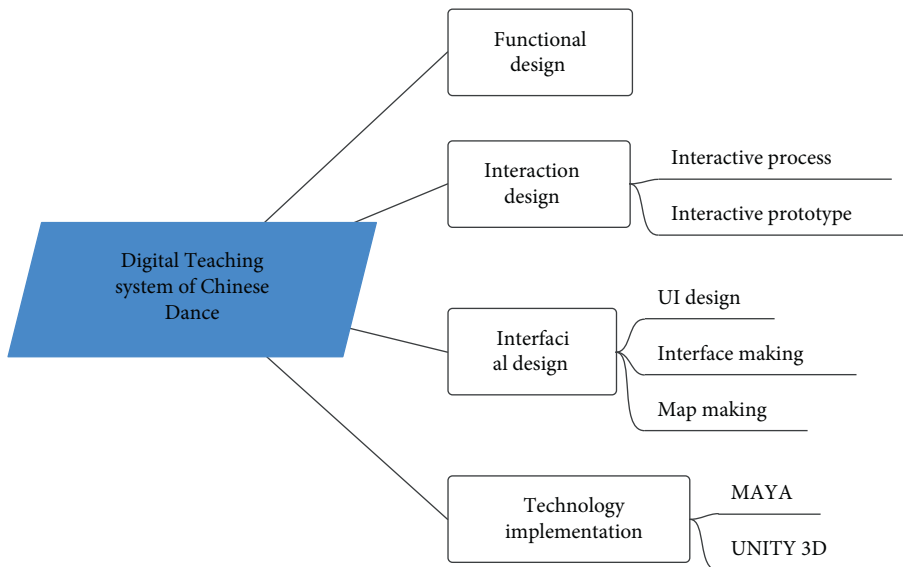


FIGURE 10: Correction model of Chinese dance training movements based on digital feature recognition technology.

- (1) After removing the root element, its corresponding heap headspace bit is compared with its two child node values. Then, the algorithm selects the smaller of the two and swaps positions with the vacancy, and the new vacancy continues to perform the above operations on its corresponding two child nodes until the vacancy reaches the bottom layer of the heap and stops the above operations.
- (2) The algorithm adds new elements to the vacancies and performs reverse and upward comparison operations according to step (1) to finally form a minimum heap data structure.

In the above process, the corresponding values of two child nodes need to be compared each time when the gap is adjusted downward, and the maximum number of comparisons is $(h-1)$. Compared with the conventional heap sorting method, the new element inserted into the vacancy needs to be compared with its parent node each time when it is adjusted upward, and the number of comparisons is $(h-1)$. The maximum number of comparisons for the above improved heap operation is $2(h-1)$,

and the time complexity of the algorithm is $T_2(n) = 2[\log_2 n]$. However, according to the characteristics of the fast forward algorithm to calculate the travel time, that is, the travel time of the newly added narrowband point is always not less than the travel time corresponding to the accepting point and the original narrowband point extending this point. Therefore, considering only one comparison with its parent node when a new element is added to the vacancy, the time complexity of the conventional and improved heap sorting algorithm is $T_1(n) = 2[\log_2 n] + 1, T_2(n) = [\log_2 n] + 1$, respectively. Figure 9 shows the data structure after regular and improved heap reconstruction.

From the analysis of Figure 8 and Figure 9, in the process of rebuilding the heap, the improved heap still maintains the structure of the minimum heap although the elements corresponding to the nodes in the heap have changed. This fully demonstrates the effectiveness of this improvement for heap sort. At the same time, the improved heap is twice as efficient as the traditional conventional heap sort in terms of its numerical comparison efficiency.

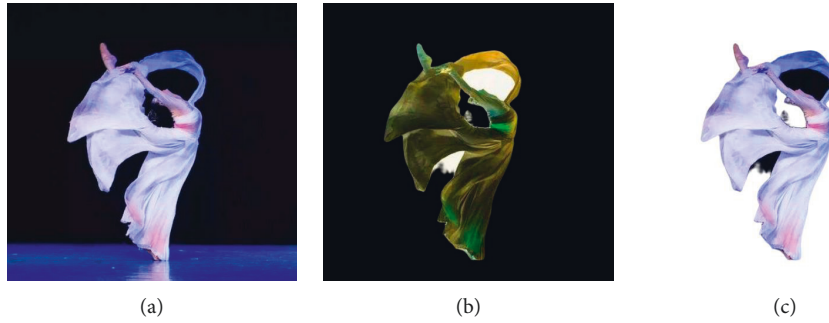


FIGURE 11: Demonstration of Chinese dance movement correction image based on digital feature recognition technology. (a) Original Chinese dance movement image. (b) Background removal of Chinese dance movement image. (c) Feature extraction of Chinese dance movement image.

TABLE 1: The effect of the correction system of Chinese dance training movements based on digital feature recognition technology.

VB	Training effect	Number	Training effect	Number	Training effect	Number	Training effect
1	87.20	21	86.73	41	80.31	61	83.85
2	86.99	22	78.57	42	83.15	62	88.70
3	85.57	23	79.37	43	87.75	63	80.52
4	80.26	24	89.58	44	86.18	64	82.59
5	80.92	25	89.97	45	78.58	65	82.06
6	78.27	26	81.64	46	80.38	66	83.84
7	84.40	27	84.93	47	84.90	67	85.22
8	81.15	28	81.47	48	80.97	68	85.60
9	85.40	29	90.50	49	90.37	69	83.71
10	81.73	30	87.20	50	86.86	70	84.63
11	88.11	31	83.42	51	80.31	71	86.61
12	79.53	32	87.08	52	87.77	72	78.64
13	89.62	33	85.42	53	81.07	73	82.65
14	80.97	34	80.71	54	86.23	74	78.62
15	82.40	35	86.95	55	82.62	75	88.94
16	89.73	36	89.72	56	84.86	76	88.61
17	81.13	37	84.17	57	90.83	77	80.98
18	80.32	38	90.00	58	87.99	78	86.79
19	83.09	39	79.05	59	85.96	79	86.34
20	90.82	40	80.68	60	79.79	80	90.45

4. Correction of Chinese Dance Training Movements Based on Digital Feature Recognition Technology

The design of the digital teaching system of Chinese classical dance is to design the function of the system according to the user's needs, and then, according to the function, the design concept will be transformed into a concrete visual representation through interactive prototypes. Then, the visual design of the interface is carried out according to the interactive prototype, and finally, the development of the system is realized by interactive technology, as shown in Figure 10.

After the above system is constructed, the practical effect of the correction model of Chinese dance training movements based on digital feature recognition technology is explored, and the demonstration image shown in Figure 11 is obtained.

On the basis of the above research, the effect evaluation of the correction system of Chinese dance training movements based on digital feature recognition technology in this paper is carried out, and the final results are counted, and the results obtained are shown in Table 1.

From the above analysis, the correction system of Chinese dance training movements based on digital feature recognition technology proposed in this paper has a good effect and can effectively promote the improvement of Chinese dance training effects.

5. Conclusion

The basic skills training of Chinese classical dance has certain standard movements and strict requirements. In the large amount of exercise and long-term training, it is required to maintain correct movements and elegant posture. If the posture of a person's body movement is not correct, not only the movement is not elegant, but, more

importantly, the dancer is prone to injury. Therefore, in the dance teaching of professional colleges, the basic training and teaching of Chinese classical dance is an extremely difficult learning process. This paper combines digital feature recognition technology to correct and analyze Chinese dance training movements and constructs an intelligent auxiliary training system. From the test analysis results, it can be seen that the correction system of Chinese dance training movements based on digital feature recognition technology proposed in this paper has a good effect and can effectively promote the improvement of Chinese dance training effects.

Data Availability

The labeled dataset used to support the findings of this study is available from the corresponding author upon request.

Conflicts of Interest

The authors declare that they have no conflicts of interest.

References

- [1] G. Hua, L. Li, and S. Liu, "Multipath affinity stacked—hourglass networks for human pose estimation," *Frontiers of Computer Science*, vol. 14, no. 4, pp. 1–12, 2020.
- [2] M. Li, Z. Zhou, and X. Liu, "Multi-person pose estimation using bounding box constraint and LSTM," *IEEE Transactions on Multimedia*, vol. 21, no. 10, pp. 2653–2663, 2019.
- [3] S. Liu, Y. Li, and G. Hua, "Human pose estimation in video via structured space learning and halfway temporal evaluation," *IEEE Transactions on Circuits and Systems for Video Technology*, vol. 29, no. 7, pp. 2029–2038, 2018.
- [4] W. McNally, A. Wong, and J. McPhee, "Action recognition using deep convolutional neural networks and compressed spatio-temporal pose encodings," *Journal of Computational Vision and Imaging Systems*, vol. 4, no. 1, p. 3, 2018.
- [5] D. Mehta, S. Sridhar, O. Sotnychenko et al., "VNect," *ACM Transactions on Graphics*, vol. 36, no. 4, pp. 1–14, 2017.
- [6] M. Nasr, H. Ayman, N. Ebrahim, R. Osama, N. Mosaad, and A. Mounir, "Realtime multi-person 2D pose estimation," *International Journal of Advanced Networking and Applications*, vol. 11, no. 6, pp. 4501–4508, 2020.
- [7] X. Nie, J. Feng, J. Xing, S. Xiao, and S. Yan, "Hierarchical contextual refinement networks for human pose estimation," *IEEE Transactions on Image Processing*, vol. 28, no. 2, pp. 924–936, 2018.
- [8] Y. Nie, J. Lee, S. Yoon, and D. S. Park, "A multi-stage convolution machine with scaling and dilation for human pose estimation," *KSII Transactions on Internet and Information Systems (TIIS)*, vol. 13, no. 6, pp. 3182–3198, 2019.
- [9] I. Petrov, V. Shakhuro, and A. Konushin, "Deep probabilistic human pose estimation," *IET Computer Vision*, vol. 12, no. 5, pp. 578–585, 2018.
- [10] G. Szűcs and B. Tamás, "Body part extraction and pose estimation method in rowing videos," *Journal of Computing and Information Technology*, vol. 26, no. 1, pp. 29–43, 2018.
- [11] N. T. Thành and P. T. Công, "An evaluation of pose estimation in video of traditional martial arts presentation," *Journal of Research and Development on Information and Communication Technology*, vol. 26, no. 2, pp. 114–126, 2019.
- [12] J. Xu, K. Tasaka, and M. Yamaguchi, "[Invited paper] fast and accurate whole-body pose estimation in the wild and its applications," *ITE Transactions on Media Technology and Applications*, vol. 9, no. 1, pp. 63–70, 2021.
- [13] A. Zarkeshev and C. Csiszár, "Rescue method based on V2X communication and human pose estimation," *Periodica Polytechnica: Civil Engineering*, vol. 63, no. 4, pp. 1139–1146, 2019.
- [14] A. Bakshi, D. Sheikh, Y. Ansari, C. Sharma, and H. Naik, "Pose estimate based yoga instructor," *International Journal of Recent Advances in Multidisciplinary Topics*, vol. 2, no. 2, pp. 70–73, 2021.
- [15] S. L. Colyer, M. Evans, D. P. Cosker, and A. I. T. Salo, "A review of the evolution of vision-based motion analysis and the integration of advanced computer vision methods towards developing a markerless system," *Sports medicine - open*, vol. 4, no. 1, pp. 24–15, 2018.
- [16] I. Sárándi, T. Linder, K. O. Arras, and B. Leibe, "Mettrabs: metric-scale truncation-robust heatmaps for absolute 3d human pose estimation," *IEEE Transactions on Biometrics, Behavior, and Identity Science*, vol. 3, no. 1, pp. 16–30, 2020.
- [17] A. Azhand, S. Rabe, S. Müller, I. Sattler, and A. Heimann-Steinert, "Algorithm based on one monocular video delivers highly valid and reliable gait parameters," *Scientific Reports*, vol. 11, no. 1, p. 10, Article ID 14065, 2021.
- [18] J. Xu and K. Tasaka, "[Papers] keep your eye on the ball: detection of kicking motions in multi-view 4K soccer videos," *ITE Transactions on Media Technology and Applications*, vol. 8, no. 2, pp. 81–88, 2020.

Research Article

Research on Intelligent Campus and Visual Teaching System Based on Internet of Things

Tao Xu , Zhi-hong Wang, and Xian-qi Zhang

Hebei Vocational University of Technology and Engineering, Xing Tai, Hebei 054000, China

Correspondence should be addressed to Tao Xu; xutaoflyice@163.com

Received 24 February 2022; Revised 29 March 2022; Accepted 7 April 2022; Published 28 April 2022

Academic Editor: Xuefeng Shao

Copyright © 2022 Tao Xu et al. This is an open access article distributed under the Creative Commons Attribution License, which permits unrestricted use, distribution, and reproduction in any medium, provided the original work is properly cited.

The rapid development of Internet of things technology provides robust conditions for building a perfect intelligent campus. A visual teaching question answering system is essential for creating a smart campus, significantly improving education quality. However, the accuracy of the existing teaching question answering system is not high. To solve this problem, this paper proposes a visual teaching system based on a knowledge map. The system mainly includes two parts: problem processing and answer search. In the part of problem processing, combined with the pretraining language model, a new model framework is constructed to deal with the problem of entity reference recognition, entity link, and relationship extraction. By setting three kinds of classification labels, the problem is divided into simple, chain, and multientity problems. Different solutions are given to the above three classification problems in the answer search part. The experimental results show that the answer accuracy of this system is higher than other comparison methods.

1. Introduction

Internet of things technology refers to various modern information sensing devices and technologies based on the Internet [1]. The process is collecting, inputting, and connecting various information of objects and carrying out intelligent perception, recognition, and management [2]. It uses the Internet to realize the information exchange between people and things. It achieves the accurate collection, exchange, and sharing of information, so it has three characteristics: overall perception, reliable transmission, and intelligent processing [3]. Overall perception refers to its use of perception equipment to perceive and obtain information to achieve a comprehensive information collection. Reliable transmission refers to the accurate sharing of object information based on the Internet, so that information can be accurately communicated and disseminated. Intelligent processing refers to a series of processes in which it can use various intelligent technologies to perceive, collect, process, and monitor object information to provide more convenience for people's lives, studies, and work.

Smart campus refers to integrating campus learning, life, and work using Internet of things technology [4], to make

the campus management, teaching, scientific research, and campus life more systematic and efficient, solve the problems existing in the traditional campus more appropriately, and promote the further development of China's education. In the construction and application of the Internet of things environment in the smart campus, based on the data processing ability of the smart campus, focus on the opening of the existing data communication channel of the smart campus [5]. The accurate collection of data in teaching and learning activities provides a data basis for the multilevel and diversified development of the school, analyzing the reasons behind academic achievements and helping teachers determine targeted teaching strategies and realize individualized education [6]. In addition, the design of smart campus Internet of things environment architecture and the development of related applications provide model reference and practical guidance for applying new technologies in smart campus.

In recent years, the development of Internet of things technology has gradually formed a scale. People have invested a lot of workforces, material resources, and energy in developing Internet of things technology [7]. It has helped all walks of life solve the problems existing in the previous

model and achieved good results. However, there are still challenges in the cost, technology, and management of Internet of things technology. Universities should understand these challenges when using Internet of things technology for smart campus construction, to avoid problems in the construction of smart campus. The challenges of Internet of things technology mainly exist in three aspects. (1) Technical standards: Internet of things technology has higher requirements for the Internet [8]. It needs to use different technologies and ports for information perception to meet the needs of object information collection, transmission, and sharing needs. However, there is no unified technical standard for Internet of things technology [9]. As a result, universities cannot have unified standards to implement when building smart campus. This is not conducive to the standardized construction of smart campus. (2) Management issues: Internet of things technology is a further improvement of the Internet [10]. With the continuous expansion of its application scope, the information of all walks of life will cross each other. This leads to the need for universities to screen all kinds of information when building smart campus [11]. It also brings difficulties to the platform management of smart campus. (3) Cost issues: The application of Internet of things technology needs a lot of financial support [12]. In the process of using the Internet of things, the school increases the investment in the construction of smart campus and increases the investment in the maintenance of smart campus, which increases the financial pressure of the school. Universities should understand the shortcomings of Internet of things technology in using Internet of things technology and build a smart campus in combination with the actual situation of the university to improve the campus teaching environment and the efficiency of teaching and management [13].

This paper proposes a visual teaching system based on a knowledge map to solve the above problems. Different tags are set for questions to use different modules to search the answers and solve chain and multientity problems in complex problems. In entity reference recognition, a method combining the pretraining language model BERT [14] and BiLSTM network [15] is proposed. In the part of relationship extraction, the complex model structure is abandoned and the similarity calculation of question and candidate relationship is realized directly based on BERT model. In the entity link part, different features are designed with the help of XGBoost model to improve the system performance [16]. By setting three kinds of classification labels, the problem is divided into simple, chain, and multientity problems. Different solutions are given to the above three classification problems in the answer search part.

2. Related Work

The development trend of smart campus at home and abroad mainly focuses on the following aspects: comprehensive informatization and creating a social learning atmosphere; using cloud computing technology to provide convenient learning space [17]. With intelligent teaching and management anytime, anywhere, big data can tailor learning

plans and analyze learning behaviors for students, build an intelligent campus based on Internet of things technology, and use renewable energy to achieve campus energy conservation and emission reduction and build a monitoring campus with sensor interconnection to realize a safe campus.

2.1. Data Problems in Smart Campus. The main technical problems in the construction of smart campus are data processing and data acquisition [18]. Due to the needs of school development, different school departments have built different management platforms at different stages, such as learning resource management platform, student management platform, educational administration management platform, logistics management platform, and teacher management platform. Due to many data sources and the lack of unified data standards and specifications, the data formats are different and the data integration and processing are difficult. In terms of data processing, to integrate the data of various departments and solve the problems of incompatible platforms and inconsistent data, [19] and others built a one-stop service center, data center, and certification (Registration) center through the cloud platform to realize business process integration and unified data planning and governance. Literature [20] and others took data aggregation as the core and changed the close coupling mode of traditional data. With the data processing problem, the acquisition of data is no longer constrained. Internet of things technology has the characteristics of comprehensive perception and reliable transmission [21]. The application of Internet of things technology in smart campus extends the traditional information transmission between people to people and things, things and things [22]. In terms of data acquisition, it realizes comprehensive perception and provides data support for decision-making analysis of smart campus.

2.2. Application of New Technology in Smart Campus. Here, the search is conducted by the theme “smart campus” through CNKI, and the query time is set from January 1, 2018, to January 31, 2022. The frequency of high-frequency keywords about smart campus in recent five years is analyzed. See Table 1. In the past five years, CNKI has collected a total of 5457 documents on “smart campus.” Through word frequency classification and merging synonymous keywords, seven high-frequency keywords related to technology are finally obtained. The top three keywords are “big data,” “Internet of things,” and “Internet plus.” Through co-occurrence matrix analysis, the frequency of “smart campus” and “Internet of things” in 5457 documents is 366, as shown in Table 1.

3. Question Answering Model Based on Knowledge Map

Given a Chinese natural language question Q , the goal of CKBQA system is to extract answer A from a teaching knowledge map knowledge base KB . The flow of the teaching knowledge Atlas question answering system proposed in this

TABLE 1: High-frequency keywords of smart campus research.

Ordering	High-frequency keywords	Frequency of occurrence
1	Smart campus	5457
2	Big data	660
3	Internet of things	640
4	Internet+	275
5	Cloud computing	209
6	Campus card	204

paper is shown in Figure 1, which includes two main modules, question processing and answer search. The question processing module involves classification model, entity reference recognition, and entity link model. The answer search module involves unified single-hop question search, chain question search, and multientity question search. The dotted line in Figure 1 indicates that the three search processes are completed in the knowledge map.

3.1. BERT Model. The BERT (Bidirectional Encoder Representations from Transformers) model is shown in Figure 2. It is a multilayer two-way language model. The model input comprises word vector, position vector, and segment vector. In addition, the head and tail of the sentence have two special marking symbols [CLS] and [SEP], respectively, to distinguish different sentences. After the semantic model is fused, the output information of each coder is the corresponding word of the semantic model. Suppose that the input sequence of a Chinese natural language question is $I = (i_1, i_2, \dots, i_t)$ and $S = ([CLS], i_1, i_2, \dots, i_t, [SEP])$ after being processed by the text word splitter. The output sequence after passing through the M-layer encoder is $B = (b_0, b_1, \dots, b_t, b_{t+1})$. The pretrained BERT model provides a powerful context-sensitive representation of sentence features. After fine-tuning, it can be used for various target tasks, including single sentence classification, sentence pair classification, and sequence annotation.

3.2. Entity Reference Identification. Entity reference recognition refers to identifying the reference of the subject entity from a given question. In this paper, entity reference recognition is regarded as a sequence annotation task, and neural network model is used for recognition. Firstly, the reference of the subject entity is found according to the SPARQL statement of the training corpus. Then construct the data used for sequence annotation and train a reference recognition model.

This paper combines the BERT language model with the bidirectional short-term memory (BiLSTM) network and input into the conditional random field (CRF) model. Proposed model is constructed to predefine the label of each character. Firstly, the BERT language model obtains the degree context representation of each character in the question. Then, the BiLSTM network is used to obtain the semantic relationship between each character's left and right sides. Finally, the CRF model is used to ensure that the result of the prerule is a legal label. The specific calculation of the above process is shown in equations (1) and (2).

$$N = \text{BiLSTM}(B), \quad (1)$$

$$K = \text{CRF}(N), \quad (2)$$

where $N \in R^{(t+2) \times 2D}$ represents the output of the encoded sentence after passing through the BiLSTM model. $K \in R^{1 \times (t+2)}$ indicates the label of CRF model prerule. D represents the hidden layer dimension output by the BERT model.

The model structure of proposed is shown in Figure 3.

3.3. Classification Model. In practical application scenarios, the questions raised by users are often not limited to simple questions. Many problems involve complex multihop problems. Therefore, this paper divides the problem into single-hop and multihop problems. Among them, the single-hop question is divided into three positions, main, predicate, and object. The multihop question can be divided into chain and entity questions.

3.3.1. Single Multihop Classification. Single-hop problem (simple problem) means that the question corresponds to a single triple query, while multihop problem (complex problem) means that the question corresponds to multiple triple queries. For the single sentence classification task, it gives the basic classification framework of BERT. That is, the output of the first tag [CLS] in the last layer of the model is directly used as the fusion representation of the whole sentence and then classified through a multilayer perceptron. The model structure is shown in Figure 4, and the calculation of the last step is shown in the following equation:

$$j = \text{softmax}(b_0 M^N + h). \quad (3)$$

Softmax represents the activation function, which calculates the probability distribution of each category. $M \in R^{Z \times D}$ is the weight of the hidden layer, $h \in R^{1 \times Z}$ is offset, and Z represents the number of categories.

3.3.2. Subject Predicate Object Classification. Subject predicate object classification means that the answer of a single jump question corresponds to one of the subject, predicate, or object in the triple. When the subject entity of a question is known, it is impossible to know whether it is in the subject position or object position in the knowledge base triplet. Therefore, this paper divides the single-hop problem into three categories, subject, predicate, and object, to find the answer. According to the position of the question mark in the SPARQL statement triplet of the single-hop problem, the data of the single-hop problem is divided into three categories. Then train a three-classification model, and the model structure is shown in Figure 4.

3.3.3. Chain Classification. Chained questions involve multiple triples of queries, and there is a progressive relationship between triples. The questions of such complex

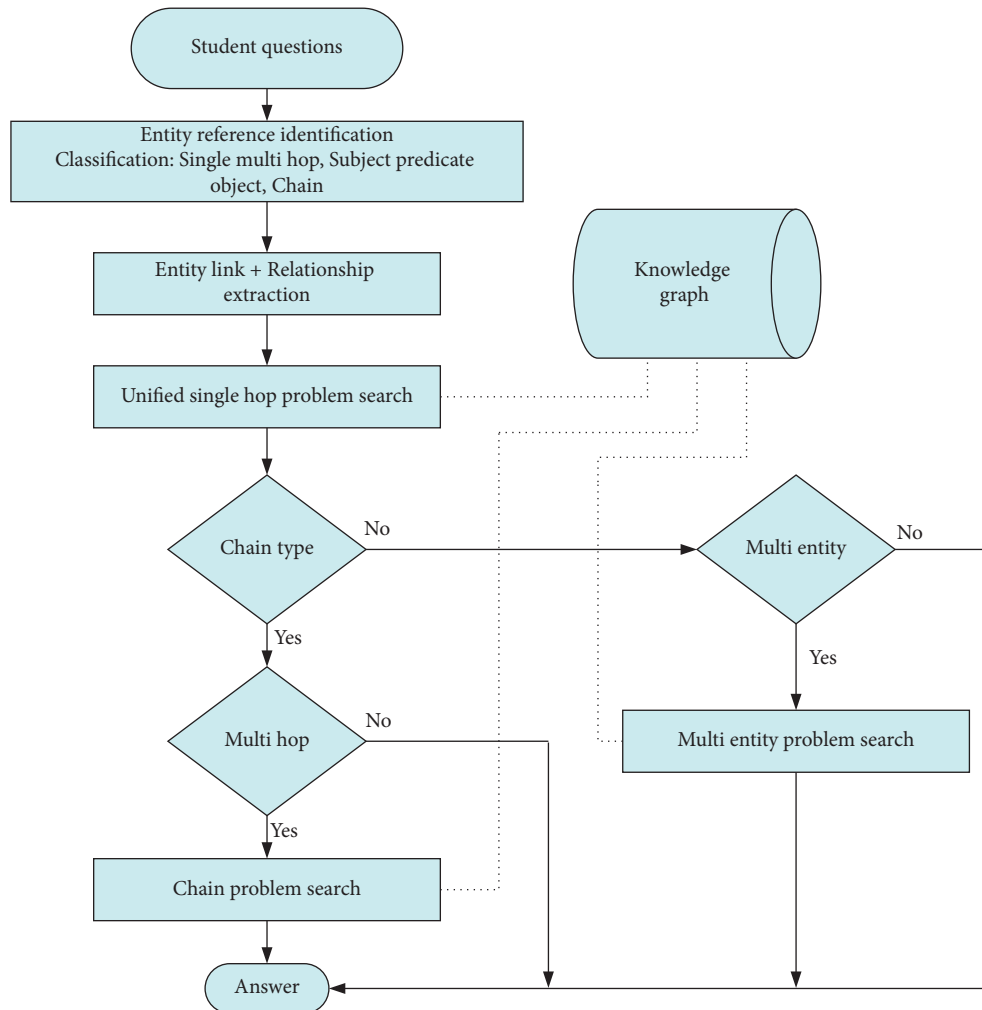


FIGURE 1: Procedure of teaching knowledge base question answering system.

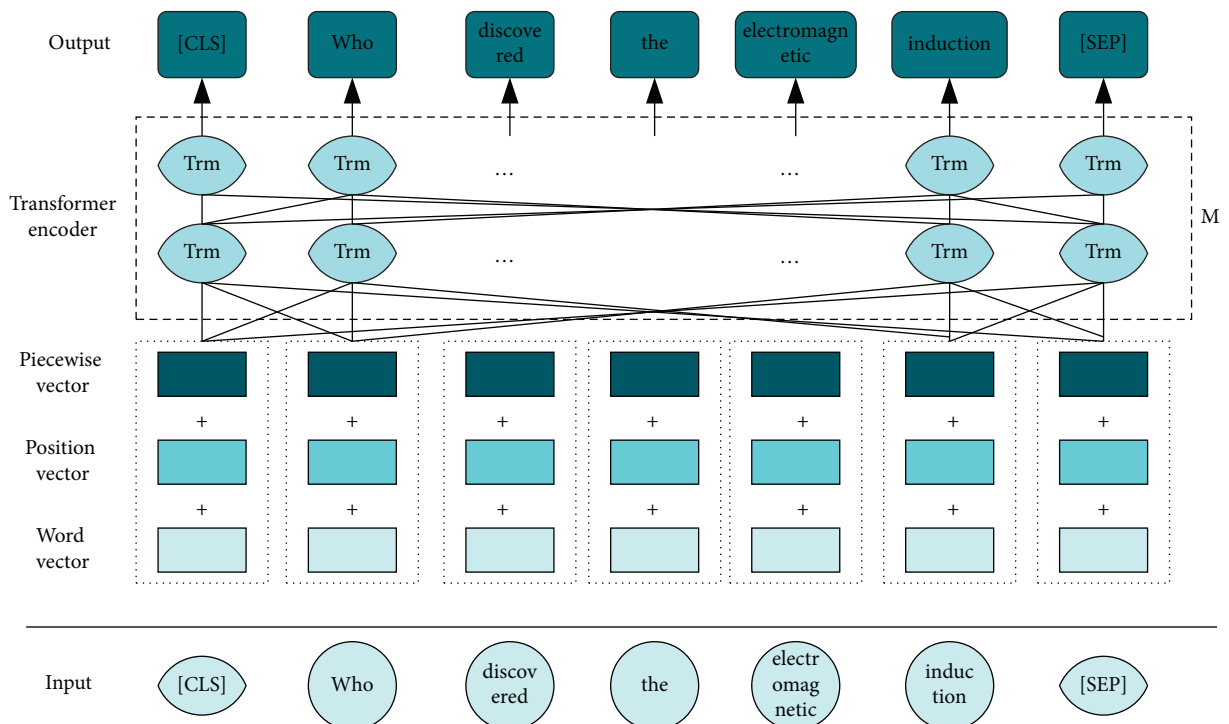


FIGURE 2: Structure of BERT model.

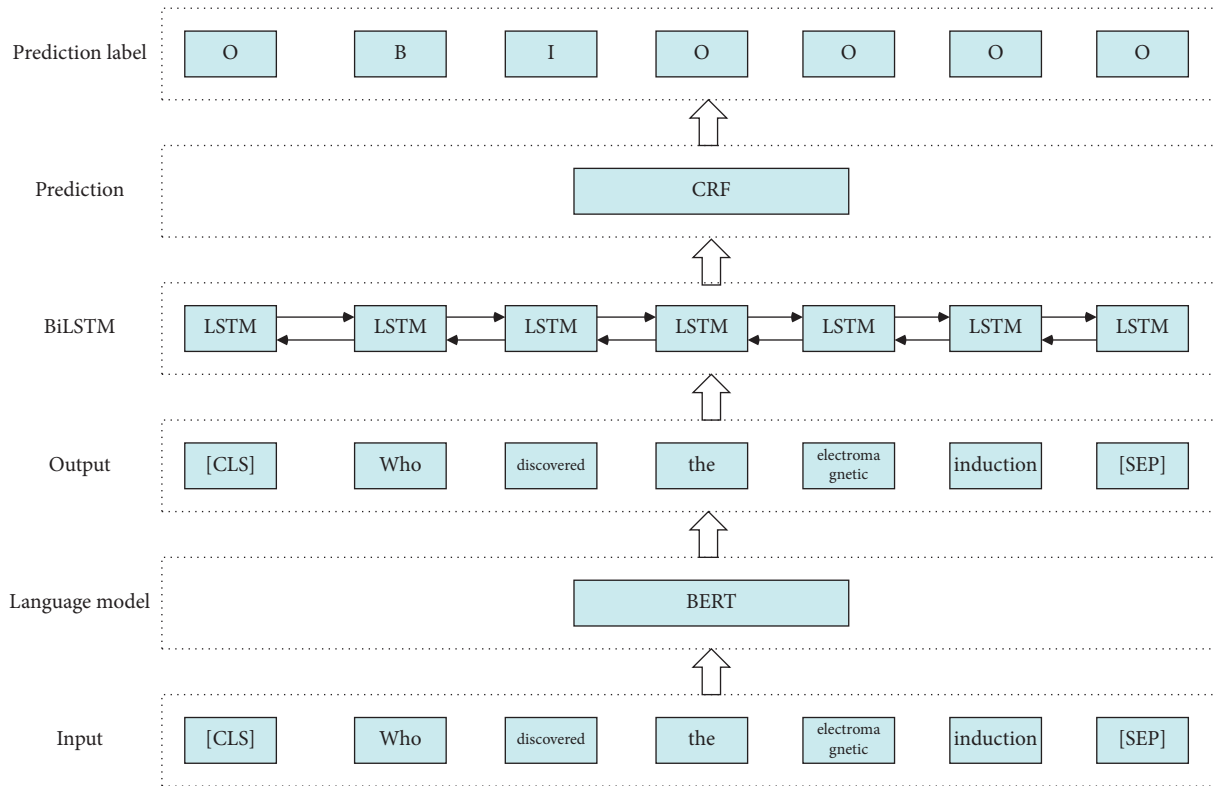


FIGURE 3: Structure of proposed model.

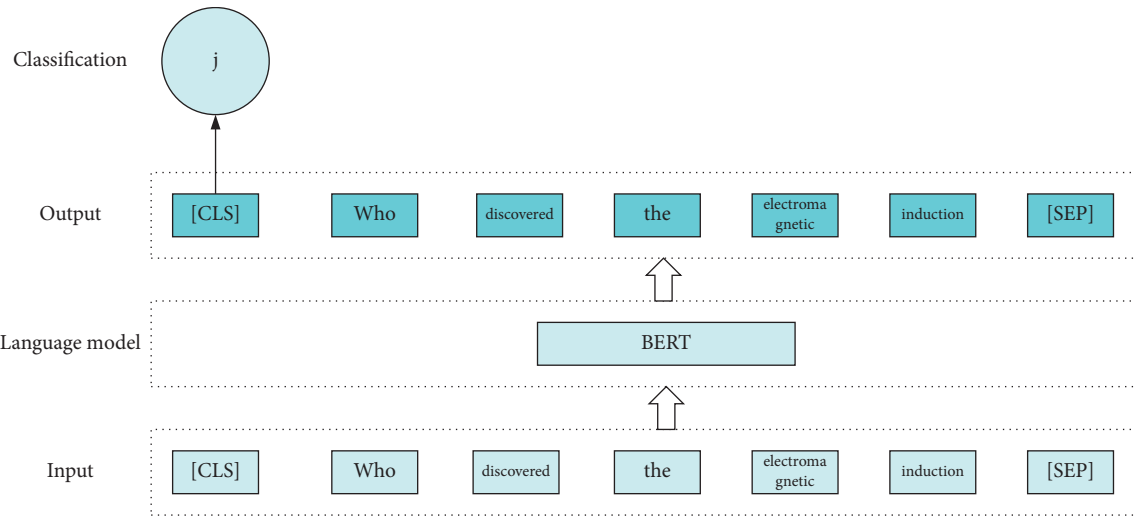


FIGURE 4: Structure of BERT classification model.

problems contain multiple relational attributes. According to whether the triples in SPARQL statement are presented, all data can be divided into chain problem and nonchain problem. Because the single-hop problem may also have multiple entities in the question, the multihop problem is not directly divided into chain and multientity problems. On this basis, a binary classification model is trained, and the model structure is shown in Figure 4.

3.3.4. Relationship Extraction. Relationship extraction refers to finding the closest relationship between the subject entity of a given question and the question’s expression among all the entity’s candidate relationships. In many cases, the relationship expression in Chinese questions is colloquial and lacking standardization, which is inconsistent with the expression in the knowledge base. It is impossible to extract the relationship directly through character alignment. Based on

BERT model, this paper designs a semantic similarity calculation method of question and relationship. For example, there is a question, “when is Leo Messi’s birthday?” The SPARQL statement knows that the subject entity is “< Rio Messi (Argentine football player).” However, the entity has many candidate relationships, including “Chinese name,” “foreign name,” “wife,” “date of birth,” “sports team,” etc. This paper constructs a similarity calculation model data. Let the label of positive examples be 1 and the label of 5 negative examples be 0. The trained model is used to calculate the similarity between the question and each candidate relationship (classified as the probability value of label 1) and then sort. Select the relationship with the highest similarity to search the final answer. The model structure is shown in Figure 4, but the difference is that the input sequence is question $V = (i_1, i_2, \dots, i_t)$ and relationship $U = (z_1, z_2, \dots, z_w)$, and then the sequence processed by BERT’s Chinese text classifier is $S = ([CLS], i_1, i_2, \dots, i_t, [SEP], z_1, z_2, \dots, z_w, [SEP])$.

3.4. Answer Search. The answer search process is shown in Figure 1, and the specific steps are as follows.

- (1) First classify the questions to determine whether they are single multihop, subject predicate object, or chain, and then realize entity reference recognition.
- (2) According to the identified references, expand or delete left and right, and search all possible candidate entities. Then, according to a set of features, the candidate entities are scored and sorted through the entity link model, and the entity with the highest score is selected.
- (3) Search all the relationships corresponding to the entity according to the subject predicate object tag of the question. The relationship extraction model calculates the semantic similarity between them and the current query. The highest score relationship is obtained. The unified single-hop question is obtained by searching the knowledge base.
- (4) If the question is a chain and a multihop question, take the answer obtained in step 3 as the subject entity and execute step 3 again to answer the multihop chain question.
- (5) If the question is nonchained and multiple entities are identified, search the database for each entity. Query all the corresponding candidate triples, and then find the intersection of two to get the answer to the multientity problem.

4. Design of Educational Problem System

4.1. Function Design. This system is an intelligent question answering system based on knowledge map, which is developed with Python programming language and GitHub

open-source intelligent question answering system code. It is necessary to realize the function of the rapid dialogue between computers and users, which can solve students’ doubts about teaching difficulties in the teaching field. Give accurate answers through intelligent analysis of background database to reduce the burden on teachers. The overall operation of the system is simple and suitable for students of different majors. The development of question answering system is divided into three functional modules, question classification, question parsing, and query results. The system framework is shown in Figure 5.

The implementation steps of question classification are as follows. Define problem classification, and define member variables such as keywords, dictionaries, domain trees, questions, and questions in the class. In addition to seven types of entity keywords, feature words also include domain words and negative words composed of these entity words. Questions and questions include difficult attribute words commonly used by students. The construction of domain tree and dictionary is realized by calling functions. The construction of domain tree function is realized through Aho-Corasick library.

Aho-Corasick is a string matching algorithm implemented by two data structures: Trie and Aho-Corasick (AC) automata. Trie is a dictionary of string index. The time to retrieve relevant items is directly proportional to the length of the string. AC automata can find all strings of a given set in one run. AC algorithm is actually to implement KMP on Trie tree, which can complete the matching of multimode strings.

The attribute function constructs a dictionary according to seven types of entities through question type, namely, keyword + keyword type. Use the function to check the user’s questions to see if there are domain words about the entity type contained in the system. If detected, filter the questions.

Question filtering matches domain words through the unique ITER function in Aho-Corasick library. Filter the domain words with the same characters, select the domain word with the longest string, and return it as the domain word in the user’s question and the entity type corresponding to the vocabulary.

After obtaining the question domain words and related fields, the entity types related to the question are integrated. Call related functions to determine the type of question. For example, if the student question is a major difficulty type, return the detailed information about the major. If the type is practice, return all the professional practice problem details. Merge all the results and return to the dictionary for placement.

Question resolution transfers the result of question classification to the main function, calls the keyword function to extract the dictionary of entity type and domain word form, and then converts each problem type to Cyper language, which is easy to query. It should be noted that the

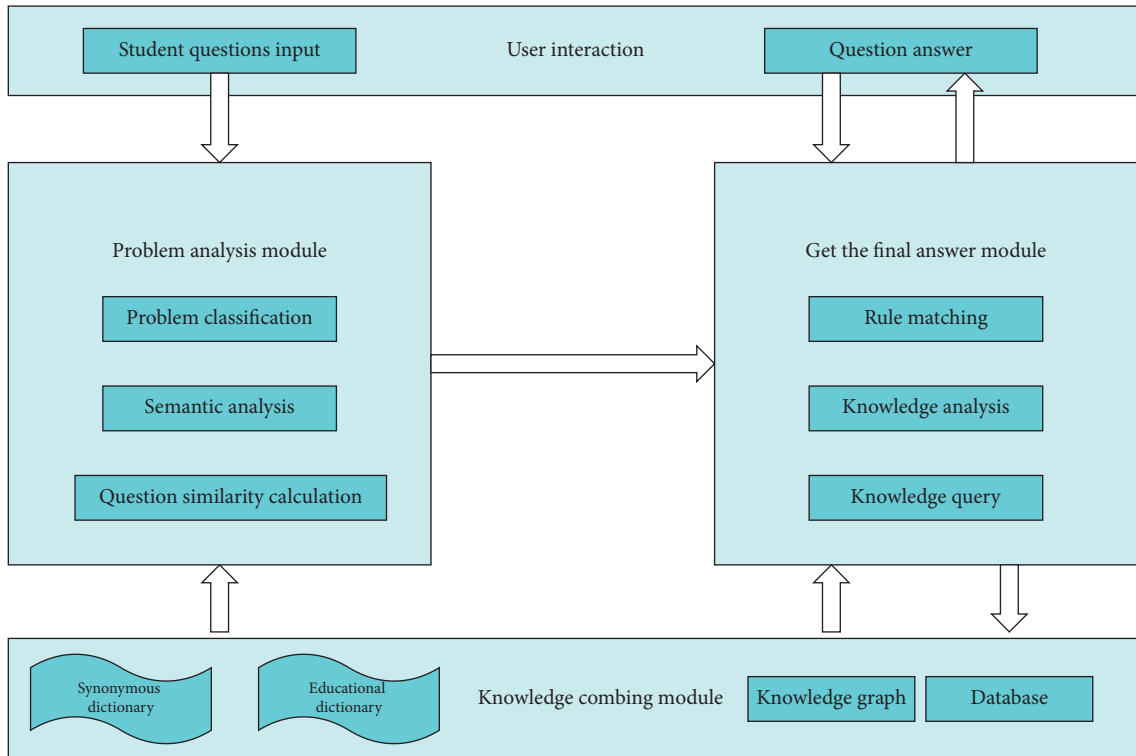


FIGURE 5: System framework.

additional problems of education need two-way query. Students' questions may be about the attributes of important and difficult questions, or they may query the connection relationship. Difficult questions include students' specific questions and relevant answers.

4.2. Function Module Design

4.2.1. Student Module. Based on deep learning, the main authority of automatic question answering system is student users, and the main function is to ask questions. The steps are as follows. Students enter the home page and log in to their own account, enter the question page and ask questions by voice, or enter the question in the text box and click submit. The system judges the problem input format after receiving the problem. If it is voice input, the original system of the company will convert the voice into text for input. The system processes the received sentences and performs word segmentation and keyword extraction operations. The system searches the problem of high similarity in the knowledge base according to keywords. Output the retrieved question answers from high to low according to the similarity. If there is no problem of high similarity, turn to the search engine search problem, and use web crawlers to grab relevant web pages at the same time.

After searching the answers, the natural language generation technology is used to return the answers to the students. At the same time, it is suggested that the answer comes from the network. After the teacher gives the standard answer through the history record, the students can get it by viewing the history record.

4.2.2. Teacher Module. In the automatic question answering system based on deep learning, the use authority of teachers is teachers' users, which are mainly responsible for answering students' questions. The specific steps of screening crawler results are as follows. If a teacher logs in on the home page, he/she needs to confirm his/her identity first. After passing the authentication, you can enter the teacher user page to manage the relevant information of students. Teachers can check the history to see if there are new questions, whether the problem exists in the existing knowledge base. If there are problems, check whether they are accurate and whether they need to be changed. If not recorded, check the search engine and web crawler results. Review whether the search and captured results are correct and whether the statement is in line with students' understanding ability. If you are satisfied with the results, you can add questions and answers to the knowledge base. If you are not satisfied, you can delete the results, write your own answers, and add them to the knowledge base.

5. Experiment and Analysis

5.1. Data Preparation

5.1.1. Knowledge Map. We use the open-source knowledge map Chinese education database in the experiment. It is constructed from six Chinese education Q&A websites, five Chinese education knowledge bases, and some electronic teaching plans. We selected six kinds of educational entities, namely, teaching, practice, feedback, search, class, and school, and 15 kinds of relationships between them for the

experiment. In addition, we also crawled multiple pictures for each entity from Baidu pictures and constructed a multimodal knowledge map.

5.1.2. Teaching Question and Answer Data Set. We obtained the question and answer data from the education and teaching network question and answer platform. There are 245123 question and answer pairs in the data set, with an average number of words of 30 questions and 76 answers, involving 18 teaching direction questions. The preprocessing process is to remove punctuation and classify.

5.1.3. Path Extraction. We use depth-first search to extract paths. During the experiment, extracting paths from the knowledge map is time-consuming and laborious, and the number of paths increases exponentially with the length of paths. However, long paths bring more possible connections and add more noise. Experiments point out that when the number of hops of the path increases from 2 to 3, the performance of the experiment decreases significantly. Therefore, we limit the length of the path to 3.

5.2. Comparison Method. We selected five methods for comparison.

- (1) Literature [23], word bag model is a simple and effective model in natural language processing.
- (2) Literature [24], it learns the representation of low dimensional vectors of sentences based on word2vec.
- (3) Literature [25], it uses similarity matrix to describe the complex relationship between question and answer pairs.
- (4) Literature [26], it describes the interaction at the word level of question and answer pairs and uses this interaction for document matching.
- (5) Proposed, it is the teaching knowledge Atlas question and answer system with multilabel strategy, which applies the knowledge Atlas to the representation of questions and answers.

5.3. Evaluation Method and Parameter Setting. We used precision and nDCG as evaluation indicators. Accuracy refers to the proportion of correct answers that get the highest score, and nDCG is used to evaluate the ranking. Because precision and nDCG need to scan the whole data set and calculate the score of each answer, it takes a lot of time. Therefore, we sample 1 positive sample and n negative samples for each question in the evaluation and then calculate the final evaluation result on this candidate set.

As for parameter setting, the embedded dimensions of questions, answers, entities, and relationships for all methods are set to 150. We tested the number of negative

samples $n=6$ and $n=20$, respectively. At the same time, in order to verify that our method can benefit from a large amount of data, we train with $p=20\%$, 40% , and 60% data, respectively, and the remaining data are used for testing.

5.4. Analysis of Experimental Results

5.4.1. Quantitative Analysis. We listed the experimental results in Tables 2 and 3, observed the experimental results, and got the following conclusions.

- (1) With the increase of training data, the performance of the method in [23] is very stable, while the performance of other methods becomes better with the increase of training data showing that the representation based method can make effective use of data.
- (2) Proposed is superior to the methods of [25] and [26], which shows that adding knowledge map is effective.
- (3) The results of [25] and [26] are better than those of [23] and [24], which shows that the retrieval performance of teaching question answering is improved after considering the interactive information between question answering pairs.

5.4.2. Elimination Analysis. To analyze the influence of multilabel strategy teaching knowledge map on the experimental results, we did elimination analysis on the data set of education and teaching network question and answer platform. As shown in Table 4, four variants are designed, including only knowledge map structure information (S), combination of structure information and text information (S/T), combination of structure information and image information (S/I), and combination of the three (S/I/T). The experimental results show that, among the four variants, the information containing three modes of structure, text, and image is the best, followed by the information containing only two modes, and is better than the model containing only single-mode information. The experimental results show that the teaching knowledge map of multilabel strategy is effective for teaching Q&A task.

5.4.3. Q&A Interaction Analysis. We analyze the weight between the connection Q&A pairs. As shown in Figure 6, the words in the question and answer can be mapped to the entities in the knowledge map. Below is the path on the multilabel strategy knowledge map. The color of the entity on the path represents the importance of the path. A path from the entity in the question to the entity in the answer can be regarded as the process of reasoning when the teacher answers the question. For example, when the user mentions "a knowledge difficulty," the teacher first thinks about the

TABLE 2: nDCG and precision on CNKI dataset when n is 6.

Method	nDCG			Precision		
	$p = 20\%$	$p = 40\%$	$p = 60\%$	$p = 20\%$	$p = 40\%$	$p = 60\%$
Literature [23]	0.6951	0.6863	0.6811	0.4145	0.4003	0.3945
Literature [24]	0.7172	0.7186	0.7282	0.4273	0.4291	0.4464
Literature [25]	0.7755	0.7958	0.7985	0.5373	0.5696	0.5757
Literature [26]	0.7326	0.7794	0.7295	0.4607	0.5431	0.4593
Proposed	0.8678	0.8726	0.8705	0.7015	0.7147	0.7087

TABLE 3: nDCG and precision on CNKI dataset when n is 20.

Method	nDCG			Precision		
	$p = 20\%$	$p = 40\%$	$p = 60\%$	$p = 20\%$	$p = 40\%$	$p = 60\%$
Literature [23]	0.5176	0.5162	0.5174	0.2433	0.2402	0.2435
Literature [24]	0.4995	0.5063	0.5158	0.1922	0.2056	0.2143
Literature [25]	0.5903	0.6202	0.6323	0.3176	0.3542	0.3685
Literature [26]	0.5301	0.5878	0.5897	0.2513	0.3206	0.3277
Proposed	0.7308	0.7305	0.7417	0.4933	0.4905	0.5067

TABLE 4: nDCG and precision on CNKI dataset with variants when n is 6.

Method	nDCG			Precision		
	$p = 20\%$	$p = 40\%$	$p = 60\%$	$p = 20\%$	$p = 40\%$	$p = 60\%$
S	0.8556	0.8735	0.8606	0.6787	0.7148	0.6889
S/T	0.8543	0.8746	0.8635	0.6743	0.7175	0.6972
S/I	0.8651	0.8735	0.8623	0.6946	0.7142	0.6917
S/I/T	0.8678	0.7087	0.8728	0.8709	0.7012	0.7145

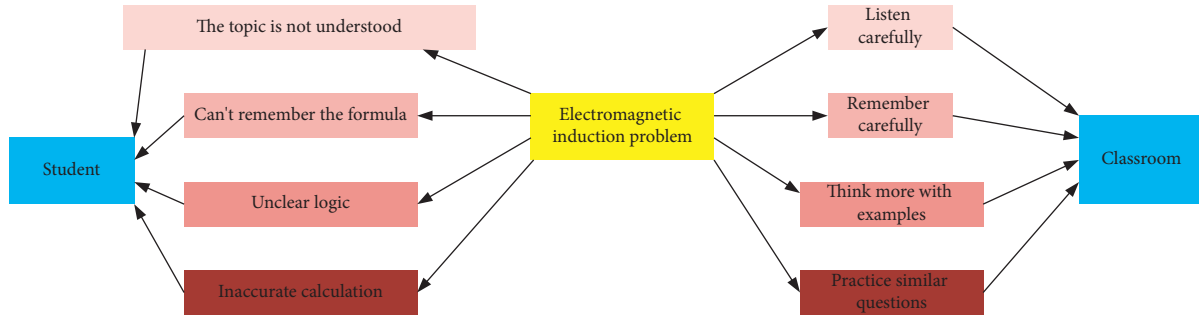


FIGURE 6: Answer example.

reasons, such as maybe not clear about the relevant concepts and problem-solving ideas, and then gives his suggestions.

6. Conclusion

This paper presents a visual teaching system based on knowledge map. The system mainly includes two parts, problem processing and answer search. Different tags are set for questions to use different modules to search the answers of questions and solve chain and multientity problems in complex problems. In the part of entity reference recognition, a method combining the pretraining language model BERT and BiLSTM network is proposed. In the part of relationship extraction, the complex model structure is

abandoned and the similarity calculation of question and candidate relationship is realized directly based on BERT model. In the entity link part, different features are designed with the help of XGBoost model to improve the system performance. By setting three kinds of classification labels, the problem is divided into simple, chain, and multientity problems. Different solutions are given to the above three classification problems in the answer search part. The experimental results show that the system can effectively solve different types of simple, chain, and multientity questions in teaching knowledge map Q&A, and the answer accuracy is higher than other comparison methods. However, there is also a disadvantage. Setting multiple labels on questions through different classification models will lead to an error

transmission process, and the system's overall performance will be affected by the performance of multiple submodules. Therefore, an end-to-end method will be studied and implemented to complete teaching knowledge map Q&A in the future. In addition, NL2SQL technology can directly convert users' natural statements into executable SQL statements. The next research direction is how to effectively introduce NL2SQL technology into the question and answer task of the teaching knowledge map.

Data Availability

The labeled dataset used to support the findings of this study is available from the corresponding author upon request.

Conflicts of Interest

The authors declare that they have no conflicts of interest.

Acknowledgments

This work was funded by Research on the Construction of Civil Construction Specialty Group in Higher Vocational Colleges Based on Intelligent Construction (no. SZ2021034).

References

- [1] D. Jiang, "The construction of smart city information system based on the Internet of Things and cloud computing," *Computer Communications*, vol. 150, pp. 158–166, 2020.
- [2] X. Shi, X. An, Q. Zhao et al., "State-of-the-art internet of things in protected agriculture," *Sensors*, vol. 19, no. 8, p. 1833, 2019.
- [3] L. Bai, D. Yang, X. Wang et al., "Chinese experts' consensus on the Internet of Things-aided diagnosis and treatment of coronavirus disease 2019 (COVID-19)," *Clinical eHealth*, vol. 3, pp. 7–15, 2020.
- [4] X. Xu, D. Li, M. Sun et al., "Research on key technologies of smart campus teaching platform based on 5G network," *IEEE Access*, vol. 7, pp. 20664–20675, 2019.
- [5] W. Li, "Design of smart campus management system based on internet of things technology," *Journal of Intelligent and Fuzzy Systems*, vol. 40, no. 2, pp. 3159–3168, 2021.
- [6] Y. Roh, G. Heo, and S. E. Whang, "A survey on data collection for machine learning: a big data-ai integration perspective," *IEEE Transactions on Knowledge and Data Engineering*, vol. 33, no. 4, pp. 1328–1347, 2019.
- [7] G. Sun, "Research on the cooperative development of university and industry economy based on Internet of Things technology," *Transactions on Emerging Telecommunications Technologies*, vol. 31, no. 12, Article ID e3917, 2020.
- [8] Z. Lv, "Security of internet of things edge devices," *Software: Practice and Experience*, vol. 51, no. 12, pp. 2446–2456, 2021.
- [9] X. Li, P. Wei, Z. J. Wei et al., "Research on security issues of military internet of things [C]//2020 17th international computer conference on wavelet active media technology and information processing (ICCWAMTIP)," *IEEE*, pp. 399–403, 2020.
- [10] M. M. Dhanvijay and S. C. Patil, "Internet of Things: a survey of enabling technologies in healthcare and its applications," *Computer Networks*, vol. 153, pp. 113–131, 2019.
- [11] W. Villegas-Ch, X. Palacios-Pacheco, and S. Luján-Mora, "Application of a smart city model to a traditional university campus with a big data architecture: a sustainable smart campus," *Sustainability*, vol. 11, no. 10, p. 2857, 2019.
- [12] Y. Ding, M. Jin, S. Li, and D. Feng, "Smart logistics based on the internet of things technology: an overview," *International Journal of Logistics Research and Applications*, vol. 24, no. 4, pp. 323–345, 2021.
- [13] S. Alrashed, "Key performance indicators for smart campus and microgrid," *Sustainable Cities and Society*, vol. 60, Article ID 102264, 2020.
- [14] C. Sung, T. Dhamecha, and S. Saha, "Pre-training BERT on domain resources for short answer grading," in *Proceedings of the 2019 Conference on Empirical Methods in Natural Language Processing and the 9th International Joint Conference on Natural Language Processing (EMNLP-IJCNLP)*, pp. 6071–6075, Hong Kong, China, November, 2019.
- [15] J.-H. Jeong, K.-H. Shim, D.-J. Kim, and S.-W. Lee, "Brain-controlled robotic arm system based on multi-directional CNN-BiLSTM network using EEG signals," *IEEE Transactions on Neural Systems and Rehabilitation Engineering*, vol. 28, no. 5, pp. 1226–1238, 2020.
- [16] D. Chakraborty and H. Elzarka, "Early detection of faults in HVAC systems using an XGBoost model with a dynamic threshold," *Energy and Buildings*, vol. 185, pp. 326–344, 2019.
- [17] Z. Y. Dong, Y. Zhang, C. Yip, S. Swift, and K. Beswick, "Smart campus: definition, framework, technologies, and services," *IET Smart Cities*, vol. 2, no. 1, pp. 43–54, 2020.
- [18] W. Villegas-Ch, A. Arias-Navarrete, and X. Palacios-Pacheco, "Proposal of an architecture for the integration of a chatbot with artificial intelligence in a smart campus for the improvement of learning," *Sustainability*, vol. 12, no. 4, p. 1500, 2020.
- [19] K. Kasemsap, "The roles of business process modeling and business process reengineering in e-government," *Open Government: Concepts, Methodologies, Tools, and Applications*, IGI Global, Hershey, PA, USA, 2020.
- [20] R. Rialti, G. Marzi, C. Ciappei, and D. Busso, "Big data and dynamic capabilities: a bibliometric analysis and systematic literature review," *Management Decision*, 2019.
- [21] C. Zhang, "Design and application of fog computing and Internet of Things service platform for smart city," *Future Generation Computer Systems*, vol. 112, pp. 630–640, 2020.
- [22] A. Ghasempour, "Internet of things in smart grid: architecture, applications, services, key technologies, and challenges," *Inventions*, vol. 4, no. 1, p. 22, 2019.
- [23] Y. Fu, Y. Feng, and J. P. Cunningham, "Paraphrase generation with latent bag of words," *Advances in Neural Information Processing Systems*, vol. 32, 2019.
- [24] A. K. Sharma, S. Chaurasia, and D. K. Srivastava, "Sentimental short sentences classification by using CNN deep learning model with fine tuned Word2Vec," *Procedia Computer Science*, vol. 167, pp. 1139–1147, 2020.
- [25] H. Sun, T. Bedrax-Weiss, and W. W. Cohen, "Pullnet: open domain question answering with iterative retrieval on knowledge bases and text," 2019, <https://arxiv.org/abs/1904.09537>.
- [26] W. Lu, X. Zhang, H. Lu, and F. Li, "Deep hierarchical encoding model for sentence semantic matching," *Journal of Visual Communication and Image Representation*, vol. 71, Article ID 102794, 2020.

Research Article

Pedestrian Fall Event Detection in Complex Scenes Based on Attention-Guided Neural Network

Peng Geng, Hui Xie, Houqin Shi, Rui Chen , and Ying Tong

School of Information and Communication Engineering, Nanjing Institute of Technology, Nanjing, China

Correspondence should be addressed to Rui Chen; j00000002555@njit.edu.cn

Received 8 February 2022; Revised 11 March 2022; Accepted 1 April 2022; Published 28 April 2022

Academic Editor: Wei Liu

Copyright © 2022 Peng Geng et al. This is an open access article distributed under the Creative Commons Attribution License, which permits unrestricted use, distribution, and reproduction in any medium, provided the original work is properly cited.

To address automatic detection of pedestrian fall events and provide feedback in emergency situations, this paper proposes an attention-guided real-time and robust method for pedestrian detection in complex scenes. First, the YOLOv3 network is used to effectively detect pedestrians in the videos. Then, an improved DeepSort algorithm is used to track by detection. After tracking, the authors extract effective features from the tracked bounding box, use the output of the last convolutional layer, and introduce the attention weight factor into the tracking module for final fall event prediction. Finally, the authors use the sliding window for storing feature maps and SVM classifier to redetect fall events. The experimental results on the CityPersons dataset, Montreal fall dataset, and self-built dataset indicate that this approach has good performance in complex scenes. The pedestrian detection rate is 87.05%, the accuracy of fall event detection reaches 98.55%, and the delay is within 120 ms.

1. Introduction

Pedestrian fall event detection is one of the challenging problems for public security, particularly in some crowded complex environments. Fall events are also the leading factor of physical injury among elderly. In the WHO report of 2020, fall-related mortality rate is 6%, so there has been much research interest in fall-alerting systems. Many research studies based on a variety of devices, such as wearable devices [1, 2] and imaging sensors [3], have been presented to detect fall events. The works based on wearable devices, including tilt sensors, accelerometers, and gyroscopes, achieve good detection performances. But it is impossible for people to wear specific equipment in crowded situations. Imaging sensor-based approaches depend on cameras, depth sensors, and infrared sensors. These methods and datasets mainly focus on detection in indoor scenarios equipped with expensive devices, and complex scenarios are not considered.

At present, various vision-based pedestrian fall detection methods have been developed and many existing problems have been solved. These proposed methods can be classified into two categories, namely, two-stage method and one-

stage method. The two-stage method is based on regional proposal, and its typical methods include Girshick's R-CNN [4] and R-CNN's various improved versions [5, 6]. As the extraction of region proposal is time consuming, even in faster R-CNN, the alternative training is still required to get shared convolutional parameters between the region proposal network and the detection network. Therefore, processing time becomes a bottleneck for real-time applications. The one-stage method is based on regression, such as YOLO (You Look Only Once) [7], SSD (Single Shot MultiBox Detector) [8], and their variants. This method has fast detection speed, but it is difficult in small target grouping processing. The above generic object detection approaches achieve the most advanced performance on the benchmark dataset. Due to lots of small-scale pedestrian instances existing in typical scenes of pedestrian detection, the application of ROI (region of interest) pool layer in the general target detection pipeline will lead to "plain" feature caused by the collapse of the dustbin. Many researchers have conducted studies to adapt generic detector to detect pedestrians. On the basis of faster R-CNN, Zhang et al. [9] revised the downstream classifier via introducing enhanced forest into the shared high-resolution convolution feature

map and using region proposal network (RPN) to process small-scale objects and hard negative samples. For occlusion problem, Dinakaran et al. [10] presented a deep learning framework to deal with partial complex occlusions, and judgments are made according to several partial detectors. As LSTM (long short-term memory) can derive temporal information from video sequence by exploiting the fact that feature vectors are connected semantically for contiguous frames, various CNN-LSTM models are proposed to obtain spatial-temporal information for better detection performance. A cascaded LSTM [11] is presented for training several partial detectors to handle the common occlusion patterns and integrated into the detection module. Since the attention mechanism can quickly focus on regions of interest in complex scenes, some approaches introduced attention mechanism into the fall event detection framework. Qi et al. [12] proposed an explicit attention-guided LSTM based framework of pedestrian fall event detection, in which YOLOv3 is used to detect pedestrians in video frames, DeepSort algorithm [13] is used to complete the tracking task, and VGG-16 is used to extract the features from the tracked bounding boxes. For occluded pedestrian detection, Zou et al. [14] proposed an attention-guided deep learning network to handle the occluded problem, which integrated the CNN, attention mechanism module, and RNN into one framework. The attention module is used to guide LSTM to generate the feature representation, so the performance deterioration caused by occlusions can be greatly decreased. Although these methods can effectively detect pedestrian fall events, the training process and RPN are very time consuming. Zhou and Yuan [15] presented a joint learning algorithm to train the part detectors and reduce training time. But the detection rate relies heavily on the occlusion pattern.

For pedestrian fall event detection, the target has the characteristics of large posture changes and fast speed. Utilizing these characteristics, a fall event detection method [16] is proposed, which is based on the finite state machine theory. However, the detection performance of this method is highly dependent on the aspect ratio, which leads to weak robustness. According to angle and distance information, Chua et al. [17] classified the fall events by the changes of posture state. Many fall event detection algorithms based on neural network have been proposed, such as PCANet [18], two-stream CNN-based action detection [19], and so on. These methods have good performance in fall event detection in solitary scene, but in complex scenes, that is, when there are severe occlusion, insufficient lighting, and scale changes, they are difficult to locate the fall event.

Focusing on fall event detection in complex environments, the authors present an attention-guided fall event detection algorithm to handle occlusion, illumination change, and scale change. The authors add an attention-guided neural network to the YOLOv3 network, which can effectively solve the problem of losing targets due to occlusion. The rest of this paper is organized as follows. Section 2 introduces the framework and implementation details of the proposed fall event detection method. The experimental results are described and

analyzed in Section 3. The conclusion of this paper is given in Section 4.

2. The Proposed Algorithm

A new attention-guided algorithm is proposed in this paper, which is used to detect fall events in complex scenes, and its framework is depicted in Figure 1. It includes three modules: pedestrian detection, target tracking, and redetection modules. The pedestrian detection module includes two branches, one is the traditional YOLOv3 network, and the other is block-based feature extraction and attention module. The attention module guides the neural network to generate an attention weight factor. The target tracking module is used to track each pedestrian for the trajectory which contains continuous event in the video sequence. The tracking module uses the DeepSort [13] algorithm to track by detection. The redetection module uses the sliding window for storing feature maps and SVM classifier to redetect fall events.

2.1. Pedestrian Detection. Tracking-by-detection is a multi-target tracking method, and selecting an appropriate and excellent detector has a great impact on the tracking effect. YOLO [20] is a target detection algorithm based on one stage, which processes and learns the target region, position, and class of the corresponding target at one time by means of direct regression. Many YOLO-based approaches have been proposed for pedestrian detection [21–23]. YOLOv3 [24] can predict 4 coordinated values for each bounding box (t_x, t_y, t_w, t_h) . Let P_W be the width and P_H be the height of bounding box; based on the deviation of the upper left corner of image (c_x, c_y) , next bounding box can be predicted by

$$\begin{cases} b_x = \sigma(t_x) + c_x \\ b_y = \sigma(t_y) + c_y \\ b_w = P_W e^{t_w} \\ b_h = P_H e^{t_h} \end{cases} \quad (1)$$

The structure of YOLOv3 is depicted in Figure 2. It includes a feature extraction module and a detection module. The former integrates YOLOv2, Darknet-53, and ResNet. Unlike the traditional CNN [5], Darknet-53 discards the commonly used pooling layers and carries the Leaky-ReLU activation function after convolutional layer. Also, no bias is utilized in Leaky-ReLU function's input, which can simplify the model and reduce the dimension and parameters of the convolution kernel. Furthermore, the feature extraction capability of the model is enhanced, and the timeliness and sensitivity of pedestrian detection are improved.

To detect small crowded targets with low resolution, the authors use multi-scale prediction. The prediction is implemented on three scales with the strides of 52, 26, and 13, respectively. Based on multi-scale characteristics of the network, the convolutional layer of different receptive fields in the network is improved to be used as a separate output

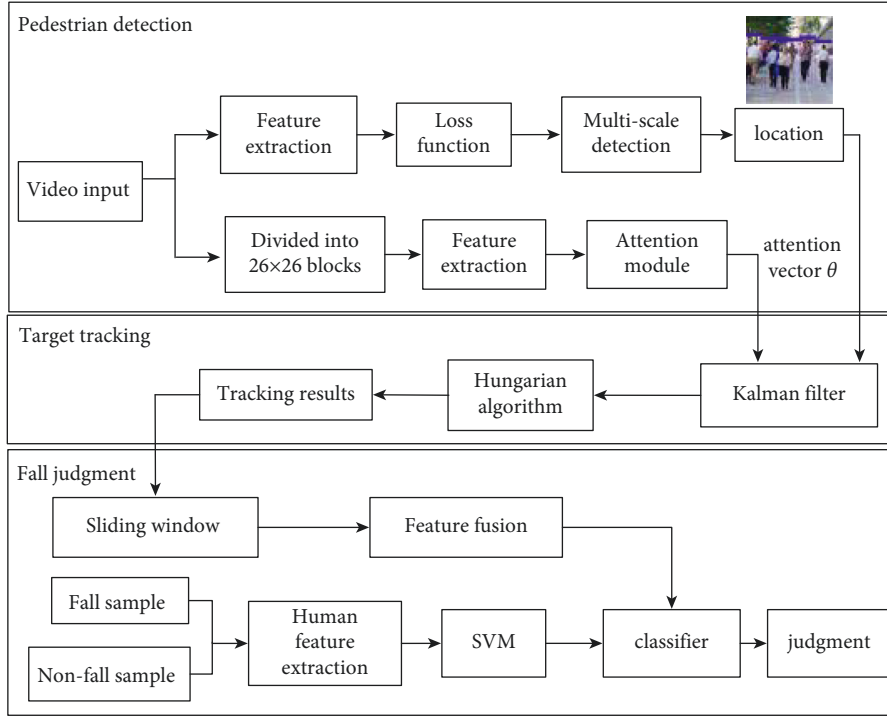


FIGURE 1: Framework of the proposed attention-guided fall event detection method.

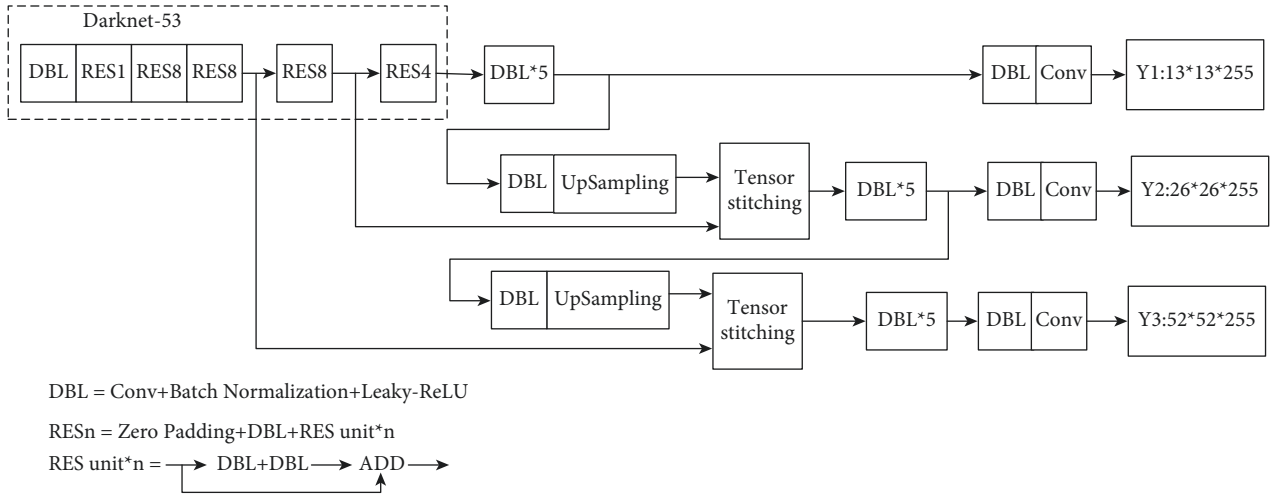


FIGURE 2: YOLOv3 network structure diagram.

for classification calculation. In addition, the network can adjust the priori box of the receiving field convolutional layer according to the value of GT (ground truth). IoU (intersection over union) is calculated by

$$\text{IoU} = \frac{\text{area}(A) \cap \text{area}(B)}{\text{area}(A) \cup \text{area}(B)}, \quad (2)$$

where $\text{area}(A)$ represents the GT bounding box area and $\text{area}(B)$ represents the candidate bounding box area. IoU close to 1 means that the candidate and the ground truth bounding boxes overlap completely. Finally, because different distances between pedestrians and cameras will

produce size differences, the detection box can be resized accordingly.

The distance between the prediction and the real bounding box is estimated by using the loss function in YOLOv3, which is multi-objective, including localization error, confidence error, and classification error:

$$\text{Loss} = l_{xy} + l_{wh} + l_{cls} + l_{conf}, \quad (3)$$

where l_{xy} and l_{wh} are localization errors calculated by sum of error square loss function and l_{conf} and l_{cls} are confidence error and classification error, respectively, calculated by binary cross entropy loss function.

2.2. Attention-Guided Tracking Module. In order to handle occlusions in pedestrian detection, the authors introduce the spatial attention module to increase the feature weight of pedestrian's body parts (such as head, trunk, feet, and so on), so that the tracker can focus on these key body parts which can avoid the influence of interference information such as background occlusion. The attention module needs to use a fixed window of 26×26 first and divide the static 416×416 image into 16 subimages by sliding from left to right for odd lines and from right to left for even lines. Then, CNN is used to extract features from these subimages to obtain a series of feature sequences.

The attention module is shown in Figure 3. First, each video frame is segmented into N subimages, denoted as $s(t) (t = 1, 2, \dots, N)$. The features of subimage sequence are extracted by CNN, denoted as $f(t) (t = 1, 2, \dots, N)$, and introduced to the attention module for generating the attention vector θ .

Attention module implements the local feature weighting and learns a mapping function F for regressing the attention vector θ as

$$\theta_t = \frac{\exp(F(x(t)))}{\sum_{i=1}^N \exp(F(x(i)))}, \quad t = 1, 2, \dots, N. \quad (4)$$

The size of θ_t represents the probability of whether $f(i)$ is a body part feature, and the element weighting of F is as follows:

$$F(i) = f(i) \odot \theta_i, \quad i = 1, 2, \dots, N, \quad (5)$$

where $F(i)$ represent weighted elements of F and \odot represents the element-wise multiplication. Through continuous learning of the attention module, the authors can update its parameters and optimize the weight θ_t in (4). The attention vector θ_t is introduced into tracking module to improve the detection and tracking efficiency of pedestrians.

For pedestrian tracking, the DeepSort method [13] is used to predict the next position of each trajectory. First, the Kalman filter is used to obtain the features of the extracted targets in the previous frame, including the center position coordinates, the aspect ratio, the height, and the speed. Then, the next location \hat{X}_K is predicted by using the error covariance matrix, and it can be corrected by $\hat{X}_K = K_K \times Z_K + (1 - K_K) \times \hat{X}_{K-1}$, where K_K is the Kalman gain and Z_K is the actual measured value which can be corrected by \hat{X}_{K-1} and K_K . The optimal estimation is the prediction.

The DeepSort algorithm is based on sort algorithm. It has the characteristics of deep correlation and conducts tracking task by the exact detection results. The DeepSort algorithm takes the detection results, bounding box, confidence, and feature as inputs, where confidence is mainly used for filtering detection boxes and bounding box and feature (ReID) are used for matching calculation with tracker. The prediction task is completed by the Kalman filter, and the update part adopts IoU to match the Hungarian algorithm. A tracking scenario is defined by an eight-dimensional state space $(\mu, \nu, \gamma, h, \dot{x}, \dot{y}, \dot{\gamma}, \dot{h})$, where (μ, ν) represents the center of the

bounding box, γ represents the rectangular aspect ratio of the target, h represents the height of the bounding box, and $(\dot{x}, \dot{y}, \dot{\gamma}, \dot{h})$ describes the motion feature. The algorithm applies the standard Kalman filter of the linear observation model and uniform model to calculate the target trajectory in the following frame and takes the boundary coordinates (μ, ν, γ, h) as the direct observation of the object state. For each trajectory, the authors record the number of frames between the last successfully detected frame and the current detected frame as a_k . The counter is incremented during Kalman filter prediction and set to zero when the trajectory is associated with the measurement. The value of a_k exceeding the threshold A_{\max} means that the trajectory has lost and the target is out of the scene, so the trajectory is removed. If no detection can match the existing trajectory in the detector, then the detector will generate a tentative trajectory. If a trajectory cannot be rematched in 3 frames, then it will be removed.

The sort tracking algorithm was first proposed in [25], aiming at real-time online tracking. When the target is occluded or missed in multiple frames, the trajectory of the same target will be suspended and a new one will be generated. The DeepSort method solves this problem, and it combines the Mahalanobis distance and cosine distance metrics to obtain the final decision information $C_{i,j}$ by weighted summation:

$$C_{i,j} = \lambda d_1(i, j) + (1 - \lambda) d_2(i, j), \quad (6)$$

where λ is a superparameter which is used to adjust the weight of different items, $d_1(i, j)$ represents the Mahalanobis distance, and $d_2(i, j)$ represents the cosine distance. The DeepSort algorithm uses the Kalman filter to calculate next position for every trajectory and then calculates the Mahalanobis distance $d_1(i, j)$ by

$$d_1(i, j) = (d_j - y_i)^T S_i^{-1} (d_j - y_i), \quad (7)$$

where d_j represents the location of j -th bounding box, y_i represents the prediction of the target location from i -th tracker, S_i represents the covariance matrix between the location of detection and tracking, and (y_i, S_i) describes the projection of the i -th tracker to the measurement space. Considering the state estimation uncertainty, the Mahalanobis distance measurement detects the standard deviation from the average track position. It retains the result of spatial distribution and is more efficient, while in order to express the correlation degree of appearance features, the least cosine distance between i -th and j -th can be calculated as

$$d_2(i, j) = \min\{1 - r_j^T r_k^{(i)} | r_k^{(i)} \in R_i\}, \quad (8)$$

where r_j is the appearance descriptor (it is calculated for each test box type) and $\|r_j\| = 1$. To ensure that the algorithm can still track the target after prolonged occlusion, the descriptors of the newest 100 frames on each trajectory are saved in R_i , i.e., R_i is the appearance feature vector set. When the cosine distance $d_2(i, j)$ is smaller than the training threshold of convolutional neural network, the association is considered to be successful.

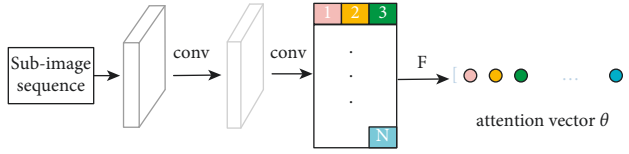


FIGURE 3: Structure of attention module.

The final decision information $C_{i,j}$ is obtained by (6) and adjusted by the superparameter λ . The smaller $C_{i,j}$, the greater the correlation between the detecting target and the tracking target. $C_{i,j}$ has a good effect on short-term prediction and matching, while the appearance feature can more efficiently measure the matching degree for long-lost tracks, which improves the robustness of the algorithm against target loss and occlusion.

2.3. Fall Judgment. According to the pedestrian detection and tracking results, the final fall events judgment is a binary classification problem. When a pedestrian is standing, the ground truth aspect ratio recognized is less than or equal to 0.4; when a pedestrian falls, the aspect ratio increases to 0.7~1.2. Meanwhile, the deflection angle is lower than a preset value (such as 37°), and the instantaneous acceleration in vertical direction is increased, which is significantly greater than that of squatting and bending. In this paper, the aspect ratio, deflection angle, and vertical instantaneous acceleration of the bounding box are comprehensively considered for the final fall judgment. These three factors not only have their own independence and meet the conditions of comprehensive judgment but also can avoid the higher dimension of feature vector space, overcomplex classifier, and poor real-time performance caused by excessive selection of feature vectors.

According to the tracking results, the authors can obtain the length H , width W , upper left point (x_L, y_L) , and lower right point (x_R, y_R) of the bounding box in each frame. Then, the aspect ratio ρ is $\rho = W/H$. The bounding box (x_P, y_P) is

$$\begin{cases} x_P = (x_L + x_R)/2 \\ y_P = (y_L + y_R)/2 \end{cases} \quad (9)$$

The deflection angle β of the bounding box is calculated by

$$\beta = \arctan \frac{y_P - y_L}{x_P - x_L} \quad (10)$$

The authors denote M_i and M_{i+1} as two adjacent frames, respectively. The centroids of M_i and M_{i+1} are (x_{P_i}, y_{P_i}) and $(x_{P_{i+1}}, y_{P_{i+1}})$, respectively, and then the vertical velocity of the target in M_{i+1} is obtained by

$$v_{i+1} = \frac{|y_{P_{i+1}} - y_{P_i}|}{t} \quad (11)$$

where t is the time interval between M_i and M_{i+1} . Then, the vertical instantaneous acceleration a_{i+1} is

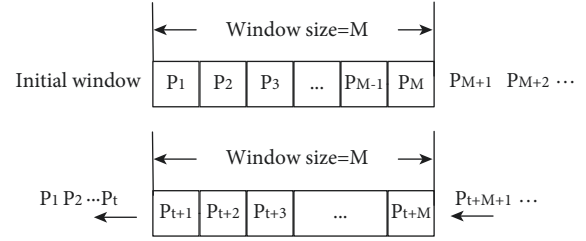


FIGURE 4: The sliding window diagram.

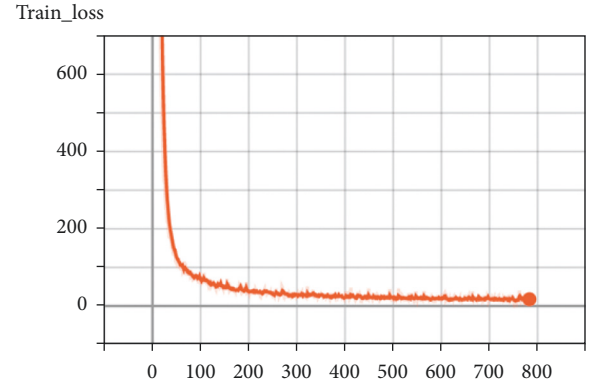


FIGURE 5: Loss curve.

$$a_{i+1} = \frac{v_{i+1} - v_i}{t} \quad (12)$$

Because the traditional fall judgment algorithm only considers the factors of a single frame and the fall behavior has time continuity, the authors use the sliding window to obtain the variation of the three factors in continuous frames. As shown in Figure 4, the factors of the first frame are stored in a fixed size sliding window. As time goes on, the factors of subsequent frames continue to enter the container. After the container is filled, the newly entered factors are added at the end of the sliding window, and the leftmost data are removed.

Figure 4 shows that the size of the sliding window is M . For video frame sequence $\{P_1, P_2, \dots, P_t, \dots\}$, the initial window contains $\{P_1, P_2, \dots, P_M\}$, where P_i stores the features obtained from moving targets, including human aspect ratio, deflection angle, and vertical instantaneous acceleration. After t frames, the content of the sliding window is $\{P_{t+1}, P_{t+2}, \dots, P_{t+M}\}$. In this paper, the window size is set according to the fall behavior period. Since the fall period is about 0.5~0.8 seconds and the experimental video frame rate is 20 fps, the empirical value of window size is 15.

According to the feature information in the sliding window, a support vector machine (SVM) classifier [26] is constructed for fall detection training to determine whether a pedestrian has fallen. The training process inputs a large number of fall sample feature data and non-fall sample feature data into the SVM module to train a fall classifier by training these samples. Since extracting feature vector which

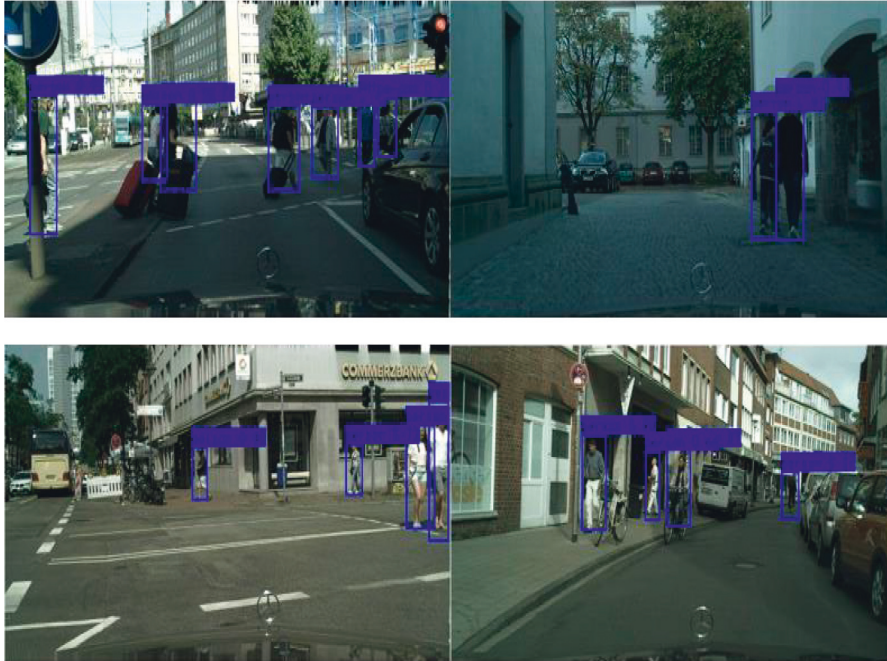


FIGURE 6: Detection results on the CityPersons dataset.



FIGURE 7: Fall event detection results on the Montreal fall dataset.

TABLE 1: Performance comparison conducted on the CityPersons dataset (%).

Algorithms	Average precision	mAP	fps
YOLOv1 [8]	96.33	76.13	67
YOLOv3 [24]	97.1	86.54	48
SSD [9]	97.27	78.37	41
Proposed	98.55	93.15	45

TABLE 2: Performance comparison conducted on the Montreal fall dataset (%).

Algorithms	Average precision
YOLOv1 [8]	96.33
YOLOv3 [24]	97.1
SSD [9]	97.27
Proposed	98.55

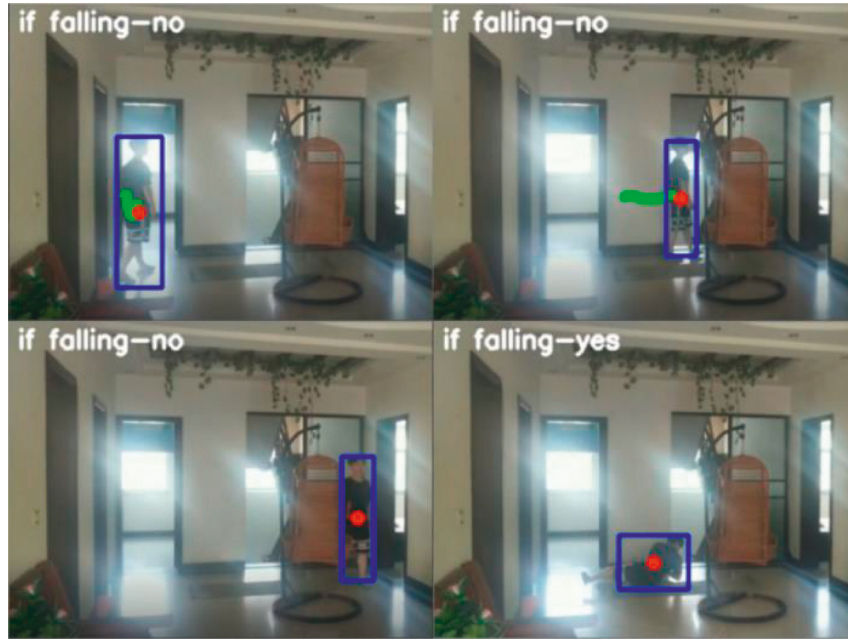


FIGURE 8: Test results of illumination change on self-built dataset in complex environments.

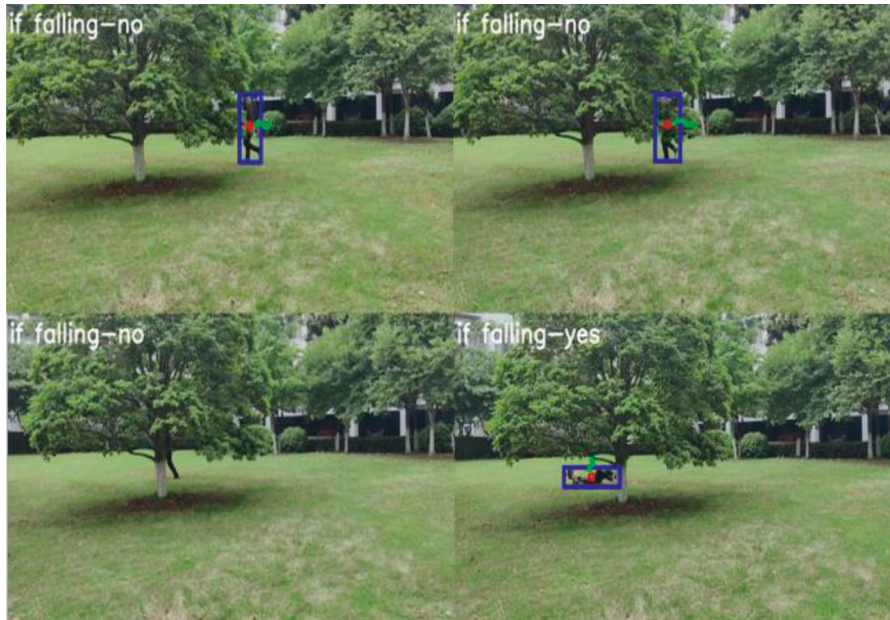


FIGURE 9: Results of outdoor occlusions.

is integrated of multiple features is a linear inseparable problem, the authors adopt the Gaussian kernel function to project the feature information into a high-dimensional space as

$$K(x, z) = e^{-\gamma \|x-z\|_2^2}, \quad (13)$$

where γ is a superparameter and $\gamma > 0$. It can be seen from, (13) that only a few parameters need to be adjusted.

3. Experiment

3.1. Dataset and Implementation. The experiments are conducted on the CityPersons [27] and the Montreal fall [28] datasets. The two datasets are built for supporting fall event detection study, and they are challenging for pedestrian detection. The CityPersons dataset is constructed based on Cityscapes dataset, which includes many video sequences, including 2975 image training sets and 1525 image test sets, with a resolution of 2048×1024 . Among them, the Montreal

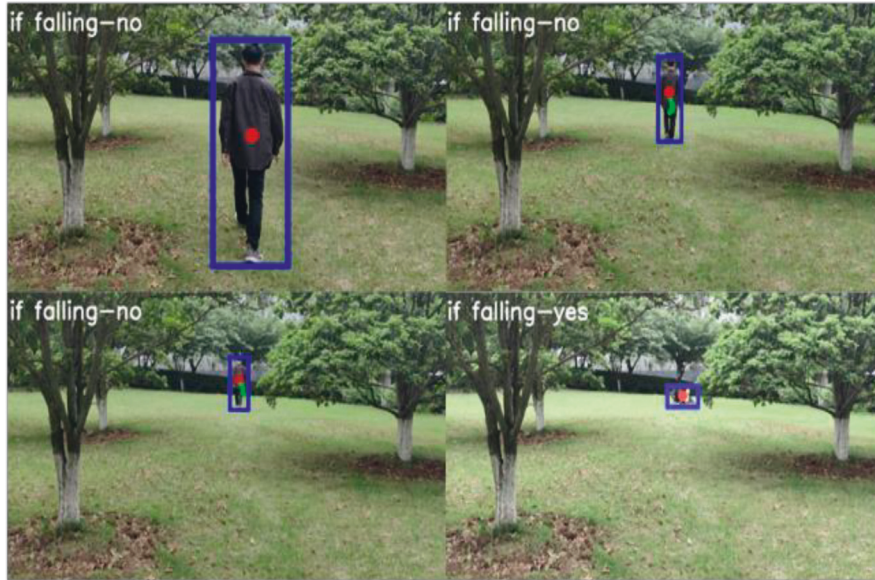


FIGURE 10: Results of outdoor scale changes.



FIGURE 11: Results of interference experiment.

autumn dataset consists of 22 autumn events and 2 mixed events, which are recorded synchronously in the simulated daily life scenes. These videos are multi-view synchronized and can be used alone as a typical autumn event dataset or as a dataset for 3D scene reconstruction.

To diminish the effect of light illumination and scale transformation, the authors extend the test dataset through randomly changing the illumination, image size, angle, and so on. Accordingly, the original label box is adjusted, and the training set is extended.

The authors use the precision and recall rate, and the calculation formulas are described as follows:

$$\begin{aligned} \text{precision} &= \frac{TP}{TP + FP}, \\ \text{recall} &= \frac{TP}{TP + FN}, \end{aligned} \quad (14)$$

where TP is true positive, FP is false positive, and FN is false negative, respectively.

In the experiment of this article, the YOLOv3 network is pretrained on the ImageNet [24] dataset. The initial learning rate, batch size, and epoch are set to 0.001, 8, and 200, respectively. Input image resolution is 416×416 . The variation of training loss with the number of iterative steps is shown in Figure 5. Obviously, the model converges with the increase of iterative steps, and it reaches a low of about 800 and then gradually tends to be stable.

3.2. Experimental Results. The authors verify the proposed detector on the CityPersons and Montreal fall video dataset. Also, the visualization of detection results is described in Figures 6 and 7, respectively. Figure 6 shows the pedestrian detection results on CityPersons dataset. In Figure 6, the challenge includes the occlusions caused by other pedestrian or road signs or cars and different lighting and scales. It can be seen that the proposed detector can efficiently overcome the partial pedestrian occlusions and has certain robustness to the light and dark environment and different scales of pedestrians.

Figure 7 describes several fall event detection results on the Montreal fall dataset. There are three typical fall behaviors in different ways and angles, and the proposed method can automatically mark the detected fall event at the top right of the image accurately.

Tables 1 and 2 describe the detection performance on the CityPersons dataset and the Montreal fall dataset, respectively. It can be seen from the tables that the method proposed by the authors is better than YOLOv1 [7], YOLOv3 [24], and SSD [8] and achieves good performance similar to the most advanced methods.

To evaluate the proposed method in handling illumination changes and scale changes, the authors conduct test experiments on the self-built dataset. Figures 8–11 show some typical test results of self-built dataset in real complex scenarios. Figure 8 displays the fall event detection results of the indoor scene with high light and partial occlusion. Figure 9 shows the results of outdoor scene with pedestrian occluded by trees. Figure 10 shows the detection results handling scale changes, and Figure 11 shows the results handling four interferences of pedestrian: standing, squatting, bending, and squatting. Figures 8–11 show that the method proposed by the authors can handle strong light interference and keep tracking occluded pedestrians. In addition, for pedestrians of different scales, the proposed method can effectively adjust the bounding box and improve the accuracy of fall judgment. Especially, the proposed fall judgment algorithm has low judgment error for squatting, bending, and other interferences.

4. Conclusions

In this paper, the authors propose an attention-guided neural network to detect pedestrian fall events in complex scenes. By introducing the attention module into the detection framework, the attention module can guide the detector to focus on the key feature sequences of pedestrians;

therefore, the detection performance is improved. In addition, the authors use the sliding window for storing feature maps and SVM classifier to redetect fall events. The experiments on CityPersons dataset, Montreal fall dataset, and the self-built dataset show the efficiency of the proposed attention-guided detection method. Although the proposed method can keep tracking occluded pedestrians well, it is necessary to develop the feature representation algorithm of pedestrians' body parts and improve detection precision for heavy occlusions.

Data Availability

The data used to support the findings of this study are included within the article.

Conflicts of Interest

The authors declare that they have no conflicts of interest.

Acknowledgments

This study was supported by the National Natural Science Foundation of China (NSFC) under grant no. 61703201, the Natural Science Foundation of Jiangsu Province under grant no. BK20170765, the Foundation of Nanjing Institute of Technology under grant no. CKJB201905, the Graduate Innovation Program of Jiangsu Province under grant no. SJCX21_0945, and the College Students' Science and Technology Innovation Fund of Jiangsu Province under grant no. 202011276039Y.

References

- [1] . Lee and Tseng, "Development of an enhanced threshold-based fall detection system using smartphones with built-in accelerometers," *IEEE Sensors Journal*, vol. 19, no. 18, pp. 8293–8302, 2019.
- [2] Kumar, Acharya, and B. Sandeep, "Wearable sensor-based human fall detection wireless system [J]," *Wireless Communication Networks and Internet of Things*, vol. 493, pp. 217–234, 2018.
- [3] P. Tsinganos and A. Skodras, "On the comparison of wearable sensor data fusion to a single sensor machine learning technique in fall detection [J]," *Sensors*, vol. 18, no. 2, pp. 592–607, 2018.
- [4] T. Xu, Y. Zhou, and J. Zhu, "New advances and challenges of fall detection systems: a survey [J]," *Applied Sciences*, vol. 8, no. 3, p. 418, 2018.
- [5] K. Ghada, M. Mohamed, and B. Ouiem, "Automatic fall detection using region-based convolutional neural network [J]," *International Journal of Injury Control and Safety Promotion*, vol. 27, no. 4, pp. 546–557, 2020.
- [6] X. Wang and K. Jia, "Human Fall Detection Algorithm Based on YOLOv3," in *Proceedings of the 5th IEEE International Conference on Image, Vision and Computing (ICIVC)*, pp. 50–54, IEEE, Beijing, China, 10 July 2020.
- [7] P. Adarsh and P. Rathi, M. Kumar, "YOLO v3-Tiny: object Detection and Recognition using one stage improved model," in *Proceedings of the 6th International Conference on Advanced Computing and Communication Systems (ICACCS)*, pp. 687–694, IEEE, Coimbatore, India, 6 March 2020.

- [8] A. Kumar and S. Srivastava, "Object detection system based on convolution neural networks using single Shot multi-box detector [J]," *Procedia Computer Science*, vol. 171, pp. 2610–2617, 2020.
- [9] L. Zhang, L. Lin, X. Liang, and K. He, "Is Faster R-CNN Doing Well for Pedestrian Detection," in *Proceedings of the Conference on Computer Vision (ECCV)*, pp. 443–457, Springer, Netherlands, 11 October 2016.
- [10] R. Dinakaran, L. Zhang, and A. Bouridane, "Deep learning based pedestrian detection at distance in smart cities," in *Proceedings of the IEEE Conference on Computer Vision and Pattern Recognition (CVPR)*, pp. 1–6, IEEE, San Francisco, CA, USA, 18 June 2018, <https://www.researchgate.net/profile/Faria-Mehboob>.
- [11] C. Rui, Y. Tong, and R. Liang, "Real-time generic object tracking via recurrent regression network [J]," *IEICE Trans. on Information and systems*, no. 3, pp. 602–611, 2020.
- [12] F. Qi, C. Gao, and W. Lan, "Spatio-temporal fall event detection in complex scenes using attention guided LSTM [J]," *Pattern Recognition Letters*, vol. 130, pp. 242–249, 2020, <https://www.sciencedirect.com/science/article/abs/pii/S016786551830504X><https://www.sciencedirect.com/science/article/abs/pii/S016786551830504X>.
- [13] A. Pramanik, S. K. Pal, J. Maiti, and P. Mitra, "Granulated RCNN and multi-class deep SORT for multi-object detection and tracking [J]," *IEEE Transactions on Emerging Topics in Computational Intelligence*, pp. 1–11, 2021.
- [14] T. Zou, S. Yang, and Y. Zhang, "Attention guided neural network models for occluded pedestrian detection [J]," *Pattern Recognition Letters*, vol. 131, pp. 91–97, 2020, <https://www.sciencedirect.com/science/article/abs/pii/S0167865519303733>.
- [15] C. Zhou and J. Yuan, "Multi-label learning of part detectors for heavily occluded pedestrian detection," *Proceedings of IEEE International Conference on Computer Vision (ICCV)*, pp. 3506–3515, 2017.
- [16] A. Fernández-Isabel, P. Peixoto, M. Isaac, C. Conde, and E. Cabello, "Combining dynamic finite state machines and text-based similarities to represent human behavior [J]," *Engineering Applications of Artificial Intelligence*, vol. 85, pp. 504–516, 2019.
- [17] J. L. Chua, Y. C. Chang, and W. K. Lim, "A simple vision-based fall detection technique for indoor video surveillance [J]," *Signal, Image and Video Processing*, pp. 623–633, 2015.
- [18] J. Wu, S. Qiu, Y. Kong, Y. Wankou, L. Senhadji, and S. Huazhong, "PCANet: an energy perspective [J]," *Neurocomputing*, vol. 313, pp. 271–287, 2018.
- [19] M. Zhang, C. Gao, and Q. Li, "Action detection based on tracklets with the two-stream CNN [J]," *Multimedia Tools and Applications*, vol. 77, no. 3, pp. 3303–3316, 2018.
- [20] R. Girshick, J. Donahue, and T. Darrell, "Rich feature hierarchies for accurate object detection and semantic segmentation [C]," *Proceedings of the IEEE Conference on Computer Vision and Pattern Recognition (CVPR)*, pp. 580–587, 2014.
- [21] Z. Yi, S. Yongliang, and Z. Jun, "An improved tiny-yolov3 pedestrian detection algorithm [J]," *Optik - International Journal for Light and Electron Optics*, vol. 183, pp. 17–23, 2019.
- [22] F. Ahmad, N. Li, and M. Tahir, "An Improved D-CNN Based on YOLOv3 for Pedestrian Detection," in *Proceedings of the IEEE 4th International Conference on Signal and Image Processing (ICSIP)*, pp. 405–409, IEEE, ECOMC, Buffalo, 19 July 2019.
- [23] E. Zdobrischi and M. Negru, "Pedestrian Detection Based on TensorFlow YOLOv3 Embedded in a Portable System Adaptable to vehicles," in *Proceedings of the 2020 International Conference On Development And Application Systems (DAS)*, pp. 21–26, IEEE, Suceava, Romania, 21 May 2020.
- [24] J. Redmon and A. Farhadi, "An Incremental Improvement," in *Proceedings of the 2018 IEEE Conference on Computer Vision and Pattern Recognition*, pp. 459–453, IEEE Computer Society, Washington, 18 June 2018.
- [25] A. Bewley, Z. Ge, and L. Ott, "Simple Online and Realtime Tracking," in *Proceedings of the IEEE International Conference on Image Processing (ICIP)*, pp. 3464–3468, IEEE, Anchorage, AK, USA, 25 September 2016.
- [26] A. Iazzi, M. Rziza, and H. Thami, "edchine," in *Proceedings of the 4th International Conference on Advanced Technologies for Signal and Image Processing (ATSIP)*, pp. 1–6, Springer, 21 March 2018.
- [27] S. Zhang, R. Benenson, and B. Schiele, "CityPersons: A Diverse Dataset for Pedestrian detection," in *Proceedings of the IEEE Conference on Computer Vision and Pattern Recognition (CVPR)*, pp. 3213–3224, IEEE, Honolulu, 21 July 2017.
- [28] E. Auvinet, C. Rougier, J. Meunier, A. St-Arnaud, and J. Rousseau, *Multiple cameras fall dataset [M]. Technical report 1350*, DIRO - Université de Montreal, Quebec, Canada, 2010.

Research Article

Personalized Music Hybrid Recommendation Algorithms Fusing Gene Features

Yixiao Cao ¹ and Peng Liu²

¹Art Education Center, Criminal Investigation Police University of China, Shenyang 110854, China

²Music Department, Cangzhou Normal University, Cangzhou, Hebei 061000, China

Correspondence should be addressed to Yixiao Cao; caoyixiao@cipuc.edu.cn

Received 26 February 2022; Revised 24 March 2022; Accepted 1 April 2022; Published 28 April 2022

Academic Editor: Wei Liu

Copyright © 2022 Yixiao Cao and Peng Liu. This is an open access article distributed under the Creative Commons Attribution License, which permits unrestricted use, distribution, and reproduction in any medium, provided the original work is properly cited.

Aiming at the shortcomings of current music recommendation algorithms, such as low accuracy and poor timeliness, a personalized hybrid recommendation algorithm incorporating genetic features is proposed. The user-based collaborative filtering (UserCF) algorithm analyzes the degree of users' preference for music genes. The improved neural matrix decomposition collaborative filtering (B-NCF) algorithm calculates the correlation between similar users and constructs the adjacency relationship between users. The results of the two algorithms are fused by using a weighted hybrid approach to generate the recommendation list. Finally, the hybrid recommendation model is built on the Spark platform. The paper's traditional and hybrid recommendation algorithms are validated using the Yahoo Music dataset. The experimental results show that the advantages of the algorithm in this paper are more significant under the MAE and F1-measure indexes, and the recommendation accuracy and precision have been greatly improved; the hybrid algorithm can ensure the diversity of the recommended contents, the recommendation hit rate is higher, and the timeliness meets the demand of personalized music recommendation.

1. Introduction

With the rapid development of mobile communication technology, the Internet has become the most effective channel for music transmission [1]. Network music provides convenience for people's entertainment and leads us into the considerable data age. In the face of vast and complex music data, if users cannot get accurate information quickly and effectively, it will inevitably cause the problem of information overload [2, 3]. At present, traditional Internet music platforms tend to focus on light operation modes such as search, collection, and selection of tracks. Users need to put forward precise song requirements independently to complete the search task, which is time consuming and easy to cause user information fatigue [4]. Based on this, some scholars use different algorithms to achieve the active recommendation of music, which can effectively solve the problem of information overload. Park and Cho [5] presented a recommendation algorithm based on SVD matrix

decomposition to predict user preferences. The accuracy is 7% higher than Netflix Cinematch, and the prediction performance is good. However, there are some shortcomings, such as high algorithm complexity and ample storage space. Ahn [6] proposed a heuristic similarity measure PIP, which can solve the cold start recommendation problem to some extent. However, there are fewer everyday scoring items among users in sparse datasets, and the recommended results are not ideal. Liu et al. [7] proposed a new heuristic algorithm, NHSM, by improving the PIP algorithm. The algorithm considers the user's rating context information and the global preferences of user behaviour. It can calculate the user's similarity with fewer scores, and the recommendation performance has been dramatically improved. He et al. [8] proposed the neural collaborative filtering (NCF) algorithm, used the neural network architecture to model the characteristics of users and projects, designed a common framework for the neural network collaborative filtering algorithm, and improved the performance of the

recommended model by introducing a multilayer sensor to make the algorithm highly nonlinear. At the same time, some researchers from the perspective of music genes put forward some feasible personalized music recommendation methods for the emotions and scenarios of music. Vignoli and Pauws [9] calculated the similarity based on the music's timbre, rhythm, mood, and genre and calculated the similarity of songs through the factor weight factor to complete the accurate music recommendation. Baltrunas et al. [10] proposed a music recommendation algorithm according to the user's mood in different scenarios which achieved good results in the experiment. Hariri et al. [11] used the user's social tags to classify music and used the user's historical playlists and collection lists to organise and recommend the user's preferred music genres and achieved good results.

In summary, the current recommendation system can better solve the information overload problem and has further improved the recommendation performance. However, there are still shortcomings such as complex implementation process, standard recommendation accuracy, and poor timeliness, and the single algorithm recommendation cannot meet the multifaceted needs of users. The recommendation effect is not ideal in practical applications. Therefore, this paper introduces the concept of music genes based on users' preferences for music genes and social tags and combines the advantages of two algorithms, UserCF and B-NCF. We design a hybrid recommendation algorithm incorporating music gene features to solve the shortcomings of current music recommendation algorithms and improve personalized music recommendations' accuracy.

2. Music Genetic Characteristics

Music genes control the basic information that expresses the auditory effects of music. They are mainly composed of four essential elements: melody, rhythm, harmony, and timbre [12]. Genetic traits can describe different characteristics of music. For a piece of music, some features can be directly felt by the user, have uniqueness, and cannot be changed. For example, lyrics and audio of music can be classified as internal genetic characteristics. However, some music features that are not unique can be classified as external gene characteristics because different users will have different perceptions, such as emotion, style, category, and other music features. The overall structure of music gene characteristics is shown in Figure 1.

According to the different nature of music, external gene characteristics can also be divided into fixed gene characteristics and free gene characteristics. Selected gene characteristics refer to the inherent characteristics of music that users cannot change, mainly including music title, album, singer, and other identifying features. Free radical gene characteristics are user-defined and can reflect the music characteristics of the user's cognition, mainly including music style, attribution category, music emotion, and other cognitive features [13]. Among them, music emotion refers to the emotional type used to describe the music, which is generally derived from analyzing the context of the lyrics or

the user's active tags. Figure 2 shows the Hevner emotional ring model, composed of strong, joyous, soothing, sad, exciting, and other eight emotions. Free radical gene characteristics can reflect users' interests, preferences, and cognitive status and play an essential role in improving the ability of personalized music recommendations.

3. Hybrid Recommendation Algorithms Combining Musical Gene

3.1. User-Based Collaborative Filtering Algorithm. The basic idea of user-based collaborative filtering algorithm is calculating the user's preference degree for a particular gene feature, searching for similar users with higher interest levels to the target user, and then recommending suitable music to the target user according to the similarity principle [14]. Suppose u is the number of users; n is the number of music genes; p_{un} denotes the preference degree of user u for a specific music gene n ; and the preference degree can be the direct or implicit evaluation of users. Then, the expression of the user-music gene matrix P in the collaborative filtering algorithm is

$$P = \begin{bmatrix} P_{11} & P_{12} & \cdots & P_{1n} \\ P_{21} & P_{22} & \cdots & P_{2n} \\ \cdots & \cdots & \cdots & \cdots \\ P_{u1} & P_{u2} & \cdots & P_{un} \end{bmatrix}. \quad (1)$$

Since users have limited usage time and experience, it is impossible to generate behaviours for most music genres, and thus P is mostly a sparse matrix. After obtaining the user-music gene scoring matrix, the similarity between the target users and similar users needs to be calculated to get the set of users with the highest similarity to the target users. There are more algorithms to calculate the similarity, and the main algorithms commonly used at present are cosine distance, Jaccard similarity coefficient, and Pearson correlation coefficient [15]. Among them, the cosine distance uses the cosine of the angle between two vectors to measure the similarity between users, focusing more on the difference of vectors in direction. Thus, the cosine distance is used to calculate the similarity between users.

Each user description file can be considered a vector, projected to a space of n dimensions to obtain a dimensional vector [16]. If the user does not evaluate the music genes, the value of the corresponding position of the user vector is set to 0. The cosine angle between the vectors measures the similarity between users. Let the vectors of user a and target user u be \vec{a} and \vec{u} , respectively; then, the similarity between the two users $\kappa_{a,u}$ is

$$\kappa_{a,u} = \frac{\vec{a} \cdot \vec{u}}{\|\vec{a}\| \cdot \|\vec{u}\|}. \quad (2)$$

The range of cosine value is $[-1, 1]$; the closer the weight tends to 1, the closer the direction of the two vectors is and the higher the similarity between users is; on the contrary, the closer the value tends to -1 , the greater the difference in the direction of the two vectors is and the lower the similarity

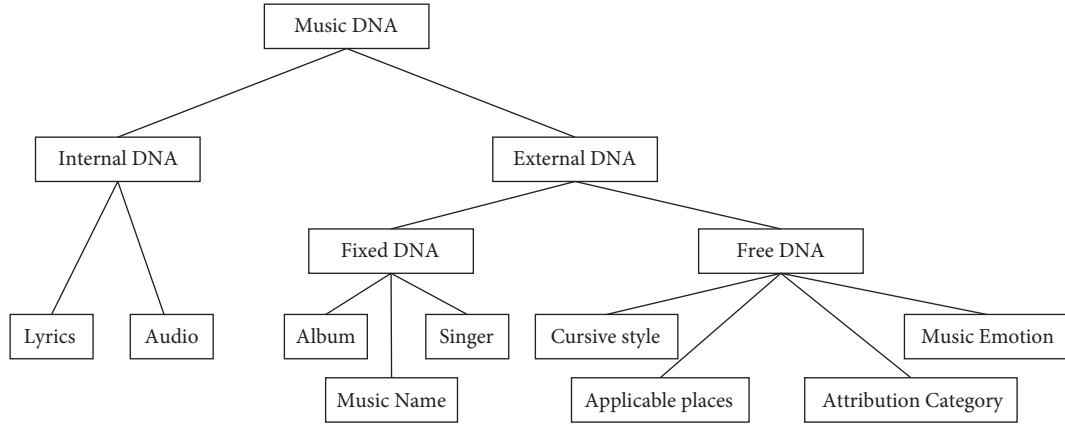


FIGURE 1: Structure of music gene characteristics.

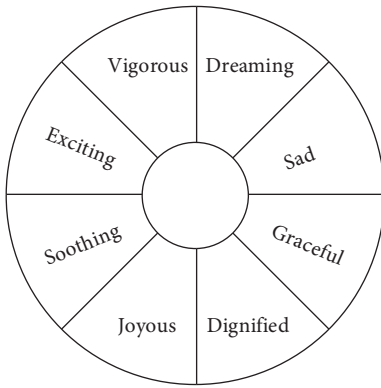


FIGURE 2: Hevner music emotion loop model.

between users is. Based on the similarity between users, the music not viewed by the target user is predicted, and the piece with the highest preference score is selected and recommended to the target user.

3.2. Improved NCF Model. A The NCF model uses “dual thread” to model the user and music genes and connects arithmetic information through two routes. The arithmetic information is connected through generalized matrix decomposition (GMF) and multilayer perceptron (MLP) to obtain the info combined with high-order implicit features and low-order features [17]. However, model learning abstraction of implicit information is prone to loss, the algorithm is poorly interpreted, and a single source of information is challenging to satisfy complex recommendation problems [18]. Therefore, the Bayesian personalized ranking (BPR) structure is used to replace the GMF structure of the neural collaborative filtering network, and the designed B-NCF model is used to complete the information mining and ranking. Figure 3 shows the structure of the B-NCF model.

In the B-NCF model, the upper layer of the input layer is the fully connected embedding layer, which is used to map the sparse representation of the input layer into a dense vector. The user ID (Uid) is mapped to the user feature vector, and the rated music ID (Rid) and the unrated music ID (Kid) are mapped to the music feature vector.

Vectors suffixed with MLP are input to the MLP layer for stitching to form new vectors that generate higher-order feature information through a multilayer perceptron. Based on the MLP layer, batch normalization (BN) and dropout layers are added. The BN layers are used to unify the variance of each layer to speed up the convergence of the model. The dropout layer improves model generalization ability and prevents overfitting. The output high-order feature information expression is

$$\vartheta_{\text{MLP}} = f(O^T s_u^U, Q^T s_{rk}^I | O, Q, \Theta_f), \quad (3)$$

where O^T represents the transpose of user feature matrix O ; Q^T represents the transpose of music feature matrix Q ; s_u^U and s_{rk}^I represent the user feature vector and music feature vector, respectively; and Θ_f defines the model parameters of the interaction function.

The vector with the suffix Emb is input to the BPR layer, and the weights of the BPR layer can be considered a user-music hidden factor matrix, which can be used to obtain the ranking scores of different users for any music. The purpose of ranking is to minimize the BPR loss and thus maximize the probability of ranking the music higher. The expression of BPR loss is

$$\begin{aligned} \max_v p &= \sum_{(u,r,k \in D)} \ln \sigma(\overline{x_{ur}} - \overline{x_{uk}}) + \lambda \|v\|^2, \\ L_{\text{BPR}} &= 1 - \max_v p, \end{aligned} \quad (4)$$

where $\max p$ denotes the posterior probability p maximized under the v model parameter v ; \ln is the natural logarithm function; x_{ur} and x_{uk} indicate the vector of users u multiplied by the vectors of music r and k , expressing the user’s preference for different music genes; σ denotes the sigmoid activation function; λ is the regularization parameter; and $\lambda \|v\|^2$ is the regularization term.

In the output layer, the ranking information of the BPR layer and the high-order feature information of the MLP layer are spliced to form a new vector. The predicted value is obtained using the sigmoid activation function. When the expected value is 1, it indicates interaction; 0 indicates no interaction. The expected value’s \hat{y}_{urk} expression is

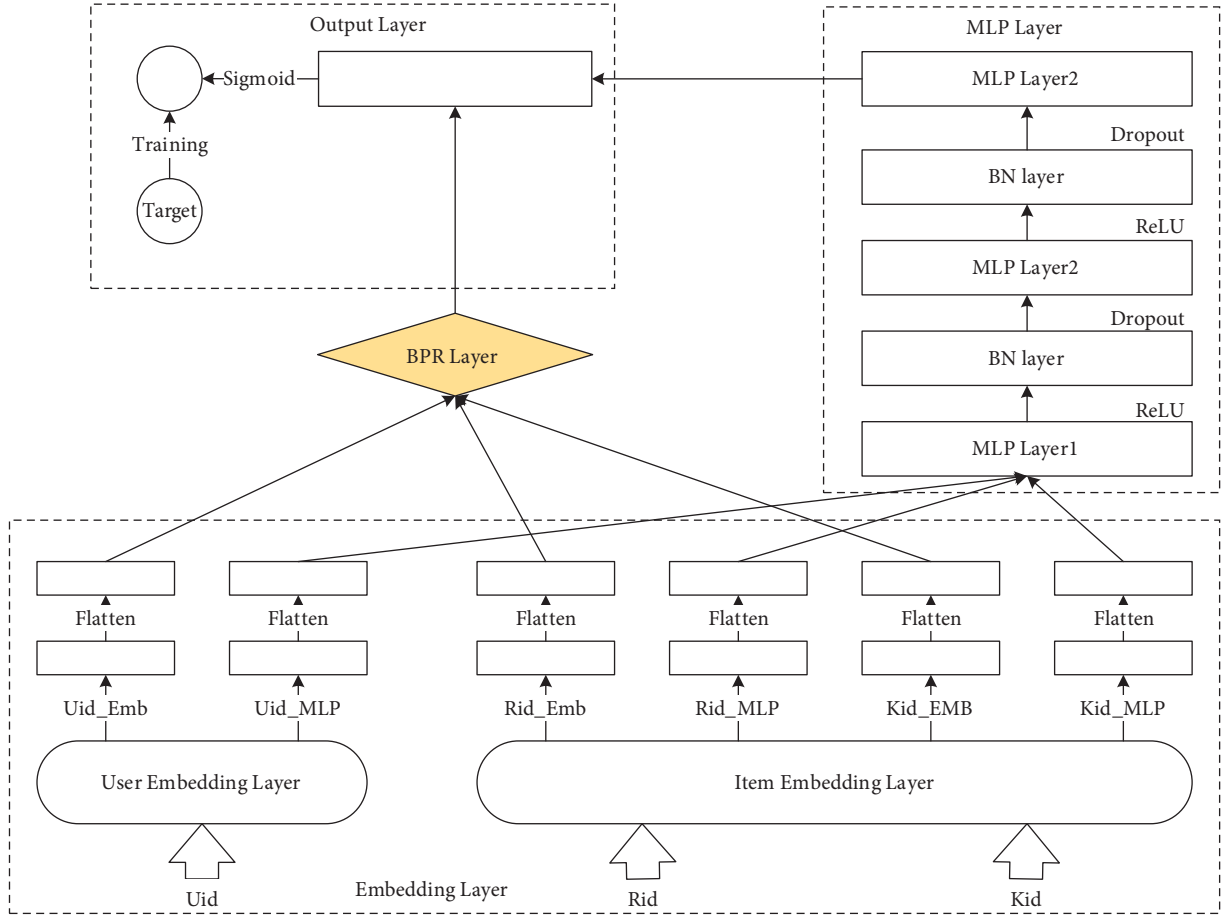


FIGURE 3: Structure of B-NCF model.

$$\hat{y}_{urk} = \sigma(h^T[\vartheta_{MLP}, \vartheta_{BPR}]). \quad (5)$$

The cross entropy between the predicted value and the target value y_{urk} is calculated, and the parameters of the model are updated with the following expression:

$$J = - \sum_{(u,r,k) \in D} [y_{urk} \log \hat{y}_{urk} + (1 - y_{urk}) \log (1 - \hat{y}_{urk})]. \quad (6)$$

3.3. Hybrid Recommendation Algorithm. A single recommendation algorithm is often challenging to meet the needs of diverse scenarios, and thus a mixture of multiple recommendation algorithms is needed to improve the accuracy of recommendations [19]. The commonly used hybrid methods are waterfall hybrid, weighted hybrid, and transform combination. Among them, the weighted mixture can set different weight factors for other models and generate dynamic weighted models through training, which can improve the accuracy of recommendation and make the recommendation model more suitable for diverse scenarios [20]. Therefore, in this paper, we use a weighted mixture to mix the two algorithms of UserCF and B-NCF.

Let the length of the list to be recommended to the user be N . X_{UserCF} and Y_{B-NCF} are the recommendation lists

derived from the collaborative filtering algorithm and the improved neural collaborative filtering model, respectively. α and β denote the recommendation weights of the two algorithms, $\alpha + \beta = 1$. Then, the algorithm's mixed recommendation list $TopN$ can be expressed as

$$TopN = \alpha X_{UserCF} + \beta Y_{B-NCF}. \quad (7)$$

Depending on the application scenarios, the way the weights of each algorithm in the hybrid model are taken varies slightly. In this paper, the hit ratio percentage situation is used as the weight, and the corresponding evaluation index is used to evaluate its performance. The hybrid algorithm flow is shown in Figure 4.

First, the user-music gene information is obtained from the music dataset, and the collaborative filtering algorithm calculates a recommendation list. At the same time, user-preferred song information is extracted from the dataset, and another recommendation list is calculated according to the B-NCF model. Then, the two recommendation lists are fused using a weighted mixture, and the recommendation list is obtained after data filtering. The two algorithms are performed simultaneously in a parallel manner, and the weights can be adapted according to the actual situation to meet the recommended requirements in different scenarios.

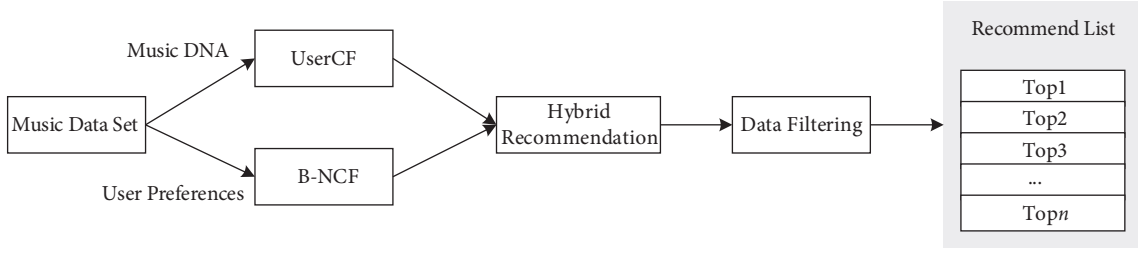


FIGURE 4: Flow of the hybrid algorithm.

TABLE 1: Experimental dataset.

Dataset	Number of users	Number of music	Number of ratings	Sparsity (%)	Gene type	Training set	Test set
Yahoo music	13270	2270	347200	2.3	14	10616	2654

4. Experiments

4.1. Experimental Dataset and Test Environment. To verify the advantages of the hybrid algorithm in this paper, the Yahoo Music dataset is used as the experimental dataset for testing the algorithm in this paper, and its performance is evaluated. The genetic types of music are added according to their attributes, including artist, song title, genre, emotion type, etc., which are 14 types in total. The dataset is divided into a training set and a test set according to the ratio of 8 : 2. The description of the relevant information of the dataset is detailed in Table 1.

The experiments were conducted under the Spark platform, containing 1 master node and 7 worker nodes. The operating system of each node computer is Linux CentOS6.5, CPU is Intel i7-12700 KF, and memory is 16 GB. Software includes Hadoop-2.8.4, Spark-2.3.2, JDK 1.8.0_171 and Python3.6.4. The code editor uses Pycharm2017.2.3 × 64.

4.2. Performance Evaluation Indicators. MAE and F1-measure are used as evaluation criteria to measure the accuracy and recommendation performance of the algorithm. MAE evaluates the recommendation accuracy of the algorithm by calculating the deviation between the predicted user-music gene scores and the actual scores. The lower the value of MAE is, the higher the recommendation performance is indicated [21]. Assuming that the predicted set of ratings is AA and the corresponding set of actual ratings is BB, the MAE can be expressed as

$$\text{MAE} = \frac{\sum_{i=1}^n |s_i - t_i|}{n} \quad (8)$$

F1-measure is a metric that combines precision and recall results to evaluate the strengths and weaknesses of a recommendation model. Assumptions: IR_1 is the predicted list of recommendations provided by the recommendation algorithm for the target user u , IR_2 is the actual list of recommendations for user u in the test set, and I_u is the number of music genes reviewed by user in the test set. The relationship between the precision, recall, and F1-measure evaluation metrics is as follows:

$$\begin{aligned} \text{precision} &= \frac{1}{m} \sum_{u=1}^m \frac{|IR_1 \cap IR_2|}{IR_1}, \\ \text{recall} &= \frac{1}{m} \sum_{u=1}^m \frac{|IR_1 \cap IR_2|}{IR_2}, \\ \text{F1-measure} &= \frac{2 \times \text{precision} \times \text{recall}}{\text{precision} + \text{recall}}. \end{aligned} \quad (9)$$

4.3. Model Parameter Optimization. The training process of the hybrid recommendation algorithm takes a lot of time and cannot guarantee the timeliness of the recommendation. Therefore, the algorithm parameters need to be optimized to ensure that the algorithm has good real-time performance, and the learning rate (LR) of the B-NCF model has a significant impact on the performance of the model. Considering the large sparsity of the dataset, the optimizer of the B-NCF model was chosen as Adam, the epoch was formed as 30, and the learning rates were 0.1, 0.05, 0.01, and 0.001 for the experiments. The results are shown in Figure 5.

Figure 5 shows that when the learning rate is 0.1 and 0.05, the network iteration loss is large, which is not conducive to model training. When the learning rate is 0.01 and 0.001, the network error is lower and stabilizes after 20 rounds of training. Considering the model training speed requirement, the learning rate of the model is taken as 0.01, the optimizer is chosen as Adam, and the epoch is set as 20. The training time is shortened based on guaranteeing the recommendation accuracy. After several trials, the weights of UserCF and B-NCF are taken as 0.37 and 0.63, respectively.

4.4. Analysis of Results. As can be seen from Figure 6, the MAE index of this method is significantly better than that of other recommendation methods. When the number of similar users K is 500, the prediction error of this method reaches the lowest, and the MAE value is 0.944. Compared with the NCF model, which has a higher prediction accuracy, the accuracy is improved by about 4%. Figure 7 shows

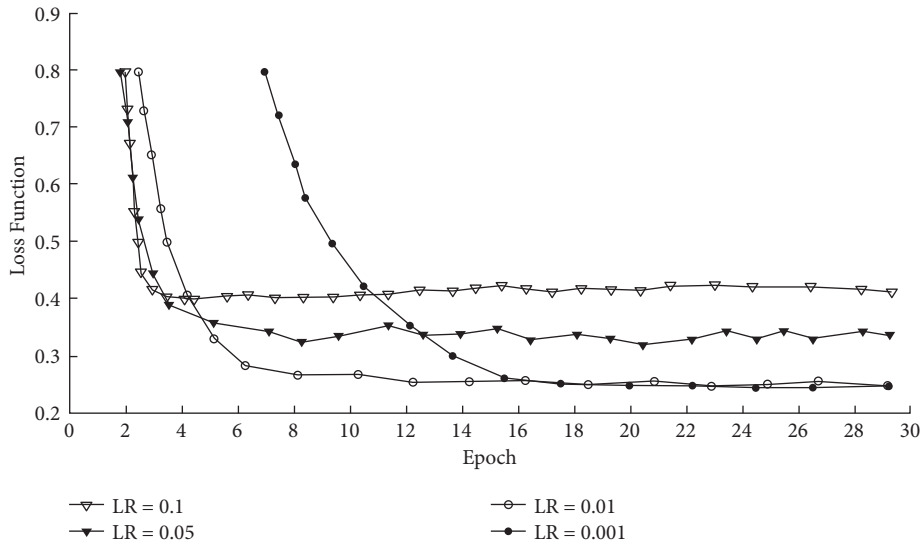


FIGURE 5: Learning rate comparison curve of B-NCF model.

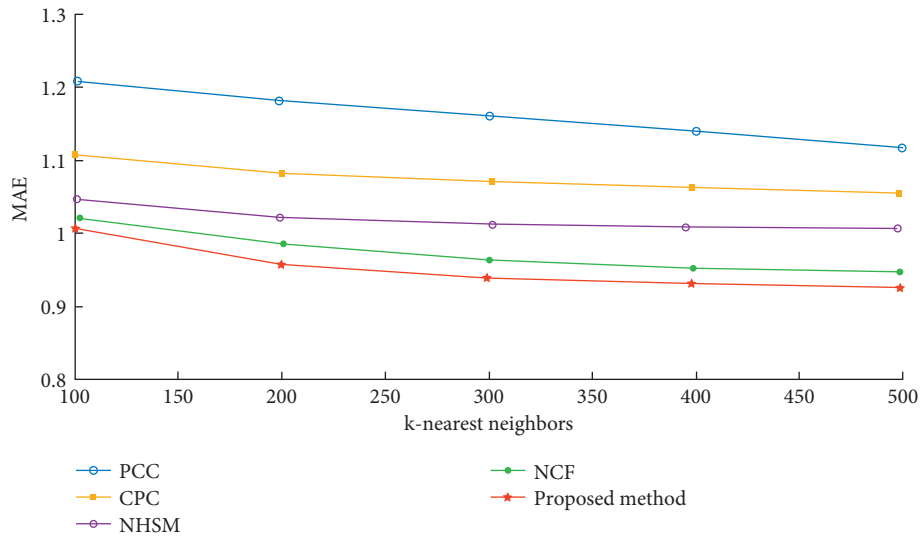


FIGURE 6: MAE comparison curves of different algorithms.

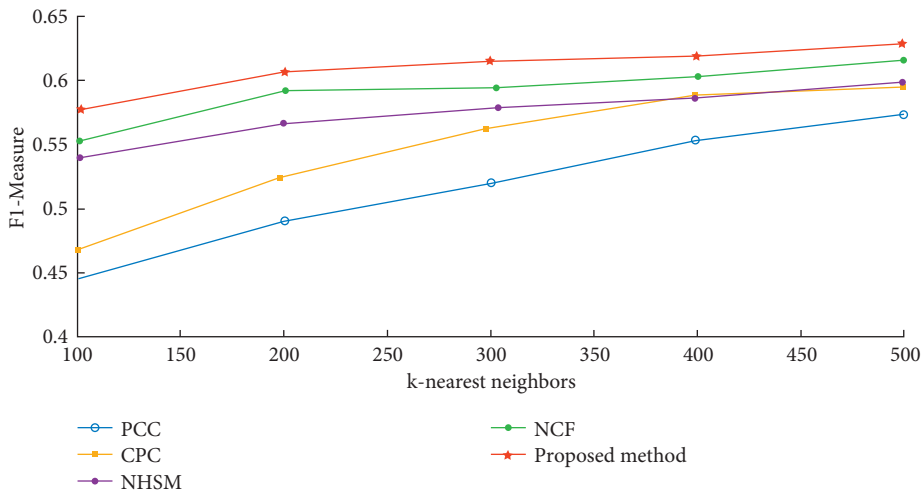


FIGURE 7: F1-measure comparison results of different algorithms.

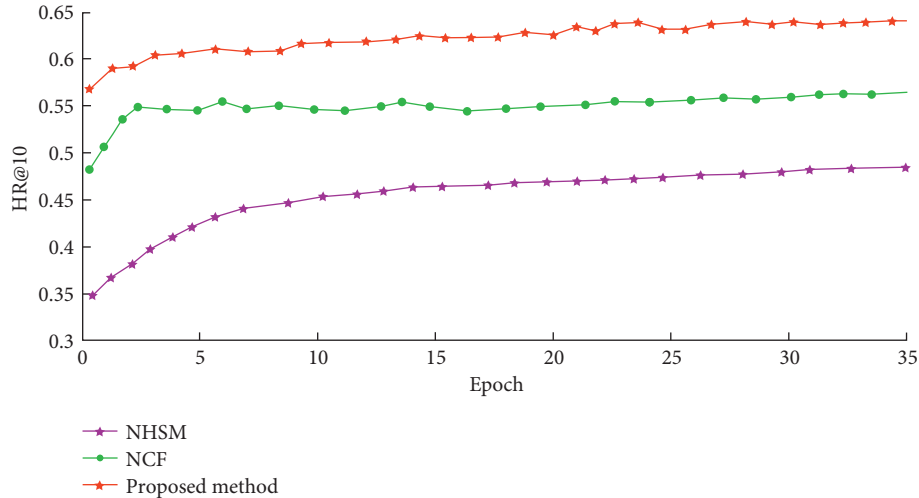


FIGURE 8: Hit rate comparison results.

the performance comparison of the algorithms under the F1-measure index.

Figure 7 shows the strengths and weaknesses of the recommendation quality of the Yahoo Music dataset. The evaluation metric F1 increases with the increase of K value. When the K value is 500, the hybrid algorithm has the highest evaluation with a value of 0.64, 2.2% and 5.3% more accurate than the NCF and NHSM algorithms, respectively. Thus, it shows that the hybrid recommendation algorithm provides more detailed music listings.

NCF, NHSM, and hybrid recommendation algorithms are used as examples, and the length of the recommendation list is set to 10 to examine the hit rate of the algorithms. The obtained results are shown in Figure 8.

Compared with NCF and NHSM algorithms, the hit rate of the hybrid recommendation algorithm is higher, which indicates that the algorithm has more vital higher-order nonlinear expression ability and can better realize the interaction between users and music genes. In the early stage of the hybrid recommendation algorithm, the hit rate of the hybrid model mainly comes from B-NCF due to the low hit rate of UserCF. As the hit rate of ALS improves and stabilizes, the hybrid model better combines the advantages of UserCF and B-NCF, and its hit rate is also improved to some extent. To further verify the performance of the hybrid algorithm in the paper, the hit rate and diversity metrics of the hybrid model are analyzed by taking different length recommendation lists. The experimental results are shown in Table 2.

From Table 2, it can be seen that the hybrid algorithm has a high hit rate for different lengths of recommendation lists, and the diversity changes steadily. Thus, it can be shown that the performance of the hybrid algorithm in terms of accuracy and recall is better than the currently used recommendation algorithms, and it can better match the relationship between users and music genes; when the length of the recommendation list is 50, the time taken is only 96.82, which meets the requirement of recommendation timeliness, and the algorithm is more feasible and can be used as a recommended method for personalized music.

TABLE 2: Performance of the hybrid algorithm with different length recommendation lists.

Recommended list length	Hit rate	Diversity	Recommended time (ms)
5	0.4924	0.5783	68.94
10	0.5941	0.5610	71.78
15	0.6218	0.5533	72.68
30	0.6337	0.5504	83.50
50	0.6672	0.5319	96.82

5. Conclusion

A personalized music hybrid recommendation algorithm based on UserCF and B-NCF is proposed to research the user's preference situation of music genres. Several metrics are used to verify the algorithm's performance. Experiments on the Yahoo Music dataset show that the algorithm improves the accuracy and precision of recommendation by 4% and 2.2%, respectively, compared with the NCF model, and the recommendation list is more reasonable and effective. For different lengths of recommendation lists, the hybrid algorithm takes less time to recommend, which can meet the requirements of hit rate, diversity, and timeliness of music recommendation. From the perspective of the depth of information mining, the hybrid algorithm can improve the effective recommendation hit rate and requires less computational resources. In terms of the breadth of information sources, the hybrid algorithm can be used as a personalized music recommendation method because it takes music genetic information into account and broadens the diversity of information sources.

Data Availability

The labeled dataset used to support the findings of this study is available from the corresponding author upon request.

Conflicts of Interest

The authors declare that they have no conflicts of interest.

References

- [1] M. Skoro and A. Roncevic, "The music industry in the context of digitization," *Economic and Social Development: Book of Proceedings*, vol. 23, pp. 279–288, 2019.
- [2] D. Xu, "Research on music culture personalized recommendation based on factor decomposition machine," *Personal and Ubiquitous Computing*, vol. 24, no. 2, pp. 247–257, 2020.
- [3] G. Li and J. Zhang, "Music personalized recommendation system based on improved KNN algorithm," in *Proceedings of the 2018 IEEE 3rd Advanced Information Technology, Electronic and Automation Control Conference (IAEAC)*, pp. 777–781, IEEE, Chongqing, China, October 2018.
- [4] S. Singh, N. P. Singh, and D. Chaudhary, "A survey on autonomous techniques for music classification based on human emotions recognition," *International Journal of Computing and Digital Systems*, vol. 9, no. 3, pp. 433–447, 2020.
- [5] H.-S. Park and S.-B. Cho, "Evolutionary attribute ordering in bayesian networks for predicting the metabolic syndrome," *Expert Systems with Applications*, vol. 39, no. 4, pp. 4240–4249, 2012.
- [6] H. J. Ahn, "A new similarity measure for collaborative filtering to alleviate the new user cold-starting problem," *Information Sciences*, vol. 178, no. 1, pp. 37–51, 2008.
- [7] H. Liu, Z. Hu, A. Mian, H. Tian, and X. Zhu, "A new user similarity model to improve the accuracy of collaborative filtering," *Knowledge-Based Systems*, vol. 56, pp. 156–166, 2014.
- [8] X. He, L. Liao, H. Zhang, L. Nie, X. Hu, and T. S. Chua, "Neural collaborative filtering," in *Proceedings of the 26th international conference on world wide web*, pp. 173–182, Perth Australia, April 2017.
- [9] F. Vignoli and S. Pauws, "A music retrieval system based on user driven similarity and its evaluation," *International Society for Music Information Retrieval*, pp. 272–279, 2005.
- [10] L. Baltrunas, M. Kaminskas, B. Ludwig et al., "Incarmusic: context-aware music recommendations in a car," in *Proceedings of the International conference on electronic commerce and web technologies*, pp. 89–100, Springer, Toulouse, France, August 2011.
- [11] N. Hariri, B. Mobasher, and R. Burke, "Using social tags to infer context in hybrid music recommendation," in *Proceedings of the twelfth international workshop on Web information and data management*, pp. 41–48, Maui, HW, USA, November 2012.
- [12] A. Y. H. Yap, H. C. Soong, and S. S. H. Tse, "Real-time evolutionary music composition using JFUGUE and genetic algorithm," in *Proceedings of the 2021 IEEE 19th Student Conference on Research and Development (SCORED)*, pp. 377–382, IEEE, Kota Kinabalu, Malaysia, November 2021.
- [13] B. P. Gold, M. T. Pearce, E. Mas-Herrero, A. Dagher, and R. J. Zatorre, "Predictability and uncertainty in the pleasure of music: a reward for learning?" *Journal of Neuroscience*, vol. 39, no. 47, pp. 9397–9409, 2019.
- [14] D. Sánchez-Moreno, J. Pérez-Marcos, A. B. Gil González, V. L. Batista, and M. N. Moreno-García, "Social influence-based similarity measures for user-user collaborative filtering applied to music recommendation," in *Proceedings of the International Symposium on Distributed Computing and Artificial Intelligence*, pp. 267–274, Springer, Bilbao, Spain, June 2018.
- [15] D. Sánchez-Moreno, M. N. Moreno-García, N. Sonboli, B. Mobasher, and R. Burke, "Inferring user expertise from social tagging in music recommender systems for streaming services," in *Proceedings of the International Conference on Hybrid Artificial Intelligence Systems*, pp. 39–49, Springer, Oviedo, Spain, June 2018.
- [16] Y. Wang, "Research on handwritten note recognition in digital music classroom based on deep learning," *Journal of Internet Technology*, vol. 22, no. 6, pp. 1443–1455, 2021.
- [17] E. Zheng, G. Y. Kondo, S. Zilora, and Q. Yu, "Tag-aware dynamic music recommendation," *Expert Systems with Applications*, vol. 106, pp. 244–251, 2018.
- [18] R. Wang, X. Ma, C. Jiang, Y. Ye, and Y. Zhang, "Heterogeneous information network-based music recommendation system in mobile networks," *Computer Communications*, vol. 150, pp. 429–437, 2020.
- [19] P. Lops, D. Jannach, C. Musto, T. Bogers, and M. Koolen, "Trends in content-based recommendation," *User Modeling and User-Adapted Interaction*, vol. 29, no. 2, pp. 239–249, 2019.
- [20] W. Zhang, Y. Wang, H. Chen, and X. Wei, "An efficient personalized video recommendation algorithm based on mixed mode," in *Proceedings of the 2019 IEEE International Conferences on Ubiquitous Computing & Communications (IUCC) and Data Science and Computational Intelligence (DSCI) and Smart Computing, Networking and Services (SmartCNS)*, pp. 367–373, IEEE, Shenyang, China, October 2019.
- [21] W. Zou, "Design and application of incremental music recommendation system based on Slope one algorithm," *Wireless Personal Communications*, vol. 102, no. 4, pp. 2785–2795, 2018.

Research Article

Substation Equipment Spare Parts' Inventory Prediction Model Based on Remaining Useful Life

Bing Tang,¹ Zhenguo Ma,¹ Keqi Zhang,¹ Danyi Cao,¹ and Jianyong Zhang ²

¹Changzhou Power Supply Branch, State Grid Jiangsu Electric Power Co., Ltd., Changzhou, Jiangsu 213003, China

²College of Science, Hohai University, Changzhou, Jiangsu 213022, China

Correspondence should be addressed to Jianyong Zhang; hohaizhangjy@hhu.edu.cn

Received 11 March 2022; Accepted 31 March 2022; Published 27 April 2022

Academic Editor: Wei Liu

Copyright © 2022 Bing Tang et al. This is an open access article distributed under the Creative Commons Attribution License, which permits unrestricted use, distribution, and reproduction in any medium, provided the original work is properly cited.

A large variety of high-value substation relay protection equipment occupies a considerable amount of inventory space and capital in electric power companies. To improve this problem, this study proposes an inventory prediction model based on the remaining useful life (RUL) of equipment. The model acquires the RUL data of equipment by using the support vector regression (SVR) algorithm, and then, by taking this data as the main factor and the environmental factors and human factors during the operation of equipment as secondary factors, the model can realize the prediction of relay protection equipment in the substation. At the same time, the nature of the enterprise and the requirements for safety inventory are considered. The comparison of calculation results and error analysis, as well as the calculation time, all indicate that the RUL-based inventory forecasting is the best one. This model not only has high prediction accuracy but also has strong stability and portability. The model can provide a strong decision basis for improving the inventory management of the enterprise, enhancing the resource allocation capability, and formulating the spare parts procurement plan under the condition that the spare parts inventory reaches the safety stock.

1. Introduction

Safety stock is an important topic in inventory management [1, 2], and its main role is to meet the uncertainty of supply and demand. The definition of safety stock varies from industry to industry. In power systems, the safety stock of spare parts means that the stock level should always be slightly redundant to the actual demand, in case there are no spare parts available when an unexpected event occurs. Spare parts inventory levels are often calculated based on certain historical data and forecasting models. The authors of [3, 4] have summarized the inventory research results of spares, and the forecasting techniques cover everything from early expert system models to the current artificial intelligence models.

The expert meeting method and the Delphi method are less practical and reliable due to their reliance on expert experience. However, this qualitative model, combined with other methods, has an excellent performance in forecasting [5–7]. With the development of computers and the demand for short-term and medium-term forecasting techniques,

quantitative forecasting models have taken the dominant position, such as gray forecasting models [8, 9], linear regression [10] and nonlinear regression [11], and autoregressive moving average (ARMA) models [12–14]. These quantitative forecasting approaches tend to have certain data requirements and also have obvious advantages and disadvantages, such as an emphasis on model improvement to improve the prediction accuracy, but less consideration is given to the factors affecting the inventory, and the information contained in the data is not sufficiently mined. With the development of artificial intelligence, forecasting models based on AI techniques began to play an important role, such as machine learning [15, 16], deep learning [17–19], support vector machine (SVM) [20, 21], backpropagation (BP) neural networks [22, 23], and long short-term memory (LSTM) [24, 25]. These intelligent prediction techniques have played an important role in various industries with the help of excellent data processing capabilities.

There is also rich research on inventory forecasting for spare parts in power systems. Zhang [26] established a smart meter inventory demand forecasting model based on analyzing

its fault characteristic and installing requirements, and an optimal management strategy [27] was developed. Ding [28] improved the BP neural network model based on the Adam optimization method to forecast the demand for materials in the Guizhou power grid, and the method can significantly reduce the error. In [25], an effective model based on the long short-term memory (LSTM) recurrent neural network was put forward to predict the requirement for maintenance of spare parts. Hamoud and Yiu [29] described a practical reliability model based on a stationary Markov process for assessing the number of spare parts. Yang [30] constructed a deep convolutional neural network based on the graph to realize multicriteria classification for spare parts, which could supply good decision support to control inventory.

As an integral part of the power grid, relay protection equipment has the main characteristics of being diverse, small in size, difficult to obtain monitoring data, and its service life is affected by various factors. Therefore, the advanced prediction techniques mentioned in the above literature, according to our review, found that few prediction models have been applied to this type of equipment. For this reason, in this study, on the basis of analyzing the characteristics of the equipment and its elimination records and safety inventory requirements of electric power enterprises, we make an innovative model of an inventory prediction algorithm according to the RUL of the equipment and applied it to the inventory management system of relay protection equipment in the Changzhou substation. The model implements the following functions:

- (i) To improve the prediction accuracy of the model, this study fully considers the factors that have direct and indirect effects on the RUL of equipment; these factors are shown in Section 3.1
- (ii) To reduce the computational difficulty, we define the new variable of the life course as the main variable to obtain the RUL of equipment
- (iii) To meet the requirement of saving inventory cost and storage space under the condition of achieving inventory safety and to provide decision support for Changzhou Power Supply Company to realize spare parts procurement on a quarterly cycle

Section 1 of this study introduces the current research status of inventory forecasting models and inventory of spare parts in power companies. Section 2 is the inventory forecasting algorithm according to the remaining useful life of equipment, including the algorithm about obtaining the RUL of equipment with the aid of support vector regression and the prediction algorithm of spare parts based on the RUL. Section 3 is a case study for inventory prediction of the central processing unit (CPU) of a substation in Changzhou City. The portability of the model is illustrated by using the predictions for the liquid crystal display (LCD) and DC 220 V Power Supply (DCPS). The validity and stability of the model are indicated by comparing the RUL model with the LSTM, ARMA, support vector machine (SVM), and SVM + BP models. At the same time, the error analyses are given. Section 4 is the conclusions and the perspective.

2. Inventory Prediction Model on the Basis of RUL

The remaining useful life [31] plays an important role in many fields. It can provide strong support for upper-level decision-making, scientifically reduce the operating cost of the system, and enhance the reliability of the system. Especially, with the gradual maturity of AI technology, RUL has been successfully applied to many practical problems [32]. Figure 1 is the main idea for this study; this framework can demonstrate our research steps.

In this section, we will discuss how to obtain the RUL of substation equipment by using SVR and the construction of an inventory prediction model based on the RUL.

2.1. Principle and Algorithm of RUL Based on SVR. In machine learning [33, 34], SVR is a nonparametric regression model that determines the regression hyperplane by optimizing the distance to nearby support vectors. We first consider the regression hyperplane that achieves the remaining useful life.

For the given training set $D = \{(\mathbf{x}_1, y_1), (\mathbf{x}_2, y_2), \dots, (\mathbf{x}_m, y_m)\}$, $y_i \in (0, 1]$, since it is difficult to determine whether the training set is linearly divisible in the original space, let the division hyperplane be

$$f(\mathbf{x}) = \mathbf{w}^T \phi(\mathbf{x}) + b, \quad (1)$$

where $\mathbf{x} = (\mathbf{x}_1, \mathbf{x}_2, \dots, \mathbf{x}_m)$, $\phi(\mathbf{x})$ is the eigenvector after mapping \mathbf{x} , $\mathbf{w} = \{w_1, w_2, \dots, w_m\}^T$ is the weight vector, and b is the bias.

The problem of solving the regression hyperplane $f(\mathbf{x})$ can be transformed into the following optimization problem:

$$\min_{\mathbf{w}, b} \frac{1}{2} \|\mathbf{w}\|^2 + C \sum_{i=1}^m l_\varepsilon(f(\mathbf{x}_i) - y_i), \quad (2)$$

where the penalty coefficient $C > 0$ and l_ε is the insensitivity loss function and its expression is

$$l_\varepsilon(z) = \begin{cases} 0, & \text{if } |z| \leq \varepsilon, \\ |z| - \varepsilon, & \text{otherwise.} \end{cases} \quad (3)$$

Introducing the slack variables ξ and $\hat{\xi}$ to normalize (2), we can obtain

$$\begin{aligned} \min_{\mathbf{w}, b, \xi, \hat{\xi}} \frac{1}{2} \|\mathbf{w}\|^2 + C \sum_{i=1}^m (\xi_i + \hat{\xi}_i), \\ f(x_i) - y_i \leq \varepsilon + \xi_i, \\ \text{s.t. } f(x_i) - y_i \geq \varepsilon + \hat{\xi}_i, \\ \xi_i \geq 0, \quad \hat{\xi}_i \geq 0, \quad i = 1, 2, \dots, m. \end{aligned} \quad (4)$$

Introducing the Lagrange multipliers $\mu_i \geq 0$, $\hat{\mu}_i \geq 0$, $\alpha_i \geq 0$, $\hat{\alpha}_i \geq 0$, we construct the Lagrange function of (4) as follows:

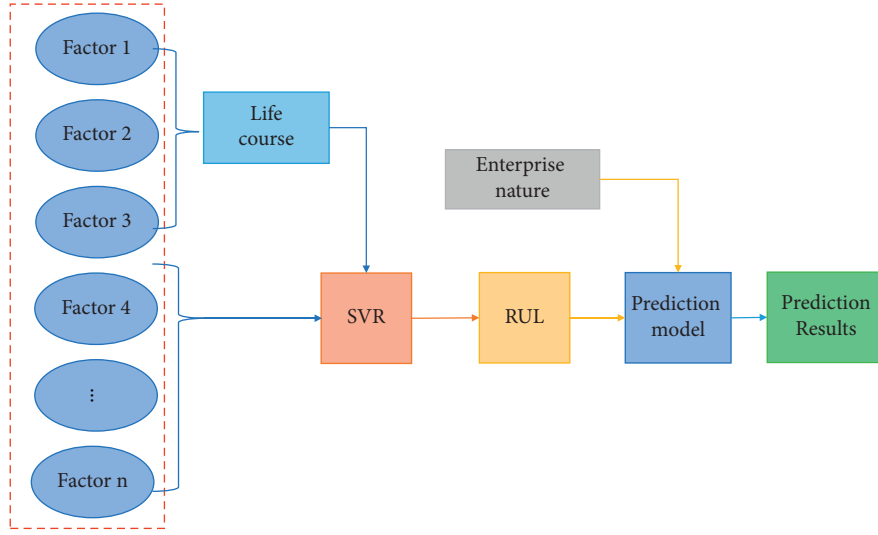


FIGURE 1: The main ideation and framework of this study.

$$\begin{aligned}
 L(\mathbf{w}, \mathbf{b}, \boldsymbol{\mu}_i, \widehat{\boldsymbol{\mu}}_i, \xi_i, \widehat{\xi}_i, \boldsymbol{\alpha}_i, \widehat{\boldsymbol{\alpha}}_i) &= \frac{1}{2} \|\mathbf{w}\|^2 + C \sum_{i=1}^m (\xi_i + \widehat{\xi}_i) \\
 &\quad - \sum_{i=1}^m \mu_i \xi_i - \sum_{i=1}^m \widehat{\mu}_i \widehat{\xi}_i \\
 &\quad + \sum_{i=1}^m \alpha_i (f(x_i) - y_i - \varepsilon - \xi_i) \\
 &\quad + \sum_{i=1}^m \widehat{\alpha}_i (f(x_i) - y_i - \varepsilon + \widehat{\xi}_i).
 \end{aligned} \tag{5}$$

Considering (1), let the derivatives of $L(\mathbf{w}, \mathbf{b}, \mu_i, \widehat{\mu}_i, \xi_i, \widehat{\xi}_i, \alpha_i, \widehat{\alpha}_i)$ with respect to $\mathbf{w}, \mathbf{b}, \xi_i, \widehat{\xi}_i$ be zeros; we can obtain

$$\mathbf{w} = \sum_{i=1}^m (\widehat{\alpha}_i - \alpha_i) \mathbf{x}_i, \tag{6}$$

$$0 = \sum_{i=1}^m (\widehat{\alpha}_i - \alpha_i), \tag{7}$$

$$C = \alpha_i + \mu_i, \tag{8}$$

$$C = \widehat{\alpha}_i + \widehat{\mu}_i. \tag{9}$$

Substituting equation (5)–(8) into (5), we obtain the dual programming problem as follows:

$$\begin{aligned}
 \max_{\boldsymbol{\alpha}, \widehat{\boldsymbol{\alpha}}} & \sum_{i=1}^m y_i (\widehat{\alpha}_i - \alpha_i) - \varepsilon (\widehat{\alpha}_i + \alpha_i) - \frac{1}{2} \sum_{i=1}^m \sum_{j=1}^m (\widehat{\alpha}_i - \alpha_i) (\widehat{\alpha}_j - \alpha_j) \mathbf{x}_i^T \mathbf{x}_j, \\
 \text{s.t.} & \sum_{j=1}^m (\widehat{\alpha}_j - \alpha_j) = 0, \\
 & 0 \leq \widehat{\alpha}_i, \alpha_i \leq C.
 \end{aligned} \tag{10}$$

With the KKT condition satisfied, the optimal solution of (1) can be obtained as

$$f(\mathbf{x}) = \mathbf{w}^{*T} \boldsymbol{\phi}(\mathbf{x}) + b^*. \tag{11}$$

(11) is the regression hyperplane used to calculate the remaining useful life.

2.2. Variables and Data Processing. Let the data matrix of a certain type of equipment be $\mathbf{Z} = (z_{ij})_{N \times 10}$, where the i th row z_i of \mathbf{Z} denotes the data vector of the i th device of that class of

devices and N is the number of devices that have been eliminated. The name and type of the variables in z_i are shown in Table 1.

To facilitate the description, several variables are introduced, and the notation and description of the variables are shown in Table 2.

To improve the accuracy of the prediction results, firstly, the data \mathbf{Z} need to be cleaned, and let $U_l(i) = z_i(9) - z_i(8)$ be the days of usage of equipment, and the mean μ and variance σ^2 of U_l are calculated, and the singular values are screened out using the Z-score method; then, the

TABLE 1: Variables, notations, and types.

Variables	Notations	Types
Manufacturers	$z_i(1)$	Text variable
Substation name	$z_i(2)$	Text variable
Interval	$z_i(3)$	Text variable
Device	$z_i(4)$	Text variable
O&M shift*	$z_i(5)$	Text variable
Temperature (°C)	$z_i(6)$	Numeric variables
Humidity (hPa)	$z_i(7)$	Numeric variables
Installation date	$z_i(8)$	Time variables
Date of damage	$z_i(9)$	Time variables
Design life/days	$z_i(10)$	Numeric variables

* O&M, operations and maintenance shift.

TABLE 2: Variables and descriptions.

Notations	Descriptions
U_l	Days of usage of equipment/day
D_{pl}	RUL prediction value of equipment/days
$x_i(8)$	The design life course of equipment
y_{ir}	The actual life course of equipment
D_t	Current date
D_{dl}	Left days of equipment by design life/day
D_{pb}	Predicted damage date of in-service equipment

elimination records containing the singular values are deleted. The formula of the Z-score is as follows:

$$\left| \frac{U_l - \mu}{\sigma} \right| \leq z_\theta. \quad (12)$$

Generally, the threshold $z_\theta \in (1, 3)$. The data satisfying the above equation are retained, and the new data set matrix is still denoted as $Z = (z_{ij})_{M \times 10}$, where $M \leq N$.

Next, we make certain variables labeled and also define a new variable named life course.

The textual variables $z_i(1)$ to $z_i(5)$ are labeled with the regular numerical values and are denoted as $x_i(1)$ to $x_i(5)$. The numerical variables $z_i(6)$ and $z_i(7)$ are denoted as $x_i(6)$ and $x_i(7)$. To reduce the dimensionality of the data and simplify the calculation, the life history course $x_i(8)$ are constructed by using the installation date $z_i(8)$, damage date $z_i(9)$, and design to life $z_i(10)$ as follows:

- (i) % M is the number of elimination records of a class of components after cleaning
- (ii) % I is the number of interval days
- (iii) $J_i = z_i(9) - z_i(8)/I$
- (iv) for i from 1 to M
- (v) $j = 1$
- (vi) $D_t = z_i(8) + I$ % Date after installation I days
- (vii) while $now < z_i(9)$ % now Indicates the current date
- (viii) $r = \sum_{k=1}^{i-1} J_k + j$
- (ix) $x_i(8) = D_t - z_i(8)/z_i(10)$ % Design life course of equipment
- (x) $y_{ir} = D_t - z_i(8)/z_i(9) - z_i(8)$ % Actual life course of equipment

$$(xi) \quad \mathbf{x}_i = (x_i(1), x_i(2), x_i(3), x_i(4), x_i(5), x_i(6), x_i(7), x_i(8)) \text{ \% update variable symbols}$$

$$(xii) \quad j = j + 1$$

$$(xiii) \quad now = now + I$$

where $z_i(9) - z_i(8)$ is expressed by the number of days. If the i th device is active, take $z_i(9)$ means the current date.

Then, the processed data matrix for this type of device is obtained as $\mathbf{X} = (\mathbf{x}_{ij})_{N \times 8}$. The data of the i th device are

$$\mathbf{x}_i = (x_i(1), x_i(2), x_i(3), x_i(4), x_i(5), x_i(6), x_i(7), x_i(8)). \quad (13)$$

2.3. Computation of RUL. Under the above theory and its data characteristics, Algorithm 1 is constructed to predict the RUL of equipment.

With Algorithm 1, the number of days of the RUL of the k th in-service device can be calculated as $D_{pl}(k)$.

2.4. Algorithm for Inventory Forecasting of Spare Parts by RUL. Once the RUL of an in-service device is obtained, we can construct Algorithm 2 to predict the inventory. The main idea of Algorithm 2 is to consider how many components have an RUL less than T in a prediction period T . Also, a correction function is added for tuning to prevent over-prediction and to protect the safety stock.

3. Experiment and Analyses

3.1. Elimination Record. The data on the defect elimination records stored in Changzhou Power Supply Company contain 10 field variables, which are listed in Table 1. The spare parts in this research are installed in relay protection equipment of the substation. They share the following common features:

- (i) A wide variety and distribution, high value, and integration.
- (ii) It is difficult to obtain monitoring data since they are board-like devices of small size. The operation and maintenance (O&M) processes require a lot of manpower. It has a long procurement cycle.
- (iii) Service life is influenced by many kinds of factors listed in Table 1.

3.2. Prediction Results Based on RUL, Comparison, and Its Error. First, we make forecasts for the CPU inventory. Combining with the proposed procurement cycle of Changzhou Power Supply Company, we set the prediction period $T = 90$ days and the interval days $I = 10$ days and make $z_\theta = 2.5$ in the Z-score during data screening and parameter $s = 2$ in the correction function $Q_s(t)$. Figure 1 shows the prediction results of CPU spare parts based on the RUL.

In Figure 2, the horizontal coordinate indicates the quarter and the vertical coordinate indicates the prediction result about CPU. From it, we can see that the prediction curve of the CPU with the quarterly cycle has almost the same trend as the real value, which means that the RUL-

Input: $\mathbf{x}_i = (x_i(1), x_i(2), x_i(3), x_i(4), x_i(5), x_i(6), x_i(7), x_i(8))$.

Output: the RUL value of the k th component $D_{pl}(k)$.

Step 1. The data matrix \mathbf{x} is assigned to training set \mathbf{x}_{train} and test set \mathbf{x}_{test} in the ratio of 4:1.

Step 2. Get the prediction model by the training data. The regression hyperplane expression is obtained by inputting a certain class of components processed data \mathbf{x}_{train} into equation (2), i.e., $f(\mathbf{x}) = \mathbf{w}^{*T}\phi(\mathbf{x}) + b^*$.

Step 3. Validity test, let T_{test} be the number of rows of test data, for the given $\Delta > 0$, if $1/T_{test} \sum_{r=1}^{T_{test}} |y_{test}(r) - f(\mathbf{x}_{test}(\mathbf{r}))| < \Delta$. go to Step4, otherwise, go to (2), and adjust the penalty coefficients C and ϵ until they are satisfied.

Step 4. Substitute the k th data of the in-use device $\mathbf{x}_k = (x_k(1), x_k(2), x_k(3), x_k(4), x_k(5), x_k(6), x_k(7), x_k(8))$ into (14) and output $f(\mathbf{x}_k)$. This is the value of the life course of the actual life of the k th component.

Step 5. Calculate the damage date $D_{pb}(k)$ of the k th in-service spare part: $D_{pb}(k) = x_k(8) + D_t - x_k(8) / f(\mathbf{x}_k)$.

Step 6. Compute the number of days $D_{pl}(k)$ left in the life of the k th in-service spare part: $D_{pl}(k) = D_{pb}(k) - D_t$.

ALGORITHM 1: Computation of RUL by SVR.

Input : RUL of the k th equipment $D_{pl}(k)$

Output : the demand for spare parts Q in the next cycle T .

Step 7. Calculate the number of days remaining in the design life of the k th component $D_{bl}(k) : D_{bl}(k) = x_k(8) + z_k(10) - D_t$.

Step 8. Set the correction function to $Q_s(t) = 1 - \tanh st = 2e^{-st} / (1 + e^{-st})$, ($s > 1, t \in R$)

Step 9. Predicting the inventory level of a certain type of component spare parts, the algorithm pseudocode is as follows:

- (i) % Q is the demand for a class of components.
- (ii) % Sum is the number of components of this class being operated in the system
- (iii) % T is the forecast period
- (iv) $Q = 0$
- (v) for $k = 1$: sum
- (vi) If $D_{pl}(k) \leq T$
- (vii) $Q = Q + 1$
- (viii) If $D_{pl}(k) > T$ and $D_{bl}(k) \leq T$
- (ix) $Q = Q + Q_s(t)$
- (x) Output Q % the demand for spare parts in the next cycle.

ALGORITHM 2: Prediction algorithm by RUL.

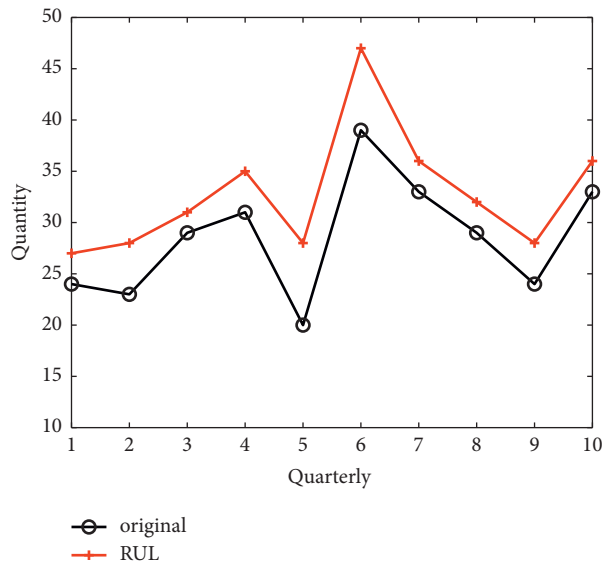


FIGURE 2: The prediction results of CPU based on RUL.

based prediction method is effective. In the graph, we will also notice that the predicted value is slightly larger than the true value, which is intended to make the spare parts slightly

more available in case there are no spare parts available when an unexpected event occurs, i.e., it is beneficial to the stability of the power system.

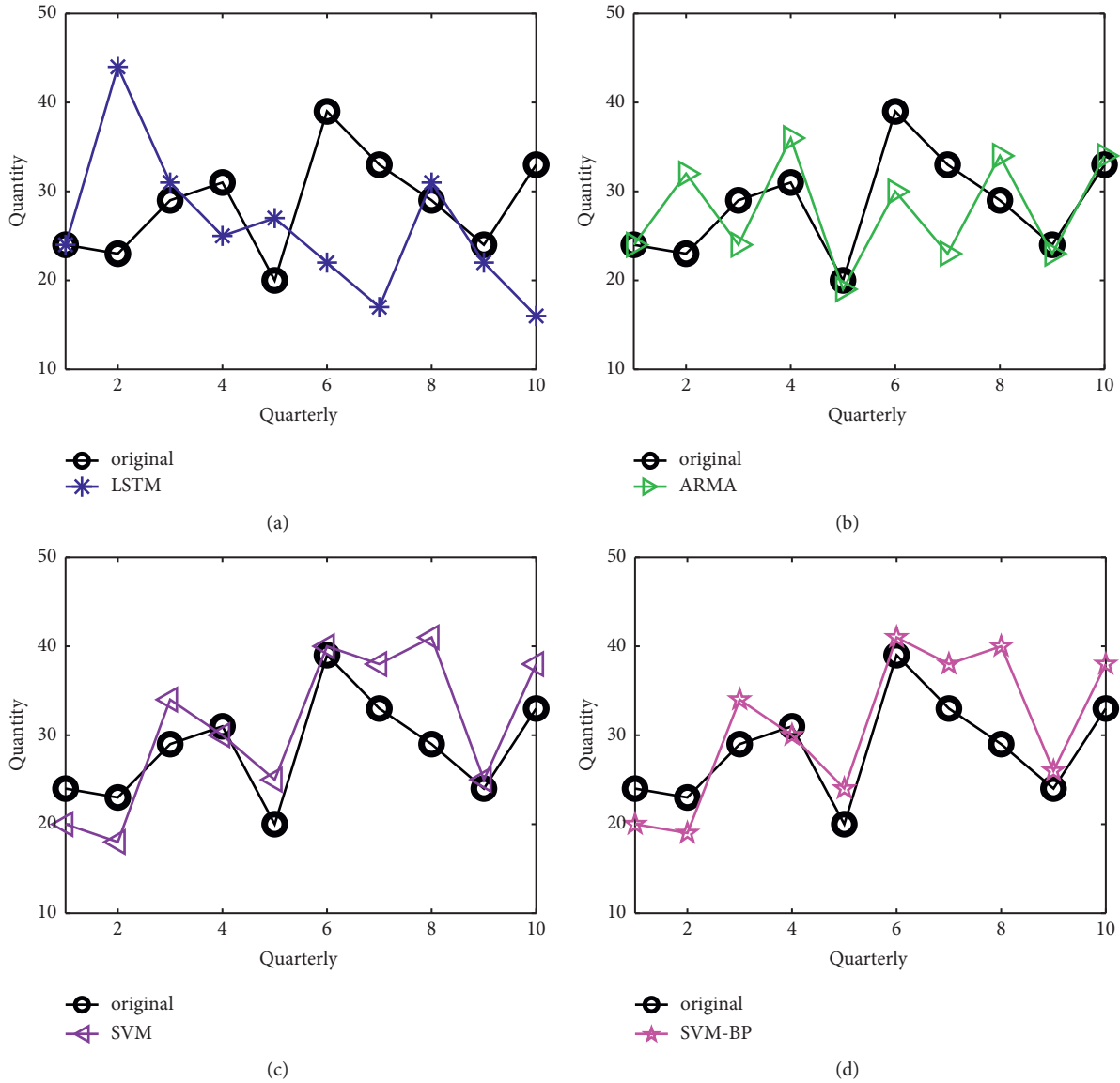


FIGURE 3: (a) to (d) The prediction results of the CPU based on LSTM, ARMA, SVM, and BP-SVM, respectively.

Second, to illustrate the effectiveness of the algorithm, we employ LSTM, ARMA, SVM, and a combined model of BP and SVM to predict the CPU inventory, and a comparison of the predicted results with the true values is shown in Figure 3.

As we can see from Figure 3, although the prediction results of these four forecasting models are the same as the true values in some quarters, the overall prediction results are not suitable for electric power companies mainly because the difference between the predicted and true values is positive and negative, which leads to the inability of Changzhou Power Supply Company to achieve the goal of purchasing by quarters, and the safe and stable operation of the electric power system cannot be guaranteed under such prediction results.

Finally, the errors of five forecasting models are compared, the root mean square error (RMSE) and mean absolute error (MAE) corresponding to the forecast values under different models are discussed, and the formulas are as follows:

$$\text{RMSE} = \sqrt{\frac{1}{n} \sum_{i=1}^n (x_a(i) - x_p(i))^2}, \quad (14)$$

$$\text{MAE} = \frac{1}{n} \sum_{i=1}^n |x_a(i) - x_p(i)|,$$

where x_p and x_a are the predicted and true values, respectively. If the values of RMSE and MAE of an algorithm are smaller, it means that the algorithm is more effective. The RMSE and MAE of the five method prediction methods are shown in Table 3.

From Table 3, it can be seen that the RUL-based prediction results have the smallest RMSE and MAE among the above five prediction models. It further illustrates the effectiveness of RUL-based CPU prediction.

TABLE 3: RMSE and MAE of CPU prediction results on different prediction models.

	RUL	LSTM	ARMA	SVM	SVM-BP
RMSE	4.7434	11.7132	5.8310	5.3666	5.0299
MAE	4.3201	9.0611	4.6517	4.411	4.3603

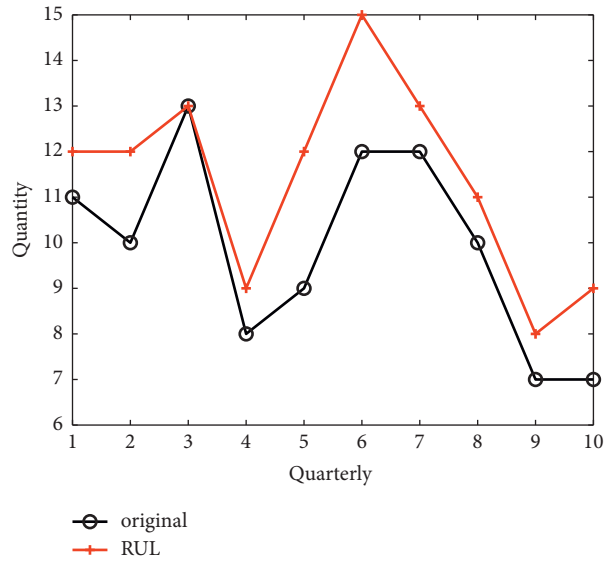


FIGURE 4: The prediction results of LCD based on RUL.

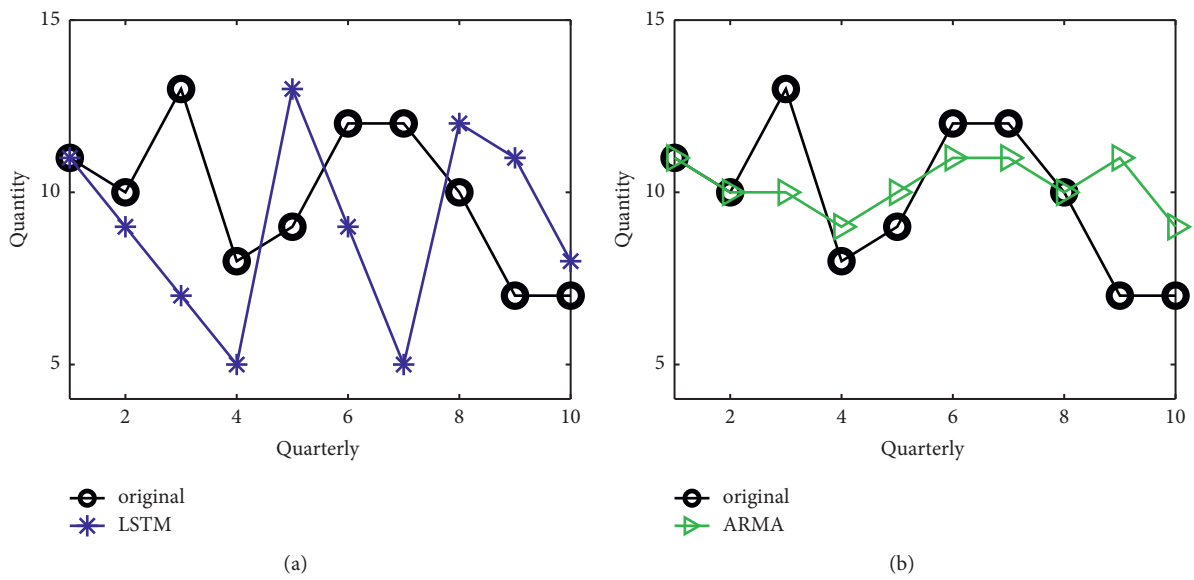


FIGURE 5: Continued.

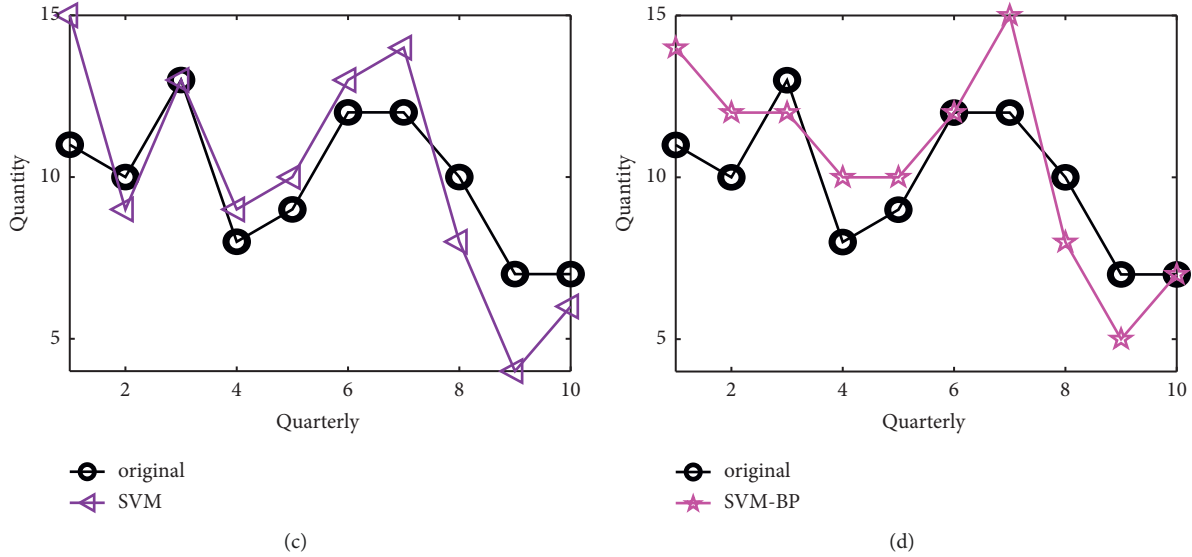


FIGURE 5: (a) to (d) Prediction results of LCD based on LSTM, ARMA, SVM, and BP-SVM, respectively.

3.3. Portability and Stability. There are many other CPU-like devices in substations that have similar characteristics to CPUs. To exemplify the portability of the model, we apply the model to the LCD and DCPS inventory predictions, respectively. The parameter settings are unchanged. Figure 4 shows the prediction results based on the RUL model for LCD. Figure 5 presents the inventory prediction results for LCD based on LSTM, ARMA, SVM, and BP-SVM. Figure 6 illustrates the prediction results of DCPS based on the RUL model. Figure 7 demonstrates the inventory prediction results for DCPS based on LSTM, ARMA, SVM, and BP+SVM. Table 4 is the error comparison of the responses.

From Figures 4 and 6, we can notice that the trend of the predicted and true values is almost the same, and the predicted values are also slightly larger than the true values, thus indicating that the RUL-based prediction model has strong portability and also strong stability. This prediction model is suitable for the corporate requirements of Changzhou Power Supply Company and the requirements for power system stability.

From Figures 5 and 7, the predicted and true value curves intersect several times. Although, in some quarters, the predicted results are almost the same as the true ones, this does not satisfy the enterprise requirements.

In Table 4, it can be found that the RMSE and MAE of the forecast results based on RUL are the smallest, except for the MAE of the forecast based on the ARMA model for LCD. For this exception, the result of our analysis is that LCDs are durable equipment in substations with a long service life, resulting in small data for elimination records and data with a strong linear nature, while the ARMA model has a high advantage in dealing with this type of prediction problem.

The purpose of forecasting on a quarterly cycle is to provide a decision basis for the procurement of spare parts for Changzhou Power Supply Company to save storage space as well as improve capital utilization.

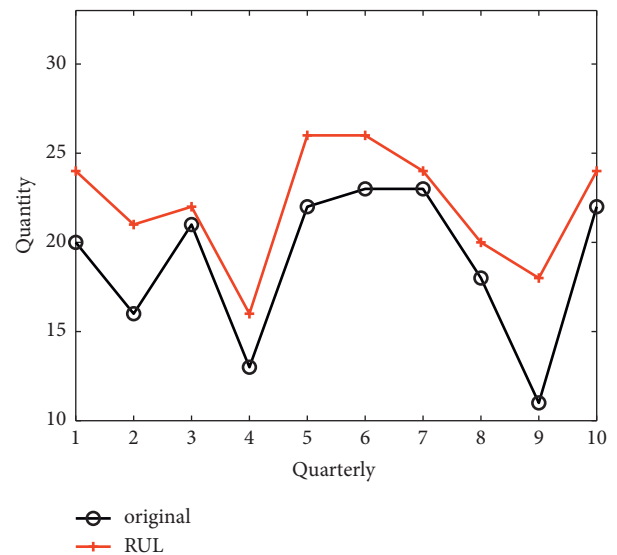


FIGURE 6: The prediction results of DCPS based on RUL.

3.4. Computation Time. The elapsed time of a model is affected by several aspects, such as the complexity of the algorithm, the dimensionality of the variables, and the code, and therefore, it is often used as a metric to assess the efficiency of the model. In this study, the elapsed time of the five algorithms involved is statistically measured, and the results are shown in Figure 8.

Figure 8 shows the time consumption for the computation of the RUL-based prediction model is not the most or the least. Combined with the previous prediction results, we can consider this time consumption to be acceptable for the following reasons: (1) For this study, we are pursuing the accuracy of the prediction and the conformity of the prediction results to the nature of the enterprise; (2) the engineering environment in which the algorithm is applied is not in a time-critical circumstance but has a very sufficient amount of time.

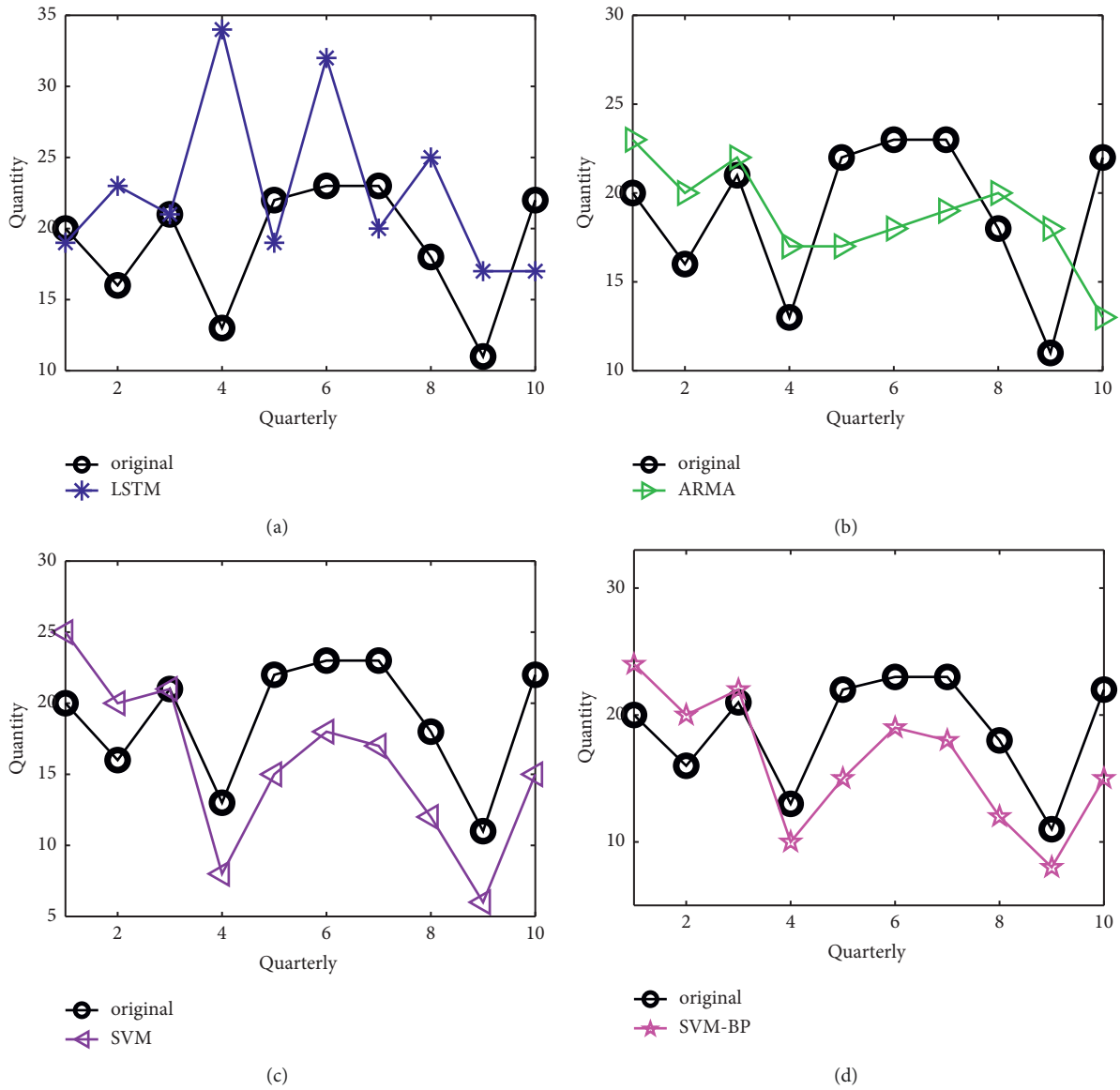


FIGURE 7: (a) to (d) Prediction results of DCPS based on LSTM, ARMA, SVM, and BP-SVM, respectively.

TABLE 4: Comparison of the errors of different models for LCD and DCPS prediction results.

		RUL	LSTM	ARMA	SVM	SVM-BP
LCD	RMSE	1.7607	3.7757	1.8166	1.9494	1.8974
	MAE	1.5123	3.2411	1.3301	1.6221	1.6000
DCPS	RMSE	3.6606	8.3666	4.9193	5.3479	4.7539
	MAE	3.202	6.2817	4.4709	5.01	4.4212

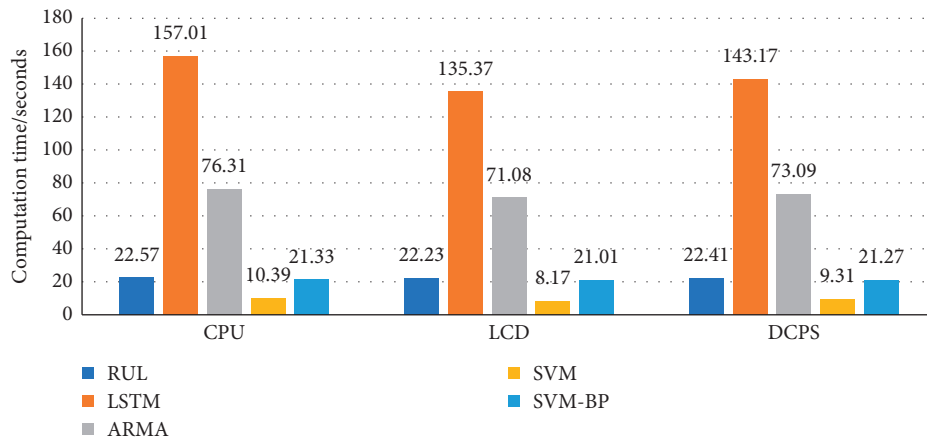


FIGURE 8: Computation time.

4. Conclusions and Perspective

In this study, a spare parts inventory forecasting model based on the remaining useful life of in-service equipment is proposed for the nature of electric power company enterprises, spare parts characteristics, and data. From the results of the case study, the model is suitable for inventory forecasting in electric power companies. The comparison of the model, the analysis of the error, and the computation time illustrate the validity, stability, and portability of the model.

According to the forecasting algorithm, the quarterly cycle is used for forecasting, which avoids the randomness of data brought by a small cycle and the large forecast error caused by a large cycle. At the same time, the quarterly cycle does not affect the annual procurement plan, while inspiring us to provide a feasible procurement proposal, i.e., to pay and supply according to the quarter, which can save inventory space and reduce holding costs.

The value of the forecasting model used in this study is reflected in three aspects: (1) accurate calculation, portability, and stability; (2) improving inventory management capability and saving inventory cost and storage space; (3) the model idea has certain generalizations, such as applying to the primary variable equipment of power system and enriching the whole life cycle management of power equipment.

The inability to obtain monitoring data makes it difficult to operate and maintain (O&M) relay protection equipment, and usually, routine maintenance does not reduce the failure rate of the device. Currently, the best maintenance strategy is predictive O&M [35–37]. An essential prerequisite for predictive O&M is to have information about the status of the health of the equipment, and the remaining useful life is an influential parameter for assessing the operational status of equipment. Therefore, we can utilize RUL to assess the health of equipment and provide a reliable basis for predictive maintenance.

Data Availability

All data included in this study are available from the corresponding author upon request.

Conflicts of Interest

The authors declare no conflicts of interest.

Acknowledgments

This paper was supported by the Science and Technology Project of the State Grid Corporation Limited (SGJSCZ00KJJS2100747).

References

- [1] J. N. C. Gonçalves, M. S. Carvalho, and P. Cortez, “Operations research models and methods for safety stock determination: a review,” *Operations Research Perspectives*, vol. 7, Article ID 100164, 2020.
- [2] B. Lei, R. Zhao, W. Wang, and H. Mou, “A research review on inventory demand forecasting methods,” *Statistics & Decisions*, vol. 37, no. 3, pp. 58–62, 2021.
- [3] A. A. Syntetos, J. E. Boylan, and S. M. Disney, “Forecasting for inventory planning: a 50-year review,” *Journal of the Operational Research Society*, vol. 60, no. 1, pp. 149–160, 2009.
- [4] S. Zhang, K. Huang, and Y. Yuan, “Spare parts inventory management: a literature review,” *Sustainability*, vol. 13, no. 5, p. 2469, 2021.
- [5] B. González-Pérez, C. Núñez, J. L. Sánchez, G. Valverde, and J. M. Velasco, “Expert system to model and forecast time series of epidemiological counts with applications to COVID-19,” *Mathematics*, vol. 9, no. 13, p. 1485, 2021.
- [6] K. Srinivasan, L. Garg, B.-Y. Chen et al., “Expert system for stable power generation prediction in microbial fuel cell,” *Intelligent Automation & Soft Computing*, vol. 29, no. 3, pp. 17–30, 2021.
- [7] N. Ghadami, M. Gheibi, Z. Kian et al., “Implementation of solar energy in smart cities using an integration of artificial neural network, photovoltaic system and classical delphi methods,” *Sustainable Cities and Society*, vol. 74, Article ID 103149, 2021.
- [8] Y. Lu, Y. Teng, and H. Wang, “Load prediction in power system with grey theory and its diagnosis of stabilization,” *Electric Power Components and Systems*, vol. 47, no. 6-7, pp. 619–628, 2019.
- [9] N. Xu, S. Ding, and Y. Gong, “Advances in grey GM (1, 1) forecasting model and its extension,” *Mathematics in Practice and Theory*, vol. 51, no. 13, pp. 52–59, 2021.

- [10] X. Huang, H. Wang, W. Luo, S. Xue, F. Hayat, and Z. Gao, "Prediction of loquat soluble solids and titratable acid content using fruit mineral elements by artificial neural network and multiple linear regression," *Scientia Horticulturae*, vol. 278, Article ID 109873, 2021.
- [11] S. W. Fleming and A. G. Goodbody, "A machine learning metasystem for robust probabilistic nonlinear regression-based forecasting of seasonal water availability in the us west," *IEEE Access*, vol. 7, pp. 119943–119964, 2019.
- [12] L. Alhmod and Q. Nawafleh, "Short-term load forecasting for Jordan power system based on narx-elman neural network and ARMA model," *IEEE Canadian Journal of Electrical and Computer Engineering*, vol. 44, no. 3, pp. 356–363, 2021.
- [13] P. M. Almeida-Junior and A. D. C. Nascimento, "ARMA process for speckled data," *Journal of Statistical Computation and Simulation*, vol. 91, no. 15, pp. 3125–3153, 2021.
- [14] Y. Zhang, H. Sun, and Y. Guo, "Wind power prediction based on pso-svr and grey combination model," *IEEE Access*, vol. 7, pp. 136254–136267, 2019.
- [15] Z. Wang, J. Zhang, and Y. Zhang, "Research on photovoltaic output power prediction method based on machine learning," *Computer Simulation*, vol. 37, no. 4, pp. 71–75, 2020.
- [16] A. Srivastava and S. K. Parida, "A robust fault detection and location prediction module using support vector machine and Gaussian process regression for AC m," *IEEE Transactions on Industry Applications*, vol. 58, no. 1, pp. 930–939, 2022.
- [17] Z. Yang, X. Peng, J. Lang, H. Wang, B. Wang, and C. Liu, "Short-term wind power prediction based on dynamic cluster division and blstm deep learning method," *High Voltage Engineering*, vol. 47, no. 4, pp. 1195–1203, 2021.
- [18] P. Jiang, Z. Liu, X. Niu, and L. Zhang, "A combined forecasting system based on statistical method, artificial neural networks, and deep learning methods for short-term wind speed forecasting," *Energy*, vol. 217, Article ID 119361, 2021.
- [19] N. Zhou, J. Liao, Q. Wang, C. Li, and J. Li, "Analysis and prospect of deep learning application in smart grid," *Automation of Electric Power Systems*, vol. 43, no. 4, pp. 180–197, 2019.
- [20] Z. L. Li, J. Xia, A. Liu, and P. Li, "States prediction for solar power and wind speed using BBA-SVM," *IET Renewable Power Generation*, vol. 13, no. 7, pp. 1115–1122, 2019.
- [21] R. Xing and X. Shi, "A BP-SVM combined model for intermittent spare parts demand prediction," in *Proceedings of the 2019 IEEE International Conference on Systems, Man and Cybernetics*, pp. 1085–1090, Bari, Italy, October 2019.
- [22] M. Du, J. Luo, S. Wang, and S. Liu, "Genetic algorithm combined with BP neural network in hospital drug inventory management system," *Neural Computing & Applications*, vol. 32, no. 7, pp. 1981–1994, 2020.
- [23] C. Han and Q. Wang, "Research on commercial logistics inventory forecasting system based on neural network," *Neural Computing & Applications*, vol. 33, no. 2, pp. 691–706, 2021.
- [24] Y. Zhang, R. Xiong, H. He, and M. G. Pecht, "Long short-term memory recurrent neural network for remaining useful life prediction of lithium-ion batteries," *IEEE Transactions on Vehicular Technology*, vol. 67, no. 7, pp. 5695–5705, 2018.
- [25] W. Song, J. Wu, J. Kang, and J. Zhang, "Research on maintenance spare parts requirement prediction based on LSTM recurrent neural network," *Open Physics*, vol. 19, no. 1, pp. 618–627, 2021.
- [26] X. Zhang, Z. Bai, X. Wang, J. Huang, Z. Lin, and J. Gan, "Joint optimal replacement and spare part provisioning for smart meter," *Operations Research and Management Science*, vol. 27, no. 10, pp. 70–75, 2018.
- [27] M. T. Hussain, D. N. B. Sulaiman, M. S. Hussain, and M. Jabir, "Optimal management strategies to solve issues of grid having electric vehicles (EV): a review," *Journal of Energy Storage*, vol. 33, Article ID 102114, 2021.
- [28] H. Ding, W. Wang, L. Wan, and J. Luo, "Research on Material Demand Prediction of Power Network Based on BP Neural Network," *Computer Technology and Development*, vol. 29, pp. 138–142, 2019.
- [29] G. A. Hamoud and C. Yiu, "Assessment of spare parts for system components using a Markov model," *IEEE Transactions on Power Systems*, vol. 35, no. 4, pp. 3114–3121, 2020.
- [30] K. Yang, Y. Wang, S. Fan, and A. Mosleh, "Multi-criteria spare parts classification using the deep convolutional neural network method," *Applied Sciences-Basel*, vol. 11, no. 5, 2021.
- [31] Z. Song, X. Jia, B. Guo, and Z. Chen, "Remaining useful life prediction of system based on Bayesian fusion and simulation," *Systems Engineering and Electronics*, vol. 43, no. 6, pp. 1706–1713, 2021.
- [32] H. Pei, C. Hu, X. Si, J. Zhang, Z. Pang, and P. Zhang, "Review of machine learning based remaining useful life prediction methods for equipment," *Journal of Mechanical Engineering*, vol. 55, no. 8, pp. 1–13, 2019.
- [33] Z. Zhou, *Machine Learning*, Tsinghua University Press, Beijing, 2016.
- [34] M. Mohri, A. Rostamizadeh, and A. Talwalkar, *Foundations of Machine Learning*, MIT Press, Boston, 2018.
- [35] W. Udo and Y. Muhammad, "Data-driven predictive maintenance of wind turbine based on SCADA data," *IEEE Access*, vol. 9, pp. 162370–162388, 2021.
- [36] J. R. Segubiense Fernandez and M. V. Dalistan Rada, "Proposed application of an iot-based predictive maintenance to improve o&m of university project by fm company: a six sigma approach," in *Proceedings of the 2021 the 5th International Conference on Robotics, Control and Automation*, pp. 107–113, Seoul Republic of Korea, March 2021.
- [37] H. Nordal and I. El-Thalji, "Modeling a predictive maintenance management architecture to meet industry 4.0 requirements: a case study," *Systems Engineering*, vol. 24, no. 1, pp. 34–50, 2021.

Research Article

A Recognition Method Based on Speech Feature Parameters-English Teaching Practice

Lili Zhu,¹ Xiuqing Yan ,¹ and Jing Wang²

¹School of Foreign Languages, Mudanjiang Medical University, Mudanjiang, Heilongjiang 157011, China

²School of Basic Medical Sciences, Mudanjiang Medical University, Mudanjiang, Heilongjiang 157011, China

Correspondence should be addressed to Xiuqing Yan; yanxiuqing@mdjmu.edu.cn

Received 22 February 2022; Revised 13 March 2022; Accepted 4 April 2022; Published 27 April 2022

Academic Editor: Wei Liu

Copyright © 2022 Lili Zhu et al. This is an open access article distributed under the Creative Commons Attribution License, which permits unrestricted use, distribution, and reproduction in any medium, provided the original work is properly cited.

In order to improve the effect of English teaching practice, this paper constructs an intelligent English phonetic teaching system combined with the method of phonetic feature parameter recognition. Moreover, this paper simulates the self-mixing interference signal containing noise by establishing a simulation, analyzes the size of the noise and its various possibilities, and selects the EEMD method as the English speech denoising algorithm. In addition, with the support of an intelligent denoising algorithm, this paper implements an English intelligent teaching system based on the recognition algorithm of English speech feature parameters. Finally, this paper evaluates the teaching effect of the intelligent English speech feature recognition algorithm proposed in this paper and the intelligent teaching system of this paper by means of simulation teaching. The research shows that the English teaching system based on the intelligent speech feature recognition algorithm proposed in this paper has a good effect.

1. Introduction

In English learning, language input and language output are closely related. Input is the premise and necessary preparation for output, and output is the ultimate goal of input and can also stimulate input. The two complement each other and jointly improve students' comprehensive language ability. Although the Internet provides a large number of online learning resources, the individual differences in English proficiency of college students are quite large. Moreover, students are not very motivated to actively obtain language input, and their ability to learn online resources independently is not good. Therefore, college students in the Internet age still have the problem of insufficient effective language input.

The teaching hours and teaching capacity of English classrooms in colleges and universities are limited. Public English courses are mostly taught in large classes. The number of students in each class ranges from fifty to sixty to hundreds of students. One class is 90 minutes, and the average output of each student is the language output. There are very few opportunities, and the students' language

output in the classroom is far less than the language input, relying on the online learning platform to realize real-time online and offline interaction between teachers and students, expand teaching space and time, increase students' language output opportunities on online platforms and offline classrooms, and help solve the dilemma of traditional English classrooms. The content and form requirements of language output are not random. It should form an organically linked whole with the content and form of language input. It is not only necessary for teachers to regulate the quantity and quality of language input. Make the content of language input materials meet the interests and needs of college students, and ensure that the difficulty level of language input materials is in line with students' learning ability and learning level. It is even more necessary for teachers to properly supervise the online and offline language input process of students in classrooms and online platforms, promote students' online and offline autonomous learning, and achieve effective language output.

Oral expression and written writings are the main forms of language output and the main way to test the validity of language input. When designing the teaching content of

speaking, audio-visual, reading, and writing, attention should be paid to the relevance of thematic cohesion between modules to ensure that, under the same learning theme, students can learn vocabulary and sentence patterns layer by layer and practice repeatedly to gradually improve [1]. Oral content is mainly arranged in the course, and under the guidance of teachers, students train their oral expression or speech ability. In the case of students with low English proficiency, we can set up oral homework after class and encourage students to assist each other offline [2]. In the writing module, short videos, microlectures, or courseware materials for preclass preview can be provided for students to learn by themselves. If students have a poor English foundation, they should not set too many preclass writing tasks that are too difficult. We can focus on the input of writing knowledge, strengthen the teacher's intensive teaching and guidance in the middle of the class, encourage students to write on the spot in the classroom, and complete effective language output [3].

In English teaching, listening teaching runs through the whole teaching process, and the application conditions of intelligent speech synthesis technology in English listening teaching are analyzed from two aspects of teaching activities and lesson types in the textbook.

This paper combines the method of speech feature parameter recognition to construct an intelligent English pronunciation teaching system and applies it in English teaching practice to improve the effect of modern English teaching.

2. Related Work

The artificial neural network essentially imitates the human neuron structure, sets some judgments between the input and output, whether it is 1 or 0, and outputs data after a series of judgments and processing. After being able to solve some simple linear problems, it falls into the stagnation of development, and the XOR problem is difficult to solve [4]. The study of backpropagation has arisen. Backpropagation helps the model to learn the weight parameters independently, which solves the training problem of artificial neural networks. With the continuous development of Internet technology, artificial neural networks accumulate more and more data, and the learning speed is getting faster and faster. It has become a research hotspot in the world [4].

The deep learning method is developed on the model of artificial neural network, and the learning speed is faster. Literature [5] designed an 8-layer convolutional neural network for speech recognition. The deep learning model has strong learning ability and good calculation results, and the training difficulty is also better than that of artificial neural network, but because it is an emerging technology, there is still less research at present, and continuous exploration and attempts are required.

Reference [6] divides the nonstationary signal into several signals with small time intervals by adding a fixed time window to the signal, and the signal can be regarded as stationary within a sufficiently narrow time window, and then the Fourier transform is performed to obtain the signal. The time-frequency correspondence of the Gabor transform

is proposed. On the basis of the Gabor transform, the signal is decomposed by using window functions of different sizes to obtain the time-frequency analysis method of the Short-Time Fourier Transform (STFT) [7]. STFT relies heavily on the selection of the size and shape of the time window, and the selection of the time window is unique, which also leads to the singularity of the resolution of the STFT, and the size of the window function cannot be adjusted according to the frequency transformation. Reference [8] proposed the Wigner-Ville Distribution (WVD), which performs Fourier transform on the signal by using the instantaneous auto-correlation function. It is also an effective method to deal with nonstationary signals because it does not use a window function. The signal is decomposed so that its time-frequency focus is high, but there are serious cross-interference terms. Reference [9] proposes a time-frequency analysis method of NLMS transform (Wavelet Transform, WT) by matching the NLMS basis function with the signal. The parent NLMS selected by the NLMS transform can be scaled and shifted, and the shape of the NLMS basis can be changed according to the frequency characteristics of the signal. Therefore, the time-frequency analysis results have a certain "zoom." The NLMS transform essentially considers the signal in the time window to be approximately stationary, and sometimes the local signal time-frequency resolution deteriorates, which limits the application of the NLMS transform in seismic signals [10]. Reference [11] proposed S transform (ST), whose time window can be adaptively adjusted with frequency, which improves the defect of fixed time-frequency resolution in STFT and better meets the time-varying characteristics of seismic signals, but the fixedness of the selected NLMS basis function leads to certain limitations in its application. Reference [12] proposed the generalized S transform (GST), the window function of the generalized S transform can be flexibly adjusted with the frequency transformation, and the time-frequency analysis results with high time-frequency focus can be obtained. At the same time, the seismic signal can be flexibly analyzed according to actual needs.

In literature [13], the Hilbert transform is proposed, which is an analysis method suitable for spectral decomposition of seismic signals, which well excavates the physical significance of seismic signals and obtains three-instantaneous parameter attributes with geological significance. Reference [14] proposed the Hilbert-Huang Transform (HHT) on the basis of the Hilbert transform, which combined the Empirical Mode Decomposition (EMD) method with the Hilbert transform. EMD decomposes the signal into several subsignals, that is, Intrinsic Mode Function (IMF), and performs Hilbert transform on each M component to obtain the instantaneous properties of each subsignal. EMD decomposition has the advantages of completeness and self-adaptation but also has the defects of mode aliasing, endpoint effect, and insufficient sieving conditions. Reference [15] applied high-order spline interpolation to EMD to improve its calculation accuracy. Reference [16] improves EMD and proposes Ensemble Empirical Mode Decomposition (EEMD), which adds white noise to the original signal, which effectively solves the problem of modal aliasing, but

also causes residual signal reconstruction and noise. Reference [17] proposed the Complete Ensemble Empirical Mode Decomposition (CEEMD), which is also a noise-assisted method. It aims to add white noise to the first segment of the decomposition, which greatly reduces the influence of noise. From the above examples, although the decomposition method of EMD has achieved certain results, the overall calculation process is complicated and difficult to handle because there is no mathematical theoretical basis in the process. Reference [18] proposes an adaptive and nonrecursive signal decomposition method, which can locate the signal homeopathic spectrum more accurately because the modes decomposed in this method have their own center frequencies, and the modes are different from the modes. It is very compact between states, which can effectively eliminate the modal aliasing phenomenon commonly found in EMD, CEEMD, and other methods.

3. Denoising and Recognition of Speech Waveform Features

Signal denoising is an important step in the whole system process, and it is a basis for the following work. Only by obtaining relatively pure self-mixing interference signals after denoising can the following theories and experiments ensure the rigor and reduce unnecessary errors.

EMD is a form of decomposing the entire signal data into multiple IMFs and then superimposing them on each other. By analyzing the IMF subsignals, respectively, a more meaningful frequency and power can be obtained. The whole is the screening process, which is to simplify the complexity. In the whole process, the signal is iterated countless times, which can eliminate its previous error and eliminate the waveform superposition. Compared with the former, it is more symmetrical, and it is also the significance of decomposing into multiple IMF subsignals.

EEMD is an Ensemble Empirical Mode Decomposition, and the EEMD algorithm is a noise-assisted data analysis algorithm proposed on the basis of the EMD algorithm, which makes up for the insufficiency of EMD. The processing method based on EEMD is to assist the analysis by adding noise. In the EMD method, the obtained IMF is the required condition, that is, the distribution of the extreme points of the signal. If the distribution of extreme points is not uniform, modal aliasing will occur.

The principle of the EEMD algorithm is similar to that of EMD, but different from EMD is that modal aliasing will occur in EEMD, which is also unique to EEMD. EEMD is based on EMD by adding white noise signals with different degrees of uniformity, and the white noise will be evenly distributed in each signal. According to the characteristics of zero-mean noise, each time the noise is removed, it is superimposed and finally averaged, which can cancel each other out. Simply put, the principle of EEMD is to add white noise on the basis of EMD and then remove it. The specific steps of the EEMD algorithm are as follows:

- (1) The algorithm introduces white Gaussian noise $\omega(t)$ with spectral mean value of 0 into the signal to be

decomposed $x(t)$ and normalizes it to obtain the signal $X(t)$, as shown in formula (1):

$$X(t) = x(t) + \omega(t). \quad (1)$$

- (2) The algorithm performs EMD operation on the signal $X(t)$ and decomposes it to obtain n IMF components $C_j(t)$ and 1 participating component $r_n(t)$, as shown in formula (2):

$$X(t) = \sum_{j=1}^n C_j(t) + r_n(t). \quad (2)$$

- (3) The algorithm repeats test steps 1 and 2 and continues to introduce white noise that satisfies the normal distribution into the signal to be processed. The total number of tests is N , which can be obtained as shown in formula (3):

$$X(t) = \sum_{j=1}^n C_{ij}(t) + r_{in}(t). \quad (3)$$

- (4) According to the characteristics of the zero-mean value made above, it can be canceled as nothing, and the influence of the added white noise on the signal can be removed. Finally, the IMF components $C_j(t)$ and $r(t)$ of each order are obtained by decomposition, as shown in formula (4):

$$\left\{ C_j(t) = \frac{1}{N} \sum_{i=1}^n C_{ij}(t) r(t) = \frac{1}{N} \sum_{i=1}^n r_{in}(t), \quad i, j = (1, 2, 3, \dots, n). \right. \quad (4)$$

- (5) The final reconstructed signal is shown in formula (5):

$$X(t) = \sum_{j=1}^n C_j(t) + r_m(t). \quad (5)$$

In the above formulas, $C_{ij}(t)$ is the j -th IMF component obtained by decomposing the i -th white noise, r is the time, N is the number of white noise sequences added, $X(t)$ is the original signal, $r_n(t)$ is the residual term after decomposition, and n is the number of times of decomposition. In formula (5), $C_j(t)$ and $r_m(t)$ are the IMF components of each order and the final residual components obtained after EEMD decomposition, respectively. For the convenience of understanding, the flowchart of EEMD decomposition is drawn as shown in Figure 1.

Signal denoising has always been a key area that people generally pay attention to. There are many denoising methods with different denoising effects and different degrees of simplicity. Therefore, how to choose a better method for denoising is very important, and denoising needs evaluation indicators to evaluate. Nowadays, the more practical evaluation indicators are signal-to-noise ratio, mean square error, and correlation coefficient. The following will use these three evaluation indicators to select and

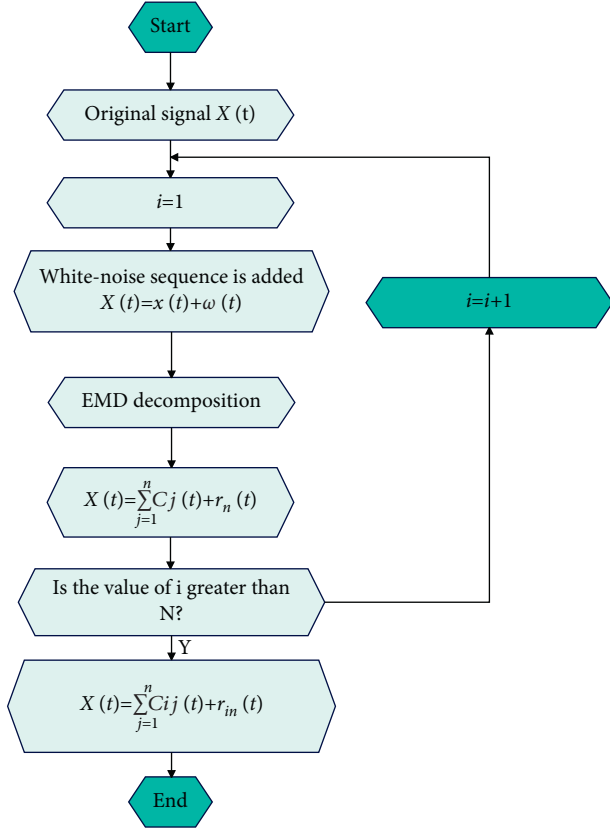


FIGURE 1: Flowchart of EEMD algorithm.

compare different denoising methods in order to select the optimal algorithm. First, the three evaluation indicators are introduced.

3.1. Signal-to-Noise Ratio (SNR). The signal-to-noise ratio can be expressed as the ratio of two energies in the mathematical sense, and the expression is

$$\text{SNR} = 10 \times \log_{10} \left(\frac{\text{Power}_{\text{signal}}}{\text{Power}_{\text{noise}}} \right). \quad (6)$$

In the formula, $\text{Power}_{\text{signal}} = (1/n) \sum_n [f(i) - \widehat{f(i)}]^2 = \text{RSME}^2$ is the frequency of the original signal; $\text{Power}_{\text{noise}} = (1/n) \sum_n [f(i) - \widehat{f(i)}]^2 = \text{RSME}^2$ is the power of the noise.

Among them, $\text{Power}_{\text{signal}} = (1/n) \sum_n f^2(n)$;

$$\text{Power}_{\text{signal}} = \frac{1}{n} \sum_n [f(i) - \widehat{f(i)}]^2 = \text{RSME}^2. \quad (7)$$

From the current research, the signal-to-noise ratio is often used as a measure of noise. It can not only reflect the size of the noise but also use it to evaluate the effect of denoising. In theory, the higher the signal-to-noise ratio, the better the denoising effect.

3.2. Root Mean Square Error (RMSE). The root mean square error usually refers to the ratio of the square of the deviation of the reconstructed signal and the original signal to the

number of measurements. It can well express the precision of the measurement process and is also called the standard error. Its expression is

$$\text{RSME} = \sqrt{\frac{\sum_n [f(i) - \widehat{f(i)}]^2}{n}}. \quad (8)$$

In the formula, $f(i)$ is the original signal, $\widehat{f(i)}$ is the decomposed reconstructed signal at a certain scale, and n is the total length of the signal.

From the current research, the mean square error is often used as a measure to remove noise. In theory, the smaller the mean square error, the better the denoising effect.

3.3. Correlation Coefficient. The correlation coefficient is a statistical indicator first designed by statistician Carl Pearson. It is a measure of the degree of linear correlation between variables. It is generally represented by the letter r , and its expression form is

$$r(X, Y) = \frac{\text{cov}(X, Y)}{\sqrt{\text{Var}[X] \text{Var}[Y]}}. \quad (9)$$

In the formula, $\text{cov}(X, Y)$ is the covariance of X and Y , $\text{Var}[X]$ is the variance of X , and $\text{Var}[Y]$ is the variance of Y .

The correlation coefficient is often used as a strong indicator of how well the noise is removed. In theory, the larger the correlation coefficient, the better the denoising effect, and the smaller the correlation coefficient, the worse the denoising effect.

We add varying degrees of noise to the pure, undisturbed simulated signal. Moreover, we add three different levels of interference with SNR of 20 dB, 25 dB, and 30 dB to the signals of $f_t = 20$ Hz, $f_s = 2000$ Hz, $a_1 = 7\pi$, $a_2 = 120\pi$, $n = 2000$, and $C = 3$, respectively, as shown in Figure 2.

It can be seen from Figure 2 that, with the increase of the added SNR, the noise becomes smaller and smaller. It can simulate different degrees of interference in real experiments, which is closer to reality and can conduct more comprehensive simulation and analysis so as to better determine the effective feasibility of the method. EEMD generates each IMF by decomposition, as shown in Figure 3.

The simulation of this paper is carried out on the operating platform of Matlab, and EEMD is used to denoise the self-mixing interference signal. In the simulation, we set $f_t = 20$ Hz, $f_s = 2000$ Hz, $a_1 = 7\pi$, $a_2 = 120\pi$, $n = 2000$, $C = 3$, and $\alpha = 3$ and add Gaussian white noise with a signal-to-noise ratio (NSR) of 20 dB.

It can be clearly seen from the first 8 IMFs in the figure that the high-frequency signals are mainly concentrated in the first 4 IMFs, and the signals decomposed later are relatively pure signals. What we mainly remove is the high-frequency signal. It can be seen from the first four IMF diagrams that the noise mainly comes from the transition point, and the interference generated by the transition point is the mainstream interference. The key point to filter out is the noise of the transition point so that the transition point can be pinpointed when processing the signal, so the first 4

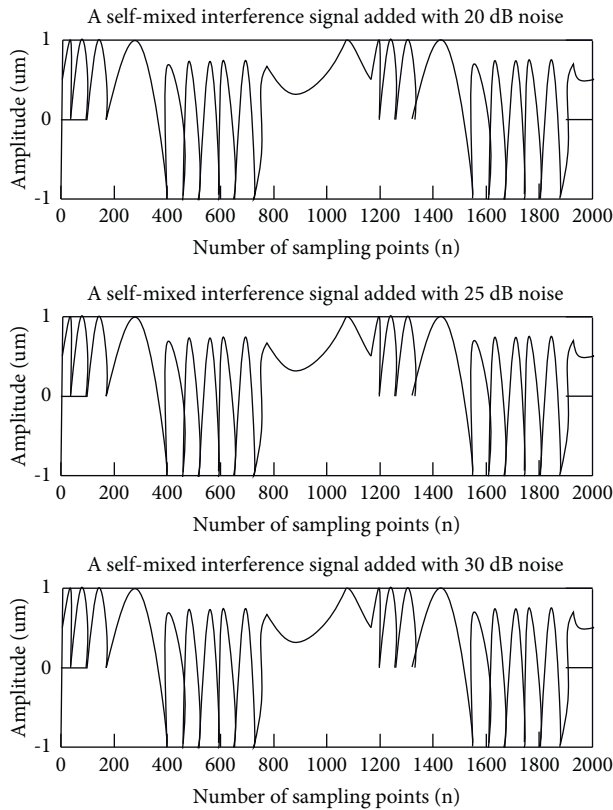


FIGURE 2: Self-mixing interference signal with different noise added.

signals are filtered out, and all the remaining IMF signals are synthesized, as shown in Figure 4.

From the above figures, it can be clearly seen that most of the noise can be basically removed, and residue is the signal that removes the residual high-frequency noise. It can be seen that the noise is negligible, a pure interference signal is obtained, and the transition point is easy to see, which lays the foundation for the subsequent phase unwrapping and displacement reconstruction.

In order to observe the simulation effect more intuitively, we comprehensively compare the influence of each signal-to-noise ratio on the signal. The simulated signal parameters are $f_t = 20$ Hz, $f_s = 2000$ Hz, $a_1 = 7\pi$, $a_2 = 120\pi$, $n = 2000$, $C = 3$, and $\alpha = 3$. Table 1 shows the data of each denoising evaluation index when $C = 3$.

4. English Teaching Based on Speech Feature Parameter Recognition

When setting up teaching units in English courses, the topics of chapters can be modularized, and each teaching unit adopts a combination mode of life themes, workplace, or post themes. In addition, the commonly used teaching content can also be selected according to the module combination of vocabulary, audio-visual, speaking, reading, writing, grammar, and translation (interpretation and translation). Each learning module is configured with teaching content according to the combination of before

class, one class and one after class, online learning + online tutoring, and offline teaching + offline activities. According to the teaching content, design various activities of online teaching and classroom teaching. At the same time, it is necessary to optimize the online learning mode and teacher-student interaction mode of the course, broaden the path of language task output, and design corresponding homework, tasks, and their supporting evaluation methods. The overall framework of the modular hybrid teaching model is shown in Figure 5.

There are four teaching layers in Figure 6, which are cognitive construction layer, embodied learning layer, situation interaction layer, and innovation generation layer. The cognitive construction layer and the embodied learning layer are the process layer of acquiring knowledge and skills, the situational interaction layer is the situational layer of problem solving, and the innovation generation layer is the practical layer of knowledge and ability. In the process layer, teachers are students' facilitators, supporters, and classroom observers. Students actively acquire tools and materials through "physical skills," actively seek help and support from human resources, and complete the construction of self-cognition through repeated iterations of action and thinking. At the situational level, teachers use examples familiar to students to introduce teaching, creating a learning atmosphere and motivation for students. Moreover, they set up problem situations to make students live in the teaching content, let students understand the truth that learning is life and life is learning, exert students' associative ability and innovative thinking, and stimulate students' strong desire to solve problems. In the practice layer, students use imagination and open thinking in brainstorming to conceive a variety of implementation plans and possibilities, open up new ideas for problem solving through hands-on practice, and creatively organize experience and knowledge to solve new problems. The implementation of teaching links, the growth and development of students, and the improvement of ability and literacy all run through the four teaching layers in the model. Each of the four teaching layers plays a different role. Among them, the cognitive construction layer is a collection of experience and creation, and experience is transferred and applied in innovation. The embodied learning layer gives full play to students' initiative and encourages students to use their hands and brains and experience learning through "doing." The situational interaction layer realizes the transfer of the situation, which can incite the emotion of the students, arouse the students' resonance, strengthen the interaction of the classroom, and make the classroom teaching start, proceed, and end under the sense of substitution of the situation. The innovation generation layer is the practice field for students to solve problems and an important activity layer for cultivating students' innovative thinking and creativity. Each layer is independent of each other but not isolated and disconnected, and multiple teaching activities may be carried out in one teaching layer. For example, in the cognitive construction layer, there will be learning activities such as experience reproduction, comprehension of new knowledge, and design and creation. At the same time, the same teaching

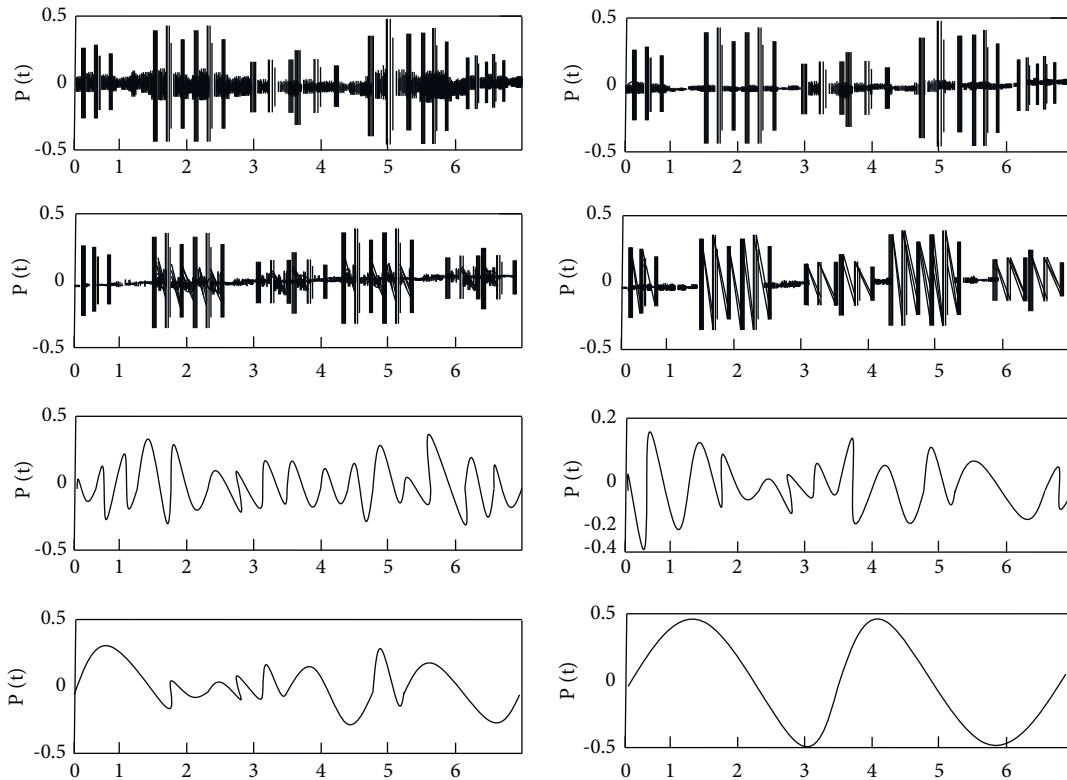


FIGURE 3: Decomposed different IMF diagrams.

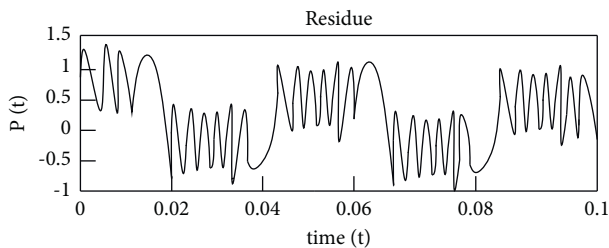


FIGURE 4: Self-mixing interference signal after filtering.

task will be completed in more than one teaching layer, such as students' inquiry activities occurring in the cognitive construction layer, the embodied learning layer, and the innovation generation layer. The four teaching layers are an important part of the migration teaching model, which echoes the top layer of the model, conforms to the theoretical concept of this study, supports the implementation of the three paths in the middle layer of the model, and is a teaching field that nurtures teaching, development, and ability literacy.

Speech recognition technology, broadly speaking, refers to semantic recognition and voiceprint recognition. In a narrow sense, it refers to the understanding and recognition of speech semantics, also known as Automatic Speech Recognition (ASR). As the most natural way of human-computer information interaction, the basic idea of speech recognition technology takes speech as the research object and converts the input speech signal into

corresponding text commands through the process of machine recognition and understanding so as to realize the control of the machine by speech. In the development of speech recognition technology, although different researchers have proposed many different solutions, the basic principles are the same. In the processing of speech signals, any speech recognition system can use Figure 7 to represent its general recognition principle. The most important modules of speech recognition system are speech feature extraction and speech pattern matching.

In the view of behaviorist learning theory, human learning is a process of stimulus-response-reinforcement. In the learning process, there is only stimulus-response, and the lack of reinforcement will greatly reduce the learning effect. However, if we blindly provide stimuli and ignore the learner's original knowledge level, learning needs, and interest in learning, it will be difficult for the stimulus to stimulate the learner's response; that is, it is difficult for learning to occur. On the other hand, because people's information processing methods are different, if only a single learning stimulus is provided and the differences in the learners' individual information processing methods are ignored, it will lead to difficulties for learners to process new knowledge using their original cognitive experience. The manifestation is that it is difficult to learn new knowledge. At the same time, in English pronunciation learning software, many learning systems lack an overall score for the learner's phonetic pronunciation, nor can they give timely and accurate feedback on the learner's pronunciation. Moreover, it does not provide corrective guidance for learners'

TABLE 1: The recognition effect of the English teaching system based on the intelligent speech feature recognition algorithm on spoken English features.

Num	Speech recognition	Num	Speech recognition	Num	Speech recognition
1	93.86	19	94.96	37	92.01
2	94.69	20	95.95	38	92.78
3	90.34	21	92.28	39	96.53
4	94.60	22	93.82	40	89.42
5	95.25	23	94.53	41	93.98
6	89.96	24	93.94	42	89.65
7	91.98	25	96.06	43	96.58
8	94.75	26	93.59	44	91.86
9	89.02	27	94.00	45	94.05
10	89.26	28	96.20	46	89.01
11	92.20	29	89.79	47	89.25
12	95.90	30	95.86	48	93.09
13	90.66	31	89.37	49	92.00
14	89.19	32	96.92	50	92.35
15	93.19	33	89.28	51	96.90
16	90.36	34	91.91	52	94.39
17	91.00	35	93.09	53	95.87
18	96.60	36	96.61	54	92.33

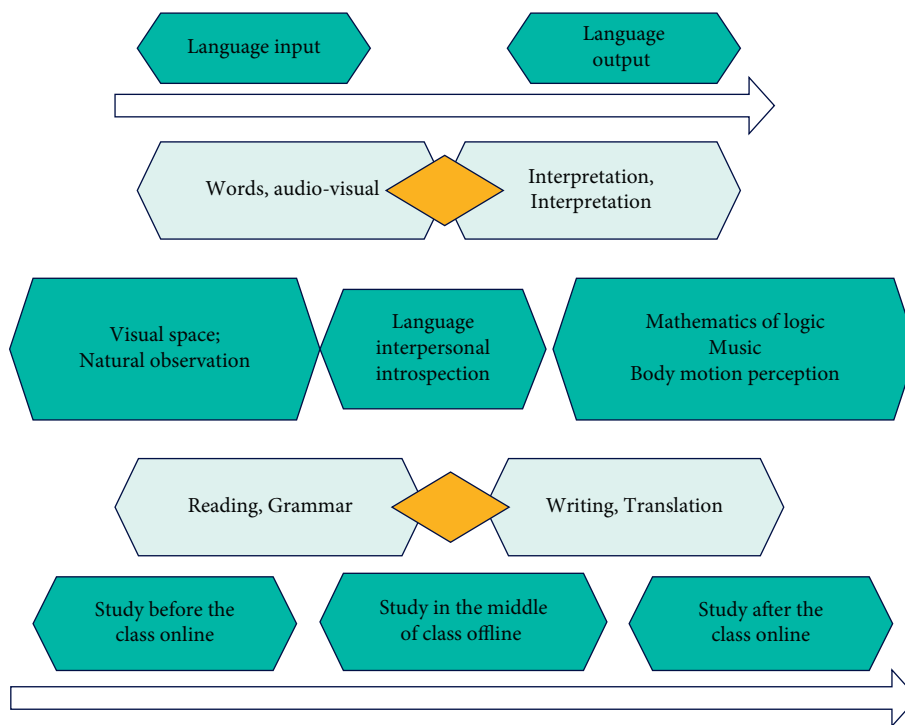


FIGURE 5: Framework diagram of the mixed mode of “language + multiple intelligences.”

mispronunciation, and it is difficult for learners to find and correct their own pronunciation errors due to their limited level.

The integration of information technology and English courses is not simply to present the learning content on the computer, but the following points need to be considered. One is to use information technology and multimedia technology to systematically integrate the knowledge of English phonetic transcription. The second is to present

knowledge to best promote learners to absorb. The third is to strengthen and consolidate the learning of the learners. In view of the problems existing in the above-mentioned English phonetic pronunciation learning software, behaviorist learning theory, multimedia cognitivist learning theory, and related theories of information technology and curriculum integration should be taken into account when designing the platform. In the implementation of the system, by constructing an English phonetic transcription learning

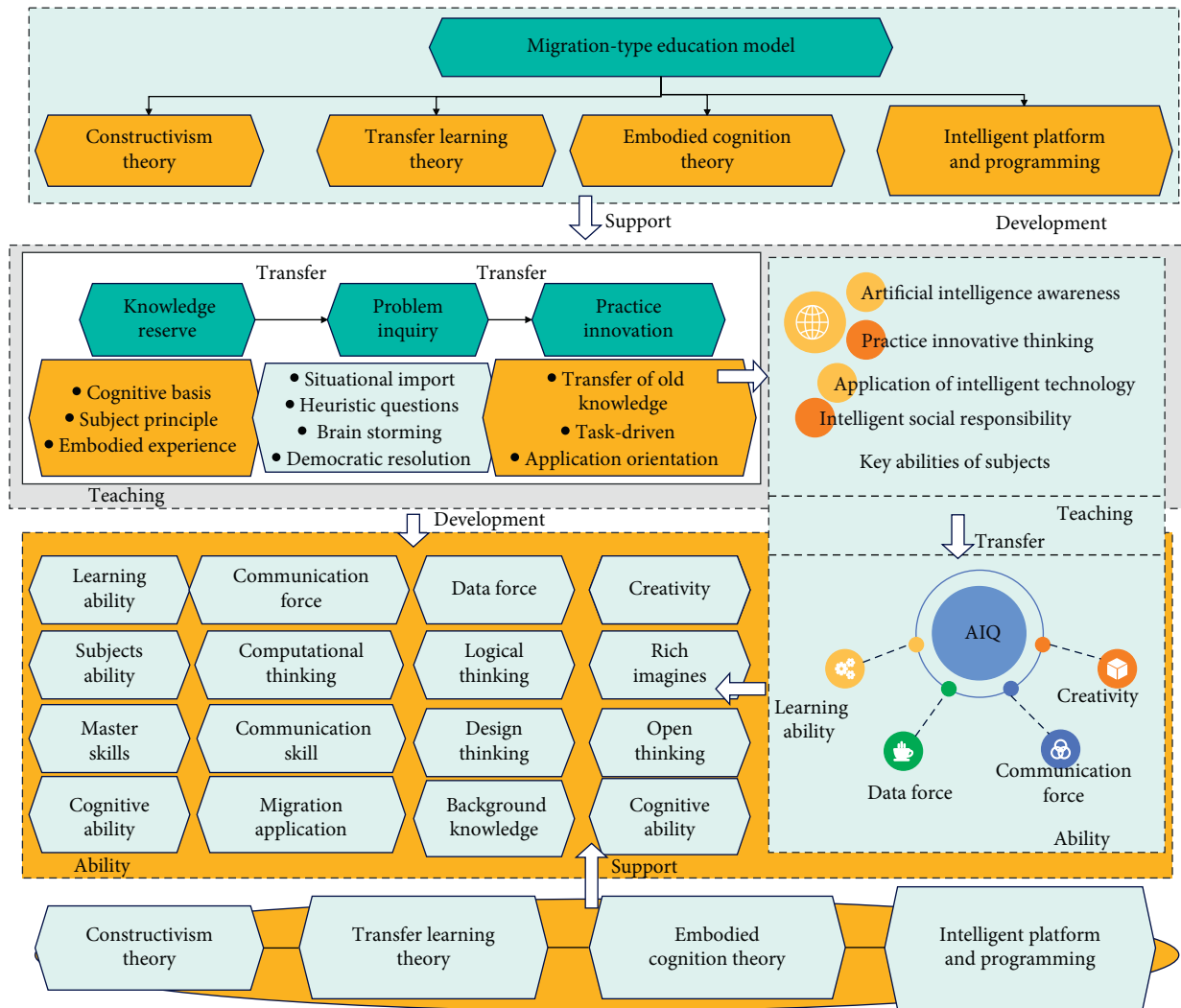


FIGURE 6: English teaching mode diagram.

environment, learners can choose the learning content independently. The system presents learners with various forms of learning stimuli, which facilitates learners to link old and new knowledge through various information processing channels and form their own knowledge structure. At the same time, the system uses template matching technology in speech recognition to compare the difference between the tester’s pronunciation and the standard pronunciation and strengthens the learning results by testing the learner’s pronunciation and giving pronunciation feedback. This process of stimulation, response, connection, and

reinforcement is more in line with the law of human learning, so it can better promote the occurrence of learning. As mentioned in the review, the English speech learning assistance platform studied in this paper is shown in Figure 8.

On the basis of the above research, the intelligent English speech feature recognition algorithm proposed in this paper and the intelligent teaching system of this paper are evaluated by means of simulation teaching, and the results shown in Table 1 and Table 2 are obtained.

From the above research, it can be seen that the English teaching system based on the intelligent speech feature

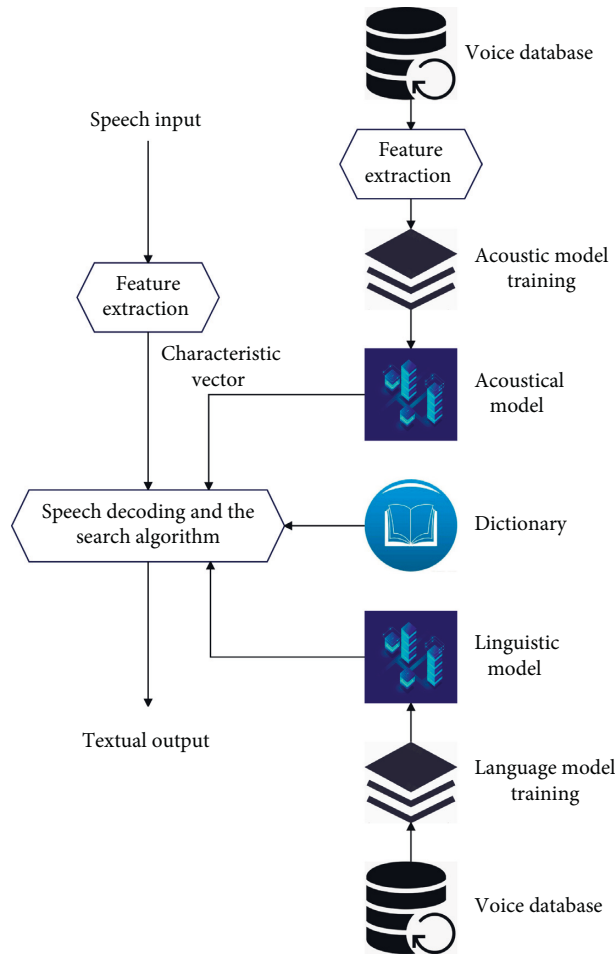


FIGURE 7: Principle block diagram of English speech recognition system.

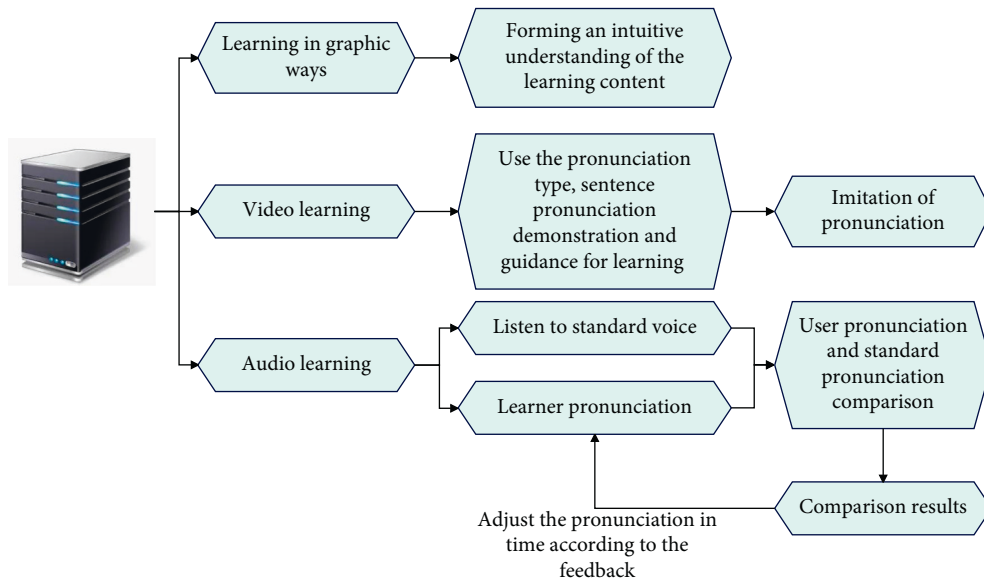


FIGURE 8: English speech learning assistance platform.

TABLE 2: Evaluation of the English teaching effect of the English teaching system based on the intelligent speech feature recognition algorithm.

Num	Teaching English	Num	Teaching English	Num	Teaching English
1	82.71	19	83.38	37	85.31
2	92.44	20	82.40	38	83.74
3	89.75	21	85.83	39	82.54
4	89.95	22	92.05	40	82.41
5	84.45	23	84.62	41	88.85
6	85.28	24	85.80	42	89.95
7	86.39	25	87.98	43	92.67
8	90.15	26	86.55	44	90.04
9	83.58	27	92.38	45	90.46
10	92.84	28	91.76	46	88.36
11	83.25	29	87.44	47	84.36
12	90.57	30	90.97	48	92.56
13	89.49	31	91.81	49	87.40
14	87.02	32	84.75	50	88.97
15	85.83	33	91.57	51	83.14
16	87.12	34	83.21	52	90.89
17	90.70	35	92.35	53	85.25
18	84.24	36	87.58	54	85.01

recognition algorithm proposed in this paper can not only effectively improve the effect of spoken English feature recognition but also effectively improve the effect of English teaching.

5. Conclusion

The application of intelligent voice technology in education and teaching is never to replace the role of teachers but to help teachers carry out teaching, make up for teachers' deficiencies, improve teaching efficiency and effect, and achieve the effect of "reducing burden and increasing efficiency." The application conditions of technology in education and teaching also need to be analyzed. Under the application conditions, teachers can play their original role, and technology can also reflect the functional advantages of technology itself. In English listening teaching links or teaching scenarios, intelligent speech technology can give full play to its technical advantages and better assist teachers in English listening teaching, so that the role of teachers and the functions of intelligent speech synthesis technology can complement each other. In this paper, an intelligent English pronunciation teaching system is constructed by combining the method of speech feature parameter recognition. The experimental study shows that the English teaching system based on the intelligent speech feature recognition algorithm proposed in this paper can not only effectively improve the recognition effect of spoken English but also effectively improve the effect of English teaching.

Data Availability

The labeled dataset used to support the findings of this study is available from the corresponding author upon request.

Conflicts of Interest

The authors declare that they have no conflicts of interest.

Acknowledgments

The study was supported by the "Teaching Reform Project of Higher Education" in Heilongjiang Province, China, and Construction of English Teaching Model Based on Blue-Ink Cloud Class + BOPPPS in Application-Oriented Universities (Grant no. SJGY20190707).

References

- [1] A. S. Fatimah, S. Santiana, and Y. Saputra, "Digital comic: an innovation of using toondoo as media technology for teaching English short story," *English Review: Journal of English Education*, vol. 7, no. 2, pp. 101–108, 2019.
- [2] B. Ayçiçek and T. Yanpar Yelken, "The effect of flipped classroom model on students' classroom engagement in teaching English," *International Journal of Instruction*, vol. 11, no. 2, pp. 385–398, 2018.
- [3] N. Guzachchova, "Zoom technology as an effective tool for distance learning in teaching English to medical students," *Bulletin of Science and Practice*, vol. 6, no. 5, pp. 457–460, 2020.
- [4] M. S. Hadi, "The use of song in teaching English for junior high school student," *English Language in Focus (ELIF)*, vol. 1, no. 2, pp. 107–112, 2019.
- [5] A. Mahboob, "Beyond global Englishes: teaching English as a dynamic language," *RELC Journal*, vol. 49, no. 1, pp. 36–57, 2018.
- [6] H. Sundari, "Classroom interaction in teaching English as foreign language at lower secondary schools in Indonesia," *Advances in Language and Literary Studies*, vol. 8, no. 6, pp. 147–154, 2017.
- [7] A. Gupta, "Principles and practices of teaching English language learners," *International Education Studies*, vol. 12, no. 7, pp. 49–57, 2019.
- [8] B. S. M. Abdelshaheed, "Using flipped learning model in teaching English language among female English majors in majmaah university," *English Language Teaching*, vol. 10, no. 11, pp. 96–110, 2017.

- [9] T. Ara Ashraf, "Teaching English as a foreign language in Saudi Arabia: struggles and strategies," *International Journal of English Language Education*, vol. 6, no. 1, pp. 133–154, 2018.
- [10] O. Tarnopolsky, "Principled pragmatism, or well-grounded eclecticism: a new paradigm in teaching English as a foreign language at Ukrainian tertiary schools?" *Advanced Education*, vol. 5, no. 10, pp. 5–11, 2018.
- [11] N. I. Sayakhan and D. H. Bradley, "A nursery rhymes as a vehicle for teaching English as a foreign language," *Journal of University of Raparin*, vol. 6, no. 1, pp. 44–55, 2019.
- [12] D. A. W. Nurhayati, "Students' perspective on innovative teaching model using e in teaching English phonology: a virtual class development," *Dinamika Ilmu*, vol. 19, no. 1, pp. 13–35, 2019.
- [13] S. Zou, "Designing and practice of a college English teaching platform based on artificial intelligence," *Journal of Computational and Theoretical Nanoscience*, vol. 14, no. 1, pp. 104–108, 2017.
- [14] F. Kong, "Application of artificial intelligence in modern art teaching," *International Journal of Emerging Technologies in Learning (iJET)*, vol. 15, no. 13, pp. 238–251, 2020.
- [15] M. Pantic, R. Zwitserloot, and R. J. Grootjans, "Teaching introductory artificial intelligence using a simple agent framework," *IEEE Transactions on Education*, vol. 48, no. 3, pp. 382–390, 2005.
- [16] C. Yang, S. Huan, and Y. Yang, "A practical teaching mode for colleges supported by artificial intelligence," *International Journal of Emerging Technologies in Learning (iJET)*, vol. 15, no. 17, pp. 195–206, 2020.
- [17] K. Kim and Y. Park, "A development and application of the teaching and learning model of artificial intelligence education for elementary students," *Journal of The Korean Association of Information Education*, vol. 21, no. 1, pp. 139–149, 2017.
- [18] O. Zawacki-Richter, V. I. Marín, M. Bond, and F. Gouverneur, "Systematic review of research on artificial intelligence applications in higher education—where are the educators?" *International Journal of Educational Technology in Higher Education*, vol. 16, no. 1, pp. 1–27, 2019.

Research Article

Ray Tracing Acceleration Algorithm Based on FaceMap

Jian Wang, Hui Xiao, and Hongbin Wang 

Faculty of Information Engineering and Automation, Kunming University of Science and Technology, Kunming 650504, China

Correspondence should be addressed to Hongbin Wang; whbin2013@kust.edu.cn

Received 7 January 2022; Revised 28 February 2022; Accepted 7 March 2022; Published 25 April 2022

Academic Editor: Wei Liu

Copyright © 2022 Jian Wang et al. This is an open access article distributed under the Creative Commons Attribution License, which permits unrestricted use, distribution, and reproduction in any medium, provided the original work is properly cited.

Raster method and ray tracing are two important algorithms in computer graphics. The former, raster method, marked by high speed and efficiency, has the disadvantage of an unrealistic rendering effect. By contrast, ray tracing requires considerable computing resources and time despite its advantages of high fidelity and simple structure, thus only suitable for offline rendering. Given such limitations, a ray-tracing acceleration algorithm that combines the raster method and ray tracing is proposed in this study based on FaceMap, a two-dimensional data structure that stores surface distribution under point light or the view of a camera. Firstly, all triangular surfaces of the 3D model are rasterized by linear surface projection to form the surface distribution of a spherical panorama. Secondly, the structure of FaceMap is adopted to store the distribution information of all the surfaces in the scene. Thirdly, the data on the intersecting surfaces in this direction are collected by projecting the ray onto FaceMap in the ray-tracing process, thus reducing the intersection and propagation operations and improving the efficiency. Four object models including chessboard, grass patch, bust, and typewriter are selected for comparative rendering experiments. Our proposed method is used to compare with Rhino and V-Ray rendering software, respectively. The results show that our proposed method obtained better rendering effects within greatly reduced rendering time (© 2018 Optical Society of America).

1. Introduction

Raster method and ray tracing are two branches of computer graphics. Raster method has the advantages of fast speed and high efficiency in scene rendering, but the disadvantage is that the rendering degree is far less than the reality; ray tracing has the advantages of high rendering reality and simple structure, and the disadvantage is that it consumes too much calculation, so it can only be used in offline rendering.

Traditional ray-tracing algorithms adopt the Monte Carlo illumination model [1], which simulates the propagation of light in the real physical environment. After the conduct of a series of operations such as specular reflection, perspective refraction, and diffuse reflection, an image is finally generated. However, it is difficult to determine which surfaces the light may intersect within the propagation process due to the relatively complex rendered scenes. Therefore, the main calculation in the ray-tracing process lies in the intersection operation of the ray and surface.

To narrow the range of surfaces requiring intersection operation, commonly used techniques are ray-tracing acceleration algorithms including the bounding box method, three-dimensional DDA (3D-DDA) algorithm, and octree division method:

- (i) Bounding box method: the basic idea of the bounding box is to use geometric objects of regular shapes to wrap each model in the scene, respectively. The adjacent bounding boxes are wrapped in larger boxes to form a tree structure [2]. The intersection operation starts from the root node of the tree and then to the subnodes. It will involve the sub-bounding boxes or the surfaces of inner models of the bounding box if there is an intersection point. Otherwise, the ray will not intersect with any surface of the inner models in the bounding box.
- (ii) 3D-DDA algorithm: the low efficiency of ray intersection operation is mainly due to the uncertainty about the surfaces that may intersect and that are closest to the ray source. DDA algorithm evenly

divides the space into three-dimensional grids, within which the corresponding surface is stored [3]. In the process of intersection operation, the ray starts from the grid where the ray source is located and successively intersects with the encountered surfaces inside other grids. If an intersection point appears, it will be the closest to the ray source.

- (iii) Octree division method: similar to the 3D-DDA algorithm, the octree division method divides the space into nonuniform grids [4]. A cube that can wrap the whole scene is divided into eight blocks, and the number of surfaces in each block is calculated. The block will be further divided into eight sub-blocks if the number is larger than the threshold; otherwise, the division stops. The above steps are repeated until the surface number of every sub-block is smaller than the threshold.

The above three methods are all based on space dividing, which means dividing the space capable of wrapping the whole scene into different grids that contain some surfaces inside. When the ray propagates between different grids, the intersection operation is conducted between the ray and the surface within a grid.

Although these methods are efficient in scene rendering, they require additional calculation of ray propagation between grids and fail to determine whether there is an intersection between surfaces in a direction before the ray leaves the scene. Such drawbacks are particularly serious when there are numerous light sources in the scene [5]. The reason is that for each intersection on a surface, a shadow test line is required to be sent out to the light source for the purpose of examining whether it would be obscured by other surfaces.

It can be seen from the above analysis that both the raster method and ray tracing have their own advantages and disadvantages. A natural idea is to combine the advantages of the two algorithms to solve the aforementioned problems. As a remedy, we propose FaceMap, a two-dimensional data structure, to store surface distribution corresponding to the point light source or camera. It is by virtue of FaceMap that the surfaces intersected in a certain direction can be rapidly determined, and the efficiency of intersection operation can thus be improved.

The rest of this paper is organized as follows: Section 2 and Section 3 introduce the raster method and the ray-tracing method, respectively. In Section 4, the ray-tracing acceleration algorithm based on FaceMap is illustrated in detail. Experimental results and analysis are presented in Section 5. Finally, conclusions are drawn in Section 6.

2. Raster Method

Raster rendering has the advantages of speed and efficiency. Because of its special rendering pipeline flow, raster rendering can be well integrated into the hardware (such as GPU). Besides, customized programming based on particular needs is made possible to obtain the desired picture effect. The pipeline flow mainly consists of vertex conversion, primitive assembly, rasterization, and interpolation coloring [6, 7].

2.1. Vertex Conversion. Each 3D rendering engine involves a space camera, whose projection result of a 3D scene is an image seen by a user. The camera itself is in the 3D space, capable of basic movement, rotation, and other different view transformations.

The basic unit of the 3D model is a triangular surface with three vertices where the 3D coordinate data are stored in accordance with the world coordinate system. The data do not change when the model remains static. However, if the model coordinates cannot be calculated according to the world coordinate system due to changing the camera's angle of view, they should be converted to the camera's space. This is called vertex conversion. When the coordinate data of the model's vertices are transformed into the visual field of the camera, the basic projection transformation can be conducted. There are two kinds of projection transformation, namely perspective projection and orthogonal projection. The former is similar to what is observed by human eyes, that is, an object is big when near and small when far, complying with the perspective principle. By comparison, the latter is similar to the scene when all models are compressed to a plane while retaining the original sizes, which is not in line with the perspective principle. Therefore, raster rendering mainly focuses on perspective projection.

2.2. Perspective Projection. The camera used in the raster method usually contains four parameters, namely viewing angle θ , near clipping plane distance n , far clipping plane distance f , and screen aspect ratio α , with the near clipping plane, serving as the projection plane, as shown in Figure 1.

For points that have been converted to the camera space, their 3D coordinates can be transformed accordingly by the projection transformation matrix M . At this point, the coordinates are not clipped in the screen space; the coordinates on the near projection plane can then be obtained. In addition, the transformation matrix can be regarded as the process of the space points being transformed into the near projection plane. Accordingly, the reverse process is to transform the points on the projection plane into the vectors in the camera space and thus is often used to solve the coordinates and rotation angles of camera. The transformation matrix M is expressed as follows:

$$M = \begin{bmatrix} \frac{\cot \theta}{\alpha} & 0 & 0 & 0 \\ 0 & \cot \theta & 0 & 0 \\ 0 & 0 & \frac{f}{f-n} & 1 \\ 0 & 0 & \frac{fn}{n-f} & 0 \end{bmatrix}. \quad (1)$$

Then, the points after perspective projection can be transferred to the screen coordinate system through the screen matrix S , and the matrix S is shown as follows:

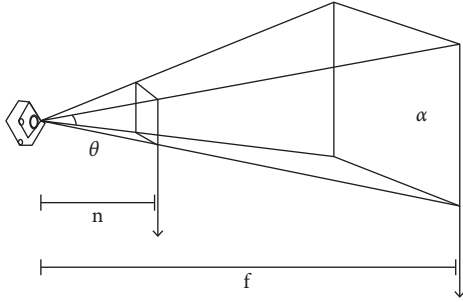


FIGURE 1: Perspective camera.

$$S = \begin{bmatrix} \frac{\text{width}}{2} & 0 & 0 & 0 \\ 0 & -\frac{\text{height}}{2} & 0 & 0 \\ 0 & 0 & 1 & 0 \\ \frac{\text{width}}{2} & \frac{\text{height}}{2} & 0 & 1 \end{bmatrix}. \quad (2)$$

2.3. Triangular Rasterization. The smallest polygon in a two-dimensional plane is a triangle, and any polygon can be viewed as a combination of several triangles. Hence, triangles are often used as basic structure for 3D models. For a triangle that has been transferred to screen coordinate system, its three edges and inside pixels need to be filled with progressive scanning being the frequently adopted method [8], as shown in Figure 2.

The pseudo-code of the process is described in Algorithm 1.

The highest and lowest points of a triangle should not exceed the scope of the display screen and, if necessary, should be reduced to 0~(height - 1). Specifically, a triangle edge intersects with a certain line y if and only if one vertex of the edge is below y and the other vertex is not. Assume the two vertices of the edge are (x_1, y_1) and (x_2, y_2) , respectively; then the equation that solves the x -coordinates of the vertices is expressed as follows:

$$x = x_2 + (x_2 - x_1) \frac{y - y_1}{y_2 - y_1}. \quad (3)$$

The two intersection points of the triangle edge and the line y can be obtained by the above method. The rasterization of the line is completed after filling the pixels between the two points. However, one drawback of triangle rasterization lies in the serious jagged edges of a triangle. A normal solution to such problem is to increase the sampling points in the edge pixels, as shown in Figure 3.

The edge pixel is divided into several pixels for rasterization, and then, the average value of the pixel color is calculated, serving as the color of the edge pixel. This approach can greatly alleviate the jag effect and meanwhile achieves low consumption since only edges require

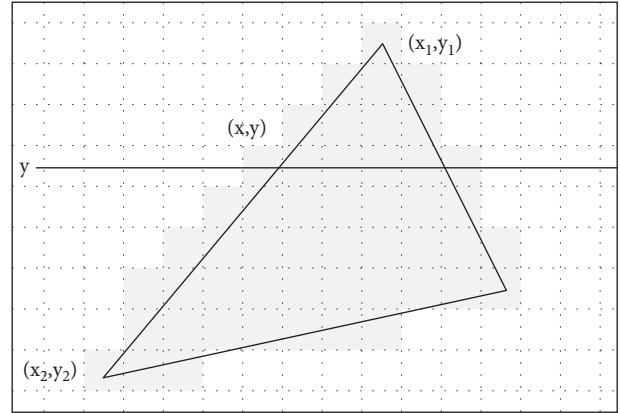


FIGURE 2: Triangle rasterization.

upsampling. Therefore, it can also be applied to mobile devices such as cell phones [9].

Given the triangular surfaces of the model, its fineness can be regarded as equivalent to the number of triangles. However, a detail-emphasized model will significantly increase rendering time due to its large number of triangular surfaces. Therefore, existing improved algorithms use a small number of points to simulate a high-accuracy model. After fitting surfaces by voxel rendering (as shown in Figure 4), the numbers of vertices and triangular surfaces are reduced, and the rendering of the model is accelerated [10].

3. Ray Tracing

Scene rendering of ray tracing mainly involves the process of sampling, reconstructing, synthesizing, and resampling the global illumination, for the virtual 3D space that can be viewed as the combination of objects and light sources. Unlike in the raster method, objects in ray tracing are not directly observed by cameras. Instead, certain light distribution forms in space after the light source and objects are illuminated by light, and what the camera captures is the reflected light as a result of the intersection of the ray and surface [11].

Ray tracing mainly computes the intersection of the point-based ray and the triangular surface in the space and then obtains u and v of the intersection point relative to the triangle vertices.

Assume the ray starts from point O , and the unit direction vector is D which intersects with the triangle (V_0, V_1, V_2) at point P . Then, P can be viewed as translated from V_0 corresponding to V_1 and V_2 , the distance between P and O being t , as displayed in Figure 5.

The equation obtained is expressed as follows [12]:

$$O + Dt = (1 - u - v)V_0 + uV_1 + vV_2 \quad \begin{cases} u \geq 0 \\ v \geq 0 \\ u + v \leq 1 \end{cases}. \quad (4)$$

By rearranging the above equation and extracting t , u , and v as unknowns, the linear equations can be described as follows:

Input: A triangle vertex information

- (1) Find the highest and lowest points of the triangle;
- (2) Traverse from the highest point to the lowest point:
 - (a) Calculate the two intersection points of the current line and the triangle edge;
 - (b) Fill from the left node to the right node;

Output: Results after transfer

ALGORITHM 1: A triangle transfer to the screen coordinate system.

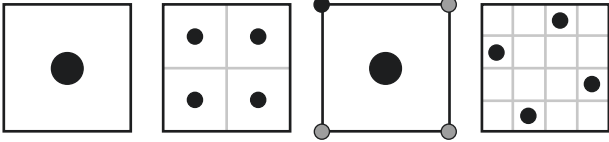


FIGURE 3: Edge pixel sampling.

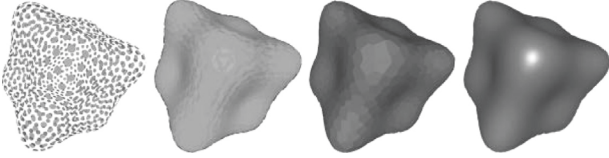


FIGURE 4: Surface simulation by the sparse point set.

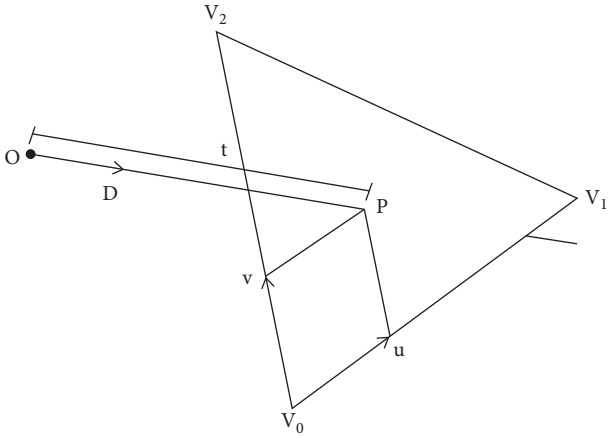


FIGURE 5: Intersection of the ray and surface.

$$[-D(V_1 - V_0)(V_2 - V_0)] \begin{bmatrix} t \\ u \\ v \end{bmatrix} = o - V_0, \quad (5)$$

$$[-D \ E_1 \ E_2] \begin{bmatrix} t \\ u \\ v \end{bmatrix} = T. \quad (6)$$

Assume $E_1 = V_1 - V_0$, $E_2 = V_2 - V_0$, and $T = O - V_0$, and then, equation (5) can be rewritten as equation (6).

Next, according to Cramer's rule and the mixed product formula, t , u , and v are solved, as expressed as follows:

$$\begin{bmatrix} t \\ u \\ v \end{bmatrix} = \frac{1}{|D \times E_2 \cdot E_1|} \begin{bmatrix} T \times E_1 \cdot E_2 \\ D \times E_2 \cdot T \\ T \times E_1 \cdot D \end{bmatrix}. \quad (7)$$

To avoid repeated operations, assume $R = D \times E_2$ and $Q = T \times E_1$, and thus, equation (7) is simplified as follows:

$$\begin{bmatrix} t \\ u \\ v \end{bmatrix} = \frac{1}{|R \cdot E_1|} \begin{bmatrix} Q \cdot E_2 \\ R \cdot T \\ Q \cdot D \end{bmatrix}. \quad (8)$$

4. Ray-Tracing Acceleration Algorithm Based on FaceMap

The raster method is characterized by high speed and efficiency but has the disadvantage of an unsatisfactory rendering effect. In contrast, the ray-tracing method features in simple mechanism and high fidelity, but it only applies to offline rendering due to its high computational complexity and time complexity. Therefore, the idea of combining the advantages of the two algorithms becomes very natural and intuitive.

4.1. Basic Idea of FaceMap. Conventional raster projection is a kind of linear plane projection, with linear variations of the distance between points relative to the origin. By contrast, the projection of FaceMap belongs to linear surface projection, with linear variations of angles between points relative to the origin. FaceMap consists of four parts as follows: linear surface projection, curve approximation by bisection method, filling of the curved triangle, and reverse solution of light vector.

Figure 6 clearly shows that in terms of ordinary plane projection, the angle between point's narrows with the decrease in the distance between points and the screen edge. Consequently, serious deformation can occur at the screen edge, and the larger the field angle is, the more serious the deformation becomes.

A typewriter model was extracted via Adobe After Effect 2015 (AE for short), and the conversions of the camera's field angle are shown in Figure 7. To go into detail, the upper left field angle was 50° , basically without deformation; the upper

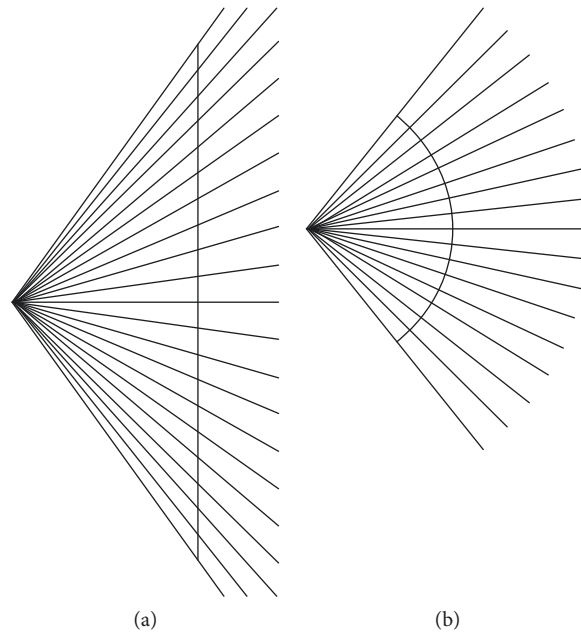


FIGURE 6: (a) Plane projection. (b) Surface projection.

right field angle was 90° , with tensile deformation near the bottom corners; the bottom left field angle was 120° , with particularly evident tensile deformation; the bottom right field angle was 170° (because AE is unable to set the field angle as 180° , or in other words, the field angle in plane projection cannot reach 180°), with the whole typewriter model being stretched to a strip.

In comparison, the linear surface projection based on FaceMap is similar to real optical lens in everyday life, with a complete 360-degree visual field. It can generate various image effects including wide-angle, fisheye, and ultra-wide-angle. As shown in Figure 8, the upper left field angle was 50° , basically without deformation (similar to that in plane projection); the upper right field angle was 90° , with an overall bent deformation; the field angles of the lower left and the lower right were 120° and 170° , respectively, both with the effect closer to that obtained by fisheye lens.

FaceMap is a two-dimensional data structure that stores the spherical panorama distribution of the scene. Therefore, after mapping the object in the scene to FaceMap, a spherical panorama can be generated. Figure 9 presents the FaceMap schematic diagram of the interior of a typewriter model with spatial origin $(0, 0, 0)$, the field angle being 360° . Each point in the figure stored the surface data in that direction. A darker color of points indicated a larger number of surfaces in the direction, and a lighter color, a smaller number of surfaces.

In the ray-tracing process, for ray vectors emitted by the camera, surfaces that might intersect can be determined directly by FaceMap. In addition, the shadow test line facing the light source can also find out whether there is any surface as an obstacle, requiring no light propagation operation.

In this study, the scene surface was projected onto FaceMap by the raster method so as to accelerate the generation. Instead of using ordinary linear plane projection whose maximum field angle is approximately 180° , this paper adopted the linear surface projection which has a 360-degree visual field for the generation of FaceMap.

As shown in Figure 10, the central point of FaceMap was O . After projecting a triangular surface in the scene onto the sphere of FaceMap, a curved triangle ABC was formed, and the three corresponding edges, denoted as a , b , and c , were all curves.

The detailed raster process is shown in Figure 11. The three vertices A , B , and C of the triangle were projected onto the two-dimensional structure of FaceMap by virtue of linear surface projection. Then, the bisection method was used to approximate any curved edge of the triangle, and finally, the scanning line filling method was employed to fill the curved triangle.

4.2. FaceMap Algorithm

4.2.1. Linear Surface Projection. The BIT-VBF left-handed 3D coordinate system was adopted in this paper. The vertex coordinate transformation was viewed as converting points from the world coordinate system to the camera coordinate system, by virtue of the transformation matrix [13]. The position coordinates of any point in 3D space were represented by (x, y, z) , while the world coordinate axes were described as axis $X(1, 0, 0)$, axis $Y(0, 1, 0)$, and axis $Z(0, 0, 1)$ successively. Similarly, a camera also possessed position coordinates and three axes. The position of the camera was assumed as camPos ,

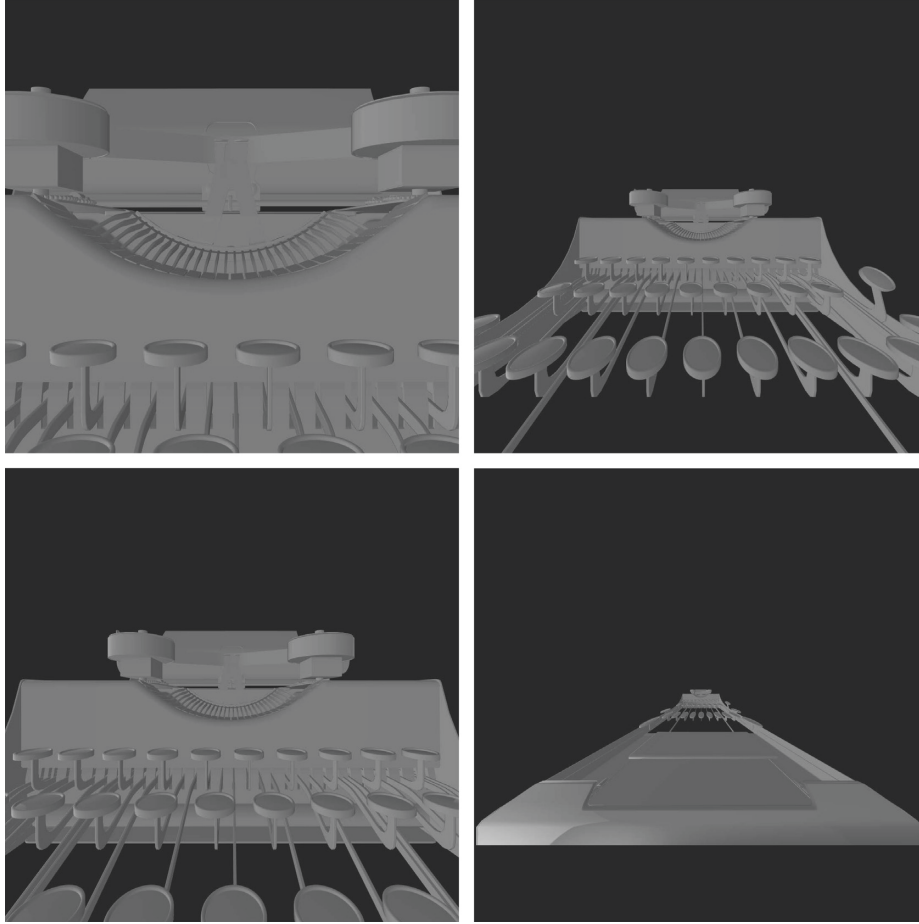


FIGURE 7: Plane projection with field angles of 50°, 90°, 120°, and 170°.

with the three axes being $camAX$, $camAY$, and $camAZ$, respectively, and the axis coordinates would change according to the rotation of the camera.

The angle changes relative to the screen center are linear in linear surface projection. In other words, if the distance between a point and the central origin is two times that of another point, then the angle between this point and the line of sight is also two times that of the other point.

The field angle of a surface was denoted as θ , the center as $camPos$, and the three axes as $camAX$, $camAY$, and $camAZ$. For a certain point v in the space, its vector cv relative to the camera was calculated by

$$\begin{aligned} cv.x &= v.x - camPos.x, \\ cv.y &= v.y - camPos.y, \\ cv.z &= v.z - camPos.z. \end{aligned} \quad (9)$$

Vector operation was expressed as

$$cv = v - camPos. \quad (10)$$

The calculated cv was the converted coordinates when the camera remained static, while the axis coordinates changed when the camera rotated, and the correspondingly converted vertex coordinates tv were calculated by

$$\begin{aligned} tv.x &= cv.x \times camAX.x + cv.y \times camAX.y \\ &\quad + cv.z \times camAX.z, \\ tv.y &= cv.x \times camAY.x + cv.y \times camAY.y \\ &\quad + cv.z \times camAY.z, \\ tv.z &= cv.x \times camAZ.x + cv.y \times camAZ.y \\ &\quad + cv.z \times camAZ.z. \end{aligned} \quad (11)$$

After simplification, the transformation matrix was expressed as

$$tv = \begin{bmatrix} camAX \\ camAY \\ camAZ \end{bmatrix} [cv]. \quad (12)$$

The transformation matrix can operate a series of transformations of the model, such as translation, rotation, and scaling. Only one point in the space is needed to move and rotate, and then, all the vertices of the model experience coordinate transformation relative to that point, thereby resulting in the converted model. Besides, scaling could be realized merely by multiplying one factor in the matrix [14].

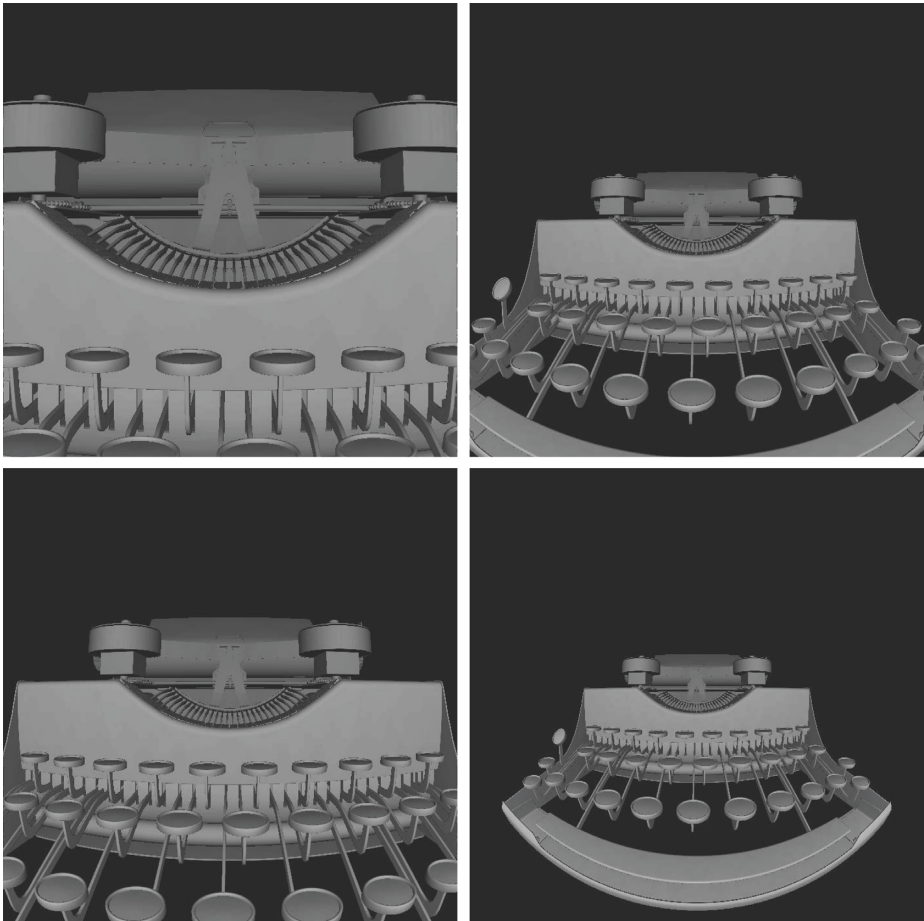


FIGURE 8: Surface projection with field angles of 50°, 90°, 120°, and 170°.



FIGURE 9: FaceMap schematic diagram.

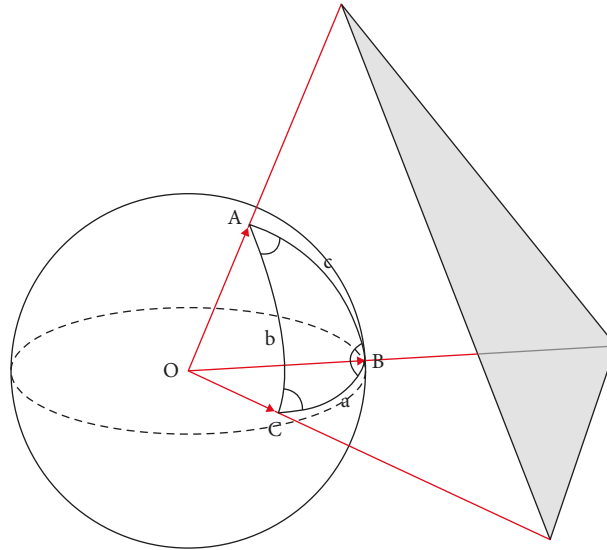


FIGURE 10: Surface projection.

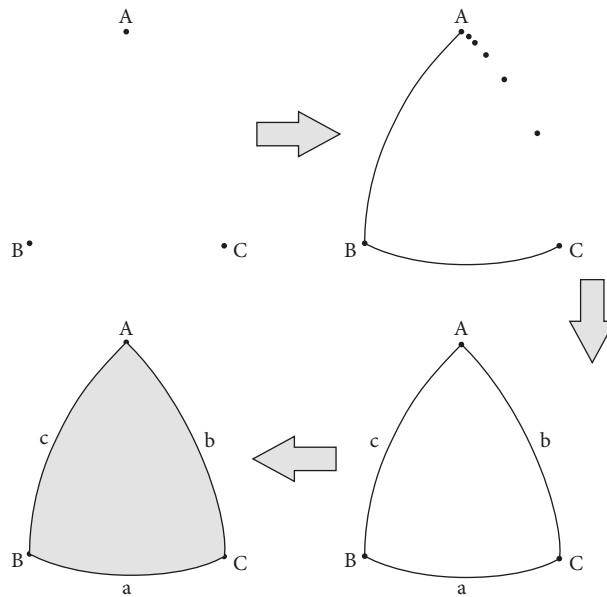


FIGURE 11: Curved triangle rasterization.

The angle β between tv and the sight axis was calculated by

$$\beta = \arccos\left(\frac{tv \cdot camAZ}{|tv||camAZ|}\right). \quad (13)$$

Next, the screen radius was assumed to be R , so the distance t between point sv after mapping and the screen center was obtained by the following equation:

$$t = \frac{2\beta}{\theta} R. \quad (14)$$

Given the x -coordinate and y -coordinate of tv , the direction of its projection on the XOY plane of FaceMap could

be determined. The distance between tv on the XOY plane and the central origin was denoted as $Dist$, and then, the ratios kx and ky of components in the OX and OY directions were obtained, as calculated by

$$\begin{aligned} Dist &= \sqrt{x^2 + y^2}, \\ kx &= \frac{x}{Dist}, \\ ky &= \frac{y}{Dist}. \end{aligned} \quad (15)$$

At last, the sx - coordinate and sy - coordinate of point sv projected onto FaceMap were calculated by

$$\begin{bmatrix} sx \\ sy \end{bmatrix} = t \begin{bmatrix} kx \\ ky \end{bmatrix}. \quad (16)$$

4.2.2. *Curve Approximation by the Bisection Method.* A curve can be seen as a collection of countless points, while a line in screen space is a collection of finite points. Therefore, curves in a space can be approximated by calculating finite pixels. Given the method of perspective projection, the curve mapping method in screen space is described in Algorithm 2.

4.2.3. *Filling of the Curved Triangle.* The curved triangle needs to be filled after all its points are obtained. Similar to the rasterization of regular triangles, the filling of the curved triangle also employed the progressive scanning method is described in Algorithm 3.

The number of intersections per row, though might more than two due to the curved triangle edges, could only be even, so the filling was conducted in pairs.

For a curved triangle, the intersection of each line and the curved edge is described in Algorithm 4.

This method is capable of conflict detection and the recognition of multipoints on the same line, thus avoiding the occurrence of odd number of intersection points on a line.

4.2.4. *Reverse Solution of the Light Vector.* In the reverse ray tracing, each pixel on the screen needs a reverse solution of the ray vector.

By the nature of surface projection, the distance from a point to the screen center is linearly correlated with the angle between the vector corresponding to the point and the sight axis camAZ. Accordingly, for a point (sx, sy) on the screen, the radius of the screen was assumed as R , and the field angle as θ . Then, the relation between the coordinates of the point and those of the screen center was $dx = sx - R$ and $dy = R - sy$. The angle β between its vector and the sight axis was calculated by

$$\beta = \frac{\sqrt{dx^2 + dy^2}}{2R} \theta. \quad (17)$$

After the normalization of both the ray vector and sight axis camAZ, its module became 1. The characteristics of the vector inner product indicated that the axis Z 's component Lz of the ray vector could be calculated by

$$Lz = \cos(\beta). \quad (18)$$

The module of the normalized ray vector was 1, as mentioned above. Next, the components of axis X and axis Y of the ray vector were assumed as Lx and Ly , respectively. According to the calculation of vector modulus, (19) could be expressed as

$$\sqrt{Lx^2 + Ly^2 + Lz^2} = 1. \quad (19)$$

With the ratio of Lx to Ly being denoted as k , (20) could be derived based on projection characteristics as

$$k = \frac{Ly}{Lx} = \frac{dy}{dx}. \quad (20)$$

Then, (19) was embedded into (20) to form (21), described as

$$Lx = \sqrt{\frac{1 - Lz^2}{1 + k^2}}. \quad (21)$$

In summary, the ray vector $L(Lx, Ly, Lz)$ was calculated by

$$\begin{cases} Lx = \sqrt{\frac{1 - \cos^2 \beta}{1 + (dy/dx)^2}}, \\ Ly = \frac{dy}{dx} Lx, \\ Lz = \cos \beta. \end{cases} \quad (22)$$

Nonetheless, this calculated ray vector L was still within FaceMap space, thus needed to be converted to a world coordinate system. Therefore, the ray vector of the world coordinate system was denoted as T , and (23) was obtained as

$$\begin{bmatrix} \text{camAX} \\ \text{camAY} \\ \text{camAZ} \end{bmatrix} [T] = [L]. \quad (23)$$

The value of the determinant was calculated according to Cramer's rule, as shown as follows:

$$\begin{aligned} D &= \begin{vmatrix} \text{camAX}.x & \text{camAX}.y & \text{camAX}.z \\ \text{camAY}.x & \text{camAY}.y & \text{camAY}.z \\ \text{camAZ}.x & \text{camAZ}.y & \text{camAZ}.z \end{vmatrix}, \\ D1 &= \begin{vmatrix} L.x & \text{camAX}.y & \text{camAX}.z \\ L.y & \text{camAY}.y & \text{camAY}.z \\ L.z & \text{camAZ}.y & \text{camAZ}.z \end{vmatrix}, \\ D2 &= \begin{vmatrix} \text{camAX}.x & L.x & \text{camAX}.z \\ \text{camAY}.x & L.y & \text{camAY}.z \\ \text{camAZ}.x & L.z & \text{camAZ}.z \end{vmatrix}, \\ D3 &= \begin{vmatrix} \text{camAX}.x & \text{camAX}.y & L.x \\ \text{camAY}.x & \text{camAY}.y & L.y \\ \text{camAZ}.x & \text{camAZ}.y & L.z \end{vmatrix}. \end{aligned} \quad (24)$$

The calculation of ray vector T in the world space was shown as follows:

Input: A curve information

- (1) Plot function of space curve (Input the two vertices of the curve):
 - (1) Project the two vertices onto the screen space as two endpoints
 - (2) Add the first endpoint
 - (3) **if** the distance between the two endpoints is longer than one pixel:
 - (i) Find the midpoint of the two vertices
 - (ii) Curve approximation function (the first vertex and the midpoint)
 - (iii) Add the endpoint after the midpoint projection
 - (iv) Curve approximation function (the midpoint and the second vertex)
 - (4) **else** Add the second endpoint
- (2) Curve approximation function (input the two 3D vertices):
 - (1) **if** the distance between endpoints after vertex projection is longer than one pixel:
 - (i) Find the midpoint of the two vertices
 - (ii) Curve approximation function (the first vertex and the midpoint)
 - (iii) Add the endpoint after the midpoint projection
 - (iv) Curve approximation function (the midpoint and the second vertex)
 - (2) **else** null

Output: Results after mapping

ALGORITHM 2: Screen space curve mapping algorithm.

Input: All point information of curve triangle

- (1) Find the highest and lowest points of the triangle;
- (2) Traverse from the highest point to the lowest point:
 - (a) Traverse from the highest point to the lowest point: Calculate all intersection points of the current line and the triangle edge;
 - (b) For every two intersect points: Fill from the left node to the right node;

Output: Results after filling

ALGORITHM 3: Filling algorithm of the curve triangle.

Input: A triangle vertex information

Traverse all points on a curve:

if the current point is online y and the next point is below line y :
 Add the x -coordinate of the current point

else null

if the next point is online y and the current point is below line y :
 Add the x -coordinate of the next point **else** null

Output: Intersection information

ALGORITHM 4: Algorithm for calculating the intersection of each line and curve edge of curve triangle.

$$\begin{bmatrix} T.x \\ T.y \\ T.z \end{bmatrix} = \frac{1}{D} \begin{bmatrix} D1 \\ D2 \\ D3 \end{bmatrix}. \quad (25)$$

In accordance with Cramer's rule, only one solution exists when D is greater than 0; innumerable solutions exist when D equals 0; no solution exists when D is less than 0. Geometrically, (23) is similar to the intersection operation of three planes, with the normal vectors of the three planes being $camAX$, $camAY$, and $camAZ$, respectively, serving as three sight axes of FaceMap. Therefore, the three normal vectors would certainly intersect at a point. Moreover, since

the sight axes were normalized unit vectors with modules of 1 and the value of D was also calculated as 1, (25) was simplified as

$$T = \begin{bmatrix} D1 \\ D2 \\ D3 \end{bmatrix}. \quad (26)$$

4.3. *Renderer Design Based on FaceMap Algorithm.* FaceMap, being abstract in the program, can be inherited by other components to obtain the panorama distribution of the scene model. Then, FaceMap can be used or modified

according to specific needs. The structure of Renderer based on the FaceMap algorithm is shown in Figure 12:

- (1) Vector class contains attribute coordinate values x , y , and z and basic vector operations such as addition, subtraction, point multiplication, and cross multiplication
- (2) Face class is used for storing basic triangular surfaces, involving vertex arrays with a length of 3 and normal arrays with a length of 3
- (3) OBJ class stores model data and helps to load Obj model files which are then converted to face object arrays
- (4) Space vector class represents a basic space point, with attributes including space position, rotation angle, and self-space coordinate axis
- (5) FaceMap class, deriving from space vector, is also abstract. However, compared with space vector, FaceMap contains additional attributes including field angle and field radius
- (6) Camera inherits FaceMap. While generating FaceMap structure, it only stores the information of surfaces closest to itself, and then, the closest intersection point can be directly calculated during rendering
- (7) Point Light also inherits FaceMap. While generating the FaceMap structure, it stores the distribution data of all surfaces. Furthermore, the point light class provides the method of `get_lighten_up()`. It judges by virtue of its FaceMap whether an entered space point will be blocked by other surfaces, namely whether the point is in shadow
- (8) Color class is used for color operation and contains the values of three components R, G, and B. While rendering a certain point, shadow test of multiple light sources should be performed. If can be irradiated, the value of illumination color should be accumulated. Color class provides several basic methods including addition, subtraction, numerical multiplication, and conversion to 24 bit color
- (9) Image class is a two-dimensional image buffer, storing scene graphs for ray-tracing rendering; [10] Renderer class controls the whole Renderer, which contains OBJ model, Camera, Point Light array, and Image buffer.

5. Experimental Results and Analysis

5.1. Experimental Environment. The computer configuration used in the experiments is as follows:

System: Windows 7 Ultimate
 Processor: Intel Core i7-4710 HQ 2.50 GHz
 Memory: 12 GB

5.2. Comparison Methods Introduction. In order to reflect the superiority of the performance of this method, this paper selects the more mature products on the market for

comparative experiments. Apart from the proposed Renderer, Rhino 5 and V-Ray 2.00.02 were also chosen for the comparative experiment. Rhino, introduced by American company Robert McNeel in 1998, is a 3D modeling software based on NURBS (nonuniform rational B-spline). It has been widely used in 3D animation, industrial manufacturing, scientific research, mechanical design, and other fields [15]. V-Ray, produced by chaos group and ASGVIS Company, is high-quality rendering software and one of the most popular rendering engines in the industry [16].

5.3. Selection of the Rendering Model in Comparative Experiment. A total of four object rendering scenes was used in the comparative experiment, with detailed data of the scene as shown in Table 1.

5.4. Experimental Results and Analysis. Rhino 5, V-Ray 2.00.02, and Renderer presented in this paper were employed successively to render the four models, and the corresponding effects are shown in Figures 13–16, mainly from the rendering effect for comparison.

Judging from the rendering effects as reflected in Figures 13–16, the effects achieved by the proposed Renderer were similar to those by Rhino and V-Ray, with main differences lying in the deformation at the edge of the visual field and the brightness. Firstly, in terms of the deformation at the field edge, since surface projection was used in the proposed Renderer, the reserve resolution of the ray vector was also based on surface distribution. As shown from the effects of rendering chessboard in Figure 13 and typewriter in Figure 16, lines close to the camera were slightly bent when using Renderer, while they were straight in the results obtained by Rhino and V-Ray. Consequently, the rendering effects by the proposed Renderer were closer to those by a real camera. The second inference consisted of the brightness of illumination. Distinct illumination models used by different renderers resulted in diverse calculations of brightness and propagation attenuation of the light source, thus causing differences in brightness and contrast degree of the whole image. Nonetheless, the difference in brightness only led to various displaying effects, with a negligible impact on computational cost.

The specific time consumption of each rendering shown in Figures 13–16 is listed in Table 2.

Table 2 demonstrates that the proposed Renderer spent the least time in total, less than half the total time spent by either of the other two renderers. The computational efficiency of Renderer was 2.34 times that of Rhino and 2.15 times that of V-Ray 2.0. It is worth noting that the rendering by Renderer was completed in a single-thread environment, indicating an even lower CPU resources occupancy and a higher speed, while Rhino and V-Ray 2.0 used multithread rendering.

In summary, in this study, the proposed FaceMap-based ray-tracing algorithm, Rhino, and V-Ray were successively used to render four object models including chessboard, grass patch, bust, and typewriter. The comparison in terms of rendering effect and rendering time indicated that the

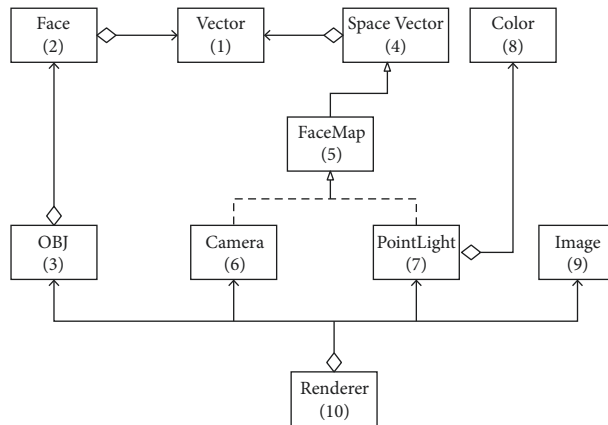
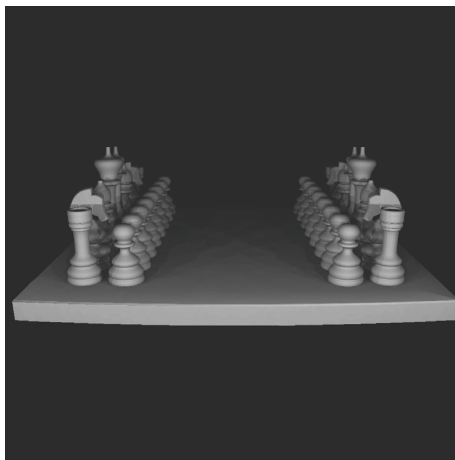


FIGURE 12: Renderer structure based on FaceMap algorithm.

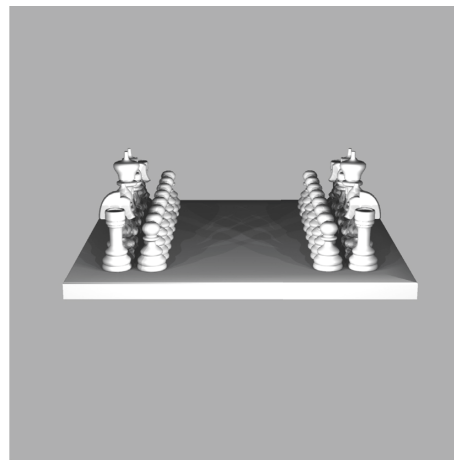
TABLE 1: Model data.

Scene name	No. of vertices	No. of surfaces	Size (MB)
Chessboard	61749	123314	11.4
Grass patch	52600	86864	6.93
Bust	22299	44590	4.01
Typewriter	73920	145558	11.3

Each scene was rendered in white mode with the same camera view, and eight point light sources were added to the scene.

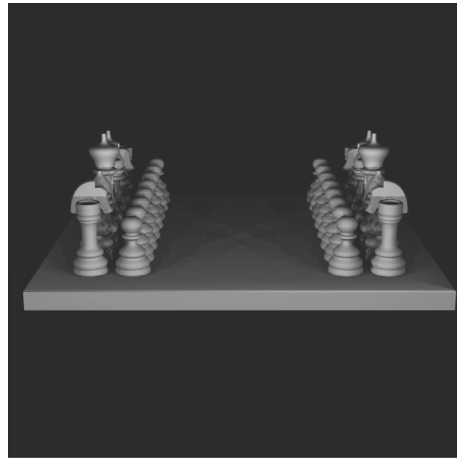


(a)



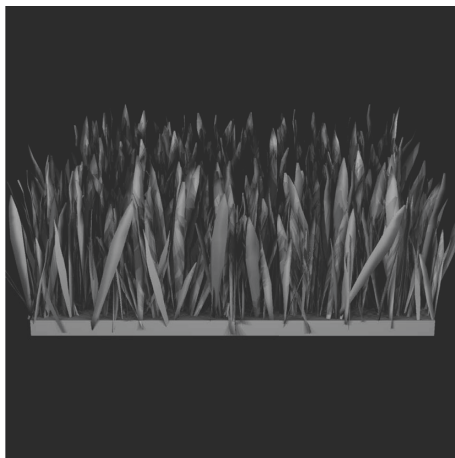
(b)

FIGURE 13: Continued.

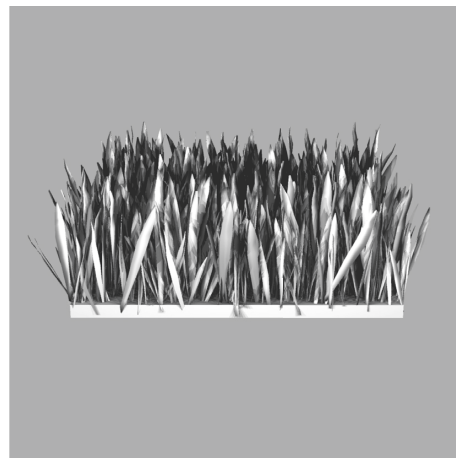


(c)

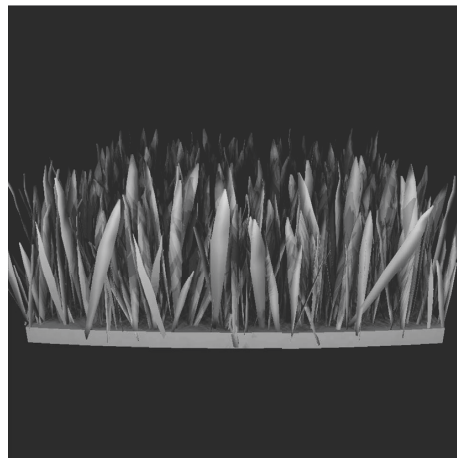
FIGURE 13: Effects of rendering chessboard. (a) Rendering effect by Rhino. (b) Rendering effect by V-Ray. (c) Rendering effect by Renderer (our method).



(a)



(b)



(c)

FIGURE 14: Effects of rendering grass patch. (a) Rendering effect by Rhino. (b) Rendering effect by V-Ray. (c) Rendering effect by Renderer.

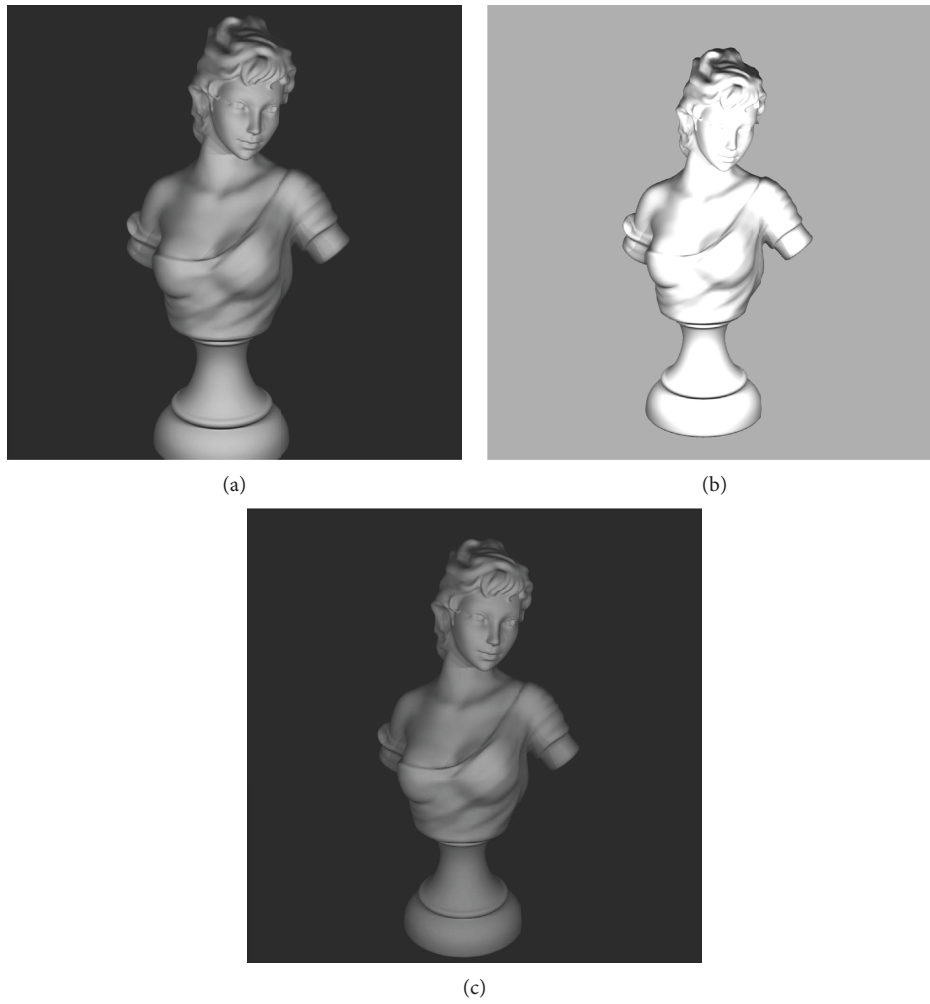


FIGURE 15: Effects of rendering a bust. (a) Rendering effect by Rhino. (b) Rendering effect by VRay. (c) Rendering effect by Renderer (our method).

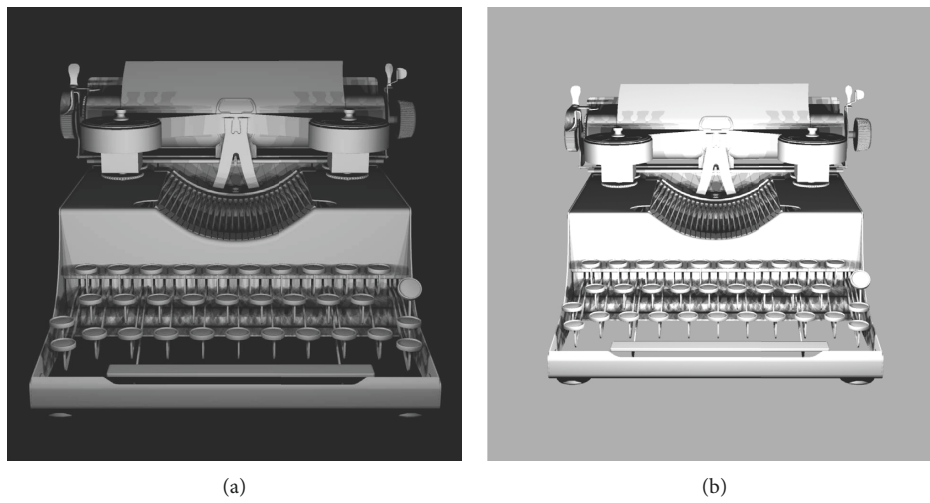


FIGURE 16: Continued.



(c)

FIGURE 16: Effects of rendering typewriter. (a) Rendering effect by Rhino. (b) Rendering effect by VRay. (c) Rendering effect by Renderer (our method).

TABLE 2: Time consumption of each rendering.

Renderer	Rendering time (s)				Total time
	Chessboard	Grass patch	Bust	Typewriter	
Rhino 5	2.2	25.2	7.1	45.2	79.7
VRay 2.0	4.7	25.6	9.2	33.7	73.2
Renderer	7.3	11.0	4.8	11.0	34.1

proposed method achieved relatively better rendering effects and significantly reduced the rendering time in the meanwhile.

6. Conclusion

This study intends to solve the shortcomings of the poor rendering effect of the raster method and the high computational complexity caused by the ray-tracing method. We propose a ray-tracing acceleration algorithm based on FaceMap by combining the raster method and ray-tracing method. FaceMap can be defined as a data structure that stores the surface distribution corresponding to a point light source or a camera. With the help of FaceMap, one can quickly determine the surfaces that may intersect in a certain direction, which can help improve the efficiency of intersection operation and thus speed up the overall rendering task and reduce computational complexity.

The novelty of this study and the advantages of the proposed method can be described as follows: (i) it can directly determine the data of a surface in a certain direction, requiring no calculation of light propagation process; (ii) the camera can rapidly determine intersection points based on FaceMap, which in turn greatly improved the speed of rendering operation; (iii) once generated, the FaceMap corresponding to a specific point light source can be reused, thus further reduces computational complexity.

To sum up, based on the theory of rendering acceleration and optimization, this paper proposes a new structure representation and corresponding projection algorithm, which provides a new research angle and an efficient technology for the actual rendering requirements and has a promising application prospect in the field of computer graphics. In spite of what stated, the present study is not without limitations, which can be addressed in future research: (i) FaceMap consumes relatively large memory and considers compression as a feasible solution; (ii) the texture and the material of rendered object have not yet been considered by the current model; (iii) the shadow processing caused by light conditions also needs to be further improved.

Data Availability

The data used to support the findings of this study are available from the corresponding author upon request.

Conflicts of Interest

The authors declare that they have no conflicts of interest regarding the publication of this paper.

Acknowledgments

This work was supported by the National Natural Science Foundation of China (61462054) and the Science and Technology Plan Projects of Yunnan Province (2015FB135).

References

- [1] H. W. Jensen and N. J. Christensen, "Photon maps in bidirectional Monte Carlo ray tracing of complex objects," *Computers & Graphics*, vol. 19, no. 2, pp. 215–224, 1995.
- [2] J. Gao, K. Xu, and J. Cui, "An algorithm based on bounding box technology to improve the light and the objects intersection efficiency," *Journal of Traffic information and security*, vol. 22, no. 6, pp. 65–68, 2004.
- [3] J. Amanatides and A. Woo, "A fast voxel traversal algorithm for ray tracing," *Eurographics*, vol. 87, no. 3, pp. 3–10, 1987.
- [4] W.-x. Wang, S. Xiao, M. Wen, and H. Dong, "Ray tracing algorithm based on octree space partition method," *Journal of Computer Applications*, vol. 28, no. 3, pp. 656–658, 2008.
- [5] H. Weghorst, G. Hooper, and D. P. Greenberg, "Improved computational methods for ray tracing," *ACM Transactions on Graphics*, vol. 3, no. 1, pp. 52–69, 1984.
- [6] A. Fujimoto and K. Iwata, "Accelerated ray tracing," *Computer Graphics*, vol. 85, pp. 41–65, 1985.
- [7] A. Fujimoto, T. Tanaka, and K. Iwata, "ARTS: accelerated ray-tracing system," *IEEE Computer Graphics and Applications*, vol. 6, no. 4, pp. 16–26, 1986.
- [8] T. L. Kay and J. T. Kajiya, "Ray tracing complex scenes," *ACM SIGGRAPH Computer Graphics*, vol. 20, no. 4, pp. 269–278, 1986.
- [9] J. G. Cleary, B. Wyvill, G. M. Birtwistle, and R. Vatti, *Multiprocessor Ray Tracing*, Department of Computer Science University of Calgary, Calgary, Canada, 1983.
- [10] A. S. Glassner, "Space subdivision for fast ray tracing," *IEEE Computer Graphics and Applications*, vol. 4, no. 10, pp. 15–24, 1984.
- [11] M. A. J. Sweeney and R. H. Bartels, "Ray tracing free-form B-spline surfaces," *IEEE Computer Graphics and Applications*, vol. 6, no. 2, pp. 41–49, 1986.
- [12] E. Haines and D. Greenberg, "The light buffer: a shadow-testing accelerator," *IEEE Computer Graphics and Applications*, vol. 6, no. 9, pp. 6–16, 1986.
- [13] T. Whitted, "An improved illumination model for shaded display," *Communications of the ACM*, vol. 23, no. 6, pp. 343–349, 1980.
- [14] S. M. Rubin and T. Whitted, "A 3-dimensional representation for fast rendering of complex scenes," *ACM SIGGRAPH Computer Graphics*, vol. 14, no. 3, pp. 110–116, 1980.
- [15] <https://baike.baidu.com/item/rhino/4065831?fr=aladdin>.
- [16] <https://baike.baidu.com/item/vray/894350?fr=aladdin>.

Research Article

Research on University Innovation and Entrepreneurship Resource Database System Based on SSH2

Libo Wu, Lili Feng , and Jianna Yan

Hebei Vocational University of Technology and Engineering, Xingtai 054000, China

Correspondence should be addressed to Lili Feng; fengll417457768@stu.ahu.edu.cn

Received 28 February 2022; Revised 14 March 2022; Accepted 25 March 2022; Published 22 April 2022

Academic Editor: Wei Liu

Copyright © 2022 Libo Wu et al. This is an open access article distributed under the Creative Commons Attribution License, which permits unrestricted use, distribution, and reproduction in any medium, provided the original work is properly cited.

With the wide application of the Internet, the entrepreneurial resources of colleges and universities have grown at an exponential rate. With the rapid accumulation of this information, it is difficult for students to find what they are interested in from a large amount of information. To accurately recommend innovation and entrepreneurship resources, this paper proposes a recommendation algorithm based on user trust and a probability matrix. After obtaining the user trust data, the PMD (probability matrix decomposition) algorithm is used to complete the trust matrix and normalize it to get the similarity matrix. At the same time, the trust factor between users is added to the calculation process of the posterior probability, and the prediction score is obtained by maximizing the posterior probability. On this basis, the weights of users in the group are normalized, and the weighting strategy based on user interaction is used to integrate the preferences of group members to obtain the final recommendation results. When designing the recommendation system, the web system of the mainstream SSH2 framework is used to design, and the B/S structure of the entrepreneurial resource recommendation system platform is realized. Experimental results show that the proposed system has a higher recommendation quality compared with other recommended algorithms.

1. Introduction

At the end of 2014, the concept of mass entrepreneurship and mass innovation was proposed for the first time [1]. Under the background of the era of “Internet +”, the innovation and entrepreneurship space, as the carrier of innovation and entrepreneurship services, conforms to the development needs of the times [2]. Taking the Internet as an important tool, the Internet platform and Internet technology provide technical support and environmental guarantee for the innovation and entrepreneurship space. Form a new ecological chain in the field of innovation and entrepreneurship [3]. The innovation and entrepreneurship space based on “Internet +” has a strategic impact on the education ecosystem of universities and even the national economic development system [4].

As the development goal of the innovation and entrepreneurship space changes from quantitative growth to quality improvement, innovation and entrepreneurship space resources based on “Internet +” have become the current hot spots in this field [5]. A large number of studies

have been conducted on the development strategy and development model of innovation and entrepreneurship space resources based on “Internet +”, but there is still a lack of a unified recommendation system for the recommendation of innovation and entrepreneurship space resources based on “Internet +” [6]. Based on this, we will build an operable and enforceable innovation and entrepreneurship space resource recommendation system based on “Internet +.” It is of great significance for guiding its development direction, improving its management quality, and promoting regional economic development.

To make the fusion results more charted, improve the reliability and interpretability of the recommended results [7]. In this paper, a group recommendation algorithm that integrates user trust is proposed, and group fusion is carried out considering the interaction relationship between users in the group [8]. After obtaining the user trust data, the trust vector and trusted vector of group members are trained, and the mean of the trusted vector is used as the benchmark vector [9]. The trust vector of each member is given the corresponding weight by doing the dot product operation

with it [10]. A list of recommendations is generated by summing the normalized weight scores to obtain a group score [11].

This paper consists of six main parts: the first part is the introduction, the second part is related work, the third part is the proposed resource recommendation algorithm, the fourth part is the university entrepreneurship resource recommendation system based on SSH2, the fifth part is the experiment and analysis, and the sixth part is the conclusion.

2. Related Work

2.1. The Necessity of Innovation and Entrepreneurship Resources in Colleges and Universities. With the spread of information technology, college students are increasingly inclined to use online learning [12]. Universities and colleges also use online tools to expand the learning resource library of innovation and entrepreneurship to provide more learning convenience for students. The innovation and entrepreneurship resource recommendation system in the new era offers students with richer learning resources, and different resources are updated in real-time, consistent with the characteristics of the innovation and entrepreneurship environment in the process of dynamic change [13].

The construction of the recommendation system for innovation and entrepreneurship resources in colleges and universities should be based on the rules of unified planning, and the software and hardware equipment in colleges and universities should be configured according to the actual educational needs [14]. In advocating the rational allocation of educational resources and enhancing the effectiveness of innovation and entrepreneurship education. The construction of the resource recommendation system needs to follow the development law of the times and cater to the learning needs of college students. Innovation and entrepreneurship are becoming important driving forces for national economic development, and it is imperative to build a resource recommendation system.

2.2. The Current Situation of Innovation and Entrepreneurship Resources in Colleges and Universities. Learning resources refer to the human and material resources that serve the main body of learning in education and teaching activities, and educational resources are rich in connotation [15]. It includes both nonlife information and physical objects and various human resources with vitality [16]. The resource recommendation system is an indispensable part of innovation and entrepreneurship education. This resource pool involves large-scale human and material resources [17]. The construction of the resource recommendation system is an essential systematic project, but there are still many problems in promoting this project.

In the context of increasingly abundant educational resources, high-quality educational resources related to innovation and entrepreneurship are still scarce. On the one hand, many colleges and universities are trying to establish a recommendation system for innovative and entrepreneurial resources, and the types of resources required for innovation

and entrepreneurship education are not clear. The scale of the innovation and entrepreneurship resource recommendation system continues to expand, but the quality of improvement has fallen into a bottleneck period. On the other hand, high-quality innovation and entrepreneurship learning resources have not fully flowed between higher schools. Under the premise that there are barriers to interuniversity cooperation between universities, many universities are not really involved in the process of developing innovative and entrepreneurial resources. Since their establishment, some innovation and entrepreneurship curriculum development projects have rarely been asked about. This causes the waste of project resources and leads to the construction of resource recommendation systems becoming more inefficient.

All kinds of networked means have not been rationally applied in building a resource recommendation system. The main body of education lacks the concept of lifelong education [18]. For example, some colleges and universities try to use microcourse and MOOC resources to enrich the innovation and entrepreneurship resource recommendation system. However, to avoid learning, students directly pulled the video progress bar to the end without carefully watching the video content. However, the video terminal still shows that the student has learned relevant content due to the existing technical conditions. The existing learning resource system design is also lacking in forward looking elements [19]. Colleges and universities follow traditional educational thinking to build a learning resource library. Lack of guidance in the design and research of online courses. The content involved in various online courses is highly repetitive and cannot meet students' differentiated innovation and entrepreneurship learning needs.

Under the concept of lifelong education, the construction of the recommendation system for innovation and entrepreneurship resources in colleges and universities should be sufficient to meet the learning needs of students at different stages of innovation and entrepreneurship. It is also necessary to study the differences between different students in innovation and entrepreneurship, and provide them with differentiated learning resources. Under the existing system, the learning resources provided by universities for students at different levels are not differentiated. The cookie-cutter innovation and entrepreneurship education resources are not highly targeted. It cannot play a role in guiding students and enhancing the orientation of education [20].

3. The Proposed Resource Recommendation Algorithm

3.1. Group Recommendation Framework. The framework of the group recommendation model proposed in this paper is shown in Figure 1. The specific process is as follows:

- (1) Obtain the user trust data, use the classical probability matrix decomposition algorithm to complete the trust matrix N , and obtain the user trust characteristic vectors L and R .
- (2) Normalize each row of the trust matrix using softmax to obtain the similarity matrix F .

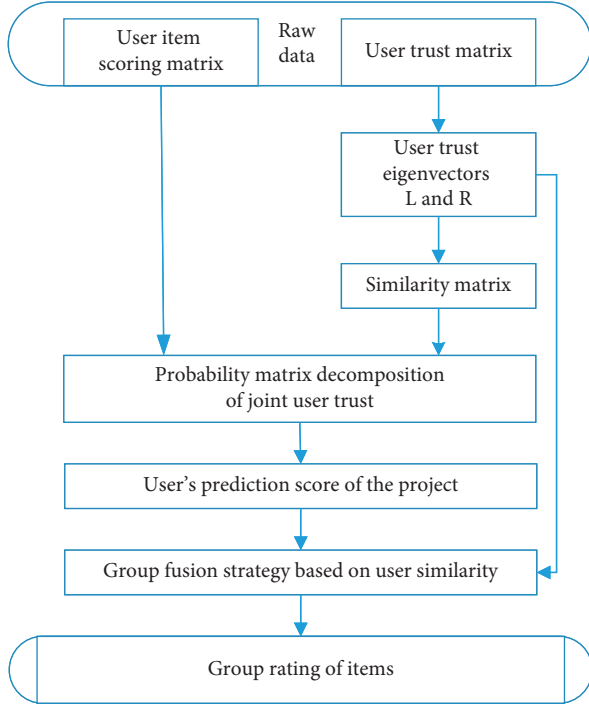


FIGURE 1: Group recommendation model framework.

- (3) Get user-item scoring data. The probability matrix decomposition algorithm of the joint similarity is used to complete the prediction score of the unrated items.
- (4) Use the confluence trust weighting strategy to combine the scores of all members of the group. It gets the ratings of items by the entire group and generates a list of recommendations based on the ratings.

3.2. User Similarity Matrix Construction. This article uses a real dataset that contains several trust relationships between users and user ratings of items. Building a user similarity matrix requires a trust relationship between two users. Therefore, the probability matrix decomposition algorithm is first used to complete the user trust matrix.

Suppose there are W users, $N_{l,r}$ represents the trust of user l to user r , forming a trust matrix of $W \times W$. The target trust matrix is decomposed into the product $L_{Z \times W}^N R_{Z \times W}$ of two matrices with lower dimensions, where Z is the potential vector dimension. L and R represent the implicit eigenvector of user trust.

Suppose that the user trust $N_{l,r}$ is determined by the inner product of the potential vector of user l and the potential vector of user r , and the trust follows a Gaussian distribution, that is, formula (1).

$$N_{l,r} \sim T(L_l^N R_r, \sigma^2). \quad (1)$$

Then, the conditional probability of the observed trust matrix is formula (2).

$$u(N|L, R, \sigma^2) \sim \prod_{l=1}^W \prod_{r=1}^W T(L_l^N R_r, \sigma^2)^{X_{lr}}, \quad (2)$$

where $X_{l,r}$ is the indicator function. If user l has trust data for user r , it is 1. Otherwise, it is 0.

Then, assume that the potential feature vectors of users obey the Gaussian prior distribution with a mean value of 0, that is, formula (3) and formula (4).

$$u(L|\sigma_L^2) \sim \prod_{l=1}^W T(L_l | 0, \sigma_L^2 X), \quad (3)$$

$$u(R|\sigma_R^2) \sim \prod_{r=1}^W T(R_r | 0, \sigma_R^2 X), \quad (4)$$

where X represents a diagonal matrix. Then, the posterior probabilities of L and R is formula (5).

$$u(L, R|N, \sigma_L^2, \sigma_R^2, \sigma^2) \propto u(N|L, R, \sigma^2) u(L|\sigma_L^2) u(R|\sigma_R^2). \quad (5)$$

Logarithms are taken from both sides to obtain formula (6).

$$\begin{aligned} \ln p(L, R|N, \sigma_L^2, \sigma_R^2, \sigma^2) &= -\frac{1}{2\sigma^2} \sum_{l=1}^W \sum_{r=1}^W X_{l,r} (N_{l,r} - L_l^N R_r)^2 \\ &\quad - \frac{1}{2\sigma_L^2} \sum_{l=1}^W L_l^N L_l - \frac{1}{2\sigma_R^2} \sum_{l=1}^W R_r^N R_r \\ &\quad - \frac{1}{2} \left(\sum_{l=1}^W \sum_{r=1}^W X_{l,r} \right) \ln \sigma^2 \\ &\quad - \frac{1}{2} WZ \ln \sigma_L^2 - \frac{1}{2} WZ \ln \sigma_R^2 + C, \end{aligned} \quad (6)$$

where C is an independent constant.

The posterior probability is maximized by minimizing the following objective function:

$$L = \frac{1}{2} \sum_l \sum_r X_{l,r} (N_{l,r} - L_l^N R_r)^2 + \frac{\lambda_L}{2} \sum_{l=1}^W L_{l,Fro}^2 + \frac{\lambda_R}{2} \sum_{l=1}^W R_{l,Fro}^2. \quad (7)$$

where $\lambda_L = \sigma^2/\sigma_L^2$, $\lambda_R = \sigma^2/\sigma_R^2$.

Equation L obtains formula (8) and formula (9) by deriving partial derivatives of L_l and R_r , respectively.

$$\frac{\partial E}{\partial L_l} = (N_{l,r} - L_l^N R_r) R_r - \lambda_L L_l, \quad (8)$$

$$\frac{\partial E}{\partial R_r} = (N_{l,r} - L_l^N R_r) L_l - \lambda_R R_r. \quad (9)$$

Then, the random gradient descent is used to update L_l and R_r until they converge or reach the maximum number of iterations.

After training, two eigenvectors L and R of each user can be obtained. The left vector L_l of any user l is multiplied by the right vector R_r of another user r to obtain L 's trust in R , that is, formula [10].

$$N_{l,r} = L_l \cdot R_r. \quad (10)$$

Firstly, the trust matrix N between each pair of users is calculated, and $N_{l,r}$ represents the trust of user l to user r . The L -to row of the matrix indicates the trust of the L -to user to other users. At this time, the softmax operation is performed on each row of data, and the sum of the trust degree of each row is normalized to obtain the similarity matrix F , that is, formula (11).

$$F_{l,r} = \frac{e^{N_{l,r}}}{\sum_{r=1}^W e^{N_{l,r}}}, \quad (11)$$

where $F_{l,r}$ represents the similarity between user l and user r .

3.3. FPMF Algorithm Combined with User Trust. Assuming that there are w users and t items, the score of each user and item is taken as a $W \times T$ matrix, and $R_{W \times T}$, $R_{x,y}$ represents the score of user x on item y . Then, assume that R obeys the Gaussian distribution with mean $P_x^N Q_y$ and variance σ_R^2 , and its probability distribution is formula (12).

$$u(R | P, Q, \sigma_R^2) = \prod_{x=1}^W \prod_{y=1}^T T(P_x^N Q_y, \sigma_R^2)^{X_{x,y}^R}. \quad (12)$$

From the similarity matrix, it can be seen that the user's feature vector and other user feature vectors in the similarity matrix F should be equal after multiplying by the weight, that is, formula [13].

$$P_x = \sum_{n=1}^W F_{x,n} P_n, \quad (13)$$

where $F_{x,n}$ represents the similarity between user x and user n . Then, the Gaussian prior distribution of the user characteristic matrix P is as shown in formula (14).

$$\begin{aligned} u(P|F, \sigma_P^2, \sigma_F^2) &\propto u(P|\sigma_P^2)u(P|F, \sigma_F^2) \\ &= \prod_{x=1}^W T(P_x|0, \sigma_P^2 X) \times \prod_{x=1}^W T\left(P_x \mid \sum_{n=1}^W F_{x,n} P_n, \sigma_F^2 X\right). \end{aligned} \quad (14)$$

Suppose again that the item eigenvector Q also obeys the Gaussian distribution, that is, formula (15).

$$u(Q|\sigma_Q^2) = \prod_{y=1}^T T(Q_y|0, \sigma_Q^2 X). \quad (15)$$

Then, the posterior probability distribution of P and Q can be obtained as follows:

$$\begin{aligned} u(P, Q|R, F, \sigma_R^2, \sigma_F^2, \sigma_P^2, \sigma_Q^2) &\propto \\ u(R|P, Q, \sigma_R^2)u(P|F, \sigma_P^2, \sigma_F^2)u(Q|\sigma_Q^2). \end{aligned} \quad (16)$$

Logarithm is taken on both sides to get formula (17).

$$\begin{aligned} \ln p(P, Q|R, F, \sigma_R^2, \sigma_F^2, \sigma_P^2, \sigma_Q^2) &= -\frac{1}{2\sigma_R^2} \sum_{x=1}^W \sum_{y=1}^T X_{x,y}^R (R_{x,y} - P_x^N Q_y)^2 \\ &\quad - \frac{1}{2\sigma_F^2} \sum_{x=1}^W \left(\left(P_x - \sum_{n=1}^W F_{x,n} P_n \right) \left(P_x - \sum_{n=1}^W F_{x,n} P_n \right) \right) \\ &\quad - \frac{1}{2\sigma_P^2} \sum_{x=1}^W P_x^N P_n - \frac{1}{2\sigma_Q^2} \sum_{y=1}^T Q_y^N Q_y - \frac{1}{2} \left(\sum_{x=1}^W \sum_{y=1}^T X_{x,y}^R \right) \ln \sigma_R^2 \\ &\quad - \frac{1}{2} WZ \ln \sigma_P^2 - \frac{1}{2} TZ \ln \sigma_Q^2 + C. \end{aligned} \quad (17)$$

The posterior probability is maximized by minimizing the following objective function:

$$\begin{aligned} L &= \frac{1}{2} \sum_{x=1}^W \sum_{y=1}^T X_{x,y}^R (R_{x,y} - P_x^N Q_y)^2 + \frac{\lambda_P}{2} \sum_{x=1}^W \|P_x\|_{Fro}^2 \\ &\quad + \frac{\lambda_Q}{2} \sum_{y=1}^T \|Q_y\|_{Fro}^2 + \frac{\lambda_F}{2} \sum_{x=1}^W \left\| P_x - \sum_{n=1}^W F_{x,n} P_n \right\|_{Fro}^2, \end{aligned} \quad (18)$$

where $\lambda_P = \sigma_R^2/\sigma_P^2$, $\lambda_Q = \sigma_R^2/\sigma_Q^2$, $\lambda_F = \sigma_R^2/\sigma_F^2$.

Then, the gradient descent method is used to update P_x and Q_y until they converge or reach the maximum number of iterations.

3.4. Convergence Strategies. This paper proposes a new fusion strategy based on user interaction in terms of group fusion. This will again leverage the previously acquired network of user trust. The specific process is further discussed.

The implicit eigenvector R of the trust degree of all users is obtained, and the average value R_{mean} of R is also obtained, that is, formula (19).

$$R_{\text{mean}} = \frac{1}{W} \sum_{l=1}^W R_l. \quad (19)$$

The left vector L of each user is multiplied by point R_{mean} to obtain the weight of the user, that is, formula (20).

$$m_x = \langle L_x \cdot R_{\text{mean}} \rangle. \quad (20)$$

When recommending a group, normalize the weight of users in the group using the softmax function, that is, formula (21).

$$m_x = \frac{e^{m_x}}{\sum_{y=1}^W e^{m_y}}. \quad (21)$$

The weight strategy is used to combine the scores of users in the group with the scores of groups, that is, formula (22).

$$R(A, y) = \sum_{x \in A} m_x R_{x,y}, \quad (22)$$

where $R(A, y)$ represents the score of group A on item y .

4. Design of University Entrepreneurship Resource Recommendation System Based on SSH2

The traditional information network resource management system adopts the C/S architecture. Each client needs to install the appropriate software for the relevant configuration. The system adopts the B/S architecture, and the user does not need to install software. Only the browser needs to be installed to access the system, and the technical requirements for the user are not high. In addition, the system uses SSH2 as the framework, uses the Java language and MySQL database, and introduces JavaScript, CSS, and other web technologies. It realizes the five functions of login verification, permission management, data retrieval, data management, and version management.

4.1. Overall Framework Design of the Resource Recommendation System. The resource recommendation system adopts a B/S architecture, and the framework diagram of the entire system is shown in Figure 2.

It is divided into 4 floors, from bottom to bottom, entity layer, DAO layer, service layer, and WEB layer. There is an interaction between the DAO layer, the service layer, and the WEB layer (3 layers). The upper layer can call the services of the lower layer, and the lower layer can return data to the upper layer.

The entity layer is mainly used to encapsulate the data of the entire repository system, including form data transmitted from the foreground page to the webserver and the web service to the database mapping data. Data transfer from the client to the webserver requires the corresponding POJO (plain ordinary Java object) variable to be defined in the controller. The corresponding get and set methods are provided for this variable. This allows Struts2 to pass data from the client form to the controller's corresponding properties in the POJO object. Data is passed from the web server to the database, mainly by defining a corresponding POJO object for each table in the database, and then configuring a mapping between the POJO and the database table in Hibernate's configuration file. This allows it possible to pass data between the web server and the database via POJO. This layer is the basis for the data exchange of the entire

system, and the data exchange of all layers is the data encapsulated using the entity layer.

The service layer is the business processing layer of the entire system, which is mainly responsible for handling the business logic. Each time the controller receives a request, it calls the corresponding processing method of the service layer. After the service receives the processing task, it calls the methods of the DAO layer, completes the logical operations required by the request, and finally passes the returned data to the controller of the WEB layer. The service layer is the brain of the entire repository system, and all the complex logic is written in this layer.

The DAO layer is the bridge between the server and the database. The data processed by the WEB server is persisted to the database by the DAO layer, and the data in the database is transmitted to the WEB server through the DAO layer. To optimize the operation of the repository on the database, the DAO layer of the repository system adopts the Hibernate framework. The framework provides a pool of database connections placed in a connection pool each time the system starts with a certain number of database connections based on Hibernate's configuration file. Each time a database connection needs to be established, it is not necessary to establish another database connection, but instead takes a database connection from the connection pool, use it up, and then put it back into the connection pool. This connection pooling pattern avoids consuming too many resources every time due to the establishment and release of connections.

4.2. Graphic Design of Entrepreneurial Resource Recommendation System. The functional module design of the startup resource recommendation system is shown in Figure 3.

5. Experiments and Analysis

This section uses real data sets and implements the algorithm in Python. The experiment is carried out on a computer configured with Windows 7, 2.5 GHz CPU, and 8 GB memory.

5.1. Datasets. The experiment uses real data sets, all from the college student innovation and entrepreneurship resource library system, based on personalized recommendations, composed of two parts: rating data ratings.txt and user trust data trust.txt. The ratings.txt contained 35497 data, with a scoring range of 0.5 to 4.0, a step size of 0.5, and an intensity of 1.044%. The trust.txt contains 1853 data with an intensity of 0.069%.

5.2. Evaluation Indicators. To test the effectiveness of the proposed algorithm, the mean absolute error (MAE), coverage rate (COV), and comprehensive evaluation index (F1) are used to evaluate the performance of the recommended system. The average absolute error refers to the average value of the difference between the resource score recommended by the recommendation system for the user and the score of

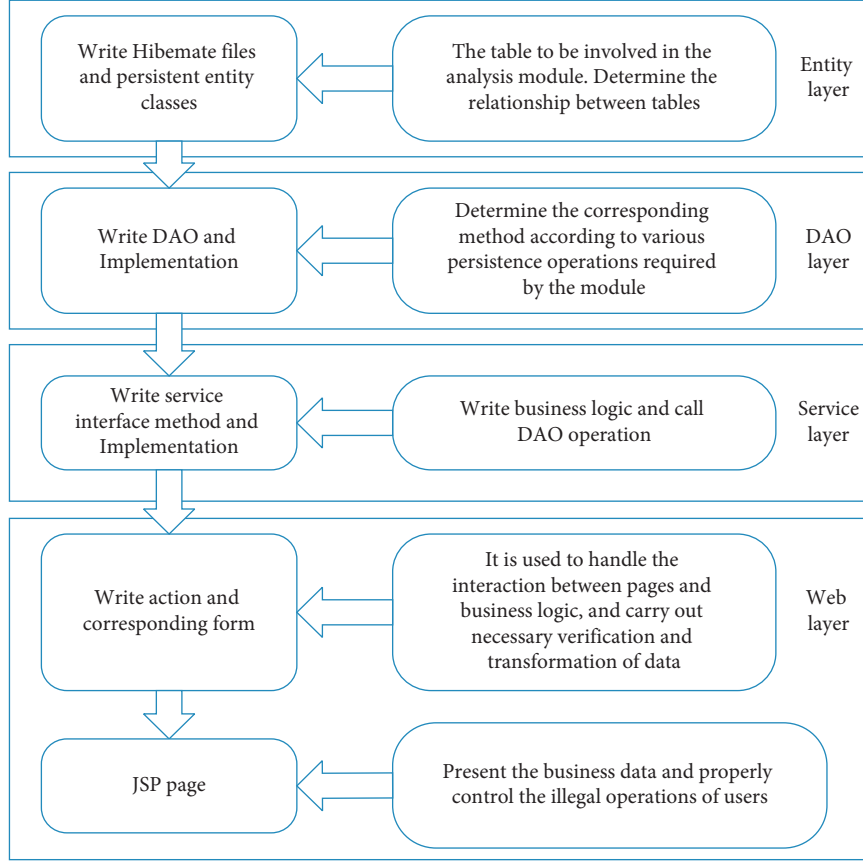


FIGURE 2: Resource recommendation system framework.

the real user resource in the test set, and the smaller the value, the more accurate the prediction score, as shown in equation (23). Coverage refers to the ratio of the number of scoring resources that the recommendation system can predict for the user to the total number of resources in the test set, the higher the value, the stronger the ability of the algorithm to mine long-tail resources, as shown in equation (24). The F1 value refers to the comprehensive evaluation index of the recommendation system, and the higher the value, the better the performance, and the calculation formula is shown in equation (25).

$$W_{MAE} = \frac{\sum_{x=1}^T |r_x - r_u|}{T}, \quad (23)$$

$$C_{COV} = \frac{|L_p|}{t}, \quad (24)$$

$$F1 = \frac{2 \times U_{Precision} \times C_{COV}}{U_{Precision} + C_{COV}}, \quad (25)$$

$$U_{Precision} = 1 - \frac{W_{MAE}}{r_{max} - r_{min}}, \quad (26)$$

where r_x is the true score of item x in the test set. r_u is the resource prediction score of the recommendation system for

the target user. $|L_p|$ represents the number of scoring resources predicted by the push system for the target user. T represents the total number of resources in the test set. r_{max} and r_{min} represent the highest score and the lowest score in the push system, respectively.

5.3. The Results and Analysis. The experiment selects 80% of the real data set as the training set and 20% as the test set, uses the recommendation system to compare the resource score recommended by the user with the resource score in the known test set, and uses the given evaluation index to measure the performance of the recommendation algorithm. Comparing the proposed algorithm with the traditional user-based recommendation algorithm literature [21], the fuzzy C -means clustering-based collaborative filtering algorithm literature [22], and the implicit trust-based recommendation algorithm literature [22], with the same parameters set, evaluate the performance of the recommendation algorithm by scoring and top-N predictions.

The algorithm of this article involves parameters α and β . Among them, the α is the proportion of the comprehensive trust value between users in the comprehensive direct trust value, and the β is the proportion of the global trust value between users in the comprehensive trust value. As shown in Figure 4, different α values have a larger impact on the

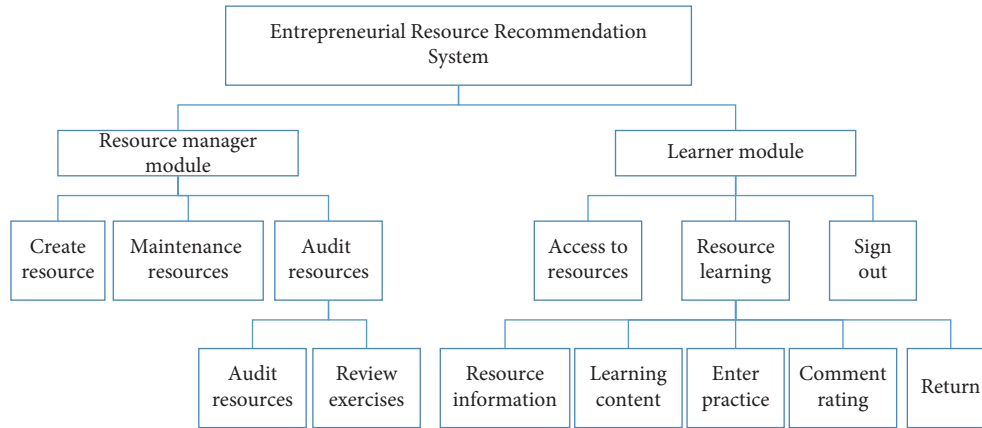


FIGURE 3: System function module.

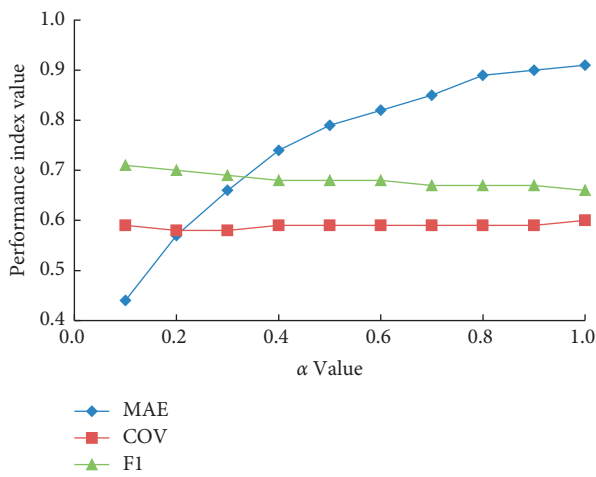


FIGURE 4: Influence of α value on recommended quality.

average absolute error of the prediction score. The average absolute error value is minimal at $\alpha = 0.1$ and $\beta = 0.9$. Coverage and F1 values are the largest, at 0.45, 0.593, and 0.715, respectively. Note that when there are many sparse data and cold-start users, the proposed algorithm relies more on obtaining the best trust neighbours through trust passing between users to achieve scoring prediction.

Figure 5 shows the recommended quality comparison of the proposed algorithm at different neighbours. As can be seen, as the number of near neighbours increases, the quality of recommendations continues to decrease and eventually flattens out. Where MAE increases with the number of neighbours, the reason is that the comprehensive trust value between users continues to decrease as the number of neighbours increases, resulting in a continuous decrease in the quality of recommendations. Eventually, the values of COV and F1 decrease with the increase of the number of neighbours, which proves that the recommended quality of the proposed algorithm is better when the number of neighbours is 5.

Figure 6 shows the variation of the proposed algorithm and the comparison algorithm under different neighbour numbers. It can be seen that when there are different numbers of neighbours, the MAE of the literature [21] and literature [22] algorithms first declines, then rises, and finally

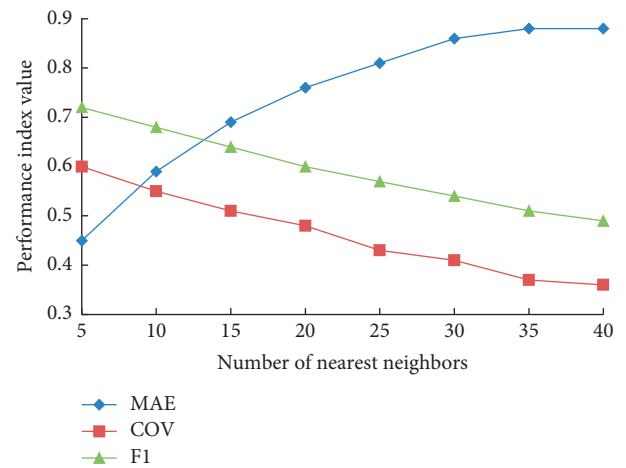


FIGURE 5: Influence of number of neighbours on recommendation quality.

tends to be stable. Moreover, the MAE value is above 1.0, and the proposed algorithm and the literature [22] algorithm are both stable as the number of neighbours increases as the MAE value increases. And the MAE is significantly smaller than the literature [21] and literature [22] algorithms.

Figures 7 and 8 show the changes of COV and F1 values of the algorithm and the comparison algorithm under different numbers of nearest neighbours. It can be seen that with the increase of the number of nearest neighbours, the long tail resources and personalized resources recommended for the target users are reduced, resulting in the continuous reduction of COV. When the number of COV is 40~35, it is not very different from the algorithm in this paper. However, when the number of nearest neighbours is 5~20, this algorithm has a better mining effect for long-tail resources and a better recommendation effect than the comparison algorithm.

Combined with the abovementioned experimental results, the results show that compared with the traditional user-based recommendation algorithm, the collaborative filtering algorithm based on fuzzy c-means clustering, and

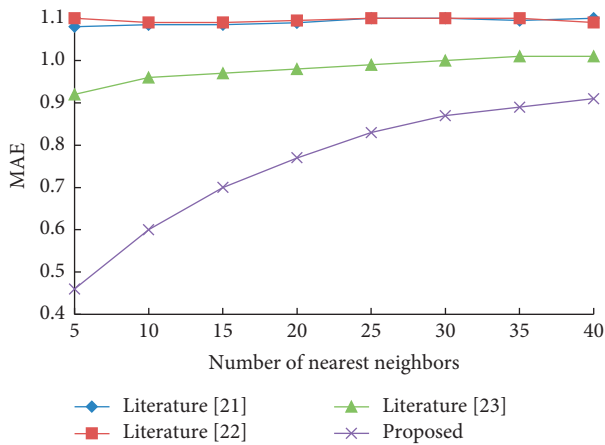


FIGURE 6: MAE comparison of four recommended algorithms.

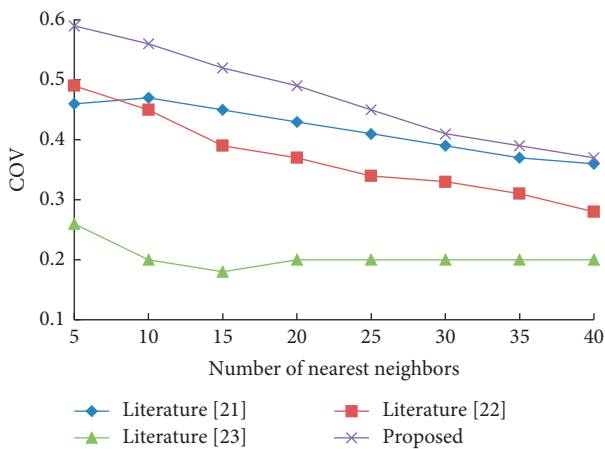


FIGURE 7: COV comparison of four recommended algorithms.

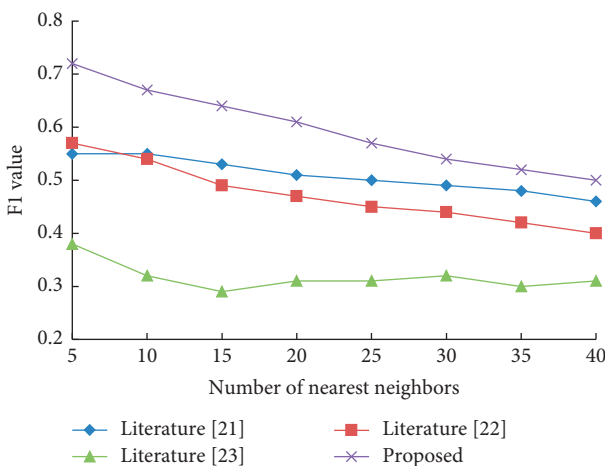


FIGURE 8: F1 comparison of four recommended algorithms.

the recommendation algorithm based on implicit trust, the proposed algorithm has better performance in terms of average absolute error, mining ability of long-tail resources, and comprehensive evaluation index. Especially in the case of a few neighbours, the proposed algorithm can still make

accurate recommendations for target users under the problems of sparse data and cold start.

6. Conclusion

An accurate and effective recommendation system for efficient entrepreneurial resources is an inevitable requirement for developing the innovation and entrepreneurship space based on “Internet +”. To accurately recommend entrepreneurial resources, this paper proposes a recommendation algorithm based on user trust and a probability matrix. To test the effectiveness of the proposed algorithm, the average absolute error (MAE), coverage rate (COV), and comprehensive evaluation index (F1) are used to evaluate the performance of the recommended system. When designing the recommendation system, the web system of the mainstream SSH2 framework is used to create, and the B/S structure of the entrepreneurial resource recommendation system platform is realized. Experimental results show that the proposed system has a higher recommendation quality compared with other recommended algorithms. In the future, the impact of trust propagation among users on the performance of the recommendation system will be studied to further improve the recommendation quality and user experience.

Data Availability

The labeled dataset used to support the findings of this study are available from the corresponding author upon request.

Conflicts of Interest

The authors declare no conflicts of interest.

Acknowledgments

This work is supported by the Hebei Federation of Social Sciences: Research on the cultivation of students’ volunteering practice based on the perspective of social governance modernization (No. 20200602034).

References

- [1] Y. Song, “Cultivation of talents for mass entrepreneurship and innovation of fine arts majors in colleges and universities from the perspective of “internet+,” *IOP Conference Series: Materials Science and Engineering*, IOP Publishing, vol. 750, no. 1, Article ID 012225, 2020.
- [2] D. Tang and X. Li, “Thoughts on innovation and entrepreneurship mode reform of college students in the context of COVID-19,” *International Journal of Electrical Engineering Education*, Article ID 002072092098431, 2021.
- [3] X. Yan, W. Liu, M. K. Lim, Y. Lin, and W. Wei, “Exploring the factors to promote circular supply chain implementation in the smart logistics ecological chain,” *Industrial Marketing Management*, vol. 101, pp. 57–70, 2022.
- [4] S. M. Pompea and P. Russo, “Astronomers engaging with the education ecosystem: a best-evidence synthesis,” *Annual Review of Astronomy and Astrophysics*, vol. 58, pp. 313–361, 2020.

- [5] R. B. Bouncken, S. M. Laudien, V. Fredrich, and L. Gormor, "Coopetition in coworking-spaces: value creation and appropriation tensions in an entrepreneurial space," *Review of Managerial Science*, vol. 12, no. 2, pp. 385–410, 2018.
- [6] P. Nagarnaik and A. Thomas, "Survey on recommendation system methods," in *Proceedings of the 2015 2nd International Conference on Electronics and Communication Systems (ICECS)*, pp. 1603–1608, IEEE, Coimbatore, India, February 2015.
- [7] A. D. Harrison, T. F. Whale, M. A. Carpenter, A. Holden, J. Murray, and T. Vergara, "Not all feldspars are equal: a survey of ice nucleating properties across the feldspar group of minerals," *Atmospheric Chemistry and Physics*, vol. 16, no. 17, pp. 10927–10940, 2016.
- [8] K. K. Brock, S. Mutic, T. R. McNutt, H. Li, and M. Kessler, "Use of image registration and fusion algorithms and techniques in radiotherapy: report of the AAPM radiation therapy committee task group no. 132," *Medical Physics*, vol. 44, no. 7, pp. e43–e76, 2017.
- [9] K. Yu, S. Berkovsky, R. Taib, J. Zhou, and F. Chen, "User trust dynamics: an investigation driven by differences in system performance," in *Proceedings of the 22nd International Conference On Intelligent User Interfaces*, pp. 307–317, Limassol, Cyprus, March 2017.
- [10] A. Zhou, J. Li, Q. Sun, and C. Fan, "A security authentication method based on trust evaluation in VANETs," *EURASIP Journal on Wireless Communications and Networking*, vol. 2015, no. 1, pp. 1–8, 2015.
- [11] A. Gonzalez-Caceres, A. K. Lassen, and T. R. Nielsen, "Barriers and challenges of the recommendation list of measures under the EPBD scheme: a critical review," *Energy and Buildings*, vol. 223, Article ID 110065, 2020.
- [12] Z. Yu and C. Zhang, "Image based static facial expression recognition with multiple deep network learning," in *Proceedings of the 2015 ACM on International Conference On Multimodal Interaction*, pp. 435–442, Seattle, WA, USA, November 2015.
- [13] E. G. Stets, L. A. Sprague, G. P. Oelsner, C. Jennifer, B. Karen, and E. Robert, "Landscape drivers of dynamic change in water quality of US rivers," *Environmental Science & Technology*, vol. 54, no. 7, pp. 4336–4343, 2020.
- [14] A. Hodkinson, *Key Issues in Special Educational Needs and Inclusion*, Sage, New York, NY, USA, 2015.
- [15] L. Wynter, A. Burgess, E. Kalman, J. Heron, and B. Jane, "Medical students: what educational resources are they using?" *BMC Medical Education*, vol. 19, no. 1, pp. 1–8, 2019.
- [16] S. M. Eknath and G. D. Janardhan, "Level of human resources development-a conceptual and review exposition," *International Journal for Research in Applied Science and Engineering Technology*, vol. 8, no. 3, pp. 687–691, 2020.
- [17] A. Kaye-Tzadok, A. Ben-Arieh, and H. Kosher, "Hope, material resources, and subjective well-being of 8-to 12-year-old children in Israel," *Child Development*, vol. 90, no. 2, pp. 344–358, 2019.
- [18] R. Burns, *Adult Learner at Work: The Challenges of Lifelong Education in the New Millennium*, Routledge, England, UK, 2020.
- [19] E. F. Rusydiyah, E. Purwati, and A. Prabowo, "How to use digital literacy as a learning resource for teacher candidates in Indonesia," *Cakrawala Pendidikan*, vol. 39, no. 2, pp. 305–318, 2020.
- [20] N. Q. Linh, N. M. Duc, and C. Yuenyong, "Developing critical thinking of students through STEM educational orientation program in Vietnam," *Journal of Physics: Conference Series*, IOP Publishing, vol. 1340, no. 1, Article ID 012025, 2019.
- [21] M. Kumar, S. Kumar, and P. K. Kashyap, "Towards data mining in IoT cloud computing networks: collaborative filtering based recommended system," *Journal of Discrete Mathematical Sciences and Cryptography*, vol. 24, no. 5, pp. 1309–1326, 2021.
- [22] L. Dincă and A. Peticilă, "How many alder species (*Alnus* sp.) exist? a statistic based on herbarium vouchers," *Scientific papers, Series B, Horticulture*, vol. 63, no. 1, pp. 613–619, 2019.

Research Article

Digital Transformation of Listed Agricultural Companies in China: Practice, Performance, and Value Creation

Ying Yang and Wenqin Cui 

Tongling University, Tongling 244061, Anhui, China

Correspondence should be addressed to Wenqin Cui; cuiwenqin27@tlu.edu.cn

Received 7 January 2022; Revised 19 February 2022; Accepted 2 March 2022; Published 14 April 2022

Academic Editor: Wei Liu

Copyright © 2022 Ying Yang and Wenqin Cui. This is an open access article distributed under the Creative Commons Attribution License, which permits unrestricted use, distribution, and reproduction in any medium, provided the original work is properly cited.

In the digital economy era, the deep integration of the digital economy and the real economy promotes high-quality economic development. The digital transformation of listed agricultural companies in China, which is in a critical period of transformation and upgrading, is an important driving force for achieving high-quality agricultural development. This article takes Xinjinnong as an example to analyze how the practice of digital transformation can improve corporate performance and achieve value creation. The analysis found that in the initial stage of digital transformation (that is, the informationization stage, the company realized financial sharing, the person in charge of the company called the company digitalization 1.0 stage), this paper try to reduce costs and increase benefits by digital transformation from aspect of each link of production and operation (production link, operation link, supply chain management link, etc.) due to the low level of digitalization, the impact of digitalization on corporate performance is limited. The chain management link has achieved cost reduction and efficiency enhancement, and has significantly improved performance. The impact of digitalization on performance in production and application links is not obvious. With the deepening of digital transformation, Xinjinnong will realize value creation in the entire industry chain of the aquaculture industry in the digital 2.0 era.

1. Introduction

In the digital economy era, the in-depth integration of the digital economy and the real economy is an important driving force to promote high-quality economic development. Digitization can increase corporate value through effective use of corporate information to effectively allocate corporate resources [1]; at the same time, after a company has built a digital system, it can interconnect all links from product design to after-sales through the digital system to achieve product innovation acceleration. At the same time grasp the market demand [2]. Enterprises realize digitalization and promote enterprise innovation activities through product innovation, process innovation, organizational innovation and business model innovation [3]. For example, Since 2008 Sany Heavy Industry Co., Ltd., as the Leading enterprises in China's construction machinery industry, has experienced three stages: prosperity, recession and recovery.

Sany has realized digital operation and digital supply chain management. Through the digital transformation, Sany successfully reduced its costs and increased its efficiency, finally realized value creating. The in-depth integration of digital economy and agricultural development in my country's agricultural enterprises, which are in a critical period of transformation and upgrading, is an important measure to accelerate the realization of agricultural modernization [4]. On May 16, 2019, the General Office of the Central Committee of the Communist Party of China and the State Council issued the "Digital Village Exhibition Strategic Outline," proposing that digital countryside is the application of networking, informatization and digitization in the economic and social development of agriculture and rural areas, as well as farmers' modern information skills The improved and endogenous agricultural and rural modernization development and transformation process is not only a strategic direction for rural revitalization, but also an

important content of building a digital China. One of the key tasks is to promote the digital transformation of agriculture. The number of Internet users in rural China is 255 million, and this number increased more than 30% over the 2015. During 13th Five-Year period, the scale of the Internet continues to expand, the application continues to deepen. The Internet has been integrated into all aspects of people's life, and has had an important impact on the law of economic operation and the model of social development [5].

Accelerate the promotion of the application of cloud computing, big data, Internet of Things, and artificial intelligence in agricultural production and management, and promote the comprehensive and in-depth integration of new-generation information technology with plantation, seed industry, animal husbandry, fishery, and agro-product processing industries to create scientific and technological agriculture, Smart agriculture, brand agriculture. Build smart farms (livestock) and promote precision agriculture (livestock) operations [6]. The application and development of the new generation of digital technology in agriculture will help restructure the agricultural industry chain, upgrade the agricultural value chain, deepen the integration of the agricultural industry, explore and innovate new agricultural models and new formats, and promote the development of agriculture to network, precision, and intelligence [7].

On the basis of expounding the basic understanding of digital transformation of agricultural enterprises, Starting from the practical understanding of the new Jinnong digital 1.0 era to the Digital 2.0 era, this paper discusses the impact of the digital transformation process of Chinese agricultural listed companies on enterprise performance, and we also try to provides a reference for the digital transformation of similar enterprises.

2. The Status Quo of Digital Transformation of Agricultural Listed Companies

The Information Center of the Ministry of Agriculture and Rural Affairs issued the "Evaluation Report on the Development Level of Digital Agriculture and Rural Areas in the Country in 2020" and pointed out that the digital level of agricultural production has risen from 18.6% in 2019 to 23.8%. Compared with the digital level of other industries, the level of digitalization of agricultural enterprises is low. However, in the development of agricultural enterprises led by agricultural listed companies, agricultural listed companies have already carried out digital transformation and upgrading in their respective fields.

There are many studies about Agricultural digital transformation, for example, Li Qixiu (2021) studied the basis, mode and future development trend of agricultural digitization from the background of 5 g Er [8]; Yin et al. [9] puts forward the realistic representation, influence mechanism and vehicle road of agricultural and rural digital transformation based on agricultural and rural digital transformation [9]; Qian [10] and Liu [11] proposed that the transformation of agricultural digitization needs to accelerate the construction of agricultural and rural big digital center, driven by technological innovation from the

perspective of digital agricultural transformation. Most of the studies which support the digital transformation of agriculture are How to carry out professional transformation in agricultural companies. The purpose of digital transformation is to improve enterprises' response to uncertainty, Improve the economic benefits of enterprises, So as to enhance their competitiveness. At present, there are relatively few studies on the performance of digital transformation of Chinese agricultural listed companies. In particular, there is less research on the performance of digital transformation of Chinese agricultural listed companies. Based on this, this paper choose xinjinnong as the study object because this company has completed the 1.0 era of digital transformation and is currently undergoing the transformation to Digital 2.0, Meet research needs.

2.1. Digital Transformation of "Dayu Water Saving" Smart Water Conservancy. Dayu Water Saving Group Co., Ltd. is a national high-tech enterprise. "Make agriculture smarter, make rural areas better, and make farmers happier" as the corporate mission; take "agricultural water-saving irrigation, rural sewage treatment, and farmers' safe drinking water" as the company's core business areas, with water network, information network, "Service Network" (referred to as "Three Networks of Agriculture, Rural Areas, Three Waters and Three Networks"), three networks integration technology and service platform, help modern agriculture development and development model of modern agriculture industry and finance integration. In August 2019, the company took water as the entrance and water saving as the starting point, relying on the new generation of digital technology to achieve solutions for precision irrigation, water and soil environment and information technology; in April 2021, Dayu Water Saving signed a strategic cooperation with Huawei The agreement relies on Dayu's water-saving expansion in the "three rural, three-water, three-network" market, and leverages Huawei's next-generation technological advantages in 5G, big data, cloud computing, artificial intelligence, and information communication to build a cloud base for smart water conservancy and water services. The aggregation of water conservancy and water affairs scenario applications and the realization of "digital scenarios, intelligent simulation, and precise decision-making" will help promote the company to accelerate the formation of a demonstration effect in the national agricultural, rural and intelligent water conservancy field, and drive the company's business upgrade and performance improvement.

2.2. Digital Transformation of "Fubon Co., Ltd." Digital Technology and Planting Industry Integration. Fubon innovates in a digital way to effectively open up the upper, middle, and lower reaches of the industrial chain. The digital smart supply chain + platform-based ecological services it builds not only connects the upstream and downstream of the enterprise, the enterprise, and the industry, but more importantly, the connection The individual and data within the enterprises on both sides are reconstructed to

reconstruct the business chain and industrial chain of traditional industries, to help enterprises reduce costs and increase efficiency, and accelerate industrial transformation and upgrading; at the same time, a new intelligent fertilizer distribution station + farmer model is created to provide farmers with a full range of Agricultural technology services.

In the digital agriculture industry, Fubon is in an important stage of transformation and upgrading. Under the guidance of national policies and the company's new-generation technology application, the digital agriculture business will become the company's new profit and value growth point.

2.3. Digital Transformation of "China Information" Agricultural Integrated Service Platform. "Shenzhou Information" takes rural government affairs as the entrance and the informatization processing of rural government affairs as the entry point. The industrial chain extends to the informatization of agriculture, rural areas and farmers, traceability of agricultural products, and large digital platforms for agricultural products. Research and develop smart agricultural projects internally, and cooperate with high-tech companies externally to build a smart management platform.

In addition to the above three listed agricultural companies that have been deployed earlier in the digital transformation of agriculture, "Dabeinong" is also engaged in the integration of digital technology and animal husbandry, and "Guanghong Holdings" is also promoting the overall scale and intensification of agricultural and rural areas. The layout of my country's high-efficiency agriculture has made positive attempts to advance to high-quality development and achieved corresponding benefits.

At present, the digital transformation of agricultural enterprises in my country is still in the layout stage, which is also a key stage of the industrial upgrading of agricultural enterprises. Most of the research on the digital transformation of agricultural enterprises is theoretical research on the path of how digitalization affects performance and value. This article takes the "Xinjinnong" represented by the digital transformation of agriculture and animal husbandry as a case to analyze the road of "New Jinnong" digital transformation and the impact of digital transformation on company performance.

3. Shenzhen New Jinnong Digital Transformation

3.1. Overview of Shenzhen New Jinnong. Shenzhen Xinjinnong is the abbreviation of Shenzhen Xinjinnong Technology Co., Ltd. The company was established in 1999 and landed on the capital market in February 2011. It is a modern technology-based listed company with three core businesses of breeding, feed and animal protection. . After more than 20 years of development, the company now has a national key agricultural industrialization leading enterprise, two national-level core breeding farms, five provincial-level agricultural leading enterprises, and six of the first batch of feed quality and safety management standards that have

passed the acceptance of the Ministry of Agriculture. Demonstration enterprise, an integrated enterprise in the pig breeding industry of seven national high-tech enterprises. In the breeding sector, with the "four modernizations" model + the "four good" goals leading the digital transformation of the company's new technology breeding business, it has successfully survived the impact of the "African Swine Fever" on the breeding industry in 2018 and the impact of the 2020 epidemic on the industry. The "Four Modernizations" model is a standardized, large-scale, intelligent, and ecological scientific breeding model; the "Four Goods" goal is to provide the market with high-quality pig products under the "Four Modernizations" scientific breeding model. Good planting, prevention, eating, and housing.

3.2. Shenzhen Securities New Jinnong Digital Transformation. SAP facilitates the digital transformation of Xinjinnong's agricultural and animal husbandry industry chain with industry-financial integration and transparent management. According to the person in charge of the company's corporate management department, Xinjinnong was successfully listed from 2011 to 2015. Xinjinnong's overall digitalization is very weak. Basically, it handles some related accounting systems manually, which is low in efficiency and poor in accuracy. 2016 to 2019 is the 1.0 era of Xinjinnong's digital transformation, and 2020 to the future will be the 2.0 era of Xinjinnong's digital transformation. The single-industry chain (SAP Business One on HANA) financial sharing platform built by Xinjinnong in 2016 was upgraded to a multi-industry, diversified (SAP S/4HANA) refined management platform after 4 years of use.

3.2.1. Digital 1.0 Era. From 2016 to 2019 is the era of New Jinnong Digital 1.0. The process from the establishment of the SAP B1 system to the deepened application of ERP as the core has gone through the digitalization from 0 to 1 in 2016, which consolidated the basic standardization and the preliminary process of combing. Completed, the digital concept, analysis and sharing in 2017, and finally the intensified application of ERP as the core in 2018 and 2019. Figure 1 describes the digital transformation process of Xinjinnong.

3.2.2. Digital 2.0 Era. In 2020, the company will carry out a comprehensive digital transformation to empower management innovation. The company has initially realized digital transformation. By opening up the entire industry chain, it simultaneously formulates feed formulas and production plans according to different stages of breeding. In this way, the numbers are transparent and the plan is good, thus ensuring the maximum economic benefits of the entire industry chain. Moreover, the integrated financial management platform can directly analyze the costs and benefits of the upstream and downstream of the entire industry chain, and guide the optimization and adjustment of the business based on the feedback information of the financial data, so as to realize the transformation and

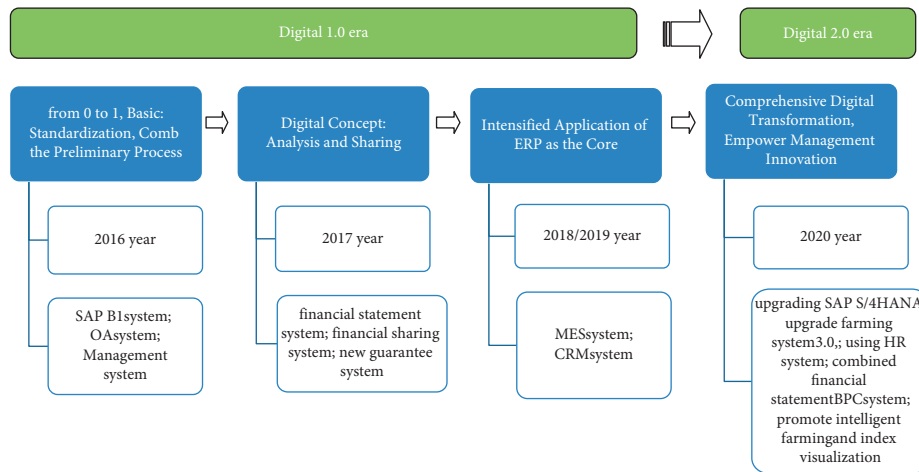


FIGURE 1: Digital transformation process of Xinjinnong (Source: CCID.com, Xu Peiyan).

transformation of the digital empowerment of the enterprise's business, and realize the business financial Converged and integrated digital transformation road. The specific practices of Xinjinnong in the company's digital transformation process are listed in.

In the digital 2.0 era, Xinjinnong will realize the goal of the construction and application of intelligent Internet of Things system, pig individual identification handheld terminal and digital management system. To achieve such a digital transformation, we need to focus on digital acquisition, data management, numerical analysis, and digital assets. The establishment of a technical and economic digital management platform in aspects such as industrialization and management decision-making to achieve digital transformation. Based on the technical and economic digital management platform, three major systems have been built based on production indicators, financial indicators, sales indicators, procurement indicators, market indicators and warehousing indicators to achieve digital transformation and upgrading. The relationship among the three major systems, indicators and platforms is shown in Figure 2. Describes the digital transformation process of Xinjinnong in digital 2.0.

4. Xinjinnong's Digital Transformation and Enterprise Performance Analysis

4.1. Cost Reduction and Efficiency Increase in All Links of Production and Operation

4.1.1. Production Process. Digital production intelligent manufacturing frees production personnel from repetitive work to focus on more valuable and beneficial work [12], and at the same time realizes the interconnection of production equipment through a digital platform, which reduces labor costs and equipment losses [13]. In the era of Digital 1.0, Xinjinnong was mainly financial digitization (Financial Shared Service Center), and the digitization of production was not completed. Therefore, the cost reduction and efficiency increase in the digital production process were not realized. Instead, as the company scale increased, related

indicators in the production process. It has not decreased, but increased. The specific data is shown in Table 1. The original value of fixed assets and the proportion of production personnel in the manufacturing process of Xinjinnong have increased significantly after 2015, especially the original value of fixed assets indicators have shown a stepwise pattern. The growth is mainly due to the fact that Xinjinnong has carried out several large-scale mergers after 2015 to realize the strategic layout of the entire industry chain of the aquaculture industry. However, compared with the substantial increase in the original value of fixed assets, the turnover rate of fixed assets does not have a corresponding proportion. Although there is a decline, the proportion of decline is much lower than the increase in the original value of fixed assets. It can be concluded that Xinjinnong's fixed assets will be optimized after 2015 to speed up the turnover of fixed assets. When the depreciation amount accounts for the proportion of operating income, it is found that this indicator continues to rise, reaching the highest level of 3.79 in 2019, and starting to decline in 2020. From the relevant indicators of the production link of Xinjinnong, it can be seen that Xinjinnong is in the era of digital 1.0. Digital transformation has not made a corresponding contribution to corporate performance. The main reason is that the new Jinnong still adopts traditional production methods in the digital 1.0 era.

Data source: The data in Tables 1–5 come from the 2011–2020 annual report of Xinjinnong. The indicators in the table refer to Wang Ziqing and Chen Jia. Digital transformation and value creation of enterprises-taking Sany Heavy Industry as an example.

4.1.2. Operations. If the company has carried out digital transformation in the operation link, according to theoretical analysis, the company should improve the turnover rate of related assets, business cycle, related management expenses and other indicators [14], reduce management costs and improve operating efficiency [10]. In the 1.0 era of the company's digital transformation, Xinjinnong is mainly financial digital transformation. In the company's operation

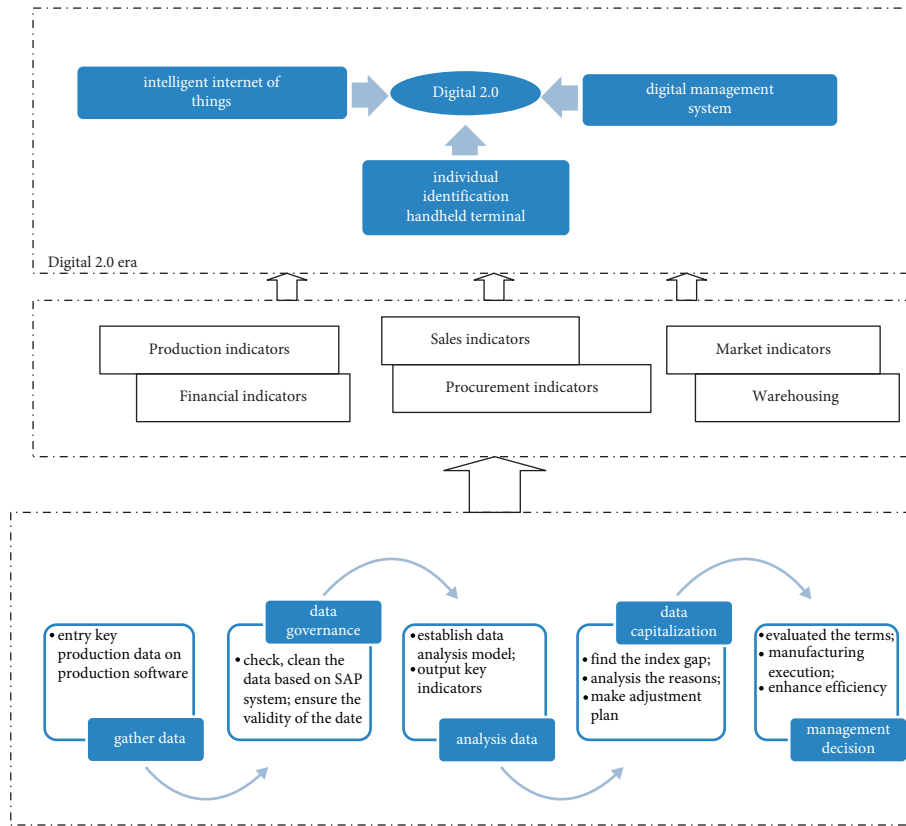


FIGURE 2: Digital transformation process of Xinjinnong in digital 2.0.

TABLE 1: Performance analysis of Xinjinnong’s production links.

year	2011	2012	2013	2014	2015	2016	2017	2018	2019	2020
Manufacturing worker rate (%)	23.87	27.83	27.84	34.25	34.15	39.24	40.91	52.36	52.37	57.64
Labor cost profit rate (%) (labor/profit)	4.04	4.47	4.98	5.61	5.16	7.28	8.73	10.16	11.34	9.54
Depreciation profit rate (%)	0.81	0.86	0.74	1.02	0.93	1.48	2.67	3.01	3.79	2.66
Plant assets of fixed assets (ten million)	10.00	10.78	18.22	25.39	32.21	80.39	90.07	94.07	130.65	182.52
Turnover of fixed assets	20.318	19.412	15.245	9.8849	9.3867	5.166	3.82297	3.3321	2.32817	2.81037

link, it is still the traditional operation model. According to the period from 2011 to 2020, the relevant indicators clearly show a phased change trend, as shown in Figure 3. According to the report, the first stage is from 2011 to 2015, the related indicators have not changed much, and are basically consistent with the company’s normal development level. Business diversification, on the one hand, is the company’s larger-scale merger business, especially the increase in the proportion of the main business of the breeding industry. The breeding industry of Xinjinnong is pig breeding, and the cycle of pig breeding is longer than that of feed processing. Due to the cycle, the number of inventory turnover days of New Jinnong in 2015 was significantly longer than before. Compared with the change in the management expense rate, although there has been an upward trend from 2016, it is less important than the expansion of the enterprise scale. The performance indicators of Xinjinnong in the operation link are shown in Table 2 shown. The financial performance of operation is shown in Figure 4.

4.1.3. Supply Chain Management. The digital transformation of enterprises in the supply chain is mainly to realize data sharing at the end of the supply chain, reduce non-value-added activities at the end of the supply chain, and realize the value creation of the entire industrial chain [15]. The digital transformation of Xinjinnong on the supply chain is mainly on the sales side, increasing online sales, greatly reducing the proportion of sales staff, and strengthening the management of accounts receivable, reducing the turnover days of accounts receivable and multiyear accounts receivable. The management of transfers can improve sales efficiency and increase company value. It can be found from Table 3 that the turnover days of accounts receivable reached a maximum of 39.31 days in 2019, and dropped to 15.61 days in 2020, which is basically the same as 2014, and the proportion of accounts receivable longer than 2 years remained basically the same before 2016, But after 2016, there have been relatively large fluctuations. In 2019, it reached the highest proportion of 58.69, and there was a significant drop in 2020. The short- and medium-term

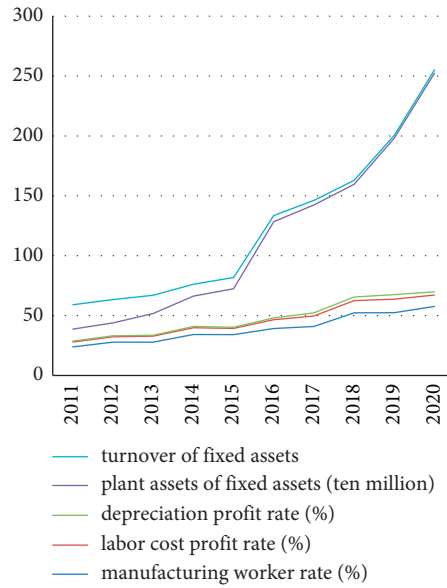


FIGURE 3: Financial performance analysis of production.

TABLE 2: Performance analysis of Xinjinnong’s operations.

year	2011	2012	2013	2014	2015	2016	2017	2018	2019	2020
Inventory turnover	30.8679	28.5588	30.7495	34.32597	25.2965	44.39374	56.92058	57.197	73.5882	83.05079
Business cycle	34.6993	32.2958	37.4263	51.62938	47.7555	70.1618	85.64266	95.2143	112.895	98.65848
Charge ratio (%)	3.9333	4.4622	5.50375	5.3814	5.0302	6.6136	8.2875	8.3118	9.0538	10.2152

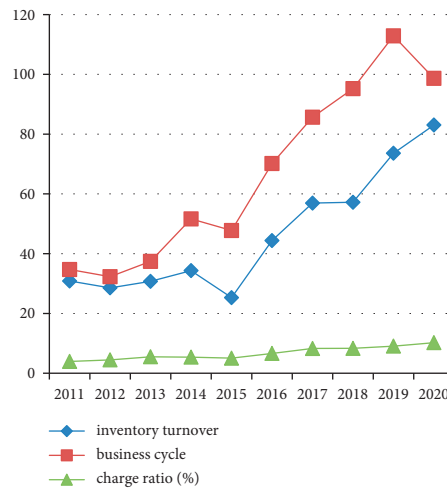


FIGURE 4: Financial performance of operation.

TABLE 3: Performance analysis of new Jinnong supply chain links.

year	2011	2012	2013	2014	2015	2016	2017	2018	2019	2020
Receivables turnover ratio	3.8314	3.73696	6.67678	17.3034	22.459	25.7681	28.7221	38.0174	39.3063	15.60769
1 year–2 year receivables (%)	2.6	5.67	2.67	4.02	4.56	8.55	7.16	11.45	13.08	24.38
Receivables over 2 year (%)	1.2	1.93	2.3	1.42	2.88	4.04	54.7	37.94	58.69	32.38
Bad debt reserve profit rate (%)	0.08	0.01	0.19	0.45	0.18	0.14	0.67	1.31	0.03	0.44
Sales (%)	44.87	40.97	41.65	30.4	27.33	23.33	25.88	21.76	18.97	10.4
Sales expense rate (%)	5.0485	4.661	5.0238	4.6246	3.8323	4.4221	4.6525	4.6929	3.9089	1.6607
Sales profit rate (million)	3.2782	3.4345	3.2837	4.8366	5.2076	4.1298	4.1994	5.4276	6.0454	12.4062

accounts receivable basically showed a slight upward trend. The proportion of customer service staff continued to decline, and as of 2020, it had dropped to 10.40, which was a 30.47 percentage point drop compared with the highest of 44.87 (2011). The main reason for the decline was that enterprises were engaged in sales of modern technology such as Internet+. With the application, the sales and customer service personnel have been greatly reduced, and the corresponding sales expense rate has also shown a downward trend, and the expense category has been reduced, so as to increase efficiency in the supply chain. The financial performance on supply chain management is shown in Figure 5.

4.2. Realizing Value Creation Based on Cost Reduction and Efficiency Enhancement. Xinjinnong is driven by the digital 1.0 era and intelligence (digital 2.0), per capita output value is an important measure of company value creation [16]. Due to the company's strategic implementation of the entire industry chain layout of the aquaculture industry, the total number of employees has increased year by year, reaching 3,150 in 2020. Compared with 1,010 in 2011, the number of employees has tripled. Per capita income has slightly changed, but in terms of the profit index created by the per capita for the company, it basically shows an increasing trend. In addition to the substantial impact of the company's main business number in 2017 and 2018, the African swine fever has shown an upward trend. The profit per capita was minus 110,300 yuan. In 2019, it achieved more than 86,500 per capita. The profit per capita in 2020 is 2.67 times that of 2013. Observation of the per capita salary index shows that it is showing a trend of increasing year by year, especially after 2016. At the same time, the company's per capita salary has shown a simultaneous increase, indicating that the company's production automation level has increased, and the per capita income generated by lean management has significantly increased, which creates more for employees value.

Specific data are listed in Table 4.

The digital transformation of enterprises is a process [17]. The digital transformation of Xinjinnong has experienced the 1.0 era of digital transformation of financial shared services (2016 to 2019) and the 2.0 era of digital transformation that began in 2020, and the 1.0 era of digital transformation of the company. The company achieves the purpose of reducing costs and increasing efficiency in the supply chain management link, and improves the company's operating performance. Judging from the various profit indicators in Table 5, Xinjinnong's operating income decreased due to the impact of African swine fever in 2018 and 2019, and showed a trend of increasing year by year. Especially in 2020, Xinjinnong's receivables reached 40.69. 100 million yuan to achieve strong growth after African swine fever. Return on net assets, net sales margin, and net sales margin appeared negative in 2018, but turned negative to positive in 2019, returning to normal levels in a short time, even after Affected by the new crown epidemic in 2020, Xinjinnong will basically maintain the level of 2019, and the digital transformation and upgrading of enterprises has

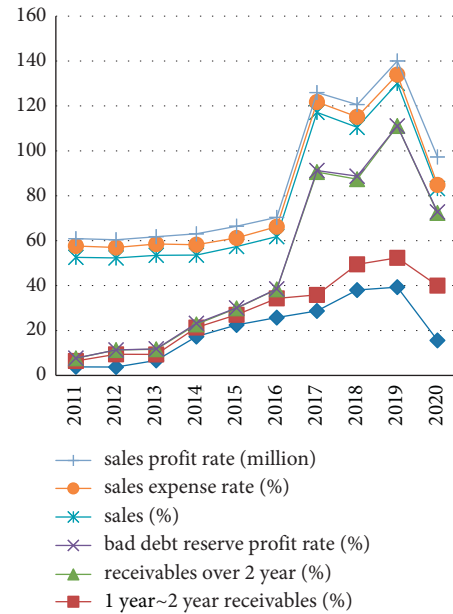


FIGURE 5: Financial performance on supply chain management.

minimized the negative impact of the new crown epidemic. While operating income has grown, the company's various profit indicators have also risen significantly, with good cost control and high earnings quality, indicating that the company's digital transformation has created value for shareholders. The Per capita output value analysis is shown in Figure 6 and the profitability analysis is shown in Figure 7.

5. Summary

From the perspective of the micromajor enterprises of market participants, digital transformation is a process. In the initial stage of transformation, the driving effect of digitalization on business performance is not obvious. As the maturity of digital transformation increases, digitalization will be realized in the entire value chain of enterprise production, operation and management. After the transformation, the cost reduction and efficiency increase of enterprises will be more obvious. Digital empowerment of all aspects of the enterprise, while reducing costs and increasing efficiency, strengthens the enterprise's response to internal and external uncertain risks [3]. This article analyzes the financial indicators of the new Jinnong digital transformation from the 1.0 era to the beginning of the 2.0 era in 2020, and concludes that the new Jinnong's digital transformation in the initial stage of digital transformation, the information phase (digital 1.0 stage), and the impact of digitization on corporate performance. Mainly in the supply chain links and per capita breakthrough level. Due to the low level of digitalization, the impact of digitalization on corporate performance is limited. The chain management link has achieved cost reduction and efficiency enhancement, and has significantly improved performance. The impact of digitalization on performance in production and application links is not obvious. With the deepening of digital transformation, Xinjinnong will realize value creation in the

TABLE 4: Analysis of per capita output value of Xinjinnong.

year	2011	2012	2013	2014	2015	2016	2017	2018	2019	2020
Total employees (thousand)	1.014	1.257	1.455	1.352	1.76	2.867	2.817	2.371	2.093	3.154
per capita sales revenue (million) (business revenue/labor quantity)	1.47	1.40712	1.3676	1.47286	1.4232	0.9637	1.0867	1.1812	1.14668	1.2902
per capita profit (ten thousand) (profit//labor quantity)	6.7019	4.4151	2.9386	4.6298	6.1087	6.0783	3.7681	-11.03	8.6532	7.7783
per capita salary (ten thousand) (labor salary/labor quantity)	5.93948	6.2856	6.8148	8.2503	7.3412	7.0163	9.4922	11.999	13.0059	12.31

TABLE 5: Analysis of new Jinnong's profitability.

year	2011	2012	2013	2014	2015	2016	2017	2018	2019	2020
Business income (hundred million)	14.92	17.69	19.90	19.88	25.05	27.63	30.61	28.01	24.00	40.69
ROE (%)	11.62	6.87	5.21	7.58	8.65	9.65	5.55	-15.54	10.2	9.6
ROA (%)	9.21	5.68	4.15	7.89	8.41	7.34	5.24	-4.81	5.91	6.84
Net profit margin on sales (%)	3.95	3.14	2.15	3.15	4.29	6.31	3.47	-9.34	7.55	6.03
Gross profit margin of sales (%)	12.69	12.1	11.81	14.17	14.03	15.04	18.46	14.75	23.36	28.32

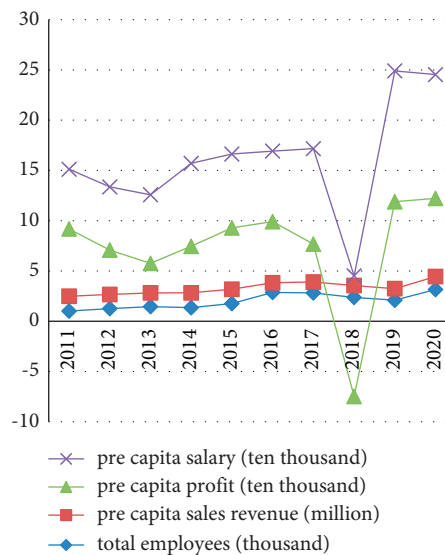


FIGURE 6: Pre capita output value analysis.

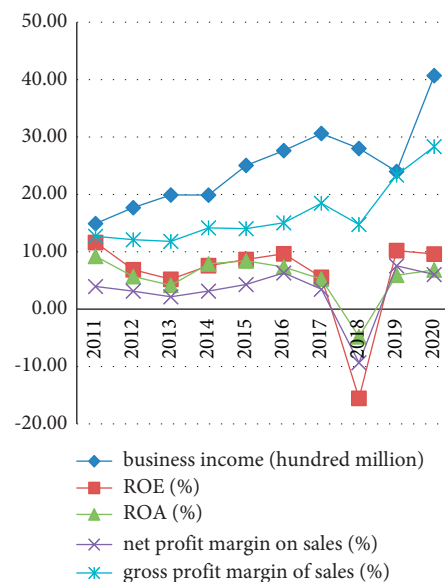


FIGURE 7: Profitability analysis.

entire industry chain of the aquaculture industry in the digital 2.0 era. As the maturity of digital transformation increases, companies will reduce costs and increase efficiency, create value, and increase corporate value in the entire industry chain of the aquaculture industry [18].

The digital transformation of agricultural enterprises is not just a handfuller, apart of the companies, a complex and systematic project. Research on the digital transformation of agricultural enterprises can further study the subdivided industries of agriculture, forestry, livestock and animal husbandry according to the characteristics of agricultural enterprises, at the same time, study how to promote their high-quality development.

Data Availability

No data were used to support this study.

Conflicts of Interest

The authors declare that there are no conflicts of interest regarding the publication of this article.

Acknowledgments

This work was supported by the Anhui Province University Young Teachers Funding Project (2008jqw135) and Tongling University Talent Research Startup Fund Project (2014tlxyrc05).

References

- [1] A. Bharadwaj, O. A. El Sawy, P. A. Pavlou, and N. Venkatraman, "Digital business strategy: Toward a next generation of insights," *MIS Quarterly*, vol. 37, no. 2, pp. 471–482, 2013.
- [2] T. Ritter and C. L. Pedersen, "Digitization capability and the digitalization of business models in business-to-business firms: P," *Industrial Marketing Management*, vol. 86, no. 4, pp. 180–190, 2020.
- [3] Y. Liu, J. Dong, and J. Wei, "Digital innovation management: Theoretical framework and future research," *Management World*, vol. 36, no. 7, pp. 198–217+219, 2020.
- [4] Y. Liu, "Efficacy analysis and countermeasures of agricultural digital transformation," *Economic Aspects*, vol. 07, 2020.
- [5] M. Li, "Research on the transformation and development of agricultural digitization," *ICT and Policy*, vol. 11, pp. 57–61, 2020.
- [6] General Office of the Central Committee of the Communist Party of China, "State Council," *Digital Village Exhibition Strategic Outline*, vol. 05, 2019.
- [7] M. Wang and D. Li, "Push for the deep integration of digital technology and agriculture and rural areas," *China Agricultural Abstracts*, vol. 32, 2020.
- [8] Lixiuqi, "Research on agricultural digital development in 5g Era," *Shanxi Agricultural Economy*, vol. 12, pp. 155–156, 2021.
- [9] H. Yin, P. Huo, and S. Wang, "Agricultural and rural digital transformation: Realistic representation. Influence mechanism and promotion strategy," *Reform*, vol. 12, pp. 48–55, 2020.
- [10] H. Qian, "Efficiency analysis and promotion path of agricultural digital transformation," *Tropical Agricultural Engineering*, vol. 12, pp. 6–8, 2020.
- [11] Y. Liu, "Efficiency analysis and Countermeasures of agricultural digital transformation," *Economic Review*, vol. 7, pp. 106–113, 2020.
- [12] S. G. Gavrilu and A. D. L. Ancillo, "Spanish SMEs' digitalization enablers: E-Receipt applications to the offline retail market," *Technological Forecasting and Social Change*, vol. 162, no. 1, Article ID 120381, 2020.
- [13] C. Legner, T. Eymann, T. Hess et al., "Digitalization: Opportunity and challenge for the business and information systems engineering community," *Business & Information Systems Engineering*, vol. 59, no. 4, pp. 301–308, 2017.
- [14] Minghua and X. Yin, "Literature review of digital transformation and enterprise value influencing factors," *Marketing Circle*, pp. 75–76, 2021.
- [15] J. Chen, S. Huang, and Y. Liu, "From enabling to enabling—enterprise operation management in a digital environment," *Management World*, vol. 36, no. 02, 2020.
- [16] F. Lv, Y. Zhu, and R. Catherine, "Overview of the innovation value chain in the context of digitalization abroad," *Science and Technology Management Research*, vol. 40, no. 14, 2020.
- [17] Z. Wang, W. Wei, W. Zhu, and J. Liao, "Exploration of Rainbow's digital transformation path from the perspective of business model," *Journal of Management*, vol. 17, no. 12, 2020.
- [18] Z. Wang and J. Chen, "Enterprise digital transformation and value creation—taking Sany Heavy industry as an example," *International Business Accounting*, vol. 10, 2021.

Research Article

Research on Basic Information of Enterprise Electronization under the Background of Big Data

Qihang Wang 

Business School, Chongqing College of Electronic Engineering, Chongqing 401331, China

Correspondence should be addressed to Qihang Wang; 200624018@cqcet.edu.cn

Received 19 February 2022; Revised 16 March 2022; Accepted 28 March 2022; Published 11 April 2022

Academic Editor: Wei Liu

Copyright © 2022 Qihang Wang. This is an open access article distributed under the Creative Commons Attribution License, which permits unrestricted use, distribution, and reproduction in any medium, provided the original work is properly cited.

Ensuring information security is a maintenance process that combines dynamic and static. First of all, you can use a series of protective tools, such as firewalls, operating system authentication, encryption, and so on. At the same time, use some dynamic detection tools. With the rapid development of Internet technology, big data, cloud computing, and other technical terms are no longer strange to people. Today's society is increasingly networked, creating a common platform for big data resource sharing and data communication in various industries. Big data and cloud computing technology have been applied to every field of human life with a strong penetration, resulting in technological innovation in various industries. Under the background of the rapid development of big data and cloud computing technology, the traditional enterprise form has been difficult to cope with the increasingly fierce competitive environment, making the electronic enterprise become the inevitable trend in the development and reform of enterprises in today's world. Electronic enterprises promote the efficient and vigorous development of enterprises, improve the speed, efficiency, and market competitiveness of enterprises, and better adapt to the changes in the market environment caused by big data and cloud computing. With big data and cloud computing as the background, this paper studies and analyzes the inevitability, basic characteristics, existing problems, countermeasures, and other basic information of enterprise electronization, so as to provide theoretical guidance for enterprise electronization. It has the ability to control the dissemination and content of information, ensure the censorship of information, and provide the basis and means of investigation for emerging network security issues.

1. Introduction

In recent years, the informatization of enterprises and the socialization of the network have gradually risen, and the corresponding derivatives such as cloud computing, the Internet of Things, and the mobile Internet have also been widely used quickly. In the era of big data, data has the characteristics of "massive, diverse, high-speed, and variable." From a large variety of massive data, through in-depth analysis by means of cloud computing and other means, to find out valuable information for enterprise development and to find new ones, laws and contents are applied to enterprise production, enterprise trade, enterprise planning, etc., to realize scientific management of enterprises and improve the operational efficiency of enterprises. The development of the times requires enterprises to change the

traditional business model and promote the electronic management of enterprises, which not only improves the management efficiency of enterprises but also is an important strategic guarantee for enterprise development [1]. Although "big data" can literally be understood as a large amount of data, it is still impossible to distinguish "big data" from "massive data" and "hyperscale data" only in the dimension of magnitude.

The emerging product "big data" in the IT field is used to rationally plan the market in this field and continuously improve new technologies and products and services. Enterprise electronization refers to the integration of data and information, such as production, operation, and trade of enterprises through advanced technologies such as big data and cloud computing, to realize informatization and digitization of enterprises, improve the operational efficiency of

enterprises, and reduce business risks and industries. Cost improves the overall management level and the ability of continuous operation and improves the comprehensive level of production, operation, management, decision-making, and service, thereby effectively improving the market competitiveness of enterprises. In the twenty-first century, advanced technologies such as big data and cloud computing have strongly promoted the rapid development of society and gradually become an important symbol of social progress [2, 3]. In the era of rapid development and application of technologies such as big data and cloud computing, the level of electronization has gradually become an important criterion for measuring the degree of modernization of an enterprise. Electronic enterprise is an inevitable choice for enterprises to adapt to the development of the times. Electronic technology has developed into an important resource for enterprises. By making full use of this resource, it can greatly enhance the efficiency of enterprises [4]. Accompanied by various information security conferences and big data security forums. While big data brings development opportunities to mankind, it also brings many security problems. There are also many cases that threaten data security.

Enterprises should manage data in an all-around way, not just to achieve the goal of preventing data leakage. Many experts and scholars at home and abroad have conducted much research on the research of enterprise electronization. Putra P. O. H. et al. [5, 6] assessed and critically analyzed a range of research frameworks and assessed the extent to which the nature of SMEs and their ability to provide practical tools for SME transformation were assessed. It provides a multifaceted overview and presents a preliminary concept for integrated e-commerce for the SME framework. Tan Xiao et al. [7, 8] analyzed the problems existing in the information construction of coal enterprises in China and proposed corresponding countermeasures to improve the level of informatization construction of coal enterprises. Lipitakis and Phillips [9, 10] studied the impact of the financial and nonfinancial performance of the organization on e-commerce strategic planning and constructed a conceptual model. The United Kingdom and Greece tested it to verify the scalability and effectiveness of the model. Chen et al. [11, 12] studied the intrinsic influence mechanism of enterprise informatization, IT capability, and innovation ability. Based on the theoretical research, the research results were fully discussed and the countermeasures were proposed. He et al. [13, 14], based on the e-commerce development index system issued by CII, through the status quo investigation and data collection, create an e-commerce development level measurement model, comprehensively apply factor analysis and cluster analysis methods to deeply analyze the development level of China's e-commerce, and put forward relevant countermeasures and suggestions. Bi et al. [15, 16] tested a theoretical model for assessing e-commerce capabilities and value in a rapidly growing small and medium-sized enterprise (SME) environment, providing a preliminary demonstration of the relationship between IT and SME performance evidence. Wei [17, 18] carried out a certain degree of analysis on the application of

computer application technology in enterprise informatization to promote enterprises to strengthen information construction. Although there has been a lot of research on enterprise electronization, the research on basic information of enterprises is not comprehensive and detailed, and there are still some shortcomings. E-commerce companies are developing rapidly, and the development of the small and microloan market with the help of the big data era has attracted close attention from all walks of life. From this point of view, big data is of great significance to the development and competition of enterprises.

Taking big data as the meeting point, the data generated from various new-generation information technology applications will be brought together, and the unified and comprehensive processing, analysis, and optimization of data from different sources will help to deeply improve the user experience. At the same time, it can excavate huge commercial value, economic value, and social value. Enterprise electronization is not only the need for enterprise development but also a key force for enterprise innovation. For enterprises, enterprise electronization has gradually become a vital component of the company's international strategic layout and effectively promotes the development and progress of the company's scale, efficiency, market advantage, culture, and work mode. Electronization is an important metric for the internationalization and modernization of traditional enterprises, and it is the boost for the rapid and all-round development of SMEs (Small and medium enterprises). Since the establishment of the Ministry of Industry and Information Technology, the state has vigorously promoted and promoted the promotion of electronic information technology. The electronization of enterprises has become the only way for enterprises in the new era to flourish. In recent years, with the development of emerging Internet technologies such as big data and cloud computing, the development of traditional enterprises has suffered a huge impact. In the face of an increasingly competitive environment, traditional companies must be electronically adapted to the new environment. The ever-changing Internet technology is triggering a storm that has revolutionized all aspects of traditional businesses. With the comprehensive development and application of big data, cloud computing, and other technologies, the demand for electronization of traditional enterprises continues to increase. In the context of big data, cloud computing, and other technologies, this paper studies the basic information of the inevitability, basic characteristics, difficulties, and countermeasures of enterprise electronization and provides theoretical guidance and suggestions for the electronic transformation of traditional enterprises.

2. The Inevitability of Enterprise Electronization in the New Era

2.1. The Development of Big Data Technology Is the Main Driving Force for Enterprise Electronization. The new opportunities brought about by big data technology and the prospect of electronization have an unstoppable temptation for enterprise development. Under the traditional enterprise

model, it is not easy for companies to develop their own business radiation range for the whole country. It is even more unrealistic to go deep into the world market. And enterprise electronization can help companies to meet these requirements easily. In short, the rapid development of Internet technology has brought a new market competition environment for enterprises. Technologies such as big data and cloud computing integrate enterprises and customers into their application systems and utilize information sharing and real-time interactive functions to minimize unnecessary links in the middle, improve operational efficiency, and achieve open and transparent information, thus constructing an open market environment [19, 20]. In this open market environment, the distance between the company and the customer becomes very close, making the competition between enterprises become open competition for customers. Various companies can compete in this open market regardless of the size of their operations. This hinders the market monopoly of some enterprises and forms a multipolarized form of competition. Especially for small and medium-sized enterprises, this is a rare opportunity for development [21]. Media technology has liberated the geographical space constraints of business operations and broke the geographical restrictions of traditional enterprise markets. The concept of geography can no longer hinder the development direction of the enterprise and the scale of the market. Customers and enterprises can conduct trading activities without leaving the house. Enterprise electronics can enable companies to reach potential customers around the world, and the market opens up to areas that were previously inaccessible. This open and transparent market competition environment has undoubtedly provided many enterprises with new development opportunities and become a great driving force for traditional enterprises to carry out electronization. The influencing factors of e-commerce system acceptance are shown in Figure 1.

At present, human beings have fully entered the era of informationization. Modern information technologies such as the popularization of the Internet, computers, the maturity of network communications, and breakthroughs in data management are rapidly infiltrating all fields of society.

$$\begin{aligned} \rho &= (\beta + \pi)h\tau_K, \\ \psi_n &= (\mu + \delta)\delta\lambda H\vartheta_M + \frac{(n + \theta)\phi HS_M}{V_B C}, \\ \beta &= \frac{K}{S - \theta(-L\phi_M/G_B C)}, \end{aligned} \quad (1)$$

ρ represents the development parameters of the Internet, ψ_n represents the challenges encountered in the development process, and β represents the speed.

The Internet occupies an important position in the market economy, plays a leading role in the economy, and has a strong guiding role in economic innovation, thereby stimulating the production vitality of the whole society $J(N)$ and promoting economic development.

$$\begin{aligned} J(N) &= N \sum_{F=0}^{\infty} (\sqrt{N})^2 \lambda_n, \\ B_S &= B_0 \left(\frac{M}{K_S} \right)^4 \frac{L}{1 - \kappa(-L\omega_M/L_B T)}, \\ Q_{aS} &= Q_0 \left(\frac{L}{\lambda_S} \right)^4 \frac{\kappa}{\exp(J\varphi_M/L_B H) - 1}. \end{aligned} \quad (2)$$

The sum of the distance traveled to visit n points is equal to the following:

$$\begin{aligned} M(N) &= \sum_{k=0}^{N-1} D(K)x(L - H), \\ z &= 2 \sum_{j=2}^n c_1. \end{aligned} \quad (3)$$

The resulting distance saving value $s(i, j)$ can be calculated as follows:

$$s(i, j) = 2c_{11} + 2c_{1j} - (c_{1i} + c_{1j} + c_{ij}). \quad (4)$$

Per-service perceived performance values for each dimension:

$$Q = \frac{1}{M} \sum_{i=1}^m p w_i. \quad (5)$$

2.2. The Urgency of Electronization of Traditional Enterprises.

In today's environment, traditional enterprises facing great threats also want to change and open up new living environments. In the tide of Big data and cloud computing technology, the Internet has challenged the traditional enterprise model, and the relationship between the enterprise and the customer and the relationship with the cooperative enterprise has undergone tremendous changes. The form of competition between enterprises has also become more open, and it has also produced many new ways of competition and competitiveness. Under such external pressure, many traditional enterprises are facing an unprecedented impact, and many shortcomings within traditional enterprises are clearly exposed. In order to improve operational efficiency and acquire new competitive quantities, traditional enterprises must promptly explore enterprise survival strategies in the new environment, and electronization is undoubtedly the best choice. The electronic trading platform is shown in Figure 2. The rapid development of information technology has promoted the process of information globalization, and information plays an important role in social and economic development. Information technology has penetrated into all walks of life in our society and affects each of us. At the same time, because of its important value, information has evolved into an important factor of production in our production process.

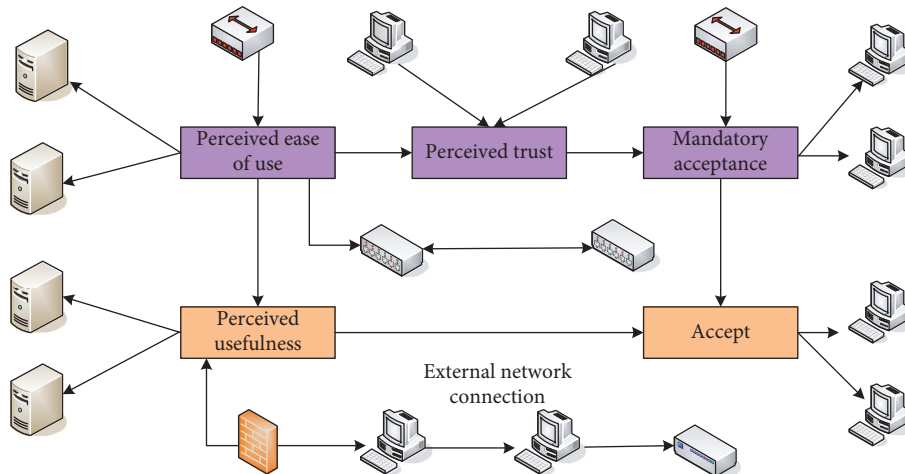


FIGURE 1: The influencing factors of e-commerce system acceptance.

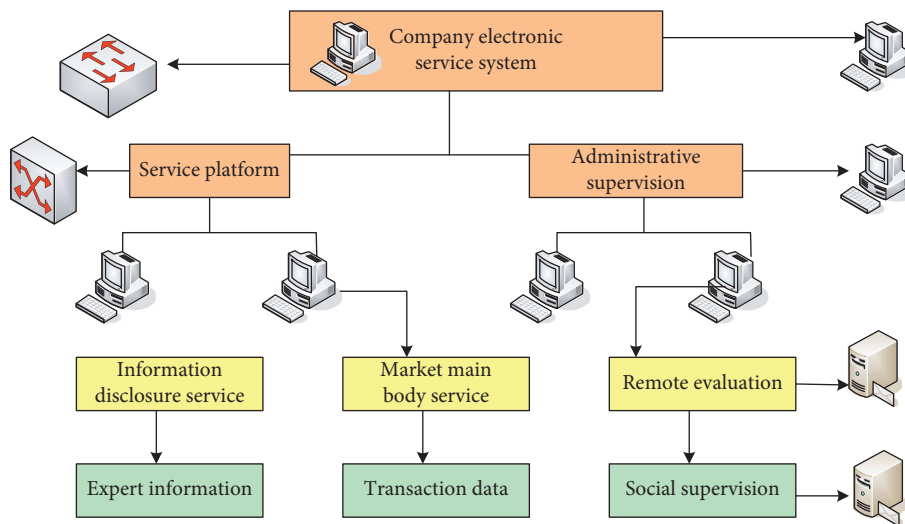


FIGURE 2: The electronic trading platform.

2.3. Enterprise Electronization Is the Requirement for Enterprises to Participate in International Competition. The current trend of global economic integration has become increasingly apparent, and information technology plays a very important role in the process of economic globalization [22]. With the development of Internet information technology such as big data, cloud computing, the management and management of multinational corporations have undergone tremendous innovation, which has caused a great impact on China’s economic market. With the continuous invasion of multinational corporations, Chinese enterprises must change their traditional modes of operation, implement enterprise electronization, gradually integrate into the international market, participate in the distribution of international resources, and seize the international market share. Traditional enterprises must realize that information resources are the lifeline of enterprises, and they must have stronger capabilities in collecting, processing, processing, and disseminating information in order to obtain better competitive advantages and seize market opportunities.

2.4. Enterprise Electronization Can Improve the Core Competitiveness of Enterprises. Enterprise electronization is a necessary means for enterprises to adapt to the ever-changing market environment. In the information age, the market is changing rapidly. The development, production, production, listing, and service rhythm of products are accelerating. The product life cycle is greatly shortened, and the production methods of enterprises have also changed. It has been reduced from the traditional production mode of large quantities and small varieties. The production mode of batch and multivariety changes. Customer demand determines the survival of the company. Meeting the increasingly individualized needs of customers with the best quality, the shortest time, the lowest cost, and the most perfect service is the premise and basis for the survival of the company. Understanding, analyzing, transforming, developing, guiding, and realizing user needs has become the focus and difficulty of corporate work. With the acceleration of global economic integration, any enterprise will face the most powerful competition and challenges from the industry, the

local domain, and even world-class enterprises, as well as the opportunity to develop its potential customers in the global park. In a sense, information resources are more important than material resources in a strategic sense. The competitiveness of enterprises depends to a large extent on the information competitiveness of enterprises. Electronic construction has become the best choice and the only way for enterprises to gain competitive advantage.

3. Basic Characteristics of Enterprise Electronization

In the context of big data, the electronic strategy of enterprises needs to use new information and thinking to carry out new layouts and construction. In addition, with the more convenient cloud computing technology resources to enhance the competitiveness of enterprises and complete the electronization of enterprises. The widespread popularity of big data technology and its applications has had a profound impact on traditional enterprise models, and corporate electronization has gradually evolved toward externalization. Enterprise electronization is not only for internal employees but also for customers at the end of the enterprise industry chain. In the process of enterprise electronization, although the influence and factors of the industry type and enterprise scale are different, different enterprises have different understanding and construction of electronization, but enterprise electronization generally has the following basic characteristics.

3.1. Deep Integration of Mobility, Socialization, and Enterprise Applications. Under the influence of the big data technology revolution, diverse Internet application forms make information exchange updates simple and fast and change the communication forms of enterprise managers, internal employees, and external partners, thus further impacting corporate decision-making, marketing, procurement, and many other aspects. Technical approach. Smartphones are currently the most important mobile terminal. In the global smart market in 2018, smartphone shipments were 1.49 billion. Combine it with the electronization of the enterprise and realize the characteristics of its mobile socialization and deep integration with enterprise applications. The popularity of smart phones has greatly improved the level of mobilization and socialization of enterprises, making mobile enterprise applications occupy an important position in enterprise electronization. Mobile enterprise applications have become the main direction of future business innovation. In particular, mobile terminal applications developed using Internet technologies such as big data and cloud computing have become an important part of enterprise electronization [23]. The use of mobile terminal applications can realize information exchange and mobile office within the enterprise and also realize the interaction and interaction between enterprises and consumers, thereby improving the scope of influence of enterprises. In addition to smart phones, mobile terminal devices that

can meet enterprise-level applications are also gradually diversified, driving the development of enterprise electronic forms toward flatness and transparency, and traditional corporate boundaries are broken.

3.2. Increased User Experience. As big data and cloud computing technologies are widely used in enterprise processes. Enterprise electronization has also produced new features. The content provided by enterprise electronic applications has changed. It is no longer just to provide products. Enterprise services have become the key content of enterprise electronic applications, and the importance of user experience has been increasing. For example, when building an ERP system, enterprises can increase the user experience, increase the interaction function, facilitate the collection of employees' suggestions, and increase the cohesiveness of the enterprise. At the same time, research and develop a supporting mobile application system to provide users with convenient communication channels and convenient decision-making tasks. The rapid delivery further enhances user satisfaction [24]. What kind of technology is used? As long as the enterprise electronization realizes the integration of internal processes and the user experience satisfaction is improved, the effectiveness of the enterprise electronization will be obvious.

3.3. Digitization of Enterprise Information. Digitization of enterprise information is an important part of the enterprise's electronic structure. Data services are mainly represented in the integration and availability of data. Due to the rise of the Internet, massive data has grown exponentially, data sources and data types have been continuously enriched, and the impact on corporate decision-making is increasingly dependent on data, not only depends on the company's operational production data but also on mobile applications, web pages, etc. Consumer behavioral information in public Internet platforms is closely related. That is to say, in the multiterminal and multiformat environment of Internet, the data to be processed by enterprise electronization will continue to increase, including not only the production data of various workflows within the traditional enterprise but also online social platforms, mobile commerce applications, news. The information in Internet application platforms such as information, the degree of digitization of enterprise information is deepening, and it is even more important in the electronization of enterprises. The rapid development of the Internet has made the scale of available data expand rapidly. Therefore, it is necessary to clean and filter huge data, analyze the data attributes and data sources in detail, and explore the inherent relationship implicit in the deep data. The auxiliary decision-making system is formed for the data with the value of use, and the intelligent decision-making of the enterprise is realized [25, 26]. The key to the electronization of traditional enterprises lies in the use of the value of information resources in business operations and business development.

3.4. Technical Service Capabilities Extended to the Industrial Chain. In the era of big data, with the increasing influence of consumers on enterprises, enterprise electronization should not only meet the needs of internal functional departments and employees but also meet the needs of external commercialization and expand enterprise electronic services from the inside to the outside. Build and integrate the entire industry chain platform [27]. Therefore, in the process of enterprise electronization, enterprise informatization will be incorporated into business services and provide external service delivery. According to the survey, 77% of CIOs' current work focuses on "integrating and optimizing systems," exploring how to build industry chain informatization and provide external services for the entire industry chain.

3.5. Technology Light Asset Model Transformation. With the development of the Internet, information communication is becoming more and more convenient, the social division of labor is further refined, services provided outside the enterprise are becoming more and more abundant, and intermediate products and services that need to be solved within the enterprise are becoming less and less. Therefore, the resources that need to be purchased within the enterprise are gradually replaced by an external supply. This means that more and more assets in the electronic process of the enterprise are provided and delivered by independent third parties. Therefore, the electronic process of enterprise in the Internet era will gradually prefer the light asset model. Taking the information technology hotspot cloud computing as an example, using a cloud service project provided by a third party to pay a fixed cloud service fee every month, you can enjoy a full set of cloud services including network dedicated line equipment, infrastructure, operation, and maintenance services. The light asset model eliminates electronic construction investment and long-term maintenance fees. In addition to the "light asset" of visible assets, the light asset model can also be expressed as "light asset" of human resources [28]. Due to the cloud computing-based information technology management model, information technology personnel are relatively concentrated in a certain area and no longer separate. Therefore, talent management will realize a centralized management mode in the electronic process of the enterprise, which will optimize the integration of human resources and achieve intensive human capital.

4. Problems in the Electronic Process of Enterprise

4.1. Insufficient Understanding of Enterprise Electronic Construction. Some enterprises have not fully understood electronic construction and have not paid enough attention to electronic construction of enterprises. They mistakenly believe that the long-term development of enterprises does not require electronic construction. Some business managers are accustomed to experience management methods and are not aware of the impact of electronic construction on enterprises. In the era of big data technology, the

information determines the future and destiny of the enterprise. Without electronic construction, enterprise development will certainly develop slowly and will not last long [29].

4.2. Basic Work Cannot Meet the Needs of Electronic Construction. On the one hand, the internal indicator system of the enterprise is not uniform, which brings great trouble to electronic construction. The indicator system is necessary for business management and is an important foundation for the company. Some internal products, materials, and equipment are not uniformly coded, and the grassroots departments have to deal with the data reports of different departments. The channel data of the indicators of the upper management departments are not the same, which seriously affects the accuracy and authenticity of the information. Secondly, the enterprise information collection channel is relatively backward, resulting in incomplete information. Traditional market research lacks innovation, cannot guarantee the timeliness and accuracy of information, and affects the reliability of information [30].

4.3. Enterprises Pay Insufficient Attention to Management and Restructuring in the Process of Electronic Construction. Some enterprises have an insufficient understanding of the role and significance of management and reorganization in the process of electronic construction. China's current enterprise management model needs to be improved. Although it has a strict hierarchical system and detailed characteristics of labor division, the functional departments are independent and lack each other. The issue of communication and collaboration cannot be ignored. Without good cooperation, it will cause wasteful internal friction and enthusiasm for employees. The lack of information exchange, affecting the efficiency of information transmission, has a great negative effect, unable to meet the needs of market customers. Second, the company did not grasp the essence of electronic construction. The essence of enterprise electronic construction is to enhance the competitiveness of enterprises through management and restructuring. Most of the electronic construction of enterprises ignores the change of management mode, so it has not achieved good results [31].

Two weeks after the questionnaires were distributed, the questionnaires were collected. In the process of inputting, the questionnaires were preliminarily tested for validity, and the invalid data (questionnaires that were not completely filled out, questionnaires that were filled in hastily) were excluded. The specific recovery results are shown in Table 1.

The sample statistics of the valid questionnaires are made, and the results are shown in Table 2.

In addition to the user behavior, the reliability test value of the factors affecting the perceived ease of use is relatively low, which does not affect the reliability of the questionnaire, but it is necessary to make simple corrections on the ease of use of information technology, trust in the system, technology trust, and mandatory acceptance. Cronbach's Alpha reliability test is shown in Table 3. Cronbach's coefficient is a

TABLE 1: The specific recovery results.

Questionnaire	The number of questionnaires issued	Number of returned questionnaires	Number of valid questionnaires
Network distribution	500	390	354
Paper questionnaire	100	60	40
Total	600	450	394

TABLE 2: The sample statistics of the valid questionnaires are made.

Questionnaire	Options	Frequency
Gender	Male	180
	Female	204
Age	Under 20	12
	20–25 years old	228
	25–30 years old	96
	30–35 years old	23
	36+	23

TABLE 3: Cronbach’s Alpha reliability test.

Options	Frequency	Cronbach’s alpha	Number of items
Accept	Use behavior	0.210	2
	Information technology	0.735	4
Perceived ease of use	Management technology	0.704	2
	Work hard to expect	0.672	2
	System functions	0.921	12
Perceived usefulness	Performance expectations	0.782	3
	Social influence	0.822	3

set of commonly used methods to measure the reliability of psychological or educational tests. It overcomes the shortcomings of the partial halving method and is the most commonly used reliability index in social research. It measures the reliability of a set of synonymous or parallel “sum.”

In the statistical analysis table of basic data, it is found that the e-commerce used by this group is mainly personal system, and the ratio of enterprise and personal e-commerce systems is 0.635 and 0.818, respectively. More than half of the people have contacted or used this type of e-commerce system, so it is feasible to analyze the influencing factors of enterprise acceptance behavior. E-commerce acceptance behavior is shown in Figure 3.

Figure 4 shows the rapid growth in the number of consignees and consignors, the number of inquiring customers, the number of foreign agents, and the number of carriers (shipping companies, airlines).

The influencing factors in this study have a high structure, and the mutual independence of the influencing factors is relatively low. In order to support the research purpose, the structural validity test of the influencing factors should be carried out to provide a basis for determining the construction of the model. The tests of KMO and Bartlett are shown in Table 4. When the sum of squares of simple correlation coefficients between all variables is much larger than the sum of squares of partial correlation coefficients, the KMO value is close to 1. The closer the KMO value is to 1, the

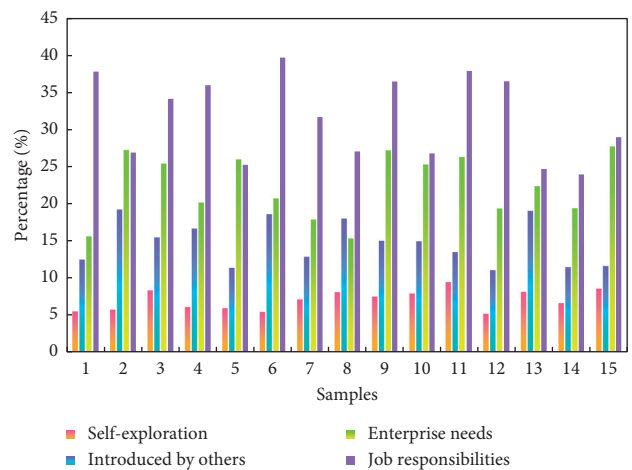


FIGURE 3: E-commerce acceptance behavior.

stronger the correlation between variables, and the more suitable the original variables are for factor analysis.

Only two coefficient values are higher than 0.6, so it is concluded that the internal correlation of the perceived ease of use variable is low. User management has a strong correlation with website technology, department management has a weak correlation with website technology, network technology, and data technology, while the correlation between user management and department management is 0.506, and the correlation between effort expectation and

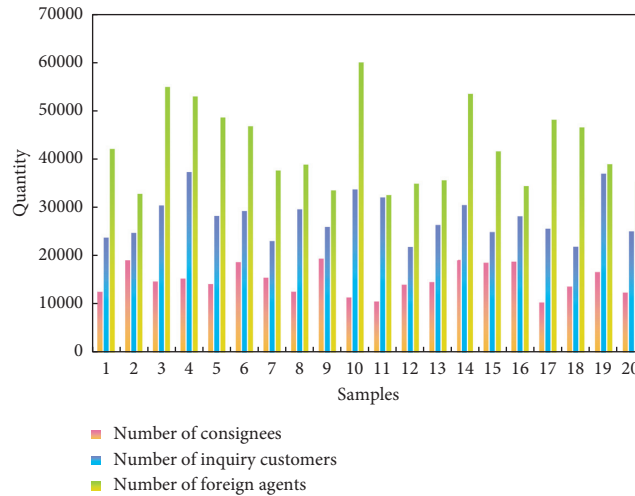


FIGURE 4: Rapid growth in the number of consignees and consignors, the number of inquiring customers, the number of foreign agents, and the number of carriers (shipping companies, airlines).

TABLE 4: The tests of KMO and Bartlett.

Perceived ease of use	KMO metrics	Number of items	
		Df	Sig
Perceived usefulness	0.700	28	0.000
Perceived trust	0.702	153	0.000
Mandatory acceptance	0.800	36	0.000
Perceived ease of use	0.767	15	0.000

TABLE 5: The correlation analysis of primary indicators.

Correlation	1	2	3
Website technology	1.000	0.502	0.761
Network technology	0.214	0.314	0.531
Data technology	0.467	0.409	0.543
User management	0.502	1.000	0.506

department management is high. Therefore, the primary factors of perceived ease of use are adjusted, and the influencing factors of perceived ease of use are divided into user-perceived usefulness and organization-perceived usefulness. The correlation analysis of primary indicators is shown in Table 5.

The rapid development of the Internet has promoted the networking of e-commerce and computer applications and set off an upsurge of Internet thinking, making it inevitable for freight forwarders to choose the e-commerce market. The relationship between the size of netizens and the penetration rate of the Internet is shown in Figure 5.

In fact, compared with personal computers, cloud computing is more reliable because cloud service providers are taking safe and effective measures all the time to ensure cloud services, such as multiple copies of data, fault tolerance, and homogeneity of computing nodes. Cloud computing features are shown in Figure 6.

According to the latest survey data from the National Bureau of Information Technology Statistics, more than 97% of foreign-funded enterprises have achieved informatization. Among them, more than 100 large companies have realized paperless, that is, office automation and many multinational companies have realized virtual office. In contrast, nearly 50% of SMEs are not equipped with computers. Less than 20% of businesses have a website. Large enterprises with more than 500 employees have initially achieved informatization. There is a big gap between the

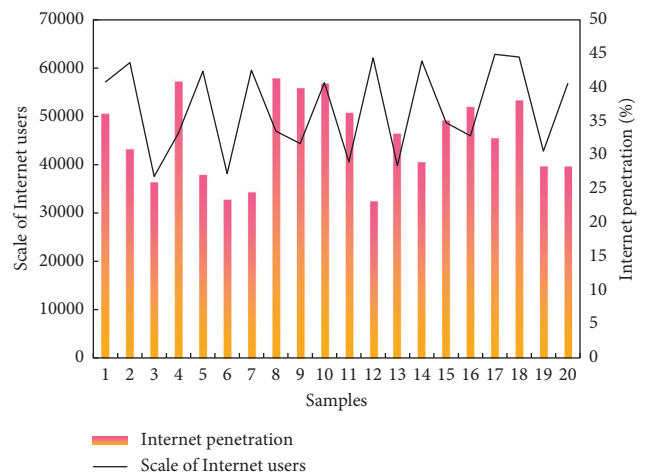


FIGURE 5: The relationship between the size of netizens and the penetration rate of the Internet.

informatization of domestic enterprises and developed countries. The comparison of information status of domestic and foreign enterprises is shown in Figure 7.

5. Countermeasures for the Electronization of Traditional Enterprises

5.1. Clearly Determining the Direction of Electronization. Traditional enterprises of any nature will eventually become electronic, with different approaches and methods. Maybe going electronic will not necessarily succeed. However, if

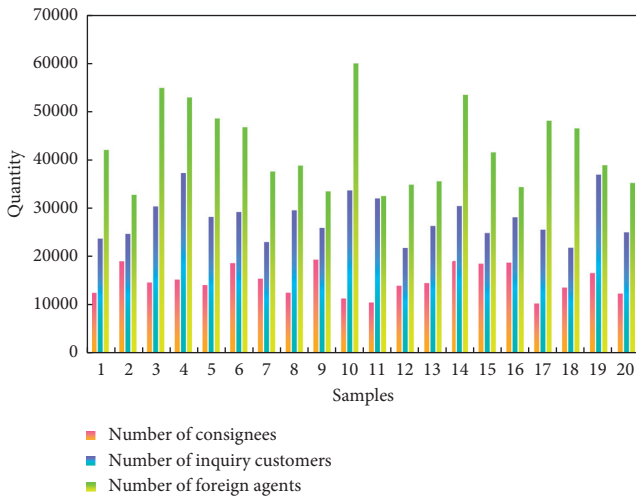


FIGURE 6: Cloud computing features.

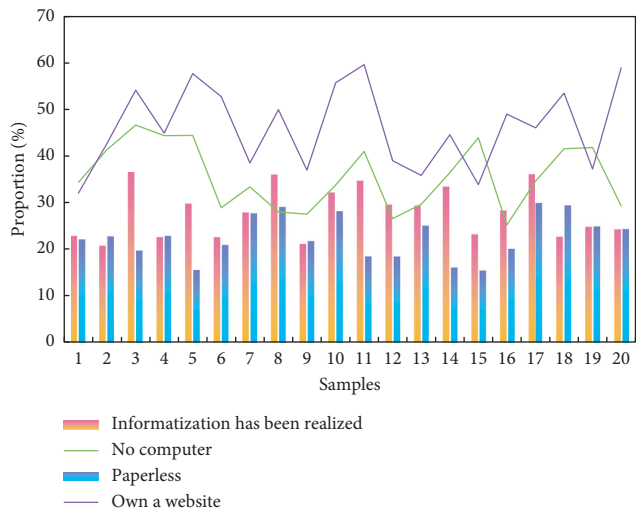


FIGURE 7: The comparison of information status of domestic and foreign enterprises.

you are not self-styled and do not go electronization, it is tantamount to sitting still and eventually being eliminated by society. In the inevitability analysis of the former enterprise electronization, we can clearly recognize the urgency and necessity of enterprise electronization. Many business leaders have seen this and are doing a variety of useful explorations, which is very gratifying. Although the road to exploration is long and sturdy, as long as you have this awareness, you may progress and succeed. There are also some business leaders who have felt that the times have changed and they are in crisis. However, due to the lack of understanding of Big data and cloud computing, the new economy is not very good, thinking that its own business has nothing to do with electronization. This kind of corporate thinking is very dangerous. In the wave of the new era of big data, traditional enterprises should seize the opportunity and move toward electronic. In particular, those enterprises that are still immersed in the traditional world and who are

indifferent to the Internet and information age should reform their corporate forms and carry out an electronic layout of enterprises to adapt to the challenges and impacts of the new era.

5.2. *Fully Developing the Electronic Construction of Enterprises.* We should regard enterprise electronization as an opportunity for enterprises to carry out technological innovation in all aspects, improve the efficiency of enterprise operation, and save enterprise cost. In the electronic construction of enterprises, it is not only to establish a corporate website but to start from the internal management of the enterprise and to deepen the electronic thinking into all aspects of the enterprise process. Correctly determine the relationship between the various parts, make electronic one step by step, and achieve significant benefits. The key part of the traditional enterprise to complete the electronic construction is to realize the electronization in the internal management mode of the enterprise. Specifically, it is to use big data technology and cloud computing technology to carry out intelligent and digital innovations in traditional production and management modes. On this basis, we will fully realize the electronization of enterprises, optimize internal operation processes, improve enterprise management efficiency, and achieve management innovation.

5.3. *Thinking in an Electronic way of Thinking.* As previously analyzed, in the current Internet development environment, enterprise development needs to face many threats, and we cannot consider all the situations in advance. Traditional corporate thinking is conservative, and it is accustomed to thinking clearly, so companies often spend a lot of time and managers in decision-making. In the Internet field, the time cost is the most important and precious, far exceeding capital, income, and talent. Although there are many situations in the process of enterprise electronization, if we are afraid of not trying, we will certainly be eliminated by the times and the market. We can learn from the experience of successful people, which can reduce the risk of exploring adventures. Do not be afraid to try enterprise electronization. Only practice can determine the effectiveness. Conservative companies are destined to be eliminated by homeopathic companies. This is an era full of opportunities and challenges. If enterprises cannot adapt to the thinking of the new era, they will be eliminated by the times.

5.4. *Starting from Reality.* It is necessary to base on the national conditions and the actual situation, analyze the actual situation of the enterprise itself, and explore and establish an electronic road that is applicable to the enterprise's own situation. Different types of businesses and scales of operations have different electronic opportunities and methods. In the process of enterprise electronization, we must consider the sensitivity of each enterprise type to big data technology and explore the best time and method of electronization. Enterprises must make electronic development plans suitable for their own enterprises according to

their actual conditions and determine the electronic form adopted by their own enterprises. Enterprises should decide the way and steps of electronic construction based on their actual needs. For some SMEs, if they just want to put relevant content about their own business on the Internet and provide corresponding network functions for people to browse, trade, and contact, then companies only need to establish their own corporate website portal. For some large enterprises, electronic construction needs to consider a relatively large number of aspects, complex technology, and high cost, and it takes a lot of time and manpower to carry out maintenance and management after completion, and it is not suitable for small and medium-sized enterprises.

5.5. Making Full Use of the Internal and External Advantages of the Company. Enterprises should try their best to realize their electronic transformation as quickly and efficiently as possible with all available external forces. Some companies are still in good shape, and some resources, capital, or brand advantages should be fully utilized when starting electronic construction. There are still many companies that have a high degree of informatization and should make full use of their internal information systems to enable enterprises to connect with the Internet as soon as possible. It can be said that in the process of e-commerce operation, the most important thing is the goal. Technology is not an obstacle. It is closely integrated with the IT industry. With the help of external technical forces, the company's own technical level can be quickly improved. Some SMEs can also consider using some websites that provide Internet services for enterprises to get online or e-commerce as soon as possible. In addition, the emerging technology can be used for strategic planning of electronic transformation to improve electronic efficiency.

6. Conclusion

Enterprise electronization is an inevitable trend of corporate strategic development and a long-term systematic process. Enterprises have transformed their traditional operating models and used advanced technologies such as big data and cloud computing to explore the potential value of enterprise data and industry data, better plan and layout the development of enterprises, and at the same time introduce enterprise resources into enterprises more quickly and effectively. To solve the problem of resource allocation of enterprises, rationally allocate enterprise resources, and operate the enterprise in a more fair, transparent, and convenient mode, which greatly improved the level of modern management capability of enterprises. By using big data and cloud computing means, it can provide fast and accurate information for enterprises, improve the correctness of enterprise management decisions, promote rapid and stable development of enterprises, and better stand in the fierce market competition environment. In addition, the basic characteristics of enterprise electronization, such as mobilization, deep integration of social and business applications, increased emphasis on user experience,

digitization of asset values, expansion of technical service capabilities to industrial chains, and transformation of technology light asset models, require enterprises. We must grasp the mainstream of the times, keep up with the wave of emerging technologies in the era, combine big data and cloud computing technologies to carry out electronization, and advance in the fierce competitive environment.

In the big data context, the necessity of electronic electronics in traditional enterprises is not to be doubted. The new opportunities brought about by cloud computing technology, and the prospect of electronization have an unstoppable temptation for enterprise development, which is the main driving force for the electronization of enterprises. In today's information era, the survival of traditional enterprises faces enormous threats. Traditional enterprises urgently need reforms to adapt to the new living environment. Electronic enterprise is the best choice and the only way for enterprises to participate in international competition and nominate the core competitiveness of enterprises.

At present, many enterprises still have many objective problems in the electronic process, such as insufficient understanding of enterprise electronic construction, basic work cannot meet the needs of information construction, and enterprises pay insufficient attention to management and restructuring in the process of electronic construction. These problems have seriously hindered the healthy and sustainable development of enterprises. On this basis, with big data and cloud computing as the background, this paper fully analyzes the problems of the above-mentioned enterprise electronization and proposes countermeasures for electronic enterprises. This countermeasure is to clearly determine the direction of electronization, fully develop electronic construction, think in an electronic way of thinking, start from reality, and make full use of the internal and external advantages of the enterprise.

This paper studies and analyzes the basic information of enterprise electronization, summarizes the necessity, basic characteristics, and existing problems of enterprise electronization, and proposes new countermeasures for enterprise electronization. This research hopes to make a contribution to promoting the development of electronic enterprises.

Data Availability

The data that support the findings of this study are available from the corresponding author upon reasonable request.

Conflicts of Interest

The authors declare that they have no conflicts of interest.

Acknowledgments


This work was supported by the Chongqing Education Science Planning Project (2020-Gx-035) "An Empirical Study on the Correlation between Professional Settings of Higher Vocational Colleges and Big Health Industry in the Three Gorges Reservoir Area."

References

- [1] J. Wang, "How to transform Traditional enterprises in the "Internet+" background," *China Opening Journal*, vol. 198, no. 3, pp. 93–96, 2018.
- [2] J. Wang, "Application status and development of multimedia technology," *Electronic Technology & Software Engineering*, vol. 11, p. 86, 2017.
- [3] K. Wu, "Application status and development prospect of computer multimedia technology," *Industrial & Science Tribune*, vol. 17, no. 7, pp. 53–54, 2018.
- [4] N. Lei, "Discussion on the predicament and future development trend of E-commerce enterprises," *Modern Economic Information*, vol. 21, p. 295, 2017.
- [5] P. O. H. Putra and Z. A. Hasibuan, "E-Business framework for small and medium enterprises: a critical review," in *Proceedings of the 2015 3rd International Conference on Information and Communication Technology (ICoICT)*, pp. 516–521, IEEE, Nusa Dua, Indonesia, May 2015.
- [6] S. Rajendran, O. I. Khalaf, Y. Alotaibi, and S. Alghamdi, "MapReduce-based big data classification model using feature subset selection and hyperparameter tuned deep belief network," *Scientific Reports*, vol. 11, no. 1, p. 24138, 2021.
- [7] Z. Tan and C. Xiao, "Discussion on situation and development countermeasures of coal enterprise informatization construction," *Industry and Mine Automation*, vol. 42, no. 7, pp. 63–65, 2016.
- [8] A. F. Metwaly, M. Z. Rashad, F. A. Omara, and A. A. Megahed, "Architecture of multicast centralized key management scheme using quantum key distribution and classical symmetric encryption," *The European Physical Journal - Special Topics*, vol. 223, no. 8, pp. 1711–1728, 2014.
- [9] A. Lipitakis and P. Phillips, "On E-business strategy planning and performance: a comparative study of the UK and Greece," *Technology Analysis & Strategic Management*, vol. 28, no. 3, pp. 266–289, 2016.
- [10] M. Lee, L. Mesicek, and K. Bae, "AI Advisor Platform for Disaster Response Based on Big Data," *Concurrency and Computation-Practice & Experience*, vol. 2021, p. e6215, 2021.
- [11] C. Sheng, Z. Liu, and N. Zhang, "The empirical study on influence of enterprise informatization on innovation capability in resource-oriented regions-based on resource view theory," *Soft Science*, vol. 31, no. 11, pp. 44–48, 2017.
- [12] K. Lee, H. Ko, H. Kim, S. Y. Lee, and J. Choi, "Practical vulnerability analysis of mouse data according to offensive security based on machine learning," *Entropy*, vol. 7, p. 50, 2020.
- [13] H. Sheng-yu, H. Ma, and T. Xi-hua, "Study on the level of development of E-commerce in China based on factor Analysis and cluster Analysis," *Reform of Economic System*, vol. 2017, no. 2, pp. 196–200, 2017.
- [14] M. Adil, J. Ali, M. Attique et al., "Three byte-based mutual authentication scheme for autonomous Internet of Vehicles," *IEEE Transactions on Intelligent Transportation Systems*, vol. 2021, Article ID 3114507, 2021.
- [15] R. Bi, R. M. Davison, and K. X. Smyrniotis, "E-business and fast growth SMEs," *Small Business Economics*, vol. 48, no. 3, pp. 559–576, 2017.
- [16] M. Adil, M. A. Jan, S. Mastorakis et al., "Hash-MAC-DSDV: mutual authentication for intelligent IoT-based cyber-physical systems," *IEEE Internet of Things Journal*, 2021.
- [17] Y. Wei, "Computer application technology in enterprise informatization," in *Proceedings of the International Conference on Application of Intelligent Systems in Multi-modal Information Analytics*, Springer, Cham, 2019.
- [18] A. Farouk, A. Alahmadi, S. Ghose, and A. Mashatan, "Blockchain platform for industrial healthcare: vision and future opportunities," *Computer Communications*, vol. 154, no. 9, pp. 66–67, 2020.
- [19] J. M. Xie and Q. Qin, "Research on the small and medium sized enterprise informatization's model and strategy of development," *Applied Mechanics and Materials*, vol. 63–64, pp. 309–312, 2011.
- [20] O. P. Singh, C. Kumar, A. K. Singh, M. P. Singh, and C. A. K. Singh, "Fuzzy-based secure exchange of digital data using watermarking in nsct-rdwt-svd domain," *Concurrency and Computation: Practice and Experience*, pp. 1–11, 2021.
- [21] D. Marin and T. Verdier, "Globalization and the new enterprise," *Journal of the European Economic Association*, vol. 1, no. 2–3, pp. 337–344, 2011.
- [22] B. Unhelkar and S. Murugesan, "The enterprise mobile applications development framework," *It Professional*, vol. 12, no. 3, pp. 33–39, 2010.
- [23] Yi Zhang, "Research on the application of ERP in electronic commerce," *China Science and Technology Information*, vol. 21, pp. 29–20, 2004.
- [24] Z. Wang, "Rebuilding enterprises' competitiveness in the era of big data," *China Business and Market*, vol. 12, pp. 3–13, 2017.
- [25] S.-C. Huang, S. Mcintosh, S. Sobolevsky, and P. C. K. Hung, "Big data analytics and business intelligence in industry," *Information Systems Frontiers*, vol. 19, no. 6, pp. 1229–1232, 2017.
- [26] F. Vendrell-Herrero, O. F. Bustinza, and G. Parry, "Servitization, digitization and supply chain interdependency," *Industrial Marketing Management*, vol. 60, pp. 69–81, 2016.
- [27] Y. Tang and Y. Jiang, "Asset-light operation and control allocation of enterprises in the Internet era," *Enterprise Economy*, vol. 36, no. 6, pp. 49–54, 2017.
- [28] X. Wang, "Problems and countermeasures in enterprise informatization construction," *Electronics World*, vol. 547, no. 13, pp. 76–77, 2018.
- [29] H. Li, Y. Yang, Y. Dai, S. Yu, and Y. Xiang, "Achieving secure and efficient dynamic searchable symmetric encryption over medical cloud data," *IEEE Transactions on Cloud Computing*, vol. 8, no. 2, pp. 484–494, 2020.
- [30] J. Kisielnicki and M. M. Markowski, "Real time enterprise as a platform of support management systems," *Foundations of Management*, vol. 13, no. 1, pp. 7–20, 2021.
- [31] U. Meyer and Z. Abedjan, "Algorithms for Big Data," *it - Information Technology*, vol. 62, no. 3–4, pp. 117–118, 2020.

Research Article

Research and Application of Haar Wavelet Transformation in Train Positioning

Pengfei Wang ^{1,2} and Xiuhui Diao²

¹*School of Mechanical Engineering, Dalian Jiaotong University, Dalian 116028, Liaoning, China*

²*School of Mechanical Engineering, Henan Institute of Technology, Xinxiang 453000, Henan, China*

Correspondence should be addressed to Pengfei Wang; steve@hait.edu.cn

Received 12 January 2022; Accepted 14 March 2022; Published 11 April 2022

Academic Editor: Wei Liu

Copyright © 2022 Pengfei Wang and Xiuhui Diao. This is an open access article distributed under the Creative Commons Attribution License, which permits unrestricted use, distribution, and reproduction in any medium, provided the original work is properly cited.

With the continuous increase of the urban population, urban traffic problems have become increasingly prominent. The subway and light rail have the characteristics of large passenger volume and low pollution, which are the preferred solutions to solve the traffic problems in large and medium cities. Due to the high density of rail transit trains, the close distance between stations, and the high safety requirements, the real-time and accurate determination of the train's position on the line is the premise to ensure safety, maximize efficiency, and provide the best service. How to accurately detect the speed and position of the train to control its the operation is the core content of the rail transit system. Therefore, the in-depth study of train positioning methods has great and far-reaching significance for promoting the research of train operation control system and the development of rail transit system. It has become a research hotspot to rely on computer technology and image recognition technology to realize precise positioning of trains. In order to realize the real-time precise positioning of the train, this paper proposes a train positioning method based on Haar wavelet transform. First, the samples are obtained by the method of video acquisition, and the video images are initially processed by binarization. Second, the image is compressed, denoised, and enhanced by Haar wavelet transform, and the train number is determined. Finally, the orbital electronic map and satellite assistance are used to determine the position of the train and realize the train positioning. The simulation experiments show that the image acquired by Haar wavelet transform can accurately identify the train and track. Based on the satellite aid of the orbital electronic map, the train positioning can be accurately realized, and the proposed Haar wavelet transform is proposed and has good positioning accuracy.

1. Introduction

With the rapid development of railways and the increasing speed of operation, safety has become the primary issue accompanying the development of railways. The safety guarantee is first and foremost an accurate and efficient train positioning system. The train positioning system is a very important link in the railway operation automation system. It makes the integration of dispatching command and operation more automatic and improves the operation efficiency and safety. In short, the train positioning system can determine the specific position of the train on the line and has the functions of supervising and controlling the speed of the train. The key to ensuring the safe operation of railways

[1–3] is to have a high-performance train operation control system. The train control system passes the train speed. The information such as the train position is accurately grasped to realize the safety report on the train operation. As the train continues to increase speed, the equipment and system related to the safe driving must also be guaranteed, such as the positioning accuracy and reliability of the train. At present, train control systems in many countries adopt ground transponder-assisted wheel sensors to achieve train positioning. Due to the large amount of ground equipment used, this requires not only a large amount of capital to build facilities, but also a large amount of personnel management costs and material costs. And it takes a lot of time to maintain it constantly. At the same time, the construction

cycle is relatively long, which will increase the cost of railway operations. Therefore, there is a need to find new ways to optimize train positioning. In order to prevent sudden power equipment failures and safety accidents, it is necessary to conduct regular and irregular regular inspections of important substations and lines. It is possible to detect potential safety hazards in time and eliminate the safety accidents in the bud. As a result, the reliability of the grid operation will be improved. In recent years, the Beidou satellite navigation [4, 5] system independently designed and developed by China has been continuously improved and developed, which promotes the further development of GNSS, and its application range is more spreading, such as in surveying, transportation, public safety, agriculture, and natural disaster detection. Therefore, the application of Beidou satellite navigation system in train positioning has also received extensive attention. In order to improve the autonomy of China's railway train control system, more and more people are studying the research of Beidou satellite navigation system in train positioning.

Image-based positioning methods in current technology fall into three categories. (1) A region-based approach: this type of method divides the image into multiple regions by utilizing grayscale similarity or clustering of colors and then acquires the target region for certain characteristics. However, the method is highly targeted and utilizes the characteristics that the background is relatively simple and the color information is rich. When the car number color is determined and there is a large difference from the vehicle body, the candidate feature can be quickly determined employing the color feature and its shape characteristics. However, this method has higher requirements for the contrast between the target and the background, and the anti-interference ability is weak. Therefore, the application of this algorithm is narrow and needs to rely on excellent image quality. (2) Edge-based positioning method: the edges contain information such as direction and step properties. The extraction of such information is often done by using edge operators (Canny, Sobel, Robert) [6–11]. This type of method takes advantage of the high contrast between the target and the background at the edge of the target to obtain the gradient information; at the same time, it also has a good performance in resisting noise interference. However, if the edge information is proliferated in a complex scenario, then only the edge information is used as the judgment basis without excluding the irrelevant area in advance, which greatly increases the calculation amount of the character area positioning, reduces the positioning efficiency and accuracy, and increases the candidate area. It is difficult to determine the final license plate location. (3) Texture-based [12–14] positioning method: this method completes the positioning by distinguishing the background by the unique texture features of the target area. That is, when the target texture is strong and the texture of the background is relatively weak, this method can be adopted. However, when the texture is similar, it is easy to extract the pseudo target. At the same time, the biggest disadvantage of this method is the high computational complexity.

At present, the most commonly used positioning algorithms based on the above three methods are as follows:

- (1) Edge detection method: the method is based on the fact that the license plate area has more dense edges than the background. Through the vertical edge detection, the area in which the edge density is within a certain threshold is found in the image, and the geometric features of the license plate are filtered according to these areas to complete the positioning. However, in the case where the background image is complicated, the method is susceptible to interference and affects the positioning accuracy.
- (2) Interlaced statistical edge method: the method is also carried out by enriching the edge information of the license plate area, scanning the image every N lines, obtaining the number of edge points of the line, and determining whether the threshold value is exceeded, thereby determining whether the license plate area is found. The positioning accuracy is closely related to the shooting distance and the size of the license plate, which has greater limitations and is greatly affected by the background image.
- (3) Straight line detection method: this method uses the Hough transform to detect the license plate frame for positioning. But this method will be difficult to work with when the license plate border is blurred, tilted, or twisted.
- (4) A positioning method based on mathematical morphology: this method employs the geometric characteristics of the license plate and its characters for positioning. This method is fast, but when the image is rotated, it will greatly affect the accuracy of the positioning.
- (5) Color-based positioning method. The key to the success of this method is the uniqueness of the license plate color. However, in the natural scene, the complexity of the background and the diversity of the license plate make the lack of accuracy and robustness of the method difficult to use.

During the running of the train, the data obtained by the accelerometer, the gyroscope, and the GPS receiver are subjected to discrete wavelet transform, and the components of different frequencies in each signal are decomposed into mutually nonoverlapping frequency bands. The processed data are subjected to data fusion by Kalman filtering, inputting the output of the filter to the map matching module, and determining the most likely driving section and the most likely position of the train in the section by an appropriate matching process. Finally, the matching position result is used to estimate and correct the GPS error through the negative feedback module to realize the effectiveness of the train combination positioning data. During the research, it was found that the Beidou navigation system realizes the train positioning. Like the problems faced by the global satellite navigation system, the Beidou satellite navigation is encountered when the train

encounters more and more complicated geographical conditions during the whole journey. As a new positioning system, the system is also affected. Therefore, in view of the above situation, the researchers began to explore the use of other auxiliary methods to solve the problems of these navigation systems, such as the use of inertial navigation system to assist the positioning of the train, but in the process of use, it is found that the positioning method has integral error in the use process. As the error increases, it will eventually cause deviations in the positioning results.

Wavelet Transform [15] is an analysis method different from Fourier transform. It inherits and develops the idea of Fourier transform, but it also overcomes the shortcomings of the window size of Fourier transform and frequency conversion. A time-frequency analysis window that varies with frequency can be provided. The multiresolution analysis of wavelet transform has good characteristics of time domain and spatial domain. It can focus on the arbitrary details of the analysis object by using the gradually refined time domain or spatial wavelength of different frequency segments of the signal. It is therefore particularly suitable for handling nonstationary signals. In addition, wavelet transform has been applied to many fields such as speech recognition, computer vision, signal detection, and image processing. Wavelet transforms can also be divided into many classes, including classic wavelets, also known as primitive wavelets. Such wavelet transforms include Haar wavelet [16], Morlet wavelet [17–19], Mexican hat wavelet [20, 21], and Gaussian wavelet [22, 23]. The second type is orthogonal wavelets constructed by Daubechies. These orthogonal wavelets are different from classical wavelets. They are generally not given by a simple expression, but are generated by a weighted combination of expressions called “scalar functions”. The third is a biorthogonal wavelet constructed by Cohen and Daubechies. The wavelet is proposed to obtain a linear phase wavelet and a corresponding filter bank under the condition of relaxing wavelet orthogonality.

Compared with the Fourier transform, the wavelet transform is a local transform of space (time) and frequency, so it can effectively extract information from the signal. Multiscale detailed analysis of functions or signals can be carried out by means of operations such as scaling and translation, which solves many difficult problems that cannot be solved by Fourier transform. Wavelet transform links applied mathematics, physics, computer science, signal and information processing, image processing, seismic exploration, and other disciplines. Mathematicians believe that wavelet analysis is a new branch of mathematics, which is the perfect crystallization of functional analysis, Fourier analysis, spline analysis, and numerical analysis; signal and information processing experts believe that wavelet analysis is time-scale analysis and multiresolution analysis. It has achieved scientifically meaningful and valuable results in research on signal analysis, speech synthesis, image recognition, computer vision, data compression, seismic exploration, and atmospheric and ocean wave analysis. The main purpose of signal analysis is to find a simple and effective signal transformation method, so that the important information contained in the signal can be revealed.

In order to realize the precise positioning of the train, this paper proposes a train positioning technology based on Haar wavelet transform combined with Haar wavelet transform. The specific contributions of this paper are as follows:

- (1) The sampled samples are obtained by the method of video acquisition, and the video images are initially processed by binarization
- (2) The image is compressed, denoised, and enhanced by Haar wavelet transform, and the train number is determined by identifying the train number of the train
- (3) The position of the train is determined by matching the electronic map of the track and satellite assistance to achieve train positioning

2. Wavelet Transform Method for Train Positioning

A wavelet is a function defined at a finite interval and whose mean is zero. It has a finite duration and abrupt frequency and amplitude, and the waveform can be either irregular or asymmetrical, but with an average amplitude of zero over the entire time range. The basic idea of wavelet transform is to utilize a family of functions to represent or approximate a signal. In wavelet transform, the approximation is the coefficient produced by the large scaling factor, representing the low frequency component of the signal; the detail value is a coefficient produced by a small scaling factor, denoting the high-frequency component of the signal. The wavelet transform is actually a combination of windowing techniques and variable-size windows, which allows large windows to be employed when it is desired to accurately observe low-frequency information, and small windows when observing high-frequency information. After wavelet transform, the signal can reveal many aspects of the signal, such as signal trend, break point, and discontinuity generated by high-frequency part and self-similarity, which are often ignored in other analysis methods. In addition, because wavelet transform can provide different observation angles of signals than other traditional methods, it can often compress and denoise signals without significantly reducing the quality.

2.1. Wavelet Transform. Wavelet transform is an important analysis tool applied to image processing. The multi-resolution characteristic of wavelet analysis makes the high-frequency wavelet coefficients of the wavelet decomposition coefficients have different characteristics in different directions. Therefore, it is one of the development trends of wavelet denoising to use directional wavelet to reflect the situation that the image changes in any direction at different resolutions to use local closed values for denoising. The multiscale decomposition characteristics of wavelet transform are more in line with the human visual mechanism. After the character image is transformed by wavelet, it is very easy to extract the horizontal and vertical strokes, and it is

concise and clear. Wavelet grid feature extraction and wavelet elastic grid feature extraction based on wavelet transform combine the advantages of statistical features and structural features. It is suitable for the classification idea from coarse to fine in character recognition, so it has become a development trend.

In fact, the application fields of wavelet analysis are very wide, including many subjects in the field of mathematics; signal analysis, image processing; quantum mechanics, theoretical physics; military electronic countermeasures and intelligence of weapons; computer classification and recognition; music and language artificial synthesis; medical imaging and diagnosis; seismic exploration data processing; and fault diagnosis of large machinery. For example, in mathematics, it has been used for construction of fast numerical methods, curved surface construction, differential equation solving, and cybernetics in numerical analysis; filtering, denoising, compression, and transmission in signal analysis; and image compression, classification, recognition and diagnosis, and decontamination in image processing. In medical imaging, it can reduce the time of B-ultrasound, CT, and MRI and improve the resolution.

From the point of view of image processing, wavelet transform has the following advantages:

- (1) Wavelet decomposition can cover the entire frequency domain
- (2) Wavelet transform can greatly reduce or remove the correlation between different extracted features by selecting appropriate filters
- (3) The wavelet transform has the “zoom” feature, which can use high frequency resolution and low time resolution (wide analysis window) in low frequency bands, and low frequency resolution and high time resolution (narrow analysis window) in high-frequency bands
- (4) There is a fast algorithm in the realization of wavelet transform

Multiresolution analysis is also called multiscale analysis by many scholars, which is a very prominent feature of using wavelet transform in signal processing. The basic idea of multiresolution analysis is to divide the data signal into several signals according to different resolutions and then process them on the signals corresponding to different resolutions or required resolutions. There is a more appropriate analogy; that is, the scale can be understood as the lens of the camera. If the scale changes from large to small, then it is equivalent to the lens of the camera approaching the object from far to near and vice versa; it is moving away from the object from near to far. In the large-scale space, it is shown as observing the target at a distance, and at this time, only the basic situation of the target can be seen roughly; in the small-scale space, it is shown as detecting the target at a closer distance, and at this time, it can be seen carefully, a specific part of the target. Therefore, when we convert the scale from large to small, we can detect the target data signal from rough to fine, which is the basic idea of multiresolution analysis.

Wavelet transform is a localized analysis of spatial (time) frequency, and its mathematical description is as follows.

The function $\Phi(t) \in L^2(R)$ is called a basic wavelet or a mother wavelet, and the function cluster $\Phi_{a,b}(t) = 1/\sqrt{|a|}\Phi(t-b/a)$ of the basic wavelet that is shifted and stretched is called a continuous wavelet, where a is the scale parameter, $a \in R, a \neq 0$; b is the translation parameter, $b \in R$. The wavelet transform of a function or signal $f(x) \in L^2(R)$ is

$$W_f(a, b) = \langle f, \Phi_{a,b} \rangle = \frac{1}{\sqrt{|a|}} \int_{-\infty}^{\infty} f(t) \Phi\left(\frac{x-b}{a}\right) dx. \quad (1)$$

For mathematical convenience, the wavelet transform can also be expressed as

$$W_s f(x) = f(x) \times \Phi_s(x) = \frac{1}{s} \int_{-\infty}^{\infty} f(t) \Phi\left(\frac{x-t}{s}\right) dt, \quad (2)$$

a is the stretch factor, b is the translation factor, where $\Phi_s(x) = 1/s\Phi(x/s)$, and s is still a scale parameter.

2.2. Haar Wavelet Transform. The Haar wavelet function is the simplest orthogonal function. Compared with other orthogonal functions, it has the characteristics of simple structure and convenient calculation. Therefore, the Haar wavelet function has attracted widespread attention. Alfréd proposed Haar wavelet transform in 1909, which is the simplest method in wavelet transform. It is a special case of wavelet $N = 2$, which can be called D_2 .

The mother wavelet of the Haar wavelet can be expressed as

$$\psi(t) = \begin{cases} 1, & 0 \leq t < 0.5, \\ -1, & 0.5 \leq t < 1, \\ 0, & \text{otherwise.} \end{cases} \quad (3)$$

And the corresponding scaling function can be represented as

$$\Phi(t) = \begin{cases} 1, & 0 \leq t < 1, \\ 0, & \text{otherwise.} \end{cases} \quad (4)$$

Its filter $h[n]$ is defined as

$$h[n] = \begin{cases} \frac{1}{\sqrt{2}}, & \text{if } (n = 0, 1), \\ 0, & \text{otherwise.} \end{cases} \quad (5)$$

Among all orthogonal wavelet transforms, wavelet transform is the simplest one. It is the only orthogonal wavelet with both symmetry and finite support, and it has applicable features of simple calculation, high efficiency, and better programming.

2.3. Selection of Optimal Wavelet Basis. The GPS data processing based on wavelet transform is based on the wavelet transform of wavelet transform phase double-difference

observation, and the selection of wavelet base affects the distribution of wavelet coefficients to some extent. Thus, good or bad wavelet base will directly affect the outcome of the process.

In the process of noise reduction, we need to focus on two points when determining the wavelet to be used. First, the wavelet needs to have good noise reduction correlation; that is, the wavelet coefficients that approach zero after wavelet transformation should be as many as possible. Second, after using the wavelet for noise reduction, our viewing effect needs to be considered. Therefore, it is very important to determine the wavelet that meets the actual needs.

The choice of wavelet basis usually considers the following five criteria. (1) Orthogonality: strict normative orthogonality is beneficial to the accurate reconstruction of wavelet decomposition coefficients. Orthogonal and bi-orthogonal are necessary conditions for selecting wavelet base in multiscale analysis methods. (2) Tight support: the tightly supported wavelet satisfies the requirement of spatial locality. The narrower the support width, the better the localization characteristics of the wavelet, the lower the computational complexity of the wavelet transform and the faster implementation. (3) Regularity: it is a kind of description of the smoothness of the wavelet function. It is very useful for the reconstruction of the signal to obtain a better smoothing effect. The larger the regularity order, the better the regularity. (4) Symmetry: choosing a wavelet function with symmetry or antisymmetry can avoid distortion of the signal in multiscale decomposition and reconstruction, thus obtaining high quality reconstructed signals. (5) Vanishing Moment: the vanishing moment indicates the concentration of energy after wavelet transform. When the order of vanishing moment is large, the values of the high-frequency part at the fine scale are negligibly small. Therefore, after the wavelet base with larger vanishing moment is decomposed, the signal concentrates the energy more.

The eight wavelet bases (wavelet systems) commonly utilized in the MATLAB toolbox are Haar, dbN, biorNr, Nd, CoifN, symN, morl, mexh, and meyer, and their main features can be found in the literature. The GPS data processing based on wavelet transform depends on carrier phase double-difference measurement for wavelet decomposition and reconstruction. Therefore, the selected wavelet base should have the characteristics of discrete wavelet transform, and it has orthogonality and symmetry. In the GPS fast precision positioning data processing, four wavelet basis functions such as Haar, dbN, CoifN, and symN can be selected.

2.4. Establishment of Train Positioning System Model

2.4.1. The Role of Train Positioning. The train position information plays an important role in the train automatic control technology. The realization of almost every subfunction requires the position information of the train as one of the parameters. Train positioning is a very important part of the train control system.

- (1) Provide a basis for ensuring safe train separation
- (2) Provide accurate position information for the train automatic protection (ATP) subsystem, as the basis for calculating the speed curve of the train, opening the door after the train stops at the station, and shielding the door inside the station
- (3) The train precise position information is provided for the automatic train operation (ATO) subsystem as the main parameter for automatic speed control
- (4) Train position information is provided for the automatic train monitoring (ATS) subsystem as basic information for displaying the running status of the train
- (5) In some CBTC systems, it is used as the basis for wireless base station connection
- (6) In some ATC systems, section occupancy/clearing information is provided as a basis for sending track detection information and speed control information

2.4.2. Train Positioning Technical Requirements

- (1) Accuracy: the accuracy of the train positioning system needs to meet two different requirements: one is the longitudinal positioning accuracy of the train on the same track and the other is the lateral positioning accuracy of the train between different tracks
- (2) Continuity: the positioning system must have the ability to perform train positioning without any interruptions; that is, it has good availability over time
- (3) Coverage: regardless of whether the train is operating in any geographic area, the location information must be provided to the ATC system without interruption; that is, there is good availability in space
- (4) Reliability and safety: the positioning system is independent of other subsystems of the train automatic control system. It has the ability to work continuously and can detect and report its own failures
- (5) Maintainability: the design and utilization of the positioning system must take into account factors such as preventive maintenance and corrective maintenance, thus minimizing the life cycle cost of the positioning system
- (6) Failure-safety: when the positioning system fails, the system cannot detect the "no car" notification information, but must have corresponding measures to ensure the safety of the train.

2.4.3. Train Positioning System Features. Unlike conventional road vehicles that project in two-dimensional planes, high-speed trains are one-dimensional motions on existing orbits, and the presence of rails has a strong constraint on trains. Thus, compared with the social vehicle positioning

system, the train positioning system has several remarkable features.

(1) *How the Coordinate System Is Defined.* The train operation can be described as a reference point of the track, extending in a one-dimensional position along the running direction of the train. Therefore, the coordinate system in which the train runs can be regarded as taking the position of the track as the origin (generally taking the kilometer as 0). The one-dimensional reference system is along the track direction, and the description of the train position refers to the relative distance between the train running on the track and the origin.

Therefore, in the position calculation result, the traditional vehicle positioning coordinate system describes the three-dimensional space (navigation coordinate system) in the ellipsoid coordinate system. For high-speed trains, the position estimation result requires to be mapped to the special coordinate system of the train operation by means of coordinate conversion.

(2) *Operating Environment.* Compared with road vehicles, trains have long running time, fast speed, wide distance extension, long radiation, and large vibration. Their motion cannot be regarded as a translation of a mass point. Rails have strong restraint ability for train operation. Therefore, the positioning system needs to consider the processing of multisource noise and propose a reliable information fusion and fault handling strategy. In order to ensure the continuity of positioning, it is necessary to consider the positioning system to be safe and reliable under different harsh environments (such as satellite signal loss and sensor failure).

(3) *Security Level.* Safety is the primary prerequisite for railway operation. Compared with road vehicles, its safety level is higher, and its location service is closely related to railway system safety applications. Due to the higher running speed of the train and the longer body, it is necessary to add a longer safety redundancy distance at the front and the rear of the train after calculating the train position, forming a one-dimensional safety envelope and reducing the impact of calculation error on the safety of position information.

After the above analysis of the characteristics of the system, there is a big difference between the high-speed train combined positioning system and the traditional road vehicle positioning system. Therefore, we must comprehensively consider the characteristics of the train operation and the functions expected to be realized. On the basis of the traditional navigation framework, considering the particularity of the train, we cannot simply copy the original combined positioning method. Based on the premise of safety, we design a train combination positioning system with high precision, strong real-time, and high continuity.

2.4.4. Car Number Positioning and Binarization. Due to the large color of the body and the number of the passenger train, the illumination changes greatly, and the traditional positioning algorithm is often not ideal. In this paper,

wavelet decomposition and morphological processing are introduced to complete the car number location, and the binarization algorithm based on local gray mean and standard deviation is used to threshold the car number. According to the texture analysis experiment of the car number region, this paper selects the two-layer decomposition detail signal for the car number positioning after the preprocessed car number image. The algorithm steps are as follows.

- (1) The Haar wavelet is utilized to perform two-layer decomposition on the preprocessed image to extract vertical high-frequency components.
- (2) Edge detection employs the improved Canny edge detection algorithm.
- (3) Morphological processing [24–28] utilizes linear operators to perform closed operations, so that the detected edge information is connected into a connected region. According to the length of the car number in the image and the experiment, the selected linear operator is $[1, 1, 1, 1, 1, 1, 1, 1, 1, 1]$.
- (4) According to the brushing rules of the passenger train number and the prior knowledge of the length and width of the car number in the actual captured image, combined with the wavelet transform image size transformation relationship, the minimum circumscribed rectangle segmentation is used to extract the region that satisfies the constraint condition and complete the car number positioning. Constraint: car size is 250×250 , and the error in length and width is 5 pixels.

2.4.5. Establishment of Station Equation. In urban rail transit, the momentum of the train is large, and the operation of the train must follow relevant guidelines and regulations. Under normal conditions, it is a constant speed operation and equal acceleration operation, and the uniform motion model can be considered as a uniform acceleration motion model with acceleration of Gaussian white noise. Therefore, it is more suitable to describe the motion state of trains in urban rail transit by using uniform acceleration motion model. That is,

$$\begin{bmatrix} \dot{l} \\ \dot{v} \\ \dot{a} \end{bmatrix} = \begin{bmatrix} 0 & 1 & 0 \\ 0 & 0 & 1 \\ 0 & 0 & 0 \end{bmatrix} \begin{bmatrix} l \\ v \\ a \end{bmatrix} + \begin{bmatrix} 0 \\ 0 \\ 1 \end{bmatrix} \begin{bmatrix} l \\ v \\ a \end{bmatrix} + \begin{bmatrix} 0 \\ 0 \\ 1 \end{bmatrix} w(t), \quad (6)$$

where lva are the position, velocity, and acceleration components of the train. Let $w(t)$ be a Gaussian white noise, which is equivalent to the random disturbance acceleration. It can be seen that the acceleration of the train is the source of changing the train state.

$$X = [l \ v \ a]^T, \quad A = \begin{bmatrix} 0 & 1 & 0 \\ 0 & 0 & 1 \\ 0 & 0 & 0 \end{bmatrix}, \quad B = [0 \ 0 \ 1]^T. \quad (7)$$

Then the station equation is

$$\dot{X}(t) = AX(t) + Bw(t). \quad (8)$$

Discretization is done, taking $T = t_k - t_{k-1}$, an iterative formula based on velocity and acceleration:

$$l(k) = l(k-1) + T \cdot v(k-1) + \left(\frac{T^2}{2}\right) \cdot a(k-1) + w_l(k-1),$$

$$v(k) = v(k-1) + T \cdot a(k-1) + w_v(k-1),$$

$$a(k) = a(k-1) + w_a(k-1),$$

(9)

where $l(k)$, $v(k)$ and $a(k)$ are the position, velocity, and acceleration components of the train at time k ; $w_l(k)$, $w_v(k)$ and $w_a(k)$ are system noises that affect train position, velocity, and acceleration at time k , respectively. It is expressed as the following matrix:

$$\begin{bmatrix} l(k) \\ v(k) \\ a(k) \end{bmatrix} = \begin{bmatrix} 1 & T & \frac{T^2}{2} \\ 0 & 1 & T \\ 0 & 0 & 1 \end{bmatrix} \begin{bmatrix} l(k-1) \\ v(k-1) \\ a(k-1) \end{bmatrix} + \begin{bmatrix} 1 & 0 & 0 \\ 0 & 1 & 0 \\ 0 & 0 & 1 \end{bmatrix} \begin{bmatrix} w_l(k-1) \\ w_v(k-1) \\ w_a(k-1) \end{bmatrix}, \quad (10)$$

$$X(k) = \begin{bmatrix} l(k) \\ v(k) \\ a(k) \end{bmatrix}, \Phi = \begin{bmatrix} 1 & T & \frac{T^2}{2} \\ 0 & 1 & T \\ 0 & 0 & 1 \end{bmatrix}, \Gamma = \begin{bmatrix} 1 & 0 & 0 \\ 0 & 1 & 0 \\ 0 & 0 & 1 \end{bmatrix}, W(k) = \begin{bmatrix} w_l(k) \\ w_v(k) \\ w_a(k) \end{bmatrix}.$$

Then, $X(k) = \Phi X(k-1) + \Gamma W(k-1)$.

2.4.6. Establishment of Measurement Equation. The measurement equation for the axle speed sensor is

$$Z_L(k) = H_L X(k) + V_L(k). \quad (11)$$

The accelerometer's measurement equation is

$$Z_A(k) = H_A X(k) + V_A(k). \quad (12)$$

The measurement equation of the Doppler radar speed sensor is

$$Z_R(k) = H_R X(k) + V_R(k), \quad (13)$$

where $V(k)$ is measurement noise, and $H(k)$ is the measurement matrix.

In summary, the common station equation of the system is

$$X_i(k) = \Phi X_i(k-1) + \Gamma W(k-1). \quad (14)$$

The observation equation for each sensor is

$$Z_i(k) = H_i X(k) + V_i(k), \quad (i = L, A, R). \quad (15)$$

2.5. Map Matching Positioning Technology. Since the train runs on a definite track, the motion of the train can be seen as moving back and forth on a definite line—i.e., “one-dimensionality.” According to railway conventions, the location of trains on railway lines is expressed using kilometer markers; when using the navigation system for positioning, the receiver receives three-dimensional information (latitude, longitude, and altitude). Therefore, when using the navigation system to determine the train position, the latitude and longitude information of the receiver needs to be converted into the kilometer mark required by the railway. The storage method of digital track map is to use the collection of sampling points to form railway lines from points to lines. This approach can not only describe the information of the railway line completely, but also help to realize the transformation of geographic information coordinates and one-dimensional coordinates of the railway line. The digital map is involved in train positioning, which can effectively correct errors and improve the integrity of the entire system.

Map matching is a positioning method based on software correction. The train positioning trajectory measured by the GPS/DR is associated with the road network in the digital map, and thereby the position of the vehicle is determined relative to the map. Further correction of the GPS/DR combined positioning result by map matching can improve the accuracy of the entire system again. The map matching principle is shown in Figure 1.

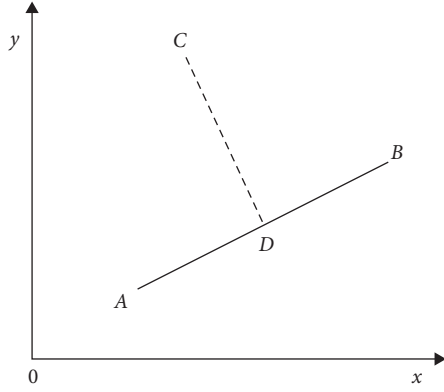


FIGURE 1: Location point matching principle.

As shown in Figure 1, the line is simple due to the multiline and easing curve of the railway line. Utilizing the vertical projection method, the coordinates of the position of the train measured under the GPS/DR combined positioning condition are (X_C, Y_C) . Query the digital electronic map database of the train is to find the two-point coordinates closest to the measurement position on the trajectory $A(X_A, Y_A)$ 和 $B(X_B, Y_B)$.

3. Experiments

3.1. Simulation Environment and Parameter Settings. The algorithm proposed in this paper is carried out in the Intel Core i5-3230M CPU, 2.6 GHz, 4 GB memory platform, Matlab2.14a simulation environment. In the experiment, a train track with a length of 1000 m (where both linear and curved tracks are 1000 m) is selected, and a certain number of anchor nodes are deployed beside the track. The parameters are set as follows.

- (1) Anchor node communication radius: in this experiment, the communication radius of the anchor node is set to $R = 50m$ for the first time; then, the communication radius of the anchor node is changed sequentially in the range $[30, 70]$ at $5m$ intervals, and the influence of the communication radius on the positioning accuracy of the train is observed.
- (2) The location information of the anchor node itself has been hard coded into its control chip prior to deployment. The error of the anchor node's own position and the influence of environmental factors are not considered.
- (3) Anchor node deployment density. In the experiment, the deployment density of the anchor nodes (the distance between adjacent anchor nodes) is set to $d_1 = 1m$, and then the deployment density is changed within the range $[1, 15]$ to observe its influence on the train positioning error.
- (4) The running speed of the train: set the running speed of the train to $v = 30m/s$ for the first time, then change the running speed in the range $[10, 45]$ and observe its influence on the train positioning error.

Here, the maximum running speed of a normal train is $160km/h$ (i.e., $45m/s$).

- (5) The scanning period of the gateway sensor is $T = 1s$. At each prediction step, the noise in the motion model is randomly selected from the range $(0.5, 1)$.

The parameter settings used for the specific algorithm simulation are shown in Table 1.

4. Discussion

4.1. Simulation Analysis. In the simulation experiment, the root mean square error (RMSE) is used to measure the positioning accuracy, which is defined as

$$RMSE = \sqrt{(\hat{x}_k - x_k)^2 + (\hat{y}_k - y_k)^2}, \quad (16)$$

where (x_k, y_k) and (\hat{x}_k, \hat{y}_k) are the true position and estimated position of the train at time k , respectively.

4.2. Image Preprocessing. In the whole process of image processing, noise has a certain influence on all steps, including input and output and steps in all aspects. Therefore, a good image processing system will put noise reduction in a very critical position. Basically, most of the noise cannot be described by a certain rule, so no filter can be effective for any kind of noise in the past. According to different methods, it can be divided into many kinds: additive noise model, multiplicative noise model, Gaussian noise model, and so on.

Subjective evaluation and objective evaluation are two more common evaluation criteria for image noise reduction. The subjective evaluation method requires us to directly observe the target with the naked eye and judge the visual effect of the target according to a specific standard, which is a qualitative evaluation. For subjective evaluation, let a certain number of testers observe the target image after noise reduction with the naked eye and then score according to established criteria, such as sharpness, brightness, hue, and softness, and then combine the scores of all testers, so that an evaluation result of the noise reduction effect of the target image can be generated. The objective evaluation method is to use the objective indicators of the image after noise reduction to measure the noise reduction effect of the image, including the measurement of noise reduction ability and image clarity after noise reduction, which is a quantitative evaluation.

In order to highlight the useful features in the image of the power device, it is necessary to preprocess the image. The following is a simulation to illustrate the preprocessing of the power equipment image, which is beneficial to the subsequent image feature extraction.

In the paper, the image is grayed out before filtering the image. The result is shown in Figure 2, where Figure 2(a) is the original image and Figure 2(b) is the grayscale image. As can be seen from Figure 2, the grayscale processing reduces the three-dimensional original image to a two-dimensional grayscale image, but the image basic information is retained without affecting the contour change of the image.

TABLE 1: Simulation parameter settings.

Parameter name	Parameter value
Path loss factor	4
Simulation area	1000 m
Anchor node deployment density	1 m
Anchor node communication radius	50 m
Train speed	30 m/s
Maximum train speed	45 m/s
Minimum number of anchor nodes	3
Test count	50 times
Node communication model	Lognormal shadow model
Scanning wave emission period T	1 s
Linear region train initial position	(0, 0)
Curve region train initial position	(1000, 5000)

In digital image processing, binary image occupies a very important position. First, the binarization of the image facilitates further processing of the image, making the image simple, and the amount of data is reduced, which can highlight the contour of the target of interest. Secondly, to process and analyze the binary image, firstly, the grayscale image is binarized to obtain a binarized image. All pixels whose gradation is greater than or equal to the threshold are determined to belong to a specific object, and their gradation value is 255. Otherwise, these pixels are excluded from the object region, and the gradation value is 0, indicating a background or an exceptional object region.

At the same time, before the image processing, the image is binarized. The result is shown in Figure 3. Figure 3(a) is the original image, and Figure 3(b) is the grayscale image. Image binarization is to set the gray value of the pixel on the image to 0 or 255, which is to show the whole image a distinct black and white effect. A grayscale image of 256 brightness levels is selected by appropriate thresholds to obtain a binarized image that still reflects the overall and local features of the image.

Neighborhood mean filter is a noise reduction algorithm that appeared earlier and is easier to implement. It belongs to a linear low-pass filter. The brief idea of this method is to replace the value of the unknown point with the mean value of multiple points near the desired point, and the number of pixel points used to obtain the mean value is determined by itself according to the specific situation. The median filter is a relatively good image noise reduction algorithm. It is similar to the neighborhood mean filter described above in that it also belongs to window type noise reduction. The difference is that the mean was replaced by the median.

The basic idea of threshold noise reduction is related to the properties of the coefficients used in the noise reduction process. First, the original input data are not uniformly distributed, so at each scale, its high-frequency coefficients only appear larger in fewer individual areas. Value and the region where it is located is the edge detail part of the input image, and the remaining high-frequency wavelet coefficients have smaller amplitudes. The second point is that after the main part of the noise in the image is decomposed, it still obeys the Gaussian distribution, so its decomposition coefficients at each scale are uniformly distributed, and the amplitude decreases as the scale increases.

Figure 4 shows the experimental results of the filtering process in this paper, where Figure 4(a) is an image containing noise and Figure 4(b) is a filtered image. It can be seen from the figure that this paper utilizes the simple and easy noise threshold to filter the image, effectively filtering out the noise in the image and avoiding the noise to deteriorate the image quality. After filtering, the image quality is improved, which is beneficial to extract object features for analysis.

4.3. Algorithm Comparison

4.3.1. Algorithm Localization Performance under Linear Motion Model. Figure 5 shows the trajectory curve of the following models of the linear motion model in different deployment modes. Figures 5(a) and 5(b) are the trajectory diagrams of the uniform linear deployment of the anchor node on one side and the uniform deployment of the two sides. It can be seen that the EKF positioning algorithm will generate large fluctuations regardless of the deployment mode. With the change of time, the positioning trajectory of the train is far from the real trajectory. The positioning trajectory of the proposed algorithm is close to the true trajectory of the train. It has good matching and robustness and is more stable than the other two algorithms.

Figure 6 shows the positioning error of the following vehicles in the linear motion model. Figures 6(a) and 6(b) show the positioning error of the anchor node on one-side straight line uniform deployment and double-sided cross-uniform deployment. It can be seen that under the same conditions, the proposed algorithm has higher filtering accuracy than the other two algorithms. The calculation of the positioning error proves the superiority of the algorithm. Because the algorithm is based on Bayesian theory, the extended Kalman filter algorithm is used to overcome the linearization error of the algorithm. When the rail-side anchor nodes are evenly distributed on both sides, the train positioning error is the smallest. This is because when the anchor nodes are evenly distributed on both sides, the possibility that the anchor sensor has a communication coverage blind zone is smaller than the other deployment mode. At the same time, due to different deployment modes,



FIGURE 2: Grayscale processing: (a) original image and (b) grayscale image.



FIGURE 3: Binary processing: (a) original image and (b) binarized image.

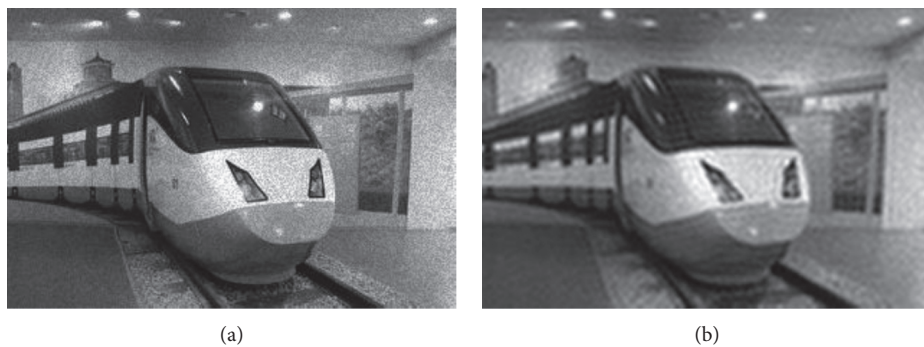


FIGURE 4: Image filtering processing: (a) noisy image and (b) filtered image.

the anchor node information received by the gateway node is different at each moment. The two-sided cross-uniform deployment can receive more information, and then more positioning anchor nodes can be selected to improve the positioning accuracy.

4.3.2. Algorithm Localization Performance under Curve Motion Model. Figure 7 shows the positioning trajectory curves corresponding to the three algorithms under the curve motion model. It can be seen that during the start of the turning maneuver (curving motion) of the train, the tracking and positioning curve of the EKF has fluctuated greatly and deviated from the real trajectory, and the positioning error gradually increased. However, the

particle filter algorithm and the proposed algorithm can still maintain a good positioning trajectory, but as the running time increases, the positioning trajectory of the particle filter algorithm will gradually deviate. The algorithm of this paper can still maintain good matching with the real track of the train and has good positioning accuracy.

4.3.3. Real-Time Positioning of Algorithm. Figure 8 shows the real-time nature of the three train positioning algorithms. That is, the calculation time of the positioning algorithm in each positioning period, which is the indicator of the real-time nature of the train positioning. It can be observed that since the algorithm needs to select the

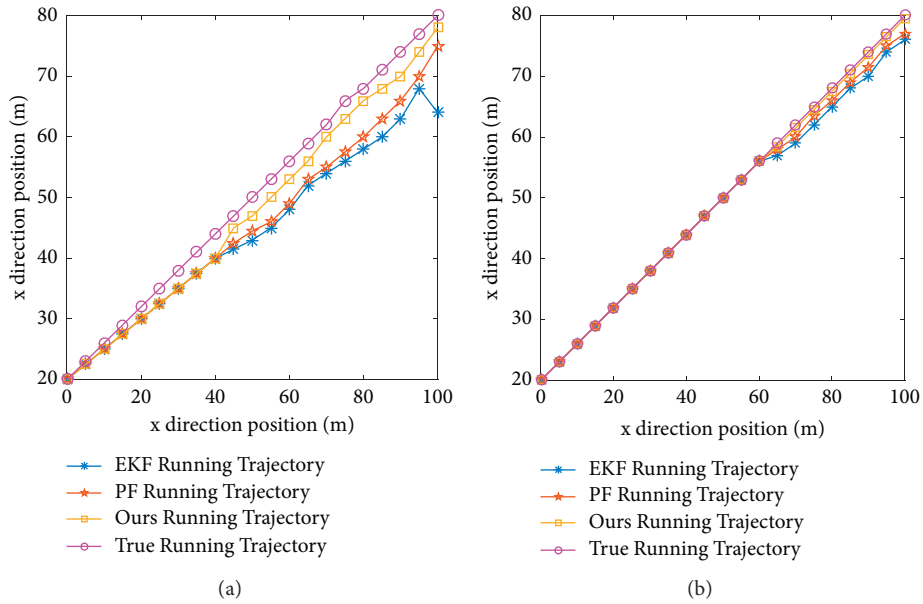


FIGURE 5: Train linear motion trajectory. (a) Unilateral straight line uniform deployment motion trajectory and (b) double-sided cross-uniform deployment motion trajectory.

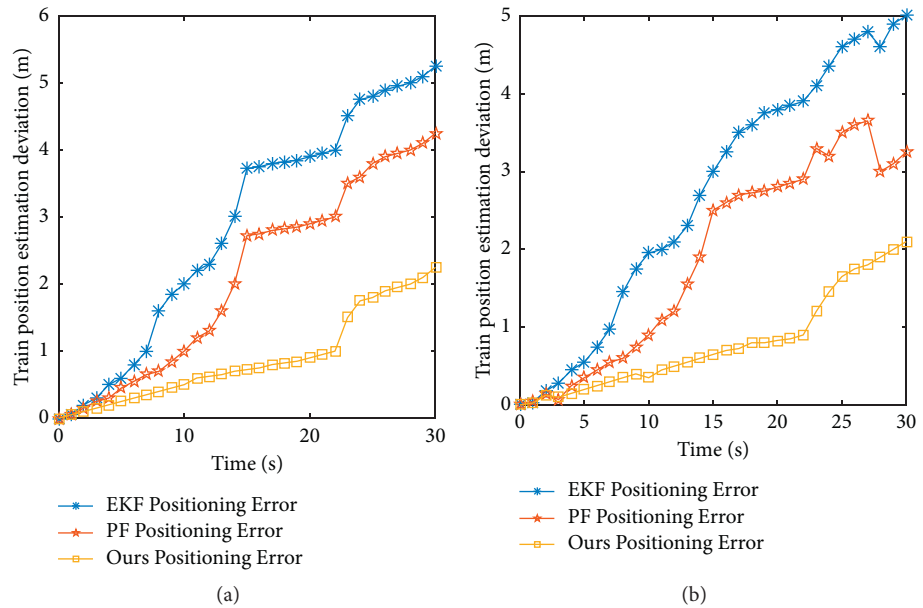


FIGURE 6: Train linear motion positioning error map. (a) Uniform straight line deployment positioning error map and (b) double-sided cross-uniform deployment positioning error map.

positioning anchor node in the anchor node that receives the information and because the train motion state changes, the algorithm needs to continuously resample to determine the motion state of the train at the current moment. Therefore, it leads to an increase in the complexity of the algorithm and an increase in the amount of calculation. Therefore, the

running time of this algorithm is longer than the other two algorithms. Although the real-time performance of the positioning algorithm is poor, it has higher accuracy from the positioning accuracy. For the safe operation of the train, the comprehensive performance of the algorithm is better than the other two algorithms.

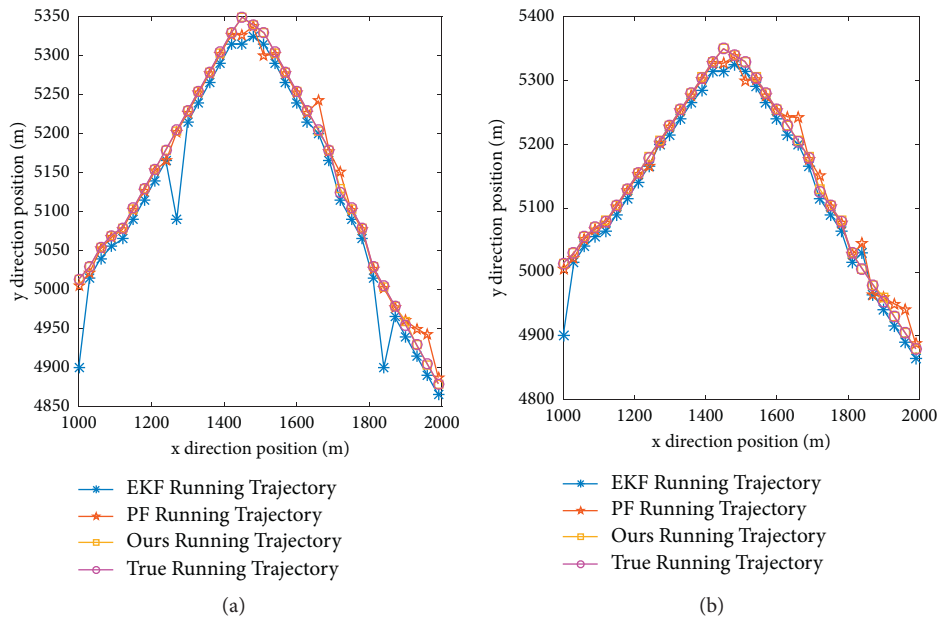


FIGURE 7: Train curve motion map. (a) One-sided uniform deployment curve motion trajectory and (b) unilaterally deployed curve motion trajectory.

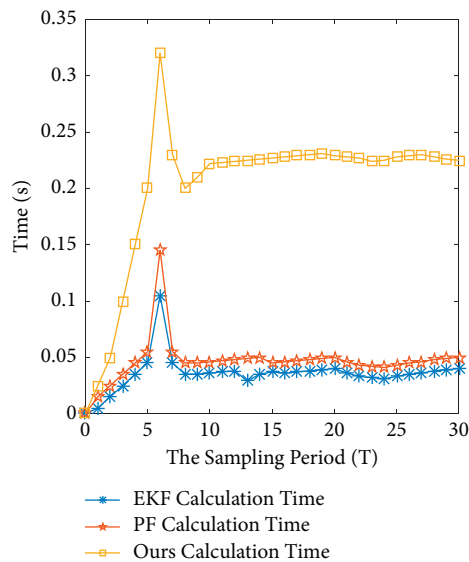


FIGURE 8: Train positioning algorithm real-time.

5. Conclusion

Utilizing the MATLAB simulation tool, the EKF algorithm, PF algorithm, and the proposed algorithm under two different deployment modes and train motion models are used from the positioning trajectory of the train, the positioning error, the running speed of the train, and the real-time performance of the algorithm. The performance was simulated and analyzed. The simulation results show that the Haar algorithm is less affected by the environment and the positioning accuracy is higher than the traditional algorithm. Although this paper analyzes and discusses the wavelet noise reduction algorithm in depth and systematically, it is still unable to achieve complete separation of image and noise. Therefore, future

research should balance the requirements of protecting the original image and filtering noise and try to achieve a better good performance.

Data Availability

The data that support the findings of this study are available from the corresponding author upon reasonable request.

Conflicts of Interest

The authors declare no potential conflicts of interest with respect to the research, authorship, and/or publication of this article.

References

- [1] G. Yu, W. Zheng, L. Wang, and Z. Zhang, "Identification of significant factors contributing to multi-attribute railway accidents dataset (MARA-D) using SOM data mining," in *Proceedings of the 2018 21st International Conference on Intelligent Transportation Systems (ITSC)*, p. 170, Maui, HI, USA, November 2018.
- [2] P. Stankaitis and A. Iliassov, "Safety verification of modern railway signaling with the SafeCap platform," in *Proceedings of the 2017 IEEE International Symposium on Software Reliability Engineering Workshops (ISSREW)*, p. 153, Toulouse, France, October 2017.
- [3] S. Liu, J. Mu, D. Zhou, and A. G. Hessami, "Model safety standard of railway signaling system for assessing the conformity of safety critical software based weighted factors analysis," in *Proceedings of the 2017 4th International Conference on Transportation Information and Safety (ICTIS)*, p. 779, Banff, AB, August 2017.
- [4] Z. Dong, J. Duan, M. Wang, J. Zhao, and H. Wang, "On Agricultural machinery operation system of Beidou navigation system," in *Proceedings of the 2018 IEEE 3rd Advanced Information Technology, Electronic and Automation Control Conference (IAEAC)*, p. 1748, Chongqing, China, October 2018.
- [5] L. Deng, S. Ye, and H. Qiu, "Transmission security platform for transportation information based on BeiDou navigation satellite system," in *Proceedings of the 2018 IEEE 3rd Advanced Information Technology, Electronic and Automation Control Conference (IAEAC)*, p. 2110, Chongqing, China, October 2018.
- [6] P. Prathusha, S. Jyothi, and D. M. Mamatha, "Enhanced image edge detection methods for crab species identification," in *Proceedings of the 2018 International Conference on Soft-computing and Network Security (ICSNS)*, p. 1, Coimbatore, India, February 2018.
- [7] D. Xiaoheng, L. Minghang, M. Jiashu, and W. Zhengyu, "Edge detection operator for underwater target image," in *Proceedings of the 2018 IEEE 3rd International Conference on Image, Vision and Computing (ICIVC)*, p. 91, Chongqing, China, June 2018.
- [8] Y. Zhang, X. Han, H. Zhang, and L. Zhao, "Edge detection algorithm of image fusion based on improved Sobel operator," in *Proceedings of the 2017 IEEE 3rd Information Technology and Mechatronics Engineering Conference (ITOEC)*, p. 457, Chongqing, China, October 2017.
- [9] W. Chen, Y. J. Yu, and H. Shi, "An improvement of edge-adaptive image scaling algorithm based on Sobel operator," in *Proceedings of the 2017 4th International Conference on Information Science and Control Engineering (ICISCE)*, p. 183, Changsha, China, July 2017.
- [10] Y. Zhai, G. Wang, H. Yu, and G. Wei, "Research on the application of the edge detection method for the UAVs icing monitoring of transmission lines," in *Proceedings of the 2017 IEEE International Conference on Mechatronics and Automation (ICMA)*, p. 1110, Takamatsu, Japan, August 2017.
- [11] W. Xiong, X. Nie, X. Zou, Z. Yang, and X. He, "Face illumination invariant feature extraction based on edge detection operator," in *Proceedings of the 2017 IEEE International Conference on Imaging Systems and Techniques (IST)*, p. 1, Beijing, China, October 2017.
- [12] T. You and Y. Tang, "Visual saliency detection based on adaptive fusion of color and texture features," in *Proceedings of the 2017 3rd IEEE International Conference on Computer and Communications (ICCC)*, p. 2034, Chengdu, China, December 2017.
- [13] E. Temizkan and H. Ş. Bilge, "Airport detection by combining geometric and texture features on RASAT satellite images," in *Proceedings of the 2017 25th Signal Processing and Communications Applications Conference (SIU)*, p. 1, Antalya, Turkey, May 2017.
- [14] H. S. Lee, H. Hong, and J. Kim, "Detection and segmentation of small renal masses in contrast-enhanced CT images using texture and context feature classification," in *Proceedings of the 2017 IEEE 14th International Symposium on Biomedical Imaging (ISBI 2017)*, p. 583, Melbourne, VIC, Australia, April 2017.
- [15] B. J. Adigun, A. G. Buchan, A. Adam, S. Dargaville, M. A. Goffin, and C. C. Pain, "A haar wavelet method for angularly discretising the boltzmann transport equation," *Progress in Nuclear Energy*, pp. 108–295, 2018.
- [16] F. Li, Q. Mao, and C. Chang, "Reversible data hiding scheme based on the Haar discrete wavelet transform and interleaving prediction method," *Multimedia Tools and Applications*, vol. 77, p. 5149, 2018.
- [17] R. M. Al Abdi and M. Jarrah, "Cardiac disease classification using total variation denoising and morlet continuous wavelet transformation of ECG signals," in *Proceedings of the 2018 IEEE 14th International Colloquium on Signal Processing & Its Applications (CSPA)*, p. 57, Penang, Malaysia, March 2018.
- [18] D. Gao, Y. Zhu, X. Wang, K. Yan, and J. Hong, "A fault diagnosis method of rolling bearing based on complex morlet CWT and CNN," in *Proceedings of the 2018 Prognostics and System Health Management Conference (PHM-Chongqing)*, p. 1101, Chongqing, China, October 2018.
- [19] J. Jw, J. Jh, and T. Q., W. Ht, "Study on nanosecond impulse frequency response for detecting transformer winding deformation based on morlet wavelet transform," in *Proceedings of the 2018 International Conference on Power System Technology (POWERCON)*, p. 3479, Guangzhou, China, November 2018.
- [20] Š. Džakmić, T. Namas, and A. Husagić-Selman, "Combined fourier transform and Mexican hat wavelet for fault detection in distribution networks," in *Proceedings of the 2017 9th IEEE-GCC Conference and Exhibition (GCCCE)*, p. 1, Manama, Bahrain, May 2017.
- [21] P. Liu, Z. Zeng, and J. Wang, "Multistability of delayed recurrent neural networks with Mexican hat activation functions," *Neural Computation*, vol. 29, p. 423, 2017.
- [22] G. Qiaoman, W. Guoxin, and X. Xiaoli, "Application of adaptive median filter and wavelet transform to dongba manuscript images denoising," in *Proceedings of the 2017 13th IEEE International Conference on Electronic Measurement & Instruments (ICEMI)*, p. 335, Yangzhou, China, October 2017.
- [23] L. Nadal, M. S. Moreolo, J. M. Fàbrega, and F. J. Vilchez, "Hybrid electro-optical MCM as multi-flow generation enabler for elastic optical networks," in *Proceedings of the 2017 Conference on Lasers and Electro-Optics Europe & European Quantum Electronics Conference (CLEO/Europe-EQEC)*, p. 1, Munich, Germany, June 2017.
- [24] B. Villarini, H. Asaturyan, E. L. Thomas, R. Mould, and J. D. Bell, "A framework for morphological feature extraction of organs from MR images for detection and classification of abnormalities," in *Proceedings of the 2017 IEEE 30th International Symposium on Computer-Based Medical Systems (CBMS)*, p. 666, Thessaloniki, Greece, June 2017.
- [25] J. Almotiri, K. Elleithy, and A. Elleithy, "A multi-anatomical retinal structure segmentation system for automatic eye

- screening using morphological adaptive fuzzy thresholding,” *IEEE Journal of Translational Engineering in Health and Medicine*, vol. 6, p. 1, 2018.
- [26] M. Ghatge, G. Walters, T. Nishida, and R. Tabrizian, “Phononic detection of morphological phase transition in atomic-layered Hafnium-Zirconium-Oxide,” in *Proceedings of the 2017 19th International Conference on Solid-State Sensors, Actuators and Microsystems (TRANSDUCERS)*, p. 746, Kaohsiung, Taiwan, June 2017.
- [27] M. H. O. Rashid, M. A. Mamun, M. A. Hossain, and M. P. Uddin, “Brain tumor detection using anisotropic filtering, SVM classifier and morphological operation from MR images,” in *Proceedings of the 2018 International Conference on Computer, Communication, Chemical, Material and Electronic Engineering (IC4ME2)*, p. 1, Rajshahi, Bangladesh, February 2018.
- [28] U. Niemann, P. Berg, A. Niemann et al., “Rupture status classification of intracranial aneurysms using morphological parameters,” in *Proceedings of the 2018 IEEE 31st International Symposium on Computer-Based Medical Systems (CBMS)*, p. 48, Karlstad, Sweden, June 2018.

Research Article

Thermal Analysis of Axial-Flux Permanent Magnet Motors for Vehicles Based on Fast Two-Way Magneto-Thermal Coupling

Xiaoting Zhang ¹, Bingyi Zhang,¹ Xin Chen,² and Simeng Zhong¹

¹School of Electrical Engineering, Shenyang University of Technology, Shenyang 110870, China

²Zhejiang CRRC Shangchi Electric Co., Ltd., Jiaxing, China

Correspondence should be addressed to Xiaoting Zhang; zhangxt@smail.sut.edu.cn

Received 8 January 2022; Revised 22 February 2022; Accepted 3 March 2022; Published 7 April 2022

Academic Editor: Wei Liu

Copyright © 2022 Xiaoting Zhang et al. This is an open access article distributed under the Creative Commons Attribution License, which permits unrestricted use, distribution, and reproduction in any medium, provided the original work is properly cited.

Axial-flux permanent magnet motor (AFPMM) have small size and high power density. It has a good application prospect in the field of new energy vehicle driving. In this paper, based on a 56 kW AFPMM, the magnetic circuit characteristics are calculated by the split loop method, considering the influence of pulse width modulated (PWM) power supply. The loss is taken as the heat source, combined with the motor structure characteristics and cooling conditions, the lumped-parameter thermal network model of the motor is established to solve the steady-state and transient temperature distribution of each structure. By this way, fast and accurate thermal calculation of the motor is realized in design stage. The accuracy of the lumped-parameter thermal network model is verified by experiment. At the same time, the effects of splitting the permanent magnet (PM) into pieces, flow rate of cooling water, and loss distribution on temperature rise are analyzed. This research work provides an effective fast thermal calculation method for AFPMM and provides a reference basis for the design of similar motors. It has important value of theoretical significance and engineering practical.

1. Introduction

Owing to the demand for light weight and miniaturization of new energy vehicles, drive motors need to have the characteristics of high speed, high frequency, and high power density. AFPMM have great superiority in terms of power density and material utilization because of their unique magnetic circuit structure. The loss of high-frequency motors increase under PWM-powered, and the thermal load of high-power-density motors increase with the decrease of relative heat dissipation area, make temperature rise higher, which will pose a certain challenge to the temperature resistance of insulating materials and PM [1]; at the same time, changes in temperature rise have a greater impact on the electromagnetic parameters of main materials such as PM, copper wires, silicon steel sheets and so on, thereby affecting loss of motor, and then having an iterative effect on temperature rise. In order to solve the above problems, thermal analysis based on the two-way

magneto-thermal coupling is very necessary for the research and application of AFPMM for vehicles.

The current analysis methods for motor temperature rise mainly include simplified analytical method, finite element method (FEM) and thermal network method. The simplified analytical method has poor calculation accuracy [2]. The FEM can obtain the overall temperature distribution of the motor, and the calculation accuracy is high, but it is necessary to establish a finite element model, carry out corresponding meshing and parameter settings, especially for axial-flux motors often require the establishment of a three-dimensional finite element model, which takes a long time and requires high computer performance, it is not conducive to parameter adjustment and optimal design in the initial design stage of the motor. Kamiya et al. analyzed the loss of motor and temperature rise of PM in the hybrid electric vehicle used the three-dimensional FEM under the power supply condition of the PWM controller [3]. Li et al. proposed a three-dimensional flow-thermal

coupling model, using the FEM to solve the different flow velocity and temperature of the high-voltage linear motor [4]. The thermal network method replaces the real heat source and thermal resistance with a small amount of concentrated heat source and equivalent thermal resistance, and converts the temperature field into a heat circuit with concentrated parameters for calculation. Wrobel et al. used the thermal network method to study the thermal characteristics of the outer rotor brushless permanent magnet motor, analyzed the advantages of modular windings in reducing temperature rise, and verified them through experiments [5]. Camilleri et al. established a motor fluid network and an equivalent thermal network, and used the thermal network method to predict the overall temperature distribution of the segmented stator [6]. Scholars from various countries have achieved certain results in the calculation of motor temperature rise [7–11], but they have not considered the two-way magnetic-thermal coupling of AFPMM and there are few studies on its transient thermal analysis.

Based on the idea of two-way coupling, this paper fully considers the interactions and influencing factors among multiple physical fields such as electricity, magnetism, fluid, and heat, conduct an in-depth study on the temperature rise of AFPMM for new energy vehicles; The method and the equivalent thermal network method respectively simplify the calculation models of motor loss and temperature rise, and fully consider different factors such as PWM power supply harmonics, permanent magnet block, cooling water flow rate, loss distribution and other factors to affect the steady-state and transient temperature of the motor. The influence of temperature rise; the magnetic-thermal coupling model was established, and the temperature rise calculation was corrected through coupling iterations, which achieved a small accuracy error; the temperature rise calculation results were verified and compared through experiments, and the test results proved the calculation method High accuracy, meeting the design calculation requirements, has important guiding significance for the subsequent design and development of AFPMM.

2. Loss Analysis

2.1. Establishment of Magnetic Circuit Model Based on Split Loop Method. In this paper, the AFPMM adopt dual-stator and single-rotor structure as shown in Figure 1, which can offset the unbalanced axial magnetic pull between stator and rotor, and has high structural stability, it is suitable for vehicles in the working conditions of frequent starting. The rotor has no core support structure with magnetic steel embedded on the surface, which has higher power density and higher efficiency.

The magnetic flux starts from the N pole of the PM, passes through the air gap, the stator teeth, and the stator yoke back to the S pole, forming a closed loop. The magnetic circuit structure and equivalent magnetic circuit model are shown in Figure 2. The relationship of magnetomotive force on a magnetic circuit is shown in formula.

$$F_m = H_m h_m = 4F_\delta + 2F_{j1} + 4F_{t1}, \quad (1)$$

where F_m , H_m , and h_m , respectively, represent the magnetomotive force, magnetic field strength, and length of the PM; F_δ , F_{j1} , and F_{t1} are magnetic potential drop of air gap, yoke, and the tooth.

The magnetic field of AFPMM is distributed along the axial direction. As the increase of radius and tooth pitch, the magnetic circuit length, tooth width also increase gradually, and the saturability of magnetic circuit changed at the same time. The calculation method equivalent to a one-dimensional magnetic circuit is unreliable, and the use of the three-dimensional finite element method consumes a lot of time. In this paper, the split-loop method is proposed to calculate the magnetic circuit characteristics of the motor. Ignoring the edge effect, the AFPMM is cut into several small annular belts in the radial direction, and the magnetic circuit characteristics of each small annular belt are calculated separately.

2.2. The Calculation of Loss. Ignoring the additional copper consumption of winding, the basic copper consumption of motor is

$$P_{Cu} = mI^2R, \quad (2)$$

where m is the number of phases of the winding; I is the effective value of phase current passing through the winding; and R is winding resistance.

The iron loss of stator core mainly includes hysteresis loss and eddy current loss. The magnetic circuit split-loop method is adopted to call the data of tooth magnetic density B_{tn} and yoke magnetic density B_{jn} in each split loop. According to Steinmetz iron loss model and standard sinusoidal power supply, the iron loss in each split loop is calculated to obtain the total iron loss of the motor:

$$\begin{aligned} P_{Fe} &= \sum_{k=1}^n P_{Fek} \\ &= \sum_{k=1}^n P_{hk} + \sum_{k=1}^n P_{ek} \\ &= \sum_{k=1}^n K_h f B_k^\alpha + \sum_{k=1}^n K_e (f B_{mk})^2, \end{aligned} \quad (3)$$

where k represents the number of split loops; P_h is hysteresis loss; P_e is eddy current loss; K_h is hysteresis loss coefficient; B_m is the maximum magnetic induction intensity; f is frequency; and α is the Steinmetz coefficient, generally in the range of 1.5–2.5.

2.3. The Loss Calculation under PWM Power Supply. The vehicle motor is controlled by the controller (inverter) taking power from the DC bus, and equivalent sine wave magnetic field in the form of PWM chopper. It will introduce a large number of high-order current harmonics, especially when the motor frequency is high, due to the

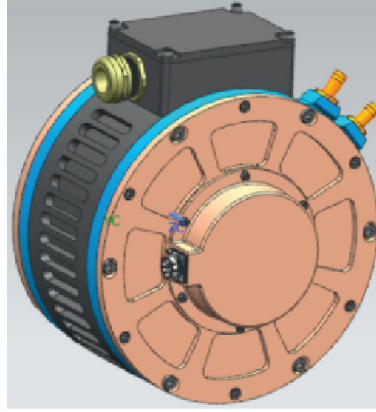


FIGURE 1: Motor structure.

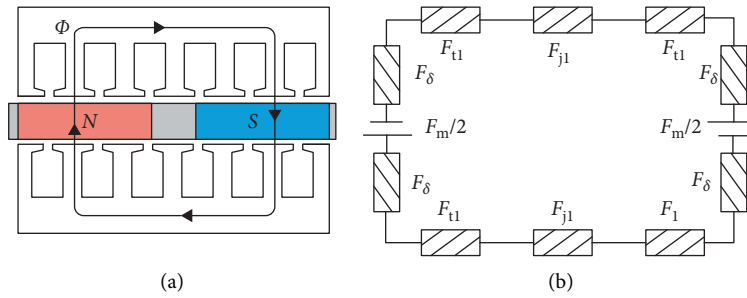


FIGURE 2: Magnetic circuit model of AFPMM. (a) Magnetic circuit structure. (b) Equivalent magnetic circuit model.

limitation of the highest switching frequency of IGBT, the harmonic proportion will increase, resulting in the increase of harmonic loss, thus increasing the heating power. When under PWM power supply, the eddy current loss generated by each harmonic is

$$P_{ePWM} = k_e \sum_{k=1}^{\infty} (k f B_k)^2. \quad (4)$$

That is, the overall eddy current loss can be expressed as the sum of eddy current losses generated by each harmonic magnetic field.

The ratio of total harmonic eddy current loss to fundamental eddy current loss can be expressed as

$$\begin{aligned} \chi &= \frac{\sum_{k=2}^{\infty} P_{ek}}{P_{e1}} \\ &= \frac{\sum_{k=2}^{\infty} k_e (u_k/k_u)^2}{k_e (u_1/k_u)^2} \\ &= \frac{\sum_{k=2}^{\infty} u_k^2}{u_1^2} \\ &= \text{THD}^2, \end{aligned} \quad (5)$$

where, u_k is the inductive voltage of winding by the k -th harmonic magnetic field, when the resistance voltage drop is ignored, and THD is the total distortion rate of harmonic voltage.

Therefore, in the case of PWM power supply, the total eddy current loss caused by fundamental voltage and time harmonic voltage can be expressed as

$$\begin{aligned} P_{FePWM} &= p_h + P_{ePWM} \\ &= (1 + \kappa) p_{Fe}, \end{aligned} \quad (6)$$

where $\kappa = (\chi/k_{h/e}) + 1$ is the iron loss increase coefficient. As the carrier ratio increases, the loss decreases, but limited by the switching loss of power devices, the carrier ratio of inverter cannot be too large. The loss under different carrier ratios is shown in Figure 3.

Considering the influence of PWM power supply, the loss of motor under 36 kW and 5600 rpm is calculated, and the results are shown in Table 1.

2.4. Simulation Verification. In order to verify the accuracy of the calculated loss derived by the split loop method in this paper, the finite element model of the motor is established as shown in Figure 4. The no-load loss of the motor at different speeds is obtained through calculation, and the simulation results are compared with the results calculated by the split loop method, as shown in Figure 5. When the motor speed is higher than 4800 rpm, the calculation results of split loop method are very close to those of finite element method; When the motor speed is lower than 4800 rpm, there is a large error between the calculation results of analytical method and finite element method, the maximum error is 97.6 W. When the rotating speed is low, the hysteresis loss is

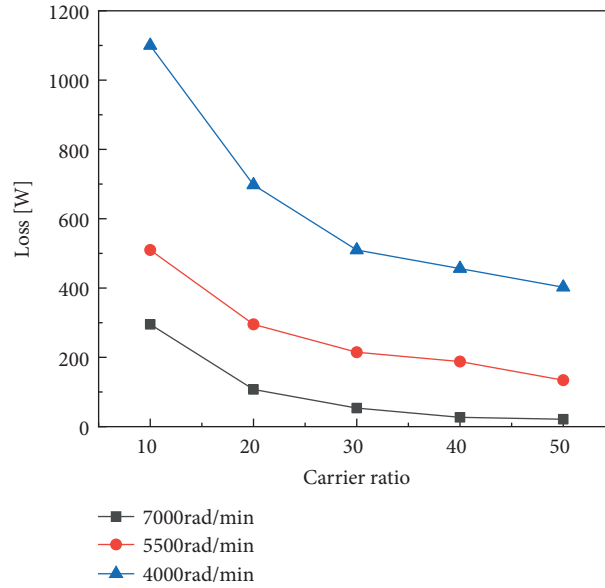


FIGURE 3: Loss corresponding to different carrier wave ratios.

TABLE 1: Loss distribution of prototype at rated power.

Location	Stator teeth	Stator yoke	Stator winding	PM	Rotor core	Bearing
Loss/W	402	564	430	139	10	34

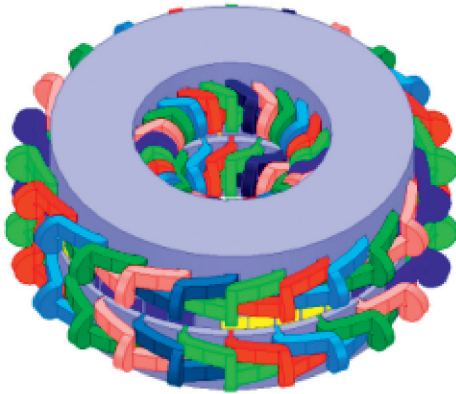


FIGURE 4: Finite element analysis model.

dominant. Using the traditional iron loss calculation mathematical model, there is a problem that the selection of material hysteresis loss coefficient and Steinmetz coefficient is not accurate enough.

3. Thermal Network Model

When the equivalent thermal network method is used to mesh and calculate the temperature field of AFPMM, the following assumptions are made:

- (1) The cooling conditions of the motor in the circumferential direction are the same, and the motor temperature is symmetrical along the circumferential direction

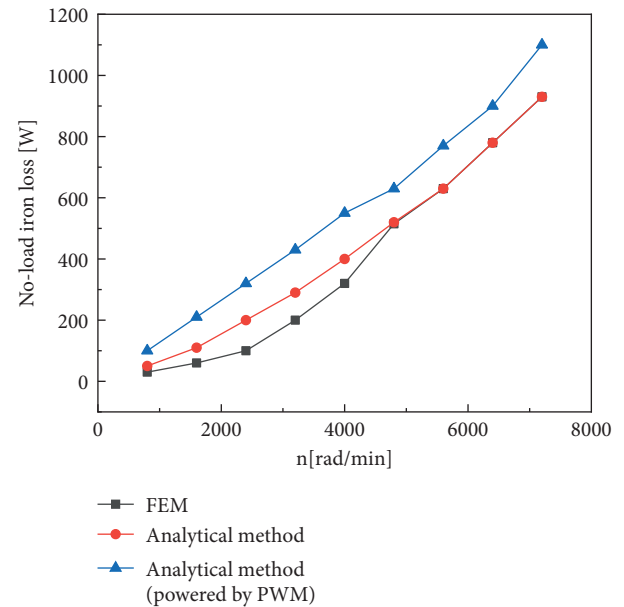


FIGURE 5: No-load iron loss comparison.

- (2) The temperature field of the motor is symmetrical along the axial centerline of the rotor
- (3) The temperature of each air node in the motor cavity is the same, that is, it is divided by the same node

The main structures of the motor include waterway, End cap, stator yoke, stator teeth, winding, PM, rotor, bearing and so on. The temperature nodes are divided according to

the characteristics of each part, and the nodes are connected according to the heat flow direction to form a heat network, as shown in Table 2.

3.1. Steady State Thermal Analysis. The motor in this paper is a fully enclosed motor with water cooling and natural cooling outside the motor. The thermal resistance parameters of the equivalent thermal network model are mainly conduction thermal resistance and convection thermal resistance, and radiation thermal resistance can be ignored. Distribution of thermal network node is shown in Figure 6.

3.1.1. Thermal Conductivity and Thermal Resistance

(1) *Cylinder Structure.* The heat conduction between the main parts of the motor can be equivalent to a cylindrical structure. R_1 , R_2 are the inner and outer diameters of the cylinder, T_1 , T_2 are the temperatures on both sides of the cylinder, and L is the length of the cylinder. According to the basic theory of heat conduction, the radial heat conduction can be obtained. The resistance is

$$R_a = \frac{1}{2\pi\lambda L} \ln \frac{R_2}{R_1}. \quad (7)$$

Axial heat conduction resistance:

$$R_b = \frac{1}{\lambda\pi(R_2 - R_1)} \ln \frac{R_2}{(R_1 + R_2)/2}. \quad (8)$$

(2) *Winding.* The position distribution of each conductor in the winding is random, and the equivalent thermal conductivity of the winding K_s is introduced. Node 3 (stator yoke) and node 7 (slot winding) exchange heat through the slot bottom section. The thermal conductivity and thermal resistance between the stator yoke and the slot winding are

$$G_{37} = K_{s1}S_{37},$$

$$R_{s1} = \frac{\delta_i}{\lambda_i} + \frac{1}{4} \left[\frac{b_1(1-S_f)}{\lambda_L} K_L + \frac{b_1(1-S_f)}{\lambda_L} \cdot \left(1 - K_L \right) + \frac{d-d_w}{\lambda_d} \frac{b_1\sqrt{S_f}}{d} \right]. \quad (9)$$

In the formula, Q_1 is the number of stator slots; b_1 is the width of the slot bottom; K_{s1} is the equivalent thermal conductivity of the slot winding; δ_i is the insulation thickness of the slot; S_f is the slot full rate; d is the elongation of the straight part of the coil after exiting the slot; d_w is the diameter of the parallel wire; λ_i is the insulation thermal conductivity of the groove; λ_L is the thermal conductivity of the dipping varnish; λ_d is the thermal conductivity of the wire paint.

3.1.2. Thermal Convection Thermal Resistance

(1) *Case and Air.* The casing is in direct contact with the outside air, where air flows slowly, the convective thermal resistance is

TABLE 2: Corresponding nodes of each part of the motor.

Location	Node	Location	Node
Chassis	1-2	PM	15-17
Stator yoke	3-5	Air of end part	19-21
Winding	6-10, 33-37	Shaft	22-24
Stator teeth	11-13	Bearing	25
Rotor core	14, 18, 30-32	End cap	26-29

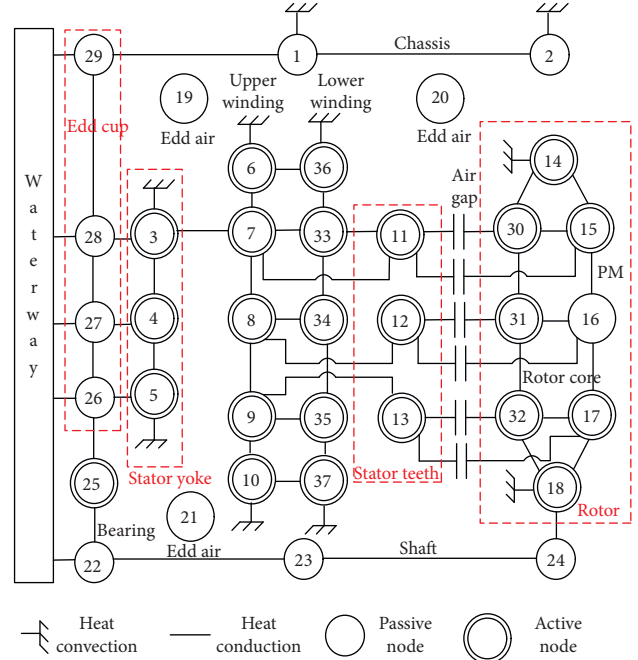


FIGURE 6: Distribution of thermal network node.

$$R_{1a-1} = \frac{1}{S_1\alpha}. \quad (10)$$

According to the definition of the heat transfer coefficient in the case of natural heat transfer between the casing wall and the surrounding space, the heat dissipation coefficient of the chassis surface is

$$\alpha = 14(1 + 0.5\sqrt{\omega_w})^3 \sqrt{\frac{\theta}{25}}. \quad (11)$$

In the formula, α is the heat transfer coefficient of the chassis surface, $W/(m^2 \cdot K)$; ω_w is the wind speed blowing on the inner wall of the chassis; θ is the temperature of the outer surface of the chassis, K .

(2) *The Space between Stator Teeth and Air Gap.* The node 11 and the node 15 exchange heat through an air gap. The heat dissipation coefficient of this part is related to the air gap fluid velocity. The key to calculating the air gap convective thermal resistance is the selection and calculation of the Nusselt number. For a smooth air gap, when the Taylor number is small, that is, $Ta < 1700$, the fluid is laminar, and the air gap is dominated by heat conduction; when $1700 < Ta < 10^4$, the air gap fluid is not only laminar,

but also accompanied by eddy currents; When $10^4 < Ta < 10^7$, the fluid state of air gap is turbulent, the Nusselt coefficient and the corresponding convective heat dissipation coefficient under different fluid states are calculated as follows:

$$\begin{aligned} Re_\delta &= \frac{v_r g}{\mu_{air}}, \\ Ta &= \frac{Re_\delta^2 g}{r}, \\ Nu &= \begin{cases} 2, & Ta < 1700, \\ 0.128Ta^{0.367}, & 1700 < Ta < 10^4, \\ 0.409Ta^{0.241}, & 10^4 < Ta < 10^7, \end{cases} \quad (12) \\ \alpha_{air} &= \frac{Nu \cdot \lambda_{air}}{g}. \end{aligned}$$

(3) *Waterway*. The convective heat transfer coefficient of the waterway is calculated as follows:

$$\begin{aligned} D_h &= \frac{2HW}{(H+W)}, \\ Re_w &= \frac{\rho_w v_w D_w}{\mu_w}, \quad (13) \\ Pr &= \frac{\mu_w C_w}{\lambda_w}, \end{aligned}$$

where H and W are the height and width of the waterway outlet; D_h is the hydraulic diameter of the waterway; Re_w is the Reynolds number of the waterway fluid; C_w , ρ_w , v_w and μ_w are the specific heat capacity, density, flow velocity and dynamic viscosity of the fluid;

When $Re_w < 2300$, the fluid in waterway is laminar, and its Nusselt number is calculated as

$$\begin{aligned} Nu_{sd} &= 7.46 - 17.02 \left(\frac{H}{W} \right) + 22.43 \left(\frac{H}{W} \right)^2 \\ &\quad - 9.94 \left(\frac{H}{W} \right)^3 + \frac{(0.065 D_h Re_w Pr / L_w)}{1 + 0.04 (D_h Re_w Pr / L_w)^{2/3}}, \end{aligned} \quad (14)$$

where L_w is the length of the waterway.

When $2300 < Re_w < 10^6$, the fluid in the waterway is turbulent, and its Nusselt number is calculated as

$$\begin{aligned} f_w &= [0.79 \ln(Re_w) - 1.64]^{-2}, \\ Nu_{sd} &= \frac{(f_w/8)(Re_w - 1000)Pr}{1 + 12.7(f_w/8)^{1/2}(Pr^{2/3} - 1)}. \end{aligned} \quad (15)$$

where f_w is the friction factor of the smooth waterway.

The convective heat transfer coefficient of the waterway is

$$\alpha_{sd} = \frac{Nu_{sd} \lambda_w}{D_h}. \quad (16)$$

(4) *Rotor Core*. The Reynolds number, Nusselt heat number and heat dissipation coefficient of the rotor along the radial end face are

$$\begin{aligned} Re_{1420} &= \frac{\pi D_2^2 n}{120 \mu_{air}}, \\ Nu_{1420} &= 1.67 Re_{1420}^{0.385}, \quad (17) \\ \alpha_{1420} &= \frac{Nu_{1420} \lambda_{air}}{2D_2}. \end{aligned}$$

Through the heat transfer relationship of each node of the motor, the heat balance equations related to the nodes can be listed, and the heat balance equations of the motor can be obtained by combining these equations. The matrix form is

$$[T] = [G][W]. \quad (18)$$

In the formula, $[G]$ is the thermal conductivity matrix of each node; $[T]$ is the temperature rise matrix of each node; $[W]$ is the heat source matrix of each node. By solving this linear equation system, the temperature rise of each node can be obtained, as shown in Table 3. The thermal resistance of different parts of the motor obtains an $n \times n$ thermal conductivity matrix related to the node:

$$G = \begin{bmatrix} \sum_{i=1}^n \frac{1}{R_{1,i}} & -\frac{1}{R_{1,2}} & \cdots & -\frac{1}{R_{1,n}} \\ -\frac{1}{R_{2,1}} & \sum_{i=1}^n \frac{1}{R_{2,i}} & \cdots & -\frac{1}{R_{2,n}} \\ \vdots & \vdots & \ddots & \vdots \\ -\frac{1}{R_{n,1}} & -\frac{1}{R_{n,2}} & \cdots & \sum_{i=1}^n \frac{1}{R_{n,i}} \end{bmatrix}. \quad (19)$$

3.2. Transient Thermal Analysis. When the motor is in a short-term acceleration state, the output power exceeds the rated power. At this time, it is obviously unreasonable to use the steady-state thermal network equation to calculate the motor temperature rise. Therefore, it is effective to use the transient thermal network to calculate the temperature change of the motor during short-term overload. Evaluate the safety performance of the motor.

TABLE 3: The temperature rise of each node at the rated power of the prototype.

Location	Node	Temperature rise (K)	Node	Temperature rise (K)	Node	Temperature rise (K)
Stator yoke	3	12.5	4	12.8	5	12.0
Stator teeth	11	29.3	12	31.3	13	34.0
Stator winding	6	60.3	8	56.1	10	59.0
PM	15	77.9	16	84.4	17	85.6
Shaft	22	43.0	23	48.6	24	53.9
Rotor core	14	63.8	18	59.4		

Under transient conditions, for any temperature node, the net heat flow into the node at all times is equal to the increase in the internal energy of the node's relevant volume:

$$q_i = \rho_i C_i V_i \frac{dT_i}{dt}, \quad (20)$$

where q_i is the net heat flow of the i -th node; ρ_i is the density of the unit represented by the i -th node; C_i is the specific heat capacity of the unit represented by the i -th node; V_i is the volume of the unit represented by the i -th node; dT_i/dt is the temperature rise rate of the i -th node. The initial condition of the first-order nonlinear differential equation is the initial temperature of each node. Solving the differential equation can obtain the characteristics of temperature change of each node with time.

If the temperature of node i at time t_{k+1} is T_i^{k+1} ($i = 1, 2, 3, 4, \dots, n$), then the temperature T_i^k of node i at time t_k can be used to recursively obtain T_i^{k+1} :

$$\begin{aligned} T_i^{k+1} &= T_i^k + \frac{dT_i^k}{dt} \Delta t \\ &= T_i^k + \frac{q_i^k}{\rho_i^k C_i^k V_i^k} \Delta t, \end{aligned} \quad (21)$$

$$q_i^k = Q_i^k - Q_{oi}^k.$$

In the formula, Q_i^k is the calorific value of the node at time k , which is an $m \times 1$ matrix; Q_{oi}^k is the heat outflow of the node at time k , which is an $m \times 1$ matrix; m is the number of nodes divided by the thermal network. V_i is a fixed value, and only q_i^k , C_i^k , ρ_i and T_i^k at time t_k are calculated, T_i^{k+1} can be obtained. Therefore, as long as the initial temperature of the node is obtained, the node temperature at each time can be obtained.

Taking nodes 3, 6, and 7 as examples, construct their transient thermal network solving equations:

$$\begin{aligned} Q_3 - \left(\frac{T_3^{k+1} - T_{28}^{k+1}}{R_{328}} + \frac{T_3^{k+1} - T_7^{k+1}}{R_{37}} + \frac{T_3^{k+1} - T_{11}^{k+1}}{R_{311}} + \frac{T_3^{k+1} - T_{19}^{k+1}}{R_{319}} + \frac{T_3^{k+1} - T_4^{k+1}}{R_{34}} \right) &= \rho_3 C_3 V_3 \frac{dT_3^k}{dt}, \\ Q_6 - \frac{T_6^{k+1} - T_7^{k+1}}{R_{67}} + \frac{T_6^{k+1} - T_{19}^{k+1}}{R_{619}} &= \rho_6 C_6 V_6 \frac{dT_6^k}{dt}, \\ Q_7 - \left(\frac{T_7^{k+1} - T_3^{k+1}}{R_{73}} + \frac{T_7^{k+1} - T_6^{k+1}}{R_{76}} + \frac{T_7^{k+1} - T_8^{k+1}}{R_{78}} + \frac{T_7^{k+1} - T_{11}^{k+1}}{R_{711}} \right) &= \rho_7 C_7 V_7 \frac{dT_7^k}{dt}. \end{aligned} \quad (22)$$

It should be noted that, due to the presence of windings and dipping varnish in the stator slots, the calculation of the heat capacity of the windings is more complicated. The calculation method of the equivalent specific heat capacity of the winding nodes in reference [12] in this article is as follows:

$$C_{eff} = \frac{S_f (\rho_w C_w - \rho_{in} C_{in}) + \rho_{in} C_{in}}{S_f (\rho_w - \rho_{in}) + \rho_{in}}. \quad (23)$$

In the formula, C_{eff} is the equivalent specific heat capacity; S_f is the slot full rate; ρ_w is the winding density; ρ_{in} is the dipping varnish density; C_w is the winding specific heat capacity; C_{in} is specific heat capacity of dipping varnish.

The initial temperature is the ambient temperature, and the motor runs at rated power. The transient temperature changes of each node are shown in Figure 7. The stable

temperature reached by each node is the same as the calculation result of the steady-state thermal network. The temperature of each node is stable in about 2000 s, and the temperature of the PM rises fastest.

In order to fit the actual situation of the motor operation better, the motor operating state is given as shown in Figure 8, the temperature changes of each node over time are shown in Figure 9. It can be seen that when the output torque of the motor increased, the winding temperature increases rapidly with the increase of the winding current, and the permanent magnet temperature decreases with the decrease of the speed. The change trend of the rotor temperature is the same as that of the permanent magnet temperature. The transient temperature of the winding does not affect the transient temperature of the permanent magnet basically.

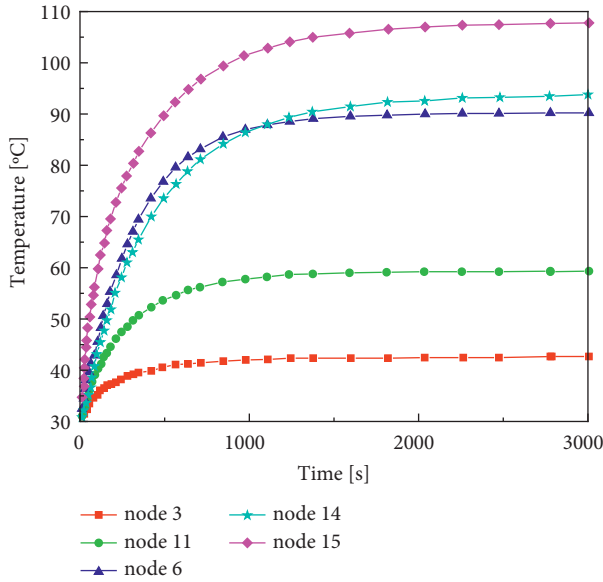


FIGURE 7: The temperature change curve of each part of the motor when running at rated power.

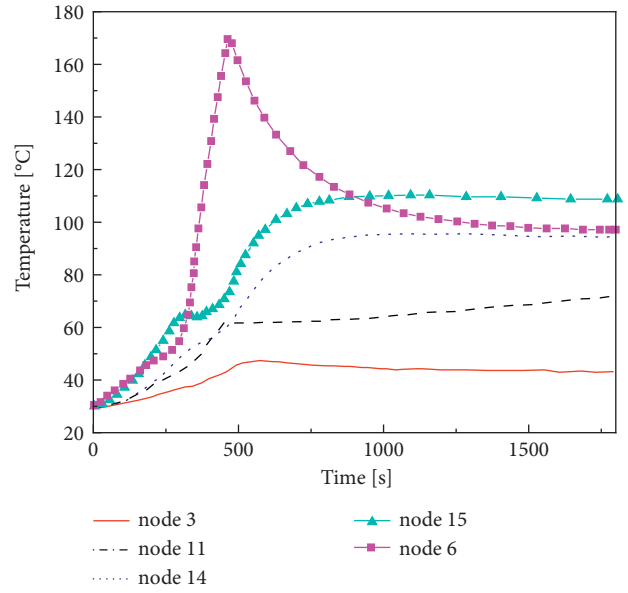


FIGURE 9: The temperature change curve of each part of the motor under the working condition shown in Figure 8.

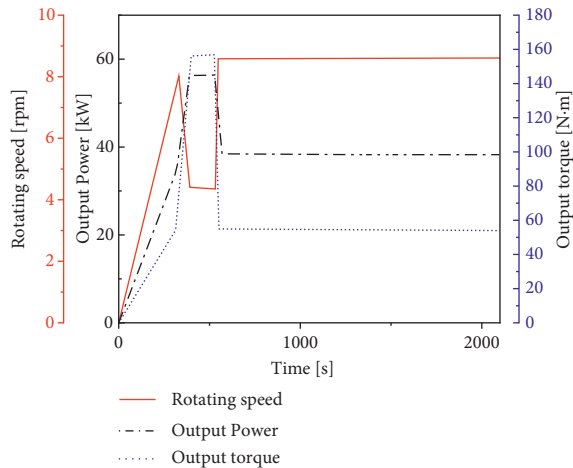


FIGURE 8: Motor operating conditions.

The temperature changes of the windings and permanent magnets at maximum power are shown in Figure 10. The maximum temperature of the winding is 235°C, and the maximum temperature of the permanent magnet is 140°C. The temperature of the permanent magnet changes smoothly during short-term overload. Due to the short time, the heat in the winding is not enough to be taken away by the cooling medium, so the temperature of the winding basically rises linearly. According to the insulation specification, the maximum overload time can be solved.

3.3. The Effect of Permanent Magnet Segmentation on Eddy Current and Temperature Rise. The eddy current loss of the permanent magnet is related to the eddy current path, magnetic induction intensity, permanent magnet material and shape, and can be calculated by the following formula:

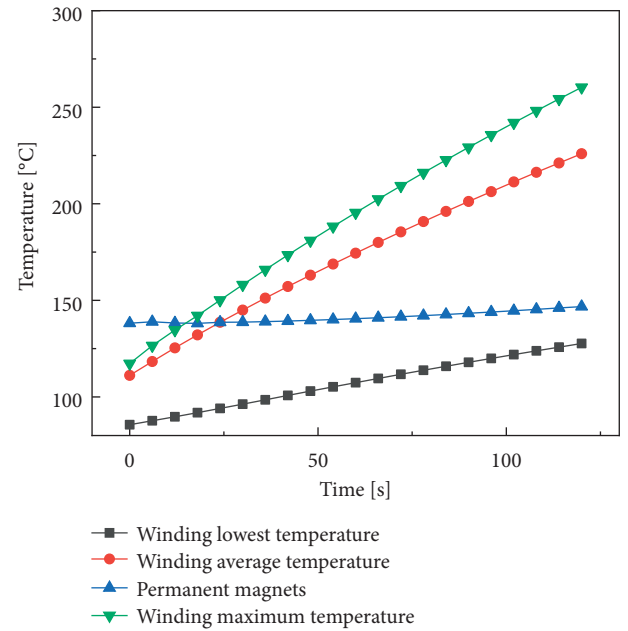


FIGURE 10: Temperature changes of windings and permanent magnets within 2 minutes at peak power.

$$\begin{aligned}
 P_{\text{eddy}} &= \int_V E \cdot J dV \\
 &= \int_V \rho J^2 dV,
 \end{aligned}
 \tag{24}$$

where E is eddy current intensity; J is eddy current density; ρ is permanent magnet resistivity; and V is permanent magnet volume.

The permanent magnet is divided into pieces along the axial and radial directions, and an insulating layer is added in the middle to block the eddy current loss path. The eddy

current loss of the permanent magnet decreases with the increase of the number of segments, as shown in Figure 11. The number of segments cannot be increased indefinitely due to factors such as the manufacturing process, changes in the effective size of the permanent magnet, and the utilization rate of the permanent magnet material. When the motors in this paper are divided into two pieces, the loss has a clear tendency to decrease. The distribution and size of the eddy current loss under different divide methods are shown in Figures 12 and 13. The radial blocking has a significant effect on reducing loss, so as to reduce the temperature rise of the permanent magnet. Because the AFPMM magnetic field is distributed in the three-dimensional space, there is an axial eddy current loss component, but the content is small, so the effect of splitting block loss in the axial direction is not obvious. Steady-state temperature rise of permanent magnets and windings with different block methods is shown in Figure 14. Dividing the permanent magnet into four pieces can reduce the temperature rise by 23% compared with the permanent magnet not divided, and dividing the permanent magnet has little effect on the winding temperature.

3.4. The Influence of Cooling Water Speed on the Temperature Rise of the Motor. Under steady-state conditions, the temperature rise curves of permanent magnets and winding with the change of cooling water flow rate are shown in Figure 15(a), the change curve of cooling coefficient in waterway is shown in Figure 15(b). With the flow rate increase of the cooling water, during the period of 0–1.5 m/s, the cooling coefficient of the waterway increases, and the temperature rise of windings and permanent magnets decreases. After 1.5 m/s, the cooling water enters the turbulent flow stage, the more flow rate increases, the more slowly speed decreases. the saturated water speed will eventually be reached, and then increasing the water speed has little effect on heat dissipation. Therefore, choosing a reasonable cooling water speed can not only ensure the safe operation of the motor, but also reduce the power of the water pump.

Under transient conditions, the temperature of the permanent magnet and winding changes with the cooling water flow rate when the motor runs for 180 s at 56 kW and 3000 rpm. As shown in Figure 16, the temperature of the winding and permanent magnet basically does not change, and the temperature of the permanent magnet does not change, it is about 77°C, and the winding is about 183°C. From the principle of the transient thermal network equation in section III(B) of this paper, it can be seen that the transient temperature rise speed is mainly affected by the heat of the input node and the heat capacity of the node itself. It is easy to know that in this working state, the short-term heating power of the winding is large, and the thermal resistance of the heat dissipation circuit is large, and the balance of the cooling power cannot be achieved before a large temperature difference occurs, and the heat capacity of the winding and insulating paint is limited, resulting in the winding temperature rise rapidly.

3.5. The Influence of Loss Distribution on Motor Temperature Rise. Assuming that the sum of copper loss and iron loss of the motor is constant, the ratio of copper loss to iron loss is changed, and the change curve of the steady temperature rise of permanent magnets and windings with the ratio is shown in Figure 17. Under steady-state conditions, when the ratio of copper loss to iron loss increases, the copper loss increases, the temperature of winding rise rapidly, and the temperature rise of the permanent magnet slowly increases. When the sum of copper consumption and iron consumption of the motor is constant, other factors are ignored. Reducing the proportion of the copper consumption of the motor is beneficial to reduce the temperature rise of the motor, but a lower proportion of the copper consumption requires a larger amount of copper and a larger slot area, so that the material utilization rate and power density are reduced. Under transient conditions, the temperature rise speed of the permanent magnet is basically not affected by the change in the ratio of copper loss to iron loss, while the winding temperature rise speed decreases as the ratio of copper loss to iron loss decreases, reducing the copper loss of the motor. The proportion is conducive to reducing the temperature rise rate of the motor.

4. Magneto-Thermal Coupling Analysis Model

The change of temperature in motor affect the characteristics of windings and permanent magnets, changes of resistance and magnetic field strength affect the loss of motor, and the changes in loss will be fed back to the temperature field calculation. Therefore, the two-way magneto-thermal coupling calculation of the motor can effectively improve the accuracy of the calculation.

The temperature change of the conductor causes the change of resistance value, and the copper loss of the stator also changes:

$$R_T = R_0 (1 + \alpha_T T), \quad (25)$$

where α_T is the temperature coefficient of the copper wire, R_0 is the resistance at the initial temperature, and T is the operating temperature. In addition, the remanence of permanent magnets decreases as the temperature of the motor rises:

$$B_{rT} = B_{r20} [1 + \alpha_{Br} (T - 20)], \quad (26)$$

where B_{rT} and B_{r20} are the residual magnetism at temperature T and 20°C, respectively, and α_{Br} is the reversible temperature coefficient of the permanent magnet.

Considering the mutual influence between the electromagnetism and temperature rise of the motor, a magneto-thermal coupling calculation model is established to iteratively correct the input temperature. The calculation process is shown in Figure 18. In the figure, $m\%$ is the allowable error between the calculated temperature and the input temperature rise. When the input starting temperature of the permanent magnet and the winding is 95°C and 115°C, and the allowable error is 5% and 1%, the number of iterations are 4 and 7 respectively, and the allowable error is 1% in this paper.

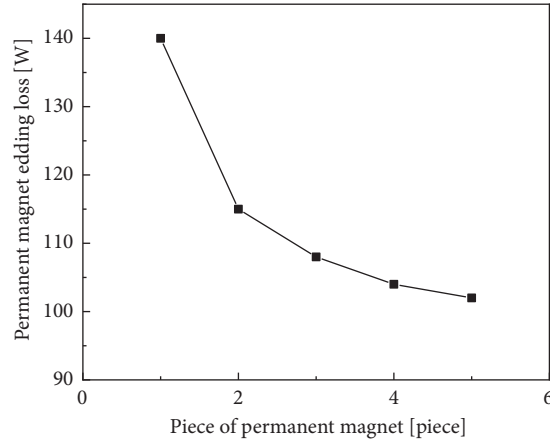


FIGURE 11: The relationship between the eddy current loss and the pieces of permanent magnets.

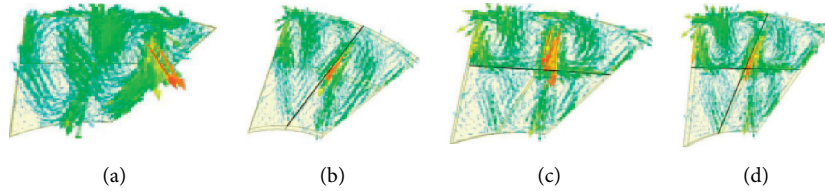


FIGURE 12: Eddy current distribution when permanent magnet is divided into pieces. (a) Undivided. (b) Divided into two pieces in the circumferential direction. (c) Divided into two pieces in the radial direction. (d) Divided into four pieces.

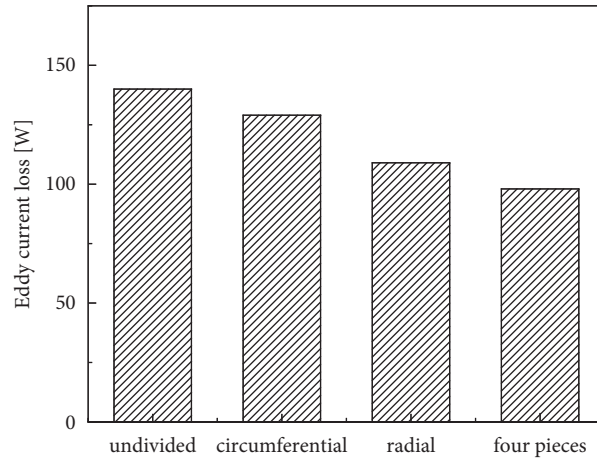


FIGURE 13: Eddy current losses of permanent magnets in different block methods.

Among them, the permanent magnet temperature rise T_p is taken as the average temperature rise of each node:

$$T_p = T_{15} \frac{V_{15}}{V_{PM}} + T_{16} \frac{V_{16}}{V_{PM}} + T_{17} \frac{V_{17}}{V_{PM}}. \quad (27)$$

The temperature rise of the stator winding T_w is taken as the average temperature rise of each node:

$$T_w = (T_6 + T_{10} + T_{36} + T_{37})k_{end} + (T_7 + T_8 + T_9 + T_{33} + T_{34})(1 - k_{end}). \quad (28)$$

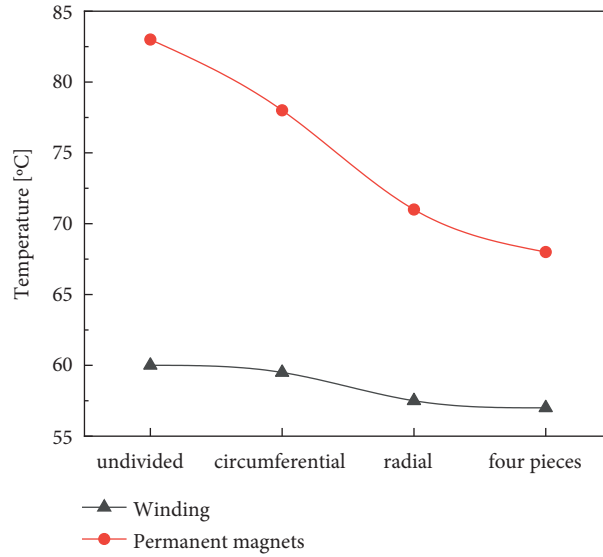


FIGURE 14: Steady-state temperature rise of permanent magnets and windings with different block methods.

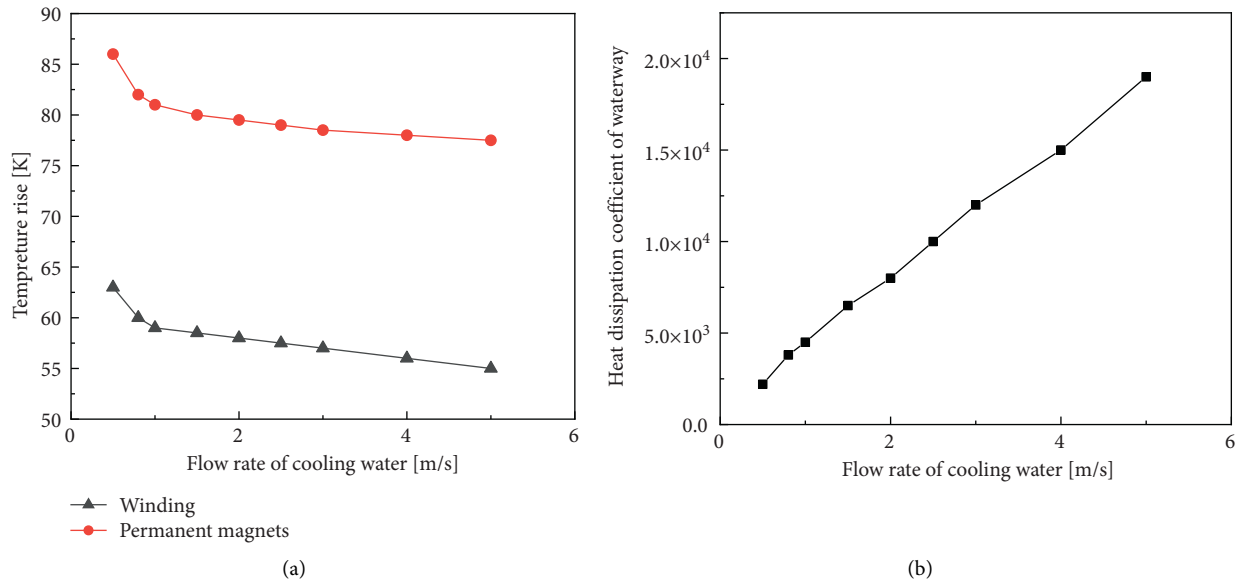


FIGURE 15: The influence of the cooling water flow rate at the rated power of the motor on the temperature rise of the permanent magnets and windings and the heat dissipation coefficient of the waterway. (a) Temperature rise of winding and permanent magnet. (b) Waterway heat dissipation coefficient.

In the formula, V_{PM} is the volume of the permanent magnet, and k_{end} is the ratio of the volume of the winding end to the total volume of the winding.

5. Experimental Test

In order to verify the calculation accuracy of the thermal network method, the temperature rise test was conducted on the prototype. The prototype and experimental platform are shown as Figure 19. The motor windings were embedded with thermal resistance, the bearing caps, shafts and other structural parts were measured with infrared thermometer, and the highest temperature of rotor was measured with

temperature stickers. The rated conditions of the experimental test are: stator current is 75 A, rotor speed is 5600 r/min, and cooling water flow rate is 2 m/s. According to the characteristic that the no-load back electric potential of the motor is inversely proportional to the permanent magnet temperature, in the prototype experiment, the no-load back electric potential measured when the motor just runs at 5600 rpm at 20°C is 368 V. After the motor runs for a period of time, the temperature reaches stable. At this time, the hot no-load back electric potential is 335 V, and the temperature rise of the permanent magnet is 84.4°C calculated according to formulas (29)–(31). When the ambient temperature is 30°C, the temperature rise of the winding is 53°C by

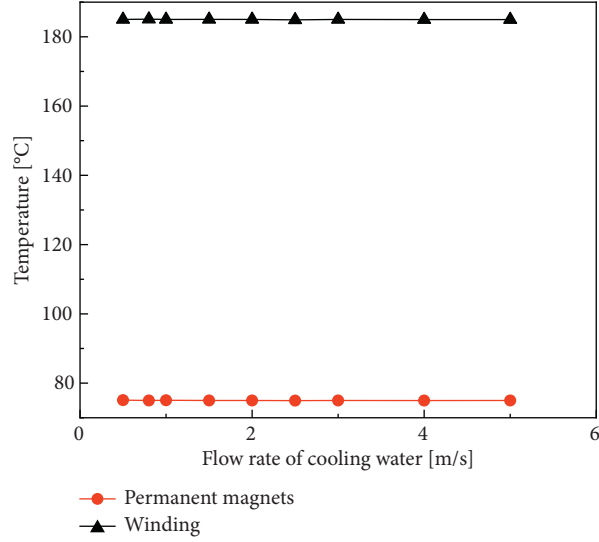


FIGURE 16: Changes of temperature of permanent magnet and winding with cooling water flow rate when the motor is running for 180 s at peak power.

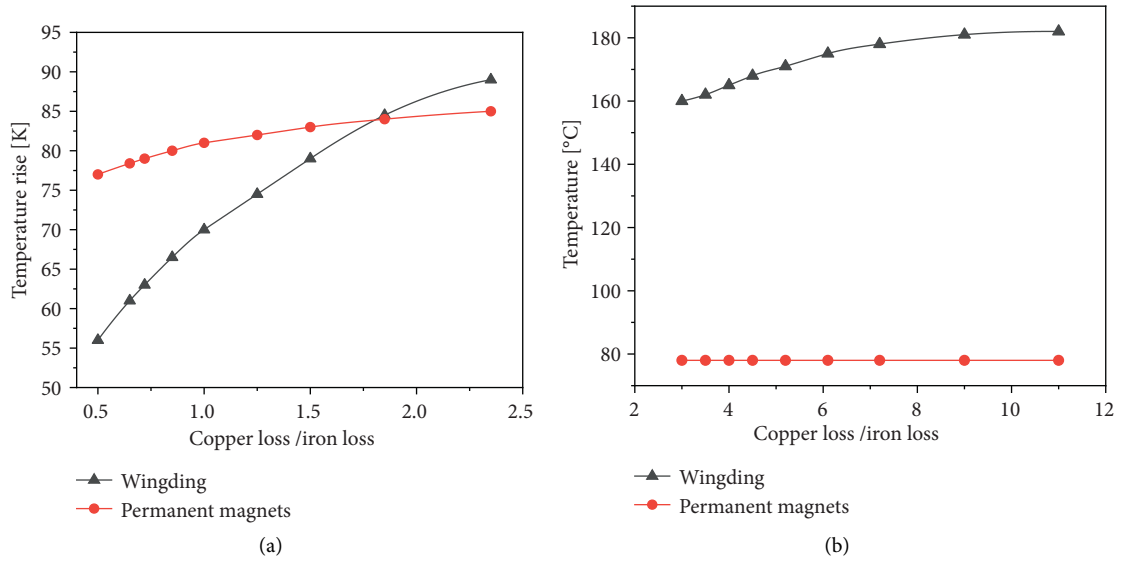


FIGURE 17: The temperature rise of permanent magnets and windings varies with the ratio of copper loss to iron loss. (a) Steady-state temperature rise. (b) Transient temperature rise.

measuring the thermocouple. Tables 4 and 5 show the comparison of the temperature distribution of each component of motor. The maximum error appears on the winding, but the error is small, all within a reasonable range, which proves the accuracy of the calculation results in the article. Figure 20 shows the efficiency map obtained by experimental testing and calculation, the accuracy of efficiency calculation is verified.

$$B_r = \left[1 + (T - 20) \frac{\alpha_{Br}}{100} \right] \left(1 - \frac{IL}{100} \right) B_{r20}, \quad (29)$$

$$\Phi_0 = \frac{b_{m0} B_r A_m}{\sigma_0}, \quad (30)$$

$$E_0 = 4.44 f N K_{dq} K_\Phi \Phi_0. \quad (31)$$

In the formula, B_{r20} is the residual magnetism of the permanent magnet at 20°C; α is the reversible temperature coefficient of the permanent magnet; IL is the irreversible loss rate of B_r ; T is the operating temperature; b_{m0} is the operating point of the permanent magnet; A_m is the cross-sectional area of pole of magnetism flux which is provided by permanent magnet; σ_0 is the magnetic leakage coefficient; f is the operating frequency; N is the number of series turns of each phase winding; K_{dq} is the winding factor; K_Φ is the air gap flux waveform coefficient; Φ_0 is the no-load main magnetic flux; E_0 is the no-load back electromotive force.

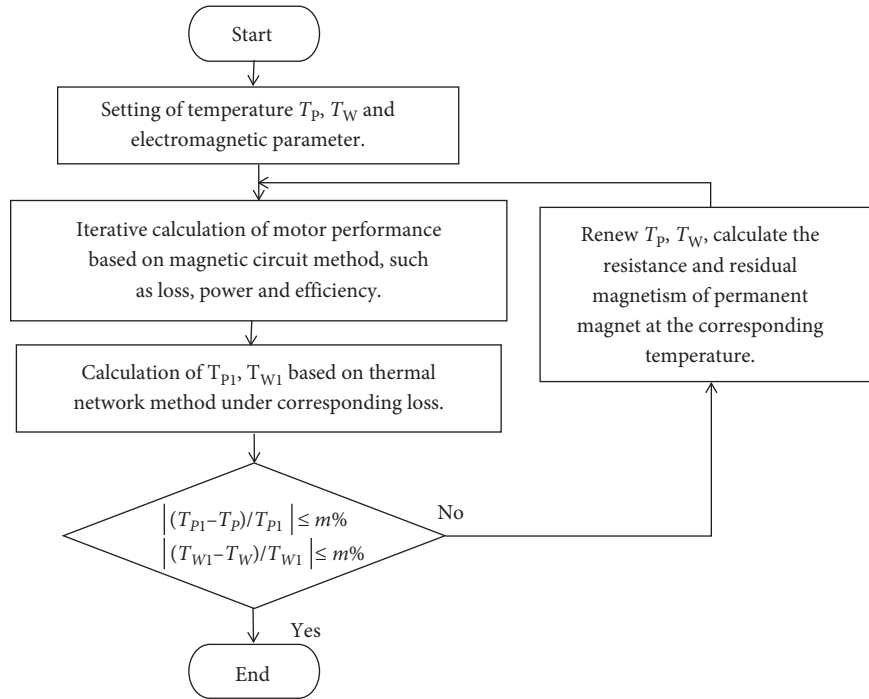


FIGURE 18: Flow chart of magnetic-thermal coupling calculation of motor characteristics.

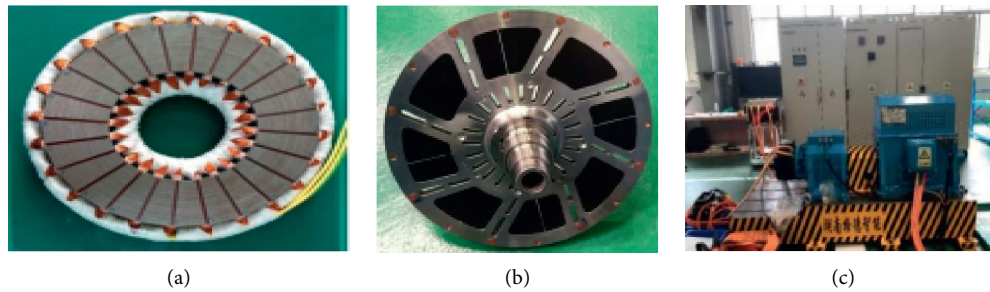


FIGURE 19: The prototype and experimental platform. (a) The stator. (b) The rotor. (c) Experimental platform.

TABLE 4: Comparison of steady-state temperature rise of various structural components.

Location	Stator			Permanent magnets	Shaft	Rotor core
	Yoke	Teeth	Winding			
Thermal network method (K)	12.8	31.3	56.1	84.4	48.6	59.4
Measurements (K)	12.5	30.3	53	81.3	47.9	56.7
Error rate	2.4%	3.3%	5.85%	3.81%	1.46%	4.76%

TABLE 5: Comparison of transient temperature rise of winding and permanent magnet.

Time (s)	Stator winding			Permanent magnets		
	Thermal network method	Measurements	Error rate (%)	Thermal network method	Measurements	Error rate (%)
280	27.2	26.1	4.21	35.3	34.6	2.02
338	58.6	56.7	3.35	36.4	35.3	3.12
458	118.3	114.3	3.50	39.3	38.1	3.15
467	140.7	135.2	4.07	40.9	39.4	3.81
1500	56.0	53.0	5.66	80.9	78.5	3.06

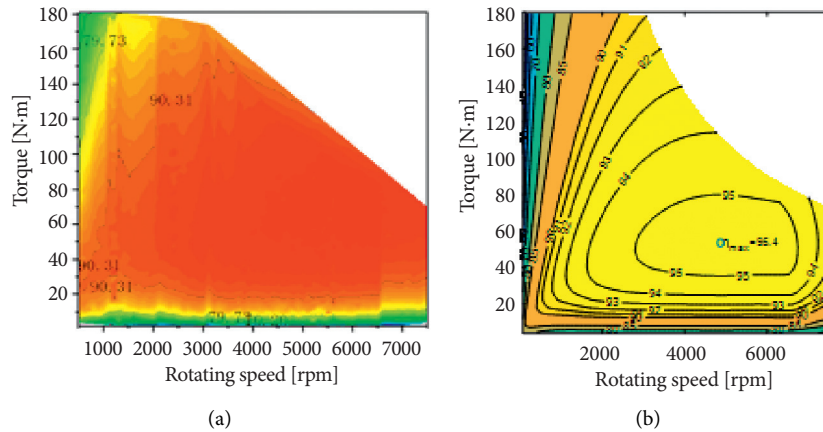


FIGURE 20: The efficiency map of prototype. (a) The test result. (b) The calculation result.

6. Conclusion

In this paper, the split-loop method is proposed to analyse the loss considering the influence of the harmonics under PWM power. The thermal network method is embodied and applied to the steady-state and transient temperature rise of the AFPMM calculate. Get the following conclusions:

- (1) By establishing a mathematical model of magneto-thermal coupling, a fast iterative temperature rise calculation method for AFPMM is proposed, and the influence of PWM power supply on loss and temperature rise is analyzed. The calculation results are more accurate and can provide guidance on the design and calculation of similar motors.
- (2) The effects of dividing PM into pieces, cooling water flow rate, and loss distribution on the steady-state and transient temperature rise of the motor are analyzed. The results showed that within a certain range, the selection of different parameters will have a great impact on motor efficiency and temperature rise, which can provide a reference for the selection of motor parameters.
- (3) The loss and temperature rise models of the AFPMM are simplified by the split-loop method and the thermal network method, which can fully ensure the calculation accuracy and avoid heavy dependence on computer software and hardware. And a serious waste of time by the finite element method.

The calculation results are verified by prototype test, and the results show that the calculation method used in this paper has high calculation accuracy. Based on the idea of two-way coupling, the interaction relations and influencing factors among electric, magnetic, fluid and thermal fields are fully considered in this paper, the rapid analysis of temperature rise is realized, and consumes less time, occupies little computer resources by the method proposed, it has extremely high application prospects for motor design and optimization.

Data Availability

No data were used to support this study.

Conflicts of Interest

The authors declare no conflicts of interest.

References

- [1] Q. Li, B. Zhang, and A. Liu, "Cogging torque computation and optimization in dual-stator axial flux permanent magnet machines," *IEEJ Transactions on Electrical and Electronic Engineering*, vol. 15, no. 10, pp. 1414–1422, 2020.
- [2] A. Boglietti, A. Cavagnino, D. Staton, M. Shanel, M. Mueller, and C. Mejuto, "Evolution and modern approaches for thermal analysis of electrical machines," *IEEE Transactions on Industrial Electronics*, vol. 56, no. 3, pp. 871–882, 2009.
- [3] M. Kamiya, Y. Kawase, and N. Matsui, "Temperature distribution analysis of permanent magnet in interior permanent magnet synchronous motor considering PWM carrier harmonics," in *Proceedings of the International Conference on Electrical Machines and Systems*, pp. 8–11, Seoul, Korea, October 2007.
- [4] W. Li, Z. Cao, and X. Zhang, "Thermal analysis of the solid rotor permanent magnet synchronous motors with air-cooled hybrid ventilation systems," *IEEE Transactions on Industrial Electronics*, vol. 69, no. 2, pp. 1146–1156, 2022.
- [5] R. Wrobel, P. H. Mellor, N. McNeill, and D. A. Staton, "Thermal performance of an open-slot modular-wound machine with external rotor," *IEEE Transactions on Energy Conversion*, vol. 25, no. 2, pp. 403–411, 2010.
- [6] R. Camilleri, D. A. Howey, and M. D. McCulloch, "Predicting the temperature and flow distribution in a direct oil-cooled electrical machine with segmented stator," *IEEE Transactions on Industrial Electronics*, vol. 63, no. 1, pp. 82–91, 2016.
- [7] Q. Gao, X. Wang, C. Gu, S. Liu, and D. Li, "Design of ultra high speed micro permanent magnet motor with integrated support type based on multi coupling characteristics," *Transactions of China Electrotechnical Society*, vol. 36, no. 14, pp. 2989–2999, 2021.
- [8] Y. Liu, L. Li, J. Cao, Q. Gao, and Z. Sun, "Electromagnetic thermal analysis for short-term high-overload permanent magnet synchronous motor," *Transactions of China Electrotechnical Society*, vol. 34, no. 11, pp. 2296–2305, 2019.

- [9] H. Li and Y. Shen, "Thermal analysis of the permanent-magnet spherical motor," *IEEE Transactions on Energy Conversion*, vol. 30, no. 3, pp. 991–998, 2015.
- [10] J. Zhang, Z. Zhang, Y. Xia, and L. Yu, "Thermal analysis and management for doubly salient brushless DC generator with flat wire winding," *IEEE Transactions on Energy Conversion*, vol. 35, no. 2, pp. 1110–1119, 2020.
- [11] J. Zhang, Z. Zhang, and L. Yu, "Thermal deformation analysis of water cooling doubly salient brushless DC generator with stator field winding," *IEEE Transactions on Industrial Electronics*, vol. 67, no. 4, pp. 2700–2710, 2020.
- [12] P. H. Mellor, D. Roberts, and D. R. Turner, "Lumped parameter thermal model for electrical machines of TEFC design," *IEE Proceedings B Electric Power Applications*, vol. 138, no. 5, pp. 205–218, 1991.

Research Article

Influence of Vertical Downward Annulus Eccentricity on Steam-Water Two-Phase Flow Pressure Drop

Chuan Ma , Xiaoyan Liu, Haiqian Zhao, and Guangfu Cui

School of Mechanical Science and Engineering, Northeast Petroleum University, Daqing 163318, Heilongjiang, China

Correspondence should be addressed to Chuan Ma; mcnepu@nepu.edu.cn

Received 11 January 2022; Revised 24 February 2022; Accepted 3 March 2022; Published 7 April 2022

Academic Editor: Wei Liu

Copyright © 2022 Chuan Ma et al. This is an open access article distributed under the Creative Commons Attribution License, which permits unrestricted use, distribution, and reproduction in any medium, provided the original work is properly cited.

Concentric dual-tubing steam injection technique is one of the main methods to improve heavy oil recovery efficiency. From field data, it was discovered that hot fluid at high temperature and pressure caused steam injection casing to have elongation strain and “necking” eccentric buckling, and the eccentricity change affected the accurate prediction of steam-water two-phase flow pressure drop in the steam injection casing. This paper established a coupling model for the steam-water two-phase flow pressure drop in vertical downward eccentric annulus and the wellbore heat transfer and developed a mathematical model calculation program, to validate the accuracy of calculating the liquid holdup and pressure gradient of fully eccentric annulus. This revealed the influential law of eccentricity on the annulus steam-water two-phase pressure, dryness, and enthalpy value. The results indicated that when the eccentricity e increased from 0 to 1, the saturation pressure of steam at annulus wellbore bottom increased by 0.265 MPa, and the dryness and enthalpy value decreased by 8.54×10^{-3} and 11.22 kJ kg^{-1} , respectively. Compared to the concentric layout, the eccentrically arranged steam injection inner tube cannot promote the wet steam dryness at annulus wellbore bottom.

1. Introduction

The International Energy Agency (IEA) predicted [1] that the heavy oil resource occupies at least half of the world's exploitable oil resources, but its hyperviscosity and complex components make it harder to exploit. In order to increase heavy oil recovery efficiency, the oil fields have adopted the concentric steam flooding technique. However, in practical work condition, the heat strain from injected steam makes the steam injection inner tube have elongation strain and “necking” eccentric buckling, and the concentric dual-tubing steam injection will change to irregular eccentric dual-tubing steam injection. For the dual-tubing steam injection wellbores in oil fields, studying the influence of eccentricity on steam-water two-phase flow pressure drop is the key to accurately figuring out the wet steam pressure at annulus wellbore bottom.

The complex movement of the two-phase fluid in eccentric annulus wellbore makes it very difficult to predict the pressure drop of two-phase fluid. Gu et al. [2] used the semianalytical method to raise a model for predicting

the steam-water mixture pressure in concentric dual-tubing steam injection wellbore, which mainly investigated the thermophysical properties of saturated steam and the wellbore heat loss. Based on the actual gas state equation as well as the mass, momentum, and energy conservation equations, Sun et al. [3–6] used the finite difference method and the iteration technique to disclose the change rules of on-way thermophysical property curves of multicomponent super-heated fluid, super-heated steam, and supercritical water in the concentric dual-tubing steam injection wellbore. Dong et al. [7] developed a model for the flowing and heat transfer of multicomponent hot fluids (including super-heated water vapor, nitrogen, and carbon dioxide) in the concentric dual-tubing wellbore and parallel dual-tubing wellbore, taking the impact of wellbore temperature and pressure on its thermophysical properties into consideration. Li et al. [8] explored the influential law of steam injection well structure, steam injection proportion, and steam injection time on the physical properties of steam in the SAGD dual-tubing horizontal wellbore. On the basis of the flowing and heat transfer model of concentric dual-

tubing wellbore, Han et al. [9] considered the phase state variation of CO₂ and explored the pressure and temperature distribution of CO₂ in concentric casing. Wang and Su [10] got a numerical solution of pressure drop when the Bingham fluid moved axially in eccentric annulus, and obtained the empirical calculation formula through parametric regression, but they did not propose an empirical solution to the pressure drop formula applicable to the axial movement of Newtonian fluid. Ibarra et al. [11, 12] put forward a model for predicting the gas-liquid two-phase flow holdup and pressure drop at the slug flow state of horizontal concentric and fully eccentric tube sections, but this model was not universal for all flow patterns. In the field of concentric dual-tubing steam injection wellbore, the studies of wellbore two-phase pressure drop model are developing rapidly, while the calculation model of steam-water two-phase pressure drop in eccentric annulus still needs to be improved. To sum up, the method to solve the pressure drop of steam-water two-phase flow in vertical eccentric annulus has not been reported yet, and the influential law of eccentricity on the steam-water two-phase pressure drop within concentric dual-tubing steam injection wellbore is not clear.

Regarding the concentric dual-tubing steam injection wellbore, this paper built a coupling model for steam-water two-phase flow pressure drop in vertical eccentric annulus and wellbore heat transfer. Then, a calculation program was prepared to conduct simulation calculation of annulus water vapor pressure drop, which revealed the influential law of eccentricity on water vapor pressure, dryness, and enthalpy value in vertical annulus downcomer.

2. Model Establishment and Verification

2.1. Physical Model. Take concentric dual-tubing steam injection wellbore as an example. Due to the symmetry of cylindrical coordinate system, the physical model of vertical downward annulus was selected as shown in Figure 1. The wellbore structure includes steam injection inner tube, steam injection outer tube, insulated tubing, casing annular space (filled with low-pressure air), cement sheath, and formation from inside to outside. The water vapor at high temperature and pressure is injected into the steam injection casing at a certain flow velocity and dryness and dissipates heat to surrounding formation, which contains the calculation problem of steam-water two-phase flow pressure drop and the wellbore heat transfer problem. With the increase of well depth, the gas content of steam-water two-phase flow in the steam injection wellbore gradually decreases, and the flow patterns of the steam-water two-phase flow from well mouth to well bottom are annular flow, erratic flow, slug flow, and bubbly flow. Regarding the wellbore heat dissipation problem, at the initial steam injection period (less than 1 day), heat shall dissipate unstably in the wellbore, and both the steam injection time and the specific heat capacity of wellbore can greatly affect the heat flow density. When the steam injection time is more than 7 days, heat transfer can be deemed as stable inside the wellbore. For the steam injection wellbore using

steam flooding technique, heat transfers stably; for the wellbores using steam stimulation techniques such as closing-in, well completion, and well soaking, the heat transfer should be transient. The on-way pressure of water vapor in the wellbore bears the impact from flow pattern and dryness at the same time. By dividing the wellbore into several infinitesimal sections and analyzing the radial heat transfer process of each section, the wellbore-formation coupled radial heat transfer includes condensation heat transfer of the steam in steam injection casing, heat conduction of insulated tubing, free convection and radiation heat exchange of the casing annular space, heat conduction of cement sheath, and transient heat conduction of formation.

Eccentricity is one of the structural parameters of annulus tube, which represents the offset distance from inner tube center to outer tube center [13]. See its definition in (1), and eccentricity value changes within 0~1. Figure 2 shows the cross-sectional view of annulus tube under a certain annulus tube diameter ratio when the eccentricity is 0, 0.5, and 1.

$$e = \frac{2 DBC}{D_C - D_T}, \quad (1)$$

In the above equation, e is the eccentricity of annulus tube, dimensionless; D_C is the outer diameter of tubing, in meters; D_T is the inner diameter of steam injection casing, in meters; and DBC is the distance between inner tube center and outer tube center, in meters.

2.2. Mathematical Model. The coupling model for the steam-water two-phase flow pressure drop in vertical eccentric annulus and the wellbore heat transfer consists of two parts: pressure drop and wellbore heat transfer. By virtue of the relationship between water vapor's saturation temperature and saturation pressure, the wellbore heat dissipation was coupled with the pressure drop, and the calculation of the water vapor pressure in eccentric annulus was coupled with the calculation of dryness and temperature.

To simplify the mathematical model, we made the following assumptions: (1) heat transfer from the wellbore to outer edge of cement sheath is at a one-dimensional steady state, and heat transfer from cement sheath to formation is at a one-dimensional nonsteady state, while the axial heat transfer of water vapor along well depth direction is ignored; (2) the heat conductivity coefficient of the formation is deemed as a constant; (3) the water vapor is at a one-dimensional two-phase steady flowing state; (4) the heat dissipation of isolated tubing coupling is ignored; (5) the wellbore-formation coupling heat transfer condition is constant heat flow; and (6) the boundary of the heat-affected zone of the formation is an insulated boundary.

The pressure drop calculation model gave preference to the Caetano prediction model for steam-liquid two-phase flow pressure drop in vertical downward eccentric annulus and the drift-flux model based on Bhagwat's sectional void fraction correlation [13].

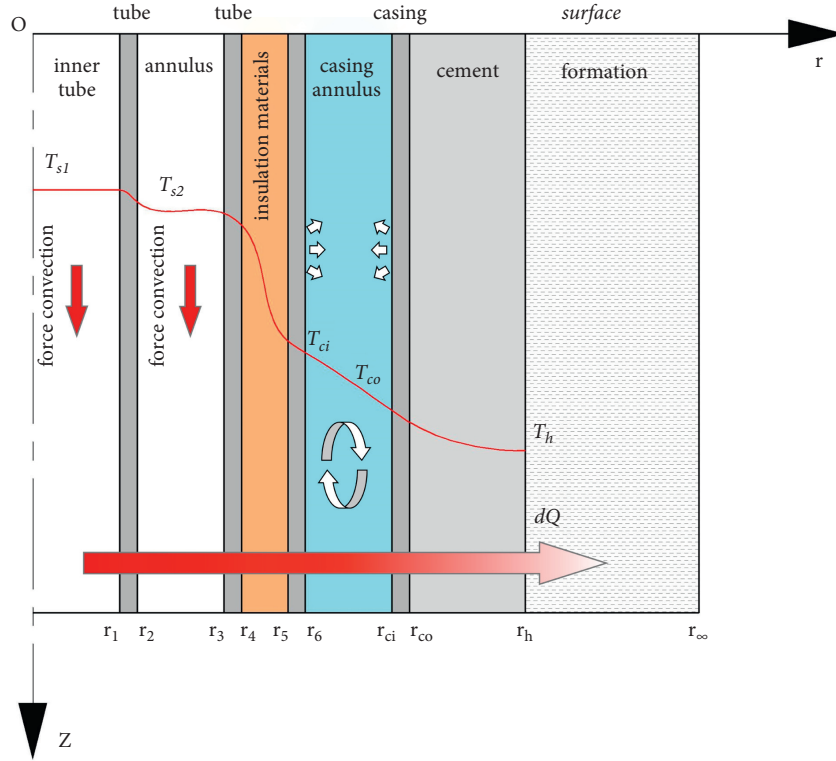


FIGURE 1: Physical model of the concentric steam flooding wellbore system.

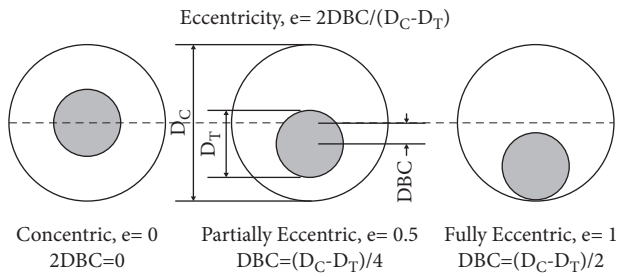


FIGURE 2: Annulus tube structure.

2.2.1. Optimal Pressure Drop Model

- (1) Calculation of sectional void fraction [13]

Calculation of distribution coefficient C_0 is as below:

$$C_0 \approx 1 + \left(0.2 - 0.2\sqrt{\rho_g/\rho_l}\right) \cdot \left[(2.6 - \beta)^{0.15} - \sqrt{f_{tp}}\right] (1 - x)^{1.5}. \quad (2)$$

Calculation of drift velocity v_{gj} is as below:

$$v_{gj} = (0.35 \sin \theta + 0.45 \cos \theta) \sqrt{g D_h (\rho_l - \rho_g) / \rho_l} \cdot (1 - \alpha)^{0.5} C_2 C_3 C_4. \quad (3)$$

Calculation of sectional void fraction α is as below:

$$\alpha = \frac{\beta}{C_0 + v_{gj}/v_m}, \quad (4)$$

$$H_L = 1 - \frac{\beta}{C_0 + (v_{gj}/v_m)}.$$

In the above equations, C_2 , C_3 , and C_4 are the correction coefficients in drift velocity calculation; f_{tp} is the friction factor; β is the volumetric void fraction; α is the sectional void fraction; H_L is the liquid holdup; the detailed calculation of above dimensionless parameters is shown in the literature [13]; ρ_g is the gas phase density, in $\text{kg}\cdot\text{m}^{-3}$; ρ_l is the liquid phase density, in $\text{kg}\cdot\text{m}^{-3}$; x is the dryness; and D_h is the hydraulic diameter, in meters.

- (2) Calculation of pressure gradient

Based on the previous flow pattern division and transition criterion theories for vertical annulus gas-liquid two-phase flow [14, 15], the flow patterns are divided into annular flow, slug flow, and bubbly flow. The transition condition from slug flow to annular flow is the sectional void fraction $\alpha=0.7$, and the transition condition from bubbly flow to slug flow is $\alpha=0.2$ under concentric annulus. The transition condition from slug flow to annular flow is the sectional void fraction $\alpha=0.8$, and the transition condition from bubbly flow to slug flow is $\alpha=0.15$

under fully eccentric condition. Figure 3 shows the flow pattern of annulus gas-fluid two-phase flow under fully eccentric condition. The division of gas-liquid two-phase flow pattern of fully eccentric annulus is similar to that of concentric annulus, while the existence of eccentric annulus breaks the symmetric distribution characteristics of bubbles along tube center. In a wide annular space, the local sections have a higher void fraction. In a narrow annular space, the local void fraction is lower. This makes the transition boundary from bubbly flow to slug flow move to the direction with decreasing average sectional void fraction, untimely forming the slug flow.

In view of the complexity of annular channel, the circular tube pressure drop theory expressed in form of equivalent hydraulic diameter cannot concretely describe the structural feature and flowing characteristic of annulus tube. Therefore, the Caetano annulus pressure drop correlation was introduced; see the calculation model in (5)~(7):

(a) The slug flow is as follows:

$$\begin{aligned} \frac{dp}{dz} &= \rho_m g \frac{L_{LS}}{L_{SU}} - \lambda \frac{\rho_m v_m^2}{2D_h} \frac{L_{LS}}{L_{SU}} \\ &+ \rho_m v_m dv_m, \\ \rho_m &= \alpha \rho_g + (1 - \alpha) \rho_l, \quad \mu_m = \alpha \mu_g \\ &+ (1 - \alpha) \mu_l, \quad h_m = x h_g + (1 - x) h_l. \end{aligned} \quad (5)$$

In the above equations, λ is the friction resistance coefficient, dimensionless; L_{LS} is the liquid slug length, in meters; and L_{SU} is the length of slug unit, in meters [16]. The presentation form of two-phase mixture parameters is shown in (8), where ρ_m is the density of two-phase mixture, in $\text{kg}\cdot\text{m}^{-3}$; α is the sectional void fraction, dimensionless; μ_m is the viscosity of two-phase mixture, in $\text{Pa}\cdot\text{s}$; v_m is the velocity of two-phase mixture, in $\text{m}\cdot\text{s}^{-1}$; h_m is the enthalpy value of two-phase mixture, in $\text{kJ}\cdot\text{kg}^{-1}$; μ_g is the viscosity coefficient of gas phase, in $\text{Pa}\cdot\text{s}$; μ_l is the viscosity coefficient of liquid phase, in $\text{Pa}\cdot\text{s}$; h_l is the enthalpy value of liquid phase, in $\text{kJ}\cdot\text{kg}^{-1}$; and h_g is the enthalpy value of gas phase, in $\text{kJ}\cdot\text{kg}^{-1}$.

(b) The annular flow is as follows:

$$\left(\frac{dp}{dz}\right)_{\text{core}} = \rho_{\text{core}} g - \tau_{CI} \frac{S_{CI}}{A_{\text{core}}} - \tau_{TI} \frac{S_{TI}}{A_{\text{core}}}. \quad (7)$$

Under a stable gas-liquid interface of annular flow, the pressure drops are equal at gas core,

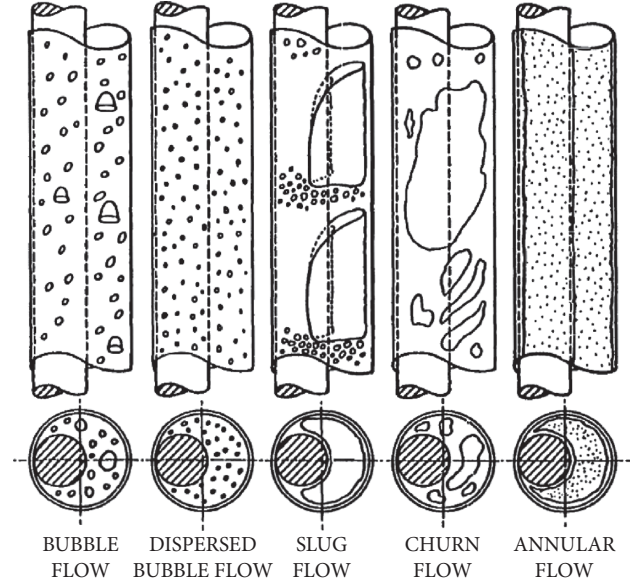


FIGURE 3: Flow pattern diagrams of fully eccentric annular upward tube, Caetano et al. [16].

inner tube's liquid film, and outer tube's liquid film, and the pressure drop at gas core represents the pressure drop of gas-liquid two-phase flow. The drift-flux model is based on the idea of weighted average to figure out the mean value of two-phase flow parameters distributed along the cross section. Thus, the calculated value of the above sectional void fraction, as well as the calculated pressure, temperature, dryness, and steam enthalpy values, is a mean value distributed along the cross section.

(b) The annular flow is as follows:

Under a stable gas-liquid interface of annular flow, the pressure drops are equal at gas core, inner tube's liquid film, and outer tube's liquid film, and the pressure drop at gas core represents the pressure drop of gas-liquid two-phase flow. The drift-flux model is based on the idea of weighted average to figure out the mean value of two-phase flow parameters distributed along the cross section. Thus, the calculated value of the above sectional void fraction, as well as the calculated pressure, temperature, dryness, and steam enthalpy values, is a mean value distributed along the cross section.

Under a stable gas-liquid interface of annular flow, the pressure drops are equal at gas core, inner tube's liquid film, and outer tube's liquid film, and the pressure drop at gas core represents the pressure drop of gas-liquid two-phase flow. The drift-flux model is based on the idea of weighted average to figure out the mean value of

two-phase flow parameters distributed along the cross section. Thus, the calculated value of the above sectional void fraction, as well as the calculated pressure, temperature, dryness, and steam enthalpy values, is a mean value distributed along the cross section.

- (3) Calculation of tubing/casing liquid film thickness ratio

The plane angle toward the tubing wall is one of the main parameters to solve the tubing/casing liquid film thickness ratio in eccentric annular structure. Caetano pointed out that solving the plane angle in eccentric annulus is different from that in concentric annulus. See the calculation of plane angle in (8), where e is the eccentricity, dimensionless; K is the radius ratio of annulus tube, dimensionless, $K = D_T / D_C$; and W_T' is the plane angle toward the tubing wall, in rad. The symbol $\langle \cdot \rangle$ denotes the mean values along the annular cross section. Since (8) has no analytical solution, the approximate solution can only be obtained by using numerical algorithm such as the complexification Simpson rule.

$$\langle W_T' \rangle = \frac{1}{\pi(1 - K^2)} \int_0^\pi \left[8a^2 \sin^{-1} \left(\frac{K}{2a} \right) + 2K \sqrt{4a^2 - K^2} - K^2 \pi \right] d\theta, \quad (8)$$

$$a = \frac{e}{2} (1 - K) \cos \theta + \frac{1}{2} \sqrt{e^2 (1 - K)^2 (\cos^2 \theta - 1) + 1}.$$

2.2.2. Quasi-Stable Heat Transfer Model for Dual-Tubing Steam Injection Wellbore

- (1) The formula of dryness gradient

$$\frac{dx}{dz} = -\frac{1}{h_g - h_l} \left[\frac{1}{W} \frac{dQ}{dz} + \left(x \frac{dh_g}{dT} + (1 - x) \frac{dh_l}{dT} \right) \frac{dT}{dP} \frac{dP}{dz} - \frac{v_m v_{sg}}{P} \frac{dP}{dz} + g \right]. \quad (9)$$

- (2) The formula of heat transfer coefficient from inside the wellbore to outer edge of cement sheath

By working out the wellbore structural data in relevant literature [17], the heat resistance of thermal insulation layer, casing annulus layer, and cement annulus accounts for 99.68% of the heat resistance of wellbore inner layer, in which the steel tube and condensation heat transfer resistance are ignored. The simplified heat transfer coefficient from inside the wellbore to cement annulus is shown as follows:

$$U = \left(\frac{r_2}{\lambda_{ins}} \ln \frac{r_5}{r_4} + \frac{r_2}{(h_c + h_r)r_6} + \frac{r_2}{\lambda_{cem}} \ln \frac{r_{cem}}{r_{co}} \right)^{-1}. \quad (10)$$

- (3) Condition of wellbore-transformation coupling heat transfer

$$dQ = 2\pi r_2 [U(T_{S1} - T_h)] dz = \frac{2\pi \lambda_e (T_h - T_e)}{f(t)} dz. \quad (11)$$

In (11), the left side of the equation denotes the quasi-stable heat transfer from wellbore to outer edge of cement annulus, and the right side of the equation denotes the transient heat conduction of the formation. This can be interpreted as follows: the heat flow density inside the wellbore is equal to that at the formation contact boundary.

In the above equation, λ_{ins} is the heat conductivity coefficient of thermal isolation materials, in $W \cdot m^{-1} K^{-1}$; λ_{cem} is the heat conductivity coefficient of cement annulus, in $W \cdot m^{-1} K^{-1}$; λ_e is the heat conductivity coefficient of the formation, in $W \cdot m^{-1} K^{-1}$; h_r is the radiation heat exchange coefficient of casing annular layer, in $W \cdot m^{-2} K^{-1}$; h_c is the natural-convection heat transfer coefficient of casing annular layer, in $W \cdot m^{-2} K^{-1}$; W is the mass velocity, in $kg \cdot s^{-1}$; Q is the heat flow density, in $W \cdot m^{-2}$; v_{sg} is the apparent gas phase velocity, in $m \cdot s^{-1}$; v_m is the flow velocity of two-phase mixture, in $m \cdot s^{-1}$; T_h is the temperature of the outer edge of cement annulus, in K; T_e is the temperature of the formation, in K; T_{S1} is the steam temperature in the steam injection inner tube, in K; and $f(t)$ is the formation thermal conduction time function, dimensionless.

- (4) Differential equation of the formation's transient thermal conduction

The differential equation of one-dimensional radial formation transient thermal conduction can be interpreted mathematically as below:

$$\frac{\partial^2 t}{\partial r^2} + \frac{1}{r} \frac{\partial t}{\partial r} = \frac{1}{\alpha} \frac{\partial t}{\partial \tau}. \quad (12)$$

The initial condition is as follows:

$$\text{When } \tau = 0: \quad t_e = t_0 + mz. \quad (13)$$

The boundary condition is as follows:

$$\text{When } r = r_\infty: \quad \frac{\partial t}{\partial r} = 0, \quad (14)$$

$$r = r_h: \quad dQ = -2\pi r_h dz \lambda_e \frac{\partial t}{\partial r} \Big|_{r=r_h}.$$

In the above equations, t is the formation temperature distribution, $t = f(\tau, r)$, in K; t_0 is the surface temperature, in K; m is the surface temperature

gradient, in K m^{-1} ; λ_e is the formation thermal conductivity coefficient, in $\text{W}\cdot\text{m}^{-1}\text{K}^{-1}$; and α is the formation thermal diffusion coefficient, in m^2s^{-1} .

The solution of the differential equation of formation transient thermal conduction is detailed in literature [17], in which the formation transient thermal conduction function $f(t)$ has taken the Chiu semi-empirical correlation for reference.

2.3. Model Validation

2.3.1. Validation of Liquid Holdup H_L . The relationship of liquid holdup H_L and sectional void fraction α is as follows: $H_L = 1 - \alpha$. The 49 groups of experimental data of fully eccentric annulus are selected [16, 18], and the predicted and measured liquid holdup values of air-water two-phase flow in vertical upward fully eccentric annulus are compared in Figure 4. It can be seen from Figure 4 that *MRD* and *Std* are the average relative error and standard deviation, respectively. On account of that, the void fraction is higher and the liquid holdup is lower in the annular flow condition, so it is suitable to measure the accurate calculation of liquid holdup by using absolute error. Therein, the average relative error of bubbly flow and slug flow is -2.6% . Except several data points falling outside the error band of 20%, 95% of the data points fall within the 20% error band, and 87% of the data points have an error less than 10%; the average absolute error of annular flow is 0.0226. The results indicate that the predicted liquid holdup value fits well with the Caetano measured value and that the Bhagwat correlation can meet the allowable error in engineering calculation of liquid holdup.

$$\text{MRD} (\%) = \frac{1}{N} \sum_{i=1}^N \frac{x_{i,\text{predicted}} - x_{i,\text{measured}}}{x_{i,\text{measured}}}, \quad (15)$$

$$\text{Std} (\%) = \sqrt{\frac{1}{N} \sum_{i=1}^N (x_{i,\text{predicted}} - x_{i,\text{measured}})^2}.$$

Compared to concentric annulus, the existence of eccentric inner tube can lead to a smaller local liquid holdup in wider annular space, a larger local liquid holdup in narrower gap, and a greater impact on average sectional liquid holdup from annulus eccentricity. This is also the reason for the prediction error of liquid holdup.

2.3.2. Validation of Pressure Gradient. In Figure 5, the predicted value and measured value of pressure drop of air-water two-phase flow in vertical upward fully eccentric annulus were compared [18]. The work condition of Caetano experiment is as follows: inner diameter of 0.0422 m, outer diameter of 0.0762 m, temperature of 28.7°C , system pressure of 0.315 MPa, and air-water two-phase flow of vertical upward fully eccentric annulus in adiabatic work condition. It can be seen from Figure 5 that the average relative error of pressure gradient is -21.15% , and the model can predict the pressure

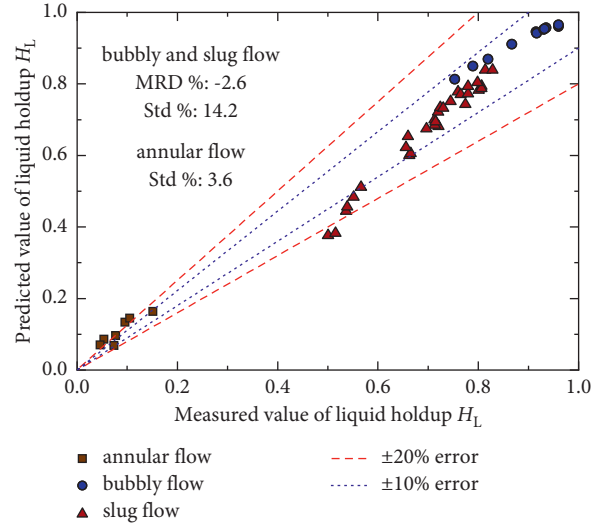


FIGURE 4: Comparison of predicted value and measured value of liquid holdup of fully eccentric annulus.

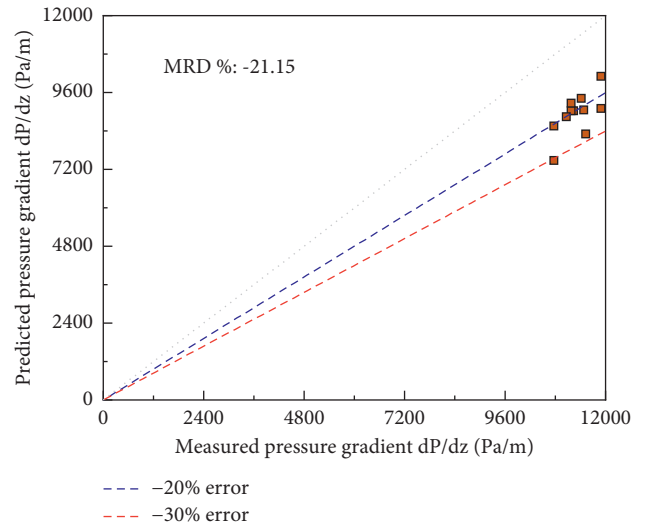


FIGURE 5: Comparison of predicted value and measured value of pressure gradient of fully eccentric annulus.

drop of eccentric annulus, which verifies the accurate calculation of pressure drop in eccentric annulus model.

Some of the prediction errors are caused by friction factors f_{CI} and f_{TI} . The tubing/casing liquid film thickness ratio reduces, which changes the Fanning friction factors, thereby affecting the frictional pressure drop. The existence of eccentric inner tube breaks the symmetry of bubble distribution in gas-liquid two-phase flow, inevitably changing the friction factor of eccentric annulus. Recently, an empirical formula for friction factor of gas-liquid two-phase flow in the fully eccentric annulus with a wide range of Reynolds numbers is still lacking, so only the empirical formula for friction factor of concentric annulus can be used to approximately calculate the frictional pressure drop of fully eccentric annulus.

The above research contents verify the accuracy of predicting liquid holdup and pressure drop through the pressure drop calculation model for gas-liquid two-phase flow in eccentric annulus. The calculation model can satisfy the allowable error in the engineering calculation of liquid holdup and pressure gradient.

3. Influential Analysis of Eccentricity on the Pressure Drop of Gas-Liquid Two-Phase Flow in Vertical Annulus

The basic parameters of dual-tubing steam injection wellbore are shown in Table 1 [16]. A simulation analysis was made on the influential rule of eccentricity on the water vapor pressure in vertical annulus, as well as the change law of water vapor's on-way pressure in annulus tube under a certain eccentricity.

3.1. Influential Law of Eccentricity on the Water Vapor On-Way Pressure in Vertical Annulus. In an annular geometric structure with the eccentricity $e = 0/0.5/1$, the influence of eccentricity on the water vapor on-way pressure of wellbore annulus is demonstrated in Figure 6.

As can be seen from Figure 6, when the well depth is 1000 m, due to the superposition of on-way frictional pressure drop in the wellbore, the influence of eccentricity on the steam pressure at wellbore bottom is more obvious in comparison with on-way pressure. With the increase of depth, the water vapor pressure along the wellbore annulus decreases gradually, and the higher the eccentricity, the greater the pressure along the wellbore annulus. The steam pressure at well bottom is the key to steam flood power, so it is necessary to make in-depth analysis of it.

3.2. Influential Law of Eccentricity on the Water Vapor Pressure at Vertical Annulus Bottom. When the dryness of injected steam is greater than 0.2, the steam-water two-phase flow pattern is determined as annular flow. See Figure 7 for the influence of eccentricity on the steam-water mixture pressure and frictional pressure drop at well bottom. See Figure 8 for the tubing/casing liquid film thickness ratio at well bottom under different eccentricity.

Figure 7 shows that the eccentricity e of vertical annulus increases from 0 to 1, causing the water vapor pressure at well bottom to increase by 0.265 MPa. Apparently, the frictional pressure drop decreases by 31.42 kPa, but actually, the tubing/casing liquid film thickness ratio reduces by 0.099 as shown in Figure 8. This changes the wet perimeters S_{CI} and S_{TI} of gas-liquid interface at tubing side and casing side as well as the Fanning friction factors f_{CI} and f_{TB} , thereby affecting the frictional pressure drop. From concentric to fully eccentric annulus structure, the frictional pressure drop at well bottom is lowered. Some scholars [10, 11] also obtained similar results through experiments. Ibarra et al. [11] considered that the frictional pressure drop of concentric annulus is larger than that of fully eccentric annulus and completed its validation through experiment. Similarly, Wang and Su [10] studied the calculation of the flowing

pressure drop of Bingham fluid in eccentric annulus and discovered that the increase of eccentricity can bring down the frictional pressure drop of annulus fluid, and the larger the radius ratio K of annulus is, the greater the frictional pressure drop decreases.

When the eccentricity becomes larger, the sectional void fraction at annulus bottom turns lower. The decreasing trend of the section gas holdup is similar to the liquid film thickness ratio of the casing shown in Figure 8. When the mass velocity is constant, a lowered sectional void fraction can cause the density of steam-water two-phase mixture to increase, the flowing velocity of two-phase mixture to decrease, the interaction of gas core and wall liquid film in an annular flow to weaken, and the frictional pressure drop to become smaller. The structural change of annulus has little impact on the wellbore heat transfer, and the influence of eccentricity on the wellbore on-way heat loss and dryness can be ignored. It is known from Figure 7 that, compared to frictional pressure drop, the dynamic pressure at well bottom is smaller than the frictional pressure drop by an order of magnitude. This indicates that the frictional pressure drop is the main reason for the change of steam saturation pressure and temperature at well bottom.

From the above analysis, the results express the following: when the eccentricity e increases from 0 to 1, the wet steam saturation pressure at annulus bottom rises by 0.265 MPa, the dryness decreases slightly by 8.54×10^{-3} , the enthalpy value decreases by 11.22 kJ kg^{-1} , and the wellbore heat loss basically remains unchanged. Therefore, for a concentric dual-tubing steam injection wellbore, the scheme is theoretically infeasible to promote the wet steam dryness at annulus bottom by an eccentric arrangement of steam injection inner tube. Increasing the eccentricity can slightly reduce the wet steam dryness at annulus bottom, and a concentric arrangement of steam injection inner tube can help to obtain a higher dryness at annulus bottom. Starting with the wellbore insulation effect, increasing the thermal resistance of insulated tubing, improving tubing annulus, and promoting the insulation performance of tubing coupling can effectively improve the steam dryness at wellbore bottom. Eccentrically arranged inner tube can raise the wet steam saturation pressure at annulus bottom and improve steam flooding capability.

3.3. Change Rules of On-Way Pressure of Annulus Wet Steam under Constant Eccentricity. When the eccentricity $e = 0.5$, the change of steam on-way pressure in eccentric annulus is shown in Figure 9.

Figure 9 shows that the steam on-way pressure decreases quickly with the increase of well depth. In the figure, the dotted line represents the minimal apparent gas phase velocity v_{sgcr} required in the transition of water vapor from erratic flow to annular flow. For a vertical upward tube, the physical significance of critical apparent gas velocity is the minimal apparent gas velocity required by the liquid drop carried in the gas core to move upward, and its value is determined by the balance between the gravity and drag force of the largest and most stable liquid drop in the gas core. For a vertical

TABLE 1: Basic wellbore parameters.

Basic parameters	Value, unit	Basic parameters	Value, unit
Inner diameter of steam injection inner tube (r_1)	0.027 m	Thermal conductivity of tubing and casing ($\lambda_{tube, \lambda_{cas}}$)	$45W \cdot m^{-1} K^{-1}$
Outer diameter of steam injection inner tube (r_2)	0.038 m	Thermal conductivity of insulation materials (λ_{ins})	$0.076 W \cdot m^{-1} K^{-1}$
Inner diameter of steam injection annulus tube (r_3)	0.062 m	Thermal conductivity of cement annulus (λ_{cem})	$0.933 W \cdot m^{-1} K^{-1}$
Outer diameter of steam injection annulus tube (r_4)	0.073 m	Thermal conductivity of formation (λ_e)	$1.7305 W \cdot m^{-1} K^{-1}$
Inner diameter of insulated tubing (r_5)	0.1003 m	Thermal diffusion coefficient of formation (α_e)	$1.75 \times 10^{-6} m s^{-2}$
Outer diameter of insulated tubing (r_6)	0.1143 m	Surface temperature gradient ($T_{gradient}$)	$0.03 K \cdot m^{-1}$
Inner diameter of casing (r_{ci})	0.1594 m	Surface temperature ($T_{surface}$)	302.15 K
Outer diameter of casing (r_{co})	0.1778 m	Tubing outer wall blackness (ϵ_6)	0.8
Outer diameter of cement annulus (r_h)	0.2410 m	Casing inner wall blackness (ϵ_{ci})	0.1

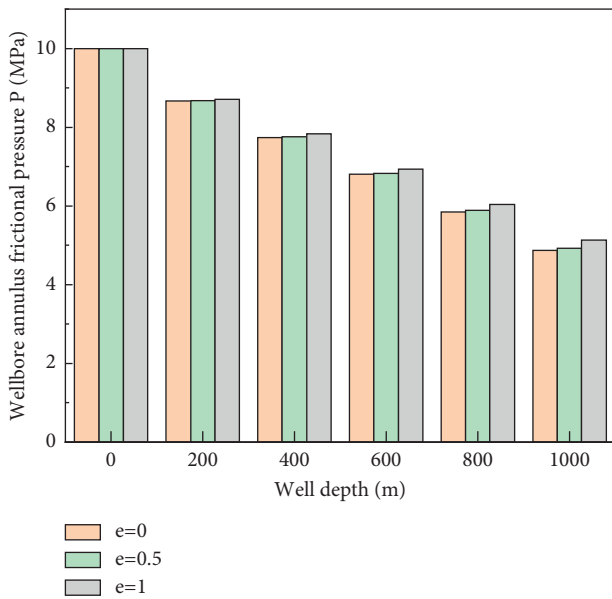


FIGURE 6: Influential law of eccentricity on the water vapor on-way pressure in annulus tube.

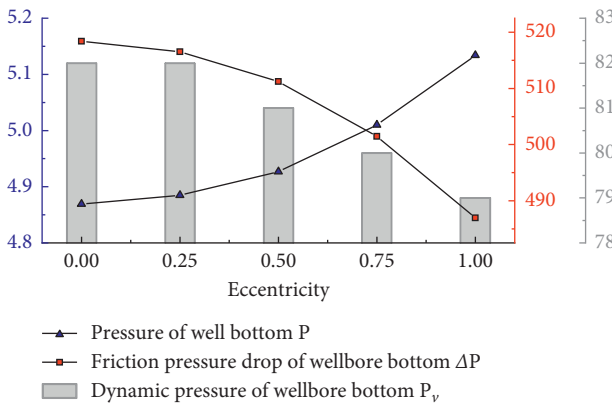


FIGURE 7: Influence of eccentricity on the steam-water mixture pressure and frictional pressure drop at well bottom.

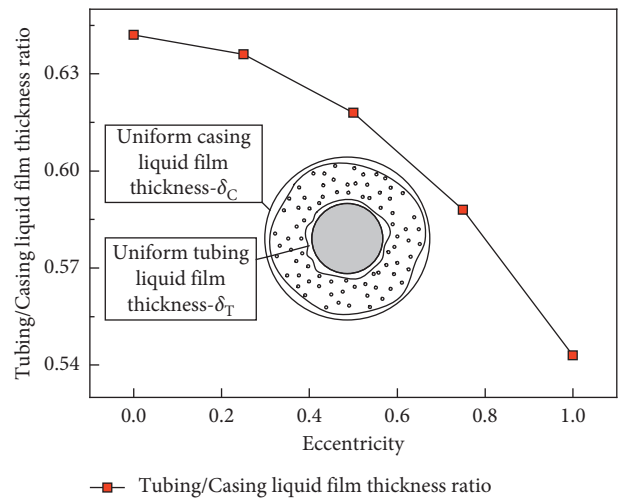


FIGURE 8: Tubing/casing liquid film thickness ratio at well bottom under different eccentricity.

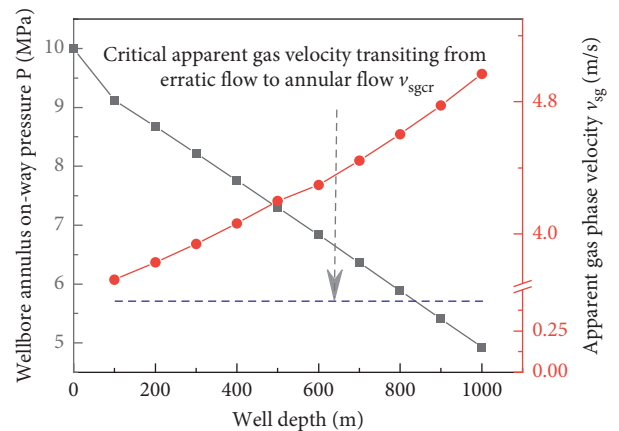


FIGURE 9: Change rule of steam on-way pressure in eccentric annulus.

downward tube, the directions of the gravity and drag force borne by the liquid drops carried are all downward, making it hard to form falling film, whose critical apparent gas velocity v_{sgcr} is lower than that of an upward tube.

In Figure 9, the critical apparent gas velocity v_{sgcr} is 0.433 m s^{-1} , the apparent gas velocity at annulus inlet v_{sg} is 3.72 m s^{-1} , and the water vapor flow pattern has already turned into annular flow. When the well depth increases, the apparent gas velocity of water vapor continue to rise to 4.97 m s^{-1} . At this time, the water vapor flow pattern transits to a fully developed annular flow. The friction effect between gas core and wall liquid film becomes larger, frictional pressure drop takes a bigger and bigger proportion in total pressure drop, and the dynamic pressure increases by about 32%, as shown in Figure 10. Thus, the steam on-way pressure declines dramatically with well depth.

As shown in Figure 10, because the water vapor flow pattern gradually transits to a fully developed annular flow, the on-way frictional pressure drop of steam quickly rises at the well depth of 500 m, fluctuates up and down within the well depth of 600~1000 m, and shows an extreme value in this depth range. These are caused by the on-way change of shear stress of gas core and steam injection inner/outer tube liquid film, and the friction factor of gas core and wall falling film is the main factor. When the eccentricity $e = 0.5$, the on-way distribution law of the frictional shear stress between gas core and the inner and outer wall liquid film of steam injection annulus (as shown in Figure 11) is similar to the on-way frictional pressure drop as shown in Figure 10.

The solid lines in Figure 11 represent the on-way distribution of shear stress between the inner wall liquid film of steam injection annulus and gas core, and the dotted lines represent the on-way distribution of shear stress between the outer wall liquid film of steam injection annulus and gas core. It is known from Figure 11 that, whether the annular geometric structure is concentric or eccentric with $e = 0.5$, the shear stress between the inner wall liquid film of steam injection annulus and gas core is always larger than that of the outer wall of steam injection annulus; that is to say, $\tau_{TI} > \tau_{CI}$. Caetano found out by experiment that, under annular flow condition, the tubing wall liquid film δ_T is thinner than casing wall liquid film δ_C . The fact that the tubing/casing liquid film thickness ratio is less than 1 (Figure 8) also conforms to this conclusion, which makes the shear stress between the inner wall liquid film of steam injection annulus and gas core always larger than that of the outer wall of steam injection annulus. It is precisely because the shear stress between the inner wall liquid film of steam injection annulus and gas core τ_{TI} is larger, in the annular flow, the gas core exerts a greater drag force on the liquid falling film of annulus inner wall, and more small droplets are carried, causing the liquid film of annulus inner wall to become thinner. In Figure 11, take well depth of 400 m as an example; as the eccentricity increases from 0 to 0.5, the shear stress between the annulus inner wall liquid film and gas core τ_{TI} reduces by 1.35 Pa, and the shear stress between the annulus outer wall liquid film and gas core τ_{CI} rises by 0.316 Pa. This indicates that the eccentricity exerts different impact on the shear stress between gas core and annulus

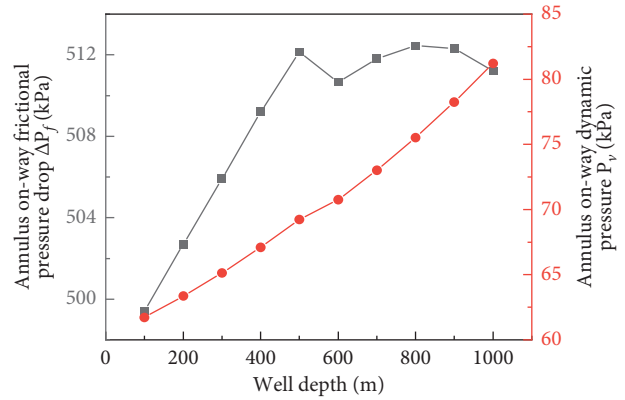


FIGURE 10: Steam on-way frictional pressure drop and dynamic pressure in eccentric annulus.

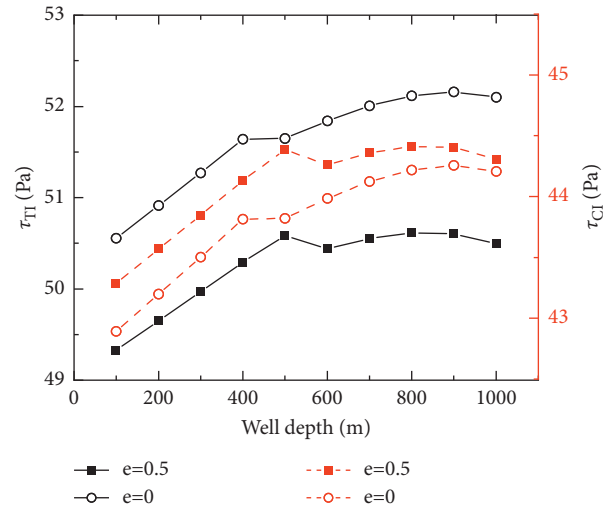


FIGURE 11: On-way distribution of frictional shear stress between gas core and casing inner/outer walls.

inner/outer wall liquid film. However, the change rule of the shear stress between liquid film and gas core with well depth displays a rapid rise at first, followed by a steady change ($e = 0$) or a slight down-fluctuation ($e = 0.5$), and finally a gentle rise ($e = 0$) or the appearance of an extreme value ($e = 0.5$).

In order to reveal the influence law of pipe diameter, mass flow rate, and steam injection dryness on wet steam pressure at the bottom of annulus pipe under concentric and certain eccentricity conditions, the analysis of influencing factors of wet steam pressure at the bottom of annulus pipe under concentric and eccentricity conditions will be carried out below.

3.4. Influence of Steam Injection Inner Tube Diameter on Wet Steam Pressure at Annulus Bottom. The influence of steam injection inner tube diameter on the wet steam pressure at annulus bottom under concentric and given eccentricity conditions is demonstrated in Figure 12. The histogram ordinate denotes the wet steam saturation pressure at well bottom, and the ordinate of point plot represents the

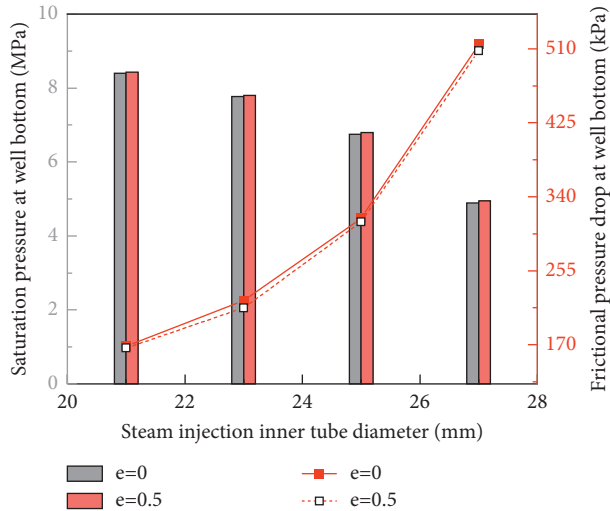


FIGURE 12: Influence of steam injection inner tube diameter on the wet steam pressure at well bottom.

frictional pressure drop at well bottom. In Figure 12, when the eccentricity remains unchanged, as the inner tube diameter rises, the wet steam saturation pressure at annulus bottom declines, and the frictional pressure drop of wet steam increases. Therefore, under a constant tube diameter, the eccentricity has little impact on the wet steam saturation pressure and frictional pressure drop at well bottom.

From the results of Figure 7, we can know that an increased eccentricity can result in a slight rise in the wet steam saturation pressure at well bottom and a slight decline in frictional pressure drop. Take the steam injection inner tube radius of 21 mm as an example; as the eccentricity rises by 0.5, the wet steam frictional pressure drop at well bottom reduces by about 2.3 kPa, which basically will not change the wet steam saturation pressure at well bottom by an order of magnitude of 1 MPa. Accordingly, the influence of the eccentricity on the wet steam saturation pressure and frictional pressure drop at annulus bottom can be ignored.

3.5. Influence of Steam Injection Outer Tube's Mass Flow Rate on the Wet Steam Pressure at Annulus Bottom. The influence of steam injection velocity on wet steam pressure at annulus bottom is shown in Figure 13. The histogram ordinate denotes the wet steam saturation pressure at well bottom, and the ordinate of point plot represents the frictional pressure drop at well bottom. It can be seen from the figure that, as the steam injection velocity accelerates, the wet steam saturation pressure at annulus bottom declines, but the frictional pressure drop of wet steam is enlarged. Under a certain steam injection velocity, when the eccentricity rises, the wet steam pressure at annulus bottom increases slightly, while the frictional pressure drop is lowered slightly.

When the steam injection velocity is 35 t/d, as the eccentricity increases by 0.5, the steam frictional pressure drop declines by 1.26 kPa. If the steam injection velocity is accelerated to 50 t/d, the steam frictional pressure drop in eccentric annulus will reduce by 7.1 kPa. With the increase of

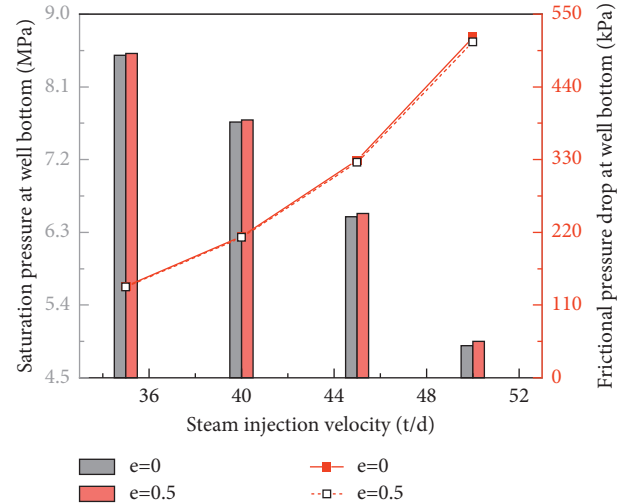


FIGURE 13: Influence of steam injection velocity on wet steam pressure at annulus bottom.

steam injection velocity, the decreasing value of frictional pressure drop will rise. Combining the analytical results of the influential factors of concentric annulus steam injection parameters, we come to the conclusion that, under eccentric annular state, the influential law of mass velocity on the wellbore steam saturation pressure is identical with that of concentric annulus.

3.6. Influence of Steam Injection Outer Tube Dryness on Wet Steam Pressure at Annulus Bottom. The influence of steam injection out tube dryness on the wet steam pressure at annulus bottom is shown in Figure 14.

Figure 14 illustrates that when steam injection dryness is constant, the eccentricity rises by 0.5, and the wet steam saturation pressure at well bottom reduces by 0.02 MPa. As steam injection dryness is increased, the wet steam saturation pressure at annulus bottom significantly declines. Integrating the analytical results of influential factors of annulus steam injection dryness, under an eccentric annular structure, the influential law of steam injection dryness on wellbore steam saturation pressure is the same as that of concentric annulus.

The influence of steam injection outer tube dryness on the wet steam frictional pressure drop at annulus bottom is shown in Figure 15.

Figure 15 demonstrates that when steam injection dryness is 0.5, the eccentricity rises by 0.5, while the eccentric annulus steam frictional pressure drop falls by 0.79 kPa. As the steam injection dryness rises to 0.7, the eccentric annulus steam frictional pressure drop will decline by 7.11 kPa. The change of eccentricity has little impact on wet steam frictional pressure drop.

After comprehensively analyzing Figures 12~15, we know that when the steam injection pressure at annulus reaches an order of magnitude of 1 MPa, the eccentricity can increase from 0 to 0.5, and the steam frictional pressure drop at well bottom only changes within 0~10 kPa. Hence, the eccentricity change has little impact on steam saturation pressure at well bottom.

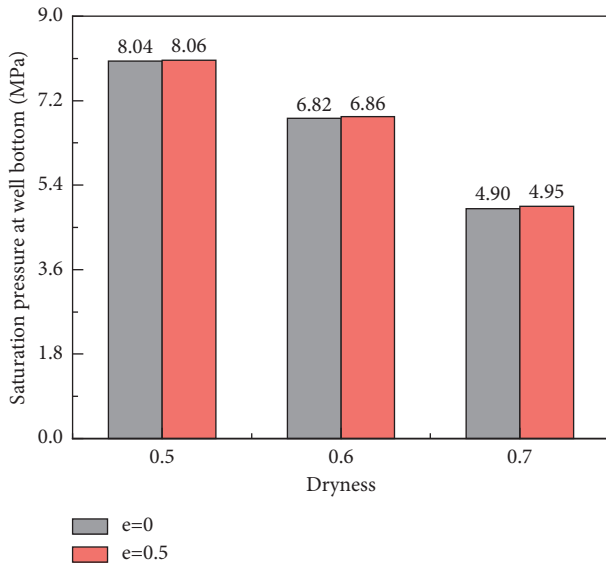


FIGURE 14: Influence of steam injection out tube dryness on the wet steam pressure at annulus bottom.

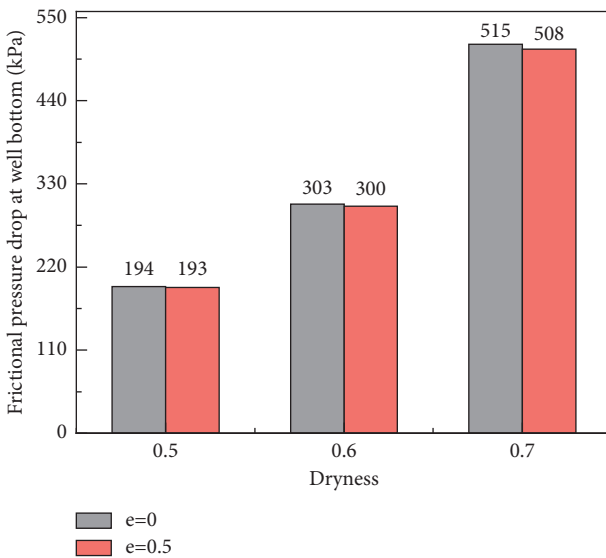


FIGURE 15: Influence of steam injection outer tube dryness on the wet steam frictional pressure drop at annulus bottom.

4. Conclusions

In this paper, a calculation model for steam-water two-phase flow pressure drop in vertical downward eccentric annulus was established, and a simulation calculation program was prepared. Through investigation, the influential law of the eccentricity on the steam-water two-phase flow pressure drop in vertical downward annulus was revealed, the change trend of steam on-way pressure in an annular geometric structure with eccentricity $e = 0.5$ was explored, and the accurate calculation of fully eccentric annulus liquid holdup and pressure gradient was validated. From simulation calculation, it is discovered that when the eccentricity e increases from 0 to 1, the steam frictional pressure drop at

annulus bottom declines by 31.42 kPa, the saturation pressure rises by 0.265 MPa, the dryness slightly reduces by 8.54×10^{-3} , and the enthalpy value decreases by $11.22 \text{ kJ} \cdot \text{kg}^{-1}$, but the wellbore heat loss is basically not affected. Therefore, we have come to the conclusion that when the steam injection pressure of dual-tube steam injection wellbore reaches an order of magnitude of 1 MPa, compared to concentrically arranged inner tube, the eccentrically arranged steam injection inner tube fails to improve the wet steam dryness at annulus bottom.

Data Availability

No data were used to support this study.

Conflicts of Interest

The authors declare that there are no potential conflicts of interest in this study.

Acknowledgments

The authors acknowledge the support from the Surface Project of National Natural Science Foundation of China (52076036) and the Northeast Petroleum University Leading Innovative Fund Project (2019YDL-12).


References

- [1] R Martinezpalou, M. D Mosqueira, and B Zapatarendon, "Transportation of heavy and extra-heavy crude oil by pipeline: a review[J]," *Journal of Petroleum Science and Engineering*, vol. 75, no. 3, pp. 274–282, 2011.
- [2] H. Gu, L. Cheng, S. Huang, B. Du, and C. Hu, "Prediction of thermophysical properties of saturated steam and wellbore heat losses in concentric dual-tubing steam injection wells," *Energy*, vol. 75, no. oct, pp. 419–429, 2014.
- [3] F. Sun, Y. Yao, X. Li, P. Yu, L. Zhao, and Y. Zhang, "A numerical approach for obtaining type curves of superheated multi-component thermal fluid flow in concentric dual-tubing wells," *International Journal of Heat and Mass Transfer*, vol. 111, pp. 41–53, 2017.
- [4] F. Sun, Y. Yao, X. Li, J. Tian, G. Zhu, and Z. Chen, "The flow and heat transfer characteristics of superheated steam in concentric dual-tubing wells," *International Journal of Heat and Mass Transfer*, vol. 115, pp. 1099–1108, 2017.
- [5] F. R Sun, Y. D Yao, and X. F Li, "Numerical simulation of superheated steam flow in dual-tubing wells[J]," *Journal of Petroleum Exploration & Production Technology*, vol. 8, no. 3, pp. 1–13, 2017.
- [6] F. R Sun, Y. D Yao, G Li et al., "Numerical simulation of supercritical-water flow in concentric-dual-tubing wells[C]," *America: SPE 191363-PA*, vol. 23, no. 6, pp. 1–14, 2018.
- [7] X. Dong, H. Liu, Z. Pang, C. Wang, and C. Lu, "Flow and heat transfer characteristics of multi-thermal fluid in a dual-string horizontal well," *Numerical Heat Transfer, Part A: Applications*, vol. 66, no. 2, pp. 185–204, 2014.
- [8] P. Li, Y. Zhang, X. Sun, H. Chen, and Y. Liu, "A numerical model for investigating the steam conformance along the dual-string horizontal wells in SAGD o," *Energies*, vol. 13, no. 15, p. 3981, 2020.

- [9] Wu Han, X. Wu, and Q. Wang, "A shaft flow model of CO₂ separate injection with concentric dualtubes and its affecting factors[J]," *Acta Petrolei Sinica*, vol. 32, no. 1, pp. 723–727, 2011.
- [10] H. Wang and Y. Su, "A practical method of determination of pressure loss in eccentric annulus[J]," *Oil Drilling & Production Technology*, vol. 19, no. 06, pp. 5–9, 1997.
- [11] R. Ibarra, J. Nossen, and M. Tutkun, "Two-phase gas-liquid flow in concentric and fully eccentric annuli. Part I: flow patterns, holdup, slip ratio and pressure gradient," *Chemical Engineering Science*, vol. 203, pp. 489–500, 2019.
- [12] R. Ibarra, J. Nossen, and M. Tutkun, "Two-phase gas-liquid flow in concentric and fully eccentric annuli. Part II: model development, flow regime transition algorithm and pressure gradient," *Chemical Engineering Science*, vol. 203, pp. 501–510, 2019.
- [13] S. M. Bhagwat and A. J. Ghajar, "A flow pattern independent drift flux model based void fraction correlation for a wide range of gas-liquid two phase flow," *International Journal of Multiphase Flow*, vol. 59, pp. 186–205, 2014.
- [14] V. C. Kelessidis and A. E. Dukler, "Modeling flow pattern transitions for upward gas-liquid flow in vertical concentric and eccentric annuli," *International Journal of Multiphase Flow*, vol. 15, no. 2, pp. 173–191, 1989.
- [15] J. E. Julia, B. Ozar, J.-J. Jeong, T. Hibiki, and M. Ishii, "Flow regime development analysis in adiabatic upward two-phase flow in a vertical annulus," *International Journal of Heat and Fluid Flow*, vol. 32, no. 1, pp. 164–175, 2011.
- [16] E. F. Caetano, O. Shoham, and J. P. Brill, "Upward vertical two-phase flow through an annulus-Part I: single-phase friction factor, taylor bubble rise velocity, and flow pattern prediction," *Journal of Energy Resources Technology*, vol. 114, no. 1, pp. 1–13, 1992.
- [17] M. Wang, "The determination of overall heat transfer coefficient of isolated tubing steam injection wellbore—a supplement and discussion of the paper written by Hu Zhimian [J]," *Oil Drilling & Production Technology*, no. 6, pp. 75–78+85, 1985.
- [18] E. F. Caetano, O. Shoham, and J. P. Brill, "Upward vertical two-phase flow through an annulus-Part II: m bubble, slug, and annular flow," *Journal of Energy Resources Technology*, vol. 114, no. 1, pp. 14–30, 1992.

Research Article

Judgment of Athlete Action Safety in Sports Competition Based on LSTM Recurrent Neural Network Algorithm

Yanying Liu,¹ Lijun Wang ,^{2,3} Yuanjin Tang ,³ and Bo Ren⁴

¹Institute of Physical Education and Health, Zhaoqing University, Zhaoqing 526000, Guangdong, China

²Institute of Physical Education, Soochow University, Suzhou 215000, Jiangsu, China

³Institute of Physical Education and Health, Yulin Normal University, Yulin 537000, Guangxi, China

⁴School of Economics and Management, Shanghai University of Sport, Shanghai 200438, China

Correspondence should be addressed to Lijun Wang; wanglj567@126.com and Yuanjin Tang; hubiaolch@yku.edu.cn

Received 6 January 2022; Revised 25 February 2022; Accepted 3 March 2022; Published 30 March 2022

Academic Editor: Wei Liu

Copyright © 2022 Yanying Liu et al. This is an open access article distributed under the Creative Commons Attribution License, which permits unrestricted use, distribution, and reproduction in any medium, provided the original work is properly cited.

Athlete injury has always been an important factor that plagues sports. In order to reduce the probability of athletes' sports injury and improve the judgment of athletes' action safety, the inherent laws of sports actions are fully excavated, the development of action safety is promoted, and learners and instructors are caused to fully understand the safety of actions. This study uses the LSTM (long short-term memory) cyclic neural network algorithm to judge the safety of athletes in sports competitions. The experiment verifies the effectiveness of the LSTM cyclic neural network algorithm in basketball segmentation and recognition. Sports injury is one of the important factors affecting the performance of all sports, and the problem of athletes' injury is worrying, so it is very necessary to effectively prevent potential sports injuries. Through the investigation of different professional athletes, the LSTM cyclic neural network algorithm is used for the whole process of extracting an independent motion action including continuous actions. It is used to distinguish key postures and nonkey postures in an action, and to judge the correctness of the action. Basketball skills here are mainly the movements of basic skills such as moving, passing the ball, dribbling, shooting, breaking with the ball, personal defense, grabbing the ball, stealing the ball, and grabbing the ball. The research results prove that the LSTM recurrent neural network algorithm has a good effect on the safety of athletes. For athletes, 41.9% of people can improve the safety of their movements by strengthening strength training.

1. Introduction

Physical education coaches ignore the general laws of human body movement and play football games with high intensity without warm-up. According to the characteristics of physical education and training, the preparatory activities should follow the principle of step by step. In recent years, due to the frequent occurrence of sports safety accidents, the safety of sports competitions has attracted extensive attention from all walks of life. In particular, the occurrence of school sports accidents not only endangers students' health but also puts a certain pressure on the school's teaching control. There are constant disputes between parents and schools, endangering students' lives. Because the nonprofessional athletes do not understand the sports safety

knowledge, the evaluation of sports ability is insufficient, they often carry out some sports beyond their scope, and the identification of external risk factors is insufficient. These reasons lead to frequent sports safety accidents in recent years. The occurrence of sports safety accidents will bring a series of problems.

Deep learning evolved from machine learning, and deep neural networks evolved from artificial neural networks with deep network structures. The LSTM recurrent neural network is an improved version of the RNN neural network. It mainly solves the problem of gradient disappearance, which can make the network remember the content for a longer time and make the network more reliable. This feature of LSTM is caused by the improvement of its hidden neuron structure and does not need to change the training method of the network.

For action recognition, many experts at home and abroad have been researched. Guo et al. extracted features from the initial 200 ms EMG, applied Kohonen and the supervised Kohonen neural network, and compared the results with the BP neural network. Experimental results show that the supervised Kohonen neural network is better than the other two algorithms, and the average recognition rate can be increased to 88.4% [1]. Zaborski et al. believe that standard-based morphometric methods or modern genetic analyses are not always reliable enough and may be replaced by multivariate statistical methods, especially discriminant analysis and cluster analysis, and the Kohonen artificial neural network included in data mining. The hypothesis of the complex species of *Amidostomum acutum* is divided into three different species [2]. Yong et al. use the local mean decomposition (LMD) method and supervised Kohonen neural network (SKNN) for sound signal analysis. The optimal SKNN model is obtained after training samples. Experimental results show that the comprehensive recognition rate of the coal-rock interface is as high as 89%. The interface can be effectively identified through sound signal analysis [3]. Martin et al. proposed a new dual-temporal convolutional neural network (TSTCNN). When applied to table tennis, it can detect and recognize 20 table tennis shots. The model has been trained on a specific dataset, the so-called TTStroke-21, which was recorded under the natural conditions of the School of Physical Education of the University of Bordeaux [4]. In order to improve the recognition rate of sports athletes, this study analyzes the motion recognition system based on clustering regression and improved ISA deep network. The network data collection method is used to construct the athlete's action video library, the basketball event is taken as an example for analysis, and identification is performed through feature judgment [5]. Shih and Lin compared the expected performance of taekwondo athletes, weightlifters, and non-athletes and then linked these performances to their emotional recognition performance. This study mainly found that accurate motion prediction does not necessarily depend on the dynamic information of the motion. The results show that facial emotion recognition plays an important role in the action prediction of fighting sports such as taekwondo [6]. Ramesh and Mahesh initially tried to evaluate the performance of the deep convolutional neural network architecture on the ordered frame sequence of sports video. It believes that the main purpose of sports video classification is to help viewers find videos they are interested in for training and improving performance. Convolutional neural networks can be widely used as a powerful classification model for image recognition problems [7]. These studies have improved the effective reference for this study, but due to the limitations of related experiments, such as data sources and too many variables in the experiment process, the results of the experiment are questionable.

Compared with the total score of the FMS test, there is no significant difference in the total score of the FMS test of athletes with different competitive abilities, training years, and BMI. Feature action recognition methods based on gesture selection, most human action recognition

algorithms contain many parameters that need to be manually adjusted, which seriously affects the realization of the algorithm's real-time function. In this study, the LSTM recurrent neural network is used to extract the features of the human body. It solves the problem of traditional feature extraction. The clustered keyframes are used as the hidden state, and the parameters are initialized to enhance the applicability of the algorithm. It is helpful to take differentiated processing according to the weight of the information contained in the subsequent recognition work, focusing on the recognition and calculation of those gestures of great significance, which helps to improve the degree of automatic analysis and reduce the complexity of analysis. Guided by the theory of sports injury risk assessment, combined with the results of expert interviews, the indicators were designed to form the screening indicators and methods for the risk of sports injuries in youth; the scientificity of the screening indicators for the risk of sports injuries in adolescents was verified, and the evaluation standards were established.

2. Judgment Method of Operation Safety

2.1. LSTM Recurrent Neural Network. An artificial neural network is a system that intelligently processes input information by imitating the functions of the human brain. The basic processing unit of a neural network is a neuron, which is often called a "processing unit" [8, 9]. Artificial neuron abstracts the process of biological neuron processing information and then describes it in mathematical language. It is a simulation of the structure and function of the biological neuron and finally expressed by a model [10].

The LSTM transforms the skeleton into another coordinate system, replacing the original skeleton as input, to gain robustness to scale, rotation, and translation, and then extracts salient motion features from them. The sigmoid forget gate in LSTM determines whether the information is retained during the process of information transmission between neurons. As shown in Figures 1–5, the dots represent allowed information transmission, and the crosses represent information truncation [11]. If allowed, the information will continue to be passed to the next node or the next hidden layer; if not allowed, the information will be ignored. In LSTM, the truncated information will not affect the calculation of subsequent neurons, and the released information will affect the subsequent calculations. It is through these switches that we can decide whether to pass on the influence of previous information. The LSTM memory valve is shown in Figure 6:

The advantages of the Kohonen network: the Kohonen network can map the human input pattern into a one-dimensional or two-dimensional graph at the output layer and keep its topology unchanged; the network can make the weight vector space and the probability of the input pattern through repeated learning of the input pattern. The distribution area is consistent, that is, probability retention. Each neuron in the input layer sends the input information to each neuron in the output layer through the weight coefficient vector. The neural network through repeated self-

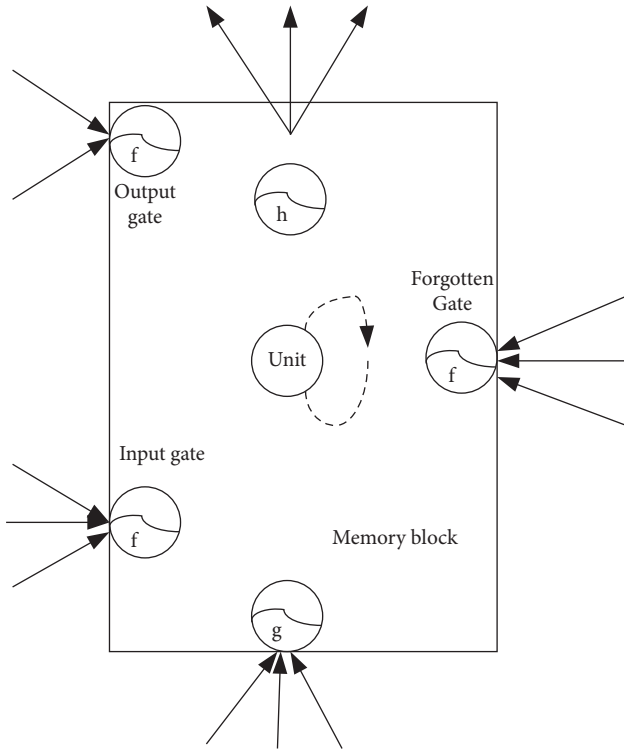


FIGURE 1: The internal structure of the LSTM memory block.

organization learning of the input layer mode connects the spatial distribution density of the weight coefficient with the input mode. The probability distribution tends to be the same. At this time, the spatial distribution density distribution of the connection weight coefficient can reflect the characteristics of the input mode [12, 13].

This study uses the sigmoid function. According to the characteristics of the sigmoid function, the value is between 0 and 1. g is the input function of the unit, and h is the output function of the unit. They usually use the tanh function or the sigmoid function%. The tanh function is generally used in the state and output, which is the processing of data. The multiplication gate will provide the output value to the nodes in the other network of the memory block. The activation functions of the input gate, output gate, and forget gate all use the sigmoid function to generate values between 0 and 1. The internal structure of the memory block of LSTM is shown in Figure 1:

We can regard the basic processing unit of the LSMT recurrent neural network as a neuron. For an n -dimensional input pattern, then, there are n input neurons. These neurons are connected to the output neurons to a certain degree, and the degree of weighting varies. The connection, that is, the connection right, is different. The output layer is a two-layer neural network structure, the neurons in the output layer are also connected to each other, and these connections have a certain weight [14].

One mode pk among the M learning modes is randomly selected as the input layer of the network, and the input mode is normalized.

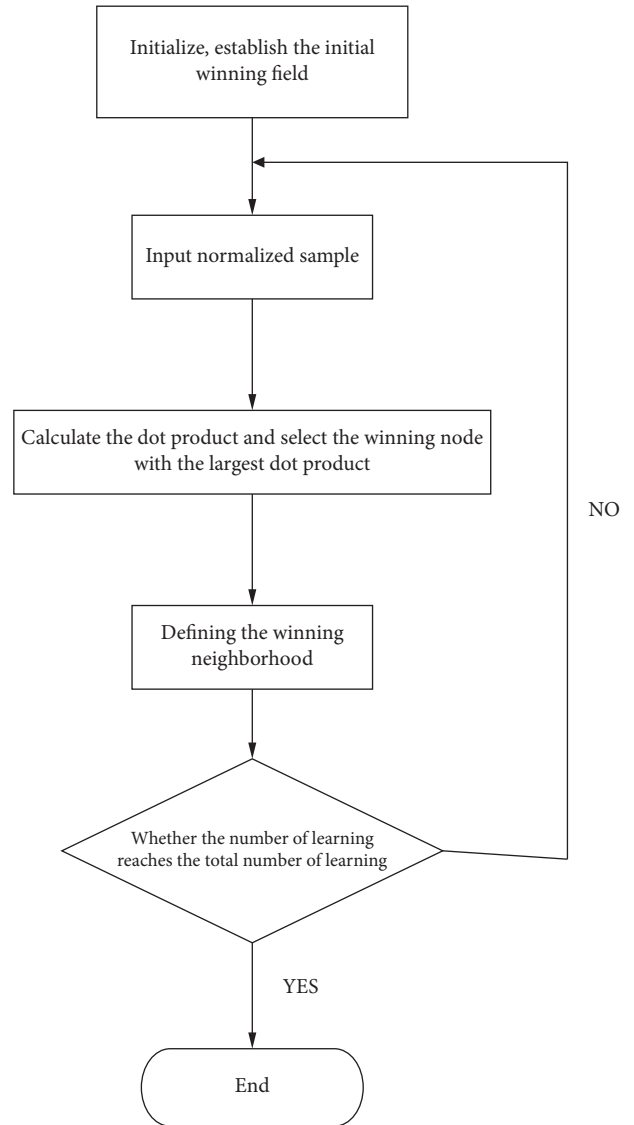


FIGURE 2: Kohonen neural network algorithm flow.

$$\bar{P}_k = \frac{Pk}{|Pk|} = \frac{(P_1^k, P_2^k, \dots, P_n^k)}{\left[(P_1^k)^2 + (P_2^k)^2 + \dots + (P_n^k)^2 \right]^{1/2}} \quad (1)$$

At the same time, the connection weight vector is normalized, and then, the Euclidean distance between \bar{P}_k and \bar{W}_j is calculated as follows:

$$\bar{W}_j = \frac{W_j}{|W_j|} = \frac{W_{j1}, W_{j2}, \dots, W_{jm}}{\left[(W_{j1})^2 + (W_{j2})^2 + \dots + (W_{jm})^2 \right]^{1/2}} \quad (2)$$

$$dj = \left[\sum_{i=1}^N (\bar{P}_i^k - \bar{W}_{ji})^2 \right]^{1/2}$$

After all the N inputs are calculated, the minimum Euclidean distance d_k is found to determine the optimal matching neuron g . The calculation formula is as follows:

$$d_g = \min [d_j], j = 1, 2, \dots, M. \quad (3)$$

The connection weights are adjusted, and the connection weights between all neurons $N_g(t)$ in the neighborhood of the output layer and the neurons in the input layer are modified.

$$\overline{W}_{ji}(t+1) = \overline{W}_{ji}(t) + \eta(t) * [\overline{P}_i^k - W_{ji}(t)]. \quad (4)$$

Correspondingly, $\eta(t)$ and $N_g(t)$ are updated, that is, the learning rate and neighborhood range are updated.

$$\eta(t) = \eta(0) \left(1 - \frac{t}{T}\right). \quad (5)$$

Among them, $\eta(0)$ is the initial learning rate, t is the number of learning, and T is the total number of learning.

The correction formula of the neighborhood function is as follows:

$$N_g(t) = INT \left(Ng(0) \left(1 - \frac{t}{T}\right) \right). \quad (6)$$

This kind of network simulates the function of self-organizing feature mapping of the brain nervous system. It is a kind of competitive learning network, which can conduct unsupervised self-organizing learning in learning. The role is played by the neighborhood and its adjustment. In the SOM network, the neighborhood defines the range of neurons that can adjust the connection weight at the same time as the winning neuron. In the initial stage of learning, the range covered by the neighborhood is relatively large, generally within the amplitude of the output layer array, or it can cover the entire output layer [15]. As the learning progresses further, the range of the neighborhood gradually $N_g(t)$ becomes smaller, eventually reaching the expected range. The algorithm flow is shown in Figure 2:

At present, the traditional moving image collection or feature extraction method generally uses a horizontal camera or an overhead camera to collect video images with moving actions. Since the horizontal camera detects the moving image of a target above a certain height in the horizontal direction, there will be many interference images, so it is difficult to set a clear detection area. The input of the system training data is X , the expected output is Y , and then, the general input of each neuron in the hidden layer is as follows:

$$H_j = \sum_{i=1}^n \phi_{ij} x_i. \quad (7)$$

In order to simplify the calculation, the output results of each hidden node can be obtained:

$$net_j = f(H_j), \quad j = 1, 2, \dots, l. \quad (8)$$

The input of each output node is as follows:

$$O_k = \sum_{j=1}^l H_j w_{jk} \quad k = 1, 2, \dots, m. \quad (9)$$

Suppose we expect the value of the i -th output neuron to be d_i , then, the prediction error of the i -th neuron is $e_i = d_i - y_i$, and then, the error function of the output layer is as follows:

$$E = \frac{1}{2} \sum_i e_i^2 = \frac{1}{2} (d_i - y_i)^2. \quad (10)$$

For each input $X(k)$, the output $Y(k)$ of each layer is calculated:

$$Y(k) = [y_1(k), y_n(k)], y_j^i(k) = \phi(s_j^i(k)) = \frac{1}{1 + e^{-s_j^i(k)}},$$

$$s_j^i(k) = \sum_{i=0}^{N_{i-1}} W_{ji}^i y_i^{i-1}(k) = (W_{ji}^i)^t Y^{i1}(k),$$

$$\begin{aligned} (W_j^l)^T &= [w_{j0}^i, w_{j1}^i, \dots, w_{jN-1}^i], w_{j0}^i = -\theta_j^i, (Y^l(k))^t \\ &= [1, y_1^i(k), \dots, y_{N1}^i(k)]. \end{aligned} \quad (11)$$

Therefore, the general situation can be obtained, that is, for any i -th layer, there is the following:

$$\Delta w_{ji}^l(k) = \delta_j^l(k) y_i^{l-1}(k). \quad (12)$$

Therefore, the error data transfer equation between the input layer and the hidden layer is as follows:

$$\Delta \phi_{ij} = -\eta \frac{\partial E}{\partial \phi_{ij}} \quad i = 1, 2, \dots, n. \quad (13)$$

Because of the sigmoid function $f'(x) = f(x)(1 - f(x))$, the result obtained is as follows:

$$\Delta w_{jk} = -\eta (d_i - y_i) y_i (1 - y_i) net_j. \quad (14)$$

Also because

$$\frac{\partial y_k}{\partial net_j} = \frac{\partial y_k}{\partial O_k} \frac{\partial O_k}{\partial net_j} = y_k (1 - y_i) u_{ki}, \quad (15)$$

$$\frac{\partial net_j}{\partial w_{ij}} = \frac{\partial net_j}{\partial H_i} \frac{\partial H_i}{\partial w_{ij}} = net_j (1 - net_j) w_j.$$

Then, the formula can be further expressed as follows:

$$w_{ij}(t+1) = w_{ij}(t) + \eta \sum_{k=1}^m (d_k - y_k) y_k u_k net_i (1 - net_i) x_j. \quad (16)$$

The neural network is used to train the data according to the above steps. Due to the characteristic that errors can be transmitted backward, in the process of using data to train the network, the weights between each layer are continuously adjusted until the obtained data are close to the expected result. The centroid of the variables of the samples corresponding to each neuron after classification is calculated, the median of the variables of the corresponding

samples is used as the centroids, and the centroids of the variables of the corresponding samples are used to update the connection weights of each neuron.

2.2. Sports Action Safety. Usually due to irregular movement, adverse climate factors, or sudden environmental factors, such as wet road after rain, insufficient light, high or low temperature, jet lag factors, and altitude changes, sports safety is threatened. As an important part of human life, sports become one of the values pursued by human society because it can meet the different needs of human society [16, 17]. Sports competition is a basic form of sports, which is determined by the competitive nature of sports and sports competition as a social and cultural system. All practical activities of competitive sports are guided by competitive competitions. The selection and training of athletes must be based on the requirements of modern sports competitions for the intensity of competitive competitions, determine the direction and standards of selection and training, and form sports teams through competitive sports. The role of sports competitions in various sports academies is very common. With the rapid development of sports, many competitions also appear from time to time.

At present, the distribution of sports injuries in track and field events is mainly on the limbs and trunk, and soft tissue injuries are more common. Lack of knowledge of sports healthcare and insufficient attention to the prevention of sports injuries are the potential factors causing sports injuries [18]. Sports specialty students' training time is short, the training system is not strong, coupled with factors such as unreasonable training arrangements, improper preparation activities, poor physical fitness, and movement skills, and difficult training environments, and they are prone to sports injuries. Without adequate rest and treatment, training with injuries is more likely to lead to aggravation of injuries or induce new injuries. Therefore, the prevention of sports injuries and the treatment and recovery after sports injuries are particularly important for sports specialties [19]. In addition to the above points, the reasons for athletes' sports injuries are the movement problems that this study wants to discuss. Sports movements are generally divided into regular movements, unconventional movements, and wrong movements. Conventional actions generally refer to standard actions. Unconventional technical actions are different from wrong actions. Unconventional technical actions are a kind of performance in the game, and wrong actions are contrary to the standard of action and are easily injured by athletes [20].

As the main body of competitive sports, the country has invested a lot of mental, human, and financial resources to train an outstanding athlete. Athletes have invested precious youth and hard work to achieve good results and reflect their social value by virtue of their own competitive ability. The development of competitive sports athletes and the improvement of competitive sports levels may be restricted due to sports injuries, hindering the career development of athletes. Therefore, having a healthy body is one of the important reasons for athletes to extend their sports career

life, and the prevention and rehabilitation of sports injuries are very important [21]. Therefore, the research of sports movements also appears to be particularly critical.

In recent years, more and more attention has been paid to the training of sports injury prevention and treatment personnel, but the injury protection system of athletes has not been perfected. At this time, athletes' own sports injury prevention is more important. Athletes' awareness of sports injury prevention may affect their time and method of medical treatment and their attitude toward treatment, which in turn affects their recovery speed after injury. Therefore, understanding athletes' cognition of sports injury knowledge and discussing related influencing factors can provide important information for coaches or people involved in sports injury protection.

2.3. Action Feature Extraction. The current action feature extraction methods can be roughly divided into two categories: (1) extraction based on feature parameters; (2) extraction methods based on model measurement [22]. The basis of this classification is whether they used the model, and the model is equivalent to the advanced processing products after feature parameter extraction, so the model method obviously has higher reliability based on the feature parameter method, but the corresponding processing calculation method is more complex, so which feature extraction method should also be selected according to the specific situation of the studied problem [23].

The feature-based extraction method is a relatively basic extraction method that has been studied for a long time and is relatively mature and simple. This extraction method does not involve the establishment of a human body model, so the amount of calculation is usually much smaller than that of model-based extraction methods. Because of the nature of the extracted feature parameters, the apparent features are usually extracted from the area of the moving human body, usually some two-dimensional information such as contours, colors, heights and widths, and perimeters [24]. Then, these characteristic parameters are used to match with the human body movement to achieve the purpose of recognition and analysis.

In the feature-based extraction method, various apparent feature parameters are extracted, and the contour feature is one of several important ones. Although the methods are different, their steps are relatively similar. They can usually be divided into background subtraction, human body monitoring, processing to eliminate noise, and feature extraction.

For video information, color information occupies a very important role as one of the information. The information contained in color information when information is usually obtained through human vision occupies a large proportion of the total amount of information obtained from video. Therefore, in the research of automatic recognition of action behavior, color is often selected as the characteristic parameter because of its characteristics [25]. The application of color in the research is diverse. Researchers have set up human bodies and backgrounds with large color differences

to more highly extract human bodies from video. This ideal situation is relatively rare in reality. Therefore, in order to solve the problem of complex background colors, methods for marking colors in images were proposed. For example, based on RGB and HSV color space and grayscale-based colors are two more popular marking methods.

There are significant differences in the FMS test scores of athletes of different genders, age-groups, with or without injury history, and training bases. There are significant differences in the patterns. Based on the model method to identify the characteristic information of the moving human body, the first step is to establish a human body model. The establishment of this model requires a lot of preliminary work. It needs to use human body structure and a large number of examples to verify to establish a human body model. The second part is to extract feature parameters from the underlying features to match this model to drive this model, so as to obtain various information that was about the moving human body. This model can be used to characterize any individual, so it has a better recognition effect than the feature method for humans with different shapes, and even if the feature acquisition is inaccurate and it is difficult to match the model, the motion law can be made according to the estimation of the human body posture. The real human movement is restored to the greatest extent. These advantages are also the reason why the model method is becoming more and more common and gradually becoming the main direction of the development of human movement consciousness.

3. Judgment Experiment and Results of Action Safety

3.1. Database. Functional movement screening is a screening system that predicts exercise risk based on the basic movement patterns of the body. It is widely used in various fields due to its easy operation and remarkable screening effect. In the database conceptual design stage, it considers the constraints and processing requirements of the data in the position of all participants in the competition and designs a data model based on the concept of system participants—a conceptual model. The conceptual model is concretized to refine the requirements analysis. The conceptual structure abstracts the real world. By abstracting things in reality into an information structure independent of specific machines, the tasks at each stage are single, reduced in complexity, and independent of a certain DBMS. We use the statistics of student athletes in a middle school in this city, combined with the widely used human motion data in human motion recognition. The database service can record and alert database risk operation behaviors such as database injection and risk operation. The athlete action database and ECS self-built database are supported and provide security diagnosis, maintenance, and management capabilities for the action database. The motion database is shown in Figure 3:

Let us take a basketball player as an example. We use sensors to analyze the player's movements. The experiment starts at an angle of 0 degrees and continues to rotate the

sensor node at an angle of 1,080 degrees, sampling data every 90 degrees. The experiment is divided into two groups. In order to compare the compensation effect of the Kalman filter on the angle calculation, the first group of the experiment does not use any compensation method and directly obtains the rotation angle of the sensor through the angular velocity integration; the second group uses the extended Kalman. The filtering method compensates for the angle output of the sensor node. The compensation results are shown in Table 1.

The comparison of the error data before and after compensation is shown in the table. After rotating by 1,080 degrees, the angle calculation error without any compensation method has reached 10 degrees, while the compensated angle calculation error is only 0.37 degrees. It can be seen that the algorithm can effectively compensate for the error caused by the angular velocity integral and improve the human body.

Some athletes have weak shoulder and hip flexibility, stability and core strength, poor coordination, and serious body asymmetry. In the process of data collection, the tester's 9 types of actions such as walking, running, jumping without the ball, standing dribbling, walking dribbling, running dribbling, shooting, passing, and receiving the ball when the tester is without the ball are collected. The basketball action is shown in Figure 4:

As the basketball action progresses, the aspect ratio of the moving human body in the image sequence will also change. These changes in the aspect ratio can reflect information such as the speed of movement outside of the contour feature, and the human body in action can be drawn according to the amount of change. The result is shown in Figure 5:

In the data collection process, according to the different placement positions of the sensor nodes on the body, the collected upper limb movement and lower limb movement data will be separately discussed and identified. Therefore, for upper and lower extremity movements, classifiers are separately constructed for recognition. Through the combination of upper and lower extremity movements, the movements made by athletes can be determined. In this study, the classification characteristics of different classifiers are analyzed and the basketball gesture recognition of different classifiers is compared. For classification performance, according to the movement data of different limbs, the corresponding classification algorithm is constructed for training, and the recognition effect is analyzed from the accuracy rate and recall rate. The upper and lower limb movement test results are shown in Tables 2 and 3:

It can be seen from the table that the recognition effect achieved by the LSTM cyclic neural network is better for the classification of different limb movements. The average accuracy rate of upper limb movements reaches 93%, the average recall rate reaches 92.1%, the average accuracy rate of lower limb movements reaches 98.1%, and the average recall rate reaches 99%.

3.2. Action Comparison. We express the recognition result in the form of a confusion matrix graph, where the diagonal line is the correct recognition rate of the corresponding category, and the off-diagonal line is the recognition rate of



FIGURE 3: Movement database.

TABLE 1: Error before and after output angle compensation.

Rotation angle	Error after compensation	Error before compensation
0	0.24	0.01
90	0.31	0.03
180	-0.01	-0.51
270	-0.03	-0.07
360	-0.43	2.69
450	0.14	2.02
540	-0.03	3.02
630	0	3.51
720	-0.04	8.27
810	-0.01	9.13
900	-0.69	7.89
990	-0.03	8.85
1080	0.36	9.15

the wrong category. From the comparison of the two confusion matrix diagrams, it can be seen that the recognition result using only static features is significantly lower than the recognition result of combining static features and dynamic features. The addition of dynamic features can improve the recognition effect, and the combination of dynamic features and static features can improve the recognition effect. Strong ability to characterize actions is more suitable for action recognition, as shown in Figure 7:

We compare the recognition results without frame selection and after frame selection, where the abscissa is the specific eight types of actions, and the ordinate is the recognition rate. The result is shown in Figure 8:

Due to the different levels of exercise, the sports skills they accept are also different, the injuries caused and the number of injured parts experienced are also different, and there are obvious differences in the recognition of sports injury names. Figure 9 shows the analysis of differences in cognition of injury names among physical education students of different specialties:

It can be seen that there is little difference in the scores of sports majors of different specialties for injury names. The highest score is 4.90 for “basketball”; the lowest score is 4.81 for “wushu.” The one-way analysis of variance on the cognitive differences of sports majors in different specialties showed that there was no significant difference between the groups.

For basketballs that are prone to action safety, we surveyed professional athletes and counted the training they believe can effectively prevent related work. The results are shown in Figure 10:

It can be seen that most athletes believe that the prevention of physical factors such as strengthening strength training and agility training is very important. Among them, 41.9% felt that strengthening strength training had a great effect on preventing injury, 35.3% felt that the effect was large, and 21.1% felt that the effect was general. From the aspect of project characteristics, the prerequisite for successfully completing difficult movements is to ensure sufficient muscle strength and good physical agility, which requires strengthening of strength and agility.

4. Discuss

With the rapid development of the electronic information industry today, artificial intelligence has been greatly improved compared to the past. With the popularization of video capture equipment and the improvement of computer performance, computer vision technology has also ushered in a rapid development period. At the same time, human body action recognition is closely related to our lives and has huge potential value. Human action recognition technology based on computer technology and image recognition technology is also a hot field of research today. The application of the LSTM recurrent neural network to the safety recognition of sports actions has also become a trend.

This study selects a segmentation method of continuous motion human motion in video based on human motion



FIGURE 4: Basketball action collection diagram.

feature parameters to realize a sports motion recognition method with simple calculation and better real-time performance. In order to reduce the workload and improve the real-time performance during the video processing and analysis, the noncritical gestures can be eliminated for the

key gestures. Through the analysis of the specific actions of the moving human body, the extraction method based on the motion feature parameters is adopted. It is different from the model method in that it does not need to build a human body model, usually the calculation complexity is relatively

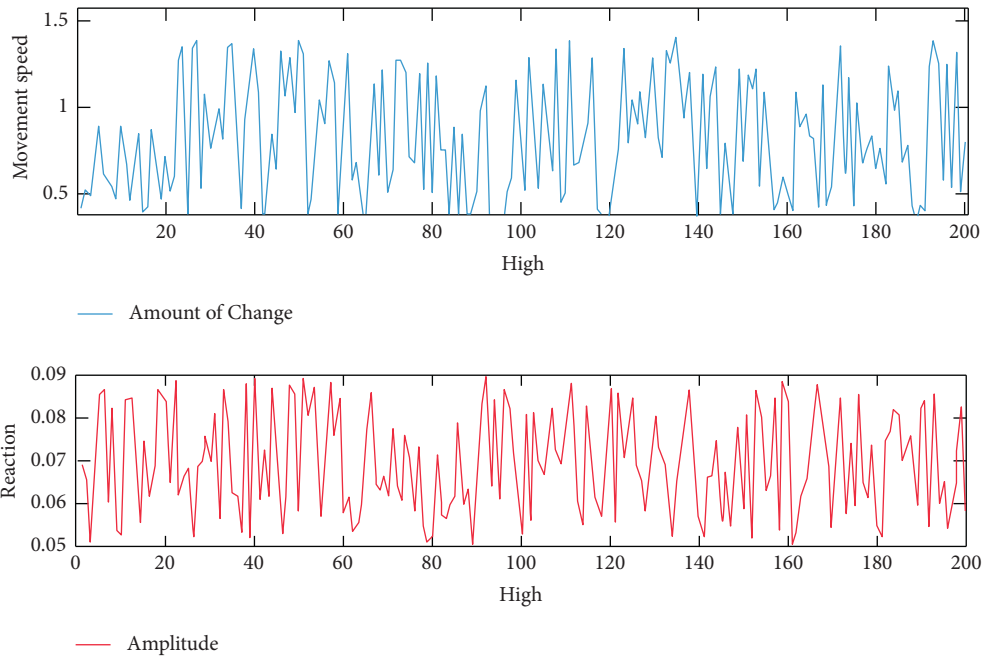


FIGURE 5: Basketball action speed curve.

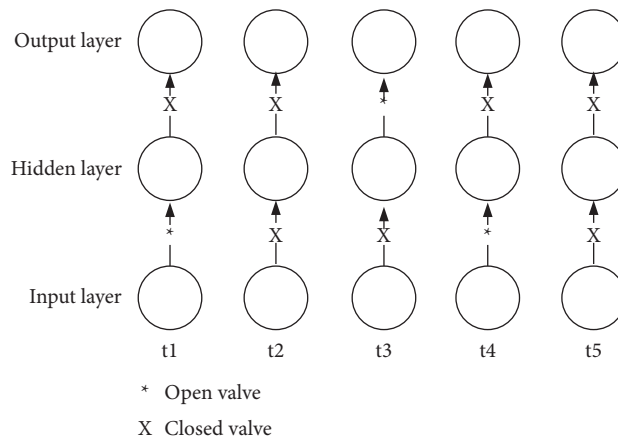


FIGURE 6: LSTM memory valve.

TABLE 2: Basketball upper limb movement test.

Action	C4.5		SVM		BN		LSTM	
	Recall rate	Accuracy	Recall rate	Accuracy	Recall rate	Accuracy	Recall rate	Accuracy
Catch the ball	0.928	0.943	0.954	0.965	0.884	0.918	0.954	0.967
Pass	0.909	0.921	0.965	0.989	0.925	0.945	0.972	0.971
Shot	0.914	0.908	0.977	0.983	0.947	0.904	0.968	0.971
Walking dribble	0.876	0.852	0.921	0.907	0.789	0.934	0.922	0.907
Standing dribble	0.775	0.756	0.806	0.548	0.768	0.702	0.894	0.866
Running dribble	0.771	0.811	0.681	0.851	0.803	0.746	0.864	0.886

low, and the motion feature can carry enough parameters that can be used for the recognition and analysis of the moving human body. Due to the serious jump problem when extracting the feature parameters, the method of

increasing the dimension to reduce the sensitivity of the vector modulus is used for optimization.

For sports, it is necessary to establish a sound competition operation mechanism. The operation mechanism

TABLE 3: Lower limb movement test results.

Action	C4.5		SVM		BN		LSTM	
	Recall rate	Accuracy	Recall rate	Accuracy	Recall rate	Accuracy	Recall rate	Accuracy
Jump	0.986	0.983	0.972	0.988	0.968	0.965	0.974	0.988
Run	0.972	0.971	0.987	0.968	0.944	0.964	0.986	0.974
Walk	0.969	0.965	0.977	0.985	0.979	0.947	0.992	0.983
Average	0.973	0.973	0.989	0.987	0.971	0.969	0.981	0.989

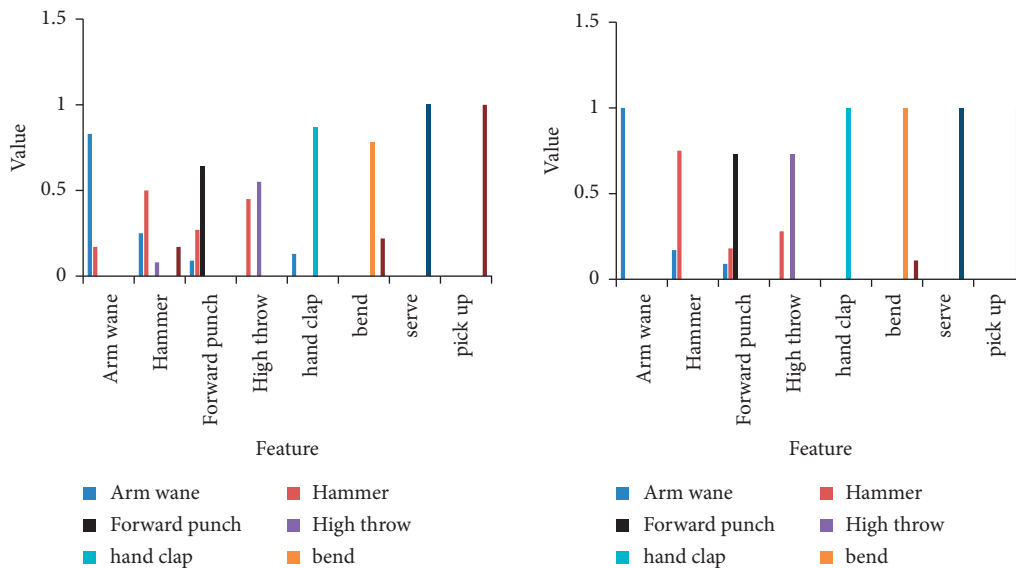


FIGURE 7: Dynamic recognition and static recognition.

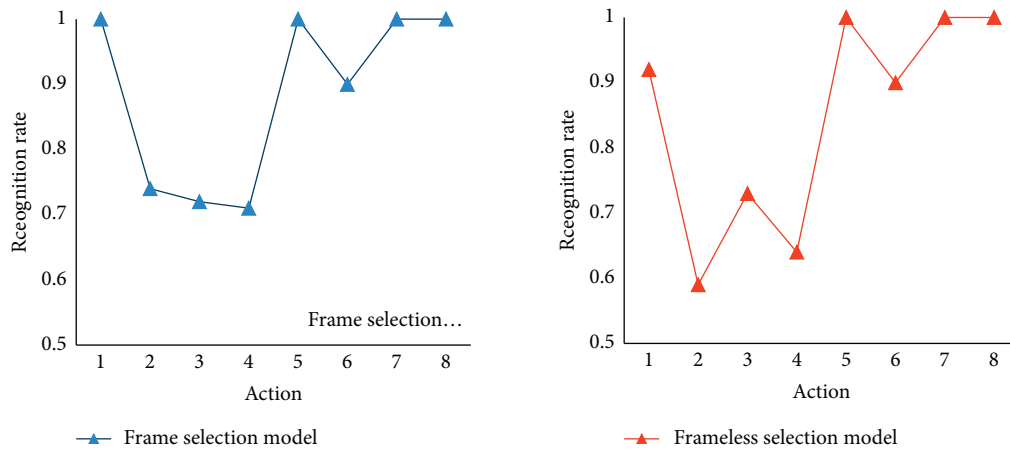


FIGURE 8: The action is recognized in the presence or the absence of frame selection.

refers to a mechanism in that people try to establish a certain goal and realize a certain desire and demand as the starting point and ending point. The national sports academies' competition operation mechanism is the process in which the various constituent factors have an impact and play a role in the process of completing the development goals of the cooperative association competition. The development of national sports college competition activities meets the needs of three different levels: one is the highest level, that is,

it meets the needs of the country's education and sports development; the other is the need for the middle level, that is, the development of each cooperative unit, the need for mutual communication to promote and improve; the third is the need for microlevel, that is, to meet the personal development needs of participating athletes and coaches. These three different levels of needs that constitute the needs of the development of competition activities in national sports colleges and universities and are the power source to

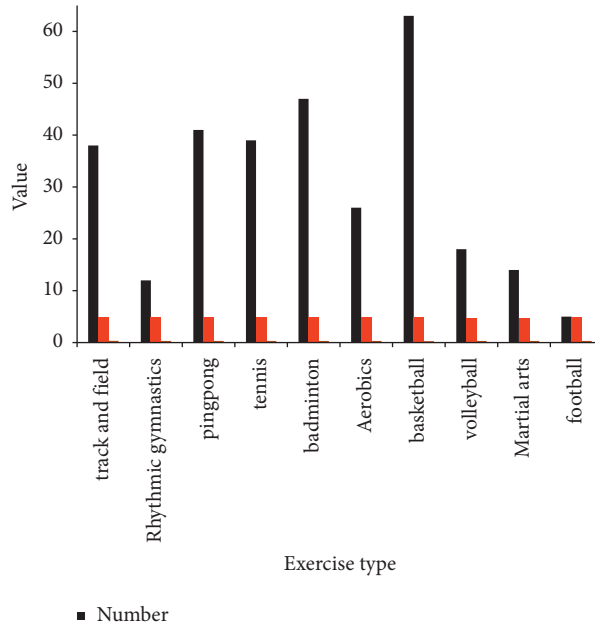


FIGURE 9: Cognitive difference analysis diagram.

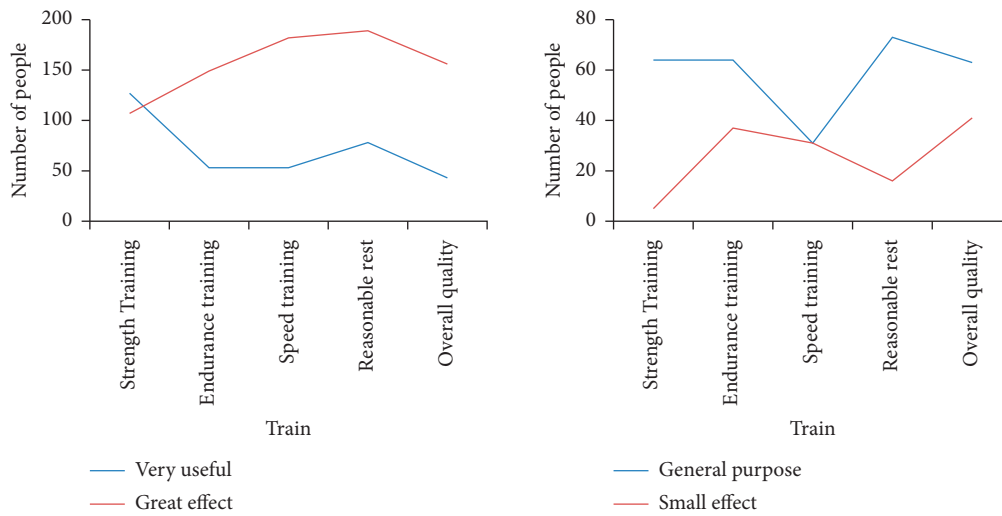


FIGURE 10: Training to prevent wrong movements.

promote their development. Only by meeting the needs of these three levels and integrating them, the operation of national sports colleges and universities can be unblocked and the competition development goal of national sports colleges and universities can be realized.

In terms of the implementation of corrective training, due to the influence of competition, technical, and tactical training content, athletes cannot complete corrective training content in quality and quantity during the correction period and are affected by various objective factors, so they should pay attention to the preparation work before class, competition, and activities. Sports equipment is complete, and physical condition is good. Establishing a reasonable competition operation mechanism is a guarantee system for the development of competition activities

in sports colleges across the country. The further improvement of the competition system is to fully mobilize the enthusiasm of schools, society, and the country to participate, improve the level of competition, make the competition better serve education and sports, and serve the development of individuals and society. Therefore, the arrangement of competition activities should be scientific and reasonable, and the needs of systematic teaching and training should be met to the greatest extent. At the same time, multiperiod competition activities should be developed to meet the needs of different levels and different levels of competition teams, and necessary single competitions should be carried out. The reform meets the needs of market competition and makes the development of the project realize a virtuous cycle. Through the

continuous improvement of the competition system, the competition management goal of conforming to the market and serving teaching, scientific research, and training is achieved.

For athletes, attention should be paid to body relaxation and physical recovery after exercise. The study of professional courses for undergraduates majoring in physical education is particularly important, but the study of technical courses cannot be ignored. The level of physical fitness of students greatly varies. For students with average physical fitness, thin or obese students, they should pay attention to relaxation after class and physical recovery to ensure the normal progress of the next class to avoid excessive fatigue and cause sports injuries. A good job of self-monitoring is done. Before class, before the game, before the activity need to check whether the sports equipment is complete, whether the physical condition is good (no discomfort symptoms, injury recovery), and whether the warm-up activity is sufficient. If you realize that your current physical condition is not able to complete the task, you must not force yourself instead of making self-adjustment and consulting a teacher or see a doctor in time.

5. Conclusions

Due to the limitation of monitoring and correction training time, only one training base was selected for intervention, and the sample size was too small. In addition, this study only compared a single group of experiments before and after, and no control group was designed, which could not prove the effect of the correction training program to a certain extent. Human action recognition is a research direction that combines computer vision and artificial intelligence. Kohonen neural network has been applied in the fields of abnormal human behavior recognition, intelligent nursing, and action comparison. It is one of the important technologies for the intelligent development of people's lives and has great practical significance. From the experiments in this study, it can also be seen that the LSTM recurrent neural network can play an important role in sports action recognition. The recognition of simple actions has obtained good results, but the recognition of actions in complex environments, complex interactive actions, and group action recognition still faces many difficulties and challenges. There is still a lot of room for improvement in the recognition rate. The deep features of the Kohonen neural network alone cannot accurately identify the movements of the human body. Combining the extracted human body features with the surrounding environment can eliminate ambiguity and more accurately recognize complex scenes and human body movements. In addition, in many real scenes, it is the interaction of multiple people. How to track and recognize the actions of multiple people still face great challenges.

Data Availability

No data were used to support this study.

Conflicts of Interest

The authors declare that there are no conflicts of interest regarding the publication of this article.

References

- [1] X. Guo, L. Wang, B. K. Xuan, and C.-P. Li, "Gait recognition based on supervised kohonen neural network," *Zidonghua Xuebao/Acta Automatica Sinica*, vol. 43, no. 3, pp. 430–438, 2017.
- [2] D. Zaborski, K. M. Kavetska, W. Grzesiak, K. Królaczyk, and E. Dzierzba, "The use of selected statistical methods and Kohonen networks in the revision and redescription of parasites," *Ann Parasitol*, vol. 62, no. 4, pp. 285–293, 2016.
- [3] L. Yong, C. Gang, X. Chen, and C. Liu, "Coal-rock interface recognition based on permutation entropy of LMD and supervised kohonen neural network," *Current Science*, vol. 116, no. 1, pp. 96–103, 2019.
- [4] P. E. Martin, J. Benois-Pineau, R. Péteri, and J. Morlier, "Fine grained sport action recognition with Twin spatio-temporal convolutional neural networks," *Multimedia Tools and Applications*, vol. 79, no. 27, pp. 20429–20447, 2020.
- [5] H. Xu and R. Yan, "Research on sports action recognition system based on cluster regression and improved ISA deep network," *Journal of Intelligent and Fuzzy Systems*, vol. 39, no. 4, pp. 5871–5881, 2020.
- [6] Y.-L. Shih and C.-Y. Lin, "The relationship between action anticipation and emotion recognition in athletes of open skill sports," *Cognitive Processing*, vol. 17, no. 3, pp. 259–268, 2016.
- [7] M. Ramesh and K. Mahesh, "Sports video classification with deep convolution neural network: a test on UCF101 dataset," *International Journal of Engineering and Advanced Technology*, vol. 8, no. 4S2, pp. 2249–8958, 2019.
- [8] K. S. Koltai and K. R. Fleischmann, "Questioning science with science: the evolution of the vaccine safety movement," in *Proceedings of the Association for Information Science and Technology*, vol. 54, no. 1, pp. 232–240, 2017.
- [9] M. Seo, T. G. Gweon, C. W. Huh, J. S. Ji, and H. Choi, "Comparison of bowel cleansing efficacy, safety, bowel movement kinetics, and patient tolerability of same-day and split-dose bowel preparation using 4L of polyethylene glycol: A prospective randomized study," *Diseases of the Colon & Rectum*, vol. 62, no. 12, pp. 1518–1527, 2019.
- [10] A. Ananenkov, A. Konovaltsev, V. Nuzhdin, V. Rastorguev, and P. Sokolov, "Radio vision systems ensuring movement safety for ground, airborne and sea vehicles," *Journal of Telecommunications and Information Technology*, vol. 8, no. 4, pp. 54–63, 2019.
- [11] M. Płóciennik, A. Kruk, D. J. Michczyńska, and H. J. B. Birks, "Kohonen artificial neural networks and the IndVal index as supplementary tools for the quantitative analysis of palaeoecological data," *Nephron Clinical Practice*, vol. 44, no. 1, p. 111, 2017.
- [12] D. S. Hong, J. H. Lee, and E. J. Kim, "A comparative study on the survey and recognition of life sports safety accidents in Korea and Germany," *Korean Journal of Sports Science*, vol. 27, no. 4, pp. 891–900, 2018.
- [13] A. Abdulmunem, Y.-K. Lai, and X. Sun, "Saliency guided local and global descriptors for effective action recognition," *Computational Visual Media*, vol. 2, no. 1, pp. 97–106, 2016.
- [14] Y. N. Chung, "A study on the facility operators recognition for establishing marine leisure activation plan," *Korean Journal of Sports Science*, vol. 26, no. 6, pp. 815–830, 2017.

- [15] P. C. Bulhes and I. C. Condessa, "A criana e o seu desenvolvimento em atividades lúdicas e físico-motoras uma reflexo sobre instituies de tempos livres," *International Journal of Developmental and Educational Psychology Revista INFAD de psicología*, vol. 1, no. 2, pp. 23–32, 2019.
- [16] J. Y. Son, "A study on influence of social support of elderly participating in leisure sports on successful aging recognition and resilience relation," *Korean Journal of Leisure Recreation & Park*, vol. 43, no. 4, pp. 17–34, 2019.
- [17] Y. J. Lee, "The effects of leisure perception on Korean dance performance recognition and visitor intention," *Korean Journal of Sports Science*, vol. 27, no. 6, pp. 845–856, 2018.
- [18] I. T. Ko and J. H. Han, "Snowboard recognition and future development plan as leisure sports based on big data," *Journal of Tourism and Leisure Research*, vol. 33, no. 2, pp. 295–309, 2021.
- [19] X. Ji, Z. Lu, N. Qin, and Y. Li, "A simple and fast action recognition method based on AdaBoost algorithm," *International Journal of Multimedia and Ubiquitous Engineering*, vol. 11, no. 8, pp. 225–236, 2016.
- [20] C. Li, Y. Hou, P. Wang, and W. Li, "Joint distance maps based action recognition with convolutional neural networks," *IEEE Signal Processing Letters*, vol. 24, no. 5, pp. 624–628, 2017.
- [21] H. J. A. Park, "Study on the relations VR training, Recognition effect and Safety action: focusing on the Mediation effects of recognition effect," *Journal of Tourism Management Research*, vol. 23, no. 5, pp. 761–781, 2019.
- [22] L. Chen, N. Ma, P. Wang et al., "Survey of pedestrian action recognition techniques for autonomous driving," *Tsinghua Science and Technology*, vol. 25, no. 4, pp. 458–470, 2020.
- [23] P. Li, Z. Zhou, Q. Liu, and X. Sun, "Machine learning-based emotional recognition in surveillance video images in the context of smart city safety," *Traitement du Signal*, vol. 38, no. 2, pp. 359–368, 2021.
- [24] J. K. Hrica and B. M. Eiter, "Competencies for the competent person: Defining workplace examiner competencies from the health and safety leader's perspective," *Mining, Metallurgy & Exploration*, vol. 37, no. 6, pp. 1951–1959, 2020.
- [25] C. Seok and Sun-Lyoung, "The effects of safety awareness of child sports instructors based on experience of accident on safty environment," *Korean Journal of Sports Science*, vol. 25, no. 2, pp. 159–172, 2016.

Research Article

Global COVID-19 Epidemic Prediction and Analysis Based on Improved Dynamic Transmission Rate Model with Neural Networks

Yanyu Ding,¹ Jiaxing Li,² Weiliang Song,² Xiaojin Xie,³ and Guoqiang Wang³ 

¹School of Chemistry and Chemical Engineering, Shanghai University of Engineering Science, Shanghai 201620, China

²School of Electronic and Electrical Engineering, Shanghai University of Engineering Science, Shanghai 201620, China

³School of Mathematics, Physics and Statistics, Shanghai University of Engineering Science, Shanghai 201620, China

Correspondence should be addressed to Guoqiang Wang; guoq_wang@hotmail.com

Received 7 January 2022; Accepted 22 February 2022; Published 30 March 2022

Academic Editor: Wei Liu

Copyright © 2022 Yanyu Ding et al. This is an open access article distributed under the Creative Commons Attribution License, which permits unrestricted use, distribution, and reproduction in any medium, provided the original work is properly cited.

The cross-regional spread of COVID-19 had a huge impact on the normal global social order. This paper aims to build an improved dynamic transmission rate model based on the conjugate gradient neural network predicting and analyzing the global COVID-19 epidemic. First, we conduct an exploratory analysis of the COVID-19 epidemic from Canada, Germany, France, the United States, South Korea, Iran, Spain, and Italy. Second, a two-parameter power function is used for the nonlinear fitting of the dynamic transmission rate on account of data-driven approaches. Third, we correct the residual error and construct an improved nonlinear dynamic transmission rate model utilizing the conjugate gradient neural network. Finally, the inflection points of the global COVID-19 epidemic and new outbreaks, as well as the corresponding existing cases are predicted under the optimal sliding window period. The experimental results show that the model presented in this paper has higher prediction accuracy and robustness than some other existing methods.

1. Introduction

With the acceleration of globalization and the development of science and technology, the population is moving rapidly, and the world has become interdependent and interconnected, making it possible for infectious diseases to spread rapidly. In early December 2019, the first case of a new type of coronavirus was reported in Wuhan, China, and it was named corona virus disease 2019 (COVID-19) on February 11, 2020. Subsequently, the COVID-19 epidemic spread rapidly from Hubei Province to many provinces across China and brought serious harm to the lives and health of Chinese, as well as to social and economic development. Until late February 2020, the COVID-19 epidemic prevention and control work in China had achieved a phased victory. Unfortunately, due to the lack of awareness regarding the COVID-19 epidemic in many overseas countries and inadequate prevention and control measures, the COVID-19 epidemic began to spread rapidly in Asia, the

Middle East, Europe, and North America in late February and early March of 2020. In particular, the introduction of the concept of “herd immunity” by the British government has exacerbated the spread of the COVID-19 epidemic in Europe. Ferguson et al. [1] pointed out that if the British government does not change the current situation with respect to “herd immunity” approach, this wave of the COVID-19 epidemic will even cause 510,000 British deaths, and the number of deaths in the United States will be even greater, with possibly 2.2 million deaths. According to a report from Johns Hopkins University, as of January 24, 2022 (Beijing time), there were 351,983,072 confirmed cases and 5,614,569 deaths from the COVID-19 worldwide. More than 200 countries and regions in the world have confirmed the presence of the COVID-19 epidemic. More seriously, there have been 71,925,931 confirmed cases and 889197 deaths in the United States (USA). The top ten countries in terms of cumulative confirmed cases and deaths are shown in Figure 1.

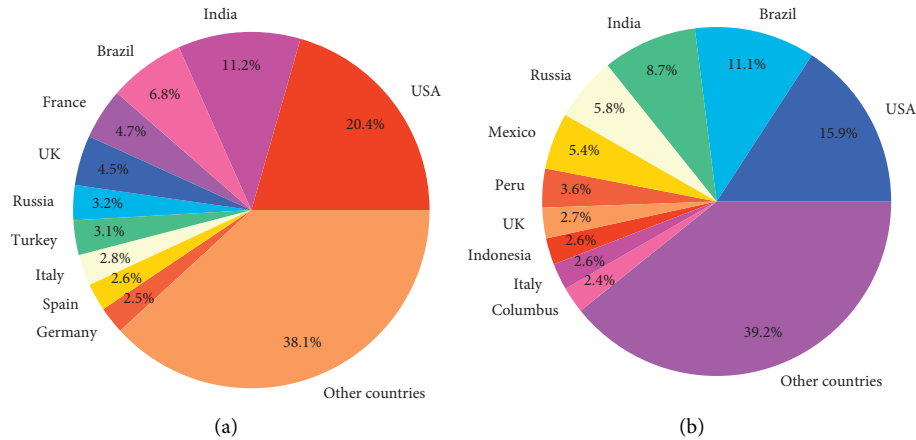


FIGURE 1: Top ten countries with cumulative confirmed cases and deaths.

Figure 1 shows that the United States is the country with the largest cumulative number of confirmed cases and deaths, accounting for approximately 20.4% and 15.9% of the global totals, respectively.

Statistics from Johns Hopkins University show that the cumulative number of confirmed cases worldwide exceeded 100 million cases on January 26, 2021, more than 200 million cases on August 4, 2021, more than 300 million cases on January 7, 2022. It is notable that it took 370 days from January 20, 2020 to reached 100 million cases. However, the increase rate of cumulative confirmed cases of the global COVID-19 epidemic has accelerated since October 2020. It took 190 days to increase from 100 million to 200 million cases. More seriously, it only took 156 days to go from 200 million cases to 300 million cases. The details is displayed in Figure 2.

From Figure 2, it takes about 10–25 days for every 10 million increase from October 18, 2020, to December 12, 2021. Recently, with the new Omicron variant of COVID-19, the global spread of the COVID-19 epidemic has once again set a new record. It only took 14 days to increase from 270 million to 280 million cases, 7 days to increase from 280 million to 290 million cases, 4 days to increase from 290 million to 300 million cases, 4 days to increase from 300 million to 310 million cases, 3 days to increase from 310 million to 320 million cases, 4 days to increase from 320 million to 330 million cases, 3 days to increase from 330 million to 340 million cases, and 3 days to increase from 340 million to 350 million cases. However, there is no sign of improvement at present.

There are a lot of work have been studied on the transmission mechanism and prediction models of the COVID-19 epidemic, with the aim revealing the governing law of the epidemic, predicting changes and developmental trends, analyzing the causes and key factors of the epidemic, and seeking the best strategy for prevention and control. In particular, the SEIR model and its extensions are favoured by researchers. Wu et al. [2] used the SEIR model to predict the domestic and international spread of the COVID-19 epidemic in the short-term and long-term. The numerical results show that in order to avoid outbreaks in large cities with strong transport links in China, a large number of

public health interventions must be implemented immediately at the population and individual levels. Caetano et al. [3] used an age-structured SEIR model to determine the impact of the implementation of past non-pharmaceutical interventions on the COVID-19 epidemic. Ghostine et al. [4] achieved encouraging results in small-scale short-term predictions by an extended SEIR model.

Based on the SEIR model, Wang et al. [5] constructed a complex network model for the spread of the COVID-19 epidemic in 15 cities with severe epidemics in Wuhan and the surrounding areas, focusing on the analysis of the possible time points at which the resumption of work in Wuhan and the surrounding areas could occur and the impact of resumption on the risk of secondary outbreaks. Yang et al. [6] used a modified SEIR model to predict the trend of the COVID-19 epidemic in China under public health interventions. Li et al. [7] studied the estimation of the scale of the COVID-19 epidemic in the United States based on air travel data from Wuhan. Liu et al. [8] used mathematical models to analyze the developmental trends of the COVID-19 epidemic in South Korea, Italy, France, and Germany. Hermanowicz [9] used a logistic model to conduct a systematic evaluation for predicting the growth of the COVID-19 epidemic in the United States based on 87-day data from China as of March 13, 2020 and 70-day data from the United States as of March 31, 2020. In the meantime, models based on data-driven statistics have also been widely used for the prediction and analysis of the COVID-19 epidemic, including function fitting [10, 11], machine learning [12–15], deep learning [16–18] and time series models [19, 20].

In particular, in view of the difficulty of accurately estimating the basic infection number R_0 in traditional infectious disease epidemiology, Huang et al. [21] proposed a data-driven concise and practical method for calculating the dynamic transmission rate of an epidemic to replace the basic infection number. Subsequently, Hu et al. [22, 23] used dynamic transmission rate model (DTRM) and dynamic growth rate model (DGRM) to predict and empirically analyze the domestic and global COVID-19 epidemics, respectively, and the experimental results show that the prediction accuracies of both models were greatly improved.

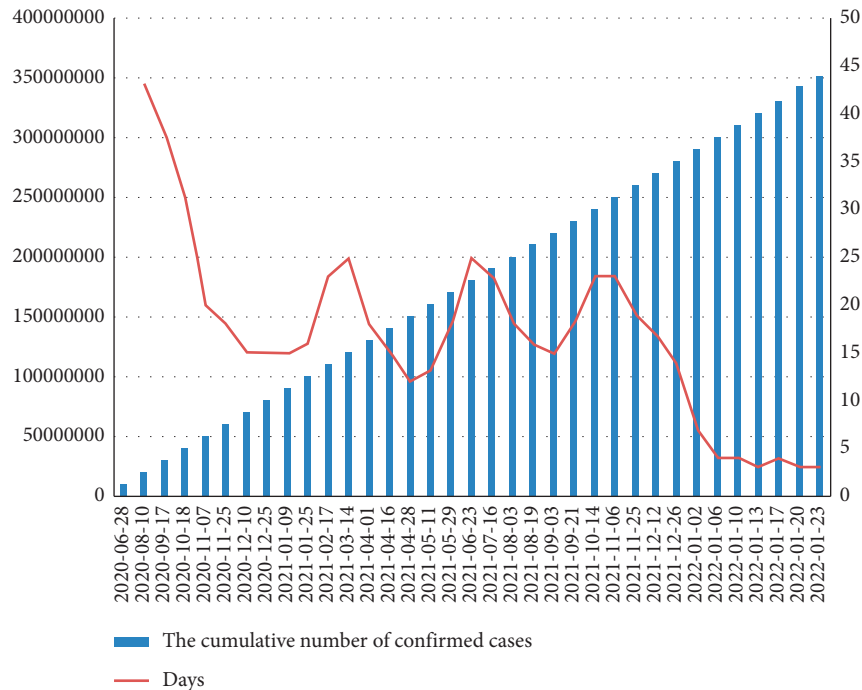


FIGURE 2: Global COVID-19 epidemic.

Compared with the SIR model [24], the SEIR model [2] and their extensions [5, 6], the DTRM based on a data-driven approach has a wider application range, higher prediction accuracy and stronger robustness. Xie et al. [25] used an nonlinear combinational DTRM (NCDTRM) based on support vector regression (SVR) to predict the COVID-19 epidemic in China. The experimental results demonstrate that NCDTRM effectively overcomes the shortcomings of insufficient information extraction and insufficient prediction accuracy of the single model. Xie et al. [26] presented an improved NCDTRM (INCDTRM) based on forecasting effective measure and SVR for analyzing and predicting the COVID-19 pandemic in eight countries. The experimental results reveal that INCDTRM has smaller prediction error and stronger generalization ability than the single prediction models, DGRM and NCDTRM that have been used previously.

Undoubtedly, the COVID-19 epidemic is a major public health emergency, that poses major challenge to the medical and health systems of all countries in the world and has a major impact on the global economic order. However, people are only concerned about the source, host, and spread of the COVID-19 epidemic, but the method of spreading, the pathogenic mechanism, the harmfulness, the lethality, the diagnosis and treatment plan, the treatment drugs, whether a given patient has sequelae after recovery, etc. have not been fully understood [27]. Therefore, in the face of the global COVID-19 epidemic, how to construct an effective and reasonable mathematical model for quickly, accurately and quantitatively evaluating the current stage of the epidemic, determining the effects of control measures, predicting future trends, and controlling the spread of the epidemic to avoid the collapse of the medical system has become a major

issue and an urgent task for the government, the scientific community, and the public.

Existing research results show that when the sample size is not large enough, the DTRM model estimation parameter method has a large deviation [28]. Therefore, the paper aims to build an improved DTRM based on the conjugate gradient neural network (CGNN) (abbreviated as IDTRM-CGNN) to predict the inflection point of the COVID-19 epidemic in Canada, Germany, France, the United States, South Korea, Iran, Spain and Italy. The corresponding existing confirmed cases are also reported. The core idea of the IDTRM-CGNN is to use the CGNN to correct the residuals for improving the prediction accuracy. The empirical results show that our model has higher prediction accuracy and robustness than some other existing methods, and can provide scientific decision-making for the prevention and control of the global COVID-19 epidemic. Furthermore, these results can also provide a study and judgement of the effects of the epidemic control measures employed in different countries.

The rest of this paper is organized as follows: Section 2 briefly recalls some well-known results on the dynamic transmission rate, the inflection point of the COVID-19 epidemic, and the neural network based on the conjugate gradient method. Section 3, the IDTRM-CGNN is proposed to predict and analyze the global COVID-19 epidemic. Conclusions and remarks are made in Section 4.

2. Preliminary Knowledge

2.1. Dynamic Transmission Rate. In this subsection, we introduce the basic idea of the dynamic transmission rate, which plays an important role in the COVID-19 epidemic

predictions and analysis. For the details can be referred to [21–23, 25, 26].

Let $N(t)$ be the number of existing confirmed cases at time t . Then,

$$N(t) = L(t) - K(t) - D(t), \quad (1)$$

where $L(t)$, $K(t)$, and $D(t)$ are the numbers of cumulative confirmed cases, cumulative deaths and cumulative cures at time t , respectively.

It is well-known that the natural growth model is defined by

$$\frac{dN(t)}{dt} = q(t)N(t), \quad (2)$$

where $q(t) \geq 0$ is the growth rate of the number of existing confirmed cases at time t .

Let

$$q(t) = g(t) - 1. \quad (3)$$

It follows from (2) and (3) that

$$\ln N(t) - \ln N(t_0) = \int_{t_0}^t g(x)dx - (t - t_0). \quad (4)$$

Then, the number of existing confirmed cases is obtained by

$$N(t) = N(t_0)\exp\{a_t(t - t_0)\}, \quad (5)$$

where

$$a_t = \frac{\int_{t_0}^t g(x)dx}{(t - t_0) - 1}. \quad (6)$$

For the sake of analysis, we introduce the dynamic transmission rate, i.e.,

$$c_t = 1 + a_t, \quad (7)$$

which was first studied in [21]. Then, we have

$$c_t = 1 + \frac{1}{t - t_0} \ln \frac{N(t)}{N(t_0)}. \quad (8)$$

This implies that

$$c_t = 1 + \frac{1}{k} \ln \frac{N(t)}{N(t - k)}, \quad (9)$$

where $k = t - t_0$ represents the sliding window period, see [22, 23, 25, 26] or Section 3.3 for details.

2.2. Inflection Point of the COVID-19 Epidemic. The inflection point of the COVID-19 epidemic in this paper refers to the moment when the number of existing confirmed cases reaches a peak within a certain period of time [22]. Therefore, the inflection point of the COVID-19 epidemic is the key point for the prevention and control of the COVID-19 epidemic, so it is an important factor for measuring whether the COVID-19 epidemic is under control. The following are the trend charts of the numbers of existing confirmed cases in

Canada, Germany, France, the United States, South Korea, Iran, Spain and Italy from the outbreak of the COVID-19 epidemic to April 7, 2020, as shown in Figure 3.

Figure 3 shows that the first wave of the COVID-19 epidemic inflection point in South Korea arrived on March 12, 2020. This means that South Korea has achieved good momentum with regard to the prevention and control of the first wave of the COVID-19 epidemic. However, the numbers of existing confirmed cases in other countries are still increasing, and the first wave of the COVID-19 epidemic was not effectively controlled before April 7, 2020; that is, there was no inflection point in the COVID-19 epidemic.

2.3. Neural Network Based on Conjugate Gradient Method.

Artificial neural networks (ANNs), also known as neural networks, are mathematical models that imitate the behaviour characteristics of animal neural networks and perform distributed parallel information processing. They are widely used in pattern recognition, signal processing, knowledge engineering, expert systems, robot control and other fields [29]. In view of the local convergence of neural networks and the difficulty of slow convergence speeds, the study of the CGNN has attracted the attention of many scholars [30]. In what follows, we briefly introduce the basic idea of the CGNN, which updates the weight and bias values according to the scaled conjugate gradient method.

Considering the neural networks were composed of an input layer, $(L - 1)$ hidden layers, and an output layer. Let $x \in R^n$ and $y \in R^m$ be the input and output of the given neural network, respectively. Furthermore, we denote $x^{(0)} \in R^n$ be the initial input of the neural network. Then the output of the k -th hidden layer of the neural network is obtained from

$$\begin{cases} u^{(k)} = W^{(k)}x^{(k-1)} + b^{(k)}, \\ x^{(k)} = f_k(u^{(k)}), k = 1, 2, \dots, L, \end{cases} \quad (10)$$

where $f_k(\cdot)$ is the activation function of the k -th hidden layer, $x^{(k-1)} \in R^{N_{k-1}}$ is the output of the $(k - 1)$ -th hidden layer, also is the input of the k -th hidden layer, $W^{(k)} = (w_{ij}^{(k)}) \in R^{N_j \times N_i}$ is the weight matrix between the $(k - 1)$ -th hidden layer and the k -th hidden layer, in whose $w_{ij}^{(k)}$ is the weight from the j -th neuron in the $(k - 1)$ -th hidden layer to the i -th neuron in the k -th hidden layer and N_k is the number of the neurons in the k -th hidden layers, $b^{(k)}$ is the bias vector of the k -th hidden layer.

The basic block diagram of the neural network is shown in Figure 4.

Suppose there are n train samples (x_i, y_i) , where $x_i \in R^n$ and $y_i \in R^m$ are the input vector and the label vector, respectively. For the given neural network, the global error function, i.e., the sum of the squared differences of all the training samples, is defined by

$$E(w) := E(W^{(k)}, b^{(k)}) = \frac{1}{2n} \sum_{i=1}^n \|x_i^{(L)} - y_i\|^2, \quad (11)$$

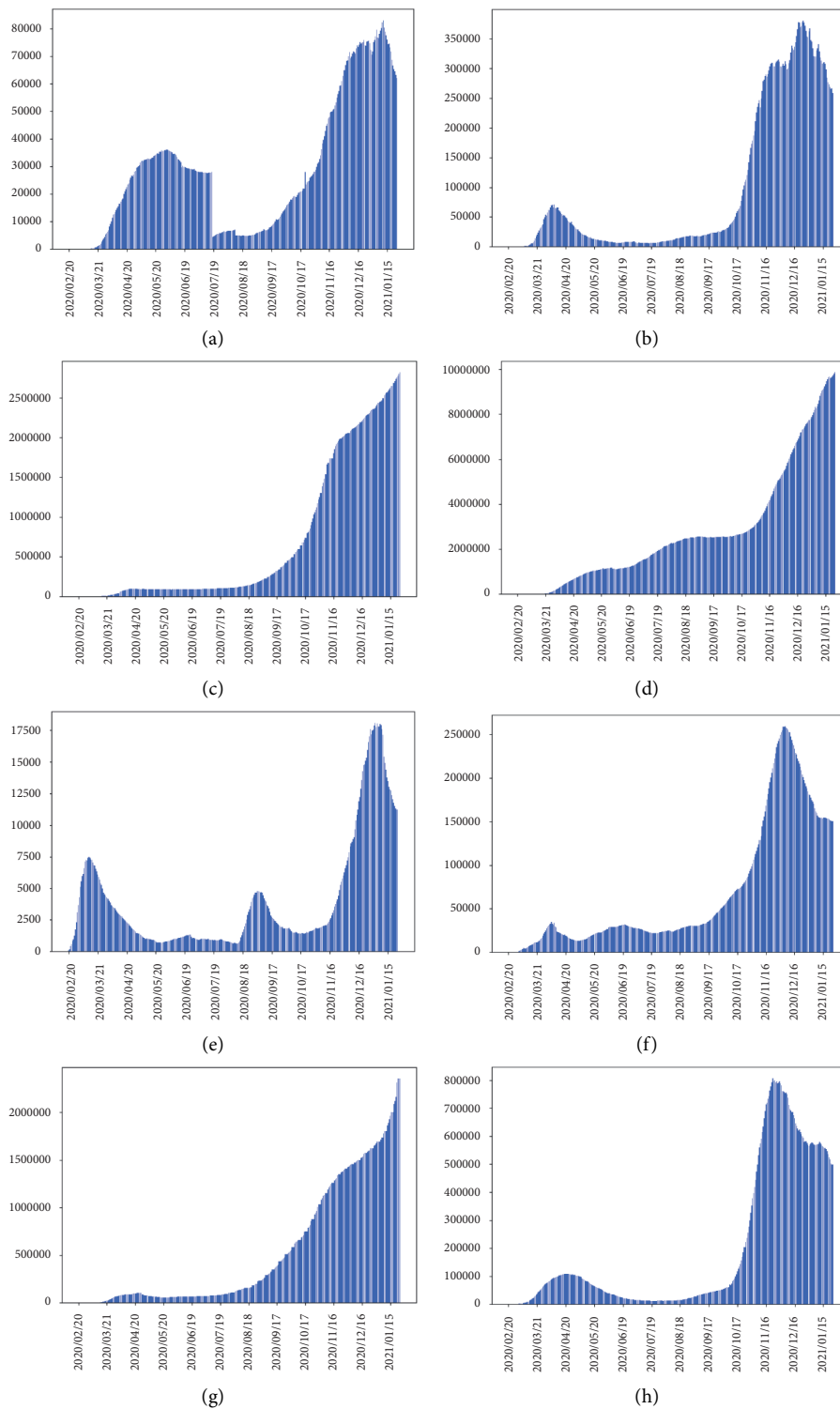


FIGURE 3: Trends of the numbers of existing confirmed cases in eight countries. (a) Canada (b) Germany (c) France (d) The United States (e) South Korea (f) Iran (g) Spain and (h) Italy.

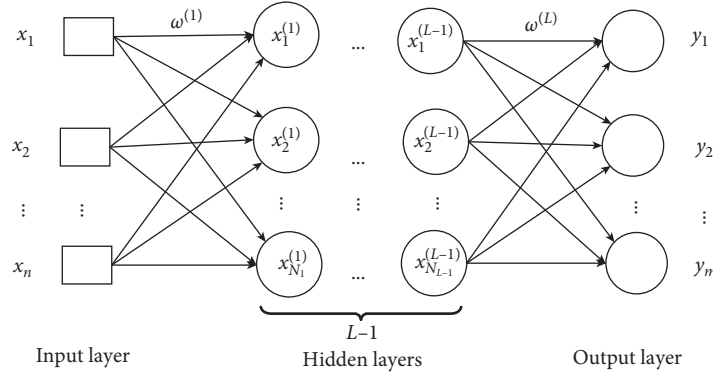


FIGURE 4: Diagram of the neural network.

where w is the set of all parameters of the neural network, including the weight matrix $W^{(k)}$ and biases $b^{(k)}$ are attached to the neural network, $x_i^{(L)}$ is the actual output in the output layer associated with the input vector x_i .

Mathematically, the problem of training a neural network can be expressed as finding the minimum w^* to minimize the global error function $E(w)$, that is,

$$\min E(w) = E(W^{(k)}, b^{(k)}). \quad (12)$$

Unfortunately, there is no guarantee that the objective function $E(w)$ is convex function with respect to $W^{(k)}$ and $b^{(k)}$. This easily leads to the risk of falling into local minima.

In general, one can apply the gradient descent method or other optimization methods to minimize the objective function. The conjugate gradient method is an efficient gradient descent algorithm for solving large-scale linear equations and nonlinear optimization problems [31]. It not only uses the first derivative information, but also overcomes the slow convergence of the steepest descent method and avoids the need to store and calculate the Hesse matrix for the Newton method for calculating its inverse matrix.

In this paper, we consider the neural network based on the scaled conjugate gradient method [30]. For the given neural network, the scaled conjugate gradient method generates a sequence of weights $\{w_k\}$ from the following iterative formula, i.e.,

$$w_{k+1} = w_k + \eta_k d_k, \quad k = 0, 1, \dots, \quad (13)$$

where w_0 is a given initial weight vector, $\eta_k > 0$ is the learning rate, and d_k is the descent search direction of the k th iteration defined by

$$d_k = \begin{cases} -g_k, & k = 0, \\ -g_k + \beta_{k-1} d_{k-1}, & k \geq 1, \end{cases} \quad (14)$$

where $g_k = \nabla E(w_k)$ and $\beta_{k-1} \in \mathbb{R}$. In the literature, there have been proposed several choices for β_k which give rise to distinct conjugate gradient methods with quite different computational efficiency and theoretical properties [31].

The search direction of each iteration of the CGNN is the conjugate combination of the negative gradient direction and the search direction of the previous iteration, and it therefore has the advantages of low storage, few calculations,

and high stability. The choice for β_k used in the scaled conjugate gradient is given by

$$\beta_{k-1} = \frac{|-g_k|^2 - g_k g_{k-1}}{d_{k-1}^T g_{k-1}}. \quad (15)$$

For a more detailed discussion of the CGNN, we refer to [30, 32–35] and the references within.

3. Global COVID-19 Epidemic Prediction and Analysis

The algorithms and models used in this paper are developed in Windows 10 with Python 3.6.0 and MATLAB R2018a, the SVR regression model, and Least Absolute Shrinkage and Selection Operator (LASSO) model are imported from the SVM class of sklearn python library and LASSO class of sklearn python library, respectively. The fitting methods and CGNN model are developed in MATLAB.

3.1. Optimal Fitting Function. It is well-known that the fitting function plays an important role in the accuracy of prediction. Some well-known fitting functions have been considered in the literature, including the four-parameter polynomial function, the normal distribution function, the three-parameter exponential function, the three-parameter hyperbolic function, the two-parameter power function and the four-parameter logical function [11, 22, 23, 25]. The details can be found in Table 1.

Through observation and experimentation, we finally choose the two-parameter power function $f_5(t)$ as the fitting function for fitting c_t . It is the same fitting function to the fitting function considered in [22].

3.2. Dataset. The COVID-19 data repository (<https://github.com/CSSEGISandData/COVID-19>, accessed on 24 January 2022) used in the study was obtained from the Johns Hopkins University Center for Systems Science and Engineering. In this paper, we consider the COVID-19 epidemic data from eight countries including Canada, Germany, France, the United States, South Korea, Iran, Spain and Italy. The starting and ending dates are shown in Table 2.

TABLE 1: Fitting functions.

Fitting function	References
$f_1(t) = \alpha_1 + \alpha_2 t + \alpha_3 t^2 + \alpha_4 t^3$	[23]
$f_2(t) = (1/\sqrt{2\pi}\sigma)\exp(-((t-\mu)^2/2\sigma^2))$	New
$f_3(t) = \alpha_1 \exp(\alpha_2 t) + \alpha_3$	[23]
$f_4(t) = (\alpha_1 + t/\alpha_2 + \alpha_3 t)$	[25]
$f_5(t) = ut^{v-1}$	[22]
$f_6(t) = (\alpha_1/(1 - \alpha_2 \exp(-\alpha_3 t)) + \alpha_4)$	[11]

TABLE 2: Date of COVID-19 outbreak data start and end.

Country	Start of dataset	End of dataset
Canada	2020/01/28	2020/04/07
Germany	2020/01/28	2020/04/07
France	2020/01/28	2020/04/07
The United States	2020/01/28	2020/04/07
South Korea	2020/01/28	2020/04/07
Iran	2020/02/19	2020/04/07
Spain	2020/02/01	2020/04/07
Italy	2020/01/31	2020/04/07

3.3. *Optimal Sliding Window Period.* To avoid inflection point prediction lag due to an excessively large sliding window period, we choose the optimal sliding window period from the integer set $\{1, \dots, 7\}$, i.e., the maximum sliding window period does not exceed one week [22]. Based on the available global COVID-19 epidemic data, we calculate the dynamic transmission rate every k days, and use this value to replace the dynamic transmission rate for these k days. This strategy can reduce the volatility of the data, and overcome the lack of training data.

In this paper, we use the MAE and RMSE as the evaluation indicators for selecting the best sliding window period, and they are defined by

$$MAE = \frac{1}{N} \sum_{t=1}^N |c_t - \hat{c}_t|. \quad (16)$$

and

$$RMSE = \left[\frac{1}{N} \sum_{t=1}^N (c_t - \hat{c}_t)^2 \right]^{(1/2)}, \quad (17)$$

respectively, where \hat{c}_t is the predictive value of the dynamic transmission rate at time t , and N is the length of the time series of the predictive value.

The steps for selecting the optimal sliding window period are provided as follows:

Input: numbers of cumulative confirmed cases $L(t)$, cumulative deaths $D(t)$, and cumulative cures $K(t)$, $t = 1, 2, \dots, N$

Output: optimal sliding window period k

Step 1: calculate the number of existing cases from Equation (1), $t = 1, \dots, N$.

Step 2: calculate the dynamic transmission rate c_t using

$$c_t = 1 + \frac{1}{k} \ln \frac{N(T)}{N(T-k)}, \quad (18)$$

under different values of k , where $t \in [T-k, T-1]$, $T = sk$, $s = 1, 2, \dots$, $k \in \{1, 2, \dots, 7\}$.

Step 3: divide the data set c_t into the training data set and the testing data set, and the ratio of the training set to the testing set is 7:3.

Step 4: fit the training data set based on $f_5(t)$ under different sliding window periods $k, k = 1, 2, \dots, 7$.

Step 5: calculate the predicted values obtained different sliding window periods $k, k = 1, 2, \dots, 7$.

Step 6: calculate the MAE and RMSE of each predicted value under different sliding window periods $k, k = 1, 2, \dots, 7$.

Step 7: calculate the average MAE and RMSE under different sliding window periods, and then select the optimal sliding window period k . Connect the training set and testing set to make it a fitting set, and refit the fitting set under the selected optimal sliding window period.

In what follows, we list the optimal fitting parameters of the fitting function $f_5(t)$, the optimal sliding window period and its evaluation indicators in eight countries as shown in Table 3.

3.4. *Global COVID-19 Epidemic Prediction and Analysis Based on IDTRM.* In order to better reveal the trend of c_t crossing the sliding window period, we consider the so-called IDTRM proposed in [22]. The calculation method of c_t in this paper is improved, as shown in (18). The value of the fitting parameter of the two-parameter power function $f_5(t)$ can reflect the severity of the epidemic in a given country to a certain extent, and can reflect the effect of the development and control of the COVID-19 epidemic [22]. According to the fitting curve expression obtained based on the optimal sliding window period, the solution of $\hat{f}_5(t) = 1$ is the inflection point of the COVID-19 epidemic.

The estimated inflection points of the global COVID-19 epidemic based on IDTRM with the improved dynamic transmission rate c_t calculated from (18) is shown in Table 4.

From Table 4, through a comparison with the actual inflection point, the predicted result shows that the calculated dynamic transmission rate in this paper is suitable for the real situation, but the accuracy rate still needs to be improved.

For this purpose, we will use the CGNN to correct the residuals for improving the predictions accuracy, and to make the model more practical and instructive for the prediction of the global COVID-19 epidemic and new waves of the outbreaks. The details see the below.

3.5. *Global COVID-19 Epidemic Prediction and Analysis Based on IDTRM_CGNN.* To improve the prediction accuracy of IDTRM, we use IDTRM_CGNN to predict the global COVID-19 epidemic. In view of the good self-learning abilities of neural networks, we choose the CGNN to train the early residual set for obtaining the calibrated and predicted residual sets.

TABLE 3: Fitting parameters, optimal sliding window period and evaluation indicators.

Country	u	v	k	MAE	RMSE
Canada	1.3241	0.941	3	0.0241	0.0246
Germany	1.9939	0.8325	2	0.0450	0.0526
France	1.8440	0.8519	6	0.0115	0.0138
The United States	1.4116	0.9264	5	0.0363	0.0376
South Korea	1.8040	0.8288	4	0.0220	0.0239
Iran	1.8880	0.8426	5	0.0228	0.0255
Spain	2.3148	0.7770	1	0.0150	0.0201
Italy	2.1015	0.8060	5	0.0182	0.0195

TABLE 4: Actual and estimated inflection points.

Country	Actual inflection point (A.I.P)	Estimated inflection point (E.I.P)
Canada	2020/05/31	2020/08/01
Germany	2020/04/08	2020/04/17
France	2020/04/16	2020/04/26
The United States	2020/05/31	2020/05/27
South Korea	2020/03/12	2020/03/19
Iran	2020/04/05	2020/04/16
Spain	2020/04/26	2020/04/08
Italy	2020/04/20	2020/04/07

The main steps of IDTRM_CGNN are as follows:

Input: numbers of cumulative confirmed cases $L(t)$, cumulative deaths $D(t)$, and cumulative cures $K(t)$, $t = 1, 2, \dots, N$

Output: estimated inflection points and their corresponding existing confirmed cases

Step 1: calculate the number of existing confirmed cases $N(t)$ from equation (1), $t = 1, \dots, N$.

Step 2: choose $f_5(t)$ as the optimal fitting function, see Section 3.1.

Step 3: calculate the dynamic transmission rate c_t using equation (18)

Step 4: choose the optimal sliding window period k^* , see Section 3.3.

Step 5: calculate the dynamic transmission rate \hat{c}_t by means of $f_5(t)$.

Step 6: calculate the residual of the dynamic transmission rate c_t from

$$\delta_t = c_t - \hat{c}_t, \quad t = 1, 2, \dots, N. \quad (19)$$

Step 7: predict the residual of the dynamic transmission rate δ'_t by means of the CGNN.

The residual sequence $\{\delta_t\}$ of the dynamic transmission rate is divided into the training set and the test set as the input layer variables of the neural network according to a ratio of 7 : 3; the hidden layer contains 2 layers in our experiments; the initial weight vector w_0 in the scaled conjugate gradient method is randomly initialized; the hidden layer activation function of the neural network selects the double curve tangent function, i.e.,

$$\tan hx = \frac{\sin hx}{\cos hx} = \frac{e^x - e^{-x}}{e^x + e^{-x}}, \quad (20)$$

The activation function of the output layer is an identity; the modified residual sequence $\{\delta'_t\}$ and the predicted residual sequence of the dynamic transmission rate are output. All the experiments are repeated 100 times to demonstrate the robustness of the method.

Step 8: calculate the corrected dynamic transmission rate using

$$c'_t = \hat{c}_t + \delta'_t, \quad (21)$$

which is equivalents to

$$\hat{f}'_5(t) = \hat{f}_5(t) + \delta'_t. \quad (22)$$

Step 9: predict the inflection point t^* using $\hat{f}'_5(t) = 1$.

Step 10: predict the number of existing confirmed cases at time t ($t = N + 1, N + 2, \dots$) using

$$\hat{N}(t) = \frac{1}{k} \sum_{i=1}^k \hat{N}(t-i) \exp\{i(c'_t - 1)\}, \quad (23)$$

where $\hat{N}(t)$ represents the estimated numbers of existing confirmed cases at time t . When $N(t-i)$ is unknown, $\hat{N}(t-i)$ is used to instead of it [22].

To verify the robustness and generalization ability of the model, the residuals of the fitted curve and the dynamic transmission rate obtained are used to correct and predict the residuals in combination with the CGNN. The prediction results of the inflection point of the global COVID-19 epidemic based on IDTRM_CGNN are shown in Figure 5.

Figure 5 compares the prediction results regarding the inflection point of the COVID-19 epidemic before and after

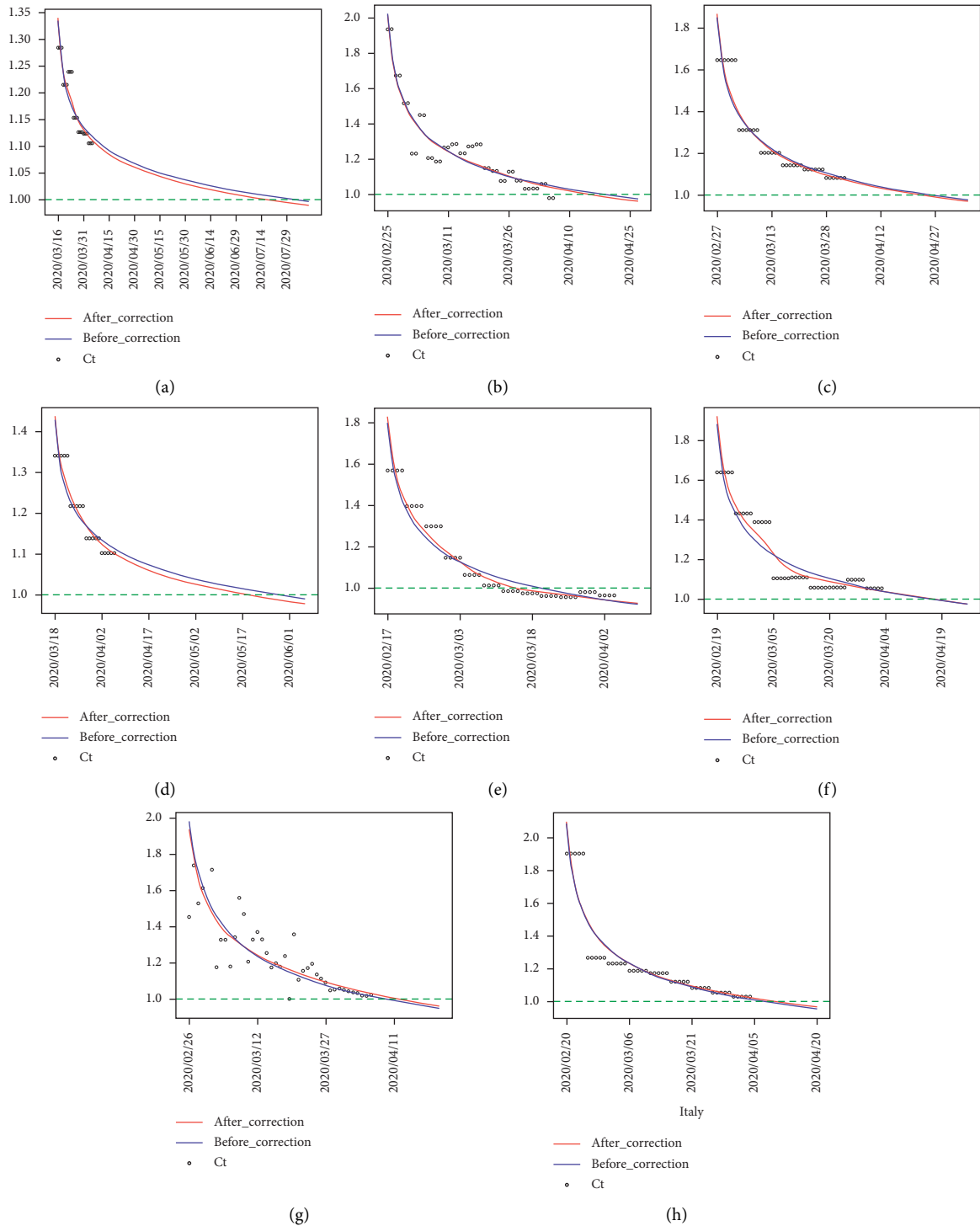


FIGURE 5: Prediction results based on IDTRM_CGNN. (a) Canada (b) Germany (c) France (d) The United States (e) South Korea (f) Iran (g) Spain and (h) Italy.

using the CGNN in Canada, Germany, France, the United States, South Korea, Iran, Spain and Italy. The overall prediction effect of the new model is better than those of some other existing methods, and it can effectively capture the fitting curve with smaller errors while maintaining the original trend. In order to demonstrate the advantages of the model, we use LASSO [36], SVR [37] and DTRM [22] to

process the residuals, In addition, we also add the sliding window period steps to DTRM considered in [22], other unchanged, and the date of inflection point is calculated.

Table 5 provides the predictive inflection point of the COVID-19 epidemic based on LASSO, SVR, DTRM and IDTRM_CGNN. As can be seen from Table 5, our model has a good correction effect on the original curve which deviates

TABLE 5: The inflection point.

Country	A.I.P	IDTRM_CGNN	LASSO	SVR	DTRM [22]
Canada	2020/05/31	2020/07/16	2020/08/04	2020/07/26	2020/06/14
Germany	2020/04/08	2020/04/14	2020/04/17	2020/04/17	2020/04/21
France	2020/04/16	2020/04/22	2020/04/25	2020/04/24	2020/05/29
The United States	2020/05/31	2020/05/17	2020/05/27	2020/05/21	2020/05/08
South Korea	2020/03/12	2020/03/14	2020/03/18	2020/03/14	2020/03/20
Iran	2020/04/05	2020/04/16	2020/04/09	2020/04/17	2020/04/15
Spain	2020/04/26	2020/04/11	2020/04/13	2020/04/09	2020/04/16
Italy	2020/04/20	2020/04/10	2020/04/07	2020/04/07	2020/04/20

TABLE 6: Existing confirmed cases accumulated in 7 days.

Country	ALL(RECC)	ALL(PECC)	MAPE
Canada	108211	117414	8.62 %
Germany	451867	501200	11.42 %
France	608544	522295	14.06 %
The United States	3123671	2902818	7.11 %
South Korea	21416	18928	11.58 %
Iran	183693	247453	37.85 %
Spain	601975	599185	0.99 %
Italy	690617	631831	8.40 %

greatly. For example, the error of the inflection point of the COVID-19 epidemic in Canada has been corrected by half a month. In addition, other curves that deviated less sharply were also corrected to varying degrees, most of which were closer to the true inflection point. Compared with those of DTRM and other statistical models, the predicted inflection points of the COVID-19 epidemic based on IDTRM_CGNN in most countries are closer to reality, indicating that IDTRM after residual correction has higher accuracy and robustness.

In the meantime, IDTRM_CGNN is used to predict the daily number of confirmed cases for 7 days after April 7, 2020 (2020/04/08–2020/04/15), and the mean absolute percentage error (MAPE) is used as the performance index, which is defined by

$$MAPE = \frac{1}{N} \sum_{t=1}^N \frac{|N(t) - \hat{N}(t)|}{N(t)} \times 100\%. \quad (24)$$

In general, we can divide the predictive ability of the model into four levels: high prediction (the error rate is between 0%–10%), good prediction (the error rate is between 10%–20%), feasible prediction (the error rate is between 20%–50%) and poor prediction accuracy (the error rate > 50%).

The real number of existing confirmed cases accumulated (ALL(RECC)) in 7 days, the predicted value of the number of existing confirmed cases (ALL(PECC)) in 7 days and the corresponding MAPE are shown in Table 6.

Table 6 shows that all MAPEs are within a suitable accuracy range. It is worth mentioning that our model achieves high prediction accuracies for Canada, the United States, Spain and Italy, in which their MAPEs are 8.62%, 7.11%, 0.99% and 8.40%, respectively. In addition, the average MAPE for the epidemic prediction in all countries is 10.81 %. This further validates the effectiveness of IDTRM_CGNN.

4. Conclusions and remarks

Aiming at the shortcomings of the traditional SIR and SEIR models in which the basic infection number is difficult to accurately estimate, this paper constructs IDTRM_CGNN to predict the inflection points and the corresponding number of existing confirmed cases of the COVID-19 epidemic in eight countries. The numerical results show that the model proposed in this paper has higher prediction accuracy and robustness. Furthermore, our model can also provide a certain reference value for countries around the world to effectively predict and grasp the development trend of the upcoming wave of the global COVID-19 epidemic.

However, the treatment of various complex influencing factors in this paper is relatively weak, and it is only applicable to countries with a monotonically decreasing trend of the dynamic transmission rate. Due to the characteristics of the fitting function, in cases with few data, IDTRM_CGNN is prone to overfitting.

The future research direction of this paper: Whether IDTRM_CGNN is universal for other infectious diseases is a topic worthy of continuing research. In addition, studying the use of rolling prediction technology to characterize the epidemic in real time, and performing online correction and updating of the dynamic transmission rate with the help of data assimilation methods are also future research directions of this article.

Data Availability

The data used to support the findings of this study are available from the corresponding author upon request.

Conflicts of Interest

The authors declare that there are no potential conflicts of interest in this study.

Authors' Contributions

All the authors have seen and approved the manuscript to be published.

Acknowledgments

This work was supported by the National Natural Science Foundation of China (no. 11971302), the National Statistical Science Research Project of China (no. 2020LY067), and National Innovation and Entrepreneurship Training Program for College Students (no. 202110856037).

References

- [1] N. M. Ferguson, D. Laydon, G. Nedjati-Gilani, N. Imai, and A. C. Ghani, "Impact of non-pharmaceutical interventions (NPIs) to reduce COVID-19 mortality and healthcare demand," *British Medical Journal*, vol. 82, no. 5, pp. 201–157, 2020.
- [2] J. T. Wu, K. Leung, and G. M. Leung, "Nowcasting and forecasting the potential domestic and international spread of the 2019-nCoV outbreak originating in Wuhan, China: a modelling study," *The Lancet*, vol. 395, no. 10225, pp. 689–697, 2020.
- [3] C. Caetano, M. L. Morgado, P. Patricio, J. F. Pereira, and B. Nunes, "Mathematical modelling of the impact of non-pharmacological strategies to control the COVID-19 epidemic in Portugal," *Mathematics*, vol. 9, no. 10, 2021.
- [4] R. Ghostine, M. Gharamti, S. Hassrouny, and I. Hoteit, "An extended SEIR model with vaccination for forecasting the covid-19 pandemic in Saudi Arabia using an ensemble kalman filter," *Mathematics*, vol. 9, no. 6, 2020.
- [5] Y. Xiao, X. Feng, Z. Xu, X. Wang, and S. Tang, "When will be the resumption of work in Wuhan and its surrounding areas during COVID-19 epidemic? A data-driven network modeling analysis," *Scientia Sinica Mathematica*, vol. 50, no. 7, pp. 969–978, 2020, In Chinese.
- [6] Z. Yang, Z. Zeng, K. Wang, S. Wong, and J. He, "Modified SEIR and AI prediction of the epidemics trend of COVID-19 in China under public health interventions," *Journal of Thoracic Disease*, vol. 12, no. 2, pp. 165–174, 2020.
- [7] D. Li, J. Lv, G. Botwin, J. Braun, and D. P. B. Mcgovern, "Estimating the Scale of COVID-19 Epidemic in the United States: Simulations Based on Air Traffic Directly from Wuhan, China," *MedRxiv*, 2020.
- [8] Z. Liu, P. Magal, and G. Webb, "Predicting the number of reported and unreported cases for the COVID-19 epidemics in China, South Korea, Italy, France, Germany and United Kingdom," *Journal of Theoretical Biology*, vol. 509, Article ID 110501, 2021.
- [9] S. W. Hermanowicz, "Simple Model for COVID-19 Epidemics-Back-Casting in China and Forecasting in the US," *MedRxiv*, 2020.
- [10] H. Ankarali, S. Ankarali, H. Caskurlu, Y. Cag, and H. Vahaboglu, "A statistical modeling of the course of COVID-19 (SARS-CoV-2) outbreak: a comparative analysis," *Asia-Pacific Journal of Public Health*, vol. 32, no. 4, pp. 157–160, 2020.
- [11] Z. Liu, "Uncertain growth model for the cumulative number of COVID-19 infections in China," *Fuzzy Optimization and Decision Making*, vol. 20, no. 2, pp. 229–242, 2021.
- [12] D. Parbat and M. Chakraborty, "A python based support vector regression model for prediction of COVID19 cases in India," *Chaos, Solitons & Fractals*, vol. 138, Article ID 109942, 2020.
- [13] C. Yesilkanat, "Spatio-temporal estimation of the daily cases of COVID-19 in worldwide using random forest machine learning algorithm," *Chaos, Solitons & Fractals*, vol. 140, Article ID 110210, 2020.
- [14] S. F. Ardabili, A. Mosavi, P. Ghamisi, and F. Ferdinand, A. R. Varkonyi-Koczy, U. Reuter, T. Rabczuk, and P. M. Atkinson, "COVID-19 outbreak prediction with machine learning," *Algorithms*, vol. 13, no. 10, 2020.
- [15] F. Rustam, A. A. Reshi, A. Mehmood, S. Ullah, and G. S. Choi, "COVID-19 future forecasting using supervised machine learning models," *IEEE Access*, vol. 8, no. 1, Article ID 101489, 2020.
- [16] F. Shahid, A. Zameer, and M. Muneeb, "Predictions for COVID-19 with deep learning models of LSTM, GRU and Bi-LSTM," *Chaos, Solitons & Fractals*, vol. 140, Article ID 110212, 2020.
- [17] A. Zeroual, F. Harrou, A. Dairi, and Y. Sun, "Deep learning methods for forecasting COVID-19 time-series data: a comparative study," *Chaos, Solitons & Fractals*, vol. 140, Article ID 110121, 2020.
- [18] H. Abbasimehr and R. Paki, "Prediction of COVID-19 confirmed cases combining deep learning methods and Bayesian optimization," *Chaos, Solitons & Fractals*, vol. 142, Article ID 110511, 2021.
- [19] A. Bezerra and E. Santos, "Prediction the daily number of confirmed cases of COVID-19 in Sudan with ARIMA and holt winter exponential smoothing," *International Journal of Development Research*, vol. 10, no. 8, Article ID 39408, 2020.
- [20] M. Maleki, M. R. Mahmoudi, M. H. Heydari, and K. -H. Pho, "Modeling and forecasting the spread and death rate of coronavirus (COVID-19) in the world using time series models," *Chaos, Solitons & Fractals*, vol. 140, Article ID 110151, 2020.
- [21] N. E. Huang and F. Qiao, "A data driven time-dependent transmission rate for tracking an epidemic: a case study of 2019-nCoV," *Science Bulletin*, vol. 65, no. 6, pp. 425–427, 2020.
- [22] Y. Hu, Y. Liu, L. Wu et al., "A dynamic transmission rate model and its application in epidemic analysis," *Operations Research Transactions*, vol. 24, no. 3, pp. 27–42, 2020, In Chinese.
- [23] Y. Hu, J. Kong, L. Yang et al., "A dynamic growth rate model and its application in global COVID-19 epidemic analysis," *Acta Mathematicae Applicatae Sinica*, vol. 43, no. 2, pp. 452–467, 2020, In Chinese.
- [24] Y. Zhang and J. Li, "Prediction and analysis of propagation of novel coronavirus pneumonia epidemic based on SIR model," *Journal of Anhui University of Technology*, vol. 37, no. 1, pp. 94–101, 2020, In Chinese.
- [25] X. Xie, K. Luo, Y. Zhang et al., "Nonlinear combinational dynamic transmission rate model and COVID-19 epidemic analysis and prediction in China," *Operations Research Transactions*, vol. 25, no. 1, pp. 17–30, 2020, In Chinese.
- [26] X. Xie, K. Luo, Z. Yin, and G. Wang, "Nonlinear combinational dynamic transmission rate model and its application in global COVID-19 epidemic prediction and analysis," *Mathematics*, vol. 9, no. 18, 2021.
- [27] S. Layne, J. Hyman, D. Morens, and J. Taubenberger, "New coronavirus outbreak: framing questions for pandemic

- prevention," *Science Translational Medicine*, vol. 12, no. 534, Article ID eabb1469, 2020.
- [28] J. Guan, "The Parameter Estimation and Bias Correction of Short-Term Interest Rate Model," *Southwestern University of Finance and Economic*, Doctoral Dissertation, In Chinese, 2014.
- [29] Z. Waszczyszyn, *Fundamentals of Artificial Neural Networks*, MIT Press, Cambridge, MA, USA, 1999.
- [30] M. F. Moller, "A scaled conjugate gradient algorithm for fast supervised learning," *Neural Networks*, vol. 6, no. 4, pp. 525–533, 1993.
- [31] W. Sun and Y. Yuan, *Optimization Theory and Methods*, Springer US, Philadelphia, NY, USA, 2006.
- [32] E. M. Johansson, F. U. Dowla, and D. M. Goodman, "Backpropagation learning for multilayer feed-forward neural networks using the conjugate gradient method," *International Journal of Neural Systems*, vol. 2, no. 4, pp. 291–301, 1991.
- [33] X. Zhang, S. L. Broschat, and P. J. Flynn, "Inverse imaging of the breast using a conjugate gradient-neural network technique," *Journal of the Acoustical Society of America*, vol. 103, no. 5, pp. 2792–2793, 1998.
- [34] J. Wang, W. Wu, and J. M. Zurada, "Deterministic convergence of conjugate gradient method for feedforward neural networks," *Neurocomputing*, vol. 74, no. 14–15, pp. 2368–2376, 2011.
- [35] E. Ioannis and P. Panagiotis, "A new conjugate gradient algorithm for training neural networks based on a modified secant equation," *Applied Mathematics and Computation*, vol. 221, pp. 491–502, 2013.
- [36] R. Tibshirani, "Regression shrinkage and selection via the lasso," *Journal of the Royal Statistical Society: Series B*, vol. 58, no. 1, pp. 267–288, 1996.
- [37] A. J. Smola and B. Schölkopf, "A tutorial on support vector regression," *Statistics and Computing*, vol. 14, no. 3, pp. 199–222, 2004.

Research Article

Pattern Recognition Characteristics and Neural Mechanism of Basketball Players' Dribbling Tactics Based on Artificial Intelligence and Deep Learning

Xuhui Song¹ and Linyuan Fan ²

¹Department of Sports, Capital University of Economics and Business, Beijing 100070, China

²College of Mathematics and Data Science, Minjiang University, Fuzhou 350108, Fujian, China

Correspondence should be addressed to Linyuan Fan; fanlinyuan@mju.edu.cn

Received 23 January 2022; Revised 21 February 2022; Accepted 5 March 2022; Published 27 March 2022

Academic Editor: Wei Liu

Copyright © 2022 Xuhui Song and Linyuan Fan. This is an open access article distributed under the Creative Commons Attribution License, which permits unrestricted use, distribution, and reproduction in any medium, provided the original work is properly cited.

There are many factors that affect a player's overall basketball ability, and different factors will have different effects. The effect is mainly manifested in the difference of offensive and defensive data of basketball players in basketball games. In the basketball field, the formulation of existing training plans mainly relies on the manual observation and personal experience of coaches. This method is inevitably subjective. The pattern recognition of dribbling tactics is one of the important factors. A proper dribbling tactic can make the team achieve better results. In order to discover different dribbling characteristics, reanalyze the connotation and manifestation of basketball speed and strive to analyze the factors that affect basketball speed reasonably and accurately. The deep learning algorithm simulates the thinking process of the human brain neurons through the computer method and then realizes the function of the computer to automatically learn the data characteristics and complete the complex data analysis task. We use artificial intelligence and deep learning to simulate various dribbling tactics of players and find out the rules to improve players' abilities. The results of the study prove that developing a suitable dribbling tactical model for basketball players can increase their competitive ability by more than 10%, reduce the damage to players, and prolong their careers. Generally speaking, athletes' injuries can be reduced by more than 15%. This shows that the pattern recognition characteristics and neural mechanisms of dribbling tactics are extremely important to basketball players.

1. Introduction

With the rapid developments of economic globalization and the expanding exchanges between countries, the level of development of sports has become an important indicia to measure the social development of a country or region and the progress of human civilization [1]. There are many forms of sports classification, which can be broadly divided and classified into mass sports and voluntary sports, mainly including sports culture, sports education, sports-related activities, sports competitions, sports infrastructure, sports organizations, sports technology, and many other elements [2].

By being part of the social infrastructure, the sports business is an important part of the modern service business.

The high-speed development of the sports sector is a new economic and employment driver for the socioeconomic growth of the region [3]. It is now the pillar for developed economic world. In North America, Western Europe, and Japan, the industrial value of sports and its related industries has been located among the top ten of the national industries in terms of years of production. Under the environment of sustained and stable development of our country's macro-economic economy, with the increase in per capita income of residents, the substantial improvement of people's living standards and people's growing spiritual, cultural, and material needs will continue to promote the development of sports in the country. The dribbling tactics pattern recognition feature can provide suitable training methods according to the individual characteristics of the athletes,

improve the training level of basketball players, and provide support for high-level basketball games [4]. Scholars at home and abroad have related research on the pattern recognition characteristics and neural mechanisms of athletes' dribbling tactics; Taniguchi fixed a type of sensor equipment on the back of a player's hand in basketball to collect accumulative and angular accelerations data of the player's hand over the jump shot process. The jump throw process is divided into a four phase process, and the pitch position of each phase is analyzed and remedied by voice feedback to help the athlete correct his shooting posture. However, the jump shot posture of the athlete is reflected by the motion of his arm and leg postures [5]. Paul compared the physical performance of performers in different forms of competition and training, proving that wearables are effective. The quantification of basketball is very helpful but does not involve specific basketball quantification studies [6]. Nguyen and Yang used acceleration sensors to construct a basketball gesture recognition system, collected the lower limb data of basketball players, and completed the basketball movement. For the recognition of 8 kinds of actions, the article only uses acceleration data as a reference, the constructed data set has a single feature, and its average recognition accuracy is less than 70% [7].

Deep learning is not originally a stand-alone learning method but itself uses both supervised and unsupervised learning methods to train deep neural networks. However, due to the rapid development of the field in recent years and the introduction of specific learning tools (such as residual networks), it is increasingly seen as a separate learning method. Initially, deep learning was a learning process that used deep neural networks to solve feature representations. Deep neural networks themselves are not a completely new concept and can be broadly understood as a neural network structure containing multiple hidden layers. In order to improve the training of deep neural networks, adjustments have been made to aspects such as the method of connecting neurons and the activation function. Many of these ideas have been developed in the early years, but due to the lack of training data and computational power at the time, the results were not as good as they could have been. Deep learning has decimated a wide range of tasks, making seemingly every machine-assisted function possible. Driverless cars, preventative healthcare, and even better movie recommendations are all close at hand, or on the horizon.

This article aims to study some of the ideas that we have generated based on previous research results. In recent studies at home and abroad, few have included the dribbling mode of basketball players into the comprehensive evaluation of players. This article highlights the role of players' dribbling patterns in the comprehensive evaluation. When evaluating the offensive and defensive abilities of players, some new variables are also added to replace outdated variables. This paper analyses the characteristics of basketball players' technical and tactical use, particularly in relation to key games and key points, in order to discover the common characteristics of basketball players' technical and tactical use. Through comprehensive and detailed research and analysis, the future directions are drawn in the

conclusion part, a new method of comprehensive evaluation of basketball players is drawn, and the structural equation of comprehensive evaluation constructed is used to analyze the relative importance of various indicators of players and conclude the determinants of player value. Cluster analysis was used to calculate the dribbling patterns of the athletes and a new cluster evaluation function was added to guide the cluster analysis process. The scientific validity of the experimental protocol was verified by comparing the experimental group with the control group.

2. Dribbling Tactics Pattern Recognition Characteristics and Neural Mechanism Research Methods

2.1. Basketball. Sports itself has its own unique characteristics: physical activity is used as a means to exercise the body. In basketball training, the basic skills training mainly includes technical training such as ball control, dribbling, passing, catching, shooting, and step adjustment [8, 9]. In specific training, the coaches need to carefully explain the basic movements and demonstrate the correct technical movements and promptly correct various problems that arise during the training of the athletes, so as to encourage the athletes to master the correct and standardized technical movements [10]. In the training practice of basketball shooting techniques, many athletes often have irregular technical movements during the training process due to their own movement habits and do not fully respect the objectiveness of basketball shooting. The law cannot realize the reasonable control of the ball by the body, thus affecting the improvement of basketball technical training results and the improvement of shooting percentage. In order to ensure that athletes are proficient in basic basketball movements, athletes spend most of their training time on repetitive training of single movements [11].

Sport is about developing healthy behaviours, appreciating the spirit of sport, and regulating the rhythm of the mind and body. Sport is a behavioural activity involving a set of rules, bound by habits, involving physical strength and skill, often of a competitive nature. Whether you are a professional athlete or an ordinary person, a certain amount of daily exercise is good for your physical and mental health and relaxes you.

It is very important to make sure that the cardinal action is performed with standard accuracy. In the training practice of basketball shooting techniques, many athletes often have irregular technical movements during the training process due to their own movement habits and do not fully respect the objectiveness of basketball shooting. The law cannot realize the reasonable control of the ball by the body, thus affecting the improvement of basketball technical training results and the improvement of shooting percentage. In order to ensure that athletes are proficient in basic basketball movements, athletes spend most of their training time on repetitive training of individual movements. For the specification of basic movements, it is a necessity to have the supervision and tutorials of a coach to provide real-time guidance and advice to the athletes [12]. This manmade

guidance requires a lot of time and is a complex work for the coaches. Basketball players have great training intensity. A reasonable intensity is conducive to improving the athlete's competitive ability. However, too high intensity can easily cause damage to the athletes:

One-handed approach: take a right-handed in situ one-handed over-the-shoulder shot as an example. Start by holding the ball with both hands; then, lead the ball over the front of the right shoulder with the right arm bent at the elbow, the elbow joint slightly inward, the upper arm about level with the shoulder joint and the forearm about 90 degrees to the upper arm. The five fingers of the right hand are naturally open, the wrist is bent back, the palm is free, the outer edge of the palm and the part above the root of the fingers are used to hold the ball at the bottom of the back, and the left hand holds the left side of the ball.

How to hold the ball with both hands: take a two-handed chest shot in situ as an example. The five fingers of both hands are naturally open, and the ball is held by the back side of the ball above the root of the fingers, with the two thumbs forming a figure of eight opposite each other and the palm hollowed out. Both elbows are naturally down and the shoulders are relaxed, placing the ball between the chest and jaw.

Direct hit aiming point: usually aim for the point of the basketball rim closest to you. This method aims at a solid target and is suitable for shooting hollow-point baskets from any position on the court. It is also advocated to aim at the centre of the rim, a target that is consistent with where the ball will land and facilitates force.

The aiming point for a touchboard shot: this is the point at which the ball is thrown at the rim to make it rebound into the basket. If the shooter is located in an area with an angle of 15 to 45 degrees to the rim, the effect of the touchboard shot is better, especially in areas close to the 30 degree angle. The aiming point of the touchboard shot should be reasonably chosen according to the angle, distance, and curvature of the shot. The general rule is that the smaller the angle, the further the distance and the higher the arc and the further and higher the touchboard point is from the rim; conversely, the closer and lower it is.

Low arc: the ball's flight path is short and the power is easy to control, but because the flight path is low and flat, the basketball rim is exposed to a small area under the ball and it is not easy to shoot. **Medium arc:** the highest point of the ball's flight arc is roughly on a horizontal line with the top edge of the rim, with most of the basket exposed underneath the ball, making it a more suitable throw. **High arc:** the ball falls close to vertical direction, the area of the rim is almost completely exposed underneath the ball, and the ball can easily get into the basket. However, the flight path of the ball is too long and not easily controlled, which can actually reduce the hitting rate.

2.2. Basketball Player Injury Detection. Various injuries that occur in sports are called sports injuries. Basketball is a high-frequency sports event with sports injuries due to its multiple physical contact, fast speed, and strong antagonism [13]. However, there are many reasons for sports injuries, such as an insufficient sense of self-protection, preparatory activities, incorrect technical movements, and poor physical condition. Among them, there are reasons that account for a larger number of factors. Whether in an incidental movement in training or competition, most sports injuries are so unpredictable that it becomes crucial to reduce them. Action patterning is the process by which the muscles, fascia, and histotoconia execute the corresponding action program stored in the brain under the control of the mesocortical system. This executed process takes part in certain temporal and spatial steps [14].

There are many actions to prevent basketball sports impairment. Traditional preventions of basketball sports injuries mainly be concentrated on pregame warm-up, postgame relaxation, and flexibility and strength training; however, the appearances of functional exercise have brought new ideas and functions to the prevention of sports and athletic injuries. Training is stressed on the importance of movement, that is "space is movement," and the correct movement pattern is the key to the prevention of sports injury. From this perspectival point of view, simply stretching and strengthening muscles do not change their original mis-sporting habits. Wrong motion habits are the key culprit of sports injuries. Therefore, in athletic injury prevention, it is necessary to improve the nerves. Further correction of faulty motor patterns or habits based on flexibility and stability can truly reduce the odds of sports injuries [15].

Current procedures for measuring body mass include overall body mass measurement and select body mass measurement. Among them, the measurement the whole body composition includes measurement methods of bio-resistance resistance, total potassium estimation algorithm, body water treatment, DXA method, and a submersible weighing method.

Bioresistance immunoassay: it is a method to determine the fat content of the human body that is derived from the electrical resistivity of the human body. Its basic approach is to use the electrical resistance of human cells and the organization to determine the electrical conductivity of the human body components and then test its resistance level; the more the water from the organization, the stronger its electrical conductivity and the lower its resistivity, and conversely, the less the water from the organization, the weaker its electrical conductivity and the higher its electrical resistivity. For example, the fatter the body's tissue with a low water concentration, the lower its conductive properties and the higher the electric resistivity. The higher the water content of muscle muscles, the more conductive they are and the lower their resistivity [16, 17]. The fat mass of the body is then estimated by inference. This method is in an economic and practical

way and is widely used in various medical institutions and in general for households.

Total potassium algorithm for calculation: this method focuses on determining the body fat levels and lean body masses based on the total potassium content of the body. It is generally accepted that the potassium content in the fat-free body weight of the human body is constant, so that the body fat content and lean weight can be calculated by calculating the total potassium in the body (mainly by having measured the 40k content in the body; this is in view of the fact that 40k represents 0.00118% of the total potassium composition) [18]:

$$q = \beta * \partial * \left[\left(\frac{t_1}{100} \right)^4 - \left(\frac{t_2}{100} \right)^4 \right]. \quad (1)$$

Body water technique: this is a procedure to estimate both the body's lean body mass and body fat by a measurement of the total amount of body water. The reason for this has been that the water content is stable for lean body mass. By delivering certain chemicals (bilin, ethanol, etc.) to the body, the degree of dilution of these chemicals can be used to estimate the total amount of volume of fluid in the body and then the body fat weight and slender body mass of the body can be also to be calculated [19].

$$Q = \frac{Y}{t} A_n (T_m - T_n). \quad (2)$$

The DXA is the method of calculating the body component (bone mineral content, body fat, muscle, etc.) by an absorption measurement of X-rays. The basic technique is to use high and low with low-energy X-rays to determine the absorption of human and fatty tissues, including dual-energy X-ray absorptiometry and spectroscopic photon assays [20].

$$\alpha = \frac{2.057 f * (v * p)^{0.8}}{d^{0.2}}. \quad (3)$$

Underwater weighing method: use water as a medium to measure the body's volume and body density and then calculate the proportion of body fat to calculate the body fat and lean body weight. This is a more classic body composition method [21].

$$T = \sqrt{\frac{(a_{x1} - a_{x-1})^2 + (a_{y1} - a_{y-1})^2 + (a_{z1} - a_{z-1})^2}{100}}. \quad (4)$$

Sports can improve body composition and reduce body fat. Especially for people who often insist on physical exercises, not only can their various functions of the body be greatly improved but their athletic ability can also be significantly improved, so athletic ability and body composition can influence and promote each other, thereby improving people's good health and physical fitness.

2.3. Neural Mechanism. The concept of neural mechanism is opposite of biological neural network. People are inspired by the organization of biological neurons and build artificial neural networks. Therefore, there are similarities in the organization of the entire network from the most basic unit neuron. A neuron receives different signals from different neurons from several dendrites and performs a complex summation process in the cell body. The output of neurons is

$$y = f \left(\sum_{i=1}^n w_i x_i - \delta \right), \quad (5)$$

where δ represents the threshold, assuming that there are q pairs of samples; for the p -th sample, the error is defined as

$$J(W, b)_p = \frac{1}{2} \|y^n - y\|^2. \quad (6)$$

Find the average loss for the entire sample set, and then perform a uniform gradient descent:

$$J(W, b) = \frac{1}{q} \sum_{p=1}^q J(W, b)_p. \quad (7)$$

Find the partial derivatives and find out their respective contributions to the final error. This process can be expressed by the following formula:

$$w_{ij}^{(l)} = w_{ij}^{(l)} - lr \frac{\partial (j(W, b))}{\partial w_{ij}^{(l)}}. \quad (8)$$

The convolutional layer is different from the ordinary fully connected layer in that it uses the method of local connection and weight sharing.

2.4. Model Recognition. For athletes' dribbling patterns, we can calculate them through cluster analysis. In general cluster analysis, because the distribution characteristics of the clustered data sets are unknown, the limitations of individual cluster evaluations make the calculation results unclear. Ideally, usually the function that guides the trend of clustering results or the evaluation function of clustering results is often only one; that is, the analysis process is actually a single-objective optimization process, and the clustering results obtained often depend on an evaluation index. Its distribution characteristics are not known in advance, so the evaluation mechanism for clustering processing should not be determined and the applicability of the clustering algorithm is not high. The intraclass distance and the interclass distance of each cluster can be considered at the same time as the evaluation mechanism of clustering. Therefore, this paper adds a new cluster evaluation function to guide the cluster analysis process. It can be processed with the following functions:

$$F(u) = \int |Du| dx dy + \frac{1}{2} \lambda \|u - u_0\|^2. \quad (9)$$

The corresponding equation is

$$-\operatorname{div}\left(\frac{\nabla u}{|\nabla u|}\right) - \lambda(u_0 - u) = 0. \quad (10)$$

An optimization problem can be transformed into a function; let the error function be

$$E(x, y) = \operatorname{div}\left(\frac{\nabla u}{|\nabla u|}\right) - \lambda(u - u_0). \quad (11)$$

Assuming that the final output is an ideal model, we can get

$$\begin{aligned} u(x, y) &= N(u_0(x, y), w), \\ t(s) &= \exp\left(-\int_0^s \kappa(t) dt\right). \end{aligned} \quad (12)$$

From it, we see that

$$\partial = 1 - t(s) = 1 - \exp\left(-\int_0^s \kappa(t) dt\right). \quad (13)$$

When Δs approaches zero, use the following differential equation to illustrate the change:

$$\frac{dI}{ds} = T(s) * \rho(s) * A = T(s) * \kappa(s). \quad (14)$$

We used generally the following equations:

$$x(k+1) = Ix(k) + Jv(k), k = 1, 2, \dots \quad (15)$$

The two-party group has the following targets for performing the test:

$$K = \sum_{k=1}^{\infty} [x^i(k)Jx(k) + r^i(k)cJ], \quad (16)$$

where the weighting matrix Q is

$$Q = \frac{1}{2a^2r^{-1}} \left(\frac{2b^2}{a^2r^{-1}} p - t \right)^{-1} [a^2r^{-1}t^2 + 2(1-b^2)t]. \quad (17)$$

Clustering is an important technique and method in the process of data mining and is a crucial part of the data mining process, which makes it an important research direction in the field of data mining. The process of clustering means that objects are grouped into a certain category or objects with similar properties are grouped together according to their characteristics. The essence of cluster analysis is to use an effective clustering algorithm to obtain classes of data and to group the data with large differences into different clusters, so that the resulting clusters are a collection of data objects. Cluster analysis does not require knowledge guidance, and it obtains meaningful data classification directly from the data and is a form of unsupervised learning. Clustering techniques generally start from the data, and there is no fixed classification standard. Clustering results usually vary depending on the clustering method, and the same data set may show different clustering results if different clustering methods are used.

The difference between clustering and classification is that the classes required for clustering are unknown. Cluster analysis is very rich and includes systematic clustering, ordered sample clustering, dynamic clustering, fuzzy clustering, graphical clustering, and cluster forecasting. Classification refers to the grouping of species, classes, or properties.

Characteristics of clustering methods: cluster analysis is simple and intuitive. Cluster analysis is mainly used in exploratory research, the results of its analysis can provide several possible solutions, and the selection of the final solution requires the subjective judgment of the researcher and subsequent analysis; regardless of whether there are really different categories in the actual data, using cluster analysis can obtain a solution divided into several categories; the solution of cluster analysis depends entirely on the clustering variables selected by the researcher, and adding or deleting some variables may have a substantial impact on the final solution. The researcher should pay particular attention to the various factors that may affect the results when using cluster analysis. Outliers and special variables have a large impact on clustering. When categorical variables are measured on inconsistent scales, prior standardisation is required.

In general, the clustering analysis algorithm is divided into the following steps: data preprocessing including data standardisation, data denoising, data feature selection, etc. The main role is to transform the original data into a form of data that can be easily processed, so as to improve the quality of the clustering results. This process gives the data new features by extracting the data features, selecting a suitable feature set, effectively removing isolated points, and preparing the groundwork for subsequent processing. Definition of data similarity: the measure of similarity between different data objects in the same feature space has a great impact on clustering, and due to the diversity of data features and types, similarity must be defined carefully. Typically, differences between data are assessed by defining a distance measure in the feature space, with Euclidean distance being the most commonly used method. Clustering or grouping: this step is used to group data objects into classes, commonly used in division-based and hierarchical methods. This step is the core of the cluster analysis process, and the choice of cluster analysis algorithm is crucial. In addition to the two clustering methods mentioned above, there are model-based clustering algorithms, density-based clustering algorithms, and grid-based clustering algorithms. The data stream clustering analysis algorithm studied in this paper is the grid density-based data stream clustering algorithm. Output and evaluation of results: after the above steps, the results are output and evaluated, i.e., the evaluation of the quality of clustering, and the results are analysed according to certain evaluation rules, which is also the process of measuring the merits of clustering algorithms. The output of the results is generally presented to the user certain clustering results, including clustering accuracy, clustering efficiency, clustering results shape, etc., and different clustering analysis algorithms play to present different forms.

3. Athletes' Dribbling Tactics Pattern Recognition Characteristics and Neural Mechanism Experiments

3.1. Subject. This article first randomly selects 5 members of the school team as the experimental group and the remaining 5 members of the school team as the control group. Combined with the current level of players' dribbling, a three-week experiment was conducted using the developed training plan. The training plan was developed by the same coach, and the training and testing were carried out in their respective training venues. The experimental group used new indicators for intervention training. Its difference and effectiveness are compared, and they are analyzed with reference to the coach's observation and evaluation of the athletes. The control group adopts traditional training methods, strictly controls the entire experimental process, and allocates phase tasks reasonably. After the third week of training, the experimental subjects will be tested on all indicators again, and the experimental group and the control will be compared qualitatively through the athletes' performance in the competition. Differences between groups are used to verify the scientific nature of the experimental program.

3.2. Data Collection. The data were collected by E-Prime software, and the analysis index is the reaction time and accuracy rate of sports decision-making. The data obtained in the formal experiment only are analyzed. Data (1.5%) for which decision-making response time and correct response time were greater than or less than three standard deviations were excluded. Due to the "biological wall" time of simple visual reaction, the limit time of reaction was 220 ms. Therefore, the data that were less than 220 ms in response time (accounting for 2.51%) were removed. SPSS17.0 statistical software package was used to perform repeated measures analysis of variance on behavioral data. We will display some of the collected data, as shown in Figure 1.

3.3. Experimental Purpose. This study uses general situational decision-making tasks to explore the behavioral characteristics and cognitive mechanisms of high-level basketball players in colleges and universities.

4. Athletes' Dribbling Tactics Pattern Recognition Characteristics and Neural Mechanism Experimental Analysis

4.1. Status of Players. We first make statistics on the current basketball level of the two groups of players in order to compare the changes in various data after receiving the dribbling pattern and tactical recognition, as shown in Table 1.

As shown in Figure 2, before the athletes selected in our school undergo separate training, although there is a certain gap in the parameters of their dribbling, in general, the gap is not obvious. The athletes dribble on the spot and turn

around to dribble. Such skill levels are basically around 2. We also conduct statistics on the physical fitness of these athletes and compare their changes before and after tactical pattern recognition. The details are shown in Table 2.

As shown in Figure 3, the physical fitness of basketball players is higher than the average level of the average person. There is not much difference between the players selected this time, and the contrast changes are more representative. In general, the players maintain a good level of physique and muscles, the value is basically around 2.2, the performance of the lower limbs is not very satisfactory, and the score is only about 1.9 and needs to be strengthened.

4.2. Data Preprocessing. In the data acquisition stage, the data signals collected by the sensor equipment are usually affected by external or own interference. These interferences include jitter generated by the body during human movement or irregular signals generated by the peripheral environment; the signal acquisition equipment itself having measurement errors; and the signal being inaccurate due to the displacement of the node position during the movement. In practical applications, the collected raw data cannot be directly used for analysis and calculation. In order to obtain a more accurate signal, it needs to be preprocessed after the signal is collected. The collected data required for basketball are shown in Figure 4.

As for the dribbling mode, generally speaking, it can be divided into five types, namely, high dribble, low dribble, emergency stop dribble, reverse dribble, and turn dribble. Statistics of skills and difficulty are shown in Table 3.

As shown in Figure 5, different dribbling methods have different requirements and the physical needs of athletes are also different. We can see that in turn dribble, the skills and physical fitness required by athletes are the highest overall, more than 15% higher than other dribbling methods. The high and low dribble requires the least, so the high and low dribble is the most common dribbling method in basketball. We make statistics on the mastery of each dribbling mode of the school basketball team members, as shown in Table 4.

As shown in Figure 6, in the two groups of athletes tested, people have the best mastery of the simplest high and low dribble, with an average of about 2.2, and the mastery of stopping dribbling and turning dribbling is also about 2, reaching the passing line. The higher the overall strength of the player, the higher the overall level of the player and even the overall level of the team.

4.3. Changes after Training. We divided the players into groups and trained for 3 weeks. We tested the indicators of the two groups of players again and compared the changes of the two groups of players, as shown in Table 5.

After group training, the players using the traditional training method have little improvement in various indicators, only less than 20%, while the training indicators of the players after the dribble tactical pattern recognition are of quality. The improvement of dribbling tactics by more than 50% shows that pattern recognition of dribbling tactics can have a huge effect on the competitiveness of players.

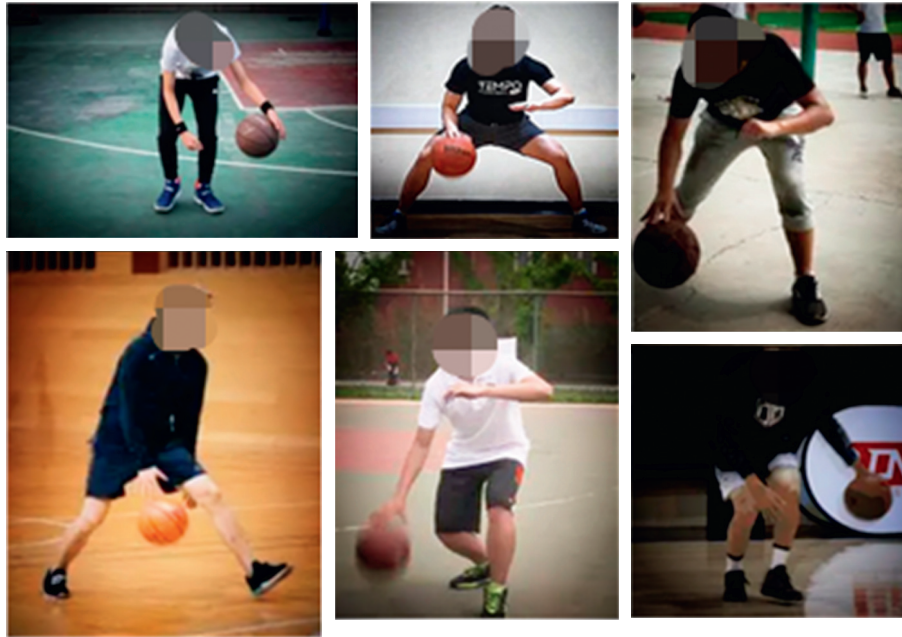


FIGURE 1: Part of the collected data.

TABLE 1: Current level of athletes.

	Test group					Control group				
	1	2	3	4	5	1	2	3	4	5
Dribble	2.38	2.06	1.92	1.81	2.08	2.48	2.08	2	2.43	1.89
Travel height	2.02	1.99	1.92	1.93	2.4	2.35	2.09	1.98	2.42	2.48
Low dribble	2.41	2.13	1.98	1.82	2.25	2.17	2.05	2.16	1.91	2.36
Dribble	1.86	1.85	2.18	2.25	1.96	2.32	1.83	1.83	2.14	2.01
Turn dribble	2.5	2.18	2.48	2.5	2.26	2.47	2.25	2.15	2.27	2.28

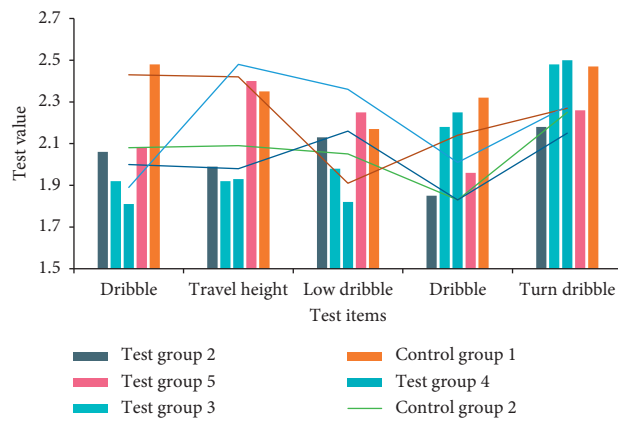


FIGURE 2: Athlete level test.

TABLE 2: Physical fitness of basketball players.

	Test group					Control group				
	1	2	3	4	5	1	2	3	4	5
Muscle	2.27	2.28	2.13	1.89	1.92	2.03	2.28	1.83	1.97	1.96
Fascia	1.89	2.09	1.81	1.91	2.34	2.21	1.88	2	2.18	1.81
Joint	2.39	2.42	1.84	2.14	2.24	2.29	1.98	2.24	2.01	2.23
Body fat	1.97	2.24	2.12	2.25	1.92	2.16	1.82	1.96	2.26	1.84
Lower limb ability	1.86	2.23	2.42	2.49	1.86	2.39	2.2	2.25	1.92	2.1

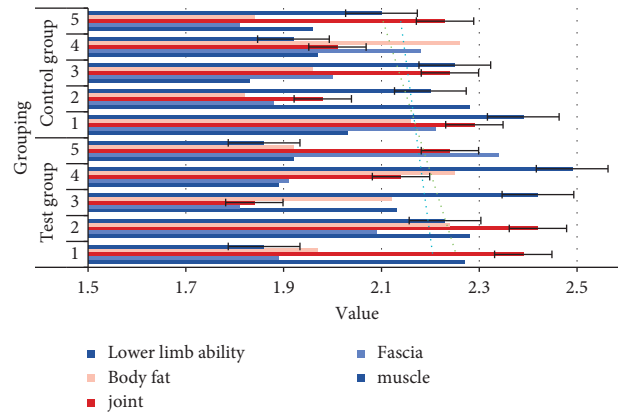


FIGURE 3: Physical fitness statistics of athletes.

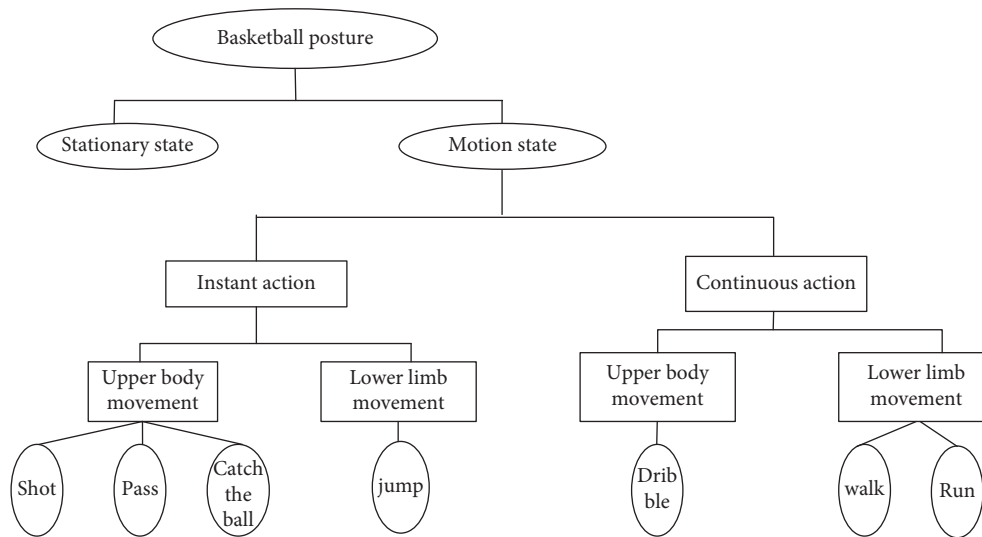


FIGURE 4: Basketball gesture recognition.

TABLE 3: Ways of dribbling.

	Skill	Training time	Lower limb ability	Physical coordination	Difficulty
High dribble	4.56	4.35	4.96	4.34	4.89
Low dribble	5.38	4.96	4.74	5.15	5.21
Emergency stop dribble	5.77	5.3	5.57	5.19	5.35
Reverse dribble	6.16	6.2	6.18	6.3	6.03
Turn dribble	6.45	6.68	7	6.42	6.89

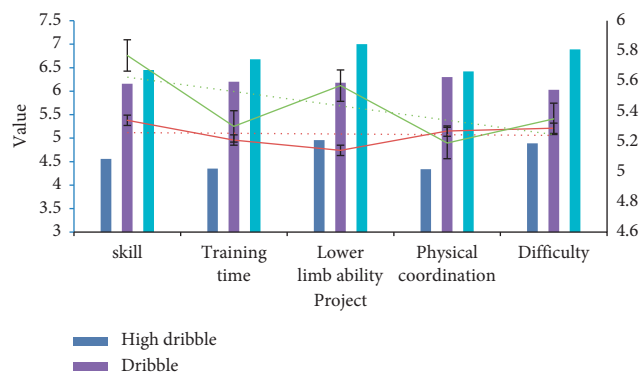


FIGURE 5: Skills required for different dribbling methods.

TABLE 4: Players' mastery of dribbling methods.

	Test group					Control group				
	1	2	3	4	5	1	2	3	4	5
High dribble	2.24	1.99	2.1	2.16	2.01	2	2.13	1.88	2.28	2.01
Low dribble	1.93	2.47	2.21	2.27	1.94	2.09	1.81	2.15	1.85	2.21
Emergency stop dribble	1.97	2	2.13	2.5	2.24	2.48	2.18	1.94	2.35	2.43
Reverse dribble	1.92	2.09	1.98	2.17	2.33	1.97	2	1.89	2.38	2.44
Turn dribble	1.95	2.37	1.89	2.41	2.03	2.46	2.26	2.21	2.32	2.26

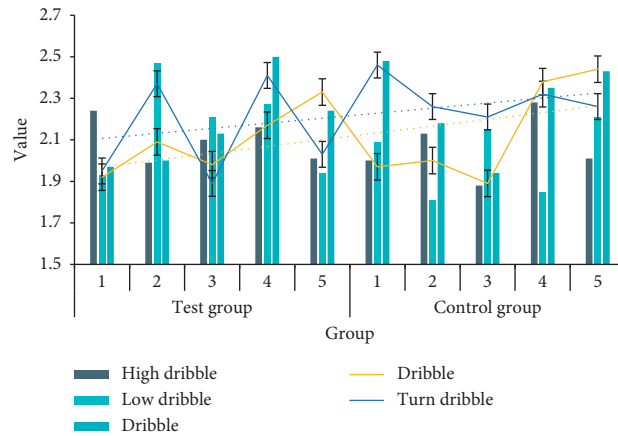


FIGURE 6: Players' mastery of different dribbling methods.

TABLE 5: Changes in players after training.

	Test group					Control group				
	1	2	3	4	5	1	2	3	4	5
Dribble	2.29	2.28	1.85	2.33	2.05	4.74	5.15	5.21	5.14	5.33
Travel height	2.88	2.53	2.7	2.53	2.95	5.57	5.19	5.35	5.55	5.69
Low dribble	3.16	3.47	3.21	3.42	3.59	6.18	6.3	6.03	5.86	4.27
Dribble	3.85	3.41	3.77	3.86	3.34	5.12	4.42	4.89	4.47	4.51
Turn dribble	3.14	3.31	3.28	3.07	3.18	5.52	5.85	5.21	5.72	5.82

TABLE 6: Injury degree of different groups of players after training.

	Test group					Control group				
	1	2	3	4	5	1	2	3	4	5
Muscle	4.7	5.37	5.12	5.38	4.96	2.08	1.83	2.01	2.02	2.35
Fascia	5.81	5.16	5.95	5.77	5.3	2.03	2.28	1.83	1.97	1.96
Joint	5.78	5.82	6.07	6.16	6.2	2.21	1.88	2	2.18	1.81
Body fat	6.78	6.47	6.88	6.45	6.68	2.29	1.98	2.24	2.01	2.23
Lower limb ability	7.62	7.98	7.93	7.7	7.68	2.16	1.82	1.96	2.26	1.84

And, after finding a suitable dribbling method for the player, the player's injury was also effectively contained, as shown in Table 6.

From Figure 7, we can see that after the training of two groups, the physical injury indicators of the players using the traditional training method are much higher than

those of the players after the tactical pattern recognition. This is because after the dribble, there is pattern recognition. According to the athlete's own situation, the coach allows the players to adopt a suitable dribbling method, which improves training efficiency and reduces physical injury.

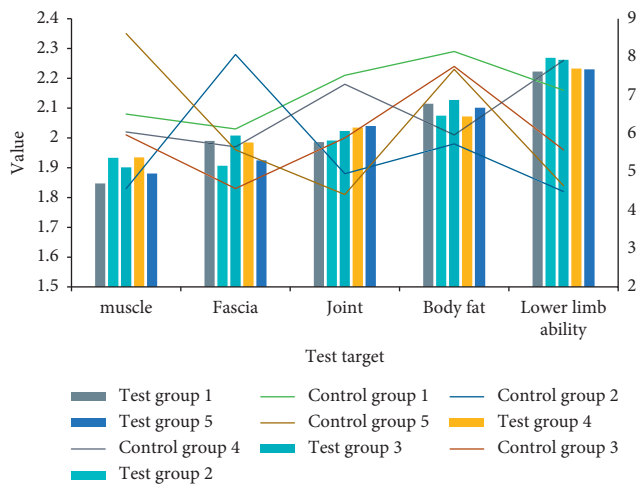


FIGURE 7: Two groups of injuries after training.

5. Conclusion

In recent years, with the development of wireless sensor network and microelectronic equipment technology, body area network technology has been extensively developed and human body recognition has attracted much attention in various fields, such as medical treatment, sports, games, movies, etc. Based on the human body gesture recognition, this paper studies and analyzes the movement gesture recognition of athletes in the field of basketball sports. By detecting the movement state information of the human arms and legs, the recognition of basketball dribbling patterns is completed, a method of basketball gesture recognition based on unit action division.

The analysis done in this paper is just for posing, and there are many shortcomings in the evaluation of players' overall ability. For example, the valuation of potential influencing factors is incomplete, and three factors are initially selected for such evaluation. In this way, the evaluation is rather single and incomplete in consideration of the player's overall ability. There may be some potential factors that are worth noting here. The acquisition of data for measurable variables is not comprehensive, and the measured variables identified for the relevant latent polarities are not comprehensive enough to fully reflect the meaning of the latent variables. The obtain analysis results are not very satisfactory. There is still a lot of work waiting for us to do, which needs to be continued by the latecomers. We hope that the research results of this paper can enlighten the later ones and better contribute to the game development of basketball. Future research should refine the assessment of athletes' overall ability, with comprehensive data collection on measurable variables.

Data Availability

No data were used to support this study.

Conflicts of Interest

The authors declare that they have no conflicts of interest.

Acknowledgments

This work was supported by a special fund granted by Minjiang University.

References

- [1] L. Li, "A brief analysis of the content of physical education in junior high school: taking basketball dribbling as an example," *Middle School Curriculum Guidance (Teaching Research)*, vol. 12, no. 19, pp. 49–52, 2018.
- [2] C.-Y. Chang, C.-S. Ho, H.-Y. Yang, and C.-T. Chan, "The effect of single whole body vibration training and different elastic basketballs on basketball players' dribbling speed and specific physical fitness," *Journal of Sports and Leisure Management*, vol. 13, no. 1, pp. 1–8, 2016.
- [3] A. Liu, "Analysis of the influence of core strength training on basketball specific physical fitness," *Peasant staff*, vol. 595, no. 18, pp. 253–255, 2018.
- [4] B. H. Wu, H. Tsai, and C. Y. Yang, "Effects of physical training mode on single training performance and physiological response," *Journal of sports performance*, vol. 4, no. 1, pp. 33–41, 2017.
- [5] X. L. Taniguchi and S. Xu, "Physiological and biomechanical factors affecting running endurance," *Chinese tissue engineering research*, vol. 24, no. 20, pp. 130–137, 2020.
- [6] Paul, "Analysis on the characteristics of volleyball players' physical training," *Industry and Technology Forum*, vol. 16, no. 17, pp. 140–141, 2017.
- [7] J. Liu, J. Niu, L. Yang, Z. Niu, P. Zhan, and X. Yu, Literature review of sports biomechanics on basketball, *Wushu Studies*.
- [8] J. Zhan, "Analysis of body shape and physical function factors in outdoor rock climbing," *Biology teaching in middle school*, vol. 1, no. 22, pp. 71–72, 2015.
- [9] Y. Chen, "Research on the interaction between protein and sports," *Qiuzhi guide*, vol. 13, no. 11, pp. 37–39, 2016.
- [10] W. Zhang, "Sociological attribution and strategy of adolescent physical health promotion in China," *Sports world*, vol. 24, no. 11, pp. 176–178, 2016.
- [11] P. Zhang, L. Yang, and L. Wang, "Research on the joint force of adolescent physical health promotion," *Journal of Hebei Institute of physical education*, vol. 29, no. 1, pp. 5–8, 2015.
- [12] H. Yan, C. Liang, Y. Zhang, Y. Y. Geng, and G. E. Qing, "Adjustment of youth physical health promotion policy: Japanese experience and China's reference," *Education and teaching forum*, vol. 37, no. 4, pp. 67–68, 2017.
- [13] Y. Zhang and Y. Xu, "Research on the promotion of adolescent physical health," *Contemporary sports science and technology*, vol. 5, no. 36, pp. 121–125, 2015.
- [14] L. Chong and S. Shi, "Analysis on the formulation and implementation of youth physical health promotion policy from the perspective of game theory," *Journal of Hebei Institute of physical education*, vol. 33, no. 4, pp. 1–5, 2019.
- [15] Z. Guo and D. sun, "Investigation and influencing factors of physical fitness of adolescent students in different urban areas of Xi'an," *Journal of Xi'an Institute of physical education*, vol. 1, no. 2, pp. 98–102, 2017.
- [16] J. Jia and B. Li, "Physical Health of Teenagers and the Biological Characteristics Affecting Sports-Related Physical Fitness," *Network Modeling Analysis in Health Informatics and Bioinformatics*, vol. 10, no. 1, pp. 1–12, 2021.
- [17] H. Yan, Y. Yang, and H. Liu, "Based on the analysis of the current situation of sports behavior and physical health of adolescents in four cities and eight districts of Shanxi

- Province,” *Contemporary sports science and technology*, vol. 9, no. 17, pp. 17-18, 2019.
- [18] L. Gai, X. Xia, T. Liao, and P. Huo, “Research on adolescent physical health: concept, evaluation and intervention promotion,” *Hubei Sports Science and technology*, vol. 36, no. 7, pp. 585-590, 2017.
- [19] T. Chen, “Research on adolescent physical health promotion under the guidance of healthy China,” *Electronic Journal of new education era (Student Edition)*, vol. 3, no. 30, pp. 13-15, 2019.
- [20] R. Han, “Research on Influencing Factors of physical health of Chinese adolescents,” *Adolescent sports*, vol. 15, no. 2, pp. 37-38, 2020.
- [21] C. Zhang, “Research on influencing factors and coping strategies of adolescent physical health in China,” *Sports teachers and friends*, vol. 39, no. 6, pp. 53-55, 2016.

Research Article

Computer Analysis and Automatic Recognition Technology of Music Emotion

Yuehua Xiang 

Center for College Students' Cultural Quality Education, Central South University, Changsha 410083, Hunan, China

Correspondence should be addressed to Yuehua Xiang; xyh10070207@163.com

Received 7 January 2022; Revised 21 February 2022; Accepted 5 March 2022; Published 23 March 2022

Academic Editor: Wei Liu

Copyright © 2022 Yuehua Xiang. This is an open access article distributed under the Creative Commons Attribution License, which permits unrestricted use, distribution, and reproduction in any medium, provided the original work is properly cited.

With the rapid development of the related computer industry, the use of computer-related technologies has become more and more frequent. The music industry is no exception. The research and analysis of music emotions has been a problem since ancient times. Due to the diversification of music emotions, people with different music in the same piece of music will have different feelings. The research topic of this article is to make a comprehensive analysis of the computer's automatic identification technology, combined with the powerful subcapacity of the computer, so that the research on music emotion can be developed rapidly. The article analyzes the technical research of the automatic recognition and analysis of music emotion in the computer, and conducts a comprehensive analysis of the music emotion through the research of the computer-related automatic recognition technology. This paper focuses on the computer automatic recognition model of music emotion, and successfully realizes the design and simulation of the automatic recognition system based on the MATLAB platform. An automatic identification model using BP neural network algorithm is proposed. By comparing it with the statistical classification algorithm, the experimental results verify the effectiveness of the designed BP network in music emotion recognition.

1. Introduction

Different from the traditional media, the core of new media is the digital media using digital technology, Music plays an important connecting role in emotional communication in different cultural contexts such as age, ethnicity, music, cultural experience, etc. [1]. With its massive information, wide coverage, fast speed, and strong interaction [2, 3], new media has become a carrier for more and more audiences to receive information [4]. Nowadays, digital technology has irresistibly penetrated into every corner of life [5, 6], making people equal between extremely low cost and huge amount of information [7]. The achievements of digital revolution such as digital television and digital CD-ROM enable information to be disseminated in a simple way, accessed in a larger capacity, and communicated with recipients in a more personalized way [8]. Simple interpersonal relationship is being replaced by two-way communication between people, people and groups, so that people can selectively obtain the information they need [9].

At present, the traditional media is gradually becoming digital, and the information exchange between media is more and more accomplished by digital. Internet music relies on new media to quickly become a unique cultural landscape [10]. Numerous netizens forget to return and get their own place in the creation and sharing of "grassroots" music art. Bukharin's Theory of Historical Materialism regards art as the result of reflection of social life, a special "spiritual" activity and spiritual production [11]. It holds that science is the result of systematization of people's thoughts and art is the result of systematization of emotions in images. Art is a means of transferring feelings, and its direct function is to promote emotional socialization. Art is an activity that expresses emotion by artistic image and words, sound, action or other means [12]. It has great vitality and potential, and has become an important means of the development of today's music art, and has a far-reaching impact on music creation, dissemination, appreciation and even the whole music culture [13]. Digital network provides a new way of music creation, production, dissemination and

communication, which deeply influences the way of music creation, performance and its existence in society, and forms a unique aesthetic culture [14]. Even people's ideas and attitudes towards music art are changing quietly [15]. The support of high-tech means of new media culture meets the sensory needs of human beings. The creative impulse of creators can be accurately expressed. The online music world is connected with the imaginary world and the real world. At this time, the form of music art is more perceptual products, and the appreciation activities are more perceptual. Entertainment has become the first demand of network music.

The use of computer's automatic identification technology can well promote the development of human music. Music is a special way of expressing emotions, and his communication method must be highly consistent with the way that humans can accept. And no matter what kind of music, what era of music, his development cannot be separated from technological innovation, especially in this era of rapid technological development, once the development of music and high-tech technology are out of track, it will definitely be leading to the backwardness of music. Through the rational use of computers, this article promotes the innovation and development of music on the one hand, and hopes to have a systematic understanding of the expression of music emotions on the other. The relationship between new media and computer network is very close, and the two influence each other and promote each other. From a technical point of view, computer network applications provide technological impetus for new media, and take the characteristics of new media technology as the research and development point. For example, the most popular new media software WeChat, Weibo, official account, etc. of new media technology. Although the emergence of these new media platforms has brought a huge impact on traditional media, they can still play a relatively positive role in guiding social public opinion. From the perspective of application promotion, new media has a large number of audiences in the Internet environment, and these audiences are the recipients of computer networks, prompting new media to innovate in promoting computer network technology and promoting computer network applications. And under the interaction and feedback mechanism of new media, it provides reference for the realization of technological reform of computer network applications.

2. The Present Situation of Music Communication in the New Media Age

(1) In this age, the use of mobile phones is becoming more and more frequent, and this has also led to mobile phones becoming an important carrier of music expression. Music, as one of the carriers rich in emotions, has always been. It is highly valued by people from all walks of life, especially for artists. Since music was invented, people's research on him has not been interrupted. As of 2018, the penetration rate of smartphone users in China has reached about 70%, and this has further promoted the development of music. Among them, the music media in the new

media era is shown in Figure 1. According to the Expressway Research Institute's Mobile Music Market Report 2018, music applications ranked fourth with 77.2% usage in all kinds of applications, and first in leisure and entertainment software. In addition to the basic needs of netizens such as interaction and information acquisition on the mobile Internet, netizens have a higher demand for music. Users' music listening habits are gradually shifting to the mobile end. From network statistics, we can know that 56.6% of users are used to listening to music on the mobile end, while only 22.4% are used to listening to music on the PC side. 17.3% of users use mixed music on the mobile end and the PC side. 3.7% of users say they don't listen to music very much. The statistics of the specific situation are shown in Table 1.

Combining with the development trend of mobile Internet users and their strong demand for music, mobile music has broad prospects for development in the future. In addition, with the development of APP application of smart phone, which matches the music playing software of smart phone, there will always be a music app playing software in every mobile phone, no matter whether the audience is a music enthusiast or not, such as Cool Dog Music, Cool Me Music, Daily Beauty, NetEasy Cloud Music, QQ Music, and so on. Mi Music, Baidu Music, etc. The market share survey of major apps is shown in Table 2.

Music APP broadcasting software has various functions, including original music (Domi music), music + social networking (NetEase cloud music), original + voice music (5 sing mobile client) and other different types, which indicates that "everyone can have a microphone, everyone can have their own music media communication platform, and everyone can interact with music." The era of mobile Internet, a new media of communication, has begun to mature day by day. The melody of music is also called tune, which is organized by a series of notes that can reflect the theme of the music according to a certain mode relationship and rhythm-rhythm relationship. Melody is the foundation and soul of music, especially the main melody, which embodies the main ideas contained in music and the main emotional information that music wants to express. But for computer-aided sentiment analysis, these sentiment information cannot be obtained directly, and can only be represented by the melody characteristic parameters of the musical work itself. Therefore, the research on the characteristics of the main theme of music is an important prerequisite for sentiment analysis.

(2) Digital control and processing capabilities make communication terminals gradually accepted by people, and can become human-computer interactive media; third, the rich music resources in the Internet are very cheap and even free. Self-media refers to the media form in which information publishers use intelligent terminal devices to disseminate microinformation to the social units, social groups and public users with specific symbols



FIGURE 1: Music media in the new media age.

TABLE 1: Music listening habits of users.

	Male (%)	Female (%)	Total (%)
PC side	18.4	4	22.4
Mobile	21.4	35.2	56.6
Don't listen to music	15	6	21

TABLE 2: Market share of major apps.

	Downloads	Percentage (%)
qq music	460 million	27.4
NetEase cloud music	570 million	31.9
Kugou music	120 million	8.2
Mobile phone users	560 million	65
PC users	320 million	35

through the Internet channels, thus enabling the re-dissemination of microinformation among these audiences. Information disseminated by self-Media includes text, pictures, audio and video. From the point of view of its dissemination technology, self-Media dissemination has the convenience that traditional network media does not have. That is, everyone can register self-Media platform to achieve point-to-point and point-to-point interactive

dissemination of music information. Table 3 shows the amount of music reposted on major platforms.

For the user, sharing his favorite music through his mobile phone is a happy thing for him, and he can do it very happily. While the utilization rate of mobile phones continues to increase, there are more and more listeners to online music. The emergence of a large number of music software has deepened this situation. People have also begun to use various channels to learn about their favorite music. To listen. The development of computer technology is also one of the reasons to promote the development of this convenient thing. People can more conveniently listen to their favorite music accurately and share it with their friends. It is also better for the development of music. Great effect. At the same time, the application field of music is also relatively extensive, as shown in Figure 2:

3. Characteristics of Music Communication in the New Media Era

In the new media era, the form of music information dissemination represented by WeChat media can be summarized and analyzed according to the "five W" model of the famous American scholar Lasswell. The new media music

TABLE 3: The amount of music reprinted on each platform.

	Reprint	Frequency	Percentage (%)
WeChat	3500million	2-3	31
Weibo	4821million	5-8	42
Blog	891million	1-2	11

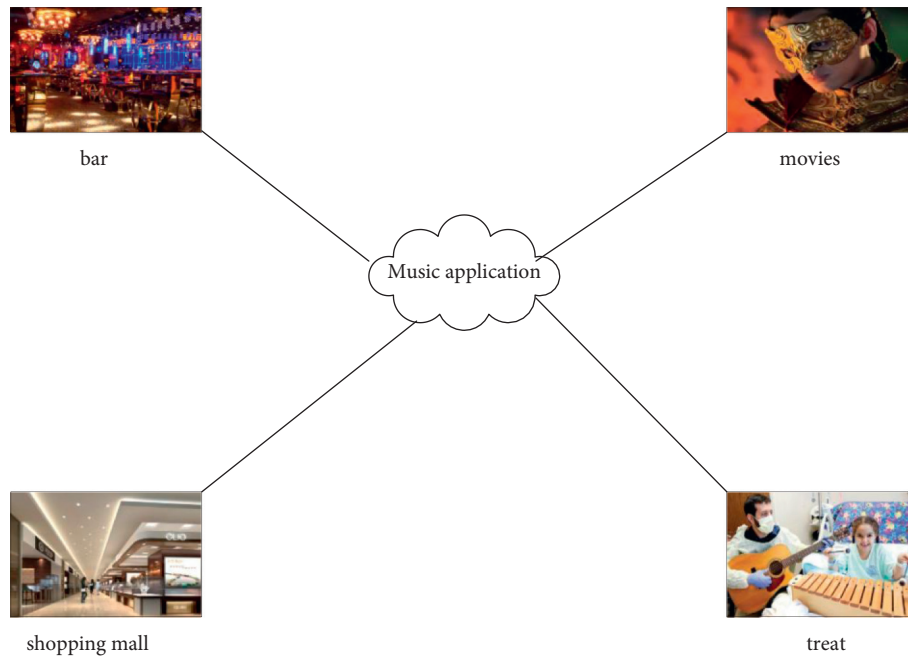


FIGURE 2: Application areas of music.

dissemination gradually presents the following main features. 1. The diversity of music communicators. In the new media communication environment, the source of music has begun to present a variety of characteristics of network interlacing. First, the traditional singularity of music communication sources has gradually disappeared. New media music is transmitted through smart client update. The rate has been greatly improved, and the content of music information has shown a quantitative upward trend. Just taking the original Chinese music base website as an example, as of now, there are more than 30 million registered users, including more than 200,000 original artists; 15,000 new songs are uploaded every day, including more than 2000 original songs; original cover accompaniment content library More than 10 million, including more than 1 million original works; more than 1.5 million uniquely accessed music users per day, more than 6 million page views, music information in both content and form, showing a quantitative feature. In addition to the mainstream primary colors, the live light color can also be matched with a virtual studio software system to control the lighting parameters, which can be adjusted in the software environment according to changes in music rhythm, timbre, speed and other elements. It enables the on-site comprehensive effects such as lighting projection to undertake the task of expressing the emotion of music, expressing the emotion, and rendering and emphasizing it, so as to better convey it to the audience and

achieve a better audio-visual effect. The survey of uploading songs on various platforms is shown in Table 4:

- (3) With the rapid development of music, the development method of music has also undergone tremendous changes. From the original word of mouth to the current record, MP3, mobile phone listening to music, various methods of listening to music emerge in endlessly. People can choose the way they like to listen to their favorite music as they like, so as to enrich their emotions and cultivate their sentiment. The changes in the way of listening to music have also led to more and more accurate music that people can listen to, and they can accurately find the yinyue that suits their tastes. The characteristics of music communication in the new era are shown in Figure 3.

It is also a business model that currently dominates the mainstream market. However, due to the low stickiness of this type of service users, its future business development needs further observation. Typical representatives such as Cool Dog, Cool Me, QQ Music, Baidu Music, etc.; The main feature is that the user actively listens to passive listening. With the increasing content of music, in order to better meet the user's preferences, the life cycle of the product is specifically compressed, typical representatives such as Jing.FM, Douban FM, etc.; Fourth, in the music store

TABLE 4: Status of uploaded songs.

	Upload song	Original song	Percentage (%)
WeChat	210000	12000	29.4
Weibo	360000	70000	47.1
Blog	80000	11000	2.9

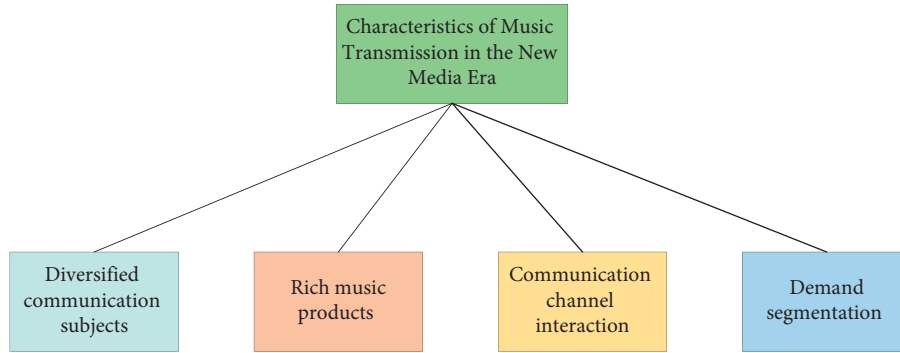


FIGURE 3: Characteristics of music communication in the new era.

category, users are still accustomed to using pirated copies when piracy is not well contained. Such models have a high threshold in terms of user scale expansion and revenue growth. Domestic typical enterprises include Jingdong Mall, Amazon China, Taobao, etc. Class operators, mainly refers to the operator’s music-related products, including ring tones, ring, etc., as well as the operator’s music client software products. Typical products of operators include Mi Mi music, Wo music, and love music. Second, in the form of music dissemination, there is a diversified trend. The spread of music is no longer a “point-to-face” broadcast, but an “peer-to-peer” interactive spread. For example, in terms of music socialization, Domi music and singer are the first to make breakthroughs: Domi music is on the basic needs of listening, allowing users to freely create song lists and share them interactively around songs, through users and users. Communication, to help users find better music; singing to meet the needs of users to practice songs through mobile phones, through the form of community, let users interact, become an interactive platform to show personal charm. 5. The intelligence of music communication effects. In the “music cloud” era, audiences only need to use smart mobile terminals through the Internet, and a huge amount of music information is at your fingertips.

4. The Change of Music Communication in the New Media Age

At present, the development of new media technology has not only changed the form of music information received by audiences, but also exerted a subtle change on the development of music communication. Understanding the changing trend of music communication in the new media era will certainly play a deeper role in promoting the prosperity and development of China’s music industry.

(1) The change of the environment of music media. As McLuhan said, “Media is the extension of human beings.” People’s expression in the new media environment has the characteristics of “transmission-reception” integration. Intrahuman communication, interpersonal communication, organizational communication and mass communication all have new characteristics: the “one-to-one” and “one-to-many” expression forms of instant messaging, the most typical of which are Wechat and Wechat. QQ and other products, their expression and communication can be “one-to-one” or “group” group discussed by many people. Therefore, with the change of media environment, the environment of music communication should also change accordingly. First, music communicators should not only consider creating better works, but also consider how to use the current media environment to disseminate their own works. Secondly, we should make good use of new social media such as WeChat, QQ, blog and so on. Music creation is disseminated through social media. Its effect is very remarkable. Music audiences use WeChat, QQ, blog, microblog, and other platforms to comment, forward and share new works. Music works can quickly become popular works of the times through the spread of “one-to-one” and “one-to-many” by countless disseminators. For example, the popular chopsticks brothers’ Little Apple in 2014 has become a Divine Song widely sung by online and offline audiences with the help of the promotion of the new media environment. Thirdly, we should make good use of smart mobile phone platform. Mobile media has become a new platform for music creation, appreciation and communication. In the future, music audio-visual has changed from the fixed mode to the mobile mode, and the new mode of music communication, channel and industry has gradually become perfect. The proportion of music

media and the trend of music communication are shown in Figures 4 and 5.

- (2) The change of music communication platform. Music communication platform began to change from a single platform to a multimedia, multichannel composite platform. First of all, new media and traditional media platform began to gradually integrate. Taking music communication on TV platform as an example, a large number of music programs such as “Good Voice of China,” “China Dream Show,” and “Most Beautiful Harmony” have been closely integrated with the mobile network, thus constantly refreshing the ratings and improving the effect of music transmission. Secondly, self-Media has gradually become a new platform for music communication. With the continuous improvement of the functions of smartphone Wechat and APP, new media clients have moved from simple content packages to “content + interactive services”. The content of music communication is not limited to content-based state. Self-media music communication should redefine the relationship between audiences and media, change the relationship chain of music communication from music audiences to music users, and on the basis of the new communication relationship, introduce music products that meet the requirements of the industry. Finally, all media platforms should be integrated. In the new communication environment, music communication platform still exists. How to effectively integrate the new platform with the old platform has become the key to expand the effect of music communication. Therefore, the new platform gradually determines the direction of future music communication development with the idea of “Internet +.” Through the effective means of “Internet + newspapers and magazines” and “Internet + Radio and television media,” we will identify new ideas for the development of music communication platform.
- (3) The transformation of the mode of music communication industry. From the perspective of the model of the music communication industry, domestic streaming music still cannot escape the curse of genuine free. In this mode, streaming media providers cannot get compensation from users. Therefore, the new media platform will encounter a series of problems such as how to protect music copyright. Therefore, in the mode of music communication industry, first of all, the state should amend the Copyright Law and other relevant laws in time to promote the transformation of illegal music websites and P2P websites to the mode of music genuine fees. Secondly, music industry practitioners should systematically safeguard their legitimate rights and interests, and promote the closed-loop of music copyright to gradually take shape. Finally, in the level of payment mode, we need to form a closed-loop payment system for genuine online music. In the

period of digital music development, online music payment in China develops slowly, and online music matching payment channels are absent. The survey on music copyright awareness is shown in Table 5:

There is no significant difference in user experience between genuine and pirated music. Even genuine paid music products are more troublesome to use. These three closed-loops well explain the historical reasons for the lag of the construction of the genuine music system in China, and they are also a lesson to be added to the development of the genuine music business model in the new media era. Like the passive old media and interactive new media mentioned by Nicolas Nigroponte in *Digital Survival*, interaction is the most essential feature of the new media.

The influence of digital networking on music is profound, and music has become unprecedented open. Music under the influence of new media has the following characteristics: Virtualization makes the global dissemination of art products inevitable. From the creator’s point of view, professional creators are subject to such restrictions as record companies or media. There are restrictions on their publication of their works. In contrast, individual composers are free to publish their works on the Internet as long as they want, as long as there are certain groups of people to visit. The survey on music dissemination trends is shown in Table 6:

Hegel believes that the initial need of art is to embody the ideas or ideas produced by the spirit in his works. On the one hand, the works of art presented in the sense organs should have an inherent meaning. On the other hand, they should express the content meaning and its image as the products of artistic activities of thought and spirit, rather than the real things that exist directly. In the face of the audience, the new media directly removes the utilitarian content and moves towards the natural transmission. The creators and appreciators regard the creation, dissemination and appreciation of music as a pure artistic act, full of artistic creativity and vitality. Where possible, people with the same interest orientation can establish their own ideological community in the virtual community and exchange ideas with voice and color. 2. Timeliness and popularity as far as the timeliness of music communication is concerned. The new media makes the network music free from space restriction and content updating without fixed cycle, which is extremely easy to operate. Many network music itself is not a professional music creation. New media can quickly transmit the music, sound and image of netizens by means of “always ready” transmission, which is not limited by cost, technology and distribution. The widespread popularity of grassroots music on the Internet is the embodiment of this phenomenon. The great increase of individualized artistic creators will inevitably make the world colorful and dazzling. 3. The interaction and synthesis of music and personalized products appear simultaneously. Multimedia music is a challenge to the pure music form. The involvement of visual media makes the pure music form which requires high quality of the audience develop towards multilevel and planar direction. The deep meaning of music is often expressed directly by

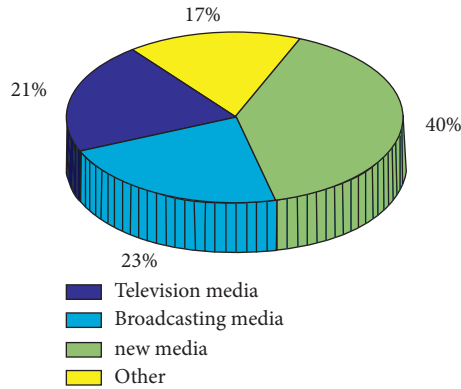


FIGURE 4: The proportion of Music Media.

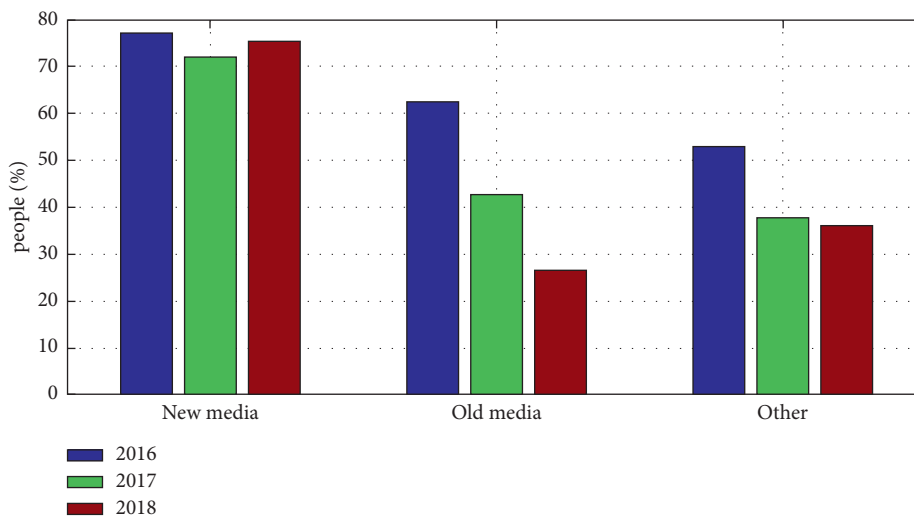


FIGURE 5: The trend of music communication.

TABLE 5: Survey of music copyright awareness.

Gender	Genuine (%)	Piracy (%)	Total (%)
Male	64	36	100
Female	28	72	100
Total	92	108	200

TABLE 6: Survey results of music dissemination trends.

	2016	2017	2018
New media	77	72	75
Old media	62	42	26
Other	53	38	35

means of visual aids. In the way of multimedia appreciation, appreciation changes from simple audio-visual to comprehensive audio-visual acceptance, and then expresses feelings freely on the information platform. The perfection of audio-visual experience is the need of people to accept network music. In the creation and appreciation of the popularity of network music, the creator only experiences the pleasure of existence of “I speak therefore I am,” and the audience does not need to think about the subtle meaning of the works.

Network music creators often use humorous and personalized language to construct works with lively rhythm and clear structure. Most of the audience and audience want to vent their emotions, relax their body and mind in a limited time, and get aesthetic pleasure that makes them happy. As a result, online browsing provides them with a pleasant aesthetic experience, which is easy to appreciate without burden and pressure. Network music uses frank, perceptual and fragmentary voices to dispel the existing discourse authority in the field of aesthetics, bringing people into the virtual aesthetic space the simplest pleasant aesthetic experience. Some people think that this kind of appreciation pleasure is low-level, not aesthetic. However, there is no difference between pleasure and aesthetic feeling. The real aesthetic feeling is the aesthetic feeling after blending all kinds of complex aesthetic psychological pleasure. It brings people a kind of spiritual intoxication. The virtuality, timeliness and interaction of new media music communication are shown in Figure 6.

In terms of the timeliness of music dissemination, traditional media can hardly compare with new media. Due to the influence of many factors such as cost, technology and mainstream ideology, the timeliness of traditional music

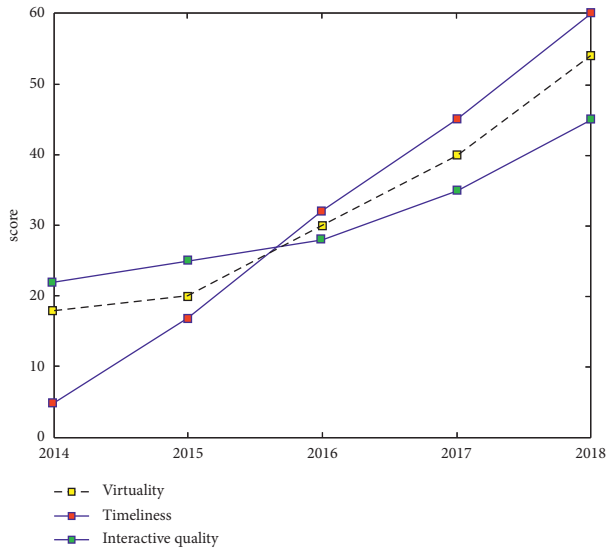


FIGURE 6: The virtual, timeliness and interaction of music communication in new media operations.

media is restricted. The new media makes online music not limited by space, and the content update does not have a fixed period. It is extremely easy to operate. Many online music itself is not a professional music creation, and new media quickly transmits the music, sound and image of netizens in the way of “always ready”, which is not limited by cost, technology and distribution. The widespread popularity of grassroots music on the Internet is a manifestation of this phenomenon. The popularity of many Internet songs and the overnight fame of Internet singers are closely related to the timeliness and popularity of new media. The development of the network enables people to get the latest information as long as they are connected to the network, and virtualization makes the global dissemination of art products inevitable. From the creator’s point of view, professional creators are subject to restrictions such as record companies or media, and they are restricted in publishing their own works. Compared with individual composers, they can freely publish their works on the Internet. As long as he wants, as long as there is a certain crowd to visit. Hegel believed that the original need of art is that people should embody the concepts or ideas generated by the spirit in his works, just as people use language to convey ideas, so that others can understand. On the one hand, a work of art presented to the senses should contain an inner meaning, and on the other hand, it should express this content meaning and its image as something that appears to be not just a directly existing reality, but a mental and spiritual thing. Products for artistic activities: what emerges with personalized products is the vividness and synthesis of music. Multimedia music is a challenge to the pure music form. The intervention of visual media makes the pure music form, which has high requirements on the appreciator’s own quality, develop towards a multilevel plane, and the deep meaning of music is often expressed directly with the aid of visual aids. In the multimedia joyful way, appreciation changes from simple listening to a comprehensive acceptance of audio-visual

integration, and then freely expresses feelings on the information platform. This interaction and comprehensiveness are also the characteristics of new media communication methods. Mature composing techniques and omnipotent digital means make the concept and listening habits of the Voice of Entertainment deeply affect all people who come into contact with digital life. The perfect audio-visual experience is what people need to accept online music.

5. Conclusions

The emergence of new media has greatly promoted the spread and development of music culture. The influence of the media on music culture is firstly manifested in the way in which the works exist, and then expands its scope of influence, eventually expanding to the whole field of music culture. Throughout the development process of music culture, it is actually a process to meet people’s changing perceptual needs, so music culture must put people’s aesthetic needs first. The emergence of new media provides a platform for the spread and development of network music, meets the aesthetic needs of people, and is an indispensable important carrier in the process of the spread of network music culture. As a means of communication, the new media has a tremendous impact on music and its culture. The process of research on the development of music emotion is also relatively difficult. Countless people have invested in this research. The research on music emotion in this article is also a new way, through the use of high-tech technology, such as computer analysis technology and automatic identification technology. Use it to automatically research and recognize music emotions. The changes of the media first affect the way music works exist, and then expand to the whole field of music culture, forming a new way of music interpretation. From this point of view, the modernization of the means of music communication is carried out on the premise of the development of human social science and technology, and is a clear representation of human development. Network music pays more attention to people’s livelihood, people’s cultural and aesthetic needs. In fact, the development of the whole music culture is aimed at satisfying the human perceptual needs. The human musical aesthetic needs are always the first and unconditional. The arrival of the new media era greatly meets the needs of music perceptual aesthetics in new ways. Any music works or even related cultures are used materials. People who live in such media have few burdens left by history because they firmly believe that only aesthetics and perception are always right. Artists use certain material materials and tools, and use their own aesthetic ability and skills to express their worship emotions. Then, art appreciators feel the author’s adoration from the works of art. This kind of worship emotion combined with the appreciator’s own understanding constitutes the appreciator’s own unique interpretation and evaluation. How we judge a work of art comes from whether we feel what the author wants to express in it. Everyone is more or less adored. This is a deeply rooted tradition that we have inherited from time immemorial. Artists use this

adoration as a bridge for emotional transmission. Based on the worship of something, the author's thoughts and emotions are extended. The research focus is on the music emotion recognition system, and the melody feature space for emotion is based on the selection of relatively simple MIDI music. However, a large number of existing music forms are audio files such as MP3 and CD, so this is lacking in practical application. The research method of this paper can be applied to music types such as MP3, the only difference is that it needs to use signal processing, spectral analysis and other means to extract music features, which is also an important direction for further research.

Data Availability

No data were used to support this study.

Conflicts of Interest


The authors declare that they have no conflicts of interest.

References

- [1] Y. E. Linna, "On the musical emotion processing of college student in different cultural background," *Journal of Ningbo Institute of Education*, 2019.
- [2] A. A. Elegza and B. E. zad, "New media scholarship in africa: an evaluation of africa-focused blog related research from 2006 to 2016," *Quality & Quantity International Journal of Methodology*, vol. 52, no. 1, pp. 1–16, 2018.
- [3] R. Emms and N. Crossley, "Translocality, network structure, and music worlds: underground metal in the United Kingdom," *Canadian Review of Sociology/Revue canadienne de sociologie*, vol. 55, no. 1, pp. 111–135, 2018.
- [4] W. C. Ihejirika, "Autorita' and autorevolezza: explaining contestations between political and religious leaders in the age, of the new media," *The Politics and Religion Journal - Serbian Edition*, vol. 5, no. 1, p. 22, 2017.
- [5] H.-I. Kwon, H.-S. Kim, and J. Jang, "Service value network model for the classical music market in South Korea," *Advanced Science Letters*, vol. 23, no. 1, pp. 75–77, 2017.
- [6] D. J. Park and J. David, "United States news media and climate change in the era of US President Trump," *Integrated Environmental Assessment and Management*, vol. 14, no. 2, pp. 202–204, 2018.
- [7] S. Sigtia, E. Benetos, and S. Dixon, "An end-to-end neural network for polyphonic piano music transcription," *IEEE/ACM Transactions on Audio Speech & Language Processing*, vol. 24, no. 5, pp. 927–939, 2017.
- [8] X. Gong, Y. Zhu, H. Zhu, and H. Wei, *Chmusic: A Traditional Chinese Music Dataset for Evaluation of Instrument Recognition*, Engineering and Systems Science>Audio and Speech Processing, 2021.
- [9] L. Taruffi, C. Pehrs, S. Skouras, and S. Koelsch, "Effects of sad and happy music on mind-wandering and the default mode network," *Scientific Reports*, vol. 7, no. 1, Article ID 14396, 2017.
- [10] Y. T. Chen, C. H. Chen, S. Wu, and C. C. Lo, "A two-step approach for classifying music genre on the strength of AHP weighted musical features," *Mathematics*, vol. 7, no. 1, p. 19, 2019.
- [11] J. Li, D. Chen, Y. Ning, Z. Zhao, and Z. Lv, "Emotion recognition of Chinese paintings at the thirteenth national exhibition of fines arts in China based on advanced affective computing," *Frontiers in Psychology*, vol. 12, Article ID 741665, 2021.
- [12] T.-Y. Kim, H. Ko, S.-H. Kim, and H.-D. Kim, "Modeling of recommendation system based on emotional information and collaborative filtering," *Sensors*, vol. 21, no. 6, p. 1997, 2021.
- [13] G. Thompson, "The 'music therapy with families network': creating a community of practice via social media," *British Journal of Music Therapy*, vol. 31, no. 1, pp. 50–52, 2017.
- [14] S. Namasudra and P. Roy, "PpBAC," *Journal of Organizational and End User Computing*, vol. 30, no. 4, pp. 14–31, 2018.
- [15] V. Tolz and Y. Teper, "Broadcasting agittainment: a new media strategy of Putin'S third presidency," *Post-soviet Affairs*, vol. 34, no. 2, pp. 1–15, 2018.

Research Article

Continuance Intention Mechanism of Middle School Student Users on Online Learning Platform Based on Qualitative Comparative Analysis Method

Guomin Chen,¹ Pengrun Chen,² Wenxia Huang,¹ and Jie Zhai ¹

¹Guilin University of Aerospace Technology, Guilin, China

²The University of Manchester, Manchester, UK

Correspondence should be addressed to Jie Zhai; 2020143@guat.edu.cn

Received 18 January 2022; Revised 23 February 2022; Accepted 2 March 2022; Published 20 March 2022

Academic Editor: Wei Liu

Copyright © 2022 Guomin Chen et al. This is an open access article distributed under the Creative Commons Attribution License, which permits unrestricted use, distribution, and reproduction in any medium, provided the original work is properly cited.

The research on the users' continuance intention behavior of online learning platforms is not a new topic. In the past, more studies were conducted on users of MOOC online learning platforms, which are based on symmetric causality. This study adopts the qualitative comparison analysis method to build configuration model by combining platforms, students, parents, teachers (4 level seven elements) with middle school students' continuance intention. The configuration analysis identifies the user' retention path of middle school students on online learning platform under the collaborative influence of multi-level elements, summarizes the online learning platform of continuance intention mechanism and implementation path for middle school students and reveals that the users of online learning platform for middle school students keep clear of the mechanism of action and realistic choice. In the end, the user retention mechanism of middle school students' online learning platform is summarized, including platform quality orientation, platform interaction orientation, and "parent-teacher" dual drive.

1. Introduction

With the development of information technology, especially the popularity of mobile Internet terminal devices, and the spread of COVID-19, online learning has become one of the common learning methods for middle school students. In the past, most studies focused on the influencing factors of single-level users. In fact, for middle school students' online learning, its continuance intention are affected by many level factors. The research of single-level elements often follows deductive logic and hypothesis test, which is suitable for the analysis of net effect relationship at the variable level. The research on the continuance intention of multi-level elements for middle school students is based on abduction logic to identify the configuration causes of specific results (such as continuance intention), which is suitable for the research on the complex relationship of hierarchical configuration shaping continuance intention behavior [1]. Based on the perspective of level-element configuration, combined with

Fs-QCA (fuzzy set Qualitative Comparative Analysis) method, this paper analyzes the necessary and sufficient causal relationships [2], explores the causes of level configuration of results (continuance intention) according to abduction logic, and then obtains the path of middle school students' continuance intention behavior.

2. Research Basis

2.1. Community of Inquiry. Community of Inquiry (CoI), is a valid theoretical framework for the study of online learning cocreated by Garrison and Arbaugh [3]. This theory mainly emphasizes the importance of interaction between teachers and students or between students and students in the process of online learning, and aims to promote the construction of students' knowledge, the discovery of students' ability and the cultivation of students' skills under the teachers' feedback when students learn online. The theory can be divided into cognitive

presence, social presence and teaching presence. Cognitive presence which considers students as the main object, takes advantage of their own learning efficiency and learning engagement to explore learning tasks, to integrate the application of solving problems, thus obtaining the acquisition and application of advanced knowledge. Social presence means students display their personal characteristics in the trustworthy inquiry learning community through communication media, so as to interact with others, realize the purpose of developing interpersonal relationships, and enrich their social interaction experience. Teaching presence is the design, promotion and guidance of students' cognitive processes, including curriculum design and organization, facilitating dialogue and direct teaching, in order to achieve personally meaningful learning results. In the theory, the main subject of cognitive presence is students, while parents only participate in online learning process as supporters and supervisors, mainly to check the completion of its task. Social presence and teaching presence both require parents to guide and help students in family education environment. The significance of the above theory for this study mainly lies in students' self-learning efficacy and the performance of observing students' perception of parental involvement in online learning.

2.2. Overlapping Spheres of Influence. The theory of Overlapping Spheres of Influence was proposed by Epstein based on the ecological theory of school-family relationship, to establish family-school partnership, mainly the one between school, family and community [4]. In this study, the theory of community is defined as the online learning platform, on which the collaborative relationship is expected to be based on. Through the method of online study, the family, school, and platform establish the same goal for the children's occupational planning, undertake the common task and establish a new type of cooperative relationship between the student, family and school. To sum up, users' continuance intention of using online learning platforms is a dynamic process that covers multiple factors such as macro environment and micro-individual characteristics, and this process is affected by many precursors, including family, school, platform and individual characteristics [5–7]. In particular, compared with adults, there exists a realistic situation of "middle school students-parents" role separation. However, existing studies are often limited to a certain level, which ignores the possible influence of multiple factors concurrency on users' continuance intention behavior in the context of role separation, leading to the inconsistency of existing conclusions [8]. The internal mechanism of multi-level synergy affecting users' continuance intention of online learning platform remains unclear. In view of this, this study integrated four levels to explore the multiple concurrent factors and causal complex mechanism.

3. Relationship and Research Model between Level Factors and Continuance Intention

3.1. Relationship between Student-Level Factors and Continuance Intention

3.1.1. Relationship between Online Learning Self-Efficacy and Continuance Intention. The concept of "online learning self-efficacy" is derived from the concept of "self-efficacy" proposed by Bandura. From the perspective of its development, this concept has gone through the process of "self-efficacy," "learning self-efficacy," and then "online learning self-efficacy" [9]. It can be seen that he regarded it as a subjective cognitive variable of people's ability to complete a certain task. He regarded it as a key factor of human motivation system and explored its influence mechanism on individual behavior. With the deepening of research, many studies have clarified and expanded the role of self-efficacy as the basic mechanism for the change, maintenance and generalization of individual actions. The concept of "self-efficacy in learning" is just the application and development of "self-efficacy" in the field of learning. At the same time, he discussed the operation mechanism of self-efficacy in the process of learning, pointing out that learning motivation is discussed according to self-efficacy, that is, learners' judgment of their ability to perform specific learning behaviors. With the rapid development of information technology and the deepening of research, the study of "learning self-efficacy" has been gradually extended to the field of online learning, resulting in the concept of "online learning self-efficacy." In 2006, Pituch defined self-efficacy in the context of e-learning as learners' confidence in their ability to perform specific learning tasks using e-learning systems. Chinese researcher Guo Li et al. described it as "Learners' subjective judgment of their own network learning ability" [10]. Based on this, this study believes that the self-efficacy of online learning of middle school students will affect their continuance intention.

3.1.2. Relationship between Online Learning Engagement and Middle School Students' Continuance Intention. The word "input" originates from the research on input in the field of work. The researchers regard employees' engagement in the work environment as an internal psychological structure, and "engagement" refers to employees' total commitment to work. Although the environments and places where employees perform tasks are different, their underlying psychological structures are similar to some extent. Therefore, this paper introduces the concept of work engagement into the field of learning, resulting in the concept of "learning engagement." "Learning engagement" is described as "learners show an active and persistent state in the learning process, as well as a universal and persistent state." With the rapid development of online learning, the effect of middle school students' online learning has aroused widespread concern and discussion among researchers. More and more

researchers regard the level of learning engagement as an important indicator to measure the quality of online learning process, and a large number of studies have been carried out. As the online learning of middle school students is characterized by the situation of role separation, the importance of learning engagement for middle school students online learning is self-evident. Whether online learning can happen, whether it can be persevered and focused, and whether it can achieve good learning results is worth discussing. Based on previous research results, this study defined the concept of “online learning engagement” as “whether the online learning of middle school students can be sustained and focused is the performance of the online learning process of middle school students.” Therefore, online learning involvement of middle school students will definitely affect their continuance intention behavior.

3.2. Relationship between Parent-Level Factors and Continuance Intention. The parents mentioned in this study refer to the parents of middle school students, or a small number of them are other guardians in addition to their parents. Parental participation means that parents pay attention to the learning process of middle school students, participate in the learning style of middle school students, affect the choice of learning style of middle school students, and then affect the learning effect. Parents’ participation can be divided into in school educational activities and out of school educational activities according to their behavior. Parents’ participation in school educational activities can be divided into direct participation and indirect participation. Direct participation refers to guiding students’ after-school learning, assisting students to complete their homework, paying attention to students’ psychological changes, providing material support and ensuring the learning environment. Indirect participation refers to understanding children’s learning status through interaction and communication with teachers and other teaching staff, feeding back students’ learning status to teachers, and helping children make progress in quality, study, behavior and so on. Parents’ participation in extracurricular educational activities includes learning habit formation, learning method training, quality improvement etc. The behavior of participation can be divided into direct participation and indirect participation. Direct participation refers to parents’ tutoring their children’s homework at home; indirect participation means that parents provide conditional support for their children’s learning, including high-quality learning resources and valuable guidance. In this study, parents’ participation in children’s online learning mainly refers to parents’ support or involvement in the learning process of middle school students, which affects the learning effect. Participation usually includes time companionship, necessary supervision, material supply and emotional encouragement and support. Therefore, parental participation will certainly affect the continuance intention of middle school students.

3.3. Relationship between Teacher-Level Factors and Continuance Intention. As a specific professional role behavior, teacher behavior not only has the common characteristics of

human behavior, but also has the unique characteristics of teacher role. From the perspective of teacher quality, scholars Lin and others believe that teacher behavior is the external embodiment of a comprehensive quality such as teaching philosophy, teaching by example and teaching ability in specific teaching. The teacher behavior understood by Bai is sometimes called teacher performance [11]. Therefore, whether expressed by teacher behavior or discussed by teacher performance, they all express the implicit concept of teachers’ internal quality through explicit behavior. The relativity of teacher behavior determines that whether they experience from the perspective of explicit behavior or from the perspective of implicit behavior, their object is always learners, which needs learners’ real experience and perception to judge. The teacher behavior in this study is mostly replaced by teacher support behavior, which can better highlight the directivity and purpose of teaching behavior. In order to further standardize the research, teacher support behavior is defined as: Based on their own teaching ideas, teaching ideas, teaching experience and individual level, and with the support of external educational environment (including teaching materials, teaching tools, physical environment, etc.), teachers carry out teaching design and teaching management. A series of teaching activities, such as teaching evaluation, expressed through words, actions and expressions, which have an impact on students’ instrumental guidance, knowledge guidance, emotional help and social interaction. It can be seen that the continuance intention of middle school students’ online learning, if supported by teachers, will inevitably encourage students to continue to use it. Therefore, teacher support will affect the continuance intention of middle school students.

3.4. Relationship between Platform-Level Factors and Continuance Intention

3.4.1. Relationship between Platform Interaction and Middle School Students’ Continuance Intention. In traditional communication and cybernetics, interaction refers to a process in which the receiver reads, understands, processes and gives feedback to the information obtained [12]. Nowadays, the concept of interactivity has been gradually used by other disciplines, and its meaning has also been more extensive. For the interaction, the current academic community has not given a unified definition. After close scrutiny and research, Cho and Leckenby believes that these interactions should be summarized as follows: there are three types of interaction: user-machine, user-user, and user-message. The interaction between users and devices was the research field that early scholars paid more attention to, which emphasized the human-computer interaction process [13]. In this study, it refers to the user’s perceived satisfaction of teacher-student interaction and student-student interaction when using online learning platforms. In the traditional school-based education mode, teachers’ attention and communication to students will positively affect personal learning effect to a certain extent. The higher the user’s awareness of platform interaction, the problems will be

solved in time. When they have ideas, they can communicate happily. At the same time, their needs will be better met. Therefore, the interaction of the platform will definitely affect the continuance intention of middle school students.

3.4.2. Relationship between Platform Service Quality and Middle School Students' Continuance Intention. Service quality is also an important variable in the success model of information system. Initially, it refers to the speed and effect of relevant operation and maintenance personnel to solve problems in the event of operation problems of information system. Combined with the actual situational characteristics of students using online learning platforms, this paper thinks that service quality means that when online learning platforms provide matched platform support (such as the timely response of the customer service, teaching assistant of the work on teaching etc.) for learning products (such as courses) and when the technical problems arise in the process of using the platform, the speed and quality of solving problems will affect middle school students' continuance intention. Therefore, the service quality of the platform will definitely affect middle school students' continuance intention.

3.4.3. Relationship between Content Quality of Platforms and Middle School Students' Continuance Intention. In this study, quality of content refers to the adequacy of learning resources on online learning platforms, the rationality of course arrangement, and the quality of relevant videos and materials. Related scholars have carried out studies in this field. Zhang et al. confirms that content quality can positively affect the expectation confirmation of users of online learning platform [14], while Yang points out that the more satisfied MOOC users are with course quality and auxiliary effect, the higher users' perceived ease of use and expected confirmation are [15]. Rich content quality can better meet the expected needs of users, while reasonable course arrangement and high-quality audio auxiliary materials can enable users to better experience the information system, that is, users' perception of the content quality of the platform can affect users' continuous use. Therefore, the quality of the platform content will definitely affect middle school students' continuance intention.

3.5. Research Model. The middle school students' continuance intention on online learning platforms is not a single and direct influence, but the result of many causal conditions. Therefore, this paper uses Qualitative comparative analysis (QCA) to conduct in-depth research and discussion on this issue. The QCA method proposed by Ragin, an American scholar, in the 1980s, explored how the combination paths of different antecedent variables affect the outcome variables, based on the cross-case comparison between qualitative and quantitative methods of Boolean algebra and set theory [16]. Therefore, it is of good applicability and scientific to apply the configuration view and holistic view of QCA analysis method to the research of

students' continuance intention on online learning platforms. The relationship mechanism between antecedent variables and outcome variables is explored through analysis from a configuration perspective. The specific configuration analysis research model in this chapter is shown in Figure 1.

4. Research Design and Data Collection

4.1. Research Design. The subjects of this study are paired (parent-student). According to the characteristics of the research problem and the three characteristics of qualitative comparative analysis: conjectural causation, equifinality and causal asymmetry, fuzzy set qualitative comparative analysis (Fs-QCA) is chosen as the main research method in this study. In this study, semistructured interview and fuzzy set qualitative comparative analysis are used to determine the conditional variables and outcome variables of the configuration response. First of all, interviews are conducted with middle school students and parents who use online learning platforms, and the obtained data are analyzed to further summarize and refine their respective influencing factors. Secondly, interviews are conducted with middle school students and their parents who frequently used online learning platforms in the past 12 months. Finally, based on the interview results, the Fs-QCA3.0 software is used for configuration, and the configuration analysis model of high continuance intention is constructed.

4.2. Research Method. Qualitative Comparative Analysis (QCA) was first proposed by Ragin, an American social scientist, in the 1980s, and is a research method combining Qualitative and quantitative Analysis [17]. The basic idea of qualitative comparative analysis method is to apply set theory and Boolean to explore how the combination of antecedent conditions affects the results, aiming at solving the phenomenon with complex causal relationship.

Different from the traditional quantitative analysis method, the qualitative comparative analysis method thinks whether the result occurs is the result of the comprehensive action of different factors on the basis of examining the net effect of factors, and calls the combination of various factors "configuration." As the cornerstone of QCA method, configuration thinking is used to analyze results along the whole and system approach, that is, case-level configuration is adopted instead of single independent variables. QCA integrates the advantages of qualitative analysis and quantitative analysis to some extent. QCA solves causal complexity problems that large sample analysis cannot solve through overall configuration analysis. It is not only suitable for small sample studies with less than 15 cases, but also suitable for large samples with more than 100 cases. As a research method different from quantitative and qualitative research, QCA has gradually been recognized by economic management scholars at home and abroad [2].

Qualitative comparative analysis methods generally include several steps: calibrating variables, generating matrix, essential analysis, counterfactual analysis, and solution.

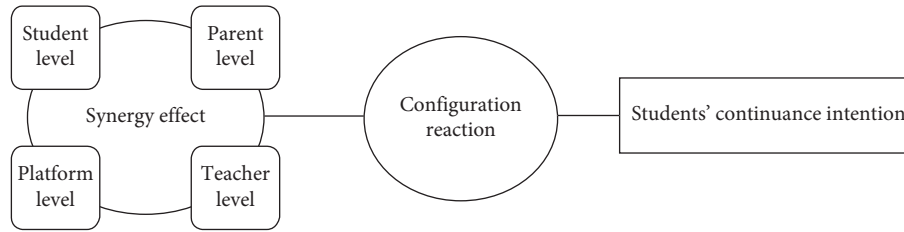


FIGURE 1: Configuration analysis model.

- (1) Calibrate variables: QCA uses direct or indirect calibration to transform antecedent factors and interpreted results into aggregate data. Fs-QCA adjusts fuzzy set variables to be assigned to the closed interval from 0 to 1 by calibration. In Fs-QCA, calibration needs to set three critical values according to the actual needs, namely, the complete membership point, the complete nonmembership point and the crossing point, according to which to calibrate the antecedent conditions and the standards of the interpreted results in each set.
- (2) Generating matrix: according to the “set-subset” relationship, the relationship between antecedent factors and explained results is explored and analyzed to find the corresponding combination of antecedent conditions and generate matrix. The combination of antecedent conditions for the explicable results in the matrix of all potential configurations is analyzed based on set consistency and case frequency.
- (3) Essential analysis: to determine the extent to which the configuration is a sufficient and necessary condition for the result variable, and to explain the explained result, QCA reflects through consistency and coverage. Generally, the consistency is greater than or equal to 0.75 and the coverage value is between 0 and 1, which is considered acceptable.
- (4) Counterfactual analysis and solution: in order to avoid possible complex solutions, QCA also needs to conduct counterfactual analysis on the configuration to arrive at parsimonious and intermediate solutions. Among them, the antecedent conditions involved in both the reductive and intermediate solutions are the core conditions, and only the antecedent conditions in the intermediate solutions are the auxiliary conditions. In the current research on QCA method, Marx and Dusa stipulated the relationship between the number of influencing factors and the number of samples of Cs-QCA based on data simulation [16].

4.3. Data Collection. The data collection of this study was completed from September 2020 to February in 2021. The respondents of semistructured interviews were middle school students and parents who frequently used online learning platform products in the last 12 months. Firstly, the author and the research group selected 4 middle schools in

Zhongshan District, Xigang District, Ganjingzi District and high-tech zone of Dalian, and randomly selected 10 pairs of students and parents who kept using the online learning platform. Among them, students, as actual users of online learning platform, have personal experience and feelings about the use of online learning platforms. Parents, as decision makers and participants of online learning platform, determine the students' continuance intention of online learning platforms. The author and members of the research group interviewed these 10 groups from September to October in 2020. The average individual interview time lasted more than 30 minutes. The main information of the 10 groups of respondents is shown in Table 1.

During the interview, the interviewees were asked three kinds of questions through semistructured interviews: first, the learning characteristics of the interviewees and their use of the online learning platform; second, describe the adoption of online learning platforms, continuance intention, specific process of continuance intention, and describe the situation and feelings therein; third, list the factors that may affect the attitude of middle school students' parents on online learning platforms. The main purpose of asking questions is to inspire the respondents to describe the factors that promote the continuous intention of online learning platform users based on their own actual experience and feelings.

In terms of students, the interview content mainly includes four aspects: (1) middle school students themselves. It mainly includes their learning attitude, self-confidence, ability and time invested; (2) platform. Because middle school students have been using it for 12 months or more, the interview questions mainly focus on the content and service quality of the platform and the real-time interaction of the platform; (3) parents. The interview content is about whether online learning needs the company of parents and whether parents can provide help in case of problems etc.; (4) Schools. Considering that the teachers have a great impact on middle school students' online learning, the interview focuses on whether they need teachers' encouragement, help and support for online learning. Finally, the research group collected and sorted out 20 descriptive data.

Twenty valid descriptive data were processed. The data processing process is mainly divided into the following steps: first, sort out 20 descriptive data into text format and import it into NVivo system to start text processing of the data; Second, make use of the different node types provided by NVivo to create nodes, tree nodes, cases and relationships with different levels and connotations, and merge the

TABLE 1: Main information of the interviewee.S

Data number	Middle school (abbreviation)	Area	Number of interviews	Role/identity
001-006	ZXJNM	Zhongshan district	6	Student, parent
007-010	XGYHJ	Xigang district	4	Student, parent
011-016	GZZJEJ	Ganjingzi district	6	Student, parent
017-020	GXXYY	High-tech zone	4	Student, parent

description data with similar content to form data fragments for further analysis; Third, through the query function of NVivo, find the frequency and source of text data, count the material source value and reference point value, and filter and retain the data with material source value greater than 3; Fourth, the group function of NVivo is used to induce and refine the retained data. After many times of induction and refinement, the causal factors of multi-level factors and high continuance intention behavior of online learning platforms are finally obtained, including learning self-efficacy (SE), learning engagement (LE), interactivity quality (IQ), service quality (SQ), content quality (CQ), parental participation (PP), teacher influence (TI), and continuance intention (CI).

After the preliminary survey and interview, the large sample case survey of this study was concentrated between October 2020 and February 2021. In the formal case study, due to the epidemic situation, all data were collected by telephone and network, including semistructured interview by telephone and questionnaire distribution by network. In order to avoid the influence of common method bias, this study carried out program control in the questionnaire design and distribution: on the one hand, the anonymity and confidentiality commitment to the respondents were marked in bold on the questionnaire, and the psychological pressure of the respondents was reduced and the social approval deviation of the respondents is minimized by covering up stories when the questionnaire is distributed; On the other hand, in addition to Likert's five level measurement model, judgment questions and semantic difference questions were added in the questionnaire design to reduce the consistency motivation of the respondents.

A total of 400 groups were entrusted to contact students and parents through their head teachers. 400 groups of students and parents were interviewed separately by telephone, and 400 sets of questionnaires were distributed. Based on the combination of telephone interview records and manual screening of returned questionnaires, unqualified questionnaires with too many missed answers, non-standard answers and obviously halfhearted answers were deleted. Finally, 300 groups of valid samples were obtained, and the effective rate of data collection was 75%. After sorting out interview records and questionnaires, they were marked and sorted for relevance. Firstly, independent sample *T*-test was performed on the data and the results showed no significant difference ($P > 0.050$). Secondly, Harman single-factor method was used to test the common method bias. It was found that the variance explanation rate of the first factor was 21.93% (lower than 50%), which verified that there was no significant common method bias in this study.

4.4. Data Calibration and Configuration Construction. The data analysis process of this study is mainly divided into two stages: data calibration and configuration construction.

The first stage: data calibration. Based on the calibration method suggested by Rihoux and Ragin [17] and Fiss et al. [18], the influencing factors of each sample and the attribution degree of the interpreted results are calibrated. In this study, the causal factors of continuance intention and antecedent conditions of middle school students on online learning platforms are measured by 5-point Likert method. The fuzzy data set adopted in this paper, referring to the practice of Jia and Du [1], takes the upper quartile, the mean of the upper quartile and the lower quartile, and the lower quartile of the data of 7 antecedents and 1 outcome variable as the complete membership, intersection and complete nonmembership of the data set.

The second stage: configuration construction. Fs-QCA3.0 software is used to analyze the calibrated data. First of all, the necessary conditions of causal factors are tested. When the necessity of the current cause condition exceeds 0.9, the core condition is formed, indicating that the explanatory power of the result variable is strong and should be taken into account in the subsequent analysis. Secondly, Ragin's suggestions are taken into account in the selection of the threshold value of the consistency rate, and the threshold value of the consistency rate is set at 0.8. Finally, Fs-QCA3.0 software gives the solution based on Boolean algebra and set analysis operation, and draws the corresponding configuration table.

In order to ensure the robustness of the results, following the suggestion of Epstein [4], the consistency rate threshold is lowered to 0.75 in Fs-QCA3.0 software and the configuration construction is carried out again. Three new configurations are obtained, but the consistency rates of the three new configurations are all lower than 0.75, and there is no fundamental change in the interpretation of the results, so the configurations obtained in this study are credible. In addition, in view of the high proportion of female parents in 246 pairs of respondents (82.3%), in order to ensure that the conclusions of this study are not affected by parental gender, two samples with male parents ($n = 54$) and female parents ($n = 246$) are constructed respectively, and there is no significant difference in the results in terms of factors. Therefore, the configuration obtained in this study is not affected by the factor of parental gender.

5. Sample Description and Data Processing

5.1. Descriptive Statistics of Data. In this study, Fs-QCA method is used to analyze the combination of antecedent conditions of students' continuance intention. Fs-QCA is

suitable for explaining which combination of conditions causes occurrence of consequences and which condition configuration causes lack of consequences. There are many antecedent conditions of students' continuance intention, and the causality of various antecedent conditions is complex, so it is suitable to use Fs-QCA method to study it. Based on a configuration perspective in this study, antecedent variables are selected from four aspects: student characteristics, platform characteristics, teacher influence and parent involvement, that is, learning self-efficacy (SE), online learning investment (LE), platform service quality (SQ), platform content quality (CQ), interactivity quality (IQ), teachers influence (TI) and parents participation (PP). The study variables included 300 cases. First, descriptive statistical analysis of variables conducted in this study to calculate the mean, standard deviation, maximum and minimum values of each variable. The above statistical indicators are shown in Table 2.

In addition, although the robustness of the analysis results of the QCA method has nothing to do with sample size, Rihoux and Ragin also suggest that "a good balance must be reached between the number of cases and the number of conditions, and the ideal balance state has no absolute numerical range and is mostly obtained through trial and error" [17]. However, there is still a lack of similar research on Fs-QCA. When the final sample size is 300, the probability of the results being affected by random data is 1%, which can clearly distinguish random data from real data and ensure the accuracy of the analysis results.

5.2. Data Calibration. Following the steps of the Fs-QCA method, first, we transform the values of the set consisting of antecedent variables and outcome variables, and set 3 critical values based on the actual conditions: complete membership, intersection, and complete nonmembership. After the transformation, the collective value is introduced between 0 and 1. With reference to previous studies, set 3 anchor points as the upper quartile of the sample data, the mean of the upper and lower quartiles, and the lower quartile. The calibration anchor points of the research variables are shown in Table 3.

Secondly, we constructed a truth table, and 7 antecedent conditions constituted 128 antecedent condition combinations. Since the combinations are only theoretically all possible solutions, we further determine which antecedent combinations are subsets of the results by evaluating the consistency of the combinations and the number of cases. According to Ragin [2], we set the original consistency score to 0.8 and the case frequency threshold to 1. PRI consistency threshold is set as 0.70 [19]. The combination consistency score above or equal to the critical value is indeed defined as fuzzy subset and coded as 1, while the combination below the critical value does not constitute fuzzy subset and coded as 0.

5.3. Antecedent Condition Necessity Test. A necessary condition is a condition that must exist to cause the result to occur. If the necessary condition does not exist in the

configuration, the corresponding result will not happen, and other conditions cannot make up for the influence of the nonexistence of the necessary condition. However, the existence of necessary conditions does not guarantee the inevitable occurrence of the result. It still needs to be combined with other factors to produce a corresponding result. Before fuzzy qualitative comparative analysis, necessity analysis should be conducted on each antecedent variable. If the necessity is greater than 0.9, it is the core condition, indicating strong explanatory power for the result variable and should be taken into consideration in subsequent analysis. The necessity analysis of each antecedent condition is shown in Table 4. The necessity of each antecedent variable studied in this paper is less than 0.9, indicating that a single antecedent variable cannot explain the formation mechanism of each high-outcome variable. Therefore, fuzzy qualitative comparative analysis is needed to further explore its formation mechanism.

6. Configuration Result and Analysis

6.1. Configuration Result. Simplify the truth table and get the configuration of the outcome variable. For the study of high school students' continuance intention, no logical remainder is used, and the complex solution of the outcome variable is directly obtained. On this basis, the logical remainder is introduced to simplify the truth table, and the logical remainder is "IQ*CQ*SE*LE~PP" and "IQ*CQ*SE*LE*TI*PP" to obtain a simple solution. Then the logical remainders "~PP*TI*LE*SE*CQ*IQ" and "PP*TI*LE*SE*CQ*IQ" are added based on theory and practical knowledge to obtain intermediate solutions. For the study of nonsenior students' continuance intention, the logical remainder is not used, and the complex solution of the result variable is directly obtained. On this basis, the logic remainder is introduced to simplify the truth table, and the logic remainder is "~TI*~LE*~SE*~SQ*~CQ*~TP" to obtain a simple solution. Then the logical remainders "PP*~LE*SE~CQ*~IQ" and "PP*~LE*~SE*~SQ*~CQ*~IQ" is added based on theory and practical knowledge to obtain intermediate solutions. Through the comparison of the nested relationship between the intermediate solution and the reduced solution, the core condition of each solution is identified: the condition that appears in the intermediate solution and the reduced solution at the same time is the core condition of the solution, and the condition that only appears in the intermediate solution is the edge condition.

In this study, Fs-QCA3.0 software is used to process and analyze the data according to the above steps. After passing the necessity test, the consistency threshold is set as 0.8, PRI consistency threshold is set as 0.75, and case threshold is set as 1. Among them, there are 4 configurations with high continuance intention, and the consistency of each configuration is 0.902, 0.920, 0.908 and 0.900 respectively. The overall consistency reaches 0.901, and the overall coverage reaches 0.457 shown in Table 5.

This study follows the configuration representation method in Fiss et al. [20] and subsequent studies. ● and ● indicate that the condition exists while ⊗ and ⊗ indicate that

TABLE 2: Descriptive statistical analysis results of research variables.

Statistical indicator	Condition variable							Result variable
	Student level		Platform level			School level	Parent level	
	SE	LE	SQ	CQ	IQ	TI	PP	
Mean	3.101	3.491	3.552	3.277	2.891	3.602	3.854	3.012
Standard deviation	0.930	0.914	0.770	0.866	0.931	0.991	1.019	0.973
Minimum	1	1	1	1	1	1	1	1
Maximum	5	5	5	5	5	5	5	5

TABLE 3: Calibration anchor points for each variable.

Research variable	Anchor point				
	Complete membership	Intersection	Complete nonmembership		
Condition variable	Student level	SE	3.67	3	2.67
		LE	4	3.67	3
		SQ	4	3.5	3
	Platform level	CQ	4	3.33	3
		IQ	3.33	3	2.33
		Teacher level	TI	4.33	3.67
Parent level	PP	5	4	3	
Outcome variable	CI	3.67	3	2.33	

TABLE 4: Necessity test of students' continuous learning intention.

Condition variable	High continuance intention	Non-high continuance intention	
Student level	SE	0.839	0.413
	~SE	0.344	0.771
	LE	0.678	0.383
	~LE	0.415	0.710
Platform level	SQ	0.692	0.431
	~SQ	0.416	0.677
	CQ	0.658	0.314
	~CQ	0.445	0.789
	IQ	0.743	0.432
	~IQ	0.438	0.749
Teacher level	TI	0.470	0.511
	~TI	0.598	0.557
Parent level	PP	0.532	0.562
	~PP	0.593	0.563

TABLE 5: Configuration analysis of continuance intention.

Condition variable	High and medium continuance intention				Non-high continuance intention				
	S1a	S1b	S2	S3	H1a	H1b	H1c	H1d	H2
SE	●	●	●	•	⊗	⊗	⊗	⊗	⊗
LE		•	●	●	⊗	⊗	⊗	⊗	
CQ	●	●				⊗	⊗	⊗	●
SQ	●	●	●	●				⊗	⊗
IQ			●	●	⊗	⊗	⊗	⊗	⊗
TI	⊗	⊗	•	●	⊗	⊗	•	⊗	•
PP	⊗		⊗	●	⊗	⊗	•		●
Consistency	0.902	0.920	0.908	0.900	0.927	0.959	0.938	0.936	0.932
Coverage scale	0.269	0.268	0.228	0.184	0.256	0.228	0.223	0.122	0.247
Unique coverage	0.037	0.029	0.018	0.133	0.033	0.008	0.129	0.055	0.021
Overall consistency		0.901					0.924		
Overall coverage		0.457					0.504		

Note. ● and • indicate that condition exists, ⊗ and ⊙ indicate that condition does not exist; ● and ⊗ indicate core condition, • and ⊙ indicate edge condition.

the condition does not exist. ● And ⊗ indicate the core condition w • and ⊗ indicate the edge condition. And “blank” indicates whether the condition exists or not in the configuration (there is no direct causal relationship with the result). The coverage in the table indicates the proportion of all samples that can be explained by this configuration. It should be noted that some samples can also be explained by other configurations. Net coverage indicates the proportion of the number of samples explained by a single configuration to the total number of samples. Therefore, net coverage is usually far less than the coverage, but it can more intuitively reflect the importance of a single configuration. As the research object of this study is individual, in order to facilitate analysis and discussion, Fs-QCA3.0 software is used to analyze the configurations leading to high and low continuance intention respectively. Different configurations represent different environmental ecology that achieves the same result (high or low continuance intention).

Qualitative comparison and analysis of fuzzy sets will get three types of solutions: complex solution (without logical residual term), reduced solution (including logical residual term, but without evaluating its rationality), and intermediate solution (only including the logical residual term consistent with theoretical and practical knowledge into the solution). An important advantage of intermediate solutions is that they do not allow the elimination of necessary conditions. In general, intermediate solutions are superior to the other two solutions. The core condition and edge condition of grouping states are distinguished according to the reduced solution and the intermediate solution. If an antecedent condition occurs in both the reduced solution and the intermediate solution, it is the core condition, which has an important influence on the results. If this condition only appears in the intermediate solution, it will be recorded as the edge condition, which is the condition of auxiliary contribution [1]. The middle solution is obtained through counterfactual analysis, that is, assuming that the presence of each condition variable (present) is likely to promote the continuance intention of middle school students, fuzzy set analysis shows that there are four configurations (paths) to produce the continuance intention of middle school students (as shown in Table 5). The consistency indexes of the four configurations are 0.902, 0.920, 0.908 and 0.900 respectively, indicating that the four configurations are sufficient conditions for the continuance intention of high school students. The overall consistency index is 0.901, which further indicates that the four configurations covering most cases are also sufficient conditions for the continuance intention of high school students. The overall coverage of the model is 0.497, indicating that the four configurations explain about 50% of the high persistence. At the same time, assuming that each condition variable (absent) may result in the high continuance intention, fuzzy set analysis shows that there are 5 configurations (paths) that produce high school students' non-high continuance intention, which covers the vast majority of cases, not only constitute the noncontinuous intention of sufficient condition, and explain about 50% of the causes of the high continuance intention.

6.2. High Persistence Path Analysis. In view of various core conditions involved in each group, in order to better compare the differences of different configurations, this paper summarizes the following four configurations (paths) that middle school students' continuance intention, shown in Table 5: Service quality and content quality of platforms and self-learning efficacy of middle school students are dominant; Service quality and content quality of platforms and self-learning efficacy of middle school students are dominant while learning engagement is auxiliary; Interaction between students and teachers and platforms is dominant while the service quality is auxiliary; Parents' participation, platform interaction and platform service quality are dominant while teachers' support is auxiliary.

- (1) Service quality and content quality of platforms and self-learning efficacy of middle school students are dominant. S1a shows that middle school students with strong learning self-efficacy will continue to use online learning platforms as long as the content quality and service quality of online learning platform are high, no matter whether the platform has good interaction or not, whether parents participate in it or not and whether teachers support it or not. Specifically, when middle school students with high learning self-efficacy find the content and quality of online learning platform are good, they will continue to use it. In fact, if middle school students want to continue to use online learning platform, they will also be affected by the factors such as parental participation, teacher support and self-learning investment. When these factors are available, the continuance intention will be constantly strengthened, thus driving continuance intention behavior. This path can also be used to explain that middle school students with strong self-learning efficiency pay more attention to the content and services of platforms when they use online learning platforms, which is also the same reason that we usually see that students with strong ability knows how to study. These students have their own evaluation criteria when choosing online learning platforms. They can decide their own learning problems without asking parents or teachers. But this type of middle school students, in real life is rare. This paper verifies the positive effects of the platform content quality and service quality on middle school students' continuance intention, and also shows that the platform content quality, service quality and learning self-efficacy have synergistic effects on middle school students' continuance intention. The typical case of this configuration is Beijing No. 4 Online School. Since it was founded in 2001, the online learning platform with the purpose of “let more children get better education,” has constantly strengthened the platform content and at the same time set up more than 100 branch offices all over the country, which

can quickly provide online and offline integrated services for local online learning students.

It should be noted that this configuration also shows that when the content quality and service quality of online learning platforms promote the continuance intention of middle school students, the interaction of the platform has nothing to do with the high continuance intention of middle students. Specifically, when the content quality and service quality of platforms can meet the learning needs of middle school students, those with learning self-efficacy will choose the online learning platform for continuous learning. When they have puzzles, technical problems or other problems related to learning and life in other aspects, users of online learning platforms can solve problems in time through online and offline services. To some extent, this service replaces parents' participation and teachers' support. On the contrary, if the online learning platform can not provide timely and high-quality services, teacher support and parent participation may be more important.

- (2) Service quality and content quality of platforms and self-learning efficacy of middle school students are dominant while learning engagement is auxiliary. S1b and S1a are basically the same. The two paths only differ in the learning input elements of middle school students. Learning input belongs to the edge core condition element in this path, which plays an auxiliary role. This is because, in a broad way, the two paths can be regarded as the same path, because the element of learning engagement only appears in the intermediate solution and reduced solution of the two paths. Therefore, in this paper, S1A and S1b are used to represent the two paths, and there is not too much explanation here. The author collectively refers to S1A and S1b as S1 path below. Through the above comprehensive analysis of configuration, S1 path is the type that service quality and content quality of platforms and middle school students' self-learning efficacy are dominant.
- (3) Interaction between students and teachers and platforms is dominant while the service quality is auxiliary. S2 shows that the middle school students' continuance intention of online learning platforms not only requires strong learning self-efficacy, but also requires a lot of learning engagement. At the same time, middle school students prefer to interact with online teachers on the platform to obtain the learning support from online teachers. However, when middle school students study online, The length of time teachers spend online is limited. Specifically, online teachers leave the platform after online teaching, but the support students need to get exists for a long time, which leads to the contradiction that students and teachers cannot be online at the same time. Therefore, the service of the online learning platform is particularly important. This

service can resolve the contradiction that teachers and students can not communicate online at the same time, which is the reason why the service quality of platforms plays a major role in the S2 path. On the other hand, S2 path also shows that no matter what the content quality of online learning platforms is, whether parents participate or not, and whether school teachers give offline support, it will not affect the use of the online learning platforms by middle school students. This is because the participation of parents is mainly in the period of after-school education and students' independent learning. Parents only provide necessary material guarantee and supervision for students, while the offline support of school teachers is replaced by the online interaction with teachers in S2 configuration. And middle school students in this path devote more time to online learning. Therefore, they have more opportunities to communicate with online teachers, so as to solve some puzzles in learning.

In addition, students do not care about content quality of online platforms a lot, because the interaction of online learning platforms is strong, which allows students to more focus on the communication and exchange with online teachers, thus solving the learning problems in class. At the same time, if the problems are not solved in class, students can always turn to the service department provided by the platform for help at any time. Therefore, parental involvement and content quality of the platform have no impact on the continuance intention of their online learning platform. This paper verifies the positive effects of platform interaction and platform service quality on students' continuance intention of online learning platforms, and also shows that there is synergistic effect of platform interaction, platform service quality and online learning investment on students' continuance intention. The typical case of this configuration is Intelligent Practice System Online School. This online learning platform, with live teaching method is given priority to, emphasizes more on the digestion of knowledge in class, so more attention is paid to the interaction. This will allow students to ask questions at any time, and get on-site solution. At the same time, the platform also provides a large number of platform customer service, which can answer and solve students' difficulties in time, providing a powerful aid to online learning.

- (4) Parents' participation, platform interaction and platform service quality are dominant while teachers' support is auxiliary. The S3 path shows that even when middle school students are more engaged in learning, their continuance intention is also affected by both parental involvement and teacher support, which is particularly important in this path. To be specific, although such students have more engagement in online learning, their learning self-efficacy is not prominent, so they need more

participation of parents in online learning, and parents play a role of companionship, supervision and encouragement in the whole process. These middle school students have correct learning attitude and average ability, and they need more interaction and offline communication with teachers in online learning to complete their learning tasks. They are also more dependent on the services provided by the platform and always want help in the first place when they encounter problems.

It is worth noting that the S3 path also shows that the quality of platform content has nothing to do with the middle school students' continuance intention of online learning platforms. As long as online interaction and parental supervision are well created, and teachers can support and help offline, middle school students' continuance intention of online learning platforms will be affected. To be specific, if online learning can be interactive in a timely manner, teachers can provide strong support offline, and service departments of platforms can be supplemented in time, these factors can synergistically affect the middle school students' continuance intention of online learning platform. Therefore, the content quality of online learning platform is not so important. On the other hand, if the platform is not interactive enough, parents cannot participate in it and teachers do not support it, no matter how high the content quality of platforms is, it will not motivate middle school students to continue to use the online learning platform. The typical case of this configuration is New Oriental Online School, which has launched a dual-teacher class—there are two classroom situations in one course—Teachers of New Oriental Headquarters use online learning platform as the main teacher; students of the same grade and subject are required to study in the same classroom, where auxiliary teachers are equipped to maintain classroom discipline. If students have any questions in the learning process, first of all, the auxiliary teacher can make records and sort them out. After sorting them out, the teacher can use the network to transfer them to the lecturer, who can then answer the students' questions. Auxiliary teachers in dual-teacher classes play both the role of platform service and parental participation.

By comparing the three configuration paths (S1a and S1b have been mentioned in the above analysis: S1a and S1b can be regarded as one path S1), according to the coverage index, the coverage of S1 and S2 reaches about 77%, which explains 77% of the outcome variable and covers about 230 cases. On the whole, a majority of middle school students have the willingness of high continuance intention through S1 and S2 paths. This fully shows that online learning platforms should not only have good interaction, high-quality platform content and high-quality services, but also adopt the integration of online and offline development and school teachers' support, so as to have a deep and powerful influence on the middle school students' continuance intention. By comparing the three configurations, it is also found that S3 path is different from S1 and S2. S3 path requires more roles to participate at the same time, especially teachers

and parents, with relatively high requirements. For most families, the time for parents to accompany their children to study is also "relatively" limited. Especially at the middle school stage, children's learning time is long and the number of subjects is large, which makes it difficult for parents to meet their children's requirements. Whether teachers can support students' online learning depends on the specific situation. Most online learning is carried out after class. Whether teachers have enough practical support for students after class needs more discussion. The low coverage and interpretation rate of S3 paths is also the reason.

7. Conclusion

The research analyzes the configuration of middle school students' continuance intention from the student level, parent level, teacher level and platform level. Based on the configuration analysis model, by comparing the configuration analysis data and the configuration path of middle school students' willingness of continuance intention, the user retention mechanism of online learning platform under the collaborative influence of multi-level elements is finally identified and summarized.

The main conclusions are as follows:

- (1) Through data analysis, this paper finds that a single element at each level does not constitute a necessary condition for the middle school students' continuance intention.

The data analysis structure shows that the necessary condition analysis results of each antecedent variable studied in this paper do not exceed 0.9, indicating that a single antecedent variable cannot explain the formation mechanism of high outcome variables. The necessary condition is the one that must exist to cause the result. If the necessary condition does not exist in the configuration, the corresponding result will not occur, and other conditions cannot make up for the impact of the absence of necessary conditions. However, even if the existence of the necessary conditions does not guarantee the inevitable occurrence of the results, it still needs to be combined with other factors to produce the corresponding results. Therefore, this paper takes four levels and multiple elements as antecedent variables for configuration analysis.

- (2) This paper adopts the configuration perspective and Fs-QCA method to analyze the configuration of 7 factors from 4 levels of students, parents, teachers and platforms respectively, and obtains 3 configurations.
 - ① Service quality and content quality of platforms and self-learning efficacy of middle school students are dominant
 - ② Service quality and content quality of platforms and self-learning efficacy of middle school students are dominant while learning engagement is auxiliary

- ③ Parents' participation, platform interaction and platform service quality are dominant while teachers' support is auxiliary
- (3) Based on the configuration analysis model, three kinds of student user retention mechanisms of online learning platforms are finally identified and summarized by comparing the configuration analysis data table in this paper.
- ① Middle school student user retention mechanism based on online learning platforms dominated by platform quality.
This user retention mechanism is suitable for middle school students with strong self-learning efficiency and independent learning ability, so the online platform only needs to consider the content quality and service quality of the platform.
- ② Middle school student user retention mechanism based on online learning platforms dominated by platform interaction.
The user retention mechanism is suitable for middle school students who have strong self-learning efficiency and are willing to devote more time and energy to online learning. Therefore, the online learning platform only needs to consider the interactivity of the platform and take the service quality into account.
- ③ Middle school student user retention mechanism based on online learning platforms dominated by "Parent-teacher" dual drive, platform interaction and service quality.

The user retention mechanism is suitable for middle school students with weak self-learning efficiency but correct learning attitude and willing to devote themselves to learning. These middle school students attach great importance to the platform's interactivity, service quality and parents' participation, and are also concerned about whether school teachers support them.

Data Availability

Data sharing is not applicable to this article as no new data were created or analyzed in this study.

Conflicts of Interest

The authors declare that they have no conflicts of interest.

References

- [1] Y. Du and L. Jia, "QCA: a new approach to management research," *Management World*, vol. 6, pp. 155–167, 2017.
- [2] C. C. Ragin, "Qualitative comparative analysis using fuzzy sets (Fs QCA)," *Configurational Comparative Methods: Qualitative Comparative Analysis (QCA) and Related Techniques*, vol. 51, pp. 87–121, 2009.
- [3] D. R. Garrison and J. B. Arbaugh, "Researching the community of inquiry framework: review, issues, and future directions," *The Internet and Higher Education*, vol. 10, no. 3, pp. 157–172, 2007.
- [4] J. L. Epstein, *School, Family, and Community Partnerships: Preparing Educators and Improving Schools*[M], Routledge, New York, 2018.
- [5] X. Li and X. Xiao, "Institutional Escape or Innovation Drive? Institutional constraints and foreign direct investment by private enterprises," *Management World*, vol. 10, pp. 99–112, 2017.
- [6] X. Zhao and H. Li, "National differences in entrepreneurial activities: the interaction between culture and national economic development level," *Management World*, vol. 8, pp. 78–90, 2012.
- [7] X. Zheng, X. Zhou, and L. Zhang, "Social norms and entrepreneurship: an analysis based on entrepreneurship data from 62 countries," *Economic Research Journal*, vol. 52, no. 11, pp. 59–73, 2017.
- [8] A. N. Kiss, W. M. Danis, and S. T. Cavusgil, "International entrepreneurship research in emerging economies: a critical review and research agenda," *Journal of Business Venturing*, vol. 27, no. 2, pp. 266–290, 2012.
- [9] Y. J. Wong, K. A. Pituch, and A. B. Rochlen, "Men's restrictive emotionality: an investigation of associations with other emotion-related constructs, anxiety, and underlying dimensions," *Psychology of Men & Masculinity*, vol. 7, no. 2, pp. 113–126, 2006.
- [10] L. Guo, Y. Wang, L. Fan, and Y. Li, "Research on cultivation strategies of self-efficacy of Network learners in online education," *China Education Informatization*, vol. 5, pp. 18–21, 2016.
- [11] Y. Bai, "Research on the behavioral characteristics of highly effective Teachers," *Educational Research and Experiment*, vol. 4, pp. 33–39, 2000.
- [12] N. Wiener, "Contributions aux problèmes de L'intégration sensorio motrice et de La cybernétique: some maxims for biologists and psychologists," *Dialectica*, vol. 4, no. 3, pp. 186–191, 1950.
- [13] C. H. Cho and J. D. Leckenby, "Internet-related programming technology and advertising," in *Proceedings of the Conference-American Academy of Advertising*, pp. 69–79, St. Louis, MO, USA, January 1997.
- [14] N. Zhang, Q. Yuan, and Q. Zhu, "The impact of social network platform management on user perceived information quality: an empirical study from Research Gate," *Journal of information science*, vol. 39, no. 8, pp. 829–844, 2020.
- [15] G. Yang, "Research on the influencing factors of MOOC users' continuous use behavior," *Open Education Research*, vol. 1, pp. 100–111, 2016.
- [16] A. Marx and A. Dusa, "Crisp-set qualitative comparative analysis (csQCA), contradictions and consistency benchmarks for model specification," *Methodological Innovations Online*, vol. 6, no. 2, pp. 103–148, 2011.
- [17] B. Rihoux and C. C. Ragin, *Configurational Comparative Methods: Qualitative Comparative Analysis (QCA) and Related techniques*, Sage Publications, Los Angeles, London, 2008.
- [18] P. C. Fiss, D. Sharapov, and L. Cronqvist, "Opposites attract? Opportunities and challenges for integrating large-N QCA and econometric analysis," *Political Research Quarterly*, vol. 66, no. 1, pp. 191–198, 2013.
- [19] Y. Du, Q. Liu, and J. Cheng, "What kind of business environment ecology produces high entrepreneurial activity in cities?" *Management World*, vol. 36, no. 9, pp. 141–155, 2020.
- [20] P. C. Fiss, A. Marx, and B. Rihoux, "Comment," *Sociological Methodology*, vol. 44, no. 1, pp. 95–100, 2014.